# Thu. May 30, 2019

[J] Oral | U (Union )：Union

9:00 AM - 10:30 AM JST | 12:00 AM - 1:30 AM UTC | IC 2F

## [U-06] Japan's contribution to IUGG celebrating 100th anniversary

convener:Setsuya Nakada(National Research Institute for Earth Science and Disaster Resilience), Kenji Satake(Earthquake Research Institute, University of Tokyo), Kumiko Goto-Azuma(National Institute of Polar Research), Chairperson:Kumiko Goto-Azuma(National Institute of Polar Research), Setsuya Nakada(NIED)

9:00 AM - 9:20 AM JST | 12:00 AM - 12:20 AM UTC

[U06-01] **Centennial of the International Cooperation in Earth and Space Sciences**

★Invited Papers

*Alik Ismail-Zadeh[1,2,3] (1.Karlsruhe Institute of Technology, 2.International Union of Geodesy and Geophysics, 3.International Science Council)

---

9:20 AM - 9:40 AM JST | 12:20 AM - 12:40 AM UTC

[U06-02] IUGG and Japan: the past, the present, and the way to go from now

★Invited Papers

*Masaru Kono[1] (1.Tokyo Institute of Technology)

---

9:40 AM - 9:55 AM JST | 12:40 AM - 12:55 AM UTC

[U06-03] **Contributions from the Science Council of Japan to international cooperation in the field of Earth and planetary science**

*Hisashi Nakamura[1] (1.Research Center for Advanced Science and Technology, University of Tokyo)

---

9:55 AM - 10:15 AM JST | 12:55 AM - 1:15 AM UTC

[U06-04] History and Japanese contribution to the International Association of Cryospheric Sciences IACS

★Invited Papers

*Ralf Greve[1] (1.Institute of Low Temperature Science, Hokkaido University)

---

10:15 AM - 10:30 AM JST | 1:15 AM - 1:30 AM UTC

[U06-05] **Japan's Contributions to IAG**

*Yoichi Fukuda[1] (1.Department of Geophysics, Graduate School of Science, Kyoto University)

[J] Oral | U (Union )：Union

10:45 AM - 12:15 PM JST | 1:45 AM - 3:15 AM UTC | IC 2F

## [U-06] Japan's contribution to IUGG celebrating 100th anniversary

convener:Setsuya Nakada(National Research Institute for Earth Science and Disaster Resilience), Kenji Satake(Earthquake Research Institute, University of Tokyo), Kumiko Goto-Azuma(National Institute of Polar Research), Chairperson:Kumiko Goto-Azuma(National Institute of Polar Research), Kenji Satake(Earthquake Research Institute, the University of Tokyo)

10:45 AM - 11:00 AM JST | 1:45 AM - 2:00 AM UTC

[U06-06] IAGA activities in the era of too many international conferences

*Toshihiko Iyemori[1] (1.Kyoto University)

---

11:00 AM - 11:15 AM JST | 2:00 AM - 2:15 AM UTC

[U06-07] The role of IAHS in education, research, social issues concerning water and future perspective

*Maki Tsujimura[1] (1.Faculty of Life and Environmental Sciences, University of Tsukuba)

---

11:15 AM - 11:30 AM JST | 2:15 AM - 2:30 AM UTC

[U06-08] Centenary of the atmospheric sciences: Its progress and future issues

*Teruyuki Nakajima[1] (1.Japan Aerospace Exploration Agency)

---

11:30 AM - 11:45 AM JST | 2:30 AM - 2:45 AM UTC

[U06-09] Contributuins of Japan to IAPSO

*Yukio Masumoto[1] (1.Graduate School of Science, The University of Tokyo)

---

11:45 AM - 12:00 PM JST | 2:45 AM - 3:00 AM UTC

[U06-10] IASPEI- activities, history and Japan’s contribution

*Kenji Satake[1], Thorne Lay[2], Johannes Schweitzer[3] (1.Earthquake Research Institute, University of Tokyo, 2.IASPEI President , 3.IASPEI Secretary General)

---

12:00 PM - 12:15 PM JST | 3:00 AM - 3:15 AM UTC

[U06-11] Recent history of IAVCEI in Japan and young researchers’ response to IUGG and IAVCEI

*Setsuya Nakada[1] (1.National Research Institute for Earth Science and Disaster Resilience)

[J] Oral | U (Union )：Union

1:45 PM - 3:15 PM JST | 4:45 AM - 6:15 AM UTC | 101 1F

## [U-08] Opinions and recommendations from meeting participants to the future of the Japan Geoscience Union

convener:Yozo Hamano(KOBE Ocean-Bottom Exploration Center, Kobe University), Eiichi Tajika(Department of Earth and Planetary Science, Graduate School of Science, The University of Tokyo), Koji Wada(Planetary Exploration Research Center, Chiba Institute of Technology), Ikuro Sumita(Geosciences and Civil Engineering, Institute of Science and Engineering, Kanazawa University), Chairperson:Koji Wada(Planetary Exploration Research Center, Chiba Institute of Technology), Ikuro Sumita

1:51 PM - 2:03 PM JST | 4:51 AM - 5:03 AM UTC

[U08-01] Request and proposal from the Committee on Earth and Planetary Sciences of the Science Council of Japan to JpGU

*Ryoichi Fujii[1] (1.Research Organization of Information and Systems)

2:03 PM - 2:15 PM JST | 5:03 AM - 5:15 AM UTC

[U08-02] Geography in JpGU: current status and future perspectives

*Takashi Oguchi[1], Ikuho Yamada[2], Yuichi S. Hayakawa[3], Daichi Kohmoto[4], Hitoshi Saito[5] (1.Center for Spatial Information Science, The University of Tokyo, 2.Faculty of Science and Engineering, Chuo University, 3.Graduate School of Env.Science, Hokkaido University , 4.Nara University of Education, 5.College of Economics, Kanto Gakuin University)

2:15 PM - 2:27 PM JST | 5:15 AM - 5:27 AM UTC

[U08-03] Biogeoscineces will connect everthing together

*Takeshi Kakegawa[1] (1.Graduate School of Science, Tohoku University)

2:27 PM - 2:39 PM JST | 5:27 AM - 5:39 AM UTC

[U08-04] Coverage of JpGU

*Yukihiro Takahashi[1] (1.Department of Cosmosciences, Graduate School of Science, Hokkaido University)

2:39 PM - 2:51 PM JST | 5:39 AM - 5:51 AM UTC

[U08-05] Is he a bit overkill for English?

*Yoshi-Yuki Hayashi[1] (1.Department of Planetology/CPS, Graduate School of Science, Kobe University)

2:51 PM - 3:03 PM JST | 5:51 AM - 6:03 AM UTC

[U08-06] Globalization of Japan Geoscience Union

*Hirokuni Oda[1] (1.Institute of Geology and Geoinformation, Geological Survey of Japan, AIST)

3:03 PM - 3:15 PM JST | 6:03 AM - 6:15 AM UTC

[U08-07] A proposal for JpGU based on the questionaires to SSJ members

*Koshun Yamaoka[1] (1.Earthquake and Volcano Research Center, Graduate School of Environmental Studies, Nagoya University)

[J] Oral | U (Union )：Union

3:30 PM - 5:00 PM JST | 6:30 AM - 8:00 AM UTC | 101 1F

## [U-08] Opinions and recommendations from meeting participants to the future of the Japan Geoscience Union

convener:Yozo Hamano(KOBE Ocean-Bottom Exploration Center, Kobe University), Eiichi Tajika(Department of Earth and Planetary Science, Graduate School of Science, The University of Tokyo), Koji Wada(Planetary Exploration Research Center, Chiba Institute of Technology), Ikuro Sumita(Geosciences and Civil Engineering, Institute of Science and Engineering, Kanazawa University), Chairperson:Koji Wada(Planetary Exploration Research Center, Chiba Institute of Technology), Ikuro Sumita

3:30 PM - 3:42 PM JST | 6:30 AM - 6:42 AM UTC

[U08-08] Opinions and recommendations to the Japan Geoscience Union from Society of Geomagnetism and Earth, Planetary and Space Sciences

Yoshiharu Omura[2], Shigeto Watanabe[3], *Yuto Katoh[1], Takuya Tsugawa[4], Yuichi Otsuka[5], SGEPSS steering committee (1.Graduate School of Science, Tohoku University, 2.Research Institute for Sustainable Humanosphere, Kyoto University, 3.Hokkaido Information University, 4.National Institute of Information and Communications Technology, 5.Institute for Space–Earth Environmental Research, Nagoya University)

3:42 PM - 3:54 PM JST | 6:42 AM - 6:54 AM UTC

[U08-09] Collaboration between Earth & Planetary Science and Information Science ~A trial of mutual benefit in the interdisciplinary field~

*Hirohide Demura[1] (1.The University of Aizu)

3:54 PM - 4:06 PM JST | 6:54 AM - 7:06 AM UTC

[U08-10] Comments from young planetary scientists

*Shunichi Kamata[1], Keiko Hamano[2], Go Murakami[3], Ryuki Hyodo[2], Yusuke Nakauchi[3] (1.Hokkaido University, 2.Tokyo Institute of Technology, 3.JAXA/ISAS)

4:06 PM - 4:18 PM JST | 7:06 AM - 7:18 AM UTC

[U08-11] Japan Geoscience Union should operate based on the perspective of individual academic society and fulfill accountability

*Naoji Koizumi[1] (1.School of Environmental Science,the University of Shiga Prefecture)

4:18 PM - 4:30 PM JST | 7:18 AM - 7:30 AM UTC

[U08-12] A proposal from a representative of General Geoscience Sector on a possible direction to future JpGU: actions for domestic activities could be weighted

*Hidenori Kumagai[1] (1.Japan Agency for Marine-Earth Science and Technology)

4:30 PM - 4:42 PM JST | 7:30 AM - 7:42 AM UTC

[U08-13] Fifteen years of Japan Geoscience Letters and its future

*Shogo Tachibana[1], Eiichi Tajika[2] (1.UTokyo Organization for Planetary and Space Science, University of Tokyo , 2.Dept. Earth and Planetary Science, University of Tokyo)

[J] Oral | P (Space and Planetary Sciences)：P-PS Planetary Sciences

9:00 AM - 10:30 AM JST | 12:00 AM - 1:30 AM UTC | 103 1F

## [P-PS08] Lunar science and exploration

convener:Hiroshi Nagaoka(Japan Aerospace Exploration Agency), Masahiro KAYAMA(Department of Earth and Planetary Material Sciences, Faculty of Science, Tohoku University), Masaki N Nishino(Japan Aerospace Exploration Agency, Institute of Space and Astronautical Science), Tomokatsu Morota(Graduate School of Environmental Studies, Nagoya University), Chairperson:Satoshi Tanaka, Masaki Nishino(名古屋大学宇宙地球環境研究所)

9:00 AM - 9:15 AM JST | 12:00 AM - 12:15 AM UTC

[PPS08-01] Observing simulations of impact-induced moonquakes combined with the lunar impact flash observation data for future lunar seismic explorations

*Keisuke Onodera[1,2], Taichi Kawamura[3], Satoshi Tanaka[2], Yoshiaki Ishihara[4], Takuto Maeda[5], Masahisa Yanagisawa[6], Yuki Uchida[6], Shinsuke Abe[7], Ryuhei Yamada[8], Takaya Okamoto[2] (1.SOKENDAI (The Graduate University for Advanced Studies), 2.Institute of Space and Astronautical Science / Japan Aerospace Exploration Agency, 3.Insitut de Physique du Globe de Paris, 4.National Institute for Environmental Studies, 5.Hirosaki University, 6.The University of Electro-Communications, 7.Nihon University, 8.University of Aizu)

9:15 AM - 9:30 AM JST | 12:15 AM - 12:30 AM UTC

[PPS08-02] New Results from Restored Apollo Magnetic Field Records

*Peter J Chi[1] (1.University of California Los Angeles)

9:30 AM - 9:45 AM JST | 12:30 AM - 12:45 AM UTC

[PPS08-03] Analysis of the High Latitude Region of the Moon with Spectral Profiler Data: Possible Presence of Water Ice

Haramitsu Kyoda[3], *Satoshi Tanaka[1], Makiko Ohtake[1], Hiroshi Nagaoka[2], Yusuke Nakauchi[2], Keisuke Onodera[4] (1.Department of Solid Planetary Sciences Institute of Space and Astronautical Science, 2.Japan Aerospace Exploration Agency, 3.Department of Complexity Science and Enginnering, the University of Tokyo, 4.Department of Space and Astronautical Science, SOKENDAI)

9:45 AM - 10:00 AM JST | 12:45 AM - 1:00 AM UTC

[PPS08-04] **Detection of Dark Regions on the Lunar Surface with Shadow Masked Multiband Imager Data**

*Riho Ito[1], Hiroka Inoue[2], Makiko Ohtake[2], Hisashi Otake[2], Ryosuke Nakamura[1] (1.National Institute of Advanced Industrial Science and Technology, 2.Japan Aerospace Exploration Agency)

10:00 AM - 10:15 AM JST | 1:00 AM - 1:15 AM UTC

[PPS08-05] Estimation of Moho depth under lunar basins by using only the GRAIL gravity data

*Gaku Nishiyama[1], Noriyuki Namiki[2] (1.Department of Earth and Planetary Science, The University of Tokyo, 2.RISE Project, National Astronomical Observatory of Japan)

10:15 AM - 10:30 AM JST | 1:15 AM - 1:30 AM UTC

[PPS08-06] Ejecta Thickness Distribution of Lunar Schrödinger Basin

*Luyuan Xu[1], Minggang Xie[1] (1.State Key Laboratory of Lunar and Planetary Sciences, Macau University of Science and Technology)

[J] Oral | P (Space and Planetary Sciences)：P-PS Planetary Sciences

10:45 AM - 12:15 PM JST | 1:45 AM - 3:15 AM UTC | 103 1F

## [P-PS08] Lunar science and exploration

convener:Hiroshi Nagaoka(Japan Aerospace Exploration Agency), Masahiro KAYAMA(Department of Earth and Planetary Material Sciences, Faculty of Science, Tohoku University), Masaki N Nishino(Japan Aerospace Exploration Agency, Institute of Space and Astronautical Science), Tomokatsu Morota(Graduate School of Environmental Studies, Nagoya University), Chairperson:Ko Hashizume, Hiroshi Nagaoka

10:45 AM - 11:00 AM JST | 1:45 AM - 2:00 AM UTC

[PPS08-07] Possible evolution paths of the lunar orbit based on tidal response in the global ocean model of the early Earth

*Mai Motoyama[1], Hideo Tsunakawa[1], Futoshi Takahashi[2] (1.Department of Earth and Planetary Sciences, School of Science, Tokyo Institute of Technology, 2.Department of Earth and Planetary Sciences, Faculty of Science, Kyushu University)

11:00 AM - 11:15 AM JST | 2:00 AM - 2:15 AM UTC

[PPS08-08] Geochemical and Petrological Investigations of Lunar Feldspathic Crust by Lunar Sample Studies and Remote Sensing Data

*Hiroshi Nagaoka[1], Yuzuru Karouji[1], Makiko Ohtake[1] (1.Japan Aerospace Exploration Agency)

11:15 AM - 11:30 AM JST | 2:15 AM - 2:30 AM UTC

[PPS08-09] Development of frosting system for lunar simulant and the detectability of ice growing on the simulant by NIR measurement

*Aoi Ogishima[1], Kazuto Saiki[1] (1.Department of Earth and Space Science, Graduate School of Science, Osaka University)

11:30 AM - 11:45 AM JST | 2:30 AM - 2:45 AM UTC

[PPS08-10] Volatile studies on Moon - A review toward future exploration programs

*Ko Hashizume[1] (1.Faculty of Science, Ibaraki University)

11:45 AM - 12:00 PM JST | 2:45 AM - 3:00 AM UTC

[PPS08-11] Scientific approach for the promotion of lunar polar exploration mission

*Masahiro KAYAMA[1], Ko Hashizume[2], Hiroshi Nagaoka[3], Kazuto Saiki[4], Chihiro Yamanaka[4], Makoto Hareyama[5], Makiko Ohtake[3] (1.Tohoku University, 2.Ibaraki University, 3.Japan Aerospace Exploration Agency, 4.Osaka University, 5.St. Marianna University School of Medicine)

12:00 PM - 12:15 PM JST | 3:00 AM - 3:15 AM UTC

[PPS08-12] Feasibility study of detection of the lunar subsurface ice with UHF-band GPR based on FDTD electromagnetic simulation

*Atsushi Kumamoto[1], Hideaki Miyamoto[2], Toshifumi Nishibori[3], Takafumi Niihara[2], Fuminori Tsuchiya[1], Ken Ishiyama[3] (1.Tohoku University, 2.University of Tokyo, 3.JAXA)

[J] Oral | P (Space and Planetary Sciences)：P-PS Planetary Sciences

1:45 PM - 3:15 PM JST | 4:45 AM - 6:15 AM UTC | 103 1F

## [P-PS08] Lunar science and exploration

convener:Hiroshi Nagaoka(Japan Aerospace Exploration Agency), Masahiro KAYAMA(Department of Earth and Planetary Material Sciences, Faculty of Science, Tohoku University), Masaki N Nishino(Japan Aerospace Exploration Agency, Institute of Space and Astronautical Science), Tomokatsu Morota(Graduate School of Environmental Studies, Nagoya University), Chairperson:Masahiro Kayama(東北大学), Yusuke Nakauchi(JAXA/ISAS)

1:45 PM - 2:00 PM JST | 4:45 AM - 5:00 AM UTC

[PPS08-13] **Geology of the SLIM landing site on the Moon**

★Invited Papers

*Makiko Ohtake[1], Kazuto Saiki[2], Yusuke Nakauchi[1], Hiroaki Shiraishi[1], Yoshiaki Ishihara[3], Hiroyuki Sato[1], Chikatoshi Honda[4] (1.Institute of Space and Astronautical Science, Japan Aerospace Exploration Agency, 2.Osaka University, 3.National Institute for Environmental Studies, 4.University of Aizu)

2:00 PM - 2:15 PM JST | 5:00 AM - 5:15 AM UTC

[PPS08-14] Observing scenario for the Multi-Band Camera onboard SLIM

*Kazuto Saiki[1], Yuya Igarashi[1], Yusuke Nakauchi[2], Chikatoshi Honda[3], Makiko Ohtake[2], Hiroaki Shiraishi[2], Hiroyuki Satoh[2], Yoshiaki Ishihara[4], Takao Maeda[5], Chihiro Yamanaka[1] (1.Osaka Univ., 2.JAXA, 3.Univ. Aizu, 4.National Institute for Environmental Studies, 5.Chuo Univ.)

2:15 PM - 2:30 PM JST | 5:15 AM - 5:30 AM UTC

[PPS08-15] **Current status of a Japanese lunar polar exploration mission**

*Takeshi Hoshino[1], Makiko Ohtake[1], Yuzuru Karouji[1], Hiroaki Shiraishi[1] (1.Japan Aerospace Exploration Agency)

2:30 PM - 2:45 PM JST | 5:30 AM - 5:45 AM UTC

[PPS08-16] HERACLES mission: Returning to the Moon by an ESA-JAXA-CSA Joint Study

*Yuzuru Karouji[1], Hiroshi Nagaoka[1], Yoshiaki Ishihara[2], Masahiro KAYAMA[3], Satoru Yamamoto[4], Nobuyuki Hasebe[5], Ko Hashizume[6], Yoshiko Ogawa[7], Toru Yada[1], Junichi Haruyama[1], Masanao Abe[1], Makiko Ohtake[1], HERACLES Science Working Group, HERACLES International Science Definition Team (1.Japan Aerospace Exploration Agency, 2.National Institute for Environmental Studies, 3.Faculty of Science, Tohoku University, 4.J-spacesystems, 5.Advanced Research Institute for Science and Engineering, Waseda University, 6.Faculty of Science, Ibaraki University, 7.The University of Aizu)

2:45 PM - 3:00 PM JST | 5:45 AM - 6:00 AM UTC

[PPS08-17] **Lunar Science for Landed Missions – High-Priority Landing Sites Visualized with NASA's Moon Trek**

*Brian Hamilton Day[1], Emily Law[2] (1.NASA Solar System Exploration Research Virtual Institute, NASA Ames Research Center, 2.NASA Jet Propulsion Laboratory, California Institute of Technology)

3:00 PM - 3:15 PM JST | 6:00 AM - 6:15 AM UTC

[PPS08-18] NASA SSERVI: Merging Science and Human Exploration

*Brad Eugene Bailey[1], Kristina Gibbs[1], Gregory Schmidt[1] (1.NASA)

[J] Poster | P (Space and Planetary Sciences)：P-PS Planetary Sciences

3:30 PM - 5:00 PM JST | 6:30 AM - 8:00 AM UTC | Poster Hall International Exhibition Hall8, Makuhari Messe_1

## [P-PS08] Lunar science and exploration

convener:Hiroshi Nagaoka(Japan Aerospace Exploration Agency), Masahiro KAYAMA(Department of Earth and Planetary Material Sciences, Faculty of Science, Tohoku University), Masaki N Nishino(Japan Aerospace Exploration Agency, Institute of Space and Astronautical Science), Tomokatsu Morota(Graduate School of Environmental Studies, Nagoya University)

[PPS08-P01] Estimation of lava tube cave height below the vertical hole from the surface topography of the Moon

*Tsutomu Honda[1] (1.Vulcano-speleological Society)

[PPS08-P02] Detecting mare basalts intruded into the crust on the early Moon

*Ayame Ikeda[1], Tomokatsu Morota[2], Hiroshi Nagaoka[3] (1.Department of Science, Nagoya University, 2.Graduate School of Enviromental Studies, Nagoya University, 3.Japan Aerospace Exploration Agency)

[PPS08-P03] Distribution of major minerals around the Crisium and Moscoviense basins of the Moon revealed by SELENE Multiband Imager

Yuji Agatsuma[1], *Naru Hirata[1], Satoru Yamamoto[2], Makiko Ohtake[3] (1.Dep. of Computer Science and Engineering, Univ. of Aizu, 2.J-spacesystems, 3.Department of Planetary Science, Institute of Space and Astronautical Science, Japan Aerospace Exploration Agency)

[PPS08-P04] Searching for lunar swirls with deep learning

*Yurika Iwabuchi[1], Yoshiko Ogawa[1] (1.The University of Aizu)

[PPS08-P05] Lunar surface feature reconstruction by deep learning using synthetic data

*Koichi Tsuru[1], Toru Kouyama[1], Ryosuke Nakamura[1] (1.National Institute of Advanced Industrial Science and Technology)

[PPS08-P06] Evaluation of the influence of alkali elements on hydrogen solubility of clinopyroxene for estimating water content of lunar mantle

*Miki Muranushi[1], Akio Suzuki[1], Masahiro KAYAMA[1], Tsuyoshi MIYAMOTO[2] (1.Graduate school of Science, Tohoku university , 2.Center for Northeast Asian Studies, Tohoku university)

[PPS08-P07] Preliminary examination of mineral structure effect on relative permittivity

*Makito Kobayashi[1], Takafumi Niihara[2], Hideaki Miyamoto[2,1] (1.Department of Earth and Planetary Science, School of Science, University of Tokyo, 2.Department of Systems Innovation, School of Engineering, University of Tokyo)

[PPS08-P08] Lunar surface magnetic field intensity in the solar wind inferred from electron reflectometry

*Tomoki Kawaguchi[1], Yuki Harada[1], Yoshifumi Saito[2], Shoichiro Yokota[3], Masaki N Nishino[4], Hideyuki Usui[5], Yohei Miyake[6], Hideo Tsunakawa[7], Daiba Kato[8] (1.Dept. Geophysics, Kyoto Univ., 2.Solar System Science Division, Institute of Space and Astronautical Science, Japan Aerospace Exploration Agency, 3.Graduate School of Science, Osaka University, 4.Institute for Space-Earth Environmental Research, Nagoya University, 5.Graduate school of system informatics Kobe University, 6.Education Center on Computational Science and Engineering, Kobe University, 7.Deparment of Earth and Planetary Sciences, Tokyo Institute of Technology, 8.The University of Tokyo)

[PPS08-P09] Objective and Current Development Status of Multi-Band Camera on SLIM

*Yusuke Nakauchi[1], Kazuto Saiki[2], Makiko Ohtake[1], Hiroaki Shiraishi[1], Chikatoshi Honda[3], Hiroyuki Sato[1], Yoshiaki Ishihara[4], Takao Maeda[5], Masatsugu Otsuki[1], Sin-ichiro Sakai[1], Shujiro Sawai[1], SLIM Project Team (1.Japan Aerospace Exploration Agency, 2.Osaka University, 3.Aizu University, 4.National Institute for Environmental Studie, 5.Chuo University)

[PPS08-P10] Monte Carlo simulation of neutron production and transport in the Moon: Effect of lunar subsurface water

*Hiroki Kusano[1], Yuzuru Karouji[1], Hiroshi Nagaoka[1], Naoyuki Yamashita[2], Makoto Hareyama[3] (1.Japan Aerospace Exploration Agency, 2.Planetary Science Institute, 3.St. Marianna University School of Medicine)

[PPS08-P11] **Exploration of ice deposits on the Moon using continuous seismic source system**

*Yuichiro Nagata[1], Takeshi Tsuji[1,2], Hideaki Miyamoto[9], Taichi Kawamura[3], Akito Araya[4], Yoshiaki Ishihara[5], Kazunori Ogawa[6], Taizo Kobayashi[7], Yuzuru Karouji[8], Satoshi Tanaka[10] (1.Department of Earth Resources Engineering,

Kyushu University, 2.International Institute for Carbon-Neutral Energy Research (WPI-I2CNER), Kyushu University, 3.Institut de Physique du Globe de Paris, 4.Earthquake Research Institute, University of Tokyo, 5.National Institute for Environmental Studies, 6.Kobe University, 7.Ritsumeikan University, 8.Japan Aerospace Exploration Agency, 9.University of Tokyo, 10.Department of Solid Planetary Sciences Institute of Space and Astronautical Science)

[PPS08-P12] Orbit determination of the Chang'E-5 Test 1 and a new gravity field model

*shanhong liu[1], Jianguo Yan[1] (1.Wuhan University)

[J] Poster | P (Space and Planetary Sciences)：P-PS Planetary Sciences

5:15 PM - 6:30 PM JST | 8:15 AM - 9:30 AM UTC | Poster Hall International Exhibition Hall8, Makuhari Messe_1

## [P-PS08] Lunar science and exploration

convener:Hiroshi Nagaoka(Japan Aerospace Exploration Agency), Masahiro KAYAMA(Department of Earth and Planetary Material Sciences, Faculty of Science, Tohoku University), Masaki N Nishino(Japan Aerospace Exploration Agency, Institute of Space and Astronautical Science), Tomokatsu Morota(Graduate School of Environmental Studies, Nagoya University)

[PPS08-P01] Estimation of lava tube cave height below the vertical hole from the surface topography of the Moon

*Tsutomu Honda[1] (1.Vulcano-speleological Society)

[PPS08-P02] Detecting mare basalts intruded into the crust on the early Moon

*Ayame Ikeda[1], Tomokatsu Morota[2], Hiroshi Nagaoka[3] (1.Department of Science, Nagoya University, 2.Graduate School of Enviromental Studies, Nagoya University, 3.Japan Aerospace Exploration Agency)

[PPS08-P03] Distribution of major minerals around the Crisium and Moscoviense basins of the Moon revealed by SELENE Multiband Imager

Yuji Agatsuma[1], *Naru Hirata[1], Satoru Yamamoto[2], Makiko Ohtake[3] (1.Dep. of Computer Science and Engineering, Univ. of Aizu, 2.J-spacesystems, 3.Department of Planetary Science, Institute of Space and Astronautical Science, Japan Aerospace Exploration Agency)

[PPS08-P04] Searching for lunar swirls with deep learning

*Yurika Iwabuchi[1], Yoshiko Ogawa[1] (1.The University of Aizu)

[PPS08-P05] Lunar surface feature reconstruction by deep learning using synthetic data

*Koichi Tsuru[1], Toru Kouyama[1], Ryosuke Nakamura[1] (1.National Institute of Advanced Industrial Science and Technology)

[PPS08-P06] Evaluation of the influence of alkali elements on hydrogen solubility of clinopyroxene for estimating water content of lunar mantle

*Miki Muranushi[1], Akio Suzuki[1], Masahiro KAYAMA[1], Tsuyoshi MIYAMOTO[2] (1.Graduate school of Science, Tohoku university , 2.Center for Northeast Asian Studies, Tohoku university)

[PPS08-P07] Preliminary examination of mineral structure effect on relative permittivity

*Makito Kobayashi[1], Takafumi Niihara[2], Hideaki Miyamoto[2,1] (1.Department of Earth and Planetary Science, School of Science, University of Tokyo, 2.Department of Systems Innovation, School of Engineering, University of Tokyo)

[PPS08-P08] Lunar surface magnetic field intensity in the solar wind inferred from electron reflectometry

*Tomoki Kawaguchi[1], Yuki Harada[1], Yoshifumi Saito[2], Shoichiro Yokota[3], Masaki N Nishino[4], Hideyuki Usui[5], Yohei Miyake[6], Hideo Tsunakawa[7], Daiba Kato[8] (1.Dept. Geophysics, Kyoto Univ., 2.Solar System Science Division, Institute of Space and Astronautical Science, Japan Aerospace Exploration Agency, 3.Graduate School of Science, Osaka University, 4.Institute for Space-Earth Environmental Research, Nagoya University, 5.Graduate school of system informatics Kobe University, 6.Education Center on Computational Science and Engineering, Kobe University, 7.Deparment of Earth and Planetary Sciences, Tokyo Institute of Technology, 8.The University of Tokyo)

[PPS08-P09] Objective and Current Development Status of Multi-Band Camera on SLIM

*Yusuke Nakauchi[1], Kazuto Saiki[2], Makiko Ohtake[1], Hiroaki Shiraishi[1], Chikatoshi Honda[3], Hiroyuki Sato[1], Yoshiaki Ishihara[4], Takao Maeda[5], Masatsugu Otsuki[1], Sin-ichiro Sakai[1], Shujiro Sawai[1], SLIM Project Team (1.Japan Aerospace Exploration Agency, 2.Osaka University, 3.Aizu University, 4.National Institute for Environmental Studie, 5.Chuo University)

[PPS08-P10] Monte Carlo simulation of neutron production and transport in the Moon: Effect of lunar subsurface water

*Hiroki Kusano[1], Yuzuru Karouji[1], Hiroshi Nagaoka[1], Naoyuki Yamashita[2], Makoto Hareyama[3] (1.Japan Aerospace Exploration Agency, 2.Planetary Science Institute, 3.St. Marianna University School of Medicine)

[PPS08-P11] **Exploration of ice deposits on the Moon using continuous seismic source system**

*Yuichiro Nagata[1], Takeshi Tsuji[1,2], Hideaki Miyamoto[9], Taichi Kawamura[3], Akito Araya[4], Yoshiaki Ishihara[5], Kazunori Ogawa[6], Taizo Kobayashi[7], Yuzuru Karouji[8], Satoshi Tanaka[10] (1.Department of Earth Resources Engineering,

Kyushu University, 2.International Institute for Carbon-Neutral Energy Research (WPI-I2CNER), Kyushu University, 3.Institut de Physique du Globe de Paris, 4.Earthquake Research Institute, University of Tokyo, 5.National Institute for Environmental Studies, 6.Kobe University, 7.Ritsumeikan University, 8.Japan Aerospace Exploration Agency, 9.University of Tokyo, 10.Department of Solid Planetary Sciences Institute of Space and Astronautical Science)

[PPS08-P12] Orbit determination of the Chang'E-5 Test 1 and a new gravity field model

*shanhong liu[1], Jianguo Yan[1] (1.Wuhan University)

[E] Oral | P (Space and Planetary Sciences )：P-EM Solar-Terrestrial Sciences, Space Electromagnetism & Space Environment

9:00 AM - 10:30 AM JST | 12:00 AM - 1:30 AM UTC | A03 TOKYO BAY MAKUHARI HALL

## [P-EM09] Vertical coupling in the atmosphere and Ionosphere

convener:Huixin Liu(Earth and Planetary Science Division, Kyushu University SERC, Kyushu University), Loren Chang(Institute of Space Science, National Central University), Yuichi Otsuka(Institute for Space-Earth Environmental Research, Nagoya University), Chairperson:Huixin Liu(Kyushu University, Japan), Stan Solomon(National Center for Atmospheric Research, US)

9:00 AM - 9:20 AM JST | 12:00 AM - 12:20 AM UTC

[PEM09-11] Assimilation products of thermospheric and ionospheric measurements by the NASA Ionopsheric Connection Explorer

★Invited Papers

*Thomas J Immel[1], Chihoko Cullens[1], Yen-Jung Wu[1], Gary Bust[2], Jeffrey Forbes[3], Scott L England[4] (1.University of California, Berkeley, 2.Johns Hopkins University, 3.University of Colorado, 4.Virginia Tech)

9:20 AM - 9:35 AM JST | 12:20 AM - 12:35 AM UTC

[PEM09-12] petitSat - A 6U CubeSat to examine the link between MSTIDS and ionospheric plasma density enhancements

*Jeffrey Klenzing[1], Ryan L Davidson[2], Gregory D Earle[3], Alexa J Halford[4], Sarah L Jones[1], Carlos Martinis[5], Nikolaos Paschalidis[1], Robert F Pfaff[1], Jonathon M Smith[1,6] (1.NASA Goddard Space Flight Center, Greenbelt, MD, USA, 2.Utah State University, Logan, UT, USA, 3.Virginia Tech, Blacksburg, VA, USA, 4.The Aerospace Corporation, Chantilly, VA, USA, 5.Boston University, Boston, MA, USA, 6.Catholic Universtiy of America, Washington, DC, USA)

9:35 AM - 9:55 AM JST | 12:35 AM - 12:55 AM UTC

[PEM09-13] A three-dimensional ionospheric electrodynamics model

★Invited Papers

*Astrid I Maute[1], Arthur D Richmond[1] (1.High Altitude Observatory, National Center for Atmospheric Research, Boulder CO, USA.)

9:55 AM - 10:10 AM JST | 12:55 AM - 1:10 AM UTC

[PEM09-14] **Spatial Fluctuation of TEC Index: A new index of ionospheric irregularities**

*Guanyi Ma[1], Takashi Maruyama[2] (1.National Astronomical Observatories, Chinese Academy of Sciences, 2.National Institute of Information and Communications Technology)

10:10 AM - 10:25 AM JST | 1:10 AM - 1:25 AM UTC

[PEM09-15] Coupling of lower thermosphere planetary wave energy into the ionosphere

*Patrick J Espy[1,2], Nora Stray[1,2,3], Robert Hibbins[1,2] (1.Norwegian University of Science and Technology, Trondheim, Norway, 2.Birkeland Centre for Space Science, Bergen, Norway, 3.Teknova AS, Tordenskjolds Gate 9, 4612 Kristiansand, Norway)

[E] Oral | P (Space and Planetary Sciences)：P-EM Solar-Terrestrial Sciences, Space Electromagnetism & Space Environment

10:45 AM - 12:15 PM JST | 1:45 AM - 3:15 AM UTC | A03 TOKYO BAY MAKUHARI HALL

## [P-EM09] Vertical coupling in the atmosphere and Ionosphere

convener:Huixin Liu(Earth and Planetary Science Division, Kyushu University SERC, Kyushu University), Loren Chang(Institute of Space Science, National Central University), Yuichi Otsuka(Institute for Space-Earth Environmental Research, Nagoya University), Chairperson:Jann-Yenq Liu(National Central University, Taiwan), Loren Chang(National Central University, Taiwan)

10:45 AM - 11:00 AM JST | 1:45 AM - 2:00 AM UTC

[PEM09-16] Modulation of Lightning Occurrence by the Solar Wind

*Omar Angelo Nava[1], Daniel Emmons[1], Robert Loper[1] (1.Air Force Institute of Technology)

11:00 AM - 11:15 AM JST | 2:00 AM - 2:15 AM UTC

[PEM09-17] Long Term Mesopause Temperature Variations resolved by SD-WACCM, MSISE-00,TIMED SABER and Local Observations in Irkutsk (52.29o, 104.29o), Russia

*Yi Chung Chiu[1], Loren Chang[1], Yi Duann[1], ALEXEI DMITRIEV[1], Irina Medvedeva[2], Konstantin Ratovsky[2], Jia Yue[3] (1.Institute of Space Science, National Central University, 2.Russian Academy of Sciences, Russian Federation, 3.Hampton University, USA)

11:15 AM - 11:30 AM JST | 2:15 AM - 2:30 AM UTC

[PEM09-18] ISS-IMAP observation of the mesospheric disturbances generated by tropical cyclones

*Akinori Saito[1], Takeshi Sakanoi[2], Septi Perwitasari[4], Yuta Hozumi[3], Ryota Okada[1], Ryo Murakami[1] (1.Department of Geophysics, Graduate School of Science, Kyoto University, 2.Planetary Plasma and Atmospheric Research Center, Graduate School of Science, Tohoku University, 3.University of Electro-Communications, 4.Space and Upper Atmospheric Sciences Group, National Institute of Polar Research)

11:30 AM - 11:45 AM JST | 2:30 AM - 2:45 AM UTC

[PEM09-19] A fast acoustic wave detected in GNSS total electron content after the foreshock of the 2011 Tohoku Earthquake

*Yoshihiro Kakinami[1], Hiroaki Saito[2], Tetsuo Yamamoto[3], Chia-Hung Chen[4], Masa-yuki Yamamoto[2], Kensuke Nakajima[5], JANN-YENQ Liu[6] (1.Hokkaido Information University, 2.Kochi University of Technology, 3.Hokkaido University, 4.National Cheng Kung University, 5.Kyushu University, 6.National Central University)

11:45 AM - 12:00 PM JST | 2:45 AM - 3:00 AM UTC

[PEM09-20] **Study of quiet-time high-latitude thermospheric winds using a Fabry-Perot interferometer at Tromsoe: Averages and exceptional events**

*Heqiucen XU[1], Kazuo Shiokawa[1], Shin-ichiro Oyama[1] (1.Institute for Space-Earth Environmental Research, Nagoya University)

12:00 PM - 12:15 PM JST | 3:00 AM - 3:15 AM UTC

[PEM09-21] **The longitudinal differences of lunar tidal characteristics between East Asian and American sectors during stratospheric sudden warming events: 2009-2018.**

*Jing Liu[1], Donghe Zhang[1] (1.Peking University)

[E] Oral | P (Space and Planetary Sciences )：P-EM Solar-Terrestrial Sciences, Space Electromagnetism & Space Environment

9:00 AM - 10:30 AM JST | 12:00 AM - 1:30 AM UTC | A04 TOKYO BAY MAKUHARI HALL

## [P-EM11] Dynamics of Magnetosphere and Ionosphere

convener:Aoi Nakamizo(Applied Electromagnetic Research Institute, National Institute of Information and Communications Technology), Mitsunori Ozaki(Faculty of Electrical and Computer Engineering, Institute of Science and Engineering, Kanazawa University), Akiko Fujimoto(Kyushu Institute of Technology), Tomoaki Hori(Institute for Space-Earth Environmental Research, Nagoya University), Chairperson:Shin'ya Nakano(情報・システム研究機構 統計数理研究所), Motoharu Nowada(Shandong University)

9:00 AM - 9:15 AM JST | 12:00 AM - 12:15 AM UTC

[PEM11-07] **Nightside Distorted Transpolar Arcs and Their Possible Formation Process Model**

*Nowada Motoharu[1], Jun Yang[1], Benoit Hubert[2], Qiu-Gang Zong[3], Quan-Qi Shi[1], Yong-Fu Wang[3], Xu-Zhi Zhou[3], Zhao Hua-Yu[3] (1.Shandong University at Weihai, 2.Université de Liège, 3.Peking University)

9:15 AM - 9:30 AM JST | 12:15 AM - 12:30 AM UTC

[PEM11-08] Ionospheric Conductivity Dependence of the Subauroral Polarization Streams Observed by the SuperDARN HF Radars

Yuting Zhang[1], *Nozomu Nishitani[1], Tomoaki Hori[1], Simon G. Shepherd[2], William A. Bristow[3] (1.Institute for Space-Earth Environmental Research, Nagoya University, 2.Thayer School of Engineering, Dartmouth College, 3.University of Alaska Fairbanks)

9:30 AM - 9:45 AM JST | 12:30 AM - 12:45 AM UTC

[PEM11-09] Ionospheric convection modeling based on convolution with a localized vector-valued basis function

*Shin ya Nakano[1], Tomoaki Hori[2], Kanako Seki[3], Nozomu Nishitani[2] (1.The Institute of Statistical Mathematics, 2.Institute for Space-Earth Environmental Research, Nagoya University, 3.Graduate School of Science, University of Tokyo)

9:45 AM - 10:00 AM JST | 12:45 AM - 1:00 AM UTC

[PEM11-10] **Occurrence Statistics and Driving Mechanisms of Ionospheric ULF Waves Observed by SuperDARN Radars**

★Invited Papers

*Xueling Shi[1], Joseph B. H. Baker[1], John Michael Ruohoniemi[1], Dong Lin[1], Michael Hartinger[1,2] (1.Virginia Tech, 2.Space Science Institute)

10:00 AM - 10:15 AM JST | 1:00 AM - 1:15 AM UTC

[PEM11-11] Magnetic Field Oscillations Observed by Swarm Satellites in the Nightside Upper Ionosphere During Low-latitude Pi2 Pulsations

*Khan-Hyuk Kim[1], Jae-Hee Park[1] (1.School of Space Research, Kyung Hee Univ.)

10:15 AM - 10:30 AM JST | 1:15 AM - 1:30 AM UTC

[PEM11-12] Magnetospheric Multiscale observations of ULF waves and correlated low-energy ion monoenergetic acceleration

*Bin Li[1], De-sheng Han[2], Ze-jun Hu[1], Jian-jun Liu[1], Lei Dai[3] (1.Polar Research Institute of China, 2.Tongji University, 3.National Space Science Center, Chinese Academy of Sciences)

[E] Oral | P (Space and Planetary Sciences )：P-EM Solar-Terrestrial Sciences, Space Electromagnetism & Space Environment

10:45 AM - 12:15 PM JST | 1:45 AM - 3:15 AM UTC | A04 TOKYO BAY MAKUHARI HALL

## [P-EM11] Dynamics of Magnetosphere and Ionosphere

convener:Aoi Nakamizo(Applied Electromagnetic Research Institute, National Institute of Information and Communications Technology), Mitsunori Ozaki(Faculty of Electrical and Computer Engineering, Institute of Science and Engineering, Kanazawa University), Akiko Fujimoto(Kyushu Institute of Technology), Tomoaki Hori(Institute for Space-Earth Environmental Research, Nagoya University), Chairperson:Kunuhiro Keika(東京大学大学院理学系研究科), Shin'ya Nakano(情報・システム研究機構 統計数理研究所), Motoharu Nowada(Shandong University)

10:45 AM - 11:00 AM JST | 1:45 AM - 2:00 AM UTC

[PEM11-13] Statistical study on warm plasma in the magnetotail based on two-component fits of distribution functions

*Kunihiro Keika[1], Ryuta Asami[1], Masahiro Hoshino[1] (1.Department of Earth and Planetary Science, Graduate School of Science, The University of Tokyo)

11:00 AM - 11:15 AM JST | 2:00 AM - 2:15 AM UTC

[PEM11-14] Analysis on anisotropy variations for pitch angle distributions of electrons with various parameters at dipolarization sites in the inner plasma sheet

*Kaiti Wang[1], Zhuo-Ren Lang[2], Ching-Huei Lin[3], Tohru Hada[4], Toshi Nishimura[5] (1.Tamkang Univ., 2.National Cheng Kung Univ., 3.Chien-Hsin Univ. of Sci. & Tech., 4.Kyushu Univ., 5.Boston Univ.)

11:15 AM - 11:30 AM JST | 2:15 AM - 2:30 AM UTC

[PEM11-15] Study of slow-mode shock formation in the symmetric magnetic reconnection based on hybrid simulations

*Nehpreet Kaur Walia[1], Kanako Seki[1], Takanobu Amano[1] (1. Department of Earth & Planetary Science, Graduate School of Science, University of Tokyo)

11:30 AM - 11:45 AM JST | 2:30 AM - 2:45 AM UTC

[PEM11-16] Reconstruction of the electron diffusion region of magnetotail reconnection seen by the Magnetospheric Multiscale spacecraft

*Hiroshi Hasegawa[1], Richard E. Denton[2], Rumi Nakamura[3], Kevin J. Genestreti[4], Takuma Nakamura[3], Kyoung Joo Hwang[5], Tai D. Phan[6], Roy B. Torbert[4], Jim L. Burch[5], Barbara L. Giles[7], Dan J. Gershman[7], Chris T. Russell[8], Bob J. Strangeway[8], Per Arne Lindqvist[9], Yuri V. Khotyaintsev[10], Robert E. Ergun[11], Naritoshi Kitamura[12], Yoshifumi Saito[1] (1.Institute of Space and Astronautical Science, Japan Aerospace Exploration Agency, 2.Dartmouth College, 3.Space Research Institute, Austrian Academy of Science, 4.University of New Hampshire, 5.Southwest Research Institute, 6.University of California Berkeley, 7.NASA Goddard Space Flight Center, 8.University of California Los Angeles, 9.Royal Institute of Technology, 10.Swedish Institute of Space Physics, 11.University of Colorado, 12.University of Tokyo)

11:45 AM - 12:00 PM JST | 2:45 AM - 3:00 AM UTC

[PEM11-17] **MMS observations of the dense high speed flow in the magnetotail**

*Mingyu Wu[1], Tielong Zhang[1] (1.Harbin Insitute of Technology, Shenzhen)

12:00 PM - 12:15 PM JST | 3:00 AM - 3:15 AM UTC

[PEM11-18] The spatio-temporal development of lightning-induced electron precipitation events

★Invited Papers

*Robert C Moore[1], Dooyoung Kim[1] (1.University of Florida)

[E] Oral | P (Space and Planetary Sciences )：P-EM Solar-Terrestrial Sciences, Space Electromagnetism & Space Environment

1:45 PM - 3:15 PM JST | 4:45 AM - 6:15 AM UTC | A04 TOKYO BAY MAKUHARI HALL

## [P-EM11] Dynamics of Magnetosphere and Ionosphere

convener:Aoi Nakamizo(Applied Electromagnetic Research Institute, National Institute of Information and Communications Technology), Mitsunori Ozaki(Faculty of Electrical and Computer Engineering, Institute of Science and Engineering, Kanazawa University), Akiko Fujimoto(Kyushu Institute of Technology), Tomoaki Hori(Institute for Space-Earth Environmental Research, Nagoya University), Chairperson:Naritoshi Kitamura(東京大学大学院理学系研究科), Yuka Sato(日本工業大学)

1:45 PM - 2:00 PM JST | 4:45 AM - 5:00 AM UTC

[PEM11-19] Energy flow, dynamo and field-aligned current during a substorm

*Yusuke Ebihara[1], Takashi Tanaka[2] (1.Research Institute for Sustainable Humanosphere, Kyoto University, 2.Kyushu University)

2:00 PM - 2:15 PM JST | 5:00 AM - 5:15 AM UTC

[PEM11-20] **Electron flux and field-aligned current associated with Pc5 auroral arc pulsations observed onboard THEMIS and DMSP satellites**

*Natsuo Sato[1], Akira S Yukimatu[1,2], Yoshimasa Tanaka[1,2], Tomoaki Hori[3], Akira Kadokura[1,2], Tohru Sakurai[4], Desheng Han[5], Yuzhang Ma[6], Qinghe Zhang[6] (1.National Institute of Polar Research, 2.SOKENDAI, 3.Nagoya University, 4.Tokai University, 5.Tongji University, 6.Shandong University)

2:15 PM - 2:30 PM JST | 5:15 AM - 5:30 AM UTC

[PEM11-21] Multiple spots of enhanced electron precipitation near the equatorward boundary of the cusp

*Satoshi Taguchi[1], Satoshi Kose[1], Kohei Takasu[1], Morio Tanaka[1], Keisuke Hosokawa[2], Yasunobu Ogawa[3] (1.Department of Geophysics, Graduate School of Science, Kyoto University, 2.Department of Communication Engineering and Informatics, University of Electro-Communications, 3.National Institute of Polar Research)

2:30 PM - 2:45 PM JST | 5:30 AM - 5:45 AM UTC

[PEM11-22] Statistical study of auroral/resonant-scattering 427.8-nm emission observed at subauroral latitudes over 14 years

*Kazuo Shiokawa[1], Yuichi Otsuka[1], Martin Connors[2] (1.Institute for Space-Earth Environmental Research, Nagoya University, 2.Athabasca University)

2:45 PM - 3:00 PM JST | 5:45 AM - 6:00 AM UTC

[PEM11-23] Antarctic large area network observation of auroral phenomena using unmanned system: Conjugate auroral event studies (2)

*Akira Kadokura[1], Hisao Yamagishi[1], Masaki Okada[1], Yasunobu Ogawa[1], Yoshimasa Tanaka[1], Ryuho Kataoka[1], Herbert Akihito Uchida[1], Yuichi Otsuka[2] (1.National Institute of Polar Research, 2.Nagoya University)

3:00 PM - 3:15 PM JST | 6:00 AM - 6:15 AM UTC

[PEM11-24] **Dawn-Dusk Asymmetry in Dayside and Nightside auroral Ovals: Surveys of auroral emissions based on the all-sky imagers in Arctic and Antarctic**

★Invited Papers

*Zejun Hu[1] (1.Polar Research Institute of China)

[E] Oral | P (Space and Planetary Sciences )：P-EM Solar-Terrestrial Sciences, Space Electromagnetism & Space Environment

3:30 PM - 5:00 PM JST | 6:30 AM - 8:00 AM UTC | A04 TOKYO BAY MAKUHARI HALL

## [P-EM11] Dynamics of Magnetosphere and Ionosphere

convener:Aoi Nakamizo(Applied Electromagnetic Research Institute, National Institute of Information and Communications Technology), Mitsunori Ozaki(Faculty of Electrical and Computer Engineering, Institute of Science and Engineering, Kanazawa University), Akiko Fujimoto(Kyushu Institute of Technology), Tomoaki Hori(Institute for Space-Earth Environmental Research, Nagoya University), Chairperson:Naritoshi Kitamura(東京大学大学院理学系研究科), Yuka Sato(日本工業大学), Masaki Nishino(名古屋大学宇宙地球環境研究所)

3:30 PM - 3:45 PM JST | 6:30 AM - 6:45 AM UTC

[PEM11-25] Enhancement of 10MeV protons associated with a change of magnetic field configuration at geosynchronous orbit

*Takahiro Obara[1] (1.Planetary Plasma and Atmospheric Research Center,Tohoku University)

3:45 PM - 4:00 PM JST | 6:45 AM - 7:00 AM UTC

[PEM11-26] Solar-cycle variations of >30 keV proton flux enhancements under the inner radiation belt

*ALLA SUVOROVA[1] (1.National Central University)

4:00 PM - 4:15 PM JST | 7:00 AM - 7:15 AM UTC

[PEM11-27] Auroral Imaging with Commercial DSLR Cameras near Athabasca, Canada

*Martin G Connors[1,2], Ian Schofield[1], Mike Noble[2], Alister Ling[2], Ryuho Kataoka[3], Ken Murata[4], Kazunori Yamamoto[4] (1.Athabasca University, 2.Edmonton Centre, Royal Astronomical Society of Canada, 3.National Institute for Polar Research, 4.National Institute for Communications Technology)

4:15 PM - 4:30 PM JST | 7:15 AM - 7:30 AM UTC

[PEM11-28] PARM: Investigation of precipitating high-energy electrons into the auroral ionosphere with sounding rockets

*Kazushi Asamura[1], Yoshizumi Miyoshi[2], Keisuke Hosokawa[3], Takefumi Mitani[1], Taku Namekawa[1,5], Takeshi Sakanoi[4], Naoshi Yagi[4], Mizuki Fukizawa[4], Genki Ishizawa[4], Satoshi Kasahara[5], Shin Sugo[5], Oya Kawashima[5], Reiko Nomura[6], Masahito Nose[2], Mariko Teramoto[2], Yasunobu Ogawa[7], Shinji Saito[2], Ryoichi Fujii[8] (1.ISAS / JAXA, 2.ISEE, Nagoya University, 3.The University of Electro-Communications, 4.Tohoku University, 5.The University of Tokyo, 6.NAOJ / NINS, 7.NiPR / ROIS, 8.ROIS)

4:30 PM - 4:45 PM JST | 7:30 AM - 7:45 AM UTC

[PEM11-30] Development of a miniaturized X-ray imager for GEOspace X-ray imager (GEO-X)

*Kumi Ishikawa[1], Yuichiro Ezoe[2], Masaki Numazawa[2], Daiki Ishi[2], Maiko Fujitani[2], Ryota Otsubo[2], Aoto Fukushima[2], Hikari Suzuki[2], Tatsuya Yuasa[2], Hiroshi Nakajima[3], Junko Hiraga[4], Yoshizumi Miyoshi[5], Satoshi Kasahara[6], Kazuhisa Mitsuda[1] (1.Japan Aerospace Exploration Agency/Institute of Space and Astronautical Science , 2.Tokyo Metropolitan University, 3.Kanto Gakuin University, 4.Kwansei Gakuin University, 5.Nagoya University, 6.The university of Tokyo)

[E] Oral | P (Space and Planetary Sciences)：P-EM Solar-Terrestrial Sciences, Space Electromagnetism & Space Environment

9:00 AM - 10:30 AM JST | 12:00 AM - 1:30 AM UTC | A01 TOKYO BAY MAKUHARI HALL

## [P-EM15] Study of coupling processes in solar-terrestrial system

convener:Mamoru Yamamoto(Research Institute for Sustainable Humanosphere, Kyoto University), Yasunobu Ogawa(National Institute of Polar Research), Satonori Nozawa(Institute for Space-Earth Environment Research), Akimasa Yoshikawa(Department of Earth and Planetary Sciences, Kyushu University), Chairperson:Mamoru Yamamoto

9:00 AM - 9:15 AM JST | 12:00 AM - 12:15 AM UTC

### [PEM15-01] Status of Equatorial MU Radar project in 2019

*Mamoru Yamamoto[1], Hiroyuki Hashiguchi[1], Tatsuhiro Yokoyama[1], Toshitaka Tsuda[1] (1.Research Institute for Sustainable Humanosphere, Kyoto University)

9:15 AM - 9:30 AM JST | 12:15 AM - 12:30 AM UTC

### [PEM15-02] Recent Progress and Current Status of EISCAT_3D in 2018-2019

*Hiroshi Miyaoka[1], Yasunobu Ogawa[1], Satonori Nozawa[2], Koji Nishimura[1], Shin-ichiro Oyama[2], Takuji Nakamura[1], Ryoichi Fujii[2], Craig James Heinselman[3] (1.National Institute of Polar Research, 2.Institute for Space-Earth Environmental Research, Nagoya University, 3.European Incoherent Scatter Scientific Association)

9:30 AM - 9:45 AM JST | 12:30 AM - 12:45 AM UTC

### [PEM15-03] Current status of the ground-based multi-point network observation of the upper atmosphere, ionosphere, and magnetosphere by the PWING Project and the Optical Mesosphere Thermosphere Imagers (OMTIs)

*Kazuo Shiokawa[1], Yuichi Otsuka[1], PWING Team (1.Institute for Space-Earth Environmental Research, Nagoya University)

9:45 AM - 10:00 AM JST | 12:45 AM - 1:00 AM UTC

### [PEM15-04] Development of MAGDAS project: Search for global electromagnetic coupling from polar to equatorial ionosphere

*Akimasa Yoshikawa[1], Taisei Kabasawa[2], Teiji Uozumi[3], Akiko Fujimoto[4], Shuji Abe[3] (1.Department of Earth and Planetary Sciences, Kyushu University, 2.Graduate school of Sciences, Kyushu Univerity, 3.International center for Space weather science and education, Kyushu University, 4.Kyushu Institute of Technology)

10:00 AM - 10:15 AM JST | 1:00 AM - 1:15 AM UTC

### [PEM15-05] IUGONET data analysis system for a study of coupling processes in the solar-terrestrial system

*Atsuki Shinbori[1], Yoshimasa Tanaka[2], Norio Umemura[1], Shuji Abe[3], Masahito Nose[1], Satoru UeNo[4] (1.Institute for Space-Earth Environment Research (ISEE), Nagoya University, 2.National institute of Polar Research, 3.International Center for Space Weather Science and Education Kyushu University, 4.Observatory, Kyoto University)

10:15 AM - 10:30 AM JST | 1:15 AM - 1:30 AM UTC

### [PEM15-06] Discussion on large-scale research project "Study of coupling processes in solar-terrestrial system" (1)

*Mamoru Yamamoto[1] (1.Research Institute for Sustainable Humanosphere, Kyoto University)

[E] Oral | P (Space and Planetary Sciences )：P-EM Solar-Terrestrial Sciences, Space Electromagnetism & Space Environment

10:45 AM - 12:15 PM JST | 1:45 AM - 3:15 AM UTC | A01 TOKYO BAY MAKUHARI HALL

## [P-EM15] Study of coupling processes in solar-terrestrial system

convener:Mamoru Yamamoto(Research Institute for Sustainable Humanosphere, Kyoto University), Yasunobu Ogawa(National Institute of Polar Research), Satonori Nozawa(Institute for Space-Earth Environment Research), Akimasa Yoshikawa(Department of Earth and Planetary Sciences, Kyushu University), Chairperson:Satonori Nozawa

10:45 AM - 11:15 AM JST | 1:45 AM - 2:15 AM UTC

[PEM15-07] Numerical Experiments on Stratosphere-Troposphere Two-Way Dynamical Coupling in the Tropics through Organizations of Moist Convective Systems

★Invited Papers

*Shigeo Yoden[1], Hai Bui[2], Takahiro Banno[1] (1.Division of Earth and Planetary Sciences, Graduate School of Science, Kyoto University, 2.Geophysical Institute, University of Bergen)

11:15 AM - 11:30 AM JST | 2:15 AM - 2:30 AM UTC

[PEM15-08] Future development of numerical simualtion of equatorial plasma bubbles

*Tatsuhiro Yokoyama[1] (1.Kyoto University)

11:30 AM - 11:45 AM JST | 2:30 AM - 2:45 AM UTC

[PEM15-09] Characteristics of CME- and CIR-driven ion upflows in the polar ionosphere

*Yasunobu Ogawa[1], Kanako Seki[2], Kunihiro Keika[2], Yusuke Ebihara[3] (1.National Institute of Polar Research, 2.School of Science, the University of Tokyo, 3.Research Institute for Sustainable Humanosphere, Kyoto University)

11:45 AM - 12:00 PM JST | 2:45 AM - 3:00 AM UTC

[PEM15-10] SuperDARN Hokkaido Pair of (HOP) radars and mid-latitude SuperDARN: today and future

*Nozomu Nishitani[1] (1.Institute for Space-Earth Environmental Research, Nagoya University)

12:00 PM - 12:15 PM JST | 3:00 AM - 3:15 AM UTC

[PEM15-11] Simultaneous observation of Ionospheric Incoherent Scatter and Field Aligned Irregularities using adaptive signal processing techniques by the PANSY radar at Antarctic Syowa Station (39.6°E, 69.0°S)

*Taishi Hashimoto[1], Akinori Saito[2], Koji Nishimura[3], Masaki Tsutsumi[3], Kaoru Sato[4], Toru Sato[1] (1.Graduate School of Informatics, Kyoto University, 2.Graduate School of Science, Kyoto University, 3.National Institute of Polar Research, 4.Graduate School of Science, The University of Tokyo)

[E] Oral | P (Space and Planetary Sciences )：P-EM Solar-Terrestrial Sciences, Space Electromagnetism & Space Environment

1:45 PM - 3:15 PM JST | 4:45 AM - 6:15 AM UTC | A01 TOKYO BAY MAKUHARI HALL

## [P-EM15] Study of coupling processes in solar-terrestrial system

convener:Mamoru Yamamoto(Research Institute for Sustainable Humanosphere, Kyoto University), Yasunobu Ogawa(National Institute of Polar Research), Satonori Nozawa(Institute for Space-Earth Environment Research), Akimasa Yoshikawa(Department of Earth and Planetary Sciences, Kyushu University), Chairperson:Yasunobu Ogawa

1:45 PM - 2:00 PM JST | 4:45 AM - 5:00 AM UTC

[PEM15-12] Mini/Micro Satellite Constelaltion for the study of LAI coupling

*Koichiro Oyama[1,2,3] (1.Institute of Plasma and Space Sciences,National Cheng Kung Univ., Taiwan, 2.International Ceneter for Space Weather Sudy and Education, Kyushu Univ.,, 3.CoLtd. Asia Space Environment Research Consortium, Japan)

2:00 PM - 2:15 PM JST | 5:00 AM - 5:15 AM UTC

[PEM15-13] Statistical study of daily and seasonal variation of the equatorial anomaly in Asia based on satellite-ground beacon experiment

*Yuki Sakamoto[1], Mamoru Yamamoto[1], Kornyanat Hozumi[2] (1.Research Institute for Sustainable Humanosphere, Kyoto University, 2.National Institute of Information and Communications Technology)

2:15 PM - 2:30 PM JST | 5:15 AM - 5:30 AM UTC

[PEM15-14] Latest installation of FM-CW radar in Peru

*Akiko Fujimoto[1], Akihiro Ikeda[2], Akimasa Yoshikawa[3] (1.Kyushu Institute of Technology, 2.National Institute of Technology,Kagoshima College, 3.Kyushu University)

2:30 PM - 2:45 PM JST | 5:30 AM - 5:45 AM UTC

[PEM15-15] **Understanding the OH Meinel Band Emissions on the Terrestrial Planets**

*Konstantinos S. Kalogerakis[1] (1.Center for Geospace Studies, SRI International, Menlo Park, California, U.S.A.)

2:45 PM - 3:00 PM JST | 5:45 AM - 6:00 AM UTC

[PEM15-16] Statistical study of Sporadic Sodium Layer (SSL) observed at Tromsø

*Satonori Nozawa[1], Takuo T. Tsuda[2], Norihito Saito[3], Toru Takahashi[4], Takuya Kawahara[5], Yasunobu Ogawa[4], Hitoshi Fujiwara[6], Satoshi Wada[3], Youhei Ogawa[1], Chris Hall[7], Asgeir Brekke[7] (1.Institute for Space-Earth Environment Research, 2.The University of Electro-Communications, 3.RIKEN Center for Advanced Photonics, 4.National Institute of Polar Research, 5.Faculty of Engineering, Shinshu University, 6.Faculty of Science and Technology, Seikei University, 7.UiT The Arctic University of Norway)

3:00 PM - 3:15 PM JST | 6:00 AM - 6:15 AM UTC

[PEM15-17] Discussion on large-scale research project "Study of coupling processes in solar-terrestrial system" (2)

*Mamoru Yamamoto[1] (1.Research Institute for Sustainable Humanosphere, Kyoto University)

[E] Poster | P (Space and Planetary Sciences )：P-EM Solar-Terrestrial Sciences, Space Electromagnetism & Space Environment

3:30 PM - 5:00 PM JST | 6:30 AM - 8:00 AM UTC | Poster Hall International Exhibition Hall8, Makuhari Messe_2

## [P-EM15] Study of coupling processes in solar-terrestrial system

convener:Mamoru Yamamoto(Research Institute for Sustainable Humanosphere, Kyoto University), Yasunobu Ogawa(National Institute of Polar Research), Satonori Nozawa(Institute for Space-Earth Environment Research), Akimasa Yoshikawa(Department of Earth and Planetary Sciences, Kyushu University)

### [PEM15-P01] Study on adaptive clutter rejection system using external receiving antennas for the MU radar

*Hiroyuki Hashiguchi[1], Issei Terada[1], Mamoru Yamamoto[1] (1.Research Institute for Sustainable Humanosphere, Kyoto University)

### [PEM15-P02] Detached cusp aurora for southward IMF

*Kohei Takasu[1], Satoshi Taguchi[1], Keisuke Hosokawa[2] (1.Department of Geophysics, Graduate School of Science, Kyoto University, 2.Department of Communication Engineering and Informatics, University of Electro-Communications)

### [PEM15-P03] Motion of the inverted-V structure during an isolated substorm

*Morio Tanaka[1], Satoshi Taguchi[1], Kohei Takasu[1], Tomokazu Oigawa[1], Keisuke Hosokawa[2] (1.Department of Geophysics, Graduate school of science, Kyoto University, 2.Department of Communication Engineering and Informatics, University of Electro-Communications)

### [PEM15-P04] Observation and modeling of Na layer response to energetic particle precipitation

*Takuo T. Tsuda[1], Kyogo Takizawa[1], Ryo Tozu[1], Takuya Kawahara[2], Yoshimasa Tanaka[3], Mitsumu K. Ejiri[3], Takanori Nishiyama[3], Takuji Nakamura[3] (1.The University of Electro-Communications, 2.Shinshu University, 3.National Institute of Polar Research)

### [PEM15-P05] Lidar data analysis of the sodium atoms in the thermosphere observed at Tromsoe, Norway

*Takuya Kawahara[1], Satonori Nozawa[2], Norihito Saito[3], Takuo T. Tsuda[4], Toru Takahashi[5], Testuya Kawabata[2], Miki Nishimura[1], Yoshitaka Kobayashi[1] (1.Faculty of Engineering, Shinshu University, 2.ISEE, Nagoya University, 3.RIKEN, Center for Advanced Photonics, 4.The University of Electro-Communications, 5.National Institute of Polar Research)

### [PEM15-P06] Spatial-temporal distribution of anomalous enhancement of ambipolar diffusion coefficient observed by meteor radars installed in the polar region

*Toru Takahashi[1], Masaki Tsutsumi[1,2], Yasunobu Ogawa[1,2,3], Satonori Nozawa[3], Chris Hall[4], Hiroshi Miyaoka[1,2] (1.National Institute of Polar Research, 2.SOKENDAI, 3.Institute for Space-Earth Environmental Research, 4.TGO, The Arctic University of Norway)

### [PEM15-P07] Progress of ICSWSE and MAGDAS project in recent years

*Shuji Abe[1], Akimasa Yoshikawa[2,1], Teiji Uozumi[1], Akiko Fujimoto[3] (1.International Center for Space Weather Science and Education, Japan, 2.Department of Earth and Planetary Sciences, Kyushu University, 3.Kyushu Institute of Technology)

### [PEM15-P08] Status of GNU Radio Beacon Receiver 2 (GRBR2) development

*Mamoru Yamamoto[1], Mayumi Matsunaga[2], Roland Tsunoda[3] (1.Research Institute for Sustainable Humanosphere, Kyoto University, 2.Tokyo University of Technology, 3.SRI International)

### [PEM15-P09] Statistical comparison between plasma bubble day-to-day variability and neutral atmosphere by using GPS scintillation and GAIA model

*Mamoru Yamamoto[1], Keigo Kono[1] (1.Research Institute for Sustainable Humanosphere, Kyoto University)

### [PEM15-P10] Redevelopment of the MU radar transceiver-module control system

*Mamoru Yamamoto[1], Koki Kurokawa[1], Hiroyuki Hashiguchi[1] (1.Research Institute for Sustainable Humanosphere, Kyoto University)

[E] Poster | P (Space and Planetary Sciences )：P-EM Solar-Terrestrial Sciences, Space Electromagnetism & Space Environment

5:15 PM - 6:30 PM JST | 8:15 AM - 9:30 AM UTC | Poster Hall International Exhibition Hall8, Makuhari Messe_2

## [P-EM15] Study of coupling processes in solar-terrestrial system

convener:Mamoru Yamamoto(Research Institute for Sustainable Humanosphere, Kyoto University), Yasunobu Ogawa(National Institute of Polar Research), Satonori Nozawa(Institute for Space-Earth Environment Research), Akimasa Yoshikawa(Department of Earth and Planetary Sciences, Kyushu University)

### [PEM15-P01] Study on adaptive clutter rejection system using external receiving antennas for the MU radar

*Hiroyuki Hashiguchi[1], Issei Terada[1], Mamoru Yamamoto[1] (1.Research Institute for Sustainable Humanosphere, Kyoto University)

### [PEM15-P02] Detached cusp aurora for southward IMF

*Kohei Takasu[1], Satoshi Taguchi[1], Keisuke Hosokawa[2] (1.Department of Geophysics, Graduate School of Science, Kyoto University, 2.Department of Communication Engineering and Informatics, University of Electro-Communications)

### [PEM15-P03] Motion of the inverted-V structure during an isolated substorm

*Morio Tanaka[1], Satoshi Taguchi[1], Kohei Takasu[1], Tomokazu Oigawa[1], Keisuke Hosokawa[2] (1.Department of Geophysics, Graduate school of science, Kyoto University, 2.Department of Communication Engineering and Informatics, University of Electro-Communications)

### [PEM15-P04] Observation and modeling of Na layer response to energetic particle precipitation

*Takuo T. Tsuda[1], Kyogo Takizawa[1], Ryo Tozu[1], Takuya Kawahara[2], Yoshimasa Tanaka[3], Mitsumu K. Ejiri[3], Takanori Nishiyama[3], Takuji Nakamura[3] (1.The University of Electro-Communications, 2.Shinshu University, 3.National Institute of Polar Research)

### [PEM15-P05] Lidar data analysis of the sodium atoms in the thermosphere observed at Tromsoe, Norway

*Takuya Kawahara[1], Satonori Nozawa[2], Norihito Saito[3], Takuo T. Tsuda[4], Toru Takahashi[5], Testuya Kawabata[2], Miki Nishimura[1], Yoshitaka Kobayashi[1] (1.Faculty of Engineering, Shinshu University, 2.ISEE, Nagoya University, 3.RIKEN, Center for Advanced Photonics, 4.The University of Electro-Communications, 5.National Institute of Polar Research)

### [PEM15-P06] Spatial-temporal distribution of anomalous enhancement of ambipolar diffusion coefficient observed by meteor radars installed in the polar region

*Toru Takahashi[1], Masaki Tsutsumi[1,2], Yasunobu Ogawa[1,2,3], Satonori Nozawa[3], Chris Hall[4], Hiroshi Miyaoka[1,2] (1.National Institute of Polar Research, 2.SOKENDAI, 3.Institute for Space-Earth Environmental Research, 4.TGO, The Arctic University of Norway)

### [PEM15-P07] Progress of ICSWSE and MAGDAS project in recent years

*Shuji Abe[1], Akimasa Yoshikawa[2,1], Teiji Uozumi[1], Akiko Fujimoto[3] (1.International Center for Space Weather Science and Education, Japan, 2.Department of Earth and Planetary Sciences, Kyushu University, 3.Kyushu Institute of Technology)

### [PEM15-P08] Status of GNU Radio Beacon Receiver 2 (GRBR2) development

*Mamoru Yamamoto[1], Mayumi Matsunaga[2], Roland Tsunoda[3] (1.Research Institute for Sustainable Humanosphere, Kyoto University, 2.Tokyo University of Technology, 3.SRI International)

### [PEM15-P09] Statistical comparison between plasma bubble day-to-day variability and neutral atmosphere by using GPS scintillation and GAIA model

*Mamoru Yamamoto[1], Keigo Kono[1] (1.Research Institute for Sustainable Humanosphere, Kyoto University)

### [PEM15-P10] Redevelopment of the MU radar transceiver-module control system

*Mamoru Yamamoto[1], Koki Kurokawa[1], Hiroyuki Hashiguchi[1] (1.Research Institute for Sustainable Humanosphere, Kyoto University)

[J] Poster | P (Space and Planetary Sciences )：P-EM Solar-Terrestrial Sciences, Space Electromagnetism & Space Environment

3:30 PM - 5:00 PM JST | 6:30 AM - 8:00 AM UTC | Poster Hall International Exhibition Hall8, Makuhari Messe_3

## [P-EM16] Physics and Chemistry in the Atmosphere and Ionosphere

convener:Yuichi Otsuka(Institute for Space-Earth Environmental Research, Nagoya University), Takuya Tsugawa(National Institute of Information and Communications Technology), Seiji Kawamura(National Institute of Information and Communications Technology)

### [PEM16-P01] Temporal and spatial variation of GPS phase scintillation during substorms and auroral breakups

*Paul Prikryl[1,2], James M. Weygand[3], Reza Ghoddousi-Fard[4], P. Thayyil Jayachandran[1], David R. Themens[1], Anthony M. McCaffrey[1], Bharat S. R. Kunduri[5], Emma Spanswick[6], Yongliang Zhang[7], Akira Sessai Yukimatu[8] (1.Physics Department, University of New Brunswick, Fredericton, NB, Canada, 2.Geomagnetic Laboratory, Natural Resources Canada, Ottawa, ON, Canada, 3.Earth Planetary and Space Sciences, University of California, Los Angeles, CA, USA, 4.Canadian Geodetic Survey, Natural Resources Canada, Ottawa, ON, Canada, 5.Bradley Dept. of Electrical and Computer Engineering, Virginia Tech, USA, 6.Dept. of Physics and Astronomy, University of Calgary, AB, Canada, 7.Johns Hopkins University Applied Physics Laboratory, Laurel, MD, USA, 8.National Institute of Polar Research, Tokyo, Japan)

### [PEM16-P02] Statistical study of SAPS occurrence characteristics using the SuperDARN Hokkaido HF radar

*Kento Oya[1], Nozomu Nishitani[1], Tomoaki Hori[1] (1.Institute for Space-Earth Environmental Research, Nagoya University)

### [PEM16-P03] Spectral investigations of near infrared aurora and airglow at 1.0-1.6 microns: 1-year ground-based imaging spectroscopic observation at Syowa station (69.0°S, 39.6°E)

*Takanori Nishiyama[1], Takeshi Sakanoi[2], Makoto Taguchi[3], Hidehiko Suzuki[4] (1.National Institute of Polar Research, 2.Planetary Plasma and Atmospheric Research Center, Tohoku University, 3.Rikkyo University, 4.Department of Physics, Meiji University)

### [PEM16-P04] The study of the lower ionosphere in the South Atlantic Anomaly (SAA) Region

*Chih-Yu Chiang[1], Tzu-Fang Chang[2,1], Sunny W. Y. Tam[1] (1.Institute of Space and Plasma Sciences, National Cheng Kung University, Tainan, Taiwan, 2.Institute for Space-Earth Environmental Research, Nagoya University, Japan)

### [PEM16-P05] Multi-GNSS observation of LSTID in Japan and its link with auroral activities

*Mayumi Hashimoto[1], Kosuke Heki[1] (1.Hokkaido University)

### [PEM16-P06] Basic development of accurate analytical method in order to determine coordinates of artificial illuminating clouds of Barium and Strontium for chemical-release rocket experiments

*Taro Watanabe[1], Masa-yuki Yamamoto[1], Yoshihiro Kakinami[2] (1.Kochi University of Technology, 2.Hokkaido Information University)

### [PEM16-P07] Neutral and plasma density perturbations in the top-/bottom-side ionosphere associated with MSTIDs

*Shin Suzuki[1], Jaeheung Park[2], Yuichi Otsuka[3], Kazuo Shiokawa[3], Huixin Liu[4], Hermann Luehr[5] (1.Faculty of Regional Policy, Aichi University, 2.Korea Astronomy and Space Science Institute, 3.Institute for Space-Earth Environmental Research, Nagoya University, 4.Earth and Planetary Science Division, Kyushu University SERC, Kyushu University, 5.Helmholtz Centre Potsdam, GFZ, German Research Centre for Geosciences)

### [PEM16-P08] Analysis of ionospheric TEC fluctuation by rocket

*Tsuyoshi Takegawa[1], Hiroyuki Nakata[1], Hiroyo Ohya[1], Toshiaki Takano[1], Takuya Tsugawa[2], Michi Nishioka[2] (1.Graduate School of Integrated Science and Technology, Chiba University, 2.National Institute of Information and Communications Technology)

### [PEM16-P09] Examinations of the ionospheric perturbation associated with H-IIA rockets launching

*Junpei Yamazaki[1], Hiroyuki Nakata[1], Hiroyo Ohya[1], Toshiaki Takano[1], Keisuke Hosokawa[2], Ichiro Tomizawa[2] (1.Graduate School of Engineering, Chiba University, 2.Department of Communication Engineering and Informatics, University of Electro-Communications)

[PEM16-P10] Explosion energy derived from the 2015 Kuchinoerabujima eruption: Estimation from infrasound less than 0.01 Hz detected by barometers, seismometers, and TEC

*Yuki Nakashima[1], Kiwamu Nishida[1], Yosuke Aoki[1], Kosuke Heki[2] (1.Earthquake Research Institute, 2.Natural History Sciences, Hokkaido University)

---

[PEM16-P11] Detection of spread-F echoes in ionograms using machine learning

*Hiroyuki Nakata[1], Yuta Goto[2], Hiroyo Ohya[1], Toshiaki Takano[1] (1.Graduate School of Engineering, Chiba University, 2.Department of Electrical and Electronics Engineering)

---

[PEM16-P12] Evaluation of GNSS-TEC receiver performance for sounding rocket installation

*Makoto Okumura[1], Yuki Ashihara[1] (1.National Institute of Technology, Nara College)

---

[PEM16-P13] Relationship between mesosperical airglow disturbance and occurrence of equatorial plasma bubbles

*Ryota Okada[1], Akinori Saito[1], Takafumi Ikeda[1], Hiroyuki Shinagawa[2], Takuya Tsugawa[2], Takeshi Sakanoi[3] (1.Department of Geophysics, Graduate School of Science, Kyoto University, 2.National Institute of Information and Communications Technology, 3.Planetary Plasma and Atmospheric Research Center, Graduate School of Science, Tohoku University)

---

[PEM16-P14] Analysis of parameters controlling the occurrence and growth of equatorial plasma bubbles using GAIA

*Hiroyuki Shinagawa[1], Hidekatsu Jin[1], Yasunobu Miyoshi[2], Hitoshi Fujiwara[3], Tatsuhiro Yokoyama[4], Yuichi Otsuka[5] (1.National Institute of Information and Communications Technology, 2.Department of Earth and Planetary Sciences, Faculty of Sciences, Kyushu University, 3.Faculty of Science and Technology, Seikei University, 4.Kyoto University, 5.Institute for Space-Earth Environmental Research, Nagoya University)

---

[PEM16-P15] A three-dimensional numerical model to study the modulation of midlatitude $E_s$-layers

*Satoshi Andoh[1], Akinori Saito[1], Hiroyuki Shinagawa[2], Shin'ichi Miyazaki[1] (1.Graduate School of Science, Kyoto University, 2.National Institute of Information and Communications Technology)

---

[PEM16-P16] Statistical analysis of the horizontal phase velocity distribution of mesospheric and ionospheric waves observed in airglow images in Hawaii

*Hideto Naito[1], Kazuo Shiokawa[1], Yuichi Otsuka[1], Takeshi Sakanoi[2], Akinori Saito[3], Takuji Nakamura[4] (1.Institute for Space-Earth Environmental Research, Nagoya University, 2.Planetary Plasma and Atmospheric Research Center, Graduate School of Science, Tohoku University, 3.Department of Geophysics, Graduate school of science, Kyoto University, 4.National Institute of Polar Research)

---

[PEM16-P17] Estimation of mesospheric OH temperature by observation data by ISS-IMAP VISI

*Ryo Murakami[1], Akinori Saito[1], Takeshi Sakanoi[2], Yuta Hozumi[3] (1.Kyoto University, 2.Tohoku University, 3.University of Electro-Communications)

---

[PEM16-P18] Implementation of photochemical process of NOx and HOx into a whole atmosphere GCM

*Yasunobu Miyoshi[1], Hitoshi Fujiwara[2] (1.Department of Earth and Planetary Sciences, Faculty of Sciences, Kyushu University, 2.Seikei University)

---

[PEM16-P19] Development of a Lagrangian chemical transport model to understand the mechanism of composition change due to change in atmospheric environment

*Shingo Nakanishi[1], Tomoo Nagahama[1], Akira Mizuno[1], Tac Nakajima[1], Riku Ishijima[1] (1.Institute for Space-Earth Environmental Research, Nagoya University)

[J] Poster | P (Space and Planetary Sciences )：P-EM Solar-Terrestrial Sciences, Space Electromagnetism & Space Environment

5:15 PM - 6:30 PM JST | 8:15 AM - 9:30 AM UTC | Poster Hall International Exhibition Hall8, Makuhari Messe_3

## [P-EM16] Physics and Chemistry in the Atmosphere and Ionosphere

convener:Yuichi Otsuka(Institute for Space-Earth Environmental Research, Nagoya University), Takuya Tsugawa(National Institute of Information and Communications Technology), Seiji Kawamura(National Institute of Information and Communications Technology)

### [PEM16-P01] Temporal and spatial variation of GPS phase scintillation during substorms and auroral breakups

*Paul Prikryl[1,2], James M. Weygand[3], Reza Ghoddousi-Fard[4], P. Thayyil Jayachandran[1], David R. Themens[1], Anthony M. McCaffrey[1], Bharat S. R. Kunduri[5], Emma Spanswick[6], Yongliang Zhang[7], Akira Sessai Yukimatu[8] (1.Physics Department, University of New Brunswick, Fredericton, NB, Canada, 2.Geomagnetic Laboratory, Natural Resources Canada, Ottawa, ON, Canada, 3.Earth Planetary and Space Sciences, University of California, Los Angeles, CA, USA, 4.Canadian Geodetic Survey, Natural Resources Canada, Ottawa, ON, Canada, 5.Bradley Dept. of Electrical and Computer Engineering, Virginia Tech, USA, 6.Dept. of Physics and Astronomy, University of Calgary, AB, Canada, 7.Johns Hopkins University Applied Physics Laboratory, Laurel, MD, USA, 8.National Institute of Polar Research, Tokyo, Japan)

### [PEM16-P02] Statistical study of SAPS occurrence characteristics using the SuperDARN Hokkaido HF radar

*Kento Oya[1], Nozomu Nishitani[1], Tomoaki Hori[1] (1.Institute for Space-Earth Environmental Research, Nagoya University)

### [PEM16-P03] Spectral investigations of near infrared aurora and airglow at 1.0-1.6 microns: 1-year ground-based imaging spectroscopic observation at Syowa station (69.0°S, 39.6°E)

*Takanori Nishiyama[1], Takeshi Sakanoi[2], Makoto Taguchi[3], Hidehiko Suzuki[4] (1.National Institute of Polar Research, 2.Planetary Plasma and Atmospheric Research Center, Tohoku University, 3.Rikkyo University, 4.Department of Physics, Meiji University)

### [PEM16-P04] The study of the lower ionosphere in the South Atlantic Anomaly (SAA) Region

*Chih-Yu Chiang[1], Tzu-Fang Chang[2,1], Sunny W. Y. Tam[1] (1.Institute of Space and Plasma Sciences, National Cheng Kung University, Tainan, Taiwan, 2.Institute for Space-Earth Environmental Research, Nagoya University, Japan)

### [PEM16-P05] Multi-GNSS observation of LSTID in Japan and its link with auroral activities

*Mayumi Hashimoto[1], Kosuke Heki[1] (1.Hokkaido University)

### [PEM16-P06] Basic development of accurate analytical method in order to determine coordinates of artificial illuminating clouds of Barium and Strontium for chemical-release rocket experiments

*Taro Watanabe[1], Masa-yuki Yamamoto[1], Yoshihiro Kakinami[2] (1.Kochi University of Technology, 2.Hokkaido Information University)

### [PEM16-P07] Neutral and plasma density perturbations in the top-/bottom-side ionosphere associated with MSTIDs

*Shin Suzuki[1], Jaeheung Park[2], Yuichi Otsuka[3], Kazuo Shiokawa[3], Huixin Liu[4], Hermann Luehr[5] (1.Faculty of Regional Policy, Aichi University, 2.Korea Astronomy and Space Science Institute, 3.Institute for Space-Earth Environmental Research, Nagoya University, 4.Earth and Planetary Science Division, Kyushu University SERC, Kyushu University, 5.Helmholtz Centre Potsdam, GFZ, German Research Centre for Geosciences)

### [PEM16-P08] Analysis of ionospheric TEC fluctuation by rocket

*Tsuyoshi Takegawa[1], Hiroyuki Nakata[1], Hiroyo Ohya[1], Toshiaki Takano[1], Takuya Tsugawa[2], Michi Nishioka[2] (1.Graduate School of Integrated Science and Technology, Chiba University, 2.National Institute of Information and Communications Technology)

### [PEM16-P09] Examinations of the ionospheric perturbation associated with H-IIA rockets launching

*Junpei Yamazaki[1], Hiroyuki Nakata[1], Hiroyo Ohya[1], Toshiaki Takano[1], Keisuke Hosokawa[2], Ichiro Tomizawa[2] (1.Graduate School of Engineering, Chiba University, 2.Department of Communication Engineering and Informatics, University of Electro-Communications)

[PEM16-P10] Explosion energy derived from the 2015 Kuchinoerabujima eruption: Estimation from infrasound less than 0.01 Hz detected by barometers, seismometers, and TEC

*Yuki Nakashima[1], Kiwamu Nishida[1], Yosuke Aoki[1], Kosuke Heki[2] (1.Earthquake Research Institute, 2.Natural History Sciences, Hokkaido University)

---

[PEM16-P11] Detection of spread-F echoes in ionograms using machine learning

*Hiroyuki Nakata[1], Yuta Goto[2], Hiroyo Ohya[1], Toshiaki Takano[1] (1.Graduate School of Engineering, Chiba University, 2.Department of Electrical and Electronics Engineering)

---

[PEM16-P12] Evaluation of GNSS-TEC receiver performance for sounding rocket installation

*Makoto Okumura[1], Yuki Ashihara[1] (1.National Institute of Technology, Nara College)

---

[PEM16-P13] Relationship between mesosperical airglow disturbance and occurrence of equatorial plasma bubbles

*Ryota Okada[1], Akinori Saito[1], Takafumi Ikeda[1], Hiroyuki Shinagawa[2], Takuya Tsugawa[2], Takeshi Sakanoi[3] (1.Department of Geophysics, Graduate School of Science, Kyoto University, 2.National Institute of Information and Communications Technology, 3.Planetary Plasma and Atmospheric Research Center, Graduate School of Science, Tohoku University)

---

[PEM16-P14] Analysis of parameters controlling the occurrence and growth of equatorial plasma bubbles using GAIA

*Hiroyuki Shinagawa[1], Hidekatsu Jin[1], Yasunobu Miyoshi[2], Hitoshi Fujiwara[3], Tatsuhiro Yokoyama[4], Yuichi Otsuka[5] (1.National Institute of Information and Communications Technology, 2.Department of Earth and Planetary Sciences, Faculty of Sciences, Kyushu University, 3.Faculty of Science and Technology, Seikei University, 4.Kyoto University, 5.Institute for Space-Earth Environmental Research, Nagoya University)

---

[PEM16-P15] A three-dimensional numerical model to study the modulation of midlatitude $E_s$-layers

*Satoshi Andoh[1], Akinori Saito[1], Hiroyuki Shinagawa[2], Shin'ichi Miyazaki[1] (1.Graduate School of Science, Kyoto University, 2.National Institute of Information and Communications Technology)

---

[PEM16-P16] Statistical analysis of the horizontal phase velocity distribution of mesospheric and ionospheric waves observed in airglow images in Hawaii

*Hideto Naito[1], Kazuo Shiokawa[1], Yuichi Otsuka[1], Takeshi Sakanoi[2], Akinori Saito[3], Takuji Nakamura[4] (1.Institute for Space-Earth Environmental Research, Nagoya University, 2.Planetary Plasma and Atmospheric Research Center, Graduate School of Science, Tohoku University, 3.Department of Geophysics, Graduate school of science, Kyoto University, 4.National Institute of Polar Research)

---

[PEM16-P17] Estimation of mesospheric OH temperature by observation data by ISS-IMAP VISI

*Ryo Murakami[1], Akinori Saito[1], Takeshi Sakanoi[2], Yuta Hozumi[3] (1.Kyoto University, 2.Tohoku University, 3.University of Electro-Communications)

---

[PEM16-P18] Implementation of photochemical process of NOx and HOx into a whole atmosphere GCM

*Yasunobu Miyoshi[1], Hitoshi Fujiwara[2] (1.Department of Earth and Planetary Sciences, Faculty of Sciences, Kyushu University, 2.Seikei University)

---

[PEM16-P19] Development of a Lagrangian chemical transport model to understand the mechanism of composition change due to change in atmospheric environment

*Shingo Nakanishi[1], Tomoo Nagahama[1], Akira Mizuno[1], Tac Nakajima[1], Riku Ishijima[1] (1.Institute for Space-Earth Environmental Research, Nagoya University)

[J] Poster | P (Space and Planetary Sciences )：P-EM Solar-Terrestrial Sciences, Space Electromagnetism & Space Environment

10:45 AM - 12:15 PM JST | 1:45 AM - 3:15 AM UTC | Poster Hall International Exhibition Hall8, Makuhari Messe_1

## [P-EM17] Space Plasma Physics: Theory and Simulation

convener:Takayuki Umeda(Institute for Space-Earth Environmental Research, Nagoya University), Takanobu Amano(Department of Earth and Planetary Science, University of Tokyo), Yasuhiro Nariyuki(Faculty of Human Development, University of Toyama), Tadas Nakamura(Fukui Prefectural University)

[PEM17-P01] PIC Simulation on nonlinear development of lower-hybrid instabilities driven by energetic ions.

*Tsubasa Kotani[1], Mieko Toida[2], Toseo Moritaka[2], Satoshi Taguchi[1] (1.Graduate School of Science, Kyoto University, 2.National Insititute for Fusion Science)

[PEM17-P02] **Study of Kinetic Alfven waves in space plasmas with electron having Kappa distribution**

*SATYAVIR SINGH[1], Krushna Chandra Barik[1], Yoshiharu Omura[2], Gurbax Singh Lakhina[1] (1.Indian Institute of Geomagnetism, New Panvel, India, 2.Research Institute for Sustainable Humanosphere, Kyoto University, Kyoto, Japan)

[PEM17-P03] A high-order divergence-free weighted finite difference scheme for the two-fluid plasma equations

*Takahiro Miyoshi[1], Takashi Minoshima[2], Yosuke Matsumoto[3] (1.Graduate School of Science, Hiroshima University, 2.Department of Mathematical Science and Advanced Technology, Japan Agency for Marine-Earth Science and Technology, 3.Graduate School of Science, Chiba University)

[PEM17-P04] Electromagnetic linear dispersion relation for plasma with a drift across magnetic field

*Takayuki Umeda[1], Takuma Nakamura[2] (1.Institute for Space-Earth Environmental Research, Nagoya University, 2.Space Research Institute, Austrian Academy of Sciences)

[J] Poster | P (Space and Planetary Sciences )：P-EM Solar-Terrestrial Sciences, Space Electromagnetism & Space Environment

5:15 PM - 6:30 PM JST | 8:15 AM - 9:30 AM UTC | Poster Hall International Exhibition Hall8, Makuhari Messe_4

## [P-EM17] Space Plasma Physics: Theory and Simulation

convener:Takayuki Umeda(Institute for Space-Earth Environmental Research, Nagoya University), Takanobu Amano(Department of Earth and Planetary Science, University of Tokyo), Yasuhiro Nariyuki(Faculty of Human Development, University of Toyama), Tadas Nakamura(Fukui Prefectural University)

[PEM17-P01] PIC Simulation on nonlinear development of lower-hybrid instabilities driven by energetic ions.

*Tsubasa Kotani[1], Mieko Toida[2], Toseo Moritaka[2], Satoshi Taguchi[1] (1.Graduate School of Science, Kyoto University, 2.National Insititute for Fusion Science)

[PEM17-P02] **Study of Kinetic Alfven waves in space plasmas with electron having Kappa distribution**

*SATYAVIR SINGH[1], Krushna Chandra Barik[1], Yoshiharu Omura[2], Gurbax Singh Lakhina[1] (1.Indian Institute of Geomagnetism, New Panvel, India, 2.Research Institute for Sustainable Humanosphere, Kyoto University, Kyoto, Japan)

[PEM17-P03] A high-order divergence-free weighted finite difference scheme for the two-fluid plasma equations

*Takahiro Miyoshi[1], Takashi Minoshima[2], Yosuke Matsumoto[3] (1.Graduate School of Science, Hiroshima University, 2.Department of Mathematical Science and Advanced Technology, Japan Agency for Marine-Earth Science and Technology, 3.Graduate School of Science, Chiba University)

[PEM17-P04] Electromagnetic linear dispersion relation for plasma with a drift across magnetic field

*Takayuki Umeda[1], Takuma Nakamura[2] (1.Institute for Space-Earth Environmental Research, Nagoya University, 2.Space Research Institute, Austrian Academy of Sciences)

[J] Oral | P (Space and Planetary Sciences )：P-EM Solar-Terrestrial Sciences, Space Electromagnetism & Space Environment

1:45 PM - 3:15 PM JST | 4:45 AM - 6:15 AM UTC | A03 TOKYO BAY MAKUHARI HALL

## [P-EM17] Space Plasma Physics: Theory and Simulation

convener:Takayuki Umeda(Institute for Space-Earth Environmental Research, Nagoya University), Takanobu Amano(Department of Earth and Planetary Science, University of Tokyo), Yasuhiro Nariyuki(Faculty of Human Development, University of Toyama), Tadas Nakamura(Fukui Prefectural University), Chairperson:Takayuki Umeda(Institute for Space-Earth Environmental Research, Nagoya University), Takanobu Amano(Department of Earth and Planetary Science, University of Tokyo)

1:45 PM - 2:00 PM JST | 4:45 AM - 5:00 AM UTC

[PEM17-01] Prediction of the high-resolution numerical flux by using a deep neural network

*Yosuke Matsumoto[1] (1.Graduate School of Science, Chiba University)

2:00 PM - 2:15 PM JST | 5:00 AM - 5:15 AM UTC

[PEM17-02] Multiple Boris integrators for particle-in-cell simulation

*Seiji Zenitani[1], Tsunehiko N Kato[2] (1.Kyoto University, 2.National Astronomical Observatory of Japan)

2:15 PM - 2:30 PM JST | 5:15 AM - 5:30 AM UTC

[PEM17-03] Contour Dynamics for Vlasov–Poisson Plasma with the Periodic Boundary

*Hiroki Sato[1], Tomo-Hiko Watanabe[1], Shinya Maeyama[1] (1.Nagoya University)

2:30 PM - 2:45 PM JST | 5:30 AM - 5:45 AM UTC

[PEM17-04] Simulation methods and visualization tools for MHD simulations in a sphere

*Akira Kageyama[1], Kumiko Hori[1], Naohisa Sakamoto[1] (1.Graduate School of System Informatics, Kobe University)

2:45 PM - 3:00 PM JST | 5:45 AM - 6:00 AM UTC

[PEM17-05] Kármán Vortex Street, Strouhal Number, Hairpin Vortex in 3D global Magnetohydrodynamic MHD simulations in Northward IMF

*DongSheng CAI[1] (1.University of Tsukuba)

3:00 PM - 3:15 PM JST | 6:00 AM - 6:15 AM UTC

[PEM17-06] Correlations between plasma density and magnetic field strength in MHD turbulence in space

*Tohru Hada[1], Yasuhito Narita[2], Yasuhiro Nariyuki[3] (1.Interdisciplinary Graduate School of Engineering Sciences, Kyushu University, 2.Space Research Institute, Austrian Academy of Sciences, 3.Faculty of Human Development, University of Toyama)

[J] Oral | P (Space and Planetary Sciences )：P-EM Solar-Terrestrial Sciences, Space Electromagnetism & Space Environment

3:30 PM - 5:00 PM JST | 6:30 AM - 8:00 AM UTC | A03 TOKYO BAY MAKUHARI HALL

## [P-EM17] Space Plasma Physics: Theory and Simulation

convener:Takayuki Umeda(Institute for Space-Earth Environmental Research, Nagoya University), Takanobu Amano(Department of Earth and Planetary Science, University of Tokyo), Yasuhiro Nariyuki(Faculty of Human Development, University of Toyama), Tadas Nakamura(Fukui Prefectural University), Chairperson:Tadas Nakamura(Fukui Prefectural University), Yasuhiro Nariyuki

3:30 PM - 3:45 PM JST | 6:30 AM - 6:45 AM UTC

[PEM17-07] Stochastic models of phase space diffusion via wave-particle interaction with parallel propagating electromagnetic waves

*Yasuhiro Nariyuki[1] (1.Faculty of Human Development, University of Toyama)

3:45 PM - 4:00 PM JST | 6:45 AM - 7:00 AM UTC

[PEM17-08] Electron beam instability in collisionless magnetic reconnection with a strong guide field

*Kazuya Shimomura[1], Tomo-Hiko Watanabe[1], Shinya Maeyama[1], Akihiro Ishizawa[2] (1.Nagoya Univertsity, 2.Kyoto University)

4:00 PM - 4:15 PM JST | 7:00 AM - 7:15 AM UTC

[PEM17-09] Particle acceleration with precursor wave driven wakefield in relativistic shocks

*Masanori Iwamoto[1], Takanobu Amano[1], Masahiro Hoshino[1], Yosuke Matsumoto[2] (1.Graduate School of Science,The University of Tokyo, 2.Graduate School of Science, Chiba University)

4:15 PM - 4:30 PM JST | 7:15 AM - 7:30 AM UTC

[PEM17-10] Stochastic Shock Drift Acceleration in the Shock Transition Region with Finite Pitch-Angle Anisotropy

*Takuma Katou[1], Takanobu Amano[1] (1.The University of Tokyo)

4:30 PM - 4:45 PM JST | 7:30 AM - 7:45 AM UTC

[PEM17-11] Near-fields and its Applications in Space Plasmas

*Tadas Nakamura[1] (1.Fukui Prefectural University)

4:45 PM - 5:00 PM JST | 7:45 AM - 8:00 AM UTC

[PEM17-12] Problems of Gravitational Waves and Origin of Gravitational Fields Raised by Studies on Binary Black Hole

*Hiroshi Oya[1] (1.Department of Geophysics Graduate School for Science Tohoku University)

[E] Oral | A (Atmospheric and Hydrospheric Sciences )：A-AS Atmospheric Sciences, Meteorology & Atmospheric Environment

9:00 AM - 10:30 AM JST | 12:00 AM - 1:30 AM UTC | 104 1F

## [A-AS02] Advances in Tropical Cyclone Research: Past, Present, and Future

convener:Sachie Kanada(Nagoya University), Akiyoshi Wada(Department of Typhoon and Severe Weather Research, Meteorological Research Institute), Kosuke Ito(University of the Ryukyus), Yoshiaki Miyamoto(Faculty of Environment and Information Studies, Keio University), Chairperson:Sachie Kanada(Nagoya University), Akiyoshi Wada(Meteorological Research Institute)

9:00 AM - 9:15 AM JST | 12:00 AM - 12:15 AM UTC

[AAS02-01] A GRAPES-based mesoscale EPS for TC forecasting: configuration and performance

*Xubin Zhang[1] (1.Institute of Tropical and Marine Meteorology, CMA)

9:15 AM - 9:30 AM JST | 12:15 AM - 12:30 AM UTC

[AAS02-02] **Evaluation of operational Ensemble based Global Forecast System prediction for Tropical Cyclones over the North Indian Ocean**

*Medha Deshpande[1], Radhika Kanase[1], R P M Krishna[1], Emmanuel Rongmie[1], P Mukhopadhyay[1] (1.IITM, Pune, INDIA)

9:30 AM - 9:45 AM JST | 12:30 AM - 12:45 AM UTC

[AAS02-03] Structural Changes Preceding Rapid Intensification in Tropical Cyclones as shown in a Large Ensemble of Idealized Simulations

*Yoshiaki Miyamoto[1], David S Nolan[2] (1.Faculty of Environment and Information Studies, Keio University, 2.Rosenstiel School of Marine and Atmospheric Science, University of Miami)

9:45 AM - 10:00 AM JST | 12:45 AM - 1:00 AM UTC

[AAS02-04] Potential impacts of tropical cyclone inner-core convective activity on the predictability of rapid intensification

*Masashi Minamide[1], Derek J. Posselt[1] (1.Jet Propulsion Laboratory, california institute of technology)

10:00 AM - 10:15 AM JST | 1:00 AM - 1:15 AM UTC

[AAS02-05] A link between high-speed solar wind streams and rapid intensification of tropical cyclones

*Paul Prikryl[1,2], Lidia Nikitina[2], Vojto Rušin[3] (1.Physics Department, University of New Brunswick, Fredericton, NB, Canada, 2.Geomagnetic Laboratory, Natural Resources Canada, Ottawa, ON, Canada, 3.Astronomical Institute, Slovak Academy of Sciences, Tatranská Lomnica, Slovak Republic)

10:15 AM - 10:30 AM JST | 1:15 AM - 1:30 AM UTC

[AAS02-06] Influence of Tropical Lower Stratospheric Cooling on Extreme Deep Convective Activity and Tropical Cyclones

*Kunihiko Kodera[1], Nawo Eguchi[2], Rei Ueyama[3], Beatriz M Funatsu[4], Chantal Claud[5] (1.Meteorological Research Institute, 2.Kyushu University, 3.NASA Ames Research Center, 4.Université de Nantes, 5.Ecole Polytechnique)

[E] Oral | A (Atmospheric and Hydrospheric Sciences )：A-AS Atmospheric Sciences, Meteorology & Atmospheric Environment

10:45 AM - 12:15 PM JST | 1:45 AM - 3:15 AM UTC | 104 1F

## [A-AS02] Advances in Tropical Cyclone Research: Past, Present, and Future

convener:Sachie Kanada(Nagoya University), Akiyoshi Wada(Department of Typhoon and Severe Weather Research, Meteorological Research Institute), Kosuke Ito(University of the Ryukyus), Yoshiaki Miyamoto(Faculty of Environment and Information Studies, Keio University), Chairperson:Yoshiaki Miyamoto, Kosuke Ito(University of Ryukyus)

10:45 AM - 11:15 AM JST | 1:45 AM - 2:15 AM UTC

[AAS02-07] A change in the inner-core structure of Typhoon Trami (2018) as observed through upper-tropospheric aircraft reconnaissance of T-PARCII

★Invited Papers

*Hiroyuki Yamada[1], Kazuhisa Tsuboki[2], Taro Shinoda[2], Hisayuki Kubota[3], Yukihiro Takahashi[3], Norio Nagahama[4], Kensaku Shimizu[4], Tadayasu Ohigashi[5], Kosuke Ito[1], Munehiko Yamaguchi[6], Tetsuo Nakazawa[6] (1.University of the Ryukyus, 2.Nagoya University, 3.Hokkaido University, 4.Meisei Electric, 5.National Research Institute for Earth Science and Disaster Resilience, 6.Meteorological Research Institute, Japan Meteorological Agency)

---

11:15 AM - 11:30 AM JST | 2:15 AM - 2:30 AM UTC

[AAS02-08] **Dramatic changes in the inner-core structure of Typhoon Jebi (2018) at landfall and relationship between a mesovortex and strong wind gusts**

*Udai Shimada[1], Ryo OYAMA[1], shingo shimizu[2] (1.Meteorological Research Institute, 2.National Research Institute for Earth Science and Disaster Prevention)

---

11:30 AM - 11:45 AM JST | 2:30 AM - 2:45 AM UTC

[AAS02-09] **Revisiting Asymmetric CAPE in Sheared Tropical Cyclones**

*Qingqing Li[1] (1.NUIST Nanjing University of Information Science and Technology)

---

11:45 AM - 12:00 PM JST | 2:45 AM - 3:00 AM UTC

[AAS02-10] **Observed rainfall asymmetry of tropical cyclone in the process of making landfall in Guangdong, South China**

*Guanhuan Wen[1] (1.Guangzhou Institute of Tropical and Marine Meteorology, China Meteorological Administation)

---

12:00 PM - 12:15 PM JST | 3:00 AM - 3:15 AM UTC

[AAS02-11] Volumetric Detection of Tornadic Vortices Associated with Typhoon Nanmadol (2017) Using PAWR and Deep Learning

*Toru Adachi[1], Naoki Ishitsu[2], Kenichi Kusunoki[1], Hanako Inoue[1], Ken-ichiro Arai[2], Chusei Fujiwara[3], Hiroto Suzuki[3] (1.Meteorological Research Institute, 2.Alpha Denshi/Meteorological Research Institute, 3.East Japan Railway Company)

[E] Poster | A (Atmospheric and Hydrospheric Sciences )：A-AS Atmospheric Sciences, Meteorology & Atmospheric Environment

1:45 PM - 3:15 PM JST | 4:45 AM - 6:15 AM UTC | Poster Hall International Exhibition Hall8, Makuhari Messe_1

## [A-AS02] Advances in Tropical Cyclone Research: Past, Present, and Future

convener:Sachie Kanada(Nagoya University), Akiyoshi Wada(Department of Typhoon and Severe Weather Research, Meteorological Research Institute), Kosuke Ito(University of the Ryukyus), Yoshiaki Miyamoto(Faculty of Environment and Information Studies, Keio University)

[AAS02-P01] Numerical study on lightning frequency in a tropical cyclone

*Yousuke Sato[1,3], Yoshiaki Miyamoto[2,3], Tomita Hirofumi[3] (1.Department of Applied Energy, Nagoya University, 2.Faculty of Environment and Information Studies, Keio University, 3.RIKEN Center for Computational Science)

[AAS02-P02] **Sensitivity of Numerical Simulation of Typhoon Nepartak (2016) to Cloud Condensation Nuclei Concentration**

*Yu-De Wu[1], Jian-Liang Wang[1] (1.Dept. of Environmental Informational and Engineering, Chung Cheng Institute of Technology, National Defense University, Taiwan)

[AAS02-P03] Moisture Budget Analysis for Hurricane Precipitation on Texas

*Satoshi Iizuka[1], Naoki Sakai[1] (1.National Research Institute for Earth Science and Disaster Resilience)

[AAS02-P04] Remote response of a developing tropical cyclone over the western North Pacific to large-scale vapor transport from the Kuroshio in boreal fall

*Keita Fujiwara[1], Ryuichi Kawamura[2], Tetsuya Kawano[2] (1.Graduate School of Science, Kyushu University, 2.Faculty of Science, Kyushu University)

[AAS02-P05] Asymmetrically Intensifying Processes of a Category 4 Super Typhoon Lan (2017) during High Vertical Wind Shear

*Sachie Kanada[1], Akiyoshi Wada[2], Kazuhisa Tsuboki[1] (1.Nagoya University, 2.Meteorological Research Institute)

[AAS02-P06] Roles of preexisting oceanic condition and ocean coupling processes in the intensity prediction during the mature phase of Typhoon Trami (2018)

*Akiyoshi Wada[1] (1.Typhoon Research Department Meteorological Research Institute)

[AAS02-P07] Development and assessment of the probabilistic storm surge forecast system in Taiwan: Case Study of Typhoon Maria in 2018

*Chun-Wei Lin[1], Tso-Ren Wu[1], Yu-Lin Tsai[1], Shu-Chun Chuang[1], Chi-Hao Chu[2], Chuen-Teyr Terng[2] (1.Graduate Institute of Hydrological and Oceanic Sciences, National Central University, Chungli, Taiwan, 2.Marine Meteorology Center, Central Weather Bureau, Taipei, Taiwan)

[AAS02-P08] Basic Data Construction for a Typhoon Disaster Prevention Model : Analysis and Changes by El Nino and La Nina year

*HANA NA[1], Woo-Sik Jung[1] (1.Department of Atmospheric Environment Information Engineering, Atmospheric Environment Information Research Center, Inje University, Gimhae 50834, Korea)

[AAS02-P09] Basic Data Construction for a Typhoon Disaster Prevention Model : Analysis According to the Typhoon Path Type

*HANA NA[1], Woo-Sik JUNG[1] (1.Department of Atmospheric Environment Information Engineering, Atmospheric Environment Information Research Center, Inje University, Gimhae 50834, Korea)

[AAS02-P10] Basic Data Construction for a Typhoon Disaster Prevention Model : Monthly Characteristics of Typhoon Rusa, Maemi, Kompasu, and Bolaven

*HANA NA[1], Woo-Sik Jung[1] (1.Department of Atmospheric Environment Information Engineering, Atmospheric Environment Information Research Center, Inje University, Gimhae 50834, Korea)

[AAS02-P11] The mechanism of typhoon generated in the earth that rotates in the space where the solar wind blows

*Shinji Karasawa[1] (1.Miyagi National College of Technology Professor emeritus)

[E] Poster | A (Atmospheric and Hydrospheric Sciences )：A-AS Atmospheric Sciences, Meteorology & Atmospheric Environment

5:15 PM - 6:30 PM JST | 8:15 AM - 9:30 AM UTC | Poster Hall International Exhibition Hall8, Makuhari Messe_5

## [A-AS02] Advances in Tropical Cyclone Research: Past, Present, and Future

convener:Sachie Kanada(Nagoya University), Akiyoshi Wada(Department of Typhoon and Severe Weather Research, Meteorological Research Institute), Kosuke Ito(University of the Ryukyus), Yoshiaki Miyamoto(Faculty of Environment and Information Studies, Keio University)

[AAS02-P01] Numerical study on lightning frequency in a tropical cyclone

*Yousuke Sato[1,3], Yoshiaki Miyamoto[2,3], Tomita Hirofumi[3] (1.Department of Applied Energy, Nagoya University, 2.Faculty of Environment and Information Studies, Keio University, 3.RIKEN Center for Computational Science)

[AAS02-P02] **Sensitivity of Numerical Simulation of Typhoon Nepartak (2016) to Cloud Condensation Nuclei Concentration**

*Yu-De Wu[1], Jian-Liang Wang[1] (1.Dept. of Environmental Informational and Engineering, Chung Cheng Institute of Technology, National Defense University, Taiwan)

[AAS02-P03] Moisture Budget Analysis for Hurricane Precipitation on Texas

*Satoshi Iizuka[1], Naoki Sakai[1] (1.National Research Institute for Earth Science and Disaster Resilience)

[AAS02-P04] Remote response of a developing tropical cyclone over the western North Pacific to large-scale vapor transport from the Kuroshio in boreal fall

*Keita Fujiwara[1], Ryuichi Kawamura[2], Tetsuya Kawano[2] (1.Graduate School of Science, Kyushu University, 2.Faculty of Science, Kyushu University)

[AAS02-P05] Asymmetrically Intensifying Processes of a Category 4 Super Typhoon Lan (2017) during High Vertical Wind Shear

*Sachie Kanada[1], Akiyoshi Wada[2], Kazuhisa Tsuboki[1] (1.Nagoya University, 2.Meteorological Research Institute)

[AAS02-P06] Roles of preexisting oceanic condition and ocean coupling processes in the intensity prediction during the mature phase of Typhoon Trami (2018)

*Akiyoshi Wada[1] (1.Typhoon Research Department Meteorological Research Institute)

[AAS02-P07] Development and assessment of the probabilistic storm surge forecast system in Taiwan: Case Study of Typhoon Maria in 2018

*Chun-Wei Lin[1], Tso-Ren Wu[1], Yu-Lin Tsai[1], Shu-Chun Chuang[1], Chi-Hao Chu[2], Chuen-Teyr Terng[2] (1.Graduate Institute of Hydrological and Oceanic Sciences, National Central University, Chungli, Taiwan, 2.Marine Meteorology Center, Central Weather Bureau, Taipei, Taiwan)

[AAS02-P08] Basic Data Construction for a Typhoon Disaster Prevention Model : Analysis and Changes by El Nino and La Nina year

*HANA NA[1], Woo-Sik Jung[1] (1.Department of Atmospheric Environment Information Engineering, Atmospheric Environment Information Research Center, Inje University, Gimhae 50834, Korea)

[AAS02-P09] Basic Data Construction for a Typhoon Disaster Prevention Model : Analysis According to the Typhoon Path Type

*HANA NA[1], Woo-Sik JUNG[1] (1.Department of Atmospheric Environment Information Engineering, Atmospheric Environment Information Research Center, Inje University, Gimhae 50834, Korea)

[AAS02-P10] Basic Data Construction for a Typhoon Disaster Prevention Model : Monthly Characteristics of Typhoon Rusa, Maemi, Kompasu, and Bolaven

*HANA NA[1], Woo-Sik Jung[1] (1.Department of Atmospheric Environment Information Engineering, Atmospheric Environment Information Research Center, Inje University, Gimhae 50834, Korea)

[AAS02-P11] The mechanism of typhoon generated in the earth that rotates in the space where the solar wind blows

*Shinji Karasawa[1] (1.Miyagi National College of Technology Professor emeritus)

[E] Oral | A (Atmospheric and Hydrospheric Sciences )：A-AS Atmospheric Sciences, Meteorology & Atmospheric Environment

3:30 PM - 5:00 PM JST | 6:30 AM - 8:00 AM UTC | 104 1F

## [A-AS02] Advances in Tropical Cyclone Research: Past, Present, and Future

convener:Sachie Kanada(Nagoya University), Akiyoshi Wada(Department of Typhoon and Severe Weather Research, Meteorological Research Institute), Kosuke Ito(University of the Ryukyus), Yoshiaki Miyamoto(Faculty of Environment and Information Studies, Keio University), Chairperson:Sachie Kanada(Nagoya University), Yoshiaki Miyamoto

3:30 PM - 3:45 PM JST | 6:30 AM - 6:45 AM UTC

[AAS02-12] Evaluation of the monthly Potential of the 2018 typhoon activity and the effect of the positive PMM and SST of the eastern northwestern Pacific

*Takahiro Ishiyama[1], Masaki Satoh[1] (1.Atmosphere and Ocean Research Institute, The University of Tokyo)

3:45 PM - 4:00 PM JST | 6:45 AM - 7:00 AM UTC

[AAS02-13] **Contributions of different time scale variations to tropical cyclogenesis over the western North Pacific**

*Xi Cao[1] (1. Institute of Atmospheric Physics, Chinese Academy of Sciences)

4:00 PM - 4:15 PM JST | 7:00 AM - 7:15 AM UTC

[AAS02-14] Binary interaction between TC Chanthu (2016) and a nearby cold low

*Kosuke Ito[1], Miyabi Higa[1], Johnny Chan[2] (1.University of the Ryukyus, 2.City University of Hong Kong)

4:15 PM - 4:30 PM JST | 7:15 AM - 7:30 AM UTC

[AAS02-15] **Response of landfalling North Indian Ocean cyclonic disturbances to warming climate and associated environmental parameters**

*JAGABANDHU PANDA[1], KASTURI SINGH[1] (1.Department of Earth and Atmospheric Sciences, National Institute of Technology Rourkela, India)

4:30 PM - 4:45 PM JST | 7:30 AM - 7:45 AM UTC

[AAS02-16] **Rainfall contribution of North Indian Ocean cyclonic disturbances over India in a warming climate**

*KASTURI SINGH[1], JAGABANDHU PANDA[1] (1.Department of Earth and Atmospheric Sciences, National Institute of Technology Rourkela, India)

4:45 PM - 5:00 PM JST | 7:45 AM - 8:00 AM UTC

[AAS02-17] Analysis of typhoon tracks and associated precipitation amount over western Japan: A case study with Typhoon Nancy and Typhoon Jebi

*Sridhara Nayak[1], Tetsuya Takemi[1] (1.Disaster Prevention Research Institute, Kyoto University)

[J] Oral | A (Atmospheric and Hydrospheric Sciences )：A-AS Atmospheric Sciences, Meteorology & Atmospheric Environment

9:00 AM - 10:30 AM JST | 12:00 AM - 1:30 AM UTC | 102 1F

## [A-AS04] Atmospheric Chemistry

convener:Tomoki Nakayama(Graduate School of Fisheries and Environmental Sciences, Nagasaki University), Yoko Iwamoto(Graduate School of Biosphere Science, Hiroshima University), Sakae Toyoda(Department of Chemical Science and Engineering, Tokyo Institute of Technology), Nawo Eguchi(Kyushu University), Chairperson:Hisahiro Takashima(福岡大学)

9:00 AM - 9:15 AM JST | 12:00 AM - 12:15 AM UTC

[AAS04-16] Toward the Reduction of Radiative Forcing of Methane and Tropospheric Ozone: Aiming at the Emission Control of $CH_4$, $NO_x$and NMVOC in Asia

*Hajime Akimoto[1], Tatsuya NNagashima[1], Hiroshi Tanimoto[1], Zig Klimont[2], Markus Amann[2] (1.National Institute for Environmental Studies, 2.International Institute for Applied Systems Analysis)

9:15 AM - 9:30 AM JST | 12:15 AM - 12:30 AM UTC

[AAS04-17] **Determination of atmospheric $NO_2$ column densities using a Pandora instrument measuring direct-sun spectra at Yokosuka, Japan: Improved validation of TROPOMI satellite observations**

*Yugo Kanaya[1], Hisahiro Takashima[2,1], Masato I. Nodzu[3], Takashi Sekiya[7], Kazuyuki Miyazaki[1], Henk Eskes[4], Gaia Pinardi[5], Daniel Santana Diaz[6], Moritz Müller[6], Alexander Cede[6] (1.Research and Development Center for Global Change, Japan Agency for Marine-Earth Science and Technology (JAMSTEC), 2.Fukuoka University, 3.Tokyo Metropolitan University, 4.KNMI, 5.BIRA-IASB, 6.LuftBlick, 7.Japan Agency for Marine-Earth Science and Technology (JAMSTEC))

9:30 AM - 9:45 AM JST | 12:30 AM - 12:45 AM UTC

[AAS04-18] A high-resolution global data assimilation for air pollution analysis on megacity scale using multi-sensor satellite measurements including TROPOMI $NO_2$ data

*Takashi Sekiya[1], Kazuyuki Miyazaki[2,1], Henk Eskes[3], Folkert Boersma[3], Koji Ogochi[1], Kengo Sudo[4,1], Masayuki Takigawa[1] (1.Japan Agency for Marine-Earth Science and Technology, 2.Jet Propulsion Laboratory/California Institute for Technology, 3.Royal Netherlands Meteorological Institute (KNMI), 4.Graduate School of Environmental Studies, Nagoya University)

9:45 AM - 10:00 AM JST | 12:45 AM - 1:00 AM UTC

[AAS04-19] Recent trends of $NO_2$, VOC, and tropospheric ozone concentrations observed around Chiba, Japan in 2013-2018

*Daichi Yonekawa[1], Hitoshi Irie[2] (1.Chiba university Graduate school, 2.Chiba university)

10:00 AM - 10:15 AM JST | 1:00 AM - 1:15 AM UTC

[AAS04-20] Long-term seasonal changes in tropospheric ozone over Japan

*Natsumi Kawano[1], Tatsuya Nagashima[1], Seiji Sugata[1] (1.National Institute for Environmental Studies)

10:15 AM - 10:30 AM JST | 1:15 AM - 1:30 AM UTC

[AAS04-21] **Characteristics of Atmospheric Photochemical Pollution at a Comprehensive Site in Guangzhou, China**

*Yu Zou[1] (1.Institute of Tropical and Marine Meteorology, CMA,Guangzhou,China)

[J] Oral | A (Atmospheric and Hydrospheric Sciences )：A-AS Atmospheric Sciences, Meteorology & Atmospheric Environment

10:45 AM - 12:15 PM JST | 1:45 AM - 3:15 AM UTC | 102 1F

## [A-AS04] Atmospheric Chemistry

convener:Tomoki Nakayama(Graduate School of Fisheries and Environmental Sciences, Nagasaki University), Yoko Iwamoto(Graduate School of Biosphere Science, Hiroshima University), Sakae Toyoda(Department of Chemical Science and Engineering, Tokyo Institute of Technology), Nawo Eguchi(Kyushu University), Chairperson:Fumikazu Taketani(海洋研究開発機構), Michihiro Mochida(名古屋大学)

10:45 AM - 11:00 AM JST | 1:45 AM - 2:00 AM UTC

[AAS04-22] LC/MS analysis of molecular markers present in biogenic secondary organic aerosols collected during year-round observations at a cool-temperature forest

*Kei Sato[1], Sathiyamurthi Ramasamy[1], Satoshi Inomata[1], Yuzo Miyazaki[2] (1.National Institute for Environmental Studies, 2.Hokkaido University)

---

11:00 AM - 11:15 AM JST | 2:00 AM - 2:15 AM UTC

[AAS04-23] Surfactant Effects on Acid-Catalyzed Reactions at Aqueous Aerosol Surfaces

*Shinnosuke Ishizuka[1], Tetsuya Hama[2], Shinichi Enami[1] (1.National Institute for Environmental Studies, 2.Institute for Low Temperature Science, Hokkaido University)

---

11:15 AM - 11:30 AM JST | 2:15 AM - 2:30 AM UTC

[AAS04-24] Roles of heterogeneous reactions in the tropospheric chemistry: a global modeling study

*Phuc Thi Minh Ha[1], Fumikazu Taketani[2], Yugo Kanaya[2], Kengo Sudo[1,2] (1.Graduate School of Environmental Studies, Nagoya University, 2.Research and Development Center for Global Change, JAMSTEC)

---

11:30 AM - 11:45 AM JST | 2:30 AM - 2:45 AM UTC

[AAS04-25] Sensitivity of regional deposition of inhaled atmospheric aerosols in human respiratory tract to their size distribution and hygroscopicity: A case study

*Minrui Wang[1], Toshiyuki Mihara[2,4], Mizuo Kajino[5], Kaori Kawana[2,6], Michihiro Mochida[1,2,3] (1.Institute for Space Earth Environmental Research, 2.Graduate School of Environmental Studies, Nagoya University, 3.Institute for Advanced Research, Nagoya University, 4.Now at Gifu Prefectural Industrial Research Institute, 5.Meteorological Research Institute, Japan Meteorological Agency, 6.Now at Research and Development Center for Global Change, JAMASTEC)

---

11:45 AM - 12:00 PM JST | 2:45 AM - 3:00 AM UTC

[AAS04-26] Biogeochemical cycle between atmosphere and ocean via particulate matters
-Award lecture for JpSAC Young Scientist Award-

★Invited Papers

*Yoko Iwamoto[1] (1.Graduate School of Biosphere Science, Hiroshima University)

---

12:00 PM - 12:15 PM JST | 3:00 AM - 3:15 AM UTC

[AAS04-27] Kinetic Studies for Quantitative Elucidation of Heterogeneous Halogen Chemistry in the Troposphere
-JpSAC Early Career Scientist Award Lecure-

★Invited Papers

*Yosuke Sakamoto[1,2] (1.Graduate School of Global Environmental Studies, Kyoto University , 2.Graduate School of Human and Environmental Studies, Kyoto University)

[J] Poster | A (Atmospheric and Hydrospheric Sciences )：A-AS Atmospheric Sciences, Meteorology & Atmospheric Environment

1:45 PM - 3:15 PM JST | 4:45 AM - 6:15 AM UTC | Poster Hall International Exhibition Hall8, Makuhari Messe_2

## [A-AS04] Atmospheric Chemistry

convener:Tomoki Nakayama(Graduate School of Fisheries and Environmental Sciences, Nagasaki University), Yoko Iwamoto(Graduate School of Biosphere Science, Hiroshima University), Sakae Toyoda(Department of Chemical Science and Engineering, Tokyo Institute of Technology), Nawo Eguchi(Kyushu University)

[AAS04-P01] Validation of GOSAT cloud judgement by using Himawari-8 data

*Kitamura Katsuki[1], Naoko Saitoh[2] (1.Chiba University Graduate School of Science and Engineering Division of Earth Environmental Science , 2.Center for Environmental Remote Sensing Chiba University)

[AAS04-P02] Measurement of temperature that fungal spores form ice nuclei

*Kazuyuki Kita[1], Kansei Sasaki[1], Koutaro Minami[1], Takeshi Kinase[2], Kouji Adachi[2], Yuji Zaizen[2], Kentaro Hosaka[3], Teruya Maki[4], Yasuhito Igarashi[1,5] (1.Ibaraki University, 2.Meteorological Research Laboratory, 3.National Musium of Nature and Science, 4.Kanazawa University, 5.Kyoto University)

[AAS04-P03] **Investigation of Atmospheric Aerosol Particles and gases by R/V Mirai cruise over the Arctic Ocean on 2017**

*Fumikazu Taketani[1], Saki Kato[1,2], Takuma Miyakawa[1], Masayuki Takigawa[1], Masahiro Yamaguchi[1], Hisahiro Takashima[1,2], Petr Mordovskoi[1], Yugo Kanaya[1] (1.Japan Agency for Marine-Earth Science and Technology, 2.Fukuoka University)

[AAS04-P04] Characterization of carbonaceous aerosols in East Asia in the spring of 2015: Importance of non-fossil fuel sources

*Takuma Miyakawa[1], Yuichi Komazaki[1], Fumikazu Taketani[1], Xiaole PAN[2], Zifa Wang[2], Yugo Kanaya[1] (1.Japan Agency for Marine-Earth Science and Technology, 2.Institute for Atmospheric Physics, Chinese Academy of Science)

[AAS04-P05] **Analyzing the influence of biomass burning on ambient air pollution in mainland Southeast Asia from 2001 to 2016**

*Shuai Yin[1] (1.National Institute for Environmental Studies)

[AAS04-P06] High-resolution and multi-year inventory of mercury emissions from biomass burning in tropical continents during 2001–2017

*Yusheng Shi[1] (1.Aerospace Information Research Institute, Chinese Academy of Sciences)

[AAS04-P07] Simultaneous observations by sky radiometer and MAX-DOAS for characterization of biomass burning plumes in central Thailand in January-April 2016

*Hitoshi Irie[1], Syedul Hoque[1], Alessandro Damiani[1], Al Mashroor Fatmi[1], Pradeep Khatri[2], Tamio Takamura[1], Thanawat Jarupongsakul[3] (1.Chiba University, 2.Tohoku University, 3.Chulalongkorn University)

[AAS04-P08] Quantifying PM2.5 from long-range transport and local pollution in Taiwan during winter monsoon.

*Ming-Tung Chuang[1] (1.Research Center for Environmental Changes, Academia Sinica)

[AAS04-P09] Vertical characterization of $PM_{2.5}$ based on observation using compact sensors on and around Mt. Unzen in Nagasaki Prefecture

*Tomoki Nakayama[1], Ayane Ueno[1], Kenta Kanegae[1], Kazuaki Kawamoto[1], Kodo Umakoshi[1], Takayuki Yamasaki[2], Wataru Okamoto[2], Yutaka Matsumi[2] (1.Faculty of Environmental Science, Nagasaki University, 2.ISEE, Nagoya University)

[AAS04-P10] Observation of NPF events at the summit of Mt. Fuji during daytime and nighttime

*Hiroki Igarashi[1], Takenori Sato[1], Tatsuhiro Mori[1], Kazuhiko Miura[1], Yoko Iwamoto[2], Ryuichi Wada[3], Shungo Kato[4], Hiroshi Okochi[5] (1.Tokyo University of Science, 2.Hiroshima University, 3.Teikyo University of Science, 4.Tokyo Metropolitan University, 5.Waseda University)

[AAS04-P11] Measurement of atmospheric metal particles using an ICP-MS and TEM.

*Takeshi Kinase[1], Kouji Adachi[1], Mizuo Kajino[1], Masahiko Hayashi[2], Keiichiro Hara[2] (1.Meteorological Research Institute, 2.Fukuoka)

[AAS04-P12] Experimental results on measuring device of complex refractive index using the single particle extinction and scattering method

*TAKASAGO YUYA[1] (1.Tokyo university)

[AAS04-P13] **Evaluation of BC and CO emission inventory based on long-term in-situ observations over East Asia**

*Yongjoo Choi[1], Yugo Kanaya[1], Hye-Jung Shin[2], Seung-Myong Park[2], Atsushi Matsuki[3], Yasuhiro Sadanaga[4], Sang-woo Kim[5], Itsushi Uno[6], Xiaole Pan[7] (1.Development Center for Global Change, Japan Agency for Marine-Earth Science and Technology, 2.Division of Climate & Air Quality Research, National Institute of Environmental Research, Korea, 3.Institute of Nature and Environmental Technology, Kanazawa University, 4.Department of Applied Chemistry, Graduate School of Engineering, Osaka Prefecture University, 5.School of Earth and Environmental Sciences, Seoul National University, Seoul, Korea, 6.Research Institute for Applied Mechanics, Kyushu University, 7.Institute of Atmospheric Physics, CAS, Beijing, China)

[AAS04-P14] **Inverse modeling of black carbon emissions over China using ensemble data assimilation**

*Ping Wang[1] (1. Chinese Academy of Meteorological Sciences)

[AAS04-P15] Analysis of BC emissions in East Asia using inverse model

*Takashi Maki[1], Taichu Y Tanaka[1], Naga Oshima[1], Thomas Sekiyama[1], Keiichi Kondo[1], Jun-ichi Kurokawa[2], Keiya Yumimoto[3], Toshimasa Ohara[4] (1.Meteorological Research Institute, 2.Asia Center for AirPollution Research, 3.Kyushu University, 4.National Institute for Environmental Studies)

[AAS04-P16] Source attribution of BC in the northern Pacific and Arctic Ocean by chemistry climate model

*Takato Onishi[1], Kengo Sudo[1,2], Yugo Kanaya[2], Fumikazu Taketani[2] (1. Graduate School of Environmental Studies, Nagoya University, 2.Japan Agency for Marine-Earth Science and Technology)

[AAS04-P17] Evaluation of a mobile $PM_{2.5}$ sensor and application to the measurements along the National route 1 and around Nagasaki University

*Kenta Kanegae[1], Takayuki Yamasaki[2], Wataru Okamoto[2], Yutaka Matsumi[2], Tomoki Nakayama[1] (1.Nagasaki University, 2.Nagoya University)

[AAS04-P18] Analysis on the Relationship between the Concentration of Particulate Matter and Mortality from Respiratory and Cardiovascular Diseases

*Woo-Sik JUNG[1], Woo-Gon Do[2] (1.Department of Atmospheric Environment Information Engineering, Atmospheric Environment Information Research Center, Inje University, Gimhae 50834, Korea, 2.Busan Metropolitan City of Institute of Health and Environment Busan, Korea)

[AAS04-P19] A Study on the Estimation of Contribution Rate of Odour Substances Using CALPUFF model

*Woo-Sik JUNG[1], Woo-Gon Do[2] (1.Department of Atmospheric Environment Information Engineering, Atmospheric Environment Information Research Center, Inje University, Gimhae 50834, Korea, 2.Busan Metropolitan City of Institute of Health and Environment Busan, Korea)

[AAS04-P20] Stepwise decrease in atmospheric trace gases near the ground associated with rapid vertical mixing observed by 3-D coherent Doppler lidar and in-situ gas measurements

*Hisahiro Takashima[1], Keiichiro Hara[1], Yuki Ohira[1], Akinori Takami[2], Ayako Yoshino[2], Yasushi Fujiyoshi[3] (1.Fukuoka University, 2.National Institute for Environmental Studies, 3.Hokaido University)

[AAS04-P21] Spatiotemporal variations of nitrogen dioxide ($NO_2$) over Fukuoka , observed by multiple MAX-DOAS instruments and 3-D coherent Doppler lidar

*Hironobu Ueki[1], Hisahiro Takashima[1], Martina M. Friedrich[2] (1.Fukuoka university, 2.Belgian Institute for Space Aeronomy (BIRA-IASB), Belgium)

[AAS04-P22] Measurement on the $^{17}O$-excess of tropospheric nitrogen oxides

*Fumiko Nakagawa[1], Dong Ding[1], Urumu Tsunogai[1], Takashi Yamaguchi[2], Izumi Noguchi[2] (1.Graduate School of Environmental Studies, Nagoya University, 2.Institute of Environment Sciences, Hokkaido Research Organization)

[AAS04-P23] Long-term measurements of the column-averaged mixing ratios of tropospheric substances related to the air pollution using ground-based FTIRs at Rikubetsu, Japan

*Tomoo Nagahama[1], Isamu Morino[2], Shingo Nakanishi[1] (1.Institute for Space-Earth Environmental Research, Nagoya University, 2.National Institute for Environmental Studies)

[AAS04-P24] Impacts of Biogenic and Anthropogenic Emissions on Summertime Ozone Formation in the Guanzhong Basin, China

*Nan Li[1] (1.Nanjing University of Information Science & Technology)

[AAS04-P25] **Comprehensive monitoring project of greenhouse gases and air pollutants around Jakarta megacity in Indonesia**

*Masahide Nishihashi[1], Hitoshi Mukai[1], Yukio Terao[1], Shigeru Hashimoto[1], Rizaldi Boer[2], Muhammad Ardiansyah[2], Bregas Budianto[2], Gito Sugih Immanuel[2], Adi Rakhman[2], Rudi Nugroho[3], Nawa Suwedi[3], Agus Rifai[3], Iif Miftahul Ihsan[3], Anies Marufatin[3], Albert Sulaiman[3], Dodo Gunawan[4], Eka Suharguniyawan[4], Asep Firman Ilahi[4], Muharam Syam Nugraha[4], Ronald Christian Wattimena[4], Bayu Feriaji[4], Thomas Lauvaux[5], Tomohiro Oda[6] (1.National Institute for Environmental Studies, 2.Bogor Agricultural University (IPB), Indonesia, 3.Agency for the Assessment and Application of Technology (BPPT), Indonesia, 4.Meteorological, Climatological, and Geophysical Agency (BMKG), Indonesia, 5.Laboratory for Sciences of Climate and Environment (LSCE), France, 6.Universities Space Research Association/NASA Goddard Space Flight Center, USA)

[AAS04-P26] **Seasonality of short-term variations in atmospheric $CH_4$ observed at Hateruma and relationship with the reginal emissions from East Asia**

*Yasunori Tohjima[1], Jiye Zeng[1], Tomoko Shirai[1], Akihiko Ito[1], Motoki Sasakawa[1], Toshinobu Machida[1] (1.National Institute for Environmental Studies)

[AAS04-P27] A cryogen-free automated measurement system of stable carbon isotope ratio of atmospheric methane

*Taku Umezawa[1], Takuya Saito[1] (1.National Institute of Environmental Studies)

[AAS04-P28] Global inverse analysis of $CH_4$ fluxes using NICAM-TM 4D-Var

*Yosuke Niwa[1,2], Akihiko Ito[1], Toshinobu Machida[1], Motoki Sasakawa[1], Yasunori Tohjima[1], Taku Umezawa[1], Shinji Morimoto[3], Shuji Aoki[3], Yousuke Sawa[2], Kazuhiro Tsuboi[2], Hidekazu Matsueda[2], Ed Dlugokencky[4], Christina Harth[5], Paul B Krummel[6], Ray L Langenfelds[6], Zoe M Loh[6], Jens Mühle[5], Simon O'Doherty[7], Ronald G Prinn[8], Michel Ramonet[9], Peter Salameh[5], Colm Sweeney[4], Ray Weiss[5], Dickon Young[7], Simona Castaldi[10,11], Sergio Noce[12], Marielle Saunois[9], Ann R Stavert[13] (1.National Institute for Environmental Studies, 2.Meteorological Research Institute, 3.Tohoku University, 4.Earth System Research Laboratory, National Oceanic and Atmospheric Administration, 5.Scripps Institution of Oceanography, University of California, 6.Climate Science Centre, CSIRO Oceans and Atmosphere, 7.School of Chemistry, University of Bristol, 8.Massachusetts Institute of Technology, 9.Laboratoire des Sciences du Climat et de l'Environnement, LSCE-IPSL (CEA-CNRS-UVSQ), 10.DISTABIF, Università degli studi della Campania Luigi Vanvitelli, 11.Department Landscape Design & Sustainable Ecosystems RUDN University, 12.IAFES, Euro-Mediterranean Center on Climate Change, 13.Global Carbon Project, CSIRO Oceans and Atmosphere)

[AAS04-P29] Scientific findings from observations of GOSAT/TANSO−FTS TIR band

*Naoko Saitoh[1], Shingo Kosaka[1], Masato Shiraki[1], Hinako Kobayashi[1] (1.Center for Environmental Remote Sensing)

[AAS04-P30] **Continuous measurements of atmospheric $CO_2$ and its $\delta^{13}C$ and $\delta^{18}O$ at Minamitorishima Island**

*Shohei Murayama[1], Kazuhiro Tsuboi[2], Shigeyuki Ishidoya[1], Hidekazu Matsueda[2], Yosuke Niwa[3], Yousuke Sawa[2], Kentaro Ishijima[2], Kentaro Kozumi[4], Genta Umezawa[4], Kazuya Yukita[4], Shigeharu Nishida[4], Megumi Yamamoto[4], Tetsuyuki Usami[1], Shinji Morimoto[5] (1.National Institute of Advanced Industrial Science and Technology (AIST), 2.Meteorological Research Institute, 3.National Institute for Environmental Studies, 4.Japan Meteorological Agency, 5.Tohoku University)

[AAS04-P31] Variations of atmospheric Radon-222 concentration observed at JMA stations

*Kentaro Ishijima[1], Kazuhiro Tsuboi[1], Hidekazu Matsueda[1], Yousuke Sawa[1], Yosuke Niwa[2,1], Takashi Maki[1], Takashi Nakamura[3] (1.Meteorological Research Institute, 2.National Institute for Environmental Studies, 3.Japan Meteorological Agency)

[AAS04-P32] Long-term variations of CFCs and HCFCs observed with ground-based FTIR spectrometers at Rikubetsu, Syowa Station, and Tsukuba since 1995

*Hideaki Nakajima[1,2], Masanori Takeda[2,1], Isao Murata[2], Takafumi Sugita[1], Tomoo Nagahama[3], Isamu Morino[1], Takeshi Kinase[4] (1.National Institute for Environmental Studies, 2.Graduate School of Environmental Studies, Tohoku University, 3.Institute for Space-Earth Environmental Research, Nagoya University, 4.Meteorological Research Institute)

---

## [AAS04-P33] Millimeter-wave observation of stratospheric ozone in 2015-2017 in Rio Gallegos at the southern tip of South America

*Akira Mizuno[1], Hironori Seki[1], Tomoo Nagahama[1], Hirofumi Ohyama[2], Jacobo Salvador[3], Facundo Orte[3], Elian Walfram[3] (1.Institute for Space-Earth Environmental Research, Nagoya University, 2.National Institute for Environmental Studies, 3.Laser and Applications Research Center, UNIDEF (CITEDEF-CONICET))

[J] Poster | A (Atmospheric and Hydrospheric Sciences )：A-AS Atmospheric Sciences, Meteorology & Atmospheric Environment

5:15 PM - 6:30 PM JST | 8:15 AM - 9:30 AM UTC | Poster Hall International Exhibition Hall8, Makuhari Messe_6

## [A-AS04] Atmospheric Chemistry

convener:Tomoki Nakayama(Graduate School of Fisheries and Environmental Sciences, Nagasaki University), Yoko Iwamoto(Graduate School of Biosphere Science, Hiroshima University), Sakae Toyoda(Department of Chemical Science and Engineering, Tokyo Institute of Technology), Nawo Eguchi(Kyushu University)

[AAS04-P01] Validation of GOSAT cloud judgement by using Himawari-8 data

*Kitamura Katsuki[1], Naoko Saitoh[2] (1.Chiba University Graduate School of Science and Engineering Division of Earth Environmental Science , 2.Center for Environmental Remote Sensing Chiba University)

[AAS04-P02] Measurement of temperature that fungal spores form ice nuclei

*Kazuyuki Kita[1], Kansei Sasaki[1], Koutaro Minami[1], Takeshi Kinase[2], Kouji Adachi[2], Yuji Zaizen[2], Kentaro Hosaka[3], Teruya Maki[4], Yasuhito Igarashi[1,5] (1.Ibaraki University, 2.Meteorological Research Laboratory, 3.National Musium of Nature and Science, 4.Kanazawa University, 5.Kyoto University)

[AAS04-P03] **Investigation of Atmospheric Aerosol Particles and gases by R/V Mirai cruise over the Arctic Ocean on 2017**

*Fumikazu Taketani[1], Saki Kato[1,2], Takuma Miyakawa[1], Masayuki Takigawa[1], Masahiro Yamaguchi[1], Hisahiro Takashima[1,2], Petr Mordovskoi[1], Yugo Kanaya[1] (1.Japan Agency for Marine-Earth Science and Technology, 2.Fukuoka University)

[AAS04-P04] Characterization of carbonaceous aerosols in East Asia in the spring of 2015: Importance of non-fossil fuel sources

*Takuma Miyakawa[1], Yuichi Komazaki[1], Fumikazu Taketani[1], Xiaole PAN[2], Zifa Wang[2], Yugo Kanaya[1] (1.Japan Agency for Marine-Earth Science and Technology, 2.Institute for Atmospheric Physics, Chinese Academy of Science)

[AAS04-P05] **Analyzing the influence of biomass burning on ambient air pollution in mainland Southeast Asia from 2001 to 2016**

*Shuai Yin[1] (1.National Institute for Environmental Studies)

[AAS04-P06] High-resolution and multi-year inventory of mercury emissions from biomass burning in tropical continents during 2001–2017

*Yusheng Shi[1] (1.Aerospace Information Research Institute, Chinese Academy of Sciences)

[AAS04-P07] Simultaneous observations by sky radiometer and MAX-DOAS for characterization of biomass burning plumes in central Thailand in January-April 2016

*Hitoshi Irie[1], Syedul Hoque[1], Alessandro Damiani[1], Al Mashroor Fatmi[1], Pradeep Khatri[2], Tamio Takamura[1], Thanawat Jarupongsakul[3] (1.Chiba University, 2.Tohoku University, 3.Chulalongkorn University)

[AAS04-P08] Quantifying PM2.5 from long-range transport and local pollution in Taiwan during winter monsoon.

*Ming-Tung Chuang[1] (1.Research Center for Environmental Changes, Academia Sinica)

[AAS04-P09] Vertical characterization of $PM_{2.5}$ based on observation using compact sensors on and around Mt. Unzen in Nagasaki Prefecture

*Tomoki Nakayama[1], Ayane Ueno[1], Kenta Kanegae[1], Kazuaki Kawamoto[1], Kodo Umakoshi[1], Takayuki Yamasaki[2], Wataru Okamoto[2], Yutaka Matsumi[2] (1.Faculty of Environmental Science, Nagasaki University, 2.ISEE, Nagoya University)

[AAS04-P10] Observation of NPF events at the summit of Mt. Fuji during daytime and nighttime

*Hiroki Igarashi[1], Takenori Sato[1], Tatsuhiro Mori[1], Kazuhiko Miura[1], Yoko Iwamoto[2], Ryuichi Wada[3], Shungo Kato[4], Hiroshi Okochi[5] (1.Tokyo University of Science, 2.Hiroshima University, 3.Teikyo University of Science, 4.Tokyo Metropolitan University, 5.Waseda University)

[AAS04-P11] Measurement of atmospheric metal particles using an ICP-MS and TEM.

*Takeshi Kinase[1], Kouji Adachi[1], Mizuo Kajino[1], Masahiko Hayashi[2], Keiichiro Hara[2] (1.Meteorological Research Institute, 2.Fukuoka)

[AAS04-P12] Experimental results on measuring device of complex refractive index using the single particle extinction and scattering method

*TAKASAGO YUYA[1] (1.Tokyo university)

[AAS04-P13] **Evaluation of BC and CO emission inventory based on long-term in-situ observations over East Asia**

*Yongjoo Choi[1], Yugo Kanaya[1], Hye-Jung Shin[2], Seung-Myong Park[2], Atsushi Matsuki[3], Yasuhiro Sadanaga[4], Sang-woo Kim[5], Itsushi Uno[6], Xiaole Pan[7] (1.Development Center for Global Change, Japan Agency for Marine-Earth Science and Technology, 2.Division of Climate & Air Quality Research, National Institute of Environmental Research, Korea, 3.Institute of Nature and Environmental Technology, Kanazawa University, 4.Department of Applied Chemistry, Graduate School of Engineering, Osaka Prefecture University, 5.School of Earth and Environmental Sciences, Seoul National University, Seoul, Korea, 6.Research Institute for Applied Mechanics, Kyushu University, 7.Institute of Atmospheric Physics, CAS, Beijing, China)

[AAS04-P14] **Inverse modeling of black carbon emissions over China using ensemble data assimilation**

*Ping Wang[1] (1. Chinese Academy of Meteorological Sciences)

[AAS04-P15] Analysis of BC emissions in East Asia using inverse model

*Takashi Maki[1], Taichu Y Tanaka[1], Naga Oshima[1], Thomas Sekiyama[1], Keiichi Kondo[1], Jun-ichi Kurokawa[2], Keiya Yumimoto[3], Toshimasa Ohara[4] (1.Meteorological Research Institute, 2.Asia Center for AirPollution Research, 3.Kyushu University, 4.National Institute for Environmental Studies)

[AAS04-P16] Source attribution of BC in the northern Pacific and Arctic Ocean by chemistry climate model

*Takato Onishi[1], Kengo Sudo[1,2], Yugo Kanaya[2], Fumikazu Taketani[2] (1. Graduate School of Environmental Studies, Nagoya University, 2.Japan Agency for Marine-Earth Science and Technology)

[AAS04-P17] Evaluation of a mobile $PM_{2.5}$ sensor and application to the measurements along the National route 1 and around Nagasaki University

*Kenta Kanegae[1], Takayuki Yamasaki[2], Wataru Okamoto[2], Yutaka Matsumi[2], Tomoki Nakayama[1] (1.Nagasaki University, 2.Nagoya University)

[AAS04-P18] Analysis on the Relationship between the Concentration of Particulate Matter and Mortality from Respiratory and Cardiovascular Diseases

*Woo-Sik JUNG[1], Woo-Gon Do[2] (1.Department of Atmospheric Environment Information Engineering, Atmospheric Environment Information Research Center, Inje University, Gimhae 50834, Korea, 2.Busan Metropolitan City of Institute of Health and Environment Busan, Korea)

[AAS04-P19] A Study on the Estimation of Contribution Rate of Odour Substances Using CALPUFF model

*Woo-Sik JUNG[1], Woo-Gon Do[2] (1.Department of Atmospheric Environment Information Engineering, Atmospheric Environment Information Research Center, Inje University, Gimhae 50834, Korea, 2.Busan Metropolitan City of Institute of Health and Environment Busan, Korea)

[AAS04-P20] Stepwise decrease in atmospheric trace gases near the ground associated with rapid vertical mixing observed by 3-D coherent Doppler lidar and in-situ gas measurements

*Hisahiro Takashima[1], Keiichiro Hara[1], Yuki Ohira[1], Akinori Takami[2], Ayako Yoshino[2], Yasushi Fujiyoshi[3] (1.Fukuoka University, 2.National Institute for Environmental Studies, 3.Hokaido University)

[AAS04-P21] Spatiotemporal variations of nitrogen dioxide ($NO_2$) over Fukuoka , observed by multiple MAX-DOAS instruments and 3-D coherent Doppler lidar

*Hironobu Ueki[1], Hisahiro Takashima[1], Martina M. Friedrich[2] (1.Fukuoka university, 2.Belgian Institute for Space Aeronomy (BIRA-IASB), Belgium)

[AAS04-P22] Measurement on the $^{17}O$-excess of tropospheric nitrogen oxides

*Fumiko Nakagawa[1], Dong Ding[1], Urumu Tsunogai[1], Takashi Yamaguchi[2], Izumi Noguchi[2] (1.Graduate School of Environmental Studies, Nagoya University, 2.Institute of Environment Sciences, Hokkaido Research Organization)

[AAS04-P23] Long-term measurements of the column-averaged mixing ratios of tropospheric substances related to the air pollution using ground-based FTIRs at Rikubetsu, Japan

*Tomoo Nagahama[1], Isamu Morino[2], Shingo Nakanishi[1] (1.Institute for Space-Earth Environmental Research, Nagoya University, 2.National Institute for Environmental Studies)

[AAS04-P24] Impacts of Biogenic and Anthropogenic Emissions on Summertime Ozone Formation in the Guanzhong Basin, China

*Nan Li[1] (1.Nanjing University of Information Science & Technology)

[AAS04-P25] **Comprehensive monitoring project of greenhouse gases and air pollutants around Jakarta megacity in Indonesia**

*Masahide Nishihashi[1], Hitoshi Mukai[1], Yukio Terao[1], Shigeru Hashimoto[1], Rizaldi Boer[2], Muhammad Ardiansyah[2], Bregas Budianto[2], Gito Sugih Immanuel[2], Adi Rakhman[2], Rudi Nugroho[3], Nawa Suwedi[3], Agus Rifai[3], Iif Miftahul Ihsan[3], Anies Marufatin[3], Albert Sulaiman[3], Dodo Gunawan[4], Eka Suharguniyawan[4], Asep Firman Ilahi[4], Muharam Syam Nugraha[4], Ronald Christian Wattimena[4], Bayu Feriaji[4], Thomas Lauvaux[5], Tomohiro Oda[6] (1.National Institute for Environmental Studies, 2.Bogor Agricultural University (IPB), Indonesia, 3.Agency for the Assessment and Application of Technology (BPPT), Indonesia, 4.Meteorological, Climatological, and Geophysical Agency (BMKG), Indonesia, 5.Laboratory for Sciences of Climate and Environment (LSCE), France, 6.Universities Space Research Association/NASA Goddard Space Flight Center, USA)

[AAS04-P26] **Seasonality of short-term variations in atmospheric $CH_4$ observed at Hateruma and relationship with the reginal emissions from East Asia**

*Yasunori Tohjima[1], Jiye Zeng[1], Tomoko Shirai[1], Akihiko Ito[1], Motoki Sasakawa[1], Toshinobu Machida[1] (1.National Institute for Environmental Studies)

[AAS04-P27] A cryogen-free automated measurement system of stable carbon isotope ratio of atmospheric methane

*Taku Umezawa[1], Takuya Saito[1] (1.National Institute of Environmental Studies)

[AAS04-P28] Global inverse analysis of $CH_4$ fluxes using NICAM-TM 4D-Var

*Yosuke Niwa[1,2], Akihiko Ito[1], Toshinobu Machida[1], Motoki Sasakawa[1], Yasunori Tohjima[1], Taku Umezawa[1], Shinji Morimoto[3], Shuji Aoki[3], Yousuke Sawa[2], Kazuhiro Tsuboi[2], Hidekazu Matsueda[2], Ed Dlugokencky[4], Christina Harth[5], Paul B Krummel[6], Ray L Langenfelds[6], Zoe M Loh[6], Jens Mühle[5], Simon O'Doherty[7], Ronald G Prinn[8], Michel Ramonet[9], Peter Salameh[5], Colm Sweeney[4], Ray Weiss[5], Dickon Young[7], Simona Castaldi[10,11], Sergio Noce[12], Marielle Saunois[9], Ann R Stavert[13] (1.National Institute for Environmental Studies, 2.Meteorological Research Institute, 3.Tohoku University, 4.Earth System Research Laboratory, National Oceanic and Atmospheric Administration, 5.Scripps Institution of Oceanography, University of California, 6.Climate Science Centre, CSIRO Oceans and Atmosphere, 7.School of Chemistry, University of Bristol, 8.Massachusetts Institute of Technology, 9.Laboratoire des Sciences du Climat et de l'Environnement, LSCE-IPSL (CEA-CNRS-UVSQ), 10.DISTABIF, Università degli studi della Campania Luigi Vanvitelli, 11.Department Landscape Design & Sustainable Ecosystems RUDN University, 12.IAFES, Euro-Mediterranean Center on Climate Change, 13.Global Carbon Project, CSIRO Oceans and Atmosphere)

[AAS04-P29] Scientific findings from observations of GOSAT/TANSO−FTS TIR band

*Naoko Saitoh[1], Shingo Kosaka[1], Masato Shiraki[1], Hinako Kobayashi[1] (1.Center for Environmental Remote Sensing)

[AAS04-P30] **Continuous measurements of atmospheric $CO_2$ and its $\delta^{13}C$ and $\delta^{18}O$ at Minamitorishima Island**

*Shohei Murayama[1], Kazuhiro Tsuboi[2], Shigeyuki Ishidoya[1], Hidekazu Matsueda[2], Yosuke Niwa[3], Yousuke Sawa[2], Kentaro Ishijima[2], Kentaro Kozumi[4], Genta Umezawa[4], Kazuya Yukita[4], Shigeharu Nishida[4], Megumi Yamamoto[4], Tetsuyuki Usami[1], Shinji Morimoto[5] (1.National Institute of Advanced Industrial Science and Technology (AIST), 2.Meteorological Research Institute, 3.National Institute for Environmental Studies, 4.Japan Meteorological Agency, 5.Tohoku University)

[AAS04-P31] Variations of atmospheric Radon-222 concentration observed at JMA stations

*Kentaro Ishijima[1], Kazuhiro Tsuboi[1], Hidekazu Matsueda[1], Yousuke Sawa[1], Yosuke Niwa[2,1], Takashi Maki[1], Takashi Nakamura[3] (1.Meteorological Research Institute, 2.National Institute for Environmental Studies, 3.Japan Meteorological Agency)

[AAS04-P32] Long-term variations of CFCs and HCFCs observed with ground-based FTIR spectrometers at Rikubetsu, Syowa Station, and Tsukuba since 1995

*Hideaki Nakajima[1,2], Masanori Takeda[2,1], Isao Murata[2], Takafumi Sugita[1], Tomoo Nagahama[3], Isamu Morino[1], Takeshi Kinase[4] (1.National Institute for Environmental Studies, 2.Graduate School of Environmental Studies, Tohoku University, 3.Institute for Space-Earth Environmental Research, Nagoya University, 4.Meteorological Research Institute)

[AAS04-P33] Millimeter-wave observation of stratospheric ozone in 2015-2017 in Rio Gallegos at the southern tip of South America

*Akira Mizuno[1], Hironori Seki[1], Tomoo Nagahama[1], Hirofumi Ohyama[2], Jacobo Salvador[3], Facundo Orte[3], Elian Walfram[3] (1.Institute for Space-Earth Environmental Research, Nagoya University, 2.National Institute for Environmental Studies, 3.Laser and Applications Research Center, UNIDEF (CITEDEF-CONICET))

[J] Oral | A (Atmospheric and Hydrospheric Sciences )：A-AS Atmospheric Sciences, Meteorology & Atmospheric Environment

3:30 PM - 5:00 PM JST | 6:30 AM - 8:00 AM UTC | 103 1F

## [A-AS04] Atmospheric Chemistry

convener:Tomoki Nakayama(Graduate School of Fisheries and Environmental Sciences, Nagasaki University), Yoko Iwamoto(Graduate School of Biosphere Science, Hiroshima University), Sakae Toyoda(Department of Chemical Science and Engineering, Tokyo Institute of Technology), Nawo Eguchi(Kyushu University), Chairperson:Hideaki Nakajima(国立環境研究所)

3:30 PM - 4:00 PM JST | 6:30 AM - 7:00 AM UTC

[AAS04-28] Planetary atmosphere - Mars and Venus -

★Invited Papers

*Hiroyuki Maezawa[1] (1.Department of Physical Science Osaka Prefecture University)

4:00 PM - 4:15 PM JST | 7:00 AM - 7:15 AM UTC

[AAS04-29] Validation of methane profile observed with FTIR at Tsukuba

Yuki Dai[2], *Isao Murata[1], Hideaki Nakajima[3], Isamu Morino[3] (1.Graduate School of Environmental Studies, Tohoku University, 2.Graduate School of Science, Tohoku University, 3.National Institute for Environmental Studies)

4:15 PM - 4:30 PM JST | 7:15 AM - 7:30 AM UTC

[AAS04-30] **Retrieval of HFC-23 from FTIR observations at Syowa Station, Rikubetsu and Tsukuba**

*Masanori Takeda[1,2], Hideaki Nakajima[2,1], Isao Murata[1], Tomoo Nagahama[3], Isamu Morino[2] (1.Graduate School of Environmental Studies, Tohoku University, 2.Center for Global Environmental Research, National Institute for Environmental Studies, 3.Institute for Space-Earth Environmental Research, Nagoya University)

4:30 PM - 4:45 PM JST | 7:30 AM - 7:45 AM UTC

[AAS04-31] Roles of cloud distribution in global atmospheric photochemistry

*Ryoki Matsuda[1], Kengo Sudo[1,2] (1.Graduate School of Environmental Studies, Nagoya University , 2.Japan Marine-Earth Science and Technology)

4:45 PM - 5:00 PM JST | 7:45 AM - 8:00 AM UTC

[AAS04-32] Evaluating global distribution and interannual variation of stratosphere-troposphere exchange of ozone: impacts of climate variabilities

*Kengo Sudo[1,2], Xin Li[1] (1.Graduate School of Environmental Studies, Nagoya University, 2.Research and Development Center for Global Change, JAMSTEC)

[E] Poster | A (Atmospheric and Hydrospheric Sciences )：A-OS Ocean Sciences & Ocean Environment

10:45 AM - 12:15 PM JST | 1:45 AM - 3:15 AM UTC | Poster Hall International Exhibition Hall8, Makuhari Messe_2

## [A-OS07] Climate variability and predictability on subseasonal to decadal timescales

convener:Takashi Mochizuki(Japan Agency for Marine-Earth Science and Technology), V Ramaswamy(NOAA GFDL), Doug Smith(Met Office), Yushi Morioka(Japan Agency for Marine-Earth Science and Technology)

[AOS07-P01] Changes in North American and European Heatwave Characteristics

*Szandra A. Peter[1], Ben Kirtman[1] (1.Rosenstiel School of Marine and Atmospheric Science)

[AOS07-P02] **The effects of the "New Climate" Warming on Western Mediterranean: Situation of the Recent Extreme Events**

*Mohammed-Said KARROUK[1] (1.Hassan II University of Casablanca)

[AOS07-P03] **Month-to-month Difference of the Western Pacific Subtropical High Simulated by CMIP5 Models**

*Xiao Dong[1], Renping Lin[1] (1.Institute of Atmospheric Physics)

[AOS07-P04] Potential regulation on the climatic effect of Tibetan Plateau heating by tropical air–sea coupling

*Ziqian Wang[1], Anmin Duan[2], Song Yang[1] (1.School of Atmospheric Sciences, Sun Yat-sen University, 2.Institute of Atmospheric Physics, Chinese Academy of Sciences)

[AOS07-P05] Intraseasonal variation of the South Asian high and its role in connecting the Indian and East Asian summer monsoons

*Wei Wei[1] (1.Sun Yat-sen University)

[AOS07-P06] Mean Surface Air Temperatures in Japan - Regional Classification and Interranual Variability

*Pascal Oettli[1], Masami Nonaka[1], Swadhin Behera[1] (1.Japan Agency for Marine-Earth Science and Technology)

[AOS07-P07] Inter-Annual Variability of the Indonesian Rainfall and Air-Sea Interaction over the Indian-Pacific Ocean Associated with Regime Shift

*Murni Ngestu Nurutami[1], Tadahiro Hayasaka[1] (1.Center for Atmospheric and Oceanic Studies, Graduate School of Science, Tohoku University)

[AOS07-P08] Exploring synoptic-scale drivers of interannual rainfall variability over Africa

*Piotr Wolski[1], Chris Jack[1], Waarith Abrahams[1], Stefaan Conradie[1] (1.University of Cape Town)

[AOS07-P09] **Effect of El Niño on the response ratio of Hadley circulation to different SST meridional structures**

*Juan Feng[1] (1.Beijing Normal University)

[AOS07-P10] **Novel data-driven approach for ENSO prediction**

*Dmitri Kondrashov[1], Evgeniy Loskutov[2], Andrei Gavrilov[2], Dmitry Mukhin[2], Alexander Feigin[2] (1.University of California, Los Angeles, United States, 2.Institute of Applied Physics of the Russian Academy of Sciences, Nizhny Novgorod, Russian Federation)

[AOS07-P11] Experimental seasonal climate prediction using CFES: Comparison with the SINTEX-F systems

*Nobumasa Komori[1], Bunmei Taguchi[2], Akira Kuwano-Yoshida[3,1], Takeshi Doi[1], Masami Nonaka[1] (1.Japan Agency for Marine-Earth Science and Technology, 2.Research Center for Advanced Science and Technology, The University of Tokyo, 3.Disaster Prevention Research Institute, Kyoto University)

[AOS07-P12] Exploring the SST error growth during ENSO developing phase by using BCC_CSM1.1(m)

*Ben Tian[1], Hongli Ren[1] (1.National Climate Center, China Meteorological Administration)

[AOS07-P13] Role of sea-ice initialization in climate predictability over the Weddell Sea

*Yushi Morioka[1], Takeshi Doi[1], Doroteaciro Iovino[2], Simona Masina[2], Swadhin Behera[1] (1.Japan Agency for Marine-Earth Science and Technology (JAMSTEC), 2.Centro Euro-Mediterraneo sui Cambiamenti Climatici (CMCC))

[AOS07-P14] Observed and hindcasted subdecadal variability of the tropical Pacific climate

*Takashi Mochizuki[1], Masahiro Watanabe[2] (1.Japan Agency for Marine-Earth Science and Technology, 2.Atmosphere-Ocean Research Institute, The University of Tokyo)

[E] Poster | A (Atmospheric and Hydrospheric Sciences )：A-OS Ocean Sciences & Ocean Environment

5:15 PM - 6:30 PM JST | 8:15 AM - 9:30 AM UTC | Poster Hall International Exhibition Hall8, Makuhari Messe_7

## [A-OS07] Climate variability and predictability on subseasonal to decadal timescales

convener:Takashi Mochizuki(Japan Agency for Marine-Earth Science and Technology), V Ramaswamy(NOAA GFDL), Doug Smith(Met Office), Yushi Morioka(Japan Agency for Marine-Earth Science and Technology)

[AOS07-P01] Changes in North American and European Heatwave Characteristics

*Szandra A. Peter[1], Ben Kirtman[1] (1.Rosenstiel School of Marine and Atmospheric Science)

[AOS07-P02] **The effects of the "New Climate" Warming on Western Mediterranean: Situation of the Recent Extreme Events**

*Mohammed-Said KARROUK[1] (1.Hassan II University of Casablanca)

[AOS07-P03] **Month-to-month Difference of the Western Pacific Subtropical High Simulated by CMIP5 Models**

*Xiao Dong[1], Renping Lin[1] (1.Institute of Atmospheric Physics)

[AOS07-P04] Potential regulation on the climatic effect of Tibetan Plateau heating by tropical air–sea coupling

*Ziqian Wang[1], Anmin Duan[2], Song Yang[1] (1.School of Atmospheric Sciences, Sun Yat-sen University, 2.Institute of Atmospheric Physics, Chinese Academy of Sciences)

[AOS07-P05] Intraseasonal variation of the South Asian high and its role in connecting the Indian and East Asian summer monsoons

*Wei Wei[1] (1.Sun Yat-sen University)

[AOS07-P06] Mean Surface Air Temperatures in Japan - Regional Classification and Interranual Variability

*Pascal Oettli[1], Masami Nonaka[1], Swadhin Behera[1] (1.Japan Agency for Marine-Earth Science and Technology)

[AOS07-P07] Inter-Annual Variability of the Indonesian Rainfall and Air-Sea Interaction over the Indian-Pacific Ocean Associated with Regime Shift

*Murni Ngestu Nurutami[1], Tadahiro Hayasaka[1] (1.Center for Atmospheric and Oceanic Studies, Graduate School of Science, Tohoku University)

[AOS07-P08] Exploring synoptic-scale drivers of interannual rainfall variability over Africa

*Piotr Wolski[1], Chris Jack[1], Waarith Abrahams[1], Stefaan Conradie[1] (1.University of Cape Town)

[AOS07-P09] **Effect of El Niño on the response ratio of Hadley circulation to different SST meridional structures**

*Juan Feng[1] (1.Beijing Normal University)

[AOS07-P10] **Novel data-driven approach for ENSO prediction**

*Dmitri Kondrashov[1], Evgeniy Loskutov[2], Andrei Gavrilov[2], Dmitry Mukhin[2], Alexander Feigin[2] (1.University of California, Los Angeles, United States, 2.Institute of Applied Physics of the Russian Academy of Sciences, Nizhny Novgorod, Russian Federation)

[AOS07-P11] Experimental seasonal climate prediction using CFES: Comparison with the SINTEX-F systems

*Nobumasa Komori[1], Bunmei Taguchi[2], Akira Kuwano-Yoshida[3,1], Takeshi Doi[1], Masami Nonaka[1] (1.Japan Agency for Marine-Earth Science and Technology, 2.Research Center for Advanced Science and Technology, The University of Tokyo, 3.Disaster Prevention Research Institute, Kyoto University)

[AOS07-P12] Exploring the SST error growth during ENSO developing phase by using BCC_CSM1.1(m)

*Ben Tian[1], Hongli Ren[1] (1.National Climate Center, China Meteorological Administration)

[AOS07-P13] Role of sea-ice initialization in climate predictability over the Weddell Sea

*Yushi Morioka[1], Takeshi Doi[1], Doroteaciro Iovino[2], Simona Masina[2], Swadhin Behera[1] (1.Japan Agency for Marine-Earth Science and Technology (JAMSTEC), 2.Centro Euro-Mediterraneo sui Cambiamenti Climatici (CMCC))

[AOS07-P14] Observed and hindcasted subdecadal variability of the tropical Pacific climate

*Takashi Mochizuki[1], Masahiro Watanabe[2] (1.Japan Agency for Marine-Earth Science and Technology, 2.Atmosphere-Ocean Research Institute, The University of Tokyo)

[E] Oral | A (Atmospheric and Hydrospheric Sciences )：A-OS Ocean Sciences & Ocean Environment

1:45 PM - 3:15 PM JST | 4:45 AM - 6:15 AM UTC | 105 1F

## [A-OS07] Climate variability and predictability on subseasonal to decadal timescales

convener:Takashi Mochizuki(Japan Agency for Marine-Earth Science and Technology), V Ramaswamy(NOAA GFDL), Doug Smith(Met Office), Yushi Morioka(Japan Agency for Marine-Earth Science and Technology), Chairperson:V Ramaswamy(NOAA GFDL), Takashi Mochizuki(Japan Agency for Marine-Earth Science and Technology)

1:45 PM - 2:00 PM JST | 4:45 AM - 5:00 AM UTC

[AOS07-01] Seasonal Predictions of Tropical Cyclones in 2018 using GFDL and NICAM High-Resolution Global Models

★Invited Papers

*Hiroyuki Murakami[1,2], Masuo Nakano[3], V Ramaswamy[1], Thomas Delworth[1], Sarah Kapnick[1], Rich Gudgel[1], Takashi Mochizuki[3], Takeshi Doi[3], Yushi Morioka[3] (1.Geophysical Fluid Dynamics Laboratory, 2.University Corporation for Atmospheric Research, 3.JAMSTEC)

2:00 PM - 2:15 PM JST | 5:00 AM - 5:15 AM UTC

[AOS07-02] **Future change of tropical cyclone-induced waves in the Indian Ocean; An analysis based on super-high-resolution MRI-AGCM3.2 climate model**

*Bahareh Kamranzad[1,2], Nobuhito Mori[1] (1.Disaster Prevention Research Institute, Kyoto University, 2.Hakubi Center for Advanced Research, Kyoto University)

2:15 PM - 2:30 PM JST | 5:15 AM - 5:30 AM UTC

[AOS07-03] The ocean-coupled global cloud-resolving modeling era

★Invited Papers

*Tomoki Miyakawa[1] (1.Atmosphere and Ocean Research Institute University of Tokyo)

2:30 PM - 2:45 PM JST | 5:30 AM - 5:45 AM UTC

[AOS07-04] Westerly Wind Burst (WWB)/Easterly Wind Surge (EWS)-like stochastic forcing and the effects on ENSO prediction by the SINTEX-F system

*Takeshi Doi[1], Swadhin Behera[1], Toshio Yamagata[1] (1.JAMSTEC)

2:45 PM - 3:00 PM JST | 5:45 AM - 6:00 AM UTC

[AOS07-05] **The life-cycle of annual waves in the Pacific Ocean as identified by a seamless diagnosis for the energy flux**

*Hidenori AIKI[1], Takahiro Shimura[2] (1.Institute for Space-Earth Environmental Research, Nagoya University, 2.Graduate School for Environmental Studies, Nagoya University)

3:00 PM - 3:15 PM JST | 6:00 AM - 6:15 AM UTC

[AOS07-06] Development of weakly coupled atmosphere-ocean data assimilation system and the evaluation of the coupled reanalysis in JMA/MRI

★Invited Papers

*Yosuke Fujii[1], Chiaki Kobayashi[1], Toshiyuki Ishibashi[1], Yuhei Takaya[1] (1.Meteorological Research Institute, Japan Meteorological Agency)

[E] Oral | A (Atmospheric and Hydrospheric Sciences)：A-OS Ocean Sciences & Ocean Environment

3:30 PM - 5:00 PM JST | 6:30 AM - 8:00 AM UTC | 105 1F

## [A-OS07] Climate variability and predictability on subseasonal to decadal timescales

convener:Takashi Mochizuki(Japan Agency for Marine-Earth Science and Technology), V Ramaswamy(NOAA GFDL), Doug Smith(Met Office), Yushi Morioka(Japan Agency for Marine-Earth Science and Technology), Chairperson:Yushi Morioka(Japan Agency for Marine-Earth Science and Technology), Takashi Mochizuki(Japan Agency for Marine-Earth Science and Technology)

3:30 PM - 3:45 PM JST | 6:30 AM - 6:45 AM UTC

[AOS07-07] Decadal variability and predictability of the North Atlantic Oscillation

★Invited Papers

*Rosemary Eade[1,2], David Stephenson[2], Doug Smith[1], Adam Scaife[1,2], Leon Hermanson[1], Nick Dunstone[1] (1.Met Office Hadley Centre, 2.University of Exeter)

---

3:45 PM - 4:00 PM JST | 6:45 AM - 7:00 AM UTC

[AOS07-08] Seasonal to multi-year climate predictability in a climate model MIROC6

*Takahito Kataoka[1], Hiroaki Tatebe[1], Hiroshi Koyama[1], Takashi Mochizuki[1] (1.JAMSTEC Japan Agency for Marine-Earth Science and Technology)

---

4:00 PM - 4:15 PM JST | 7:00 AM - 7:15 AM UTC

[AOS07-09] Identifying the early 2000s hiatus associated with internal climate variability

*Xin-Gang Dai[1], Ping Wang[2] (1.Institute of Atmospheric Physics, Chinese Academy of Sciences, 2.Chinese Academy of Meteorological Sciences)

---

4:15 PM - 4:30 PM JST | 7:15 AM - 7:30 AM UTC

[AOS07-10] Decadal Evolution of the Surface Energy Budget during the Fast Warming and Global Warming Hiatus Periods in the ERA-Interim

*XIAOMING HU[1] (1.Sun Yat-sen University)

---

4:30 PM - 4:45 PM JST | 7:30 AM - 7:45 AM UTC

[AOS07-11] **The role of ocean variability for multi-year droughts in Australia**

*Andrea Taschetto[1,2], Alex Sen Gupta[1,2], Caroline C Ummenhofer[3], Matthew H England[1,2] (1.Climate Change Research Centre, University of New South Wales, Sydney, Australia, 2.ARC Centre of Excellence for Climate Extremes, University of New South Wales, Sydney, Australia, 3.Department of Physical Oceanography, Woods Hole Oceanographic Institution, Woods Hole, MA, USA)

---

4:45 PM - 5:00 PM JST | 7:45 AM - 8:00 AM UTC

[AOS07-12] Decadal variability and predictability in the Southern Ocean - implications for interpreting recent observed trends

★Invited Papers

*Liping Zhang[1,2], Thomas L Delworth[2], William Cooke[2,3], Xiaosong Yang[2,3] (1.Princeton University, 2.Geophysical Fluid Dynamics Laboratory, 3.UCAR)

[E] Oral | A (Atmospheric and Hydrospheric Sciences )：A-OS Ocean Sciences & Ocean Environment

9:00 AM - 10:30 AM JST | 12:00 AM - 1:30 AM UTC | 105 1F

## [A-OS10] Atlantic climate variability, and its global impacts and predictability

convener:Ingo Richter(JAMSTEC Japan Agency for Marine-Earth Science and Technology), Hiroki Tokinaga(Research Institute for Applied Mechanics, Kyushu University), Noel S Keenlyside(Geophysical Institute Bergen), Carlos R Mechoso(University of California Los Angeles), Chairperson:Hiroki Tokinaga(京都大学白眉センター), Ingo Richter

9:00 AM - 9:15 AM JST | 12:00 AM - 12:15 AM UTC

[AOS10-01] Atlantic impacts on the tropical Pacific climate in the 2000s

*Takashi Mochizuki[1], Masahiro Watanabe[2], Masahide Kimoto[2] (1.Japan Agency for Marine-Earth Science and Technology, 2.Atmosphere-Ocean Research Institute, The University of Tokyo)

9:15 AM - 9:30 AM JST | 12:15 AM - 12:30 AM UTC

[AOS10-02] Recent acceleration of Arabian Sea warming induced by the Atlantic-western Pacific trans-basin multidecadal variability

*Cheng Sun[1] (1.Beijing Normal University)

9:30 AM - 9:45 AM JST | 12:30 AM - 12:45 AM UTC

[AOS10-03] **Westward Wind Changes over the Tropical and Mid-latitude Pacific in the Past Three Decades Driven by the Inter-basin Teleconnections**

★Invited Papers

*Xichen Li[1] (1.Institute of Atmospheric Physics)

9:45 AM - 10:00 AM JST | 12:45 AM - 1:00 AM UTC

[AOS10-04] On the Usefulness of the Atlantic Multidecadal Oscillation Index for Identifying Origins of North Atlantic Sea Surface Temperature Variability

*Jing Sun[1,2], Mojib Latif[1,3], Wonsun Park[1], Taewook Park[1,4] (1.GEOMAR Helmholtz Centre for Ocean Research Kiel, 2.Ocean University of China, 3.University of Kiel, 4.Korea Polar Research Institute)

10:00 AM - 10:15 AM JST | 1:00 AM - 1:15 AM UTC

[AOS10-05] Atlantic Multidecadal SST Signal Modulated by the Low-Frequency Mixed Layer Depth Variability

*Ayako Yamamoto[1], Hiroaki Tatebe[1], Masami Nonaka[1] (1.Japan Agency for Marine-Earth Science and Technology)

10:15 AM - 10:30 AM JST | 1:15 AM - 1:30 AM UTC

[AOS10-06] A High-Resolution Future Wave Climate Projection for the Northwestern Atlantic

*Adrean Webb[1], Tomoya Shimura[1], Nobuhito Mori[1] (1.Kyoto University, Disaster Prevention Research Institute)

[E] Oral | A (Atmospheric and Hydrospheric Sciences )：A-OS Ocean Sciences & Ocean Environment

10:45 AM - 12:15 PM JST | 1:45 AM - 3:15 AM UTC | 105 1F

## [A-OS10] Atlantic climate variability, and its global impacts and predictability

convener:Ingo Richter(JAMSTEC Japan Agency for Marine-Earth Science and Technology), Hiroki Tokinaga(Research Institute for Applied Mechanics, Kyushu University), Noel S Keenlyside(Geophysical Institute Bergen), Carlos R Mechoso(University of California Los Angeles), Chairperson:Ingo Richter, Hiroki Tokinaga(京都大学白眉センター)

10:45 AM - 11:00 AM JST | 1:45 AM - 2:00 AM UTC

[AOS10-07] Tropical Atlantic Impact on ENSO predictability

★Invited Papers

*Belen Rodriguez-Fonseca[1,2], Irene - Polo[1], Elsa - Mohino[1], Teresa - Losada[1], Marta - Martin-Rey[5], Roberto - Mechoso[3], Noel - Keenlyside[4] (1.Department of Physics of the Earth and Astrophysics, UCM, Madrid, Spain, 2.Institute of Geosciences, IGEO, UCM-CSIC, Madrid, Spain, 3.Department of Atmospheric and Oceanic Sciences, UCLA, Los Angeles, USA, 4.Geophysical Institute, University of Bergen, Norway, 5.Instituto de Ciencias del Mar, Barcelona, Spain)

11:00 AM - 11:15 AM JST | 2:00 AM - 2:15 AM UTC

[AOS10-08] **Interannual variability of Antarctic Intermediate Water in the tropical North Atlantic**

*Yao Fu[1], Chunzai Wang[1], Peter Brandt[2,3], Richard J. Greatbatch[2,3] (1.State Key Laboratory of Tropical Oceanography, South China Sea Institute of Oceanology, Chinese Academy of Sciences, Guangzhou, China, 2.GEOMAR Helmholtz Centre for Ocean Research Kiel, Kiel, Germany , 3.Christian-Albrechts-Universität zu Kiel, Kiel, Germany)

11:15 AM - 11:30 AM JST | 2:15 AM - 2:30 AM UTC

[AOS10-09] **Understanding the mechanisms of the Atlantic meridional climate variability**

*Hyacinth C Nnamchi[1], Riccardo Farneti[2], Noel S Keenlyside[3], Fred Fred Kucharski[2], Mojib Latif[1] (1.GEOMAR Helmholtz Centre for Ocean Research Kiel, Kiel, Germany, 2.Abdus Salam International Centre for Theoretical Physics, Trieste, Italy, 3.Geophysical Institute, University of Bergen, and Bjerknes Centre for Climate Research, Bergen, Norway)

11:30 AM - 11:45 AM JST | 2:30 AM - 2:45 AM UTC

[AOS10-10] The corss-equatorical gradient variability: The role of heat, momentum, and freshwater flux

*Takahito Kataoka[1] (1.JAMSTEC Japan Agency for Marine-Earth Science and Technology)

11:45 AM - 12:00 PM JST | 2:45 AM - 3:00 AM UTC

[AOS10-11] Generation mechanisms of the Benguela Nino with a focus on local amplification

*Tomoki Tozuka[1], Ryo Kobayashi[1] (1.Department of Earth and Planetary Science, Graduate School of Science, The University of Tokyo)

12:00 PM - 12:15 PM JST | 3:00 AM - 3:15 AM UTC

[AOS10-12] **Seasonal energy analysis for baroclinic waves in equatorial Atlantic through a diagnostic scheme for energy flux**

*Qingyang Song[1], Hidenori AIKI[1] (1.Institute of space-earth environmental research, Nagoya University)

[E] Poster | A (Atmospheric and Hydrospheric Sciences )：A-OS Ocean Sciences & Ocean Environment

3:30 PM - 5:00 PM JST | 6:30 AM - 8:00 AM UTC | Poster Hall International Exhibition Hall8, Makuhari Messe_4

## [A-OS10] Atlantic climate variability, and its global impacts and predictability

convener:Ingo Richter(JAMSTEC Japan Agency for Marine-Earth Science and Technology), Hiroki Tokinaga(Research Institute for Applied Mechanics, Kyushu University), Noel S Keenlyside(Geophysical Institute Bergen), Carlos R Mechoso(University of California Los Angeles)

[AOS10-P01] The strengthening of Amazonian precipitation during the wet season driven by tropical sea surface temperature forcing

*Xinyue Wang[1], Xichen Li[1], Jiang Zhu[1], Clemente A S Tanajura[2] (1.Institute of Atmospheric Physics, Chinese Academy of Sciences, 2.Institute of Physics, Federal University of Bahia, Salvador, Brazil)

[AOS10-P02] **Linear inverse modeling of the tropical Atlantic**

*Ingo Richter[1], Ping Chang[2] (1.JAMSTEC Japan Agency for Marine-Earth Science and Technology, 2.Texas A&M University)

[AOS10-P03] Relationships Among Inter-model Spread and Biases in Tropical Atlantic Sea Surface Temperatures

Elsa - Mohino Harris[1], *Belen Rodriguez-Fonseca[1,2], Teresa - Losada[1], Irene - Polo[1], Roberto - Mechoso[3] (1.Department of Physics of the Earth and Astrophysics, Universidad Complutense de Madrid, 28040, Madrid, Spain. , 2.Institute of Geosciences IGEO,UCM-CSIC, 28040, Madrid, Spain., 3.Department of Atmospheric and Oceanic Sciences, UCLA, Los Angeles, USA)

[AOS10-P04] **Revisiting the CMIP5 Thermocline in the Equatorial Pacific and Atlantic Oceans**

Antonio - Castaño[1,2], Elsa - Mohino[1], *Belen Rodriguez-Fonseca[1,2], Teresa - Losada[1] (1.Department of Physics of the Earth and Astrophysics, Universidad Complutense de Madrid, 28040, Madrid, Spain., 2.Institute of Geosciences, IGEO, UCM-CSIC 28040, Madrid, Spain.)

[AOS10-P05] Lagged Effects of North Atlantic SST Anomalies on Weather in Remote Areas

*Natalia Gnatiuk[1], Timo Vihma[2], Leonid Bobylev[1] (1.Nansen International Environmental and Remote Sensing Centre, 2.Finnish Meteorological Institute)

[AOS10-P06] **SST anomalies in the northern tropical Atlantic as a negative feedback to ENSO development**

*Ingo Richter[1], Hiroki Tokinaga[2], Yu Kosaka[3], Takeshi Doi[1] (1.JAMSTEC Japan Agency for Marine-Earth Science and Technology, 2.Kyoto University, 3.University of Tokyo)

[E] Poster | A (Atmospheric and Hydrospheric Sciences )：A-OS Ocean Sciences & Ocean Environment

5:15 PM - 6:30 PM JST | 8:15 AM - 9:30 AM UTC | Poster Hall International Exhibition Hall8, Makuhari Messe_8

## [A-OS10] Atlantic climate variability, and its global impacts and predictability

convener:Ingo Richter(JAMSTEC Japan Agency for Marine-Earth Science and Technology), Hiroki Tokinaga(Research Institute for Applied Mechanics, Kyushu University), Noel S Keenlyside(Geophysical Institute Bergen), Carlos R Mechoso(University of California Los Angeles)

[AOS10-P01] The strengthening of Amazonian precipitation during the wet season driven by tropical sea surface temperature forcing

*Xinyue Wang[1], Xichen Li[1], Jiang Zhu[1], Clemente A S Tanajura[2] (1.Institute of Atmospheric Physics, Chinese Academy of Sciences, 2.Institute of Physics, Federal University of Bahia, Salvador, Brazil)

[AOS10-P02] **Linear inverse modeling of the tropical Atlantic**

*Ingo Richter[1], Ping Chang[2] (1.JAMSTEC Japan Agency for Marine-Earth Science and Technology, 2.Texas A&M University)

[AOS10-P03] Relationships Among Inter-model Spread and Biases in Tropical Atlantic Sea Surface Temperatures

Elsa - Mohino Harris[1], *Belen Rodriguez-Fonseca[1,2], Teresa - Losada[1], Irene - Polo[1], Roberto - Mechoso[3] (1.Department of Physics of the Earth and Astrophysics, Universidad Complutense de Madrid, 28040, Madrid, Spain. , 2.Institute of Geosciences IGEO,UCM-CSIC, 28040, Madrid, Spain., 3.Department of Atmospheric and Oceanic Sciences, UCLA, Los Angeles, USA)

[AOS10-P04] **Revisiting the CMIP5 Thermocline in the Equatorial Pacific and Atlantic Oceans**

Antonio - Castaño[1,2], Elsa - Mohino[1], *Belen Rodriguez-Fonseca[1,2], Teresa - Losada[1] (1.Department of Physics of the Earth and Astrophysics, Universidad Complutense de Madrid, 28040, Madrid, Spain., 2.Institute of Geosciences, IGEO, UCM-CSIC 28040, Madrid, Spain.)

[AOS10-P05] Lagged Effects of North Atlantic SST Anomalies on Weather in Remote Areas

*Natalia Gnatiuk[1], Timo Vihma[2], Leonid Bobylev[1] (1.Nansen International Environmental and Remote Sensing Centre, 2.Finnish Meteorological Institute)

[AOS10-P06] **SST anomalies in the northern tropical Atlantic as a negative feedback to ENSO development**

*Ingo Richter[1], Hiroki Tokinaga[2], Yu Kosaka[3], Takeshi Doi[1] (1.JAMSTEC Japan Agency for Marine-Earth Science and Technology, 2.Kyoto University, 3.University of Tokyo)

[E] Oral | A (Atmospheric and Hydrospheric Sciences)：A-HW Hydrology & Water Environment

9:00 AM - 10:30 AM JST | 12:00 AM - 1:30 AM UTC | 201B 2F

## [A-HW22] Materials transport and nutrient cycles in watersheds; from headwaters to coastal seas

convener:Masahiro Kobayashi(Forestry and Forest Products Research Institute), Seiko Yoshikawa(Institute for Agro-environmental Sciences, National Agriculture and Food Research Organization), Jun Yasumoto(University of the Ryukyus, Faculty of Agriculuture), Adina Paytan(University of California Santa Cruz), Chairperson:Adina Paytan(University of California, Santa Cruz)

9:00 AM - 9:15 AM JST | 12:00 AM - 12:15 AM UTC

### [AHW22-06] Biodiversity increases integrated trophic position of macroinvertebrate communities in coastal food webs: testing the vertical diversity hypothesis

*Noboru Okuda[1], Jin'ichi Karube[2], Yoichiro Sakai[3], Tomohiro Takeyama[4], Ichiro Tayasu[1], Chikage Yoshimizu[1], Toshi Nagata[5] (1.Research Institute for Humanity and Nature, 2.Kindai University, 3.Lake Biwa Environmental Research Institute, 4.Okayama University of Science, 5.University of Tokyo)

9:15 AM - 9:30 AM JST | 12:15 AM - 12:30 AM UTC

### [AHW22-07] The analysis of the community composition of riverine bacteria and microalgae in relation to nutrient status and diversity: the case in irrigation season in the Yasu River, Japan

*Tohru Ikeya[1], Takuya Ishida[1], Yoshitoshi Uehara[1], Satoshi Asano[2], Ichiro Tayasu[1], Noboru Okuda[1], Masayuki Ushio[3,4,5], Shohei Fujinaga[4], Chia-Ying Ko[6], Elfritzson Martin Peralta[7], Naoto F. Ishikawa[8], Tomoya Iwata[9] (1.Research Institute for Humanity and Nature, 2.Lake Biwa Environmental Research Institute, 3.Hakubi Center, Kyoto University, 4.Center for Ecological Research, Kyoto University, 5.PRESTO, Japan Science and Technology Agency, 6.National Taiwan University, 7.University of Santo Tomas, 8.Department of Biogeochemistry, Japan Agency for Marine-Earth Science and Technology, 9.Faculty of Life and Environmental Sciences, Yamanashi University)

9:30 AM - 9:45 AM JST | 12:30 AM - 12:45 AM UTC

### [AHW22-08] Multiple stressors and protection efforts in highly urbanized watersheds in the Philippines

*Elfritzson M. Peralta[1,3], Leocris S. Batucan Jr.[4,6], Alexis E. Belen[2,3], Irisse Bianca B. De Jesus[1,3], Takuya Ishida[5], Chia-Ying Ko[7], Yuki Kobayashi[5], Tohru Ikeya[5], Yoshitoshi Uehara[5], Tomoya Iwata[8], Adelina S. Borja[9], Jonathan Carlo A. Briones[1,2,3], Francis S. Magbanua[4], Rey Donne S. Papa[1,2,3], Noboru Okuda[5] (1.Research Center for the Natural and Applied Sciences, University of Santo Tomas, PH, 2.Department of Biological Sciences, University of Santo Tomas, PH, 3.The Graduate School, University of Santo Tomas, PH, 4.Institute of Biology, University of the Philippines Diliman, PH, 5.Research Institute for Humanity and Nature, JP, 6.Academia Sinica and Department of Life Science, National Taiwan Normal University, TW, 7.Institute of Fisheries Science and Department of Life Science, National Taiwan University, TW, 8.Faculty of Life and Environmental Sciences, University of Yamanashi, JP, 9.Resource Management and Development Department, Laguna Lake Development Authority, PH)

9:45 AM - 10:00 AM JST | 12:45 AM - 1:00 AM UTC

### [AHW22-09] Ammonium contamination of shallow groundwater beneath vegetable fields in Central Vietnam

★Invited Papers

*Maeda Morihiro[1], Takuya Fujimura[1], Van Ngoc Tuong Hoang[2], Daisuke Inoue[3], Hidetaka Chikamori[1], Fujio Hyodo[1] (1.Okayama University, 2.Hue University, 3.Osaka University)

10:00 AM - 10:15 AM JST | 1:00 AM - 1:15 AM UTC

### [AHW22-10] Modelling nutrient and organic waste behaviour in a tropical wetland in Singapore under projected anthropogenic scenarios

*Swee Yang Edmund Low[1], Dong Eon Kim[1], Canh Tien Trinh Nguyen[1], Yixiong Cai, Shie-Yui Liong[1] (1.National University of Singapore)

10:15 AM - 10:30 AM JST | 1:15 AM - 1:30 AM UTC

### [AHW22-11] Benthic macroinvertebrate assemblages and water quality reflect the impacts of land use and land cover in Marikina Watershed, Philippines

*Julie - An N. Gregorio[1,2], Elfritzson M. Peralta[3,5], Irisse Bianca B. de Jesus[3,5], Tohru Ikeya[6], Jonathan Carlo A. Briones[3,4,5], Rey Donne S. Papa[3,4,5], Francis S. Magbanua[1], Noboru Okuda[6] (1.Institute of Biology, University of the Philippines, Diliman, Quezon City, 1101 Philippines, 2.Institute of Environmental Science and Meteorology, University of the Philippines, Diliman, Quezon City 1101 Philippines, 3.Research Center for the Natural and Applied Sciences, University of Santo Tomas, España Boulevard, Manila, 1015, Philippines, 4.Department of Biological Sciences,

University of Santo Tomas, España Boulevard, Manila, 1015, Philippines, 5.The Graduate School, University of Santo Tomas, España Boulevard, Manila, 1015, Philippines, 6.Research Institute for Humanity and Nature, 457-4 Motoyama, Kamigamo, Kyoto, 603-8047, Japan)

[E] Oral | A (Atmospheric and Hydrospheric Sciences )：A-HW Hydrology & Water Environment

10:45 AM - 12:15 PM JST | 1:45 AM - 3:15 AM UTC | 201B 2F

## [A-HW22] Materials transport and nutrient cycles in watersheds; from headwaters to coastal seas

convener:Masahiro Kobayashi(Forestry and Forest Products Research Institute), Seiko Yoshikawa(Institute for Agro-environmental Sciences, National Agriculture and Food Research Organization), Jun Yasumoto(University of the Ryukyus, Faculty of Agriculuture), Adina Paytan(University of California Santa Cruz), Chairperson:Yasumoto Jun(University of the Ryukyus, Faculty of Agriculuture Department of Regional Agricultural Engineering)

10:45 AM - 11:00 AM JST | 1:45 AM - 2:00 AM UTC

[AHW22-12] **Characterization, distribution and degradation of environmental plastics in inland river system of Mongolia**

*Batdulam Battulga[1], Masayuki Kawahigashi[1], Bolormaa Oyuntsetseg[2] (1.Department of Geography, Tokyo Metropolitan University, Tokyo, 192-0397, Japan , 2.Department of Chemistry, National University of Mongolia, Ulaanbaatar, 210646, Mongolia)

11:00 AM - 11:15 AM JST | 2:00 AM - 2:15 AM UTC

[AHW22-13] Multi-site and multi-approach sediment transport modeling in tropical watersheds

★Invited Papers

*Assefa M Melesse[1], Alemu Osore Aga[2], Hagos Gebreselassie[2] (1.Florida International University, 2.Addis Ababa University)

11:15 AM - 11:30 AM JST | 2:15 AM - 2:30 AM UTC

[AHW22-14] Calculation of SS concentration coefficients of river water for each land use by a simple watershed model.

*Seiko Yoshikawa[1], Donglai Ma[1,2], Tadamasa Saito[1,3], Kenji Matsumori[4], Yuko Itoh[5], Masahiro Kobayashi[5] (1.Institute for Agro-environmental Sciences, National Agriculture and Food Research Organization, 2.Graduate Scool, Tsukuba University , 3.Faculty of Agriculture, Ibaraki University , 4.Western Region Agricultural Research Center, National Agriculture and Food Research Organization, 5.Forestry and Forest Products Research Institute)

11:30 AM - 11:45 AM JST | 2:30 AM - 2:45 AM UTC

[AHW22-15] Evaluation of long term variation in water balance and discharge of sediment and nitrogen in the urbanized catchment of Yamato River, using SWAT model

*Kunyang Wang[1,2], Yuta Shimizu[3], Shin-ichi Onodera[1], Mitsuyo Saito[4], Yusuke Tomozawa[1] (1.Graduate School of Integrated Arts and Science, Hiroshima University, 2.Capital Normal University, 3.National Agriculture and Food Research Organization, 4.Okayama University)

11:45 AM - 12:00 PM JST | 2:45 AM - 3:00 AM UTC

[AHW22-16] Causal correlation between water-use of the Tedori River and coastal erosion of Chirihama Nagisa Driveway, Ishikawa, Japan

*Toshihiko Momose[1] (1.Ishikawa Prefectural University)

12:00 PM - 12:15 PM JST | 3:00 AM - 3:15 AM UTC

[AHW22-17] Role of suspended solids on elemental dynamics in the Selenga River system

★Invited Papers

*Masayuki Kawahigashi[1], Orgilbold Myangan[2], Bolormaa Oyuntsetseg[2] (1.Tokyo Metropolitan University, 2.National University of Mongolia)

[E] Oral | A (Atmospheric and Hydrospheric Sciences )：A-HW Hydrology & Water Environment

1:45 PM - 3:15 PM JST | 4:45 AM - 6:15 AM UTC | 201B 2F

## [A-HW22] Materials transport and nutrient cycles in watersheds; from headwaters to coastal seas

convener:Masahiro Kobayashi(Forestry and Forest Products Research Institute), Seiko Yoshikawa(Institute for Agro-environmental Sciences, National Agriculture and Food Research Organization), Jun Yasumoto(University of the Ryukyus, Faculty of Agriculuture), Adina Paytan(University of California Santa Cruz), Chairperson:Yoshikawa Seiko(Institute for Agro-environmental Sciences, National Agriculture and Food Research Organization)

1:45 PM - 2:00 PM JST | 4:45 AM - 5:00 AM UTC

[AHW22-18] Relationship between topographical characteristics in catchment area and dissolved iron concentration of river in permafrost area

*Yuto Tashiro[1], Muneoki Yoh[1], Takayuki Shiraiwa[2], Takeo Onishi[3] (1.Tokyo University of Agriculture and Technology, 2.Hokkaido University, 3.Gifu University)

2:00 PM - 2:15 PM JST | 5:00 AM - 5:15 AM UTC

[AHW22-19] Water Source Zones and Hydrochemical Properties of Fluoride Water in Mt. Meru Watershed, Tanzania

*Shinji Nakaya[1], Ryogo Takada[1], Jun Yasumoto[2], Junichi Yoshitani[1], Innocent Lugodisha[3], Zuberi Dominicus Lwimbo[3], Hans Komakech[4], Thomas Reuben Mollel[5] (1.Department of Water Environment and Civil Engineering, Faculty of Engineering, Shinshu University, Japan, 2.Department of Regional Agriculture Engineering, University of the Rykuyus, Japan, 3.School of Materials, Energy, Water and Environmental Sciences, NM-AIST, Tanzania, 4.WISE-Future, NM-AIST, Tanzania, 5.SGSS and Institute of resources assessment-UDSM, Tanzania)

2:15 PM - 2:30 PM JST | 5:15 AM - 5:30 AM UTC

[AHW22-20] Development and Application of a System for Measurement of Total Load of Water Quality

★Invited Papers

*Keiji Takase[1], Yuko Itoh[2] (1.Ishikawa Prefectual University, 2.Forestry and Forest Products research Institute, Japan)

2:30 PM - 2:45 PM JST | 5:30 AM - 5:45 AM UTC

[AHW22-21] Water infiltration and uptake around a Japanese cypress growing on a flat upland

*Masahiro Kobayashi[1], Shin-ichi Onodera[2], Yuko Itoh[1], Tadashi Sakata[1] (1.Forestry and Forest Products Research Institute, 2.Graduate School of Integrated and Arts Sciences, Hiroshima University)

2:45 PM - 3:00 PM JST | 5:45 AM - 6:00 AM UTC

[AHW22-22] Innovative Rainfall Simulator Design for Moving Storm Scenarios with Different Storm Patterns

*RAVI KUMAR MEENA[1], SUMIT SEN[2] (1.M.Tech Student, Department of Hydrology, Indian Institute of Technology Roorkee, Roorkee, Uttarakhand, India, 2. Associate Professor, Department of Hydrology, Indian Institute of Technology Roorkee, Roorkee, Uttarakhand, India)

[E] Poster | A (Atmospheric and Hydrospheric Sciences )：A-HW Hydrology & Water Environment

3:30 PM - 5:00 PM JST | 6:30 AM - 8:00 AM UTC | Poster Hall International Exhibition Hall8, Makuhari Messe_5

## [A-HW22] Materials transport and nutrient cycles in watersheds; from headwaters to coastal seas

convener:Masahiro Kobayashi(Forestry and Forest Products Research Institute), Seiko Yoshikawa(Institute for Agro-environmental Sciences, National Agriculture and Food Research Organization), Jun Yasumoto(University of the Ryukyus, Faculty of Agriculuture), Adina Paytan(University of California Santa Cruz)

[AHW22-P01] Phosphate Enrichment Hampers Development of Juvenile Acropora digitifera Coral by Inhibiting Skeleton Formation

Mariko Iijima[1], *Yasumoto Ko[1], Jun Yasumoto[2], Mina Hirose[3], Mitsuru Jimbo[1], Shugo Watabe[1] (1.Kitasato University School of Marine Biosciences, 2.Faculty of Agriculture, University of the Ryukyus, 3.Tropical Technology Plus)

[AHW22-P02] Modeling chlorophyll-a concentration using remote sensing in shallow water systems: Comparison of sensors

*Assefa M Melesse[1], Tara Blakey[1], Mohammad Haji Gholizadeh[1], Mohd Manzar Abbas[1] (1.Florida International University)

[AHW22-P03] Dynamics in groundwater flow system with seasonal water table variation in a coastal and island

*Yusuke Tomozawa[1], Shin-ichi Onodera[1], Mitsuyo Saito[2] (1.Graduate School of Integrated Arts and Sciences Hiroshima University, 2.Graduate School of Environmental and Life Science, Okayama University)

[AHW22-P04] **The Tracing of Groundwater Contamination Sources in Indonesian Coastal Alluvial Groundwater using $\delta^{34}S$ and $\delta^{15}N$ Isotopes**

*Anna Fadliah Rusydi[1,4], Mitsuyo Saito[2], Seiichiro Ioka[3], Shin-ichi Onodera[1] (1.Graduate School of Integrated Arts and Sciences, Hiroshima University, Japan, 2.Graduate School of Environmental and Life Sciences, Okayama University, Japan, 3.Research Institute for Sustainable Energy, Hirosaki University, Japan, 4.Research Center for Geotechnology, Indonesian Institute of Sciences, Indonesia)

[AHW22-P05] Spatio-temporal dynamics of orthophosphate with implications for limitation of phytoplankton growth in north basin of Lake Biwa, Japan

*Xin Liu[1], Rong Yi[1], Masahiro Maruo[1], Syuhei Ban[1] (1.The University of Shiga Prefecture)

[AHW22-P06] Microbial phase analysis in aquifer of Ryukyu Limestone Zone using next generation sequencer

*Umi Murao[1], Jun Yasumoto[1], Yasumoto Ko[3], Mina Hirose[2], Nanami Mizusawa[3], Ryo Iguchi[4], Bam H.N. Razafindrabe[5], Syugo Watabe[3] (1.University of the Ryukyus, Faculty of Agriculuture Department of Regional Agricultural Engineering, 2.Tropical Tecnology Plus, 3.Kitasato University School of Marine Biosciences, 4.National Institute of Advanced Industrial Science and Technology, 5.University of the Ryukyus, Faculty of Agriculuture Department of Subtropical Agro-Environmental Sciences)

[AHW22-P07] Evaluation for temporal variation in groundwater inflow to the lagoons connected to Lake Biwa by radon ($^{222}Rn$) tracer analysis

*Mitsuyo Saito[1], Shin-ichi Onodera[2], Yusuke Tomozawa[2], Kunyang Wang[2], Syuhei Ban[3], Noboru Okuda[4] (1.Graduate School of Environmental and Life Science, Okayama University, 2.Graduate School of Integrated Arts and Sciences, Hiroshima University, 3.School of Environmental Sciences, The University of Shiga Prefecture, 4.Research Institute for Humanity and Nature)

[AHW22-P08] Br/Cl ratio characteristics of groundwater in coastal areas in Indonesia

*Seiichiro Ioka[1], Shin-ichi Onodera[2], Mitsuyo Saito[3], Anna Fadliah Rusydi[2,4] (1.Institute of Regional Innovation, Hirosaki University, Japan, 2.Graduate School of Integrated Arts and Sciences, Hiroshima University, Japan, 3.Graduate School of Environmental and Life Sciences, Okayama University, Japan, 4.Research Center for Geotechnology, Indonesian Institute of Sciences, Indonesia)

[AHW22-P09] Estimation of groundwater recharge and phosphorus transport under different precipitation conditions in a suburban catchment, using SWAT model

*Kunyang Wang[1,2], Shin-ichi Onodera[1], Mitsuyo Saito[3], Noboru Okuda[4], Takuya Okubo[5] (1.Graduate School of Integrated Arts and Science, Hiroshima University, 2.Capital Normal University, 3.Okayama University, 4.Research

Institute for Humanity and Nature, 5.University of the Shiga Prefecture)

[AHW22-P10] Losses of phosphorus with soil erosion and nitrate with groundwater recharge in an agricultural catchment, subtropical small island

*Shin-ichi Onodera[1], Mitsuyo Saito[2], Yang Cao[1], Anna Fadliah Rusydi[1], Hide Omae[3], Yoshiko Iizumi[4], Yusuke Tomozawa[1] (1.Graduate School of Integrated and Arts Sciences, Hiroshima University, 2.Graduate School of Environmental and Life Science, Okayama University, 3.JIRCAS TARF, 4.JIRCAS HQ)

[AHW22-P11] Phosphate solubilizing bacteria as an indicator of sediment phosphorus in freshwater lakes

*Sreekumari Kurissery[1], Katelynn Crawford[1], Nandakumar Kanavillil[1] (1.Lakehead University, Canada)

[AHW22-P12] A Study on the dynamics of various phosphate forms in soil and groundwater in Ryukyu limestone regions

*Masashi Nozaki[1], Jun Yasumoto[2], Yasumoto Ko[3], Hirose Mina[4], Iijima Mariko[3], Ryuichi Shinjo[5], Bam H.N. Razafindrabe[6] (1.University of The Ryukyus, Graduate School of Agriculture,, 2.University of the Ryukyus, Faculty of Agriculture, Department of Regional Agricultural Engineering, 3.Kitasato University School of Marine Biosciences, 4.Tropical Technology Plus, 5.Department of Physics and Earth Sciences, University of the Ryukyus, 6.University of the Ryukyus, Faculty of Agriculture, Department of Subtropical Agro-Environmental Sciences)

[AHW22-P13] Impacts of highly concentrated turbid water on the groundwater in the Tedori River alluvial fan, Japan

*Yoichi Fujihara[1], Shunsuke Chono[1], Keiji Takase[1], Eiji Ichion[1] (1.Department of Environmental Science, Ishikawa Prefectural University)

[AHW22-P14] Altitude effect of water stable isotopic ratio of ravine water and its contribution to groundwater in alluvial plains - Comparison in east and west side catchments of Lake Biwa –

*Yusuke Tomozawa[1], Kunyang Wang[1], Mitsuyo Saito[2], Syuhei Ban[3], Noboru Okuda[4], Shin-ichi Onodera[1] (1.Graduate School of Integrated Arts and Sciences Hiroshima University, 2.Graduate School of Environmental and Life Science, Okayama University, 3.School of Environmental Science, The University of Shiga Prefecture, 4.Research Institute for Humanity and Nature)

[AHW22-P15] Calculation of TN and TP concentration coefficients of river water for each land use by a simple watershed model.

*Seiko Yoshikawa[1], Donglai Ma[1,4], Tadamasa Saito[1,5], Kenji Matsumori[2], Yuko Itoh[3], Masahiro Kobayashi[3] (1.Institute for Agro-environmental Sciences, National Agriculture and Food Research Organization, 2.Western Region Agricultural Research Center, National Agriculture and Food Research Organization, 3.Forestry and Forest Products Research Institute, 4.Graduate school,Tsukuba University, 5.Faculty of Agriculture, Ibaraki University)

[AHW22-P16] **Possibility of nutrients transportation from littoral slope for enhancement of phytoplankton growth in north basin of Lake Biwa**

*Syuhei Ban[1], Rong YI[1], Xin Liu[1], Masahiro Maruo[1], Miki Sudo[1], Naoshige Goto[1], Jun Murase[2] (1.The University of Shiga Prefecture, 2.Nagoya University)

[AHW22-P17] SWAT model analysis for confirming the effects of crop growth on the suspended sediment concentration from a settling basin catchment on Ishigaki island

*Yang Cao[1], Shin-ichi Onodera[1], Mitsuyo Saito[2], Hide Omae[3], Yoshiko Iizumi[3] (1.Graduate School of Integrate Arts and Sciences, Hiroshima University, 2.Graduate School of Environmental and life Science, Okayama University, 3.Tropical Agriculture Research Front (TARF), Japan International Research Center for Agricultural Sciences (JIRCAS))

[AHW22-P18] Estimating the runoff of water, sediment, and nutrient using SWAT model in Kikuchi-river watershed, Kumamoto, and the influence of the forest

*Soichiro Fujii[1], Masahiko Kanamori[1], Yuko Nagano[1], Maki Kinoshita[2], Yuta Shimizu[3], Shin-ichi Onodera[4] (1.Japan Forest Technology Association, 2.PASCO Corporation, 3.Western Region Agricultural Research Center, National Agriculture and Food Research Organization, 4.Graduate School of Integrated and Arts Sciences, Hiroshima University)

[AHW22-P19] Atmospheric depositions on forest ecosystems in areas along the Sea of Japan

*Yuko Itoh[1], Keiji Takase[2], Yoichi Fujihara[2], Toru Okamoto[1] (1.Forestry and Forest Products Research Institute, Japan, 2.Ishikawa Prefectural University)

[AHW22-P20] Continuous and simultaneous flux measurement of $N_2O$ and $CO_2$ from agricultural soil using a portable multi-turn time-of-flight mass spectrometer

*Noriko Nakayama[1], Yusuke Iwai[1], Yo Toma[2], Hiroshi Furutani[1], Ryusuke Hatano[3], Michisato Toyoda[1] (1.Osaka University, 2.Ehime University, 3.Hokkaido University)

---

[AHW22-P21] Effects of introduction of cyclic irrigation system on mass balances of SS and T-P in Lake Inbanuma, Chiba, Japan

*Tomijiro Kubota[1] (1.National Agriculture and Food Research Organization, Institute for Rural Engineering)

[E] Poster | A (Atmospheric and Hydrospheric Sciences )：A-HW Hydrology & Water Environment

5:15 PM - 6:30 PM JST | 8:15 AM - 9:30 AM UTC | Poster Hall International Exhibition Hall8, Makuhari Messe_9

## [A-HW22] Materials transport and nutrient cycles in watersheds; from headwaters to coastal seas

convener:Masahiro Kobayashi(Forestry and Forest Products Research Institute), Seiko Yoshikawa(Institute for Agro-environmental Sciences, National Agriculture and Food Research Organization), Jun Yasumoto(University of the Ryukyus, Faculty of Agriculuture), Adina Paytan(University of California Santa Cruz)

[AHW22-P01] Phosphate Enrichment Hampers Development of Juvenile Acropora digitifera Coral by Inhibiting Skeleton Formation

Mariko Iijima[1], *Yasumoto Ko[1], Jun Yasumoto[2], Mina Hirose[3], Mitsuru Jimbo[1], Shugo Watabe[1] (1.Kitasato University School of Marine Biosciences, 2.Faculty of Agriculture, University of the Ryukyus, 3.Tropical Technology Plus)

[AHW22-P02] Modeling chlorophyll-a concentration using remote sensing in shallow water systems: Comparison of sensors

*Assefa M Melesse[1], Tara Blakey[1], Mohammad Haji Gholizadeh[1], Mohd Manzar Abbas[1] (1.Florida International University)

[AHW22-P03] Dynamics in groundwater flow system with seasonal water table variation in a coastal and island

*Yusuke Tomozawa[1], Shin-ichi Onodera[1], Mitsuyo Saito[2] (1.Graduate School of Integrated Arts and Sciences Hiroshima University, 2.Graduate School of Environmental and Life Science, Okayama University)

[AHW22-P04] **The Tracing of Groundwater Contamination Sources in Indonesian Coastal Alluvial Groundwater using $\delta^{34}S$ and $\delta^{15}N$ Isotopes**

*Anna Fadliah Rusydi[1,4], Mitsuyo Saito[2], Seiichiro Ioka[3], Shin-ichi Onodera[1] (1.Graduate School of Integrated Arts and Sciences, Hiroshima University, Japan, 2.Graduate School of Environmental and Life Sciences, Okayama University, Japan, 3.Research Institute for Sustainable Energy, Hirosaki University, Japan, 4.Research Center for Geotechnology, Indonesian Institute of Sciences, Indonesia)

[AHW22-P05] Spatio-temporal dynamics of orthophosphate with implications for limitation of phytoplankton growth in north basin of Lake Biwa, Japan

*Xin Liu[1], Rong Yi[1], Masahiro Maruo[1], Syuhei Ban[1] (1.The University of Shiga Prefecture)

[AHW22-P06] Microbial phase analysis in aquifer of Ryukyu Limestone Zone using next generation sequencer

*Umi Murao[1], Jun Yasumoto[1], Yasumoto Ko[3], Mina Hirose[2], Nanami Mizusawa[3], Ryo Iguchi[4], Bam H.N. Razafindrabe[5], Syugo Watabe[3] (1.University of the Ryukyus, Faculty of Agriculuture Department of Regional Agricultural Engineering, 2.Tropical Tecnology Plus, 3.Kitasato University School of Marine Biosciences, 4.National Institute of Advanced Industrial Science and Technology, 5.University of the Ryukyus, Faculty of Agriculuture Department of Subtropical Agro-Environmental Sciences)

[AHW22-P07] Evaluation for temporal variation in groundwater inflow to the lagoons connected to Lake Biwa by radon ($^{222}Rn$) tracer analysis

*Mitsuyo Saito[1], Shin-ichi Onodera[2], Yusuke Tomozawa[2], Kunyang Wang[2], Syuhei Ban[3], Noboru Okuda[4] (1.Graduate School of Environmental and Life Science, Okayama University, 2.Graduate School of Integrated Arts and Sciences, Hiroshima University, 3.School of Environmental Sciences, The University of Shiga Prefecture, 4.Research Institute for Humanity and Nature)

[AHW22-P08] Br/Cl ratio characteristics of groundwater in coastal areas in Indonesia

*Seiichiro Ioka[1], Shin-ichi Onodera[2], Mitsuyo Saito[3], Anna Fadliah Rusydi[2,4] (1.Institute of Regional Innovation, Hirosaki University, Japan, 2.Graduate School of Integrated Arts and Sciences, Hiroshima University, Japan, 3.Graduate School of Environmental and Life Sciences, Okayama University, Japan, 4.Research Center for Geotechnology, Indonesian Institute of Sciences, Indonesia)

[AHW22-P09] Estimation of groundwater recharge and phosphorus transport under different precipitation conditions in a suburban catchment, using SWAT model

*Kunyang Wang[1,2], Shin-ichi Onodera[1], Mitsuyo Saito[3], Noboru Okuda[4], Takuya Okubo[5] (1.Graduate School of Integrated Arts and Science, Hiroshima University, 2.Capital Normal University, 3.Okayama University, 4.Research

Institute for Humanity and Nature, 5.University of the Shiga Prefecture)

[AHW22-P10] Losses of phosphorus with soil erosion and nitrate with groundwater recharge in an agricultural catchment, subtropical small island

*Shin-ichi Onodera[1], Mitsuyo Saito[2], Yang Cao[1], Anna Fadliah Rusydi[1], Hide Omae[3], Yoshiko Iizumi[4], Yusuke Tomozawa[1] (1.Graduate School of Integrated and Arts Sciences, Hiroshima University, 2.Graduate School of Environmental and Life Science, Okayama University, 3.JIRCAS TARF, 4.JIRCAS HQ)

[AHW22-P11] Phosphate solubilizing bacteria as an indicator of sediment phosphorus in freshwater lakes

*Sreekumari Kurissery[1], Katelynn Crawford[1], Nandakumar Kanavillil[1] (1.Lakehead University, Canada)

[AHW22-P12] A Study on the dynamics of various phosphate forms in soil and groundwater in Ryukyu limestone regions

*Masashi Nozaki[1], Jun Yasumoto[2], Yasumoto Ko[3], Hirose Mina[4], Iijima Mariko[3], Ryuichi Shinjo[5], Bam H.N. Razafindrabe[6] (1.University of The Ryukyus, Graduate School of Agriculture,, 2.University of the Ryukyus, Faculty of Agriculture, Department of Regional Agricultural Engineering, 3.Kitasato University School of Marine Biosciences, 4.Tropical Technology Plus, 5.Department of Physics and Earth Sciences, University of the Ryukyus, 6.University of the Ryukyus, Faculty of Agriculture, Department of Subtropical Agro-Environmental Sciences)

[AHW22-P13] Impacts of highly concentrated turbid water on the groundwater in the Tedori River alluvial fan, Japan

*Yoichi Fujihara[1], Shunsuke Chono[1], Keiji Takase[1], Eiji Ichion[1] (1.Department of Environmental Science, Ishikawa Prefectural University)

[AHW22-P14] Altitude effect of water stable isotopic ratio of ravine water and its contribution to groundwater in alluvial plains - Comparison in east and west side catchments of Lake Biwa –

*Yusuke Tomozawa[1], Kunyang Wang[1], Mitsuyo Saito[2], Syuhei Ban[3], Noboru Okuda[4], Shin-ichi Onodera[1] (1.Graduate School of Integrated Arts and Sciences Hiroshima University, 2.Graduate School of Environmental and Life Science, Okayama University, 3.School of Environmental Science, The University of Shiga Prefecture, 4.Research Institute for Humanity and Nature)

[AHW22-P15] Calculation of TN and TP concentration coefficients of river water for each land use by a simple watershed model.

*Seiko Yoshikawa[1], Donglai Ma[1,4], Tadamasa Saito[1,5], Kenji Matsumori[2], Yuko Itoh[3], Masahiro Kobayashi[3] (1.Institute for Agro-environmental Sciences, National Agriculture and Food Research Organization, 2.Western Region Agricultural Research Center, National Agriculture and Food Research Organization, 3.Forestry and Forest Products Research Institute, 4.Graduate school,Tsukuba University, 5.Faculty of Agriculture, Ibaraki University)

[AHW22-P16] **Possibility of nutrients transportation from littoral slope for enhancement of phytoplankton growth in north basin of Lake Biwa**

*Syuhei Ban[1], Rong YI[1], Xin Liu[1], Masahiro Maruo[1], Miki Sudo[1], Naoshige Goto[1], Jun Murase[2] (1.The University of Shiga Prefecture, 2.Nagoya University)

[AHW22-P17] SWAT model analysis for confirming the effects of crop growth on the suspended sediment concentration from a settling basin catchment on Ishigaki island

*Yang Cao[1], Shin-ichi Onodera[1], Mitsuyo Saito[2], Hide Omae[3], Yoshiko Iizumi[3] (1.Graduate School of Integrate Arts and Sciences, Hiroshima University, 2.Graduate School of Environmental and life Science, Okayama University, 3.Tropical Agriculture Research Front (TARF), Japan International Research Center for Agricultural Sciences (JIRCAS))

[AHW22-P18] Estimating the runoff of water, sediment, and nutrient using SWAT model in Kikuchi-river watershed, Kumamoto, and the influence of the forest

*Soichiro Fujii[1], Masahiko Kanamori[1], Yuko Nagano[1], Maki Kinoshita[2], Yuta Shimizu[3], Shin-ichi Onodera[4] (1.Japan Forest Technology Association, 2.PASCO Corporation, 3.Western Region Agricultural Research Center, National Agriculture and Food Research Organization, 4.Graduate School of Integrated and Arts Sciences, Hiroshima University)

[AHW22-P19] Atmospheric depositions on forest ecosystems in areas along the Sea of Japan

*Yuko Itoh[1], Keiji Takase[2], Yoichi Fujihara[2], Toru Okamoto[1] (1.Forestry and Forest Products Research Institute, Japan, 2.Ishikawa Prefectural University)

[AHW22-P20] Continuous and simultaneous flux measurement of $N_2O$ and $CO_2$ from agricultural soil using a portable multi-turn time-of-flight mass spectrometer

*Noriko Nakayama[1], Yusuke Iwai[1], Yo Toma[2], Hiroshi Furutani[1], Ryusuke Hatano[3], Michisato Toyoda[1] (1.Osaka University, 2.Ehime University, 3.Hokkaido University)

---

[AHW22-P21] Effects of introduction of cyclic irrigation system on mass balances of SS and T-P in Lake Inbanuma, Chiba, Japan

*Tomijiro Kubota[1] (1.National Agriculture and Food Research Organization, Institute for Rural Engineering)

[E] Oral | A (Atmospheric and Hydrospheric Sciences)：A-GE Geological & Soil Environment

9:00 AM - 10:30 AM JST | 12:00 AM - 1:30 AM UTC | 301A 3F

## [A-GE28] Subsurface Mass Transport, Material Cycle, and Environmental Assessment

convener:Yuki Kojima(Department of Civil Engineering, Gifu University), Shoichiro Hamamoto(Department of Biological and Environmental Engineering, The University of Tokyo), Hirotaka Saito(Department of Ecoregion Science, Tokyo University of Agriculture and Technology), Yasushi Mori(Graduate School of Environmental and Life Science, Okayama University), Chairperson:Yuki Kojima(Gifu University), Shoichiro Hamamoto(The University of Tokyo), Yasushi Mori(Okayama University), Hirotaka Saito(Tokyo University of Agriculture and Technology)

9:00 AM - 9:25 AM JST | 12:00 AM - 12:25 AM UTC

[AGE28-01] **Humic substances in deep sedimentary groundwater**

★Invited Papers

*Takumi Saito[1] (1.School of Engineering, The University of Tokyo)

---

9:25 AM - 9:40 AM JST | 12:25 AM - 12:40 AM UTC

[AGE28-02] Nano-Bubble Retention in Saturated Porous Media under Different Solution Chemistry

*Shoichiro Hamamoto[1], Takuya Sugimoto[1], Takato Takemura[2], Taku Nishimura[1], Scott A Bradford[3] (1.Department of Biological and Environmental Engineering, The University of Tokyo, 2.College of Humanities and Sciences, Nihon University, 3.U. S. Salinity Laboratory)

---

9:40 AM - 9:55 AM JST | 12:40 AM - 12:55 AM UTC

[AGE28-03] **Geochemical Investigation of Metals and Trace Elements around the Abandoned Cu – Ni Mine Site in Selibe Phikwe, Botswana**

*Fiona Segolame Motswaiso[1], Kengo - Nakamura[1], Noriaki - Watanabe[1], Takeshi - Komai[1] (1.Tohoku Univeristy Graduate School of Environmental Studies)

---

9:55 AM - 10:10 AM JST | 12:55 AM - 1:10 AM UTC

[AGE28-04] Removal of Arsenic (III) From Aqueous Solution Using Pumice and Zeolite Supported Zero-Valent Iron Nanoparticle

*Shashi Ranjan[1], Brijesh kumar yadav[1], Himanshu Joshi[1] (1.Indian Institute of Technology Roorkee)

---

10:10 AM - 10:25 AM JST | 1:10 AM - 1:25 AM UTC

[AGE28-05] **Unsaturated Hydraulic Conductivity Estimation from Multi-step Centrifuge Outflow**

*Thanh Long Bui[1], Yasushi Mori[1] (1.Graduate School of Environmental and Life Science, Okayama University)

[E] Poster | A (Atmospheric and Hydrospheric Sciences )：A-GE Geological & Soil Environment

5:15 PM - 6:30 PM JST | 8:15 AM - 9:30 AM UTC | Poster Hall International Exhibition Hall8, Makuhari Messe_10

## [A-GE28] Subsurface Mass Transport, Material Cycle, and Environmental Assessment

convener:Yuki Kojima(Department of Civil Engineering, Gifu University), Shoichiro Hamamoto(Department of Biological and Environmental Engineering, The University of Tokyo), Hirotaka Saito(Department of Ecoregion Science, Tokyo University of Agriculture and Technology), Yasushi Mori(Graduate School of Environmental and Life Science, Okayama University)

### [AGE28-P01] Vegetation pellets development and feasibility evaluation for unmanned-aerial-vehicle seeding on post-landslide sites

*Kai-Chi Hsu[1], Guo-Zhang M. Song[1], Shin-Hwei Lin[1], Chi-Hao Chang[2] (1.Department of Soil and Water Conservation, National Chung Hsing University, 2.Department of Landscape Architecture, Tunghai University)

### [AGE28-P02] Characterizing Soil Environment in The Rice Terraces of the Philippine Cordilleras

*Tomoyo Kurozumi[1], Yasushi Mori[2], Hiroaki Somura[2], Milagros Ong How[3] (1.Faculty of Environmental Science and Technology, Okayama University, 2.Graduate School of Environmental and Life Science, Okayama University , 3.Universal Harvested Incorporated)

### [AGE28-P03] Web-based interactive platform for analysis of regional-scale groundwater resources

*Chuen-Fa Ni[1], I-Hsien Lee[1], Chi-Ping Lin[1], Wi-Ci Li[1] (1.National Central University)

### [AGE28-P04] Development of simultaneous measurement system of viscosity and permeability for highly accurate evaluation of flow characteristic of Geofluid

*Tomoya Muramoto[1], Yoshitaka Fujita[1], Hiroaki Kajikawa[1], Hideaki Iizumi[1], Kazunori Ide[1] (1.National Institute of Advanced Industrial Science and Technology, National Metrology Institute of Japan)

### [AGE28-P05] Soil hydraulic parameter estimation by evaporation method

Shintaro Kubota[1], *Hirotaka Saito[1] (1.Graduate School of Agriculture, Tokyo University of Agriculture and Technology)

### [AGE28-P06] Measurement of apparent gas diffusion coefficient in poorly tilled seedbed under windy condition.

*Yoshihiro Matsumoto[1], Shuichiro Yoshida[1], Hiroyuki Sekiya[2], Kazuhiro Nishida[1] (1.Graduate School of Agricultural and Life Sciences, The University of Tokyo, 2.National Agricultural Research Center NARO)

### [AGE28-P07] Evaluating improvement techniques for phytosuction separation method to remove heavy metals from contaminated soils

*Yuki Kojima[1], Hayata Terada[1], Masahiko Katoh[2], Kohji Kamiya[1] (1.Department of Civil Engineering, Gifu University, 2.School of Agriculture, Meiji University)

### [AGE28-P08] Transport of Colloidal Particles in Saturated Toyoura Sand: Effects of Flow Rate on Importance of Electrostatic Repulsion

*Takuya Sugimoto[1], Shoichiro Hamamoto[1], Taku Nishimura[1], Yasuhisa Adachi[2], Motoyoshi Kobayashi[2] (1.Graduate School of Agricultural and Life Sciences, The University of Tokyo, 2.Faculty of Life and Environmental Sciences, University of Tsukuba)

### [AGE28-P09] Leaching behavior of As, Pb, Cd and Se in subsurface marine and nonmarine sedimentary environment in central Kanto plain, Japan

*SUSHMITA HOSSAIN[1], Takashi Ishiyama[2], Shoichi Hachinohe[2], Chiaki T. Oguchi[1] (1.Graduate school of Science and Engineering, Saitama University, 2.Center for Environmental Science in Saitama)

### [AGE28-P10] Colloid transport in a quasi-saturated porous media

*Yushi Ooko[1], Takuya Sugimoto[2], Shoichiro Hamamoto[2], Taku Nishimura[2] (1.The University of Tokyo, 2.Graduate School of Agricultural and Life Sciences, The University of Tokyo)

[E] Oral | A (Atmospheric and Hydrospheric Sciences)：A-GE Geological & Soil Environment

10:45 AM - 12:15 PM JST | 1:45 AM - 3:15 AM UTC | 301A 3F

## [A-GE29] Energy-Environment-Water Nexus and Sustainable Development

convener:Ming Zhang(Institute for Geo-Resources and Environment, Geological Survey of Japan, AIST), Ken Kawamoto(Graduate School of Science and Engineering, Saitama University), Jet-Chau Wen(National Yunlin University of Science and Technology), Yonghong Hao(Tianjin Normal University), Chairperson:Ming Zhang(AIST), Hirotaka Saito(Tokyo University of Agriculture and Technology), Yonghong Hao(Tianjin Normal University)

10:50 AM - 11:05 AM JST | 1:50 AM - 2:05 AM UTC

[AGE29-01] Input-Output Analysis of Taiwan's Food-Energy-Water Risk

*CHU-CHUN YAO[1], Gene Jiing-yun You[1] (1.National Taiwan University)

---

11:05 AM - 11:20 AM JST | 2:05 AM - 2:20 AM UTC

[AGE29-02] **Groundwater potential analysis using the multiple spatiotemporal remote sensing approach in fractured rock of mountainous region**

*Jung-Jun Lin[1,2], Yuei-An Liou[1], Chien-Chung Ke[2], Su-Yun Chi[2], Jia-Hung Liang[3] (1.National Central Univ., 2.Sinotech Engineering Consultants, Inc., 3.Ministry of Economic Affairs)

---

11:20 AM - 11:35 AM JST | 2:20 AM - 2:35 AM UTC

[AGE29-03] Estimating Soil Water Content with Color Calibration Method in the Image of Remote Sensing by Unmanned Aerial Vehicle

*Hong-Yi Li[1], Hong-Ru Lin[1], Jyun-Lin Chen[1], Shao-Yang Huang[1], Jet-Chau Wen[1] (1.National Yunlin University of Science and Technology)

---

11:35 AM - 11:50 AM JST | 2:35 AM - 2:50 AM UTC

[AGE29-04] **Characterizing Geotechnical Properties of Drinking Water Sludge Blended with Graded Crushed Clay Brick for Road Subgrade: Effects of Gradation and Mixing Proportion of Crushed Clay Brick on CBR and Water Permeability**

*Muhammad Rashid Iqbal[1], Akihiro Matsuno[1], Ken Kawamoto[1] (1.Graduate School of Science and Engineering, Saitama University)

---

11:50 AM - 12:05 PM JST | 2:50 AM - 3:05 AM UTC

[AGE29-05] Investigation and Evaluation of the Multiple-liquefaction Site at the Southern Taiwan

*Chih-Sheng KU[1] (1.I-Shou University)

[E] Oral | A (Atmospheric and Hydrospheric Sciences )：A-GE Geological & Soil Environment

1:45 PM - 3:15 PM JST | 4:45 AM - 6:15 AM UTC | 301A 3F

## [A-GE29] Energy-Environment-Water Nexus and Sustainable Development

convener:Ming Zhang(Institute for Geo-Resources and Environment, Geological Survey of Japan, AIST), Ken Kawamoto(Graduate School of Science and Engineering, Saitama University), Jet-Chau Wen(National Yunlin University of Science and Technology), Yonghong Hao(Tianjin Normal University), Chairperson:Ken Kawamoto(Saitama University), Jet- Chau Wen(National Yunlin University of Science and Technology, Taiwan)

1:50 PM - 2:05 PM JST | 4:50 AM - 5:05 AM UTC

[AGE29-06] Investigating the Reproducibility of Hydraulic Tomography Estimates with Time-Variable Boundary Conditions

*Jian-Dao Li[1], Jyun-Lin Chen[1], Hong-Ru Lin[1], Shao-Yang Huang [1], Tian-Chyi Jim Yeh[2], Jet-Chau Wen[1] (1.National Yunlin University of Science and Technology, 2.The University of Arizona)

---

2:05 PM - 2:20 PM JST | 5:05 AM - 5:20 AM UTC

[AGE29-07] **Applying river pollution index and QUAL2K model for water quality assessment and management in Ke-Ya river, Taiwan**

*Hong-Syuan Li[1], Yu-Chih Lin[1] (1.Department of Environmental Engineering & Health, Yuanpei University of Medical Technology)

---

2:20 PM - 2:35 PM JST | 5:20 AM - 5:35 AM UTC

[AGE29-08] Environmental assessment at CDW disposal sites in Vietnam: Case study in Thanh Tri landfill, Hanoi

*Thanh Ha Ngo[1], Akihiro Matsuno[1], Ken Kawamoto[1] (1.Graduate School of Science and Engineering, Saitama University)

---

2:35 PM - 2:50 PM JST | 5:35 AM - 5:50 AM UTC

[AGE29-09] **Modeling Study on the Impacts of Groundwater Pumping to Regional Hydroclimatology in 37 World Major Aquifers**

*Pat J.-F. Yeh[1] (1.Monash University Malaysia)

---

2:50 PM - 3:05 PM JST | 5:50 AM - 6:05 AM UTC

[AGE29-10] CHRATERIZING BURIED WASTE COMPOSITION AT CONSTRUCTION AND DEMOLITION WASTE (CDW) DISPOSAL SITE IN VIETNAM: A CASE STUDY IN THANH TRI LANDFILL IN HANOI

*Tselmeg Aldarjav[1], Akira Kato[1], Akihiro Matsuno[1], Ken Kawamoto[1,2] (1.Graduate School of Science and Engineering, Saitama University, Japan , 2.International Institute for Resilient Society, Saitama University, Japan)

[E] Poster | A (Atmospheric and Hydrospheric Sciences )：A-GE Geological & Soil Environment

5:15 PM - 6:30 PM JST | 8:15 AM - 9:30 AM UTC | Poster Hall International Exhibition Hall8, Makuhari Messe_11

## [A-GE29] Energy-Environment-Water Nexus and Sustainable Development

convener:Ming Zhang(Institute for Geo-Resources and Environment, Geological Survey of Japan, AIST), Ken Kawamoto(Graduate School of Science and Engineering, Saitama University), Jet-Chau Wen(National Yunlin University of Science and Technology), Yonghong Hao(Tianjin Normal University)

[AGE29-P01] **The role of anthropogenic activities in spring discharge cessation: Jinci Springs China**

Yaru Guo[1], *Yonghong Hao[1], Chun Zhao[1], Huan Lian[1] (1.Tianjin Normal University)

[AGE29-P02] **Groundwater response to tidal fluctuations in a leaky confined coastal aquifer with finite length**

*Zhi-Xue Zhao[1], Tongke Wang[1], Jun Li[1] (1.Tianjin Normal University, Tianjin, China)

[AGE29-P03] Relationship between "source and sink"landscape patterns and river nutrient discharge in a peri-urban watershed

*Chongwei Li[1] (1.Tianjin Normal University)

[AGE29-P04] Assessing the Urban Storm-Flood Disaster of Zhengzhou city Based on Fuzzy Methods

*Caihong Hu[1], Xian Du[1], Ying Zhang[1], SHAN E HYDER ALIAS TAHIR[1], Shengqi Jian[1] (1.School of water conservancy and environment, Zhengzhou University, Zhengzhou City, Henan Province, P.R. China, 450001)

[AGE29-P05] Application of RAMMS Software to Predict the submerged area of Debris Flow: A Case Study of Feng-Chiou torrent in Taiwan

*Hsin-Ying Hsieh[1], Chun-Yi Wu[1] (1.Department of Soil and Water Conservation, National Chung Hsing University)

[AGE29-P06] Applications of the Cholesteric Liquid Crystal (CLC) Sensor to Rapidly Measure the Volatile Organic Compounds in the Atmosphere Environment

Ruey-Fang YU[1], *GUAN-BO CHAO[1], Jian-cheng XU[1], KUANG-PENG HSIEH[1] (1.Department of Safety, Health and Environmental Engineering, National United University, Taiwan, R. O. C.)

[AGE29-P07] Solar Ag/P3HT@$TiO_2$ Photocatalysis of Phenol Wastewater by a Pilot-Scale Fresnel Lens Assisted IPCC Reactor

*An-Chi Chen[1], Ting-Yu Zeng [1], Wen-Shiuh Kuo[1] (1.National United University,Department of Safety, Health and Environmental Engineering)

[AGE29-P08] Using fluorescence quenching effect to investigate the electrical neutralization ability for different aromatic organic compounds

*Yu-Ting Chen[1], Wen-Po Cheng[1] (1.National United University,Department of Safety, Health and Environmental Engineering)

[AGE29-P09] **Sustainable recovery of sugarcane biowastes to prepare biochar-derived electrodes for recycling of brackish water**

*Shou-Heng Liu[1] (1.National Cheng Kung University)

[AGE29-P10] The National Survey of POPs in Soil: A study of polybrominated diethyl ethers (PBDEs) in Soil in Taiwan

*Shyh-Wei Chen[1], Ming-Yang Syue[2], I HSIN LEE[3], Chia Hsin Li[3], Yihsin Lai[3], Bo-Wei Power Liang[3] (1.Chung Yuan Christian Univ. Taiwan, 2.Soil and Groundwater Pollution Remediation Fund Management Board, EPA, Taiwan, 3.Sinotech Engineering Service LTD., Taiwan)

[AGE29-P11] **Remediation of Total Peteoleum Hydrocarbons in Soils by Combining Cyclodextrin and Microbubble Ozonation**

*Kuan-Yi Kuo[1], Meng-hau Sung[1], Fu-yin Xie[1] (1.Department of Environmental Science and Engineering,Tunghai University,Taiwan)

[AGE29-P12] **Treatment of organic pollutants in wastewater by ozone microbubbles and cyclodextrins**

*Fu-Yin XIE[1], Meng-hau Sung[1] (1.Department of Environmental Science and Engineering,Tunghai University,Taichung City,Taiwan)

[AGE29-P13] High Addition Valued Recycling Technology of Lithium-ion Battery

*YI-CHEN TSENG[1], TIEN-CHIN CHANG[1], YI-HSIANG HONG[1] (1.Institute of Environmental Engineering and Management, National Taipei University of Technology, No. 1, Sec. 3, Zhongxiao E. Rd., Da'an Dist., Taipei City 106, Taiwan (R.O.C.))

[AGE29-P14] Applying GIS Site Suitability Analysis to Optimize Landfill Selection in Mozambique

*Chelsea Adelina Langa[1] (1.Tohoku University, Graduate School of Environmental Studies)

[AGE29-P15] Effectiveness of Solidification/Stabilization of a Heavy Metal-Contaminated Soil Using a Sustainable Binder

*Yasong Feng[1,2,3], Weiyi Xia[1], Shiji Zhou[1], Ming Zhang[2], Yanjun Du[1] (1.Southeast Univ., 2.AIST, 3.Tohoku Univ.)

[AGE29-P16] **Determining diffusive parameters using out-diffusion experiment with consideration of sampling effect**

*Ranran Song[1], Chihiro Inoue[1], Ming Zhang[2] (1. Tohoku University, 2.Geological Survey of Japan, AIST)

[AGE29-P17] **Exploring the removal characteristics of heavy metals employing Nanofiltration (NF) technique**

*Jagdeesh Kumar[1], Himanshu Joshi[1] (1.INDIAN INSTITUTE OF TECHNOLOGY ROORKEE)

[AGE29-P18] **Potential of Potash Recovery Employing Electrodialysis(ED) Technique from Distillery Effluent**

*SUNIL YADAV[1], HIMANSHU JOSHI[1] (1.INDIAN INSTITUTE OF TECHNOLOGY ROORKEE)

[AGE29-P19] CHARACTERIZATION OF WATER RETENTION AND MASS TRANSPORT PROPERTIES FOR RECYCLED ROADBED MATERIALS BLENDED WITH AAC FINES

*Ryohei ITO[1], Akira KATO[1], Akihiro MATSUNO[1], Ken KAWAMOTO[1,2] (1.Graduate School of Science and Engineering, Saitama University, 2.National University of Civil Engineering, Vietnam)

[AGE29-P20] **Characterizing Geotechnical Properties of Drinking Water Sludge Blended with Graded Crushed Clay Brick for Road Subgrade: Effects of Gradation and Mixing Proportion of Crushed Clay Brick on Compaction Property**

*Tserenlkham lkhagvasuren[1], Muhammad Rashid Iqbal[1], Ken Kawamoto[1] (1.Graduate school of science and engineering Saitama University, Japan)

[AGE29-P21] CHARACTERIZING PHYSICAL AND CHEMICAL PROPERTIES OF RESIDUES GENERATED FROM CONSTRUCTION AND DEMOLITION WASTE

*NINGNING HAO[1], Ken Kawamoto[1], Akihiro Matsuno[1] (1.Saitama University)

[AGE29-P22] CHARACTERIZATION OF PORE-STRUCTURE PARAMETERS FOR UNDISTURBED AND REPACKED SAMPLES AT FIELD WATER CONTENTS

*Arjun Baniya[1], Akihiro Matsuno[1], Ken Kawamoto[1] (1.Saitama University , Graduate school of Science and Engineering)

[AGE29-P23] **CHECK SHEET SURVEY FOR ESTIMATING CDW GENERATION AND CASH FLOW AT BUILDING DEMOLISHING SITES IN HANOI, VIETNAM**

*Cuong Viet Tran[1], Kawamoto Ken[1] (1.Graduate School of Science and Engineering, Saitama University)

[AGE29-P24] APPLICATION OF CRUSHED GRAINS OF LATERITE AND AUTOCLAVED AERATED CONCRETE FOR HEAVY METAL REMOVAL FROM WASTEWATER

*Buddhika Priyadarshani Bandara Arachchillage[1], Yuki Yoshida[1], Pradeep Kumara Gajanayake Mudalige[1], Akihiro Matsuno[1], Ken Kawamoto[1] (1.Graduate School of Science and Engineering, Saitama University)

[AGE29-P25] Effects of Silicic Acid on Environmental Stability of Spent Calcium-based Arsenic Adsorbents

*Hajime Sugita[1], Terumi Oguma[1], Ming Zhang[1], Junko Hara[1], Yoshishige Kawabe[1] (1.National Institute of Advanced Industrial Science and Technology)

[AGE29-P26] The Fate of Chloroethene in Geo-environment

*Ming Zhang[1], Miho Yoshikawa[1] (1.Institute for Geo-Resources and Environment, Geological Survey of Japan, AIST)

[E] Oral | A (Atmospheric and Hydrospheric Sciences )：A-CG Complex & General

9:00 AM - 10:30 AM JST | 12:00 AM - 1:30 AM UTC | 302 3F

## [A-CG34] Satellite Earth Environment Observation

convener:Riko Oki(Japan Aerospace Exploration Agency), Yoshiaki HONDA(Center for Environmental Remote Sensing, Chiba University), Yukari Takayabu(Atmosphere and Ocean Research Institute, the University of Tokyo), Tsuneo Matsunaga(Center for Global Environmental Research and Satellite Observation Center, National Institute for Environmental Studies), Chairperson:Kentaroh Suzuki

9:00 AM - 9:15 AM JST | 12:00 AM - 12:15 AM UTC

### [ACG34-07] GCOM-C “Shikisai” FIRST YEAR OBSERVATIONS

★Invited Papers

*Hiroshi Murakami[1], Masahiro Hori[1], Risa Miyazaki[1], Toshiyuki Kobayashi[1], Takashi M. Nagao[1], Kazunori Ogata[1], Rigen Shimada[1], Junichi Takaku[2] (1.Earth Observation Research Center, Japan Aerospace Exploration Agency, 2.Remote Sensing Technology Center of Japan)

9:15 AM - 9:30 AM JST | 12:15 AM - 12:30 AM UTC

### [ACG34-08] Algorithm improvement for GCOM-C/SGLI Above Ground Biomass Standard product.

*KAJIWARA Koji[1], Yoshiaki HONDA[1] (1.Chiba University)

9:30 AM - 9:45 AM JST | 12:30 AM - 12:45 AM UTC

### [ACG34-09] Common retrieval of Atmospheric Aerosol Properties for geostationary and polar-orbital Satellite Imaging Sensors: Himawari8/AHI and GCOM-C/SGLI results

*Yoshida Mayumi[1], Maki Kikuchi[1], Takashi M. Nagao[1], Hiroshi Murakami[1], Keiya Yumimoto[2] (1.Japan Aerospace Exploration Agency, 2.Kyusyu University)

9:45 AM - 10:00 AM JST | 12:45 AM - 1:00 AM UTC

### [ACG34-10] Cloud optical properties from various ground and satellite instruments evaluated during an intensive campaign

*Alessandro Damiani[1], Hitoshi Irie[1], Takashi Horio[1], Tamio Takamura[1], Rei Kudo[2], Pradeep Khatri[3], Hironobu Iwabuchi[3], Ryosuke Masuda[3], Takashi M. Nagao[4] (1.CEReS, Chiba University, 2.Meteorological Research Institute, Japan Meteorological Agency, 3.Graduate School of Science, Tohoku University, 4.Earth Observation Research Center, JAXA)

10:00 AM - 10:15 AM JST | 1:00 AM - 1:15 AM UTC

### [ACG34-11] Issues in aerosol-cloud-climate interaction: Needs for future satellite mission

★Invited Papers

*Kentaroh Suzuki[1] (1.Atmosphere and Ocean Research Institute, University of Tokyo)

10:15 AM - 10:30 AM JST | 1:15 AM - 1:30 AM UTC

### [ACG34-12] Impact of aerosol vertical profile and optical parameters on the accuracy of satellite AOD retrieval

*Jing Li[1], Chong Li[1] (1.Peking University)

[E] Oral | A (Atmospheric and Hydrospheric Sciences )：A-CG Complex & General

10:45 AM - 12:15 PM JST | 1:45 AM - 3:15 AM UTC | 302 3F

## [A-CG34] Satellite Earth Environment Observation

convener:Riko Oki(Japan Aerospace Exploration Agency), Yoshiaki HONDA(Center for Environmental Remote Sensing, Chiba University), Yukari Takayabu(Atmosphere and Ocean Research Institute, the University of Tokyo), Tsuneo Matsunaga(Center for Global Environmental Research and Satellite Observation Center, National Institute for Environmental Studies), Chairperson:Nobuhiro Takahashi(Institute for Space-Earth Environmental Research, Nagoya University)

10:45 AM - 11:00 AM JST | 1:45 AM - 2:00 AM UTC

[ACG34-13] Statistical validation of drop size distribution estimated by GPM/DPR

*Nobuhiro Takahashi[1] (1.Institute for Space-Earth Environmental Research, Nagoya University)

---

11:00 AM - 11:15 AM JST | 2:00 AM - 2:15 AM UTC

[ACG34-14] Impact study of DPR SLH nudging method for data assimilation in the JMA Local NWP system

★Invited Papers

*Yasutaka Ikuta[1] (1.Japan Meteorological Agency)

---

11:15 AM - 11:30 AM JST | 2:15 AM - 2:30 AM UTC

[ACG34-15] Precipitation Extremes Monitoring using Global Satellite Mapping of Precipitation (GSMaP) Product

*Takuji Kubota[1], Tashima Tomoko[1], Riko Oki[1], Tomoaki Mega[2], Tomoo Ushio[2] (1.Earth Observation Research Center,Japan Aerospace Exploration Agency, 2.Department of Aerospace Engineering, Tokyo Metropolitan University)

---

11:30 AM - 11:45 AM JST | 2:30 AM - 2:45 AM UTC

[ACG34-16] Estimation of cloud water content over land using satellite-based passive microwave observations with a coupled land and atmosphere assimilation method

*Rie Seto[1], Shinjiro Kanae[1] (1.Tokyo Institute of Technology)

---

11:45 AM - 12:00 PM JST | 2:45 AM - 3:00 AM UTC

[ACG34-17] Ensemble-Based Data Assimilation of GPM/DPR Reflectivity into the Nonhydrostatic Icosahedral Atmospheric Model NICAM

*Shunji Kotsuki[1], Koji Terasaki[1], Takemasa Miyoshi[1] (1.RIKEN Center for Computational Science)

---

12:00 PM - 12:15 PM JST | 3:00 AM - 3:15 AM UTC

[ACG34-18] **An ecohydrological land reanalysis by integrating simulation and satellite observations**

*Yohei Sawada[1], Tosiyuki Nakaegawa[1], Kozo Okamoto[1], Takeshi Iriguchi[1], Hideyuki Fujii[2] (1.Meteorological Research Institute, 2.Japan Aerospace Exploration Agency)

[E] Poster | A (Atmospheric and Hydrospheric Sciences )：A-CG Complex & General

1:45 PM - 3:15 PM JST | 4:45 AM - 6:15 AM UTC | Poster Hall International Exhibition Hall8, Makuhari Messe_3

## [A-CG34] Satellite Earth Environment Observation

convener:Riko Oki(Japan Aerospace Exploration Agency), Yoshiaki HONDA(Center for Environmental Remote Sensing, Chiba University), Yukari Takayabu(Atmosphere and Ocean Research Institute, the University of Tokyo), Tsuneo Matsunaga(Center for Global Environmental Research and Satellite Observation Center, National Institute for Environmental Studies)

[ACG34-P01] **Impact of usage of multiple-satellite sensors on accuracy of daily-mean sea surface wind data**

*Ayumi Koizumi[1], Masahisa Kubota[2], Kunio Kutsuwada[3], Hiroyuki Tomita[4], Tsutomu Hihara[5] (1.Tokai University, 2.Tokai University, Institute of Ocean Research and Development, 3.School of Marine Science and Technology, Tokai University, 4.Institute for Space-Earth Environmental, Nagoya University, 5.Japan Agency for Marine-Erth Science and Technology)

[ACG34-P02] Temperature and Size Variability of Warm Pools in the Global Oceans

*ChunYi Lin[1] (1.National Museum of Marine Science & Technology)

[ACG34-P03] Sea surface temperature from SGLI aboard the GCOM-C satellite of JAXA

*Yukio Kurihara[1], Kazunori Ogata[2], Hiroshi Murakami[2], Misako Kachi[2] (1.Tripli-I Co., Ltd., 2.JAXA EORC)

[ACG34-P04] Concept of small satellite UV/visible imaging spectrometer optimized for tropospheric $NO_2$ measurements in air quality monitoring

*Tamaki Fujinawa[1,5], Katsuyuki Noguchi[2], Akihiko Kuze[3], Andreas Richter[4], John P. Burrows[4], Andreas C. Meier[4], Tomohiro Sato[1], Takeshi Kuroda[1], Naohiro Yoshida[5], YASUKO KASAI[1,5] (1.National Institute of Information and Communications Technology, 2.Nara Women's University, 3.Japan Aerospace Exploration Agency, 4.University of Bremen, 5.Tokyo Institute of Technology)

[ACG34-P05] EarthCARE L2 algorithms for cloud and precipitation

*Kaori Sato[1], Hajime Okamoto[1], Hiroshi Ishimoto[2] (1.Research Institute for Applied Mechanics, Kyushu University, 2.Meteorological Research Institute)

[ACG34-P06] Analysis of the Surface Echo Characteristics Derived from GPM/DPR Wide Swath Observation Experiment

*Kosuke Yamamoto[1], Kinji Furukawa[1], Nobuhiro Takahashi[2], Takuji Kubota[1] (1.Japan Aerospace Exploration Agency, 2.Nagoya University)

[ACG34-P07] The Recent Results from the Global Precipitation Measurement (GPM) mission in Japan

*Riko Oki[1], Takuji Kubota[1], Kinji Furukawa[1], Yuki Kaneko[1], Moeka Yamaji[1], Kosuke Yamamoto[1], Toshio Iguchi[2], Yukari Takayabu[3] (1.Japan Aerospace Exploration Agency, 2.NICT, 3.the University of Tokyo)

[ACG34-P08] **Verification of Global Satellite Mapping of precipitation (GSMaP) for providing its error information**

*Moeka Yamaji[1], Takuji Kubota[1] (1.Earth Observation Research Center, Japan Aerospace Exploration Agency)

[ACG34-P09] Detection of the mixed phase top using the measured dual-frequency ratio of reflectivity with GPM/DPR

*Yuki Kaneko[1], Toshio Iguchi[2] (1.Japan Aerospace Exploration Agency, 2.National Institute of Information and Communications Technology)

[ACG34-P10] **Comparison between high frequency satellite rainfall estimation and APHRODITE-2 ground rain gauge observation**

*Hitoshi Hirose[1], Koichi Toyoshima[1], Atsushi Higuchi[1], Akiyo Yatagai[2], Natsuko Yasutomi[3] (1.Center for Environmental Remote Sensing, Chiba University, 2.Hirosaki University, 3.Disaster Prevention Research Institute, Kyoto University)

[ACG34-P11] Development of the high resolution GSMaP by the Himawari-8

*Tomoaki Mega[1], Tomoo Ushio[1] (1.Tokyo Metropolitan University)

[ACG34-P12] Preliminary results of on-orbit estimation for polarization sensitivity of GCOM-C/SGLI

*Risa Miyazaki[1], Hiroshi Murakami[1], Masahiro Hori[1] (1.Japan Aerospace Exploration Agency)

[ACG34-P13] Analysis of SGLI validation datas based on the effects of the growth and ground types for the AGB development

*Ryota Ishibashi[1], Koji KAJIWARA[1], Yoshiaki HONDA[1] (1.Center for environmental remote sensing, Chiba University)

[ACG34-P14] Remote sensing of aerosol optical properties and water-leaving radiance based on the optimal estimation approach

*Chong Shi[1], Teruyuki Nakajima[1], Makiko Hashimoto[1], Hideaki Takenaka[1] (1.Japan Aerospace Exploration Agency)

[ACG34-P15] Aerosol retrieval and PM2.5 from space using GOSAT/TANSO-CAI

*Makiko Hashimoto[1], Hideaki Takenaka[1], Teruyuki Nakajima[1], Akiko Higurashi[2] (1.Japan Aerospace Explortion Agency, 2.NIES)

[ACG34-P16] **Establishing a high resolution road fugitive dust emission inventory in Kaifeng City, China**

*Yiming Xu[1], Shili Liu[1], Xinyue Cao[1], Xianbao Shen[1], Zhiliang Yao[1] (1.Department of Environmental Science and Engineering, Beijing Technology and Business University)

[ACG34-P17] A Relationship between Diurnal Change Patterns of Land Surface Temperature and Spatial Configuration of the Osaka Metropolitan Area Captured by Himawari-8

*Yuhei Yamamoto[1], Hirohiko Ishikawa[1] (1.Disaster Prevention Research Institute, Kyoto University)

[E] Poster | A (Atmospheric and Hydrospheric Sciences )：A-CG Complex & General

5:15 PM - 6:30 PM JST | 8:15 AM - 9:30 AM UTC | Poster Hall International Exhibition Hall8, Makuhari Messe_12

## [A-CG34] Satellite Earth Environment Observation

convener:Riko Oki(Japan Aerospace Exploration Agency), Yoshiaki HONDA(Center for Environmental Remote Sensing, Chiba University), Yukari Takayabu(Atmosphere and Ocean Research Institute, the University of Tokyo), Tsuneo Matsunaga(Center for Global Environmental Research and Satellite Observation Center, National Institute for Environmental Studies)

[ACG34-P01] **Impact of usage of multiple-satellite sensors on accuracy of daily-mean sea surface wind data**

*Ayumi Koizumi[1], Masahisa Kubota[2], Kunio Kutsuwada[3], Hiroyuki Tomita[4], Tsutomu Hihara[5] (1.Tokai University, 2.Tokai University, Institute of Ocean Research and Development, 3.School of Marine Science and Technology, Tokai University, 4.Institute for Space-Earth Environmental, Nagoya University, 5.Japan Agency for Marine-Erth Science and Technology)

[ACG34-P02] Temperature and Size Variability of Warm Pools in the Global Oceans

*ChunYi Lin[1] (1.National Museum of Marine Science & Technology)

[ACG34-P03] Sea surface temperature from SGLI aboard the GCOM-C satellite of JAXA

*Yukio Kurihara[1], Kazunori Ogata[2], Hiroshi Murakami[2], Misako Kachi[2] (1.Tripli-I Co., Ltd., 2.JAXA EORC)

[ACG34-P04] Concept of small satellite UV/visible imaging spectrometer optimized for tropospheric $NO_2$ measurements in air quality monitoring

*Tamaki Fujinawa[1,5], Katsuyuki Noguchi[2], Akihiko Kuze[3], Andreas Richter[4], John P. Burrows[4], Andreas C. Meier[4], Tomohiro Sato[1], Takeshi Kuroda[1], Naohiro Yoshida[5], YASUKO KASAI[1,5] (1.National Institute of Information and Communications Technology, 2.Nara Women's University, 3.Japan Aerospace Exploration Agency, 4.University of Bremen, 5.Tokyo Institute of Technology)

[ACG34-P05] EarthCARE L2 algorithms for cloud and precipitation

*Kaori Sato[1], Hajime Okamoto[1], Hiroshi Ishimoto[2] (1.Research Institute for Applied Mechanics, Kyushu University, 2.Meteorological Research Institute)

[ACG34-P06] Analysis of the Surface Echo Characteristics Derived from GPM/DPR Wide Swath Observation Experiment

*Kosuke Yamamoto[1], Kinji Furukawa[1], Nobuhiro Takahashi[2], Takuji Kubota[1] (1.Japan Aerospace Exploration Agency, 2.Nagoya University)

[ACG34-P07] The Recent Results from the Global Precipitation Measurement (GPM) mission in Japan

*Riko Oki[1], Takuji Kubota[1], Kinji Furukawa[1], Yuki Kaneko[1], Moeka Yamaji[1], Kosuke Yamamoto[1], Toshio Iguchi[2], Yukari Takayabu[3] (1.Japan Aerospace Exploration Agency, 2.NICT, 3.the University of Tokyo)

[ACG34-P08] **Verification of Global Satellite Mapping of precipitation (GSMaP) for providing its error information**

*Moeka Yamaji[1], Takuji Kubota[1] (1.Earth Observation Research Center, Japan Aerospace Exploration Agency)

[ACG34-P09] Detection of the mixed phase top using the measured dual-frequency ratio of reflectivity with GPM/DPR

*Yuki Kaneko[1], Toshio Iguchi[2] (1.Japan Aerospace Exploration Agency, 2.National Institute of Information and Communications Technology)

[ACG34-P10] **Comparison between high frequency satellite rainfall estimation and APHRODITE-2 ground rain gauge observation**

*Hitoshi Hirose[1], Koichi Toyoshima[1], Atsushi Higuchi[1], Akiyo Yatagai[2], Natsuko Yasutomi[3] (1.Center for Environmental Remote Sensing, Chiba University, 2.Hirosaki University, 3.Disaster Prevention Research Institute, Kyoto University)

[ACG34-P11] Development of the high resolution GSMaP by the Himawari-8

*Tomoaki Mega[1], Tomoo Ushio[1] (1.Tokyo Metropolitan University)

[ACG34-P12] Preliminary results of on-orbit estimation for polarization sensitivity of GCOM-C/SGLI

*Risa Miyazaki[1], Hiroshi Murakami[1], Masahiro Hori[1] (1.Japan Aerospace Exploration Agency)

[ACG34-P13] Analysis of SGLI validation datas based on the effects of the growth and ground types for the AGB development

*Ryota Ishibashi[1], Koji KAJIWARA[1], Yoshiaki HONDA[1] (1.Center for environmental remote sensing, Chiba University)

[ACG34-P14] Remote sensing of aerosol optical properties and water-leaving radiance based on the optimal estimation approach

*Chong Shi[1], Teruyuki Nakajima[1], Makiko Hashimoto[1], Hideaki Takenaka[1] (1.Japan Aerospace Exploration Agency)

[ACG34-P15] Aerosol retrieval and PM2.5 from space using GOSAT/TANSO-CAI

*Makiko Hashimoto[1], Hideaki Takenaka[1], Teruyuki Nakajima[1], Akiko Higurashi[2] (1.Japan Aerospace Explortion Agency, 2.NIES)

[ACG34-P16] **Establishing a high resolution road fugitive dust emission inventory in Kaifeng City, China**

*Yiming Xu[1], Shili Liu[1], Xinyue Cao[1], Xianbao Shen[1], Zhiliang Yao[1] (1.Department of Environmental Science and Engineering, Beijing Technology and Business University)

[ACG34-P17] A Relationship between Diurnal Change Patterns of Land Surface Temperature and Spatial Configuration of the Osaka Metropolitan Area Captured by Himawari-8

*Yuhei Yamamoto[1], Hirohiko Ishikawa[1] (1.Disaster Prevention Research Institute, Kyoto University)

[E] Oral | A (Atmospheric and Hydrospheric Sciences )：A-CG Complex & General

3:30 PM - 5:00 PM JST | 6:30 AM - 8:00 AM UTC | 302 3F

## [A-CG34] Satellite Earth Environment Observation

convener:Riko Oki(Japan Aerospace Exploration Agency), Yoshiaki HONDA(Center for Environmental Remote Sensing, Chiba University), Yukari Takayabu(Atmosphere and Ocean Research Institute, the University of Tokyo), Tsuneo Matsunaga(Center for Global Environmental Research and Satellite Observation Center, National Institute for Environmental Studies), Chairperson:Tsuneo Matsunaga

3:30 PM - 3:45 PM JST | 6:30 AM - 6:45 AM UTC

[ACG34-19] How GOSAT has survived in-orbit anomalies and calibrated radiance spectra for 10 years.

★Invited Papers

*Akihiko Kuze[1], hiroshi Suto[1], Kei Shiomi[1], Nobuhiro Kikuchi[1], Makiko Hashimoto[1], Fumie Kataoka[2] (1.Japan Aerospace Exploration Agency, 2.RESTEC)

---

3:45 PM - 4:00 PM JST | 6:45 AM - 7:00 AM UTC

[ACG34-20] Estimating regional anthropogenic methane emissions with GOSAT satellite retrievals and ground-based observations

*Shamil Maksyutov[1], Aki Tsuruta[2], Rajesh Janardanan[1], Fenjuan Wang[1], Akihiko Ito[1], Motoki Sasakawa[1], Toshinobu Machida[1], Isamu Morino[1], Yukio Yoshida[1], Johannes Kaiser[3], Greet Janssens-Maenhout[4], Ed Dlugokencky[5], Tsuneo Matsunaga[1] (1.National Institute for Environmental Studies, 2.Finnish Meteorological Institute, 3.Deutscher Wetterdienst, 4.European Commission, Joint Research Centre , 5.National Oceanic and Atmospheric Administration, Global Monitoring Division)

---

4:00 PM - 4:15 PM JST | 7:00 AM - 7:15 AM UTC

[ACG34-21] The Status and the Future Plan of GOSAT-2 Level 2 and 4 Products

★Invited Papers

*Tsuneo Matsunaga[1], Isamu Morino[1], Yukio Yoshida[1], Makoto Saito[1], Hibiki M Noda[1], Hirofumi Ohyama[1], Akihide Kamei[1], Fumie Kawazoe[1], Ryoichi Imasu[2], Teruyuki Nakajima[4], Takashi Nakajima[5], Naoko Saitoh[3], Makiko Hashimoto[4] (1.Center for Global Environmental Research and Satellite Observation Center, National Institute for Environmental Studies, 2.The University of Tokyo, 3.Chiba University, 4.Japan Aerospace Exploration Agency, 5.Tokai University)

---

4:15 PM - 4:30 PM JST | 7:15 AM - 7:30 AM UTC

[ACG34-22] A preliminary initial check of the cloud discrimination products by CAI-2 onboard GOSAT-2

*Yoshiaki Ishihara[1], Yu Oishi[2], Haruma Ishida[3], Takashi Nakajima[4] (1.NIES, 2.NARO, 3.JMA, 4.Tokai Univ.)

---

4:30 PM - 4:45 PM JST | 7:30 AM - 7:45 AM UTC

[ACG34-23] **Drought monitoring and evaluation performance of temperature vegetation drought index (TVDI) over Eurasia**

*Fengmei Yao[1], Siqi Shi[1], Jiahua Zhang[2] (1.UCAS University of Chinese Academy of Sciences, 2.Institute of Remote Sensing and Digital Earth, Chinese Academy of Sciences)

---

4:45 PM - 5:00 PM JST | 7:45 AM - 8:00 AM UTC

[ACG34-24] **IMPACT OF CHANGE IN LAND USE AND LAND COVER PATTERN ON LAND SURFACE TEMPERATURE AND THERMAL COMFORT USING MICRO-SCALE AREA MODEL: CASE STUDY OF AN EDUCATIONAL CAMPUS.**

*DILJIT KUMAR NAYAK[1], MANJU MOHAN[1] (1.IIT DELHI)

[J] Oral | A (Atmospheric and Hydrospheric Sciences)：A-CG Complex & General

10:45 AM - 12:15 PM JST | 1:45 AM - 3:15 AM UTC | 106 1F

## [A-CG36] Earth & Environmental Sciences and Artificial Intelligence

convener:Tomohiko Tomita(Faculty of Advanced Science and Technology, Kumamoto University), Ken-ichi Fukui(Osaka University), Daisuke Matsuoka(Japan Agency for Marine-Earth Science and Technology), Satoshi Ono(Kagoshima University), Chairperson:Tomohiko Tomita(Kumamoto University, Faculty of Advanced Science and Technology)

10:50 AM - 11:20 AM JST | 1:50 AM - 2:20 AM UTC

[ACG36-01] Recent Progress in Deep Neural Network Architectures and their Applications

★Invited Papers

*Shinichi Shirakawa[1] (1.Yokohama National University)

---

11:20 AM - 11:35 AM JST | 2:20 AM - 2:35 AM UTC

[ACG36-02] Improving performance of oxidant prediction using machine learning by optimizing input data based on atmospheric science knowledge

*Tomohiro Sato[1], Peijiang Zhao[1], Koji Zettsu[1] (1.National Institute of Information and Communications Technology)

---

11:35 AM - 11:50 AM JST | 2:35 AM - 2:50 AM UTC

[ACG36-03] Spatiotemporal Climate Forecasting with ConvLSTM

*Ekasit Phermphoonphiphat[1], Tomohiko Tomita[3], Masayuki Numao[2], Ken-ichi Fukui[2] (1.Graduate School of Information Science and Technology, Osaka University, 2.The Institute of Scientific and Industrial Research, Osaka University, 3.Faculty of Advanced Science and Technology, Kumamoto University)

---

11:50 AM - 12:05 PM JST | 2:50 AM - 3:05 AM UTC

[ACG36-04] Deep-Learning Based Short-Term Prediction Method for Sea Ice Concentration Using Explanatory Variables

*Issei Kawashima[1], Toru Kouyama[1], Ryu Sugimoto[1], Ryosuke Nakamura[1] (1.National Institute of Advanced Industrial Science and Technology)

[J] Oral | A (Atmospheric and Hydrospheric Sciences)：A-CG Complex & General

1:45 PM - 3:15 PM JST | 4:45 AM - 6:15 AM UTC | 104 1F

## [A-CG36] Earth & Environmental Sciences and Artificial Intelligence

convener:Tomohiko Tomita(Faculty of Advanced Science and Technology, Kumamoto University), Ken-ichi Fukui(Osaka University), Daisuke Matsuoka(Japan Agency for Marine-Earth Science and Technology), Satoshi Ono(Kagoshima University), Chairperson:Tomohiko Tomita(Kumamoto University, Faculty of Advanced Science and Technology)

1:45 PM - 2:00 PM JST | 4:45 AM - 5:00 AM UTC

[ACG36-05] **Remote sensing of cloud using the deep learning based on three-dimensional radiative transfer**

*Hironobu Iwabuchi[1], Ryosuke Masuda[1], K. Sebastian Schmidt[2,3], Alessandro Damiani[4], Rei Kudo[5] (1.Graduate School of Science, Tohoku University, 2.Department of Atmospheric and Oceanic Sciences, University of Colorado, 3.Laboratory for Atmospheric and Space Physics, University of Colorado, 4.Center for Environmental Remote Sensing, Chiba University, 5.Meteorological Research Institute, Japan Meteorological Agency)

2:00 PM - 2:15 PM JST | 5:00 AM - 5:15 AM UTC

[ACG36-06] Time series of cloud cover during the night derived from an omnidirectional camera

*Karin miyabe[1], Kazunori Ogohara[1] (1.University of Shiga Prefecture)

2:15 PM - 2:30 PM JST | 5:15 AM - 5:30 AM UTC

[ACG36-07] Time series prediction of cloud cover using whole-sky images and meteorological elements

*Kazunori Ogohara[1], Teppei Sonoda[2] (1.School of Engineering, University of Shiga Prefecture, 2.Graduate School of Engineering, University of Shiga Prefecture)

2:30 PM - 2:45 PM JST | 5:30 AM - 5:45 AM UTC

[ACG36-08] Fundamental investigation about the inductive prediction of precipitation based on the time series data

*Naoki Matsumoto[1], Tomohiko Tomita[1], Kenichi Fukui[2] (1.Kumamoto Univ., 2.Osaka Univ.)

2:45 PM - 3:00 PM JST | 5:45 AM - 6:00 AM UTC

[ACG36-09] Identification of ships image on SAR data using machine learning

*Takashi Sonoke[1], Hirohide Demura[1] (1.University of Aizu)

[J] Poster | A (Atmospheric and Hydrospheric Sciences )：A-CG Complex & General

3:30 PM - 5:00 PM JST | 6:30 AM - 8:00 AM UTC | Poster Hall International Exhibition Hall8, Makuhari Messe_6

## [A-CG36] Earth & Environmental Sciences and Artificial Intelligence

convener:Tomohiko Tomita(Faculty of Advanced Science and Technology, Kumamoto University), Ken-ichi Fukui(Osaka University), Daisuke Matsuoka(Japan Agency for Marine-Earth Science and Technology), Satoshi Ono(Kagoshima University)

[ACG36-P01] **Automatic Detection of Illegal Waste Sites in UAS Orthoimages**

Wei-De Chen[1], *Yu-Ching Lin[1], Hsien-Min Wu[1] (1.Chung Cheng Institute of Technology, Taiwan)

[ACG36-P02] Using machine learning models to predict the benefits of solar power generation in northern Taiwan

*SHIH-CHIAO TSAI[1], KUO-CHIH HUANG[1], DUN-REN GUO[1] (1.National Defense Univ.)

[ACG36-P03] Change Point Detection and Visualization of Region of Interests on Weather Time Series Data Using Three-dimensional Convolutional Neural Network

*Satoshi Ono[1], Sotaro Maehara[1], Takahiro Kinoshita[1], Ken-ichi Fukui[2], Tomohiko Tomita[3] (1.Kagoshima University, 2.Osaka University, 3.Kumamoto University)

[ACG36-P04] Estimation of sediment disaster risk around the Fuji River Basin using a machine learning method that considers trigger and inherent factors

*Kazuyoshi Souma[1], Sei Kuroda[2], Takeru Kurakami[2], Takashi Miyamoto[1] (1.Interdisciplinary Graduate School, University of Yamanashi, 2.Integrated Graduate School of Medicine, Engineering, and Agricultural Sciences)

[ACG36-P05] Application of deep learning techniques to precipitation guidance in short-term weather predictions

*TAKERU KURAKAMI[1], Kazuyoshi Souma[1], Takashi Miyamoto[1], Takahiko Huruya[1], Jun Magome[1], Hiroshi Ishidaira[1] (1.University of Yamanashi)

[ACG36-P06] Characteristics of precipitation in Japan evaluated from the ratio of precipitation events

*Kenta Ogino[1], Tomohiko Tomita[1], Naoki Matsumoto[1] (1.Kumamoto University)

[J] Poster | A (Atmospheric and Hydrospheric Sciences )：A-CG Complex & General

5:15 PM - 6:30 PM JST | 8:15 AM - 9:30 AM UTC | Poster Hall International Exhibition Hall8, Makuhari Messe_13

## [A-CG36] Earth & Environmental Sciences and Artificial Intelligence

convener:Tomohiko Tomita(Faculty of Advanced Science and Technology, Kumamoto University), Ken-ichi Fukui(Osaka University), Daisuke Matsuoka(Japan Agency for Marine-Earth Science and Technology), Satoshi Ono(Kagoshima University)

[ACG36-P01] **Automatic Detection of Illegal Waste Sites in UAS Orthoimages**

Wei-De Chen[1], *Yu-Ching Lin[1], Hsien-Min Wu[1] (1.Chung Cheng Institute of Technology, Taiwan)

[ACG36-P02] Using machine learning models to predict the benefits of solar power generation in northern Taiwan

*SHIH-CHIAO TSAI[1], KUO-CHIH HUANG[1], DUN-REN GUO[1] (1.National Defense Univ.)

[ACG36-P03] Change Point Detection and Visualization of Region of Interests on Weather Time Series Data Using Three-dimensional Convolutional Neural Network

*Satoshi Ono[1], Sotaro Maehara[1], Takahiro Kinoshita[1], Ken-ichi Fukui[2], Tomohiko Tomita[3] (1.Kagoshima University, 2.Osaka University, 3.Kumamoto University)

[ACG36-P04] Estimation of sediment disaster risk around the Fuji River Basin using a machine learning method that considers trigger and inherent factors

*Kazuyoshi Souma[1], Sei Kuroda[2], Takeru Kurakami[2], Takashi Miyamoto[1] (1.Interdisciplinary Graduate School, University of Yamanashi, 2.Integrated Graduate School of Medicine, Engineering, and Agricultural Sciences)

[ACG36-P05] Application of deep learning techniques to precipitation guidance in short-term weather predictions

*TAKERU KURAKAMI[1], Kazuyoshi Souma[1], Takashi Miyamoto[1], Takahiko Huruya[1], Jun Magome[1], Hiroshi Ishidaira[1] (1.University of Yamanashi)

[ACG36-P06] Characteristics of precipitation in Japan evaluated from the ratio of precipitation events

*Kenta Ogino[1], Tomohiko Tomita[1], Naoki Matsumoto[1] (1.Kumamoto University)

[J] Oral | A (Atmospheric and Hydrospheric Sciences)：A-CG Complex & General

9:00 AM - 10:30 AM JST | 12:00 AM - 1:30 AM UTC | 303 3F

## [A-CG37] Science in the Arctic Region

convener:NAOYA KANNA(Arctic Research Center, Hokkaido University), Masashi Niwano(Meteorological Research Institute), Tetsu Nakamura(Faculty of Environmental Earth Science, Hokkaido University), Shunsuke Tei(Arctic Research Center, Hokkaido University), Chairperson:Tetsu Nakamura(Faculty of Earth Environmental Science, Hokkaido University), Shunsuke Tei(Arctic Research Center, Hokkaido University)

9:00 AM - 9:15 AM JST | 12:00 AM - 12:15 AM UTC

[ACG37-01] **Arctic midlatitude linkage modulated by the QBO**

*Jinro Ukita[1], Kazuhiro Hoshi[1], Meiji Honda[1], Tetsu Nakamura[2], Koji Yamazaki[2] (1.Niigata University, 2.Hokkaido University)

9:15 AM - 9:30 AM JST | 12:15 AM - 12:30 AM UTC

[ACG37-02] **Interhemispheric synchronization between the AO and the AAO**

*Yoshihiro Tachibana[1], Yusuke Inoue[1], Kensuke K komatsu[1], Tetsu Nakamura[2], Meiji Honda[3], Koto Ogata[1,4], Koji Yamazaki[2] (1.Mie University, 2.Hokkaido University, 3.Niigata University, 4.Japan Meteorological Agency)

9:30 AM - 9:45 AM JST | 12:30 AM - 12:45 AM UTC

[ACG37-03] Marginal ice zone sea ice observations in the refreezing Chukchi Sea

*Takehiko Nose[1], Tsubasa Kodaira[1], Takuji Waseda[1], Jun Inoue[2] (1.The university of Tokyo, 2.National Institute of Polar Research)

9:45 AM - 10:00 AM JST | 12:45 AM - 1:00 AM UTC

[ACG37-04] **Prediction of wildfire and air pollution with machine learning over the five domains of Eastern Eurasia**

*Teppei J Yasunari[1,2], Ichigaku Takigawa[3], Kyu-Myong Kim[4], Arlindo M da Silva[4] (1.Faculty of Engineering, Hokkaido University, 2.Arctic Research Center, Hokkaido University, 3.Graduate School of Information Science and Technology, Hokkaido University, 4.NASA Goddard Space Flight Center)

10:00 AM - 10:15 AM JST | 1:00 AM - 1:15 AM UTC

[ACG37-05] Hydrological Changes in the Four Largest Siberian Arctic River Basins

*Kazuyoshi Suzuki[1], Tetsuya Hiyama[2], Kazuhito Ichii[3], Yoshihiro Iijima[4], Koji Matsuo[5], Dai Yamazaki[6,1] (1.Japan Agency for Marine-Earth Science and Technology, 2.Institute for Space-Earth Environmental Research, Nagoya University, 3.Chiba University, 4.Graduate School of Bioresources, Mie University, 5.Geospatial Information Authority of Japan, 6.Institute of Industrial Sciences, The University of Tokyo)

10:15 AM - 10:30 AM JST | 1:15 AM - 1:30 AM UTC

[ACG37-06] Mapping thermokarst subsidence in Central Yakutia using L-band SAR interferometry

*Takahiro Abe[1], Go Iwahana[2,3], Takeo Tadono[1] (1.Earth Observation Research Center, Japan Aerospace Exploration Agency, 2.International Arctic Research Center, University of Alaska, Fairbanks, 3.Arctic Research Center, Hokkaido University)

[J] Oral | A (Atmospheric and Hydrospheric Sciences)：A-CG Complex & General

10:45 AM - 12:15 PM JST | 1:45 AM - 3:15 AM UTC | 303 3F

## [A-CG37] Science in the Arctic Region

convener:NAOYA KANNA(Arctic Research Center, Hokkaido University), Masashi Niwano(Meteorological Research Institute), Tetsu Nakamura(Faculty of Environmental Earth Science, Hokkaido University), Shunsuke Tei(Arctic Research Center, Hokkaido University), Chairperson:Shunsuke Tei(Arctic Research Center, Hokkaido University), Masashi Niwano(Meteorological Research Institute)

10:45 AM - 11:00 AM JST | 1:45 AM - 2:00 AM UTC

[ACG37-07] Spatiotemporal variation of thaw subsidence and frost heave of permafrost caused by wildfire around Batagay, East Siberia

*Kazuki Yanagiya[1], Masato Furuya[2] (1.Graduate School of Science, Hokkiado University, 2.Faculty of Science, Hokkaido University)

---

11:00 AM - 11:15 AM JST | 2:00 AM - 2:15 AM UTC

[ACG37-08] Influence of recent climate change on permafrost coast dynamics in the Kara Sea, Russian Arctic Ocean

*A. Kioka[1,2], V. S. Isaev[2], A. V. Koshurnikov[2], A. Pogorelov[2], R. M. Amangurov[2], O. Podchasov[2], D. O. Sergeev[3], S. N. Buldovich[2], D. M. Aleksyutina[4], E. A. Grishakina[5] (1.Institut für Geologie, Leopold-Franzens-Universität Innsbruck, Austria, 2.Department of Geocryology, Lomonosov Moscow State University, Russia, 3.Sergeev Institute of Environmental Geoscience, Russian Academy of Science, Russia, 4.Research Laboratory of Geoecology of the Northern Territories, Lomonosov Moscow State University, Russia, 5.Vernadsky Institute of Geochemistry and Analytical Chemistry, Russian Academy of Science, Russia)

---

11:15 AM - 11:30 AM JST | 2:15 AM - 2:30 AM UTC

[ACG37-09] Ice front variations of Heilprin Glacier in northwestern Greenland controlled by the ocean and glacier bed geometries

*Izumi Asaji[1,2], Daiki Sakakibara[3], Takuto Ando[3], Shin Sugiyama[1] (1.Institute of Low Temperature Science, Hokkaido University, 2.Graduate School of Environmental Science, Hokkaido University, 3.Arctic Research Center, Hokkaido University)

---

11:30 AM - 11:45 AM JST | 2:30 AM - 2:45 AM UTC

[ACG37-10] Meltwater discharge and flooding of the outlet stream of Qaanaaq Glacier, northwestern Greenland

*Ken Kondo[1,2], Daiki Sakakibara[3,2], Shungo Fukumoto[1,2], Shin Sugiyama[2] (1.Graduate School of Environmental Science, Hokkaido University, 2.Institute of Low Temperature Science, Hokkaido University, 3.Arctic Research Center, Hokkaido University)

---

11:45 AM - 12:00 PM JST | 2:45 AM - 3:00 AM UTC

[ACG37-11] Occurrence frequency of lee-side downslope winds near Siorapaluk in northwest Greenland

*Akihiro Hashimoto[1], Tetsuhide Yamasaki[2], Teruo Aoki[3,1], Masashi Niwano[1], Satoru Yamaguchi[4] (1.Meteorological Research Institute, 2.Avangnaq, 3.The Graduate School of Natural Science and Technology, Okayama University, 4.Snow and Ice Research Center, National Research Institute for Earth Science and Disaster Resilience)

---

12:00 PM - 12:15 PM JST | 3:00 AM - 3:15 AM UTC

[ACG37-12] **Impacts of clouds on the Greenland ice sheet surface melt and mass balance**

*Masashi Niwano[1], Akihiro Hashimoto[1], Teruo Aoki[2] (1.Meteorological Research Institute, 2.Graduate School of Natural Science and Technology, Okayama University)

[J] Poster | A (Atmospheric and Hydrospheric Sciences )：A-CG Complex & General

1:45 PM - 3:15 PM JST | 4:45 AM - 6:15 AM UTC | Poster Hall International Exhibition Hall8, Makuhari Messe_4

## [A-CG37] Science in the Arctic Region

convener:NAOYA KANNA(Arctic Research Center, Hokkaido University), Masashi Niwano(Meteorological Research Institute), Tetsu Nakamura(Faculty of Environmental Earth Science, Hokkaido University), Shunsuke Tei(Arctic Research Center, Hokkaido University)

### [ACG37-P01] Increasing trend of downward long-wave radiation at the surface in the winter Arctic

*Yuta Miwa[1], Toru Nozawa[2] (1.Faculty of Science, Okayama University , 2.Graduate School of Natural Science and Technology, Okayama University)

### [ACG37-P02] Climate memory of the Eurasian land process for the Arctic amplification

*Tetsu Nakamura[1], Koji Yamazaki[1], Tomonori Sato[1], Jinro Ukita[2] (1.Faculty of Environmental Earth Science, Hokkaido University, 2.Faculty of Science , Niigata University)

### [ACG37-P03] Interannual variation of summer precipitation and atmospheric water circulation over and around Alaska

*Shohei Morino[1], Tetsuya Hiyama[2], Hatsuki Fujinami[2], Hironari Kanamori[2], Masahito Ueyama[3] (1. Graduate School of Environmental Studies, Nagoya University, 2.Institute for Space-Earth Environmental Research, Nagoya University, 3.Graduate School of Life and Environmental Sciences, Osaka Prefecture University)

### [ACG37-P04] Detection of a climatological short break in the polar night jet in early winter and its relation to cooling over Siberia

*Yuta Ando[1], Koji Yamazaki[2], Yoshihiro Tachibana[1], Masayo Ogi[3], Jinro Ukita[4] (1.Graduate School of Bioresources, Mie University, 2.Hokkaido University, 3.Centre for Earth Observation Science, University of Manitoba, 4.Faculty of Science, Niigata University)

### [ACG37-P05] Recent breakdown of the seasonal linkage between the winter North Atlantic Oscillation/Northern Annular Mode and summer Northern Annular Mode

*Koji Yamazaki[1], Yoshihiro Tachibana[2], Masayo Ogi[1], Tetsu Nakamura[1], Kazuhiro Oshima[3] (1.Hokkaido University, 2.Mie University, 3.Institute of Environmental Sciences)

### [ACG37-P06] Did an Arctic sea-ice hole cause hemispheric extreme cold winter in 2017/18?

*Keisuke Ota[1], Yoshihiro Tachibana[1], Kensuke K. Komatsu[1], Alexeev A. Vladimir[2], Cai Lei[2], Yuta Ando[1] (1.Graduate School of Bioresources, Mie University, 2.International Arctic Research Center, University of Alaska Fairbanks)

### [ACG37-P07] Flood affects vegetation at plant species level to regional level: *Arctagrostis latifolia* increased one year after flooding in Indigirka lowland, northeastern Siberia

*Tomoki Morozumi[1,2], Shihong Zhong[1], Ryo Shingubara[5,1], Shunsuke Tei[2], Shinya Takano[1], Rong Fan[1,2], Yumiko Miyamoto[2], Ruslan Shakhmatov[1], Shin Nagai[3], Hideki Kobayashi[3], Rikie Suzuki[3], Trofim C Maximov[4,6], Atsuko Sugimoto[2,7] (1.Graduate School of Environmental Science, Hokkaido University, 2.Arctic Research Center, Hokkaido University, 3.Japan Agency for Marine-Earth Science and Technology, 4.Institute for Biological Problems of Cryolithozone SB RAS, 5.Graduate School of Environmental Studies, Nagoya University, 6.North Eastern Federal University, 7.Station for Arctic Research, Global Institution for Collaborative Research and Education, Hokkaido University)

### [ACG37-P08] Extent and cause of an extreme flooding occurred in spring - summer 2017 over the Indigirka River lowland in Northeastern Siberia

*Shunsuke Tei[1], Tomoki Morozumi[2], Shin Nagai[3], Shinya Takano[2], Atsuko Sugimoto[1], Ryo Shingubara[4], RONG FAN[2], Alexander Fedorov[5], Trofim Maximov[6] (1.Arctic Research Center, Hokkaido University, 2.Graduate School of Environmental Science, Hokkaido University, 3.Japan Agency for Marine Earth Science and Technology, 4.Graduate School of Environmental studies, Nagoya University, 5.Melnikov Permafrost Institute, 6.North-Eastern Federal University)

### [ACG37-P09] Monitoring of the light absorbing aerosols and the impact on radiation budget of atmosphere and snow

*Masahiro Hosaka[1], Hiroshi Ishimoto[1], Tomonori Tanikawa[1], Masashi Niwano[1], Kouji Adachi[1], Naga Oshima[1], Mizuo Kajino[1], Taichu Y Tanaka[1], Sumito Matoba[2] (1.Meteorological Research Institute, 2.Hokkaido University)

[ACG37-P10] Mass concertation and particle number of black carbon on glaciers in the eastern Alaskan Range, Alaska USA

*Keiko Konya[1], Takuma Miyakawa[1], Masayuki Takigawa[1], Masahiro Yamaguchi[1], Shad O'neel[2], Martin Truffer[3] (1.Japan Agency for Marine-Earth Science and Technology, 2.USGS, 3.University of Alaska, Fairbanks)

[ACG37-P11] Remote estimation of phenological shifts in phytoplankton community in the Pacific Arctic Region

*Hisatomo Waga[1], Toru Hirawake[1] (1.Hokkaido University)

[ACG37-P12] Seasonality of diatom and silicoflagellate assemblages observed in settling particles of the western Arctic Ocean

*Jonaotaro Onodera[1,2], EIJI WATANABE[2], Naomi Harada[1,2] (1.Research and Development Center for Global Change, JAMSTEC, 2.Institute of Arctic Climate and Environment Change Research, JAMSTEC)

[ACG37-P13] Iron and macronutrient distributions near the fronts of marine-terminating glaciers in Inglefield Gulf, northwestern Greenland

*NAOYA KANNA[1], Shin Sugiyama[2], Takuto Ando[1], Izumi Asaji[3,2], Yoshiki Fujishi[3,2], Jun Nishioka[2] (1.Arctic Research Center, Hokkaido University, 2.Institute of Low Temperature Science, Hokkaido University, 3.Graduate School of Environmental Science, Hokkaido University)

[ACG37-P14] Paleoenvironmental reconstruction from sediments of Bowdoin fjord, northwestern Greenland

*Takuto Ando[1], NAOYA KANNA[1], Izumi Asaji[2,3], Yoshiki Fujishi[2,3], Shin Sugiyama[1,2,3] (1.Arctic Research Center, Hokkaido University, 2.Institute of Low Temperature Science, Hokkaido University, 3.Graduate School of Environmental Science, Hokkaido University)

[ACG37-P15] A large-eddy simulation of upwelling meltwater plume at marine-terminating glacier fronts

*Yoshimasa Matsumura[1], Naoya Kanna[2], Shin Sugiyama[3,2] (1.Atmosphere and Ocean Research Institute, University of Tokyo, 2.Arctic Research Center, Hokkaido University, 3.Institute of Low Temperature Science, Hokkaido University)

[ACG37-P16] Impact of observation-based snow/ice albedo with starting temperature of −2°C for surface melting effect on a global ocean simulation

*Takahiro Toyoda[1], Teruo Aoki[1,2], Masashi Niwano[1], Tomonori Tanikawa[1], Shogo Urakawa[1], Hiroyuki Tsujino[1], Hideyuki Nakano[1], Kei Sakamoto[1], Nariaki Hirose[1], Goro Yamanaka[1] (1.Meteorological Research Institute, Japan Meteorological Agency, 2.Graduate School of Natural Science and Technology, Okayama University)

[J] Poster | A (Atmospheric and Hydrospheric Sciences )：A-CG Complex & General

5:15 PM - 6:30 PM JST | 8:15 AM - 9:30 AM UTC | Poster Hall International Exhibition Hall8, Makuhari Messe_14

## [A-CG37] Science in the Arctic Region

convener:NAOYA KANNA(Arctic Research Center, Hokkaido University), Masashi Niwano(Meteorological Research Institute), Tetsu Nakamura(Faculty of Environmental Earth Science, Hokkaido University), Shunsuke Tei(Arctic Research Center, Hokkaido University)

### [ACG37-P01] Increasing trend of downward long-wave radiation at the surface in the winter Arctic

*Yuta Miwa[1], Toru Nozawa[2] (1.Faculty of Science, Okayama University , 2.Graduate School of Natural Science and Technology, Okayama University)

### [ACG37-P02] Climate memory of the Eurasian land process for the Arctic amplification

*Tetsu Nakamura[1], Koji Yamazaki[1], Tomonori Sato[1], Jinro Ukita[2] (1.Faculty of Environmental Earth Science, Hokkaido University, 2.Faculty of Science , Niigata University)

### [ACG37-P03] Interannual variation of summer precipitation and atmospheric water circulation over and around Alaska

*Shohei Morino[1], Tetsuya Hiyama[2], Hatsuki Fujinami[2], Hironari Kanamori[2], Masahito Ueyama[3] (1. Graduate School of Environmental Studies, Nagoya University, 2.Institute for Space-Earth Environmental Research, Nagoya University, 3.Graduate School of Life and Environmental Sciences, Osaka Prefecture University)

### [ACG37-P04] Detection of a climatological short break in the polar night jet in early winter and its relation to cooling over Siberia

*Yuta Ando[1], Koji Yamazaki[2], Yoshihiro Tachibana[1], Masayo Ogi[3], Jinro Ukita[4] (1.Graduate School of Bioresources, Mie University, 2.Hokkaido University, 3.Centre for Earth Observation Science, University of Manitoba, 4.Faculty of Science, Niigata University)

### [ACG37-P05] Recent breakdown of the seasonal linkage between the winter North Atlantic Oscillation/Northern Annular Mode and summer Northern Annular Mode

*Koji Yamazaki[1], Yoshihiro Tachibana[2], Masayo Ogi[1], Tetsu Nakamura[1], Kazuhiro Oshima[3] (1.Hokkaido University, 2.Mie University, 3.Institute of Environmental Sciences)

### [ACG37-P06] Did an Arctic sea-ice hole cause hemispheric extreme cold winter in 2017/18?

*Keisuke Ota[1], Yoshihiro Tachibana[1], Kensuke K. Komatsu[1], Alexeev A. Vladimir[2], Cai Lei[2], Yuta Ando[1] (1.Graduate School of Bioresources, Mie University, 2.International Arctic Research Center, University of Alaska Fairbanks)

### [ACG37-P07] Flood affects vegetation at plant species level to regional level: *Arctagrostis latifolia* increased one year after flooding in Indigirka lowland, northeastern Siberia

*Tomoki Morozumi[1,2], Shihong Zhong[1], Ryo Shingubara[5,1], Shunsuke Tei[2], Shinya Takano[1], Rong Fan[1,2], Yumiko Miyamoto[2], Ruslan Shakhmatov[1], Shin Nagai[3], Hideki Kobayashi[3], Rikie Suzuki[3], Trofim C Maximov[4,6], Atsuko Sugimoto[2,7] (1.Graduate School of Environmental Science, Hokkaido University, 2.Arctic Research Center, Hokkaido University, 3.Japan Agency for Marine-Earth Science and Technology, 4.Institute for Biological Problems of Cryolithozone SB RAS, 5.Graduate School of Environmental Studies, Nagoya University, 6.North Eastern Federal University, 7.Station for Arctic Research, Global Institution for Collaborative Research and Education, Hokkaido University)

### [ACG37-P08] Extent and cause of an extreme flooding occurred in spring - summer 2017 over the Indigirka River lowland in Northeastern Siberia

*Shunsuke Tei[1], Tomoki Morozumi[2], Shin Nagai[3], Shinya Takano[2], Atsuko Sugimoto[1], Ryo Shingubara[4], RONG FAN[2], Alexander Fedorov[5], Trofim Maximov[6] (1.Arctic Research Center, Hokkaido University, 2.Graduate School of Environmental Science, Hokkaido University, 3.Japan Agency for Marine Earth Science and Technology, 4.Graduate School of Environmental studies, Nagoya University, 5.Melnikov Permafrost Institute, 6.North-Eastern Federal University)

### [ACG37-P09] Monitoring of the light absorbing aerosols and the impact on radiation budget of atmosphere and snow

*Masahiro Hosaka[1], Hiroshi Ishimoto[1], Tomonori Tanikawa[1], Masashi Niwano[1], Kouji Adachi[1], Naga Oshima[1], Mizuo Kajino[1], Taichu Y Tanaka[1], Sumito Matoba[2] (1.Meteorological Research Institute, 2.Hokkaido University)

[ACG37-P10] Mass concertation and particle number of black carbon on glaciers in the eastern Alaskan Range, Alaska USA

*Keiko Konya[1], Takuma Miyakawa[1], Masayuki Takigawa[1], Masahiro Yamaguchi[1], Shad O'neel[2], Martin Truffer[3] (1.Japan Agency for Marine-Earth Science and Technology, 2.USGS, 3.University of Alaska, Fairbanks)

[ACG37-P11] Remote estimation of phenological shifts in phytoplankton community in the Pacific Arctic Region

*Hisatomo Waga[1], Toru Hirawake[1] (1.Hokkaido University)

[ACG37-P12] Seasonality of diatom and silicoflagellate assemblages observed in settling particles of the western Arctic Ocean

*Jonaotaro Onodera[1,2], EIJI WATANABE[2], Naomi Harada[1,2] (1.Research and Development Center for Global Change, JAMSTEC, 2.Institute of Arctic Climate and Environment Change Research, JAMSTEC)

[ACG37-P13] Iron and macronutrient distributions near the fronts of marine-terminating glaciers in Inglefield Gulf, northwestern Greenland

*NAOYA KANNA[1], Shin Sugiyama[2], Takuto Ando[1], Izumi Asaji[3,2], Yoshiki Fujishi[3,2], Jun Nishioka[2] (1.Arctic Research Center, Hokkaido University, 2.Institute of Low Temperature Science, Hokkaido University, 3.Graduate School of Environmental Science, Hokkaido University)

[ACG37-P14] Paleoenvironmental reconstruction from sediments of Bowdoin fjord, northwestern Greenland

*Takuto Ando[1], NAOYA KANNA[1], Izumi Asaji[2,3], Yoshiki Fujishi[2,3], Shin Sugiyama[1,2,3] (1.Arctic Research Center, Hokkaido University, 2.Institute of Low Temperature Science, Hokkaido University, 3.Graduate School of Environmental Science, Hokkaido University)

[ACG37-P15] A large-eddy simulation of upwelling meltwater plume at marine-terminating glacier fronts

*Yoshimasa Matsumura[1], Naoya Kanna[2], Shin Sugiyama[3,2] (1.Atmosphere and Ocean Research Institute, University of Tokyo, 2.Arctic Research Center, Hokkaido University, 3.Institute of Low Temperature Science, Hokkaido University)

[ACG37-P16] Impact of observation-based snow/ice albedo with starting temperature of −2°C for surface melting effect on a global ocean simulation

*Takahiro Toyoda[1], Teruo Aoki[1,2], Masashi Niwano[1], Tomonori Tanikawa[1], Shogo Urakawa[1], Hiroyuki Tsujino[1], Hideyuki Nakano[1], Kei Sakamoto[1], Nariaki Hirose[1], Goro Yamanaka[1] (1.Meteorological Research Institute, Japan Meteorological Agency, 2.Graduate School of Natural Science and Technology, Okayama University)

[J] Oral | A (Atmospheric and Hydrospheric Sciences )：A-CG Complex & General

3:30 PM - 5:00 PM JST | 6:30 AM - 8:00 AM UTC | 303 3F

## [A-CG37] Science in the Arctic Region

convener:NAOYA KANNA(Arctic Research Center, Hokkaido University), Masashi Niwano(Meteorological Research Institute), Tetsu Nakamura(Faculty of Environmental Earth Science, Hokkaido University), Shunsuke Tei(Arctic Research Center, Hokkaido University), Chairperson:Naoya Kanna(Arctic Research Center, Hokkaido University)

3:30 PM - 3:45 PM JST | 6:30 AM - 6:45 AM UTC

[ACG37-13] Introduction of the IASC project "T-MOSAiC"

Masaki Uchida[1], *Tetsuo Sueyoshi[1] (1.National Institute of Polar Research)

3:45 PM - 4:00 PM JST | 6:45 AM - 7:00 AM UTC

[ACG37-14] Estimation of ice thickness and volume in the Sea of Okhotsk using ICESat and CryoSat-2 data

*Sohey Nihashi[1], Nathan T. Kurtz[2], Takenobu Toyota[3] (1.National Institute of Technology, Tomakomai College, 2.NASA GSFC, 3.Institute of Low Temperature Science, Hokkaido University)

4:00 PM - 4:15 PM JST | 7:00 AM - 7:15 AM UTC

[ACG37-15] Arctic Sea Ice Changes in the DAMIP experiments using the MRI Earth System Model

*Takuro Aizawa[1], Masayoshi Ishii[2], Naga Oshima[2], Seiji Yukimoto[2], Hiroyasu Hasumi[1] (1.Atmosphere and Ocean Research Institute, The University of Tokyo, 2.Meteorological Reseaerch Institute)

4:15 PM - 4:30 PM JST | 7:15 AM - 7:30 AM UTC

[ACG37-16] **Oceanographic Observation in the Refreezing Warm Chukchi Sea during 2018 Mirai Cruise**

*Tsubasa Kodaira[1], Takehiko Nose[1], Takuji Waseda[1], Jun Inoue[2] (1.The University of Tokyo, 2.National Institute of Polar Research)

4:30 PM - 4:45 PM JST | 7:30 AM - 7:45 AM UTC

[ACG37-17] **Observed Waves in the refreezing eastern Chukchi Sea during 2018 Mirai Cruise**

*Takuji Waseda[1], Takehiko Nose[1], Tsubasa Kodaira[1], Alison Kohout[2], Johannes Gemmrich[3], Hui Shen[4], Jun Inoue[5] (1.The University of Tokyo, 2.National Institute of Water and Atmospheric Research, 3.University of Victoria, 4.Bedford Institute of Oceanography, 5.National Institute for Polar Research)

4:45 PM - 5:00 PM JST | 7:45 AM - 8:00 AM UTC

[ACG37-18] Mooring measurement near a marine-terminating glacier in Bowdoin Fjord in northwestern Greenland

*Yoshiki Fujishi[1,2], Yasushi Fukamachi[1,3], NAOYA KANNA[3], Shin Sugiyama[1,3] (1.Institute of Low Temperature Science, Hokkaido University, 2.Graduate School of Environmental Science, Hokkaido University , 3.Arctic Research Center, Hokkaido University)

[J] Oral | H (Human Geosciences )：H-DS Disaster geosciences

1:45 PM - 3:15 PM JST | 4:45 AM - 6:15 AM UTC | 106 1F

## [H-DS15] Human environment and disaster risk

convener:Tatsuto Aoki(School of Regional Development Studies, Kanazawa University), Hisao Kondo(Geological Survey of Japan, National Institute of Advanced Industrial Science and Technology), Chairperson:Tatsuto Aoki(金沢大学地域創造学類)

1:45 PM - 2:00 PM JST | 4:45 AM - 5:00 AM UTC

[HDS15-01] Influence of inhomogeneous structure in surficial reclaimed body traced by aerial photos and delineated by near surface geophysical survey at Makuhari-Kaihin Park liquefied by the 2011 off the Pacific coast of Tohoku earthquake.

*Tomio INAZAKI[1], Takanori Ogahara[1] (1.Public Works Research Institute, Tsukuba Central Institute)

2:00 PM - 2:15 PM JST | 5:00 AM - 5:15 AM UTC

[HDS15-02] Distribution morphology of deformed reclaimed valley associated with the 2018 Hokkaido Eastern Iburi Earthquake

*Takayuki Nakano[1], Satoshi Fujiwara[1], Hiroshi Une[1] (1.GSI of Japan)

2:15 PM - 2:30 PM JST | 5:15 AM - 5:30 AM UTC

[HDS15-03] Liquefaction risk evaluation using relative height data of natural levee

*Mamoru Koarai[1], Kouta Uchiyama[1], Takayuki Nakano[2] (1.Earth Science course, College of Science, Ibaraki University, 2.Geospatial Information Authority of Japan)

2:30 PM - 2:45 PM JST | 5:30 AM - 5:45 AM UTC

[HDS15-04] **Spatial Analysis of Social Vulnerability to large-scale flood: a case study on the Katsushika Ward, Tokyo**

*LIAN XIAO[1] (1.University of Tsukuba)

2:45 PM - 3:00 PM JST | 5:45 AM - 6:00 AM UTC

[HDS15-05] Importance and method of visualization of future occurrence possibilities of giant earthquakes along the Nankai trough

*Yo Fukushima[1] (1.International Research Institute of Disaster Science, Tohoku University)

3:00 PM - 3:15 PM JST | 6:00 AM - 6:15 AM UTC

[HDS15-06] Investigation of efficient tsunami evacuation using real-time disaster information

*Yusuke Oishi[1,2,3], Takashi Furumura[2], Fumihiko Imamura[3], Yoshiteru Mihara[4], Fumiyasu Makinoshima[3], Yamashita Kei[3], Takao Higashiyama[5], Tomonori Goto[5], Makoto Oomura[4], Mitsuyuki Nagayama[4] (1.Fujitsu Laboratories Ltd., 2.Earthquake Research Institute, the University of Tokyo, 3.IRIDeS, Tohoku University, 4.Kawasaki City, 5.Fujitsu Ltd.)

[J] Poster | H (Human Geosciences )：H-DS Disaster geosciences

3:30 PM - 5:00 PM JST | 6:30 AM - 8:00 AM UTC | Poster Hall International Exhibition Hall8, Makuhari Messe_7

## [H-DS15] Human environment and disaster risk

convener:Tatsuto Aoki(School of Regional Development Studies, Kanazawa University), Hisao Kondo(Geological Survey of Japan, National Institute of Advanced Industrial Science and Technology)

[HDS15-P01] Validity Verification in Typhoon Disaster Prevention Model for Typhoon Damage Reduction– GUST Wind Speed, Maximum Wind Speed -

*Woo-Sik JUNG[1], Hana Na[1] (1.Department of Atmospheric Environment Information Engineering, Atmospheric Environment Information Research Center, Inje University, Gimhae 50834, Korea)

[HDS15-P02] A Study on the Assimilation of Meteorological Data and Sea Surface Temperature Data for Improving the Accuracy of WRF Prediction during Typhoon periods on the Korean Peninsula

*Woo-Sik JUNG[1], Hana Na[1] (1.Department of Atmospheric Environment Information Engineering, Atmospheric Environment Information Research Center, Inje University, Gimhae 50834, Korea)

[HDS15-P03] Validation and application of a finite element approach on field mechanically stabilized earth walls with secondary reinforcement

*BING-RU WU[1], CHIH-HSUAN LIU[1], CHING HUNG[1] (1.National Cheng Kung University)

[HDS15-P04] **EXPERIMENTAL STUDY ON POLYUREA-COATED RC SLAB SUBJECTED TO CONTACT EXPLOSIONS**

*Minghsien Wu[1], Yingkuan Tsai[1], Chien-Hsien Liu[1], Pang-Ting Pai[1], Feng-Cheng Yang[1], Chun-Chia Huang[1] (1.Chung Cheng Institute of Technology National Defense University)

[HDS15-P05] Simulation and field investigation of scour and sediment transport after Dam removal in the mountainous creek in Central Taiwan

*Chunhung WU[1] (1.Feng Chia University)

[HDS15-P06] Examination and systematization of predispositions to floods in the Heavy Rain in July 2018

*Kanako Kimura[1], Toshihiko Sugai[2] (1.The University of Tokyo, 2.Graduate School of Frontier Sciences, the University of Tokyo)

[HDS15-P07] Expand various disaster risk information and sophisticate methods to disseminate on the Hazard Map Portal Site

*Takuya Ueshiba[1], Yumeka Fujii[1], Naoki Yoshimatsu[1], Noriyuki Takakuwa[1], Wataru Yamasaki[1], Jun Suwabe[1] (1.GSI of Japan)

[HDS15-P08] A study on evaluation formulae of the principal fault in PFDHA- In consideration of a relevance to known active faults-

*Tsuyoshi Kanda[1], Makoto Takao[1], Toshimichi Kaneto[1], Takehisa Arakawa[1] (1.Tokyo Electoric Power Company Holdings, Inc)

[HDS15-P09] Characteristics of sediment deposition distribution in debris flow disasters in caused by heavy rain in August 2014 Hiroshima, Japan

*Shoichiro Uchiyama[1], Toshihiko Sugai[2] (1.National Research Institute for Earth Science and Disaster Resilience, 2.The University of Tokyo)

[HDS15-P10] Land use change after tsunami and its problems in Kii peninsula

*Kenta Okidate[1], Tatsuto Aoki[2] (1.School of Humanities, Kanazawa University, 2.School of Regional Development Studies, Kanazawa University)

[HDS15-P11] Reconstruction of the building damages caused by the Typhoon Kathleen and analyses of their land conditions at the southern foot of the Akagi Volcano using U.S. military aerial photographs

*Masafumi Aoyama[1], Yoshiki Saito[2] (1.Faculty of Education, Gunma University, 2.Graduate Student, Gunma University)

[J] Poster | H (Human Geosciences )：H-DS Disaster geosciences

5:15 PM - 6:30 PM JST | 8:15 AM - 9:30 AM UTC | Poster Hall International Exhibition Hall8, Makuhari Messe_15

## [H-DS15] Human environment and disaster risk

convener:Tatsuto Aoki(School of Regional Development Studies, Kanazawa University), Hisao Kondo(Geological Survey of Japan, National Institute of Advanced Industrial Science and Technology)

[HDS15-P01] Validity Verification in Typhoon Disaster Prevention Model for Typhoon Damage Reduction– GUST Wind Speed, Maximum Wind Speed -

*Woo-Sik JUNG[1], Hana Na[1] (1.Department of Atmospheric Environment Information Engineering, Atmospheric Environment Information Research Center, Inje University, Gimhae 50834, Korea)

[HDS15-P02] A Study on the Assimilation of Meteorological Data and Sea Surface Temperature Data for Improving the Accuracy of WRF Prediction during Typhoon periods on the Korean Peninsula

*Woo-Sik JUNG[1], Hana Na[1] (1.Department of Atmospheric Environment Information Engineering, Atmospheric Environment Information Research Center, Inje University, Gimhae 50834, Korea)

[HDS15-P03] Validation and application of a finite element approach on field mechanically stabilized earth walls with secondary reinforcement

*BING-RU WU[1], CHIH-HSUAN LIU[1], CHING HUNG[1] (1.National Cheng Kung University)

[HDS15-P04] **EXPERIMENTAL STUDY ON POLYUREA-COATED RC SLAB SUBJECTED TO CONTACT EXPLOSIONS**

*Minghsien Wu[1], Yingkuan Tsai[1], Chien-Hsien Liu[1], Pang-Ting Pai[1], Feng-Cheng Yang[1], Chun-Chia Huang[1] (1.Chung Cheng Institute of Technology National Defense University)

[HDS15-P05] Simulation and field investigation of scour and sediment transport after Dam removal in the mountainous creek in Central Taiwan

*Chunhung WU[1] (1.Feng Chia University)

[HDS15-P06] Examination and systematization of predispositions to floods in the Heavy Rain in July 2018

*Kanako Kimura[1], Toshihiko Sugai[2] (1.The University of Tokyo, 2.Graduate School of Frontier Sciences, the University of Tokyo)

[HDS15-P07] Expand various disaster risk information and sophisticate methods to disseminate on the Hazard Map Portal Site

*Takuya Ueshiba[1], Yumeka Fujii[1], Naoki Yoshimatsu[1], Noriyuki Takakuwa[1], Wataru Yamasaki[1], Jun Suwabe[1] (1.GSI of Japan)

[HDS15-P08] A study on evaluation formulae of the principal fault in PFDHA- In consideration of a relevance to known active faults-

*Tsuyoshi Kanda[1], Makoto Takao[1], Toshimichi Kaneto[1], Takehisa Arakawa[1] (1.Tokyo Electoric Power Company Holdings, Inc)

[HDS15-P09] Characteristics of sediment deposition distribution in debris flow disasters in caused by heavy rain in August 2014 Hiroshima, Japan

*Shoichiro Uchiyama[1], Toshihiko Sugai[2] (1.National Research Institute for Earth Science and Disaster Resilience, 2.The University of Tokyo)

[HDS15-P10] Land use change after tsunami and its problems in Kii peninsula

*Kenta Okidate[1], Tatsuto Aoki[2] (1.School of Humanities, Kanazawa University, 2.School of Regional Development Studies, Kanazawa University)

[HDS15-P11] Reconstruction of the building damages caused by the Typhoon Kathleen and analyses of their land conditions at the southern foot of the Akagi Volcano using U.S. military aerial photographs

*Masafumi Aoyama[1], Yoshiki Saito[2] (1.Faculty of Education, Gunma University, 2.Graduate Student, Gunma University)

[E] Poster | H (Human Geosciences )：H-TT Technology & Techniques

10:45 AM - 12:15 PM JST | 1:45 AM - 3:15 AM UTC | Poster Hall International Exhibition Hall8, Makuhari Messe_3

## [H-TT19] Geographic Information Systems and Cartography

convener:Takashi Oguchi(Center for Spatial Information Science, The University of Tokyo), Yuji Murayama(Graduate School of Life and Environmental Sciences), Yoshiki Wakabayashi(Graduate School of Urban Environmental Sciences, Tokyo Metropolitan University)

[HTT19-P01] **Monitoring and Simulating Land Use/Cover Changes and its Impact on Land Surface Temperature in Sapporo City, Japan**

*RUCI WANG[1], YUJI MURAYAMA[1] (1.University of Tsukuba)

---

[HTT19-P02] **Spatiotemporal Variations of Land Cover/Use and Sustainable Urban Heat Island (UHI) Mitigation Strategies: A Case Study of Chinese Bay Megacities**

★Invited Papers

*Fei LIU[1], Yuji MURAYAMA[1] (1. University of Tsukuba)

---

[HTT19-P03] A LST Study of the Seoul Metropolitan City, South Korea, Based on Landsat Data (1996 – 2017)

*Prabath Priyankara[1,3], Manjula Ranagalage[1,4], DMSLB Dissanayake[1,4], Takehiro Morimoto[1,2], Yuji Murayama[1,2] (1.Graduate School of Life and Environmental Sciences, University of Tsukuba, Japan, 2.Faculty of Life and Environmental Sciences, University of Tsukuba, Japan, 3.Faculty of Agriculture, University of Ruhuna, Sri Lanka, 4.Faculty of Social Sciences and Humanities, Rajarata University of Sri Lanka, Sri Lanka)

---

[HTT19-P04] Improvement of GIS exercise classes using the GIS open educational resources based on questionnaire surveys

★Invited Papers

*Hiroyuki Yamauchi[1], Takashi Oguchi[1], Yuichi S. Hayakawa[2,1], Kotaro Iizuka[1] (1.Center for Spatial Information Science, The University of Tokyo, 2.Environmental Geography, Faculty of Environmental Earth Science, Hokkaido University)

---

[HTT19-P05] **The Development of COP for Tzu Chi Disaster Prevention System by Using QGIS-Taking 2018 Hualien Earthquake as an Example**

*kuan-wen tseng[1], Ming-Ta Tsai[1], Yun-Ching Wang[1], Ming-Chih Wang[1], Chien-Hsien Liu[1] (1.03-3809093)

---

[HTT19-P06] Comparative study on shape and distribution of landslides caused by the 2012 Northern Kyushu heavy rainfall and the 2016 Kumamoto earthquake in the Aso region, Kumamoto, Japan

*Yasutaka Haneda[1], Takashi Oguchi[2], Kotaro Iizuka[2], Hitoshi SAITO[3,2], Yuichi S. Hayakawa[4,2], Shoichiro Uchiyama[5] (1.Graduate School of Frontier Science, The University of Tokyo, 2.Center for Spatial Information Science, The University of Tokyo, 3.College of Economics, Kanto Gakuin University, 4.Faculty of Environmental Earth Science, Hokkaido University, 5.National Research Institute for Earth Science and Disaster Resilience)

---

[HTT19-P07] Using GIS and remote sensing to assess relationships between landslides and land cover changes in the Sanbagawa and Mikabu Belts, Shikoku, Japan

*Roxanne Lai[1], Takashi Oguchi[1] (1.University of Tokyo)

---

[HTT19-P08] **Analysis of Morphometric Parameters for Mountains Ranges and Landslides due to the July 2018 Heavy Rain in Western Japan Using GIS Data**

*Toshikazu Fukuba[1], Takashi Oguchi[2] (1.Department of Earth and Planetary Environmental Science, The University of Tokyo, 2.Center for Spatial Information Science, The University of Tokyo)

---

[HTT19-P09] Analyzing short-term topographic change in coastal sand dunes using UAS-SfM photogrammetry: A case study in Northern Kujukuri, Japan

*Seulgi Lee[1], Yasutaka Nakata[2], Kotaro Iizuka[3], Takashi Oguchi[3] (1.Graduate School of Frontier Sciences, The University of Tokyo, 2.Forest Research Department, Forestry Research Institute, Hokkaido Research Organization, 3.Center for Spatial Information Science, The University of Tokyo)

---

[HTT19-P10] **Responses of suspended sediment yield to precipitation, topography and dam control in the Yellow River Basin, China**

*Ruiqi Zhang[1], Takashi Oguchi[2] (1. Department of Natural Environmental Studies, Graduate School of Frontier Sciences, The University of Tokyo, 2.Center for Spatial Information Science, The University of Tokyo)

[E] Poster | H (Human Geosciences )：H-TT Technology & Techniques

5:15 PM - 6:30 PM JST | 8:15 AM - 9:30 AM UTC | Poster Hall International Exhibition Hall8, Makuhari Messe_16

## [H-TT19] Geographic Information Systems and Cartography

convener:Takashi Oguchi(Center for Spatial Information Science, The University of Tokyo), Yuji Murayama(Graduate School of Life and Environmental Sciences), Yoshiki Wakabayashi(Graduate School of Urban Environmental Sciences, Tokyo Metropolitan University)

[HTT19-P01] **Monitoring and Simulating Land Use/Cover Changes and its Impact on Land Surface Temperature in Sapporo City, Japan**

*RUCI WANG[1], YUJI MURAYAMA[1] (1.University of Tsukuba)

[HTT19-P02] **Spatiotemporal Variations of Land Cover/Use and Sustainable Urban Heat Island (UHI) Mitigation Strategies: A Case Study of Chinese Bay Megacities**

★Invited Papers

*Fei LIU[1], Yuji MURAYAMA[1] (1. University of Tsukuba)

[HTT19-P03] A LST Study of the Seoul Metropolitan City, South Korea, Based on Landsat Data (1996 – 2017)

*Prabath Priyankara[1,3], Manjula Ranagalage[1,4], DMSLB Dissanayake[1,4], Takehiro Morimoto[1,2], Yuji Murayama[1,2] (1.Graduate School of Life and Environmental Sciences, University of Tsukuba, Japan, 2.Faculty of Life and Environmental Sciences, University of Tsukuba, Japan, 3.Faculty of Agriculture, University of Ruhuna, Sri Lanka, 4.Faculty of Social Sciences and Humanities, Rajarata University of Sri Lanka, Sri Lanka)

[HTT19-P04] Improvement of GIS exercise classes using the GIS open educational resources based on questionnaire surveys

★Invited Papers

*Hiroyuki Yamauchi[1], Takashi Oguchi[1], Yuichi S. Hayakawa[2,1], Kotaro Iizuka[1] (1.Center for Spatial Information Science, The University of Tokyo, 2.Environmental Geography, Faculty of Environmental Earth Science, Hokkaido University)

[HTT19-P05] **The Development of COP for Tzu Chi Disaster Prevention System by Using QGIS-Taking 2018 Hualien Earthquake as an Example**

*kuan-wen tseng[1], Ming-Ta Tsai[1], Yun-Ching Wang[1], Ming-Chih Wang[1], Chien-Hsien Liu[1] (1.03-3809093)

[HTT19-P06] Comparative study on shape and distribution of landslides caused by the 2012 Northern Kyushu heavy rainfall and the 2016 Kumamoto earthquake in the Aso region, Kumamoto, Japan

*Yasutaka Haneda[1], Takashi Oguchi[2], Kotaro Iizuka[2], Hitoshi SAITO[3,2], Yuichi S. Hayakawa[4,2], Shoichiro Uchiyama[5] (1.Graduate School of Frontier Science, The University of Tokyo, 2.Center for Spatial Information Science, The University of Tokyo, 3.College of Economics, Kanto Gakuin University, 4.Faculty of Environmental Earth Science, Hokkaido University, 5.National Research Institute for Earth Science and Disaster Resilience)

[HTT19-P07] Using GIS and remote sensing to assess relationships between landslides and land cover changes in the Sanbagawa and Mikabu Belts, Shikoku, Japan

*Roxanne Lai[1], Takashi Oguchi[1] (1.University of Tokyo)

[HTT19-P08] **Analysis of Morphometric Parameters for Mountains Ranges and Landslides due to the July 2018 Heavy Rain in Western Japan Using GIS Data**

*Toshikazu Fukuba[1], Takashi Oguchi[2] (1.Department of Earth and Planetary Environmental Science, The University of Tokyo, 2.Center for Spatial Information Science, The University of Tokyo)

[HTT19-P09] Analyzing short-term topographic change in coastal sand dunes using UAS-SfM photogrammetry: A case study in Northern Kujukuri, Japan

*Seulgi Lee[1], Yasutaka Nakata[2], Kotaro Iizuka[3], Takashi Oguchi[3] (1.Graduate School of Frontier Sciences, The University of Tokyo, 2.Forest Research Department, Forestry Research Institute, Hokkaido Research Organization, 3.Center for Spatial Information Science, The University of Tokyo)

[HTT19-P10] **Responses of suspended sediment yield to precipitation, topography and dam control in the Yellow River Basin, China**

*Ruiqi Zhang[1], Takashi Oguchi[2] (1. Department of Natural Environmental Studies, Graduate School of Frontier Sciences, The University of Tokyo, 2.Center for Spatial Information Science, The University of Tokyo)

[E] Oral | H (Human Geosciences)：H-TT Technology & Techniques

1:45 PM - 3:15 PM JST | 4:45 AM - 6:15 AM UTC | 301B 3F

## [H-TT19] Geographic Information Systems and Cartography

convener:Takashi Oguchi(Center for Spatial Information Science, The University of Tokyo), Yuji Murayama(Graduate School of Life and Environmental Sciences), Yoshiki Wakabayashi(Graduate School of Urban Environmental Sciences, Tokyo Metropolitan University), Chairperson:Yuji Murayama, Yoshiki Wakabayashi

1:45 PM - 2:00 PM JST | 4:45 AM - 5:00 AM UTC

[HTT19-01] **A study on geographical changes in main roads and coastlines in the 200 years in Japan**

*Yuki IWAI[1], Yuji Murayama[1] (1.Graduate School of Life and Environmental Sciences, University of Tsukuba)

2:00 PM - 2:15 PM JST | 5:00 AM - 5:15 AM UTC

[HTT19-02] Comparative analysis of foreign tourists' spatial behavior in Tokyo using locational data from the photo-sharing service of Flickr

*Bochra Bettaieb[1], Yoshiki Wakabayashi[1] (1.Tokyo Metropolitan University)

2:15 PM - 2:30 PM JST | 5:15 AM - 5:30 AM UTC

[HTT19-03] Neighborhood Walkability and its Potential Associations with Residents' Walking Habits

★Invited Papers

*Ikuho Yamada[1], Keiichiro Sanada[2] (1.Faculty of Science and Engineering, Chuo University, 2.Graduate School of Science and Engineering, Chuo University)

2:30 PM - 2:45 PM JST | 5:30 AM - 5:45 AM UTC

[HTT19-04] **THE STUDY OF USING PARTICLE FILTER METHOD COMBINED INDOOR MAGNETIC MAP AND PEDESTRIAN DEAD RECKONING FOR INDOOR POSITIONING.**

*Yu-Chun Chen[1] (1.Department of Land Economics, National Chengchi University)

2:45 PM - 3:00 PM JST | 5:45 AM - 6:00 AM UTC

[HTT19-05] Assessing the Agriculture Sustainability based on Geospatial Technique in a Tropical Mountain Area : A Case Study in Kotmale Catchment in Sri Lanka.

*DM Sanjeewa Lasantha Bandara[1], Takehiro Morimoto [2] (1.Division of Spatial Information Science, Graduate School of Life and Environmental Sciences, University of Tsukuba, 2.Faculty of Life and Environmental Sciences, University of Tsukuba)

3:00 PM - 3:15 PM JST | 6:00 AM - 6:15 AM UTC

[HTT19-06] **Spatial Evaluation of Potential Tsunami Vertical Evacuation: A Case Study of the Western Coastal Belt in Sri Lanka**

*Ranagalage Mahinda Manjula[1], Yuji Murayama[1] (1.Division of Spatial Science, Graduate School of Life and Environmental Sciences, University of Tsukuba, Japan)

[E] Oral | H (Human Geosciences)：H-TT Technology & Techniques

3:30 PM - 5:00 PM JST | 6:30 AM - 8:00 AM UTC | 301B 3F

## [H-TT19] Geographic Information Systems and Cartography

convener:Takashi Oguchi(Center for Spatial Information Science, The University of Tokyo), Yuji Murayama(Graduate School of Life and Environmental Sciences), Yoshiki Wakabayashi(Graduate School of Urban Environmental Sciences, Tokyo Metropolitan University), Chairperson:Takashi Oguchi, Ikuho Yamada(Chuo University)

3:30 PM - 3:45 PM JST | 6:30 AM - 6:45 AM UTC

[HTT19-07] A Framework for Assessing the Spatial Distribution of Vulnerability of Communities to Landslides in Tropical Mountainous Region: A Case study from Kegalle District – Sri Lanka.

★Invited Papers

*Nimala Chinthake Perera[1] (1.SANASA CAMPUS - SRI LANKA, IHRA - UNIVERSITY OF COLOMBO - SRI LANKA)

---

3:45 PM - 4:00 PM JST | 6:45 AM - 7:00 AM UTC

[HTT19-08] Applications of WebGIS to Educating Disaster Risk Reduction for Chinese and Japanese Students

*Jiali SONG[1], Takashi Oguchi[2], Hiroyuki Yamauchi[2], Takuro Ogura[1] (1.Graduate School of Frontier Sciences, The University of Tokyo, 2.Center for Spatial Information Science, The University of Tokyo)

---

4:00 PM - 4:15 PM JST | 7:00 AM - 7:15 AM UTC

[HTT19-09] Solar System Treks - GIS that provides interactive visualization and analysis for planetary science and exploration

★Invited Papers

*Emily Law[1], Brian Hamilton Day[2] (1.NASA Jet Propulsion Laboratory, 2.NASA Ames Research Center)

---

4:15 PM - 4:30 PM JST | 7:15 AM - 7:30 AM UTC

[HTT19-10] **Landslide Recognition using Remote Sensing Images and PCANet**

*Yimei Wei[1], Takashi Oguchi[1] (1.Graduate School of Frontier Science, the University of Tokyo)

---

4:30 PM - 4:45 PM JST | 7:30 AM - 7:45 AM UTC

[HTT19-11] Estimating the fractional vegetation cover using fixed-wing drone and multiple vegetation indices

★Invited Papers

*Kotaro Iizuka[1] (1.Center for Spatial Information Science, The University of Tokyo)

---

4:45 PM - 5:00 PM JST | 7:45 AM - 8:00 AM UTC

[HTT19-12] Topographic surveys in Ny-Alesund, Svalbard, and improvement of mapping methods

*Jaeyong Lee[1], Takashi Oguchi[2] (1.Department of Environmental Studies, Graduate School of Frontier Sciences, The University of Tokyo, 2.Center for Spatial Information Science, The University of Tokyo)

[J] Oral | H (Human Geosciences )：H-TT Technology & Techniques

10:45 AM - 12:15 PM JST | 1:45 AM - 3:15 AM UTC | 301B 3F

## [H-TT23] Geographic Information System and Cartography

convener:Mamoru Koarai(Earth Science course, College of Science, Ibaraki University), Kazunari Tanka(Department of Civil Engineering and Urban Design, Faculty of Engineering, Osaka Institute of Technology), Kazuhiko Nakamura(The University of Tokyo), Chairperson:Mamoru KOARAI(Ibaraki University), Kazunari Tanaka(大阪工業大学)

10:45 AM - 11:00 AM JST | 1:45 AM - 2:00 AM UTC

[HTT23-01] **An analysis of the year-round distribution of $PM_{2.5}$ and Oxidant by (Web)GIS and R**

★Invited Papers

*Junji Yamakawa[1] (1.Graduate School of Natural Science and Technology, Okayama University)

---

11:00 AM - 11:15 AM JST | 2:00 AM - 2:15 AM UTC

[HTT23-02] Development Process and Spatial Structure of Urban Villages in Shenzhen City China

*YARONG LUAN

---

11:15 AM - 11:30 AM JST | 2:15 AM - 2:30 AM UTC

[HTT23-03] An analysis on the location characteristic of alley spaces in Tokyo

*Ryo Taniguchi[1], Go Ishikawa[1], Mayumi Oka[2] (1.Tokyo Map Research Inc., 2.Research Organization of Information and Systems The Institute of Statistical Mathematics)

---

11:30 AM - 11:45 AM JST | 2:30 AM - 2:45 AM UTC

[HTT23-04] Image analysis of night scape using lyrics

*Hiroki Komai[1], Kazunari Tanaka[1] (1.Osaka Institute of Technology)

---

11:45 AM - 12:00 PM JST | 2:45 AM - 3:00 AM UTC

[HTT23-05] On the Method to Evaluate Signboards based on the Relationship with the Surrounding Space

*Akihiro Kishikawa[1], Kazunari Tanaka[1] (1.Osaka Institute of Technology)

---

12:00 PM - 12:15 PM JST | 3:00 AM - 3:15 AM UTC

[HTT23-06] ON THE LANDSCAPES ELEMENTS FROM A BIRD'S-EYE VIEW SCAPE

*Nobuaki Tanaka[1], kazunari Tanaka[1] (1.Osaka Institute of Technology)

[J] Poster | H (Human Geosciences )：H-TT Technology & Techniques

3:30 PM - 5:00 PM JST | 6:30 AM - 8:00 AM UTC | Poster Hall International Exhibition Hall8, Makuhari Messe_8

## [H-TT23] Geographic Information System and Cartography

convener:Mamoru Koarai(Earth Science course, College of Science, Ibaraki University), Kazunari Tanka(Department of Civil Engineering and Urban Design, Faculty of Engineering, Osaka Institute of Technology), Kazuhiko Nakamura(The University of Tokyo)

### [HTT23-P01] Development of 3D Web map making service, MyMap3D

★Invited Papers

*Yoshiharu Nishioka[1], Kaoru Kitao[2] (1.National Insititute of Advanced Industrial Science and Technology, 2.CubeWorks Inc.)

### [HTT23-P02] Experimental hazard map for accurate communication

*Ryo Endo[1], Takayuki Nakano[1] (1.GSI of Japan)

### [HTT23-P03] Effectiveness of color hillshade with multiple light sources for geopark guide maps : A case of the North Ibaraki Geopark Project

*Keiko SUZUKI[1], Go ISHIKAWA[1], Mamoru KOARAI[2], Rika IMAIZUMI[3], Naoki TAKEDA[4] (1.Tokyo Map Research Inc., 2.Ibaraki University, 3.Aero Asahi Co., Ltd., 4.Association for Promotion of North Ibaraki Geopark Project)

### [HTT23-P04] Estimation of three-dimensional structure of forest using LiDAR data in Abukuma mountainous region

Akane Narikiyo[1], *Mamoru Koarai[1], Wataru Murakami[2], Yasuhiro Ogawa[2] (1.Earth Science course, College of Science, Ibaraki University, 2.Forest Research Institute)

### [HTT23-P05] Disaster information sharing of welfare service workers based on knowledge from experience in a tsunami disaster area

*ARISA INOUE[1], Yoshiki Wakabayashi[1] (1.Graduate School of Urban Environmental Sciences, Tokyo Metropolitan University)

### [HTT23-P06] Spatial analysis of children's commuting space - a case study of Toyama city elementary school -

*Koji Ohnishi[1] (1.Department of Humanities, University of Toyama)

[J] Poster | H (Human Geosciences )：H-TT Technology & Techniques

5:15 PM - 6:30 PM JST | 8:15 AM - 9:30 AM UTC | Poster Hall International Exhibition Hall8, Makuhari Messe_17

## [H-TT23] Geographic Information System and Cartography

convener:Mamoru Koarai(Earth Science course, College of Science, Ibaraki University), Kazunari Tanka(Department of Civil Engineering and Urban Design, Faculty of Engineering, Osaka Institute of Technology), Kazuhiko Nakamura(The University of Tokyo)

### [HTT23-P01] Development of 3D Web map making service, MyMap3D

★Invited Papers

*Yoshiharu Nishioka[1], Kaoru Kitao[2] (1.National Insititute of Advanced Industrial Science and Technology, 2.CubeWorks Inc.)

### [HTT23-P02] Experimental hazard map for accurate communication

*Ryo Endo[1], Takayuki Nakano[1] (1.GSI of Japan)

### [HTT23-P03] Effectiveness of color hillshade with multiple light sources for geopark guide maps : A case of the North Ibaraki Geopark Project

*Keiko SUZUKI[1], Go ISHIKAWA[1], Mamoru KOARAI[2], Rika IMAIZUMI[3], Naoki TAKEDA[4] (1.Tokyo Map Research Inc., 2.Ibaraki University, 3.Aero Asahi Co., Ltd., 4.Association for Promotion of North Ibaraki Geopark Project)

### [HTT23-P04] Estimation of three-dimensional structure of forest using LiDAR data in Abukuma mountainous region

Akane Narikiyo[1], *Mamoru Koarai[1], Wataru Murakami[2], Yasuhiro Ogawa[2] (1.Earth Science course, College of Science, Ibaraki University, 2.Forest Research Institute)

### [HTT23-P05] Disaster information sharing of welfare service workers based on knowledge from experience in a tsunami disaster area

*ARISA INOUE[1], Yoshiki Wakabayashi[1] (1.Graduate School of Urban Environmental Sciences, Tokyo Metropolitan University)

### [HTT23-P06] Spatial analysis of children's commuting space - a case study of Toyama city elementary school -

*Koji Ohnishi[1] (1.Department of Humanities, University of Toyama)

[J] Oral | H (Human Geosciences)：H-CG Complex & General

9:00 AM - 10:30 AM JST | 12:00 AM - 1:30 AM UTC | 101 1F

## [H-CG31] Nuclear Energy and Geoscience

convener:Eiji Sasao(Tono Geoscience Center, Japan Atomic Energy Agency), Ryuta Hataya(Central Research Institute of Electric Power Industry), Shinji Takeuchi(Department of Earth and Environmental Sciences, College of Humanities & Sciences, Nihon University), Chairperson:Tadafumi Niizato

9:00 AM - 9:15 AM JST | 12:00 AM - 12:15 AM UTC

[HCG31-01] **Uplift estimation in coastal sea area by extrapolation of the land area model and its uncertainty**

*Ryuta Hataya[1], Takaomi Hamada[1], Yohei Shimizu[1] (1.Central Research Institute of Electric Power Industry)

9:15 AM - 9:30 AM JST | 12:15 AM - 12:30 AM UTC

[HCG31-02] Deep groundwater mobility at costal area estimated by groundwater dating

*Takuma HASEGAWA[1], Kotaro NAKATA[1], Yuichi Tomioka[1], Tomoko Ota[1], Atsunao Marui[2], Isao Machida[2], Reo Ikawa[2], Masahiko Ono[2], Shinji Matsumoto[2] (1.Central Research Institute of Electric Power Industry, 2.The National Institute of Advanced Industrial Science and Technology)

9:30 AM - 9:45 AM JST | 12:30 AM - 12:45 AM UTC

[HCG31-03] Attempt to Estimate permeability of rock mass based on elasticity and resistivity measurement in underground tunnel

*Sota Kawaguchi[1], Tada-nori Goto[1], Koki Kashiwaya[1] (1.Graduate School of Engineering, Kyoto University)

9:45 AM - 10:00 AM JST | 12:45 AM - 1:00 AM UTC

[HCG31-04] Study on relationship between pathway of groundwater and mass transport, and cooling process of granitic rock

*Eiji Sasao[1], Takashi Yuguchi[2], Masayuki Ishibashi[1] (1.Tono Geoscience Center, Japan Atomic Energy Agency, 2.Faculty of Science, Yamagata University)

10:00 AM - 10:15 AM JST | 1:00 AM - 1:15 AM UTC

[HCG31-05] Fracture characterization in the accretionary complex from the view point of mass transfer

*Shinji Takeuchi[1], Chikara Kurata[1], Masakazu Niwa[2], Tadamasa Ueki[2] (1.Department of Earth and Environmental Sciences, College of Humanities & Sciences, Nihon University, 2.Japan Atomic Energy Agency)

10:15 AM - 10:30 AM JST | 1:15 AM - 1:30 AM UTC

[HCG31-06] Retardation of Cs and Sr leachings by geopolymer matrices with zeolte and titanate adsorbent

*Kazuma Kuroda[1], Soonthornwiphat Natatsawas[1], Chaerun Raudhatul Islam[1], Hnin Wint Wint Two[1], Kanako Toda[1], Yutaro Kobayashi[1], Tsutomu Sato[2], Tsubasa Otake[2] (1.Graduate school of Engineering, Hokkaido University, 2.Faculty of Engineering, Hokkaido University)

[J] Oral | H (Human Geosciences )：H-CG Complex & General

10:45 AM - 12:15 PM JST | 1:45 AM - 3:15 AM UTC | 101 1F

## [H-CG31] Nuclear Energy and Geoscience

convener:Eiji Sasao(Tono Geoscience Center, Japan Atomic Energy Agency), Ryuta Hataya(Central Research Institute of Electric Power Industry), Shinji Takeuchi(Department of Earth and Environmental Sciences, College of Humanities & Sciences, Nihon University), Chairperson:Shinji Takeuchi

10:45 AM - 11:00 AM JST | 1:45 AM - 2:00 AM UTC

[HCG31-07] Focus points of post-closure monitoring in geological disposal

*Hiroaki Murakami[1], Yusuke Watanabe[1], Kenji Fukuda[1], Teruki Iwatsuki[1] (1.Japan Atomic Energy Agency)

---

11:00 AM - 11:15 AM JST | 2:00 AM - 2:15 AM UTC

[HCG31-08] 5 years monitoring results for the environmental dynamics of radiocesium in mountainous forest of the Abukuma Mountains, Fukushima

*Tadafumi Niizato[1], Takayoshi Watanabe[1], Yoshito Sasaki[1], Katsuaki Mitachi[2], Satomi Ito[1], Hironobu Abe[1] (1.Japan Atomic Energy Agency, 2.ATOM TRANSPORT SERVICE CO., LTD)

---

11:15 AM - 11:30 AM JST | 2:15 AM - 2:30 AM UTC

[HCG31-09] Problems of geological disposal based on the contaminated water issues at Fukushima Daiichi NPS

*Naoaki Shibasaki[1] (1.Fukushima University)

---

11:30 AM - 11:45 AM JST | 2:30 AM - 2:45 AM UTC

[HCG31-10] Examination of "Nationalwide Map of Scientific Features" for HLRW geological disposal in case of Niigata Prefecture and fundamental problems in the fair discussion on this task

*Junji Akai[1], Ryuichiro Ohno (1.Emeritus Professor of Niigata University)

---

11:45 AM - 12:00 PM JST | 2:45 AM - 3:00 AM UTC

[HCG31-11] Problems of the "Nationwide Map of Scientific Features for Geological Disposal" in Saitama prefecture and storage method of High-level Radioactive Waste (HLW)

*Kazuaki SEKINE[1], Kazuyuki SUENAGA[2], Tadao KOBAYASHI (1.Saitama Prefectural Chichibu High School, 2.SUENAGA Environmental Geology)

[J] Poster | H (Human Geosciences )：H-CG Complex & General

3:30 PM - 5:00 PM JST | 6:30 AM - 8:00 AM UTC | Poster Hall International Exhibition Hall8, Makuhari Messe_9

## [H-CG31] Nuclear Energy and Geoscience

convener:Eiji Sasao(Tono Geoscience Center, Japan Atomic Energy Agency), Ryuta Hataya(Central Research Institute of Electric Power Industry), Shinji Takeuchi(Department of Earth and Environmental Sciences, College of Humanities & Sciences, Nihon University)

[HCG31-P01] Better identification of submerged terraces based on digital terrain analysis

*Hiura Yuki[1], Tetsuya Komatsu[1], Toshihiko Sugai[2] (1.Japan Atomic Energy Agency, 2.Graduate School of Frontier Sciences, The University of Tokyo)

[HCG31-P02] Advanced examination technique for river erosion in inland area – a case study of the Kii Peninsula, Japan –

*Nakanishi Toshimichi[1], Tetsuya Komatsu[1], Manabu Ogata[1], Takashi Hosoya[2], Takumi Kaga[2] (1.Japan Atomic Energy Agency, 2.Chuo Kaihatsu Corporation)

[HCG31-P03] Hydrothermal experiment on quartz hydration: Toward a development of new dating method for natural phenomena

*Masakazu Niwa[1], Koji Shimada[1] (1.Japan Atomic Energy Agency)

[HCG31-P04] **Diffusion Coefficient and Porosity of Granite for Evaluation of Mobility Parameter**

*Kenji Fukuda[1], Hiroaki Murakami[1], Kaori Itai[2], Masayuki Ishibashi[1], Eiji Sasao[1] (1.Japan Atomic Energy Agency, 2.C・TECH corporation)

[HCG31-P05] Hydrogeological structure of hydraulic conductive fractures in gallery scale and their rock matrix

*Ai Hamada[1] (1.Central Research Institute of Electric Power Industry)

[J] Poster | H (Human Geosciences )：H-CG Complex & General

5:15 PM - 6:30 PM JST | 8:15 AM - 9:30 AM UTC | Poster Hall International Exhibition Hall8, Makuhari Messe_18

## [H-CG31] Nuclear Energy and Geoscience

convener:Eiji Sasao(Tono Geoscience Center, Japan Atomic Energy Agency), Ryuta Hataya(Central Research Institute of Electric Power Industry), Shinji Takeuchi(Department of Earth and Environmental Sciences, College of Humanities & Sciences, Nihon University)

[HCG31-P01] Better identification of submerged terraces based on digital terrain analysis

*Hiura Yuki[1], Tetsuya Komatsu[1], Toshihiko Sugai[2] (1.Japan Atomic Energy Agency, 2.Graduate School of Frontier Sciences, The University of Tokyo)

[HCG31-P02] Advanced examination technique for river erosion in inland area – a case study of the Kii Peninsula, Japan –

*Nakanishi Toshimichi[1], Tetsuya Komatsu[1], Manabu Ogata[1], Takashi Hosoya[2], Takumi Kaga[2] (1.Japan Atomic Energy Agency, 2.Chuo Kaihatsu Corporation)

[HCG31-P03] Hydrothermal experiment on quartz hydration: Toward a development of new dating method for natural phenomena

*Masakazu Niwa[1], Koji Shimada[1] (1.Japan Atomic Energy Agency)

[HCG31-P04] **Diffusion Coefficient and Porosity of Granite for Evaluation of Mobility Parameter**

*Kenji Fukuda[1], Hiroaki Murakami[1], Kaori Itai[2], Masayuki Ishibashi[1], Eiji Sasao[1] (1.Japan Atomic Energy Agency, 2.C・TECH corporation)

[HCG31-P05] Hydrogeological structure of hydraulic conductive fractures in gallery scale and their rock matrix

*Ai Hamada[1] (1.Central Research Institute of Electric Power Industry)

[J] Poster | H (Human Geosciences )：H-CG Complex & General

1:45 PM - 3:15 PM JST | 4:45 AM - 6:15 AM UTC | Poster Hall International Exhibition Hall8, Makuhari Messe_5

## [H-CG34] Education and research for rehabilitation of agriculture against harmful rumors in nuclear disaster areas

convener:Masaru Mizoguchi(Graduate school of Agricultural and Life Sciences, The University of Tokyo)

[HCG34-P01] Calculation of water and sediment discharge from a small forested catchment for evaluating load of the particulate radioactive cesium

*Takuhei Yamasaki[1], Shoichiro Hamamoto[1], Taku Nishimura[1] (1.University of Tokyo)

[HCG34-P02] Radiocesium Inter-Annual Variations and Spatial Dynamics in Watershed in Iitate, Fukushima, Japan

*Saito Mari[1], Kazutoshi Osawa[1], Naoto Nihei[2] (1.Utsunomiya University, 2.Tokyuo University)

[HCG34-P03] Efforts in university to keep consciousness of disaster caused by The Great East Japan Earthquake for resurrection of agriculture at Iitate village

*Junko NISHIWAKI[1], Masaru Mizoguchi[2] (1.College of Agriculture, Ibaraki University, 2.Graduate School of Agricultural and Life Sciences, The University of Tokyo)

[HCG34-P04] Effects of remaining radiocesium in bunds and slopes of paddy fields on ambient dose and downstream environment.

*Yoshida Shuichiro[1], Kazuhiro Nishida[1], Taku Fukui[1] (1.The University of Tokyo)

[J] Poster | H (Human Geosciences )：H-CG Complex & General

5:15 PM - 6:30 PM JST | 8:15 AM - 9:30 AM UTC | Poster Hall International Exhibition Hall8, Makuhari Messe_19

## [H-CG34] Education and research for rehabilitation of agriculture against harmful rumors in nuclear disaster areas

convener:Masaru Mizoguchi(Graduate school of Agricultural and Life Sciences, The University of Tokyo)

[HCG34-P01] Calculation of water and sediment discharge from a small forested catchment for evaluating load of the particulate radioactive cesium

*Takuhei Yamasaki[1], Shoichiro Hamamoto[1], Taku Nishimura[1] (1.University of Tokyo)

[HCG34-P02] Radiocesium Inter-Annual Variations and Spatial Dynamics in Watershed in Iitate, Fukushima, Japan

*Saito Mari[1], Kazutoshi Osawa[1], Naoto Nihei[2] (1.Utsunomiya University, 2.Tokyuo University)

[HCG34-P03] Efforts in university to keep consciousness of disaster caused by The Great East Japan Earthquake for resurrection of agriculture at Iitate village

*Junko NISHIWAKI[1], Masaru Mizoguchi[2] (1.College of Agriculture, Ibaraki University, 2.Graduate School of Agricultural and Life Sciences, The University of Tokyo)

[HCG34-P04] Effects of remaining radiocesium in bunds and slopes of paddy fields on ambient dose and downstream environment.

*Yoshida Shuichiro[1], Kazuhiro Nishida[1], Taku Fukui[1] (1.The University of Tokyo)

[J] Oral | H (Human Geosciences)：H-CG Complex & General

3:30 PM - 5:00 PM JST | 6:30 AM - 8:00 AM UTC | 202 2F

## [H-CG34] Education and research for rehabilitation of agriculture against harmful rumors in nuclear disaster areas

convener:Masaru Mizoguchi(Graduate school of Agricultural and Life Sciences, The University of Tokyo), Chairperson:Masaru Mizoguchi(The University of Tokyo), Kousuke Noborio(School of Agricultural Science, Meiji University)

3:30 PM - 3:45 PM JST | 6:30 AM - 6:45 AM UTC

[HCG34-01] Education and research for rehabilitation of agriculture against harmful rumors in nuclear disaster areas

*Masaru Mizoguchi[1] (1.Graduate school of Agricultural and Life Sciences, The University of Tokyo)

---

3:45 PM - 4:00 PM JST | 6:45 AM - 7:00 AM UTC

[HCG34-02] Towards the reborn of Iitate village 'Agriculture'

★Invited Papers

Makoto Sugisoka[2], *Masaru Mizoguchi[1] (1.Graduate school of Agricultural and Life Sciences, The University of Tokyo, 2.Division of Reconstruction Measures, Iitate Village)

---

4:00 PM - 4:15 PM JST | 7:00 AM - 7:15 AM UTC

[HCG34-03] Difference among crop species by radiocesium absorption from different soil fractions

*Nihei Naoto[1], Yoshimi Ohmae[1], Makoto Furukawa[1], Syuichiro Yoshida[1] (1.The University of Tokyo, Graduate School of Agricultural and Life Sciences)

---

4:15 PM - 4:30 PM JST | 7:15 AM - 7:30 AM UTC

[HCG34-04] Wild vegetables and mushrooms retrieving agriculter in Iitate Village, Fukushima Prefecture

*Kosuke Noborio[1], Yudai Fukuyama[2], Satoko Fujita[1], Hiroaki Sugino[2], Masaru Mizoguchi[2] (1.Meiji University, 2.the Univewrsity of Tokyo)

---

4:30 PM - 4:45 PM JST | 7:30 AM - 7:45 AM UTC

[HCG34-05] Effect of Study Tour toward Participants' Attachment on the Study Site - Case Study of University Student Tour to
Iitate Village, Fukushiima Prefecture -

*Natsumi Ebitani[1], Masaru Mizoguchi[1], Hiroaki Sugino[1] (1.Graduate school of Agricultural and Life Sciences, The University of Tokyo)

[J] Poster | S (Solid Earth Sciences )：S-SS Seismology

10:45 AM - 12:15 PM JST | 1:45 AM - 3:15 AM UTC | Poster Hall International Exhibition Hall8, Makuhari Messe_4

## [S-SS12] Crustal Structure

convener:Kazuo Nakahigashi(Tokyo University of Marine Science and Technology)

[SSS12-P01] Regional difference in long period surface wave phase velocity by an explosive phenomenon generated in North Korea on September 3, 2017

*Koji Yamada[1] (1.Hanshin Consultants co., ltd.)

---

[SSS12-P02] Phase velocity estimation based on spatial gradient of surface wave arrival time of teleseismic earthquakes observed by S-net

*Akira Ishigami[1], Ryota Takagi[1] (1.Research Center for Prediction of Earthquakes and Volcanic Eruptions, Graduate School of Science)

---

[SSS12-P03] Crustal seismic velocity structure in the Japanese Islands from receiver function analysis using similar earthquakes

*Toshihiro Igarashi[1] (1.Earthquake Research Institute, University of Tokyo)

---

[SSS12-P04] **Estimation of the Crustal Structure beneath the Broadband Seismic Network in the Eskisehir Region, Turkey, by Using Receiver Function Method**

*Pinar Duran[1], Asim Oguz Ozel[1], Hiroaki Yamanaka[2] (1.ISTANBUL UNIVERSITY-CERRAHPASA, 2.TOKYO INSTITUTE OF TECHNOLOGY)

---

[SSS12-P05] Three-dimensional S-wave attenuation structure in and around Hokkaido, Japan

*Ryoichi Nakamura[1], Takahiro Shiina[1] (1.Earthquake Research Institute, The University of Tokyo)

---

[SSS12-P06] Reexamination for the subsurface structure beneath the southern part of the Hidaka Collision Zone, Hokkaido, Japan by using a numerical test of wave propagation

*Masahiro Shimazaki[1], Noriko Tsumura[2] (1.Graduate School of Science and Engineering, Chiba University, 2.Graduate School of Science, Chiba University)

---

[SSS12-P07] High resolution seismic surveys in the Kuril trench off Hokkaido

*Yasuyuki Nakamura[1], Shuichi Kodaira[1], Mikiya Yamashita[1], Seiichi Miura[1], Gou Fujie[1] (1.Japan Agency for Marine Earth Science and Technology)

---

[SSS12-P08] Subsurface Structure at the North of the Yokosuka Fault by Seismic Reflection Survey

*Shinobu Ito[1] (1.Geological Survey of Japan, AIST)

---

[SSS12-P09] **Crust and Uppermost mantle P-wave velocity structure of the Ordos block and its neighbors based on travel time tomography**

*Yaning Liu[1], Jianping Wu[1], Shuxian Bao[1], Xiaohong Meng[2] (1.Institute of Geophysics, China Earthquake Administration, 2.China University of Geosciences (Beijing))

---

[SSS12-P10] Seismic imaging of the 2016 Kumamoto earthquake area using P and PmP data

*Dapeng Zhao[1], Haibo Wang[2], Zhouchuan Huang[2], Mingjie Xu[2], Liangshu Wang[2] (1.Department of Geophysics, Tohoku University, 2.School of Earth Sciences and Engineering, Nanjing University)

---

[SSS12-P11] Estimation of 3D velocity structure in Kyushu region by the seismic tomography

*Toya Mitsuhiro[1], Koji Yamada[1] (1.Hanshin Consultants Co., Ltd.)

---

[SSS12-P12] Estimation of the structure of the Philippine Sea slab under south Kyushu using receiver function analysis

*Masaki Uchida[1], Takahiro Ohkura[1], Takuo Shibutani[1], Yuki Abe[2], Shintaro Komatsu[1], Ken'ichi Yamazaki[1], Yusuke Yamashita[1], Shin Yoshikawa[1], Masato Iguchi[1], Takeshi Tameguri[1], Tadaomi Sonoda[1] (1.Kyoto Univ., 2.Hot Springs Research Institute)

---

[SSS12-P13] Imaging subduction structure beneath the eastern part of Kii Peninsula, SW Japan, using an earthquake reflection method

*Eiji Kurashimo[1], Takashi Iidaka[1], Noriko Tsumura[2], Takaya Iwasaki[1] (1.Earthquake Research Institute, the University of Tokyo, 2.Chiba University)

[SSS12-P14] **Tomography of Mejillones Peninsula using cross-correlation of ambient seismic noise**

*Kellen Azua Quezada[1], Sergio Ruiz[1], Francisco Pasten-Araya[2,3], José Salomón[4], Pablo Salazar[2,3], Miguel Saez[1], César Pastén[4], Felipe Leyton[5], Wasja Bloch[6] (1.DGF, UChile, 2.DG, UCN, 3.CIGIDEN, 4.DIC, UChile, 5.CSN, Chile, 6.GFZ)

[SSS12-P15] **Crustal thickness beneath Central Indonesia by the cross-correlation analysis of seismic ambient noise (2)**

*Masyitha Retno Budiati[1], Genti Toyokuni[1], Tomomi Okada[1], Toru Matsuzawa[1] (1.Graduate School of Science, Geophysics Department, Tohoku University)

[SSS12-P16] Subsurface structure below the southernmost area of South Japanese Alps estimated by seismic interferometry imaging

*Toshiki Watanabe[1], Hasegawa Daima[1], Tanio Ito[2], Ken'ichi Kano[3], Susumu Abe[4], Akira Fujiwara[5], Yoshinori Kouchi[6] (1.Graduate School of Environmental Studies, Nagoya University, 2.Association for the Development of Earthquake Prediction, 3.Shizuoka Univertity, 4.JAPEX, Co. Ltd., 5.JOGMEC, 6.Geosys, Inc.)

[SSS12-P17] Strong variations of near-surface seismic anisotropy of Taiwan revealed by coda interferometry

*Hsin-Yu Lee[1], Yuancheng Gung[1], Li-Wei Chen[2], Ling-Yun Chiao[3] (1.Department of Geosciences, National Taiwan University, Taiwan, 2.Department of Earth and Planetary Science, University of California at Berkeley, CA, USA, 3.Institute of Oceanography, National Taiwan University, Taiwan)

[SSS12-P18] Investigating anomalous crustal structures along the convergent zone in eastern Taiwan with the new airborne magnetic survey and updated seismic tomographic models

*Chi-Hsuan Chen[1], Hsin-Hua Huang[2], Lun-Tao Tong[3], Wayne Lin[3], Po-Tsun Lee[1], Shou-Fang Chang[1], Jin-Fa Lee[1] (1.Cntrl. Geo. Surv., MOEA, Taiwan, 2.Inst. Earth. Sc., Acad. Sinica, Taiwan , 3.Industr. Technol. Res. Inst., Taiwan)

[J] Poster | S (Solid Earth Sciences )：S-SS Seismology

5:15 PM - 6:30 PM JST | 8:15 AM - 9:30 AM UTC | Poster Hall International Exhibition Hall8, Makuhari Messe_20

## [S-SS12] Crustal Structure

convener:Kazuo Nakahigashi(Tokyo University of Marine Science and Technology)

[SSS12-P01] Regional difference in long period surface wave phase velocity by an explosive phenomenon generated in North Korea on September 3, 2017

*Koji Yamada[1] (1.Hanshin Consultants co., ltd.)

---

[SSS12-P02] Phase velocity estimation based on spatial gradient of surface wave arrival time of teleseismic earthquakes observed by S-net

*Akira Ishigami[1], Ryota Takagi[1] (1.Research Center for Prediction of Earthquakes and Volcanic Eruptions, Graduate School of Science)

---

[SSS12-P03] Crustal seismic velocity structure in the Japanese Islands from receiver function analysis using similar earthquakes

*Toshihiro Igarashi[1] (1.Earthquake Research Institute, University of Tokyo)

---

[SSS12-P04] **Estimation of the Crustal Structure beneath the Broadband Seismic Network in the Eskisehir Region, Turkey, by Using Receiver Function Method**

*Pinar Duran[1], Asim Oguz Ozel[1], Hiroaki Yamanaka[2] (1.ISTANBUL UNIVERSITY-CERRAHPASA, 2.TOKYO INSTITUTE OF TECHNOLOGY)

---

[SSS12-P05] Three-dimensional S-wave attenuation structure in and around Hokkaido, Japan

*Ryoichi Nakamura[1], Takahiro Shiina[1] (1.Earthquake Research Institute, The University of Tokyo)

---

[SSS12-P06] Reexamination for the subsurface structure beneath the southern part of the Hidaka Collision Zone, Hokkaido, Japan by using a numerical test of wave propagation

*Masahiro Shimazaki[1], Noriko Tsumura[2] (1.Graduate School of Science and Engineering, Chiba University, 2.Graduate School of Science, Chiba University)

---

[SSS12-P07] High resolution seismic surveys in the Kuril trench off Hokkaido

*Yasuyuki Nakamura[1], Shuichi Kodaira[1], Mikiya Yamashita[1], Seiichi Miura[1], Gou Fujie[1] (1.Japan Agency for Marine Earth Science and Technology)

---

[SSS12-P08] Subsurface Structure at the North of the Yokosuka Fault by Seismic Reflection Survey

*Shinobu Ito[1] (1.Geological Survey of Japan, AIST)

---

[SSS12-P09] **Crust and Uppermost mantle P-wave velocity structure of the Ordos block and its neighbors based on travel time tomography**

*Yaning Liu[1], Jianping Wu[1], Shuxian Bao[1], Xiaohong Meng[2] (1.Institute of Geophysics, China Earthquake Administration, 2.China University of Geosciences (Beijing))

---

[SSS12-P10] Seismic imaging of the 2016 Kumamoto earthquake area using P and PmP data

*Dapeng Zhao[1], Haibo Wang[2], Zhouchuan Huang[2], Mingjie Xu[2], Liangshu Wang[2] (1.Department of Geophysics, Tohoku University, 2.School of Earth Sciences and Engineering, Nanjing University)

---

[SSS12-P11] Estimation of 3D velocity structure in Kyushu region by the seismic tomography

*Toya Mitsuhiro[1], Koji Yamada[1] (1.Hanshin Consultants Co., Ltd.)

---

[SSS12-P12] Estimation of the structure of the Philippine Sea slab under south Kyushu using receiver function analysis

*Masaki Uchida[1], Takahiro Ohkura[1], Takuo Shibutani[1], Yuki Abe[2], Shintaro Komatsu[1], Ken'ichi Yamazaki[1], Yusuke Yamashita[1], Shin Yoshikawa[1], Masato Iguchi[1], Takeshi Tameguri[1], Tadaomi Sonoda[1] (1.Kyoto Univ., 2.Hot Springs Research Institute)

---

[SSS12-P13] Imaging subduction structure beneath the eastern part of Kii Peninsula, SW Japan, using an earthquake reflection method

*Eiji Kurashimo[1], Takashi Iidaka[1], Noriko Tsumura[2], Takaya Iwasaki[1] (1.Earthquake Research Institute, the University of Tokyo, 2.Chiba University)

[SSS12-P14] **Tomography of Mejillones Peninsula using cross-correlation of ambient seismic noise**

*Kellen Azua Quezada[1], Sergio Ruiz[1], Francisco Pasten-Araya[2,3], José Salomón[4], Pablo Salazar[2,3], Miguel Saez[1], César Pastén[4], Felipe Leyton[5], Wasja Bloch[6] (1.DGF, UChile, 2.DG, UCN, 3.CIGIDEN, 4.DIC, UChile, 5.CSN, Chile, 6.GFZ)

[SSS12-P15] **Crustal thickness beneath Central Indonesia by the cross-correlation analysis of seismic ambient noise (2)**

*Masyitha Retno Budiati[1], Genti Toyokuni[1], Tomomi Okada[1], Toru Matsuzawa[1] (1.Graduate School of Science, Geophysics Department, Tohoku University)

[SSS12-P16] Subsurface structure below the southernmost area of South Japanese Alps estimated by seismic interferometry imaging

*Toshiki Watanabe[1], Hasegawa Daima[1], Tanio Ito[2], Ken'ichi Kano[3], Susumu Abe[4], Akira Fujiwara[5], Yoshinori Kouchi[6] (1.Graduate School of Environmental Studies, Nagoya University, 2.Association for the Development of Earthquake Prediction, 3.Shizuoka Univertity, 4.JAPEX, Co. Ltd., 5.JOGMEC, 6.Geosys, Inc.)

[SSS12-P17] Strong variations of near-surface seismic anisotropy of Taiwan revealed by coda interferometry

*Hsin-Yu Lee[1], Yuancheng Gung[1], Li-Wei Chen[2], Ling-Yun Chiao[3] (1.Department of Geosciences, National Taiwan University, Taiwan, 2.Department of Earth and Planetary Science, University of California at Berkeley, CA, USA, 3.Institute of Oceanography, National Taiwan University, Taiwan)

[SSS12-P18] Investigating anomalous crustal structures along the convergent zone in eastern Taiwan with the new airborne magnetic survey and updated seismic tomographic models

*Chi-Hsuan Chen[1], Hsin-Hua Huang[2], Lun-Tao Tong[3], Wayne Lin[3], Po-Tsun Lee[1], Shou-Fang Chang[1], Jin-Fa Lee[1] (1.Cntrl. Geo. Surv., MOEA, Taiwan, 2.Inst. Earth. Sc., Acad. Sinica, Taiwan , 3.Industr. Technol. Res. Inst., Taiwan)

[J] Oral | S (Solid Earth Sciences )：S-SS Seismology

1:45 PM - 3:15 PM JST | 4:45 AM - 6:15 AM UTC | A05 TOKYO BAY MAKUHARI HALL

## [S-SS12] Crustal Structure

convener:Kazuo Nakahigashi(Tokyo University of Marine Science and Technology), Chairperson:Yoshio Murai(Hokkaido University), Genti Toyokuni(東北大学)

1:45 PM - 2:00 PM JST | 4:45 AM - 5:00 AM UTC

[SSS12-01] Shrinking and draining continental lower crust: its binary effects of stress and fluid on crustal activities

*Takehito Koyama[1] (1.Institute of Industrial Science, the University of Tokyo)

---

2:00 PM - 2:15 PM JST | 5:00 AM - 5:15 AM UTC

[SSS12-02] Seismic velocity structure in southern Hokkaido deduced from ocean-bottom seismographic and land observations

*Yoshio Murai[1], Kei Katsumata[1], Tetsuo Takanami[2], Tomoki Watanabe[3], Tadashi Yamashina[4], Ikuo Cho[5], Masayuki Tanaka[6], Ryosuke Azuma[7] (1.Institute of Seismology and Volcanology, Faculty of Science, Hokkaido University, 2.Department of Terrestrial Magnetism, Carnegie Institution of Washington, 3.Marine Works Japan LTD, 4.Kochi University, 5.National Institute of Advanced Industrial Science and Technology, 6.Meteorological Research Institute, 7.Research Center for Prediction of Earthquakes and Volcanic Eruptions, Graduate School of Science, Tohoku University)

---

2:15 PM - 2:30 PM JST | 5:15 AM - 5:30 AM UTC

[SSS12-03] Structural Complexity Associated with Arc-Arc Collision in Hokkaido Island, Japan - Review on Controlled-Source Seismic Researches in Western and Central Hokkaido -

★Invited Papers

*Takaya Iwasaki[1], Noriko Tsumura[2], Tanio Ito[3], Kazunori Arita[4], Hiroshi Sato[1] (1.Eathquake Research Institute, the University of Tokyo, 2.Graduate School of Science, Chiba University, 3.Association for the Development of Earthquake Prediction, 4.Hokkaido Research Center of Geology)

---

2:30 PM - 2:45 PM JST | 5:30 AM - 5:45 AM UTC

[SSS12-04] **Seismic imaging of the eastern Japan forearc region using S-net data**

*Genti Toyokuni[1], Dapeng Zhao[1], Naoki Uchida[1], Takashi NAKAYAMA[1] (1.RCPEVE, Tohoku Univ.)

---

2:45 PM - 3:00 PM JST | 5:45 AM - 6:00 AM UTC

[SSS12-05] The relationship between the location of the mid crustal reflector and seismicity in Iwaki area, northeastern Japan

*Takashi Iidaka[1], Shin'ichi Sakai[1], Toshihiro Igarashi[1], Kazushige Obara[1], Aitaro Kato[1], Tetsuya Takeda[2], Shigeki Nakagawa[1] (1.Earthquake Research Institute, University of Tokyo, 2.National Research Institute for Earth Science and Disaster Resilience)

---

3:00 PM - 3:15 PM JST | 6:00 AM - 6:15 AM UTC

[SSS12-06] Abnormal Seismic Anisotropy beneath the Tokyo Metropolitan Area (1) Mantle of the Philippine Sea Slab

*Motoko Ishise[1], Shin'ichi Sakai[1], Aitaro Kato[1], Shin Aoi[2], Makoto MATSUBARA[2] (1.Earthquake Reseach Institute, University of Tokyo, 2.National Research Institute for EarthScience and Disaster Resillience)

[J] Oral | S (Solid Earth Sciences )：S-SS Seismology

3:30 PM - 5:00 PM JST | 6:30 AM - 8:00 AM UTC | A05 TOKYO BAY MAKUHARI HALL

## [S-SS12] Crustal Structure

convener:Kazuo Nakahigashi(Tokyo University of Marine Science and Technology), Chairperson:Tsuruga Kayoko(Tokyo University of Marine Science and Technology), Yojiro Yamamoto(Japan Agency for Marine-Earth Science and Technology)

3:30 PM - 3:45 PM JST | 6:30 AM - 6:45 AM UTC

### [SSS12-07] Deep seismic reflection profiling across the Suruga trough, Shizuoka, Japan

*Hiroshi Sato[1], Kayoko Tsuruga[2], Hisatoshi Baba[3], Tatsuya Ishiyama[1], Shinji Kawasaki[4], Yasuhisa Tanaka[4], Toshifumi Hayashi[2], Yoshihiro Sekino[2], Masanao Shinohara[1], Takaya Iwasaki[1], Makoto MATSUBARA[5], Naoshi Hirata[1,5] (1.Earthquake Research Institute, The University of Tokyo, 2.Tokyo University of Marine Science and Technology, 3.Tokai Univerisity, 4.JGI Inc., 5.National Research Institute for Earth Science and Disaster Resilience)

3:45 PM - 4:00 PM JST | 6:45 AM - 7:00 AM UTC

### [SSS12-08] Multi-channel seismic profiling in the northern part of Suruga bay using the Shiyomaru-vessel of Tokyo University of Marine Science and Technology (Preliminary report)

*Kayoko Tsuruga[1], Hiroshi Sato[2], Hisatoshi Baba[3], Yoshihiro Sekino[1], Toshifumi Hayashi[1], Hayato Kondotec[1], Chiharu Aoyama[1], Tetsutaro Aikawa[1], Tatsuya Ishiyama[2], Masanao Shinohara[2], Shinji Kawasaki[4], Yasuhisa Tanaka[4] (1.Tokyo University of Marine Science and Technology, 2.University of Tokyo, 3.Tokai University, 4.JGI, Inc.)

4:00 PM - 4:15 PM JST | 7:00 AM - 7:15 AM UTC

### [SSS12-09] Crustal structure refraction survey using Airgun-OBS in the northern part of Suruga Bay -Fujikawa fault zone- (Preliminary Report)

*Hisatoshi Baba[1], Kayoko Tsuruga[2], Hiroshi Sato[3], Tatsuya Ishiyama[3], Masanao Shinohara[3], Takahito Nishimiya[4], Shintaro Abe[5] (1.Department of Marine and Earth Science, Tokai University, 2.Tokyo University of Marine Science and Technology, 3.Earthquake Research Institute, University of Tokyo, 4.Meteorological Research Institute, Japan Meteorological Agency, 5.Association for the Development of Earthquake Prediction)

4:15 PM - 4:30 PM JST | 7:15 AM - 7:30 AM UTC

### [SSS12-10] 3D seismic attenuation profiling for imaging an active fault in Uchiura wan

*Tetsuro Tsuru[1], Shio Shimizu[1], Mayu Ogawa[1], Jin-Oh Park[2], Seishiro Furuyama[1], Kosaku Arai[3], Takahiko Inoue[3], Chen Guo[2] (1.Tokyo University of Marine Science and Technology, 2.Atmosphere and Ocean Research Institute, The University of Tokyo, 3.National Institute of Advanced Industrial Science and Technology)

4:30 PM - 4:45 PM JST | 7:30 AM - 7:45 AM UTC

### [SSS12-11] Gravity survey at the extension of the Takahama fault and the Yokosuka fault in Nishio City, Aichi Prefecture

*Tokunosuke Tatsuzawa[1,2], Tatsuya Sumita[2], Shinobu Ito[2], Tomoya Abe[2] (1.Department of Earth Sciences, Resources and Environmental Engineering, Creative Science and Engineering, Faculty of Science and Engineering, Waseda University, 2.National Institute of Advanced Industrial Science and Technology)

4:45 PM - 5:00 PM JST | 7:45 AM - 8:00 AM UTC

### [SSS12-12] Subduction geometry and seismicity around northern Ryukyu subduction zone

*Yojiro Yamamoto[1], Tsutomu Takahashi[1], Yasushi Ishihara[1], Koichiro Obana[1], Seiichi Miura[1], Shuichi Kodaira[1], Yoshiyuki Kaneda[2] (1.Japan Agency for Marine-Earth Science and Technology (JAMSTEC), 2.Kagawa University)

[E] Oral | S (Solid Earth Sciences)：S-IT Science of the Earth's Interior & Techtonophysics

9:00 AM - 10:30 AM JST | 12:00 AM - 1:30 AM UTC | A09 TOKYO BAY MAKUHARI HALL

## [S-IT25] Planetary cores: Structure, formation, and evolution

convener:Hidenori Terasaki(Graduate School of Science, Osaka University), Eiji Ohtani(Department of Earth and Planetary Materials Science, Graduate School of Science, Tohoku University), William F McDonough(University of Maryland College Park), George Helffrich(Earth-Life Science Institute, Tokyo Institute of Technology), Chairperson:George Helffrich(ELSI, Tokyo Institute of Technology), Hidenori Terasaki

9:00 AM - 9:15 AM JST | 12:00 AM - 12:15 AM UTC

[SIT25-01] **High-pressure Equation of State of Schreibersite $Fe_{2.15}Ni_{0.85}P$: Implications for the Martian Core**

*Xuejing He[1], Jiazeng Guo[2], Xiang Wu[3], Shengxuan Huang[1], Fei Qin[1], Xiangping Gu[4], Shan Qin[1] (1.Peking Univ., 2.Nanyang Normal Univ., 3.China Univ. of Geosciences, 4.Central South Univ.)

9:15 AM - 9:30 AM JST | 12:15 AM - 12:30 AM UTC

[SIT25-02] Bottom-up solidification versus top-down solidification of the liquid core of the relatively small planetary bodies

*Satoru Urakawa[1], Hidenori Terasaki[2] (1.Department of Earth Sciences, Okayama University, 2.Department of Earth and Space Science, Osaka University)

9:30 AM - 9:45 AM JST | 12:30 AM - 12:45 AM UTC

[SIT25-03] P-wave velocity of $Fe_3S$ under high pressure and temperature

*Seiji Kamada[1,2], Hidenori Terasaki[3], Hiroshi Fukui[4,5], Tatsuya Sakamaki[2], Hiroshi Uchiyama[6], Satoshi Tsutsui[6], Eiji Ohtani[2], Alfred Q.R. Baron[5] (1.Frontier Research Institute for Interdisciplinary Sciences, Tohoku University, 2.Department of Earth Science, Graduate School of Science, Tohoku University, 3.Department of Earth and Space Science, Graduate School of Science, Osaka University, 4.Graduate School of Material Science, University of Hyogo, 5.RIKEN, 6.JASRI)

9:45 AM - 10:00 AM JST | 12:45 AM - 1:00 AM UTC

[SIT25-04] The sound velocity of liquid Fe-Ni-S-Si alloys under Mercury's core condition

*Iori Yamada[1], Hidenori Terasaki[1], Asaka Kamiya[1], Ryo Tsuruoka[1], Yuji Higo[2], Akihiko Machida[3] (1.Graduate School of Science, Osaka University, 2.Japan Synchrotron Radiation Research Institute, 3.National Institute for Quantum and Radiological Science and Technology)

10:00 AM - 10:15 AM JST | 1:00 AM - 1:15 AM UTC

[SIT25-05] In situ observation of Rayleigh–Taylor instability growth of liquid Fe-Si using laser shock

*Hidenori Terasaki[1], Tatsuhiro Sakaiya[1], Keisuke Shigemori[2], Hiroki Kato[2], Yoichiro Hironaka[2], Tadashi Kondo[1] (1.Graduate School of Science, Osaka University, 2.Institute of Laser Engineering, Osaka University)

[E] Oral | S (Solid Earth Sciences )：S-IT Science of the Earth's Interior & Techtonophysics

10:45 AM - 12:15 PM JST | 1:45 AM - 3:15 AM UTC | A09 TOKYO BAY MAKUHARI HALL

## [S-IT25] Planetary cores: Structure, formation, and evolution

convener:Hidenori Terasaki(Graduate School of Science, Osaka University), Eiji Ohtani(Department of Earth and Planetary Materials Science, Graduate School of Science, Tohoku University), William F McDonough(University of Maryland College Park), George Helffrich(Earth-Life Science Institute, Tokyo Institute of Technology), Chairperson:William McDonough(University of Maryland / Tohoku University), Eiji Ohtani(Tohoku University)

10:45 AM - 11:00 AM JST | 1:45 AM - 2:00 AM UTC

[SIT25-06] *P-V-T* equation-of-state of liquid Fe from *ab-initio* simulations to the TPa regime

*Gerd Steinle-Neumann[1], Fabian Wagle[1] (1.Bayerisches Geoinstitut, University of Bayreuth, Germany)

---

11:00 AM - 11:15 AM JST | 2:00 AM - 2:15 AM UTC

[SIT25-07] ***Ab initio* study of Iron-Nickel alloys in Super-Earths cores**

*Francois Soubiran[1], Razvan Caracas[1] (1.Ecole normale superieure de Lyon, Laboratoire de Géologie de Lyon, Université Lyon 1, CNRS UMR 5276, Lyon, France)

---

11:15 AM - 11:30 AM JST | 2:15 AM - 2:30 AM UTC

[SIT25-08] **Impurity effect on the iron's transport properties at Earth's core conditions: A key constraint for the evolution of the Earth's core**

*Youjun Zhang[1], Mingqiang Hou[2], Nilesh Salke[2], Jung-Fu Lin[3] (1.Sichuan University, 2.HPSTAR, 3.University of Texas at Austin)

---

11:30 AM - 11:45 AM JST | 2:30 AM - 2:45 AM UTC

[SIT25-09] Melting in the Fe-FeO system to 214 GPa

*Kenta Oka[1], Yuto Kidokoro, Kei Hirose[1], Yoichi Nakajima[2], Guillaume Morard[3], Guillaume Fiquet[3], Nicolas Coudurier[3] (1.Department of Earth and Planetary Science, The University of Tokyo, 2.Priority Organization for Innobation and Excellence, 3.Sorbonne Université)

---

11:45 AM - 12:00 PM JST | 2:45 AM - 3:00 AM UTC

[SIT25-10] B2 phase in the inner core: constraints from high pressure experiments

*Eiji Ohtani[1], Daijo Ikuta[1], Seiji Kamada[2], Tatsuya Sakamaki[1], Naohisa Hirao[3] (1.Department of Earth and Planetary Materials Science, Graduate School of Science, Tohoku University, 2.Frontier Institute for Interdisciplinary Research, Tohoku University, 3.SRring-8, Japan Synchrotron Research Institute)

[E] Poster | S (Solid Earth Sciences)：S-IT Science of the Earth's Interior & Techtonophysics

3:30 PM - 5:00 PM JST | 6:30 AM - 8:00 AM UTC | Poster Hall International Exhibition Hall8, Makuhari Messe_10

## [S-IT25] Planetary cores: Structure, formation, and evolution

convener:Hidenori Terasaki(Graduate School of Science, Osaka University), Eiji Ohtani(Department of Earth and Planetary Materials Science, Graduate School of Science, Tohoku University), William F McDonough(University of Maryland College Park), George Helffrich(Earth-Life Science Institute, Tokyo Institute of Technology)

[SIT25-P01] Stratification of the Earth's core by $SiO_2$ crystallisation

*George Helffrich[1], Satoshi Kaneshima[2], Kei Hirose[1,3] (1.Earth-Life Science Institute, Tokyo Institute of Technology, 2.Earth and Planetary Sciences, Kyushu University, 3.Earth and Planetary Sciences Department, University of Tokyo)

[SIT25-P02] Relation between sound velocity and density for liquid iron alloys under Earth's core pressures by laser-shock compression

*Tatsuhiro Sakaiya[1], Tadashi Kondo[1], Hidenori Terasaki[1], Keisuke Shigemori[2], Yoichiro Hironaka[2] (1.Graduate School of Science, Osaka University, 2.Institute of Laser Engineering, Osaka University)

[SIT25-P03] **Geochemical estimates of Earth's core heat content at the end of accretion**

*Vincent Clesi[1], Renaud Deguen[1] (1.Laboratoire de Geologie de Lyon - Terre, Planètes, Environnement, Université Claude Bernard Lyon 1, CNRS, ENS-Lyon, 69622 Villeurbanne, France.)

[SIT25-P04] The effect of temperature on density of solid metals

*Asaka Kamiya[1], Hidenori Terasaki[1], Tadashi Kondo[1] (1.Osaka University)

[SIT25-P05] Phase relations in the Fe-Ni-Si system at high pressures and high temperatures

*Daijo Ikuta[1], Eiji Ohtani[1], Saori Kawaguchi[2], Naohisa Hirao[2], Yasuo Ohishi[2] (1.Department of Earth Science, Tohoku University, 2.JASRI)

[E] Poster | S (Solid Earth Sciences)：S-IT Science of the Earth's Interior & Techtonophysics

5:15 PM - 6:30 PM JST | 8:15 AM - 9:30 AM UTC | Poster Hall International Exhibition Hall8, Makuhari Messe_21

## [S-IT25] Planetary cores: Structure, formation, and evolution

convener:Hidenori Terasaki(Graduate School of Science, Osaka University), Eiji Ohtani(Department of Earth and Planetary Materials Science, Graduate School of Science, Tohoku University), William F McDonough(University of Maryland College Park), George Helffrich(Earth-Life Science Institute, Tokyo Institute of Technology)

[SIT25-P01] Stratification of the Earth's core by $SiO_2$ crystallisation

*George Helffrich[1], Satoshi Kaneshima[2], Kei Hirose[1,3] (1.Earth-Life Science Institute, Tokyo Institute of Technology, 2.Earth and Planetary Sciences, Kyushu University, 3.Earth and Planetary Sciences Department, University of Tokyo)

[SIT25-P02] Relation between sound velocity and density for liquid iron alloys under Earth's core pressures by laser-shock compression

*Tatsuhiro Sakaiya[1], Tadashi Kondo[1], Hidenori Terasaki[1], Keisuke Shigemori[2], Yoichiro Hironaka[2] (1.Graduate School of Science, Osaka University, 2.Institute of Laser Engineering, Osaka University)

[SIT25-P03] **Geochemical estimates of Earth's core heat content at the end of accretion**

*Vincent Clesi[1], Renaud Deguen[1] (1.Laboratoire de Geologie de Lyon - Terre, Planètes, Environnement, Université Claude Bernard Lyon 1, CNRS, ENS-Lyon, 69622 Villeurbanne, France.)

[SIT25-P04] The effect of temperature on density of solid metals

*Asaka Kamiya[1], Hidenori Terasaki[1], Tadashi Kondo[1] (1.Osaka University)

[SIT25-P05] Phase relations in the Fe-Ni-Si system at high pressures and high temperatures

*Daijo Ikuta[1], Eiji Ohtani[1], Saori Kawaguchi[2], Naohisa Hirao[2], Yasuo Ohishi[2] (1.Department of Earth Science, Tohoku University, 2.JASRI)

[J] Oral | S (Solid Earth Sciences )：S-GL Geology

9:00 AM - 10:30 AM JST | 12:00 AM - 1:30 AM UTC | A10 TOKYO BAY MAKUHARI HALL

## [S-GL27] Geochronology and Isotope Geology

convener:Takahiro Tagami(Graduate School of Science, Kyoto University), Yuji Sano(Division of Ocean and Earth Systems, Atmosphere and Ocean Research Institute, University of Tokyo), Chairperson:Takahiro Tagami, Yuji Sano

9:00 AM - 9:30 AM JST | 12:00 AM - 12:30 AM UTC

### [SGL27-01] Terrestrial cosmogenic nuclides as a dating tool of landforms and near-surface materials: applicability and limitations

★Invited Papers

*Yuki Matsushi[1] (1.Disaster Prevention Research Institute, Kyoto University)

---

9:30 AM - 9:45 AM JST | 12:30 AM - 12:45 AM UTC

### [SGL27-02] Dating of marine erosional terraces using cosmogenic nuclides: A case study of the Hyuga City, Miyazaki Prefecture, southwest Japan (preliminary results)

*Shigeru Sueoka[1], Tetsuya Komatsu[1], Yuki Matsushi[2], Yusuke Yonaga[1], Naomi Sano[1], Noriaki Hirao[1], Tadamasa Ueki[1], Natsuko Fujita[1], Yoko Kokubu[1], Masakazu Niwa[1] (1.Japan Atomic Energy Agency, 2.Disaster Prevention Research Institute, Kyoto University)

---

9:45 AM - 10:00 AM JST | 12:45 AM - 1:00 AM UTC

### [SGL27-03] Estimation of thermal history of Toki granite over 0.1Myr timescale by Multi-OSL-thermochronometry

*Manabu Ogata[1], Georgina E King[2], Frédéric Herman[2], Shigeru Sueoka[1] (1.Tono Geoscience Center, Japan Atomic Energy Agency, 2.University of Lausanne)

---

10:00 AM - 10:15 AM JST | 1:00 AM - 1:15 AM UTC

### [SGL27-04] Depth condition under which OSL signal of quartz gouge experiences coseismic zeroing

*Yuki Minomo[1], Kiyokazu Oohashi[1], Noriko Hasebe[2], Kazumasa Miura[3] (1.Graduate School of science and Technology for Innovation, Yamaguchi University , 2.Institute of Nature and Environmental Technology, Kanazawa University, 3.Kanazawa University)

---

10:15 AM - 10:30 AM JST | 1:15 AM - 1:30 AM UTC

### [SGL27-05] Result of age determination of samples from Hokuriku Group

*Noriko Hasebe[1], Ryo Kamiguchi[2] (1.Institute of Nature and Environmental Technology, Kanazawa University, 2.Department of Earth Sciences, Kanazawa University)

[J] Oral | S (Solid Earth Sciences)：S-GL Geology

10:45 AM - 12:15 PM JST | 1:45 AM - 3:15 AM UTC | A10 TOKYO BAY MAKUHARI HALL

## [S-GL27] Geochronology and Isotope Geology

convener:Takahiro Tagami(Graduate School of Science, Kyoto University), Yuji Sano(Division of Ocean and Earth Systems, Atmosphere and Ocean Research Institute, University of Tokyo), Chairperson:Yuji Sano, Takahiro Tagami

10:45 AM - 11:15 AM JST | 1:45 AM - 2:15 AM UTC

[SGL27-06] **Geochemical origin/cycle analysis with isotopologues and isotopomers**

★Invited Papers

*Naohiro Yoshida[1] (1.Department of Chemical Science and Engineering, Earth-Life Science Institute, Tokyo Institute of Technology)

---

11:15 AM - 11:30 AM JST | 2:15 AM - 2:30 AM UTC

[SGL27-07] Estimation of Paleoenvironment by sedimentary rocks in Labrador, Cacada

*katsutaka sudo[1], Yuji Sano[1], Tsuyoshi Komiya[1], Bakert David[2], Michael Broadley[2], Bernard Marty[2] (1.University of Tokyo, 2.CRPG-CNRS, Université de Lorraine)

---

11:30 AM - 11:45 AM JST | 2:30 AM - 2:45 AM UTC

[SGL27-08] Hf-W dating of zircons from mesosiderites with high-pressure sintered sample

*Yuta Koyama[1], Naoto Takahata[1], Yuji Sano[1], Naoji Sugiura[1], Mizuho Koike[2], Makiko K. Haba[3], Sakata Shuhei[4], Hideharu Kuwahara[5], Tetsuo Irifune[5] (1.the University of Tokyo, 2.Japan Aerospace Exploration Agency, 3.Tokyo Institute of Technology, 4.Gakushuin University, 5.Geodynamics Research Center, Ehime University)

---

11:45 AM - 12:15 PM JST | 2:45 AM - 3:15 AM UTC

[SGL27-09] Radiometric ages *vs.* astrophysical ages -with regard to the numerical age in the International Stratigraphic Chart

★Invited Papers

*Ichiro Kaneoka[1] (1.Earthquake Research Institute, University of Tokyo)

[J] Poster | S (Solid Earth Sciences )：S-GL Geology

3:30 PM - 5:00 PM JST | 6:30 AM - 8:00 AM UTC | Poster Hall International Exhibition Hall8, Makuhari Messe_11

## [S-GL27] Geochronology and Isotope Geology

convener:Takahiro Tagami(Graduate School of Science, Kyoto University), Yuji Sano(Division of Ocean and Earth Systems, Atmosphere and Ocean Research Institute, University of Tokyo)

[SGL27-P01] Research report on long-term stability of geological environments and LA-ICP-MS-based age dating

★Invited Papers

*Tatsunori Yokoyama[1], Takehiro Mitsucuchi[1], Shigeru Sueoka[1] (1.Japan Atomic Energy Agency)

---

[SGL27-P02] **U-Pb detrital zircon age dating from the Aileu Formation of Timor-Leste; Estimate depositional age and provenance of the sediment**

*Jovita Elisa Fatima da Costa[1], Shoichi Kiyokawa[1], Yukiyasu Tsutsumi[2] (1.Kyushu University, 2.National Museum of Nature and Science)

---

[SGL27-P03] Petrological, geochemical, and geochronological characteristics of the Oritate travertine from Unazuki area, Toyama, Japan: possibility of U-Pb geochronology of carbonates with high common Pb.

*Mayuko Fukuyama[1], Masatsugu Ogasawara[2] (1.Graduate School of Engineering Science, Akita University, 2.Geological Survey of Japan, National Institute of Advanced Industrial Science and Technology)

---

[SGL27-P04] Zircon U-Pb age and tectonics of shirakamidake granitic complex

*Hiroki Sato[1], Koji Umeda[1] (1.Hirosaki University)

---

[SGL27-P05] Zircon U-Pb dating of plutonic rocks from Yamizo Area, northeast Japan

*Terumi Ejima[1,2], Yoshiaki Kon[2], Daisuke Araoka[2], Shigenori Kawano[3], Yutaka Takahashi[2] (1.Shinshu University, 2.Geological Survey of Japan, 3.Tochigi Prefectural Museum)

---

[SGL27-P06] Denudation history of the Higher Himalayan Crystallines in West-Central Nepal: insights from zircon fission-track dating and thermokinematic modeling

*Nakajima Toru[1], Harutaka Sakai[1], Hideki Iwano[2], Tohru Danhara[2], Takafumi Hirata[3] (1.Division of Earth and Planetary Sciences, Graduate School of Science, Kyoto University, 2.Kyoto Fission-Track Co., Ltd., 3. Geochemical Research Center, The University of Tokyo)

---

[SGL27-P07] Thermochronology on the fore-arc side of Northeast Japan Arc

*Yuya Kajita[1], Shigeru Sueoka[2], Shoma Fukuda[1], Noriko Hasebe[3], Akihiro Tomoaki[4], Tomoaki Morishita[4], Barry P. Kohn[5], Tatsunori Yokoyama[2], Takahiro Tagami[1] (1.Graduate School of Science, Kyoto University , 2.Japan Atomic Energy Agency, 3.Institute of Nature and Environmental Technology, Kanazawa University, 4.Department of Sciences, Kanazawa University, 5.School of Earth Sciences, University of Melbourne)

---

[SGL27-P08] Argon diffusion in rocks - classical approach in view of heating and relaxation

Horst Zwingmann[1], *Hironobu Hyodo[2] (1.KUEPS, Kyoto University, 2.Research Institute of Natural Sciences, Okayama University of Science)

---

[SGL27-P09] $^{4}$He/U-Th dating of pore waters from Quaternary sediments in Switzerland: potential and challenges

*Yama Tomonaga[1], Edith Horstmann[1], Gaudenz Deplazes[2], Rolf Kipfer[1] (1.Swiss Federal Institute of Aquatic Science and Technology (Eawag), 2.National Cooperative for the Disposal of Radioactive Waste (Nagra))

---

[SGL27-P10] Compound-specific radiocarbon analysis of lipid biomarkers in surface sediment from Lake Kawaguchi, central Japan

*Shinya Yamamoto[1], Yosuke Miyairi[2], Yusuke Yokoyama[2], Hisami Suga[3], Nanako O. Ogawa[3], Naohiko Ohkouchi[3] (1.Mount Fuji Research Institute, Yamanashi Prefectural Government, 2.Atmosphere and Ocean Research Institute, The University of Tokyo, 3.Japan Agency for Marine-Earth Science and Technology)

---

[SGL27-P11] Reestablishment of the Mesozoic and Cenozoic Stratigraphic Events of the Fergana Basin, Uzbekistan

*OTABEK ULUGBEK OGLI ANVAROV[1], Ken-ichiro Hisada[1], Teruyuki Maruoka[1], Junichiro Kuroda[2], Sherzod Makhmudov[3] (1.UNIVERSITY OF TSUKUBA, 2.Atmosphere and Ocean Research Institute, the University of Tokyo , 3.State Comittee of Geology and Mineral Resources of Uzbekistan)

[J] Poster | S (Solid Earth Sciences )：S-GL Geology

5:15 PM - 6:30 PM JST | 8:15 AM - 9:30 AM UTC | Poster Hall International Exhibition Hall8, Makuhari Messe_22

## [S-GL27] Geochronology and Isotope Geology

convener:Takahiro Tagami(Graduate School of Science, Kyoto University), Yuji Sano(Division of Ocean and Earth Systems, Atmosphere and Ocean Research Institute, University of Tokyo)

### [SGL27-P01] Research report on long-term stability of geological environments and LA-ICP-MS-based age dating

★Invited Papers

*Tatsunori Yokoyama[1], Takehiro Mitsucuchi[1], Shigeru Sueoka[1] (1.Japan Atomic Energy Agency)

### [SGL27-P02] U-Pb detrital zircon age dating from the Aileu Formation of Timor-Leste; Estimate depositional age and provenance of the sediment

*Jovita Elisa Fatima da Costa[1], Shoichi Kiyokawa[1], Yukiyasu Tsutsumi[2] (1.Kyushu University, 2.National Museum of Nature and Science)

### [SGL27-P03] Petrological, geochemical, and geochronological characteristics of the Oritate travertine from Unazuki area, Toyama, Japan: possibility of U-Pb geochronology of carbonates with high common Pb.

*Mayuko Fukuyama[1], Masatsugu Ogasawara[2] (1.Graduate School of Engineering Science, Akita University, 2.Geological Survey of Japan, National Institute of Advanced Industrial Science and Technology)

### [SGL27-P04] Zircon U-Pb age and tectonics of shirakamidake granitic complex

*Hiroki Sato[1], Koji Umeda[1] (1.Hirosaki University)

### [SGL27-P05] Zircon U-Pb dating of plutonic rocks from Yamizo Area, northeast Japan

*Terumi Ejima[1,2], Yoshiaki Kon[2], Daisuke Araoka[2], Shigenori Kawano[3], Yutaka Takahashi[2] (1.Shinshu University, 2.Geological Survey of Japan, 3.Tochigi Prefectural Museum)

### [SGL27-P06] Denudation history of the Higher Himalayan Crystallines in West-Central Nepal: insights from zircon fission-track dating and thermokinematic modeling

*Nakajima Toru[1], Harutaka Sakai[1], Hideki Iwano[2], Tohru Danhara[2], Takafumi Hirata[3] (1.Division of Earth and Planetary Sciences, Graduate School of Science, Kyoto University, 2.Kyoto Fission-Track Co., Ltd., 3. Geochemical Research Center, The University of Tokyo)

### [SGL27-P07] Thermochronology on the fore-arc side of Northeast Japan Arc

*Yuya Kajita[1], Shigeru Sueoka[2], Shoma Fukuda[1], Noriko Hasebe[3], Akihiro Tomoaki[4], Tomoaki Morishita[4], Barry P. Kohn[5], Tatsunori Yokoyama[2], Takahiro Tagami[1] (1.Graduate School of Science, Kyoto University , 2.Japan Atomic Energy Agency, 3.Institute of Nature and Environmental Technology, Kanazawa University, 4.Department of Sciences, Kanazawa University, 5.School of Earth Sciences, University of Melbourne)

### [SGL27-P08] Argon diffusion in rocks - classical approach in view of heating and relaxation

Horst Zwingmann[1], *Hironobu Hyodo[2] (1.KUEPS, Kyoto University, 2.Research Institute of Natural Sciences, Okayama University of Science)

### [SGL27-P09] $^{4}$He/U-Th dating of pore waters from Quaternary sediments in Switzerland: potential and challenges

*Yama Tomonaga[1], Edith Horstmann[1], Gaudenz Deplazes[2], Rolf Kipfer[1] (1.Swiss Federal Institute of Aquatic Science and Technology (Eawag), 2.National Cooperative for the Disposal of Radioactive Waste (Nagra))

### [SGL27-P10] Compound-specific radiocarbon analysis of lipid biomarkers in surface sediment from Lake Kawaguchi, central Japan

*Shinya Yamamoto[1], Yosuke Miyairi[2], Yusuke Yokoyama[2], Hisami Suga[3], Nanako O. Ogawa[3], Naohiko Ohkouchi[3] (1.Mount Fuji Research Institute, Yamanashi Prefectural Government, 2.Atmosphere and Ocean Research Institute, The University of Tokyo, 3.Japan Agency for Marine-Earth Science and Technology)

[J] Oral | S (Solid Earth Sciences )：S-MP Mineralogy & Petrology

9:00 AM - 10:30 AM JST | 12:00 AM - 1:30 AM UTC | 301B 3F

## [S-MP32] Deformed rocks, Metamorphic rocks and Tectonics

convener:Yumiko Harigane(Geological Survey of Japan, National Institute of Advanced Industrial Science and Technology (AIST)), Yoshihiro Nakamura(Geological Survey of Japan, National Institute of Advanced Industrial Science and Technology), Chairperson:Yoshihiro Nakamura(産総研), Yumiko Harigane(産総研)

9:00 AM - 9:15 AM JST | 12:00 AM - 12:15 AM UTC

[SMP32-19] Thermal interaction of the lithosphere and asthenosphere revealed from internal variations of pressure-temperature history in orogenic peridotite complexes

*Kazuhito Ozawa[1], Carlos J. Garrido[2], Karoly Hidas[2], Jean-Louis Bodinier[3] (1.Department of Earth and Planetary Science, Graduate School of Science, University of Tokyo, 2.Instituto Andaluz de Ciencias de la Tierra (IACT), CSIC – UGR, Armilla, Granada, Spain, 3.Geosciences Montpellier, Montpellier, France)

9:15 AM - 9:30 AM JST | 12:15 AM - 12:30 AM UTC

[SMP32-20] **Hydration and Ca-metasomatism in Mantle Wedge: An evidence from the Alag Khadny Accretionary Wedge, Western Mongolia**

*OTGONBAYAR DANDAR[1], Atsushi Okamoto[1], Masaoki Uno[1], Noriyoshi Tsuchiya[1] (1.Graduate School of Environmental Studies, Tohoku University)

9:30 AM - 9:45 AM JST | 12:30 AM - 12:45 AM UTC

[SMP32-21] **Attenuated Total Reflection Infrared (ATR-IR) Spectroscopy of Antigorite, Chrysotile and Lizardite**

*Ilona Talvikki Sakaguchi[1] (1.Nagoya University)

9:45 AM - 10:00 AM JST | 12:45 AM - 1:00 AM UTC

[SMP32-22] Fabric and petrological characteristics of sheared peridotites in Marion transform fault, Southwest Indian Ridge

*Kakihata Yuki[1], Katsuyoshi Michibayashi[2], Henry Dick[3] (1.Shizuoka University Graduate School of Science, 2.Nagoya University Graduate School of Environmental Studies, 3.Woods Hole Oceanographic Institution)

10:00 AM - 10:15 AM JST | 1:00 AM - 1:15 AM UTC

[SMP32-23] Structure and formation mechanism of lithosphere-asthenosphere boundary decoded from Ichinomegata peridotite xenoliths

*Yuto Sato[1], Kazuhito Ozawa[1] (1.Department of Earth and Planetary Science, Graduate School of Science, The University of Tokyo)

10:15 AM - 10:30 AM JST | 1:15 AM - 1:30 AM UTC

[SMP32-24] Metasomatic banding and deformation instability in the metamorphic rocks

*mitsuhiro toriumi[1] (1.Japan agency of marine science and technology)

[E] Oral | S (Solid Earth Sciences)：S-VC Volcanology

9:00 AM - 10:30 AM JST | 12:00 AM - 1:30 AM UTC | A07 TOKYO BAY MAKUHARI HALL

## [S-VC34] Connecting magma dynamics in vent-conduit system with surface expression of volcanic eruption

convener:Takahiro Miwa(National research institute for earth science and disaster prevention), Nobuo Geshi(Geological Survey of Japan, The National Institute of Advanced Industrial Science and Technology), Chairperson:Takahiro Miwa, Jacopo Taddeucci

9:00 AM - 9:15 AM JST | 12:00 AM - 12:15 AM UTC

[SVC34-01] An experimental basis for estimating particle properties following volcanic ash emissions

★Invited Papers

*Adrian Hornby[1], Ulrich Kueppers[1], Hanna Horsch[2], Paul Ayris[1], Nick Varley[3], Daniele Andronico[4], Boris Behncke[4], Yan Lavallée[5], Jackie E Kendrick[5], James Utley[5], Amy Hughes[5], David Damby[6], Benedikt Maurer[1], Marlin Juchem[1], Donald B Dingwell[1] (1.Ludwig-Maximilians-Universität München, DE, 2.Hazen Research, Golden, USA, 3.University of Colima, MX, 4.INGV Catania, IT, 5.University of Liverpool, UK, 6.USGS Cascades Volcano Observatory, USA)

9:15 AM - 9:30 AM JST | 12:15 AM - 12:30 AM UTC

[SVC34-02] **Vapor transport in shallow intruded magmas: insights from diktytaxitic texture**

*Ryosuke Sakurai[1], Michihiko Nakamura[2], Satoshi Okumura[2], Mayumi Mujin[2], Takayuki Nakatani[2] (1.Division of Earth and Planetary Materials Science, Faculty of Science, Tohoku University, 2.Division of Earth and Planetary Materials Science, Department of Earth Science, Graduate School of Science, Tohoku University)

9:30 AM - 9:45 AM JST | 12:30 AM - 12:45 AM UTC

[SVC34-03] First observation of nanolites and ultrananolites in alkaline volcanic glasses (Eifel, Germany)

*Marija Putak Juricek[1], Michihiko Nakamura[2], Mayumi Mujin[2], Hans-Ulrich Schmincke[3], Mari Sumita[3], Nobuyoshi Miyajima[1] (1.BGI, 2.Tohoku Univ., 3.GEOMAR)

9:45 AM - 10:00 AM JST | 12:45 AM - 1:00 AM UTC

[SVC34-04] Textural Study of Pumice Clasts from The Youngest Toba Tuff Eruption

*Gabriela Nogo Retnaningtyas Bunga Naen[1], Atsushi Toramaru[1], Tomoharu Miyamoto[1], Haryo Edi Wibowo[2] (1.Department Earth and Planetary Sciences, Graduate School of Sciences, Kyushu University, Nishiku, 744, Motooka, Fukuoka, 819-0395, Japan, 2.Geological Engineering Department, Universitas Gadjah Mada, 55284, Yogyakarta, Indonesia)

10:00 AM - 10:15 AM JST | 1:00 AM - 1:15 AM UTC

[SVC34-05] **Oomurodashi volcano: Past effusive and phreatomagmatic activity revealed by submarine and subaerial deposits**

*Iona McIntosh[1], Kenichiro Tani[2], Alexander Nichols[3], Qing Chang[1], Jun-Ichi Kimura[1] (1.Japan Agency for Marine-Earth Science and Technology, Yokosuka, 2.National Museum of Nature and Science, Tsukuba, 3.University of Canterbury, Christchurch, New Zealand)

10:15 AM - 10:30 AM JST | 1:15 AM - 1:30 AM UTC

[SVC34-06] Mechanism of volatile transport from mafic to silicic magma upon mixing

*Shumpei Yoshimura[1], Akiko Matsumoto[1], Mitsuhiro Nakagawa[1] (1.Department of Earth and Planetary Sciences, Hokkaido University)

[E] Oral | S (Solid Earth Sciences)：S-VC Volcanology

10:45 AM - 12:15 PM JST | 1:45 AM - 3:15 AM UTC | A07 TOKYO BAY MAKUHARI HALL

## [S-VC34] Connecting magma dynamics in vent-conduit system with surface expression of volcanic eruption

convener:Takahiro Miwa(National research institute for earth science and disaster prevention), Nobuo Geshi(Geological Survey of Japan, The National Institute of Advanced Industrial Science and Technology), Chairperson:Nobuo Geshi(GSJ/AIST), Adrian Hornby(Ludwig-Maximilians-University Munich)

10:45 AM - 11:00 AM JST | 1:45 AM - 2:00 AM UTC

[SVC34-07] The in-flight grain size distribution of lapilli and bombs from Strombolian explosions

*Jacopo Taddeucci[1], Piergiorgio Scarlato[1], Elisabetta Del Bello[1], Tullio Ricci[1], Ulrich Kueppers[2], Bruce Houghton[3] (1.Istituto Nazionale di Geofisica e Vulcanologia, Rome, Italy, 2.Department of Earth and Environmental Sciences. Ludwig-Maximilians-Universität (LMU). Munich, Germany, 3.Department of Earth Sciences, University of Hawai‘i at Mānoa, Honolulu, USA)

11:00 AM - 11:15 AM JST | 2:00 AM - 2:15 AM UTC

[SVC34-08] **Pyrrotite oxidation as a proxy for air entrainment in eruption columns**

*Keiko Matsumoto[1], Michihiko Nakamura[2] (1.Geological Survey of Japan, The National Institute of Advanced Industrial Science and Technology, 2.Faculty of Science, Tohoku University)

11:15 AM - 11:30 AM JST | 2:15 AM - 2:30 AM UTC

[SVC34-09] **Thermal signals in volcano monitoring: combining MODIS-MIROVA data with ground-based measurements at Aso Volcano, Japan**

*Corrado CIGOLINI[1], Akihiko Yokoo[2], Diego Coppola[1], Marco Laiolo[1] (1.Department of Earth Sciences, University of Torino, Italy, 2.Aso Volcanological Laboratory, Institute for Geothermal Sciences, Kyoto University, Japan)

11:30 AM - 11:45 AM JST | 2:30 AM - 2:45 AM UTC

[SVC34-10] Magma transfer processes in the NE Japan arc: insights from crustal ambient noise tomography combined with volcanic eruption records

*Georg F Zellmer[1], Kai-Xun Chen[2], Yuancheng Gung[2], Ban-Yuan Kuo[3], Takeyoshi Yoshida[4] (1.Massey University, Palmerston North, New Zealand, 2.National Taiwan University, Taipei, Taiwan, 3.Academia Sinica, Taipei, Taiwan, 4.Tohoku University, Sendai, Japan)

11:45 AM - 12:00 PM JST | 2:45 AM - 3:00 AM UTC

[SVC34-11] **STRATIGRAPHY RENEWAL, MAGMA CHAMBER STRATIFICATION, AND CONDUIT PROCESS OF THE 1815 TAMBORA CALDERA FORMING ERUPTION**

*Indranova Suhendro[1], Atsushi Toramaru[1], Yasuo Miyabuchi[2], Tomoharu Miyamoto[1] (1.Department of Earth and Planetary Sciences, Graduate School of Sciences, Kyushu University, Japan, 2.Faculty of Advanced Science and Technology, Kumamoto University, Kurokami 2-40-1, Chuo-ku, Kumamoto 860-8555, Japan)

[E] Poster | S (Solid Earth Sciences)：S-VC Volcanology

3:30 PM - 5:00 PM JST | 6:30 AM - 8:00 AM UTC | Poster Hall International Exhibition Hall8, Makuhari Messe_12

## [S-VC34] Connecting magma dynamics in vent-conduit system with surface expression of volcanic eruption

convener:Takahiro Miwa(National research institute for earth science and disaster prevention), Nobuo Geshi(Geological Survey of Japan, The National Institute of Advanced Industrial Science and Technology)

[SVC34-P01] A new formulation of viscosity-included bubble nucleation rate in ascending magmas and re-estimation of bubble number density (2)

*Mizuki Nishiwaki[1], Atsushi Toramaru[2] (1.Department of Earth and Planetary Sciences, Graduate School of Sciences, Kyushu University, 2.Department of Earth and Planetary Sciences, Faculty of Sciences, Kyushu University)

[SVC34-P02] Kinetic delay of crystal growth controls plagioclase-basaltic melt apparent disequilibrium

*Ryoya Oida[1], Hidemi Ishibashi[1], ATSUSHI YASUDA[2], Natsumi Hokanishi[2] (1.Faculty of Science, Shizuoka University, 2.Earthquake Research Institute, University of Tokyo)

[SVC34-P03] **Eruptive trends and dynamics of remote volcanoes detected form space-based thermal data and $SO_2$ emissions: a comparative analysis of Stromboli, Batu Tara and Tinakula volcanoes**

*Corrado CIGOLINI[1], Marco Laiolo[1], Francesco Massimetti[1,2], Maurizio Ripepe[2], Diego Coppola[1] (1.Department of Earth Sciences, University of Torino, Italy, 2.Department of Earth Sciences, University of Firenze, Italy)

[SVC34-P04] The source depth of Strombolian explosions: a multiparametric approach and comparison

*Jacopo Taddeucci[1], Miguel Angel Alatorre-Ibarguengoitia[2], Valeria Cigala[3], Elisabetta Del Bello[1], Damien Gaudin[4], Ulrich Kueppers[4], Tullio Ricci[1], Valentino Salvatore[5], Piergiorgio Scarlato[1] (1.Istituto Nazionale di Geofisica e Vulcanologia, Rome, Italy, 2.Centro de Investigación en Gestión de Riesgo y Cambio Climático, Universidad de Ciencias y Artes de Chiapas, Tuxtla Gutiérrez, Mexico, 3.Department of Geosciences, Università degli Studi di Padova, Padua, Italy, 4.Department of Earth and Environmental Sciences. Ludwig-Maximilians-Universität (LMU). Munich, Germany, 5.Dipartimento di Scienze della Terra, Sapienza Università di Roma, Rome, Italy)

[SVC34-P05] Magmatic aggregate of basaltic ash particles

*Takahiro Miwa[1], Nobuo Geshi[2] (1.National research institute for earth science and disaster prevention, 2.National Institute of Advanced Industrial Science and Technology)

[SVC34-P06] Melt inclusion study on the eruption process of Izu-Omuroyama monogenetic volcano, Japan

Risako Hatada[1], *Hidemi Ishibashi[1], Yusuke Suzuki[2], ATSUSHI YASUDA[3], Natsumi Hokanishi[3] (1.Faculty of Science, Shizuoka University, 2.Izu Peninsula Geopark, 3.Earthquake Research Institute, University of Tokyo)

[SVC34-P07] Time-series variation in the textures of ejecta of the An'ei eruption, Izu-Oshima

*Yuya Ikenaga[1], Fukashi Maeno[1], ATSUSHI YASUDA[1] (1.Earthquake Research Institute, The University of Tokyo)

[SVC34-P08] The textural analysis of pumice from the Plinian eruption of Taupo volcano: implications for tube pumice

*Masatoshi Ohashi[1], Mie Ichihara[2], Fukashi Maeno[2], Ben Kennedy[3], Darren Gravley[3] (1.Department of Earth and Planetary Science, Graduate School of Science, The University of Tokyo, 2.Earthquake Research Institute, The University of Tokyo, 3.Department of Geological Sciences, The University of Canterbury)

[E] Poster | S (Solid Earth Sciences)：S-VC Volcanology

5:15 PM - 6:30 PM JST | 8:15 AM - 9:30 AM UTC | Poster Hall International Exhibition Hall8, Makuhari Messe_23

## [S-VC34] Connecting magma dynamics in vent-conduit system with surface expression of volcanic eruption

convener:Takahiro Miwa(National research institute for earth science and disaster prevention), Nobuo Geshi(Geological Survey of Japan, The National Institute of Advanced Industrial Science and Technology)

[SVC34-P01] A new formulation of viscosity-included bubble nucleation rate in ascending magmas and re-estimation of bubble number density (2)

*Mizuki Nishiwaki[1], Atsushi Toramaru[2] (1.Department of Earth and Planetary Sciences, Graduate School of Sciences, Kyushu University, 2.Department of Earth and Planetary Sciences, Faculty of Sciences, Kyushu University)

[SVC34-P02] Kinetic delay of crystal growth controls plagioclase-basaltic melt apparent disequilibrium

*Ryoya Oida[1], Hidemi Ishibashi[1], ATSUSHI YASUDA[2], Natsumi Hokanishi[2] (1.Faculty of Science, Shizuoka University, 2.Earthquake Research Institute, University of Tokyo)

[SVC34-P03] **Eruptive trends and dynamics of remote volcanoes detected form space-based thermal data and $SO_2$ emissions: a comparative analysis of Stromboli, Batu Tara and Tinakula volcanoes**

*Corrado CIGOLINI[1], Marco Laiolo[1], Francesco Massimetti[1,2], Maurizio Ripepe[2], Diego Coppola[1] (1.Department of Earth Sciences, University of Torino, Italy, 2.Department of Earth Sciences, University of Firenze, Italy)

[SVC34-P04] The source depth of Strombolian explosions: a multiparametric approach and comparison

*Jacopo Taddeucci[1], Miguel Angel Alatorre-Ibarguengoitia[2], Valeria Cigala[3], Elisabetta Del Bello[1], Damien Gaudin[4], Ulrich Kueppers[4], Tullio Ricci[1], Valentino Salvatore[5], Piergiorgio Scarlato[1] (1.Istituto Nazionale di Geofisica e Vulcanologia, Rome, Italy, 2.Centro de Investigación en Gestión de Riesgo y Cambio Climático, Universidad de Ciencias y Artes de Chiapas, Tuxtla Gutiérrez, Mexico, 3.Department of Geosciences, Università degli Studi di Padova, Padua, Italy, 4.Department of Earth and Environmental Sciences. Ludwig-Maximilians-Universität (LMU). Munich, Germany, 5.Dipartimento di Scienze della Terra, Sapienza Università di Roma, Rome, Italy)

[SVC34-P05] Magmatic aggregate of basaltic ash particles

*Takahiro Miwa[1], Nobuo Geshi[2] (1.National research institute for earth science and disaster prevention, 2.National Institute of Advanced Industrial Science and Technology)

[SVC34-P06] Melt inclusion study on the eruption process of Izu-Omuroyama monogenetic volcano, Japan

Risako Hatada[1], *Hidemi Ishibashi[1], Yusuke Suzuki[2], ATSUSHI YASUDA[3], Natsumi Hokanishi[3] (1.Faculty of Science, Shizuoka University, 2.Izu Peninsula Geopark, 3.Earthquake Research Institute, University of Tokyo)

[SVC34-P07] Time-series variation in the textures of ejecta of the An'ei eruption, Izu-Oshima

*Yuya Ikenaga[1], Fukashi Maeno[1], ATSUSHI YASUDA[1] (1.Earthquake Research Institute, The University of Tokyo)

[SVC34-P08] The textural analysis of pumice from the Plinian eruption of Taupo volcano: implications for tube pumice

*Masatoshi Ohashi[1], Mie Ichihara[2], Fukashi Maeno[2], Ben Kennedy[3], Darren Gravley[3] (1.Department of Earth and Planetary Science, Graduate School of Science, The University of Tokyo, 2.Earthquake Research Institute, The University of Tokyo, 3.Department of Geological Sciences, The University of Canterbury)

[J] Poster | S (Solid Earth Sciences )：S-VC Volcanology

10:45 AM - 12:15 PM JST | 1:45 AM - 3:15 AM UTC | Poster Hall International Exhibition Hall8, Makuhari Messe_5

## [S-VC37] Dynamics of volcanic eruptions and their physical and chemical processes

convener:Yujiro Suzuki(Earthquake Research Institute, The University of Tokyo)

[SVC37-P01] **Geochemical interpretation of Ulleung Island volcanic rocks: Implication for the new magmatic model for plume-slab interaction in East Asia**

*Chungwan LIM[1], Dohyun Kim[1] (1.Kongju National University)

[SVC37-P02] 1D particle model for vertiacal non-uniform bubble coalescence

*Maruishi Takafumi[1] (1.Department of Earth and Planetary Sciences, Faculty of Sciences, Kyushu University)

[SVC37-P03] The formation process of a 100m thick basaltic lava flow in the Kitamatsuura basalts, northwestern Kyushu

*Ryotaro Araki[1], Tetsuya Sakuyama[1] (1.Osaka City University)

[SVC37-P04] An introduction to the observation method of imaging volcanoes by using cosmic-ray muons

*Seigo Miyamoto[1] (1.Earth Reasearch Institute, University of Tokyo)

[SVC37-P05] Simulation and test observation for omni-directional muography at Omuro-yama

*Shogo Nagahara[1], Seigo Miyamoto[1], Kunihiro Morishima[2], Toshiyuki Nakano[2], Masato Koyama[3], Yusuke Suzuki[4] (1.Earthquake Research Institute,the University of Tokyo, 2.Nagoya University, 3.Shizuoka University, 4.Izu Peninsula Geopark Promotion Council)

[SVC37-P06] Estimation of pressure source occurring volcanic crustal deformation with FEM considering topography

*Shinya Yamada[1], Tomokazu Kobayashi[1] (1.GSI of Japan)

[J] Poster | S (Solid Earth Sciences )：S-VC Volcanology

5:15 PM - 6:30 PM JST | 8:15 AM - 9:30 AM UTC | Poster Hall International Exhibition Hall8, Makuhari Messe_24

## [S-VC37] Dynamics of volcanic eruptions and their physical and chemical processes

convener:Yujiro Suzuki(Earthquake Research Institute, The University of Tokyo)

[SVC37-P01] **Geochemical interpretation of Ulleung Island volcanic rocks: Implication for the new magmatic model for plume-slab interaction in East Asia**

*Chungwan LIM[1], Dohyun Kim[1] (1.Kongju National University)

[SVC37-P02] 1D particle model for vertiacal non-uniform bubble coalescence

*Maruishi Takafumi[1] (1.Department of Earth and Planetary Sciences, Faculty of Sciences, Kyushu University)

[SVC37-P03] The formation process of a 100m thick basaltic lava flow in the Kitamatsuura basalts, northwestern Kyushu

*Ryotaro Araki[1], Tetsuya Sakuyama[1] (1.Osaka City University)

[SVC37-P04] An introduction to the observation method of imaging volcanoes by using cosmic-ray muons

*Seigo Miyamoto[1] (1.Earth Reasearch Institute, University of Tokyo)

[SVC37-P05] Simulation and test observation for omni-directional muography at Omuro-yama

*Shogo Nagahara[1], Seigo Miyamoto[1], Kunihiro Morishima[2], Toshiyuki Nakano[2], Masato Koyama[3], Yusuke Suzuki[4] (1.Earthquake Research Institute,the University of Tokyo, 2.Nagoya University, 3.Shizuoka University, 4.Izu Peninsula Geopark Promotion Council)

[SVC37-P06] Estimation of pressure source occurring volcanic crustal deformation with FEM considering topography

*Shinya Yamada[1], Tomokazu Kobayashi[1] (1.GSI of Japan)

[J] Oral | S (Solid Earth Sciences )：S-VC Volcanology

1:45 PM - 3:15 PM JST | 4:45 AM - 6:15 AM UTC | A07 TOKYO BAY MAKUHARI HALL

## [S-VC37] Dynamics of volcanic eruptions and their physical and chemical processes

convener:Yujiro Suzuki(Earthquake Research Institute, The University of Tokyo), Chairperson:Yujiro Suzuki(Earthquake Research Institute, The University of Tokyo), Hiroyuki Shimizu(Earthquake Research Institute, The University of Tokyo)

1:45 PM - 2:00 PM JST | 4:45 AM - 5:00 AM UTC

[SVC37-01] Volcanic activities triggered or inhibited by resonance of volcanic edifices to large earthquakes

*Atsuko Namiki[1], Eleonora Rivalta[2], Heiko Woith[2], Timothy Willey[2], Stefano Parolai[3], Thomas R Walter[2] (1.Graduate School of Integrated Arts and Sciences, Hiroshima University, 2.GFZ, 3.OGS)

2:00 PM - 2:15 PM JST | 5:00 AM - 5:15 AM UTC

[SVC37-02] **Groundmass crystallization experiments of an andesitic pumice under low vapor pressure.**

*Yasukawa Hiroki[1], Mayumi Mujin[1], Michihiko Nakamura[1], Shizuka Otsuki[2] (1.Division of Earth and Planetary Materials Science, Department of Earth Science, Graduate School of Science, Tohoku University., 2.National Institute of Advanced Industrial Science and Technology)

2:15 PM - 2:30 PM JST | 5:15 AM - 5:30 AM UTC

[SVC37-03] Decoding pre-eruptive magma evolution and water behavior from plagioclase phenocrysts: Application to the Hoei eruption of Mt. Fuji

*Tsuyoshi Iizuka[1], Chiyo Harada[1], Kenji Shimizu[2], Takayuki Ushikubo[2], Morihisa Hamada[2], Mitsuhiro Yoshimoto[3] (1.University of Tokyo, 2.JAMSTEC, 3.Mount Fuji Research Institute)

2:30 PM - 2:45 PM JST | 5:30 AM - 5:45 AM UTC

[SVC37-04] Probing magmatic processes just prior to historic eruptions at Sakurajima volcano: Toward understanding “magma pre-charge”

*Naoki Araya[1], Michihiko Nakamura[1], Satoshi Okumura[1] (1.Division of Earth and Planetary Materials Science, Department of Earth Science, Graduate School of Science, Tohoku UniversityUniversity)

2:45 PM - 3:00 PM JST | 5:45 AM - 6:00 AM UTC

[SVC37-05] Magmatic processes prior to the Vulcanian eruptions of Sakurajima volcano: A combined petrologic and geophysical approach

*Sakauchi Nono[2], Michihiko Nakamura[2], ATSUSHI YASUDA[1], Satoshi Okumura[2], Naoki Araya[2], Masato Iguchi[3], Daisuke Miki[3], Nobuo Geshi[4] (1.Earthquake Research Institute, University of Tokyo, 2.Division of Earth and Planetary Materials Science, Department of Earth Science, Graduate School of Science, Tohoku University, 3.Sakurajima Volcano Research Center, Disaster Prevention Research Institute, Kyoto University, 4.Geological Survey of Japan, The National Institute of Advanced Industrial Science and Technology)

3:00 PM - 3:15 PM JST | 6:00 AM - 6:15 AM UTC

[SVC37-06] Cyclic degassing behavior accompanying dome-forming lava effusion at Shinmoedake volcano in the 2018 eruption

★Invited Papers

*Taishi Yamada[1], Hideki Ueda[1], Toshiya Mori[2], Toshikazu Tanada[1] (1.National Research Institute for Earth Science and Disaster Resilience, 2.Geochemical Research Center, Graduate School of Science, The University of Tokyo)

[J] Oral | S (Solid Earth Sciences )：S-VC Volcanology

3:30 PM - 5:00 PM JST | 6:30 AM - 8:00 AM UTC | A07 TOKYO BAY MAKUHARI HALL

## [S-VC37] Dynamics of volcanic eruptions and their physical and chemical processes

convener:Yujiro Suzuki(Earthquake Research Institute, The University of Tokyo), Chairperson:Yujiro Suzuki(Earthquake Research Institute, The University of Tokyo), Taishi Yamada

3:30 PM - 3:45 PM JST | 6:30 AM - 6:45 AM UTC

[SVC37-07] Estimation of the amplitude of infrasoundsignal based on sound diffraction

*Kyoka Ishii[1], Akihiko Yokoo[1] (1.Graduate School of Science, Kyoto University)

3:45 PM - 4:00 PM JST | 6:45 AM - 7:00 AM UTC

[SVC37-08] Mechanism and frequency change of pressure oscillation in the laboratory geyser system

*Noriko Teshima[1], Atsushi Toramaru[2] (1.Department of Earth and Planetary Sciences, Graduate School of Sciences, Kyushu University, 2.Department of Earth and Planetary Sciences, Faculty of Sciences, Kyushu University)

4:00 PM - 4:15 PM JST | 7:00 AM - 7:15 AM UTC

[SVC37-09] Effects of temperature on the run-out distance of large-scale pyroclastic density currents: Numerical simulation of a two-layer depth-averaged model

*Hiroyuki A. Shimizu[1], Takehiro Koyaguchi[1], Yujiro J. Suzuki[1] (1.Earthquake Research Institute, The University of Tokyo)

4:15 PM - 4:30 PM JST | 7:15 AM - 7:30 AM UTC

[SVC37-10] **Total grain-size distribution of pumice fallout deposits (Kj-P1) from 54 ka plinian eruption at Kuju Volcano**

*Tomohiro Tsuji[1], Kishimoto Hiroshi[2], Fujita Kouji[2], Chisato Nakamura[3], Nagata Tomohiro[3], Kimura Kazunari[3], Michiharu Ikeda[1], Naoki Nishizaka[4], Kozo Onishi[4] (1.Shikoku Research Institute Inc., 2.Asia Air Survey Co. Ltd., 3.Naiba, 4.Shikoku Electric Power Co. Inc.)

4:30 PM - 4:45 PM JST | 7:30 AM - 7:45 AM UTC

[SVC37-11] Estimating ashfall volumes for the 2018 Shinmoedake eruptions using the Ellipse Approximated Isopach (EAI) method - How to quantify ashfall volumes from limited ashfall observation locations

*Yasuhisa Tajima[1], Setsuya Nakada[2], Masashi NAGAI[2], Fukashi Maeno[3], Jun Oikawa[3], Teruki Oikawa[4], Yasuo Miyabuchi[5], Toshiaki Hasenaka[5], Masataka Kawaguchi[5] (1.NIPPON KOEI CO.,LTD., 2.NIED, 3.ERI, the Univ. Tokyo, 4.Geological Survey of Japan, AIST, 5.Kumamoto Univ.)

4:45 PM - 5:00 PM JST | 7:45 AM - 8:00 AM UTC

[SVC37-12] Optical disdrometer measurement of tephra fall: Constraints on radar parameters for eruption cloud observations

★Invited Papers

*Tomofumi Kozono[1], Masato Iguchi[2], Takahiro Miwa[3], Masayuki Maki[4], Takeshi Maesaka[3], Daisuke Miki[2], Takeshi Nishimura[1] (1.Department of Geophysics, Graduate School of Science, Tohoku University, 2.Sakurajima Volcano Research Center, Disaster Prevention Research Institute, Kyoto University, 3.National Research Institute for Earth Science and Disaster Resilience, 4.Research and Education Center for Natural Hazards, Kagoshima University)

[J] Oral | S (Solid Earth Sciences )：S-TT Technology & Techniques

10:45 AM - 12:15 PM JST | 1:45 AM - 3:15 AM UTC | A11 TOKYO BAY MAKUHARI HALL

## [S-TT43] seismic monitoring and processing system

convener:Takahiro Maeda(National Research Institute for Earth Science and Disaster Resilience), Chairperson:Masanao Shinohara(Earthquake Research Institute, The University of Tokyo)

10:45 AM - 11:00 AM JST | 1:45 AM - 2:00 AM UTC

[STT43-01] Summary and Considerations about Characteristics of Borehole Stress Meter for Continuous Observation

*Hiroshi Ishii[1], Yasuhiro Asai[1] (1.Tono Research Institute of Earthquake Science, Association for the Development of Earthquake Prediction)

11:00 AM - 11:15 AM JST | 2:00 AM - 2:15 AM UTC

[STT43-02] Seismic monitoring by an autonomous robotic float equipped with a hydrophone: MERMAID

*Masayuki Obayashi[1], Hiroko Sugioka[2] (1.Japan Agency for Marine-Earth Science and Technology, 2.Department of Planetology, Kobe University)

11:15 AM - 11:30 AM JST | 2:15 AM - 2:30 AM UTC

[STT43-03] Earthquake observation in a borehole over 250 °C using high temperature optical fiber and DAS technology

*Tsunehisa KIMURA[1] (1.Schlumberger)

11:30 AM - 11:45 AM JST | 2:30 AM - 2:45 AM UTC

[STT43-04] Distributed Acoustic Sensing measurement by using seafloor optical fiber cable system off Sanriku for dense seismic observation

*Masanao Shinohara[1], Tomoaki Yamada[1], Takeshi Akuhara[1], Kimihiro Mochizuki[1], Takeo Kasajima[2], Takahiro Arioka[2], Masayuki Hamakawa[3], Shunsuke Kubota[4] (1.Earthquake Research Institute, University of Tokyo, 2.Fujitsu Laboratories Ltd., 3.Fujitsu Limited, 4.YK Giken Co., Ltd.)

[J] Poster | S (Solid Earth Sciences )：S-TT Technology & Techniques

3:30 PM - 5:00 PM JST | 6:30 AM - 8:00 AM UTC | Poster Hall International Exhibition Hall8, Makuhari Messe_13

## [S-TT43] seismic monitoring and processing system

convener:Takahiro Maeda(National Research Institute for Earth Science and Disaster Resilience)

[STT43-P01] Proposal of the low cost seismometer network system

*Takamori Ito[1], Takashi Akazawa[2], Koichi Kusunoki[3], Masato Yazawa[4] (1.aLab Inc., 2.Geo-Research Institute, 3.ERI, The University of Tokyo, 4.MAD Lab.)

[STT43-P02] Experimental observation toward the realization of low-cost and high-density strong-motion observation network

*Takashi Akazawa[1], Takamori Ito[2] (1.Geo-Research Institute, 2.aLab Inc.)

[STT43-P03] Comparison of noise levels of the JMA and F-net broadband seismographs / strong motion velocity-type seismographs in long-period range for the purpose of magnitude estimation of tsunami earthquakes

*Masayuki Tanaka[1], Akio Katsumata[1] (1.Meteorological Research Institute)

[STT43-P04] Estimation of seismic wave velocity of seafloor surface and installation orientation at S-net station based on observed waveform of air gun: Toward sound source localization of large baleen whale

*Ryoichi Iwase[1] (1.National Research and Development Agency, Japan Agency for Marine-Earth Science and Technology)

[STT43-P05] **Parametric time series – video sincronization tool**

*Gerardo Manuel Mendo Pérez[1], Alejandra Arciniega Ceballos[1,2], Alejandro Rosado Fuentes[1] (1.Earth Science Graduate Program, National Autonomous University of Mexico, 2.Department of Volcanology, Institute of Geophysics, National Autonomus University of Mexico)

[J] Poster | S (Solid Earth Sciences )：S-TT Technology & Techniques

5:15 PM - 6:30 PM JST | 8:15 AM - 9:30 AM UTC | Poster Hall International Exhibition Hall8, Makuhari Messe_25

## [S-TT43] seismic monitoring and processing system

convener:Takahiro Maeda(National Research Institute for Earth Science and Disaster Resilience)

[STT43-P01] Proposal of the low cost seismometer network system

*Takamori Ito[1], Takashi Akazawa[2], Koichi Kusunoki[3], Masato Yazawa[4] (1.aLab Inc., 2.Geo-Research Institute, 3.ERI, The University of Tokyo, 4.MAD Lab.)

[STT43-P02] Experimental observation toward the realization of low-cost and high-density strong-motion observation network

*Takashi Akazawa[1], Takamori Ito[2] (1.Geo-Research Institute, 2.aLab Inc.)

[STT43-P03] Comparison of noise levels of the JMA and F-net broadband seismographs / strong motion velocity-type seismographs in long-period range for the purpose of magnitude estimation of tsunami earthquakes

*Masayuki Tanaka[1], Akio Katsumata[1] (1.Meteorological Research Institute)

[STT43-P04] Estimation of seismic wave velocity of seafloor surface and installation orientation at S-net station based on observed waveform of air gun: Toward sound source localization of large baleen whale

*Ryoichi Iwase[1] (1.National Research and Development Agency, Japan Agency for Marine-Earth Science and Technology)

[STT43-P05] **Parametric time series – video sincronization tool**

*Gerardo Manuel Mendo Pérez[1], Alejandra Arciniega Ceballos[1,2], Alejandro Rosado Fuentes[1] (1.Earth Science Graduate Program, National Autonomous University of Mexico, 2.Department of Volcanology, Institute of Geophysics, National Autonomus University of Mexico)

[E] Oral | S (Solid Earth Sciences )：S-CG Complex & General

9:00 AM - 10:30 AM JST | 12:00 AM - 1:30 AM UTC | Convention Hall A 2F

## [S-CG48] Science of slow earthquakes: Toward unified understandings of whole earthquake process

convener:Satoshi Ide(Department of Earth an Planetary Science, University of Tokyo), Hitoshi Hirose(Research Center for Urban Safety and Security, Kobe University), Kohtaro Ujiie(Graduate School of Life and Environmental Sciences, University of Tsukuba), Takahiro Hatano(Earthquake Research Institute, University of Tokyo), Chairperson:Kimihiro Mochizuki(Earthquake Research Institute, University of Tokyo), Ryuta Arai

9:00 AM - 9:15 AM JST | 12:00 AM - 12:15 AM UTC

[SCG48-17] Three-dimensional seismic structure of the shallow plate boundary in the northern Hikurangi margin from NZ3D OBS data

*Ryuta Arai[1], Shuichi Kodaira[1], Richard Kellett[2], Valerie Stucker[2], Dan Bassett[2], Stuart Henrys[2], Koichiro Obana[1], Nathan Bangs[3], Dan Barker[2], Rebecca Bell[4], Kimihiro Mochizuki[5], Gou Fujie[1], Seiichi Miura[1], Bill Fry[2], team NZ3D (1.Japan Agency for Marine-Earth Science and Technology, 2.GNS Science, 3.University of Texas Institute for Geophysics, 4.Imperial College London, 5.Earthquake Research Institute, University of Tokyo)

9:15 AM - 9:45 AM JST | 12:15 AM - 12:45 AM UTC

[SCG48-18] **Using earthquake focal mechanisms to investigate slow slip driving forces in the northern Hikurangi**

★Invited Papers

*Emily Warren-Smith[1], Bill Fry[1], Laura Wallace[1] (1.GNS Science)

9:45 AM - 10:00 AM JST | 12:45 AM - 1:00 AM UTC

[SCG48-19] Seismological structural changes around source regions of slow earthquakes in Nankai subduction zone inferred from broadband receiver functions

*Yasunori Sawaki[1], Yoshihiro Ito[2], Kazuaki Ohta[2], Takuo Shibutani[2], Tomotaka Iwata[2] (1.Graduate School of Science, Kyoto University , 2.Disaster Prevention Research Institute, Kyoto University)

10:00 AM - 10:15 AM JST | 1:00 AM - 1:15 AM UTC

[SCG48-20] Slip tendency maps for compressional and extensional stress states on a shallow decollement in Nankai Trough

*Yoshitaka Hashimoto[1], Shigeyuki Sato[1], Gregory F Moore[2], Masataka Kinoshita[3], Gaku Kimura[4], Ayumu Miyakawa[5], Kazuya Shiraishi[6], Yasuhiro Yamada[6] (1.Kochi University, 2.University of Hawaii, 3.University of Tokyo, 4.Tokyo University of Marine Science and Technology, 5.AIST, 6.JAMSTEC)

10:15 AM - 10:30 AM JST | 1:15 AM - 1:30 AM UTC

[SCG48-21] Permeability and its anisotropy on creeping Chihshang Fault, Taiwan

*Tyas Dwi Aprilniadi[1], Wen-Jie Wu[1], Li-Wei Kuo[1], Jian-Cheng Lee[2], Jia-Jyun Dong[3] (1.Department of Earth Sciences, National Central University, 2.Institute of Earth Sciences, Academia Sinica, 3.Graduate Institute of Applied Geology, National Central University)

[E] Oral | S (Solid Earth Sciences )：S-CG Complex & General

10:45 AM - 12:15 PM JST | 1:45 AM - 3:15 AM UTC | Convention Hall A 2F

## [S-CG48] Science of slow earthquakes: Toward unified understandings of whole earthquake process

convener:Satoshi Ide(Department of Earth an Planetary Science, University of Tokyo), Hitoshi Hirose(Research Center for Urban Safety and Security, Kobe University), Kohtaro Ujiie(Graduate School of Life and Environmental Sciences, University of Tsukuba), Takahiro Hatano(Earthquake Research Institute, University of Tokyo), Chairperson:Kohtaro Ujiie(Graduate School of Life and Environmental Sciences, University of Tsukuba), Simon Wallis(Nagoya University)

10:45 AM - 11:00 AM JST | 1:45 AM - 2:00 AM UTC

[SCG48-22] Short fluid infiltration events in the low permeable metamorphic rocks triggered by crustal fracturing at amphibolite–granulite facies conditions

*Diana Mindaleva[1], Masaoki Uno[1], Fumiko Higashino[1], Atsushi Okamoto[1], Noriyoshi Tsuchiya[1] (1.Graduate school of environmental studies, Tohoku University)

11:00 AM - 11:15 AM JST | 2:00 AM - 2:15 AM UTC

[SCG48-23] Generation of high fluid pressure at the base of the shallow mantle wedge—evidence from serpentinite of the Sanbagawa belt, SW Japan

*Simon Richard Wallis[1], Yui Kouketsu[2], Mari Yokota[1,2] (1.University of Tokyo, 2.Nagoya University)

11:15 AM - 11:30 AM JST | 2:15 AM - 2:30 AM UTC

[SCG48-24] **Overpressured subduction plate boundary caused by infiltration of mantle-derived fluids: Evidence from helium isotope analysis on veins in subduction mélange**

*Naoki Nishiyama[1], Kohtaro Ujiie[1], Hirochika Sumino[2] (1.University of Tsukuba, 2.The University of Tokyo)

11:30 AM - 11:45 AM JST | 2:30 AM - 2:45 AM UTC

[SCG48-25] **Geological and rheological conditions of subduction plate boundary between the seismogenic zone and the ETS zone in warm-slab environments**

*Kohtaro Ujiie[1], Kazuya Noro[1], Norio Shigematsu[2], Ake Fagereng[3], Naoki Nishiyama[1], Christopher Tulley[3], Haruna MASUYAMA[1], Yasushi Mori[4] (1.Graduate School of Life and Environmental Sciences, University of Tsukuba, 2.Research Institute of Earthquake and Volcano Geology, National Institute of Advanced Industrial Science and Technology, Japan, 3.Cardiff University, 4.Kitakyushu Museum of Natural History and Human History)

11:45 AM - 12:00 PM JST | 2:45 AM - 3:00 AM UTC

[SCG48-26] Temperature variation in tectonic mélanges of the Shimanto Belt, SW Japan

*Tsai-Wei Chen[1], Donald M Fisher[1], Andrew J Smye[1], Yoshitaka Hashimoto[2] (1.Penn State Univ., 2.Kochi Univ.)

12:00 PM - 12:15 PM JST | 3:00 AM - 3:15 AM UTC

[SCG48-27] Frictional properties of opal gouge at low-temperature hydrothermal conditions and their implications for seismogenic faulting along subduction-zone megathrusts

*Kyuichi Kanagawa[1], Tomoya Nakanishi[2], Morito Kuwana[3], Michiyo Sawai[1], Takehiro Hirose[4] (1.School of Science, Chiba University, 2.Graduate School of Science and Engineering, Chiba University, 3.Faculty of Science, Chiba University, 4.Kochi Institute for Core Sample Research, Japan Agency for Marine-Earth Science and Technology)

[E] Oral | S (Solid Earth Sciences)：S-CG Complex & General

1:45 PM - 3:15 PM JST | 4:45 AM - 6:15 AM UTC | Convention Hall A 2F

## [S-CG48] Science of slow earthquakes: Toward unified understandings of whole earthquake process

convener:Satoshi Ide(Department of Earth an Planetary Science, University of Tokyo), Hitoshi Hirose(Research Center for Urban Safety and Security, Kobe University), Kohtaro Ujiie(Graduate School of Life and Environmental Sciences, University of Tsukuba), Takahiro Hatano(Earthquake Research Institute, University of Tokyo), Chairperson:Takahiro Hatano, Takehito Suzuki

1:45 PM - 2:00 PM JST | 4:45 AM - 5:00 AM UTC

[SCG48-28] **Rate and State Dependent Friction Law and Static Friction Force**

*Hiroshi Matsukawa [1] (1.Aoyama Gakuin University)

---

2:00 PM - 2:30 PM JST | 5:00 AM - 5:30 AM UTC

[SCG48-29] **Stable sliding, slow and silent slip events and laboratory earthquakes across the brittle ductile transition**

★Invited Papers

*Alexandre Schubnel[1], Aubry Jérôme[1], François Passelègue[2] (1.Laboratoire de Géologie, ENS, PARIS, France, 2.EPFL, Switzerland)

---

2:30 PM - 2:45 PM JST | 5:30 AM - 5:45 AM UTC

[SCG48-30] Dramatic velocity weakening of dry quartz friction at relatively slow slip velocities

*Akito Tsutsumi[1], Hirotaka Iida[2], Yuko Onoe[1] (1.Graduate School of Science, Kyoto University, 2.Geothermal Engineering. Co. Ltd.)

---

2:45 PM - 3:00 PM JST | 5:45 AM - 6:00 AM UTC

[SCG48-31] Rupture nucleation processes accompanying tremor and slow slip in gel friction experiments

*Tetsuo Yamaguchi[1] (1.Graduate school of Engineering, Kyushu University)

---

3:00 PM - 3:15 PM JST | 6:00 AM - 6:15 AM UTC

[SCG48-32] Solution Orbit for k and epsilon Model for Turbulent Flow in Porous Media

*Takehito Suzuki[1] (1.Department of Physics and Mathematics, Aoyama Gakuin University)

[E] Oral | S (Solid Earth Sciences )：S-CG Complex & General

3:30 PM - 5:00 PM JST | 6:30 AM - 8:00 AM UTC | Convention Hall A 2F

## [S-CG48] Science of slow earthquakes: Toward unified understandings of whole earthquake process

convener:Satoshi Ide(Department of Earth an Planetary Science, University of Tokyo), Hitoshi Hirose(Research Center for Urban Safety and Security, Kobe University), Kohtaro Ujiie(Graduate School of Life and Environmental Sciences, University of Tsukuba), Takahiro Hatano(Earthquake Research Institute, University of Tokyo), Chairperson:Naofumi Aso, Takahiro Hatano

3:30 PM - 4:00 PM JST | 6:30 AM - 7:00 AM UTC

[SCG48-33] **Modelling precursory seismicity in the laboratory using a roughness derived rate and state friction model**

★Invited Papers

*Paul A Selvadurai[1], Percy Galvez[2], Stefan Wiemer[1], P. Martin Mai[2] (1.Swiss Seismological service, ETH Zurich, Switzerland, 2.King Abdullah University of Science and Technology, Thuwal, Saudi Arabia)

---

4:00 PM - 4:15 PM JST | 7:00 AM - 7:15 AM UTC

[SCG48-34] Exponential dependence on perturbation stress of earthquake nucleation

*Saito Takuya[1], Takahiro Hatano[1] (1.The University of Tokyo)

---

4:15 PM - 4:30 PM JST | 7:15 AM - 7:30 AM UTC

[SCG48-35] Stochastic modeling of slow earthquakes comparable to observations

*Naofumi Aso[1], Ryosuke Ando[2], Satoshi Ide[2] (1.Tokyo Institute of Technology, 2.University of Tokyo)

---

4:30 PM - 4:45 PM JST | 7:30 AM - 7:45 AM UTC

[SCG48-36] Migration of aqueous fluid near the subducting plate interface

*Manabu Morishige[1] (1.Japan Agency for Marine-Earth Science and Technology)

---

4:45 PM - 5:00 PM JST | 7:45 AM - 8:00 AM UTC

[SCG48-37] EnKF estimation of frictional properties and slip evolution on a LSSE fault and the changing slip deficit rate on a megathrust fault

*Kazuro Hirahara[1,2] (1.Institute of Education, Research and Regional Cooperation for crisis Management Shikoku, Kagawa University , 2.Riken, AIP center)

[E] Oral | S (Solid Earth Sciences )：S-CG Complex & General

9:00 AM - 10:30 AM JST | 12:00 AM - 1:30 AM UTC | A02 TOKYO BAY MAKUHARI HALL

## [S-CG50] Intraslab and intraplate earthquakes

convener:Saeko Kita(International Institute of Seismology and Earthquake Engineering, BRI), Tomohiro Ohuchi(Geodynamics Research Center, Ehime University), Marcel Thielmann(Bavarian Geoinstitute, University of Bayreuth), Ryo Okuwaki(Research Institute of Earthquake and Volcano Geology, Geological Survey of Japan, National Institute of Advanced Industrial Science and Technology), Chairperson:Saeko Kita(Building Research Insitute), Tomohiro Ohuchi(Geodynamics Research Center, Ehime University), Marcel Thielmann(University of Bayreuth), Ryo Okuwaki(筑波大学), Thomas Ferrand(UC San Diego)

9:00 AM - 9:15 AM JST | 12:00 AM - 12:15 AM UTC

### [SCG50-01] On a reversely-dipping low-velocity layer in the Tohoku-slab beneath the forearc: unbending induced fluid pathway?

★Invited Papers
# Cancelled

*Hitoshi Kawakatsu[1], HyeJeong Kim[1] (1.Earthquake Research Institute, University of Tokyo)

9:15 AM - 9:30 AM JST | 12:15 AM - 12:30 AM UTC

### [SCG50-02] Evidence for transient fluid pathways in the mantle of the subducting Nazca slab from seismological observations and modeling of the Poisson's ratio

★Invited Papers

*Wasja Bloch[1,2], Timm John[2], Jörn Kummerow[2], Bernd Schurr[1], Pablo Salazar[3,4], Serge A. Shapiro[2] (1.GeoForschungszentrum GFZ, Potsdam, Germany, 2.Freie Universität Berlin, Germany, 3.Universidád Católica del Norte, Antofagasta, Chile, 4.National Research Center for Integrated Natural Disasters Management (CIGIDEN), Santiago, Chile)

9:30 AM - 9:45 AM JST | 12:30 AM - 12:45 AM UTC

### [SCG50-03] Numerical simulation of water transportation along subducting slabs and implications for intraslab earthquakes

★Invited Papers

*Atsushi Nakao[1], Hikaru Iwamori[1,2,3], Tomoeki Nakakuki[4], Yujiro Suzuki[1], Takashi Nakagawa[5], Hitomi Nakamura[2,3,6,7] (1.Earthquake Research Institute, University of Tokyo, 2.Department of Solid Earth Geochemistry, Japan Agency for Marine-Earth Science and Technology, 3.Department of Earth and Planetary Sciences, Tokyo Institute of Technology, 4.Department of Earth and Planetary Systems Science, Hiroshima University, 5.Department of Earth Sciences, The University of Hong Kong, 6.Geological Survey of Japan, National Institute of Advanced Industrial Science and Technology, 7.Ocean Resource Research Center for Next Generation, Chiba Institute of Technology)

9:45 AM - 10:00 AM JST | 12:45 AM - 1:00 AM UTC

### [SCG50-04] Subduction of serpentinized fracture zone and intraslab earthquakes in southern Mexico

★Invited Papers

*Marina Manea[1,2] (1.Computational Geodynamics Laboratory, Geosciences Center, National Autonomous University of Mexico, 2.Institute of Astronomy, Romanian Academy)

10:00 AM - 10:15 AM JST | 1:00 AM - 1:15 AM UTC

### [SCG50-05] Reaction-induced embrittlement of the lower continental crust

*Alexandre Schubnel[1], Sarah Incel[2], Julien Gasc[1], Nadège Hilairet[5], Yanbin Wang[3], Feng Shi[3], Loic Labrousse[4] (1.Laboratoire de Géologie, ENS, 2.University of Oslo, 3.GCECARS, University of Chicago, 4.ISTEP, Sorbonne Université, 5.UMET, Université de Lille)

10:15 AM - 10:30 AM JST | 1:15 AM - 1:30 AM UTC

### [SCG50-06] Transformation-induced, melt-enhanced faulting in orthoenstatite: implications for global intermediate-depth earthquakes

Feng Shi[1], Jianguo Wen[2], Tony Yu[1], Lupei Zhu[3], *Yanbin Wang[1] (1.Center for Advanced Radiation Sources, University of Chicago, Chicago, IL, USA, 2.Center for Nanoscale Materials, Argonne National Laboratory, Argonne, IL, USA, 3.Department of Earth & Atmospheric Sciences, Saint Louis University, St. Louis, MO, USA)

[E] Oral | S (Solid Earth Sciences )：S-CG Complex & General

10:45 AM - 12:15 PM JST | 1:45 AM - 3:15 AM UTC | A02 TOKYO BAY MAKUHARI HALL

## [S-CG50] Intraslab and intraplate earthquakes

convener:Saeko Kita(International Institute of Seismology and Earthquake Engineering, BRI), Tomohiro Ohuchi(Geodynamics Research Center, Ehime University), Marcel Thielmann(Bavarian Geoinstitute, University of Bayreuth), Ryo Okuwaki(Research Institute of Earthquake and Volcano Geology, Geological Survey of Japan, National Institute of Advanced Industrial Science and Technology), Chairperson:Saeko Kita(Building Research Insitute), Tomohiro Ohuchi(Geodynamics Research Center, Ehime University), Marcel Thielmann(University of Bayreuth), Ryo Okuwaki(筑波大学), Thomas Ferrand(UC San Diego)

10:45 AM - 11:00 AM JST | 1:45 AM - 2:00 AM UTC

[SCG50-07] The Isolated M7.9 Deep Earthquake of 30 May 2015 Under the Present Bonin Wadati-Benioff Zone: Evidence from the New ISC-EHB Earthquake Catalogue (1930-2015) and CMT Focal Mechanisms

*Stephen Kirby[1], E. Robert Engdahl[2], Emile Andre Okal[3] (1.United States Geological Survey, Menlo Park, 2.University of Colorado, 3.Northwestern University)

11:00 AM - 11:15 AM JST | 2:00 AM - 2:15 AM UTC

[SCG50-08] What Can $M_W$ –4 Lab-Quakes Teach Us About Deep-Focus Earthquakes?

★Invited Papers

*Julien Gasc[1], Julien Fauconnier[1], Clémence Daigre[1], Arefeh Moarefvand[1], Damien Deldicque[1], Blandine Gardonio[1], Alexandre Schubnel[1], Pamela Burnley[2] (1.Laboratoire de Géologie, ENS-CNRS, Paris, FRANCE, 2.University of Nevada Las Vegas, Las Vegas, USA)

11:15 AM - 11:30 AM JST | 2:15 AM - 2:30 AM UTC

[SCG50-09] Deep intraslab earthquake rupture due to grain size assisted thermal runaway

*Marcel Thielmann[1], Thibault Duretz[2] (1.Bavarian Geoinstitute, University of Bayreuth, Germany, 2.Université de Rennes, Rennes, France)

11:30 AM - 11:45 AM JST | 2:30 AM - 2:45 AM UTC

[SCG50-10] Fault model of the 2012 off-Miyagi intraslab earthquake doublet and its implication for rheological signature of incoming Pacific plate

*Tatsuya Kubota[1], Ryota Hino[2], Syuichi Suzuki[2] (1.National Research Institute for Earth Science and Disaster Resilience, 2.Graduate School of Science, Tohoku University)

11:45 AM - 12:00 PM JST | 2:45 AM - 3:00 AM UTC

[SCG50-11] Source-rupture process of the intraplate earthquake; its diversity related to the fault geometry and damaged fault zone

*Ryo Okuwaki[1], Yuji Yagi[1] (1.Graduate School of Life and Environmental Sciences, University of Tsukuba)

12:00 PM - 12:15 PM JST | 3:00 AM - 3:15 AM UTC

[SCG50-12] **Aftershocks of the NEXT Cascadia Intraslab Earthquake**

*Paul Bodin[1,2] (1.University of Washington Seattle, 2.Pacific Northwest Seismic Network)

[E] Poster | S (Solid Earth Sciences)：S-CG Complex & General

3:30 PM - 5:00 PM JST | 6:30 AM - 8:00 AM UTC | Poster Hall International Exhibition Hall8, Makuhari Messe_14

## [S-CG50] Intraslab and intraplate earthquakes

convener:Saeko Kita(International Institute of Seismology and Earthquake Engineering, BRI), Tomohiro Ohuchi(Geodynamics Research Center, Ehime University), Marcel Thielmann(Bavarian Geoinstitute, University of Bayreuth), Ryo Okuwaki(Research Institute of Earthquake and Volcano Geology, Geological Survey of Japan, National Institute of Advanced Industrial Science and Technology)

[SCG50-P01] Changes in seismicity rate, stress orientations, and b-values before and after ETS events in the Philippine sea plate under Kii Peninsula

*Saeko Kita[1], Heidi Houston[2], Sachiko Tanaka[3], Youichi Asano[3], Takuo Shibutani[4], Naoki Suda[5] (1.Building Research Institute, 2.USC, 3.NIED, 4.DPRI, Kyoto University, 5.Hiroshima University)

[SCG50-P02] **Inhomogeneous conduit across slab controlled by intraslab stress heterogeneity in the Nankai subduction zone**

*Makoto Otsubo[1], Ayumu Miyakawa[2], Ikuo Katayama[3], Keishi Okazaki[4] (1.Geological Survey of Japan, Research Institute of Earthquake and Volcano Geology, 2.Geological Survey of Japan, Research Institute of Geology and Geoinformation, 3.Hiroshima University, 4.JAMSTEC)

[SCG50-P03] New insights into the mechanism of deep-focus earthquakes

*Ayako Tsuchiyama[1], Junichi Nakajima[1] (1.Tokyo Institute of Technology)

[SCG50-P04] Faulting in deforming harzburgite under wet conditions

*Tomohiro Ohuchi[1], Xinglin Lei[2], Yuji Higo[3], Yoshinori Tange[3], Takeshi Sakai[1] (1.Geodynamics Research Center, Ehime University, 2.National Institute of Advanced Industrial Science and Technology, 3.Japan Synchrotron Radiation Research Institute)

[SCG50-P05] Semi-brittle behavior of olivine single crystals under the conditions of Earth's mantle transition zone

Yoshihisa Naruse[1], *Tomohiro Ohuchi[1] (1.Geodynamics Research Center, Ehime University)

[SCG50-P06] High-pressure deformation experiments on peridotite gouges under hydrothermal conditions, using a deformation-DIA apparatus

*Maki Semba[1], Ken-ichi Hirauchi[1], Tomohiro Ohuchi[2], Katsuyoshi Michibayashi[3] (1.Department of Geosciences, Faculty of Science, Shizuoka University, 2.Geodynamics Research Center, Ehime University, 3.Department of Earth and Planetary Sciences, Nagoya university)

[SCG50-P07] Stable fault slip in antigorite-olivine aggregates at high pressures

Mai Ikehara[1], *Tomoaki Kubo[1], Takuya Iwasato[2], Yuji Higo[3], Masahiro Imamura[1], Yoshinori Tange[3] (1.Kyushu University, 2.Shin-Nippon Nondestructive Inspection Co., Ltd., 3.JASRI)

[SCG50-P08] Rheology and frictional instability of lawsonite in high pressure deformation experiments

*Rei Shiraishi[1], Jun Muto[1], Akihiro Tsunoda[2], Sando Sawa[1], Akio Suzuki[1] (1.Department of Earth Science, Graduate School of Science, Tohoku University, 2.Earthquake Research Institute, University of Tokyo)

[SCG50-P09] Grain Size Dependency of Olivine-Spinel Phase Transformational Mechanism Responsible for Deep-focus Earthquakes

*Sando Sawa[1], Jun Muto[1], Nobuyoshi Miyajima[2], Hiroyuki Nagahama[1] (1.Department of Earth Science, Tohoku University, 2.Bayerisches Geoinstitut, University of Bayreuth)

[SCG50-P10] **Seismicity and mineral destabilizations in the subducting mantle up to 6 GPa, 200 km depth**

*Thomas P. Ferrand[1] (1.Earthquake Research Institute)

[SCG50-P11] Receiver function imaging of subducting Pacific plate and mantle wedge under Japanese islands using denser network of stations

*HyeJeong Kim[1], Hitoshi Kawakatsu[1], Takeshi Akuhara[1], Masanao Shinohara[1] (1.Earthquake Research Institute, The University of Tokyo)

[SCG50-P12] Strong S-wave attenuation in the mantle wedge beneath the NE Japan and interpretations of high-frequency wave propagation path of intraslab earthquakes

*Takahiro Shiina[1,2], Kei Katsumata[2], Kiyoshi Yomogida[3], Aitaro Kato[1] (1.Earthquake Research Institute, The University of Tokyo, 2.Institute of Seismology and Volcanology, Graduate School of Science, Hokkaido University, 3.Graduate School of Science, Hokkaido University)

[E] Poster | S (Solid Earth Sciences)：S-CG Complex & General

5:15 PM - 6:30 PM JST | 8:15 AM - 9:30 AM UTC | Poster Hall International Exhibition Hall8, Makuhari Messe_26

## [S-CG50] Intraslab and intraplate earthquakes

convener:Saeko Kita(International Institute of Seismology and Earthquake Engineering, BRI), Tomohiro Ohuchi(Geodynamics Research Center, Ehime University), Marcel Thielmann(Bavarian Geoinstitute, University of Bayreuth), Ryo Okuwaki(Research Institute of Earthquake and Volcano Geology, Geological Survey of Japan, National Institute of Advanced Industrial Science and Technology)

[SCG50-P01] Changes in seismicity rate, stress orientations, and b-values before and after ETS events in the Philippine sea plate under Kii Peninsula

*Saeko Kita[1], Heidi Houston[2], Sachiko Tanaka[3], Youichi Asano[3], Takuo Shibutani[4], Naoki Suda[5] (1.Building Research Institute, 2.USC, 3.NIED, 4.DPRI, Kyoto University, 5.Hiroshima University)

[SCG50-P02] **Inhomogeneous conduit across slab controlled by intraslab stress heterogeneity in the Nankai subduction zone**

*Makoto Otsubo[1], Ayumu Miyakawa[2], Ikuo Katayama[3], Keishi Okazaki[4] (1.Geological Survey of Japan, Research Institute of Earthquake and Volcano Geology, 2.Geological Survey of Japan, Research Institute of Geology and Geoinformation, 3.Hiroshima University, 4.JAMSTEC)

[SCG50-P03] New insights into the mechanism of deep-focus earthquakes

*Ayako Tsuchiyama[1], Junichi Nakajima[1] (1.Tokyo Institute of Technology)

[SCG50-P04] Faulting in deforming harzburgite under wet conditions

*Tomohiro Ohuchi[1], Xinglin Lei[2], Yuji Higo[3], Yoshinori Tange[3], Takeshi Sakai[1] (1.Geodynamics Research Center, Ehime University, 2.National Institute of Advanced Industrial Science and Technology, 3.Japan Synchrotron Radiation Research Institute)

[SCG50-P05] Semi-brittle behavior of olivine single crystals under the conditions of Earth's mantle transition zone

Yoshihisa Naruse[1], *Tomohiro Ohuchi[1] (1.Geodynamics Research Center, Ehime University)

[SCG50-P06] High-pressure deformation experiments on peridotite gouges under hydrothermal conditions, using a deformation-DIA apparatus

*Maki Semba[1], Ken-ichi Hirauchi[1], Tomohiro Ohuchi[2], Katsuyoshi Michibayashi[3] (1.Department of Geosciences, Faculty of Science, Shizuoka University, 2.Geodynamics Research Center, Ehime University, 3.Department of Earth and Planetary Sciences, Nagoya university)

[SCG50-P07] Stable fault slip in antigorite-olivine aggregates at high pressures

Mai Ikehara[1], *Tomoaki Kubo[1], Takuya Iwasato[2], Yuji Higo[3], Masahiro Imamura[1], Yoshinori Tange[3] (1.Kyushu University, 2.Shin-Nippon Nondestructive Inspection Co., Ltd., 3.JASRI)

[SCG50-P08] Rheology and frictional instability of lawsonite in high pressure deformation experiments

*Rei Shiraishi[1], Jun Muto[1], Akihiro Tsunoda[2], Sando Sawa[1], Akio Suzuki[1] (1.Department of Earth Science, Graduate School of Science, Tohoku University, 2.Earthquake Research Institute, University of Tokyo)

[SCG50-P09] Grain Size Dependency of Olivine-Spinel Phase Transformational Mechanism Responsible for Deep-focus Earthquakes

*Sando Sawa[1], Jun Muto[1], Nobuyoshi Miyajima[2], Hiroyuki Nagahama[1] (1.Department of Earth Science, Tohoku University, 2.Bayerisches Geoinstitut, University of Bayreuth)

[SCG50-P10] **Seismicity and mineral destabilizations in the subducting mantle up to 6 GPa, 200 km depth**

*Thomas P. Ferrand[1] (1.Earthquake Research Institute)

[SCG50-P11] Receiver function imaging of subducting Pacific plate and mantle wedge under Japanese islands using denser network of stations

*HyeJeong Kim[1], Hitoshi Kawakatsu[1], Takeshi Akuhara[1], Masanao Shinohara[1] (1.Earthquake Research Institute, The University of Tokyo)

[SCG50-P12] Strong S-wave attenuation in the mantle wedge beneath the NE Japan and interpretations of high-frequency wave propagation path of intraslab earthquakes

*Takahiro Shiina[1,2], Kei Katsumata[2], Kiyoshi Yomogida[3], Aitaro Kato[1] (1.Earthquake Research Institute, The University of Tokyo, 2.Institute of Seismology and Volcanology, Graduate School of Science, Hokkaido University, 3.Graduate School of Science, Hokkaido University)

[E] Poster | S (Solid Earth Sciences)：S-CG Complex & General

10:45 AM - 12:15 PM JST | 1:45 AM - 3:15 AM UTC | Poster Hall International Exhibition Hall8, Makuhari Messe_6

## [S-CG51] Role of volatiles on Earth and planetary dynamics

convener:Takayuki Ishii(Bavarian Research Institute, University of Bayreuth), Eiji Ohtani(Department of Earth and Planetary Materials Science, Graduate School of Science, Tohoku University), Michihiko Nakamura(Division of Earth and Planetary Materials Science, Department of Earth Science, Graduate School of Science, Tohoku University), Bjorn Mysen(Geophysical Laboratory, Carnegie Inst. Washington)

[SCG51-P01] Permeability prediction of porous media with the finite difference Stokes solver LaMEM

*Philipp Eichheimer[1], Wakana Fujita[2], Marcel Thielmann[1], Anton Popov[3], Gregor Golabek[1], Boris Kaus[3], Maximilian Kottwitz[3] (1.Bayerisches Geoinstitut, University of Bayreuth, 2.Department of Earth Science, Tohoku University, Sendai, 3.Institute of Geosciences, Johannes Gutenberg University Mainz)

[SCG51-P02] Grain growth-induced fluid localization and permeability reduction

*Wakana Fujita[1], Michihiko Nakamura[1], Kentaro Uesugi[2] (1.Graduate School of Science, Tohoku University, 2.JASRI/SPring-8)

[SCG51-P03] Pargasite stability in the upper mantle at $H_2O$-undersaturated conditions

*Marija Putak Juricek[1], Hans Keppler[1] (1.BGI)

[SCG51-P04] **Constraining the water content at the top of the mantle transition zone with the elasticity of wadsleyite and olivine**

*Zhongqing Wu[1] (1.University of Science and Technology of China)

[SCG51-P05] ***Single crystal elasticity of Fe-bearing phase E by Brillouin spectroscopy***

*Niccolo Satta[1], Hauke Marquardt [2], Alexander Kurnosov[1], Tiziana Boffa Ballaran [1], Johannes Buchen[3], Catherine McCammon[1], Takaaki Kawazoe[4] (1.Bayerisches Geoinstitut, University of Bayreuth, 95440 Bayreuth, Germany, 2.Department of Earth Sciences, University of Oxford, South Parks Road, Oxford, UK., 3.Seismological Laboratory, California Institute of Technology, Pasadena, CA 91125, USA., 4.Department of Earth and Planetary Systems Science, Hiroshima University, Hiroshima 739-8526, Japan.)

[SCG51-P06] Discovery of two hexagonal phases in (Fe,Al)OOH under the P-T conditions of the deep lower mantle

*Lu Liu[1,2], Li Zhang[1], Hongsheng Yuan[1] (1.Center for High Pressure Science and Technology Advanced Research, 2.University of Science and Technology of China)

[SCG51-P07] **Effect of grid resolution on tectonic regimes in global-scale convection models**

*Enrico Marzotto[1], Marcel Thielmann[1], Gregor Golabek[1] (1.Bayerisches Geoinstitut)

[SCG51-P08] A 3-D crust and uppermost mantle electrical conductivity model of subduction zone beneath NE Japan

*Masahiro Ichiki[1,2], Toshiki Kaida[1], Yasuo Ogawa[3] (1.Graduate School of Science, Tohoku University, 2.International Research Institute of Disaster Science, 3.School of Science, Tokyo Institute of Technology)

[SCG51-P09] *The conditions of sublithospheric diamond formation constrained from ferric iron-rich exsolution from ferropericlase inclusions.*

*Caterina Melai[1], Daniel Frost[1], Tiziana Boffa Ballaran[1], Catherine McCammon[1] (1.Bayerisches Geoinstitute)

[SCG51-P10] **Probing the variation of the oxygen fugacity in diamond anvil cells using the Fe-Ir alloy as redox sensor**

*Serena Dominijanni[1], Catherine McCammon[1], Leonid Dubrovinsky[1], Dan Frost[1], Nobuyoshi Miyajima[1] (1.Bayerisches Geoinstitut)

[SCG51-P11] Goethite behavior at Earth's lower mantle conditions

*Egor Gennadievich Koemets[1], Maxim Bykov[1], George Aprilis[2], Timofey Fedotenko[2], Stella Chariton[1], Saiana Khandarkhaeva[1], Iuliia Koemets[1], Marcel Thielmann[1], Natalia Dubrovinsaia[2], Leonid Dubrovinsky[1] (1.BGI (Bayerisches Geoinstitut), Universität Bayreuth, Germany, 2.Material Physics and Technology at Extreme Conditions, Laboratory of Crystallography, Universität Bayreuth, Germany)

[SCG51-P12] The oxygen content of sulphides in the mantle and a geothermometer for diamond formation

*Sumith Abeykoon[1], Dan Frost[1], Vera Laurenz[1] (1.Bayerisches Geoinstitut, University of Bayreuth)

[E] Poster | S (Solid Earth Sciences)：S-CG Complex & General

5:15 PM - 6:30 PM JST | 8:15 AM - 9:30 AM UTC | Poster Hall International Exhibition Hall8, Makuhari Messe_27

## [S-CG51] Role of volatiles on Earth and planetary dynamics

convener:Takayuki Ishii(Bavarian Research Institute, University of Bayreuth), Eiji Ohtani(Department of Earth and Planetary Materials Science, Graduate School of Science, Tohoku University), Michihiko Nakamura(Division of Earth and Planetary Materials Science, Department of Earth Science, Graduate School of Science, Tohoku University), Bjorn Mysen(Geophysical Laboratory, Carnegie Inst. Washington)

[SCG51-P01] Permeability prediction of porous media with the finite difference Stokes solver LaMEM

*Philipp Eichheimer[1], Wakana Fujita[2], Marcel Thielmann[1], Anton Popov[3], Gregor Golabek[1], Boris Kaus[3], Maximilian Kottwitz[3] (1.Bayerisches Geoinstitut, University of Bayreuth, 2.Department of Earth Science, Tohoku University, Sendai, 3.Institute of Geosciences, Johannes Gutenberg University Mainz)

[SCG51-P02] Grain growth-induced fluid localization and permeability reduction

*Wakana Fujita[1], Michihiko Nakamura[1], Kentaro Uesugi[2] (1.Graduate School of Science, Tohoku University, 2.JASRI/SPring-8)

[SCG51-P03] Pargasite stability in the upper mantle at $H_2O$-undersaturated conditions

*Marija Putak Juricek[1], Hans Keppler[1] (1.BGI)

[SCG51-P04] **Constraining the water content at the top of the mantle transition zone with the elasticity of wadsleyite and olivine**

*Zhongqing Wu[1] (1.University of Science and Technology of China)

[SCG51-P05] ***Single crystal elasticity of Fe-bearing phase E by Brillouin spectroscopy***

*Niccolo Satta[1], Hauke Marquardt [2], Alexander Kurnosov[1], Tiziana Boffa Ballaran [1], Johannes Buchen[3], Catherine McCammon[1], Takaaki Kawazoe[4] (1.Bayerisches Geoinstitut, University of Bayreuth, 95440 Bayreuth, Germany, 2.Department of Earth Sciences, University of Oxford, South Parks Road, Oxford, UK., 3.Seismological Laboratory, California Institute of Technology, Pasadena, CA 91125, USA., 4.Department of Earth and Planetary Systems Science, Hiroshima University, Hiroshima 739-8526, Japan.)

[SCG51-P06] Discovery of two hexagonal phases in (Fe,Al)OOH under the P-T conditions of the deep lower mantle

*Lu Liu[1,2], Li Zhang[1], Hongsheng Yuan[1] (1.Center for High Pressure Science and Technology Advanced Research, 2.University of Science and Technology of China)

[SCG51-P07] **Effect of grid resolution on tectonic regimes in global-scale convection models**

*Enrico Marzotto[1], Marcel Thielmann[1], Gregor Golabek[1] (1.Bayerisches Geoinstitut)

[SCG51-P08] A 3-D crust and uppermost mantle electrical conductivity model of subduction zone beneath NE Japan

*Masahiro Ichiki[1,2], Toshiki Kaida[1], Yasuo Ogawa[3] (1.Graduate School of Science, Tohoku University, 2.International Research Institute of Disaster Science, 3.School of Science, Tokyo Institute of Technology)

[SCG51-P09] *The conditions of sublithospheric diamond formation constrained from ferric iron-rich exsolution from ferropericlase inclusions.*

*Caterina Melai[1], Daniel Frost[1], Tiziana Boffa Ballaran[1], Catherine McCammon[1] (1.Bayerisches Geoinstitute)

[SCG51-P10] **Probing the variation of the oxygen fugacity in diamond anvil cells using the Fe-Ir alloy as redox sensor**

*Serena Dominijanni[1], Catherine McCammon[1], Leonid Dubrovinsky[1], Dan Frost[1], Nobuyoshi Miyajima[1] (1.Bayerisches Geoinstitut)

[SCG51-P11] Goethite behavior at Earth's lower mantle conditions

*Egor Gennadievich Koemets[1], Maxim Bykov[1], George Aprilis[2], Timofey Fedotenko[2], Stella Chariton[1], Saiana Khandarkhaeva[1], Iuliia Koemets[1], Marcel Thielmann[1], Natalia Dubrovinsaia[2], Leonid Dubrovinsky[1] (1.BGI (Bayerisches Geoinstitut), Universität Bayreuth, Germany, 2.Material Physics and Technology at Extreme Conditions, Laboratory of Crystallography, Universität Bayreuth, Germany)

[SCG51-P12] The oxygen content of sulphides in the mantle and a geothermometer for diamond formation

*Sumith Abeykoon[1], Dan Frost[1], Vera Laurenz[1] (1.Bayerisches Geoinstitut, University of Bayreuth)

[E] Oral | S (Solid Earth Sciences)：S-CG Complex & General

1:45 PM - 3:15 PM JST | 4:45 AM - 6:15 AM UTC | A11 TOKYO BAY MAKUHARI HALL

## [S-CG51] Role of volatiles on Earth and planetary dynamics

convener:Takayuki Ishii(Bavarian Research Institute, University of Bayreuth), Eiji Ohtani(Department of Earth and Planetary Materials Science, Graduate School of Science, Tohoku University), Michihiko Nakamura(Division of Earth and Planetary Materials Science, Department of Earth Science, Graduate School of Science, Tohoku University), Bjorn Mysen(Geophysical Laboratory, Carnegie Inst. Washington), Chairperson:Michihiko Nakamura, Eiji Ohtani(Tohoku University)

1:45 PM - 2:00 PM JST | 4:45 AM - 5:00 AM UTC

[SCG51-01] Constraining the degassing rate of the mantle since 3 Ga using the deficit of xenon-129 in the ancient atmosphere

★Invited Papers

*Bernard Marty[1], David Bekaert[1], Michael Broadley[1] (1.Centre de Recherches Pétrographiques et Géochimiques/ CNRS - Universite de Lorraine France)

2:00 PM - 2:15 PM JST | 5:00 AM - 5:15 AM UTC

[SCG51-02] **Investigating volatile cycles in the terrestrial mantle by incorporating He and Ar isotopes into geodynamical models of mantle convection**

★Invited Papers

*Rosie Ellen Jones[1], Peter van Keken[2], Jonathan M Tucker[2], Chris J Ballentine[1] (1.Department of Earth Sciences, University of Oxford, Oxford, UK, 2.Department of Terrestrial Magnetism, Carnegie Institution of Washington, Washington, USA)

2:15 PM - 2:30 PM JST | 5:15 AM - 5:30 AM UTC

[SCG51-03] Fluid circulation in the forearc mantle wedge inferred from the dihedral angle in an olivine-$H_2O$-NaCl system

*Yongsheng HUANG[1], Takayuki Nakatani[1], Michihiko Nakamura[1], Catherine McCammon[2] (1.Graduate School of Science, Tohoku University, 2.Byerisches Geoinstitut, University of Bayreuth)

2:30 PM - 2:45 PM JST | 5:30 AM - 5:45 AM UTC

[SCG51-04] The oxygen fugacity of serpentinites: implications for subduction zone redox evolution

*Lisa Eberhard[1], Dan Frost[1], Catherine McCammon[1] (1.BGI)

2:45 PM - 3:00 PM JST | 5:45 AM - 6:00 AM UTC

[SCG51-05] Experimental study of the effect of composition on water solubility in natural silicate melts

*Shigeru Yamashita[1] (1.Institute for Planetary Materials, Okayama University)

3:00 PM - 3:15 PM JST | 6:00 AM - 6:15 AM UTC

[SCG51-06] Deep mantle volatile cycle and plate tectonics: Impact to the climate evolution

*Takashi Nakagawa[1], Shintaro Kadoya[2], Eiichi Tajika[3] (1.Department of Earth Sciences, The University of Hong Kong, 2.Department of Earth and Space Sciences, University of Washington, 3.Department of Earth and Planetary Sciences, The University of Tokyo)

[E] Oral | S (Solid Earth Sciences )：S-CG Complex & General

3:30 PM - 5:00 PM JST | 6:30 AM - 8:00 AM UTC | A11 TOKYO BAY MAKUHARI HALL

## [S-CG51] Role of volatiles on Earth and planetary dynamics

convener:Takayuki Ishii(Bavarian Research Institute, University of Bayreuth), Eiji Ohtani(Department of Earth and Planetary Materials Science, Graduate School of Science, Tohoku University), Michihiko Nakamura(Division of Earth and Planetary Materials Science, Department of Earth Science, Graduate School of Science, Tohoku University), Bjorn Mysen(Geophysical Laboratory, Carnegie Inst. Washington), Chairperson:Takayuki Ishii(Bavarian Research Institute, University of Bayreuth), Bjorn Mysen(Carnegie Institution of Washington)

3:30 PM - 3:45 PM JST | 6:30 AM - 6:45 AM UTC

[SCG51-07] The nature of water induced small degree melts in the deep mantle

★Invited Papers

*Daniel James Frost[1], Pierre Condamine[3], Davide Novella[2], Rong Huang[1] (1.University of Bayreuth, 2.University of Cambridge, 3.Université de Lorraine)

---

3:45 PM - 4:00 PM JST | 6:45 AM - 7:00 AM UTC

[SCG51-08] **Phase separation of hydrous Vesuvius melt: vesicle nucleation or spinodal decomposition?**

★Invited Papers

*Anja Allabar[1], Marcus Nowak[1] (1.University of Tuebingen)

---

4:00 PM - 4:15 PM JST | 7:00 AM - 7:15 AM UTC

[SCG51-09] Role of water on dynamics in the lower mantle and core-mantle boundary regions

*Eiji Ohtani[1], Takayuki Ishii[2], Liang Yuan[1], Daijo Ikuta[1], Tomoo Katsura[2], Dan Frost[2] (1.Department of Earth and Planetary Materials Science, Graduate School of Science, Tohoku University, 2.Bavarian Research Institute, University of Bayreuth)

---

4:15 PM - 4:30 PM JST | 7:15 AM - 7:30 AM UTC

[SCG51-10] Stability of Fe-bearing hydrous phases and element partitioning in the system MgO-$Al_2O_3$-$Fe_2O_3$-$SiO_2$-$H_2O$ in Earth's lowermost mantle

*Hongsheng Yuan[1], Li Zhang[1], Eiji Ohtani[2], Yue Meng[3], Eran Greenberg[4], Vitali B. Prakapenka [4] (1.Center for High Pressure Science and Technology Advanced Research, 2.Department of Earth Science, Graduate School of Science, Tohoku University, 3.HPCAT, X-Ray Science Division, Argonne National Laboratory, 4.Center for Advanced Radiation Sources, University of Chicago)

---

4:30 PM - 4:45 PM JST | 7:30 AM - 7:45 AM UTC

[SCG51-11] **Laboratory Micro-Seismicity during Serpentinite Deformation as a Potential Analogue for Lower Wadati-Benioff Plane Seismicity**

*Julien Gasc[1,3], Nadège Hilairet[2], Tony Yu[3], Yanbin Wang[3], Thomas P. Ferrand[1], Alexandre Schubnel[1] (1.Laboratoire de Géologie, CNRS - ENS, Paris, FRANCE, 2.Unité Matériaux et Transformations, CNRS - Lille University, Villeneuve d'Ascq, FRANCE, 3.GeoSoilEnviro-CARS, University of Chicago, Argonne IL, USA)

---

4:45 PM - 5:00 PM JST | 7:45 AM - 8:00 AM UTC

[SCG51-12] Water transport and mixing in the whole-mantle scale convection

*Takeo Kaneko[1], Tomoeki Nakakuki[1], Masanori Kameyama[2], Hikaru Iwamori[3] (1.Department of Earth and Planetary Systems Science, Graduate School of Science, Hiroshima University, 2.Geodynamics Research Center, Ehime University, 3.Earthquake Research Institute, University of Tokyo)

[J] Oral | S (Solid Earth Sciences )：S-CG Complex & General

10:45 AM - 12:15 PM JST | 1:45 AM - 3:15 AM UTC | A08 TOKYO BAY MAKUHARI HALL

## [S-CG52] Petrology, Mineralogy & Resource Geology

convener:Tatsuo Nozaki(Research and Development Center for Submarine Resources, Japan Agency for Marine-Earth Science and Technology), Satoshi SAITO(Graduate School of Science and Engineering, Ehime University), Koichi Momma(National Museum of Nature and Science), Nobutaka Tsuchiya(Department of Geology, Faculty of Education, Iwate University), Chairperson:Tatsuo Nozaki(JAMSTEC), Satoshi Saito

10:45 AM - 11:00 AM JST | 1:45 AM - 2:00 AM UTC

### [SCG52-01] Coordinated sample preparation with cryo-FIB-SEM and X-ray CT: Applications to chemical analysis for fluid inclusions in minerals

*Yu Kodama[1], Naotaka Tomioka[2], Tatsuhiko Kawamoto[3], Junichiro Kuroda[4], Masafumi MURAYAMA[5], Motoo Ito[2] (1.Marine Works Japan Ltd., 2.Kochi Institute for Core Sample Research, JAMSTEC, 3.Department of Geoscience, Faculty of Science, Shizuoka University, 4.Atmosphere and Ocean Research Institute, the University of Tokyo, 5.Faculty of Agriculture and Marine Science, Kochi University)

11:00 AM - 11:15 AM JST | 2:00 AM - 2:15 AM UTC

### [SCG52-02] Feasibility Study for Precise Particle Characterization of Fine Clay Particle Using An Automated Particle Image Analysis and Nanotrakcking Analysis.

*Daisuke Sasakura[1], Aiko Hayauchi[1], Sho Kimura[2] (1.MalvernPanalytical Japan ,Div of Spectris Co.Ltd,., 2.Faculty of Agriculture, University of the Ryukyu)

11:15 AM - 11:30 AM JST | 2:15 AM - 2:30 AM UTC

### [SCG52-03] Crystal structure and local structures of natural perovskite-type (Na,REE,Ca)(Ti, Nb)$O_3$ loparite by single crystal diffraction and XAFS analyses

*Ginga Kitahara[1], Akira Yoshiasa[1], Makoto Tokuda[1], Kazumasa Sugiyama[2] (1.Kumamoto University, 2.Tohoku University)

11:30 AM - 11:45 AM JST | 2:30 AM - 2:45 AM UTC

### [SCG52-04] Crystal Size Distributions based on crystal habit of groundmass pyroxene crystals in the ejecta of the Shinmoedake 2011 eruption

*Shota Okumura[1], Mayumi Mujin[2], Akira Tsuchiyama[1], Norimasa Shimobayashi[1], Akira Miyake[1] (1.Department of Geology and Mineralogy, Graduate School of Science, Kyoto University, 2.Division of Earth and Planetary Materials Science, Department of Earth Science, Tohoku University)

11:45 AM - 12:00 PM JST | 2:45 AM - 3:00 AM UTC

### [SCG52-05] Petrochemistry and zircon U-Pb age of ``lateritic'' metamorphic rocks from the Kitakami Mountains

*Nobutaka Tsuchiya[1], Yamato Kumagai[1], Tatsuro Adachi[2], Nobuhiko Nakano[2], Yasuhito Osanai[2] (1.Department of Geology, Faculty of Education, Iwate University, 2.Department of Earth Sciences, Faculty of Social and Cultural Studies, Kyushu University)

12:00 PM - 12:15 PM JST | 3:00 AM - 3:15 AM UTC

### [SCG52-06] How to make 'syn-plutonic dike' - - - Another story from the Ryoke granitic province, Southwest Japan

*Takashi Nakajima[1], Hiroyuki Kamiyama[2], Ian S. Williams[3] (1.Geological Survey of Japan, 2.Ueyama-Shisui, Co. Ltd., 3.Australian National University)

[J] Poster | S (Solid Earth Sciences )：S-CG Complex & General

3:30 PM - 5:00 PM JST | 6:30 AM - 8:00 AM UTC | Poster Hall International Exhibition Hall8, Makuhari Messe_15

## [S-CG52] Petrology, Mineralogy & Resource Geology

convener:Tatsuo Nozaki(Research and Development Center for Submarine Resources, Japan Agency for Marine-Earth Science and Technology), Satoshi SAITO(Graduate School of Science and Engineering, Ehime University), Koichi Momma(National Museum of Nature and Science), Nobutaka Tsuchiya(Department of Geology, Faculty of Education, Iwate University)

[SCG52-P01] Combined microspectroscopic characterization of a red-colored granite rock sample

*Katsuya Okada[1], Satoru Nakashima[1] (1.Department of Earth and Space Science, Graduate School of Science, Osaka University)

[SCG52-P02] Crystal chemistry of synthetic mukhinite, V-analogue of clinozoisite, on the join $Ca_2Al_3Si_3O_{12}(OH)$-$Ca_2Al_2VSi_3O_{12}(OH)$

*Mariko Nagashima[1], Daisuke Nishio-Hamane[2], Nobuhiko Nakano[3], Toshisuke Kawasaki[4] (1.Graduate school of Sciences and Technology for Innovation, Yamaguchi University, 2.The institute for Solid State Physics, the University of Tokyo, 3.Department of Environmental Changes, Faculty of Social and Cultural Studies, Kyushu University, 4.Faculty of Science, Ehime University)

[SCG52-P03] High temperature In-situ TEM observation of crystallization in Sakurajima volcanic glass

*Akira Miyake[1], Shota Okumura[1] (1.Department of Geology and Mineralogy, Graduate School of Science, Kyoto University)

[SCG52-P04] Timing of intrusion and Sr isotopic composition of granodiorite porphyrites in the Noko Island, western part of northern Kyushu

*Masaki Yuhara[1], Yoshinobu Kawano[2], Osamu Okano[3] (1.Department of Earth System Science, Faculty of Science, Fukuoka University, 2.Department of Environment Systems, Faculty of Geo-environmental Science, Rissho University, 3.Department of Earth Sciences, Faculty of Science, Okayama University)

[SCG52-P05] Petrological study of crystallization process of a composite dike in the Ryoke belt (Mie Prefecture, SW Japan)

*Ayu Yamazaki[1], Tetsuo Kawakami[1], Fumiko Higashino[2] (1.Department of Geology and Mineralogy, Graduate school of Science, Kyoto University , 2.Graduate school of Environmental Studies, Tohoku University)

[SCG52-P06] Petrography and Zircon U-Pb ages of the Ryoke Granitoids distributed in the Takanawa Peninsula, Ehime Prefecture.

*Kazuya Shimooka[1], Satoshi SAITO[1], Kenichiro Tani[2] (1.Graduate School of Science and Engineering, Ehime University, 2.Department of Geology and Paleontology, National Museum of Nature and Science)

[SCG52-P07] Neoproterozoic arc magmatism and high-grade metamorphism of the basement rocks in southern Malawi

*Toshiaki Tsunogae[1], Sam Uthup[1], Mzee Wandembo Nyirongo[2], Md. Sazzadur Rahman[1], Yusuke Takamura[1], Kazuki Takahashi[1] (1.University of Tsukuba, 2.Malawi University of Science and Technology)

[SCG52-P08] Geochemical features of Quaternary rhyolitic magma and xenolith from Hime-shima volcanic group

*Takehiro Hirayama[1], Tomoyuki Shibata[1], Masako Yoshikawa[1], Yasutaka Hayasaka[1], Keiji Takemura[2] (1.Department of Earth and Planetary Systems Science, Graduate School of Science, Hiroshima University, 2.Kyoto university)

[SCG52-P09] Petrological study on the intrusive contact of a Setouchi volcanic rock dike in the Nakajima Island, Ehime Prefecture

*Taiki Omori[1], Satoshi SAITO[2] (1.Department of Earth Science, Faculty of Science, Ehime University , 2.Department of Earth Science, Graduate Schoole of Science, Ehime University)

[SCG52-P10] **Fundamental evaluation for making simulated sea bed floc**

*AIKO HAYAUCHI[1], Daisuke Sasakura[1], Hisato Yasuda[2], Shinya Nakamura[3], Sho Kimura[3], Shohei Noda[4] (1.Malvern Panalytical division of Spectris Co., Ltd, 2.Kochi University, 3.UNIVERSITY OF THE RYUKYU, 4.TOKYO UNIVESITY OF SCIENCE)

[SCG52-P11] Petrology of the Morobe Granodiorite in the Kuper Range, Morobe Province, Papua New Guinea

Angela Lynett Bokuik[1], *Takashi Hoshide[1] (1.Faculty of International Resource Sciences, Akita University)

---

[SCG52-P12] Sr–Nd isotopic compositions of the San-yo Belt, Southwest Japan: Implications for the Cretaceous enriched mantle

*Shogo Kodama[1], Masaaki Owada[1], Teruyoshi Imaoka[1], Atsushi Kamei[2] (1.Yamaguchi University, 2.Shimane University)

---

[SCG52-P13] Lithological variation of massive serpentinites in marginal zone of serpentinite body in Kamuikotan belt, Hokkaido, Japan: Analysis of advanced-boring cores for tunnel construction

*Shusaku Yamazaki[1], Kenji Okazaki[1], Toshiyuki Kurahashi[1] (1.Civil Engineering Research Institute for Cold Region, Public Works Research Institute, National Research and Development Agancy)

[J] Poster | S (Solid Earth Sciences )：S-CG Complex & General

5:15 PM - 6:30 PM JST | 8:15 AM - 9:30 AM UTC | Poster Hall International Exhibition Hall8, Makuhari Messe_28

## [S-CG52] Petrology, Mineralogy & Resource Geology

convener:Tatsuo Nozaki(Research and Development Center for Submarine Resources, Japan Agency for Marine-Earth Science and Technology), Satoshi SAITO(Graduate School of Science and Engineering, Ehime University), Koichi Momma(National Museum of Nature and Science), Nobutaka Tsuchiya(Department of Geology, Faculty of Education, Iwate University)

[SCG52-P01] Combined microspectroscopic characterization of a red-colored granite rock sample

*Katsuya Okada[1], Satoru Nakashima[1] (1.Department of Earth and Space Science, Graduate School of Science, Osaka University)

[SCG52-P02] Crystal chemistry of synthetic mukhinite, V-analogue of clinozoisite, on the join $Ca_2Al_3Si_3O_{12}(OH)$-$Ca_2Al_2VSi_3O_{12}(OH)$

*Mariko Nagashima[1], Daisuke Nishio-Hamane[2], Nobuhiko Nakano[3], Toshisuke Kawasaki[4] (1.Graduate school of Sciences and Technology for Innovation, Yamaguchi University, 2.The institute for Solid State Physics, the University of Tokyo, 3.Department of Environmental Changes, Faculty of Social and Cultural Studies, Kyushu University, 4.Faculty of Science, Ehime University)

[SCG52-P03] High temperature In-situ TEM observation of crystallization in Sakurajima volcanic glass

*Akira Miyake[1], Shota Okumura[1] (1.Department of Geology and Mineralogy, Graduate School of Science, Kyoto University)

[SCG52-P04] Timing of intrusion and Sr isotopic composition of granodiorite porphyrites in the Noko Island, western part of northern Kyushu

*Masaki Yuhara[1], Yoshinobu Kawano[2], Osamu Okano[3] (1.Department of Earth System Science, Faculty of Science, Fukuoka University, 2.Department of Environment Systems, Faculty of Geo-environmental Science, Rissho University, 3.Department of Earth Sciences, Faculty of Science, Okayama University)

[SCG52-P05] Petrological study of crystallization process of a composite dike in the Ryoke belt (Mie Prefecture, SW Japan)

*Ayu Yamazaki[1], Tetsuo Kawakami[1], Fumiko Higashino[2] (1.Department of Geology and Mineralogy, Graduate school of Science, Kyoto University , 2.Graduate school of Environmental Studies, Tohoku University)

[SCG52-P06] Petrography and Zircon U-Pb ages of the Ryoke Granitoids distributed in the Takanawa Peninsula, Ehime Prefecture.

*Kazuya Shimooka[1], Satoshi SAITO[1], Kenichiro Tani[2] (1.Graduate School of Science and Engineering, Ehime University, 2.Department of Geology and Paleontology, National Museum of Nature and Science)

[SCG52-P07] Neoproterozoic arc magmatism and high-grade metamorphism of the basement rocks in southern Malawi

*Toshiaki Tsunogae[1], Sam Uthup[1], Mzee Wandembo Nyirongo[2], Md. Sazzadur Rahman[1], Yusuke Takamura[1], Kazuki Takahashi[1] (1.University of Tsukuba, 2.Malawi University of Science and Technology)

[SCG52-P08] Geochemical features of Quaternary rhyolitic magma and xenolith from Hime-shima volcanic group

*Takehiro Hirayama[1], Tomoyuki Shibata[1], Masako Yoshikawa[1], Yasutaka Hayasaka[1], Keiji Takemura[2] (1.Department of Earth and Planetary Systems Science, Graduate School of Science, Hiroshima University, 2.Kyoto university)

[SCG52-P09] Petrological study on the intrusive contact of a Setouchi volcanic rock dike in the Nakajima Island, Ehime Prefecture

*Taiki Omori[1], Satoshi SAITO[2] (1.Department of Earth Science, Faculty of Science, Ehime University , 2.Department of Earth Science, Graduate Schoole of Science, Ehime University)

[SCG52-P10] **Fundamental evaluation for making simulated sea bed floc**

*AIKO HAYAUCHI[1], Daisuke Sasakura[1], Hisato Yasuda[2], Shinya Nakamura[3], Sho Kimura[3], Shohei Noda[4] (1.Malvern Panalytical division of Spectris Co., Ltd, 2.Kochi University, 3.UNIVERSITY OF THE RYUKYU, 4.TOKYO UNIVESITY OF SCIENCE)

[SCG52-P11] Petrology of the Morobe Granodiorite in the Kuper Range, Morobe Province, Papua New Guinea

Angela Lynett Bokuik[1], *Takashi Hoshide[1] (1.Faculty of International Resource Sciences, Akita University)

[SCG52-P12] Sr–Nd isotopic compositions of the San-yo Belt, Southwest Japan: Implications for the Cretaceous enriched mantle

*Shogo Kodama[1], Masaaki Owada[1], Teruyoshi Imaoka[1], Atsushi Kamei[2] (1.Yamaguchi University, 2.Shimane University)

[SCG52-P13] Lithological variation of massive serpentinites in marginal zone of serpentinite body in Kamuikotan belt, Hokkaido, Japan: Analysis of advanced-boring cores for tunnel construction

*Shusaku Yamazaki[1], Kenji Okazaki[1], Toshiyuki Kurahashi[1] (1.Civil Engineering Research Institute for Cold Region, Public Works Research Institute, National Research and Development Agancy)

[J] Oral | S (Solid Earth Sciences )：S-CG Complex & General

10:45 AM - 12:15 PM JST | 1:45 AM - 3:15 AM UTC | A05 TOKYO BAY MAKUHARI HALL

## [S-CG53] Environment formed and maintained by active faults

convener:Naoji Koizumi(School of Environmental Science,the University of Shiga Prefecture), Makoto Yamano(Earthquake Research Institute, the University of Tokyo), Takafumi Kasaya(Japan Agency for Marine-Earth Science and Technology), Hideki Hamamoto(Center for Environmental Science in Saitama), Chairperson:NAOJI KOIZUMI, TADANORI GOTO(Graduate School of Engineering, Kyoto University)

10:45 AM - 11:00 AM JST | 1:45 AM - 2:00 AM UTC

[SCG53-01] **Effect of the Hanaore fault and Biwako-seigan fault on the water quality of the Ado river in Shiga Prefecture**

*Naoji Koizumi[1], Masahiro Ueda[1], Shinsuke Minote[1], Tatsuya Tanaka[1], Masahiro Maruo[1], Kanto Mitani[2] (1.School of Environmental Science,the University of Shiga Prefecture, 2.Daikokuten Bussan Co., Ltd.)

11:00 AM - 11:15 AM JST | 2:00 AM - 2:15 AM UTC

[SCG53-02] **Hydrothermal vents in the deep basin of Lake Biwa**

★Invited Papers

*Michio Kumagai[1] (1.Ritsumeikan University)

11:15 AM - 11:30 AM JST | 2:15 AM - 2:30 AM UTC

[SCG53-03] Heat flow anomalies observed on the seafloor in the vicinity of faults: indication of fluid flow

*Makoto Yamano[1], Shusaku Goto[2], Yoshifumi Kawada[3], Hideki Hamamoto[4] (1.Earthq. Res. Inst., Univ. Tokyo, 2.Geol. Surv. Japan, AIST, 3.IRIDeS, Tohoku Univ., 4.Center Environ. Sci. Saitama)

11:30 AM - 11:45 AM JST | 2:30 AM - 2:45 AM UTC

[SCG53-04] How can we quantify the hydraulic permeability of fault based on geophysical survey?

*Tada-nori Goto[1], Sota Kawaguchi[1] (1.Graduate School of Engineering, Kyoto University)

11:45 AM - 12:00 PM JST | 2:45 AM - 3:00 AM UTC

[SCG53-05] Healing process of the Nojima Fault zone after 1995 Hyogo-ken Nanbu earthquake

*Hideki Murakami[1], Naoto Oshiman[2], Ryokei Yoshimura[2], Tsutomu Miura[2], Masato Kamo[2] (1.Research and Education Faculty,Kochi University, 2.Disaster Prevention Research Institute,Kyoto University)

12:00 PM - 12:15 PM JST | 3:00 AM - 3:15 AM UTC

[SCG53-06] Discussion on the environment formed and maintained by active faults

*Naoji Koizumi[1] (1.School of Environmental Science,the University of Shiga Prefecture)

[J] Poster | S (Solid Earth Sciences )：S-CG Complex & General

3:30 PM - 5:00 PM JST | 6:30 AM - 8:00 AM UTC | Poster Hall International Exhibition Hall8, Makuhari Messe_16

## [S-CG53] Environment formed and maintained by active faults

convener:Naoji Koizumi(School of Environmental Science,the University of Shiga Prefecture), Makoto Yamano(Earthquake Research Institute, the University of Tokyo), Takafumi Kasaya(Japan Agency for Marine-Earth Science and Technology), Hideki Hamamoto(Center for Environmental Science in Saitama)

### [SCG53-P01] Heat flow measurement in Lake Biwa

*Hideki Hamamoto[1], Makoto Yamano[2] (1.Center for Environmental Science in Saitama, 2.Earthquake Research Institute, University of Tokyo)

### [SCG53-P02] Shallow Resistivity Structure across the Futagawa-Fault Nishihara Area and the Reliability

*Tada-nori Goto[1], Hisatoshi Koji[1], Sota Kawaguchi[1], Satoru Yamaguchi[2], Yuto Yamalaka[2], Daigo Furukawa[2], Koki Aizawa[3] (1.Graduate School of Engineering, Kyoto University, 2.Graduate School of Science, Osaka City University, 3.Institute of Seismology and Volcanology, Faculty of Sciences, Kyushu University)

### [SCG53-P03] Detailed topography and sub-surface structure around the 2016 Fukushima Earthquake

*Takafumi Kasaya[1], Toshiya Fujiwara[1], Toshiya Kanamatsu[1], Katsunori FUJIKURA[1] (1.Japan Agency for Marine-Earth Science and Technology)

[J] Poster | S (Solid Earth Sciences )：S-CG Complex & General

5:15 PM - 6:30 PM JST | 8:15 AM - 9:30 AM UTC | Poster Hall International Exhibition Hall8, Makuhari Messe_29

## [S-CG53] Environment formed and maintained by active faults

convener:Naoji Koizumi(School of Environmental Science,the University of Shiga Prefecture), Makoto Yamano(Earthquake Research Institute, the University of Tokyo), Takafumi Kasaya(Japan Agency for Marine-Earth Science and Technology), Hideki Hamamoto(Center for Environmental Science in Saitama)

### [SCG53-P01] Heat flow measurement in Lake Biwa

*Hideki Hamamoto[1], Makoto Yamano[2] (1.Center for Environmental Science in Saitama, 2.Earthquake Research Institute, University of Tokyo)

### [SCG53-P02] Shallow Resistivity Structure across the Futagawa-Fault Nishihara Area and the Reliability

*Tada-nori Goto[1], Hisatoshi Koji[1], Sota Kawaguchi[1], Satoru Yamaguchi[2], Yuto Yamalaka[2], Daigo Furukawa[2], Koki Aizawa[3] (1.Graduate School of Engineering, Kyoto University, 2.Graduate School of Science, Osaka City University, 3.Institute of Seismology and Volcanology, Faculty of Sciences, Kyushu University)

### [SCG53-P03] Detailed topography and sub-surface structure around the 2016 Fukushima Earthquake

*Takafumi Kasaya[1], Toshiya Fujiwara[1], Toshiya Kanamatsu[1], Katsunori FUJIKURA[1] (1.Japan Agency for Marine-Earth Science and Technology)

[J] Oral | S (Solid Earth Sciences )：S-CG Complex & General

9:00 AM - 10:30 AM JST | 12:00 AM - 1:30 AM UTC | A11 TOKYO BAY MAKUHARI HALL

## [S-CG55] Crustal fluids and deformation

convener:Yuichi Kitagawa(Tectono-Hydrology Research Group, Geological Survey of Japan, National Institute of Advanced Industrial Science and Technology), Naoji Koizumi(School of Environmental Science,the University of Shiga Prefecture), Koji Umeda(Hirosaki University), Fumiaki Tsunomori(Geochemical Research Center, Graduate School of Science, University of Tokyo), Chairperson:Yuichi Kitagawa(産業技術総合研究所地質調査総合センター地震地下水研究グループ), Fumiaki Tsunomori(東京大学大学院理学系研究科地殻化学実験施設)

9:00 AM - 9:15 AM JST | 12:00 AM - 12:15 AM UTC

### [SCG55-01] Estimation of fault models of the short-term SSE using groundwater pressures at the Hokusei observation site

*Yuichi Kitagawa[1], Norio Matsumoto[1] (1.Tectono-Hydrology Research Group, Geological Survey of Japan, National Institute of Advanced Industrial Science and Technology)

---

9:15 AM - 9:35 AM JST | 12:15 AM - 12:35 AM UTC

### [SCG55-02] Groundwater level changes during the 2018 Hokkaido Eastern Iburi earthquake

★Invited Papers

*Tomo Shibata[1], Ryo Takahashi[2], Hiroaki Takahashi[3], Takanori Kagoshima[4], Yuji Sano[4], Daniele Pinti[5] (1.Graduate School of Science, Kyoto University, 2.Geological Survey of Hokkaido, Hokkaido Research Organization, 3.Graduate School of Science, Hokkaido University, 4.Atmosphere and Ocean Research Institute, The University of Tokyo, 5.GEOTOP, Université du Québec)

---

9:35 AM - 9:50 AM JST | 12:35 AM - 12:50 AM UTC

### [SCG55-03] Postseismic streamflow changes after the 2016 Kumamoto earthquake

*Naoji Koizumi[1], Shinsuke Minote[1], Tatusya Tanaka[1] (1.School of Environmental Science,the University of Shiga Prefecture)

---

9:50 AM - 10:05 AM JST | 12:50 AM - 1:05 AM UTC

### [SCG55-04] Development of Radium Concentration Monitoring System based on Gamma-Ray Spectroscopy

*Fumiaki Tsunomori[1], Shigekazu Nagai[2], Junji Yoshii[3], Yoshihide Kimura[4], Yoriyuki Kamakura[5], Yuki Inoue[5], Norihito Sato[6], Shiro Sakuragi[7], Ryuichi Shimizu[8], V N Gluchschenko[9] (1.Geochemical Research Center, Graduate School of Science, University of Tokyo, 2.Graduate School of Engineering, Mie University, 3.Advanced Clinical Research Center, Fukushima Medical University, 4.Graduate School of Engineering, Osaka University, 5.Faculty of Information Science and Technology, Osaka Institute of Technology, 6.Chiyoda Technol corp., 7.Union Material Inc., 8.Office for University-Industry Collaboration, Osaka University, 9.Institute of Nuclear Physics, Almaty, Republic of Kazakhstan)

---

10:05 AM - 10:25 AM JST | 1:05 AM - 1:25 AM UTC

### [SCG55-05] $^{222}$Rn concentration distribution in Yatsushiro Sea

★Invited Papers

*Kuniyo Kawabata[1], Fumiaki Tsunomori[2], Yujin Kitamura[1], Hakuho-Maru K18-3 scientists (1.Graduate School of Science and Engineering, KAGOSHIMA UNIVERSITY, 2.Geochemical Research Center, Graduate School of Science, University of Tokyo)

[J] Poster | S (Solid Earth Sciences )：S-CG Complex & General

3:30 PM - 5:00 PM JST | 6:30 AM - 8:00 AM UTC | Poster Hall International Exhibition Hall8, Makuhari Messe_17

## [S-CG55] Crustal fluids and deformation

convener:Yuichi Kitagawa(Tectono-Hydrology Research Group, Geological Survey of Japan, National Institute of Advanced Industrial Science and Technology), Naoji Koizumi(School of Environmental Science,the University of Shiga Prefecture), Koji Umeda(Hirosaki University), Fumiaki Tsunomori(Geochemical Research Center, Graduate School of Science, University of Tokyo)

[SCG55-P01] Application of slug test model to earthquake-related groundwater-level change in the Oi well Kanagawa Prefecture, Center Japan

*Yang Li[1], Motoo Ukawa[1], Kazuhiro Itadera[2], Masatake Harada[2] (1.Nihon University, 2.Hot Spring Research Institute of Kanagawa Prefecture)

[SCG55-P02] Changes in groundwater level and borehole strain data associated with the 2018 Osaka Hokubu earthquake (M6.1) at the Takarazuka observatory

*Norio Matsumoto[1], Tsutomu Kiguchi[1] (1.Geological Survey of Japan, National Institute of Advanced Industrial Science and Technology (AIST))

[SCG55-P03] Changes in groundwater level at the Kusanagi observatory

*Norio Matsumoto[1] (1.Tectono-Hydrology Research Group, Geological Survey of Japan, National Institute of Advanced Industrial Science and Technology (AIST))

[SCG55-P04] Spatial and temporal changes of $^{3}He/^{4}He$ ratios around a source region before and after an inland earthquake

*Koji Umeda[1] (1.Hirosaki University)

[J] Poster | S (Solid Earth Sciences )：S-CG Complex & General

5:15 PM - 6:30 PM JST | 8:15 AM - 9:30 AM UTC | Poster Hall International Exhibition Hall8, Makuhari Messe_30

## [S-CG55] Crustal fluids and deformation

convener:Yuichi Kitagawa(Tectono-Hydrology Research Group, Geological Survey of Japan, National Institute of Advanced Industrial Science and Technology), Naoji Koizumi(School of Environmental Science,the University of Shiga Prefecture), Koji Umeda(Hirosaki University), Fumiaki Tsunomori(Geochemical Research Center, Graduate School of Science, University of Tokyo)

[SCG55-P01] Application of slug test model to earthquake-related groundwater-level change in the Oi well Kanagawa Prefecture, Center Japan

*Yang Li[1], Motoo Ukawa[1], Kazuhiro Itadera[2], Masatake Harada[2] (1.Nihon University, 2.Hot Spring Research Institute of Kanagawa Prefecture)

[SCG55-P02] Changes in groundwater level and borehole strain data associated with the 2018 Osaka Hokubu earthquake (M6.1) at the Takarazuka observatory

*Norio Matsumoto[1], Tsutomu Kiguchi[1] (1.Geological Survey of Japan, National Institute of Advanced Industrial Science and Technology (AIST))

[SCG55-P03] Changes in groundwater level at the Kusanagi observatory

*Norio Matsumoto[1] (1.Tectono-Hydrology Research Group, Geological Survey of Japan, National Institute of Advanced Industrial Science and Technology (AIST))

[SCG55-P04] Spatial and temporal changes of $^{3}He/^{4}He$ ratios around a source region before and after an inland earthquake

*Koji Umeda[1] (1.Hirosaki University)

[J] Poster | S (Solid Earth Sciences )：S-CG Complex & General

10:45 AM - 12:15 PM JST | 1:45 AM - 3:15 AM UTC | Poster Hall International Exhibition Hall8, Makuhari Messe_7

## [S-CG58] Brittle-Ductile Transition and Supercritical Geofluids for Crustal Energy in Island Arc

convener:Noriyoshi Tsuchiya(Graduate School of Environmental Studies, Tohoku University), Hiroshi Asanuma(AIST), Yasuo Ogawa(Volcanic Fluid Research Center, School of Science, Tokyo Institute of Technology), Shigemi Naganawa(Akita University)

[SCG58-P01] Mechanical and hydrological properties of granite under supercritical fluid conditions

*Manami Kitamura[1], Miki Takahashi[1] (1.National Institute of Advanced Industrial Science and Technology)

[SCG58-P02] Three-dimensional electrical resistivity structure of kuju Volcano, Central Kyushu, Japan revealed by Magnetotelluric survey data

*Sabry Abdallah[1], Mitsuru Utsugi [1], Koki Aizawa[2], Makoto Uyeshima[3], Wataru Kanda[4], Takao Koyama[3] (1.Institute of geothermal science, Faculty of Science, Kyoto University, 2.Institute of Seismology and Volcanology, Faculty of Sciences, Kyushu University, 3.Earthquake Research Institute, The University of Tokyo, 4.Volcanic Fluid Research Center, School of Science, Tokyo Institute of Technology)

[SCG58-P03] Preliminary Report on Themoluminescence Geothermal Exploration in Northern Area of Mt. Kurikoma (Akayumata-River), NE Japan.

*Hiroki Okano[1], Nobuo Hirano[1], Noriyoshi Tsuchiya[1] (1.Graduate School of Environmental Studies Tohoku University)

[SCG58-P04] Experimental Study of Critical Point Determination for Multicomponent Fluids using light-scattering Spectroscopic Method

*Nobuo Hirano[1], Yuta Oshima[1], Atsushi Okamoto[1], Noriyoshi Tsuchiya[1] (1.Graduate School of Environmental studies, Tohoku University)

[SCG58-P05] Transport and Reaction Behavior of Supercritical Geofluid Revealed by Porphyry Copper Deposit

*Geri Agroli[1], Noriyoshi Tsuchiya[1] (1.Tohoku University)

[SCG58-P06] Characteristics of precipitation of amorphous silica and its influences on permeability of fractured granite in superhot geothermal environments

*Hikaru Abe[1], Noriaki Watanabe[1], Kengo Nakamura[1], Atsushi Okamoto[1], Takeshi Komai[1] (1.Graduate School of Environmental Studies, Tohoku University)

[SCG58-P07] **Evolution and The Total Budget of Fluid in Granitic Magma through Magmatism and Volcanism in The Subduction Zone, NE Japan**

*Fajar Febiani Amanda[1], Ryoichi Yamada[2], Satoshi Okumura[2], Masaoki Uno[1], Noriyoshi Tsuchiya[1] (1.Graduate School of Environmental Studies, Tohoku University, 2.Graduate School of Science, Tohoku University)

[SCG58-P08] **Porosity generation during feldspar replacement as the mark of potassium-rich supercritical fluids on the top of granitic intrusion**

*Astin Nurdiana[1], Atsushi Okamoto[1], Masaoki Uno[1], Kenta Yoshida[2], Noriyoshi Tsuchiya[1] (1.Tohoku University, 2.Japan Agency for Marine-earth Science and Technology)

[SCG58-P09] Quantitative evaluation of fracture distribution in granite and the relationship between fracture distribution and physical properties

*Manami Kadono[1], Shin-ichi Uehara[2], Miki Takahashi[3], Manami Kitamura[3] (1.Department of Environment Systems, Graduate School of frontier Science, The University of Tokyo, 2.Department of Enviroment Science, Faculty of Science, Toho University, 3.National Institute of Advanced Industrial Science and Technology)

[J] Poster | S (Solid Earth Sciences )：S-CG Complex & General

5:15 PM - 6:30 PM JST | 8:15 AM - 9:30 AM UTC | Poster Hall International Exhibition Hall8, Makuhari Messe_31

## [S-CG58] Brittle-Ductile Transition and Supercritical Geofluids for Crustal Energy in Island Arc

convener:Noriyoshi Tsuchiya(Graduate School of Environmental Studies, Tohoku University), Hiroshi Asanuma(AIST), Yasuo Ogawa(Volcanic Fluid Research Center, School of Science, Tokyo Institute of Technology), Shigemi Naganawa(Akita University)

[SCG58-P01] Mechanical and hydrological properties of granite under supercritical fluid conditions

*Manami Kitamura[1], Miki Takahashi[1] (1.National Institute of Advanced Industrial Science and Technology)

---

[SCG58-P02] Three-dimensional electrical resistivity structure of kuju Volcano, Central Kyushu, Japan revealed by Magnetotelluric survey data

*Sabry Abdallah[1], Mitsuru Utsugi [1], Koki Aizawa[2], Makoto Uyeshima[3], Wataru Kanda[4], Takao Koyama[3] (1.Institute of geothermal science, Faculty of Science, Kyoto University, 2.Institute of Seismology and Volcanology, Faculty of Sciences, Kyushu University, 3.Earthquake Research Institute, The University of Tokyo, 4.Volcanic Fluid Research Center, School of Science, Tokyo Institute of Technology)

---

[SCG58-P03] Preliminary Report on Themoluminescence Geothermal Exploration in Northern Area of Mt. Kurikoma (Akayumata-River), NE Japan.

*Hiroki Okano[1], Nobuo Hirano[1], Noriyoshi Tsuchiya[1] (1.Graduate School of Environmental Studies Tohoku University)

---

[SCG58-P04] Experimental Study of Critical Point Determination for Multicomponent Fluids using light-scattering Spectroscopic Method

*Nobuo Hirano[1], Yuta Oshima[1], Atsushi Okamoto[1], Noriyoshi Tsuchiya[1] (1.Graduate School of Environmental studies, Tohoku University)

---

[SCG58-P05] Transport and Reaction Behavior of Supercritical Geofluid Revealed by Porphyry Copper Deposit

*Geri Agroli[1], Noriyoshi Tsuchiya[1] (1.Tohoku University)

---

[SCG58-P06] Characteristics of precipitation of amorphous silica and its influences on permeability of fractured granite in superhot geothermal environments

*Hikaru Abe[1], Noriaki Watanabe[1], Kengo Nakamura[1], Atsushi Okamoto[1], Takeshi Komai[1] (1.Graduate School of Environmental Studies, Tohoku University)

---

[SCG58-P07] **Evolution and The Total Budget of Fluid in Granitic Magma through Magmatism and Volcanism in The Subduction Zone, NE Japan**

*Fajar Febiani Amanda[1], Ryoichi Yamada[2], Satoshi Okumura[2], Masaoki Uno[1], Noriyoshi Tsuchiya[1] (1.Graduate School of Environmental Studies, Tohoku University, 2.Graduate School of Science, Tohoku University)

---

[SCG58-P08] **Porosity generation during feldspar replacement as the mark of potassium-rich supercritical fluids on the top of granitic intrusion**

*Astin Nurdiana[1], Atsushi Okamoto[1], Masaoki Uno[1], Kenta Yoshida[2], Noriyoshi Tsuchiya[1] (1.Tohoku University, 2.Japan Agency for Marine-earth Science and Technology)

---

[SCG58-P09] Quantitative evaluation of fracture distribution in granite and the relationship between fracture distribution and physical properties

*Manami Kadono[1], Shin-ichi Uehara[2], Miki Takahashi[3], Manami Kitamura[3] (1.Department of Environment Systems, Graduate School of frontier Science, The University of Tokyo, 2.Department of Enviroment Science, Faculty of Science, Toho University, 3.National Institute of Advanced Industrial Science and Technology)

[J] Oral | S (Solid Earth Sciences )：S-CG Complex & General

1:45 PM - 3:15 PM JST | 4:45 AM - 6:15 AM UTC | A09 TOKYO BAY MAKUHARI HALL

## [S-CG58] Brittle-Ductile Transition and Supercritical Geofluids for Crustal Energy in Island Arc

convener:Noriyoshi Tsuchiya(Graduate School of Environmental Studies, Tohoku University), Hiroshi Asanuma(AIST), Yasuo Ogawa(Volcanic Fluid Research Center, School of Science, Tokyo Institute of Technology), Shigemi Naganawa(Akita University), Chairperson:Noriyoshi Tsuchiya, Atsushi Okamoto

1:45 PM - 1:55 PM JST | 4:45 AM - 4:55 AM UTC

[SCG58-01] Supercritical Geothermal Resources as a Function of Mass and Energy Transport in Subduction Zone

*Noriyoshi Tsuchiya[1] (1.Graduate School of Environmental Studies, Tohoku University)

1:55 PM - 2:05 PM JST | 4:55 AM - 5:05 AM UTC

[SCG58-02] Outline of NEDO Supercritical Geothermal Project

*Hiroshi Asanuma[1] (1.AIST)

2:05 PM - 2:30 PM JST | 5:05 AM - 5:30 AM UTC

[SCG58-03] Mineral precipitation/dissolution from water and brine with decreasing temperatures along hydrostatic pressures

★Invited Papers

*Kenichi Hoshino[1] (1.Department of Earth and Planetary Systems Science, Hiroshima University)

2:30 PM - 2:45 PM JST | 5:30 AM - 5:45 AM UTC

[SCG58-04] Thermodynamic data of aqueous species for supercritical water–rock interaction: dissolution experiments and density-based extrapolation

*Atsushi Okamoto[1], Hajime Ishii[1], Ryosuke Oyanagi[2], Noriyoshi Tsuchiya[1] (1.Graduate School of Environmental Studies, 2.JAMSTEC)

2:45 PM - 3:00 PM JST | 5:45 AM - 6:00 AM UTC

[SCG58-05] Nitrogen isotope ratios of ammonium in hypersaline hot spring waters distributed along Arima-Takatsuki fault zone.

*Kazuhiro Amita[1], Takashi Nakamura[2], Shinji Ohsawa[3] (1.Faculty of Engineering Science, Akita University, 2.International Research Center for River Basin Environment, University of YAMANASHI, 3.Institute for Geothermal Sciences, Graduate School of Science, Kyoto University)

3:00 PM - 3:15 PM JST | 6:00 AM - 6:15 AM UTC

[SCG58-06] **Crustal fluid pressure gradients and permeability estimated from fluid-rock reaction zones**

*Masaoki Uno[1], Diana Mindaleva[1], Noriyoshi Tsuchiya[1] (1.Graduate School of Environmental Studies, Tohoku University)

[J] Oral | S (Solid Earth Sciences )：S-CG Complex & General

3:30 PM - 5:00 PM JST | 6:30 AM - 8:00 AM UTC | A09 TOKYO BAY MAKUHARI HALL

## [S-CG58] Brittle-Ductile Transition and Supercritical Geofluids for Crustal Energy in Island Arc

convener:Noriyoshi Tsuchiya(Graduate School of Environmental Studies, Tohoku University), Hiroshi Asanuma(AIST), Yasuo Ogawa(Volcanic Fluid Research Center, School of Science, Tokyo Institute of Technology), Shigemi Naganawa(Akita University), Chairperson:Noriyoshi Tsuchiya

3:30 PM - 3:45 PM JST | 6:30 AM - 6:45 AM UTC

[SCG58-07] 3D S-wave velocity structure in volcanic region using surface-wave tomography

*Hiro Nimiya[1], Tatsunori Ikeda[1], Takeshi Tsuji[1] (1.Kyushu University)

---

3:45 PM - 4:00 PM JST | 6:45 AM - 7:00 AM UTC

[SCG58-08] Resistivity-Based Temperature and Permeability Estimation of the Kakkonda Geothermal Field, Japan, Using a Neural Network

*Ugou Tsubasa[1], Kazuya Ishitsuka[2], Toru Mogi[3] (1.Department of Socio-Environmental Engineering Scool of Engineering Hokkaido University, 2.Division of Urban Management, Grduate School of Engineering, Kyoto University, 3.Division of Sustinable Resources Enginieering, Faculty of Engineering, Hokkaido University)

---

4:00 PM - 4:15 PM JST | 7:00 AM - 7:15 AM UTC

[SCG58-09] Preliminary report on geothermal structure revealed by geological and MT surveys around Akayumatasawa river in Sanzugawa caldera, NE Japan

*Keishi Nunohara[1], Kuo Hsuan Tseng[2], Hiroki Okano[1], Yasuo Ogawa[2], Noriyoshi Tsuchiya[1] (1.Graduate school of Environmental Studies Tohoku University , 2.Graduate school of Science , Tokyo Institute of Technology)

---

4:15 PM - 4:30 PM JST | 7:15 AM - 7:30 AM UTC

[SCG58-10] Characterization of hydraulic fracturing phenomena in supercritical geothermal environments revealed by elastic wave measurements

*Miura Takahiro[1], Noriaki Watanabe[1], Kiyotoshi Sakaguchi[1], Ryota Goto, Kota Yamane, Takeshi Komai[1], Youqing CHEN[2], Takuya ISHIBASHI[3], Noriyoshi Tsuchiya[1] (1. Graduate School of Environmental Studies, Tohoku University, 2.Graduate School of Energy Science, Kyoto University, 3.AIST, FREA)

---

4:30 PM - 4:45 PM JST | 7:30 AM - 7:45 AM UTC

[SCG58-11] Experimental measurements of transport pore radius of thermally cracked granite and the relationship of pore structure to permeability

*Sueyoshi Kazumasa[1], Tadashi Yokoyama[2], Ikuo Katayama[1] (1.Department of Earth and Planetary Systems Science, Hiroshima University, 2.Graduate School of Integrated Arts and Sciences, Hiroshima University)

---

4:45 PM - 5:00 PM JST | 7:45 AM - 8:00 AM UTC

[SCG58-12] Geothermal reservoir evaluation by using TL of Quartz and Fluid Flow Simulation Model of the Kakkonda system in Japan

*Alvaro Josue Amaya[1], Nobuo Hirano[1], Noriyoshi Tsuchiya[1] (1.Tohoku University. Graduate School of Environmental Studies)

[J] Poster | S (Solid Earth Sciences )：S-CG Complex & General

10:45 AM - 12:15 PM JST | 1:45 AM - 3:15 AM UTC | Poster Hall International Exhibition Hall8, Makuhari Messe_8

## [S-CG59] Reducing risks from earthquakes, tsunamis & volcanoes: new applications of realtime geophysical data

convener:Masashi Ogiso(Meteorological Research Institute, Japan Meteorological Agency), Naotaka YAMAMOTO CHIKASADA(National Research Institute for Earth Science and Disaster Resilience), Satoshi Kawamoto(Geospatial Information Authority of Japan), Mitsuyuki Hoshiba(Meteorological Research Institute)

[SCG59-P01] Numerical Shake Prediction for earthquake early warning: prediction of distant future using Green function method

*Mitsuyuki Hoshiba[1] (1.Meteorological Research Institute)

[SCG59-P02] Introduction of forward scattering model into the Numerical Shake Prediction scheme

*Masashi Ogiso[1] (1.Meteorological Research Institute, Japan Meteorological Agency)

[SCG59-P03] Magnitude estimation by using ocean-bottom pressure gauge data

*Takeshi Nakamura[1], Eiichiro Araki[2], Narumi Takahashi[1], Kensuke Suzuki[2], Shunroku Yamamoto[3], Masahiro Korenaga[3], Shunta Noda[3] (1.National Research Institute for Earth Science and Disaster Resilience, 2.Japan Agency for Marine-Earth Science and Technology, 3.Railway Technical Research Institute)

[SCG59-P04] Calculation of tsunami propagation by applying ray tracing based on the shortest path method to tsunamis

*Shoji Sekiguchi[1] (1.National Research Institute for Earth Science and Disaster Prevention)

[SCG59-P05] Derivation of the series expansion of Kajiura filter, Green's function of a tsunami

*Nobuki Kame[1], Tetsuya Kusakabe[1], Shingo Watada[1] (1.Earthquake Research Institute, the University of Tokyo)

[J] Poster | S (Solid Earth Sciences )：S-CG Complex & General

5:15 PM - 6:30 PM JST | 8:15 AM - 9:30 AM UTC | Poster Hall International Exhibition Hall8, Makuhari Messe_32

## [S-CG59] Reducing risks from earthquakes, tsunamis & volcanoes: new applications of realtime geophysical data

convener:Masashi Ogiso(Meteorological Research Institute, Japan Meteorological Agency), Naotaka YAMAMOTO CHIKASADA(National Research Institute for Earth Science and Disaster Resilience), Satoshi Kawamoto(Geospatial Information Authority of Japan), Mitsuyuki Hoshiba(Meteorological Research Institute)

[SCG59-P01] Numerical Shake Prediction for earthquake early warning: prediction of distant future using Green function method

*Mitsuyuki Hoshiba[1] (1.Meteorological Research Institute)

[SCG59-P02] Introduction of forward scattering model into the Numerical Shake Prediction scheme

*Masashi Ogiso[1] (1.Meteorological Research Institute, Japan Meteorological Agency)

[SCG59-P03] Magnitude estimation by using ocean-bottom pressure gauge data

*Takeshi Nakamura[1], Eiichiro Araki[2], Narumi Takahashi[1], Kensuke Suzuki[2], Shunroku Yamamoto[3], Masahiro Korenaga[3], Shunta Noda[3] (1.National Research Institute for Earth Science and Disaster Resilience, 2.Japan Agency for Marine-Earth Science and Technology, 3.Railway Technical Research Institute)

[SCG59-P04] Calculation of tsunami propagation by applying ray tracing based on the shortest path method to tsunamis

*Shoji Sekiguchi[1] (1.National Research Institute for Earth Science and Disaster Prevention)

[SCG59-P05] Derivation of the series expansion of Kajiura filter, Green's function of a tsunami

*Nobuki Kame[1], Tetsuya Kusakabe[1], Shingo Watada[1] (1.Earthquake Research Institute, the University of Tokyo)

[J] Oral | S (Solid Earth Sciences )：S-CG Complex & General

1:45 PM - 3:15 PM JST | 4:45 AM - 6:15 AM UTC | A08 TOKYO BAY MAKUHARI HALL

## [S-CG59] Reducing risks from earthquakes, tsunamis & volcanoes: new applications of realtime geophysical data

convener:Masashi Ogiso(Meteorological Research Institute, Japan Meteorological Agency), Naotaka YAMAMOTO CHIKASADA(National Research Institute for Earth Science and Disaster Resilience), Satoshi Kawamoto(Geospatial Information Authority of Japan), Mitsuyuki Hoshiba(Meteorological Research Institute), Chairperson:Mitsuyuki Hoshiba(Meteorological Res. Inst., JMA, Japan), Satoshi Kawamoto(Geospatial Information Authority of Japan )

1:45 PM - 2:00 PM JST | 4:45 AM - 5:00 AM UTC

[SCG59-01] Earthquake early warning in the United States and beyond

★Invited Papers

*Richard M Allen[1] (1.University of California Berkeley)

---

2:00 PM - 2:15 PM JST | 5:00 AM - 5:15 AM UTC

[SCG59-02] Study on the relationship between seismometer site environment and earthquake early warning seismic parameter estimation accuracy

*Katsutomo Niwa[1], Naoyasu Iwata[1], Shunroku Yamamoto[1] (1.Railway Technical Research Institute)

---

2:15 PM - 2:30 PM JST | 5:15 AM - 5:30 AM UTC

[SCG59-03] **Prediction of surface ground motion using underground seismic records based on data assimilation (2)**

*Masaya Ishihara[1], Hisashi Nakahara[1] (1.Solid Earth Physics Laboratory, Department of Geophysics, Graduate School of Science, Tohoku University)

---

2:30 PM - 2:45 PM JST | 5:30 AM - 5:45 AM UTC

[SCG59-04] Development of Realtlime Long-Period Ground-Motion Prediction System and Demonstration Experiment

★Invited Papers

*Shin Aoi[1], Takeshi Kimura[1], Takashi Kunugi[1], Wataru Suzuki[1], Yadab Prasad Dhakal[1], Naoto Kojya[2] (1.National Research Institute for Earth Science and Disaster Resilience, 2.Japan Meteorological Agency)

---

2:45 PM - 3:00 PM JST | 5:45 AM - 6:00 AM UTC

[SCG59-05] Real-time forecasting of long-period ground motions for the Nankai Trough earthquake: The effectivity of the Green function-based data assimilation method

*Atsuki Oba[1], Takashi Furumura[1], Takuto Maeda[2] (1.Earthquake Research Institute, University of Tokyo, 2.Graduate School of Science and Technology, Hirosaki University)

---

3:00 PM - 3:15 PM JST | 6:00 AM - 6:15 AM UTC

[SCG59-06] Development of EEW system exchanging real-time seismic intensity and seismic waveform

*Shigeki Horiuchi[1], Yuko Sato[1], Taku Urabe[2], Yamaimaiti Nizhamudong[3], Kazuo Sasaki[3] (1.Home Seismometer Corporation, 2.telemetra , 3.Challenge)

[J] Oral | S (Solid Earth Sciences )：S-CG Complex & General

3:30 PM - 5:00 PM JST | 6:30 AM - 8:00 AM UTC | A08 TOKYO BAY MAKUHARI HALL

## [S-CG59] Reducing risks from earthquakes, tsunamis & volcanoes: new applications of realtime geophysical data

convener:Masashi Ogiso(Meteorological Research Institute, Japan Meteorological Agency), Naotaka YAMAMOTO CHIKASADA(National Research Institute for Earth Science and Disaster Resilience), Satoshi Kawamoto(Geospatial Information Authority of Japan), Mitsuyuki Hoshiba(Meteorological Research Institute), Chairperson:Naotaka Chikasada(National Res. Inst. for Earth Science and Disaster Resilience), Masashi Ogiso(Meteorological Research Institute, JMA)

3:30 PM - 3:45 PM JST | 6:30 AM - 6:45 AM UTC

[SCG59-07] Enhancements of real time seismic intensity estimation using seismic intensity meters maintained by a local government – Case study on Tottori prefecture -

*Takao Kagawa[1] (1.Tottori University Graduate School of Engineering)

---

3:45 PM - 4:00 PM JST | 6:45 AM - 7:00 AM UTC

[SCG59-08] **Drawig of the realtime seismic intesity on live screen and maximum distribution map for the Earthquak disaster prevension.**
**-Planar indication of seismic intensity using surface ground amplification factor-**

*Kenji Kanjo[1], Isao Takahashi[1], Yoshinori Shinohara[1], Rami Ibrahim[2] (1.Takamisawa cybernetics Co. Ltd, 2.Earthquake Research Institute, University of Tokyo)

---

4:00 PM - 4:15 PM JST | 7:00 AM - 7:15 AM UTC

[SCG59-09] Improvements of the GEONET real-time analysis system (REGARD) for more reliable operation

*Kazuyuki Ohashi[1], Satoshi Abe[1], Yasuaki Kakiage[1], Satoshi Kawamoto[1], Hiroshi Munekane[1] (1.GSI of Japan)

---

4:15 PM - 4:30 PM JST | 7:15 AM - 7:30 AM UTC

[SCG59-10] Development of “real-time” uncertainty evaluation algorithm for the estimated coseismic fault model using MCMC approach

*Keitaro Ohno[1], Yusaku Ohta[1] (1.Recerch Center for Prediction of Earthquakes and Volcanic Eruptions, Graduate School of Science, Tohoku University)

---

4:30 PM - 4:45 PM JST | 7:30 AM - 7:45 AM UTC

[SCG59-11] Drifting float measurement of pressure change by tsunami

*Masayuki Obayashi[1], Shingo Watada[2], Hiroko Sugioka[3] (1.Japan Agency for Marine-Earth Science and Technology, 2.Earthquake Research Institute, University of Tokyo, 3.Department of Planetology, Kobe University)

---

4:45 PM - 5:00 PM JST | 7:45 AM - 8:00 AM UTC

[SCG59-12] Development of the Real-time Forecasting for Meteorite Impact Tsunami

*Naotaka YAMAMOTO CHIKASADA[1], Toshitaka Baba[2], Tetsuharu Fuse[3] (1.NIED, 2.Tokushima University, 3.NICT)

[J] Oral | B (Biogeosciences) : B-PT Paleontology

1:45 PM - 3:15 PM JST | 4:45 AM - 6:15 AM UTC | 201A 2F

## [B-PT05] Biotic History

convener:Isao Motoyama(Department of Earth and Environmental Sciences, Yamagata University), Takao Ubukata(Division of Geology & Mineralogy, Department of Earth & Planetary Sciences, Kyoto University), Kazuyoshi Moriya(Department of Earth Sciences, Faculty of Education and Integrated Arts and Sciences, Waseda University), Chairperson:Isao Motoyama, Takao Ubukata, Kazuyoshi Moriya

1:45 PM - 2:00 PM JST | 4:45 AM - 5:00 AM UTC

### [BPT05-01] Cause of accelerated evolution of Earth's life; four-layered underground robust bio-communities played a critical role for the accelerated genome evolution as a response of mass extinction

*Shigenori Maruyama[1], Akio Kanai[2], Issay Narumi[3] (1.Earth-Life Science Institute, Tokyo Institute of Technology, 2.keio University, 3.Toyo University)

2:00 PM - 2:15 PM JST | 5:00 AM - 5:15 AM UTC

### [BPT05-02] Amino acid composition in molluscan shells and its relation to taxa and shell microstructure ~ Toward reconstruction of ancient trophic level using compound specific isotope analysis of amino acids ~

*Naoki Yugami[1], Akiko Goto[2], Robert Jenkins[2] (1.Graduate School of Natural Science & Technology. Kanazawa Univercity, 2.Institute of Science & Engineering . Kanazawa Univercity)

2:15 PM - 2:30 PM JST | 5:15 AM - 5:30 AM UTC

### [BPT05-03] Relation of shell form to rocking motion in planispiral cephalopods

*Takao Ubukata[1] (1.Division of Geology & Mineralogy, Department of Earth & Planetary Sciences, Kyoto University)

2:30 PM - 2:45 PM JST | 5:30 AM - 5:45 AM UTC

### [BPT05-04] Paleoenvironment aross the Meddle Eocene Climatic Optimum

Hiroki Masui[1], *Kazuyoshi Moriya[1] (1.Department of Earth Sciences, Faculty of Education and Integrated Arts and Sciences, Waseda University)

2:45 PM - 3:00 PM JST | 5:45 AM - 6:00 AM UTC

### [BPT05-05] Reconstruction of the North Pacific subtropical gyre from the Middle to Late Miocene as inferred from radiolarian assemblages

*Shin-ichi Kamikuri[1], Isao Motoyama[2], Taiki Sawada[3] (1.Faculty of Education, Ibaraki University, 2.Faculty of Science, Yamagata University, 3.Japan Petroleum Exploration Co.,Ltd.)

3:00 PM - 3:15 PM JST | 6:00 AM - 6:15 AM UTC

### [BPT05-06] Fossilization processes of Pliocene tree fossils from the Yasu River, Shiga Prefecture, Japan: Organic geochemical approach

*Jinya Nakamura[1], Ken Sawada[2], Masashi A Ikeda[1], Hideto Nakamura[3], Minoru Tsukagoshi[4] (1.Graduate School of Science, Hokkaido University, 2.Department of Earth and Planetary Sciences, Faculty of Science, Hokkaido University, 3.Faculty of Science, Osaka City Univerisity, 4.Osaka Museum of Natural History)

[J] Poster | B (Biogeosciences )：B-PT Paleontology

3:30 PM - 5:00 PM JST | 6:30 AM - 8:00 AM UTC | Poster Hall International Exhibition Hall8, Makuhari Messe_18

## [B-PT05] Biotic History

convener:Isao Motoyama(Department of Earth and Environmental Sciences, Yamagata University), Takao Ubukata(Division of Geology & Mineralogy, Department of Earth & Planetary Sciences, Kyoto University), Kazuyoshi Moriya(Department of Earth Sciences, Faculty of Education and Integrated Arts and Sciences, Waseda University)

[BPT05-P01] Simultaneous observations of both hard and soft tissues of *Oulastrea crispata* (Cnidaria: Scleractinia)

*Rie Tajiri[1], Yuki Tokuda[2], Yoichi Ezaki[1] (1.Osaka City University, 2.Tottori University of Environment Studies)

---

[BPT05-P02] Coral-based paleoenvironmental interpretation and depositional history of the late middle Pleistocene Minatogawa Formation, southern Okinawa-jima, Japan

*Riho Tomatsu[1], Marc Humblet[1], Kazuhiko Fujita[2] (1.Graduate School of Environmental Studies, Nagoya University, 2.Department of Physics and Earth Sciences, University of the Ryukyus)

---

[BPT05-P03] Calcareous nannofossil biostratigraphy and oxygen isotope stratigraphy of the lower part of the Pleistocene formation distributed in the central part of the Pacific side of Japan

*Daisuke Kuwano[1], Yoshimi Kubota[2], Kanako Mantoku[2], Koji Kameo[3] (1.Division of Earth and Environmental Sciences, Graduate School of Science and Engineering, Chiba University, 2.National Museum of Nature and Science, 3.Department of Earth Sciences, faculty of Science, Chiba University)

---

[BPT05-P04] Cretaceous and Miocene geology and paleontology of the Tounai River region, Biratori, Hokkaido

*Isao Motoyama[1], Kotaro Uchimura[2], Tomohiro Nishimura[3], Yojiro Taketani (1.Department of Earth and Environmental Sciences, Yamagata University, 2.JCE Co.,LTD, 3.Hobetsu Museum)

---

[BPT05-P05] Response of benthic organisms to oceanic anoxic event in the Early Jurasic (T-OAE): Insights from quantitative analysis of the trace fossil Phycosiphon from the Nishinakayama Formation, Toyora Group

*Kyosuke Kitabatake[1,2], Kentaro Izumi[3], Kenji Okoshi[1] (1.Department of Environmental Science, Faculty of Science, Toho University, 2.Department of Earth Sciences, College of Science, Ibaraki University, 3.Faculty & Graduate School of Education, Chiba University)

[J] Poster | B (Biogeosciences )：B-PT Paleontology

5:15 PM - 6:30 PM JST | 8:15 AM - 9:30 AM UTC | Poster Hall International Exhibition Hall8, Makuhari Messe_33

## [B-PT05] Biotic History

convener:Isao Motoyama(Department of Earth and Environmental Sciences, Yamagata University), Takao Ubukata(Division of Geology & Mineralogy, Department of Earth & Planetary Sciences, Kyoto University), Kazuyoshi Moriya(Department of Earth Sciences, Faculty of Education and Integrated Arts and Sciences, Waseda University)

[BPT05-P01] Simultaneous observations of both hard and soft tissues of *Oulastrea crispata* (Cnidaria: Scleractinia)

*Rie Tajiri[1], Yuki Tokuda[2], Yoichi Ezaki[1] (1.Osaka City University, 2.Tottori University of Environment Studies)

---

[BPT05-P02] Coral-based paleoenvironmental interpretation and depositional history of the late middle Pleistocene Minatogawa Formation, southern Okinawa-jima, Japan

*Riho Tomatsu[1], Marc Humblet[1], Kazuhiko Fujita[2] (1.Graduate School of Environmental Studies, Nagoya University, 2.Department of Physics and Earth Sciences, University of the Ryukyus)

---

[BPT05-P03] Calcareous nannofossil biostratigraphy and oxygen isotope stratigraphy of the lower part of the Pleistocene formation distributed in the central part of the Pacific side of Japan

*Daisuke Kuwano[1], Yoshimi Kubota[2], Kanako Mantoku[2], Koji Kameo[3] (1.Division of Earth and Environmental Sciences, Graduate School of Science and Engineering, Chiba University, 2.National Museum of Nature and Science, 3.Department of Earth Sciences, faculty of Science, Chiba University)

---

[BPT05-P04] Cretaceous and Miocene geology and paleontology of the Tounai River region, Biratori, Hokkaido

*Isao Motoyama[1], Kotaro Uchimura[2], Tomohiro Nishimura[3], Yojiro Taketani (1.Department of Earth and Environmental Sciences, Yamagata University, 2.JCE Co.,LTD, 3.Hobetsu Museum)

---

[BPT05-P05] Response of benthic organisms to oceanic anoxic event in the Early Jurasic (T-OAE): Insights from quantitative analysis of the trace fossil Phycosiphon from the Nishinakayama Formation, Toyora Group

*Kyosuke Kitabatake[1,2], Kentaro Izumi[3], Kenji Okoshi[1] (1.Department of Environmental Science, Faculty of Science, Toho University, 2.Department of Earth Sciences, College of Science, Ibaraki University, 3.Faculty & Graduate School of Education, Chiba University)

[E] Poster | M (Multidisciplinary and Interdisciplinary)：M-IS Intersection

10:45 AM - 12:15 PM JST | 1:45 AM - 3:15 AM UTC | Poster Hall International Exhibition Hall8, Makuhari Messe_9

## [M-IS03] Evolution and variability of the Asian monsoon in Cenozoic global climate changes

convener:Masanobu Yamamoto(Faculty of Environmental Earth Science, Hokkaido University), Ryuji Tada(Department of Earth and Planetary Science, Graduate School of Science, The Univeristy of Tokyo)

[MIS03-P01] Asian dust source variability since 10 Ma based on grain size specific mineral composition at IODP Site U1425 in the Japan Sea

*Mui Fa Alison Lee[1], Tomohisa Irino[1] (1.Faculty of Environmental Earth Science, Hokkaido University)

[MIS03-P02] Sources and formation environment of biomass burning products in Pliocene and Pleistocene marine sediments in the Japan Sea

*Song Lu[1], Youhei Yamashita[2], Tomohisa Irino[2] (1.Graduate School of Environmental Science, Hokkaido University , 2.Faculty of Environmental Earth Science, Hokkaido University)

[MIS03-P03] Variation of mineral dust flux in peat at a high moor on the Mt. Daisetsu during Holocene

*Tomohisa Irino[1], Keisuke Hirai[1], Osamu Seki[1], James Hooper[2], Samuel Marx[2] (1.Hokkaido University, 2.University of Wollongong)

[MIS03-P04] Variations in sea surface environments recorded by algal biomarkers in the Japan Sea off the western coast of Hokkaido (IODP Site U1422) over the last 250 ka

*Asako Suzuki[1], Ken Sawada[2], Satoshi Furota[3], Yaeko Igarashi[4], Tomohisa Irino[5] (1.Graduate School of Science, Hokkaido University, 2.Department of Earth and Planetary Sciences, Faculty of Science, Hokkaido University, 3.Japan Agency for Marine-Earth Science and Technology, 4.Institute for Paleoenvironment of Northern Regions, 5.Faculty of Environmental Earth Science, Hokkaido University)

[MIS03-P05] **Decadal oscillation in hydrogen stable isotope ratio of long chain fatty acids in Lake Suigetsu sediment core**

*Masaya Inagaki[1], Masanobu Yamamoto[1,2], Takeshi Nakagawa[3] (1.Graduate School of Environmental Science, Hokkaido University, 2.Faculty of Environmental Earth Science, Hokkaido University, 3.Research Center for Palaeoclimatology, Ritsumeikan University)

[MIS03-P06] **Amplitude modulation of sea surface temperature variability in the Bay of Bengal by 400-kyr eccentricity cycle**

*Masanobu Yamamoto[1], Yuko Tsuchiya[1], Steven Clemens[2] (1.Faculty of Environmental Earth Science, Hokkaido University, 2.Department of Earth, Planetary and Environmental Sciences, Brown University)

[E] Poster | M (Multidisciplinary and Interdisciplinary)：M-IS Intersection

5:15 PM - 6:30 PM JST | 8:15 AM - 9:30 AM UTC | Poster Hall International Exhibition Hall8, Makuhari Messe_34

## [M-IS03] Evolution and variability of the Asian monsoon in Cenozoic global climate changes

convener:Masanobu Yamamoto(Faculty of Environmental Earth Science, Hokkaido University), Ryuji Tada(Department of Earth and Planetary Science, Graduate School of Science, The Univeristy of Tokyo)

[MIS03-P01] Asian dust source variability since 10 Ma based on grain size specific mineral composition at IODP Site U1425 in the Japan Sea

*Mui Fa Alison Lee[1], Tomohisa Irino[1] (1.Faculty of Environmental Earth Science, Hokkaido University)

[MIS03-P02] Sources and formation environment of biomass burning products in Pliocene and Pleistocene marine sediments in the Japan Sea

*Song Lu[1], Youhei Yamashita[2], Tomohisa Irino[2] (1.Graduate School of Environmental Science, Hokkaido University , 2.Faculty of Environmental Earth Science, Hokkaido University)

[MIS03-P03] Variation of mineral dust flux in peat at a high moor on the Mt. Daisetsu during Holocene

*Tomohisa Irino[1], Keisuke Hirai[1], Osamu Seki[1], James Hooper[2], Samuel Marx[2] (1.Hokkaido University, 2.University of Wollongong)

[MIS03-P04] Variations in sea surface environments recorded by algal biomarkers in the Japan Sea off the western coast of Hokkaido (IODP Site U1422) over the last 250 ka

*Asako Suzuki[1], Ken Sawada[2], Satoshi Furota[3], Yaeko Igarashi[4], Tomohisa Irino[5] (1.Graduate School of Science, Hokkaido University, 2.Department of Earth and Planetary Sciences, Faculty of Science, Hokkaido University, 3.Japan Agency for Marine-Earth Science and Technology, 4.Institute for Paleoenvironment of Northern Regions, 5.Faculty of Environmental Earth Science, Hokkaido University)

[MIS03-P05] **Decadal oscillation in hydrogen stable isotope ratio of long chain fatty acids in Lake Suigetsu sediment core**

*Masaya Inagaki[1], Masanobu Yamamoto[1,2], Takeshi Nakagawa[3] (1.Graduate School of Environmental Science, Hokkaido University, 2.Faculty of Environmental Earth Science, Hokkaido University, 3.Research Center for Palaeoclimatology, Ritsumeikan University)

[MIS03-P06] **Amplitude modulation of sea surface temperature variability in the Bay of Bengal by 400-kyr eccentricity cycle**

*Masanobu Yamamoto[1], Yuko Tsuchiya[1], Steven Clemens[2] (1.Faculty of Environmental Earth Science, Hokkaido University, 2.Department of Earth, Planetary and Environmental Sciences, Brown University)

[E] Oral | M (Multidisciplinary and Interdisciplinary) : M-IS Intersection

1:45 PM - 3:15 PM JST | 4:45 AM - 6:15 AM UTC | 304 3F

## [M-IS03] Evolution and variability of the Asian monsoon in Cenozoic global climate changes

convener:Masanobu Yamamoto(Faculty of Environmental Earth Science, Hokkaido University), Ryuji Tada(Department of Earth and Planetary Science, Graduate School of Science, The Univeristy of Tokyo), Chairperson:Masanobu Yamamoto(Hokkaido University), Tomohisa Irino, Yoshimi Kubota(National Science Museum), Ryuji Tada(The University of Tokyo)

1:45 PM - 2:00 PM JST | 4:45 AM - 5:00 AM UTC

[MIS03-01] **Reconstruction of Indian summer monsoon variability during the last 1,460,000 years**

*Masanobu Yamamoto[1], Steven Clemens[2] (1.Faculty of Environmental Earth Science, Hokkaido University, 2.Department of Earth, Environmental and Planetary Sciences, Brown University)

---

2:00 PM - 2:20 PM JST | 5:00 AM - 5:20 AM UTC

[MIS03-02] Pleistocene Seawater $\delta^{18}O$ reconstructions from the Indian and East Asian Monsoon Regions

★Invited Papers

*Steven C Clemens[1], Masanobu Yamamoto[2] (1.Brown University, 2.Hokkaido University)

---

2:20 PM - 2:40 PM JST | 5:20 AM - 5:40 AM UTC

[MIS03-03] The Monsoon Erosion Pump

★Invited Papers
# Cancelled

*Liviu Giosan[1] (1.Woods Hole Oceanographic Institution)

---

2:40 PM - 3:00 PM JST | 5:40 AM - 6:00 AM UTC

[MIS03-04] East Asian winter monsoon intensity in the Pleistocene based on seasonal land snail shell stable isotope ratios

★Invited Papers

*David L Dettman[1,3], Xin Wang[2], Mi Wang[2], Junhui Zhang[2] (1.University of Arizona, Geosciences Dept., Environmental Isotope Lab., 2.Lanzhou University, Key Laboratory of Western China's Environmental Systems, College of Earth and Environmental Sciences, 3.Shimane University, Estuary Research Center)

---

3:00 PM - 3:15 PM JST | 6:00 AM - 6:15 AM UTC

[MIS03-05] Reconstruction of ventilation history of the Japan Sea based on physical properties data collected during IODP Exp. 346

*Tomohisa Irino[1], Liviu Giosan[2], Ryuji Tada[3], Ken Ikehara[4] (1.Faculty of Environmental Earth Science, Hokkaido University, 2.Woods Hole Oceanographic Institution, 3.Graduate School of Science, University of Tokyo, 4.Institute of Geology and Geoinformation, National Institute of Advanced Industrial Science and Technology)

[E] Oral | M (Multidisciplinary and Interdisciplinary) : M-IS Intersection

3:30 PM - 5:00 PM JST | 6:30 AM - 8:00 AM UTC | 304 3F

## [M-IS03] Evolution and variability of the Asian monsoon in Cenozoic global climate changes

convener:Masanobu Yamamoto(Faculty of Environmental Earth Science, Hokkaido University), Ryuji Tada(Department of Earth and Planetary Science, Graduate School of Science, The Univeristy of Tokyo), Chairperson:Ryuji Tada(The University of Tokyo), Yoshimi Kubota(National Science Museum), Masanobu Yamamoto(Hokkaido University)

3:30 PM - 3:45 PM JST | 6:30 AM - 6:45 AM UTC

[MIS03-06] The spatial-temporal patterns of Indian monsoonal variations during the past 80 kyr recorded in NGHP-02 Hole 19B, western Bay of Bengal: Implications from chemical and mineral properties

*Yuki Ota[1,2,3,4], Hodaka Kawahata[4], Junichiro Kuroda[4,3], Atsushi Suzuki[2], Daisuke Araoka[2], Asuka Yamaguchi[4], Ayako Abe-Ouchi[4] (1.Department of Earth and Planetary Science, The University of Tokyo, 2.Geological Survey of Japan, National Institute of Advanced Industrial Science and Technology, 3.Department of Biogeochemistry, Japan Agency for Marine-Earth Science and Technology, 4.Atmosphere and Ocean Research Institute, The University of Tokyo)

3:45 PM - 4:05 PM JST | 6:45 AM - 7:05 AM UTC

[MIS03-07] **400,000 years millennial scale temperature and rainfall in East Asia deduced from paired Mg/Ca and oxygen isotope of planktic foraminifera from the East China Sea**

★Invited Papers

*Yoshimi Kubota[1], Steven Clemens[2], Kyung-Eun Lee[3], Ann Holbourn[4], Etsuko Wakisaka[5], Keiji Horikawa[5], Ryuji Tada[6], Katsunori Kimoto[7] (1.National Museum of Nature and Science, 2.Brown University, 3.Korea Maritime and Ocean University, 4.Christian-Albrechts-University, 5.University of Toyama, 6.The University of Tokyo, 7.Japan Agency for Marine-Earth Science and Technology)

4:05 PM - 4:20 PM JST | 7:05 AM - 7:20 AM UTC

[MIS03-08] Onset and evolution of millennial-scale variability of East Asian Monsoon recorded in the Japan Sea sediments: New data with new interpretation

*Ryuji Tada[1], Tomohisa Irino[2], Arisa Seki[3], Masafumi Murayama[4], Kaz Mitake[1], Masayuki Ikeda[5] (1.Department of Earth and Planetary Science, Graduate School of Science, The Univeristy of Tokyo, 2.Faculty of Environmental Earth Science, Hokkaido University, 3.Faculty of Science, Shinshu University, 4.Faculty of Agriculture and Marine Science, 5.Shizuoka University)

4:20 PM - 4:40 PM JST | 7:20 AM - 7:40 AM UTC

[MIS03-09] Interhemispheric linkages of Australian and Asian monsoons on a warmer-than-modern Earth

★Invited Papers

*Ann E Holbourn[1], Wolfgang Kuhnt[1], Janika Joehnck[1], Sebastian Beil[1], Julia Luebbers[1], Kenji Marc Raymond Matsuzaki[2], Yair Rosenthal[3], Denise Kulhanek[4], IODP Expedition 363 Scientists (1.University of Kiel, 2.University of Tokyo, 3.Rutgers University, 4.Texas A&M University)

4:40 PM - 5:00 PM JST | 7:40 AM - 8:00 AM UTC

[MIS03-10] **Miocene evolution of the Asian Monsoon from climate and productivity proxies in the Bay of Bengal and South China Sea**

★Invited Papers

*Wolfgang Kuhnt[1], Julia Luebbers[1], Ann Holbourn[1], Karlos GD Kochhann[2], Steven C Clemens[3], Clara T Bolton[4], Yoichi Usui[5] (1.University of Kiel, 2.UNISINOS University, 3.Brown University, 4.Aix-Marseille Université, 5.Japan Agency for Marine-Earth Science and Technology)

[E] Poster | M (Multidisciplinary and Interdisciplinary)：M-IS Intersection

10:45 AM - 12:15 PM JST | 1:45 AM - 3:15 AM UTC | Poster Hall International Exhibition Hall8, Makuhari Messe_10

## [M-IS04] Interdisciplinary studies on pre-earthquake processes

convener:Katsumi Hattori(Department of Earth Sciences, Graduate School of Science, Chiba University), JANN-YENQ Liu(Institute of Space Science, National Central University, Taiwan), Dimitar Ouzounov(Center of Excellence in Earth Systems Modeling & Observations (CEESMO) , Schmid College of Science & Technology Chapman University, Orange, California, USA), Qinghua Huang(Peking University)

### [MIS04-P01] Statistical analysis and Evaluation of ULF seismo-magnetic phenomena at Kakioka, Japan, during 1983-2017

*Kei Takahashi[1], Katsumi Hattori[2], Peng Han[3] (1.Faculty of Science, Chiba University, 2.Graduate School of Science, Chiba University, 3.Southern University of Science and Technology, China)

### [MIS04-P02] Pre-seismic anomalies on Earth's magnetic field and ionosphere electron density using Swarm data

*Amune Yamazaki[1], Katsumi Hattori[1], Rui Song[1] (1.Chiba University)

### [MIS04-P03] Measurement of radon density in the atmosphere at Okayama, Kochi, Choshi and Kiyosumi, II

*Tohru Okabayashi[1], Kiyotaka Ninagawa[2], Isao Yamamoto[3], Katsumi Hattori[4], Chie Yoshino[4], Haruna Kojima[4], Nobuhiro Maeda (1.Department of Merical Risk and Crisis Management, Faculty of Risk and Crisis Management, Chiba Institute of Science, 2.Faculty of Science, Okayama University of Science, 3.Falcuty of Engineering, Okayama University of Science, 4.Graduate school of Science, Chiba University)

### [MIS04-P04] Possible anomalous changes in solar quiet-daily geomagnetic variation *Sq* related to the 2011 off the Pacific coast of Tohoku earthquake (Mw 9.0)

*Xiaocan Liu[1], Katsumi Hattori[2,3], Peng Han[4], Huaran Chen[1] (1.Institute of geophysics China Earthquake Administrition, 2.Graduate School of Science, Chiba University, Chiba, Japan, 3. Center for Environmental Remote Sensing, Chiba University, Chiba, Japan, 4.Department of Earth and Space Sciences, Southern University of Science and Technology, ShenZhen, China)

### [MIS04-P05] Co-seismic geomagnetic fluctuations and atmospheric disturbances during the 2018 M6.2 Hualien Earthquake

*Chun-Rong Chen[1], JANN-YENQ Liu[1] (1.Graduate Institute of Space Science, National Central University)

### [MIS04-P06] Multi-sensor monitoring network for earthquake precursor study near subduction zone at Boso, Japan

*Katsumi Hattori[1], Chie Yoshino[1], WEIYUN XIE[2], Sanaka Saito[2], Haruna Kojima[2], Rui Song[2], Peng Han[3], Toru Mogi[4], Tada-nori Goto[5], Ichi Takumi[6], Hiroshi Yasukawa[7], Motoaki Mouri[8], Jun Izutsu[9], Tadashi Takano[10], Chihiro Yamanaka[11], Masashi Kamogawa[12], Yoshiaki Ando[13], JANN-YENQ Liu[14], Dimitar Ouzounov[15], Valery Tramutoli[16] (1.Department of Earth Sciences, Graduate School of Science, Chiba University, 2.Graduate School of Science and Engineering, Chiba University, 3.Southern University of Science and Technology, China, 4.Hokkaido University, 5.Kyoto University, 6.Nagoya Institute of Technology, 7.Aichi Prefectural University, 8.Aichi University, 9.Chubu University, 10.Nihon University, 11.Osaka University, 12.Tokyo Gakugei University, 13.The University of Electro-Communications, 14.National Central University, Taiwan, 15.Chapman University, US, 16.University of Basilicagta, Italy)

### [MIS04-P07] Transient Effects in Atmosphere and Ionosphere Associated with 2018 Mw 7.5 Sulawesi Indonesia Earthquake and Triggered Tsunami and Volcano Activities

★Invited Papers

*Dimitar Ouzounov[1], Sergey Pulinets[2], Dmitry Davidenko[2], Alexander Rozhnoi[3], Maria Solovieva[3], Tiger Liu[4] (1.Center of Excellence in Earth Systems Modeling & Observations (CEESMO) , Schmid College of Science & Technology Chapman University, Orange, California, USA, 2.Space Research Institute, RAS, Moscow, Russia, 3.The Schmidt Institute of Physics of the Earth, RAS, Moscow, Russia, 4.Center for Astronautical Physics and Engineering, National Central University, Taoyuan City, Taiwan)

### [MIS04-P08] Seismicity change and b value variation prior to the Wenchuan earthquake (*Ms 8.0*)

*Peng Han[1], Rui Wang[1], Ying Chang[1], Miao Miao[1], Haixia Shi[2], Lingyuan Meng[2], Xuemei Zhang[2], Weiyun Xie[3], Katsumi Hattori[3] (1.Southern University of Science and Technology, Shenzhen, China, 2.China Earthquake Networks

Center, Beijing 100045, China, 3.Chiba University, Chiba, Japan)

[E] Poster | M (Multidisciplinary and Interdisciplinary)：M-IS Intersection

5:15 PM - 6:30 PM JST | 8:15 AM - 9:30 AM UTC | Poster Hall International Exhibition Hall8, Makuhari Messe_35

## [M-IS04] Interdisciplinary studies on pre-earthquake processes

convener:Katsumi Hattori(Department of Earth Sciences, Graduate School of Science, Chiba University), JANN-YENQ Liu(Institute of Space Science, National Central University, Taiwan), Dimitar Ouzounov(Center of Excellence in Earth Systems Modeling & Observations (CEESMO) , Schmid College of Science & Technology Chapman University, Orange, California, USA), Qinghua Huang(Peking University)

### [MIS04-P01] Statistical analysis and Evaluation of ULF seismo-magnetic phenomena at Kakioka, Japan, during 1983-2017

*Kei Takahashi[1], Katsumi Hattori[2], Peng Han[3] (1.Faculty of Science, Chiba University, 2.Graduate School of Science, Chiba University, 3.Southern University of Science and Technology, China)

### [MIS04-P02] Pre-seismic anomalies on Earth's magnetic field and ionosphere electron density using Swarm data

*Amune Yamazaki[1], Katsumi Hattori[1], Rui Song[1] (1.Chiba University)

### [MIS04-P03] Measurement of radon density in the atmosphere at Okayama, Kochi, Choshi and Kiyosumi, II

*Tohru Okabayashi[1], Kiyotaka Ninagawa[2], Isao Yamamoto[3], Katsumi Hattori[4], Chie Yoshino[4], Haruna Kojima[4], Nobuhiro Maeda (1.Department of Merical Risk and Crisis Management, Faculty of Risk and Crisis Management, Chiba Institute of Science, 2.Faculty of Science, Okayama University of Science, 3.Falcuty of Engineering, Okayama University of Science, 4.Graduate school of Science, Chiba University)

### [MIS04-P04] Possible anomalous changes in solar quiet-daily geomagnetic variation *Sq* related to the 2011 off the Pacific coast of Tohoku earthquake (Mw 9.0)

*Xiaocan Liu[1], Katsumi Hattori[2,3], Peng Han[4], Huaran Chen[1] (1.Institute of geophysics China Earthquake Administrition, 2.Graduate School of Science, Chiba University, Chiba, Japan, 3. Center for Environmental Remote Sensing, Chiba University, Chiba, Japan, 4.Department of Earth and Space Sciences, Southern University of Science and Technology, ShenZhen, China)

### [MIS04-P05] Co-seismic geomagnetic fluctuations and atmospheric disturbances during the 2018 M6.2 Hualien Earthquake

*Chun-Rong Chen[1], JANN-YENQ Liu[1] (1.Graduate Institute of Space Science, National Central University)

### [MIS04-P06] Multi-sensor monitoring network for earthquake precursor study near subduction zone at Boso, Japan

*Katsumi Hattori[1], Chie Yoshino[1], WEIYUN XIE[2], Sanaka Saito[2], Haruna Kojima[2], Rui Song[2], Peng Han[3], Toru Mogi[4], Tada-nori Goto[5], Ichi Takumi[6], Hiroshi Yasukawa[7], Motoaki Mouri[8], Jun Izutsu[9], Tadashi Takano[10], Chihiro Yamanaka[11], Masashi Kamogawa[12], Yoshiaki Ando[13], JANN-YENQ Liu[14], Dimitar Ouzounov[15], Valery Tramutoli[16] (1.Department of Earth Sciences, Graduate School of Science, Chiba University, 2.Graduate School of Science and Engineering, Chiba University, 3.Southern University of Science and Technology, China, 4.Hokkaido University, 5.Kyoto University, 6.Nagoya Institute of Technology, 7.Aichi Prefectural University, 8.Aichi University, 9.Chubu University, 10.Nihon University, 11.Osaka University, 12.Tokyo Gakugei University, 13.The University of Electro-Communications, 14.National Central University, Taiwan, 15.Chapman University, US, 16.University of Basilicagta, Italy)

### [MIS04-P07] Transient Effects in Atmosphere and Ionosphere Associated with 2018 Mw 7.5 Sulawesi Indonesia Earthquake and Triggered Tsunami and Volcano Activities

★Invited Papers

*Dimitar Ouzounov[1], Sergey Pulinets[2], Dmitry Davidenko[2], Alexander Rozhnoi[3], Maria Solovieva[3], Tiger Liu[4] (1.Center of Excellence in Earth Systems Modeling & Observations (CEESMO) , Schmid College of Science & Technology Chapman University, Orange, California, USA, 2.Space Research Institute, RAS, Moscow, Russia, 3.The Schmidt Institute of Physics of the Earth, RAS, Moscow, Russia, 4.Center for Astronautical Physics and Engineering, National Central University, Taoyuan City, Taiwan)

### [MIS04-P08] Seismicity change and b value variation prior to the Wenchuan earthquake (*Ms 8.0*)

*Peng Han[1], Rui Wang[1], Ying Chang[1], Miao Miao[1], Haixia Shi[2], Lingyuan Meng[2], Xuemei Zhang[2], Weiyun Xie[3], Katsumi Hattori[3] (1.Southern University of Science and Technology, Shenzhen, China, 2.China Earthquake Networks Center, Beijing 100045, China, 3.Chiba University, Chiba, Japan)

[E] Oral | M (Multidisciplinary and Interdisciplinary) : M-IS Intersection

1:45 PM - 3:15 PM JST | 4:45 AM - 6:15 AM UTC | A02 TOKYO BAY MAKUHARI HALL

## [M-IS04] Interdisciplinary studies on pre-earthquake processes

convener:Katsumi Hattori(Department of Earth Sciences, Graduate School of Science, Chiba University), JANN-YENQ Liu(Institute of Space Science, National Central University, Taiwan), Dimitar Ouzounov(Center of Excellence in Earth Systems Modeling & Observations (CEESMO) , Schmid College of Science & Technology Chapman University, Orange, California, USA), Qinghua Huang(Peking University), Chairperson:Jann-Yenq Liu(National Central University, Taiwan), Toshiyasu Nagao

1:45 PM - 2:00 PM JST | 4:45 AM - 5:00 AM UTC

[MIS04-01] Application of blind source separation method in seismo-magnetic data analysis

★Invited Papers

*Peng Han[1], Yi Zhong[1], Yuanyuan Zhou[1], Yonghui Ma[2], Chengliang Xie[3], Katsumi Hattori[4], Chie Yoshino[4] (1.Southern University of Science and Technology, Shenzhen, China, 2.Harbin Institute of Technology (Shenzhen), Shenzhen 518055, China, 3.China University of Geosciences (Beijing), Beijing, 100083, China, 4.Chiba University, Chiba, Japan)

2:00 PM - 2:15 PM JST | 5:00 AM - 5:15 AM UTC

[MIS04-02] Rn flux anomaly and local seiemicity around Asahi station,Boso,Japan

*Haruna Kojima[1], Katsumi Hattori[2], Chie Yoshino[2], Michikuni Shimo[3], Toshiharu Konishi[4], Ryuichi Furuya[5] (1.Graduate School of Science and Engineering,Chiba University, 2.Department of Earth Sciences,Graduate School of Science,Chiba University, 3.Fujita Hearth University, 4.OHYO KOKEN KOGYO Co.,Ltd, 5.COM SYSTEM ,INC.)

2:15 PM - 2:30 PM JST | 5:15 AM - 5:30 AM UTC

[MIS04-03] Geochemical evidence for the occurrence of 2018 Hualien earthquake triggered by earlier earthquake swarm

*Ching-Chou Fu[1], Lou-Chuang Lee[1], Cheng-Horng Lin[1], Vivek Walia[2], Dimitar Ouzounov[3] (1.Institute of Earth Sciences, Academia Sinica, 2.National Center for Research on Earthquake Engineering, NARL, Taiwan, 3.Chapman University, One University Drive, Orange, CA, USA)

2:30 PM - 2:45 PM JST | 5:30 AM - 5:45 AM UTC

[MIS04-04] Temporal Variation and Statistical Assessment of b value

*weiyun xie[1], Katsumi Hattori[1], Peng Han[2] (1.chiba university, 2. Southern University of Science and Technology)

2:45 PM - 3:00 PM JST | 5:45 AM - 6:00 AM UTC

[MIS04-05] The S-K characteristics of the borehole areal strains associated with the Ms 8.0 Wenchuan and Ms 7.0 Lushan earthquakes

★Invited Papers

*Kaiguang Zhu[1], Zining Yu[1], Chenquan Chi[1], Mengxuan Fan[1], Kaiyan Lii[1] (1.Jilin University)

3:00 PM - 3:15 PM JST | 6:00 AM - 6:15 AM UTC

[MIS04-06] The Relationship between Earthquakes and Lightning Events of the globe during 2009-2017

*Ching-Chung Cheng[1], JANN-YENQ Liu[1,2,3] (1.Graduate Institute of Space Science, National Central University, TAIWAN, 2.Center for Astronautical Physics and Engineering, National Central University, TAIWAN, 3.Center for Space and Remote Sensing Research, National Central University, TAIWAN)

[E] Oral | M (Multidisciplinary and Interdisciplinary)：M-IS Intersection

3:30 PM - 5:00 PM JST | 6:30 AM - 8:00 AM UTC | A02 TOKYO BAY MAKUHARI HALL

## [M-IS04] Interdisciplinary studies on pre-earthquake processes

convener:Katsumi Hattori(Department of Earth Sciences, Graduate School of Science, Chiba University), JANN-YENQ Liu(Institute of Space Science, National Central University, Taiwan), Dimitar Ouzounov(Center of Excellence in Earth Systems Modeling & Observations (CEESMO) , Schmid College of Science & Technology Chapman University, Orange, California, USA), Qinghua Huang(Peking University), Chairperson:Peng Han, Katsumi Hattori

3:30 PM - 3:45 PM JST | 6:30 AM - 6:45 AM UTC

[MIS04-07] 3D-Tomography of the Ionospheric Anomalies Preceding the 2011 Tohoku-Oki ($M_w$9.0) Earthquake

*Ihsan Naufal Muafiry[1,2], Kosuke Heki[1] (1.Hokkaido University, Japan, 2.Universitas Esa Unggul, Indonesia)

3:45 PM - 4:00 PM JST | 6:45 AM - 7:00 AM UTC

[MIS04-08] Statistical Analysis of Pre-seismic Ionospheric Electron Density Anomalies and Investigation of Precursor

*Sanaka Saito[1], Chie Yoshino[1], Katsumi Hattori[1] (1.Chiba University)

4:00 PM - 4:15 PM JST | 7:00 AM - 7:15 AM UTC

[MIS04-09] Spatial clustering of pre-earthquake anomalies as an indicator of the preparation/activation zone

*Dimitar Ouzounov[1], Sergey Pulinets[2], Tiger Liu[3], Katsumi Hattori[4] (1.Center of Excellence in Earth Systems Modeling & Observations (CEESMO) , Schmid College of Science & Technology Chapman University, Orange, California, USA, 2.Space Research Institute, RAS, Moscow, Russia, 3.National Central University, Taoyuan City, Taiwan, 4. Chiba University, Chiba, Japan)

4:15 PM - 4:30 PM JST | 7:15 AM - 7:30 AM UTC

[MIS04-10] **Application of the ionospheric parameters on the seismic research**- -Seismic-ionospheric effect detected from China Seismo-Electromagnetic Satellite

★Invited Papers

*Rui Song[1], Hattori Katsumi[2], Xuemin Zhang[3] (1.Graduate School of Science and Engeering, Chiba University, 2.Graduate School of Science, Chiba University, 3.Institute of Earthquake Science, China Earthquake Administration)

4:30 PM - 4:45 PM JST | 7:30 AM - 7:45 AM UTC

[MIS04-11] ROC curve analyses on the ionospheric TEC of M>=6.0 earthquakes in Japan during 1998-2015

★Invited Papers

*JANN-YENQ Liu[1], Yuh-Ing Chen[2], Pei-Jung Lee[1] (1.Center for Astronautical Physics and Engineering; Graduate Institute of Space Science, National Central University, Taiwan, 2.Graduate Institute of Statistics, National Central University, Taiwan)

4:45 PM - 5:00 PM JST | 7:45 AM - 8:00 AM UTC

[MIS04-12] FORMOSAT-5/AIP observes seismo-ionospheric precursors

*JANN-YENQ Liu[1], Chi-Kuang Chao[1] (1.Center for Astronautical Physics and Engineering; and Graduate Institute of Space Science, National Central University, TAIWAN)

[E] Oral | M (Multidisciplinary and Interdisciplinary)：M-IS Intersection

1:45 PM - 3:15 PM JST | 4:45 AM - 6:15 AM UTC | 202 2F

## [M-IS06] Conservation of geoparks, natural geosites and cultural heritage: weathering process and damage assessment

convener:Chiaki T. Oguchi(Institute for Environmental Science and Technology, Graduate School of Science and Engineering, Saitama University), Tetsuya Waragai(Graduate School of Science and Engineering, Nihon University), Kuniyasu Mokudai(Tohoku Gakuin University), Magdalini Theodoridou(School of Engineering, Cardiff University), Chairperson:Tetsuya Waragai(日本大学大学院　理工学研究科), Kuniyasu Mokudai(Japan Geoservicee)

1:45 PM - 2:00 PM JST | 4:45 AM - 5:00 AM UTC

[MIS06-01] Geopark's response to conservation of geosites from natural hazards

*Kuniyasu Mokudai[1], Shuichi Hasegawa[2] (1.Japan Geoservice Incorporated, 2.Kagawa Univ.)

2:00 PM - 2:15 PM JST | 5:00 AM - 5:15 AM UTC

[MIS06-02] Physical and mechanical properties for damage assesment of Taya Cave rocks, central Japan

*Chiaki T. Oguchi[1], Yurina Akimoto[2], Yasuhiko TAMURA[3], Kaisei Sakane[1] (1.Institute for Environmental Science and Technology, Graduate School of Science and Engineering, Saitama University, 2.Faculty of Engineering, Saitama University, 3.The Exective Committee for the Preservation of TAYA CAVERN)

2:15 PM - 2:30 PM JST | 5:15 AM - 5:30 AM UTC

[MIS06-03] Interdisciplinary approaches on conservation of underground geoheritage for community development of Taya Cave and its adjacent area

★Invited Papers

*Yasuhiko TAMURA[1,2], Chiaki T. Oguchi[4], Yuichi S. Hayakawa[5,2], Takuro Ogura[2], OGATA KEISUKE[6], Masashi MORITA[3] (1.The Executive Committee for the Preservation of TAYA CAVERN , 2.The University of Tokyo, Center for Spatial Information Science, 3.Yokohama National University, Institute of Urban Innovation, 4.Saitama University, Graduate School of Science and Engineering, 5.Hokkaido University, Faculty of Environmental Earth Science, 6.Tsurumi University, The Department of Cultural Properties)

2:30 PM - 2:45 PM JST | 5:30 AM - 5:45 AM UTC

[MIS06-04] Italian underground cultural heritage: from monitoring to enhancement

★Invited Papers

*Mario Parise[1], Tiziana Vitolo[2], Roberta Varriale[2] (1.Univ. Aldo Moro, Dept. Earth and Environmental Sciences, Bari, Italy, 2.CNR-ISSM, Italy)

2:45 PM - 3:00 PM JST | 5:45 AM - 6:00 AM UTC

[MIS06-05] Possibility of insolation weathering of sandstone blocks composing Angkor temples, Cambodia

*Tetsuya Waragai[1] (1.Graduate School of Science and Engineering, Nihon University)

3:00 PM - 3:15 PM JST | 6:00 AM - 6:15 AM UTC

[MIS06-06] Durability evaluation of pyroclastic rocks used in the historical built environment of Hungary

*Luigi Germinario[1,2], Ákos Török[1] (1.Budapest University of Technology and Economics, Hungary, 2.Saitama University, Japan)

[E] Poster | M (Multidisciplinary and Interdisciplinary)：M-IS Intersection

3:30 PM - 5:00 PM JST | 6:30 AM - 8:00 AM UTC | Poster Hall International Exhibition Hall8, Makuhari Messe_19

## [M-IS06] Conservation of geoparks, natural geosites and cultural heritage: weathering process and damage assessment

convener:Chiaki T. Oguchi(Institute for Environmental Science and Technology, Graduate School of Science and Engineering, Saitama University), Tetsuya Waragai(Graduate School of Science and Engineering, Nihon University), Kuniyasu Mokudai(Tohoku Gakuin University), Magdalini Theodoridou(School of Engineering, Cardiff University)

[MIS06-P01] The artistic qualities of religion reliefs in Taya-cave.Japan

*OGATA KEISUKE[1] (1.TSURUMI UNIVERSITY)

---

[MIS06-P02] Effect of stress concentration on the Weathering Mechanism of Sandstone Pillars of Angkor Wat, Cambodia by means of numerical simulation

*Takato Takemura[1], Tetsuya Waragai[2] (1.Nihon Univ., 2.Nihon University)

---

[MIS06-P03] Meaning to preserve evidence of large scale landslide

*Kuniyasu Mokudai[1], Hidekazu Sato[2] (1.Japan Geoservice Incorporated, 2.Mt. Kurikoma Area Geopark)

[E] Poster | M (Multidisciplinary and Interdisciplinary)：M-IS Intersection

5:15 PM - 6:30 PM JST | 8:15 AM - 9:30 AM UTC | Poster Hall International Exhibition Hall8, Makuhari Messe_36

## [M-IS06] Conservation of geoparks, natural geosites and cultural heritage: weathering process and damage assessment

convener:Chiaki T. Oguchi(Institute for Environmental Science and Technology, Graduate School of Science and Engineering, Saitama University), Tetsuya Waragai(Graduate School of Science and Engineering, Nihon University), Kuniyasu Mokudai(Tohoku Gakuin University), Magdalini Theodoridou(School of Engineering, Cardiff University)

[MIS06-P01] The artistic qualities of religion reliefs in Taya-cave.Japan

*OGATA KEISUKE[1] (1.TSURUMI UNIVERSITY)

---

[MIS06-P02] Effect of stress concentration on the Weathering Mechanism of Sandstone Pillars of Angkor Wat, Cambodia by means of numerical simulation

*Takato Takemura[1], Tetsuya Waragai[2] (1.Nihon Univ., 2.Nihon University)

---

[MIS06-P03] Meaning to preserve evidence of large scale landslide

*Kuniyasu Mokudai[1], Hidekazu Sato[2] (1.Japan Geoservice Incorporated, 2.Mt. Kurikoma Area Geopark)

[E] Oral | M (Multidisciplinary and Interdisciplinary)：M-IS Intersection

9:00 AM - 10:30 AM JST | 12:00 AM - 1:30 AM UTC | 201A 2F

## [M-IS07] Astrobiology

convener:Hikaru Yabuta(Hiroshima University, Department of Earth and Planetary Systems Science), Seiji Sugita(Department of Earth and Planetary Science, Graduate School of Science Sciece, The University of Tokyo), Misato Fukagawa(National Astronomical Observatory of Japan), Fujishima Kosuke(Tokyo Institute of Technology, Earth-Life Science Institute), Chairperson:Hikaru Yabuta(Hiroshima University), Seiji Sugita(東京大学大学院 理学系研究科), Misato Fukagawa(名古屋大学大学院 理学研究科), Kosuke Fujishima(ELSI 地球生命研究所)

9:00 AM - 9:20 AM JST | 12:00 AM - 12:20 AM UTC

[MIS07-06] How to find and characterize nearby habitable exoplanets

★Invited Papers

*Norio Narita[1] (1.Astrobiology Center)

---

9:20 AM - 9:40 AM JST | 12:20 AM - 12:40 AM UTC

[MIS07-07] **Organic Matter Preserved in Mudstones of a 3-Billion-Year-Old Lake Deposit in Gale Crater, Mars**

★Invited Papers

*Jennifer L Eigenbrode[1], Roger E Summons[2], Andrew Steele[3], Caroline Freissinet[4], Maëva Millan[5], Rafael Navarro-González[6], Paul Mahaffy[1] (1.NASA Goddard Space Flight Center, 2.Massachusetts Institute of Technology, 3.Carnegie Institution of Washington, 4.Institut Pierre Simon Laplace, CNRS, 5.Georgetown University, 6.Universidad Nacional Autónoma de México)

---

9:40 AM - 9:55 AM JST | 12:40 AM - 12:55 AM UTC

[MIS07-08] **The third year sample return of Tanpopo: Capture and Exposure Experiment of Micrometeorite and Microbes on Exposure Facility of International Space Station**

*Akihiko Yamagishi[1], Hirofumi Hashimoto[2], Hajime Yano[2], Shin-ichi Yokobori[3], Kensei Kobayashi[4], Hajime Mita[5], Hikaru Yabuta[6], Masumi Higashide[7], Makoto Tabata[8], Hideyuki Kawai[8], Eiichi Imai[9] (1.Tokyo University of Pharmacy and Life Science, Department of Molecular Biology, 2.ISAS/JAXA, Sagamihara, Japan, 3.Tokyo University of Pharmacy and Life Science, Tokyo, Japan, 4.Yokohama National University, Yokohama, Japan, 5.Fukuoka Institute of Technology, Fukuoka, Japan, 6.Hiroshima University, Hirosima, Japan, 7.Japan Aerospace Exploration Agency (JAXA), Tokyo, Japan, 8.Chiba University, Chiba, Japan, 9.Nagaoka University of Technology, Nagaoka, Japan)

---

9:55 AM - 10:10 AM JST | 12:55 AM - 1:10 AM UTC

[MIS07-09] Theoretical search for photosynthetic pigments applicable around low temperature stars: Modulation of physical-chemical properties by central metals

*Yu Komatsu[1,2], Kenji Takizawa[1,3] (1.Astrobiology Center, 2.National Astronomical Observatory of Japan, 3.National Institute for Basic Biology)

---

10:10 AM - 10:25 AM JST | 1:10 AM - 1:25 AM UTC

[MIS07-10] Effects of the formation of hydrocarbon aerosols on the climate stability of Earth-like planets and their habitability

*Yasuto Watanabe[1], Eiichi Tajika[1], Kazumi Ozaki[2], Peng Hong[3] (1.The University of Tokyo, 2.Toho University, 3.Chiba Institute of Technology)

[E] Oral | M (Multidisciplinary and Interdisciplinary)：M-IS Intersection

10:45 AM - 12:15 PM JST | 1:45 AM - 3:15 AM UTC | 201A 2F

## [M-IS07] Astrobiology

convener:Hikaru Yabuta(Hiroshima University, Department of Earth and Planetary Systems Science), Seiji Sugita(Department of Earth and Planetary Science, Graduate School of Science Sciece, The University of Tokyo), Misato Fukagawa(National Astronomical Observatory of Japan), Fujishima Kosuke(Tokyo Institute of Technology, Earth-Life Science Institute), Chairperson:Kosuke Fujishima(ELSI 地球生命研究所), Misato Fukagawa(名古屋大学大学院 理学研究科), Seiji Sugita(東京大学大学院 理学系研究科), Hikaru Yabuta(Hiroshima University)

10:45 AM - 11:05 AM JST | 1:45 AM - 2:05 AM UTC

[MIS07-11] the emergence of iron-sulfur protometabolism

★Invited Papers

*Sheref Mansy[1] (1.University of Trento)

---

11:05 AM - 11:25 AM JST | 2:05 AM - 2:25 AM UTC

[MIS07-12] Life-water-mineral interactions and their products

★Invited Papers

*Fumito Shiraishi[1] (1.Hiroshima University)

---

11:25 AM - 11:40 AM JST | 2:25 AM - 2:40 AM UTC

[MIS07-13] How much can we learn about ancient cells from sequence analysis? New metrics on an old problem.

*Shawn E McGlynn[1], Sarah J Berkemer[2,3] (1.Earth-Life Science Institute, Tokyo Institute of Technology, 2.Bioinformatics Group, Department of Computer Science, Interdisciplinary Center for Bioinformatics, University of Leipzig, 3.Max Planck Institute for Mathematics in the Sciences, Leipzig, Germany)

---

11:40 AM - 11:55 AM JST | 2:40 AM - 2:55 AM UTC

[MIS07-14] Scientific significance of searching living cells on Mars surface by Life Detection Microscope (LDM )

*Yoshitaka Yoshimura[1], Akihiko Yamagishi[2], Takehiko Satoh[3], Atsuo Miyakawa[2], Eiichi Imai[4], Satoshi Sasaki[5], Kensei Kobayashi[6], Yoko Kebukawa[6], Tomoka Okada[6], Keigo Enya[3], Hikaru Yabuta[7], Takeshi Naganuma[7], Hajime Mita[8], Kazuhisa Fujita[3], Tomohiro Usui[3] (1.College of Agriculture, Tamagawa University, 2.Tokyo University of Pharmacy and Life Science, 3.Japan Aerospace Exploration Agency, 4.Nagaoka University of Technology, 5.Tokyo University of Technology, 6.Yokohama National University, 7.Hiroshima University, 8.Fukuoka Institute of Technology)

---

11:55 AM - 12:10 PM JST | 2:55 AM - 3:10 AM UTC

[MIS07-15] Civilization-bearing planets in the Milky-Way Galaxy; 50 necessary conditions must be satisfied in order

*Shigenori Maruyama[1] (1.Earth-Life Science Institute, Tokyo Institute of Technology)

[E] Poster | M (Multidisciplinary and Interdisciplinary)：M-IS Intersection

3:30 PM - 5:00 PM JST | 6:30 AM - 8:00 AM UTC | Poster Hall International Exhibition Hall8, Makuhari Messe_20

## [M-IS07] Astrobiology

convener:Hikaru Yabuta(Hiroshima University, Department of Earth and Planetary Systems Science), Seiji Sugita(Department of Earth and Planetary Science, Graduate School of Science Sciece, The University of Tokyo), Misato Fukagawa(National Astronomical Observatory of Japan), Fujishima Kosuke(Tokyo Institute of Technology, Earth-Life Science Institute)

### [MIS07-P01] Exoplanets Revealed by High-Precision Infrared Doppler Technique Using IRD: Large Exploration for Planets around Cool M-type Stars Begins

*Masayuki Kuzuhara[1,3], Bunei Sato[4], Motohide Tamura[2,1,3], Takayuki Kotani[1,3,5], Nagayoshi Ohashi[3,6], Masashi Omiya[1,3], Teruyuki Hirano[4], Hiroki Harakawa[6,3,1], Wako Aoki[3,5], Norio Narita[2,1], Yasunori Hori[1,3], Akitoshi Ueda[3,5], Akihiko Fukui[2], Hiroyuki Tako Ishikawa[5,3], Ishizuka Masato[2], Takashi Kurokawa[1,7], Nobuhiko Kusakabe[1,3], Tomoyuki Kudo[6,3,1], Eiichiro Kokubo[3], Mihoko Konishi[1,3], Tadashi Nakajima[1,3,5], Jun Nishikawa[3,5,1], Masahiro Ogihara[3], Takuma Serizawa[7] (1.Astrobiology Center of NINS, 2.The University of Tokyo, Graduate School of Science, 3.National Astronomical Observatory of Japan, 4.Tokyo Institute of Technology, 5.SOKENDAI, 6.Subaru Telescope, 7.Tokyo University of Agriculture and Technology)

### [MIS07-P02] Discrimination of organic compounds and mineral particles by fluorescent microscopy for the detection of Martian life.

*Tomoka Okada[1], Yoshitaka Yoshimura[2], Atsuo Miyakawa[3], Yuka Murano[3], Shin-ichi Yokobori[3], Akihiko Yamagishi[3], Kensei Kobayashi[1], Yoko Kebukawa[1] (1.YOKOHAMA National university, 2.Tamagawa University, 3.Tokyo University of Pharmacy and Life Sciences)

### [MIS07-P03] Morphological and spectroscopic characteristics of organic matter in Banded Iron Formation, Barberton Greenstone Belt, South Africa

*Hiroki Amemiya[1], Ryo Nakajima[1], Yoko Ohtomo[1], Tsubasa Otake[1], Tsutomu Sato[1] (1.Division of sustainable Resources Engineering, Faculty of Engineering, Hokkaido University)

### [MIS07-P04] Understanding peptide sequence selectivity on iron sulfide (FeS) nanoparticle surfaces

*Fujishima Kosuke[1], Norio Kitadai[1], Kenji Kasama[1] (1.Earth-Life Science Institute, Tokyo Institute of Technology)

### [MIS07-P05] A process model of L-homochiral peptides formation initiated with L-alanine

*Toratane Munegumi[1], Taisuke Yamaga[1] (1.Department of Science Education, Naruto University of Education)

### [MIS07-P06] Possible Formation of Amino Acids and Carboxylic Acids in Slightly-Reducing Primitive Earth Atmospheres

*Miei Kinoshita[1], Shintaro Ikeda[1], Kimitaka Kawamura[2], Bhagawati Kunwar[2], Hitoshi Fukuda[3], Yoshiyuki Oguri[3], Hiromi Shibata[4], Junichi Takahashi[1], Vladimir Airapetian[5], Yoko Kebukawa[1], Kensei Kobayashi[1] (1.Yokohama National University, 2.Chubu University, 3.Tokyo Institute of Technology, 4.Osaka University, 5.NASA Goddard SFC)

### [MIS07-P07] Application of Machine learning and software development for initial analysis in the TANPOPO mission

*Kyoko Okudaira[1], Yuto Toda[1], Takashi Sonoke[1], Yuichi Yaguchi[1], Masashi Yoshida[1], Junya Imani[2], Satoshi Sasaki[3], Hajime Yano[4], Hirohide Demura[1], Makoto Tabata[5], Akihiko Yamagishi[6] (1.The University of Aizu, 2.YUKI Precision, 3.Tokyo University of Technology, 4.JAXA, 5.Chiba University, 6.Tokyo University of Pharmacy and Life Science)

### [MIS07-P08] Structure analysis of the hyper velocity impact tracks of the particles captured by silica aerogel on the International Space Station

*Mizuho Nishi[1], Akira Tsuchiyama[1], Hajime Yano[2], Hikaru Yabuta[3], Kyoko Okudaira[4], Junya Matsuno[1], Masayuki Uesugi[5], Uesugi Kentaro[5], Nakano Tukasa[6], Takaaki Noguchi[7], MITA Hajime[8], Akihiko Yamagishi[9] (1.Kyoto University, 2.Institute of Space and Astronautical Science, Japan Aerospace Exploration Agency, 3.Hiroshima University, 4.The University of Aizu, 5.JASRI/SPring-8, 6.National Institute of Advanced Industrial Science and Technology, 7.Kyusyu University, 8.Fukuoka Institute of Technology, 9.Tokyo University of Pharmacy and Life Science)

### [MIS07-P09] High-Angular-Resolution Observations of Protoplanetary Disks

*Misato Fukagawa[1] (1.National Astronomical Observatory of Japan)

[MIS07-P10] Characterization of high molecular weight amino acid precursors formed in interstellar ice analog

*Soushi Kuramoto[1], Tomohito Sato[1], Hitoshi Fukuda[2], Yoshiyuki Oguri[2], Kotaro Kondo[2], Hiromi Shibata[3], Yoko Kebukawa[1], Kensei Kobayashi[1], Satoshi Yoshida[4] (1.Yokohama National University, 2.Tokyo Institute of Technology, 3.University of Osaka, 4.National Institutes for Quantum Radiological Science and Technology)

---

[MIS07-P11] Theoretical elucidation of prebiotic formation processes into nucleobases

*Yu Komatsu[1,2], Taiki Suzuki[1,2] (1.Astrobiology Center, 2.National Astronomical Observatory of Japan)

---

[MIS07-P12] Formation Process of A Glycine's Precursor Candidate, CH3NH2

*Taiki Suzuki[1,2], Liton Majumdar[3], Masatoshi Ohishi[2] (1.National Institutes of Natural Sciences Astrobiology Center, 2.National Astronomical Observatory of Japan, 3.NASA Jet Propulsion Laboratory (JPL))

---

[MIS07-P13] Numerical study on the stellar atmosphere & wind of Cool Stars

*Takahito Sakaue[1], Kazunari Shibata[1] (1.Kyoto University)

---

[MIS07-P14] Design of space exposure experiments of organic matter in Tanpopo 2

*Takuya Yokoo[1], tomohito sato[1], Itsuki Sakon[2], Kazumichi Nakagawa[3], Hajime Yano[4], Miki Nakayama[5], Hajime Mita[5], Yoko Kebukawa[1], Kensei Kobayashi[1] (1.Yokohama National University, 2.University of Tokyo, 3.Kobe University, 4.JAXA, 5.Fukuoka Institute of Technology)

[E] Poster | M (Multidisciplinary and Interdisciplinary)：M-IS Intersection

5:15 PM - 6:30 PM JST | 8:15 AM - 9:30 AM UTC | Poster Hall International Exhibition Hall8, Makuhari Messe_37

## [M-IS07] Astrobiology

convener:Hikaru Yabuta(Hiroshima University, Department of Earth and Planetary Systems Science), Seiji Sugita(Department of Earth and Planetary Science, Graduate School of Science Sciece, The University of Tokyo), Misato Fukagawa(National Astronomical Observatory of Japan), Fujishima Kosuke(Tokyo Institute of Technology, Earth-Life Science Institute)

### [MIS07-P01] Exoplanets Revealed by High-Precision Infrared Doppler Technique Using IRD: Large Exploration for Planets around Cool M-type Stars Begins

*Masayuki Kuzuhara[1,3], Bunei Sato[4], Motohide Tamura[2,1,3], Takayuki Kotani[1,3,5], Nagayoshi Ohashi[3,6], Masashi Omiya[1,3], Teruyuki Hirano[4], Hiroki Harakawa[6,3,1], Wako Aoki[3,5], Norio Narita[2,1], Yasunori Hori[1,3], Akitoshi Ueda[3,5], Akihiko Fukui[2], Hiroyuki Tako Ishikawa[5,3], Ishizuka Masato[2], Takashi Kurokawa[1,7], Nobuhiko Kusakabe[1,3], Tomoyuki Kudo[6,3,1], Eiichiro Kokubo[3], Mihoko Konishi[1,3], Tadashi Nakajima[1,3,5], Jun Nishikawa[3,5,1], Masahiro Ogihara[3], Takuma Serizawa[7] (1.Astrobiology Center of NINS, 2.The University of Tokyo, Graduate School of Science, 3.National Astronomical Observatory of Japan, 4.Tokyo Institute of Technology, 5.SOKENDAI, 6.Subaru Telescope, 7.Tokyo University of Agriculture and Technology)

### [MIS07-P02] Discrimination of organic compounds and mineral particles by fluorescent microscopy for the detection of Martian life.

*Tomoka Okada[1], Yoshitaka Yoshimura[2], Atsuo Miyakawa[3], Yuka Murano[3], Shin-ichi Yokobori[3], Akihiko Yamagishi[3], Kensei Kobayashi[1], Yoko Kebukawa[1] (1.YOKOHAMA National university, 2.Tamagawa University, 3.Tokyo University of Pharmacy and Life Sciences)

### [MIS07-P03] Morphological and spectroscopic characteristics of organic matter in Banded Iron Formation, Barberton Greenstone Belt, South Africa

*Hiroki Amemiya[1], Ryo Nakajima[1], Yoko Ohtomo[1], Tsubasa Otake[1], Tsutomu Sato[1] (1.Division of sustainable Resources Engineering, Faculty of Engineering, Hokkaido University)

### [MIS07-P04] Understanding peptide sequence selectivity on iron sulfide (FeS) nanoparticle surfaces

*Fujishima Kosuke[1], Norio Kitadai[1], Kenji Kasama[1] (1.Earth-Life Science Institute, Tokyo Institute of Technology)

### [MIS07-P05] A process model of L-homochiral peptides formation initiated with L-alanine

*Toratane Munegumi[1], Taisuke Yamaga[1] (1.Department of Science Education, Naruto University of Education)

### [MIS07-P06] Possible Formation of Amino Acids and Carboxylic Acids in Slightly-Reducing Primitive Earth Atmospheres

*Miei Kinoshita[1], Shintaro Ikeda[1], Kimitaka Kawamura[2], Bhagawati Kunwar[2], Hitoshi Fukuda[3], Yoshiyuki Oguri[3], Hiromi Shibata[4], Junichi Takahashi[1], Vladimir Airapetian[5], Yoko Kebukawa[1], Kensei Kobayashi[1] (1.Yokohama National University, 2.Chubu University, 3.Tokyo Institute of Technology, 4.Osaka University, 5.NASA Goddard SFC)

### [MIS07-P07] Application of Machine learning and software development for initial analysis in the TANPOPO mission

*Kyoko Okudaira[1], Yuto Toda[1], Takashi Sonoke[1], Yuichi Yaguchi[1], Masashi Yoshida[1], Junya Imani[2], Satoshi Sasaki[3], Hajime Yano[4], Hirohide Demura[1], Makoto Tabata[5], Akihiko Yamagishi[6] (1.The University of Aizu, 2.YUKI Precision, 3.Tokyo University of Technology, 4.JAXA, 5.Chiba University, 6.Tokyo University of Pharmacy and Life Science)

### [MIS07-P08] Structure analysis of the hyper velocity impact tracks of the particles captured by silica aerogel on the International Space Station

*Mizuho Nishi[1], Akira Tsuchiyama[1], Hajime Yano[2], Hikaru Yabuta[3], Kyoko Okudaira[4], Junya Matsuno[1], Masayuki Uesugi[5], Uesugi Kentaro[5], Nakano Tukasa[6], Takaaki Noguchi[7], MITA Hajime[8], Akihiko Yamagishi[9] (1.Kyoto University, 2.Institute of Space and Astronautical Science, Japan Aerospace Exploration Agency, 3.Hiroshima University, 4.The University of Aizu, 5.JASRI/SPring-8, 6.National Institute of Advanced Industrial Science and Technology, 7.Kyusyu University, 8.Fukuoka Institute of Technology, 9.Tokyo University of Pharmacy and Life Science)

### [MIS07-P09] High-Angular-Resolution Observations of Protoplanetary Disks

*Misato Fukagawa[1] (1.National Astronomical Observatory of Japan)

[MIS07-P10] Characterization of high molecular weight amino acid precursors formed in interstellar ice analog

*Soushi Kuramoto[1], Tomohito Sato[1], Hitoshi Fukuda[2], Yoshiyuki Oguri[2], Kotaro Kondo[2], Hiromi Shibata[3], Yoko Kebukawa[1], Kensei Kobayashi[1], Satoshi Yoshida[4] (1.Yokohama National University, 2.Tokyo Institute of Technology, 3.University of Osaka, 4.National Institutes for Quantum Radiological Science and Technology)

---

[MIS07-P11] Theoretical elucidation of prebiotic formation processes into nucleobases

*Yu Komatsu[1,2], Taiki Suzuki[1,2] (1.Astrobiology Center, 2.National Astronomical Observatory of Japan)

---

[MIS07-P12] Formation Process of A Glycine's Precursor Candidate, CH3NH2

*Taiki Suzuki[1,2], Liton Majumdar[3], Masatoshi Ohishi[2] (1.National Institutes of Natural Sciences Astrobiology Center, 2.National Astronomical Observatory of Japan, 3.NASA Jet Propulsion Laboratory (JPL))

---

[MIS07-P13] Numerical study on the stellar atmosphere & wind of Cool Stars

*Takahito Sakaue[1], Kazunari Shibata[1] (1.Kyoto University)

---

[MIS07-P14] Design of space exposure experiments of organic matter in Tanpopo 2

*Takuya Yokoo[1], tomohito sato[1], Itsuki Sakon[2], Kazumichi Nakagawa[3], Hajime Yano[4], Miki Nakayama[5], Hajime Mita[5], Yoko Kebukawa[1], Kensei Kobayashi[1] (1.Yokohama National University, 2.University of Tokyo, 3.Kobe University, 4.JAXA, 5.Fukuoka Institute of Technology)

[J] Oral | M (Multidisciplinary and Interdisciplinary)：M-IS Intersection

1:45 PM - 3:15 PM JST | 4:45 AM - 6:15 AM UTC | 102 1F

## [M-IS09] dust

convener:Ishizuka Masahide(Kagawa University), Yasunori Kurosaki(Arid Land Research Center, Tottori University), Thomas Sekiyama(Meteorological Research Institute), Kana Nagashima(Japan Agency for Marine-Earth Science and Technology, Research and Development Center for Global Change), Chairperson:Tsuyoshi Sekiyama

1:55 PM - 2:15 PM JST | 4:55 AM - 5:15 AM UTC

### [MIS09-01] Global modeling study of atmospheric supply of lithogenic and pyrogenic Fe-containing aerosols to the ocean

★Invited Papers

*Akinori Ito[1], Akitomo Yamamoto[1], Michio Watanabe[1], Maki Noguchi Aita[1], Ying Ye[2] (1.Japan Agency for Marine-Earth Science and Technology, 2.Alfred Wegener Institute for Polar and Marine Research)

---

2:15 PM - 2:30 PM JST | 5:15 AM - 5:30 AM UTC

### [MIS09-02] Regional variations in the elemental and mineral compositions of solid particles in rainwater in Iran

*Yoriko Yokoo[1], Chihiro Sakamoto[1], Atsushi Kitamura[1], Ryo Anma[2], Shiva Mehrabani[3] (1.Faculty of Science and Engineering, Doshisha University, 2.Tokushima University, 3.Kurdistan University)

---

2:30 PM - 2:45 PM JST | 5:30 AM - 5:45 AM UTC

### [MIS09-03] Comparison of airborne microbial variations in air samples from Asian-dust source and arrival regions

*Teruya Maki[1], Tatsuyuki Fujita[1], Yuuma Mastuba[1], Yasunori Kurosaki[2], Masahide Ishizuka[3], Kei Kawai[4], Yasunobu Iwasaka[5] (1.College of Science and Engineering, Kanazawa University, 2.Arid Land Research Center, Tottori University, Tottori University, 3.Faculty of Engineering, Kagawa University, 4.Graduate School of Environmental Studies, Nagoya Universit, 5.Center for Environmental Creative Studies)

---

2:45 PM - 3:00 PM JST | 5:45 AM - 6:00 AM UTC

### [MIS09-04] Prediction of health effects of cross-border atmospheric pollutants using the Model of Aerosol Species in the Global Atmosphere (MASINGAR)

*Kazunari Onishi[1], Thomas Sekiyama[2], Yasunori Kurosaki[3], Masato Shinoda[4] (1.Graduate School of Public Health, Support Unit for Conducting Clinically Essential Studies, St.Luke's International University, 2.Meteorological Research Institute, 3.Arid Land Research Center, Tottori University, 4.Graduate School of Environmental Studies Nagoya University)

---

3:00 PM - 3:15 PM JST | 6:00 AM - 6:15 AM UTC

### [MIS09-05] Dust layer captured by an inversion layer over the Gobi Desert on 29–30 April 2015

*Kei Kawai[1], Yuta Nishio[2], Kenji Kai[1,3], Jun Noda[4], Erdenebadrakh Munkhjargal[1,5], Masato Shinoda[1], Nobuo Sugimoto[6], Atsushi Shimizu[6], Enkhbaatar Davaanyam[5,7], Dashdondog Batdorj[8] (1.Nagoya University, 2.Japan Meteorological Agency, 3.Ibaraki University, 4.Rakuno Gakuen University, 5.Information and Research Institute of Meteorology, Hydrology and Environment, Mongolia, 6.National Institute for Environmental Studies, 7.University of Tsukuba, 8.National Agency for Meteorology and Environmental Monitoring, Mongolia)

[J] Oral | M (Multidisciplinary and Interdisciplinary)：M-IS Intersection

3:30 PM - 5:00 PM JST | 6:30 AM - 8:00 AM UTC | 102 1F

## [M-IS09] dust

convener:Ishizuka Masahide(Kagawa University), Yasunori Kurosaki(Arid Land Research Center, Tottori University), Thomas Sekiyama(Meteorological Research Institute), Kana Nagashima(Japan Agency for Marine-Earth Science and Technology, Research and Development Center for Global Change), Chairperson:Kana Nagashima

3:30 PM - 3:45 PM JST | 6:30 AM - 6:45 AM UTC

[MIS09-06] Favorable regions for dust haze transport revealed by ensemble simulations

*Kazunori Ogohara[1], Shogo Isoda[1] (1.School of Engineering, University of Shiga Prefecture)

3:45 PM - 4:00 PM JST | 6:45 AM - 7:00 AM UTC

[MIS09-07] Measurement of adhesion force of individual aerosol particles by atomic force microscopy

*Kohei Ono[1], Yuki Mizushima[4], Ayumi Iwata[3], Furuya Masaki[1], Nozomu Tsuchiya[1], Atsushi Matsuki[2] (1.Graduate School of Natural Science and Technology, Kanazawa University, 2.Institute of Nature and Environmental Technology, Kanazawa University, 3.Faculty of Science and Technology, Keio University, 4.College of Science and Technology, Kanazawa University)

4:00 PM - 4:15 PM JST | 7:00 AM - 7:15 AM UTC

[MIS09-08] Occurrence of micro-meso scale dust storms and its relationship to the vegetation and topography in Mongolian grassland and Gobi Desert

*Kenji Kai[1], Kei Kawai[2], Teruya Maki[3], Jun Noda[4] (1.College of Education, Ibaraki University , 2.Nagoya University, 3.Kanazawa University, 4.Rakuno-Gakuen University)

4:15 PM - 4:30 PM JST | 7:15 AM - 7:30 AM UTC

[MIS09-09] A trial of elucidation for dust emission conditions in East Asia by synoptic data analyses and a field observation

*Yasunori Kurosaki[1], Jing Wu[1], Batjargal Buyantogtokh[1], Ishizuka Masahide[2], Batdelger Gantsetseg[3] (1.Tottori University, 2.Kagawa University, 3.IRIMHE, Mongolia)

4:30 PM - 4:45 PM JST | 7:30 AM - 7:45 AM UTC

[MIS09-10] Monitoring and assessing aeolian desertification processes based on a dust erodibility index – A case study in the Xilingol grassland, China

*Jing Wu[1], Yasunori Kurosaki[1], Chunling Du[2], Tao Wang[3] (1. Arid Land Research Center, Tottori University, 2.School of Economics and Management, Inner Mongolia Agricultural University, 3.Northwest Institute of Eco-Environment and Resources, Chinese Academy of Sciences)

4:45 PM - 5:00 PM JST | 7:45 AM - 8:00 AM UTC

[MIS09-11] Influences of land surface conditions and human activities on dust events in Inner Mongolian grasslands, China

*Mei Yong[1], Masato Shinoda[2], Nandintsetseg Banzragch[2] (1.Inner Mongolia normal university, 2.Nagoya university)

[J] Poster | M (Multidisciplinary and Interdisciplinary)：M-IS Intersection

5:15 PM - 6:30 PM JST | 8:15 AM - 9:30 AM UTC | Poster Hall International Exhibition Hall8, Makuhari Messe_38

## [M-IS09] dust

convener:Ishizuka Masahide(Kagawa University), Yasunori Kurosaki(Arid Land Research Center, Tottori University), Thomas Sekiyama(Meteorological Research Institute), Kana Nagashima(Japan Agency for Marine-Earth Science and Technology, Research and Development Center for Global Change)

[MIS09-P01] Study on decadal influencing of the teleconnection pattern EA and SCAND on major atmospheric circulation systems of the northern China dust storms during the past 65 years (1954-2018)

*Gao Tao[1], Mei Yong[2] (1.Inner Mongolia Meteorological Institute, 2.Inner Mongolia Normal University)

[MIS09-P02] **Effects of freeze-thaw and land-surface processes on dust occurrence in the Mongolian desert steppe**

*Kaman kong[1], Masato Shinoda[1], Banzragch Nandintsetseg[1,2,3], Yasunori Kurosaki[4] (1.Nagoya Unviserity, 2.Information and Research Institute of Meteorology, Hydrology, and Environment, 3.National University of Mongolia, 4.Tottori University)

[MIS09-P03] Mineral particles suspending in the surface waters of the North Pacific and its marginal seas – atmospheric dust deposition as investigated from seawater analysis

*Yoko Iwamoto[1], Mitsuo Uematsu[2] (1.Graduate School of Biosphere Science, Hiroshima University, 2.Atmosphere and Ocean Research Institute, the University of Tokyo)

[MIS09-P04] Seasonal change of the Asian dust provenance within the Canadian ice core estimated from cathodoluminescence spectra of single quartz grains

*Kana Nagashima[1], Kumiko Goto-Azuma[2] (1.Japan Agency for Marine-Earth Science and Technology, Research and Development Center for Global Change, 2.National Institute of Polar Research)

[MIS09-P05] Wind tunnel experiments for saltation and dust emission under weak crusted Mongolian soil

*Ishizuka Masahide[1], Yusuke Nakahara[5], Hitomi Masaoka[6], Genki Nakao[6], Tomoyuki Ishii[6], Yasunori Kurosaki[2], Hagino Hiroaki[3], Kouichi Nakamura[7], Batdelger Gantsetseg[4], Kazuki Nanko[9], Eiji Nishihara[8], Satoru Suzuki[9] (1.Kagawa University, Faculty of Engineering and Design, 2.Tottori University, Arid land research center, 3.Forestry and Forest Products Research Institute, Tohoku Research Center, 4.Information and Research Institute of Meteorology Hydrology and Environment, 5.Kagawa University, Graduate school of Engineering, 6.Kagawa University, Faculty of Engineering, 7.Tottori University, Faculty of Engineering, 8.Tottori University, Faculty of Agriculture, 9.Forestry and Forest Products Research Institute, Meteorology and Hydrology)

[MIS09-P06] **Effect of stone on sand saltation in Tsogt-Ovoo, Mongolia: Observation and Model simulation**

*Batjargal Buyantogtokh[1], Yasunori Kurosaki[1], Masahide Ishizuka[2], Tsuyoshi Sekiyama[3] (1.Arid Land Research Center, Tottori University, 2.Faculty of Engineering and Design, Kagawa University, 3.Japan Meteorological Agency, Meteorological Research Institute)

[J] Oral | M (Multidisciplinary and Interdisciplinary)：M-IS Intersection

9:00 AM - 10:30 AM JST | 12:00 AM - 1:30 AM UTC | Convention Hall B 2F

## [M-IS12] tsunami deposit

convener:Takashi Chiba(Faculty of Bioresource Sciences, Akita Prefectural University), Tetsuya Shinozaki(Center for Research in Isotopes and Environmental Dynamics (CRiED), University of Tsukuba), Daisuke Ishimura(Department of Geography, Tokyo Metropolitan University), Chairperson:Daisuke Ishimura(Department of Geography, Tokyo Metropolitan University)

9:00 AM - 9:15 AM JST | 12:00 AM - 12:15 AM UTC

### [MIS12-01] Geological Record of Tsunamis and Storms Influenced by Relative Sea-Level Change, Southern Hidaka Coast, Hokkaido, Japan.

*RYO NAKANISHI[1], Satoshi Okamura[1,2], Tsumoru Sagayama[3], Yusuke Yokoyama[4], Yosuke Miyairi[4] (1.Hokkaido Edu. Univ., 2.Hokkaido Soil Res. Co-op., 3.HRCG, 4.Univ. Tokyo)

9:15 AM - 9:30 AM JST | 12:15 AM - 12:30 AM UTC

### [MIS12-02] Before and after relationship between the seismic uplift and the large tsunami due to the seventeenth-century giant earthquake observed in the seismic barrier systems around the Kuril subduction zone

*Futoshi Nanayama[1,5], Kazuaki Watanabe[1], Keita Fukatsu[2], Takeshi Hasegawa[4], Kiyoyuki Shigeno[3], Masayuki Ishii[6], Kazuhito Ishiwata[7], Shigeto Inokuma[8] (1.Geological Survey of Japan, AIST, 2.Notsuke Peninsula Nature Center, 3.Meiji consultant Co., Ltd., 4.Ibaraki University, 5.CWMD, Kumamoto Univ., 6.Ishii Professional Engineer Office, 7.Betsukai municipal museum, 8.Nemuro City museum history and nature)

9:30 AM - 9:45 AM JST | 12:30 AM - 12:45 AM UTC

### [MIS12-03] Coastal landform changes and Washover deposits due to high waves generated by anatmospheric low-pressure system in June 2016 at Horokayanto, Hokkaido, Japan

*Takashi Chiba[1], Yuichi Nishimura[2] (1.Faculty of Bioresource Sciences, Akita Prefectural University, 2.Graduate School of Science, Hokkaido University)

9:45 AM - 10:00 AM JST | 12:45 AM - 1:00 AM UTC

### [MIS12-04] Survey of tsunami deposits in Kunashiri Island: Results obtained in the 2015-2018 projects

*Yuichi Nishimura[1], Yasuhiro Takashimizu[2], Daisuke Sugawara[3], Takafumi Enya[4], Takashi Chiba[5], Ryo Nakanishi[6], Alexander Shishkin[7], Alexey Gorbunov[8], Victor Kaistrenko[8], Asuka Takahashi[9], Hiroki Muramatsu[10], Yasuyuki Kawazoe[11], Naofumi Takamatsu[11] (1.Graduate School of Science, Hokkaido University, 2.Institute of Humanities, Social Sciences and Education, Niigata University, 3.Museum of Natural and Environmental History, Shizuoka, 4.Hokkaido Museum, 5.Faculty of Bioresource Sciences, Akita Prefectural University, 6.Hokkaido Education University, 7.Shikotan Geophysical Observatory, 8.Institute of Marine Geology and Geophysics, Russian Academy of Sciences, 9.Japan Meteorological Agency, 10.Geospatial Information Authority of Japan, 11.Ministry of Education, Culture, Sports, Science and Technology)

10:00 AM - 10:15 AM JST | 1:00 AM - 1:15 AM UTC

### [MIS12-05] Deposit-based assessment of tsunami size: example from Nankai-Trough earthquakes

*Daisuke Sugawara[1], Kentaro Imai[2], Shinsuke Okada[3], Takuto Maeda[4] (1.Museum of Natural and Environmental History, Shizuoka, 2.JAMSTEC, 3.Tohoku University, 4.Hirosaki University)

10:15 AM - 10:30 AM JST | 1:15 AM - 1:30 AM UTC

### [MIS12-06] Flume experiments for understanding variety of tsunami deposit

★Invited Papers

*Naofumi Yamaguchi[1] (1.Center for Water Environment Studies, Ibaraki University)

[J] Oral | M (Multidisciplinary and Interdisciplinary)：M-IS Intersection

10:45 AM - 12:15 PM JST | 1:45 AM - 3:15 AM UTC | Convention Hall B 2F

## [M-IS12] tsunami deposit

convener:Takashi Chiba(Faculty of Bioresource Sciences, Akita Prefectural University), Tetsuya Shinozaki(Center for Research in Isotopes and Environmental Dynamics (CRiED), University of Tsukuba), Daisuke Ishimura(Department of Geography, Tokyo Metropolitan University), Chairperson:Tetsuya Shinozaki(Center for Research in Isotopes and Environmental Dynamics, University of Tsukuba)

10:45 AM - 11:00 AM JST | 1:45 AM - 2:00 AM UTC

[MIS12-07] **Inverse modeling of Tsunami deposit using Deep Learning Neural Network**

*Rimali Mitra[1], Hajime Naruse[1] (1.Kyoto University, Graduate School of Science)

---

11:00 AM - 11:15 AM JST | 2:00 AM - 2:15 AM UTC

[MIS12-08] Numerical estimation of tsunami size using boulders deposited by the 2011 Tohoku-oki tsunami at Settai, Miyako city, Japan

*Tatsuya Takei[1,4], Kazuhisa Goto[2], Masaki Yamada[3] (1.Department of Earth Sciences, Graduate School of Science, Tohoku University, 2.International Research Institute of Disaster Science (IRIDeS), Tohoku University, 3.Earthquake Research Institute, University of Tokyo, 4.Department of Complexity Science and Engineering, Graduate School of Frontier Sciences, Tokyo University)

---

11:15 AM - 11:30 AM JST | 2:15 AM - 2:30 AM UTC

[MIS12-09] Constraint of the ages of historical tsunami deposits on the Ishinomaki Plain

*Hiroshi Tetsuka[1], Kazuhisa Goto[2], Takashi Ishizawa[1], Daisuke Sugawara[3], Yusuke Yokoyama[4], Yosuke Miyairi[4] (1.Department of Earth Science, Tohoku University, 2.International Research Institute of Disaster Science, Tohoku University, 3.Museum of Natural and Environmental History, Shizuoka, 4.Atmosphere and Ocean Research Institute, University of Tokyo)

---

11:30 AM - 11:45 AM JST | 2:30 AM - 2:45 AM UTC

[MIS12-10] Non-destructive analyzes of sediments to discern tsunami-related mud cap and overlying muds to improve age determination of tsunami deposits

*Takashi Ishizawa[1], Kazuhisa Goto[2], Yusuke Yokoyama[3], Yosuke Miyairi[3] (1.Department of Earth Science, Tohoku University, 2.International Research Institute of Disaster Science, Tohoku University, 3.Atmosphere and Ocean Research Institute, The University of Tokyo)

---

11:45 AM - 12:00 PM JST | 2:45 AM - 3:00 AM UTC

[MIS12-11] Sedimentological and paleontological studies of storm surge deposits in intertidal mud floor -case study of Ena Bay on Miura Peninsula, Central Japan.

*Akihisa Kitamura[1], yamamoto yuka[1], Takashi Toyofuku[2] (1.Institute of Geosciences, Faculty of Science, Shizuoka University, 2.Japan Agency for Marine-Earth Science and Technology (JAMSTEC))

---

12:00 PM - 12:15 PM JST | 3:00 AM - 3:15 AM UTC

[MIS12-12] Shallow marine tsunami deposits and bioturbation

★Invited Papers

*Koji Seike[1] (1.Geological Survey of Japan, AIST)

[J] Poster | M (Multidisciplinary and Interdisciplinary)：M-IS Intersection

3:30 PM - 5:00 PM JST | 6:30 AM - 8:00 AM UTC | Poster Hall International Exhibition Hall8, Makuhari Messe_21

## [M-IS12] tsunami deposit

convener:Takashi Chiba(Faculty of Bioresource Sciences, Akita Prefectural University), Tetsuya Shinozaki(Center for Research in Isotopes and Environmental Dynamics (CRiED), University of Tsukuba), Daisuke Ishimura(Department of Geography, Tokyo Metropolitan University)

[MIS12-P01] Discussion of tsunami age estimation using coralline tsunami deposits

*Ryosuke Fujita[1], Kazuhisa Goto[1], Yasufumi Iryu[1], Takashi Ishizawa[1], Yusuke Yokoyama[2], Yosuke Miyairi[2] (1.TOHOKU University, 2.Atmosphere and Ocean Research Institute, the University of Tokyo)

[MIS12-P02] Identification method of event deposits caused by natural hazards

*Takumi Yoshii[1], Shiro Tanaka[1], Yuki Ito[1], Takaomi Hamada[1], Masafumi Matsuyama[1] (1.Central Research Institute of Electric Power Industry)

[MIS12-P03] Investigation of event deposits for construction of tsunami deposit discriminating method

*Shiro Tanaka[1], Takumi Yoshii[1], Yasuto Hirata[1], Takaomi Hamada[1], Masafumi Matsuyama[1], Yuki Ito[1] (1.Central Research Institute of Electric Power Industry)

[MIS12-P04] Lateral variation of mud clasts in onshore tsunami deposits

*Yasuhiro Takashimizu[1], Daichi Ito (1.Niigata University)

[MIS12-P05] Examination of model validity and sensitivity of tsunami sediment transport modeling using the 2011 Tohoku tsunami deposits in Iwate, Miyagi, and Fukushima Prefectures

*Satoshi Kusumoto[1], Aditya Gusman[2], Kenji Satake[1] (1.Earthquake Research Institute, the Univ. of Tokyo, 2.GNS Science)

[MIS12-P06] Paleotsunami History in Hachinohe, Aomori Prefecture, northern Japan

*Erick Velasco R.[1], Kazuhisa Goto[2], Takahiro Shinohara[1], Daisuke Sugawara[3], Yuichi Nishimura[4], Takashi Chiba[5] (1.Earth Science Department, Graduate Faculty of Science, Tohoku Univ., 2.International Research Institute of Disaster Science (IRIDeS), Tohoku Univ., 3.Museum of Natural and Environmental History, Shizuoka, 4.Graduate School of Science, Hokkaido Univ., 5.Faculty of Bioresource Sciences, Akita Prefectural Univ.)

[MIS12-P07] Characteristics of event deposits and their source in Sekine-hama, Mutsu city, Aomori prefecture

# Cancelled

*Daisuke Ishimura[1], Kaori Aoki[2] (1.Department of Geography, Tokyo Metropolitan University, 2.Research Center for Volcanic Hazards and Their Mitigation, Tokyo Metropolitan University)

[MIS12-P08] **Sedimentary structure and composition of sand blows and sand dikes formed by the 2018 Iburi-Tobu Earthquake, Hokkaido, Japan**

*Yuichi Nishimura[1], Takashi Chiba[2] (1.Graduate School of Science, Hokkaido University, 2.Faculty of Bioresource Sciences, Akita Prefectural University)

[MIS12-P09] Tsunami deposits and tsunami wave source of the southern part of Okushiri Island, Hokkaido

*Atsushi Urabe[1], Yoshihiro Kase[2], Gentaro Kawakami[2], Kenji Nishina[2], Hiromichi Koyasu[2] (1.Research Institute for Natural Hazards and Disaster Recovery, Niigata University, 2.Geological Survey of Hokkaido, Hokkaido Research Organization)

[MIS12-P10] Inter-seismic and post-seismic tectonic movements detected during the 17th century earthquake and inferred from diatom analysis in Tokachi area, Hokkaido, Japan

*Takashi Chiba[1], Yuichi Nishimura[2] (1.Faculty of Bioresource Sciences, Akita Prefectural University, 2.Graduate School of Science, Hokkaido University)

[J] Poster | M (Multidisciplinary and Interdisciplinary)：M-IS Intersection

5:15 PM - 6:30 PM JST | 8:15 AM - 9:30 AM UTC | Poster Hall International Exhibition Hall8, Makuhari Messe_39

## [M-IS12] tsunami deposit

convener:Takashi Chiba(Faculty of Bioresource Sciences, Akita Prefectural University), Tetsuya Shinozaki(Center for Research in Isotopes and Environmental Dynamics (CRiED), University of Tsukuba), Daisuke Ishimura(Department of Geography, Tokyo Metropolitan University)

[MIS12-P01] Discussion of tsunami age estimation using coralline tsunami deposits

*Ryosuke Fujita[1], Kazuhisa Goto[1], Yasufumi Iryu[1], Takashi Ishizawa[1], Yusuke Yokoyama[2], Yosuke Miyairi[2] (1.TOHOKU University, 2.Atmosphere and Ocean Research Institute, the University of Tokyo)

[MIS12-P02] Identification method of event deposits caused by natural hazards

*Takumi Yoshii[1], Shiro Tanaka[1], Yuki Ito[1], Takaomi Hamada[1], Masafumi Matsuyama[1] (1.Central Research Institute of Electric Power Industry)

[MIS12-P03] Investigation of event deposits for construction of tsunami deposit discriminating method

*Shiro Tanaka[1], Takumi Yoshii[1], Yasuto Hirata[1], Takaomi Hamada[1], Masafumi Matsuyama[1], Yuki Ito[1] (1.Central Research Institute of Electric Power Industry)

[MIS12-P04] Lateral variation of mud clasts in onshore tsunami deposits

*Yasuhiro Takashimizu[1], Daichi Ito (1.Niigata University)

[MIS12-P05] Examination of model validity and sensitivity of tsunami sediment transport modeling using the 2011 Tohoku tsunami deposits in Iwate, Miyagi, and Fukushima Prefectures

*Satoshi Kusumoto[1], Aditya Gusman[2], Kenji Satake[1] (1.Earthquake Research Institute, the Univ. of Tokyo, 2.GNS Science)

[MIS12-P06] Paleotsunami History in Hachinohe, Aomori Prefecture, northern Japan

*Erick Velasco R.[1], Kazuhisa Goto[2], Takahiro Shinohara[1], Daisuke Sugawara[3], Yuichi Nishimura[4], Takashi Chiba[5] (1.Earth Science Department, Graduate Faculty of Science, Tohoku Univ., 2.International Research Institute of Disaster Science (IRIDeS), Tohoku Univ., 3.Museum of Natural and Environmental History, Shizuoka, 4.Graduate School of Science, Hokkaido Univ., 5.Faculty of Bioresource Sciences, Akita Prefectural Univ.)

[MIS12-P07] Characteristics of event deposits and their source in Sekine-hama, Mutsu city, Aomori prefecture

*Daisuke Ishimura[1], Kaori Aoki[2] (1.Department of Geography, Tokyo Metropolitan University, 2.Research Center for Volcanic Hazards and Their Mitigation, Tokyo Metropolitan University)

[MIS12-P08] **Sedimentary structure and composition of sand blows and sand dikes formed by the 2018 Iburi-Tobu Earthquake, Hokkaido, Japan**

*Yuichi Nishimura[1], Takashi Chiba[2] (1.Graduate School of Science, Hokkaido University, 2.Faculty of Bioresource Sciences, Akita Prefectural University)

[MIS12-P09] Tsunami deposits and tsunami wave source of the southern part of Okushiri Island, Hokkaido

*Atsushi Urabe[1], Yoshihiro Kase[2], Gentaro Kawakami[2], Kenji Nishina[2], Hiromichi Koyasu[2] (1.Research Institute for Natural Hazards and Disaster Recovery, Niigata University, 2.Geological Survey of Hokkaido, Hokkaido Research Organization)

[MIS12-P10] Inter-seismic and post-seismic tectonic movements detected during the 17th century earthquake and inferred from diatom analysis in Tokachi area, Hokkaido, Japan

*Takashi Chiba[1], Yuichi Nishimura[2] (1.Faculty of Bioresource Sciences, Akita Prefectural University, 2.Graduate School of Science, Hokkaido University)

[J] Oral | M (Multidisciplinary and Interdisciplinary)：M-IS Intersection

9:00 AM - 10:30 AM JST | 12:00 AM - 1:30 AM UTC | A05 TOKYO BAY MAKUHARI HALL

## [M-IS16] Dynamics of eruption cloud and cumulonimbus; modelling and observation

convener:Eiichi Sato(Meteorological Research Institute), Fukashi Maeno(Earthquake Research Institute, University of Tokyo), Takeshi Maesaka(National Research Institute for Earth Science and Disaster Resilience), Chairperson:Eiichi Sato(Meteorological Research Institute)

9:00 AM - 9:15 AM JST | 12:00 AM - 12:15 AM UTC

[MIS16-01] **Observations of Volcanic Eruption Columns with Different Types of Weather Radars**

★Invited Papers

*Masayuki Maki[1], Takehiko KOBORI[1], Yura Kim[1], Yasushi Fujiyoshi[2], Eiichi Sato[3], Hidehiko Tokushima[4], Masato Iguchi[5] (1.Kagoshima University, 2.Hokkaido University, 3.Meteorological Research Institute, 4.Field Researchers Corporation, 5.Kyoto University)

9:15 AM - 9:30 AM JST | 12:15 AM - 12:30 AM UTC

[MIS16-02] Observation of Eruption Plumes by X-Band MP radar and Lidar at Sakurajima and Kuchinoerabujima

*Haruhisa Nakamichi[1], Atsushi Shimizu[2], Makoto Shimomura[1], Magfira Syarifuddin[1], Masato Iguchi[1] (1.Sakurajima Volcano Research Center, Disaster Prevention Research Institute, Kyoto University, 2.National Institute for Environmental Studies)

9:30 AM - 9:45 AM JST | 12:30 AM - 12:45 AM UTC

[MIS16-03] 2018-2019 Kuchinoerabu-jima eruption plume/cloud echoes observed by JMA weather radar network

*Eiichi Sato[1], Keiichi Fukui[2], Toshiki Shimbori[1] (1.Meteorological Research Institute, 2.Japan Meteorological Agency)

9:45 AM - 10:00 AM JST | 12:45 AM - 1:00 AM UTC

[MIS16-04] Numerical Study on the Ejection Conditions of Ash Clouds during Recent Eruptions of Kuchinoerabujima Volcano

*Yasuhiro Ishimine[1], Teruki Oikawa[2], Nobuo Geshi[2] (1.Research and Education Center for Natural Hazards, Kagoshima University, 2.Geological Survey of Japan, AIST)

10:00 AM - 10:15 AM JST | 1:00 AM - 1:15 AM UTC

[MIS16-05] Image analysis of volcanic clouds during the 2011 Kirishima Shinmoedake eruption

*Takehiko KOBORI[1], Kisei KINOSHITA[1], Naoko IINO[2], Masayuki MAKI[1], Seiji FUKUSHIMA[1] (1.Kagoshima University, 2.Kumamoto University)

10:15 AM - 10:30 AM JST | 1:15 AM - 1:30 AM UTC

[MIS16-06] Cloud Radar Network for Early Detection of Cumulonimbus Generation

*Takeshi Maesaka[1], Tadayasu Ohigashi[1], Koyuru Iwanami[1], Shin-Ichi Suzuki[1], Yukari Shusse[1], Namiko Sakurai[1] (1.National Research Institute for Earth Science and Disaster Resilience)

[J] Poster | M (Multidisciplinary and Interdisciplinary)：M-IS Intersection

3:30 PM - 5:00 PM JST | 6:30 AM - 8:00 AM UTC | Poster Hall International Exhibition Hall8, Makuhari Messe_22

## [M-IS16] Dynamics of eruption cloud and cumulonimbus; modelling and observation

convener:Eiichi Sato(Meteorological Research Institute), Fukashi Maeno(Earthquake Research Institute, University of Tokyo), Takeshi Maesaka(National Research Institute for Earth Science and Disaster Resilience)

[MIS16-P01] Redesign of the Japan Meteorological Agency Atmospheric Transport Model

*Toshiki Shimbori[1], Kensuke Ishii[1] (1.Volcanology Research Department, Meteorological Research Institute)

[MIS16-P02] Mathematical mechanism of an inverse problem for tephra transport and dispersal model

*Kensuke Ishii[1], Takehiro Koyaguchi[2] (1.Meteorological Research Institute, 2.Earthquake Research Institute, the University of Tokyo)

[MIS16-P03] Development of the plume source model for inversion of tephra fallout

*Akira Nishijo[1], Takehiro Koyaguchi[1], Yujiro Suzuki[1] (1.The University of Tokyo Earthquake Research Institute)

[MIS16-P04] Segregation height and size distribution of volcanic ash of Sakurajima eruptions inferred by observed settling velocity

*Kosei Takishita[1], Masato Iguchi[2], Tadaomi Sonoda[2] (1.Graduate School of Science, Kyoto Univ., 2.DPRI, Kyoto Univ.)

[MIS16-P05] Distant tracking of maximum pumice diameter in pumice-fall of the Tenmei eruption of Asama volcano: An attempt to draw isopleth lines of mm scale-maximum pumice diameter in the Kanto Plain

*Shingo Takeuchi[1], Shimpei Uesawa[1] (1.Central Research Institute of Electric Power Industry, Civil Engineering Research Laboratory, Geosphere Sciences)

[MIS16-P06] Degassing activity of Aso volcano, Japan, before the 8 October 2016 eruption measured by satellite and ground-based remote sensing techniques

*Masaaki Morita[1] (1.Geological Survey of Japan, AIST)

[MIS16-P07] Characteristics of polarimetric radar parameters of dry volcanic ash clouds

*Yura Kim[1], Masayuki Maki[1], Masato Iguchi[2], Dong-In Lee[3] (1.Research and Education Center for Natural Hazards, Kagoshima University, Korimoto, Kagoshima, Japan, 2.Sakurajima Volcano Research Center/DPRI, Kyoto University, Sakurajima, Kagoshima, Japan, 3.Department of Atmospheric Sciences, Pukyong National University, Namgu, Busan, Republic of Korea)

[MIS16-P08] Development of easy tools for volcanic eruption plume/cloud analysis using weather radars

*Eiichi Sato[1], Ryutaro Senba[2] (1.Meteorological Research Institute, 2.Fukuoka Regional Headquarter, Japan Meteorological Agency)

[J] Poster | M (Multidisciplinary and Interdisciplinary)：M-IS Intersection

5:15 PM - 6:30 PM JST | 8:15 AM - 9:30 AM UTC | Poster Hall International Exhibition Hall8, Makuhari Messe_40

## [M-IS16] Dynamics of eruption cloud and cumulonimbus; modelling and observation

convener:Eiichi Sato(Meteorological Research Institute), Fukashi Maeno(Earthquake Research Institute, University of Tokyo), Takeshi Maesaka(National Research Institute for Earth Science and Disaster Resilience)

[MIS16-P01] Redesign of the Japan Meteorological Agency Atmospheric Transport Model

*Toshiki Shimbori[1], Kensuke Ishii[1] (1.Volcanology Research Department, Meteorological Research Institute)

[MIS16-P02] Mathematical mechanism of an inverse problem for tephra transport and dispersal model

*Kensuke Ishii[1], Takehiro Koyaguchi[2] (1.Meteorological Research Institute, 2.Earthquake Research Institute, the University of Tokyo)

[MIS16-P03] Development of the plume source model for inversion of tephra fallout

*Akira Nishijo[1], Takehiro Koyaguchi[1], Yujiro Suzuki[1] (1.The University of Tokyo Earthquake Research Institute)

[MIS16-P04] Segregation height and size distribution of volcanic ash of Sakurajima eruptions inferred by observed settling velocity

*Kosei Takishita[1], Masato Iguchi[2], Tadaomi Sonoda[2] (1.Graduate School of Science, Kyoto Univ., 2.DPRI, Kyoto Univ.)

[MIS16-P05] Distant tracking of maximum pumice diameter in pumice-fall of the Tenmei eruption of Asama volcano: An attempt to draw isopleth lines of mm scale-maximum pumice diameter in the Kanto Plain

*Shingo Takeuchi[1], Shimpei Uesawa[1] (1.Central Research Institute of Electric Power Industry, Civil Engineering Research Laboratory, Geosphere Sciences)

[MIS16-P06] Degassing activity of Aso volcano, Japan, before the 8 October 2016 eruption measured by satellite and ground-based remote sensing techniques

*Masaaki Morita[1] (1.Geological Survey of Japan, AIST)

[MIS16-P07] Characteristics of polarimetric radar parameters of dry volcanic ash clouds

*Yura Kim[1], Masayuki Maki[1], Masato Iguchi[2], Dong-In Lee[3] (1.Research and Education Center for Natural Hazards, Kagoshima University, Korimoto, Kagoshima, Japan, 2.Sakurajima Volcano Research Center/DPRI, Kyoto University, Sakurajima, Kagoshima, Japan, 3.Department of Atmospheric Sciences, Pukyong National University, Namgu, Busan, Republic of Korea)

[MIS16-P08] Development of easy tools for volcanic eruption plume/cloud analysis using weather radars

*Eiichi Sato[1], Ryutaro Senba[2] (1.Meteorological Research Institute, 2.Fukuoka Regional Headquarter, Japan Meteorological Agency)

[J] Oral | M (Multidisciplinary and Interdisciplinary) : M-IS Intersection

9:00 AM - 10:30 AM JST | 12:00 AM - 1:30 AM UTC | 304 3F

## [M-IS19] Paleoclimatology and paleoceanography

convener:Yusuke Okazaki(Department of Earth and Planetary Sciences, Graduate School of Science, Kyushu University), Akira Oka(Atmosphere and Ocean Research Institute, The University of Tokyo), Michinobu Kuwae(Center for Marine Environmental Studies), Hitoshi Hasegawa(Faculty of Science and Technology, Kochi University), Chairperson:Hitoshi Hasegawa

9:00 AM - 9:15 AM JST | 12:00 AM - 12:15 AM UTC

### [MIS19-17] Paleotemperature and precipitation history (18.1–4.5 ka) in stalagmite bulk and clumped isotopes from Hiroshima, Japan

*Hirokazu Kato[1], Shota Amekawa[1], Akihiro Kano[1] (1.Department of Earth and Planetary Science, The University of Tokyo)

---

9:15 AM - 9:30 AM JST | 12:15 AM - 12:30 AM UTC

### [MIS19-18] Terrestrial paleoclimate since 80 ka recorded in stable and clumped isotopes of two stalagmites obtained from the Pacific side of the Japanese islands

*Shota Amekawa[1], Hirokazu Kato[1], Akihiro Kano[1], Kenji Kashiwagi[2], Taiki Mori[3], Ryoko Senda[3], Chuan–Chou Shen[4] (1.Graduate School of Science, The University of Tokyo, 2.Graduate School of Science and Engineering for Research, University of Toyama, 3.Graduate School of Integrated Sciences for Global Society, Kyushu University, 4.Department of Geosciences, National Taiwan University)

---

9:30 AM - 9:45 AM JST | 12:30 AM - 12:45 AM UTC

### [MIS19-19] Seasonal changes in Li/Ca ratio and inferred phytoplankton abundance as analyzed by daily growth increments of *Pecten albicans* (Bivalvia)

*Kondo Yasuo[1], Hondo Shutaro, Hasegawa Hitoshi[1], Nshio Yoshiro[1], Hirota Takayoshi (1.National University Corporation Kochi University)

---

9:45 AM - 10:00 AM JST | 12:45 AM - 1:00 AM UTC

### [MIS19-20] Geological reconstruction of Antarctic Ice Sheet deglaciation on Soya Coast, East Antarctica since the Last Glacial Maximum

*Moto Kawamata[1], Yusuke Suganuma[2,1], Koichiro Doi[2,1], Takanobu Sawagaki[3], Akihisa Hattori[1] (1.Department of Polar Science, School of Multidisciplinary Science, SOKENDAI (The Graduate Unversity for Advanced Studies), 2.National Institute of Polar Research, 3.Hosei University)

---

10:00 AM - 10:15 AM JST | 1:00 AM - 1:15 AM UTC

### [MIS19-21] Os isotope record of the Quaternary seawater derived from pelagic sediment in the Lau Basin, western South Pacific Ocean, and its implications for global climate changes

*Yusuke Kuwahara[1], Kazutaka Yasukawa[1,2], Koichiro Fujinaga[2,3], Tatsuo Nozaki[4,3,5,2], Junichiro Ohta[2,6,3], Honami Sato[2,4], Jun-Ichi Kimura[6], Kentaro Nakamura[1], Yasuhiro Kato[3,1,2] (1.Department of Systems Innovation, School of Engineering, The University of Tokyo, 2.Ocean Resources Research Center for Next Generation, Chiba Institute of Technology, 3.Frontier Research Center for Energy and Resources, School of Engineering, The University of Tokyo, 4.Research and Development Center for Submarine Resources, Japan Agency for Marine-Earth Science and Technology , 5.Department of Planetology, Graduate School of Science, Kobe University, 6.Department of Solid Earth Geochemistry, Japan Agency for Marine-Earth Science and Technology)

---

10:15 AM - 10:30 AM JST | 1:15 AM - 1:30 AM UTC

### [MIS19-22] Rapid glaciation and sea level changes during the Last Glacial Maximum and the deglaciation

*Yusuke Yokoyama[1], Tezer M Esat[9], William G Thompson[10], Alexandar L Thomas[11], Jody W Webster[2], Yosuke Miyairi[1], Chikako Sawada[1], Takahiro AZE[1], Hiroyuki Matsuzaki[1], Jun'ichi Okuno[3], Stewart Fallon[9], Juan-Carlos Braga[12], Marc Humblet[4], Yasufumi Iryu[5], Donald C Potts[13], Kazuhiko Fujita[6], Atsushi Suzuki[7], Hironobu Kan[8] (1.Atmosphere and Ocean Research Institute, University of Tokyo, 2.University of Sydney, Australia, 3.National Institute of Polar Research, 4.Nagoya University, 5.Tohoku University, 6.University of the Ryukyus, 7.The Geological Survey of Japan, AIST, 8.Kyushu University, 9.Research School of Earth Sciences, The Australian National University, Australia, 10.Woods Hole Oceanographic Institute, USA, 11.University of Edinburgh, UK, 12.Universidad de Granada, Spain, 13.University of California Santa Cruise, USA)

[J] Oral | M (Multidisciplinary and Interdisciplinary)：M-IS Intersection

10:45 AM - 12:15 PM JST | 1:45 AM - 3:15 AM UTC | 304 3F

## [M-IS19] Paleoclimatology and paleoceanography

convener:Yusuke Okazaki(Department of Earth and Planetary Sciences, Graduate School of Science, Kyushu University), Akira Oka(Atmosphere and Ocean Research Institute, The University of Tokyo), Michinobu Kuwae(Center for Marine Environmental Studies), Hitoshi Hasegawa(Faculty of Science and Technology, Kochi University), Chairperson:Yusuke Okazaki

10:45 AM - 11:00 AM JST | 1:45 AM - 2:00 AM UTC

[MIS19-23] Long-chain alkenediones found from marine sediments and their unsaturation ratios: key compounds to study the evolution of alkenone biosynthetic pathway?

*Satoshi Furota[1], Hideto Nakamura[2], Ken Sawada[3] (1.Department of Biogeochemistry, Japan Agency for Marine-Earth Science and Technology (JAMSTEC), 2.Faculty of Science, Osaka City University, 3.Department of Earth and Planetary Sciences, Faculty of Science, Hokkaido University)

11:00 AM - 11:15 AM JST | 2:00 AM - 2:15 AM UTC

[MIS19-24] **Geomorphic and pedogenic forcing on the distribution of organic matter from vegetation to soil- a concern for paleoenvironment studies**

*Biswajit Roy[1], Kanva Goyal[1], Prasanta Sanyal[1] (1.Indian Institute of Science Education Research Kolkata)

11:15 AM - 11:30 AM JST | 2:15 AM - 2:30 AM UTC

[MIS19-25] Sea surface salinity of the Kuroshio Current along the Nansei Islands in the mid-Holocene inferred from fossil corals

*Kohki Sowa[1], Chuki Hongo[2], Kentaro Tanaka[3], Takuma Fujii[4], Saburo Sakai[1], Kosei E. Yamaguchi[6,5] (1.Japan Agency for Marine-Earth Science and Technology, 2.Ryukyu University, 3.The University of Tokyo , 4.Kagoshima University, 5.Toho University, 6.NASA Astrobiology Institute)

11:30 AM - 11:45 AM JST | 2:30 AM - 2:45 AM UTC

[MIS19-26] An ocean-dynamic model for the periodic inflow of Tsushima Current in the early Holocene

*Atsuhiko Isobe[1] (1.Research Institute for Applied Mechanics, Kyushu University)

11:45 AM - 12:00 PM JST | 2:45 AM - 3:00 AM UTC

[MIS19-27] Centennial to millennial scale variability of the Aleutian Low and Westerly Jet during the Holocene

*Kana Nagashima[1], Naomi Harada[1] (1.Japan Agency for Marine-Earth Science and Technology, Research and Development Center for Global Change)

12:00 PM - 12:15 PM JST | 3:00 AM - 3:15 AM UTC

[MIS19-28] **Monsoon-related errors in paleotemperature estimation based on leaf margin analysis in central Japan**

*Yuqing Wang[1], Arata Momohara[1], Yongjiang Huang[2] (1.Graduate School of Horticulture, Chiba University, 2.Key Laboratory for Plant Diversity and Biogeography of East Asia, Kunming Institute of Botany, CAS)

[J] Poster | M (Multidisciplinary and Interdisciplinary)：M-IS Intersection

3:30 PM - 5:00 PM JST | 6:30 AM - 8:00 AM UTC | Poster Hall International Exhibition Hall8, Makuhari Messe_23

## [M-IS19] Paleoclimatology and paleoceanography

convener:Yusuke Okazaki(Department of Earth and Planetary Sciences, Graduate School of Science, Kyushu University), Akira Oka(Atmosphere and Ocean Research Institute, The University of Tokyo), Michinobu Kuwae(Center for Marine Environmental Studies), Hitoshi Hasegawa(Faculty of Science and Technology, Kochi University)

### [MIS19-P01] Orbital-scale changes in redox condition and biogenic silica/detrital fluxes of the Jurassic Radiolarite: Possible link with glaciation?

*Masayuki Ikeda[1] (1.Shizuoka University)

### [MIS19-P02] Evaluation of hinterland weathering and paleoclimate of the Cretaceous strata in the Sichuan basin, central China

*Tenichi Cho[1], Hideaki Mantani[1], Tohru Ohta[1], Gang Li[2] (1.Waseda University, 2.Nanjing Institute of Geology and Paleontology)

### [MIS19-P03] Productivity-induced lacustrine bedded chert formation in the Eocene Green River Formation

*Ryusei Kuma[1], Hitoshi Hasegawa[2], Koshi Yamamoto[1], Hidekazu Yoshida[1], Masayuki Ikeda[3], Nagayoshi Katsuta[4], J. Whiteside[5] (1.Nagoya University, 2.Kochi University, 3.Shizuoka University, 4.Gifu University, 5.Southampton University)

### [MIS19-P04] Extraction of the sedimentary cycles and application of cyclostratigraphy to the Middle Miocene Onnagawa Formation in Yashima District, Akita Prefecture, Japan

*Jumpei Yoshioka[1], Ryuji Tada[1,3], Kenji Marc Raymond Matsuzaki[2], Toshihiro Tada[1], Aki Sakuma[1], Yusuke Umemiya[1], Shunsuke Kurokawa (1.Department of Earth and Planetary Science, the University of Tokyo, 2.Atmosphere and Ocean Research Institute, the University of Tokyo, 3.Yunnan University)

### [MIS19-P05] Pliocene magneto–oxygen isotope stratigraphy from the Anno Formation, Awa Group, central Japan

*Yuki Haneda[1], Makoto Okada[1] (1.College of Science, Ibaraki University)

### [MIS19-P06] Planktonic foraminiferal assemblage and paleoceanography of the Plio-Pleistocene sequence at IODP Site U1499 in the northern South China Sea

*Mizuki Kitamura[1], Akira Furusawa[1], Hiroki Hayashi[1] (1.SHIMANE University)

### [MIS19-P07] Reconstruction of the surface water mass fluctuation during the late Pliocene to early Pleistocene based on planktonic foraminiferal fossils from the Mera Formation, Chikura Group, in the southernmost part of the Boso Peninsula

*Makoto Okada[1], Daisuke Hasegawa[2] (1.Department of Earth Sciences, Faculty of Science, Ibaraki University, 2.Graduate School of Scinece and Engineering, Ibaraki University)

### [MIS19-P08] Centennial-scale bioproductivity changes during the earliest Middle-Pleistocene

*Waka Fujii[1], Masayuki Hyodo[1], Shigehiro Katoh[2], Yosuke Miyairi[3], Haruka Yamaguchi[1], Yusuke Yokoyama[3] (1.Kobe University, 2.Hyogo Museum of Nature and Human Activities, 3.University of Tokyo)

### [MIS19-P09] Development of new-paleoceanographic proxies based on oxygen isotope analysis of sponge spicule

*Hitomi Uchimura Wakaki[1], Akira Ijiri[2], Minoru Ikehara[1], Sangmin Hyun[3] (1.Center for Advanced Marine Core Research, Kochi University, 2.Japan Agency for Marine-Earth Science and Technology, 3.Korea Institute of Ocean Science & Technology)

### [MIS19-P10] A system for automatic collection of specific microfossil species using a deep learning classification

*Takuya Itaki[1], Yosuke Taira[2], Naoki Kuwamori[2], Toshinori Maebayashi[3], Satoshi Takeshima[4], Kenji Toya[4] (1.Geological Survey of Japan, AIST, 2.NEC Corporation, 3.Microsupport Co.Ltd, 4.Mitani-Corporation)

[MIS19-P11] Towards reconstructing environmental conditions related to Australian Great Barrier Reef initiation

*Stephen Obrochta[1], Wataru Miwa[1], Kotaro Shirai[2], Yusuke Yokoyama[2], Yosuke Miyairi[2], Jody Webster[2,3], Albert Hine[4] (1.Akita University, 2.University of Tokyo Atmosphere and Ocean Research Institute, 3.University of Sydney, 4.University of South Florida College of Marine Science)

[MIS19-P12] An 8,000-year climate record from Lake Motosu, Japan: Implications for the East Asian Monsoon

Sarah McDonlad[3], Jonathan Tyler[3], *Stephen Obrochta[1], Yusuke Yokoyama[2], Yosuke Miyairi[2], Kosuke Ota[2] (1.Akita University, 2.University of Tokyo Atmosphere and Ocean Research Institute, 3.Department of Earth Sciences, The University of Adelaide)

[MIS19-P13] Environmental changes in northern Mongolia in During the Late Pleistocene: chemical analyses of lacustrine sedimentary sequences in Darhad basin

Yumiko Ohno[1], Sayuri Naito[1], *Nagayoshi Katsuta[1], Takuma Murakami[3], Shinya Ochiai[2], Noriko Hasebe[2], Shin-ichi kawaka[4] (1.Faculty of Education, Gifu University, 2.Institute of Natural and Environmental Technology, Kanazawa University, 3.Horonobe Research Inst. for the Subsurface Environment, 4.Faculty of Education, Gifu Shotoku Gakuen University)

[MIS19-P14] Paleoenvironmental changes recorded in Orog Lake, southwestern Mongolia during MIS 3 and its relationship with *Homo sapiens*'s migration into northern Asia

*Hitoshi Hasegawa[1], Nanase Noma[1], Nagayoshi Katsuta[2], Masafumi MURAYAMA[3], Toru Tamura[4], Masami Izuho[5], Niiden Ichinnorov[6], Davaasuren Davaadorj[7], Noriko Hasebe[8], Miho Sasaoka[9], Masao Iwai[9] (1.Faculty of Science and Technology, Kochi Univ., 2.Faculty of Education, Gifu Univ., 3.Faculty of Agriculture and Marine Science, Kochi Univ., 4.Geological Survey of Japan, AIST, 5.Faculty of Social Sciences and Humanities, Tokyo Metropolitan Univ., 6.Mongolian Academy of Sciences, 7.National University of Mongolia, 8.Institute of Nature and Environmental Technology, Kanazawa Univ., 9.Center for Advanced Marine Core Research, Kochi Univ.)

[MIS19-P15] Reconstruction for water-mass structure of the Okhotsk Sea for the past 1.5 million years based on radiolarian assemblages

*Tatuya Sakamoto[1], Yusuke Okazaki[1] (1.Department of Earth and Planetary Sciences, School of Science, Kyushu University)

[MIS19-P16] Silicoflagellate assemblages in the Okhotsk Sea during the interglacial periods

*Kazuki Egashira[1], Yusuke Okazaki[2], Tatsuhiko Sakamoto[3] (1.Department of Earth and Planetary Sciences, Kyushu University, 2.Department of Earth and Planetary Sciences, Graduate School of Science, Kyushu University , 3.Mie University)

[MIS19-P17] Role of wind stress and sea surface thermal forcing in the formation of the Atlantic meridional overturning circulation at the Last Glacial Maximum

*Akira Oka[1], Kazuki Togawa[1] (1.Atmosphere and Ocean Research Institute, The University of Tokyo)

[MIS19-P18] Comparison of the Kuroshio during LGM simulated by an ocean general circulation model driven by multiple paleoclimate models

*Kensho Ichikawa[1], Haiyan Yang[2], Xinyu Guo[2], Yasumasa Miyazawa[3] (1.Graduate School of Science and Engineering,Ehime University, 2.Center for Marine Environmental Studies,Ehime University, 3.Japan Agency for Marine-Earth Science and Technology)

[MIS19-P19] The changes of the Kuroshio path in the Northwest Pacific since 35ka

*Haiyan Yang[1], Xinyu Guo[1], Ayako Abe-Ouchi[2], Yasumasa Miyazawa[3], Sergey Varlamov[4], Wing-Le Chan[2] (1.Center for Marine Environmental Studies, Ehime University, 2.Atmosphere and Ocean Research Institute, University of Tokyo, 3.Research Institute for Global Change, Japan Agency for Marine-Earth Science and Technology, 4.Application Laboratory, Japan Agency for Marine-Earth Science and Technology)

[MIS19-P20] Temperature reconstruction in the late Pleistocene using fossil terrestrial snails and a stalagmite from an archaeological cave in Okinawa

*Ryuji Asami[1], Rikuto Hondoh[2], Ryu Uemura[3], Ryuichi Shinjo[3], Akihiro Kano[4], Masaki Fujita[5], Shinji Yamasaki[6], Hideko Takayanagi[1], Yasufumi Iryu[1] (1.Graduate School of Science, Tohoku University, 2.Faculty of Science, Tohoku University, 3.Faculty of Science, University of the Ryukyus, 4.School of Science, the University of Tokyo, 5.National Museum of Nature and Science, 6.Okinawa Prefectural Museum and Art Museum)

[MIS19-P21] Silicoflagellate and *Actiniscus* response to meltwater during the last deglaciation in the Alaska margin

*Asuka Tomokawa[1], Yusuke Okazaki[1], Jonaotaro Onodera[2], Keiji Horikawa[3] (1.Department of Earth and Planetary Sciences, Kyushu University, 2.Research and Development Center for Global Change, JAMSTEC, 3.Graduate School of Engineer and Science, University of Toyama)

---

[MIS19-P22] Application of the ramped pyrolysis $^{14}C$ dating to postglacial sediments from the Alaskan margin, Arctic Ocean

*Kenta Suzuki[1], Masanobu Yamamoto[1,2], Brad Rosenheim[3], Takayuki Omori[4], Leonid Polyak[5] (1.Graduate School of Environmental Science, Hokkaido University, 2.Faculty of Environmental Earth Science, Hokkaido University, 3.College of Marine Science, University of South Florida, 4.The University Museum, The University of Tokyo, 5.Bard Polar and Climate Research Center, Ohio State University)

---

[MIS19-P23] Utility of sedimentary environmental DNA for indices of past pelagic fish species populations

*Hiromichi Tamai[1], Michinobu Kuwae[2], Hideyuki Doi[3], Toshihumi Minamoto[4] (1.Graduate School of Science and Engineering, Ehime university, 2.Center for Marine Environmental Studies, Ehime university, 3.Graduate School of Simulation Studies, University of Hyogo, 4.Graduate School of Human Development and Environment, Kobe University)

---

[MIS19-P24] Improvements of extraction methods of sedimentary fish-origin DNA for reconstruction of marine fish communities

*Jun Kurata[1], Hiromichi Tamai[2], Hideyuki Doi[3], Toshihumi Minamoto[4], Michinobu Kuwae[5] (1. department of earth science, Ehime university, 2.Graduate School of Science and Engineering, Ehime university, 3.Graduate School of Simulation Studies, University of Hyogo, 4.Graduate School of Human Development and Environment, Kobe University, 5.Center for Marine Environmental Studies, Ehime university)

---

[MIS19-P25] The paleotemperature reconstruction during the late-Holocene using the sediment core recovered from the Tokyo Bay, Japan

*Hiroto Kajita[1,2,3,4], Naomi Harada[5], Miyako Sato[5], Nanako Ogawa[1], Yusuke Yokoyama[1,2,4], Chikako Sawada[1], Yosuke Miyairi[1], Masayuki Utsunomiya[3], Atsushi Suzuki[3], Hodaka Kawahata[1,2,3] (1.Atmosphere and Ocean Research Institute, The University of Tokyo, Japan, 2.Department of Earth and Planetary Science, Graduate school of Science, The University of Tokyo, Japan, 3. Research Institute of Geology and Geoinformation, Geological Survey of Japan, National Institute of Advanced Industrial Science and Technology (AIST), Japan, 4.Department of Biochemistry, Japan Agency for Marine-Earth Science and Technology (JAMSTEC), Japan, 5.Research and Development Center for Global Change, Japan Agency for Marine-Earth Science and Technology (JAMSTEC), Japan)

---

[MIS19-P26] Summer monsoon variability over the past 400 years in Tateyama, Japan, as reconstructed from tree-ring oxygen isotope data

*Masaki Sano[1], Kota Mori[1], Akane Tsushima[2], Zhen Li[3], Koh Yasue[4], Takeshi Nakatsuka[2,3] (1.Faculty of Human Sciences, Waseda University, 2.Nagoya University, 3.Research Institute for Humanity and Nature, 4.Shinshu University)

---

[MIS19-P27] Eventural Layers of anciant disasters during these 4500 years at Lake Ikeda (Lake Daijya), western coast of Kyushu Island presumed by diatom assemblages in lake deposits

*Kaoru Kashima[1], Tomokazu Mita[1], Yu Fukumoto[3], Tsuyoshi Haraguchi[2], Kazuyoshi Yamada[4] (1.Department of Earth and Planetary Sciences, Kyushu University, 2.Department of Geosicneces, Graduate School of Science, Osaka City University, 3.Ritsumeikan University, 4.Museum of Natural and Environmental History, Shizuoka)

---

[MIS19-P28] Variability of hemipelagic and event depositions in the Beppu Bay during Holocene

*Tomohisa Irino[1], Airi Maruyama[1], Ken Ikehara[2], Masanobu Yamamoto[1], Michinobu Kuwae[3] (1.Graduate School of Environmental Science, Hokkaido University, 2.Institute of Geology and Geoinformation, National Institute of Advanced Industrial Science and Technology, 3. Center for Marine Environmental Studies, Ehime University)

---

[MIS19-P29] The composition of laminae in the sediment of Beppu-Bay and potential as annual laminations

*Yoshiaki Suzuki[1], Michinobu Kuwae[2], Kazuno Arai[3], Ken Ikehara[4], Masafumi MURAYAMA[3] (1.Waseda University, 2.Ehime University, 3.Kochi University, 4.AIST)

---

[MIS19-P30] Simulation of global distribution of Pa/Th using an ocean general circulation model

*Yusuke Sasaki[1], Akira Oka[1] (1.Atmosphere and Ocean Research Institute, The University of Tokyo)

[MIS19-P31] Construction of modern silicoflagellate assemblage dataset in the North Pacific for paleo sea-surface temperature and its application for sediment cores

*Yusuke Okazaki[1], fumiaki nishizono[1], Tanizaki Kyohei[1] (1.Department of Earth and Planetary Sciences, Graduate School of Science, Kyushu University)

[MIS19-P32] Microplastics in surface sediments of the Ariake Bay

Hiroki Sonoda[1], *Yusuke Okazaki[1], Atsuhiko Isobe[2] (1.Department of Earth and Planetary Sciences, Graduate School of Science, Kyushu University, 2.Research Institute for Applied Mechanics, Kyushu University)

[J] Poster | M (Multidisciplinary and Interdisciplinary)：M-IS Intersection

5:15 PM - 6:30 PM JST | 8:15 AM - 9:30 AM UTC | Poster Hall International Exhibition Hall8, Makuhari Messe_41

## [M-IS19] Paleoclimatology and paleoceanography

convener:Yusuke Okazaki(Department of Earth and Planetary Sciences, Graduate School of Science, Kyushu University), Akira Oka(Atmosphere and Ocean Research Institute, The University of Tokyo), Michinobu Kuwae(Center for Marine Environmental Studies), Hitoshi Hasegawa(Faculty of Science and Technology, Kochi University)

### [MIS19-P01] Orbital-scale changes in redox condition and biogenic silica/detrital fluxes of the Jurassic Radiolarite: Possible link with glaciation?

*Masayuki Ikeda[1] (1.Shizuoka University)

### [MIS19-P02] Evaluation of hinterland weathering and paleoclimate of the Cretaceous strata in the Sichuan basin, central China

*Tenichi Cho[1], Hideaki Mantani[1], Tohru Ohta[1], Gang Li[2] (1.Waseda University, 2.Nanjing Institute of Geology and Paleontology)

### [MIS19-P03] Productivity-induced lacustrine bedded chert formation in the Eocene Green River Formation

*Ryusei Kuma[1], Hitoshi Hasegawa[2], Koshi Yamamoto[1], Hidekazu Yoshida[1], Masayuki Ikeda[3], Nagayoshi Katsuta[4], J. Whiteside[5] (1.Nagoya University, 2.Kochi University, 3.Shizuoka University, 4.Gifu University, 5.Southampton University)

### [MIS19-P04] Extraction of the sedimentary cycles and application of cyclostratigraphy to the Middle Miocene Onnagawa Formation in Yashima District, Akita Prefecture, Japan

*Jumpei Yoshioka[1], Ryuji Tada[1,3], Kenji Marc Raymond Matsuzaki[2], Toshihiro Tada[1], Aki Sakuma[1], Yusuke Umemiya[1], Shunsuke Kurokawa (1.Department of Earth and Planetary Science, the University of Tokyo, 2.Atmosphere and Ocean Research Institute, the University of Tokyo, 3.Yunnan University)

### [MIS19-P05] Pliocene magneto–oxygen isotope stratigraphy from the Anno Formation, Awa Group, central Japan

*Yuki Haneda[1], Makoto Okada[1] (1.College of Science, Ibaraki University)

### [MIS19-P06] Planktonic foraminiferal assemblage and paleoceanography of the Plio-Pleistocene sequence at IODP Site U1499 in the northern South China Sea

*Mizuki Kitamura[1], Akira Furusawa[1], Hiroki Hayashi[1] (1.SHIMANE University)

### [MIS19-P07] Reconstruction of the surface water mass fluctuation during the late Pliocene to early Pleistocene based on planktonic foraminiferal fossils from the Mera Formation, Chikura Group, in the southernmost part of the Boso Peninsula

*Makoto Okada[1], Daisuke Hasegawa[2] (1.Department of Earth Sciences, Faculty of Science, Ibaraki University, 2.Graduate School of Scinece and Engineering, Ibaraki University)

### [MIS19-P08] Centennial-scale bioproductivity changes during the earliest Middle-Pleistocene

*Waka Fujii[1], Masayuki Hyodo[1], Shigehiro Katoh[2], Yosuke Miyairi[3], Haruka Yamaguchi[1], Yusuke Yokoyama[3] (1.Kobe University, 2.Hyogo Museum of Nature and Human Activities, 3.University of Tokyo)

### [MIS19-P09] Development of new-paleoceanographic proxies based on oxygen isotope analysis of sponge spicule

*Hitomi Uchimura Wakaki[1], Akira Ijiri[2], Minoru Ikehara[1], Sangmin Hyun[3] (1.Center for Advanced Marine Core Research, Kochi University, 2.Japan Agency for Marine-Earth Science and Technology, 3.Korea Institute of Ocean Science & Technology)

### [MIS19-P10] A system for automatic collection of specific microfossil species using a deep learning classification

*Takuya Itaki[1], Yosuke Taira[2], Naoki Kuwamori[2], Toshinori Maebayashi[3], Satoshi Takeshima[4], Kenji Toya[4] (1.Geological Survey of Japan, AIST, 2.NEC Corporation, 3.Microsupport Co.Ltd, 4.Mitani-Corporation)

[MIS19-P11] Towards reconstructing environmental conditions related to Australian Great Barrier Reef initiation

*Stephen Obrochta[1], Wataru Miwa[1], Kotaro Shirai[2], Yusuke Yokoyama[2], Yosuke Miyairi[2], Jody Webster[2,3], Albert Hine[4] (1.Akita University, 2.University of Tokyo Atmosphere and Ocean Research Institute, 3.University of Sydney, 4.University of South Florida College of Marine Science)

[MIS19-P12] An 8,000-year climate record from Lake Motosu, Japan: Implications for the East Asian Monsoon

Sarah McDonlad[3], Jonathan Tyler[3], *Stephen Obrochta[1], Yusuke Yokoyama[2], Yosuke Miyairi[2], Kosuke Ota[2] (1.Akita University, 2.University of Tokyo Atmosphere and Ocean Research Institute, 3.Department of Earth Sciences, The University of Adelaide)

[MIS19-P13] Environmental changes in northern Mongolia in During the Late Pleistocene: chemical analyses of lacustrine sedimentary sequences in Darhad basin

Yumiko Ohno[1], Sayuri Naito[1], *Nagayoshi Katsuta[1], Takuma Murakami[3], Shinya Ochiai[2], Noriko Hasebe[2], Shin-ichi kawaka[4] (1.Faculty of Education, Gifu University, 2.Institute of Natural and Environmental Technology, Kanazawa University, 3.Horonobe Research Inst. for the Subsurface Environment, 4.Faculty of Education, Gifu Shotoku Gakuen University)

[MIS19-P14] Paleoenvironmental changes recorded in Orog Lake, southwestern Mongolia during MIS 3 and its relationship with *Homo sapiens*'s migration into northern Asia

*Hitoshi Hasegawa[1], Nanase Noma[1], Nagayoshi Katsuta[2], Masafumi MURAYAMA[3], Toru Tamura[4], Masami Izuho[5], Niiden Ichinnorov[6], Davaasuren Davaadorj[7], Noriko Hasebe[8], Miho Sasaoka[9], Masao Iwai[9] (1.Faculty of Science and Technology, Kochi Univ., 2.Faculty of Education, Gifu Univ., 3.Faculty of Agriculture and Marine Science, Kochi Univ., 4.Geological Survey of Japan, AIST, 5.Faculty of Social Sciences and Humanities, Tokyo Metropolitan Univ., 6.Mongolian Academy of Sciences, 7.National University of Mongolia, 8.Institute of Nature and Environmental Technology, Kanazawa Univ., 9.Center for Advanced Marine Core Research, Kochi Univ.)

[MIS19-P15] Reconstruction for water-mass structure of the Okhotsk Sea for the past 1.5 million years based on radiolarian assemblages

*Tatuya Sakamoto[1], Yusuke Okazaki[1] (1.Department of Earth and Planetary Sciences, School of Science, Kyushu University)

[MIS19-P16] Silicoflagellate assemblages in the Okhotsk Sea during the interglacial periods

*Kazuki Egashira[1], Yusuke Okazaki[2], Tatsuhiko Sakamoto[3] (1.Department of Earth and Planetary Sciences, Kyushu University, 2.Department of Earth and Planetary Sciences, Graduate School of Science, Kyushu University , 3.Mie University)

[MIS19-P17] Role of wind stress and sea surface thermal forcing in the formation of the Atlantic meridional overturning circulation at the Last Glacial Maximum

*Akira Oka[1], Kazuki Togawa[1] (1.Atmosphere and Ocean Research Institute, The University of Tokyo)

[MIS19-P18] Comparison of the Kuroshio during LGM simulated by an ocean general circulation model driven by multiple paleoclimate models

*Kensho Ichikawa[1], Haiyan Yang[2], Xinyu Guo[2], Yasumasa Miyazawa[3] (1.Graduate School of Science and Engineering,Ehime University, 2.Center for Marine Environmental Studies,Ehime University, 3.Japan Agency for Marine-Earth Science and Technology)

[MIS19-P19] The changes of the Kuroshio path in the Northwest Pacific since 35ka

*Haiyan Yang[1], Xinyu Guo[1], Ayako Abe-Ouchi[2], Yasumasa Miyazawa[3], Sergey Varlamov[4], Wing-Le Chan[2] (1.Center for Marine Environmental Studies, Ehime University, 2.Atmosphere and Ocean Research Institute, University of Tokyo, 3.Research Institute for Global Change, Japan Agency for Marine-Earth Science and Technology, 4.Application Laboratory, Japan Agency for Marine-Earth Science and Technology)

[MIS19-P20] Temperature reconstruction in the late Pleistocene using fossil terrestrial snails and a stalagmite from an archaeological cave in Okinawa

*Ryuji Asami[1], Rikuto Hondoh[2], Ryu Uemura[3], Ryuichi Shinjo[3], Akihiro Kano[4], Masaki Fujita[5], Shinji Yamasaki[6], Hideko Takayanagi[1], Yasufumi Iryu[1] (1.Graduate School of Science, Tohoku University, 2.Faculty of Science, Tohoku University, 3.Faculty of Science, University of the Ryukyus, 4.School of Science, the University of Tokyo, 5.National Museum of Nature and Science, 6.Okinawa Prefectural Museum and Art Museum)

[MIS19-P21] Silicoflagellate and *Actiniscus* response to meltwater during the last deglaciation in the Alaska margin

*Asuka Tomokawa[1], Yusuke Okazaki[1], Jonaotaro Onodera[2], Keiji Horikawa[3] (1.Department of Earth and Planetary Sciences, Kyushu University, 2.Research and Development Center for Global Change, JAMSTEC, 3.Graduate School of Engineer and Science, University of Toyama)

[MIS19-P22] Application of the ramped pyrolysis $^{14}C$ dating to postglacial sediments from the Alaskan margin, Arctic Ocean

*Kenta Suzuki[1], Masanobu Yamamoto[1,2], Brad Rosenheim[3], Takayuki Omori[4], Leonid Polyak[5] (1.Graduate School of Environmental Science, Hokkaido University, 2.Faculty of Environmental Earth Science, Hokkaido University, 3.College of Marine Science, University of South Florida, 4.The University Museum, The University of Tokyo, 5.Bard Polar and Climate Research Center, Ohio State University)

[MIS19-P23] Utility of sedimentary environmental DNA for indices of past pelagic fish species populations

*Hiromichi Tamai[1], Michinobu Kuwae[2], Hideyuki Doi[3], Toshihumi Minamoto[4] (1.Graduate School of Science and Engineering, Ehime university, 2.Center for Marine Environmental Studies, Ehime university, 3.Graduate School of Simulation Studies, University of Hyogo, 4.Graduate School of Human Development and Environment, Kobe University)

[MIS19-P24] Improvements of extraction methods of sedimentary fish-origin DNA for reconstruction of marine fish communities

*Jun Kurata[1], Hiromichi Tamai[2], Hideyuki Doi[3], Toshihumi Minamoto[4], Michinobu Kuwae[5] (1. department of earth science, Ehime university, 2.Graduate School of Science and Engineering, Ehime university, 3.Graduate School of Simulation Studies, University of Hyogo, 4.Graduate School of Human Development and Environment, Kobe University, 5.Center for Marine Environmental Studies, Ehime university)

[MIS19-P25] The paleotemperature reconstruction during the late-Holocene using the sediment core recovered from the Tokyo Bay, Japan

*Hiroto Kajita[1,2,3,4], Naomi Harada[5], Miyako Sato[5], Nanako Ogawa[1], Yusuke Yokoyama[1,2,4], Chikako Sawada[1], Yosuke Miyairi[1], Masayuki Utsunomiya[3], Atsushi Suzuki[3], Hodaka Kawahata[1,2,3] (1.Atmosphere and Ocean Research Institute, The University of Tokyo, Japan, 2.Department of Earth and Planetary Science, Graduate school of Science, The University of Tokyo, Japan, 3. Research Institute of Geology and Geoinformation, Geological Survey of Japan, National Institute of Advanced Industrial Science and Technology (AIST), Japan, 4.Department of Biochemistry, Japan Agency for Marine-Earth Science and Technology (JAMSTEC), Japan, 5.Research and Development Center for Global Change, Japan Agency for Marine-Earth Science and Technology (JAMSTEC), Japan)

[MIS19-P26] Summer monsoon variability over the past 400 years in Tateyama, Japan, as reconstructed from tree-ring oxygen isotope data

*Masaki Sano[1], Kota Mori[1], Akane Tsushima[2], Zhen Li[3], Koh Yasue[4], Takeshi Nakatsuka[2,3] (1.Faculty of Human Sciences, Waseda University, 2.Nagoya University, 3.Research Institute for Humanity and Nature, 4.Shinshu University)

[MIS19-P27] Eventural Layers of anciant disasters during these 4500 years at Lake Ikeda (Lake Daijya), western coast of Kyushu Island presumed by diatom assemblages in lake deposits

*Kaoru Kashima[1], Tomokazu Mita[1], Yu Fukumoto[3], Tsuyoshi Haraguchi[2], Kazuyoshi Yamada[4] (1.Department of Earth and Planetary Sciences, Kyushu University, 2.Department of Geosicneces, Graduate School of Science, Osaka City University, 3.Ritsumeikan University, 4.Museum of Natural and Environmental History, Shizuoka)

[MIS19-P28] Variability of hemipelagic and event depositions in the Beppu Bay during Holocene

*Tomohisa Irino[1], Airi Maruyama[1], Ken Ikehara[2], Masanobu Yamamoto[1], Michinobu Kuwae[3] (1.Graduate School of Environmental Science, Hokkaido University, 2.Institute of Geology and Geoinformation, National Institute of Advanced Industrial Science and Technology, 3. Center for Marine Environmental Studies, Ehime University)

[MIS19-P29] The composition of laminae in the sediment of Beppu-Bay and potential as annual laminations

*Yoshiaki Suzuki[1], Michinobu Kuwae[2], Kazuno Arai[3], Ken Ikehara[4], Masafumi MURAYAMA[3] (1.Waseda University, 2.Ehime University, 3.Kochi University, 4.AIST)

[MIS19-P30] Simulation of global distribution of Pa/Th using an ocean general circulation model

*Yusuke Sasaki[1], Akira Oka[1] (1.Atmosphere and Ocean Research Institute, The University of Tokyo)

[MIS19-P31] Construction of modern silicoflagellate assemblage dataset in the North Pacific for paleo sea-surface temperature and its application for sediment cores

*Yusuke Okazaki[1], fumiaki nishizono[1], Tanizaki Kyohei[1] (1.Department of Earth and Planetary Sciences, Graduate School of Science, Kyushu University)

[MIS19-P32] Microplastics in surface sediments of the Ariake Bay

Hiroki Sonoda[1], *Yusuke Okazaki[1], Atsuhiko Isobe[2] (1.Department of Earth and Planetary Sciences, Graduate School of Science, Kyushu University, 2.Research Institute for Applied Mechanics, Kyushu University)

[J] Oral | M (Multidisciplinary and Interdisciplinary)：M-IS Intersection

1:45 PM - 3:15 PM JST | 4:45 AM - 6:15 AM UTC | 303 3F

## [M-IS26] Arctic and Antarctic Science and Future Plan

convener:Yoshifumi Nogi(National Institute of Polar Research), Takuji Nakamura(National Institute of Polar Research), Atsuko Sugimoto(Arctic Research Center, Hokkaido University), Shin Sugiyama(Institute of Low Temperature Science, Hokkaido University), Chairperson:Tetsuo Sueyoshi(National Institute of Polar Research), Yoshifumi Nogi(National Institute of Polar Research)

1:45 PM - 2:00 PM JST | 4:45 AM - 5:00 AM UTC

[MIS26-01] Antarctic Circumpolar Interdisciplinary Survey - ACIS

★Invited Papers

*Robin Elizabeth Bell[1], Kirsteen Tinto[1], Xiaojun Yuan[1] (1.Lamont Doherty Earth Observatory of Columbia University)

2:00 PM - 2:15 PM JST | 5:00 AM - 5:15 AM UTC

[MIS26-02] Proposal of Polar Science to Master Plan 2020

*Takuji Nakamura[1], Atsuko Sugimoto[2], Shin Sugiyama[2], Yoshifumi Nogi[1], Tetsuo Sueyoshi[1] (1.National Institute of Polar Research, 2.Hokkaido University)

2:15 PM - 2:30 PM JST | 5:15 AM - 5:30 AM UTC

[MIS26-03] Towards the understanding of mass balance variation of Arctic and Antarctic ice sheets

Teruo Aoki[1,2,4], Masashi Niwano[4], *Tetsuo Sueyoshi[2,3] (1.Okayama Univ., 2.National Institute of Polar Research, 3.Japan Agency for Marine-Earth Science and Technology, 4.Meteorological Research Institute)

2:30 PM - 2:45 PM JST | 5:30 AM - 5:45 AM UTC

[MIS26-04] **Modelling Perspective for the Past and Future tipping points of ice-sheets and climate**

*Ayako Abe-Ouchi[1,2,3], Fuyuki SAITO[2], Takashi Obase[1], Ralf Greve[4], Sam Sherriff-Tadano[1] (1.Atmosphere and Ocean Research Institute, The University of Tokyo, 2.JAMSTEC, 3.NIPR, 4.Hokkaido University)

2:45 PM - 3:00 PM JST | 5:45 AM - 6:00 AM UTC

[MIS26-05] Prediction of sea level rise caused by ice sheet melt

*Takeshi Tamura[1], Junichi Okuno[1], Yusuke Suganuma[1], Tetsuo Sueyoshi[1], Yoshifumi Nogi[1], Takuji Nakamura[1] (1.NIPR National Institute of Polar Research)

3:00 PM - 3:15 PM JST | 6:00 AM - 6:15 AM UTC

[MIS26-06] Future Research Plan in the Polar region

*Yoshifumi Nogi[1], Tetsuo Sueyoshi[1], Takuji Nakamura[1] (1.National Institute of Polar Research)

[J] Poster | M (Multidisciplinary and Interdisciplinary)：M-IS Intersection

3:30 PM - 5:00 PM JST | 6:30 AM - 8:00 AM UTC | Poster Hall International Exhibition Hall8, Makuhari Messe_24

## [M-IS26] Arctic and Antarctic Science and Future Plan

convener:Yoshifumi Nogi(National Institute of Polar Research), Takuji Nakamura(National Institute of Polar Research), Atsuko Sugimoto(Arctic Research Center, Hokkaido University), Shin Sugiyama(Institute of Low Temperature Science, Hokkaido University)

[MIS26-P01] Towards sustained ice–ocean observation network of East Antarctica

*Shigeru Aoki[1], Takeshi Tamura[2], Toshihiro Maki[3], Shin Sugiyama[1] (1.Hokkaido University, 2.National Institute of Polar Research, 3.The University of Tokyo)

[MIS26-P02] Deep ice corings in Antarctica and Greenland

*Kenji Kawamura[1,2,3], Kumiko Goto-Azuma[1,2], Shuji Fujita[1,2], Fumio Nakazawa[1,2], Ikumi Oyabu[1], Hideaki Motoyama[1,2], Ayako Abe-Ouchi[4,3] (1.National Institute of Polar Research, Research Organization of Information and Systems, 2.SOKENDAI (The Graduate University of Advanced Studies), 3.JAMSTEC, 4.University of Tokyo)

[MIS26-P03] **Understanding of whole history of Antarctic ice sheet, sea ice, and bottom water based on core-seismic integrated investigation from Antarctic continental shelf to deep sea floor**

*Minoru Ikehara[1], Takuya Itaki[2], Masakazu Fujii[3] (1.Center for Advanced Marine Core Research, Kochi University, 2.GSJ, AIST, 3.National Institute of Polar Research)

[MIS26-P04] Impacts of the interaction between ice sheets and solid Earth on the prediction of sea-level change

*Jun'ichi Okuno[1,2], Yoshifumi Nogi[1,2] (1.National Institute of Polar Research, 2.SOKENDAI)

[MIS26-P05] International organization's science plan and Japan's Arctic policy

*Yuji Kodama[1], Tetsuo Ohata[1] (1.National Institute of Polar Research)

[J] Poster | M (Multidisciplinary and Interdisciplinary)：M-IS Intersection

5:15 PM - 6:30 PM JST | 8:15 AM - 9:30 AM UTC | Poster Hall International Exhibition Hall8, Makuhari Messe_42

## [M-IS26] Arctic and Antarctic Science and Future Plan

convener:Yoshifumi Nogi(National Institute of Polar Research), Takuji Nakamura(National Institute of Polar Research), Atsuko Sugimoto(Arctic Research Center, Hokkaido University), Shin Sugiyama(Institute of Low Temperature Science, Hokkaido University)

[MIS26-P01] Towards sustained ice–ocean observation network of East Antarctica

*Shigeru Aoki[1], Takeshi Tamura[2], Toshihiro Maki[3], Shin Sugiyama[1] (1.Hokkaido University, 2.National Institute of Polar Research, 3.The University of Tokyo)

[MIS26-P02] Deep ice corings in Antarctica and Greenland

*Kenji Kawamura[1,2,3], Kumiko Goto-Azuma[1,2], Shuji Fujita[1,2], Fumio Nakazawa[1,2], Ikumi Oyabu[1], Hideaki Motoyama[1,2], Ayako Abe-Ouchi[4,3] (1.National Institute of Polar Research, Research Organization of Information and Systems, 2.SOKENDAI (The Graduate University of Advanced Studies), 3.JAMSTEC, 4.University of Tokyo)

[MIS26-P03] **Understanding of whole history of Antarctic ice sheet, sea ice, and bottom water based on core-seismic integrated investigation from Antarctic continental shelf to deep sea floor**

*Minoru Ikehara[1], Takuya Itaki[2], Masakazu Fujii[3] (1.Center for Advanced Marine Core Research, Kochi University, 2.GSJ, AIST, 3.National Institute of Polar Research)

[MIS26-P04] Impacts of the interaction between ice sheets and solid Earth on the prediction of sea-level change

*Jun'ichi Okuno[1,2], Yoshifumi Nogi[1,2] (1.National Institute of Polar Research, 2.SOKENDAI)

[MIS26-P05] International organization's science plan and Japan's Arctic policy

*Yuji Kodama[1], Tetsuo Ohata[1] (1.National Institute of Polar Research)

[E] Poster | M (Multidisciplinary and Interdisciplinary)：M-AG Applied Geosciences

10:45 AM - 12:15 PM JST | 1:45 AM - 3:15 AM UTC | Poster Hall International Exhibition Hall8, Makuhari Messe_11

## [M-AG38] Satellite Land Physical Processes Monitoring at Medium/High/Very High Resolution

convener:Jean-Claude Roger(University of Maryland College Park), Shinichi Sobue(Japan Aerospace Exploration Agency), Eric Vermote(NASA Goddard Space Flight Center)

[MAG38-P01] Improving the AVHRR LTDR BRDF correction

*Jose Luis Villaescusa[1,2], Belen Franch[1,2], Jean-Claude Roger[1,2], Eric Vermote[2] (1.University of Maryland College Park, 2.NASA Goddard Space Flight Center)

[MAG38-P02] Winter wheat yield model based on remote sensing data

*Belen Franch[1,2], Eric Vermote[2,1], Sergii Skakun[1,2], Jean-Claude Roger[1,2], Inbal Becker-Reshef[1], Chris Justice[1] (1.Department of Geographical Sciences, University of Maryland, 2.NASA Goddard Space Flight Center)

[MAG38-P03] Agricultural monitoring from Optical and SAR data

*Andrés Eduardo Santamaría-Artigas[1,2], Sergii Skakun[1,2], Belen Franch[1,2], Jean-Claude Roger[1,2], Eric Vermote[2] (1.University of Maryland College Park, 2.NASA Goddard Space Flight Center)

[MAG38-P04] **Eco-hydrological modeling using field-based and Earth Observations to assess water use efficiency and support agricultural water resources management**

pierre Guillevic[2,1], *Jean-Claude Roger[1,2] (1.University of Maryland, College Park, USA, 2.NASA Goddard Space flight Center, Greenbelt, USA)

[MAG38-P05] Detecting and quantifying forest dynamics using SAR time-series data in Indonesia

*Pedro Rodriguez-Veiga[1,2,3], Narumasa Tsutsumida[3] (1.Centre for Landscape and Climate Research, University of Leicester, Leicester, UK, 2.NERC National Centre for Earth Observation (NCEO), Leicester, UK, 3.Graduate School of Global Environmental Studies, Kyoto University, Japan)

[E] Poster | M (Multidisciplinary and Interdisciplinary)：M-AG Applied Geosciences

5:15 PM - 6:30 PM JST | 8:15 AM - 9:30 AM UTC | Poster Hall International Exhibition Hall8, Makuhari Messe_43

## [M-AG38] Satellite Land Physical Processes Monitoring at Medium/High/Very High Resolution

convener:Jean-Claude Roger(University of Maryland College Park), Shinichi Sobue(Japan Aerospace Exploration Agency), Eric Vermote(NASA Goddard Space Flight Center)

[MAG38-P01] Improving the AVHRR LTDR BRDF correction

*Jose Luis Villaescusa[1,2], Belen Franch[1,2], Jean-Claude Roger[1,2], Eric Vermote[2] (1.University of Maryland College Park, 2.NASA Goddard Space Flight Center)

[MAG38-P02] Winter wheat yield model based on remote sensing data

*Belen Franch[1,2], Eric Vermote[2,1], Sergii Skakun[1,2], Jean-Claude Roger[1,2], Inbal Becker-Reshef[1], Chris Justice[1] (1.Department of Geographical Sciences, University of Maryland, 2.NASA Goddard Space Flight Center)

[MAG38-P03] Agricultural monitoring from Optical and SAR data

*Andrés Eduardo Santamaría-Artigas[1,2], Sergii Skakun[1,2], Belen Franch[1,2], Jean-Claude Roger[1,2], Eric Vermote[2] (1.University of Maryland College Park, 2.NASA Goddard Space Flight Center)

[MAG38-P04] **Eco-hydrological modeling using field-based and Earth Observations to assess water use efficiency and support agricultural water resources management**

pierre Guillevic[2,1], *Jean-Claude Roger[1,2] (1.University of Maryland, College Park, USA, 2.NASA Goddard Space flight Center, Greenbelt, USA)

[MAG38-P05] Detecting and quantifying forest dynamics using SAR time-series data in Indonesia

*Pedro Rodriguez-Veiga[1,2,3], Narumasa Tsutsumida[3] (1.Centre for Landscape and Climate Research, University of Leicester, Leicester, UK, 2.NERC National Centre for Earth Observation (NCEO), Leicester, UK, 3.Graduate School of Global Environmental Studies, Kyoto University, Japan)

[E] Oral | M (Multidisciplinary and Interdisciplinary)：M-AG Applied Geosciences

1:45 PM - 3:15 PM JST | 4:45 AM - 6:15 AM UTC | 302 3F

## [M-AG38] Satellite Land Physical Processes Monitoring at Medium/High/Very High Resolution

convener:Jean-Claude Roger(University of Maryland College Park), Shinichi Sobue(Japan Aerospace Exploration Agency), Eric Vermote(NASA Goddard Space Flight Center), Chairperson:Jean-Claude Roger, Eric Vermote

1:50 PM - 2:05 PM JST | 4:50 AM - 5:05 AM UTC

[MAG38-01] 15-years of LSA-SAF/Eumetsat satellite-derived albedo products: method for retrieval validation, and recent advances using neural networks during spectral integration

*Florian Pinault[1], Dominique Carrer[1], Xavier Ceamanos[1], Gabriel Lellouch[1], Catherine Meurey[1], Suman Moparthy[1], Chloé Vincent[1], Sandra Coelho[2], Isabel Trigo[2] (1.Météo France, CNRM-GAME, UMR3589, Toulouse, France, 2.IPMA, Lisbon, Portugal)

---

2:05 PM - 2:20 PM JST | 5:05 AM - 5:20 AM UTC

[MAG38-02] **Toward a Consistent Land Long Term Climate Data Records from Large Field of View Polar Orbiting Earth Observation Satellites**

*Eric Vermote[1], Jean-Claude Roger[1,2], Belen Franch[1,2], Christopher Justice[2], Ivan Csiszar[3], Sadashiva Devadiga[1], Edward Masuoka[1] (1.NASA Goddard Space Flight Center, 2.University of Maryland, Dept. of Geographical Sciences, 3.NOAA/NESDIS/STAR)

---

2:20 PM - 2:35 PM JST | 5:20 AM - 5:35 AM UTC

[MAG38-03] **LaSRC Cloud Detection Algorithm for Landsat 8 and Sentinel-2 Data**

*Sergii Skakun[1], Eric Vermote[2], Jean-Claude Roger[1] (1.University of Maryland College Park, 2.NASA Goddard Space Flight Center)

---

2:35 PM - 2:50 PM JST | 5:35 AM - 5:50 AM UTC

[MAG38-04] **Aerosol models for the validation of Surface Reflectances for MODIS, VIIRS, Landsat-8, Sentinel-2 from LaSRC**

*Jean-Claude Roger[1,2], Eric Vermote[2], Sergii Skakun[1,2], Belen Franch[1,2], Georgia Doxani[4], William Rountree[1,2], Ferran Gascon[4], chris justice[1], oleg dubovik[3], Brent holben[2] (1.University of Maryland, College Park, USA, 2.NASA Goddard Space flight Center, Greenbelt, USA, 3.LOA, University of Lille, Villeneuve d'Ascq, France, 4.ESA, Frascati, Italy)

---

2:50 PM - 3:05 PM JST | 5:50 AM - 6:05 AM UTC

[MAG38-05] Quantity and spatial distribution of aboveground biomass carbon in Colombia’s forest

*Pedro Rodriguez-Veiga[1,2], Adriana Paola Barbosa-Herrera[3], Edersson Cabrera[3], Gustavo Galindo[3], Valentin Louis[1], Pilar Lozano[3], Pacheco-Pascagaza Ana Maria[1], Indira Pachon-Cendales[3], Salinas Nelso Ricardo[3], Heiko Balzter[1,2] (1.Centre for Landscape and Climate Research, University of Leicester, Leicester, UK, 2.NERC National Centre for Earth Observation (NCEO), Leicester, UK, 3.Institute of Hydrology, Meteorology and Environmental Studies (IDEAM), Bogota, Colombia)

[E] Oral | M (Multidisciplinary and Interdisciplinary)：M-AG Applied Geosciences

3:30 PM - 5:00 PM JST | 6:30 AM - 8:00 AM UTC | 201B 2F

## [M-AG38] Satellite Land Physical Processes Monitoring at Medium/High/Very High Resolution

convener:Jean-Claude Roger(University of Maryland College Park), Shinichi Sobue(Japan Aerospace Exploration Agency), Eric Vermote(NASA Goddard Space Flight Center), Chairperson:Sergii Skakun(University of Mrayland, USA), Eric Vermote

3:35 PM - 3:50 PM JST | 6:35 AM - 6:50 AM UTC

[MAG38-06] Introduction of GCOM-C/SGLI Leaf Area Index & Fraction of Absorbed Photosynthetically Active Radiation products

*Toshiyuki Kobayashi[1], Yoshiaki HONDA[2], Yuhsaku Ono[2], Hideki Kobayashi[3], Wei Yang[2], Shin Nagai[3], Tomoko Akitsu[4], Kenlo Nasahara[4], Risa Miyazaki[1], Masahiro Hori[1], Hiroshi Murakami[1] (1.Japan Aerospace Exploration Agency, 2.Center for Environmental Remote Sensing, Chiba University, 3.Japan Agency for Marine-Earth Science and Technology, 4.University of Tsukuba)

3:50 PM - 4:05 PM JST | 6:50 AM - 7:05 AM UTC

[MAG38-07] **35-years of Land Surface Albedo and 15-years of Down-Welling Short-Wave Radiation Retrievals from Satellites through the EUMETSAT/LSA-SAF and ECMWF/C3S projects**

*Dominique Carrer[1], Florian Pinault[1], Iskander Benhadj[2], Xavier Ceamanos[1], Sandra Coelho[3], Gabriel Lellouch[1], Catherine Meurey[1], Suman Moparthy[1], Else Swinnen[2], Chloé Vincent[1], Isabel Trigo[3] (1.Meteo France, CNRM, France, 2.VITO, Belgium, 3.IPMA, Portugal)

4:05 PM - 4:20 PM JST | 7:05 AM - 7:20 AM UTC

[MAG38-08] **Integrating the satellite-based biophysical model and environmental zonation scheme to estimate rice yield gap in Northeast China**

*Jiahua Zhang[1,3], Jingwen Wang[1,2,3] (1.Institute of Remote Sensing and Digital Earth, Chinese Academy of Sciences, 2.University of Chinese Academy of Sciences, 3.Aerospace Information Research Institute, Chinese Academy of Sciences)

4:20 PM - 4:35 PM JST | 7:20 AM - 7:35 AM UTC

[MAG38-09] Landsat-based Phenological Classification Mapping in Japan

*Narumasa Tsutsumida[1], Shin Nagai[2], Pedro Rodriguez-Veiga[3,4,1], Tomoaki Miura[5] (1.Graduate School of Global Environmental Studies, Kyoto Univeristy, 2.Research and Development Center for Global Change, Japan Agency for Marine-Earth Science and Technology, 3.Centre for Landscape and Climate Research, University of Leicester, 4. National Centre for Earth Observation, University of Leicester, 5.Department of Natural Resources and Environmental Management University of Hawaii at Manoa)

4:35 PM - 4:50 PM JST | 7:35 AM - 7:50 AM UTC

[MAG38-10] **Incorporating satellite-retrieved canopy nitrogen content into the biophysical process model for estimating crop yield and N fertilizer recommendation**

*Jingwen Wang[1,2,3], Jiahua Zhang[1,3] (1.Institute of Remote Sensing and Digital Earth, Chinese Academy of Sciences, 2.University of Chinese Academy of Sciences, 3.Aerospace Information Research Institute, Chinese Academy of Sciences)

[J] Poster | M (Multidisciplinary and Interdisciplinary)：M-AG Applied Geosciences

10:45 AM - 12:15 PM JST | 1:45 AM - 3:15 AM UTC | Poster Hall International Exhibition Hall8, Makuhari Messe_12

## [M-AG39] Marine-Earth Informatics

convener:Seiji Tsuboi(JAMSTEC, Center for Earth Information Science and Technology), Keiko Takahashi(Japan Agency for Marine and Earth Science and Technology), Masaki Kanao(National Institute of Polar Research), Daisuke Matsuoka(Japan Agency for Marine-Earth Science and Technology)

[MAG39-P01] A bottleneck against industrial distribution of atmosphere-ocean product from the Earth Simulator

*Shinya Kakuta[1], Hajime Nishimura[1] (1.JAMSTEC Japan Agency for Marine-Earth Science and Technology)

[MAG39-P02] GANSEKI: Long-Term Strategy of JAMSTEC Deep Seafloor Rock Sample Curation

*Takayuki Tomiyama[1] (1.Japan Agency for Marine-Earth Science and Technology)

[MAG39-P03] Running global seismic waveform simulation on Windows10

*Seiji Tsuboi[1] (1.JAMSTEC, Center for Earth Information Science and Technology)

[MAG39-P04] Synthetic seismograms of explosive sources calculated by the Earth Simulator

*Seiji Tsuboi[1] (1.JAMSTEC, Center for Earth Information Science and Technology)

[J] Poster | M (Multidisciplinary and Interdisciplinary)：M-AG Applied Geosciences

5:15 PM - 6:30 PM JST | 8:15 AM - 9:30 AM UTC | Poster Hall International Exhibition Hall8, Makuhari Messe_44

## [M-AG39] Marine-Earth Informatics

convener:Seiji Tsuboi(JAMSTEC, Center for Earth Information Science and Technology), Keiko Takahashi(Japan Agency for Marine and Earth Science and Technology), Masaki Kanao(National Institute of Polar Research), Daisuke Matsuoka(Japan Agency for Marine-Earth Science and Technology)

[MAG39-P01] A bottleneck against industrial distribution of atmosphere-ocean product from the Earth Simulator

*Shinya Kakuta[1], Hajime Nishimura[1] (1.JAMSTEC Japan Agency for Marine-Earth Science and Technology)

[MAG39-P02] GANSEKI: Long-Term Strategy of JAMSTEC Deep Seafloor Rock Sample Curation

*Takayuki Tomiyama[1] (1.Japan Agency for Marine-Earth Science and Technology)

[MAG39-P03] Running global seismic waveform simulation on Windows10

*Seiji Tsuboi[1] (1.JAMSTEC, Center for Earth Information Science and Technology)

[MAG39-P04] Synthetic seismograms of explosive sources calculated by the Earth Simulator

*Seiji Tsuboi[1] (1.JAMSTEC, Center for Earth Information Science and Technology)

[J] Oral | M (Multidisciplinary and Interdisciplinary)：M-AG Applied Geosciences

1:45 PM - 3:15 PM JST | 4:45 AM - 6:15 AM UTC | A10 TOKYO BAY MAKUHARI HALL

## [M-AG39] Marine-Earth Informatics

convener:Seiji Tsuboi(JAMSTEC, Center for Earth Information Science and Technology), Keiko Takahashi(Japan Agency for Marine and Earth Science and Technology), Masaki Kanao(National Institute of Polar Research), Daisuke Matsuoka(Japan Agency for Marine-Earth Science and Technology), Chairperson:Daisuke Matsuoka, Seiji Tsuboi

1:45 PM - 2:00 PM JST | 4:45 AM - 5:00 AM UTC

[MAG39-01] Future direction of Marine Earth Informatics

*Keiko Takahashi[1] (1.Japan Agency for Marine and Earth Science and Technology)

---

2:00 PM - 2:15 PM JST | 5:00 AM - 5:15 AM UTC

[MAG39-02] Extraction method of weather informations from camera image using Deep Neural Network

*DAISUKE SUGIYAMA[1], RYO ONISHI[1], HIDENORI FUDEYASU[2] (1.Japan Agency for Marine-Earth Science and Technology, 2.Yokohama National University)

---

2:15 PM - 2:30 PM JST | 5:15 AM - 5:30 AM UTC

[MAG39-03] Automatic detection of weather front around Japan using deep convolutional neural network

*Daisuke Matsuoka[1,2], Shiori Sugimoto[1], Yujin Nakagawa[1], Fumiaki Araki[1], Shintaro Kawahara[1], Yosuke Onoue[4], Masaaki Iiyama[3], Koji Koyamada[3] (1.Japan Agency for Marine-Earth Science and Technology, 2.Japan Science and Technology Agency, 3.Nihon University, 4.Kyoto University)

---

2:30 PM - 2:45 PM JST | 5:30 AM - 5:45 AM UTC

[MAG39-04] Detection of multiple earthquakes by using theoretical seismograms as training dataset of machine learning

*Seiji Tsuboi[1], DAISUKE SUGIYAMA[1] (1.JAMSTEC, Center for Earth Information Science and Technology)

---

2:45 PM - 3:00 PM JST | 5:45 AM - 6:00 AM UTC

[MAG39-05] Classification with imbalanced cloud data using deep convolutional neural network

*Daisuke Matsuoka[1,2], Masuo Nakano[1], Daisuke Sugiyama[1], Seiichi Uchida[3] (1.Japan Agency for Marine-Earth Science and Technology, 2.Japan Science and Technology Agency, 3.Kyushu University)

---

3:00 PM - 3:15 PM JST | 6:00 AM - 6:15 AM UTC

[MAG39-06] discussion

*Seiji Tsuboi[1] (1.JAMSTEC, Center for Earth Information Science and Technology)

[J] Oral | M (Multidisciplinary and Interdisciplinary)：M-AG Applied Geosciences

3:30 PM - 5:00 PM JST | 6:30 AM - 8:00 AM UTC | A10 TOKYO BAY MAKUHARI HALL

## [M-AG39] Marine-Earth Informatics

convener:Seiji Tsuboi(JAMSTEC, Center for Earth Information Science and Technology), Keiko Takahashi(Japan Agency for Marine and Earth Science and Technology), Masaki Kanao(National Institute of Polar Research), Daisuke Matsuoka(Japan Agency for Marine-Earth Science and Technology), Chairperson:Seiji Tsuboi, Daisuke Matsuoka

3:30 PM - 3:50 PM JST | 6:30 AM - 6:50 AM UTC

[MAG39-07] Farmed fish management: integration of observation and simulation

★Invited Papers

*Haruka Nishikawa[1] (1.Japan Agency for Marine-Earth Science and Technology)

---

3:50 PM - 4:05 PM JST | 6:50 AM - 7:05 AM UTC

[MAG39-08] **Q-factor estimation for Greenland ice sheet using 3-D seismic waveform modeling**

*Genti Toyokuni[1], Hiroshi Takenaka[2], Masanao Komatsu[2], Ryota Takagi[1], Masaki Kanao[3], Seiji Tsuboi[4] (1.RCPEVE, Tohoku Univ., 2.Okayama Univ., 3.NIPR, 4.JAMSTEC)

---

4:05 PM - 4:20 PM JST | 7:05 AM - 7:20 AM UTC

[MAG39-09] CLCL: CAVELib Compatible Library for Head-mounted Displays

*Shintaro Kawahara[1] (1.Japan Agency for Marine-Earth Science and Technology)

---

4:20 PM - 4:35 PM JST | 7:20 AM - 7:35 AM UTC

[MAG39-10] Super-Resolution Simulation for Real-Time Prediction of Urban Micrometeorology

*Ryo Onishi[1], DAISUKE SUGIYAMA[1], Keigo Matsuda[1] (1.Japan Agency for Marine-Earth Science and Technology)

---

4:35 PM - 4:50 PM JST | 7:35 AM - 7:50 AM UTC

[MAG39-11] Proposal of adaptation measures for the anthropogenic heat release to improve the summer heat environment in a district

*Toru Sugiyama[1], Xiaoran Tong[2], Satoshi Yoshida[2], Satoru Sadohara[2] (1.Japan Agency for Marine-Earth Science and Technology Center for Earth Information Science and Technology, 2.Yokohama National Univercity Institute of Urban Innovation)

[E] Oral | M (Multidisciplinary and Interdisciplinary)：M-AG Applied Geosciences

9:00 AM - 10:30 AM JST | 12:00 AM - 1:30 AM UTC | 202 2F

## [M-AG40] CTBT IMS Technologies for Detecting Nuclear Explosion and Their Applications to Earth Science

convener:Nurcan Meral Ozel(Comprehensive Nuclear-Test-Ban Treaty Organization), Hiroyuki Matsumoto(Japan Agency for Marine-Earth Science and Technology), Yosuke Naoi(Japan Atomic Energy Agency), Chairperson:Nurcan Meral Özel(Comprehensive Nuclear-Test-Ban Treaty Organization), Hiroyuki Matsumoto(JAMSTEC), Noriko Kamaya(ERI, University of Tokyo)

9:00 AM - 9:15 AM JST | 12:00 AM - 12:15 AM UTC

[MAG40-01] Japanese Contributions and Collaborations for IMS Technologies and the Verification Regime

*Nurcan Meral Ozel[1], David Jepsen[1], Naoko Nakashima[1], Hideaki Komiyama[1], Hiroyuki Matsumoto[1,2] (1.Comprehensive Nuclear-Test-Ban Treaty Organization (CTBTO), 2.Japan Agency for Marine-Earth Science and Technology (JAMSTEC))

---

9:15 AM - 9:30 AM JST | 12:15 AM - 12:30 AM UTC

[MAG40-02] Review: Researches on detection of nuclear tests by seismic waves in Japan

★Invited Papers

*Noriko Kamaya[1] (1.Earthquake Research Institute, the University of Tokyo)

---

9:30 AM - 9:45 AM JST | 12:30 AM - 12:45 AM UTC

[MAG40-03] Waveform Analysis on Induced Earthquakes after the 2017 Nuclear Test and Detected Mining Events in DPRK

*Masashi Motohashi[1], Takanari Fujii[1], Takayuki Otsu[1] (1.Japan Weather Association)

---

9:45 AM - 10:00 AM JST | 12:45 AM - 1:00 AM UTC

[MAG40-04] Submarine volcanoes and where to find them: Harnessing IMS hydroacoustic data

★Invited Papers

*Dirk Metz[1] (1.Japan Agency for Marine-Earth Science and Technology)

---

10:00 AM - 10:15 AM JST | 1:00 AM - 1:15 AM UTC

[MAG40-05] **Importance of noble gas monitoring in CTBT verification technology and observation results in Takasaki radionuclide monitoring station**

*Yoichi Yamamoto[1], Yuichi Kijima[1], Yutaka Tomita[1] (1.Japan Atomic Energy Agency)

---

10:15 AM - 10:30 AM JST | 1:15 AM - 1:30 AM UTC

[MAG40-06] ATM analysis results on radioxenons detected in Japan

*Yuichi Kijima[1], Yoichi Yamamoto[1], Yutaka Tomita[1] (1.Japan Atomic Energy Agency)

[E] Poster | M (Multidisciplinary and Interdisciplinary)：M-AG Applied Geosciences

3:30 PM - 5:00 PM JST | 6:30 AM - 8:00 AM UTC | Poster Hall International Exhibition Hall8, Makuhari Messe_25

## [M-AG40] CTBT IMS Technologies for Detecting Nuclear Explosion and Their Applications to Earth Science

convener:Nurcan Meral Ozel(Comprehensive Nuclear-Test-Ban Treaty Organization), Hiroyuki Matsumoto(Japan Agency for Marine-Earth Science and Technology), Yosuke Naoi(Japan Atomic Energy Agency)

### [MAG40-P01] Overview of the Japanese National Data Centre-1 (NDC-1)

*RYOHEI EMURA[1], Takayuki Otsu[1], Toyomi Sakamoto[1], Soshi Iwata[1], Takanari Fujii[1], Mami Nogami[1], Makiko Iwakuni[1], Masashi Motohashi[1] (1.Japan Weather Association)

### [MAG40-P02] Challenging to utilize the infrasound technologies for civil and science application

*Masashi Motohashi[1], Nobuo Arai[2], Takayuki Otsu[1], Mami Nogami[1], Makiko Iwakuni[1], Ryohei Emura[1] (1.Japan Weather Association, 2.Disaster Mitigation Research Center, Nagoya Unicersity)

### [MAG40-P03] CTBT IMS hydroacoustic signal detections from the Ioto volcanic island in the northwest Pacific Ocean

*Hiroyuki Matsumoto[1,2], Mario Zampolli[1], Georgios Haralabus[1], Jerry Stanley[1], James Mattila[1], Nurcan Meral Ozel[1] (1.Comprehensive Nuclear-Test-Ban Treaty Organization (CTBTO), 2.Japan Agency for Marine-Earth Science and Technology (JAMSTEC))

### [MAG40-P04] Installation of a floating hydrophone system within the SOFAR channel

*Hiroko Sugioka[1], Masayuki Obayashi[2] (1.Kobe University, 2.JAMSTEC)

### [MAG40-P05] Fin whale signals observed at S-net seismic stations

*Takeshi Nakamura[1], Ryoichi Iwase[2] (1.National Research Institute for Earth Science and Disaster Resilience, 2.Japan Agency for Marine-Earth Science and Technology)

### [MAG40-P06] Implementation of integrated observation from seafloor through atmosphere – past, current, and future plans

*Keisuke Ariyoshi[1], Akira Nagano[1], Hiroyuki Matsumoto[1], Nurcan Meral Ozel[2] (1.Japan Agency for Marine-Earth Science and Technology, 2.Comprehensive Nuclear-Test-Ban Treaty Organization)

[E] Poster | M (Multidisciplinary and Interdisciplinary)：M-AG Applied Geosciences

5:15 PM - 6:30 PM JST | 8:15 AM - 9:30 AM UTC | Poster Hall International Exhibition Hall8, Makuhari Messe_45

## [M-AG40] CTBT IMS Technologies for Detecting Nuclear Explosion and Their Applications to Earth Science

convener:Nurcan Meral Ozel(Comprehensive Nuclear-Test-Ban Treaty Organization), Hiroyuki Matsumoto(Japan Agency for Marine-Earth Science and Technology), Yosuke Naoi(Japan Atomic Energy Agency)

### [MAG40-P01] Overview of the Japanese National Data Centre-1 (NDC-1)

*RYOHEI EMURA[1], Takayuki Otsu[1], Toyomi Sakamoto[1], Soshi Iwata[1], Takanari Fujii[1], Mami Nogami[1], Makiko Iwakuni[1], Masashi Motohashi[1] (1.Japan Weather Association)

### [MAG40-P02] Challenging to utilize the infrasound technologies for civil and science application

*Masashi Motohashi[1], Nobuo Arai[2], Takayuki Otsu[1], Mami Nogami[1], Makiko Iwakuni[1], Ryohei Emura[1] (1.Japan Weather Association, 2.Disaster Mitigation Research Center, Nagoya Unicersity)

### [MAG40-P03] CTBT IMS hydroacoustic signal detections from the Ioto volcanic island in the northwest Pacific Ocean

*Hiroyuki Matsumoto[1,2], Mario Zampolli[1], Georgios Haralabus[1], Jerry Stanley[1], James Mattila[1], Nurcan Meral Ozel[1] (1.Comprehensive Nuclear-Test-Ban Treaty Organization (CTBTO), 2.Japan Agency for Marine-Earth Science and Technology (JAMSTEC))

### [MAG40-P04] Installation of a floating hydrophone system within the SOFAR channel

*Hiroko Sugioka[1], Masayuki Obayashi[2] (1.Kobe University, 2.JAMSTEC)

### [MAG40-P05] Fin whale signals observed at S-net seismic stations

*Takeshi Nakamura[1], Ryoichi Iwase[2] (1.National Research Institute for Earth Science and Disaster Resilience, 2.Japan Agency for Marine-Earth Science and Technology)

### [MAG40-P06] Implementation of integrated observation from seafloor through atmosphere – past, current, and future plans

*Keisuke Ariyoshi[1], Akira Nagano[1], Hiroyuki Matsumoto[1], Nurcan Meral Ozel[2] (1.Japan Agency for Marine-Earth Science and Technology, 2.Comprehensive Nuclear-Test-Ban Treaty Organization)

[J] Oral | M (Multidisciplinary and Interdisciplinary)：M-TT Technology & Techniques

10:45 AM - 12:15 PM JST | 1:45 AM - 3:15 AM UTC | 202 2F

## [M-TT49] Brand-new scope of coupling geophysics being established by infrasound and associated waves

convener:Masa-yuki Yamamoto(Department of systems engineering, Kochi University of Technology), Mie Ichihara(Earthquake Research Institute, University of Tokyo), Nobuo Arai(Disaster Mitigation Research Center, Nagoya University), Chairperson:Masa-yuki Yamamoto(Kochi University of Technology), Hiroaki Saito(Kochi University of Technology)

10:45 AM - 11:00 AM JST | 1:45 AM - 2:00 AM UTC

[MTT49-01] A two-step amplification mechanism of infrasound waves in the ocean-atmosphere system

★Invited Papers

*Hiroyuki Shinagawa[1] (1.National Institute of Information and Communications Technology)

---

11:00 AM - 11:15 AM JST | 2:00 AM - 2:15 AM UTC

[MTT49-02] Propagation of infrasound generated by an explosive eruption of Mt. Shinmoedake on 10 March 2018

*Hiroaki Saito[1], Tetsuo Yamamoto[2], Masa-yuki Yamamoto[1] (1.School of Systems Engineering, Kochi University of Technology, 2.Hokkaido University)

---

11:15 AM - 11:30 AM JST | 2:15 AM - 2:30 AM UTC

[MTT49-03] Infrasound observations of atmospheric disturbances due to a sequence of 2018 explosive volcano eruptions in Japan.

*Mario Batubara[1], Masa-yuki Yamamoto[1], Saito Hiroaki[1] (1.Kochi University of Technology)

---

11:30 AM - 11:45 AM JST | 2:30 AM - 2:45 AM UTC

[MTT49-04] Comparison of seismic waveforms observed by co-located seismometer and barometer installed indoors 2nd report

*Makiko Iwakuni[1], Nobuo Arai[2], Takayuki Otsu[1], Masashi Motohashi[1], Toyomi Sakamoto[1], Takanari Fujii[1], Ryohei Emura[1], Mami Nogami[1], Takahiko Murayama[1], Takuma Oi[3] (1.Japan Weather Association, 2.Disaster Mitigation Research Center, Nagoya University, 3.Toho Mercantile co., Ltd.)

---

11:45 AM - 12:00 PM JST | 2:45 AM - 3:00 AM UTC

[MTT49-05] Ionospheric disturbances associated with typhoons and a tornado observed by HF doppler sounding

★Invited Papers

*Hiroyuki Nakata[1], Ryuichi Mashiko[1], Hiroyo Ohya[1], Toshiaki Takano[1], Keisuke Hosokawa[2], Ichiro Tomizawa[3], Hiromichi Nagao[4] (1.Graduate School of Science and Engineering, Chiba University, 2.Graduate School of Communication Engineering and Informatics, the University of Electro-Communications, 3.Center for Space Science and Radio Engineering, the University of Electro-Communications, 4.Earthquake Research Institute, the University of Tokyo.)

---

12:00 PM - 12:15 PM JST | 3:00 AM - 3:15 AM UTC

[MTT49-06] Two-year infrasound monitoring by using a prefectural-level sensor network in Kochi

*Masa-yuki Yamamoto[1] (1.Department of systems engineering, Kochi University of Technology)

[J] Poster | M (Multidisciplinary and Interdisciplinary)：M-TT Technology & Techniques

3:30 PM - 5:00 PM JST | 6:30 AM - 8:00 AM UTC | Poster Hall International Exhibition Hall8, Makuhari Messe_26

## [M-TT49] Brand-new scope of coupling geophysics being established by infrasound and associated waves

convener:Masa-yuki Yamamoto(Department of systems engineering, Kochi University of Technology), Mie Ichihara(Earthquake Research Institute, University of Tokyo), Nobuo Arai(Disaster Mitigation Research Center, Nagoya University)

[MTT49-P01] Infrasound signals in Cocos Islands (I06AU) associated with eruption or volcanic body collapse of the Anak Krakatau Volcano or tsunami

*Makiko Iwakuni[1], Nobuo Arai[2], Takayuki Otsu[1], Masashi Motohashi[1], Takanari Fujii[1], Mami Nogami[1], Takahiko Murayama[1], Takuma Oi[3] (1.Japan Weather Association, 2.Disaster Mitigation Research Center, Nagoya University, 3.Toho Mercantile co., Ltd.)

---

[MTT49-P02] A try of origin identification estimated from 2 CTBTO stations detected infrasound signals excited by “The 2018 Hokkaido Eastern Iburi Earthquake”

*Mami Nogami[1], Takayuki Otsu[1], Takahiko Murayama[1], Masashi Motohashi[1], Makiko Iwakuni[1] (1.Japan Weather Association)

---

[MTT49-P03] Quantitative evaluation of blast pressure in the atmosphere and direct measurement of infrasonic/acoustic wave propagation characteristics

*Yusuke Yasukochi[1], Masa-yuki Yamamoto[1], Hiroaki Saito[1] (1.Kochi University of Technology)

---

[MTT49-P04] A case study on relationship with infrasonic wave and auroral activity in the polar region

*Ohata Haruka[1], Masa-yuki Yamamoto[1] (1.KOCHI UNIVERSITY OF TECHNOLOGY)

---

[MTT49-P05] Development of a data-handling platform for simultaneous observation using multiple-type infrasound sensors

*Yuichiro Inoue[1], Masa-yuki Yamamoto[1] (1.Kochi University of Technology)

[J] Poster | M (Multidisciplinary and Interdisciplinary)：M-TT Technology & Techniques

5:15 PM - 6:30 PM JST | 8:15 AM - 9:30 AM UTC | Poster Hall International Exhibition Hall8, Makuhari Messe_46

## [M-TT49] Brand-new scope of coupling geophysics being established by infrasound and associated waves

convener:Masa-yuki Yamamoto(Department of systems engineering, Kochi University of Technology), Mie Ichihara(Earthquake Research Institute, University of Tokyo), Nobuo Arai(Disaster Mitigation Research Center, Nagoya University)

[MTT49-P01] Infrasound signals in Cocos Islands (I06AU) associated with eruption or volcanic body collapse of the Anak Krakatau Volcano or tsunami

*Makiko Iwakuni[1], Nobuo Arai[2], Takayuki Otsu[1], Masashi Motohashi[1], Takanari Fujii[1], Mami Nogami[1], Takahiko Murayama[1], Takuma Oi[3] (1.Japan Weather Association, 2.Disaster Mitigation Research Center, Nagoya University, 3.Toho Mercantile co., Ltd.)

---

[MTT49-P02] A try of origin identification estimated from 2 CTBTO stations detected infrasound signals excited by “The 2018 Hokkaido Eastern Iburi Earthquake”

*Mami Nogami[1], Takayuki Otsu[1], Takahiko Murayama[1], Masashi Motohashi[1], Makiko Iwakuni[1] (1.Japan Weather Association)

---

[MTT49-P03] Quantitative evaluation of blast pressure in the atmosphere and direct measurement of infrasonic/acoustic wave propagation characteristics

*Yusuke Yasukochi[1], Masa-yuki Yamamoto[1], Hiroaki Saito[1] (1.Kochi University of Technology)

---

[MTT49-P04] A case study on relationship with infrasonic wave and auroral activity in the polar region

*Ohata Haruka[1], Masa-yuki Yamamoto[1] (1.KOCHI UNIVERSITY OF TECHNOLOGY)

---

[MTT49-P05] Development of a data-handling platform for simultaneous observation using multiple-type infrasound sensors

*Yuichiro Inoue[1], Masa-yuki Yamamoto[1] (1.Kochi University of Technology)

[J] Oral | U (Union )：Union

Thu. May 30, 2019 9:00 AM - 10:30 AM JST | Thu. May 30, 2019 12:00 AM - 1:30 AM UTC | IC 2F

## [U-06] Japan's contribution to IUGG celebrating 100th anniversary

convener:Setsuya Nakada(National Research Institute for Earth Science and Disaster Resilience), Kenji Satake(Earthquake Research Institute, University of Tokyo), Kumiko Goto-Azuma(National Institute of Polar Research), Chairperson:Kumiko Goto-Azuma(National Institute of Polar Research), Setsuya Nakada(NIED)

International Union of Geodesy and Geophysics (IUGG) is one of the 40 unions in the International Science Council (ISC), celebrating its 100th anniversary in 2019. IUGG promotes and coordinates research on the interior and the periphery of the Earth. The IUGG has associations of eight research fields (IACS, IAG, IAGA, IAHS, IAMAS, IAPSO, IASPEI, and IAVCEI), which carry out semi-autonomously activities in cooperation with each other. In addition, IUGG encourages research to respond to social needs such as reduction of natural disasters and environmental conservation. The IUGG Subcommittee at the Japan Science Council's Earth and Planetary Science Committee and the eight association-committees under the former serve as representatives of Japan for the IUGG and 8 Associations.<br/> In this session, as IUGG celebrates its 100th anniversary, researchers related to each association exchange the ideas on the role of IUGG in earth science and the contribution that Japanese researchers should make to IUGG.

9:00 AM - 9:20 AM JST | 12:00 AM - 12:20 AM UTC

[U06-01] **Centennial of the International Cooperation in Earth and Space Sciences**

★Invited Papers

*Alik Ismail-Zadeh[1,2,3] (1.Karlsruhe Institute of Technology, 2.International Union of Geodesy and Geophysics, 3.International Science Council)

---

9:20 AM - 9:40 AM JST | 12:20 AM - 12:40 AM UTC

[U06-02] IUGG and Japan: the past, the present, and the way to go from now

★Invited Papers

*Masaru Kono[1] (1.Tokyo Institute of Technology)

---

9:40 AM - 9:55 AM JST | 12:40 AM - 12:55 AM UTC

[U06-03] **Contributions from the Science Council of Japan to international cooperation in the field of Earth and planetary science**

*Hisashi Nakamura[1] (1.Research Center for Advanced Science and Technology, University of Tokyo)

---

9:55 AM - 10:15 AM JST | 12:55 AM - 1:15 AM UTC

[U06-04] History and Japanese contribution to the International Association of Cryospheric Sciences IACS

★Invited Papers

*Ralf Greve[1] (1.Institute of Low Temperature Science, Hokkaido University)

---

10:15 AM - 10:30 AM JST | 1:15 AM - 1:30 AM UTC

[U06-05] **Japan's Contributions to IAG**

*Yoichi Fukuda[1] (1.Department of Geophysics, Graduate School of Science, Kyoto University)

# Centennial of the International Cooperation in Earth and Space Sciences

*Alik Ismail-Zadeh[1,2,3]

1. Karlsruhe Institute of Technology, 2. International Union of Geodesy and Geophysics, 3. International Science Council

The International Union of Geodesy and Geophysics (IUGG) was established in 1919 under the umbrella of the International Research Council (later ICSU, and now the International Science Council) as one of the unions to promote activities of existing associations dealing with geodesy, terrestrial magnetism and electricity, hydrology, meteorology, physical oceanography, seismology, volcanology. This presentation describes the origin and the development of the Union for the last century and until today. During the initial period (1919-1939), the number of member countries increased from nine founding Member countries to 35 Member countries; general assemblies were held every three years, each in a different international venue, and the number of delegates attending the assemblies increased from a few dozen to several hundred scientists. The World War II (WWII) interrupted the cooperation, and international scientific activities were resumed in 1946. The Union continued cooperation with many international scientific organizations of ICSU, and began cooperation with new intergovernmental organizations such as UNESCO and the World Meteorological Organization, and their programs. The technologies developed during the WWII were brought to bear in the extraordinary global scientific effort that was the International Geophysical Year (1957-1958). Changes in the geopolitical landscape brought about changes in the IUGG's structure. International campaigns encompassing multiple disciplines became commonplace, and international scientific bodies were organized. At the beginning of the 21st century IUGG added an eighth association on cryospheric sciences, developed new grants, science education, and recognition programs, and added new commissions on geophysical risk & sustainability, climatic & environmental change, data & information, and planetary sciences to existing commissions on mathematical geophysics and study of the Earth's deep interior. IUGG has been initiating, developing, and implementing international cooperative programs, setting scientific standards, developing research tools, educating and building capacity, and contributing to science for policy. Today, IUGG is a vibrant modern scientific union of 72 nations and scientists from all over the world promoting research, linking scientific knowledge to societal needs, and working toward a sustainable Earth.

Keywords: international cooperation, IUGG, Earth and space sciences

©2019. Japan Geoscience Union. All Right Reserved. 

# IUGG and Japan: the past, the present, and the way to go from now

*Masaru Kono[1]

1. Tokyo Institute of Technology

International Union of Geodesy and Geophysics (IUGG) was formed in 1919 and held its first General Assembly in 1922. A hundred years has passed since then. Japan was one of the seven member countries which joined IUGG at the inauguration. Prof. A. Tanakadate of Tokyo University represented Japan at that time, and he was elected as one of three Vice-Presidents for 1919-1922. Since then, except the period that Japan was vetoed to take part in the Assemblies after Japan was defeated in 1945, Japan has consistently been a strong supporter of the IUGG activities.

Because of the "cold war" after the end of the world war, there were very few chances that east and west scientists meet at the same place, IUGG and other international scientific organizations were playing an important role in providing such opportunities. In particular the International Geophysical Year (IGY) of 1957-1958 was a splendid opportunity for cooperation between east and west countries. Japan took part in this project in many subject including the rocket observation, but among them, the start of the antarctic research which was carried out with the concent of the international community, was a highlight of this project.

Several decades have passed since then. In these years, the status of IUGG became quite low. IUGG holds it General Assembly every four years, collecting 3000 to 4000 scientists, but AGU Fall meeting is held every year, and nowadays they receive about 30,000 participants while keeping the scientific standards quite high. Nowadays, there are EGU, JpGU, and others which collect more than 10,000 participants. These societies also have well-cited jounals to output scientific results in printed form. It looks that there is little possibility that IUGG can compete with these societies in the scientific merit.

With these situations in mind, which way should IUGG go in the future? One possibility is to work in problems which concerns the whole Earth, and thus it is impossible to find the solution in a single country. A clear example of such a problem is the Global Warming. The international scientific organization which deals with this is IPCC, but the scientists working in IPCC have strong ties with some of the Associations in IUGG (eg., IAMAS, IAPSO, IAHS). Another possibility is to look for a scientifically important probem, which usually has small number of scientists engaged in the problem. A good example in IUGG is SEDI which works in the deep interior of the Earth. It is also an interdisciplinary science including seismology, geomagnetism and others. SEDI seems to prosper by providing an interdisciplinary platform for these hundred or so very high-level scientists.

Keywords: IUGG, International cooperation, Way to go from now

©2019. Japan Geoscience Union. All Right Reserved. 

# Contributions from the Science Council of Japan to international cooperation in the field of Earth and planetary science

*Hisashi Nakamura[1]

1. Research Center for Advanced Science and Technology, University of Tokyo

Since its establishment in 1949, the Science Council of Japan (SCJ) has made a variety of contributions to international academic cooperation in every field of natural and social sciences as an official member of the International Science Council (ICSU: currently InterAcademy Council). The budget for international commitment has been stable in spite of continuous decline of the entire budget of SCJ. Recognizing that international cooperation is essential for research activities in the field of Earth and planetary science, ICSU has promoted the International Geophysical Year (IGY: 1957-58) and the 4th International Polar Year (IPY: 2007-08), while offering its membership to 12 international unions/associations in our field, including the International Union of Geodesy and Geophysics (IUGG). Under this international framework, the Japanese government has been offering financial support to those unions/associations through SCJ, in which 12 branch committees are organized under the Earth and Planetary Science Committee to appoint some members as delegates to executive meetings of those unions/associations and promote related domestic activities. In addition, SCJ co-hosts a general assembly of an international union/association held in Japan under the approval of the SCJ International Affairs Committee, as exemplified by the 2017 IAG-IASPEI Joint Scientific Assembly in Kobe. This presentation offers an overview of specific contributions from SCJ to international cooperation in the field of Earth and planetary science.

Keywords: Science Council of Japan, international cooperation, IUGG

©2019. Japan Geoscience Union. All Right Reserved. 

# History and Japanese contribution to the International Association of Cryospheric Sciences IACS

*Ralf Greve[1]

1. Institute of Low Temperature Science, Hokkaido University

The International Association of Cryospheric Sciences, or IACS, is the eighth association of the International Union of Geodesy and Geophysics (IUGG), launched by the IUGG Council on 2007-07-04. Despite being the latest of the IUGG associations, IACS looks back on a history of 125 years, starting with the International Commission on Glaciers (Commission Internationale des Glaciers) founded in 1894. It then evolved via the International Commission of Snow and Ice (ICSI) of the International Association of Hydrological Sciences (IAHS) and the transitional Union Commission for the Cryospheric Sciences (UCCS) into its current constitution as an independent IUGG association, recognizing the increased importance of cryospheric sciences within the context of Global Change. In this presentation, we will outline the history of IACS and its precursor organizations, describe the current activities of IACS and highlight the Japanese links with IACS in the form of contributions to its governance, divisions and research activities.

Keywords: IUGG, IACS, Cryosphere, Cryospheric sciences, Earth sciences

©2019. Japan Geoscience Union. All Right Reserved. 

# Japan's Contributions to IAG

*Yoichi Fukuda[1]

1. Department of Geophysics, Graduate School of Science, Kyoto University

In this presentation we introduce the roles of the modern geodesy and the activities of IAG (the International Association of Geodesy) as well as the Japan's contributions to IAG.

Keywords: International Association of Geodesy, GGOS

©2019. Japan Geoscience Union. All Right Reserved. 

[J] Oral | U (Union )：Union

Thu. May 30, 2019 10:45 AM - 12:15 PM JST | Thu. May 30, 2019 1:45 AM - 3:15 AM UTC | IC 2F

## [U-06] Japan's contribution to IUGG celebrating 100th anniversary

convener:Setsuya Nakada(National Research Institute for Earth Science and Disaster Resilience), Kenji Satake(Earthquake Research Institute, University of Tokyo), Kumiko Goto-Azuma(National Institute of Polar Research), Chairperson:Kumiko Goto-Azuma(National Institute of Polar Research), Kenji Satake(Earthquake Research Institute, the University of Tokyo)

International Union of Geodesy and Geophysics (IUGG) is one of the 40 unions in the International Science Council (ISC), celebrating its 100th anniversary in 2019. IUGG promotes and coordinates research on the interior and the periphery of the Earth. The IUGG has associations of eight research fields (IACS, IAG, IAGA, IAHS, IAMAS, IAPSO, IASPEI, and IAVCEI), which carry out semi-autonomously activities in cooperation with each other. In addition, IUGG encourages research to respond to social needs such as reduction of natural disasters and environmental conservation. The IUGG Subcommittee at the Japan Science Council's Earth and Planetary Science Committee and the eight association-committees under the former serve as representatives of Japan for the IUGG and 8 Associations.<br/> In this session, as IUGG celebrates its 100th anniversary, researchers related to each association exchange the ideas on the role of IUGG in earth science and the contribution that Japanese researchers should make to IUGG.

10:45 AM - 11:00 AM JST | 1:45 AM - 2:00 AM UTC

[U06-06] IAGA activities in the era of too many international conferences

*Toshihiko Iyemori[1] (1.Kyoto University)

11:00 AM - 11:15 AM JST | 2:00 AM - 2:15 AM UTC

[U06-07] The role of IAHS in education, research, social issues concerning water and future perspective

*Maki Tsujimura[1] (1.Faculty of Life and Environmental Sciences, University of Tsukuba)

11:15 AM - 11:30 AM JST | 2:15 AM - 2:30 AM UTC

[U06-08] Centenary of the atmospheric sciences: Its progress and future issues

*Teruyuki Nakajima[1] (1.Japan Aerospace Exploration Agency)

11:30 AM - 11:45 AM JST | 2:30 AM - 2:45 AM UTC

[U06-09] Contributuins of Japan to IAPSO

*Yukio Masumoto[1] (1.Graduate School of Science, The University of Tokyo)

11:45 AM - 12:00 PM JST | 2:45 AM - 3:00 AM UTC

[U06-10] IASPEI- activities, history and Japan’s contribution

*Kenji Satake[1], Thorne Lay[2], Johannes Schweitzer[3] (1.Earthquake Research Institute, University of Tokyo, 2.IASPEI President , 3.IASPEI Secretary General)

12:00 PM - 12:15 PM JST | 3:00 AM - 3:15 AM UTC

[U06-11] Recent history of IAVCEI in Japan and young researchers’ response to IUGG and IAVCEI

*Setsuya Nakada[1] (1.National Research Institute for Earth Science and Disaster Resilience)

# IAGA activities in the era of too many international conferences

*Toshihiko Iyemori[1]

1. Kyoto University

During the last 20 years, the size of international meeting such as AGU, EGU and AOGS has been getting larger and larger, and they are now the major place for the researchers in geoscience and space science to show their results and collect new information. This tendency is the same also for the scientists in our country, and the role of IAGA need to change its role. In this presentation, IAGA activities and our contribution in the last 20 years will be presented.

Keywords: geomagnetism and aeronomy, international conference

©2019. Japan Geoscience Union. All Right Reserved. 

# The role of IAHS in education, research, social issues concerning water and future perspective

*Maki Tsujimura[1]

1. Faculty of Life and Environmental Sciences, University of Tsukuba

IAHS (International Association of Hydrological Sciences) was launched in 1922, and now have approximately 5500 individuals, 10 commissions and 3 working groups. The Scientific Assembly is held every 4 years and held in Yokohama, Japan 1993. Professor in Emeritus Dr. Kuniyoshi Takeuchi, Yamanashi University has served as a president of IAHS from 2001 through 2005, thus Japan has taken an important role in IAHS.

The commission consists of Continental Erosion, Coupled Land-Atmosphere Systems, Groundwater, Remote Sensing, Statistical Hydrology, Snow and Ice Hydrology, Surface Water, Tracers, Water Quality, Water Resources Systems, and it covers a variety of field in hydrology. Also, a working group “PANTA RHEI –Change in Hydrology and Society” has been launched in 2013 focusing on changing hydrological cycle system with changing human system.

The Japan National Committee of IAHS in cooperation with Japan National Committee of IHP (International Hydrology Programme) hold a symposium “Japan Water 2012: International Contribution from Japan in education/ research of water science and technology”. Also, Japan Association of Hydrology and Water Resources, Japanese Association of Hydrological Sciences, Japanese Association of Groundwater Hydrology and Japan Society of Physical Hydrology collaborated to publish Hydrological Research Letters (HRL) since 2017. Additionally, IAEA (International Atomic Energy Agency) Regional Training Course on Isotopic Data Processing and Interpretation –Hands on Exercises is held in March 2019, Tsukuba, Japan supported by Japan National Committee of IAHS and Japan National Committee of IHP.
On the other hand, the changing environment in hydrology and water resources in Japan and the world requires the change of the role in IAHS. We need to promote a collaboration between IAHS and IHP, early career support and career paths developments in future.

Keywords: IAHS

©2019. Japan Geoscience Union. All Right Reserved. 

# Centenary of the atmospheric sciences: Its progress and future issues

*Teruyuki Nakajima[1]

1. Japan Aerospace Exploration Agency

IAMAS (International Association of Meteorology and Atmospheric Sciences), one of associations of IUGG (International Union of Geodesy and Geophysics), celebrates in 2019 its centenary after establishment with IUGG. Held are commemorative projects and memorial events at the IUGG general meeting in Montreal in this July. Atmospheric science has long been developed as a science related to various weather phenomena related to the lives of mankind. As a result, there are many important issues related to society. Especially over the past 100 years, there are major developments such as establishment of weather prediction infrastructure, researches to global warming problem and environmental problems such as ozone hole etc. An overview of these progresses will be important for us to think about what we should do next. In particular, in this era, as climate and environment changes have become apparent and disasters increase, observation and understanding of the phenomena is increasingly necessary through collaborations with other areas such as the social science etc. I like to discuss that point.

Keywords: Atmospheric sciences, 100 years

©2019. Japan Geoscience Union. All Right Reserved. 

# Contributuins of Japan to IAPSO

*Yukio Masumoto[1]

1. Graduate School of Science, The University of Tokyo

The International Association for the Physical Sciences of the Oceans (IAPSO) is one of eight associations of the International Union of Geodesy and Geophysics (IUGG). IAPSO is promoting the study of scientific problems relating to the oceans and the interactions taking places at the sea floor, coastal, and atmospheric boundaries insofar as such research is conducted by the use of mathematics, physics, and chemistry. IAPSO has addressed this goal through four fundamental objectives: (1) Organize, sponsor, and co-sponsor formal and informal international forums permitting ready means of communication amongst ocean scientists throughout the world; (2) Establish commissions, sub-committees, and organize commensurate workshops to encourage, stimulate, and coordinate new and advanced international research activities; (3) Provide basic services significant to the conduct of physical oceanography, and (4) Publish proceedings of symposia, meetings, and workshops, and fundamental references on the current state-of-the art and knowledge of physical oceanography.
The Japanese ocean research communities have been contributing to IAPSO mainly through their research activities at the IAPSO assemblies and through administrative works by taking a position of the exective committee member for about 20 years, with the president position by Prof. Imawaki for four years from 2003. This presentation summarizes the Japanese contributions to IAPSO and discuss on future relation between the Japanese research communities and IAPSO.

Keywords: Ocean Sciences, IAPSO, the Decade of Ocean Science for Sustainable Development

©2019. Japan Geoscience Union. All Right Reserved. 

# IASPEI- activities, history and Japan’s contribution

*Kenji Satake[1], Thorne Lay[2], Johannes Schweitzer[3]

1. Earthquake Research Institute, University of Tokyo, 2. IASPEI President , 3. IASPEI Secretary General

IASPEI (International Association of Seismology and Physics of the Earth’s Interior) is one of the eight associations of IUGG, and promotes the study of earthquakes and other seismic sources, the propagation of seismic waves, and the Earth's internal structure, properties, and processes. IASPEI has seven commissions on seismological observation and interpretation, on tectonophysics and crustal structure, on earthquake generation process - physics, modelling, and monitoring for forecast, on earth structure and geodynamics, on earthquake hazard, risk and strong ground motion, on earthquake source mechanics, and on education and outreach. Besides these topical commissions, IASPEI has their regional commissions in Europe (since 1951), Asia (since 1996), Africa (since 2011) and Latin America (since 2013). These regional commissions meet bi-annually, typically with training courses, to promote seismology in each region.

Seismology started as national scale for describing the earthquake phenomena and their effects. First seismological societies were established in Switzerland (1878), in Italy (1879) and in Japan (1880). After the first teleseismic recording in Germany from an earthquake in Japan (1889), seismology became an international science, and Frist International Seismological Conference was held in Strasbourg in 1901, representing 8 countries including Japan. In 1904, International Seismological Society was established. In 1922, it became a part of IUGG (established in 1919), with changing name to IAS in 1930 and IASPEI in 1951.

IASPEI plays important roles in unifying seismological observations, such as naming seismic phases, defining measurement procedures, or improving the network of seismic stations, and published Manuals of Seismological Observatory Practice (the latest version in 2012). IASPEI has a close relation with International Seismological Centre, which has produced seismological bulletins based on the IASPEI standard. IASPEI also provided standard seismic velocity structure models of the earth, such as iasp91 or ak135. Global distribution of earthquakes in the earth and the reference earth models have been important basic data for developing the science such as plate tectonics, or structure and dynamics of the earth’s interior. IASPEI also conducted peer reviews and evaluated the published precursory phenomena for earthquakes. IASPEI developed and distributed seismological software, and International Handbook of Earthquake and Engineering Seismology.

IASPEI supports FDSN (International Federation of Digital Seismograph Networks) which is composed of groups responsible for installation and maintenance of seismological networks, and activities of CTBTO (Comprehensive Test-Ban Treaty Organization) which uses seismic data to detect nuclear explosions. IASPEI also supports joint commissions with other associations of IUGG, such as ILP (International Lithosphere Project), on tsunamis, volcanology or on space geodesy.

The IASPEI commission of Seismological Society of Japan practically acts as the national committee of IASPEI, and disseminates IASPEI information to Japanese seismological community, nominates officers and award candidates. SSJ has made financial supports to ASC (Asian Seismological Commission) and IASPEI, for travel support of participants and for management of the ASC meetings. Several members of executive committees and chairs of commission are elected from Japan. The last scientific assembly of

©2019. Japan Geoscience Union. All Right Reserved. 

IASPEI, joint with IAG, was held in Kobe, Japan, in 2017 with great success.

Keywords: IASPEI, Seismology, IUGG

©2019. Japan Geoscience Union. All Right Reserved. 

# Recent history of IAVCEI in Japan and young researchers' response to IUGG and IAVCEI

*Setsuya Nakada[1]

1. National Research Institute for Earth Science and Disaster Resilience

Japanese volcano researchers, especially young scientists, do not recognize well the relationship of IAVCEI with IUGG. IUGG is less visible than IAVCEI to them. The latter used to be introduced first as the international conference that they can challenge. IAVCEI is visible also in the Volcanological Society of Japan (VSJ) of which they are members. Japanese researchers served as the executive board members of IAVCEI, such as its presidents by Hisashi Kuno, Shigeo Aramaki, and Setsuya Nakada for these 100 years. Scientific Assemblies of IAVCEI were held in Japan in 1962, 1981, and 2013. The Cities on Volcanoes (COV) is the second largest international conference of IAVCEI, held every two years between the years of IAVCEI Scientific Assembly and IUGG General Assembly since 1998. COV conference originates from the International Volcano Conference, which was held in the Kagoshima City in 1988, as a forum between scientists and non-scientists for mitigating volcanic disasters. The fifth COV conference was held in the Shimabara City in 2007.

In spite of the fact that IUGG General Assembly was held in Sapporo in 2003, it seems that IUGG has not become well known among young, possibly middle-aged volcano researchers. For example, recent IAVCEI Science Assembly gathers over 1000 participants, while there are only about 300 participants at General Assemble of IAVCEI when IUGG. The latter number is much smaller than around 1000 participants of recent COV. Though one of the reasons may be few excursions for volcanologists, organized in IUGG conferences, it is likely that a simple reason is the size of fields covered by the conferences. Each association itself is wide in fields enough and the assemble of 8 associations will be too wide for young researchers to attend. They may feel not comfortable like business even in AGU and EGU, contrasting to comfort in own associational conference.

This may be similar to the relationship between JpGU and individual national societies. We have to confirm and share the merit of assemblage of large international associations having fields related to but different from each other. In addition, roles of government-contributing organization like IUGG and International Science Council (ISC) should be confirmed among us. In this case, increasing the number of participants to the conference is not the first priority. Global climate change and regional geological hazards such as large earthquakes and volcanic eruptions have become worldwide high priority issues to reduce the risks. Under this situation, the United Nation clarified the sustainable development goals (SDGs) until 2030, therefore, the missions by IUGG and ISC, which are guaranteed by governments, have expanded to solve these issues.

Keywords: IAVCEI, IUGG, geohazard, SDGs

©2019. Japan Geoscience Union. All Right Reserved. 

[J] Oral | U (Union )：Union

Thu. May 30, 2019 1:45 PM - 3:15 PM JST | Thu. May 30, 2019 4:45 AM - 6:15 AM UTC | 101 1F

## [U-08] Opinions and recommendations from meeting participants to the future of the Japan Geoscience Union

convener:Yozo Hamano(KOBE Ocean-Bottom Exploration Center, Kobe University), Eiichi Tajika(Department of Earth and Planetary Science, Graduate School of Science, The University of Tokyo), Koji Wada(Planetary Exploration Research Center, Chiba Institute of Technology), Ikuro Sumita(Geosciences and Civil Engineering, Institute of Science and Engineering, Kanazawa University), Chairperson:Koji Wada(Planetary Exploration Research Center, Chiba Institute of Technology), Ikuro Sumita

The JpGU meeting 2019 will be the 30th since the start of the Joint Meeting of the Earth and Planetary Science societies, and 15th after the foundation of the Japan Geoscience Union (JpGU).Today, JpGU is becoming indispensable for the Earth and Planetary Science community due to the significant increase in the number of participants and the progress towards one of the International Organization of Geosciences. However, since the voluntary group that originally started aggregating the individual's intentions of the community, grew to a huge organization of about 10,000 members, it becomes rather difficult to reflect requests and opinions as individuals. In addition, by becoming a public interest corporation, it is rather difficult to operate as an academic organization under the constraints of the public interest corporation law. In aiming for further development of JpGU in the future, we would like to invite all the participants of the meeting to express their strict opinion and constructive proposal for the future of JpGU. The opinions of participants will be valuable materials for considering the direction of JpGU after 2020. We would like to invite many participants to present opinions and recommendations from various viewpoints, returning to the bottom-up spirit which is the basic philosophy of the science community.

1:45 PM - 1:51 PM JST | 4:45 AM - 4:51 AM UTC

Introduction

---

1:51 PM - 2:03 PM JST | 4:51 AM - 5:03 AM UTC

[U08-01] Request and proposal from the Committee on Earth and Planetary Sciences of the Science Council of Japan to JpGU

*Ryoichi Fujii[1] (1.Research Organization of Information and Systems)

---

2:03 PM - 2:15 PM JST | 5:03 AM - 5:15 AM UTC

[U08-02] Geography in JpGU: current status and future perspectives

*Takashi Oguchi[1], Ikuho Yamada[2], Yuichi S. Hayakawa[3], Daichi Kohmoto[4], Hitoshi Saito[5] (1.Center for Spatial Information Science, The University of Tokyo, 2.Faculty of Science and Engineering, Chuo University, 3.Graduate School of Env.Science, Hokkaido University , 4.Nara University of Education, 5.College of Economics, Kanto Gakuin University)

---

2:15 PM - 2:27 PM JST | 5:15 AM - 5:27 AM UTC

[U08-03] Biogeoscineces will connect everthing together

*Takeshi Kakegawa[1] (1.Graduate School of Science, Tohoku University)

---

2:27 PM - 2:39 PM JST | 5:27 AM - 5:39 AM UTC

[U08-04] Coverage of JpGU

*Yukihiro Takahashi[1] (1.Department of Cosmosciences, Graduate School of Science, Hokkaido University)

---

2:39 PM - 2:51 PM JST | 5:39 AM - 5:51 AM UTC

[U08-05] Is he a bit overkill for English?

*Yoshi-Yuki Hayashi[1] (1.Department of Planetology/CPS, Graduate School of Science, Kobe University)

---

2:51 PM - 3:03 PM JST | 5:51 AM - 6:03 AM UTC

[U08-06] Globalization of Japan Geoscience Union

*Hirokuni Oda[1] (1.Institute of Geology and Geoinformation, Geological Survey of Japan, AIST)

3:03 PM - 3:15 PM JST | 6:03 AM - 6:15 AM UTC

[U08-07] A proposal for JpGU based on the questionaires to SSJ members

*Koshun Yamaoka[1] (1.Earthquake and Volcano Research Center, Graduate School of Environmental Studies, Nagoya University)

# Request and proposal from the Committee on Earth and Planetary Sciences of the Science Council of Japan to JpGU

*Ryoichi Fujii[1]

1. Research Organization of Information and Systems

Japan Geoscience Union (JpGU) and the Committee on Earth and Planetary Sciences (EPS) of the Science Council of Japan (SCJ) has long been collaborating closely for the wide developments of earth and planetary sciences. Recent collaborations are being done, e.g., for the revision of the dream roadmap and the proposal of the large-scale research programs.
In this presentation we would like to present our request and proposal to JpGU and to discuss in depth the future, closer collaborations between the two organizations.

Keywords: JpGU, Dream roadmap, Science Council of Japan

©2019. Japan Geoscience Union. All Right Reserved. 

# Geography in JpGU: current status and future perspectives

*Takashi Oguchi[1], Ikuho Yamada[2], Yuichi S. Hayakawa[3], Daichi Kohmoto[4], Hitoshi Saito[5]

1. Center for Spatial Information Science, The University of Tokyo, 2. Faculty of Science and Engineering, Chuo University, 3. Graduate School of Env.Science, Hokkaido University , 4. Nara University of Education, 5. College of Economics, Kanto Gakuin University

Although some geographers and geographical societies have been members of JpGU, the majority of geographers in Japan seldom contribute to JpGU activities. One reason for this is that more than half of Japanese geographers are specialized in human geography, whereas JpGU focuses on physical sciences. However, interdisciplinary studies integrating arts and sciences are becoming all the more important, and modern geography linked to natural hazards and global environmental issues requires knowledge of earth sciences. Therefore, geography in JpGU should play an increasing role. This presentation aims to discuss how to strengthen collaborative relationships between JpGU and geographers.

Keywords: Geography, JpGU, Collaboration

©2019. Japan Geoscience Union. All Right Reserved. 

# Biogeoscineces will connect everthing together

*Takeshi Kakegawa[1]

1. Graduate School of Science, Tohoku University

Biogeosciences Section is unique compared to other sections at JPGU. Other sections have strong affiliation with big national projects, such as wide-sale observation of earthquake, space mission, climate change observation, etc. As a result, Biogeosciences Section has difficulty to establish main or leading subjects in JPGU. Scientific subjects and themes are often overlapped between Biogeosciences Section and other sections. This makes presence of Biogeosciences Section unclear at JPGU. In order to promote Biogeosciences Sections, I am going to suggest some points. It will be important to establish strategic collaborations with other sections of JPGU and other communities, such as microbiology, ecology, agriculture, and /or bio-engineering fields. I think that organizing temporal sections with other communities or having invite speaker from other community will be effective. Biogeosciences Sections should have more functions as an interface with others.

Keywords: Earth, Life

©2019. Japan Geoscience Union. All Right Reserved. 

# Coverage of JpGU

*Yukihiro Takahashi[1]

1. Department of Cosmosciences, Graduate School of Science, Hokkaido University

Geoscience unions originally started from classical several categories, namely, solid earth, atmosphere, land and ocean water, upper atmosphere and space, and plant. However, in AGU or EGU, adding to those conventional fields, many new science targets or methodologies are becoming important player in the union. Especially, biology including agriculture and natural hazard became one of the largest communities. On the other hand, such movement in JpGU is going at very slow speed. Here we discuss the strategy about this matter.

Keywords: Coverage , Union

©2019. Japan Geoscience Union. All Right Reserved. 

# Is he a bit overkill for English?

*Yoshi-Yuki Hayashi[1]

1. Department of Planetology/CPS, Graduate School of Science, Kobe University

English is taught in English or a special subject is also taught in English, indeed, English has been introduced to elementary school, and English examination of college entrance examination has become to be said to be four skill test today, lead this The importance of "international" importance of the leadership including not only the Keidanren that causes it but also the academic community, the direction of individuals' shooting spirit towards these, ... ... that socioeconomic and cultural academic background I do not know that the various aspects of JpGU are no exception.

However, has not underestimated the influence of stopping recharging of the Japanese space which I have been working diligently since the Meiji era so that education and practice up to the research level can be conducted in my mother tongue almost exclusively in European languages? Do you think that a Japanese language space and its operation ability are natural there and there is nothing to think that it is acquired naturally? As a mother tongue is being trained, we have a wide width and deep depth Although I am able to acquire imagination comprehension ability with, but because it is too "nature" its cost and power can not be forecasted easily, but I am worried that the power is rapidly declining.The language is recharged It goes without saying that training is necessary in order to master this.

I can not predict how far the convergence of language (Englishization) will proceed.The leap in China may brake somebody, but if it keeps it as it is, it will be several generations and Japanese will become a daily word It is a momentum to degenerate into a language that can only be used for the languages of European languages Unlike the multilingualization of the European languages group, it is not easy for the language system to respond at a high level to multilingualization between different languages If you try to secure the breadth and depth of thinking you will have to concentrate on a specific language system and you may be made to choose to switch at the language selection stage. I do not like being there, so I wonder if there can be an avalanche decline.
Advanced knowledge is accumulated in the English space Today, it is desirable to improve the management system to ensure that it contributes to the participation in the Japanese-English system, and it is also wonderful to build an operational system that can accept English sessions. I would like to have English, I would like to forcibrate that the material must be in English, eliminate Japanese sessions that emphasize Japanese language spaces and emphasize provision of knowledge to those with their native language. I would like to be able to accept it rather than it.

By the way I put a raw google translation in English abstract AI seems to need a little time to engage in this issue.

Keywords: Englishization problem

©2019. Japan Geoscience Union. All Right Reserved. 

# Globalization of Japan Geoscience Union

*Hirokuni Oda[1]

1. Institute of Geology and Geoinformation, Geological Survey of Japan, AIST

In the presentation, globalization of Japan Geoscience Union (JpGU) is going to be discussed as a member. Although activities of JpGU is broad, JpGU annual meeting and academic publishing are considered as the key pillars. Also, the necessity of globalization on these two have been emphasized. On academic publishing, journal PEPS has been started on 2014 supported by Grant-in-Aid for Publication of Scientific Research Results "Enchancement of International Dissemination of Information" of JSPS. In addition, Impact Factor 2017 has been given to the journal and its future is promising. JpGU meeting was jointly organized successfully with AGU in 2017 and the next JpGU-AGU meeting will be held in 2020. Although globalization of JpGU meeting has been promoted, Japanese language is also considered as important. The burden on the participants and organizers of the meeting by the requirements both in English and Japanese cannot be ignored. Also, there seems to be a barrier in inviting researchers to JpGU meeting from abroad, where number of international sessions and attendees are limited. Number of international meetings on geosciences has been increasing and relative importance of JpGU meeting in the world is decreasing. Thus, the meaning of globalization for JpGU and significant increase of the number of English sessions (or significant decrease of the number of Japanese sessions) of JpGU meeting will be discussed.

Keywords: globalization, academic publishing, JpGU meeting, attendees from abroad, Joint meeting with AGU

©2019. Japan Geoscience Union. All Right Reserved. 

# A proposal for JpGU based on the questionaires to SSJ members

*Koshun Yamaoka[1]

1. Earthquake and Volcano Research Center, Graduate School of Environmental Studies, Nagoya University

The Seismological Society of Japan (hereafter, SSJ) is one of the original members of the group which is ancestral of present JpGU. The group consists of several societies including SSJ organized a joint meeting instead of independent meetings which were usually held in early April every year. In this historical circumstances SSJ expects JpGU meeting as one of the regular meetings of SSJ in addition to the SSJ fall meeting. In this regard, sessions that are equivalent to those in the SSJ fall meeting are proposed for JpGU meeting every year.
Academic society exists because members expect benefits in participating the society. Similarly member societies such as SSJ also expect benefits in participating JpGU. JpGU is expected to represent academic community of earth and planetary science, which is sometimes called geoscience, of Japan to raise visibility and recognition in Japan’ s society. Visibility of geoscience, especially in high school education, is still low in spite of Japan’ s geological unstableness. This is one reason that Japan has underestimated the risk of geohazards. Academic characteristics of geoscience which inevitably need tackle the complexity, irreversibility and unrepeatability of earth’ s process is sometimes unreasonably degraded relative to other fields. JpGU also works for encouraging collaboratory researches beyond conventional discipline and national boundaries.
The results of such function of JpGU are sometimes opposed to by members. One member of SSJ make an opposition of the management of JpGU meeting, saying that JpGU meeting is too long, too expensive and too much obsequious to English language. The first issue come from the recent condition of universities, in which academic schedule is getting more and more tight. SSJ send questionnaires asking for such an opinion is common or not. Half of the answers favor the opinion although 2/3 of the answers express the satisfaction in participating JpGU meeting. More effort should be made on the session scheduling by considering the participants’ needs. 90% of the answer favors variety of JpGU sessions which cannot be enjoyed in the independent society meeting. I am personally happy to be able to have sessions in English in regular scientific meetings in Japan because English is de facto common language in science community, and because it is what I dreamed when joint meeting started when I was young.
Another function to be expected to JpGU is providing inter-society communication opportunity. Recently many societies suffer gradual decline of members, especially of young generation. Sharing administration may be one of the measures against financial decline. Merging of societies can also be a solution. We need to look for a relation between JpGU and each societies for the development of science.

Keywords: Seismological Society of Japan, questionnaire

©2019. Japan Geoscience Union. All Right Reserved. 

[J] Oral | U (Union )：Union

Thu. May 30, 2019 3:30 PM - 5:00 PM JST | Thu. May 30, 2019 6:30 AM - 8:00 AM UTC | 101 1F

## [U-08] Opinions and recommendations from meeting participants to the future of the Japan Geoscience Union

convener:Yozo Hamano(KOBE Ocean-Bottom Exploration Center, Kobe University), Eiichi Tajika(Department of Earth and Planetary Science, Graduate School of Science, The University of Tokyo), Koji Wada(Planetary Exploration Research Center, Chiba Institute of Technology), Ikuro Sumita(Geosciences and Civil Engineering, Institute of Science and Engineering, Kanazawa University), Chairperson:Koji Wada(Planetary Exploration Research Center, Chiba Institute of Technology), Ikuro Sumita

The JpGU meeting 2019 will be the 30th since the start of the Joint Meeting of the Earth and Planetary Science societies, and 15th after the foundation of the Japan Geoscience Union (JpGU).Today, JpGU is becoming indispensable for the Earth and Planetary Science community due to the significant increase in the number of participants and the progress towards one of the International Organization of Geosciences. However, since the voluntary group that originally started aggregating the individual's intentions of the community, grew to a huge organization of about 10,000 members, it becomes rather difficult to reflect requests and opinions as individuals. In addition, by becoming a public interest corporation, it is rather difficult to operate as an academic organization under the constraints of the public interest corporation law. In aiming for further development of JpGU in the future, we would like to invite all the participants of the meeting to express their strict opinion and constructive proposal for the future of JpGU. The opinions of participants will be valuable materials for considering the direction of JpGU after 2020. We would like to invite many participants to present opinions and recommendations from various viewpoints, returning to the bottom-up spirit which is the basic philosophy of the science community.

3:30 PM - 3:42 PM JST | 6:30 AM - 6:42 AM UTC

### [U08-08] Opinions and recommendations to the Japan Geoscience Union from Society of Geomagnetism and Earth, Planetary and Space Sciences

Yoshiharu Omura[2], Shigeto Watanabe[3], *Yuto Katoh[1], Takuya Tsugawa[4], Yuichi Otsuka[5], SGEPSS steering committee (1.Graduate School of Science, Tohoku University, 2.Research Institute for Sustainable Humanosphere, Kyoto University, 3.Hokkaido Information University, 4.National Institute of Information and Communications Technology, 5.Institute for Space–Earth Environmental Research, Nagoya University)

3:42 PM - 3:54 PM JST | 6:42 AM - 6:54 AM UTC

### [U08-09] Collaboration between Earth & Planetary Science and Information Science ~A trial of mutual benefit in the interdisciplinary field~

*Hirohide Demura[1] (1.The University of Aizu)

3:54 PM - 4:06 PM JST | 6:54 AM - 7:06 AM UTC

### [U08-10] Comments from young planetary scientists

*Shunichi Kamata[1], Keiko Hamano[2], Go Murakami[3], Ryuki Hyodo[2], Yusuke Nakauchi[3] (1.Hokkaido University, 2.Tokyo Institute of Technology, 3.JAXA/ISAS)

4:06 PM - 4:18 PM JST | 7:06 AM - 7:18 AM UTC

### [U08-11] Japan Geoscience Union should operate based on the perspective of individual academic society and fulfill accountability

*Naoji Koizumi[1] (1.School of Environmental Science,the University of Shiga Prefecture)

4:18 PM - 4:30 PM JST | 7:18 AM - 7:30 AM UTC

### [U08-12] A proposal from a representative of General Geoscience Sector on a possible direction to future JpGU: actions for domestic activities could be weighted

*Hidenori Kumagai[1] (1.Japan Agency for Marine-Earth Science and Technology)

4:30 PM - 4:42 PM JST | 7:30 AM - 7:42 AM UTC

[U08-13] Fifteen years of Japan Geoscience Letters and its future

*Shogo Tachibana[1], Eiichi Tajika[2] (1.UTokyo Organization for Planetary and Space Science, University of Tokyo , 2.Dept. Earth and Planetary Science, University of Tokyo)

---

4:42 PM - 5:00 PM JST | 7:42 AM - 8:00 AM UTC

Discussion

# Opinions and recommendations to the Japan Geoscience Union from Society of Geomagnetism and Earth, Planetary and Space Sciences

Yoshiharu Omura[2], Shigeto Watanabe[3], *Yuto Katoh[1], Takuya Tsugawa[4], Yuichi Otsuka[5], SGEPSS steering committee

1. Graduate School of Science, Tohoku University, 2. Research Institute for Sustainable Humanosphere, Kyoto University, 3. Hokkaido Information University, 4. National Institute of Information and Communications Technology, 5. Institute for Space–Earth Environmental Research, Nagoya University

We present opinions and recommendations to the future of the Japan Geoscience Union (JpGU) from members of Society of Geomagnetism and Earth, Planetary and Space Sciences (SGEPSS). The opinions and recommendations are categorized into (1) opinions for the future perspective of JpGU and (2) comments and requests to the organization of the JpGU meeting.

- Future perspective of JpGU as an international meeting and the relation with AOGS

- Increase the number of sessions jointly organized by multiple societies

- Official channel of opinions/suggestions from participants/conveners to JpGU

In this presentation, we summarize the opinions and recommendations from the members of SGEPSS.

Keywords: Opinions and recommendations, Society of Geomagnetism and Earth, Planetary and Space Sciences

©2019. Japan Geoscience Union. All Right Reserved. 

# Collaboration between Earth & Planetary Science and Information Science ~A trial of mutual benefit in the interdisciplinary field~

*Hirohide Demura[1]

1. The University of Aizu

Earth and planetary science is interdisciplinary one. This introduces collaboration between Earth & Planetary Science and Information Science in the University of Aizu as a trial of mutual benefit in the interdisciplinary field. I hope exchanging frank opinions about the future of our JpGU.

Keywords: Earth and Planetary Science , Information Science, interdisciplinary field

©2019. Japan Geoscience Union. All Right Reserved. 

# Comments from young planetary scientists

*Shunichi Kamata[1], Keiko Hamano[2], Go Murakami[3], Ryuki Hyodo[2], Yusuke Nakauchi[3]

1. Hokkaido University, 2. Tokyo Institute of Technology, 3. JAXA/ISAS

We will present comments to JpGU from young researchers in planetary sciences.

Keywords: JpGU, Future

©2019. Japan Geoscience Union. All Right Reserved. 

# Japan Geoscience Union should operate based on the perspective of individual academic society and fulfill accountability

*Naoji Koizumi[1]

1. School of Environmental Science,the University of Shiga Prefecture

Japan Geoscience Union (JpGU) is no longer a bottom-up organization but a top-down organization. JpGU should recognize it and operate based on the perspective of individual academic society and fulfill accountability

Keywords: Japan Geoscience Union

©2019. Japan Geoscience Union. All Right Reserved. 

# A proposal from a representative of General Geoscience Sector on a possible direction to future JpGU: actions for domestic activities could be weighted

*Hidenori Kumagai[1]

1. Japan Agency for Marine-Earth Science and Technology

As one of the representative of General Geoscience Sector, here I pointed following items as to be discussed in order to strengthen foundations of JpGU through activation and diversification of domestic earth science community: 1) too much internationalization is to be suppressed, 2) accessibility for the members outside the metropolitan area or the member societies, 3) support for member societies and 4) enhance the function as the "Union." Details described in Japanese (see abstract written in Japanese).

Keywords: General Geoscience Sector, diversify earth science community, focus to domestic activity

©2019. Japan Geoscience Union. All Right Reserved. 

# Fifteen years of Japan Geoscience Letters and its future

*Shogo Tachibana[1], Eiichi Tajika[2]

1. UTokyo Organization for Planetary and Space Science, University of Tokyo , 2. Dept. Earth and Planetary Science, University of Tokyo

It has been 15 years since the first issue of Japan Geoscience Letters (JGL), which is a newsletter of JpGU. Fifty-five issues have been published with 157 articles on hot topics in the Earth and planetary science field. The JGL has been a window into various disciplines in Earth and planetary science and is potentially be a good outreach tool to the society. There are many things to do to make the JGL better as the newsletter of JpGU that has been expanding as the largest geoscience community in Japan. However, it is not possible to make them a reality because of limited human resources. In this talk, we will discuss the 15-year publication activity of JGL and its future.

Keywords: Japan Geoscience Letters , Outreach

©2019. Japan Geoscience Union. All Right Reserved. 

[J] Oral | P (Space and Planetary Sciences )：P-PS Planetary Sciences

Thu. May 30, 2019 9:00 AM - 10:30 AM JST | Thu. May 30, 2019 12:00 AM - 1:30 AM UTC | 103 1F

## [P-PS08] Lunar science and exploration

convener:Hiroshi Nagaoka(Japan Aerospace Exploration Agency), Masahiro KAYAMA(Department of Earth and Planetary Material Sciences, Faculty of Science, Tohoku University), Masaki N Nishino(Japan Aerospace Exploration Agency, Institute of Space and Astronautical Science), Tomokatsu Morota(Graduate School of Environmental Studies, Nagoya University), Chairperson:Satoshi Tanaka, Masaki Nishino(名古屋大学宇宙地球環境研究所)

Scientific data sets acquired by not only Japanese lunar mission SELENE (Kaguya), but also other countries' missions, have become new standard for lunar science. Analyses of these data have been providing several new knowledge and changing some hypotheses into the truth of the Moon. In concurrence with these studies, some countries including Japan are planning future lunar missions. In this session, we will discuss scientific results based on newly acquired lunar data, strategy for future missions including SLIM, and theoretical and experimental studies for lunar science.<br/>

9:00 AM - 9:15 AM JST | 12:00 AM - 12:15 AM UTC

### [PPS08-01] Observing simulations of impact-induced moonquakes combined with the lunar impact flash observation data for future lunar seismic explorations

*Keisuke Onodera[1,2], Taichi Kawamura[3], Satoshi Tanaka[2], Yoshiaki Ishihara[4], Takuto Maeda[5], Masahisa Yanagisawa[6], Yuki Uchida[6], Shinsuke Abe[7], Ryuhei Yamada[8], Takaya Okamoto[2] (1.SOKENDAI (The Graduate University for Advanced Studies), 2.Institute of Space and Astronautical Science / Japan Aerospace Exploration Agency, 3.Insitut de Physique du Globe de Paris, 4.National Institute for Environmental Studies, 5.Hirosaki University, 6.The University of Electro-Communications, 7.Nihon University, 8.University of Aizu)

9:15 AM - 9:30 AM JST | 12:15 AM - 12:30 AM UTC

### [PPS08-02] New Results from Restored Apollo Magnetic Field Records

*Peter J Chi[1] (1.University of California Los Angeles)

9:30 AM - 9:45 AM JST | 12:30 AM - 12:45 AM UTC

### [PPS08-03] Analysis of the High Latitude Region of the Moon with Spectral Profiler Data: Possible Presence of Water Ice

Haramitsu Kyoda[3], *Satoshi Tanaka[1], Makiko Ohtake[1], Hiroshi Nagaoka[2], Yusuke Nakauchi[2], Keisuke Onodera[4] (1.Department of Solid Planetary Sciences Institute of Space and Astronautical Science, 2.Japan Aerospace Exploration Agency, 3.Department of Complexity Science and Enginnering, the University of Tokyo, 4.Department of Space and Astronautical Science, SOKENDAI)

9:45 AM - 10:00 AM JST | 12:45 AM - 1:00 AM UTC

### [PPS08-04] Detection of Dark Regions on the Lunar Surface with Shadow Masked Multiband Imager Data

*Riho Ito[1], Hiroka Inoue[2], Makiko Ohtake[2], Hisashi Otake[2], Ryosuke Nakamura[1] (1.National Institute of Advanced Industrial Science and Technology, 2.Japan Aerospace Exploration Agency)

10:00 AM - 10:15 AM JST | 1:00 AM - 1:15 AM UTC

### [PPS08-05] Estimation of Moho depth under lunar basins by using only the GRAIL gravity data

*Gaku Nishiyama[1], Noriyuki Namiki[2] (1.Department of Earth and Planetary Science, The University of Tokyo, 2.RISE Project, National Astronomical Observatory of Japan)

10:15 AM - 10:30 AM JST | 1:15 AM - 1:30 AM UTC

### [PPS08-06] Ejecta Thickness Distribution of Lunar Schrödinger Basin

*Luyuan Xu[1], Minggang Xie[1] (1.State Key Laboratory of Lunar and Planetary Sciences, Macau University of Science and Technology)

# Observing simulations of impact-induced moonquakes combined with the lunar impact flash observation data for future lunar seismic explorations

*Keisuke Onodera[1,2], Taichi Kawamura[3], Satoshi Tanaka[2], Yoshiaki Ishihara[4], Takuto Maeda[5], Masahisa Yanagisawa[6], Yuki Uchida[6], Shinsuke Abe[7], Ryuhei Yamada[8], Takaya Okamoto[2]

1. SOKENDAI (The Graduate University for Advanced Studies), 2. Institute of Space and Astronautical Science / Japan Aerospace Exploration Agency, 3. Insitut de Physique du Globe de Paris, 4. National Institute for Environmental Studies, 5. Hirosaki University, 6. The University of Electro-Communications, 7. Nihon University, 8. University of Aizu

Over the past 50 years, the lunar interior has been investigated by analyzing the Apollo lunar seismic data (e.g. [1]-[3]). However, currently proposed models of the internal structure are not in accordance with each other although each model can explain the Apollo seismic data. This means there still exists a large uncertainty in the lunar internal structure because the Apollo data does not have enough quality to determine the inner structure precisely. Since the internal structure is a significant factor to elucidate the origin of the Moon, it is essential to obtain new seismic data in order to improve our knowledge of the lunar internal structure.

In particular, the lunar crustal structure (e.g. elastic velocity, density, layer-thickness) is significant when discussing the thermal environment at the initial stage of the lunar formation. From the observation results of KAGUYA (SELENE), it is suggested that the lunar crust consists of very pure anorthosite, which means the refractory element Al concentrates within the crust (e.g. [4][5]). Since the bulk amount of refractory elements gives a strong constraint on the thermal condition of the lunar formation, revealing the lunar crustal structure will lead to better understanding of the history of the Moon.

When determining the lunar crustal structure, impact-induced seismic waves are usually used [6]. Generally, at least 3 seismic stations are required to determine seismic source locations. In the case of the Apollo, although 4 seismic stations were placed and made a network on the nearside of the Moon, it was difficult to determine the impact locations (seismic source locations) precisely due to uncertain arrival time readings and unknown origin times. In future seismic explorations, it is required to carry out seismic observations even at a single point since it is difficult to deploy multi-seismic stations at once. In this situation, the precise determination of origin times and impact locations will play an important role in order to improve the crustal structure. However, as described above, it is considered that a single seismic station is not adequate for the precise determination of origin times and impact locations. This is one of the serious problems when performing a future seismic exploration.

In order to overcome this problem, it has been proposed to apply ground observation data of lunar impact flashes to seismic observations on the Moon [7][8]. Since the basic recording system of the impact flash observation allows us to determine impact times and locations more precisely compared to seismological approaches, it will enable to realize seismic observation at single point. However, these fields of study (lunar impact flash and lunar seismology) have been carried out independently in the past. In this study, we bring these two field together by performing observing simulations of impact-induced seismic waves by combining a seismological simulation with the lunar impact flash observation data as a first step for the consideration of a future seismic exploration.

©2019. Japan Geoscience Union. All Right Reserved. 

In the presentation, we will report the simulation results of the lunar seismic observations and discuss the requirements for a future seismic instrument and landing site.

References

[1] Toksöz et al. (1974), *Rev. Geophys. Space Phys.*, 12, 539-567.
[2] Lognonné et al. (2003), *Earth Plant. Sci. Lett.*, 211, 27 –44.
[3] Garcia et al. (2011), *Phys. Earth Planet. Inter.*,188, 96 –113.
[4] Ohtake et al. (2009), *nature*, 461, 236-241.
[5] Yamamoto et al. (2012), *Geophys. Res. Lett.*, 39, L13201.
[6] Chenet et al. (2006), *Earth Planet. Sci. Lett.*, 243, 1-14.
[7] Tanaka et al. (2018), *Proc.NVM2-Asia*, #6025.
[8] Yamada et al. (2019), *Proc.Lunar Planet. Science Conf., 50*th, #1770.

Keywords: Moon, Moonquake, Future Exploration, Impact, Lunar Impact Flash

©2019. Japan Geoscience Union. All Right Reserved. 

# New Results from Restored Apollo Magnetic Field Records

*Peter J Chi[1]

1. University of California Los Angeles

Three Apollo missions collected digital magnetic field measurements by the Lunar Surface Magnetometers on the surface (Apollo 12, 15, and 16) and by Subsatellite Biaxial Magnetometers in orbit surrounding the Moon (Apollo 15 and 16). After approximately a half century, the Apollo 15 and 16 missions are still the only lunar missions conducting simultaneous surface and orbital magnetic field experiments. The Apollo magnetic field experiments enabled many first discoveries, such as the lunar magnetic anomalies and the electrical conductivity of the Moon.

A recent effort has restored all the Apollo magnetic field records from the archaic data format originally archived. The restored LSM data have revealed many narrowband ion cyclotron waves in the Earth’s magnetotail that were not investigated during Apollo years. The restored data also allow re-analyses for the Moon-solar wind interaction and magnetic sounding of the lunar interior. We find that the observed transfer function responses in both tangential and radial components on the lunar surface are consistent with theoretical expectations at least for frequencies greater than $10^{-4}$ Hz. The comparison between SBM and LSM data indicates that, when the Moon is in the solar wind, the surface magnetic field is slightly enhanced on the sunward side. This paper summarizes the recent findings from the restored Apollo magnetic field data and discusses the unexplored topics for future magnetic field measurements on the lunar surface.

Keywords: Moon, Apollo magnetic field experiments, plasma waves at the Moon, magnetic sounding of lunar interior, solar wind interaction with the Moon

©2019. Japan Geoscience Union. All Right Reserved. 

# Analysis of the High Latitude Region of the Moon with Spectral Profiler Data: Possible Presence of Water Ice

Haramitsu Kyoda[3], *Satoshi Tanaka[1], Makiko Ohtake[1], Hiroshi Nagaoka[2], Yusuke Nakauchi[2], Keisuke Onodera[4]

1. Department of Solid Planetary Sciences Institute of Space and Astronautical Science, 2. Japan Aerospace Exploration Agency, 3. Department of Complexity Science and Enginnering, the University of Tokyo, 4. Department of Space and Astronautical Science, SOKENDAI

Recently, space agencies such as NASA and JAXA are actively planning to explore the polar region of the Moon since its usability as lunar base and possible existence of volatile elements([1],[2]). Landing site selection should be taken into consideration of the sunshine rate, existence of volatile materials in the vicinity [3], and so on. Therefore, geological and geomorphological studies in the polar region of the Moon have become more important. In this paper, we focused on detecting of water ice in the polar region using Spectral Proler(SP) data obtained by KAGUYA. Li et al.,(2018)[4] reported exposed water in the permanently shaded area by $M^3$ data. It is possible to detect more distinct feature of water absorption by the SP data with high S/N ratio. Data analysis by the SP data in the polar region is still difficult due to the large solar incidence angle, however, we reported that the data could be handled with high-accuracy by estimation of insolation area for each spectrum using deep learning method [5]. Based on the SP data in the fully shaded area classied by the method above, we investigated the spectrum having absorption at 1260 nm and 1500 nm both of which are featured by ice and frost of water. As a result, we found about 300 spectrum data having distinct water absorption. One of the data with this absorption obtained in the middle of April, 2009 was located at around (lat. , lon.)=(-85, 50) at where Li et al., (2018) indicated the presence of water ice, but most of the data locations are not overlapped. Moreover, the solar incident angles of all selected data are too high to detect the direct nor the secondary reflected light from the surface of the target area. It is possible that the floating dust at a distance of several tens of kilometers the Moon originated from the impacts or levitation may have been detected[6].

References

[1] Heldmann et al., (2016) Acta Astronautica, 127, 308-320.
[2] Ivanov et al., (2015) Planetary and Space Science, 117, 45-63.
[3]Sanin et al., 2016, Icarus 283 20{30.
[4]Li et al., 2018, PNAS 115 (36) 8907-8912.
[5]Kyoda et al., 2018, 49th Lunar and Planetary Science Conference 2018 (LPI Contrib. No. 2083).
[6]Wooden et al., 2016, Nature Geoscience volume 9, pages 665{668

Keywords: Moon, spectral profiler, water ice

©2019. Japan Geoscience Union. All Right Reserved. 

# Detection of Dark Regions on the Lunar Surface with Shadow Masked Multiband Imager Data

*Riho Ito[1], Hiroka Inoue[2], Makiko Ohtake[2], Hisashi Otake[2], Ryosuke Nakamura[1]

1. National Institute of Advanced Industrial Science and Technology, 2. Japan Aerospace Exploration Agency

The lunar low-reflectance regions, such as Dark Mantle Deposits (DMDs), iron or titanium rich regions, or weathered older mare, have important information for clarifying the process of lunar evolution. To locate the global distribution of the low-reflectance (dark) region is one of important studies for lunar geological science. Since even small dark regions can be detected based on high-resolution lunar images such as Kaguya's Multiband Imager (MI) images, a goal of this research is to identify candidates of the darkest region with various spatial scale on the global lunar surface. However, a simple automatic identification of small dark regions from Kaguya's MI images, such as using a threshold value, may be hindered by shadows. Therefore, in this research, dark regions other than shadows were identified after removing the shadow regions from the MI images.

The areas that have relatively lower reflectance than the surrounding area due to the difference in the local solar incidence angle are treated as same as actual shadows cast by being hidden from sunshine because the areas often show abnormal spectrum patterns. In the first step, to detect shadow regions, we employed conditional generative adversarial networks (cGAN) which is deep learning method. The cGAN is composed of the generator neatwork and the discriminator network. The Generator is trained to generate realistic fake images that cannot be distinguished from real images by the Discriminator, whereas the Discriminator is trained to detect the fake images generated by the Generator. We prepared supervised data which are pair of MI images and correct shadow masks for training the cGAN networks. In this step, Generator was trained for generating a realistic shadow mask as much as possible according to an input MI image. After the training, our Generator successfully provide a shadow mask in which we can detect high contrast shadows and shadows by craters or other land features. On the other hand, we found that our network had low accuracy for smaller shadows and surround regions of invalid values, and these detected shadow masks included many noises.

In the next step, we employed simple thresholding to detect candidates of DMD from the MI images with shadow masks generated by the trained Generator. Since the results of shadow detection are not stable when an image has many invalid values., regions higher than ±60 ˚including relatively many invalid values were excluded from target regions. The threshold value was determined from a histogram of the reflectance which calculated from the band 2 (750 nm) of the MI image after the shadow removal, and regions where the reflectance was lower than the threshold were detected as candidate of the dark region. In this study, because dark regions with a small size in the detected candidates may be mis-detection of the small shadow regions that could not be distinguished and removed by the trained network, dark regions which area are smaller than 900 pixels (0.36 $km^2$) were excluded from candidates. Though this process may exclude candidates for actual small dark regions that are not shadows, we decided to focus on locating candidates that can be more reliably determined as dark regions. As threshold processing and noise removal method are important factors greatly affecting the detection of the final candidate points, we will consider the improvements for detecting smaller dark regions in the future work.

In the result of applying this method, although some noise remained, some known DMDs, in the Sinus Aestuum, Taurus-Littrow, Sulpicius-Gallus and Mare Vaporum, were detected as candidates of dark regions. Most of the other detected points were also located in the region of high titanium. In this work, analysis results of detected dark regions and utility of the detection methods will be reported and

©2019. Japan Geoscience Union. All Right Reserved. 

discussed.

Keywords: deep learning, shadow detection, Multiband Imager, Dark Mantle Deposit

©2019. Japan Geoscience Union. All Right Reserved. 

# Estimation of Moho depth under lunar basins by using only the GRAIL gravity data

*Gaku Nishiyama[1], Noriyuki Namiki[2]

1. Department of Earth and Planetary Science, The University of Tokyo, 2. RISE Project, National Astronomical Observatory of Japan

In order to unravel the formation of solar-system, the subsurface structure of planets and moons will be a key to constrain early differentiation and subsequent thermal evolution. In particular, lunar crustal thickness is of importance for understanding the volume of the ancient magma ocean. Conventionally planetary crustal thickness is estimated by analyzing gravity anomaly data derived from tracking data of spacecrafts using downward continuation filter. In this method, the relief of crust-mantle interface (Moho) are calculated as a variation of surface density anomalies under the condition that a mean crustal thickness or crustal thickness at a specific location has been already known from seismic observation. In this study, however, we demonstrate that the calculation is theoretically incorrect in the point that the Moho relief is imposed on the surface density at certain depth. Downward continuation filter is mathematical trick to stabilize the previous calculation, but it indeed violating gravity theory.

In this study, we show a new method which doesn't require ad hoc assumptions of crustal thickness nor downward continuation filter, but assumes the simple shape of Moho uplift. Under the assumption that the Moho is uplifted like an axisymmetric cylinder beneath Crisium basins , the observed Bouguer gravity anomalies can be expanded in the Bessel-Fourier coefficients . Then we find the best fit parameters such as radius, height and depth of cylinder. Thus, the depth of surrounding crust is estimated to be 37.9±7.7 km. Our estimate is consistent with that of the analysis result of moonquake data measured at Apollo 12 & 14 landing sites. This result indicates that the new method can estimate crustal thicknessby gravity data alone and independently from seismic data. Here we assumed a simple morphology of mass anomalies beneath Crisium basin, however, the top surface of the cylinder as well as surrounding Moho boundary shall be laterally variable. In further research we evaluate an influence of the shape, crustal flexure, and other effects.

Keywords: moon, crust, gravity, GRAIL, Moholovicic discontinuity

©2019. Japan Geoscience Union. All Right Reserved. 

# Ejecta Thickness Distribution of Lunar Schrödinger Basin

*Luyuan Xu[1], Minggang Xie[1]

1. State Key Laboratory of Lunar and Planetary Sciences, Macau University of Science and Technology

A hypervelocity impact on a target with solid surface forms an impact crater, and a fraction of debris is ejected and emplaced ballistically from the crater. The thickness distribution of primary ejecta gives insight into the processes of impact cratering, the stratigraphy of planetary crust, the evolution of planetary surface, and the source of lunar samples. However, the widely used empirical ejecta thickness distribution model of McGetchin et al. (1973) is inconsistent with recent observations of complex craters and the Orientale basin.

As a typical case to address this problem, here we conducted detailed measurements of ejecta thickness distribution for Schrödinger Basin, which is a large impact basin located near the lunar south pole, the best-preserved peak-ring basin, and the second youngest one on the Moon.

Based on LROC WAC, Kaguya TC, and LOLA DTM data, the thickness of primary ejecta is estimated indirectly from the measurements of partially filled pre-basin craters using crater morphometry and the effect of crater degradation is taken into considerations. The results show that the ejecta thickness distribution of Schrödinger Basin is more consistent with Pike (1974)’s model rather than McGetchin et al. (1973)’s, the excavation of Schrödinger basin-forming impact does not penetrate through lunar crust, and the rim relief of Schrödinger Basin consists mostly of rim uplift rather than the primary ejecta.

Keywords: Impact ejecta, rim uplift, Schrödinger Basin

©2019. Japan Geoscience Union. All Right Reserved. 

[J] Oral | P (Space and Planetary Sciences )：P-PS Planetary Sciences

Thu. May 30, 2019 10:45 AM - 12:15 PM JST | Thu. May 30, 2019 1:45 AM - 3:15 AM UTC | 103 1F

## [P-PS08] Lunar science and exploration

convener:Hiroshi Nagaoka(Japan Aerospace Exploration Agency), Masahiro KAYAMA(Department of Earth and Planetary Material Sciences, Faculty of Science, Tohoku University), Masaki N Nishino(Japan Aerospace Exploration Agency, Institute of Space and Astronautical Science), Tomokatsu Morota(Graduate School of Environmental Studies, Nagoya University), Chairperson:Ko Hashizume, Hiroshi Nagaoka

Scientific data sets acquired by not only Japanese lunar mission SELENE (Kaguya), but also other countries' missions, have become new standard for lunar science. Analyses of these data have been providing several new knowledge and changing some hypotheses into the truth of the Moon. In concurrence with these studies, some countries including Japan are planning future lunar missions. In this session, we will discuss scientific results based on newly acquired lunar data, strategy for future missions including SLIM, and theoretical and experimental studies for lunar science.<br/>

10:45 AM - 11:00 AM JST | 1:45 AM - 2:00 AM UTC

### [PPS08-07] Possible evolution paths of the lunar orbit based on tidal response in the global ocean model of the early Earth

*Mai Motoyama[1], Hideo Tsunakawa[1], Futoshi Takahashi[2] (1.Department of Earth and Planetary Sciences, School of Science, Tokyo Institute of Technology, 2.Department of Earth and Planetary Sciences, Faculty of Science, Kyushu University)

11:00 AM - 11:15 AM JST | 2:00 AM - 2:15 AM UTC

### [PPS08-08] Geochemical and Petrological Investigations of Lunar Feldspathic Crust by Lunar Sample Studies and Remote Sensing Data

*Hiroshi Nagaoka[1], Yuzuru Karouji[1], Makiko Ohtake[1] (1.Japan Aerospace Exploration Agency)

11:15 AM - 11:30 AM JST | 2:15 AM - 2:30 AM UTC

### [PPS08-09] Development of frosting system for lunar simulant and the detectability of ice growing on the simulant by NIR measurement

*Aoi Ogishima[1], Kazuto Saiki[1] (1.Department of Earth and Space Science, Graduate School of Science, Osaka University)

11:30 AM - 11:45 AM JST | 2:30 AM - 2:45 AM UTC

### [PPS08-10] Volatile studies on Moon - A review toward future exploration programs

*Ko Hashizume[1] (1.Faculty of Science, Ibaraki University)

11:45 AM - 12:00 PM JST | 2:45 AM - 3:00 AM UTC

### [PPS08-11] Scientific approach for the promotion of lunar polar exploration mission

*Masahiro KAYAMA[1], Ko Hashizume[2], Hiroshi Nagaoka[3], Kazuto Saiki[4], Chihiro Yamanaka[4], Makoto Hareyama[5], Makiko Ohtake[3] (1.Tohoku University, 2.Ibaraki University, 3.Japan Aerospace Exploration Agency, 4.Osaka University, 5.St. Marianna University School of Medicine)

12:00 PM - 12:15 PM JST | 3:00 AM - 3:15 AM UTC

### [PPS08-12] Feasibility study of detection of the lunar subsurface ice with UHF-band GPR based on FDTD electromagnetic simulation

*Atsushi Kumamoto[1], Hideaki Miyamoto[2], Toshifumi Nishibori[3], Takafumi Niihara[2], Fuminori Tsuchiya[1], Ken Ishiyama[3] (1.Tohoku University, 2.University of Tokyo, 3.JAXA)

# Possible evolution paths of the lunar orbit based on tidal response in the global ocean model of the early Earth

*Mai Motoyama[1], Hideo Tsunakawa[1], Futoshi Takahashi[2]

1. Department of Earth and Planetary Sciences, School of Science, Tokyo Institute of Technology, 2. Department of Earth and Planetary Sciences, Faculty of Science, Kyushu University

The Moon's orbital evolution has been affected by the Earth's ocean tide as well as the solid Earth's tide (e.g. MacDonald, 1964, Kaula, 1964). Many previous studies pointed out that the continental crusts would be few amounts in the early Earth (e.g. Stein & Ben-Avraham, 2007, Rino et. al., 2004), possibly with larger seawater volume than the present day (e.g. Kurokawa et al., 2018, Korenaga et. al., 2017). Thus the early Earth is considered to have been covered by the global ocean for a long time, strongly implying the importance of the ocean tide for the early evolution of the Earth-Moon system. Most of previous studies of the evolution of the Earth-Moon system calculated back to the past with the initial condition of the present state (e.g. Abe et. al., 1997, Rubincam, 2015). The backward calculation is inappropriate to estimate the effects of various parameters concerning the early Earth’s ocean, since there are many uncertain factors such as continental drift. Thus we carried out forward calculation of the lunar orbit from the past for the first 2 billion years to understand characteristic effects of the ocean state in the global ocean model.
Energy dissipation mechanism of the ocean is one of the critical factors in the Moon’s orbital evolution (e.g. Webb, 1982, Lambeck, 1977). Recent studies have revealed that the internal gravity wave, so-called internal tide, is a main mechanism of tidal energy dissipation in the deep ocean (e.g. Taguchi et. al., 2014, Egbert & Ray, 2000). In this study, we considered its effect on the early evolution, assuming the early ocean is as deep as the present abyssal depth.
Our results show that the eigenmode resonance occurs once or more for the first 2 billion years. The Earth-Moon distance rapidly increases with a step-like change at the eigenmode resonance. In the case of the ocean depth decreasing linearly to the time, it is found that the torque due to the oceanic tidal bulge causes continuous increase in the Earth-Moon distance with an especial response of eigenmode oscillation. These acceleration effects could work in the coevolution of the early Earth-Moon system.

Keywords: Moon, Earth, ocean, tide, resonance, orbit

©2019. Japan Geoscience Union. All Right Reserved. 

# Geochemical and Petrological Investigations of Lunar Feldspathic Crust by Lunar Sample Studies and Remote Sensing Data

*Hiroshi Nagaoka[1], Yuzuru Karouji[1], Makiko Ohtake[1]

1. Japan Aerospace Exploration Agency

Feldspathic highland crust deriving from ferroan anorthosite (FAN) have been assumed to be formed by the lunar magma ocean (LMO) model, whose the early crust was accumulated by the crystallization and flotation of plagioclase (Warren, 1985). However, the studies of lunar meteorites which originated from the highlands not covered by the Apollo missions, found more magnesian anorthosites than FAN (e.g., Takeda et al., 2006). Furthermore, Kaguya observation revealed feldspathic crust with higher Mg# (= molar 100 ×Mg/(Mg + Fe)) than FAN (Ohtake et al., 2012).
Furthermore, purest anorthosite (PAN) (>98% plagioclase) lithology was found in central peak of several large craters by Kaguya observation. On the basis of Kaguya results, the massive PAN layer are assumed to be distributed under mafic-rich mixing layer in highlands (Ohtake et al., 2009; Yamamoto et al., 2012).
Like this, lunar meteorite studies and global remote sensing data have provided new global information on geological features of lunar crust.

Feldspathic meteorites from lunar highlands are brecciated by impacts on the lunar surface.
The 10-30% mafic minerals (pyroxene and olivine) are included in the meteorites.
These feldspathic meteorites is similar with the surface composition of mafic-rich mixing layer of feldspathic crust in elemental composition (e.g., FeO, Th).
On the other hand, several highly pure anorthosite (PAN) clasts were found among some of feldspathic lunar meteorites (Nagaoka et al., 2014). They are correspond with PAN lithology observed by Kaguya.

In this work, we have measured and summarized the elemental and mineral composition of feldspahtic lunar meteorites, by bulk chemical analyses, electron micro-probe analyses, and UV-VIS-NIR reflectance spectroscopy. In this presentation, we report and discuss geochemical and petrological features of lunar crust on the basis of recent geochemical and petrological studies combined the above lunar samples analyses data and the recent remote sensing data.

Keywords: Lunar Feldspathic Crust, Lunar Meteorites, Remote Sensing

©2019. Japan Geoscience Union. All Right Reserved. 

# Development of frosting system for lunar simulant and the detectability of ice growing on the simulant by NIR measurement

*Aoi Ogishima[1], Kazuto Saiki[1]

1. Department of Earth and Space Science, Graduate School of Science, Osaka University

In recent years, many remote sensing studies have suggested the existence of lunar water, but it is still an open issue how or how much water is on the Moon. Lunar prospector launched in 1998 found the concentration of proton around lunar poles. In 2009 Lunar Crater Observation and Sensing Satellite (LCROSS) project observed ejecting debris from Cabeus crater and estimated that concentration of water ice is 5.6±2.9 wt%. Chandrayaan-1 data suggested the abundance of water could be as high as 0.077wt%. After these results, Japan’ s space agency JAXA and India’ s space agency ISRO have signed an Implementation Arrangement (IA) for a Joint Lunar Polar Expedition in December 2017. In preparation for this mission, assuming that the grains of lunar regolith are covered by water frost on the lunar permanently shadowed regions, we made minute ice on lunar simulants and measured their Near-Infrared reflectance spectra. As lunar simulant we use olivine (from San Carlos, 125-250um, Fo90) and lunar simulant FJS-1 (Shimizu Corporation). We developed a frosting system. It’ s a kind of cooling stage in which simulant grains cooled with liquid N2 can be mixed with highly humid air and vibrated. In the stage, water frosts condensed and cover the surface of grains. The top of the stage is covered with silica glass plate, so we can observe the spectra without taking out samples from the stage. We observed the reflectance spectra of the frosted simulants with a Near-Infrared imaging spectrometer developed by Saiki at 950-1600 nm, angle of incidence = 30˚, angle of viewing = 0˚. After the measurement, we weighed the mass of frosts. In order to prevent additional frost during weighing, we made a vinyl house and weighed frosted samples in the house purged with dry N2 gas. Then, the samples were heated and the frosts on them evaporated. After heating we weighed the samples again, regarded the decreased mass as the mass of frosts, and calculated mass fraction of frosts. We succeeded in making the minute ice less than 1wt% on the simulant, but it is difficult to make ice homogeneously and to control the amount. In order to address these problems, we developed a new fall-type frosting system. In this system cooled simulant fall down in humid air and covered by minute ice homogeneously.We continue trial and error on falling distance and humid air volume aiming to control the amount of frost on the order of 0.1 wt%. Latest results will be reported.

Keywords: Lunar polar mission, frosting experiment

©2019. Japan Geoscience Union. All Right Reserved. 

# Volatile studies on Moon - A review toward future exploration programs

*Ko Hashizume[1]

1. Faculty of Science, Ibaraki University

I would like to first review the recent findings regarding the water detected on Moon's surface, point out the current issues, then discuss necessary actions in the future exploration programs.

Keywords: Exploration, Isotope Compositions, Volatile Compounds

©2019. Japan Geoscience Union. All Right Reserved. 

# Scientific approach for the promotion of lunar polar exploration mission

*Masahiro KAYAMA[1], Ko Hashizume[2], Hiroshi Nagaoka[3], Kazuto Saiki[4], Chihiro Yamanaka[4], Makoto Hareyama[5], Makiko Ohtake[3]

1. Tohoku University, 2. Ibaraki University, 3. Japan Aerospace Exploration Agency, 4. Osaka University, 5. St. Marianna University School of Medicine

Remote sensing spacecraft missions (e.g., LCROSS and Deep Impact), lunar sample studies, and theoretical simulations suggest the existence of various water species (e.g., $H_2O$ ice, hydroxyl and molecular water, and aqueous phase) on the lunar surface and in the subsurface. Lunar water is thought to originate from solar wind, meteorite/asteroid/comet collisions, and/or volcanic eruptions and concentrated locally on the lunar surface to subsurface, especially permanently shadowed regions near the lunar poles. These findings indicate the possibility of the presence of available water resources for future human activity on the Moon. Moreover, lunar water is significant because it is closely related to a formation process of the lunar magma ocean and its differentiation to the mantle. Therefore, Lunar Polar Exploration Mission is planned to be launched in the 2020’s to survey lunar water. From the viewpoint of resources, science and engineering, this mission provides new insights into lunar evolutionary history and lunar base construction. Here, we will discuss analytical techniques for in-situ water analyses on the lunar poles and experiments simulating low-temperature and high-vacuum lunar environment.

Keywords: Lunar polar exploration mission, Lunar water, Infrared spectroscopy, Thermogravimetric analysis, Cavity ring-down spectroscopy, Neutron spectrometry

©2019. Japan Geoscience Union. All Right Reserved. 

# Feasibility study of detection of the lunar subsurface ice with UHF-band GPR based on FDTD electromagnetic simulation

*Atsushi Kumamoto[1], Hideaki Miyamoto[2], Toshifumi Nishibori[3], Takafumi Niihara[2], Fuminori Tsuchiya[1], Ken Ishiyama[3]

1. Tohoku University, 2. University of Tokyo, 3. JAXA

Detectability of the subsurface ice by UHF-band (0.5-3 GHz) ground penetrating radar (GPR) onboard the rover in the lunar polar region was investigated based on electromagnetic simulation using finite-difference time-domain (FDTD) method. The water brought on the lunar surface is lost within 1 day due to photodissociation. However, if a part of water molecules jump to polar region within 1 day, they can be kept in the polar shadowed region [Arnord, 1979]. Some observations such as impact experiment in LCROSS mission [Colaprete et al., 2010] and SAR polarization measurements in Chandrayaan mission [Spudis et al., 2010] suggests the existence of the water in the lunar polar region.

In this study, we used Meep code [Oskooi et al., 2010] for FDTD simulation. The simulation space with a size of 0.25 m x 1.25 m is divided into meshes with a size of 0.3 mm x 0.3 mm. The uppermost part with a height of 0.5 m is filled with vacuum (permittivity: 1). The second part with a thickness of 0.5 m is filled with dry regolith, basalt (permittivity: 7) including voids (vacuum). The lowermost part with a thickness of 0.25 m is filled with several kind of media such as (i) cavity (vacuum), (ii) rocks (basalt without pores), (iii) pure ice (permittivity: 3), and (iv) icy regolith, regolith whose voids are filled ice. The porosity of the dry and icy regolith layers was determined based on the report from Apollo missions on the vertical profile of the bulk density of the lunar subsurface soils up to depth of 3 m [Carrier et al., 1991]. Chirp pulse in a frequency range from 0.5 to 3 GHz was transmitted for 167 ns from 0.4 m above the dry regolith surface. The electromagnetic fields in simulation space were evolved with time step of 0.52 ps. At the transmission point, the waveform of electric field component of the echoes was recorded at an interval of 33 ps.

Calculation results suggests that subsurface echoes from (i) cavity, (iii) rocks, and (iv) icy regolith at a depth of 0.5 m can be detected with enough echo powers while the echo power from (iii) pure ice were as large as volume scatters due to inhomogeneity in the regolith. They are a little different from the results of our previous calculation performed in a frequency range 1-15 GHz with subsurface materials at a depth of 0.1 m: The echo powers from ice and icy regolith were as large as volume scatters. We can consider that the difference is from (a) the decrease of the volume scatters power by changing the operation frequency range, and (b) the depth dependence of permittivity contrast in inhomogeneous regolith.

Keywords: Lunar polar exploration, Lunar water ice, Ground penetrating radar (GPR), Finite difference time domain (FDTD) method

©2019. Japan Geoscience Union. All Right Reserved. 

[J] Oral | P (Space and Planetary Sciences )：P-PS Planetary Sciences

Thu. May 30, 2019 1:45 PM - 3:15 PM JST | Thu. May 30, 2019 4:45 AM - 6:15 AM UTC | 103 1F

## [P-PS08] Lunar science and exploration

convener:Hiroshi Nagaoka(Japan Aerospace Exploration Agency), Masahiro KAYAMA(Department of Earth and Planetary Material Sciences, Faculty of Science, Tohoku University), Masaki N Nishino(Japan Aerospace Exploration Agency, Institute of Space and Astronautical Science), Tomokatsu Morota(Graduate School of Environmental Studies, Nagoya University), Chairperson:Masahiro Kayama(東北大学), Yusuke Nakauchi(JAXA/ISAS)

Scientific data sets acquired by not only Japanese lunar mission SELENE (Kaguya), but also other countries' missions, have become new standard for lunar science. Analyses of these data have been providing several new knowledge and changing some hypotheses into the truth of the Moon. In concurrence with these studies, some countries including Japan are planning future lunar missions. In this session, we will discuss scientific results based on newly acquired lunar data, strategy for future missions including SLIM, and theoretical and experimental studies for lunar science.<br/>

1:45 PM - 2:00 PM JST | 4:45 AM - 5:00 AM UTC

### [PPS08-13] Geology of the SLIM landing site on the Moon

★Invited Papers

*Makiko Ohtake[1], Kazuto Saiki[2], Yusuke Nakauchi[1], Hiroaki Shiraishi[1], Yoshiaki Ishihara[3], Hiroyuki Sato[1], Chikatoshi Honda[4] (1.Institute of Space and Astronautical Science, Japan Aerospace Exploration Agency, 2.Osaka University, 3.National Institute for Environmental Studies, 4.University of Aizu)

2:00 PM - 2:15 PM JST | 5:00 AM - 5:15 AM UTC

### [PPS08-14] Observing scenario for the Multi-Band Camera onboard SLIM

*Kazuto Saiki[1], Yuya Igarashi[1], Yusuke Nakauchi[2], Chikatoshi Honda[3], Makiko Ohtake[2], Hiroaki Shiraishi[2], Hiroyuki Satoh[2], Yoshiaki Ishihara[4], Takao Maeda[5], Chihiro Yamanaka[1] (1.Osaka Univ., 2.JAXA, 3.Univ. Aizu, 4.National Institute for Environmental Studies, 5.Chuo Univ.)

2:15 PM - 2:30 PM JST | 5:15 AM - 5:30 AM UTC

### [PPS08-15] Current status of a Japanese lunar polar exploration mission

*Takeshi Hoshino[1], Makiko Ohtake[1], Yuzuru Karouji[1], Hiroaki Shiraishi[1] (1.Japan Aerospace Exploration Agency)

2:30 PM - 2:45 PM JST | 5:30 AM - 5:45 AM UTC

### [PPS08-16] HERACLES mission: Returning to the Moon by an ESA-JAXA-CSA Joint Study

*Yuzuru Karouji[1], Hiroshi Nagaoka[1], Yoshiaki Ishihara[2], Masahiro KAYAMA[3], Satoru Yamamoto[4], Nobuyuki Hasebe[5], Ko Hashizume[6], Yoshiko Ogawa[7], Toru Yada[1], Junichi Haruyama[1], Masanao Abe[1], Makiko Ohtake[1], HERACLES Science Working Group, HERACLES International Science Definition Team (1.Japan Aerospace Exploration Agency, 2.National Institute for Environmental Studies, 3.Faculty of Science, Tohoku University, 4.J-spacesystems, 5.Advanced Research Institute for Science and Engineering, Waseda University, 6.Faculty of Science, Ibaraki University, 7.The University of Aizu)

2:45 PM - 3:00 PM JST | 5:45 AM - 6:00 AM UTC

### [PPS08-17] Lunar Science for Landed Missions – High-Priority Landing Sites Visualized with NASA's Moon Trek

*Brian Hamilton Day[1], Emily Law[2] (1.NASA Solar System Exploration Research Virtual Institute, NASA Ames Research Center, 2.NASA Jet Propulsion Laboratory, California Institute of Technology)

3:00 PM - 3:15 PM JST | 6:00 AM - 6:15 AM UTC

### [PPS08-18] NASA SSERVI: Merging Science and Human Exploration

*Brad Eugene Bailey[1], Kristina Gibbs[1], Gregory Schmidt[1] (1.NASA)

# Geology of the SLIM landing site on the Moon

*Makiko Ohtake[1], Kazuto Saiki[2], Yusuke Nakauchi[1], Hiroaki Shiraishi[1], Yoshiaki Ishihara[3], Hiroyuki Sato[1], Chikatoshi Honda[4]

1. Institute of Space and Astronautical Science, Japan Aerospace Exploration Agency, 2. Osaka University, 3. National Institute for Environmental Studies, 4. University of Aizu

**Introduction:** Smart Lander for Investigating Moon (SLIM) is a Japanese technology demonstration mission to pinpoint landing within a hundred meters in radius, which will be launched in fiscal year 2021. The lander carries one small instrument (high-resolution Multiband Camera; see Saiki et al. in this conference) to derive the detailed mineralogy of the olivine-rich exposure to investigate a olivine bearing lithology for understanding their origin and investigating the composition of the lunar unsampled mantle or deep crustal material. To directly explore this unexplored lithology, one of the small fresh craters just outside of the Theophilus crater is selected as a landing site for the SLIM mission. In this study, we analyzed geology of Theophilus crater and the selected landing site.

Crater Theophilus (11.4˚S, 26.4˚E) is located in the immediate vicinity (northwest) of the Mare Nectaris on the Moon. It is on the ring of the Nectaris basin. Its diameter is 110 km, and it has a clear central peak at the center of the crater. Previous study revealed the central peak’ s compositional diversity [1][2]. However, the origin of other lithologies and the relation of these rare geologic lithologies in this unique central peak are still not clear. In addition to their geological (mineralogical) diversity.

**Data and Results:**We used remote sensing reflectance spectra and spectral images obtained by the SELENE (Kaguya) Spectral Profiler (SP) and Multiband Imager (MI). Olivine-dominant lithology at the central peak have clear diagnostic absorption of olivine. Percentage of olivine among olivine and pyroxene of the olivine dominant lithology is estimated to be more than 70. The FeO abundance of the olivine-dominant lithology estimated ranges from 5 to 8 wt.%. Olivine-dominantlithology appears to be present as a basal lithology of the central peak blocks. Olivine dominantlithology is also observed as localized exposures at many small but fresh craters throughout the wall and ejecta region. These fresh craters commonly have a very clear olivine absorption feature, and the FeO abundance of these localized olivine exposures ranges up to 12 wt.%,which corresponds to a nearly pure olivine rock, if Mg# (Mg/(Mg+Fe) in mole per cent) of the olivine is assumed to be similar to the olivine-rich rock types (troctolite and dunite) among the Apollo samples.

**Discussion:** Based on the modal abundance, FeO abundance, distribution, and morphological information of the observed lithologies, we believe that the central peak of Theophilus crater mainly consists of olivine-dominant lithologies with lesser amounts of purest anorthosite (PAN) and Mg-spinel bearing lithologies. Distribution of Mg-spinel bearing lithology is limited in our datasets and they tend to have a relatively sharp vertical boundary with the adjacent lithology. Therefore, we interpret it is not presented as a laterally extensive unit before the formation of the Theophilus crater as suggested [1]. Observed olivine-rich composition comparable to dunite and a sharp boundary with the adjacent PAN lithology suggest that it is not a part of the continuous crustal material. Instead, it is probably mantle (or the lower part of the crustal) origin, which is excavated by the Nectaris basin forming impact as suggested by the global distribution of the olivine-rich sites [2], well before the formation of the Theophlius.

**References:**[1] Dhingra D. et al. (2011) *Geophys. Res. Let., 38*, L11201, doi:10.1029/2011GL047314. [2]

©2019. Japan Geoscience Union. All Right Reserved. 

Yamamoto S. et al. (2012) *Geophys. Res. Let., 39*, L13201, doi:10.1029/2012GL052098.

Keywords: Moon, olivine, SLIM, mantle

©2019. Japan Geoscience Union. All Right Reserved. 

# Observing scenario for the Multi-Band Camera onboard SLIM

*Kazuto Saiki[1], Yuya Igarashi[1], Yusuke Nakauchi[2], Chikatoshi Honda[3], Makiko Ohtake[2], Hiroaki Shiraishi[2], Hiroyuki Satoh[2], Yoshiaki Ishihara[4], Takao Maeda[5], Chihiro Yamanaka[1]

1. Osaka Univ., 2. JAXA, 3. Univ. Aizu, 4. National Institute for Environmental Studies, 5. Chuo Univ.

Smart Lander for Investigating Moon (SLIM) is being planned by Japan Aerospace Exploration Agency (JAXA). SLIM aims to research and demonstrate the engineering key issues related to the smart landing on the gravitational planets. They are precise guidance algorithm, vision based navigation, smart landing gear. By doing SLIM mission, we expect to achieve the paradigm shift in the field of celestial body landing from ‘landing where easy to land’ to ‘landing where desire to land’. We proposed Multi-Band Camera (MBC) for SLIM lander. MBC is a compact VIS-NIR camera composed of an imaging sensor (InGaAs), a filter-wheel with 10 band-pass filters, and a movable mirror for panning and tilting. Scientific objectives of MBC are the identification of rocks and rock-forming minerals around the lander and the estimation of Mg#(=Mg/(Mg+Fe)) of olivines that might have come from lunar mantle.

MBC has a telescopic optical system and is a camera with a new concept of spectroscopic observation of rock rather than powder called regolith, so various innovative methods are required for its operation. Among them, we will introduce the methodology of scan operation, on-site calibration, autofocus system, spectroscopic observation of rocks, and Mg # estimation.

Since it is dangerous to land on a place covered with rocks, SLIM landing site was carefully selected. The landing site should be the site where the rock distribution does not become an obstacle to landing and the distribution is as much as rocks can be observed. Since MBC is a telephoto optical system in which the horizontal viewing angle is 4 degrees, rocks would not be observed in random shots. Therefore, it has a function to create a map with a combined low resolution scanned images of around 300 shots that can cover the all observable field of view. After specifying the location of the rock to be observed, we will perform spectroscopic observations efficiently. SLIM, a small unmanned spacecraft, arrives at the moon after a much longer period of time than a manned rocket, so it will be attacked much higher levels of radiation. Because there is a possibility that the background signal of the imaging device increases or the transmittance of the filter changes, we plan to calibrate on the moon. Specifically, MBC has a function to acquire deep space images as dark background data and subtract it from observed image. We also plan to carry out luminance calibration by installing a standard diffuse reflection plate. Since MBC is a telephoto optical system, a focus adjustment mechanism is also indispensable. We realized an automatic focus adjustment function using the fact that the file-size compression rate of the acquired image decreases when approaching the best focus. Although spectroscopic observation of rocks in the near infrared range is thought to be inherently difficult, we are planning to make use of the observable conditions obtained by observation experiments of natural rocks and rock-analogs. In addition, we are planning to spline-fit the data of each band intensity and detect subtle change in wavelength of the absorption peak of $Fe^{2+}$ to estimate Mg # of olivine.

Keywords: Moon, SLIM, multiband camera

©2019. Japan Geoscience Union. All Right Reserved. 

# Current status of a Japanese lunar polar exploration mission

*Takeshi Hoshino[1], Makiko Ohtake[1], Yuzuru Karouji[1], Hiroaki Shiraishi[1]

1. Japan Aerospace Exploration Agency

## Introduction:

Recently, it has been suggested that water ice might be present in the lunar polar region based on spectral measurements of artificial-impact-induced plumes in the permanently shadowed region, and remote sensing observation of the lunar surface using a neutron spectrometer [1], [2] and visible to infrared spectrometer [3]. In addition to the scientific interest about the origin and concentration mechanism of the water ice, there is strong interest in using water ice (if present) as an in-situ resources. Specifically, using water ice as a propellant will significantly affect future exploration scenarios and activities because the propellant generated from the water can be used for ascent from the lunar surface and can reduce the mass of the launched spacecraft of lunar landing missions.

However, currently it is unclear if water ice is really present in the polar region because of the currently limited available data. Therefore, we need to learn that by directly measuring on the lunar surface. If there is water ice, we also need to know it’ s quantity (how much), quality (is it pure water or does it contain other phases such as $CO_2$ and $CH_4$), and usability (how deep do we need to drill or how much energy is required to derive the water) for assessing if we can use it as resources. Therefore, JAXA is studying a lunar polar exploration mission that aims to gain the above information and to establish the technology for planetary surface exploration [4]. JAXA is also studying possibility of implementing it within the framework of international collaboration with Indian Space Research Organisation (ISRO).

## Spacecraft configuration:

The spacecraft system comprises a lander system and a rover system. The system does not have a communication relay satellite but is based on direct communication with the Earth. The minimum target for the landing payload mass is several-hundred kilograms. The launch orbit is the lunar transfer orbit (LTO). After the spacecraft reaches the Moon it is inserted into a circular orbit having a 100km altitude via a few orbital changes. During powered-descent phase, the position of the lander is estimated by landmark navigation using shadows created by the terrain. After landing, the rover is deployed on the lunar surface using ramps. The rover then prospects water ice with its observation instruments..

## Spacecraft configuration:

The spacecraft system comprises a lander system and a rover system. The system does not have a communication relay satellite but is based on direct communication with the Earth. The minimum target for the landing payload mass is several-hundred kilograms. The launch orbit is the lunar transfer orbit (LTO). After the spacecraft reaches the Moon it is inserted into a circular orbit having a 100km altitude via

©2019. Japan Geoscience Union. All Right Reserved. 

a few orbital changes. During powered-descent phase, the position of the lander is estimated by landmark navigation using shadows created by the terrain. After landing, the rover is deployed on the lunar surface using ramps. The rover then prospects water ice with its observation instruments..

**Landing site selection:**

Considering the mission objectives and condition of the lunar polar region, we listed the following parameters as constraints.
- Presence of water
- Surface topography
- Communication capability
- Duration of sunshine

As a first trial of the landing site selection, sunshine is simulated using digital elevation models to obtain the sunlight days per year and the number of continuous sunshine periods at each site. Also, slope and the simulated communication visibility map from the Earth are created. These conditions can be superimposed to select the landing site candidate.

**Current status:**
Recently, we finished joint mission definition review (JMDR) with ISRO, in which JAXA provide a launch rocket and a rover while ISRO provide a lander system. Related to the instruments which will be carried on the rover or the lander, JAXA selected several candidate instrument study teams for accelerating development of these instruments. In this presentation, we are going to introduce current status of the mission planning.

**References:**
[1] Feldman W. C. et al. (1998) *Science*, 281, 1496-1500.
[2] Sanin A. B. et al. (2017) *Icarus*, 283, 20-30.
[3] Pieters C. M. et al. (2009) *Science,* 326, 568-572.
[4] Hoshino T. et al. (2017) 68$^{th}$ IAC, IAC-17-3.2B.4.

Keywords: lunar polar exploration , lunar water, volatile

©2019. Japan Geoscience Union. All Right Reserved. 

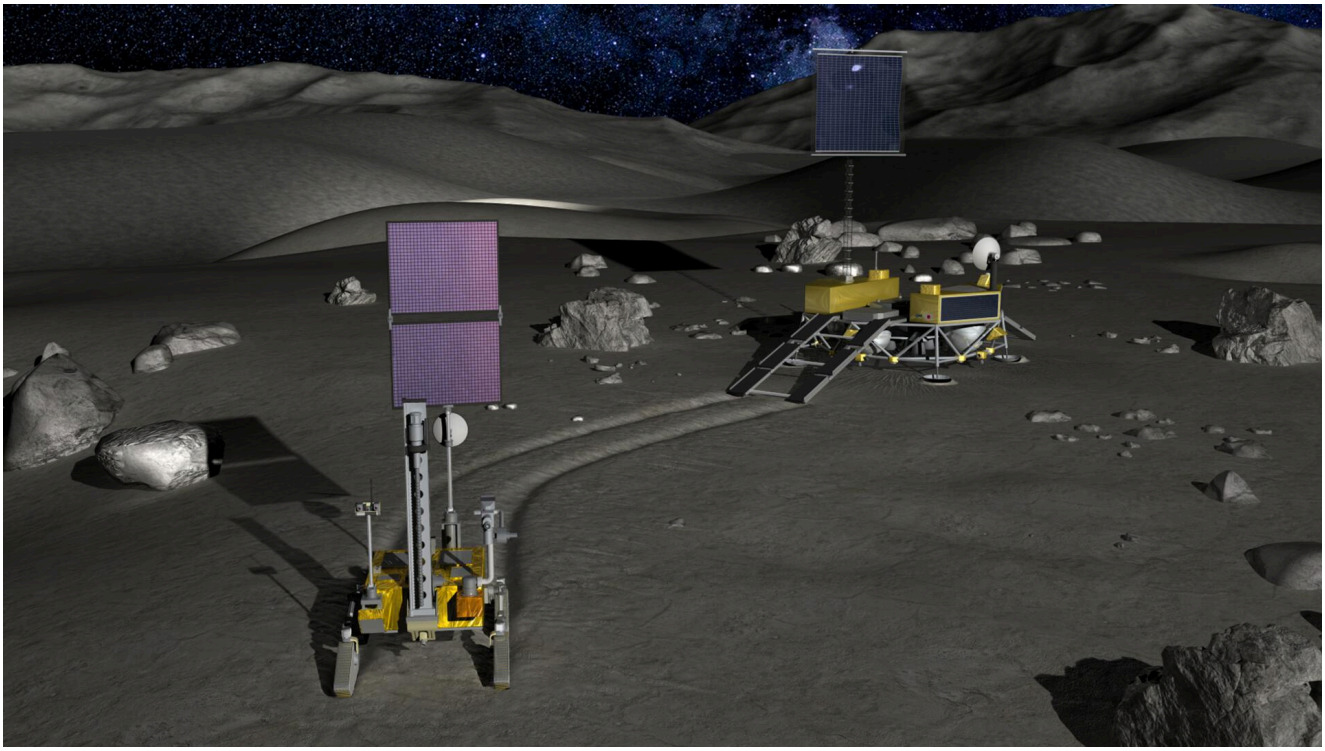

©2019. Japan Geoscience Union. All Right Reserved. 

# HERACLES mission: Returning to the Moon by an ESA-JAXA-CSA Joint Study

*Yuzuru Karouji[1], Hiroshi Nagaoka[1], Yoshiaki Ishihara[2], Masahiro KAYAMA[3], Satoru Yamamoto[4], Nobuyuki Hasebe[5], Ko Hashizume[6], Yoshiko Ogawa[7], Toru Yada[1], Junichi Haruyama[1], Masanao Abe[1], Makiko Ohtake[1], HERACLES Science Working Group, HERACLES International Science Definition Team

1. Japan Aerospace Exploration Agency, 2. National Institute for Environmental Studies, 3. Faculty of Science, Tohoku University, 4. J-spacesystems, 5. Advanced Research Institute for Science and Engineering, Waseda University, 6. Faculty of Science, Ibaraki University, 7. The University of Aizu

Global Exploration Roadmap published in January 2018 by the International Space Exploration Coordination Group (ISECG) clearly identify the Moon as the next logical destination and defined strategic goals and objectives for its exploration. Returning to the Moon not only yields fundamentally important science opportunities for our understanding of the Solar System but also allows us to test hardware and operational procedures for the exploration and utilization of space beyond Low Earth Orbit (LEO). The Human-Enhanced Robotic Architecture and Capability for Lunar Exploration and Science (HERACLES) is a joint mission under study by European Space Agency (ESA), Japan Aerospace Exploration Agency (JAXA) and Canadian Space Agency (CSA) with NASA and Roscosmos having observer status [e.g., 1]. Thus, HERACLES is an international effort in preparation of returning humans to the Moon and providing opportunities for unprecedented science utilizing the Lunar Orbital Platform-Gateway (Gateway). It is a sub-scale demonstration mission of human lunar exploration aiming for launch in the mid-2020's, and the vehicle is composed to test key components including the three following elements: The Lunar Ascent Element (LAE) will be provided by the ESA, the Lunar Descent Element (LDE) will be provided by the JAXA, and the rover will be provided by the CSA.

The coordination of the planning of science opportunities is performed by the multi-agency HERACLES Science Working Group (SWG). The SWG is also responsible for developing a mission science management plan to describe science themes and science payload instruments selection processes, and data/sample allocation policies. The SWG engaged the science communities of each country and organized the HERACLES international Science Definition Team (iSDT). The iSDT will generate a prioritized list of investigations and will provide input for the landing site selection.

Recently, the iSDT discussed the science scope of the HERACLES mission. The iSDT agreed that the following five non-prioritized topics are the most important lunar science themes that should be addressed by HERACLES; (1) crustal anorthosite composition and crystallization age, (2) mantle composition, (3) improvement of chronology with crater counting of young basalts (<2.5 Ga), (4) internal structure: surface, subsurface, crust, mantle and core, (5) mechanism of material transport (e.g., water) to the Moon. Furthermore, the iSDT has identified several potential landing areas to accomplish these science themes: Jackson crater, Moscoviense basin, Copernicus crater, Schrödinger basin and some young basalts in the Flamsteed region [2, 3].

By the way, the International Space Exploration Program Committee of the Advisory Committee for Space Science and Engineering organized the HERACLES Task Force and independently of SWG, is compiling to recommendations on science and engineering of HERACLES mission. These reports will be submitted at the end of February 2019. These recommentdations will also be taken deeply as opinions of the Japanese scientific community and SWG will discuss how to reflect it in the SWG discussion in the future. In this presentation, we are going to report outcom of previous activities related to the HERACLES SWG and planned discussion within Japanese lunar science community of study in this SWG.

©2019. Japan Geoscience Union. All Right Reserved. 

[1] Landgraf et al. (2018) LPSC 50th, abstract 1030; [2] Hiesinger et al. (2018) LPSC 50th, abstract 1327; [3] Karouji et al. (2018) LPSC 50th, abstract 1736.

Keywords: HERACLES, Lunar Exploration, Sample Return mission

©2019. Japan Geoscience Union. All Right Reserved. 

# Lunar Science for Landed Missions –High-Priority Landing Sites Visualized with NASA’ s Moon Trek

*Brian Hamilton Day[1], Emily Law[2]

1. NASA Solar System Exploration Research Virtual Institute, NASA Ames Research Center, 2. NASA Jet Propulsion Laboratory, California Institute of Technology

The Lunar Science for Landed Missions workshop was held on 10–12 January, 2018 at NASA Ames Research Center and was attended by lunar scientists, representatives from commercial companies, and representative of various international space agencies including the Japan Aerospace Exploration Agency and the European Space Agency. The workshop was cosponsored by the Solar System Exploration Research Virtual Institute (SSERVI) and the Lunar Exploration Analysis Group (LEAG). The primary goal of the workshop was to produce a set of high-priority landing site targets, generated by the lunar science community, for near-term lunar missions. The scope of such missions was aimed primarily, but not exclusively, at commercial exploration companies with interests in pursuing ventures on the surface of the Moon. The results of this workshop were published in a report that summarized the findings of the workshop and provided an analysis of priority landing sites and how missions to these sites would meet key science and exploration goals determined by NASA and the scientific community (Jawin, et al, 2019). This presentation for JpGU will review the landing sites advocated by the workshop, highlight characteristics that make them high-priority sites, and showcase the sites using visualizations generated using NASA’ s Moon Trek data visualization and analysis portal (Day and Law, 2017).

Jawin, E. R., Valencia, S. N., Watkins, R. N., Crowell, J. M., Neal, C. R., & Schmidt, G. (2019). Lunar science for landed missions workshop findings report. Earth and Space Science, 6.

Day, B. H., Law, E. S., 2017, Moon Trek: An Interactive Web Portal for Current and Future Lunar Missions. EPSC Abstracts, Vol. 11, EPSC2017-100, European Planetary Science Congress 2017

Keywords: Moon, Lunar, Landing

©2019. Japan Geoscience Union. All Right Reserved. 

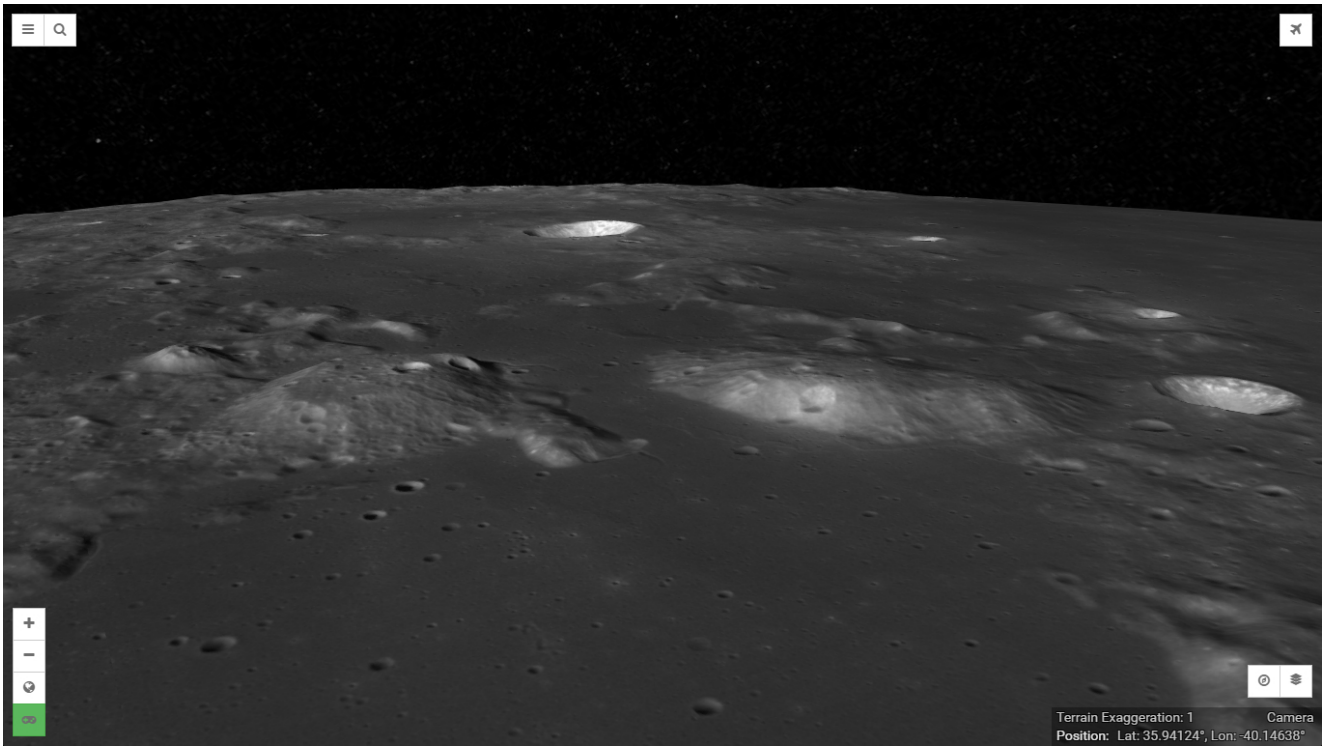


©2019. Japan Geoscience Union. All Right Reserved. 

# NASA SSERVI: Merging Science and Human Exploration

*Brad Eugene Bailey[1], Kristina Gibbs[1], Gregory Schmidt[1]

1. NASA

NASA's Solar System Exploration Research Virtual Institute (SSERVI) represents a close collaboration between science, technology and exploration, and was created to enable a deeper understanding of the Moon and other airless bodies. SSERVI is supported jointly by NASA’ s Science Mission Directorate and Human Exploration and Operations Mission Directorate. The institute currently focuses on the scientific asp ects of exploration as they pertain to the Moon, Near Earth Asteroids (NEAs) and the moons of Mars, but the institute goals may expand, depending on NASA's needs, in the future. The nine initial teams, selected in late 2013 were funded from 2014 - 2019, have expertise across the broad spectrum of lunar, NEA, and Martian moon sciences. An additional four teams were selected in 2017.

The research includes various aspects of the surface, interior, exosphere, near - space environments, and dynamics of these bodies. In addition, SSERVI has ten International Partners which collaborate with US teams NASA anticipates additional team selections in mid 2019 from the 3rd SSERVI Cooperative Agreement Notice call for proposals. Calls for proposals are issued every 2-3 years to allow overlap between generations of institute teams, but the intent for each team is to provide a stable base of funding for a five-year period.

SSERVI's mission includes acting as a bridge between several groups, joining together researchers from:

1) scientific and exploration communities, 2) multiple disciplines across a wide range of planetary sciences, and 3) domestic and international communities and partnerships.

The SSERVI central office is located at NASA Ames Research Center in Mountain View, CA. The administrative staff at the central office forms the organizational hub for the domestic and international teams and enables the virtual collaborative environment. Interactions with geographically dispersed teams across the U.S., and global partners, occur easily and frequently in a collaborative virtual environment. This talk will consist of an overview of SSERVI’ s mission, current US teams and International Partners.

Keywords: Moon, Asteroids, Lunar, Exploration

©2019. Japan Geoscience Union. All Right Reserved. 

[J] Poster | P (Space and Planetary Sciences )：P-PS Planetary Sciences

Thu. May 30, 2019 3:30 PM - 5:00 PM JST | Thu. May 30, 2019 6:30 AM - 8:00 AM UTC | Poster Hall International Exhibition Hall8, Makuhari Messe_1

## [P-PS08] Lunar science and exploration

convener:Hiroshi Nagaoka(Japan Aerospace Exploration Agency), Masahiro KAYAMA(Department of Earth and Planetary Material Sciences, Faculty of Science, Tohoku University), Masaki N Nishino(Japan Aerospace Exploration Agency, Institute of Space and Astronautical Science), Tomokatsu Morota(Graduate School of Environmental Studies, Nagoya University)

Scientific data sets acquired by not only Japanese lunar mission SELENE (Kaguya), but also other countries' missions, have become new standard for lunar science. Analyses of these data have been providing several new knowledge and changing some hypotheses into the truth of the Moon. In concurrence with these studies, some countries including Japan are planning future lunar missions. In this session, we will discuss scientific results based on newly acquired lunar data, strategy for future missions including SLIM, and theoretical and experimental studies for lunar science.<br/>

### [PPS08-P01] Estimation of lava tube cave height below the vertical hole from the surface topography of the Moon

*Tsutomu Honda[1] (1.Vulcano-speleological Society)

### [PPS08-P02] Detecting mare basalts intruded into the crust on the early Moon

*Ayame Ikeda[1], Tomokatsu Morota[2], Hiroshi Nagaoka[3] (1.Department of Science, Nagoya University, 2.Graduate School of Enviromental Studies, Nagoya University, 3.Japan Aerospace Exploration Agency)

### [PPS08-P03] Distribution of major minerals around the Crisium and Moscoviense basins of the Moon revealed by SELENE Multiband Imager

Yuji Agatsuma[1], *Naru Hirata[1], Satoru Yamamoto[2], Makiko Ohtake[3] (1.Dep. of Computer Science and Engineering, Univ. of Aizu, 2.J-spacesystems, 3.Department of Planetary Science, Institute of Space and Astronautical Science, Japan Aerospace Exploration Agency)

### [PPS08-P04] Searching for lunar swirls with deep learning

*Yurika Iwabuchi[1], Yoshiko Ogawa[1] (1.The University of Aizu)

### [PPS08-P05] Lunar surface feature reconstruction by deep learning using synthetic data

*Koichi Tsuru[1], Toru Kouyama[1], Ryosuke Nakamura[1] (1.National Institute of Advanced Industrial Science and Technology)

### [PPS08-P06] Evaluation of the influence of alkali elements on hydrogen solubility of clinopyroxene for estimating water content of lunar mantle

*Miki Muranushi[1], Akio Suzuki[1], Masahiro KAYAMA[1], Tsuyoshi MIYAMOTO[2] (1.Graduate school of Science, Tohoku university , 2.Center for Northeast Asian Studies, Tohoku university)

### [PPS08-P07] Preliminary examination of mineral structure effect on relative permittivity

*Makito Kobayashi[1], Takafumi Niihara[2], Hideaki Miyamoto[2,1] (1.Department of Earth and Planetary Science, School of Science, University of Tokyo, 2.Department of Systems Innovation, School of Engineering, University of Tokyo)

### [PPS08-P08] Lunar surface magnetic field intensity in the solar wind inferred from electron reflectometry

*Tomoki Kawaguchi[1], Yuki Harada[1], Yoshifumi Saito[2], Shoichiro Yokota[3], Masaki N Nishino[4], Hideyuki Usui[5], Yohei Miyake[6], Hideo Tsunakawa[7], Daiba Kato[8] (1.Dept. Geophysics, Kyoto Univ., 2.Solar System Science Division, Institute of Space and Astronautical Science, Japan Aerospace Exploration Agency, 3.Graduate School of Science, Osaka University, 4.Institute for Space-Earth Environmental Research,

Nagoya University, 5.Graduate school of system informatics Kobe University, 6.Education Center on Computational Science and Engineering, Kobe University, 7.Deparment of Earth and Planetary Sciences, Tokyo Institute of Technology, 8.The University of Tokyo)

---

[PPS08-P09] Objective and Current Development Status of Multi-Band Camera on SLIM

*Yusuke Nakauchi[1], Kazuto Saiki[2], Makiko Ohtake[1], Hiroaki Shiraishi[1], Chikatoshi Honda[3], Hiroyuki Sato[1], Yoshiaki Ishihara[4], Takao Maeda[5], Masatsugu Otsuki[1], Sin-ichiro Sakai[1], Shujiro Sawai[1], SLIM Project Team (1.Japan Aerospace Exploration Agency, 2.Osaka University, 3.Aizu University, 4.National Institute for Environmental Studie, 5.Chuo University)

---

[PPS08-P10] Monte Carlo simulation of neutron production and transport in the Moon: Effect of lunar subsurface water

*Hiroki Kusano[1], Yuzuru Karouji[1], Hiroshi Nagaoka[1], Naoyuki Yamashita[2], Makoto Hareyama[3] (1.Japan Aerospace Exploration Agency, 2.Planetary Science Institute, 3.St. Marianna University School of Medicine)

---

[PPS08-P11] **Exploration of ice deposits on the Moon using continuous seismic source system**

*Yuichiro Nagata[1], Takeshi Tsuji[1,2], Hideaki Miyamoto[9], Taichi Kawamura[3], Akito Araya[4], Yoshiaki Ishihara[5], Kazunori Ogawa[6], Taizo Kobayashi[7], Yuzuru Karouji[8], Satoshi Tanaka[10] (1.Department of Earth Resources Engineering, Kyushu University, 2.International Institute for Carbon-Neutral Energy Research (WPI-I2CNER), Kyushu University, 3.Institut de Physique du Globe de Paris, 4.Earthquake Research Institute, University of Tokyo, 5.National Institute for Environmental Studies, 6.Kobe University, 7.Ritsumeikan University, 8.Japan Aerospace Exploration Agency, 9.University of Tokyo, 10.Department of Solid Planetary Sciences Institute of Space and Astronautical Science)

---

[PPS08-P12] Orbit determination of the Chang'E-5 Test 1 and a new gravity field model

*shanhong liu[1], Jianguo Yan[1] (1.Wuhan University)

# Estimation of lava tube cave height below the vertical hole from the surface topography of the Moon

*Tsutomu Honda[1]

1. Vulcano-speleological Society

**[Introduction]** The inclination(sin $\alpha$) and slope angle($\alpha$) of the near surface of the vertical hole and the rille,where the cavity of the lava tube cave is assumed to be under it, can be obtained from the LROC Quick Map[(1)] made from the data of the US LRO. Marius Hills Hole (MHH), Mare Tranquillitatis Hole (MTH), Mare Ingenii Hole (MIH)[(2~5)] discovered by Haruyama et al., furthermore Lacus Mortis vertical holes[(6,7)], Rille structure discovered by Chandrayaan-1[(8)], and Sinus Iridum Pit [(9)] were examined. For the case where the direction of flow of the lava is unknown, the direction showing the angle at which the highest inclination angle of the surrounding is adopted. The cavity height is obtained from the lava (Bingham fluid) flow limit condition H = nfb / ($\rho$ gsin $\alpha$) in the tube [(10~12)], where for n = 4 , H is a tube height with circular section, for n = 3,H is a tube height with finite width rectangular cross section, for n= 2 , H is a tube height with infinite width rectangular section. Here, the gravitational acceleration g = 1.62 m / $sec^2$, the lava density $\rho$ = 2500 kg / $m^3$, and the yield strength values fb = 100 Pa and 200 Pa [(13)].**[Marius Hills Hole (MHH)]** MHH has a diameter of 57 m ×48 m, a depth of 48 m, a ceiling thickness of 31 m, and a cavity height of 17 m. The inclination angle of the rille surface in the vicinity where MHH exists is considered to be in the range of 0.28 degree to 0.69 degree and the tube height was obtained with the lava yield strength value 100 Pa to 200 Pa. For a finite width rectangular section tube, the height is 15.4 m at 100 Pa, which is close to the cavity height of 17 m of MHH.**[Mare Tranquilitatis Hole (MTH)]** MTH has a diameter of 99 m ×84 m, a depth of 107 m, a ceiling thickness of 47 m, and a cave cavity height of 60 m. The inclination angle in the highest direction near MTH was 0.62 degree. A finite width rectangular section tube height is 6.7 m to 13.5 m at 100 Pa to 200 Pa, which is smaller than the cavity height 60 m. The actual angle of the inclination of the tube may be lower.**[Mare Ingenii Hole (MIH)]** MIH has a diameter of 103 mx 66 m and a depth of 37 - 63 m. As the highest inclination angle is 0.21 degree around MIH, the finite width rectangular cross section tube height is estimated as 20 to 40 m at 100 Pa to 200 Pa. As the vertical hole depth is 37 to 63 m, so the ceiling thickness is considered to be about 20 m.**[Pit of Lacus Mortis]** Lacus Mortis's pit has a diameter of 60 m ×100 m and a depth of 114 m. The highest inclination angle around the pit is 1.2 degrees. So,the finite width rectangular cross section tube height is estimated as 3.7 m - 7.4 m at 100 Pa - 200 Pa. As the vertical hole depth is 114 m, so the ceiling thickness seems to be quite thick.**[Rille discovered by Chandrayaan - 1]** The inclination angle of the undamaged portion in the central part of the rille is 0.93 degree. The height of the finite width rectangular cross section tube height is estimated as 4.6 m to 9.2 m at 100 Pa to 200 Pa. Considering that the rille depth at both ends of the undamaged portion is 8 m to 17 m, the ceiling thickness is considered to be extremely thin if there is a cavity under the undeflected ceiling of the rille.**[Pit of Sinus Iridum]** Sinus Iridum Pit has a diameter of 70 m ×30 m and a depth of 20 m. The maximum inclination angle around the Sinus Iridum Pit is 0.83 degree. The height of the finite width rectangular section tube is estimated as 5.1 m to 10.2 m at 100 Pa to 200 Pa. The ceiling thickness will be on the order of 10 to 15 meters.

**[Conclusion]** Table 1 shows a summary of estimates of cavity heights of possible lava tube caves under the holes or pits and rilles. Lava tube cave height was estimated from the LROC Quick Map by measuring the slope of the surface. However, due to the possible lunar crustal deformation after tube formation, there is a possibility that the used slope angle may be different from the actual slope angle of the lava tube below the surface. The estimated cavity height is only a rough estimate and it is expected to be demonstrated by further detailed examination and exploration.

©2019. Japan Geoscience Union. All Right Reserved. 

**References:see japanese version.**

Keywords: Moon, pit, lava tube

表１　縦孔/**Rille**下に想定される溶岩チューブ洞窟の空洞高さの推定値

| 縦孔/Rille | 降伏値: fb | 傾斜率:sinα | 傾斜角度: α | 円形断面チューブ高さ: H=4fb/(ρgsinα) | 有限幅矩形断面チューブ高さ: H=3fb/(ρgsinα) | 無限幅矩形断面チューブ高さ: H=2fb/(ρgsinα) |
|---|---|---|---|---|---|---|
| Marius Hills Hole(MHH) 直径57mx48m,深さ48m, 天井厚さ31m, 空洞高さ17m | 100Pa | 0.0128 | 0.78° | 7.7m | 5.8m | 3.9m |
| | 200Pa | 0.0128 | 0.78° | 15.4m | 11.6m | 7.7m |
| | 100Pa | 0.0048 | 0.28° | 20.6m | 15.4m | 10.3m |
| | 200Pa | 0.0048 | 0.28° | 41.2m | 30.9m | 20.6m |
| Mare Tranquillitatis Hole (MTH) 直径99mx84m, 深さ107m,天井厚さ47m, 空洞高さ60m | 100Pa | 0.0110 | 0.62° | 9.0m | 6.7m | 4.5m |
| | 200Pa | 0.0110 | 0.62° | 18.0m | 13.5m | 9.0m |
| Mare Ingenii Hole(MIH) 直径103mx66m, 深さ37m~63m | 100Pa | 0.0037 | 0.21° | 26.7m | 20m | 13.3m |
| | 200Pa | 0.0037 | 0.21° | 53.4m | 40m | 26.7m |
| Lacus Mortis Pit 直径60mx100m, 深さ114m | 100Pa | 0.0201 | 1.2° | 4.9m | 3.7m | 2.5m |
| | 200Pa | 0.0201 | 1.2° | 9.8m | 7.4m | 4.9m |
| Rille found by Chandrayaan-I 深さ8m~17m | 100Pa | 0.0162 | 0.93° | 6.1m | 4.6m | 3.1m |
| | 200Pa | 0.0162 | 0.93° | 12.2m | 9.2m | 6.2m |
| Sinus Iridum Pit 直径70mx30m, 深さ20m | 100Pa | 0.0145 | 0.83° | 6.8m | 5.1m | 3.4m |
| | 200Pa | 0.0145 | 0.83° | 13.6m | 10.2m | 6.8m |

©2019. Japan Geoscience Union. All Right Reserved. 

# Detecting mare basalts intruded into the crust on the early Moon

*Ayame Ikeda[1], Tomokatsu Morota[2], Hiroshi Nagaoka[3]

1. Department of Science, Nagoya University, 2. Graduate School of Enviromental Studies, Nagoya University, 3. Japan Aerospace Exploration Agency

To understand the lunar thermal evolution, unraveling the eruption rate of mare basalts and its temporal variation is important. Absolute dating of lunar basalt samples returned by the Apollo and Luna missions indicated that lunar magma eruptions were active from 3.9 to 3.0 Ga [e.g., Nyquist and Shih, 1992]. Also, the age of basalt fragments in the lunar meteorite is estimated to be 4.35 Ga by radiometric dating [Terada et al., 2007], implying that mare magmatism already started at that time. However, the magnitude of magma activity before the basin-forming period (>3.9 Ga) remains unknown, because these magmas could hardly extrude to the surface before topographic lows were formed by basin-forming impacts.

In order to verify the existence of pre-basin basalts and estimate its total volume we investigated the inner ring of the Crisium basin, which consists of deposits of crustal materials ejected by the Crisium-forming impact. In this study, we used topographic data and multiband images obtained by Terrain Camera and Multiband Imager onboard Kaguya. The inner-ring area was defined as area with an altitude higher than -1.3 km. Mare basalts in the inner-ring area were identified based on the optical matuality, the FeO content, and the spectral absorption depths at 950nm, 1050 nm and 1250 nm.

The mean FeO content of the fresh regions in the inner-ring area was calculated to be 6.75 wt%, suggesting the limited amount of basalts in the area. However, we found some basaltic outcrops at interior and ejecta of smaller craters excavating part of the ring materials. The surface area of the basaltic outcrops is estimated to be $1.3\times10^{-3}$ % of the inner-ring area. By assuming that the area abundance of the basalts in the inner ring is equal to the volume abundance, we estimated to be the total volume of basaltic intrusions of $1.2\times10^{5}$ $km^3$. Based on comparison with the total volume of Mare Crisium ($2.0\times10^{5}$–$7.2\times10^{5}$ $km^3$) [Mulis et al., 1992; Solomon and Head, 1980], we conclude that mare volcanism before the Crisium-forming impact was less active than post-Crisium volcanism.

Keywords: the Moon, Crisium basin, Mare basalt

©2019. Japan Geoscience Union. All Right Reserved. 

# Distribution of major minerals around the Crisium and Moscoviense basins of the Moon revealed by SELENE Multiband Imager

Yuji Agatsuma[1], *Naru Hirata[1], Satoru Yamamoto[2], Makiko Ohtake[3]

1. Dep. of Computer Science and Engineering, Univ. of Aizu, 2. J-spacesystems, 3. Department of Planetary Science, Institute of Space and Astronautical Science, Japan Aerospace Exploration Agency

Distribution of major minerals consisting the lunar crust and mantle (olivine, plagioclase, Hi-Ca pyroxene, and Low-Ca pyroxene) around the Crisium and Moscoviense basins of the Moon is revealed by SELENE Multiband Imager.

Keywords: Moon, multiband imager, olivine, plagioclase, HCP, LCP

©2019. Japan Geoscience Union. All Right Reserved. 

# Searching for lunar swirls with deep learning

*Yurika Iwabuchi[1], Yoshiko Ogawa[1]

1. The University of Aizu

Lunar swirls are winding high albedo patterns not-correlated with topography.They have irregular shapes, distributions, and various spatial scales. About 10 swirls have been discovered so far by visual inspection. However, it is expected there would be more swirls. We have been working on applying Deep Learning to automaticallyfind lunar swirls candidates of small-medium size especially.

The objective of this study is building and updating learning models for automatic identification of lunar swirls and evaluating the models. We aim to search for lunar swirls with Deep Learning. We set the target area in Mare Ingenii area (20˚-50˚S, 150˚-180˚E).

The point to identifying swirl is to distinguish albedo features (swirls) from shading patterns (non-swirls). Therefore, we allocated two kinds of data to the 3 bands in RGB image: Camera imager for R band, and topography data for G and B bands following Kato et al. [2018].As camera image, we use the Multi-band Imager (MI) data from Kaguya satellite. As for DEM data, the data of SLDEM2013 are used. By creating such unique “Combined Image”, we can combine different kinds of information collectively as one image.

We built learning models using the framework of Caffe. We increased variation and quantity of training data to collect data from all confirmed swirl areas and to rotate original images in 3 directions. Totally 212 images (each image covers 1 by 1 deg.) were used as training data. We prepared correct answer data in target area and conduct cross validation for evaluation of results and models. The model building and evaluation were sequentially cycled.

Running the latest learning model, we found 275 images as swirl candidate scenes out of 832 images in the Mare Ingenii. Focusing on True positive rate, the best swirl detection was performed by the learning model built based on training data set which increases variation and quantity of swirl images and ratio of swirl images to non-swirl images.

Keywords: swirl, deep learning, Moon, automatic detection, exploration data

©2019. Japan Geoscience Union. All Right Reserved. 

# Lunar surface feature reconstruction by deep learning using synthetic data

*Koichi Tsuru[1], Toru Kouyama[1], Ryosuke Nakamura[1]

1. National Institute of Advanced Industrial Science and Technology

Various machine learning methods have been proposed to detect lunar surface features such as craters and boulders from satellite imagery. However, many of them need a huge manual effort to create a training data set even to solve one task.

Hence, so far, we have focused on several algorithms based on Generative Adversarial Networks (GANs) that enable highly accurate image generation even from a small amount of training set, and we examined to use Cycle-Consistency Adversarial Networks (CycleGAN) which can learn translation relationship between two image groups, such as a group of Moon surface images and a group of crater maps, for crater detection on the Moon surface. The CycleGAN does not require paired images, whereas it learns the relationship between the two image groups with an unpaired training manner, and images in one of the two groups can be simulated label data.

Initially, we tried to translate a satellite imagery to a labeled image (i.e. crater map), in which the labeled image is produced by simulations based on statistical crater size-frequency distribution. Although it could reduce the annotation cost drastically by the automatic generation of the label data, we found that the learning was not stable and not precise because the texture was too different between the satellite imagery and the simple labeled image. Then, we considered that, in order to improve the performance, it is necessary to train a network with multiple feature labels (i.e. lunar surface elevation, albedo, and shadow maps, and crater and boulder distributions) that characterize the appearance of the Moon surface to be observed.

In this work, we adopted a two-step deep learning framework with fine-tune models trained by 1) generating feature labels from a modeled surface image which is based on given feature labels, and synthesizing the labels to generate a lunar surface image that is compared with the original one to check the network performance (at the same time the generated feature labels are also compared with given ones), and then 2) generating feature labels from actual observed data and again synthesizing the labels to generate a lunar surface image to be compared with the actual image. The good advantage of using modeled data and labels as training data is that it becomes easier to cover complicated and enormous amount of possible observation conditions which is necessary for analyzing actual observation data. In addition, highly precise inference can be possible by the simulation even when the existing observation data of a target object covers only insufficient observation conditions.

In the proposed framework, we employed two generative networks that reconstruct terrain features from satellite imagery and to synthesize satellite imagery from terrain features. By applying cycle-consistency for the training that is measured from similarity between the resynthesized satellite image from “reconstructed” features and the original, the actual terrain features are not required in the training phase.

We prepared DEM, albedo map, crater map, boulder map, and shadow map as features for the reconstruction of a target region. In this presentation, we show the results of feature reconstruction from

©2019. Japan Geoscience Union. All Right Reserved. 

the actual observed SELENE Terrain Camera imagery.

Keywords: Moon, Feature Detection, Deep Learning, SELENE

©2019. Japan Geoscience Union. All Right Reserved. 

# Evaluation of the influence of alkali elements on hydrogen solubility of clinopyroxene for estimating water content of lunar mantle

*Miki Muranushi[1], Akio Suzuki[1], Masahiro KAYAMA[1], Tsuyoshi MIYAMOTO[2]

1. Graduate school of Science, Tohoku university , 2. Center for Northeast Asian Studies, Tohoku university

In the early history of lunar exploration, lunar samples returned by the Apollo missions revealed that volatile elements are depleted on the Moon. Almost all volatile components were thought to be eliminated by the giant impact event that probably led to the formation of the Moon. However, recent microanalyses of lunar samples have discovered hydroxyl or water in the constituent minerals. These observations suggest that the lunar mantle may not be entirely dry and contain water to same extent as the Earth’ s mantle. The lunar volcanic glasses of Apollo 15 and 17 were measured by SIMS and about 4-46 ppm water were detected (Saal et al., 2008). Hui et al. (2013, Nature Geosci.) detected up to 2.7 ppm water in plagioclase grains from the lunar highland crust sample. They suggest that the initial water content of the lunar magma ocean (LMO) reaches approximately 320 ppm water content. As a result of these studies, water content and the process that the moon got water has attracted a lot of attention.
Since no indigenous hydrous minerals have been found in the moon, it is likely that anhydrous mineral possess water as a reservoir in the lunar mantle. Water exists in the Earth’ s mantle as hydrous mineral, anhydrous mineral, silicate melt, liquid water, and their intermediate form. In the Earth’ s mantle, hydrogen may be incorporated as defects in nominally anhydrous minerals (NAMs) such as Olivine, pyroxene and garnet. (e.g., Smyth et al., 1991). Especially, clinopyroxene (Cpx) shows the maximum water content in the upper mantle xenolith (Inglin and Skogby, 2000). Cpx has possibility of being water reservoir in the lunar mantle due to its crystal structure and chemical composition.
Nakamura et al. (2012) confirmed the presence of calcium rich pyroxene in the South Pole-Aitken (SPA). It is possible that the lunar upper mantle has been excavated and exposed in SPA (Cintala and Grieve, 1998; Lucey et al., 1998). Cpx is likely to be one of the major minerals of the lunar mantle as well as the earth.
Since there is less hydrous mineral in the Moon, water should concentrated in KREEPy basalt that assumed to be the final part of the lunar magma ocean solidification. In this study, we target the measurement of hydrogen solubility of Cpx crystallized from alkali-rich magma.
We conducted a high temperature and high pressure experiment at 1 GPa using a piston cylinder apparatus at Bayreiches Geoinstitut, Germany. Starting material is the natural alkali basalt powder (Haku-4 reported by Kuritani et al., 2009), adding ~5 wt. % water with a micro-syringe. For the Fourier Transform Infrared (FT-IR) analysis, it is necessary to produce Cpx crystals larger than 50 μm. Therefore, in order to considerate conditions suitable for sample synthesis, we conducted several experiments that the initial temperature, cooling rate, the temperature after cooling and the retention time were changed. We report the conditions that succeeded in creating the Cpx large enough for FT-IR analysis and the future plans.
Funding acknowledgment: This work was partially supported by the JSPS Japanese-German Graduate Externship.

Keywords: nominally anhydrous minerals , lunar mantle , alkali basalt

©2019. Japan Geoscience Union. All Right Reserved. 

# Preliminary examination of mineral structure effect on relative permittivity

*Makito Kobayashi[1], Takafumi Niihara[2], Hideaki Miyamoto[2,1]

1. Department of Earth and Planetary Science, School of Science, University of Tokyo, 2. Department of Systems Innovation, School of Engineering, University of Tokyo

The surface of the Moon is covered with regolith formed by the bombardment of meteorites and micro-meteorites. Although drill core samples collected during Apollo missions revealed that the subsurface (1-2 m) structure changes vertically over centimeter to meter scales at landing sites, deeper (> 10 m) structure and spatial continuity is still unknown. Ground Penetrating Radar (GPR) can detect potential variations in subsurface structure which result in permittivity contrasts, therefore, understanding of factors that affect the permittivity of the regolithis important.

Relative permittivity depends on multiple factors such as radar frequency, porosity, temperature, moisture content and chemical composition (e.g., Campbell and Ulrichs, 1969). Correlation between Ti and Fe concentration and the relative permittivity of Apollo samples was previously addressed by Shkuratov and Bondarenko(2001). On the other hand, Fa and Wieczorek (2012) reported that there was no correlation between chemical composition and relative permittivity althoughthe bulk density varied between samples in this study. Because previous workshave not focused specifically on the influence of mineral composition (while keeping bulk density and composition constant), we prepared samples to isolate the influence of mineral composition on relative permittivity.

Bulk density of regolith mostly depends on porosity and the constituent minerals among samples which have the same bulk chemical composition. Lunar regolith contains Fe- and/or Ti-bearing spinel minerals and other oxide minerals (e.g. ilmenite, magnetite, armarcolite), andthe abundance of those minerals depends on the sample. Differences in abundance of constituent minerals indicate different origins of precursor rocks. If we can detect the permittivity contrast resulting from those mineral differences, it could help further our understanding of the subsurface structure and evolution of surface of the Moon. Therefore, we examine whether crystal types of opaque minerals with the samechemicalcomposition affect the relative permittivity.

We prepare a mixture of rutile and iron oxide (II) to create same chemical composition as ilmenite. Porosities of samples are uniform (40%), therefore, densities of the mixture and ilmenite samples are 2.96 and 2.90, respectively. In order to avoid the effect of moisture content, samples are dried for a few days, and we then measure the relative permittivity using a coaxial probe in the range of 1 MHz to 6 GHz at room temperature.

There is a difference of relative permittivity of about 3.6-4.2 when comparing the mixture (10.6-10.7) with ilmenite (6.4-7.0). This result indicates that crystal structure can affect the relative permitivity.In this presentation, we will discuss the effect in more detail.

References:

©2019. Japan Geoscience Union. All Right Reserved. 

Campbell, Malcolm J., and Juris Ulrichs. "Electrical properties of rocks and their significance for lunar radar observations." *Journal of Geophysical Research* 74.25 (1969): 5867-5881.

Fa, Wenzhe, and Mark A. Wieczorek. "Regolith thickness over the lunar nearside: Results from Earth-based 70-cm Arecibo radar observations." *Icarus* 218.2 (2012): 771-787.

Shkuratov, Yurij G., and Nataliya V. Bondarenko. "Regolith layer thickness mapping of the Moon by radar and optical data." *Icarus*149.2 (2001): 329-338.

Keywords: relative permittivity, GPR, lunar regolith, ilmenite

©2019. Japan Geoscience Union. All Right Reserved. 

# Lunar surface magnetic field intensity in the solar wind inferred from electron reflectometry

*Tomoki Kawaguchi[1], Yuki Harada[1], Yoshifumi Saito[2], Shoichiro Yokota[3], Masaki N Nishino[4], Hideyuki Usui[5], Yohei Miyake[6], Hideo Tsunakawa[7], Daiba Kato[8]

1. Dept. Geophysics, Kyoto Univ., 2. Solar System Science Division, Institute of Space and Astronautical Science, Japan Aerospace Exploration Agency, 3. Graduate School of Science, Osaka University, 4. Institute for Space-Earth Environmental Research, Nagoya University, 5. Graduate school of system informatics Kobe University, 6. Education Center on Computational Science and Engineering, Kobe University, 7. Deparment of Earth and Planetary Sciences, Tokyo Institute of Technology, 8. The University of Tokyo

The Moon is classified as a nonmagnetized celestial body that does not hold a global, intrinsic magnetic field and atmosphere, and most of the dayside lunar surface is bombarded by the solar wind plasma. Therefore, most of the solar wind collides with the lunar surface and is absorbed. Meanwhile, some regions called magnetic anomaly of the lunar surface are locally shielded from the solar wind by magnetic fields of crustal origin. The interaction between the lunar crustal magnetic fields and the solar wind is an important topic relevant to the plasma environment around the Moon. Research on the interaction between the solar wind and the strong magnetic anomaly has been advanced so far, but it remains unclear how the magnetic field strength on the dayside lunar surface varies globally.

The global distribution of crustal magnetic field strength has been investigated by electron reflectometry, which remotely infers the surface magnetic field strength from the loss cone angle of reflected electrons from the lunar crustal magnetic field, using the magnetic mirror effect of the moon periphery electron. As the aim of the conventional electron reflectometry is measurements of the strength of the lunar crustal magnetic field itself, a standard practice is to use data obtained on the night side of the Moon and within the terrestrial magnetotail lobes with less influence of the solar wind plasma. Here we apply the electron reflectometry to the data obtained on the day side of the Moon in the solar wind, thereby investigating variations of the surface magnetic field strength caused by the interaction with the solar wind. By applying this method to the data of Kaguya when exposed to the solar wind on the lunar day side, the magnetic field became stronger globally.

We utilized data obtained by the electron spectrum analyzers (MAP-PACE-ESA) and magnetometer (MAP-LMAG) on board Kaguya. We investigated a surface magnetic field intensity by analyzing electron pitch angle distributions of each different energy band measured when the day side lunar surface was exposed to the solar wind. As a result, we revealed energy dependence on the pitch angle distribution of electrons. This suggests that the cutoff pitch angles are influenced by the potential difference between the lunar surface and the satellite and the electric field generated by decoupling of electrons and ions. We will discuss the solar wind dynamic pressure control of the lunar surface magnetic field intensity with energy dependence.

©2019. Japan Geoscience Union. All Right Reserved. 

# Objective and Current Development Status of Multi-Band Camera on SLIM

*Yusuke Nakauchi[1], Kazuto Saiki[2], Makiko Ohtake[1], Hiroaki Shiraishi[1], Chikatoshi Honda[3], Hiroyuki Sato[1], Yoshiaki Ishihara[4], Takao Maeda[5], Masatsugu Otsuki[1], Sin-ichiro Sakai[1], Shujiro Sawai[1], SLIM Project Team

1. Japan Aerospace Exploration Agency, 2. Osaka University, 3. Aizu University, 4. National Institute for Environmental Studie, 5. Chuo University

Smart Lander for Investigating Moon (SLIM) project is on going in JAXA. The main objective of this project is to demonstrate various techniques for “pin-point landing” on the moon. SLIM spacecraft is a small lander. It is designed to achieve “pin-point landing” to 100 meter-order error circle. In order to “pin-point landing” of this level, SLIM mission will demonstrate new image-based onboard navigation system and autonomous landing along with several other new technologies (e.g. “tow stage” landing sequence, metal shock absorbers). The SLIM spacecraft weight is ~730 kg wet mass and ~200 kg class dry mass, both of which are more lightweight than previous lunar landers. The spacecraft will be launched with a Japanese rocket H-IIA in 2021 or 2022. Landing on (25.2ºE, 13.3ºS) located in the west of Mare Nectaris is planned.

After landing, SLIM project is planning to observe around landing site using Multi-Band Camera (MBC). The observational mission is positioned as extra success. MBC will observe olivine and estimate Mg# of it. MBC is a compact VIS-NIR camera composed of an imaging sensor (InGaAs), a filter-wheel with 10 band-pass filters, a telephoto optical system, and a movable mirror for panning and tilting. The sensor has sensitivity at wavelength from 700 to 1700 nm, which covers the characteristic ab-sorption bands of lunar minerals. The telephoto optical system can focus on an object from 1.5 to 30 m distance. The imaging sensor has 640 ×512 pixels with 20 $\mu$m pitch. The 4º field of view corresponds to the spatial sampling of 1.3 mm per pixel at 10 m from the lander. Using the movable mirror, observable scanning area is ~50º in azimuth and ~70º in elevation. This makes it possible to observe the size distribution of boulders around the lander. The observation wavelength of band pass filters were selected 10 bands: 750, 920, 950, 970, 1000, 1050, 1100, 1250, 1550, and 1650 nm. The width of their bands is 30nm.

Keywords: Moon, SLIM, reflectance spectra, Olivine

©2019. Japan Geoscience Union. All Right Reserved. 

# Monte Carlo simulation of neutron production and transport in the Moon: Effect of lunar subsurface water

*Hiroki Kusano[1], Yuzuru Karouji[1], Hiroshi Nagaoka[1], Naoyuki Yamashita[2], Makoto Hareyama[3]

1. Japan Aerospace Exploration Agency, 2. Planetary Science Institute, 3. St. Marianna University School of Medicine

The intensity of thermal, epithermal, and fast neutrons emitted from a planetary surface provides information on the surface elemental composition, particularly on the hydrogen abundance. In an airless planetary surface, the galactic cosmic rays produce fast neutrons via nuclear interactions in the subsurface materials within a depth of tens centimeters. Then, the fast neutrons are moderated by interactions with subsurface materials including the secondary neutron production. This neutron transport process is terminated at the thermal neutron capture or the neutron leakage from surface. Because the hydrogen atom has a large elastic scattering cross section for a neutron and a nearly identical mass as a neutron, neutrons are efficiently moderated by the elastic scattering with hydrogen atoms. Therefore, the leakage neutron intensity strongly depends on the hydrogen abundance as well as the surface elemental composition. Neutron spectroscopy is thus well suited to detect subsurface water which may present at the lunar polar region. It is essential to obtain the abundance and distribution of lunar subsurface water from the viewpoint of planetary science and space resources for future manned activities.

In this study, the neutron production and transport in the Moon was modeled by Monte Carlo simulation with Geant4 10.3.p03. The effect of subsurface hydrogen abundance and spatial distribution was studied for in-situ water search in future lunar polar landing explorations. The leakage neutron intensity produced by protons and alpha particles in galactic cosmic rays was calculated for the lunar highland composition mixed with various amounts of hydrogen. The production depth and flux of subsurface neutrons, and the production depth of leakage thermal, epithermal, and fast neutrons were also calculated. It was confirmed that the leakage neutron intensity depends on the subsurface hydrogen abundance. The epithermal neutron intensity is particularly sensitive to the presence of subsurface hydrogen. Most of the leakage neutrons were produced within a depth of about 100 g/cm$^2$, which means that the neutron spectroscopy is mainly sensitive to the subsurface water in the top of surface with about 50 cm in depth depending on the surface density. When a dry layer presents at the top of surface, the leakage neutron intensity was found to depend on the dry layer thickness. The variation of leakage neutron intensity was detectable for the dry layer thickness less than about 80 g/cm$^2$. The behavior of lunar subsurface neutrons and its sensitivity for lunar subsurface water will be presented and discussed.

Keywords: Lunar water, Lunar polar region, Lunar landing exploration, Neutron spectroscopy, Galactic cosmic ray, Monte Carlo simulation

©2019. Japan Geoscience Union. All Right Reserved. 

# Exploration of ice deposits on the Moon using continuous seismic source system

*Yuichiro Nagata[1], Takeshi Tsuji[1,2], Hideaki Miyamoto[9], Taichi Kawamura[3], Akito Araya[4], Yoshiaki Ishihara[5], Kazunori Ogawa[6], Taizo Kobayashi[7], Yuzuru Karouji[8], Satoshi Tanaka[10]

1. Department of Earth Resources Engineering, Kyushu University, 2. International Institute for Carbon-Neutral Energy Research (WPI-I2CNER), Kyushu University, 3. Institut de Physique du Globe de Paris, 4. Earthquake Research Institute, University of Tokyo, 5. National Institute for Environmental Studies, 6. Kobe University, 7. Ritsumeikan University, 8. Japan Aerospace Exploration Agency, 9. University of Tokyo, 10. Department of Solid Planetary Sciences Institute of Space and Astronautical Science

We have been designing and developing an active seismic exploration package with seismometers, active seismic source and anchoring system. Our seismic exploration package was designed to investigate from shallow formation (i.e., ice saturation) to deep formation (i.e., thickness of regolith) of the Moon. Here we present the basic concept of our seismic exploration package and its experimental results. We then discuss the possibilities of future space missions. We evaluate the relation between the S-wave velocity and the ice saturation, and found that S-wave velocity largely increase due to ice deposition (low ice saturation). To evaluate our active-source seismic exploration system, furthermore, we conducted seismic exploration in the test field in JAXA. The test field is filled with loose sands of ~50cm thickness. In this experiment, we conducted seismic survey with several acquisition parameters. When we applied the active seismic survey for small-size receiver array, we retrieved clear shot gather. We further calculated dispersion curve from the shot gather and obtained S-wave velocity profile beneath the array using inversion. In addition, we could detect the cushioning material whose S wave velocity is lower than sand by surface wave analysis and compare the result with the dispersion curve which has no buried material. These results demonstrate that S-wave velocity in shallow formation was accurately estimated, suggesting that ice can be identified as anomalous high S-wave velocity via our seismic system. When the seismometer interval is long, the attenuation of the surface wave is large. However, the refracted P-wave can arrive at far offset receivers. Using the refracted wave, we can estimate P-wave velocity of the basement.

©2019. Japan Geoscience Union. All Right Reserved. 

# Orbit determination of the Chang’E-5 Test 1 and a new gravity field model

*shanhong liu[1], Jianguo Yan[1]

1. Wuhan University

We introduce the recently Chang’E 5-Test 1 (CE-5T1) mission overall and its orbit characteristic and present the results on precision orbit determination from the radio science investigation of the CE-5T1 spacecraft. We describe the data, modeling and methods used to achieve position knowledge several times better than the required demand (in total position) for most of arcs, over the period from 10 March 2014 to 28 December 2018. In addition to we try to use the near-continuous radiometric tracking data of CE-5T1 to develop a new lunar gravity field up to degree and order 100, which is solved independently using about four years tracking data. The accuracy of the gravity field model is assessed by multi means, such as gravity spectrum, observational residuals after precision orbit determination, lunar surface gravity anomaly character, admittance/coherence with topography model, and the corresponding physical feature and effect are analyzed. We also make a comparison between this model and the previously models we ever solved, CEGM-01 and CEGM-02. The results indicate the effectiveness and reasonability of this solution process. On the basis of current work, with the Chang’E 5, 6, and 7 under implementing and planning, the prospect of future development of Chinese lunar gravity field detection is presented.

Keywords: Lunar, Chang'E 5T1, precise orbit determination, gravity field model

©2019. Japan Geoscience Union. All Right Reserved. 

[J] Poster | P (Space and Planetary Sciences )：P-PS Planetary Sciences

Thu. May 30, 2019 5:15 PM - 6:30 PM JST | Thu. May 30, 2019 8:15 AM - 9:30 AM UTC | Poster Hall International Exhibition Hall8, Makuhari Messe_1

## [P-PS08] Lunar science and exploration

convener:Hiroshi Nagaoka(Japan Aerospace Exploration Agency), Masahiro KAYAMA(Department of Earth and Planetary Material Sciences, Faculty of Science, Tohoku University), Masaki N Nishino(Japan Aerospace Exploration Agency, Institute of Space and Astronautical Science), Tomokatsu Morota(Graduate School of Environmental Studies, Nagoya University)

Scientific data sets acquired by not only Japanese lunar mission SELENE (Kaguya), but also other countries' missions, have become new standard for lunar science. Analyses of these data have been providing several new knowledge and changing some hypotheses into the truth of the Moon. In concurrence with these studies, some countries including Japan are planning future lunar missions. In this session, we will discuss scientific results based on newly acquired lunar data, strategy for future missions including SLIM, and theoretical and experimental studies for lunar science.<br/>

### [PPS08-P01] Estimation of lava tube cave height below the vertical hole from the surface topography of the Moon

*Tsutomu Honda[1] (1.Vulcano-speleological Society)

### [PPS08-P02] Detecting mare basalts intruded into the crust on the early Moon

*Ayame Ikeda[1], Tomokatsu Morota[2], Hiroshi Nagaoka[3] (1.Department of Science, Nagoya University, 2.Graduate School of Enviromental Studies, Nagoya University, 3.Japan Aerospace Exploration Agency)

### [PPS08-P03] Distribution of major minerals around the Crisium and Moscoviense basins of the Moon revealed by SELENE Multiband Imager

Yuji Agatsuma[1], *Naru Hirata[1], Satoru Yamamoto[2], Makiko Ohtake[3] (1.Dep. of Computer Science and Engineering, Univ. of Aizu, 2.J-spacesystems, 3.Department of Planetary Science, Institute of Space and Astronautical Science, Japan Aerospace Exploration Agency)

### [PPS08-P04] Searching for lunar swirls with deep learning

*Yurika Iwabuchi[1], Yoshiko Ogawa[1] (1.The University of Aizu)

### [PPS08-P05] Lunar surface feature reconstruction by deep learning using synthetic data

*Koichi Tsuru[1], Toru Kouyama[1], Ryosuke Nakamura[1] (1.National Institute of Advanced Industrial Science and Technology)

### [PPS08-P06] Evaluation of the influence of alkali elements on hydrogen solubility of clinopyroxene for estimating water content of lunar mantle

*Miki Muranushi[1], Akio Suzuki[1], Masahiro KAYAMA[1], Tsuyoshi MIYAMOTO[2] (1.Graduate school of Science, Tohoku university , 2.Center for Northeast Asian Studies, Tohoku university)

### [PPS08-P07] Preliminary examination of mineral structure effect on relative permittivity

*Makito Kobayashi[1], Takafumi Niihara[2], Hideaki Miyamoto[2,1] (1.Department of Earth and Planetary Science, School of Science, University of Tokyo, 2.Department of Systems Innovation, School of Engineering, University of Tokyo)

### [PPS08-P08] Lunar surface magnetic field intensity in the solar wind inferred from electron reflectometry

*Tomoki Kawaguchi[1], Yuki Harada[1], Yoshifumi Saito[2], Shoichiro Yokota[3], Masaki N Nishino[4], Hideyuki Usui[5], Yohei Miyake[6], Hideo Tsunakawa[7], Daiba Kato[8] (1.Dept. Geophysics, Kyoto Univ., 2.Solar System Science Division, Institute of Space and Astronautical Science, Japan Aerospace Exploration Agency, 3.Graduate School of Science, Osaka University, 4.Institute for Space-Earth Environmental Research,

Nagoya University, 5.Graduate school of system informatics Kobe University, 6.Education Center on Computational Science and Engineering, Kobe University, 7.Deparment of Earth and Planetary Sciences, Tokyo Institute of Technology, 8.The University of Tokyo)

---

[PPS08-P09] Objective and Current Development Status of Multi-Band Camera on SLIM

*Yusuke Nakauchi[1], Kazuto Saiki[2], Makiko Ohtake[1], Hiroaki Shiraishi[1], Chikatoshi Honda[3], Hiroyuki Sato[1], Yoshiaki Ishihara[4], Takao Maeda[5], Masatsugu Otsuki[1], Sin-ichiro Sakai[1], Shujiro Sawai[1], SLIM Project Team (1.Japan Aerospace Exploration Agency, 2.Osaka University, 3.Aizu University, 4.National Institute for Environmental Studie, 5.Chuo University)

---

[PPS08-P10] Monte Carlo simulation of neutron production and transport in the Moon: Effect of lunar subsurface water

*Hiroki Kusano[1], Yuzuru Karouji[1], Hiroshi Nagaoka[1], Naoyuki Yamashita[2], Makoto Hareyama[3] (1.Japan Aerospace Exploration Agency, 2.Planetary Science Institute, 3.St. Marianna University School of Medicine)

---

[PPS08-P11] **Exploration of ice deposits on the Moon using continuous seismic source system**

*Yuichiro Nagata[1], Takeshi Tsuji[1,2], Hideaki Miyamoto[9], Taichi Kawamura[3], Akito Araya[4], Yoshiaki Ishihara[5], Kazunori Ogawa[6], Taizo Kobayashi[7], Yuzuru Karouji[8], Satoshi Tanaka[10] (1.Department of Earth Resources Engineering, Kyushu University, 2.International Institute for Carbon-Neutral Energy Research (WPI-I2CNER), Kyushu University, 3.Institut de Physique du Globe de Paris, 4.Earthquake Research Institute, University of Tokyo, 5.National Institute for Environmental Studies, 6.Kobe University, 7.Ritsumeikan University, 8.Japan Aerospace Exploration Agency, 9.University of Tokyo, 10.Department of Solid Planetary Sciences Institute of Space and Astronautical Science)

---

[PPS08-P12] Orbit determination of the Chang'E-5 Test 1 and a new gravity field model

*shanhong liu[1], Jianguo Yan[1] (1.Wuhan University)

# Estimation of lava tube cave height below the vertical hole from the surface topography of the Moon

*Tsutomu Honda[1]

1. Vulcano-speleological Society

**[Introduction]** The inclination(sin $\alpha$) and slope angle($\alpha$) of the near surface of the vertical hole and the rille,where the cavity of the lava tube cave is assumed to be under it, can be obtained from the LROC Quick Map[(1)] made from the data of the US LRO. Marius Hills Hole (MHH), Mare Tranquillitatis Hole (MTH), Mare Ingenii Hole (MIH)[(2~5)] discovered by Haruyama et al., furthermore Lacus Mortis vertical holes[(6,7)], Rille structure discovered by Chandrayaan-1[(8)], and Sinus Iridum Pit [(9)] were examined. For the case where the direction of flow of the lava is unknown, the direction showing the angle at which the highest inclination angle of the surrounding is adopted. The cavity height is obtained from the lava (Bingham fluid) flow limit condition H = nfb / ($\rho$ gsin $\alpha$) in the tube [(10~12)], where for n = 4 , H is a tube height with circular section, for n = 3,H is a tube height with finite width rectangular cross section, for n= 2 , H is a tube height with infinite width rectangular section. Here, the gravitational acceleration g = 1.62 m / $sec^2$, the lava density $\rho$ = 2500 kg / $m^3$, and the yield strength values fb = 100 Pa and 200 Pa [(13)].**[Marius Hills Hole (MHH)]** MHH has a diameter of 57 m ×48 m, a depth of 48 m, a ceiling thickness of 31 m, and a cavity height of 17 m. The inclination angle of the rille surface in the vicinity where MHH exists is considered to be in the range of 0.28 degree to 0.69 degree and the tube height was obtained with the lava yield strength value 100 Pa to 200 Pa. For a finite width rectangular section tube, the height is 15.4 m at 100 Pa, which is close to the cavity height of 17 m of MHH.**[Mare Tranquilitatis Hole (MTH)]** MTH has a diameter of 99 m ×84 m, a depth of 107 m, a ceiling thickness of 47 m, and a cave cavity height of 60 m. The inclination angle in the highest direction near MTH was 0.62 degree. A finite width rectangular section tube height is 6.7 m to 13.5 m at 100 Pa to 200 Pa, which is smaller than the cavity height 60 m. The actual angle of the inclination of the tube may be lower.**[Mare Ingenii Hole (MIH)]** MIH has a diameter of 103 mx 66 m and a depth of 37 - 63 m. As the highest inclination angle is 0.21 degree around MIH, the finite width rectangular cross section tube height is estimated as 20 to 40 m at 100 Pa to 200 Pa. As the vertical hole depth is 37 to 63 m, so the ceiling thickness is considered to be about 20 m.**[Pit of Lacus Mortis]** Lacus Mortis's pit has a diameter of 60 m ×100 m and a depth of 114 m. The highest inclination angle around the pit is 1.2 degrees. So,the finite width rectangular cross section tube height is estimated as 3.7 m - 7.4 m at 100 Pa - 200 Pa. As the vertical hole depth is 114 m, so the ceiling thickness seems to be quite thick.**[Rille discovered by Chandrayaan - 1]** The inclination angle of the undamaged portion in the central part of the rille is 0.93 degree. The height of the finite width rectangular cross section tube height is estimated as 4.6 m to 9.2 m at 100 Pa to 200 Pa. Considering that the rille depth at both ends of the undamaged portion is 8 m to 17 m, the ceiling thickness is considered to be extremely thin if there is a cavity under the undeflected ceiling of the rille.**[Pit of Sinus Iridum]** Sinus Iridum Pit has a diameter of 70 m ×30 m and a depth of 20 m. The maximum inclination angle around the Sinus Iridum Pit is 0.83 degree. The height of the finite width rectangular section tube is estimated as 5.1 m to 10.2 m at 100 Pa to 200 Pa. The ceiling thickness will be on the order of 10 to 15 meters.

**[Conclusion]** Table 1 shows a summary of estimates of cavity heights of possible lava tube caves under the holes or pits and rilles. Lava tube cave height was estimated from the LROC Quick Map by measuring the slope of the surface. However, due to the possible lunar crustal deformation after tube formation, there is a possibility that the used slope angle may be different from the actual slope angle of the lava tube below the surface. The estimated cavity height is only a rough estimate and it is expected to be demonstrated by further detailed examination and exploration.

©2019. Japan Geoscience Union. All Right Reserved. 

**References:see japanese version.**

Keywords: Moon, pit, lava tube

表１　縦孔/**Rille**下に想定される溶岩チューブ洞窟の空洞高さの推定値

| 縦孔/Rille | 降伏値: fb | 傾斜率:sinα | 傾斜角度: α | 円形断面チューブ高さ: H=4fb/(ρgsinα) | 有限幅矩形断面チューブ高さ: H=3fb/(ρgsinα) | 無限幅矩形断面チューブ高さ: H=2fb/(ρgsinα) |
|---|---|---|---|---|---|---|
| Marius Hills Hole(MHH) 直径57mx48m,深さ48m, 天井厚さ31m, 空洞高さ17m | 100Pa | 0.0128 | 0.78° | 7.7m | 5.8m | 3.9m |
| | 200Pa | 0.0128 | 0.78° | 15.4m | 11.6m | 7.7m |
| | 100Pa | 0.0048 | 0.28° | 20.6m | 15.4m | 10.3m |
| | 200Pa | 0.0048 | 0.28° | 41.2m | 30.9m | 20.6m |
| Mare Tranquillitatis Hole (MTH) 直径99mx84m, 深さ107m,天井厚さ47m, 空洞高さ60m | 100Pa | 0.0110 | 0.62° | 9.0m | 6.7m | 4.5m |
| | 200Pa | 0.0110 | 0.62° | 18.0m | 13.5m | 9.0m |
| Mare Ingenii Hole(MIH) 直径103mx66m, 深さ37m~63m | 100Pa | 0.0037 | 0.21° | 26.7m | 20m | 13.3m |
| | 200Pa | 0.0037 | 0.21° | 53.4m | 40m | 26.7m |
| Lacus Mortis Pit 直径60mx100m, 深さ114m | 100Pa | 0.0201 | 1.2° | 4.9m | 3.7m | 2.5m |
| | 200Pa | 0.0201 | 1.2° | 9.8m | 7.4m | 4.9m |
| Rille found by Chandrayaan-I 深さ8m~17m | 100Pa | 0.0162 | 0.93° | 6.1m | 4.6m | 3.1m |
| | 200Pa | 0.0162 | 0.93° | 12.2m | 9.2m | 6.2m |
| Sinus Iridum Pit 直径70mx30m, 深さ20m | 100Pa | 0.0145 | 0.83° | 6.8m | 5.1m | 3.4m |
| | 200Pa | 0.0145 | 0.83° | 13.6m | 10.2m | 6.8m |

©2019. Japan Geoscience Union. All Right Reserved. 

# Detecting mare basalts intruded into the crust on the early Moon

*Ayame Ikeda[1], Tomokatsu Morota[2], Hiroshi Nagaoka[3]

1. Department of Science, Nagoya University, 2. Graduate School of Enviromental Studies, Nagoya University, 3. Japan Aerospace Exploration Agency

To understand the lunar thermal evolution, unraveling the eruption rate of mare basalts and its temporal variation is important. Absolute dating of lunar basalt samples returned by the Apollo and Luna missions indicated that lunar magma eruptions were active from 3.9 to 3.0 Ga [e.g., Nyquist and Shih, 1992]. Also, the age of basalt fragments in the lunar meteorite is estimated to be 4.35 Ga by radiometric dating [Terada et al., 2007], implying that mare magmatism already started at that time. However, the magnitude of magma activity before the basin-forming period (>3.9 Ga) remains unknown, because these magmas could hardly extrude to the surface before topographic lows were formed by basin-forming impacts.

In order to verify the existence of pre-basin basalts and estimate its total volume we investigated the inner ring of the Crisium basin, which consists of deposits of crustal materials ejected by the Crisium-forming impact. In this study, we used topographic data and multiband images obtained by Terrain Camera and Multiband Imager onboard Kaguya. The inner-ring area was defined as area with an altitude higher than -1.3 km. Mare basalts in the inner-ring area were identified based on the optical matuality, the FeO content, and the spectral absorption depths at 950nm, 1050 nm and 1250 nm.

The mean FeO content of the fresh regions in the inner-ring area was calculated to be 6.75 wt%, suggesting the limited amount of basalts in the area. However, we found some basaltic outcrops at interior and ejecta of smaller craters excavating part of the ring materials. The surface area of the basaltic outcrops is estimated to be $1.3\times10^{-3}$ % of the inner-ring area. By assuming that the area abundance of the basalts in the inner ring is equal to the volume abundance, we estimated to be the total volume of basaltic intrusions of $1.2\times10^{5}$ $km^3$. Based on comparison with the total volume of Mare Crisium ($2.0\times10^{5}$–$7.2\times10^{5}$ $km^3$) [Mulis et al., 1992; Solomon and Head, 1980], we conclude that mare volcanism before the Crisium-forming impact was less active than post-Crisium volcanism.

Keywords: the Moon, Crisium basin, Mare basalt

©2019. Japan Geoscience Union. All Right Reserved. 

# Distribution of major minerals around the Crisium and Moscoviense basins of the Moon revealed by SELENE Multiband Imager

Yuji Agatsuma[1], *Naru Hirata[1], Satoru Yamamoto[2], Makiko Ohtake[3]

1. Dep. of Computer Science and Engineering, Univ. of Aizu, 2. J-spacesystems, 3. Department of Planetary Science, Institute of Space and Astronautical Science, Japan Aerospace Exploration Agency

Distribution of major minerals consisting the lunar crust and mantle (olivine, plagioclase, Hi-Ca pyroxene, and Low-Ca pyroxene) around the Crisium and Moscoviense basins of the Moon is revealed by SELENE Multiband Imager.

Keywords: Moon, multiband imager, olivine, plagioclase, HCP, LCP

©2019. Japan Geoscience Union. All Right Reserved. 

# Searching for lunar swirls with deep learning

*Yurika Iwabuchi[1], Yoshiko Ogawa[1]

1. The University of Aizu

Lunar swirls are winding high albedo patterns not-correlated with topography.They have irregular shapes, distributions, and various spatial scales. About 10 swirls have been discovered so far by visual inspection. However, it is expected there would be more swirls. We have been working on applying Deep Learning to automaticallyfind lunar swirls candidates of small-medium size especially.

The objective of this study is building and updating learning models for automatic identification of lunar swirls and evaluating the models. We aim to search for lunar swirls with Deep Learning. We set the target area in Mare Ingenii area (20˚-50˚S, 150˚-180˚E).

The point to identifying swirl is to distinguish albedo features (swirls) from shading patterns (non-swirls). Therefore, we allocated two kinds of data to the 3 bands in RGB image: Camera imager for R band, and topography data for G and B bands following Kato et al. [2018].As camera image, we use the Multi-band Imager (MI) data from Kaguya satellite. As for DEM data, the data of SLDEM2013 are used. By creating such unique “Combined Image”, we can combine different kinds of information collectively as one image.

We built learning models using the framework of Caffe. We increased variation and quantity of training data to collect data from all confirmed swirl areas and to rotate original images in 3 directions. Totally 212 images (each image covers 1 by 1 deg.) were used as training data. We prepared correct answer data in target area and conduct cross validation for evaluation of results and models. The model building and evaluation were sequentially cycled.

Running the latest learning model, we found 275 images as swirl candidate scenes out of 832 images in the Mare Ingenii. Focusing on True positive rate, the best swirl detection was performed by the learning model built based on training data set which increases variation and quantity of swirl images and ratio of swirl images to non-swirl images.

Keywords: swirl, deep learning, Moon, automatic detection, exploration data

©2019. Japan Geoscience Union. All Right Reserved. 

# Lunar surface feature reconstruction by deep learning using synthetic data

*Koichi Tsuru[1], Toru Kouyama[1], Ryosuke Nakamura[1]

1. National Institute of Advanced Industrial Science and Technology

Various machine learning methods have been proposed to detect lunar surface features such as craters and boulders from satellite imagery. However, many of them need a huge manual effort to create a training data set even to solve one task.

Hence, so far, we have focused on several algorithms based on Generative Adversarial Networks (GANs) that enable highly accurate image generation even from a small amount of training set, and we examined to use Cycle-Consistency Adversarial Networks (CycleGAN) which can learn translation relationship between two image groups, such as a group of Moon surface images and a group of crater maps, for crater detection on the Moon surface. The CycleGAN does not require paired images, whereas it learns the relationship between the two image groups with an unpaired training manner, and images in one of the two groups can be simulated label data.

Initially, we tried to translate a satellite imagery to a labeled image (i.e. crater map), in which the labeled image is produced by simulations based on statistical crater size-frequency distribution. Although it could reduce the annotation cost drastically by the automatic generation of the label data, we found that the learning was not stable and not precise because the texture was too different between the satellite imagery and the simple labeled image. Then, we considered that, in order to improve the performance, it is necessary to train a network with multiple feature labels (i.e. lunar surface elevation, albedo, and shadow maps, and crater and boulder distributions) that characterize the appearance of the Moon surface to be observed.

In this work, we adopted a two-step deep learning framework with fine-tune models trained by 1) generating feature labels from a modeled surface image which is based on given feature labels, and synthesizing the labels to generate a lunar surface image that is compared with the original one to check the network performance (at the same time the generated feature labels are also compared with given ones), and then 2) generating feature labels from actual observed data and again synthesizing the labels to generate a lunar surface image to be compared with the actual image. The good advantage of using modeled data and labels as training data is that it becomes easier to cover complicated and enormous amount of possible observation conditions which is necessary for analyzing actual observation data. In addition, highly precise inference can be possible by the simulation even when the existing observation data of a target object covers only insufficient observation conditions.

In the proposed framework, we employed two generative networks that reconstruct terrain features from satellite imagery and to synthesize satellite imagery from terrain features. By applying cycle-consistency for the training that is measured from similarity between the resynthesized satellite image from “reconstructed” features and the original, the actual terrain features are not required in the training phase.

We prepared DEM, albedo map, crater map, boulder map, and shadow map as features for the reconstruction of a target region. In this presentation, we show the results of feature reconstruction from

©2019. Japan Geoscience Union. All Right Reserved. 

the actual observed SELENE Terrain Camera imagery.

Keywords: Moon, Feature Detection, Deep Learning, SELENE

©2019. Japan Geoscience Union. All Right Reserved. 

# Evaluation of the influence of alkali elements on hydrogen solubility of clinopyroxene for estimating water content of lunar mantle

*Miki Muranushi[1], Akio Suzuki[1], Masahiro KAYAMA[1], Tsuyoshi MIYAMOTO[2]

1. Graduate school of Science, Tohoku university , 2. Center for Northeast Asian Studies, Tohoku university

In the early history of lunar exploration, lunar samples returned by the Apollo missions revealed that volatile elements are depleted on the Moon. Almost all volatile components were thought to be eliminated by the giant impact event that probably led to the formation of the Moon. However, recent microanalyses of lunar samples have discovered hydroxyl or water in the constituent minerals. These observations suggest that the lunar mantle may not be entirely dry and contain water to same extent as the Earth’ s mantle. The lunar volcanic glasses of Apollo 15 and 17 were measured by SIMS and about 4-46 ppm water were detected (Saal et al., 2008). Hui et al. (2013, Nature Geosci.) detected up to 2.7 ppm water in plagioclase grains from the lunar highland crust sample. They suggest that the initial water content of the lunar magma ocean (LMO) reaches approximately 320 ppm water content. As a result of these studies, water content and the process that the moon got water has attracted a lot of attention.
Since no indigenous hydrous minerals have been found in the moon, it is likely that anhydrous mineral possess water as a reservoir in the lunar mantle. Water exists in the Earth’ s mantle as hydrous mineral, anhydrous mineral, silicate melt, liquid water, and their intermediate form. In the Earth’ s mantle, hydrogen may be incorporated as defects in nominally anhydrous minerals (NAMs) such as Olivine, pyroxene and garnet. (e.g., Smyth et al., 1991). Especially, clinopyroxene (Cpx) shows the maximum water content in the upper mantle xenolith (Inglin and Skogby, 2000). Cpx has possibility of being water reservoir in the lunar mantle due to its crystal structure and chemical composition.
Nakamura et al. (2012) confirmed the presence of calcium rich pyroxene in the South Pole-Aitken (SPA). It is possible that the lunar upper mantle has been excavated and exposed in SPA (Cintala and Grieve, 1998; Lucey et al., 1998). Cpx is likely to be one of the major minerals of the lunar mantle as well as the earth.
Since there is less hydrous mineral in the Moon, water should concentrated in KREEPy basalt that assumed to be the final part of the lunar magma ocean solidification. In this study, we target the measurement of hydrogen solubility of Cpx crystallized from alkali-rich magma.
We conducted a high temperature and high pressure experiment at 1 GPa using a piston cylinder apparatus at Bayreiches Geoinstitut, Germany. Starting material is the natural alkali basalt powder (Haku-4 reported by Kuritani et al., 2009), adding ~5 wt. % water with a micro-syringe. For the Fourier Transform Infrared (FT-IR) analysis, it is necessary to produce Cpx crystals larger than 50 μm. Therefore, in order to considerate conditions suitable for sample synthesis, we conducted several experiments that the initial temperature, cooling rate, the temperature after cooling and the retention time were changed. We report the conditions that succeeded in creating the Cpx large enough for FT-IR analysis and the future plans.
Funding acknowledgment: This work was partially supported by the JSPS Japanese-German Graduate Externship.

Keywords: nominally anhydrous minerals , lunar mantle , alkali basalt

©2019. Japan Geoscience Union. All Right Reserved. 

# Preliminary examination of mineral structure effect on relative permittivity

*Makito Kobayashi[1], Takafumi Niihara[2], Hideaki Miyamoto[2,1]

1. Department of Earth and Planetary Science, School of Science, University of Tokyo, 2. Department of Systems Innovation, School of Engineering, University of Tokyo

The surface of the Moon is covered with regolith formed by the bombardment of meteorites and micro-meteorites. Although drill core samples collected during Apollo missions revealed that the subsurface (1-2 m) structure changes vertically over centimeter to meter scales at landing sites, deeper (> 10 m) structure and spatial continuity is still unknown. Ground Penetrating Radar (GPR) can detect potential variations in subsurface structure which result in permittivity contrasts, therefore, understanding of factors that affect the permittivity of the regolithis important.

Relative permittivity depends on multiple factors such as radar frequency, porosity, temperature, moisture content and chemical composition (e.g., Campbell and Ulrichs, 1969). Correlation between Ti and Fe concentration and the relative permittivity of Apollo samples was previously addressed by Shkuratov and Bondarenko(2001). On the other hand, Fa and Wieczorek (2012) reported that there was no correlation between chemical composition and relative permittivity althoughthe bulk density varied between samples in this study. Because previous workshave not focused specifically on the influence of mineral composition (while keeping bulk density and composition constant), we prepared samples to isolate the influence of mineral composition on relative permittivity.

Bulk density of regolith mostly depends on porosity and the constituent minerals among samples which have the same bulk chemical composition. Lunar regolith contains Fe- and/or Ti-bearing spinel minerals and other oxide minerals (e.g. ilmenite, magnetite, armarcolite), andthe abundance of those minerals depends on the sample. Differences in abundance of constituent minerals indicate different origins of precursor rocks. If we can detect the permittivity contrast resulting from those mineral differences, it could help further our understanding of the subsurface structure and evolution of surface of the Moon. Therefore, we examine whether crystal types of opaque minerals with the samechemicalcomposition affect the relative permittivity.

We prepare a mixture of rutile and iron oxide (II) to create same chemical composition as ilmenite. Porosities of samples are uniform (40%), therefore, densities of the mixture and ilmenite samples are 2.96 and 2.90, respectively. In order to avoid the effect of moisture content, samples are dried for a few days, and we then measure the relative permittivity using a coaxial probe in the range of 1 MHz to 6 GHz at room temperature.

There is a difference of relative permittivity of about 3.6-4.2 when comparing the mixture (10.6-10.7) with ilmenite (6.4-7.0). This result indicates that crystal structure can affect the relative permitivity.In this presentation, we will discuss the effect in more detail.

References:

©2019. Japan Geoscience Union. All Right Reserved. 

Campbell, Malcolm J., and Juris Ulrichs. "Electrical properties of rocks and their significance for lunar radar observations." *Journal of Geophysical Research* 74.25 (1969): 5867-5881.

Fa, Wenzhe, and Mark A. Wieczorek. "Regolith thickness over the lunar nearside: Results from Earth-based 70-cm Arecibo radar observations." *Icarus* 218.2 (2012): 771-787.

Shkuratov, Yurij G., and Nataliya V. Bondarenko. "Regolith layer thickness mapping of the Moon by radar and optical data." *Icarus*149.2 (2001): 329-338.

Keywords: relative permittivity, GPR, lunar regolith, ilmenite

©2019. Japan Geoscience Union. All Right Reserved. 

# Lunar surface magnetic field intensity in the solar wind inferred from electron reflectometry

*Tomoki Kawaguchi[1], Yuki Harada[1], Yoshifumi Saito[2], Shoichiro Yokota[3], Masaki N Nishino[4], Hideyuki Usui[5], Yohei Miyake[6], Hideo Tsunakawa[7], Daiba Kato[8]

1. Dept. Geophysics, Kyoto Univ., 2. Solar System Science Division, Institute of Space and Astronautical Science, Japan Aerospace Exploration Agency, 3. Graduate School of Science, Osaka University, 4. Institute for Space-Earth Environmental Research, Nagoya University, 5. Graduate school of system informatics Kobe University, 6. Education Center on Computational Science and Engineering, Kobe University, 7. Deparment of Earth and Planetary Sciences, Tokyo Institute of Technology, 8. The University of Tokyo

The Moon is classified as a nonmagnetized celestial body that does not hold a global, intrinsic magnetic field and atmosphere, and most of the dayside lunar surface is bombarded by the solar wind plasma. Therefore, most of the solar wind collides with the lunar surface and is absorbed. Meanwhile, some regions called magnetic anomaly of the lunar surface are locally shielded from the solar wind by magnetic fields of crustal origin. The interaction between the lunar crustal magnetic fields and the solar wind is an important topic relevant to the plasma environment around the Moon. Research on the interaction between the solar wind and the strong magnetic anomaly has been advanced so far, but it remains unclear how the magnetic field strength on the dayside lunar surface varies globally.

The global distribution of crustal magnetic field strength has been investigated by electron reflectometry, which remotely infers the surface magnetic field strength from the loss cone angle of reflected electrons from the lunar crustal magnetic field, using the magnetic mirror effect of the moon periphery electron. As the aim of the conventional electron reflectometry is measurements of the strength of the lunar crustal magnetic field itself, a standard practice is to use data obtained on the night side of the Moon and within the terrestrial magnetotail lobes with less influence of the solar wind plasma. Here we apply the electron reflectometry to the data obtained on the day side of the Moon in the solar wind, thereby investigating variations of the surface magnetic field strength caused by the interaction with the solar wind. By applying this method to the data of Kaguya when exposed to the solar wind on the lunar day side, the magnetic field became stronger globally.

We utilized data obtained by the electron spectrum analyzers (MAP-PACE-ESA) and magnetometer (MAP-LMAG) on board Kaguya. We investigated a surface magnetic field intensity by analyzing electron pitch angle distributions of each different energy band measured when the day side lunar surface was exposed to the solar wind. As a result, we revealed energy dependence on the pitch angle distribution of electrons. This suggests that the cutoff pitch angles are influenced by the potential difference between the lunar surface and the satellite and the electric field generated by decoupling of electrons and ions. We will discuss the solar wind dynamic pressure control of the lunar surface magnetic field intensity with energy dependence.

©2019. Japan Geoscience Union. All Right Reserved. 

# Objective and Current Development Status of Multi-Band Camera on SLIM

*Yusuke Nakauchi[1], Kazuto Saiki[2], Makiko Ohtake[1], Hiroaki Shiraishi[1], Chikatoshi Honda[3], Hiroyuki Sato[1], Yoshiaki Ishihara[4], Takao Maeda[5], Masatsugu Otsuki[1], Sin-ichiro Sakai[1], Shujiro Sawai[1], SLIM Project Team

1. Japan Aerospace Exploration Agency, 2. Osaka University, 3. Aizu University, 4. National Institute for Environmental Studie, 5. Chuo University

Smart Lander for Investigating Moon (SLIM) project is on going in JAXA. The main objective of this project is to demonstrate various techniques for “pin-point landing” on the moon. SLIM spacecraft is a small lander. It is designed to achieve “pin-point landing” to 100 meter-order error circle. In order to “pin-point landing” of this level, SLIM mission will demonstrate new image-based onboard navigation system and autonomous landing along with several other new technologies (e.g. “tow stage” landing sequence, metal shock absorbers). The SLIM spacecraft weight is ~730 kg wet mass and ~200 kg class dry mass, both of which are more lightweight than previous lunar landers. The spacecraft will be launched with a Japanese rocket H-IIA in 2021 or 2022. Landing on (25.2ºE, 13.3ºS) located in the west of Mare Nectaris is planned.

After landing, SLIM project is planning to observe around landing site using Multi-Band Camera (MBC). The observational mission is positioned as extra success. MBC will observe olivine and estimate Mg# of it. MBC is a compact VIS-NIR camera composed of an imaging sensor (InGaAs), a filter-wheel with 10 band-pass filters, a telephoto optical system, and a movable mirror for panning and tilting. The sensor has sensitivity at wavelength from 700 to 1700 nm, which covers the characteristic ab-sorption bands of lunar minerals. The telephoto optical system can focus on an object from 1.5 to 30 m distance. The imaging sensor has 640 ×512 pixels with 20 $\mu$m pitch. The 4º field of view corresponds to the spatial sampling of 1.3 mm per pixel at 10 m from the lander. Using the movable mirror, observable scanning area is ~50º in azimuth and ~70º in elevation. This makes it possible to observe the size distribution of boulders around the lander. The observation wavelength of band pass filters were selected 10 bands: 750, 920, 950, 970, 1000, 1050, 1100, 1250, 1550, and 1650 nm. The width of their bands is 30nm.

Keywords: Moon, SLIM, reflectance spectra, Olivine

©2019. Japan Geoscience Union. All Right Reserved. 

# Monte Carlo simulation of neutron production and transport in the Moon: Effect of lunar subsurface water

*Hiroki Kusano[1], Yuzuru Karouji[1], Hiroshi Nagaoka[1], Naoyuki Yamashita[2], Makoto Hareyama[3]

1. Japan Aerospace Exploration Agency, 2. Planetary Science Institute, 3. St. Marianna University School of Medicine

The intensity of thermal, epithermal, and fast neutrons emitted from a planetary surface provides information on the surface elemental composition, particularly on the hydrogen abundance. In an airless planetary surface, the galactic cosmic rays produce fast neutrons via nuclear interactions in the subsurface materials within a depth of tens centimeters. Then, the fast neutrons are moderated by interactions with subsurface materials including the secondary neutron production. This neutron transport process is terminated at the thermal neutron capture or the neutron leakage from surface. Because the hydrogen atom has a large elastic scattering cross section for a neutron and a nearly identical mass as a neutron, neutrons are efficiently moderated by the elastic scattering with hydrogen atoms. Therefore, the leakage neutron intensity strongly depends on the hydrogen abundance as well as the surface elemental composition. Neutron spectroscopy is thus well suited to detect subsurface water which may present at the lunar polar region. It is essential to obtain the abundance and distribution of lunar subsurface water from the viewpoint of planetary science and space resources for future manned activities.

In this study, the neutron production and transport in the Moon was modeled by Monte Carlo simulation with Geant4 10.3.p03. The effect of subsurface hydrogen abundance and spatial distribution was studied for in-situ water search in future lunar polar landing explorations. The leakage neutron intensity produced by protons and alpha particles in galactic cosmic rays was calculated for the lunar highland composition mixed with various amounts of hydrogen. The production depth and flux of subsurface neutrons, and the production depth of leakage thermal, epithermal, and fast neutrons were also calculated. It was confirmed that the leakage neutron intensity depends on the subsurface hydrogen abundance. The epithermal neutron intensity is particularly sensitive to the presence of subsurface hydrogen. Most of the leakage neutrons were produced within a depth of about 100 g/cm$^2$, which means that the neutron spectroscopy is mainly sensitive to the subsurface water in the top of surface with about 50 cm in depth depending on the surface density. When a dry layer presents at the top of surface, the leakage neutron intensity was found to depend on the dry layer thickness. The variation of leakage neutron intensity was detectable for the dry layer thickness less than about 80 g/cm$^2$. The behavior of lunar subsurface neutrons and its sensitivity for lunar subsurface water will be presented and discussed.

Keywords: Lunar water, Lunar polar region, Lunar landing exploration, Neutron spectroscopy, Galactic cosmic ray, Monte Carlo simulation

©2019. Japan Geoscience Union. All Right Reserved. 

# Exploration of ice deposits on the Moon using continuous seismic source system

*Yuichiro Nagata[1], Takeshi Tsuji[1,2], Hideaki Miyamoto[9], Taichi Kawamura[3], Akito Araya[4], Yoshiaki Ishihara[5], Kazunori Ogawa[6], Taizo Kobayashi[7], Yuzuru Karouji[8], Satoshi Tanaka[10]

1. Department of Earth Resources Engineering, Kyushu University, 2. International Institute for Carbon-Neutral Energy Research (WPI-I2CNER), Kyushu University, 3. Institut de Physique du Globe de Paris, 4. Earthquake Research Institute, University of Tokyo, 5. National Institute for Environmental Studies, 6. Kobe University, 7. Ritsumeikan University, 8. Japan Aerospace Exploration Agency, 9. University of Tokyo, 10. Department of Solid Planetary Sciences Institute of Space and Astronautical Science

We have been designing and developing an active seismic exploration package with seismometers, active seismic source and anchoring system. Our seismic exploration package was designed to investigate from shallow formation (i.e., ice saturation) to deep formation (i.e., thickness of regolith) of the Moon. Here we present the basic concept of our seismic exploration package and its experimental results. We then discuss the possibilities of future space missions. We evaluate the relation between the S-wave velocity and the ice saturation, and found that S-wave velocity largely increase due to ice deposition (low ice saturation). To evaluate our active-source seismic exploration system, furthermore, we conducted seismic exploration in the test field in JAXA. The test field is filled with loose sands of ~50cm thickness. In this experiment, we conducted seismic survey with several acquisition parameters. When we applied the active seismic survey for small-size receiver array, we retrieved clear shot gather. We further calculated dispersion curve from the shot gather and obtained S-wave velocity profile beneath the array using inversion. In addition, we could detect the cushioning material whose S wave velocity is lower than sand by surface wave analysis and compare the result with the dispersion curve which has no buried material. These results demonstrate that S-wave velocity in shallow formation was accurately estimated, suggesting that ice can be identified as anomalous high S-wave velocity via our seismic system. When the seismometer interval is long, the attenuation of the surface wave is large. However, the refracted P-wave can arrive at far offset receivers. Using the refracted wave, we can estimate P-wave velocity of the basement.

©2019. Japan Geoscience Union. All Right Reserved. 

# Orbit determination of the Chang’E-5 Test 1 and a new gravity field model

*shanhong liu[1], Jianguo Yan[1]

1. Wuhan University

We introduce the recently Chang’E 5-Test 1 (CE-5T1) mission overall and its orbit characteristic and present the results on precision orbit determination from the radio science investigation of the CE-5T1 spacecraft. We describe the data, modeling and methods used to achieve position knowledge several times better than the required demand (in total position) for most of arcs, over the period from 10 March 2014 to 28 December 2018. In addition to we try to use the near-continuous radiometric tracking data of CE-5T1 to develop a new lunar gravity field up to degree and order 100, which is solved independently using about four years tracking data. The accuracy of the gravity field model is assessed by multi means, such as gravity spectrum, observational residuals after precision orbit determination, lunar surface gravity anomaly character, admittance/coherence with topography model, and the corresponding physical feature and effect are analyzed. We also make a comparison between this model and the previously models we ever solved, CEGM-01 and CEGM-02. The results indicate the effectiveness and reasonability of this solution process. On the basis of current work, with the Chang’E 5, 6, and 7 under implementing and planning, the prospect of future development of Chinese lunar gravity field detection is presented.

Keywords: Lunar, Chang'E 5T1, precise orbit determination, gravity field model

©2019. Japan Geoscience Union. All Right Reserved. 

[E] Oral | P (Space and Planetary Sciences )：P-EM Solar-Terrestrial Sciences, Space Electromagnetism & Space Environment

Thu. May 30, 2019 9:00 AM - 10:30 AM JST | Thu. May 30, 2019 12:00 AM - 1:30 AM UTC | A03 TOKYO BAY MAKUHARI HALL

## [P-EM09] Vertical coupling in the atmosphere and Ionosphere

convener:Huixin Liu(Earth and Planetary Science Division, Kyushu University SERC, Kyushu University), Loren Chang(Institute of Space Science, National Central University), Yuichi Otsuka(Institute for Space-Earth Environmental Research, Nagoya University), Chairperson:Huixin Liu(Kyushu University, Japan), Stan Solomon(National Center for Atmospheric Research, US)

Vertical coupling mechanisms throughout the whole atmosphere are critical to understanding the near Earth space environment, as well as its sensitivity to the solar, geomagnetic, and atmospheric drivers. This international session focuses on physical/chemical processes occurring in the mesosphere, thermosphere, and ionosphere (MTI). Both quiet and disturbed states in response to lower atmospheric forcing or solar forcing are important for understanding the MTI system and its coupling to other regions. We invite presentations of observations and observational concepts with ground-based and/or space-borne instruments, theoretical studies, numerical simulations, and development of data analysis systems for various kinds of temporal and spatial variations in atmosphere-ionosphere coupled system.

9:00 AM - 9:20 AM JST | 12:00 AM - 12:20 AM UTC

[PEM09-11] Assimilation products of thermospheric and ionospheric measurements by the NASA Ionopsheric Connection Explorer

★Invited Papers

*Thomas J Immel[1], Chihoko Cullens[1], Yen-Jung Wu[1], Gary Bust[2], Jeffrey Forbes[3], Scott L England[4] (1.University of California, Berkeley, 2.Johns Hopkins University, 3.University of Colorado, 4.Virginia Tech)

9:20 AM - 9:35 AM JST | 12:20 AM - 12:35 AM UTC

[PEM09-12] petitSat - A 6U CubeSat to examine the link between MSTIDS and ionospheric plasma density enhancements

*Jeffrey Klenzing[1], Ryan L Davidson[2], Gregory D Earle[3], Alexa J Halford[4], Sarah L Jones[1], Carlos Martinis[5], Nikolaos Paschalidis[1], Robert F Pfaff[1], Jonathon M Smith[1,6] (1.NASA Goddard Space Flight Center, Greenbelt, MD, USA, 2.Utah State University, Logan, UT, USA, 3.Virginia Tech, Blacksburg, VA, USA, 4.The Aerospace Corporation, Chantilly, VA, USA, 5.Boston University, Boston, MA, USA, 6.Catholic Universtiy of America, Washington, DC, USA)

9:35 AM - 9:55 AM JST | 12:35 AM - 12:55 AM UTC

[PEM09-13] A three-dimensional ionospheric electrodynamics model

★Invited Papers

*Astrid I Maute[1], Arthur D Richmond[1] (1.High Altitude Observatory, National Center for Atmospheric Research, Boulder CO, USA.)

9:55 AM - 10:10 AM JST | 12:55 AM - 1:10 AM UTC

[PEM09-14] **Spatial Fluctuation of TEC Index: A new index of ionospheric irregularities**

*Guanyi Ma[1], Takashi Maruyama[2] (1.National Astronomical Observatories, Chinese Academy of Sciences, 2.National Institute of Information and Communications Technology)

10:10 AM - 10:25 AM JST | 1:10 AM - 1:25 AM UTC

[PEM09-15] Coupling of lower thermosphere planetary wave energy into the ionosphere

*Patrick J Espy[1,2], Nora Stray[1,2,3], Robert Hibbins[1,2] (1.Norwegian University of Science and Technology, Trondheim, Norway, 2.Birkeland Centre for Space Science, Bergen, Norway, 3.Teknova AS, Tordenskjolds Gate 9, 4612 Kristiansand, Norway)

10:25 AM - 10:30 AM JST | 1:25 AM - 1:30 AM UTC

Discussion

# Assimilation products of thermospheric and ionospheric measurements by the NASA Ionopsheric Connection Explorer

*Thomas J Immel[1], Chihoko Cullens[1], Yen-Jung Wu[1], Gary Bust[2], Jeffrey Forbes[3], Scott L England[4]

1. University of California, Berkeley, 2. Johns Hopkins University, 3. University of Colorado, 4. Virginia Tech

ICON is an orbiting NASA observatory built to simultaneously observe the characteristics of the ionosphere and thermosphere in order to understand the connection between conditions in space and energy sources in the atmosphere below. Ready for launch in 2019 into a 27 degree inclination, 575 km altitude orbit, it will provide neutral wind, density and temperature products as well as in-situ and remotely-sensed ionospheric densities. These products will inform the conditions of two models that assimilate the data in different ways, and be available on the ICON website. The first is the TIEGCM, where assimilation is accomplished through modification of the winds and temperatures at the lower boundary as prescribed by observations . The second is the IDA4D model, that through a Gauss-Markhov scheme modifies a background ionosphere with actual observations that include many different sources including ICON. Given the expected sampling and data uncertainties from ICON, the expected performance of these models is reported. ICON expects a launch in 2019.

Keywords: ionosphere , thermosphere, atmospheric tides

©2019. Japan Geoscience Union. All Right Reserved.

©2019. Japan Geoscience Union. All Right Reserved. 

# petitSat - A 6U CubeSat to examine the link between MSTIDS and ionospheric plasma density enhancements

*Jeffrey Klenzing[1], Ryan L Davidson[2], Gregory D Earle[3], Alexa J Halford[4], Sarah L Jones[1], Carlos Martinis[5], Nikolaos Paschalidis[1], Robert F Pfaff[1], Jonathon M Smith[1,6]

1. NASA Goddard Space Flight Center, Greenbelt, MD, USA, 2. Utah State University, Logan, UT, USA, 3. Virginia Tech, Blacksburg, VA, USA, 4. The Aerospace Corporation, Chantilly, VA, USA, 5. Boston University, Boston, MA, USA, 6. Catholic Universtiy of America, Washington, DC, USA

The mid- and low-latitude ionosphere is home to a variety of plasma density irregularities, including depletions (bubbles), enhancements (blobs), and small-scale scintillation, which result in the distortion of radio wave propagation. Recent observations from the C/NOFS satellite suggest that multiple mechanisms are responsible for forming plasma density enhancements, with wave action in the thermosphere as a significant driver of the enhanced densities. Indeed, statistical analysis of enhancements observed from satellites resembles the statistics of Medium-Scale Traveling Ionosphere Disturbances (MSTIDs) with respect to seasonal variability and solar activity. In order to investigate the link between these two phenomena, both in-situ data of the plasma enhancement and remote data of the MSTID at the magnetic footpoint are required. petitSat is a CubeSat mission designed to provide in situ measurements of the plasma density, 3D ion drift, as well as ion and neutral composition. The instrument suite includes a combined retarding potential analyzer and cross-track drift meter and an ion neutral mass spectrometer. This instrument suite will provide comprehensive information about the fluctuations in plasma, as well as changes in the neutral profile. petitSat will launch into a 51 deg inclination orbit at 400 km (consistent with an International Space Station deployment), allowing for numerous conjunctions with the Boston University All-Sky Imager network and GPS receivers from the International Global Navigation Satellite Systems (GNSS) Service (IGS) network over the mission lifetime.

Keywords: Ionosphere, CubeSat, MSTIDs

©2019. Japan Geoscience Union. All Right Reserved. 

# A three-dimensional ionospheric electrodynamics model

*Astrid I Maute[1], Arthur D Richmond[1]

1. High Altitude Observatory, National Center for Atmospheric Research, Boulder CO, USA.

Ionospheric electric fields and currents are driven by collisional interaction between thermospheric winds and ions, by magnetospherically driven convection and field-aligned currents at high latitudes, by gravitational and pressure-gradient forces on the ionospheric plasma, and by weak currents from the lower atmosphere. The electrodynamics of the ionospheric E and F regions are strongly coupled. For time scales longer than a few minutes the electric field is electrostatic. The electric potential is nearly constant along geomagnetic-field lines, and can be represented in two dimensions in a coordinate system aligned with the magnetic field. The current density, however, varies in all three dimensions. Knowing the ionospheric current flow in three dimension is important for determining the magnetic perturbations at Low Earth Orbit (LEO) satellite height.

We are developing a model of ionospheric electrodynamics that takes into account all of the sources and calculates the three-dimensional structure of currents and their associated magnetic perturbation fields. This model will be used to simulate ionospheric drifts, currents, and ground and LEO geomagnetic perturbations. In this presentation we discuss the modeling principles and present results relevant to the electrodynamics of the middle and low latitude ionosphere, including the effects of coupling with F-region electrodynamics and the expected observable effects at low Earth orbit satellites.

Keywords: Ionospheric electrodynamics, ionospheric current, magnetic perturbations

©2019. Japan Geoscience Union. All Right Reserved. 

# Spatial Fluctuation of TEC Index: A new index of ionospheric irregularities

*Guanyi Ma[1], Takashi Maruyama[2]

1. National Astronomical Observatories, Chinese Academy of Sciences, 2. National Institute of Information and Communications Technology

This study presents a new spatial fluctuation of total electron content (TEC) index (SFTI) to identify and analyze ionospheric irregularities. SFTI is defined as the dispersion of vertical TEC (VTEC) within a specific area at a given time. With the data from the Global Navigation Satellite System (GNSS) Earth Observation Network of Japan (GEONET), the size of the specific area for SFTI calculation can be chosen as 0.8˚× 0.8˚ in longitude and latitude. An SFTI map generated by sliding window shows the spatial variation of the ionospheric irregularities in two dimensions. It can be used to obtain the size, shape, orientation and intensity distribution of the irregularity structures. With a series of SFTI maps, we analyzed three strong irregularity events on 12 February 2000, 20 March 2001 and 10 November 2004. The irregularities are found to consist of branching structures, which are anisotropic and elongate along longitudinal direction when first seen at low latitudes. The structures can drift and eventually move perpendicular to their orientations. It is concluded that SFTI will provide an unprecedented view of irregularity development and help to understand the process of irregularity generation.

Keywords: ionospheric irregularities, GNSS observation, SFTI

©2019. Japan Geoscience Union. All Right Reserved. 

# Coupling of lower thermosphere planetary wave energy into the ionosphere

*Patrick J Espy[1,2], Nora Stray[1,2,3], Robert Hibbins[1,2]

1. Norwegian University of Science and Technology, Trondheim, Norway, 2. Birkeland Centre for Space Science, Bergen, Norway, 3. Teknova AS, Tordenskjolds Gate 9, 4612 Kristiansand, Norway

Neutral atmosphere winds derived from meteor trail drifts observed by a longitudinal chain of Super Dual Auroral Radar Network (SuperDARN) radars have characterized planetary waves with wavenumber 1 and 2 in the lower thermosphere near 95 km. The simultaneous wind observations at stations between 50$^{o}$ and 66$^{o}$ N removes the temporal-spatial aliasing associated with satellite observations and shows the continuous evolution of the planetary waves near the turbopause. A similar technique has been applied to a longitudinal chain of ionosondes in the same latitude band, and the same wavenumber components were observed in $f_{o}$F2. An analysis of the two signals shows them to be highly correlated, with the ionospheric waves lagging behind those in the lower thermosphere. We will describe the technique to extract the waves and compare it with other observations. We will also show the relationship of the ionospheric waves with magnetic and solar activity, and describe a process, commensurate with our measurements, by which planetary wave signals near the turbopause can be transmitted into the ionospheric electron density.

Keywords: dynamics, turbopause, ionosphere

©2019. Japan Geoscience Union. All Right Reserved. 

[E] Oral | P (Space and Planetary Sciences )：P-EM Solar-Terrestrial Sciences, Space Electromagnetism & Space Environment

Thu. May 30, 2019 10:45 AM - 12:15 PM JST | Thu. May 30, 2019 1:45 AM - 3:15 AM UTC | A03 TOKYO BAY MAKUHARI HALL

## [P-EM09] Vertical coupling in the atmosphere and Ionosphere

convener:Huixin Liu(Earth and Planetary Science Division, Kyushu University SERC, Kyushu University), Loren Chang(Institute of Space Science, National Central University), Yuichi Otsuka(Institute for Space-Earth Environmental Research, Nagoya University), Chairperson:Jann-Yenq Liu(National Central University, Taiwan), Loren Chang(National Central University, Taiwan)

Vertical coupling mechanisms throughout the whole atmosphere are critical to understanding the near Earth space environment, as well as its sensitivity to the solar, geomagnetic, and atmospheric drivers. This international session focuses on physical/chemical processes occurring in the mesosphere, thermosphere, and ionosphere (MTI). Both quiet and disturbed states in response to lower atmospheric forcing or solar forcing are important for understanding the MTI system and its coupling to other regions. We invite presentations of observations and observational concepts with ground-based and/or space-borne instruments, theoretical studies, numerical simulations, and development of data analysis systems for various kinds of temporal and spatial variations in atmosphere-ionosphere coupled system.

10:45 AM - 11:00 AM JST | 1:45 AM - 2:00 AM UTC

[PEM09-16] Modulation of Lightning Occurrence by the Solar Wind

*Omar Angelo Nava[1], Daniel Emmons[1], Robert Loper[1] (1.Air Force Institute of Technology)

---

11:00 AM - 11:15 AM JST | 2:00 AM - 2:15 AM UTC

[PEM09-17] Long Term Mesopause Temperature Variations resolved by SD-WACCM, MSISE-00,TIMED SABER and Local Observations in Irkutsk (52.29o, 104.29o), Russia

*Yi Chung Chiu[1], Loren Chang[1], Yi Duann[1], ALEXEI DMITRIEV[1], Irina Medvedeva[2], Konstantin Ratovsky[2], Jia Yue[3] (1.Institute of Space Science, National Central University, 2.Russian Academy of Sciences, Russian Federation, 3.Hampton University, USA)

---

11:15 AM - 11:30 AM JST | 2:15 AM - 2:30 AM UTC

[PEM09-18] ISS-IMAP observation of the mesospheric disturbances generated by tropical cyclones

*Akinori Saito[1], Takeshi Sakanoi[2], Septi Perwitasari[4], Yuta Hozumi[3], Ryota Okada[1], Ryo Murakami[1] (1.Department of Geophysics, Graduate School of Science, Kyoto University, 2.Planetary Plasma and Atmospheric Research Center, Graduate School of Science, Tohoku University, 3.University of Electro-Communications, 4.Space and Upper Atmospheric Sciences Group, National Institute of Polar Research)

---

11:30 AM - 11:45 AM JST | 2:30 AM - 2:45 AM UTC

[PEM09-19] A fast acoustic wave detected in GNSS total electron content after the foreshock of the 2011 Tohoku Earthquake

*Yoshihiro Kakinami[1], Hiroaki Saito[2], Tetsuo Yamamoto[3], Chia-Hung Chen[4], Masa-yuki Yamamoto[2], Kensuke Nakajima[5], JANN-YENQ Liu[6] (1.Hokkaido Information University, 2.Kochi University of Technology, 3.Hokkaido University, 4.National Cheng Kung University, 5.Kyushu University, 6.National Central University)

---

11:45 AM - 12:00 PM JST | 2:45 AM - 3:00 AM UTC

[PEM09-20] **Study of quiet-time high-latitude thermospheric winds using a Fabry-Perot interferometer at Tromsoe: Averages and exceptional events**

*Heqiucen XU[1], Kazuo Shiokawa[1], Shin-ichiro Oyama[1] (1.Institute for Space-Earth Environmental Research, Nagoya University)

---

12:00 PM - 12:15 PM JST | 3:00 AM - 3:15 AM UTC

[PEM09-21] **The longitudinal differences of lunar tidal characteristics between East Asian and American sectors during stratospheric sudden warming events: 2009-2018.**

*Jing Liu[1], Donghe Zhang[1] (1.Peking University)

# Modulation of Lightning Occurrence by the Solar Wind

*Omar Angelo Nava[1], Daniel Emmons[1], Robert Loper[1]

1. Air Force Institute of Technology

The connection between terrestrial and space weather phenomena is an emerging field of study with implications for different aspects of operational weather forecasting. This study investigates the influence of solar wind events on the frequency of lightning occurrence over North America. Empirical mode decomposition (EMD) is applied to National Lightning Detection Network (NLDN) data from 1996 to 2012 and correlated against various solar wind parameters. EMD performs operations that partition the lightning time series data into modes or Intrinsic Mode Functions (IMFs). Using composite analysis, we identified an IMF that corresponds to a 27-day co-rotating interaction region (CIR) that results in a statistically significant decrease in thunderstorm occurrence across the entire NLDN for approximately three to nine days. This finding is consistent with previous studies indicating that faster solar wind speeds are correlated with a decrease in galactic cosmic ray (GCR) flux and a reduction in lightning reports. However, the analysis also highlighted a latitudinal stratification in the thunderstorm response. In the mid-latitudes (30-38 deg N), faster solar wind speeds initially increased the number of lightning occurrences before decreasing significantly over the next 14 days. In the upper mid-latitudes (38-46 deg N), the response was reversed with an increase in thunderstorm events followed by a significant decrease. Additional “lightning response reversals” are noted at even higher latitudes. It is hypothesized that solar energetic particles associated with the CIRs are able to penetrate to tropospheric altitudes and increase lightning rates at higher latitudes, while at lower latitudes, the solar wind modulated GCR flux drives the decrease in lightning occurrence. Overall, understanding the electrodynamic connection between the lower and upper atmospheres has important implications for both space physics and atmospheric science communities.

Keywords: Lightning, Solar Wind, Empirical Mode Decomposition, National Lightning Detection Network

©2019. Japan Geoscience Union. All Right Reserved. 

# Long Term Mesopause Temperature Variations resolved by SD-WACCM, MSISE-00,TIMED SABER and Local Observations in Irkutsk (52.29o, 104.29o), Russia

*Yi Chung Chiu[1], Loren Chang[1], Yi Duann[1], ALEXEI DMITRIEV[1], Irina Medvedeva[2], Konstantin Ratovsky[2], Jia Yue[3]

1. Institute of Space Science, National Central University, 2. Russian Academy of Sciences, Russian Federation, 3. Hampton University, USA

Measurements of mesopause temperature are quite challenging and must rely on remote sensing methods. As part of the Taiwan-Russia joint research cooperation program, we carry out an analysis comparing mesopause temperature measurements made by the Irkutsk spectrophotometer between 2008 - 2018 and those resolved by the SD-WACCM data assimilation model, the empirical MSISE-00 model, and TIMED SABER satellite measurements. Spectral decomposition is performed on the datasets to determine the differences between the different observed and modelled seasonal and inter-annual variability, as well as to resolve long term trends.

Keywords: Mesopause, Temperature variability

©2019. Japan Geoscience Union. All Right Reserved. 

# ISS-IMAP observation of the mesospheric disturbances generated by tropical cyclones

*Akinori Saito[1], Takeshi Sakanoi[2], Septi Perwitasari[4], Yuta Hozumi[3], Ryota Okada[1], Ryo Murakami[1]

1. Department of Geophysics, Graduate School of Science, Kyoto University, 2. Planetary Plasma and Atmospheric Research Center, Graduate School of Science, Tohoku University, 3. University of Electro-Communications, 4. Space and Upper Atmospheric Sciences Group, National Institute of Polar Research

Troposphere was investigated to elucidate the vertical atmospheric coupling process using the global observational data from the International Space Station (ISS). The vertical coupling between the lower and the upper atmospheres has been revealed to be significant to control the dynamics and disturbances in the upper atmosphere by recent studies. The phenomena generated by the vertical coupling processes have been detected with various observational instruments, and studied with numerical simulations. TC, such as typhoon, hurricane and cyclone, is regarded as one of the intense sources in the Troposphere to affect the Mesosphere, the Thermosphere and the Ionosphere. There is a plenty of studies that reports the observation of the upper atmospheric disturbances associating with TC using ground-based instruments, such as HF doppler radars, IS radars, GNSS receiver arrays, and optical imagers. Because the ground-based observation cannot track the movement of TC, and TC is much active over the ocean, the observational opportunity is limited for the ground-based instruments. ISS-Ionosphere, Mesosphere, upper Atmosphere, and Plasmasphere (ISS-IMAP) mapping mission made a global observation of the airglow in the mesosphere and the ionosphere for three years. The data set of visible-light and infrared spectrum imager (VISI) of ISS-IMAP is idealistic to investigate the effect of TC on the Mesosphere and the Ionosphere. Mesospheric disturbances were detected by the airglow from the molecular oxygen in 762nm of wavelength, and the ionospheric disturbances were detected by the airglow from the atomic oxygen in 630nm of wavelength. In its three years observation, the number of TC that ISS-IMAP/VISI made the conjugate observation was 171. It was found that more than 20% of TC was associated with the mesospheric disturbances that seems to be generated by TC. The duration of these disturbances was one or two days in spite of the lifetime of TC is longer than a week. The relationship among TC, the mesospheric and the ionospheric disturbances will be discussed in the presentation.

Keywords: ISS-IMAP, Tropical cyclone, airglow, Mesosphere, Ionosphere

©2019. Japan Geoscience Union. All Right Reserved. 

# A fast acoustic wave detected in GNSS total electron content after the foreshock of the 2011 Tohoku Earthquake

*Yoshihiro Kakinami[1], Hiroaki Saito[2], Tetsuo Yamamoto[3], Chia-Hung Chen[4], Masa-yuki Yamamoto[2], Kensuke Nakajima[5], JANN-YENQ Liu[6]

1. Hokkaido Information University, 2. Kochi University of Technology, 3. Hokkaido University, 4. National Cheng Kung University, 5. Kyushu University, 6. National Central University

Acoustic waves are often emitted from large earthquakes, reach the thermosphere and disturb the ionosphere. The disturbances are observed by using of GNSS total electron content (TEC). After the foreshock of the 2011 Tohoku Earthquake, which occurred on 9 March 2011, traveling ionospheric disturbance induced by tsunami was detected. When vertical propagation of acoustic wave from the tsunami source area is assumed, the onset points of co-seismic ionospheric disturbance (CID) must coincide. However, the onset points of the co- CID were detected at different locations in different satellite data assuming that the altitude of CID were the same (ex. at 300 km). Furthermore, we found the onset times were different in the different satellite data. The results suggest that the altitudes of CID are different and timings of observation are also different in the different satellite data. By changing the altitudes of CID, we found coinciding onset point. Once the coinciding onset point is found in the different data sets, the altitudes of the CID are also estimated because the sub-ionospheric point is a function of the altitude of observation. The CID altitude were found at 155.4 and 234.9 km. Considering the time difference of the onset time (399.9 s to the altitude of 155.4 km and 476.1 s to 234.9 km), the acoustic wave velocity is estimated to be 1.04 km/s which is 1.4 times higher than the velocity calculated using the empirical model NRLMSISE-00. The fast acoustic wave would arise from temperature elevated by the limited degrees of freedom of motion of atmospheric molecules, and dissipation of the acoustic wave. Especially, the neutral temperature with heating by the dissipation of the acoustic wave would increase by a factor of 3 for acoustic waves with 0.1 Hz and a pressure at sea level of ~2 Pa, which is on the order of the pressure of the acoustic wave emitted from the sea surface during the observed event. The elevated temperature explains the fast acoustic wave.

Keywords: fast acoustic wave, the foreshock of the 2011 Tohoku Earthquake, co-seismic ionospheric disturbance , GNSS total electron content, altitude estimation of ionospheric disturbance , heating of the thermosphere

©2019. Japan Geoscience Union. All Right Reserved. 

# Study of quiet-time high-latitude thermospheric winds using a Fabry-Perot interferometer at Tromsoe: Averages and exceptional events

*Heqiucen XU[1], Kazuo Shiokawa[1], Shin-ichiro Oyama[1]

1. Institute for Space-Earth Environmental Research, Nagoya University

In the previous reports, we studied the dependences of average winds on Kp and F10.7 indices by using a Fabry-Perot interferometer (FPI) at Tromsoe, Norway. In this study, we have further focused on the winds during both globally (Kp < 1+) and locally quiet times in order to provide a baseline wind without magnetic disturbances at latitude of Tromsoe. The wind variations were measured from the Doppler shift of both red-line (630.0 nm, altitudes: 200-300 km, upper thermosphere) and green-line (557.7 nm, altitudes: 90-100 km, mesopause region) emissions with a time resolution of ~13 min. The wind data were collected from 2009 to 2015. In the upper thermosphere, the quiet-time average zonal wind shows westward acceleration at pre-midnight side at ~21-24 LT, while the meridional wind has a minimum around the midnight. In the mesopause region, the average wind tends to show a westward and eastward flow at dusk and dawn side, respectively. By applying sinusoidal regression to the mesospheric average zonal wind, we found that the semidiurnal component has a dominant amplitude of 12.1 m/s. During quiet time, we also found a few exceptional events of more than 100 m/s westward at dusk side in the upper thermosphere. We speculate these exceptional westward winds are related to local plasma convection under quiet time or substorm activities occurred at some other latitudes/local times.

Keywords: Thermosphere, Fabry-Perot interferometer

©2019. Japan Geoscience Union. All Right Reserved. 

# The longitudinal differences of lunar tidal characteristics between East Asian and American sectors during stratospheric sudden warming events: 2009-2018.

*Jing Liu[1], Donghe Zhang[1]

1. Peking University

With data of total electron content (TEC), equatorial electrojet (EEJ), stratospheric temperature and wind field, variations of the low-latitudinal ionosphere in East Asian and American sectors were investigated during stratospheric sudden warming events from 2009-2018. The lunar tidal amplitudes (M2) were derived with the least-square method. Then their features were compared separately during outstanding major events, moderate major events, minor events, and a non-SSW winter. Brief results are listed as follows: (1) In the American sector, the M2 tides appeared to be dominant over solar tides in all major events since distinct time-shifted semi-diurnal patterns could always be detected during those periods. (2) In the East Asian sector, the M2 characteristics were less clear, and sometimes even hard to identify, which means the relative strengths of lunar and solar tides are more complex in this sector. (3) The M2 amplitudes in TEC tend to be larger in the American sector than in East Asian sector during the same event. (4) The longitudinal differences tend to be lessened in minor SSWs compared to major SSWs. (5) During the non-SSW winter, lunitidal features could still be detected in both sectors. Similar results can be found in previous works for different kinds of parameters. Such longitudinal differences were attributed to combined effects of the geomagnetic field configuration, the latitudinal dependence of lunar and solar tides, the changes of atmospheric circulation, and the coupling process from the lower-atmosphere to the F region ionosphere.

Keywords: Stratospheric Sudden Warming, Low-latitudinal Ionosphere, Longitudinal Differences, Lunitidal Characteristics

©2019. Japan Geoscience Union. All Right Reserved. 

[E] Oral | P (Space and Planetary Sciences )：P-EM Solar-Terrestrial Sciences, Space Electromagnetism & Space Environment

Thu. May 30, 2019 9:00 AM - 10:30 AM JST | Thu. May 30, 2019 12:00 AM - 1:30 AM UTC | A04 TOKYO BAY MAKUHARI HALL

## [P-EM11] Dynamics of Magnetosphere and Ionosphere

convener:Aoi Nakamizo(Applied Electromagnetic Research Institute, National Institute of Information and Communications Technology), Mitsunori Ozaki(Faculty of Electrical and Computer Engineering, Institute of Science and Engineering, Kanazawa University), Akiko Fujimoto(Kyushu Institute of Technology), Tomoaki Hori(Institute for Space-Earth Environmental Research, Nagoya University), Chairperson:Shin'ya Nakano(情報・システム研究機構 統計数理研究所), Motoharu Nowada(Shandong University)

This session provides an opportunity to present recent results from satellite and ground-based observations and theoretical and simulation studies on the magnetosphere, ionosphere, and their coupling processes. We invite talks and posters discussing various phenomena related to the magnetosphere-ionosphere system: solar wind-magnetosphere interaction, magnetosphere-ionosphere convection, field-aligned current, magnetic storms/substorms, neutral-plasma interaction, ionospheric ion inflow and outflow, aurora phenomena, and so forth. Discussions on planetary and satellite ionosphere and magnetospheres, future missions and instrument developments are also welcome.

9:00 AM - 9:15 AM JST | 12:00 AM - 12:15 AM UTC

[PEM11-07] **Nightside Distorted Transpolar Arcs and Their Possible Formation Process Model**

*Nowada Motoharu[1], Jun Yang[1], Benoit Hubert[2], Qiu-Gang Zong[3], Quan-Qi Shi[1], Yong-Fu Wang[3], Xu-Zhi Zhou[3], Zhao Hua-Yu[3] (1.Shandong University at Weihai, 2.Université de Liège, 3.Peking University)

9:15 AM - 9:30 AM JST | 12:15 AM - 12:30 AM UTC

[PEM11-08] Ionospheric Conductivity Dependence of the Subauroral Polarization Streams Observed by the SuperDARN HF Radars

Yuting Zhang[1], *Nozomu Nishitani[1], Tomoaki Hori[1], Simon G. Shepherd[2], William A. Bristow[3] (1.Institute for Space-Earth Environmental Research, Nagoya University, 2.Thayer School of Engineering, Dartmouth College, 3.University of Alaska Fairbanks)

9:30 AM - 9:45 AM JST | 12:30 AM - 12:45 AM UTC

[PEM11-09] Ionospheric convection modeling based on convolution with a localized vector-valued basis function

*Shin ya Nakano[1], Tomoaki Hori[2], Kanako Seki[3], Nozomu Nishitani[2] (1.The Institute of Statistical Mathematics, 2.Institute for Space-Earth Environmental Research, Nagoya University, 3.Graduate School of Science, University of Tokyo)

9:45 AM - 10:00 AM JST | 12:45 AM - 1:00 AM UTC

[PEM11-10] **Occurrence Statistics and Driving Mechanisms of Ionospheric ULF Waves Observed by SuperDARN Radars**

★Invited Papers

*Xueling Shi[1], Joseph B. H. Baker[1], John Michael Ruohoniemi[1], Dong Lin[1], Michael Hartinger[1,2] (1.Virginia Tech, 2.Space Science Institute)

10:00 AM - 10:15 AM JST | 1:00 AM - 1:15 AM UTC

[PEM11-11] Magnetic Field Oscillations Observed by Swarm Satellites in the Nightside Upper Ionosphere During Low-latitude Pi2 Pulsations

*Khan-Hyuk Kim[1], Jae-Hee Park[1] (1.School of Space Research, Kyung Hee Univ.)

10:15 AM - 10:30 AM JST | 1:15 AM - 1:30 AM UTC

[PEM11-12] Magnetospheric Multiscale observations of ULF waves and correlated low-energy ion monoenergetic acceleration

*Bin Li[1], De-sheng Han[2], Ze-jun Hu[1], Jian-jun Liu[1], Lei Dai[3] (1.Polar Research Institute of China, 2.Tongji University, 3.National Space Science Center, Chinese Academy of Sciences)

# Nightside Distorted Transpolar Arcs and Their Possible Formation Process Model

*Nowada Motoharu[1], Jun Yang[1], Benoit Hubert[2], Qiu-Gang Zong[3], Quan-Qi Shi[1], Yong-Fu Wang[3], Xu-Zhi Zhou[3], Zhao Hua-Yu[3]

1. Shandong University at Weihai, 2. Université de Liège, 3. Peking University

Transpolar Arc (TPA) is an important auroral phenomenon when considering how the energy stored in magnetotail is transported to ionosphere via magnetic reconnection under the northward interplanetary magnetic field. Magnetotail reconnection is considered to play a crucial role in TPA formation. Reconnection X-points are expected to retreat tailward as TPA grows from nightside auroral oval to the dayside. Usually, they straightforwardly retreat tailward, and reconnection-formed TPA morphology is straight-bar shape. However, we wonder how the TPA shape would be expected when traces of the tailward X-point retreats were not straightforward. The Wideband Imaging Camera (WIC), which is a part of Far Ultraviolet (FUV) instrument, onboard the Imager for Magnetopause-to-Aurora Global Exploration (IMAGE) satellite detected an interesting type of TPAs, which are identified as “nightside distorted TPAs”. Their main bar-shaped parts were located at the dawn or dusk sides, and the nightside ends of them got distorted toward pre- or post-midnight sectors. Because these TPAs look like the shape of an alphabetical letter of “J” or “L”, we distinguished the nightside distorted TPAs from “J”- and “L”-shaped TPAs. We followed the time sequence of the evolutions of several nightside distorted TPAs with the IMAGE FUV-WIC imager data. In most cases, the “J” and “L”-shaped TPAs started to grow from the nightside main auroral oval, and protruded to the dayside auroral oval via the experience of distortion, suggesting that magnetotail magnetic reconnection was closely be related with the formation of the nightside distorted TPAs. In this study, we have proposed a model to explain the nightside distorted TPA formation, in order to discuss that TPAs with their nightside ends distorted toward pre- or post-midnight were formed through how physical process. Furthermore, we have tried to verify whether or not our model proposed is appropriate to adequately explain formation process of nightside distorted TPA based on the global MHD simulation using the BATS-R-US codes.

Keywords: Nightside distorted transpolar arc: “J”- and “L”-shaped TPAs, Nightside magnetic reconnection, Straightforward or wry tailward retreats of X-points , State of dynamic equilibrium, Magnetospheric convection

©2019. Japan Geoscience Union. All Right Reserved. 

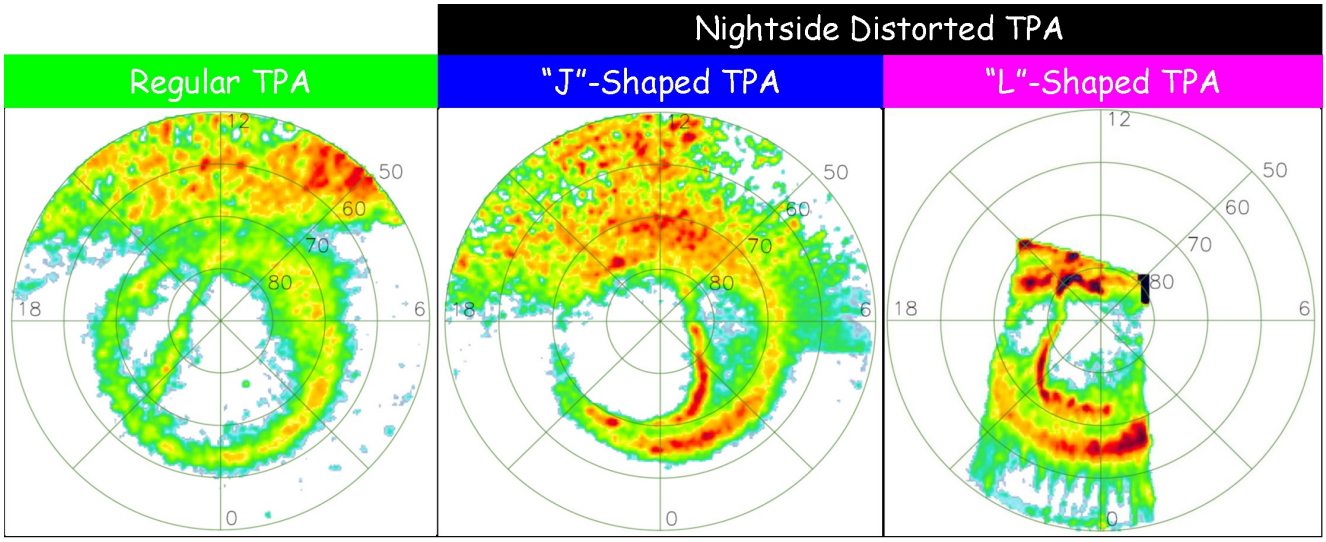


©2019. Japan Geoscience Union. All Right Reserved.

# Ionospheric Conductivity Dependence of the Subauroral Polarization Streams Observed by the SuperDARN HF Radars

Yuting Zhang[1], *Nozomu Nishitani[1], Tomoaki Hori[1], Simon G. Shepherd[2], William A. Bristow[3]

1. Institute for Space-Earth Environmental Research, Nagoya University, 2. Thayer School of Engineering, Dartmouth College, 3. University of Alaska Fairbanks

We investigate the characteristics of the subauroral polarization stream (SAPS), with a main focus on the solar zenith angle (SZA) dependence using the Super Dual Auroral Radar Network (SuperDARN) HF radars and NOAA POES spacecraft data. In this study, we used 3 SuperDARN radars (HOK / CVE / ADW), and checked data from 2008 to 2017 and found 124 SAPS events where the line-of-sight velocity is larger than 150m/s, magnetic local time is 13 to 19 hours and the flow regions are identified to be equatorward of the auroral precipitation region. For each event, we examined the SZA using the geographic latitude, longitude and the UT span of SAPS. We found that the results of CVE radar are different from the result of HOK and ADW radar, the SAPS observed by CVE radar can happen in high conductivity occasion when both hemispheres are illuminated. However, we found that these illuminated SAPS could only occur under geomagnetically disturbed condition and mostly in spring and fall. In addition, when the geomagnetic activity is low, SAPS tends to appear when the minimum threshold of illuminated ionospheric altitude is 130 km or more, which is near and slightly above the altitude of the peak of Pedersen conductivity. These results suggest that the generation mechanism of SAPS is affected by both geomagnetic activity and the Pedersen conductivity. Results of detailed discussion will be presented.

Keywords: SuperDARN Hokkaido East radar, solar zenith angle, sub-auroral polarization stream (SAPS), magnetosphere-ionosphere coupling, Pedersen conductivity

©2019. Japan Geoscience Union. All Right Reserved. 

# Ionospheric convection modeling based on convolution with a localized vector-valued basis function

*Shin ya Nakano[1], Tomoaki Hori[2], Kanako Seki[3], Nozomu Nishitani[2]

1. The Institute of Statistical Mathematics, 2. Institute for Space-Earth Environmental Research, Nagoya University, 3. Graduate School of Science, University of Tokyo

Divergence free assumption is useful for modeling the flow velocity distribution in the ionosphere where plasma velocity can be assumed to be orthogonal to a potential electric field. If the divergence of two-dimensional plasma velocity is assumed to be zero, we can consider a stream function yielding the plasma velocity distribution. In order to estimate the two-dimensional flow velocity distribution in the ionosphere, we propose a framework which expresses the stream function by a convolution with a spherical Gaussian function. From this spherical Gaussian function, we can obtain a localized vector-valued basis function for flow velocity distribution satisfying the divergence-free condition. Accordingly, flow velocity distribution can be represented by a convolution with the vector-valued basis functions. We combine this model with a state space model and estimate a temporal evolution using the Kalman filter algorithm. Hyperparameters of the model are determined by maximizing marginal likelihood.

The proposed framework is applied for estimating the two-dimensional ionospheric convection pattern from the Super Dual Auroral Radar Network (SuperDARN) data. Although there are some wide gaps in the spatial coverage of the SuperDARN radar network for ionospheric observation, the use of the localized basis function enhances the robustness of the estimate. This basis function also enables us to evaluate the uncertainty of the estimate which would be helpful for incorporating other observations. Some results of the analysis of the SuperDARN data will be demonstrated.

Keywords: ionospheric convection, SuperDARN, spherical Gaussian function

©2019. Japan Geoscience Union. All Right Reserved. 

# Occurrence Statistics and Driving Mechanisms of Ionospheric ULF Waves Observed by SuperDARN Radars

*Xueling Shi[1], Joseph B. H. Baker[1], John Michael Ruohoniemi[1], Dong Lin[1], Michael Hartinger[1,2]

1. Virginia Tech, 2. Space Science Institute

Ultra-low frequency (ULF; 1 mHz - 5 Hz) waves are known to play an important role in the transfer of energy from the solar wind to Earth's magnetosphere and ionosphere. The Super Dual Auroral Radar Network (SuperDARN) is an international network consisting of 35 low-power high frequency coherent scatter radars at middle to polar latitudes that look into Earth's upper atmosphere and ionosphere. In this study, we use Doppler velocity measurements obtained by the SuperDARN radars and coordinated spacecraft observations to investigate the occurrence statistics and driving mechanisms of ionospheric ULF waves. Pc3-5 band (1.7-40.0 mHz) ULF waves were surveyed using high time resolution radar data from 2010 to 2016. Specifically, we have investigated the wave spatial occurrence, frequency characteristics, seasonal factors, and dependence on solar wind and geomagnetic conditions. We note two particular findings: (i) an internal wave-particle interaction source is responsible for Pc4 waves at high latitudes in the duskside ionosphere; and, (ii) a source associated with the magnetotail dynamics during active geomagnetic times is suggested for Pc3-4/Pi2 waves at midlatitudes in the nightside ionosphere. A few interesting ULF wave events will be further analyzed for their driving mechanisms via coordinated observations from spacecraft. Collectively, these research findings provide better constraints on where and when ionospheric ULF waves occur and how they might affect magnetospheric and ionospheric dynamics.

Keywords: ULF Waves, SuperDARN, Ionosphere

©2019. Japan Geoscience Union. All Right Reserved. 

# Magnetic Field Oscillations Observed by Swarm Satellites in the Nightside Upper Ionosphere During Low-latitude Pi2 Pulsations

*Khan-Hyuk Kim[1], Jae-Hee Park[1]

1. School of Space Research, Kyung Hee Univ.

Pi2-associated geomagnetic oscillations in the nighside upper ionosphere are studied using magnetic field data acquired by low-Earth orbiting multispacecraft Swarm and at the low-latitude Bohyun (BOH) station located at magnetic shell of L = 1.3 on 22 October 2014. Four Pi2 events were identified from the BOH data near midnight (MLT = 1.5) while Swarm A, B, and C spacecraft were orbiting on the nightside (MLT = 21-22) upper ionosphere from 70˚ to --60˚ in magnetic latitude (MLAT) at 450-500 km altitudes. It is found that the horizontal H component of BOH data is well correlated with the radial ($B_x$) and compressional ($B_z$) components of ionospheric magnetic fields when Swarm spacecraft were at |MLAT| < 30˚. Both $B_x$ and $B_z$ components exhibit in phase or out of phase with the BOH H oscillations depending on the location of the spacecraft (i.e., in the Northern Hemisphere or in the Southern Hemisphere). This indicates that Pi2-associated magnetic oscillation in the ionosphere is the consequence of field line displacement that is symmetric or odd mode about the magnetic equator. We also find that stationary magnetic field perturbation, which is similar to Pi2 oscillation but not associated Pi2 signals, in the upper ionosphere near magnetic equator. A statistical analysis for the global distribution of static/spatial magnetic field perturbations using low-latitude Pi2 oscillation as a reference is a subject of future work.

Keywords: Pi2 pulsation

©2019. Japan Geoscience Union. All Right Reserved. 

# Magnetospheric Multiscale observations of ULF waves and correlated low-energy ion monoenergetic acceleration

*Bin Li[1], De-sheng Han[2], Ze-jun Hu[1], Jian-jun Liu[1], Lei Dai[3]

1. Polar Research Institute of China, 2. Tongji University, 3. National Space Science Center, Chinese Academy of Sciences

Low-energy ions of ionospheric origin with energies below tens of eV dominate most of the volume and mass of the terrestrial magnetosphere. However, sunlit spacecraft often become positively charged to several tens of volts, which prevents low-energy ions from reaching the particle detectors on the spacecraft. Magnetospheric multiscale spacecraft (MMS) observations show that ultralow-frequency (ULF) waves drive low-energy ions to drift in the E×B direction with a drift velocity equal to $V_{E\times B}$, and low-energy ions were accelerated to a higher energy level to reach the detection range of the MMS/Fast Plasma Investigation (FPI). The maximum ion flux energy level detected by MMS1 DIS agreed perfectly with the theoretical calculation of $H^+$ ion E×B drift energy. The density of ions in the energy range below 2 eV was between 1 $cm^{-3}$ and 3 $cm^{-3}$ in the magnetosphere subsolar region in this event.

Keywords: low-energy ion monoenergetic acceleration, ultralow-frequency wave, E×B drift

©2019. Japan Geoscience Union. All Right Reserved. 

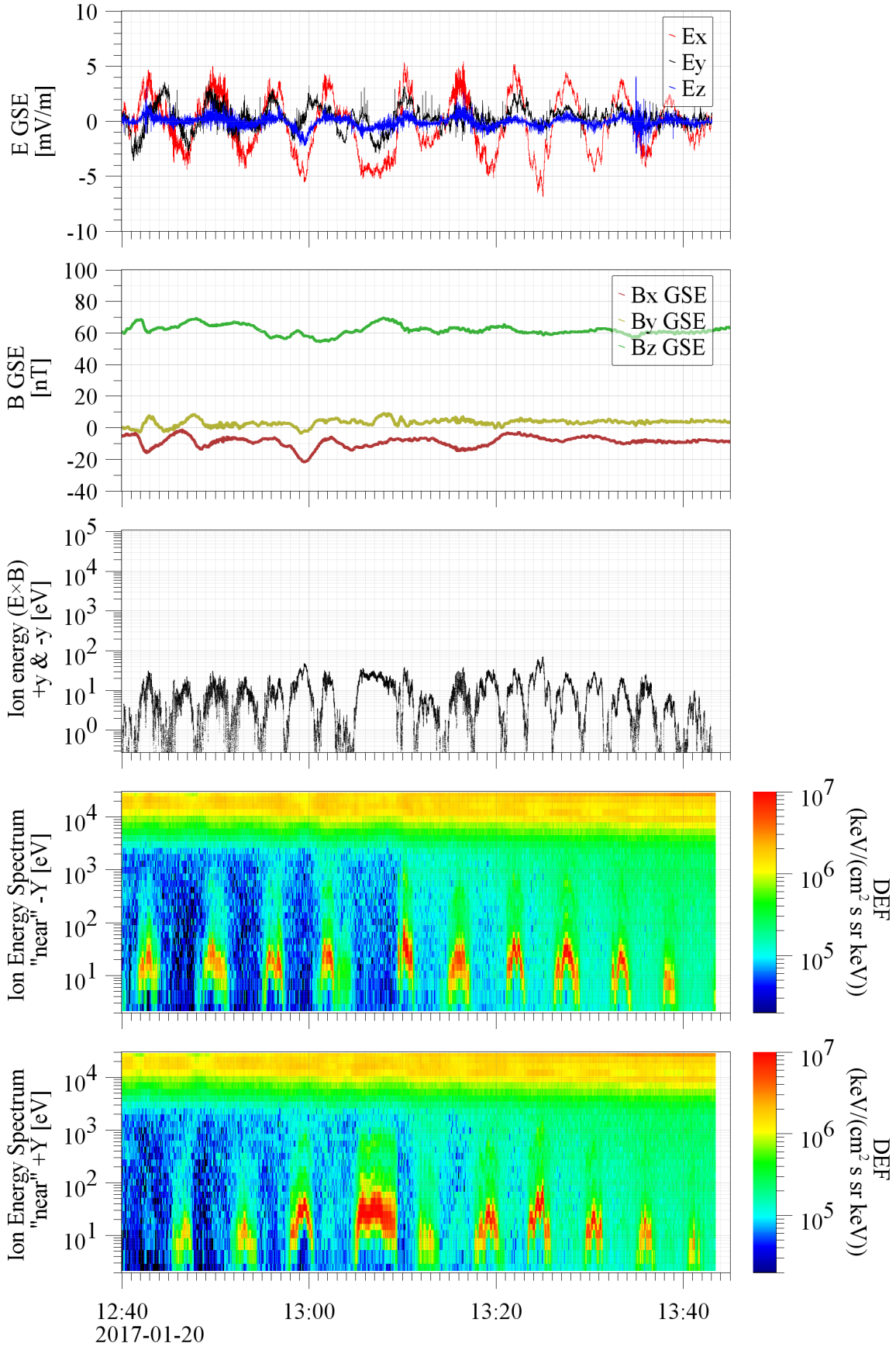


©2019. Japan Geoscience Union. All Right Reserved.

[E] Oral | P (Space and Planetary Sciences )：P-EM Solar-Terrestrial Sciences, Space Electromagnetism & Space Environment

Thu. May 30, 2019 10:45 AM - 12:15 PM JST | Thu. May 30, 2019 1:45 AM - 3:15 AM UTC | A04 TOKYO BAY MAKUHARI HALL

## [P-EM11] Dynamics of Magnetosphere and Ionosphere

convener:Aoi Nakamizo(Applied Electromagnetic Research Institute, National Institute of Information and Communications Technology), Mitsunori Ozaki(Faculty of Electrical and Computer Engineering, Institute of Science and Engineering, Kanazawa University), Akiko Fujimoto(Kyushu Institute of Technology), Tomoaki Hori(Institute for Space-Earth Environmental Research, Nagoya University), Chairperson:Kunuhiro Keika(東京大学大学院理学系研究科), Shin'ya Nakano(情報・システム研究機構 統計数理研究所), Motoharu Nowada(Shandong University)

This session provides an opportunity to present recent results from satellite and ground-based observations and theoretical and simulation studies on the magnetosphere, ionosphere, and their coupling processes. We invite talks and posters discussing various phenomena related to the magnetosphere-ionosphere system: solar wind-magnetosphere interaction, magnetosphere-ionosphere convection, field-aligned current, magnetic storms/substorms, neutral-plasma interaction, ionospheric ion inflow and outflow, aurora phenomena, and so forth. Discussions on planetary and satellite ionosphere and magnetospheres, future missions and instrument developments are also welcome.

10:45 AM - 11:00 AM JST | 1:45 AM - 2:00 AM UTC

[PEM11-13] Statistical study on warm plasma in the magnetotail based on two-component fits of distribution functions

*Kunihiro Keika[1], Ryuta Asami[1], Masahiro Hoshino[1] (1.Department of Earth and Planetary Science, Graduate School of Science, The University of Tokyo)

11:00 AM - 11:15 AM JST | 2:00 AM - 2:15 AM UTC

[PEM11-14] Analysis on anisotropy variations for pitch angle distributions of electrons with various parameters at dipolarization sites in the inner plasma sheet

*Kaiti Wang[1], Zhuo-Ren Lang[2], Ching-Huei Lin[3], Tohru Hada[4], Toshi Nishimura[5] (1.Tamkang Univ., 2.National Cheng Kung Univ., 3.Chien-Hsin Univ. of Sci. & Tech., 4.Kyushu Univ., 5.Boston Univ.)

11:15 AM - 11:30 AM JST | 2:15 AM - 2:30 AM UTC

[PEM11-15] Study of slow-mode shock formation in the symmetric magnetic reconnection based on hybrid simulations

*Nehpreet Kaur Walia[1], Kanako Seki[1], Takanobu Amano[1] (1. Department of Earth & Planetary Science, Graduate School of Science, University of Tokyo)

11:30 AM - 11:45 AM JST | 2:30 AM - 2:45 AM UTC

[PEM11-16] Reconstruction of the electron diffusion region of magnetotail reconnection seen by the Magnetospheric Multiscale spacecraft

*Hiroshi Hasegawa[1], Richard E. Denton[2], Rumi Nakamura[3], Kevin J. Genestreti[4], Takuma Nakamura[3], Kyoung Joo Hwang[5], Tai D. Phan[6], Roy B. Torbert[4], Jim L. Burch[5], Barbara L. Giles[7], Dan J. Gershman[7], Chris T. Russell[8], Bob J. Strangeway[8], Per Arne Lindqvist[9], Yuri V. Khotyaintsev[10], Robert E. Ergun[11], Naritoshi Kitamura[12], Yoshifumi Saito[1] (1.Institute of Space and Astronautical Science, Japan Aerospace Exploration Agency, 2.Dartmouth College, 3.Space Research Institute, Austrian Academy of Science, 4.University of New Hampshire, 5.Southwest Research Institute, 6.University of California Berkeley, 7.NASA Goddard Space Flight Center, 8.University of California Los Angeles, 9.Royal Institute of Technology, 10.Swedish Institute of Space Physics, 11.University of Colorado, 12.University of Tokyo)

11:45 AM - 12:00 PM JST | 2:45 AM - 3:00 AM UTC

[PEM11-17] **MMS observations of the dense high speed flow in the magnetotail**

*Mingyu Wu[1], Tielong Zhang[1] (1.Harbin Insitute of Technology, Shenzhen)

12:00 PM - 12:15 PM JST | 3:00 AM - 3:15 AM UTC

## [PEM11-18] The spatio-temporal development of lightning-induced electron precipitation events

★Invited Papers

*Robert C Moore[1], Dooyoung Kim[1] (1.University of Florida)

# Statistical study on warm plasma in the magnetotail based on two-component fits of distribution functions

*Kunihiro Keika[1], Ryuta Asami[1], Masahiro Hoshino[1]

1. Department of Earth and Planetary Science, Graduate School of Science, The University of Tokyo

A large number of observations reported two distinct plasma populations with different temperatures in the Earth's magnetotail: 1-10 keV for the hotter component and <1 keV for the colder. It is well accepted that plasma of solar wind origin can enter into the magnetosphere due to tailward convection of magnetic field lines that were reconnected at the dayside magnetopause, or due to instabilities or waves that develop on the dawn and dusk flanks. Cold plasma of ionospheric origin can be also transported into the plasma sheet predominantly along the field lines. Such cold plasma can be then heated/accelerated to 1 keV or higher. The dominant transport region(s) and heating mechanism(s) are, however, not well understood. This study investigates global characteristics of warm (10-1000 eV) plasma populations observed in the magnetotail in order to better understand transport regions of solar wind and ionospheric plasma.

We use data from plasma observations made by the Hot Plasma Composition Analyzer (HPCA) on board the Magnetospheric Multiscale (MMS) spacecraft. HPCA measures ions with energies of a few eV to ~40 keV with the determination of ion mass. We perform a one-component Maxwellian fit and a two-component Maxwellian fit to a distribution function of the omni-directional proton flux during intervals of slow flow speed (<~70 km/s). The best fit provides density and temperature of one-component Maxwellian plasma or density and temperature for each component of two-component Maxwellian plasma. This study is focused most on the colder (hotter) component of the two-component plasma, which we term a cold (normal) population. We apply this analysis and categorization to HPCA proton data obtained for a period of May 1 to August 31 of Year 2017. MMS dwelled in the magnetotail for the period, and HPCA data are available in the regions of 6 Re < r < 24 Re.

We examine dependence of density and temperature on plasma beta, which is the ratio of plasma thermal pressure to the magnetic pressure and thus represents the distance from the current sheet. The normal population shows clear positive correlations of density and temperature to plasma beta. This indicates adiabatic heating of lobe plasma transported toward the central plasma sheet. The cold population, on the other hand, does not show clear correlations. It is separated into three different types. Type 1 is characterized by positive correlations of density to plasma beta, similar to the normal population. Density is between 0.01 and 0.1 $cm^{-3}$ at a beta range of 0.001 to 0.01, and increases to ~1 $cm^{-3}$ at beta of >0.1. We confirm that the relation between density and temperature is well explained by adiabatic heating with the specific heat ratio of 5/3. Type 2 is seen only in the high beta (>0.1) regions, with density of ~0.01 $cm^{-3}$. Type 3 can be identified by a different relation between density and beta; density is between 0.01 and 1.0 with the highest occurrence frequency at 0.1 $cm^{-3}$, and temperature is a few 10s to 100s eV. Spatial distributions of each type show that Types 1 and 2 are observed at the radial distance of >10 Re. Type 1 shows no clear dawn-dusk asymmetry of occurrence frequency or average temperature, while Type 2 is more frequently observed on the dusk and dawn sides than around midnight. Type 3 occupies the region closer to 10 Re and is also observed at the radial distance of 10-20 Re with lower occurrence.

We interpret that Type 1 is dominated by plasma of solar wind origin transported over the polar regions, through the lobe toward the plasma sheet. Type 2 is likely solar wind plasma that enters through the flank

©2019. Japan Geoscience Union. All Right Reserved. 

magnetopauses. Type 3 is of ionospheric origin, presumably from nightside auroral regions. We suggest that the north-south component of magnetospheric convection over the polar cap becomes dominant at the radial distance of 10 Re or further. Instabilities or waves that allow solar wind plasma to enter the plasma sheet are likely to sufficiently develop on the night side (i.e., $X < 0$).

Keywords: Entry of solar wind plasma, Supply of ionospheric plasma , plasma mixing, magnetospheric cold plasma

©2019. Japan Geoscience Union. All Right Reserved. 

# Analysis on anisotropy variations for pitch angle distributions of electrons with various parameters at dipolarization sites in the inner plasma sheet

*Kaiti Wang[1], Zhuo-Ren Lang[2], Ching-Huei Lin[3], Tohru Hada[4], Toshi Nishimura[5]

1. Tamkang Univ., 2. National Cheng Kung Univ., 3. Chien-Hsin Univ. of Sci. & Tech., 4. Kyushu Univ., 5. Boston Univ.

During geomagnetic activities, dipolarization of geomagnetic fields can been found to occur at tailside. In this study, we investigate variations in anisotropies of pitch angle distributions for electrons at 63 observed dipolarization sites around distance of 10 $R_E$ (Earth radii) near the magnetic equator in the inner plasma sheet when auroral electrojet AL index decreases. Observational data from 2008 to 2011 for electrons below ~26 keV from the instrument ESA (ElectroStatic Analyzer) onboard of THEMIS mission are adopted. Followed from our previous presentation in which the dependence of these variations on field line lengths (FLL) was focused on [*Wang et al.*, 2018], we present new analysis results concentrating on the dependence of the changes as well as the rates of changes in FLL, magnetic field strengths, and dipolarization angles, during a dipolarizaion period. Comparisons between the anisotropy variations in pitch angle distributions of electrons and the associated bounce time of electrons, event dipolarization time, and measured environmental electric fields will also be presented and discussed.

References

Wang, K., Z. R. Lang, C. H. Lin, T. Hada, A. B. C. Chen, Y. Nishimura (2018). On the field line length dependence of variations in anisotropies for pitch angle distributions of keV electrons at dipolarization sites in the tailside. PEM16-25, JpGU Meeting 2018, Chiba, Japan.

Keywords: dipolarization, anisotropy of pitch angle distributions of electrons , observations of THEMIS mission

©2019. Japan Geoscience Union. All Right Reserved. 

# Study of slow-mode shock formation in the symmetric magnetic reconnection based on hybrid simulations

*Nehpreet Kaur Walia[1], Kanako Seki[1], Takanobu Amano[1]

1. Department of Earth & Planetary Science, Graduate School of Science, University of Tokyo

Fast magnetic reconnection is achieved in the Petschek' s reconnection theory [1964] via a pair of slow-mode shocks on each side of the diffusion region. The occurrence of these slow-mode shocks has been established in MHD regime by the various MHD and Hall-MHD simulation studies [e.g., e.g., Hoshino and Nishida, 1983; Biernat et al., 1989; Lin and Lee, 1993; Hau and Wang, 2016]. However, in the kinetic regime, their existence is still debated. Some of the hybrid and PIC simulations studies of magnetic reconnection region show slow-shock like structures, where either all the Rankine-Hugoniot (RH) or the Mach number conditions are not satisfied [e.g., Krauss-Varban and Omidi, 1995; Lottermoser et al. 1998; Higashimori and Hoshino, 2012], while some show the presence of Petschek like slow-mode shocks [e.g., Lin and Swift, 1996; Liu et al. 2012; Innocenti et al., 2015]. With satellite observations, the presence of slow-mode shocks have been confirmed for both asymmetric dayside magnetopause reconnection [Walia et al., 2018 and Sonnerup at al., 2016] and symmetric magnetotail reconnection [e.g. Feldman et al., 1987; Saito et al., 1995; Eriksson et al., 2004]. Walia et al. [2018] and Saito et al. [1995] reported that the detection probability of slow-mode shocks at around 20% and 10% in the dayside magnetopause and the magnetotail, respectively. One of the reasons for low detection probability of slow-mode shocks can be that the non-slow mode shock crossings used in the observational studies are very close to the X-point, and hence the slow-mode structure has not developed fully. The error in the determination of the shock normal direction and the shock frame of reference can be another reason for lack of observations of slow-mode shocks. In situ measurements via the use of the satellite data, can help us to look into the detailed structure of a magnetic reconnection crossing, but if one wants to look at the whole structure of magnetic reconnection region, simulation studies are needed. Especially, if one wants to look into the transition from the kinetic scales to MHD scales to find out how the structure of reconnection region changes and slow-mode shocks or other discontinuities form and develop.

In the present study we use 2D hybrid simulations for symmetric magnetic reconnection with isotropic temperature to investigate the formation of slow-mode shocks. The presence of slow-shocks in the magnetic reconnection region is established by checking the satisfaction of the RH conditions and specific conditions of Mach numbers, normal angles etc. [e.g., Seon et al., 1995, 1996]. We check the set of 12 slow-mode shock conditions and use the 30% satisfaction criteria [e.g., Walia et al., 2018; Eriksson et al., 2004] at all distances from the X-point to study the formation of slow-mode shocks from the ion inertial length scales to MHD scale. We found that the Petschek like slow-mode shocks can be identified as close as ~10 $\lambda_i$ ($\lambda_i$ = ion inertial length) to the X-point. Below, 10 $\lambda i$ slow-mode shocks are not fully developed, and rather slow shock-like structure is present. Also, it is found that the slow-mode shock identification is sensitive to the slow-shock normal determination. We will also report the differences in the satisfaction of various conditions (e.g., RH conditions, Mach numbers) and the characteristics of the ion distribution functions between the regions with slow-mode shocks and slow shock-like structures.

Keywords: Magnetic reconnection, Slow-mode shocks

©2019. Japan Geoscience Union. All Right Reserved. 

# Reconstruction of the electron diffusion region of magnetotail reconnection seen by the Magnetospheric Multiscale spacecraft

*Hiroshi Hasegawa[1], Richard E. Denton[2], Rumi Nakamura[3], Kevin J. Genestreti[4], Takuma Nakamura[3], Kyoung Joo Hwang[5], Tai D. Phan[6], Roy B. Torbert[4], Jim L. Burch[5], Barbara L. Giles[7], Dan J. Gershman[7], Chris T. Russell[8], Bob J. Strangeway[8], Per Arne Lindqvist[9], Yuri V. Khotyaintsev[10], Robert E. Ergun[11], Naritoshi Kitamura[12], Yoshifumi Saito[1]

1. Institute of Space and Astronautical Science, Japan Aerospace Exploration Agency, 2. Dartmouth College, 3. Space Research Institute, Austrian Academy of Science, 4. University of New Hampshire, 5. Southwest Research Institute, 6. University of California Berkeley, 7. NASA Goddard Space Flight Center, 8. University of California Los Angeles, 9. Royal Institute of Technology, 10. Swedish Institute of Space Physics, 11. University of Colorado, 12. University of Tokyo

Magnetic reconnection is a fundamental plasma process that controls transfer of solar wind energy and mass to planetary magnetospheres and causes explosive energy release associated with solar flares and sudden auroral brightening. NASA's Magnetospheric Multiscale (MMS) mission, which consists of four identical spacecraft launched in March 2015, aims at elucidating how magnetic reconnection works with unprecedented high temporal and spatial resolution measurements of charged particles and electromagnetic fields in space. MMS has been observing Earth's magnetotail since May 2017, and encountered the central region of magnetic reconnection, called the electron diffusion region (EDR), on 11 July 2017 (Torbert et al., Science, 2018). We present results from the reconstruction of the electron diffusion region (EDR) observed in this event. The conditions were suited for the reconstruction technique, developed by Sonnerup et al. (JGR, 2016), that produces magnetic field and electron streamline maps based on a two-dimensional (2-D), time independent, inertia-less form of electron magnetohydrodynamic equation, assuming an approximately symmetric current sheet and negligible guide magnetic field. Our reconstruction results (Hasegawa et al., JGR, 2019) indicate that although the X point was not captured inside its tetrahedron, MMS approached the X point as close as one electron inertial length ~27 km. The opening angle of the recovered separatrix field line, combined with theory, suggests that the dimensionless reconnection rate was 0.17, which is consistent with the measured reconnection electric field 2–4 mV/m. The stagnation point of the reconstructed electron flow is shifted earthward of the X point by ~90 km, one possible interpretation of which is discussed. The energy conversion rate $\mathbf{j}^{*}\mathbf{E}'$ in the electron frame tends to be higher near the stagnation point, consistent with earlier observations and simulations, and is not correlated with the amplitude of broadband electrostatic waves observed in the upper-hybrid frequency range. The latter suggests that the waves did not contribute to energy dissipation in this particular EDR.

References:
Hasegawa, H., Denton, R. E., Nakamura, R., Genestreti, K. J., Nakamura, T. K. M., Hwang, K.-J., et al., Reconstruction of the electron diffusion region of magnetotail reconnection seen by the MMS spacecraft on 11 July 2017. Journal of Geophysical Research: Space Physics, 124. https://doi.org/10.1029/2018JA026051, 2019.
Sonnerup, B. U. O., H. Hasegawa, R. E. Denton, and T. K. M. Nakamura, Reconstruction of the electron diffusion region, J. Geophys. Res. Space Physics, 121, 4279-4290, doi:10.1002/2016JA022430, 2016.
Torbert, R. B., J. L. Burch, T. D. Phan, ... Y. Saito, Electron-scale dynamics of the diffusion region during symmetric magnetic reconnection in space, Science, doi:10.1126/science.aat2998, 2018.

©2019. Japan Geoscience Union. All Right Reserved. 

Keywords: magnetic reconnection, magnetotail, electron diffusion region

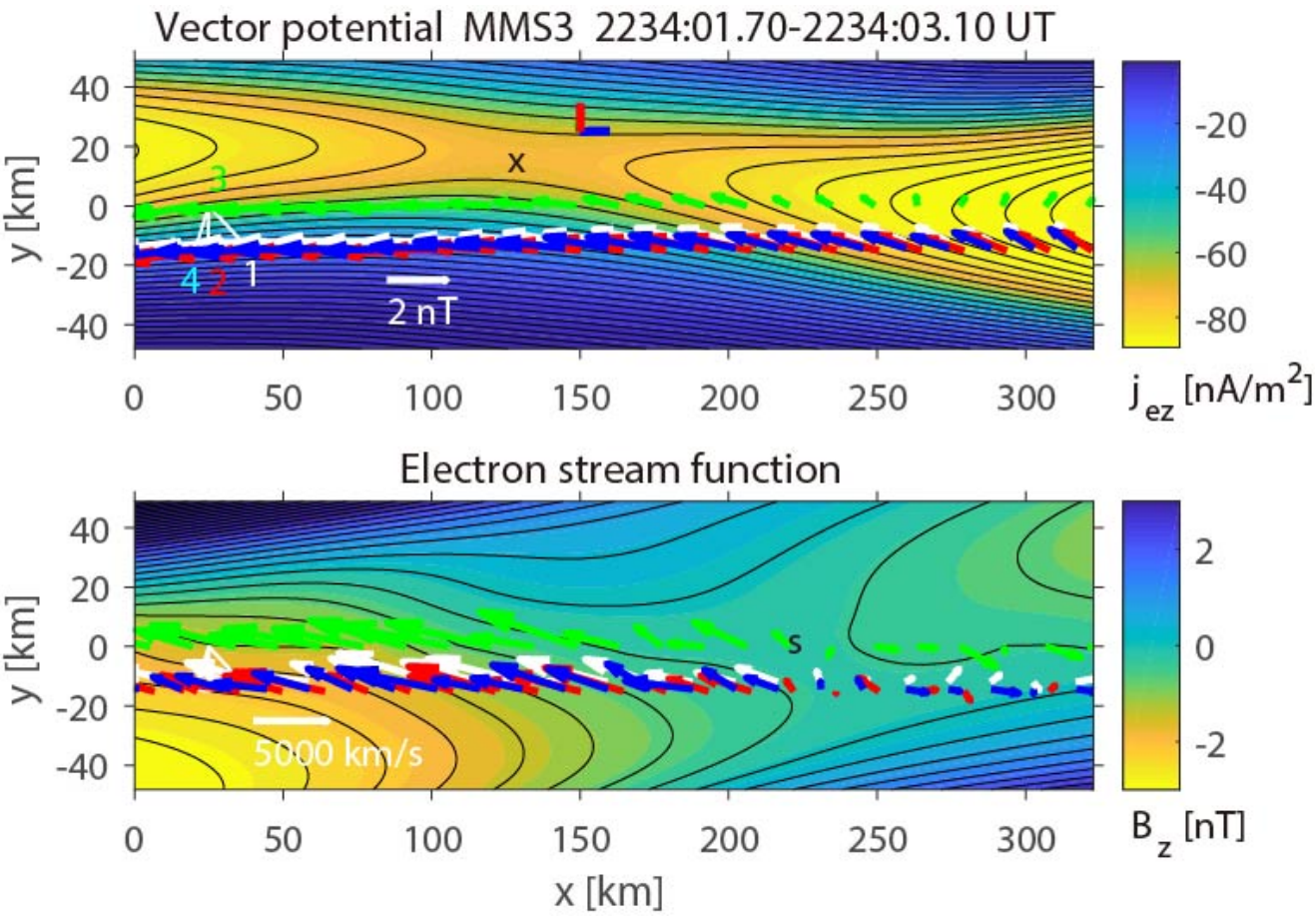


©2019. Japan Geoscience Union. All Right Reserved. 

# MMS observations of the dense high speed flow in the magnetotail

*Mingyu Wu[1], Tielong Zhang[1]

1. Harbin Insitute of Technology, Shenzhen

With the MMS observations in the magnetotail, we report a earthward, dense, high speed, bulk flow event. In this event, two dense high speed flows (DHSF) are observed. Compared with the plasma sheet, DHSF contains much denser and colder plasma. Ion density of DHSF is about 8 times higher to plasma sheet density, while temperature of DHSF is several times lower to plasma sheet plasma. Due to the high density, DHSF can transport mass more effective than normal bursty bulk flows. Such DHSF can be generated by Magnetic reconnection, but the generation mechanism is still unclear.

Keywords: High-density bulk flow, Plasma sheet, Magnetic reconnection

©2019. Japan Geoscience Union. All Right Reserved. 

# The spatio-temporal development of lightning-induced electron precipitation events

*Robert C Moore[1], Dooyoung Kim[1]

1. University of Florida

Lightning-induced electron precipitation (LEP) events occur when the electromagnetic energy radiated by lightning couples to the magnetosphere and scatters ¬stably trapped radiation belt electrons. A portion of these scattered electrons in turn precipitate into the underlying ionosphere, producing electron density disturbances in the D-region ionosphere which can be detected by VLF remote sensing. When LEP events are observed nearly simultaneously at both the northern and southern ends of a field line, the LEP event is known as a conjugate LEP event. In this paper, an array of VLF receivers in the northern hemisphere is used to measure the spatial-temporal development of the LEP-related ionization patch produced within the D-region ionosphere. During one interesting event, LEP-associated VLF signal perturbations were observed at three receiver sites in the northern hemisphere (Florida, North Carolina, and Connecticut) and at one receiver in the conjugate hemisphere (Palmer Station, Antarctica). The LEP-related disturbance is observed to move poleward with time, consistent with many past observations. A second interesting event indicates the detection of an eastward expansion (with time) of the LEP-related disturbance, however. Together, these observations indicate that previous large-scale statistics compiled for conjugate LEP events may be seriously impacted by the spatio-temporal development of the LEP-associated ionospheric disturbances in the two hemispheres. Perhaps equally importantly, these observations indicate that VLF remote sensing can be used to measure the temporal and spatial development of energetic electron precipitation from the Earth's radiation belts.

Keywords: Lightning-induced electron precipitation, Radiation belts, Ionosphere

©2019. Japan Geoscience Union. All Right Reserved. 

[E] Oral | P (Space and Planetary Sciences )：P-EM Solar-Terrestrial Sciences, Space Electromagnetism & Space Environment

Thu. May 30, 2019 1:45 PM - 3:15 PM JST | Thu. May 30, 2019 4:45 AM - 6:15 AM UTC | A04 TOKYO BAY MAKUHARI HALL

## [P-EM11] Dynamics of Magnetosphere and Ionosphere

convener:Aoi Nakamizo(Applied Electromagnetic Research Institute, National Institute of Information and Communications Technology), Mitsunori Ozaki(Faculty of Electrical and Computer Engineering, Institute of Science and Engineering, Kanazawa University), Akiko Fujimoto(Kyushu Institute of Technology), Tomoaki Hori(Institute for Space-Earth Environmental Research, Nagoya University), Chairperson:Naritoshi Kitamura(東京大学大学院理学系研究科), Yuka Sato(日本工業大学)

This session provides an opportunity to present recent results from satellite and ground-based observations and theoretical and simulation studies on the magnetosphere, ionosphere, and their coupling processes. We invite talks and posters discussing various phenomena related to the magnetosphere-ionosphere system: solar wind-magnetosphere interaction, magnetosphere-ionosphere convection, field-aligned current, magnetic storms/substorms, neutral-plasma interaction, ionospheric ion inflow and outflow, aurora phenomena, and so forth. Discussions on planetary and satellite ionosphere and magnetospheres, future missions and instrument developments are also welcome.

1:45 PM - 2:00 PM JST | 4:45 AM - 5:00 AM UTC

[PEM11-19] Energy flow, dynamo and field-aligned current during a substorm

*Yusuke Ebihara[1], Takashi Tanaka[2] (1.Research Institute for Sustainable Humanosphere, Kyoto University, 2.Kyushu University)

2:00 PM - 2:15 PM JST | 5:00 AM - 5:15 AM UTC

[PEM11-20] **Electron flux and field-aligned current associated with Pc5 auroral arc pulsations observed onboard THEMIS and DMSP satellites**

*Natsuo Sato[1], Akira S Yukimatu[1,2], Yoshimasa Tanaka[1,2], Tomoaki Hori[3], Akira Kadokura[1,2], Tohru Sakurai[4], Desheng Han[5], Yuzhang Ma[6], Qinghe Zhang[6] (1.National Institute of Polar Research, 2.SOKENDAI, 3.Nagoya University, 4.Tokai University, 5.Tongji University, 6.Shandong University)

2:15 PM - 2:30 PM JST | 5:15 AM - 5:30 AM UTC

[PEM11-21] Multiple spots of enhanced electron precipitation near the equatorward boundary of the cusp

*Satoshi Taguchi[1], Satoshi Kose[1], Kohei Takasu[1], Morio Tanaka[1], Keisuke Hosokawa[2], Yasunobu Ogawa[3] (1.Department of Geophysics, Graduate School of Science, Kyoto University, 2.Department of Communication Engineering and Informatics, University of Electro-Communications, 3.National Institute of Polar Research)

2:30 PM - 2:45 PM JST | 5:30 AM - 5:45 AM UTC

[PEM11-22] Statistical study of auroral/resonant-scattering 427.8-nm emission observed at subauroral latitudes over 14 years

*Kazuo Shiokawa[1], Yuichi Otsuka[1], Martin Connors[2] (1.Institute for Space-Earth Environmental Research, Nagoya University, 2.Athabasca University)

2:45 PM - 3:00 PM JST | 5:45 AM - 6:00 AM UTC

[PEM11-23] Antarctic large area network observation of auroral phenomena using unmanned system: Conjugate auroral event studies (2)

*Akira Kadokura[1], Hisao Yamagishi[1], Masaki Okada[1], Yasunobu Ogawa[1], Yoshimasa Tanaka[1], Ryuho Kataoka[1], Herbert Akihito Uchida[1], Yuichi Otsuka[2] (1.National Institute of Polar Research, 2.Nagoya University)

3:00 PM - 3:15 PM JST | 6:00 AM - 6:15 AM UTC

[PEM11-24] **Dawn-Dusk Asymmetry in Dayside and Nightside auroral Ovals: Surveys of auroral emissions based on the all-sky imagers in Arctic and Antarctic**

★Invited Papers

*Zejun Hu[1] (1.Polar Research Institute of China)

# Energy flow, dynamo and field-aligned current during a substorm

*Yusuke Ebihara[1], Takashi Tanaka[2]

1. Research Institute for Sustainable Humanosphere, Kyoto University, 2. Kyushu University

A substorm is one of the most severe disturbances that occur in the magnetosphere. Extremely bright aurora is a great manifestation of the substorm. Since the bright aurora is caused by precipitating electrons, the bright aurora is closely associated with the upward field-aligned currents (FACs). Simultaneously, a large amount of energy, of the order of $10^{11}$ watts, is consumed in the auroral ionosphere due to Joule dissipation during the substorm. The dissipating energy is brought by the FACs that are rapidly intensified. Thus, the formation of the FACs is a key to understand the substorm. The generation of the FACs is accompanied with conversion of energy (dynamo). The energy comes from the solar wind. The purpose of this study is to provide a unified view of a substorm in terms of the energy flow, energy conversion (dynamo) and field-aligned current on the basis of a global magnetohydrodynamics (MHD) simulation. The recent global MHD simulation tells us that, at least, some dynamo regions appear one by one in association with the substorm. The first dynamo region is found in the bow shock where the solar wind kinetic energy is converted to the magnetic energy and the internal energy. However, the role of the bow shock dynamo is suggested to be minor. The second dynamo region is found in the lobe region when the interplanetary magnetic field (IMF) is northward. A complicated structure of the plasma pressure in the lobe gives rise to the generation of FACs that could manifest high-latitude auroral arcs during the growth phase. The third dynamo region appears in the mantle region when IMF is southward. The internal energy is converted to the magnetic energy by way of the kinetic energy in the mantle dynamo. Simultaneously, a large-scale FACs (known as Region 1 FACs) are generated in association with the mantle dynamo, which is probably responsible to the formation of a quiet auroral arc during growth phase. The fourth dynamo appears in the near-Earth magnetosphere on the nightside as a consequence of the formation of the near-Earth neutral line. The magnetic energy (coming from the lobe region) is converted to the internal energy, followed by the kinetic energy and the magnetic energy. The near-Earth dynamo is associated with the onset of the sudden intensification of the upward FACs that are related to the initiation of the auroral breakup. The fifth dynamo is located near the leading/trailing edges of the bright auroral surge where charge separation takes place due to the gradient of the ionospheric Hall conductivity. A localized upward FAC is generated, which probably manifests the bright auroral surge traveling westward. It is concluded that the evolution of the substorm can be understood to the evolution of the dynamo regions in the magnetosphere and the ionosphere.

Keywords: Substorm, Energy conversion, MHD simulation

©2019. Japan Geoscience Union. All Right Reserved. 

# Electron flux and field-aligned current associated with Pc5 auroral arc pulsations observed onboard THEMIS and DMSP satellites

*Natsuo Sato[1], Akira S Yukimatu[1,2], Yoshimasa Tanaka[1,2], Tomoaki Hori[3], Akira Kadokura[1,2], Tohru Sakurai[4], Desheng Han[5], Yuzhang Ma[6], Qinghe Zhang[6]

1. National Institute of Polar Research, 2. SOKENDAI, 3. Nagoya University, 4. Tokai University, 5. Tongji University, 6. Shandong University

Pc5 poleward moving auroral arc (PMAA) pulsations observed on the ground in the post-midnight sector exhibit east-west-aligned auroral arcs elongated ~ 1000-3000 km and behave poleward moving form with a recurrence period of ~ 2-10 minutes (Pc5 range). They appear just poleward side of common type pulsating auroras. We examined the space-ground coordinated observations with the THEMIS-A, D, and E spacecraft whose footprints were located near the PMAA observed with the all-sky imager on the ground. The latitudinal wave amplitudes and phase structures are consistent with the field-line resonance (FLR) model, while the period of oscillation was longer at the higher latitude side (not a monochromatic wave). The electron flux in the higher energy range of ~ 2–20 keV showed decreasing modulation in conjunction with the FLR oscillations. The intensity of the electric field and the velocity showed a spatial gradient that suggests the existence of a field-aligned current flow around the region of the satellites. The period of FLR oscillations in the magnetosphere was ~ 15–25% longer than that of the auroral pulsations in the ionosphere, and the enhancement of FLR oscillations was ~ 3–4 minutes ahead of the auroral pulsations. These signals imply that the FLR oscillations could not directly enhance the luminosity oscillation but needed some other process that could enhance the luminosity pulsation. We will examine the mechanism of how to produce the field-aligned electric field in association with the PMAA. In this study we focus on the characteristics of the electron flux variations observed onboard the THEMIS and DMSP satellites. The THEMIS satellites were located near the equatorial plane in the magnetosphere, and the DMSP satellites traversed in the ionosphere and crossed over the field of view of all-sky imager at observatories in Canada and Alaska and Syowa Station in Antarctica. It is found that the DMSP satellites observed the precipitating electron flux that behaved the feature of field-aligned acceleration and also observed the field-aligned currents when the DMSP satellite crossed the region of the PMAA.

Keywords: auroral arc pulsation, Pc 5 pulsation, pulsating aurora, field-line resonance, THEMIS spacecraft, DMSP satellite

©2019. Japan Geoscience Union. All Right Reserved. 

# Multiple spots of enhanced electron precipitation near the equatorward boundary of the cusp

*Satoshi Taguchi[1], Satoshi Kose[1], Kohei Takasu[1], Morio Tanaka[1], Keisuke Hosokawa[2], Yasunobu Ogawa[3]

1. Department of Geophysics, Graduate School of Science, Kyoto University, 2. Department of Communication Engineering and Informatics, University of Electro-Communications, 3. National Institute of Polar Research

Localized enhancements of electron precipitation near the equatorward boundary of the cusp is thought to be caused by enhanced fluxes of soft magnetosheath electrons in the flux tube immediately after localized intermitted reconnection on the dayside magnetopause. A recent study based on an all-sky imager has reported an event which shows that enhanced electron precipitation appears in two separate locations along the equatorward boundary of the cusp, and that the distance between them is approximately 0.2 MLT. In this study we have examined if there is any characteristic scale in the distance between neighboring electron precipitation spots near the equatorward of the cusp to understand the characteristics of the occurrence point of intermittent reconnection. We analyzed 630-nm aurora data from an all-sky imager at Longyearbyen, Svalbard, and electron precipitation and field-aligned current data from DMSP spacecraft, which flied in the field-of-view of the auroral imager. A simultaneous observation event shows that six enhanced electron precipitation regions, each of which is accompanied with an upward/downward pair of mesoscale field-aligned currents, were observed along the pass of the DMSP satellite, and that all of those enhanced electron precipitation regions were also identified as auroral spots in the 630-nm auroral image data. By examining auroral image data obtained before the simultaneous observation event, we traced back to the initial brightening for each auroral spot. The result of analysis has shown that the longitudinal distance between the neighboring spots near the equatorward boundary of the cusp lies between 0.15 and 0.4 MLT. The statistical analysis with data obtained for longer period of time on the same day has also shown a similar tendency. We discuss why localized intermittent reconnection tends to occur in such locations.

Keywords: cusp, aurora, electron precipitation, reconnection

©2019. Japan Geoscience Union. All Right Reserved. 

# Statistical study of auroral/resonant-scattering 427.8-nm emission observed at subauroral latitudes over 14 years

*Kazuo Shiokawa[1], Yuichi Otsuka[1], Martin Connors[2]

1. Institute for Space-Earth Environmental Research, Nagoya University, 2. Athabasca University

Auroral emission at 427.8-nm from $N_2^+$ ions is caused by precipitation of energetic electrons, or by resonant scattering of sunlight at high altitudes by $N_2^+$ ions. The latter often causes impressive purple aurora at high altitudes. However, statistical characteristics of auroral 427.8-nm emission have not well been understood. In this paper we report occurrence characteristics of high 427.8-nm emission intensities (more than 100 R) at subauroral latitudes, based on measurements by a filter-tilting photometer over 14 years (2005-2018) at Athabasca, Canada (magnetic latitude: ~62°). We divided the dataset into the elevation angles ($\theta$s) of the sun more than and less than -24° (shadow height of sunlight: 600 km) to separate the 427.8-nm emissions caused by resonant scattering of sunlight and those excited by auroral electrons, respectively. The occurrence rate of 427.8-nm emissions of more than 100 R is 10.6 % and 7.65 % for $\theta$s more than and less than -24°, respectively. The occurrence rate is high in the post-midnight sector, and increases with increasing geomagnetic activity, solar-wind speed, and density. The occurrence rate is highest in summer. A high occurrence rate was also observed in 2015-2018, from the maximum to the declining phase of the 11-year solar activity. Superposed epoch analysis indicates that the 427.8-nm emission exceeds 100 R when solar wind speed increases and solar wind density concurrently decreases, suggesting that the solar wind structures typically observed at the arrival of corotating interaction regions (CIR) can be responsible for the high 427.8-nm emission.

Keywords: 427.8 nm emission, resonant scattering of sunlight, purple aurora

©2019. Japan Geoscience Union. All Right Reserved. 

# Antarctic large area network observation of auroral phenomena using unmanned system: Conjugate auroral event studies (2)

*Akira Kadokura[1], Hisao Yamagishi[1], Masaki Okada[1], Yasunobu Ogawa[1], Yoshimasa Tanaka[1], Ryuho Kataoka[1], Herbert Akihito Uchida[1], Yuichi Otsuka[2]

1. National Institute of Polar Research, 2. Nagoya University

Conjugate auroral events observed at Syowa Station, Antarctica and observatories in Iceland on September 28 in 2017 are analyzed. During this period, auroral data obtained by the all-sky auroral imager of the Unmanned Auroral Observation system (UAO) at Amundsen Bay, which is located about 500 km eastward from Syowa Station, are also available. We will discuss development of the conjugate auroral activities in a broader longitudinal area than before.

Keywords: aurora, conjugate observation, substorm

©2019. Japan Geoscience Union. All Right Reserved. 

# Dawn-Dusk Asymmetry in Dayside and Nightside auroral Ovals: Surveys of auroral emissions based on the all-sky imagers in Arctic and Antarctic

*Zejun Hu[1]

1. Polar Research Institute of China

The synoptic distributions of dayside aurora in the Northern and Southern Hemispheres, acquired from all-sky imagers at Yellow River Station in Arctic and South Pole Station in Antarctica, respectively, present the same two-peak structure, namely, the prenoon 09:00 MLT and postnoon 14:00-15:00 MLT peaks. The auroral intensity presents a hemispheric asymmetry, i.e., the postnoon intensity is less than the prenoon intensity in the Southern Hemisphere but more in the Northern Hemisphere. The hemispheric asymmetry is not changed with the change of IMF’ s polarity, although 1) the negative (positive) IMF By favors the postnoon 557.7/630.0-nm auroral emissions, and the positive (negative) By favor to the excitation of 630.0-nm auroral on prenoon oval in the Northern (Southern) Hemisphere; 2) the 630.0-nm auroral intensity in dayside oval increases dramatically during the negative IMF Bz. We suggested that 1) the two-peak structure in the dayside oval are predominantly related with the prenoon/postnoon antiparallel reconnection in high-latitude magnetopause produced to the prenoon and postnoon peaks; 2) the IMF By should modulate the dayside aurora through the inter-hemispheric current, which is produced by a north-south oriented electric field , and changing the distribution of midday R0-R1 current; 3) the opposite prenoon-postnoon asymmetries of dayside auroral distributions in the two hemispheres are the combined effect of the prenoon-postnoon variations of the magnetosheath density and the variation of the local ionospheric conductivity in the two ground-based observatories.

The synoptic distributions of nightside aurora in the Northern Hemisphere, acquired from all-sky imagers at China-Iceland joint Aurora Observatory (CIAO) in Iceland, present that there are different characteristics on 427.8, 557.7, and 630.0 nm: 1) There is a two-peak structure on 427.8 and 557.7 nm, namely the pre-midnight 20:00- 21:00 MLT and post-midnight 04:00 peaks. For 427.8-nm auroral emission, the intensity of two peaks are same. For 557.7-nm emission, the maximal intensity is at peak 21:00 MLT. 2) There is only on peak on 630.0 nm, namely the pre-midnight 20:00-21:00 MLT. The dawn-dusk asymmetry in the nightside auroral oval should be related with the asymmetries of field-aligned currents and plasma waves in magnetosphere.

Keywords: dawn-dusk asymmetry, dayside & nightside auroral oval, particle precipitation, auroral morphology

©2019. Japan Geoscience Union. All Right Reserved. 

[E] Oral | P (Space and Planetary Sciences )：P-EM Solar-Terrestrial Sciences, Space Electromagnetism & Space Environment

Thu. May 30, 2019 3:30 PM - 5:00 PM JST | Thu. May 30, 2019 6:30 AM - 8:00 AM UTC | A04 TOKYO BAY MAKUHARI HALL

## [P-EM11] Dynamics of Magnetosphere and Ionosphere

convener:Aoi Nakamizo(Applied Electromagnetic Research Institute, National Institute of Information and Communications Technology), Mitsunori Ozaki(Faculty of Electrical and Computer Engineering, Institute of Science and Engineering, Kanazawa University), Akiko Fujimoto(Kyushu Institute of Technology), Tomoaki Hori(Institute for Space-Earth Environmental Research, Nagoya University), Chairperson:Naritoshi Kitamura(東京大学大学院理学系研究科), Yuka Sato(日本工業大学), Masaki Nishino(名古屋大学宇宙地球環境研究所)

This session provides an opportunity to present recent results from satellite and ground-based observations and theoretical and simulation studies on the magnetosphere, ionosphere, and their coupling processes. We invite talks and posters discussing various phenomena related to the magnetosphere-ionosphere system: solar wind-magnetosphere interaction, magnetosphere-ionosphere convection, field-aligned current, magnetic storms/substorms, neutral-plasma interaction, ionospheric ion inflow and outflow, aurora phenomena, and so forth. Discussions on planetary and satellite ionosphere and magnetospheres, future missions and instrument developments are also welcome.

3:30 PM - 3:45 PM JST | 6:30 AM - 6:45 AM UTC

### [PEM11-25] Enhancement of 10MeV protons associated with a change of magnetic field configuration at geosynchronous orbit

*Takahiro Obara[1] (1.Planetary Plasma and Atmospheric Research Center,Tohoku University)

3:45 PM - 4:00 PM JST | 6:45 AM - 7:00 AM UTC

### [PEM11-26] Solar-cycle variations of >30 keV proton flux enhancements under the inner radiation belt

*ALLA SUVOROVA[1] (1.National Central University)

4:00 PM - 4:15 PM JST | 7:00 AM - 7:15 AM UTC

### [PEM11-27] Auroral Imaging with Commercial DSLR Cameras near Athabasca, Canada

*Martin G Connors[1,2], Ian Schofield[1], Mike Noble[2], Alister Ling[2], Ryuho Kataoka[3], Ken Murata[4], Kazunori Yamamoto[4] (1.Athabasca University, 2.Edmonton Centre, Royal Astronomical Society of Canada, 3.National Institute for Polar Research, 4.National Institute for Communications Technology)

4:15 PM - 4:30 PM JST | 7:15 AM - 7:30 AM UTC

### [PEM11-28] PARM: Investigation of precipitating high-energy electrons into the auroral ionosphere with sounding rockets

*Kazushi Asamura[1], Yoshizumi Miyoshi[2], Keisuke Hosokawa[3], Takefumi Mitani[1], Taku Namekawa[1,5], Takeshi Sakanoi[4], Naoshi Yagi[4], Mizuki Fukizawa[4], Genki Ishizawa[4], Satoshi Kasahara[5], Shin Sugo[5], Oya Kawashima[5], Reiko Nomura[6], Masahito Nose[2], Mariko Teramoto[2], Yasunobu Ogawa[7], Shinji Saito[2], Ryoichi Fujii[8] (1.ISAS / JAXA, 2.ISEE, Nagoya University, 3.The University of Electro-Communications, 4.Tohoku University, 5.The University of Tokyo, 6.NAOJ / NINS, 7.NiPR / ROIS, 8.ROIS)

4:30 PM - 4:45 PM JST | 7:30 AM - 7:45 AM UTC

### [PEM11-30] Development of a miniaturized X-ray imager for GEOspace X-ray imager (GEO-X)

*Kumi Ishikawa[1], Yuichiro Ezoe[2], Masaki Numazawa[2], Daiki Ishi[2], Maiko Fujitani[2], Ryota Otsubo[2], Aoto Fukushima[2], Hikari Suzuki[2], Tatsuya Yuasa[2], Hiroshi Nakajima[3], Junko Hiraga[4], Yoshizumi Miyoshi[5], Satoshi Kasahara[6], Kazuhisa Mitsuda[1] (1.Japan Aerospace Exploration Agency/Institute of Space and Astronautical Science , 2.Tokyo Metropolitan University, 3.Kanto Gakuin University, 4.Kwansei Gakuin University, 5.Nagoya University, 6.The university of Tokyo)

4:45 PM - 5:00 PM JST | 7:45 AM - 8:00 AM UTC
Discussion

# Enhancement of 10MeV protons associated with a change of magnetic field configuration at geosynchronous orbit

*Takahiro Obara[1]

1. Planetary Plasma and Atmospheric Research Center,Tohoku University

It was found that 10MeV proton flux enhanced at geosynchronous orbit during the thinning of the magnetic field configuration. Since no significant enhancement of 10MeV proton flux was observed outside of the magnetosphere, the 10MeV protons seem to be of magnetospheric origin. Drastic decrease of 2MeV electron flux was observed at the geosynchronous orbit when the thinning of the magnetic field commenced. The 2MeV electron flux recovered when the dipolarization of the magnetic field occurred, while 10MeV proton flux remained almost constant. Three hours before the increase of 10MeV protons, shock structure of the solar wind hit the Earth’ s magnetosphere. At that time, increase of 6.5MeV protons was observed at geosynchronous orbit. Low energy (1~10MeV) protons are thought to be produced by the interaction of the solar wind shock and the magnetopause (Shimazu and Tanaka, 2005). In this event, only 6.5 MeV protons could reach geosynchronous orbit just after the production. Due to the thinning of the magnetic field configuration, 10MeV protons could then reach geosynchronous orbit. Low energy (1~10MeV) protons will be probes of the magnetosphere configuration weather the magnetosphere is truly quiet when the first protons (6.5MeV protons) arrive at geosynchronous orbit altitude and time delay of second protons (10MeV protons) was accompanied by the magnetic field changes in the magnetosphere. This type of event will be interesting from the view of the magnetosphere configuration change during the solar wind shock arrival. We are collecting more events to confirm above mentioned scenario.

Keywords: Geosynchronous orbit, Enhancement of 10MeV protons , Magnetic field change

©2019. Japan Geoscience Union. All Right Reserved. 

# Solar-cycle variations of >30 keV proton flux enhancements under the inner radiation belt

*ALLA SUVOROVA[1]

1. National Central University

Upper atmosphere is continually affected by intense fluxes of energetic electrons and protons penetrating from the magnetosphere to low altitudes. The energetic particles ionize and excite neutral species altering local characteristics of the ionosphere. Continuous monitoring of energetic particles at low heights of ~850 km with the MEPED instrument onboard the NOAA/POES satellites allows studying of particle flux variations with geomagnetic activity and solar cycle. The instrument measures precipitating/trapped electrons and protons in the wide energy range. In the previous study, we revealed enhancements of electrons with energies 30 - 300 keV at low latitudes in a so-called forbidden zone. It was established that the electrons were injected from the inner radiation belt probably due to a mechanism of fast radial transport in the crossed electric and magnetic fields. In the current work, we study fluxes of >30 keV protons in the forbidden zone. We distinguish two types of proton enhancements, which have different spatial-temporal characteristics. One type of proton enhancements occurs due to the charge-exchange mechanism of the ring current and is always observed during magnetic storms. Another type is due to injections from the inner radiation belt. The last enhancements are similar to the electron enhancements. Results of long-term analysis of proton injections will be presented.

Keywords: magnetosphere-ionosphere, energetic protons, low latitudes, solar cycle

©2019. Japan Geoscience Union. All Right Reserved. 

# Auroral Imaging with Commercial DSLR Cameras near Athabasca, Canada

*Martin G Connors[1,2], Ian Schofield[1], Mike Noble[2], Alister Ling[2], Ryuho Kataoka[3], Ken Murata[4], Kazunori Yamamoto[4]

1. Athabasca University, 2. Edmonton Centre, Royal Astronomical Society of Canada, 3. National Institute for Polar Research, 4. National Institute for Communications Technology

Commercial DSLR Cameras have permitted a revolution in auroral imaging, due to their digital nature, low cost, high sensitivity, and other advantages. Athabasca University Geophysical Observatory is in the subauroral zone, but due to the high altitude of auroras, usually has optical auroral activity visible on its northern horizon. We have operated mostly northward-pointing DSLR cameras, either with a field of view of about 50 degrees, or nearly allsky coverage. Since the “allsky” cameras we have used in fact do not cover the whole sky, we have tilted them northward to cover that horizon preferentially. We have livestreamed images to http://autumn.athabascau.ca/auroracamhd.htm. Ironically, the northward orientation of cameras at the observatory has precluded us capturing images of the newly-recognized STEVE phenomenon, which is normally located south of our location. However, STEVE events found on auroral imaging campaigns in the Edmonton area can often be identified on EMCCD images from our Keo Scientific intensified allsky camera. Then we can combine the images, showing for example, that STEVE is roughly 200 km above the surface. The auroral imaging campaigns have used three fullframe DSLRs to produce partial sky images that are then stitched together using software to produce approximately 10k-pixel color auroral movies, suited for use with modem planetarium projector systems as impressive high resolution sky shows. Most recently we have used a Sony Alpha 7000 camera, taking advantage of the fiber optic internet link to the Athabasca site, to make livecasting of auroras to Japan possible. Since reliability of cameras with moving parts has been a problem, we hope that the direct imaging Sony Alpha camera will be more reliable than the “reflex” cameras previously used. To get around the problem of moving parts wearing out under the very high frame rate, we also tested inexpensive CMOS-type sensors controlled by single-board computers, and sending a digital image stream, but so far with different, but still present, reliability problems. Another issue faced is that in continuous operation, a large amount of data is produced due to the high pixel count of the cameras. We will discuss technical issues and challenges, but also show some results of DSLR operation over the years, including auroral movies and high resolution still frames.

Keywords: aurora, imaging, STEVE

©2019. Japan Geoscience Union. All Right Reserved. 

[E] Oral | P (Space and Planetary Sciences ) | P-EM Solar-Terrestrial Sciences, Space Electromagnetism & Space Environment

# [P-EM11] Dynamics of Magnetosphere and Ionosphere

convener:Aoi Nakamizo(Applied Electromagnetic Research Institute, National Institute of Information and Communications Technology), Mitsunori Ozaki(Faculty of Electrical and Computer Engineering, Institute of Science and Engineering, Kanazawa University), Akiko Fujimoto(Kyushu Institute of Technology), Tomoaki Hori(Institute for Space-Earth Environmental Research, Nagoya University), Chairperson:Naritoshi Kitamura(東京大学大学院理学系研究科), Yuka Sato(日本工業大学), Masaki Nishino(名古屋大学宇宙地球環境研究所)

Thu. May 30, 2019 3:30 PM - 5:00 PM A04 (TOKYO BAY MAKUHARI HALL)

This session provides an opportunity to present recent results from satellite and ground-based observations and theoretical and simulation studies on the magnetosphere, ionosphere, and their coupling processes. We invite talks and posters discussing various phenomena related to the magnetosphere-ionosphere system: solar wind-magnetosphere interaction, magnetosphere-ionosphere convection, field-aligned current, magnetic storms/substorms, neutral-plasma interaction, ionospheric ion inflow and outflow, aurora phenomena, and so forth. Discussions on planetary and satellite ionosphere and magnetospheres, future missions and instrument developments are also welcome.

4:15 PM - 4:30 PM

# [PEM11-28]PARM: Investigation of precipitating high-energy electrons into the auroral ionosphere with sounding rockets

*Kazushi Asamura[1], Yoshizumi Miyoshi[2], Keisuke Hosokawa[3], Takefumi Mitani[1], Taku Namekawa[1,5], Takeshi Sakanoi[4], Naoshi Yagi[4], Mizuki Fukizawa[4], Genki Ishizawa[4], Satoshi Kasahara[5], Shin Sugo[5], Oya Kawashima[5], Reiko Nomura[6], Masahito Nose[2], Mariko Teramoto[2], Yasunobu Ogawa[7], Shinji Saito[2], Ryoichi Fujii[8] (1.ISAS / JAXA, 2.ISEE, Nagoya University, 3.The University of Electro-Communications, 4.Tohoku University, 5.The University of Tokyo, 6.NAOJ / NINS, 7.NiPR / ROIS, 8.ROIS)

Keywords: electron microburst precipitation, sounding rocket, pulsating aurora

Bursty precipitations of high-energy electrons into the polar ionopshere have been observed by low-altitude satellite, for example, SAMPEX and FIREBIRD II. These precipitations, called microburst, may contribute to the loss of the terrestrial radiation belt through the collisional energy loss with the dense, cold atmospheric particles. Recent numerical simulations successfully reproduce these microburst precipitations with a few Hz modulations by taking into account the pitch angle scattering with the whistler chorus elements at off-equator regions in the inner magnetosphere. Therefore, one can expect that the miscroburst precipitations have properties depending on auroral activities especially the pulsating auroras. In order to investigate the mechanisms of the microburst precipitations by in-situ observations, we are developing two instrument packages: PARM (Pulsating AuRora and Microbursts; already developed) and PARM-2 (being developed), both of which are designed suitable for sounding rocket experiments. PARM consists of four sensors; HEP (high-energy electron energy spectrometer), MED (medium-energy electron detector), AIC (auroral camera), and AFG (ASIC-based fluxgate magnetometer). PARM was onboard the NASA's RockSat-XN sounding rocket, and launched from Andoya, Norway at 09:13UT, Jan 13, 2019. On the other hand, PARM-2 is under development. It consists of HEP, two AICs, and MIM (magneto-impedance magnetometer). PARM-2 is to be onboard the NASA's LAMP sounding rocket which will fly from Poker Flat, Alaska in the period between the end of 2019 and the

©Japan Geoscience Union

beginning of 2020.

We will present the overview of PARM missions including the initial results of RockSat-XN/PARM with ground-based observations and preparation status of LAMP/PARM-2.

©Japan Geoscience Union

# Development of a miniaturized X-ray imager for GEOspace X-ray imager (GEO-X)

*Kumi Ishikawa[1], Yuichiro Ezoe[2], Masaki Numazawa[2], Daiki Ishi[2], Maiko Fujitani[2], Ryota Otsubo[2], Aoto Fukushima[2], Hikari Suzuki[2], Tatsuya Yuasa[2], Hiroshi Nakajima[3], Junko Hiraga[4], Yoshizumi Miyoshi[5], Satoshi Kasahara[6], Kazuhisa Mitsuda[1]

1. Japan Aerospace Exploration Agency/Institute of Space and Astronautical Science , 2. Tokyo Metropolitan University, 3. Kanto Gakuin University, 4. Kwansei Gakuin University, 5. Nagoya University, 6. The university of Tokyo

A reduction in weight of instrument, especially optics, is a key technique for explorers or small satellite missions. GEO-X (GEOspace X-ray imager) is a Japanese small satellite mission for X-ray observations of the dayside boundaries of the Earth’ s magnetosphere. An instrument is composed of a X-ray telescope
and a radio hard semiconductor pixel detector. Conventional X-ray optics have a trend that optics with better angular resolution have larger ratio of the weight to effective area. Therefore, it is difficult to utilize them for the X-ray planetary mission which has a severe weight limit. Micro pore optics are being developed based on a concept of a miniature optics. An original micro pore optics based on Si micromachining technologies will be used. A CMOS image sensor and a DEPFET (DEPleted P-Channle FET) are candidates for the X-ray detector. These new type semiconductor detectors are radiation hard and have optical light resistance, which are crucial in GEO-X to observe magnetosheaths and cusps near the dayside of the Earth. We report a summary of the instrument design and development for GEO-X.

Keywords: X-ray, magnetosphere

©2019. Japan Geoscience Union. All Right Reserved. 

[E] Oral | P (Space and Planetary Sciences )：P-EM Solar-Terrestrial Sciences, Space Electromagnetism & Space Environment

Thu. May 30, 2019 9:00 AM - 10:30 AM JST | Thu. May 30, 2019 12:00 AM - 1:30 AM UTC | A01 TOKYO BAY MAKUHARI HALL

## [P-EM15] Study of coupling processes in solar-terrestrial system

convener:Mamoru Yamamoto(Research Institute for Sustainable Humanosphere, Kyoto University), Yasunobu Ogawa(National Institute of Polar Research), Satonori Nozawa(Institute for Space-Earth Environment Research), Akimasa Yoshikawa(Department of Earth and Planetary Sciences, Kyushu University), Chairperson:Mamoru Yamamoto

The Earth accepts vast input of energy and material from the Sun. The Earth's environment is maintained by the balance between their inputs and outputs. It is therefore important to study energy and mass transport on the Earth. This is an international session that discusses studies of the coupling processes in the Sun-Earth system based on the project "Study of coupling processes in solar-terrestrial system" that was approved by the Master Plan 2011/2014/2017 of Science Council of Japan. We continue proposing the project to the Master Plan 2020. The facilities and networks included are Equatorial MU Radar (EMU) in Indonesia to study the whole equatorial atmosphere, the EISCAT_3D radar system in northern Scandinavia to study detailed structures and elementary processes of the magnetosphere-ionosphere coupling in the polar region, and global networks of various ground-based instruments and observation data. We will show the current status of the project and discuss sciences by soliciting variety papers. This session is open to the world, and we strongly encourage submission of papers related to other facilities and projects, i.e., atmospheric or incoherent scatter radars, observation networks, satellites, and simulation or theoretical studies, etc.

9:00 AM - 9:15 AM JST | 12:00 AM - 12:15 AM UTC

### [PEM15-01] Status of Equatorial MU Radar project in 2019

*Mamoru Yamamoto[1], Hiroyuki Hashiguchi[1], Tatsuhiro Yokoyama[1], Toshitaka Tsuda[1] (1.Research Institute for Sustainable Humanosphere, Kyoto University)

---

9:15 AM - 9:30 AM JST | 12:15 AM - 12:30 AM UTC

### [PEM15-02] Recent Progress and Current Status of EISCAT_3D in 2018-2019

*Hiroshi Miyaoka[1], Yasunobu Ogawa[1], Satonori Nozawa[2], Koji Nishimura[1], Shin-ichiro Oyama[2], Takuji Nakamura[1], Ryoichi Fujii[2], Craig James Heinselman[3] (1.National Institute of Polar Research, 2.Institute for Space-Earth Environmental Research, Nagoya University, 3.European Incoherent Scatter Scientific Association)

---

9:30 AM - 9:45 AM JST | 12:30 AM - 12:45 AM UTC

### [PEM15-03] Current status of the ground-based multi-point network observation of the upper atmosphere, ionosphere, and magnetosphere by the PWING Project and the Optical Mesosphere Thermosphere Imagers (OMTIs)

*Kazuo Shiokawa[1], Yuichi Otsuka[1], PWING Team (1.Institute for Space-Earth Environmental Research, Nagoya University)

---

9:45 AM - 10:00 AM JST | 12:45 AM - 1:00 AM UTC

### [PEM15-04] Development of MAGDAS project: Search for global electromagnetic coupling from polar to equatorial ionosphere

*Akimasa Yoshikawa[1], Taisei Kabasawa[2], Teiji Uozumi[3], Akiko Fujimoto[4], Shuji Abe[3] (1.Department of Earth and Planetary Sciences, Kyushu University, 2.Graduate school of Sciences, Kyushu Univerity, 3.International center for Space weather science and education, Kyushu University, 4.Kyushu Institute of Technology)

---

10:00 AM - 10:15 AM JST | 1:00 AM - 1:15 AM UTC

### [PEM15-05] IUGONET data analysis system for a study of coupling processes in the solar-terrestrial system

*Atsuki Shinbori[1], Yoshimasa Tanaka[2], Norio Umemura[1], Shuji Abe[3], Masahito Nose[1], Satoru UeNo[4] (1.Institute for Space-Earth Environment Research (ISEE), Nagoya University, 2.National institute of Polar Research, 3.International Center for Space Weather Science and Education Kyushu University, 4.Observatory, Kyoto University)

---

10:15 AM - 10:30 AM JST | 1:15 AM - 1:30 AM UTC

## [PEM15-06] Discussion on large-scale research project "Study of coupling processes in solar-terrestrial system" (1)

*Mamoru Yamamoto[1] (1.Research Institute for Sustainable Humanosphere, Kyoto University)

# Status of Equatorial MU Radar project in 2019

*Mamoru Yamamoto[1], Hiroyuki Hashiguchi[1], Tatsuhiro Yokoyama[1], Toshitaka Tsuda[1]

1. Research Institute for Sustainable Humanosphere, Kyoto University

Research Institute for Sustainable Humanosphere, Kyoto University (RISH) has been studying the atmosphere and ionosphere by using radars. The first big facility was the MU (Middle and Upper atmosphere) radar installed in Shiga, Japan in 1984. This is one of the most powerful and multi-functional radar, and is successful of revealing importance of atmospheric waves for the dynamical vertical coupling processes. The next big radar was the Equatorial Atmosphere Radar (EAR) installed at Kototabang, West Sumatra, Indonesia in 2001. The EAR was operated under close collaboration with LAPAN (Indonesia National Institute for Aeronautics and Space), and conducted the long-term continuous observations of the equatorial atmosphere/ionosphere. The EAR, however, had a limited sensitivity to the MU radar as the total output power is just 1/10 to the MU radar. Our new project is to establish "Equatorial MU (EMU) Radar" just next to the EAR site in Indonesia. The EMU will have an active phased array antenna with the 163 m diameter and 1055 cross-element Yagis. Total output power of the EMU will be more than 500 kW. The EMU is the "MU radar class" facility, and can detect turbulent echoes from the mesosphere (60-80 km). In the ionosphere incoherent-scatter observations of plasma density, drift, and temperature would be possible. Multi-channel receivers will realizes radar-imaging observations. Preparation for the EMU progress in many aspect including site survey for the construction, discussion with local government, etc. In March 2019, RISH and LAPAN have 1st Internal School on Equatorial Atmosphere (ISQUAR) 2019 with more than 100 participants at Bandung, Indonesia. ISQUAR aims to promote interesting studies of the equatorial atmosphere and use of the atmospheric radar including the EMU. The EMU is one of the key element in the project "Study of coupling processes in the solar-terrestrial system" that is one of the important project in the Master Plan 2014 and 2017 of the Science Council of Japan (SCJ). We continue proposing the project to the SCJ Masterplan 2020.

Keywords: Atmospheric radar, Equatorial atmosphere, Low-latitude ionosphere

©2019. Japan Geoscience Union. All Right Reserved. 

# Recent Progress and Current Status of EISCAT_3D in 2018-2019

*Hiroshi Miyaoka[1], Yasunobu Ogawa[1], Satonori Nozawa[2], Koji Nishimura[1], Shin-ichiro Oyama[2], Takuji Nakamura[1], Ryoichi Fujii[2], Craig James Heinselman[3]

1. National Institute of Polar Research, 2. Institute for Space-Earth Environmental Research, Nagoya University, 3. European Incoherent Scatter Scientific Association

The European Incoherent Scatter(EISCAT) Scientific Association with associate members from Sweden, Norway, Finland, UK, China and Japan, has officially started the construction of the 1st stage of EISCAT_3D from September 2017 toward its completion by the end of 2021, including the commissioning of the radar system. EISCAT 3D is the major upgrade of the existing EISCAT mainland radars, with a multi-static phased array system composed of one central active (transmit-receive) site and 4 receive-only sites to provide us 50-100 times higher temporal resolution than the present system. The construction of EISCAT 3D is planned to implement by 4-staged approach, starting from the core site with half transmitting power about 5MW at Skibotn (Norway) and 2 receiving sites at Kaiseniemi (Sweden) and Karesuvanto (Finland) at the 1st stage. As for site preparation, geotechnical surveys have been completed at three sites, and ground cleaning with trenching for power lines and optical fiber cables have almost finished at the core site, Skibotn. All site buildings are scheduled to be built in 2019 to start installation of the radar system from 2020.

Through the international tendering process led by the EISCAT headquarter, antenna units with housing containers, first stage receiver units, sub-array transmitter units and pulse and steering control units have been completed and contracted providers have just started their preparation for productions to meet the EISCAT_3D implementation plan for sub-systems in 2020.

National Institute of Polar Research has been pursuing the opportunity to contribute in-kind to the construction of EISCAT_3D by supplying radar transmitter units in cooperation with the EISCAT Headquarters and ISEE/Nagoya University. The EISCAT_3D program in Japan was successfully granted as as one of high-priority programs of the Master Plan 2014/2017 and the Roadmap 2014 program, as a core facility of ’Study of Coupling Processes in the Solar-Terrestrial System’ (PI: Prof. Toshitaka Tsuda, ROIS/Kyoto Univ.). Supported by these positive evaluations, high energy-efficient transmitter power amplifiers (SSPAs) has been developed and produced for the engineering verification test at the EISCAT Tromso site with partial fundings for development since 2016.
In this paper, we will overview the recent progress and current status of the project including our strategy for the transmitter units as our national contribution to the EISCAT_3D project.

Keywords: incoherent scatter radar, space weather, arctic, master plan

©2019. Japan Geoscience Union. All Right Reserved. 

# Current status of the ground-based multi-point network observation of the upper atmosphere, ionosphere, and magnetosphere by the PWING Project and the Optical Mesosphere Thermosphere Imagers (OMTIs)

*Kazuo Shiokawa[1], Yuichi Otsuka[1], PWING Team

1. Institute for Space-Earth Environmental Research, Nagoya University

The Optical Mesosphere Thermosphere Imagers (OMTIs) consist of ~20 all-sky cooled-CCD imagers, 5 Fabry-Perot interferometers, 3 airglow temperature photometers, and 3 meridian-scanning photometers. They measure two-dimensional airglow images in the mesopause region and in the thermosphere, wind and temperatures in the lower thermosphere, and airglow rotational temperatures in the mesopause region. Details of the OMTIs project can be seen at http://stdb2.isee.nagoya-u.ac.jp/omti/. The PWING stands for "study of dynamical variation of Particles and Waves in the INner magnetosphere using Ground-based network observations." The PWING project started on April 2016 as a 5-year project of the Grant-in-Aid for Specially Promoted Research of the Japan Society for the Promotion of Science (JSPS) (16H06286). The PWING project deploy OMTIs all-sky cooled-CCD airglow imagers, 64-Hz sampled induction magnetometers, 40-kHz VLF receivers, and 64-Hz riometers at 8 stations at magnetic latitudes of ~60 degree around the north-pole to cover longitudinal variation of aurora and electromagnetic disturbances in the inner magnetosphere. Details of the PWING project can be seen at http://www.isee.nagoya-u.ac.jp/dimr/PWING/PWING_web_e.htm. These PWING and OMTIs instruments are in automatic operation at various locations from high to equatorial latitudes in Canada, US (Alaska), Russia, Norway, Finland, Iceland, Japan, Thailand, Indonesia, Nigeria, and Australia. In the presentation, we introduce current status and some recent results obtained by these multi-instrument ground networks around the world.

PWING Team: http://www.isee.nagoya-u.ac.jp/dimr/PWING/en/

Keywords: Optical Mesosphere Thermosphere Imagers (OMTIs) , PWING Project, upper atmosphere , ionosphere and magnetosphere

©2019. Japan Geoscience Union. All Right Reserved. 

# Development of MAGDAS project: Search for global electromagnetic coupling from polar to equatorial ionosphere

*Akimasa Yoshikawa[1], Taisei Kabasawa[2], Teiji Uozumi[3], Akiko Fujimoto[4], Shuji Abe[3]

1. Department of Earth and Planetary Sciences, Kyushu University, 2. Graduate school of Sciences, Kyushu Univerity, 3. International center for Space weather science and education, Kyushu University, 4. Kyushu Institute of Technology

The equatorial ionosphere is a final destination of electromagnetic energy brought about by energy incidence to the polar ionosphere. Distribution of geomagnetic disturbance accompanying such a coupling phenomenon shows strong asymmetry. Such an aspect suggests that the magnetosphere-ionosphere form a unique transmission and / or propagation system depending on each event.
The MAGDAS project investigates such a global electromagnetic coupling system by combining global geomagnetic field network observation with electric field observation using ionosonde installed at low and dip-equator region.
Recently, by using 250Hz sampling and 10Hz averaged MAGDAS 9 magnetometer data, we found that when the auroral substorm were enhanced during geomagnetic storm, together with enhancement of Pc1 wave at the polar region, the global Pc2 type disturbances (period range from 5 to 20 sec) can be captured from polar to equatorial region. In this talk, we will present recent update of MAGDAS project and of which scientific results.

Keywords: global electromagnetic coupling, Pc2 pulsation, Magnetosphere-ionosphere Coupling

©2019. Japan Geoscience Union. All Right Reserved. 

# IUGONET data analysis system for a study of coupling processes in the solar-terrestrial system

*Atsuki Shinbori[1], Yoshimasa Tanaka[2], Norio Umemura[1], Shuji Abe[3], Masahito Nose[1], Satoru UeNo[4]

1. Institute for Space-Earth Environment Research (ISEE), Nagoya University, 2. National institute of Polar Research, 3. International Center for Space Weather Science and Education Kyushu University, 4. Observatory, Kyoto University

The earth’s atmosphere in a height range of more than 80 km is called the upper atmosphere, and the atmospheric layer is influenced by both the solar activity and the atmospheric waves propagating from the lower atmosphere. Therefore, in order to understand the physical mechanism of the short-term and long-term variations in the upper atmosphere, we need to perform an integrated analysis of various kinds of ground-based and satellite observation data taken by different instruments. Since these observation data were separately being managed by each institute, it was difficult for users to effectively find and analyze them for promotion of an interdisciplinary study. In order to solve this problem, the Inter-university Upper atmosphere Global Observation NETwork (IUGONET) project has been initiated in 2009, consisting of five institutes (Tohoku University, National Institute of Polar Research, Nagoya University, Kyoto University, and Kyushu University). In this project, we have added data information (metadata) for various kinds of ground-based observation data in the solar-terrestrial physics and built a practical database (IUGONET Type-A) to share them on the Internet. We have also developed an integrated data analysis tool (IUGONET Data Analysis Software: UDAS) written in an Interactive Data Language (IDL). This analysis tool is a plugin software for Space Physics Environment Data Analysis Software (SPEDAS) to analyze and visualize various kinds of ground-based and satellite observation data. In the IUGONET Type-A, users can easily learn characteristics of observation data through the quick look images/plots and how to use several basic commands to visualize the data. Recently, we developed a UDAS EGG (UDAS Easy Guide to Generate your load routines) to provide users with the templates for IDL procedures that can load their own data in CSV and CDF format into SPEDAS/IDL. In order to enhance an international use of these IUGONET products and to promote an interdisciplinary study of coupling processes on the sun-earth system, we have held tutorial seminars and workshops several times in Japan and foreign countries (India, Indonesia, Nigeria, Malaysia etc.). As a result, many scientific papers [e.g., Dao et al., 2017; Batubara et al., 2018; Koushik et al., 2018] and Master/Doctor theses become published by preparing an analysis environment, and the IUGONET products effectively works as an international platform. This fact suggests that the IUGONET project is in the position enough to serve the subjects of a large research project: Study of coupling processes in the solar-terrestrial system (Master Plan 2014/2017, Load Map 2014) through a collaboration with other ground-based and satellite observation plans and international programs as already planned by Master Plan 2014/2017. Judging from the above situations, the IUGONET project has a potential possibility to extend human development and strong international cooperation to a whole equatorial region (South America, Africa) in addition to India and Indonesia in future. Therefore, it can be concluded that the IUGONET activity effectively promotes the equatorial and polar atmospheric observations, international collaboration and data science (data assimilation), which are three main subjects of Master Plan (2014/2017).

Reference:

©2019. Japan Geoscience Union. All Right Reserved. 

Batubara. M, et al., Long-term distribution of meteors in a solar cycle period observed by VHF meteor radars at near-equatorial latitudes, J. Geophysical Res., doi:10.1029/2018JA025906, 2018.

Koushik, N., et al., Response of equatorial and low latitude mesosphere lower thermospheric dynamics to the northern hemispheric sudden stratospheric warming events, JAtmos.Solar-Terr. Phys., 169, 66-77, doi:10.1016/j.jastp.2018.01.021, 2018.
Dao, T., et al., Coordinated observations of postmidnight irregularities and thermospheric neutral winds and temperatures at low latitudes, J. Geophys. Res. Space Physics, 122, 7, 7504-7518, doi:10.1002/2017JA024048, 2017.

Keywords: IUGONET, Study of coupling process in the solar-terrestrial system, International collaboration, Database, Analysis tool (SPEDAS/UDAS), Equatorial atmosphere

©2019. Japan Geoscience Union. All Right Reserved. 

# Discussion on large-scale research project "Study of coupling processes in solar-terrestrial system" (1)

*Mamoru Yamamoto[1]

1. Research Institute for Sustainable Humanosphere, Kyoto University

The large-scale research plan "Study of coupling processes in solar-terrestrial system" is recognized in the important projects in Master Plan 2014 and 2017. We are currently preparing for a continuous proposal to Master Plan 2020. In this international session, we will apply discussion time in order to proceed the research plan.

©2019. Japan Geoscience Union. All Right Reserved. 

[E] Oral | P (Space and Planetary Sciences )：P-EM Solar-Terrestrial Sciences, Space Electromagnetism & Space Environment

Thu. May 30, 2019 10:45 AM - 12:15 PM JST | Thu. May 30, 2019 1:45 AM - 3:15 AM UTC | A01 TOKYO BAY MAKUHARI HALL

## [P-EM15] Study of coupling processes in solar-terrestrial system

convener:Mamoru Yamamoto(Research Institute for Sustainable Humanosphere, Kyoto University), Yasunobu Ogawa(National Institute of Polar Research), Satonori Nozawa(Institute for Space-Earth Environment Research), Akimasa Yoshikawa(Department of Earth and Planetary Sciences, Kyushu University), Chairperson:Satonori Nozawa

The Earth accepts vast input of energy and material from the Sun. The Earth's environment is maintained by the balance between their inputs and outputs. It is therefore important to study energy and mass transport on the Earth. This is an international session that discusses studies of the coupling processes in the Sun-Earth system based on the project "Study of coupling processes in solar-terrestrial system" that was approved by the Master Plan 2011/2014/2017 of Science Council of Japan. We continue proposing the project to the Master Plan 2020. The facilities and networks included are Equatorial MU Radar (EMU) in Indonesia to study the whole equatorial atmosphere, the EISCAT_3D radar system in northern Scandinavia to study detailed structures and elementary processes of the magnetosphere-ionosphere coupling in the polar region, and global networks of various ground-based instruments and observation data. We will show the current status of the project and discuss sciences by soliciting variety papers. This session is open to the world, and we strongly encourage submission of papers related to other facilities and projects, i.e., atmospheric or incoherent scatter radars, observation networks, satellites, and simulation or theoretical studies, etc.

10:45 AM - 11:15 AM JST | 1:45 AM - 2:15 AM UTC

### [PEM15-07] Numerical Experiments on Stratosphere-Troposphere Two-Way Dynamical Coupling in the Tropics through Organizations of Moist Convective Systems

★Invited Papers

*Shigeo Yoden[1], Hai Bui[2], Takahiro Banno[1] (1.Division of Earth and Planetary Sciences, Graduate School of Science, Kyoto University, 2.Geophysical Institute, University of Bergen)

11:15 AM - 11:30 AM JST | 2:15 AM - 2:30 AM UTC

### [PEM15-08] Future development of numerical simualtion of equatorial plasma bubbles

*Tatsuhiro Yokoyama[1] (1.Kyoto University)

11:30 AM - 11:45 AM JST | 2:30 AM - 2:45 AM UTC

### [PEM15-09] Characteristics of CME- and CIR-driven ion upflows in the polar ionosphere

*Yasunobu Ogawa[1], Kanako Seki[2], Kunihiro Keika[2], Yusuke Ebihara[3] (1.National Institute of Polar Research, 2.School of Science, the University of Tokyo, 3.Research Institute for Sustainable Humanosphere, Kyoto University)

11:45 AM - 12:00 PM JST | 2:45 AM - 3:00 AM UTC

### [PEM15-10] SuperDARN Hokkaido Pair of (HOP) radars and mid-latitude SuperDARN: today and future

*Nozomu Nishitani[1] (1.Institute for Space-Earth Environmental Research, Nagoya University)

12:00 PM - 12:15 PM JST | 3:00 AM - 3:15 AM UTC

### [PEM15-11] Simultaneous observation of Ionospheric Incoherent Scatter and Field Aligned Irregularities using adaptive signal processing techniques by the PANSY radar at Antarctic Syowa Station (39.6°E, 69.0°S)

*Taishi Hashimoto[1], Akinori Saito[2], Koji Nishimura[3], Masaki Tsutsumi[3], Kaoru Sato[4], Toru Sato[1] (1.Graduate School of Informatics, Kyoto University, 2.Graduate School of Science, Kyoto University, 3.National Institute of Polar Research, 4.Graduate School of Science, The University of Tokyo)

# Numerical Experiments on Stratosphere-Troposphere Two-Way Dynamical Coupling in the Tropics through Organizations of Moist Convective Systems

*Shigeo Yoden[1], Hai Bui[2], Takahiro Banno[1]

1. Division of Earth and Planetary Sciences, Graduate School of Science, Kyoto University, 2. Geophysical Institute, University of Bergen

Recently, we started a new international research activity on Stratospheric And Tropospheric Influences on Tropical Convective Systems (SATIO-TCS) under WCRP/SPARC. It focuses on stratosphere-troposphere (S-T) two-way dynamical coupling in the tropics, where moist convection and its large-scale organization in the troposphere could be influenced by the stratospheric variations, such as stratospheric sudden warming events, the equatorial quasi-biennial oscillation (QBO), or anthropogenic cooling trend in the lower stratosphere, as revealed by some observational studies. For example, Nishimoto and Yoden (2017) made a statistical analysis on the influence of QBO on the Madden-Julian oscillation (MJO) during boreal winter in neutral ENSO periods from 1979 to 2013, and showed that the composite OLR anomaly for a particular MJO phase over the Maritime Continent has a larger negative value and slower eastward propagation with a prolonged period of active convection in the easterly phase of QBO than in the westerly phase.

The tropical dynamics is largely different from the counterpart in the extratropics where dry quasi-geostrophic dynamics prevail. Multi-scale dynamics of moist convection and its organizations are likely to play a vital role in determining the tropospheric response to the stratospheric variations, but numerical model studies from such viewpoint are still limited. Thus, we had performed a series of numerical experiments on radiative-moist convective quasi-equilibrium states in a highly-idealized two-dimensional regional model of an S-T coupled system with explicit moist convection under a periodic lateral boundary condition without Coriolis effects, in which self-sustained oscillations dynamically analogous to the QBO were obtained (Yoden et al. 2014). Modulation of moist convective systems is associated with the QBO-like oscillation of the mean zonal wind, as alternative appearance of squall-line- or back-building-type precipitation patterns, and vertical momentum transports associated with slant-wise moist convection and convectively generated gravity waves are periodically modulated in the oscillation (Nishimoto et al. 2016). Downward influence of the QBO-like oscillation on organized moist convective systems was further investigated in a series of experiments that control the vertical shear of the mean zonal wind with a nudging term (Bui et al. 2017).

Recently, we have performed numerical experiments in a three-dimensional minimal model framework that produces a QBO-like oscillation in a radiative-moist convective quasi-equilibrium state. The computational domain is rectangular (640 km x 160 km, 5 km grid size; Bui et al., 2019), or square (100 km x 100 km, 1 km grid size), without Coriolis effects under doubly periodic boundary conditions. In these experiments, an oscillation with a period of about 300 days emerges in the stratosphere, both in the domain-averaged zonal wind and meridional wind. Synchronization of the zonal and meridional winds is characterized as an anti-clockwise rotation of a skewed spiral feature with height in the horizontal wind hodograph. The QBO-like wind oscillation penetrates into the troposphere with large reduction of oscillation amplitude, and influences tropospheric temperature anomalies and precipitation with an irregular period of about 100 days. Heavy precipitation is associated with positive temperature anomalies.

©2019. Japan Geoscience Union. All Right Reserved. 

The simulation reveals three types of precipitation patterns; fast-moving back-building- and squall-line-type patterns, and isolated quasi-stationary type clusters, which is newly identified in this three-dimensional model. The zonal-height cross sections of the meridionally averaged clouds and relative humidity for this pattern show clear-sky areas with low humidity without shallow clouds, whereas shallow clouds exist over the entire domain including non-precipitating areas with high humidity for the fast-moving two patterns. Intermittent self-organization of convective systems into quasi-stationary type and transition back to the fast-moving back-building- or squall-line-type patterns are fundamental characteristics of self-aggregation in the three-dimensional model.

## References

Bui, H.-H., E. Nishimoto, and S. Yoden, 2017: *J. Atmos. Sci.*, 74, 3635–3655.

Bui H., S. Yoden, and E. Nishimoto, 2019: *SOLA*, **15**, 59–62.

Nishimoto, E., and S. Yoden, 2017: *J. Atmos. Sci.*, **74**, 1105–1125.

Nishimoto, E., S. Yoden, and H.-H. Bui, 2016: *J. Atmos. Sci.*, **73**, 2935–2957.

Yoden, S., H.-H. Bui, and E. Nishimoto, 2014: *SOLA*, **10**, 112–116.

Keywords: Stratosphere-Troposphere Dynamical Coupling, Moist Convective Systems, Tropical Meteorology

©2019. Japan Geoscience Union. All Right Reserved. 

# Future development of numerical simualtion of equatorial plasma bubbles

*Tatsuhiro Yokoyama[1]

1. Kyoto University

Equatorial plasma bubbles (EPBs) have been a longstanding and increasingly important subject because they cause severe scintillations in radio waves from Global Navigation Satellite System satellites. The phenomenon was found in the 1930s as irregular ionosonde observations and was termed equatorial spread F (ESF). ESF is interpreted as plasma density irregularities associated with EPBs that have nonlinearly evolved into the topside ionosphere. Since late 1970s, numerical simulations have been powerful tools to study the fully nonlinear evolution of EPBs, which cannot be wholly understood from theoretical predictions. The most recent model, High-Resolution Bubble (HIRB) model, could reproduce very turbulent structures inside EPBs such as bufurcation, zonal asymmetry, and two-component power law spectral characteristics. Future directions toward scintillation evaluation and forecasting are discussed.

Keywords: equatorial plasma bubble, simulation, ionosphere

©2019. Japan Geoscience Union. All Right Reserved. 

# Characteristics of CME- and CIR-driven ion upflows in the polar ionosphere

*Yasunobu Ogawa[1], Kanako Seki[2], Kunihiro Keika[2], Yusuke Ebihara[3]

1. National Institute of Polar Research, 2. School of Science, the University of Tokyo, 3. Research Institute for Sustainable Humanosphere, Kyoto University

We investigated how velocity and flux of ionospheric ion upflows vary during magnetic storms driven by corotating interaction regions (CIRs) and coronal mass ejections (CMEs), using data from the European Incoherent Scatter (EISCAT) Tromsø UHF and Svalbard radars between 1996 and 2015. The characteristics of ion upflows were compared with ion and electron temperature variations measured with the EISCAT radars, and also joule heating rate, electric field, and field-aligned current (FAC) distribution derived from the Weimer model. Upward ion velocity increases in the nighttime at Tromsø (66.2 ° N geomagnetic latitude) just after the CIR- and CME-driven storms, corresponding to electron temperature enhancements due to soft particle precipitation and also ion temperature enhancements in the strong westward electric field region. The CME-driven storms have larger upward ion flux (~$1.7\times10^{13}$ $m^{-2}s^{-1}$) than those under the CIR-driven storms (~$0.3\times10^{13}$ $m^{-2}s^{-1}$). In the daytime, ion upflows are seen at Longyearbyen, Svalbard (75.2 ° N geomagnetic latitude), with an upward flux of typically $10^{13}$ $m^{-2}s^{-1}$ for small CIR and CME storm cases. Substantial ion upflows last for a few days after the storm onsets under small CIR storms, whereas they last for only a day under small CME storms. Under both the cases, the substantial ion upflows are associated with an enhancement of the Region 1 FAC, eastward electric field and Joule heating rate. For large CME storms, substantial ion upflows are absent in the daytime probably due to equatorward expansion of the auroral oval.

Keywords: polar ionosphere, M-I coupling, EISCAT

©2019. Japan Geoscience Union. All Right Reserved. 

# SuperDARN Hokkaido Pair of (HOP) radars and mid-latitude SuperDARN: today and future

*Nozomu Nishitani[1]

1. Institute for Space-Earth Environmental Research, Nagoya University

The Super Dural Auroral Radar Network (SuperDARN) is a network of HF radars. At present there are total of 36 SuperDARN radars located in high- to mid-latitude regions of both northern (23) and southern (13) hemispheres. Mid-latitude SuperDARN radars started operation about 15 years ago and have been acquiring scientific data, which could be obtained using the pre-existing high-latitude radars. The SuperDARN Hokkaido Pair of (HOP) radars consisting of Hokkaido East / West radars are located equatorward of 40 degrees geomagnetic latitude (currently located at the lowest geomagnetic latitude) and have been storing important scientific data during quiet to very active periods. In this presentation accomplishments, present status and future directions of the SuperDARN HOP radars and mid-latitude SuperDARN be reviewed.

Keywords: mid-latitude SuperDARN

©2019. Japan Geoscience Union. All Right Reserved. 

# Simultaneous observation of Ionospheric Incoherent Scatter and Field Aligned Irregularities using adaptive signal processing techniques by the PANSY radar at Antarctic Syowa Station (39.6˚E, 69.0˚S)

*Taishi Hashimoto[1], Akinori Saito[2], Koji Nishimura[3], Masaki Tsutsumi[3], Kaoru Sato[4], Toru Sato[1]

1. Graduate School of Informatics, Kyoto University, 2. Graduate School of Science, Kyoto University, 3. National Institute of Polar Research, 4. Graduate School of Science, The University of Tokyo

The Program of Antarctic Syowa Mesosphere-Stratosphere-Troposphere (MST) / Incoherent Scatter (IS) radar (the PANSY radar) is a large VHF-band atmospheric radar located at Antarctic Syowa Station. Besides the general functionalities of MST radars, the PANSY radar is also capable of observing IS from 100 km to 500 km in altitude to estimate ionospheric plasma parameters. The ionospheric observation was successfully performed in 2015, which was the first in the Antarctic region.

In contrast to existing IS radars using higher frequencies, the ionospheric observation of the PANSY radar suffers contamination from E-region Field Aligned Irregularities (FAIs). Because the perpendicular condition between the line of sight and the geomagnetic field is satisfied around 100 km in altitude using the VHF-band at this latitude, strong coherent echoes from FAIs fall into the same range gates with the F-region peak of IS.

To mitigate the contamination of FAIs in IS observation of the PANSY radar, we have developed a signal processing procedure using adaptive beamforming techniques [1]. The PANSY radar has two peripheral linear antenna arrays, each with twelve three-element antennas for the Directionally Constrained Minimization of Power approach, to separate signals from different directions. Hence, this technique makes it possible not only to measure the background electron densities accurately, but also to observe the structure and motion of FAIs simultaneously.

In this presentation, we briefly overview the signal processing procedure applied to the ionospheric observation of the PANSY radar, and show recent results from simultaneous observations of IS and FAIs, including some radar images of FAIs obtained by adaptive beamforming techniques.

[1] Hashimoto et al., 2018: “First incoherent scatter measurements and adaptive suppression of field-aligned irregularities by the PANSY radar at Syowa Station, Antarctic”, *J. Atmos. Oceanic Technol.*, conditional acceptance.

Keywords: PANSY, ionospheric incoherent scatter, adaptive signal processing, field aligned irregularities, Antarctic Syowa Station, IS radar

©2019. Japan Geoscience Union. All Right Reserved. 

[E] Oral | P (Space and Planetary Sciences )：P-EM Solar-Terrestrial Sciences, Space Electromagnetism & Space Environment

Thu. May 30, 2019 1:45 PM - 3:15 PM JST | Thu. May 30, 2019 4:45 AM - 6:15 AM UTC | A01 TOKYO BAY MAKUHARI HALL

## [P-EM15] Study of coupling processes in solar-terrestrial system

convener:Mamoru Yamamoto(Research Institute for Sustainable Humanosphere, Kyoto University), Yasunobu Ogawa(National Institute of Polar Research), Satonori Nozawa(Institute for Space-Earth Environment Research), Akimasa Yoshikawa(Department of Earth and Planetary Sciences, Kyushu University), Chairperson:Yasunobu Ogawa

The Earth accepts vast input of energy and material from the Sun. The Earth's environment is maintained by the balance between their inputs and outputs. It is therefore important to study energy and mass transport on the Earth. This is an international session that discusses studies of the coupling processes in the Sun-Earth system based on the project "Study of coupling processes in solar-terrestrial system" that was approved by the Master Plan 2011/2014/2017 of Science Council of Japan. We continue proposing the project to the Master Plan 2020. The facilities and networks included are Equatorial MU Radar (EMU) in Indonesia to study the whole equatorial atmosphere, the EISCAT_3D radar system in northern Scandinavia to study detailed structures and elementary processes of the magnetosphere-ionosphere coupling in the polar region, and global networks of various ground-based instruments and observation data. We will show the current status of the project and discuss sciences by soliciting variety papers. This session is open to the world, and we strongly encourage submission of papers related to other facilities and projects, i.e., atmospheric or incoherent scatter radars, observation networks, satellites, and simulation or theoretical studies, etc.

1:45 PM - 2:00 PM JST | 4:45 AM - 5:00 AM UTC

[PEM15-12] Mini/Micro Satellite Constelaltion for the study of LAI coupling

*Koichiro Oyama[1,2,3] (1.Institute of Plasma and Space Sciences,National Cheng Kung Univ., Taiwan, 2.International Ceneter for Space Weather Sudy and Education, Kyushu Univ.,, 3.CoLtd. Asia Space Environment Research Consortium, Japan)

2:00 PM - 2:15 PM JST | 5:00 AM - 5:15 AM UTC

[PEM15-13] Statistical study of daily and seasonal variation of the equatorial anomaly in Asia based on satellite-ground beacon experiment

*Yuki Sakamoto[1], Mamoru Yamamoto[1], Kornyanat Hozumi[2] (1.Research Institute for Sustainable Humanosphere, Kyoto University, 2.National Institute of Information and Communications Technology)

2:15 PM - 2:30 PM JST | 5:15 AM - 5:30 AM UTC

[PEM15-14] Latest installation of FM-CW radar in Peru

*Akiko Fujimoto[1], Akihiro Ikeda[2], Akimasa Yoshikawa[3] (1.Kyushu Institute of Technology, 2.National Institute of Technology,Kagoshima College, 3.Kyushu University)

2:30 PM - 2:45 PM JST | 5:30 AM - 5:45 AM UTC

[PEM15-15] **Understanding the OH Meinel Band Emissions on the Terrestrial Planets**

*Konstantinos S. Kalogerakis[1] (1.Center for Geospace Studies, SRI International, Menlo Park, California, U.S.A.)

2:45 PM - 3:00 PM JST | 5:45 AM - 6:00 AM UTC

[PEM15-16] Statistical study of Sporadic Sodium Layer (SSL) observed at Tromsø

*Satonori Nozawa[1], Takuo T. Tsuda[2], Norihito Saito[3], Toru Takahashi[4], Takuya Kawahara[5], Yasunobu Ogawa[4], Hitoshi Fujiwara[6], Satoshi Wada[3], Youhei Ogawa[1], Chris Hall[7], Asgeir Brekke[7] (1.Institute for Space-Earth Environment Research, 2.The University of Electro-Communications, 3.RIKEN Center for Advanced Photonics, 4.National Institute of Polar Research, 5.Faculty of Engineering, Shinshu University, 6.Faculty of Science and Technology, Seikei University, 7.UiT The Arctic University of Norway)

3:00 PM - 3:15 PM JST | 6:00 AM - 6:15 AM UTC

[PEM15-17] Discussion on large-scale research project "Study of coupling processes in solar-terrestrial system" (2)

*Mamoru Yamamoto[1] (1.Research Institute for Sustainable Humanosphere, Kyoto University)

# Mini/Micro Satellite Constelaltion for the study of LAI coupling

*Koichiro Oyama[1,2,3]

1. Institute of Plasma and Space Sciences,National Cheng Kung Univ., Taiwan, 2. International Ceneter for Space Weather Sudy and Education, Kyushu Univ.,, 3. CoLtd. Asia Space Environment Research Consortium, Japan

Recent Studies show that ionosphere influenced by Thunder cloud, Typhoon, Sudden Stratosphere warming, Earth quake, and so on. Possible atmosphere perturbation to generate Radio wave scintillation is still not confirmed by observation in spite of the long history of radio scintillation research. Since 1970’ s, no break through is found in ionosphere physics. The reason is the lack of information of the atmosphere below which is needed simultaneously with ionopshere information. We propose here the satellite constellation of /Pico /mini satellites combined with one /two small satellite (200-500 Kg). Pico/mini satellite should be constellation to measure basic ionosphere parameter. These are electron density, temperature, ion temperature, ion mass, electric field, and neutral wind at ionosphere height. Information on the atmospheric wind down to ground surface below 120 km should be simultaneously measured. This means that we need photometric instruments such as TIDI and SABAR accommodated in TIMED satellite or instruments to measure electromagnetic waves radiated by neutral particles. These observations can be done through international collaboration.

References

Oyama, K.-I., J. T. Jhou, J. T. Lin, M. L. Hsu , C. Lin ,Y. S. Wu, H. Liu, and K.Yumoto, Behavior of the northern ionosphere during 2009 Sudden Stratosphere Warming, J.Geophys.Res., doi:10.1002/2014JA020014, 2014

Chou, M. Y., C. C. H. Lin, J. Yue, H. F. Tsai, Y. Y. Sun, J. Y. Liu, and C. H. Chen (2017), Concentric traveling ionosphere disturbances triggered by Super Typhoon Meranti (2016), Geophys. Res. Lett., 44, 1219–1226, doi:10.1002/2016GL072205.

Oyama, K. -I., Y.Kakinami, ,J.Y.Liu, T.Kodama, and C.Y.Chen, Micro/mini satellites for earthquake studies - toward international collaboration, Advances in Geoscience, 21, 251- 256, 2010.

Oyama, K.-I., Y. Kakinami, J. Y. Liu, M. A. Abdu, and C. Z. Cheng, Anomalous Ion Density Latitudinal Distribution as a precursor of large earthquake, J.Geophys. Res., 116, A04319, doi:10.1029/2010JA015948, 2011

Keywords: EAI coupling, Satellite Obserbation, International Collaboartion

©2019. Japan Geoscience Union. All Right Reserved. 

# Statistical study of daily and seasonal variation of the equatorial anomaly in Asia based on satellite-ground beacon experiment

*Yuki Sakamoto[1], Mamoru Yamamoto[1], Kornyanat Hozumi[2]

1. Research Institute for Sustainable Humanosphere, Kyoto University, 2. National Institute of Information and Communications Technology

Studies of ionospheric structures by the satellite-ground beacon experiment were conducted in southeast Asia. We have deployed a meridional chain of five beacon receivers from 8S to 27N along 100E meridian, they showed meridional distribution of total-electron content (TEC) of the ionosphere. We revealed time and spatial variabilities of the equatorial anomaly in a certain period of time (Watthanasangmechai et al., 2014, 2015). The data analysis was, however, not easy mainly because of difficulty in estimating bias of the measurement to get the absolute TEC.
In this study, we developed the method of bias estimation. As a result, we can get TEC distribution by computers automatically. Using this method, we analyzed latitude distribution of TEC from Thai to Indonesia in 2012-2015. It is valuable to measure such latitudinal distribution of TEC in the wide latitudinal range from the ground fixed sites.
Using these data, we classified TEC distribution with the equatorial anomaly. It shows some distribution patterns depends on season or time. Classifying the TEC distribution data of LT14-17 and LT20-23, assuming after the formation of the equatorial anomaly (EIA), we take the average in 2012-2015. The plasma fountain makes the 2 peaks (northern and southern of the magnetic equator) in the TEC-Lat graph. In the northern hemisphere summer, the northern peak is larger than the southern one. In winter, the southern peak is larger than the northern one. Classifying the data of LT10-13, assuming the right after formation of the EIA. It shows the opposite result. In summer, the southern one is larger. In winter, the northern one is larger. We will compare these analysis results with atmospheric parameters from the whole atmosphere model GAIA and MSIS.

Keywords: total-electron content, equatorial anomaly

©2019. Japan Geoscience Union. All Right Reserved. 

# Latest installation of FM-CW radar in Peru

*Akiko Fujimoto[1], Akihiro Ikeda[2], Akimasa Yoshikawa[3]

1. Kyushu Institute of Technology, 2. National Institute of Technology,Kagoshima College, 3. Kyushu University

An FM-CW (Frequency Modulated Continuous Wave) radar is a type of HF (High Frequency) radar. The FM-CW radar can measure the range of target as well as Doppler shift for reflected radio waves from the target (e.g., ionized layer). From the observed Doppler shift, we can estimate east-west electric field in the ionosphere. Poole (1985) and Poole and Evans (1985) first used FM-CW radar for Doppler observation. Nozaki and Kikuchi (1987, 1988) made improvements to the design. We have installed three FM-CW stations along the Japanese longitude, at Japan, Russia and Philippine, in order to measure the electric fields that penetrate the ionosphere (Yumoto, 2006).

Our goals are, (i) to estimate EEJ (Equatorial Electrojet) structure including the generation, variance and modulation of EEJ, (ii) to understand the electrodynamics of EEJ and the generation mechanism of the Equatorial Spread F (ESF) associated with Plasma Bubbles (PBs) and (iii) to reveal the generation mechanisms of ULF pulsation waves at the lower and equatorial latitudes.

In 2018, the new FM-CW radar has been installed in Peru. This FM-CW observation will give the opportunity of the simultaneous ionospheric observation at the Japan local time and the opposite side of Japan (for example dayside and nightside). ICSWSE (International Center for Space Weather Science and Education, Kyushu University) also have the ground-based magnetometer network (MAGDAS) on the world including Peru MAGDAS chain. With the both magnetometer and FM-CW observations, we try to understand the energy transfer and propagation process from the poles to the equator, in the terms of the coupling the solar-magnetosphere-ionosphere-atmosphere.

We will give the detail and current status of FM-CW radar project.

©2019. Japan Geoscience Union. All Right Reserved. 

# Understanding the OH Meinel Band Emissions on the Terrestrial Planets

*Konstantinos S. Kalogerakis[1]

1. Center for Geospace Studies, SRI International, Menlo Park, California, U.S.A.

The OH Meinel band emissions, originating from vibrationally excited hydroxyl radicals, OH(v), represent some of the most important airglow features in the Earth's upper atmosphere. Such emissions were also observed on the night side of Venus during the Venus Express mission [*Piccioni et al.*, A&A 483, L29-L33 (2008)]. Data obtained by CRISM (Compact Reconnaissance Imaging Spectrometer for Mars) aboard the MRO (Mars Reconnaissance Orbiter) revealed OH(v) emissions in the nightglow of Mars [*Clancy et al.*, Icarus 226, 272-281 (2013)]. Modeling studies have shown that the predicted OH(v) emission intensities can vary dramatically depending on the nature of the vibrational relaxation mechanism assumed [e.g., *García Muñoz et al.*, Icarus 176, 75-95 (2005)]. Despite several investigations, the details of all the relevant OH(v) relaxation kinetics and pathways are not well understood.

Our recent studies demonstrated a previously unknown, efficient pathway for vibrational relaxation of OH(v) by O atoms that couples the mesospheric OH(v) emissions with the $CO_2$ 4.3-micron emission and resolves a long-standing problem of severe discrepancies between model predictions and observations of the 4.3-micron emission in the Earth's atmosphere [*Panka et al.* , ACP 17, 9751-9760 (2017); *Kalogerakis et al.*, GRL 43, 8835-8843 (2016)]. This recent breakthrough development highlights the importance of investigating the mechanistic details of OH(v) collisional energy transfer.

We will discuss our efforts to investigate OH(v) vibrational relaxation relevant to the atmospheres of the terrestrial planets. Important areas of interest are the key OH(v) vibrational relaxation rate constants at temperatures relevant to the altitude of the emission layer and the pathways of OH(v) vibrational energy relaxation. The Meinel OH(v) emissions can be used as an indicator of atmospheric composition, variability, circulation, gravity waves, and as a probe of local temperature. A detailed understanding of the sources and sinks of these emissions is a prerequisite before they can be reliably used as a proxy for the aforementioned processes.

Keywords: OH Meinel band emission, Nightglow, vibrational relaxation, Terrestrial planets

©2019. Japan Geoscience Union. All Right Reserved. 

# Statistical study of Sporadic Sodium Layer (SSL) observed at Tromsø

*Satonori Nozawa[1], Takuo T. Tsuda[2], Norihito Saito[3], Toru Takahashi[4], Takuya Kawahara[5], Yasunobu Ogawa[4], Hitoshi Fujiwara[6], Satoshi Wada[3], Youhei Ogawa[1], Chris Hall[7], Asgeir Brekke[7]

1. Institute for Space-Earth Environment Research, 2. The University of Electro-Communications, 3. RIKEN Center for Advanced Photonics, 4. National Institute of Polar Research, 5. Faculty of Engineering, Shinshu University, 6. Faculty of Science and Technology, Seikei University, 7. UiT The Arctic University of Norway

Based on about 3000 hours of sodium density data obtained with the Tromsø sodium LIDAR over 7 year seasons between 2012 and 2018, we have identified about 40 events of Sporadic Sodium Layer (SSL) in the polar mesosphere and lower thermosphere (MLT) region. A SSL is a thin sodium layer (about 1-2 km) with high sodium density (usually factor of 2 or more higher than that of a normal layer), and its life time is about a few minutes to a few hours. We have investigated an occurrence rate of sporadic sodium layer (SSL) as well as necessary conditions for a SSL to form in the polar MLT region. SSLs appeared for shorter than 5 % of the overall observational time, indicating it is a rare event. Auroral electron precipitation as well as appearance of a sporadic E layer would be necessary conditions to form a SSL.

The sodium LIDAR at Tromsø (69.6 deg N, 19.2 deg E) has made simultaneous five directional (vertical position, plus 4 horizontal positions with zenith angle = 30 deg or 12.5 deg and azimuth = 0, 90, 180, 270 deg) observations, and has obtained about 3000 hours of temperature, sodium density, and wind data between October 2012 and February 2019. Analyzing the datasets with temporal and height resolutions of 3 min and 500 m, respectively, we have identified about 40 SSL events over the seven winter seasons. By utilizing five point observations, we have determined if a SSL was in-situ generated or was advected. Most SSLs show feature of advection (systematic and similar temporal variations of sodium density), indicating associated sharp rise of sodium density, whose mechanism has long been not understood, can be explained with an advection effect.

Observational results can be summarized as follows:
(1) most SSLs found are probably advected, (2) ionization of aurora would be a necessary condition, (3) sporadic E (Es) layers are almost always associated, (4) local time dependence of appearance of SSL is found, suggesting convectional electric field and semidiurnal tide would play an important role. We will address a generation mechanism of SSL.

Keywords: Sodium layer, Tromso, SSL, Es layer, Sodium LIDAR

©2019. Japan Geoscience Union. All Right Reserved. 

# Discussion on large-scale research project "Study of coupling processes in solar-terrestrial system" (2)

*Mamoru Yamamoto[1]

1. Research Institute for Sustainable Humanosphere, Kyoto University

The large-scale research plan "Study of coupling processes in solar-terrestrial system" is recognized in the important projects in Master Plan 2014 and 2017. We are currently preparing for a continuous proposal to Master Plan 2020. In this international session, we will apply discussion time in order to proceed the research plan.

©2019. Japan Geoscience Union. All Right Reserved. 

[E] Poster | P (Space and Planetary Sciences )：P-EM Solar-Terrestrial Sciences, Space Electromagnetism & Space Environment

Thu. May 30, 2019 3:30 PM - 5:00 PM JST | Thu. May 30, 2019 6:30 AM - 8:00 AM UTC | Poster Hall International Exhibition Hall8, Makuhari Messe_2

## [P-EM15] Study of coupling processes in solar-terrestrial system

convener:Mamoru Yamamoto(Research Institute for Sustainable Humanosphere, Kyoto University), Yasunobu Ogawa(National Institute of Polar Research), Satonori Nozawa(Institute for Space-Earth Environment Research), Akimasa Yoshikawa(Department of Earth and Planetary Sciences, Kyushu University)

The Earth accepts vast input of energy and material from the Sun. The Earth's environment is maintained by the balance between their inputs and outputs. It is therefore important to study energy and mass transport on the Earth. This is an international session that discusses studies of the coupling processes in the Sun-Earth system based on the project "Study of coupling processes in solar-terrestrial system" that was approved by the Master Plan 2011/2014/2017 of Science Council of Japan. We continue proposing the project to the Master Plan 2020. The facilities and networks included are Equatorial MU Radar (EMU) in Indonesia to study the whole equatorial atmosphere, the EISCAT_3D radar system in northern Scandinavia to study detailed structures and elementary processes of the magnetosphere-ionosphere coupling in the polar region, and global networks of various ground-based instruments and observation data. We will show the current status of the project and discuss sciences by soliciting variety papers. This session is open to the world, and we strongly encourage submission of papers related to other facilities and projects, i.e., atmospheric or incoherent scatter radars, observation networks, satellites, and simulation or theoretical studies, etc.

### [PEM15-P01] Study on adaptive clutter rejection system using external receiving antennas for the MU radar

*Hiroyuki Hashiguchi[1], Issei Terada[1], Mamoru Yamamoto[1] (1.Research Institute for Sustainable Humanosphere, Kyoto University)

### [PEM15-P02] Detached cusp aurora for southward IMF

*Kohei Takasu[1], Satoshi Taguchi[1], Keisuke Hosokawa[2] (1.Department of Geophysics, Graduate School of Science, Kyoto University, 2.Department of Communication Engineering and Informatics, University of Electro-Communications)

### [PEM15-P03] Motion of the inverted-V structure during an isolated substorm

*Morio Tanaka[1], Satoshi Taguchi[1], Kohei Takasu[1], Tomokazu Oigawa[1], Keisuke Hosokawa[2] (1.Department of Geophysics, Graduate school of science, Kyoto University, 2.Department of Communication Engineering and Informatics, University of Electro-Communications)

### [PEM15-P04] Observation and modeling of Na layer response to energetic particle precipitation

*Takuo T. Tsuda[1], Kyogo Takizawa[1], Ryo Tozu[1], Takuya Kawahara[2], Yoshimasa Tanaka[3], Mitsumu K. Ejiri[3], Takanori Nishiyama[3], Takuji Nakamura[3] (1.The University of Electro-Communications, 2.Shinshu University, 3.National Institute of Polar Research)

### [PEM15-P05] Lidar data analysis of the sodium atoms in the thermosphere observed at Tromsoe, Norway

*Takuya Kawahara[1], Satonori Nozawa[2], Norihito Saito[3], Takuo T. Tsuda[4], Toru Takahashi[5], Testuya Kawabata[2], Miki Nishimura[1], Yoshitaka Kobayashi[1] (1.Faculty of Engineering, Shinshu University, 2.ISEE, Nagoya University, 3.RIKEN, Center for Advanced Photonics, 4.The University of Electro-Communications, 5.National Institute of Polar Research)

### [PEM15-P06] Spatial-temporal distribution of anomalous enhancement of ambipolar diffusion coefficient observed by meteor radars installed in the polar region

*Toru Takahashi[1], Masaki Tsutsumi[1,2], Yasunobu Ogawa[1,2,3], Satonori Nozawa[3], Chris Hall[4], Hiroshi Miyaoka[1,2] (1.National Institute of Polar Research, 2.SOKENDAI, 3.Institute for Space-Earth Environmental Research, 4.TGO, The Arctic University of Norway)

## [PEM15-P07] Progress of ICSWSE and MAGDAS project in recent years

*Shuji Abe[1], Akimasa Yoshikawa[2,1], Teiji Uozumi[1], Akiko Fujimoto[3] (1.International Center for Space Weather Science and Education, Japan, 2.Department of Earth and Planetary Sciences, Kyushu University, 3.Kyushu Institute of Technology)

## [PEM15-P08] Status of GNU Radio Beacon Receiver 2 (GRBR2) development

*Mamoru Yamamoto[1], Mayumi Matsunaga[2], Roland Tsunoda[3] (1.Research Institute for Sustainable Humanosphere, Kyoto University, 2.Tokyo University of Technology, 3.SRI International)

## [PEM15-P09] Statistical comparison between plasma bubble day-to-day variability and neutral atmosphere by using GPS scintillation and GAIA model

*Mamoru Yamamoto[1], Keigo Kono[1] (1.Research Institute for Sustainable Humanosphere, Kyoto University)

## [PEM15-P10] Redevelopment of the MU radar transceiver-module control system

*Mamoru Yamamoto[1], Koki Kurokawa[1], Hiroyuki Hashiguchi[1] (1.Research Institute for Sustainable Humanosphere, Kyoto University)

# Study on adaptive clutter rejection system using external receiving antennas for the MU radar

*Hiroyuki Hashiguchi[1], Issei Terada[1], Mamoru Yamamoto[1]

1. Research Institute for Sustainable Humanosphere, Kyoto University

Strong clutter echoes from a hard target such as a mountain or building sometimes cause problems of observations with atmospheric radars. In order to reject or suppress ground clutter echoes, it is effective to use NC-DCMP (Norm Constrained- Directionally Constrained Minimum Power) method, which makes null toward the direction of the clutter, if we can receive signals independently from plural antennas [Nishimura et al., JTech., 2012]. It has been demonstrated that the NC-DCMP method is effective to real observation data with the MU (Middle and Upper atmosphere) radar [Hashiguchi et al., Radio Sci., 2018]. Although NC-DCMP method suppresses clutter echoes with almost maintaining the shape of main lobe to add pseudo-noise compared with the conventional DCMP method, the signal-to-noise ratio (S/N) of atmospheric echoes is somewhat degraded. We studied the clutter suppression method with little S/N degradation by using external antennas.

Four turnstile antennas are installed in the MU radar site. The signal from the antenna is sent to the MU radar observation room through the coaxial cable after amplified by the LNA with the limiter and BPF. It is further amplified by the LNA in the observation room, and then down-converted to intermediate frequency (5 MHz) signal to input to the multi-channel receiving system of the MU radar.

We compared the NC-DCMP method using the each received data of 25 channels, which is a conventional clutter suppression method, and the NC-DCMP method using the simple combination of 25 channels and 4 channels of external antennas. In the former case, the S/N of the atmospheric echoes is somewhat degraded, but in the latter case the main lobe shape is guaranteed by 25 channel simple synthesis, so the S/N degradation is not observed. In the latter case, the clutter suppression is sometimes insufficient. This cause is considered to be that the current positions of external antennas are biased to the north side. Antenna positions should be optimized in the future.

We can apply the achievement of this study to the Equatorial MU radar (EMU), which is proposed to be constructed at West Sumatera, Indonesia. The EMU system is the similar as the MU radar, but its antenna consists of 1045 Yagi antennas with 55 groups and it has 64 receiver channels.

Keywords: Atmospheric radar, Clutter rejection, NC-DCMP method, MU radar

©2019. Japan Geoscience Union. All Right Reserved. 

# Detached cusp aurora for southward IMF

*Kohei Takasu[1], Satoshi Taguchi[1], Keisuke Hosokawa[2]

1. Department of Geophysics, Graduate School of Science, Kyoto University, 2. Department of Communication Engineering and Informatics, University of Electro-Communications

A poleward-moving aurora is a typical phenomenon in the dayside cusp of the high-latitude ionosphere. This aurora usually originates near the equatorward boundary of the cusp, and diminishes near the poleward boundary of the persistent cusp auroral emissions. In this study we have examined faint poleward-moving auroras that are detached from the persistent cusp emissions by analyzing 630-nm aurora image data from an all-sky imager at Longyearbyen, Svalbard, and precipitating electron data from DMSP spacecraft. These auroras occur for southward IMF, and are located at latitudes higher than 80 MLAT. The intensities are very weak (less than 1 kilo Rayleigh). The result of the analysis shows that the speed of the auroral motion is 1 to 2 km/s, which is faster than typical convection speed in the dayside polar cap. We show the similarities and differences between the faint aurora and the typical poleward moving cusp aurora, and discuss how soft electron precipitation occurs in the region that is well separated from the cusp.

Keywords: Aurora, cusp, plasma convection, IMF

©2019. Japan Geoscience Union. All Right Reserved. 

# Motion of the inverted-V structure during an isolated substorm

*Morio Tanaka[1], Satoshi Taguchi[1], Kohei Takasu[1], Tomokazu Oigawa[1], Keisuke Hosokawa[2]

1. Department of Geophysics, Graduate school of science, Kyoto University, 2. Department of Communication Engineering and Informatics, University of Electro-Communications

The inverted-V is an energetic electron precipitation event, which can be seen as a V-shape structure in electron flux spectrograms, and causes intense auroral arcs. Previous studies have suggested that the inverted-V structure can move fast poleward or equatorward. However, we still do not understand what drives its motion. In this study we have investigated the detailed characteristics of an inverted-V structure moving poleward, which occurred during an isolated substorm, using simultaneous observations of auroras, precipitating electrons, and field-aligned currents. We analyzed aurora data (630-nm and 557.7-nm) from an all-sky imager at Longyearbyen, Svalbard, and precipitating electrons and magnetic field data from the DMSP spacecraft (F16, F17, F18, F19). One of the interesting characteristics of the poleward-moving inverted-V is the appearance of a downward field-aligned current equatorward of and adjacent to the inverted-V. We discuss how the region of the downward field-aligned current evolves in association with the motion and growth/decay of the inverted V structure, and possibility of a role of the downward field-aligned current for the latitudinal motion of the inverted V.

Keywords: Field-aligned current, aurora, inverted-V, isolated substorm

©2019. Japan Geoscience Union. All Right Reserved. 

# Observation and modeling of Na layer response to energetic particle precipitation

*Takuo T. Tsuda[1], Kyogo Takizawa[1], Ryo Tozu[1], Takuya Kawahara[2], Yoshimasa Tanaka[3], Mitsumu K. Ejiri[3], Takanori Nishiyama[3], Takuji Nakamura[3]

1. The University of Electro-Communications, 2. Shinshu University, 3. National Institute of Polar Research

Metallic layers, such as Na, Fe, Mg, K, and Ca layers, exist in the mesosphere and lower thermosphere (MLT). The height range of the MLT region corresponds to the ionospheric *D* and *E* regions, and in the polar region energetic particles precipitating from the magnetosphere can often penetrate into the *E* region and even into the *D* region. Therefore, the influence of energetic particles on the metallic layers is of interest regarding changes in atmospheric composition accompanied by auroral activity or geomagnetic activity.

In this study, we have performed a statistical investigation on relationship between Na density and cosmic noise absorption (CNA), which were obtained from 2000 to 2002 at Syowa Station, Antarctic (69.0ºS, 39.6ºE). From the investigation, we found the Na density decrease in accordance with the CNA increase, i.e., increase in the energetic particle precipitation. In the presentation, we will show these observational results, and discuss causality about the observed relationship based on numerical caculations using our Na chemistry model.

Keywords: Na layer, Energetic particle precipitation, Syowa Station, Na chemistry model

©2019. Japan Geoscience Union. All Right Reserved. 

# Lidar data analysis of the sodium atoms in the thermosphere observed at Tromsoe, Norway

*Takuya Kawahara[1], Satonori Nozawa[2], Norihito Saito[3], Takuo T. Tsuda[4], Toru Takahashi[5], Testuya Kawabata[2], Miki Nishimura[1], Yoshitaka Kobayashi[1]

1. Faculty of Engineering, Shinshu University, 2. ISEE, Nagoya University, 3. RIKEN, Center for Advanced Photonics, 4. The University of Electro-Communications, 5. National Institute of Polar Research

Distribution of low-density Na atoms in the thermosphere is interesting because of the capability of measuring neutral temperature and wind into the lower thermosphere up to 140 km. The thermospheric Na atoms significantly made the altitude range of Na lidar measurements expanded from the 80–105 km to 80–140 km, covering almost the entire E region (Liu et al., GRL, 2016).

The measurements of wind and temperature by a Na lidar in the northern mesosphere (80-105 km) at Tromsoe, Norway (69.6˚N, 19.2˚E) have been carried out in Polar winter season since 2010. However, thermospheric Na has not been seen in our data so far. This is because the automatic analysis program calculates the background signal level using the 140-150 km signals which possibly include a small amount of thermospheric Na signal. Deriving thermospheric Na is done by lowering the background signal level to emphasize thermospheric Na signals. The data at the new moon are selected which have a low background signal. Also, we calculated signal intensity from the Na atoms in the thermosphere based on our lidar parameters such as laser power, a telescope aperture area etc. by using the lidar equation. The results are summarized as follows. (1) Assuming that the Na density is 10 /cm^3, the signal from the Na atoms between 120 and 140 km is expected 300-400 photons, (2) The background signal observed is about 4,400 counts which means the noise level is about 220. So the signal intensity from the Na is nearly comparable to the noise level. (3) Thermospheric Na was not clearly seen in the re-calculated data. However, it depends on the smoothing technique to the original lidar data.

In this talk, we show the results derived by varying the binning time and discuss it.

Keywords: Na lidar, thermosphere, Tromsoe

©2019. Japan Geoscience Union. All Right Reserved. 

# Spatial-temporal distribution of anomalous enhancement of ambipolar diffusion coefficient observed by meteor radars installed in the polar region

*Toru Takahashi[1], Masaki Tsutsumi[1,2], Yasunobu Ogawa[1,2,3], Satonori Nozawa[3], Chris Hall[4], Hiroshi Miyaoka[1,2]

1. National Institute of Polar Research, 2. SOKENDAI, 3. Institute for Space-Earth Environmental Research, 4. TGO, The Arctic University of Norway

The meteor radar detected echoes of meteor tails as a tracer of neutral wind from 75 to 100 km altitudes (Hall et al., 2005). In addition, by using a decay time of the echo power, the meteor radar also estimated the ambipolar diffusion coefficient, which depends on the ion and electron temperature. The ambipolar diffusion coefficient was utilized to estimate the neutral temperature because the ion and electron temperature are generally in the thermal equilibrium with the neutral temperature. Recently, an anomalous enhancement of the ambipolar diffusion coefficient which could not be explained by the neutral temperature enhancement (hereafter called the anomalous enhancement) was observed by the meteor radar installed at Tromsoe, Norway (69.6 deg. N, 19.2 deg. E)
A previous study compared the anomalous enhancement with the ion velocity and the ion and electron temperature observed by EISCAT radar (Tsutsumi et al. 2017, Proceedings of the 30th Atmospheric Science Symposium, 2017). They reported that the anomalous enhancement tended to appear with the enhancement of ion velocity and electron temperature and frequently appeared at 16 UT. Furthermore, the anomalous enhancement was not seen during an event of the high energy particle precipitation on November 17, 2012 although one case study. Thus, the anomalous enhancement seems to be generated by the intense electric field and the high energy particle precipitation is not always necessary for its generation. As mentioned above, the previous study revealed a fundamental characteristics of the anomalous enhancement, however the generation mechanisms of the anomalous enhancement is still unclear. To clarify this, the comparison the spatial distribution of the anomalous enhancement with the convective electric field are needed. However, to date the latitudinal and local time occurrence of the anomalous enhancement was not revealed in the polar region.
Three meteor radars have been installed at Tromsoe, Bear island (74.5 deg. N, 19.0 deg. E), and Longyearbyen (78.2 deg. N, 16.2 deg. E). These meteor radars almost align on the same longitude line and can provide the spatial distribution of the anomalous enhancement. All meteor radars are a commercially produced VHF system (ENDR8-20) manufactured by ATRAD Pty Ltd. The antennas were produced by the Arctic University of Norway (Nozawa et al., 2012, JGR; Hall et al., 2002, GRL, Hall et al., 2006, JASTP). In this study, the spatial distribution and the occurrence rate of the anomalous enhancement was derived by these meteor radars.
Peaks of occurrence rate was seen at 20-22, 19-21, 16-19 MLT (~UT+3) at Tromsoe, Bear island, and Longyearbyen latitudes, respectively. This indicates that the anomalous enhancement appeared sequentially from high to low latitudes. In the morning sector, the peak of occurrence rate was only seen at 2-6 MLT above Bear island. In the case of high geomagnetic activity (Kp>3), the evening peaks of the occurrence rate shifted to an earlier time. On the other hand, clear peaks of the occurrence rate in the morning sector appeared at 3-5, 4-8, 7-10 MLT, respectively. Furthermore, the anomalous enhancement appeared with high possibility of 90% around 100 km south of Tromsoe. These characteristics which are seen during the time interval of high geomagnetic activity showed good agreement with the geomagnetic activity dependences of convective electric field.

©2019. Japan Geoscience Union. All Right Reserved. 

We found another interesting characteristic in the geomagnetic dependence of the occurrence of the anomalous enhancement. The peak of occurrence rate in the evening sector was larger than it observed in the morning sector. This is considered to be related that auroral arcs appearing with intense electric field mainly observed in the evening sector. Thus, the generation of anomalous enhancement seems to relate both the convective electric field and the appearance of auroral arcs.
In this presentation, we will show the spatial distribution, MLT and geomagnetic activity dependence of the anomalous enhancement. We will also intend to present the comparison it with the electric filed observed by EISCAT and EISCAT Svalbard radars

Keywords: meteor radar, Tromsø, EISCAT radar

©2019. Japan Geoscience Union. All Right Reserved. 

# Progress of ICSWSE and MAGDAS project in recent years

*Shuji Abe[1], Akimasa Yoshikawa[2,1], Teiji Uozumi[1], Akiko Fujimoto[3]

1. International Center for Space Weather Science and Education, Japan, 2. Department of Earth and Planetary Sciences, Kyushu University, 3. Kyushu Institute of Technology

International Center for Space Weather Science and Education (ICSWSE), Kyushu University is the research institute for conducting research and education in space weather. Our magnetometer array named as "MAGDAS/CPMN (MAGnetic Data Acquisition System/Circum-pan Pacific Magnetometer Network)" (Principal Investigator: Dr. A. Yoshikawa) has over seventy fluxgate magnetometers, one induction magnetometer, and four FM-CW (Frequency Modulated Continuous Wave) radars around the world. One of our recent research topics is Equatorial Electrojet (EEJ). We calculate EE-index (Uozumi et al, 2008; Fujimoto et al., 2016) for space weather nowcast/forecast using realtime magnetometer data along the magnetic equator, and update it at each hour on the website (http://data.icswse.kyushu-u.ac.jp/eeindex/). To accelerate the understanding of EEJ structure, we constructed dense magnetometer array near magnetic equator at Peru and Malaysia in recent year. In addition, we finished to install new FM-CW radar at Sicaya, Peru. The instrument works well current now. We are providing our observational information and data including old project via our website ( http://data.icswse.kyushu-u.ac.jp/). We also provide them via IUGONET (Inter-university Upper Atmosphere Observation NETwork) Type-A (http://search.iugonet.org/) which is one-stop web service system for researchers to search data, get the information of data, and plot data, and SPEDAS (Space Physics Environment Data Analysis System)/UDAS (iUgonet Data Analysis System). We will provide them via SuperMAG (http://supermag.jhuapl.edu/) in the near future. For accelerating the usage of MAGDAS and its science, we held a tutorial session in International Conference on Space Weather and Satellite Application 2018 at Malaysia, for handling MAGDAS and other data related our research field by using IUGONET system. We believe researchers use MAGDAS data on proper rule and develop their science. We will introduce other research activities in ICSWSE and MAGDAS project, for example, plasma bubble, geomagnetically induced current, and so on.

©2019. Japan Geoscience Union. All Right Reserved. 

# Status of GNU Radio Beacon Receiver 2 (GRBR2) development

*Mamoru Yamamoto[1], Mayumi Matsunaga[2], Roland Tsunoda[3]

1. Research Institute for Sustainable Humanosphere, Kyoto University, 2. Tokyo University of Technology, 3. SRI International

GNU Radio Beacon Receiver (GRBR) is the very successful digital receiver developed for dual-band (150/400MHz) beacon experiment. We were successfully conducted observations of total-electron content (TEC) of the ionosphere over Japan and in southeast Asia. However, many beacon satellites is now aging, and its number is decreasing. We now have a project to start new satellite-ground beacon experiment with new satellite constellations. One of them is TBEx (Tandem Beacon Explorer), a project by SRI International, to fly a constellation of two 3U cubesats with triband beacon transmitters. Another one is a project of FORMOSAT-7/COSMIC-2 by Taiwan/USA. Well-known mission of COSMIC-2 is GNSS occultation experiment, but the satellites carry triband beacon transmitters. All of these satellites will be placed into low-inclination orbits by the same launch vehicle in 2018, which will give us great opportunities to enhance studies of the low-latitude ionosphere. We develop a new digital receiver, GRBR2, for these new satellite beacon. GRBR2 is a four channel receiver at 150/400/965/1067MHz beacon signals from two satellite constellations. Now The reveiver system was finally fixed. Problem of the project of delay of the satellite launch. But it is now on schedule for launch by 2019 summer. We start deploying GRBR2 in southeast Asian countries. In this presentaiton, we will report GRBR2 system and its performance including results from test experiment in the field.

Keywords: Satellite beacon experiment, Digital receiver development, Total electron content

©2019. Japan Geoscience Union. All Right Reserved. 

# Statistical comparison between plasma bubble day-to-day variability and neutral atmosphere by using GPS scintillation and GAIA model

*Mamoru Yamamoto[1], Keigo Kono[1]

1. Research Institute for Sustainable Humanosphere, Kyoto University

Equational plasma bubble is one of the most intense irregularities in the ionosphere. The occurrence of the plasma bubble is considered related to weak changes of the underlying atmosphere which is called large-scale wavelike structure (LSWS). The LSWS is expected formed by penetration of the atmospheric wave into the ionosphere. But its real effect is not yet known in detail. The purpose of this research is to investigate the correlation between the neutral atmosphere and day-to-day variability of equatorial plasma bubbles mainly in the Southeast Asia region. We based on the study by Yamamoto et al (2018) that showed relationship between 40-km height temperature variation and S4 index over Kototabang, Indonesia. In this study we tried to extend the observation region and also tried to elucidate atmospheric waves that are related to the plasma bubble. For indicating activity of the plasma bubble, we used S4 index of GPS scintillation measured by ISEE, Nagoya Univ. at Kototabang, Indonesia. Atmospheric data were taken from GAIA database prepared by NICT. We analyzed data from 2003, 2004, 2012, and 2013 where the solar activity was high. Overall correlation between S4 index and the atmospheric temperature showed similar feature throughout these years. However, even when we tried to extract atmospheric wave components from the GAIA data, the correlation between the wave parameter to S4 index did not show large change. This means that the elucidation of the atmospheric wave component was not very successful so far. Further analyses are required.

Reference
Yamamoto, M., Y. Otsuka, H. Jin, Y. Miyoshi (2018) Relationship between day-to-day variability of equatorial plasma bubble activity from GPS scintillation and atmospheric properties from GAIA assimilation, Progress in Earth and Planetary Science, Vol. 5, page 26, doi: 10.1186/s40645-018-0184-7.

©2019. Japan Geoscience Union. All Right Reserved. 

# Redevelopment of the MU radar transceiver-module control system

*Mamoru Yamamoto[1], Koki Kurokawa[1], Hiroyuki Hashiguchi[1]

1. Research Institute for Sustainable Humanosphere, Kyoto University

The MU radar was installed in Shigaraki, Japan in 1984 as the world first atmospheric radar with active phased-array antenna system. The MU radar consists of 475 Yagi antennas in the circular field of about 100m diameter. By the electronic phase shift of each Yagi, the antenna beam is steered to one of pre-selected 2048 directions in the transmitting pulse-to-pulse basis. Success of the MU radar in the atmospheric/ionospheric research is well known, and its active phased-array configuration was followed by many other radar systems. The phase control of the MU radar is realized by the control of its transceiver-module (TR-module) that are equipped with each Yagi antenna. They are gathered into 25 groups of each 19 modules. One CPU (microcomputer board) is used for control of one group of modules. A weak point of the MU radar exists in this point because we are using the original 8085 CPU board that is connected to the host computer by 1200-baud (!) serial line. This control is very slow, and we could not meet demands for rapid change of observation parameters for long time. This time we tried to re-develop the new TR-module controller by using recent CPU board and electronic devices. In the presentation, we show hardware/software of the newly developed prototype of the MU radar TR-module controller.

Keywords: MU radar, control system, redevelopment

©2019. Japan Geoscience Union. All Right Reserved. 

[E] Poster | P (Space and Planetary Sciences )：P-EM Solar-Terrestrial Sciences, Space Electromagnetism & Space Environment

Thu. May 30, 2019 5:15 PM - 6:30 PM JST | Thu. May 30, 2019 8:15 AM - 9:30 AM UTC | Poster Hall International Exhibition Hall8, Makuhari Messe_2

## [P-EM15] Study of coupling processes in solar-terrestrial system

convener:Mamoru Yamamoto(Research Institute for Sustainable Humanosphere, Kyoto University), Yasunobu Ogawa(National Institute of Polar Research), Satonori Nozawa(Institute for Space-Earth Environment Research), Akimasa Yoshikawa(Department of Earth and Planetary Sciences, Kyushu University)

The Earth accepts vast input of energy and material from the Sun. The Earth's environment is maintained by the balance between their inputs and outputs. It is therefore important to study energy and mass transport on the Earth. This is an international session that discusses studies of the coupling processes in the Sun-Earth system based on the project "Study of coupling processes in solar-terrestrial system" that was approved by the Master Plan 2011/2014/2017 of Science Council of Japan. We continue proposing the project to the Master Plan 2020. The facilities and networks included are Equatorial MU Radar (EMU) in Indonesia to study the whole equatorial atmosphere, the EISCAT_3D radar system in northern Scandinavia to study detailed structures and elementary processes of the magnetosphere-ionosphere coupling in the polar region, and global networks of various ground-based instruments and observation data. We will show the current status of the project and discuss sciences by soliciting variety papers. This session is open to the world, and we strongly encourage submission of papers related to other facilities and projects, i.e., atmospheric or incoherent scatter radars, observation networks, satellites, and simulation or theoretical studies, etc.

### [PEM15-P01] Study on adaptive clutter rejection system using external receiving antennas for the MU radar

*Hiroyuki Hashiguchi[1], Issei Terada[1], Mamoru Yamamoto[1] (1.Research Institute for Sustainable Humanosphere, Kyoto University)

### [PEM15-P02] Detached cusp aurora for southward IMF

*Kohei Takasu[1], Satoshi Taguchi[1], Keisuke Hosokawa[2] (1.Department of Geophysics, Graduate School of Science, Kyoto University, 2.Department of Communication Engineering and Informatics, University of Electro-Communications)

### [PEM15-P03] Motion of the inverted-V structure during an isolated substorm

*Morio Tanaka[1], Satoshi Taguchi[1], Kohei Takasu[1], Tomokazu Oigawa[1], Keisuke Hosokawa[2] (1.Department of Geophysics, Graduate school of science, Kyoto University, 2.Department of Communication Engineering and Informatics, University of Electro-Communications)

### [PEM15-P04] Observation and modeling of Na layer response to energetic particle precipitation

*Takuo T. Tsuda[1], Kyogo Takizawa[1], Ryo Tozu[1], Takuya Kawahara[2], Yoshimasa Tanaka[3], Mitsumu K. Ejiri[3], Takanori Nishiyama[3], Takuji Nakamura[3] (1.The University of Electro-Communications, 2.Shinshu University, 3.National Institute of Polar Research)

### [PEM15-P05] Lidar data analysis of the sodium atoms in the thermosphere observed at Tromsoe, Norway

*Takuya Kawahara[1], Satonori Nozawa[2], Norihito Saito[3], Takuo T. Tsuda[4], Toru Takahashi[5], Testuya Kawabata[2], Miki Nishimura[1], Yoshitaka Kobayashi[1] (1.Faculty of Engineering, Shinshu University, 2.ISEE, Nagoya University, 3.RIKEN, Center for Advanced Photonics, 4.The University of Electro-Communications, 5.National Institute of Polar Research)

### [PEM15-P06] Spatial-temporal distribution of anomalous enhancement of ambipolar diffusion coefficient observed by meteor radars installed in the polar region

*Toru Takahashi[1], Masaki Tsutsumi[1,2], Yasunobu Ogawa[1,2,3], Satonori Nozawa[3], Chris Hall[4], Hiroshi Miyaoka[1,2] (1.National Institute of Polar Research, 2.SOKENDAI, 3.Institute for Space-Earth Environmental Research, 4.TGO, The Arctic University of Norway)

## [PEM15-P07] Progress of ICSWSE and MAGDAS project in recent years

*Shuji Abe[1], Akimasa Yoshikawa[2,1], Teiji Uozumi[1], Akiko Fujimoto[3] (1.International Center for Space Weather Science and Education, Japan, 2.Department of Earth and Planetary Sciences, Kyushu University, 3.Kyushu Institute of Technology)

## [PEM15-P08] Status of GNU Radio Beacon Receiver 2 (GRBR2) development

*Mamoru Yamamoto[1], Mayumi Matsunaga[2], Roland Tsunoda[3] (1.Research Institute for Sustainable Humanosphere, Kyoto University, 2.Tokyo University of Technology, 3.SRI International)

## [PEM15-P09] Statistical comparison between plasma bubble day-to-day variability and neutral atmosphere by using GPS scintillation and GAIA model

*Mamoru Yamamoto[1], Keigo Kono[1] (1.Research Institute for Sustainable Humanosphere, Kyoto University)

## [PEM15-P10] Redevelopment of the MU radar transceiver-module control system

*Mamoru Yamamoto[1], Koki Kurokawa[1], Hiroyuki Hashiguchi[1] (1.Research Institute for Sustainable Humanosphere, Kyoto University)

# Study on adaptive clutter rejection system using external receiving antennas for the MU radar

*Hiroyuki Hashiguchi[1], Issei Terada[1], Mamoru Yamamoto[1]

1. Research Institute for Sustainable Humanosphere, Kyoto University

Strong clutter echoes from a hard target such as a mountain or building sometimes cause problems of observations with atmospheric radars. In order to reject or suppress ground clutter echoes, it is effective to use NC-DCMP (Norm Constrained- Directionally Constrained Minimum Power) method, which makes null toward the direction of the clutter, if we can receive signals independently from plural antennas [Nishimura et al., JTech., 2012]. It has been demonstrated that the NC-DCMP method is effective to real observation data with the MU (Middle and Upper atmosphere) radar [Hashiguchi et al., Radio Sci., 2018]. Although NC-DCMP method suppresses clutter echoes with almost maintaining the shape of main lobe to add pseudo-noise compared with the conventional DCMP method, the signal-to-noise ratio (S/N) of atmospheric echoes is somewhat degraded. We studied the clutter suppression method with little S/N degradation by using external antennas.

Four turnstile antennas are installed in the MU radar site. The signal from the antenna is sent to the MU radar observation room through the coaxial cable after amplified by the LNA with the limiter and BPF. It is further amplified by the LNA in the observation room, and then down-converted to intermediate frequency (5 MHz) signal to input to the multi-channel receiving system of the MU radar.

We compared the NC-DCMP method using the each received data of 25 channels, which is a conventional clutter suppression method, and the NC-DCMP method using the simple combination of 25 channels and 4 channels of external antennas. In the former case, the S/N of the atmospheric echoes is somewhat degraded, but in the latter case the main lobe shape is guaranteed by 25 channel simple synthesis, so the S/N degradation is not observed. In the latter case, the clutter suppression is sometimes insufficient. This cause is considered to be that the current positions of external antennas are biased to the north side. Antenna positions should be optimized in the future.

We can apply the achievement of this study to the Equatorial MU radar (EMU), which is proposed to be constructed at West Sumatera, Indonesia. The EMU system is the similar as the MU radar, but its antenna consists of 1045 Yagi antennas with 55 groups and it has 64 receiver channels.

Keywords: Atmospheric radar, Clutter rejection, NC-DCMP method, MU radar

©2019. Japan Geoscience Union. All Right Reserved. 

# Detached cusp aurora for southward IMF

*Kohei Takasu[1], Satoshi Taguchi[1], Keisuke Hosokawa[2]

1. Department of Geophysics, Graduate School of Science, Kyoto University, 2. Department of Communication Engineering and Informatics, University of Electro-Communications

A poleward-moving aurora is a typical phenomenon in the dayside cusp of the high-latitude ionosphere. This aurora usually originates near the equatorward boundary of the cusp, and diminishes near the poleward boundary of the persistent cusp auroral emissions. In this study we have examined faint poleward-moving auroras that are detached from the persistent cusp emissions by analyzing 630-nm aurora image data from an all-sky imager at Longyearbyen, Svalbard, and precipitating electron data from DMSP spacecraft. These auroras occur for southward IMF, and are located at latitudes higher than 80 MLAT. The intensities are very weak (less than 1 kilo Rayleigh). The result of the analysis shows that the speed of the auroral motion is 1 to 2 km/s, which is faster than typical convection speed in the dayside polar cap. We show the similarities and differences between the faint aurora and the typical poleward moving cusp aurora, and discuss how soft electron precipitation occurs in the region that is well separated from the cusp.

Keywords: Aurora, cusp, plasma convection, IMF

©2019. Japan Geoscience Union. All Right Reserved. 

# Motion of the inverted-V structure during an isolated substorm

*Morio Tanaka[1], Satoshi Taguchi[1], Kohei Takasu[1], Tomokazu Oigawa[1], Keisuke Hosokawa[2]

1. Department of Geophysics, Graduate school of science, Kyoto University, 2. Department of Communication Engineering and Informatics, University of Electro-Communications

The inverted-V is an energetic electron precipitation event, which can be seen as a V-shape structure in electron flux spectrograms, and causes intense auroral arcs. Previous studies have suggested that the inverted-V structure can move fast poleward or equatorward. However, we still do not understand what drives its motion. In this study we have investigated the detailed characteristics of an inverted-V structure moving poleward, which occurred during an isolated substorm, using simultaneous observations of auroras, precipitating electrons, and field-aligned currents. We analyzed aurora data (630-nm and 557.7-nm) from an all-sky imager at Longyearbyen, Svalbard, and precipitating electrons and magnetic field data from the DMSP spacecraft (F16, F17, F18, F19). One of the interesting characteristics of the poleward-moving inverted-V is the appearance of a downward field-aligned current equatorward of and adjacent to the inverted-V. We discuss how the region of the downward field-aligned current evolves in association with the motion and growth/decay of the inverted V structure, and possibility of a role of the downward field-aligned current for the latitudinal motion of the inverted V.

Keywords: Field-aligned current, aurora, inverted-V, isolated substorm

©2019. Japan Geoscience Union. All Right Reserved. 

# Observation and modeling of Na layer response to energetic particle precipitation

*Takuo T. Tsuda[1], Kyogo Takizawa[1], Ryo Tozu[1], Takuya Kawahara[2], Yoshimasa Tanaka[3], Mitsumu K. Ejiri[3], Takanori Nishiyama[3], Takuji Nakamura[3]

1. The University of Electro-Communications, 2. Shinshu University, 3. National Institute of Polar Research

Metallic layers, such as Na, Fe, Mg, K, and Ca layers, exist in the mesosphere and lower thermosphere (MLT). The height range of the MLT region corresponds to the ionospheric *D* and *E* regions, and in the polar region energetic particles precipitating from the magnetosphere can often penetrate into the *E* region and even into the *D* region. Therefore, the influence of energetic particles on the metallic layers is of interest regarding changes in atmospheric composition accompanied by auroral activity or geomagnetic activity.

In this study, we have performed a statistical investigation on relationship between Na density and cosmic noise absorption (CNA), which were obtained from 2000 to 2002 at Syowa Station, Antarctic (69.0ºS, 39.6ºE). From the investigation, we found the Na density decrease in accordance with the CNA increase, i.e., increase in the energetic particle precipitation. In the presentation, we will show these observational results, and discuss causality about the observed relationship based on numerical caculations using our Na chemistry model.

Keywords: Na layer, Energetic particle precipitation, Syowa Station, Na chemistry model

©2019. Japan Geoscience Union. All Right Reserved. 

# Lidar data analysis of the sodium atoms in the thermosphere observed at Tromsoe, Norway

*Takuya Kawahara[1], Satonori Nozawa[2], Norihito Saito[3], Takuo T. Tsuda[4], Toru Takahashi[5], Testuya Kawabata[2], Miki Nishimura[1], Yoshitaka Kobayashi[1]

1. Faculty of Engineering, Shinshu University, 2. ISEE, Nagoya University, 3. RIKEN, Center for Advanced Photonics, 4. The University of Electro-Communications, 5. National Institute of Polar Research

Distribution of low-density Na atoms in the thermosphere is interesting because of the capability of measuring neutral temperature and wind into the lower thermosphere up to 140 km. The thermospheric Na atoms significantly made the altitude range of Na lidar measurements expanded from the 80–105 km to 80–140 km, covering almost the entire E region (Liu et al., GRL, 2016).

The measurements of wind and temperature by a Na lidar in the northern mesosphere (80-105 km) at Tromsoe, Norway (69.6˚N, 19.2˚E) have been carried out in Polar winter season since 2010. However, thermospheric Na has not been seen in our data so far. This is because the automatic analysis program calculates the background signal level using the 140-150 km signals which possibly include a small amount of thermospheric Na signal. Deriving thermospheric Na is done by lowering the background signal level to emphasize thermospheric Na signals. The data at the new moon are selected which have a low background signal. Also, we calculated signal intensity from the Na atoms in the thermosphere based on our lidar parameters such as laser power, a telescope aperture area etc. by using the lidar equation. The results are summarized as follows. (1) Assuming that the Na density is 10 /cm^3, the signal from the Na atoms between 120 and 140 km is expected 300-400 photons, (2) The background signal observed is about 4,400 counts which means the noise level is about 220. So the signal intensity from the Na is nearly comparable to the noise level. (3) Thermospheric Na was not clearly seen in the re-calculated data. However, it depends on the smoothing technique to the original lidar data.

In this talk, we show the results derived by varying the binning time and discuss it.

Keywords: Na lidar, thermosphere, Tromsoe

©2019. Japan Geoscience Union. All Right Reserved. 

# Spatial-temporal distribution of anomalous enhancement of ambipolar diffusion coefficient observed by meteor radars installed in the polar region

*Toru Takahashi[1], Masaki Tsutsumi[1,2], Yasunobu Ogawa[1,2,3], Satonori Nozawa[3], Chris Hall[4], Hiroshi Miyaoka[1,2]

1. National Institute of Polar Research, 2. SOKENDAI, 3. Institute for Space-Earth Environmental Research, 4. TGO, The Arctic University of Norway

The meteor radar detected echoes of meteor tails as a tracer of neutral wind from 75 to 100 km altitudes (Hall et al., 2005). In addition, by using a decay time of the echo power, the meteor radar also estimated the ambipolar diffusion coefficient, which depends on the ion and electron temperature. The ambipolar diffusion coefficient was utilized to estimate the neutral temperature because the ion and electron temperature are generally in the thermal equilibrium with the neutral temperature. Recently, an anomalous enhancement of the ambipolar diffusion coefficient which could not be explained by the neutral temperature enhancement (hereafter called the anomalous enhancement) was observed by the meteor radar installed at Tromsoe, Norway (69.6 deg. N, 19.2 deg. E)
A previous study compared the anomalous enhancement with the ion velocity and the ion and electron temperature observed by EISCAT radar (Tsutsumi et al. 2017, Proceedings of the 30th Atmospheric Science Symposium, 2017). They reported that the anomalous enhancement tended to appear with the enhancement of ion velocity and electron temperature and frequently appeared at 16 UT. Furthermore, the anomalous enhancement was not seen during an event of the high energy particle precipitation on November 17, 2012 although one case study. Thus, the anomalous enhancement seems to be generated by the intense electric field and the high energy particle precipitation is not always necessary for its generation. As mentioned above, the previous study revealed a fundamental characteristics of the anomalous enhancement, however the generation mechanisms of the anomalous enhancement is still unclear. To clarify this, the comparison the spatial distribution of the anomalous enhancement with the convective electric field are needed. However, to date the latitudinal and local time occurrence of the anomalous enhancement was not revealed in the polar region.
Three meteor radars have been installed at Tromsoe, Bear island (74.5 deg. N, 19.0 deg. E), and Longyearbyen (78.2 deg. N, 16.2 deg. E). These meteor radars almost align on the same longitude line and can provide the spatial distribution of the anomalous enhancement. All meteor radars are a commercially produced VHF system (ENDR8-20) manufactured by ATRAD Pty Ltd. The antennas were produced by the Arctic University of Norway (Nozawa et al., 2012, JGR; Hall et al., 2002, GRL, Hall et al., 2006, JASTP). In this study, the spatial distribution and the occurrence rate of the anomalous enhancement was derived by these meteor radars.
Peaks of occurrence rate was seen at 20-22, 19-21, 16-19 MLT (~UT+3) at Tromsoe, Bear island, and Longyearbyen latitudes, respectively. This indicates that the anomalous enhancement appeared sequentially from high to low latitudes. In the morning sector, the peak of occurrence rate was only seen at 2-6 MLT above Bear island. In the case of high geomagnetic activity (Kp>3), the evening peaks of the occurrence rate shifted to an earlier time. On the other hand, clear peaks of the occurrence rate in the morning sector appeared at 3-5, 4-8, 7-10 MLT, respectively. Furthermore, the anomalous enhancement appeared with high possibility of 90% around 100 km south of Tromsoe. These characteristics which are seen during the time interval of high geomagnetic activity showed good agreement with the geomagnetic activity dependences of convective electric field.

©2019. Japan Geoscience Union. All Right Reserved. 

We found another interesting characteristic in the geomagnetic dependence of the occurrence of the anomalous enhancement. The peak of occurrence rate in the evening sector was larger than it observed in the morning sector. This is considered to be related that auroral arcs appearing with intense electric field mainly observed in the evening sector. Thus, the generation of anomalous enhancement seems to relate both the convective electric field and the appearance of auroral arcs.
In this presentation, we will show the spatial distribution, MLT and geomagnetic activity dependence of the anomalous enhancement. We will also intend to present the comparison it with the electric filed observed by EISCAT and EISCAT Svalbard radars

Keywords: meteor radar, Tromsø, EISCAT radar

©2019. Japan Geoscience Union. All Right Reserved. 

# Progress of ICSWSE and MAGDAS project in recent years

*Shuji Abe[1], Akimasa Yoshikawa[2,1], Teiji Uozumi[1], Akiko Fujimoto[3]

1. International Center for Space Weather Science and Education, Japan, 2. Department of Earth and Planetary Sciences, Kyushu University, 3. Kyushu Institute of Technology

International Center for Space Weather Science and Education (ICSWSE), Kyushu University is the research institute for conducting research and education in space weather. Our magnetometer array named as "MAGDAS/CPMN (MAGnetic Data Acquisition System/Circum-pan Pacific Magnetometer Network)" (Principal Investigator: Dr. A. Yoshikawa) has over seventy fluxgate magnetometers, one induction magnetometer, and four FM-CW (Frequency Modulated Continuous Wave) radars around the world. One of our recent research topics is Equatorial Electrojet (EEJ). We calculate EE-index (Uozumi et al, 2008; Fujimoto et al., 2016) for space weather nowcast/forecast using realtime magnetometer data along the magnetic equator, and update it at each hour on the website (http://data.icswse.kyushu-u.ac.jp/eeindex/). To accelerate the understanding of EEJ structure, we constructed dense magnetometer array near magnetic equator at Peru and Malaysia in recent year. In addition, we finished to install new FM-CW radar at Sicaya, Peru. The instrument works well current now. We are providing our observational information and data including old project via our website ( http://data.icswse.kyushu-u.ac.jp/). We also provide them via IUGONET (Inter-university Upper Atmosphere Observation NETwork) Type-A (http://search.iugonet.org/) which is one-stop web service system for researchers to search data, get the information of data, and plot data, and SPEDAS (Space Physics Environment Data Analysis System)/UDAS (iUgonet Data Analysis System). We will provide them via SuperMAG (http://supermag.jhuapl.edu/) in the near future. For accelerating the usage of MAGDAS and its science, we held a tutorial session in International Conference on Space Weather and Satellite Application 2018 at Malaysia, for handling MAGDAS and other data related our research field by using IUGONET system. We believe researchers use MAGDAS data on proper rule and develop their science. We will introduce other research activities in ICSWSE and MAGDAS project, for example, plasma bubble, geomagnetically induced current, and so on.

©2019. Japan Geoscience Union. All Right Reserved. 

# Status of GNU Radio Beacon Receiver 2 (GRBR2) development

*Mamoru Yamamoto[1], Mayumi Matsunaga[2], Roland Tsunoda[3]

1. Research Institute for Sustainable Humanosphere, Kyoto University, 2. Tokyo University of Technology, 3. SRI International

GNU Radio Beacon Receiver (GRBR) is the very successful digital receiver developed for dual-band (150/400MHz) beacon experiment. We were successfully conducted observations of total-electron content (TEC) of the ionosphere over Japan and in southeast Asia. However, many beacon satellites is now aging, and its number is decreasing. We now have a project to start new satellite-ground beacon experiment with new satellite constellations. One of them is TBEx (Tandem Beacon Explorer), a project by SRI International, to fly a constellation of two 3U cubesats with triband beacon transmitters. Another one is a project of FORMOSAT-7/COSMIC-2 by Taiwan/USA. Well-known mission of COSMIC-2 is GNSS occultation experiment, but the satellites carry triband beacon transmitters. All of these satellites will be placed into low-inclination orbits by the same launch vehicle in 2018, which will give us great opportunities to enhance studies of the low-latitude ionosphere. We develop a new digital receiver, GRBR2, for these new satellite beacon. GRBR2 is a four channel receiver at 150/400/965/1067MHz beacon signals from two satellite constellations. Now The reveiver system was finally fixed. Problem of the project of delay of the satellite launch. But it is now on schedule for launch by 2019 summer. We start deploying GRBR2 in southeast Asian countries. In this presentaiton, we will report GRBR2 system and its performance including results from test experiment in the field.

Keywords: Satellite beacon experiment, Digital receiver development, Total electron content

©2019. Japan Geoscience Union. All Right Reserved. 

# Statistical comparison between plasma bubble day-to-day variability and neutral atmosphere by using GPS scintillation and GAIA model

*Mamoru Yamamoto[1], Keigo Kono[1]

1. Research Institute for Sustainable Humanosphere, Kyoto University

Equational plasma bubble is one of the most intense irregularities in the ionosphere. The occurrence of the plasma bubble is considered related to weak changes of the underlying atmosphere which is called large-scale wavelike structure (LSWS). The LSWS is expected formed by penetration of the atmospheric wave into the ionosphere. But its real effect is not yet known in detail. The purpose of this research is to investigate the correlation between the neutral atmosphere and day-to-day variability of equatorial plasma bubbles mainly in the Southeast Asia region. We based on the study by Yamamoto et al (2018) that showed relationship between 40-km height temperature variation and S4 index over Kototabang, Indonesia. In this study we tried to extend the observation region and also tried to elucidate atmospheric waves that are related to the plasma bubble. For indicating activity of the plasma bubble, we used S4 index of GPS scintillation measured by ISEE, Nagoya Univ. at Kototabang, Indonesia. Atmospheric data were taken from GAIA database prepared by NICT. We analyzed data from 2003, 2004, 2012, and 2013 where the solar activity was high. Overall correlation between S4 index and the atmospheric temperature showed similar feature throughout these years. However, even when we tried to extract atmospheric wave components from the GAIA data, the correlation between the wave parameter to S4 index did not show large change. This means that the elucidation of the atmospheric wave component was not very successful so far. Further analyses are required.

Reference
Yamamoto, M., Y. Otsuka, H. Jin, Y. Miyoshi (2018) Relationship between day-to-day variability of equatorial plasma bubble activity from GPS scintillation and atmospheric properties from GAIA assimilation, Progress in Earth and Planetary Science, Vol. 5, page 26, doi: 10.1186/s40645-018-0184-7.

©2019. Japan Geoscience Union. All Right Reserved. 

# Redevelopment of the MU radar transceiver-module control system

*Mamoru Yamamoto[1], Koki Kurokawa[1], Hiroyuki Hashiguchi[1]

1. Research Institute for Sustainable Humanosphere, Kyoto University

The MU radar was installed in Shigaraki, Japan in 1984 as the world first atmospheric radar with active phased-array antenna system. The MU radar consists of 475 Yagi antennas in the circular field of about 100m diameter. By the electronic phase shift of each Yagi, the antenna beam is steered to one of pre-selected 2048 directions in the transmitting pulse-to-pulse basis. Success of the MU radar in the atmospheric/ionospheric research is well known, and its active phased-array configuration was followed by many other radar systems. The phase control of the MU radar is realized by the control of its transceiver-module (TR-module) that are equipped with each Yagi antenna. They are gathered into 25 groups of each 19 modules. One CPU (microcomputer board) is used for control of one group of modules. A weak point of the MU radar exists in this point because we are using the original 8085 CPU board that is connected to the host computer by 1200-baud (!) serial line. This control is very slow, and we could not meet demands for rapid change of observation parameters for long time. This time we tried to re-develop the new TR-module controller by using recent CPU board and electronic devices. In the presentation, we show hardware/software of the newly developed prototype of the MU radar TR-module controller.

Keywords: MU radar, control system, redevelopment

©2019. Japan Geoscience Union. All Right Reserved. 

[J] Poster | P (Space and Planetary Sciences )：P-EM Solar-Terrestrial Sciences, Space Electromagnetism & Space Environment

Thu. May 30, 2019 3:30 PM - 5:00 PM JST | Thu. May 30, 2019 6:30 AM - 8:00 AM UTC | Poster Hall International Exhibition Hall8, Makuhari Messe_3

## [P-EM16] Physics and Chemistry in the Atmosphere and Ionosphere

convener:Yuichi Otsuka(Institute for Space-Earth Environmental Research, Nagoya University), Takuya Tsugawa(National Institute of Information and Communications Technology), Seiji Kawamura(National Institute of Information and Communications Technology)

This session covers a broad scope of studies of physics and chemistry in the atmosphere and the ionosphere. Coupling processes between plasma and neutral species, and upward and downward coupling among lower/upper atmosphere, and ionosphere/mesosphere/thermosphere including magnetosphere are discussed. We solicit papers based on experiments with ground-based and/or space-borne instruments, theoretical studies, numerical simulations, and development of new observation techniques.

### [PEM16-P01] Temporal and spatial variation of GPS phase scintillation during substorms and auroral breakups

*Paul Prikryl[1,2], James M. Weygand[3], Reza Ghoddousi-Fard[4], P. Thayyil Jayachandran[1], David R. Themens[1], Anthony M. McCaffrey[1], Bharat S. R. Kunduri[5], Emma Spanswick[6], Yongliang Zhang[7], Akira Sessai Yukimatu[8] (1.Physics Department, University of New Brunswick, Fredericton, NB, Canada, 2.Geomagnetic Laboratory, Natural Resources Canada, Ottawa, ON, Canada, 3.Earth Planetary and Space Sciences, University of California, Los Angeles, CA, USA, 4.Canadian Geodetic Survey, Natural Resources Canada, Ottawa, ON, Canada, 5.Bradley Dept. of Electrical and Computer Engineering, Virginia Tech, USA, 6.Dept. of Physics and Astronomy, University of Calgary, AB, Canada, 7.Johns Hopkins University Applied Physics Laboratory, Laurel, MD, USA, 8.National Institute of Polar Research, Tokyo, Japan)

### [PEM16-P02] Statistical study of SAPS occurrence characteristics using the SuperDARN Hokkaido HF radar

*Kento Oya[1], Nozomu Nishitani[1], Tomoaki Hori[1] (1.Institute for Space-Earth Environmental Research, Nagoya University)

### [PEM16-P03] Spectral investigations of near infrared aurora and airglow at 1.0-1.6 microns: 1-year ground-based imaging spectroscopic observation at Syowa station (69.0°S, 39.6°E)

*Takanori Nishiyama[1], Takeshi Sakanoi[2], Makoto Taguchi[3], Hidehiko Suzuki[4] (1.National Institute of Polar Research, 2.Planetary Plasma and Atmospheric Research Center, Tohoku University, 3.Rikkyo University, 4.Department of Physics, Meiji University)

### [PEM16-P04] The study of the lower ionosphere in the South Atlantic Anomaly (SAA) Region

*Chih-Yu Chiang[1], Tzu-Fang Chang[2,1], Sunny W. Y. Tam[1] (1.Institute of Space and Plasma Sciences, National Cheng Kung University, Tainan, Taiwan, 2.Institute for Space-Earth Environmental Research, Nagoya University, Japan)

### [PEM16-P05] Multi-GNSS observation of LSTID in Japan and its link with auroral activities

*Mayumi Hashimoto[1], Kosuke Heki[1] (1.Hokkaido University)

### [PEM16-P06] Basic development of accurate analytical method in order to determine coordinates of artificial illuminating clouds of Barium and Strontium for chemical-release rocket experiments

*Taro Watanabe[1], Masa-yuki Yamamoto[1], Yoshihiro Kakinami[2] (1.Kochi University of Technology, 2.Hokkaido Information University)

### [PEM16-P07] Neutral and plasma density perturbations in the top-/bottom-side ionosphere associated with MSTIDs

*Shin Suzuki[1], Jaeheung Park[2], Yuichi Otsuka[3], Kazuo Shiokawa[3], Huixin Liu[4], Hermann Luehr[5] (1.Faculty of Regional Policy, Aichi University, 2.Korea Astronomy and Space Science Institute, 3.Institute for Space-Earth Environmental Research, Nagoya University, 4.Earth and Planetary Science Division, Kyushu University SERC, Kyushu University, 5.Helmholtz Centre Potsdam, GFZ, German Research Centre for Geosciences)

[PEM16-P08] Analysis of ionospheric TEC fluctuation by rocket

*Tsuyoshi Takegawa[1], Hiroyuki Nakata[1], Hiroyo Ohya[1], Toshiaki Takano[1], Takuya Tsugawa[2], Michi Nishioka[2] (1.Graduate School of Integrated Science and Technology, Chiba University, 2.National Institute of Information and Communications Technology)

[PEM16-P09] Examinations of the ionospheric perturbation associated with H-IIA rockets launching

*Junpei Yamazaki[1], Hiroyuki Nakata[1], Hiroyo Ohya[1], Toshiaki Takano[1], Keisuke Hosokawa[2], Ichiro Tomizawa[2] (1.Graduate School of Engineering, Chiba University, 2.Department of Communication Engineering and Informatics, University of Electro-Communications)

[PEM16-P10] Explosion energy derived from the 2015 Kuchinoerabujima eruption: Estimation from infrasound less than 0.01 Hz detected by barometers, seismometers, and TEC

*Yuki Nakashima[1], Kiwamu Nishida[1], Yosuke Aoki[1], Kosuke Heki[2] (1.Earthquake Research Institute, 2.Natural History Sciences, Hokkaido University)

[PEM16-P11] Detection of spread-F echoes in ionograms using machine learning

*Hiroyuki Nakata[1], Yuta Goto[2], Hiroyo Ohya[1], Toshiaki Takano[1] (1.Graduate School of Engineering, Chiba University, 2.Department of Electrical and Electronics Engineering)

[PEM16-P12] Evaluation of GNSS-TEC receiver performance for sounding rocket installation

*Makoto Okumura[1], Yuki Ashihara[1] (1.National Institute of Technology, Nara College)

[PEM16-P13] Relationship between mesosperical airglow disturbance and occurrence of equatorial plasma bubbles

*Ryota Okada[1], Akinori Saito[1], Takafumi Ikeda[1], Hiroyuki Shinagawa[2], Takuya Tsugawa[2], Takeshi Sakanoi[3] (1.Department of Geophysics, Graduate School of Science, Kyoto University, 2.National Institute of Information and Communications Technology, 3.Planetary Plasma and Atmospheric Research Center, Graduate School of Science, Tohoku University)

[PEM16-P14] Analysis of parameters controlling the occurrence and growth of equatorial plasma bubbles using GAIA

*Hiroyuki Shinagawa[1], Hidekatsu Jin[1], Yasunobu Miyoshi[2], Hitoshi Fujiwara[3], Tatsuhiro Yokoyama[4], Yuichi Otsuka[5] (1.National Institute of Information and Communications Technology, 2.Department of Earth and Planetary Sciences, Faculty of Sciences, Kyushu University, 3.Faculty of Science and Technology, Seikei University, 4.Kyoto University, 5.Institute for Space-Earth Environmental Research, Nagoya University)

[PEM16-P15] A three-dimensional numerical model to study the modulation of midlatitude $E_s$-layers

*Satoshi Andoh[1], Akinori Saito[1], Hiroyuki Shinagawa[2], Shin'ichi Miyazaki[1] (1.Graduate School of Science, Kyoto University, 2.National Institute of Information and Communications Technology)

[PEM16-P16] Statistical analysis of the horizontal phase velocity distribution of mesospheric and ionospheric waves observed in airglow images in Hawaii

*Hideto Naito[1], Kazuo Shiokawa[1], Yuichi Otsuka[1], Takeshi Sakanoi[2], Akinori Saito[3], Takuji Nakamura[4] (1.Institute for Space-Earth Environmental Research, Nagoya University, 2.Planetary Plasma and Atmospheric Research Center, Graduate School of Science, Tohoku University, 3.Department of Geophysics, Graduate school of science, Kyoto University, 4.National Institute of Polar Research)

## [PEM16-P17] Estimation of mesospheric OH temperature by observation data by ISS-IMAP VISI

*Ryo Murakami[1], Akinori Saito[1], Takeshi Sakanoi[2], Yuta Hozumi[3] (1.Kyoto University, 2.Tohoku University, 3.University of Electro-Communications)

## [PEM16-P18] Implementation of photochemical process of NOx and HOx into a whole atmosphere GCM

*Yasunobu Miyoshi[1], Hitoshi Fujiwara[2] (1.Department of Earth and Planetary Sciences, Faculty of Sciences, Kyushu University, 2.Seikei University)

## [PEM16-P19] Development of a Lagrangian chemical transport model to understand the mechanism of composition change due to change in atmospheric environment

*Shingo Nakanishi[1], Tomoo Nagahama[1], Akira Mizuno[1], Tac Nakajima[1], Riku Ishijima[1] (1.Institute for Space-Earth Environmental Research, Nagoya University)

# Temporal and spatial variation of GPS phase scintillation during substorms and auroral breakups

*Paul Prikryl[1,2], James M. Weygand[3], Reza Ghoddousi-Fard[4], P. Thayyil Jayachandran[1], David R. Themens[1], Anthony M. McCaffrey[1], Bharat S. R. Kunduri[5], Emma Spanswick[6], Yongliang Zhang[7], Akira Sessai Yukimatu[8]

1. Physics Department, University of New Brunswick, Fredericton, NB, Canada, 2. Geomagnetic Laboratory, Natural Resources Canada, Ottawa, ON, Canada, 3. Earth Planetary and Space Sciences, University of California, Los Angeles, CA, USA, 4. Canadian Geodetic Survey, Natural Resources Canada, Ottawa, ON, Canada, 5. Bradley Dept. of Electrical and Computer Engineering, Virginia Tech, USA, 6. Dept. of Physics and Astronomy, University of Calgary, AB, Canada, 7. Johns Hopkins University Applied Physics Laboratory, Laurel, MD, USA, 8. National Institute of Polar Research, Tokyo, Japan

The ionospheric structure caused by precipitation of high energy particles can adversely affect the GPS causing phase scintillation and cycle slip (loss of lock). GPS phase scintillation correlates with the intensity of the aurora, especially the rapid change in the auroral brightness [1,2,3]. Enhancement of the total electron content (TEC) observed during the substorm expansion phase in the night side downward region 1 current seems to be related to intense precipitation particle flux [4]. Such TEC enhancements cause phase scintillation that is most intense just after substorm onsets and auroral breakups. Phase scintillation index is computed for sampling rate of 50 Hz by specialized GPS scintillation receivers from the Canadian High Arctic Ionospheric Network (CHAIN). A proxy scintillation index is obtained from dual frequency measurements of geodetic-quality GPS receivers sampling at 1 Hz, which include globally distributed receivers of RT-IGS network that are monitored by the Canadian Geodetic Survey in near-real-time. Temporal and spatial changes of TEC and phase scintillation are investigated in the context of equivalent ionospheric currents derived from ground magnetometer network using the spherical elementary current method [5,6]. The relation of phase scintillation with auroral emission is also examined. In general, GPS phase scintillation maps to regions of strong westward electrojet and to the poleward edge of the eastward electrojet. Following substorm onsets and auroral breakups, strong phase scintillation associated with TEC enhancements are mapped mainly to the upward region 2 current or the equatorward edge of the downward region 1 current at or near the Harang discontinuity region [7].

[1] Kinrade J., et al., J. Geophys. Res., 118, 2490–2502, 2013. https://doi.org/10.1002/jgra.50214
[2] Semeter J., et al., Geophys. Res. Lett., 44, 9539–9546, 2013.
https://doi.org/10.1002/2017GL073570
[3] Mushini S., et al., Space Wea., 16, 838–848, 2018. https://doi.org/10.1029/2018SW001919
[4] Weygand J.M., et al., Abstract SA41B-3484, presented at 2018 AGU Fall Meeting
[5] Amm O., and A. Viljanen, Earth Planets Space, 51, 431–440, 1999, doi:10.1186/BF03352247
[6] Weygand J.M., et al., J. Geophys. Res., 116, A03305, 2011. doi:10.1029/2010JA016177
[7] Weygand J.M., et al., J. Geophys. Res.. 113, A04213, 2008. doi:10.1029/2007JA012537

Keywords: High-latitude ionosphere, GPS TEC and phase scintillation, Ionospheric currents

©2019. Japan Geoscience Union. All Right Reserved. 

# Statistical study of SAPS occurrence characteristics using the SuperDARN Hokkaido HF radar

*Kento Oya[1], Nozomu Nishitani[1], Tomoaki Hori[1]

1. Institute for Space-Earth Environmental Research, Nagoya University

We investigate the occurrence characteristics of Sub-Auroral Polarization Streams (SAPS), using the Super Dual Auroral Radar Network (SuperDARN) Hokkaido East radar. The ultimate goal is to clarify the longitudinal dependence of SAPS occurrence characteristics using the whole SuperDARN radars. In this study, we statistically analyzed about 10-year data from 2007/1/1 to 2016/12/31 and studied the occurrence rate of the flow that can be considered as SAPS, vs MLT and MLAT. Assuming that the flows are east-west oriented, we set the criteria for line of sight velocity of > 80 m/s and echo power of > 3dB. We obtained the overall characteristics of SAPS, i.e., equatorward shift of high occurrence rate region with increasing MLT and geomagnetic activity. Some of the characteristics are different from previous studies. The SAPS regions seem to be located at higher latitudes than the previous studies and the SAPS occurrence peak regions are located at later MLT. These differences might be due to the difference in geographic longitude (Far-East Siberia to Pacific vs North American region). We also found new feature, i.e, westward flows from midnight to morning at relatively low geomagnetic latitudes, that could not be caught in the previous studies probably due to the limitation of radars fields of view, especially lower latitude boundary.

Keywords: magnetosphere-ionosphere coupling, SAPS, SuperDARN, geomagnetic activity

©2019. Japan Geoscience Union. All Right Reserved. 

# Spectral investigations of near infrared aurora and airglow at 1.0-1.6 microns: 1-year ground-based imaging spectroscopic observation at Syowa station (69.0˚S, 39.6˚E)

*Takanori Nishiyama[1], Takeshi Sakanoi[2], Makoto Taguchi[3], Hidehiko Suzuki[4]

1. National Institute of Polar Research, 2. Planetary Plasma and Atmospheric Research Center, Tohoku University, 3. Rikkyo University, 4. Department of Physics, Meiji University

The motivation of this study is further understanding of dayside magnetosphere and terrestrial atmosphere coupling system by using continuous observation. Dayside aurora, polar patch, and airglow should be key phenomena for the understanding. In particular, those phenomena in near infrared (NIR) wavelength are crucially important because lower background sky luminosity by Rayleigh scattering may allow us to conduct ground-based optical observation even in dayside. Continuous dayside optical monitoring with high temporal and spatial resolutions in aurora region and cusp give us a clue to understanding of substorm pre-onset sequences at cusp region, magnetopause dynamics related to solar wind shocks, and wave-particle interactions due to electromagnetic ion cyclotron waves and whistler mode chorus. However, NIR aurora has a total lack of its spectral information with enough resolution to make a feasibility study in comparison to that in visible wavelength.

We designed a narrow field spectrometer with medium-high spectral resolution that mainly consists of Czerny-Turner type imaging spectrometer (HORIBA, iHR320) with one entry port and two exit ports. This spectrometer has two mirrors and three diffractive gratings in a rotating turret. A toroidal mirror for collimating corrects for astigmatism so that the tangential (resolution optimized) and sagittal (imaging optimized) focal planes cross at the center of the focal plane. Another larger focus mirror allows the entire flat field to be used without vignetting. Collecting optics, equipped outside the spectrometer, are a gold coated off-axis parabolic mirror and a NIR longpass filter for removal of secondary diffracted light in visible wavelength. Using 1-d InGaAs array (1024 pixels) and 600 gr/mm grating, spectral range and spectral range per pixel are 119 nm and 0.11 nm/pixel, respectively.

We started ground-based spectroscopic observation in NIR wavelength ranging from 1.0 to 1.6 microns, which covers strong OH airglow emissions and auroral emissions in $N_2$1st Positive (1.2 microns) and $N_2^+$ Meinel (1.1 and 1.5 microns) [Jones 1974; Zhou et al., 2007], at Syowa Station (69.0˚S, 39.6˚E) in Antarctica from March 2018. OH airglow spectrum in NIR can be well resolved even in water vapor absorption region. OH rotational temperature is successfully estimated using OH 3-1 band P1(2) and P1(4) emissions. However, auroral emissions were not clearly identified at 1.52 micron (N2+ Meinel) so far. Further investigations are needed including 1.10 micron (N2+ Meinel) and 1.24 micron (N2 1P). In this presentation, we are going to report results in more detail based on one year observation.

Keywords: Near Infrared, Spectral observation, Aurora, Airglow, Mesopause, Antarctica

©2019. Japan Geoscience Union. All Right Reserved. 

# The study of the lower ionosphere in the South Atlantic Anomaly (SAA) Region

*Chih-Yu Chiang[1], Tzu-Fang Chang[2,1], Sunny W. Y. Tam[1]

1. Institute of Space and Plasma Sciences, National Cheng Kung University, Tainan, Taiwan, 2. Institute for Space-Earth Environmental Research, Nagoya University, Japan

South Atlantic Anomaly (SAA) corresponds to a region where the geomagnetic field is relatively weak; such a magnetic field enables energetic particles from the inner radiation belt to penetrate closer to the Earth's surface more easily, thus resulting in relatively high level of radiation in the environment. In this study, we analyze the nighttime airglows in 2007 to 2008 in the SAA region by using the data from the ISUAL (Imager of Sprites and Upper Atmospheric Lightning) experiment aboard the FORMOSAT-2 satellite. We focus specifically on the measurements by the six spectrophotometers and the CCD Imager, which overall cover the spectrum from ultraviolet to infrared wavelengths. Based on our analysis, features of clear enhancements and annual variations at 337 nm, 391.4 nm and 777.4 nm are identified in the SAA region. Through comparing these multiple-band emissions, we can identify energy variation of incident particles and atmospheric compositions of SAA region.

Keywords: South Atlantic Anomaly, SAA, airglow, ISUAL, FORMOSAT-2

©2019. Japan Geoscience Union. All Right Reserved. 

# Multi-GNSS observation of LSTID in Japan and its link with auroral activities

*Mayumi Hashimoto[1], Kosuke Heki[1]

1. Hokkaido University

Interaction between southward magnetic field in solar winds and the Earth’ s magnetosphere causes geomagnetic activities and auroral substorms. The auroral activity is associated with strong electric currents (auroral jet) within the auroral oval. This disturbs the geomagnetic field at high latitude region and is reflected in changes in the AE (Auroral Electrojet) index. At this time, atmospheric gravity waves, generated as a result of the heating of the atmosphere by electric currents, propagate toward the middle and low latitudinal regions and make Large-Scale Traveling Ionospheric Disturbances (LSTID). In this study, we observed ionospheric disturbance in Japan located in middle and low latitudes as the changes in TEC (Total Electron Content). Here we study the relationship between LSTID observed with multiple-GNSS (Global Navigation Satellite System), GPS, GLONASS, Galileo, and QZSS, and short-term changes in the high time resolution AE index time series.

In this study, we used the AE index one minute values from Kyoto University, World Data Center for Geomagnetism (wdc.kugi.kyoto-u.ac.jp). As the GNSS observation point, we used Tsukuba (tskb), one of the IGS observation points in Japan with inter-frequency bias values available. To examine the relationship, we first identified the day when the AE index exceeded 2,000 nT between 2011 and 2017. Then, we converted the RINEX data files of tskb on these days to TEC, removed satellite and receiver biases, and converted them to vertical TEC (VTEC). We compared the AE index and VTEC for 22 cases, and the occurrences of LSTID were confirmed in 5 of them. In these cases, LSTIDs were observed 1 or 2 hours after the peak of the AE index. We estimated the propagation velocity in two ways, i.e. by calculating the time lag between the AE peak and LSTID arrivals in Japan and the distance between the auroral oval and Japan, and by comparing the times of TEC peaks within Japan. Both approaches showed the velocity of ~0.7 km/sec.

Since 2018 summer, the Japanese GNSS network started to track multiple GNSS including the Japanese Quasi-zenith Satellite System (QZSS) and to open the raw data on-line by RINEX 3.02 format. discuss the relationship LSTID and AE index. QZSS includes three satellites with quasi-zenith orbits (PRN01, 02, 03) and one satellite with geostationary orbit (PRN07). Generally speaking, GNSS-TEC data changes by the three reasons, (1) temporal change in ionosphere, (2) spatial change in ionosphere, and (3) apparent change by changes in satellite elevation angle. However, QZSS-TEC includes only (1), and useful in studying ionospheric disturbances without bothering about (2) and (3).

Keywords: LSTID, TEC, GNSS

©2019. Japan Geoscience Union. All Right Reserved. 

# Basic development of accurate analytical method in order to determine coordinates of artificial illuminating clouds of Barium and Strontium for chemical-release rocket experiments

*Taro Watanabe[1], Masa-yuki Yamamoto[1], Yoshihiro Kakinami[2]

1. Kochi University of Technology, 2. Hokkaido Information University

In order to investigate neutral atmospheric heating phenomenon in the polar cusp, it is necessary to estimate Joule heating and fluctuation of electric field in the cusp. To accomplish this, we conducted a US-Japan joint rocket experiment called the Cusp Region Experiment 1 (CREX-1) in the Arctic region in November 2014, with releasing Ba (to be ionized in a short time by extreme ultraviolet (EUV) from the Sun) and Sr (not ionized in a short time). And then, we observed resonance scattering emission of $Ba^+$ and Sr simultaneously from two sites on ground so as to obtain fluctuation of the electric field and Joule heating. However, we could not release the gases in the cusp at that time. We are planning additional space experiments, based on the CREX-1 results, using two sounding rockets of the Cusp Region Experiment 2 (CREX-2) and the Joint Japan-US Cusp Heating Investigation (CHI) aiming at observing of the cusp in December 2019.

In this study, we developed a basis of accurate analytical method in order to determine coordinates of artificial illuminating cloud with applying observed data of CREX-1. At the beginning of the analysis, we made calibration data from the RAW images taken at a previous optical system tests. We compared the exposure input-output characteristics of JPEG and RAW to establish an analysis method using RAW images instead of JPEG. Next, we investigated whether it is possible to replace the work of determining centers of the illuminating clouds, which has been carried out by hand, by a method of uniquely determining the luminance maximal by gradient descent method. In addition, we made a background image by a darken composition method and attempted to remove the background brightness gradient trend.

As a result, the characteristics of JPEG image reported by Kakinami et al. (2015) were thought to be arcuate gamma curves, but in RAW images, they were obtained as linear characteristics. Regarding the gradient descent method, although it is possible to uniquely determine the luminance maximal without any human factors, it was found that there is a possibility that the local maximum is not the true center. For background removal by the darken composition method, it is effective for background light gradient removal. However, there is a problem that the shadow of the illuminating clouds appearing in the background image affects the remained shape of the illuminating clouds when removing the background.

Furthermore, we developed an algorithm tracing the three-dimensional position of $Ba^+$/Sr cloud uniquely without any human factors.

References:
Y. Kakinami, S. Watanabe, M.-Y. Yamamoto, D. Kihara, M. Conde and M.F. Larsen, Measurement of thermospheric wind and plasma drift using barium strontium in cusp region, the 138th SGEPSS Meeting, 2015.

©2019. Japan Geoscience Union. All Right Reserved. 

Keywords: Sounding Rocket, Polar Cusp, Neutral Atmospheric Wind, Plasma Drift, Thermosphere

©2019. Japan Geoscience Union. All Right Reserved. 

# Neutral and plasma density perturbations in the top-/bottom-side ionosphere associated with MSTIDs

*Shin Suzuki[1], Jaeheung Park[2], Yuichi Otsuka[3], Kazuo Shiokawa[3], Huixin Liu[4], Hermann Luehr[5]

1. Faculty of Regional Policy, Aichi University, 2. Korea Astronomy and Space Science Institute, 3. Institute for Space-Earth Environmental Research, Nagoya University, 4. Earth and Planetary Science Division, Kyushu University SERC, Kyushu University, 5. Helmholtz Centre Potsdam, GFZ, German Research Centre for Geosciences

Medium-scale traveling ionospheric disturbances (MSTIDs) are a well-known wavy structure in the F-region ionosphere. They typically have a horizontal wavelength of several hundred kilometers and a periodicity of about one hour. Although, the MSTIDs were considered to be caused by atmospheric gravity waves, recent studies have suggested that the generation of the MSTID in nighttime is highly associated with coupling processes between the E- and F-region electrodynamics. To confirm the different processes in the MSTID generation in daytime and nighttime, CHAMP satellite measurements would be greatly helpful; CHAMP plasma and neutral density data obtained in the day- and night-side sector can monitor the phase relations between the neutral (i.e., atmospheric gravity wave) and ionospheric plasma perturbations simultaneously at the top-side F-region (approximately 400 km).

As the first step in the abovementioned research, we compared the MSTID signatures between the CHAMP and ground-based 630-nm airglow measurements to validate the MSTID detection by CHAMP. Airglow imaging is a quite useful technique to investigate two-dimensional characteristics of the nighttime MSTIDs. Horizontal parameters of the MSTIDs (such as wavelengths, motions, and their spatial extent) can be estimated directly with a high spatial and temporal resolutions through the 630-nm airglow emission in the bottom-side F-region. Previous study by Park et al. [2009, JGR] made an investigation of spatial signatures regarding one MSTID event using airglow images along the CHAMP orbit. The Institute for Space-Earth Environmental Research, Nagoya University, has operated airglow imaging network, as the OMTI system, around the world since 2000; this network gives much more chance to make coordinated measurements with CHAMP. We found three clear MSTID events (March 15, 2004, February 15, 2007, and January 12, 2007) in which CHAMP passed over the field-of-views of the OMTI camera.

In this presentation, we will report phase relations between the neutral and plasma density perturbations associated with the MSTID events.

Keywords: MSTID

©2019. Japan Geoscience Union. All Right Reserved. 

# Analysis of ionospheric TEC fluctuation by rocket

*Tsuyoshi Takegawa[1], Hiroyuki Nakata[1], Hiroyo Ohya[1], Toshiaki Takano[1], Takuya Tsugawa[2], Michi Nishioka[2]

1. Graduate School of Integrated Science and Technology, Chiba University, 2. National Institute of Information and Communications Technology

It is known that atmospheric waves arised by massive earthquakes, typhoons and volcanic eruptions cause the ionospheric variation. In recent years, ionospheric fluctuations excited by rocket launches have been confirmed (Lin et al., 2014,2017). In case of Taepodong 2, the first wave of TEC fluctuations is confirmed due to the chemical reaction with ionospheric plasmas and the exhaust of the rocket about 5 minutes after the launch and the second wave was confirmed after about 30 minutes from the launch. To examine the ionospheric disturbances apart from the trajectories of rockets, in this study, TEC fluctuation due to the launches of H2A rocket No.25 and No. 29 we examined using GEONET data. The first waves of the TEC fluctuations were confirmed around hundreds kilometers from the rocket trajectory 5 minutes after launch of both of H2A rockets. The first waves appeared as large decreases in VTEC, which is consistent with the previous study of Taepodong 2. Calculating the propagation time of the sound waves from the points on the trajectories of the rockets, the delays correspond to the propagation times from the trajectories to the pierce points of TEC. The second waves were also observed around the 30 minutes after the rocket launches. Calculating the arrival time of sound waves for the second waves, the seconds waves once reflected on the ground were affected by the second waves.

Keywords: ionospheric, rocket, TEC

©2019. Japan Geoscience Union. All Right Reserved. 

# Examinations of the ionospheric perturbation associated with H-IIA rockets launching

*Junpei Yamazaki[1], Hiroyuki Nakata[1], Hiroyo Ohya[1], Toshiaki Takano[1], Keisuke Hosokawa[2], Ichiro Tomizawa[2]

1. Graduate School of Engineering, Chiba University, 2. Department of Communication Engineering and Informatics, University of Electro-Communications

It is reported that ionospheric perturbation are caused by natural hazards, such as giant earthquakes, olcanic eruptions and so on. This is because the infrasound waves generated by natural hazards propagate to the ionospheric. Since rocket launches also generate the atmospheric waves, it is reported that passage and exhaust plumes generate TEC perturbations determined by GEONET data(Lin et al.,2014,2017).
On the other hand, there is few studies about ionospheric perturbation associated with rocket launch away from rocket’ s trajectory. Then, in this study, we analyzed ionospheric perturbations associated with H IIA(No.25 and 26) relatively far trajectory from the Japanese islands using HF Doppler sounding.
The perturbations of Doppler shifts associated with H-IIA No.25 were observed at Kakioka and Sugadaira observatories and those of H-IIA No.26 were observed at Kakioka,Fujisawa and Sugadaira observatories about 35 minutes after the launch. It is confirmed that this delay corresponds to the propagation time of the infrasound wave from the launch site to observation points once reflected on the ground. The frequencies of the disturbance of Doppler shift were 5~10 mHz. Similar disturbances were reported in Lin et al (2014) which examined the TEC disturbances associated with Taepodong. The Doppler shift perturbation is clear when the infrasound wave reached the observation point after reflection on the ground as compared to the case where the infrasound wave reached the observation point directly. When the infrasound wave directly reaches the observation point, it passed through about 200~250km altitude. Where the amplitude of infrasound waves with several 10mHz tend to attenuate. Therefore, ionospheric perturbation at the moment corresponding to the arrived at the direct wave become small.

©2019. Japan Geoscience Union. All Right Reserved. 

# Explosion energy derived from the 2015 Kuchinoerabujima eruption: Estimation from infrasound less than 0.01 Hz detected by barometers, seismometers, and TEC

*Yuki Nakashima[1], Kiwamu Nishida[1], Yosuke Aoki[1], Kosuke Heki[2]

1. Earthquake Research Institute, 2. Natural History Sciences, Hokkaido University

This study discusses the amount of energy emitted to the atmosphere as acoustic waves of less than 0.01 Hz by the 2015 Kuchinoerabujima volcano, southwest Japan, eruption derived from barometers, broadband seismometers, and GNSS-TEC observations.
Kuchinoerabujima is one of the volcanic islands of active recently. The volcano erupted at 0:59 UT on 25th May 2015. Many previous studies pointed out that this is a phreatomagmatic eruption and involves a lateral signal (e.g., Kobayashi, 2017; Matsuzawa et al., 2016; Yamada et al., 2017). Yamada et al. (2017) found that barometric data include two phases in about 20 sec. In the first stage, the volcanic plume went up with a pressure pulse, and the second another pulse corresponds to the plume growing laterally. The seismic source time function of that has a component of north-south direction obviously (Matsuzawa et al. 2016).
We found atmospheric disturbances with a characteristic frequency of ~0.01 Hz in all the observations. The frequency range is equivalent to the highest part of the detectable band in the ionosphere. We detected the signal of lower atmospheric perturbation from F-net, an array of broadband seismometers installed by NIED, and a barometer array along the Japanese coastline in front of the Pacific ocean by AIST. As the ionospheric observation, we used GNSS-TEC time series extracted from GEONET 1 Hz sampling data. The waveform feature is very similar to ionospheric disturbances excited by Asama volcano on 1st September 2004 (Heki, 2006; Chonan et al., 2017).
We tried to reproduce the observed signal and estimate the magnitude of the energy source using the ray-tracing method. Atmospheric parameters are inputted from NRLMSISE-00 (Picone et al., 2002), HWM-14 (Drob et al., 2015), IRI2016 (Billitza et al., 2016), and IGRF-12 (Thébault et al., 2015). We put an isotropic energy source on the ground in the windy atmosphere.
The estimated travel time by ray-tracing is consistent with the observation, indicating that the excited atmospheric perturbation simply propagates isotropically without wave broadening due to dispersion discussed in Dautermann et al. (2009a).
If we choose the source energy as $10^8$ J, our model expects about one-third of the observed signal in both the lower atmosphere in the far field and the ionosphere. This amount of energy is $10^{1-2}$ times larger than that of the 2004 Asama eruption estimated from TEC observation (Heki, 2006). It seems to depend on not only the difference of volcanic eruption magnitude but also the crude assumption like ignoring the geomagnetic effect and geometrical spreading same as Dautermann et al. (2009) suggested.
We were not able to find any evidence for anisotropic radiation of energy as stated in some previous studies, suggesting that infrasound of such very low frequencies infrasound (< ~0.01 Hz) responds to with a longer time constant such as the growth of the thermal plume.
Acknowledgment
We would thank GSI, JMA, AIST, and NIED which provide GNSS, barometer, microphone, and broadband seismometer data.

Keywords: GPS-TEC, GNSS-TEC, Volcanic eruption, Infrasound, Broadband seismometer

©2019. Japan Geoscience Union. All Right Reserved. 

©2019. Japan Geoscience Union. All Right Reserved. 

# Detection of spread-F echoes in ionograms using machine learning

*Hiroyuki Nakata[1], Yuta Goto[2], Hiroyo Ohya[1], Toshiaki Takano[1]

1. Graduate School of Engineering, Chiba University, 2. Department of Electrical and Electronics Engineering

Ionospheric irregularities referred to as equatorial spread-F is very important phenomena in terms of radio wave propagation because their spatial scales are from centimeters to tens of kilometer and they affects wide-band radio waves. Therefore, they influence the reliability of satellite-ground communications, navigation systems and so on. The ionogram is one of the important observation system of spread-F. Because the detection of spread-F in the ionogram is done manually, detection of spread-F could be replaced with automatic detection by developing an excellent machine learning system. In this study, therefore, we have developed a method to detect spread-F in the ionogram automatically using machine learning.

In this detection process, we have arranged two classifiers for typical frequency-type and mixed (frequency-type and range-type) spread-F echoes in the ionograms. A number of correct images must be prepared for these classifiers to learn the feature values of spread-F. To do so, ten thousands of correct images were generated by create_samples utility provided by OpenCV library. Using these classifiers, we have detected the both types of spread-F echos in the ionograms observed at 4 observatories (Wakkanai, Kokubunji, Yamagawa, Ogimi) utilized by National Institute of Information and Communications Technology. The detection rates of both types of spread-F echos are from 50% to 73% and both classifier detected both types of spread-F echos similarly. Namely, the classifier for the frequency-type spread-F echo detected both of the frequency-type and mixed-type echos, and vice versa. In case where the two types of spread-F echos are not distinguished, on the other hand, both of classifiers detect 80% of total spread-F echos. In addition, the classifiers also picked up some other phenomenon , such as overlapped traces of O-mode and X-mode, multi-hop trace.

As for the future plan, there might be several way to improve the detection rate; to use more classifiers, to make the classifiers be precisely with more training data, and so on. However, a number of correct images are inevitable in machine learning. In order to prepare such a number of images, it may be effective to generate training data using deep generative model.

Keywords: spread F, ionogram, machine learning

©2019. Japan Geoscience Union. All Right Reserved. 

# Evaluation of GNSS-TEC receiver performance for sounding rocket installation

*Makoto Okumura[1], Yuki Ashihara[1]

1. National Institute of Technology, Nara College

Earth's atmospheric region ionized electrons by X-rays and ultraviolet rays involved in sunlight is called ionosphere. Ionospheric disturbance causes some problems, e.g., which are terrestrial satellite communication impairment and positioning error of GNSS. For elucidating the generation mechanism of the ionospheric disturbance, we need to observe spatial structure of ionospheric electron density. Ionosphere observation is generally implemented with remote sensing method such as Ionosonde, GNSS-TEC and others. Ionosonde can observe the electron density vertical structure below the altitude of electron density peak in F region, and GNSS-TEC can obtain the total electron content along the radio wave propagation path. However, these methods cannot observe the spatial structure. In this paper, we propose a rocket GNSS-TEC tomography method as a new approach to the ionosphere observation. In this method, we install the GNSS-TEC receiver onboard a sounding rocket, and it is flying the boundary region between the ionospheric E and the F region. It is possible to acquire the TEC data only for the F region.
In case of a combining antenna system installed on the side on sounding rocket, it is simulated that the received signal becomes unstable since the sounding rocket spins at the speed of 1 to 2 Hz. Therefore, we built a structure model of the sounding rocket, and conducted a ground-based rotation experiment. In this experiment, the GNSS carrier phase data was approximately obtained for the steady rotation speed, but TEC value had the variation more than 60 TECU. As the results, we understood that a combining antenna system cannot useful for a rocket GNSS-TEC.

Keywords: ionosphere, GNSS-TEC, sounding rocket

©2019. Japan Geoscience Union. All Right Reserved. 

# Relationship between mesosperical airglow disturbance and occurrence of equatorial plasma bubbles

*Ryota Okada[1], Akinori Saito[1], Takafumi Ikeda[1], Hiroyuki Shinagawa[2], Takuya Tsugawa[2], Takeshi Sakanoi[3]

1. Department of Geophysics, Graduate School of Science, Kyoto University, 2. National Institute of Information and Communications Technology, 3. Planetary Plasma and Atmospheric Research Center, Graduate School of Science, Tohoku University

762 nm airglow data observed by Ionosphere, Mesosphere, upper Atmosphere and Plasmasphere mapping mission from the ISS / Visible and near Infrared Spectral Imager (ISS-IMAP/VISI) to investigate relationship between mesospheric gravity waves and the occurrence of Equatorial Plasma Bubbles (EPBs). EPBs are depletion of electron density in the equatorial ionosphere. According to the previous study EPBs can be generated through the Rayleigh-Taylor (R-T) instability in the ionosphere. Medium-scale gravity waves with horizontal scales of a few hundred kilometers in the bottom side of the F region have been frequently suggested to play a key role in EPBs seeding. Gravity wave occurrence may depend on seasonal and longitudinal variation and may have oscillation whose period is few days. This several days oscillation of gravity wave may affect the variation of EPBs occurrence that can not be explained only by the R-T growth rate. Previous research of concentric gravity waves (CGWs) using observed by ISS-IMAP/VISI shows more mesospheric CGW events occur in the west side of the African continent than the east side of the African content. It indicate occurrence of CGWs is different between nearby areas. Objective of this study is to elucidate relationship between mesospheric gravity waves and longitudinal dependence of EPB occurrences. ISS-IMAP/VISI was operated for three years from September 2012 to August 2015. ISS-IMAP/VISI observed the airglow in the nadir direction on the nightside with two FOVs facing 45 degrees in the forward and backward of the orbital direction. We analyzed 762nm airglow data and compared with occurrence rate of EPBs and Growth rate of R-T instability. Occurrence rate of EPBs using Rate of TEC Index (ROTI) that is standard deviation of differential of GPS-TEC. Growth rate of R-T instability was calculated by using parameters from Ground-to-topside model of Atmosphere and Ionosphere for Aeronomy (GAIA). In this study, we investigated relationship between occurrence of EPBs observed by GPS-TEC data, linear growth rate of the R-T instability in the ionosphere obtained with GAIA, and mesospheric gravity wave activities observed by ISS-IMAP/VISI.

Keywords: Equatorial Plasma Bubbles, Airglow

©2019. Japan Geoscience Union. All Right Reserved. 

# Analysis of parameters controlling the occurrence and growth of equatorial plasma bubbles using GAIA

*Hiroyuki Shinagawa[1], Hidekatsu Jin[1], Yasunobu Miyoshi[2], Hitoshi Fujiwara[3], Tatsuhiro Yokoyama[4], Yuichi Otsuka[5]

1. National Institute of Information and Communications Technology, 2. Department of Earth and Planetary Sciences, Faculty of Sciences, Kyushu University, 3. Faculty of Science and Technology, Seikei University, 4. Kyoto University, 5. Institute for Space-Earth Environmental Research, Nagoya University

In our previous studies, the linear growth rates of the Rayleigh-Taylor (R-T) instability in the ionosphere were obtained with a whole atmosphere-ionosphere coupled model GAIA, and the growth rates were compared with observations [Shinagawa et al., 2018]. We found that a high growth rate of R-T instability tends to correspond to the actual equatorial plasma bubble (EPB) occurrence. The result suggests that the occurrence and growth of EPB are controlled both by atmospheric waves propagating from the lower atmosphere and by geomagnetic activities. However, dependence of various parameters such as electric fields, electron and neutral densities, and neutral wind velocities on the EPB occurrence and growth has not been quantitatively understood. We will discuss how those parameters affect the linear growth rates of the R-T instability using GAIA simulation data, and report the importance of the parameters in controlling the EPB occurrence and growth.

Keywords: Ionosphere, Atmosphere, Model, Plasma bubble, Linear growth rate, Parameter

©2019. Japan Geoscience Union. All Right Reserved. 

# A three-dimensional numerical model to study the modulation of midlatitude $E_s$-layers

*Satoshi Andoh[1], Akinori Saito[1], Hiroyuki Shinagawa[2], Shin'ichi Miyazaki[1]

1. Graduate School of Science, Kyoto University, 2. National Institute of Information and Communications Technology

We develop a three-dimensional numerical model to shed light on the generation, growth and diffusion mechanisms of the sporadic E layers in the midlatitude.

The Es layer is a high-density layer of plasma formed at around 100 kilometers high. It is affected by both the atmospheric waves generated in the troposphere and mesosphere, and the electromagnetic interaction between the E region and the F region, so that it is a very important phenomena to understand the physics of the upper atmosphere.

The mechanism of Es layer formation is described through the Windshear Theory. According to the theory, factors affecting the Es layer formation are zonal windshears and meridional windshears. Which one can make more effects depends on the altitude of Es layer.

Lately, there has been some new structures of the Es layer detected by several observations (e.g. Lidar observation). They cannot be explained only by Windshear Theory. It is considered that there are three factors of the structures: atmospheric waves, Kelvin-Helmholtz instability and Es layer instability. Several models have been developed to study each factor, but no model includes all three factors. Such a model is necessary to give a consistent explanation for which factor is the most effective for modulation of the Es layers.

Our model includes six kinds of ions of $O^+$, $O_2^+$, $N^+$, $N_2^+$, $NO^+$, $Ca^+$, and in both the transport process and the chemical process of ions in the uniform geomagnetic field solve. In addition, NRLMSISE-00 is used as a background field of neutral atmospheric density. This model uses three-dimensional polar coordinate system. Altitude coverage is from 85 km to 305 km and horizontal domain size is 5 degree ×5 degree in the longitude and latitude direction. The vertical and horizontal resolutions are 1 km and 0.1 degrees, respectively and the time resolution is 1 second.
By inputting latitude, longitude and UT into this model, it is possible to simulate ionosphere in midlatitude within the above calculation area.

In this presentation, as a pseudo-zonal and meridional neutral windshear, we employed a sinusoidal windsear in the vertical direction and reevaluated which component of the neutral windshear will affect more to form Es layers.
As a result, we obtained results consistent with the previous study that the influence of the zonal windshear is large at the low altitude and the influence of the meridional windshear is large at the high altitude.
Moreover, by incorporating the neutral winds of GSWM model and HWM14 model into ours, we examined the mechanism of generation of Es layer in the more real condition.

Based on these, we will introduce the future view in the presentation.

©2019. Japan Geoscience Union. All Right Reserved. 

Keywords: sporadic E layer, midlatitude, simulation, ionosphere

©2019. Japan Geoscience Union. All Right Reserved. 

# Statistical analysis of the horizontal phase velocity distribution of mesospheric and ionospheric waves observed in airglow images in Hawaii

*Hideto Naito[1], Kazuo Shiokawa[1], Yuichi Otsuka[1], Takeshi Sakanoi[2], Akinori Saito[3], Takuji Nakamura[4]

1. Institute for Space-Earth Environmental Research, Nagoya University, 2. Planetary Plasma and Atmospheric Research Center, Graduate School of Science, Tohoku University, 3. Department of Geophysics, Graduate school of science, Kyoto University, 4. National Institute of Polar Research

Matsuda et al. [JGR, 2014] proposed a method of deriving the horizontal phase velocity and propagation direction of the power spectral density of waves found in images using three-dimensional fast Fourier transform. Takeo et al. [JGR, 2017] and Tsuchiya et al. [JGR, 2018] applied this method to the airglow images obtained at Shigaraki and Rikubetsu, Japan, and reported 16-year variability of atmospheric waves at middle latitudes. However, there is no report using this method for analyzing airglow images obtained at low latitudes near the equator. In this study, we applied the analysis method of Matsuda et al. [2014] to airglow images obtained at wavelengths of 557.7 and 630.0 nm during the three years from 2013 to 2016 at Haleakala (20.7°N, 203.7°E) in Hawaii, where the latitude, longitude and orography are greatly different those of Shigaraki (34.8°N, 136.1°E) and Rikubetsu (43.5°N, 143.8°E). We clarified the statistical features of atmospheric gravity waves (AGWs) and medium-scale traveling ionospheric disturbances (MSTIDs) in the low latitude region near the equator, and compared it with features seen in Shigaraki and Rikubetsu (Takeo et al., JGR, 2017 and Tsuchiya et al., JGR, 2018).

The three-year average of the phase velocity spectra of AGWs observed in airglow images at wavelength of 557.7 nm show less propagation in due eastward and due westward in summer. The dominant propagation direction was southward in winter. The power spectral density was strongest in spring and summer, and weakest in winter. In Shigaraki and Rikubetsu, the direction of propagation changes from east in summer to west in winter, while in Haleakala there was no such seasonal change in the propagation in summer and winter. This is probably because Haleakala is located at latitudes away from the peak of the mesospheric jet, so the wind filtering effect by the mesosphere jet is smaller than that at Rikubetsu and Shigaraki.

The MSTIDs observed in airglow images at wavelength of 630.0 nm showed strong spectra in four particular nights, and we found that the average spectra largely affected by these strong spectra. Thus we removed these strong nights and calculated the three-year average horizontal phase velocity spectra for four seasons. From the average spectra, MSTIDs propagate from northwestward to southward in summer and from northward to southeastward in fall. In winter, the power spectral density was strongest, and the MSTIDs propagate mainly in the east-west direction. Spring power spectrum density was weakest. We note that dominant propagation direction of MSTIDs at Shigaraki and Rikubetsu was southwestward regardless of the season, which is very different from Haleakala. The power spectral density was weaker at Haleakala than those at Shigaraki and Rikubetsu. These results may be because polarization electric fields

©2019. Japan Geoscience Union. All Right Reserved. 

associated with MSTIDs tends to be attenuated by the equatorial ionization anomaly crest, which exists at low latitudes before midnight and by the MBW (Midnight Brightness Wave) moving poleward from low latitudes associated with the MPB (midnight pressure bulge) even after midnight, as suggested by Narayanan et al. [JGR, 2014].

Keywords: Atmospheric gravity waves, Medium-scale traveling ionospheric disturbances, Hawaii

©2019. Japan Geoscience Union. All Right Reserved. 

# Estimation of mesospheric OH temperature by observation data by ISS-IMAP VISI

*Ryo Murakami[1], Akinori Saito[1], Takeshi Sakanoi[2], Yuta Hozumi[3]

1. Kyoto University, 2. Tohoku University, 3. University of Electro-Communications

In general, the data of satellite observation is inferior in resolution to ground observation data and its wavelength resolution is inferior, so it is difficult to analyze. In this research, from 2012 to 2015, data of atmospheric light emission in the mesosphere by the Visible / Near Infrared Spectroscopic Imager (VISI), which is an observation device mounted on the International Space Station in the ISS-IMAP mission, Temperature estimation of the OH luminescent layer in the mesosphere near 85 km is tried. It is known from the previous study that the relative existence distribution of the rotation level when the OH molecule transitions between certain vibration levels follows the Boltzmann distribution and this distribution is determined by the rotation temperature of the OH molecule. Research using this property to try to estimate temperature from OH multiwavelength data has been used only for ground observation data so far. In this research, we apply this method to observation data from outer space and aim to obtain a spatially large temperature distribution map which has never been obtained. For analysis, data in two modes, Calibration mode and Spectral mode are used. In the calibration mode data, the observation data is recorded using the whole light receiving part of the observation equipment in the wavelength range of 500 to 900 nm, and the data of the spectral mode is narrowed down to the wavelength range of six ROI (Region of interest) And observation data are recorded together with spatial position information. Analysis is based on data in Spectral mode. Removal of salt-and-pepper-noise by cosmic rays and removal of artificial noise-containing data using random sample consensus algorithm for multi-wavelength data of OH around 828 nm, In order to compensate for the low resolution of the wavelength resolution, we tried fitting by Gaussian function and tried to estimate the temperature.

Keywords: ionosphere, airglow, mesosphere, hydroxyl, ISS-IMAP, temperature

©2019. Japan Geoscience Union. All Right Reserved. 

# Implementation of photochemical process of NOx and HOx into a whole atmosphere GCM

*Yasunobu Miyoshi[1], Hitoshi Fujiwara[2]

1. Department of Earth and Planetary Sciences, Faculty of Sciences, Kyushu University, 2. Seikei University

Photochemical process associated with NOx and HOx plays an important role on the energy budged and general circulation in the mesosphere and lower thermosphere (MLT). For example, NO is important for the infrared cooling in the MLT region. Photochemical process associated with HOx is essential for accurate estimate of the O3 distribution in the mesopause region. We implemented photochemical process of HOx and NOx into a whole atmosphere general circulation model (GCM). Using this GCM, effects of the solar activity on the general circulation in the MLT region are studied. Furthermore, this GCM can provide accurate estimate of the energy budget due to the global cooling due to the increase of CO2. In this study, preliminary results will be shown, and further development of the GCM will be discussed.

Keywords: the general circulation of the atmosphere, photochemical process

©2019. Japan Geoscience Union. All Right Reserved. 

# Development of a Lagrangian chemical transport model to understand the mechanism of composition change due to change in atmospheric environment

*Shingo Nakanishi[1], Tomoo Nagahama[1], Akira Mizuno[1], Tac Nakajima[1], Riku Ishijima[1]

1. Institute for Space-Earth Environmental Research, Nagoya University

Mesospheric chemical composition largely varies caused by environmental changes from the earth inside and outside. Recent studies reported enhancement of $NO_x$ and $HO_x$ and ozone depletion in the polar mesospheric region at a large solar proton event. These suggest that precipitation of other high energy particles such as a high energy electron from the magnetosphere also has influence on the chemical composition in the mesosphere. For these reasons, we have installed millimeter-wave spectrometers in Rikubetsu-cho, Hokkaido (Japan), Syowa Station (Antarctic), Atacama (Chile), Rio Gallegos (Argentine) and Tromso (Norway), and have been observing steady atmospheric minor molecules such as Ozone, $NO_x$, $HO_x$ and ozone-depleting substances in the stratosphere and mesosphere to understand the atmospheric composition changes caused by natural phenomena such as Energetic Particle Precipitation (EPP).

In addition to these observations, we have been developing a Lagrangian chemical transport model, which is suitable for a simulation of a sudden and a local event to evaluate the influence of the atmospheric composition mechanism in the stratosphere and mesosphere. Our developing model is an extension of the Lagrangian particle dispersion model (FLEXPART) by incorporating meteorological fields data and chemical reactions in the mesosphere. FLEXPART can analyze a trajectory from the ground to about 40 km in altitude using the reanalysis data of NCEP and ECMWF as meteorological fields input data. In this study, we incorporated a new reanalysis dataset (MERRA2) as meteorological fields input data to extend the analysis range toward the mesosphere, and as a result, trajectory a analysis ranging from the ground to about 80 km in altitude can be made. In order to evaluate the analysis accuracy of our developing model, we calculated trajectories for a single position at altitudes of 15, 45, 55, 70 km, and compared the results with another trajectory analysis model. Moreover, only OH reactions are considered in FLEXPART, although it needs to calculate non-linear chemical reactions separately in this study because chemical reactions caused by EPP include not only reactions by natural molecules but also ion-molecular reaction, ionization, dissociation and ion recombination, and so on. For this reason, we incorporated chemical reactions of the stratosphere and mesosphere in FLEXPART using Kinetic Preprocessor (KPP) which is chemical reaction computation software. We previously calculated chemical reactions of the stratosphere and mesosphere using KPP alone and confirmed the amount of mesosphere ozone variation in day and night.
In this presentation, we will report the results of comparison bet between our developing model and other trajectory models as well as the simulation results about some EPP events using our model.

Keywords: mesosphere, ozone, high energy particle, chemical transport model

©2019. Japan Geoscience Union. All Right Reserved. 

[J] Poster | P (Space and Planetary Sciences )：P-EM Solar-Terrestrial Sciences, Space Electromagnetism & Space Environment

Thu. May 30, 2019 5:15 PM - 6:30 PM JST | Thu. May 30, 2019 8:15 AM - 9:30 AM UTC | Poster Hall International Exhibition Hall8, Makuhari Messe_3

## [P-EM16] Physics and Chemistry in the Atmosphere and Ionosphere

convener:Yuichi Otsuka(Institute for Space-Earth Environmental Research, Nagoya University), Takuya Tsugawa(National Institute of Information and Communications Technology), Seiji Kawamura(National Institute of Information and Communications Technology)

This session covers a broad scope of studies of physics and chemistry in the atmosphere and the ionosphere. Coupling processes between plasma and neutral species, and upward and downward coupling among lower/upper atmosphere, and ionosphere/mesosphere/thermosphere including magnetosphere are discussed. We solicit papers based on experiments with ground-based and/or space-borne instruments, theoretical studies, numerical simulations, and development of new observation techniques.

### [PEM16-P01] Temporal and spatial variation of GPS phase scintillation during substorms and auroral breakups

*Paul Prikryl[1,2], James M. Weygand[3], Reza Ghoddousi-Fard[4], P. Thayyil Jayachandran[1], David R. Themens[1], Anthony M. McCaffrey[1], Bharat S. R. Kunduri[5], Emma Spanswick[6], Yongliang Zhang[7], Akira Sessai Yukimatu[8] (1.Physics Department, University of New Brunswick, Fredericton, NB, Canada, 2.Geomagnetic Laboratory, Natural Resources Canada, Ottawa, ON, Canada, 3.Earth Planetary and Space Sciences, University of California, Los Angeles, CA, USA, 4.Canadian Geodetic Survey, Natural Resources Canada, Ottawa, ON, Canada, 5.Bradley Dept. of Electrical and Computer Engineering, Virginia Tech, USA, 6.Dept. of Physics and Astronomy, University of Calgary, AB, Canada, 7.Johns Hopkins University Applied Physics Laboratory, Laurel, MD, USA, 8.National Institute of Polar Research, Tokyo, Japan)

### [PEM16-P02] Statistical study of SAPS occurrence characteristics using the SuperDARN Hokkaido HF radar

*Kento Oya[1], Nozomu Nishitani[1], Tomoaki Hori[1] (1.Institute for Space-Earth Environmental Research, Nagoya University)

### [PEM16-P03] Spectral investigations of near infrared aurora and airglow at 1.0-1.6 microns: 1-year ground-based imaging spectroscopic observation at Syowa station (69.0°S, 39.6°E)

*Takanori Nishiyama[1], Takeshi Sakanoi[2], Makoto Taguchi[3], Hidehiko Suzuki[4] (1.National Institute of Polar Research, 2.Planetary Plasma and Atmospheric Research Center, Tohoku University, 3.Rikkyo University, 4.Department of Physics, Meiji University)

### [PEM16-P04] The study of the lower ionosphere in the South Atlantic Anomaly (SAA) Region

*Chih-Yu Chiang[1], Tzu-Fang Chang[2,1], Sunny W. Y. Tam[1] (1.Institute of Space and Plasma Sciences, National Cheng Kung University, Tainan, Taiwan, 2.Institute for Space-Earth Environmental Research, Nagoya University, Japan)

### [PEM16-P05] Multi-GNSS observation of LSTID in Japan and its link with auroral activities

*Mayumi Hashimoto[1], Kosuke Heki[1] (1.Hokkaido University)

### [PEM16-P06] Basic development of accurate analytical method in order to determine coordinates of artificial illuminating clouds of Barium and Strontium for chemical-release rocket experiments

*Taro Watanabe[1], Masa-yuki Yamamoto[1], Yoshihiro Kakinami[2] (1.Kochi University of Technology, 2.Hokkaido Information University)

### [PEM16-P07] Neutral and plasma density perturbations in the top-/bottom-side ionosphere associated with MSTIDs

*Shin Suzuki[1], Jaeheung Park[2], Yuichi Otsuka[3], Kazuo Shiokawa[3], Huixin Liu[4], Hermann Luehr[5] (1.Faculty of Regional Policy, Aichi University, 2.Korea Astronomy and Space Science Institute, 3.Institute for Space-Earth Environmental Research, Nagoya University, 4.Earth and Planetary Science Division, Kyushu University SERC, Kyushu University, 5.Helmholtz Centre Potsdam, GFZ, German Research Centre for Geosciences)

[PEM16-P08] Analysis of ionospheric TEC fluctuation by rocket

*Tsuyoshi Takegawa[1], Hiroyuki Nakata[1], Hiroyo Ohya[1], Toshiaki Takano[1], Takuya Tsugawa[2], Michi Nishioka[2] (1.Graduate School of Integrated Science and Technology, Chiba University, 2.National Institute of Information and Communications Technology)

[PEM16-P09] Examinations of the ionospheric perturbation associated with H-IIA rockets launching

*Junpei Yamazaki[1], Hiroyuki Nakata[1], Hiroyo Ohya[1], Toshiaki Takano[1], Keisuke Hosokawa[2], Ichiro Tomizawa[2] (1.Graduate School of Engineering, Chiba University, 2.Department of Communication Engineering and Informatics, University of Electro-Communications)

[PEM16-P10] Explosion energy derived from the 2015 Kuchinoerabujima eruption: Estimation from infrasound less than 0.01 Hz detected by barometers, seismometers, and TEC

*Yuki Nakashima[1], Kiwamu Nishida[1], Yosuke Aoki[1], Kosuke Heki[2] (1.Earthquake Research Institute, 2.Natural History Sciences, Hokkaido University)

[PEM16-P11] Detection of spread-F echoes in ionograms using machine learning

*Hiroyuki Nakata[1], Yuta Goto[2], Hiroyo Ohya[1], Toshiaki Takano[1] (1.Graduate School of Engineering, Chiba University, 2.Department of Electrical and Electronics Engineering)

[PEM16-P12] Evaluation of GNSS-TEC receiver performance for sounding rocket installation

*Makoto Okumura[1], Yuki Ashihara[1] (1.National Institute of Technology, Nara College)

[PEM16-P13] Relationship between mesosperical airglow disturbance and occurrence of equatorial plasma bubbles

*Ryota Okada[1], Akinori Saito[1], Takafumi Ikeda[1], Hiroyuki Shinagawa[2], Takuya Tsugawa[2], Takeshi Sakanoi[3] (1.Department of Geophysics, Graduate School of Science, Kyoto University, 2.National Institute of Information and Communications Technology, 3.Planetary Plasma and Atmospheric Research Center, Graduate School of Science, Tohoku University)

[PEM16-P14] Analysis of parameters controlling the occurrence and growth of equatorial plasma bubbles using GAIA

*Hiroyuki Shinagawa[1], Hidekatsu Jin[1], Yasunobu Miyoshi[2], Hitoshi Fujiwara[3], Tatsuhiro Yokoyama[4], Yuichi Otsuka[5] (1.National Institute of Information and Communications Technology, 2.Department of Earth and Planetary Sciences, Faculty of Sciences, Kyushu University, 3.Faculty of Science and Technology, Seikei University, 4.Kyoto University, 5.Institute for Space-Earth Environmental Research, Nagoya University)

[PEM16-P15] A three-dimensional numerical model to study the modulation of midlatitude $E_s$-layers

*Satoshi Andoh[1], Akinori Saito[1], Hiroyuki Shinagawa[2], Shin'ichi Miyazaki[1] (1.Graduate School of Science, Kyoto University, 2.National Institute of Information and Communications Technology)

[PEM16-P16] Statistical analysis of the horizontal phase velocity distribution of mesospheric and ionospheric waves observed in airglow images in Hawaii

*Hideto Naito[1], Kazuo Shiokawa[1], Yuichi Otsuka[1], Takeshi Sakanoi[2], Akinori Saito[3], Takuji Nakamura[4] (1.Institute for Space-Earth Environmental Research, Nagoya University, 2.Planetary Plasma and Atmospheric Research Center, Graduate School of Science, Tohoku University, 3.Department of Geophysics, Graduate school of science, Kyoto University, 4.National Institute of Polar Research)

## [PEM16-P17] Estimation of mesospheric OH temperature by observation data by ISS-IMAP VISI

*Ryo Murakami[1], Akinori Saito[1], Takeshi Sakanoi[2], Yuta Hozumi[3] (1.Kyoto University, 2.Tohoku University, 3.University of Electro-Communications)

## [PEM16-P18] Implementation of photochemical process of NOx and HOx into a whole atmosphere GCM

*Yasunobu Miyoshi[1], Hitoshi Fujiwara[2] (1.Department of Earth and Planetary Sciences, Faculty of Sciences, Kyushu University, 2.Seikei University)

## [PEM16-P19] Development of a Lagrangian chemical transport model to understand the mechanism of composition change due to change in atmospheric environment

*Shingo Nakanishi[1], Tomoo Nagahama[1], Akira Mizuno[1], Tac Nakajima[1], Riku Ishijima[1] (1.Institute for Space-Earth Environmental Research, Nagoya University)

# Temporal and spatial variation of GPS phase scintillation during substorms and auroral breakups

*Paul Prikryl[1,2], James M. Weygand[3], Reza Ghoddousi-Fard[4], P. Thayyil Jayachandran[1], David R. Themens[1], Anthony M. McCaffrey[1], Bharat S. R. Kunduri[5], Emma Spanswick[6], Yongliang Zhang[7], Akira Sessai Yukimatu[8]

1. Physics Department, University of New Brunswick, Fredericton, NB, Canada, 2. Geomagnetic Laboratory, Natural Resources Canada, Ottawa, ON, Canada, 3. Earth Planetary and Space Sciences, University of California, Los Angeles, CA, USA, 4. Canadian Geodetic Survey, Natural Resources Canada, Ottawa, ON, Canada, 5. Bradley Dept. of Electrical and Computer Engineering, Virginia Tech, USA, 6. Dept. of Physics and Astronomy, University of Calgary, AB, Canada, 7. Johns Hopkins University Applied Physics Laboratory, Laurel, MD, USA, 8. National Institute of Polar Research, Tokyo, Japan

The ionospheric structure caused by precipitation of high energy particles can adversely affect the GPS causing phase scintillation and cycle slip (loss of lock). GPS phase scintillation correlates with the intensity of the aurora, especially the rapid change in the auroral brightness [1,2,3]. Enhancement of the total electron content (TEC) observed during the substorm expansion phase in the night side downward region 1 current seems to be related to intense precipitation particle flux [4]. Such TEC enhancements cause phase scintillation that is most intense just after substorm onsets and auroral breakups. Phase scintillation index is computed for sampling rate of 50 Hz by specialized GPS scintillation receivers from the Canadian High Arctic Ionospheric Network (CHAIN). A proxy scintillation index is obtained from dual frequency measurements of geodetic-quality GPS receivers sampling at 1 Hz, which include globally distributed receivers of RT-IGS network that are monitored by the Canadian Geodetic Survey in near-real-time. Temporal and spatial changes of TEC and phase scintillation are investigated in the context of equivalent ionospheric currents derived from ground magnetometer network using the spherical elementary current method [5,6]. The relation of phase scintillation with auroral emission is also examined. In general, GPS phase scintillation maps to regions of strong westward electrojet and to the poleward edge of the eastward electrojet. Following substorm onsets and auroral breakups, strong phase scintillation associated with TEC enhancements are mapped mainly to the upward region 2 current or the equatorward edge of the downward region 1 current at or near the Harang discontinuity region [7].

[1] Kinrade J., et al., J. Geophys. Res., 118, 2490–2502, 2013. https://doi.org/10.1002/jgra.50214
[2] Semeter J., et al., Geophys. Res. Lett., 44, 9539–9546, 2013.
https://doi.org/10.1002/2017GL073570
[3] Mushini S., et al., Space Wea., 16, 838–848, 2018. https://doi.org/10.1029/2018SW001919
[4] Weygand J.M., et al., Abstract SA41B-3484, presented at 2018 AGU Fall Meeting
[5] Amm O., and A. Viljanen, Earth Planets Space, 51, 431–440, 1999, doi:10.1186/BF03352247
[6] Weygand J.M., et al., J. Geophys. Res., 116, A03305, 2011. doi:10.1029/2010JA016177
[7] Weygand J.M., et al., J. Geophys. Res.. 113, A04213, 2008. doi:10.1029/2007JA012537

Keywords: High-latitude ionosphere, GPS TEC and phase scintillation, Ionospheric currents

©2019. Japan Geoscience Union. All Right Reserved. 

# Statistical study of SAPS occurrence characteristics using the SuperDARN Hokkaido HF radar

*Kento Oya[1], Nozomu Nishitani[1], Tomoaki Hori[1]

1. Institute for Space-Earth Environmental Research, Nagoya University

We investigate the occurrence characteristics of Sub-Auroral Polarization Streams (SAPS), using the Super Dual Auroral Radar Network (SuperDARN) Hokkaido East radar. The ultimate goal is to clarify the longitudinal dependence of SAPS occurrence characteristics using the whole SuperDARN radars. In this study, we statistically analyzed about 10-year data from 2007/1/1 to 2016/12/31 and studied the occurrence rate of the flow that can be considered as SAPS, vs MLT and MLAT. Assuming that the flows are east-west oriented, we set the criteria for line of sight velocity of > 80 m/s and echo power of > 3dB. We obtained the overall characteristics of SAPS, i.e., equatorward shift of high occurrence rate region with increasing MLT and geomagnetic activity. Some of the characteristics are different from previous studies. The SAPS regions seem to be located at higher latitudes than the previous studies and the SAPS occurrence peak regions are located at later MLT. These differences might be due to the difference in geographic longitude (Far-East Siberia to Pacific vs North American region). We also found new feature, i.e, westward flows from midnight to morning at relatively low geomagnetic latitudes, that could not be caught in the previous studies probably due to the limitation of radars fields of view, especially lower latitude boundary.

Keywords: magnetosphere-ionosphere coupling, SAPS, SuperDARN, geomagnetic activity

©2019. Japan Geoscience Union. All Right Reserved. 

# Spectral investigations of near infrared aurora and airglow at 1.0-1.6 microns: 1-year ground-based imaging spectroscopic observation at Syowa station (69.0˚S, 39.6˚E)

*Takanori Nishiyama[1], Takeshi Sakanoi[2], Makoto Taguchi[3], Hidehiko Suzuki[4]

1. National Institute of Polar Research, 2. Planetary Plasma and Atmospheric Research Center, Tohoku University, 3. Rikkyo University, 4. Department of Physics, Meiji University

The motivation of this study is further understanding of dayside magnetosphere and terrestrial atmosphere coupling system by using continuous observation. Dayside aurora, polar patch, and airglow should be key phenomena for the understanding. In particular, those phenomena in near infrared (NIR) wavelength are crucially important because lower background sky luminosity by Rayleigh scattering may allow us to conduct ground-based optical observation even in dayside. Continuous dayside optical monitoring with high temporal and spatial resolutions in aurora region and cusp give us a clue to understanding of substorm pre-onset sequences at cusp region, magnetopause dynamics related to solar wind shocks, and wave-particle interactions due to electromagnetic ion cyclotron waves and whistler mode chorus. However, NIR aurora has a total lack of its spectral information with enough resolution to make a feasibility study in comparison to that in visible wavelength.

We designed a narrow field spectrometer with medium-high spectral resolution that mainly consists of Czerny-Turner type imaging spectrometer (HORIBA, iHR320) with one entry port and two exit ports. This spectrometer has two mirrors and three diffractive gratings in a rotating turret. A toroidal mirror for collimating corrects for astigmatism so that the tangential (resolution optimized) and sagittal (imaging optimized) focal planes cross at the center of the focal plane. Another larger focus mirror allows the entire flat field to be used without vignetting. Collecting optics, equipped outside the spectrometer, are a gold coated off-axis parabolic mirror and a NIR longpass filter for removal of secondary diffracted light in visible wavelength. Using 1-d InGaAs array (1024 pixels) and 600 gr/mm grating, spectral range and spectral range per pixel are 119 nm and 0.11 nm/pixel, respectively.

We started ground-based spectroscopic observation in NIR wavelength ranging from 1.0 to 1.6 microns, which covers strong OH airglow emissions and auroral emissions in $N_2$1st Positive (1.2 microns) and $N_2^+$ Meinel (1.1 and 1.5 microns) [Jones 1974; Zhou et al., 2007], at Syowa Station (69.0˚S, 39.6˚E) in Antarctica from March 2018. OH airglow spectrum in NIR can be well resolved even in water vapor absorption region. OH rotational temperature is successfully estimated using OH 3-1 band P1(2) and P1(4) emissions. However, auroral emissions were not clearly identified at 1.52 micron (N2+ Meinel) so far. Further investigations are needed including 1.10 micron (N2+ Meinel) and 1.24 micron (N2 1P). In this presentation, we are going to report results in more detail based on one year observation.

Keywords: Near Infrared, Spectral observation, Aurora, Airglow, Mesopause, Antarctica

©2019. Japan Geoscience Union. All Right Reserved. 

# The study of the lower ionosphere in the South Atlantic Anomaly (SAA) Region

*Chih-Yu Chiang[1], Tzu-Fang Chang[2,1], Sunny W. Y. Tam[1]

1. Institute of Space and Plasma Sciences, National Cheng Kung University, Tainan, Taiwan, 2. Institute for Space-Earth Environmental Research, Nagoya University, Japan

South Atlantic Anomaly (SAA) corresponds to a region where the geomagnetic field is relatively weak; such a magnetic field enables energetic particles from the inner radiation belt to penetrate closer to the Earth's surface more easily, thus resulting in relatively high level of radiation in the environment. In this study, we analyze the nighttime airglows in 2007 to 2008 in the SAA region by using the data from the ISUAL (Imager of Sprites and Upper Atmospheric Lightning) experiment aboard the FORMOSAT-2 satellite. We focus specifically on the measurements by the six spectrophotometers and the CCD Imager, which overall cover the spectrum from ultraviolet to infrared wavelengths. Based on our analysis, features of clear enhancements and annual variations at 337 nm, 391.4 nm and 777.4 nm are identified in the SAA region. Through comparing these multiple-band emissions, we can identify energy variation of incident particles and atmospheric compositions of SAA region.

Keywords: South Atlantic Anomaly, SAA, airglow, ISUAL, FORMOSAT-2

©2019. Japan Geoscience Union. All Right Reserved. 

# Multi-GNSS observation of LSTID in Japan and its link with auroral activities

*Mayumi Hashimoto[1], Kosuke Heki[1]

1. Hokkaido University

Interaction between southward magnetic field in solar winds and the Earth’ s magnetosphere causes geomagnetic activities and auroral substorms. The auroral activity is associated with strong electric currents (auroral jet) within the auroral oval. This disturbs the geomagnetic field at high latitude region and is reflected in changes in the AE (Auroral Electrojet) index. At this time, atmospheric gravity waves, generated as a result of the heating of the atmosphere by electric currents, propagate toward the middle and low latitudinal regions and make Large-Scale Traveling Ionospheric Disturbances (LSTID). In this study, we observed ionospheric disturbance in Japan located in middle and low latitudes as the changes in TEC (Total Electron Content). Here we study the relationship between LSTID observed with multiple-GNSS (Global Navigation Satellite System), GPS, GLONASS, Galileo, and QZSS, and short-term changes in the high time resolution AE index time series.

In this study, we used the AE index one minute values from Kyoto University, World Data Center for Geomagnetism (wdc.kugi.kyoto-u.ac.jp). As the GNSS observation point, we used Tsukuba (tskb), one of the IGS observation points in Japan with inter-frequency bias values available. To examine the relationship, we first identified the day when the AE index exceeded 2,000 nT between 2011 and 2017. Then, we converted the RINEX data files of tskb on these days to TEC, removed satellite and receiver biases, and converted them to vertical TEC (VTEC). We compared the AE index and VTEC for 22 cases, and the occurrences of LSTID were confirmed in 5 of them. In these cases, LSTIDs were observed 1 or 2 hours after the peak of the AE index. We estimated the propagation velocity in two ways, i.e. by calculating the time lag between the AE peak and LSTID arrivals in Japan and the distance between the auroral oval and Japan, and by comparing the times of TEC peaks within Japan. Both approaches showed the velocity of ~0.7 km/sec.

Since 2018 summer, the Japanese GNSS network started to track multiple GNSS including the Japanese Quasi-zenith Satellite System (QZSS) and to open the raw data on-line by RINEX 3.02 format. discuss the relationship LSTID and AE index. QZSS includes three satellites with quasi-zenith orbits (PRN01, 02, 03) and one satellite with geostationary orbit (PRN07). Generally speaking, GNSS-TEC data changes by the three reasons, (1) temporal change in ionosphere, (2) spatial change in ionosphere, and (3) apparent change by changes in satellite elevation angle. However, QZSS-TEC includes only (1), and useful in studying ionospheric disturbances without bothering about (2) and (3).

Keywords: LSTID, TEC, GNSS

©2019. Japan Geoscience Union. All Right Reserved. 

# Basic development of accurate analytical method in order to determine coordinates of artificial illuminating clouds of Barium and Strontium for chemical-release rocket experiments

*Taro Watanabe[1], Masa-yuki Yamamoto[1], Yoshihiro Kakinami[2]

1. Kochi University of Technology, 2. Hokkaido Information University

In order to investigate neutral atmospheric heating phenomenon in the polar cusp, it is necessary to estimate Joule heating and fluctuation of electric field in the cusp. To accomplish this, we conducted a US-Japan joint rocket experiment called the Cusp Region Experiment 1 (CREX-1) in the Arctic region in November 2014, with releasing Ba (to be ionized in a short time by extreme ultraviolet (EUV) from the Sun) and Sr (not ionized in a short time). And then, we observed resonance scattering emission of $Ba^+$ and Sr simultaneously from two sites on ground so as to obtain fluctuation of the electric field and Joule heating. However, we could not release the gases in the cusp at that time. We are planning additional space experiments, based on the CREX-1 results, using two sounding rockets of the Cusp Region Experiment 2 (CREX-2) and the Joint Japan-US Cusp Heating Investigation (CHI) aiming at observing of the cusp in December 2019.

In this study, we developed a basis of accurate analytical method in order to determine coordinates of artificial illuminating cloud with applying observed data of CREX-1. At the beginning of the analysis, we made calibration data from the RAW images taken at a previous optical system tests. We compared the exposure input-output characteristics of JPEG and RAW to establish an analysis method using RAW images instead of JPEG. Next, we investigated whether it is possible to replace the work of determining centers of the illuminating clouds, which has been carried out by hand, by a method of uniquely determining the luminance maximal by gradient descent method. In addition, we made a background image by a darken composition method and attempted to remove the background brightness gradient trend.

As a result, the characteristics of JPEG image reported by Kakinami et al. (2015) were thought to be arcuate gamma curves, but in RAW images, they were obtained as linear characteristics. Regarding the gradient descent method, although it is possible to uniquely determine the luminance maximal without any human factors, it was found that there is a possibility that the local maximum is not the true center. For background removal by the darken composition method, it is effective for background light gradient removal. However, there is a problem that the shadow of the illuminating clouds appearing in the background image affects the remained shape of the illuminating clouds when removing the background.

Furthermore, we developed an algorithm tracing the three-dimensional position of $Ba^+$/Sr cloud uniquely without any human factors.

References:
Y. Kakinami, S. Watanabe, M.-Y. Yamamoto, D. Kihara, M. Conde and M.F. Larsen, Measurement of thermospheric wind and plasma drift using barium strontium in cusp region, the 138th SGEPSS Meeting, 2015.

©2019. Japan Geoscience Union. All Right Reserved. 

Keywords: Sounding Rocket, Polar Cusp, Neutral Atmospheric Wind, Plasma Drift, Thermosphere

©2019. Japan Geoscience Union. All Right Reserved. 

# Neutral and plasma density perturbations in the top-/bottom-side ionosphere associated with MSTIDs

*Shin Suzuki[1], Jaeheung Park[2], Yuichi Otsuka[3], Kazuo Shiokawa[3], Huixin Liu[4], Hermann Luehr[5]

1. Faculty of Regional Policy, Aichi University, 2. Korea Astronomy and Space Science Institute, 3. Institute for Space-Earth Environmental Research, Nagoya University, 4. Earth and Planetary Science Division, Kyushu University SERC, Kyushu University, 5. Helmholtz Centre Potsdam, GFZ, German Research Centre for Geosciences

Medium-scale traveling ionospheric disturbances (MSTIDs) are a well-known wavy structure in the F-region ionosphere. They typically have a horizontal wavelength of several hundred kilometers and a periodicity of about one hour. Although, the MSTIDs were considered to be caused by atmospheric gravity waves, recent studies have suggested that the generation of the MSTID in nighttime is highly associated with coupling processes between the E- and F-region electrodynamics. To confirm the different processes in the MSTID generation in daytime and nighttime, CHAMP satellite measurements would be greatly helpful; CHAMP plasma and neutral density data obtained in the day- and night-side sector can monitor the phase relations between the neutral (i.e., atmospheric gravity wave) and ionospheric plasma perturbations simultaneously at the top-side F-region (approximately 400 km).

As the first step in the abovementioned research, we compared the MSTID signatures between the CHAMP and ground-based 630-nm airglow measurements to validate the MSTID detection by CHAMP. Airglow imaging is a quite useful technique to investigate two-dimensional characteristics of the nighttime MSTIDs. Horizontal parameters of the MSTIDs (such as wavelengths, motions, and their spatial extent) can be estimated directly with a high spatial and temporal resolutions through the 630-nm airglow emission in the bottom-side F-region. Previous study by Park et al. [2009, JGR] made an investigation of spatial signatures regarding one MSTID event using airglow images along the CHAMP orbit. The Institute for Space-Earth Environmental Research, Nagoya University, has operated airglow imaging network, as the OMTI system, around the world since 2000; this network gives much more chance to make coordinated measurements with CHAMP. We found three clear MSTID events (March 15, 2004, February 15, 2007, and January 12, 2007) in which CHAMP passed over the field-of-views of the OMTI camera.

In this presentation, we will report phase relations between the neutral and plasma density perturbations associated with the MSTID events.

Keywords: MSTID

©2019. Japan Geoscience Union. All Right Reserved. 

# Analysis of ionospheric TEC fluctuation by rocket

*Tsuyoshi Takegawa[1], Hiroyuki Nakata[1], Hiroyo Ohya[1], Toshiaki Takano[1], Takuya Tsugawa[2], Michi Nishioka[2]

1. Graduate School of Integrated Science and Technology, Chiba University, 2. National Institute of Information and Communications Technology

It is known that atmospheric waves arised by massive earthquakes, typhoons and volcanic eruptions cause the ionospheric variation. In recent years, ionospheric fluctuations excited by rocket launches have been confirmed (Lin et al., 2014,2017). In case of Taepodong 2, the first wave of TEC fluctuations is confirmed due to the chemical reaction with ionospheric plasmas and the exhaust of the rocket about 5 minutes after the launch and the second wave was confirmed after about 30 minutes from the launch. To examine the ionospheric disturbances apart from the trajectories of rockets, in this study, TEC fluctuation due to the launches of H2A rocket No.25 and No. 29 we examined using GEONET data. The first waves of the TEC fluctuations were confirmed around hundreds kilometers from the rocket trajectory 5 minutes after launch of both of H2A rockets. The first waves appeared as large decreases in VTEC, which is consistent with the previous study of Taepodong 2. Calculating the propagation time of the sound waves from the points on the trajectories of the rockets, the delays correspond to the propagation times from the trajectories to the pierce points of TEC. The second waves were also observed around the 30 minutes after the rocket launches. Calculating the arrival time of sound waves for the second waves, the seconds waves once reflected on the ground were affected by the second waves.

Keywords: ionospheric, rocket, TEC

©2019. Japan Geoscience Union. All Right Reserved. 

# Examinations of the ionospheric perturbation associated with H-IIA rockets launching

*Junpei Yamazaki[1], Hiroyuki Nakata[1], Hiroyo Ohya[1], Toshiaki Takano[1], Keisuke Hosokawa[2], Ichiro Tomizawa[2]

1. Graduate School of Engineering, Chiba University, 2. Department of Communication Engineering and Informatics, University of Electro-Communications

It is reported that ionospheric perturbation are caused by natural hazards, such as giant earthquakes, olcanic eruptions and so on. This is because the infrasound waves generated by natural hazards propagate to the ionospheric. Since rocket launches also generate the atmospheric waves, it is reported that passage and exhaust plumes generate TEC perturbations determined by GEONET data(Lin et al.,2014,2017).
On the other hand, there is few studies about ionospheric perturbation associated with rocket launch away from rocket’ s trajectory. Then, in this study, we analyzed ionospheric perturbations associated with H IIA(No.25 and 26) relatively far trajectory from the Japanese islands using HF Doppler sounding.
The perturbations of Doppler shifts associated with H-IIA No.25 were observed at Kakioka and Sugadaira observatories and those of H-IIA No.26 were observed at Kakioka,Fujisawa and Sugadaira observatories about 35 minutes after the launch. It is confirmed that this delay corresponds to the propagation time of the infrasound wave from the launch site to observation points once reflected on the ground. The frequencies of the disturbance of Doppler shift were 5~10 mHz. Similar disturbances were reported in Lin et al (2014) which examined the TEC disturbances associated with Taepodong. The Doppler shift perturbation is clear when the infrasound wave reached the observation point after reflection on the ground as compared to the case where the infrasound wave reached the observation point directly. When the infrasound wave directly reaches the observation point, it passed through about 200~250km altitude. Where the amplitude of infrasound waves with several 10mHz tend to attenuate. Therefore, ionospheric perturbation at the moment corresponding to the arrived at the direct wave become small.

©2019. Japan Geoscience Union. All Right Reserved. 

# Explosion energy derived from the 2015 Kuchinoerabujima eruption: Estimation from infrasound less than 0.01 Hz detected by barometers, seismometers, and TEC

*Yuki Nakashima[1], Kiwamu Nishida[1], Yosuke Aoki[1], Kosuke Heki[2]

1. Earthquake Research Institute, 2. Natural History Sciences, Hokkaido University

This study discusses the amount of energy emitted to the atmosphere as acoustic waves of less than 0.01 Hz by the 2015 Kuchinoerabujima volcano, southwest Japan, eruption derived from barometers, broadband seismometers, and GNSS-TEC observations.
Kuchinoerabujima is one of the volcanic islands of active recently. The volcano erupted at 0:59 UT on 25th May 2015. Many previous studies pointed out that this is a phreatomagmatic eruption and involves a lateral signal (e.g., Kobayashi, 2017; Matsuzawa et al., 2016; Yamada et al., 2017). Yamada et al. (2017) found that barometric data include two phases in about 20 sec. In the first stage, the volcanic plume went up with a pressure pulse, and the second another pulse corresponds to the plume growing laterally. The seismic source time function of that has a component of north-south direction obviously (Matsuzawa et al. 2016).
We found atmospheric disturbances with a characteristic frequency of ~0.01 Hz in all the observations. The frequency range is equivalent to the highest part of the detectable band in the ionosphere. We detected the signal of lower atmospheric perturbation from F-net, an array of broadband seismometers installed by NIED, and a barometer array along the Japanese coastline in front of the Pacific ocean by AIST. As the ionospheric observation, we used GNSS-TEC time series extracted from GEONET 1 Hz sampling data. The waveform feature is very similar to ionospheric disturbances excited by Asama volcano on 1st September 2004 (Heki, 2006; Chonan et al., 2017).
We tried to reproduce the observed signal and estimate the magnitude of the energy source using the ray-tracing method. Atmospheric parameters are inputted from NRLMSISE-00 (Picone et al., 2002), HWM-14 (Drob et al., 2015), IRI2016 (Billitza et al., 2016), and IGRF-12 (Thébault et al., 2015). We put an isotropic energy source on the ground in the windy atmosphere.
The estimated travel time by ray-tracing is consistent with the observation, indicating that the excited atmospheric perturbation simply propagates isotropically without wave broadening due to dispersion discussed in Dautermann et al. (2009a).
If we choose the source energy as $10^8$ J, our model expects about one-third of the observed signal in both the lower atmosphere in the far field and the ionosphere. This amount of energy is $10^{1-2}$ times larger than that of the 2004 Asama eruption estimated from TEC observation (Heki, 2006). It seems to depend on not only the difference of volcanic eruption magnitude but also the crude assumption like ignoring the geomagnetic effect and geometrical spreading same as Dautermann et al. (2009) suggested.
We were not able to find any evidence for anisotropic radiation of energy as stated in some previous studies, suggesting that infrasound of such very low frequencies infrasound (< ~0.01 Hz) responds to with a longer time constant such as the growth of the thermal plume.
Acknowledgment
We would thank GSI, JMA, AIST, and NIED which provide GNSS, barometer, microphone, and broadband seismometer data.

Keywords: GPS-TEC, GNSS-TEC, Volcanic eruption, Infrasound, Broadband seismometer

©2019. Japan Geoscience Union. All Right Reserved. 

©2019. Japan Geoscience Union. All Right Reserved. 

# Detection of spread-F echoes in ionograms using machine learning

*Hiroyuki Nakata[1], Yuta Goto[2], Hiroyo Ohya[1], Toshiaki Takano[1]

1. Graduate School of Engineering, Chiba University, 2. Department of Electrical and Electronics Engineering

Ionospheric irregularities referred to as equatorial spread-F is very important phenomena in terms of radio wave propagation because their spatial scales are from centimeters to tens of kilometer and they affects wide-band radio waves. Therefore, they influence the reliability of satellite-ground communications, navigation systems and so on. The ionogram is one of the important observation system of spread-F. Because the detection of spread-F in the ionogram is done manually, detection of spread-F could be replaced with automatic detection by developing an excellent machine learning system. In this study, therefore, we have developed a method to detect spread-F in the ionogram automatically using machine learning.

In this detection process, we have arranged two classifiers for typical frequency-type and mixed (frequency-type and range-type) spread-F echoes in the ionograms. A number of correct images must be prepared for these classifiers to learn the feature values of spread-F. To do so, ten thousands of correct images were generated by create_samples utility provided by OpenCV library. Using these classifiers, we have detected the both types of spread-F echos in the ionograms observed at 4 observatories (Wakkanai, Kokubunji, Yamagawa, Ogimi) utilized by National Institute of Information and Communications Technology. The detection rates of both types of spread-F echos are from 50% to 73% and both classifier detected both types of spread-F echos similarly. Namely, the classifier for the frequency-type spread-F echo detected both of the frequency-type and mixed-type echos, and vice versa. In case where the two types of spread-F echos are not distinguished, on the other hand, both of classifiers detect 80% of total spread-F echos. In addition, the classifiers also picked up some other phenomenon , such as overlapped traces of O-mode and X-mode, multi-hop trace.

As for the future plan, there might be several way to improve the detection rate; to use more classifiers, to make the classifiers be precisely with more training data, and so on. However, a number of correct images are inevitable in machine learning. In order to prepare such a number of images, it may be effective to generate training data using deep generative model.

Keywords: spread F, ionogram, machine learning

©2019. Japan Geoscience Union. All Right Reserved. 

# Evaluation of GNSS-TEC receiver performance for sounding rocket installation

*Makoto Okumura[1], Yuki Ashihara[1]

1. National Institute of Technology, Nara College

Earth's atmospheric region ionized electrons by X-rays and ultraviolet rays involved in sunlight is called ionosphere. Ionospheric disturbance causes some problems, e.g., which are terrestrial satellite communication impairment and positioning error of GNSS. For elucidating the generation mechanism of the ionospheric disturbance, we need to observe spatial structure of ionospheric electron density. Ionosphere observation is generally implemented with remote sensing method such as Ionosonde, GNSS-TEC and others. Ionosonde can observe the electron density vertical structure below the altitude of electron density peak in F region, and GNSS-TEC can obtain the total electron content along the radio wave propagation path. However, these methods cannot observe the spatial structure. In this paper, we propose a rocket GNSS-TEC tomography method as a new approach to the ionosphere observation. In this method, we install the GNSS-TEC receiver onboard a sounding rocket, and it is flying the boundary region between the ionospheric E and the F region. It is possible to acquire the TEC data only for the F region.
In case of a combining antenna system installed on the side on sounding rocket, it is simulated that the received signal becomes unstable since the sounding rocket spins at the speed of 1 to 2 Hz. Therefore, we built a structure model of the sounding rocket, and conducted a ground-based rotation experiment. In this experiment, the GNSS carrier phase data was approximately obtained for the steady rotation speed, but TEC value had the variation more than 60 TECU. As the results, we understood that a combining antenna system cannot useful for a rocket GNSS-TEC.

Keywords: ionosphere, GNSS-TEC, sounding rocket

©2019. Japan Geoscience Union. All Right Reserved. 

# Relationship between mesosperical airglow disturbance and occurrence of equatorial plasma bubbles

*Ryota Okada[1], Akinori Saito[1], Takafumi Ikeda[1], Hiroyuki Shinagawa[2], Takuya Tsugawa[2], Takeshi Sakanoi[3]

1. Department of Geophysics, Graduate School of Science, Kyoto University, 2. National Institute of Information and Communications Technology, 3. Planetary Plasma and Atmospheric Research Center, Graduate School of Science, Tohoku University

762 nm airglow data observed by Ionosphere, Mesosphere, upper Atmosphere and Plasmasphere mapping mission from the ISS / Visible and near Infrared Spectral Imager (ISS-IMAP/VISI) to investigate relationship between mesospheric gravity waves and the occurrence of Equatorial Plasma Bubbles (EPBs). EPBs are depletion of electron density in the equatorial ionosphere. According to the previous study EPBs can be generated through the Rayleigh-Taylor (R-T) instability in the ionosphere. Medium-scale gravity waves with horizontal scales of a few hundred kilometers in the bottom side of the F region have been frequently suggested to play a key role in EPBs seeding. Gravity wave occurrence may depend on seasonal and longitudinal variation and may have oscillation whose period is few days. This several days oscillation of gravity wave may affect the variation of EPBs occurrence that can not be explained only by the R-T growth rate. Previous research of concentric gravity waves (CGWs) using observed by ISS-IMAP/VISI shows more mesospheric CGW events occur in the west side of the African continent than the east side of the African content. It indicate occurrence of CGWs is different between nearby areas. Objective of this study is to elucidate relationship between mesospheric gravity waves and longitudinal dependence of EPB occurrences. ISS-IMAP/VISI was operated for three years from September 2012 to August 2015. ISS-IMAP/VISI observed the airglow in the nadir direction on the nightside with two FOVs facing 45 degrees in the forward and backward of the orbital direction. We analyzed 762nm airglow data and compared with occurrence rate of EPBs and Growth rate of R-T instability. Occurrence rate of EPBs using Rate of TEC Index (ROTI) that is standard deviation of differential of GPS-TEC. Growth rate of R-T instability was calculated by using parameters from Ground-to-topside model of Atmosphere and Ionosphere for Aeronomy (GAIA). In this study, we investigated relationship between occurrence of EPBs observed by GPS-TEC data, linear growth rate of the R-T instability in the ionosphere obtained with GAIA, and mesospheric gravity wave activities observed by ISS-IMAP/VISI.

Keywords: Equatorial Plasma Bubbles, Airglow

©2019. Japan Geoscience Union. All Right Reserved. 

# Analysis of parameters controlling the occurrence and growth of equatorial plasma bubbles using GAIA

*Hiroyuki Shinagawa[1], Hidekatsu Jin[1], Yasunobu Miyoshi[2], Hitoshi Fujiwara[3], Tatsuhiro Yokoyama[4], Yuichi Otsuka[5]

1. National Institute of Information and Communications Technology, 2. Department of Earth and Planetary Sciences, Faculty of Sciences, Kyushu University, 3. Faculty of Science and Technology, Seikei University, 4. Kyoto University, 5. Institute for Space-Earth Environmental Research, Nagoya University

In our previous studies, the linear growth rates of the Rayleigh-Taylor (R-T) instability in the ionosphere were obtained with a whole atmosphere-ionosphere coupled model GAIA, and the growth rates were compared with observations [Shinagawa et al., 2018]. We found that a high growth rate of R-T instability tends to correspond to the actual equatorial plasma bubble (EPB) occurrence. The result suggests that the occurrence and growth of EPB are controlled both by atmospheric waves propagating from the lower atmosphere and by geomagnetic activities. However, dependence of various parameters such as electric fields, electron and neutral densities, and neutral wind velocities on the EPB occurrence and growth has not been quantitatively understood. We will discuss how those parameters affect the linear growth rates of the R-T instability using GAIA simulation data, and report the importance of the parameters in controlling the EPB occurrence and growth.

Keywords: Ionosphere, Atmosphere, Model, Plasma bubble, Linear growth rate, Parameter

©2019. Japan Geoscience Union. All Right Reserved. 

# A three-dimensional numerical model to study the modulation of midlatitude $E_s$-layers

*Satoshi Andoh[1], Akinori Saito[1], Hiroyuki Shinagawa[2], Shin'ichi Miyazaki[1]

1. Graduate School of Science, Kyoto University, 2. National Institute of Information and Communications Technology

We develop a three-dimensional numerical model to shed light on the generation, growth and diffusion mechanisms of the sporadic E layers in the midlatitude.

The Es layer is a high-density layer of plasma formed at around 100 kilometers high. It is affected by both the atmospheric waves generated in the troposphere and mesosphere, and the electromagnetic interaction between the E region and the F region, so that it is a very important phenomena to understand the physics of the upper atmosphere.

The mechanism of Es layer formation is described through the Windshear Theory. According to the theory, factors affecting the Es layer formation are zonal windshears and meridional windshears. Which one can make more effects depends on the altitude of Es layer.

Lately, there has been some new structures of the Es layer detected by several observations (e.g. Lidar observation). They cannot be explained only by Windshear Theory. It is considered that there are three factors of the structures: atmospheric waves, Kelvin-Helmholtz instability and Es layer instability. Several models have been developed to study each factor, but no model includes all three factors. Such a model is necessary to give a consistent explanation for which factor is the most effective for modulation of the Es layers.

Our model includes six kinds of ions of $O^+$, $O_2^+$, $N^+$, $N_2^+$, $NO^+$, $Ca^+$, and in both the transport process and the chemical process of ions in the uniform geomagnetic field solve. In addition, NRLMSISE-00 is used as a background field of neutral atmospheric density. This model uses three-dimensional polar coordinate system. Altitude coverage is from 85 km to 305 km and horizontal domain size is 5 degree ×5 degree in the longitude and latitude direction. The vertical and horizontal resolutions are 1 km and 0.1 degrees, respectively and the time resolution is 1 second.
By inputting latitude, longitude and UT into this model, it is possible to simulate ionosphere in midlatitude within the above calculation area.

In this presentation, as a pseudo-zonal and meridional neutral windshear, we employed a sinusoidal windsear in the vertical direction and reevaluated which component of the neutral windshear will affect more to form Es layers.
As a result, we obtained results consistent with the previous study that the influence of the zonal windshear is large at the low altitude and the influence of the meridional windshear is large at the high altitude.
Moreover, by incorporating the neutral winds of GSWM model and HWM14 model into ours, we examined the mechanism of generation of Es layer in the more real condition.

Based on these, we will introduce the future view in the presentation.

©2019. Japan Geoscience Union. All Right Reserved. 

Keywords: sporadic E layer, midlatitude, simulation, ionosphere

©2019. Japan Geoscience Union. All Right Reserved. 

# Statistical analysis of the horizontal phase velocity distribution of mesospheric and ionospheric waves observed in airglow images in Hawaii

*Hideto Naito[1], Kazuo Shiokawa[1], Yuichi Otsuka[1], Takeshi Sakanoi[2], Akinori Saito[3], Takuji Nakamura[4]

1. Institute for Space-Earth Environmental Research, Nagoya University, 2. Planetary Plasma and Atmospheric Research Center, Graduate School of Science, Tohoku University, 3. Department of Geophysics, Graduate school of science, Kyoto University, 4. National Institute of Polar Research

Matsuda et al. [JGR, 2014] proposed a method of deriving the horizontal phase velocity and propagation direction of the power spectral density of waves found in images using three-dimensional fast Fourier transform. Takeo et al. [JGR, 2017] and Tsuchiya et al. [JGR, 2018] applied this method to the airglow images obtained at Shigaraki and Rikubetsu, Japan, and reported 16-year variability of atmospheric waves at middle latitudes. However, there is no report using this method for analyzing airglow images obtained at low latitudes near the equator. In this study, we applied the analysis method of Matsuda et al. [2014] to airglow images obtained at wavelengths of 557.7 and 630.0 nm during the three years from 2013 to 2016 at Haleakala (20.7°N, 203.7°E) in Hawaii, where the latitude, longitude and orography are greatly different those of Shigaraki (34.8°N, 136.1°E) and Rikubetsu (43.5°N, 143.8°E). We clarified the statistical features of atmospheric gravity waves (AGWs) and medium-scale traveling ionospheric disturbances (MSTIDs) in the low latitude region near the equator, and compared it with features seen in Shigaraki and Rikubetsu (Takeo et al., JGR, 2017 and Tsuchiya et al., JGR, 2018).

The three-year average of the phase velocity spectra of AGWs observed in airglow images at wavelength of 557.7 nm show less propagation in due eastward and due westward in summer. The dominant propagation direction was southward in winter. The power spectral density was strongest in spring and summer, and weakest in winter. In Shigaraki and Rikubetsu, the direction of propagation changes from east in summer to west in winter, while in Haleakala there was no such seasonal change in the propagation in summer and winter. This is probably because Haleakala is located at latitudes away from the peak of the mesospheric jet, so the wind filtering effect by the mesosphere jet is smaller than that at Rikubetsu and Shigaraki.

The MSTIDs observed in airglow images at wavelength of 630.0 nm showed strong spectra in four particular nights, and we found that the average spectra largely affected by these strong spectra. Thus we removed these strong nights and calculated the three-year average horizontal phase velocity spectra for four seasons. From the average spectra, MSTIDs propagate from northwestward to southward in summer and from northward to southeastward in fall. In winter, the power spectral density was strongest, and the MSTIDs propagate mainly in the east-west direction. Spring power spectrum density was weakest. We note that dominant propagation direction of MSTIDs at Shigaraki and Rikubetsu was southwestward regardless of the season, which is very different from Haleakala. The power spectral density was weaker at Haleakala than those at Shigaraki and Rikubetsu. These results may be because polarization electric fields

©2019. Japan Geoscience Union. All Right Reserved. 

associated with MSTIDs tends to be attenuated by the equatorial ionization anomaly crest, which exists at low latitudes before midnight and by the MBW (Midnight Brightness Wave) moving poleward from low latitudes associated with the MPB (midnight pressure bulge) even after midnight, as suggested by Narayanan et al. [JGR, 2014].

Keywords: Atmospheric gravity waves, Medium-scale traveling ionospheric disturbances, Hawaii

©2019. Japan Geoscience Union. All Right Reserved. 

# Estimation of mesospheric OH temperature by observation data by ISS-IMAP VISI

*Ryo Murakami[1], Akinori Saito[1], Takeshi Sakanoi[2], Yuta Hozumi[3]

1. Kyoto University, 2. Tohoku University, 3. University of Electro-Communications

In general, the data of satellite observation is inferior in resolution to ground observation data and its wavelength resolution is inferior, so it is difficult to analyze. In this research, from 2012 to 2015, data of atmospheric light emission in the mesosphere by the Visible / Near Infrared Spectroscopic Imager (VISI), which is an observation device mounted on the International Space Station in the ISS-IMAP mission, Temperature estimation of the OH luminescent layer in the mesosphere near 85 km is tried. It is known from the previous study that the relative existence distribution of the rotation level when the OH molecule transitions between certain vibration levels follows the Boltzmann distribution and this distribution is determined by the rotation temperature of the OH molecule. Research using this property to try to estimate temperature from OH multiwavelength data has been used only for ground observation data so far. In this research, we apply this method to observation data from outer space and aim to obtain a spatially large temperature distribution map which has never been obtained. For analysis, data in two modes, Calibration mode and Spectral mode are used. In the calibration mode data, the observation data is recorded using the whole light receiving part of the observation equipment in the wavelength range of 500 to 900 nm, and the data of the spectral mode is narrowed down to the wavelength range of six ROI (Region of interest) And observation data are recorded together with spatial position information. Analysis is based on data in Spectral mode. Removal of salt-and-pepper-noise by cosmic rays and removal of artificial noise-containing data using random sample consensus algorithm for multi-wavelength data of OH around 828 nm, In order to compensate for the low resolution of the wavelength resolution, we tried fitting by Gaussian function and tried to estimate the temperature.

Keywords: ionosphere, airglow, mesosphere, hydroxyl, ISS-IMAP, temperature

©2019. Japan Geoscience Union. All Right Reserved. 

# Implementation of photochemical process of NOx and HOx into a whole atmosphere GCM

*Yasunobu Miyoshi[1], Hitoshi Fujiwara[2]

1. Department of Earth and Planetary Sciences, Faculty of Sciences, Kyushu University, 2. Seikei University

Photochemical process associated with NOx and HOx plays an important role on the energy budged and general circulation in the mesosphere and lower thermosphere (MLT). For example, NO is important for the infrared cooling in the MLT region. Photochemical process associated with HOx is essential for accurate estimate of the O3 distribution in the mesopause region. We implemented photochemical process of HOx and NOx into a whole atmosphere general circulation model (GCM). Using this GCM, effects of the solar activity on the general circulation in the MLT region are studied. Furthermore, this GCM can provide accurate estimate of the energy budget due to the global cooling due to the increase of CO2. In this study, preliminary results will be shown, and further development of the GCM will be discussed.

Keywords: the general circulation of the atmosphere, photochemical process

©2019. Japan Geoscience Union. All Right Reserved. 

# Development of a Lagrangian chemical transport model to understand the mechanism of composition change due to change in atmospheric environment

*Shingo Nakanishi[1], Tomoo Nagahama[1], Akira Mizuno[1], Tac Nakajima[1], Riku Ishijima[1]

1. Institute for Space-Earth Environmental Research, Nagoya University

Mesospheric chemical composition largely varies caused by environmental changes from the earth inside and outside. Recent studies reported enhancement of $NO_x$ and $HO_x$ and ozone depletion in the polar mesospheric region at a large solar proton event. These suggest that precipitation of other high energy particles such as a high energy electron from the magnetosphere also has influence on the chemical composition in the mesosphere. For these reasons, we have installed millimeter-wave spectrometers in Rikubetsu-cho, Hokkaido (Japan), Syowa Station (Antarctic), Atacama (Chile), Rio Gallegos (Argentine) and Tromso (Norway), and have been observing steady atmospheric minor molecules such as Ozone, $NO_x$, $HO_x$ and ozone-depleting substances in the stratosphere and mesosphere to understand the atmospheric composition changes caused by natural phenomena such as Energetic Particle Precipitation (EPP).

In addition to these observations, we have been developing a Lagrangian chemical transport model, which is suitable for a simulation of a sudden and a local event to evaluate the influence of the atmospheric composition mechanism in the stratosphere and mesosphere. Our developing model is an extension of the Lagrangian particle dispersion model (FLEXPART) by incorporating meteorological fields data and chemical reactions in the mesosphere. FLEXPART can analyze a trajectory from the ground to about 40 km in altitude using the reanalysis data of NCEP and ECMWF as meteorological fields input data. In this study, we incorporated a new reanalysis dataset (MERRA2) as meteorological fields input data to extend the analysis range toward the mesosphere, and as a result, trajectory a analysis ranging from the ground to about 80 km in altitude can be made. In order to evaluate the analysis accuracy of our developing model, we calculated trajectories for a single position at altitudes of 15, 45, 55, 70 km, and compared the results with another trajectory analysis model. Moreover, only OH reactions are considered in FLEXPART, although it needs to calculate non-linear chemical reactions separately in this study because chemical reactions caused by EPP include not only reactions by natural molecules but also ion-molecular reaction, ionization, dissociation and ion recombination, and so on. For this reason, we incorporated chemical reactions of the stratosphere and mesosphere in FLEXPART using Kinetic Preprocessor (KPP) which is chemical reaction computation software. We previously calculated chemical reactions of the stratosphere and mesosphere using KPP alone and confirmed the amount of mesosphere ozone variation in day and night.
In this presentation, we will report the results of comparison bet between our developing model and other trajectory models as well as the simulation results about some EPP events using our model.

Keywords: mesosphere, ozone, high energy particle, chemical transport model

©2019. Japan Geoscience Union. All Right Reserved. 

[J] Poster | P (Space and Planetary Sciences )：P-EM Solar-Terrestrial Sciences, Space Electromagnetism & Space Environment

Thu. May 30, 2019 10:45 AM - 12:15 PM JST | Thu. May 30, 2019 1:45 AM - 3:15 AM UTC | Poster Hall International Exhibition Hall8, Makuhari Messe_1

## [P-EM17] Space Plasma Physics: Theory and Simulation

convener:Takayuki Umeda(Institute for Space-Earth Environmental Research, Nagoya University), Takanobu Amano(Department of Earth and Planetary Science, University of Tokyo), Yasuhiro Nariyuki(Faculty of Human Development, University of Toyama), Tadas Nakamura(Fukui Prefectural University)

This session focuses on studies of space plasma physics via theoretical and numerical approaches. Papers on a wide variety of topics from natural phenomena to artificial plasma environment as well as theoretical and computational methodologies are welcome.

[PEM17-P01] PIC Simulation on nonlinear development of lower-hybrid instabilities driven by energetic ions.

*Tsubasa Kotani[1], Mieko Toida[2], Toseo Moritaka[2], Satoshi Taguchi[1] (1.Graduate School of Science, Kyoto University, 2.National Insititute for Fusion Science)

[PEM17-P02] **Study of Kinetic Alfven waves in space plasmas with electron having Kappa distribution**

*SATYAVIR SINGH[1], Krushna Chandra Barik[1], Yoshiharu Omura[2], Gurbax Singh Lakhina[1] (1.Indian Institute of Geomagnetism, New Panvel, India, 2.Research Institute for Sustainable Humanosphere, Kyoto University, Kyoto, Japan)

[PEM17-P03] A high-order divergence-free weighted finite difference scheme for the two-fluid plasma equations

*Takahiro Miyoshi[1], Takashi Minoshima[2], Yosuke Matsumoto[3] (1.Graduate School of Science, Hiroshima University, 2.Department of Mathematical Science and Advanced Technology, Japan Agency for Marine-Earth Science and Technology, 3.Graduate School of Science, Chiba University)

[PEM17-P04] Electromagnetic linear dispersion relation for plasma with a drift across magnetic field

*Takayuki Umeda[1], Takuma Nakamura[2] (1.Institute for Space-Earth Environmental Research, Nagoya University, 2.Space Research Institute, Austrian Academy of Sciences)

# PIC Simulation on nonlinear development of lower-hybrid instabilities driven by energetic ions.

*Tsubasa Kotani[1], Mieko Toida[2], Toseo Moritaka[2], Satoshi Taguchi[1]

1. Graduate School of Science, Kyoto University, 2. National Insititute for Fusion Science

Instabilities driven by energetic ions are important issues both for space plasmas and magnetic fusion plasmas. Radio Frequency (RF) waves in the range from the ion cyclotron frequency to the lower hybrid resonance frequency are often observed during the period of neutral beam injection (NBI) in Large Helical Device (LHD) plasmas. The experimental results showed that the peak frequency in the Lower Hybrid Wave (LHW) region has a positive correlation with the electron density and the ion cyclotron emissions (ICEs) have much larger amplitudes than LHW. These waves can be excited by instabilities due to energetic ions generated by the NBI perpendicular to the magnetic field.

Using a one-dimensional, electromagnetic, Particle-In-Cell (PIC) code, we study instabilities driven by energetic ions assuming that the energetic ions have a non-Maxwellian ring-like distribution in the velocity space perpendicular to the magnetic field. This PIC code enables us to self-consistently simulate full dynamics of electrons and ions and evolution of electromagnetic fields, using the full Maxwell's equations and the equations of motion of particles. We focus on the nonlinear evolution of LHW and ICEs caused by continuous energetic-ion injection into a plasma.

The simulation results are as follows. After the rapid growth of the LHW in the early stage, the ICEs gradually become intense. Finally, the ICEs have larger amplitudes than LHW.

Keywords: lower-hybrid instabilities, ion-cyclotron emissions, non-linear development, Particle-In-Cell simulation

©2019. Japan Geoscience Union. All Right Reserved. 

# Study of Kinetic Alfven waves in space plasmas with electron having Kappa distribution

*SATYAVIR SINGH[1], Krushna Chandra Barik[1], Yoshiharu Omura[2], Gurbax Singh Lakhina[1]

1. Indian Institute of Geomagnetism, New Panvel, India, 2. Research Institute for Sustainable Humanosphere, Kyoto University, Kyoto, Japan

A theoretical model is developed by assuming a three component plasma comprising of the cold background ions, hot electrons having kappa distribution and hot ion beams to study the generation of kinetic Alfvén waves (KAWs).The background ions and beam ions are considered Maxwellian and the ion beam is only allowed to have velocity shear and non-uniform streaming. A dispersion relation for the excitation of the kinetic Alfven waves (KAWs) is analyzed. The effect of plasma parameters like number density, propagation angle, temperature, kappa etc. on the excitation of KAWs is examined. A comparative study of the results obtained from this model will be carried out with a plasma model having all the three species as Maxwellian. Further, an application of the theoretical model will be discussed relevant in the Earth’ s magnetosphere.

Keywords: Earth, Magnetosphere, kinetic Alfven waves

©2019. Japan Geoscience Union. All Right Reserved. 

# A high-order divergence-free weighted finite difference scheme for the two-fluid plasma equations

*Takahiro Miyoshi[1], Takashi Minoshima[2], Yosuke Matsumoto[3]

1. Graduate School of Science, Hiroshima University, 2. Department of Mathematical Science and Advanced Technology, Japan Agency for Marine-Earth Science and Technology, 3. Graduate School of Science, Chiba University

Recent development of numerical techniques for magnetohydrodynamics (MHD) enables us to simultaneously simulate fine structures created by shock-vortex interactions and a large-scale MHD structure. On the other hand, the scales of the fine structures can become so small that the MHD approximation breaks down. Thus, a new macroscopic plasma simulation model beyond MHD is strongly required. In particular, the full two-fluid plasma model including local charge separation is considered in this study. According to the growth of computing power, the full two-fluid plasma simulation model will be scope of a standard model in the near future.

Since the full two-fluid plasma equations are hyperbolic conservation laws with stiff source terms, i.e., hyperbolic balance laws, state-of-the-art numerical techniques for the neutral fluid and MHD models can be applied. Recently, Minoshima et al. [1] developed high-order, non-oscillatory, and divergence-free finite difference schemes for MHD. In their schemes, the magnetic fields are defined on staggered grids, and the induction equation is discretized using high-order centered finite differences of the electric fields that correspond to numerical fluxes for the induction equation weightedly interpolated to the vertices of the grids. We apply this approach such that the Maxwell equations are discretized on the staggered grids using high-order centered finite differences of the electric and magnetic fields interpolated to the grid vertices and construct a high-order non-oscillatory divergence-free scheme for the full two-fluid plasma equations. A comparative study with other schemes is presented in this talk. We also discuss the time integration method.

[1] T. Minoshima, T. Miyoshi, Y. Matsumoto, submitted to Astrophys. J. Suppl.

Keywords: two-fluid plasma equations, high-order finite difference, weighted interpolation, divergence-free

©2019. Japan Geoscience Union. All Right Reserved. 

# Electromagnetic linear dispersion relation for plasma with a drift across magnetic field

*Takayuki Umeda[1], Takuma Nakamura[2]

1. Institute for Space-Earth Environmental Research, Nagoya University, 2. Space Research Institute, Austrian Academy of Sciences

A current across the magnetic field is formed in various situations in plasma. The relative drift between ions and electrons due to the cross-field current becomes a source of various microscopic instabilities. A fully electromagnetic and kinetic linear dispersion relation for plasma with a drift across magnetic field is derived by assuming a uniform background plasma. The dielectric permittivity tensor for shifted Maxwellian velocity distributions is also presented.

Keywords: plasma waves, linear theory, dispersion relation

©2019. Japan Geoscience Union. All Right Reserved. 

[J] Poster | P (Space and Planetary Sciences )：P-EM Solar-Terrestrial Sciences, Space Electromagnetism & Space Environment

Thu. May 30, 2019 5:15 PM - 6:30 PM JST | Thu. May 30, 2019 8:15 AM - 9:30 AM UTC | Poster Hall International Exhibition Hall8, Makuhari Messe_4

## [P-EM17] Space Plasma Physics: Theory and Simulation

convener:Takayuki Umeda(Institute for Space-Earth Environmental Research, Nagoya University), Takanobu Amano(Department of Earth and Planetary Science, University of Tokyo), Yasuhiro Nariyuki(Faculty of Human Development, University of Toyama), Tadas Nakamura(Fukui Prefectural University)

This session focuses on studies of space plasma physics via theoretical and numerical approaches. Papers on a wide variety of topics from natural phenomena to artificial plasma environment as well as theoretical and computational methodologies are welcome.

[PEM17-P01] PIC Simulation on nonlinear development of lower-hybrid instabilities driven by energetic ions.

*Tsubasa Kotani[1], Mieko Toida[2], Toseo Moritaka[2], Satoshi Taguchi[1] (1.Graduate School of Science, Kyoto University, 2.National Insititute for Fusion Science)

[PEM17-P02] **Study of Kinetic Alfven waves in space plasmas with electron having Kappa distribution**

*SATYAVIR SINGH[1], Krushna Chandra Barik[1], Yoshiharu Omura[2], Gurbax Singh Lakhina[1] (1.Indian Institute of Geomagnetism, New Panvel, India, 2.Research Institute for Sustainable Humanosphere, Kyoto University, Kyoto, Japan)

[PEM17-P03] A high-order divergence-free weighted finite difference scheme for the two-fluid plasma equations

*Takahiro Miyoshi[1], Takashi Minoshima[2], Yosuke Matsumoto[3] (1.Graduate School of Science, Hiroshima University, 2.Department of Mathematical Science and Advanced Technology, Japan Agency for Marine-Earth Science and Technology, 3.Graduate School of Science, Chiba University)

[PEM17-P04] Electromagnetic linear dispersion relation for plasma with a drift across magnetic field

*Takayuki Umeda[1], Takuma Nakamura[2] (1.Institute for Space-Earth Environmental Research, Nagoya University, 2.Space Research Institute, Austrian Academy of Sciences)

# PIC Simulation on nonlinear development of lower-hybrid instabilities driven by energetic ions.

*Tsubasa Kotani[1], Mieko Toida[2], Toseo Moritaka[2], Satoshi Taguchi[1]

1. Graduate School of Science, Kyoto University, 2. National Insititute for Fusion Science

Instabilities driven by energetic ions are important issues both for space plasmas and magnetic fusion plasmas. Radio Frequency (RF) waves in the range from the ion cyclotron frequency to the lower hybrid resonance frequency are often observed during the period of neutral beam injection (NBI) in Large Helical Device (LHD) plasmas. The experimental results showed that the peak frequency in the Lower Hybrid Wave (LHW) region has a positive correlation with the electron density and the ion cyclotron emissions (ICEs) have much larger amplitudes than LHW. These waves can be excited by instabilities due to energetic ions generated by the NBI perpendicular to the magnetic field.

Using a one-dimensional, electromagnetic, Particle-In-Cell (PIC) code, we study instabilities driven by energetic ions assuming that the energetic ions have a non-Maxwellian ring-like distribution in the velocity space perpendicular to the magnetic field. This PIC code enables us to self-consistently simulate full dynamics of electrons and ions and evolution of electromagnetic fields, using the full Maxwell's equations and the equations of motion of particles. We focus on the nonlinear evolution of LHW and ICEs caused by continuous energetic-ion injection into a plasma.

The simulation results are as follows. After the rapid growth of the LHW in the early stage, the ICEs gradually become intense. Finally, the ICEs have larger amplitudes than LHW.

Keywords: lower-hybrid instabilities, ion-cyclotron emissions, non-linear development, Particle-In-Cell simulation

©2019. Japan Geoscience Union. All Right Reserved. 

# Study of Kinetic Alfven waves in space plasmas with electron having Kappa distribution

*SATYAVIR SINGH[1], Krushna Chandra Barik[1], Yoshiharu Omura[2], Gurbax Singh Lakhina[1]

1. Indian Institute of Geomagnetism, New Panvel, India, 2. Research Institute for Sustainable Humanosphere, Kyoto University, Kyoto, Japan

A theoretical model is developed by assuming a three component plasma comprising of the cold background ions, hot electrons having kappa distribution and hot ion beams to study the generation of kinetic Alfvén waves (KAWs).The background ions and beam ions are considered Maxwellian and the ion beam is only allowed to have velocity shear and non-uniform streaming. A dispersion relation for the excitation of the kinetic Alfven waves (KAWs) is analyzed. The effect of plasma parameters like number density, propagation angle, temperature, kappa etc. on the excitation of KAWs is examined. A comparative study of the results obtained from this model will be carried out with a plasma model having all the three species as Maxwellian. Further, an application of the theoretical model will be discussed relevant in the Earth’ s magnetosphere.

Keywords: Earth, Magnetosphere, kinetic Alfven waves

©2019. Japan Geoscience Union. All Right Reserved. 

# A high-order divergence-free weighted finite difference scheme for the two-fluid plasma equations

*Takahiro Miyoshi[1], Takashi Minoshima[2], Yosuke Matsumoto[3]

1. Graduate School of Science, Hiroshima University, 2. Department of Mathematical Science and Advanced Technology, Japan Agency for Marine-Earth Science and Technology, 3. Graduate School of Science, Chiba University

Recent development of numerical techniques for magnetohydrodynamics (MHD) enables us to simultaneously simulate fine structures created by shock-vortex interactions and a large-scale MHD structure. On the other hand, the scales of the fine structures can become so small that the MHD approximation breaks down. Thus, a new macroscopic plasma simulation model beyond MHD is strongly required. In particular, the full two-fluid plasma model including local charge separation is considered in this study. According to the growth of computing power, the full two-fluid plasma simulation model will be scope of a standard model in the near future.

Since the full two-fluid plasma equations are hyperbolic conservation laws with stiff source terms, i.e., hyperbolic balance laws, state-of-the-art numerical techniques for the neutral fluid and MHD models can be applied. Recently, Minoshima et al. [1] developed high-order, non-oscillatory, and divergence-free finite difference schemes for MHD. In their schemes, the magnetic fields are defined on staggered grids, and the induction equation is discretized using high-order centered finite differences of the electric fields that correspond to numerical fluxes for the induction equation weightedly interpolated to the vertices of the grids. We apply this approach such that the Maxwell equations are discretized on the staggered grids using high-order centered finite differences of the electric and magnetic fields interpolated to the grid vertices and construct a high-order non-oscillatory divergence-free scheme for the full two-fluid plasma equations. A comparative study with other schemes is presented in this talk. We also discuss the time integration method.

[1] T. Minoshima, T. Miyoshi, Y. Matsumoto, submitted to Astrophys. J. Suppl.

Keywords: two-fluid plasma equations, high-order finite difference, weighted interpolation, divergence-free

©2019. Japan Geoscience Union. All Right Reserved. 

# Electromagnetic linear dispersion relation for plasma with a drift across magnetic field

*Takayuki Umeda[1], Takuma Nakamura[2]

1. Institute for Space-Earth Environmental Research, Nagoya University, 2. Space Research Institute, Austrian Academy of Sciences

A current across the magnetic field is formed in various situations in plasma. The relative drift between ions and electrons due to the cross-field current becomes a source of various microscopic instabilities. A fully electromagnetic and kinetic linear dispersion relation for plasma with a drift across magnetic field is derived by assuming a uniform background plasma. The dielectric permittivity tensor for shifted Maxwellian velocity distributions is also presented.

Keywords: plasma waves, linear theory, dispersion relation

©2019. Japan Geoscience Union. All Right Reserved. 

[J] Oral | P (Space and Planetary Sciences )：P-EM Solar-Terrestrial Sciences, Space Electromagnetism & Space Environment

Thu. May 30, 2019 1:45 PM - 3:15 PM JST | Thu. May 30, 2019 4:45 AM - 6:15 AM UTC | A03 TOKYO BAY MAKUHARI HALL

## [P-EM17] Space Plasma Physics: Theory and Simulation

convener:Takayuki Umeda(Institute for Space-Earth Environmental Research, Nagoya University), Takanobu Amano(Department of Earth and Planetary Science, University of Tokyo), Yasuhiro Nariyuki(Faculty of Human Development, University of Toyama), Tadas Nakamura(Fukui Prefectural University), Chairperson:Takayuki Umeda(Institute for Space-Earth Environmental Research, Nagoya University), Takanobu Amano(Department of Earth and Planetary Science, University of Tokyo)

This session focuses on studies of space plasma physics via theoretical and numerical approaches. Papers on a wide variety of topics from natural phenomena to artificial plasma environment as well as theoretical and computational methodologies are welcome.

1:45 PM - 2:00 PM JST | 4:45 AM - 5:00 AM UTC

[PEM17-01] Prediction of the high-resolution numerical flux by using a deep neural network

*Yosuke Matsumoto[1] (1.Graduate School of Science, Chiba University)

2:00 PM - 2:15 PM JST | 5:00 AM - 5:15 AM UTC

[PEM17-02] Multiple Boris integrators for particle-in-cell simulation

*Seiji Zenitani[1], Tsunehiko N Kato[2] (1.Kyoto University, 2.National Astronomical Observatory of Japan)

2:15 PM - 2:30 PM JST | 5:15 AM - 5:30 AM UTC

[PEM17-03] Contour Dynamics for Vlasov–Poisson Plasma with the Periodic Boundary

*Hiroki Sato[1], Tomo-Hiko Watanabe[1], Shinya Maeyama[1] (1.Nagoya University)

2:30 PM - 2:45 PM JST | 5:30 AM - 5:45 AM UTC

[PEM17-04] Simulation methods and visualization tools for MHD simulations in a sphere

*Akira Kageyama[1], Kumiko Hori[1], Naohisa Sakamoto[1] (1.Graduate School of System Informatics, Kobe University)

2:45 PM - 3:00 PM JST | 5:45 AM - 6:00 AM UTC

[PEM17-05] Kármán Vortex Street, Strouhal Number, Hairpin Vortex in 3D global Magnetohydrodynamic MHD simulations in Northward IMF

*DongSheng CAI[1] (1.University of Tsukuba)

3:00 PM - 3:15 PM JST | 6:00 AM - 6:15 AM UTC

[PEM17-06] Correlations between plasma density and magnetic field strength in MHD turbulence in space

*Tohru Hada[1], Yasuhito Narita[2], Yasuhiro Nariyuki[3] (1.Interdisciplinary Graduate School of Engineering Sciences, Kyushu University, 2.Space Research Institute, Austrian Academy of Sciences, 3.Faculty of Human Development, University of Toyama)

# Prediction of the high-resolution numerical flux by using a deep neural network

*Yosuke Matsumoto[1]

1. Graduate School of Science, Chiba University

Magnetohydrodynamic simulations have played important roles for understanding space and astrophysical phenomena. In such circumstances, shock waves and turbulence are inherent properties, and both aspects equally affect evolution of the whole system. Therefore development of numerical algorithms capable of solving both shock waves (discontinuities) and turbulence (waves) with high resolution is a challenging task to tackle violent phenomena in space and astrophysical plasmas.

High-order (greater than the fifth) spatial interpolation coupled with approximate Riemann solvers is a promising solution to such problems (Matsumoto et al., 2016; Minoshima, Miyoshi, Matsumoto, 2019). CANS+ (Matsumoto et al., 2016) employs the fifth order MP5 reconstruction scheme coupled with the HLLD approximate Riemann solver (Miyoshi and Kusano, 2005), and it successfully provided highly resolved solutions for both shock waves and turbulence. A drawback of adopting high-order schemes is its large and complex floating-point operations for obtaining the numerical flux at the cell surface, including minmod (with four arguments) limiters and conversion from the primitive to the characteristic variables. These numerical operations in addition to calculation of the HLLD numerical flux dominated overall computational loads.

In this paper, we propose a different way of calculating the numerical flux by adopting supervised learning algorithms. A deep (multilayer) neural network consists of input and output layers, whose sizes are determined by the problem of interest, and arbitrary numbers and sizes of hidden layers. These layers are connected by linear operations followed by a mapping through nonlinear functions such as a sigmoid function (fully connected networks). Weighting parameters used in the linear operations in each layer are updated repeatedly so that the loss function between the output and the label data (true value) becomes a minimum value. In the present particular problem, we prepared learning data by examining a 1-D shock tube problem which contains rarefaction waves and discontinuities by using CANS+. The input and label data are cell states for all primitive variables in six-point stencils centered on a cell and the numerical flux on the right-hand side of the cell, respectively. We have implemented a multi-layer, fully-connected network by using the Chainer framework for the prepared learning data. With the given data set we successfully obtained a network that can predict the numerical flux with 99% accuracy. In this talk we present detailed algorithms and learning data, and discuss future perspectives including application to multidimensional simulations.

Keywords: neural network, MHD simulations

©2019. Japan Geoscience Union. All Right Reserved. 

# Multiple Boris integrators for particle-in-cell simulation

*Seiji Zenitani[1], Tsunehiko N Kato[2]

1. Kyoto University, 2. National Astronomical Observatory of Japan

We construct Boris-type schemes for integrating the gyration of charged particles in particle-in-cell (PIC) simulation. The new solvers virtually combine the classic 2-step Boris solver arbitrary $n$ times, and then they provide $n^2$ times smaller errors. We derive a single-step form of the multiple Boris solvers, whose coefficients are given by polynomials. We carry out numerical tests of the new solvers, in comparison with other particle integrators.

Keywords: Particle-in-Cell (PIC) simulation, Numerical scheme, Boris integrator

©2019. Japan Geoscience Union. All Right Reserved. 

# Contour Dynamics for Vlasov–Poisson Plasma with the Periodic Boundary

*Hiroki Sato[1], Tomo-Hiko Watanabe[1], Shinya Maeyama[1]

1. Nagoya University

Zabusky, Hughes, and Roberts presented a contour dynamics algorithm for the Euler equations of fluid dynamics in two dimensions [1].On the paper, they succeed in calculating time development of contours of vorticity on the x-y plane with the contour dynamics(CD) algorithm, which is a method by using contours of vorticity, piece-wise constant function, and line integrals of Green’ s function on the contours. The CD method does not use underlying lattice, but uses nodes on the contours, and it can lead to more accurate calculation for complex deformation of vorticity.

This method is also applied to Vlasov–Poisson system. In order to study the CD in the Vlasov–Poisson plasma, we have developed a method to implement the periodic of potential and its derivative are satisfied.To check validity of out method, we test the Linear Landau damping by means of the CD scheme.While discretization of the distribution function might lead to some difference from that with continuous distribution, soundness of our new scheme is confirmed in comparison with analytical solutions.

We are also investigating in behaviors of the CD in the continuous limit, and in the nonlinear Landau damping as well.

Reference 1. Contour dynamics for the Euler equations in two Dimensions (1978)

©2019. Japan Geoscience Union. All Right Reserved. 

# Simulation methods and visualization tools for MHD simulations in a sphere

*Akira Kageyama[1], Kumiko Hori[1], Naohisa Sakamoto[1]

1. Graduate School of System Informatics, Kobe University

In recent years, we have been developing a set of simulation and visualization tools for magnetohydrodynamics (MHD) simulations in the spherical geometry. The adopted numerical scheme is a finite-difference method on the Yin-Yang-Zhong grid [1], which is an overset grid system in the spherical geometry.

The codes are written in Fortran 2003 or in eFortran [2], which is a dialect of Fortran 2008 language. The features of eFortran include; the period "." as the member access operator; block comments, addition/subtraction/multiplication assignment, pre-defined and user-defined aliases, automatic check of "implicit none" call, "just once" block, and "skip" block. We have developed a preprocessor to convert the dialect into the legitimate Fortran. It is a simple text converter in Python that keeps the line numbers of the input dialect and the output standard codes.

We have performed MHD simulations of relaxation process in a sphere [5]. Since the spherical geometry is free from the lateral dynamic pressure on the spherical boundary, we can observe MHD relaxation process in which flow and the magnetic field coexist. Intriguing structures of magnetic/flow fields are observed after relaxations.

One of interesting applications of the spherical MHD solver is the spherical shell convection with resistive inner core. Magnetic field generated by dynamo process in the convective spherical layer can diffuse into the inner solid core. We have solved slowly rotating spherical thin shell convection system and confirmed that the resistive inner core plays important roles to keep the dynamo operating in convection rolls in the ring- or spiral-shape.

We have also applied the Yin-Yang-Zhong simulation code to simulate MHD flows in a precessing sphere. We have confirmed that magnetic field is generated in spherical precession flows in some parameter regimes that are reported in previous studies. The structure and the generation mechanism of the magnetic field is analyzed in detail.

For the visualization purposes, we have developed two kinds of visualization tools for simulation data produced on the Yin-Yang or Yin-Yang-Zhong grid : (a) Two dimensional (cross sectional) in-situ visualization library with vector graphics format (EPS) [3], and (b) three dimensional visualization methods based on an advanced visualization framework KVS (Kyoto Visualization System) [4].

References

[1] Hiroshi Hayashi and Akira Kageyama. Yin-Yang-Zhong grid: An overset grid system for a sphere. Journal of Computational Physics, 305:895– 905, 2016.
[2] Shin' Ya Hosoyamada and Akira Kageyama. A Dialect of Modern Fortran for Computer Simulations. Proceedings of AsiaSim 2018, CCIS 946, 90:439–448, 2018.
[3] Akira Kageyama. Magnetohydrodynamics Simulation in a Sphere by Yin-Yang-Zhong Grid. Proceedings of the 6th International Conference on Simulation and Modeling Methodologies, Technologies and

©2019. Japan Geoscience Union. All Right Reserved. 

Applications, (Simultech):239–243, 2016.
[4] Naohisa Sakamoto and Koji Koyamada. KVS: A simple and effective framework for scientific visualization. J. Adv. Simulation. Sci. Eng., 2(1):76–95, 2015.
[5] Kohei Yamamoto and Akira Kageyama. MHD relaxation with flow in a sphere. Procedia Computer Science, 80(2):1374–1381, 2016.

Keywords: magnetohydrodynamics, sphere, MHD simulation, visualization

©2019. Japan Geoscience Union. All Right Reserved. 

# Kármán Vortex Street, Strouhal Number, Hairpin Vortex in 3D global Magnetohydrodynamic MHD simulations in Northward IMF

*DongSheng CAI[1]

1. University of Tsukuba

A Kármán vortex street is a repeating pattern of two rows of paired swirling vortices and appears after some obstacles or stagnation areas in fluid or plasma flows. It is caused by a process known as a vortex shedding where vortices leave the shear layer. Recently, several studies have discussed the Kelvin-Helmholtz (K-H) instability and its related waves and vortex structures by using 2D / 3D global (Magneto Hydro Dynamics) MHD simulations in the northward IMF (Interplanetary Magnetic Field). These found a double-vortex sheet in which a vortex train propagates, respectively, along the inner and outer edges of the magnetopause. In the present paper, we show that these two rows of vortices form the Kármán vortex street, and we discuss its generation mechanism with the help of 3D global MHD simulations. These Kármán vortex stretches and elongates in the night side and becomes to be the so-called the Hairpin vortex that is essential for the coherent structure. We also identify the non-dimensional number vortex so-called the Strouhal number in our simulation. The Stouhal number is ubiquitous and represents one of the most significant features in the Kármán vortex street.

Keywords: Kármán vortex street, Strouhal Number, Hairpin Vortex

©2019. Japan Geoscience Union. All Right Reserved. 

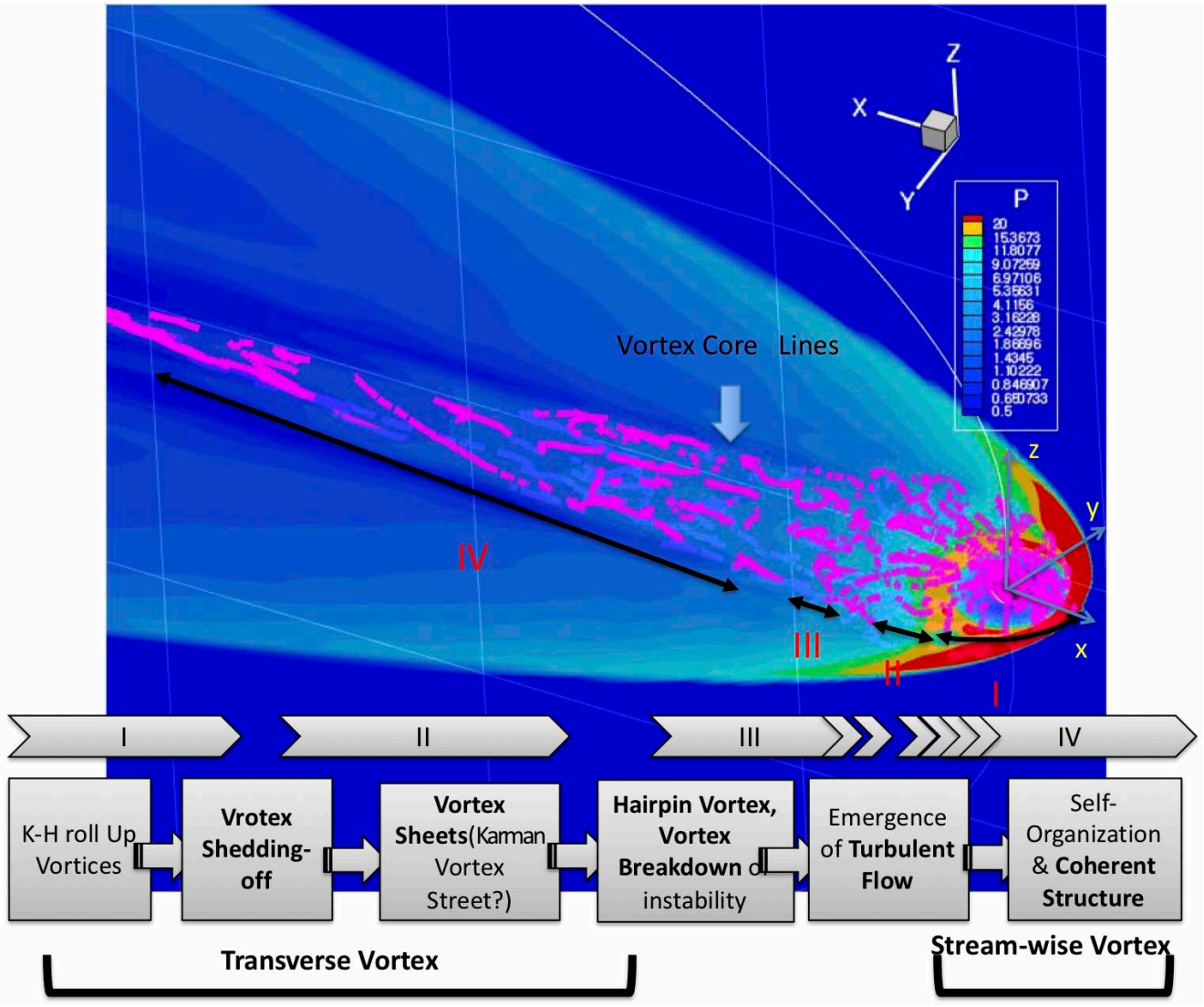


©2019. Japan Geoscience Union. All Right Reserved. 

# Correlations between plasma density and magnetic field strength in MHD turbulence in space

*Tohru Hada[1], Yasuhito Narita[2], Yasuhiro Nariyuki[3]

1. Interdisciplinary Graduate School of Engineering Sciences, Kyushu University, 2. Space Research Institute, Austrian Academy of Sciences, 3. Faculty of Human Development, University of Toyama

Large amplitude magnetohydrodynamic (MHD) turbulence is ubiquitous in space plasma, for example, in the solar wind, in the foreshock region (Narita, World Scientific, 2010) and in the sheath region of the earth's bowshock (e.g., Pollock et al., J. Atmosph. Solar Terr. Phys, 2018). Moreover, recent Voyager observations of large amplitude density and magnetic field fluctuations in the heliosheath behind the termination shock arouse a vivid discussion on the compressible nature and the origin of the observed turbulence (Burlaga and Ness, ApJ, 2009; Gutynska et al., ApJ, 2010). An obvious way of generating the density fluctuations is via the presence of compressive wave modes, such as obliquely propagating MHD waves. The density response is linear to the magnetic field perturbations in this case, and it vanishes in the limit of parallel wave propagation. In a finite (large) amplitude Alfvenic turbulence the density perturbation may be mainly generated via the "frozen-in" of the magnetic field to the plasma or the static balance between the plasma pressure and the magnetic field. Both of these processes result in the quadratic response of the density to the magnetic field perturbations, although their correlation is positive for the former and negative for the latter. This simple fluid picture, sometimes referred to as the "quasi-static" approximation, is known to be significantly modified when the ion response to the turbulence is kinetically treated (Mjolhus and Wyller, Phys. Scripta, 1986; Medvedev and Diamond, Phys. Plasmas, 1996). In this presentation, we address this unsolved issue of the correlations between the plasma density and the magnetic field amplitude in the presence of finite amplitude MHD turbulence by performing hybrid simulations (kinetic ions + fluid electrons), and by examining the in situ Cluster spacecraft data of the foreshock plasma (Narita and Hada, Earth, Planets and Space, 2018).

Keywords: MHD turbulence, quasi-static approximation

©2019. Japan Geoscience Union. All Right Reserved. 

[J] Oral | P (Space and Planetary Sciences )：P-EM Solar-Terrestrial Sciences, Space Electromagnetism & Space Environment

Thu. May 30, 2019 3:30 PM - 5:00 PM JST | Thu. May 30, 2019 6:30 AM - 8:00 AM UTC | A03 TOKYO BAY MAKUHARI HALL

## [P-EM17] Space Plasma Physics: Theory and Simulation

convener:Takayuki Umeda(Institute for Space-Earth Environmental Research, Nagoya University), Takanobu Amano(Department of Earth and Planetary Science, University of Tokyo), Yasuhiro Nariyuki(Faculty of Human Development, University of Toyama), Tadas Nakamura(Fukui Prefectural University), Chairperson:Tadas Nakamura(Fukui Prefectural University), Yasuhiro Nariyuki

This session focuses on studies of space plasma physics via theoretical and numerical approaches. Papers on a wide variety of topics from natural phenomena to artificial plasma environment as well as theoretical and computational methodologies are welcome.

3:30 PM - 3:45 PM JST | 6:30 AM - 6:45 AM UTC

[PEM17-07] Stochastic models of phase space diffusion via wave-particle interaction with parallel propagating electromagnetic waves

*Yasuhiro Nariyuki[1] (1.Faculty of Human Development, University of Toyama)

3:45 PM - 4:00 PM JST | 6:45 AM - 7:00 AM UTC

[PEM17-08] Electron beam instability in collisionless magnetic reconnection with a strong guide field

*Kazuya Shimomura[1], Tomo-Hiko Watanabe[1], Shinya Maeyama[1], Akihiro Ishizawa[2] (1.Nagoya Univertsity, 2.Kyoto University)

4:00 PM - 4:15 PM JST | 7:00 AM - 7:15 AM UTC

[PEM17-09] Particle acceleration with precursor wave driven wakefield in relativistic shocks

*Masanori Iwamoto[1], Takanobu Amano[1], Masahiro Hoshino[1], Yosuke Matsumoto[2] (1.Graduate School of Science,The University of Tokyo, 2.Graduate School of Science, Chiba University)

4:15 PM - 4:30 PM JST | 7:15 AM - 7:30 AM UTC

[PEM17-10] Stochastic Shock Drift Acceleration in the Shock Transition Region with Finite Pitch-Angle Anisotropy

*Takuma Katou[1], Takanobu Amano[1] (1.The University of Tokyo)

4:30 PM - 4:45 PM JST | 7:30 AM - 7:45 AM UTC

[PEM17-11] Near-fields and its Applications in Space Plasmas

*Tadas Nakamura[1] (1.Fukui Prefectural University)

4:45 PM - 5:00 PM JST | 7:45 AM - 8:00 AM UTC

[PEM17-12] Problems of Gravitational Waves and Origin of Gravitational Fields Raised by Studies on Binary Black Hole

*Hiroshi Oya[1] (1.Department of Geophysics Graduate School for Science Tohoku University)

# Stochastic models of phase space diffusion via wave-particle interaction with parallel propagating electromagnetic waves

*Yasuhiro Nariyuki[1]

1. Faculty of Human Development, University of Toyama

Particle diffusion due to electromagnetic waves is one of fundamental processes in various phenome in space plasms such as electron acceleration in the outer radiation belt [e.g., Saito et al, JGR, 2016], astrophysical shock [e.g., Yamazaki, JHEA, 2015], and solar wind [e.g., Seough et al, APJ, 2015]. Although quasi-linear theories are widely used as a standard theory of particle scattering, nonlinear wave-particle interactions such as particle trapping also affect particle diffusions in the presence of finite amplitude waves. Saito et al [JGR, 2016] demonstrated that nonlinearity of whistler chorus waves plays a significant role in electron diffusion though nonlinear wave-particle interactions.

In Saito et al [JGR, 2016], the artificial randomization of gyrophases (phase breaking) is incorporated to discuss suppression of coherent wave-particle interactions. Remark that such a randomization corresponds to a noise term in equations of motion of each particles. In this sense, phase breaking causes not only the suppression of coherent processes but also diffusions in phase space. In the present study, we discuss the generalization of phase breaking. It is shown that particle diffusion depends on probability density functions of noises and their parameters. Noise terms in equations of the pitch angle are also necessary to describe diffusion in phase space. Treatment of phase breaking as a stochastic differential equation is also discussed.

Keywords: particle diffusion, wave-particle interactions, stochastic model, whistler waves, magnetohydrodynamic waves

©2019. Japan Geoscience Union. All Right Reserved. 

# Electron beam instability in collisionless magnetic reconnection with a strong guide field

*Kazuya Shimomura[1], Tomo-Hiko Watanabe[1], Shinya Maeyama[1], Akihiro Ishizawa[2]

1. Nagoya Univertsity, 2. Kyoto University

Magnetic reconnection is a fundamental physics mechanism in magnetized plasma that causes a topological change of magnetic field lines and a conversion of magnetic energy to kinetic energy, leading to a self-organization of plasmas in laboratory and space. It is considered that the two-fluid effects or the kinetic effects facilitate the fast reconnection of magnetic field lines in colllisionless plasmas. Anomalous resistivity (AR) is one of the candidates that contributes to continuously drive the magnetic reconnection. A recent simulation study reports that AR induced by the Buneman instability accelerates the magnetic reconnection [1]. However, it is not clear how the instability causing the AR is spontaneously driven during the reconnection.
In our study so far, we have carried out numerical simulations of the collisionless magnetic reconnection by means of the gyrokinetic model of a slab plasma with a strong guide field [2][3]. During the reconnection, the parallel electric field is induced by the electron inertia at the X-point where electrons are acccelerated along the guide field. A liner analysis by use of the dispersion releation shows that the kinetic Alfvén waves (KAWs) are destabilized when the electron beam velocity exceeds the Alfvén speed, where, we assumed a plane wave in an uniform background profile. Furthermore, in this $\delta f$ gyrokinetic model, the total distribution function F is approximately described as $F=FM+\delta f=(1+Uv)FM\tilde{}1/2pi\ exp(-(v-U)^2/2)$, where $FM$, $\delta f$ and $U$ are the Maxwellian, perturbed distribution function, and a beam velocity component, respectively. In order to analyze a stability of the KAWs in an inhomogeneous background profile during the collisionless magnetic reconnection, we must use the total distribution function rather than $\delta f$, since the KAWs are stable for $(1+Uv)FM$, according to the Nyquist criteria. Therefore, in this study, the magnetic reconnection process triggered by the electron inertia is simulated by use of a full-f gyrokinetic model of a slab plasma with the guide field. As a result, the shifted Maxwellian is formed at the X-point self-consistently by the parallel electric field. The attached figure shows distribution of the parallel electron beam on the reconnection plane in the nonlinear phase during the reconnection. It is possible to carry out the stability analysis in an inhomogeneous background by use of this simulation results. Results of the stability analysis will also be discussed at the meeting.

[1] H. Che, Phys. Plasmas (2017) 24, 082115
[2] A. Ishizawa, T.-H. Watanabe, Phys. Plasmas (2013) 20, 102116
[3] K. Shimomura, T.-H. Watanabe, et al, submitted to Phys. Plasmas (2019)

Keywords: magnetic reconnection, distribution function, instability, kinetic Alfven wave, gyrokinetic

©2019. Japan Geoscience Union. All Right Reserved. 

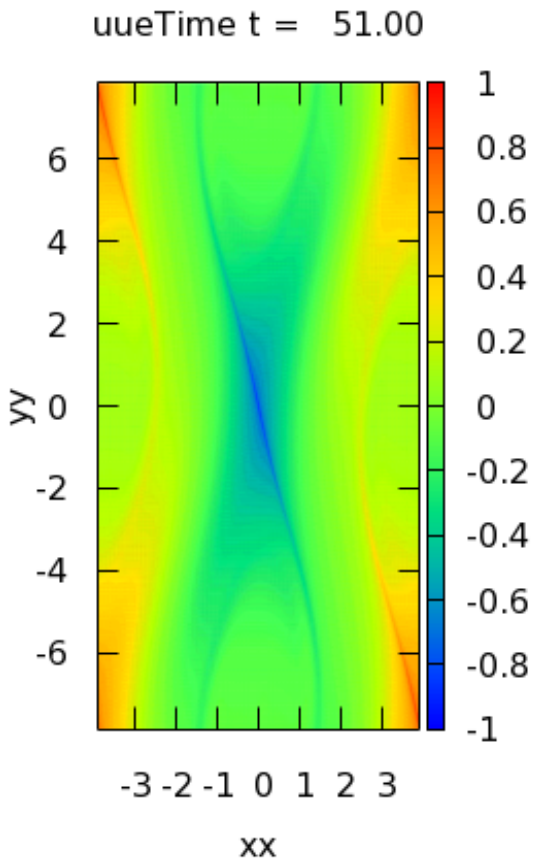


©2019. Japan Geoscience Union. All Right Reserved. 

# Particle acceleration with precursor wave driven wakefield in relativistic shocks

*Masanori Iwamoto[1], Takanobu Amano[1], Masahiro Hoshino[1], Yosuke Matsumoto[2]

1. Graduate School of Science,The University of Tokyo, 2. Graduate School of Science, Chiba University

The acceleration mechanism for generating ultra-high-energy cosmic rays (UHECRs) with energies above $10^{18}$eV is one of the most important unsolved problems in astrophysics. Relativistic shocks in extragalactic astrophysical objects such as jets from active galactic nuclei (AGNs) and gamma-ray bursts (GRBs) are considered as efficient acceleration sites and commonly proposed sources for UHECRs. Observations of anisotropy in the arrival direction of the UHECRs favor the extragalactic origin.

In relativistic shocks, large-amplitude electromagnetic waves are excited by synchrotron maser instability (SMI) in the shock transition and propagate upstream (Hoshino & Arons 1991). The precursor wave emission via the SMI is widely studied by means of 1D particle-in-cell (PIC) simulations. Hoshino (2008) demonstrated that the pump electromagnetic wave decays into a Langmuir wave via parametric decay instability and found that nonthermal particles are generated in the manner analogous to wakefield acceleration (WFA) during the nonlinear process of the Langmuir wave collapse. The WFA is first proposed in laboratory plasmas (Tajima & Dawson 1979) and recently applied for UHECR acceleration (e.g., Chen et al. 2002). The WFA in the context of relativistic shocks is considered a promising candidate for UHECR acceleration.

It was believed that in multidimensional shocks, the intense wave emission via the SMI would cease soon due to inhomogeneity along the shock surface. Recently, however, our high-resolution 2D PIC simulations in pair plasmas showed that the wave emission continues (Iwamoto et al. 2017, 2018). Although our studies give positive results for the WFA in relativistic shocks, we could not directly demonstrate it because finite mass difference of two opposite charges is essential for exciting the wakefield.

In this presentation, by performing 2D PIC simulation of ion-electron shocks, we will demonstrate that the wakefield is indeed induced by the large-amplitude precursor wave. Especially for relatively high magnetization, the precursor wave amplitude is significantly amplified and exceeds that in pair plasmas due to a positive feedback process associated with ion-electron coupling through the wakefield. Nonthermal electrons and ions are generated during the nonlinear process of the wakefield collapse and the particle energy spectrum shows a power-law distribution. We will discuss the particle acceleration mechanism in details.

Keywords: cosmic rays, shock waves, acceleration of particles

©2019. Japan Geoscience Union. All Right Reserved. 

# Stochastic Shock Drift Acceleration in the Shock Transition Region with Finite Pitch-Angle Anisotropy

*Takuma Katou[1], Takanobu Amano[1]

1. The University of Tokyo

The acceleration of non-thermal electrons is one of the important subjects in space physics. The shock accelerated non-thermal electrons have been observed at Earth's bow shocks (Gostling et al. 1989). These electrons are supra-thermal (with energies from 1keV to 100keV), and their distribution is power-law. However, acceleration models proposed in the past could not reproduce such observed spectra. Recent in-situ satellite observations of Earth's bow shock found wave-particle interactions between whistler waves and electrons at the shock transition region (Oka et.al. 2017). These results indicate that whistler waves play an important role for the acceleration of supra-thermal electrons.

We propose the stochastic shock drift acceleration (SSDA) model as a new acceleration mechanism for non-thermal electrons. It takes into account the effect of stochastic pitch-angle scatterings by whistler waves during the course of the Shock Drift Accelerations (SDA), which is a classical acceleration model for supra-thermal electrons at the shock transition region (Wu 1984, Leroy and Mangeney 1984). By introducing stochasticity with pitch-angle scatterings, the acceleration efficiency may be improved. We theoretically analyzed this acceleration model. We showed that the electron energy spectrum becomes a power-law consistent with observations in the limit of strong scatterings. We also found the maximum energy attainable through the proposed model, and it scales linearly with the pitch-angle scattering coefficient which represents the strength of scatterings. In our previous study, we have assumed the electron pitch-angle distribution is isotropic, and an effective shock speed $u/\cos\theta$ (u: shock speed, $\theta$: shock normal angle) is non-relativistic. The SSDA model cannot consider an anisotropy of the electron pitch-angle distribution. It is well known that the shock with a relativistic effective shock speed has a finite pitch-angle anisotropy. Therefore it is difficult to compare the SSDA model with full particle-in-cell (PIC) simulations which can reproduce only the shock with a relativistic effective shock speed because of the limitation of parameters we can take. To fix this problem, we extend the SSDA model so that it can be applied to such a shock. In this presentation, we discuss the consistency between the extended SSDA model and PIC simulation results.

Keywords: acceleration of particle, Earth, shock waves

©2019. Japan Geoscience Union. All Right Reserved. 

# Near-fields and its Applications in Space Plasmas

*Tadas Nakamura[1]

1. Fukui Prefectural University

Solutions to Maxwell's equations consists of two parts: propagating components (electromagnetic waves) and the so-called near-field. Unfortunately, there seems to be considerable confusion on the latter, and the words "near-field" have different meanings depending on authors. For example, Coulomb interaction is often explained as the result of the interchange of virtual photons, however, the Coulomb field is not a photon but a near-field in the sense of this talk. Also, little attention is paid to the difference between propagating plasma waves and plasma near-fields in space physics.

The near-field in the present talk is understood as the off-shell solution to the inhomogeneous linear equations; the term "off-shell" means solutions that do not satisfy the dispersion relation. When the field source is static (Coulomb field or magnetic dipole, for example), it is easy to decompose the field into waves and off-shell near-fields. Here in this talk, the way to do this decomposition for time-dependent field source is explained. When we solve Maxwell's equations, usually we make use of Fourier-Laplace transform to obtain the dispersion relation. The time dependence of the fields is obtained by the inverse Laplace transform using the residue theorem; the wave components are obtained from the residue at the pole of the dispersion relation. One can obtain the near-field component by subtracting this residue contribution from the solution of the inhomogeneous equations.

The author reported the derivation of this result at the fall meeting of SGEPSS last year, and will report its application to space physics this time. The talk at the fall meeting was mainly about the electromagnetic fields in a vacuum; fields in plasmas will be discussed this time. The athematical structure of the fields in plasmas are essentially the same as that in a vaccum, however, currents and charges in plasmas cause a wide variety of phenomena in space. Phenomena such as current generation around small bodies in space plasma flows, the return currents genereted by energetic auroral electrons, and several others will be examined as examples.

Keywords: plasma waves, Laplace transform, near field

©2019. Japan Geoscience Union. All Right Reserved. 

# Problems of Gravitational Waves and Origin of Gravitational Fields Raised by Studies on Binary Black Hole

*Hiroshi Oya[1]

1. Department of Geophysics Graduate School for Science Tohoku University

1.INTRODUCTION
As results of a study on the observations and analyses of the decameter radio wave pulses from the center of our Galaxy, it has been concluded that the super massive objects at the center of our Galaxy consist of two black holes which are forming a binary system rotating with common period of 2200sec; two black holes called Gaa and Gab, here, are associated with spin with rotation periods of 176.4±1.7 sec and 148.6±1.0 sec with orbiting velocities 18% and 21% of the light velocity, respectively. The radius of the orbits of Gaa and Gab are 0.13 AU and 0.15 AU ; applying Newtonian dynamics with assumption of coincidence of the orbital plane surfaces with the observing direction, it has been concluded that Gaa and Gab have masses of (2.27±0.06)x10∧6 SM and 1.94±0.03)x10∧6 SM with unit of solar mass ( SM).
2.THE THEORETICAL INVESTIGATION OF THE GRAVITATIONAL WAVE PROPAGATION
Considering the all parameters deduced for the Gaa and Gab binary system, fast reduction of the radii of the orbits of the binary due to emissions of gravitational waves is inevitable in so far as we follow the traditional theory of the generation of the gravitational wave from the black hole. In the present studies, the propagation of wave general across the event horizon have been theoretically investigated using the spacetime of Minkowski which is realized in the frame that is making free fall in the black hole space time. The results has indicated, both for Shwarzschild and Kerr black holes, that the waves are ceased to propagate at the event horizon. Then we concluded that black hole is not able to be origin of the gravitational wave.
3.DISCUSSION AND CONCLUSION
For the LIGO results that reported observations of the gravitational wave from the stellar mass black hole mergers, an alternative interpretation of the possible origin of the merger is the merger of the compact stars which have no event horizon. By the result of our study, the existence of the graviton which is currently assumed as origin of gravitational force meets problem because the graviton is also a wave in the regime of the quantum mechanics. We suggest the necessity of new concept otherwise than graviton hypothesis for origin of the gravitational fields.

Keywords: Black Hole Binary, Galaxy Center, Decameter Radio Wave, gravitational Wave, Origin of Gravitational Field

©2019. Japan Geoscience Union. All Right Reserved. 

[E] Oral | A (Atmospheric and Hydrospheric Sciences )：A-AS Atmospheric Sciences, Meteorology & Atmospheric Environment

Thu. May 30, 2019 9:00 AM - 10:30 AM JST | Thu. May 30, 2019 12:00 AM - 1:30 AM UTC | 104 1F

## [A-AS02] Advances in Tropical Cyclone Research: Past, Present, and Future

convener:Sachie Kanada(Nagoya University), Akiyoshi Wada(Department of Typhoon and Severe Weather Research, Meteorological Research Institute), Kosuke Ito(University of the Ryukyus), Yoshiaki Miyamoto(Faculty of Environment and Information Studies, Keio University), Chairperson:Sachie Kanada(Nagoya University), Akiyoshi Wada(Meteorological Research Institute)

Tropical cyclones (TC) sometimes cause destructive disasters in many countries by torrential rainfall, strong wind, storm surge, and high surf. In 2008, the western Japan suffered a record-breaking heavy rainfall related to Typhoon Prapirooon (2018) in July. Furthermore, two Category 4 typhoons, typhoons Jebi (2018) and Trami (2018), made landfalls on the western Japan in September and caused devastating disasters over the Japanese Islands. In the Northern Atlantic, Hurricane Florence caused catastrophic damage in the eastern side of U.S. Recent studies reported a northward shift of the location where a TC achieved the peak intensity and also reported increases in the frequency of rapidly intensifying storms. Thus, understanding the TC processes related to translation, intensity change and precipitation in the changing climate, and to provide more accurate forecasts and long-term projections are essential for the earth and planetary science.<br/>Advances in innovative observations such as meteorological aircraft, weather satellite, supercomputer systems such as the Earth Simulator and K-computer, and introduction of new methods such as the deep-learning, have led to novel development of numerical weather forecasting and understanding of the phenomena related to TCs in the past, present and future climates. In this session, we welcome papers on various aspects of TC studies. We hope that the session will provide a new direction for future TC researches.

9:00 AM - 9:15 AM JST | 12:00 AM - 12:15 AM UTC

[AAS02-01] A GRAPES-based mesoscale EPS for TC forecasting: configuration and performance

*Xubin Zhang[1] (1.Institute of Tropical and Marine Meteorology, CMA)

9:15 AM - 9:30 AM JST | 12:15 AM - 12:30 AM UTC

[AAS02-02] **Evaluation of operational Ensemble based Global Forecast System prediction for Tropical Cyclones over the North Indian Ocean**

*Medha Deshpande[1], Radhika Kanase[1], R P M Krishna[1], Emmanuel Rongmie[1], P Mukhopadhyay[1] (1.IITM, Pune, INDIA)

9:30 AM - 9:45 AM JST | 12:30 AM - 12:45 AM UTC

[AAS02-03] Structural Changes Preceding Rapid Intensification in Tropical Cyclones as shown in a Large Ensemble of Idealized Simulations

*Yoshiaki Miyamoto[1], David S Nolan[2] (1.Faculty of Environment and Information Studies, Keio University, 2.Rosenstiel School of Marine and Atmospheric Science, University of Miami)

9:45 AM - 10:00 AM JST | 12:45 AM - 1:00 AM UTC

[AAS02-04] Potential impacts of tropical cyclone inner-core convective activity on the predictability of rapid intensification

*Masashi Minamide[1], Derek J. Posselt[1] (1.Jet Propulsion Laboratory, california institute of technology)

10:00 AM - 10:15 AM JST | 1:00 AM - 1:15 AM UTC

[AAS02-05] A link between high-speed solar wind streams and rapid intensification of tropical cyclones

*Paul Prikryl[1,2], Lidia Nikitina[2], Vojto Rušin[3] (1.Physics Department, University of New Brunswick, Fredericton, NB, Canada, 2.Geomagnetic Laboratory, Natural Resources Canada, Ottawa, ON, Canada, 3.Astronomical Institute, Slovak Academy of Sciences, Tatranská Lomnica, Slovak Republic)

10:15 AM - 10:30 AM JST | 1:15 AM - 1:30 AM UTC

## [AAS02-06] Influence of Tropical Lower Stratospheric Cooling on Extreme Deep Convective Activity and Tropical Cyclones

*Kunihiko Kodera[1], Nawo Eguchi[2], Rei Ueyama[3], Beatriz M Funatsu[4], Chantal Claud[5] (1.Meteorological Research Institute, 2.Kyushu University, 3.NASA Ames Research Center, 4.Université de Nantes, 5.Ecole Polytechnique)

# A GRAPES-based mesoscale EPS for TC forecasting: configuration and performance

*Xubin Zhang[1]

1. Institute of Tropical and Marine Meteorology, CMA

To improve short-range tropical cyclone (TC) forecasting in China from both deterministic and probabilistic standpoints, a mesoscale ensemble prediction system (TREPS) based on the Global/Regional Assimilation and Prediction System (GRAPES) is constructed as a planned operational system. TREPS comprises one unperturbed and 30 perturbed forecasts ranging up to 60 h at horizontal resolution of 9 km. Downscaling perturbations from the ECMWF ensemble prediction system (ENS) are used to generate initial perturbations by blending them with balanced random perturbations implemented around the TC and to generate perturbations for lateral boundary conditions. The surface temperature around the TC is also perturbed, with a combination of multi-physics and stochastically perturbed parametrization tendencies considered to represent uncertainties in the model physics. These perturbation methods contribute a full-area, multi-scale and multi-variable mutual complement to increasing forecast perturbations. TREPS is evaluated for 19 TCs making landfall in China during 2014–2016. For deterministic guidance, TREPS significantly improves TC forecasting for intensity, rainfall and wind compared to ECMWF deterministic and ensemble forecasts. TREPS demonstrates significant advantages over its deterministic forecasts in predicting track, intensity, (extremely) heavy rainfall and wind. Furthermore, TREPS effectively reduces the degree of underdispersion in intensity forecasting compared to ENS. For probabilistic forecasting, TREPS outperforms ENS in accurately predicting extremely heavy rainfall and (extremely) strong wind owing to its better discriminating ability, but performs worse in predicting modest wind, light and heavy rainfall. Two post-processing techniques –optimal member and optimal probability –to improve, respectively, deterministic and probabilistic guidance of TREPS in rainfall and wind forecasting are proposed. The former is shown to be effective only for light rainfall, while the latter demonstrates consistent (partial) improvements in rainfall (wind). The superiorities and inferiorities of TREPS, as well as possible reasons for these, are intuitively illustrated in a case-study for Rammasun.

Keywords: ensemble prediction system, mesoscale, tropical cyclone

©2019. Japan Geoscience Union. All Right Reserved. 

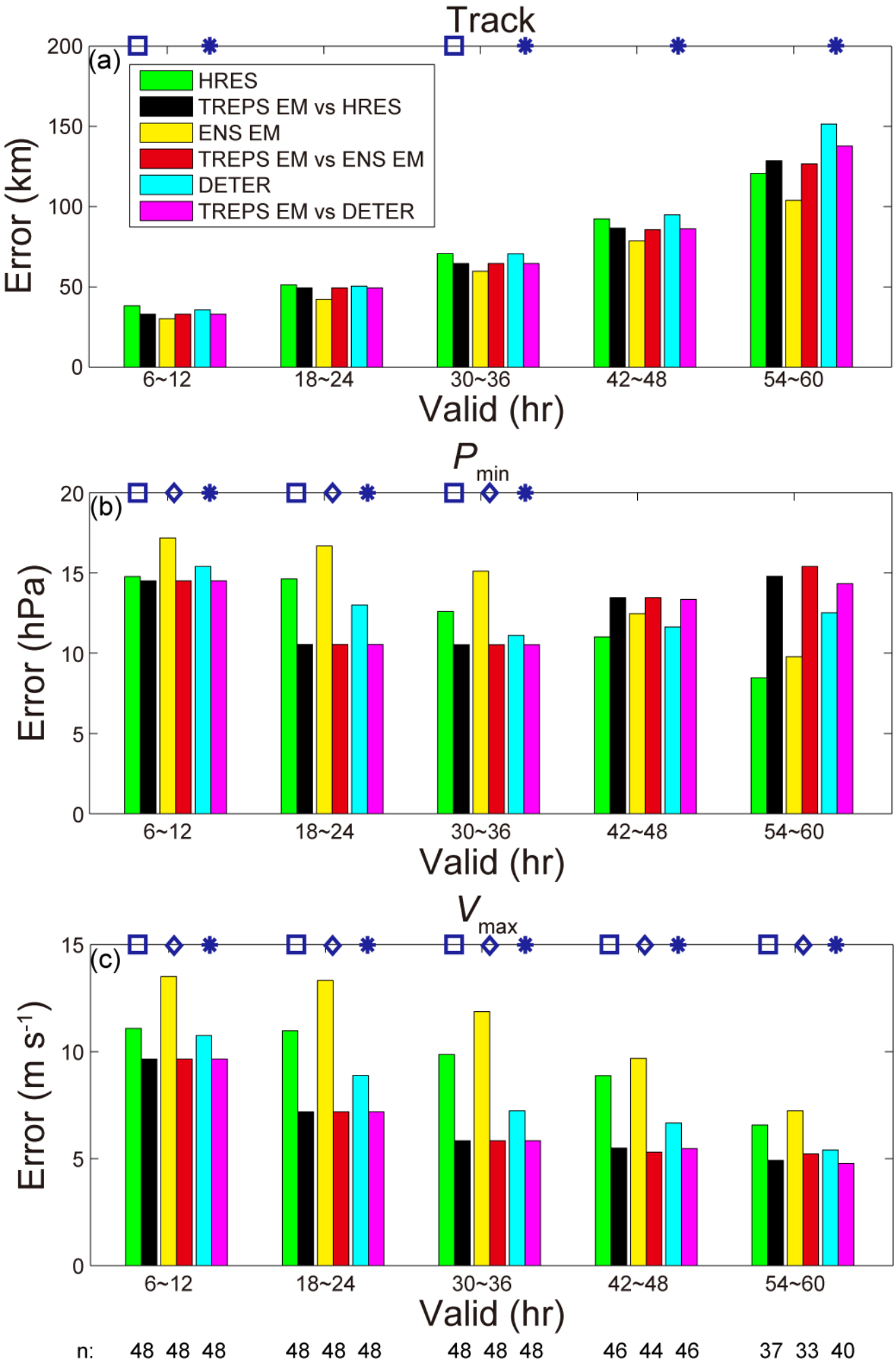


©2019. Japan Geoscience Union. All Right Reserved. 

©2019. Japan Geoscience Union. All Right Reserved. 

# Evaluation of operational Ensemble based Global Forecast System prediction for Tropical Cyclones over the North Indian Ocean

*Medha Deshpande[1], Radhika Kanase[1], R P M Krishna[1], Emmanuel Rongmie[1], P Mukhopadhyay[1]

1. IITM, Pune, INDIA

The importance of accurate prediction of Tropical Cyclone (TC) genesis, rapid intensity changes, location and intensity during landfall is well known. Reliable prediction of these at 3-5 days lead time is crucial for disaster managing point of view. Bearing in mind the uncertainty in initial condition and model physics there was a need for high resolution ensemble based forecast system for region specific probabilistic prediction of weather over India. Considering this along with the existing Global Forecast System deterministic model (GFS T1534), the ensemble forecast system GEFS (T 1534) with 20 members is implemented and is in operation since June 2018 for the probabilistic prediction.

This paper evaluates the skill of operational high resolution (12.5 km) modelling system in predicting track and intensity of recent cases of TCs over North Indian Ocean at various lead time. Ensemble prediction of tracks of cyclones and its strike probability are evaluated. Ensemble mean track is better than the deterministic track particularly at longer lead time (figure 1). The vertical thermo-dynamic structure at the mature stage of the cyclone is well captured by the deterministic model. Evaluation of deterministic model (figure 2) specify average track error is ranging from < 100 km at Day 1 lead up to about 280 km at day 5 lead time and average error in intensity prediction is ranging from 10 kt –20 kts. In general model indicates early intensification and slightly overestimates the peak intensity in majority of the cases. It is challenging to predict the variation in the intensity. Skill in the prediction of genesis is also evaluated by calculating Genesis Potential Index (GPI). Further developments like improving the physics and dynamics of the model along with use of proper land use land cover data are underway.

Keywords: Tropical Cyclones, North Indian Ocean, High Resolution ensemble Prediction System

©2019. Japan Geoscience Union. All Right Reserved. 

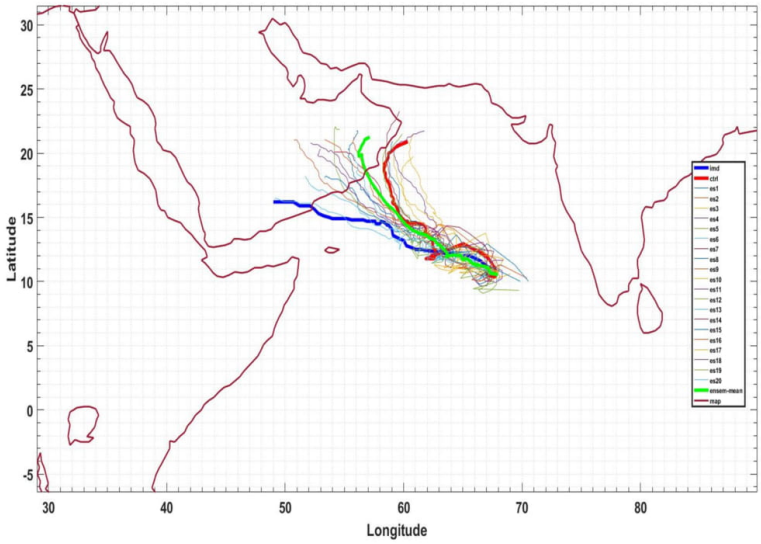


**Figure1: Ensemble prediction of tracks based on 6 Oct Initial Condition for the case of Luban (6-14 Oct 2018)**

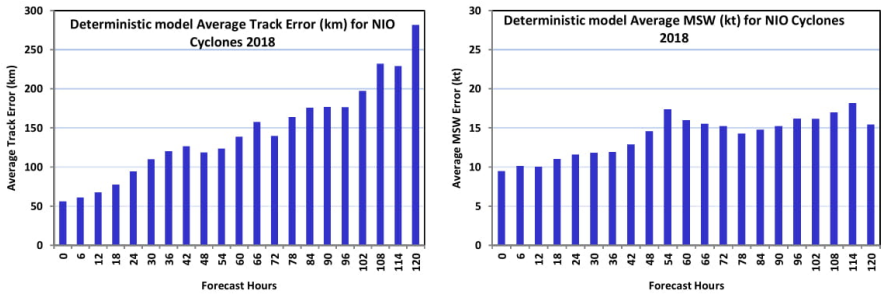


**Figure 2: Deterministic model (GFS (T1534) average Track and intensity error for NIO cyclones 2018**

©2019. Japan Geoscience Union. All Right Reserved. 

# Structural Changes Preceding Rapid Intensification in Tropical Cyclones as shown in a Large Ensemble of Idealized Simulations

*Yoshiaki Miyamoto[1], David S Nolan[2]

1. Faculty of Environment and Information Studies, Keio University, 2. Rosenstiel School of Marine and Atmospheric Science, University of Miami

Structural changes that precede rapid intensification (RI) of tropical cyclones (TCs) are examined in a full physics model by conducting a large ensemble (270) of simulations.

The processes leading to RI in a representative case with moderate shear are consistent with previous studies for weakly sheared cases. The most distinct changes are that the vortex tilt and the vortex size begin to decrease more rapidly 6 h before the onset of RI.

A vorticity budget analysis for the upper layer around the low--level center reveals that the vertical vorticity is increased by vertical advection, stretching, and tilting terms before RI, whereas the horizontal advection is small. Thus, the upright vortex structure is not achieved through a vortex alignment process, but rather is built upward by deep convection.

The ensemble simulations are generated by changing the intensity and size of the initial vortex, the magnitude of vertical wind shear, and the translation speed. The ensemble members that show RI are consistent with the control case and many previous studies:

before the onset of RI, the intensity gradually increases, the radius of maximum tangential velocity (RMW) decreases, the flow structure becomes more symmetric, the vortex tilt decreases, and the radius of maximum convergence approaches the radius of maximum winds.

A dimensionless parameter representing a tendency for the formation of the vertically upright structure is considered.

The product of this parameter and the local Rossby number is significantly larger for TCs that exhibit RI in the next 24 hours.

Keywords: Tropical Cyclone, Rapid Intensification

©2019. Japan Geoscience Union. All Right Reserved. 

# Potential impacts of tropical cyclone inner-core convective activity on the predictability of rapid intensification

*Masashi Minamide[1], Derek J. Posselt[1]

1. Jet Propulsion Laboratory, california institute of technology

Predictions of significant changes in tropical cyclone (TC) intensity, such as rapid intensification (RI), have emerged as a more challenging topic than forecasting TC tracks, since intensification of TCs involves multi-scale physical processes with significant contributions from convective-scale phenomena. Before the onset of RI, intensifying TCs are known to experience a precession process, in which tilted vortex rotates counter-clockwise to develop axisymmetric structure. From both modeling and observational studies, there is an agreement in the qualitative features of precession process among TCs, but the quantitative features, such as the vortex tilt magnitude, the duration of the precession process and whether or not the vortex is able to complete the precession process, vary among TCs. The predictability of the variety of precession process and subsequent RI is reported to be ultimately dominated by the chaotic nature of moist convection. Given the large influence of RI on the TC intensity forecasts, the further understandings in its uncertainty sources are necessary.

In this study, mechanisms that determine the variability of these precession processes are explored through sets of sensitivity and ensemble forecast experiments. We have used the Pennsylvania State University's experimental real-time ensemble Kalman filter analysis of Hurricane Harvey (2017) that assimilated GOES-16 all-sky satellite radiances (which has an equivalent monitoring capability to Himawari-8) in convection-permitting Weather Research and Forecasting model (WRF-ARW) simulations. This analysis resulted in a highly accurate forecast of intensity and track, and realistically represented the storm's rapid intensification. Starting with an analysis based on 18 hours of cycling data assimilation, we have conducted sensitivity experiments in which we reduced the initial atmospheric moisture amount by 5 to 20 %. Even initialized with the same wind field, and with fully developed convective updrafts and organization, the vortex tilt magnitude and the duration of precession are significantly modified by the inner-core moist processes. We explore the characteristics of the vortex structures that underwent short/long/uncompleted precession process, together with the theoretical background for these varieties of precession process by using a simplified toy-model. The results have implications for the design of future observation networks tasked with providing constraint on predictions of convections and rapidly intensifying tropical cyclones.

Keywords: tropical cyclones, numerical weather prediction, all-sky satellite radiance, convection

©2019. Japan Geoscience Union. All Right Reserved. 

# A link between high-speed solar wind streams and rapid intensification of tropical cyclones

*Paul Prikryl[1,2], Lidia Nikitina[2], Vojto Rušin[3]

1. Physics Department, University of New Brunswick, Fredericton, NB, Canada, 2. Geomagnetic Laboratory, Natural Resources Canada, Ottawa, ON, Canada, 3. Astronomical Institute, Slovak Academy of Sciences, Tatranská Lomnica, Slovak Republic

Physical processes responsible for changes of tropical cyclone intensity are not well understood [1]. To improve the current understanding of tropical cyclone structure and intensity changes the future research needs to focus on response to all external forcing [2]. We examined rapid intensification of tropical storms in the context of solar wind coupling to the magnetosphere-ionosphere-atmosphere system. Tropical cyclone “best tracks” in the southern and northern hemispheres are used in the superposed epoch analysis of time series of solar wind parameters. The results indicate that rapid intensification of tropical storms tends to follow arrivals of high-speed solar wind from coronal holes and coronal mass ejections [3]. The ensuing auroral and polar cap activity including ionospheric currents and ionospheric convection generates atmospheric gravity waves that propagate from the high-latitude lower thermosphere both upward and downward [4,5,6]. If ducted in the lower atmosphere, they can reach tropical troposphere. Despite significantly reduced wave amplitude, but subject to amplification upon reflection in the upper troposphere, these gravity waves can trigger/release moist instabilities to initiate convective bursts, with the latent heat release leading to intensification of storms [7]. Convective bursts have been linked to rapid intensification of tropical cyclones. Tropical cyclone intensifications are preceded by atmospheric gravity waves generated by the solar wind magnetosphere-ionosphere-atmosphere coupling process. The gravity waves are observed in the ionosphere as traveling ionospheric disturbances. Their propagation in the lower atmosphere is examined by ray tracing in a model atmosphere to show that they can reach tropical cyclones. It is suggested that the interaction of aurorally-generated gravity waves with the tropical cyclone vortex and the inner primary eyewall could play a role in the intensification process. Assuming that quasi-periodic convective bursts lead to vortex waves, a two-dimensional barotropic approximation [8] is used to obtain asymptotic solutions representing propagation of vortex waves. The absorption of vortex waves by the mean flow in the critical layer leads to formation of the secondary eyewall and ultimately to a process of eyewall replacement cycle, one of the well-established paradigms of intensity changes in tropical cyclones [9].

[1] Kaplan J., et al., Wea. Forecasting, 25, 220–241, 2010. https://doi.org/10.1175/2009WAF2222280.1
[2] Wang Y., Wu C.-C., Meteor. Atmos. Phys., 87, 257–278, 2004.
[3] Prikryl P., et al., J. Atmos. Sol.-Terr. Phys., 183, 36-60, 2019.
https://doi.org/10.1016/j.jastp.2018.12.009.
[4] Mayr H.G., et al., J. Geophys. Res., 89, 10929–10959, 1984.
[5] Mayr H.G., et al., Space Sci. Rev. 54, 297–375, 1990.
[6] Prikryl P., et al., Ann. Geophys., 23, 401–417, 2005. doi:10.5194/angeo-23-401-2005
[7] Prikryl P., et al., Ann. Geophys. 27, 31–57, 2009. https://doi.org/10.5194/angeo-27-31-2009.
[8] Nikitina L.V., Campbell L.J., Stud. Appl. Math., 135, 377–446, 2015.
[9] Willoughby H.E., et al., J. Atmos. Sci., 39, 395–411, 1982.

Keywords: Solar wind-magnetosphere-ionosphere-atmosphere coupling, High-speed solar wind stream, Atmospheric gravity wave, Extratropical and tropical cyclones

©2019. Japan Geoscience Union. All Right Reserved. 

©2019. Japan Geoscience Union. All Right Reserved. 

# Influence of Tropical Lower Stratospheric Cooling on Extreme Deep Convective Activity and Tropical Cyclones

*Kunihiko Kodera[1], Nawo Eguchi[2], Rei Ueyama[3], Beatriz M Funatsu[4], Chantal Claud[5]

1. Meteorological Research Institute, 2. Kyushu University, 3. NASA Ames Research Center, 4. Université de Nantes, 5. Ecole Polytechnique

In previous studies we showed that stratospheric sudden warming (SSW) event can induce rapid cooling in the tropical stratosphere and impact on the tropical convective activity. Case studies on two large SSWs in January 2009 and January 2010, showed that convective activity increased along ascending branch of the Hadley circulation in the austral summer hemisphere. It is also found that frequency of the convective overshooting clouds, and the tropical cyclones (TCs) increased following the tropical stratospheric cooling. Detailed analysis on the relationship between the tropical stratospheric cooling and tropical cyclones are made for 2010 January case. In January 2010, TCs have been generated one after another over Indian Ocean, Maritime continent, and Pacific sectors following a eastward propagation of convective active center associated with the Madden-Julian Oscillation (MJO) until rapid cooling started in the tropical stratosphere in late January. Then, after that, MJO became stationary over the central Pacific and TCs developed or re-developed simultaneously over 3 different sectors: Southwest Indian Ocean, Australia, and central Pacific. TC does not form over the lands, however, extreme deep convective activity simultaneously enhanced with the TCs over African and South American continents. It is suggested that a decrease of static stability in the tropical tropopause layer (TTL) due to a cooling in the lower stratosphere, produced favorable condition for the development of extreme deep convection. The increase of extreme deep convection around 15° S latitudinal zone following the tropical stratospheric cooling can be characterized as a strengthening of deep ascending branch of the Hadley circulation connected to the Brewer-Dobson circulation.

Keywords: tropical cyclone, stratosphere, deep convection

©2019. Japan Geoscience Union. All Right Reserved. 

[E] Oral | A (Atmospheric and Hydrospheric Sciences )：A-AS Atmospheric Sciences, Meteorology & Atmospheric Environment

Thu. May 30, 2019 10:45 AM - 12:15 PM JST | Thu. May 30, 2019 1:45 AM - 3:15 AM UTC | 104 1F

## [A-AS02] Advances in Tropical Cyclone Research: Past, Present, and Future

convener:Sachie Kanada(Nagoya University), Akiyoshi Wada(Department of Typhoon and Severe Weather Research, Meteorological Research Institute), Kosuke Ito(University of the Ryukyus), Yoshiaki Miyamoto(Faculty of Environment and Information Studies, Keio University), Chairperson:Yoshiaki Miyamoto, Kosuke Ito(University of Ryukyus)

Tropical cyclones (TC) sometimes cause destructive disasters in many countries by torrential rainfall, strong wind, storm surge, and high surf. In 2008, the western Japan suffered a record-breaking heavy rainfall related to Typhoon Prapirooon (2018) in July. Furthermore, two Category 4 typhoons, typhoons Jebi (2018) and Trami (2018), made landfalls on the western Japan in September and caused devastating disasters over the Japanese Islands. In the Northern Atlantic, Hurricane Florence caused catastrophic damage in the eastern side of U.S. Recent studies reported a northward shift of the location where a TC achieved the peak intensity and also reported increases in the frequency of rapidly intensifying storms. Thus, understanding the TC processes related to translation, intensity change and precipitation in the changing climate, and to provide more accurate forecasts and long-term projections are essential for the earth and planetary science.<br/>Advances in innovative observations such as meteorological aircraft, weather satellite, supercomputer systems such as the Earth Simulator and K-computer, and introduction of new methods such as the deep-learning, have led to novel development of numerical weather forecasting and understanding of the phenomena related to TCs in the past, present and future climates. In this session, we welcome papers on various aspects of TC studies. We hope that the session will provide a new direction for future TC researches.

10:45 AM - 11:15 AM JST | 1:45 AM - 2:15 AM UTC

[AAS02-07] A change in the inner-core structure of Typhoon Trami (2018) as observed through upper-tropospheric aircraft reconnaissance of T-PARCII

★Invited Papers

*Hiroyuki Yamada[1], Kazuhisa Tsuboki[2], Taro Shinoda[2], Hisayuki Kubota[3], Yukihiro Takahashi[3], Norio Nagahama[4], Kensaku Shimizu[4], Tadayasu Ohigashi[5], Kosuke Ito[1], Munehiko Yamaguchi[6], Tetsuo Nakazawa[6] (1.University of the Ryukyus, 2.Nagoya University, 3.Hokkaido University, 4.Meisei Electric, 5.National Research Institute for Earth Science and Disaster Resilience, 6.Meteorological Research Institute, Japan Meteorological Agency)

11:15 AM - 11:30 AM JST | 2:15 AM - 2:30 AM UTC

[AAS02-08] **Dramatic changes in the inner-core structure of Typhoon Jebi (2018) at landfall and relationship between a mesovortex and strong wind gusts**

*Udai Shimada[1], Ryo OYAMA[1], shingo shimizu[2] (1.Meteorological Research Institute, 2.National Research Institute for Earth Science and Disaster Prevention)

11:30 AM - 11:45 AM JST | 2:30 AM - 2:45 AM UTC

[AAS02-09] **Revisiting Asymmetric CAPE in Sheared Tropical Cyclones**

*Qingqing Li[1] (1.NUIST Nanjing University of Information Science and Technology)

11:45 AM - 12:00 PM JST | 2:45 AM - 3:00 AM UTC

[AAS02-10] **Observed rainfall asymmetry of tropical cyclone in the process of making landfall in Guangdong, South China**

*Guanhuan Wen[1] (1.Guangzhou Institute of Tropical and Marine Meteorology, China Meteorological Administation)

12:00 PM - 12:15 PM JST | 3:00 AM - 3:15 AM UTC

[AAS02-11] Volumetric Detection of Tornadic Vortices Associated with Typhoon Nanmadol (2017) Using PAWR and Deep Learning

*Toru Adachi[1], Naoki Ishitsu[2], Kenichi Kusunoki[1], Hanako Inoue[1], Ken-ichiro Arai[2], Chusei Fujiwara[3], Hiroto Suzuki[3] (1.Meteorological Research Institute, 2.Alpha Denshi/Meteorological Research Institute, 3.East Japan Railway Company)

# A change in the inner-core structure of Typhoon Trami (2018) as observed through upper-tropospheric aircraft reconnaissance of T-PARCII

*Hiroyuki Yamada[1], Kazuhisa Tsuboki[2], Taro Shinoda[2], Hisayuki Kubota[3], Yukihiro Takahashi[3], Norio Nagahama[4], Kensaku Shimizu[4], Tadayasu Ohigashi[5], Kosuke Ito[1], Munehiko Yamaguchi[6], Tetsuo Nakazawa[6]

1. University of the Ryukyus, 2. Nagoya University, 3. Hokkaido University, 4. Meisei Electric, 5. National Research Institute for Earth Science and Disaster Resilience, 6. Meteorological Research Institute, Japan Meteorological Agency

Upper-tropospheric aircraft reconnaissance with dropsonde deployment using a Gulfstream-II aircraft was carried out for the inner core of Typhoon Trami on four successive days since 25 September 2018. According to the JMA best track, the central pressure reached its minimum value of 915 hPa on the first day and was subsequently maintained at 950 hPa for three days. Using dropsonde data, this study examined the change in the inner-core structure associated with the intensity change. Based on satellite imagery, this intensity change was associated with the rapid expansion of the eye (with radius increasing from 35 to 90 km) and the gradual increase in the eyewall cloud-top height. A composite analysis of dropsonde profiles in the radius-height domain on each day revealed a change in the flow structure, with the decrease (increase) in the tangential wind component near the radius of 40 km (120 km). This caused an increase in the radial gradient of angular momentum, corresponding to an increase in inertial stability. These results suggest that this typhoon underwent the structural change similar to eyewall replacement cycle while the central pressure was maintained.

Acknowledgements: This work was supported by JSPS KAKENHI Grant Numbers JP16H06311, JP16H04053, JP18H03805, and the Science and Technology Research Partnership for Sustainable Development (SATREPS) Understanding Lightning and Thunderstorm (ULAT) project.

Keywords: aircraft reconnaissance, tropical cyclone, western North Pacific

©2019. Japan Geoscience Union. All Right Reserved. 

# Dramatic changes in the inner-core structure of Typhoon Jebi (2018) at landfall and relationship between a mesovortex and strong wind gusts

*Udai Shimada[1], Ryo OYAMA[1], shingo shimizu[2]

1. Meteorological Research Institute, 2. National Research Institute for Earth Science and Disaster Prevention

Landfalling tropical cyclones experience dramatic structural changes due to increased friction, topography, reduced surface heat fluxes, and reduced moisture supply. Typhoon Jebi (2018) made landfall in Shikoku Island on September 4, 2018, and then it caused record-breaking gust wind speeds greater than 40 m $s^{-1}$ and heavy rainfall greater than 50 mm $h^{-1}$ along its track. Dramatic changes in the inner-core structure of Jebi at landfall and the relationship between heavy rainfall and strong wind gusts, and structural features were examined by using observations. The azimuthal-mean structure of Jebi after landfall shows that while the tangential wind at 1-km altitude decreased from 45 m $s^{-1}$ to 30 m $s^{-1}$, the structure became more compact, with the radius of maximum wind (RMW) at ~50 km and radar reflectivity increasing inside the RMW at altitudes from 1 to 5 km. Because of increasing forward speed and active convection inside the RMW, maximum wind speed below 6-km altitude did not decrease significantly even after landfall. Inside the RMW, a mesovortex with a scale of 50 km formed in the downshear-left quadrant. The formation of the mesovortex was likely attributed to dynamically forced updraft associated with the storm vortex tilted by vertical wind shear and attributed to tilting of horizontal vorticity associated with the convergence of enhanced frictional inflow. The mesovortex contributed to the strong wind gusts and heavy rainfall. Also, the fast forward speed of more than 15 m $s^{-1}$ increased wind gusts on the right-hand side of Jebi’ s track.

Keywords: landfalling tropical cyclones, radar analysis, mesovortices

©2019. Japan Geoscience Union. All Right Reserved. 

# Revisiting Asymmetric CAPE in Sheared Tropical Cyclones

*Qingqing Li[1]

1. NUIST Nanjing University of Information Science and Technology

This study numerically revisits the characteristics and physical processes of azimuthally asymmetric convective available potential energy (CAPE) in the outer cores of vertically sheared tropical cyclones (TCs), which has been observed previously. The results indicate that a downshear-upshear contrast in CAPE occurs in weakly sheared TCs as pointed out in prior studies, while an enhanced downshear left-downshear right contrast is found in strongly sheared storms. Specifically, less (larger) CAPE values arise downshear left (right) under large shear environments. Downward transport of low entropy by the convective and mesoscale downdrafts in principal rainbands reduces the equivalent potential temperature ($\theta e$) in the downshear-left boundary layer, whereas positive horizontal advection by the asymmetric outflow contributes to the presence of a mid-level maximum of $\theta e$ in the same quadrant. Resultantly, lower outer-core CAPE is present downshear left. In the downshear-right quadrant, a lack of convective downdrafts together with surface fluxes leads to higher $\theta e$ in the boundary layer. The intrusion of dry air by ventilation produces lower $\theta e$ in the upper troposphere on the right of the shear. Larger CAPE values thus arise downshear right. The effects of such azimuthally asymmetric CAPE on TC structure and intensity are also discussed.

Keywords: tropical cyclone, CAPE, shear

©2019. Japan Geoscience Union. All Right Reserved. 

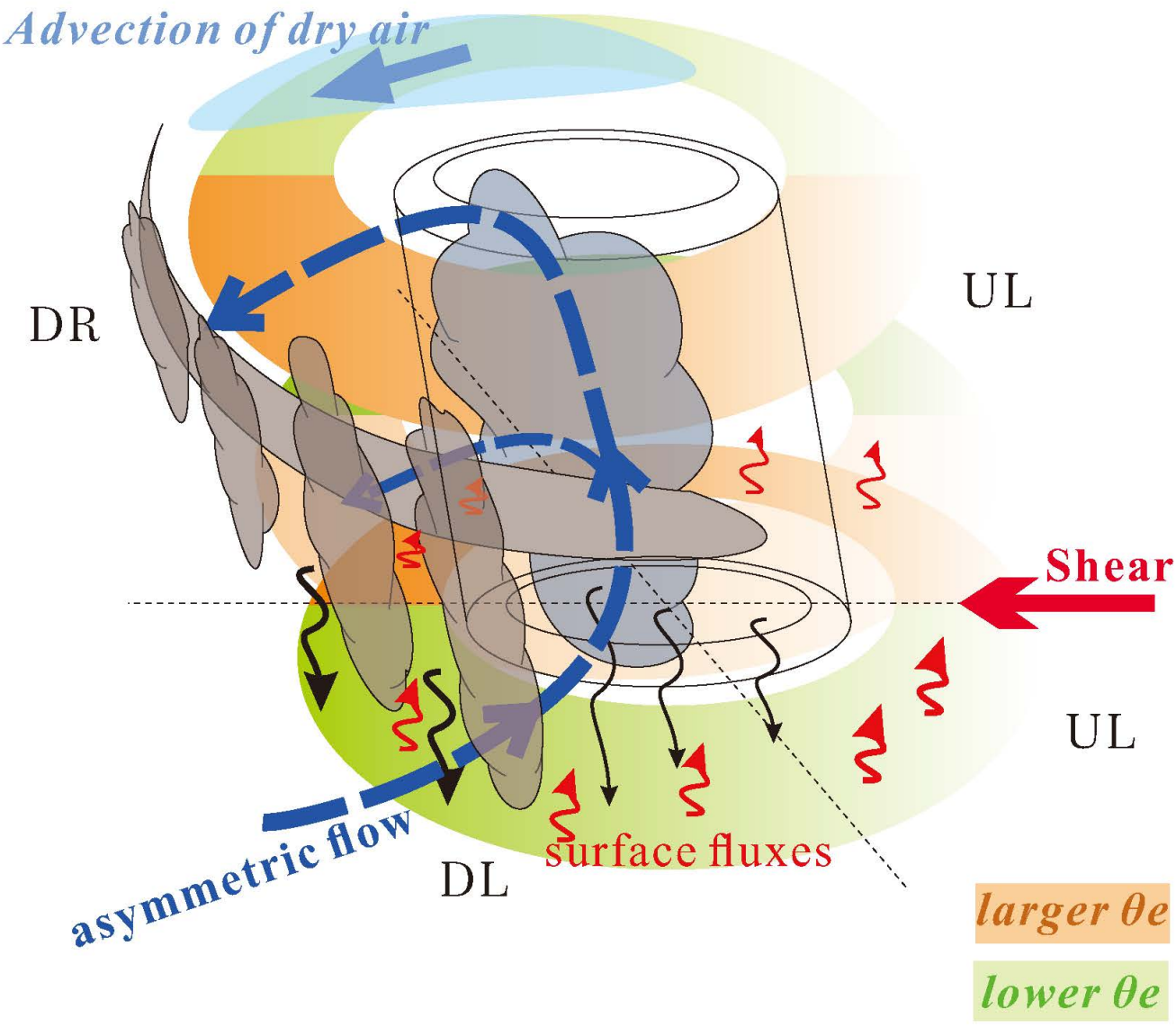


©2019. Japan Geoscience Union. All Right Reserved. 

# Observed rainfall asymmetry of tropical cyclone in the process of making landfall in Guangdong, South China

*Guanhuan Wen[1]

1. Guangzhou Institute of Tropical and Marine Meteorology, China Meteorological Administation

This study investigates the rainfall asymmetry of tropical cyclones (TCs) in the process of making landfall in Guangdong (GD), South China, on the basis of satellite-based and reanalysis precipitation data. We mainly focus on TC rainfall asymmetry, its main influencing factor, and its change in the process of landfall, and the difference between different ENSO phases. The results reveal that vertical wind shear (VWS) is the dominant influencing factor of TC rainfall asymmetry in GD. The rainfall maximum is located in downshear left of VWS. The TC rainfall asymmetry has little change in the process of making landfall, though the rain rate decreases. Both the phase and amplitude of TC rainfall asymmetry have no significant change from 24 hours prior to landfall to 12 hours after landfall. The rainfall maximum steadily lies in downshear left. The amplitude of rainfall asymmetry is about 50%, suggesting that the asymmetric rainfall is about half of the axisymmetric rainfall. There is no obvious difference in TC rainfall asymmetry between El Niño, La Niña, and neutral years.

Keywords: Tropical cyclone, Rainfall asymmetry, TRMM, Vertical wind shear

©2019. Japan Geoscience Union. All Right Reserved. 

# Volumetric Detection of Tornadic Vortices Associated with Typhoon Nanmadol (2017) Using PAWR and Deep Learning

*Toru Adachi[1], Naoki Ishitsu[2], Kenichi Kusunoki[1], Hanako Inoue[1], Ken-ichiro Arai[2], Chusei Fujiwara[3], Hiroto Suzuki[3]

1. Meteorological Research Institute, 2. Alpha Denshi/Meteorological Research Institute, 3. East Japan Railway Company

Tornadoes spawned by miniature supercells associated with typhoon are one of critical issues for disaster risk reduction in Japan. However, it is not easy to monitor and predict their occurrence because the parent storm is considerably small compared with classic-type tornadic supercell. We try to overcome this problem by combining cutting-edge technologies using rapid-scan phased array weather radar (PAWR) and deep learning analysis. We present a case study of tornado-like vortices which caused damages in Souka city, Saitama, during the approach of Typhoon Nanmadol (2017). We performed data analysis of two rapid-scan phased array weather radars operated by Meteorological Research Institute in Tsukuba and operated by Japan Radio Co., Ltd. in Chiba. To detect vortices from the PAWR-observed Doppler velocity data, we employed a vortex pattern finding scheme using convolutional neural network. Since PAWR carries out quasi-simultaneous observation of multi-elevational angles, we considered a group of vortices located in a radius of 4-km as a single vertically-extending volumetric vortex. By analyzing the spatiotemporal structure, we found a significant growth of a tornadic vortex about five minutes prior to its passage over the ground damage area. This finding suggests that a combination of rapid-scan PAWR observation and deep learning analysis is useful for monitoring and short-term forecasting of tornadoes associated with typhoon.

Acknowledgement: This work is supported by JSPS KAKENHI Grant 17K13007. In this analysis, we used PAWR data operated by Japan Radio Co., Ltd.

Keywords: Typhoon, Tornado, Phased Array Weather Radar, Deep Learning

©2019. Japan Geoscience Union. All Right Reserved. 

[E] Poster | A (Atmospheric and Hydrospheric Sciences)：A-AS Atmospheric Sciences, Meteorology & Atmospheric Environment

Thu. May 30, 2019 1:45 PM - 3:15 PM JST | Thu. May 30, 2019 4:45 AM - 6:15 AM UTC | Poster Hall International Exhibition Hall8, Makuhari Messe_1

## [A-AS02] Advances in Tropical Cyclone Research: Past, Present, and Future

convener:Sachie Kanada(Nagoya University), Akiyoshi Wada(Department of Typhoon and Severe Weather Research, Meteorological Research Institute), Kosuke Ito(University of the Ryukyus), Yoshiaki Miyamoto(Faculty of Environment and Information Studies, Keio University)

Tropical cyclones (TC) sometimes cause destructive disasters in many countries by torrential rainfall, strong wind, storm surge, and high surf. In 2008, the western Japan suffered a record-breaking heavy rainfall related to Typhoon Prapirooon (2018) in July. Furthermore, two Category 4 typhoons, typhoons Jebi (2018) and Trami (2018), made landfalls on the western Japan in September and caused devastating disasters over the Japanese Islands. In the Northern Atlantic, Hurricane Florence caused catastrophic damage in the eastern side of U.S. Recent studies reported a northward shift of the location where a TC achieved the peak intensity and also reported increases in the frequency of rapidly intensifying storms. Thus, understanding the TC processes related to translation, intensity change and precipitation in the changing climate, and to provide more accurate forecasts and long-term projections are essential for the earth and planetary science.<br/>Advances in innovative observations such as meteorological aircraft, weather satellite, supercomputer systems such as the Earth Simulator and K-computer, and introduction of new methods such as the deep-learning, have led to novel development of numerical weather forecasting and understanding of the phenomena related to TCs in the past, present and future climates. In this session, we welcome papers on various aspects of TC studies. We hope that the session will provide a new direction for future TC researches.

[AAS02-P01] Numerical study on lightning frequency in a tropical cyclone

*Yousuke Sato[1,3], Yoshiaki Miyamoto[2,3], Tomita Hirofumi[3] (1.Department of Applied Energy, Nagoya University, 2.Faculty of Environment and Information Studies, Keio University, 3.RIKEN Center for Computational Science)

[AAS02-P02] **Sensitivity of Numerical Simulation of Typhoon Nepartak (2016) to Cloud Condensation Nuclei Concentration**

*Yu-De Wu[1], Jian-Liang Wang[1] (1.Dept. of Environmental Informational and Engineering, Chung Cheng Institute of Technology, National Defense University, Taiwan)

[AAS02-P03] Moisture Budget Analysis for Hurricane Precipitation on Texas

*Satoshi Iizuka[1], Naoki Sakai[1] (1.National Research Institute for Earth Science and Disaster Resilience)

[AAS02-P04] Remote response of a developing tropical cyclone over the western North Pacific to large-scale vapor transport from the Kuroshio in boreal fall

*Keita Fujiwara[1], Ryuichi Kawamura[2], Tetsuya Kawano[2] (1.Graduate School of Science, Kyushu University, 2.Faculty of Science, Kyushu University)

[AAS02-P05] Asymmetrically Intensifying Processes of a Category 4 Super Typhoon Lan (2017) during High Vertical Wind Shear

*Sachie Kanada[1], Akiyoshi Wada[2], Kazuhisa Tsuboki[1] (1.Nagoya University, 2.Meteorological Research Institute)

[AAS02-P06] Roles of preexisting oceanic condition and ocean coupling processes in the intensity prediction during the mature phase of Typhoon Trami (2018)

*Akiyoshi Wada[1] (1.Typhoon Research Department Meteorological Research Institute)

[AAS02-P07] Development and assessment of the probabilistic storm surge forecast system in Taiwan: Case Study of Typhoon Maria in 2018

*Chun-Wei Lin[1], Tso-Ren Wu[1], Yu-Lin Tsai[1], Shu-Chun Chuang[1], Chi-Hao Chu[2], Chuen-Teyr Terng[2] (1.Graduate Institute of Hydrological and Oceanic Sciences, National Central University, Chungli, Taiwan, 2.Marine Meteorology Center, Central Weather Bureau, Taipei, Taiwan)

[AAS02-P08] Basic Data Construction for a Typhoon Disaster Prevention Model : Analysis and Changes by El Nino and La Nina year

*HANA NA[1], Woo-Sik Jung[1] (1.Department of Atmospheric Environment Information Engineering, Atmospheric Environment Information Research Center, Inje University, Gimhae 50834, Korea)

[AAS02-P09] Basic Data Construction for a Typhoon Disaster Prevention Model : Analysis According to the Typhoon Path Type

*HANA NA[1], Woo-Sik JUNG[1] (1.Department of Atmospheric Environment Information Engineering, Atmospheric Environment Information Research Center, Inje University, Gimhae 50834, Korea)

[AAS02-P10] Basic Data Construction for a Typhoon Disaster Prevention Model : Monthly Characteristics of Typhoon Rusa, Maemi, Kompasu, and Bolaven

*HANA NA[1], Woo-Sik Jung[1] (1.Department of Atmospheric Environment Information Engineering, Atmospheric Environment Information Research Center, Inje University, Gimhae 50834, Korea)

[AAS02-P11] The mechanism of typhoon generated in the earth that rotates in the space where the solar wind blows

*Shinji Karasawa[1] (1.Miyagi National College of Technology Professor emeritus)

# Numerical study on lightning frequency in a tropical cyclone

*Yousuke Sato[1,3], Yoshiaki Miyamoto[2,3], Tomita Hirofumi[3]

1. Department of Applied Energy, Nagoya University, 2. Faculty of Environment and Information Studies, Keio University, 3. RIKEN Center for Computational Science

This study investigates frequency of lightning in each stage of lifecycle of tropical cyclone (TC) using the next generation weather and climate library called Scalable Computing for Advanced Library and Environment (SCALE; Sato et al. 2015, Nishizawa et al. 2015). Lightning component was developed and implemented into SCALE in this study. An idealized experiment based on an experimental setup of Miyamoto and Takemi (2013) was conducted by SCALE coupled with lightning component. The results of the simulation indicate that the lightning frequency is maximum before rapid intensification (RI) of TC, which supports the report of Price et al. (2009) derived from satellite observation. The frequency of lightning decreases after RI and it keeps small until the TC reaches steady state. Our analyses elucidate that the dependency of the lightning frequency upon the developing stage of TC is originated from the type of convection dominating at each growth stage. Before the RI, the convection generated by consuming convective available potential energy (CAPE) transport hydrometeors upward, and the charge split and the lightning frequently occur. During the steady state, the hydrometeors are mainly transported by the fast rotating flow in the simulated TC, which resulted in the weak charge split and small frequency of lightning.

Keywords: Tropical cyclone, Lightning

©2019. Japan Geoscience Union. All Right Reserved. 

# Sensitivity of Numerical Simulation of Typhoon Nepartak (2016) to Cloud Condensation Nuclei Concentration

*Yu-De Wu[1], Jian-Liang Wang[1]

1. Dept. of Environmental Informational and Engineering, Chung Cheng Institute of Technology, National Defense University, Taiwan

The study is carried out using the WRF model and the Cloud Condensation Nuclei, CCN, in the WDM6 microphysics scheme has been modified to test its impacts on typhoon simulations. The simulated track, intensity, and rainfall distribution of Typhoon Nepartak (2016) over Pacific Ocean are compared among numerical experiments of different initial concentration of CCN (wdm6_ctr, wdm6_10, and wdm6_50, where wdm6_10 and wdm6_50 represent that CCN are respectively 10 and 50 times of the value used in wdm6_ctr).

The simulated tracks in three runs are similar, but the intensity and the maximum dBz increase both in wdm6_10 and wdm6_50, but it takes more time for wdm6_50 to intensify. The comparison of mixing ratios of five water species shows that the cloud droplets mixing ratios increase as CCN is increased. The mixing ratios of rain, cloud ice, snow and graupel are enhanced more rapidly in wdm6_10 compared with wdm6_50. The same situation happens in the divergence field and upward motions. It is suggested that the increase of CCN will result in stronger typhoon, but the intensification will be slowed down with too much CCN.

Keywords: Cloud Condensation Nuclei, Typhoon Nepartak, Microphysics Scheme

©2019. Japan Geoscience Union. All Right Reserved. 

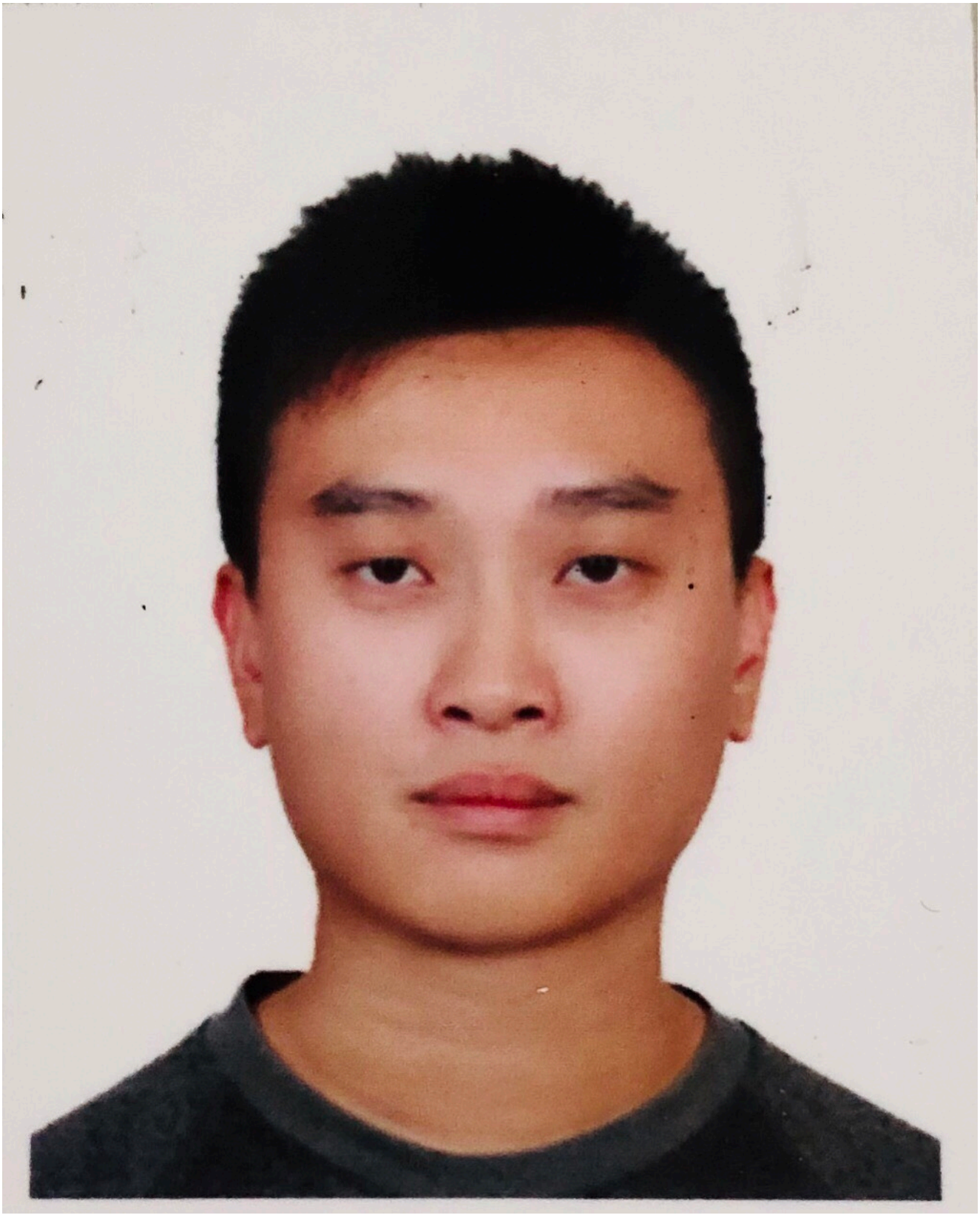

©2019. Japan Geoscience Union. All Right Reserved. 

# Moisture Budget Analysis for Hurricane Precipitation on Texas

*Satoshi Iizuka[1], Naoki Sakai[1]

1. National Research Institute for Earth Science and Disaster Resilience

In August 2017, Hurricane Harvey brought the unprecedented amount of rainfall and catastrophic flooding on the Houston metropolitan area, as it stagnated near the coast of Texas for several days after its decline to a tropical storm intensity. The present study compares the moisture budget for rainfall associated with Harvey with those of past hurricanes making landfall on Texas. It seems that the high pressure over the west coast region of the US, along with the meandering of the subtropical jet starting from the periphery of Hawaii and toward the south in Texas, stagnated Hurricane Harvey around the coast of Texas for several days. The meandering of the subtropical jet toward the south in Texas also caused the largest convergence of moisture advected from the Gulf of Mexico efficiently over Texas, although the accompanied high pressure was not extraordinary event. Therefore, it is suggested that surrounding meteorological conditions can greatly affect rainfall related to tropical cyclones.

Keywords: Hurricane Harvey, Precipitation, Moisture Budget

©2019. Japan Geoscience Union. All Right Reserved. 

# Remote response of a developing tropical cyclone over the western North Pacific to large-scale vapor transport from the Kuroshio in boreal fall

*Keita Fujiwara[1], Ryuichi Kawamura[2], Tetsuya Kawano[2]

1. Graduate School of Science, Kyushu University, 2. Faculty of Science, Kyushu University

A remote linkage between the development of tropical cyclone (TC) over the western North Pacific and moisture transport from the Kuroshio Current due to environmental flow toward TC was examined by using regional cloud resolving model and Lagrangian diagnostics. In this study, we specially highlighted a prototypical TC (Typhoon Chaba 2010), which developed and migrated northward over the Philippines Sea in boreal fall, and conducted sensitivity experiments that modified surface turbulent latent heat flux (LHF) over the Kuroshio. The large-scale environment was characterized by a combination of two synoptic systems, eastward-migrating anticyclone from the Asian continent and TC approaching Japan, bringing low-level northeasterly flows over the Kuroshio through an enhanced meridional pressure gradient in that region. Trajectory analyses suggested that air parcels along the northeasterlies modified by receiving abundant water vapor from the underlying Kuroshio may contribute to latent heating within Chaba’s inner core region as a remote effect, leading to TC development.

When LHF was removed or reduced over the Kuroshio under the dominance of the northwesterly flow, TC intensity attenuated during its developing stage even though TC was fairly far away from the Kuroshio. Since no or little modification of dry air parcels occurred in the atmospheric boundary layer over the Kuroshio, contribution of those parcels to latent heat release around Chaba’s eyewall become small. Furthermore, dry air penetration into TC’s inner core region may act as an inhibitor of convection within that region, resulting in deceleration of the TC development. These findings were consistent with another TC (Typhoon Toakge 2004) with a similar synoptic environment, increasing reliability of remote impact of moisture import from the Kuroshio on TC development.

Keywords: tropical cyclone, moisture transport, Kuroshio Current

©2019. Japan Geoscience Union. All Right Reserved. 

# Asymmetrically Intensifying Processes of a Category 4 Super Typhoon Lan (2017) during High Vertical Wind Shear

*Sachie Kanada[1], Akiyoshi Wada[2], Kazuhisa Tsuboki[1]

1. Nagoya University, 2. Meteorological Research Institute

On 21 October 2017, Typhoon Lan developed to a Category 4 super typhoon with the minimum central pressure (MCP) of 915 hPa at 25.6 degrees north latitude and maintained the peak intensity until the storm arrived at 29.9˚N under a strong environmental vertical wind shear (VWS) of 14 m $s^{-1}$. To understand the intensification processes of an intense typhoon with such high VWS, numerical simulations on Typhoon Lan were conducted using a high-resolution three-dimensional atmosphere regional model, the Cloud Resolving Storm Simulator (CReSS; Tsuboki and Sakakibara, 2002). Two sensitivity experiments, 1dO and FO, were conducted with different SST representations. In the 1dO experiment, a simple thermal diffusion model was used to express temperature changes due to ocean vertical mixing. The FO experiment with a time-fixed SST did not consider the evolution of SST. Both experiments used the same initial and boundary conditions and model specifications for the atmosphere, started at 0000 UTC 18 October 2017, and had an integration time of 5 days. The computational domain was 2˚N–37.8˚N and 115˚E–145˚E. The number of horizontal grids in the computational domain was 752×896 with the horizontal grid size of 0.04 longitude by 0.04 latitude.

The typhoon simulated in the 1dO experiment successfully achieved the MCP of 910 hPa at 29.5˚N, exhibiting strong asymmetric precipitation pattern as observed by the satellites. The intensification processes were accompanied by rapid developments of the strong winds and warm core in the low-levels. The strong northeast VWS forced to tilt the storm axis to downshear side (northeast) and, in the downshear quadrants, tall, intense and upstanding eyewall updrafts (CBs) formed from the low-level convergence of the storm travelling northeastward with a relatively fast translation speed of 10 m $s^{-1}$. Meanwhile, dry subsidence from the upper-levels intensified the low-level warm core in the upshear side of the eye. Despite the inner-core convection and precipitation exhibited strong asymmetric structures, the axisymmetricity of the storm circulation was maintained in the mid-to-low levels and abundant water vapor enclosed in the eye allowed to develop CBs around the radius of the maximum wind speeds. Although the FO storm overestimated the MCP of 879hPa, the similar asymmetric patterns in precipitation and convection were also found in the FO storm. The results indicated that the storm structures of typhoon Lan would be less sensitive to the SST-cooling effect.

Keywords: Typhoon, numerical model

©2019. Japan Geoscience Union. All Right Reserved. 

# Roles of preexisting oceanic condition and ocean coupling processes in the intensity prediction during the mature phase of Typhoon Trami (2018)

*Akiyoshi Wada[1]

1. Typhoon Research Department Meteorological Research Institute

Typhoon Trami (2018) is one of the typhoons that made landfall in Japan. According to the Regional Specialized Meteorological Center (RSMC) Tokyo best track analysis, the central pressure reached 915 hPa at 18 UTC on 24 September around 20˚N and then rapidly increased by 950 hPa in 18 hours. After the rapid increases in the central pressure, intensity forecasts announced further intensification to 935 hPa, but the typhoon could not intensify again. In order to clarify the impact of the cold eddies over the ocean on this forecast error, we conducted numerical simulations with different oceanic initial conditions (daily data from 19 to 25 September were used so that the number of ensemble members is seven) using a 2 km-mesh nonhydrostatic atmosphere model coupled with ocean surface wave and multilayer ocean models with the Japan Meteorological Agency (JMA) global objective analysis with horizontal resolution of 20 km and the JMA North Pacific Ocean analysis with horizontal resolution of 0.5˚. In addition, a sensitivity numerical experiment was conducted with the oceanic initial condition on 23 September merged with an artificial cold vortex centered at 21˚N, 129˚E of which both a mixed layer and thermocline was 50 m shallower than the control experiment. Moreover, a simulation with a 2 km-mesh nonhydrostatic atmosphere model was performed with the oceanic initial condition on 23 September. The initial time and integration period are 00 UTC on 23 September and 180 hours with the time interval of 3 seconds.

The results of simulated tracks were reasonable compared with the RSMC best track analysis, while the rapid decrease in the central pressure could not be simulated due to a large difference in central pressure at the initial time so that the simulated minimum central pressure was higher than the best track central pressure. From the analysis with the ratio of a difference to the standard deviation obtained from the ensemble experiments, the impact of different oceanic initial conditions on central pressure was different from that on the maximum wind speed particularly from 25 to 27 September when the typhoon passed near the cold eddy. The impact of ocean coupling on simulated central pressure and maximum wind speed was considerably greater than that of the artificial cold eddy and that of different oceanic initial conditions. The impact of the artificial cold eddy was a few times greater than that of different oceanic initial conditions around 26 September. The result indicates that more detailed observation and more accurate analysis regarding the cold eddy over the ocean will contribute to the improvement of typhoon intensity predictions.

Keywords: tropical cyclone, atmosphere-wave-ocean coupled model, intensity forecast, preexisting cold eddy

©2019. Japan Geoscience Union. All Right Reserved. 

# Development and assessment of the probabilistic storm surge forecast system in Taiwan: Case Study of Typhoon Maria in 2018

*Chun-Wei Lin[1], Tso-Ren Wu[1], Yu-Lin Tsai[1], Shu-Chun Chuang[1], Chi-Hao Chu[2], Chuen-Teyr Terng[2]

1. Graduate Institute of Hydrological and Oceanic Sciences, National Central University, Chungli, Taiwan, 2. Marine Meteorology Center, Central Weather Bureau, Taipei, Taiwan

From the forecast and the analyzed typhoon tracks in Taiwan, it is found that if the forecast track errors are greater than 100 km, roughly a quarter of the length of Taiwan, significant variability of storm surge elevation can be seen.
In order to consider the uncertainty of the atmospheric forecast, this study aims to develop the probabilistic storm surge forecast system. The coastal storm surge model applied in this study is COMCOT-SS (COrnell Multi-Grid COupled Tsunami Model –Storm Surge), which is the kernel of the operating deterministic storm surge forecast system in CWB, Taiwan. It solves nonlinear shallow water equations in the nested-grid scheme. Two ensemble methods are adopted in this study, one is Deterministic Track Error Distribution Method, D-TED Method. The other one is the Ensemble Track Analysis Method, ETA Method. D-TED Method is generated from the deterministic forecast, while the ETA Method obtains typhoon tracks and parameters from the CWB WEPS (CWB WRF Ensemble Prediction System).
From the case study of typhoon Maria in 2018, it shows that as the typhoon approaching Taiwan, the coverage of the tracks from ETA Method would be more convergence comparing to the tracks from D-TED Method, and it provides a more concentrated surge elevation distribution.

Keywords: storm surge, ensemble forecast, COMCOT-SS

©2019. Japan Geoscience Union. All Right Reserved. 

# Basic Data Construction for a Typhoon Disaster Prevention Model : Analysis and Changes by El Nino and La Nina year

*HANA NA[1], Woo-Sik Jung[1]

1. Department of Atmospheric Environment Information Engineering, Atmospheric Environment Information Research Center, Inje University, Gimhae 50834, Korea

Among the typhoons that affected the Korean Peninsula for approximately 110 years from 1904, when weather observation began until 2018, all of the top five typhoons in terms of the maximum wind speed and property damage record occurred after 2000. This implies that the intensity of typhoons is becoming stronger and the damage is more severe compared to the past. Moreover, typhoons are significantly affected by the sea temperature. The El Nino and La Nina phenomena, in which significant changes in the sea temperature occur, may significantly affect the occurrence and intensity of typhoons affecting the Korean Peninsula. Therefore, this study aims to analyze changes by year, and the years of El Nino and La Nina occurrences by estimating the maximum wind speed that can be generated during typhoon period based on the typhoons that affected the Korean Peninsula. This study was conducted for the period between 2002 and 2015. As a result of analyzing the maximum wind speed of the typhoons that affected the Korean Peninsula by year, high 3-second gusts tended to occur in the Gyeongsang-do area including the southeast coast of the Korean Peninsula from 2002 to 2006. Subsequently, the strong wind area of the 3-second gusts expanded, and high 3-second gusts occurred in the Seoul metropolitan area. Moreover, as a result of investigating the 3-second gust characteristics for the years of El Nino and La Nina occurrences, a higher maximum wind speed was observed from the typhoons that affected the Korean Peninsula in the years of El Nino occurrence.

This research was supported by Basic Science Research Program through the National Research Foundation of Korea(NRF) funded by the Ministry of Education(2017R1D1A3B03036152)

Keywords: Typhoon Disaster Prevention Model, 3-Second gust, El Nino, La Nina

©2019. Japan Geoscience Union. All Right Reserved. 

# Basic Data Construction for a Typhoon Disaster Prevention Model : Analysis and Changes by El Nino and La Nina year

Hana Na, Woo-Sik Jung

Among the typhoons that affected the Korean Peninsula for approximately 110 years from 1904, when weather observation began until 2018, all of the top five typhoons in terms of the maximum wind speed and property damage record occurred after 2000. This implies that the intensity of typhoons is becoming stronger and the damage is more severe compared to the past. Moreover, typhoons are significantly affected by the sea temperature. The El Nino and La Nina phenomena, in which significant changes in the sea temperature occur, may significantly affect the occurrence and intensity of typhoons affecting the Korean Peninsula. Therefore, this study aims to analyze changes by year, and the years of El Nino and La Nina occurrences by estimating the maximum wind speed that can be generated during typhoon period based on the typhoons that affected the Korean Peninsula. This study was conducted for the period between 2002 and 2015. As a result of analyzing the maximum wind speed of the typhoons that affected the Korean Peninsula by year, high 3-second gusts tended to occur in the Gyeongsang-do area including the southeast coast of the Korean Peninsula from 2002 to 2006. Subsequently, the strong wind area of the 3-second gusts expanded, and high 3-second gusts occurred in the Seoul metropolitan area. Moreover, as a result of investigating the 3-second gust characteristics for the years of El Nino and La Nina occurrences, a higher maximum wind speed was observed from the typhoons that affected the Korean Peninsula in the years of El Nino occurrence.

This research was supported by Basic Science Research Program through the National Research Foundation of Korea(NRF) funded by the Ministry of Education(2017R1D1A3B03036152)

Key words : Typhoon Disaster Prevention Model, WRF, 3-Second gust, El Nino, La Nina

©2019. Japan Geoscience Union. All Right Reserved. 

# Basic Data Construction for a Typhoon Disaster Prevention Model : Analysis According to the Typhoon Path Type

*HANA NA[1], Woo-Sik JUNG[1]

1. Department of Atmospheric Environment Information Engineering, Atmospheric Environment Information Research Center, Inje University, Gimhae 50834, Korea

In this study, a typhoon disaster prevention model was used to estimate the maximum wind speed during typhoon period by path type from all typhoons that affected the Korean Peninsula from 2002 to 2015. For the typhoon information and upper wind information used as input data, the results of the WRF numerical model, which utilized the Best Track data of the RSMC Tokyo Typhoon Center and the RDAPS data of the Korea Meteorological Administration, were applied. From analyzing the path type impact frequency using all typhoons that affected the Korean Peninsula during the study period (2002–2015), Type 7 that affected the Korean Peninsula through Japan was the most frequent, followed by Type 2 that directly landed on the Korean Peninsula through the southern coast. From analyzing the monthly path types of the typhoons that affected the Korean Peninsula, Type 2 that affected the Korean Peninsula by landing on the southern coast and Type 7 that affected the Korean Peninsula through Japan were the most frequent for the recently increasing September typhoons. The analysis of the maximum wind speed of the 3-second gust that may occur during typhoon period by path type revealed that Type 2 that affected the Korean Peninsula by landing on the southern coast exhibited the highest 3-second gust. As a result of examining the distribution of Type 2, high 3-second gusts occurred throughout the Korean Peninsula, including the southeast coast. As for the path of Type 2 that directly affected the Korean Peninsula by landing on the southern coast, the occurrence frequency was the second highest during the entire study period and the value of the 3-second gust, which was the maximum wind speed that may occur during typhoon period, was the highest.

This research was supported by Basic Science Research Program through the National Research Foundation of Korea(NRF) funded by the Ministry of Education(2017R1D1A3B03036152)

Keywords: Typhoon Path, 3-Second gust, Typhoon Disaster Prevention Model

©2019. Japan Geoscience Union. All Right Reserved. 

# Basic Data Construction for a Typhoon Disaster Prevention Model : Analysis According to the Typhoon Path Type

Hana Na, Woo-Sik Jung

In this study, a typhoon disaster prevention model was used to estimate the maximum wind speed during typhoon period by path type from all typhoons that affected the Korean Peninsula from 2002 to 2015. For the typhoon information and upper wind information used as input data, the results of the WRF numerical model, which utilized the Best Track data of the RSMC Tokyo Typhoon Center and the RDAPS data of the Korea Meteorological Administration, were applied. From analyzing the path type impact frequency using all typhoons that affected the Korean Peninsula during the study period (2002–2015), Type 7 that affected the Korean Peninsula through Japan was the most frequent, followed by Type 2 that directly landed on the Korean Peninsula through the southern coast. From analyzing the monthly path types of the typhoons that affected the Korean Peninsula, Type 2 that affected the Korean Peninsula by landing on the southern coast and Type 7 that affected the Korean Peninsula through Japan were the most frequent for the recently increasing September typhoons. The analysis of the maximum wind speed of the 3-second gust that may occur during typhoon period by path type revealed that Type 2 that affected the Korean Peninsula by landing on the southern coast exhibited the highest 3-second gust. As a result of examining the distribution of Type 2, high 3-second gusts occurred throughout the Korean Peninsula, including the southeast coast. As for the path of Type 2 that directly affected the Korean Peninsula by landing on the southern coast, the occurrence frequency was the second highest during the entire study period and the value of the 3-second gust, which was the maximum wind speed that may occur during typhoon period, was the highest.

This research was supported by Basic Science Research Program through the National Research Foundation of Korea(NRF) funded by the Ministry of Education(2017R1D1A3B03036152)

Keywords : Typhoon Disaster Prevention Model, WRF, Typhoon Track, 3-Second gust

©2019. Japan Geoscience Union. All Right Reserved. 

# Basic Data Construction for a Typhoon Disaster Prevention Model : Monthly Characteristics of Typhoon Rusa, Maemi, Kompasu, and Bolaven

*HANA NA[1], Woo-Sik Jung[1]

1. Department of Atmospheric Environment Information Engineering, Atmospheric Environment Information Research Center, Inje University, Gimhae 50834, Korea

According to a typhoon report that summarized the typhoons that had affected the Korean Peninsula for approximately 100 years since the start of weather observation in the Korean Peninsula, the number of typhoons that affected the Korean Peninsula was the highest in August, followed by July, and September. A study that analyzed the period between 1953 and 2003 revealed that the number of typhoons that affected the Korean Peninsula was 62 in August, 49 in July, and 45 in September. As shown, previous studies that analyzed the typhoons that affected the Korean Peninsula by month were primarily focused on the impact frequency. This study aims to estimate the monthly impact frequency of the typhoons that affected the Korean Peninsula as well as the maximum wind speed that accompanied the typhoons. It also aims to construct the basic data of a typhoon disaster prevention model by estimating the maximum wind speed during typhoon period using Typhoon Rusa that resulted in the highest property damage, Typhoon Maemi that recorded the maximum wind speed, Typhoon Kompasu that significantly affected the Seoul metropolitan area, and Typhoon Bolaven that recently recorded severe damages. A typhoon disaster prevention model was used to estimate the maximum wind speed of the 3-second gust that may occur, and the 700 hPa wind speed estimated through WRF(Weather Research and Forecasting) numerical simulation was used as input data.

Unlike the target period reported in the white paper on typhoons (1904–2010), this study analyzed the monthly impact frequency of the typhoons that affected the Korean Peninsula from 2002 and 2015. The result indicated that the impact frequency was the highest in August, followed by July and September. This result was the same as that of the typhoon report. An analysis by year revealed that typhoon period increased in September. The 3-second gust was found to be the highest in September, followed by August and July. When this result was analyzed in relation to the recently increasing autumn typhoons (September and October), the 3-second gust result was the highest in September, indicating disaster prevention must be emphasized. By additionally analyzing the maximum wind speed distributions of Typhoon Rusa, Maemi, Kompasu, and Bolaven, the area with the maximum wind speed varied depending on the typhoon path, and the 3-second gust was higher than 44 m/s based on the typhoon intensity classification and accounted for approximately10%.

This research was supported by Basic Science Research Program through the National Research Foundation of Korea(NRF) funded by the Ministry of Education(2017R1D1A3B03036152)

Keywords: Typhoon Disaster Prevention Model, WRF, 3-Second gust

©2019. Japan Geoscience Union. All Right Reserved. 

# Basic Data Construction for a Typhoon Disaster Prevention Model : Monthly Characteristics of Typhoon Rusa, Maemi, Kompasu, and Bolaven

Hana Na, Woo-Sik Jung

According to a typhoon report that summarized the typhoons that had affected the Korean Peninsula for approximately 100 years since the start of weather observation in the Korean Peninsula, the number of typhoons that affected the Korean Peninsula was the highest in August, followed by July, and September. A study that analyzed the period between 1953 and 2003 revealed that the number of typhoons that affected the Korean Peninsula was 62 in August, 49 in July, and 45 in September. As shown, previous studies that analyzed the typhoons that affected the Korean Peninsula by month were primarily focused on the impact frequency. This study aims to estimate the monthly impact frequency of the typhoons that affected the Korean Peninsula as well as the maximum wind speed that accompanied the typhoons. It also aims to construct the basic data of a typhoon disaster prevention model by estimating the maximum wind speed during typhoon period using Typhoon Rusa that resulted in the highest property damage, Typhoon Maemi that recorded the maximum wind speed, Typhoon Kompasu that significantly affected the Seoul metropolitan area, and Typhoon Bolaven that recently recorded severe damages. A typhoon disaster prevention model was used to estimate the maximum wind speed of the 3-second gust that may occur, and the 700 hPa wind speed estimated through WRF(Weather Research and Forecasting) numerical simulation was used as input data.

Unlike the target period reported in the white paper on typhoons (1904–2010), this study analyzed the monthly impact frequency of the typhoons that affected the Korean Peninsula from 2002 and 2015. The result indicated that the impact frequency was the highest in August, followed by July and September. This result was the same as that of the typhoon report. An analysis by year revealed that typhoon period increased in September. The 3-second gust was found to be the highest in September, followed by August and July. When this result was analyzed in relation to the recently increasing autumn typhoons (September and October), the 3-second gust result was the highest in September, indicating disaster prevention must be emphasized. By additionally analyzing the maximum wind speed distributions of Typhoon Rusa, Maemi, Kompasu, and Bolaven, the area with the maximum wind speed varied depending on the typhoon path, and the 3-second gust was higher than 44 m/s based on the typhoon intensity classification and accounted for approximately10%.

This research was supported by Basic Science Research Program through the National Research Foundation of Korea(NRF) funded by the Ministry of Education(2017R1D1A3B03036152)

Keywords : Typhoon Disaster Prevention Model, WRF, 3-Second gust, RUSA, MAEMI, KOMPASU, BOLAVEN

©2019. Japan Geoscience Union. All Right Reserved. 

# The mechanism of typhoon generated in the earth that rotates in the space where the solar wind blows

*Shinji Karasawa[1]

1. Miyagi National College of Technology Professor emeritus

The atmosphere in the upper tropical cyclone (TC) rotates the clock-wise direction by the trade winds and westerlies. The rotation speed near the center increases, because the angular momentum of the atmospheric molecule is transported. The eye of the typhoon is appeared at the place where the centrifugal force of the rotation on the flow exceeds compared with the difference of the pressure. The atmosphere including the vapor of water in the cumulonimbus are mixed with the cold air flow swirling in the clockwise direction at the eye of typhoon, where the water vapors become to the rain, and the cumulonimbus rotates in anticlockwise direction.
The solar wind includes rotational momentum and the rotational momentum of the solar wind generates the trade winds. On the other hand, the westerlies are caused by the solar wind that rotates the tail of Earth's magnetosphere on the opposite side of the Sun in anticlockwise rotation, and it gives the driving force of the westerlies. Ref. S. Karasawa.
https://www.youtube.com/watch?v=bzCup63G8z8&feature=youtu.be

Keywords: tropical cyclone, westerlies, trade winds, solar wind, Earth’ s rotation, Sun’ s rotation

©2019. Japan Geoscience Union. All Right Reserved. 

[E] Poster | A (Atmospheric and Hydrospheric Sciences)：A-AS Atmospheric Sciences, Meteorology & Atmospheric Environment

Thu. May 30, 2019 5:15 PM - 6:30 PM JST | Thu. May 30, 2019 8:15 AM - 9:30 AM UTC | Poster Hall International Exhibition Hall8, Makuhari Messe_5

## [A-AS02] Advances in Tropical Cyclone Research: Past, Present, and Future

convener:Sachie Kanada(Nagoya University), Akiyoshi Wada(Department of Typhoon and Severe Weather Research, Meteorological Research Institute), Kosuke Ito(University of the Ryukyus), Yoshiaki Miyamoto(Faculty of Environment and Information Studies, Keio University)

Tropical cyclones (TC) sometimes cause destructive disasters in many countries by torrential rainfall, strong wind, storm surge, and high surf. In 2008, the western Japan suffered a record-breaking heavy rainfall related to Typhoon Prapirooon (2018) in July. Furthermore, two Category 4 typhoons, typhoons Jebi (2018) and Trami (2018), made landfalls on the western Japan in September and caused devastating disasters over the Japanese Islands. In the Northern Atlantic, Hurricane Florence caused catastrophic damage in the eastern side of U.S. Recent studies reported a northward shift of the location where a TC achieved the peak intensity and also reported increases in the frequency of rapidly intensifying storms. Thus, understanding the TC processes related to translation, intensity change and precipitation in the changing climate, and to provide more accurate forecasts and long-term projections are essential for the earth and planetary science.<br/>Advances in innovative observations such as meteorological aircraft, weather satellite, supercomputer systems such as the Earth Simulator and K-computer, and introduction of new methods such as the deep-learning, have led to novel development of numerical weather forecasting and understanding of the phenomena related to TCs in the past, present and future climates. In this session, we welcome papers on various aspects of TC studies. We hope that the session will provide a new direction for future TC researches.

[AAS02-P01] Numerical study on lightning frequency in a tropical cyclone

*Yousuke Sato[1,3], Yoshiaki Miyamoto[2,3], Tomita Hirofumi[3] (1.Department of Applied Energy, Nagoya University, 2.Faculty of Environment and Information Studies, Keio University, 3.RIKEN Center for Computational Science)

[AAS02-P02] **Sensitivity of Numerical Simulation of Typhoon Nepartak (2016) to Cloud Condensation Nuclei Concentration**

*Yu-De Wu[1], Jian-Liang Wang[1] (1.Dept. of Environmental Informational and Engineering, Chung Cheng Institute of Technology, National Defense University, Taiwan)

[AAS02-P03] Moisture Budget Analysis for Hurricane Precipitation on Texas

*Satoshi Iizuka[1], Naoki Sakai[1] (1.National Research Institute for Earth Science and Disaster Resilience)

[AAS02-P04] Remote response of a developing tropical cyclone over the western North Pacific to large-scale vapor transport from the Kuroshio in boreal fall

*Keita Fujiwara[1], Ryuichi Kawamura[2], Tetsuya Kawano[2] (1.Graduate School of Science, Kyushu University, 2.Faculty of Science, Kyushu University)

[AAS02-P05] Asymmetrically Intensifying Processes of a Category 4 Super Typhoon Lan (2017) during High Vertical Wind Shear

*Sachie Kanada[1], Akiyoshi Wada[2], Kazuhisa Tsuboki[1] (1.Nagoya University, 2.Meteorological Research Institute)

[AAS02-P06] Roles of preexisting oceanic condition and ocean coupling processes in the intensity prediction during the mature phase of Typhoon Trami (2018)

*Akiyoshi Wada[1] (1.Typhoon Research Department Meteorological Research Institute)

[AAS02-P07] Development and assessment of the probabilistic storm surge forecast system in Taiwan: Case Study of Typhoon Maria in 2018

*Chun-Wei Lin[1], Tso-Ren Wu[1], Yu-Lin Tsai[1], Shu-Chun Chuang[1], Chi-Hao Chu[2], Chuen-Teyr Terng[2] (1.Graduate Institute of Hydrological and Oceanic Sciences, National Central University, Chungli, Taiwan, 2.Marine Meteorology Center, Central Weather Bureau, Taipei, Taiwan)

[AAS02-P08] Basic Data Construction for a Typhoon Disaster Prevention Model : Analysis and Changes by El Nino and La Nina year

*HANA NA[1], Woo-Sik Jung[1] (1.Department of Atmospheric Environment Information Engineering, Atmospheric Environment Information Research Center, Inje University, Gimhae 50834, Korea)

[AAS02-P09] Basic Data Construction for a Typhoon Disaster Prevention Model : Analysis According to the Typhoon Path Type

*HANA NA[1], Woo-Sik JUNG[1] (1.Department of Atmospheric Environment Information Engineering, Atmospheric Environment Information Research Center, Inje University, Gimhae 50834, Korea)

[AAS02-P10] Basic Data Construction for a Typhoon Disaster Prevention Model : Monthly Characteristics of Typhoon Rusa, Maemi, Kompasu, and Bolaven

*HANA NA[1], Woo-Sik Jung[1] (1.Department of Atmospheric Environment Information Engineering, Atmospheric Environment Information Research Center, Inje University, Gimhae 50834, Korea)

[AAS02-P11] The mechanism of typhoon generated in the earth that rotates in the space where the solar wind blows

*Shinji Karasawa[1] (1.Miyagi National College of Technology Professor emeritus)

# Numerical study on lightning frequency in a tropical cyclone

*Yousuke Sato[1,3], Yoshiaki Miyamoto[2,3], Tomita Hirofumi[3]

1. Department of Applied Energy, Nagoya University, 2. Faculty of Environment and Information Studies, Keio University, 3. RIKEN Center for Computational Science

This study investigates frequency of lightning in each stage of lifecycle of tropical cyclone (TC) using the next generation weather and climate library called Scalable Computing for Advanced Library and Environment (SCALE; Sato et al. 2015, Nishizawa et al. 2015). Lightning component was developed and implemented into SCALE in this study. An idealized experiment based on an experimental setup of Miyamoto and Takemi (2013) was conducted by SCALE coupled with lightning component. The results of the simulation indicate that the lightning frequency is maximum before rapid intensification (RI) of TC, which supports the report of Price et al. (2009) derived from satellite observation. The frequency of lightning decreases after RI and it keeps small until the TC reaches steady state. Our analyses elucidate that the dependency of the lightning frequency upon the developing stage of TC is originated from the type of convection dominating at each growth stage. Before the RI, the convection generated by consuming convective available potential energy (CAPE) transport hydrometeors upward, and the charge split and the lightning frequently occur. During the steady state, the hydrometeors are mainly transported by the fast rotating flow in the simulated TC, which resulted in the weak charge split and small frequency of lightning.

Keywords: Tropical cyclone, Lightning

©2019. Japan Geoscience Union. All Right Reserved. 

# Sensitivity of Numerical Simulation of Typhoon Nepartak (2016) to Cloud Condensation Nuclei Concentration

*Yu-De Wu[1], Jian-Liang Wang[1]

1. Dept. of Environmental Informational and Engineering, Chung Cheng Institute of Technology, National Defense University, Taiwan

The study is carried out using the WRF model and the Cloud Condensation Nuclei, CCN, in the WDM6 microphysics scheme has been modified to test its impacts on typhoon simulations. The simulated track, intensity, and rainfall distribution of Typhoon Nepartak (2016) over Pacific Ocean are compared among numerical experiments of different initial concentration of CCN (wdm6_ctr, wdm6_10, and wdm6_50, where wdm6_10 and wdm6_50 represent that CCN are respectively 10 and 50 times of the value used in wdm6_ctr).

The simulated tracks in three runs are similar, but the intensity and the maximum dBz increase both in wdm6_10 and wdm6_50, but it takes more time for wdm6_50 to intensify. The comparison of mixing ratios of five water species shows that the cloud droplets mixing ratios increase as CCN is increased. The mixing ratios of rain, cloud ice, snow and graupel are enhanced more rapidly in wdm6_10 compared with wdm6_50. The same situation happens in the divergence field and upward motions. It is suggested that the increase of CCN will result in stronger typhoon, but the intensification will be slowed down with too much CCN.

Keywords: Cloud Condensation Nuclei, Typhoon Nepartak, Microphysics Scheme

©2019. Japan Geoscience Union. All Right Reserved. 

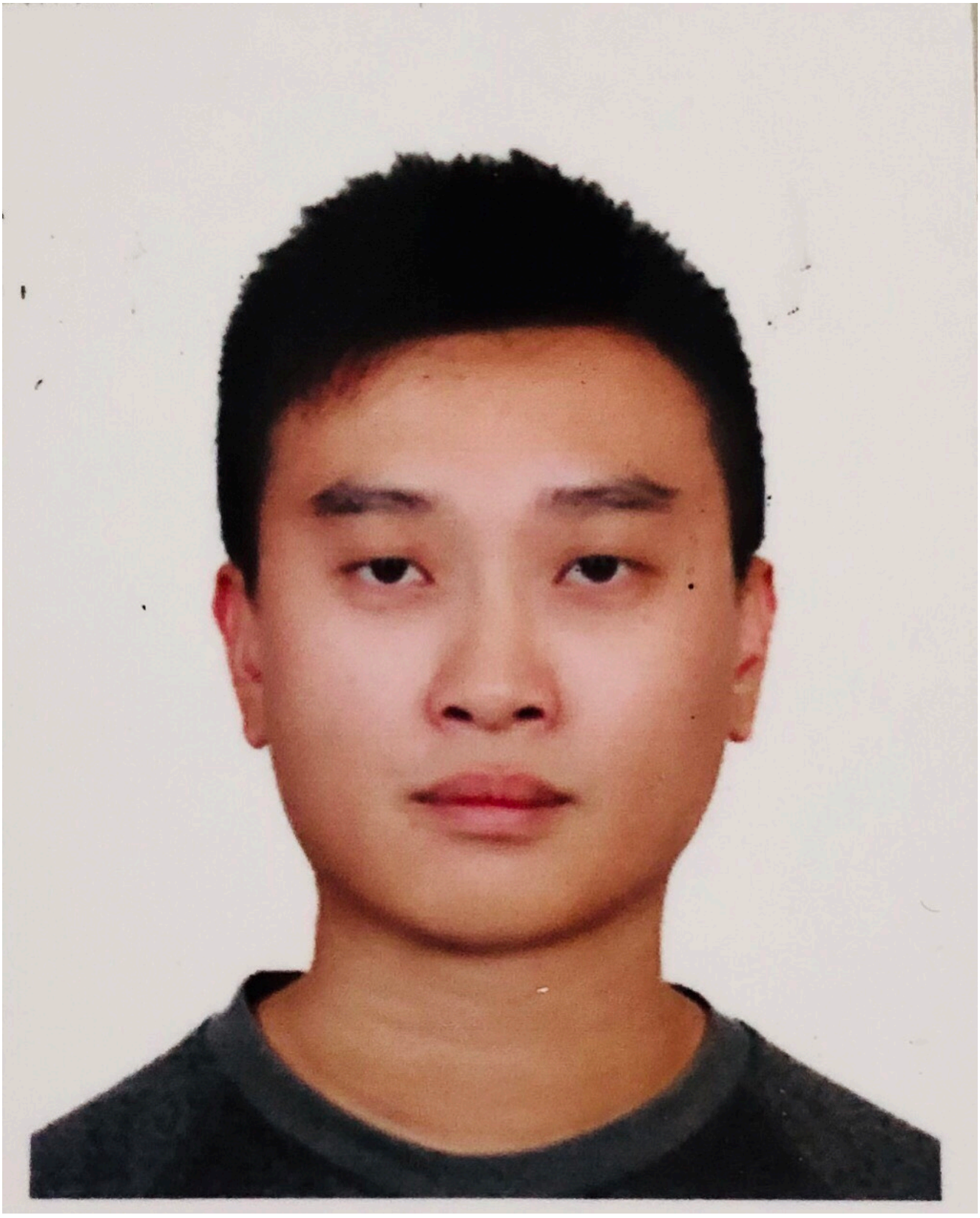

©2019. Japan Geoscience Union. All Right Reserved. 

# Moisture Budget Analysis for Hurricane Precipitation on Texas

*Satoshi Iizuka[1], Naoki Sakai[1]

1. National Research Institute for Earth Science and Disaster Resilience

In August 2017, Hurricane Harvey brought the unprecedented amount of rainfall and catastrophic flooding on the Houston metropolitan area, as it stagnated near the coast of Texas for several days after its decline to a tropical storm intensity. The present study compares the moisture budget for rainfall associated with Harvey with those of past hurricanes making landfall on Texas. It seems that the high pressure over the west coast region of the US, along with the meandering of the subtropical jet starting from the periphery of Hawaii and toward the south in Texas, stagnated Hurricane Harvey around the coast of Texas for several days. The meandering of the subtropical jet toward the south in Texas also caused the largest convergence of moisture advected from the Gulf of Mexico efficiently over Texas, although the accompanied high pressure was not extraordinary event. Therefore, it is suggested that surrounding meteorological conditions can greatly affect rainfall related to tropical cyclones.

Keywords: Hurricane Harvey, Precipitation, Moisture Budget

©2019. Japan Geoscience Union. All Right Reserved. 

# Remote response of a developing tropical cyclone over the western North Pacific to large-scale vapor transport from the Kuroshio in boreal fall

*Keita Fujiwara[1], Ryuichi Kawamura[2], Tetsuya Kawano[2]

1. Graduate School of Science, Kyushu University, 2. Faculty of Science, Kyushu University

A remote linkage between the development of tropical cyclone (TC) over the western North Pacific and moisture transport from the Kuroshio Current due to environmental flow toward TC was examined by using regional cloud resolving model and Lagrangian diagnostics. In this study, we specially highlighted a prototypical TC (Typhoon Chaba 2010), which developed and migrated northward over the Philippines Sea in boreal fall, and conducted sensitivity experiments that modified surface turbulent latent heat flux (LHF) over the Kuroshio. The large-scale environment was characterized by a combination of two synoptic systems, eastward-migrating anticyclone from the Asian continent and TC approaching Japan, bringing low-level northeasterly flows over the Kuroshio through an enhanced meridional pressure gradient in that region. Trajectory analyses suggested that air parcels along the northeasterlies modified by receiving abundant water vapor from the underlying Kuroshio may contribute to latent heating within Chaba’s inner core region as a remote effect, leading to TC development.

When LHF was removed or reduced over the Kuroshio under the dominance of the northwesterly flow, TC intensity attenuated during its developing stage even though TC was fairly far away from the Kuroshio. Since no or little modification of dry air parcels occurred in the atmospheric boundary layer over the Kuroshio, contribution of those parcels to latent heat release around Chaba’s eyewall become small. Furthermore, dry air penetration into TC’s inner core region may act as an inhibitor of convection within that region, resulting in deceleration of the TC development. These findings were consistent with another TC (Typhoon Toakge 2004) with a similar synoptic environment, increasing reliability of remote impact of moisture import from the Kuroshio on TC development.

Keywords: tropical cyclone, moisture transport, Kuroshio Current

©2019. Japan Geoscience Union. All Right Reserved. 

# Asymmetrically Intensifying Processes of a Category 4 Super Typhoon Lan (2017) during High Vertical Wind Shear

*Sachie Kanada[1], Akiyoshi Wada[2], Kazuhisa Tsuboki[1]

1. Nagoya University, 2. Meteorological Research Institute

On 21 October 2017, Typhoon Lan developed to a Category 4 super typhoon with the minimum central pressure (MCP) of 915 hPa at 25.6 degrees north latitude and maintained the peak intensity until the storm arrived at 29.9˚N under a strong environmental vertical wind shear (VWS) of 14 m $s^{-1}$. To understand the intensification processes of an intense typhoon with such high VWS, numerical simulations on Typhoon Lan were conducted using a high-resolution three-dimensional atmosphere regional model, the Cloud Resolving Storm Simulator (CReSS; Tsuboki and Sakakibara, 2002). Two sensitivity experiments, 1dO and FO, were conducted with different SST representations. In the 1dO experiment, a simple thermal diffusion model was used to express temperature changes due to ocean vertical mixing. The FO experiment with a time-fixed SST did not consider the evolution of SST. Both experiments used the same initial and boundary conditions and model specifications for the atmosphere, started at 0000 UTC 18 October 2017, and had an integration time of 5 days. The computational domain was 2˚N–37.8˚N and 115˚E–145˚E. The number of horizontal grids in the computational domain was 752×896 with the horizontal grid size of 0.04 longitude by 0.04 latitude.

The typhoon simulated in the 1dO experiment successfully achieved the MCP of 910 hPa at 29.5˚N, exhibiting strong asymmetric precipitation pattern as observed by the satellites. The intensification processes were accompanied by rapid developments of the strong winds and warm core in the low-levels. The strong northeast VWS forced to tilt the storm axis to downshear side (northeast) and, in the downshear quadrants, tall, intense and upstanding eyewall updrafts (CBs) formed from the low-level convergence of the storm travelling northeastward with a relatively fast translation speed of 10 m $s^{-1}$. Meanwhile, dry subsidence from the upper-levels intensified the low-level warm core in the upshear side of the eye. Despite the inner-core convection and precipitation exhibited strong asymmetric structures, the axisymmetricity of the storm circulation was maintained in the mid-to-low levels and abundant water vapor enclosed in the eye allowed to develop CBs around the radius of the maximum wind speeds. Although the FO storm overestimated the MCP of 879hPa, the similar asymmetric patterns in precipitation and convection were also found in the FO storm. The results indicated that the storm structures of typhoon Lan would be less sensitive to the SST-cooling effect.

Keywords: Typhoon, numerical model

©2019. Japan Geoscience Union. All Right Reserved. 

# Roles of preexisting oceanic condition and ocean coupling processes in the intensity prediction during the mature phase of Typhoon Trami (2018)

*Akiyoshi Wada[1]

1. Typhoon Research Department Meteorological Research Institute

Typhoon Trami (2018) is one of the typhoons that made landfall in Japan. According to the Regional Specialized Meteorological Center (RSMC) Tokyo best track analysis, the central pressure reached 915 hPa at 18 UTC on 24 September around 20˚N and then rapidly increased by 950 hPa in 18 hours. After the rapid increases in the central pressure, intensity forecasts announced further intensification to 935 hPa, but the typhoon could not intensify again. In order to clarify the impact of the cold eddies over the ocean on this forecast error, we conducted numerical simulations with different oceanic initial conditions (daily data from 19 to 25 September were used so that the number of ensemble members is seven) using a 2 km-mesh nonhydrostatic atmosphere model coupled with ocean surface wave and multilayer ocean models with the Japan Meteorological Agency (JMA) global objective analysis with horizontal resolution of 20 km and the JMA North Pacific Ocean analysis with horizontal resolution of 0.5˚. In addition, a sensitivity numerical experiment was conducted with the oceanic initial condition on 23 September merged with an artificial cold vortex centered at 21˚N, 129˚E of which both a mixed layer and thermocline was 50 m shallower than the control experiment. Moreover, a simulation with a 2 km-mesh nonhydrostatic atmosphere model was performed with the oceanic initial condition on 23 September. The initial time and integration period are 00 UTC on 23 September and 180 hours with the time interval of 3 seconds.

The results of simulated tracks were reasonable compared with the RSMC best track analysis, while the rapid decrease in the central pressure could not be simulated due to a large difference in central pressure at the initial time so that the simulated minimum central pressure was higher than the best track central pressure. From the analysis with the ratio of a difference to the standard deviation obtained from the ensemble experiments, the impact of different oceanic initial conditions on central pressure was different from that on the maximum wind speed particularly from 25 to 27 September when the typhoon passed near the cold eddy. The impact of ocean coupling on simulated central pressure and maximum wind speed was considerably greater than that of the artificial cold eddy and that of different oceanic initial conditions. The impact of the artificial cold eddy was a few times greater than that of different oceanic initial conditions around 26 September. The result indicates that more detailed observation and more accurate analysis regarding the cold eddy over the ocean will contribute to the improvement of typhoon intensity predictions.

Keywords: tropical cyclone, atmosphere-wave-ocean coupled model, intensity forecast, preexisting cold eddy

©2019. Japan Geoscience Union. All Right Reserved. 

# Development and assessment of the probabilistic storm surge forecast system in Taiwan: Case Study of Typhoon Maria in 2018

*Chun-Wei Lin[1], Tso-Ren Wu[1], Yu-Lin Tsai[1], Shu-Chun Chuang[1], Chi-Hao Chu[2], Chuen-Teyr Terng[2]

1. Graduate Institute of Hydrological and Oceanic Sciences, National Central University, Chungli, Taiwan, 2. Marine Meteorology Center, Central Weather Bureau, Taipei, Taiwan

From the forecast and the analyzed typhoon tracks in Taiwan, it is found that if the forecast track errors are greater than 100 km, roughly a quarter of the length of Taiwan, significant variability of storm surge elevation can be seen.
In order to consider the uncertainty of the atmospheric forecast, this study aims to develop the probabilistic storm surge forecast system. The coastal storm surge model applied in this study is COMCOT-SS (COrnell Multi-Grid COupled Tsunami Model –Storm Surge), which is the kernel of the operating deterministic storm surge forecast system in CWB, Taiwan. It solves nonlinear shallow water equations in the nested-grid scheme. Two ensemble methods are adopted in this study, one is Deterministic Track Error Distribution Method, D-TED Method. The other one is the Ensemble Track Analysis Method, ETA Method. D-TED Method is generated from the deterministic forecast, while the ETA Method obtains typhoon tracks and parameters from the CWB WEPS (CWB WRF Ensemble Prediction System).
From the case study of typhoon Maria in 2018, it shows that as the typhoon approaching Taiwan, the coverage of the tracks from ETA Method would be more convergence comparing to the tracks from D-TED Method, and it provides a more concentrated surge elevation distribution.

Keywords: storm surge, ensemble forecast, COMCOT-SS

©2019. Japan Geoscience Union. All Right Reserved. 

# Basic Data Construction for a Typhoon Disaster Prevention Model : Analysis and Changes by El Nino and La Nina year

*HANA NA[1], Woo-Sik Jung[1]

1. Department of Atmospheric Environment Information Engineering, Atmospheric Environment Information Research Center, Inje University, Gimhae 50834, Korea

Among the typhoons that affected the Korean Peninsula for approximately 110 years from 1904, when weather observation began until 2018, all of the top five typhoons in terms of the maximum wind speed and property damage record occurred after 2000. This implies that the intensity of typhoons is becoming stronger and the damage is more severe compared to the past. Moreover, typhoons are significantly affected by the sea temperature. The El Nino and La Nina phenomena, in which significant changes in the sea temperature occur, may significantly affect the occurrence and intensity of typhoons affecting the Korean Peninsula. Therefore, this study aims to analyze changes by year, and the years of El Nino and La Nina occurrences by estimating the maximum wind speed that can be generated during typhoon period based on the typhoons that affected the Korean Peninsula. This study was conducted for the period between 2002 and 2015. As a result of analyzing the maximum wind speed of the typhoons that affected the Korean Peninsula by year, high 3-second gusts tended to occur in the Gyeongsang-do area including the southeast coast of the Korean Peninsula from 2002 to 2006. Subsequently, the strong wind area of the 3-second gusts expanded, and high 3-second gusts occurred in the Seoul metropolitan area. Moreover, as a result of investigating the 3-second gust characteristics for the years of El Nino and La Nina occurrences, a higher maximum wind speed was observed from the typhoons that affected the Korean Peninsula in the years of El Nino occurrence.

This research was supported by Basic Science Research Program through the National Research Foundation of Korea(NRF) funded by the Ministry of Education(2017R1D1A3B03036152)

Keywords: Typhoon Disaster Prevention Model, 3-Second gust, El Nino, La Nina

©2019. Japan Geoscience Union. All Right Reserved. 

# Basic Data Construction for a Typhoon Disaster Prevention Model : Analysis and Changes by El Nino and La Nina year

Hana Na, Woo-Sik Jung

Among the typhoons that affected the Korean Peninsula for approximately 110 years from 1904, when weather observation began until 2018, all of the top five typhoons in terms of the maximum wind speed and property damage record occurred after 2000. This implies that the intensity of typhoons is becoming stronger and the damage is more severe compared to the past. Moreover, typhoons are significantly affected by the sea temperature. The El Nino and La Nina phenomena, in which significant changes in the sea temperature occur, may significantly affect the occurrence and intensity of typhoons affecting the Korean Peninsula. Therefore, this study aims to analyze changes by year, and the years of El Nino and La Nina occurrences by estimating the maximum wind speed that can be generated during typhoon period based on the typhoons that affected the Korean Peninsula. This study was conducted for the period between 2002 and 2015. As a result of analyzing the maximum wind speed of the typhoons that affected the Korean Peninsula by year, high 3-second gusts tended to occur in the Gyeongsang-do area including the southeast coast of the Korean Peninsula from 2002 to 2006. Subsequently, the strong wind area of the 3-second gusts expanded, and high 3-second gusts occurred in the Seoul metropolitan area. Moreover, as a result of investigating the 3-second gust characteristics for the years of El Nino and La Nina occurrences, a higher maximum wind speed was observed from the typhoons that affected the Korean Peninsula in the years of El Nino occurrence.

This research was supported by Basic Science Research Program through the National Research Foundation of Korea(NRF) funded by the Ministry of Education(2017R1D1A3B03036152)

Key words : Typhoon Disaster Prevention Model, WRF, 3-Second gust, El Nino, La Nina

©2019. Japan Geoscience Union. All Right Reserved. 

# Basic Data Construction for a Typhoon Disaster Prevention Model : Analysis According to the Typhoon Path Type

*HANA NA[1], Woo-Sik JUNG[1]

1. Department of Atmospheric Environment Information Engineering, Atmospheric Environment Information Research Center, Inje University, Gimhae 50834, Korea

In this study, a typhoon disaster prevention model was used to estimate the maximum wind speed during typhoon period by path type from all typhoons that affected the Korean Peninsula from 2002 to 2015. For the typhoon information and upper wind information used as input data, the results of the WRF numerical model, which utilized the Best Track data of the RSMC Tokyo Typhoon Center and the RDAPS data of the Korea Meteorological Administration, were applied. From analyzing the path type impact frequency using all typhoons that affected the Korean Peninsula during the study period (2002–2015), Type 7 that affected the Korean Peninsula through Japan was the most frequent, followed by Type 2 that directly landed on the Korean Peninsula through the southern coast. From analyzing the monthly path types of the typhoons that affected the Korean Peninsula, Type 2 that affected the Korean Peninsula by landing on the southern coast and Type 7 that affected the Korean Peninsula through Japan were the most frequent for the recently increasing September typhoons. The analysis of the maximum wind speed of the 3-second gust that may occur during typhoon period by path type revealed that Type 2 that affected the Korean Peninsula by landing on the southern coast exhibited the highest 3-second gust. As a result of examining the distribution of Type 2, high 3-second gusts occurred throughout the Korean Peninsula, including the southeast coast. As for the path of Type 2 that directly affected the Korean Peninsula by landing on the southern coast, the occurrence frequency was the second highest during the entire study period and the value of the 3-second gust, which was the maximum wind speed that may occur during typhoon period, was the highest.

This research was supported by Basic Science Research Program through the National Research Foundation of Korea(NRF) funded by the Ministry of Education(2017R1D1A3B03036152)

Keywords: Typhoon Path, 3-Second gust, Typhoon Disaster Prevention Model

©2019. Japan Geoscience Union. All Right Reserved. 

# Basic Data Construction for a Typhoon Disaster Prevention Model : Analysis According to the Typhoon Path Type

Hana Na, Woo-Sik Jung

In this study, a typhoon disaster prevention model was used to estimate the maximum wind speed during typhoon period by path type from all typhoons that affected the Korean Peninsula from 2002 to 2015. For the typhoon information and upper wind information used as input data, the results of the WRF numerical model, which utilized the Best Track data of the RSMC Tokyo Typhoon Center and the RDAPS data of the Korea Meteorological Administration, were applied. From analyzing the path type impact frequency using all typhoons that affected the Korean Peninsula during the study period (2002–2015), Type 7 that affected the Korean Peninsula through Japan was the most frequent, followed by Type 2 that directly landed on the Korean Peninsula through the southern coast. From analyzing the monthly path types of the typhoons that affected the Korean Peninsula, Type 2 that affected the Korean Peninsula by landing on the southern coast and Type 7 that affected the Korean Peninsula through Japan were the most frequent for the recently increasing September typhoons. The analysis of the maximum wind speed of the 3-second gust that may occur during typhoon period by path type revealed that Type 2 that affected the Korean Peninsula by landing on the southern coast exhibited the highest 3-second gust. As a result of examining the distribution of Type 2, high 3-second gusts occurred throughout the Korean Peninsula, including the southeast coast. As for the path of Type 2 that directly affected the Korean Peninsula by landing on the southern coast, the occurrence frequency was the second highest during the entire study period and the value of the 3-second gust, which was the maximum wind speed that may occur during typhoon period, was the highest.

This research was supported by Basic Science Research Program through the National Research Foundation of Korea(NRF) funded by the Ministry of Education(2017R1D1A3B03036152)

Keywords : Typhoon Disaster Prevention Model, WRF, Typhoon Track, 3-Second gust

©2019. Japan Geoscience Union. All Right Reserved. 

# Basic Data Construction for a Typhoon Disaster Prevention Model : Monthly Characteristics of Typhoon Rusa, Maemi, Kompasu, and Bolaven

*HANA NA[1], Woo-Sik Jung[1]

1. Department of Atmospheric Environment Information Engineering, Atmospheric Environment Information Research Center, Inje University, Gimhae 50834, Korea

According to a typhoon report that summarized the typhoons that had affected the Korean Peninsula for approximately 100 years since the start of weather observation in the Korean Peninsula, the number of typhoons that affected the Korean Peninsula was the highest in August, followed by July, and September. A study that analyzed the period between 1953 and 2003 revealed that the number of typhoons that affected the Korean Peninsula was 62 in August, 49 in July, and 45 in September. As shown, previous studies that analyzed the typhoons that affected the Korean Peninsula by month were primarily focused on the impact frequency. This study aims to estimate the monthly impact frequency of the typhoons that affected the Korean Peninsula as well as the maximum wind speed that accompanied the typhoons. It also aims to construct the basic data of a typhoon disaster prevention model by estimating the maximum wind speed during typhoon period using Typhoon Rusa that resulted in the highest property damage, Typhoon Maemi that recorded the maximum wind speed, Typhoon Kompasu that significantly affected the Seoul metropolitan area, and Typhoon Bolaven that recently recorded severe damages. A typhoon disaster prevention model was used to estimate the maximum wind speed of the 3-second gust that may occur, and the 700 hPa wind speed estimated through WRF(Weather Research and Forecasting) numerical simulation was used as input data.

Unlike the target period reported in the white paper on typhoons (1904–2010), this study analyzed the monthly impact frequency of the typhoons that affected the Korean Peninsula from 2002 and 2015. The result indicated that the impact frequency was the highest in August, followed by July and September. This result was the same as that of the typhoon report. An analysis by year revealed that typhoon period increased in September. The 3-second gust was found to be the highest in September, followed by August and July. When this result was analyzed in relation to the recently increasing autumn typhoons (September and October), the 3-second gust result was the highest in September, indicating disaster prevention must be emphasized. By additionally analyzing the maximum wind speed distributions of Typhoon Rusa, Maemi, Kompasu, and Bolaven, the area with the maximum wind speed varied depending on the typhoon path, and the 3-second gust was higher than 44 m/s based on the typhoon intensity classification and accounted for approximately10%.

This research was supported by Basic Science Research Program through the National Research Foundation of Korea(NRF) funded by the Ministry of Education(2017R1D1A3B03036152)

Keywords: Typhoon Disaster Prevention Model, WRF, 3-Second gust

©2019. Japan Geoscience Union. All Right Reserved. 

# Basic Data Construction for a Typhoon Disaster Prevention Model : Monthly Characteristics of Typhoon Rusa, Maemi, Kompasu, and Bolaven

Hana Na, Woo-Sik Jung

According to a typhoon report that summarized the typhoons that had affected the Korean Peninsula for approximately 100 years since the start of weather observation in the Korean Peninsula, the number of typhoons that affected the Korean Peninsula was the highest in August, followed by July, and September. A study that analyzed the period between 1953 and 2003 revealed that the number of typhoons that affected the Korean Peninsula was 62 in August, 49 in July, and 45 in September. As shown, previous studies that analyzed the typhoons that affected the Korean Peninsula by month were primarily focused on the impact frequency. This study aims to estimate the monthly impact frequency of the typhoons that affected the Korean Peninsula as well as the maximum wind speed that accompanied the typhoons. It also aims to construct the basic data of a typhoon disaster prevention model by estimating the maximum wind speed during typhoon period using Typhoon Rusa that resulted in the highest property damage, Typhoon Maemi that recorded the maximum wind speed, Typhoon Kompasu that significantly affected the Seoul metropolitan area, and Typhoon Bolaven that recently recorded severe damages. A typhoon disaster prevention model was used to estimate the maximum wind speed of the 3-second gust that may occur, and the 700 hPa wind speed estimated through WRF(Weather Research and Forecasting) numerical simulation was used as input data.

Unlike the target period reported in the white paper on typhoons (1904–2010), this study analyzed the monthly impact frequency of the typhoons that affected the Korean Peninsula from 2002 and 2015. The result indicated that the impact frequency was the highest in August, followed by July and September. This result was the same as that of the typhoon report. An analysis by year revealed that typhoon period increased in September. The 3-second gust was found to be the highest in September, followed by August and July. When this result was analyzed in relation to the recently increasing autumn typhoons (September and October), the 3-second gust result was the highest in September, indicating disaster prevention must be emphasized. By additionally analyzing the maximum wind speed distributions of Typhoon Rusa, Maemi, Kompasu, and Bolaven, the area with the maximum wind speed varied depending on the typhoon path, and the 3-second gust was higher than 44 m/s based on the typhoon intensity classification and accounted for approximately10%.

This research was supported by Basic Science Research Program through the National Research Foundation of Korea(NRF) funded by the Ministry of Education(2017R1D1A3B03036152)

Keywords : Typhoon Disaster Prevention Model, WRF, 3-Second gust, RUSA, MAEMI, KOMPASU, BOLAVEN

©2019. Japan Geoscience Union. All Right Reserved. 

# The mechanism of typhoon generated in the earth that rotates in the space where the solar wind blows

*Shinji Karasawa[1]

1. Miyagi National College of Technology Professor emeritus

The atmosphere in the upper tropical cyclone (TC) rotates the clock-wise direction by the trade winds and westerlies. The rotation speed near the center increases, because the angular momentum of the atmospheric molecule is transported. The eye of the typhoon is appeared at the place where the centrifugal force of the rotation on the flow exceeds compared with the difference of the pressure. The atmosphere including the vapor of water in the cumulonimbus are mixed with the cold air flow swirling in the clockwise direction at the eye of typhoon, where the water vapors become to the rain, and the cumulonimbus rotates in anticlockwise direction.
The solar wind includes rotational momentum and the rotational momentum of the solar wind generates the trade winds. On the other hand, the westerlies are caused by the solar wind that rotates the tail of Earth's magnetosphere on the opposite side of the Sun in anticlockwise rotation, and it gives the driving force of the westerlies. Ref. S. Karasawa.
https://www.youtube.com/watch?v=bzCup63G8z8&feature=youtu.be

Keywords: tropical cyclone, westerlies, trade winds, solar wind, Earth’ s rotation, Sun’ s rotation

©2019. Japan Geoscience Union. All Right Reserved. 

[E] Oral | A (Atmospheric and Hydrospheric Sciences )：A-AS Atmospheric Sciences, Meteorology & Atmospheric Environment

Thu. May 30, 2019 3:30 PM - 5:00 PM JST | Thu. May 30, 2019 6:30 AM - 8:00 AM UTC | 104 1F

## [A-AS02] Advances in Tropical Cyclone Research: Past, Present, and Future

convener:Sachie Kanada(Nagoya University), Akiyoshi Wada(Department of Typhoon and Severe Weather Research, Meteorological Research Institute), Kosuke Ito(University of the Ryukyus), Yoshiaki Miyamoto(Faculty of Environment and Information Studies, Keio University), Chairperson:Sachie Kanada(Nagoya University), Yoshiaki Miyamoto

Tropical cyclones (TC) sometimes cause destructive disasters in many countries by torrential rainfall, strong wind, storm surge, and high surf. In 2008, the western Japan suffered a record-breaking heavy rainfall related to Typhoon Prapirooon (2018) in July. Furthermore, two Category 4 typhoons, typhoons Jebi (2018) and Trami (2018), made landfalls on the western Japan in September and caused devastating disasters over the Japanese Islands. In the Northern Atlantic, Hurricane Florence caused catastrophic damage in the eastern side of U.S. Recent studies reported a northward shift of the location where a TC achieved the peak intensity and also reported increases in the frequency of rapidly intensifying storms. Thus, understanding the TC processes related to translation, intensity change and precipitation in the changing climate, and to provide more accurate forecasts and long-term projections are essential for the earth and planetary science.<br/>Advances in innovative observations such as meteorological aircraft, weather satellite, supercomputer systems such as the Earth Simulator and K-computer, and introduction of new methods such as the deep-learning, have led to novel development of numerical weather forecasting and understanding of the phenomena related to TCs in the past, present and future climates. In this session, we welcome papers on various aspects of TC studies. We hope that the session will provide a new direction for future TC researches.

3:30 PM - 3:45 PM JST | 6:30 AM - 6:45 AM UTC

[AAS02-12] Evaluation of the monthly Potential of the 2018 typhoon activity and the effect of the positive PMM and SST of the eastern northwestern Pacific

*Takahiro Ishiyama[1], Masaki Satoh[1] (1.Atmosphere and Ocean Research Institute, The University of Tokyo)

3:45 PM - 4:00 PM JST | 6:45 AM - 7:00 AM UTC

[AAS02-13] **Contributions of different time scale variations to tropical cyclogenesis over the western North Pacific**

*Xi Cao[1] (1. Institute of Atmospheric Physics, Chinese Academy of Sciences)

4:00 PM - 4:15 PM JST | 7:00 AM - 7:15 AM UTC

[AAS02-14] Binary interaction between TC Chanthu (2016) and a nearby cold low

*Kosuke Ito[1], Miyabi Higa[1], Johnny Chan[2] (1.University of the Ryukyus, 2.City University of Hong Kong)

4:15 PM - 4:30 PM JST | 7:15 AM - 7:30 AM UTC

[AAS02-15] **Response of landfalling North Indian Ocean cyclonic disturbances to warming climate and associated environmental parameters**

*JAGABANDHU PANDA[1], KASTURI SINGH[1] (1.Department of Earth and Atmospheric Sciences, National Institute of Technology Rourkela, India)

4:30 PM - 4:45 PM JST | 7:30 AM - 7:45 AM UTC

[AAS02-16] **Rainfall contribution of North Indian Ocean cyclonic disturbances over India in a warming climate**

*KASTURI SINGH[1], JAGABANDHU PANDA[1] (1.Department of Earth and Atmospheric Sciences, National Institute of Technology Rourkela, India)

4:45 PM - 5:00 PM JST | 7:45 AM - 8:00 AM UTC

[AAS02-17] Analysis of typhoon tracks and associated precipitation amount over western Japan: A case study with Typhoon Nancy and Typhoon Jebi

*Sridhara Nayak[1], Tetsuya Takemi[1] (1.Disaster Prevention Research Institute, Kyoto University)

# Evaluation of the monthly Potential of the 2018 typhoon activity and the effect of the positive PMM and SST of the eastern northwestern Pacific

*Takahiro Ishiyama[1], Masaki Satoh[1]

1. Atmosphere and Ocean Research Institute, The University of Tokyo

Typhoons in the northwest Pacific in 2018 exceeded the average for 29 occurrences, the number of landings to Japan to 5, and for the typhoon which became extreme strength it was updated with the most record and the activity was active. In the ENSO phase, La Niña phenomenon occurred in the beginning of 2018 but converged by early spring and El Niño phenomenon occurred in October. However, during the most active period of the typhoon (from June to November), the ENSO phase was still in a neutral state. Therefore, Pacific Meridional Mode (hereafter PMM) (Chiang and Vimont 2004) is focused recently. At the positive phase of PMM, a zone of warming sea surface temperature (hereafter SST) is formed in the northeast - southwest direction of 20 degrees north latitude, 120 degrees west latitude to 0 degrees north latitude and 180 degrees west longitude. Previous studies have pointed out that this positive PMM favors TC activities in the northwest Pacific (Zhang et al. 2016). Looking at the PMM index (SST) from 1948 to 2018, there was positive PMM in 2018 and the intensity was strong enough to be within 15th place of 71 in each month of active typhoon season. Especially, in August and September, strong positive PMM phenomenon was developed in 4th place and 2nd place.

The purpose of this research is to focus on the monthly SST variation such as ENSO and PMM and to evaluate the Potential of the 2018 typhoon activity. We also focus on the PMM and the SST over the eastern of northwest Pacific, and investigate how they affect the 2018 typhoon activity.

For the above purpose, we conducted perpetual experiments in which boundary conditions were fixed from July to October, respectively, using a nonhydrostatic model NICAM. The horizontal resolution was 56 km, and the number of vertical layers was 38 layers. In sensitivity experiments, PMM region and PMM + eastern northwest Pacific regions of SST in July 2018 sensitivity experiment 1 and sensitivity experiment 2 replaced with climate value were conducted. Comparing the experimental result of sea level pressure (hereafter SLP) with JRA-55, although the position of the maximum value of the high pressure in July is misaligned, the position and overhang of the high pressure does not differ greatly in each month, and perpetual experiments also reproduce the reality well. Both reanalysis and perpetual experiments have more typhoons in July and August than in September and October. Also, the occurrence position of the typhoon occurs more frequently in the eastern side of the northwestern Pacific in order of July, August, September. The same tendency was observed. Such differences in active areas of typhoon activity had an effect on the monsoon trough.
Subsequently, the SLPs of the 2018 experiment, sensitivity experiment 1 and sensitivity experiment 2 were compared. In comparison with the sensitivity experiment 1, the sensitivity experiment 1 became a lower pressure deviation in the west side of the northwest Pacific than 2018 experiment, whereas in the sensitivity experiment 2, the sensitivity experiment 2 had higher SLP in the whole northwest Pacific than 2018 experiment. From this, it was found that the positive SST deviation in the eastern northwest Pacific was more involved in the typhoon activity of 2018.

©2019. Japan Geoscience Union. All Right Reserved. 

Keywords: tropical cyclone, Pacific Meridional Mode, nonhydrostatic model

©2019. Japan Geoscience Union. All Right Reserved. 

# Contributions of different time scale variations to tropical cyclogenesis over the western North Pacific

*Xi Cao[1]

1. Institute of Atmospheric Physics, Chinese Academy of Sciences

The present study investigates relative contributions of different time scale variations of environmental factors to the tropical cyclone (TC) genesis over the western North Pacific (WNP) during July-August-September-October (JASO). Distinct from previous studies that are concerned with large-scale spatial patterns during a certain period, the present study focuses on local and instantaneous conditions of the TC genesis. Analysis shows that the contribution of convection and lower-level vorticity to the TC genesis is mainly due to intraseasonal and synoptic variations. The contribution of vertical wind shear is largely related to synoptic variations. The contribution of mid-level specific humidity is almost two times more from intraseasonal variations than from synoptic variations. The contribution of sea surface temperature (SST) to the TC genesis is mainly due to interannual and intraseasonal variations. The barotropic energy for synoptic-scale disturbances during the TC genesis comes mainly from climatological mean flows over the southwest quadrant and from intraseasonal wind variations over the northeast quadrant of the WNP, respectively. The contribution of interannual variations to the TC genesis is enhanced over the southeast quadrant of the WNP. More TCs form under weak easterly and westerly vertical shears, respectively, during El Niño developing and decaying JASO. The contribution of interannual variations of SST tends to be larger during the El Niño decaying than developing JASO.

Keywords: tropical cyclone genesis, western North Pacific , different time scales

©2019. Japan Geoscience Union. All Right Reserved. 

# Binary interaction between TC Chanthu (2016) and a nearby cold low

*Kosuke Ito[1], Miyabi Higa[1], Johnny Chan[2]

1. University of the Ryukyus, 2. City University of Hong Kong

Tropical cyclone (TC) Chanthu (2016) caused the heavy rainfall and strong wind on Hokkaido Prefecture, Japan. However, this was one of the "busted" cases in which the track forecast error reached up to 900 km in a 72-h forecast by the Regional Specialized Meteorological Center (RSMC) Tokyo. In fact, the re-forecast experiment with Japan Meterological Agency Non-Hydrostatic Model (JMA-NHM) that employed Kain-Fritsch scheme as a convective parameterization correctly captured the observed northward translation speed of TC Chanthu, while the JMA Global Spectral Model (JMA-GSM) and JMA-NHM that employed Arakawa-Schubert scheme failed to predict the accurate northward translation speed. The mesoscale analysis showed that there was a cold low located at 200km west of TC Chanthu (2016). With Kain-Frische scheme, the binary interaction between TC Chanthu and the nearby cold low was reproduced so that it contributed the faster translation to the north as consistent with the best track. In contrast, the binary interaction was not reproduced in the simulations with Arakawa-Schubert scheme because a triggered large-scale convection made TC Chanthu and the nearby cold low merged. It exemplifies that the reproduction of fine-scale features diminishes "busted" cases, which contributes to the disaster prevention and mitigation.

Keywords: tropical cyclone, Fujiwhara effect, track forecast

©2019. Japan Geoscience Union. All Right Reserved. 

# Response of landfalling North Indian Ocean cyclonic disturbances to warming climate and associated environmental parameters

*JAGABANDHU PANDA[1], KASTURI SINGH[1]

1. Department of Earth and Atmospheric Sciences, National Institute of Technology Rourkela, India

Most of the studies focusing on cyclonic disturbances (CDs) concentrate on their frequency. However, the system that causes destruction to nearby coastal areas is the landfalling one. The impact of warming climate on landfalling CD activity is an interesting topic. Thus, the present study focuses on the landfalling activity of CDs formed over North Indian Ocean (NIO) and associated environmental parameters responsible for the same. The study is divided into two epochs i.e. pre-warming period (PWP) 1891-1946 and current warming period (CWP) 1947-2016 based on the sea surface temperature anomaly variation.

Over NIO, nearly 88 and 84.80% of systems made landfall over coastal areas associated with Bay of Bengal (BOB) basin and the respective percentages are 53.03 and 39% for AS during PWP and CWP respectively. The percentage of landfalling CDs shows a decreasing and stable trend respectively during PWP and CWP for BOB sub-basin. Over AS, the Kendall’ s coefficients are found to be −0.255 and −0.0024 during PWP and CWP respectively. The study reveals that Bangladesh, Andhra Pradesh (AP), and Tamil Nadu (TN) are more vulnerable to severe cyclones formed over BOB during the current warming climate. Whereas, for Arabian Sea (AS) region, Gujrat (GJ) is prone to severe cyclones and Arabian Peninsula countries are vulnerable to cyclonic storms during the current warming climate. For pre-monsoon season, among all NIO coastal states, Bangladesh and Arakan face a greater number of CD landfalls during CWP for BOB systems. Whereas, for post-monsoon season, AP, TN and Bangladesh suffered maximum landfalls. The seasonal landfalling activity of CDs over AS shows that Arabian Peninsula is more vulnerable than GJ in pre-monsoon season during CWP. However, for post-monsoon season, both Arabian Peninsula and GJ are significantly prone to landfalling CDs. During PWP, most of the systems formed over middle sector of BOB recurve in north-eastward direction. Whilst, one climatological track is found to be recurving towards Bangladesh, another one is towards AP during CWP. CDs formed over southern sector of BOB prefers two tracks, one being westward towards TN and the other is in north-east direction towards Bangladesh during CWP. The enhanced genesis over southern and middle sector of BOB is mainly responsible for more landfalls over AP, TN and Bangladesh. The CDs formed over the eastern AS basin recurve to make landfall over GJ or Oman during PWP. However, during CWP, another preferable track towards Yemen is also seen for the systems formed over eastern AS.

The climatological vertically integrated (mass-weighted) tropospheric wind pattern near TN coast has changed direction from westward during PWP to north-westward during CWP (Figure 1), favouring more landfall over AP and TN. Over the central part near the latitude 14˚N, change in the magnitude has occurred with change in the direction of the winds from NW-N to NE. Because of the prevailing wind steering pattern, the systems that formed over the middle and southern BOB do not prefer to make landfall to WB and Odisha during CWP. Over AS, the wind is mostly directed towards GJ irrespective of the period considered, which favours more landfalling of CDs over the place. These winds are primarily part of mid-latitude westerly troughs. For BOB, the SST gradient is in meridional direction and hence most of the systems formed, suffer landfall over Indian coastal states and other rim countries face less landfalls. Over AS, SST gradient is zonally distributed and therefore, the eastward deflection of CDs is more observed, making the Indian state of GJ to be the most affected region. The study is expected to be helpful in the decision-making process in view of socio-economic impacts of landfalling CDs.

©2019. Japan Geoscience Union. All Right Reserved. 

Keywords: Cyclonic disturbances, North Indian Ocean, Landfall, Bay of Bengal, Arabian Sea

©2019. Japan Geoscience Union. All Right Reserved. 

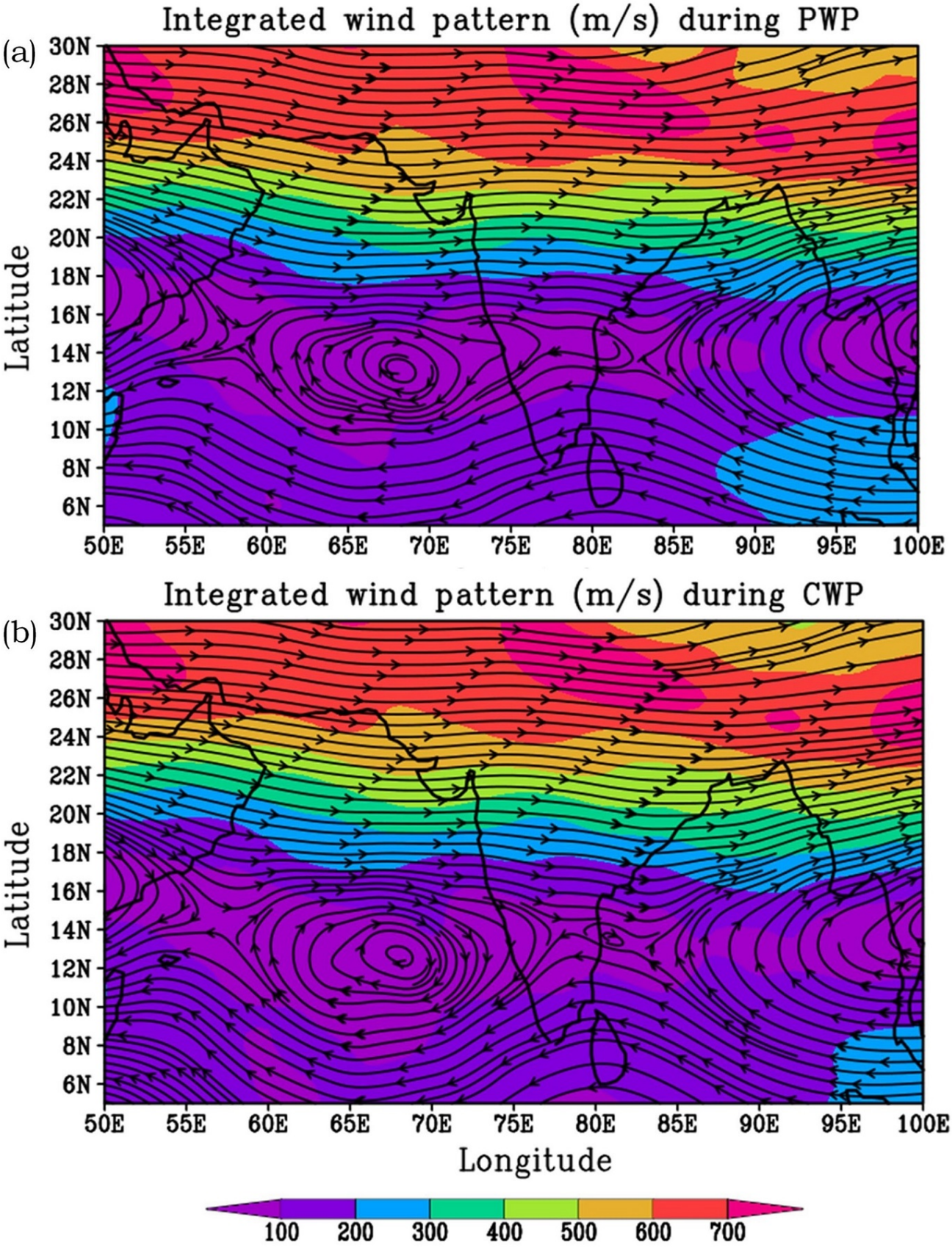


Figure 1: Climatological variation of mass weighted vertically integrated tropospheric wind magnitude (shaded) and wind pattern (vector) in m/s over NIO for the period 1891-2014 during PWP (a) and CWP (b). Here, NOAA-CIRES global re-analyses data set is used.

©2019. Japan Geoscience Union. All Right Reserved. 

# Rainfall contribution of North Indian Ocean cyclonic disturbances over India in a warming climate

*KASTURI SINGH[1], JAGABANDHU PANDA[1]

1. Department of Earth and Atmospheric Sciences, National Institute of Technology Rourkela, India

Rainfall associated with cyclonic disturbances (CDs) poses mostly significant threat to the society. Such type of systems and their remnants are capable of producing heavy rainfall, which often produce flash flooding. The warming climate is considered from 1947 onwards based on sea surface temperature anomaly variation over North Indian Ocean (NIO) basin. Nearly 71.42% of CDs in pre-monsoon and 87.07% CDs in post-monsoon season crossed or gazed the Indian coast during 140 cyclone seasons of the warming climate. The trend for annual variation of CD rainfall (CDR) anomaly is decreasing along with CD anomaly during pre-monsoon season (P=4.89901E-15). The trend for CDR anomaly is observed to be almost stable while the CD anomaly is decreasing drastically (P=1) in the post-monsoon season, indicating increased amount of rainfall is contributed by CDs over India in this period.

Among eastern coastal states, Andhra Pradesh (AP), Tamil Nadu (TN), Mizoram, Tripura and among western coastal states, Kerala (KL), Karnataka (KA) and Gujarat (GJ) received most of the accumulated rainfall in pre-monsoon season. The rainfall contributed by CDs during pre-monsoon season is limited to the coastal districts of India only. However, the rainfall occurrences during post-monsoon season could penetrate up to very interior districts. During post-monsoon season, Odisha (OD), AP and TN received the highest rainfall contribution from CDs. Jharkhand, KL, KA, parts of Maharashtra (MH) and coastal GJ received significantly higher amount of rainfall in comparison to other interior places. Up to ~70% of rainfall is contributed by CDs over GJ, nearly 20-30% over AP and 15-18% over western Rajasthan during pre-monsoon (Figure 1). During post-monsoon season, considerable rainfall (60% of annual value) contribution is seen over all states. The trend in CD rainfall is observed to be increasing over western GJ, western Rajasthan, northeast AP and southeast OD during pre-monsoon months. The spatio-temporal trend of CD rainfall over Bihar, Jharkhand, northern OD, northern Chhattisgarh, eastern Madhya Pradesh, Sikkim and Meghalaya are observed to be increasing during post-monsoon months. The rainfall contributed by CDs over the border regions of AP and TN is observed to be decreasing. Among eastern coastal states, AP has received 200cm of accumulated rainfall contribution during pre-monsoon season. The corresponding values for TN, OD and WB are 180, 140 and 140cm respectively. During post-monsoon season, AP received 1100cm of rainfall, OD and TN with 900cm of rainfall each, and WB received 450cm of accumulated rainfall contributed by CDs. For western coastal states, during pre-monsoon season, the maximum amount of accumulated rainfall contributions over GJ, MH, KA and KL are about 85, 75, 110 and 160cm respectively. During post-monsoon season, the corresponding values are nearly 134, 145, 320 and 350cm. Comparing the trend for maximum and minimum rainfall received by a coastal state, it can be concluded that even though the maximum values for some years are slightly less in comparison to other years, the minimum contribution is quite significant for those particular years. The possible reason can be due to larger and faster moving storms those result in longer precipitation durations with greater area coverage.

Further, the association of such rainfall contributions with ENSO, MJO and IOD cannot be undermined and thus, analyzed using observations and modeling output. The preliminary results indicate relative dominance of MJO in determining the CDR over Indian region during pre-monsoon months. During IOD –ve, heavy rainfall is contributed by CDs over AP and TN. The explicit discussion regarding the same will

©2019. Japan Geoscience Union. All Right Reserved. 

be included in the presentation.

Keywords: cyclonic disturbances, rainfall, North Indian Ocean, India

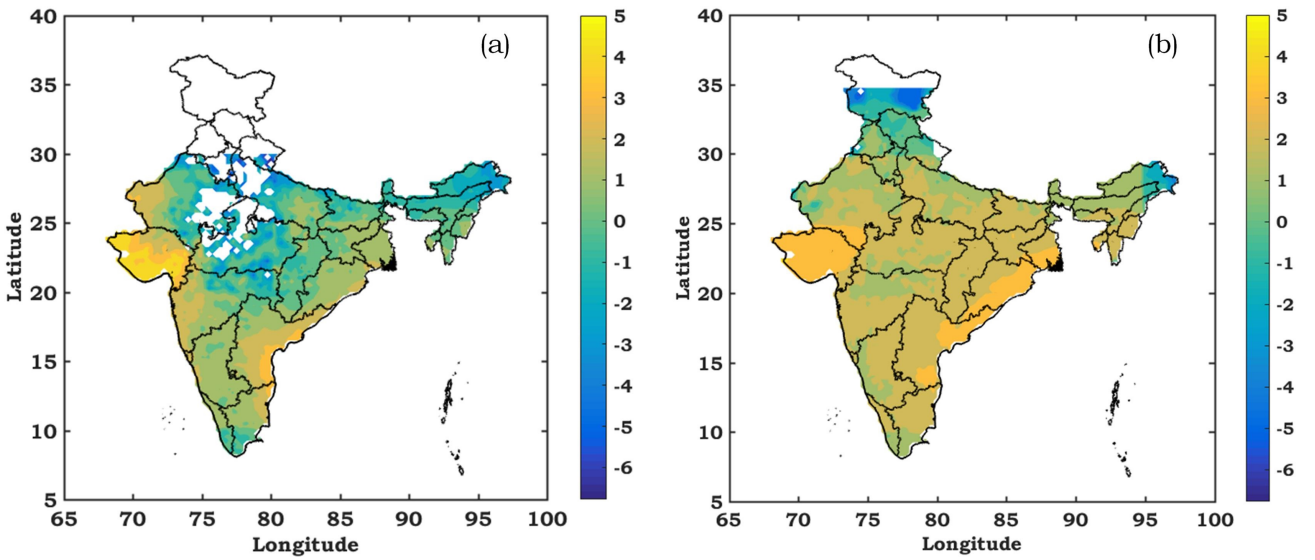


Figure 1: Percentage rainfall (cm) contributed by CDs formed over NIO during (a) pre-monsoon and (b) post-monsoon season respectively over India. Here, the percentage contribution of rainfall is shown in terms of logarithmic scale of actual value.

©2019. Japan Geoscience Union. All Right Reserved. 

# Analysis of typhoon tracks and associated precipitation amount over western Japan: A case study with Typhoon Nancy and Typhoon Jebi

*Sridhara Nayak[1], Tetsuya Takemi[1]

1. Disaster Prevention Research Institute, Kyoto University

Recent research suggests that typhoons under future warming climate will be more powerful and bring excessive precipitations to the landfall areas. In our study, we downscaled two very strong Typhoons [Typhoon Nancy (international #196118) and Typhoon Jebi (international #201821)] at 1-km grid resolution in present climate and with pseudo global warming (PGW) conditions by using Weather Research and Forecasting (WRF) model. An attempt is also made to examine whether the precipitation amounts carried by Typhoon Jebi can be projected from Typhoon Nancy with PGW conditions, because both typhoons made landfall over same region of Japan with a difference of 57 years. Our results indicate that the typhoon tracks in present climate simulation have good agreement with that of from the RSMC, Tokyo’ s best track datasets. The precipitation amounts over western Japan in the present climate simulation also follows the Radar-AMeDAS observed precipitation amounts. We again find similar typhoon tracks under PGW conditions for both typhoons with higher winds and precipitations compared to that of in present climate simulation. The precipitation amounts associated with the Typhoon Nancy in future climate is found to be higher than that of with Typhoon Jebi during the landfall. However, the 24 hours accumulated precipitation amount brought by Typhoon Nancy with PGW conditions has an overall good agreement with that of by Typhoon Jebi in present climate simulation especially over landfall region. Closer investigation on the typhoon tracks and typhoon induced precipitation amounts suggests that Typhoon Jebi is a possible projection of Typhoon Nancy although it was formed over different location.

Keywords: Typhoon Nancy, Typhoon Jebi, Typhoon track, Typhoon intensity

©2019. Japan Geoscience Union. All Right Reserved. 

[J] Oral | A (Atmospheric and Hydrospheric Sciences )：A-AS Atmospheric Sciences, Meteorology & Atmospheric Environment

Thu. May 30, 2019 9:00 AM - 10:30 AM JST | Thu. May 30, 2019 12:00 AM - 1:30 AM UTC | 102 1F

## [A-AS04] Atmospheric Chemistry

convener:Tomoki Nakayama(Graduate School of Fisheries and Environmental Sciences, Nagasaki University), Yoko Iwamoto(Graduate School of Biosphere Science, Hiroshima University), Sakae Toyoda(Department of Chemical Science and Engineering, Tokyo Institute of Technology), Nawo Eguchi(Kyushu University), Chairperson:Hisahiro Takashima(福岡大学)

This session provides a forum for the presentation of the broad spectrum of tropospheric and stratospheric chemistry, including various research topics (e.g., dynamical processes, air quality and climate), approaches (modeling, field measurements, remote sensing, and laboratory studies), and species (gas and aerosol). This session also provides an opportunity for discussing possible future collaboration with other research fields relevant to atmospheric chemistry. We strongly encourage authors to prepare presentation slides and a poster in English.

9:00 AM - 9:15 AM JST | 12:00 AM - 12:15 AM UTC

[AAS04-16] Toward the Reduction of Radiative Forcing of Methane and Tropospheric Ozone: Aiming at the Emission Control of $CH_4$, $NO_x$and NMVOC in Asia

*Hajime Akimoto[1], Tatsuya NNagashima[1], Hiroshi Tanimoto[1], Zig Klimont[2], Markus Amann[2] (1.National Institute for Environmental Studies, 2.International Institute for Applied Systems Analysis)

9:15 AM - 9:30 AM JST | 12:15 AM - 12:30 AM UTC

[AAS04-17] **Determination of atmospheric $NO_2$ column densities using a Pandora instrument measuring direct-sun spectra at Yokosuka, Japan: Improved validation of TROPOMI satellite observations**

*Yugo Kanaya[1], Hisahiro Takashima[2,1], Masato I. Nodzu[3], Takashi Sekiya[7], Kazuyuki Miyazaki[1], Henk Eskes[4], Gaia Pinardi[5], Daniel Santana Diaz[6], Moritz Müller[6], Alexander Cede[6] (1.Research and Development Center for Global Change, Japan Agency for Marine-Earth Science and Technology (JAMSTEC), 2.Fukuoka University, 3.Tokyo Metropolitan University, 4.KNMI, 5.BIRA-IASB, 6.LuftBlick, 7.Japan Agency for Marine-Earth Science and Technology (JAMSTEC))

9:30 AM - 9:45 AM JST | 12:30 AM - 12:45 AM UTC

[AAS04-18] A high-resolution global data assimilation for air pollution analysis on megacity scale using multi-sensor satellite measurements including TROPOMI $NO_2$ data

*Takashi Sekiya[1], Kazuyuki Miyazaki[2,1], Henk Eskes[3], Folkert Boersma[3], Koji Ogochi[1], Kengo Sudo[4,1], Masayuki Takigawa[1] (1.Japan Agency for Marine-Earth Science and Technology, 2.Jet Propulsion Laboratory/California Institute for Technology, 3.Royal Netherlands Meteorological Institute (KNMI), 4.Graduate School of Environmental Studies, Nagoya University)

9:45 AM - 10:00 AM JST | 12:45 AM - 1:00 AM UTC

[AAS04-19] Recent trends of $NO_2$, VOC, and tropospheric ozone concentrations observed around Chiba, Japan in 2013-2018

*Daichi Yonekawa[1], Hitoshi Irie[2] (1.Chiba university Graduate school, 2.Chiba university)

10:00 AM - 10:15 AM JST | 1:00 AM - 1:15 AM UTC

[AAS04-20] Long-term seasonal changes in tropospheric ozone over Japan

*Natsumi Kawano[1], Tatsuya Nagashima[1], Seiji Sugata[1] (1.National Institute for Environmental Studies)

10:15 AM - 10:30 AM JST | 1:15 AM - 1:30 AM UTC

[AAS04-21] **Characteristics of Atmospheric Photochemical Pollution at a Comprehensive Site in Guangzhou, China**

*Yu Zou[1] (1.Institute of Tropical and Marine Meteorology, CMA,Guangzhou,China)

# Toward the Reduction of Radiative Forcing of Methane and Tropospheric Ozone: Aiming at the Emission Control of $CH_4$, $NO_x$and NMVOC in Asia

*Hajime Akimoto[1], Tatsuya NNagashima[1], Hiroshi Tanimoto[1], Zig Klimont[2], Markus Amann[2]

1. National Institute for Environmental Studies, 2. International Institute for Applied Systems Analysis

In order to reduce impacts of climate change, including potential further increase of damages due to extreme events related to global warming, reduction of burdens of $CH_4$and tropospheric ozone in Asia are discussed. In order to mitigate the inevitable further increase of radiative forcing (RF) of ca. 0.8 W $m^{-2}$by 2040 caused by the increase of $CO_2$in 2040, feasible reduction of the industrial RF of methane ($CH_4$) and tropospheric ozone (trop-$O_3$) to the 50% of the values in 2011 are targeted to compensate 50% of the RF increase of $CO_2$. The remaining RF of $CH_4$and trop-$O_3$(0.26 and 0.22 W $m^{-2}$, respectively) correspond to the historical levels in 1960-1970. The necessary reductions of anthropogenic emissions of $CH_4$, $NO_x$and NMVOC in Asia in 2040 to the level of 1970 from that of 2010 have been estimated to be 35% $CH_4$, 44% $NO_2$, and 22% NMVOC from those of 2010 assuming the same necessary reduction ratio as for the global emissions. The estimated reductions have been compared with the reduction amount proposed in the Solution Report prepared under UN Environment Asia Pacific Office in 2018. The presumed reduction of the Asian emissions by 2030 through introducing of proven control measures are 27, 57 and 55% for $CH_4$ , $NO_x$and NMVOC. Thus, the reduction of RF of more than 50% from the reference year of 2010 is feasible for trop-$O_3$if the emissions of $NO_x$and NMVOC from other part of the world could be reduced coherently. Further efforts would be necessary for the reduction RF of $CH_4$by more than 50% of the present value.

Keywords: Extreme weather, SLCF, Asian emission control

©2019. Japan Geoscience Union. All Right Reserved. 

# Determination of atmospheric $NO_2$ column densities using a Pandora instrument measuring direct-sun spectra at Yokosuka, Japan: Improved validation of TROPOMI satellite observations

*Yugo Kanaya[1], Hisahiro Takashima[2,1], Masato I. Nodzu[3], Takashi Sekiya[7], Kazuyuki Miyazaki[1], Henk Eskes[4], Gaia Pinardi[5], Daniel Santana Diaz[6], Moritz Müller[6], Alexander Cede[6]

1. Research and Development Center for Global Change, Japan Agency for Marine-Earth Science and Technology (JAMSTEC), 2. Fukuoka University, 3. Tokyo Metropolitan University, 4. KNMI, 5. BIRA-IASB, 6. LuftBlick, 7. Japan Agency for Marine-Earth Science and Technology (JAMSTEC)

Satellite observations of $NO_2$, a key atmospheric pollutant, have provided critical information on global distribution of $NO_x$ sources and their temporal changes since 1995, and advanced understanding of atmospheric chemistry. A recent remarkable improvement is with their spatial resolution, reaching 7×3.5 km for TROPOMI (Sentinel-5P), launched in 2017. However, there is still a fundamental issue of low bias in the determined tropospheric $NO_2$ column densities (e.g., 25-50% for TROPOMI), when evaluated against ground-based spectroscopic observations. Potential causes would be (1) a-priori vertical profile shapes, (2) co-present aerosols and/or surface albedo, and (3) spatial inhomogeneity of $NO_2$, while (4) uncertainty in the ground-based observations could also be important. At Yokosuka (32.32˚N, 139.65˚E), located on the south edge of Tokyo-Yokohama metropolitan area, we newly started direct-sun Pandora spectrometer observations in November 2018 and strengthened validation capability, where the scattered-sun MAX-DOAS observations (from a JAMSTEC original instrument) had been solely referenced before. Results during winter 2018/2019 showed TROPOMI (within 0.1˚ from Yokosuka) had ~40% low bias against MAX-DOAS. The magnitude of difference was similar to the results from longer comparison during Feb-Sep 2018 for TROPOMI and earlier comparisons for OMI (QA4ECV). Pandora (in direct-sun mode) gave values ~24 % less than MAX-DOAS; the cause of difference was likely spatial inhomogeneity, as pollution levels were higher in the northeast for the sight of MAX-DOAS than in south for Pandora. This was consistent with the fact that TROPOMI gave ~18% higher values, when the averaging area was shifted to northeast by 10 km. As such, the importance of factors (3) and (4) was newly evaluated. By considering MAX-DOAS profile shapes in the recalculation of satellite products, we will discuss on factor (1), and the possibility to derive near-surface $NO_2$ concentrations from satellite observations.

Keywords: Satellite observations, Validation, Spectroscopy, Air pollution

©2019. Japan Geoscience Union. All Right Reserved. 

# A high-resolution global data assimilation for air pollution analysis on megacity scale using multi-sensor satellite measurements including TROPOMI $NO_2$ data

*Takashi Sekiya[1], Kazuyuki Miyazaki[2,1], Henk Eskes[3], Folkert Boersma[3], Koji Ogochi[1], Kengo Sudo[4,1], Masayuki Takigawa[1]

1. Japan Agency for Marine-Earth Science and Technology, 2. Jet Propulsion Laboratory/California Institute for Technology, 3. Royal Netherlands Meteorological Institute (KNMI), 4. Graduate School of Environmental Studies, Nagoya University

Intensive human activities lead to high emissions of air pollutants at megacities, causing severe damages to human health. The number of megacities is expected to rise in developing regions in the near future. Thus, it is important to provide information on air pollutants and their emissions on a megacity scale for the globe in a consistent way. In this study, we present the results from global chemical data assimilation of multi-species satellite observations with a resolution of 0.56 degree using an ensemble Kalman filter approach (Miyazaki et al., 2015) and high-resolution global chemical transport model, CHASER (Sekiya et al., 2018). Assimilated data were obtained from the OMI, GOME-2, and SCIAMACHY for tropospheric $NO_2$ column, the TES for $O_3$ profile, the MOPITT for total CO column, the MLS for $O_3$ and $HNO_3$ profiles, and the OMI for total $SO_2$ column. Data assimilation at 0.56-degree resolution largely improved agreements with the observed surface $NO_2$ pollutions on megacity scale, with reductions of the root mean square errors (RMSEs) relative to in-situ measuring networks (AirBase, AQS, Hong Kong EPD, and NIES) by 33% for Europe, by 67% for the U.S., and by 75% for East Asia, compared to the model simulations without data assimilation. With increasing horizontal resolution from 2.8 to 0.56 degree, the global total $NO_x$emission estimates became lower by 10% mainly because of the effects of non-linear $O_3$-$HO_x$-$NO_x$ chemistry, while resolving higher NOx emissions by a factor of 4-5 in most of the megacities than their surrounding areas. Using the high-resolution data assimilation system and applying advanced super-observation approach, we demonstrated that assimilation of tropospheric $NO_2$ retrievals from TROPOMI improved agreements of tropospheric $NO_2$ column with the assimilated TROPOMI data itself by 62% and with OMI by 40% (not used for data assimilation) compared to model simulation at 1.1-degree resolution for April 2018. These improvements primarily resulted from substantial emission reductions over the U.S., China and India and increases over rural regions relative to the a priori emissions (HTAP_v2.2+GFED4 +GEIA). These results demonstrated the potentials of the high-resolution global data assimilation with the combined use of advanced satellite observations to provide valuable information on spatial and temporal variations of air pollution on a megacity scale globally.

Keywords: Tropospheric NO2, Megacity, Data assimilation, Emission inversion, Satellite observation

©2019. Japan Geoscience Union. All Right Reserved. 

# Recent trends of $NO_2$, VOC, and tropospheric ozone concentrations observed around Chiba, Japan in 2013-2018

*Daichi Yonekawa[1], Hitoshi Irie[2]

1. Chiba university Graduate school, 2. Chiba university

Tropospheric ozone ($O_3$) is not only a major photochemical oxidant but also the third important greenhouse gas. In recent years its importance is widely recognized as a short-lived climate pollutant (SLCP). As nitrogen dioxide ($NO_2$) and volatile organic compounds (VOC) are both important precursors of $O_3$, they play a central role in photochemical chemistry in the atmosphere. In addition, they have negative direct effects on human health. However, recent trends of $O_3$, $NO_2$, and VOC have not been fully understood yet even in Japan.
Using the multi-axis differential optical absorption spectroscopy (MAX-DOAS), we conducted continuous observations of $NO_2$, formaldehyde (HCHO; as a substitute for VOC) and $O_3$ concentrations for altitudes of 0-1 km at the SKYNET Chiba site (35.63ºN, 140.10ºE, 21 m asl) for 6 years from 2013 to 2018. Analysis of the data showed that $NO_2$ and HCHO concentrations decreased by about 30%, but a systematic decrease in $O_3$ concentration was not observed. Similar trends were seen in tropospheric $NO_2$ column data obtained by the Ozone Monitoring Instrument (OMI) onboard the Aura satellite of the National Aeronautics and Space Administration (NASA), and concentration data of $NO_2$, non-methane hydrocarbon (NMHC; as a substitute for VOC), and photochemical oxidant (Ox; as a substitute for $O_3$) observed by the atmospheric environmental regional observation system (AEROS) called Soramamekun. These results are consistent with previous reports. In this presentation, the observed trends and their causes will also be discussed by utilizing our unique MAX-DOAS system that was directed to 4 different azimuth directions (north, east, west, and south), while traffic is heavy at the north, a residential area is located at the east, there is a sea at the west, and a factory area is located at the south around the SKYNET Chiba site.

Keywords: Nitrogen dioxide, Volatile organic compounds, Tropospheric ozone

©2019. Japan Geoscience Union. All Right Reserved. 

# Long-term seasonal changes in tropospheric ozone over Japan

*Natsumi Kawano[1], Tatsuya Nagashima[1], Seiji Sugata[1]

1. National Institute for Environmental Studies

Tropospheric $O_3$ is the primary source of OH radicals in the troposphere that contribute to the oxidation capacity of the atmosphere. According to the seasonal cycles of surface $O_3$, different behaviors at the remote and metropolitan areas in northern midlatitude have been pointed out (Parrish et al., 2013; Cooper et al., 2014; McGlynn et al., 2018; Jung et al., 2018). For example, European, American and Asian continental remote sites indicated that the seasonal cycle in the present decade had earlier annual maximum peaks than the maximum in the past decades. On the other hand, delayed maximum peaks appeared in urban locations. In spite of lots of monitoring stations, research for changes in seasonal $O_3$ cycles in Japan is still unclear. In this study, we investigate the seasonal cycle changes by using long-term continuous $O_3$ monitoring data at 265 ambient sites.
First, to clarify the annual $O_3$ maximum, sine function fitting examined by Parrish et al. (2013) was applied to monitoring data between the 1980s and 2010s. Regarding the spatial distribution of seasonal shifting between the 1980s and 2010s, most monitoring sites showed changes in a delayed shift. In particular, the stations with more than 0.2 days/decade delay belong to eastern and southwestern parts of Japan. Next, sine function was fitted to 5-years moving average over the entire data record to acquire the long-term trends of seasonal maximum in each region. All monitoring station were classified based on the 35-years averaged NOx concentration: urban, suburban and rural (Kurokawa et al., 2009). Results in all classifications showed delayed trends over analysis periods. In rural sites, $O_3$ mixing ratio reached the annual maximum in 5-days earlier than urban and suburban sites. In future work, we will conduct long-term air quality simulation and investigate the mechanism of seasonal cycle delaying.

Acknowledgement
This research was supported by the Environment Research and Technology Development Fund (S-12) of the Ministry of the Environment, Japan.

Keywords: ozone, long-term data record, seasonal cycle

©2019. Japan Geoscience Union. All Right Reserved. 

# Characteristics of Atmospheric Photochemical Pollution at a Comprehensive Site in Guangzhou, China

*Yu Zou[1]

1. Institute of Tropical and Marine Meteorology, CMA,Guangzhou,China

Guangzhou, one of China’ s megacities, is beset with frequent occurrence of atmospheric photochemistry events. In this study, online instruments were used to simultaneously monitor NMHCs, NO*x* and $O_3$ at Guangzhou Panyu Atmospheric Composition Station (GPACS) of the China Meteorological Administration (CMA), from June 2011 to May 2012, in order to obtain their characteristics, NMHCs reactivity and the control strategies for atmospheric photochemistry. The results showed that during the observation period, the seasonal variation of $O_3$ mixing ratio was lower in spring and winter compared to summer and autumn, which was opposite that for NMHCs and NO*x*. $O_3$ mixing ratio began to show a net increase at 8:00LT, likely due to the breakup of the nocturnal boundary layer and increased photochemistry, while a net decrease in $O_3$ mixing ratio occurred at about 15:00LT, due to the fact that sunlight and its associated photochemistry begin to decrease, leading to low OH radicals and the titration of $O_3$ by emissions of NO*x*. In terms of NMHCs, aromatics had the largest $O_3$ formation potential, among which toluene, xylenes, ethylbenzene, 1,2,4-trimethylbenzene and 1,3,5-trimethybenzene were the most important species, with a total contribution of about 44%. Weekday/weekend $O_3$ differences in the morning and at midday largely depend on how much the $O_3$ precursors are affected by the different intensity of anthropogenic activities. Although the increase of biogenic NMHCs emissions at midday reverses the sensitivity of $O_3$ production from NMHCs-sensitive to NO*x*-sensitive, high-reactive NMHCs and NO*x* control can be effective for reducing peak $O_3$ mixing ratios in Guangzhou. Further investigation based on numerical models is required to reach more robust conclusions.

Keywords: Photochemical Pollution, Guangzhou

©2019. Japan Geoscience Union. All Right Reserved. 

[J] Oral | A (Atmospheric and Hydrospheric Sciences)：A-AS Atmospheric Sciences, Meteorology & Atmospheric Environment

Thu. May 30, 2019 10:45 AM - 12:15 PM JST | Thu. May 30, 2019 1:45 AM - 3:15 AM UTC | 102 1F

## [A-AS04] Atmospheric Chemistry

convener:Tomoki Nakayama(Graduate School of Fisheries and Environmental Sciences, Nagasaki University), Yoko Iwamoto(Graduate School of Biosphere Science, Hiroshima University), Sakae Toyoda(Department of Chemical Science and Engineering, Tokyo Institute of Technology), Nawo Eguchi(Kyushu University), Chairperson:Fumikazu Taketani(海洋研究開発機構), Michihiro Mochida(名古屋大学)

This session provides a forum for the presentation of the broad spectrum of tropospheric and stratospheric chemistry, including various research topics (e.g., dynamical processes, air quality and climate), approaches (modeling, field measurements, remote sensing, and laboratory studies), and species (gas and aerosol). This session also provides an opportunity for discussing possible future collaboration with other research fields relevant to atmospheric chemistry. We strongly encourage authors to prepare presentation slides and a poster in English.

10:45 AM - 11:00 AM JST | 1:45 AM - 2:00 AM UTC

### [AAS04-22] LC/MS analysis of molecular markers present in biogenic secondary organic aerosols collected during year-round observations at a cool-temperature forest

*Kei Sato[1], Sathiyamurthi Ramasamy[1], Satoshi Inomata[1], Yuzo Miyazaki[2] (1.National Institute for Environmental Studies, 2.Hokkaido University)

11:00 AM - 11:15 AM JST | 2:00 AM - 2:15 AM UTC

### [AAS04-23] Surfactant Effects on Acid-Catalyzed Reactions at Aqueous Aerosol Surfaces

*Shinnosuke Ishizuka[1], Tetsuya Hama[2], Shinichi Enami[1] (1.National Institute for Environmental Studies, 2.Institute for Low Temperature Science, Hokkaido University)

11:15 AM - 11:30 AM JST | 2:15 AM - 2:30 AM UTC

### [AAS04-24] Roles of heterogeneous reactions in the tropospheric chemistry: a global modeling study

*Phuc Thi Minh Ha[1], Fumikazu Taketani[2], Yugo Kanaya[2], Kengo Sudo[1,2] (1.Graduate School of Environmental Studies, Nagoya University, 2.Research and Development Center for Global Change, JAMSTEC)

11:30 AM - 11:45 AM JST | 2:30 AM - 2:45 AM UTC

### [AAS04-25] Sensitivity of regional deposition of inhaled atmospheric aerosols in human respiratory tract to their size distribution and hygroscopicity: A case study

*Minrui Wang[1], Toshiyuki Mihara[2,4], Mizuo Kajino[5], Kaori Kawana[2,6], Michihiro Mochida[1,2,3] (1.Institute for Space Earth Environmental Research, 2.Graduate School of Environmental Studies, Nagoya University, 3.Institute for Advanced Research, Nagoya University, 4.Now at Gifu Prefectural Industrial Research Institute, 5.Meteorological Research Institute, Japan Meteorological Agency, 6.Now at Research and Development Center for Global Change, JAMASTEC)

11:45 AM - 12:00 PM JST | 2:45 AM - 3:00 AM UTC

### [AAS04-26] Biogeochemical cycle between atmosphere and ocean via particulate matters -Award lecture for JpSAC Young Scientist Award-

★Invited Papers

*Yoko Iwamoto[1] (1.Graduate School of Biosphere Science, Hiroshima University)

12:00 PM - 12:15 PM JST | 3:00 AM - 3:15 AM UTC

### [AAS04-27] Kinetic Studies for Quantitative Elucidation of Heterogeneous Halogen Chemistry in the Troposphere

-JpSAC Early Career Scientist Award Lecure-
★Invited Papers

*Yosuke Sakamoto[1,2] (1.Graduate School of Global Environmental Studies, Kyoto University , 2.Graduate School of Human and Environmental Studies, Kyoto University)

# LC/MS analysis of molecular markers present in biogenic secondary organic aerosols collected during year-round observations at a cool-temperature forest

*Kei Sato[1], Sathiyamurthi Ramasamy[1], Satoshi Inomata[1], Yuzo Miyazaki[2]

1. National Institute for Environmental Studies, 2. Hokkaido University

To understand formation processes for organic nitrogen and dimeric compounds present in forest aerosols, we analyzed molecular markers present in forest aerosols collected during year-round observations using negative/mode electrospray ionization-liquid chromatography-mass spectrometry (ESI-LC/MS). Thirty-seven aerosol filter samples were collected at Tomakomai Experimental Forest between January and December in 2013, and 33 of the collected samples were analyzed in this study. Molecular markers analyzed in this study were cis-pinic acid, 3-methyl-1,2,3-butanetricarboxylic acid (3-MBTCA), α-pinene-derived dimer detected by ESI at m/z 357 (α-pinene dimer), isoprene-derived olganosulfate detected at m/z 215 (isoprene OS), and isoprene-derived nitrooxyorganosulfate detected at m/z 260 (isoprene NOS). Each aerosol filter sample was extracted in methanol; the extract was concentrated under gentle stream of nitrogen; the concentrated extract was dissolved in an analytical solvent to obtain an analytical sample; and the analytical sample was analyzed by an LC/MS instrument (Sato et al., 2007). The seasonal change in the concentration of cis-pinic acid, formed from α-pinene oxidation, was peaked in spring and fall, whereas the seasonal change in the concentration of 3-MBTCA, formed from oxidation of pinonic acid, was peaked in summer. Very similar results were reported in a previous paper on the GC/MS analysis of the same samples (Müller et al., 2017). The seasonal change in the concentration of α-pinene dimer was similar to that of cis-pinic acid, suggesting that a major formation process of the detected dimers was the atmospheric oxidation of α-pinene. The seasonal changes in the concentrations of isoprene OS and isoprene NOS, which are derived from isoprene epoxydiol (IEPOX), were peaked at fall and summer, respectively. The seasonal change in the concentration of isoprene NOS agreed well with that of 2-methyltetrols, molecular markers of isoprene secondary organic aerosol. These results suggest that a major formation process of isoprene NOS is secondary organic aerosol formation from isoprene in the presence of air pollutants.

References

Sato, K., Hatakeyama, S., Imamura, T., Secondary organic aerosol formation during the photooxidation of toluene: NO x dependence of chemical composition, J. Phys. Chem. A 111, 9796-9808 (2007).

Müller, A., Miyazaki, Y., Tachibana, E., Kawamura, K., Hiura, T., Evidence of a reduction in cloud condensation nuclei activity of water-soluble aerosols caused by biogenic emissions in a cool-temperate forest, Sci. Rep., 7, 8452 (2017).

Keywords: Bigenic volatile organic compound, Secondary organic aerosol, Organosurfate, Nitrooxy organosulfate, Organic nitrogen

©2019. Japan Geoscience Union. All Right Reserved. 

# Surfactant Effects on Acid-Catalyzed Reactions at Aqueous Aerosol Surfaces

*Shinnosuke Ishizuka[1], Tetsuya Hama[2], Shinichi Enami[1]

1. National Institute for Environmental Studies, 2. Institute for Low Temperature Science, Hokkaido University

The outermost layer of atmospheric aqueous aerosol is covered with amphiphilic organic compounds. Volatile organic compounds (VOCs) in the gas phase should encounter them first at the air/aerosol interface, rather than solute molecules homgeneously distributed in the bulk. It may control the whole reactivity of the aqueous aerosol and play key roles in birth, growth and degradation processes of atmospheric aerosols. Here we studied activities of quaternary alkyl trimethyl ammonium cations $CH_3(CH_2)_{n-1}(CH_3)_3N^+$ (n = 1, 4, 8, 10, 12, 14) at the surfaces of water using surface-sensitive spraying ionization mass spectrometry. The longer-chain alkyl ammonium cations are detected more prominently at the water surface of the equimolar solution, expressed as an exponential function of the alkyl chain length. We suggest the occurrence of competitive adsorption among the quaternary ammonium cations at water surface. Then, the surfactant effects on the gaseous uptake and subsequent reactions of VOCs was investigated. When isoprene is exposed to acidified water surfaces, proton transfer reaction from $H_3O^+$ to isoprene occurs, which is followed by chain-propagation reactions. We found that the longer-chain ammonium cations suppressed isoprene oligomer signals but rarely hindered chain-propagation reactions even at larger concentrations, e.g., the higher surface coverage. It suggests that gaseous isoprene is directly added to the protonated species at water surface. We conclude that competitive adsorption between isoprene oligomers and the ammonium cations suppressed the acid-catalyzed reactions. Driving force leading to the adsorptive competition will be argued based on experiments performed by adding anionic and neutral surfactants.

Keywords: The Air/Water Interface, SOA

©2019. Japan Geoscience Union. All Right Reserved. 

# Roles of heterogeneous reactions in the tropospheric chemistry: a global modeling study

*Phuc Thi Minh Ha[1], Fumikazu Taketani[2], Yugo Kanaya[2], Kengo Sudo[1,2]

1. Graduate School of Environmental Studies, Nagoya University, 2. Research and Development Center for Global Change, JAMSTEC

Heterogeneous reactions in the atmosphere largely affect air quality and climate by changing tropospheric photochemical processes involving gases like $O_3$, $HO_x$, $NO_x$, $HNO_3$, CO, VOCs, and aerosols. There are many previous studies on the effects of heterogeneous reactions at regional to global scales using direct measurements, remote sensing, and simulation. For the atmospheric chemistry simulation, there is a large uncertainty from the treatment of the heterogeneous reactions in the model due to the still insufficient understanding of the mechanism of heterogeneous reactions.
This study is intended to understand the roles of the heterogeneous reactions in the global tropospheric chemistry using a chemistry-climate model CHASER (MIROCESM) (Sudo et al., 2011) which includes more than 250 chemical reactions in the troposphere and stratosphere with more than 70 chemical species. This model also includes aerosol components (SPRINTARS) for sulfate, nitrate, BC, POA/SOA, dust, and sea-salt; formation of nitrate and SOA, and ageing of BC are calculated tightly linked to the chemistry in CHASER. The present version of CHASER considers heterogeneous reactions of $N_2O_5$, $HO_2$, $RO_2$, and HCHO for surfaces of the individual aerosol components and cloud particles.
The model simulation is validated with the observational data from EANET, EMEP and the ship-based observation. Our performed sensitivity simulations with respect to the heterogeneous reactions show that the impacts of the $N_2O_5$ heterogeneous reaction may not be as large as previously reported; surface concentrations of $NO_x$, $O_3$ and OH are only reduced by 1.6%, 2.2%, 2.6%, respectively, in global mean (in regional, at most, 23%, 5.4%, and 12.8%). Whereas, the $HO_2$ reaction (to form $H_2O_2$) can cause a significant effect on distributions of $O_3$ and related species ($NO_x$, $O_3$, OH are changed by 68.7%, -21.5% and -70.1%). In addition to the polluted areas in China and India, we found that in the North Pacific region the heterogeneous reactions can play a critical role in the concentrations of $NO_x$, $O_3$, CO, OH, $HO_2$ (up to 69%, 21%, 7%, 70%, 81%, respectively). The possible large impacts of the heterogeneous reactions are also verified with the ship-based observational data for the North Pacific and Alaska regions.

Keywords: heterogeneous reaction, chemical climate model, North Pacific

©2019. Japan Geoscience Union. All Right Reserved. 

# Sensitivity of regional deposition of inhaled atmospheric aerosols in human respiratory tract to their size distribution and hygroscopicity: A case study

*Minrui Wang[1], Toshiyuki Mihara[2,4], Mizuo Kajino[5], Kaori Kawana[2,6], Michihiro Mochida[1,2,3]

1. Institute for Space Earth Environmental Research, 2. Graduate School of Environmental Studies, Nagoya University, 3. Institute for Advanced Research, Nagoya University, 4. Now at Gifu Prefectural Industrial Research Institute, 5. Meteorological Research Institute, Japan Meteorological Agency, 6. Now at Research and Development Center for Global Change, JAMASTEC

Aerosols, which inhaled to human respiratory tract, can cause various diseases that threaten one's health. In order to estimate aerosol's health risk, it is significant to elucidate the sensitivity of regional deposition of inhaled aerosols.

In this study, by applying size distribution and hygroscopic growth factor data of aerosol (measured by a scanning mobility particle sizer in September 2009 and July-August 2010) to an MPPD (Multiple-Path Particle Dosimetry) model, we calculated the regional deposition differentiated by size diameter/hygroscopicity for a resting/light exercising adult male. As a result, regional deposition ratio in intrathoracic region (both tracheobronchial airway and alveolar interstitium) showed a bimodal distribution among particle size diameter ranging between 24.1~359.0 nm, in which the maximum value was 50.1%/50.0% at 24.1 nm (during light exercise). In general, there was a decreasing trend in deposition ratio when particle size diameter increased. For mode particles (dry diameter $d_{p,dry} < 100$ nm), the regional deposition of particles that have low hygroscopicity parameter ($\kappa$) tent to be larger than those with higher $\kappa$. However, for larger particles (especially when $d_{p,dry} > 200$ nm), this trend became reversed.

In 2009 the measurement was continuous for 10 days, while daily variation was found in aerosol number-size distribution and regional deposition. Therefore, we analyzed the meteorological data of the measurement period in 2009, comparing daytime (12:00-18:00 LST) and nighttime (00:00-06:00 LST) in order to indicate meteorological matters that affect the temporal variation of regional deposition. The result showed that the relative humidity (RH) during daytime was basically lower than 50% except September 15 and September 22~23 due to continuous rain, and the distribution of regional deposition was maximum for relatively hydrophobic mode particles ($d_{p,dry} < 100$ nm, hygroscopic growth factor $g$ ranges between 1.0~1.2). On the other hand, RH during nighttime was mostly higher than 60%, and a bimodal distribution of both hydrophobic and hydrophilic ($g$ ranges between 1.2~1.4) particles was found. Meanwhile, on September 23 RH was high (over 75%) during whole day, we found a monomodal distribution of regional deposition with a maximum value for hydrophilic particles that last about 6 hours in the afternoon.

According to our results we suggested that along with the temporal variation of artificial emission, changes in ambient humidity could also influence the composition of inhaled aerosol particles to a great extent, and therefore affected the regional deposition.

Keywords: Aerosol, size distribution, hygroscopicity, regional deposition

©2019. Japan Geoscience Union. All Right Reserved. 

# Biogeochemical cycle between atmosphere and ocean via particulate matters
# -Award lecture for JpSAC Young Scientist Award-

*Yoko Iwamoto[1]

1. Graduate School of Biosphere Science, Hiroshima University

The oceans absorbs carbon dioxide which is increasing in the atmosphere and has the ability to mitigate sudden climate change. The biological pump driven by marine phytoplankton play an important role in the global carbon cycle. In order to accurately estimate the carbon absorptive capacity of the oceans, it is important to know the supply amount of nutrient elements that support the growth of phytoplankton. Despite the fact that iron is an essential element for marine phytoplankton, the concentration of dissolved iron in the surface ocean is extremely low. Iron containing aerosols such as mineral dust in the atmosphere could be important as a source of iron to the surface ocean.

In my previous work, the sporadic deposition of atmospheric mineral dust by sea fog over the North Pacific was observed during an Asian dust event. By using bulk and individual particle analyses for suspended particulate matters in seawater, the biogeochemical impact of the dust deposition was investigated. As a result, it was found that the bioavailable iron supply to the surface ocean by an Asian dust event was sufficient to promote the growth of phytoplankton, and it also contribute the carbon absorption to the northern North Pacific. In addition, from a mapping data covering the North Pacific and its marginal seas, it was revealed that mineral particles of atmospheric origin existed ubiquitously in the surface ocean even during summer when the influence of Asian dust event is small.

On the other hand, the growth of marine phytoplankton causes changes in the atmospheric environment through aerosol generation. My current research focuses on oceanic aerosols acting as cloud condensation nuclei. From the continuous observation conducted at Noto ground-based research observatory (NOTOGRO) facing the Sea of Japan, it was found that the growth rate of cloud droplets delayed when the organic mass fraction of the aerosol was high. Currently, researches on the linkage between phytoplankton species and marine biogenic aerosol and the climate effect of aerosol generated by bubble bursting at the air-sea interface are conducted.

Keywords: the North Pacific, Mineral dust, Aerosol, Biogeochemical cycles, Cloud condensation nuclei

©2019. Japan Geoscience Union. All Right Reserved. 

# Kinetic Studies for Quantitative Elucidation of Heterogeneous Halogen Chemistry in the Troposphere
# -JpSAC Early Career Scientist Award Lecure-

*Yosuke Sakamoto[1,2]

1. Graduate School of Global Environmental Studies, Kyoto University , 2. Graduate School of Human and Environmental Studies, Kyoto University

Ozone is one of the most important species in the troposphere since it has health and environmental effects, and relates to atmospheric oxidation capacity and climate change. Halogen species are deeply involved in the tropospheric ozone chemistry by forming catalytic reaction cycles. Observations, model simulations and laboratory experiments have suggested that heterogeneous reactions of gaseous oxidants such as ozone and OH radical with halide ions in sea water/ice and sea salt aerosol are important halogen emission sources. However, quantitatively we still have not had conclusions of their importance in many cases due to experimental difficulties to determine kinetic parameters for the heterogeneous reactions. To obtain quantitative kinetic parameters of gas-liquid heterogeneous oxidation reactions of halide ions which are difficult for conventional methods, this study has developed original approaches using laser spectroscopy or mass spectrometry, and applied them to kinetic studies. This presentation includes results of three reaction systems: 1. gaseous ozone with iodide solution (Sakamoto et al. 2009, 2013), 2. gaseous ozone with bromide solution (Sakamoto et al. 2018a), 3. gaseous OH radical with chloride containing deliquesced aerosol (Sakamoto et al. 2018b), and also discussion on contribution of interfacial process to total reaction rate.

## References

Sakamoto. Y., A. Yabushita, M. Kawasaki and S. Enami (2009), *J. Phys. Chem. A* 113, 7707-7711.
Sakamoto. Y., S. Enami and K. Tonokura (2013), *J. Phys. Chem. A*, 117, 2980-2986.
Sakamoto, Y., M. Goda, J. Hirokawa (2018a), *J. Phys. Chem. A*, 122, 2723-2731.
Sakamoto, Y., J. Zhou, N. Kohno, M. Nakagawa, J. Hirokawa and Y. Kajii (2018b), *J. Phys. Chem. Lett.*, 9, 4115-4119.

Keywords: earth, aerosol, oxidant

©2019. Japan Geoscience Union. All Right Reserved. 

[J] Poster | A (Atmospheric and Hydrospheric Sciences )：A-AS Atmospheric Sciences, Meteorology & Atmospheric Environment

Thu. May 30, 2019 1:45 PM - 3:15 PM JST | Thu. May 30, 2019 4:45 AM - 6:15 AM UTC | Poster Hall International Exhibition Hall8, Makuhari Messe_2

## [A-AS04] Atmospheric Chemistry

convener:Tomoki Nakayama(Graduate School of Fisheries and Environmental Sciences, Nagasaki University), Yoko Iwamoto(Graduate School of Biosphere Science, Hiroshima University), Sakae Toyoda(Department of Chemical Science and Engineering, Tokyo Institute of Technology), Nawo Eguchi(Kyushu University)

This session provides a forum for the presentation of the broad spectrum of tropospheric and stratospheric chemistry, including various research topics (e.g., dynamical processes, air quality and climate), approaches (modeling, field measurements, remote sensing, and laboratory studies), and species (gas and aerosol). This session also provides an opportunity for discussing possible future collaboration with other research fields relevant to atmospheric chemistry. We strongly encourage authors to prepare presentation slides and a poster in English.

[AAS04-P01] Validation of GOSAT cloud judgement by using Himawari-8 data

*Kitamura Katsuki[1], Naoko Saitoh[2] (1.Chiba University Graduate School of Science and Engineering Division of Earth Environmental Science , 2.Center for Environmental Remote Sensing Chiba University)

[AAS04-P02] Measurement of temperature that fungal spores form ice nuclei

*Kazuyuki Kita[1], Kansei Sasaki[1], Koutaro Minami[1], Takeshi Kinase[2], Kouji Adachi[2], Yuji Zaizen[2], Kentaro Hosaka[3], Teruya Maki[4], Yasuhito Igarashi[1,5] (1.Ibaraki University, 2.Meteorological Research Laboratory, 3.National Musium of Nature and Science, 4.Kanazawa University, 5.Kyoto University)

[AAS04-P03] **Investigation of Atmospheric Aerosol Particles and gases by R/V Mirai cruise over the Arctic Ocean on 2017**

*Fumikazu Taketani[1], Saki Kato[1,2], Takuma Miyakawa[1], Masayuki Takigawa[1], Masahiro Yamaguchi[1], Hisahiro Takashima[1,2], Petr Mordovskoi[1], Yugo Kanaya[1] (1.Japan Agency for Marine-Earth Science and Technology, 2.Fukuoka University)

[AAS04-P04] Characterization of carbonaceous aerosols in East Asia in the spring of 2015: Importance of non-fossil fuel sources

*Takuma Miyakawa[1], Yuichi Komazaki[1], Fumikazu Taketani[1], Xiaole PAN[2], Zifa Wang[2], Yugo Kanaya[1] (1.Japan Agency for Marine-Earth Science and Technology, 2.Institute for Atmospheric Physics, Chinese Academy of Science)

[AAS04-P05] **Analyzing the influence of biomass burning on ambient air pollution in mainland Southeast Asia from 2001 to 2016**

*Shuai Yin[1] (1.National Institute for Environmental Studies)

[AAS04-P06] High-resolution and multi-year inventory of mercury emissions from biomass burning in tropical continents during 2001–2017

*Yusheng Shi[1] (1.Aerospace Information Research Institute, Chinese Academy of Sciences)

[AAS04-P07] Simultaneous observations by sky radiometer and MAX-DOAS for characterization of biomass burning plumes in central Thailand in January-April 2016

*Hitoshi Irie[1], Syedul Hoque[1], Alessandro Damiani[1], Al Mashroor Fatmi[1], Pradeep Khatri[2], Tamio Takamura[1], Thanawat Jarupongsakul[3] (1.Chiba University, 2.Tohoku University, 3.Chulalongkorn University)

[AAS04-P08] Quantifying PM2.5 from long-range transport and local pollution in Taiwan during winter monsoon.

*Ming-Tung Chuang[1] (1.Research Center for Environmental Changes, Academia Sinica)

[AAS04-P09] Vertical characterization of $PM_{2.5}$ based on observation using compact sensors on and around Mt. Unzen in Nagasaki Prefecture

*Tomoki Nakayama[1], Ayane Ueno[1], Kenta Kanegae[1], Kazuaki Kawamoto[1], Kodo Umakoshi[1], Takayuki Yamasaki[2], Wataru Okamoto[2], Yutaka Matsumi[2] (1.Faculty of Environmental Science, Nagasaki University, 2.ISEE, Nagoya University)

[AAS04-P10] Observation of NPF events at the summit of Mt. Fuji during daytime and nighttime

*Hiroki Igarashi[1], Takenori Sato[1], Tatsuhiro Mori[1], Kazuhiko Miura[1], Yoko Iwamoto[2], Ryuichi Wada[3], Shungo Kato[4], Hiroshi Okochi[5] (1.Tokyo University of Science, 2.Hiroshima University, 3.Teikyo University of Science, 4.Tokyo Metropolitan University, 5.Waseda University)

[AAS04-P11] Measurement of atmospheric metal particles using an ICP-MS and TEM.

*Takeshi Kinase[1], Kouji Adachi[1], Mizuo Kajino[1], Masahiko Hayashi[2], Keiichiro Hara[2] (1.Meteorological Research Institute, 2.Fukuoka)

[AAS04-P12] Experimental results on measuring device of complex refractive index using the single particle extinction and scattering method

*TAKASAGO YUYA[1] (1.Tokyo university)

[AAS04-P13] **Evaluation of BC and CO emission inventory based on long-term in-situ observations over East Asia**

*Yongjoo Choi[1], Yugo Kanaya[1], Hye-Jung Shin[2], Seung-Myong Park[2], Atsushi Matsuki[3], Yasuhiro Sadanaga[4], Sang-woo Kim[5], Itsushi Uno[6], Xiaole Pan[7] (1.Development Center for Global Change, Japan Agency for Marine-Earth Science and Technology, 2.Division of Climate & Air Quality Research, National Institute of Environmental Research, Korea, 3.Institute of Nature and Environmental Technology, Kanazawa University, 4.Department of Applied Chemistry, Graduate School of Engineering, Osaka Prefecture University, 5.School of Earth and Environmental Sciences, Seoul National University, Seoul, Korea, 6.Research Institute for Applied Mechanics, Kyushu University, 7.Institute of Atmospheric Physics, CAS, Beijing, China)

[AAS04-P14] **Inverse modeling of black carbon emissions over China using ensemble data assimilation**

*Ping Wang[1] (1. Chinese Academy of Meteorological Sciences)

[AAS04-P15] Analysis of BC emissions in East Asia using inverse model

*Takashi Maki[1], Taichu Y Tanaka[1], Naga Oshima[1], Thomas Sekiyama[1], Keiichi Kondo[1], Jun-ichi Kurokawa[2], Keiya Yumimoto[3], Toshimasa Ohara[4] (1.Meteorological Research Institute, 2.Asia Center for AirPollution Research, 3.Kyushu University, 4.National Institute for Environmental Studies)

[AAS04-P16] Source attribution of BC in the northern Pacific and Arctic Ocean by chemistry climate model

*Takato Onishi[1], Kengo Sudo[1,2], Yugo Kanaya[2], Fumikazu Taketani[2] (1. Graduate School of Environmental Studies, Nagoya University, 2.Japan Agency for Marine-Earth Science and Technology)

[AAS04-P17] Evaluation of a mobile $PM_{2.5}$ sensor and application to the measurements along the National route 1 and around Nagasaki University

*Kenta Kanegae[1], Takayuki Yamasaki[2], Wataru Okamoto[2], Yutaka Matsumi[2], Tomoki Nakayama[1] (1.Nagasaki University, 2.Nagoya University)

[AAS04-P18] Analysis on the Relationship between the Concentration of Particulate Matter and Mortality from Respiratory and Cardiovascular Diseases

*Woo-Sik JUNG[1], Woo-Gon Do[2] (1.Department of Atmospheric Environment Information Engineering, Atmospheric Environment Information Research Center, Inje University, Gimhae 50834, Korea, 2.Busan Metropolitan City of Institute of Health and Environment Busan, Korea)

[AAS04-P19] A Study on the Estimation of Contribution Rate of Odour Substances Using CALPUFF model

*Woo-Sik JUNG[1], Woo-Gon Do[2] (1.Department of Atmospheric Environment Information Engineering, Atmospheric Environment Information Research Center, Inje University, Gimhae 50834, Korea, 2.Busan Metropolitan City of Institute of Health and Environment Busan, Korea)

[AAS04-P20] Stepwise decrease in atmospheric trace gases near the ground associated with rapid vertical mixing observed by 3-D coherent Doppler lidar and in-situ gas measurements

*Hisahiro Takashima[1], Keiichiro Hara[1], Yuki Ohira[1], Akinori Takami[2], Ayako Yoshino[2], Yasushi Fujiyoshi[3] (1.Fukuoka University, 2.National Institute for Environmental Studies, 3.Hokaido University)

[AAS04-P21] Spatiotemporal variations of nitrogen dioxide ($NO_2$) over Fukuoka , observed by multiple MAX-DOAS instruments and 3-D coherent Doppler lidar

*Hironobu Ueki[1], Hisahiro Takashima[1], Martina M. Friedrich[2] (1.Fukuoka university, 2.Belgian Institute for Space Aeronomy (BIRA-IASB), Belgium)

[AAS04-P22] Measurement on the $^{17}O$-excess of tropospheric nitrogen oxides

*Fumiko Nakagawa[1], Dong Ding[1], Urumu Tsunogai[1], Takashi Yamaguchi[2], Izumi Noguchi[2] (1.Graduate School of Environmental Studies, Nagoya University, 2.Institute of Environment Sciences, Hokkaido Research Organization)

[AAS04-P23] Long-term measurements of the column-averaged mixing ratios of tropospheric substances related to the air pollution using ground-based FTIRs at Rikubetsu, Japan

*Tomoo Nagahama[1], Isamu Morino[2], Shingo Nakanishi[1] (1.Institute for Space-Earth Environmental Research, Nagoya University, 2.National Institute for Environmental Studies)

[AAS04-P24] Impacts of Biogenic and Anthropogenic Emissions on Summertime Ozone Formation in the Guanzhong Basin, China

*Nan Li[1] (1.Nanjing University of Information Science & Technology)

[AAS04-P25] **Comprehensive monitoring project of greenhouse gases and air pollutants around Jakarta megacity in Indonesia**

*Masahide Nishihashi[1], Hitoshi Mukai[1], Yukio Terao[1], Shigeru Hashimoto[1], Rizaldi Boer[2], Muhammad Ardiansyah[2], Bregas Budianto[2], Gito Sugih Immanuel[2], Adi Rakhman[2], Rudi Nugroho[3], Nawa Suwedi[3], Agus Rifai[3], Iif Miftahul Ihsan[3], Anies Marufatin[3], Albert Sulaiman[3], Dodo Gunawan[4], Eka Suharguniyawan[4], Asep Firman Ilahi[4], Muharam Syam Nugraha[4], Ronald Christian Wattimena[4], Bayu Feriaji[4], Thomas Lauvaux[5], Tomohiro Oda[6] (1.National Institute for Environmental Studies, 2.Bogor Agricultural University (IPB), Indonesia, 3.Agency for the Assessment and Application of Technology (BPPT), Indonesia, 4.Meteorological, Climatological, and Geophysical Agency (BMKG), Indonesia, 5.Laboratory for Sciences of Climate and Environment (LSCE), France, 6.Universities Space Research Association/NASA Goddard Space Flight Center, USA)

[AAS04-P26] **Seasonality of short-term variations in atmospheric $CH_4$ observed at Hateruma and relationship with the reginal emissions from East Asia**

*Yasunori Tohjima[1], Jiye Zeng[1], Tomoko Shirai[1], Akihiko Ito[1], Motoki Sasakawa[1], Toshinobu Machida[1] (1.National Institute for Environmental Studies)

[AAS04-P27] A cryogen-free automated measurement system of stable carbon isotope ratio of atmospheric methane

*Taku Umezawa[1], Takuya Saito[1] (1.National Institute of Environmental Studies)

[AAS04-P28] Global inverse analysis of $CH_4$ fluxes using NICAM-TM 4D-Var

*Yosuke Niwa[1,2], Akihiko Ito[1], Toshinobu Machida[1], Motoki Sasakawa[1], Yasunori Tohjima[1], Taku Umezawa[1], Shinji Morimoto[3], Shuji Aoki[3], Yousuke Sawa[2], Kazuhiro Tsuboi[2], Hidekazu Matsueda[2], Ed Dlugokencky[4], Christina Harth[5], Paul B Krummel[6], Ray L Langenfelds[6], Zoe M Loh[6], Jens Mühle[5], Simon O'Doherty[7], Ronald G Prinn[8], Michel Ramonet[9], Peter Salameh[5], Colm Sweeney[4], Ray Weiss[5], Dickon Young[7], Simona Castaldi[10,11], Sergio Noce[12], Marielle Saunois[9], Ann R Stavert[13] (1.National Institute for Environmental Studies, 2.Meteorological Research Institute, 3.Tohoku University, 4.Earth System Research Laboratory, National Oceanic and Atmospheric Administration, 5.Scripps Institution of Oceanography, University of California, 6.Climate Science Centre, CSIRO Oceans and Atmosphere, 7.School of Chemistry, University of Bristol, 8.Massachusetts Institute of Technology, 9.Laboratoire des Sciences du Climat et de l'Environnement, LSCE-IPSL (CEA-CNRS-UVSQ), 10.DISTABIF, Università degli studi della Campania Luigi Vanvitelli, 11.Department Landscape Design & Sustainable Ecosystems RUDN University, 12.IAFES, Euro-Mediterranean Center on Climate Change, 13.Global Carbon Project, CSIRO Oceans and Atmosphere)

[AAS04-P29] Scientific findings from observations of GOSAT/TANSO−FTS TIR band

*Naoko Saitoh[1], Shingo Kosaka[1], Masato Shiraki[1], Hinako Kobayashi[1] (1.Center for Environmental Remote Sensing)

[AAS04-P30] **Continuous measurements of atmospheric $CO_2$ and its $\delta^{13}C$ and $\delta^{18}O$ at Minamitorishima Island**

*Shohei Murayama[1], Kazuhiro Tsuboi[2], Shigeyuki Ishidoya[1], Hidekazu Matsueda[2], Yosuke Niwa[3], Yousuke Sawa[2], Kentaro Ishijima[2], Kentaro Kozumi[4], Genta Umezawa[4], Kazuya Yukita[4], Shigeharu Nishida[4], Megumi Yamamoto[4], Tetsuyuki Usami[1], Shinji Morimoto[5] (1.National Institute of Advanced Industrial Science and Technology (AIST), 2.Meteorological Research Institute, 3.National Institute for Environmental Studies, 4.Japan Meteorological Agency, 5.Tohoku University)

[AAS04-P31] Variations of atmospheric Radon-222 concentration observed at JMA stations

*Kentaro Ishijima[1], Kazuhiro Tsuboi[1], Hidekazu Matsueda[1], Yousuke Sawa[1], Yosuke Niwa[2,1], Takashi Maki[1], Takashi Nakamura[3] (1.Meteorological Research Institute, 2.National Institute for Environmental Studies, 3.Japan Meteorological Agency)

[AAS04-P32] Long-term variations of CFCs and HCFCs observed with ground-based FTIR spectrometers at Rikubetsu, Syowa Station, and Tsukuba since 1995

*Hideaki Nakajima[1,2], Masanori Takeda[2,1], Isao Murata[2], Takafumi Sugita[1], Tomoo Nagahama[3], Isamu Morino[1], Takeshi Kinase[4] (1.National Institute for Environmental Studies, 2.Graduate School of Environmental Studies, Tohoku University, 3.Institute for Space-Earth Environmental Research, Nagoya University, 4.Meteorological Research Institute)

[AAS04-P33] Millimeter-wave observation of stratospheric ozone in 2015-2017 in Rio Gallegos at the southern tip of South America

*Akira Mizuno[1], Hironori Seki[1], Tomoo Nagahama[1], Hirofumi Ohyama[2], Jacobo Salvador[3], Facundo Orte[3], Elian Walfram[3] (1.Institute for Space-Earth Environmental Research, Nagoya University, 2.National Institute for Environmental Studies, 3.Laser and Applications Research Center, UNIDEF (CITEDEF-CONICET))

# Validation of GOSAT cloud judgement by using Himawari-8 data

*Kitamura Katsuki[1], Naoko Saitoh[2]

1. Chiba University Graduate School of Science and Engineering Division of Earth Environmental Science , 2. Center for Environmental Remote Sensing Chiba University

In the retrieval processing of greenhouse gases from the Thermal and Near Infrared Sensor for Carbon Observation (TANSO)−Fourier Transform Spectrometer (FTS) on board Greenhouse Gases Observing Satellite (GOSAT), cloud contamination in the field of views (FOVs) of TANSO−FTS has been judged by TANSO−Cloud and Aerosol Imager (CAI) in the daytime and by the thermal infrared (TIR) band of TANSO−FTS in the nighttime. This study has compared the cloud detections in the TANSO−FTS FOVs by TANSO−CAI or TANSO−FTS TIR band with cloud detections by the Advanced Himawari Imager (AHI) on board Himawari−8.

For each of all TANSO−FTS observations over the ocean in January and July in 2016, we first selected all coincident Himawari−8 data when their center positions were located in the TANSO−FTS FOVs and they were obtained within one minute before or after the TANSO−FTS observations. Next, we conducted cloud detection tests for each of the selected Himawari−8 data based on their reflectance and brightness temperature values, and then judged each of TANSO−FTS FOVs as a clear or cloudy scene by combining the cloud detection tests of the Himawari−8 data in the TANSO−FTS FOVs.

About 90% of cloud judgements by TANSO−CAI and Himawari−8 agreed with each other. TANSO−CAI used only reflectance data in visible bands for their cloud detections, whereas Himawari−8 used both reflectance and brightness temperature data in visible and infrared bands, respectively, which may cause their ~10% disagreements. In contrast, agreements in cloud judgements between TANSO−FTS TIR band and Himawari−8 got worse by 13−20% compared to the TANSO−CAI and Himawari−8 cloud judgements. This is because that the FOVs of TANSO−FTS (10.5 km) is larger than those of TANSO−CAI and Himawari−8 (0.5 km and 2 km), and cloud detections by TANSO−FTS TIR band used only brightness temperature data.

In addition, GOSAT cloud judgements (TANSO−CAI or TANSO−FTS TIR band) tended to judge TANSO−FTS FOVs as “clear”, whereas Himawari−8 judged the same TANSO−FTS FOVs as “cloud” in most cases of disagreements in their cloud judgements. This is partly because of “clear conservativeness” of our cloud detection algorithm by Himawari−8. As for TANSO−FTS FOVs judged as “clear” by TANSO−FTS TIR band and “cloud” by Himawari−8, small-scale clouds partly existed in the TANSO−FTS FOVs judging from relatively low brightness temperature values of the coincident Himawari−8 data. This suggests the possibility that TANSO−FTS TIR band cannot detect such small-scale clouds.

Keywords: GOSAT, Himawari-8, cloud judgement, validation

©2019. Japan Geoscience Union. All Right Reserved. 

# Measurement of temperature that fungal spores form ice nuclei

*Kazuyuki Kita[1], Kansei Sasaki[1], Koutaro Minami[1], Takeshi Kinase[2], Kouji Adachi[2], Yuji Zaizen[2], Kentaro Hosaka[3], Teruya Maki[4], Yasuhito Igarashi[1,5]

1. Ibaraki University, 2. Meteorological Research Laboratory, 3. National Musium of Nature and Science, 4. Kanazawa University, 5. Kyoto University

## 1. Background

Aerosols act as condensation nuclei and ice nuclei for the cloud particle formation in the atmosphere. In recent years, it was discovered that some bioaerosols can be ice-nuclei at relatively high temperatures of -15 ˚C or higher, indicating the possibility they could form ice clouds and precipitation at lower altitudes where formation mechanism of ice clouds has not been understood, and their significance in the meteorology and climate has been recognized. Although there have been many studies that measure ice nuclei formation temperature for general aerosols, it has been measured for very limited number of fungal spores in those studies. Thus, it has been not yet understood what kind of fungal spores can work as ice nuclei at relatively high temperatures.

In this research, we measured ice nucleation of spores of various kinds of fungi sampled in Japanese forests and examined the relationship between ice nucleation temperature and biological classification. We also classified patterns of ice nuclei formation, which may have information on ice nuclei formation temperature and process.

## 2. Method

In this research, spores were sampled from fungi collected during fungi surveys conducted every month from May to October in various types of woods in the Tsukuba Botanical Garden. Some fungi were also collected in the forests of Namie Town, Fukushima Prefecture. Using an optical microscope equipped with a cooling stage, ice nuclei form of generation of ice nuclei is observed.

## 3. Results and discussion

The ice nucleation temperatures of fungal spores showed large diversity, depending on their species. The ice nucleation temperature depends on the biological classification of fungi. Although there were a large variation, ice nucleation temperatures of spores of *Russulales*, ranged from -20 to -30 ˚C. The temperatures of *Boletales* spores were about -30 ˚C, and they of *Polyporales* spores were -22 ˚C. *Agaricales* can be divided into two groups: spore ice nucleation temperature was about -15 ˚C and about - 30 ˚C. The generation form of ice nuclei in spores can be categorized into 4 groups: A: ice grows from the whole spore surface after its swelling, B: ice grows suddenly from the spore surface, C: ice grows from a particular part of spores, D: ice generated around spores. Although there are a few exceptions, most of the spores that could be classified as “A” became ice nucleus at a relatively high temperature of -15 ˚C or higher. For other developmental forms, the relationship with ice nucleation temperature is not clear. Measuring the ice nucleation temperatures of various kinds of fungal spores this study found that some

©2019. Japan Geoscience Union. All Right Reserved. 

fungal spores can become ice nuclei at a relatively high temperature of -15 ˚C or so, showing a possibility that fungal spore can produce ice clouds in relatively lower atmosphere. It is also found that fungal spores forming ice at relatively high temperature mostly classified as *Agaricales* , and that they swelled just before they made ice particles. These results may have information on factors determining the ice formation temperature of spores.

Keywords: bioaerosol, fungal spore, ice nuclei

©2019. Japan Geoscience Union. All Right Reserved. 

# Investigation of Atmospheric Aerosol Particles and gases by R/V Mirai cruise over the Arctic Ocean on 2017

*Fumikazu Taketani[1], Saki Kato[1,2], Takuma Miyakawa[1], Masayuki Takigawa[1], Masahiro Yamaguchi[1], Hisahiro Takashima[1,2], Petr Mordovskoi[1], Yugo Kanaya[1]

1. Japan Agency for Marine-Earth Science and Technology, 2. Fukuoka University

Atmospheric aerosol particles play an important role in Arctic climate through the absorbing and scattering of solar radiation. Also, the deposition of light-absorbing particles on the surface reduces the Earth’ s albedo and accelerates snow/ice melting by absorbing the sunlight. However, the observational information has been still insufficient to assess their contribution over the Arctic region. In this study, we conducted the ship-based measurements of marine aerosol particles (black carbon (BC), and fluorescent property) and trace gases (ozone and carbon monoxide) using R/V Mirai during a cruise across the Arctic Ocean and Bering Sea (23 August –4 October 2017). The measured BC mass concentration over the Arctic Ocean in the latitudinal region > 70˚N was an overall mean value of 3.5 ±2.0 ng/$m^3$ . This value was almost same to the levels recorded during our previous observations in the Arctic cruise on September during 2014 -2016. We captured relatively high BC mass concentration and/or CO mixing ratio events at 4 and 7-12 September 2017. The trajectory and BC property suggested that the source of BC on 4 September could be oil field at north of Alaska. We will present further analysis on the size distribution, BC mixing state, during the cruise in the presentation.

Keywords: Black Carbon, Arctic Ocean, Ship-based Observation

©2019. Japan Geoscience Union. All Right Reserved. 

# Characterization of carbonaceous aerosols in East Asia in the spring of 2015: Importance of non-fossil fuel sources

*Takuma Miyakawa[1], Yuichi Komazaki[1], Fumikazu Taketani[1], Xiaole PAN[2], Zifa Wang[2], Yugo Kanaya[1]

1. Japan Agency for Marine-Earth Science and Technology, 2. Institute for Atmospheric Physics, Chinese Academy of Science

The sources of elemental (EC) and organic carbon (OC) aerosols in the spring of 2015 in Asian outflow were investigated in terms of the radiocarbon ($^{14}C$) for carbonaceous aerosols and organic molecular marker analyses. The contribution of fossil fuel (FF) sources to total carbonaceous aerosols (TC) significantly increased in polluted air masses with enhancements of carbon monoxide concentrations. For EC, FF sources dominated in the polluted air masses. For OC, the contributions of non-FF and non-biomass burning (BB) sources were found to be significant (comparable to or higher than those of FF sources), especially in the air masses with higher values of both the ratio of water-soluble fraction of OC ($f_{WSOC}$) and $^{14}C$ concentrations ($F^{14}C$). Positive correlation between $f_{WSOC}$ and $F^{14}C$ indicates that the origins of TC (mainly OC) have great effects on the variabilities in the water solubility and the following climatic impacts (i.e., cloud formation process) of OC in the regional scale within the time scale of a week. Multivariate analyses using metallic and ionic tracers revealed the insights into the characteristics of classified carbonaceous aerosols in Asian outflow.

Keywords: Carbonaceous aerosols, Radiocarbon analysis, Source attribution

©2019. Japan Geoscience Union. All Right Reserved. 

# Analyzing the influence of biomass burning on ambient air pollution in mainland Southeast Asia from 2001 to 2016

*Shuai Yin[1]

1. National Institute for Environmental Studies

In this study, various remote sensing data, modeling data and emission inventories were integrated to analyze the tempo-spatial distribution of biomass burning in mainland Southeast Asia and its effects on the local ambient air quality from 2001 to 2016. With such a long time span, land cover changes have been considered in dividing the biomass burning into four types: forest fires, shrubland fires, crop residue burning and other fires. The results show that the monthly average number of fire spots peaked at 34,512 in March and that the monthly variation followed a strong seasonal pattern, which was closely related to precipitation and farming activities. The four kinds of biomass burning fires presented totally different tempo-spatial distributions and forest fires and shrubland fires are more dominant than other types. Moreover, the monthly Aerosol Optical Depth (AOD), particulate matter with a diameter less than 2.5 $\mu$m ($PM_{2.5}$) and carbon monoxide (CO) concentrations also peaked in March with values of 0.62, 73.97 $\mu g/m^3$ and 426 ppb, respectively. There are significant correlations between the monthly AOD, $PM_{2.5}$, and CO concentrations and the number of fire spots. On an annual scale, we also found certain correlations between the AOD and $PM_{2.5}$ concentrations and the number of fire spots. With respect to the spatial distribution, the AOD, $PM_{2.5}$ and CO concentrations are always higher in intense biomass burning regions. Southeast Asia is one of the most populated and fastest growing economic regions in the world. Therefore, in order to objectively and accurately analyze the influence of biomass burning on local air quality over a long time span, it is imperative for this study to consider the effects of anthropogenic activities. Two anthropogenic $CO_2$ emission inventories, the Emission Database for Global Atmosphere Research (EDGAR) and the Carbon Dioxide Information Analysis Center (CDIAC), were used. The results further prove that biomass burning is the dominant cause of the variation in the local air quality in mainland Southeast Asia. Although government authorities have taken measures to control biomass burning, the number of fire spots did not decrease; the numbers exceeded 100,000 each year from 2012 to 2016.

Keywords: AOD, Anthropogenic emission, Biomass burning, Carbon monoxide, PM2.5

©2019. Japan Geoscience Union. All Right Reserved. 

# High-resolution and multi-year inventory of mercury emissions from biomass burning in tropical continents during 2001–2017

*Yusheng Shi[1]

1. Aerospace Information Research Institute, Chinese Academy of Sciences

Mercury emissions from biomass burning contribute significantly to the atmospheric mercury budget and the interannual variations of mercury concentrations in the troposphere. This study developed a high-resolution (0.1 deg) and multi-year (2001-2017) monthly inventory of mercury emissions from biomass burning in five fire types in the tropical continents (Central and South America, Africa, and South and Southeast Asia). The inventory estimates of mercury emissions from biomass burning are based on the newly released MCD61A1 version 6 Burned Area data product, satellite and observational data of biomass density, and spatial and temporal variable combustion factors. Results from the inventory demonstrated that during 2001-2017, the average annual mercury emissions from biomass burning in tropical continents was 497 Mg and ranged from 289 Mg to 681 Mg. Forest fires were the largest contributor, accounting for 61% (300 Mg) of the total mercury emissions from biomass burning, followed by fires in shrubland (30%, 151 Mg), savanna (7%, 35 Mg), peatland (1%, 6 Mg), and cropland (1%, 5 Mg). However, these proportions varied between the continents; in the Americas and Asia, the largest biomass burning emissions came from forest fires, and in Africa the largest emissions were from shrubland fires. Between the three continents, Africa released 41% of the mercury emissions from biomass burning (202 Mg $year^{-1}$), Asia released 31% (154 Mg $year^{-1}$), and the Americas released 28% (141 Mg $year^{-1}$). The total mercury emissions from biomass burning in these tropical continents exhibited strong interannual variations from 2001 to 2017, with peak emissions in March and Agust to September, and forest fires were the primary land fire type controlling the interannual variations. Soil mercury emissions released during biomass burning was determined to be 495 Mg $year^{-1}$ during 2001-2017. The biomass burning mercury emissions data in this inventory agrees with results by other studies, which suggests that it could be used as an input for atmospheric transport models.

Keywords: biomass burning, mercury emissions, forest fires, tropical continents

©2019. Japan Geoscience Union. All Right Reserved. 

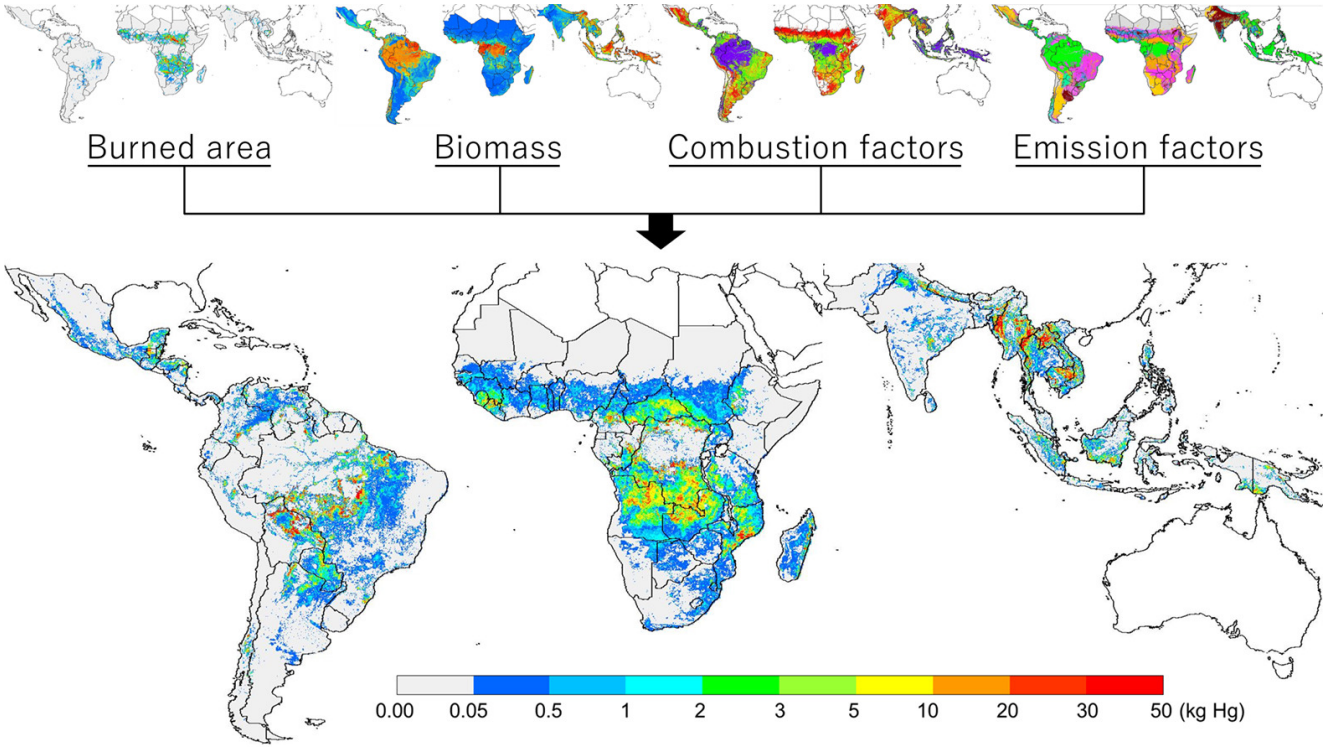


©2019. Japan Geoscience Union. All Right Reserved. 

# Simultaneous observations by sky radiometer and MAX-DOAS for characterization of biomass burning plumes in central Thailand in January-April 2016

*Hitoshi Irie[1], Syedul Hoque[1], Alessandro Damiani[1], Al Mashroor Fatmi[1], Pradeep Khatri[2], Tamio Takamura[1], Thanawat Jarupongsakul[3]

1. Chiba University, 2. Tohoku University, 3. Chulalongkorn University

The first intensive multi-component ground-based remote sensing observations by sky radiometer and Multi-Axis Differential Optical Absorption Spectroscopy (MAX-DOAS) were performed simultaneously at the SKYNET/Phimai site located in central Thailand (15.18˚N, 102.56˚E) from January to April 2016. The period corresponds to the dry season associated with the intense biomass burning (BB) activity around the site. The near-surface concentration of formaldehyde (HCHO) retrieved from MAX-DOAS was found to be a useful tracer for absorption aerosols from BB plumes, when BB was the dominant sources of HCHO and absorption aerosols over other sources. As the HCHO concentration tripled from 3 to 9 ppbv, the ratio of gaseous glyoxal to HCHO concentrations in daytime decreased from ~0.04 to ~0.03, responding presumably to the increased contribution of volatile organic compound emissions from BB. In addition, clear increases in aerosol absorption optical depths (AAODs) retrieved from sky radiometer observations were seen with the HCHO enhancement. At a HCHO of 9 ppbv, AAOD at a wavelength of 340 nm reached as high as ~0.15±0.03. The wavelength dependence of AAODs at 340-870 nm was quantified by the absorption Ångström exponent (AAE), providing evidence for the presence of brown carbon aerosols at an AAE of 1.5±0.2. Thus, our multi-component observations around central Thailand are expected to provide unique constraints for understanding physical/chemical/optical properties of BB plumes.

Keywords: Biomass burning, HCHO, CHOCHO, aerosol, sky radiometer, MAX-DOAS

©2019. Japan Geoscience Union. All Right Reserved. 

# Quantifying PM2.5 from long-range transport and local pollution in Taiwan during winter monsoon.

*Ming-Tung Chuang[1]

1. Research Center for Environmental Changes, Academia Sinica

From autumn to the following spring, annually, the northeast monsoon transports PM2.5 (particles less than
2.5 μm in aerodynamic diameter) from the Asian continent to downstream areas. Naturally, this triggered a
question: What are the contributions of PM2.5 from long-range transport (LRT) and local pollution (LP) at any
downstream location? To answer that question, the present study developed an economical and efficient method
that can easily estimate the contribution of PM2.5 from LRT (LRT-PM2.5) and PM2.5 from LP (LP-PM2.5). The
method used PM2.5 and meteorological observation data in Taiwan from 2006 to 2015 and a short-term simulation
from January to May in 2010. The analysis classified the data into three types of PM2.5 source patterns:
LRT-Event (high concentration plume at the front edge of southward moving anticyclones/strong northeast
wind), LRT-Ordinary (less concentration in common strong northeast wind), and LRT/LP Mix or Pure LP (PM2.5
was from both LRT and LP or from only LP under weak northeast wind). During the ten-year period, the average
LRT-PM2.5 values at the northern tip of Taiwan were 31–39 μgm−3, 12–16 μgm−3, and 4–13 μgm−3 for the
LRT-Event, LRT-Ordinary, and LRT/LP Mix or Pure LP patterns, respectively. The 10-year average LRT-PM2.5
and LP-PM2.5 contributions were approximately 70:30 in northern Taiwan, 50:50 in central Taiwan, and 30:70 in
southern Taiwan for the LRT-Event pattern; 60:40 in northern and 40:60 in central and southern Taiwan for the
LRT-Ordinary pattern; and 30:70 in northern and 25:75 in central and southern Taiwan for the LRT/LP Mix or
Pure LP pattern. Interestingly, LRT-PM2.5 peaked in 2013 but has decreased annually since then, whereas LPPM2.5
has roughly decreased in the past ten years.

Keywords: PM2.5, long-range transport, local pollution, CMAQ

©2019. Japan Geoscience Union. All Right Reserved. 

# Vertical characterization of $PM_{2.5}$ based on observation using compact sensors on and around Mt. Unzen in Nagasaki Prefecture

*Tomoki Nakayama[1], Ayane Ueno[1], Kenta Kanegae[1], Kazuaki Kawamoto[1], Kodo Umakoshi[1], Takayuki Yamasaki[2], Wataru Okamoto[2], Yutaka Matsumi[2]

1. Faculty of Environmental Science, Nagasaki University, 2. ISEE, Nagoya University

Aerosol particles in the atmosphere, including $PM_{2.5}$, are known to have significant impacts on climate, the atmospheric environment, ecosystems, and human health. Whereas both of domestic sources and transboundary pollution from Asian Continent possibly contribute to the $PM_{2.5}$ mass concentrations in Japan, high $PM_{2.5}$ events owing to the transboundary pollution are often observed, especially in north-western part of Kyushu region (including Nagasaki Prefecture). Although $PM_{2.5}$ mass concentrations are observed at the observatories of the Atmospheric Environmental Regional Observation System (AEROS) of the Ministry of the Environment, Japan (MOEJ), the observatory on mountain is very limited, and widely used large and expensive bate attenuation monitor (BAM) is not suitable for the multi-point observations.

We developed a compact $PM_{2.5}$ sensor with Panasonic Corporation [Nakayama et al. 2018]. This sensor can measure $PM_{2.5}$ mass concentrations by detecting light scattering intensities from individual aerosol particles with diameters greater than 0.3 $\mu$m. In this study, this sensor was applied for the observations of $PM_{2.5}$ mass concentrations around Mt. Unzen in Nagasaki Prefecture from December 2018. The $PM_{2.5}$ sensors were installed at six sites with different altitudes from 20 m to 1300 m to analyze vertical and horizontal distributions of $PM_{2.5}$. During high $PM_{2.5}$ events (>35 $\mu g/m^3$) in winter, the $PM_{2.5}$ mass concentrations at an altitude above 1000 m are similar to those at 20 m in most cases. However, in some cases, high $PM_{2.5}$ was observed only at low altitude sites, likely because of inflow of clean air with lower aerosol burden from higher altitude to the mountain sites and/or low boundary layer height. The vertical profile data obtained in this work will be compared with the lidar data obtained by NIES at Omura city, which is located 38 km north-west of Mt. Unzen, to discuss the possible sources and transport patterns of $PM_{2.5}$.

Acknowledgements

This work is supported by Unzen city, Shimabara city, Minamishimabara city, Unzen ropeway Corporation, and Eco Solutions Company, Panasonic Corporation.

Reference

T. Nakayama, Y. Matsumi, K. Kawahito, Y. Watabe, Development and evaluation of a palm-sized optical $PM_{2.5}$ sensor, *Aerosol Sci. Technol.*, 52, 2-12, doi:10.1080/02786826.2017.1375078 (2018).

Keywords: PM2.5, Transboundary Air Pollution , Compact sensor, Mountain

©2019. Japan Geoscience Union. All Right Reserved. 

# Observation of NPF events at the summit of Mt. Fuji during daytime and nighttime

*Hiroki Igarashi[1], Takenori Sato[1], Tatsuhiro Mori[1], Kazuhiko Miura[1], Yoko Iwamoto[2], Ryuichi Wada[3], Shungo Kato[4], Hiroshi Okochi[5]

1. Tokyo University of Science, 2. Hiroshima University, 3. Teikyo University of Science, 4. Tokyo Metropolitan University, 5. Waseda University

An improved understanding of a new particle formation (NPF), which is a key process controlling the spatial and temporal distributions of aerosol concentration, is needed to estimate the direct radiative forcing. However, it is difficult to quantitatively understand the mechanism of NPF because the frequency of the NPF depends on the aerosol concentration, gases, and meteorological condition. In this study, we measured number concentrations (*N*) of aerosol particles (10 to 487 nm) at the summit of Mt. Fuji (35.360˚N, 138.727˚E, 3776 m a.s.l.) between July and August during 2011-2017. We report the annual and diurnal variations of the frequency of the NPF for a long-term period. The summit of Mt. Fuji is usually located in the free troposphere and enable us to observe the long-range transport of aerosol particles. The NPF event was defined as the event that *N* increases over 1 hour for diameter smaller than 25 nm. We observed 172 NPF events (daytime and nighttime events were 90 times and 82 times, respectively) during the observation period. Most events occurred at 8 o'clock (at the peak of daytime events) and 20 to 21 o'clock (at peaks of nighttime events) in local time. In addition, the growth rate of aerosol particles was calculated. The median value of the growth rate was estimated to be 5.27 nm/h (6.03 nm/h for daytime and 4.56 nm/h for nighttime) at 40 NPF events, suggesting that aerosol particles are easily grown during daytime. Finally, using a back trajectory analysis (NOAA HYSPLIT version 4), we investigated when and where the NPF occurred. As a result, it is suggested that 62.5% of the total NPF occurred during the daytime, and the rest occurred during the nighttime (37.5%). The NPF frequently occurred during daytime over Japan although a few NPF occurred over the sea during nighttime.

Keywords: New particle formation, Mt. Fuji, Nighttime NPF event, Particle size distribution

©2019. Japan Geoscience Union. All Right Reserved. 

# Measurement of atmospheric metal particles using an ICP-MS and TEM.

*Takeshi Kinase[1], Kouji Adachi[1], Mizuo Kajino[1], Masahiko Hayashi[2], Keiichiro Hara[2]

1. Meteorological Research Institute, 2. Fukuoka

Particles containing transition metal components (hereafter, metal particle) are one of the major aerosols. Some of these metal particles have strong oxidation potential and have health effects by deposition into the human body through generating reactive oxygen and free-radical in and on cells. These reactive oxygen and free radicals cause various effects such as oxidative stress, inflammatory cell, DNA oxidative damages and cell death. However, oxidation potential for each metal particle and the magnitude of hazard to human health are not well known. In addition, colored metal particles, such as iron oxide, absorb solar radiation and contribute to the global warming. However, these effects of metal particles are not clarified because their observations and detailed features are not well known.

In this study, we measured atmospheric metal particle concentrations using an inductively coupled plasma-mass spectrometry (ICP-MS) and collected aerosol samples on the Cu grids using impactors to observe each aerosol particle using a transmission electron microscope (TEM) and an energy-dispersive X-ray spectrometry detector (EDS) with the scanning transmission electron microscopy (STEM). The ICP-MS instrument was coupled with a gas changer for air replacement in argon gas atmosphere, so that aerosol particles were directly measured using the ICP-MS in real-time. As a result, we could measure time trends of atmospheric metal particle concentrations quantitatively with high time resolutions together with their shape and mixing states by the TEM and STEM-EDS analysis.

We measured atmospheric metal particles in winter (2018/1/17–2/8) and in spring (2018/5/8–5/30) at Fukuoka University. We measured increasing events of metal particles by ICP-MS. Fe and Al were the highest concentration followed by Zn, Mn, Cr and Pb. Two different slopes were observed in relation between Fe and other metal elements such as Mn, V, and Al. On the other hand, Ag, Au, Mo and Tc did not correlate with Fe. From TEM observation of samples with high concentrations of metal particles, we found aggregated metal particles as ultrafine metal spheres (for smaller particles were several nm). These particles contained Fe, Mn and Cr as major metal elements, and most particles were internally mixed with a sulphate. Furthermore, some metal particles contained many ultrafine metal particles that distributed separately in a sulphate. Zn and Pb containing particles were also internally mixed with sulphate, however, they were observed as dissolved substances (not particle state) or crystallized state, which were decomposed by electron beam.
We found other metal particles which contained such as Ag, Sb, and Cu during their increasing periods. Our results are useful for understanding of atmospheric metal particles behaviors.

Keywords: Oxidation potential, Metal particle, ICP-MS, TEM, Feature observation

©2019. Japan Geoscience Union. All Right Reserved. 

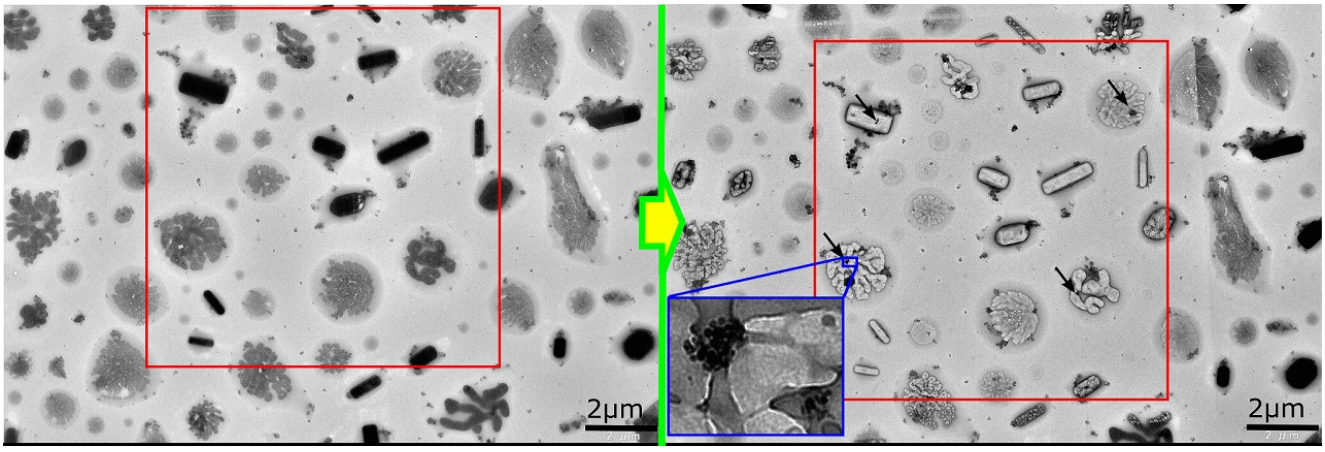


©2019. Japan Geoscience Union. All Right Reserved. 

# Experimental results on measuring device of complex refractive index using the single particle extinction and scattering method

*TAKASAGO YUYA[1]

1. Tokyo university

Changes in the type and amount of atmospheric aerosol alter the albedo, resulting in radiation budget and climate change. However, the prediction accuracy of the fluctuation range is not high at the present. The complex refractive index can estimate the type of atmospheric aerosol. In the existing method, a method of measuring the complex refractive index for each bulk is mainstream, and there are few cases to measure for each single particle. If accurate measurement data of complex refractive index for each particle type can be obtained, it is possible to improve prediction accuracy of climate change width of particle type, so measurement with complex refractive index for each single particle is important. In this study, we conducted an experiment using single particle extinction and scattering method as a method to measure the complex refractive index. The single particle extinction and scattering method is a method of measuring forward scattered light intensity generated by projecting a laser on fine particles and interference between scattered light and incident light and estimating the value of the complex refractive index of the particle from these data. We developed an experimental apparatus using this method and conducted experiments with polystyrene, BC standard particles and precipitation samples (Okinawa, Happo, Fukui). Currently, I am thinking a method to solve the inverse problem that estimates particle characteristics such as particle type and complex refractive index from forward scattering intensity obtained from experiment and interference data of incident light and scattered light. For this purpose, we are developing a method of classifying samples mixed with plural types of particles into particle type by using clustering method of machine learning.

©2019. Japan Geoscience Union. All Right Reserved. 

# Evaluation of BC and CO emission inventory based on long-term in-situ observations over East Asia

*Yongjoo Choi[1], Yugo Kanaya[1], Hye-Jung Shin[2], Seung-Myong Park[2], Atsushi Matsuki[3], Yasuhiro Sadanaga[4], Sang-woo Kim[5], Itsushi Uno[6], Xiaole Pan[7]

1. Development Center for Global Change, Japan Agency for Marine-Earth Science and Technology, 2. Division of Climate & Air Quality Research, National Institute of Environmental Research, Korea, 3. Institute of Nature and Environmental Technology, Kanazawa University, 4. Department of Applied Chemistry, Graduate School of Engineering, Osaka Prefecture University, 5. School of Earth and Environmental Sciences, Seoul National University, Seoul, Korea, 6. Research Institute for Applied Mechanics, Kyushu University, 7. Institute of Atmospheric Physics, CAS, Beijing, China

Compared to carbon dioxide ($CO_2$), which is a major long-lived greenhouse gas, the influence of black carbon (BC) to global warming is not negligible among the short-lived components. To improve the bottom-up emission inventory for enhancing the understanding level of BC, the measured ΔBC/ΔCO ratios were compared with those from the Regional Emission inventory in Asia (REAS) version 2.1 bottom-up inventory. The measurements were conducted at two sites in Korea (Baengnyeong; 124.63˚ E, 37.97˚ N, and Gosan; 126.17˚ E, 33.28˚ N) and two sites in Japan (Noto; 137.36˚ E, 37.45˚ N, and Fukuoka; 130.47˚ E, 33.52˚ N). The instruments for measuring CO concentration are same at all sites as Model 48i (Thermo Fisher Scientific), however, the instruments for BC were different depends on the sites (sunset EC/OC analyzer in Baengnyeong, Continuous Light Absorption Photometer in Gosan, Multi-Angle Absorption Photometer in Noto and Fukuoka). Based on the backward trajectories during past 120 hours calculated from HYSPLIT model, all trajectories were assigned to six study domains which divided by country and/or administrative district (East China, North China, Northeast China, South Korea, North Korea, and Japan). To exclude the wet-removal effect, the ΔBC/ΔCO ratio was considered only when the accumulated precipitation along a backward trajectory (APT) for three days is equal to zero. Also, we confirmed that the comparison of ΔBC/ΔCO by six study domains could be reasonable since there were no significant differences in ΔBC/ΔCO ratio depending on traveling time (dry deposition effects) and residence time over the emission source areas. Compared to measured ΔBC/ΔCO ratio (6.6 –8.4 ng/$m^3$·ppb), ΔBC/ΔCO from REAS emission inventory (8.0 ng/$m^3$·ppb for East China –23.2 ng/$m^3$·ppb for South Korea) were overestimated by factor 1.2 for East China to 2.9 for South Korea whereas those for North Korea (3.7 ng/$m^3$·ppb from REAS) was underestimated by factor 2.0. The measured ΔBC/ΔCO ratios in Japan (6.8 ng/$m^3$·ppb) were similar to those from REAS emission inventory (6.5 ng/$m^3$·ppb). The seasonal and spatial differences of ΔBC/ΔCO ratios between measured and emission inventory will be examined to identify the over- and under-estimated administrative districts.

Keywords: Black Carbon, Carbon monoxide, REAS emission inventory, ΔBC/ΔCO ratios

©2019. Japan Geoscience Union. All Right Reserved. 

# Inverse modeling of black carbon emissions over China using ensemble data assimilation

*Ping Wang[1]

1. Chinese Academy of Meteorological Sciences

Emissions inventories of black carbon (BC), which are traditionally constructed using a “bottom-up” approach based on activity data and emissions factors, are considered to contain a large level of uncertainty. In this paper, an ensemble optimal interpolation (EnOI) data assimilation technique is used to investigate the possibility of optimally recovering the spatially resolved emissions bias of BC. An inverse modeling system for emissions is established for an atmospheric chemistry aerosol model and two key problems related to ensemble data assimilation in the top-down emissions estimation are discussed: 1) how to obtain reasonable ensembles of prior emissions; and 2) establishing a scheme to localize the background-error matrix. An experiment involving one year long simulation cycle with EnOI inversion of BC emissions is performed for 2008. The bias of the BC emissions intensity in China at each grid point is corrected by this inverse system. The inversed emission over China in January is 240.1 Gg, and annual emission is about 2539.3 Gg, which is about 1.8 times of bottom-up emission inventory. The results show that, even though only monthly mean BC measurements are employed to inverse the emissions, the accuracy of the daily model simulation improves. Using top-down emissions, the average root-mean-square error of simulated daily BC is decreased by nearly 30%. These results are valuable and promising for a better understanding of aerosol emissions and distributions, as well as aerosol forecasting.

Keywords: Inverse modeling, black carbon, ensemble optimal interpolation

©2019. Japan Geoscience Union. All Right Reserved. 

# Analysis of BC emissions in East Asia using inverse model

*Takashi Maki[1], Taichu Y Tanaka[1], Naga Oshima[1], Thomas Sekiyama[1], Keiichi Kondo[1], Jun-ichi Kurokawa[2], Keiya Yumimoto[3], Toshimasa Ohara[4]

1. Meteorological Research Institute, 2. Asia Center for AirPollution Research, 3. Kyushu University, 4. National Institute for Environmental Studies

In addition to affecting climate change and global warming, Black Carbon (BC) brings impact on society and human health as well. However, changes in BC emissions in east Asia have yet to be fully understood. Attempts have been made by various institutions and researchers to estimate BC emission inventories from various statistics but there are problems such as lack of rapid reporting. In order to modify black carbon emissions inventory based on this statistic, we have constructed an BC emission inversion system for east Asia using aerosol transport model and surface observations. The analysis period for emissions is from 2011 to 2014. We adopt global aerosol transport model named MASINGAR mk-2 (Tanaka et al.). The model is a subset of MRI (Meteorological Research Institute) earth system model for climate research and can treat BC, OC, mineral dust, sulfate and sea-salt with external mixing. We divided tags of each province of China, South Korea, Japan into 33 regions and carried out tagged tracer transport experiments. We collected 5 surface sites daily observation data (Hedo, Fukue, Echizen, Happo and Lulin). A priori BC emission is provided by REAS 2.2 (Kurokawa et al.) at 2010. Inversion results suggested that BC emissions in East Asia between 2011 and 2014 are decreasing especially in China about 10%, compared to the 2010 emissions. There was no significant change in BC emissions in Japan and South Korea during the analysis period. However, the observation network could constrain mainly northern part of China. We need more observation data (ex. satellite data) to constrain BC emission amount.

Keywords: Inverse model, BC emission, Aerosol model

©2019. Japan Geoscience Union. All Right Reserved. 

# Source attribution of BC in the northern Pacific and Arctic Ocean by chemistry climate model

*Takato Onishi[1], Kengo Sudo[1,2], Yugo Kanaya[2], Fumikazu Taketani[2]

1. Graduate School of Environmental Studies, Nagoya University, 2. Japan Agency for Marine-Earth Science and Technology

Black Carbon (BC) is emitted from combustion of biomass and fossil fuel into the atmosphere. BC in the atmosphere absorbs visible light and heats the atmosphere contributing to global warming. The emitted BC being originally hydrophobic with low CCN activity, is not easily scavenged by precipitation allowing long-range transport of BC to remote areas. Snow or ice surfaces, when affected by deposition of BC, decrease their albedo causing further warming in the high latitudes.
This study focuses on long-range transport of BC in the northern high latitude regions and investigates BC origins (source regions and types) with a tagged tracer simulation by a global chemistry climate model CHASER. The modeled BC concentrations are validated with the BC observational data obtained from the JAMSTEC research vessel Mirai (from August to September). The model is found to be overestimating the observed BC by a factor of 1.2 to 7 in the south of 70°N in the northern Pacific. Differences between the model and observation are relatively small near Japan, but a bit larger between 160°E to 180°E in the Pacific Ocean. For the Arctic Ocean, on the other hand, the model severely overestimates BC by a factor of 13 to 70. In the model, BC in the North Pacific and Arctic Ocean is originated mainly from Siberia, North America and China.
The overestimated BC in the model probably shows an underestimate of wet deposition by precipitation. However, it is found that CHASER tends to overestimate precipitation amount when compared to the reanalysis data as the ERA-interim. This suggests that there is an inconsistency in the BC wet deposition scheme such as underestimation of BC uptake to cloud droplets. We considered correlation between precipitation and BC wet deposition flux normalized by columnar BC mass for checking relation of precipitation and BC wet removal. The correlation coefficient is about 0.4 suggesting that BC removal by precipitation is weak in the model. In addition, the ratios of internal BC to total BC for the surface to lower troposphere are calculated for the years of 2014 to 2017. In the northern pacific and Arctic Ocean, the ratios are about 30 percent indicating that the hydrophobic type of BC is dominant in the region for which CHASER overestimates BC.
As a result, it is suggested that there is much room for improvement in the simulation of aging process of BC (hydrophobic to hydrophilic conversion) and the scheme for wet deposition of external BC. In the presentation, the results from the further improved model simulations will be introduced and discussed.

Keywords: BC, chemistry-climate model, wet deposition, Arctic Ocean, Pacific Ocean

©2019. Japan Geoscience Union. All Right Reserved. 

# Evaluation of a mobile $PM_{2.5}$ sensor and application to the measurements along the National route 1 and around Nagasaki University

*Kenta Kanegae[1], Takayuki Yamasaki[2], Wataru Okamoto[2], Yutaka Matsumi[2], Tomoki Nakayama[1]

1. Nagasaki University, 2. Nagoya University

Short-term exposure of $PM_{2.5}$, negatively impacts human health through respiratory disease (such as asthma and bronchitis) and cardiovascular diseases, and leads to premature death. Because $PM_{2.5}$ is spatially and temporally variable and individuals also move in time and space, it is important to understand personal exposures of $PM_{2.5}$ for better assessment of the health impact. We developed a palm-sized optical $PM_{2.5}$ sensor with and Panasonic Corporation, and evaluated the performance for environmental monitoring at fixed sites [Nakayama et al. 2018]. This sensor was designed to measure $PM_{2.5}$ mass concentrations by detecting light scattering intensities from individual aerosol particles with diameters greater than 0.3 $\mu$m. The small size, light weight, and low power consumption of the sensor are suitable for mobile personal exposure measurement. However, the sensitivity of the sensor can be change if the sensor is tilted or swung, because aerosol particles flow into the sensor via an updraft generated by a heater and flow rate may be change during tinting or swinging.
In this study, we investigate the performance of the $PM_{2.5}$ sensor for mobile exposure measurements. The changes in the sensitivity of the sensor during tilting or swinging have been tested. Moreover, the change in the sensitivity of the sensor during walking has been investigated, by comparing the $PM_{2.5}$ data during walking with those during standing. From the results of these tests, it was found that the sensor can be applied for mobile exposure measurements of $PM_{2.5}$ mass concentration. We applied this sensor for the mobile measurements during walking along the National Route 1 (from Tokyo to Kyoto) for two weeks, and around Nagasaki University. The obtained $PM_{2.5}$ data will be compared with those obtained at the surrounding ambient air monitoring stations (AEROS) and meteorological data to discuss the sources and transportation of $PM_{2.5}$. We believe that this research will provide useful information for applications of the compact sensor to epidemiological research of health effects of $PM_{2.5}$.

Acknowledgements
This work is supported by the Eco Solutions Company, Panasonic Corporation.

Reference
T. Nakayama, Y. Matsumi, K. Kawahito, Y. Watabe, Development and evaluation of a palm-sized optical $PM_{2.5}$ sensor, *Aerosol Sci. Technol.*, 52, 2-12, doi:10.1080/02786826.2017.1375078 (2018).

Keywords: Compact PM2.5 sensor , Personal exposure, Mobile measurement

©2019. Japan Geoscience Union. All Right Reserved. 

# Analysis on the Relationship between the Concentration of Particulate Matter and Mortality from Respiratory and Cardiovascular Diseases

*Woo-Sik JUNG[1], Woo-Gon Do[2]

1. Department of Atmospheric Environment Information Engineering, Atmospheric Environment Information Research Center, Inje University, Gimhae 50834, Korea, 2. Busan Metropolitan City of Institute of Health and Environment Busan, Korea

Concerns over particulate matter are growing rapidly as the number high concentration days are increasing. Since 2015, PM2.5 has been set as a national ambient air quality standard and frequency of Asian dust or mists and precursors coming from the west of Korea has increased. Various studies have been conducted on the distribution and composition of particulate matter. The particulate matter is known to be the main cause of respiratory and cardiovascular disease, such as vascular dysfunction, asthma and the occurrence of chronic bronchitis. As the paradigm of air quality management policy changes from controlling, treating and reducing sources to taking into account the damage of a receptor including assessing health risks, it is necessary to establish scientific policies by quantitatively assessing the health effects of the particulate matter and calculating health benefits. To do this, a quantitative assessment of the health risks of particulate matter is essential. The purpose of this study is to analyze the effects of changes in the daily average concentration of particulate matter on the mortality of respiratory and cardiovascular diseases in Busan, Korea. In this study, we employed a generalized additive model (GAM) with a quasi-Poisson to assess the association between daily mean particulate matter and mortality. A penalized spline function was used to adjust the seasonal pattern and long-term trend in daily mortality and the nonlinear mortality effects of the weather. Based on this, a model between the death rate and daily average particulate matter was established and the change in the mortality rate of respiratory and cardiovascular diseases was analyzed according to the change in particulate concentration. The daily mean particulate matter were calculated using hourly PM2.5 and PM10 data provided the Environment Ministry of Korea and the causes of death from 2015 to 2017 were provided by the National Statistical Office's 'Micro Data Service'.

This research was supported by Basic Science Research Program through the National Research Foundation of Korea(NRF) funded by the Ministry of Education(2017R1D1A3B03036152)

Keywords: Particulate Matters, Mortality, Respiratory Diseases, Cardiovascular Diseases

©2019. Japan Geoscience Union. All Right Reserved. 

# Analysis on the Relationship between the Concentration of Particulate Matter and Mortality from Respiratory and Cardiovascular Diseases

**Woo-Sik Jung*, Woo-Gon Do,**

*Dept. of Atmospheric Environment Information Engineering, Inje University, Gimhae, Korea
Busan Metropolitan City of Institute of Health and Environment Busan, Korea

Concerns over particulate matter are growing rapidly as the number high concentration days are increasing. Since 2015, PM2.5 has been set as a national ambient air quality standard and frequency of Asian dust or mists and precursors coming from the west of Korea has increased. Various studies have been conducted on the distribution and composition of particulate matter. The particulate matter is known to be the main cause of respiratory and cardiovascular disease, such as vascular dysfunction, asthma and the occurrence of chronic bronchitis. As the paradigm of air quality management policy changes from controlling, treating and reducing sources to taking into account the damage of a receptor including assessing health risks, it is necessary to establish scientific policies by quantitatively assessing the health effects of the particulate matter and calculating health benefits. To do this, a quantitative assessment of the health risks of particulate matter is essential. The purpose of this study is to analyze the effects of changes in the daily average concentration of particulate matter on the mortality of respiratory and cardiovascular diseases in Busan, Korea. In this study, we employed a generalized additive model (GAM) with a quasi-Poisson to assess the association between daily mean particulate matter and mortality. A penalized spline function was used to adjust the seasonal pattern and long-term trend in daily mortality and the nonlinear mortality effects of the weather. Based on this, a model between the death rate and daily average particulate matter was established and the change in the mortality rate of respiratory and cardiovascular diseases was analyzed according to the change in particulate concentration. The daily mean particulate matter were calculated using hourly PM2.5 and PM10 data provided the Environment Ministry of Korea and the causes of death from 2015 to 2017 were provided by the National Statistical Office's 'Micro Data Service'.

Acknowledgement

This research was supported by Basic Science Research Program through the National Research Foundation of Korea(NRF) funded by the Ministry of Education(2017R1D1A3B03036152)

©2019. Japan Geoscience Union. All Right Reserved. 

# A Study on the Estimation of Contribution Rate of Odour Substances Using CALPUFF model

*Woo-Sik JUNG[1], Woo-Gon Do[2]

1. Department of Atmospheric Environment Information Engineering, Atmospheric Environment Information Research Center, Inje University, Gimhae 50834, Korea, 2. Busan Metropolitan City of Institute of Health and Environment Busan, Korea

The environmental odours produced by anthropogenic origin according to urbanization and industrialization continue to increase. These odours cause mental and physiological stress and have a variety of adverse health effects, including nausea, headaches, loss of appetite, gastrointestinal disorders, difficulty in breathing, and allergy. Therefore, the odours are degrading the quality of life for residents in nearby residential areas, causing health hazards and eventually causing economic loss in the community. Miscellaneous approaches are used internationally within odour regulatory systems, with methods and tools for management and control supported by ambient air odour concentration and individual chemicals(maximum impact standard); fixed and variable separation distances(separation distance standard); maximum emission rate for odours and individual chemicals(maximum emission standard); number of complaints or annoyance level(maximum annoyance standard); best available technologies e BAT (technology standard). However, the occurrence of odors is a very local issue that reflects the characteristics of individual sources and the subjective impact of nearby residents. Therefore, prior to these regulations, it is very important to assess the impact of individual emissions quantitatively. The CALPUFF model is a typically used model for assessing the dispersion of air pollutants or odours in various research institutes, including the U.S. EPA. This model is an optimal method for calculating the contribution rate of individual emission sources in area where odour sources are concentrated. In this study, the CALPUFF model was used to identify the contribution rate of the four adjacent emission facilities to the surrounding areas in Saenggok Industrial Complex located in Saenggok-dong, Gangseo-gu, Busan in Korea. In order to estimate the contribution rate of individual emission sources, the predicted odour concentration of each emission source was calculated respectively(S1-S4). Next, the predicted odour concentration was calculated considering four emission sources together(Base). Finally, the contribution rates of individual emission sources within the modeling domain were calculated as the ratio of S1-S4 to Base. The amount of area sources in each emission facility was indirectly calculated using the concentration measured near the emission facility. Meterological input data produced by applying the results of the WRF model to the CALMET model. As a result of the CALPUFF model, the contribution rate of sludge treatment facility was the highest at 76%, and the rest of the facilities were shown to contribute about 10% to the surrounding area.

This research was supported by Basic Science Research Program through the National Research Foundation of Korea(NRF) funded by the Ministry of Education(2017R1D1A3B03036152)

Keywords: Odour, CALPUFF

©2019. Japan Geoscience Union. All Right Reserved. 

# A Study on the Estimation of Contribution Rate of Odour Substances Using CALPUFF model

**Woo-Sik Jung*, Woo-Gon Do,**

*Dept. of Atmospheric Environment Information Engineering, Inje University, Gimhae, Korea
Busan Metropolitan City of Institute of Health and Environment Busan, Korea

The environmental odours produced by anthropogenic origin according to urbanization and industrialization continue to increase. These odours cause mental and physiological stress and have a variety of adverse health effects, including nausea, headaches, loss of appetite, gastrointestinal disorders, difficulty in breathing, and allergy. Therefore, the odours are degrading the quality of life for residents in nearby residential areas, causing health hazards and eventually causing economic loss in the community. Miscellaneous approaches are used internationally within odour regulatory systems, with methods and tools for management and control supported by ambient air odour concentration and individual chemicals(maximum impact standard); fixed and variable separation distances(separation distance standard); maximum emission rate for odours and individual chemicals(maximum emission standard); number of complaints or annoyance level(maximum annoyance standard); best available technologies e BAT (technology standard). However, the occurrence of odors is a very local issue that reflects the characteristics of individual sources and the subjective impact of nearby residents. Therefore, prior to these regulations, it is very important to assess the impact of individual emissions quantitatively. The CALPUFF model is a typically used model for assessing the dispersion of air pollutants or odours in various research institutes, including the U.S. EPA. This model is an optimal method for calculating the contribution rate of individual emission sources in area where odour sources are concentrated. In this study, the CALPUFF model was used to identify the contribution rate of the four adjacent emission facilities to the surrounding areas in Saenggok Industrial Complex located in Saenggok-dong, Gangseo-gu, Busan in Korea. In order to estimate the contribution rate of individual emission sources, the predicted odour concentration of each emission source was calculated respectively(S1-S4). Next, the predicted odour concentration was calculated considering four emission sources together(Base). Finally, the contribution rates of individual emission sources within the modeling domain were calculated as the ratio of S1-S4 to Base. The amount of area sources in each emission facility was indirectly calculated using the concentration measured near the emission facility. Meterological input data produced by applying the results of the WRF model to the CALMET model. As a result of the CALPUFF model, the contribution rate of sludge treatment facility was the highest at 76%, and the rest of the facilities were shown to contribute about 10% to the surrounding area.

Acknowledgement

This research was supported by Basic Science Research Program through the National Research Foundation of Korea(NRF) funded by the Ministry of Education(2017R1D1A3B03036152)

©2019. Japan Geoscience Union. All Right Reserved. 

# Stepwise decrease in atmospheric trace gases near the ground associated with rapid vertical mixing observed by 3-D coherent Doppler lidar and in-situ gas measurements

*Hisahiro Takashima[1], Keiichiro Hara[1], Yuki Ohira[1], Akinori Takami[2], Ayako Yoshino[2], Yasushi Fujiyoshi[3]

1. Fukuoka University, 2. National Institute for Environmental Studies, 3. Hokaido University

Stepwise decreases, which occur over several minutes, in nitrogen oxides (NOx) and carbon monoxide (CO) concentrations, in which the main source of these gases is supposed to be near the surface, are sometimes observed in Fukuoka, urban site in Japan, during the summer-winter seasons. In the most cases, ozone ($O_3$) content, which could be higher at higher altitudes, increases. Wind observations by 3-D coherent Doppler lidar suggest there is a thin surface layer (up to ~50-300 m thickness) near the ground before the stepwise change, and then rapid vertical mixing associated with the local meteorological system occurs. The surface thin layer plays a role as a cover of pollutants near the ground, and the vertical mixing within the boundary layer rapidly dilutes/reduces the pollutant contents near the ground.

©2019. Japan Geoscience Union. All Right Reserved. 

# Spatiotemporal variations of nitrogen dioxide ($NO_2$) over Fukuoka , observed by multiple MAX-DOAS instruments and 3-D coherent Doppler lidar

*Hironobu Ueki[1], Hisahiro Takashima[1], Martina M. Friedrich[2]

1. Fukuoka university, 2. Belgian Institute for Space Aeronomy (BIRA-IASB), Belgium

To understand spatiotemporal variations and transport/mixing processes in nitrogen dioxide ($NO_2$) over Fukuoka, an urban area in Japan, continuous $NO_2$ profile observations with a high temporal resolution of four minutes by MAX-DOAS (Multi Axis Differential Optical Absorption Spectroscopy) at three sites in Fukuoka have been conducted from October 2018 to January 2019. Two sites (Yakuin (33.580˚N, 130.396˚E) and Sohara (33.580˚N, 130356˚E)) are located near the city center and pointing towards the north(towards the sea), and one site (Fukuoka University (33.550˚N, 130.364˚E)) is located outside of the city center pointing towards the city center.

In the case of 29 November 2018, an air mass with a high $NO_2$ concentration was observed near the ground in the morning (until 10:30 am) and later, around 10:30 to 11:30 am, an increased concentration of $NO_2$ gradually appeared at a higher altitude over the city center. This increased $NO_2$ concentration disappeared around 13:30-14:00 pm. From the simultaneous three-dimensional (3-D) wind observations by 3-D coherent Doppler lidar installed at Fukuoka University, it is suggested that the air mass with high $NO_2$ concentration was transported upward from the ground by vertical convection, and after that, a clean air-mass was advected from sea by sea-breeze. In this presentation, we will show several results observed by the multipoint MAX-DOAS and 3-D wind observations, focusing on the 3-D transport over Fukuoka using the high $NO_2$ air mass as a tracer.

Keywords: MAX-DOAS

©2019. Japan Geoscience Union. All Right Reserved. 

# Measurement on the $^{17}O$-excess of tropospheric nitrogen oxides

*Fumiko Nakagawa[1], Dong Ding[1], Urumu Tsunogai[1], Takashi Yamaguchi[2], Izumi Noguchi[2]

1. Graduate School of Environmental Studies, Nagoya University, 2. Institute of Environment Sciences, Hokkaido Research Organization

Nitrogen oxides are important trace gases that influence the concentrations of atmospheric oxidants that drive tropospheric and stratospheric chemistry. Triple oxygen isotopes ($\Delta^{17}O$ values; deviation of $^{17}O$ from the mass dependent fractionation line) have been used to understand complex chemical systems such as the cycling and oxidation of NOx. For example, $\Delta^{17}O$ valuesof atmospheric nitrate ($HNO_3$, $NO_3^-$, and p-$NO_3^-$), indicates the proportion of NOx that reacts with ozone ($O_3$) during its oxidation (Michalski *et al.*, 2003; Tsunogai *et al.*, 2010; Nelson et al., 2018). $\Delta^{17}O$ values of atmospheric nitrous acid (HONO; recognized as a potentially important source of OH radicals) have also been used recently to decipher their production pathways. In these studies, however, predicted $\Delta^{17}O$ values were used for $NO_2$. Here, we tried to establish a method to determine $\Delta^{17}O$ values of atmospheric $NO_2$.

$\Delta^{17}O$ value of $NO_2$ was determined, together with $\Delta^{17}O$ value of HONO, by combining sensitive determination method on isotope compositions of $NO_2^-$(Komatsu *et al.*, 2008; Tsunogai *et al.*, 2010) with a slightly modified filter-pack method (Noguchi *et al.*, 2007), in which both $NO_2$ and HONO were collected simultaneously as $NO_2^-$on triethanolamine (TEA)-coated filter and alkaline ($K_2CO_3$) impregnated filter, respectively. Periodical sampling of atmospheric $NO_2$ and HONO was carried out at Hokkaido Institute of Environmental Sciences, Sapporo and at Nagoya University, which is located in a suburban area of Nagoya City. The sample collection period was fixed to one week with a flow rate of 10 L/min. In order to determine diurnal variation in $\Delta^{17}O$ value of $NO_2$ and HONO, an automated system for time-interval air sampling equipped with 6 four-stage-filter-packs were made and used it to collect atmospheric samples every 4 hours.The $\Delta^{17}O$ values of $NO_2$ and HONO showed similar diurnal variations; higher value on the day time than the night time. The result suggests that the atmospheric HONO is formed mainly by chemical reaction of NOx in the urban atmosphere.

Keywords: nitrogen oxides, troposphere, triple oxygen isotope

©2019. Japan Geoscience Union. All Right Reserved. 

# Long-term measurements of the column-averaged mixing ratios of tropospheric substances related to the air pollution using ground-based FTIRs at Rikubetsu, Japan

*Tomoo Nagahama[1], Isamu Morino[2], Shingo Nakanishi[1]

1. Institute for Space-Earth Environmental Research, Nagoya University, 2. National Institute for Environmental Studies

Air pollutants originating from carbon compounds such as reactive volatile organic compounds (VOCs) cause a serious degrading of the air quality near their sources. In addition, these are transported to remote areas with chemical composition changes, and affect air quality in urban areas and their surrounding areas, and therefore, are one of major issues in preserving the air quality. Especially, HCHO and HCOOH originating from forest fires and biogenic VOCs are distributed near their sources since their chemical lifetime is within a few days, and therefore, their distributions and time variations are one of important keys in associating the sources with the impact to the global environment. In order to understand the characteristics of long-term variation of the air quality and its influence on the global environment, the temporal variation of tropospheric substances related to the air pollution are measured with ground-based Fourier Transform InfraRed (FTIR) instrument (Bruker IFS120M and IFS120/5HR) installed at Rikubetsu observatory in Hokkaido, Japan. The cooperative measurements of solar absorption spectra using the FTIRs are conducted by the Institute for Space-Earth Environmental Research (ISEE) of Nagoya University and the National Institute for Environmental Studies (NIES) since 1995. The spectrum is obtained in a 3-15 $\mu$m band with a resolution of 0.0035 $cm^{-1}$. The vertical distribution of trace gases in troposphere and stratosphere is retrieved from the measured spectrum by using the SFIT4 (version 0.944) software. Using SFIT4, we have retrieved the total column amounts and tropospheric column-averaged mixing ratio of $O_3$, $CH_4$, $C_2H_6$, N2O, CO, HCN, HCHO, HCOOH, $C_2H_2$, $CH_3OH$, and find their seasonal and long-term variations from 1995 to 2018. The observed tropospheric column-averaged mixing ratios of $O_3$, $C_2H_6$ and CO show the maximum in March and April, although that of HCHO peaks in July and that of HCN is in May and August, respectively. These differences among the substances may reflect the source and sink processes. Especially, HCHO having a short lifetime may reflect oxidation of biogenic VOCs in summer as well as forest fires.
In the presentation, we will report the detailed features of temporal variations of these substances in troposphere and will discuss its influence on the global environment.

Keywords: Air pollutants, Column-averaged mixing ratio, Infrared spectroscopy, Seasonal variation, Long-term trend

©2019. Japan Geoscience Union. All Right Reserved. 

# Impacts of Biogenic and Anthropogenic Emissions on Summertime Ozone Formation in the Guanzhong Basin, China

*Nan Li[1]

1. Nanjing University of Information Science & Technology

This study is the first attempt to understand the synergistic impact of anthropogenic and biogenic emissions on summertime ozone ($O_3$) formation in the Guanzhong (GZ) basin where Xi’ an, the oldest and the most populous city (with a population of 9 million) in the northwest China, is located. Month-long (August 2011) WRF-Chem simulations with different sensitivity experiments were conducted and compared with near-surface measurements. Biogenic volatile organic compounds (VOCs) concentrations were characterized from 6 surface sites among the Qinling Mountains, and urban air composition was measured in the Xi’ an city at a tower 100 m above the surface. The WRF-Chem control experiment reasonably reproduced the magnitudes and variations of observed $O_3$, VOCs, $NO_x$, $PM_{2.5}$ and meteorological parameters, with normalized mean biases for each parameter within ±21%. Subsequent analysis employed the factor separation approach (FSA) to quantitatively disentangle the pure and synergistic impacts of anthropogenic and/or biogenic sources on summertime $O_3$ formation. The impact of anthropogenic sources alone was found to be dominant for $O_3$ formation. Although anthropogenic particles reduced $NO_2$ photolysis by up to 60%, the anthropogenic sources contributed 19.1 ppb $O_3$ formation on average for urban Xi’ an. The abundant biogenic VOCs from the nearby forests promoted $O_3$ formation in urban areas by interacting with the anthropogenic $NO_x$. The calculated synergistic contribution (from both biogenic and anthropogenic sources) was up to 14.4 ppb in urban Xi’ an, peaking in the afternoon. Our study reveals that the synergistic impact of individual source contributions to $O_3$ formation should be considered in the formation of air pollution control strategies, especially for big cities in the vicinity of forests.

Keywords: ozone, biogenic volatile organic compounds, WRF-Chem

©2019. Japan Geoscience Union. All Right Reserved. 

# Comprehensive monitoring project of greenhouse gases and air pollutants around Jakarta megacity in Indonesia

*Masahide Nishihashi[1], Hitoshi Mukai[1], Yukio Terao[1], Shigeru Hashimoto[1], Rizaldi Boer[2], Muhammad Ardiansyah[2], Bregas Budianto[2], Gito Sugih Immanuel[2], Adi Rakhman[2], Rudi Nugroho[3], Nawa Suwedi[3], Agus Rifai[3], Iif Miftahul Ihsan[3], Anies Marufatin[3], Albert Sulaiman[3], Dodo Gunawan[4], Eka Suharguniyawan[4], Asep Firman Ilahi[4], Muharam Syam Nugraha[4], Ronald Christian Wattimena[4], Bayu Feriaji[4], Thomas Lauvaux[5], Tomohiro Oda[6]

1. National Institute for Environmental Studies, 2. Bogor Agricultural University (IPB), Indonesia, 3. Agency for the Assessment and Application of Technology (BPPT), Indonesia, 4. Meteorological, Climatological, and Geophysical Agency (BMKG), Indonesia, 5. Laboratory for Sciences of Climate and Environment (LSCE), France, 6. Universities Space Research Association/NASA Goddard Space Flight Center, USA

The emission increases of greenhouse gases (GHGs) and air pollutants in megacities have been recognized as one of the important issues as a concern for health and climate change. Jakarta, the capital city of Indonesia, including suburban cities (Bogor, Depok, Tangerang, and Bekasi; locally known as “Jabodetabek”), has a population of 32 million people and has been listed as the second largest megacity in the world and the largest megacity in Southeast Asia. Several air quality monitoring campaigns were conducted in Jakarta. However, previous studies lacked continuous high-accuracy monitoring stations due to the limitations of environmental monitoring budgets and experts. We present here a new interdisciplinary project to expand our current understanding of the interactions between emissions, air quality, and regional/global climates.

To estimate the amount of anthropogenic emissions from Jakarta megacity and compare with city activities, we developed a ground-based comprehensive monitoring system of GHGs and air pollutants controlled remotely in addition to automated start-and-stop operations during power failures. Monitoring systems were installed at Bogor (center of Bogor city), Serpong (Jakarta suburb), and Cibeureum (mountainous area) in 2016–2017. Each monitoring system consists of system control/data acquisition units controlling multiple instruments and collecting continuously and continuous monitoring instruments of $CO_2$, $CH_4$, CO, $NO_x$, $SO_2$, $O_3$, aerosol concentrations ($PM_{2.5}$, $PM_{10}$, BC) and the chemical components ($NO_3^-$, $SO_4^{2-}$) of $PM_{2.5}$ and $PM_{10}$, and meteorological parameters. Flask sampling of air is also performed automatically once a week to analyze $N_2O$, $SF_6$, and carbon isotopes ($^{13}C$, $^{14}C$) in $CO_2$ in NIES and to validate the continuous measurement data of $CO_2$, $CH_4$, and CO.

The results show that the daytime values of $CO_2$, three hours averages from 12 to 15 local time, at Bogor and Serpong are 6.8 and 7.1 ppm higher than Cibeureum, respectively. These features are also presented in the other species, i.e., CO, $NO_x$, $SO_2$, $PM_{2.5}$, $PM_{10-2.5}$, and BC. Moreover, we found 5–10 ppm lower values of $CO_2$ during daytime at Bogor and Serpong in December and January, mid-rainy season in Jakarta, compared with the other months and frequent and extremely high $CH_4$ enhancements during nighttime (i.e., 3 to 5 ppm) at Serpong.

We present here the temporal variability observed at three monitoring sites and some preliminary results based on high-resolution $CO_2$ simulations using Weather Research and Forecasting model coupled to Chemistry (WRF-Chem).

Keywords: greenhouse gases, air pollutants, urban monitoring, Indonesia

©2019. Japan Geoscience Union. All Right Reserved. 

# Seasonality of short-term variations in atmospheric $CH_4$ observed at Hateruma and relationship with the reginal emissions from East Asia

*Yasunori Tohjima[1], Jiye Zeng[1], Tomoko Shirai[1], Akihiko Ito[1], Motoki Sasakawa[1], Toshinobu Machida[1]

1. National Institute for Environmental Studies

National Institute of Environmental Studies (NIES), Japan, has been carrying out in-situ observation of atmospheric $CH_4$ at Hateruma Island (HAT; lat. 24.1˚N, long. 123.8˚E) since 1996 by using a gas chromatographic system. Since HAT is in the marginal region of the East Asia, air masses from the continental region would cause elevated concentrations of a variety of species including $CH_4$. Such events were often observed especially during late autumn to early spring due to the Asian monsoon. In the previous studies, we revealed a secular increase in the short-term variations of $CH_4$ and its relationship with the emission increase from the continental China. Here, we examined the seasonality of the short-term variations of $CH_4$ in 1996 to 2017. First, we computed the increment of the hourly $CH_4$ ($\Delta CH_4$) over the baseline, which was the smoothed averages of $CH_4$ below the 20 percentile in a 101-hour moving time-window. Then the standard deviation of $\Delta CH_4$ for each month of each year was computed. The average monthly standard deviations of $\Delta CH_4$ show rather stable values in winter (November-February, 18~20 ppb), peaks in May (28 ppb) and September (26 ppb), and a dip in July (11 ppb). We simulated $\Delta CH_4$ by a Lagrangian particle dispersion model (LPDM) using the monthly $CH_4$ emission maps of Patra et al. (2009) and EDGAR v4.3.2, respectively. Although the monthly variability of the simulated $\Delta CH_4$ based on the Patra et al. (2009) emission maps well reconstructed the observed pattern of the monthly standard deviations, that based on the EDGAR v4.3.2 emission maps showed a maximum in March, which was not consistent with the observed pattern. The simulated maximum variability in March is related to the emission peak in March of the EDGAR v4.3.2 inventory, which is attributed to the maximum emissions from agricultural and livestock sectors. The lack of the spring peak in the observation suggests that the anthropogenic $CH_4$ emission in March of EDGAR v4.3.2 may be overestimated.

Keywords: atmospheric CH4, short-term variation, LPDM

©2019. Japan Geoscience Union. All Right Reserved. 

# A cryogen-free automated measurement system of stable carbon isotope ratio of atmospheric methane

*Taku Umezawa[1], Takuya Saito[1]

1. National Institute of Environmental Studies

Methane is an important greenhouse gas emitted from both natural and anthropogenic sources. Accurate understanding of various methane sources is needed for effective reduction of its emissions. Measurement of stable carbon isotope ratio of atmospheric methane is useful for top-down evaluation of relative contributions of various types of methane sources, because individual methane sources have characteristic isotope signatures. Isotope ratio data for atmospheric methane therefore receive increasing attention for constraining the global methane budget. To meet research community demand, it is imperative for measurement systems to achieve adequate precision and traceability as well as high measurement throughput to process number of air samples that are routinely shipped from monitoring sites to laboratory. Stable carbon isotope ratio has been measured by continuous-flow isotope ratio mass spectrometry where methane in sample air is preconcentrated in a trap filled with an adsorbent cooled by liquid nitrogen. By using a stirring cooler instead, we set up a cryogen-free measurement system, and our configuration attained reproducibility of ~0.1 per mil. This precision is comparable to those previously achieved by using liquid nitrogen; our system is however advantageous for unattended and automated measurement operation. We examined measurements for air sampled outside our laboratory, and the preliminary measurement data at ~1-hour intervals show a clear diurnal variation.

Keywords: Methane, Stable carbon isotope ratio

©2019. Japan Geoscience Union. All Right Reserved. 

# Global inverse analysis of $CH_4$ fluxes using NICAM-TM 4D-Var

*Yosuke Niwa[1,2], Akihiko Ito[1], Toshinobu Machida[1], Motoki Sasakawa[1], Yasunori Tohjima[1], Taku Umezawa[1], Shinji Morimoto[3], Shuji Aoki[3], Yousuke Sawa[2], Kazuhiro Tsuboi[2], Hidekazu Matsueda[2], Ed Dlugokencky[4], Christina Harth[5], Paul B Krummel[6], Ray L Langenfelds[6], Zoe M Loh[6], Jens Mühle[5], Simon O'Doherty[7], Ronald G Prinn[8], Michel Ramonet[9], Peter Salameh[5], Colm Sweeney[4], Ray Weiss[5], Dickon Young[7], Simona Castaldi[10,11], Sergio Noce[12], Marielle Saunois[9], Ann R Stavert[13]

1. National Institute for Environmental Studies, 2. Meteorological Research Institute, 3. Tohoku University, 4. Earth System Research Laboratory, National Oceanic and Atmospheric Administration, 5. Scripps Institution of Oceanography, University of California, 6. Climate Science Centre, CSIRO Oceans and Atmosphere, 7. School of Chemistry, University of Bristol, 8. Massachusetts Institute of Technology, 9. Laboratoire des Sciences du Climat et de l'Environnement, LSCE-IPSL (CEA-CNRS-UVSQ), 10. DISTABIF, Università degli studi della Campania Luigi Vanvitelli, 11. Department Landscape Design & Sustainable Ecosystems RUDN University, 12. IAFES, Euro-Mediterranean Center on Climate Change, 13. Global Carbon Project, CSIRO Oceans and Atmosphere

Atmospheric methane ($CH_4$) is the most important greenhouse gas after carbon dioxide. Because $CH_4$ has a relatively short lifetime due to chemical losses in the atmosphere, it is expected that reducing $CH_4$ emissions would mitigate global warming in a relatively short timeframe. However, sources of atmospheric $CH_4$ are associated with a wide variety of processes such as fossil fuel production and consumption, agriculture, natural wetlands, and biomass burning, and our understanding of the full $CH_4$ budget is limited. To better understand $CH_4$ sources, an inverse analysis is one prominent methodology that estimates spatiotemporal variations of $CH_4$ sources consistent with their prior estimates and atmospheric observations within specified uncertainties. In this study, we performed a long-term inverse analysis of $CH_4$ fluxes with an inversion system named NICAM-TM 4D-Var (Niwa et al., 2017a,b). The inversion system is based on the atmospheric transport model NICAM-TM (Niwa et al., 2011), which has a homogeneous icosahedral grid system and mass conserving property. The horizontal model grid resolution was set to 223 km and the $CH_4$ flux estimation was performed at the same resolution, though some spatial error correlations were introduced. The prior flux dataset includes wetland/rice cultivation emission and soil uptake estimated by the terrestrial ecosystem model VISIT (Ito and Inatomi, 2012). The other emission categories are provided from the ongoing Global Carbon Project (GCP)–$CH_4$. In the inversion, several emission categories are separately estimated according to their seasonal and interannual variabilities. Compared with the prior estimates, the inverse analysis with ground-based station data estimated smaller emissions from East Asia and Europe, larger and smaller northern summer emissions from West Siberia and Hudson Bay Lowlands, respectively, and larger emissions from Bengal and Indochina areas. These changes estimated by the inversion are attributed to emissions from anthropogenic categories (mainly fossil fuel related), natural wetlands, and rice cultivation, respectively. The presentation will also address the reliability of the inversion estimates using independent aircraft data and examine the independence of each category emission estimate.

## References

Niwa et al. (2011), Journal of the Meteorological Society of Japan. Ser. II, 89(3), 255–268.
Ito and Inatomi (2012), Biogeoscience, 9:759-773.
Niwa et al. (2017a), Geoscientific Model Development, 10(3), 1157–1174.
Niwa et al. (2017b), Geoscientific Model Development, 10(6), 2201–2219.

©2019. Japan Geoscience Union. All Right Reserved. 

Acknowledgement
This study is supported by the Environment Research and Technology Development Fund (2-1701) of the Ministry of the Environment, Japan. The authors acknowledge the Global Carbon Project–$CH_4$ for providing the prior flux dataset, some of which is made under the support of the RUDN project "5-100". The authors also acknowledge Doug Worthy of Environmental Canada, Juha Hatakka of Finnish Meteorological Institute, Camille Yver Kwok of Laboratoire des Sciences du Climat et de l’ Environnement, Sebastien Conil of Andra, and Kazuyuki Saito and other members of Japan Meteorological Agency for providing observational data of atmospheric $CH_4$. This study used observational data of Advanced Global Atmospheric Gases Experiment (AGAGE). Operations of the AGAGE network are principally supported by the NASA Upper Atmospheric Research Program in the US, by the Department for Business, Energy & Industrial Strategy (BEIS) in the UK, by the Commonwealth Scientific and Industrial Research Organization (CSIRO) and the Bureau of Meteorology (Australia) in Australia, with additional support from the National Oceanographic and Atmospheric Administration (NOAA) in the US. Yosuke Niwa sincerely thanks the members of the NICAM team for developing and maintaining the codes of NICAM.

Keywords: methane, inverse analysis

©2019. Japan Geoscience Union. All Right Reserved. 

# Scientific findings from observations of GOSAT/TANSO–FTS TIR band

*Naoko Saitoh[1], Shingo Kosaka[1], Masato Shiraki[1], Hinako Kobayashi[1]

1. Center for Environmental Remote Sensing

Greenhouse Gases Observing Satellite (GOSAT) has continued its observations of greenhouse gases for more than 10 years since its launch on 23 January 2009. The thermal infrared (TIR) band of the Thermal and Near Infrared Sensor for Carbon Observation (TANSO)–Fourier Transform Spectrometer (FTS) on board GOSAT has observed concentrations of $CO_2$, $CH_4$ and other greenhouse gases in several atmospheric layers. In the latest TANSO–FTS TIR Level 2 retrieval algorithm, Version 1 (V1), ozone, water vapor, and temperature have been retrieved as by-products of the $CO_2$ and $CH_4$ products (Saitoh et al., 2016). We have already evaluated the data quality of the TANSO–FTS TIR V1 $CO_2$ and $CH_4$ products (Saitoh et al., 2016, 2017; Holl et al., 2016; Zou et al., 2016; Olsen et al., 2017). We applied the evaluated bias-correction values to the TANSO–FTS TIR V1 $CO_2$ data and compared variations in concentrations of the TIR $CO_2$ data with those of Measurement Of Pollution In The Troposphere (MOPITT) CO data [Deeter et al., 2014] in upper troposphere over the northern Africa. The comparison result showed that both TANSO–FTS TIR $CO_2$ and MOPITT CO concentrations became larger there almost at the same time in March through May, which suggests air mass with high CO and $CO_2$ emitted due to biomass burning was transported to upper atmosphere. As TANSO–FTS TIR V1 $CH_4$ profiles generally agreed with aircraft $CH_4$ profiles to within ~1% in the troposphere in low and middle latitudes, we analyzed seasonal variations in $CH_4$ concentrations in each altitude layer over India by using the TIR V1 $CH_4$ data. Our results were similar to the results reported in Chandra et al. (2017), but showed larger impact of $CH_4$ variations in lower troposphere on seasonal variations in $XCH_4$ concentrations. We have conducted validation analysis of TANSO–FTS TIR $O_3$ profiles simultaneously retrieved with the TIR V1 $CO_2$ product using Atmospheric Chemistry Experiment (ACE)–FTS and ozonesonde data. Although there was slightly high bias in the TANSO–FTS TIR $O_3$ data in the lower troposphere in summer, they showed better agreements with ACE–FTS and ozonesonde data than their a priori data taken from MacPeters et al. (2007). The TANSO–FTS TIR $O_3$ data in the lowest retrieval layer (surface–857 hPa) showed clear enhancements in $O_3$ concentrations over Mainland China compared to eastern Japan, which could demonstrate the detectability of tropospheric pollutants by the TANSO–FTS TIR band.

Keywords: CO2, CH4, ozone, GOSAT/TANSO-FTS

©2019. Japan Geoscience Union. All Right Reserved. 

# Continuous measurements of atmospheric $CO_2$ and its $\delta^{13}C$ and $\delta^{18}O$ at Minamitorishima Island

*Shohei Murayama[1], Kazuhiro Tsuboi[2], Shigeyuki Ishidoya[1], Hidekazu Matsueda[2], Yosuke Niwa[3], Yousuke Sawa[2], Kentaro Ishijima[2], Kentaro Kozumi[4], Genta Umezawa[4], Kazuya Yukita[4], Shigeharu Nishida[4], Megumi Yamamoto[4], Tetsuyuki Usami[1], Shinji Morimoto[5]

1. National Institute of Advanced Industrial Science and Technology (AIST), 2. Meteorological Research Institute, 3. National Institute for Environmental Studies, 4. Japan Meteorological Agency, 5. Tohoku University

The Minamitorishima (MNM; 24°17’ N, 153°59’ E) station is uniquely located to monitor background air at northern mid latitudes; the site is located on a remote coral island in the western North Pacific, about 1,950 km southeast of Tokyo. The Japan Meteorological Agency has been making long-term continuous observations of atmospheric concentrations of major greenhouse gases at MNM. For a better understanding of mechanisms governing the observed $CO_2$ variation, systematic measurements of atmospheric $CO_2$ and its $\delta^{13}C$ and $\delta^{18}O$ have been carried out at MNM by analyzing discrete flask air samples taken at the site since 2011. The existing measurement program was enhanced by initiating continuous measurements of $CO_2$ and its $\delta^{13}C$ and $\delta^{18}O$ using a laser spectroscopy (Off-Axis Integrated-Cavity Output Spectroscopy) in March 2018.

Sample air is drawn from an air intake mounted on a tower at 20-m height above the ground surface, and introduced into a continuous isotope analyzer (Model CCIA-48, Los Gatos Research) after removing water vapor and aerosol particles. The analyzer is calibrated hourly for the concentrations of each $CO_2$ isotopologue, using 3 air-based $CO_2$ standard gases with isotopic ratios of industrial $CO_2$ and different total $CO_2$ concentrations. The isotopic ratios of these standards were determined by a mass spectrometer, and the concentrations of each $CO_2$ isotopologue of the standards were obtained from the isotopic ratios. The total $CO_2$ concentration and its $\delta^{13}C$ and $\delta^{18}O$ of sample air are calculated from the measured concentrations of each isotopologue.

The obtained $CO_2$ isotopic data are scattered, and the precisions of the $\delta^{13}C$ and $\delta^{18}O$ values measured by this analyzer estimated from hourly measurements of a target gas, which is dried natural air compressed into a 48-L gas cylinder, are about 10 times and 5 times worse than those achieved by our mass spectrometer, respectively. However, the daily mean values of atmospheric $\delta^{13}C$ and $\delta^{18}O$ show day-to-day variations in concert with those of the total $CO_2$ concentration and prominent seasonal variations. The daily mean $\delta^{13}C$ and $\delta^{18}O$ show systematic difference from the isotopic values obtained from flask sampling on the same day. However, since the differences are almost constant, the nature of the variations are very similar in both cases.

In this presentation, results of the preliminary analyses of the daily mean $CO_2$, $\delta^{13}C$ and $\delta^{18}O$ data obtained from the continuous measurement will be presented. From comparison with the flask sampling results, the effectiveness of the continuous measurement will also be discussed.

Acknowledgements

We would like to thank A. Kudo and C. Abe for their technical support for our measurements. This

©2019. Japan Geoscience Union. All Right Reserved. 

research was supported by a grant for the Global Environmental Research Coordination System from the Ministry of the Environment, Japan.

Keywords: Carbon dioxide, Stable isotopic ratio, Minamitorishima Island, Continuous measurement

©2019. Japan Geoscience Union. All Right Reserved. 

# Variations of atmospheric Radon-222 concentration observed at JMA stations

*Kentaro Ishijima[1], Kazuhiro Tsuboi[1], Hidekazu Matsueda[1], Yousuke Sawa[1], Yosuke Niwa[2,1], Takashi Maki[1], Takashi Nakamura[3]

1. Meteorological Research Institute, 2. National Institute for Environmental Studies, 3. Japan Meteorological Agency

Japan Meteorological Agency (JMA) has been operating several stations to monitor atmospheric greenhouse gases since the late 1980s under the Global Atmosphere Watch programme of the World Meteorological Organization (WMO/GAW). They show synoptic, seasonal, interannual variations, and trends due to changes in atmospheric transport and source/sink strength. To know their transport from land regions, we started the monitoring of atmospheric Radon-222 ($^{222}$Rn) in the 2000s at the JMA stations. Because $^{222}$Rn is emitted from almost only lands and chemically inert, it is useful to identify temporal variability of atmospheric greenhouse gases due to sources/sinks on land. $^{222}$Rn also radioactively decays with the half-life of 3.8 days, so is widely utilized to validate regional transport of atmospheric transport model through the model-observation comparisons. Understanding such transport process is also supported by using an atmospheric transport model. We have just started to use a newly developed on-line atmospheric tracer transport model (GSAM-TM). The tracer transport process is driven by a low-resolution version (TL95) of JMA's operational global numerical weather prediction model (GSAM).
In this study, we analyze the observed and model simulated atmospheric $^{222}$Rn concentration, to understand the transport process of land-origin atmospheric tracer as well as to validate the GSAM-TM. For example, the model well reproduces high $^{222}$Rn peaks, which are frequently observed at Minamitorishima (MNM; 24.28˚N, 153.98˚E) and Chichijima (CCJ; 27.09˚N, 142.19˚E) in winter to spring. Especially in winter, there are many cases that a high peak is first observed at CCJ and one day after at MNM. They are mainly produced by a cold front moving eastward with dense $^{222}$Rn behind the frontal line. The peak height at MNM is about two-thirds of that at CCJ. It is slightly smaller than that expected from decay by the 3.8 days half-life (about four-fifths), because dense $^{222}$Rn trapped by the front is diluted mainly by diffusion while transported. The model also well reproduces such peak attenuation degree. More details and results of $^{222}$Rn-age tracer simulations as well as of other JMA station will also be discussed in our presentation.

*Acknowledgements.* We sincerely thank all members of the JMA for operating $^{222}$Rn measurement systems at JMA monitoring stations

Keywords: radon, GSAM-TM

©2019. Japan Geoscience Union. All Right Reserved. 

# Long-term variations of CFCs and HCFCs observed with ground-based FTIR spectrometers at Rikubetsu, Syowa Station, and Tsukuba since 1995

*Hideaki Nakajima[1,2], Masanori Takeda[2,1], Isao Murata[2], Takafumi Sugita[1], Tomoo Nagahama[3], Isamu Morino[1], Takeshi Kinase[4]

1. National Institute for Environmental Studies, 2. Graduate School of Environmental Studies, Tohoku University, 3. Institute for Space-Earth Environmental Research, Nagoya University, 4. Meteorological Research Institute

We have been observing atmospheric minor constituents with ground-based Fourier-Transform InfraRed spectrometer (FTIR) at Rikubetsu (43.5N, 143.8E) since 1995, at Syowa Station, Antarctica (69.0S, 39.6E) in 2007, 2011, and 2016 with Bruker IFS-120M, and at Tsukuba (36.1N, 140.1E) since 2018 with Bruker IFS-125HR. We have analyzed vertical profiles and total columns of CFC-11, CFC-12, and HCFC-22 with SFIT4 retrieval algorithm. Production and consumption of CFCs and HCFCs have been regulated under the Montreal Protocol since 1987. Substitution to HCFCs and HFCs which do not destroy ozone layer is underway. However, illegal production of CFC-11 somewhere in Asia was recently reported (Montzka et al., Nature, 2018). Monitoring of these gases are possible not only by ground-based gas-chromatogram/mass-spectroscopy technique, but also by infrared spectroscopic measurements. Ground-based FTIR measurement has a capability to monitor multiple gas species simultaneously with vertical profile information for some gases. We retrieved vertical profiles and column amounts of CFC-11, CFC-12, and HCFC-22 since 1995 from FTIR spectra. Figure 1 shows total column amounts of HCFC-22 since 1995, while Figure 2 shows partial column amounts of HCFC-22 between 0 and 8 km. Seasonal variation which are seen in Figure 1 might be due to the change of tropopause height. However, it is removed in partial column amount in Figure 2. Trajectory calculation results of CFC-11 and other gases will be presented at the meeting.

Keywords: CFC, HCFC, FTIR

©2019. Japan Geoscience Union. All Right Reserved. 

Figure 1

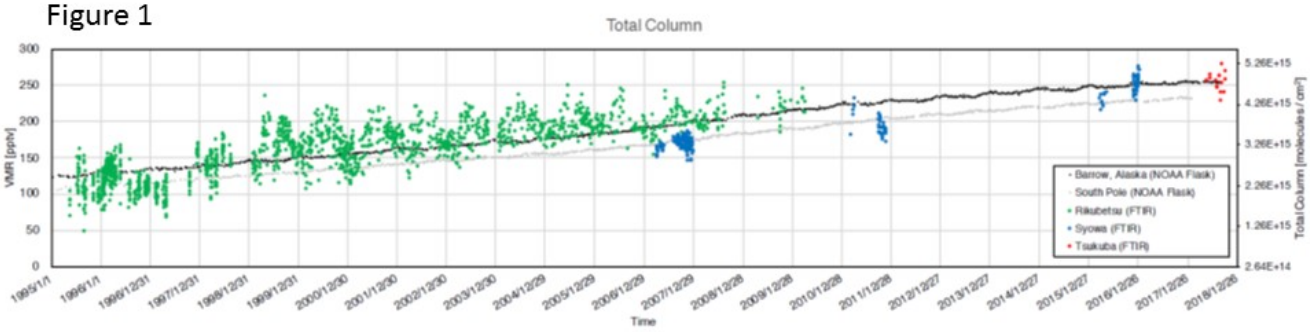


Figure 2

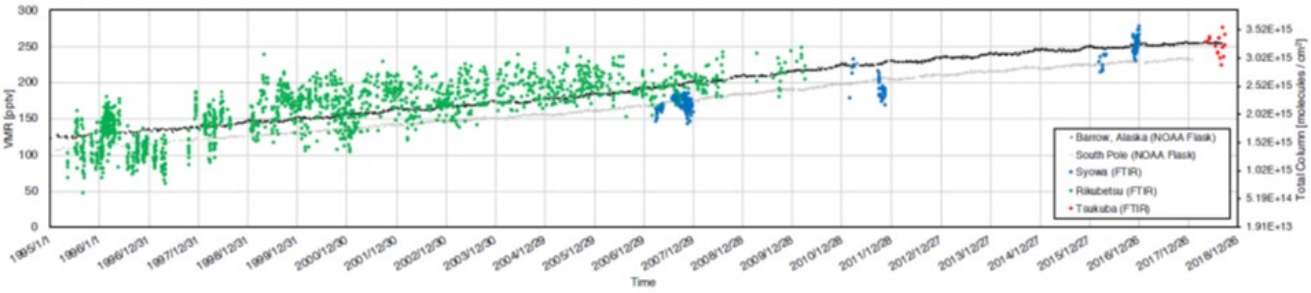


©2019. Japan Geoscience Union. All Right Reserved. 

# Millimeter-wave observation of stratospheric ozone in 2015-2017 in Rio Gallegos at the southern tip of South America

*Akira Mizuno[1], Hironori Seki[1], Tomoo Nagahama[1], Hirofumi Ohyama[2], Jacobo Salvador[3], Facundo Orte[3], Elian Walfram[3]

1. Institute for Space-Earth Environmental Research, Nagoya University, 2. National Institute for Environmental Studies, 3. Laser and Applications Research Center, UNIDEF (CITEDEF-CONICET)

We had been carried out a trilateral international collaboration among Japan, Chile, and Argentina called SAVER-Net (South American Environmental Risk Management Network) project for five years under the JST-JIICA SATREPS program. The major aim of the project was establishing an observation network of UV/ozone and aerosols over Chile and Argentina where was a blank area of the measurement stations on a global scale. The southern tip region of South America is the southernmost habitable area in the world, and the local residents in this region directly suffers from the influence of ozone hole that sometimes overpasses the region. Although the project was terminated in March 2018, we continue collaboration to develop forecast system of ozone hole and UV indices.

In this presentation, we will report the results of ozone observation by using a millimeter-wave spectrometer installed at the atmospheric observatory in southern Patagonia (OAPA) in Rio Gallegos, Argentina. The observation period was from April 2015 to March 2016 and September 2016 to August 2017, and we obtained ~ 9,400 1-hour averaged vertical profiles. We compared the time series of ozone volume mixing ratio (VMR) profile obtained in September and October when the ozone hole passes over the southern tip with the meteorological parameters, such as atmospheric temperature, potential temperature, and potential vorticities that are derived from MERRA-2 reanalysis data. As a result of the comparisons, we revealed that

・Ozone VMRs and the absolute value of potential vorticities show a good correlation below ~ 1000 K in potential temperature corresponding to ~ 35 km in altitude.

・As the ozone hole reaches above Rio Gallegos, atmospheric temperature decreases around ~ 25 km due to the horizontal advection of cool air in the polar vortex, and the temperature above ~35 km increases due to atmospheric descent inside of the polar vortex,

and we can use these quantities to easily distinguish whether Rio Gallegos is located at inside or outside of the ozone hole.

We will also present more detailed results about the ozone hole activities in 2015 and 2016.

Keywords: ozone hole, millimeter-wave spectroscopy, South America, polar vortex

©2019. Japan Geoscience Union. All Right Reserved. 

[J] Poster | A (Atmospheric and Hydrospheric Sciences )：A-AS Atmospheric Sciences, Meteorology & Atmospheric Environment

Thu. May 30, 2019 5:15 PM - 6:30 PM JST | Thu. May 30, 2019 8:15 AM - 9:30 AM UTC | Poster Hall International Exhibition Hall8, Makuhari Messe_6

## [A-AS04] Atmospheric Chemistry

convener:Tomoki Nakayama(Graduate School of Fisheries and Environmental Sciences, Nagasaki University), Yoko Iwamoto(Graduate School of Biosphere Science, Hiroshima University), Sakae Toyoda(Department of Chemical Science and Engineering, Tokyo Institute of Technology), Nawo Eguchi(Kyushu University)

This session provides a forum for the presentation of the broad spectrum of tropospheric and stratospheric chemistry, including various research topics (e.g., dynamical processes, air quality and climate), approaches (modeling, field measurements, remote sensing, and laboratory studies), and species (gas and aerosol). This session also provides an opportunity for discussing possible future collaboration with other research fields relevant to atmospheric chemistry. We strongly encourage authors to prepare presentation slides and a poster in English.

[AAS04-P01] Validation of GOSAT cloud judgement by using Himawari-8 data

*Kitamura Katsuki[1], Naoko Saitoh[2] (1.Chiba University Graduate School of Science and Engineering Division of Earth Environmental Science , 2.Center for Environmental Remote Sensing Chiba University)

[AAS04-P02] Measurement of temperature that fungal spores form ice nuclei

*Kazuyuki Kita[1], Kansei Sasaki[1], Koutaro Minami[1], Takeshi Kinase[2], Kouji Adachi[2], Yuji Zaizen[2], Kentaro Hosaka[3], Teruya Maki[4], Yasuhito Igarashi[1,5] (1.Ibaraki University, 2.Meteorological Research Laboratory, 3.National Musium of Nature and Science, 4.Kanazawa University, 5.Kyoto University)

[AAS04-P03] **Investigation of Atmospheric Aerosol Particles and gases by R/V Mirai cruise over the Arctic Ocean on 2017**

*Fumikazu Taketani[1], Saki Kato[1,2], Takuma Miyakawa[1], Masayuki Takigawa[1], Masahiro Yamaguchi[1], Hisahiro Takashima[1,2], Petr Mordovskoi[1], Yugo Kanaya[1] (1.Japan Agency for Marine-Earth Science and Technology, 2.Fukuoka University)

[AAS04-P04] Characterization of carbonaceous aerosols in East Asia in the spring of 2015: Importance of non-fossil fuel sources

*Takuma Miyakawa[1], Yuichi Komazaki[1], Fumikazu Taketani[1], Xiaole PAN[2], Zifa Wang[2], Yugo Kanaya[1] (1.Japan Agency for Marine-Earth Science and Technology, 2.Institute for Atmospheric Physics, Chinese Academy of Science)

[AAS04-P05] **Analyzing the influence of biomass burning on ambient air pollution in mainland Southeast Asia from 2001 to 2016**

*Shuai Yin[1] (1.National Institute for Environmental Studies)

[AAS04-P06] High-resolution and multi-year inventory of mercury emissions from biomass burning in tropical continents during 2001–2017

*Yusheng Shi[1] (1.Aerospace Information Research Institute, Chinese Academy of Sciences)

[AAS04-P07] Simultaneous observations by sky radiometer and MAX-DOAS for characterization of biomass burning plumes in central Thailand in January-April 2016

*Hitoshi Irie[1], Syedul Hoque[1], Alessandro Damiani[1], Al Mashroor Fatmi[1], Pradeep Khatri[2], Tamio Takamura[1], Thanawat Jarupongsakul[3] (1.Chiba University, 2.Tohoku University, 3.Chulalongkorn University)

[AAS04-P08] Quantifying PM2.5 from long-range transport and local pollution in Taiwan during winter monsoon.

*Ming-Tung Chuang[1] (1.Research Center for Environmental Changes, Academia Sinica)

[AAS04-P09] Vertical characterization of $PM_{2.5}$ based on observation using compact sensors on and around Mt. Unzen in Nagasaki Prefecture

*Tomoki Nakayama[1], Ayane Ueno[1], Kenta Kanegae[1], Kazuaki Kawamoto[1], Kodo Umakoshi[1], Takayuki Yamasaki[2], Wataru Okamoto[2], Yutaka Matsumi[2] (1.Faculty of Environmental Science, Nagasaki University, 2.ISEE, Nagoya University)

[AAS04-P10] Observation of NPF events at the summit of Mt. Fuji during daytime and nighttime

*Hiroki Igarashi[1], Takenori Sato[1], Tatsuhiro Mori[1], Kazuhiko Miura[1], Yoko Iwamoto[2], Ryuichi Wada[3], Shungo Kato[4], Hiroshi Okochi[5] (1.Tokyo University of Science, 2.Hiroshima University, 3.Teikyo University of Science, 4.Tokyo Metropolitan University, 5.Waseda University)

[AAS04-P11] Measurement of atmospheric metal particles using an ICP-MS and TEM.

*Takeshi Kinase[1], Kouji Adachi[1], Mizuo Kajino[1], Masahiko Hayashi[2], Keiichiro Hara[2] (1.Meteorological Research Institute, 2.Fukuoka)

[AAS04-P12] Experimental results on measuring device of complex refractive index using the single particle extinction and scattering method

*TAKASAGO YUYA[1] (1.Tokyo university)

[AAS04-P13] **Evaluation of BC and CO emission inventory based on long-term in-situ observations over East Asia**

*Yongjoo Choi[1], Yugo Kanaya[1], Hye-Jung Shin[2], Seung-Myong Park[2], Atsushi Matsuki[3], Yasuhiro Sadanaga[4], Sang-woo Kim[5], Itsushi Uno[6], Xiaole Pan[7] (1.Development Center for Global Change, Japan Agency for Marine-Earth Science and Technology, 2.Division of Climate & Air Quality Research, National Institute of Environmental Research, Korea, 3.Institute of Nature and Environmental Technology, Kanazawa University, 4.Department of Applied Chemistry, Graduate School of Engineering, Osaka Prefecture University, 5.School of Earth and Environmental Sciences, Seoul National University, Seoul, Korea, 6.Research Institute for Applied Mechanics, Kyushu University, 7.Institute of Atmospheric Physics, CAS, Beijing, China)

[AAS04-P14] **Inverse modeling of black carbon emissions over China using ensemble data assimilation**

*Ping Wang[1] (1. Chinese Academy of Meteorological Sciences)

[AAS04-P15] Analysis of BC emissions in East Asia using inverse model

*Takashi Maki[1], Taichu Y Tanaka[1], Naga Oshima[1], Thomas Sekiyama[1], Keiichi Kondo[1], Jun-ichi Kurokawa[2], Keiya Yumimoto[3], Toshimasa Ohara[4] (1.Meteorological Research Institute, 2.Asia Center for AirPollution Research, 3.Kyushu University, 4.National Institute for Environmental Studies)

[AAS04-P16] Source attribution of BC in the northern Pacific and Arctic Ocean by chemistry climate model

*Takato Onishi[1], Kengo Sudo[1,2], Yugo Kanaya[2], Fumikazu Taketani[2] (1. Graduate School of Environmental Studies, Nagoya University, 2.Japan Agency for Marine-Earth Science and Technology)

[AAS04-P17] Evaluation of a mobile $PM_{2.5}$ sensor and application to the measurements along the National route 1 and around Nagasaki University

*Kenta Kanegae[1], Takayuki Yamasaki[2], Wataru Okamoto[2], Yutaka Matsumi[2], Tomoki Nakayama[1] (1.Nagasaki University, 2.Nagoya University)

[AAS04-P18] Analysis on the Relationship between the Concentration of Particulate Matter and Mortality from Respiratory and Cardiovascular Diseases

*Woo-Sik JUNG[1], Woo-Gon Do[2] (1.Department of Atmospheric Environment Information Engineering, Atmospheric Environment Information Research Center, Inje University, Gimhae 50834, Korea, 2.Busan Metropolitan City of Institute of Health and Environment Busan, Korea)

[AAS04-P19] A Study on the Estimation of Contribution Rate of Odour Substances Using CALPUFF model

*Woo-Sik JUNG[1], Woo-Gon Do[2] (1.Department of Atmospheric Environment Information Engineering, Atmospheric Environment Information Research Center, Inje University, Gimhae 50834, Korea, 2.Busan Metropolitan City of Institute of Health and Environment Busan, Korea)

[AAS04-P20] Stepwise decrease in atmospheric trace gases near the ground associated with rapid vertical mixing observed by 3-D coherent Doppler lidar and in-situ gas measurements

*Hisahiro Takashima[1], Keiichiro Hara[1], Yuki Ohira[1], Akinori Takami[2], Ayako Yoshino[2], Yasushi Fujiyoshi[3] (1.Fukuoka University, 2.National Institute for Environmental Studies, 3.Hokaido University)

[AAS04-P21] Spatiotemporal variations of nitrogen dioxide ($NO_2$) over Fukuoka , observed by multiple MAX-DOAS instruments and 3-D coherent Doppler lidar

*Hironobu Ueki[1], Hisahiro Takashima[1], Martina M. Friedrich[2] (1.Fukuoka university, 2.Belgian Institute for Space Aeronomy (BIRA-IASB), Belgium)

[AAS04-P22] Measurement on the $^{17}O$-excess of tropospheric nitrogen oxides

*Fumiko Nakagawa[1], Dong Ding[1], Urumu Tsunogai[1], Takashi Yamaguchi[2], Izumi Noguchi[2] (1.Graduate School of Environmental Studies, Nagoya University, 2.Institute of Environment Sciences, Hokkaido Research Organization)

[AAS04-P23] Long-term measurements of the column-averaged mixing ratios of tropospheric substances related to the air pollution using ground-based FTIRs at Rikubetsu, Japan

*Tomoo Nagahama[1], Isamu Morino[2], Shingo Nakanishi[1] (1.Institute for Space-Earth Environmental Research, Nagoya University, 2.National Institute for Environmental Studies)

[AAS04-P24] Impacts of Biogenic and Anthropogenic Emissions on Summertime Ozone Formation in the Guanzhong Basin, China

*Nan Li[1] (1.Nanjing University of Information Science & Technology)

[AAS04-P25] **Comprehensive monitoring project of greenhouse gases and air pollutants around Jakarta megacity in Indonesia**

*Masahide Nishihashi[1], Hitoshi Mukai[1], Yukio Terao[1], Shigeru Hashimoto[1], Rizaldi Boer[2], Muhammad Ardiansyah[2], Bregas Budianto[2], Gito Sugih Immanuel[2], Adi Rakhman[2], Rudi Nugroho[3], Nawa Suwedi[3], Agus Rifai[3], Iif Miftahul Ihsan[3], Anies Marufatin[3], Albert Sulaiman[3], Dodo Gunawan[4], Eka Suharguniyawan[4], Asep Firman Ilahi[4], Muharam Syam Nugraha[4], Ronald Christian Wattimena[4], Bayu Feriaji[4], Thomas Lauvaux[5], Tomohiro Oda[6] (1.National Institute for Environmental Studies, 2.Bogor Agricultural University (IPB), Indonesia, 3.Agency for the Assessment and Application of Technology (BPPT), Indonesia, 4.Meteorological, Climatological, and Geophysical Agency (BMKG), Indonesia, 5.Laboratory for Sciences of Climate and Environment (LSCE), France, 6.Universities Space Research Association/NASA Goddard Space Flight Center, USA)

[AAS04-P26] **Seasonality of short-term variations in atmospheric $CH_4$ observed at Hateruma and relationship with the reginal emissions from East Asia**

*Yasunori Tohjima[1], Jiye Zeng[1], Tomoko Shirai[1], Akihiko Ito[1], Motoki Sasakawa[1], Toshinobu Machida[1] (1.National Institute for Environmental Studies)

[AAS04-P27] A cryogen-free automated measurement system of stable carbon isotope ratio of atmospheric methane

*Taku Umezawa[1], Takuya Saito[1] (1.National Institute of Environmental Studies)

[AAS04-P28] Global inverse analysis of $CH_4$ fluxes using NICAM-TM 4D-Var

*Yosuke Niwa[1,2], Akihiko Ito[1], Toshinobu Machida[1], Motoki Sasakawa[1], Yasunori Tohjima[1], Taku Umezawa[1], Shinji Morimoto[3], Shuji Aoki[3], Yousuke Sawa[2], Kazuhiro Tsuboi[2], Hidekazu Matsueda[2], Ed Dlugokencky[4], Christina Harth[5], Paul B Krummel[6], Ray L Langenfelds[6], Zoe M Loh[6], Jens Mühle[5], Simon O'Doherty[7], Ronald G Prinn[8], Michel Ramonet[9], Peter Salameh[5], Colm Sweeney[4], Ray Weiss[5], Dickon Young[7], Simona Castaldi[10,11], Sergio Noce[12], Marielle Saunois[9], Ann R Stavert[13] (1.National Institute for Environmental Studies, 2.Meteorological Research Institute, 3.Tohoku University, 4.Earth System Research Laboratory, National Oceanic and Atmospheric Administration, 5.Scripps Institution of Oceanography, University of California, 6.Climate Science Centre, CSIRO Oceans and Atmosphere, 7.School of Chemistry, University of Bristol, 8.Massachusetts Institute of Technology, 9.Laboratoire des Sciences du Climat et de l'Environnement, LSCE-IPSL (CEA-CNRS-UVSQ), 10.DISTABIF, Università degli studi della Campania Luigi Vanvitelli, 11.Department Landscape Design & Sustainable Ecosystems RUDN University, 12.IAFES, Euro-Mediterranean Center on Climate Change, 13.Global Carbon Project, CSIRO Oceans and Atmosphere)

[AAS04-P29] Scientific findings from observations of GOSAT/TANSO−FTS TIR band

*Naoko Saitoh[1], Shingo Kosaka[1], Masato Shiraki[1], Hinako Kobayashi[1] (1.Center for Environmental Remote Sensing)

[AAS04-P30] **Continuous measurements of atmospheric $CO_2$ and its $\delta^{13}C$ and $\delta^{18}O$ at Minamitorishima Island**

*Shohei Murayama[1], Kazuhiro Tsuboi[2], Shigeyuki Ishidoya[1], Hidekazu Matsueda[2], Yosuke Niwa[3], Yousuke Sawa[2], Kentaro Ishijima[2], Kentaro Kozumi[4], Genta Umezawa[4], Kazuya Yukita[4], Shigeharu Nishida[4], Megumi Yamamoto[4], Tetsuyuki Usami[1], Shinji Morimoto[5] (1.National Institute of Advanced Industrial Science and Technology (AIST), 2.Meteorological Research Institute, 3.National Institute for Environmental Studies, 4.Japan Meteorological Agency, 5.Tohoku University)

[AAS04-P31] Variations of atmospheric Radon-222 concentration observed at JMA stations

*Kentaro Ishijima[1], Kazuhiro Tsuboi[1], Hidekazu Matsueda[1], Yousuke Sawa[1], Yosuke Niwa[2,1], Takashi Maki[1], Takashi Nakamura[3] (1.Meteorological Research Institute, 2.National Institute for Environmental Studies, 3.Japan Meteorological Agency)

[AAS04-P32] Long-term variations of CFCs and HCFCs observed with ground-based FTIR spectrometers at Rikubetsu, Syowa Station, and Tsukuba since 1995

*Hideaki Nakajima[1,2], Masanori Takeda[2,1], Isao Murata[2], Takafumi Sugita[1], Tomoo Nagahama[3], Isamu Morino[1], Takeshi Kinase[4] (1.National Institute for Environmental Studies, 2.Graduate School of Environmental Studies, Tohoku University, 3.Institute for Space-Earth Environmental Research, Nagoya University, 4.Meteorological Research Institute)

[AAS04-P33] Millimeter-wave observation of stratospheric ozone in 2015-2017 in Rio Gallegos at the southern tip of South America

*Akira Mizuno[1], Hironori Seki[1], Tomoo Nagahama[1], Hirofumi Ohyama[2], Jacobo Salvador[3], Facundo Orte[3], Elian Walfram[3] (1.Institute for Space-Earth Environmental Research, Nagoya University, 2.National Institute for Environmental Studies, 3.Laser and Applications Research Center, UNIDEF (CITEDEF-CONICET))

# Validation of GOSAT cloud judgement by using Himawari-8 data

*Kitamura Katsuki[1], Naoko Saitoh[2]

1. Chiba University Graduate School of Science and Engineering Division of Earth Environmental Science , 2. Center for Environmental Remote Sensing Chiba University

In the retrieval processing of greenhouse gases from the Thermal and Near Infrared Sensor for Carbon Observation (TANSO)−Fourier Transform Spectrometer (FTS) on board Greenhouse Gases Observing Satellite (GOSAT), cloud contamination in the field of views (FOVs) of TANSO−FTS has been judged by TANSO−Cloud and Aerosol Imager (CAI) in the daytime and by the thermal infrared (TIR) band of TANSO−FTS in the nighttime. This study has compared the cloud detections in the TANSO−FTS FOVs by TANSO−CAI or TANSO−FTS TIR band with cloud detections by the Advanced Himawari Imager (AHI) on board Himawari−8.

For each of all TANSO−FTS observations over the ocean in January and July in 2016, we first selected all coincident Himawari−8 data when their center positions were located in the TANSO−FTS FOVs and they were obtained within one minute before or after the TANSO−FTS observations. Next, we conducted cloud detection tests for each of the selected Himawari−8 data based on their reflectance and brightness temperature values, and then judged each of TANSO−FTS FOVs as a clear or cloudy scene by combining the cloud detection tests of the Himawari−8 data in the TANSO−FTS FOVs.

About 90% of cloud judgements by TANSO−CAI and Himawari−8 agreed with each other. TANSO−CAI used only reflectance data in visible bands for their cloud detections, whereas Himawari−8 used both reflectance and brightness temperature data in visible and infrared bands, respectively, which may cause their ~10% disagreements. In contrast, agreements in cloud judgements between TANSO−FTS TIR band and Himawari−8 got worse by 13−20% compared to the TANSO−CAI and Himawari−8 cloud judgements. This is because that the FOVs of TANSO−FTS (10.5 km) is larger than those of TANSO−CAI and Himawari−8 (0.5 km and 2 km), and cloud detections by TANSO−FTS TIR band used only brightness temperature data.

In addition, GOSAT cloud judgements (TANSO−CAI or TANSO−FTS TIR band) tended to judge TANSO−FTS FOVs as “clear”, whereas Himawari−8 judged the same TANSO−FTS FOVs as “cloud” in most cases of disagreements in their cloud judgements. This is partly because of “clear conservativeness” of our cloud detection algorithm by Himawari−8. As for TANSO−FTS FOVs judged as “clear” by TANSO−FTS TIR band and “cloud” by Himawari−8, small-scale clouds partly existed in the TANSO−FTS FOVs judging from relatively low brightness temperature values of the coincident Himawari−8 data. This suggests the possibility that TANSO−FTS TIR band cannot detect such small-scale clouds.

Keywords: GOSAT, Himawari-8, cloud judgement, validation

©2019. Japan Geoscience Union. All Right Reserved. 

# Measurement of temperature that fungal spores form ice nuclei

*Kazuyuki Kita[1], Kansei Sasaki[1], Koutaro Minami[1], Takeshi Kinase[2], Kouji Adachi[2], Yuji Zaizen[2], Kentaro Hosaka[3], Teruya Maki[4], Yasuhito Igarashi[1,5]

1. Ibaraki University, 2. Meteorological Research Laboratory, 3. National Musium of Nature and Science, 4. Kanazawa University, 5. Kyoto University

## 1. Background

Aerosols act as condensation nuclei and ice nuclei for the cloud particle formation in the atmosphere. In recent years, it was discovered that some bioaerosols can be ice-nuclei at relatively high temperatures of -15 ˚C or higher, indicating the possibility they could form ice clouds and precipitation at lower altitudes where formation mechanism of ice clouds has not been understood, and their significance in the meteorology and climate has been recognized. Although there have been many studies that measure ice nuclei formation temperature for general aerosols, it has been measured for very limited number of fungal spores in those studies. Thus, it has been not yet understood what kind of fungal spores can work as ice nuclei at relatively high temperatures.

In this research, we measured ice nucleation of spores of various kinds of fungi sampled in Japanese forests and examined the relationship between ice nucleation temperature and biological classification. We also classified patterns of ice nuclei formation, which may have information on ice nuclei formation temperature and process.

## 2. Method

In this research, spores were sampled from fungi collected during fungi surveys conducted every month from May to October in various types of woods in the Tsukuba Botanical Garden. Some fungi were also collected in the forests of Namie Town, Fukushima Prefecture. Using an optical microscope equipped with a cooling stage, ice nuclei form of generation of ice nuclei is observed.

## 3. Results and discussion

The ice nucleation temperatures of fungal spores showed large diversity, depending on their species. The ice nucleation temperature depends on the biological classification of fungi. Although there were a large variation, ice nucleation temperatures of spores of *Russulales*, ranged from -20 to -30 ˚C. The temperatures of *Boletales* spores were about -30 ˚C, and they of *Polyporales* spores were -22 ˚C. *Agaricales* can be divided into two groups: spore ice nucleation temperature was about -15 ˚C and about - 30 ˚C. The generation form of ice nuclei in spores can be categorized into 4 groups: A: ice grows from the whole spore surface after its swelling, B: ice grows suddenly from the spore surface, C: ice grows from a particular part of spores, D: ice generated around spores. Although there are a few exceptions, most of the spores that could be classified as “A” became ice nucleus at a relatively high temperature of -15 ˚C or higher. For other developmental forms, the relationship with ice nucleation temperature is not clear. Measuring the ice nucleation temperatures of various kinds of fungal spores this study found that some

©2019. Japan Geoscience Union. All Right Reserved. 

fungal spores can become ice nuclei at a relatively high temperature of -15 ˚C or so, showing a possibility that fungal spore can produce ice clouds in relatively lower atmosphere. It is also found that fungal spores forming ice at relatively high temperature mostly classified as *Agaricales* , and that they swelled just before they made ice particles. These results may have information on factors determining the ice formation temperature of spores.

Keywords: bioaerosol, fungal spore, ice nuclei

©2019. Japan Geoscience Union. All Right Reserved. 

# Investigation of Atmospheric Aerosol Particles and gases by R/V Mirai cruise over the Arctic Ocean on 2017

*Fumikazu Taketani[1], Saki Kato[1,2], Takuma Miyakawa[1], Masayuki Takigawa[1], Masahiro Yamaguchi[1], Hisahiro Takashima[1,2], Petr Mordovskoi[1], Yugo Kanaya[1]

1. Japan Agency for Marine-Earth Science and Technology, 2. Fukuoka University

Atmospheric aerosol particles play an important role in Arctic climate through the absorbing and scattering of solar radiation. Also, the deposition of light-absorbing particles on the surface reduces the Earth’ s albedo and accelerates snow/ice melting by absorbing the sunlight. However, the observational information has been still insufficient to assess their contribution over the Arctic region. In this study, we conducted the ship-based measurements of marine aerosol particles (black carbon (BC), and fluorescent property) and trace gases (ozone and carbon monoxide) using R/V Mirai during a cruise across the Arctic Ocean and Bering Sea (23 August –4 October 2017). The measured BC mass concentration over the Arctic Ocean in the latitudinal region > 70˚N was an overall mean value of 3.5 ±2.0 ng/$m^3$ . This value was almost same to the levels recorded during our previous observations in the Arctic cruise on September during 2014 -2016. We captured relatively high BC mass concentration and/or CO mixing ratio events at 4 and 7-12 September 2017. The trajectory and BC property suggested that the source of BC on 4 September could be oil field at north of Alaska. We will present further analysis on the size distribution, BC mixing state, during the cruise in the presentation.

Keywords: Black Carbon, Arctic Ocean, Ship-based Observation

©2019. Japan Geoscience Union. All Right Reserved. 

# Characterization of carbonaceous aerosols in East Asia in the spring of 2015: Importance of non-fossil fuel sources

*Takuma Miyakawa[1], Yuichi Komazaki[1], Fumikazu Taketani[1], Xiaole PAN[2], Zifa Wang[2], Yugo Kanaya[1]

1. Japan Agency for Marine-Earth Science and Technology, 2. Institute for Atmospheric Physics, Chinese Academy of Science

The sources of elemental (EC) and organic carbon (OC) aerosols in the spring of 2015 in Asian outflow were investigated in terms of the radiocarbon ($^{14}C$) for carbonaceous aerosols and organic molecular marker analyses. The contribution of fossil fuel (FF) sources to total carbonaceous aerosols (TC) significantly increased in polluted air masses with enhancements of carbon monoxide concentrations. For EC, FF sources dominated in the polluted air masses. For OC, the contributions of non-FF and non-biomass burning (BB) sources were found to be significant (comparable to or higher than those of FF sources), especially in the air masses with higher values of both the ratio of water-soluble fraction of OC ($f_{WSOC}$) and $^{14}C$ concentrations ($F^{14}C$). Positive correlation between $f_{WSOC}$ and $F^{14}C$ indicates that the origins of TC (mainly OC) have great effects on the variabilities in the water solubility and the following climatic impacts (i.e., cloud formation process) of OC in the regional scale within the time scale of a week. Multivariate analyses using metallic and ionic tracers revealed the insights into the characteristics of classified carbonaceous aerosols in Asian outflow.

Keywords: Carbonaceous aerosols, Radiocarbon analysis, Source attribution

©2019. Japan Geoscience Union. All Right Reserved. 

# Analyzing the influence of biomass burning on ambient air pollution in mainland Southeast Asia from 2001 to 2016

*Shuai Yin[1]

1. National Institute for Environmental Studies

In this study, various remote sensing data, modeling data and emission inventories were integrated to analyze the tempo-spatial distribution of biomass burning in mainland Southeast Asia and its effects on the local ambient air quality from 2001 to 2016. With such a long time span, land cover changes have been considered in dividing the biomass burning into four types: forest fires, shrubland fires, crop residue burning and other fires. The results show that the monthly average number of fire spots peaked at 34,512 in March and that the monthly variation followed a strong seasonal pattern, which was closely related to precipitation and farming activities. The four kinds of biomass burning fires presented totally different tempo-spatial distributions and forest fires and shrubland fires are more dominant than other types. Moreover, the monthly Aerosol Optical Depth (AOD), particulate matter with a diameter less than 2.5 $\mu$m ($PM_{2.5}$) and carbon monoxide (CO) concentrations also peaked in March with values of 0.62, 73.97 $\mu g/m^3$ and 426 ppb, respectively. There are significant correlations between the monthly AOD, $PM_{2.5}$, and CO concentrations and the number of fire spots. On an annual scale, we also found certain correlations between the AOD and $PM_{2.5}$ concentrations and the number of fire spots. With respect to the spatial distribution, the AOD, $PM_{2.5}$ and CO concentrations are always higher in intense biomass burning regions. Southeast Asia is one of the most populated and fastest growing economic regions in the world. Therefore, in order to objectively and accurately analyze the influence of biomass burning on local air quality over a long time span, it is imperative for this study to consider the effects of anthropogenic activities. Two anthropogenic $CO_2$ emission inventories, the Emission Database for Global Atmosphere Research (EDGAR) and the Carbon Dioxide Information Analysis Center (CDIAC), were used. The results further prove that biomass burning is the dominant cause of the variation in the local air quality in mainland Southeast Asia. Although government authorities have taken measures to control biomass burning, the number of fire spots did not decrease; the numbers exceeded 100,000 each year from 2012 to 2016.

Keywords: AOD, Anthropogenic emission, Biomass burning, Carbon monoxide, PM2.5

©2019. Japan Geoscience Union. All Right Reserved. 

# High-resolution and multi-year inventory of mercury emissions from biomass burning in tropical continents during 2001–2017

*Yusheng Shi[1]

1. Aerospace Information Research Institute, Chinese Academy of Sciences

Mercury emissions from biomass burning contribute significantly to the atmospheric mercury budget and the interannual variations of mercury concentrations in the troposphere. This study developed a high-resolution (0.1 deg) and multi-year (2001-2017) monthly inventory of mercury emissions from biomass burning in five fire types in the tropical continents (Central and South America, Africa, and South and Southeast Asia). The inventory estimates of mercury emissions from biomass burning are based on the newly released MCD61A1 version 6 Burned Area data product, satellite and observational data of biomass density, and spatial and temporal variable combustion factors. Results from the inventory demonstrated that during 2001-2017, the average annual mercury emissions from biomass burning in tropical continents was 497 Mg and ranged from 289 Mg to 681 Mg. Forest fires were the largest contributor, accounting for 61% (300 Mg) of the total mercury emissions from biomass burning, followed by fires in shrubland (30%, 151 Mg), savanna (7%, 35 Mg), peatland (1%, 6 Mg), and cropland (1%, 5 Mg). However, these proportions varied between the continents; in the Americas and Asia, the largest biomass burning emissions came from forest fires, and in Africa the largest emissions were from shrubland fires. Between the three continents, Africa released 41% of the mercury emissions from biomass burning (202 Mg $year^{-1}$), Asia released 31% (154 Mg $year^{-1}$), and the Americas released 28% (141 Mg $year^{-1}$). The total mercury emissions from biomass burning in these tropical continents exhibited strong interannual variations from 2001 to 2017, with peak emissions in March and Agust to September, and forest fires were the primary land fire type controlling the interannual variations. Soil mercury emissions released during biomass burning was determined to be 495 Mg $year^{-1}$ during 2001-2017. The biomass burning mercury emissions data in this inventory agrees with results by other studies, which suggests that it could be used as an input for atmospheric transport models.

Keywords: biomass burning, mercury emissions, forest fires, tropical continents

©2019. Japan Geoscience Union. All Right Reserved. 

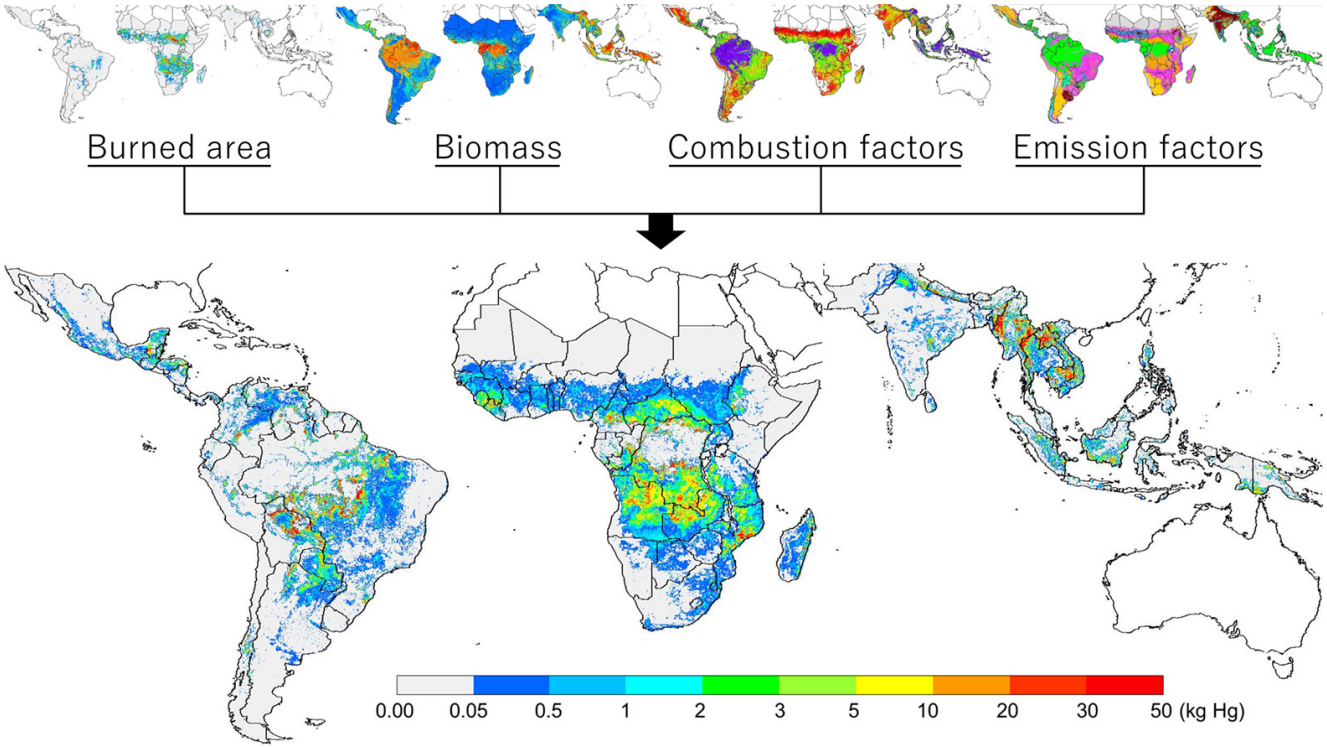


©2019. Japan Geoscience Union. All Right Reserved. 

# Simultaneous observations by sky radiometer and MAX-DOAS for characterization of biomass burning plumes in central Thailand in January-April 2016

*Hitoshi Irie[1], Syedul Hoque[1], Alessandro Damiani[1], Al Mashroor Fatmi[1], Pradeep Khatri[2], Tamio Takamura[1], Thanawat Jarupongsakul[3]

1. Chiba University, 2. Tohoku University, 3. Chulalongkorn University

The first intensive multi-component ground-based remote sensing observations by sky radiometer and Multi-Axis Differential Optical Absorption Spectroscopy (MAX-DOAS) were performed simultaneously at the SKYNET/Phimai site located in central Thailand (15.18˚N, 102.56˚E) from January to April 2016. The period corresponds to the dry season associated with the intense biomass burning (BB) activity around the site. The near-surface concentration of formaldehyde (HCHO) retrieved from MAX-DOAS was found to be a useful tracer for absorption aerosols from BB plumes, when BB was the dominant sources of HCHO and absorption aerosols over other sources. As the HCHO concentration tripled from 3 to 9 ppbv, the ratio of gaseous glyoxal to HCHO concentrations in daytime decreased from ~0.04 to ~0.03, responding presumably to the increased contribution of volatile organic compound emissions from BB. In addition, clear increases in aerosol absorption optical depths (AAODs) retrieved from sky radiometer observations were seen with the HCHO enhancement. At a HCHO of 9 ppbv, AAOD at a wavelength of 340 nm reached as high as ~0.15±0.03. The wavelength dependence of AAODs at 340-870 nm was quantified by the absorption Ångström exponent (AAE), providing evidence for the presence of brown carbon aerosols at an AAE of 1.5±0.2. Thus, our multi-component observations around central Thailand are expected to provide unique constraints for understanding physical/chemical/optical properties of BB plumes.

Keywords: Biomass burning, HCHO, CHOCHO, aerosol, sky radiometer, MAX-DOAS

©2019. Japan Geoscience Union. All Right Reserved. 

# Quantifying PM2.5 from long-range transport and local pollution in Taiwan during winter monsoon.

*Ming-Tung Chuang[1]

1. Research Center for Environmental Changes, Academia Sinica

From autumn to the following spring, annually, the northeast monsoon transports PM2.5 (particles less than
2.5 μm in aerodynamic diameter) from the Asian continent to downstream areas. Naturally, this triggered a
question: What are the contributions of PM2.5 from long-range transport (LRT) and local pollution (LP) at any
downstream location? To answer that question, the present study developed an economical and efficient method
that can easily estimate the contribution of PM2.5 from LRT (LRT-PM2.5) and PM2.5 from LP (LP-PM2.5). The
method used PM2.5 and meteorological observation data in Taiwan from 2006 to 2015 and a short-term simulation
from January to May in 2010. The analysis classified the data into three types of PM2.5 source patterns:
LRT-Event (high concentration plume at the front edge of southward moving anticyclones/strong northeast
wind), LRT-Ordinary (less concentration in common strong northeast wind), and LRT/LP Mix or Pure LP (PM2.5
was from both LRT and LP or from only LP under weak northeast wind). During the ten-year period, the average
LRT-PM2.5 values at the northern tip of Taiwan were 31–39 μgm−3, 12–16 μgm−3, and 4–13 μgm−3 for the
LRT-Event, LRT-Ordinary, and LRT/LP Mix or Pure LP patterns, respectively. The 10-year average LRT-PM2.5
and LP-PM2.5 contributions were approximately 70:30 in northern Taiwan, 50:50 in central Taiwan, and 30:70 in
southern Taiwan for the LRT-Event pattern; 60:40 in northern and 40:60 in central and southern Taiwan for the
LRT-Ordinary pattern; and 30:70 in northern and 25:75 in central and southern Taiwan for the LRT/LP Mix or
Pure LP pattern. Interestingly, LRT-PM2.5 peaked in 2013 but has decreased annually since then, whereas LPPM2.5
has roughly decreased in the past ten years.

Keywords: PM2.5, long-range transport, local pollution, CMAQ

©2019. Japan Geoscience Union. All Right Reserved. 

# Vertical characterization of $PM_{2.5}$ based on observation using compact sensors on and around Mt. Unzen in Nagasaki Prefecture

*Tomoki Nakayama[1], Ayane Ueno[1], Kenta Kanegae[1], Kazuaki Kawamoto[1], Kodo Umakoshi[1], Takayuki Yamasaki[2], Wataru Okamoto[2], Yutaka Matsumi[2]

1. Faculty of Environmental Science, Nagasaki University, 2. ISEE, Nagoya University

Aerosol particles in the atmosphere, including $PM_{2.5}$, are known to have significant impacts on climate, the atmospheric environment, ecosystems, and human health. Whereas both of domestic sources and transboundary pollution from Asian Continent possibly contribute to the $PM_{2.5}$ mass concentrations in Japan, high $PM_{2.5}$ events owing to the transboundary pollution are often observed, especially in north-western part of Kyushu region (including Nagasaki Prefecture). Although $PM_{2.5}$ mass concentrations are observed at the observatories of the Atmospheric Environmental Regional Observation System (AEROS) of the Ministry of the Environment, Japan (MOEJ), the observatory on mountain is very limited, and widely used large and expensive bate attenuation monitor (BAM) is not suitable for the multi-point observations.

We developed a compact $PM_{2.5}$ sensor with Panasonic Corporation [Nakayama et al. 2018]. This sensor can measure $PM_{2.5}$ mass concentrations by detecting light scattering intensities from individual aerosol particles with diameters greater than 0.3 $\mu$m. In this study, this sensor was applied for the observations of $PM_{2.5}$ mass concentrations around Mt. Unzen in Nagasaki Prefecture from December 2018. The $PM_{2.5}$ sensors were installed at six sites with different altitudes from 20 m to 1300 m to analyze vertical and horizontal distributions of $PM_{2.5}$. During high $PM_{2.5}$ events (>35 $\mu g/m^3$) in winter, the $PM_{2.5}$ mass concentrations at an altitude above 1000 m are similar to those at 20 m in most cases. However, in some cases, high $PM_{2.5}$ was observed only at low altitude sites, likely because of inflow of clean air with lower aerosol burden from higher altitude to the mountain sites and/or low boundary layer height. The vertical profile data obtained in this work will be compared with the lidar data obtained by NIES at Omura city, which is located 38 km north-west of Mt. Unzen, to discuss the possible sources and transport patterns of $PM_{2.5}$.

Acknowledgements

This work is supported by Unzen city, Shimabara city, Minamishimabara city, Unzen ropeway Corporation, and Eco Solutions Company, Panasonic Corporation.

Reference

T. Nakayama, Y. Matsumi, K. Kawahito, Y. Watabe, Development and evaluation of a palm-sized optical $PM_{2.5}$ sensor, *Aerosol Sci. Technol.*, 52, 2-12, doi:10.1080/02786826.2017.1375078 (2018).

Keywords: PM2.5, Transboundary Air Pollution , Compact sensor, Mountain

©2019. Japan Geoscience Union. All Right Reserved. 

# Observation of NPF events at the summit of Mt. Fuji during daytime and nighttime

*Hiroki Igarashi[1], Takenori Sato[1], Tatsuhiro Mori[1], Kazuhiko Miura[1], Yoko Iwamoto[2], Ryuichi Wada[3], Shungo Kato[4], Hiroshi Okochi[5]

1. Tokyo University of Science, 2. Hiroshima University, 3. Teikyo University of Science, 4. Tokyo Metropolitan University, 5. Waseda University

An improved understanding of a new particle formation (NPF), which is a key process controlling the spatial and temporal distributions of aerosol concentration, is needed to estimate the direct radiative forcing. However, it is difficult to quantitatively understand the mechanism of NPF because the frequency of the NPF depends on the aerosol concentration, gases, and meteorological condition. In this study, we measured number concentrations (*N*) of aerosol particles (10 to 487 nm) at the summit of Mt. Fuji (35.360˚N, 138.727˚E, 3776 m a.s.l.) between July and August during 2011-2017. We report the annual and diurnal variations of the frequency of the NPF for a long-term period. The summit of Mt. Fuji is usually located in the free troposphere and enable us to observe the long-range transport of aerosol particles. The NPF event was defined as the event that *N* increases over 1 hour for diameter smaller than 25 nm. We observed 172 NPF events (daytime and nighttime events were 90 times and 82 times, respectively) during the observation period. Most events occurred at 8 o'clock (at the peak of daytime events) and 20 to 21 o'clock (at peaks of nighttime events) in local time. In addition, the growth rate of aerosol particles was calculated. The median value of the growth rate was estimated to be 5.27 nm/h (6.03 nm/h for daytime and 4.56 nm/h for nighttime) at 40 NPF events, suggesting that aerosol particles are easily grown during daytime. Finally, using a back trajectory analysis (NOAA HYSPLIT version 4), we investigated when and where the NPF occurred. As a result, it is suggested that 62.5% of the total NPF occurred during the daytime, and the rest occurred during the nighttime (37.5%). The NPF frequently occurred during daytime over Japan although a few NPF occurred over the sea during nighttime.

Keywords: New particle formation, Mt. Fuji, Nighttime NPF event, Particle size distribution

©2019. Japan Geoscience Union. All Right Reserved. 

# Measurement of atmospheric metal particles using an ICP-MS and TEM.

*Takeshi Kinase[1], Kouji Adachi[1], Mizuo Kajino[1], Masahiko Hayashi[2], Keiichiro Hara[2]

1. Meteorological Research Institute, 2. Fukuoka

Particles containing transition metal components (hereafter, metal particle) are one of the major aerosols. Some of these metal particles have strong oxidation potential and have health effects by deposition into the human body through generating reactive oxygen and free-radical in and on cells. These reactive oxygen and free radicals cause various effects such as oxidative stress, inflammatory cell, DNA oxidative damages and cell death. However, oxidation potential for each metal particle and the magnitude of hazard to human health are not well known. In addition, colored metal particles, such as iron oxide, absorb solar radiation and contribute to the global warming. However, these effects of metal particles are not clarified because their observations and detailed features are not well known.

In this study, we measured atmospheric metal particle concentrations using an inductively coupled plasma-mass spectrometry (ICP-MS) and collected aerosol samples on the Cu grids using impactors to observe each aerosol particle using a transmission electron microscope (TEM) and an energy-dispersive X-ray spectrometry detector (EDS) with the scanning transmission electron microscopy (STEM). The ICP-MS instrument was coupled with a gas changer for air replacement in argon gas atmosphere, so that aerosol particles were directly measured using the ICP-MS in real-time. As a result, we could measure time trends of atmospheric metal particle concentrations quantitatively with high time resolutions together with their shape and mixing states by the TEM and STEM-EDS analysis.

We measured atmospheric metal particles in winter (2018/1/17–2/8) and in spring (2018/5/8–5/30) at Fukuoka University. We measured increasing events of metal particles by ICP-MS. Fe and Al were the highest concentration followed by Zn, Mn, Cr and Pb. Two different slopes were observed in relation between Fe and other metal elements such as Mn, V, and Al. On the other hand, Ag, Au, Mo and Tc did not correlate with Fe. From TEM observation of samples with high concentrations of metal particles, we found aggregated metal particles as ultrafine metal spheres (for smaller particles were several nm). These particles contained Fe, Mn and Cr as major metal elements, and most particles were internally mixed with a sulphate. Furthermore, some metal particles contained many ultrafine metal particles that distributed separately in a sulphate. Zn and Pb containing particles were also internally mixed with sulphate, however, they were observed as dissolved substances (not particle state) or crystallized state, which were decomposed by electron beam.
We found other metal particles which contained such as Ag, Sb, and Cu during their increasing periods. Our results are useful for understanding of atmospheric metal particles behaviors.

Keywords: Oxidation potential, Metal particle, ICP-MS, TEM, Feature observation

©2019. Japan Geoscience Union. All Right Reserved. 

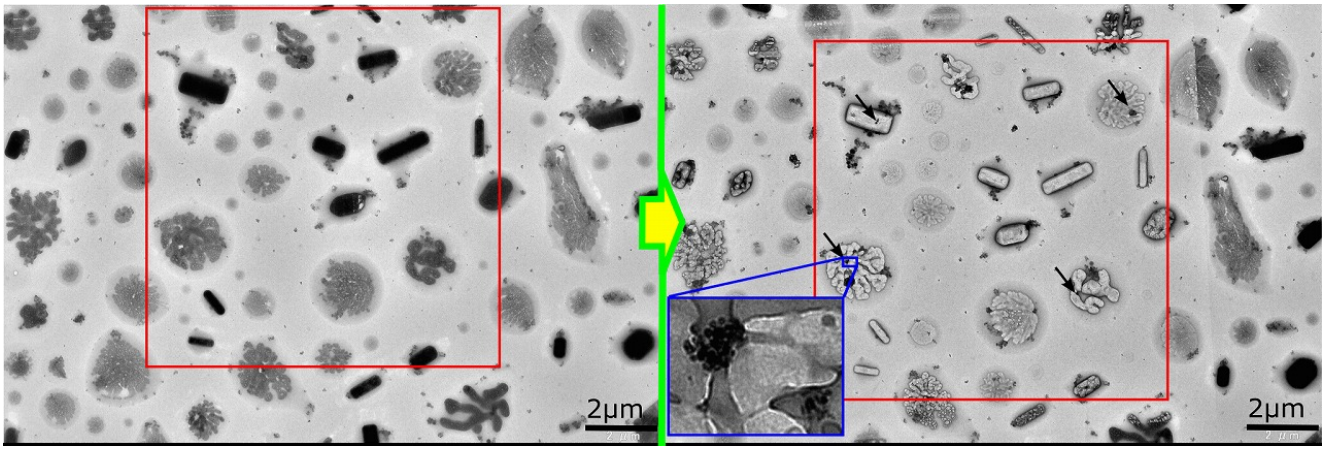


©2019. Japan Geoscience Union. All Right Reserved. 

# Experimental results on measuring device of complex refractive index using the single particle extinction and scattering method

*TAKASAGO YUYA[1]

1. Tokyo university

Changes in the type and amount of atmospheric aerosol alter the albedo, resulting in radiation budget and climate change. However, the prediction accuracy of the fluctuation range is not high at the present. The complex refractive index can estimate the type of atmospheric aerosol. In the existing method, a method of measuring the complex refractive index for each bulk is mainstream, and there are few cases to measure for each single particle. If accurate measurement data of complex refractive index for each particle type can be obtained, it is possible to improve prediction accuracy of climate change width of particle type, so measurement with complex refractive index for each single particle is important. In this study, we conducted an experiment using single particle extinction and scattering method as a method to measure the complex refractive index. The single particle extinction and scattering method is a method of measuring forward scattered light intensity generated by projecting a laser on fine particles and interference between scattered light and incident light and estimating the value of the complex refractive index of the particle from these data. We developed an experimental apparatus using this method and conducted experiments with polystyrene, BC standard particles and precipitation samples (Okinawa, Happo, Fukui). Currently, I am thinking a method to solve the inverse problem that estimates particle characteristics such as particle type and complex refractive index from forward scattering intensity obtained from experiment and interference data of incident light and scattered light. For this purpose, we are developing a method of classifying samples mixed with plural types of particles into particle type by using clustering method of machine learning.

©2019. Japan Geoscience Union. All Right Reserved. 

# Evaluation of BC and CO emission inventory based on long-term in-situ observations over East Asia

*Yongjoo Choi[1], Yugo Kanaya[1], Hye-Jung Shin[2], Seung-Myong Park[2], Atsushi Matsuki[3], Yasuhiro Sadanaga[4], Sang-woo Kim[5], Itsushi Uno[6], Xiaole Pan[7]

1. Development Center for Global Change, Japan Agency for Marine-Earth Science and Technology, 2. Division of Climate & Air Quality Research, National Institute of Environmental Research, Korea, 3. Institute of Nature and Environmental Technology, Kanazawa University, 4. Department of Applied Chemistry, Graduate School of Engineering, Osaka Prefecture University, 5. School of Earth and Environmental Sciences, Seoul National University, Seoul, Korea, 6. Research Institute for Applied Mechanics, Kyushu University, 7. Institute of Atmospheric Physics, CAS, Beijing, China

Compared to carbon dioxide ($CO_2$), which is a major long-lived greenhouse gas, the influence of black carbon (BC) to global warming is not negligible among the short-lived components. To improve the bottom-up emission inventory for enhancing the understanding level of BC, the measured ΔBC/ΔCO ratios were compared with those from the Regional Emission inventory in Asia (REAS) version 2.1 bottom-up inventory. The measurements were conducted at two sites in Korea (Baengnyeong; 124.63˚ E, 37.97˚ N, and Gosan; 126.17˚ E, 33.28˚ N) and two sites in Japan (Noto; 137.36˚ E, 37.45˚ N, and Fukuoka; 130.47˚ E, 33.52˚ N). The instruments for measuring CO concentration are same at all sites as Model 48i (Thermo Fisher Scientific), however, the instruments for BC were different depends on the sites (sunset EC/OC analyzer in Baengnyeong, Continuous Light Absorption Photometer in Gosan, Multi-Angle Absorption Photometer in Noto and Fukuoka). Based on the backward trajectories during past 120 hours calculated from HYSPLIT model, all trajectories were assigned to six study domains which divided by country and/or administrative district (East China, North China, Northeast China, South Korea, North Korea, and Japan). To exclude the wet-removal effect, the ΔBC/ΔCO ratio was considered only when the accumulated precipitation along a backward trajectory (APT) for three days is equal to zero. Also, we confirmed that the comparison of ΔBC/ΔCO by six study domains could be reasonable since there were no significant differences in ΔBC/ΔCO ratio depending on traveling time (dry deposition effects) and residence time over the emission source areas. Compared to measured ΔBC/ΔCO ratio (6.6 –8.4 ng/$m^3$·ppb), ΔBC/ΔCO from REAS emission inventory (8.0 ng/$m^3$·ppb for East China –23.2 ng/$m^3$·ppb for South Korea) were overestimated by factor 1.2 for East China to 2.9 for South Korea whereas those for North Korea (3.7 ng/$m^3$·ppb from REAS) was underestimated by factor 2.0. The measured ΔBC/ΔCO ratios in Japan (6.8 ng/$m^3$·ppb) were similar to those from REAS emission inventory (6.5 ng/$m^3$·ppb). The seasonal and spatial differences of ΔBC/ΔCO ratios between measured and emission inventory will be examined to identify the over- and under-estimated administrative districts.

Keywords: Black Carbon, Carbon monoxide, REAS emission inventory, ΔBC/ΔCO ratios

©2019. Japan Geoscience Union. All Right Reserved. 

# Inverse modeling of black carbon emissions over China using ensemble data assimilation

*Ping Wang[1]

1. Chinese Academy of Meteorological Sciences

Emissions inventories of black carbon (BC), which are traditionally constructed using a “bottom-up” approach based on activity data and emissions factors, are considered to contain a large level of uncertainty. In this paper, an ensemble optimal interpolation (EnOI) data assimilation technique is used to investigate the possibility of optimally recovering the spatially resolved emissions bias of BC. An inverse modeling system for emissions is established for an atmospheric chemistry aerosol model and two key problems related to ensemble data assimilation in the top-down emissions estimation are discussed: 1) how to obtain reasonable ensembles of prior emissions; and 2) establishing a scheme to localize the background-error matrix. An experiment involving one year long simulation cycle with EnOI inversion of BC emissions is performed for 2008. The bias of the BC emissions intensity in China at each grid point is corrected by this inverse system. The inversed emission over China in January is 240.1 Gg, and annual emission is about 2539.3 Gg, which is about 1.8 times of bottom-up emission inventory. The results show that, even though only monthly mean BC measurements are employed to inverse the emissions, the accuracy of the daily model simulation improves. Using top-down emissions, the average root-mean-square error of simulated daily BC is decreased by nearly 30%. These results are valuable and promising for a better understanding of aerosol emissions and distributions, as well as aerosol forecasting.

Keywords: Inverse modeling, black carbon, ensemble optimal interpolation

©2019. Japan Geoscience Union. All Right Reserved. 

# Analysis of BC emissions in East Asia using inverse model

*Takashi Maki[1], Taichu Y Tanaka[1], Naga Oshima[1], Thomas Sekiyama[1], Keiichi Kondo[1], Jun-ichi Kurokawa[2], Keiya Yumimoto[3], Toshimasa Ohara[4]

1. Meteorological Research Institute, 2. Asia Center for AirPollution Research, 3. Kyushu University, 4. National Institute for Environmental Studies

In addition to affecting climate change and global warming, Black Carbon (BC) brings impact on society and human health as well. However, changes in BC emissions in east Asia have yet to be fully understood. Attempts have been made by various institutions and researchers to estimate BC emission inventories from various statistics but there are problems such as lack of rapid reporting. In order to modify black carbon emissions inventory based on this statistic, we have constructed an BC emission inversion system for east Asia using aerosol transport model and surface observations. The analysis period for emissions is from 2011 to 2014. We adopt global aerosol transport model named MASINGAR mk-2 (Tanaka et al.). The model is a subset of MRI (Meteorological Research Institute) earth system model for climate research and can treat BC, OC, mineral dust, sulfate and sea-salt with external mixing. We divided tags of each province of China, South Korea, Japan into 33 regions and carried out tagged tracer transport experiments. We collected 5 surface sites daily observation data (Hedo, Fukue, Echizen, Happo and Lulin). A priori BC emission is provided by REAS 2.2 (Kurokawa et al.) at 2010. Inversion results suggested that BC emissions in East Asia between 2011 and 2014 are decreasing especially in China about 10%, compared to the 2010 emissions. There was no significant change in BC emissions in Japan and South Korea during the analysis period. However, the observation network could constrain mainly northern part of China. We need more observation data (ex. satellite data) to constrain BC emission amount.

Keywords: Inverse model, BC emission, Aerosol model

©2019. Japan Geoscience Union. All Right Reserved. 

# Source attribution of BC in the northern Pacific and Arctic Ocean by chemistry climate model

*Takato Onishi[1], Kengo Sudo[1,2], Yugo Kanaya[2], Fumikazu Taketani[2]

1. Graduate School of Environmental Studies, Nagoya University, 2. Japan Agency for Marine-Earth Science and Technology

Black Carbon (BC) is emitted from combustion of biomass and fossil fuel into the atmosphere. BC in the atmosphere absorbs visible light and heats the atmosphere contributing to global warming. The emitted BC being originally hydrophobic with low CCN activity, is not easily scavenged by precipitation allowing long-range transport of BC to remote areas. Snow or ice surfaces, when affected by deposition of BC, decrease their albedo causing further warming in the high latitudes.
This study focuses on long-range transport of BC in the northern high latitude regions and investigates BC origins (source regions and types) with a tagged tracer simulation by a global chemistry climate model CHASER. The modeled BC concentrations are validated with the BC observational data obtained from the JAMSTEC research vessel Mirai (from August to September). The model is found to be overestimating the observed BC by a factor of 1.2 to 7 in the south of 70°N in the northern Pacific. Differences between the model and observation are relatively small near Japan, but a bit larger between 160°E to 180°E in the Pacific Ocean. For the Arctic Ocean, on the other hand, the model severely overestimates BC by a factor of 13 to 70. In the model, BC in the North Pacific and Arctic Ocean is originated mainly from Siberia, North America and China.
The overestimated BC in the model probably shows an underestimate of wet deposition by precipitation. However, it is found that CHASER tends to overestimate precipitation amount when compared to the reanalysis data as the ERA-interim. This suggests that there is an inconsistency in the BC wet deposition scheme such as underestimation of BC uptake to cloud droplets. We considered correlation between precipitation and BC wet deposition flux normalized by columnar BC mass for checking relation of precipitation and BC wet removal. The correlation coefficient is about 0.4 suggesting that BC removal by precipitation is weak in the model. In addition, the ratios of internal BC to total BC for the surface to lower troposphere are calculated for the years of 2014 to 2017. In the northern pacific and Arctic Ocean, the ratios are about 30 percent indicating that the hydrophobic type of BC is dominant in the region for which CHASER overestimates BC.
As a result, it is suggested that there is much room for improvement in the simulation of aging process of BC (hydrophobic to hydrophilic conversion) and the scheme for wet deposition of external BC. In the presentation, the results from the further improved model simulations will be introduced and discussed.

Keywords: BC, chemistry-climate model, wet deposition, Arctic Ocean, Pacific Ocean

©2019. Japan Geoscience Union. All Right Reserved. 

# Evaluation of a mobile $PM_{2.5}$ sensor and application to the measurements along the National route 1 and around Nagasaki University

*Kenta Kanegae[1], Takayuki Yamasaki[2], Wataru Okamoto[2], Yutaka Matsumi[2], Tomoki Nakayama[1]

1. Nagasaki University, 2. Nagoya University

Short-term exposure of $PM_{2.5}$, negatively impacts human health through respiratory disease (such as asthma and bronchitis) and cardiovascular diseases, and leads to premature death. Because $PM_{2.5}$ is spatially and temporally variable and individuals also move in time and space, it is important to understand personal exposures of $PM_{2.5}$ for better assessment of the health impact. We developed a palm-sized optical $PM_{2.5}$ sensor with and Panasonic Corporation, and evaluated the performance for environmental monitoring at fixed sites [Nakayama et al. 2018]. This sensor was designed to measure $PM_{2.5}$ mass concentrations by detecting light scattering intensities from individual aerosol particles with diameters greater than 0.3 $\mu$m. The small size, light weight, and low power consumption of the sensor are suitable for mobile personal exposure measurement. However, the sensitivity of the sensor can be change if the sensor is tilted or swung, because aerosol particles flow into the sensor via an updraft generated by a heater and flow rate may be change during tinting or swinging.
In this study, we investigate the performance of the $PM_{2.5}$ sensor for mobile exposure measurements. The changes in the sensitivity of the sensor during tilting or swinging have been tested. Moreover, the change in the sensitivity of the sensor during walking has been investigated, by comparing the $PM_{2.5}$ data during walking with those during standing. From the results of these tests, it was found that the sensor can be applied for mobile exposure measurements of $PM_{2.5}$ mass concentration. We applied this sensor for the mobile measurements during walking along the National Route 1 (from Tokyo to Kyoto) for two weeks, and around Nagasaki University. The obtained $PM_{2.5}$ data will be compared with those obtained at the surrounding ambient air monitoring stations (AEROS) and meteorological data to discuss the sources and transportation of $PM_{2.5}$. We believe that this research will provide useful information for applications of the compact sensor to epidemiological research of health effects of $PM_{2.5}$.

Acknowledgements
This work is supported by the Eco Solutions Company, Panasonic Corporation.

Reference
T. Nakayama, Y. Matsumi, K. Kawahito, Y. Watabe, Development and evaluation of a palm-sized optical $PM_{2.5}$ sensor, *Aerosol Sci. Technol.*, 52, 2-12, doi:10.1080/02786826.2017.1375078 (2018).

Keywords: Compact PM2.5 sensor , Personal exposure, Mobile measurement

©2019. Japan Geoscience Union. All Right Reserved. 

# Analysis on the Relationship between the Concentration of Particulate Matter and Mortality from Respiratory and Cardiovascular Diseases

*Woo-Sik JUNG[1], Woo-Gon Do[2]

1. Department of Atmospheric Environment Information Engineering, Atmospheric Environment Information Research Center, Inje University, Gimhae 50834, Korea, 2. Busan Metropolitan City of Institute of Health and Environment Busan, Korea

Concerns over particulate matter are growing rapidly as the number high concentration days are increasing. Since 2015, PM2.5 has been set as a national ambient air quality standard and frequency of Asian dust or mists and precursors coming from the west of Korea has increased. Various studies have been conducted on the distribution and composition of particulate matter. The particulate matter is known to be the main cause of respiratory and cardiovascular disease, such as vascular dysfunction, asthma and the occurrence of chronic bronchitis. As the paradigm of air quality management policy changes from controlling, treating and reducing sources to taking into account the damage of a receptor including assessing health risks, it is necessary to establish scientific policies by quantitatively assessing the health effects of the particulate matter and calculating health benefits. To do this, a quantitative assessment of the health risks of particulate matter is essential. The purpose of this study is to analyze the effects of changes in the daily average concentration of particulate matter on the mortality of respiratory and cardiovascular diseases in Busan, Korea. In this study, we employed a generalized additive model (GAM) with a quasi-Poisson to assess the association between daily mean particulate matter and mortality. A penalized spline function was used to adjust the seasonal pattern and long-term trend in daily mortality and the nonlinear mortality effects of the weather. Based on this, a model between the death rate and daily average particulate matter was established and the change in the mortality rate of respiratory and cardiovascular diseases was analyzed according to the change in particulate concentration. The daily mean particulate matter were calculated using hourly PM2.5 and PM10 data provided the Environment Ministry of Korea and the causes of death from 2015 to 2017 were provided by the National Statistical Office's 'Micro Data Service'.

This research was supported by Basic Science Research Program through the National Research Foundation of Korea(NRF) funded by the Ministry of Education(2017R1D1A3B03036152)

Keywords: Particulate Matters, Mortality, Respiratory Diseases, Cardiovascular Diseases

©2019. Japan Geoscience Union. All Right Reserved. 

# Analysis on the Relationship between the Concentration of Particulate Matter and Mortality from Respiratory and Cardiovascular Diseases

**Woo-Sik Jung*, Woo-Gon Do,**

*Dept. of Atmospheric Environment Information Engineering, Inje University, Gimhae, Korea
Busan Metropolitan City of Institute of Health and Environment Busan, Korea

Concerns over particulate matter are growing rapidly as the number high concentration days are increasing. Since 2015, PM2.5 has been set as a national ambient air quality standard and frequency of Asian dust or mists and precursors coming from the west of Korea has increased. Various studies have been conducted on the distribution and composition of particulate matter. The particulate matter is known to be the main cause of respiratory and cardiovascular disease, such as vascular dysfunction, asthma and the occurrence of chronic bronchitis. As the paradigm of air quality management policy changes from controlling, treating and reducing sources to taking into account the damage of a receptor including assessing health risks, it is necessary to establish scientific policies by quantitatively assessing the health effects of the particulate matter and calculating health benefits. To do this, a quantitative assessment of the health risks of particulate matter is essential. The purpose of this study is to analyze the effects of changes in the daily average concentration of particulate matter on the mortality of respiratory and cardiovascular diseases in Busan, Korea. In this study, we employed a generalized additive model (GAM) with a quasi-Poisson to assess the association between daily mean particulate matter and mortality. A penalized spline function was used to adjust the seasonal pattern and long-term trend in daily mortality and the nonlinear mortality effects of the weather. Based on this, a model between the death rate and daily average particulate matter was established and the change in the mortality rate of respiratory and cardiovascular diseases was analyzed according to the change in particulate concentration. The daily mean particulate matter were calculated using hourly PM2.5 and PM10 data provided the Environment Ministry of Korea and the causes of death from 2015 to 2017 were provided by the National Statistical Office's 'Micro Data Service'.

Acknowledgement

This research was supported by Basic Science Research Program through the National Research Foundation of Korea(NRF) funded by the Ministry of Education(2017R1D1A3B03036152)

©2019. Japan Geoscience Union. All Right Reserved. 

# A Study on the Estimation of Contribution Rate of Odour Substances Using CALPUFF model

*Woo-Sik JUNG[1], Woo-Gon Do[2]

1. Department of Atmospheric Environment Information Engineering, Atmospheric Environment Information Research Center, Inje University, Gimhae 50834, Korea, 2. Busan Metropolitan City of Institute of Health and Environment Busan, Korea

The environmental odours produced by anthropogenic origin according to urbanization and industrialization continue to increase. These odours cause mental and physiological stress and have a variety of adverse health effects, including nausea, headaches, loss of appetite, gastrointestinal disorders, difficulty in breathing, and allergy. Therefore, the odours are degrading the quality of life for residents in nearby residential areas, causing health hazards and eventually causing economic loss in the community. Miscellaneous approaches are used internationally within odour regulatory systems, with methods and tools for management and control supported by ambient air odour concentration and individual chemicals(maximum impact standard); fixed and variable separation distances(separation distance standard); maximum emission rate for odours and individual chemicals(maximum emission standard); number of complaints or annoyance level(maximum annoyance standard); best available technologies e BAT (technology standard). However, the occurrence of odors is a very local issue that reflects the characteristics of individual sources and the subjective impact of nearby residents. Therefore, prior to these regulations, it is very important to assess the impact of individual emissions quantitatively. The CALPUFF model is a typically used model for assessing the dispersion of air pollutants or odours in various research institutes, including the U.S. EPA. This model is an optimal method for calculating the contribution rate of individual emission sources in area where odour sources are concentrated. In this study, the CALPUFF model was used to identify the contribution rate of the four adjacent emission facilities to the surrounding areas in Saenggok Industrial Complex located in Saenggok-dong, Gangseo-gu, Busan in Korea. In order to estimate the contribution rate of individual emission sources, the predicted odour concentration of each emission source was calculated respectively(S1-S4). Next, the predicted odour concentration was calculated considering four emission sources together(Base). Finally, the contribution rates of individual emission sources within the modeling domain were calculated as the ratio of S1-S4 to Base. The amount of area sources in each emission facility was indirectly calculated using the concentration measured near the emission facility. Meterological input data produced by applying the results of the WRF model to the CALMET model. As a result of the CALPUFF model, the contribution rate of sludge treatment facility was the highest at 76%, and the rest of the facilities were shown to contribute about 10% to the surrounding area.

This research was supported by Basic Science Research Program through the National Research Foundation of Korea(NRF) funded by the Ministry of Education(2017R1D1A3B03036152)

Keywords: Odour, CALPUFF

©2019. Japan Geoscience Union. All Right Reserved. 

# A Study on the Estimation of Contribution Rate of Odour Substances Using CALPUFF model

**Woo-Sik Jung*, Woo-Gon Do,**

*Dept. of Atmospheric Environment Information Engineering, Inje University, Gimhae, Korea
Busan Metropolitan City of Institute of Health and Environment Busan, Korea

The environmental odours produced by anthropogenic origin according to urbanization and industrialization continue to increase. These odours cause mental and physiological stress and have a variety of adverse health effects, including nausea, headaches, loss of appetite, gastrointestinal disorders, difficulty in breathing, and allergy. Therefore, the odours are degrading the quality of life for residents in nearby residential areas, causing health hazards and eventually causing economic loss in the community. Miscellaneous approaches are used internationally within odour regulatory systems, with methods and tools for management and control supported by ambient air odour concentration and individual chemicals(maximum impact standard); fixed and variable separation distances(separation distance standard); maximum emission rate for odours and individual chemicals(maximum emission standard); number of complaints or annoyance level(maximum annoyance standard); best available technologies e BAT (technology standard). However, the occurrence of odors is a very local issue that reflects the characteristics of individual sources and the subjective impact of nearby residents. Therefore, prior to these regulations, it is very important to assess the impact of individual emissions quantitatively. The CALPUFF model is a typically used model for assessing the dispersion of air pollutants or odours in various research institutes, including the U.S. EPA. This model is an optimal method for calculating the contribution rate of individual emission sources in area where odour sources are concentrated. In this study, the CALPUFF model was used to identify the contribution rate of the four adjacent emission facilities to the surrounding areas in Saenggok Industrial Complex located in Saenggok-dong, Gangseo-gu, Busan in Korea. In order to estimate the contribution rate of individual emission sources, the predicted odour concentration of each emission source was calculated respectively(S1-S4). Next, the predicted odour concentration was calculated considering four emission sources together(Base). Finally, the contribution rates of individual emission sources within the modeling domain were calculated as the ratio of S1-S4 to Base. The amount of area sources in each emission facility was indirectly calculated using the concentration measured near the emission facility. Meterological input data produced by applying the results of the WRF model to the CALMET model. As a result of the CALPUFF model, the contribution rate of sludge treatment facility was the highest at 76%, and the rest of the facilities were shown to contribute about 10% to the surrounding area.

Acknowledgement

This research was supported by Basic Science Research Program through the National Research Foundation of Korea(NRF) funded by the Ministry of Education(2017R1D1A3B03036152)

©2019. Japan Geoscience Union. All Right Reserved. 

# Stepwise decrease in atmospheric trace gases near the ground associated with rapid vertical mixing observed by 3-D coherent Doppler lidar and in-situ gas measurements

*Hisahiro Takashima[1], Keiichiro Hara[1], Yuki Ohira[1], Akinori Takami[2], Ayako Yoshino[2], Yasushi Fujiyoshi[3]

1. Fukuoka University, 2. National Institute for Environmental Studies, 3. Hokaido University

Stepwise decreases, which occur over several minutes, in nitrogen oxides (NOx) and carbon monoxide (CO) concentrations, in which the main source of these gases is supposed to be near the surface, are sometimes observed in Fukuoka, urban site in Japan, during the summer-winter seasons. In the most cases, ozone ($O_3$) content, which could be higher at higher altitudes, increases. Wind observations by 3-D coherent Doppler lidar suggest there is a thin surface layer (up to ~50-300 m thickness) near the ground before the stepwise change, and then rapid vertical mixing associated with the local meteorological system occurs. The surface thin layer plays a role as a cover of pollutants near the ground, and the vertical mixing within the boundary layer rapidly dilutes/reduces the pollutant contents near the ground.

©2019. Japan Geoscience Union. All Right Reserved. 

# Spatiotemporal variations of nitrogen dioxide ($NO_2$) over Fukuoka , observed by multiple MAX-DOAS instruments and 3-D coherent Doppler lidar

*Hironobu Ueki[1], Hisahiro Takashima[1], Martina M. Friedrich[2]

1. Fukuoka university, 2. Belgian Institute for Space Aeronomy (BIRA-IASB), Belgium

To understand spatiotemporal variations and transport/mixing processes in nitrogen dioxide ($NO_2$) over Fukuoka, an urban area in Japan, continuous $NO_2$ profile observations with a high temporal resolution of four minutes by MAX-DOAS (Multi Axis Differential Optical Absorption Spectroscopy) at three sites in Fukuoka have been conducted from October 2018 to January 2019. Two sites (Yakuin (33.580˚N, 130.396˚E) and Sohara (33.580˚N, 130356˚E)) are located near the city center and pointing towards the north(towards the sea), and one site (Fukuoka University (33.550˚N, 130.364˚E)) is located outside of the city center pointing towards the city center.

In the case of 29 November 2018, an air mass with a high $NO_2$ concentration was observed near the ground in the morning (until 10:30 am) and later, around 10:30 to 11:30 am, an increased concentration of $NO_2$ gradually appeared at a higher altitude over the city center. This increased $NO_2$ concentration disappeared around 13:30-14:00 pm. From the simultaneous three-dimensional (3-D) wind observations by 3-D coherent Doppler lidar installed at Fukuoka University, it is suggested that the air mass with high $NO_2$ concentration was transported upward from the ground by vertical convection, and after that, a clean air-mass was advected from sea by sea-breeze. In this presentation, we will show several results observed by the multipoint MAX-DOAS and 3-D wind observations, focusing on the 3-D transport over Fukuoka using the high $NO_2$ air mass as a tracer.

Keywords: MAX-DOAS

©2019. Japan Geoscience Union. All Right Reserved. 

# Measurement on the $^{17}O$-excess of tropospheric nitrogen oxides

*Fumiko Nakagawa[1], Dong Ding[1], Urumu Tsunogai[1], Takashi Yamaguchi[2], Izumi Noguchi[2]

1. Graduate School of Environmental Studies, Nagoya University, 2. Institute of Environment Sciences, Hokkaido Research Organization

Nitrogen oxides are important trace gases that influence the concentrations of atmospheric oxidants that drive tropospheric and stratospheric chemistry. Triple oxygen isotopes ($\Delta^{17}O$ values; deviation of $^{17}O$ from the mass dependent fractionation line) have been used to understand complex chemical systems such as the cycling and oxidation of NOx. For example, $\Delta^{17}O$ valuesof atmospheric nitrate ($HNO_3$, $NO_3^-$, and p-$NO_3^-$), indicates the proportion of NOx that reacts with ozone ($O_3$) during its oxidation (Michalski *et al.*, 2003; Tsunogai *et al.*, 2010; Nelson et al., 2018). $\Delta^{17}O$ values of atmospheric nitrous acid (HONO; recognized as a potentially important source of OH radicals) have also been used recently to decipher their production pathways. In these studies, however, predicted $\Delta^{17}O$ values were used for $NO_2$. Here, we tried to establish a method to determine $\Delta^{17}O$ values of atmospheric $NO_2$.

$\Delta^{17}O$ value of $NO_2$ was determined, together with $\Delta^{17}O$ value of HONO, by combining sensitive determination method on isotope compositions of $NO_2^-$(Komatsu *et al.*, 2008; Tsunogai *et al.*, 2010) with a slightly modified filter-pack method (Noguchi *et al.*, 2007), in which both $NO_2$ and HONO were collected simultaneously as $NO_2^-$on triethanolamine (TEA)-coated filter and alkaline ($K_2CO_3$) impregnated filter, respectively. Periodical sampling of atmospheric $NO_2$ and HONO was carried out at Hokkaido Institute of Environmental Sciences, Sapporo and at Nagoya University, which is located in a suburban area of Nagoya City. The sample collection period was fixed to one week with a flow rate of 10 L/min. In order to determine diurnal variation in $\Delta^{17}O$ value of $NO_2$ and HONO, an automated system for time-interval air sampling equipped with 6 four-stage-filter-packs were made and used it to collect atmospheric samples every 4 hours.The $\Delta^{17}O$ values of $NO_2$ and HONO showed similar diurnal variations; higher value on the day time than the night time. The result suggests that the atmospheric HONO is formed mainly by chemical reaction of NOx in the urban atmosphere.

Keywords: nitrogen oxides, troposphere, triple oxygen isotope

©2019. Japan Geoscience Union. All Right Reserved. 

# Long-term measurements of the column-averaged mixing ratios of tropospheric substances related to the air pollution using ground-based FTIRs at Rikubetsu, Japan

*Tomoo Nagahama[1], Isamu Morino[2], Shingo Nakanishi[1]

1. Institute for Space-Earth Environmental Research, Nagoya University, 2. National Institute for Environmental Studies

Air pollutants originating from carbon compounds such as reactive volatile organic compounds (VOCs) cause a serious degrading of the air quality near their sources. In addition, these are transported to remote areas with chemical composition changes, and affect air quality in urban areas and their surrounding areas, and therefore, are one of major issues in preserving the air quality. Especially, HCHO and HCOOH originating from forest fires and biogenic VOCs are distributed near their sources since their chemical lifetime is within a few days, and therefore, their distributions and time variations are one of important keys in associating the sources with the impact to the global environment. In order to understand the characteristics of long-term variation of the air quality and its influence on the global environment, the temporal variation of tropospheric substances related to the air pollution are measured with ground-based Fourier Transform InfraRed (FTIR) instrument (Bruker IFS120M and IFS120/5HR) installed at Rikubetsu observatory in Hokkaido, Japan. The cooperative measurements of solar absorption spectra using the FTIRs are conducted by the Institute for Space-Earth Environmental Research (ISEE) of Nagoya University and the National Institute for Environmental Studies (NIES) since 1995. The spectrum is obtained in a 3-15 $\mu$m band with a resolution of 0.0035 $cm^{-1}$. The vertical distribution of trace gases in troposphere and stratosphere is retrieved from the measured spectrum by using the SFIT4 (version 0.944) software. Using SFIT4, we have retrieved the total column amounts and tropospheric column-averaged mixing ratio of $O_3$, $CH_4$, $C_2H_6$, N2O, CO, HCN, HCHO, HCOOH, $C_2H_2$, $CH_3OH$, and find their seasonal and long-term variations from 1995 to 2018. The observed tropospheric column-averaged mixing ratios of $O_3$, $C_2H_6$ and CO show the maximum in March and April, although that of HCHO peaks in July and that of HCN is in May and August, respectively. These differences among the substances may reflect the source and sink processes. Especially, HCHO having a short lifetime may reflect oxidation of biogenic VOCs in summer as well as forest fires.
In the presentation, we will report the detailed features of temporal variations of these substances in troposphere and will discuss its influence on the global environment.

Keywords: Air pollutants, Column-averaged mixing ratio, Infrared spectroscopy, Seasonal variation, Long-term trend

©2019. Japan Geoscience Union. All Right Reserved. 

# Impacts of Biogenic and Anthropogenic Emissions on Summertime Ozone Formation in the Guanzhong Basin, China

*Nan Li[1]

1. Nanjing University of Information Science & Technology

This study is the first attempt to understand the synergistic impact of anthropogenic and biogenic emissions on summertime ozone ($O_3$) formation in the Guanzhong (GZ) basin where Xi’ an, the oldest and the most populous city (with a population of 9 million) in the northwest China, is located. Month-long (August 2011) WRF-Chem simulations with different sensitivity experiments were conducted and compared with near-surface measurements. Biogenic volatile organic compounds (VOCs) concentrations were characterized from 6 surface sites among the Qinling Mountains, and urban air composition was measured in the Xi’ an city at a tower 100 m above the surface. The WRF-Chem control experiment reasonably reproduced the magnitudes and variations of observed $O_3$, VOCs, $NO_x$, $PM_{2.5}$ and meteorological parameters, with normalized mean biases for each parameter within ±21%. Subsequent analysis employed the factor separation approach (FSA) to quantitatively disentangle the pure and synergistic impacts of anthropogenic and/or biogenic sources on summertime $O_3$ formation. The impact of anthropogenic sources alone was found to be dominant for $O_3$ formation. Although anthropogenic particles reduced $NO_2$ photolysis by up to 60%, the anthropogenic sources contributed 19.1 ppb $O_3$ formation on average for urban Xi’ an. The abundant biogenic VOCs from the nearby forests promoted $O_3$ formation in urban areas by interacting with the anthropogenic $NO_x$. The calculated synergistic contribution (from both biogenic and anthropogenic sources) was up to 14.4 ppb in urban Xi’ an, peaking in the afternoon. Our study reveals that the synergistic impact of individual source contributions to $O_3$ formation should be considered in the formation of air pollution control strategies, especially for big cities in the vicinity of forests.

Keywords: ozone, biogenic volatile organic compounds, WRF-Chem

©2019. Japan Geoscience Union. All Right Reserved. 

# Comprehensive monitoring project of greenhouse gases and air pollutants around Jakarta megacity in Indonesia

*Masahide Nishihashi[1], Hitoshi Mukai[1], Yukio Terao[1], Shigeru Hashimoto[1], Rizaldi Boer[2], Muhammad Ardiansyah[2], Bregas Budianto[2], Gito Sugih Immanuel[2], Adi Rakhman[2], Rudi Nugroho[3], Nawa Suwedi[3], Agus Rifai[3], Iif Miftahul Ihsan[3], Anies Marufatin[3], Albert Sulaiman[3], Dodo Gunawan[4], Eka Suharguniyawan[4], Asep Firman Ilahi[4], Muharam Syam Nugraha[4], Ronald Christian Wattimena[4], Bayu Feriaji[4], Thomas Lauvaux[5], Tomohiro Oda[6]

1. National Institute for Environmental Studies, 2. Bogor Agricultural University (IPB), Indonesia, 3. Agency for the Assessment and Application of Technology (BPPT), Indonesia, 4. Meteorological, Climatological, and Geophysical Agency (BMKG), Indonesia, 5. Laboratory for Sciences of Climate and Environment (LSCE), France, 6. Universities Space Research Association/NASA Goddard Space Flight Center, USA

The emission increases of greenhouse gases (GHGs) and air pollutants in megacities have been recognized as one of the important issues as a concern for health and climate change. Jakarta, the capital city of Indonesia, including suburban cities (Bogor, Depok, Tangerang, and Bekasi; locally known as “Jabodetabek”), has a population of 32 million people and has been listed as the second largest megacity in the world and the largest megacity in Southeast Asia. Several air quality monitoring campaigns were conducted in Jakarta. However, previous studies lacked continuous high-accuracy monitoring stations due to the limitations of environmental monitoring budgets and experts. We present here a new interdisciplinary project to expand our current understanding of the interactions between emissions, air quality, and regional/global climates.

To estimate the amount of anthropogenic emissions from Jakarta megacity and compare with city activities, we developed a ground-based comprehensive monitoring system of GHGs and air pollutants controlled remotely in addition to automated start-and-stop operations during power failures. Monitoring systems were installed at Bogor (center of Bogor city), Serpong (Jakarta suburb), and Cibeureum (mountainous area) in 2016–2017. Each monitoring system consists of system control/data acquisition units controlling multiple instruments and collecting continuously and continuous monitoring instruments of $CO_2$, $CH_4$, CO, $NO_x$, $SO_2$, $O_3$, aerosol concentrations ($PM_{2.5}$, $PM_{10}$, BC) and the chemical components ($NO_3^-$, $SO_4^{2-}$) of $PM_{2.5}$ and $PM_{10}$, and meteorological parameters. Flask sampling of air is also performed automatically once a week to analyze $N_2O$, $SF_6$, and carbon isotopes ($^{13}C$, $^{14}C$) in $CO_2$ in NIES and to validate the continuous measurement data of $CO_2$, $CH_4$, and CO.

The results show that the daytime values of $CO_2$, three hours averages from 12 to 15 local time, at Bogor and Serpong are 6.8 and 7.1 ppm higher than Cibeureum, respectively. These features are also presented in the other species, i.e., CO, $NO_x$, $SO_2$, $PM_{2.5}$, $PM_{10-2.5}$, and BC. Moreover, we found 5–10 ppm lower values of $CO_2$ during daytime at Bogor and Serpong in December and January, mid-rainy season in Jakarta, compared with the other months and frequent and extremely high $CH_4$ enhancements during nighttime (i.e., 3 to 5 ppm) at Serpong.

We present here the temporal variability observed at three monitoring sites and some preliminary results based on high-resolution $CO_2$ simulations using Weather Research and Forecasting model coupled to Chemistry (WRF-Chem).

Keywords: greenhouse gases, air pollutants, urban monitoring, Indonesia

©2019. Japan Geoscience Union. All Right Reserved. 

# Seasonality of short-term variations in atmospheric $CH_4$ observed at Hateruma and relationship with the reginal emissions from East Asia

*Yasunori Tohjima[1], Jiye Zeng[1], Tomoko Shirai[1], Akihiko Ito[1], Motoki Sasakawa[1], Toshinobu Machida[1]

1. National Institute for Environmental Studies

National Institute of Environmental Studies (NIES), Japan, has been carrying out in-situ observation of atmospheric $CH_4$ at Hateruma Island (HAT; lat. 24.1˚N, long. 123.8˚E) since 1996 by using a gas chromatographic system. Since HAT is in the marginal region of the East Asia, air masses from the continental region would cause elevated concentrations of a variety of species including $CH_4$. Such events were often observed especially during late autumn to early spring due to the Asian monsoon. In the previous studies, we revealed a secular increase in the short-term variations of $CH_4$ and its relationship with the emission increase from the continental China. Here, we examined the seasonality of the short-term variations of $CH_4$ in 1996 to 2017. First, we computed the increment of the hourly $CH_4$ ($\Delta CH_4$) over the baseline, which was the smoothed averages of $CH_4$ below the 20 percentile in a 101-hour moving time-window. Then the standard deviation of $\Delta CH_4$ for each month of each year was computed. The average monthly standard deviations of $\Delta CH_4$ show rather stable values in winter (November-February, 18~20 ppb), peaks in May (28 ppb) and September (26 ppb), and a dip in July (11 ppb). We simulated $\Delta CH_4$ by a Lagrangian particle dispersion model (LPDM) using the monthly $CH_4$ emission maps of Patra et al. (2009) and EDGAR v4.3.2, respectively. Although the monthly variability of the simulated $\Delta CH_4$ based on the Patra et al. (2009) emission maps well reconstructed the observed pattern of the monthly standard deviations, that based on the EDGAR v4.3.2 emission maps showed a maximum in March, which was not consistent with the observed pattern. The simulated maximum variability in March is related to the emission peak in March of the EDGAR v4.3.2 inventory, which is attributed to the maximum emissions from agricultural and livestock sectors. The lack of the spring peak in the observation suggests that the anthropogenic $CH_4$ emission in March of EDGAR v4.3.2 may be overestimated.

Keywords: atmospheric CH4, short-term variation, LPDM

©2019. Japan Geoscience Union. All Right Reserved. 

# A cryogen-free automated measurement system of stable carbon isotope ratio of atmospheric methane

*Taku Umezawa[1], Takuya Saito[1]

1. National Institute of Environmental Studies

Methane is an important greenhouse gas emitted from both natural and anthropogenic sources. Accurate understanding of various methane sources is needed for effective reduction of its emissions. Measurement of stable carbon isotope ratio of atmospheric methane is useful for top-down evaluation of relative contributions of various types of methane sources, because individual methane sources have characteristic isotope signatures. Isotope ratio data for atmospheric methane therefore receive increasing attention for constraining the global methane budget. To meet research community demand, it is imperative for measurement systems to achieve adequate precision and traceability as well as high measurement throughput to process number of air samples that are routinely shipped from monitoring sites to laboratory. Stable carbon isotope ratio has been measured by continuous-flow isotope ratio mass spectrometry where methane in sample air is preconcentrated in a trap filled with an adsorbent cooled by liquid nitrogen. By using a stirring cooler instead, we set up a cryogen-free measurement system, and our configuration attained reproducibility of ~0.1 per mil. This precision is comparable to those previously achieved by using liquid nitrogen; our system is however advantageous for unattended and automated measurement operation. We examined measurements for air sampled outside our laboratory, and the preliminary measurement data at ~1-hour intervals show a clear diurnal variation.

Keywords: Methane, Stable carbon isotope ratio

©2019. Japan Geoscience Union. All Right Reserved. 

# Global inverse analysis of $CH_4$ fluxes using NICAM-TM 4D-Var

*Yosuke Niwa[1,2], Akihiko Ito[1], Toshinobu Machida[1], Motoki Sasakawa[1], Yasunori Tohjima[1], Taku Umezawa[1], Shinji Morimoto[3], Shuji Aoki[3], Yousuke Sawa[2], Kazuhiro Tsuboi[2], Hidekazu Matsueda[2], Ed Dlugokencky[4], Christina Harth[5], Paul B Krummel[6], Ray L Langenfelds[6], Zoe M Loh[6], Jens Mühle[5], Simon O'Doherty[7], Ronald G Prinn[8], Michel Ramonet[9], Peter Salameh[5], Colm Sweeney[4], Ray Weiss[5], Dickon Young[7], Simona Castaldi[10,11], Sergio Noce[12], Marielle Saunois[9], Ann R Stavert[13]

1. National Institute for Environmental Studies, 2. Meteorological Research Institute, 3. Tohoku University, 4. Earth System Research Laboratory, National Oceanic and Atmospheric Administration, 5. Scripps Institution of Oceanography, University of California, 6. Climate Science Centre, CSIRO Oceans and Atmosphere, 7. School of Chemistry, University of Bristol, 8. Massachusetts Institute of Technology, 9. Laboratoire des Sciences du Climat et de l'Environnement, LSCE-IPSL (CEA-CNRS-UVSQ), 10. DISTABIF, Università degli studi della Campania Luigi Vanvitelli, 11. Department Landscape Design & Sustainable Ecosystems RUDN University, 12. IAFES, Euro-Mediterranean Center on Climate Change, 13. Global Carbon Project, CSIRO Oceans and Atmosphere

Atmospheric methane ($CH_4$) is the most important greenhouse gas after carbon dioxide. Because $CH_4$ has a relatively short lifetime due to chemical losses in the atmosphere, it is expected that reducing $CH_4$ emissions would mitigate global warming in a relatively short timeframe. However, sources of atmospheric $CH_4$ are associated with a wide variety of processes such as fossil fuel production and consumption, agriculture, natural wetlands, and biomass burning, and our understanding of the full $CH_4$ budget is limited. To better understand $CH_4$ sources, an inverse analysis is one prominent methodology that estimates spatiotemporal variations of $CH_4$ sources consistent with their prior estimates and atmospheric observations within specified uncertainties. In this study, we performed a long-term inverse analysis of $CH_4$ fluxes with an inversion system named NICAM-TM 4D-Var (Niwa et al., 2017a,b). The inversion system is based on the atmospheric transport model NICAM-TM (Niwa et al., 2011), which has a homogeneous icosahedral grid system and mass conserving property. The horizontal model grid resolution was set to 223 km and the $CH_4$ flux estimation was performed at the same resolution, though some spatial error correlations were introduced. The prior flux dataset includes wetland/rice cultivation emission and soil uptake estimated by the terrestrial ecosystem model VISIT (Ito and Inatomi, 2012). The other emission categories are provided from the ongoing Global Carbon Project (GCP)–$CH_4$. In the inversion, several emission categories are separately estimated according to their seasonal and interannual variabilities. Compared with the prior estimates, the inverse analysis with ground-based station data estimated smaller emissions from East Asia and Europe, larger and smaller northern summer emissions from West Siberia and Hudson Bay Lowlands, respectively, and larger emissions from Bengal and Indochina areas. These changes estimated by the inversion are attributed to emissions from anthropogenic categories (mainly fossil fuel related), natural wetlands, and rice cultivation, respectively. The presentation will also address the reliability of the inversion estimates using independent aircraft data and examine the independence of each category emission estimate.

## References

Niwa et al. (2011), Journal of the Meteorological Society of Japan. Ser. II, 89(3), 255–268.
Ito and Inatomi (2012), Biogeoscience, 9:759-773.
Niwa et al. (2017a), Geoscientific Model Development, 10(3), 1157–1174.
Niwa et al. (2017b), Geoscientific Model Development, 10(6), 2201–2219.

©2019. Japan Geoscience Union. All Right Reserved. 

Acknowledgement
This study is supported by the Environment Research and Technology Development Fund (2-1701) of the Ministry of the Environment, Japan. The authors acknowledge the Global Carbon Project–$CH_4$ for providing the prior flux dataset, some of which is made under the support of the RUDN project "5-100". The authors also acknowledge Doug Worthy of Environmental Canada, Juha Hatakka of Finnish Meteorological Institute, Camille Yver Kwok of Laboratoire des Sciences du Climat et de l’ Environnement, Sebastien Conil of Andra, and Kazuyuki Saito and other members of Japan Meteorological Agency for providing observational data of atmospheric $CH_4$. This study used observational data of Advanced Global Atmospheric Gases Experiment (AGAGE). Operations of the AGAGE network are principally supported by the NASA Upper Atmospheric Research Program in the US, by the Department for Business, Energy & Industrial Strategy (BEIS) in the UK, by the Commonwealth Scientific and Industrial Research Organization (CSIRO) and the Bureau of Meteorology (Australia) in Australia, with additional support from the National Oceanographic and Atmospheric Administration (NOAA) in the US. Yosuke Niwa sincerely thanks the members of the NICAM team for developing and maintaining the codes of NICAM.

Keywords: methane, inverse analysis

©2019. Japan Geoscience Union. All Right Reserved. 

# Scientific findings from observations of GOSAT/TANSO–FTS TIR band

*Naoko Saitoh[1], Shingo Kosaka[1], Masato Shiraki[1], Hinako Kobayashi[1]

1. Center for Environmental Remote Sensing

Greenhouse Gases Observing Satellite (GOSAT) has continued its observations of greenhouse gases for more than 10 years since its launch on 23 January 2009. The thermal infrared (TIR) band of the Thermal and Near Infrared Sensor for Carbon Observation (TANSO)–Fourier Transform Spectrometer (FTS) on board GOSAT has observed concentrations of $CO_2$, $CH_4$ and other greenhouse gases in several atmospheric layers. In the latest TANSO–FTS TIR Level 2 retrieval algorithm, Version 1 (V1), ozone, water vapor, and temperature have been retrieved as by-products of the $CO_2$ and $CH_4$ products (Saitoh et al., 2016). We have already evaluated the data quality of the TANSO–FTS TIR V1 $CO_2$ and $CH_4$ products (Saitoh et al., 2016, 2017; Holl et al., 2016; Zou et al., 2016; Olsen et al., 2017). We applied the evaluated bias-correction values to the TANSO–FTS TIR V1 $CO_2$ data and compared variations in concentrations of the TIR $CO_2$ data with those of Measurement Of Pollution In The Troposphere (MOPITT) CO data [Deeter et al., 2014] in upper troposphere over the northern Africa. The comparison result showed that both TANSO–FTS TIR $CO_2$ and MOPITT CO concentrations became larger there almost at the same time in March through May, which suggests air mass with high CO and $CO_2$ emitted due to biomass burning was transported to upper atmosphere. As TANSO–FTS TIR V1 $CH_4$ profiles generally agreed with aircraft $CH_4$ profiles to within ~1% in the troposphere in low and middle latitudes, we analyzed seasonal variations in $CH_4$ concentrations in each altitude layer over India by using the TIR V1 $CH_4$ data. Our results were similar to the results reported in Chandra et al. (2017), but showed larger impact of $CH_4$ variations in lower troposphere on seasonal variations in $XCH_4$ concentrations. We have conducted validation analysis of TANSO–FTS TIR $O_3$ profiles simultaneously retrieved with the TIR V1 $CO_2$ product using Atmospheric Chemistry Experiment (ACE)–FTS and ozonesonde data. Although there was slightly high bias in the TANSO–FTS TIR $O_3$ data in the lower troposphere in summer, they showed better agreements with ACE–FTS and ozonesonde data than their a priori data taken from MacPeters et al. (2007). The TANSO–FTS TIR $O_3$ data in the lowest retrieval layer (surface–857 hPa) showed clear enhancements in $O_3$ concentrations over Mainland China compared to eastern Japan, which could demonstrate the detectability of tropospheric pollutants by the TANSO–FTS TIR band.

Keywords: CO2, CH4, ozone, GOSAT/TANSO-FTS

©2019. Japan Geoscience Union. All Right Reserved. 

# Continuous measurements of atmospheric $CO_2$ and its $\delta^{13}C$ and $\delta^{18}O$ at Minamitorishima Island

*Shohei Murayama[1], Kazuhiro Tsuboi[2], Shigeyuki Ishidoya[1], Hidekazu Matsueda[2], Yosuke Niwa[3], Yousuke Sawa[2], Kentaro Ishijima[2], Kentaro Kozumi[4], Genta Umezawa[4], Kazuya Yukita[4], Shigeharu Nishida[4], Megumi Yamamoto[4], Tetsuyuki Usami[1], Shinji Morimoto[5]

1. National Institute of Advanced Industrial Science and Technology (AIST), 2. Meteorological Research Institute, 3. National Institute for Environmental Studies, 4. Japan Meteorological Agency, 5. Tohoku University

The Minamitorishima (MNM; 24°17’ N, 153°59’ E) station is uniquely located to monitor background air at northern mid latitudes; the site is located on a remote coral island in the western North Pacific, about 1,950 km southeast of Tokyo. The Japan Meteorological Agency has been making long-term continuous observations of atmospheric concentrations of major greenhouse gases at MNM. For a better understanding of mechanisms governing the observed $CO_2$ variation, systematic measurements of atmospheric $CO_2$ and its $\delta^{13}C$ and $\delta^{18}O$ have been carried out at MNM by analyzing discrete flask air samples taken at the site since 2011. The existing measurement program was enhanced by initiating continuous measurements of $CO_2$ and its $\delta^{13}C$ and $\delta^{18}O$ using a laser spectroscopy (Off-Axis Integrated-Cavity Output Spectroscopy) in March 2018.

Sample air is drawn from an air intake mounted on a tower at 20-m height above the ground surface, and introduced into a continuous isotope analyzer (Model CCIA-48, Los Gatos Research) after removing water vapor and aerosol particles. The analyzer is calibrated hourly for the concentrations of each $CO_2$ isotopologue, using 3 air-based $CO_2$ standard gases with isotopic ratios of industrial $CO_2$ and different total $CO_2$ concentrations. The isotopic ratios of these standards were determined by a mass spectrometer, and the concentrations of each $CO_2$ isotopologue of the standards were obtained from the isotopic ratios. The total $CO_2$ concentration and its $\delta^{13}C$ and $\delta^{18}O$ of sample air are calculated from the measured concentrations of each isotopologue.

The obtained $CO_2$ isotopic data are scattered, and the precisions of the $\delta^{13}C$ and $\delta^{18}O$ values measured by this analyzer estimated from hourly measurements of a target gas, which is dried natural air compressed into a 48-L gas cylinder, are about 10 times and 5 times worse than those achieved by our mass spectrometer, respectively. However, the daily mean values of atmospheric $\delta^{13}C$ and $\delta^{18}O$ show day-to-day variations in concert with those of the total $CO_2$ concentration and prominent seasonal variations. The daily mean $\delta^{13}C$ and $\delta^{18}O$ show systematic difference from the isotopic values obtained from flask sampling on the same day. However, since the differences are almost constant, the nature of the variations are very similar in both cases.

In this presentation, results of the preliminary analyses of the daily mean $CO_2$, $\delta^{13}C$ and $\delta^{18}O$ data obtained from the continuous measurement will be presented. From comparison with the flask sampling results, the effectiveness of the continuous measurement will also be discussed.

Acknowledgements

We would like to thank A. Kudo and C. Abe for their technical support for our measurements. This

©2019. Japan Geoscience Union. All Right Reserved. 

research was supported by a grant for the Global Environmental Research Coordination System from the Ministry of the Environment, Japan.

Keywords: Carbon dioxide, Stable isotopic ratio, Minamitorishima Island, Continuous measurement

©2019. Japan Geoscience Union. All Right Reserved. 

# Variations of atmospheric Radon-222 concentration observed at JMA stations

*Kentaro Ishijima[1], Kazuhiro Tsuboi[1], Hidekazu Matsueda[1], Yousuke Sawa[1], Yosuke Niwa[2,1], Takashi Maki[1], Takashi Nakamura[3]

1. Meteorological Research Institute, 2. National Institute for Environmental Studies, 3. Japan Meteorological Agency

Japan Meteorological Agency (JMA) has been operating several stations to monitor atmospheric greenhouse gases since the late 1980s under the Global Atmosphere Watch programme of the World Meteorological Organization (WMO/GAW). They show synoptic, seasonal, interannual variations, and trends due to changes in atmospheric transport and source/sink strength. To know their transport from land regions, we started the monitoring of atmospheric Radon-222 ($^{222}$Rn) in the 2000s at the JMA stations. Because $^{222}$Rn is emitted from almost only lands and chemically inert, it is useful to identify temporal variability of atmospheric greenhouse gases due to sources/sinks on land. $^{222}$Rn also radioactively decays with the half-life of 3.8 days, so is widely utilized to validate regional transport of atmospheric transport model through the model-observation comparisons. Understanding such transport process is also supported by using an atmospheric transport model. We have just started to use a newly developed on-line atmospheric tracer transport model (GSAM-TM). The tracer transport process is driven by a low-resolution version (TL95) of JMA's operational global numerical weather prediction model (GSAM).
In this study, we analyze the observed and model simulated atmospheric $^{222}$Rn concentration, to understand the transport process of land-origin atmospheric tracer as well as to validate the GSAM-TM. For example, the model well reproduces high $^{222}$Rn peaks, which are frequently observed at Minamitorishima (MNM; 24.28˚N, 153.98˚E) and Chichijima (CCJ; 27.09˚N, 142.19˚E) in winter to spring. Especially in winter, there are many cases that a high peak is first observed at CCJ and one day after at MNM. They are mainly produced by a cold front moving eastward with dense $^{222}$Rn behind the frontal line. The peak height at MNM is about two-thirds of that at CCJ. It is slightly smaller than that expected from decay by the 3.8 days half-life (about four-fifths), because dense $^{222}$Rn trapped by the front is diluted mainly by diffusion while transported. The model also well reproduces such peak attenuation degree. More details and results of $^{222}$Rn-age tracer simulations as well as of other JMA station will also be discussed in our presentation.

*Acknowledgements.* We sincerely thank all members of the JMA for operating $^{222}$Rn measurement systems at JMA monitoring stations

Keywords: radon, GSAM-TM

©2019. Japan Geoscience Union. All Right Reserved. 

# Long-term variations of CFCs and HCFCs observed with ground-based FTIR spectrometers at Rikubetsu, Syowa Station, and Tsukuba since 1995

*Hideaki Nakajima[1,2], Masanori Takeda[2,1], Isao Murata[2], Takafumi Sugita[1], Tomoo Nagahama[3], Isamu Morino[1], Takeshi Kinase[4]

1. National Institute for Environmental Studies, 2. Graduate School of Environmental Studies, Tohoku University, 3. Institute for Space-Earth Environmental Research, Nagoya University, 4. Meteorological Research Institute

We have been observing atmospheric minor constituents with ground-based Fourier-Transform InfraRed spectrometer (FTIR) at Rikubetsu (43.5N, 143.8E) since 1995, at Syowa Station, Antarctica (69.0S, 39.6E) in 2007, 2011, and 2016 with Bruker IFS-120M, and at Tsukuba (36.1N, 140.1E) since 2018 with Bruker IFS-125HR. We have analyzed vertical profiles and total columns of CFC-11, CFC-12, and HCFC-22 with SFIT4 retrieval algorithm. Production and consumption of CFCs and HCFCs have been regulated under the Montreal Protocol since 1987. Substitution to HCFCs and HFCs which do not destroy ozone layer is underway. However, illegal production of CFC-11 somewhere in Asia was recently reported (Montzka et al., Nature, 2018). Monitoring of these gases are possible not only by ground-based gas-chromatogram/mass-spectroscopy technique, but also by infrared spectroscopic measurements. Ground-based FTIR measurement has a capability to monitor multiple gas species simultaneously with vertical profile information for some gases. We retrieved vertical profiles and column amounts of CFC-11, CFC-12, and HCFC-22 since 1995 from FTIR spectra. Figure 1 shows total column amounts of HCFC-22 since 1995, while Figure 2 shows partial column amounts of HCFC-22 between 0 and 8 km. Seasonal variation which are seen in Figure 1 might be due to the change of tropopause height. However, it is removed in partial column amount in Figure 2. Trajectory calculation results of CFC-11 and other gases will be presented at the meeting.

Keywords: CFC, HCFC, FTIR

©2019. Japan Geoscience Union. All Right Reserved. 

Figure 1

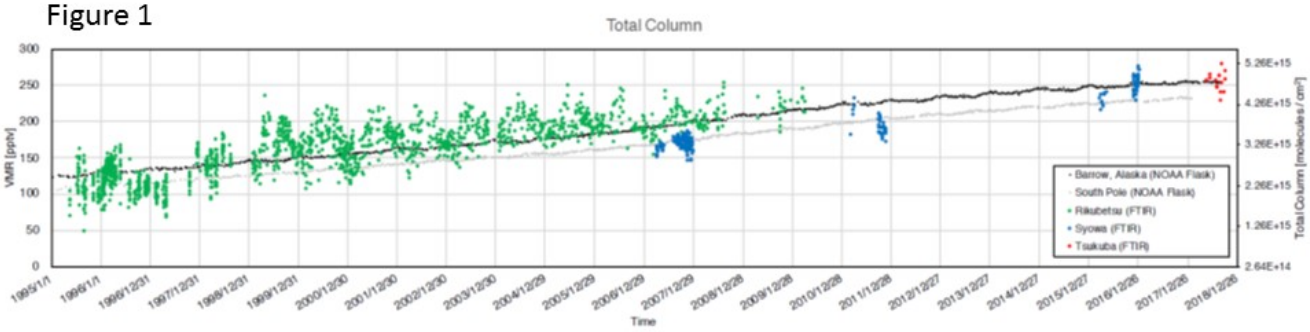


Figure 2

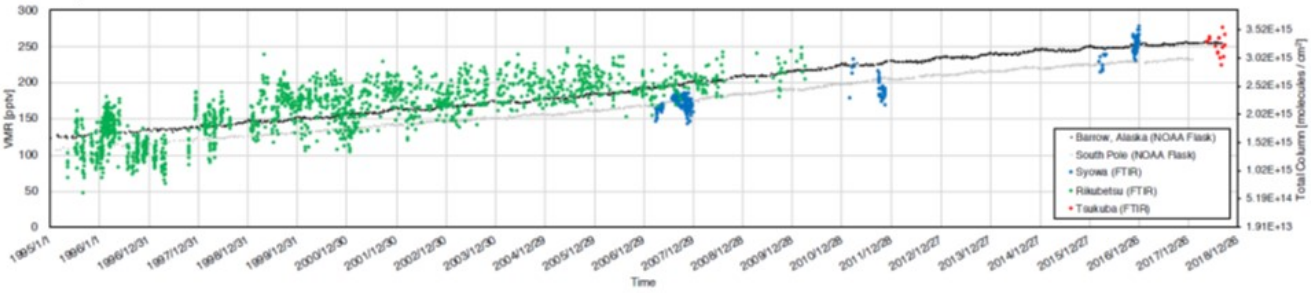


©2019. Japan Geoscience Union. All Right Reserved. 

# Millimeter-wave observation of stratospheric ozone in 2015-2017 in Rio Gallegos at the southern tip of South America

*Akira Mizuno[1], Hironori Seki[1], Tomoo Nagahama[1], Hirofumi Ohyama[2], Jacobo Salvador[3], Facundo Orte[3], Elian Walfram[3]

1. Institute for Space-Earth Environmental Research, Nagoya University, 2. National Institute for Environmental Studies, 3. Laser and Applications Research Center, UNIDEF (CITEDEF-CONICET)

We had been carried out a trilateral international collaboration among Japan, Chile, and Argentina called SAVER-Net (South American Environmental Risk Management Network) project for five years under the JST-JIICA SATREPS program. The major aim of the project was establishing an observation network of UV/ozone and aerosols over Chile and Argentina where was a blank area of the measurement stations on a global scale. The southern tip region of South America is the southernmost habitable area in the world, and the local residents in this region directly suffers from the influence of ozone hole that sometimes overpasses the region. Although the project was terminated in March 2018, we continue collaboration to develop forecast system of ozone hole and UV indices.

In this presentation, we will report the results of ozone observation by using a millimeter-wave spectrometer installed at the atmospheric observatory in southern Patagonia (OAPA) in Rio Gallegos, Argentina. The observation period was from April 2015 to March 2016 and September 2016 to August 2017, and we obtained ~ 9,400 1-hour averaged vertical profiles. We compared the time series of ozone volume mixing ratio (VMR) profile obtained in September and October when the ozone hole passes over the southern tip with the meteorological parameters, such as atmospheric temperature, potential temperature, and potential vorticities that are derived from MERRA-2 reanalysis data. As a result of the comparisons, we revealed that

・Ozone VMRs and the absolute value of potential vorticities show a good correlation below ~ 1000 K in potential temperature corresponding to ~ 35 km in altitude.

・As the ozone hole reaches above Rio Gallegos, atmospheric temperature decreases around ~ 25 km due to the horizontal advection of cool air in the polar vortex, and the temperature above ~35 km increases due to atmospheric descent inside of the polar vortex,

and we can use these quantities to easily distinguish whether Rio Gallegos is located at inside or outside of the ozone hole.

We will also present more detailed results about the ozone hole activities in 2015 and 2016.

Keywords: ozone hole, millimeter-wave spectroscopy, South America, polar vortex

©2019. Japan Geoscience Union. All Right Reserved. 

[J] Oral | A (Atmospheric and Hydrospheric Sciences)：A-AS Atmospheric Sciences, Meteorology & Atmospheric Environment

Thu. May 30, 2019 3:30 PM - 5:00 PM JST | Thu. May 30, 2019 6:30 AM - 8:00 AM UTC | 103 1F

## [A-AS04] Atmospheric Chemistry

convener:Tomoki Nakayama(Graduate School of Fisheries and Environmental Sciences, Nagasaki University), Yoko Iwamoto(Graduate School of Biosphere Science, Hiroshima University), Sakae Toyoda(Department of Chemical Science and Engineering, Tokyo Institute of Technology), Nawo Eguchi(Kyushu University), Chairperson:Hideaki Nakajima(国立環境研究所)

This session provides a forum for the presentation of the broad spectrum of tropospheric and stratospheric chemistry, including various research topics (e.g., dynamical processes, air quality and climate), approaches (modeling, field measurements, remote sensing, and laboratory studies), and species (gas and aerosol). This session also provides an opportunity for discussing possible future collaboration with other research fields relevant to atmospheric chemistry. We strongly encourage authors to prepare presentation slides and a poster in English.

3:30 PM - 4:00 PM JST | 6:30 AM - 7:00 AM UTC

[AAS04-28] Planetary atmosphere - Mars and Venus -

★Invited Papers

*Hiroyuki Maezawa[1] (1.Department of Physical Science Osaka Prefecture University)

---

4:00 PM - 4:15 PM JST | 7:00 AM - 7:15 AM UTC

[AAS04-29] Validation of methane profile observed with FTIR at Tsukuba

Yuki Dai[2], *Isao Murata[1], Hideaki Nakajima[3], Isamu Morino[3] (1.Graduate School of Environmental Studies, Tohoku University, 2.Graduate School of Science, Tohoku University, 3.National Institute for Environmental Studies)

---

4:15 PM - 4:30 PM JST | 7:15 AM - 7:30 AM UTC

[AAS04-30] **Retrieval of HFC-23 from FTIR observations at Syowa Station, Rikubetsu and Tsukuba**

*Masanori Takeda[1,2], Hideaki Nakajima[2,1], Isao Murata[1], Tomoo Nagahama[3], Isamu Morino[2] (1.Graduate School of Environmental Studies, Tohoku University, 2.Center for Global Environmental Research, National Institute for Environmental Studies, 3.Institute for Space-Earth Environmental Research, Nagoya University)

---

4:30 PM - 4:45 PM JST | 7:30 AM - 7:45 AM UTC

[AAS04-31] Roles of cloud distribution in global atmospheric photochemistry

*Ryoki Matsuda[1], Kengo Sudo[1,2] (1.Graduate School of Environmental Studies, Nagoya University , 2.Japan Marine-Earth Science and Technology)

---

4:45 PM - 5:00 PM JST | 7:45 AM - 8:00 AM UTC

[AAS04-32] Evaluating global distribution and interannual variation of stratosphere-troposphere exchange of ozone: impacts of climate variabilities

*Kengo Sudo[1,2], Xin Li[1] (1.Graduate School of Environmental Studies, Nagoya University, 2.Research and Development Center for Global Change, JAMSTEC)

# Planetary atmosphere - Mars and Venus -

*Hiroyuki Maezawa[1]

1. Department of Physical Science Osaka Prefecture University

Recently, research on extraterrestrial planets and protoplanetary disks has been rapidly increasing. Mars and Venus, lacking intrinsic magnetic fields, are valuable research targets for further understanding atmospheric environments, habitability of earth-type planets, and the influence of activity of the central star on planetary atmospheres.

On Mars, methane has been detected and research continues to investigate its originand destruction processes by oxidation reaction networks in the atmosphere and on the surface. For an Earth-type planet with an atmosphere mainly of $CO_2$, the $CO_2$ is photo-dissociated into CO and oxygen by UV radiation from the sun. Mars and Venus have small percentages of CO and oxygen, and how they are oxidized back into $CO_2$ has not yet been fully elucidated. This is known as the “$CO_2$ stability problem”. Also, in order to understand the evolutionary processes of the Martian atmosphere, detailed and systematic observations of the spatial and temporal fluctuations of $H_2O$ and oxidants, including $H_2O_2$, $O_3$, $O_2$, etc., and their altitudinal distributions are important.

Venus experiences high-speed super-rotation winds at approximately the cloud altitude and day to night circulation at higher altitudes. Recently, for example, it has gradually become clear that the latter convection does not show a similar pattern in the morning and afternoon. In addition, the Akatsuki satellite (JAXA) has captured large-scale, bow-shaped patterns induced by atmospheric gravity waves. It is also important to investigate how the complex dynamics seen in the Venusian atmosphere drive material circulations and oxidation reaction networks including those with respect to minor species such as $SO_x$, $HO_x$, $CO_x$, chloride, aerosol, sulfuric acid, etc. Venus and Mars also provide important insights into how abiotically the biomarkers, $O_2$ and $O_3$, are formed in typical terrestrial planets with mainly $CO_2$ atmospheres.

In this talk, the observations of planetary atmospheres, explored via heterodyne spectroscopy with radio telescopes such as the Atacama Large Millimeter/submillimeter-wave Array (ALMA) interferometer, as well as measurements of various wavelengths with ground-based telescopes and satellites will be also discussed. Since the wavelengths of milli/submillimeter waves are comparatively long, they are less attenuated by absorption and scattering by aerosols/dust. In addition, the Doppler shift of the spectrum obtained with heterodyne spectroscopy provides important information about the velocity fields of the mesosphere and lower thermosphere. Also, regardless of the presence or absence of background light sources such as the sun heterodyne spectroscopy allows us to observe day and night-side atmospheres of planets.

Keywords: Planetary Atmosphere, Terrestrial planet, Solar System, Mars, Venus, Heterodyne Spectroscopy

©2019. Japan Geoscience Union. All Right Reserved. 

# Validation of methane profile observed with FTIR at Tsukuba

Yuki Dai[2], *Isao Murata[1], Hideaki Nakajima[3], Isamu Morino[3]

1. Graduate School of Environmental Studies, Tohoku University, 2. Graduate School of Science, Tohoku University, 3. National Institute for Environmental Studies

$CH_4$ is the second greenhouse gas and the concentration near the surface is increasing. But there are many emission sources and the increasing rate is varying year by year. The profile of $CH_4$ can be observed with a ground-based high-resolution Fourier transform spectrometer using spectral inversion analysis. However, the validation of the retrieved profile doesn't have been performed enough. Then, we compared some retrieval parameters and validated the retrieved tropospheric partial columns using aircraft sampling measurements.
We analyzed the spectra taken at Tsukuba between 2012 and 2017. SFIT4 spectral fitting program was used to derive the profiles from spectra in 3 micrometer region. $H_2O$ as interference species affects the accuracy of the retrieved $CH_4$ profiles. Two initial profiles of $H_2O$ are provided: monthly mean (v1) and daily analyzed (v5). Two kinds of microwindows for the retrieval are also provided according to Sussmann et al. (2011): 5 microwindows (5MW) and 3 microwindows (3MW). Fitting results were compared based on the root mean square residual (RMS) and degree of freedoms (DOFs). As a result, 5MWv1 is worse for both RNS and DOFs than other 3. Then, we compared the results of 5MWv5, 3MWv1, and 3MWv5 with aircraft sampling.
The monthly mean tropospheric partial columns integrated from 0 to 8 km were compared with those calculated from aircraft sampling observed by the center for atmospheric and oceanic studies, Tohoku University near Sendai from 2012 to 2017. When all derived partial columns were compared with aircraft results, all 3 cases (5MWv5, 3MWv1, and 3MWv5) showed 5 -10 % differences in summer when $H_2O$ concentration is high. But when the derived partial columns for which RMS is less than 0.15 were compared, all 3 cases agreed with aircraft results within the uncertainty besides for the -2.9 % bias.

Keywords: FTIR, Methane, Height profile, Accuracy

©2019. Japan Geoscience Union. All Right Reserved. 

# Retrieval of HFC-23 from FTIR observations at Syowa Station, Rikubetsu and Tsukuba

*Masanori Takeda[1,2], Hideaki Nakajima[2,1], Isao Murata[1], Tomoo Nagahama[3], Isamu Morino[2]

1. Graduate School of Environmental Studies, Tohoku University, 2. Center for Global Environmental Research, National Institute for Environmental Studies, 3. Institute for Space-Earth Environmental Research, Nagoya University

The Montreal Protocol on Substances that Deplete the Ozone Layer has successfully been regulated production and consumption of chlorofluorocarbons (CFCs) and global atmospheric CFCs concentration have kept decreasing. On the other hand, production and consumption of hydrochlorofluorocarbons (HCFCs) and hydrofluorocarbons (HFCs) as alternatives for CFCs are expanding up to the present. Especially, HFC-23 ($CHF_3$) which has very high global warming potential (100yr-GWP: 12,400) is generated as unavoidable by-product of HCFC-22 ($CHClF_2$) production and their emissions into atmosphere have been increasing relevant to production of HCFC-22. Observations of these gases are possible not only by in-situ gas-chromatogram/mass-spectroscopy systems, but also by infrared spectroscopic measurements. Ground-based Fourier Transform Infrared spectrometer (FTIR) has a capability to monitor multiple gas species simultaneously. In this study, we retrieved total column abundances and vertical profiles of HFC-23 from ground-based FTIR observations with the SFIT4 version 0.9.4.4 based on the optimal estimate method (Rodgers, 2000).
We operated atmospheric solar absorption measurements using ground-based FTIR instrument at Antarctic Syowa Station (69.0ºS, 39.6ºE) in 2007, 2011 and 2016. We used two micro-windows (MWs) of 1138.5-1148.0 $cm^{-1}$(MW1) and 1154.0-1160.0 $cm^{-1}$(MW2) in this study. As the spectroscopic parameters of HFC-23, the pseudo line lists produced by G. C. Toon (NASA/JPL) were used. For other interfering species, the line parameters from HITRAN2008 were used. Temperature and pressure vertical information from surface to 40 km a.s.l. were taken by the daily temperature and pressure profiles from NCEP (National Centers for Environmental Prediction) Reanalysis-1 dataset. Meteorological information above 40 km a.s.l. were adopted from the monthly climatological profiles from the COSPAR International Reference Atmosphere (CIRA-86) dataset. The HFC-23 a priori profile was taken fromthe simulated profile by Naik et al. (2000), but that was scaled to make the concentration of the lowest level equal to 20 pptv which is the approximate value of surface concentration in southern hemisphere in 2007. For $H_2O$ and its isotopologues, the a priori profiles were taken from independent preliminarily profile retrievals for each observed spectra. For other interfering species, 40 years (1980-2020) mean profiles of the monthly profiles provided from WACCM (Whole Atmosphere Community Climate Model) version 6 were used as a priori profiles. Figure 1 shows the timeseries of the FTIR-retrieved total columns of HFC-23. According to the error analysis, mean systematic and random errors on the HFC-23 retrievals were ~40% and ~10% to retrieved HFC-23 total column, respectively. The FTIR observation is practicable to estimate the trend of atmospheric HFC-23, because the random uncertainty is relatively small.
In addition, we performed retrievals of HFC-23 from FTIR spectra at Rikubetsu (43.46ºN, 143.77ºE) and Tsukuba (36.05ºN, 140.12ºE) in Japan in the same way as the retrieval strategy at Syowa Station. In the presentation, we will discuss on the differences of HFC-23 trends among these three FTIR sites, along with the trends of HCFC-22 from FTIR observations.

## References

Naik, V., Jain, A. K., Patten, K. O. and Wuebbles, D. J., Consistent sets of atmospheric lifetimes and radiative forcings on climate for CFC replacements: HCFCs and HFCs, J. Geophys. Res.,105(D5), 6903-6914, 2000.

©2019. Japan Geoscience Union. All Right Reserved. 

Rodgers, C. D., Inverse methods for atmospheric sounding –Theory and practice, edited by: Taylor, F. W., World Scientific, Singapore, 2000.

Keywords: HFC-23, HCFC, FTIR

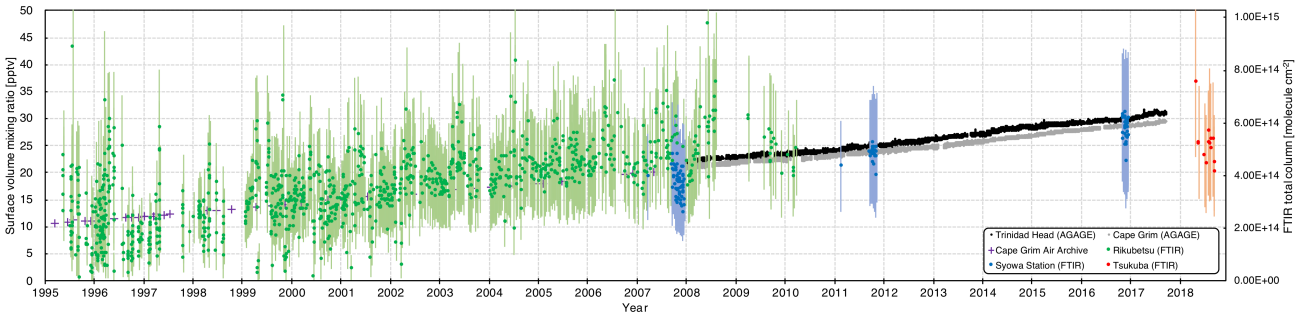


**Figure 1.** The timeseries of the FTIR-retrieved total columns of HFC-23 at Rikubetsu (green), Syowa Station (blue) and Tsukuba (red) with the retrieval uncertainties, along with ground-based in-situ measurements at Trinidad Head (41.05°N, 124.15°W; black) and Cape Grim (40.68°S, 144.69°E; grey). Also, Cape Grim Air Archive data (purple) is plotted during the period of 1995 to 2007.

©2019. Japan Geoscience Union. All Right Reserved. 

# Roles of cloud distribution in global atmospheric photochemistry

*Ryoki Matsuda[1], Kengo Sudo[1,2]

1. Graduate School of Environmental Studies, Nagoya University , 2. Japan Marine-Earth Science and Technology

Chemical reactions in the atmosphere directly affect formation and loss of ozone, methane, nitrogen oxides, sulfur oxides and aerosols, and have a great influence on the atmospheric environment and climate change. Since these reactions are driven by photodissociation of ozone and related species caused by ultraviolet radiation, they can be largely modulated by distribution of clouds. This study quantitatively investigates the photolytic impacts of clouds on atmospheric chemistry by using a global chemical transport model (chemical climate model) and observational (satellite and aircraft) data.
First, verification with satellite data (ISCCP D2) shows that the model (CHASER) reproduced well the global distribution of cloud amount as in the satellite data.
Sensitivity experiments were also performed to estimate clouds impacts on the photolytic processes and global photochemical field in the atmosphere. As a result, it was shown that OH radical (OH) concentrations decrease by 10 to 20% near the surface and increase by 10 to 20% in the upper troposphere. The changes basically reflect scattering and reflection of solar UV radiation by low-middle clouds, which is consistent with the previous studies. The global mean OH concentration, proxy of the oxidizing capacity of the atmosphere, increased by about 12% due to clouds while the global mean tropospheric ozone ($O_3$) concentration increased by about 0.7%.
The above results for clouds impacts on the atmospheric chemical field calculated in the model were verified by using aircraft observation (NASA ATOM-1). The result shows that the observed OH and $O_3$ concentrations are reproduced more accurately when clouds are properly considered in the model.
These results indicate that clouds have significant influences on the global atmospheric chemistry (especially on the OH concentration field). Since OH determines the concentrations of chemical species such as methane, carbon monoxide (CO), fluorocarbons (CFCs), etc. which are important for climate and stratospheric ozone, this study suggests that the variation and trends in clouds can largely affect the chemical species, which may give an additional influence on climate and atmospheric environment.

Keywords: Cloud, Chemistry-transport model, Ozone, OH radical

©2019. Japan Geoscience Union. All Right Reserved. 

# Evaluating global distribution and interannual variation of stratosphere-troposphere exchange of ozone: impacts of climate variabilities

*Kengo Sudo[1,2], Xin Li[1]

1. Graduate School of Environmental Studies, Nagoya University, 2. Research and Development Center for Global Change, JAMSTEC

The stratosphere-troposphere exchange (STE) of ozone ($O_3$) can have significant impacts on the interannual variability and long-term trend of global tropospheric ozone and radiation budget. This study investigates global STE of $O_3$ particularly focusing on the roles of major climate variabilities such as ENSO, PDO, and QBO and climate trend (surface temperature). Using a chemistry coupled climate model, this study estimates temporal variation in the vertical and meridional STE $O_3$ fluxes during the years of 2000-2016. For the major climate variabilities of ENSO and PDO, associated STE changes are assessed in detail using a composite analysis. The model validation shows that the model well captures the OMI-observed tropospheric column ozone (TCO) abundances (r~0.55), especially around the tropical Pacific (r~0.8). It is shown that in the tropics there is upward $O_3$ transport to the stratosphere (troposphere to stratosphere transport, TST) while in the extratropics, $O_3$ transport is downward (stratosphere to troposphere transport, STT), consistent with the Brewer-Dobson circulation in the stratosphere. Although geographical distributions of vertical and meridional STE fluxes are not changed largely by ENSO or PDO, the STE fluxes are significantly amplified by the ENSO events. Horizontal patterns of STE flux anomaly are found to be similar with respect to the El Niño episodes and the PDO warm phases (STT increased by 21% and 10%, respectively, in the northwest Pacific). These anomalies are reversed during the La Niña and PDO cold phases (STT decreased by 16% and 3%, respectively, in northeast Pacific). The anomaly of global net STE $O_3$ flux is interpreted as several key factors using a multiple-regression analysis. The result shows that the STE anomaly is explained largely by the combination of ONI, PDO, QBO, and global mean surface temperature ($R^2$~43%). Contributions of ONI and PDO to STE anomaly are estimated to be 22.3% and 23.1%, respectively. This study quantitatively reveals the possible connection between climate condition and STE.

Keywords: Stratosphere-Troposphere Exchange (STE), Ozone, chemistry climate model, chemistry-climate interaction, climate change, Budget of tropospheric ozone

©2019. Japan Geoscience Union. All Right Reserved. 

[E] Poster | A (Atmospheric and Hydrospheric Sciences)：A-OS Ocean Sciences & Ocean Environment

Thu. May 30, 2019 10:45 AM - 12:15 PM JST | Thu. May 30, 2019 1:45 AM - 3:15 AM UTC | Poster Hall International Exhibition Hall8, Makuhari Messe_2

## [A-OS07] Climate variability and predictability on subseasonal to decadal timescales

convener:Takashi Mochizuki(Japan Agency for Marine-Earth Science and Technology), V Ramaswamy(NOAA GFDL), Doug Smith(Met Office), Yushi Morioka(Japan Agency for Marine-Earth Science and Technology)

Climate variability poses growing threats to human lives and socio-economic activities through changes in frequency and intensity of abnormal weather such as cold/heat waves and floods/droughts. This involves several climate phenomena with a wide range of timescales from subseasonal to decadal variations (e.g. MJO, IOD, ENSO, PDV, AMV). Many efforts have been made for understanding and predicting climate variations on each timescale, but there remain large uncertainties in simulation and prediction of subseasonal to decadal climate variations. This highlights lack of understanding of weather and climate interaction across different spatial and temporal timescales (e.g. tropical cyclones and ENSO) as well as multiple physical processes underlying climate variations (e.g. troposphere-stratosphere coupling, air-sea-ice interaction). This session aims to share current knowledge of subseasonal to decadal climate variability and predictability in order to identify the unresolved issues for better understanding and accurate prediction. This session invites all the abstracts related to the observational, theoretical, process-level and modelling research on subseasonal to decadal climate variability and predictability.

[AOS07-P01] Changes in North American and European Heatwave Characteristics

*Szandra A. Peter[1], Ben Kirtman[1] (1.Rosenstiel School of Marine and Atmospheric Science)

[AOS07-P02] **The effects of the "New Climate" Warming on Western Mediterranean: Situation of the Recent Extreme Events**

*Mohammed-Said KARROUK[1] (1.Hassan II University of Casablanca)

[AOS07-P03] **Month-to-month Difference of the Western Pacific Subtropical High Simulated by CMIP5 Models**

*Xiao Dong[1], Renping Lin[1] (1.Institute of Atmospheric Physics)

[AOS07-P04] Potential regulation on the climatic effect of Tibetan Plateau heating by tropical air–sea coupling

*Ziqian Wang[1], Anmin Duan[2], Song Yang[1] (1.School of Atmospheric Sciences, Sun Yat-sen University, 2.Institute of Atmospheric Physics, Chinese Academy of Sciences)

[AOS07-P05] Intraseasonal variation of the South Asian high and its role in connecting the Indian and East Asian summer monsoons

*Wei Wei[1] (1.Sun Yat-sen University)

[AOS07-P06] Mean Surface Air Temperatures in Japan - Regional Classification and Interranual Variability

*Pascal Oettli[1], Masami Nonaka[1], Swadhin Behera[1] (1.Japan Agency for Marine-Earth Science and Technology)

[AOS07-P07] Inter-Annual Variability of the Indonesian Rainfall and Air-Sea Interaction over the Indian-Pacific Ocean Associated with Regime Shift

*Murni Ngestu Nurutami[1], Tadahiro Hayasaka[1] (1.Center for Atmospheric and Oceanic Studies, Graduate School of Science, Tohoku University)

[AOS07-P08] Exploring synoptic-scale drivers of interannual rainfall variability over Africa

*Piotr Wolski[1], Chris Jack[1], Waarith Abrahams[1], Stefaan Conradie[1] (1.University of Cape Town)

[AOS07-P09] **Effect of El Niño on the response ratio of Hadley circulation to different SST meridional structures**

*Juan Feng[1] (1.Beijing Normal University)

[AOS07-P10] **Novel data-driven approach for ENSO prediction**

*Dmitri Kondrashov[1], Evgeniy Loskutov[2], Andrei Gavrilov[2], Dmitry Mukhin[2], Alexander Feigin[2] (1.University of California, Los Angeles, United States, 2.Institute of Applied Physics of the Russian Academy of Sciences, Nizhny Novgorod, Russian Federation)

[AOS07-P11] Experimental seasonal climate prediction using CFES: Comparison with the SINTEX-F systems

*Nobumasa Komori[1], Bunmei Taguchi[2], Akira Kuwano-Yoshida[3,1], Takeshi Doi[1], Masami Nonaka[1] (1.Japan Agency for Marine-Earth Science and Technology, 2.Research Center for Advanced Science and Technology, The University of Tokyo, 3.Disaster Prevention Research Institute, Kyoto University)

[AOS07-P12] Exploring the SST error growth during ENSO developing phase by using BCC_CSM1.1(m)

*Ben Tian[1], Hongli Ren[1] (1.National Climate Center, China Meteorological Administration)

[AOS07-P13] Role of sea-ice initialization in climate predictability over the Weddell Sea

*Yushi Morioka[1], Takeshi Doi[1], Doroteaciro Iovino[2], Simona Masina[2], Swadhin Behera[1] (1.Japan Agency for Marine-Earth Science and Technology (JAMSTEC), 2.Centro Euro-Mediterraneo sui Cambiamenti Climatici (CMCC))

[AOS07-P14] Observed and hindcasted subdecadal variability of the tropical Pacific climate

*Takashi Mochizuki[1], Masahiro Watanabe[2] (1.Japan Agency for Marine-Earth Science and Technology, 2.Atmosphere-Ocean Research Institute, The University of Tokyo)

# Changes in North American and European Heatwave Characteristics

*Szandra A. Peter[1], Ben Kirtman[1]

1. Rosenstiel School of Marine and Atmospheric Science

Heat waves are a serious threat to ecosystems, society and the economies of the world. By calculating specific threshold values from daily maximum 2 m temperatures of the NCEP/NCAR reanalysis data (Kalnay et al. 1996), the frequency of heat waves during summer months (JJA) in Europe and the US is determined for the period of 1982 to 2017. The differences between the first and the second half of the 36-year period are discussed, and the results are compared to the North American Multi-Model Ensemble (NMME) forecast with specific focus on recent heat waves in the Pacific Northwest of North America and Central Europe. The connection between heat waves and known climate variability (i.e., the NAO, PNA) is analyzed. We strive to assess the importance of natural variability, such as the NAO, in the frequency of heat waves by comparing the first and last half of the studied 36-year period. We also examine how well the NMME retrospective and real-time forecasts capture heat waves (and cold spells), and the sources of predictability (i.e., sea surface temperature anomalies, land surface conditions), and how the predictability connects to the various modes of climate variability.

©2019. Japan Geoscience Union. All Right Reserved. 

# The effects of the "New Climate" Warming on Western Mediterranean: Situation of the Recent Extreme Events

*Mohammed-Said KARROUK[1]

1. Hassan II University of Casablanca

Since the nineties of the last century, climatological research following a great scientific advance in the field of prediction, not the variability and evolution of the different climatic parameters was beginning to be clearer!

But today, since the beginning of 2005, certainly due to oceanic thermal cumulations, and the shift of climatic zones towards poles in selective forms (more intense on the oceans present on the continents); Climatic events do not evolve according to the usual and expected rhythms: atmospheric circulation, precipitation, temperatures, seasonal phenomena, etc. These conditions are a spatiotemporal evolution and distribution, which characterize the new "global climate", by the new atmospheric regime imposing the Meridian Atmospheric Circulation (MAC), alternating the conditions of Freshness (humidity) and Heat (drought) along the year.

In this new situation, Western Mediterranean, located in the climate transition zone, is fully affected by the "New Climate". Usually, the atmospheric response to major climatic events (ENSO) in this region such as "El Niño" was characterized by the establishment of the NAO positive index, stability and drought, due to dominance Zonal Atmospheric Circulation in winter. On the other hand, in the "La Niña" episode, the negative index of the NAO and the predominant Meridian Atmospheric Circulation and precipitation became abundant.

Since the beginning of this century, qualified meteorological events of "exceptional !" causing floods have continued to occur in Western Mediterranean, with increasing recurrence, prompting us to wonder about the "new" mode of hydro-thermal function of the climate system that induces torrential rains, as well as its effect on environments and societies.

Thanks to spatial observation and monitoring of meteorological conditions over the last 15 years, these types of alternating Heat / Cold conditions have become predictable, enabling decision-makers today to prepare adequately for the management of related risks to the "New Climate" warmed.

Keywords: "New Climate" Warmed, New Atmospheric Circulation, Meridian Atmospheric Circulation (MAC) , Western Mediterranean, Heat / Cold, Drought / Flood

©2019. Japan Geoscience Union. All Right Reserved. 

# Month-to-month Difference of the Western Pacific Subtropical High Simulated by CMIP5 Models

*Xiao Dong[1], Renping Lin[1]

1. Institute of Atmospheric Physics

The western Pacific subtropical high (WPSH) is an important circulation system of the East Asian summer monsoon (EASM). Most previous studies have focused on the variability of summer mean WPSH. Note that the WPSH also experiences subseasonal variation from early to late summer. In this study we examined the month-to-month shift of the WPSH in boreal summer, that is, from June to July and from July to August, simulated by CMIP5 Atmospheric General Circulation Models (AGCMs) and coupled models. Results show that climatologically AGCMs can reproduce the northward shift of the WPSH better than eastward retreat from July to August. Compared with AGCMs, coupled models can improve the month-to-month shift simulation to some extent, indicating that the air-sea coupling processes are also important in subseasonal timescale.

Keywords: western Pacific subtropical high, CMIP5 simulation, month to month variation

©2019. Japan Geoscience Union. All Right Reserved. 

# Potential regulation on the climatic effect of Tibetan Plateau heating by tropical air–sea coupling

*Ziqian Wang[1], Anmin Duan[2], Song Yang[1]

1. School of Atmospheric Sciences, Sun Yat-sen University, 2. Institute of Atmospheric Physics, Chinese Academy of Sciences

Based on the conventional weather research and forecasting (WRF) model and the air–sea coupled mode WRF-OMLM, we investigate the potential regulation on the climatic effect of Tibetan Plateau (TP) heating by the air–sea coupling over the tropical Indian Ocean and western Pacific. Results indicate that the TP heating significantly enhances the southwesterly monsoon circulation over the northern Indian Ocean and the South Asia subcontinent. The intensified southwesterly wind cools the sea surface mainly through the wind-evaporation-SST (sea surface temperature) feedback. Cold SST anomaly then weakens monsoon convective activity, especially that over the Bay of Bengal, and less water vapor is thus transported into the TP along its southern slope from the tropical oceans. As a result, summer precipitation decreases over the TP, which further weakens the TP local heat source. Finally, the changed TP heating continues to influence the summer monsoon precipitation and atmospheric circulation. To a certain extent, the air–sea coupling over the adjacent oceans may weaken the effect of TP heating on the mean climate in summer. It is also implied that considerations of air–sea interaction are necessary in future simulation studies of the TP heating effect.

Keywords: Air–sea coupling, Tibetan Plateau, Thermal forcing, Regional model

©2019. Japan Geoscience Union. All Right Reserved. 

# Intraseasonal variation of the South Asian high and its role in connecting the Indian and East Asian summer monsoons

*Wei Wei[1]

1. Sun Yat-sen University

The South Asian high (SAH) is the most intense and persistent upper-level circulation system in the Asian monsoon region during boreal summer. It plays a crucial role in the onset and variation of the Asian summer monsoon. Ample evidence shows that the monsoon onset and activities are closely related to the intraseasonal oscillation (ISO). Previous studies have found that the ISO in the East Asian summer monsoon (EASM) is impacted by the northward or northwestward propagation of the ISO in the South China Sea and the western North Pacific, and the northeastward propagation of the ISO in the tropical Indian Ocean. However, seldom research mentioned the effect of the ISO in the SAH. Our previous studies have shown that the SAH plays an important role in connecting the Indian summer monsoon (ISM) and the EASM on the interannual time scale. However, the effect of the SAH on the connection of the ISM and the EASM on the intraseasonal time scale is still not clear. Actually, the ISO in the SAH is significant in its zonal variation. In this study, we firstly figured out the intraseasonal variation feature of the SAH. And then, we explored the upper-level signal which will lead to the onset, advance and retreat of the EASM. Considering significant ISO in the ISM, we investigated the ISO feature in the ISM and its effect on the ISO in the SAH. Finally, we addressed a new physical process that the ISO in the ISM will impact the ISO in the SAH, and further influence the advance and retreat of the EASM on the intraseasonal time scale. We try to learn about the intraseasonal variation of the EASM in a new view, and propose a new way to improve the short-term climate prediction and the extended-range weather forecast.

©2019. Japan Geoscience Union. All Right Reserved. 

# Mean Surface Air Temperatures in Japan - Regional Classification and Interranual Variability

*Pascal Oettli[1], Masami Nonaka[1], Swadhin Behera[1]

1. Japan Agency for Marine-Earth Science and Technology

Back to the year 1886, several divisions of the climate of Japan into homogeneous climatic regions have been proposed, following different approaches of the question. This includes the Köppen climate classification (Fukui in 1933; Sekiguchi in 1949), the new Thornthwaite climate classification (Isozaki in 1933; Fukui in 1957) or the similarities of weather conditions. The latter is performed either throughout the year (Nakagawa in 1899; Sekiguchi in 1959; Yoshino in 1980) or during specific seasons (Iwakiri in 1967; Murata and Yoshino in 1988), sometimes with the help of statistical techniques, such as principal component analysis and the cluster analysis (Mikami in 1975; Koizumi and Kato in 2012.)

Using a type of artificial neural network called Self-Organizing Map, or SOM, we propose another division of the climate of Japan, solely based on the mean areal surface air temperature anomalies. SOM has been successfully employed in climate studies for more than a decade and has showed its ability to extract simple features from high-dimensional data. Here, SOM is applied to group 762 AMeDAS stations, taken throughout Japan for the last 30 years, into homogeneous clusters (=regions). Clustering is performed seasonally, with a focus on boreal winter (December to February) and boreal summer (June to August). As a result, eight regions are defined and associated time series of temperature anomalies (=indices) are computed.

Subsequently, possible source(s) of the interannual variability of mean surface air temperature anomalies are explored, for a better understanding of the regional differences. For this, correlation coefficients between indices previously defined and different climatic variable anomaly fields (sea-surface temperatures, outgoing longwave radiation, geopotential height...) are calculated. Hopefully, this work would also lead to a better seasonal forecast, taking into account the specificity of each region in regard to their link to the large-scale variability.

Keywords: Japan, Air temperature, Classification, Interannual variability

©2019. Japan Geoscience Union. All Right Reserved. 

# Inter-Annual Variability of the Indonesian Rainfall and Air-Sea Interaction over the Indian-Pacific Ocean Associated with Regime Shift

*Murni Ngestu Nurutami[1], Tadahiro Hayasaka[1]

1. Center for Atmospheric and Oceanic Studies, Graduate School of Science, Tohoku University

The inter-annual and inter-decadal variability of the Indonesian rainfall are investigated in association with the interannual climate modes over Indian-Pacific Oceans and the inter-decadal modulation on inter-annual climate variability impact. Rainfall data of the Climate Research Unit (CRU) from 1901 to 2016 and the Global Precipitation Climatology Project (GPCP) from 1979 to 2016 for June –November (JJASON) are used. The empirical orthogonal function (EOF) is used to identify the dominant spatial and temporal variability patterns of rainfall and the standard and partial correlation techniques are used to compare and to quantify the linear relationship between two or more time-series datasets. Based on the first principle component (PC1) of both CRU and GPCP data, the results show that canonical El Niño Southern-Oscillation (canonical ENSO), ENSO Modoki, and Indian Ocean Dipole (IOD) are the major climate modes influencing the inter-annual variability of the Indonesian rainfall, and the Inter-decadal Pacific Oscillation (IPO) is the major decadal phenomenon which affects the decadal variability of Indonesian rainfall. All of the inter-annual climate modes and IPO have negative correlation with the Indonesian rainfall, but the spatial distributions of Indonesian rainfall change associated with each phenomenon are different. During 1970 to 2016, three phases of IPO have been identified which are strongly related to Indonesian rainfall with the correlation coefficient of -0.75. The three phases are a negative phase in 1970-1978, a positive phase in 1979-1997, and another negative phase in 1998-2015. Mostly, these climate modes occur simultaneously, and the impacts of them on rainfall are combined. The driest condition of rainfall occurs when El Niño coincides with positive IOD during positive IPO, and the wettest condition occurs when La Niña –La Niña Modoki coincides with negative IOD during negative IPO over the whole region of Indonesia. The IPO plays a role in modulating the impact of these inter-annual climate modes on their frequencies and magnitudes to Indonesian rainfall from 1970s until present. The responses of the Indonesian rainfall to each inter-annual climate mode modulated by IPO are different as based on their time series correlation coefficient. The negative correlation between canonical ENSO and Indonesian rainfall weakens during negative IPO from early 2000s and intensifies during positive IPO. On the other hand, the negative correlation between ENSO Modoki and Indonesian rainfall and between IOD and Indonesian rainfall increases during negative phase of IPO from late 1990s, and the negative correlation between ENSO Modoki and Indonesian rainfall weakens during positive IPO. Recently, the frequency of ENSO Modoki and IOD and their impacts on Indonesian rainfall increase.

Keywords: Indonesian rainfall variability, El Niño Southern-Oscillation (ENSO), ENSO Modoki, Interannual Variability, Decadal Variability, Interdecadal Pacific Oscillation

©2019. Japan Geoscience Union. All Right Reserved. 

# Exploring synoptic-scale drivers of interannual rainfall variability over Africa

*Piotr Wolski[1], Chris Jack[1], Waarith Abrahams[1], Stefaan Conradie[1]

1. University of Cape Town

Variability in local climate is a result of an interplay of multi-scale drivers –processes and feedbacks - intertwined within dependency or conditioning chain across spatial scales: from global to synoptic to meso- to local. Resolving these drivers and dependencies can be framed through the following questions: where does a deterministic signal at a particular time scale arise, how does it propagate through space and scales, and how can we maximize our ability to capture it? Here, we report on an exploratory study focusing on the synoptic-scale forcing underlying rainfall variability at the interannual time scale over Africa. In that, we systematically map, over the continent, variables and spatial scales which provide the strongest explanatory power of interannual rainfall variability. In addition, we constrast the explanatory power of mean state of synoptic fields with that of their variance, and of frequency of individual (daily) states. The analyses utilize multiple regression and CCA performed on mean de-orthogonalized fields of q,t,u,v,z at various pressure levels, with daily states of synoptic variables classified using self-organizing maps (SOM). The results are interpreted from the process perspective in terms of their agreement with the current understanding of the role of process chains affecting rainfall over various regions of the contient, and in terms of their implications to statistical downscaling of climate projections and seasonal forecasts.

Keywords: rainfall variability, statistical climatology, Africa, self organizing maps

©2019. Japan Geoscience Union. All Right Reserved. 

# Effect of El Niño on the response ratio of Hadley circulation to different SST meridional structures

*Juan Feng[1]

1. Beijing Normal University

The role of El Niño in influencing the response ratio of the Hadley circulation (HC) to different tropical sea surface temperature (SST) meridional structures is investigated over the period 1979–2016. The explained variance of the equatorially asymmetric principal mode of HC variability is enhanced during El Niño events that are characterized by equatorially symmetric El Niño SST anomalies. The reason for the enhanced explained variance is examined. It is shown that the response ratio of the HC to different SST meridional structures is greatly enhanced in El Niño events; this is because the SST over the Indo-Pacific warm pool (IPWP) shows inhomogeneous warming in El Niño events, with greater values in the southern IPWP. The asymmetric warming over the IPWP is opposite to the climatological meridional structure of the SST over the IPWP, which intensifies the equatorially symmetric variation of SST, and contributes to the enhanced response ratio of the HC to SST. This point is further verified by the suppression of this enhanced response ratio in El Niño events of the HC to SST when the effects of SST over the IPWP are removed, implying the different warming amplitude within the IPWP during the El Niño events contributes to the enhanced response ratio. The response in La Niña events is also explored, indicating a difference between El Niño and La Niña events. These results may help explain the corresponding variations of the HC during the El Niño events, and highlight the different influences of the El Niño and La Niña events on the response of the HC to SST.

Keywords: Hadley circulation, sea surface temperature, Indo-Pacific warm pool, El Niño

©2019. Japan Geoscience Union. All Right Reserved. 

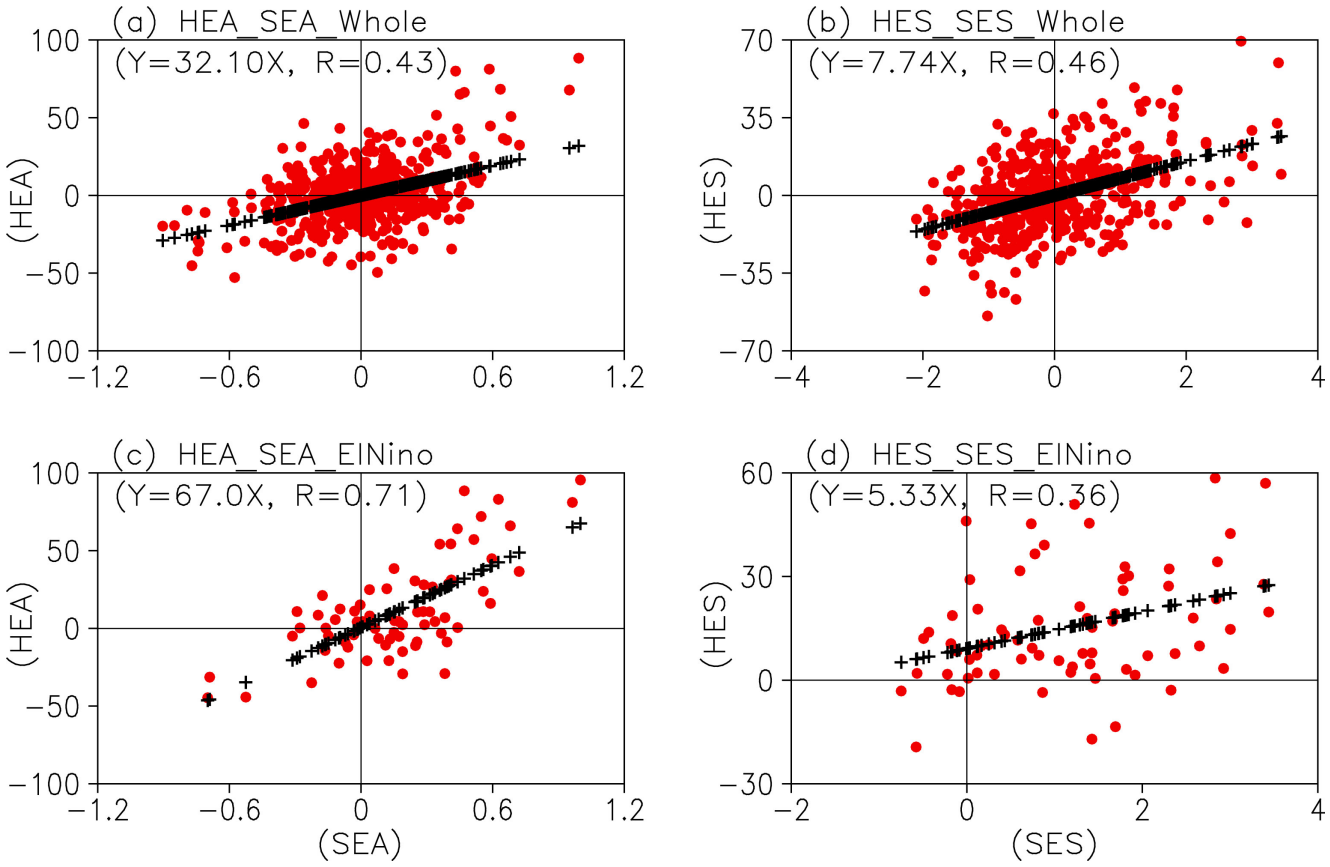


©2019. Japan Geoscience Union. All Right Reserved. 

# Novel data-driven approach for ENSO prediction

*Dmitri Kondrashov[1], Evgeniy Loskutov[2], Andrei Gavrilov[2], Dmitry Mukhin[2], Alexander Feigin[2]

1. University of California, Los Angeles, United States, 2. Institute of Applied Physics of the Russian Academy of Sciences, Nizhny Novgorod, Russian Federation

We have developed novel data-driven technique for ENSO prediction that combines two existing approaches: linear dynamical mode (LDM) decomposition of spatially distributed data, and multilevel empirical model reduction (EMR) stochastic modeling approach. The nonlinear EMR model that utilizes dynamical variables obtained by empirical orthogonal function (EOF) decomposition of tropical Pacific SST’ s (Kondrashov et al. 2005), had already achieved a very competitive skill in International Research Institute for Climate and Society (IRI) ENSO real-time multi-model plume (Barnston et al. 2012). On the other hand, Gavrilov et al. (2018) have shown that LDM decomposition provides better modes for ENSO forecast than EOFs.

In the presented results we have used LDM modes as dynamical variables at the main level of multilevel linear EMR model. The model was trained on monthly 1960 -- 2014 sea surface temperatures (30S to 30N, 2x2 deg). The results of comparing skill of the retrospective predictions of the SST-based ENSO indices obtained by EMR model with LDM and EOF modes, will be discussed.

1. Kondrashov, D., Kravtsov, S., Robertson, A. W., & Ghil, M. (2005). A Hierarchy of Data-Based ENSO Models. Journal of Climate, 18(21), 4425–4444. doi:10.1175/JCLI3567.1

2. Gavrilov, A., Seleznev, A., Mukhin, D., Loskutov, E., Feigin, A., & Kurths, J. (2018). Linear dynamical modes as new variables for data-driven ENSO forecast. Climate Dynamics, 1–18. http://doi.org/10.1007/s00382-018-4255-7.

3. Barnston, A. G., M. K. Tippett, M. L. Heureux, S. Li, and D. G. DeWitt, 2012: Skill of real-time seasonal ENSO model predictions during 2002–2011 —is our capability improving? *Bulletin of the American Meteorological Society*, **93 (5)**, 631–651, doi:10.1175/BAMS-D-11-00111.1.

Keywords: ENSO, stochastic modeling, prediction

©2019. Japan Geoscience Union. All Right Reserved. 

# Experimental seasonal climate prediction using CFES: Comparison with the SINTEX-F systems

*Nobumasa Komori[1], Bunmei Taguchi[2], Akira Kuwano-Yoshida[3,1], Takeshi Doi[1], Masami Nonaka[1]

1. Japan Agency for Marine-Earth Science and Technology, 2. Research Center for Advanced Science and Technology, The University of Tokyo, 3. Disaster Prevention Research Institute, Kyoto University

An experimental seasonal climate prediction system has been developed based on the Coupled atmosphere-ocean general circulation model for the Earth Simulator (CFES). Following the well-established systems based on the SINTEX-F model, initial conditions for seasonal climate prediction are constructed by strongly nudging sea surface temperature (SST) to observed one.

At this stage, 12-member ensemble 6-month predictions from the 1st day of March, June, September, and December have been conducted from 1983 through 2018, after 32-years of coupled spin-up integration with SST-nudging to the observed climatology. The experimental system exhibits skill in predicting variability of seasonal-mean 2-m air temperature over the tropical Pacific, and contributes to the improvement of multi-model ensemble prediction with the SINTEX-F systems.

Keywords: experimental seasonal climate prediction, global coupled atmosphere-ocean GCM, atmosphere-ocean interaction, multi-model ensemble

©2019. Japan Geoscience Union. All Right Reserved. 

# Exploring the SST error growth during ENSO developing phase by using BCC_CSM1.1(m)

*Ben Tian[1], Hongli Ren[1]

1. National Climate Center, China Meteorological Administration

Here we assess the ENSO prediction errors as a function of lead time using the seasonal hindcast of the Beijing Climate Center System Model, BCC_CSM1.1(m). The ensemble mean forecasts seems to be more challenging during the developing years of ENSO, compared with those made towards the decay phase. The composites of SST prediction errors are significantly negative and cover a large area in central-eastern tropical Pacific, thus limiting the model in forecasting the onset and intensity of El Niño. The large-scale errors, at their early stage, are generated gradually by negative anomalies in the subsurface temperature of the central-western equatorial Pacific, a process similar to El Niño decay and then transition to La Nina growth phase. Our results support others' work of "sensitive areas" for ENSO predictions, and emphasize the essential accuracy of initial fields and their early evolution, providing information for further improving the forecasting skill of ENSO.

Keywords: El Nino prediction, error evolution, sea surface temperature

©2019. Japan Geoscience Union. All Right Reserved. 

# Role of sea-ice initialization in climate predictability over the Weddell Sea

*Yushi Morioka[1], Takeshi Doi[1], Doroteaciro Iovino[2], Simona Masina[2], Swadhin Behera[1]

1. Japan Agency for Marine-Earth Science and Technology (JAMSTEC), 2. Centro Euro-Mediterraneo sui Cambiamenti Climatici (CMCC)

Potential impact of sea-ice initialization on the interannual climate predictability over the Weddell Sea is investigated using a coupled general circulation model. Climate variability in the Weddell Sea is generally believed to have association with remote forcing such as El Niño-Southern Oscillation and the Southern Annual Mode. However, sea-ice variability in the Weddell Sea has been recently suggested to play additional roles in modulating local atmospheric variability through changes in surface air temperature and near-surface baroclinicity. When both the model’s sea-surface temperature (SST) and sea-ice concentration (SIC) are initialized with observations using nudging schemes, reforecast experiments from September 1st show improvements in predicting the observed SIC anomalies in the Weddell Sea up to four months ahead, compared to the other experiments with only SST initialization. During austral spring (Oct-Dec) of lower-than-normal sea-ice years in the Weddell Sea, reforecast experiments with the SST and SIC initializations reasonably predict high surface air temperature anomalies in the Weddell Sea and high sea-level pressure anomalies over the Atlantic sector of the Southern Ocean. These results suggest that accurate initialization of sea-ice conditions during austral winter is necessary for skillful prediction of climate variability over the Weddell Sea during austral spring.

Keywords: Air-sea-ice interaction, Climate predictability, Weddell Sea

©2019. Japan Geoscience Union. All Right Reserved. 

# Observed and hindcasted subdecadal variability of the tropical Pacific climate

*Takashi Mochizuki[1], Masahiro Watanabe[2]

1. Japan Agency for Marine-Earth Science and Technology, 2. Atmosphere-Ocean Research Institute, The University of Tokyo

The tropical Pacific is highly responsible for controlling the tendencies of global climate. Here, we have found a subdecadal (i.e., 3-year-running means) variation that has been distinctively observed in the 2000s over the tropical Pacific. The warm water that originated from the positive ocean-heat-content (OHC) anomaly over the western Pacific in 2000 slowly extended eastward and stayed at the central equatorial Pacific between 2002-2005, rather than reaching the eastern edge. At the same time, an accompanying anti-cyclonic surface wind anomaly was observed in the off-equatorial North Pacific. This dynamical response of the upper ocean may have contributed to the subsequent warming in the western Pacific. In the preceding decades, in contrast, the observed OHC has usually represented a periodic fluctuation in the tropical Pacific, characterized by anomalous heat input/output in the meridional direction and slow eastward adjustment in the equatorial ocean thermocline. This subdecadal variation in the 2000s is quite distinct from our decadal hindcasts with initialization in Coupled Model Intercomparison Project Phase 5. The model predominantly simulates periodic-type fluctuations in any decade, and the resultant low predictability of the subdecadal variation in the 2000s can work to modulate the predictive skills at a lead time of several years.

Keywords: subdecadal variability, climate prediction, predictability, tropical Pacific

©2019. Japan Geoscience Union. All Right Reserved. 

[E] Poster | A (Atmospheric and Hydrospheric Sciences)：A-OS Ocean Sciences & Ocean Environment

Thu. May 30, 2019 5:15 PM - 6:30 PM JST | Thu. May 30, 2019 8:15 AM - 9:30 AM UTC | Poster Hall International Exhibition Hall8, Makuhari Messe_7

## [A-OS07] Climate variability and predictability on subseasonal to decadal timescales

convener:Takashi Mochizuki(Japan Agency for Marine-Earth Science and Technology), V Ramaswamy(NOAA GFDL), Doug Smith(Met Office), Yushi Morioka(Japan Agency for Marine-Earth Science and Technology)

Climate variability poses growing threats to human lives and socio-economic activities through changes in frequency and intensity of abnormal weather such as cold/heat waves and floods/droughts. This involves several climate phenomena with a wide range of timescales from subseasonal to decadal variations (e.g. MJO, IOD, ENSO, PDV, AMV). Many efforts have been made for understanding and predicting climate variations on each timescale, but there remain large uncertainties in simulation and prediction of subseasonal to decadal climate variations. This highlights lack of understanding of weather and climate interaction across different spatial and temporal timescales (e.g. tropical cyclones and ENSO) as well as multiple physical processes underlying climate variations (e.g. troposphere-stratosphere coupling, air-sea-ice interaction). This session aims to share current knowledge of subseasonal to decadal climate variability and predictability in order to identify the unresolved issues for better understanding and accurate prediction. This session invites all the abstracts related to the observational, theoretical, process-level and modelling research on subseasonal to decadal climate variability and predictability.

[AOS07-P01] Changes in North American and European Heatwave Characteristics

*Szandra A. Peter[1], Ben Kirtman[1] (1.Rosenstiel School of Marine and Atmospheric Science)

[AOS07-P02] **The effects of the "New Climate" Warming on Western Mediterranean: Situation of the Recent Extreme Events**

*Mohammed-Said KARROUK[1] (1.Hassan II University of Casablanca)

[AOS07-P03] **Month-to-month Difference of the Western Pacific Subtropical High Simulated by CMIP5 Models**

*Xiao Dong[1], Renping Lin[1] (1.Institute of Atmospheric Physics)

[AOS07-P04] Potential regulation on the climatic effect of Tibetan Plateau heating by tropical air–sea coupling

*Ziqian Wang[1], Anmin Duan[2], Song Yang[1] (1.School of Atmospheric Sciences, Sun Yat-sen University, 2.Institute of Atmospheric Physics, Chinese Academy of Sciences)

[AOS07-P05] Intraseasonal variation of the South Asian high and its role in connecting the Indian and East Asian summer monsoons

*Wei Wei[1] (1.Sun Yat-sen University)

[AOS07-P06] Mean Surface Air Temperatures in Japan - Regional Classification and Interranual Variability

*Pascal Oettli[1], Masami Nonaka[1], Swadhin Behera[1] (1.Japan Agency for Marine-Earth Science and Technology)

[AOS07-P07] Inter-Annual Variability of the Indonesian Rainfall and Air-Sea Interaction over the Indian-Pacific Ocean Associated with Regime Shift

*Murni Ngestu Nurutami[1], Tadahiro Hayasaka[1] (1.Center for Atmospheric and Oceanic Studies, Graduate School of Science, Tohoku University)

[AOS07-P08] Exploring synoptic-scale drivers of interannual rainfall variability over Africa

*Piotr Wolski[1], Chris Jack[1], Waarith Abrahams[1], Stefaan Conradie[1] (1.University of Cape Town)

[AOS07-P09] **Effect of El Niño on the response ratio of Hadley circulation to different SST meridional structures**

*Juan Feng[1] (1.Beijing Normal University)

[AOS07-P10] **Novel data-driven approach for ENSO prediction**

*Dmitri Kondrashov[1], Evgeniy Loskutov[2], Andrei Gavrilov[2], Dmitry Mukhin[2], Alexander Feigin[2] (1.University of California, Los Angeles, United States, 2.Institute of Applied Physics of the Russian Academy of Sciences, Nizhny Novgorod, Russian Federation)

[AOS07-P11] Experimental seasonal climate prediction using CFES: Comparison with the SINTEX-F systems

*Nobumasa Komori[1], Bunmei Taguchi[2], Akira Kuwano-Yoshida[3,1], Takeshi Doi[1], Masami Nonaka[1] (1.Japan Agency for Marine-Earth Science and Technology, 2.Research Center for Advanced Science and Technology, The University of Tokyo, 3.Disaster Prevention Research Institute, Kyoto University)

[AOS07-P12] Exploring the SST error growth during ENSO developing phase by using BCC_CSM1.1(m)

*Ben Tian[1], Hongli Ren[1] (1.National Climate Center, China Meteorological Administration)

[AOS07-P13] Role of sea-ice initialization in climate predictability over the Weddell Sea

*Yushi Morioka[1], Takeshi Doi[1], Doroteaciro Iovino[2], Simona Masina[2], Swadhin Behera[1] (1.Japan Agency for Marine-Earth Science and Technology (JAMSTEC), 2.Centro Euro-Mediterraneo sui Cambiamenti Climatici (CMCC))

[AOS07-P14] Observed and hindcasted subdecadal variability of the tropical Pacific climate

*Takashi Mochizuki[1], Masahiro Watanabe[2] (1.Japan Agency for Marine-Earth Science and Technology, 2.Atmosphere-Ocean Research Institute, The University of Tokyo)

# Changes in North American and European Heatwave Characteristics

*Szandra A. Peter[1], Ben Kirtman[1]

1. Rosenstiel School of Marine and Atmospheric Science

Heat waves are a serious threat to ecosystems, society and the economies of the world. By calculating specific threshold values from daily maximum 2 m temperatures of the NCEP/NCAR reanalysis data (Kalnay et al. 1996), the frequency of heat waves during summer months (JJA) in Europe and the US is determined for the period of 1982 to 2017. The differences between the first and the second half of the 36-year period are discussed, and the results are compared to the North American Multi-Model Ensemble (NMME) forecast with specific focus on recent heat waves in the Pacific Northwest of North America and Central Europe. The connection between heat waves and known climate variability (i.e., the NAO, PNA) is analyzed. We strive to assess the importance of natural variability, such as the NAO, in the frequency of heat waves by comparing the first and last half of the studied 36-year period. We also examine how well the NMME retrospective and real-time forecasts capture heat waves (and cold spells), and the sources of predictability (i.e., sea surface temperature anomalies, land surface conditions), and how the predictability connects to the various modes of climate variability.

©2019. Japan Geoscience Union. All Right Reserved. 

# The effects of the "New Climate" Warming on Western Mediterranean: Situation of the Recent Extreme Events

*Mohammed-Said KARROUK[1]

1. Hassan II University of Casablanca

Since the nineties of the last century, climatological research following a great scientific advance in the field of prediction, not the variability and evolution of the different climatic parameters was beginning to be clearer!

But today, since the beginning of 2005, certainly due to oceanic thermal cumulations, and the shift of climatic zones towards poles in selective forms (more intense on the oceans present on the continents); Climatic events do not evolve according to the usual and expected rhythms: atmospheric circulation, precipitation, temperatures, seasonal phenomena, etc. These conditions are a spatiotemporal evolution and distribution, which characterize the new "global climate", by the new atmospheric regime imposing the Meridian Atmospheric Circulation (MAC), alternating the conditions of Freshness (humidity) and Heat (drought) along the year.

In this new situation, Western Mediterranean, located in the climate transition zone, is fully affected by the "New Climate". Usually, the atmospheric response to major climatic events (ENSO) in this region such as "El Niño" was characterized by the establishment of the NAO positive index, stability and drought, due to dominance Zonal Atmospheric Circulation in winter. On the other hand, in the "La Niña" episode, the negative index of the NAO and the predominant Meridian Atmospheric Circulation and precipitation became abundant.

Since the beginning of this century, qualified meteorological events of "exceptional !" causing floods have continued to occur in Western Mediterranean, with increasing recurrence, prompting us to wonder about the "new" mode of hydro-thermal function of the climate system that induces torrential rains, as well as its effect on environments and societies.

Thanks to spatial observation and monitoring of meteorological conditions over the last 15 years, these types of alternating Heat / Cold conditions have become predictable, enabling decision-makers today to prepare adequately for the management of related risks to the "New Climate" warmed.

Keywords: "New Climate" Warmed, New Atmospheric Circulation, Meridian Atmospheric Circulation (MAC) , Western Mediterranean, Heat / Cold, Drought / Flood

©2019. Japan Geoscience Union. All Right Reserved. 

# Month-to-month Difference of the Western Pacific Subtropical High Simulated by CMIP5 Models

*Xiao Dong[1], Renping Lin[1]

1. Institute of Atmospheric Physics

The western Pacific subtropical high (WPSH) is an important circulation system of the East Asian summer monsoon (EASM). Most previous studies have focused on the variability of summer mean WPSH. Note that the WPSH also experiences subseasonal variation from early to late summer. In this study we examined the month-to-month shift of the WPSH in boreal summer, that is, from June to July and from July to August, simulated by CMIP5 Atmospheric General Circulation Models (AGCMs) and coupled models. Results show that climatologically AGCMs can reproduce the northward shift of the WPSH better than eastward retreat from July to August. Compared with AGCMs, coupled models can improve the month-to-month shift simulation to some extent, indicating that the air-sea coupling processes are also important in subseasonal timescale.

Keywords: western Pacific subtropical high, CMIP5 simulation, month to month variation

©2019. Japan Geoscience Union. All Right Reserved. 

# Potential regulation on the climatic effect of Tibetan Plateau heating by tropical air–sea coupling

*Ziqian Wang[1], Anmin Duan[2], Song Yang[1]

1. School of Atmospheric Sciences, Sun Yat-sen University, 2. Institute of Atmospheric Physics, Chinese Academy of Sciences

Based on the conventional weather research and forecasting (WRF) model and the air–sea coupled mode WRF-OMLM, we investigate the potential regulation on the climatic effect of Tibetan Plateau (TP) heating by the air–sea coupling over the tropical Indian Ocean and western Pacific. Results indicate that the TP heating significantly enhances the southwesterly monsoon circulation over the northern Indian Ocean and the South Asia subcontinent. The intensified southwesterly wind cools the sea surface mainly through the wind-evaporation-SST (sea surface temperature) feedback. Cold SST anomaly then weakens monsoon convective activity, especially that over the Bay of Bengal, and less water vapor is thus transported into the TP along its southern slope from the tropical oceans. As a result, summer precipitation decreases over the TP, which further weakens the TP local heat source. Finally, the changed TP heating continues to influence the summer monsoon precipitation and atmospheric circulation. To a certain extent, the air–sea coupling over the adjacent oceans may weaken the effect of TP heating on the mean climate in summer. It is also implied that considerations of air–sea interaction are necessary in future simulation studies of the TP heating effect.

Keywords: Air–sea coupling, Tibetan Plateau, Thermal forcing, Regional model

©2019. Japan Geoscience Union. All Right Reserved. 

# Intraseasonal variation of the South Asian high and its role in connecting the Indian and East Asian summer monsoons

*Wei Wei[1]

1. Sun Yat-sen University

The South Asian high (SAH) is the most intense and persistent upper-level circulation system in the Asian monsoon region during boreal summer. It plays a crucial role in the onset and variation of the Asian summer monsoon. Ample evidence shows that the monsoon onset and activities are closely related to the intraseasonal oscillation (ISO). Previous studies have found that the ISO in the East Asian summer monsoon (EASM) is impacted by the northward or northwestward propagation of the ISO in the South China Sea and the western North Pacific, and the northeastward propagation of the ISO in the tropical Indian Ocean. However, seldom research mentioned the effect of the ISO in the SAH. Our previous studies have shown that the SAH plays an important role in connecting the Indian summer monsoon (ISM) and the EASM on the interannual time scale. However, the effect of the SAH on the connection of the ISM and the EASM on the intraseasonal time scale is still not clear. Actually, the ISO in the SAH is significant in its zonal variation. In this study, we firstly figured out the intraseasonal variation feature of the SAH. And then, we explored the upper-level signal which will lead to the onset, advance and retreat of the EASM. Considering significant ISO in the ISM, we investigated the ISO feature in the ISM and its effect on the ISO in the SAH. Finally, we addressed a new physical process that the ISO in the ISM will impact the ISO in the SAH, and further influence the advance and retreat of the EASM on the intraseasonal time scale. We try to learn about the intraseasonal variation of the EASM in a new view, and propose a new way to improve the short-term climate prediction and the extended-range weather forecast.

©2019. Japan Geoscience Union. All Right Reserved. 

# Mean Surface Air Temperatures in Japan - Regional Classification and Interranual Variability

*Pascal Oettli[1], Masami Nonaka[1], Swadhin Behera[1]

1. Japan Agency for Marine-Earth Science and Technology

Back to the year 1886, several divisions of the climate of Japan into homogeneous climatic regions have been proposed, following different approaches of the question. This includes the Köppen climate classification (Fukui in 1933; Sekiguchi in 1949), the new Thornthwaite climate classification (Isozaki in 1933; Fukui in 1957) or the similarities of weather conditions. The latter is performed either throughout the year (Nakagawa in 1899; Sekiguchi in 1959; Yoshino in 1980) or during specific seasons (Iwakiri in 1967; Murata and Yoshino in 1988), sometimes with the help of statistical techniques, such as principal component analysis and the cluster analysis (Mikami in 1975; Koizumi and Kato in 2012.)

Using a type of artificial neural network called Self-Organizing Map, or SOM, we propose another division of the climate of Japan, solely based on the mean areal surface air temperature anomalies. SOM has been successfully employed in climate studies for more than a decade and has showed its ability to extract simple features from high-dimensional data. Here, SOM is applied to group 762 AMeDAS stations, taken throughout Japan for the last 30 years, into homogeneous clusters (=regions). Clustering is performed seasonally, with a focus on boreal winter (December to February) and boreal summer (June to August). As a result, eight regions are defined and associated time series of temperature anomalies (=indices) are computed.

Subsequently, possible source(s) of the interannual variability of mean surface air temperature anomalies are explored, for a better understanding of the regional differences. For this, correlation coefficients between indices previously defined and different climatic variable anomaly fields (sea-surface temperatures, outgoing longwave radiation, geopotential height...) are calculated. Hopefully, this work would also lead to a better seasonal forecast, taking into account the specificity of each region in regard to their link to the large-scale variability.

Keywords: Japan, Air temperature, Classification, Interannual variability

©2019. Japan Geoscience Union. All Right Reserved. 

# Inter-Annual Variability of the Indonesian Rainfall and Air-Sea Interaction over the Indian-Pacific Ocean Associated with Regime Shift

*Murni Ngestu Nurutami[1], Tadahiro Hayasaka[1]

1. Center for Atmospheric and Oceanic Studies, Graduate School of Science, Tohoku University

The inter-annual and inter-decadal variability of the Indonesian rainfall are investigated in association with the interannual climate modes over Indian-Pacific Oceans and the inter-decadal modulation on inter-annual climate variability impact. Rainfall data of the Climate Research Unit (CRU) from 1901 to 2016 and the Global Precipitation Climatology Project (GPCP) from 1979 to 2016 for June –November (JJASON) are used. The empirical orthogonal function (EOF) is used to identify the dominant spatial and temporal variability patterns of rainfall and the standard and partial correlation techniques are used to compare and to quantify the linear relationship between two or more time-series datasets. Based on the first principle component (PC1) of both CRU and GPCP data, the results show that canonical El Niño Southern-Oscillation (canonical ENSO), ENSO Modoki, and Indian Ocean Dipole (IOD) are the major climate modes influencing the inter-annual variability of the Indonesian rainfall, and the Inter-decadal Pacific Oscillation (IPO) is the major decadal phenomenon which affects the decadal variability of Indonesian rainfall. All of the inter-annual climate modes and IPO have negative correlation with the Indonesian rainfall, but the spatial distributions of Indonesian rainfall change associated with each phenomenon are different. During 1970 to 2016, three phases of IPO have been identified which are strongly related to Indonesian rainfall with the correlation coefficient of -0.75. The three phases are a negative phase in 1970-1978, a positive phase in 1979-1997, and another negative phase in 1998-2015. Mostly, these climate modes occur simultaneously, and the impacts of them on rainfall are combined. The driest condition of rainfall occurs when El Niño coincides with positive IOD during positive IPO, and the wettest condition occurs when La Niña –La Niña Modoki coincides with negative IOD during negative IPO over the whole region of Indonesia. The IPO plays a role in modulating the impact of these inter-annual climate modes on their frequencies and magnitudes to Indonesian rainfall from 1970s until present. The responses of the Indonesian rainfall to each inter-annual climate mode modulated by IPO are different as based on their time series correlation coefficient. The negative correlation between canonical ENSO and Indonesian rainfall weakens during negative IPO from early 2000s and intensifies during positive IPO. On the other hand, the negative correlation between ENSO Modoki and Indonesian rainfall and between IOD and Indonesian rainfall increases during negative phase of IPO from late 1990s, and the negative correlation between ENSO Modoki and Indonesian rainfall weakens during positive IPO. Recently, the frequency of ENSO Modoki and IOD and their impacts on Indonesian rainfall increase.

Keywords: Indonesian rainfall variability, El Niño Southern-Oscillation (ENSO), ENSO Modoki, Interannual Variability, Decadal Variability, Interdecadal Pacific Oscillation

©2019. Japan Geoscience Union. All Right Reserved. 

# Exploring synoptic-scale drivers of interannual rainfall variability over Africa

*Piotr Wolski[1], Chris Jack[1], Waarith Abrahams[1], Stefaan Conradie[1]

1. University of Cape Town

Variability in local climate is a result of an interplay of multi-scale drivers –processes and feedbacks - intertwined within dependency or conditioning chain across spatial scales: from global to synoptic to meso- to local. Resolving these drivers and dependencies can be framed through the following questions: where does a deterministic signal at a particular time scale arise, how does it propagate through space and scales, and how can we maximize our ability to capture it? Here, we report on an exploratory study focusing on the synoptic-scale forcing underlying rainfall variability at the interannual time scale over Africa. In that, we systematically map, over the continent, variables and spatial scales which provide the strongest explanatory power of interannual rainfall variability. In addition, we constrast the explanatory power of mean state of synoptic fields with that of their variance, and of frequency of individual (daily) states. The analyses utilize multiple regression and CCA performed on mean de-orthogonalized fields of q,t,u,v,z at various pressure levels, with daily states of synoptic variables classified using self-organizing maps (SOM). The results are interpreted from the process perspective in terms of their agreement with the current understanding of the role of process chains affecting rainfall over various regions of the contient, and in terms of their implications to statistical downscaling of climate projections and seasonal forecasts.

Keywords: rainfall variability, statistical climatology, Africa, self organizing maps

©2019. Japan Geoscience Union. All Right Reserved. 

# Effect of El Niño on the response ratio of Hadley circulation to different SST meridional structures

*Juan Feng[1]

1. Beijing Normal University

The role of El Niño in influencing the response ratio of the Hadley circulation (HC) to different tropical sea surface temperature (SST) meridional structures is investigated over the period 1979–2016. The explained variance of the equatorially asymmetric principal mode of HC variability is enhanced during El Niño events that are characterized by equatorially symmetric El Niño SST anomalies. The reason for the enhanced explained variance is examined. It is shown that the response ratio of the HC to different SST meridional structures is greatly enhanced in El Niño events; this is because the SST over the Indo-Pacific warm pool (IPWP) shows inhomogeneous warming in El Niño events, with greater values in the southern IPWP. The asymmetric warming over the IPWP is opposite to the climatological meridional structure of the SST over the IPWP, which intensifies the equatorially symmetric variation of SST, and contributes to the enhanced response ratio of the HC to SST. This point is further verified by the suppression of this enhanced response ratio in El Niño events of the HC to SST when the effects of SST over the IPWP are removed, implying the different warming amplitude within the IPWP during the El Niño events contributes to the enhanced response ratio. The response in La Niña events is also explored, indicating a difference between El Niño and La Niña events. These results may help explain the corresponding variations of the HC during the El Niño events, and highlight the different influences of the El Niño and La Niña events on the response of the HC to SST.

Keywords: Hadley circulation, sea surface temperature, Indo-Pacific warm pool, El Niño

©2019. Japan Geoscience Union. All Right Reserved. 

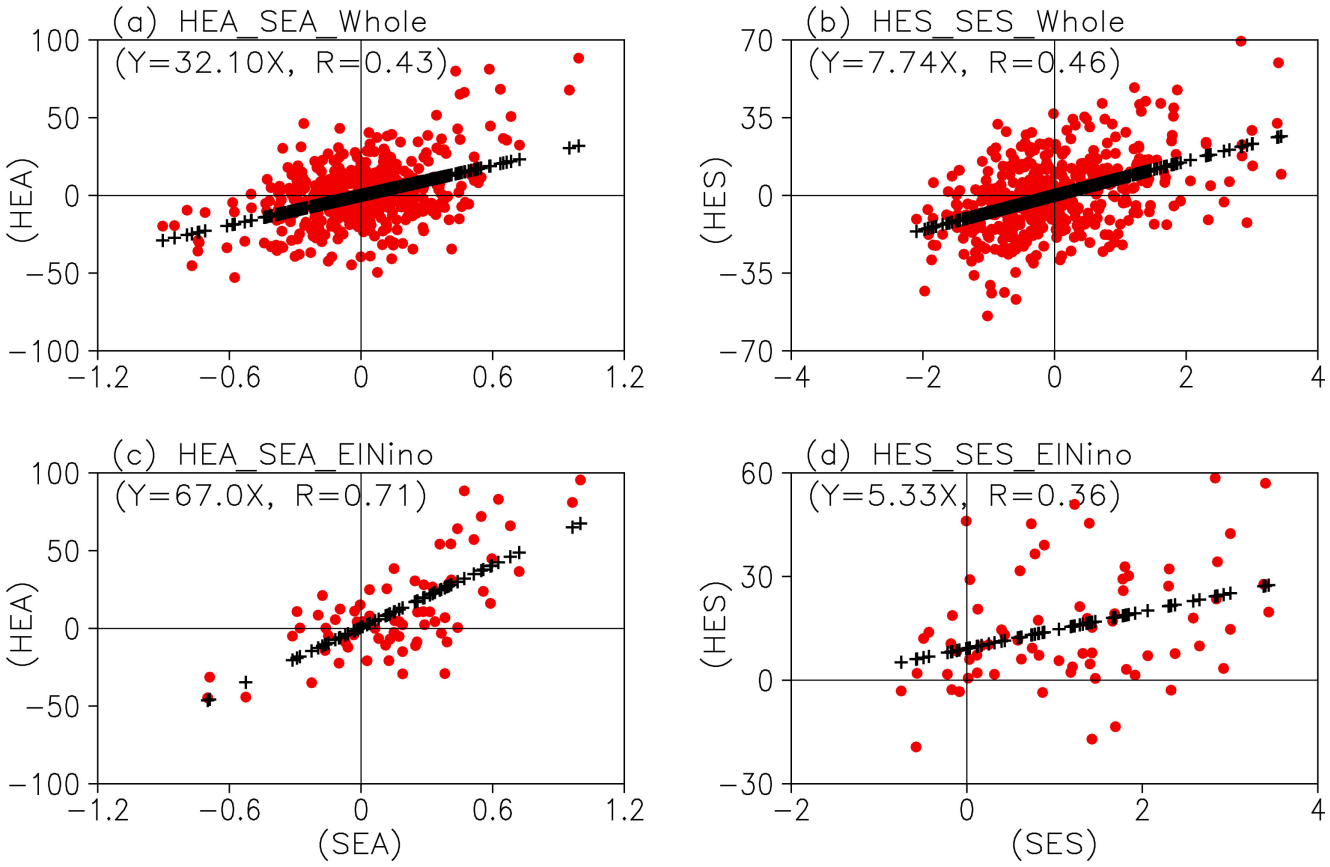


©2019. Japan Geoscience Union. All Right Reserved. 

# Novel data-driven approach for ENSO prediction

*Dmitri Kondrashov[1], Evgeniy Loskutov[2], Andrei Gavrilov[2], Dmitry Mukhin[2], Alexander Feigin[2]

1. University of California, Los Angeles, United States, 2. Institute of Applied Physics of the Russian Academy of Sciences, Nizhny Novgorod, Russian Federation

We have developed novel data-driven technique for ENSO prediction that combines two existing approaches: linear dynamical mode (LDM) decomposition of spatially distributed data, and multilevel empirical model reduction (EMR) stochastic modeling approach. The nonlinear EMR model that utilizes dynamical variables obtained by empirical orthogonal function (EOF) decomposition of tropical Pacific SST’ s (Kondrashov et al. 2005), had already achieved a very competitive skill in International Research Institute for Climate and Society (IRI) ENSO real-time multi-model plume (Barnston et al. 2012). On the other hand, Gavrilov et al. (2018) have shown that LDM decomposition provides better modes for ENSO forecast than EOFs.

In the presented results we have used LDM modes as dynamical variables at the main level of multilevel linear EMR model. The model was trained on monthly 1960 -- 2014 sea surface temperatures (30S to 30N, 2x2 deg). The results of comparing skill of the retrospective predictions of the SST-based ENSO indices obtained by EMR model with LDM and EOF modes, will be discussed.

1. Kondrashov, D., Kravtsov, S., Robertson, A. W., & Ghil, M. (2005). A Hierarchy of Data-Based ENSO Models. Journal of Climate, 18(21), 4425–4444. doi:10.1175/JCLI3567.1

2. Gavrilov, A., Seleznev, A., Mukhin, D., Loskutov, E., Feigin, A., & Kurths, J. (2018). Linear dynamical modes as new variables for data-driven ENSO forecast. Climate Dynamics, 1–18. http://doi.org/10.1007/s00382-018-4255-7.

3. Barnston, A. G., M. K. Tippett, M. L. Heureux, S. Li, and D. G. DeWitt, 2012: Skill of real-time seasonal ENSO model predictions during 2002–2011 —is our capability improving? *Bulletin of the American Meteorological Society*, **93 (5)**, 631–651, doi:10.1175/BAMS-D-11-00111.1.

Keywords: ENSO, stochastic modeling, prediction

©2019. Japan Geoscience Union. All Right Reserved. 

# Experimental seasonal climate prediction using CFES: Comparison with the SINTEX-F systems

*Nobumasa Komori[1], Bunmei Taguchi[2], Akira Kuwano-Yoshida[3,1], Takeshi Doi[1], Masami Nonaka[1]

1. Japan Agency for Marine-Earth Science and Technology, 2. Research Center for Advanced Science and Technology, The University of Tokyo, 3. Disaster Prevention Research Institute, Kyoto University

An experimental seasonal climate prediction system has been developed based on the Coupled atmosphere-ocean general circulation model for the Earth Simulator (CFES). Following the well-established systems based on the SINTEX-F model, initial conditions for seasonal climate prediction are constructed by strongly nudging sea surface temperature (SST) to observed one.

At this stage, 12-member ensemble 6-month predictions from the 1st day of March, June, September, and December have been conducted from 1983 through 2018, after 32-years of coupled spin-up integration with SST-nudging to the observed climatology. The experimental system exhibits skill in predicting variability of seasonal-mean 2-m air temperature over the tropical Pacific, and contributes to the improvement of multi-model ensemble prediction with the SINTEX-F systems.

Keywords: experimental seasonal climate prediction, global coupled atmosphere-ocean GCM, atmosphere-ocean interaction, multi-model ensemble

©2019. Japan Geoscience Union. All Right Reserved. 

# Exploring the SST error growth during ENSO developing phase by using BCC_CSM1.1(m)

*Ben Tian[1], Hongli Ren[1]

1. National Climate Center, China Meteorological Administration

Here we assess the ENSO prediction errors as a function of lead time using the seasonal hindcast of the Beijing Climate Center System Model, BCC_CSM1.1(m). The ensemble mean forecasts seems to be more challenging during the developing years of ENSO, compared with those made towards the decay phase. The composites of SST prediction errors are significantly negative and cover a large area in central-eastern tropical Pacific, thus limiting the model in forecasting the onset and intensity of El Niño. The large-scale errors, at their early stage, are generated gradually by negative anomalies in the subsurface temperature of the central-western equatorial Pacific, a process similar to El Niño decay and then transition to La Nina growth phase. Our results support others' work of "sensitive areas" for ENSO predictions, and emphasize the essential accuracy of initial fields and their early evolution, providing information for further improving the forecasting skill of ENSO.

Keywords: El Nino prediction, error evolution, sea surface temperature

©2019. Japan Geoscience Union. All Right Reserved. 

# Role of sea-ice initialization in climate predictability over the Weddell Sea

*Yushi Morioka[1], Takeshi Doi[1], Doroteaciro Iovino[2], Simona Masina[2], Swadhin Behera[1]

1. Japan Agency for Marine-Earth Science and Technology (JAMSTEC), 2. Centro Euro-Mediterraneo sui Cambiamenti Climatici (CMCC)

Potential impact of sea-ice initialization on the interannual climate predictability over the Weddell Sea is investigated using a coupled general circulation model. Climate variability in the Weddell Sea is generally believed to have association with remote forcing such as El Niño-Southern Oscillation and the Southern Annual Mode. However, sea-ice variability in the Weddell Sea has been recently suggested to play additional roles in modulating local atmospheric variability through changes in surface air temperature and near-surface baroclinicity. When both the model’s sea-surface temperature (SST) and sea-ice concentration (SIC) are initialized with observations using nudging schemes, reforecast experiments from September 1st show improvements in predicting the observed SIC anomalies in the Weddell Sea up to four months ahead, compared to the other experiments with only SST initialization. During austral spring (Oct-Dec) of lower-than-normal sea-ice years in the Weddell Sea, reforecast experiments with the SST and SIC initializations reasonably predict high surface air temperature anomalies in the Weddell Sea and high sea-level pressure anomalies over the Atlantic sector of the Southern Ocean. These results suggest that accurate initialization of sea-ice conditions during austral winter is necessary for skillful prediction of climate variability over the Weddell Sea during austral spring.

Keywords: Air-sea-ice interaction, Climate predictability, Weddell Sea

©2019. Japan Geoscience Union. All Right Reserved. 

# Observed and hindcasted subdecadal variability of the tropical Pacific climate

*Takashi Mochizuki[1], Masahiro Watanabe[2]

1. Japan Agency for Marine-Earth Science and Technology, 2. Atmosphere-Ocean Research Institute, The University of Tokyo

The tropical Pacific is highly responsible for controlling the tendencies of global climate. Here, we have found a subdecadal (i.e., 3-year-running means) variation that has been distinctively observed in the 2000s over the tropical Pacific. The warm water that originated from the positive ocean-heat-content (OHC) anomaly over the western Pacific in 2000 slowly extended eastward and stayed at the central equatorial Pacific between 2002-2005, rather than reaching the eastern edge. At the same time, an accompanying anti-cyclonic surface wind anomaly was observed in the off-equatorial North Pacific. This dynamical response of the upper ocean may have contributed to the subsequent warming in the western Pacific. In the preceding decades, in contrast, the observed OHC has usually represented a periodic fluctuation in the tropical Pacific, characterized by anomalous heat input/output in the meridional direction and slow eastward adjustment in the equatorial ocean thermocline. This subdecadal variation in the 2000s is quite distinct from our decadal hindcasts with initialization in Coupled Model Intercomparison Project Phase 5. The model predominantly simulates periodic-type fluctuations in any decade, and the resultant low predictability of the subdecadal variation in the 2000s can work to modulate the predictive skills at a lead time of several years.

Keywords: subdecadal variability, climate prediction, predictability, tropical Pacific

©2019. Japan Geoscience Union. All Right Reserved. 

[E] Oral | A (Atmospheric and Hydrospheric Sciences )：A-OS Ocean Sciences & Ocean Environment

Thu. May 30, 2019 1:45 PM - 3:15 PM JST | Thu. May 30, 2019 4:45 AM - 6:15 AM UTC | 105 1F

## [A-OS07] Climate variability and predictability on subseasonal to decadal timescales

convener:Takashi Mochizuki(Japan Agency for Marine-Earth Science and Technology), V Ramaswamy(NOAA GFDL), Doug Smith(Met Office), Yushi Morioka(Japan Agency for Marine-Earth Science and Technology), Chairperson:V Ramaswamy(NOAA GFDL), Takashi Mochizuki(Japan Agency for Marine-Earth Science and Technology)

Climate variability poses growing threats to human lives and socio-economic activities through changes in frequency and intensity of abnormal weather such as cold/heat waves and floods/droughts. This involves several climate phenomena with a wide range of timescales from subseasonal to decadal variations (e.g. MJO, IOD, ENSO, PDV, AMV). Many efforts have been made for understanding and predicting climate variations on each timescale, but there remain large uncertainties in simulation and prediction of subseasonal to decadal climate variations. This highlights lack of understanding of weather and climate interaction across different spatial and temporal timescales (e.g. tropical cyclones and ENSO) as well as multiple physical processes underlying climate variations (e.g. troposphere-stratosphere coupling, air-sea-ice interaction). This session aims to share current knowledge of subseasonal to decadal climate variability and predictability in order to identify the unresolved issues for better understanding and accurate prediction. This session invites all the abstracts related to the observational, theoretical, process-level and modelling research on subseasonal to decadal climate variability and predictability.

1:45 PM - 2:00 PM JST | 4:45 AM - 5:00 AM UTC

[AOS07-01] Seasonal Predictions of Tropical Cyclones in 2018 using GFDL and NICAM High-Resolution Global Models

★Invited Papers

*Hiroyuki Murakami[1,2], Masuo Nakano[3], V Ramaswamy[1], Thomas Delworth[1], Sarah Kapnick[1], Rich Gudgel[1], Takashi Mochizuki[3], Takeshi Doi[3], Yushi Morioka[3] (1.Geophysical Fluid Dynamics Laboratory, 2.University Corporation for Atmospheric Research, 3.JAMSTEC)

2:00 PM - 2:15 PM JST | 5:00 AM - 5:15 AM UTC

[AOS07-02] **Future change of tropical cyclone-induced waves in the Indian Ocean; An analysis based on super-high-resolution MRI-AGCM3.2 climate model**

*Bahareh Kamranzad[1,2], Nobuhito Mori[1] (1.Disaster Prevention Research Institute, Kyoto University, 2.Hakubi Center for Advanced Research, Kyoto University)

2:15 PM - 2:30 PM JST | 5:15 AM - 5:30 AM UTC

[AOS07-03] The ocean-coupled global cloud-resolving modeling era

★Invited Papers

*Tomoki Miyakawa[1] (1.Atmosphere and Ocean Research Institute University of Tokyo)

2:30 PM - 2:45 PM JST | 5:30 AM - 5:45 AM UTC

[AOS07-04] Westerly Wind Burst (WWB)/Easterly Wind Surge (EWS)-like stochastic forcing and the effects on ENSO prediction by the SINTEX-F system

*Takeshi Doi[1], Swadhin Behera[1], Toshio Yamagata[1] (1.JAMSTEC)

2:45 PM - 3:00 PM JST | 5:45 AM - 6:00 AM UTC

[AOS07-05] **The life-cycle of annual waves in the Pacific Ocean as identified by a seamless diagnosis for the energy flux**

*Hidenori AIKI[1], Takahiro Shimura[2] (1.Institute for Space-Earth Environmental Research, Nagoya University, 2.Graduate School for Environmental Studies, Nagoya University)

3:00 PM - 3:15 PM JST | 6:00 AM - 6:15 AM UTC

[AOS07-06] Development of weakly coupled atmosphere-ocean data assimilation system and the evaluation of the coupled reanalysis in JMA/MRI

★Invited Papers

*Yosuke Fujii[1], Chiaki Kobayashi[1], Toshiyuki Ishibashi[1], Yuhei Takaya[1] (1.Meteorological Research Institute, Japan Meteorological Agency)

# Seasonal Predictions of Tropical Cyclones in 2018 using GFDL and NICAM High-Resolution Global Models

*Hiroyuki Murakami[1,2], Masuo Nakano[3], V Ramaswamy[1], Thomas Delworth[1], Sarah Kapnick[1], Rich Gudgel[1], Takashi Mochizuki[3], Takeshi Doi[3], Yushi Morioka[3]

1. Geophysical Fluid Dynamics Laboratory, 2. University Corporation for Atmospheric Research, 3. JAMSTEC

We conduct real-time seasonal forecast using high-resolution global models (GFDL-FLOR, GFDL-HiFLOR, and NICAM) that have skill in predicting tropical cyclone statistics over the global ocean basins. The seasonal predictions starting from 2018 July initial conditions show above normal frequency of tropical cyclones in the Western North Pacific and Central Pacific Oceans as observed. To understand physical mechanisms behind the active storm season in the Pacific, we conducted idealized seasonal forecasts by changing sea surface temperature spatial patterns, which is so called "real-time attribution" simulations. We find out that warmer subtropical Pacific associated with positive Pacific Meridional Mode (PMM), rather than central Pacific El Nino, was responsible for the active storm season. In the presentation, we will also show preliminary results for impact of anthropogenic forcing on the 2018 active storm season.

Keywords: Tropical Cyclone, Seasonal Prediction, Pacific Meridional Mode, Anthropogenic Forcing, Typhoon, Global Warming

©2019. Japan Geoscience Union. All Right Reserved. 

# Future change of tropical cyclone-induced waves in the Indian Ocean; An analysis based on super-high-resolution MRI-AGCM3.2 climate model

*Bahareh Kamranzad[1,2], Nobuhito Mori[1]

1. Disaster Prevention Research Institute, Kyoto University, 2. Hakubi Center for Advanced Research, Kyoto University

Indian Ocean experiences intensive tropical cyclones in both northern and southern parts. The Northern Indian Ocean (NIO) includes 7% of the global tropical cyclones which results in generating severe wave climate during the extreme events. In this study, future change of tropical cyclone-induced waves due to climate change is assessed in terms of change in the spatial distribution patterns and magnitude. The cyclone seasons in NIO are divided by pre-monsoon (especially May) and northeast monsoon (October–December). Moreover, there are few cyclones form the southwest monsoon during June and September. Hence, the assessment of future change of intensity of tropical cyclones and the generated waves is necessary to be performed on a monthly scale. For this purpose, wind field obtained from super-high-resolution atmospheric global climate model MRI-AGCM3.2S of the Japan Meteorological Agency (JMA) -with horizontal spatial and temporal output resolutions of 20 km and 1 hr., respectively- was used to force a numerical wave model (SWAN) in historical (1979-2003) and future (2075-2099) periods (based on Representative Concentration Pathway (RCP) 8.5 scenario).
Spatial distribution of annual extreme events in the domain shows that the concentration of tropical cyclones is in the NIO and around Madagascar (located in the Southern Indian Ocean (SIO)) generating high waves of the magnitudes of around 20 m during the events. Spatial distribution of monthly maximum values of the historical and future wind speed (WS) and significant wave height (SWH) indicates that according to historical projection, intense cyclones happen during May and June in NIO, while they can be observed mostly during December to April in the SIO. The future monthly distribution of cyclone induced waves in SIO shows a similar pattern to the historical events, except for winter tropical cyclones (November and December), which are decreased in the future, while increasing in the intensity can be observed during October and April in NIO.
Monthly variation of maximum events in the domain was assessed in the NIO and SIO, separately. According to the past studies, due to the global warming, tropical cyclones of hurricane intensity -which currently occur only in the pre and post-monsoon seasons- will likely be formed even during the summer monsoon in NIO. Our results illustrate an increase in the intensity of cyclones in the future, not only during the summer monsoon (July) but also during the winter monsoon (September and October). Results show that the range of change in the highest SWH in NIO is between -27% (in February) and +26% (in October). In the northern part of SIO, the intensity of future tropical cyclones will increase during the southwestern inter-monsoon season (March and April), whereas it will decrease at the end of southwestern monsoon season (September). In the southern part of SIO, the intensity of tropical cyclones will increase around 20% during northeastern monsoon (February and March), which results in a future increase of 40% in maximum SWH in February. Generally, change in highest SWH in the future follows the pattern of WS except for the northern parts of SIO when the highest increase in maximum SWH (21%) occurs in March whereas the highest increase in maximum WS occurs in April (25%). There is a 20% increase in maximum WS during February in southern parts of SIO which can be a reason for the increase of SWH during March in northern parts. It can be concluded that the change in the intensity of future tropical cyclones in NIO is higher than SIO. The range of change in highest SWH in NIO is larger than SIO, except for February when the maximum wave height in southern parts of SIO will increase about 40% in

©2019. Japan Geoscience Union. All Right Reserved. 

the future. Furthermore, the change in maximum SWH in northern parts of SIO seems to be affected by the change of tropical cyclones in southern parts of SIO.

Keywords: Indian Ocean, tropical cyclone, wave climate, climate change

©2019. Japan Geoscience Union. All Right Reserved. 

# The ocean-coupled global cloud-resolving modeling era

*Tomoki Miyakawa[1]

1. Atmosphere and Ocean Research Institute University of Tokyo

Developments of global cloud/cloud-system resolving models are recently in full activity in many modeling centers, with 9 members participating in a model inter-comparison project called the DYnamics of the Atmospheric general circulation Modeled On Non-hydrostatic Domains (DYAMOND). With the aid of the supercomputers, they are eyeing to become the main-stream in the next generation models for global simulations in the seasonal to multi-decadal range. Implementation of a fully dynamical ocean model is certainly an essential component in these developments. NICAM, a front-runner in DYAMOND project, can be coupled to COCO, the ocean component of a global climate model MIROC. The coupled version is called NICAM-COCO, or NICOCO, and is now being tested in pilot studies that involve atmosphere-ocean interactions.

An overview of these early studies will be presented, including how convection is affected by the existence of fine-scale ocean fronts, and how the Madden-Julian oscillation affects the initiation and termination of ENSO.

Keywords: ocean-coupled model, global cloud-resolving model, seasonal prediction

©2019. Japan Geoscience Union. All Right Reserved. 

# Westerly Wind Burst (WWB)/Easterly Wind Surge (EWS)-like stochastic forcing and the effects on ENSO prediction by the SINTEX-F system

*Takeshi Doi[1], Swadhin Behera[1], Toshio Yamagata[1]

1. JAMSTEC

Intra-seasonal surface westerly wind bursts (WWB)/easterly wind surges (EWS) in the tropical Pacific play important roles in the onset of El Nino/La Nina. However, the latest version of the SINTEX-F seasonal prediction system tends to underestimate the chance of occurrence of those winds. This problem may cause the relatively low skill of predicting the onset of ENSO, and the over-confident problems of ENSO prediction. In this study, we developed the WWB/EWS-like stochastic forcing parameterization, and examined the effects on ENSO prediction by the SINTEX-F system. In my talk, failure of 2014 El Nino prediction is the focus.

Keywords: ENSO prediction, Westerly Wind Burst, Easterly Wind Surge

©2019. Japan Geoscience Union. All Right Reserved. 

# The life-cycle of annual waves in the Pacific Ocean as identified by a seamless diagnosis for the energy flux

*Hidenori AIKI[1], Takahiro Shimura[2]

1. Institute for Space-Earth Environmental Research, Nagoya University, 2. Graduate School for Environmental Studies, Nagoya University

Synoptic-scale waves play an important role in tropical-extratropical interactions, that has been little investigated in terms of the transfers of wave energy owing to the lack of an appropriate diagnosis scheme in previous studies. A recent theoretical study has derived a seamless scheme that is able to identify the direction of group velocity for both gravity and planetary waves at all latitudes. This new scheme has been used in the present study to provide a first-ever energetic view for the life-cycle of annual waves in the Pacific Ocean in a set of shallow-water model experiments with climatological wind forcing. The new scheme is able to show, in particular for the third baroclinic mode, the signals of eastward energy flux associated with equatorial Kelvin waves that are distributed in the eastern part of the tropical Pacific Ocean. Waves in the tropical and subtropical regions are connected each other at the eastern boundary of the Pacific Ocean that has been viewed, for the first time in the history of geophysical fluid dynamics, in terms of the circulation of wave energy. Concerning the low-pass filtered time evolution of the energy flux, the reflection of equatorial waves at the western boundary is more clearly identified than that at the eastern boundary. These results for the analysis of climatological annual waves provide a basis for the analysis of waves with interannual variations in a future study to better understand, for example, tropical-extratropical interactions during El Nino and La Nina.

Keywords: tropical-extratropical interaction, seasonal climatology experiment, group velocity

©2019. Japan Geoscience Union. All Right Reserved. 

# Development of weakly coupled atmosphere-ocean data assimilation system and the evaluation of the coupled reanalysis in JMA/MRI

*Yosuke Fujii[1], Chiaki Kobayashi[1], Toshiyuki Ishibashi[1], Yuhei Takaya[1]

1. Meteorological Research Institute, Japan Meteorological Agency

JMA/MRI have developed a weakly-coupled Data Assimilation (DA) system, MRI-CDA1, based on JMA's operational systems. MRI-CDA1 is composed of the global atmosphere Four-Dimensional Variational (4DVAR) system for numerical weather predictions, the global ocean Three-Dimensional Variational (3DVAR) system for seasonal predictions, and the coupled atmosphere-ocean model for seasonal predictions. The coupled atmosphere-ocean model is adopted as the outer model of the atmospheric 4DVAR routine although the uncoupled atmospheric model is used as the inner model. While the atmospheric 4DVAR analysis is performed every 6 hours, the oceanic 3DVAR analysis is performed every 10 days and the oceanic analysis increments are applied in the integrations of the outer (coupled) model.

Coupled reanalysis experiments based on MRI-CDA1 are conducted for the period from November 2013 to December 2015. In the coupled reanalysis the excess rainfall found in the tropics in Japanese 55-year Reanalysis (JRA-55) is effectively suppressed, particularly in the Intertropcal Convergence Zone (ITCZ) in the Pacific. We also confirmed that the coupled DA system properly reproduces the lagged-correlated variations of Sea Surface Temperature (SST) and precipitation in the far western tropical North Pacific which is not reproduced by a regular uncoupled DA system. The variation of the precipitation is improved in the coupled reanalysis over the uncoupled one when only conventional data and oceanic data are assimilated. But the coupled DA system adjusts SST to the change of precipitation, instead of correcting the precipitation field, when atmospheric data from satellite are additionally assimilated. We also conducted another coupled reanalysis experiment in which the atmospheric observation error variances set larger than the original, and found that the variation of the precipitation in the tropics is roughly improved over the original coupled reanalysis.

Keywords: coupled data assimilation, coupled analysis, Subseasonal-to-seasonal prediction, sea surface temperature, precipitation

©2019. Japan Geoscience Union. All Right Reserved. 

[E] Oral | A (Atmospheric and Hydrospheric Sciences )：A-OS Ocean Sciences & Ocean Environment

Thu. May 30, 2019 3:30 PM - 5:00 PM JST | Thu. May 30, 2019 6:30 AM - 8:00 AM UTC | 105 1F

## [A-OS07] Climate variability and predictability on subseasonal to decadal timescales

convener:Takashi Mochizuki(Japan Agency for Marine-Earth Science and Technology), V Ramaswamy(NOAA GFDL), Doug Smith(Met Office), Yushi Morioka(Japan Agency for Marine-Earth Science and Technology), Chairperson:Yushi Morioka(Japan Agency for Marine-Earth Science and Technology), Takashi Mochizuki(Japan Agency for Marine-Earth Science and Technology)

Climate variability poses growing threats to human lives and socio-economic activities through changes in frequency and intensity of abnormal weather such as cold/heat waves and floods/droughts. This involves several climate phenomena with a wide range of timescales from subseasonal to decadal variations (e.g. MJO, IOD, ENSO, PDV, AMV). Many efforts have been made for understanding and predicting climate variations on each timescale, but there remain large uncertainties in simulation and prediction of subseasonal to decadal climate variations. This highlights lack of understanding of weather and climate interaction across different spatial and temporal timescales (e.g. tropical cyclones and ENSO) as well as multiple physical processes underlying climate variations (e.g. troposphere-stratosphere coupling, air-sea-ice interaction). This session aims to share current knowledge of subseasonal to decadal climate variability and predictability in order to identify the unresolved issues for better understanding and accurate prediction. This session invites all the abstracts related to the observational, theoretical, process-level and modelling research on subseasonal to decadal climate variability and predictability.

3:30 PM - 3:45 PM JST | 6:30 AM - 6:45 AM UTC

[AOS07-07] Decadal variability and predictability of the North Atlantic Oscillation

★Invited Papers

*Rosemary Eade[1,2], David Stephenson[2], Doug Smith[1], Adam Scaife[1,2], Leon Hermanson[1], Nick Dunstone[1] (1.Met Office Hadley Centre, 2.University of Exeter)

3:45 PM - 4:00 PM JST | 6:45 AM - 7:00 AM UTC

[AOS07-08] Seasonal to multi-year climate predictability in a climate model MIROC6

*Takahito Kataoka[1], Hiroaki Tatebe[1], Hiroshi Koyama[1], Takashi Mochizuki[1] (1.JAMSTEC Japan Agency for Marine-Earth Science and Technology)

4:00 PM - 4:15 PM JST | 7:00 AM - 7:15 AM UTC

[AOS07-09] Identifying the early 2000s hiatus associated with internal climate variability

*Xin-Gang Dai[1], Ping Wang[2] (1.Institute of Atmospheric Physics, Chinese Academy of Sciences, 2.Chinese Academy of Meteorological Sciences)

4:15 PM - 4:30 PM JST | 7:15 AM - 7:30 AM UTC

[AOS07-10] Decadal Evolution of the Surface Energy Budget during the Fast Warming and Global Warming Hiatus Periods in the ERA-Interim

*XIAOMING HU[1] (1.Sun Yat-sen University)

4:30 PM - 4:45 PM JST | 7:30 AM - 7:45 AM UTC

[AOS07-11] **The role of ocean variability for multi-year droughts in Australia**

*Andrea Taschetto[1,2], Alex Sen Gupta[1,2], Caroline C Ummenhofer[3], Matthew H England[1,2] (1.Climate Change Research Centre, University of New South Wales, Sydney, Australia, 2.ARC Centre of Excellence for Climate Extremes, University of New South Wales, Sydney, Australia, 3.Department of Physical Oceanography, Woods Hole Oceanographic Institution, Woods Hole, MA, USA)

4:45 PM - 5:00 PM JST | 7:45 AM - 8:00 AM UTC

[AOS07-12] Decadal variability and predictability in the Southern Ocean - implications for interpreting recent observed trends

★Invited Papers

*Liping Zhang[1,2], Thomas L Delworth[2], William Cooke[2,3], Xiaosong Yang[2,3] (1.Princeton University, 2.Geophysical Fluid Dynamics Laboratory, 3.UCAR)

# Decadal variability and predictability of the North Atlantic Oscillation

*Rosemary Eade[1,2], David Stephenson[2], Doug Smith[1], Adam Scaife[1,2], Leon Hermanson[1], Nick Dunstone[1]

1. Met Office Hadley Centre, 2. University of Exeter

The winter of 1962/63 was the coldest in the UK in over a century while the mildest winter occurred in 1988/89. For countries to be resilient against the impacts of large weather variations in the future, it is important to assess the likelihood of seeing such extreme fluctuations and understand the physical drivers. In Europe and North America, these fluctuations are related to a combination of year-to-year variability and low-frequency variability of the North Atlantic Oscillation (NAO). The NAO is now a significant source of predictability for seasonal forecasts in these regions, however the signal-to-noise ratio of the ensemble mean to total variability in these ensemble predictions has been shown to be anomalously small, which means the real world is more predictable than our climate models suggest. Here we provide a new evaluation of the ability of climate models to simulate and predict longer-term variability and extreme trends in the NAO. For this we use statistical analyses of the observations and climate model simulations, and assess predictability with a large multi-model ensemble of decadal predictions. We also investigate the drivers of NAO variability and trends using new results from the CMIP6 Decadal Climate Prediction Project and the Polar Amplification MIP.

Keywords: Decadal variability, North Atlantic Oscillation, Polar Amplification, Trend analysis

©2019. Japan Geoscience Union. All Right Reserved. 

# Seasonal to multi-year climate predictability in a climate model MIROC6

*Takahito Kataoka[1], Hiroaki Tatebe[1], Hiroshi Koyama[1], Takashi Mochizuki[1]

1. JAMSTEC Japan Agency for Marine-Earth Science and Technology

Seasonal to multi-year climate predictability is examined in hindcast experiments using the latest version of a climate model MIROC (MIROC6). The model is initialized by assimilating observed ocean temperature and salinity anomaly fields and full-filed of sea ice concentration. In addition, the atmospheric initial conditions are replaced with variables from JRA55 reanalysis and the hindcasts are issued on November 1st. On seasonal timescales, the MIROC6 prediction system shows an improvement in Niño3.4 prediction skill from that of MIROC5, though the skill itself is still modest. SLP variability around Japan appears to have predictive skill up to second winter (lead time of about 15 month) and summer (lead time of about 21 month) possibly due to the improved ENSO prediction skill and the better representation of East Asian monsoon. On longer timescales, although the predictive component largely originates from the externally forced variability, MIROC6 shows predictive skills in the surface air temperature particularly in the North Pacific and the North Atlantic.

Keywords: near-term prediction, seasonal prediction

©2019. Japan Geoscience Union. All Right Reserved. 

# Identifying the early 2000s hiatus associated with internal climate variability

*Xin-Gang Dai[1], Ping Wang[2]

1. Institute of Atmospheric Physics, Chinese Academy of Sciences, 2. Chinese Academy of Meteorological Sciences

This study focuses on re-examining the early 2000s hiatus and the associated key components of the global mean surface temperature (GMST) using multiscale statistics for five well-known gridded surface temperature and two reanalysis datasets. The hiatus is characterized as a near-zero trend on the decadal scale corresponding to the maximum P-value via an F-test in statistics. The results reveal that the hiatus exists in both the GMST and global mean air temperature (GMAT) time series, rather than in global warming component, which has maintained an approximately constant rate of change of approximately 0.08ºC/decade over the past three decades. The hiatus' s duration is different from that of time series such as 2002-2012/2001-2013/2002-2014 in HadCRUT4, NOAA-old, ERA-Interim and NCEP-R2. The newly gridded datasets with data infilling or bias correction for interpreting the sea surface temperature (SST) measurement from the old versions show a slightly higher trend from for 2002-2012 than the hiatus, which is thus regarded as a slowdown. Comparison suggests that the hiatus should be during the period 2002-2012. Orthogonal wavelet decomposition of the temperature time series shows that the hiatus was merely a decadal balance between cooling from interannual variability and global warming, in addition to weak warming from interdecadal and multidecadal climate oscillations. In addition, the evolutions of the GMST' s interannual composite well coincided with Niño3.4 SST anomalies, which is consistent with the numerical simulation performed by Kosaka and Xie in 2013. Hence, it is the anomalous El Niño Southern Oscillation (ENSO) events in the early 2000s that caused the hiatus despite a constant rate of global warming and the maximum magnitude of the multidecadal composite that led to the limited contribution to the trend during this period. The multidecadal composite follows a downward path, which implies that future climate conditions will likely rely on competition between multidecadal cooling and global warming if the multidecadal climate cycle repeats, as was experienced during the second half of the twentieth century.

Keywords: Global mean temperature, early 2000s hiatus, multiscale decomposition, global warming, multidecadal oscillation, interannual variability

©2019. Japan Geoscience Union. All Right Reserved. 

# Decadal Evolution of the Surface Energy Budget during the Fast Warming and Global Warming Hiatus Periods in the ERA-Interim

*XIAOMING HU[1]

1. Sun Yat-sen University

The global-mean surface temperature has experienced a rapid warming from the 1980s to early-2000s but a muted warming since, referred to as the global warming hiatus in the literature. Decadal changes in deep ocean heat uptake are thought to primarily account for the accelerated warming rate and subsequent slowdown. Here, we examine the role of ocean heat uptake in establishing the fast warming and warming hiatus periods in the ERA-Interim through a decomposition of the global-mean surface energy budget. We find the increase of carbon dioxide alone yields a nearly steady increase of the downward longwave radiation at the surface from the 1980s to the present, but neither accounts for the fast warming nor warming hiatus periods. During the global warming hiatus period, the transfer of latent heat energy from the ocean to atmosphere increases and the total downward radiative energy flux to the surface decreases due to a reduction of solar absorption caused primarily by an increase of clouds. The reduction of radiative energy into the ocean and the surface latent heat flux increase cause the ocean heat uptake to decrease and thus contribute to the slowdown of the global-mean surface warming. Our analysis also indicates that in addition to a reduction of deep ocean heat uptake, the fast warming period is also driven by enhanced solar absorption due predominantly to a decrease of clouds and by enhanced longwave absorption mainly attributed to the air temperature feedback.

Keywords: global warming, global warming hiatus, surface energy budget

©2019. Japan Geoscience Union. All Right Reserved. 

# The role of ocean variability for multi-year droughts in Australia

*Andrea Taschetto[1,2], Alex Sen Gupta[1,2], Caroline C Ummenhofer[3], Matthew H England[1,2]

1. Climate Change Research Centre, University of New South Wales, Sydney, Australia, 2. ARC Centre of Excellence for Climate Extremes, University of New South Wales, Sydney, Australia, 3. Department of Physical Oceanography, Woods Hole Oceanographic Institution, Woods Hole, MA, USA

Australian climate is strongly affected by variations in sea surface temperature in the Pacific, Indian and Southern Oceans. Over the northern and eastern regions of Australia, the El Niño –Southern Oscillation (ENSO) is the main phenomenon causing profound impacts in rainfall. On the southern regions, a large proportion of rainfall comes from synoptic weather systems at the mid-latitudes, such as cold fronts and cut-off lows. The interaction between the tropical modes of variability and the atmosphere dynamics at mid-latitudes makes difficult to understand the role of the oceans for droughts relative to the atmosphere internal variability.

The contribution of ocean versus atmosphere variability for Australian rainfall is investigated in this study. Numerical experiments are performed using the National Center for Atmospheric Research (NCAR) Community Earth System Model (CESM). Three multi-century simulations are integrated to address the role of the oceans for rainfall variability: (i) a fully coupled climate system run, (ii) an run forced with climatological cycle of SST, i.e. no SST variability beyond one year, and (iii) a run forced with varying SST, i.e. containing SST variability but no air-sea feedback.

Our results show that interannual variations in sea surface temperature has a significant impact on rainfall variability and extremes, such as multi-year droughts and pluvials. Ocean variability makes droughts more intense and modulates the duration of short-term dry spells. However, interannual variability in the oceans does not significantly affect the duration of droughts longer than 3 years. On the other hand, in a world with no year-to-year ocean variability, multi-year dry spells can last longer than oceanic-driven droughts. This can be explained by the influence that ENSO has over the tropics:ENSO is a crucial phenomenon for restoring droughts and pluvials. In the absence of ocean variability, there is no dominant climate driver that can act to terminate extended dry or wet periods.

Keywords: Precipitation variability, Droughts, El Niño - Southern Oscillation, atmospheric variability , ocean variability

©2019. Japan Geoscience Union. All Right Reserved. 

# Decadal variability and predictability in the Southern Ocean - implications for interpreting recent observed trends

*Liping Zhang[1,2], Thomas L Delworth[2], William Cooke[2,3], Xiaosong Yang[2,3]

1. Princeton University, 2. Geophysical Fluid Dynamics Laboratory, 3. UCAR

While decadal variability and predictability in the North Atlantic and North Pacific have received considerable attention, there has been less work on decadal variability and predictability in the Southern Ocean. As shown previously, a coherent mode of decadal to centennial variability exists in multiple climate models. The mechanism involves a multidecadal accumulation of heat in the subsurface of the Southern Ocean, which is then rapidly discharged through intense oceanic convection when the accumulation of subsurface heat reduces the stratification of the water column. The release of this accumulated subsurface heat can have considerable regional scale climatic impacts, along with substantial impacts on ocean heat uptake. Using a large suite of perfect predictability experiments, in concert with long control simulations, we show that this variability has a high degree of predictability. We present further results that show this type of variability may play an important role for interpreting recently observed trends of sea ice and temperature in the Southern Ocean. Specifically, observed trends over the last several decades resemble a particular phase of this variability in which reduced oceanic convection leads to subsurface warming and surface cooling, with associated increases in sea ice extent. This phase of natural variability may substantially contribute to observed decadal trends, working in concert with other factors.

©2019. Japan Geoscience Union. All Right Reserved. 

[E] Oral | A (Atmospheric and Hydrospheric Sciences )：A-OS Ocean Sciences & Ocean Environment

Thu. May 30, 2019 9:00 AM - 10:30 AM JST | Thu. May 30, 2019 12:00 AM - 1:30 AM UTC | 105 1F

## [A-OS10] Atlantic climate variability, and its global impacts and predictability

convener:Ingo Richter(JAMSTEC Japan Agency for Marine-Earth Science and Technology), Hiroki Tokinaga(Research Institute for Applied Mechanics, Kyushu University), Noel S Keenlyside(Geophysical Institute Bergen), Carlos R Mechoso(University of California Los Angeles), Chairperson:Hiroki Tokinaga(京都大学白眉センター), Ingo Richter

The Atlantic Ocean is subject to pronounced climate variations that occur on a wide range of time scales, including interannual variability in the equatorial and subtropical regions, and Atlantic multi-decadal variability (AMV), which has been linked with the Atlantic meridional overturning circulation (AMOC). These are connected to other climate variations across the globe. The AMV, e.g., has long been known to have global impacts, such as changes in the Indian, Asian and South American summer monsoons, and changes in the Pacific associated with the "global hiatus". Interannual variability in the equatorial and subtropical Atlantic has also been shown to influence global climate, including over Asia, while the freshening of the North Atlantic by melting of the Greenland ice cap is expected to influence all ocean basins via atmospheric bridges. Likewise, misrepresentation of the Atlantic can have global ramifications in climate models. Misrepresentation of the AMOC, e.g., has been associated with model biases in the entire Northern Hemisphere.<br/><br/>This session seeks observational, modeling, and theoretical studies on the mechanisms that determine the Atlantic mean climate and variability, as well as the predictability and global impacts of such variability. We also seek studies that evaluate climate model performance in the region. Topics include atmosphere-ocean-cloud interactions in the tropical Atlantic and their remote impacts; relationships between tropical and mid/high latitude variability; air-sea interaction along the Gulf Stream and its influence on cyclones and storm track evolution; variability in the Benguela upwelling region; influence of Agulhas leakage on the South Atlantic; coupled climate models biases in the region and their impacts; AMOC and long-term climate change.

9:00 AM - 9:15 AM JST | 12:00 AM - 12:15 AM UTC

[AOS10-01] Atlantic impacts on the tropical Pacific climate in the 2000s

*Takashi Mochizuki[1], Masahiro Watanabe[2], Masahide Kimoto[2] (1.Japan Agency for Marine-Earth Science and Technology, 2.Atmosphere-Ocean Research Institute, The University of Tokyo)

9:15 AM - 9:30 AM JST | 12:15 AM - 12:30 AM UTC

[AOS10-02] Recent acceleration of Arabian Sea warming induced by the Atlantic-western Pacific trans-basin multidecadal variability

*Cheng Sun[1] (1.Beijing Normal University)

9:30 AM - 9:45 AM JST | 12:30 AM - 12:45 AM UTC

[AOS10-03] **Westward Wind Changes over the Tropical and Mid-latitude Pacific in the Past Three Decades Driven by the Inter-basin Teleconnections**

★Invited Papers

*Xichen Li[1] (1.Institute of Atmospheric Physics)

9:45 AM - 10:00 AM JST | 12:45 AM - 1:00 AM UTC

[AOS10-04] On the Usefulness of the Atlantic Multidecadal Oscillation Index for Identifying Origins of North Atlantic Sea Surface Temperature Variability

*Jing Sun[1,2], Mojib Latif[1,3], Wonsun Park[1], Taewook Park[1,4] (1.GEOMAR Helmholtz Centre for Ocean Research Kiel, 2.Ocean University of China, 3.University of Kiel, 4.Korea Polar Research Institute)

10:00 AM - 10:15 AM JST | 1:00 AM - 1:15 AM UTC

[AOS10-05] Atlantic Multidecadal SST Signal Modulated by the Low-Frequency Mixed Layer Depth Variability

*Ayako Yamamoto[1], Hiroaki Tatebe[1], Masami Nonaka[1] (1.Japan Agency for Marine-Earth Science and Technology)

10:15 AM - 10:30 AM JST | 1:15 AM - 1:30 AM UTC

[AOS10-06] A High-Resolution Future Wave Climate Projection for the Northwestern Atlantic

*Adrean Webb[1], Tomoya Shimura[1], Nobuhito Mori[1] (1.Kyoto University, Disaster Prevention Research Institute)

# Atlantic impacts on the tropical Pacific climate in the 2000s

*Takashi Mochizuki[1], Masahiro Watanabe[2], Masahide Kimoto[2]

1. Japan Agency for Marine-Earth Science and Technology, 2. Atmosphere-Ocean Research Institute, The University of Tokyo

A subdecadal (i.e., 3-year-running means) variation over the tropical Pacific is very distinctively observed in the 2000s. Here, we have demonstrated that sea surface temperature (SST) anomalies in the tropical Atlantic contribute to forming high ocean temperature anomalies of the tropical Pacific in the early-2000s, by performing partial data assimilation of global climate model. Low SST over the equatorial Atlantic changes the Walker circulation and the associated weakening of the Pacific trade wind raises the equatorial SST on the subdecadal timescales. At the same time, high SST anomaly is generated also in the off-equatorial North Pacific through deepening of the upper ocean thermocline due to an accompanying anti-cyclonic surface wind anomaly aloft. In addition, the north tropical Atlantic SST may help the subdecadal warming in the equatorial Pacific, similar to the common changes working as a seasonal trigger of the so-called central Pacific El Nino Southern Oscillation event.

Keywords: subdecadal variability, interbasin influence, partial data assimilation, Pacific trade wind

©2019. Japan Geoscience Union. All Right Reserved. 

# Recent acceleration of Arabian Sea warming induced by the Atlantic-western Pacific trans-basin multidecadal variability

*Cheng Sun[1]

1. Beijing Normal University

The rapid warming of the Arabian Sea (AS) brings an increased risk of extreme weather and climate events,
e.g., flood, heat wave and cyclone. AS warming has significantly accelerated since the 1990s, in particular in the
spring season, stemming from the multidecadal variability of AS sea surface temperature (SST). Here, we show
that this variability is closely related to the Atlantic multidecadal oscillation (AMO). A set of Atlantic pacemaker
experiments with slab mixed-layer ocean model successfully reproduce the AS spring multidecadal variability and
its connection with the AMO. An atmospheric teleconnection from the Atlantic to the AS in the preceding winter
and associated thermodynamic air-sea feedback are found important. The teleconnection can be recreated by the
atmospheric model when the SSTs of AMO and its trans-basin footprint over western Pacific (WP) are prescribed
simultaneously. The WP SST warming associated with AMO positive phase induces a Gill-type Rossby wave
response over the AS, showing an anomalous low and converging southerlies that weaken the winter northerly.
A positive wind-evaporation-SST feedback further develops, leading to the AS SST anomalies being formed and
maintained to the subsequent spring. The concurrent cold-to-warm phase shift of AMO and its WP SST footprint
since the 1990s contributes constructively to the rapid warming of AS. Our results suggest a key role of trans-basin
interactions in the attribution of historical regional SST warming and constraint of projected future warming.

Keywords: Atlantic multidecadal oscillation , Trans-basin variability, Arabian Sea warming

©2019. Japan Geoscience Union. All Right Reserved. 

# Westward Wind Changes over the Tropical and Mid-latitude Pacific in the Past Three Decades Driven by the Inter-basin Teleconnections

*Xichen Li[1]

1. Institute of Atmospheric Physics

Due to its active role in the atmosphere-ocean interactions and in the global climate variability, the trade wind regime over the Pacific Ocean has been receiving increased attention. Although the intensification of the equatorial trade wind in recent decades has been widely investigated, the meridional extension of this easterly wind change and the associated mechanism remain unclear. To untangle this problem, we combine observations, reanalysis datasets, and a hierarchy of climate model simulations. Analysis based on measurements and reanalysis datasets show that the intensified easterly wind anomaly is not only confined within the tropical basin, but also extends to the mid-latitude Pacific, from 40˚S to 40˚N. In the tropics, the trade wind change is primarily attributed to the enhanced Walker circulation driven by the inter-basin teleconnection and further the decadal variability over the Atlantic and the Pacific oceans, whereas in the mid-latitudes, the changes in sub-tropical highs and Aleutian Low become more dominant. While the altered winds can contribute to the observed sea surface temperature (SST) changes in both tropical and mid-latitude Pacific, they are not driven by the regional Pacific SST changes. Instead, the wind changes are mostly caused by remote influences originated from the tropical Atlantic and Indian Ocean SST changes through stationary Rossby waves. This finding builds a direct pathway linking the tropical Atlantic and Indian Ocean to the mid-latitude Pacific. This pathway has a broad implication for understanding air-sea interactions and sea level changes over the Pacific, and may have an important impact on the interannual and decadal predictability of the Pacific climate variability, such as Pacific Decadal Oscillation and El Niño –Southern Oscillation.

Keywords: Pacific, Westerly Wind, Interbasin Teleconnection

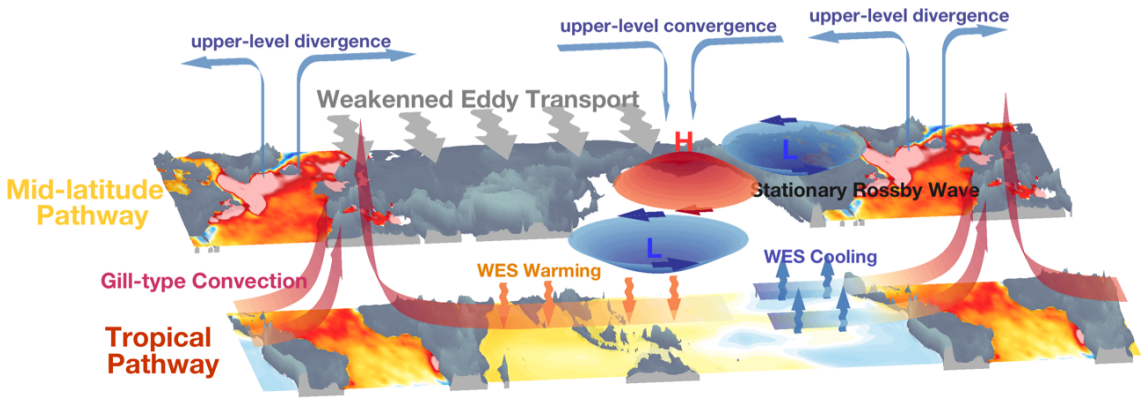


©2019. Japan Geoscience Union. All Right Reserved. 

# On the Usefulness of the Atlantic Multidecadal Oscillation Index for Identifying Origins of North Atlantic Sea Surface Temperature Variability

*Jing Sun[1,2], Mojib Latif[1,3], Wonsun Park[1], Taewook Park[1,4]

1. GEOMAR Helmholtz Centre for Ocean Research Kiel, 2. Ocean University of China, 3. University of Kiel, 4. Korea Polar Research Institute

We provide, on the basis of observations and climate models, an interpretation of the Atlantic Multidecadal Oscillation (AMO) index which is widely used in studies addressing sea surface temperature (SST) variability over the North Atlantic (NA). In particular, the AMO index is often used as an index of the Atlantic Meridional Overturning Circulation (AMOC). The AMO index, defined here as the anomalous North Atlantic SST averaged over 0˚ - 60˚ N, accounts for significant SST variability over the tropical and subpolar NA. Climate models analyzed in this study suggest that the AMOC only accounts for significant SST variability over the subpolar NA. In these models, a low-pass filtered AMO index also is associated with SST variability only over the subpolar NA and tracks well multidecadal AMOC variability. SST variability over the tropical NA has previously been suggested to be largely governed by local surface wind variability, which can be amplified the wind-evaporation-SST feedback, and remote forcing by El Niñ o/Southern Oscillation, the leading mode of interannual variability over the tropical Pacific. The AMO index lumps together SST variability associated with different physical mechanisms, which limits the usefulness of the index to understand the origins of NA SST variability. Our results may help to reconcile seemingly competing results about the role of ocean dynamics in NA SST variability.

Keywords: Atlantic Multidecadal Oscillation/Variability, Atlantic Meridional Overturning Circulation, North Atlantic sea surface temperature

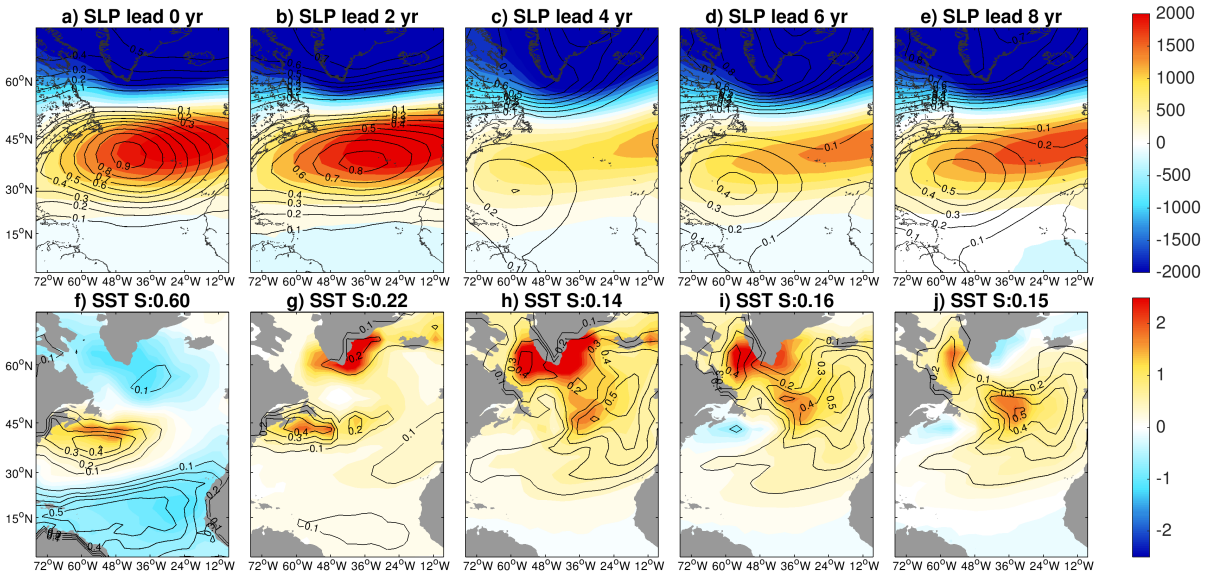


©2019. Japan Geoscience Union. All Right Reserved. 

# Atlantic Multidecadal SST Signal Modulated by the Low-Frequency Mixed Layer Depth Variability

*Ayako Yamamoto[1], Hiroaki Tatebe[1], Masami Nonaka[1]

1. Japan Agency for Marine-Earth Science and Technology

Atlantic Multidecadal Oscillation (AMO) has conventionally been attributed to the heat transport associated with the Atlantic Meridional Overturning Circulation. A recent study, however, challenged this paradigm and indicated that the North Atlantic basin-wide sea surface temperature (SST) pattern analogous to AMO can emerge owing to the atmospheric stochastic forcings in slab ocean models, without an active ocean. Subsequent studies have disputed this finding, arguing that the cause of the SST warming differ between the slab ocean models and fully-coupled models; however, a consensus is yet to be reached.

In this study, we take an approach to resolve this conundrum, by partitioning the multidecadal SST tendency into a part that is induced by the surface heat fluxes and another by the ocean, using a latest version of a fully-coupled climate model, MIROC6. We found that the heat flux term is primarily responsible for the North Atlantic subpolar SST warming, opposing the cooling caused by the oceanic term, despite that the associated heat flux anomalies are upward. Further decomposition of the heat flux term indicates that it is the mixed layer depth (MLD) deepening that makes the ocean less susceptible for cooling. This MLD variability is essentially induced by the anomalous salinity transport by the Gulf Stream modulated by the multidecadal North Atlantic Oscillation. The tropical North Atlantic SST signal, in contrast, arises due to the surface heat fluxes. Our study thus implies the key role of both air-sea fluxes and the ocean dynamics in the emergence of the AMO signal.

Keywords: Atlantic Multidecadal Oscillation/Variability, Gulf Stream, mixed-layer depth

©2019. Japan Geoscience Union. All Right Reserved. 

# A High-Resolution Future Wave Climate Projection for the Northwestern Atlantic

*Adrean Webb[1], Tomoya Shimura[1], Nobuhito Mori[1]

1. Kyoto University, Disaster Prevention Research Institute

A high-resolution wave climate projection for the Northwestern Atlantic has been conducted to help assess possible regional impacts under an RCP8.5 climate forcing scenario. Here, NOAA WAVEWATCH III is utilized to resolve the Northwestern Atlantic and US Eastern Coast at approximately 21 km and 7 km, respectively. Hourly wind field forcings are provided by MRI-AGCM 3.2S at a 21 km/lat resolution and the increased temporal frequency and spatial resolution allow for better modeling of large storm events. Climatological (25-year) significant wave height differences between future and historical periods indicate that a seesaw effect will occur, with decreases occurring in the Northwest Atlantic and Gulf of Mexico and increases occurring in the Caribbean Sea. Other notable changes include decreases in incident shoreline energy along the US East Coast. Further details of the projection will be discussed, including underlying wind field changes and extreme wave statistics.

Keywords: wave climate, Northwest Atlantic, WaveWatch III

©2019. Japan Geoscience Union. All Right Reserved. 

[E] Oral | A (Atmospheric and Hydrospheric Sciences )：A-OS Ocean Sciences & Ocean Environment

Thu. May 30, 2019 10:45 AM - 12:15 PM JST | Thu. May 30, 2019 1:45 AM - 3:15 AM UTC | 105 1F

## [A-OS10] Atlantic climate variability, and its global impacts and predictability

convener:Ingo Richter(JAMSTEC Japan Agency for Marine-Earth Science and Technology), Hiroki Tokinaga(Research Institute for Applied Mechanics, Kyushu University), Noel S Keenlyside(Geophysical Institute Bergen), Carlos R Mechoso(University of California Los Angeles), Chairperson:Ingo Richter, Hiroki Tokinaga(京都大学白眉センター)

The Atlantic Ocean is subject to pronounced climate variations that occur on a wide range of time scales, including interannual variability in the equatorial and subtropical regions, and Atlantic multi-decadal variability (AMV), which has been linked with the Atlantic meridional overturning circulation (AMOC). These are connected to other climate variations across the globe. The AMV, e.g., has long been known to have global impacts, such as changes in the Indian, Asian and South American summer monsoons, and changes in the Pacific associated with the "global hiatus". Interannual variability in the equatorial and subtropical Atlantic has also been shown to influence global climate, including over Asia, while the freshening of the North Atlantic by melting of the Greenland ice cap is expected to influence all ocean basins via atmospheric bridges. Likewise, misrepresentation of the Atlantic can have global ramifications in climate models. Misrepresentation of the AMOC, e.g., has been associated with model biases in the entire Northern Hemisphere.<br/><br/>This session seeks observational, modeling, and theoretical studies on the mechanisms that determine the Atlantic mean climate and variability, as well as the predictability and global impacts of such variability. We also seek studies that evaluate climate model performance in the region. Topics include atmosphere-ocean-cloud interactions in the tropical Atlantic and their remote impacts; relationships between tropical and mid/high latitude variability; air-sea interaction along the Gulf Stream and its influence on cyclones and storm track evolution; variability in the Benguela upwelling region; influence of Agulhas leakage on the South Atlantic; coupled climate models biases in the region and their impacts; AMOC and long-term climate change.

10:45 AM - 11:00 AM JST | 1:45 AM - 2:00 AM UTC

### [AOS10-07] Tropical Atlantic Impact on ENSO predictability

★Invited Papers

*Belen Rodriguez-Fonseca[1,2], Irene - Polo[1], Elsa - Mohino[1], Teresa - Losada[1], Marta - Martin-Rey[5], Roberto - Mechoso[3], Noel - Keenlyside[4] (1.Department of Physics of the Earth and Astrophysics, UCM, Madrid, Spain, 2.Institute of Geosciences, IGEO, UCM-CSIC, Madrid, Spain, 3.Department of Atmospheric and Oceanic Sciences, UCLA, Los Angeles, USA, 4.Geophysical Institute, University of Bergen, Norway, 5.Instituto de Ciencias del Mar, Barcelona, Spain)

---

11:00 AM - 11:15 AM JST | 2:00 AM - 2:15 AM UTC

### [AOS10-08] Interannual variability of Antarctic Intermediate Water in the tropical North Atlantic

*Yao Fu[1], Chunzai Wang[1], Peter Brandt[2,3], Richard J. Greatbatch[2,3] (1.State Key Laboratory of Tropical Oceanography, South China Sea Institute of Oceanology, Chinese Academy of Sciences, Guangzhou, China, 2.GEOMAR Helmholtz Centre for Ocean Research Kiel, Kiel, Germany , 3.Christian-Albrechts-Universität zu Kiel, Kiel, Germany)

---

11:15 AM - 11:30 AM JST | 2:15 AM - 2:30 AM UTC

### [AOS10-09] Understanding the mechanisms of the Atlantic meridional climate variability

*Hyacinth C Nnamchi[1], Riccardo Farneti[2], Noel S Keenlyside[3], Fred Fred Kucharski[2], Mojib Latif[1] (1.GEOMAR Helmholtz Centre for Ocean Research Kiel, Kiel, Germany, 2.Abdus Salam International Centre for Theoretical Physics, Trieste, Italy, 3.Geophysical Institute, University of Bergen, and Bjerknes Centre for Climate Research, Bergen, Norway)

---

11:30 AM - 11:45 AM JST | 2:30 AM - 2:45 AM UTC

### [AOS10-10] The corss-equatorical gradient variability: The role of heat, momentum, and freshwater flux

*Takahito Kataoka[1] (1.JAMSTEC Japan Agency for Marine-Earth Science and Technology)

11:45 AM - 12:00 PM JST | 2:45 AM - 3:00 AM UTC

[AOS10-11] Generation mechanisms of the Benguela Nino with a focus on local amplification

*Tomoki Tozuka[1], Ryo Kobayashi[1] (1.Department of Earth and Planetary Science, Graduate School of Science, The University of Tokyo)

12:00 PM - 12:15 PM JST | 3:00 AM - 3:15 AM UTC

[AOS10-12] **Seasonal energy analysis for baroclinic waves in equatorial Atlantic through a diagnostic scheme for energy flux**

*Qingyang Song[1], Hidenori AIKI[1] (1.Institute of space-earth environmental research, Nagoya University)

# Tropical Atlantic Impact on ENSO predictability

*Belen Rodriguez-Fonseca[1,2], Irene - Polo[1], Elsa - Mohino[1], Teresa - Losada[1], Marta - Martin-Rey[5], Roberto - Mechoso[3], Noel - Keenlyside[4]

1. Department of Physics of the Earth and Astrophysics, UCM, Madrid, Spain, 2. Institute of Geosciences, IGEO, UCM-CSIC, Madrid, Spain, 3. Department of Atmospheric and Oceanic Sciences, UCLA, Los Angeles, USA, 4. Geophysical Institute, University of Bergen, Norway, 5. Instituto de Ciencias del Mar, Barcelona, Spain

Observational studies have identified periods of enhanced ENSO predictability from tropical Atlantic variability. Some works have found that this enhancement is provided by the boreal summer Atlantic Equatorial Mode (EM) impact on the atmospheric processes that trigger the following winter ENSO phenomenon. Other works have found how the variability of sea surface temperature (SST) in the northern tropical Atlantic (NTA) during boreal spring acts as ENSOs optimal predictor. The periods of enhanced ENSO predictability appear in phase with the Atlantic Multidecadal Variability (AMV) but no physical explanation has been posed so far. Here we present a hypothesis that conciliates for the first time the existence of both relationships in observations . The results are tested in CMIP5 PI-Control simulations, which allows consideration of a large number of time-periods in which either the NTA or the EM impact ENSO are tested. Model results are consistent with our hypothesis about the switch for the inter-basin connections and the proposed mechanisms. In addition, the model bias in global SST consisting of too high values south of the equator favors some interbasin teleconnections more than others.

Keywords: Atlantic-Pacific interbasin connections, tropical Atlantic variability, ENSO predictability, CMIP5

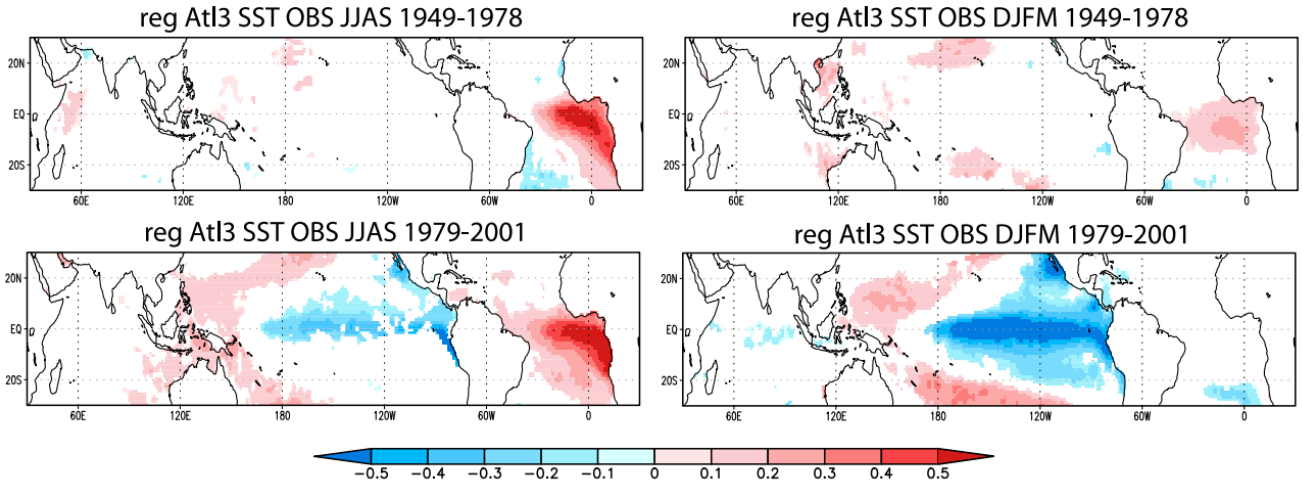


©2019. Japan Geoscience Union. All Right Reserved. 

# Interannual variability of Antarctic Intermediate Water in the tropical North Atlantic

*Yao Fu[1], Chunzai Wang[1], Peter Brandt[2,3], Richard J. Greatbatch[2,3]

1. State Key Laboratory of Tropical Oceanography, South China Sea Institute of Oceanology, Chinese Academy of Sciences, Guangzhou, China, 2. GEOMAR Helmholtz Centre for Ocean Research Kiel, Kiel, Germany , 3. Christian-Albrechts-Universität zu Kiel, Kiel, Germany

Interannual variability of Antarctic Intermediate Water (AAIW) in the tropical North Atlantic is investigated using the GECCO2 ocean state estimate and Argo data. AAIW salinity variability near the western boundary is shown to be highly correlated with the western boundary current (WBC) transport on interannual timescales. Northward propagating anomalies are associated with the WBC variability that, in turn, is related to the large-scale wind stress curl forcing by means of the Sverdrup balance. AAIW anomalies also propagate westward with the speed of baroclinic Rossby waves, indicating that the westward propagation of baroclinic Rossby waves also plays a role in the variability of AAIW characteristics. Slow eastward spreading of AAIW anomalies is also identified on decadal timescales. Understanding the observed interannual and decadal variability of AAIW salinity is important to properly interpret salinity changes with respect to changes in the hydrological cycle.

Keywords: Interannual variability of Antarctic Intermediate Water (AAIW) in the tropical North Atlantic, Meridional propagating AAIW salinity anomalies associated with the western boundary current variability, Zonal propagating AAIW anomalies related to baroclinic Rossby wave propagation

©2019. Japan Geoscience Union. All Right Reserved. 

# Understanding the mechanisms of the Atlantic meridional climate variability

*Hyacinth C Nnamchi[1], Riccardo Farneti[2], Noel S Keenlyside[3], Fred Fred Kucharski[2], Mojib Latif[1]

1. GEOMAR Helmholtz Centre for Ocean Research Kiel, Kiel, Germany, 2. Abdus Salam International Centre for Theoretical Physics, Trieste, Italy, 3. Geophysical Institute, University of Bergen, and Bjerknes Centre for Climate Research, Bergen, Norway

Decadal climate variability over tropical Atlantic is dominated by the Atlantic meridional mode (AMM). The AMM is characterized by opposite sea surface temperature anomalies to the north and south of the equator, anomalous wind flow from the cooler to the warmer hemisphere and meridional shift of the inter-tropical convergence zone. The tropical variability has also been linked to meridional variability in the South Atlantic and the extratropics of North Atlantic, with far-reaching impacts over the adjacent continents. The AMM is primarily understood in terms of the thermodynamic ocean-atmosphere interactions, particularly, the wind-evaporation sea surface feedback. Using a global ocean model forced by atmospheric observations, this study suggests that the Atlantic meridional overturning circulation may affect the Atlantic-scale meridional climate variability.

Keywords: Atlantic meridional mode, AMOC, WES feedback

©2019. Japan Geoscience Union. All Right Reserved. 

# The corss-equatorical gradient variability: The role of heat, momentum, and freshwater flux

*Takahito Kataoka[1]

1. JAMSTEC Japan Agency for Marine-Earth Science and Technology

The ocean-atmosphere feedback associated with the thermodynamic coupling among wind speed, evaporation, and sea surface temperature (SST), called the wind-evaporation-SST (WES) feedback, contributes to the cross-equatorial SST gradient over the tropical oceans. By conducting an eigenanalyses of simple linear air-sea coupled models, it is shown that three additional feedback processes are present when the variable oceanic mixed layer depth (MLD) is considered. The horizontal structures of the leading modes are similar to the WES mode, which shows a meridional dipole in the SST anomalies straddling the equator with cross-equatorial wind anomalies that represent the weakening/strengthening of the trade winds over the warm/cool SST anomalies.
In the presence of the damping term, the WES mode exists as a least damped mode consistent with previous studies. When the buoyancy flux anomaly associated with the latent heat flux anomaly is considered, a similar dipole mode in obtained, but the decaying time scale is about 40 % smaller. The freshwater flux coupling also gives a cross-equatorial gradient mode, but its stability is even smaller (decaying time scale is about 30 % of that of the WES). On the other hand, the momentum coupling allows a strongest meridional dipole variability, which is weakly unstable, indicating the importance of the wind mixing effect on the tropical meridional modes.

Keywords: air-sea interaction, tropics, ocean mixed layer

©2019. Japan Geoscience Union. All Right Reserved. 

# Generation mechanisms of the Benguela Nino with a focus on local amplification

*Tomoki Tozuka[1], Ryo Kobayashi[1]

1. Department of Earth and Planetary Science, Graduate School of Science, The University of Tokyo

Benguela Nino is associated with positive sea surface temperature (SST) anomalies off the west coast of Angola and Namibia in the South Atlantic. Although both local and remote forcing have been indicated to contribute to the development of Benguela Nino, the reason why their relative contribution varies among the events has not been clarified. Thus, the generation mechanisms of the Benguela Nino are investigated in this study by categorizing the events into locally amplified and non-locally amplified events depending on whether alongshore wind anomalies contribute to the development of the Benguela Nino. It is found that the locally events are associated with alongshore northerly wind anomalies related to anomalous weakening of the subtropical anticyclone in the South Atlantic known as St. Helena High and the continental low named Angola Low. On other hands, no alongshore wind anomalies that favor the development of SST anomalies exist in the non-locally amplified events. A mixed layer heat budget analysis reveals that the surface heat flux term is greater in the locally amplified events owing to smaller latent heat release associated with the weakening of the climatological southerly winds, while the anomalous warming by the advection term is stronger in the non-locally amplified events.

Keywords: Coastal Nino, South Atlantic, Interannual variation, St. Helena High, Angola Low

©2019. Japan Geoscience Union. All Right Reserved. 

# Seasonal energy analysis for baroclinic waves in equatorial Atlantic through a diagnostic scheme for energy flux

*Qingyang Song[1], Hidenori AIKI[1]

1. Institute of space-earth environmental research, Nagoya University

This study applied a gravity-reduced ocean model to simulate three baroclinic normal modes covering 20 years for energy analysis in Atlantic Ocean. The model, considering lateral mixing, is driven by decomposed wind forcing for each mode. Energy flux were calculated through a recently proposed diagnostic scheme with model output for all the three modes. The scheme is capable of altering pressure flux to the direction parallel to group velocities of Rossby and mixed Rossby waves in equatorial region (4° N to 4°S) without affecting the divergence. The obtained annual energy flux confirmed the dominant of westward Rossby waves in the northern and southern part of the equatorial region, while eastward Kelvin and mixed Rossby waves are most prevail in central and eastern part. The results are consistent with the fact that in the west tropical Atlantic, the most prominent signal is annual and in the central and east Atlantic, is semi-annual. Additionally, three monthly averaged energy flux revealed the seasonal energy cycle of baroclinic waves in equatorial Atlantic. Two energy sources in August and April emerged in western (around 35°W) and central part (around 15°W) of the equator in Atlantic ocean respectively. Those results suggested that the energy flux calculated by new proposed scheme in Atlantic Ocean can provide a powerful tool for energy analysis making significant contributions for further climate predictions.

Keywords: Equatorial basin mode, Energy flux, Tropical Atlantic, Seasonal variability

©2019. Japan Geoscience Union. All Right Reserved. 

[E] Poster | A (Atmospheric and Hydrospheric Sciences)：A-OS Ocean Sciences & Ocean Environment

Thu. May 30, 2019 3:30 PM - 5:00 PM JST | Thu. May 30, 2019 6:30 AM - 8:00 AM UTC | Poster Hall International Exhibition Hall8, Makuhari Messe_4

## [A-OS10] Atlantic climate variability, and its global impacts and predictability

convener:Ingo Richter(JAMSTEC Japan Agency for Marine-Earth Science and Technology), Hiroki Tokinaga(Research Institute for Applied Mechanics, Kyushu University), Noel S Keenlyside(Geophysical Institute Bergen), Carlos R Mechoso(University of California Los Angeles)

The Atlantic Ocean is subject to pronounced climate variations that occur on a wide range of time scales, including interannual variability in the equatorial and subtropical regions, and Atlantic multi-decadal variability (AMV), which has been linked with the Atlantic meridional overturning circulation (AMOC). These are connected to other climate variations across the globe. The AMV, e.g., has long been known to have global impacts, such as changes in the Indian, Asian and South American summer monsoons, and changes in the Pacific associated with the "global hiatus". Interannual variability in the equatorial and subtropical Atlantic has also been shown to influence global climate, including over Asia, while the freshening of the North Atlantic by melting of the Greenland ice cap is expected to influence all ocean basins via atmospheric bridges. Likewise, misrepresentation of the Atlantic can have global ramifications in climate models. Misrepresentation of the AMOC, e.g., has been associated with model biases in the entire Northern Hemisphere.<br/><br/>This session seeks observational, modeling, and theoretical studies on the mechanisms that determine the Atlantic mean climate and variability, as well as the predictability and global impacts of such variability. We also seek studies that evaluate climate model performance in the region. Topics include atmosphere-ocean-cloud interactions in the tropical Atlantic and their remote impacts; relationships between tropical and mid/high latitude variability; air-sea interaction along the Gulf Stream and its influence on cyclones and storm track evolution; variability in the Benguela upwelling region; influence of Agulhas leakage on the South Atlantic; coupled climate models biases in the region and their impacts; AMOC and long-term climate change.

### [AOS10-P01] The strengthening of Amazonian precipitation during the wet season driven by tropical sea surface temperature forcing

*Xinyue Wang[1], Xichen Li[1], Jiang Zhu[1], Clemente A S Tanajura[2] (1.Institute of Atmospheric Physics, Chinese Academy of Sciences, 2.Institute of Physics, Federal University of Bahia, Salvador, Brazil)

### [AOS10-P02] Linear inverse modeling of the tropical Atlantic

*Ingo Richter[1], Ping Chang[2] (1.JAMSTEC Japan Agency for Marine-Earth Science and Technology, 2.Texas A&M University)

### [AOS10-P03] Relationships Among Inter-model Spread and Biases in Tropical Atlantic Sea Surface Temperatures

Elsa - Mohino Harris[1], *Belen Rodriguez-Fonseca[1,2], Teresa - Losada[1], Irene - Polo[1], Roberto - Mechoso[3] (1.Department of Physics of the Earth and Astrophysics, Universidad Complutense de Madrid, 28040, Madrid, Spain. , 2.Institute of Geosciences IGEO,UCM-CSIC, 28040, Madrid, Spain., 3.Department of Atmospheric and Oceanic Sciences, UCLA, Los Angeles, USA)

### [AOS10-P04] Revisiting the CMIP5 Thermocline in the Equatorial Pacific and Atlantic Oceans

Antonio - Castaño[1,2], Elsa - Mohino[1], *Belen Rodriguez-Fonseca[1,2], Teresa - Losada[1] (1.Department of Physics of the Earth and Astrophysics, Universidad Complutense de Madrid, 28040, Madrid, Spain., 2.Institute of Geosciences, IGEO, UCM-CSIC 28040, Madrid, Spain.)

### [AOS10-P05] Lagged Effects of North Atlantic SST Anomalies on Weather in Remote Areas

*Natalia Gnatiuk[1], Timo Vihma[2], Leonid Bobylev[1] (1.Nansen International Environmental and Remote Sensing Centre, 2.Finnish Meteorological Institute)

## [AOS10-P06] SST anomalies in the northern tropical Atlantic as a negative feedback to ENSO development

*Ingo Richter[1], Hiroki Tokinaga[2], Yu Kosaka[3], Takeshi Doi[1] (1.JAMSTEC Japan Agency for Marine-Earth Science and Technology, 2.Kyoto University, 3.University of Tokyo)

# The strengthening of Amazonian precipitation during the wet season driven by tropical sea surface temperature forcing

*Xinyue Wang[1], Xichen Li[1], Jiang Zhu[1], Clemente A S Tanajura[2]

1. Institute of Atmospheric Physics, Chinese Academy of Sciences, 2. Institute of Physics, Federal University of Bahia, Salvador, Brazil

Amazonian rainfall plays a critical role in the global climate system and the hydrological cycle. It is thus important to quantify changes in the Amazonian rainfall and clarify its mechanism. Previous studies indicate that the interannual variability of Amazonian precipitation could be largely attributed to variabilities in the South American monsoon system and the El Niño Southern Oscillation. However, the trend of the wet season tropical Amazonian precipitation during recent decades is not very well investigated. In this study, by combining both satellite and in situ observations, it is revealed that tropical Amazonian precipitation has significantly increased by~180 to 600 mm (in different datasets) in the wet season during the satellite era from 1979 to 2015. We then use a state-of-the-art atmospheric model to simulate the impact of the tropical sea surface temperatures (SSTs) on the precipitation changes. Results show that the multidecadal warming of the tropical Atlantic has contributed more than half of this precipitation change over the past three decades, while the east Pacific cooling plays a secondary role. We finally combine the simulation results and the reanalysis data to investigate the mechanisms of this process, i.e. the SST variability dramatically increases the convergence of the moisture transport over the Amazon region. The precipitation changes over the Amazon region largely impact on the local hydrological cycle and the ecosystem, and have important impacts on the global climate system by mediating the teleconnection between the Pacific and the Atlantic oceans. Our results show that the long-term change in the wet season Amazonian precipitation is important and deserves further investigation and discussion.

Keywords: convective precipitation, Amazon, tropical Atlantic, moisture convergence

©2019. Japan Geoscience Union. All Right Reserved. 

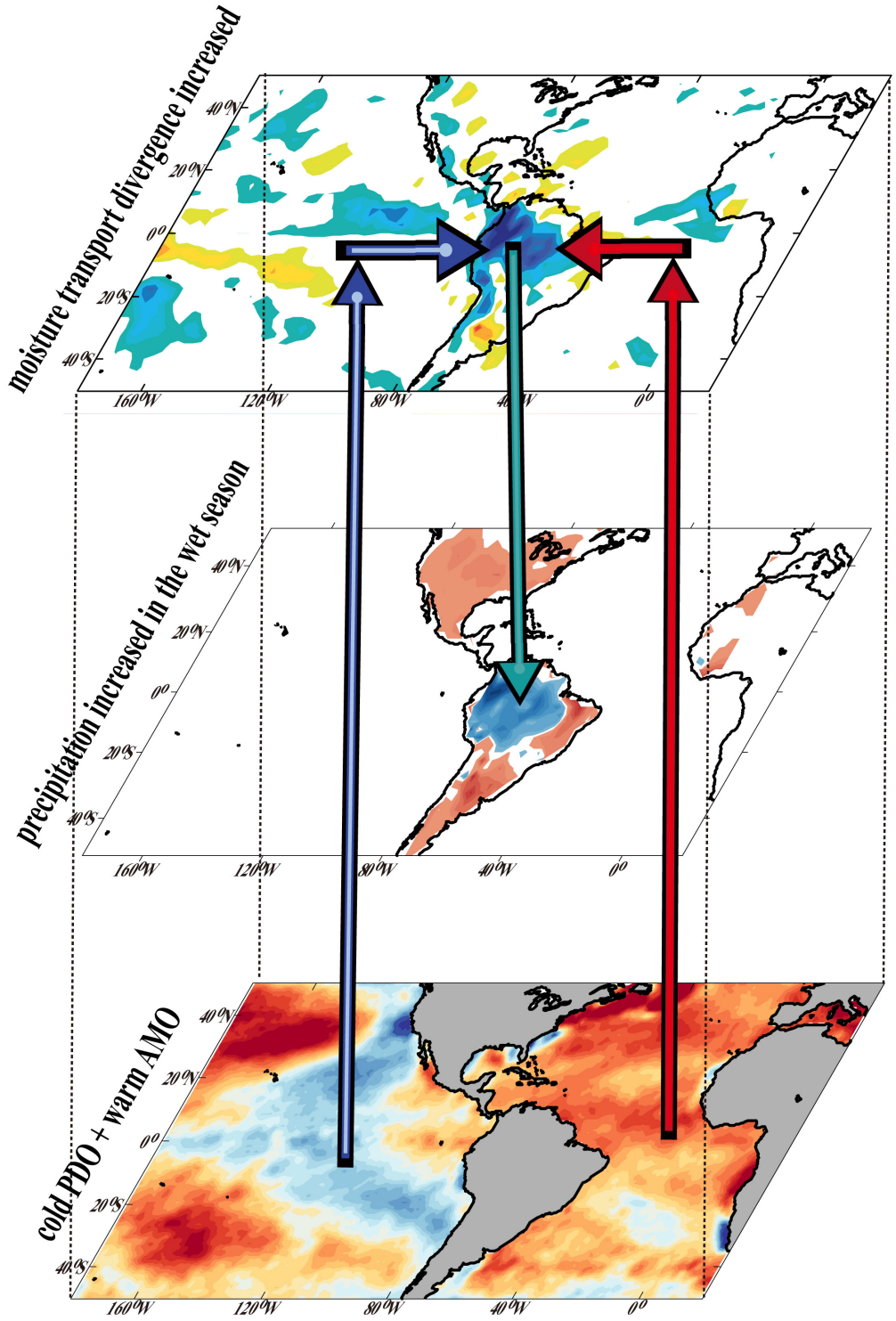


©2019. Japan Geoscience Union. All Right Reserved. 

# Linear inverse modeling of the tropical Atlantic

*Ingo Richter[1], Ping Chang[2]

1. JAMSTEC Japan Agency for Marine-Earth Science and Technology, 2. Texas A&M University

The tropical Atlantic features variability at interannual and decadal time scales that is known to have a strong influence on the surrounding continents and possibly other ocean basins. Current prediction systems, however, struggle to skillfully predict sea-surface temperature (SST), let alone its impact on rainfall over the adjacent continents. It is often assumed that this poor prediction skill is due to the severe SST biases and misrepresented variability patterns that most models feature in the region but this has recently been called into question.

In the present study, we construct a simple statistical model of the tropical Atlantic to 1) investigate the influence of model biases on prediction skill, and 2) establish a benchmark to evaluate dynamical model against. Using 35 fully coupled ocean-atmosphere GCMs from the pre-industrial control experiment (piControl) of the Coupled Model Intercomparison Project Phase 5 (CMIP5) we construct a linear inverse model (LIM) for each GCM based on tropical SSTs only. The LIM thus constructed is then used to predict SSTs for the period 2000-2017 from the NCEP/NCAR reanalysis. These predictions are compared to those from a LIM constructed using the NCEP/NCAR reference for the period 1948-1999 as training data. Since each of the model LIMs is constructed from more or less unrealistic variability patterns one would expect to see a clear impact on prediction skill.

The results, however, indicate that prediction skill in the tropical Atlantic is relatively insensitive to the tropical variability patterns of each model. Only some cases see a marked deterioration of prediction skill relative to the reference model. The LIM performs well in the subtropical north and south Atlantic. In the equatorial Atlantic, on the other hand, skill is rather poor at 3 months lead time, though clearly above persistence. Our analysis suggests that in many CMIP5 models misrepresentation of variability should not be a major stumbling block toward skillful prediction. This indicates that the current lack of prediction skill in the region is due to other factors, such as model initialization or inherent predictability limits due to noise.
Comparing several dynamical hindcast experiments with the LIM constructed from observations, we find that the LIM generally has superior prediction skill over most parts of the tropical Atlantic.

Keywords: linear inverse modeling, tropical Atlantic, seasonal prediction

©2019. Japan Geoscience Union. All Right Reserved. 

# Relationships Among Inter-model Spread and Biases in Tropical Atlantic Sea Surface Temperatures

Elsa - Mohino Harris[1], *Belen Rodriguez-Fonseca[1,2], Teresa - Losada[1], Irene - Polo[1], Roberto - Mechoso[3]

1. Department of Physics of the Earth and Astrophysics, Universidad Complutense de Madrid, 28040, Madrid, Spain. , 2. Institute of Geosciences IGEO,UCM-CSIC, 28040, Madrid, Spain., 3. Department of Atmospheric and Oceanic Sciences, UCLA, Los Angeles, USA

State-of-the-art general circulation models show important systematic errors in their simulation of sea surface temperatures (SST), especially in the Tropical Atlantic. In this work the spread in the simulation of climatological SST in the Tropical Atlantic by 24 CMIP5 models is examined, and its relationship with the mean systematic biases in the region is explored. The modes of inter-model variability are estimated by applying Principal Component (PC) analysis to the SSTs in the region 70ºW-20ºE, 20ºS-20ºN. The inter-model variability is approximately explained by the first three modes. The first mode is related to warmer SSTs in the basin, shows worldwide connections with same-signed loads over most of the tropics and is connected with lower low cloud cover over the eastern parts of the subtropical oceans. The second mode is restricted to the Atlantic, where it shows negative and positive loads to the north and south of the equator, respectively, and is connected to a too weak Atlantic Meridional Overturning Circulation (AMOC). The third mode is related to the double Intertropical Convergence Zone bias in the Pacific and to an interhemispheric asymmetry in the net radiation at the top of the atmosphere. According to the results, the most important of these contributors for SST biases spread in the Tropical Atlantic is the second mode, with models having stronger biases simulating weaker AMOCs.

Keywords: GCM bias, CMIP5, tropical Atlantic, intermodel spread

©2019. Japan Geoscience Union. All Right Reserved. 

# Revisiting the CMIP5 Thermocline in the Equatorial Pacific and Atlantic Oceans

Antonio - Castaño[1,2], Elsa - Mohino[1], *Belen Rodriguez-Fonseca[1,2], Teresa - Losada[1]

1. Department of Physics of the Earth and Astrophysics, Universidad Complutense de Madrid, 28040, Madrid, Spain., 2. Institute of Geosciences, IGEO, UCM-CSIC 28040, Madrid, Spain.

The thermocline is defined as the ocean layer for which the vertical thermal gradient is maximum. In the equatorial ocean, observations led to the use of the 20˚C isotherm depth (z20) as an estimate of the thermocline. This work compares z20 against the physical thermocline in the Equatorial Atlantic and Pacific Oceans, using SODA reanalysis and CMIP5 Pre-Industrial Control simulations. Our results show that in models z20 is systematically deeper and flatter than the thermocline and does not respond correctly to surface wind stress variations. It is also shown that the annual cycle of z20 is much weaker than that of the physical thermocline. This happens in both equatorial basins and indicates that z20 does not react to the same mechanisms as the thermocline. Possible consequences in the assessment of air-sea coupling in current GCMs and bias reduction strategies are also suggested, as well as possible effects in the representation of upwelling systems in the tropical region.

Keywords: CMIP5, defining thermocline, tropical atlantic, air-sea interactions

©2019. Japan Geoscience Union. All Right Reserved. 

# Lagged Effects of North Atlantic SST Anomalies on Weather in Remote Areas

*Natalia Gnatiuk[1], Timo Vihma[2], Leonid Bobylev[1]

1. Nansen International Environmental and Remote Sensing Centre, 2. Finnish Meteorological Institute

Polar climate has experienced dramatic changes during observed global warming. These changes in turn have, as hypothesised, strong influences on the mid-latitude weather. Many proposed linkages focus on the effects of changes in sea ice, sea surface temperature or terrestrial snow pack on the air temperature in selected mid-latitude areas. Our hypothesis is that from the point of view of the atmosphere, it does not matter whether the thermal forcing from the surface originates from sea ice melt, terrestrial snow melt, or changes in SST. Most important is to quantify how the atmosphere responds to anomalies in surface temperature, and how the local/regional responses may affect weather patterns in remote areas. By analysing these responses systematically in global scale, we can identify the regions and seasons where/when the response is strongest. Comparing these regions/seasons to observed changes in sea ice, terrestrial snow, and open ocean SST, we will obtain information on the relative importance of forcing from these three factors. For this purpose, we studied the relationships between anomalies in the surface temperature (Ts) in the Northern Hemisphere (on grid $1.5^{o}$-$1.5^{o}$) and 2-m air temperature (T2m) in selected 13 study regions in Europe, Greenland, and parts of Asia and North Africa for the period 1979-2018 based on the ERA-Interim reanalysis. Applying also detrended data, we eliminated spurious correlations resulting from similar trends in the two variables.

We detected significant correlations between the surface temperature over the Labrador Sea, Canadian archipelago and North Atlantic and 2-m air temperature in different study regions for inter-seasonal spring - summer (MAM-JJA) and autumn - winter (SON-DJF) relationships. Among the strongest correlations between the spring Ts and summer T2m were the positive correlations found between Ts in the North Atlantic and T2m in Scandinavia, Ts in the Labrador Sea and T2m in Northeast Europe, and Ts in Norther Sahara and T2m in Urals. As well, among the strongest correlations between the autumn Ts and winter T2m were the positive correlations found between Ts in the North Atlantic and the Labrador Sea and T2m in Scandinavia and Northwest Africa; and the negative correlations found between Ts in the Labrador Sea and the North Atlantic and T2m in Scandinavia, Northeast Europe, Urals, Black Sea region and Northcentral Asia.

In order to identify thermal forcing factors and to assess their relative importance, we analysed the multiyear averages and anomalies of sea-ice concentration, snow cover and surface heat fluxes. According to the results, in all identified cases, changes in SST mostly were an influencing factor.

Another big challenge was to understand the physical mechanisms responsible for the obtained statistical results. For this purpose, we analysed surface pressure, geopotential heights, wind components, air-mass trajectories, incoming solar radiation, cloud cover, and total precipitation for sub-sets of 10 coldest and 10 warmest seasons in the period 1979-2018. There is a detectable effect on anomalies in the atmospheric pressure field and wind components in these regions.

The research is granted by the “ERA.Net RUS Plus” Initiative, ID 166 and national RFBR project No. 18-55-76004; and partly by RSF grant №. 17-17-01151.

©2019. Japan Geoscience Union. All Right Reserved. 

Keywords: Sea surface temperature anomalies, Teleconnections, Mid-latitude weather, North Atlantic

©2019. Japan Geoscience Union. All Right Reserved. 

# SST anomalies in the northern tropical Atlantic as a negative feedback to ENSO development

*Ingo Richter[1], Hiroki Tokinaga[2], Yu Kosaka[3], Takeshi Doi[1]

1. JAMSTEC Japan Agency for Marine-Earth Science and Technology, 2. Kyoto University, 3. University of Tokyo

It has been known for some time that SST anomalies in the equatorial Pacific induce same-signed anomalies in the northern tropical Atlantic (NTA) through changes in the Atlantic trade winds. More recently, it has been suggested that the NTA, in turn, can influence the equatorial Pacific through changes in the surface zonal winds over the western part of the basin. The sign of these wind anomalies, however, would act to force equatorial Pacific SST anomalies that are opposite to those in the NTA. The present study takes a closer look at this apparent conundrum by conducting GCM experiments with prescribed SSTs for the period 1982-2014. In the control experiment, observed SSTs are prescribed globally, while in two sensitivity experiments SST anomalies are removed from either the tropical Atlantic or the tropical Pacific. For the control experiment, analysis suggests that NTA warming is accompanied by SST warming and westerly wind anomalies in the equatorial Pacific. When tropical Pacific SST anomalies are removed, on the other hand, NTA warming coincides with easterly anomalies. Moreover, when SST anomalies are removed from the tropical Atlantic, wind variability over the western equatorial Pacific is enhanced. These results suggest that SST anomalies in the NTA, which are strongly influenced by the tropical Pacific, act as a negative feedback to ENSO development. This interbasin link may be further complicated by other influences on the NTA, such as local air-sea coupling and the North Atlantic Oscillation.

Keywords: tropical Atlantic, ENSO, teleconnections

©2019. Japan Geoscience Union. All Right Reserved. 

[E] Poster | A (Atmospheric and Hydrospheric Sciences)：A-OS Ocean Sciences & Ocean Environment

Thu. May 30, 2019 5:15 PM - 6:30 PM JST | Thu. May 30, 2019 8:15 AM - 9:30 AM UTC | Poster Hall International Exhibition Hall8, Makuhari Messe_8

## [A-OS10] Atlantic climate variability, and its global impacts and predictability

convener:Ingo Richter(JAMSTEC Japan Agency for Marine-Earth Science and Technology), Hiroki Tokinaga(Research Institute for Applied Mechanics, Kyushu University), Noel S Keenlyside(Geophysical Institute Bergen), Carlos R Mechoso(University of California Los Angeles)

The Atlantic Ocean is subject to pronounced climate variations that occur on a wide range of time scales, including interannual variability in the equatorial and subtropical regions, and Atlantic multi-decadal variability (AMV), which has been linked with the Atlantic meridional overturning circulation (AMOC). These are connected to other climate variations across the globe. The AMV, e.g., has long been known to have global impacts, such as changes in the Indian, Asian and South American summer monsoons, and changes in the Pacific associated with the "global hiatus". Interannual variability in the equatorial and subtropical Atlantic has also been shown to influence global climate, including over Asia, while the freshening of the North Atlantic by melting of the Greenland ice cap is expected to influence all ocean basins via atmospheric bridges. Likewise, misrepresentation of the Atlantic can have global ramifications in climate models. Misrepresentation of the AMOC, e.g., has been associated with model biases in the entire Northern Hemisphere.<br/><br/>This session seeks observational, modeling, and theoretical studies on the mechanisms that determine the Atlantic mean climate and variability, as well as the predictability and global impacts of such variability. We also seek studies that evaluate climate model performance in the region. Topics include atmosphere-ocean-cloud interactions in the tropical Atlantic and their remote impacts; relationships between tropical and mid/high latitude variability; air-sea interaction along the Gulf Stream and its influence on cyclones and storm track evolution; variability in the Benguela upwelling region; influence of Agulhas leakage on the South Atlantic; coupled climate models biases in the region and their impacts; AMOC and long-term climate change.

### [AOS10-P01] The strengthening of Amazonian precipitation during the wet season driven by tropical sea surface temperature forcing

*Xinyue Wang[1], Xichen Li[1], Jiang Zhu[1], Clemente A S Tanajura[2] (1.Institute of Atmospheric Physics, Chinese Academy of Sciences, 2.Institute of Physics, Federal University of Bahia, Salvador, Brazil)

### [AOS10-P02] Linear inverse modeling of the tropical Atlantic

*Ingo Richter[1], Ping Chang[2] (1.JAMSTEC Japan Agency for Marine-Earth Science and Technology, 2.Texas A&M University)

### [AOS10-P03] Relationships Among Inter-model Spread and Biases in Tropical Atlantic Sea Surface Temperatures

Elsa - Mohino Harris[1], *Belen Rodriguez-Fonseca[1,2], Teresa - Losada[1], Irene - Polo[1], Roberto - Mechoso[3] (1.Department of Physics of the Earth and Astrophysics, Universidad Complutense de Madrid, 28040, Madrid, Spain. , 2.Institute of Geosciences IGEO,UCM-CSIC, 28040, Madrid, Spain., 3.Department of Atmospheric and Oceanic Sciences, UCLA, Los Angeles, USA)

### [AOS10-P04] Revisiting the CMIP5 Thermocline in the Equatorial Pacific and Atlantic Oceans

Antonio - Castaño[1,2], Elsa - Mohino[1], *Belen Rodriguez-Fonseca[1,2], Teresa - Losada[1] (1.Department of Physics of the Earth and Astrophysics, Universidad Complutense de Madrid, 28040, Madrid, Spain., 2.Institute of Geosciences, IGEO, UCM-CSIC 28040, Madrid, Spain.)

### [AOS10-P05] Lagged Effects of North Atlantic SST Anomalies on Weather in Remote Areas

*Natalia Gnatiuk[1], Timo Vihma[2], Leonid Bobylev[1] (1.Nansen International Environmental and Remote Sensing Centre, 2.Finnish Meteorological Institute)

## [AOS10-P06] SST anomalies in the northern tropical Atlantic as a negative feedback to ENSO development

*Ingo Richter[1], Hiroki Tokinaga[2], Yu Kosaka[3], Takeshi Doi[1] (1.JAMSTEC Japan Agency for Marine-Earth Science and Technology, 2.Kyoto University, 3.University of Tokyo)

# The strengthening of Amazonian precipitation during the wet season driven by tropical sea surface temperature forcing

*Xinyue Wang[1], Xichen Li[1], Jiang Zhu[1], Clemente A S Tanajura[2]

1. Institute of Atmospheric Physics, Chinese Academy of Sciences, 2. Institute of Physics, Federal University of Bahia, Salvador, Brazil

Amazonian rainfall plays a critical role in the global climate system and the hydrological cycle. It is thus important to quantify changes in the Amazonian rainfall and clarify its mechanism. Previous studies indicate that the interannual variability of Amazonian precipitation could be largely attributed to variabilities in the South American monsoon system and the El Niño Southern Oscillation. However, the trend of the wet season tropical Amazonian precipitation during recent decades is not very well investigated. In this study, by combining both satellite and in situ observations, it is revealed that tropical Amazonian precipitation has significantly increased by~180 to 600 mm (in different datasets) in the wet season during the satellite era from 1979 to 2015. We then use a state-of-the-art atmospheric model to simulate the impact of the tropical sea surface temperatures (SSTs) on the precipitation changes. Results show that the multidecadal warming of the tropical Atlantic has contributed more than half of this precipitation change over the past three decades, while the east Pacific cooling plays a secondary role. We finally combine the simulation results and the reanalysis data to investigate the mechanisms of this process, i.e. the SST variability dramatically increases the convergence of the moisture transport over the Amazon region. The precipitation changes over the Amazon region largely impact on the local hydrological cycle and the ecosystem, and have important impacts on the global climate system by mediating the teleconnection between the Pacific and the Atlantic oceans. Our results show that the long-term change in the wet season Amazonian precipitation is important and deserves further investigation and discussion.

Keywords: convective precipitation, Amazon, tropical Atlantic, moisture convergence

©2019. Japan Geoscience Union. All Right Reserved. 

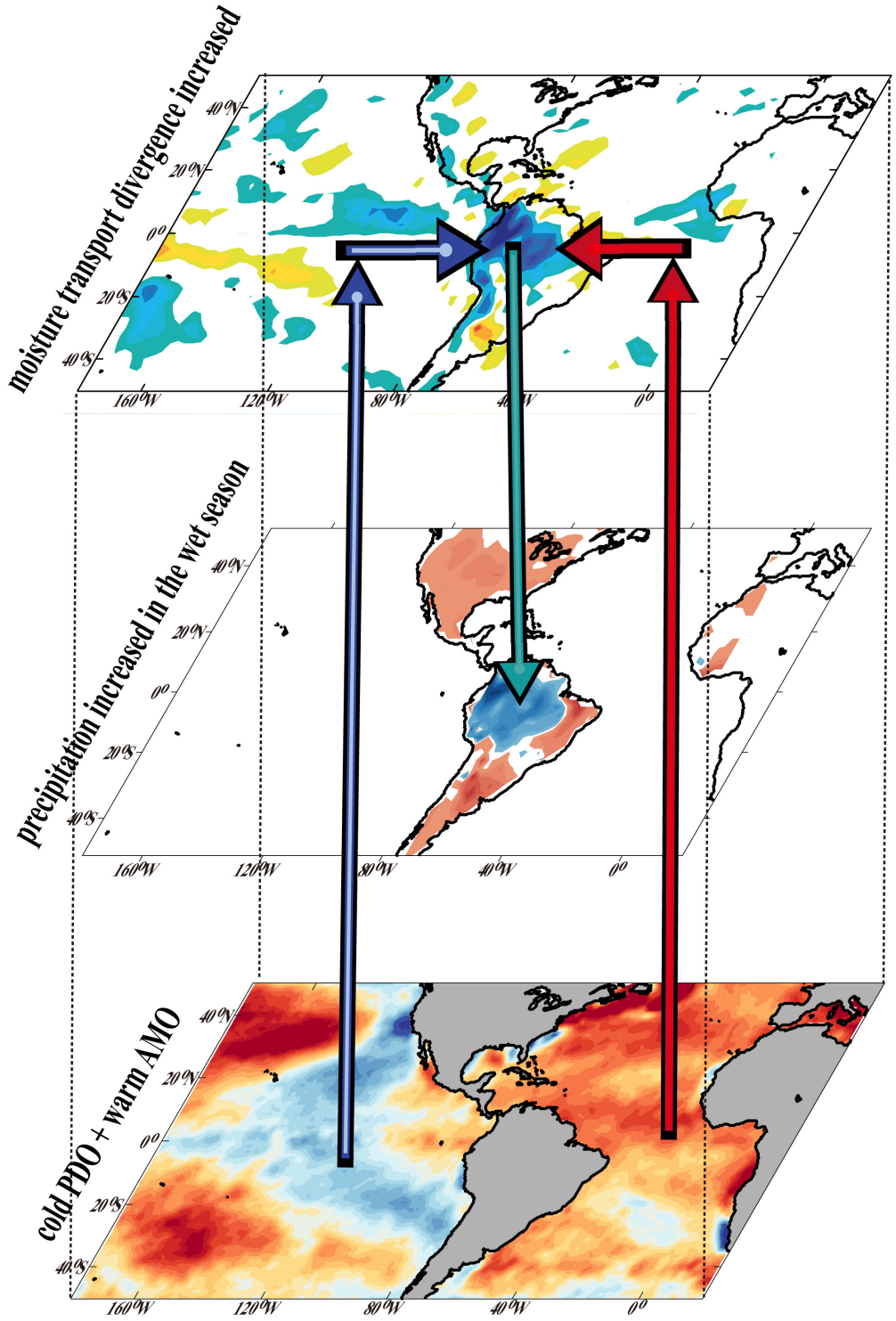


©2019. Japan Geoscience Union. All Right Reserved. 

# Linear inverse modeling of the tropical Atlantic

*Ingo Richter[1], Ping Chang[2]

1. JAMSTEC Japan Agency for Marine-Earth Science and Technology, 2. Texas A&M University

The tropical Atlantic features variability at interannual and decadal time scales that is known to have a strong influence on the surrounding continents and possibly other ocean basins. Current prediction systems, however, struggle to skillfully predict sea-surface temperature (SST), let alone its impact on rainfall over the adjacent continents. It is often assumed that this poor prediction skill is due to the severe SST biases and misrepresented variability patterns that most models feature in the region but this has recently been called into question.

In the present study, we construct a simple statistical model of the tropical Atlantic to 1) investigate the influence of model biases on prediction skill, and 2) establish a benchmark to evaluate dynamical model against. Using 35 fully coupled ocean-atmosphere GCMs from the pre-industrial control experiment (piControl) of the Coupled Model Intercomparison Project Phase 5 (CMIP5) we construct a linear inverse model (LIM) for each GCM based on tropical SSTs only. The LIM thus constructed is then used to predict SSTs for the period 2000-2017 from the NCEP/NCAR reanalysis. These predictions are compared to those from a LIM constructed using the NCEP/NCAR reference for the period 1948-1999 as training data. Since each of the model LIMs is constructed from more or less unrealistic variability patterns one would expect to see a clear impact on prediction skill.

The results, however, indicate that prediction skill in the tropical Atlantic is relatively insensitive to the tropical variability patterns of each model. Only some cases see a marked deterioration of prediction skill relative to the reference model. The LIM performs well in the subtropical north and south Atlantic. In the equatorial Atlantic, on the other hand, skill is rather poor at 3 months lead time, though clearly above persistence. Our analysis suggests that in many CMIP5 models misrepresentation of variability should not be a major stumbling block toward skillful prediction. This indicates that the current lack of prediction skill in the region is due to other factors, such as model initialization or inherent predictability limits due to noise.
Comparing several dynamical hindcast experiments with the LIM constructed from observations, we find that the LIM generally has superior prediction skill over most parts of the tropical Atlantic.

Keywords: linear inverse modeling, tropical Atlantic, seasonal prediction

©2019. Japan Geoscience Union. All Right Reserved. 

# Relationships Among Inter-model Spread and Biases in Tropical Atlantic Sea Surface Temperatures

Elsa - Mohino Harris[1], *Belen Rodriguez-Fonseca[1,2], Teresa - Losada[1], Irene - Polo[1], Roberto - Mechoso[3]

1. Department of Physics of the Earth and Astrophysics, Universidad Complutense de Madrid, 28040, Madrid, Spain. , 2. Institute of Geosciences IGEO,UCM-CSIC, 28040, Madrid, Spain., 3. Department of Atmospheric and Oceanic Sciences, UCLA, Los Angeles, USA

State-of-the-art general circulation models show important systematic errors in their simulation of sea surface temperatures (SST), especially in the Tropical Atlantic. In this work the spread in the simulation of climatological SST in the Tropical Atlantic by 24 CMIP5 models is examined, and its relationship with the mean systematic biases in the region is explored. The modes of inter-model variability are estimated by applying Principal Component (PC) analysis to the SSTs in the region 70ºW-20ºE, 20ºS-20ºN. The inter-model variability is approximately explained by the first three modes. The first mode is related to warmer SSTs in the basin, shows worldwide connections with same-signed loads over most of the tropics and is connected with lower low cloud cover over the eastern parts of the subtropical oceans. The second mode is restricted to the Atlantic, where it shows negative and positive loads to the north and south of the equator, respectively, and is connected to a too weak Atlantic Meridional Overturning Circulation (AMOC). The third mode is related to the double Intertropical Convergence Zone bias in the Pacific and to an interhemispheric asymmetry in the net radiation at the top of the atmosphere. According to the results, the most important of these contributors for SST biases spread in the Tropical Atlantic is the second mode, with models having stronger biases simulating weaker AMOCs.

Keywords: GCM bias, CMIP5, tropical Atlantic, intermodel spread

©2019. Japan Geoscience Union. All Right Reserved. 

# Revisiting the CMIP5 Thermocline in the Equatorial Pacific and Atlantic Oceans

Antonio - Castaño[1,2], Elsa - Mohino[1], *Belen Rodriguez-Fonseca[1,2], Teresa - Losada[1]

1. Department of Physics of the Earth and Astrophysics, Universidad Complutense de Madrid, 28040, Madrid, Spain., 2. Institute of Geosciences, IGEO, UCM-CSIC 28040, Madrid, Spain.

The thermocline is defined as the ocean layer for which the vertical thermal gradient is maximum. In the equatorial ocean, observations led to the use of the 20˚C isotherm depth (z20) as an estimate of the thermocline. This work compares z20 against the physical thermocline in the Equatorial Atlantic and Pacific Oceans, using SODA reanalysis and CMIP5 Pre-Industrial Control simulations. Our results show that in models z20 is systematically deeper and flatter than the thermocline and does not respond correctly to surface wind stress variations. It is also shown that the annual cycle of z20 is much weaker than that of the physical thermocline. This happens in both equatorial basins and indicates that z20 does not react to the same mechanisms as the thermocline. Possible consequences in the assessment of air-sea coupling in current GCMs and bias reduction strategies are also suggested, as well as possible effects in the representation of upwelling systems in the tropical region.

Keywords: CMIP5, defining thermocline, tropical atlantic, air-sea interactions

©2019. Japan Geoscience Union. All Right Reserved. 

# Lagged Effects of North Atlantic SST Anomalies on Weather in Remote Areas

*Natalia Gnatiuk[1], Timo Vihma[2], Leonid Bobylev[1]

1. Nansen International Environmental and Remote Sensing Centre, 2. Finnish Meteorological Institute

Polar climate has experienced dramatic changes during observed global warming. These changes in turn have, as hypothesised, strong influences on the mid-latitude weather. Many proposed linkages focus on the effects of changes in sea ice, sea surface temperature or terrestrial snow pack on the air temperature in selected mid-latitude areas. Our hypothesis is that from the point of view of the atmosphere, it does not matter whether the thermal forcing from the surface originates from sea ice melt, terrestrial snow melt, or changes in SST. Most important is to quantify how the atmosphere responds to anomalies in surface temperature, and how the local/regional responses may affect weather patterns in remote areas. By analysing these responses systematically in global scale, we can identify the regions and seasons where/when the response is strongest. Comparing these regions/seasons to observed changes in sea ice, terrestrial snow, and open ocean SST, we will obtain information on the relative importance of forcing from these three factors. For this purpose, we studied the relationships between anomalies in the surface temperature (Ts) in the Northern Hemisphere (on grid $1.5^{o}$-$1.5^{o}$) and 2-m air temperature (T2m) in selected 13 study regions in Europe, Greenland, and parts of Asia and North Africa for the period 1979-2018 based on the ERA-Interim reanalysis. Applying also detrended data, we eliminated spurious correlations resulting from similar trends in the two variables.

We detected significant correlations between the surface temperature over the Labrador Sea, Canadian archipelago and North Atlantic and 2-m air temperature in different study regions for inter-seasonal spring - summer (MAM-JJA) and autumn - winter (SON-DJF) relationships. Among the strongest correlations between the spring Ts and summer T2m were the positive correlations found between Ts in the North Atlantic and T2m in Scandinavia, Ts in the Labrador Sea and T2m in Northeast Europe, and Ts in Norther Sahara and T2m in Urals. As well, among the strongest correlations between the autumn Ts and winter T2m were the positive correlations found between Ts in the North Atlantic and the Labrador Sea and T2m in Scandinavia and Northwest Africa; and the negative correlations found between Ts in the Labrador Sea and the North Atlantic and T2m in Scandinavia, Northeast Europe, Urals, Black Sea region and Northcentral Asia.

In order to identify thermal forcing factors and to assess their relative importance, we analysed the multiyear averages and anomalies of sea-ice concentration, snow cover and surface heat fluxes. According to the results, in all identified cases, changes in SST mostly were an influencing factor.

Another big challenge was to understand the physical mechanisms responsible for the obtained statistical results. For this purpose, we analysed surface pressure, geopotential heights, wind components, air-mass trajectories, incoming solar radiation, cloud cover, and total precipitation for sub-sets of 10 coldest and 10 warmest seasons in the period 1979-2018. There is a detectable effect on anomalies in the atmospheric pressure field and wind components in these regions.

The research is granted by the “ERA.Net RUS Plus” Initiative, ID 166 and national RFBR project No. 18-55-76004; and partly by RSF grant №. 17-17-01151.

©2019. Japan Geoscience Union. All Right Reserved. 

Keywords: Sea surface temperature anomalies, Teleconnections, Mid-latitude weather, North Atlantic

©2019. Japan Geoscience Union. All Right Reserved. 

# SST anomalies in the northern tropical Atlantic as a negative feedback to ENSO development

*Ingo Richter[1], Hiroki Tokinaga[2], Yu Kosaka[3], Takeshi Doi[1]

1. JAMSTEC Japan Agency for Marine-Earth Science and Technology, 2. Kyoto University, 3. University of Tokyo

It has been known for some time that SST anomalies in the equatorial Pacific induce same-signed anomalies in the northern tropical Atlantic (NTA) through changes in the Atlantic trade winds. More recently, it has been suggested that the NTA, in turn, can influence the equatorial Pacific through changes in the surface zonal winds over the western part of the basin. The sign of these wind anomalies, however, would act to force equatorial Pacific SST anomalies that are opposite to those in the NTA. The present study takes a closer look at this apparent conundrum by conducting GCM experiments with prescribed SSTs for the period 1982-2014. In the control experiment, observed SSTs are prescribed globally, while in two sensitivity experiments SST anomalies are removed from either the tropical Atlantic or the tropical Pacific. For the control experiment, analysis suggests that NTA warming is accompanied by SST warming and westerly wind anomalies in the equatorial Pacific. When tropical Pacific SST anomalies are removed, on the other hand, NTA warming coincides with easterly anomalies. Moreover, when SST anomalies are removed from the tropical Atlantic, wind variability over the western equatorial Pacific is enhanced. These results suggest that SST anomalies in the NTA, which are strongly influenced by the tropical Pacific, act as a negative feedback to ENSO development. This interbasin link may be further complicated by other influences on the NTA, such as local air-sea coupling and the North Atlantic Oscillation.

Keywords: tropical Atlantic, ENSO, teleconnections

©2019. Japan Geoscience Union. All Right Reserved. 

[E] Oral | A (Atmospheric and Hydrospheric Sciences )：A-HW Hydrology & Water Environment

Thu. May 30, 2019 9:00 AM - 10:30 AM JST | Thu. May 30, 2019 12:00 AM - 1:30 AM UTC | 201B 2F

## [A-HW22] Materials transport and nutrient cycles in watersheds; from headwaters to coastal seas

convener:Masahiro Kobayashi(Forestry and Forest Products Research Institute), Seiko Yoshikawa(Institute for Agro-environmental Sciences, National Agriculture and Food Research Organization), Jun Yasumoto(University of the Ryukyus, Faculty of Agriculuture), Adina Paytan(University of California Santa Cruz), Chairperson:Adina Paytan(University of California, Santa Cruz)

This session aims to synthetize watershed sciences in order to understand dynamical processes of materials transport and nutrient cycles in watersheds from headwaters to coastal seas. The session will be integrating a variety of research disciplines including limnology, ground water hydrology, coastal oceanography, meteorology, pedology, sedimentology, forestry, agriculture, fishery, ecology, social science and more. This session calls for ideas on new methods for the watershed sciences, such as tracer and molecular technique, hydrological modeling, paleontological approaches, laboratory and field experiments, social-scientific evaluation of ecosystem services and social-ecological systems, and so on, in order to elucidate physical, chemical and biological mechanisms for shedding light on natural phenomena and their changes over time in complex and dynamic watershed systems under human and climate impacts. Through this session, we would like to facilitate interdisciplinary collaboration among participants to create new knowledge on watershed sciences.

9:00 AM - 9:15 AM JST | 12:00 AM - 12:15 AM UTC

[AHW22-06] Biodiversity increases integrated trophic position of macroinvertebrate communities in coastal food webs: testing the vertical diversity hypothesis

*Noboru Okuda[1], Jin'ichi Karube[2], Yoichiro Sakai[3], Tomohiro Takeyama[4], Ichiro Tayasu[1], Chikage Yoshimizu[1], Toshi Nagata[5] (1.Research Institute for Humanity and Nature, 2.Kindai University, 3.Lake Biwa Environmental Research Institute, 4.Okayama University of Science, 5.University of Tokyo)

9:15 AM - 9:30 AM JST | 12:15 AM - 12:30 AM UTC

[AHW22-07] The analysis of the community composition of riverine bacteria and microalgae in relation to nutrient status and diversity: the case in irrigation season in the Yasu River, Japan

*Tohru Ikeya[1], Takuya Ishida[1], Yoshitoshi Uehara[1], Satoshi Asano[2], Ichiro Tayasu[1], Noboru Okuda[1], Masayuki Ushio[3,4,5], Shohei Fujinaga[4], Chia-Ying Ko[6], Elfritzson Martin Peralta[7], Naoto F. Ishikawa[8], Tomoya Iwata[9] (1.Research Institute for Humanity and Nature, 2.Lake Biwa Environmental Research Institute, 3.Hakubi Center, Kyoto University, 4.Center for Ecological Research, Kyoto University, 5.PRESTO, Japan Science and Technology Agency, 6.National Taiwan University, 7.University of Santo Tomas, 8.Department of Biogeochemistry, Japan Agency for Marine-Earth Science and Technology, 9.Faculty of Life and Environmental Sciences, Yamanashi University)

9:30 AM - 9:45 AM JST | 12:30 AM - 12:45 AM UTC

[AHW22-08] **Multiple stressors and protection efforts in highly urbanized watersheds in the Philippines**

*Elfritzson M. Peralta[1,3], Leocris S. Batucan Jr.[4,6], Alexis E. Belen[2,3], Irisse Bianca B. De Jesus[1,3], Takuya Ishida[5], Chia-Ying Ko[7], Yuki Kobayashi[5], Tohru Ikeya[5], Yoshitoshi Uehara[5], Tomoya Iwata[8], Adelina S. Borja[9], Jonathan Carlo A. Briones[1,2,3], Francis S. Magbanua[4], Rey Donne S. Papa[1,2,3], Noboru Okuda[5] (1.Research Center for the Natural and Applied Sciences, University of Santo Tomas, PH, 2.Department of Biological Sciences, University of Santo Tomas, PH, 3.The Graduate School, University of Santo Tomas, PH, 4.Institute of Biology, University of the Philippines Diliman, PH, 5.Research Institute for Humanity and Nature, JP, 6.Academia Sinica and Department of Life Science, National Taiwan Normal University, TW, 7.Institute of Fisheries Science and Department of Life Science, National Taiwan University, TW, 8.Faculty of Life and Environmental Sciences, University of Yamanashi, JP, 9.Resource Management and Development Department, Laguna Lake Development Authority, PH)

9:45 AM - 10:00 AM JST | 12:45 AM - 1:00 AM UTC

[AHW22-09] Ammonium contamination of shallow groundwater beneath vegetable fields in Central Vietnam

★Invited Papers

*Maeda Morihiro[1], Takuya Fujimura[1], Van Ngoc Tuong Hoang[2], Daisuke Inoue[3], Hidetaka Chikamori[1], Fujio Hyodo[1] (1.Okayama University, 2.Hue University, 3.Osaka University)

---

10:00 AM - 10:15 AM JST | 1:00 AM - 1:15 AM UTC

[AHW22-10] Modelling nutrient and organic waste behaviour in a tropical wetland in Singapore under projected anthropogenic scenarios

*Swee Yang Edmund Low[1], Dong Eon Kim[1], Canh Tien Trinh Nguyen[1], Yixiong Cai, Shie-Yui Liong[1] (1.National University of Singapore)

---

10:15 AM - 10:30 AM JST | 1:15 AM - 1:30 AM UTC

[AHW22-11] **Benthic macroinvertebrate assemblages and water quality reflect the impacts of land use and land cover in Marikina Watershed, Philippines**

*Julie - An N. Gregorio[1,2], Elfritzson M. Peralta[3,5], Irisse Bianca B. de Jesus[3,5], Tohru Ikeya[6], Jonathan Carlo A. Briones[3,4,5], Rey Donne S. Papa[3,4,5], Francis S. Magbanua[1], Noboru Okuda[6] (1.Institute of Biology, University of the Philippines, Diliman, Quezon City, 1101 Philippines, 2.Institute of Environmental Science and Meteorology, University of the Philippines, Diliman, Quezon City 1101 Philippines, 3.Research Center for the Natural and Applied Sciences, University of Santo Tomas, España Boulevard, Manila, 1015, Philippines, 4.Department of Biological Sciences, University of Santo Tomas, España Boulevard, Manila, 1015, Philippines, 5.The Graduate School, University of Santo Tomas, España Boulevard, Manila, 1015, Philippines, 6.Research Institute for Humanity and Nature, 457-4 Motoyama, Kamigamo, Kyoto, 603-8047, Japan)

# Biodiversity increases integrated trophic position of macroinvertebrate communities in coastal food webs: testing the vertical diversity hypothesis

*Noboru Okuda[1], Jin'ichi Karube[2], Yoichiro Sakai[3], Tomohiro Takeyama[4], Ichiro Tayasu[1], Chikage Yoshimizu[1], Toshi Nagata[5]

1. Research Institute for Humanity and Nature, 2. Kindai University, 3. Lake Biwa Environmental Research Institute, 4. Okayama University of Science, 5. University of Tokyo

## Introduction

Study on relationships between biodiversity and ecosystem functioning (BEF) has attracted social as well as ecological interests because the biodiversity can affect ecosystem processes, especially productivity, which determines provisioning service for humanity. Because of difficulty in accurate measurement of the productivity, however, biomass has been traditionally used as its proxy to assess the BEF. Positive correlations between biodiversity and biomass-based productivity indices have been reported for many plants both in terrestrial and aquatic ecosystems. Such correlations are also true for consumers in terrestrial systems. In aquatic ecosystems, in contrast, the biomass-based BEF relationships are inconsistent among consumer communities: some are positive or convex and others non-significant (Waide et al. 1999).

Such an inconsistency can be explained by vertical diversity, i.e., diversity of trophic positions. In systems with multitrophic interactions, in theory, consumer biomass exponentially decreases with the increasing trophic position, while underlying more primary products. The use of the consumer biomass as a proxy of its productivity is, therefore, inappropriate to view the BEF relationships in complex multitrophic systems, as in the case of aquatic food webs. Considering the multitrophic and multifunctional nature of real food webs, Wang & Brose (2018) recently have constructed a theoretical model to test vertical diversity hypothesis (VDH), predicting that functional diversity across the TPs can enhance trophic biomass flows from basal resources to top predators.

In the multitrophic and multifunctional systems, one of better ways for full-understanding of the BEF is to estimate trophic biomass flows, using carbon ( $\delta^{13}$C) and nitrogen ( $\delta^{15}$N) stable isotope analysis, which is a powerful tool for the food web analysis. Taking advantage of this analysis, Ishikawa et al. (2017) have proposed a novel index of food web properties, integrated trophic position (hereafter, *i*TP), defined as the summed TPs of all taxa in a focal food web weighed by the relative biomass of each taxon. The *i*TP can provide appropriate estimate for ecosystem functioning of vertical diversity because it indicates how many times consumer biomass experiences metabolic turnover as a whole of community within its food web. Here we test how the biodiversity can affect *i*TP for benthic macroinvertebrates in coastal waters of Lake Biwa, focusing on within-lake variation in coastal environments which can alter their local communities and thus food web properties.

## Materials & Methods

We collected benthic macroinvertebrates and their basal food sources from 33 shallow coastal waters of Lake Biwa. For each sampling site, the macroinvertebrates were sorted, identified and counted to

©2019. Japan Geoscience Union. All Right Reserved. 

calculate Shannon-Wiener diversity index ($H'$). For each taxon at each site, its dry mass was measured to calculate its biomass per unit area. Individual taxa and their basal foods at each site were provided for $\delta^{13}C$ and $\delta^{15}N$ stable isotope analysis. After this analysis, we calculated *i*TP, according to Ishikawa et al. (2017).

## Results & Discussion

A total of 27 benthic macroinvertebrate taxa were found in coastal waters of Lake Biwa. In the coastal communities, oligochaetes and chironomids are the most dominant taxa in numerical abundance, while gazing snails and a suspension-feeding bivalve were the most dominant in biomass abundance. Most taxa of grazers and deposit feeders located around TP=2, while carnivorous leeches and a freshwater prawn had the highest TP, regarded as top predators of macroinvertebrate communities.
The community biomass tended to increase significantly but weakly with macroinvertebrate diversity $H'$. By contrast, *i*TP of coastal macroinvertebrate communities markedly increased when they have the higher $H'$ (Fig. 1). The within-lake variation in their *i*TPs was better accounted for not only by the relative biomass abundance of top predators with highest TPs and lower numerical abundance but also by that of deposit feeders with lower TP and highest numerical abundance: the former can increase the relative contribution of predator TPs to the *i*TP, while the latter can have negative effects not only on the *i*TP but also on $H'$ because of its numerical abundance. This is possible explanation for such a correlational pattern of BEF found in the coastal macroinvertebrate communities, empirically supporting the VDH. Our study demonstrated that the *i*TP rather than the consumer community biomass can be a promising indicator for BEF related to vertical diversity in aquatic food webs with multitrophic interactions.

Keywords: Biodiversity-Ecosystem functioning, Food web, Integrated trophic position, Lake Biwa, Stable isotope analysis, Vertical diversity

©2019. Japan Geoscience Union. All Right Reserved. 

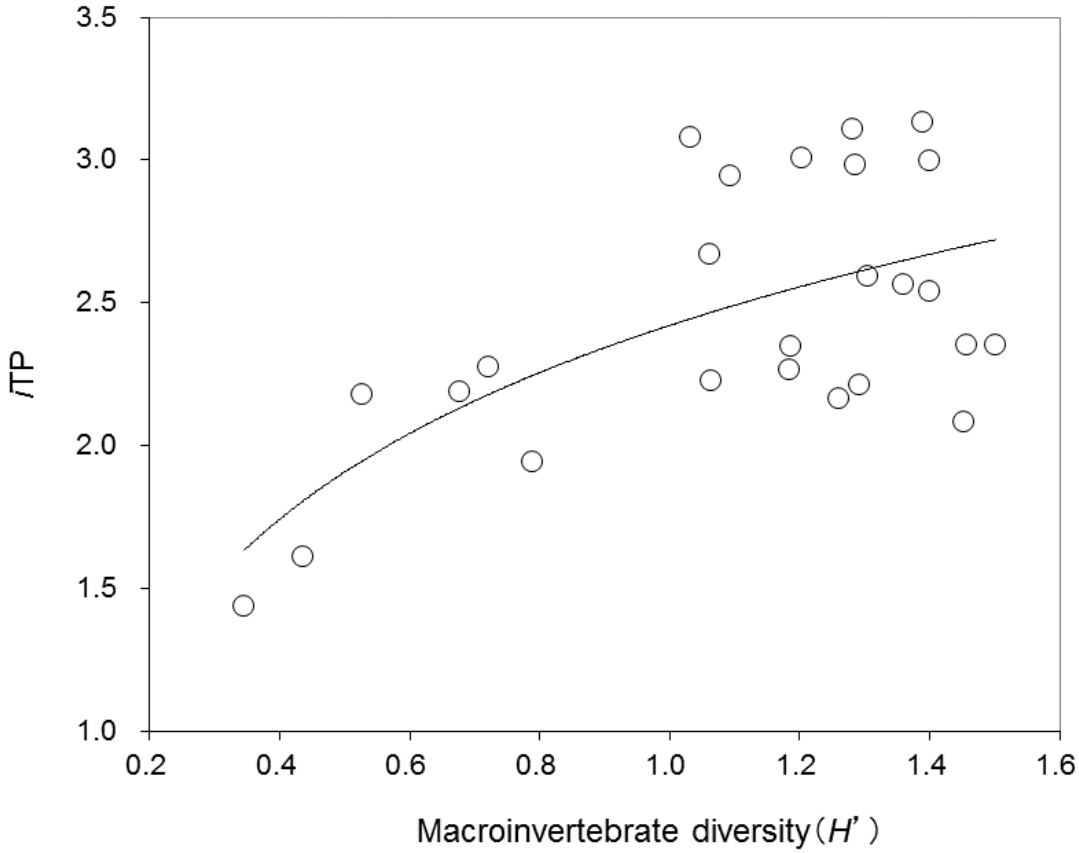


Fig. 1 A positive correlation between diversity ($H'$) and integrate trophic position ($i$TP) for benthic macroinvertebrate communities in coastal waters of Lake Biwa.

©2019. Japan Geoscience Union. All Right Reserved. 

# The analysis of the community composition of riverine bacteria and microalgae in relation to nutrient status and diversity: the case in irrigation season in the Yasu River, Japan

*Tohru Ikeya[1], Takuya Ishida[1], Yoshitoshi Uehara[1], Satoshi Asano[2], Ichiro Tayasu[1], Noboru Okuda[1], Masayuki Ushio[3,4,5], Shohei Fujinaga[4], Chia-Ying Ko[6], Elfritzson Martin Peralta[7], Naoto F. Ishikawa[8], Tomoya Iwata[9]

1. Research Institute for Humanity and Nature, 2. Lake Biwa Environmental Research Institute, 3. Hakubi Center, Kyoto University, 4. Center for Ecological Research, Kyoto University, 5. PRESTO, Japan Science and Technology Agency, 6. National Taiwan University, 7. University of Santo Tomas, 8. Department of Biogeochemistry, Japan Agency for Marine-Earth Science and Technology, 9. Faculty of Life and Environmental Sciences, Yamanashi University

The previous our analysis based on the community composition of microalgae and bacteria have shown that; 1) the beta diversity distances of algae and bacteria were significantly different between the four categories of land use in the Yasu River, 2) the ordinations of the sampling sites by the riverine microbial composition can be regressed by the environmental gradients between the sites in the watershed, 3) the diversity indices of bacteria increased with diversity index of algae. The further analyses of elemental composition of epilithic matter, most of which may be constituted from algae and bacteria, were made in order the assess the internal nutrient status of the epilithon. Both phosphorus amount per unit area and chlorophyll per carbon showed a significant positive correlation with phosphorus per carbon ($P < 10^{-8}$). Such ordination may help to realize whether phosphorus availability is limited to sustain the biofilm abundance or microbial activities so as to consider the possible impact of land use on the community composition and diversity of algae and bacteria. The richness of algae decreased with the decline of phosphorus per carbon of epilithic matter whereas that of bacteria was bifurcated. So, the richness and the Shannon diversity index ($H'$) of algae showed a significant positive relationship with the phosphorus per carbon (possible index of phosphorus availability) ($P < 10^{-4}$), whereas those of bacteria showed insignificant relationship ($P > 0.2$). Most of low bacteria richness sites at low phosphorus per carbon corresponded to those where chlorophyll abundance per unit area is relatively high in spite of low phosphorus availability.

Keywords: bacteria, microalgae, 16S, MiSeq, phosphorus

©2019. Japan Geoscience Union. All Right Reserved. 

# Multiple stressors and protection efforts in highly urbanized watersheds in the Philippines

*Elfritzson M. Peralta[1,3], Leocris S. Batucan Jr.[4,6], Alexis E. Belen[2,3], Irisse Bianca B. De Jesus[1,3], Takuya Ishida[5], Chia-Ying Ko[7], Yuki Kobayashi[5], Tohru Ikeya[5], Yoshitoshi Uehara[5], Tomoya Iwata[8], Adelina S. Borja[9], Jonathan Carlo A. Briones[1,2,3], Francis S. Magbanua[4], Rey Donne S. Papa[1,2,3], Noboru Okuda[5]

1. Research Center for the Natural and Applied Sciences, University of Santo Tomas, PH, 2. Department of Biological Sciences, University of Santo Tomas, PH, 3. The Graduate School, University of Santo Tomas, PH, 4. Institute of Biology, University of the Philippines Diliman, PH, 5. Research Institute for Humanity and Nature, JP, 6. Academia Sinica and Department of Life Science, National Taiwan Normal University, TW, 7. Institute of Fisheries Science and Department of Life Science, National Taiwan University, TW, 8. Faculty of Life and Environmental Sciences, University of Yamanashi, JP, 9. Resource Management and Development Department, Laguna Lake Development Authority, PH

Among developing countries in the tropics, urban stream syndrome is primarily driven by multiple environmental stressors, such as nutrient pollution and habitat degradation, due to social-economic developments in the catchment. To aid in environmental mitigation, improved conservation effort was recently set based on the Convention of Biological Diversity Aichi Target 11 that underscores global expansion of protected areas in terrestrial and aquatic environments. As such, this study aims to disentangle the overlaying effects of nutrient pollution and deforestation on benthic macroinvertebrate communities and assess the recent protection efforts in the watersheds of Laguna de Bay, Philippines. Study sites in Silang-Santa Rosa Subwatershed (13) and Marikina Watershed (16) were sampled for benthic macroinvertebrates and surveyed for environmental factors such as land cover and land use patterns, human population density (HPD), and stream physicochemistry including nutrient concentrations. Multivariate and multiple regression analyses on macroinvertebrate assemblages and environmental variables efficiently delineated sites according to degree of human impacts in Silang-Santa Rosa Subwatershed and the status of protection in Marikina Watershed. Canopy openness, HPD, conductivity, dissolved oxygen, and nutrients (total phosphorus, nitrates, ammonia) appeared to be the most important variables in predicting assemblages of benthic macroinvertebrates. This study effectively demonstrated how Silang-Santa Rosa Subwatershed's HPD and canopy openness, as proxies for human activities and deforestation, respectively, impact stream environments and the benthic communities. Furthermore, the recent establishment of Upper Marikina River Basin Protected Landscape inside Marikina Watershed was successfully used to show how freshwater protected areas are effective in combatting stream habitat destruction and biodiversity loss. Our findings timely show the crucial role of freshwater protected areas in conserving stream ecosystems from the effects of unsustainable urbanization in a developing country like the Philippines.

Keywords: Human population density, Deforestation, Freshwater protected area, Aichi Target 11, Biodiversity loss

©2019. Japan Geoscience Union. All Right Reserved. 

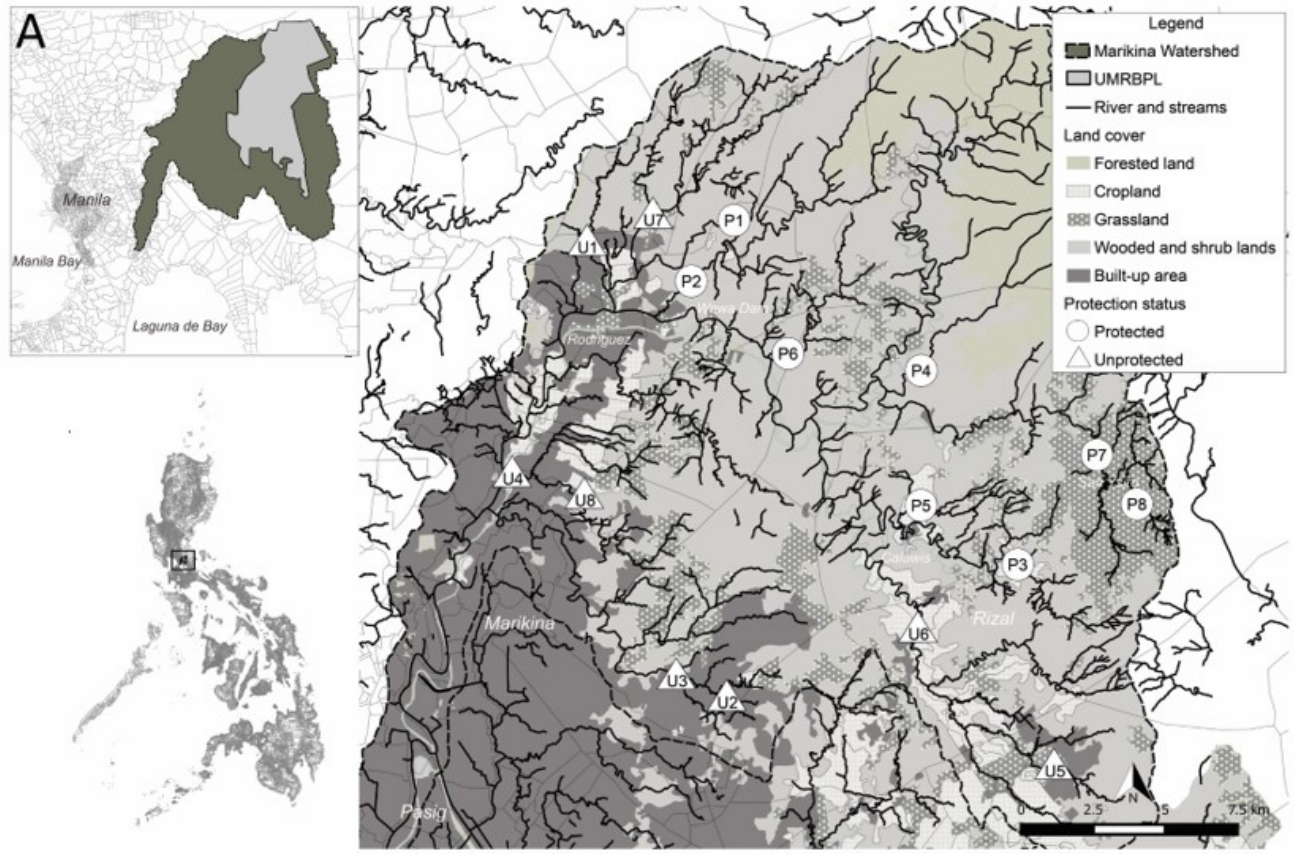


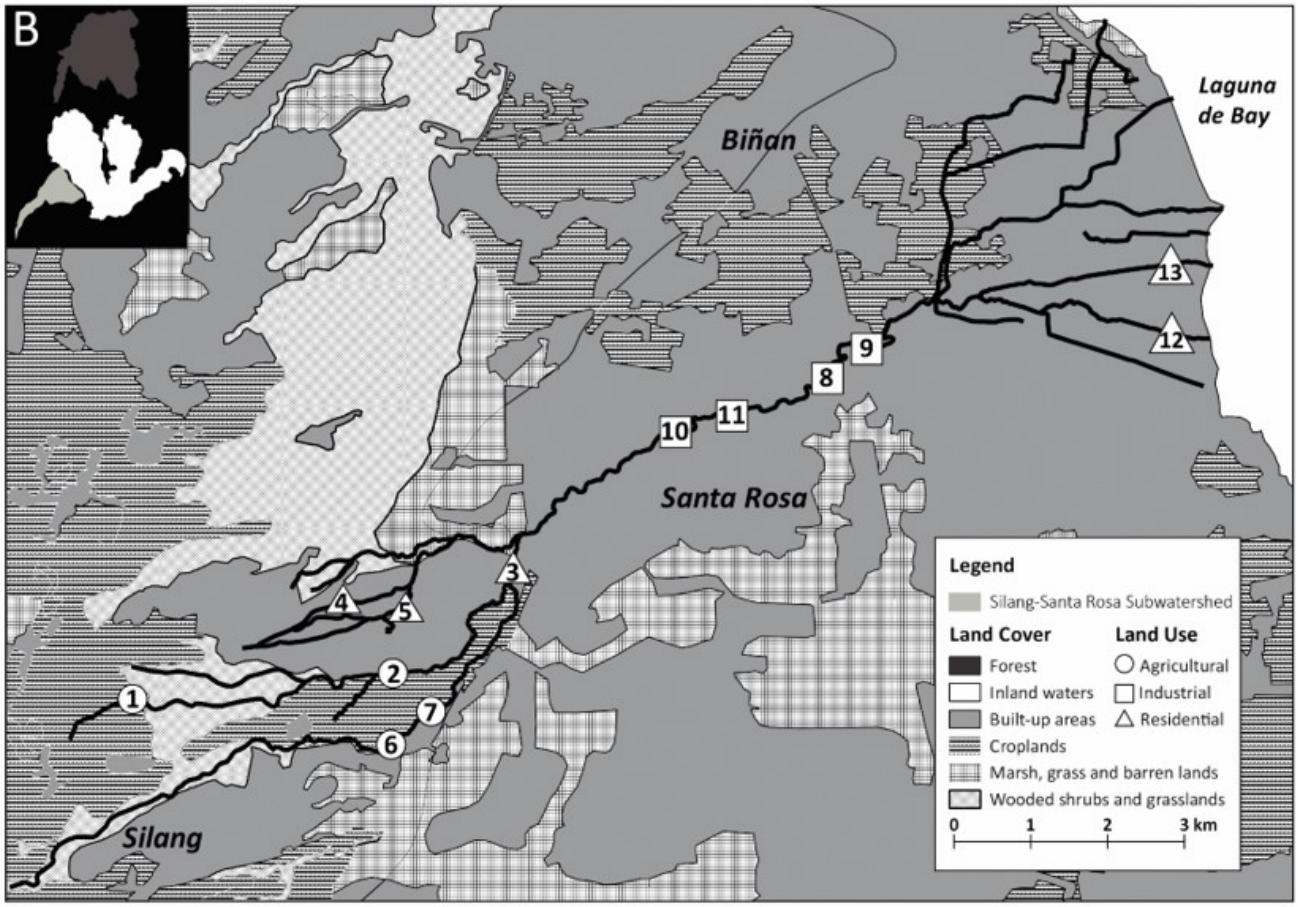


©2019. Japan Geoscience Union. All Right Reserved. 

# Ammonium contamination of shallow groundwater beneath vegetable fields in Central Vietnam

*Maeda Morihiro[1], Takuya Fujimura[1], Van Ngoc Tuong Hoang[2], Daisuke Inoue[3], Hidetaka Chikamori[1], Fujio Hyodo[1]

1. Okayama University, 2. Hue University, 3. Osaka University

Nitrogen contamination in shallow groundwater occurs in a coastal area in Central Vietnam. In agricultural fields close to the residential area, high concentrations of $NH_4^+$ and $NO_3^-$ in groundwater was attributed to unintended inflow of livestock wastes and/or domestic wastewater. On the other hand, $NH_4^+$ concentration reaches to several milligrams N per liter even in vegetable fields away from the residential area. The objective of this study was to determine $NH_4^+$ contamination mechanisms of the shallow groundwater without domestic wastewater inflow. In this study, we tested three hypotheses: (i) $NH_4^+$ derived from fertilizer or manure applied to the fields was transported to groundwater thorough soil, (ii) nitrate ($NO_3^-$) produced as a result of nitrification in topsoil was transferred to deep soil and again transformed to $NH_4^+$, or (iii) nitrogen mineralization occurred in deep soil. Soil samples were collected up to 240 cm from a vegetable production field in Quang Thang Commune, Central Vietnam in June (dry season) and November (rainy season) of 2016 and 2017. The groundwater table existed at 57 or 67 cm in June and 33 cm from the soil surface in November. Concentrations of $NH_4^+$ in PVC pipe wells fluctuated between 1 and 3 mg N $L^{-1}$ in accordance with the detection of soil $NH_4^+$ content (5-20 mg $kg^{-1}$) in the 150-240 cm layer. On the other hand, soil $NH_4^+$ was not detected in the 30-80 cm layer whereas it was 2-6 mg $kg^{-1}$ in the 0-10 cm layers, indicating that $NH_4^+$ was not transferred to layers deeper than 30 cm. The absence of a functional gene of dissimilatory nitrate reduction to $NH_4^+$ (DNRA) in the 150-240 cm soil layer shows that DNRA did not occur in this deep layer. Natural abundance values of $^{15}N$ ($\delta^{15}N$) for soil $NH_4^+$ (+3.6 to 5.5‰) were similar to those in soil total N (+1.9 to 3.6‰) in the 150-240 cm layer. In addition, anaerobically incubated soil from the 140-160 cm layer was mineralized by 1-2 mg $NH_4^+$-N $kg^{-1}$ for 8 weeks. These experimental results suggest that the high concentration of $NH_4^+$ found in wells was originated from mineralization of deep soil.

Keywords: ammonium , dissimilatory nitrate reduction to ammonium, nitrogen mineralization

©2019. Japan Geoscience Union. All Right Reserved. 

# Modelling nutrient and organic waste behaviour in a tropical wetland in Singapore under projected anthropogenic scenarios

*Swee Yang Edmund Low[1], Dong Eon Kim[1], Canh Tien Trinh Nguyen[1], Yixiong Cai, Shie-Yui Liong[1]

1. National University of Singapore

Nee Soon swamp forest is one of the last vestiges of tropical wetland in Singapore, and is important both as a site for ecological preservation, as well as a source of water for potable treatment. Understanding the hydrological regime of the swamp forest and implications for water quality is critical to guide stakeholders in implementing effective measures to preserve the wetland against anthropogenic impacts. In particular, although current field measurement data do not indicate a concern with organic or nutrient pollution, reviewing the ways in which the wetland responds to elevated waste discharges can help identify potential hotspots, and the impact on the outflow from the catchment which drains into downstream controlled watercourses. An integrated water quality model is therefore developed in this study to investigate spatial and temporal concentrations of DO levels, organic pollution (as quantified by biochemical oxygen demand, BOD), and nutrient pollution (NH3-N and NO3-N) within the catchment’s river network under projected scenarios of upstream wastewater inflow. The model was developed using MIKE HYDRO for modelling the study domain, as well as the MIKE ECO Lab numerical laboratory for characterising water quality processes. Model parameters are calibrated against time series of observed discharges and dissolved oxygen levels at measurement stations along the river network. The calibrated model was then applied to study downstream impact due to elevated BOD and ammonia from upstream wastewater discharge. Over a simulation period of April 2014 to December 2015, the model predicted that a spiked inflow of 400 mg/l BOD and 30 mg/l NH3-N upstream will elevate downstream concentrations at the catchment outlet to an average of 13 mg/l BOD, and 0.7 mg/l nitrogen (NH3-N, NO3-N), from a baseline of 0.4 mg/l BOD, 0.03 mg/l NH3-N, and 0.07 mg/l NO3-N. Levels of DO were decreased from an initial 5.4 mg/l to 3.6 mg/l. Though a scenario of spiked pollutant influx at the swamp forest’s undeveloped upstream sub-catchments is currently unlikely to occur, the outcomes nevertheless will be beneficial for future planning studies in understanding how the water quality of the catchment will be impacted should urban redevelopment works be considered around the swamp forest.

Keywords: Wetland, Organic waste impact, Nutrient impact, Water quality, Modeling

©2019. Japan Geoscience Union. All Right Reserved. 

# Benthic macroinvertebrate assemblages and water quality reflect the impacts of land use and land cover in Marikina Watershed, Philippines

*Julie - An N. Gregorio[1,2], Elfritzson M. Peralta[3,5], Irisse Bianca B. de Jesus[3,5], Tohru Ikeya[6], Jonathan Carlo A. Briones[3,4,5], Rey Donne S. Papa[3,4,5], Francis S. Magbanua[1], Noboru Okuda[6]

1. Institute of Biology, University of the Philippines, Diliman, Quezon City, 1101 Philippines, 2. Institute of Environmental Science and Meteorology, University of the Philippines, Diliman, Quezon City 1101 Philippines, 3. Research Center for the Natural and Applied Sciences, University of Santo Tomas, España Boulevard, Manila, 1015, Philippines, 4. Department of Biological Sciences, University of Santo Tomas, España Boulevard, Manila, 1015, Philippines, 5. The Graduate School, University of Santo Tomas, España Boulevard, Manila, 1015, Philippines, 6. Research Institute for Humanity and Nature, 457-4 Motoyama, Kamigamo, Kyoto, 603-8047, Japan

Watershed systems provide various ecological services such as good water quality, regulate water flow, maintain water balance and biodiversity conservation. However, human disturbances greatly affect the water quality and composition of biotic communities. Although anthropogenic changes in freshwater systems were truly evident, studies focusing on the human impacts on tropical watersheds are still limited in developing countries. Thus, this study aims to investigate the response of freshwater macroinvertebrates to varying land use patterns and land cover characteristics in Marikina Watershed, Philippines. For a total of 30 streams, which were categorized into 7 protected, 3 forested, 8 agricultural, and 12 residential streams based on land use and cover in their catchments, were collected benthic macroinvertebrates and measured environmental variables. PCA plots were not able to classify water quality according to land use and was supported with no significant difference in Kruskal –Wallis test. However, water quality of primarily vegetated and primarily non-vegetated sites as well as protected and protected streams had delineation, as accorded with the results of independent *t* - tests with significant differences ($p<0.05$) on dissolved oxygen, conductivity, total dissolved solids and salinity. While the forested streams are clustered together in the NMDS plot but there is no clear pattern in the assemblage of benthic macroinvertebrates. The similarities in the composition of macroinvertebrates could be attributed to the similar magnitude and intensity of landscape alteration of each land use among the streams. Interestingly, the nMDS plot shows strong separation of macroinvertebrate assemblages across gradient of vegetation area (Global $R = 0.388$, $P = 0.001$) and were supported independent *t*- test where with macroinvertebrate diversity, density and abundance of pollution-sensitive taxa on primarily vegetated areas exhibited significant differences from non-vegetated areas ($p < 0.05$). Additionally, biotic indices such as such as SingScore, Average Score per Taxon THAI ($ASPT^{THAI}$), Biological Monitoring Working Party ($BMWP^{THAI}$), and Stream Invertebrate Grade Number Average Level version 2 (SIGNAL 2) reveal significant differences among protection status, land use types and land cover ($p<0.05$). CCA plot also revealed pollution –sensitive taxa with primarily vegetated sites were associated with pollution-sensitive taxa and primarily non-vegetated sites are associated with pollution-tolerant organisms to on CCA plot. The findings of this study demonstrate the effects of land alteration to the macroinvertebrate community and water quality. Furthermore, it emphasizes the importance of vegetation cover and designation of protected areas to have better ecological quality in a watershed. This study thus suggests for an extensive and improved policy development and implementation. Furthermore, extensive biomonitoring and formulation of Marikina Watershed Biotic Index are recommended.

Keywords: Marikina Watershed, land use, land cover, water quality, benthic macroinvertebrates

©2019. Japan Geoscience Union. All Right Reserved. 

[E] Oral | A (Atmospheric and Hydrospheric Sciences )：A-HW Hydrology & Water Environment

Thu. May 30, 2019 10:45 AM - 12:15 PM JST | Thu. May 30, 2019 1:45 AM - 3:15 AM UTC | 201B 2F

## [A-HW22] Materials transport and nutrient cycles in watersheds; from headwaters to coastal seas

convener:Masahiro Kobayashi(Forestry and Forest Products Research Institute), Seiko Yoshikawa(Institute for Agro-environmental Sciences, National Agriculture and Food Research Organization), Jun Yasumoto(University of the Ryukyus, Faculty of Agriculuture), Adina Paytan(University of California Santa Cruz), Chairperson:Yasumoto Jun(University of the Ryukyus, Faculty of Agriculuture Department of Regional Agricultural Engineering)

This session aims to synthetize watershed sciences in order to understand dynamical processes of materials transport and nutrient cycles in watersheds from headwaters to coastal seas. The session will be integrating a variety of research disciplines including limnology, ground water hydrology, coastal oceanography, meteorology, pedology, sedimentology, forestry, agriculture, fishery, ecology, social science and more. This session calls for ideas on new methods for the watershed sciences, such as tracer and molecular technique, hydrological modeling, paleontological approaches, laboratory and field experiments, social-scientific evaluation of ecosystem services and social-ecological systems, and so on, in order to elucidate physical, chemical and biological mechanisms for shedding light on natural phenomena and their changes over time in complex and dynamic watershed systems under human and climate impacts. Through this session, we would like to facilitate interdisciplinary collaboration among participants to create new knowledge on watershed sciences.

10:45 AM - 11:00 AM JST | 1:45 AM - 2:00 AM UTC

### [AHW22-12] Characterization, distribution and degradation of environmental plastics in inland river system of Mongolia

*Batdulam Battulga[1], Masayuki Kawahigashi[1], Bolormaa Oyuntsetseg[2] (1.Department of Geography, Tokyo Metropolitan University, Tokyo, 192-0397, Japan , 2.Department of Chemistry, National University of Mongolia, Ulaanbaatar, 210646, Mongolia)

---

11:00 AM - 11:15 AM JST | 2:00 AM - 2:15 AM UTC

### [AHW22-13] Multi-site and multi-approach sediment transport modeling in tropical watersheds

★Invited Papers

*Assefa M Melesse[1], Alemu Osore Aga[2], Hagos Gebreselassie[2] (1.Florida International University, 2.Addis Ababa University)

---

11:15 AM - 11:30 AM JST | 2:15 AM - 2:30 AM UTC

### [AHW22-14] Calculation of SS concentration coefficients of river water for each land use by a simple watershed model.

*Seiko Yoshikawa[1], Donglai Ma[1,2], Tadamasa Saito[1,3], Kenji Matsumori[4], Yuko Itoh[5], Masahiro Kobayashi[5] (1.Institute for Agro-environmental Sciences, National Agriculture and Food Research Organization, 2.Graduate Scool, Tsukuba University , 3.Faculty of Agriculture, Ibaraki University , 4.Western Region Agricultural Research Center, National Agriculture and Food Research Organization, 5.Forestry and Forest Products Research Institute)

---

11:30 AM - 11:45 AM JST | 2:30 AM - 2:45 AM UTC

### [AHW22-15] Evaluation of long term variation in water balance and discharge of sediment and nitrogen in the urbanized catchment of Yamato River, using SWAT model

*Kunyang Wang[1,2], Yuta Shimizu[3], Shin-ichi Onodera[1], Mitsuyo Saito[4], Yusuke Tomozawa[1] (1.Graduate School of Integrated Arts and Science, Hiroshima University, 2.Capital Normal University, 3.National Agriculture and Food Research Organization, 4.Okayama University)

---

11:45 AM - 12:00 PM JST | 2:45 AM - 3:00 AM UTC

[AHW22-16] Causal correlation between water-use of the Tedori River and coastal erosion of Chirihama Nagisa Driveway, Ishikawa, Japan

*Toshihiko Momose[1] (1.Ishikawa Prefectural University)

---

12:00 PM - 12:15 PM JST | 3:00 AM - 3:15 AM UTC

[AHW22-17] Role of suspended solids on elemental dynamics in the Selenga River system

★Invited Papers

*Masayuki Kawahigashi[1], Orgilbold Myangan[2], Bolormaa Oyuntsetseg[2] (1.Tokyo Metropolitan University, 2.National University of Mongolia)

# Characterization, distribution and degradation of environmental plastics in inland river system of Mongolia

*Batdulam Battulga[1], Masayuki Kawahigashi[1], Bolormaa Oyuntsetseg[2]

1. Department of Geography, Tokyo Metropolitan University, Tokyo, 192-0397, Japan , 2. Department of Chemistry, National University of Mongolia, Ulaanbaatar, 210646, Mongolia

Marine plastic abundance and distribution have been reported toward increasing importance of their behavior as anthropogenic influences on aquatic environment. However, remains of plastics particularly in freshwater are largely unknown. Tributaries in the Selenga River system are important sources of fresh water in Central and Northern Mongolia, although the river system has been alarmed by various kinds of pollution because of growing population and increasing demand of land and resources. Evaluating fate of plastics in the river is vital to assess how the urban system affects plastic pollution in Selenga River. This study aimed to identify the fate of environmental plastics in the Selenga River system of Mongolia.
In 2017 and 2018, totally 18 sampling sites have been surveyed according to geographical locations from the capital city, Ulaanbaatar. Collected plastics were classified as their sizes (micro, meso, macro and mega) and materials such as films, foams, fragments and fibers. Visually sorted plastics identified by FTIR micro-spectroscopy to determine chemical characterization. Furthermore, a degradation index of collected plastics was examined using a ratio of two specific IR absorptions. Invisible microplastics (MP) attached onto the collected plastics were separated mainly from polystyrene foam (PSF), which was the most dominant environmental plastics in the research field. Characterization of the invisible MP was conducted using a digital microscope and an FTIR micro-spectroscopy.
Plastic films and foams were largely occupied in the collected plastics from the researched rivers. Surprisingly great amount of PSF were found in micro and meso size ranges. The results illustrate that on-site fragmentation and degradation of bulk PSF occurred in the research sites probably due to solar radiation and freeze-thaw cycles. A broad range of the degradation index was recorded in micro, meso and macro sized PSF, indicating that various stages of degradation occurred in the river environment. Apart from the other plastics types, PSF was considered as a carrier of invisible MP. A greater diversity of invisible MP types and numbers were found in a microscopic view using a digital microscope on the surface of PSF. Polyethylene (PE) and polystyrene (PS) were major components of the sorbed MP.
This study represents the first detailed examination of the distribution, types and degradation processes of plastics in the Mongolian river system. Environmental plastics were widespread litter in the investigated Mongolian river shores due to low-level of waste management with rapidly growing population and urbanization.

Keywords: Plastic debris, River shore, Mongolia, Degradation, Microplastics

©2019. Japan Geoscience Union. All Right Reserved. 

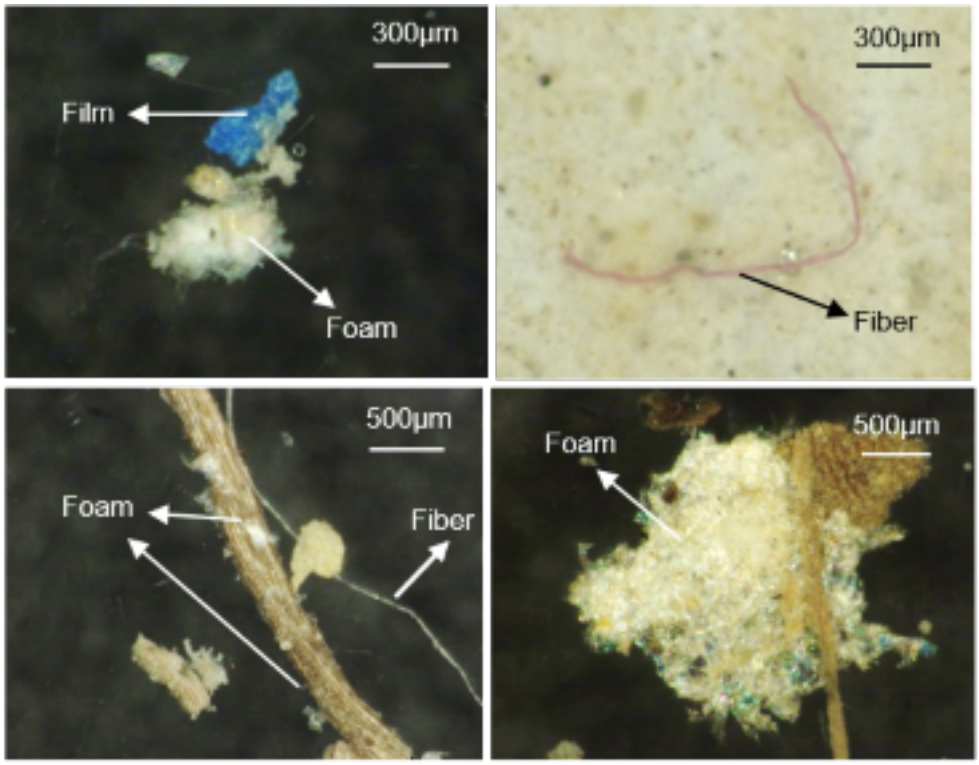


Microscopic view of microplastics attached onto visible polystyrene foam (PSF).

©2019. Japan Geoscience Union. All Right Reserved. 

# Multi-site and multi-approach sediment transport modeling in tropical watersheds

*Assefa M Melesse[1], Alemu Osore Aga[2], Hagos Gebreselassie[2]

1. Florida International University, 2. Addis Ababa University

Land degradation and poor watershed management have been the major factors that led to severe soil erosion and hence sedimentation in receiving water bodies and reservoirs. The environmental impacts of sediment transport and loading is highly pronounced in tropical watersheds where rainfall is erratic and torrential and soil and conservation measures are poor. In this study, a soil erosion, sediment yield and transport modeling were conducted in three tropical watersheds in Ethiopia and Kenya. Field plot experiment, model development and evaluation were conducted. The impact of land use, rainfall intensity and slope were evaluated at plot and watershed scales. Three models (WEPP, SWAT and Erosion 3D) were tested and compared. The results indicate that the models performed differently with Erosion 3D and WEPP performed better in sediment load simulation. In the absence of the observed sediment data, sediment rating curves developed and validated were useful and are promising.

Keywords: Sediment flux, Sediment modeling, Erosion 3D, SWAT, WEPP, Tropical watersheds

©2019. Japan Geoscience Union. All Right Reserved. 

# Calculation of SS concentration coefficients of river water for each land use by a simple watershed model.

*Seiko Yoshikawa[1], Donglai Ma[1,2], Tadamasa Saito[1,3], Kenji Matsumori[4], Yuko Itoh[5], Masahiro Kobayashi[5]

1. Institute for Agro-environmental Sciences, National Agriculture and Food Research Organization, 2. Graduate Scool, Tsukuba University , 3. Faculty of Agriculture, Ibaraki University , 4. Western Region Agricultural Research Center, National Agriculture and Food Research Organization, 5. Forestry and Forest Products Research Institute

In recent years, sediment-related disasters are increasing due to intensification and localization of rainfall caused by climate change. Although it is difficult to predict the place and extent of sediment-related disasters, we firstly grasp the average concentrations of sediment discharge in recent years and predict increase and decrease in the sediment concentrations when the way of rain changes. Sediment runoff is depend on land use and land cover, conservative measures, topography, climate condition mainly rainfall etc.. Among them, the land use and land cover is expected to be great in normal climate conditions. Here, in order to contribute to the prediction of sediment-related disasters in the future, coefficients that indicate the SS load intensity to rivers of each land use for the river watersheds across the country are calculated using a simple watershed land use model.
Watersheds whose lower ends are observation points of water quality, and whose land use ratios were determined by GIS technique using published database of DEM (GSI, 10B, raster data) and LULC mesh data (JAXA , ALOS AVNIR-2, 10m mesh data). The SS concentration coefficients of paddy, upland, forest, and urban were calculated by applying the below multiple regression equation using the land use ratios and published SS data( Ministry of Environment).

$C = a_1 x_1 + a_2 x_2 + a_3 x_3 + a_4 x_4$

$C$: SS concentration (mg $L^{-1}$) $a_i$ : SS concentration coefficient for land use $i$, $x_i$ : ratio of land use $i$, Land use $i$ : 1;paddy 2;upland fields 3;forest 4;urban

The SS concentration coefficient is 15.4 (lower limit 95% value 12.0 to upper limit 95% value 18.8), 11.5 (7.4 to 15.6), 3.9 (2.6 to 5.1), 11.2 (9.2 to 13.2) for paddy fields, upland fields, forests and urban areas respectively (n=5103).
In order to investigate further in detail, it is necessary to analyze fertilization, soil properties, livestock industry in the watershed, climatic conditions (especially rainfall amount), topographical and geographical features and so on.

Keywords: watershed land-use model, SS, concentration coefficient

©2019. Japan Geoscience Union. All Right Reserved. 

# Evaluation of long term variation in water balance and discharge of sediment and nitrogen in the urbanized catchment of Yamato River, using SWAT model

*Kunyang Wang[1,2], Yuta Shimizu[3], Shin-ichi Onodera[1], Mitsuyo Saito[4], Yusuke Tomozawa[1]

1. Graduate School of Integrated Arts and Science, Hiroshima University, 2. Capital Normal University, 3. National Agriculture and Food Research Organization, 4. Okayama University

Land-use changes, freshwater use, and the biochemical flow are important factors affecting the Earth's environmental threshold. In the research topics of Planetary Boundaries (PB), these factors have been defined as entering high-risk levels. One-third of the planet's freshwater resources come from groundwater, and now, in some countries and regions, it is also exposed to the risk of groundwater depletion. Large-scale urbanization brings economic development but also increases the possibility of urban waterlogging.

Yamato river is the highest-level river in Japan. It has a watershed area of 1067 square kilometers, covering almost half area of Nara prefecture. Yamato river catchment includes Nara basin which as an important agricultural base, Nara city and part of Sakai city. The water environment in the catchment is closely related to the healthy life of human beings. Especially in recent years, there are frequent flooding in the catchment. Therefore, the study of Yamato river is very necessary.

This thesis uses the SWAT (Soil and Water Assessment Tool) model and Geographic Information System (GIS) methodology. The SWAT model can not only simulate the water discharge and nutrient load but also find the essence of the change of water environment through the change of parameter sensitivity. Select Coefficient of determination (R2), Nash–Sutcliffe efficiency (NSE), and percentage of bias (PBIAS) as a factor of assessing results and obtained the experimental results with credibility.

It is found that the land use in the basin is mainly manifested in the change from farmland to urban land use type, which probably accounts for 1/3 of the total area of land use type changed. Over a period of 2009-2016, the average of water discharge from the total outlet in the main channel is 2.37 million m3/day while it's 2.06 million m3/day in 1971-1978. As a result of changes in land use, water yield from farmland decreased by 45% compared with the 1970s, while the yield from the city increased by 43%. Among them, Surface runoff generated increase by about 70%. In Sakai and its surrounding cities, surface runoff generated increased by 18% per 100 mm precipitation. Curb length density in the high-density urban area increased about one time. That means Sakai now, in the face of flooding caused by torrential rains, needs to take on higher risks.

Sediment yield reducing by more than 70% from 1988 to 2014. The change comes mainly from the management of the river channel. The non-point source load of nitrate increased from 1096 tons to 1534 tons, this is mainly due to the increase in precipitation and the increase in population. The growth of forests also has a certain impact. This is because the type of land used in farmland and forests, there has a large number of fertilizers on the surface of the soil from human agriculture activities or the decay of animal and plant debris. Under the driving effect of precipitation, it mainly transported by the lateral flow in farmland and forest area and the surface runoff in the urban area, a large part will enter the river channel.

©2019. Japan Geoscience Union. All Right Reserved. 

Keywords: Land use change, Water balance, Nitrogen load, SWAT Model, Long term variation

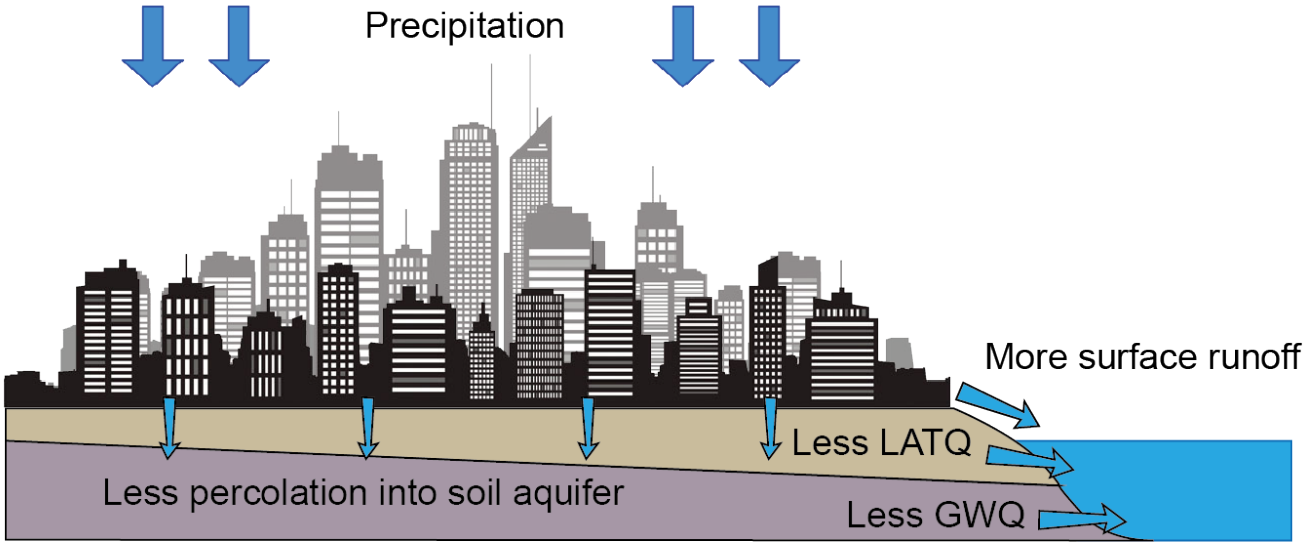


©2019. Japan Geoscience Union. All Right Reserved. 

# Causal correlation between water-use of the Tedori River and coastal erosion of Chirihama Nagisa Driveway, Ishikawa, Japan

*Toshihiko Momose[1]

1. Ishikawa Prefectural University

Awarded as the best beach of Japan (Reported by TripAdvisor, Inc. 2016), Chirihama Nagisa Driveway is a sandy beach located in Ishikawa, attracting people as the place that allows for driving cars and even large tourist buses along the shore. The source of the Chirihama sand is debris from Mt. Haku-san, which is transferred by the Tedori River and the Tsushima Current. At the river mouth, the finer sands are transferred to further offshore, and then drifted to further beach such as the Chirihama coast (50 km far from the river mouth). Due to the natural sand drifting process, the Chirihama coast is composed of the sands with fine and uniform grain size, the feature which guarantees for comfortable drive on the beach. The Chirihama coast is a treasure of Ishikawa; however, it faces a crisis of disappearance due to beach erosion.

According to Ishikawa prefectural government, the amount of sand loss of the Chirihama coast is 70000 $m^3$/year and its width decreases at 1 m/year. While the Chirihama coast is disappearing, a large-scale landslide of 1300000 $m^3$ occurred at upstream region of the Todori River in 2015 and the massive derbies moved downstream. The turbid water released for the ocean seemed to contribute to the formation of the Chirihama coast, but there are no reports on the recovery of the Chirihama coast. Where do the sands released from the Tedori River move?

Field investigations along the coast have found that the beach sediment at 4 –5 km far from the river mouth has the same feature as the Chirihama sand. From the viewpoint of recent water-use of the Tedori river, this presentation explains a possible reason why the fine sand released from the Tedori River cannot move to the Chirihama coast.

Keywords: Chirihama Nagisa Driveway, Coastal erosion, Tedori River, River structure

©2019. Japan Geoscience Union. All Right Reserved. 

# Role of suspended solids on elemental dynamics in the Selenga River system

*Masayuki Kawahigashi[1], Orgilbold Myangan[2], Bolormaa Oyuntsetseg[2]

1. Tokyo Metropolitan University, 2. National University of Mongolia

Lake Baikal is one of the cleanest lake in the world. However, there are many sources of pollution such as mining, industry and agriculture in the river basin of the main tributary, Selenga River which is flowing into Lake Baikal. Lake Baikal actually face to severe pollution affected by anthropogenic activities in the watershed. Natural cleaning mechanism can still be functioning to prevent pollutants flow into the Baikal. Since suspended solids (SS) in the Selenga River can play a role as carriers of heavy metals and organic pollutants, their dynamics should be addressed to know the mechanism.

Water and sediment samples were collected in the Russian territory from the Mongolian border to the shore of the Baikal including the Selenga Delta. SS samples were further recovered using a glass fiber filter from the water samples. Surface sediments and SS samples were digested with the mixture of nitric acid and perchloric acid for determination of elements using Inductively Coupled Plasma Atomic Emission Spectrometry (ICP-AES).

Elemental concentrations were changeable depending on SS concentration along the tributary. Changes in SS concentration can be controlled by flow rate of the tributary. The significant relationship were observed between SS and sesquioxides mainly consisting of Fe and Al. Both of Mn and Cr were also common constituents of the SS oxides despite of their low concentration in SS. In contrast, Zn and Cu have no correlation with SS, indicating that they are specifically accumulated onto SS surface at a point where the two elements were released. The concentration of SS gradually decreased accompanied by decrease in heavy metals in SS in the delta region. On the contrary, those elements in the surface sediments increased to downstream in the delta region. Deposition process of SS in the delta can be occurred due to decrease in flow rate by channel bifurcation of tributaries, back water effect from Lake Baikal and SS trapping by vegetation in the delta. The delta has a potential to trap SS, resulting that water quality in the Lake Baikal has been protected of water quality in Lake Baikal.

Keywords: Lake Baikal, SS deposition, channel bifurcation

©2019. Japan Geoscience Union. All Right Reserved. 

[E] Oral | A (Atmospheric and Hydrospheric Sciences )：A-HW Hydrology & Water Environment

Thu. May 30, 2019 1:45 PM - 3:15 PM JST | Thu. May 30, 2019 4:45 AM - 6:15 AM UTC | 201B 2F

## [A-HW22] Materials transport and nutrient cycles in watersheds; from headwaters to coastal seas

convener:Masahiro Kobayashi(Forestry and Forest Products Research Institute), Seiko Yoshikawa(Institute for Agro-environmental Sciences, National Agriculture and Food Research Organization), Jun Yasumoto(University of the Ryukyus, Faculty of Agriculuture), Adina Paytan(University of California Santa Cruz), Chairperson:Yoshikawa Seiko(Institute for Agro-environmental Sciences, National Agriculture and Food Research Organization)

This session aims to synthetize watershed sciences in order to understand dynamical processes of materials transport and nutrient cycles in watersheds from headwaters to coastal seas. The session will be integrating a variety of research disciplines including limnology, ground water hydrology, coastal oceanography, meteorology, pedology, sedimentology, forestry, agriculture, fishery, ecology, social science and more. This session calls for ideas on new methods for the watershed sciences, such as tracer and molecular technique, hydrological modeling, paleontological approaches, laboratory and field experiments, social-scientific evaluation of ecosystem services and social-ecological systems, and so on, in order to elucidate physical, chemical and biological mechanisms for shedding light on natural phenomena and their changes over time in complex and dynamic watershed systems under human and climate impacts. Through this session, we would like to facilitate interdisciplinary collaboration among participants to create new knowledge on watershed sciences.

1:45 PM - 2:00 PM JST | 4:45 AM - 5:00 AM UTC

[AHW22-18] Relationship between topographical characteristics in catchment area and dissolved iron concentration of river in permafrost area

*Yuto Tashiro[1], Muneoki Yoh[1], Takayuki Shiraiwa[2], Takeo Onishi[3] (1.Tokyo University of Agriculture and Technology, 2.Hokkaido University, 3.Gifu University)

---

2:00 PM - 2:15 PM JST | 5:00 AM - 5:15 AM UTC

[AHW22-19] Water Source Zones and Hydrochemical Properties of Fluoride Water in Mt. Meru Watershed, Tanzania

*Shinji Nakaya[1], Ryogo Takada[1], Jun Yasumoto[2], Junichi Yoshitani[1], Innocent Lugodisha[3], Zuberi Dominicus Lwimbo[3], Hans Komakech[4], Thomas Reuben Mollel[5] (1.Department of Water Environment and Civil Engineering, Faculty of Engineering, Shinshu University, Japan, 2.Department of Regional Agriculture Engineering, University of the Rykuyus, Japan, 3.School of Materials, Energy, Water and Environmental Sciences, NM-AIST, Tanzania, 4.WISE-Future, NM-AIST, Tanzania, 5.SGSS and Institute of resources assessment-UDSM, Tanzania)

---

2:15 PM - 2:30 PM JST | 5:15 AM - 5:30 AM UTC

[AHW22-20] Development and Application of a System for Measurement of Total Load of Water Quality

★Invited Papers

*Keiji Takase[1], Yuko Itoh[2] (1.Ishikawa Prefectual University, 2.Forestry and Forest Products research Institute, Japan)

---

2:30 PM - 2:45 PM JST | 5:30 AM - 5:45 AM UTC

[AHW22-21] Water infiltration and uptake around a Japanese cypress growing on a flat upland

*Masahiro Kobayashi[1], Shin-ichi Onodera[2], Yuko Itoh[1], Tadashi Sakata[1] (1.Forestry and Forest Products Research Institute, 2.Graduate School of Integrated and Arts Sciences, Hiroshima University)

---

2:45 PM - 3:00 PM JST | 5:45 AM - 6:00 AM UTC

[AHW22-22] **Innovative Rainfall Simulator Design for Moving Storm Scenarios with Different Storm Patterns**

*RAVI KUMAR MEENA[1], SUMIT SEN[2] (1.M.Tech Student, Department of Hydrology, Indian Institute of Technology Roorkee, Roorkee, Uttarakhand, India, 2. Associate Professor, Department of Hydrology, Indian Institute of Technology Roorkee, Roorkee, Uttarakhand, India)

3:00 PM - 3:15 PM JST | 6:00 AM - 6:15 AM UTC

Discussion

# Relationship between topographical characteristics in catchment area and dissolved iron concentration of river in permafrost area

*Yuto Tashiro[1], Muneoki Yoh[1], Takayuki Shiraiwa[2], Takeo Onishi[3]

1. Tokyo University of Agriculture and Technology, 2. Hokkaido University, 3. Gifu University

[Background]
Dissolved iron flowing out from the wetlands in the Amur River basin is an important nutrient that supports the primary production of phytoplankton in the Sea of Okhotsuk. Therefore, the amount of iron supplied to the sea is supposed to change due to the increase and/or decrease of the wetland area within the Amur basin. However, in the longterm observation of the dissolved iron concentration in the Amur River, the considerably high concentration, which can not be explained by the land-use change of the wetland, was observed in the latter of the 1990s. In the 1990s, because the relatively higher temperature had been continued, Shamov et al.,2014 speculated that permafrost thawing might be caution. Therefore, we hypothesized that permafrost thawing might promote the forming of humid and reductive condition which was suited to dFe generation in active layer, and have been conducting research on the mechanism of dissolved iron production and the distribution of permafrost. It has become clear that permafrost exists under the vegetation called Mari. Mari is the wetland which is covered by hygrophyte and sphagnum in a valley, and thick peat soil is accumulated underground.On the other hand, forest areas where birch or larch are densely spread with thin peat layers on the slope and ridge. Thus, the topographical features such as valley, slope and ridge in the catchment area dominate the vegetation and soil properties, and the dissolved iron cycling. In this study, we focused on the area of the valley as a topographical feature within the catchment area, and researched with the aim to discover the relationship to dissolved iron concentration in the river.
[Materials and Methods]
The research was conducted in the Tyrma River basin, which is a further tributary of the Tributary of the Amur River, in Khabarovsk. This area corresponds to the sporadic permafrost zone. In September 2018, we collected the water from 12 rivers in total; 5 rivers flowing into the Tyrma River and 5 rivers flowing into the Gujar river which is a tributary of the Tyrma River (basin area 7 to 200 km2). After sampling the water, immediately filtration was carried out with a disposable 0.45 $\mu$m filter and stored in polyethylene containers. Dissolved iron concentration was measured by the phenanthroline method after adding a few drops of HNO3- to the sample water to adjust pH <2.
We extracted the valley area using GIS soft "QGIS". The altitude data of field site, a global numerical surface model (DSM) corresponding to a resolution of 30 m by a panchromatic stereoscopic sensor (PRISM) equipped with JAXA 's Land Observing Satellite "ALOS" was used. The catchment area on the upstream side from the sampling point of each river was extracted and the Topographic Position Index (TPI) and the inclination (degree) were calculated. Next, the cells with TPI <0 - [standard deviation of TPI ×1/2] and inclination <3 (degree) were judged as a valley and these areas were calculated. The radius(R) of TPI was set to R = 500 m or R = 1000 m according to the valley width of the river. The reason why the condition of inclination <3 (degree) was added was that if only the condition of TPI was included, even the lower part of the slope was included, so that the valley area could be overestimated.
[Results and Discussion]
Dissolved iron concentrations in some rivers showed a very low concentration of <0.02 mg / L, which is below the detection limit, while others showed high concentrations of 0.37 mg / L. The relationship between these concentration differences and the valley area in the catchment area is shown in Fig.1. In the rivers whose valley area was less than 1 km2, the concentration of dissolved iron was less than 0.05

©2019. Japan Geoscience Union. All Right Reserved. 

mg / L. On the other hand, it was revealed that the concentration of dissolved iron tended to be higher with larger valley area in the catchment area. For the rivers with the low dFe concentrations, the catchment areas ware less than 15 km2, and the valley area occupied as low as 3% or less. The other rivers whose the dissolved iron concentration higher than 0.1 mg / L, the valley area accounted for 5-8% of the catchment area. The flat valley exists along the river is a typical topography in the Tyrma basin. In such places where the inclination is small, since the movement of water is also limited and make the residence time longer, the moisture and reductive environment can be maintained in the active layer on the permafrost, and wetland like Mari which is taken precedence by hygrophyte is widely formed in the valley. As the result, this study showed that Mari covering the valley has the function of dissolved iron generation and dissolved iron flow out into rivers.

Keywords: Dissolved Iron, Permafrost, Wetland

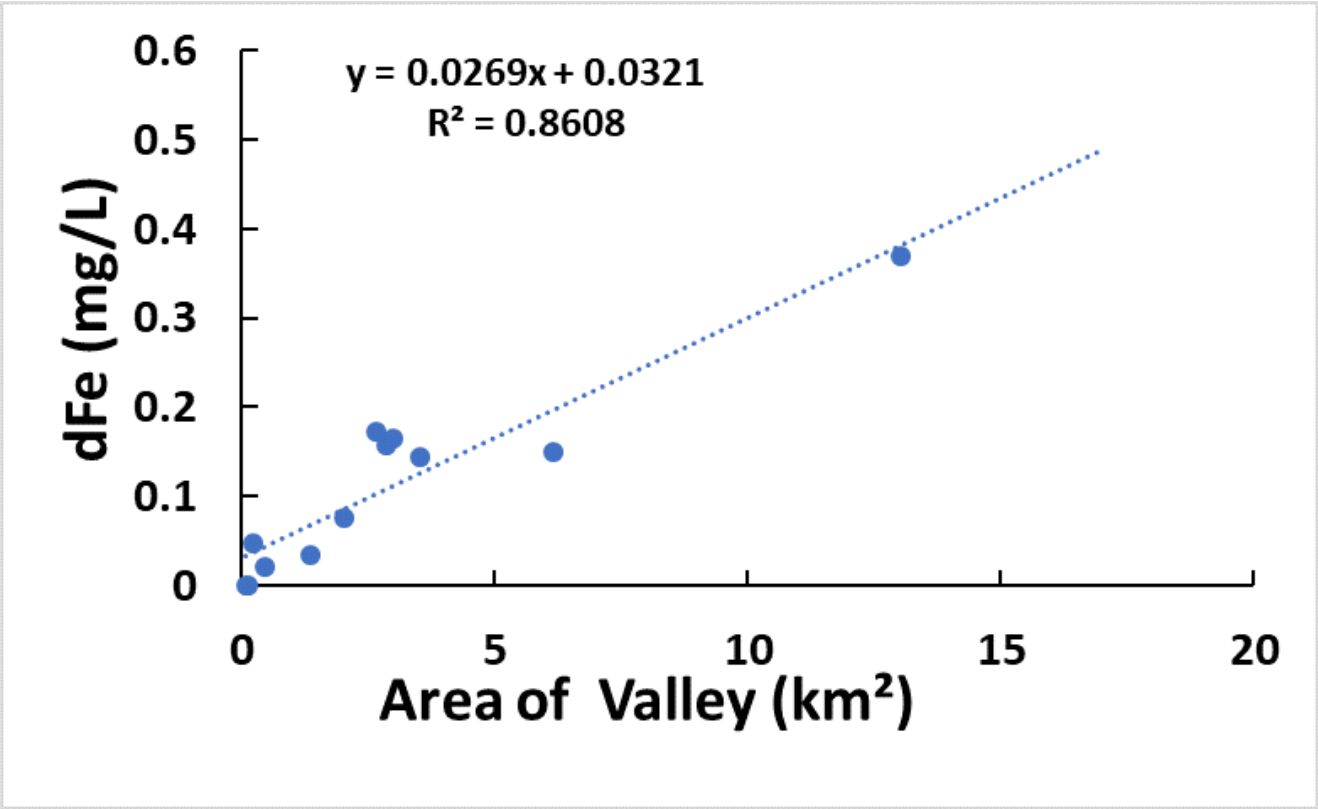


©2019. Japan Geoscience Union. All Right Reserved. 

# Water Source Zones and Hydrochemical Properties of Fluoride Water in Mt. Meru Watershed, Tanzania

*Shinji Nakaya[1], Ryogo Takada[1], Jun Yasumoto[2], Junichi Yoshitani[1], Innocent Lugodisha[3], Zuberi Dominicus Lwimbo[3], Hans Komakech[4], Thomas Reuben Mollel[5]

1. Department of Water Environment and Civil Engineering, Faculty of Engineering, Shinshu University, Japan, 2. Department of Regional Agriculture Engineering, University of the Rykuyus, Japan, 3. School of Materials, Energy, Water and Environmental Sciences, NM-AIST, Tanzania, 4. WISE-Future, NM-AIST, Tanzania, 5. SGSS and Institute of resources assessment-UDSM, Tanzania

Fluoride is leaching to natural water system from volcanic rocks and ashes with alkali volcanic activity along Great Lift Valley in east Africa. Tanzanian people in Great Lift Valley are also suffering drinking water including high fluoride ( > 1.5 mgF/L of WHO) and water shortage. We investigated the groundwater and river water fluoride pollutions in area between Arusha of Mt. Meru watershed and Moshi of Mt. Kilimanjaro watershed in September, 2018 to provide the solutions to these issues as No. 6 of SDGs. We find some results below:

1. Average fluoride content is 4.0 mgF/L in Mt. Meru watershed, and 0.5 mgF/L in Mt. Kilimanjaro watershed.

2. Fluoride concentrates in Na-$HCO_3$ type water, and Fluoride tend to increase with Na and pH.

3. Groundwater fluoride tends to be increasing with residence time, but in recent twenty five years, fluoride is
higher in younger groundwater.
4. Well waters supplied to Arusha city come from the recharge zone of 2,000 m to 3,000 m in altitude of Mt. Meru, and the fluoride content tend to increase with the recharge altitude.

Keywords: Fluoride, Great Lift Valley, Tanzania, Mt. Meru watershed

©2019. Japan Geoscience Union. All Right Reserved. 

# Development and Application of a System for Measurement of Total Load of Water Quality

*Keiji Takase[1], Yuko Itoh[2]

1. Ishikawa Prefectual University, 2. Forestry and Forest Products research Institute, Japan

Conservation and management of water quality is most important to conserve the water environment as well as to secure good water resource. Water quality has been conventionally controlled by regulation of emission concentration. On the other hand, divergence of emission material and increase of waste water in recent years indicates that the regulation of total emission will be most important. In addition, the knowledge of total load of a material such as nitrogen and phosphorous is fundamental to understand a cycle and mass balance of the material. However, the measurement of water quality load is not so easy because it requires much of time and labor well as high cost. So, we established a new system by which we could easily determine the total load of water quality. In this paper, the system is applied in a forested watershed to discuss validity of the system.

Keywords: Water Quality, Concentration, Total load of water quality, System for collecting water, Forested watershed

©2019. Japan Geoscience Union. All Right Reserved. 

# Water infiltration and uptake around a Japanese cypress growing on a flat upland

*Masahiro Kobayashi[1], Shin-ichi Onodera[2], Yuko Itoh[1], Tadashi Sakata[1]

1. Forestry and Forest Products Research Institute, 2. Graduate School of Integrated and Arts Sciences, Hiroshima University

In forest ecosystems, trees strongly influence the water movement above and below the ground. During rainfall events, some rainwater flows as stemflow, which provides concentrated water input into soil. The redistribution of soil water during periods without rainfall is affected by water uptake by roots. To clarify the effects of trees on soil water dynamics during and after rainfall events, we monitored the distribution and temporal dynamics of the soil water potential around the stem of a Japanese cypress (*Chamaecyparis obtusa*) using a two-dimensional array of tensiometers installed at multiple soil depths and distances from the tree. During rainfall events with wet antecedent moisture conditions, stemflow infiltrated into the soil and recharged the shallow groundwater near the stem. The matric potential often increased at lower positions before upper positions, indicating bypass flow through macropores. After large rainfall events, once the matric potential distribution became uniform horizontally, gravity-driven drainage proceeded. During the drying process, the matric potential decreased markedly proximal to the stem compared to distally. A horizontal gradient in the matric potential was observed in both the shallow and deeper soil layers. This indicates an intense sink caused by water uptake by roots from the deeper soil layer. Upon excavating the roots after monitoring the matric potential, dense fine roots were observed in the deeper soil layer. The tree studied may feed the deeper soil around its root zone with rainwater as stemflow and use the water advantageously following the drying process.

Keywords: tree, stemflow, water uptake

©2019. Japan Geoscience Union. All Right Reserved. 

# Innovative Rainfall Simulator Design for Moving Storm Scenarios with Different Storm Patterns

*RAVI KUMAR MEENA[1], SUMIT SEN[2]

1. M.Tech Student, Department of Hydrology, Indian Institute of Technology Roorkee, Roorkee, Uttarakhand, India, 2. Associate Professor, Department of Hydrology, Indian Institute of Technology Roorkee, Roorkee, Uttarakhand, India

Rainfall simulators are widely used in the field of hydrology, biosystem engineering, agronomy, and geomorphology to understand the processes involved in these disciplines. Usually, rainfall simulators are not able to generate spatio-temporal variation in rainfall intensity simultaneously unlike natural conditions. Majority of methods used in rainfall simulator studies assumes that the rainstorm reaches instantaneously and remains steady over an area for a certain time period. Hence, most of the rainfall experiments ignore the effect of runoff response caused by moving storm across a watershed which results in under or over estimation of runoff peaks. Considering these limitations of traditional rainfall simulators, we are developing an advanced rainfall simulator using eleven full cone nozzles to simulate moving front storm. These nozzles can generate rainfall intensity in the range of 65 to 190 mm/hr at a pressure range of 50 kPa to 180 kPa with a varying height from 1.5m to 4m above the ground surface. All the eleven nozzles are controlled by flow control valves and the valves are individually regulated by servo motors. Arduino Mega microcontroller system is used to control all the servo motors to generate variable rainfall intensities. Further, we have developed a mobile application for Android users to regulate all the valves of rainfall simulator. This simulator is able to simulate nearly natural rainfall conditions in the controlled environment in four different patterns i.e. uniform, advanced, delayed and intermediate. A tray of 250cm×140cm×50cm has also being designed and fabricated to conduct different hydrological experiments. This tray is designed with a provision to generate and record overland, subsurface and base flow. Tray area can also be divided in three partition to analyze three different soil conditions simultaneously. Slope adjustment, leachate collection unit and piezo metric head measurement unit are also incorporated in this experimental tray. Overall, the whole rainfall simulator with tray can be used to study the impact of moving storm on soil erosion, infiltration, and runoff in the simulated near natural environment along with pollutant transport mechanisms. This study is being focused on detailed analysis of moving storms and their impact on hydrograph characteristics, especially in terms of time of concentration (tc), time to peak (tp), and peak discharge (Qp) for two different storm directions (upstream and downstream) with different storm movement velocity and rainfall intensity.

Keywords: Rainfall simulator, Moving Storm experiments, Spatio-temporal variation

©2019. Japan Geoscience Union. All Right Reserved. 

[E] Poster | A (Atmospheric and Hydrospheric Sciences)：A-HW Hydrology & Water Environment

Thu. May 30, 2019 3:30 PM - 5:00 PM JST | Thu. May 30, 2019 6:30 AM - 8:00 AM UTC | Poster Hall International Exhibition Hall8, Makuhari Messe_5

## [A-HW22] Materials transport and nutrient cycles in watersheds; from headwaters to coastal seas

convener:Masahiro Kobayashi(Forestry and Forest Products Research Institute), Seiko Yoshikawa(Institute for Agro-environmental Sciences, National Agriculture and Food Research Organization), Jun Yasumoto(University of the Ryukyus, Faculty of Agriculuture), Adina Paytan(University of California Santa Cruz)

This session aims to synthetize watershed sciences in order to understand dynamical processes of materials transport and nutrient cycles in watersheds from headwaters to coastal seas. The session will be integrating a variety of research disciplines including limnology, ground water hydrology, coastal oceanography, meteorology, pedology, sedimentology, forestry, agriculture, fishery, ecology, social science and more. This session calls for ideas on new methods for the watershed sciences, such as tracer and molecular technique, hydrological modeling, paleontological approaches, laboratory and field experiments, social-scientific evaluation of ecosystem services and social-ecological systems, and so on, in order to elucidate physical, chemical and biological mechanisms for shedding light on natural phenomena and their changes over time in complex and dynamic watershed systems under human and climate impacts. Through this session, we would like to facilitate interdisciplinary collaboration among participants to create new knowledge on watershed sciences.

### [AHW22-P01] Phosphate Enrichment Hampers Development of Juvenile Acropora digitifera Coral by Inhibiting Skeleton Formation

Mariko Iijima[1], *Yasumoto Ko[1], Jun Yasumoto[2], Mina Hirose[3], Mitsuru Jimbo[1], Shugo Watabe[1] (1.Kitasato University School of Marine Biosciences, 2.Faculty of Agriculture, University of the Ryukyus, 3.Tropical Technology Plus)

### [AHW22-P02] Modeling chlorophyll-a concentration using remote sensing in shallow water systems: Comparison of sensors

*Assefa M Melesse[1], Tara Blakey[1], Mohammad Haji Gholizadeh[1], Mohd Manzar Abbas[1] (1.Florida International University)

### [AHW22-P03] Dynamics in groundwater flow system with seasonal water table variation in a coastal and island

*Yusuke Tomozawa[1], Shin-ichi Onodera[1], Mitsuyo Saito[2] (1.Graduate School of Integrated Arts and Sciences Hiroshima University, 2.Graduate School of Environmental and Life Science, Okayama University)

### [AHW22-P04] The Tracing of Groundwater Contamination Sources in Indonesian Coastal Alluvial Groundwater using $\delta^{34}S$ and $\delta^{15}N$ Isotopes

*Anna Fadliah Rusydi[1,4], Mitsuyo Saito[2], Seiichiro Ioka[3], Shin-ichi Onodera[1] (1.Graduate School of Integrated Arts and Sciences, Hiroshima University, Japan, 2.Graduate School of Environmental and Life Sciences, Okayama University, Japan, 3.Research Institute for Sustainable Energy, Hirosaki University, Japan, 4.Research Center for Geotechnology, Indonesian Institute of Sciences, Indonesia)

### [AHW22-P05] Spatio-temporal dynamics of orthophosphate with implications for limitation of phytoplankton growth in north basin of Lake Biwa, Japan

*Xin Liu[1], Rong Yi[1], Masahiro Maruo[1], Syuhei Ban[1] (1.The University of Shiga Prefecture)

### [AHW22-P06] Microbial phase analysis in aquifer of Ryukyu Limestone Zone using next generation sequencer

*Umi Murao[1], Jun Yasumoto[1], Yasumoto Ko[3], Mina Hirose[2], Nanami Mizusawa[3], Ryo Iguchi[4], Bam H.N. Razafindrabe[5], Syugo Watabe[3] (1.University of the Ryukyus, Faculty of Agriculuture Department of Regional Agricultural Engineering, 2.Tropical Tecnology Plus, 3.Kitasato University School of Marine Biosciences, 4.National Institute of Advanced Industrial Science and Technology, 5.University of the Ryukyus, Faculty of Agriculuture Department of Subtropical Agro-Environmental Sciences)

## [AHW22-P07] Evaluation for temporal variation in groundwater inflow to the lagoons connected to Lake Biwa by radon ($^{222}$Rn) tracer analysis

*Mitsuyo Saito[1], Shin-ichi Onodera[2], Yusuke Tomozawa[2], Kunyang Wang[2], Syuhei Ban[3], Noboru Okuda[4] (1.Graduate School of Environmental and Life Science, Okayama University, 2.Graduate School of Integrated Arts and Sciences, Hiroshima University, 3.School of Environmental Sciences, The University of Shiga Prefecture, 4.Research Institute for Humanity and Nature)

## [AHW22-P08] Br/Cl ratio characteristics of groundwater in coastal areas in Indonesia

*Seiichiro Ioka[1], Shin-ichi Onodera[2], Mitsuyo Saito[3], Anna Fadliah Rusydi[2,4] (1.Institute of Regional Innovation, Hirosaki University, Japan, 2.Graduate School of Integrated Arts and Sciences, Hiroshima University, Japan, 3.Graduate School of Environmental and Life Sciences, Okayama University, Japan, 4.Research Center for Geotechnology, Indonesian Institute of Sciences, Indonesia)

## [AHW22-P09] Estimation of groundwater recharge and phosphorus transport under different precipitation conditions in a suburban catchment, using SWAT model

*Kunyang Wang[1,2], Shin-ichi Onodera[1], Mitsuyo Saito[3], Noboru Okuda[4], Takuya Okubo[5] (1.Graduate School of Integrated Arts and Science, Hiroshima University, 2.Capital Normal University, 3.Okayama University, 4.Research Institute for Humanity and Nature, 5.University of the Shiga Prefecture)

## [AHW22-P10] Losses of phosphorus with soil erosion and nitrate with groundwater recharge in an agricultural catchment, subtropical small island

*Shin-ichi Onodera[1], Mitsuyo Saito[2], Yang Cao[1], Anna Fadliah Rusydi[1], Hide Omae[3], Yoshiko Iizumi[4], Yusuke Tomozawa[1] (1.Graduate School of Integrated and Arts Sciences, Hiroshima University, 2.Graduate School of Environmental and Life Science, Okayama University, 3.JIRCAS TARF, 4.JIRCAS HQ)

## [AHW22-P11] Phosphate solubilizing bacteria as an indicator of sediment phosphorus in freshwater lakes

*Sreekumari Kurissery[1], Katelynn Crawford[1], Nandakumar Kanavillil[1] (1.Lakehead University, Canada)

## [AHW22-P12] A Study on the dynamics of various phosphate forms in soil and groundwater in Ryukyu limestone regions

*Masashi Nozaki[1], Jun Yasumoto[2], Yasumoto Ko[3], Hirose Mina[4], Iijima Mariko[3], Ryuichi Shinjo[5], Bam H.N. Razafindrabe[6] (1.University of The Ryukyus, Graduate School of Agriculture,, 2.University of the Ryukyus, Faculty of Agriculture, Department of Regional Agricultural Engineering, 3.Kitasato University School of Marine Biosciences, 4.Tropical Technology Plus, 5.Department of Physics and Earth Sciences, University of the Ryukyus, 6.University of the Ryukyus, Faculty of Agriculture, Department of Subtropical Agro-Environmental Sciences)

## [AHW22-P13] Impacts of highly concentrated turbid water on the groundwater in the Tedori River alluvial fan, Japan

*Yoichi Fujihara[1], Shunsuke Chono[1], Keiji Takase[1], Eiji Ichion[1] (1.Department of Environmental Science, Ishikawa Prefectural University)

## [AHW22-P14] Altitude effect of water stable isotopic ratio of ravine water and its contribution to groundwater in alluvial plains - Comparison in east and west side catchments of Lake Biwa –

*Yusuke Tomozawa[1], Kunyang Wang[1], Mitsuyo Saito[2], Syuhei Ban[3], Noboru Okuda[4], Shin-ichi Onodera[1] (1.Graduate School of Integrated Arts and Sciences Hiroshima University, 2.Graduate School of

Environmental and Life Science, Okayama University, 3.School of Environmental Science, The University of Shiga Prefecture, 4.Research Institute for Humanity and Nature)

[AHW22-P15] Calculation of TN and TP concentration coefficients of river water for each land use by a simple watershed model.

*Seiko Yoshikawa[1], Donglai Ma[1,4], Tadamasa Saito[1,5], Kenji Matsumori[2], Yuko Itoh[3], Masahiro Kobayashi[3] (1.Institute for Agro-environmental Sciences, National Agriculture and Food Research Organization, 2.Western Region Agricultural Research Center, National Agriculture and Food Research Organization, 3.Forestry and Forest Products Research Institute, 4.Graduate school,Tsukuba University, 5.Faculty of Agriculture, Ibaraki University)

[AHW22-P16] **Possibility of nutrients transportation from littoral slope for enhancement of phytoplankton growth in north basin of Lake Biwa**

*Syuhei Ban[1], Rong YI[1], Xin Liu[1], Masahiro Maruo[1], Miki Sudo[1], Naoshige Goto[1], Jun Murase[2] (1.The University of Shiga Prefecture, 2.Nagoya University)

[AHW22-P17] SWAT model analysis for confirming the effects of crop growth on the suspended sediment concentration from a settling basin catchment on Ishigaki island

*Yang Cao[1], Shin-ichi Onodera[1], Mitsuyo Saito[2], Hide Omae[3], Yoshiko Iizumi[3] (1.Graduate School of Integrate Arts and Sciences, Hiroshima University, 2.Graduate School of Environmental and life Science, Okayama University, 3.Tropical Agriculture Research Front (TARF), Japan International Research Center for Agricultural Sciences (JIRCAS))

[AHW22-P18] Estimating the runoff of water, sediment, and nutrient using SWAT model in Kikuchi-river watershed, Kumamoto, and the influence of the forest

*Soichiro Fujii[1], Masahiko Kanamori[1], Yuko Nagano[1], Maki Kinoshita[2], Yuta Shimizu[3], Shin-ichi Onodera[4] (1.Japan Forest Technology Association, 2.PASCO Corporation, 3.Western Region Agricultural Research Center, National Agriculture and Food Research Organization, 4.Graduate School of Integrated and Arts Sciences, Hiroshima University)

[AHW22-P19] Atmospheric depositions on forest ecosystems in areas along the Sea of Japan

*Yuko Itoh[1], Keiji Takase[2], Yoichi Fujihara[2], Toru Okamoto[1] (1.Forestry and Forest Products Research Institute, Japan, 2.Ishikawa Prefectural University)

[AHW22-P20] Continuous and simultaneous flux measurement of $N_2O$ and $CO_2$ from agricultural soil using a portable multi-turn time-of-flight mass spectrometer

*Noriko Nakayama[1], Yusuke Iwai[1], Yo Toma[2], Hiroshi Furutani[1], Ryusuke Hatano[3], Michisato Toyoda[1] (1.Osaka University, 2.Ehime University, 3.Hokkaido University)

[AHW22-P21] Effects of introduction of cyclic irrigation system on mass balances of SS and T-P in Lake Inbanuma, Chiba, Japan

*Tomijiro Kubota[1] (1.National Agriculture and Food Research Organization, Institute for Rural Engineering)

# Phosphate Enrichment Hampers Development of Juvenile Acropora digitifera Coral by Inhibiting Skeleton Formation

Mariko Iijima[1], *Yasumoto Ko[1], Jun Yasumoto[2], Mina Hirose[3], Mitsuru Jimbo[1], Shugo Watabe[1]

1. Kitasato University School of Marine Biosciences, 2. Faculty of Agriculture, University of the Ryukyus, 3. Tropical Technology Plus

Coral reef degradation resulting from various types of local stress on corals such as excessive nutrient enrichment in and gravel inflow into coastal waters is of an increasing global concern. Because tropical and subtropical seawaters are generally poor in nutrients and thus oligotrophic, these stresses are thought to result in the decline of environments favorable to coral growth. Inorganic phosphates have been especially considered to possibly inhibit the formation of coral skeleton. Despite many studies available on the effects of nutrients on corals, a clear consensus for how nutrients exert deteriorative effects on the corals has not been established satisfactorily. Recently, we found that biogenic polyamines react with carbon dioxide ($CO_2$) and accelerate an aragonite formation of calcium carbonate ($CaCO_3$) in seawater. In this study, we examined the effects of phosphates and nitrates on *in vitro* aragonite formation of $CaCO_3$ by using biogenic polyamines and *in vivo* aragonite formation of juvenile coral *Acropora digitifera* skeletons, showing that phosphates clearly inhibited both *in vitro* and *in vivo* $CaCO_3$ formations at similar concentrations. In contrast, nitrates inhibited neither *in vitro* aragonite formation of $CaCO_3$ nor *in vivo* aragonite formation of juvenile coral skeletons. These findings indicate that phosphates have a detrimental effect on bioinorganic coral calcification. Furthermore, the findings that phosphate enrichment inhibits coral skeleton formation led us to conclude that enriched phosphate is adsorbed on juvenile coral skeleton surface and inhibits inorganically normal development of juvenile coral skeleton.

Keywords: phosphate, calcification

©2019. Japan Geoscience Union. All Right Reserved. 

# Modeling chlorophyll-a concentration using remote sensing in shallow water systems: Comparison of sensors

*Assefa M Melesse[1], Tara Blakey[1], Mohammad Haji Gholizadeh[1], Mohd Manzar Abbas[1]

1. Florida International University

The level of productivity in the upland and coastal water bodies is highly linked to land processes (land use, water management, water and nutrient fluxes). Understanding the linkage between these processes and the level of algal blooms in the water bodies is crucial for improving water quality. A comparative study was conducted using remote sensing data from three different sensors (SeaWIFS, MoDIS and Landsat) to evaluate the capability of reflectance data from these sensors for estimation of chl-a concentrations in three water bodies in the USA (Lake Okeechobee, Florida Bay and Chesapeake Bay). Observed chl-a data were gathered and compared with simulation results. The analysis found that all of the sensors have performed well in deeper water bodies than in shallow sections due to the bottom reflectance from non-algal blooms. For shallow water bodies, selection of the proper bands and band combinations, identification of the non-algal bloom reflectance and the corresponding algorithms can improve the simulation. Seasonality as well as spatial variability (using cross-sections) were evaluated and the results showed that chl-a values were highly variable for the selected summer months. Indicative of the effect of land surface fluxes of nutrients, chl-a values were higher closer to coastal areas in the Florida bay and Chesapeake Bay. The chl-a in the freshwater lake of Okeechobee was simulated using Landsat 8 data and the results found were very good. Comparison of the SeaWIFS and MoDIS chl-a value to that of the measured concentrations in the deeper section of Florida Bay and Chesapeake Bay, respectively showed very good agreement.

Keywords: Chl-a, SeaWIFS, Water qulity modeling, South Florida, Remote sensing

©2019. Japan Geoscience Union. All Right Reserved. 

# Dynamics in groundwater flow system with seasonal water table variation in a coastal and island

*Yusuke Tomozawa[1], Shin-ichi Onodera[1], Mitsuyo Saito[2]

1. Graduate School of Integrated Arts and Sciences Hiroshima University, 2. Graduate School of Environmental and Life Science, Okayama University

In islands, freshwater water resources are valuable as living and agricultural use, and dug wells water and reservoirs had been utilized for more than 100 years. In order to use such water resources sustainably, it is important to evaluate groundwater flow as well as water budget.

In this research, we examined to confirm the seasonal variation in water stable isotopic ratios in observation boreholes at the coastal lowland in Ikuchi Island Hiroshima prefecture. Moreover, considering that the target area is coastal, $Cl^-$ concentration was analyzed to evaluate the influence of salt fresh water boundary.

The experimental site is located on Ikuchi Island in Hiroshima prefecture. The highest altitude is 456 m. The basement rock is mainly composed of granite. Annual average precipitation is 1058.8 mm. Observation boreholes are located at the coastal lowland in the southeastern part of the island. The upper site (Site U) with the altitude of 5.1 m asl has 3 boreholes with the depths of 2 m, 15 m, 30 m, the lower site (Site D) with 2.5 m asl has 8 with the depth of 1 m, 2 m, 3 m, 10 m, 15 m, 20 m, 30 m, 40 m, respectively. The water sampling was carried out from monthly to half year interval since 2015. Every samples were analyzed for water isotopic ratios by PICARO and anion component by ion chromatography. Especially samples in January in 2019 were analyzed for CFCs and SF6.

Based on the previous study (Saito and Onodera, 2007), the distinct altitude effect of isotopic ratio in precipitation has been confirmed. Due to spatial and temporal variations in isotopic ratios, recharge process to groundwater was suggested as follows, 1) recharge on site to shallow groundwater (2-3m deep) at D ( $\delta^{18}O$: -7.8 to - 7.4 ‰), 2) river water contribution to the shallow groundwater (2-15m) at U ( $\delta^{18}O$: - 8.3 to - 7.5 ‰), 3) recharge in the mountain slope with the altitude of about 360 m to deep groundwater (30m) at U ( $\delta^{18}O$: - 8.4 to - 8.1 ‰), 4) recharge at 400 m on near the mountain top to deep groundwater (10-30 m) at D( $\delta^{18}O$: - 8.7 to - 8.4 ‰), 5) recharge of precipitation with lower isotope than in present to deeper groundwater (40 m) at D ( $\delta^{18}O$: -8.9 to - 8.8 ‰)

The deepest groundwater (40m) at D had lower isotopic ratios with higher $Cl^-$ concentration (250 to 584 mg / L) during a lower water table in the winter. This indicated the seawater –fresh water boundary rose with water table according to Gyben-Hrzberg concept. These phenomena also suggest to cause the rise of deeper and older groundwater flow line. Consequently, we suggest the lower isotopic ratio in deeper groundwater indicates the immobile water which were recharged in the glacial period. Based on other tracers (CFC, SF 6), we will discuss more.

Keywords: stable isotope, groundwater, coastal

©2019. Japan Geoscience Union. All Right Reserved. 

# The Tracing of Groundwater Contamination Sources in Indonesian Coastal Alluvial Groundwater using $\delta^{34}S$ and $\delta^{15}N$ Isotopes

*Anna Fadliah Rusydi[1,4], Mitsuyo Saito[2], Seiichiro Ioka[3], Shin-ichi Onodera[1]

1. Graduate School of Integrated Arts and Sciences, Hiroshima University, Japan, 2. Graduate School of Environmental and Life Sciences, Okayama University, Japan, 3. Research Institute for Sustainable Energy, Hirosaki University, Japan, 4. Research Center for Geotechnology, Indonesian Institute of Sciences, Indonesia

The coastal area is one of the Indonesian Government priorities as an archipelago country. The groundwater in the area is one of the most reliable clean water resources, therefore it is crucial to understanding the vulnerability of this resource. Our research area was located at Indramayu, a developing rural coastal area in Indonesia, where, the environment was relatively pristine. This research aimed was to identify the effect of natural condition and human activity to groundwater quality by using stable isotope $\delta^{34}S$ and $\delta^{15}N$.

Totally, there were 20 samples taken from groundwater (18) and river (2). The nitrate and sulfate were detected in a total of 5 and 19 samples, respectively. The isotopes composition for isotope nitrate were -11.2 ‰–+22.22‰ for $\delta^{15}N\text{-}NO_3$ and -3.4 ‰–+17.1‰ for $\delta^{18}O\text{-}NO_3$. Moreover, the values of $\delta^{34}S\text{-}SO_4$ and $\delta^{18}O\text{- }SO_4$ were varied from -4.2 ‰–+28.4‰ and +7.3 ‰–+18.8 ‰, respectively. The isotopic signatures of nitrate suggested that the used of inorganic fertilizer and animal manure give the impact to both groundwater and river. Similarly, the isotopic signatures of sulfur were showing that those detected sulfate in the groundwater were mostly coming from fertilizer. Moreover, the soil was mineralized by organic sulfate as well. At one point, located in the fishery area, the groundwater was indicated the seawater contamination. It was shown by the heavy composition of sulfur isotope (28.4‰ for $\delta^{34}S$ and 18.8‰ for $\delta^{18}O$). Lastly, our results showed those combined isotopes of $\delta^{34}S$ and $\delta^{15}N$ along with land-use evaluation could explain the possible sources of groundwater in coastal area at very early urbanization stage.

Keywords: Sulfur Isotope, Nitrate Isotope, Coastal Groundwater, Indramayu

©2019. Japan Geoscience Union. All Right Reserved. 

# Spatio-temporal dynamics of orthophosphate with implications for limitation of phytoplankton growth in north basin of Lake Biwa, Japan

*Xin Liu[1], Rong Yi[1], Masahiro Maruo[1], Syuhei Ban[1]

1. The University of Shiga Prefecture

Orthophosphate ($PO_4$-P) is the main chemical form of phosphorus (P) for phytoplankton growth, often considered as a limiting nutrient for primary production in freshwater ecosystems. However, few information on accurate measurements for $PO_4$-P concentrations in epilimnion of meso- and oligotrophic lakes due to lower than the detection limit (60 nM) of soluble reactive P using traditional spectrophotometrical method. In the present study, we measured $PO_4$-P concentrations using ion chromatography with a detection limit of 5 nM, and determined truly vertical distribution of $PO_4$-P throughout the year with other abiotic and biotic environmental factors in north basin of Lake Biwa, to accurately understand biogeochemical processes of P in this mesotrophic lake.

Field investigations were conducted monthly from April to December 2018 at station K4 (35º19'9.6"N, 136º11'2.7"E; 50 m deep). Phosphate enrichment experiments were also made at each sampling occasion to clarify P limitation for phytoplankton growth. Lake water including phytoplankton assemblage collected from epilimnion (0–20 m) was enriched with 1 $\mu$M of $PO_4$-P (+P) and incubated together with untreated one (control) for 2 days under ambient light and temperature conditions. To evaluate the effect of potentially nutrient-rich bottom water, the filtered bottom water was mixed with untreated epilimnion water including phytoplankton at 1:1 (+B) was incubated at the same conditions as the +P treatment. Phytoplankton growth rate ($g$) was calculated with equation of $g=\ln(C_t/C_0)/2$, where $C_0$ and $C_t$ are chlorophyll *a* (chl. *a*) concentrations at start and end of the experiment, respectively.

Water temperature increased in the epilimnion from May, and strict thermocline was developed from June to September. Chl. *a* concentrations increased from June to July in 10–20 m, and from October to November in 0–20 m. $PO_4$-P concentrations were always low, <20 nM, in the epilimnion from April to June. The concentrations below 30 m increased up to 140 nM in May, but decreased after that until July. In August and September, the concentrations increased up to 30–40 nM even in the epilimnion probably due to disturbance by typhoon. The concentrations below 30 m increased with depth, and the highest values were frequently observed near the bottom, up to 220 nM. On average throughout the water column, $PO_4$-P concentrations were 24–48 nM from April to June, then slightly increased up to 73 nM until September, being constant, 50–63 nM until December.

Total P, total dissolved P, dissolved organic P and particulate P exhibited similar spatio-temporal distributions, but different pattern from those of $PO_4$-P. $NH_4$-N increased in 10–20 m from May to July, whereas the $NO_3$-N increased in the hypolimnion as season progressed. Sestonic C:N:P ratios suggested a terrible P deficiency in July and October when phytoplankton biomass increased.

Phosphate enrichment experiments showed that phytoplankton in the epilimnion was mostly limited with P for its growth. Phytoplankton $g$ in control varied −0.05-0.08 $d^{-1}$, being always lower than those in +P (−0.04-0.44 $d^{-1}$) and/or +B (−0.04-0.49 $d^{-1}$) treatments except for November and December. In November, no growth was found even in +P treatment. This might be caused by nitrogen limitation because of <6 $\mu$M of $NO_3$-N in the epilimnion. The $g$ of control was similar as that of +P and +B (ca. 0.1 $d^{-1}$) in December, indicating that P deficiency for phytoplankton growth was relaxed until December by vertical convection.

©2019. Japan Geoscience Union. All Right Reserved. 

We firstly determined completely vertical distributions of $PO_4$-P in north basin of Lake Biwa from spring to winter, and detected 20–40 nM of $PO_4$-P in the epilimnion. Phosphate enrichment experiments showed that 20 nM of $PO_4$-P might be critical concentration for phytoplankton growth in the lake. No phytoplankton growth even in +P treatment in November implied that nitrogen limitation for phytoplankton growth will be possible in Autumn. Further study for clarify this will be needed.

Keywords: Orthophosphate dynamics, Phosphorus limitation, Phytoplankton growth rate, Ion chromatography, Biogeochemical processes, Freshwater ecosystem

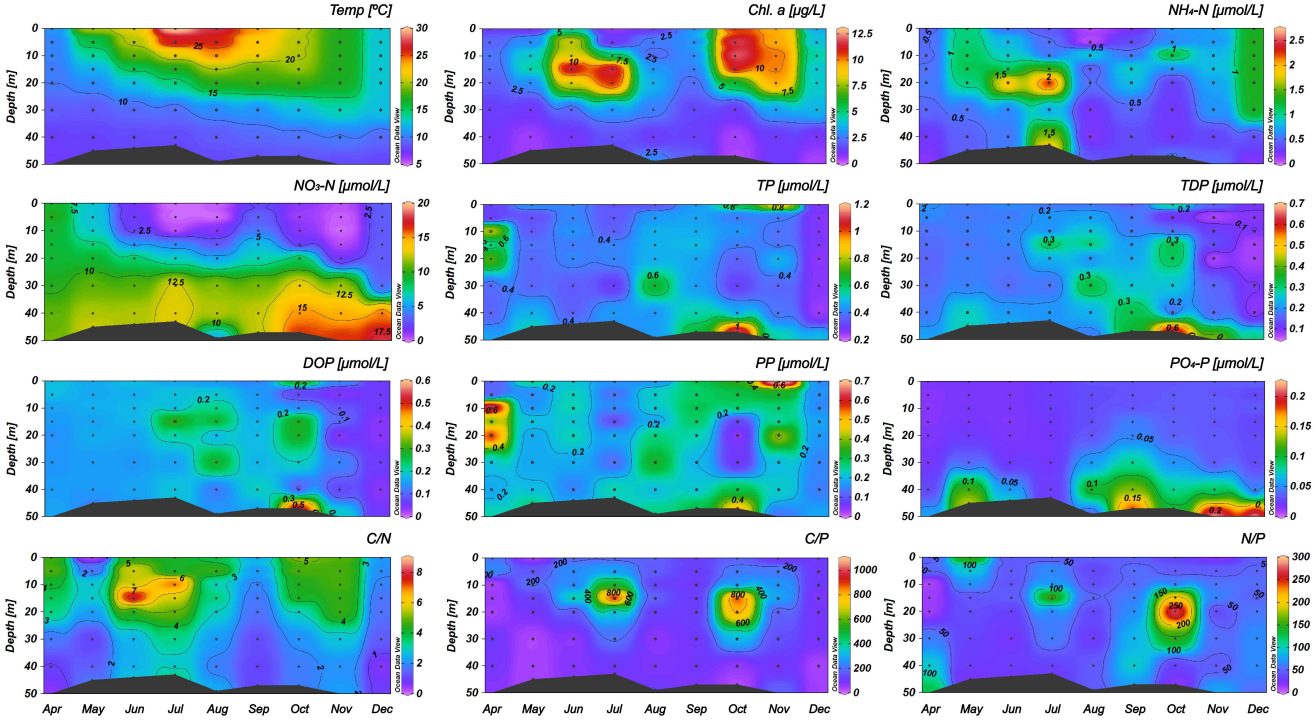


©2019. Japan Geoscience Union. All Right Reserved. 

# Microbial phase analysis in aquifer of Ryukyu Limestone Zone using next generation sequencer

*Umi Murao[1], Jun Yasumoto[1], Yasumoto Ko[3], Mina Hirose[2], Nanami Mizusawa[3], Ryo Iguchi[4], Bam H.N. Razafindrabe[5], Syugo Watabe[3]

1. University of the Ryukyus, Faculty of Agriculuture Department of Regional Agricultural Engineering, 2. Tropical Tecnology Plus, 3. Kitasato University School of Marine Biosciences, 4. National Institute of Advanced Industrial Science and Technology, 5. University of the Ryukyus, Faculty of Agriculuture Department of Subtropical Agro-Environmental Sciences

Clean water and sanitation (Sustainable development Goals (6)) is one of the world's important issues. People use groundwater in many areas as a water source, but various cases of contamination by agricultural activities and substances derived from human and animal excrements have been reported.

On the other hand, genetic analysis techniques using molecular biological methods have been applied to the analysis of microbial phase in the water environment.

In recent years, the method using the latest analysis equipment of next generation Sequencer is established, mainly for microorganisms. In addition, new monitoring indices such as environmental DNA have been developed. It is thought that the microbial phase in groundwater varies depending on the influence of various environmental factors and human activity, but the actual condition is not clear.

The next generation Sequencer is a very powerful tool used to grasp the microbial phase in groundwater. It is thought that the microbial phase can be an important indicator in water resource management of basins in the future.

The purpose of this study is to investigate the microbial species and their coexistence in groundwater in the Ryukyu Limestone area using the next generation sequencer.

Keywords: groundwater, microbial community analysis, genetic analysis

©2019. Japan Geoscience Union. All Right Reserved. 

# Evaluation for temporal variation in groundwater inflow to the lagoons connected to Lake Biwa by radon ($^{222}$Rn) tracer analysis

*Mitsuyo Saito[1], Shin-ichi Onodera[2], Yusuke Tomozawa[2], Kunyang Wang[2], Syuhei Ban[3], Noboru Okuda[4]

1. Graduate School of Environmental and Life Science, Okayama University, 2. Graduate School of Integrated Arts and Sciences, Hiroshima University, 3. School of Environmental Sciences, The University of Shiga Prefecture, 4. Research Institute for Humanity and Nature

Primary production in freshwater lakes and reservoirs are usually controlled by phosphorus (P). Lacustrine groundwater discharge (LGD), direct discharge of subsurface water to lake, is regarded as a potential nutrient paths, including phosphorus from a catchment to lake water environment. There are more than 20 lagoons around Lake Biwa which were originally a part of the lake. These lagoons are regarded to have important functions as settling ponds of inflowing loads from the catchments to Lake Biwa, refuges for shallow water ecosystems and so on. Because these lagoons are connected to Lake Biwa, evaluation of nutrient budget is important for the nutrient cycle in the lake. Some researchers have pointed out the presence of LGD in littoral area of Lake Biwa. However, it has not been evaluated for the lagoons around the lake. In the present research, we aimed to evaluate the temporal variation in groundwater inflow to a lagoon connected to Lake Biwa by radon ($^{222}$Rn) tracer analysis.

The field campaigns were conducted in December 2017, August and October 2018 for the lagoons (Noda-Numa and Hasu-Ike) located on northeastern shore of Lake Biwa. The volume of inflow and outflow, water temperature, electric conductivity, chlorophyll-a and radon ($^{222}$Rn) concentration were measured in the lagoon. $^{222}$Rn is a radioactive element of uranium ($^{238}$U) series with 3.8 day of half-life. $^{222}$Rn is a useful tracer of groundwater discharge because it generally enriched in groundwater than surface water. To examine the temporal variation in groundwater inflow, the time-series $^{222}$Rn concentration in water was obtained. Water samples were collected at the inlet, outlet and near the center of the lagoons and natural springs and groundwater wells around the lagoons. Water and $^{222}$Rn balance suggest that groundwater inflow is larger in Noda-Numa than Hasu-Ike. The catchment topography may influence on this difference. $^{222}$Rn balance-based residence time of lagoon water was estimated 10-20 days in Noda-Numa, and 4-5 days in Hasu-Ike, were similar with that based on water balance. These results suggest the groundwater inflow is a potential phosphorus path to Noda-Numa.

Keywords: Groundwater inflow, Connected lagoons, Lake Biwa, Radon (222Rn)

©2019. Japan Geoscience Union. All Right Reserved. 

# Br/Cl ratio characteristics of groundwater in coastal areas in Indonesia

*Seiichiro Ioka[1], Shin-ichi Onodera[2], Mitsuyo Saito[3], Anna Fadliah Rusydi[2,4]

1. Institute of Regional Innovation, Hirosaki University, Japan, 2. Graduate School of Integrated Arts and Sciences, Hiroshima University, Japan, 3. Graduate School of Environmental and Life Sciences, Okayama University, Japan, 4. Research Center for Geotechnology, Indonesian Institute of Sciences, Indonesia

The urban development in Indonesia’ s coastal areas has led to an increase of groundwater demand, which then has resulted in groundwater salinization. In this study, we analyze bromide and Br/Cl ratio characteristics, as index of groundwater salinization, in three cities of Indonesian coastal areas, namely: Indramayu, Mataram, and Semarang. Each research site is at different stage of urbanization. Indramayu is in very early stage of urbanization, followed by Mataram as a developing tourism area, and the last one Semarang as a heavy urbanization city. The results show that concentrations of bromide in groundwater are ranged from 0.05 to 38 mg/L in Indramayu, 0.01 to 0.8 mg/L in Mataram, and 0.02 to 8.0 mg/L in Semarang. Furthermore, the occurrence of Br is described in terms of the Br/Cl weight ratio, which allows for small changes in bromide concentrations to be assessed in terms of salinity. Median values of Br/Cl weight ratio in the groundwater of Indramayu, Mataram, and Semarang were approximately 0.0035, 0.0027, and 0.0025, respectively, while the ratio in seawater is generally around 0.0035. The relationship between Br/Cl weight ratio and chloride concentration indicate the groundwater in Indramayu is undergoing salinization due to seawater intrusion compared to the other two areas, meanwhile the groundwater in Semarang is experiencing chloride contamination due to anthropogenic activities based on the study by Andreasen and Fleck (1997).

Keywords: Indonesia, groundwater, Br/Cl ratio, coastal area

©2019. Japan Geoscience Union. All Right Reserved. 

# Estimation of groundwater recharge and phosphorus transport under different precipitation conditions in a suburban catchment, using SWAT model

*Kunyang Wang[1,2], Shin-ichi Onodera[1], Mitsuyo Saito[3], Noboru Okuda[4], Takuya Okubo[5]

1. Graduate School of Integrated Arts and Science, Hiroshima University, 2. Capital Normal University, 3. Okayama University, 4. Research Institute for Humanity and Nature, 5. University of the Shiga Prefecture

The quantification of the groundwater recharge and phosphorus transport in water is one of the most important indicators of the water cycle in lakes because these processes are related to the transport of large nutrient loads. The Yasu River is one of the important water sources of the Biwa Lake. In this paper, Geographic Information System technology is used to analyze and predict the land use change in the Yasu River Basin. The water balance was simulated using the Soil and Water Assessment Tool. Simulations of different years in different precipitation seasons were carried out. The correlation coefficient and the Nash Sutcliffe coefficient are higher than the reference values. The sensitivity analysis of the parameters reveals the different degrees of sensitivity of the parameters in different water seasons, CN2 always has a high sensitivity during all kinds of water season. The total groundwater recharge and discharge are 180 million $m^3$ and 179 million $m^3$ in the normal precipitation season, respectively. The trends differ in the dry and wet seasons. In the dry season of 2007, the groundwater recharge was below 140 million $m^3$, while it exceeded 240 million $m^3$ in the rainy season in 2003. In addition, the process of phosphorus loss in the basin and release into Lake Biwa are explained from the perspective of space and time. This is closely related to the spatial distribution of the main channel and the time distribution of precipitation. The total amount of nonpoint source pollution of phosphorus in three years is equivalent to 4.08 kg/ha of paddy fields in the watershed. The spatial distribution of phosphorus loss is related to the stream flow, it is mainly concentrated in the area with paddy fields and urban. The time distribution is related to the distribution of the precipitation. With increasing precipitation, the nonpoint source pollution of phosphorus slightly increases. This is due to the driving effect of precipitation on the phosphorus transfer and erosion of soil.

Keywords: Phosphorus transport, Groundwater recharge, Different precipitation conditions, SWAT model

©2019. Japan Geoscience Union. All Right Reserved. 

# Losses of phosphorus with soil erosion and nitrate with groundwater recharge in an agricultural catchment, subtropical small island

*Shin-ichi Onodera[1], Mitsuyo Saito[2], Yang Cao[1], Anna Fadliah Rusydi[1], Hide Omae[3], Yoshiko Iizumi[4], Yusuke Tomozawa[1]

1. Graduate School of Integrated and Arts Sciences, Hiroshima University, 2. Graduate School of Environmental and Life Science, Okayama University, 3. JIRCAS TARF, 4. JIRCAS HQ

In tropical and subtropical region, the rainfall intensity is strong and soil erosion in an agricultural land is one of big environmental issues. Especially, the impact of large sediment discharge on the coral reef is serious around small islands, such as Okinawa and Philippines. In case of Okinawa Prefecture, to reduce the sediment discharge and conserve corals, many sediment trap ponds are constructed in a downstream area of agricultural lands. However, sediment deposition rate, variation of trap effect, and component of sediment in a pond have not been confirmed.

To estimate of erosion rate and deposition process of a small pond in an agricultural catchment of a subtropical small island, we examine to observe the sediment deposition in a small pond and monitor water level and chlorophyll a in a pond and runoff and turbidity of an inflow stream in a small catchment with the area of 300m2 in Ishigaki Island, Okinawa Prefecture, Subtropical region. Our monitoring was started from February 2017 after removing all sediment in a pond in January, and up to April 2018. Observation of sediment deposition was conducted with collecting the samples at 5 sites in June 2017 and January 2018. Inflow and outflow water samples were collected every one month.
The sediment deposition was extremely large from January to May 2017, the average erosion rate in all catchment area was estimated to be 6mm. On the other hand, the sediment deposition was nothing from June 2017 to January 2018. Based on the monitoring of stream runoff and turbidity, one big storm event in April with strong intensity mainly contributes to sediment discharge and overflow of the pond occurred. On the other hand, the later period had also big events. This difference is suggested to be the difference of land cover by crops and availability of sediment trap in this pond. In addition, the sediment component mainly was composed of surface soft layer, subsurface sandy layer, and bottom gravel layer. The average thickness was 2cm in surface layer, 100cm in mid sandy layer, and 10cm in gravel layer, respectively. Especially, the surface soft layer had high nutrient content. The dissolved nutrient of inflow stream water and pond water were high concentration. But the 10% of nutrient in the inflow decreased in pond. This means the plankton was produced, using this nutrient and that was deposited later. The soft layer is suggested to be effect of organic fertilizer, it is expected to apply to agricultural lands.

Keywords: Phosphorus, groundwater, nitrate

©2019. Japan Geoscience Union. All Right Reserved. 

# Phosphate solubilizing bacteria as an indicator of sediment phosphorus in freshwater lakes

*Sreekumari Kurissery[1], Katelynn Crawford[1], Nandakumar Kanavillil[1]

1. Lakehead University, Canada

It has been well documented that phosphorus pollution is one of the most significant factors impeding the overall health of freshwater lakes. Various measures are being taken to reduce phosphorus input into the lakes by anthropogenic activities and thus to maintain a healthy ecosystem. However, it is well known that bioavailable phosphorus tends to bind with substances such as ferric iron and calcium present in the water, become insoluble, and settles into the sediments. The presentstudy has been carried out to understand the relationship between the sediment phosphorus concentration and density of phosphate solubilizing bacteria (PSB) in two lakes in Ontario, Canada, namely, Lake Simcoe and Sparrow Lake. In September 2017, 20cm sediment cores were collected from the nearshore sites of these two lakes to determine the presence of PSB in relation to the sediment phosphorus concentration. PSB could potentially release phosphorus back into the water column through a process called internal phosphorus loading from the inorganic phosphates in the sediment when the right conditions are present. PSB were isolated from the sediment cores at 5 cm intervals by plating on to Pikovskaya’ s agar. Five grams of sediment was used to analyze total reactive phosphorus in the sediment. In Lake Simcoe, PSB ranged from $3x10^1$ to $1.1x10^1$ cfu/g, and the amount of total reactive phosphorus ranged from 0.19 to 0.46 mg/g. In Sparrow Lake, PSB ranged from $4x10^0$ to $3x10^1$ cfu/g and the amount of total reactive phosphorus ranged from 0.21 to 0.39 mg/g. A linear regression was completed to determine the relationship between total reactive phosphorus and PSB for each core. The results showed a negative relationship between these two tested parameters (Lake Simcoe: $r^2$=0.23, $y = -35.34x + 30.811$ $p$=0.5206, and Sparrow Lake: $r^2$ =0.87, $y = -155.9x + 62.322$, $p$=0.067). While PSB density decreased with core depth, the concentration of reactive phosphorus increased. This indicates that the density of PSB in lake sediment may indicate the concentration of total reactive phosphorus and thus the internal phosphorus loading. More study is recommended to confirm the results.

Keywords: Phosphate Solubilizing Bacteria, Freshwater Lakes , Sediment Phosphorus , Canada

©2019. Japan Geoscience Union. All Right Reserved. 

# A Study on the dynamics of various phosphate forms in soil and groundwater in Ryukyu limestone regions

*Masashi Nozaki[1], Jun Yasumoto[2], Yasumoto Ko[3], Hirose Mina[4], Iijima Mariko[3], Ryuichi Shinjo[5], Bam H.N. Razafindrabe[6]

1. University of The Ryukyus, Graduate School of Agriculture,, 2. University of the Ryukyus, Faculty of Agriculture, Department of Regional Agricultural Engineering, 3. Kitasato University School of Marine Biosciences, 4. Tropical Technology Plus, 5. Department of Physics and Earth Sciences, University of the Ryukyus, 6. University of the Ryukyus, Faculty of Agriculture, Department of Subtropical Agro-Environmental Sciences

Phosphorus in water environment exists in various forms and size, such as dissolved, particulate, organic and inorganic forms. However, there are many unclear points in Phosphorus in groundwater. In this study, we tried to understand the dynamics of various phosphate forms in soil and groundwater in Ryukyu limestone regions by combining Inductively Coupled Plasma Atomic Emission Spectrometry (ICP-AES) and $^{31}$P Nuclear Magnetic Resonance ($^{31}$P-NMR), in addition to Colorimetric (molybdenum blue method). From August 2017 to August 2018, we took groundwater samples in southern part of Okinawa, Japan, with Ryukyu limestone distribution on a monthly basis. We measured pH, electronic conductivity (EC), Oxidation-Reduction Potential (ORP), dissolved oxygen (DO) and alkalinity ($HCO_3^-$) on site, and analyzed major dissolved ion ($Cl^-$, $HCO_3^-$, $NO_2^-$, $NO_3^-$, $SO_4^{2-}$, $Na^+$, $K^+$, $Mg^{2+}$, $Ca^{2+}$), suspended solid (SS) and phosphorus concentration. Phosphorus concentration analyzed 3 different method to molybdenum blue method (Col-P), ICP-AES (ICP-P) and Total P (T-P). Phosphate form analysis used $^{31}$P-NMR.
We compared Col-P and ICP-P in order to understand dissolved phosphorus spatial distribution. The results show that ICP-P is 1.06~49.24 times larger than Col-P. It is inferred that ICP-P is also measuring fine particulate phosphorus and organic phosphorus. As a result, several forms of phosphate without orthophosphate were found in groundwater. Particulate phosphorus was determined by subtracting ICP-P from T-P. A positive correlation (r= 0.78) was found between P-P and SS. According to these results, it is thought that PP adsorbs various forms of phosphate including orthophosphate. We analyzed the correlation between dissolved phosphorus (Col-P, ICP-P) and all measured value in order to understand the characteristics of seasonal variation to dissolved phosphorus. There was a negative correlation between Col-P to water temperature. When focusing on seasonal variation of Col-P, we found that Col-P concentration decreases when water temperature increases. Moreover, Col-P concentration increases as water temperature increases. Through the analysis of various forms of phosphate in soil and SS by using $^{31}$P-NMR, along with orthophosphate, pyrophosphate, pyrophosphate ester, orthophosphate monoester were also detected. It is thus suggested that the phosphate of polymeric or organic forms other than orthophosphate are from plant origin, as a result of microbial activities and microorganism decomposition.

Keywords: Phosphorus, 31P-NMR, Groundwater

©2019. Japan Geoscience Union. All Right Reserved. 

# Impacts of highly concentrated turbid water on the groundwater in the Tedori River alluvial fan, Japan

*Yoichi Fujihara[1], Shunsuke Chono[1], Keiji Takase[1], Eiji Ichion[1]

1. Department of Environmental Science, Ishikawa Prefectural University

The Tedori River alluvial fan in the Ishikawa prefecture is a representative alluvial fan in the Hokuriku region in Japan. The river water is taken by a headworks located at the top of the alluvial fan and is used for irrigation in paddy fields with a total area of about 7,500 ha. Seepages from the riverbed and percolations from the paddy area are the main sources of groundwater in the Tedori River alluvial fan. In 2015, large-scale landslides in the upper reaches of the Tedori River caused a long period of high turbidity in the river. Highly concentrated turbid water with an average concentration of 585 mg/L (a maximum of 4,012 mg/L) has been discharged continuously into the river since May, 2015. This turbidity has caused concerns about the recharge functions of groundwater in the alluvial fan.

In this study, the measurements of paddy percolations and riverbed seepages, before and after the occurrence of high turbidity, were used to examine the influence of these phenomena on groundwater recharge functions in the alluvial fan. We measured water requirement rates in the paddy area in the Tedori River alluvial fan. The measurements were conducted before and after the midsummer-drainage period at >100 paddy fields. We also measured the river discharges in the cross-sections of the river throughout the alluvial fan. The number of cross-sections was 16 and we estimated the riverbed seepages by calculating the discharge differences between the cross-sections.

The results revealed that the amount of paddy percolation decreased significantly due to the turbidity of the river water. The average percolation in the paddy area was found to be 12.4 mm/day in 2014 and 7.9 mm/day in 2016 before the midsummer-drainage period. Moreover, the average percolation in the paddy was found to be 19.6 mm/day in 2014 and 13.7 mm/day in 2016 after the midsummer-drainage period. The volume of the riverbed seepage was observed to have reduced and the seepage section were also observed to have shortened. The observed seepages from the river bed were 4.72 m3/s in 2009 and 3.33 m3/s in 2016 for the irrigation period, whereas for the non-irrigation period, these values were 5.92 m3/s in 2009 and 1.25 m3/s in 2016. Furthermore, the seepage section was found to shorten from 14.2 km to 8.0 km, due to the high turbidity of the water.

Finally, we estimated the amount of groundwater recharge based on these measurements, which revealed that the groundwater recharge from paddy percolation decreased by 270 mm/year (36%), and the recharge from riverbed decreased by 591 mm/year (61%). The total groundwater recharge decreased by 861 mm/year (36%), a value that corresponded to the groundwater level measurements. From these results, we can conclude that the effects of highly concentrated turbid water on the groundwater are quite serious in the Tedori River alluvial fan.

Keywords: groundwater, paddy percolation, riverbed seepage

©2019. Japan Geoscience Union. All Right Reserved. 

# Altitude effect of water stable isotopic ratio of ravine water and its contribution to groundwater in alluvial plains - Comparison in east and west side catchments of Lake Biwa –

*Yusuke Tomozawa[1], Kunyang Wang[1], Mitsuyo Saito[2], Syuhei Ban[3], Noboru Okuda[4], Shin-ichi Onodera[1]

1. Graduate School of Integrated Arts and Sciences Hiroshima University, 2. Graduate School of Environmental and Life Science, Okayama University, 3. School of Environmental Science, The University of Shiga Prefecture, 4. Research Institute for Humanity and Nature

The stable isotope ratio of hydrogen and oxygen in water is one of useful tracers for hydrological cycle and processes in the catchment scale as well as global. The typical characteristics are spatial or geographical distribution trend such as “altitude effect” or “inland effect”, which are lower in the higher altitude or more inland. Based on these trend, the groundwater recharge area had been estimated. However, the merger of these effects and additional effect such as the seasonal variation of isotopic ratio in precipitation or vapor causes various trend.
In this study, we examined to confirm the altitude effect of water stable isotope ratio and estimate recharge altitude to groundwater in alluvial plains, with comparing in the east and west side catchments of Lake Biwa .
Sampling of spring water in the Serikawa upstream area on the east side of Lake Biwa was conducted in July 2017, December 2017, August 2018. Sampling of ravine water in the Adogawa / Ukawa upstream area on the west side of Lake Biwa was conducted in August 2018. Water samples of spring in the head water and groundwater in the alluvial plain were collected at 11 and 2 sites in the east and at 13 and 2 in the west with measuring EC, pH and DO, respectively. The water stable isotopic ratios were analyzed by PICARO.
Stable isotopic ratios in groundwater were lower than surface water in both east and west. Altitude effects of spring water in the head water were recognizable. This means the surface water in the alluvial plain was mainly contributed from Lake Biwa, whereas groundwater was from the head water. The altitude effect of oxygen stable isotopic ratio was 0.15 - 0.13 ‰/ 100 m on the east side and 0.15 ‰/ 100 m on the west side (only in the upper stream of the Ado River). In addition, the d value of isotopic ratio in the precipitation was 23‰ in the upper Adokawa in August 2018, 18 ‰in Ugawa, and 20 ‰in Serikawa.
We also estimated groundwater recharge elevation and water contribution rate in the upstream region based on these.

Keywords: stable isotope, altitude effect, groundwater recharge

©2019. Japan Geoscience Union. All Right Reserved. 

# Calculation of TN and TP concentration coefficients of river water for each land use by a simple watershed model.

*Seiko Yoshikawa[1], Donglai Ma[1,4], Tadamasa Saito[1,5], Kenji Matsumori[2], Yuko Itoh[3], Masahiro Kobayashi[3]

1. Institute for Agro-environmental Sciences, National Agriculture and Food Research Organization, 2. Western Region Agricultural Research Center, National Agriculture and Food Research Organization, 3. Forestry and Forest Products Research Institute, 4. Graduate school,Tsukuba University, 5. Faculty of Agriculture, Ibaraki University

Water quality deterioration of rivers caused by leakage of fertilizer components such as nitrogen and phosphorus from paddy and upland fields is a environmental problem. Also, runoff of fertilizer components are expected to increase with the accelerated water and sediment runoff by intensification and localization of rainfall caused by climate change. Although it is difficult to predict the place and extent of heavy-rainfall-related disasters, we firstly grasp the average concentrations of nitrogen and phosphorus and predict increase and decrease in those concentrations when the way of rain changes. Nitrogen and phosphorus runoff is depend on land use and land cover, conservative measures, topography, climate condition mainly rainfall etc.. Among them, the land use and land cover is expected to be a main factor in normal climate conditions. In order to contribute to the prediction of heavy-rain related disasters in the future, coefficients that indicate the total nitrogen (TN) and total phosphorus (TP) load intensity to rivers of each land use for the river watersheds across the country are calculated using a simple watershed land use model. Watersheds whose lower ends are observation points of water quality, and whose land use ratios were determined by GIS technique using published database of DEM (GSI, 10B) and LULC mesh data (JAXA , ALOS AVNIR-2). The TN and TP concentration coefficients of paddy, upland, forest, and urban were calculated by applying the below multiple regression equation using the land use ratios and published TN and TP data( Ministry of Environment).

$c = a_1 x_1 + a_2 x_2 + a_3 x_3 + a_4 x_4$

*C:* TN or TP concentration (mg $L^{-1}$) $a_i$ : TN or TP concentration coefficient for land use *I,* $x_i$ : ratio of land use *I,* Land use: 1;paddy, 2;upland fields, 3;forest, 4;urban

TN concentration coefficient across Japan is 1.67 (from lower limit 95% value 1.34 to upper limit 95% value 2.01), 4.08 (from 3.64 to 4.51), 0.76 (from 0.67 to 0.90), 3.57 (from 3.38 to 3.76) for paddy fields, upland fields, forests and urban areas respectively (n=3256). The TP concentration coefficient is 0.146 (lower limit 95% value 0.119 to upper limit 95% value 0.172), 0.172 (0.138 to 0.206), 0.044 (0.033 to 0.055), 0.267 (0.253 to 0.282) for paddy fields, upland fields, forests and urban areas respectively (n=3256,). Prefectural TN and TP concentration coefficients for paddy and upland fields related only loosely to prefectural surplus N and surplus P. On the other hand, prefectural TN and TP concentration coefficients for forests and urban related to prefectural population densities by logarithmic functions with determination coefficients $R^2$ from 0.45 to 0.48.

Keywords: watershed land-use model, TN, TP, concentration coefficient

©2019. Japan Geoscience Union. All Right Reserved. 

# Possibility of nutrients transportation from littoral slope for enhancement of phytoplankton growth in north basin of Lake Biwa

*Syuhei Ban[1], Rong YI[1], Xin Liu[1], Masahiro Maruo[1], Miki Sudo[1], Naoshige Goto[1], Jun Murase[2]

1. The University of Shiga Prefecture, 2. Nagoya University

Nutrient loading from non-point source in a lake ecosystem has not been well recognized yet. In Lake Biwa, total phosphorus (TP) does not decline to the level before eutrophication period, 1960s to 1970s, despite of decreasing the loading from point sources surrounding the lake after that. One of the reasons for no well lowering TP in the lake is attributed to agricultural runoff, in which suspended materials including phosphorus would be deposited to the littoral bottom. In our previous study, subsurface maximum of ammonium as a proxy of dissolved materials from anaerobic interstitial waters in the littoral bottom sediments was found along a transect from littoral to pelagic regions, implying horizontal transportation of nutrients from littoral sediments. There were no such evidences of soluble reactive phosphorus (SRP) yet due to always below the detection limit in the pelagic waters. Recently, we developed modified protocol using an ion chromatography for measuring orthophosphate concentration at nano-molar levels. In this presentation, we’ d like to provide several evidences for horizontal transportation of dissolved nutrients including orthophosphate along a transect from littoral to pelagic sites in north basin of Lake Biwa.

Total of the 6 times transect surveys for determining vertical profiles of nutrients, methane and herbicides were made in 2010-2011. Additional two transect surveys for determining those of nutrients including orthophosphate were made in 16 May and 25 July of 2018. During the 2010-2011 campaigns, *in situ* phytoplankton primary production was measured during the stagnation period using light intensity and chlorophyll *a*concentration monitored by sensors attached to a mooring buoy situated at an offshore station in north basin of Lake Biwa and an equation of photosynthesis - light intensity (P-I) curve.

In 2010-2011 campaigns, we detected sub-surface maximum layer, 20-30 m, of ammonium and methane as a proxy of dissolved materials transported from interstitial water in the sediment of littoral slope. Herbicides, which were used in rice paddy during the rice planting and proxy of materials transported from terrestrial environments surrounding the lake, were also detected in 20-30 m even at the offshore regions in the lake. Primary production monitoring suggested that phytoplankton production depended on some environmental variables other than solar irradiance, e.g. nutrients, until summer months. These results suggested that nutrients for enhancing algal growth might be horizontally transported from sediment in the littoral slope, and that the source of the nutrients might be provided from the drainage of rice paddy.

In 2018 campaigns, sub-surface maximum of ammonium was clearly found along a transect from littoral to pelagic sites in both May and July, but no such sub-surface maximum of orthophosphate was found. Several reasons for failure to find sub-surface maximum of orthophosphate might be proposed. Phosphate would be used by both phytoplankton and bacteria, while ammonium would be used by phytoplankton alone in the euphotic layer. In phosphate limited environment, such as pelagic areas in north basin of Lake Biwa, sub-surface maximum could not be easily detected due to rapid absorption by both phytoplankton and bacteria. Or, a transportation of nutrients from the littoral sloop would sporadically occur, and then we simply missed to detect it. This is on-going research project, and then further studies will be conducted to clarify this issue.

©2019. Japan Geoscience Union. All Right Reserved. 

Keywords: Horizontal nutrient transportation, non-point source loading, agricultural runoff, Lake Biwa

©2019. Japan Geoscience Union. All Right Reserved. 

# SWAT model analysis for confirming the effects of crop growth on the suspended sediment concentration from a settling basin catchment on Ishigaki island

*Yang Cao[1], Shin-ichi Onodera[1], Mitsuyo Saito[2], Hide Omae[3], Yoshiko Iizumi[3]

1. Graduate School of Integrate Arts and Sciences, Hiroshima University, 2. Graduate School of Environmental and life Science, Okayama University, 3. Tropical Agriculture Research Front (TARF), Japan International Research Center for Agricultural Sciences (JIRCAS)

Crop growth has a significant effect on soil erosion in small watersheds. Exploring the characteristics and occurrences of soil erosion in small watersheds assists in our understanding of the water and material cycles in agricultural areas. The small catchment on the tropical island of Ishigaki, Japan, was chosen as the research area. The effects of sugarcane growth at different stages on the suspended sediment concentration in the basin from January 2017 to July 2018 were analyzed based on the Soil and Water Assessment Tool (SWAT) model. This study will explore the possible driving factors of these phenomena. The results show that the suspended sediment concentration in the basin reached its highest value on a rainy day near the sugarcane planting period because of the soil relaxation caused by tillage and cultivation. At the end of the sugarcane growth period, the sediment concentration was not at a high level when the rainfall reached 150 mm, because of the effective protection of the soil by sugarcane. The simulated sediment concentration of precipitation per mm showed that the simulated sediment concentration was at its highest during the crop planting period, followed by the period of bare land, and at the lowest during the crop growth period.

Keywords: SWAT model, Small catchment, Sugarcane, Sediment, Ishigaki

©2019. Japan Geoscience Union. All Right Reserved. 

# Estimating the runoff of water, sediment, and nutrient using SWAT model in Kikuchi-river watershed, Kumamoto, and the influence of the forest

*Soichiro Fujii[1], Masahiko Kanamori[1], Yuko Nagano[1], Maki Kinoshita[2], Yuta Shimizu[3], Shin-ichi Onodera[4]

1. Japan Forest Technology Association, 2. PASCO Corporation, 3. Western Region Agricultural Research Center, National Agriculture and Food Research Organization, 4. Graduate School of Integrated and Arts Sciences, Hiroshima University

Recently, enclosed sea area such as Ariake-sea have severe nutrient enrichment problem and is decreasing the produce of fishery industry. Such enclosed sea area is commonly affected by river water quality discharged from the land area. Therefore, estimating the load of sediment and nutrient from its land area is important. However, most of researches estimating discharge from land area is conducted by simple method using primary load factor. These method only can provide the estimates in annual scale regardless of the land use. On the other hand, the positive effect of forest to water quality in the river, so-called green dam, is paid attention recently, and supposed to play important roll on improvement to sea environment. However, the effect of forest to water quality is not explained enough, and few research has conducted in watershed scale. In this study, we aim to simulate water, sediment, and nutrient runoff in order to provide more detail information about discharge from land area, and to estimate the influence of the forest to water quality. We use Soil and Water Assessment Tool (SWAT) and chose Kikuchi-river as a model watershed, which has the third largest watershed area among the rivers drain into Ariake-sea.

We set Komoda observatory as the most downstream point of Kikuchi-river and the model watershed is the upstream side from there. More than half of this watershed is covered by forest. We collected land use data, soil data, climate data and 30m mesh digital elevation model (DEM) data of this watershed in order to establish the model. In order to calibrate and validate the model performance, observed data of daily stream flow from 2008 to 2016, and sampling data of sediment and nutrient were collected. Moreover, we measured the amount of sediment, phosphorus and nitrogen during flood situation in 2016 and 2017. The parameters in the model were modified according to the result of calibration, and the performance of the model was evaluated from three indices such as Nash-Sutcliffe index.

The model performance was evaluated as more than satisfactory for all materials: water, sediment, phosphorus and nitrogen. Therefore, this model can simulate daily runoff from 2008 to 2017. The runoff rate of sediment and most of nutrient from forest was less than 30% of the annual average in whole watershed, although water discharge was the same level to the rate of forest area, which indicates the function of forest to provide low concentrate water of sediment and nutrient to the river. In conclusion, modelling the runoff from land area using SWAT model has potential to provide detail information about land area discharge and estimate the influence of forest to river water quality.

Keywords: SWAT model, Runoff estimation

©2019. Japan Geoscience Union. All Right Reserved. 

# Atmospheric depositions on forest ecosystems in areas along the Sea of Japan

*Yuko Itoh[1], Keiji Takase[2], Yoichi Fujihara[2], Toru Okamoto[1]

1. Forestry and Forest Products Research Institute, Japan, 2. Ishikawa Prefectural University

In recent years, concerns about the effects of excess-nitrogen usage by human activities on terrestrial environment, including forest ecosystems, have been increasing at a global scale. The phenomenon of high-nitrate efflux from several forest watersheds has already been reported in the surroundings of metropolitan areas in Japan. Furthermore, concerns regarding the effects of transboundary air pollution on areas along the Sea of Japan with expanding economic activities have been increasing in Asian countries. However, on-site monitoring throughout the year is difficult in most of these areas because of heavy snow, especially in the mountainous area. Therefore, the behaviors of elements within forest ecosystems throughout a year have primarily not yet been elucidated in this district. This study was conducted to determine the influxes and effluxes of elements in this heavy snowy region and to understand the contribution of transboundary air pollution to the quantity of atmospheric deposition. We also carried out rainfall and stream water investigations from the headwater area to the lower stream area in the Tedori River Basin and an inland mountainous area to understand the geographical distribution of the actual conditions of elements' influxes and effluxes in this region. We started monitoring the major and minor elements in a small forested watershed in the middle part of the Tedori River Basin, Ishikawa prefecture, Japan, in 2013. In this study site, we observed a large amount of precipitation throughout the year. Regarding the annual snowfall amount, there were extensive variations among the years. Seasonal fluctuations were observed in the influx of atmospheric deposition; in particular, the distribution of most of the elements increased during winter. The annual deposition average of inorganic nitrogen ($NH_4$-N + $NO_3$-N) in this site was 15.8 kg $ha^{-1}$. The contribution of winter season deposition to the annual inputs was high. The influx of nitrogen by bulk precipitation during winter season was 2.3 times that of summer, and that of sulfur sulfate was 3.7 times. The nitrogen influx quantity was similar to or more than that reported in nitrogen-saturated forested areas of the Kanto district. Therefore, similar to that in the Kanto district, higher nitrogen deposition loads from the atmosphere could also be influenced on the effect of nitrogen dynamics and the increase in nitrogen efflux at these forest watersheds. However, the efflux concentrations of most of the dissolved elements in stream water did not show clear seasonal fluctuations. Stream water nitrate concentration was stable and low. In addition to the seasonal fluctuation of nitrogen and sulfur, the ratios among some trace elements, which are anthropogenic substances (Pb, V, As, etc.), and sea salts and yellow sand could be useful indicators to elucidate the contribution of transboundary air pollution to these regions. We compared the element inputs associated with precipitation during the non-snowy season (July–November) at six locations in the Tedori River Basin and one location in the inland area. The inorganic nitrogen and sulfuric acid sulfur influxes were the largest at the middle reaches of the Tedori River Basin. The inflow amount of inorganic nitrogen and sulfuric acid sulfur at two points in the mountainous area was approximately half or less than that at the middle region and was approximately the same as the inflow amount at the inland mountainous area. Furthermore, we investigated stream water, spring water, and ground water samples from the headwater area to the lower stream area in the Tedori River Basin. The nitrate concentrations in all the samples ranged from 0.00 to 2.93 $mgL^{-1}$ (median value: 0.69 $mgL^{-1}$). In contrast, the nitrate concentrations of stream water in the Tsukuba experimental forest watershed, which has been reported as a nitrogen-saturated forested area of the Kanto district, were much higher (average value: 7.56 $mgL^{-1}$) than those in the Tedori River Basin. Compared with the influx, the efflux concentrations of nitrate in the water

©2019. Japan Geoscience Union. All Right Reserved. 

samples were generally very low around this basin. Therefore, higher nitrogen depositions have not yet distinctly influenced the nitrate concentrations of stream water in this area. To elucidate the influence of transboundary air pollutant influx on the entire Tedori River Basin, it is necessary to evaluate the inflow amount during the snowy season in the mountainous area. Therefore, it is important to establish a method that can be used to observe the influx and efflux of elements throughout the year even in mountainous areas with heavy snow.

©2019. Japan Geoscience Union. All Right Reserved. 

# Continuous and simultaneous flux measurement of $N_2O$ and $CO_2$ from agricultural soil using a portable multi-turn time-of-flight mass spectrometer

*Noriko Nakayama[1], Yusuke Iwai[1], Yo Toma[2], Hiroshi Furutani[1], Ryusuke Hatano[3], Michisato Toyoda[1]

1. Osaka University, 2. Ehime University, 3. Hokkaido University

Agricultural soil is one of the important sources/sinks of greenhouse gases such as $N_2O$, $CO_2$, and $CH_4$. The formation and consumption of such greenhouse gases in agricultural soils are dependent on not only the chemical and biological properties of the soil, but also their variations. Hence continuous monitoring of such greenhouse gases as tracer gases are quite useful to track chemical and biological processes and variations of soil properties.

In this paper, we describe a new field-deployable gas flux measurement system for the continuous monitoring of multiple agricultural soil gases ($N_2O$, $CO_2$, and $CH_4$) using a high resolution multi-turn time-of-flight mass spectrometer (MULTUM) combined with an automated flux chamber system. The new system measured the soil gases every 2.5 min with the precisions of ~6% for $N_2O$, $CH_4$, and 2% or better for $CO_2$ and $O_2$ at atmospheric concentrations with one relative standard deviation (RSD) for n = 10.

To demonstrate the utility of the continuous multi-gas flux measurement system, we conducted a field study at the Ehime University farm (Ehime, Japan) from September 3$^{rd}$ to 8$^{th}$, 2018. In the field study, an automated flux chamber was placed in the agricultural field and the soil gas concentrations in the chamber were continuously monitored by the MULTUM system. Soil temperature/moisture sensor were also monitored at the depth of 7.5 cm underground in addition to a weather information (wind speed, precipitation, solar radiation). The continuous measurement had been continued with operators almost unattended except for a daily system check.

For one flux measurement (20 min), eight gas samples were taken every 2.5 min with the flux chamber closed. Gas flux of $N_2O$ and $CO_2$ had been carried out by applying linear regression to the eight gas measurements. We found that a significant correlation of $N_2O$ flux with soil electrical conductivity and water content, although no significant correlation of $CO_2$ flux to soil electrical conductivity was observed. Significant and rapid decreases in $N_2O$ and $CO_2$ flux during rainfall events were also observed. Our preliminary result shows that high time-resolution flux data obtained by MULTUM system is quite useful for tracking the variation in soil properties and biological processes and their activity in soil environment.

Keywords: on-site mass spectorometry, MULTUM, soil-to-atmospher gas flux

©2019. Japan Geoscience Union. All Right Reserved. 

# Effects of introduction of cyclic irrigation system on mass balances of SS and T-P in Lake Inbanuma, Chiba, Japan

*Tomijiro Kubota[1]

1. National Agriculture and Food Research Organization, Institute for Rural Engineering

## Introduction

The introduction of cyclic irrigation has been advanced since 2010 in the Lake Inbanuma as part of the update project of the irrigation facilities. In the present study, mass balances of SS and T-P were examined before and after the introduction of the cyclic irrigation.

## Materials and methods

The irrigation block where the cyclic irrigation began in 2015 was selected as the investigation site, and the investigation was executed to the irrigation period in 2014 and 2015. The hydrological and water quality investigation was executed at ① division works of irrigation canal and ② drainage pumping station. Water samples were taken at the two points and the TOC, SS, TN, NO3-N, NO2-N, NH4-N, TP, and PO4-P were analyzed in the regular investigation executed about once a month. Besides regular investigation, water samples were taken once a day (8:00AM or noon) by the automatic water sampler and SS and T-P were analysed. The turbidity and water level were measured every ten minutes by using data loggers at same sites. The turbidity data were converted into the concentration of SS and TP by using the regression curve. The quantity of water intaken from the lake and drainage to the lake were obtained from the records of the facility manager.

## Result and discussion

The inflow and outflow loads and the balance were calculated before and after the introduction of the cyclic irrigation. In 2014, before the start of cyclic irrigation, both the outflow loads of SS and T-P were small to compare with those inflow loads. The amount of accumulation of SS and T-P were about 1.3t and 2kg respectively when having no rainfall in the irrigation block. On the other hand, the outflow of SS and T-P were about 3.5t/day and 20kg/day respectively in rainy days. If 2015 year is compared to 2014, it had increased in T-P though the load of irrigation water each day at no rainfall periods and it had not been change in SS though an accurate comparison is difficult according to the missing value. However, after the cyclic irrigation had been started, the amount of the outflow loads had decreased greatly like 35% in SS and 38% in T-P. The balance of the outflow loads during the irrigation periods of 2014 were -470kg/day in SS, which meant the purification type, while +2.6kg/day in T-P. as a result, it was found that the introduction of cyclic irrigation system had worked for water purification in SS and T-P effectively.

Keywords: cyclic irrigation system, water pollution, suspended solid, total phosphorus

©2019. Japan Geoscience Union. All Right Reserved. 

[E] Poster | A (Atmospheric and Hydrospheric Sciences)：A-HW Hydrology & Water Environment

Thu. May 30, 2019 5:15 PM - 6:30 PM JST | Thu. May 30, 2019 8:15 AM - 9:30 AM UTC | Poster Hall International Exhibition Hall8, Makuhari Messe_9

## [A-HW22] Materials transport and nutrient cycles in watersheds; from headwaters to coastal seas

convener:Masahiro Kobayashi(Forestry and Forest Products Research Institute), Seiko Yoshikawa(Institute for Agro-environmental Sciences, National Agriculture and Food Research Organization), Jun Yasumoto(University of the Ryukyus, Faculty of Agriculuture), Adina Paytan(University of California Santa Cruz)

This session aims to synthetize watershed sciences in order to understand dynamical processes of materials transport and nutrient cycles in watersheds from headwaters to coastal seas. The session will be integrating a variety of research disciplines including limnology, ground water hydrology, coastal oceanography, meteorology, pedology, sedimentology, forestry, agriculture, fishery, ecology, social science and more. This session calls for ideas on new methods for the watershed sciences, such as tracer and molecular technique, hydrological modeling, paleontological approaches, laboratory and field experiments, social-scientific evaluation of ecosystem services and social-ecological systems, and so on, in order to elucidate physical, chemical and biological mechanisms for shedding light on natural phenomena and their changes over time in complex and dynamic watershed systems under human and climate impacts. Through this session, we would like to facilitate interdisciplinary collaboration among participants to create new knowledge on watershed sciences.

### [AHW22-P01] Phosphate Enrichment Hampers Development of Juvenile Acropora digitifera Coral by Inhibiting Skeleton Formation

Mariko Iijima[1], *Yasumoto Ko[1], Jun Yasumoto[2], Mina Hirose[3], Mitsuru Jimbo[1], Shugo Watabe[1] (1.Kitasato University School of Marine Biosciences, 2.Faculty of Agriculture, University of the Ryukyus, 3.Tropical Technology Plus)

### [AHW22-P02] Modeling chlorophyll-a concentration using remote sensing in shallow water systems: Comparison of sensors

*Assefa M Melesse[1], Tara Blakey[1], Mohammad Haji Gholizadeh[1], Mohd Manzar Abbas[1] (1.Florida International University)

### [AHW22-P03] Dynamics in groundwater flow system with seasonal water table variation in a coastal and island

*Yusuke Tomozawa[1], Shin-ichi Onodera[1], Mitsuyo Saito[2] (1.Graduate School of Integrated Arts and Sciences Hiroshima University, 2.Graduate School of Environmental and Life Science, Okayama University)

### [AHW22-P04] The Tracing of Groundwater Contamination Sources in Indonesian Coastal Alluvial Groundwater using $\delta^{34}S$ and $\delta^{15}N$ Isotopes

*Anna Fadliah Rusydi[1,4], Mitsuyo Saito[2], Seiichiro Ioka[3], Shin-ichi Onodera[1] (1.Graduate School of Integrated Arts and Sciences, Hiroshima University, Japan, 2.Graduate School of Environmental and Life Sciences, Okayama University, Japan, 3.Research Institute for Sustainable Energy, Hirosaki University, Japan, 4.Research Center for Geotechnology, Indonesian Institute of Sciences, Indonesia)

### [AHW22-P05] Spatio-temporal dynamics of orthophosphate with implications for limitation of phytoplankton growth in north basin of Lake Biwa, Japan

*Xin Liu[1], Rong Yi[1], Masahiro Maruo[1], Syuhei Ban[1] (1.The University of Shiga Prefecture)

### [AHW22-P06] Microbial phase analysis in aquifer of Ryukyu Limestone Zone using next generation sequencer

*Umi Murao[1], Jun Yasumoto[1], Yasumoto Ko[3], Mina Hirose[2], Nanami Mizusawa[3], Ryo Iguchi[4], Bam H.N. Razafindrabe[5], Syugo Watabe[3] (1.University of the Ryukyus, Faculty of Agriculuture Department of Regional Agricultural Engineering, 2.Tropical Tecnology Plus, 3.Kitasato University School of Marine Biosciences, 4.National Institute of Advanced Industrial Science and Technology, 5.University of the Ryukyus, Faculty of Agriculuture Department of Subtropical Agro-Environmental Sciences)

## [AHW22-P07] Evaluation for temporal variation in groundwater inflow to the lagoons connected to Lake Biwa by radon ($^{222}$Rn) tracer analysis

*Mitsuyo Saito[1], Shin-ichi Onodera[2], Yusuke Tomozawa[2], Kunyang Wang[2], Syuhei Ban[3], Noboru Okuda[4] (1.Graduate School of Environmental and Life Science, Okayama University, 2.Graduate School of Integrated Arts and Sciences, Hiroshima University, 3.School of Environmental Sciences, The University of Shiga Prefecture, 4.Research Institute for Humanity and Nature)

## [AHW22-P08] Br/Cl ratio characteristics of groundwater in coastal areas in Indonesia

*Seiichiro Ioka[1], Shin-ichi Onodera[2], Mitsuyo Saito[3], Anna Fadliah Rusydi[2,4] (1.Institute of Regional Innovation, Hirosaki University, Japan, 2.Graduate School of Integrated Arts and Sciences, Hiroshima University, Japan, 3.Graduate School of Environmental and Life Sciences, Okayama University, Japan, 4.Research Center for Geotechnology, Indonesian Institute of Sciences, Indonesia)

## [AHW22-P09] Estimation of groundwater recharge and phosphorus transport under different precipitation conditions in a suburban catchment, using SWAT model

*Kunyang Wang[1,2], Shin-ichi Onodera[1], Mitsuyo Saito[3], Noboru Okuda[4], Takuya Okubo[5] (1.Graduate School of Integrated Arts and Science, Hiroshima University, 2.Capital Normal University, 3.Okayama University, 4.Research Institute for Humanity and Nature, 5.University of the Shiga Prefecture)

## [AHW22-P10] Losses of phosphorus with soil erosion and nitrate with groundwater recharge in an agricultural catchment, subtropical small island

*Shin-ichi Onodera[1], Mitsuyo Saito[2], Yang Cao[1], Anna Fadliah Rusydi[1], Hide Omae[3], Yoshiko Iizumi[4], Yusuke Tomozawa[1] (1.Graduate School of Integrated and Arts Sciences, Hiroshima University, 2.Graduate School of Environmental and Life Science, Okayama University, 3.JIRCAS TARF, 4.JIRCAS HQ)

## [AHW22-P11] Phosphate solubilizing bacteria as an indicator of sediment phosphorus in freshwater lakes

*Sreekumari Kurissery[1], Katelynn Crawford[1], Nandakumar Kanavillil[1] (1.Lakehead University, Canada)

## [AHW22-P12] A Study on the dynamics of various phosphate forms in soil and groundwater in Ryukyu limestone regions

*Masashi Nozaki[1], Jun Yasumoto[2], Yasumoto Ko[3], Hirose Mina[4], Iijima Mariko[3], Ryuichi Shinjo[5], Bam H.N. Razafindrabe[6] (1.University of The Ryukyus, Graduate School of Agriculture,, 2.University of the Ryukyus, Faculty of Agriculture, Department of Regional Agricultural Engineering, 3.Kitasato University School of Marine Biosciences, 4.Tropical Technology Plus, 5.Department of Physics and Earth Sciences, University of the Ryukyus, 6.University of the Ryukyus, Faculty of Agriculture, Department of Subtropical Agro-Environmental Sciences)

## [AHW22-P13] Impacts of highly concentrated turbid water on the groundwater in the Tedori River alluvial fan, Japan

*Yoichi Fujihara[1], Shunsuke Chono[1], Keiji Takase[1], Eiji Ichion[1] (1.Department of Environmental Science, Ishikawa Prefectural University)

## [AHW22-P14] Altitude effect of water stable isotopic ratio of ravine water and its contribution to groundwater in alluvial plains - Comparison in east and west side catchments of Lake Biwa –

*Yusuke Tomozawa[1], Kunyang Wang[1], Mitsuyo Saito[2], Syuhei Ban[3], Noboru Okuda[4], Shin-ichi Onodera[1] (1.Graduate School of Integrated Arts and Sciences Hiroshima University, 2.Graduate School of

Environmental and Life Science, Okayama University, 3.School of Environmental Science, The University of Shiga Prefecture, 4.Research Institute for Humanity and Nature)

[AHW22-P15] Calculation of TN and TP concentration coefficients of river water for each land use by a simple watershed model.

*Seiko Yoshikawa[1], Donglai Ma[1,4], Tadamasa Saito[1,5], Kenji Matsumori[2], Yuko Itoh[3], Masahiro Kobayashi[3] (1.Institute for Agro-environmental Sciences, National Agriculture and Food Research Organization, 2.Western Region Agricultural Research Center, National Agriculture and Food Research Organization, 3.Forestry and Forest Products Research Institute, 4.Graduate school,Tsukuba University, 5.Faculty of Agriculture, Ibaraki University)

[AHW22-P16] **Possibility of nutrients transportation from littoral slope for enhancement of phytoplankton growth in north basin of Lake Biwa**

*Syuhei Ban[1], Rong YI[1], Xin Liu[1], Masahiro Maruo[1], Miki Sudo[1], Naoshige Goto[1], Jun Murase[2] (1.The University of Shiga Prefecture, 2.Nagoya University)

[AHW22-P17] SWAT model analysis for confirming the effects of crop growth on the suspended sediment concentration from a settling basin catchment on Ishigaki island

*Yang Cao[1], Shin-ichi Onodera[1], Mitsuyo Saito[2], Hide Omae[3], Yoshiko Iizumi[3] (1.Graduate School of Integrate Arts and Sciences, Hiroshima University, 2.Graduate School of Environmental and life Science, Okayama University, 3.Tropical Agriculture Research Front (TARF), Japan International Research Center for Agricultural Sciences (JIRCAS))

[AHW22-P18] Estimating the runoff of water, sediment, and nutrient using SWAT model in Kikuchi-river watershed, Kumamoto, and the influence of the forest

*Soichiro Fujii[1], Masahiko Kanamori[1], Yuko Nagano[1], Maki Kinoshita[2], Yuta Shimizu[3], Shin-ichi Onodera[4] (1.Japan Forest Technology Association, 2.PASCO Corporation, 3.Western Region Agricultural Research Center, National Agriculture and Food Research Organization, 4.Graduate School of Integrated and Arts Sciences, Hiroshima University)

[AHW22-P19] Atmospheric depositions on forest ecosystems in areas along the Sea of Japan

*Yuko Itoh[1], Keiji Takase[2], Yoichi Fujihara[2], Toru Okamoto[1] (1.Forestry and Forest Products Research Institute, Japan, 2.Ishikawa Prefectural University)

[AHW22-P20] Continuous and simultaneous flux measurement of $N_2O$ and $CO_2$ from agricultural soil using a portable multi-turn time-of-flight mass spectrometer

*Noriko Nakayama[1], Yusuke Iwai[1], Yo Toma[2], Hiroshi Furutani[1], Ryusuke Hatano[3], Michisato Toyoda[1] (1.Osaka University, 2.Ehime University, 3.Hokkaido University)

[AHW22-P21] Effects of introduction of cyclic irrigation system on mass balances of SS and T-P in Lake Inbanuma, Chiba, Japan

*Tomijiro Kubota[1] (1.National Agriculture and Food Research Organization, Institute for Rural Engineering)

# Phosphate Enrichment Hampers Development of Juvenile Acropora digitifera Coral by Inhibiting Skeleton Formation

Mariko Iijima[1], *Yasumoto Ko[1], Jun Yasumoto[2], Mina Hirose[3], Mitsuru Jimbo[1], Shugo Watabe[1]

1. Kitasato University School of Marine Biosciences, 2. Faculty of Agriculture, University of the Ryukyus, 3. Tropical Technology Plus

Coral reef degradation resulting from various types of local stress on corals such as excessive nutrient enrichment in and gravel inflow into coastal waters is of an increasing global concern. Because tropical and subtropical seawaters are generally poor in nutrients and thus oligotrophic, these stresses are thought to result in the decline of environments favorable to coral growth. Inorganic phosphates have been especially considered to possibly inhibit the formation of coral skeleton. Despite many studies available on the effects of nutrients on corals, a clear consensus for how nutrients exert deteriorative effects on the corals has not been established satisfactorily. Recently, we found that biogenic polyamines react with carbon dioxide ($CO_2$) and accelerate an aragonite formation of calcium carbonate ($CaCO_3$) in seawater. In this study, we examined the effects of phosphates and nitrates on *in vitro* aragonite formation of $CaCO_3$ by using biogenic polyamines and *in vivo* aragonite formation of juvenile coral *Acropora digitifera* skeletons, showing that phosphates clearly inhibited both *in vitro* and *in vivo* $CaCO_3$ formations at similar concentrations. In contrast, nitrates inhibited neither *in vitro* aragonite formation of $CaCO_3$ nor *in vivo* aragonite formation of juvenile coral skeletons. These findings indicate that phosphates have a detrimental effect on bioinorganic coral calcification. Furthermore, the findings that phosphate enrichment inhibits coral skeleton formation led us to conclude that enriched phosphate is adsorbed on juvenile coral skeleton surface and inhibits inorganically normal development of juvenile coral skeleton.

Keywords: phosphate, calcification

©2019. Japan Geoscience Union. All Right Reserved. 

# Modeling chlorophyll-a concentration using remote sensing in shallow water systems: Comparison of sensors

*Assefa M Melesse[1], Tara Blakey[1], Mohammad Haji Gholizadeh[1], Mohd Manzar Abbas[1]

1. Florida International University

The level of productivity in the upland and coastal water bodies is highly linked to land processes (land use, water management, water and nutrient fluxes). Understanding the linkage between these processes and the level of algal blooms in the water bodies is crucial for improving water quality. A comparative study was conducted using remote sensing data from three different sensors (SeaWIFS, MoDIS and Landsat) to evaluate the capability of reflectance data from these sensors for estimation of chl-a concentrations in three water bodies in the USA (Lake Okeechobee, Florida Bay and Chesapeake Bay). Observed chl-a data were gathered and compared with simulation results. The analysis found that all of the sensors have performed well in deeper water bodies than in shallow sections due to the bottom reflectance from non-algal blooms. For shallow water bodies, selection of the proper bands and band combinations, identification of the non-algal bloom reflectance and the corresponding algorithms can improve the simulation. Seasonality as well as spatial variability (using cross-sections) were evaluated and the results showed that chl-a values were highly variable for the selected summer months. Indicative of the effect of land surface fluxes of nutrients, chl-a values were higher closer to coastal areas in the Florida bay and Chesapeake Bay. The chl-a in the freshwater lake of Okeechobee was simulated using Landsat 8 data and the results found were very good. Comparison of the SeaWIFS and MoDIS chl-a value to that of the measured concentrations in the deeper section of Florida Bay and Chesapeake Bay, respectively showed very good agreement.

Keywords: Chl-a, SeaWIFS, Water qulity modeling, South Florida, Remote sensing

©2019. Japan Geoscience Union. All Right Reserved. 

# Dynamics in groundwater flow system with seasonal water table variation in a coastal and island

*Yusuke Tomozawa[1], Shin-ichi Onodera[1], Mitsuyo Saito[2]

1. Graduate School of Integrated Arts and Sciences Hiroshima University, 2. Graduate School of Environmental and Life Science, Okayama University

In islands, freshwater water resources are valuable as living and agricultural use, and dug wells water and reservoirs had been utilized for more than 100 years. In order to use such water resources sustainably, it is important to evaluate groundwater flow as well as water budget.

In this research, we examined to confirm the seasonal variation in water stable isotopic ratios in observation boreholes at the coastal lowland in Ikuchi Island Hiroshima prefecture. Moreover, considering that the target area is coastal, $Cl^-$ concentration was analyzed to evaluate the influence of salt fresh water boundary.

The experimental site is located on Ikuchi Island in Hiroshima prefecture. The highest altitude is 456 m. The basement rock is mainly composed of granite. Annual average precipitation is 1058.8 mm. Observation boreholes are located at the coastal lowland in the southeastern part of the island. The upper site (Site U) with the altitude of 5.1 m asl has 3 boreholes with the depths of 2 m, 15 m, 30 m, the lower site (Site D) with 2.5 m asl has 8 with the depth of 1 m, 2 m, 3 m, 10 m, 15 m, 20 m, 30 m, 40 m, respectively. The water sampling was carried out from monthly to half year interval since 2015. Every samples were analyzed for water isotopic ratios by PICARO and anion component by ion chromatography. Especially samples in January in 2019 were analyzed for CFCs and SF6.

Based on the previous study (Saito and Onodera, 2007), the distinct altitude effect of isotopic ratio in precipitation has been confirmed. Due to spatial and temporal variations in isotopic ratios, recharge process to groundwater was suggested as follows, 1) recharge on site to shallow groundwater (2-3m deep) at D ( $\delta^{18}O$: -7.8 to - 7.4 ‰), 2) river water contribution to the shallow groundwater (2-15m) at U ( $\delta^{18}O$: - 8.3 to - 7.5 ‰), 3) recharge in the mountain slope with the altitude of about 360 m to deep groundwater (30m) at U ( $\delta^{18}O$: - 8.4 to - 8.1 ‰), 4) recharge at 400 m on near the mountain top to deep groundwater (10-30 m) at D( $\delta^{18}O$: - 8.7 to - 8.4 ‰), 5) recharge of precipitation with lower isotope than in present to deeper groundwater (40 m) at D ( $\delta^{18}O$: -8.9 to - 8.8 ‰)

The deepest groundwater (40m) at D had lower isotopic ratios with higher $Cl^-$ concentration (250 to 584 mg / L) during a lower water table in the winter. This indicated the seawater –fresh water boundary rose with water table according to Gyben-Hrzberg concept. These phenomena also suggest to cause the rise of deeper and older groundwater flow line. Consequently, we suggest the lower isotopic ratio in deeper groundwater indicates the immobile water which were recharged in the glacial period. Based on other tracers (CFC, SF 6), we will discuss more.

Keywords: stable isotope, groundwater, coastal

©2019. Japan Geoscience Union. All Right Reserved. 

# The Tracing of Groundwater Contamination Sources in Indonesian Coastal Alluvial Groundwater using $\delta^{34}S$ and $\delta^{15}N$ Isotopes

*Anna Fadliah Rusydi[1,4], Mitsuyo Saito[2], Seiichiro Ioka[3], Shin-ichi Onodera[1]

1. Graduate School of Integrated Arts and Sciences, Hiroshima University, Japan, 2. Graduate School of Environmental and Life Sciences, Okayama University, Japan, 3. Research Institute for Sustainable Energy, Hirosaki University, Japan, 4. Research Center for Geotechnology, Indonesian Institute of Sciences, Indonesia

The coastal area is one of the Indonesian Government priorities as an archipelago country. The groundwater in the area is one of the most reliable clean water resources, therefore it is crucial to understanding the vulnerability of this resource. Our research area was located at Indramayu, a developing rural coastal area in Indonesia, where, the environment was relatively pristine. This research aimed was to identify the effect of natural condition and human activity to groundwater quality by using stable isotope $\delta^{34}S$ and $\delta^{15}N$.

Totally, there were 20 samples taken from groundwater (18) and river (2). The nitrate and sulfate were detected in a total of 5 and 19 samples, respectively. The isotopes composition for isotope nitrate were -11.2 ‰–+22.22‰ for $\delta^{15}N\text{-}NO_3$ and -3.4 ‰–+17.1‰ for $\delta^{18}O\text{-}NO_3$. Moreover, the values of $\delta^{34}S\text{-}SO_4$ and $\delta^{18}O\text{- }SO_4$ were varied from -4.2 ‰–+28.4‰ and +7.3 ‰–+18.8 ‰, respectively. The isotopic signatures of nitrate suggested that the used of inorganic fertilizer and animal manure give the impact to both groundwater and river. Similarly, the isotopic signatures of sulfur were showing that those detected sulfate in the groundwater were mostly coming from fertilizer. Moreover, the soil was mineralized by organic sulfate as well. At one point, located in the fishery area, the groundwater was indicated the seawater contamination. It was shown by the heavy composition of sulfur isotope (28.4‰ for $\delta^{34}S$ and 18.8‰ for $\delta^{18}O$). Lastly, our results showed those combined isotopes of $\delta^{34}S$ and $\delta^{15}N$ along with land-use evaluation could explain the possible sources of groundwater in coastal area at very early urbanization stage.

Keywords: Sulfur Isotope, Nitrate Isotope, Coastal Groundwater, Indramayu

©2019. Japan Geoscience Union. All Right Reserved. 

# Spatio-temporal dynamics of orthophosphate with implications for limitation of phytoplankton growth in north basin of Lake Biwa, Japan

*Xin Liu[1], Rong Yi[1], Masahiro Maruo[1], Syuhei Ban[1]

1. The University of Shiga Prefecture

Orthophosphate ($PO_4$-P) is the main chemical form of phosphorus (P) for phytoplankton growth, often considered as a limiting nutrient for primary production in freshwater ecosystems. However, few information on accurate measurements for $PO_4$-P concentrations in epilimnion of meso- and oligotrophic lakes due to lower than the detection limit (60 nM) of soluble reactive P using traditional spectrophotometrical method. In the present study, we measured $PO_4$-P concentrations using ion chromatography with a detection limit of 5 nM, and determined truly vertical distribution of $PO_4$-P throughout the year with other abiotic and biotic environmental factors in north basin of Lake Biwa, to accurately understand biogeochemical processes of P in this mesotrophic lake.

Field investigations were conducted monthly from April to December 2018 at station K4 (35º19'9.6"N, 136º11'2.7"E; 50 m deep). Phosphate enrichment experiments were also made at each sampling occasion to clarify P limitation for phytoplankton growth. Lake water including phytoplankton assemblage collected from epilimnion (0–20 m) was enriched with 1 $\mu$M of $PO_4$-P (+P) and incubated together with untreated one (control) for 2 days under ambient light and temperature conditions. To evaluate the effect of potentially nutrient-rich bottom water, the filtered bottom water was mixed with untreated epilimnion water including phytoplankton at 1:1 (+B) was incubated at the same conditions as the +P treatment. Phytoplankton growth rate ($g$) was calculated with equation of $g=\ln(C_t/C_0)/2$, where $C_0$ and $C_t$ are chlorophyll *a* (chl. *a*) concentrations at start and end of the experiment, respectively.

Water temperature increased in the epilimnion from May, and strict thermocline was developed from June to September. Chl. *a* concentrations increased from June to July in 10–20 m, and from October to November in 0–20 m. $PO_4$-P concentrations were always low, <20 nM, in the epilimnion from April to June. The concentrations below 30 m increased up to 140 nM in May, but decreased after that until July. In August and September, the concentrations increased up to 30–40 nM even in the epilimnion probably due to disturbance by typhoon. The concentrations below 30 m increased with depth, and the highest values were frequently observed near the bottom, up to 220 nM. On average throughout the water column, $PO_4$-P concentrations were 24–48 nM from April to June, then slightly increased up to 73 nM until September, being constant, 50–63 nM until December.

Total P, total dissolved P, dissolved organic P and particulate P exhibited similar spatio-temporal distributions, but different pattern from those of $PO_4$-P. $NH_4$-N increased in 10–20 m from May to July, whereas the $NO_3$-N increased in the hypolimnion as season progressed. Sestonic C:N:P ratios suggested a terrible P deficiency in July and October when phytoplankton biomass increased.

Phosphate enrichment experiments showed that phytoplankton in the epilimnion was mostly limited with P for its growth. Phytoplankton $g$ in control varied −0.05-0.08 $d^{-1}$, being always lower than those in +P (−0.04-0.44 $d^{-1}$) and/or +B (−0.04-0.49 $d^{-1}$) treatments except for November and December. In November, no growth was found even in +P treatment. This might be caused by nitrogen limitation because of <6 $\mu$M of $NO_3$-N in the epilimnion. The $g$ of control was similar as that of +P and +B (ca. 0.1 $d^{-1}$) in December, indicating that P deficiency for phytoplankton growth was relaxed until December by vertical convection.

©2019. Japan Geoscience Union. All Right Reserved. 

We firstly determined completely vertical distributions of $PO_4$-P in north basin of Lake Biwa from spring to winter, and detected 20–40 nM of $PO_4$-P in the epilimnion. Phosphate enrichment experiments showed that 20 nM of $PO_4$-P might be critical concentration for phytoplankton growth in the lake. No phytoplankton growth even in +P treatment in November implied that nitrogen limitation for phytoplankton growth will be possible in Autumn. Further study for clarify this will be needed.

Keywords: Orthophosphate dynamics, Phosphorus limitation, Phytoplankton growth rate, Ion chromatography, Biogeochemical processes, Freshwater ecosystem

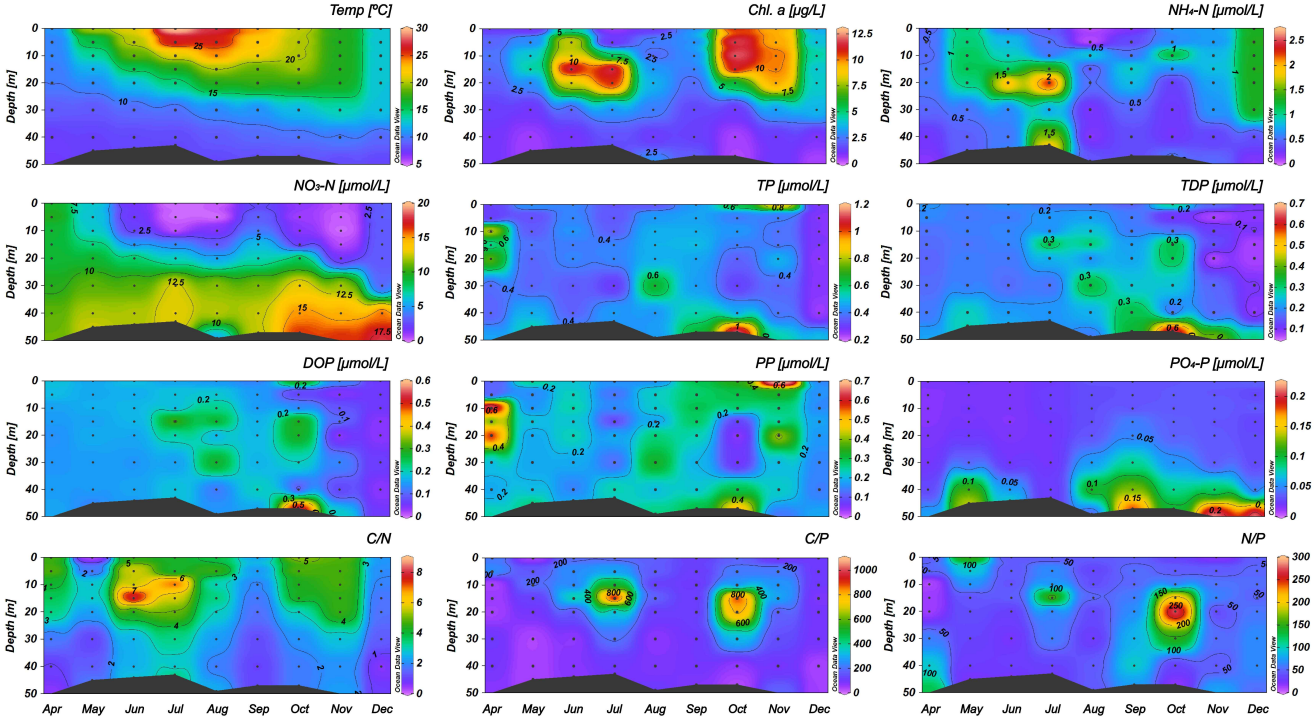


©2019. Japan Geoscience Union. All Right Reserved. 

# Microbial phase analysis in aquifer of Ryukyu Limestone Zone using next generation sequencer

*Umi Murao[1], Jun Yasumoto[1], Yasumoto Ko[3], Mina Hirose[2], Nanami Mizusawa[3], Ryo Iguchi[4], Bam H.N. Razafindrabe[5], Syugo Watabe[3]

1. University of the Ryukyus, Faculty of Agriculuture Department of Regional Agricultural Engineering, 2. Tropical Tecnology Plus, 3. Kitasato University School of Marine Biosciences, 4. National Institute of Advanced Industrial Science and Technology, 5. University of the Ryukyus, Faculty of Agriculuture Department of Subtropical Agro-Environmental Sciences

Clean water and sanitation (Sustainable development Goals (6)) is one of the world's important issues. People use groundwater in many areas as a water source, but various cases of contamination by agricultural activities and substances derived from human and animal excrements have been reported.

On the other hand, genetic analysis techniques using molecular biological methods have been applied to the analysis of microbial phase in the water environment.

In recent years, the method using the latest analysis equipment of next generation Sequencer is established, mainly for microorganisms. In addition, new monitoring indices such as environmental DNA have been developed. It is thought that the microbial phase in groundwater varies depending on the influence of various environmental factors and human activity, but the actual condition is not clear.

The next generation Sequencer is a very powerful tool used to grasp the microbial phase in groundwater. It is thought that the microbial phase can be an important indicator in water resource management of basins in the future.

The purpose of this study is to investigate the microbial species and their coexistence in groundwater in the Ryukyu Limestone area using the next generation sequencer.

Keywords: groundwater, microbial community analysis, genetic analysis

©2019. Japan Geoscience Union. All Right Reserved. 

# Evaluation for temporal variation in groundwater inflow to the lagoons connected to Lake Biwa by radon ($^{222}$Rn) tracer analysis

*Mitsuyo Saito[1], Shin-ichi Onodera[2], Yusuke Tomozawa[2], Kunyang Wang[2], Syuhei Ban[3], Noboru Okuda[4]

1. Graduate School of Environmental and Life Science, Okayama University, 2. Graduate School of Integrated Arts and Sciences, Hiroshima University, 3. School of Environmental Sciences, The University of Shiga Prefecture, 4. Research Institute for Humanity and Nature

Primary production in freshwater lakes and reservoirs are usually controlled by phosphorus (P). Lacustrine groundwater discharge (LGD), direct discharge of subsurface water to lake, is regarded as a potential nutrient paths, including phosphorus from a catchment to lake water environment. There are more than 20 lagoons around Lake Biwa which were originally a part of the lake. These lagoons are regarded to have important functions as settling ponds of inflowing loads from the catchments to Lake Biwa, refuges for shallow water ecosystems and so on. Because these lagoons are connected to Lake Biwa, evaluation of nutrient budget is important for the nutrient cycle in the lake. Some researchers have pointed out the presence of LGD in littoral area of Lake Biwa. However, it has not been evaluated for the lagoons around the lake. In the present research, we aimed to evaluate the temporal variation in groundwater inflow to a lagoon connected to Lake Biwa by radon ($^{222}$Rn) tracer analysis.

The field campaigns were conducted in December 2017, August and October 2018 for the lagoons (Noda-Numa and Hasu-Ike) located on northeastern shore of Lake Biwa. The volume of inflow and outflow, water temperature, electric conductivity, chlorophyll-a and radon ($^{222}$Rn) concentration were measured in the lagoon. $^{222}$Rn is a radioactive element of uranium ($^{238}$U) series with 3.8 day of half-life. $^{222}$Rn is a useful tracer of groundwater discharge because it generally enriched in groundwater than surface water. To examine the temporal variation in groundwater inflow, the time-series $^{222}$Rn concentration in water was obtained. Water samples were collected at the inlet, outlet and near the center of the lagoons and natural springs and groundwater wells around the lagoons. Water and $^{222}$Rn balance suggest that groundwater inflow is larger in Noda-Numa than Hasu-Ike. The catchment topography may influence on this difference. $^{222}$Rn balance-based residence time of lagoon water was estimated 10-20 days in Noda-Numa, and 4-5 days in Hasu-Ike, were similar with that based on water balance. These results suggest the groundwater inflow is a potential phosphorus path to Noda-Numa.

Keywords: Groundwater inflow, Connected lagoons, Lake Biwa, Radon (222Rn)

©2019. Japan Geoscience Union. All Right Reserved. 

# Br/Cl ratio characteristics of groundwater in coastal areas in Indonesia

*Seiichiro Ioka[1], Shin-ichi Onodera[2], Mitsuyo Saito[3], Anna Fadliah Rusydi[2,4]

1. Institute of Regional Innovation, Hirosaki University, Japan, 2. Graduate School of Integrated Arts and Sciences, Hiroshima University, Japan, 3. Graduate School of Environmental and Life Sciences, Okayama University, Japan, 4. Research Center for Geotechnology, Indonesian Institute of Sciences, Indonesia

The urban development in Indonesia’ s coastal areas has led to an increase of groundwater demand, which then has resulted in groundwater salinization. In this study, we analyze bromide and Br/Cl ratio characteristics, as index of groundwater salinization, in three cities of Indonesian coastal areas, namely: Indramayu, Mataram, and Semarang. Each research site is at different stage of urbanization. Indramayu is in very early stage of urbanization, followed by Mataram as a developing tourism area, and the last one Semarang as a heavy urbanization city. The results show that concentrations of bromide in groundwater are ranged from 0.05 to 38 mg/L in Indramayu, 0.01 to 0.8 mg/L in Mataram, and 0.02 to 8.0 mg/L in Semarang. Furthermore, the occurrence of Br is described in terms of the Br/Cl weight ratio, which allows for small changes in bromide concentrations to be assessed in terms of salinity. Median values of Br/Cl weight ratio in the groundwater of Indramayu, Mataram, and Semarang were approximately 0.0035, 0.0027, and 0.0025, respectively, while the ratio in seawater is generally around 0.0035. The relationship between Br/Cl weight ratio and chloride concentration indicate the groundwater in Indramayu is undergoing salinization due to seawater intrusion compared to the other two areas, meanwhile the groundwater in Semarang is experiencing chloride contamination due to anthropogenic activities based on the study by Andreasen and Fleck (1997).

Keywords: Indonesia, groundwater, Br/Cl ratio, coastal area

©2019. Japan Geoscience Union. All Right Reserved. 

# Estimation of groundwater recharge and phosphorus transport under different precipitation conditions in a suburban catchment, using SWAT model

*Kunyang Wang[1,2], Shin-ichi Onodera[1], Mitsuyo Saito[3], Noboru Okuda[4], Takuya Okubo[5]

1. Graduate School of Integrated Arts and Science, Hiroshima University, 2. Capital Normal University, 3. Okayama University, 4. Research Institute for Humanity and Nature, 5. University of the Shiga Prefecture

The quantification of the groundwater recharge and phosphorus transport in water is one of the most important indicators of the water cycle in lakes because these processes are related to the transport of large nutrient loads. The Yasu River is one of the important water sources of the Biwa Lake. In this paper, Geographic Information System technology is used to analyze and predict the land use change in the Yasu River Basin. The water balance was simulated using the Soil and Water Assessment Tool. Simulations of different years in different precipitation seasons were carried out. The correlation coefficient and the Nash Sutcliffe coefficient are higher than the reference values. The sensitivity analysis of the parameters reveals the different degrees of sensitivity of the parameters in different water seasons, CN2 always has a high sensitivity during all kinds of water season. The total groundwater recharge and discharge are 180 million $m^3$ and 179 million $m^3$ in the normal precipitation season, respectively. The trends differ in the dry and wet seasons. In the dry season of 2007, the groundwater recharge was below 140 million $m^3$, while it exceeded 240 million $m^3$ in the rainy season in 2003. In addition, the process of phosphorus loss in the basin and release into Lake Biwa are explained from the perspective of space and time. This is closely related to the spatial distribution of the main channel and the time distribution of precipitation. The total amount of nonpoint source pollution of phosphorus in three years is equivalent to 4.08 kg/ha of paddy fields in the watershed. The spatial distribution of phosphorus loss is related to the stream flow, it is mainly concentrated in the area with paddy fields and urban. The time distribution is related to the distribution of the precipitation. With increasing precipitation, the nonpoint source pollution of phosphorus slightly increases. This is due to the driving effect of precipitation on the phosphorus transfer and erosion of soil.

Keywords: Phosphorus transport, Groundwater recharge, Different precipitation conditions, SWAT model

©2019. Japan Geoscience Union. All Right Reserved. 

# Losses of phosphorus with soil erosion and nitrate with groundwater recharge in an agricultural catchment, subtropical small island

*Shin-ichi Onodera[1], Mitsuyo Saito[2], Yang Cao[1], Anna Fadliah Rusydi[1], Hide Omae[3], Yoshiko Iizumi[4], Yusuke Tomozawa[1]

1. Graduate School of Integrated and Arts Sciences, Hiroshima University, 2. Graduate School of Environmental and Life Science, Okayama University, 3. JIRCAS TARF, 4. JIRCAS HQ

In tropical and subtropical region, the rainfall intensity is strong and soil erosion in an agricultural land is one of big environmental issues. Especially, the impact of large sediment discharge on the coral reef is serious around small islands, such as Okinawa and Philippines. In case of Okinawa Prefecture, to reduce the sediment discharge and conserve corals, many sediment trap ponds are constructed in a downstream area of agricultural lands. However, sediment deposition rate, variation of trap effect, and component of sediment in a pond have not been confirmed.

To estimate of erosion rate and deposition process of a small pond in an agricultural catchment of a subtropical small island, we examine to observe the sediment deposition in a small pond and monitor water level and chlorophyll a in a pond and runoff and turbidity of an inflow stream in a small catchment with the area of 300m2 in Ishigaki Island, Okinawa Prefecture, Subtropical region. Our monitoring was started from February 2017 after removing all sediment in a pond in January, and up to April 2018. Observation of sediment deposition was conducted with collecting the samples at 5 sites in June 2017 and January 2018. Inflow and outflow water samples were collected every one month.
The sediment deposition was extremely large from January to May 2017, the average erosion rate in all catchment area was estimated to be 6mm. On the other hand, the sediment deposition was nothing from June 2017 to January 2018. Based on the monitoring of stream runoff and turbidity, one big storm event in April with strong intensity mainly contributes to sediment discharge and overflow of the pond occurred. On the other hand, the later period had also big events. This difference is suggested to be the difference of land cover by crops and availability of sediment trap in this pond. In addition, the sediment component mainly was composed of surface soft layer, subsurface sandy layer, and bottom gravel layer. The average thickness was 2cm in surface layer, 100cm in mid sandy layer, and 10cm in gravel layer, respectively. Especially, the surface soft layer had high nutrient content. The dissolved nutrient of inflow stream water and pond water were high concentration. But the 10% of nutrient in the inflow decreased in pond. This means the plankton was produced, using this nutrient and that was deposited later. The soft layer is suggested to be effect of organic fertilizer, it is expected to apply to agricultural lands.

Keywords: Phosphorus, groundwater, nitrate

©2019. Japan Geoscience Union. All Right Reserved. 

# Phosphate solubilizing bacteria as an indicator of sediment phosphorus in freshwater lakes

*Sreekumari Kurissery[1], Katelynn Crawford[1], Nandakumar Kanavillil[1]

1. Lakehead University, Canada

It has been well documented that phosphorus pollution is one of the most significant factors impeding the overall health of freshwater lakes. Various measures are being taken to reduce phosphorus input into the lakes by anthropogenic activities and thus to maintain a healthy ecosystem. However, it is well known that bioavailable phosphorus tends to bind with substances such as ferric iron and calcium present in the water, become insoluble, and settles into the sediments. The presentstudy has been carried out to understand the relationship between the sediment phosphorus concentration and density of phosphate solubilizing bacteria (PSB) in two lakes in Ontario, Canada, namely, Lake Simcoe and Sparrow Lake. In September 2017, 20cm sediment cores were collected from the nearshore sites of these two lakes to determine the presence of PSB in relation to the sediment phosphorus concentration. PSB could potentially release phosphorus back into the water column through a process called internal phosphorus loading from the inorganic phosphates in the sediment when the right conditions are present. PSB were isolated from the sediment cores at 5 cm intervals by plating on to Pikovskaya’ s agar. Five grams of sediment was used to analyze total reactive phosphorus in the sediment. In Lake Simcoe, PSB ranged from $3x10^1$ to $1.1x10^1$ cfu/g, and the amount of total reactive phosphorus ranged from 0.19 to 0.46 mg/g. In Sparrow Lake, PSB ranged from $4x10^0$ to $3x10^1$ cfu/g and the amount of total reactive phosphorus ranged from 0.21 to 0.39 mg/g. A linear regression was completed to determine the relationship between total reactive phosphorus and PSB for each core. The results showed a negative relationship between these two tested parameters (Lake Simcoe: $r^2$=0.23, $y = -35.34x + 30.811$ $p$=0.5206, and Sparrow Lake: $r^2$ =0.87, $y = -155.9x + 62.322$, $p$=0.067). While PSB density decreased with core depth, the concentration of reactive phosphorus increased. This indicates that the density of PSB in lake sediment may indicate the concentration of total reactive phosphorus and thus the internal phosphorus loading. More study is recommended to confirm the results.

Keywords: Phosphate Solubilizing Bacteria, Freshwater Lakes , Sediment Phosphorus , Canada

©2019. Japan Geoscience Union. All Right Reserved. 

# A Study on the dynamics of various phosphate forms in soil and groundwater in Ryukyu limestone regions

*Masashi Nozaki[1], Jun Yasumoto[2], Yasumoto Ko[3], Hirose Mina[4], Iijima Mariko[3], Ryuichi Shinjo[5], Bam H.N. Razafindrabe[6]

1. University of The Ryukyus, Graduate School of Agriculture,, 2. University of the Ryukyus, Faculty of Agriculture, Department of Regional Agricultural Engineering, 3. Kitasato University School of Marine Biosciences, 4. Tropical Technology Plus, 5. Department of Physics and Earth Sciences, University of the Ryukyus, 6. University of the Ryukyus, Faculty of Agriculture, Department of Subtropical Agro-Environmental Sciences

Phosphorus in water environment exists in various forms and size, such as dissolved, particulate, organic and inorganic forms. However, there are many unclear points in Phosphorus in groundwater. In this study, we tried to understand the dynamics of various phosphate forms in soil and groundwater in Ryukyu limestone regions by combining Inductively Coupled Plasma Atomic Emission Spectrometry (ICP-AES) and $^{31}$P Nuclear Magnetic Resonance ($^{31}$P-NMR), in addition to Colorimetric (molybdenum blue method). From August 2017 to August 2018, we took groundwater samples in southern part of Okinawa, Japan, with Ryukyu limestone distribution on a monthly basis. We measured pH, electronic conductivity (EC), Oxidation-Reduction Potential (ORP), dissolved oxygen (DO) and alkalinity ($HCO_3^-$) on site, and analyzed major dissolved ion ($Cl^-$, $HCO_3^-$, $NO_2^-$, $NO_3^-$, $SO_4^{2-}$, $Na^+$, $K^+$, $Mg^{2+}$, $Ca^{2+}$), suspended solid (SS) and phosphorus concentration. Phosphorus concentration analyzed 3 different method to molybdenum blue method (Col-P), ICP-AES (ICP-P) and Total P (T-P). Phosphate form analysis used $^{31}$P-NMR.
We compared Col-P and ICP-P in order to understand dissolved phosphorus spatial distribution. The results show that ICP-P is 1.06~49.24 times larger than Col-P. It is inferred that ICP-P is also measuring fine particulate phosphorus and organic phosphorus. As a result, several forms of phosphate without orthophosphate were found in groundwater. Particulate phosphorus was determined by subtracting ICP-P from T-P. A positive correlation (r= 0.78) was found between P-P and SS. According to these results, it is thought that PP adsorbs various forms of phosphate including orthophosphate. We analyzed the correlation between dissolved phosphorus (Col-P, ICP-P) and all measured value in order to understand the characteristics of seasonal variation to dissolved phosphorus. There was a negative correlation between Col-P to water temperature. When focusing on seasonal variation of Col-P, we found that Col-P concentration decreases when water temperature increases. Moreover, Col-P concentration increases as water temperature increases. Through the analysis of various forms of phosphate in soil and SS by using $^{31}$P-NMR, along with orthophosphate, pyrophosphate, pyrophosphate ester, orthophosphate monoester were also detected. It is thus suggested that the phosphate of polymeric or organic forms other than orthophosphate are from plant origin, as a result of microbial activities and microorganism decomposition.

Keywords: Phosphorus, 31P-NMR, Groundwater

©2019. Japan Geoscience Union. All Right Reserved. 

# Impacts of highly concentrated turbid water on the groundwater in the Tedori River alluvial fan, Japan

*Yoichi Fujihara[1], Shunsuke Chono[1], Keiji Takase[1], Eiji Ichion[1]

1. Department of Environmental Science, Ishikawa Prefectural University

The Tedori River alluvial fan in the Ishikawa prefecture is a representative alluvial fan in the Hokuriku region in Japan. The river water is taken by a headworks located at the top of the alluvial fan and is used for irrigation in paddy fields with a total area of about 7,500 ha. Seepages from the riverbed and percolations from the paddy area are the main sources of groundwater in the Tedori River alluvial fan. In 2015, large-scale landslides in the upper reaches of the Tedori River caused a long period of high turbidity in the river. Highly concentrated turbid water with an average concentration of 585 mg/L (a maximum of 4,012 mg/L) has been discharged continuously into the river since May, 2015. This turbidity has caused concerns about the recharge functions of groundwater in the alluvial fan.

In this study, the measurements of paddy percolations and riverbed seepages, before and after the occurrence of high turbidity, were used to examine the influence of these phenomena on groundwater recharge functions in the alluvial fan. We measured water requirement rates in the paddy area in the Tedori River alluvial fan. The measurements were conducted before and after the midsummer-drainage period at >100 paddy fields. We also measured the river discharges in the cross-sections of the river throughout the alluvial fan. The number of cross-sections was 16 and we estimated the riverbed seepages by calculating the discharge differences between the cross-sections.

The results revealed that the amount of paddy percolation decreased significantly due to the turbidity of the river water. The average percolation in the paddy area was found to be 12.4 mm/day in 2014 and 7.9 mm/day in 2016 before the midsummer-drainage period. Moreover, the average percolation in the paddy was found to be 19.6 mm/day in 2014 and 13.7 mm/day in 2016 after the midsummer-drainage period. The volume of the riverbed seepage was observed to have reduced and the seepage section were also observed to have shortened. The observed seepages from the river bed were 4.72 m3/s in 2009 and 3.33 m3/s in 2016 for the irrigation period, whereas for the non-irrigation period, these values were 5.92 m3/s in 2009 and 1.25 m3/s in 2016. Furthermore, the seepage section was found to shorten from 14.2 km to 8.0 km, due to the high turbidity of the water.

Finally, we estimated the amount of groundwater recharge based on these measurements, which revealed that the groundwater recharge from paddy percolation decreased by 270 mm/year (36%), and the recharge from riverbed decreased by 591 mm/year (61%). The total groundwater recharge decreased by 861 mm/year (36%), a value that corresponded to the groundwater level measurements. From these results, we can conclude that the effects of highly concentrated turbid water on the groundwater are quite serious in the Tedori River alluvial fan.

Keywords: groundwater, paddy percolation, riverbed seepage

©2019. Japan Geoscience Union. All Right Reserved. 

# Altitude effect of water stable isotopic ratio of ravine water and its contribution to groundwater in alluvial plains - Comparison in east and west side catchments of Lake Biwa –

*Yusuke Tomozawa[1], Kunyang Wang[1], Mitsuyo Saito[2], Syuhei Ban[3], Noboru Okuda[4], Shin-ichi Onodera[1]

1. Graduate School of Integrated Arts and Sciences Hiroshima University, 2. Graduate School of Environmental and Life Science, Okayama University, 3. School of Environmental Science, The University of Shiga Prefecture, 4. Research Institute for Humanity and Nature

The stable isotope ratio of hydrogen and oxygen in water is one of useful tracers for hydrological cycle and processes in the catchment scale as well as global. The typical characteristics are spatial or geographical distribution trend such as “altitude effect” or “inland effect”, which are lower in the higher altitude or more inland. Based on these trend, the groundwater recharge area had been estimated. However, the merger of these effects and additional effect such as the seasonal variation of isotopic ratio in precipitation or vapor causes various trend.
In this study, we examined to confirm the altitude effect of water stable isotope ratio and estimate recharge altitude to groundwater in alluvial plains, with comparing in the east and west side catchments of Lake Biwa .
Sampling of spring water in the Serikawa upstream area on the east side of Lake Biwa was conducted in July 2017, December 2017, August 2018. Sampling of ravine water in the Adogawa / Ukawa upstream area on the west side of Lake Biwa was conducted in August 2018. Water samples of spring in the head water and groundwater in the alluvial plain were collected at 11 and 2 sites in the east and at 13 and 2 in the west with measuring EC, pH and DO, respectively. The water stable isotopic ratios were analyzed by PICARO.
Stable isotopic ratios in groundwater were lower than surface water in both east and west. Altitude effects of spring water in the head water were recognizable. This means the surface water in the alluvial plain was mainly contributed from Lake Biwa, whereas groundwater was from the head water. The altitude effect of oxygen stable isotopic ratio was 0.15 - 0.13 ‰/ 100 m on the east side and 0.15 ‰/ 100 m on the west side (only in the upper stream of the Ado River). In addition, the d value of isotopic ratio in the precipitation was 23‰ in the upper Adokawa in August 2018, 18 ‰in Ugawa, and 20 ‰in Serikawa.
We also estimated groundwater recharge elevation and water contribution rate in the upstream region based on these.

Keywords: stable isotope, altitude effect, groundwater recharge

©2019. Japan Geoscience Union. All Right Reserved. 

# Calculation of TN and TP concentration coefficients of river water for each land use by a simple watershed model.

*Seiko Yoshikawa[1], Donglai Ma[1,4], Tadamasa Saito[1,5], Kenji Matsumori[2], Yuko Itoh[3], Masahiro Kobayashi[3]

1. Institute for Agro-environmental Sciences, National Agriculture and Food Research Organization, 2. Western Region Agricultural Research Center, National Agriculture and Food Research Organization, 3. Forestry and Forest Products Research Institute, 4. Graduate school,Tsukuba University, 5. Faculty of Agriculture, Ibaraki University

Water quality deterioration of rivers caused by leakage of fertilizer components such as nitrogen and phosphorus from paddy and upland fields is a environmental problem. Also, runoff of fertilizer components are expected to increase with the accelerated water and sediment runoff by intensification and localization of rainfall caused by climate change. Although it is difficult to predict the place and extent of heavy-rainfall-related disasters, we firstly grasp the average concentrations of nitrogen and phosphorus and predict increase and decrease in those concentrations when the way of rain changes. Nitrogen and phosphorus runoff is depend on land use and land cover, conservative measures, topography, climate condition mainly rainfall etc.. Among them, the land use and land cover is expected to be a main factor in normal climate conditions. In order to contribute to the prediction of heavy-rain related disasters in the future, coefficients that indicate the total nitrogen (TN) and total phosphorus (TP) load intensity to rivers of each land use for the river watersheds across the country are calculated using a simple watershed land use model. Watersheds whose lower ends are observation points of water quality, and whose land use ratios were determined by GIS technique using published database of DEM (GSI, 10B) and LULC mesh data (JAXA , ALOS AVNIR-2). The TN and TP concentration coefficients of paddy, upland, forest, and urban were calculated by applying the below multiple regression equation using the land use ratios and published TN and TP data( Ministry of Environment).

$c = a_1 x_1 + a_2 x_2 + a_3 x_3 + a_4 x_4$

*C:* TN or TP concentration (mg $L^{-1}$) $a_i$ : TN or TP concentration coefficient for land use *I,* $x_i$ : ratio of land use *I,* Land use: 1;paddy, 2;upland fields, 3;forest, 4;urban

TN concentration coefficient across Japan is 1.67 (from lower limit 95% value 1.34 to upper limit 95% value 2.01), 4.08 (from 3.64 to 4.51), 0.76 (from 0.67 to 0.90), 3.57 (from 3.38 to 3.76) for paddy fields, upland fields, forests and urban areas respectively (n=3256). The TP concentration coefficient is 0.146 (lower limit 95% value 0.119 to upper limit 95% value 0.172), 0.172 (0.138 to 0.206), 0.044 (0.033 to 0.055), 0.267 (0.253 to 0.282) for paddy fields, upland fields, forests and urban areas respectively (n=3256,). Prefectural TN and TP concentration coefficients for paddy and upland fields related only loosely to prefectural surplus N and surplus P. On the other hand, prefectural TN and TP concentration coefficients for forests and urban related to prefectural population densities by logarithmic functions with determination coefficients $R^2$ from 0.45 to 0.48.

Keywords: watershed land-use model, TN, TP, concentration coefficient

©2019. Japan Geoscience Union. All Right Reserved. 

# Possibility of nutrients transportation from littoral slope for enhancement of phytoplankton growth in north basin of Lake Biwa

*Syuhei Ban[1], Rong YI[1], Xin Liu[1], Masahiro Maruo[1], Miki Sudo[1], Naoshige Goto[1], Jun Murase[2]

1. The University of Shiga Prefecture, 2. Nagoya University

Nutrient loading from non-point source in a lake ecosystem has not been well recognized yet. In Lake Biwa, total phosphorus (TP) does not decline to the level before eutrophication period, 1960s to 1970s, despite of decreasing the loading from point sources surrounding the lake after that. One of the reasons for no well lowering TP in the lake is attributed to agricultural runoff, in which suspended materials including phosphorus would be deposited to the littoral bottom. In our previous study, subsurface maximum of ammonium as a proxy of dissolved materials from anaerobic interstitial waters in the littoral bottom sediments was found along a transect from littoral to pelagic regions, implying horizontal transportation of nutrients from littoral sediments. There were no such evidences of soluble reactive phosphorus (SRP) yet due to always below the detection limit in the pelagic waters. Recently, we developed modified protocol using an ion chromatography for measuring orthophosphate concentration at nano-molar levels. In this presentation, we’ d like to provide several evidences for horizontal transportation of dissolved nutrients including orthophosphate along a transect from littoral to pelagic sites in north basin of Lake Biwa.

Total of the 6 times transect surveys for determining vertical profiles of nutrients, methane and herbicides were made in 2010-2011. Additional two transect surveys for determining those of nutrients including orthophosphate were made in 16 May and 25 July of 2018. During the 2010-2011 campaigns, *in situ* phytoplankton primary production was measured during the stagnation period using light intensity and chlorophyll *a*concentration monitored by sensors attached to a mooring buoy situated at an offshore station in north basin of Lake Biwa and an equation of photosynthesis - light intensity (P-I) curve.

In 2010-2011 campaigns, we detected sub-surface maximum layer, 20-30 m, of ammonium and methane as a proxy of dissolved materials transported from interstitial water in the sediment of littoral slope. Herbicides, which were used in rice paddy during the rice planting and proxy of materials transported from terrestrial environments surrounding the lake, were also detected in 20-30 m even at the offshore regions in the lake. Primary production monitoring suggested that phytoplankton production depended on some environmental variables other than solar irradiance, e.g. nutrients, until summer months. These results suggested that nutrients for enhancing algal growth might be horizontally transported from sediment in the littoral slope, and that the source of the nutrients might be provided from the drainage of rice paddy.

In 2018 campaigns, sub-surface maximum of ammonium was clearly found along a transect from littoral to pelagic sites in both May and July, but no such sub-surface maximum of orthophosphate was found. Several reasons for failure to find sub-surface maximum of orthophosphate might be proposed. Phosphate would be used by both phytoplankton and bacteria, while ammonium would be used by phytoplankton alone in the euphotic layer. In phosphate limited environment, such as pelagic areas in north basin of Lake Biwa, sub-surface maximum could not be easily detected due to rapid absorption by both phytoplankton and bacteria. Or, a transportation of nutrients from the littoral sloop would sporadically occur, and then we simply missed to detect it. This is on-going research project, and then further studies will be conducted to clarify this issue.

©2019. Japan Geoscience Union. All Right Reserved. 

Keywords: Horizontal nutrient transportation, non-point source loading, agricultural runoff, Lake Biwa

©2019. Japan Geoscience Union. All Right Reserved. 

# SWAT model analysis for confirming the effects of crop growth on the suspended sediment concentration from a settling basin catchment on Ishigaki island

*Yang Cao[1], Shin-ichi Onodera[1], Mitsuyo Saito[2], Hide Omae[3], Yoshiko Iizumi[3]

1. Graduate School of Integrate Arts and Sciences, Hiroshima University, 2. Graduate School of Environmental and life Science, Okayama University, 3. Tropical Agriculture Research Front (TARF), Japan International Research Center for Agricultural Sciences (JIRCAS)

Crop growth has a significant effect on soil erosion in small watersheds. Exploring the characteristics and occurrences of soil erosion in small watersheds assists in our understanding of the water and material cycles in agricultural areas. The small catchment on the tropical island of Ishigaki, Japan, was chosen as the research area. The effects of sugarcane growth at different stages on the suspended sediment concentration in the basin from January 2017 to July 2018 were analyzed based on the Soil and Water Assessment Tool (SWAT) model. This study will explore the possible driving factors of these phenomena. The results show that the suspended sediment concentration in the basin reached its highest value on a rainy day near the sugarcane planting period because of the soil relaxation caused by tillage and cultivation. At the end of the sugarcane growth period, the sediment concentration was not at a high level when the rainfall reached 150 mm, because of the effective protection of the soil by sugarcane. The simulated sediment concentration of precipitation per mm showed that the simulated sediment concentration was at its highest during the crop planting period, followed by the period of bare land, and at the lowest during the crop growth period.

Keywords: SWAT model, Small catchment, Sugarcane, Sediment, Ishigaki

©2019. Japan Geoscience Union. All Right Reserved. 

# Estimating the runoff of water, sediment, and nutrient using SWAT model in Kikuchi-river watershed, Kumamoto, and the influence of the forest

*Soichiro Fujii[1], Masahiko Kanamori[1], Yuko Nagano[1], Maki Kinoshita[2], Yuta Shimizu[3], Shin-ichi Onodera[4]

1. Japan Forest Technology Association, 2. PASCO Corporation, 3. Western Region Agricultural Research Center, National Agriculture and Food Research Organization, 4. Graduate School of Integrated and Arts Sciences, Hiroshima University

Recently, enclosed sea area such as Ariake-sea have severe nutrient enrichment problem and is decreasing the produce of fishery industry. Such enclosed sea area is commonly affected by river water quality discharged from the land area. Therefore, estimating the load of sediment and nutrient from its land area is important. However, most of researches estimating discharge from land area is conducted by simple method using primary load factor. These method only can provide the estimates in annual scale regardless of the land use. On the other hand, the positive effect of forest to water quality in the river, so-called green dam, is paid attention recently, and supposed to play important roll on improvement to sea environment. However, the effect of forest to water quality is not explained enough, and few research has conducted in watershed scale. In this study, we aim to simulate water, sediment, and nutrient runoff in order to provide more detail information about discharge from land area, and to estimate the influence of the forest to water quality. We use Soil and Water Assessment Tool (SWAT) and chose Kikuchi-river as a model watershed, which has the third largest watershed area among the rivers drain into Ariake-sea.

We set Komoda observatory as the most downstream point of Kikuchi-river and the model watershed is the upstream side from there. More than half of this watershed is covered by forest. We collected land use data, soil data, climate data and 30m mesh digital elevation model (DEM) data of this watershed in order to establish the model. In order to calibrate and validate the model performance, observed data of daily stream flow from 2008 to 2016, and sampling data of sediment and nutrient were collected. Moreover, we measured the amount of sediment, phosphorus and nitrogen during flood situation in 2016 and 2017. The parameters in the model were modified according to the result of calibration, and the performance of the model was evaluated from three indices such as Nash-Sutcliffe index.

The model performance was evaluated as more than satisfactory for all materials: water, sediment, phosphorus and nitrogen. Therefore, this model can simulate daily runoff from 2008 to 2017. The runoff rate of sediment and most of nutrient from forest was less than 30% of the annual average in whole watershed, although water discharge was the same level to the rate of forest area, which indicates the function of forest to provide low concentrate water of sediment and nutrient to the river. In conclusion, modelling the runoff from land area using SWAT model has potential to provide detail information about land area discharge and estimate the influence of forest to river water quality.

Keywords: SWAT model, Runoff estimation

©2019. Japan Geoscience Union. All Right Reserved. 

# Atmospheric depositions on forest ecosystems in areas along the Sea of Japan

*Yuko Itoh[1], Keiji Takase[2], Yoichi Fujihara[2], Toru Okamoto[1]

1. Forestry and Forest Products Research Institute, Japan, 2. Ishikawa Prefectural University

In recent years, concerns about the effects of excess-nitrogen usage by human activities on terrestrial environment, including forest ecosystems, have been increasing at a global scale. The phenomenon of high-nitrate efflux from several forest watersheds has already been reported in the surroundings of metropolitan areas in Japan. Furthermore, concerns regarding the effects of transboundary air pollution on areas along the Sea of Japan with expanding economic activities have been increasing in Asian countries. However, on-site monitoring throughout the year is difficult in most of these areas because of heavy snow, especially in the mountainous area. Therefore, the behaviors of elements within forest ecosystems throughout a year have primarily not yet been elucidated in this district. This study was conducted to determine the influxes and effluxes of elements in this heavy snowy region and to understand the contribution of transboundary air pollution to the quantity of atmospheric deposition. We also carried out rainfall and stream water investigations from the headwater area to the lower stream area in the Tedori River Basin and an inland mountainous area to understand the geographical distribution of the actual conditions of elements' influxes and effluxes in this region. We started monitoring the major and minor elements in a small forested watershed in the middle part of the Tedori River Basin, Ishikawa prefecture, Japan, in 2013. In this study site, we observed a large amount of precipitation throughout the year. Regarding the annual snowfall amount, there were extensive variations among the years. Seasonal fluctuations were observed in the influx of atmospheric deposition; in particular, the distribution of most of the elements increased during winter. The annual deposition average of inorganic nitrogen ($NH_4$-N + $NO_3$-N) in this site was 15.8 kg $ha^{-1}$. The contribution of winter season deposition to the annual inputs was high. The influx of nitrogen by bulk precipitation during winter season was 2.3 times that of summer, and that of sulfur sulfate was 3.7 times. The nitrogen influx quantity was similar to or more than that reported in nitrogen-saturated forested areas of the Kanto district. Therefore, similar to that in the Kanto district, higher nitrogen deposition loads from the atmosphere could also be influenced on the effect of nitrogen dynamics and the increase in nitrogen efflux at these forest watersheds. However, the efflux concentrations of most of the dissolved elements in stream water did not show clear seasonal fluctuations. Stream water nitrate concentration was stable and low. In addition to the seasonal fluctuation of nitrogen and sulfur, the ratios among some trace elements, which are anthropogenic substances (Pb, V, As, etc.), and sea salts and yellow sand could be useful indicators to elucidate the contribution of transboundary air pollution to these regions. We compared the element inputs associated with precipitation during the non-snowy season (July–November) at six locations in the Tedori River Basin and one location in the inland area. The inorganic nitrogen and sulfuric acid sulfur influxes were the largest at the middle reaches of the Tedori River Basin. The inflow amount of inorganic nitrogen and sulfuric acid sulfur at two points in the mountainous area was approximately half or less than that at the middle region and was approximately the same as the inflow amount at the inland mountainous area. Furthermore, we investigated stream water, spring water, and ground water samples from the headwater area to the lower stream area in the Tedori River Basin. The nitrate concentrations in all the samples ranged from 0.00 to 2.93 $mgL^{-1}$ (median value: 0.69 $mgL^{-1}$). In contrast, the nitrate concentrations of stream water in the Tsukuba experimental forest watershed, which has been reported as a nitrogen-saturated forested area of the Kanto district, were much higher (average value: 7.56 $mgL^{-1}$) than those in the Tedori River Basin. Compared with the influx, the efflux concentrations of nitrate in the water

©2019. Japan Geoscience Union. All Right Reserved. 

samples were generally very low around this basin. Therefore, higher nitrogen depositions have not yet distinctly influenced the nitrate concentrations of stream water in this area. To elucidate the influence of transboundary air pollutant influx on the entire Tedori River Basin, it is necessary to evaluate the inflow amount during the snowy season in the mountainous area. Therefore, it is important to establish a method that can be used to observe the influx and efflux of elements throughout the year even in mountainous areas with heavy snow.

©2019. Japan Geoscience Union. All Right Reserved. 

# Continuous and simultaneous flux measurement of $N_2O$ and $CO_2$ from agricultural soil using a portable multi-turn time-of-flight mass spectrometer

*Noriko Nakayama[1], Yusuke Iwai[1], Yo Toma[2], Hiroshi Furutani[1], Ryusuke Hatano[3], Michisato Toyoda[1]

1. Osaka University, 2. Ehime University, 3. Hokkaido University

Agricultural soil is one of the important sources/sinks of greenhouse gases such as $N_2O$, $CO_2$, and $CH_4$. The formation and consumption of such greenhouse gases in agricultural soils are dependent on not only the chemical and biological properties of the soil, but also their variations. Hence continuous monitoring of such greenhouse gases as tracer gases are quite useful to track chemical and biological processes and variations of soil properties.

In this paper, we describe a new field-deployable gas flux measurement system for the continuous monitoring of multiple agricultural soil gases ($N_2O$, $CO_2$, and $CH_4$) using a high resolution multi-turn time-of-flight mass spectrometer (MULTUM) combined with an automated flux chamber system. The new system measured the soil gases every 2.5 min with the precisions of ~6% for $N_2O$, $CH_4$, and 2% or better for $CO_2$ and $O_2$ at atmospheric concentrations with one relative standard deviation (RSD) for n = 10.

To demonstrate the utility of the continuous multi-gas flux measurement system, we conducted a field study at the Ehime University farm (Ehime, Japan) from September 3$^{rd}$ to 8$^{th}$, 2018. In the field study, an automated flux chamber was placed in the agricultural field and the soil gas concentrations in the chamber were continuously monitored by the MULTUM system. Soil temperature/moisture sensor were also monitored at the depth of 7.5 cm underground in addition to a weather information (wind speed, precipitation, solar radiation). The continuous measurement had been continued with operators almost unattended except for a daily system check.

For one flux measurement (20 min), eight gas samples were taken every 2.5 min with the flux chamber closed. Gas flux of $N_2O$ and $CO_2$ had been carried out by applying linear regression to the eight gas measurements. We found that a significant correlation of $N_2O$ flux with soil electrical conductivity and water content, although no significant correlation of $CO_2$ flux to soil electrical conductivity was observed. Significant and rapid decreases in $N_2O$ and $CO_2$ flux during rainfall events were also observed. Our preliminary result shows that high time-resolution flux data obtained by MULTUM system is quite useful for tracking the variation in soil properties and biological processes and their activity in soil environment.

Keywords: on-site mass spectorometry, MULTUM, soil-to-atmospher gas flux

©2019. Japan Geoscience Union. All Right Reserved. 

# Effects of introduction of cyclic irrigation system on mass balances of SS and T-P in Lake Inbanuma, Chiba, Japan

*Tomijiro Kubota[1]

1. National Agriculture and Food Research Organization, Institute for Rural Engineering

## Introduction

The introduction of cyclic irrigation has been advanced since 2010 in the Lake Inbanuma as part of the update project of the irrigation facilities. In the present study, mass balances of SS and T-P were examined before and after the introduction of the cyclic irrigation.

## Materials and methods

The irrigation block where the cyclic irrigation began in 2015 was selected as the investigation site, and the investigation was executed to the irrigation period in 2014 and 2015. The hydrological and water quality investigation was executed at ① division works of irrigation canal and ② drainage pumping station. Water samples were taken at the two points and the TOC, SS, TN, NO3-N, NO2-N, NH4-N, TP, and PO4-P were analyzed in the regular investigation executed about once a month. Besides regular investigation, water samples were taken once a day (8:00AM or noon) by the automatic water sampler and SS and T-P were analysed. The turbidity and water level were measured every ten minutes by using data loggers at same sites. The turbidity data were converted into the concentration of SS and TP by using the regression curve. The quantity of water intaken from the lake and drainage to the lake were obtained from the records of the facility manager.

## Result and discussion

The inflow and outflow loads and the balance were calculated before and after the introduction of the cyclic irrigation. In 2014, before the start of cyclic irrigation, both the outflow loads of SS and T-P were small to compare with those inflow loads. The amount of accumulation of SS and T-P were about 1.3t and 2kg respectively when having no rainfall in the irrigation block. On the other hand, the outflow of SS and T-P were about 3.5t/day and 20kg/day respectively in rainy days. If 2015 year is compared to 2014, it had increased in T-P though the load of irrigation water each day at no rainfall periods and it had not been change in SS though an accurate comparison is difficult according to the missing value. However, after the cyclic irrigation had been started, the amount of the outflow loads had decreased greatly like 35% in SS and 38% in T-P. The balance of the outflow loads during the irrigation periods of 2014 were -470kg/day in SS, which meant the purification type, while +2.6kg/day in T-P. as a result, it was found that the introduction of cyclic irrigation system had worked for water purification in SS and T-P effectively.

Keywords: cyclic irrigation system, water pollution, suspended solid, total phosphorus

©2019. Japan Geoscience Union. All Right Reserved. 

[E] Oral | A (Atmospheric and Hydrospheric Sciences)：A-GE Geological & Soil Environment

Thu. May 30, 2019 9:00 AM - 10:30 AM JST | Thu. May 30, 2019 12:00 AM - 1:30 AM UTC | 301A 3F

## [A-GE28] Subsurface Mass Transport, Material Cycle, and Environmental Assessment

convener:Yuki Kojima(Department of Civil Engineering, Gifu University), Shoichiro Hamamoto(Department of Biological and Environmental Engineering, The University of Tokyo), Hirotaka Saito(Department of Ecoregion Science, Tokyo University of Agriculture and Technology), Yasushi Mori(Graduate School of Environmental and Life Science, Okayama University), Chairperson:Yuki Kojima(Gifu University), Shoichiro Hamamoto(The University of Tokyo), Yasushi Mori(Okayama University), Hirotaka Saito(Tokyo University of Agriculture and Technology)

This session covers the topics on mass transport, water and energy cycles in geoenvironment. Subjects related to laboratory and field measurements, theoretical analysis, and numerical modeling will be discussed. Presentations on geo-pollution, remediation, geological disposal of hazardous wastes, ground source heat utilization, mass transport in vadose zone, soil-water monitoring, and environmental assessment are encouraged.

9:00 AM - 9:25 AM JST | 12:00 AM - 12:25 AM UTC

[AGE28-01] **Humic substances in deep sedimentary groundwater**

★Invited Papers

*Takumi Saito[1] (1.School of Engineering, The University of Tokyo)

---

9:25 AM - 9:40 AM JST | 12:25 AM - 12:40 AM UTC

[AGE28-02] Nano-Bubble Retention in Saturated Porous Media under Different Solution Chemistry

*Shoichiro Hamamoto[1], Takuya Sugimoto[1], Takato Takemura[2], Taku Nishimura[1], Scott A Bradford[3] (1.Department of Biological and Environmental Engineering, The University of Tokyo, 2.College of Humanities and Sciences, Nihon University, 3.U. S. Salinity Laboratory)

---

9:40 AM - 9:55 AM JST | 12:40 AM - 12:55 AM UTC

[AGE28-03] **Geochemical Investigation of Metals and Trace Elements around the Abandoned Cu – Ni Mine Site in Selibe Phikwe, Botswana**

*Fiona Segolame Motswaiso[1], Kengo - Nakamura[1], Noriaki - Watanabe[1], Takeshi - Komai[1] (1.Tohoku Univeristy Graduate School of Environmental Studies)

---

9:55 AM - 10:10 AM JST | 12:55 AM - 1:10 AM UTC

[AGE28-04] Removal of Arsenic (III) From Aqueous Solution Using Pumice and Zeolite Supported Zero-Valent Iron Nanoparticle

*Shashi Ranjan[1], Brijesh kumar yadav[1], Himanshu Joshi[1] (1.Indian Institute of Technology Roorkee)

---

10:10 AM - 10:25 AM JST | 1:10 AM - 1:25 AM UTC

[AGE28-05] **Unsaturated Hydraulic Conductivity Estimation from Multi-step Centrifuge Outflow**

*Thanh Long Bui[1], Yasushi Mori[1] (1.Graduate School of Environmental and Life Science, Okayama University)

---

10:25 AM - 10:30 AM JST | 1:25 AM - 1:30 AM UTC

Discussion

# Humic substances in deep sedimentary groundwater

*Takumi Saito[1]

1. School of Engineering, The University of Tokyo

Humic substances (HSs) are ubiquitous in various environments and play important roles for the fate of nutrients and pollutants. Deep underground environment is not an exception, although the properties of HSs there are largely unknown due to their limited availability. Recently, we reported the physicochemical and ion-binding properties of HSs extracted from sedimentary groundwater at -250 m below ground surface of the Horonobe underground research center operated by the Japan Atomic Energy Agency. The Horonobe HSs (HHSs) consist of relatively small organic molecules rich in aliphatic carbon and reduced sulfur. The densities of acidic functional groups such as carboxylic groups are relatively high for HHSs, and they are chemically homogenous. Nevertheless, the binding of $Cu^{2+}$ to HHSs are smaller than that to surface HSs, suggesting the presence of different coordination environments for $Cu^{2+}$ in HHSs. Cadmium, a thiophilic metal, tends to form CdS(s) nano-particles with HHSs likely due to the high concentrations of reduced sulfur. In this talk, the particularity of the HHSs will be discussed, comparing their properties with those of their counterparts in surface environments.

Keywords: Humic substance, Groundwater

©2019. Japan Geoscience Union. All Right Reserved. 

# Nano-Bubble Retention in Saturated Porous Media under Different Solution Chemistry

*Shoichiro Hamamoto[1], Takuya Sugimoto[1], Takato Takemura[2], Taku Nishimura[1], Scott A Bradford[3]

1. Department of Biological and Environmental Engineering, The University of Tokyo, 2. College of Humanities and Sciences, Nihon University, 3. U. S. Salinity Laboratory

An understanding of nano-bubble (NB) migration in porous media is needed for potential environmental applications. This research investigates factors that control the transport, retention, and release of air NBs in repacked glass beads. One-dimensional column transport studies with air NBs were conducted under different solution IS, ionic composition, and pH conditions. Collected data were simulated using a mathematical model that considered advective and dispersive transport, first-order kinetic retention, and transient release. Results were interpreted with the aid of interaction energy calculations that considered electric double layer, van der Waals, and Lewis acid-base interactions on surfaces with different amounts of nanoscale roughness. NB concentrations in the effluent were reduced with an increase in ionic strength (IS) or a decrease in pH due to a reduction in the repulsive force between the glass surface and NBs, especially when the solution contained $Ca^{2+}$ as compared to $Na^{+}$ and for larger NBs. NB retention on the surface was explained by ubiquitous nanoscale roughness on the glass beads that significantly lowered the energy barrier, and localized attractive charge heterogeneity and/or hydrophobic interactions.

Keywords: Nano bubble, Transport, Porous media, Solution chemistry

©2019. Japan Geoscience Union. All Right Reserved. 

# Geochemical Investigation of Metals and Trace Elements around the Abandoned Cu –Ni Mine Site in Selibe Phikwe, Botswana

*Fiona Segolame Motswaiso[1], Kengo - Nakamura[1], Noriaki - Watanabe[1], Takeshi - Komai[1]

1. Tohoku Univeristy Graduate School of Environmental Studies

Metals and trace elements may occur naturally in rocks and soils, but elevated quantities of them are gradually released into the environment by anthropogenic activities such as mining. In order to address issues of trace element water and soil pollution, a distinction needs to be made between natural and anthropogenic anomalies. The current study aims at characterizing the spatial distribution of trace elements and evaluate site-specific geochemical background concentrations of trace elements in the mine soils and river sediments and also to discriminate between lithogenic and anthropogenic sources of enrichment around a copper-nickel mining town in Selibe-Phikwe, Botswana.

A total of 43 soil, 30 river sediments, and 9 river water samples were collected from an area of 500m2 within the precincts of the mine. The total concentration of Cu, Ni, Pb, Cr, As, and Co in soils and sediments were determined using ED-XRF while river water samples were analyzed by ICP-AES. Geochemical pollution indices such as Geo-accumulation Index (Igeo), Enrichment Factor (EF) and Integrated Pollution Index (IPI) were employed for the assessment of metal and trace element contamination. The average metal concentration in soil of Cu, Ni, Pb, Cr, As, and Co in the study area were 73.27, 78.10, 25.83, 61.43, 4.28 and 6.43 mg/kg, respectively. To calculate the geochemical baseline, Relative cumulative frequency curves and the 4 s -outlier test methods suggested by Matschullat (2000) were incorporated. The estimated average baseline concentrations of Cr, Cu, Ni, Co, Zn and As are 53.8, 51.85, 53.95, 5.6, 32.36 and 4.27 mg kg 1, respectively. Soil leachate, sediment leachate, and river water pH levels ranged from basic (9) to very acidic (3) in areas closer to the mine. There is high variation in heavy metal concentration, eg. Cu, depicting regional natural background concentrations while others depict anthropogenic sources. The calculated Igeo values revealed moderate pollution level by the same metals. The result of integrated pollution indices suggested a generally deteriorating site quality. The results of chemical analysis also indicate that the trace elements in soils decreased with respect to distance from the mine; controlled mainly by water movement, wind direction, and topography.

Keywords: Soil Contamination, Geochemical baseline, Pollution indices, Trace elements

©2019. Japan Geoscience Union. All Right Reserved. 

# Removal of Arsenic (III) From Aqueous Solution Using Pumice and Zeolite Supported Zero-Valent Iron Nanoparticle

*Shashi Ranjan[1], Brijesh kumar yadav[1], Himanshu Joshi[1]

1. Indian Institute of Technology Roorkee

Arsenic is a naturally occurring toxic element and is widely distributed in natural ecosystems. Due to the natural as well as human-induced actions, its presence in groundwater is expanding its horizons and is becoming a major concern in lower Gangetic plains. Large active surface area and high arsenic adsorption capacity make nano-zero valent iron nanoparticle (nZVI) a promising adsorbent to remove arsenic species but due to high surface energy and the inherent magnetic forces of nZVI, it gets agglomerated and reduces its efficiency for adsorption. The objective of the present study was to develop supported nZVI over the porous material (pumice and zeolite) and their use for As (III) removal from aqueous solution. The chemical approach, i.e., Liquid Phase Synthesis, was used to infuse the iron nanoparticle on the surface of the porous material via reduction of iron in the presence of the base material by sodium borohydride. The shape, size, and surface morphology studied by Fe-SEM and shows a uniform distribution of nZVI over the surface of granular (0.5-1 mm) base materials. Batch studies were performed to determine the applicability of prepared composites as an adsorbent for As (III) removal at varying initial As (III) concentration (0.5 -5 mg/L), adsorbent dose (1-10 g/L) and pH (3-12). Adsorption kinetics and isotherms were studied in detail for the synthesized adsorbent to deduce the overall performance. Batch experiments demonstrated the quick removal of As (III) at initial stages followed by a slower removal rate, making it a two-stage process. The supported nZVI was found to be an effective adsorbent for As (III) removal and due to its mechanical strength, it can be applied for in-situ remediation of arsenic-polluted groundwater

Keywords: Arsenic, Nano Zerovalent Iron, Remediation, Pumice and Zeolite

©2019. Japan Geoscience Union. All Right Reserved. 

# Unsaturated Hydraulic Conductivity Estimation from Multi-step Centrifuge Outflow

*Thanh Long Bui[1], Yasushi Mori[1]

1. Graduate School of Environmental and Life Science, Okayama University

In the age of blooming technologies, direct and indirect laboratory methods, which identified soil function, are developed to shorten experiment time. In developing countries of Asia area, research on soil physic is sometimes limited because it is not easy to bring samples from those countries. In addition, it is impossible to identify soil function from the soil sample without original structure. Therefore if we can measure soil hydraulic conductivity or water holding capacity with small volume of samples, it is very beneficial for the region where soil data is limited. In this study, centrifuge multi-step outflow method was examined to estimate drainage process, i.e., unsaturated hydraulic properties.

The experiment was conducted using 2-mL centrifuge tube with two pin-holes at the top and bottom of the tube. After saturated from the bottom, multi-step pressurized outflow was performed on four kinds of soil samples including standard soil, granite decomposed soil, rice paddy field soil and volcanic ash soil. Transient outflow volume was measured using small centrifuge machine within 5 and 15 minutes at room temperature (25oC). The centrifuge pressure step was 1000, 2000, 3000, 4000, and 5000rpm, which was approximately 90, 360, 810, 1400, and 2250cmH2O respectively. Based on the outflow volume and accumulated time as input data for inverse solution model (HYDRUS 1D v4.6), hydraulic conductivity was optimized.

We found out that the optimization was successful with clayey soils and volcanic ash soils, but not with granite decomposed soil and standard sandy soils. The more sand particles it contained, the less convergence for hydraulic conductivity optimization we had obtained.

Keywords: Unsaturated Hydraulic Conductivity, Multi-step outflow, Centrifuge

©2019. Japan Geoscience Union. All Right Reserved. 

[E] Poster | A (Atmospheric and Hydrospheric Sciences)：A-GE Geological & Soil Environment

Thu. May 30, 2019 5:15 PM - 6:30 PM JST | Thu. May 30, 2019 8:15 AM - 9:30 AM UTC | Poster Hall International Exhibition Hall8, Makuhari Messe_10

## [A-GE28] Subsurface Mass Transport, Material Cycle, and Environmental Assessment

convener:Yuki Kojima(Department of Civil Engineering, Gifu University), Shoichiro Hamamoto(Department of Biological and Environmental Engineering, The University of Tokyo), Hirotaka Saito(Department of Ecoregion Science, Tokyo University of Agriculture and Technology), Yasushi Mori(Graduate School of Environmental and Life Science, Okayama University)

This session covers the topics on mass transport, water and energy cycles in geoenvironment. Subjects related to laboratory and field measurements, theoretical analysis, and numerical modeling will be discussed. Presentations on geo-pollution, remediation, geological disposal of hazardous wastes, ground source heat utilization, mass transport in vadose zone, soil-water monitoring, and environmental assessment are encouraged.

### [AGE28-P01] Vegetation pellets development and feasibility evaluation for unmanned-aerial-vehicle seeding on post-landslide sites

*Kai-Chi Hsu[1], Guo-Zhang M. Song[1], Shin-Hwei Lin[1], Chi-Hao Chang[2] (1.Department of Soil and Water Conservation, National Chung Hsing University, 2.Department of Landscape Architecture, Tunghai University)

### [AGE28-P02] Characterizing Soil Environment in The Rice Terraces of the Philippine Cordilleras

*Tomoyo Kurozumi[1], Yasushi Mori[2], Hiroaki Somura[2], Milagros Ong How[3] (1.Faculty of Environmental Science and Technology, Okayama University, 2.Graduate School of Environmental and Life Science, Okayama University , 3.Universal Harvested Incorporated)

### [AGE28-P03] Web-based interactive platform for analysis of regional-scale groundwater resources

*Chuen-Fa Ni[1], I-Hsien Lee[1], Chi-Ping Lin[1], Wi-Ci Li[1] (1.National Central University)

### [AGE28-P04] Development of simultaneous measurement system of viscosity and permeability for highly accurate evaluation of flow characteristic of Geofluid

*Tomoya Muramoto[1], Yoshitaka Fujita[1], Hiroaki Kajikawa[1], Hideaki Iizumi[1], Kazunori Ide[1] (1.National Institute of Advanced Industrial Science and Technology, National Metrology Institute of Japan)

### [AGE28-P05] Soil hydraulic parameter estimation by evaporation method

Shintaro Kubota[1], *Hirotaka Saito[1] (1.Graduate School of Agriculture, Tokyo University of Agriculture and Technology)

### [AGE28-P06] Measurement of apparent gas diffusion coefficient in poorly tilled seedbed under windy condition.

*Yoshihiro Matsumoto[1], Shuichiro Yoshida[1], Hiroyuki Sekiya[2], Kazuhiro Nishida[1] (1.Graduate School of Agricultural and Life Sciences, The University of Tokyo, 2.National Agricultural Research Center NARO)

### [AGE28-P07] Evaluating improvement techniques for phytosuction separation method to remove heavy metals from contaminated soils

*Yuki Kojima[1], Hayata Terada[1], Masahiko Katoh[2], Kohji Kamiya[1] (1.Department of Civil Engineering, Gifu University, 2.School of Agriculture, Meiji University)

### [AGE28-P08] Transport of Colloidal Particles in Saturated Toyoura Sand: Effects of Flow Rate on Importance of Electrostatic Repulsion

*Takuya Sugimoto[1], Shoichiro Hamamoto[1], Taku Nishimura[1], Yasuhisa Adachi[2], Motoyoshi Kobayashi[2] (1.Graduate School of Agricultural and Life Sciences, The University of Tokyo, 2.Faculty of Life and

Environmental Sciences, University of Tsukuba)

[AGE28-P09] Leaching behavior of As, Pb, Cd and Se in subsurface marine and nonmarine sedimentary environment in central Kanto plain, Japan

*SUSHMITA HOSSAIN[1], Takashi Ishiyama[2], Shoichi Hachinohe[2], Chiaki T. Oguchi[1] (1.Graduate school of Science and Engineering, Saitama University, 2.Center for Environmental Science in Saitama)

[AGE28-P10] Colloid transport in a quasi-saturated porous media

*Yushi Ooko[1], Takuya Sugimoto[2], Shoichiro Hamamoto[2], Taku Nishimura[2] (1.The University of Tokyo, 2.Graduate School of Agricultural and Life Sciences, The University of Tokyo)

# Vegetation pellets development and feasibility evaluation for unmanned-aerial-vehicle seeding on post-landslide sites

*Kai-Chi Hsu[1], Guo-Zhang M. Song[1], Shin-Hwei Lin[1], Chi-Hao Chang[2]

1. Department of Soil and Water Conservation, National Chung Hsing University, 2. Department of Landscape Architecture, Tunghai University

Frequent disturbances of typhoons, earthquakes and heavy rains have resulted in many landslides scattering over steep terrains and remote areas of Taiwan. As a result, the general engineering methods may not work well.

In the past, helicopters were used for aerial hydroseeding on such landslides. However, the remediation method with helicopters is complicated. This method takes a lot of manpower and materials. Additionally, the remediation timing is often missed because its preparation is time-consuming.

In recent years, the relevant research and technology of unmanned aerial vehicles (UAVs) are approaching maturity. Compare to helicopters, UAVs have the advantages of mobility and instantaneity. UAVs has many potentials to deliver vegetating materials to landslides.

Traditionally, vegetating materials (liquid or dry powder types) are sprayed to landslide sites through compressors. However, the load of UAVs is limited. They can't carry too much liquid or compressors. In other words, traditional vegetating materials won’ t work for UAV methods.

This study was to develop several types of agglomerates by mixing vegetating materials. The agglomerates look like a pellet, so it is called "vegetation pellet". To make sure which pellets can be applied to what environmental conditions, the water characteristics, pH value, nutrient content and seed germination rate of pellets with different ingredients were analyzed. In the field experiment, seed germination of pellets was monitored after pellets were applied to three different landslide sites.

Results showed that seed germination of pellets is directly related to the level of environmental moisture. If pellets were applied to landslides where rainfall and soil moisture were high, seed germination rates of pellets could reach 80% within three weeks. There were 1~3 germinating woody plants per square meter. Although germination rates of pellets applied during the dry season were nearly nill, seeds in pellets could germinate vigorously after the first wave of rainfall.

Although this study is still in the initial phase of the pellet development, the preliminary experiments showed that using UAVs to deliver vegetation pellets has considerable potentials for landslide remediation. Further studies can vary the fraction of ingredients and the size of pellets to maximize remediation effects.

Keywords: Aerial hydroseeding, engineering, remediation, UAV, vegetating material

©2019. Japan Geoscience Union. All Right Reserved.

©2019. Japan Geoscience Union. All Right Reserved. 

# Characterizing Soil Environment in The Rice Terraces of the Philippine Cordilleras

*Tomoyo Kurozumi[1], Yasushi Mori[2], Hiroaki Somura[2], Milagros Ong How[3]

1. Faculty of Environmental Science and Technology, Okayama University, 2. Graduate School of Environmental and Life Science, Okayama University , 3. Universal Harvested Incorporated

Rice terraces of the Philippine Cordilleras, located in northern Luzon Island, are contribute to the food production as well as water and carbon storage. The rice terraces, which have been designated as the World Heritage and should be protected as a cultural heritage, were in danger of collapse. Thus we need to clarify the mechanism of collapse from the perspective of natural science and protect them efficiently. We made a hypothesis that rice terraces are water storage structures physically, so the weight of paddy affects the stability, which determined by levee length, the depth of hardpan, and water ponding depth. Mainly in Banaue, rice terraces in three location: Viewdeck; Bangaan; and Hapao were investigated. Sometimes, ponding water on the rice terraces had fermentation odor, and the hard pan was detected at deeper depth. During the in situ infiltration test, gas was coming up from the soil and the hydraulic conductivity was low or unmeasurable. Excess amount of organic matter was considered to cause the gas emission which disturbs the soil sedimentation and compression, resulting in hardpan formation failure. Although organic matter application was important to soil nutrition and high crop yields, it might result in reductive condition which causes mineral leaky paddy and harmful gas emission.

Keywords: rice terraces, hard pan, Philippines, World Heritage

©2019. Japan Geoscience Union. All Right Reserved. 

# Web-based interactive platform for analysis of regional-scale groundwater resources

*Chuen-Fa Ni[1], I-Hsien Lee[1], Chi-Ping Lin[1], Wi-Ci Li[1]

1. National Central University

With the increasing variability of climate conditions, the sustainable management of groundwater resources has become a challenging task. Accurate assessment of groundwater resources relies on sufficient measurements and efficient analysis tools. The integrated technologies and multidisciplinary knowledge for groundwater have enhance the understanding of dynamics in groundwater systems. Taking advantages of widely developments in computer sciences and web service, the web platform provides an excellent open environment for groundwater investigations. However, most groundwater relevant web platforms are mainly focusing on the data visualization. The data (points, polylines, and polygons) and pre-analysis results (i.e., the figures) overlap a street map to indicate the location of interests and quantify the influenced regions of groundwater hazards. Such one-way interaction framework has significantly limited the implementations of measurement data and groundwater relevant applications. The study aims to develop an online web-based platform for groundwater data visualization, temporal and spatial data analysis, mesh generation and flow modeling. The study integrates multiple program languages such as Java, C, Python, and FORTRAN to bridge the data flow and online visualization. The interactive real-time web environment enables users to screen temporal and spatial measurements on the web map, conduct online data analyses, and develop numerical groundwater models. With well-designed database and numerous modules for data analyses and modeling, the platform allows users to share data and develop collaborative activities. The built-in analysis tools can also improve the efficiency of groundwater management and decision-making processes.

Keywords: groundwater resources, Web-based platform, data visualization, groundwater model

©2019. Japan Geoscience Union. All Right Reserved. 

# Development of simultaneous measurement system of viscosity and permeability for highly accurate evaluation of flow characteristic of Geofluid

*Tomoya Muramoto[1], Yoshitaka Fujita[1], Hiroaki Kajikawa[1], Hideaki Iizumi[1], Kazunori Ide[1]

1. National Institute of Advanced Industrial Science and Technology, National Metrology Institute of Japan

In this study, we will develop a high precision simulutaneous measurement system of high temperature - high pressure viscosity and permeability to strictly evaluate the behavior of Geofluid. In this system, we combine high precision viscosity measurement technique and high pressure generation technique of National Metrology Institute of Japan. One of the features of the porous medium like crust is that the fluid can be transmitted through a cavity having a complicated geometric shape inside it. That is, the porous medium has hydraulic properties. Recently, in evaluating the long-term stability of disposal system for high-level radioactive wastes, and also, to reveal the relationship between fluid characteristic and tectonic deformation of crust, the need to know the permeability / substance transport characteristics of the target rock or stratum in detail has been emphasized. A lot of research and development has been done to grasp the flow characteristics of the Geofluid under high pressure, however, the pressure dependence of the viscosity of the crustal fluid tends to be overlooked, and also the permeability coefficient of the rock accompanying it tends to be ignored. So, there are few studies which strictly evaluated of it. Technical development of high precision measurement of permeability in terms of Metrology has not been done so far. In addition, no quantitive study has been done on the generally used Darcy’ s law from Metrology viewpoint. In this study, we focus on the similarity between flow field descriptions beased on Hagen-Poiseulle’ s law used for highly accurate viscosity measurements by capillary method and Darcy’ s law. We will develop simultaneous measurement system of high temperature - high pressure viscosity and permeability, leading to an essential understanding of flow characteristics of Geofluid.

Keywords: Hagen-Poiseulle law, Darcy's law, Permeability

©2019. Japan Geoscience Union. All Right Reserved. 

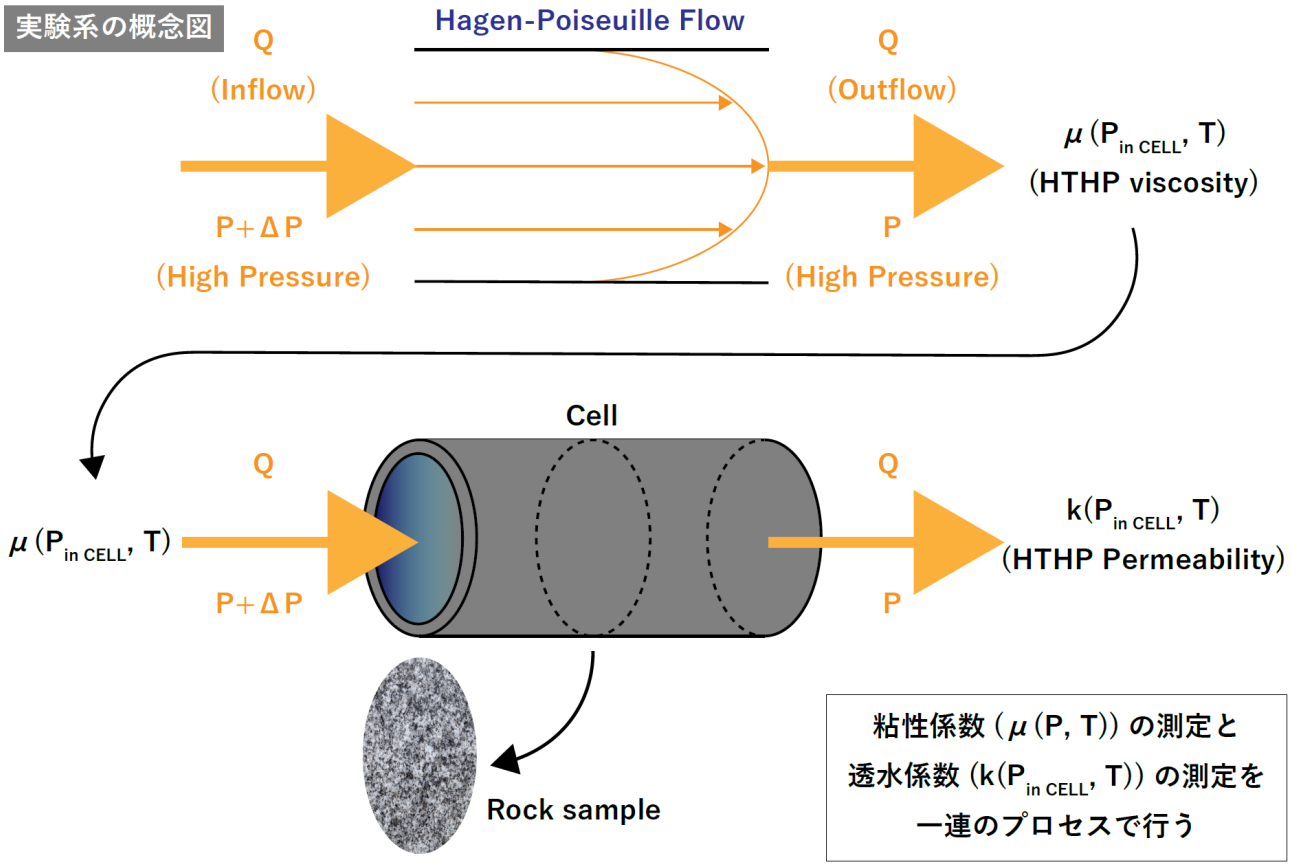


©2019. Japan Geoscience Union. All Right Reserved. 

# Soil hydraulic parameter estimation by evaporation method

Shintaro Kubota[1], *Hirotaka Saito[1]

1. Graduate School of Agriculture, Tokyo University of Agriculture and Technology

An evaporation method to estimate soil hydraulic properties, such as soil water retention curve and unsaturated hydraulic conductivity, has been receiving attention because of its simplicity and flexibility. Depending upon experimental setup, there are several approaches available for data analysis. In this study, a so-called simplified method and a more common but more involved inverse method were compared in terms of estimating soil hydraulic parameters. In the simplified method, soil water retention curve and unsaturated hydraulic conductivity were approximated by assuming that soil water pressure heads measured at two locations within the soil sample were linearly distributed. Parameter $\alpha$ and $n$ which were used in the van Genuchten (VG) soil water retention model were determined by fitting it to the curve obtained by the simplified method. Unsaturated hydraulic conductivity function was then predicted by the van Genuchten-Maulen model with the obtained $\alpha$ and $n$. For the inverse method, the $\alpha$ and $n$ parameters were directly optimized using a numerical analysis by fitting to measured pressure heads.
In this study, Toyoura sand, Tottori dune sand, glass beads and silt were used. After soil water retention curves were determined using the simplified method, the VG parameters were estimated to predict unsaturated hydraulic conductivity. With the inverse method, the VG parameters were inversely estimated using HYDRUS-1D program. Results showed that the parameters estimated from both the simplified and inverse methods predicted unsaturated hydraulic conductivity well compared to that determined from the simplified method. On the other hand, those for Toyoura sand, Tottori dune sand and glass beads were not well predicted. In general, the unsaturated hydraulic conductivity in the wet region was overpredicted, while that in the dry region was underestimated when the simplified method was used. Overall, this study shows that the simplified method needs to be carefully used especially for coarse materials, such as sand and glass beads.

Keywords: Soil hydraulic properties

©2019. Japan Geoscience Union. All Right Reserved. 

# Measurement of apparent gas diffusion coefficient in poorly tilled seedbed under windy condition.

*Yoshihiro Matsumoto[1], Shuichiro Yoshida[1], Hiroyuki Sekiya[2], Kazuhiro Nishida[1]

1. Graduate School of Agricultural and Life Sciences, The University of Tokyo, 2. National Agricultural Research Center NARO

In the cultivation of soybean in clayey paddy fields, huge clods with diameters of some centimeters are formed by tillage. In soil, movement of gas is usually assumed to be governed by molecular diffusion. On the other hand, in soil layer with huge clods, movement of gas can be enhanced by wind-induced pressure-pumping through large inter-clod pore space under windy condition. Although pressure-pumping is not a diffusive process, this phenomenon can be represented as a diffusive process by the Fick's law with the apparent gas diffusion coefficient under windy condition ($D_a$). However, little work has been done on $D_a$ in poorly tilled soil, especially in situ. This study aimed to compare $D_a$ and molecular gas diffusion coefficient ($D_m$) in poorly tilled seedbed and quantify how many times $D_a$ is larger than $D_m$.

The undisturbed poorly tilled soil was sampled on June 2018 just after tillage from the surface of the clayey field where conversion from flooded rice to soybean was conducted this year using the soil column with a diameter of 15.3 cm and a height of 9.7 cm. The porosity and mean clod diameter of the soil were 0.69 and 2.8 cm, respectively. As a control, Mikawa silica sand was packed into the column with a porosity of 0.49. The empty cap with a height of 2.9 cm were attached to the lower end of the column to conduct gas diffusion experiments. The oxygen concentration sensors were installed to the column and cap at 4.7 and 11.7 cm depth from the top of the column, respectively. The top of the column was closed, and then $CO_2$ gas was injected from the cap to saturate the column with $CO_2$. After opening the top of the column, $O_2$ concentration was continuously measured. The gas diffusion coefficient ($D_a$ or $D_m$) was estimated by fitting the measured $O_2$ concentration at 4.7 cm and 11.7 cm depth to the numerical solution of the diffusion equation. The diffusion tests under the wind for evaluating $D_a$ was conducted on November 2018 at the field where the soil specimen were taken. Three-dimensional wind velocity at 2 m above the column ($U_2$) was measured by the ultrasonic anemometer. The diffusion tests without the effect of wind for evaluating $D_m$ was conducted in the laboratory in the same manner.

Under the wind speed $U_2$ of 1.0 and 1.4 m $s^{-1}$, the apparent diffusion coefficients $D_a$ for the sand column were both 0.020 $cm^2$ $s^{-1}$, which was close to the measured $D_m$ for the column: 0.019 $cm^2$ $s^{-1}$. Thus, the gas diffusion in the sand column was governed by the molecular diffusion alone. On the other hand, the $D_a$s for the poorly tilled soil column under $U_2$ of 1.5, 2.3, and 4.1 m $s^{-1}$ were 0.065, 0.075, and 0.097 $cm^2$ $s^{-1}$, respectively, while the $D_m$ for the column was 0.036 $cm^2$ $s^{-1}$. This result shows the wind induced two to three-fold increase of apparent gas diffusion coefficient through the inter-clod pores of the poorly tilled soil, while the effect does not work on the sand layer.

Keywords: clayey rotational paddy field, tillage, clod, movement of gas, pressure-pumping

©2019. Japan Geoscience Union. All Right Reserved. 

# Evaluating improvement techniques for phytosuction separation method to remove heavy metals from contaminated soils

*Yuki Kojima[1], Hayata Terada[1], Masahiko Katoh[2], Kohji Kamiya[1]

1. Department of Civil Engineering, Gifu University, 2. School of Agriculture, Meiji University

Soil contamination by heavy metals has been a critical issue because heavy metals are bonded with soil particles tightly and are difficult to remove. Phytoextraction is one of the soil decontamination methods that plants growing at contaminated sites extract contaminants with soil moisture. Although the phytoextraction is environmentally friendly and low in cost, removal rates of contaminants are limited because plants growth is inhibited due to the toxicity of contaminants. Katoh et al. (2016) proposed a new method for heavy metal decontamination, phytosuction separation (PSS), which utilizes plant water uptake and an immobilization material (they used hydroxyapatite). In PSS, a immobilization material for heavy metals was placed on a contaminated soil, and plants grow in non-contaminated soil mounded on the immobilization material. Plant water uptake induces heavy metal transfer from contaminated soil toward the immobilization materials. Since plants are protected from the toxicity of heavy metals in this method, the removal rates of heavy metals are much higher than that with phytoextraction. In this study, we aimed to improve the PSS method by i) using new immobilization materials, ii) inducing soil water cycle between the contaminated and non-contaminated soils, and iii) applying organic fertilizer to enhance plant growth and to increase mobility of heavy metals.

We performed pot experiments to evaluate each improvement techniques with lead contaminated soil collected from a shooting range. As a new immobilization material, we examined iron slag and commercialized adsorption sheet. Water cycle between contaminated and non-contaminated soils are induced by changing position of water supply. Katoh et al. (2016) supplied water from contaminated soil, but we supplied from non-contaminated soils. The water supplied to non-contaminated soil move downward by gravity and reach contaminated soil, and then go back to the non-contaminated soil by plant water uptake. Plant roots produce organic acid and it will be transferred to the contaminated soil with water. Since organic acid increase mobility of lead, the water cycle possibly improve the efficiency of PSS method.

The results showed poor plant growth when slag and commercialized sheet are used as a immobilization material compared with when hydroxyapatite was used. Obviously the plants growth was inhibited by the toxicity of lead. The slag did not have enough ability to immobilize the lead, possibly due to the small soil moisture content in PSS method. The commercialized sheet allowed plant roots penetrate itself and the roots reached contaminated soil. The water cycle increased soluble lead content in contaminated. It means that organic acid produced by roots reached the contaminated soil. Applying organic fertilizer did not increase soluble lead content in the contaminated soil, but it improved plant growth. Therefore, water cycle and organic fertilizer improves the PSS method, but immobilization materials still need to be investigated.

Keywords: phytosuction separation, heavy metals, soil water cycle

©2019. Japan Geoscience Union. All Right Reserved. 

# Transport of Colloidal Particles in Saturated Toyoura Sand: Effects of Flow Rate on Importance of Electrostatic Repulsion

*Takuya Sugimoto[1], Shoichiro Hamamoto[1], Taku Nishimura[1], Yasuhisa Adachi[2], Motoyoshi Kobayashi[2]

1. Graduate School of Agricultural and Life Sciences, The University of Tokyo, 2. Faculty of Life and Environmental Sciences, University of Tsukuba

There are substantial colloidal particles such as clay minerals and metal oxides in soil environments. Such colloidal particles have been considered as a potential carrier of contaminants in vadose zone and aquifer, due to their surface charges and high specific surface area. Therefore, understanding the transport mechanisms of colloidal particles in soils is essential to predict the fate of the contaminants in the environments. In this study, we analyze deposition rate coefficients of polystyrene latex particles with a diameter of 1 $\mu$m in a column packed with Toyoura sand with an average diameter of 0.274 mm as a function of NaCl concentration at three different flow rates. The concentration of the colloids in the effluent was quantified using a spectrometer photometer. The experimental results showed that the deposition rate coefficients of the colloids increased with increasing NaCl concentrations and reached a plateau above a certain NaCl concentration, called the critical deposition concentration (CDC). The CDCs shifts to higher salt concentrations with increasing injected flow rates. We show that this experimental trend can be captured by a simplified model including physico-chemical interactions based on the DLVO theory.

Keywords: Colloidal particles, Transport, Porous media, Ionic strength, Flow rate

©2019. Japan Geoscience Union. All Right Reserved. 

# Leaching behavior of As, Pb, Cd and Se in subsurface marine and nonmarine sedimentary environment in central Kanto plain, Japan

*SUSHMITA HOSSAIN[1], Takashi Ishiyama[2], Shoichi Hachinohe[2], Chiaki T. Oguchi[1]

1. Graduate school of Science and Engineering, Saitama University, 2. Center for Environmental Science in Saitama

Leaching behavior of trace element and heavy metal strongly depends on the physicochemical form termed as chemical speciation in soil and sediment. So that, sediment and soil act as scavenger to transfer naturally or anthropogenically occurring element to subsurface environment with changing environmental conditions. In this research, total 25 boring core sediment samples were investigated at 1 m interval from lowland valley of Yono area, Saitama in Kanto Plain for chemical speciation and potential risk assessment of arsenic (As), lead (Pb), cadmium (Cd) and Selenium (Se) with other metals. Samples were kept in near natural or not oxidized condition applying special preservation technique. A four steps sequential extraction method was adopted to determine chemical speciation. Boring core consist of surface clayey silt, peat, organic rich silt and clay, tuffaceous clay and medium to coarse sand with gravel layer of nonmarine sediment up to 17 m depth, where as from depth of 17 to 20 m transitional sediment are underlain by marine sediment up to 26 m. Total metal concentration, mineral content and chemical speciation concentration were determined by using X-ray Florescence(XRF), X-ray diffractometer (XRD), Inductively coupled plasma mass spectrometer (ICP-MS) and Inductively coupled plasma atomic emission spectrometer (ICP-AES) respectively. Clay minerals distributions were determined specially after application of heat and ethylene glycol treatment and XRD peak analysis. Pore water were collected from each samples and element concentration were measured by ICP-MS and ICP-AES. Under natural condition, pH of the leachate from sediment are not significantly different in nonmarine and marine environment which are ranged from pH 6.55 to 8.04. However, the electrical conductivity (EC) concentration range 53.9 to 72.1 μS/cm in marine and 77.9 to 104.7 μS/cm in surface silty clay sediment, that is quite higher than (7.83 to 25.4 μS/cm) of nonmarine fluvial, peat and tuffaceous clay. Chemical speciation trend for As in marine and nonmarine sediment is Fe-Mn oxide bound > Carbonate bound > Ion-exchangeable bound > water soluble where more than 95-98 % are consist of residual and organic bound in all samples indicates their occurrence are of natural origin. The potential mobile fractions (Fe-Mn oxide bound + Carbonate bound + Ion-exchangeable bound + water soluble) of Se and Cd are less than 5 % of total concentration whereas for Pb, it is less than 1%. Chemical speciation trend for Se is Fe-Mn oxide bound > Carbonate bound > Ion-exchangeable bound > water soluble in fluvial nonmarine sediment differs from the trend in marine environment which seems more bioavailable. For Cd, the trend is Carbonate bound > Ion exchangeable bound > Fe- Mn oxide bound >> water soluble. The speciation trend of Pb and As is similar. In pore water also, the concentration trend is As > Se > Cd >Pb. However, only As conc. in pore water exceeds several times from environmental standard (10 μg/l) of WHO and Japan in leachate and drinking water of both non marine and marine sediment. The highest concentration is 116.42 μg/l at depth of 17.2-17.4 m, 86.14 μg/l at 24.2-24.4 m and 63.12 μg/l at 10.2-10.4 m in transitional, marine and fluvial environment respectively. Pore water concentration of Pb, Cd and Se have not exceeded the environmental standard of leachate and drinking water quality. According to risk assessment, the bioavailable fraction of As, Pb, Se and Cd in both marine and nonmarine sediment is less than 1-5 % of the total concentration indicating low or no risk. However, results suggest that leaching behavior of As differs from Se, Cd and Pb even though according to risk assessment on speciation, they have similar conditions. Pore water as well as groundwater As in fluvial aquifer shows higher concentration which is related to higher potential mobile fractions and enrichment.

©2019. Japan Geoscience Union. All Right Reserved. 

Keywords: Trace element, Chemical speciation, Marine sediment, Risk assessment

©2019. Japan Geoscience Union. All Right Reserved. 

# Colloid transport in a quasi-saturated porous media

*Yushi Ooko[1], Takuya Sugimoto[2], Shoichiro Hamamoto[2], Taku Nishimura[2]

1. The University of Tokyo, 2. Graduate School of Agricultural and Life Sciences, The University of Tokyo

Colloidal particles in soils have been considered as one of the transport carriers for contaminants through groundwater (saturated zone). In natural soil system, repeated wetting-drying cycles often leads to entrapped air in the pores of a water-saturated zone, namely, quasi-saturated condition. However, there are few studies on colloidal transport process in quasi-saturated condition. Therefore, studying the colloidal transport in such quasi-saturated condition is important to understand the phenomenon of colloidal migration in the environments. In this study, we aimed to investigate the effects of entrapped air on colloid transport in porous media based on one-dimensional column experiments. We also characterized entrapped air in the porous media by X-ray CT measurements.
Two different sand columns (1. i.d. 0.9-cm, height 10-cm, 2. i.d. 5-cm, height 10-cm) were prepared for X-ray CT measurements and column transport experiments, respectively. Columns repacked with Toyoura sand were completely water-saturated by applying degassed water to the dry-sand repacked column under vacuum condition. The soil water was drained by applying a suction of 70-cm H2O to the column. By hanging water table, the sand columns were then re-saturated by immersing them in water tank, resulting in quasi-saturated sand columns. In the X-ray CT measurements, the sand column was scanned by X-ray CT device (Metrotom 1500, Carl Zeiss) with spatial resolution of 11.3 micron. In the column transport experiments, the suspension of silica particles (SL) with a diameter of 100 nm in diameter was injected to the columns under saturated and quasi-saturated condition at a constant flow rate. Effluents were collected periodically to measure the turbidity, which represents SL concentrations.
X-ray- CT measurements and subsequent CT image analysis showed the decreased fraction of entrapped air in pore volume and the increased fraction of smaller entrapped air at lower part of the column. Pore-network tortuosity analysis based on the CT images revealed that more tortuous liquid-phase network formed in the quasi-saturated condition as compared to the one under water-saturated condition. As a result of column experiments, the colloid transport was facilitated in the presence of entrapped air compared to the fully -saturated condition. It was suggested that the presence of entrapped air would inhibit the deposition of silica particles at the favorable site on the sand particles.

Acknowledgement: This work was supported by Grant-in-Aid for Scientific Research of Japan Society for the Promotion of Science (JSPS) (Leading Initiative for Excellent Young Researchers, and 16H04411)

Keywords: quasi-saturated condition, colloid, porous media, transport

©2019. Japan Geoscience Union. All Right Reserved. 

[E] Oral | A (Atmospheric and Hydrospheric Sciences)：A-GE Geological & Soil Environment

Thu. May 30, 2019 10:45 AM - 12:15 PM JST | Thu. May 30, 2019 1:45 AM - 3:15 AM UTC | 301A 3F

## [A-GE29] Energy-Environment-Water Nexus and Sustainable Development

convener:Ming Zhang(Institute for Geo-Resources and Environment, Geological Survey of Japan, AIST), Ken Kawamoto(Graduate School of Science and Engineering, Saitama University), Jet-Chau Wen(National Yunlin University of Science and Technology), Yonghong Hao(Tianjin Normal University), Chairperson:Ming Zhang(AIST), Hirotaka Saito(Tokyo University of Agriculture and Technology), Yonghong Hao(Tianjin Normal University)

This session provides a broad platform for discussion and presentation of fundamental and up-to-date scientific results related to clean energy production, environmental remediation and restoration, waste management, water cycle, monitoring of water quality, management of water resources and interconnections among them for sustainable development. Presentations on the topics associated with social science that enhance public awareness, stakeholder empowerment and involvement, and policy decisions regarding the management of water, energy and the environment are also encouraged.

10:45 AM - 10:50 AM JST | 1:45 AM - 1:50 AM UTC

Introduction

---

10:50 AM - 11:05 AM JST | 1:50 AM - 2:05 AM UTC

[AGE29-01] Input-Output Analysis of Taiwan’s Food-Energy-Water Risk

*CHU-CHUN YAO[1], Gene Jiing-yun You[1] (1.National Taiwan University)

---

11:05 AM - 11:20 AM JST | 2:05 AM - 2:20 AM UTC

[AGE29-02] **Groundwater potential analysis using the multiple spatiotemporal remote sensing approach in fractured rock of mountainous region**

*Jung-Jun Lin[1,2], Yuei-An Liou[1], Chien-Chung Ke[2], Su-Yun Chi[2], Jia-Hung Liang[3] (1.National Central Univ., 2.Sinotech Engineering Consultants, Inc., 3.Ministry of Economic Affairs)

---

11:20 AM - 11:35 AM JST | 2:20 AM - 2:35 AM UTC

[AGE29-03] Estimating Soil Water Content with Color Calibration Method in the Image of Remote Sensing by Unmanned Aerial Vehicle

*Hong-Yi Li[1], Hong-Ru Lin[1], Jyun-Lin Chen[1], Shao-Yang Huang[1], Jet-Chau Wen[1] (1.National Yunlin University of Science and Technology)

---

11:35 AM - 11:50 AM JST | 2:35 AM - 2:50 AM UTC

[AGE29-04] **Characterizing Geotechnical Properties of Drinking Water Sludge Blended with Graded Crushed Clay Brick for Road Subgrade: Effects of Gradation and Mixing Proportion of Crushed Clay Brick on CBR and Water Permeability**

*Muhammad Rashid Iqbal[1], Akihiro Matsuno[1], Ken Kawamoto[1] (1.Graduate School of Science and Engineering, Saitama University)

---

11:50 AM - 12:05 PM JST | 2:50 AM - 3:05 AM UTC

[AGE29-05] Investigation and Evaluation of the Multiple-liquefaction Site at the Southern Taiwan

*Chih-Sheng KU[1] (1.I-Shou University)

---

12:05 PM - 12:15 PM JST | 3:05 AM - 3:15 AM UTC

Discussion

# Input-Output Analysis of Taiwan’s Food-Energy-Water Risk

*CHU-CHUN YAO[1], Gene Jiing-yun You[1]

1. National Taiwan University

The water, energy, and food (WEF) nexus means that the three sectors are inextricably linked and that actions in one area more often than not have impacts in one or both of the others. From a national planning perspective, it is necessary to more precisely investigate the relationships among food-energy-water sectors. This study applies input-output analysis based on interdependencies between economic sectors or industries in Taiwan’s food-energy-water challenge and risk. In this study, the research data is based on Taiwan’s trade association tables of 52 economic sectors (including food, energy, and water-related sectors) for the year 1996, 2001, 2006, and 2011. We develop the extrapolation method to produce available I-O table. The future I-O table can be forecasted by applying different predictive models (e.g., linear or nonlinear regressions). We will observe the changes in Taiwan’s economic structures during the time period (e.g., between 1996 and 2001) and also investigate the uncertainty of economic impact focusing on food, energy, and water. Based on the results of analysis of Taiwan’s trade association tables, we can predict the risks that Taiwan’s industries may face under different conditions in the future and might provide some useful information to the government for taking countermeasures.

Keywords: WEF, input-output analysis, extrapolation, I-O table, economic structures, risk

©2019. Japan Geoscience Union. All Right Reserved. 

# Groundwater potential analysis using the multiple spatiotemporal remote sensing approach in fractured rock of mountainous region

*Jung-Jun Lin[1,2], Yuei-An Liou[1], Chien-Chung Ke[2], Su-Yun Chi[2], Jia-Hung Liang[3]

1. National Central Univ., 2. Sinotech Engineering Consultants, Inc., 3. Ministry of Economic Affairs

Because of the costly field investigation, an optimum benefit technique, the multiple spatiotemporal remote sensing analysis, was used for long-term monitoring and assessment of groundwater potential capacity. In this study, we used the mentioned approach to derive the spatiotemporal index from Landsat imagery for identifying the land use change and understanding the regional hydrogeological characteristics, such as normalized difference vegetation index (NDVI), soil moisture index (SMI), land surface temperature (LST) and so on. To verify the index evaluation results, the hydrogeological properties including the core inspection, geophysical logging and hydraulic testing of totally 108 boreholes drilling in the fractured rock mass in mountainous region were collected. The pumping test results such as well capacity from 76 groundwater monitoring wells were also used to compare the potential groundwater capacity evaluated from remote sensing analysis. It was found a good agreement between the field investigation data and remote sensing analysis results. Therefore, the multi-scaled comprehensive analyses of natural and anthropogenic geomorphic features are suitable for providing more information to qualify and estimate the selections of investigated sites in the future.

Keywords: groundwater, fractured rock, remote sensing

©2019. Japan Geoscience Union. All Right Reserved. 

# Estimating Soil Water Content with Color Calibration Method in the Image of Remote Sensing by Unmanned Aerial Vehicle

*Hong-Yi Li[1], Hong-Ru Lin[1], Jyun-Lin Chen[1], Shao-Yang Huang[1], Jet-Chau Wen[1]

1. National Yunlin University of Science and Technology

From the previous research results, there are many methods for measuring soil water content (SWC), but most of the SWC measurement methods are destructive methods for soil structure. Moreover, it takes a lot of time and manpower. In recent years, the method of estimating SWC from digital images of unmanned aerial vehicle (UAV) is a novel and rapid for measuring SWC non-destructive. While estimating SWC in the field using digital images, the effects are produced sunlight and climates and setting of the camera white balance. While estimating the SWC by digital images, these influences will let these methods have a bias between the hue value of digital images and the color of actual soil. So, the purpose of this study is to add a color calibration method while the process of estimating to remove the influences of sunlight, climates and white balance of camera, to improve the accuracy of estimating SWC by digital images.

At first, this study collected the surface soil samples from 0 to 5 cm below the ground surface at the study site which is the sampling range of in-situ planning. A standard color card (ColorChecker) is placed at the study site as a basis for image color calibration. After that, this study used UAV to take a photo-shooting at 30 meters above the ground, and obtain the digital images of the study site. After the sampling is completed, the surface soil sample is obtained its gravimetric water content by thermogravimetry in the laboratory. Next, the digital images taken by the UAV is used to cut the study area and image color calibration using the image processing software.

Then, using Matlab 2018b software to calculates the hue value of RGB color space (Red (R), Green (G), and Blue (B)) of the digital images before and after the color calibration separately, and transforms them into other six color spaces (normalized RGB, HIS, I1I2I3, Lab, YCbCr, and Lch). At last, this study used multiple linear regression to establish the SWC estimation models separately, and then compare the influences which before and after color calibration.

The results of this study show the influences of sunlight, climates and white balance of camera make a significant bias when estimating SWC using the digital images before color calibration. However, this study which added color calibration improves the accuracy in the estimation of SWC by digital images. Finally, the achievements of this study can apply in reducing the number of water resources of the agriculture irrigation widely.

Keywords: Surface soil, Aerial photo-shooting, Digital image processing, Color calibration

©2019. Japan Geoscience Union. All Right Reserved. 

# Characterizing Geotechnical Properties of Drinking Water Sludge Blended with Graded Crushed Clay Brick for Road Subgrade: Effects of Gradation and Mixing Proportion of Crushed Clay Brick on CBR and Water Permeability

*Muhammad Rashid Iqbal[1], Akihiro Matsuno[1], Ken Kawamoto[1]

1. Graduate School of Science and Engineering, Saitama University

Effective uses of construction and demolition waste, sludge, and industrial by-products for engineering purposes are highly demanded in developing countries. Currently, these materials are used for other construction works such as ground levelling and backfilling without any quality control of materials and/or directly dumped at the landfill site. In this research, an attempt was made to use drinking water sludge (DWS) by blending with crushed clay bricks (CCB) to propose their utilization for constructing road subgrade. DWS with less than 2-mm was blended with CCB with three different particles range; (a) finer fraction having particle size 2-10mm, (b) Coarser fraction 10-30mm, and (c) graded fraction 2-30mm. The mixing proportion has been controlled from 0 to 100% on the dry mass basis. Geotechnical properties such as California bearing ratio (CBR) and water permeability were investigated in the laboratory. Experimental results showed that addition of a finer fraction of CCB from 0 to 100% with DWS improved CBR values from 45% to 88% which was almost double than the DWS itself and captured a well linear relationship. Up to 60% addition of a coarser and graded fraction of CCB increased CBR value from 45% to 110% which was 2.44 times higher than the DWS itself. However, at 80% addition of CCB, graded fraction enhanced the CBR value more as compared to coarser fraction which was due to the well packing and reduction of the voids. On the other hand, at 100% blend of CCB coarser fraction showed quite higher values which could be due to the breakage of the bigger particles and filling the voids effectively. The water permeabilities of all these blended samples showed a very well relationship with Hazen model as compared to Kozeny-Carman model. It can be concluded that graded and coarser fraction 60% blend had an equal or superiority effect than the 100% of the finer fraction blends. All the tested sample fulfilled the improved subgrade requirement to utilize for the road subgrade.

Keywords: Drinking water sludge, Crushed Clay bricks, California Bearing Ratio (CBR), Water Permeability

©2019. Japan Geoscience Union. All Right Reserved. 

# Investigation and Evaluation of the Multiple-liquefaction Site at the Southern Taiwan

*Chih-Sheng KU[1]

1. I-Shou University

Southern Taiwan experienced several large earthquakes on 5 December 1946 ($M_w$=6.3), 4 March 2010 ($M_w$=6.4) and 6 February 2016 ($M_w$=6.6), respectively. Liquefaction phenomenon evidences was observed at Hsinhwa district, Tainan city, Taiwan during the 1964, 2010, and 2016 earthquake. Re-liquefaction at this site was confirmed by GPS surveying at the sand boiling locations after last two earthquakes. Seismic cone penetration test (SCPT) and boring were conducted at this site after 2010, and 2016 earthquake. The recurrence of liquefaction, availability of pre-earthquake logging, and high fine content in the liquefied soil stratum make this case valuable for detail study. This paper presents the results of the investigation and evaluates the liquefaction potential of the reliquefied site by different period exploration data. The comparison of the SCPT strength profile before and after the last earthquakes seems to indicate that no significant variation has occurred in this multiple liquefied site, making the area vulnerable to liquefaction induced sand boiling in future large-scale earthquakes. Liquefaction analyses with in situ test data show that this site is still highly susceptible to liquefaction.

Keywords: Earthquake, Liquefaction, Seismic Cone Penetration Test

03-05-2010

02-13-2016

©2019. Japan Geoscience Union. All Right Reserved. 

[E] Oral | A (Atmospheric and Hydrospheric Sciences )：A-GE Geological & Soil Environment

Thu. May 30, 2019 1:45 PM - 3:15 PM JST | Thu. May 30, 2019 4:45 AM - 6:15 AM UTC | 301A 3F

## [A-GE29] Energy-Environment-Water Nexus and Sustainable Development

convener:Ming Zhang(Institute for Geo-Resources and Environment, Geological Survey of Japan, AIST), Ken Kawamoto(Graduate School of Science and Engineering, Saitama University), Jet-Chau Wen(National Yunlin University of Science and Technology), Yonghong Hao(Tianjin Normal University), Chairperson:Ken Kawamoto(Saitama University), Jet- Chau Wen(National Yunlin University of Science and Technology, Taiwan)

This session provides a broad platform for discussion and presentation of fundamental and up-to-date scientific results related to clean energy production, environmental remediation and restoration, waste management, water cycle, monitoring of water quality, management of water resources and interconnections among them for sustainable development. Presentations on the topics associated with social science that enhance public awareness, stakeholder empowerment and involvement, and policy decisions regarding the management of water, energy and the environment are also encouraged.

1:45 PM - 1:50 PM JST | 4:45 AM - 4:50 AM UTC

Introduction

---

1:50 PM - 2:05 PM JST | 4:50 AM - 5:05 AM UTC

[AGE29-06] Investigating the Reproducibility of Hydraulic Tomography Estimates with Time-Variable Boundary Conditions

*Jian-Dao Li[1], Jyun-Lin Chen[1], Hong-Ru Lin[1], Shao-Yang Huang [1], Tian-Chyi Jim Yeh[2], Jet-Chau Wen[1] (1.National Yunlin University of Science and Technology, 2.The University of Arizona)

---

2:05 PM - 2:20 PM JST | 5:05 AM - 5:20 AM UTC

[AGE29-07] **Applying river pollution index and QUAL2K model for water quality assessment and management in Ke-Ya river, Taiwan**

*Hong-Syuan Li[1], Yu-Chih Lin[1] (1.Department of Environmental Engineering & Health, Yuanpei University of Medical Technology)

---

2:20 PM - 2:35 PM JST | 5:20 AM - 5:35 AM UTC

[AGE29-08] Environmental assessment at CDW disposal sites in Vietnam: Case study in Thanh Tri landfill, Hanoi

*Thanh Ha Ngo[1], Akihiro Matsuno[1], Ken Kawamoto[1] (1.Graduate School of Science and Engineering, Saitama University)

---

2:35 PM - 2:50 PM JST | 5:35 AM - 5:50 AM UTC

[AGE29-09] **Modeling Study on the Impacts of Groundwater Pumping to Regional Hydroclimatology in 37 World Major Aquifers**

*Pat J.-F. Yeh[1] (1.Monash University Malaysia)

---

2:50 PM - 3:05 PM JST | 5:50 AM - 6:05 AM UTC

[AGE29-10] CHRATERIZING BURIED WASTE COMPOSITION AT CONSTRUCTION AND DEMOLITION WASTE (CDW) DISPOSAL SITE IN VIETNAM: A CASE STUDY IN THANH TRI LANDFILL IN HANOI

*Tselmeg Aldarjav[1], Akira Kato[1], Akihiro Matsuno[1], Ken Kawamoto[1,2] (1.Graduate School of Science and Engineering, Saitama University, Japan , 2.International Institute for Resilient Society, Saitama University, Japan)

---

3:05 PM - 3:15 PM JST | 6:05 AM - 6:15 AM UTC

Discussion

# Investigating the Reproducibility of Hydraulic Tomography Estimates with Time-Variable Boundary Conditions

*Jian-Dao Li[1], Jyun-Lin Chen[1], Hong-Ru Lin[1], Shao-Yang Huang [1], Tian-Chyi Jim Yeh[2], Jet-Chau Wen[1]

1. National Yunlin University of Science and Technology, 2. The University of Arizona

In recent years, the hydraulic tomography (HT) is a popular method for the delineation of the spatial distributions of hydraulic properties in the groundwater aquifer. Previous researches investigated the spatial distributions of hydraulic properties by the HT survey using the constant head boundary condition. However, the constant head is not the real condition in the boundary condition at the field. The study purpose is the case studies of two years at the same site using the time-variable boundary conditions to delineate the reproducibility of hydraulic properties.

The study area is located in National Yunlin University of Science and Technology (NYSUT) campus in Taiwan. The sequential pumping test is carried in 2010 and 2012 were used for the inverse modeling effort to estimate the hydraulic properties. The boundary condition is applied to the HT method using the sensitivity equation method (SEM) to calibrate the time-variable heads. Then, the reproducibility of estimates and prediction were analyzed in two different years. The results show that the more heterogeneity of hydraulic properties. The HT method can be improved using the time-variable boundary conditions.

Keywords: Sensitivity equation method, Boundary condition, Hydraulic tomography, Sequential pumping test, Heterogeneity, Hydraulic property

©2019. Japan Geoscience Union. All Right Reserved. 

# Applying river pollution index and QUAL2K model for water quality assessment and management in Ke-Ya river, Taiwan

*Hong-Syuan Li[1], Yu-Chih Lin[1]

1. Department of Environmental Engineering & Health, Yuanpei University of Medical Technology

Waste water from hundreds of factories in Hsiang-Shan industrial park, Hsinchu Science Park, animal husbandry, metal surface electroplating industries, and domestic sewage are discharged into Keiya River HshinChu, Taiwan. In this study, monitoring data of the Keya River was collected, the river pollution index (RPI) and QUAL2K models were utilized for analysis and assessment of water quality. The divide of pollution collection area and evaluation of the assimilative capacity were also discussed.
The results indicated that the main pollutant in the water quality of Keiya River was ammonia nitrogen, which was contained in wastewater discharged from residential areas and Hsinchu Science Park etc., the second was biochemical oxygen demand (BOD). In order to improve the problem of ammonia nitrogen in the rivers, the Taiwan Environmental Protection Agency has tightened the emission limits of ammonia and nitrogen concentrations in wastewater discharges from 2012. The ammonia nitrogen wastewater treatment modules were also installed in the Hsinchu Science Park to reduce ammonia nitrogen emissions into rivers. In addition, the Hsinchu City Environmental Protection Bureau has strengthened the control of the copper standard for discharge water upto 1.5mg/L from 2017, so that the copper concentration in the current river water was maintained at <0.001-0.03mg/L, which was compliance with the environmental standards related to human health protection.

Keywords: river pollution index, assimilative capacity, ammonia nitrogen

©2019. Japan Geoscience Union. All Right Reserved. 

# Environmental assessment at CDW disposal sites in Vietnam: Case study in Thanh Tri landfill, Hanoi

*Thanh Ha Ngo[1], Akihiro Matsuno[1], Ken Kawamoto[1]

1. Graduate School of Science and Engineering, Saitama University

In the last recent decade, Vietnam has become one of most developing countries within South East Asia. Due to a rapid increasing of economic and industrial, the amount of construction and demolition waste (CDW) in Vietnam also increasing fast and becoming one of the biggest issue for the surrounding environment. According to MONRE, in 2015, Vietnam produced 1.9 million tons of CDW, while the recycling rate was only accounted for 1 −2%. In particularly, 30% of total solid waste generated in Hanoi was reported as CDW during the period of 2010 −2014. Currently, most of generated CDW from construction and demolition sites is reused on-/off sites without any quality control of materials and dumped at disposal sites along with collected waste from town cleaning (e.g., sludge and soil). At CDW disposal site, there is a potential risk of accepting hazardous and scheduled waste together with non-hazardous waste due to lack of management and control of waste acceptance. Therefore, in order to have environmental risk assessment of CDW disposal sites in Vietnam, it is important to identify the current environmental status of CDW dumping sites according to an appropriate monitoring program. In this study, we assessed qualities of water, gas, and fine residues (soil and fines of dumped CDW) inside the disposal site and its surrounding at Thanh Tri Landfill CDW disposal site in Hanoi as a case study. The final goal of study is to develop a standard monitoring/operating procedure for environmental assessment of CDW disposal sites in Vietnam. The field monitoring of surface gas emission and the sampling of internal gas, water, and fine residues, and investigation of dumped scheduled waste at the site were carried out on December 2018. The internal gas samples were collected at six different points from 0.5 - 1m depth and a flux chamber method applied to determine surface gas emission. The groundwater sample was taken from a well inside the disposal site. Results showed very low concentration of methane (CH4) and Carbon Dioxide (CO2). In the meantime, groundwater quality showed that the amount of Ferrous and Arsenic became higher than Vietnam technical regulation on drinking water (QCVN 01:2009/BYT) and Vietnam technical regulation on domestic water (QCVN 02:2009/BYT).

Keywords: Environmental assessment, CDW disposal sites

©2019. Japan Geoscience Union. All Right Reserved. 

# Modeling Study on the Impacts of Groundwater Pumping to Regional Hydroclimatology in 37 World Major Aquifers

*Pat J.-F. Yeh[1]

1. Monash University Malaysia

Groundwater pumping (GWP) introduces dormant fossil waters into the active hydrologic cycle and alters the mand and atmosphere water budgets, but its effects are poorly understood due to the lack of large-scale GWP information and hydrometeorological data to estimate these changes. In this study, two sets of global-scale model simulations by a fully-coupled climate-hydrologic model, one with GWP and the other one without, are conducted for the 1900-1999 period. The effects of GWP in affecting the land and atmospheric water budgets are investigated over the selected 37 major aquifers worldwide by analyzing the output data from both sets of simulations. The entire set of the internally-consistent water budget components, includ precipitation (P), evaporation (E), runoff (R), atmospheric vapor convergence (C), and changes in land, ocean and atmosphere water storages, are analyzed, and their differences between tow simulations are considered the effects due to GWP. The contribution of GWP to global sea level rise (GSLR) as a result of the changes in the land and atmospheric water budgets is also estimated via (1) the direct R contribution from land to ocean and (2) the indirect C contribution via atmospheric interactions.

Keywords: groundwater, water budget, sea level rise, model simulations

©2019. Japan Geoscience Union. All Right Reserved. 

# CHRATERIZING BURIED WASTE COMPOSITION AT CONSTRUCTION AND DEMOLITION WASTE (CDW) DISPOSAL SITE IN VIETNAM: A CASE STUDY IN THANH TRI LANDFILL IN HANOI

*Tselmeg Aldarjav[1], Akira Kato[1], Akihiro Matsuno[1], Ken Kawamoto[1,2]

1. Graduate School of Science and Engineering, Saitama University, Japan , 2. International Institute for Resilient Society, Saitama University, Japan

In recent years building and construction work has been growing rapidly in Vietnam, as construction sector expanded simultaneously the waste generated have increased as well. Due to increasing cost and handling availability of CDW disposal the landfilling approach is the most common and cost-efficient way of disposal in developing countries, including Vietnam. On the other hand, due to lack of technical and management abilities, it is very difficult to collect the data on amount and composition of CDW dumped to the landfilling site. The data on amount and composition of dumped CDW is necessary to evaluate the remaining lifetime of present CDW landfills and to examine the possible recycling strategy and method of CDW fills in future. Besides, the waste composition data contributes to classify the type of CDW landfills. The data on the ratio of each amount is currently not available. In this study, a field survey including pit sampling of buried waste, size grading, weighting of graded fractions, and categorization of waste has been done at Thanh Tri landfill site located on the south-eastern side of Hanoi, Vietnam. The final goals of study are 1) to develop a technical manual to investigate buried CDW at disposal sites, and 2) to characterize waste composition, physical and chemical characteristics of dumped waste in Vietnam. The overall procedure of the manual includes 5 parts: 1. Preliminary survey work, 2. Design of CDW composition survey, 3. Set-up of CDW composition survey, 4. Excursion of CDW composition survey, and 5. data analysis. The proposed manual enables not only to measure the waste composition but also to characterize particle size distribution of buried waste.

Keywords: Construction and Demolition Waste , Waste composition, Landfill, Survey, Manual, Vietnam

©2019. Japan Geoscience Union. All Right Reserved. 

[E] Poster | A (Atmospheric and Hydrospheric Sciences)：A-GE Geological & Soil Environment

Thu. May 30, 2019 5:15 PM - 6:30 PM JST | Thu. May 30, 2019 8:15 AM - 9:30 AM UTC | Poster Hall International Exhibition Hall8, Makuhari Messe_11

## [A-GE29] Energy-Environment-Water Nexus and Sustainable Development

convener:Ming Zhang(Institute for Geo-Resources and Environment, Geological Survey of Japan, AIST), Ken Kawamoto(Graduate School of Science and Engineering, Saitama University), Jet-Chau Wen(National Yunlin University of Science and Technology), Yonghong Hao(Tianjin Normal University)

This session provides a broad platform for discussion and presentation of fundamental and up-to-date scientific results related to clean energy production, environmental remediation and restoration, waste management, water cycle, monitoring of water quality, management of water resources and interconnections among them for sustainable development. Presentations on the topics associated with social science that enhance public awareness, stakeholder empowerment and involvement, and policy decisions regarding the management of water, energy and the environment are also encouraged.

### [AGE29-P01] The role of anthropogenic activities in spring discharge cessation: Jinci Springs China

Yaru Guo[1], *Yonghong Hao[1], Chun Zhao[1], Huan Lian[1] (1.Tianjin Normal University)

### [AGE29-P02] Groundwater response to tidal fluctuations in a leaky confined coastal aquifer with finite length

*Zhi-Xue Zhao[1], Tongke Wang[1], Jun Li[1] (1.Tianjin Normal University, Tianjin, China)

### [AGE29-P03] Relationship between "source and sink"landscape patterns and river nutrient discharge in a peri-urban watershed

*Chongwei Li[1] (1.Tianjin Normal University)

### [AGE29-P04] Assessing the Urban Storm-Flood Disaster of Zhengzhou city Based on Fuzzy Methods

*Caihong Hu[1], Xian Du[1], Ying Zhang[1], SHAN E HYDER ALIAS TAHIR[1], Shengqi Jian[1] (1.School of water conservancy and environment, Zhengzhou University, Zhengzhou City, Henan Province, P.R. China, 450001)

### [AGE29-P05] Application of RAMMS Software to Predict the submerged area of Debris Flow: A Case Study of Feng-Chiou torrent in Taiwan

*Hsin-Ying Hsieh[1], Chun-Yi Wu[1] (1.Department of Soil and Water Conservation, National Chung Hsing University)

### [AGE29-P06] Applications of the Cholesteric Liquid Crystal (CLC) Sensor to Rapidly Measure the Volatile Organic Compounds in the Atmosphere Environment

Ruey-Fang YU[1], *GUAN-BO CHAO[1], Jian-cheng XU[1], KUANG-PENG HSIEH[1] (1.Department of Safety, Health and Environmental Engineering, National United University, Taiwan, R. O. C.)

### [AGE29-P07] Solar Ag/P3HT@$TiO_2$ Photocatalysis of Phenol Wastewater by a Pilot-Scale Fresnel Lens Assisted IPCC Reactor

*An-Chi Chen[1], Ting-Yu Zeng [1], Wen-Shiuh Kuo[1] (1.National United University,Department of Safety, Health and Environmental Engineering)

### [AGE29-P08] Using fluorescence quenching effect to investigate the electrical neutralization ability for different aromatic organic compounds

*Yu-Ting Chen[1], Wen-Po Cheng[1] (1.National United University,Department of Safety, Health and Environmental Engineering)

[AGE29-P09] **Sustainable recovery of sugarcane biowastes to prepare biochar-derived electrodes for recycling of brackish water**

*Shou-Heng Liu[1] (1.National Cheng Kung University)

[AGE29-P10] The National Survey of POPs in Soil: A study of polybrominated diethyl ethers (PBDEs) in Soil in Taiwan

*Shyh-Wei Chen[1], Ming-Yang Syue[2], I HSIN LEE[3], Chia Hsin Li[3], Yihsin Lai[3], Bo-Wei Power Liang[3] (1.Chung Yuan Christian Univ. Taiwan, 2.Soil and Groundwater Pollution Remediation Fund Management Board, EPA, Taiwan, 3.Sinotech Engineering Service LTD., Taiwan)

[AGE29-P11] **Remediation of Total Peteoleum Hydrocarbons in Soils by Combining Cyclodextrin and Microbubble Ozonation**

*Kuan-Yi Kuo[1], Meng-hau Sung[1], Fu-yin Xie[1] (1.Department of Environmental Science and Engineering,Tunghai University,Taiwan)

[AGE29-P12] **Treatment of organic pollutants in wastewater by ozone microbubbles and cyclodextrins**

*Fu-Yin XIE[1], Meng-hau Sung[1] (1.Department of Environmental Science and Engineering,Tunghai University,Taichung City,Taiwan)

[AGE29-P13] High Addition Valued Recycling Technology of Lithium-ion Battery

*YI-CHEN TSENG[1], TIEN-CHIN CHANG[1], YI-HSIANG HONG[1] (1.Institute of Environmental Engineering and Management, National Taipei University of Technology, No. 1, Sec. 3, Zhongxiao E. Rd., Da'an Dist., Taipei City 106, Taiwan (R.O.C.))

[AGE29-P14] Applying GIS Site Suitability Analysis to Optimize Landfill Selection in Mozambique

*Chelsea Adelina Langa[1] (1.Tohoku University, Graduate School of Environmental Studies)

[AGE29-P15] Effectiveness of Solidification/Stabilization of a Heavy Metal-Contaminated Soil Using a Sustainable Binder

*Yasong Feng[1,2,3], Weiyi Xia[1], Shiji Zhou[1], Ming Zhang[2], Yanjun Du[1] (1.Southeast Univ., 2.AIST, 3.Tohoku Univ.)

[AGE29-P16] **Determining diffusive parameters using out-diffusion experiment with consideration of sampling effect**

*Ranran Song[1], Chihiro Inoue[1], Ming Zhang[2] (1. Tohoku University, 2.Geological Survey of Japan, AIST)

[AGE29-P17] **Exploring the removal characteristics of heavy metals employing Nanofiltration (NF) technique**

*Jagdeesh Kumar[1], Himanshu Joshi[1] (1.INDIAN INSTITUTE OF TECHNOLOGY ROORKEE)

[AGE29-P18] **Potential of Potash Recovery Employing Electrodialysis(ED) Technique from Distillery Effluent**

*SUNIL YADAV[1], HIMANSHU JOSHI[1] (1.INDIAN INSTITUTE OF TECHNOLOGY ROORKEE)

[AGE29-P19] CHARACTERIZATION OF WATER RETENTION AND MASS TRANSPORT PROPERTIES FOR RECYCLED ROADBED MATERIALS BLENDED WITH AAC FINES

*Ryohei ITO[1], Akira KATO[1], Akihiro MATSUNO[1], Ken KAWAMOTO[1,2] (1.Graduate School of Science and Engineering, Saitama University, 2.National University of Civil Engineering, Vietnam)

[AGE29-P20] **Characterizing Geotechnical Properties of Drinking Water Sludge Blended with Graded Crushed Clay Brick for Road Subgrade: Effects of Gradation and Mixing Proportion of Crushed Clay Brick on Compaction Property**

*Tserenlkham lkhagvasuren[1], Muhammad Rashid Iqbal[1], Ken Kawamoto[1] (1.Graduate school of science and engineering Saitama University, Japan)

[AGE29-P21] CHARACTERIZING PHYSICAL AND CHEMICAL PROPERTIES OF RESIDUES GENERATED FROM CONSTRUCTION AND DEMOLITION WASTE

*NINGNING HAO[1], Ken Kawamoto[1], Akihiro Matsuno[1] (1.Saitama University)

[AGE29-P22] CHARACTERIZATION OF PORE-STRUCTURE PARAMETERS FOR UNDISTURBED AND REPACKED SAMPLES AT FIELD WATER CONTENTS

*Arjun Baniya[1], Akihiro Matsuno[1], Ken Kawamoto[1] (1.Saitama University , Graduate school of Science and Engineering)

[AGE29-P23] **CHECK SHEET SURVEY FOR ESTIMATING CDW GENERATION AND CASH FLOW AT BUILDING DEMOLISHING SITES IN HANOI, VIETNAM**

*Cuong Viet Tran[1], Kawamoto Ken[1] (1.Graduate School of Science and Engineering, Saitama University)

[AGE29-P24] APPLICATION OF CRUSHED GRAINS OF LATERITE AND AUTOCLAVED AERATED CONCRETE FOR HEAVY METAL REMOVAL FROM WASTEWATER

*Buddhika Priyadarshani Bandara Arachchillage[1], Yuki Yoshida[1], Pradeep Kumara Gajanayake Mudalige[1], Akihiro Matsuno[1], Ken Kawamoto[1] (1.Graduate School of Science and Engineering, Saitama University)

[AGE29-P25] Effects of Silicic Acid on Environmental Stability of Spent Calcium-based Arsenic Adsorbents

*Hajime Sugita[1], Terumi Oguma[1], Ming Zhang[1], Junko Hara[1], Yoshishige Kawabe[1] (1.National Institute of Advanced Industrial Science and Technology)

[AGE29-P26] The Fate of Chloroethene in Geo-environment

*Ming Zhang[1], Miho Yoshikawa[1] (1.Institute for Geo-Resources and Environment, Geological Survey of Japan, AIST)

# The role of anthropogenic activities in spring discharge cessation: Jinci Springs China

Yaru Guo[1], *Yonghong Hao[1], Chun Zhao[1], Huan Lian[1]

1. Tianjin Normal University

Most of the karst spring discharge in northern China has been declining since 1950s. Jinci Springs, as one of the typical karst springs in northern China, has dried up in May 1994. In this study, we proposed grey relational analysis with time lag to calculate the delay between spring discharge and precipitation, and set up GM (1, N) model to simulate the spring discharge. The methods were applied to investigate the drying-up of Jinci Springs. Based on its characteristics of the Jinci Springs discharge, we divided the spring discharge into two stages: in the first stage (1954-1960), the spring discharge only affected by climate variations, and in the second stage (1961-1994), the spring discharge impacted by both climate variations and anthropogenic activities. In the first stage, the Jinci Springs discharge had large grey relational degrees with precipitation ahead of one year and three years. Then the GM (1, 3) model with time lag of one year and three years was set up to simulate the spring discharge of the second stage under sole effect of climate variations. Subtracted the observed spring discharge from the simulated spring discharge, we obtained the contribution of human activities to Jinci Springs cessation. Results showed that the contribution of human activities to the cessation of Jinci Springs was 1.456$m^3$/s, accounting for 70%. The contribution of climate variations was 0.624$m^3$/s, accounting for 30%. The impact of human activities on the spring cessation surpassed climate variations and became the major factor. The contribution of the groundwater exploitation increment was 0.97$m^3$/s, the dewatering from coal mining increment was 0.60$m^3$/s, and the leakage reduction of Fenhe River was 0.19$m^3$/s. The total amount was 1.76$m^3$/s. After the Jinci Springs dried up, human further overexploited groundwater about 0.304$m^3$/s.

Keywords: spring discharge, anthropogenic activities , drying-up, Jinci Springs

©2019. Japan Geoscience Union. All Right Reserved. 

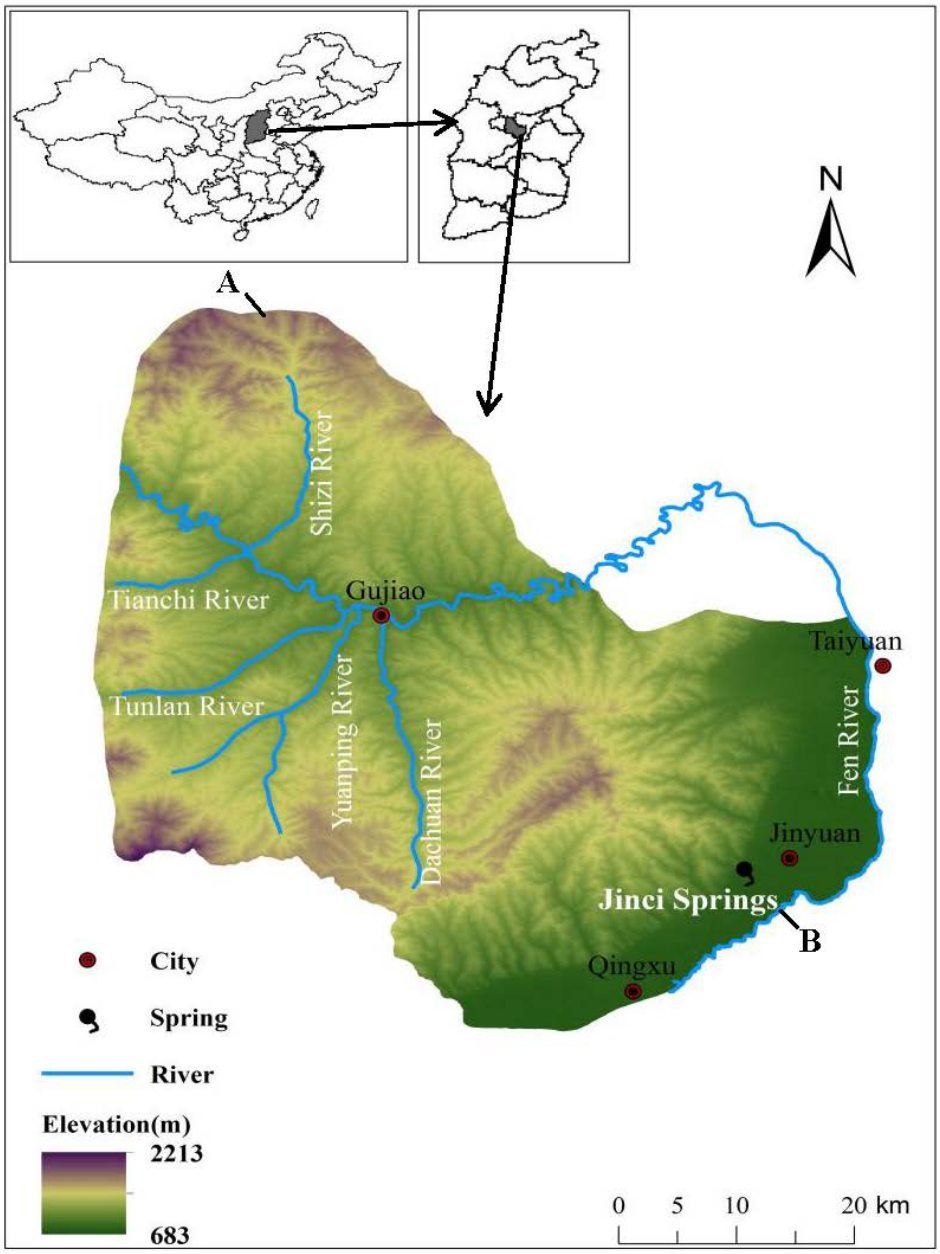


**Figure 1** Location and digital elevation model (DEM) of Jinci Springs catchmen

©2019. Japan Geoscience Union. All Right Reserved. 

# Groundwater response to tidal fluctuations in a leaky confined coastal aquifer with finite length

*Zhi-Xue Zhao[1], Tongke Wang[1], Jun Li[1]

1. Tianjin Normal University, Tianjin, China

We derive an analytical solution to calculate the groundwater response to tidal fluctuations in a horizontally-finite, leaky, coastal aquifer system. Our solution represents a generalized formulation that encompasses previous results as special cases. Based on the solution, we investigate the joint effects of the leakage and inland aquifer length on the behavior of the groundwater level fluctuation. We show that neglecting the finite-length effect may lead to significant errors in parameter estimations. Moreover, the range where the finite-length effect dominates is quantitatively determined by a characteristic dimensionless parameter. Finally, we demonstrate the usage of the proposed solution in calculating hydraulic properties through an application to a field experiment conducted at the Seine River estuary, France.

Keywords: Coastal aquifer, Analytical solution, Leakage, Tidal effect

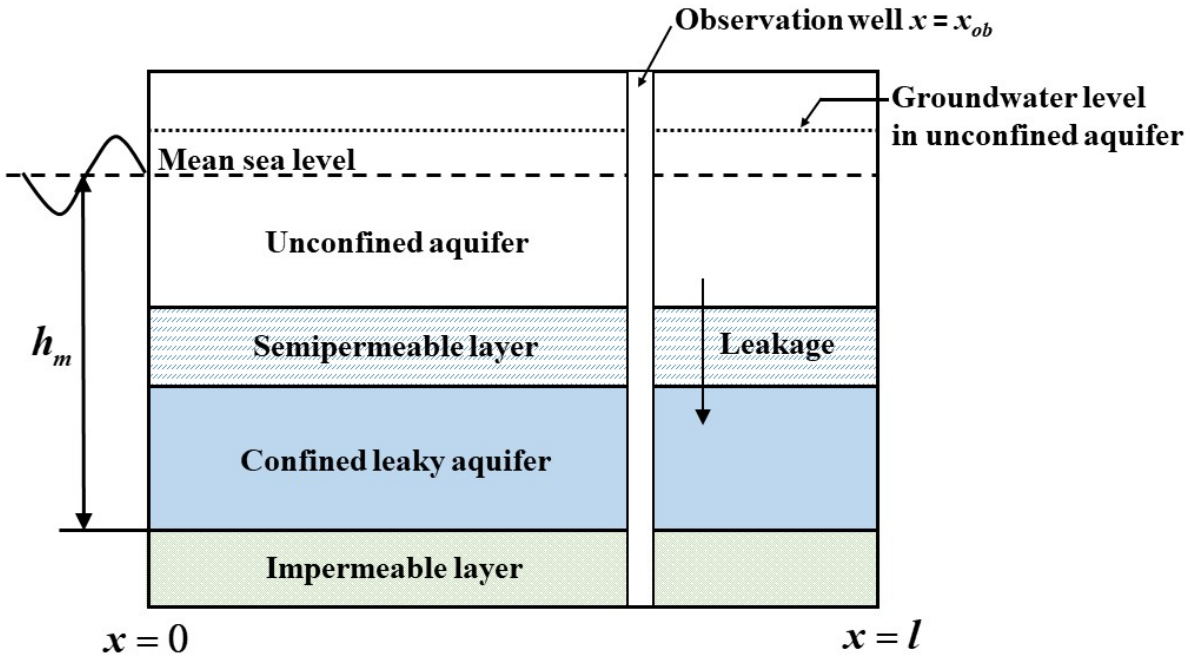


**Figure 1** Schematic diagram of the leaky confined aquifer system in coastal areas

©2019. Japan Geoscience Union. All Right Reserved. 

# Relationship between "source and sink"landscape patterns and river nutrient discharge in a peri-urban watershed

*Chongwei Li[1]

1. Tianjin Normal University

Better understanding of landscape pattern affects water quality in the peri-urban watershed are essential for sustainable development and utilization of water resources.A peri-urban watershed refers to a watershed located in the transition or interaction zone, landscape features aresubject to rapid modifications induced by human activities.Humans alter land uses and the landscape patterns both temporally and spatially.Land uses in a watershed can be functionally grouped into “source” or “sink” landscapes based on their contribution to the formation of nonpoint-source pollution in the watershed.As a result, the surface runoff and nutrient loading from a watershed are affected not only by the proportion of “source” and “sink” landscapes but also by their spatial arrangement and distribution.The assessment of non-point source pollution in peri-urban and urban watersheds is challenging but crucial for bothwater resource managers and urban planners.
The Yuqiao Watershed located in northern Tianjin City and southern part of Hebei Province, China ,which was chosen as an example of a peri-urban watershed. Based on the "source-sink" landscape characteristic index of the river basin and combined with the water quality data of 33 sub-basins in the river basin of the bridge reservoir in recent years, The relationship between landscape pattern and water quality was analyzed by spatial analysis, correlation analysis and redundancy analysis (RDA) using landscape use and landscape index as explanatory variables and nitrogen and phosphorus load as dependent variables.Results show that Under the influence of urbanization, From 1984 to 2013, the percentage of "sink" landscape (forest and grassland) decreased from 46.5% to 31.9%, entirely the result of the sharp reduction in forested area from 37.5% to 18.9%. In contrast, the percentage of "source" landscape (urban, orchard, and cultivated land) increased from 49.6% to 62.5%. Among them, the urban land increased from 11.6% to 18.1%. The global Moran's I value of landscape spatial load comparison index (LWLI) is 0.637, $P < 0.01$, and tends to cluster in space.LWLI was significantly correlated with the spatial distribution of nitrogen and phosphorus in the basin. The complex correlation coefficient $R^2$ of TN and LWLI in peacetime was 0.811, and that of LWLI and TP in wet season was 0.741.The axial angles among patch density (PD) , Shannon Diversity index (SHID) and TN,TP were smaller,indicating that PD and SHID had more influence on the nitrogen and phosphorus in the catchment.Compared with other landscape characteristics indexes, LWLI has the largest impact on nitrogen and phosphorus in rivers, and urban residential land is an important contributor to water pollution in watershed. The results could potentially provide a thoretical support for the optimization of the landscape paterrn in watershed.

Keywords: watershed, landscape pattern, nitrogen and phosphorus , spatial analysis, urbanization

©2019. Japan Geoscience Union. All Right Reserved. 

# Assessing the Urban Storm-Flood Disaster of Zhengzhou city Based on Fuzzy Methods

*Caihong Hu[1], Xian Du[1], Ying Zhang[1], SHAN E HYDER ALIAS TAHIR[1], Shengqi Jian[1]

1. School of water conservancy and environment, Zhengzhou University, Zhengzhou City, Henan Province, P.R. China, 450001

The frequency of urban waterlogging floods increased year by year with the accelerating process of urbanization in China. It is very important for us to study the urban waterlogging warning and emergency management. Four flood evaluation indexes, which are the 3h cumulative rainfall, submergence and waterlogging disaster degree and comprehensive management efficiency, are selected as the accessing indexes based on the DPSIR (Driving forces, Pressure, State, Impact and Responses model) model. Fuzzy comprehensive evaluation method is applied to evaluate the urban disaster degree based on the index weight determined by the analytic hierarchy process (AHP). Zhengzhou city, which located in the middle of China, is taken as an example for our study. Based on the SWMM model, this paper divides the urban area of Zhengzhou into 2200 unit areas. Four grades were divided for disaster degrees. The results show that Zhengzhou city will encounter different grades of waterlogging disasters with different precipitation. 469, 708, 1006 and 1057 units area of the city will encounter the second grades for warning when the rain of half a year, one year, two years and five years return period happen. The results show that the method is scientific and reasonable and can be applied to practical work.

Keywords: waterlogging warning grade, DPSIR model, evaluation index, fuzzy comprehensive evaluation method

©2019. Japan Geoscience Union. All Right Reserved. 

# Application of RAMMS Software to Predict the submerged area of Debris Flow: A Case Study of Feng-Chiou torrent in Taiwan

*Hsin-Ying Hsieh[1], Chun-Yi Wu[1]

1. Department of Soil and Water Conservation, National Chung Hsing University

Predicting the submerged area of debris flow hazard events can effectively reduce the extent of catastrophe. In this study, we used three-dimensional debris flow runout model, RAMMS (Rapid mass movements simulation), to simulate the debris flow of Feng-Chiou torrent in Feng-Chiou Village, Xinyi Township, Nantou County, Taiwan. The RAMMS is based on the Voellmy-Salm rheology theory and describes the flow development of debris flow in a depth-averaged equation. The RAMMS can be used to simulate the debris flow phenomenon caused by landslide in the study area. We use the well-documented debris-flow event to calibrate the model parameters by back analysis, so that the simulation results are more realistic. Then we used parameters of the total volume (M), flow height (H), dry-Coulomb type friction (coefficient $\mu$) and viscous-turbulent friction (coefficient $\xi$) of the debris flow event for sensitivity analysis and discussed the effect of each parameter on the simulation results. Further, we used the rational formula to estimate the discharges corresponding to the rainfall intensities of different recurrence intervals. We used simply hydrograph method as the initial condition to predict the possible submerged area of debris flow events caused by different recurrence intervals.

Keywords: RAMMS, debris flow, Feng-Chiou torrent, landslide

©2019. Japan Geoscience Union. All Right Reserved. 

# Applications of the Cholesteric Liquid Crystal (CLC) Sensor to Rapidly Measure the Volatile Organic Compounds in the Atmosphere Environment

Ruey-Fang YU[1], *GUAN-BO CHAO[1], Jian-cheng XU[1], KUANG-PENG HSIEH[1]

1. Department of Safety, Health and Environmental Engineering, National United University, Taiwan, R. O. C.

The Volatile Organic Compounds (VOCs) are one of the most important air pollutants emitted from industries. Some of the emitted Volatile Organic Compounds are carcinogenic which are harmful the health of both the human and environments. Typically, the concentrations of the VOCs in the atmosphere environment were measured by a Gas Chromatography (GC). However, these methods are expensive, complex, and difficult to be used for on-line application. According to the literatures, there is a lack of simple and economy detection methods for rapidly measure the VOCs in the atmosphere environment. The purpose of this study was to develop a Cholesterol Liquid Crystal (GLC) sensor for rapidly measure the concentrations of volatile organic compounds (VOCs) in the atmosphere environment.

According to the experimental results of this study, the physical directions of the GLC molecules will be changed when the prepared CLC sensor contact with the VOCs, and resulting the color on the surface of the CLC sensor changed from a Green or Red color to colorless, therefore, the target VOCs can be identified. By using a UV-VIS spectrophotometer or digital image analysis, the color can be identified. Moreover, it was also found that the color change from Green to colorless is rapid when contact with higher concentrations of VOCs. The durations of color change from Green to colorless was also found presented a liner relationship with the concentrations of VOCs, therefore, the concentrations of VOCs in the atmosphere environment can be identified. The CLC sensor was arranged to contact the VOCs by the controlled of different temperatures of 22±0.3$^0$C, 24± 0.3$^0$C, 27 ±0.3$^0$C and 30± 0.3$^0$C, respectively. The concentrations of VOCs can be measured from 19,955 ppm to 36,585 ppm with a linear relationship of $R^2$ =0.97 at 22±0.3$^0$C, the concentrations of VOCs from 9,978 ppm to 26,607 ppm ($R^2$=0.97) can be measured the GLC sensor at 24±0.3$^0$C, the concentrations of VOCs from 26,607 ppm to 43,237 ppm ($R^2$ =0.90) by the GLC sensor at 27±0.3$^0$C, as well as the concentrations of VOCs from 8,315 ppm to 19,955 ppm ($R^2$=0.90) by the GLC sensor at 30±0.3$^0$C. As a result, the VOCs concentrations can be easy and rapid identified by the prepared CLC sensor using the analysis data from both UV-VIS and image analysis.

Keywords: Cholesteric Liquid Crystal, sensors, Volatile organic compounds(VOCs), Image analysis

©2019. Japan Geoscience Union. All Right Reserved. 

# Solar Ag/P3HT@$TiO_2$ Photocatalysis of Phenol Wastewater by a Pilot-Scale Fresnel Lens Assisted IPCC Reactor

*An-Chi Chen[1], Ting-Yu Zeng [1], Wen-Shiuh Kuo[1]

1. National United University,Department of Safety, Health and Environmental Engineering

One of advanced oxidation processes (AOPs) - solar photocatalysis with novel Ag/P3HT@$TiO_2$ as catalyst was used to treat phenol wastewater (10 mg/L) in this study. Moreover, a pilot-scale Fresnel lens mounted inclined plate curvature channel (IPCC) reactor was well design, established and evaluated for the treatment of phenol wastewater. 5 Fresnel lens which were made of PMMA with a thickness of 2 mm, a pitch of 0.5 mm, a facet depth of 0.2 mm, and Fresnel circles of 395 were used and mounted on IPCC. Results showed that the degradation efficiency of phenol wastewater could reach 98.35% with a dosage of 0.5 g/L Ag/P3HT@$TiO_2$ and a reaction time of 3 h under solar light irradiation (average $UV_{a+b}$ : 42.90 $W/m^2$). In addition, the intensity of solar light was found to be focused with an increase of 1.86 to 3.91 times and the temperature of wastewater could be raised for 3 to 5˚C with the assistance of Fresnel lens, leading to that the degradation rate of phenol molecule in Ag/P3HT@$TiO_2$ photocatalytic process increases 1.66 times as compared to without Fresnel lens system. The molecules of phenol were more efficiently decomposed into low-molecular-weight organic acids which were further mineralized into $CO_2$ and $H_2O$. Accordingly, the Fresnel lens enhanced IPCC reactor showed a synergistic effect on the solar photocatalytic process not only in effectively dealing with a large amount of industrial organic wastewater, but also in the sector of energy conservation in terms of effective utilization of solar energy.

Keywords: Solar Photocatalysis, Ag/P3HT@TiO2, IPCC, Phenol, Fresnel lens

©2019. Japan Geoscience Union. All Right Reserved. 

# Using fluorescence quenching effect to investigate the electrical neutralization ability for different aromatic organic compounds

*Yu-Ting Chen[1], Wen-Po Cheng[1]

1. National United University,Department of Safety, Health and Environmental Engineering

The sources of organic matter in water include natural organic matter and synthetic organic matter. Most part of natural organic matter in water is humic acid which molecular weight is counted for hundreds to hundreds of thousands. The existence of humic acid not only affects the color and smell of water, but also produces toxic disinfection by-products. In addition, in synthetic organic matter, dye is used in the textile industry and the issue of process that produced waste water has been aware of increasingly. Therefore, effectively removing organic matter from water through the chemical coagulation process continues to be considered as a fairly important index of water purification efficiency.When the organic matter contains an aromatic heterocyclic structure and is excited by absorbing a specific radiation, it will eventually release the absorbed energy to the lower electronic energy level. Normally, the energy is released in the form of fluorescence. On the other hand, if the organic matter and metal ions are bonded to each other, the fluorescence intensity will be reduced. This phenomenon is known as the fluorescence quenching effect. In this study, the Stern-Volmer formula $F0F=1+K_q[M]$ will be used to evaluate the ability of the $Al^{3+}$ coagulant complex with organic matter. Where $F_0$ is the fluorescence intensity in the absence of $Al^{3+}$ quencher and F is the fluorescence intensity in the presence of $Al^{3+}$quencher, [M] is the concentration of the quencher, and $K_q$ is the equilibrium constant or quenching constant. Furthermore, the value of $K_q$ also represents the electrical neutralization capacity of coagulant under different conditions such as pH, molecular weight, hydrophilicity, functional groups of organic compound and coagulant dosage etc.The results in this study show that (1) under conditions of solution pH=6, the order of Kq values with different aluminum chloride dosage are Humic acid > Quinic acid > Salicylic Acid. Indicating that the molecular weight of organic matter is an important factor causing the degree of electrical neutralization ability; (2) under different solution pH, Reactive Blue 49 obtains the maximum Kq values than Direct Red 28 and Disperse Red 60 those often used in textile industry demonstrating the more number of sulfonic groups in the dye molecule, the more intensify electrical neutralization ability. (3) The Kq value of hydrophilic molecule (Direct Red 28) is higher than hydrophobic molecule (Disperse Red 60). These results indicate that the hydrophilicity of organic matter has a certain influence on the electrical neutralization by aluminum ions.All of results in this study show that the Stern-Volmer formula is a viable and simple method in operation to find the influencing factor of electrical neutralization ability between organic matter and aluminum coagulant and find the optimum coagulation conditions.

Keywords: Aluminum chloride, Coagulation, Aromatic orgain compounds, Fluorescence quenching effect, Electrical neutralization

©2019. Japan Geoscience Union. All Right Reserved. 

# Sustainable recovery of sugarcane biowastes to prepare biochar-derived electrodes for recycling of brackish water

*Shou-Heng Liu[1]

1. National Cheng Kung University

Membrane capacitive deionization (MCDI) is an emerging technology for the energy-efficient and cost-effective removal of ions from salt water by electrosorption. To further enhance the capacitive deionization performance, sugarcane bagasse biowastes are used as raw materials to synthesize biochars by microwave-assisted carbonization and activation with potassium hydroxide in the flows of carbon dioxide, which has the advantages of reducing preparation time and saving energy. Experimentally, the effect of microwave power (500-800 W) has been studied on the morphology, the ratios of mesoporosity in the biochars and their corresponding desalination performance of MCDI. Accordingly, the biochars which are activated at 700 W of microwave irradiation under carbon dioxide atmosphere (denoted as SB-$CO_2$-700) possess the ratios of mesopores to total pore volume ratio ($V_{meso}/V_{total}$) of ca. 64.1% with surface areas of 764 $m^2$ $g^{-1}$. By using cyclic voltammetry, the specific capacitance of SB-$CO_2$-700 is calculated to be ca. 123 F $g^{-1}$ at 5 mV $s^{-1}$. From the desalination tests at 1.2 V, the electrosorption capacity of SB-$CO_2$-700 samples is estimated to be 15.8 mg $g^{-1}$ in 5 mM of NaCl solution. The enhancement in the desalination performance of SB-$CO_2$-700 is possibly due to the greater $V_{meso}/V_{total}$ ratio, reasonable surface area and hierarchically porous structure.

Keywords: capacitive deionization, biomass, microwave-assisted CO2 activation, biochars

©2019. Japan Geoscience Union. All Right Reserved. 

# The National Survey of POPs in Soil: A study of polybrominated diethyl ethers (PBDEs) in Soil in Taiwan

*Shyh-Wei Chen[1], Ming-Yang Syue[2], I HSIN LEE[3], Chia Hsin Li[3], Yihsin Lai[3], Bo-Wei Power Liang[3]

1. Chung Yuan Christian Univ. Taiwan, 2. Soil and Groundwater Pollution Remediation Fund Management Board, EPA, Taiwan, 3. Sinotech Engineering Service LTD., Taiwan

The United Nations Environment Programme (UNEP) elaborates the Stockholm Convention on Persistent Organic Pollutants (Stockholm Convention) to protect human health and the environment through a range of measures aimed at reducing and eliminating the production and use of POPs. In order to understand the distribution of POPs in soil, a national soil quality survey has been carried out by Taiwan Environmental Protection Administration (EPA). The survey result can serve as the basis for promoting the management measures and evaluation of management effectiveness. In Taiwan, decabromodiphenyl ether (decaBDE) is still being used as flame retardants that are mostly used in electronic and electrical products. This study discusses the survey result of PBDEs in soil as one of the achievements of soil quality survey.

The strategy of soil quality survey involved investigation for potential pollution sources areas and baseline soil quality areas (Figure 1). Industries handled with a large quantity of decaBDE, large waste treatment facilities for waste electrical and electronic equipments and industrial parks were identified as potential pollution sources which were selected and soils sampled were collected at their surrounding areas. The baseline soil quality survey were undertaken to understand the environmental soil quality without the effect of potential pollution sources. Sixty composite soil samples were collected at surrounding areas of potential pollution sources and 60 composite soil samples were collected at baseline survey areas. Soil samples were analyzed for 24 PBDE congeners by gas chromatography /high resolution mass spectrometer (GC/HRMS).

The survey result shows that PBDEs concentration of all soil samples, collected from surrounding areas of the potential pollution sources and baseline survey areas, are ranged from 0.189 μg/kg to 656 μg/kg (the mean concentration is 39.6 μg/kg) and 0.268 μg/kg to 41.9 μg/kg (the mean concentration is 6.25 μg/kg), respectively (Table 1 and Figure 2). The levels of PBDEs in all soil samples are far lower than U.S. EPA's Regional Screening Levels. The study also performed hypothesis test and the result shows that the concentration at surrounding areas of potential pollution sources is significant higher than that at baseline survey areas. It means that the industrials with high polluting potential may have impact on their surrounding environment. In addition, this study compares the spatial distribution of soil surrounding potential pollution sources and baseline survey areas. The higher PBDEs concentrations are detected in soil at surrounding areas of the industrials using decaBDE. It is speculated that decaBDE which is an additive type flame retardant is affected their surrounding soil by emissions during the use of the addition process. The soil concentrations at the surrounding areas of waste treatment facilities for waste electrical and electronic appliances are on an equal level with baseline areas. Furthermore, the PBDE congener pattern is analyzed. The BDE congener pattern is dominated by BDE-209 and account for more than 80% of the total PBDEs concentration. It is speculated that it may be related to the use of decaBDE in recent years in Taiwan and accumulate easier than other BDEs with low bromine number in soil due to their solubility.
To monitoring the condition of the soil quality, assessing the effect of the potential pollution sources on soil quality, a systematic survey and monitoring plan for POPs in the Stockholm Convention was

©2019. Japan Geoscience Union. All Right Reserved. 

established by Taiwan EPA. The survey and monitoring works will be conducted in accordance with latest chemical lists of Stockholm Convention. The achievement of soil quality monitoring will help to tracking the influence of potential pollution sources and changes on environmental quality. It also can provide information to assess the effectiveness of control measures, strengthen the soil quality management and ensure the sustainable use of land resources.

Keywords: PBDEs, Soil, Taiwan

©2019. Japan Geoscience Union. All Right Reserved. 

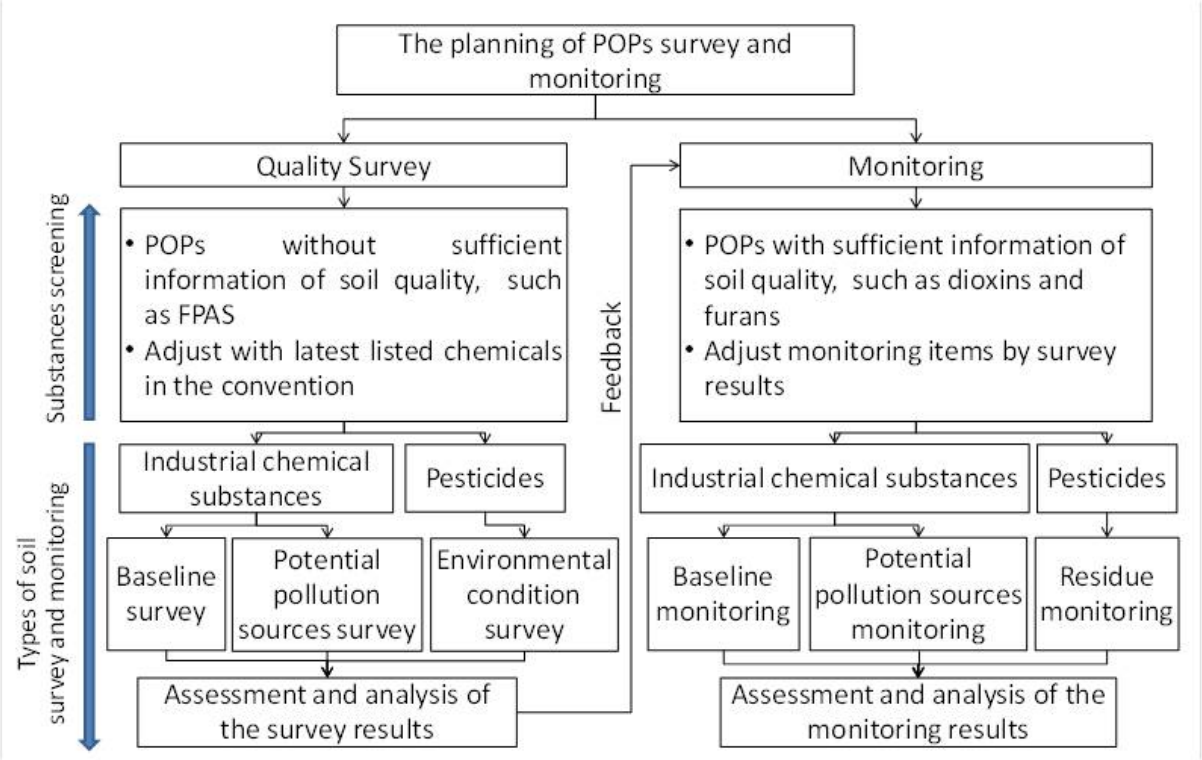


Figure 1 Framework of soil survey and monitoring plan

Table 1 Investigation results of PBDEs in soil in Taiwan

| POPs | Type of soil survey | No. of samples | Results (μg/kg) | |
|---|---|---|---|---|
| | | | Range | Average |
| PBDEs | Surrounding areas of potential pollution sources | 60 | 0.189~656 | 39.6 |
| | Baseline survey | 60 | 0.268~41.9 | 6.25 |

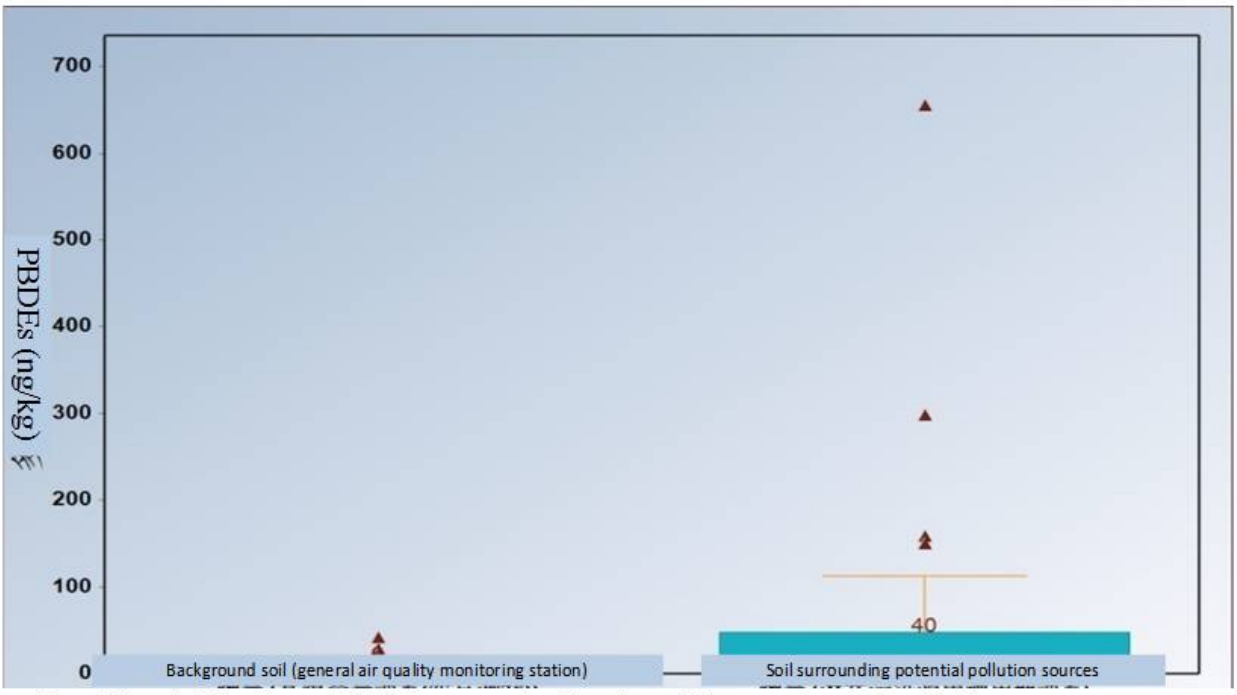


Figure 2 The distribution of PBDEs concentration in soil from potential pollution sources areas and baseline survey areas

©2019. Japan Geoscience Union. All Right Reserved. 

# Remediation of Total Peteoleum Hydrocarbons in Soils by Combining Cyclodextrin and Microbubble Ozonation

*Kuan-Yi Kuo[1], Meng-hau Sung[1], Fu-yin Xie[1]

1. Department of Environmental Science and Engineering,Tunghai University,Taiwan

In recent years, there have been many studies to increase the solubility of ozone by ozone-binding microbubbles or cyclodextrins, so that ozone has a better treatment effect. At present, no research has been conducted on the treatment of ozone in combination with microbubbles and cyclodextrins. Therefore, this study hopes to use ozone combined with microbubbles and cyclodextrin to treat the total petroleum hydrocarbons (TPH) in soil, and hopes to have better treatment effect than using microbubbles or cyclodextrin alone. This method is also a green remediation method that does not cause secondary pollution to the environment. In this study, ozone was first produced by an ozone generator and passed into a microbubble generator. Micron bubble ozone was then introduced into a water sample containing cyclodextrin, and finally the water sample was passed through a soil contaminated with TPH. In this study, different forms and concentrations of cyclodextrin were tested to examine their pertinent effects, so that the overall treatment efficiency of this method can be optimized. The instruments used in this study include spectrophotometer for the detection of ozone, LC with RID for the detection of cyclodextrin, and GC for the detection of TPH. It is expected that using microbubbles together with cyclodextrins simultaneously will improve the green remediation process.

Keywords: green remediation, soil treatment, total petroleum hydrocarbon, cyclodextrin, ozone microbubbles

©2019. Japan Geoscience Union. All Right Reserved. 

# Treatment of organic pollutants in wastewater by ozone microbubbles and cyclodextrins

*Fu-Yin XIE[1], Meng-hau Sung[1]

1. Department of Environmental Science and Engineering,Tunghai University,Taichung City,Taiwan

The hydroxyl radicals generated during ozonation can be used to oxidize organic pollutants in water. However, ozone gas is only slightly soluble in water. To increase the treatment efficiency, ozone microbubbles and cyclodextrins can be applied to increase the solubility. Microbubbles have high surface area and long residence time in aqueous solution. If they are combined with ozone gas to form ozone microbubbles, the solubility and half-life of gaseous ozone in water can be significantly improved. In definition, microbubbles refers to bubbles with a diameter between 1 micrometer and 1 millimeter. In addition to oxidative hydroxyl radicals generated, at the moment when the microbubble bursts, the pressure will be released, resulting in a high-speed microjet and ultra-high temperature locally. Under this condition, organic pollutants can also be degraded by pyrolysis. Cyclodextrins are often used in foods and are not harmful to humans. Adding cyclodextrin to the ozone microbubble system can increase the residence time of ozone in water and increase the half-life of ozone in water. Consequently, the combination of microbubbles and cyclodextrins appears to be a promising method for effective degradation of organic pollutants in water. Pesticides are common organic pollutants in water. After application, it may enter the environment via surface runoff, which may directly or indirectly enters water resources such as lakes or reservoirs. It has a certain impact on the environment and ecology, and may enter the groundwater system, which may affect the drinking water quality. The objective of this study is to establish an ozone microbubble system with cyclodextrin to treat organic pollutants in water. A variety of tests are conducted to examine its performance. Parameters considered in the experiments are pH and dosages of ozone microbubbles and cyclodextrin. The best condition for efficient degradation will be determined.

Keywords: wastewater treatment, green remediation, ozone microbubbles, cyclodextrin

©2019. Japan Geoscience Union. All Right Reserved. 

# High Addition Valued Recycling Technology of Lithium-ion Battery

*YI-CHEN TSENG[1], TIEN-CHIN CHANG[1], YI-HSIANG HONG[1]

1. Institute of Environmental Engineering and Management, National Taipei University of Technology, No. 1, Sec. 3, Zhongxiao E. Rd., Da’an Dist., Taipei City 106, Taiwan (R.O.C.)

Due to the development of lithium-ion batteries and the advancement of its technology, industrial applications such as that in electric vehicles become its leading application. The demand of lithium-ion battery increases dramatically in respond to the growing market of electric vehicles or other carriers. Under the circumstance that environmental resources are limited, high-value recycling technology is and considerably urgent need to accommodate the trend of the market. Though the differences in recycling technology exist across the countries in terms of efficiency, techniques, and feasibility of commercialization, the extracted noble metals can all be utilized in various products nowadays. No doubt, this technology and noble metals play significant roles in the perspective of industrial development in Taiwan. Other than industrial development, environmental concern due to the toxic waste coming from wasted batteries is of the same importance. Toxicants generated from rubbish lithium-ion batteries can corrode everything on this planet, therefore, policies and regulations to have good control of the waste materials should be developed along with the evolving technology.Due to the development of lithium-ion batteries and the advancement of its technology, industrial applications such as that in electric vehicles become its leading application. The demand of lithium-ion battery increases dramatically in respond to the growing market of electric vehicles or other carriers. Under the circumstance that environmental resources are limited, high-value recycling technology is and considerably urgent need to accommodate the trend of the market. Though the differences in recycling technology exist across the countries in terms of efficiency, techniques, and feasibility of commercialization, the extracted noble metals can all be utilized in various products nowadays. No doubt, this technology and noble metals play significant roles in the perspective of industrial development in Taiwan. Other than industrial development, environmental concern due to the toxic waste coming from wasted batteries is of the same importance. Toxicants generated from rubbish lithium-ion batteries can corrode everything on this planet, therefore, policies and regulations to have good control of the waste materials should be developed along with the evolving technology.

Keywords: Lithium-ion Battery, Circular Economy, Recycling Techonology

©2019. Japan Geoscience Union. All Right Reserved. 

# Applying GIS Site Suitability Analysis to Optimize Landfill Selection in Mozambique

*Chelsea Adelina Langa[1]

1. Tohoku University, Graduate School of Environmental Studies

Proper selection of landfills is a complex task. However, with the application of GIS technology, it is possible to aid in the selection of an optimal site, one that ensures environmental and social standards for potential landfills. In Maputo city, site selection of landfills is difficult due to land restrictions resulting from the land conflicts and groundwater presence. However, in the need of improving waste disposal conditions, a new landfill site has been selected. The goal of this study was to identify potential areas for landfill and evaluate the suitability of the new landfill. Environmental and social criteria were combined to firstly identifying potential disposal sites. By making a cross-reference of criteria map, three types of areas were selected, unsuitable, subjected to special evaluation and suitable areas. It was possible to estimate how the current landfill is in terms of environmental and social safety, based on the AHP ranking process. GIS and its aided tools were proved to be efficient in this process and of great value for the improvement of the municipal solid waste management in Maputo, however, due to the characteristics of the area, on-site studies are still necessary in order to validate landfills.

Keywords: Landfill, Selection, GIS

©2019. Japan Geoscience Union. All Right Reserved. 

# Effectiveness of Solidification/Stabilization of a Heavy Metal-Contaminated Soil Using a Sustainable Binder

*Yasong Feng[1,2,3], Weiyi Xia[1], Shiji Zhou[1], Ming Zhang[2], Yanjun Du[1]

1. Southeast Univ., 2. AIST, 3. Tohoku Univ.

Cement and lime are currently extensively used in solidifying/stabilizing heavy metals contaminated soils. However, cement and lime production is associated with intensive consumption of energy and nonrenewable resources. Under the drive of environmental friendliness, some by-products-based binders such as ground granulated blast furnace slag, pulverized fuel ash, and cement kiln dust have been successfully used in the remediation of contaminated soil. The authors have recently developed a sustainable binder, basic oxygen furnace slag (BOFS) activated by calcium carbide residue (CCR) and phosphogypsum (PG). The binder has almost no negative environmental impacts, and it can be used as an excellent substitute for cement.

This study presents a preliminary evaluation of the effectiveness of the BOF-based binder to stabilize mixed nickel (Ni) and zinc (Zn) contaminated soil collected from a vacant lot of an electroplating plant. The effects of binder dosage and curing time on soil pH, leachability and strength properties of the stabilized soils were examined. In addition, modified European Communities Bureau of Reference (BCR) sequential extraction procedure (SEP) and mercury intrusion porosimetry (MIP) analyses were performed to investigate the mechanisms that control the variations in heavy metal speciation and soil structure.

The results showed that soil pH and unconfined compressive strength (UCS) increased with increasing binder dosage and curing time. After 90 days of curing, the UCS of stabilized soils was approximately 2.9 - 6.6 times higher compared with those of untreated soil. Leaching concentrations of Ni and Zn were significantly reduced with increases in binder dosage and curing time. With 8% of binder addition and 28 days of curing, the leaching concentrations of both Ni and Zn were well below their corresponding remediation goals. The SEP results indicated that the binder addition significantly reduced the acid-soluble fractions of heavy metals while increased their residual fractions. The MIP test results showed that the soil pore volume reduced notably and soil structure changed remarkably after stabilization, inducing higher UCS compared with the untreated soil.

Keywords: Solidification/Stabilization, Heavy metal, Contaminated soil, Sustainable binder

©2019. Japan Geoscience Union. All Right Reserved. 

# Determining diffusive parameters using out-diffusion experiment with consideration of sampling effect

*Ranran Song[1], Chihiro Inoue[1], Ming Zhang[2]

1. Tohoku University, 2. Geological Survey of Japan, AIST

To know the details of diffusive properties of geo-materials is vital in geological disposal engineering projects. Out-diffusion experiment involves the process of heavy metal when diffuses out of geometries. It has simple structure and easy-operational experiment procedure. A theoretical solution considering the adsorption effect and sampling effect was developed. By applying theoretical analyses, we can estimate and decrease the errors induced by sampling. Sensitive analyses were also conducted to estimate a reasonable sampling time range and frequency. With the assist of theoretical analyses, a proper experiment can be designed. In this study, we assumed that heavy metal is linearly adsorpted on the surface of geo-material and linearly desorpted into the porous solution. We tested clay samples to get the effective diffusion-coefficient and capacity factor and examined the effect of sampling. As the linearly adsorption assumption may not be sufficient, especially to describe heavy-metals which easily adsorpted, we also try to discuss the effect of the heavy metal adoption effect to the diffusive process in these experiments.

Keywords: mass transport, diffusion, out-diffusion experiment, contaminants, heavy metal

©2019. Japan Geoscience Union. All Right Reserved. 

# Exploring the removal characteristics of heavy metals employing Nanofiltration (NF) technique

*Jagdeesh Kumar[1], Himanshu Joshi[1]

1. INDIAN INSTITUTE OF TECHNOLOGY ROORKEE

Heavy metals are serious environmental concern in recent industrial era, release from different industrial process. These are non-degradable, persistent, highly toxic and tendency of bioaccumulation into body tissues of organism, which causes several health consequences. Various technologies have been reported to develop so far in the removal of these contaminants which primarily include adsorption, chemical precipitation, and phytoremediation. These are conventional techniques of treatment process, which have several disadvantages such as high treatment cost, generation of sludge in bulk and requirement of large amount of adsorbent. From last few decades, usage of nanofiltration membrane (NF) during treatment process has gained significant attention in chemical processing, biotechnology and desalination industries. Recently, nanofiltration technique has been reported to be employed for the treatment of heavy metals in electroplating industries, due to its high efficiency, less energy consumption and minimum generation of toxic sludge. Therefore, a synergistic approach has been explored for the removal of concerned metals in combination with the electrocoagulation technique.

In present study, synthetic waste water was formulated containing different concentration of Zn, Cu and Ni metal ions for the treatment process. A central composite design was explored to study the effect of variable such as pH, concentration, pressure temperature ranges from the value of 4.5-9.5, 10-20 bar, 10-25 ppm and 15-35-degree C, respectively. A set of 30 experimental runs was examined for the removal. Further, the Response Surface Methodology (RSM) was adopted to optimize the removal percentage (maximize) by minimizing the pressure and maximizing the concentration. The experiments were also performed at the optimize conditions which have shown significant co-relation with the predicted values.

The removal percentage (%) of 99.96, 99.82 and 99.93 was observed at temperature of 15 -degree C for Cu, Ni and Zn metal ions, respectively. At low pH, high copper removal was observed as compared to those nickel and zinc ions. The high removal of copper occurred due to the formation of its precipitates at lower pH. The results show that the value of pH and metal concentration are not significantly affected the flux while pressure and temperature increase flux increase. This can be attributed to the fact that increased temperature decreased the viscosity and increase in the diffusion rate of solute through the membrane. The effect of pH and concentration on removal efficiency shows that the removal efficiency increases as pH increases while it decreases with the increased concentration. At desirability 0.993, the maximum removal of Zn, Ni, Cu were observed to be 101.53, 97.81 and 102.48, respectively. The maximum flux 225.88 was achieved at ambient temperature of 25-degree C. A good correlation of 0.9823 was observed for the experimental outcomes among the optimised experimental runs and predicted values.

Keywords: Nanofiltration, Response Surface Methodology (RSM), Electroplating Industry

©2019. Japan Geoscience Union. All Right Reserved. 

# Potential of Potash Recovery Employing Electrodialysis(ED) Technique from Distillery Effluent

*SUNIL YADAV[1], HIMANSHU JOSHI[1]

1. INDIAN INSTITUTE OF TECHNOLOGY ROORKEE

Sugarcane is one of the major cash crop of north-western and central part of India. Distillery industry coupled with sugar industry provides an economic and social infrastructure to the rural economy. The byproduct of sugar industry known as Molasses, utilized as raw material for the production of ethanol. The ethanol is a major source of beverages, biofuels and organic solvent production. It generates a large volume (approx. 8-10 L/L) complex, highly colored and concentrated organic stream alongwith high concentration of total dissolved solids as spent wash, which is a great concern as for treatment and disposal. Waste management and resource recovery has become a major task for large volume effluent generating industry to achieve long term sustainable economic development.

The characterization of spent wash shows a high concentration of potassium up to 8-10 g/L. High level of potassium concentration in the spent wash provide a way for economic utilization of the effluent. Several conventional technologies have been reported so far in recovering the potash from spent wash using incineration, ion exchange and chemical precipitation. These are having several disadvantageous in respect to high energy consumption, economically nonviable and less environmental significant. Presently, most of the industries depend on membrane processes alongwith anaerobic digestion techniques for the treatment of spent wash. However, the effluent is rich in potassium which can be recovered in the form of potash for its usage in agriculture production, as fertilizer.

In the present study, desalination experiments were carried out for nanofiltration membrane (NF) treated effluent, containing the concentration of potassium upto 6,000 mg $L^{-1}$ and electrical conductivity (EC) upto 28 mS $cm^{-1}$. The reject stream after the Nano filtration treatment was passed as feed through the Electrodialysis (ED). The main objective of the study is to separate the feed stream into dilute and concentrate stream with the aim of generating a highly saline effluent. A laboratory scale electrodialysis stack (mega EDR-Z) containing eleven cation exchange membranes and ten anion-exchange membranes of 64 $cm^2$ effective area was investigated for potassium removal. Two stream generated during the process one is the concentrated brine and the second one is the deionized effluent. The influence of applied voltage (10, 15, and 18 V) on removal efficiency was also examined. From these analyses, the potassium removal up to 92, 96 and 97 % has been observed at operating time of 120, 90 and 75 min, respectively. Similarly, the salinity removal upto 83, 95 and 97 % were observed. A desalinated effluent i.e. the dilute stream with conductivity less than 1mS $cm^{-1}$ and potassium level less than 150mg/l was generated. It is concluded that the increases in the voltage led to salt and potassium separation. This is due to the increase in current induces migration movement of all the dissolved ions in the process solutions. So, with the addition of an ED system with NF, a highly concentrated brine stream can be generated that can be further subjected to advance electrochemical process for potassium separation and crystallization.

Keywords: Electrodialysis, Potash Recovery, Spent wash , Ethanol Production

©2019. Japan Geoscience Union. All Right Reserved. 

# CHARACTERIZATION OF WATER RETENTION AND MASS TRANSPORT PROPERTIES FOR RECYCLED ROADBED MATERIALS BLENDED WITH AAC FINES

*Ryohei ITO[1], Akira KATO[1], Akihiro MATSUNO[1], Ken KAWAMOTO[1,2]

1. Graduate School of Science and Engineering, Saitama University, 2. National University of Civil Engineering, Vietnam

Permeable pavement systems (PPS) contribute to reduce surface runoff during heavy rainfall and to mitigate urban heat island effect.

The purpose of this study is to improve water retention capacity for recycled road-base materials utilizing fines (typically under 2 mm) from industrial by-products. Especially, the effects of mixing of fine grains made from autoclave aerated concrete (AAC; 0.106-2 mm) with graded recycled concrete (RC; 0.075-31.5 mm) and steel slag for roadbed construction (SS; 0.075-31.5 mm) were examined. Besides, mass transport parameters such as gas diffusion coefficient, air permeability, thermal conductivity, and heat capacity were measured for tested samples to characterize gas and heat exchange properties and pore structural properties of gas flow. After compacting the samples by Proctor D method, water retention curves were obtained through the drying process from water saturation. The gas and heat transport parameters were also measured at each suction stage and air-dried condition.

As a result, the mixing of AAC fines contributed highly to increase water retention capacities for both graded RC and SS. The mixing of AAC fine grains, on the other hand, did not affect the pore structural properties such as equivalent diameter and tortuosity for gas flow, suggesting the retained water in AAC fine grains would not impede the gas flow in graded roadbed materials mixed with AAC fine grains.

Keywords: Recycled Road-base Materials, Autoclave Aerated Concrete, Gas Transport

©2019. Japan Geoscience Union. All Right Reserved. 

# Characterizing Geotechnical Properties of Drinking Water Sludge Blended with Graded Crushed Clay Brick for Road Subgrade: Effects of Gradation and Mixing Proportion of Crushed Clay Brick on Compaction Property

*Tserenlkham Ikhagvasuren[1], Muhammad Rashid Iqbal[1], Ken Kawamoto[1]

1. Graduate school of science and engineering Saitama University, Japan

With rapid construction and renovation works, a huge amount of construction and demolition waste (CDW) is generated in urban areas of developing countries. The CDW is mostly dumped at the landfill sites directly and/or reused for construction works such as ground levelling and backfilling without any quality control of materials. Effective use and recycling of CDW is highly required to establish sustainable urban development. In this study, drinking water sludge (DWS) blended with crushed clay brick (CCB) was tested for the possible application to road subgrade. Especially, the effects of gradation/particle size of CCB and its mixing proportion to DWS on compaction properties have been examined using laboratory tests. A series of the modified Proctor compaction test was conducted using testing samples with three different particles of CCB; the finer (2-10 mm), coarser fraction (10-30 mm), and graded fraction (2-30 mm) and with different mixing proportions to DWS; 20, 40, 60, 80 and 100% on the dry mass basis. The tested results showed that particle breakage of all the above-mentioned fraction was almost the same up to 40% addition of CCB to DWS and was independent of particle size as well. A coarser fraction of CB showed the highest value of particle breakage (45.7%) which was almost double than that of finer (26.9%) and graded fraction breakage (22.8%) respectively. Measured compaction curves of all the mixed samples showed a linear relationship between maximum dry density and mixing proportion of the blended samples. The CCB mixing proportions more than 40% did not show any peak in the compaction curve probably due to a higher quantity of the cohesionless material (i.e., CCB).

Keywords: Drinking water sludge, Crushed clay bricks, Compaction, Particle breakage

©2019. Japan Geoscience Union. All Right Reserved. 

# CHARACTERIZING PHYSICAL AND CHEMICAL PROPERTIES OF RESIDUES GENERATED FROM CONSTRUCTION AND DEMOLITION WASTE

*NINGNING HAO[1], Ken Kawamoto[1], Akihiro Matsuno[1]

1. Saitama University

Due to rapid urbanization and population increase, the generation of Construction and Demolition Waste (CDW) is increasing in urban areas and industrial zones in developing countries. In order to promote sustainable development, it is important to have sound CDW management and recycling. Among of generated and dumped CDW, general masonry such as concrete and clay brick can be recycled for road construction and backfilling materials after suitable treatments like crushing and sieving. On the other hand, the reuse of fine residues (typically < 10 mm) faces some difficulties with regards to quality control and potential risk of hazardous materials. Based on the background, this study aims to characterize chemical and physical properties of CDW fines (especially for mortar samples). The testing samples were taken from 3 different demolition sites in Hanoi and Haiphong and a CDW dumping site in Hanoi. For the testing samples, two different fractions, one is bigger than 2mm and the other is grounded and sieved less than 2mm, were used for SEM-EDS analysis. Results showed that the samples with less than 2mm observed by 100 magnification of SEM became more stable (less spatial variability and following normal distribution). The measured Ca/Si values varied widely from 1.36 to 2.60 and became lower than that from a control mortar sample except for one sample from Hanoi demolition site. Further studies are planned to determine the mixing per cents of mortar and clay brick in CDW fines for characterizing the chemical composition and for promoting effective and safe use of recycled fines from CDW.

Keywords: Construction and Demolition Waste, Fine Residue, SEM-EDS

©2019. Japan Geoscience Union. All Right Reserved. 

# CHARACTERIZATION OF PORE-STRUCTURE PARAMETERS FOR UNDISTURBED AND REPACKED SAMPLES AT FIELD WATER CONTENTS

*Arjun Baniya[1], Akihiro Matsuno[1], Ken Kawamoto[1]

1. Saitama University , Graduate school of Science and Engineering

Mass transport in soils occurs through the soil pore network, which is highly influence by pore structure parameters (i.e. pore size distribution, porosity, pore tortuosity and pore coordination number). Micro-focus X-ray computed tomography (CT) has emerged as a powerful non-destructive tool for the direct visualization and better understand soil pore geometry. However, there have been few studies on visualization and quantification of soil pore network and soil pore networks linked to indirect pore parameters for gas flow based on measured gas diffusion coefficient and air permeability. In this study we visualized soil-pore networks for different soils, a sandy loam from Saitama, Japan and silty clay loam from Hawke’ s Bay, New Zealand. The study aimed to identify pore structure parameters using a microfocus X-ray computed tomography (MFXCT) system and compare indirect pore parameters such as tortuosity-connectivity parameter and equivalent pore diameter for gas flow. Undisturbed and repacked samples were used for characterizing soil pore networking and structure. For repacked soil samples, particle size (d<2mm) with field water content were used with different dry bulk densities by hand compaction. Soil samples were scanned by MFXCT system with different scanning resolutions of 12,30 and 50 μm/voxels. Then, 3-dimensional models were reconstructed with different regions of interest (ROI) of 50, 100, 200 and 300 voxels. Finally, soil pore-structural parameters such as effective pore radius, coordination number, and tortuosity in z direction were analyzed. With increasing ROI, the pore structure parameters of undisturbed and repacked samples showed less variation. The pore connectivity-tortuosity factors derived from MFXCT were well correlated with the indirect connectivity tortuosities from measured soil gas diffusion. However, it was observed that there were some variations between effective pore diameters from MFXCT and equivalent pore diameters for gas flow estimated by gas transport parameters depending on scanning resolutions (ranging from 1:1 to 1:3 for SR =12 μm/voxels and 1:1 to 4:1 for SR = 30 μm/voxels).

Keywords: Microfocus X-ray Computed Tomography (MFXCT), Gas Transport Parameters, Pore structural parameters

©2019. Japan Geoscience Union. All Right Reserved. 

# CHECK SHEET SURVEY FOR ESTIMATING CDW GENERATION AND CASH FLOW AT BUILDING DEMOLISHING SITES IN HANOI, VIETNAM

*Cuong Viet Tran[1], Kawamoto Ken[1]

1. Graduate School of Science and Engineering, Saitama University

## Abstract

A number of studies on reuse and recycling of construction demolition waste (CDW) for construction works as well as the properties of building materials using recycled aggregates have been carried out in many developed countries. However, in Vietnam, there are many difficulties to classify and recycle the CDW after demolition construction at site. Because the generation of CDW is increasing in Vietnam due to rapid urbanization and economic growth and CDW was dumped without any quality control of material at disposal site. It is highly demanded to promote the recycling of CDW in a sustainable manner.

In this study, in order to identify the CDW generation and cash flow at actual demolition sites in Vietnam. Firstly, we proposed a check sheet survey to discuss suitable CDW separation and treatment methods. The survey sheet enables to collect data on demolition period, number of labors and equipment, volume of CDW, number of trucks which brought the generated waste from the site, total floor areas, total cost for the demolition work, and so on. Then, using the survey sheet, actual survey works carried out at 3 different building demolishing sites in Hanoi. Finally, utilizing the collected data, we determined waste components and waste generation rates of typical materials such as concrete, brick, valuables (e.g., steel).

Results showed that most CDW generated from demolishing sites was sold to other contractors/buyers for the purpose of construction works (e.g., ground leveling). The generation rates of CDW including valuables varied widely from 0.29 to 1.22 tons/ ($m^2$ of total ground floor) depending on the building type and scale, and smaller building demolition gave a higher generation rate. As a result of cash flow, the estimated cost for selling valuables and CDW masonry to buyers became much higher than those for the contract cost of demolition work from land owner/client.

Keywords: Construction Demolition Waste (CDW)

©2019. Japan Geoscience Union. All Right Reserved. 

# APPLICATION OF CRUSHED GRAINS OF LATERITE AND AUTOCLAVED AERATED CONCRETE FOR HEAVY METAL REMOVAL FROM WASTEWATER

*Buddhika Priyadarshani Bandara Arachchillage[1], Yuki Yoshida[1], Pradeep Kumara Gajanayake Mudalige[1], Akihiro Matsuno[1], Ken Kawamoto[1]

1. Graduate School of Science and Engineering, Saitama University

Adverse effects on the environment and human health is highly influence by heavy metal contamination in water is a global significance problem. Among conventional treatment technologies for treating wastewater, a particular attention is given to adsorption process, considering as low-cost and easy technical applicability. In this study, in order to examine the applicability of locally available geo-materials and industrial by-products as cost-effective adsorbents in the treatment technology of heavy metal-contaminated water, laterite made from Vietnam and autoclaved aerated concrete were tested for the removal of arsenic and chromium in wastewater. Zeolite made from Japan was also used as a reference material. The testing samples were first grounded and sieved to be 0.105-2 mm grain size. The standard batch adsorption method by Organization of Economic Cooperation and Development (OECD 2000) was applied to determine adsorption isotherms. The isotherm experiments were evaluated for 1:10 solid liquid ratio at natural pH and 20 $^{0}$C temperature for solutions with initial concentrations ranging from 100 –2000 mg/L for both metals. The results indicated that Langmuir isotherm described the experimental data the best. Laterite removed arsenic and chromium in solutions up to 8.21 and 1.33 mg/g respectively. It revealed that laterite had higher adsorption capacity for arsenic than autoclaved aerated concrete. The measured removal percentages decreased with increasing in initial ion concentrations. Future, the adsorption mechanism will be suggested by correlating both laterite and autoclaved aerated concrete for heavy metal removal from wastewater.

Keywords: Adsorption , Heavy metals, Industrial by-products, Low-cost adsorbents, Wastewater

©2019. Japan Geoscience Union. All Right Reserved. 

# Effects of Silicic Acid on Environmental Stability of Spent Calcium-based Arsenic Adsorbents

*Hajime Sugita[1], Terumi Oguma[1], Ming Zhang[1], Junko Hara[1], Yoshishige Kawabe[1]

1. National Institute of Advanced Industrial Science and Technology

In some areas of developing countries, health effects caused by arsenic contained in groundwater used as drinking water have been a serious problem. Calcium compounds show promise for arsenic removal as effective and inexpensive adsorbents. However, the spent adsorbent would contain a great amount of arsenic. When the spent adsorbent is not properly recovered and is discarded near residences, secondary environmental pollution due to arsenic leaching from the spent adsorbent may occur. In our previous studies (leaching tests with soils), it was suggested silicic acid which leached from soils greatly affects leaching behavior of arsenic from the spent adsorbents. In this study, in order to examine the influence of silicic acid on the environmental stability of spent adsorbents in detail, leaching tests with silicic acid solution and 2 kinds of spent calcium-based adsorbent (CaO and $Ca(OH)_2$) were carried out. This study revealed that when the initial silicic acid concentration in solution is high, the leaching rate of arsenic decreases. This was inferred that when the silicic acid component in the solution reacted with the calcium component eluted from the spent adsorbents to form the calcium silicate species, the arsenate component leached from the spent adsorbents was taken into the products.

Keywords: Arsenic Leaching, Spent Adsorbent, Calcium Oxide, Calcium Hydroxide, Silicic Acid

©2019. Japan Geoscience Union. All Right Reserved. 

# The Fate of Chloroethene in Geo-environment

*Ming Zhang[1], Miho Yoshikawa[1]

1. Institute for Geo-Resources and Environment, Geological Survey of Japan, AIST

Chloroethene, also has the names of chloroethylene, ethylene monochloride, vinyl chloride monomer (VCM) or vinyl chloride (VC), is an important chemical substance widely used to produce polymer polyvinyl chloride (PVC) in plastic industry. Due to its high volatility, the pollution induced by the use of chloroethene itself is principally limited to air pollution. In geo-environment, such as soils and groundwater, the occurrence of chloroethene is mainly from biodegradation of its parent compound, like *cis*- Dichloroethene (*cis*-DCE), *trans*-DCE or 1,1-DCE, an intermediate product of biodegradation of trichloroethylene (TCE) and/or tetrachloroethylene (PCE). Either TCE or PCE has been widely used as an industrial solvent both in developed and developing countries.

To understand the fate of chloroethene in geo-environment, this presentation overviews the pathways, microorganisms, and degrading rates associated with biodegradation of chloroethene, the pollutant newly specified by the Japanese Soil Contamination Countermeasures Act. In natural environment, biodegradation of chloroethene is very slow and distribution of chloroethene around or downstream a source of pollution is dominantly affected by advection and dispersion. An advection-dispersion equation and sensitive analysis were, therefore, used to examine possible distances of chloroethene which may spread downstream of a source point over long time period. The control of groundwater flow can be an effective countermeasure against further spreading of pollutant plume.

Keywords: Chloroethene, biodegradation, pathway, microorganism, fate

©2019. Japan Geoscience Union. All Right Reserved. 

[E] Oral | A (Atmospheric and Hydrospheric Sciences )：A-CG Complex & General

Thu. May 30, 2019 9:00 AM - 10:30 AM JST | Thu. May 30, 2019 12:00 AM - 1:30 AM UTC | 302 3F

## [A-CG34] Satellite Earth Environment Observation

convener:Riko Oki(Japan Aerospace Exploration Agency), Yoshiaki HONDA(Center for Environmental Remote Sensing, Chiba University), Yukari Takayabu(Atmosphere and Ocean Research Institute, the University of Tokyo), Tsuneo Matsunaga(Center for Global Environmental Research and Satellite Observation Center, National Institute for Environmental Studies), Chairperson:Kentaroh Suzuki

In recent years, we cannot avoid facing issues on global environmental changes that occur in various spatiotemporal scales. The earth environmental observation data by satellites became the necessary basic data to tackle and solve those issues. Due to the recent advancement in the observation sensor technique and the data processing technique, the satellite observation has been showing rapid progress, and the time is changing from examining the accuracy of the observation sensor data to the advancement of the data application, leading to broaden potential users. In these days application became synergetic, so we comprehensively pick<br/>up this topic in the Atmospheric and Hydrospheric Sciences Session of this Union Meeting that enables to comprise the atmospheric, oceanic and land sciences; by combining the intelligence and the knowledge of the party, we propose a session that aims to prompt further studies towards the issues on earth environmental change, the advancement in the data application and future plans of Earth Observation missions.

9:00 AM - 9:15 AM JST | 12:00 AM - 12:15 AM UTC

### [ACG34-07] GCOM-C “Shikisai” FIRST YEAR OBSERVATIONS

★Invited Papers

*Hiroshi Murakami[1], Masahiro Hori[1], Risa Miyazaki[1], Toshiyuki Kobayashi[1], Takashi M. Nagao[1], Kazunori Ogata[1], Rigen Shimada[1], Junichi Takaku[2] (1.Earth Observation Research Center, Japan Aerospace Exploration Agency, 2.Remote Sensing Technology Center of Japan)

9:15 AM - 9:30 AM JST | 12:15 AM - 12:30 AM UTC

### [ACG34-08] Algorithm improvement for GCOM-C/SGLI Above Ground Biomass Standard product.

*KAJIWARA Koji[1], Yoshiaki HONDA[1] (1.Chiba University)

9:30 AM - 9:45 AM JST | 12:30 AM - 12:45 AM UTC

### [ACG34-09] Common retrieval of Atmospheric Aerosol Properties for geostationary and polar-orbital Satellite Imaging Sensors: Himawari8/AHI and GCOM-C/SGLI results

*Yoshida Mayumi[1], Maki Kikuchi[1], Takashi M. Nagao[1], Hiroshi Murakami[1], Keiya Yumimoto[2] (1.Japan Aerospace Exploration Agency, 2.Kyusyu University)

9:45 AM - 10:00 AM JST | 12:45 AM - 1:00 AM UTC

### [ACG34-10] Cloud optical properties from various ground and satellite instruments evaluated during an intensive campaign

*Alessandro Damiani[1], Hitoshi Irie[1], Takashi Horio[1], Tamio Takamura[1], Rei Kudo[2], Pradeep Khatri[3], Hironobu Iwabuchi[3], Ryosuke Masuda[3], Takashi M. Nagao[4] (1.CEReS, Chiba University, 2.Meteorological Research Institute, Japan Meteorological Agency, 3.Graduate School of Science, Tohoku University, 4.Earth Observation Research Center, JAXA)

10:00 AM - 10:15 AM JST | 1:00 AM - 1:15 AM UTC

### [ACG34-11] Issues in aerosol-cloud-climate interaction: Needs for future satellite mission

★Invited Papers

*Kentaroh Suzuki[1] (1.Atmosphere and Ocean Research Institute, University of Tokyo)

10:15 AM - 10:30 AM JST | 1:15 AM - 1:30 AM UTC

### [ACG34-12] Impact of aerosol vertical profile and optical parameters on the accuracy of satellite AOD retrieval

*Jing Li[1], Chong Li[1] (1.Peking University)

# GCOM-C “Shikisai” FIRST YEAR OBSERVATIONS

*Hiroshi Murakami[1], Masahiro Hori[1], Risa Miyazaki[1], Toshiyuki Kobayashi[1], Takashi M. Nagao[1], Kazunori Ogata[1], Rigen Shimada[1], Junichi Takaku[2]

1. Earth Observation Research Center, Japan Aerospace Exploration Agency, 2. Remote Sensing Technology Center of Japan

One-year observation results of Global Change Observation Mission-Climate (GCOM-C) called “SHIKISAI” are introduced.

JAXA polar-orbit satellite, GCOM-C, which carries Second-generation Global Imager (SGLI), has been launched on 23 Dec. 2017, and operated in orbit during 2018. The key characteristics of the SGLI are (1) 250-m spatial resolution with 1150 km or 1400 km swath, and (2) nineteen bands in 0.38-12 um including two polarimetry bands (at 672 nm and 866 nm) with +/- 45 degree along-track tilt.

The SGLI radiometric gain was evaluated by the on-board calibration functions (solar, lamp, lunar, and electric calibrations) and vicarious calibration over the land, ocean and ice sheet. The radiometric gain was stable during the first year except for slight degradation (<2 %/year) in 380-565 nm bands. The geometric correction accuracy was evaluated by the Ground Control Point (GCP) matching. The deviation from the GCPs was stable and kept less than about 0.3 pixels.

The SGLI 250-m bands could capture seasonal change of the vegetation and the snow cover, the large-scale red tide, and the fine structures of land-surface temperature and coastal sea-surface temperature. Especially, unique functions of SGLI, the 380-nm band and polarimetry revealed the fine-mode aerosol distribution around wild fires (e.g., California, Africa, and Siberia) and Asian city areas (e.g., North India, and East China). The polarimetry seemed to improve estimation of the aerosols emitted densely from the fires. Difference of the 250-m land-surface temperature between the day and nighttime may give us information about the heat budget in the various land covers including city and crop areas. The GCOM-C standard products have been evaluated and open to public freely through JAXA data portal, G-portal, since Dec. 2018. The re-process of the 2018 data will be completed in the early summer 2019. The accumulating GCOM-C data products are expected to be used in the wide areas of the earth environment researches.

Keywords: GCOM-C, SGLI, remote sensing

©2019. Japan Geoscience Union. All Right Reserved. 

# Algorithm improvement for GCOM-C/SGLI Above Ground Biomass Standard product.

*KAJIWARA Koji[1], Yoshiaki HONDA[1]

1. Chiba University

On 23rd Dec., 2017, Japan Aerospace Exploration Agency (JAXA) has launched new Earth observation satellite GCOM-C . GCOM-C equips Second-generation Global Land Imager (SGLI) as core sensor. Since SGLI can observe nadir and off-nadir angle with along-track direction simultaneously, it is expected to retrieve forest Above Ground Biomass (AGB) using bi-directional spectral data.

For the estimation of forest AGB, difference of bi-directional reflectance of each observation angle caused by forest canopy structure will be key information.

Authors have been developed basic AGB estimation algorithm for SGLI AGB standard product. This algorithm is based on the empirical model related to the relationship between reflectance shift on the Red-NIR plane for different viewing angle and AGB. The algorithm requires optimum approximation coefficients directly related AGB amount in observed area for each forest type. In 1st stage product algorithm, we have decided these coefficients using AGB in-situ dataset collected from literature survey which work has been conducted by JAMSTEC. While the AGB estimation results using SGLI reflectance data achieved success criteria for initial stage, it is required for getting better accuracy to achieve the full success criteria.
In this paper, development of algorithm for aimed at improving accuracy was discussed. The improved algorithm which adopting the rasterized AGB existed data base and change the zoning method, has been tested. The result of the trial, the accuracy of estimation has been confirmed.

Keywords: Second Generation Global Imager (SGLI), Multi-angular observation, Forest canopy, Biomass Estimation

©2019. Japan Geoscience Union. All Right Reserved. 

# Common retrieval of Atmospheric Aerosol Properties for geostationary and polar-orbital Satellite Imaging Sensors: Himawari8/AHI and GCOM-C/SGLI results

*Yoshida Mayumi[1], Maki Kikuchi[1], Takashi M. Nagao[1], Hiroshi Murakami[1], Keiya Yumimoto[2]

1. Japan Aerospace Exploration Agency, 2. Kyusyu University

Aerosols influence the energy budget of the earth’ s climate system through scattering and absorbing solar radiation. The Intergovernmental Panel on Climate Change Fifth Assessment Report (IPCC, 2014) reported that the radiative forcing of the total aerosol effect in the atmosphere, which includes cloud adjustments due to aerosols, is −0.9 W $m^{-2}$ and results from a negative forcing from most aerosols with a positive contribution from black carbon absorption of solar radiation. However, the range of the uncertainties remains large (−1.9 W $m^{-2}$ to −0.1 W $m^{-2}$).

For a more precise estimation of the impact of aerosols on climate systems, investigation of the behavior of aerosols on a global scale is essential but challenging because aerosol amounts and characteristics vary over space and time.

Aerosol remote sensing studies have been carried out using polar-orbital Earth observation satellites. JAXA has launched Global Change Observation Mission-Climate (GCOM-C)/Second-generation GLobal Imager (SGLI) at the end of 2017, and Greenhouse gases Observing SATellite- 2 (GOSAT-2)/Cloud and Aerosol Imager 2 (CAI-2) in 2018. In several years, Earth Clouds Aerosols and Radiation Explorer (EarthCARE)/ Multi-Spectral Imager (MSI) will be launched.

In addition, the next-generation geostationary satellite of the Japan Meteorology Agency (JMA), Himawari-8, was launched on October 7, 2014. It carries the Advanced Himawari Imager (AHI), which has six bands from visible to near-infrared wavelengths. It is significantly different from the previous Himawari-6/7 having only one channel in the wavelengths, which made the estimation of aerosol difficult because the assumption of aerosol type is necessary. Himawari-8/AHI observes the top of atmosphere (TOA) visible and near-infrared radiance at a resolution of 0.5–2.0 km over Asia and Oceania at every 10 min, which enables frequent aerosol estimation over the same ground targets.

The synergistic uses of these various imaging sensors on both geostationary and polar-orbital satellites are helpful to understand a complete picture of aerosol distribution in the global scale. For this purpose, we developed the common retrieval algorithm of the atmospheric aerosol properties for various satellite sensors and over both land and ocean.

The algorithm is based on the method developed by Higurashi and Nakajima (1998) and Fukuda et al. (2013). The three main features in the concept of this algorithm are as follows: (1) automatic selection of the optimum channels for aerosol retrieval by introducing a weight for each channel to the object function, (2) setting common candidate aerosol models over land and ocean, and (3) preparation of lookup tables for every 1 nm in the range of 300 to 2500 nm of wavelength and weighting the radiance using the response function for each sensor.

The method was applied to Himawari-8/AHI and GCOM-C/SGLI. The validation study indicated that

©2019. Japan Geoscience Union. All Right Reserved. 

aerosol optical thickness estimated from our algorithm was generally consistent with the products from Moderate Resolution Imaging Spectro-radiometer (MODIS) and Aerosol Robotic Network, and SKYNET.

In addition, the utilization of the aerosol properties forecasted by a global aerosol transport model for the retrieval are discussed.

Keywords: earosol, remote-sensing, Himawari, SGLI

©2019. Japan Geoscience Union. All Right Reserved. 

# Cloud optical properties from various ground and satellite instruments evaluated during an intensive campaign

*Alessandro Damiani[1], Hitoshi Irie[1], Takashi Horio[1], Tamio Takamura[1], Rei Kudo[2], Pradeep Khatri[3], Hironobu Iwabuchi[3], Ryosuke Masuda[3], Takashi M. Nagao[4]

1. CEReS, Chiba University, 2. Meteorological Research Institute, Japan Meteorological Agency, 3. Graduate School of Science, Tohoku University, 4. Earth Observation Research Center, JAXA

An intensive campaign to monitor the atmospheric environment (i.e., aerosols, clouds, and gases) has been carried out at the SKYNET station of Chiba University in November 2018. The station is equipped with a broad range of meteorological instruments as well as sky radiometers and is part of various international research networks. Due to their challenging estimation from ground observations and the typical discrepancy between satellite and surface-based estimates, here we focus on cloud optical properties taking a particular interest in cloud optical depth (COD). First, we conducted a careful evaluation of four COD datasets retrieved from surface observations of i) zenith radiance recorded by a sky-radiometer (based on two independent algorithms), ii) solar radiation taken by a pyranometer and iii) spatial distribution of radiance recorded by a camera system equipped with fisheyes lens. Then, we assessed satellite-based estimations of COD retrieved from AHI/Himawari-8 and SGLI/GCOM-C observations trying to explain the differences between satellite and ground data in term of atmospheric conditions, acquisition geometry and COD spatial distribution. Preliminary results achieved from this activity will be presented.

Keywords: satellite, clouds, solar radiation

©2019. Japan Geoscience Union. All Right Reserved. 

# Issues in aerosol-cloud-climate interaction: Needs for future satellite mission

*Kentaroh Suzuki[1]

1. Atmosphere and Ocean Research Institute, University of Tokyo

The aerosol forcing is the largest source of uncertainty in determining climate forcing that drives global climate change. The aerosol forcing consists of the so-called direct (aerosol-radiation interaction) and indirect (aerosol-cloud interaction) effects, both of which are subject to significant uncertainty. This uncertainty arises from our lack of understanding on key processes that govern interactions between aerosol, cloud and climate. Precipitation, among those processes, is central to the aerosol-cloud-climate interaction through its effect of depleting both clouds and aerosols. The aerosol-induced precipitation change influences the cloud lifetime and amount, whereas the precipitation change also modulates the wet removal of aerosols. This underscores a fundamental role of precipitation in shaping the aerosol-cloud-climate interaction. Recent advance in satellite observations by multiple sensors and platforms enabled us to observationally diagnose the precipitation processes on the global scale particularly, which also offers a process-level constraint on model representation of the processes. Such a “bottom-up” model constraint, however, turned out to be inconsistent with “top-down” energy balance requirement on model performance, exposing error compensations in state-of-the-art climate models at a fundamental level. This proposes that there is still a gap in our understanding of the aerosol-cloud-climate processes that hampers their reliable modeling. This presentation discusses what is required to observe in future satellite missions for filling the gap in understanding and modeling the aerosol-cloud-climate interaction. In particular, observational needs for aerosol, cloud and precipitation will be argued to better quantify aerosol-induced climate forcing in the context of recent Aerosol-Cloud-Convection-Precipitation (A-CCP) discussion emerging from the US Decadal Survey and multiple community efforts for process-oriented model diagnostics in an attempt to advance climate modeling.

Keywords: Aerosol, Cloud and precipitation, Climate modeling, Satellite observation

©2019. Japan Geoscience Union. All Right Reserved. 

# Impact of aerosol vertical profile and optical parameters on the accuracy of satellite AOD retrieval

*Jing Li[1], Chong Li[1]

1. Peking University

Satellite sensors are widely used to monitor large scale aerosol variability from space. However, current aerosol retrieval algorithm used by passive sensors still suffers from uncertainties in a series of assumptions, with two important ones being aerosol vertical distribution and scattering/absorbing parameters. In this study, we investigate the effect of these two assumptions on the accuracy of retrieved aerosol optical depth (AOD) using both sensitivity experiments and actual retrieval practices. Using the 6S and Modtran radiative transfer model, we find that the retrieved AOD is very sensitive to the height of absorbing aerosols, and the effect increases with surface albedo. In extreme cases, the error can be as large as 80%. The retrieval results are also quite sensitive to aerosol single scattering albedo, compared to other parameters such as asymmetry parameter and effective radius. Using the aerosol profiles and optical parameters measured by lidar and sunphotometer at the PKU site, we find that the retrieval accuracy can be greatly improved by ~50%. Our results highlight the necessity to refined aerosol profile and optical parameters in the passive retrieval algorithms, possibly through space born lidars and ground based observations.

Keywords: aerosol satellite retrieval, aerosol vertical profile, aerosol single scattering abledo, lidar

©2019. Japan Geoscience Union. All Right Reserved. 

[E] Oral | A (Atmospheric and Hydrospheric Sciences )：A-CG Complex & General

Thu. May 30, 2019 10:45 AM - 12:15 PM JST | Thu. May 30, 2019 1:45 AM - 3:15 AM UTC | 302 3F

## [A-CG34] Satellite Earth Environment Observation

convener:Riko Oki(Japan Aerospace Exploration Agency), Yoshiaki HONDA(Center for Environmental Remote Sensing, Chiba University), Yukari Takayabu(Atmosphere and Ocean Research Institute, the University of Tokyo), Tsuneo Matsunaga(Center for Global Environmental Research and Satellite Observation Center, National Institute for Environmental Studies), Chairperson:Nobuhiro Takahashi(Institute for Space-Earth Environmental Research, Nagoya University)

In recent years, we cannot avoid facing issues on global environmental changes that occur in various spatiotemporal scales. The earth environmental observation data by satellites became the necessary basic data to tackle and solve those issues. Due to the recent advancement in the observation sensor technique and the data processing technique, the satellite observation has been showing rapid progress, and the time is changing from examining the accuracy of the observation sensor data to the advancement of the data application, leading to broaden potential users. In these days application became synergetic, so we comprehensively pick<br/>up this topic in the Atmospheric and Hydrospheric Sciences Session of this Union Meeting that enables to comprise the atmospheric, oceanic and land sciences; by combining the intelligence and the knowledge of the party, we propose a session that aims to prompt further studies towards the issues on earth environmental change, the advancement in the data application and future plans of Earth Observation missions.

10:45 AM - 11:00 AM JST | 1:45 AM - 2:00 AM UTC

[ACG34-13] Statistical validation of drop size distribution estimated by GPM/DPR

*Nobuhiro Takahashi[1] (1.Institute for Space-Earth Environmental Research, Nagoya University)

11:00 AM - 11:15 AM JST | 2:00 AM - 2:15 AM UTC

[ACG34-14] Impact study of DPR SLH nudging method for data assimilation in the JMA Local NWP system

★Invited Papers

*Yasutaka Ikuta[1] (1.Japan Meteorological Agency)

11:15 AM - 11:30 AM JST | 2:15 AM - 2:30 AM UTC

[ACG34-15] Precipitation Extremes Monitoring using Global Satellite Mapping of Precipitation (GSMaP) Product

*Takuji Kubota[1], Tashima Tomoko[1], Riko Oki[1], Tomoaki Mega[2], Tomoo Ushio[2] (1.Earth Observation Research Center,Japan Aerospace Exploration Agency, 2.Department of Aerospace Engineering, Tokyo Metropolitan University)

11:30 AM - 11:45 AM JST | 2:30 AM - 2:45 AM UTC

[ACG34-16] Estimation of cloud water content over land using satellite-based passive microwave observations with a coupled land and atmosphere assimilation method

*Rie Seto[1], Shinjiro Kanae[1] (1.Tokyo Institute of Technology)

11:45 AM - 12:00 PM JST | 2:45 AM - 3:00 AM UTC

[ACG34-17] Ensemble-Based Data Assimilation of GPM/DPR Reflectivity into the Nonhydrostatic Icosahedral Atmospheric Model NICAM

*Shunji Kotsuki[1], Koji Terasaki[1], Takemasa Miyoshi[1] (1.RIKEN Center for Computational Science)

12:00 PM - 12:15 PM JST | 3:00 AM - 3:15 AM UTC

[ACG34-18] **An ecohydrological land reanalysis by integrating simulation and satellite observations**

*Yohei Sawada[1], Tosiyuki Nakaegawa[1], Kozo Okamoto[1], Takeshi Iriguchi[1], Hideyuki Fujii[2] (1.Meteorological Research Institute, 2.Japan Aerospace Exploration Agency)

# Statistical validation of drop size distribution estimated by GPM/DPR

*Nobuhiro Takahashi[1]

1. Institute for Space-Earth Environmental Research, Nagoya University

The dual-frequency precipitation radar (DPR) onboard Global Precipitation Measurement (GPM) core satellite provides the information of the model parameter of the drop size distribution (DSD) assuming the Gamma type DSD model by using Ku-band (KuPR) and Ka-band (KaPR) radar observations. In the current DPR algorithm introduces $\varepsilon$ (epsilon) as a DSD parameter that is constant in the vertical profile. The $\varepsilon$ is defined as a control parameter in k-Z relationship as $k=\varepsilon \alpha Z^{\wedge}\beta$, where k is specific attenuation in (dB/km) and, $\alpha$ and $\beta$ is constant value, respectively. Therefore, once $\varepsilon$ and Z are determined, DSD (and then R) and Z(Ku) - Z (Ka) relationship are determined.

The purpose of this study is to evaluate $\varepsilon$ estimated from DPR algorithm by statistical approach. In this study, two methods are implemented: 1) Histogram matching between Z from KuPR and KaPR, and 2) Estimation of $\varepsilon$ from PIA-zeta relationship that can be calculated both KuPR and KaPR individually (single frequency method).

Data used in this study are DPR level-2 (Matched swath) in 2015, 2016 and 2017. Before applying the methods, backscattering database for Ku, Ka and W band using Mie theory and Z(Ku)-Z(Ka), Z(Ku)-Z(W) table for various $\varepsilon$ ranging from 0.3 to 2.0 with 0.05 intervals, are prepared.

The histogram method compares histograms of Z (Ku) and Z (Ka). In this analysis, the average $\varepsilon$ at a certain area (e.g. 10 x 10 degrees box in latitude and longitude) represent the typical value of the area. Since the difference in the histograms of Z both from the KuPR and KaPR reflects the difference in Mie effect between KuPR and KaPR and therefore $\varepsilon$ represents the corresponding DSD model. In other words, if we know the $\varepsilon$, we can reproduce the KaPR histogram from KuPR histogram. In this analysis, starting from KuPR histogram, the most appropriate KaPR histogram is tried to find by changing the $\varepsilon$. The advantage of this approach is that $\varepsilon$ can be estimated various height (e.g. 1 km, 2 km) if the both KuPR and KaPR data exist. This method, however, is not independent estimation of $\varepsilon$ from the standard algorithm of DPR because this method uses the attenuation corrected Z by the standard algorithm that implicitly include the $\varepsilon$. For the calculation of $\varepsilon$, exceedance probability of Z histogram is used. This method can be utilized for different orbital sensors such as the comparison between CloudSat and TRMM/PR.

The next method is to utilize the path integrated attenuation (PIA)- zeta($\zeta$) relationship (regression method). According to Iguchi et al. (2000),
$1-10^{\wedge}(-PIA\beta/10)=\varepsilon\zeta$, where $\zeta$ is the integral of specific attenuation using the observed Z(Zm) instead of attenuation corrected Z multiplied by $0.2\ln(10)\beta$. PIA is estimated by the observation of the surface echo (surface reference method). By making a scatter plot of $1-10^{\wedge}(-PIA\beta/10)$ and $\zeta$, $\varepsilon$ corresponds to the slope of this plot. The slope in Ku-band corresponds to the $\varepsilon$ in this study. Ka-band epsilon is calculated using the same k-Z relationship with Ku-band.

The $\varepsilon$ estimated by these two methods are compared with the average value of $\varepsilon$ from standard algorithm. Basically $\varepsilon$ from both methods correlate well with the $\varepsilon$ from the standard algorithm. Note that the variance $\varepsilon$ from the regression method is twice large as the standard algorithm. This result may be

©2019. Japan Geoscience Union. All Right Reserved. 

caused by that the standard algorithm not to determine the $\varepsilon$ under less attenuated situation. The regression method can be utilized to assess the k-Z relationship between Ku and Ka and the histogram method of various height indicates the constant $\varepsilon$ of the throughout the profile may not be valid.

Keywords: Precipitation, radar, drop size distribution

©2019. Japan Geoscience Union. All Right Reserved. 

# Impact study of DPR SLH nudging method for data assimilation in the JMA Local NWP system

*Yasutaka Ikuta[1]

1. Japan Meteorological Agency

GPM DPR Spectral Latent Heating (GPM-SLH) profile is a very valuable product with three-dimensional latent heating information of precipitation system. The data assimilation of this GPM-SLH is expected to improve the precipitation prediction in numerical weather prediction. The impact of SLH data assimilation is investigated in the Local NWP system which includes the high-resolution numerical prediction model called Local Forecast Model (LFM) of Japan Meteorological Agency.

The purpose of the operation of LFM is to provide information on very-short range precipitation forecast and aviation weather forecasting. The initial condition for the LFM is created by hourly data assimilation in the Local NWP system because the forecast immediacy is important for the achievement of the LFM's aims. Thus the forecast of LFM from the initial condition has latest information of real atmosphere by the hourly assimilation. However, this data assimilation system consists of simple 3D-VAR combined with prediction which is capable of performing speedy calculation for rapidly updating the forecast.

GPM-SLH nudging method corrects the latent heating in cloud microphysics scheme while the numerical prediction model is running in the assimilation window. It is a very efficient method that can input SLH information into the model with keeping immediacy of forecast. In the Local NWP system, the nudging method was implemented and impact studies of SLH assimilation were conducted in typical cases of mid-latitude precipitation system. In this presentation, I will show the result of impact study of GPM-SLH assimilation and the problems to be addressed.

©2019. Japan Geoscience Union. All Right Reserved. 

# Precipitation Extremes Monitoring using Global Satellite Mapping of Precipitation (GSMaP) Product

*Takuji Kubota[1], Tashima Tomoko[1], Riko Oki[1], Tomoaki Mega[2], Tomoo Ushio[2]

1. Earth Observation Research Center,Japan Aerospace Exploration Agency, 2. Department of Aerospace Engineering, Tokyo Metropolitan University

Natural hazards caused by weather and climate tend to increase in recent years, and it is recognized that there is a need to better utilize and improve the monitoring of extreme weather and climate events from space. Recently, satellite-based precipitation datasets have been developed to achieve higher spatial and temporal resolutions using combined data from passive microwave (PMW) sensors in low Earth orbit and infrared (IR) radiometers in geostationary Earth orbit. Global Satellite Mapping of Precipitation (GSMaP) is a blended PMW–IR precipitation product and has been developed in Japan for the Global Precipitation Measurement (GPM) mission. In this study, detections of drought and heavy precipitation events are examined using standardised precipitation index (SPI) and a statistical value, to demonstrate a capability of the GSMaP. Such efforts will contribute to precipitation extremes monitoring activities using satellite data, such as the World Meteorological Organization (WMO) Space-based Weather and Climate Extremes Monitoring Demonstration Project (SEMDP) with focus on monitoring drought and heavy precipitation in countries of the South-East Asia and the Pacific.

In this study, GSMaP Near-real-time Gauge-adjusted Rainfall Product (GSMaP_Gauge_NRT) for algorithm version 6 is used. This product is adjusted using an optimization model with parameters calculated from data during the past 30 days. As for weather and climate extremes, here it is defined as an extreme precipitation, when a mean rainfall for a specified period is higher than a threshold based on the percentiles (ex. 95th, 99th percentile). Whereas, drought is diagnosed based on SPI over 1, 2 and 3 months. Percentiles and SPI are calculated in 0.1x0.1 grid at lat/lon resolution from the dataset during 18 years from April 2000 to March 2018. To demonstrate feasibilities of GSMaP_Gauge_NRT (v6) for climate extremes monitoring, we evaluated past cases of drought and heavy rainfall.

The first case is drought in south-eastern Australia during July-September 2007. A drought area where 3-month SPI is less than -1.2 spreads widely around the south of Australia. The detected drought area is roughly consistent with an area above 9$^{th}$ decile (Very Much Below Average) shown by the Bureau of Meteorology (BoM) in Australia. However, because there are few rain gauges in Western Australia’s eastern part, distributions between both are different. The second case is heavy rainfall events in western and eastern Australia in December 2010. Monthly mean precipitation exceeds 95$^{th}$ percentile in western and eastern Australia. These detected heavy rainfall area roughly corresponds to an area below 2$^{nd}$ decile (Very Much Above Average) shown by the BoM. The last case is heavy rainfall events in Malay Peninsula in December 2014, which extreme rainfall caused widespread flooding over Thailand and the east coast of Peninsular Malaysia. Time-fluctuation of GSMaP_Gauge_NRT (v6) daily precipitation averaged over these areas is roughly in good agreement with that of CPC Gauge Analysis. A series of heavy rainfall events beginning on 14 December 2014 can be confirmed from space-based observations. Especially, pentad precipitation for 22-26 December 2014, is higher than 99$^{th}$ percentile over large portion of Peninsular Malaysia. Actually, floods caused by heavy rain hit in this area.

Keywords: Precipitation, Satellite, Extreme

©2019. Japan Geoscience Union. All Right Reserved. 

©2019. Japan Geoscience Union. All Right Reserved. 

# Estimation of cloud water content over land using satellite-based passive microwave observations with a coupled land and atmosphere assimilation method

*Rie Seto[1], Shinjiro Kanae[1]

1. Tokyo Institute of Technology

We proposed a method to estimate the cloud water content (CWC) over land at multiple-kilometer resolutions and to concurrently assimilate the estimated CWC into the model by using multi-frequency satellite-based passive microwave brightness temperatures (TBs) and coupled land and atmosphere assimilation.
The need for a better understanding and more accurate representation of clouds in atmospheric models has been apparent for decades. However, a lack of sufficient observations and reanalysis products is a major obstacle. The use of TBs is an effective way to retrieve CWC of extensive and heterogeneous cloud systems all at once, but it is challenging to estimate CWC over land due to complexities of cloud processes and uncertainties in strong and heterogeneous land emissions. Our method overcomes the difficulty of retrieving clouds over land from TBs and representing them in models by simultaneously optimizing land emissions and CWC over land, and assimilating the estimations into models.
The estimated CWC was in good accordance with vertical two-dimensional products of CloudSat in terms of cloud water path and the vertical distribution of CWC. In addition, we examined the uncertainties of this method by sensitivity analysis of CWC estimates of TBs and cloud top height. The results suggested that the error in TBs is not large, and that cloud top height affects the estimated CWC more sensitively than TBs. The addition of cloud top height information from other satellite observations as a constraint of optimization allows further improvement of the vertical distributions of CWC.
This study revealed that the proposed method has great potential to provide unprecedented data for CWC with adequate accuracy, which are continuously distributed over land and ocean.

Keywords: estimation of cloud water content over land, satellite-based passive microwave brightness temperature, coupled assimilation of land and atmosphere

©2019. Japan Geoscience Union. All Right Reserved. 

# Ensemble-Based Data Assimilation of GPM/DPR Reflectivity into the Nonhydrostatic Icosahedral Atmospheric Model NICAM

*Shunji Kotsuki[1], Koji Terasaki[1], Takemasa Miyoshi[1]

1. RIKEN Center for Computational Science

This study aims to improve the precipitation forecasts from numerical weather prediction models through effective assimilation of satellite-observed precipitation data. The assimilation of precipitation data is known to be difficult mainly due to highly non-Gaussian statistics of precipitation-related variables. We have been developing a global atmospheric data assimilation system NICAM-LETKF, which comprises the Nonhydrostatic ICosahedral Atmospheric Model (NICAM) and Local Ensemble Transform Kalman Filter (LETKF). Using the NICAM-LETKF system, Kotsuki et al. (2017, JGR) successfully improved the weather forecasts by assimilating the Japan Aerospace eXploration Agency (JAXA)' s Global Satellite Mapping of Precipitation (GSMaP) data into the NICAM at 112-km horizontal resolution. However, assimilating space-borne precipitation radar data remains to be a challenging issue.

This study pioneers to assimilate radar reflectivity measured by the Dual-frequency Precipitation Radar (DPR) onboard the Global Precipitation Measurement (GPM) core satellite into the NICAM. We conduct the NICAM-LETKF experiments at 28-km horizontal resolution with explicit cloud microphysics of a single-moment 6-class bulk microphysics scheme. To simulate GPM/DPR reflectivity from NICAM model outputs, the joint-simulator (Hashino et al. 2013; JGR) is used. Our initial tests showed a better match with the observed reflectivity by assimilating GPM/DPR reflectivity into NICAM forecasts. However, the results from a 1-month data assimilation cycle experiment showed general degradation by assimilating GPM/DPR reflectivity. For better use of GPM/DPR reflectivity data, we are exploring to estimate model cloud physics parameters by assimilating them. This presentation will include the most recent progress up to the time of the meeting.

Keywords: GPM, Data Assimilation, NICAM-LETKF, Precipitation, Radar Reflectivity, Ensemble Kalman Filter

©2019. Japan Geoscience Union. All Right Reserved. 

# An ecohydrological land reanalysis by integrating simulation and satellite observations

*Yohei Sawada[1], Tosiyuki Nakaegawa[1], Kozo Okamoto[1], Takeshi Iriguchi[1], Hideyuki Fujii[2]

1. Meteorological Research Institute, 2. Japan Aerospace Exploration Agency

Monitoring terrestrial water, energy, and ecosystem is crucially important to understand global environmental changes. Land reanalysis, in which a land surface model (LSM) is driven by bias-corrected atmospheric forcing based on an atmospheric reanalysis dataset, has greatly contributed to generating the long-term and spatiotemporally homogeneous dataset of terrestrial environmental condition. Here we propose a new land reanalysis called ECoHydrological Land reAnalysis (ECHLA). Compared with the other existing land reanalyses, the characteristics of ECHLA are: (1) ECHLA can simulate not only water and energy, but also vegetation dynamics; (2) ECHLA is generated by sequential data assimilation of satellite microwave observation, which is sensitive to soil moisture and vegetation water content, into a LSM; (3) ECHLA can quantify the uncertainty in its simulated variables by an ensemble method. In this presentation, we will show the concept of ECHLA and the preliminary results of the validation of the ECHLA’ s prototype and its application to drought quantification.

**Sawada, Y.** (2018), Quantifying drought propagation from soil moisture to vegetation dynamics using a newly developed ecohydrological land reanalysis, ***Remote Sensing****, 10,* 1197

Keywords: land reanalysis, microwave remote sensing, satellite data assimilation

©2019. Japan Geoscience Union. All Right Reserved. 

[E] Poster | A (Atmospheric and Hydrospheric Sciences)：A-CG Complex & General

Thu. May 30, 2019 1:45 PM - 3:15 PM JST | Thu. May 30, 2019 4:45 AM - 6:15 AM UTC | Poster Hall International Exhibition Hall8, Makuhari Messe_3

## [A-CG34] Satellite Earth Environment Observation

convener:Riko Oki(Japan Aerospace Exploration Agency), Yoshiaki HONDA(Center for Environmental Remote Sensing, Chiba University), Yukari Takayabu(Atmosphere and Ocean Research Institute, the University of Tokyo), Tsuneo Matsunaga(Center for Global Environmental Research and Satellite Observation Center, National Institute for Environmental Studies)

In recent years, we cannot avoid facing issues on global environmental changes that occur in various spatiotemporal scales. The earth environmental observation data by satellites became the necessary basic data to tackle and solve those issues. Due to the recent advancement in the observation sensor technique and the data processing technique, the satellite observation has been showing rapid progress, and the time is changing from examining the accuracy of the observation sensor data to the advancement of the data application, leading to broaden potential users. In these days application became synergetic, so we comprehensively pick<br/>up this topic in the Atmospheric and Hydrospheric Sciences Session of this Union Meeting that enables to comprise the atmospheric, oceanic and land sciences; by combining the intelligence and the knowledge of the party, we propose a session that aims to prompt further studies towards the issues on earth environmental change, the advancement in the data application and future plans of Earth Observation missions.

### [ACG34-P01] Impact of usage of multiple-satellite sensors on accuracy of daily-mean sea surface wind data

*Ayumi Koizumi[1], Masahisa Kubota[2], Kunio Kutsuwada[3], Hiroyuki Tomita[4], Tsutomu Hihara[5] (1.Tokai University, 2.Tokai University, Institute of Ocean Research and Development, 3.School of Marine Science and Technology, Tokai University, 4.Institute for Space-Earth Environmental, Nagoya University, 5.Japan Agency for Marine-Erth Science and Technology)

### [ACG34-P02] Temperature and Size Variability of Warm Pools in the Global Oceans

*ChunYi Lin[1] (1.National Museum of Marine Science & Technology)

### [ACG34-P03] Sea surface temperature from SGLI aboard the GCOM-C satellite of JAXA

*Yukio Kurihara[1], Kazunori Ogata[2], Hiroshi Murakami[2], Misako Kachi[2] (1.Tripli-I Co., Ltd., 2.JAXA EORC)

### [ACG34-P04] Concept of small satellite UV/visible imaging spectrometer optimized for tropospheric $NO_2$ measurements in air quality monitoring

*Tamaki Fujinawa[1,5], Katsuyuki Noguchi[2], Akihiko Kuze[3], Andreas Richter[4], John P. Burrows[4], Andreas C. Meier[4], Tomohiro Sato[1], Takeshi Kuroda[1], Naohiro Yoshida[5], YASUKO KASAI[1,5] (1.National Institute of Information and Communications Technology, 2.Nara Women's University, 3.Japan Aerospace Exploration Agency, 4.University of Bremen, 5.Tokyo Institute of Technology)

### [ACG34-P05] EarthCARE L2 algorithms for cloud and precipitation

*Kaori Sato[1], Hajime Okamoto[1], Hiroshi Ishimoto[2] (1.Research Institute for Applied Mechanics, Kyushu University, 2.Meteorological Research Institute)

### [ACG34-P06] Analysis of the Surface Echo Characteristics Derived from GPM/DPR Wide Swath Observation Experiment

*Kosuke Yamamoto[1], Kinji Furukawa[1], Nobuhiro Takahashi[2], Takuji Kubota[1] (1.Japan Aerospace Exploration Agency, 2.Nagoya University)

### [ACG34-P07] The Recent Results from the Global Precipitation Measurement (GPM) mission in Japan

*Riko Oki[1], Takuji Kubota[1], Kinji Furukawa[1], Yuki Kaneko[1], Moeka Yamaji[1], Kosuke Yamamoto[1], Toshio Iguchi[2], Yukari Takayabu[3] (1.Japan Aerospace Exploration Agency, 2.NICT, 3.the University of Tokyo)

[ACG34-P08] **Verification of Global Satellite Mapping of precipitation (GSMaP) for providing its error information**

*Moeka Yamaji[1], Takuji Kubota[1] (1.Earth Observation Research Center, Japan Aerospace Exploration Agency)

[ACG34-P09] Detection of the mixed phase top using the measured dual-frequency ratio of reflectivity with GPM/DPR

*Yuki Kaneko[1], Toshio Iguchi[2] (1.Japan Aerospace Exploration Agency, 2.National Institute of Information and Communications Technology)

[ACG34-P10] **Comparison between high frequency satellite rainfall estimation and APHRODITE-2 ground rain gauge observation**

*Hitoshi Hirose[1], Koichi Toyoshima[1], Atsushi Higuchi[1], Akiyo Yatagai[2], Natsuko Yasutomi[3] (1.Center for Environmental Remote Sensing, Chiba University, 2.Hirosaki University, 3.Disaster Prevention Research Institute, Kyoto University)

[ACG34-P11] Development of the high resolution GSMaP by the Himawari-8

*Tomoaki Mega[1], Tomoo Ushio[1] (1.Tokyo Metropolitan University)

[ACG34-P12] Preliminary results of on-orbit estimation for polarization sensitivity of GCOM-C/SGLI

*Risa Miyazaki[1], Hiroshi Murakami[1], Masahiro Hori[1] (1.Japan Aerospace Exploration Agency)

[ACG34-P13] Analysis of SGLI validation datas based on the effects of the growth and ground types for the AGB development

*Ryota Ishibashi[1], Koji KAJIWARA[1], Yoshiaki HONDA[1] (1.Center for environmental remote sensing, Chiba University)

[ACG34-P14] Remote sensing of aerosol optical properties and water-leaving radiance based on the optimal estimation approach

*Chong Shi[1], Teruyuki Nakajima[1], Makiko Hashimoto[1], Hideaki Takenaka[1] (1.Japan Aerospace Exploration Agency)

[ACG34-P15] Aerosol retrieval and PM2.5 from space using GOSAT/TANSO-CAI

*Makiko Hashimoto[1], Hideaki Takenaka[1], Teruyuki Nakajima[1], Akiko Higurashi[2] (1.Japan Aerospace Explortion Agency, 2.NIES)

[ACG34-P16] **Establishing a high resolution road fugitive dust emission inventory in Kaifeng City, China**

*Yiming Xu[1], Shili Liu[1], Xinyue Cao[1], Xianbao Shen[1], Zhiliang Yao[1] (1.Department of Environmental Science and Engineering, Beijing Technology and Business University)

[ACG34-P17] A Relationship between Diurnal Change Patterns of Land Surface Temperature and Spatial Configuration of the Osaka Metropolitan Area Captured by Himawari-8

*Yuhei Yamamoto[1], Hirohiko Ishikawa[1] (1.Disaster Prevention Research Institute, Kyoto University)

# Impact of usage of multiple-satellite sensors on accuracy of daily-mean sea surface wind data

*Ayumi Koizumi[1], Masahisa Kubota[2], Kunio Kutsuwada[3], Hiroyuki Tomita[4], Tsutomu Hihara[5]

1. Tokai University, 2. Tokai University, Institute of Ocean Research and Development, 3. School of Marine Science and Technology, Tokai University, 4. Institute for Space-Earth Environmental, Nagoya University, 5. Japan Agency for Marine-Erth Science and Technology

Most satellites observing sea surface winds have sun-synchronous orbits and provide observation data at the same place two times per a day. We can expect that daily-mean values estimated from these data have some errors when diurnal changes in wind field cannot be neglected. For this problem, use of multiple satellites is helpful. Since the number of sensors used to construct daily-mean data is different among the years, it is expected that the accuracy of a daily-mean value changes from year to year.

The purpose of this study is to describe time variation of accuracy in daily-mean wind data in the Japanese Ocean Flux Data Sets with Use of Remote Sensing Observation (J-OFURO)-3 and to investigate its causes by comparing with in-situ measurement data by moored buoys and calculating three statistical values.

Results reveal that the statistical values are improved with year. To examine the relationship between the yearly statistics and the yearly number of satellite sensors, we plotted a scatter diagram between the number of satellites and three statistical values in each year. We found that the correlations between them are very high. We also focused on a time interval of the satellite wind observation, namely maximum missing time within a day. The result showed that the correlation between three statistical values and maximum missing time intervals is high. Since the relation between these two factors is not independent, we analyzed by considering both factors together. First, we chose five buoys with various standard deviations for a daily-mean value. Next, we picked up data from buoy's hourly data using random numbers, and calculated the daily mean value using the random data, and then determined the number of observations and the maximum missing time interval each day. Assuming the daily mean value calculated from 24 hourly data as a true value, the RMSE between this true value and the daily mean created from random data was calculated. From the result of this analysis, it was found that the value of Root Mean Square Error(RMSE) depends on the maximum missing time interval rather than the number of observations. Furthermore, when RMSE was normalized by standard deviation, the same figures were obtained for all buoys. This result implies that the RMSE of the daily mean value of the buoy station can be estimated if the magnitude of diurnal variation is known by giving the number of satellites used for observation and the maximum missing time interval, Moreover, by applying this result, we think that it is possible to show the optimal number of sensors and observation time for target accuracy. This result gives very breakthrough information to the design of the satellite observation system for sea surface wind.

Keywords: Multiple-satellite sensors, Sea surface wind

©2019. Japan Geoscience Union. All Right Reserved. 

# Temperature and Size Variability of Warm Pools in the Global Oceans

*ChunYi Lin[1]

1. National Museum of Marine Science & Technology

Using advance satellite-derived Sea surface height anomaly, sea surface temperature (SST) data, and heat flux data, we investigate the thermal variability, temperature and size variability of warm pools in the global oceans, the Pacific, the Atlantic, and the Indian Ocean, respectively. Because of the high density and specific heat of seawater, water can store and transport large amounts of heat. High SST has particular influence on global climate system. Furthermore previous studies focused on the global warming or area warming, in this investigation we present results of warm pool SST binned into 1 ˚C interval. Detecting temperature and size variability of warm pools in the global oceans, it suggests that the high SST area (SST ≧ 28˚C) has faster increasing rate than surrounding area (SST 20˚C - 27˚C) in the global oceans, the Pacific, the Atlantic, and the Indian Ocean, respectively. To understand the role of surface heat flux in the tropical SST fluctuation, we analyze the mixed layer heat balance equation. Upper ocean heat budget between the heat advection and heat diffusion term are compared and heat diffusion processes may be a mechanism for transporting excessive amount of heat that the warm pool through enhancing the SST gradient around the edge of the warm pool. In order to find out dominant period components and the relationship of energy-frequency distribution without influenced induced by nonlinear and nonstationary signals, the Hilbert-Huang Transform applied by ensemble empirical mode decomposition is employed. The ensemble empirical mode decomposition analysis indicates that the interannual component has strong influence on the variability of the warm core pool in the Pacific, presumably because of the presence of El Niño phenomenon, while the annual cycle dominates the variability in the Indian and the Atlantic Ocean.

Keywords: warm pool, SST, heat flux

©2019. Japan Geoscience Union. All Right Reserved. 

# Sea surface temperature from SGLI aboard the GCOM-C satellite of JAXA

*Yukio Kurihara[1], Kazunori Ogata[2], Hiroshi Murakami[2], Misako Kachi[2]

1. Tripli-I Co., Ltd., 2. JAXA EORC

The Global Change Observation Mission-Climate (GCOM-C) satellite, which is one of two satellites for the GCOM mission of the Japan Aerospace and Exploration Agency (JAXA), was launched on 23 December 2017. The Second Generation Global Imager (SGLI) is the optical sensor aboard GCOM-C which consists of two components: the Visible and Near-infrared Radiometer (VNR) and the Infrared Scanner (IRS). SGLI has switchable spatial resolution from 250 m x 250 m to 1 km x 1 km. The resolution of 250 m x 250 m is expected to reveal complicated structure of geophysical parameters. Sea surface temperature (SST), which is one of the important parameters in the geophysical field, is also determinable by using split window data of SGLI. SGLI SST is retrieved by utilization of newly developed cloud masking method and a modified SST method originally developed for Himawari-8. Considering combined utilization of satellite SSTs, the methods developed for SGLI SST will be applied back to Himawari-8 data as well as the data from the Visible Infrared Imaging Radiometer Suite (VIIRS) aboard the Suomi National Polar-orbiting Partnership (Suomi NPP) satellite. SGLI SST is validated by comparison with buoy data. The comparison result shows RMSD of ~0.4 K, good agreement between SGLI SSTs and buoy data. Triple comparison with Himawari-8 and VIIRS SSTs is being started. Operational retrieval of SGLI SST started at the end of 2018. The products are available at the G-Portal site of JAXA and the JAXA Satellite Monitoring and Environmental Studies (JASMES) site of the Earth Observation Center (EORC) of JAXA.

©2019. Japan Geoscience Union. All Right Reserved. 

# Concept of small satellite UV/visible imaging spectrometer optimized for tropospheric $NO_2$ measurements in air quality monitoring

*Tamaki Fujinawa[1,5], Katsuyuki Noguchi[2], Akihiko Kuze[3], Andreas Richter[4], John P. Burrows[4], Andreas C. Meier[4], Tomohiro Sato[1], Takeshi Kuroda[1], Naohiro Yoshida[5], YASUKO KASAI[1,5]

1. National Institute of Information and Communications Technology, 2. Nara Women's University, 3. Japan Aerospace Exploration Agency, 4. University of Bremen, 5. Tokyo Institute of Technology

Satellite observations at nadir can potentially facilitate a better understanding of the emissions and distribution of tropospheric nitrogen dioxide, $NO_2$. The identification of emissions requires adequate spatiotemporal resolution measurements of the total column amounts of $NO_2$. The spatial resolution of previous and current observations is insufficient for the identification of $NO_2$ hot-spots. Switching to a spatial resolution of ~1 km x ~1 km can improve the identification of local sources of $NO_2$ and their emissions. To investigate the feasibility of observations with such a high spatial resolution, we simulated radiance spectra for different cases under varying parameters, such as area, season, satellite altitude, and surface reflectance by using the radiative transfer model SCIATRAN. We subsequently retrieved $NO_2$ slant column densities (SCDs) using the differential optical absorption spectroscopy (DOAS) technique with several fit windows. For test cases associated with polluted conditions, we found that the conceptual nadir-observing instrument on a satellite at an altitude of ~300 km involved the lowest retrieval errors for signal-to-noise ratios of around 1000 with accuracy better than the required 5% for tropospheric $NO_2$ SCD and that the fit window of 425--497 nm met the scientific requirements for both surface reflectance cases.

Keywords: Nitrogen dioxide, Earth observation, Radiative transfer model, Remote sensing

©2019. Japan Geoscience Union. All Right Reserved. 

# EarthCARE L2 algorithms for cloud and precipitation

*Kaori Sato[1], Hajime Okamoto[1], Hiroshi Ishimoto[2]

1. Research Institute for Applied Mechanics, Kyushu University, 2. Meteorological Research Institute

The EarthCARE (Earth Clouds, Aerosols and Radiation Explorer, JAXA-ESA) mission will carry the first 94GHz Doppler Cloud Profiling Radar (CPR) with a high spectral resolution atmospheric lidar (ATLID) at 355nm. Recent progresses in EarthCARE L2 cloud/precipitation algorithms for the treatment of multiple scattering and cloud particle nonsphericity are presented.

Keywords: spaceborne active sensor, cloud

©2019. Japan Geoscience Union. All Right Reserved. 

# Analysis of the Surface Echo Characteristics Derived from GPM/DPR Wide Swath Observation Experiment

*Kosuke Yamamoto[1], Kinji Furukawa[1], Nobuhiro Takahashi[2], Takuji Kubota[1]

1. Japan Aerospace Exploration Agency, 2. Nagoya University

The observation from spaceborne precipitation radar has been contributed to better understanding of earth climate system. Global Precipitation Measurement (GPM) core satellite Dual-frequency Precipitation Radar (DPR) provides us 3-dimentional information of precipitation by the scan width of about 250 km, but there have been arguments that to bring systematic impact on the weather monitoring through global rainfall map such as GSMaP, wider swath observation by precipitation radar is necessary.

Based on those requirements, the scan pattern of GPM/DPR was experimentally changed for 1 day from 13UTC on September 26th. In this experiment, the scan angle was changed to observe from nadir to about +34˚ assuming future spaceborne precipitation radar with wider swath width, while in the normal observation DPR scans ±17˚. The height and strength of the mainlobe clutter with larger incident angle were assessed statistically to examine the possibility of the rainfall retrieval with wide swath observation by DPR.

In order to examine mainlobe clutter height, it is inevitable to reduce sidelobe and grating lobe effect. In this study, clutter-free observation data is extracted based on following procedures; 1) extract bins above mainlobe clutter; 2) extract bins under non-precipitation condition from 1); 3) extract bins that satisfy |received power −averaged noise power| < 2 sigma of the noise power from 2). Note that this procedure was applied only for KuPR observation since sidelobe and grating lobe clutter is not prominent in KaPR.

The result for KuPR observation shows that the mainlobe clutter top height at the larger incident angle over ocean is somehow suppressed at around 4 km while over land it increases almost linearly up to around 5 km due to the strong surface scattering. The same tendency is found on the KaPR observation, but it has lower clutter top height of around 2.5 km and 3.5 km, over ocean and land respectively. Suppression is clearer over ocean thanks to the specular reflection. The results also indicate that relatively intense rainfall can be retrieved while shallow rainfall with weak echo power may not be acceptable for retrieval because it should be masked by the surface clutter.

Keywords: precipitation radar, radar clutter, GPM core satellite

©2019. Japan Geoscience Union. All Right Reserved. 

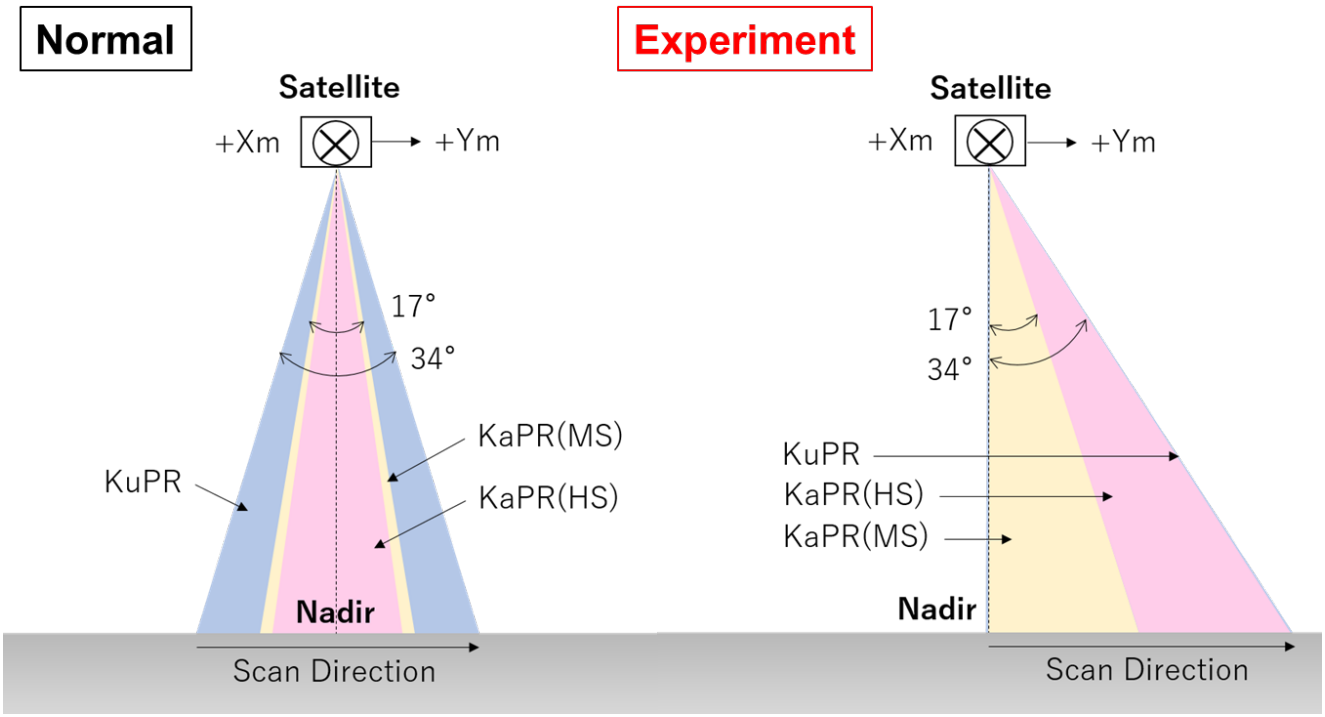


©2019. Japan Geoscience Union. All Right Reserved. 

# The Recent Results from the Global Precipitation Measurement (GPM) mission in Japan

*Riko Oki[1], Takuji Kubota[1], Kinji Furukawa[1], Yuki Kaneko[1], Moeka Yamaji[1], Kosuke Yamamoto[1], Toshio Iguchi[2], Yukari Takayabu[3]

1. Japan Aerospace Exploration Agency, 2. NICT, 3. the University of Tokyo

The Global Precipitation Measurement (GPM) mission is an international cooperate satellite project to achieve highly accurate and highly frequent global precipitation observations. The GPM mission consists of the GPM Core satellite jointly developed by the U.S. and Japan and Constellation Satellites that carry microwave radiometers and provided by the GPM partner agencies. The GPM Core satellite carries the Dual-frequency Precipitation Radar (DPR) by the Japan Aerospace Exploration Agency (JAXA) and the National Institute of Information and Communications Technology (NICT) and the GPM Microwave Imager (GMI) provided by National Aeronautics and Space Administration (NASA). The GPM Core satellite was launched in February 2014 and achieved its prime mission period planned for 3 years in 2017.

It has been continuing its observation as the extended mission phase after that.

JAXA develops the DPR Level 1 algorithm and the NASA-JAXA Joint Algorithm Team develops the DPR Level 2 and DPR-GMI combined Level 2 algorithms. The DPR, the DPR-GMI combined algorithms and the latent heating algorithm were updated, and those products were released in October 2018 as Version 0.6. Using dual frequency information of DPR, the latest Level 2 products include information such as precipitation phase at surface, heavy ice precipitation and so on. Also, the calibration factors of TRMM/PR were re-examined to have consistency between DPR/Ku. The same GPM Ku-band radar L2 algorithm now applies to the TRMM/PR, so that the long radar precipitation data exceeding more than 20 years are now available. From May 2018 in the extended mission period, the scan pattern of the Ka-band radar has been changed to realize matched beam observation in full swath. The new algorithm applying to the changed scan pattern is now under development.

JAXA also develops the Global Satellite Mapping of Precipitation (GSMaP), that is hourly and 0.1-degree horizontal resolution global rainfall map. It is available through the “JAXA Global Rainfall Watch” website (https://sharaku.eorc.jaxa.jp/GSMaP/index.htm). GSMaP product family includes different data latency products and rain gauge calibrated products and so on. The GSMaP near-real-time version (GSMaP_NRT) product provides global rainfall map in 4-hour after observation, and an improved version of GSMaP near-real-time gauge-adjusted (GSMaP_Gauge_NRT) product has been released since Dec. 2018.

The GSMaP real-time product called GSMaP_NOW now product is providing data at the earliest timing. It has been realized using the geostationary satellite Himawari-8 operated by the Japan Meteorological Agency (JMA) since November 2015. Since Nov. 2018 the domain of GSMaP_NOW has been extended to the region of the geostationary satellite Meteosat operated by the European Organization for the Exploitation of Meteorological Satellites (EUMETSAT) in November 2018. JAXA is further developing the GSMaP_NOW to provide global real-time rainfall product.

Keywords: GPM, Satellite Remote Sensing, Precipitation

©2019. Japan Geoscience Union. All Right Reserved. 

©2019. Japan Geoscience Union. All Right Reserved. 

# Verification of Global Satellite Mapping of precipitation (GSMaP) for providing its error information

*Moeka Yamaji[1], Takuji Kubota[1]

1. Earth Observation Research Center, Japan Aerospace Exploration Agency

Precipitation is one of the most essential parameters in the Earth system. Due to address water issues like water shortage or floods, JAXA has developed and provided Global Satellite Mapping of Precipitation (GSMaP), which is hourly global precipitation dataset. It is under the Global Precipitation Measurement (GPM) mission and contributes.
GSMaP allows us to capture the hourly horizontal distribution of precipitation with good latency after observation. The spatial resolution is 0.1 x 0.1 degrees latitude/longitude. It has been used for various kinds of utilization purposes.
In terms of accuracy, GSMaP algorithms were updated in several times, and GSMaP has been getting more accurate day by day, however, it is known that the inhomogeneous of accuracy is existed depending on algorithm characteristics. It has been needed to provide information about the uncertainty and accuracy of GSMaP by users.
In this study, verification result of GSMaP near-realtime product version 6 (GSMaP_NRT) is reported. The radar/raingauge analysed precipitation data by Japan Meteorological Agency, which is an hourly rainfall analysis generated from ground-based precipitation radars corrected by automated rain gauges, are used as the reference data. Since the purpose of this study is for providing generalized error information, root mean square errors (RMSE) is statistically calculated for each precipitation level and each reliability flag during May-June-July-August-September-October in 2015-2018. Some initial results showed that the RMSE qualitatively represented the error for each precipitation level and reliability flag. The RMSE ratio to the average precipitation rate got larger as the precipitation rate became smaller while it became stable around 60 –80 % when precipitation rate was more than 10 mm/h. We report the validation results in detail, such as land/ocean difference or sampling dependence, and focus on the effectiveness of it.

Keywords: precipitation, GPM, GSMaP, validation

©2019. Japan Geoscience Union. All Right Reserved. 

# Detection of the mixed phase top using the measured dual-frequency ratio of reflectivity with GPM/DPR

*Yuki Kaneko[1], Toshio Iguchi[2]

1. Japan Aerospace Exploration Agency, 2. National Institute of Information and Communications Technology

The core observatory of the Global Precipitation Measurement (GPM) mission was launched in 2014 and has been observing rain and snow between 65˚S and 65˚N by the Dual Frequency Precipitation Radar (DPR) and the GPM Microwave Imager (GMI). The DPR provides three-dimensional structure of storms derived from reflected energy from precipitation particles. Precipitation echoes at the two frequencies of the DPR, Ka-band (25GHz) and Ku-band (14GHz), make it possible to infer the mean size and physical property of precipitation particles. The swath width of Ka-band scanning was 125 kilometers centered at nadir and was nested within the Ku-band’ s wider scan width of 254 kilometers. On May 21 2018, the Ka-band scan pattern was changed to match with the Ku-band’ s. Dual frequency radar reflectivity factors are available for full swath of 254 kilometers now.

The classification (CSF) module in the standard DPR level2 algorithm detects a bright band (BB) and classifies precipitation into three types, stratiform, convective, and other. Rain types affect the retrievals of rain amount and latent heating in the DPR algorithm. Accurate classification is also important in the Global Satellite Mapping of Precipitation (GSMaP) algorithm because it affects the rain profile database used in the rain retrieval with microwave radiometers. The BB detectability by the standard CSF algorithm is lower at and near the swath edges than near nadir because only Ku-band data was available in the outer swath before and because slant incidence of radar beams smears the vertical profiles.

As the Ka-band scan pattern has changed to cover the full swath, we can apply a dual-frequency method to detect a BB now. We have developed a method that uses the dual frequency ratio (DFR) to detect the mixed phase top. It looks at the slope of DFR as a function of range to identify the transition height from ice to water. DFR itself is estimated from measured DFR (DFRm) with attenuation correction. Preliminary experiments show that the developed method can detect the BB in stratiform rain over the swath almost uniformly. This method also has a potential to identify the transition height even in some convective cases. In this research we evaluate the performance of the algorithm by comparing the altitude of BB and the transition height with those estimated by using X-band multi-parameter radar (XRAIN) data.

Keywords: GPM, Melting Layer, Precipitation Radar

©2019. Japan Geoscience Union. All Right Reserved. 

# Comparison between high frequency satellite rainfall estimation and APHRODITE-2 ground rain gauge observation

*Hitoshi Hirose[1], Koichi Toyoshima[1], Atsushi Higuchi[1], Akiyo Yatagai[2], Natsuko Yasutomi[3]

1. Center for Environmental Remote Sensing, Chiba University, 2. Hirosaki University, 3. Disaster Prevention Research Institute, Kyoto University

APHRODITE project collects daily precipitation observation data from ground rain gauges in each country, and then performs appropriate quality control and converts it into gridded data. APHRODITE holds long-term data from the 1960s to the present and focuses on analyzes such as changes in characteristics of extreme rainfall due to long-term climate change. However, ground-based daily rain observations has a problem which end of the day (EOD) in each country is different from each other. To estimate the EOD in each country, we developed a Rain Potential Map (RPM) which is a product that can estimate global rain probability using geostationary meteorological satellites (GEO) (Hirose et al., 2016, JMSJ). In this study, we used the RPM, GSMaP and CMORPH which are global satellite rain estimation data based on microwave satellite and GEO observations.

Since the above satellite rainfall observation data can estimate global precipitation every hour, it is possible to create daily average data in which the average section is shifted by one hour. By correlating the satellite daily precipitation observation time series with the APHRODITE daily precipitation observation time series, the EOD value in each country was estimated from the time when the correlation coefficient is largest. We confirmed that the reliability of this method is high by a verification analysis in the field where true value of EOD is already known. Moreover, we made pseudo hourly rain time series of APHRODITE by inserting APHDOITE daily rain time series to satellite hourly rain time series. By this method, we will try to make a new APHRODITE data that is corrected for the EOD difference between each country.

Keywords: Precipitaition, Satellite, APHRODITE

©2019. Japan Geoscience Union. All Right Reserved. 

# Development of the high resolution GSMaP by the Himawari-8

*Tomoaki Mega[1], Tomoo Ushio[1]

1. Tokyo Metropolitan University

There is a new generation infrared (IR) imager on new-generation gestationary weather-satellite such as the Himawari-8 and the Geostationary Operational Environmental Satellite-R series. The imagers observe multi-channel passive imaging radiometer. The imagers observe wave a full disk with several km in about ten minutes. In Near-future, the IR imager observation should cover the globe.

Global precipitation information is an important tool for water management or earth science. Spaceborne sensors is one of the most convenient tools of global observation. The sensors cover global and provide uniform quality data. Precipitation estimation use microwave radiometer in low earth orbit (LOE). A microwave radiometer has high spatial resolution. However, one drawback of the microwave radiometer in LOE is narrow observation area. Whole earth observation by a microwave radiometer on a LOE satellite need some days. Therefore, global precipitation map is made from combined satellite data. However, combined data of microwave radiometer on LOE don’ t cover global in one hour. One of the global precipitation map is the Global satellite mapping of Precipitation (GSMaP). Precipitation estimation of the GSMaP made from microwave radiometer data. The GSMaP Moving Vector with Kalmanfilter (MVK) and Near real time compensate precipitation of no observation area by IR information. Spatial and temporal resolution of the GSMaP MVK achives 0.1 degree and one hour. This study shows downscale technique for GSMaP precipitation map by High-spatial and temporal resolution IR data of the Himawari-8. IR datasets of Himawari-8 are available every 2.5 minutes in the Japan region. In the presentation, we will also show validation the high resolution GSMaP and ground-radar network in Japan.

Keywords: Precipitation, GSMaP, Microwave Radiometer, Infrared Radiometer, Algorithm

©2019. Japan Geoscience Union. All Right Reserved. 

# Preliminary results of on-orbit estimation for polarization sensitivity of GCOM-C/SGLI

*Risa Miyazaki[1], Hiroshi Murakami[1], Masahiro Hori[1]

1. Japan Aerospace Exploration Agency

The GCOM-C has been launched successfully on 23th Dec. 2017 from the Tanegashima Space Center by H-IIA vehicle No.37. After the initial calibration/validation phase of one year after launch, all SGLI standard products have been released from JAXA’s data providing service (G-Portal) from Dec. 20, 2018.

In generally, the radiance reflected by the sea surface and the atmosphere is strongly polarized. When observing a large polarized light, the output radiance vary from the actual radiance because of the polarization sensitivity characteristic of the optical sensor. Especially for ocean color products, it is important to evaluate the effect of polarization sensitivity because it is necessary to extract the weak water-leaving reflectance (<10% of the whole) by the accurate atmospheric correction.
The polarization sensitivity of GCOM-C/SGLI of each NP (Non-Polarization) band has been measured in the pre-launch ground test. The ground test results of polarization sensitivity were shown to be <3.5% on average in the pixel direction in all bands. In this study, we evaluate whether the polarization sensitivity estimated from on-orbit observation data is consistent with the pre-launch test results. In this work, we report on the RED bands (VN07, VN08) and the NIR bands (VN10, VN11) of SGLI.
Polarization sensitivity on-orbit was evaluated based on Gordon and Zhang (1997) and Meister et al. (2005). We use the observation data by SGLI/PL (Polarization) band to estimate the real stokes vector components at the top of atmosphere (TOA). In order to obtain the polarization sensitivity with respect to directly observed radiance at TOA, L1B before inter-pixel sensitivity correction and before inter-telescope sensitivity correction was self-made from L1A data.
We analyzed the observation data of 12 path that PL band is observed nadir direction. The characteristics of the instrument for polarization sensitivity (polarization factor) were estimated by the least squares method. On the east side of the observation image, the error is large because of Sun-Glint. Although the variation in the pixel direction was still large, the estimated polarization factors (3 to 5 %) were consisted with the prelaunch ground test (~ 3.5%). However, sensitivity patterns in the pixel direction could not be identified, so we will continue to improve the evaluation in the future.

Keywords: GCOM-C, SGLI, Polarization sensitivity

©2019. Japan Geoscience Union. All Right Reserved. 

# Analysis of SGLI validation datas based on the effects of the growth and ground types for the AGB development

*Ryota Ishibashi[1], Koji KAJIWARA[1], Yoshiaki HONDA[1]

1. Center for environmental remote sensing, Chiba University

The effects of the earth of the time variant system should be difficult to detect the influence of the growth types and also the effects of the growth field’s variations. The research may occur the SGLI’s RSRF datas of the calculated AGB data accuracy analysis that observed between every kinds of the growth and also the ground types. The significance area of the SGLI observed, each of detected datas accuracy have to be considered. We show observation ways for the ground truth of the reflectance, LAI and fAPAR. The first case we use is a case of vegetation at the grassland. And then, based of reflectance values, we compare the other type as the Mixed coniferous forest example. The influence of an effect of the type of growth may occur the reflectance of the distributed area. We will detect these effects of the growth type. The influence at the observed area be necessarily to be verified.

The research topic includes the ground truth observation for the accuracy verification of a SGLI data obtained. For development of ground truth, the way to obtain datas were important. This paper explains how to examine growth (such as a second growth forest and other) and the slope factor of the second growth forest area and also the reflectance of each forest types. Then, this paper make ground truth observation scheme for the high accuracy AGB referenced data development at ground cover area. We explain the method of examine the error detection way including observation devices and also the problem of the research topic to be examined. Results may occur an example case of such kinds of the sloped forest and the kinds of the plane. The results shows a typical difference between the sloped and the plane, and then the results may occur the possibility that comparison of standard deviation may be an effective way to detect the volume of the forest type between every ground truth.

The case of we use as the sloped fields, reflectance of each wavelength were low and then the near 400 to 700 nm area will be higher than other wavelength (ANOVA values of results: $p < 0.001$). And then, we can see the effects of slope should be detected at total values of the reflectance. The reflectance of a wavelength were obtained that aimed to detect the verification of the slope and the growth type’s reflectance. When the mixed coniferous forest, static observation develop same reflectance values but the effect of the sloped factor occur the high value of the standard deviations. Then, our method applied to the method of the SGLI’s data calculation scheme, and then the growth factor of the area be affects the influence of the from 400 to 700 nm wavelength and also the factor of slope region be affects the wavelength of reflectance. SGLI data analysis, the factor of these parameters were used to remake the size of RSRF data from 250 m to 1000 m resolution. The future, we investigate more and then, the mask area of high value difference around the nearest 16 pixels be considered. Datas were significant at some pixels, such as a steep sloped, growth types, or error detected area. Data development of RSRF, the reflectance of each cells are detected as the values of the every ground types by the standard deviation.

Keywords: SGLI's data verifications, Reflectance maps, Statistical ANOVA analysis

©2019. Japan Geoscience Union. All Right Reserved. 

## Factor analysis of variable results (Three-way ANOVA)

Sloped factors: Mean values of the SD of each (dynamic/semi-static)
Canopy factors: Difference of each SD of the every SD
Growth typed factors: Difference of each Mean and SD

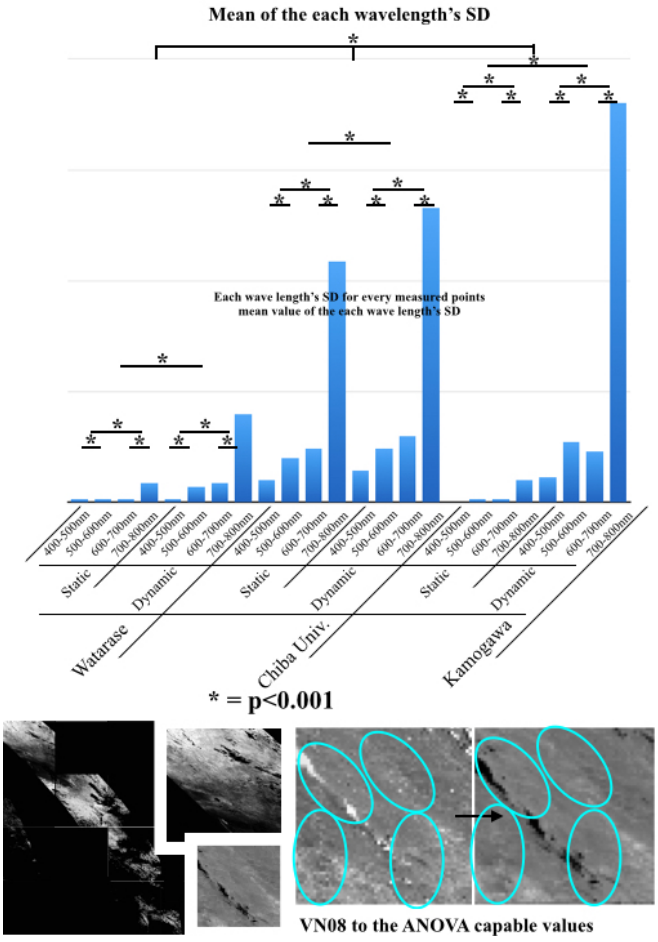


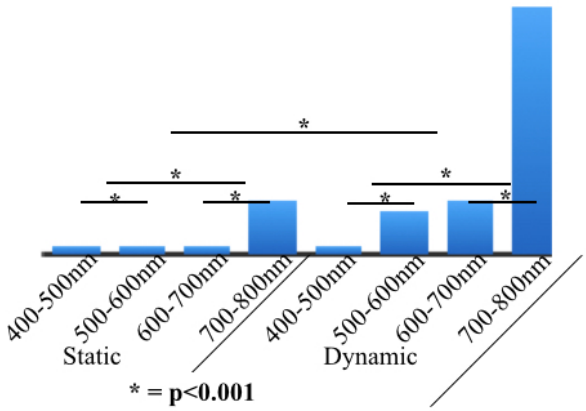


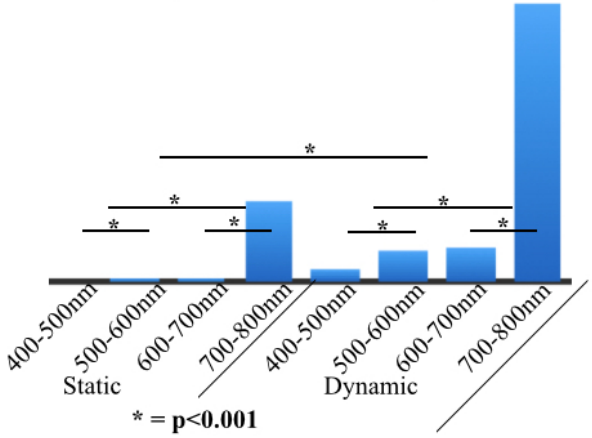





©2019. Japan Geoscience Union. All Right Reserved. 

# Remote sensing of aerosol optical properties and water-leaving radiance based on the optimal estimation approach

*Chong Shi[1], Teruyuki Nakajima[1], Makiko Hashimoto[1], Hideaki Takenaka[1]

1. Japan Aerospace Exploration Agency

A flexible inversion algorithm is proposed for jointly retrieving aerosol optical properties and water-leaving radiance from multispectral instrument over the ocean. A combined multi-wavelength and multi-pixel constraint approach is used to estimate aerosol and hydrosol over clear and turbid waters, based on the forward simulation from a coupled atmospher-ocean radiative transfer model. This sort of simultaneous inversion helps to correct the biases induced by the neglect of water-leaving radiance in the traditional aerosol retrieval algorithms, in addition, it can provide more aerosol information than the standard ocean color approach. To investigate the availability of current scheme, we conduct the retrieval in the process of MODIS, GOSAT/CAI and GCOM-C/SGLI instruments.

©2019. Japan Geoscience Union. All Right Reserved. 

# Aerosol retrieval and PM2.5 from space using GOSAT/TANSO-CAI

*Makiko Hashimoto[1], Hideaki Takenaka[1], Teruyuki Nakajima[1], Akiko Higurashi[2]

1. Japan Aerospace Explortion Agency, 2. NIES

Aerosol in the atmosphere has a great impact not only for the Earth’ s radiation budget and changing the Earth’ s climate, but also on human health. Especially, the fine particle, which is often called PM2.5, has drawn attention as a cause of health damage.

The urban area is a source of anthropogenic aerosol, which is mostly composed of small particles, and the particles are transported to other regions. Satellite remote sensing provides effective means to monitor the atmospheric aerosols in wide area including urban areas.

Accurate retrieval of fine mode aerosol optical thickness (AOT) is necessary to calculate an equivalent value of PM2.5 from space. Therefore, an aerosol retrieval algorithm for satellite remote sensing of urban areas to improve the retrieval accuracy of aerosol properties, which is called MWPM (Multiple wavelengths and pixels method) (Hashimoto and Nakajima, 2017), was developed. The method simultaneously retrieves fine and coarse mode AOT and single scattering albedo by using several wavelengths and spatial difference of surface reflectance. The method is useful for aerosol retrieval over spatially inhomogeneous surface like an urban area.

The algorithm was applied to GOSAT (Greenhouse Gases Observing Satellite) / TANSO-CAI (Cloud and Aerosol Imager, CAI) data. The GOSAT launched ten years ago (on January 23th, 2009) is a satellite to monitor greenhouse gases (GHG) such as carbon dioxide and methane with TANSO-FTS (Fourier Transform Spectrometer, FTS). The CAI is a supplementarysensor of the FTS, detecting cloud and deriving aerosol optical properties.

PM2.5 using retrieved fine mode AOT by MWPM in East Asian region from 2009 was calculated. The poster presents a retrieval result of PM2.5 over the East Asian region from space in several years and discusses the seasonal and annual variations.
Monitoring of aerosol properties such as AOT, PM2.5 and soot mixing ratio over land is added to the mission of GOSAT-2 that was launched on Otober 29th 2018. As a near-future plan, the algorithm will be applied to GOSAT-2/TANSO-CAI-2 data to generate standard PM2.5 data products.

Keywords: Remote sensing , Aerosol

©2019. Japan Geoscience Union. All Right Reserved. 

# Establishing a high resolution road fugitive dust emission inventory in Kaifeng City, China

*Yiming Xu[1], Shili Liu[1], Xinyue Cao[1], Xianbao Shen[1], Zhiliang Yao[1]

1. Department of Environmental Science and Engineering, Beijing Technology and Business University

Due to the rapid urbanization and industrialization in many Chinese cities, ambient particulate matter pollution such as road fugitive dust pollution becomes a serious environmental problem. However, the emission of road fugitive dust is relatively difficult to quantify as it is of high uncertainty and spatial heterogeneity. The research aims to build a high resolution road fugitive dust emission inventory which is transferrable and applicable to other cities in China. High spatial resolution images were utilized to digitalize whole road network of Kaifeng City, Henan Province, China. Vehicle flows of the whole road network were estimated by incorporating the whole road network, field measured data and GPS data on an hourly, daily, weekly, monthly and yearly basis at city level. By fusing the road network information, vehicle flow, road dust load, average vehicle weight, a high resolution road fugitive dust emission inventory was established. The results showed that the total emissions of $PM_{10}$, $PM_{2.5}$ and Total Suspended Particulate from road fugitive dust at commuter time and downtown were much higher compared with other time and location in Kaifeng City. The framework of this road fugitive dust emission inventory can be applied to other cities, and it can provide data support and guide fugitive dust management in China.

Keywords: Road Fugitive Dust, High Resolution Remote Sensing, Satellite Data, Air Pollutant Emission Inventory

©2019. Japan Geoscience Union. All Right Reserved. 

# A Relationship between Diurnal Change Patterns of Land Surface Temperature and Spatial Configuration of the Osaka Metropolitan Area Captured by Himawari-8

*Yuhei Yamamoto[1], Hirohiko Ishikawa[1]

1. Disaster Prevention Research Institute, Kyoto University

Land surface temperature (LST) is a physical quantity that greatly contributes to the formation of an urban thermal environment. Therefore, understanding the spatiotemporal characteristics of LST is necessary for constructing a sustainable urban environment. The spatial distribution relationship between the instantaneous LST and urban land use has been investigated using polar-orbiting satellite/airborne sensors. This study explored how the urban spatial configuration and meteorological field affect the temporal changes of LST by using Japanese geostationary satellite (Himawari-8) sensor.
The study area is the Osaka metropolitan area in Japan and target days are three days that were clear-sky throughout the day in summer (August 12, 2016, July 19, 2018, and August 4, 2018). We used 100 m-mesh urban land use data and ground-based meteorological observation data to examine the urban spatial configuration and meteorological fields, respectively. The temporal changes of LST are the amplitude and phase mainly forming the diurnal change of LST. These two temporal changes were extracted by applying principal component analysis to the diurnal changes of LST represented by the 10-minute LST dataset retrieved from Himawari-8 data.
Our results showed that the spatial variations in the amplitude and phase corresponded to the penetration time and duration of the sea breeze and the thermal inertia of surface materials. Besides, it was found that the LST change during daytime was larger in the high-density low-building areas than in the low-density low-building areas. This result suggests that the increase in building density increases the LST change during the daytime. These findings lead to a deeper understanding of an urban hot environment and are helpful for urban planning to mitigate the deterioration of a hot environment.

Keywords: Land Surface Temperature, Himawari-8, Urban Heat Island

©2019. Japan Geoscience Union. All Right Reserved. 

[E] Poster | A (Atmospheric and Hydrospheric Sciences)：A-CG Complex & General

Thu. May 30, 2019 5:15 PM - 6:30 PM JST | Thu. May 30, 2019 8:15 AM - 9:30 AM UTC | Poster Hall International Exhibition Hall8, Makuhari Messe_12

## [A-CG34] Satellite Earth Environment Observation

convener:Riko Oki(Japan Aerospace Exploration Agency), Yoshiaki HONDA(Center for Environmental Remote Sensing, Chiba University), Yukari Takayabu(Atmosphere and Ocean Research Institute, the University of Tokyo), Tsuneo Matsunaga(Center for Global Environmental Research and Satellite Observation Center, National Institute for Environmental Studies)

In recent years, we cannot avoid facing issues on global environmental changes that occur in various spatiotemporal scales. The earth environmental observation data by satellites became the necessary basic data to tackle and solve those issues. Due to the recent advancement in the observation sensor technique and the data processing technique, the satellite observation has been showing rapid progress, and the time is changing from examining the accuracy of the observation sensor data to the advancement of the data application, leading to broaden potential users. In these days application became synergetic, so we comprehensively pick<br/>up this topic in the Atmospheric and Hydrospheric Sciences Session of this Union Meeting that enables to comprise the atmospheric, oceanic and land sciences; by combining the intelligence and the knowledge of the party, we propose a session that aims to prompt further studies towards the issues on earth environmental change, the advancement in the data application and future plans of Earth Observation missions.

### [ACG34-P01] Impact of usage of multiple-satellite sensors on accuracy of daily-mean sea surface wind data

*Ayumi Koizumi[1], Masahisa Kubota[2], Kunio Kutsuwada[3], Hiroyuki Tomita[4], Tsutomu Hihara[5] (1.Tokai University, 2.Tokai University, Institute of Ocean Research and Development, 3.School of Marine Science and Technology, Tokai University, 4.Institute for Space-Earth Environmental, Nagoya University, 5.Japan Agency for Marine-Erth Science and Technology)

### [ACG34-P02] Temperature and Size Variability of Warm Pools in the Global Oceans

*ChunYi Lin[1] (1.National Museum of Marine Science & Technology)

### [ACG34-P03] Sea surface temperature from SGLI aboard the GCOM-C satellite of JAXA

*Yukio Kurihara[1], Kazunori Ogata[2], Hiroshi Murakami[2], Misako Kachi[2] (1.Tripli-I Co., Ltd., 2.JAXA EORC)

### [ACG34-P04] Concept of small satellite UV/visible imaging spectrometer optimized for tropospheric $NO_2$ measurements in air quality monitoring

*Tamaki Fujinawa[1,5], Katsuyuki Noguchi[2], Akihiko Kuze[3], Andreas Richter[4], John P. Burrows[4], Andreas C. Meier[4], Tomohiro Sato[1], Takeshi Kuroda[1], Naohiro Yoshida[5], YASUKO KASAI[1,5] (1.National Institute of Information and Communications Technology, 2.Nara Women's University, 3.Japan Aerospace Exploration Agency, 4.University of Bremen, 5.Tokyo Institute of Technology)

### [ACG34-P05] EarthCARE L2 algorithms for cloud and precipitation

*Kaori Sato[1], Hajime Okamoto[1], Hiroshi Ishimoto[2] (1.Research Institute for Applied Mechanics, Kyushu University, 2.Meteorological Research Institute)

### [ACG34-P06] Analysis of the Surface Echo Characteristics Derived from GPM/DPR Wide Swath Observation Experiment

*Kosuke Yamamoto[1], Kinji Furukawa[1], Nobuhiro Takahashi[2], Takuji Kubota[1] (1.Japan Aerospace Exploration Agency, 2.Nagoya University)

### [ACG34-P07] The Recent Results from the Global Precipitation Measurement (GPM) mission in Japan

*Riko Oki[1], Takuji Kubota[1], Kinji Furukawa[1], Yuki Kaneko[1], Moeka Yamaji[1], Kosuke Yamamoto[1], Toshio Iguchi[2], Yukari Takayabu[3] (1.Japan Aerospace Exploration Agency, 2.NICT, 3.the University of Tokyo)

[ACG34-P08] **Verification of Global Satellite Mapping of precipitation (GSMaP) for providing its error information**

*Moeka Yamaji[1], Takuji Kubota[1] (1.Earth Observation Research Center, Japan Aerospace Exploration Agency)

[ACG34-P09] Detection of the mixed phase top using the measured dual-frequency ratio of reflectivity with GPM/DPR

*Yuki Kaneko[1], Toshio Iguchi[2] (1.Japan Aerospace Exploration Agency, 2.National Institute of Information and Communications Technology)

[ACG34-P10] **Comparison between high frequency satellite rainfall estimation and APHRODITE-2 ground rain gauge observation**

*Hitoshi Hirose[1], Koichi Toyoshima[1], Atsushi Higuchi[1], Akiyo Yatagai[2], Natsuko Yasutomi[3] (1.Center for Environmental Remote Sensing, Chiba University, 2.Hirosaki University, 3.Disaster Prevention Research Institute, Kyoto University)

[ACG34-P11] Development of the high resolution GSMaP by the Himawari-8

*Tomoaki Mega[1], Tomoo Ushio[1] (1.Tokyo Metropolitan University)

[ACG34-P12] Preliminary results of on-orbit estimation for polarization sensitivity of GCOM-C/SGLI

*Risa Miyazaki[1], Hiroshi Murakami[1], Masahiro Hori[1] (1.Japan Aerospace Exploration Agency)

[ACG34-P13] Analysis of SGLI validation datas based on the effects of the growth and ground types for the AGB development

*Ryota Ishibashi[1], Koji KAJIWARA[1], Yoshiaki HONDA[1] (1.Center for environmental remote sensing, Chiba University)

[ACG34-P14] Remote sensing of aerosol optical properties and water-leaving radiance based on the optimal estimation approach

*Chong Shi[1], Teruyuki Nakajima[1], Makiko Hashimoto[1], Hideaki Takenaka[1] (1.Japan Aerospace Exploration Agency)

[ACG34-P15] Aerosol retrieval and PM2.5 from space using GOSAT/TANSO-CAI

*Makiko Hashimoto[1], Hideaki Takenaka[1], Teruyuki Nakajima[1], Akiko Higurashi[2] (1.Japan Aerospace Explortion Agency, 2.NIES)

[ACG34-P16] **Establishing a high resolution road fugitive dust emission inventory in Kaifeng City, China**

*Yiming Xu[1], Shili Liu[1], Xinyue Cao[1], Xianbao Shen[1], Zhiliang Yao[1] (1.Department of Environmental Science and Engineering, Beijing Technology and Business University)

[ACG34-P17] A Relationship between Diurnal Change Patterns of Land Surface Temperature and Spatial Configuration of the Osaka Metropolitan Area Captured by Himawari-8

*Yuhei Yamamoto[1], Hirohiko Ishikawa[1] (1.Disaster Prevention Research Institute, Kyoto University)

# Impact of usage of multiple-satellite sensors on accuracy of daily-mean sea surface wind data

*Ayumi Koizumi[1], Masahisa Kubota[2], Kunio Kutsuwada[3], Hiroyuki Tomita[4], Tsutomu Hihara[5]

1. Tokai University, 2. Tokai University, Institute of Ocean Research and Development, 3. School of Marine Science and Technology, Tokai University, 4. Institute for Space-Earth Environmental, Nagoya University, 5. Japan Agency for Marine-Erth Science and Technology

Most satellites observing sea surface winds have sun-synchronous orbits and provide observation data at the same place two times per a day. We can expect that daily-mean values estimated from these data have some errors when diurnal changes in wind field cannot be neglected. For this problem, use of multiple satellites is helpful. Since the number of sensors used to construct daily-mean data is different among the years, it is expected that the accuracy of a daily-mean value changes from year to year.

The purpose of this study is to describe time variation of accuracy in daily-mean wind data in the Japanese Ocean Flux Data Sets with Use of Remote Sensing Observation (J-OFURO)-3 and to investigate its causes by comparing with in-situ measurement data by moored buoys and calculating three statistical values.

Results reveal that the statistical values are improved with year. To examine the relationship between the yearly statistics and the yearly number of satellite sensors, we plotted a scatter diagram between the number of satellites and three statistical values in each year. We found that the correlations between them are very high. We also focused on a time interval of the satellite wind observation, namely maximum missing time within a day. The result showed that the correlation between three statistical values and maximum missing time intervals is high. Since the relation between these two factors is not independent, we analyzed by considering both factors together. First, we chose five buoys with various standard deviations for a daily-mean value. Next, we picked up data from buoy's hourly data using random numbers, and calculated the daily mean value using the random data, and then determined the number of observations and the maximum missing time interval each day. Assuming the daily mean value calculated from 24 hourly data as a true value, the RMSE between this true value and the daily mean created from random data was calculated. From the result of this analysis, it was found that the value of Root Mean Square Error(RMSE) depends on the maximum missing time interval rather than the number of observations. Furthermore, when RMSE was normalized by standard deviation, the same figures were obtained for all buoys. This result implies that the RMSE of the daily mean value of the buoy station can be estimated if the magnitude of diurnal variation is known by giving the number of satellites used for observation and the maximum missing time interval, Moreover, by applying this result, we think that it is possible to show the optimal number of sensors and observation time for target accuracy. This result gives very breakthrough information to the design of the satellite observation system for sea surface wind.

Keywords: Multiple-satellite sensors, Sea surface wind

©2019. Japan Geoscience Union. All Right Reserved. 

# Temperature and Size Variability of Warm Pools in the Global Oceans

*ChunYi Lin[1]

1. National Museum of Marine Science & Technology

Using advance satellite-derived Sea surface height anomaly, sea surface temperature (SST) data, and heat flux data, we investigate the thermal variability, temperature and size variability of warm pools in the global oceans, the Pacific, the Atlantic, and the Indian Ocean, respectively. Because of the high density and specific heat of seawater, water can store and transport large amounts of heat. High SST has particular influence on global climate system. Furthermore previous studies focused on the global warming or area warming, in this investigation we present results of warm pool SST binned into 1 ˚C interval. Detecting temperature and size variability of warm pools in the global oceans, it suggests that the high SST area (SST ≧ 28˚C) has faster increasing rate than surrounding area (SST 20˚C - 27˚C) in the global oceans, the Pacific, the Atlantic, and the Indian Ocean, respectively. To understand the role of surface heat flux in the tropical SST fluctuation, we analyze the mixed layer heat balance equation. Upper ocean heat budget between the heat advection and heat diffusion term are compared and heat diffusion processes may be a mechanism for transporting excessive amount of heat that the warm pool through enhancing the SST gradient around the edge of the warm pool. In order to find out dominant period components and the relationship of energy-frequency distribution without influenced induced by nonlinear and nonstationary signals, the Hilbert-Huang Transform applied by ensemble empirical mode decomposition is employed. The ensemble empirical mode decomposition analysis indicates that the interannual component has strong influence on the variability of the warm core pool in the Pacific, presumably because of the presence of El Niño phenomenon, while the annual cycle dominates the variability in the Indian and the Atlantic Ocean.

Keywords: warm pool, SST, heat flux

©2019. Japan Geoscience Union. All Right Reserved. 

# Sea surface temperature from SGLI aboard the GCOM-C satellite of JAXA

*Yukio Kurihara[1], Kazunori Ogata[2], Hiroshi Murakami[2], Misako Kachi[2]

1. Tripli-I Co., Ltd., 2. JAXA EORC

The Global Change Observation Mission-Climate (GCOM-C) satellite, which is one of two satellites for the GCOM mission of the Japan Aerospace and Exploration Agency (JAXA), was launched on 23 December 2017. The Second Generation Global Imager (SGLI) is the optical sensor aboard GCOM-C which consists of two components: the Visible and Near-infrared Radiometer (VNR) and the Infrared Scanner (IRS). SGLI has switchable spatial resolution from 250 m x 250 m to 1 km x 1 km. The resolution of 250 m x 250 m is expected to reveal complicated structure of geophysical parameters. Sea surface temperature (SST), which is one of the important parameters in the geophysical field, is also determinable by using split window data of SGLI. SGLI SST is retrieved by utilization of newly developed cloud masking method and a modified SST method originally developed for Himawari-8. Considering combined utilization of satellite SSTs, the methods developed for SGLI SST will be applied back to Himawari-8 data as well as the data from the Visible Infrared Imaging Radiometer Suite (VIIRS) aboard the Suomi National Polar-orbiting Partnership (Suomi NPP) satellite. SGLI SST is validated by comparison with buoy data. The comparison result shows RMSD of ~0.4 K, good agreement between SGLI SSTs and buoy data. Triple comparison with Himawari-8 and VIIRS SSTs is being started. Operational retrieval of SGLI SST started at the end of 2018. The products are available at the G-Portal site of JAXA and the JAXA Satellite Monitoring and Environmental Studies (JASMES) site of the Earth Observation Center (EORC) of JAXA.

©2019. Japan Geoscience Union. All Right Reserved. 

# Concept of small satellite UV/visible imaging spectrometer optimized for tropospheric $NO_2$ measurements in air quality monitoring

*Tamaki Fujinawa[1,5], Katsuyuki Noguchi[2], Akihiko Kuze[3], Andreas Richter[4], John P. Burrows[4], Andreas C. Meier[4], Tomohiro Sato[1], Takeshi Kuroda[1], Naohiro Yoshida[5], YASUKO KASAI[1,5]

1. National Institute of Information and Communications Technology, 2. Nara Women's University, 3. Japan Aerospace Exploration Agency, 4. University of Bremen, 5. Tokyo Institute of Technology

Satellite observations at nadir can potentially facilitate a better understanding of the emissions and distribution of tropospheric nitrogen dioxide, $NO_2$. The identification of emissions requires adequate spatiotemporal resolution measurements of the total column amounts of $NO_2$. The spatial resolution of previous and current observations is insufficient for the identification of $NO_2$ hot-spots. Switching to a spatial resolution of ~1 km x ~1 km can improve the identification of local sources of $NO_2$ and their emissions. To investigate the feasibility of observations with such a high spatial resolution, we simulated radiance spectra for different cases under varying parameters, such as area, season, satellite altitude, and surface reflectance by using the radiative transfer model SCIATRAN. We subsequently retrieved $NO_2$ slant column densities (SCDs) using the differential optical absorption spectroscopy (DOAS) technique with several fit windows. For test cases associated with polluted conditions, we found that the conceptual nadir-observing instrument on a satellite at an altitude of ~300 km involved the lowest retrieval errors for signal-to-noise ratios of around 1000 with accuracy better than the required 5% for tropospheric $NO_2$ SCD and that the fit window of 425--497 nm met the scientific requirements for both surface reflectance cases.

Keywords: Nitrogen dioxide, Earth observation, Radiative transfer model, Remote sensing

©2019. Japan Geoscience Union. All Right Reserved. 

# EarthCARE L2 algorithms for cloud and precipitation

*Kaori Sato[1], Hajime Okamoto[1], Hiroshi Ishimoto[2]

1. Research Institute for Applied Mechanics, Kyushu University, 2. Meteorological Research Institute

The EarthCARE (Earth Clouds, Aerosols and Radiation Explorer, JAXA-ESA) mission will carry the first 94GHz Doppler Cloud Profiling Radar (CPR) with a high spectral resolution atmospheric lidar (ATLID) at 355nm. Recent progresses in EarthCARE L2 cloud/precipitation algorithms for the treatment of multiple scattering and cloud particle nonsphericity are presented.

Keywords: spaceborne active sensor, cloud

©2019. Japan Geoscience Union. All Right Reserved. 

# Analysis of the Surface Echo Characteristics Derived from GPM/DPR Wide Swath Observation Experiment

*Kosuke Yamamoto[1], Kinji Furukawa[1], Nobuhiro Takahashi[2], Takuji Kubota[1]

1. Japan Aerospace Exploration Agency, 2. Nagoya University

The observation from spaceborne precipitation radar has been contributed to better understanding of earth climate system. Global Precipitation Measurement (GPM) core satellite Dual-frequency Precipitation Radar (DPR) provides us 3-dimentional information of precipitation by the scan width of about 250 km, but there have been arguments that to bring systematic impact on the weather monitoring through global rainfall map such as GSMaP, wider swath observation by precipitation radar is necessary.

Based on those requirements, the scan pattern of GPM/DPR was experimentally changed for 1 day from 13UTC on September 26th. In this experiment, the scan angle was changed to observe from nadir to about +34˚ assuming future spaceborne precipitation radar with wider swath width, while in the normal observation DPR scans ±17˚. The height and strength of the mainlobe clutter with larger incident angle were assessed statistically to examine the possibility of the rainfall retrieval with wide swath observation by DPR.

In order to examine mainlobe clutter height, it is inevitable to reduce sidelobe and grating lobe effect. In this study, clutter-free observation data is extracted based on following procedures; 1) extract bins above mainlobe clutter; 2) extract bins under non-precipitation condition from 1); 3) extract bins that satisfy |received power −averaged noise power| < 2 sigma of the noise power from 2). Note that this procedure was applied only for KuPR observation since sidelobe and grating lobe clutter is not prominent in KaPR.

The result for KuPR observation shows that the mainlobe clutter top height at the larger incident angle over ocean is somehow suppressed at around 4 km while over land it increases almost linearly up to around 5 km due to the strong surface scattering. The same tendency is found on the KaPR observation, but it has lower clutter top height of around 2.5 km and 3.5 km, over ocean and land respectively. Suppression is clearer over ocean thanks to the specular reflection. The results also indicate that relatively intense rainfall can be retrieved while shallow rainfall with weak echo power may not be acceptable for retrieval because it should be masked by the surface clutter.

Keywords: precipitation radar, radar clutter, GPM core satellite

©2019. Japan Geoscience Union. All Right Reserved. 

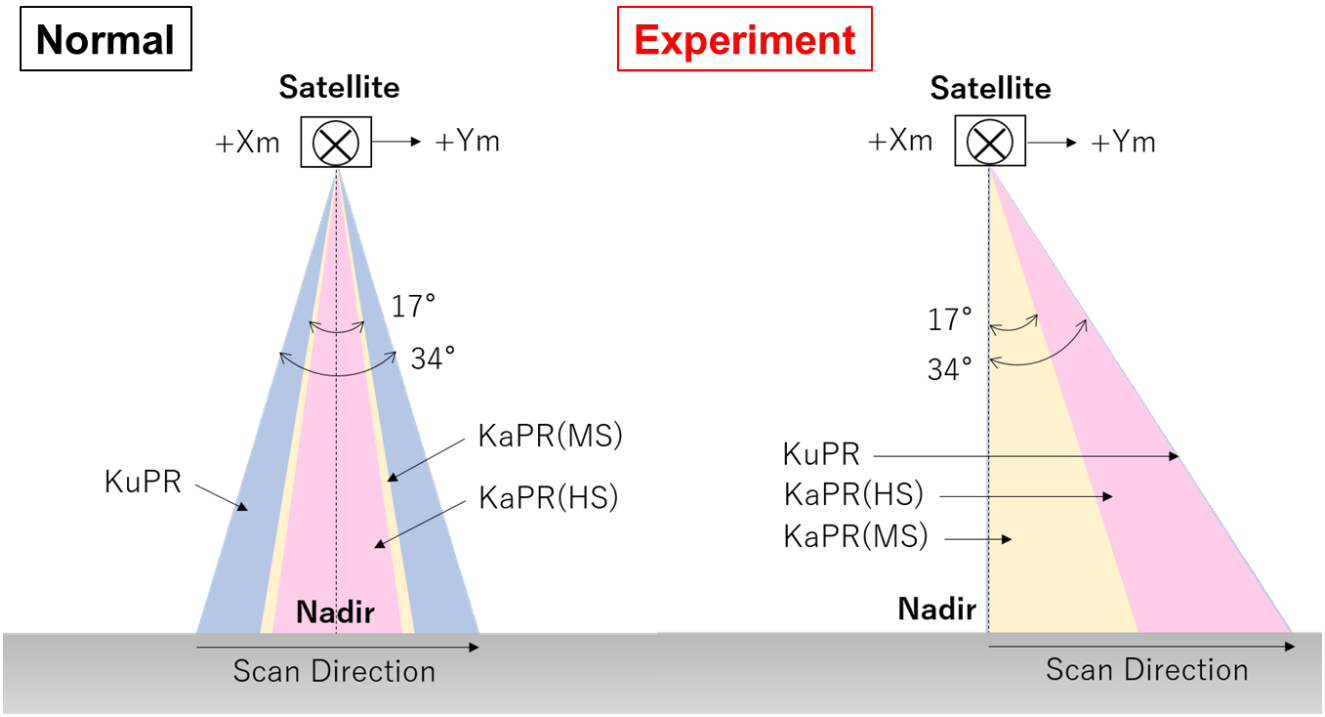


©2019. Japan Geoscience Union. All Right Reserved. 

# The Recent Results from the Global Precipitation Measurement (GPM) mission in Japan

*Riko Oki[1], Takuji Kubota[1], Kinji Furukawa[1], Yuki Kaneko[1], Moeka Yamaji[1], Kosuke Yamamoto[1], Toshio Iguchi[2], Yukari Takayabu[3]

1. Japan Aerospace Exploration Agency, 2. NICT, 3. the University of Tokyo

The Global Precipitation Measurement (GPM) mission is an international cooperate satellite project to achieve highly accurate and highly frequent global precipitation observations. The GPM mission consists of the GPM Core satellite jointly developed by the U.S. and Japan and Constellation Satellites that carry microwave radiometers and provided by the GPM partner agencies. The GPM Core satellite carries the Dual-frequency Precipitation Radar (DPR) by the Japan Aerospace Exploration Agency (JAXA) and the National Institute of Information and Communications Technology (NICT) and the GPM Microwave Imager (GMI) provided by National Aeronautics and Space Administration (NASA). The GPM Core satellite was launched in February 2014 and achieved its prime mission period planned for 3 years in 2017.

It has been continuing its observation as the extended mission phase after that.

JAXA develops the DPR Level 1 algorithm and the NASA-JAXA Joint Algorithm Team develops the DPR Level 2 and DPR-GMI combined Level 2 algorithms. The DPR, the DPR-GMI combined algorithms and the latent heating algorithm were updated, and those products were released in October 2018 as Version 0.6. Using dual frequency information of DPR, the latest Level 2 products include information such as precipitation phase at surface, heavy ice precipitation and so on. Also, the calibration factors of TRMM/PR were re-examined to have consistency between DPR/Ku. The same GPM Ku-band radar L2 algorithm now applies to the TRMM/PR, so that the long radar precipitation data exceeding more than 20 years are now available. From May 2018 in the extended mission period, the scan pattern of the Ka-band radar has been changed to realize matched beam observation in full swath. The new algorithm applying to the changed scan pattern is now under development.

JAXA also develops the Global Satellite Mapping of Precipitation (GSMaP), that is hourly and 0.1-degree horizontal resolution global rainfall map. It is available through the “JAXA Global Rainfall Watch” website (https://sharaku.eorc.jaxa.jp/GSMaP/index.htm). GSMaP product family includes different data latency products and rain gauge calibrated products and so on. The GSMaP near-real-time version (GSMaP_NRT) product provides global rainfall map in 4-hour after observation, and an improved version of GSMaP near-real-time gauge-adjusted (GSMaP_Gauge_NRT) product has been released since Dec. 2018.

The GSMaP real-time product called GSMaP_NOW now product is providing data at the earliest timing. It has been realized using the geostationary satellite Himawari-8 operated by the Japan Meteorological Agency (JMA) since November 2015. Since Nov. 2018 the domain of GSMaP_NOW has been extended to the region of the geostationary satellite Meteosat operated by the European Organization for the Exploitation of Meteorological Satellites (EUMETSAT) in November 2018. JAXA is further developing the GSMaP_NOW to provide global real-time rainfall product.

Keywords: GPM, Satellite Remote Sensing, Precipitation

©2019. Japan Geoscience Union. All Right Reserved. 

©2019. Japan Geoscience Union. All Right Reserved. 

# Verification of Global Satellite Mapping of precipitation (GSMaP) for providing its error information

*Moeka Yamaji[1], Takuji Kubota[1]

1. Earth Observation Research Center, Japan Aerospace Exploration Agency

Precipitation is one of the most essential parameters in the Earth system. Due to address water issues like water shortage or floods, JAXA has developed and provided Global Satellite Mapping of Precipitation (GSMaP), which is hourly global precipitation dataset. It is under the Global Precipitation Measurement (GPM) mission and contributes.
GSMaP allows us to capture the hourly horizontal distribution of precipitation with good latency after observation. The spatial resolution is 0.1 x 0.1 degrees latitude/longitude. It has been used for various kinds of utilization purposes.
In terms of accuracy, GSMaP algorithms were updated in several times, and GSMaP has been getting more accurate day by day, however, it is known that the inhomogeneous of accuracy is existed depending on algorithm characteristics. It has been needed to provide information about the uncertainty and accuracy of GSMaP by users.
In this study, verification result of GSMaP near-realtime product version 6 (GSMaP_NRT) is reported. The radar/raingauge analysed precipitation data by Japan Meteorological Agency, which is an hourly rainfall analysis generated from ground-based precipitation radars corrected by automated rain gauges, are used as the reference data. Since the purpose of this study is for providing generalized error information, root mean square errors (RMSE) is statistically calculated for each precipitation level and each reliability flag during May-June-July-August-September-October in 2015-2018. Some initial results showed that the RMSE qualitatively represented the error for each precipitation level and reliability flag. The RMSE ratio to the average precipitation rate got larger as the precipitation rate became smaller while it became stable around 60 –80 % when precipitation rate was more than 10 mm/h. We report the validation results in detail, such as land/ocean difference or sampling dependence, and focus on the effectiveness of it.

Keywords: precipitation, GPM, GSMaP, validation

©2019. Japan Geoscience Union. All Right Reserved. 

# Detection of the mixed phase top using the measured dual-frequency ratio of reflectivity with GPM/DPR

*Yuki Kaneko[1], Toshio Iguchi[2]

1. Japan Aerospace Exploration Agency, 2. National Institute of Information and Communications Technology

The core observatory of the Global Precipitation Measurement (GPM) mission was launched in 2014 and has been observing rain and snow between 65˚S and 65˚N by the Dual Frequency Precipitation Radar (DPR) and the GPM Microwave Imager (GMI). The DPR provides three-dimensional structure of storms derived from reflected energy from precipitation particles. Precipitation echoes at the two frequencies of the DPR, Ka-band (25GHz) and Ku-band (14GHz), make it possible to infer the mean size and physical property of precipitation particles. The swath width of Ka-band scanning was 125 kilometers centered at nadir and was nested within the Ku-band’ s wider scan width of 254 kilometers. On May 21 2018, the Ka-band scan pattern was changed to match with the Ku-band’ s. Dual frequency radar reflectivity factors are available for full swath of 254 kilometers now.

The classification (CSF) module in the standard DPR level2 algorithm detects a bright band (BB) and classifies precipitation into three types, stratiform, convective, and other. Rain types affect the retrievals of rain amount and latent heating in the DPR algorithm. Accurate classification is also important in the Global Satellite Mapping of Precipitation (GSMaP) algorithm because it affects the rain profile database used in the rain retrieval with microwave radiometers. The BB detectability by the standard CSF algorithm is lower at and near the swath edges than near nadir because only Ku-band data was available in the outer swath before and because slant incidence of radar beams smears the vertical profiles.

As the Ka-band scan pattern has changed to cover the full swath, we can apply a dual-frequency method to detect a BB now. We have developed a method that uses the dual frequency ratio (DFR) to detect the mixed phase top. It looks at the slope of DFR as a function of range to identify the transition height from ice to water. DFR itself is estimated from measured DFR (DFRm) with attenuation correction. Preliminary experiments show that the developed method can detect the BB in stratiform rain over the swath almost uniformly. This method also has a potential to identify the transition height even in some convective cases. In this research we evaluate the performance of the algorithm by comparing the altitude of BB and the transition height with those estimated by using X-band multi-parameter radar (XRAIN) data.

Keywords: GPM, Melting Layer, Precipitation Radar

©2019. Japan Geoscience Union. All Right Reserved. 

# Comparison between high frequency satellite rainfall estimation and APHRODITE-2 ground rain gauge observation

*Hitoshi Hirose[1], Koichi Toyoshima[1], Atsushi Higuchi[1], Akiyo Yatagai[2], Natsuko Yasutomi[3]

1. Center for Environmental Remote Sensing, Chiba University, 2. Hirosaki University, 3. Disaster Prevention Research Institute, Kyoto University

APHRODITE project collects daily precipitation observation data from ground rain gauges in each country, and then performs appropriate quality control and converts it into gridded data. APHRODITE holds long-term data from the 1960s to the present and focuses on analyzes such as changes in characteristics of extreme rainfall due to long-term climate change. However, ground-based daily rain observations has a problem which end of the day (EOD) in each country is different from each other. To estimate the EOD in each country, we developed a Rain Potential Map (RPM) which is a product that can estimate global rain probability using geostationary meteorological satellites (GEO) (Hirose et al., 2016, JMSJ). In this study, we used the RPM, GSMaP and CMORPH which are global satellite rain estimation data based on microwave satellite and GEO observations.

Since the above satellite rainfall observation data can estimate global precipitation every hour, it is possible to create daily average data in which the average section is shifted by one hour. By correlating the satellite daily precipitation observation time series with the APHRODITE daily precipitation observation time series, the EOD value in each country was estimated from the time when the correlation coefficient is largest. We confirmed that the reliability of this method is high by a verification analysis in the field where true value of EOD is already known. Moreover, we made pseudo hourly rain time series of APHRODITE by inserting APHDOITE daily rain time series to satellite hourly rain time series. By this method, we will try to make a new APHRODITE data that is corrected for the EOD difference between each country.

Keywords: Precipitaition, Satellite, APHRODITE

©2019. Japan Geoscience Union. All Right Reserved. 

# Development of the high resolution GSMaP by the Himawari-8

*Tomoaki Mega[1], Tomoo Ushio[1]

1. Tokyo Metropolitan University

There is a new generation infrared (IR) imager on new-generation gestationary weather-satellite such as the Himawari-8 and the Geostationary Operational Environmental Satellite-R series. The imagers observe multi-channel passive imaging radiometer. The imagers observe wave a full disk with several km in about ten minutes. In Near-future, the IR imager observation should cover the globe.

Global precipitation information is an important tool for water management or earth science. Spaceborne sensors is one of the most convenient tools of global observation. The sensors cover global and provide uniform quality data. Precipitation estimation use microwave radiometer in low earth orbit (LOE). A microwave radiometer has high spatial resolution. However, one drawback of the microwave radiometer in LOE is narrow observation area. Whole earth observation by a microwave radiometer on a LOE satellite need some days. Therefore, global precipitation map is made from combined satellite data. However, combined data of microwave radiometer on LOE don’ t cover global in one hour. One of the global precipitation map is the Global satellite mapping of Precipitation (GSMaP). Precipitation estimation of the GSMaP made from microwave radiometer data. The GSMaP Moving Vector with Kalmanfilter (MVK) and Near real time compensate precipitation of no observation area by IR information. Spatial and temporal resolution of the GSMaP MVK achives 0.1 degree and one hour. This study shows downscale technique for GSMaP precipitation map by High-spatial and temporal resolution IR data of the Himawari-8. IR datasets of Himawari-8 are available every 2.5 minutes in the Japan region. In the presentation, we will also show validation the high resolution GSMaP and ground-radar network in Japan.

Keywords: Precipitation, GSMaP, Microwave Radiometer, Infrared Radiometer, Algorithm

©2019. Japan Geoscience Union. All Right Reserved. 

# Preliminary results of on-orbit estimation for polarization sensitivity of GCOM-C/SGLI

*Risa Miyazaki[1], Hiroshi Murakami[1], Masahiro Hori[1]

1. Japan Aerospace Exploration Agency

The GCOM-C has been launched successfully on 23th Dec. 2017 from the Tanegashima Space Center by H-IIA vehicle No.37. After the initial calibration/validation phase of one year after launch, all SGLI standard products have been released from JAXA’s data providing service (G-Portal) from Dec. 20, 2018.

In generally, the radiance reflected by the sea surface and the atmosphere is strongly polarized. When observing a large polarized light, the output radiance vary from the actual radiance because of the polarization sensitivity characteristic of the optical sensor. Especially for ocean color products, it is important to evaluate the effect of polarization sensitivity because it is necessary to extract the weak water-leaving reflectance (<10% of the whole) by the accurate atmospheric correction.
The polarization sensitivity of GCOM-C/SGLI of each NP (Non-Polarization) band has been measured in the pre-launch ground test. The ground test results of polarization sensitivity were shown to be <3.5% on average in the pixel direction in all bands. In this study, we evaluate whether the polarization sensitivity estimated from on-orbit observation data is consistent with the pre-launch test results. In this work, we report on the RED bands (VN07, VN08) and the NIR bands (VN10, VN11) of SGLI.
Polarization sensitivity on-orbit was evaluated based on Gordon and Zhang (1997) and Meister et al. (2005). We use the observation data by SGLI/PL (Polarization) band to estimate the real stokes vector components at the top of atmosphere (TOA). In order to obtain the polarization sensitivity with respect to directly observed radiance at TOA, L1B before inter-pixel sensitivity correction and before inter-telescope sensitivity correction was self-made from L1A data.
We analyzed the observation data of 12 path that PL band is observed nadir direction. The characteristics of the instrument for polarization sensitivity (polarization factor) were estimated by the least squares method. On the east side of the observation image, the error is large because of Sun-Glint. Although the variation in the pixel direction was still large, the estimated polarization factors (3 to 5 %) were consisted with the prelaunch ground test (~ 3.5%). However, sensitivity patterns in the pixel direction could not be identified, so we will continue to improve the evaluation in the future.

Keywords: GCOM-C, SGLI, Polarization sensitivity

©2019. Japan Geoscience Union. All Right Reserved. 

# Analysis of SGLI validation datas based on the effects of the growth and ground types for the AGB development

*Ryota Ishibashi[1], Koji KAJIWARA[1], Yoshiaki HONDA[1]

1. Center for environmental remote sensing, Chiba University

The effects of the earth of the time variant system should be difficult to detect the influence of the growth types and also the effects of the growth field’s variations. The research may occur the SGLI’s RSRF datas of the calculated AGB data accuracy analysis that observed between every kinds of the growth and also the ground types. The significance area of the SGLI observed, each of detected datas accuracy have to be considered. We show observation ways for the ground truth of the reflectance, LAI and fAPAR. The first case we use is a case of vegetation at the grassland. And then, based of reflectance values, we compare the other type as the Mixed coniferous forest example. The influence of an effect of the type of growth may occur the reflectance of the distributed area. We will detect these effects of the growth type. The influence at the observed area be necessarily to be verified.

The research topic includes the ground truth observation for the accuracy verification of a SGLI data obtained. For development of ground truth, the way to obtain datas were important. This paper explains how to examine growth (such as a second growth forest and other) and the slope factor of the second growth forest area and also the reflectance of each forest types. Then, this paper make ground truth observation scheme for the high accuracy AGB referenced data development at ground cover area. We explain the method of examine the error detection way including observation devices and also the problem of the research topic to be examined. Results may occur an example case of such kinds of the sloped forest and the kinds of the plane. The results shows a typical difference between the sloped and the plane, and then the results may occur the possibility that comparison of standard deviation may be an effective way to detect the volume of the forest type between every ground truth.

The case of we use as the sloped fields, reflectance of each wavelength were low and then the near 400 to 700 nm area will be higher than other wavelength (ANOVA values of results: $p < 0.001$). And then, we can see the effects of slope should be detected at total values of the reflectance. The reflectance of a wavelength were obtained that aimed to detect the verification of the slope and the growth type’s reflectance. When the mixed coniferous forest, static observation develop same reflectance values but the effect of the sloped factor occur the high value of the standard deviations. Then, our method applied to the method of the SGLI’s data calculation scheme, and then the growth factor of the area be affects the influence of the from 400 to 700 nm wavelength and also the factor of slope region be affects the wavelength of reflectance. SGLI data analysis, the factor of these parameters were used to remake the size of RSRF data from 250 m to 1000 m resolution. The future, we investigate more and then, the mask area of high value difference around the nearest 16 pixels be considered. Datas were significant at some pixels, such as a steep sloped, growth types, or error detected area. Data development of RSRF, the reflectance of each cells are detected as the values of the every ground types by the standard deviation.

Keywords: SGLI's data verifications, Reflectance maps, Statistical ANOVA analysis

©2019. Japan Geoscience Union. All Right Reserved. 

## Factor analysis of variable results (Three-way ANOVA)

Sloped factors: Mean values of the SD of each (dynamic/semi-static)
Canopy factors: Difference of each SD of the every SD
Growth typed factors: Difference of each Mean and SD

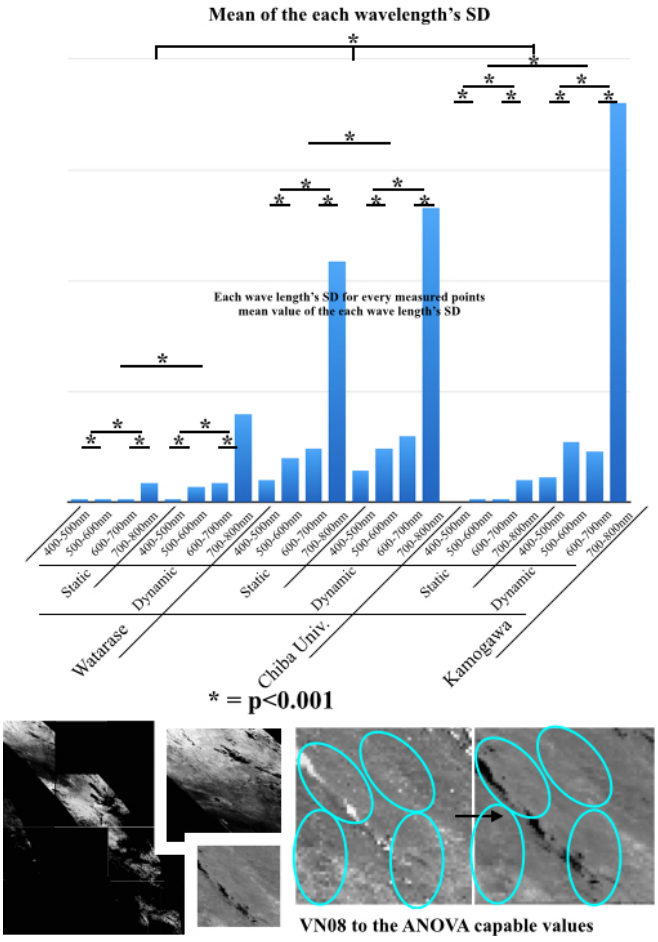


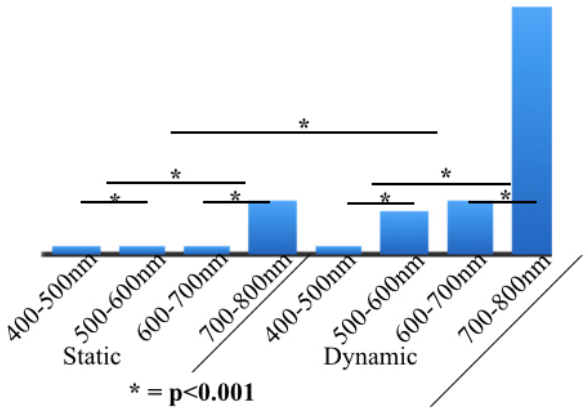


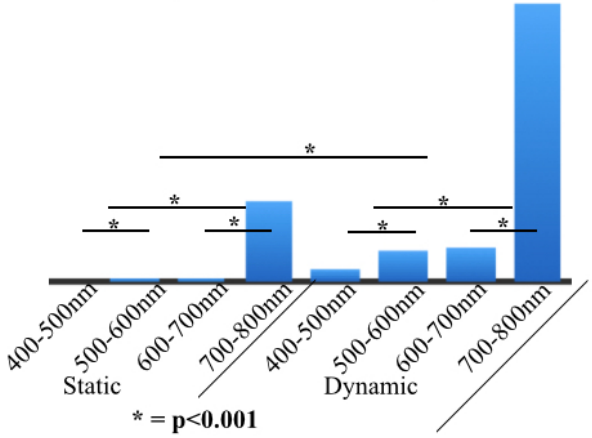





©2019. Japan Geoscience Union. All Right Reserved. 

# Remote sensing of aerosol optical properties and water-leaving radiance based on the optimal estimation approach

*Chong Shi[1], Teruyuki Nakajima[1], Makiko Hashimoto[1], Hideaki Takenaka[1]

1. Japan Aerospace Exploration Agency

A flexible inversion algorithm is proposed for jointly retrieving aerosol optical properties and water-leaving radiance from multispectral instrument over the ocean. A combined multi-wavelength and multi-pixel constraint approach is used to estimate aerosol and hydrosol over clear and turbid waters, based on the forward simulation from a coupled atmospher-ocean radiative transfer model. This sort of simultaneous inversion helps to correct the biases induced by the neglect of water-leaving radiance in the traditional aerosol retrieval algorithms, in addition, it can provide more aerosol information than the standard ocean color approach. To investigate the availability of current scheme, we conduct the retrieval in the process of MODIS, GOSAT/CAI and GCOM-C/SGLI instruments.

©2019. Japan Geoscience Union. All Right Reserved. 

# Aerosol retrieval and PM2.5 from space using GOSAT/TANSO-CAI

*Makiko Hashimoto[1], Hideaki Takenaka[1], Teruyuki Nakajima[1], Akiko Higurashi[2]

1. Japan Aerospace Explortion Agency, 2. NIES

Aerosol in the atmosphere has a great impact not only for the Earth’ s radiation budget and changing the Earth’ s climate, but also on human health. Especially, the fine particle, which is often called PM2.5, has drawn attention as a cause of health damage.

The urban area is a source of anthropogenic aerosol, which is mostly composed of small particles, and the particles are transported to other regions. Satellite remote sensing provides effective means to monitor the atmospheric aerosols in wide area including urban areas.

Accurate retrieval of fine mode aerosol optical thickness (AOT) is necessary to calculate an equivalent value of PM2.5 from space. Therefore, an aerosol retrieval algorithm for satellite remote sensing of urban areas to improve the retrieval accuracy of aerosol properties, which is called MWPM (Multiple wavelengths and pixels method) (Hashimoto and Nakajima, 2017), was developed. The method simultaneously retrieves fine and coarse mode AOT and single scattering albedo by using several wavelengths and spatial difference of surface reflectance. The method is useful for aerosol retrieval over spatially inhomogeneous surface like an urban area.

The algorithm was applied to GOSAT (Greenhouse Gases Observing Satellite) / TANSO-CAI (Cloud and Aerosol Imager, CAI) data. The GOSAT launched ten years ago (on January 23th, 2009) is a satellite to monitor greenhouse gases (GHG) such as carbon dioxide and methane with TANSO-FTS (Fourier Transform Spectrometer, FTS). The CAI is a supplementarysensor of the FTS, detecting cloud and deriving aerosol optical properties.

PM2.5 using retrieved fine mode AOT by MWPM in East Asian region from 2009 was calculated. The poster presents a retrieval result of PM2.5 over the East Asian region from space in several years and discusses the seasonal and annual variations.
Monitoring of aerosol properties such as AOT, PM2.5 and soot mixing ratio over land is added to the mission of GOSAT-2 that was launched on Otober 29th 2018. As a near-future plan, the algorithm will be applied to GOSAT-2/TANSO-CAI-2 data to generate standard PM2.5 data products.

Keywords: Remote sensing , Aerosol

©2019. Japan Geoscience Union. All Right Reserved. 

# Establishing a high resolution road fugitive dust emission inventory in Kaifeng City, China

*Yiming Xu[1], Shili Liu[1], Xinyue Cao[1], Xianbao Shen[1], Zhiliang Yao[1]

1. Department of Environmental Science and Engineering, Beijing Technology and Business University

Due to the rapid urbanization and industrialization in many Chinese cities, ambient particulate matter pollution such as road fugitive dust pollution becomes a serious environmental problem. However, the emission of road fugitive dust is relatively difficult to quantify as it is of high uncertainty and spatial heterogeneity. The research aims to build a high resolution road fugitive dust emission inventory which is transferrable and applicable to other cities in China. High spatial resolution images were utilized to digitalize whole road network of Kaifeng City, Henan Province, China. Vehicle flows of the whole road network were estimated by incorporating the whole road network, field measured data and GPS data on an hourly, daily, weekly, monthly and yearly basis at city level. By fusing the road network information, vehicle flow, road dust load, average vehicle weight, a high resolution road fugitive dust emission inventory was established. The results showed that the total emissions of $PM_{10}$, $PM_{2.5}$ and Total Suspended Particulate from road fugitive dust at commuter time and downtown were much higher compared with other time and location in Kaifeng City. The framework of this road fugitive dust emission inventory can be applied to other cities, and it can provide data support and guide fugitive dust management in China.

Keywords: Road Fugitive Dust, High Resolution Remote Sensing, Satellite Data, Air Pollutant Emission Inventory

©2019. Japan Geoscience Union. All Right Reserved. 

# A Relationship between Diurnal Change Patterns of Land Surface Temperature and Spatial Configuration of the Osaka Metropolitan Area Captured by Himawari-8

*Yuhei Yamamoto[1], Hirohiko Ishikawa[1]

1. Disaster Prevention Research Institute, Kyoto University

Land surface temperature (LST) is a physical quantity that greatly contributes to the formation of an urban thermal environment. Therefore, understanding the spatiotemporal characteristics of LST is necessary for constructing a sustainable urban environment. The spatial distribution relationship between the instantaneous LST and urban land use has been investigated using polar-orbiting satellite/airborne sensors. This study explored how the urban spatial configuration and meteorological field affect the temporal changes of LST by using Japanese geostationary satellite (Himawari-8) sensor.
The study area is the Osaka metropolitan area in Japan and target days are three days that were clear-sky throughout the day in summer (August 12, 2016, July 19, 2018, and August 4, 2018). We used 100 m-mesh urban land use data and ground-based meteorological observation data to examine the urban spatial configuration and meteorological fields, respectively. The temporal changes of LST are the amplitude and phase mainly forming the diurnal change of LST. These two temporal changes were extracted by applying principal component analysis to the diurnal changes of LST represented by the 10-minute LST dataset retrieved from Himawari-8 data.
Our results showed that the spatial variations in the amplitude and phase corresponded to the penetration time and duration of the sea breeze and the thermal inertia of surface materials. Besides, it was found that the LST change during daytime was larger in the high-density low-building areas than in the low-density low-building areas. This result suggests that the increase in building density increases the LST change during the daytime. These findings lead to a deeper understanding of an urban hot environment and are helpful for urban planning to mitigate the deterioration of a hot environment.

Keywords: Land Surface Temperature, Himawari-8, Urban Heat Island

©2019. Japan Geoscience Union. All Right Reserved. 

[E] Oral | A (Atmospheric and Hydrospheric Sciences )：A-CG Complex & General

Thu. May 30, 2019 3:30 PM - 5:00 PM JST | Thu. May 30, 2019 6:30 AM - 8:00 AM UTC | 302 3F

## [A-CG34] Satellite Earth Environment Observation

convener:Riko Oki(Japan Aerospace Exploration Agency), Yoshiaki HONDA(Center for Environmental Remote Sensing, Chiba University), Yukari Takayabu(Atmosphere and Ocean Research Institute, the University of Tokyo), Tsuneo Matsunaga(Center for Global Environmental Research and Satellite Observation Center, National Institute for Environmental Studies), Chairperson:Tsuneo Matsunaga

In recent years, we cannot avoid facing issues on global environmental changes that occur in various spatiotemporal scales. The earth environmental observation data by satellites became the necessary basic data to tackle and solve those issues. Due to the recent advancement in the observation sensor technique and the data processing technique, the satellite observation has been showing rapid progress, and the time is changing from examining the accuracy of the observation sensor data to the advancement of the data application, leading to broaden potential users. In these days application became synergetic, so we comprehensively pick<br/>up this topic in the Atmospheric and Hydrospheric Sciences Session of this Union Meeting that enables to comprise the atmospheric, oceanic and land sciences; by combining the intelligence and the knowledge of the party, we propose a session that aims to prompt further studies towards the issues on earth environmental change, the advancement in the data application and future plans of Earth Observation missions.

3:30 PM - 3:45 PM JST | 6:30 AM - 6:45 AM UTC

### [ACG34-19] How GOSAT has survived in-orbit anomalies and calibrated radiance spectra for 10 years.

★Invited Papers

*Akihiko Kuze[1], hiroshi Suto[1], Kei Shiomi[1], Nobuhiro Kikuchi[1], Makiko Hashimoto[1], Fumie Kataoka[2] (1.Japan Aerospace Exploration Agency, 2.RESTEC)

3:45 PM - 4:00 PM JST | 6:45 AM - 7:00 AM UTC

### [ACG34-20] Estimating regional anthropogenic methane emissions with GOSAT satellite retrievals and ground-based observations

*Shamil Maksyutov[1], Aki Tsuruta[2], Rajesh Janardanan[1], Fenjuan Wang[1], Akihiko Ito[1], Motoki Sasakawa[1], Toshinobu Machida[1], Isamu Morino[1], Yukio Yoshida[1], Johannes Kaiser[3], Greet Janssens-Maenhout[4], Ed Dlugokencky[5], Tsuneo Matsunaga[1] (1.National Institute for Environmental Studies, 2.Finnish Meteorological Institute, 3.Deutscher Wetterdienst, 4.European Commission, Joint Research Centre , 5.National Oceanic and Atmospheric Administration, Global Monitoring Division)

4:00 PM - 4:15 PM JST | 7:00 AM - 7:15 AM UTC

### [ACG34-21] The Status and the Future Plan of GOSAT-2 Level 2 and 4 Products

★Invited Papers

*Tsuneo Matsunaga[1], Isamu Morino[1], Yukio Yoshida[1], Makoto Saito[1], Hibiki M Noda[1], Hirofumi Ohyama[1], Akihide Kamei[1], Fumie Kawazoe[1], Ryoichi Imasu[2], Teruyuki Nakajima[4], Takashi Nakajima[5], Naoko Saitoh[3], Makiko Hashimoto[4] (1.Center for Global Environmental Research and Satellite Observation Center, National Institute for Environmental Studies, 2.The University of Tokyo, 3.Chiba University, 4.Japan Aerospace Exploration Agency, 5.Tokai University)

4:15 PM - 4:30 PM JST | 7:15 AM - 7:30 AM UTC

### [ACG34-22] A preliminary initial check of the cloud discrimination products by CAI-2 onboard GOSAT-2

*Yoshiaki Ishihara[1], Yu Oishi[2], Haruma Ishida[3], Takashi Nakajima[4] (1.NIES, 2.NARO, 3.JMA, 4.Tokai Univ.)

4:30 PM - 4:45 PM JST | 7:30 AM - 7:45 AM UTC

### [ACG34-23] Drought monitoring and evaluation performance of temperature vegetation drought index (TVDI) over Eurasia

*Fengmei Yao[1], Siqi Shi[1], Jiahua Zhang[2] (1.UCAS University of Chinese Academy of Sciences, 2.Institute of Remote Sensing and Digital Earth, Chinese Academy of Sciences)

4:45 PM - 5:00 PM JST | 7:45 AM - 8:00 AM UTC

[ACG34-24] **IMPACT OF CHANGE IN LAND USE AND LAND COVER PATTERN ON LAND SURFACE TEMPERATURE AND THERMAL COMFORT USING MICRO-SCALE AREA MODEL: CASE STUDY OF AN EDUCATIONAL CAMPUS.**

*DILJIT KUMAR NAYAK[1], MANJU MOHAN[1] (1.IIT DELHI)

# How GOSAT has survived in-orbit anomalies and calibrated radiance spectra for 10 years.

*Akihiko Kuze[1], hiroshi Suto[1], Kei Shiomi[1], Nobuhiro Kikuchi[1], Makiko Hashimoto[1], Fumie Kataoka[2]

1. Japan Aerospace Exploration Agency, 2. RESTEC

Since 2009 Thermal And Near infrared Sensor for carbon Observation Fourier-Transform Spectrometer (TANSO-FTS) onboard the Greenhouse gases Observing SATellite (GOSAT) TANSO-FTS onboard GOSAT has provided 0.2 cm-1-step radiance spectra from solar reflected light in shortwave infrared (SWIR) to thermal infrared (TIR) light using the FTS multiplex-advantage.
The SWIR light passes from the top of the atmosphere to the Earth’ s surface providing column-averaged dry air mole fractions of carbon dioxide (CO2) and methane (CH4). TIR light is the thermal emission from the Earth’ s atmosphere and surface. By combining these wide spectral data, GOSAT can extract the partial column density of lower troposphere, which shows enhanced density from local anthropogenic emission sources.
For SWIR data analysis, we use robust algorithm of differential optical absorption spectroscopy and optical path modification by thin clouds and aerosol can be calibrated by simultaneously observed oxygen (O2) data. On the other hand, thermal emission measurements need absolute radiometric calibration. Furthermore, the PC-MCT detector for TIR is less linear than the Si and InGaAs detectors for SIWR.
During the 10-year operation in orbit, TANSO-FTS had system-shut-down in May 2014, May 2018, and November 2018 due to satellite anomalies and cryo-cooler shutdown in August 2018. Every time TANSO-FTS restarted, the thermal condition of the TIR detector and optics had changed and parameters for non-linearity corrections had to be updated. We present how we can calibrate SWIR and TIR spectra for 10 years for decade-long uniform quality.

Keywords: Green House Gases, Fourier Transform Spectrometer, CO2, CH4, Thermal Infrared, Shortwave Infrared

©2019. Japan Geoscience Union. All Right Reserved. 

# Estimating regional anthropogenic methane emissions with GOSAT satellite retrievals and ground-based observations

*Shamil Maksyutov[1], Aki Tsuruta[2], Rajesh Janardanan[1], Fenjuan Wang[1], Akihiko Ito[1], Motoki Sasakawa[1], Toshinobu Machida[1], Isamu Morino[1], Yukio Yoshida[1], Johannes Kaiser[3], Greet Janssens-Maenhout[4], Ed Dlugokencky[5], Tsuneo Matsunaga[1]

1. National Institute for Environmental Studies, 2. Finnish Meteorological Institute, 3. Deutscher Wetterdienst, 4. European Commission, Joint Research Centre , 5. National Oceanic and Atmospheric Administration, Global Monitoring Division

GOSAT satellite observations of methane are being used for regional and national methane emission estimates in a number of studies using either high resolution regional inverse models or global medium resolution models. We perform global high-resolution methane flux inversion to estimate global methane emissions using atmospheric methane data collected at global in-situ network, which is archived at WDCGG and NIES, and GOSAT satellite retrievals. High resolution tracer transport is implemented by coupling Lagrangian model FLEXPART to a global atmospheric tracer transport model (NIES-TM) and its adjoint. Prior fluxes at 0.1˚ resolution were prepared for anthropogenic emissions (EDGAR 4.3.2), biomass burning (GFAS), and wetlands (VISIT). The inverse model based on NIES-TM-FLEXPART applies variational optimization to two categories of fluxes: anthropogenic and natural (wetlands). Bi-weekly emissions are estimated for years 2009 to 2017. To reduce GOSAT retrieval biases, the monthly mean difference between GOSAT data and the inversion-optimized forward simulation is estimated for each 5˚ latitude band and it is subtracted from GOSAT retrievals (NIES Level 2 retrievals, v. 02.72) before including them in the inversion. The bias correction is designed to remove large scale biases in GOSAT retrievals, while retaining local scale variability that contains most information on anthropogenic emissions from intense sources such as megacities. Estimated anthropogenic emissions over large regions (US, China, India) are compared to GCP-CH4 top-down estimates. The sensitivity of the estimated emissions to prior fluxes is tested by adjusting the prior fluxes to match UNFCCC reports for selected large countries.

Keywords: methane , inverse model, GOSAT, anthropogenic emissions

©2019. Japan Geoscience Union. All Right Reserved. 

# The Status and the Future Plan of GOSAT-2 Level 2 and 4 Products

*Tsuneo Matsunaga[1], Isamu Morino[1], Yukio Yoshida[1], Makoto Saito[1], Hibiki M Noda[1], Hirofumi Ohyama[1], Akihide Kamei[1], Fumie Kawazoe[1], Ryoichi Imasu[2], Teruyuki Nakajima[4], Takashi Nakajima[5], Naoko Saitoh[3], Makiko Hashimoto[4]

1. Center for Global Environmental Research and Satellite Observation Center, National Institute for Environmental Studies, 2. The University of Tokyo, 3. Chiba University, 4. Japan Aerospace Exploration Agency, 5. Tokai University

GOSAT-2 (Greenhouse Gases Observing Satellite 2), launched in October, 2018, is the second Japanese Earth observation satellite for greenhouse gas observation from space. It is a joint mission promoted by Ministry of the Environment, JAXA (Japan Aerospace Exploration Agency), and NIES (National Institute for Environmental Studies) as similar to the first satellite, GOSAT, launched in and operated since 2009. Both satellites are designed to measure atmospheric concentrations of carbon dioxide ($CO_2$) and methane ($CH_4$) using Fourier transform spectrometers, FTS and FTS-2, with a help of moderate resolution imagers, CAI and CAI-2, for aerosol and cloud observation. The design lifetime of GOSAT-2 is five years and the 15-year record of atmospheric $CO_2$and $CH_4$is now expected from these two satellites.

NIES is responsible for the generation of GOSAT-2's Level 2 and Level 4 standard products which are

1) GOSAT-2 TANSO-CAI-2 L2 Cloud Discrimination Product
2) GOSAT-2 TANSO-CAI-2 L2 Aerosol Property Product
3) GOSAT-2 TANSO-FTS-2 SWIR L2 Chlorophyll Fluorescence and Proxy-method Product
4) GOSAT-2 TANSO-FTS-2 SWIR L2 Column-averaged Dry-air Mole Fraction Product
5) GOSAT-2 TANSO-FTS-2 TIR L2 Cloud and Aerosol Property Product
6) GOSAT-2 TANSO-FTS-2 TIR L2 Temperature and Gas Profile Product
7) GOSAT-2 L4A Global CO2 Flux Product
8) GOSAT-2 L4A Global CH4 Flux Product
9) GOSAT-2 L4B Global CO2 Distribution Product
10) GOSAT-2 L4B Global CH4 Distribution Product

The public release of GOSAT-2 Level 2 and Level 4 products will start by the end of October 2019 and 2020, respectively.

In this presentation, the latest status and the future plan of these products will be introduced.

Keywords: greenhouse gas, climate change, satellite

©2019. Japan Geoscience Union. All Right Reserved. 

# A preliminary initial check of the cloud discrimination products by CAI-2 onboard GOSAT-2

*Yoshiaki Ishihara[1], Yu Oishi[2], Haruma Ishida[3], Takashi Nakajima[4]

1. NIES, 2. NARO, 3. JMA, 4. Tokai Univ.

GOSAT-2, which is a successor of Japanese GOSAT (Greenhouse Gases Observing Satellite) which was launched in January 2009 and has been operated for about ten years, is successfully launched on Oct. 29, 2018. Both satellites are jointly developed and operated by Ministry of the Environment, Japan Aerospace Exploration Agency, and National Institute for Environmental Studies. GOSAT-2 carries two mission instruments, Fourier Transform Spectrometer 2 (FTS-2) and Cloud and Aerosol Imager 2 (CAI-2). They are successors of GOSAT FTS and CAI.

Several publicly available standard products will be generated from GOSAT-2 FTS-2 and CAI-2 data. One of these is CAI-2 Level 2 Cloud Discrimination Product and will be used for the detection of clouds within the field of view of FTS-2. CAI-2 cloud discrimination product is generated by one of two different algorithms. One of those is CLAUDIA1 used for GOSAT CAI Level 2 cloud mask product and the other is newly developed CLAUDIA3. And CLAUDIA3 is default algorithm for CAI-2 cloud discrimination product generation.

In this presentation, we will present a very preliminary initial check results of CAI-2 Level 2 cloud discrimination products, including comparison of cloud discrimination results by CLAUDIA1 and CLAUDIA3.

Keywords: GOSAT-2, Cloud Discrimination

©2019. Japan Geoscience Union. All Right Reserved. 

# Drought monitoring and evaluation performance of temperature vegetation drought index (TVDI) over Eurasia

*Fengmei Yao[1], Siqi Shi[1], Jiahua Zhang[2]

1. UCAS University of Chinese Academy of Sciences, 2. Institute of Remote Sensing and Digital Earth, Chinese Academy of Sciences

Drought has been a common concern recent years as it is one of the high frequent nature disasters in Eurasia that is included in the Belt and Road Initiative under the background of global warming. Thus, it is of great significance to study the drought monitoring and assessment in the region to develop effective plans to mitigate the effects of disasters. This study explored applicability of Temperature Vegetation Drought Index (TVDI) derived from MODIS normalized difference vegetation index (NDVI) and land surface temperature (LST) data as an index for drought monitoring in Eurasia in growing season (April - September) from 2005 to 2014. Three methods were used to compare TVDI against Standardized Precipitation Evapotranspiration Index in three time scales (SPEI-01, SPEI-03, SPEI-06) and the Essential Climate Variable surface soil moisture product (ECV-SM) at continental scales and Land Cover scales, as well as records of drought events from Emergency Events Database (EM-DAT) and relative literatures. The results indicated acceptable correlations between TVDI and SPEIs, ECV-SM in most areas, and TVDI had higher coefficients of correlation with ECV-SM than SPEIs at continental scale. Then we found that the correlation coefficient maps at continental scales were visually consistent with the land cover types, thus correlations between TVDI and SPEIs, ECV-SM were analyzed at Land Cover scales. TVDI showed strong correlation with SPEIs and ECV-SM in evergreen Needle leaf forest, deciduous broad leaf forest and grasslands. However, the accuracy of TVDI in open shrub lands that mainly distributed at high-latitudes remains to be further validated in the future. Finally, a comparison with typical drought-year and typical drought events also demonstrated TVDI could be used as a drought index to monitor drought events in study area over study time.

Keywords: drought monitoring, Temperature Vegetation Drought Index, growing season, continental scale, land cover, drought records

©2019. Japan Geoscience Union. All Right Reserved. 

# IMPACT OF CHANGE IN LAND USE AND LAND COVER PATTERN ON LAND SURFACE TEMPERATURE AND THERMAL COMFORT USING MICRO-SCALE AREA MODEL: CASE STUDY OF AN EDUCATIONAL CAMPUS.

*DILJIT KUMAR NAYAK[1], MANJU MOHAN[1]

1. IIT DELHI

The influence of change in Land Use Land Cover pattern of an area due to rapid urbanization, over the increment in the Land Surface Temperature (LST) has always been a challenging area for research. This study covers the analysis of the influence of freshly built structure and the storey increment on the thermal comfort of the outdoor environment and Land Surface Temperature with a periodic remotely sensed observation for every three years at IIT Delhi (an educational institute campus). Numerical modelling approach using a 3D microclimate model ENVIMET is implemented for simulating the surface temperature in the presence of hostel residences and in the absence of hostel residences during a summer month of May during the period from 2002 to 2018. The effect of the Sky View Factor on Mean Radiant Temperature is likely to play a key role in influencing the thermal comfort of the residents of the campus. The entire IIT Delhi was classified under open high-rise as per Local Climate Zone (LCZ) categories. It was classified into 17 classes which included eight types of building classification from 4m to 36m and the rest of the nine classes included soil layer, asphalt roads, vegetation cover like trees, dense and light bushes, concrete roads, granite concrete and swimming pool PVC liner. The building class was sub-divided into different classes based on their height to study the effect of high rise buildings on the surface temperature. The model validation is carried out with the LST values obtained from the satellite observation of LANDSAT thermal band. The model estimated the surface temperature giving a correlation of (r=0.95) with the observed values. The RMSE value was found to be 1.28 for the student residence and 2.34 for the non-building structures. Temperature difference over the years as built structure influence was assessed approximately to the tune of 10 degrees. The model performed well in estimating the surface temperature with an accuracy of 94.97 per cent.

Keywords: ENVI-met, 3D microclimate model, Land surface temperature(LST), Land Use Land Cover(LULC), Local Climate Zone(LCZ), Landsat

©2019. Japan Geoscience Union. All Right Reserved. 

# IMPACT OF CHANGE IN LAND USE AND LAND COVER PATTERN ON LAND SURFACE TEMPERATURE AND THERMAL COMFORT USING MICRO-SCALE AREA MODEL: CASE STUDY OF AN EDUCATIONAL CAMPUS

DILJIT KUMAR NAYAK AND MANJUMOHAN

Centre for Atmospheric Sciences,

Indian Institute of Technology Delhi, Hauz Khas,

New Delhi, India 110016

**ABSTRACT**

The influence of change in Land Use Land Cover pattern of an area due to rapid urbanization, over the increment in the Land Surface Temperature (LST) has always been a challenging area for research. This study covers the analysis of the influence of freshly built structure and the storey increment on the thermal comfort of the outdoor environment and Land Surface Temperature with a periodic remotely sensed observation for every three years at IIT Delhi (an educational institute campus). Numerical modelling approach using a 3D microclimate model ENVIMET is implemented for simulating the surface temperature in the presence of hostel residences and in the absence of hostel residences during a summer month of May during the period from 2002 to 2018. The effect of the Sky View Factor on Mean Radiant Temperature is likely to play a key role in influencing the thermal comfort of the residents of the campus. The entire IIT Delhi was classified under open high-rise as per Local Climate Zone (LCZ) categories. It was classified into 17 classes which included eight types of building classification from 4m to 36m and the rest of the nine classes included soil layer, asphalt roads, vegetation cover like trees, dense and light bushes, concrete roads, granite concrete and swimming pool PVC liner. The building class was sub-divided into different classes based on their height to study the effect of high rise buildings on the surface temperature. The model validation is carried out with the LST values obtained from the satellite observation of LANDSAT thermal band. The model estimated the surface temperature giving a correlation of (r=0.95) with the observed values. The RMSE value was found to be 1.28 for the student residence and 2.34 for the non-building structures. Temperature difference over the years as built structure influence was assessed approximately to the tune of 10 degrees. The model performed well in estimating the surface temperature with an accuracy of 94.97 per cent.

***Key Words*:** ENVI-met, 3D microclimate model, Land surface temperature(LST), Landsat, Land Use Land Cover, Local Climate Zone(LCZ)

©2019. Japan Geoscience Union. All Right Reserved. 

[J] Oral | A (Atmospheric and Hydrospheric Sciences)：A-CG Complex & General

Thu. May 30, 2019 10:45 AM - 12:15 PM JST | Thu. May 30, 2019 1:45 AM - 3:15 AM UTC | 106 1F

## [A-CG36] Earth & Environmental Sciences and Artificial Intelligence

convener:Tomohiko Tomita(Faculty of Advanced Science and Technology, Kumamoto University), Ken-ichi Fukui(Osaka University), Daisuke Matsuoka(Japan Agency for Marine-Earth Science and Technology), Satoshi Ono(Kagoshima University), Chairperson:Tomohiko Tomita(Kumamoto University, Faculty of Advanced Science and Technology)

In recent years, we have been required to explore the gigantic environmental data leading global environmental studies of modern meteorology, oceanography, and hydrology to accomplish Society 5.0 and Sustainable Development Goals (SDGs). Such environmental data, which are typical "big data," include the reliable long-term observatory data, ground radar data, satellite observation, oceanographic observation, global objective analysis data, and so on. However, it is hard to say that such big data are fully utilized, or nobody may have examined many of them. Therefore, to examine the global environment more faithfully, we need to apply the techniques of artificial intelligence/machine learning on such big data, that is, spatiotemporal data modeling of artificial intelligence, prediction and detection by machine learning, techniques of automated data mining, and so forth. Only cross-cutting diagnosis of the gigantic environmental data could resolve a wide variety of environmental problems including measures against global warming. In addition, the application of artificial intelligence/machine learning on the big data would raise us to the 4th paradigm of science (the 1st paradigm, observation/experiment; 2nd, theory; 3rd, simulation; 4th, data driven). This session sincerely invites various research initiatives that accelerate the application of artificial intelligence/machine learning on such gigantic environmental data.

10:45 AM - 10:50 AM JST | 1:45 AM - 1:50 AM UTC

Introduction

---

10:50 AM - 11:20 AM JST | 1:50 AM - 2:20 AM UTC

[ACG36-01] Recent Progress in Deep Neural Network Architectures and their Applications

★Invited Papers

*Shinichi Shirakawa[1] (1.Yokohama National University)

---

11:20 AM - 11:35 AM JST | 2:20 AM - 2:35 AM UTC

[ACG36-02] Improving performance of oxidant prediction using machine learning by optimizing input data based on atmospheric science knowledge

*Tomohiro Sato[1], Peijiang Zhao[1], Koji Zettsu[1] (1.National Institute of Information and Communications Technology)

---

11:35 AM - 11:50 AM JST | 2:35 AM - 2:50 AM UTC

[ACG36-03] Spatiotemporal Climate Forecasting with ConvLSTM

*Ekasit Phermphoonphiphat[1], Tomohiko Tomita[3], Masayuki Numao[2], Ken-ichi Fukui[2] (1.Graduate School of Information Science and Technology, Osaka University, 2.The Institute of Scientific and Industrial Research, Osaka University, 3.Faculty of Advanced Science and Technology, Kumamoto University)

---

11:50 AM - 12:05 PM JST | 2:50 AM - 3:05 AM UTC

[ACG36-04] Deep-Learning Based Short-Term Prediction Method for Sea Ice Concentration Using Explanatory Variables

*Issei Kawashima[1], Toru Kouyama[1], Ryu Sugimoto[1], Ryosuke Nakamura[1] (1.National Institute of Advanced Industrial Science and Technology)

---

12:05 PM - 12:15 PM JST | 3:05 AM - 3:15 AM UTC

Discussion

# Recent Progress in Deep Neural Network Architectures and their Applications

*Shinichi Shirakawa[1]

1. Yokohama National University

A deep neural network (DNN) is a powerful machine learning model that shows remarkable performance in various artificial intelligence domains such as computer vision and natural language processing. A DNN is composed of a number of non-linear, differentiable units that have tunable parameters. In the training phase, DNN parameters (called connection weights) are trained so as to minimize training loss. After training the DNN, we expect it to be able to produce the generalized rule for the target task, i.e., the trained DNN is expected to return the ideal outputs from inputs for unknown data.

Researchers in the deep learning community are actively proposing a novel DNN architecture (i.e., the network structure of DNNs) to improve the performance and applicability of DNNs. For instance, a convolutional neural network (CNN) is frequently used as the network model for computer vision tasks, and the recurrent connection and long short-term memory (LSTM) cell is suitable for treating time series and sequential data. Besides these network structures, many extended network modules and architectures have been developed.

In this talk, we provide an overview of the recent progress in deep neural network architectures and their amazing applications. We also overview how to handle multimodal data in DNNs and present several studies on modality translation such as image-to-text (image captioning) and text-to-speech.

Although a lot of DNN architectures have been proposed so far, the selection and design of the architectures are still the users' task. Such a task is not trivial because the appropriate architecture heavily depends on the target problem and dataset, meaning that trial and error and expert knowledge are required for users. The second topic of this talk is the automatic design of DNN architectures, called neural architecture search (NAS). Recent studies show that NAS can improve the performance of DNNs depending on the dataset. Particularly, we present the computationally efficient NAS methods that can work on a single GPU with reasonable computational time.

At the end of this talk, we would like to discuss the applicability of deep neural networks to the field of global environmental science.

Keywords: Deep Learning, Deep Neural Network, Machine Learning, Artificial Intelligence

©2019. Japan Geoscience Union. All Right Reserved. 

# Improving performance of oxidant prediction using machine learning by optimizing input data based on atmospheric science knowledge

*Tomohiro Sato[1], Peijiang Zhao[1], Koji Zettsu[1]

1. National Institute of Information and Communications Technology

[Background] Air pollution was the cause of 3.7 million premature deaths globally in 2012 (WHO, 2014). In Japan, the amount of oxidant (Ox) keeps high level or has been still increasing, although other air pollutants, such as $NO_2$ and $PM_{2.5}$. has been decreasing. High level of Ox affects human health and crop yields (e.g., Zheng et al., 2018). There are many factors for Ox generation, such as precursors especially $NO_2$ and VOC, sunlight and wind. They are non-linearly connected, thus, modeling of physical and chemical processes for Ox amount prediction is difficult and requires large calculation costs. There are many studies for Ox prediction using machine learning (ML) as an alternative of traditional modeling. Keller et al., (2017) showed that the random forest demonstrated the GEOS-Chem model calculation of ozone ($O_3$), major component of Ox, within an error less than 10% during the first 10 days with a 1/100 calculation cost. Other ML methods have been tested for $O_3$ prediction, Multi Linear Regression, Artificial Neural Network (Pires and Martins, 2011), Gene Expression Programming (Samadianfard et al., 2013).

[Aim] Previous studies of air pollution prediction by ML have well developed the model algorithm. Guennec et al., (2016) reported that improvement of input data, such as data augmentation, also increased the prediction performance. In this study, we approached to improve the Ox prediction using ML technique by optimizing the input data.

[Dataset and Method] Ox, especially $O_3$, is formed via photo-chemical reaction. The $O_3$ amount increases after the sunrise (e.g., $NO_2 + hn \rightarrow NO + O$, $O + O_2 + M \rightarrow O_3 + M$), takes a maximum during the day, and decreases during the night due to collision with surface and other species. This $O_3$ trend is observed throughout a year with a variation depending on whether, season and human activity. In this study, we compared the predicted results of Ox amount using two types of input data; in case 1, the Ox amount data itself ($V_{obs}$) and case 2, difference ($DeltaV = V_{obs} - V_{diurnal}$) from the reference diurnal variation ($V_{diurnal}$). We used data of amounts of major air pollutants (such as Ox, $NO_2$, SPM, $PM_{2.5}$, $SO_2$, CO), temperature, humidity, and wind at 16 points in Fukuoka city in 2014 to 2016 (Atmospheric Environmental Regional Observation System). The reference diurnal variation $V_{diurnal}$ was mean in each local hour and year. The ML model that we employed was a Convolutional Recurrent Neural Network (CRNN) based on a Convolutional Neural Network (CNN) and Long Short-Term Memory (LSTM) (Zhao and Zettsu, 2018). The value of measurement at each point was translated into 2-D map based on the longitude and latitude in the CNN part and the spatial features was extracted. A short-term prediction was performed by the LSTM part. We used the data for the last 24 hours as an input. The output was mean value of Ox amount in all points after six hours.

[Results and Discussion] We demonstrated the Ox prediction using the CRNN model with two types of input data ($V_{obs}$ for Case 1 and DeltaV for Case 2). Root mean squared error and accuracy for the two predictions were compared; Case 1: 10.3 ppb/75.4%, Case 2: 6.7ppb/84.7% (in 2014), Case 1: 11.0 ppb/72.7%, Case 2: 8.3ppb/79.6% (in 2015), Case 1: 9.4 ppb/76.7%, Case 2: 8.6ppb/79.4% (in 2016). Using DeltaV, the accuracy was increased at most 10%. We also compared the predictions in terms of time in a day. In case 1, the model overestimated the Ox amount during the night and underestimated during the day. This bias was significantly improved in case 2 for all years.

©2019. Japan Geoscience Union. All Right Reserved. 

[Conclusion and remarks] We demonstrated an optimization of input data for Ox prediction using the CRNN model. Our approach showed the accuracy of the Ox prediction was improved at most 10% using a difference from the reference diurnal variation instead of using a raw data. This study indicates an importance to optimize input data based on atmospheric science knowledge for air pollution prediction by ML.

Keywords: Air pollution, Oxidant, Machine learning, Optimization, Short-term prediction

©2019. Japan Geoscience Union. All Right Reserved. 

# Spatiotemporal Climate Forecasting with ConvLSTM

*Ekasit Phermphoonphiphat[1], Tomohiko Tomita[3], Masayuki Numao[2], Ken-ichi Fukui[2]

1. Graduate School of Information Science and Technology, Osaka University, 2. The Institute of Scientific and Industrial Research, Osaka University, 3. Faculty of Advanced Science and Technology, Kumamoto University

Recent years, climate forecasting techniques with machine learning have been developing to get high accuracy result, unlike physical simulation that uses the techniques of ensemble mean and has already been employed by JMA (Japan Meteorological Agency) which cannot perform well for long term prediction because climate data is a very high non-linear relationship. Machine learning techniques can build a forecasting model by learning patterns from prior data while maintaining the spatial correlation that very important for climate data because the variable from one area could affect other areas. In this paper, we studied the spatial-temporal pattern of machine learning techniques can improve the forecasting result. The experiment compares 3 forecasting models. Linear regression model is a simple forecasting linear model that try to produce linear formula from the training dataset, we use this model with non-spatial correlation setup. CNN (Convolutional Neural Network) is a class of deep learning, the key idea is convolutional layer that is able to maintain spatial correlation through the network. ConvLSTM (Convolutional Long Short-Term Memory) is the improvement version of Fully Connected Long Short-Term Memory that combines convolution operator inside every gate (the control unit that measures how much information will pass through) in the memory cell; therefore, spatial correlation is preferably maintained on the arbitrary of times. We run the experiment to forecast temperature at 2 meter height of the Japan area, we used the monthly mean data of ERA-Interim dataset that started from 1979 to the present. The result has shown that ConvLSTM performs the best accuracy compares to CNN and non-spatial correlation setup linear regression model.

Keywords: Climate Forecasting, ConvLSTM, Spatial Correlation

©2019. Japan Geoscience Union. All Right Reserved. 

# Deep-Learning Based Short-Term Prediction Method for Sea Ice Concentration Using Explanatory Variables

*Issei Kawashima[1], Toru Kouyama[1], Ryu Sugimoto[1], Ryosuke Nakamura[1]

1. National Institute of Advanced Industrial Science and Technology

Importance of short-term future and middle-term future prediction techniques of sea ice concentration (SIC) has been significantly increasing for navigation of vessels which uses the Northern Sea Route. High frequent updating of the short-term prediction for adopting to SIC is required and thus its calculation load is an important issue same as the accuracy of the prediction. We have been developing a deep-learning based sea ice prediction method and adopting it to Sea of Okhotsk where sea ice coverage dramatically changes during a season. The proposed method can predict SIC immediately once we have sufficient observation or simulation data and the calculation time is very short. In addition, we have confirmed that the predicted SIC has basically good correlation with actual SIC, even though this method only uses previous and current observed SIC by AMSR2. However, considering actual applications, such as navigation for vessels, it is necessary to improve the accuracy of the proposed method as much as possible.

In this study, we proposed a new short-term prediction method for temporal variation of SIC. The new method uses not only SIC but also other variables which can be obtained from observations and/or simulations. The new method can improve the prediction accuracy than that in the previous method.

Keywords: Sea Ice Concentration, Deep Learning, LSTM

©2019. Japan Geoscience Union. All Right Reserved. 

[J] Oral | A (Atmospheric and Hydrospheric Sciences)：A-CG Complex & General

Thu. May 30, 2019 1:45 PM - 3:15 PM JST | Thu. May 30, 2019 4:45 AM - 6:15 AM UTC | 104 1F

## [A-CG36] Earth & Environmental Sciences and Artificial Intelligence

convener:Tomohiko Tomita(Faculty of Advanced Science and Technology, Kumamoto University), Kenichi Fukui(Osaka University), Daisuke Matsuoka(Japan Agency for Marine-Earth Science and Technology), Satoshi Ono(Kagoshima University), Chairperson:Tomohiko Tomita(Kumamoto University, Faculty of Advanced Science and Technology)

In recent years, we have been required to explore the gigantic environmental data leading global environmental studies of modern meteorology, oceanography, and hydrology to accomplish Society 5.0 and Sustainable Development Goals (SDGs). Such environmental data, which are typical "big data," include the reliable long-term observatory data, ground radar data, satellite observation, oceanographic observation, global objective analysis data, and so on. However, it is hard to say that such big data are fully utilized, or nobody may have examined many of them. Therefore, to examine the global environment more faithfully, we need to apply the techniques of artificial intelligence/machine learning on such big data, that is, spatiotemporal data modeling of artificial intelligence, prediction and detection by machine learning, techniques of automated data mining, and so forth. Only cross-cutting diagnosis of the gigantic environmental data could resolve a wide variety of environmental problems including measures against global warming. In addition, the application of artificial intelligence/machine learning on the big data would raise us to the 4th paradigm of science (the 1st paradigm, observation/experiment; 2nd, theory; 3rd, simulation; 4th, data driven). This session sincerely invites various research initiatives that accelerate the application of artificial intelligence/machine learning on such gigantic environmental data.

1:45 PM - 2:00 PM JST | 4:45 AM - 5:00 AM UTC

### [ACG36-05] Remote sensing of cloud using the deep learning based on three-dimensional radiative transfer

*Hironobu Iwabuchi[1], Ryosuke Masuda[1], K. Sebastian Schmidt[2,3], Alessandro Damiani[4], Rei Kudo[5] (1.Graduate School of Science, Tohoku University, 2.Department of Atmospheric and Oceanic Sciences, University of Colorado, 3.Laboratory for Atmospheric and Space Physics, University of Colorado, 4.Center for Environmental Remote Sensing, Chiba University, 5.Meteorological Research Institute, Japan Meteorological Agency)

2:00 PM - 2:15 PM JST | 5:00 AM - 5:15 AM UTC

### [ACG36-06] Time series of cloud cover during the night derived from an omnidirectional camera

*Karin miyabe[1], Kazunori Ogohara[1] (1.University of Shiga Prefecture)

2:15 PM - 2:30 PM JST | 5:15 AM - 5:30 AM UTC

### [ACG36-07] Time series prediction of cloud cover using whole-sky images and meteorological elements

*Kazunori Ogohara[1], Teppei Sonoda[2] (1.School of Engineering, University of Shiga Prefecture, 2.Graduate School of Engineering, University of Shiga Prefecture)

2:30 PM - 2:45 PM JST | 5:30 AM - 5:45 AM UTC

### [ACG36-08] Fundamental investigation about the inductive prediction of precipitation based on the time series data

*Naoki Matsumoto[1], Tomohiko Tomita[1], Kenichi Fukui[2] (1.Kumamoto Univ., 2.Osaka Univ.)

2:45 PM - 3:00 PM JST | 5:45 AM - 6:00 AM UTC

### [ACG36-09] Identification of ships image on SAR data using machine learning

*Takashi Sonoke[1], Hirohide Demura[1] (1.University of Aizu)

3:00 PM - 3:15 PM JST | 6:00 AM - 6:15 AM UTC

Discussion

# Remote sensing of cloud using the deep learning based on three-dimensional radiative transfer

*Hironobu Iwabuchi[1], Ryosuke Masuda[1], K. Sebastian Schmidt[2,3], Alessandro Damiani[4], Rei Kudo[5]

1. Graduate School of Science, Tohoku University, 2. Department of Atmospheric and Oceanic Sciences, University of Colorado, 3. Laboratory for Atmospheric and Space Physics, University of Colorado, 4. Center for Environmental Remote Sensing, Chiba University, 5. Meteorological Research Institute, Japan Meteorological Agency

Remote sensing is a field of active research to which the machine learning techniques are applied. Machine learning models can be trained to detect characteristics and estimate properties of spatial and temporal variations of geophysical features. The deep learning uses a deep neural network and is rapidly developing in wide areas of industrial applications and scientific research. The deep neural network generally offers high capabilities of automatic feature extraction from multi-variate, multi-modal data and a good approximation of non-linear functions. If a deep learning model is trained well, its advantages are high accuracy with reasonable speed of calculation, which is suitable for practical applications to processing a large amount of data.

We will present a few applications of the deep learning to remote sensing of cloud from satellite- and ground-based optical measurements. In optical remote sensing of clouds, three-dimensional (3-D) radiative transfer effects are a major source of retrieval errors. Radiative interactions operate across spatial elements of the cloudy atmosphere at a wide range of spatial scales. Radiance measured at each pixel of an image taken by a satellite-based imager or ground-based camera is influenced by not only cloud density and microphysical properties along the line of sight but also the spatial distribution of clouds in a wide domain surrounding the line of sight. Although the retrieval of cloud properties is usually based on the independent pixel approximation assuming a plane-parallel, homogeneous cloud for each image pixel, the 3-D radiative interaction makes it difficult to retrieve cloud properties at pixel level if one uses single-pixel radiances solely. Thus, use of multiple pixels looks attractive, offering a great potential to accurately retrieve cloud properties from an image. Convolutional neural networks (CNNs) naturally traces the 3-D radiative effects that appear across image pixels, which traditional single-pixel approaches cannot capture. We have thus developed deep learning models to estimate the spatial distribution of cloud properties from multi-spectral, multi-pixel cloud retrieval from satellite imagery and images taken by a ground-based digital camera. Training data of pseudo-observation radiances are made from simulations using a Monte Carlo 3-D radiative transfer model for cloud fields simulated by a large eddy simulation model with high spatial resolution. In this case, the deep learning model is trained to learn the multi-scale spatial structure of clouds in addition to the complicated relationships between cloud properties and radiances. Deep CNNs show high retrieval accuracy for cloud properties such as cloud optical thickness and effective droplet radius from multi-spectral images of visible, near-infrared, and shortwave infrared channels, efficiently deriving the spatial distribution of cloud properties at multiple pixels all at once from radiances at multiple pixels. By using multi-scale features in the images, it is possible to recover the information lost in 3-D radiative transfer. Results show significantly better accuracy compared with traditional approaches.

Keywords: deep learning, remote sensing, cloud, radiative transfer

©2019. Japan Geoscience Union. All Right Reserved. 

# Time series of cloud cover during the night derived from an omnidirectional camera

*Karin miyabe[1], Kazunori Ogohara[1]

1. University of Shiga Prefecture

Surrounding atmospheric environment have a big influence on our lives. For example, fog causes various accidents due to poor isibility. Leisure facilities must be stopped when wind speed is high. Meteoropathy tends to increase depending on perature or weather. Therefore, environmental prediction with higher temporal and spatial resolution than that of daily ather forecast is needed. Cloud cover (CC) will have a large impact on prediction of environmental changes in other tities (e.g. temperature, humidity, wind speed and direction). The method for deriving CC from RGB images taken by an omnidirectional camera has been investigated so far. However, it was not applicable to nighttime images, which is usually grayscale images, due to low SN and low brightness. Therefore, we develop a method for deriving CC from grayscale images taken by an omnidirectional camera during the night using deep learning. Also, we investigate he distortion of the whole-sky images because CC measured in the celestial sphere has a different value from that measured in whole-sky images.We separate cloud areas from sky areas in the whole-sky images using a deep learning technique for semantic segmentation, U-net. U-net is a encoder-decoder type of convolutional neural network. Area under an ROC curve (AUC), which is an evaluation index commonly used in the discipline of machine learning, for nighttime images is 0.985 and that for rainy images during the night is 0.984. However, that for evening and morning images is lower than them, 0.952. Therefore, the proposed method may not be applicable to evening and morning images.

Keywords: Cloud cover

©2019. Japan Geoscience Union. All Right Reserved. 

# Time series prediction of cloud cover using whole-sky images and meteorological elements

*Kazunori Ogohara[1], Teppei Sonoda[2]

1. School of Engineering, University of Shiga Prefecture, 2. Graduate School of Engineering, University of Shiga Prefecture

Prediction of the sky conditions is becoming important in several sectors of society. The most typical codition of the sky is cloud cover (CC). CC should have a correlation to air temperature, ground temperature, humidity, and solar radiation, etc. Therefore, prediction of CC is highly significant from the perspective of social application and should have a large impact on accuracy of time-series prediction of other variables.
We have developed a novel method for segmentation of cloud areas in whole-sky images using an encoder-decoder based convolutional neural network to derive CC from images observed by an omnidirectional camera. F-measure for cloud obtained by 10-fold cross validatoin was 0.86. We could generate time series of daytime CC for 1.5 years using the proposed method.
We have tried to predict CC after one hour based on time series of CC itself and solar radiation using recurrent neural network. RMSE of CC between the observed and predicted time series is 0.022 and the predicted time series of CC is more accurate than the persistence model. However, predicted CC tends to get close to 0.4-0.5 and the phase shift like the persistence model is partially seen.

Keywords: time-series prediction, image segmentation, deep learning

©2019. Japan Geoscience Union. All Right Reserved. 

# Fundamental investigation about the inductive prediction of precipitation based on the time series data

*Naoki Matsumoto[1], Tomohiko Tomita[1], Kenichi Fukui[2]

1. Kumamoto Univ., 2. Osaka Univ.

This work applied the artificial neural network (ANN) to observatory data and conducted a fundamental investigation about improving the prediction accuracy in precipitation. Especially, this work focused on the improvement of training data for the short-term prediction in precipitation.
The used data were precipitation, temperature, pressure, vapor pressure, wind speed, and wind direction with hourly interval edited by the Japan Meteorological Agency, and the ANN prediction model was constructed based on multilayer perceptron. Using these data and the ANN prediction model, this work tentatively predicted the time variation of hourly precipitation at Kumamoto, Japan. Then, through systematic changes of the training data, this work investigated how the accuracy of short-term predicton was improved. Especially, the contributions of each observation parameter and of increase of observatories were investigated. For the evaluation of prediction, this work emploied the verification by comparing the peak values between prediction and observation and the appearance time of the peak that are both important for heavy rainfall prediction, and the sum of squared errors between predicted and real values.
This work found that setting the data to the west into the training data is effective for predicting Kumamoto's hourly precipitation. This work also found that the peak value in prediction was greatly improved from 30% to 80% by deleting the data at the time when no precipitation occurs in the training data. Then, the contribution of vapor pressure increases. We will continue to investigate how the precipitation prediction can be improved through the changes of parameters, observatories, and forecast lead times in the training data.
The results of this work will contribute to the construction of a simple precipitation prediction scheme at the location where sophisticated observation data can not be obtained.

Keywords: artificial neural network, prediction of hourly precipitation

©2019. Japan Geoscience Union. All Right Reserved. 

# Identification of ships image on SAR data using machine learning

*Takashi Sonoke[1], Hirohide Demura[1]

1. University of Aizu

SAR(Synthetic Aperture Radar) has been popular in Earth remote sensing because this is available for all-weather and night time, unlike optical sensors. The identification of ships has been remarked from viewpoints of coast guard such as finding and monitoring marine accidents and poaching boats without Automatic Identification System (AIS). Current monitoring such situations still has been a visual inspection. This brings some difficulties such as too huge area, too time-consuming processes and so on to monitor them. So, screening candidates of ships have been required for helping the watchers. Machine learning is one of the best solutions because usual visual inspections have been substituted by the recent AI trend.
This research adopts the Convolutional Neural Network (CNN) because this is the most popular approach in image analysis. We have many uses with CNN in image recognition. This research verifies whether a ship image on SAR can be identified by CNN. This research used SAR images of PALSAR2/ALOS2 with a resolution of 10 m/pixel, polarization is HV (horizontal transmitting, vertical receiving) for the identification of ships. This machine learning needs a set of labeled data with positive/negative. The label is given to ship image on SAR using AIS. Results with PALSAR 2 data with a resolution of 10 m / pixel showed high accuracy of 95%. This research showed the availability of a method to discover ships from SAR images using CNN. In the future, this research will classification of ships not only identification. This research will examine how the change of SAR image due to marine weather affect machine learning. I would like to discuss with marine weather experts at JpGU.

Keywords: SAR, Deep learning, CNN, Ship

©2019. Japan Geoscience Union. All Right Reserved. 

[J] Poster | A (Atmospheric and Hydrospheric Sciences )：A-CG Complex & General

Thu. May 30, 2019 3:30 PM - 5:00 PM JST | Thu. May 30, 2019 6:30 AM - 8:00 AM UTC | Poster Hall International Exhibition Hall8, Makuhari Messe_6

## [A-CG36] Earth & Environmental Sciences and Artificial Intelligence

convener:Tomohiko Tomita(Faculty of Advanced Science and Technology, Kumamoto University), Ken-ichi Fukui(Osaka University), Daisuke Matsuoka(Japan Agency for Marine-Earth Science and Technology), Satoshi Ono(Kagoshima University)

In recent years, we have been required to explore the gigantic environmental data leading global environmental studies of modern meteorology, oceanography, and hydrology to accomplish Society 5.0 and Sustainable Development Goals (SDGs). Such environmental data, which are typical "big data," include the reliable long-term observatory data, ground radar data, satellite observation, oceanographic observation, global objective analysis data, and so on. However, it is hard to say that such big data are fully utilized, or nobody may have examined many of them. Therefore, to examine the global environment more faithfully, we need to apply the techniques of artificial intelligence/machine learning on such big data, that is, spatiotemporal data modeling of artificial intelligence, prediction and detection by machine learning, techniques of automated data mining, and so forth. Only cross-cutting diagnosis of the gigantic environmental data could resolve a wide variety of environmental problems including measures against global warming. In addition, the application of artificial intelligence/machine learning on the big data would raise us to the 4th paradigm of science (the 1st paradigm, observation/experiment; 2nd, theory; 3rd, simulation; 4th, data driven). This session sincerely invites various research initiatives that accelerate the application of artificial intelligence/machine learning on such gigantic environmental data.

### [ACG36-P01] Automatic Detection of Illegal Waste Sites in UAS Orthoimages

Wei-De Chen[1], *Yu-Ching Lin[1], Hsien-Min Wu[1] (1.Chung Cheng Institute of Technology, Taiwan)

### [ACG36-P02] Using machine learning models to predict the benefits of solar power generation in northern Taiwan

*SHIH-CHIAO TSAI[1], KUO-CHIH HUANG[1], DUN-REN GUO[1] (1.National Defense Univ.)

### [ACG36-P03] Change Point Detection and Visualization of Region of Interests on Weather Time Series Data Using Three-dimensional Convolutional Neural Network

*Satoshi Ono[1], Sotaro Maehara[1], Takahiro Kinoshita[1], Ken-ichi Fukui[2], Tomohiko Tomita[3] (1.Kagoshima University, 2.Osaka University, 3.Kumamoto University)

### [ACG36-P04] Estimation of sediment disaster risk around the Fuji River Basin using a machine learning method that considers trigger and inherent factors

*Kazuyoshi Souma[1], Sei Kuroda[2], Takeru Kurakami[2], Takashi Miyamoto[1] (1.Interdisciplinary Graduate School, University of Yamanashi, 2.Integrated Graduate School of Medicine, Engineering, and Agricultural Sciences)

### [ACG36-P05] Application of deep learning techniques to precipitation guidance in short-term weather predictions

*TAKERU KURAKAMI[1], Kazuyoshi Souma[1], Takashi Miyamoto[1], Takahiko Huruya[1], Jun Magome[1], Hiroshi Ishidaira[1] (1.University of Yamanashi)

### [ACG36-P06] Characteristics of precipitation in Japan evaluated from the ratio of precipitation events

*Kenta Ogino[1], Tomohiko Tomita[1], Naoki Matsumoto[1] (1.Kumamoto University)

# Automatic Detection of Illegal Waste Sites in UAS Orthoimages

Wei-De Chen[1], *Yu-Ching Lin[1], Hsien-Min Wu[1]

1. Chung Cheng Institute of Technology, Taiwan

With the force of technological development and growing human population, it is important for the government to understand the rate of land use/land-cover change. Remotely sensed data has been popularly employed for land use monitoring, in order to avoid improper land use or illegal expansion. Over the past decade, medium-resolution satellite images have been exploited to find out where illegal waste disposal sites are in Taiwan. However, acquiring satellite imagery often takes long revisit time. In recent years, Unmanned Aircraft System (UAS) attached with a non-metric camera has become a popular platform for acquisition of aerial images. It is cost-effective for acquiring temporal images over large geographic areas. This study employed a sensfly Ebee drone to acquire aerial images for monitoring land use activity. An orthoimage can be generated using state-of-the-art Structure-from-Motion (SfM) photogrammetry. With the help of object detection technique in artificial intelligence, illegal activity can be rapidly identified in the orthoimages. The Tensorflow Object Detection API was applied. In this study, a faster region-based Convolutional Neural Network (R-CNN) with Resnet-101model was retrained for detecting the location of illegal waste. The results achieved a recall of 86.9% and a precision of 72.2%. This study demonstrated that it is possible for department of land monitoring to know the hot spot of illegal waste sites. Surveillance operations become active and effective. In the future, hard sampling mining method would be investigated to reduce false alarm cases. Also, a faster detection procedure, such as YOU ONLY LOOK ONCE (YOLO) v3 will be further assessed.

Keywords: Object Detection, UAS

©2019. Japan Geoscience Union. All Right Reserved. 

# Using machine learning models to predict the benefits of solar power generation in northern Taiwan

*SHIH-CHIAO TSAI[1], KUO-CHIH HUANG[1], DUN-REN GUO[1]

1. National Defense Univ.

In recent years, the use and development of solar power has been promoted due to climate change and energy crisis. However, solar power generation is highly dependent on local weather characteristics, since the amount of solar radiation is closely related to the atmospheric transparency, water vapor content, cloud coverage and suspended particulate content. In particular, the problem of air pollution in Taiwan is getting worse, and the aerosol in the atmosphere can reflect, scatter or absorb solar radiation, reducing the amount of solar power generation. Therefore, if we want to increase the proportion of solar power generation, it is important to develop a solar energy forecasting technology that combines environmental parameters. This study utilized meteorological data from the Banqiao, Hsinchu, and Xinwu observatories of the Central Weather Bureau, and PM2.5 observation data from the Longtan Station of the Environmental Protection Administration from July 2013 to June 2018, to analysis the relationship between various environmental factors and solar radiation. Then put the data into the mechanical learning models to obtain the solar radiation prediction value (the first half of the data is used for model training and the second half is used for model testing), and compare with the measured values of solar radiation to find the best performing parameter series and model. The results show that a series of 10 weather parameter used in the decision tree algorithm has better training and test scores on the 8th floor (training score 0.821261, test score 0.674572), and the random forest algorithm has the best training and test performance (training score 0.964738, test score 0.716649).

Keywords: Machine learning, Decision tree, Random forest, Solar radiation

©2019. Japan Geoscience Union. All Right Reserved. 

# Change Point Detection and Visualization of Region of Interests on Weather Time Series Data Using Three-dimensional Convolutional Neural Network

*Satoshi Ono[1], Sotaro Maehara[1], Takahiro Kinoshita[1], Ken-ichi Fukui[2], Tomohiko Tomita[3]

1. Kagoshima University, 2. Osaka University, 3. Kumamoto University

To understand long-term natural variation on meteorological observation data, it is necessary to exclude artificial variation factors. This research proposes a 3D Convolutional Neural Network (3D-CNN)–based method to detect changes caused by artificial factors such as relocation of an observation station which appear small perturbation patterns in observed data. The proposed method allows supervised learning by synthesizing training data with supervisory signal. This research conducts experiments with observation data by Automated Meteorological Data Acquisition System (AMeDAS). By cutting off the temperature change pattern observed at two neighboring stations at a certain time and exchanging the subsequent observation data, training data can be synthesized including the virtual observation station movements. Experimental results showed that it is possible to detect the observation station movements in a short distance of several kilometers or less even when using training data synthesized from observation stations that are several tens of kilometers away. In addition, by using guided gradient-weighted class activation mapping, the proposed method could visualize the region of interests on the observation data when detecting change points.

Keywords: Observation data by AMeDAS, 3D convolutional neural network, Change point detection, Visualization

©2019. Japan Geoscience Union. All Right Reserved. 

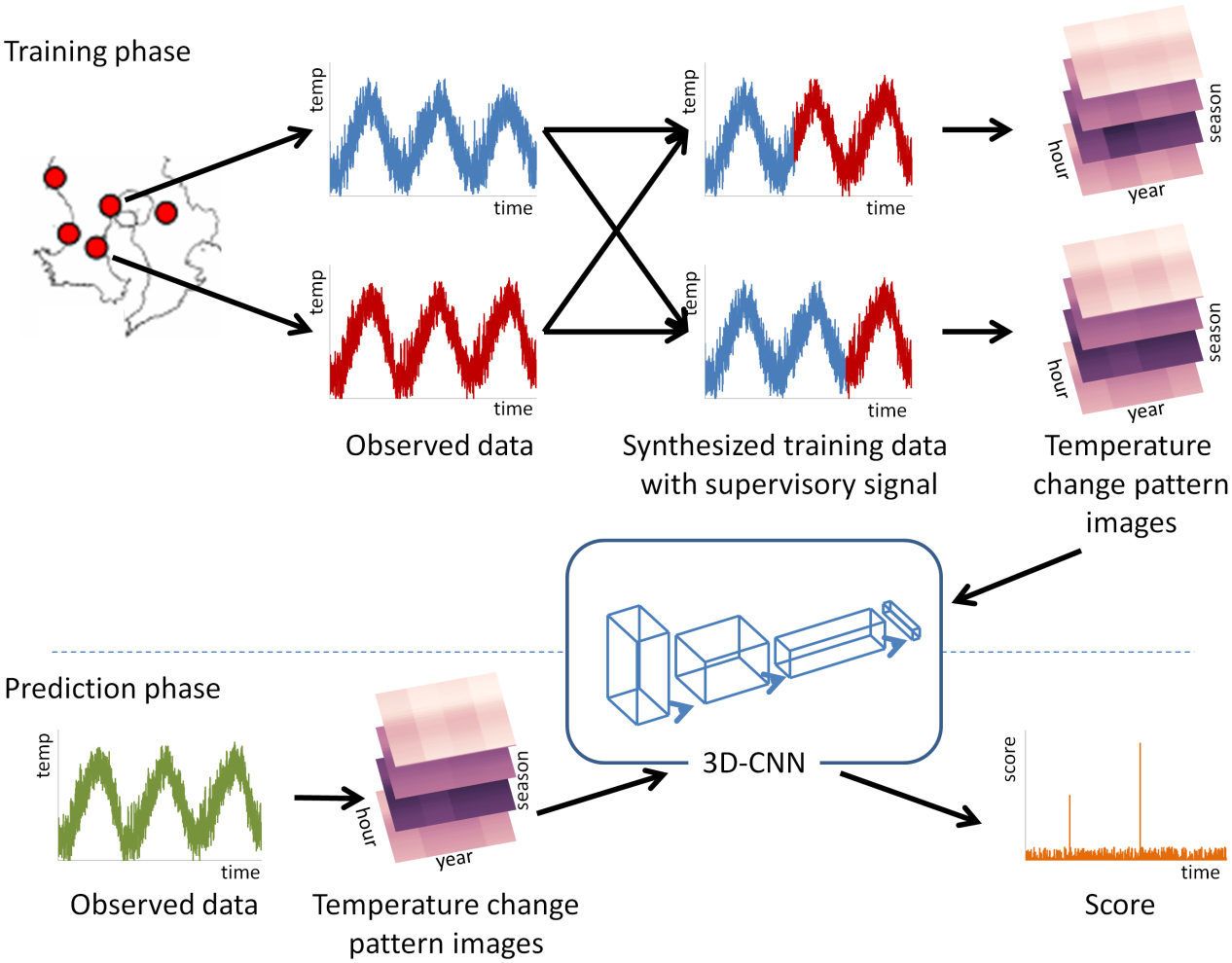


©2019. Japan Geoscience Union. All Right Reserved. 

# Estimation of sediment disaster risk around the Fuji River Basin using a machine learning method that considers trigger and inherent factors

*Kazuyoshi Souma[1], Sei Kuroda[2], Takeru Kurakami[2], Takashi Miyamoto[1]

1. Interdisciplinary Graduate School, University of Yamanashi, 2. Integrated Graduate School of Medicine, Engineering, and Agricultural Sciences

Many regions within the Fuji River Basin are vulnerable to sediment disasters. The Fuji River flows through Shizuoka, Yamanashi, and Nagano prefectures and includes the Itoigawa–Shizuoka structural line. As a non-structural countermeasure, the Japan Meteorological Agency (JMA) and prefectural governments operate the Sediment Disaster Alert Information System, which considers detailed rainfall information based on weather radar to determine trigger factors of sediment disasters. However, this system does not directly consider inherent factors such as slope gradient and land surface geology. It is therefore necessary to develop a sediment disaster risk estimation method that considers both trigger and inherent factors.

In this study, we developed a method to estimate sediment disaster risk that considers trigger and inherent factors in the areas around the Fuji River Basin (Yamanashi and Shizuoka prefectures) using neural network and k-means method. The targets of this method are shallow landslides, including debris flows and large slope failures.

As a target for training and validation, we selected the typhoons ROKE (September 21, 2011) and TALAS (September 2-4, 2011), which caused severe damage due to sediment disasters in Yamanashi and Shizuoka prefectures. To determine the inherent factors, we collected 1-km-resolution data for Yamanashi and Shizuoka prefectures using the Elevation Degree of Slope Tertiary Mesh Data, Land Use Tertiary Mesh, and Land Classification Mesh (surface layer geology) products from National Land Numerical Information. To obtain trigger factors, we extracted 60-minute accumulated rainfall (ca. 1-km resolution) from C-band radar data provided by the JMA. We also calculated the soil water index (SWI) using the 3-layer tank model. As training data, we used the occurrence of shallow landslides within each 1-km cell based on disaster reports provided by Yamanashi and Shizuoka prefectures. In this dataset, cells where shallow landslides occurred were assigned a value of 0, and those where shallow landslides did not occur were assigned a value of 1.

We began with binary classification, using a neural network to output values from 0 to 1. We then inputted trigger factors (2 elements) and inherent factors (30 elements) to the neural network. The error (loss function) of the training process did not decrease as epochs increased, due to the presence of several 0 values in the training dataset, which indicated a lack of sediment disaster. We then applied an undersampling method to the input data; however, the error still did not decrease.

In the next step, we reconstructed the neural network (which had two hidden layers) for a regression problem using risk levels from 0 to 1 for each 1-km cell as training data. The input data were classified into 40 clusters using the k-means method, and the risk level for each cell was determined based on the ratio of sediment disaster occurrence cells in each cluster. To equalize the weights of the trigger and inherent factors used in the k-means method, two trigger factors (60-minute accumulated rainfall and SWI) and two inherent factors (slope gradient, fault presence) were selected. The error of the training process (using data for 15:00 Japan Standard Time [JST], September 21, 2011) decreased as the number

©2019. Japan Geoscience Union. All Right Reserved. 

of epochs increased. In the validation phase (using data for 11:00 JST on September 3, 2011), the neural network output showed high values in cells where debris flows actually occurred.

In conclusion, we found that the outputs of the proposed method can be used to determine sediment disaster risk. Adequate selection of input data was important to the validity of the results, as was assignment of equal weight to trigger and inherent factors. Future studies should increase the number of sediment disasters used in the training process.

Keywords: Sediment disasters, Neural network, Clustering, Inherent factors, Trigger factors

©2019. Japan Geoscience Union. All Right Reserved. 

# Application of deep learning techniques to precipitation guidance in short-term weather predictions

*TAKERU KURAKAMI[1], Kazuyoshi Souma[1], Takashi Miyamoto[1], Takahiko Huruya[1], Jun Magome[1], Hiroshi Ishidaira[1]

1. University of Yamanashi

Introduction
Although numerical weather prediction models are useful methods for predicting rainfall in the short-term, it is difficult to avoid errors when making these predictions. The application of deep learning techniques, which have had remarkable results in processing big data, can effectively correct the outputs of numerical weather prediction models.

Objectives
In this study, we developed a method using deep learning techniques to correct numerical weather prediction model outputs. Using this method, the output rainfall amounts can be used as precipitation guidance.

Methods
We used a Convolutional Neural Network (CNN) as the deep learning model. The data augmentation and data selection (rejection of no rainfall data) were applied. We assumed a regression problem and the sum of squared errors was adopted as the loss function in the CNN. The rainfall amount should not be zero and should be a continuous value, so the Rectified Linear Unit (ReLU) was adopted as the activation function.
The input data for the deep learning model was acquired from numerical weather prediction models between August 1-to 31 2001 in the Keihanshin region of Japan. As input variable, vertical near-ground wind speeds was selected. For the numerical weather prediction model, we used the Heavy Rainfall Event by a CReSiBUC, which consists of Cloud resolving atmospheric model CReSS and a land surface model SiBUC. CReSiBUC considers detailed information regarding urban activity.
For the training data we used observed rainfall amounts based on Radar/Raingauge-Analyzed Precipitation data provide by the Japan Meteorological Agency. The observed data were interpolated, using the nearest neighbor method into the same meshes simultaneously with the prediction results.

Results and discussions
The two-dimensional rainfall distributions before and after being corrected by the deep learning method were compared with the observed data from the Radar Raingauge Analyzed Precipitation. The accuracy was improved by the introduction of the deep learning technique at 01:00JST (Japan Standard Time) on August 21, 2001 during a typhoon rainfall event. We found that the introduction of the deep learning technique effectively improved the accuracy of a precipitation event at a large spatial scale during a typhoon. Conversely, the deep learning technique did not improve the accuracy at 14:00JST on August 6, 2001 during a localized heavy rainfall event. Therefore, errors in the position of the precipitation area cannot be completely corrected in the case of rainfall events at small spatial scales.

Summary
In this study, we have used deep learning techniques to develop a method of precipitation guidance to correct numerical weather prediction model outputs. When comparing these results with observed rainfall

©2019. Japan Geoscience Union. All Right Reserved. 

distribution, the method is effective for large spatial scale precipitation events such as typhoons. However, errors in the position of the area of precipitation cannot be corrected completely in the case of precipitation events at small spatial scales and this needs to be investigated in future research.

Keywords: Short-term weather prediction, Machine learning, Deep learning, Numerical prediction model, Precipitation guidance

©2019. Japan Geoscience Union. All Right Reserved. 

# Characteristics of precipitation in Japan evaluated from the ratio of precipitation events

*Kenta Ogino[1], Tomohiko Tomita[1], Naoki Matsumoto[1]

1. Kumamoto University

This study quantitatively evaluated the spatial difference in characteristics of precipitation in Japan based on the time variability in precipitation events and the occurrence ratio of each of clustered events at 47 points (prefectural capitals) in Japan. First, the time variation patterns in precipitation events were classified by the method of hierarchical clustering. In this study, the precipitation event was been defined as follows: (1) the total precipitation is 0.5 mm and over; (2) the start value is 0 mm/h; (3) the time period of a precipitation event is set to be 72 hours; (4) when two-hour break appears, the value of 0 mm/h is set into the subsequent period in the 72 hours. Based on this definition, the precipitation events were extracted in the time period from 1978 to 2018. Then, the precipitation events were separately investigated for “warm” (May to October) and “cold” (November to April) seasons.
The results show that the number of annual precipitation events tends to be large in the area with heavy snowfall and to the south of Kagoshima. In addition, in the warm season, light rain events account for 60 % and more at all points in Japan, and the events lasting for one day are less than 10 %. On the other hand, in the cold season, light rain events are more than 60 % at all points in Japan, and the events lasting for one day are less than 15 %.
From the above results, the characteristics of precipitation in Japan is divided into five; (1) winter light rain area, (2) summer light rain area, (3) summer long-term rain area, (4) winter long-term rain area, (5) all year round rain area.

Keywords: precipitation events, time variation patterns of precipitation, precipitation characteristics in Japan, hierarchical clustering

©2019. Japan Geoscience Union. All Right Reserved. 

[J] Poster | A (Atmospheric and Hydrospheric Sciences )：A-CG Complex & General

Thu. May 30, 2019 5:15 PM - 6:30 PM JST | Thu. May 30, 2019 8:15 AM - 9:30 AM UTC | Poster Hall International Exhibition Hall8, Makuhari Messe_13

## [A-CG36] Earth & Environmental Sciences and Artificial Intelligence

convener:Tomohiko Tomita(Faculty of Advanced Science and Technology, Kumamoto University), Ken-ichi Fukui(Osaka University), Daisuke Matsuoka(Japan Agency for Marine-Earth Science and Technology), Satoshi Ono(Kagoshima University)

In recent years, we have been required to explore the gigantic environmental data leading global environmental studies of modern meteorology, oceanography, and hydrology to accomplish Society 5.0 and Sustainable Development Goals (SDGs). Such environmental data, which are typical "big data," include the reliable long-term observatory data, ground radar data, satellite observation, oceanographic observation, global objective analysis data, and so on. However, it is hard to say that such big data are fully utilized, or nobody may have examined many of them. Therefore, to examine the global environment more faithfully, we need to apply the techniques of artificial intelligence/machine learning on such big data, that is, spatiotemporal data modeling of artificial intelligence, prediction and detection by machine learning, techniques of automated data mining, and so forth. Only cross-cutting diagnosis of the gigantic environmental data could resolve a wide variety of environmental problems including measures against global warming. In addition, the application of artificial intelligence/machine learning on the big data would raise us to the 4th paradigm of science (the 1st paradigm, observation/experiment; 2nd, theory; 3rd, simulation; 4th, data driven). This session sincerely invites various research initiatives that accelerate the application of artificial intelligence/machine learning on such gigantic environmental data.

### [ACG36-P01] Automatic Detection of Illegal Waste Sites in UAS Orthoimages

Wei-De Chen[1], *Yu-Ching Lin[1], Hsien-Min Wu[1] (1.Chung Cheng Institute of Technology, Taiwan)

### [ACG36-P02] Using machine learning models to predict the benefits of solar power generation in northern Taiwan

*SHIH-CHIAO TSAI[1], KUO-CHIH HUANG[1], DUN-REN GUO[1] (1.National Defense Univ.)

### [ACG36-P03] Change Point Detection and Visualization of Region of Interests on Weather Time Series Data Using Three-dimensional Convolutional Neural Network

*Satoshi Ono[1], Sotaro Maehara[1], Takahiro Kinoshita[1], Ken-ichi Fukui[2], Tomohiko Tomita[3] (1.Kagoshima University, 2.Osaka University, 3.Kumamoto University)

### [ACG36-P04] Estimation of sediment disaster risk around the Fuji River Basin using a machine learning method that considers trigger and inherent factors

*Kazuyoshi Souma[1], Sei Kuroda[2], Takeru Kurakami[2], Takashi Miyamoto[1] (1.Interdisciplinary Graduate School, University of Yamanashi, 2.Integrated Graduate School of Medicine, Engineering, and Agricultural Sciences)

### [ACG36-P05] Application of deep learning techniques to precipitation guidance in short-term weather predictions

*TAKERU KURAKAMI[1], Kazuyoshi Souma[1], Takashi Miyamoto[1], Takahiko Huruya[1], Jun Magome[1], Hiroshi Ishidaira[1] (1.University of Yamanashi)

### [ACG36-P06] Characteristics of precipitation in Japan evaluated from the ratio of precipitation events

*Kenta Ogino[1], Tomohiko Tomita[1], Naoki Matsumoto[1] (1.Kumamoto University)

# Automatic Detection of Illegal Waste Sites in UAS Orthoimages

Wei-De Chen[1], *Yu-Ching Lin[1], Hsien-Min Wu[1]

1. Chung Cheng Institute of Technology, Taiwan

With the force of technological development and growing human population, it is important for the government to understand the rate of land use/land-cover change. Remotely sensed data has been popularly employed for land use monitoring, in order to avoid improper land use or illegal expansion. Over the past decade, medium-resolution satellite images have been exploited to find out where illegal waste disposal sites are in Taiwan. However, acquiring satellite imagery often takes long revisit time. In recent years, Unmanned Aircraft System (UAS) attached with a non-metric camera has become a popular platform for acquisition of aerial images. It is cost-effective for acquiring temporal images over large geographic areas. This study employed a sensfly Ebee drone to acquire aerial images for monitoring land use activity. An orthoimage can be generated using state-of-the-art Structure-from-Motion (SfM) photogrammetry. With the help of object detection technique in artificial intelligence, illegal activity can be rapidly identified in the orthoimages. The Tensorflow Object Detection API was applied. In this study, a faster region-based Convolutional Neural Network (R-CNN) with Resnet-101model was retrained for detecting the location of illegal waste. The results achieved a recall of 86.9% and a precision of 72.2%. This study demonstrated that it is possible for department of land monitoring to know the hot spot of illegal waste sites. Surveillance operations become active and effective. In the future, hard sampling mining method would be investigated to reduce false alarm cases. Also, a faster detection procedure, such as YOU ONLY LOOK ONCE (YOLO) v3 will be further assessed.

Keywords: Object Detection, UAS

©2019. Japan Geoscience Union. All Right Reserved. 

# Using machine learning models to predict the benefits of solar power generation in northern Taiwan

*SHIH-CHIAO TSAI[1], KUO-CHIH HUANG[1], DUN-REN GUO[1]

1. National Defense Univ.

In recent years, the use and development of solar power has been promoted due to climate change and energy crisis. However, solar power generation is highly dependent on local weather characteristics, since the amount of solar radiation is closely related to the atmospheric transparency, water vapor content, cloud coverage and suspended particulate content. In particular, the problem of air pollution in Taiwan is getting worse, and the aerosol in the atmosphere can reflect, scatter or absorb solar radiation, reducing the amount of solar power generation. Therefore, if we want to increase the proportion of solar power generation, it is important to develop a solar energy forecasting technology that combines environmental parameters. This study utilized meteorological data from the Banqiao, Hsinchu, and Xinwu observatories of the Central Weather Bureau, and PM2.5 observation data from the Longtan Station of the Environmental Protection Administration from July 2013 to June 2018, to analysis the relationship between various environmental factors and solar radiation. Then put the data into the mechanical learning models to obtain the solar radiation prediction value (the first half of the data is used for model training and the second half is used for model testing), and compare with the measured values of solar radiation to find the best performing parameter series and model. The results show that a series of 10 weather parameter used in the decision tree algorithm has better training and test scores on the 8th floor (training score 0.821261, test score 0.674572), and the random forest algorithm has the best training and test performance (training score 0.964738, test score 0.716649).

Keywords: Machine learning, Decision tree, Random forest, Solar radiation

©2019. Japan Geoscience Union. All Right Reserved. 

# Change Point Detection and Visualization of Region of Interests on Weather Time Series Data Using Three-dimensional Convolutional Neural Network

*Satoshi Ono[1], Sotaro Maehara[1], Takahiro Kinoshita[1], Ken-ichi Fukui[2], Tomohiko Tomita[3]

1. Kagoshima University, 2. Osaka University, 3. Kumamoto University

To understand long-term natural variation on meteorological observation data, it is necessary to exclude artificial variation factors. This research proposes a 3D Convolutional Neural Network (3D-CNN)–based method to detect changes caused by artificial factors such as relocation of an observation station which appear small perturbation patterns in observed data. The proposed method allows supervised learning by synthesizing training data with supervisory signal. This research conducts experiments with observation data by Automated Meteorological Data Acquisition System (AMeDAS). By cutting off the temperature change pattern observed at two neighboring stations at a certain time and exchanging the subsequent observation data, training data can be synthesized including the virtual observation station movements. Experimental results showed that it is possible to detect the observation station movements in a short distance of several kilometers or less even when using training data synthesized from observation stations that are several tens of kilometers away. In addition, by using guided gradient-weighted class activation mapping, the proposed method could visualize the region of interests on the observation data when detecting change points.

Keywords: Observation data by AMeDAS, 3D convolutional neural network, Change point detection, Visualization

©2019. Japan Geoscience Union. All Right Reserved. 

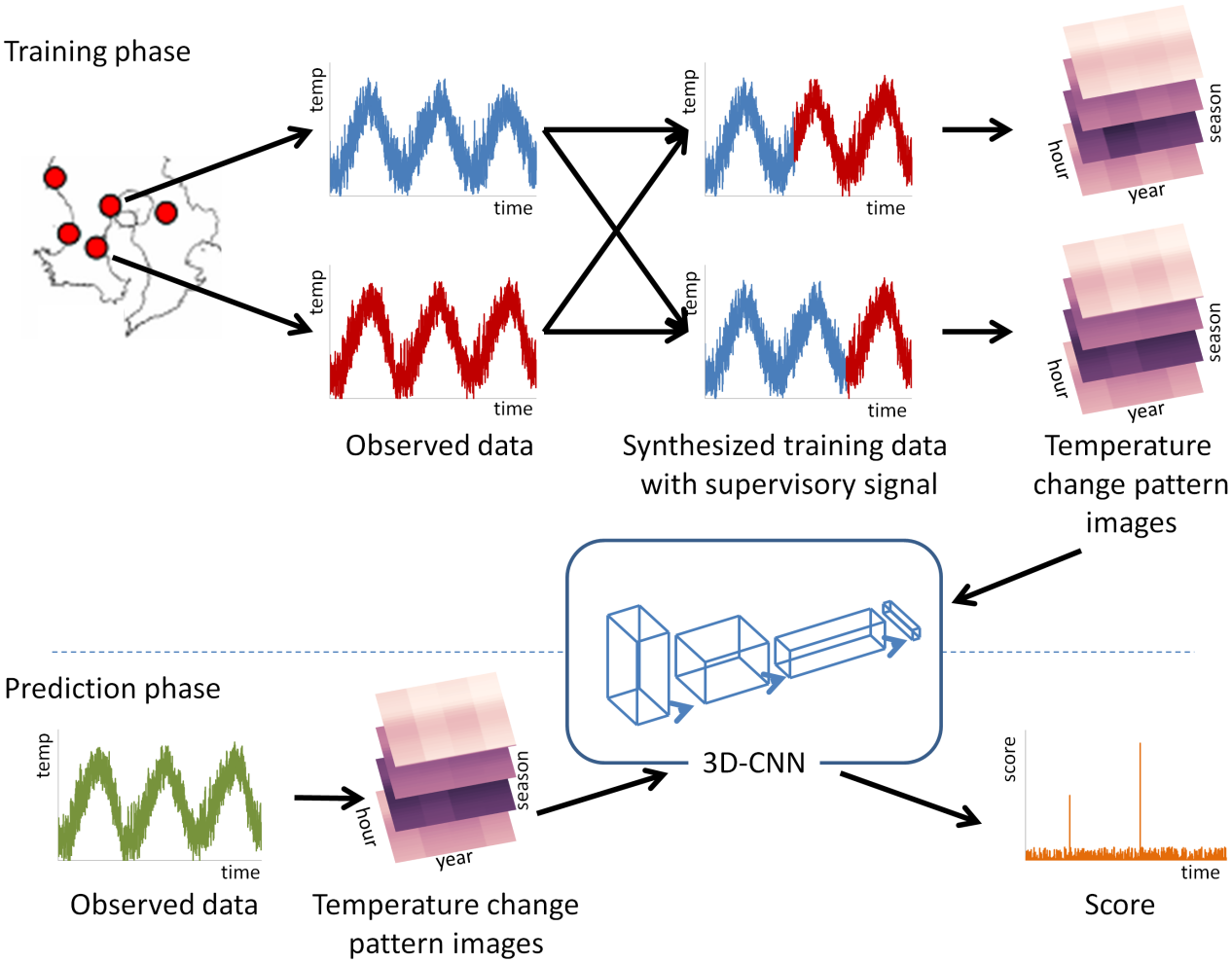


©2019. Japan Geoscience Union. All Right Reserved. 

# Estimation of sediment disaster risk around the Fuji River Basin using a machine learning method that considers trigger and inherent factors

*Kazuyoshi Souma[1], Sei Kuroda[2], Takeru Kurakami[2], Takashi Miyamoto[1]

1. Interdisciplinary Graduate School, University of Yamanashi, 2. Integrated Graduate School of Medicine, Engineering, and Agricultural Sciences

Many regions within the Fuji River Basin are vulnerable to sediment disasters. The Fuji River flows through Shizuoka, Yamanashi, and Nagano prefectures and includes the Itoigawa–Shizuoka structural line. As a non-structural countermeasure, the Japan Meteorological Agency (JMA) and prefectural governments operate the Sediment Disaster Alert Information System, which considers detailed rainfall information based on weather radar to determine trigger factors of sediment disasters. However, this system does not directly consider inherent factors such as slope gradient and land surface geology. It is therefore necessary to develop a sediment disaster risk estimation method that considers both trigger and inherent factors.

In this study, we developed a method to estimate sediment disaster risk that considers trigger and inherent factors in the areas around the Fuji River Basin (Yamanashi and Shizuoka prefectures) using neural network and k-means method. The targets of this method are shallow landslides, including debris flows and large slope failures.

As a target for training and validation, we selected the typhoons ROKE (September 21, 2011) and TALAS (September 2-4, 2011), which caused severe damage due to sediment disasters in Yamanashi and Shizuoka prefectures. To determine the inherent factors, we collected 1-km-resolution data for Yamanashi and Shizuoka prefectures using the Elevation Degree of Slope Tertiary Mesh Data, Land Use Tertiary Mesh, and Land Classification Mesh (surface layer geology) products from National Land Numerical Information. To obtain trigger factors, we extracted 60-minute accumulated rainfall (ca. 1-km resolution) from C-band radar data provided by the JMA. We also calculated the soil water index (SWI) using the 3-layer tank model. As training data, we used the occurrence of shallow landslides within each 1-km cell based on disaster reports provided by Yamanashi and Shizuoka prefectures. In this dataset, cells where shallow landslides occurred were assigned a value of 0, and those where shallow landslides did not occur were assigned a value of 1.

We began with binary classification, using a neural network to output values from 0 to 1. We then inputted trigger factors (2 elements) and inherent factors (30 elements) to the neural network. The error (loss function) of the training process did not decrease as epochs increased, due to the presence of several 0 values in the training dataset, which indicated a lack of sediment disaster. We then applied an undersampling method to the input data; however, the error still did not decrease.

In the next step, we reconstructed the neural network (which had two hidden layers) for a regression problem using risk levels from 0 to 1 for each 1-km cell as training data. The input data were classified into 40 clusters using the k-means method, and the risk level for each cell was determined based on the ratio of sediment disaster occurrence cells in each cluster. To equalize the weights of the trigger and inherent factors used in the k-means method, two trigger factors (60-minute accumulated rainfall and SWI) and two inherent factors (slope gradient, fault presence) were selected. The error of the training process (using data for 15:00 Japan Standard Time [JST], September 21, 2011) decreased as the number

©2019. Japan Geoscience Union. All Right Reserved. 

of epochs increased. In the validation phase (using data for 11:00 JST on September 3, 2011), the neural network output showed high values in cells where debris flows actually occurred.

In conclusion, we found that the outputs of the proposed method can be used to determine sediment disaster risk. Adequate selection of input data was important to the validity of the results, as was assignment of equal weight to trigger and inherent factors. Future studies should increase the number of sediment disasters used in the training process.

Keywords: Sediment disasters, Neural network, Clustering, Inherent factors, Trigger factors

©2019. Japan Geoscience Union. All Right Reserved. 

# Application of deep learning techniques to precipitation guidance in short-term weather predictions

*TAKERU KURAKAMI[1], Kazuyoshi Souma[1], Takashi Miyamoto[1], Takahiko Huruya[1], Jun Magome[1], Hiroshi Ishidaira[1]

1. University of Yamanashi

Introduction
Although numerical weather prediction models are useful methods for predicting rainfall in the short-term, it is difficult to avoid errors when making these predictions. The application of deep learning techniques, which have had remarkable results in processing big data, can effectively correct the outputs of numerical weather prediction models.

Objectives
In this study, we developed a method using deep learning techniques to correct numerical weather prediction model outputs. Using this method, the output rainfall amounts can be used as precipitation guidance.

Methods
We used a Convolutional Neural Network (CNN) as the deep learning model. The data augmentation and data selection (rejection of no rainfall data) were applied. We assumed a regression problem and the sum of squared errors was adopted as the loss function in the CNN. The rainfall amount should not be zero and should be a continuous value, so the Rectified Linear Unit (ReLU) was adopted as the activation function.
The input data for the deep learning model was acquired from numerical weather prediction models between August 1-to 31 2001 in the Keihanshin region of Japan. As input variable, vertical near-ground wind speeds was selected. For the numerical weather prediction model, we used the Heavy Rainfall Event by a CReSiBUC, which consists of Cloud resolving atmospheric model CReSS and a land surface model SiBUC. CReSiBUC considers detailed information regarding urban activity.
For the training data we used observed rainfall amounts based on Radar/Raingauge-Analyzed Precipitation data provide by the Japan Meteorological Agency. The observed data were interpolated, using the nearest neighbor method into the same meshes simultaneously with the prediction results.

Results and discussions
The two-dimensional rainfall distributions before and after being corrected by the deep learning method were compared with the observed data from the Radar Raingauge Analyzed Precipitation. The accuracy was improved by the introduction of the deep learning technique at 01:00JST (Japan Standard Time) on August 21, 2001 during a typhoon rainfall event. We found that the introduction of the deep learning technique effectively improved the accuracy of a precipitation event at a large spatial scale during a typhoon. Conversely, the deep learning technique did not improve the accuracy at 14:00JST on August 6, 2001 during a localized heavy rainfall event. Therefore, errors in the position of the precipitation area cannot be completely corrected in the case of rainfall events at small spatial scales.

Summary
In this study, we have used deep learning techniques to develop a method of precipitation guidance to correct numerical weather prediction model outputs. When comparing these results with observed rainfall

©2019. Japan Geoscience Union. All Right Reserved. 

distribution, the method is effective for large spatial scale precipitation events such as typhoons. However, errors in the position of the area of precipitation cannot be corrected completely in the case of precipitation events at small spatial scales and this needs to be investigated in future research.

Keywords: Short-term weather prediction, Machine learning, Deep learning, Numerical prediction model, Precipitation guidance

©2019. Japan Geoscience Union. All Right Reserved. 

# Characteristics of precipitation in Japan evaluated from the ratio of precipitation events

*Kenta Ogino[1], Tomohiko Tomita[1], Naoki Matsumoto[1]

1. Kumamoto University

This study quantitatively evaluated the spatial difference in characteristics of precipitation in Japan based on the time variability in precipitation events and the occurrence ratio of each of clustered events at 47 points (prefectural capitals) in Japan. First, the time variation patterns in precipitation events were classified by the method of hierarchical clustering. In this study, the precipitation event was been defined as follows: (1) the total precipitation is 0.5 mm and over; (2) the start value is 0 mm/h; (3) the time period of a precipitation event is set to be 72 hours; (4) when two-hour break appears, the value of 0 mm/h is set into the subsequent period in the 72 hours. Based on this definition, the precipitation events were extracted in the time period from 1978 to 2018. Then, the precipitation events were separately investigated for “warm” (May to October) and “cold” (November to April) seasons.
The results show that the number of annual precipitation events tends to be large in the area with heavy snowfall and to the south of Kagoshima. In addition, in the warm season, light rain events account for 60 % and more at all points in Japan, and the events lasting for one day are less than 10 %. On the other hand, in the cold season, light rain events are more than 60 % at all points in Japan, and the events lasting for one day are less than 15 %.
From the above results, the characteristics of precipitation in Japan is divided into five; (1) winter light rain area, (2) summer light rain area, (3) summer long-term rain area, (4) winter long-term rain area, (5) all year round rain area.

Keywords: precipitation events, time variation patterns of precipitation, precipitation characteristics in Japan, hierarchical clustering

©2019. Japan Geoscience Union. All Right Reserved. 

[J] Oral | A (Atmospheric and Hydrospheric Sciences)：A-CG Complex & General

Thu. May 30, 2019 9:00 AM - 10:30 AM JST | Thu. May 30, 2019 12:00 AM - 1:30 AM UTC | 303 3F

## [A-CG37] Science in the Arctic Region

convener:NAOYA KANNA(Arctic Research Center, Hokkaido University), Masashi Niwano(Meteorological Research Institute), Tetsu Nakamura(Faculty of Environmental Earth Science, Hokkaido University), Shunsuke Tei(Arctic Research Center, Hokkaido University), Chairperson:Tetsu Nakamura(Faculty of Earth Environmental Science, Hokkaido University), Shunsuke Tei(Arctic Research Center, Hokkaido University)

The Arctic and circumpolar region is the key area for the study of global change because the anthropogenic impact is projected to be the largest in this area due to the complicated feedback processes of the nature. A number of international and interdisciplinary research projects have been conducted for the studies on the land-atmosphere-ocean system. In order to understand the feedback processes occurring in the Arctic and to project the global warming in the future, we need to establish the intense observational network and to exchange the knowledge and information by combining the different scientific communities under the common interest of the Arctic. The objectives of this session are 1) to exchange our knowledge on the observational facts and integrated modelling and 2) to deepen our understanding on wide range of natural sciences related to the Arctic and the circumpolar region. Studies on humanities, social sciences, and interdisciplinary fields are also welcomed.

9:00 AM - 9:15 AM JST | 12:00 AM - 12:15 AM UTC

### [ACG37-01] Arctic midlatitude linkage modulated by the QBO

*Jinro Ukita[1], Kazuhiro Hoshi[1], Meiji Honda[1], Tetsu Nakamura[2], Koji Yamazaki[2] (1.Niigata University, 2.Hokkaido University)

9:15 AM - 9:30 AM JST | 12:15 AM - 12:30 AM UTC

### [ACG37-02] Interhemispheric synchronization between the AO and the AAO

*Yoshihiro Tachibana[1], Yusuke Inoue[1], Kensuke K komatsu[1], Tetsu Nakamura[2], Meiji Honda[3], Koto Ogata[1,4], Koji Yamazaki[2] (1.Mie University, 2.Hokkaido University, 3.Niigata University, 4.Japan Meteorological Agency)

9:30 AM - 9:45 AM JST | 12:30 AM - 12:45 AM UTC

### [ACG37-03] Marginal ice zone sea ice observations in the refreezing Chukchi Sea

*Takehiko Nose[1], Tsubasa Kodaira[1], Takuji Waseda[1], Jun Inoue[2] (1.The university of Tokyo, 2.National Institute of Polar Research)

9:45 AM - 10:00 AM JST | 12:45 AM - 1:00 AM UTC

### [ACG37-04] Prediction of wildfire and air pollution with machine learning over the five domains of Eastern Eurasia

*Teppei J Yasunari[1,2], Ichigaku Takigawa[3], Kyu-Myong Kim[4], Arlindo M da Silva[4] (1.Faculty of Engineering, Hokkaido University, 2.Arctic Research Center, Hokkaido University, 3.Graduate School of Information Science and Technology, Hokkaido University, 4.NASA Goddard Space Flight Center)

10:00 AM - 10:15 AM JST | 1:00 AM - 1:15 AM UTC

### [ACG37-05] Hydrological Changes in the Four Largest Siberian Arctic River Basins

*Kazuyoshi Suzuki[1], Tetsuya Hiyama[2], Kazuhito Ichii[3], Yoshihiro Iijima[4], Koji Matsuo[5], Dai Yamazaki[6,1] (1.Japan Agency for Marine-Earth Science and Technology, 2.Institute for Space-Earth Environmental Research, Nagoya University, 3.Chiba University, 4.Graduate School of Bioresources, Mie University, 5.Geospatial Information Authority of Japan, 6.Institute of Industrial Sciences, The University of Tokyo)

10:15 AM - 10:30 AM JST | 1:15 AM - 1:30 AM UTC

### [ACG37-06] Mapping thermokarst subsidence in Central Yakutia using L-band SAR interferometry

*Takahiro Abe[1], Go Iwahana[2,3], Takeo Tadono[1] (1.Earth Observation Research Center, Japan Aerospace Exploration Agency, 2.International Arctic Research Center, University of Alaska, Fairbanks, 3.Arctic Research Center, Hokkaido University)

# Arctic midlatitude linkage modulated by the QBO

*Jinro Ukita[1], Kazuhiro Hoshi[1], Meiji Honda[1], Tetsu Nakamura[2], Koji Yamazaki[2]

1. Niigata University, 2. Hokkaido University

We examined an observed relationship between the BKS sea ice variability and the midlatitudes cold anomaly and found that this relationship is highly dependent on the QBO phase, easerly (QBO-E) or westerly (QBO-W). For the QBO-E winters midlatitude cold (warm) anomalies appear significantly under the low (high) sea ice condition. On the other hand, such a relationship is not found in the QBO-W winters. This dependence is a robust feature. Atmospheric circulation anomalies related to the high and low sea ice conditions are also different between the two QBO phases. In the troposphere, stationary Rossby wave propagation from the BKS region and the negative NAO appear in QBO-E, along with weakened stratospheric polar vortex and downward propagation of the signals. For QBO-W, such tropospheric and stratospheric signals are mainly absent. Our results may provide an explanation for why some simulations suggest the presence of Arctic sea ice impacts on midlatitude surface temperature while others do not. The most important implication is that in the Arctic-midlatitudes climate linkage tropics also plays a key role.

Keywords: Arctic, QBO, sea ice, stratosphere, polar vortex

©2019. Japan Geoscience Union. All Right Reserved. 

# Interhemispheric synchronization between the AO and the AAO

*Yoshihiro Tachibana[1], Yusuke Inoue[1], Kensuke K komatsu[1], Tetsu Nakamura[2], Meiji Honda[3], Koto Ogata[1,4], Koji Yamazaki[2]

1. Mie University, 2. Hokkaido University, 3. Niigata University, 4. Japan Meteorological Agency

**Abstract**

Teleconnections between lower and higher latitude regions are widely known in both the Northern and Southern Hemispheres. To broaden our view of these teleconnections, we searched a reanalysis dataset for evidence of a teleconnection between the Arctic Oscillation (AO) and the Antarctic Oscillation (AAO), two widely separated circumpolar phenomena. Statistical analysis of the Japanese 55-year reanalysis dataset showed significant in-phase synchronization between the AO and AAO, particularly in October and February, with a vertical structure extending from the troposphere to the stratosphere. This vertical structure may suggest a stratospheric control, and we did not find a significant signature indicating a tropical ocean control. We also observed decadal-scale modulation of the synchronicity. Observational evidence implies that the stratospheric meridional circulation may be responsible for AO–AAO synchronization. This paper was published in ***GRL,*** 45, DOI:10.1029/2018GL081002 by Tachibana et al., 2018.

**Plain Language summary**

The Arctic Oscillation (AO) and the Antarctic Oscillation (AAO) are dominant atmospheric variability patterns in the Northern and Southern hemispheres, respectively. Each is a pressure seesaw between the pole and the midlatitudes that remotely affects weather, climate, and environment around the world. We showed interhemispheric in-phase synchronization between the AO and AAO in October and February, and we also found decadal-scale variation of the synchronicity. Because the vertical structure of the AO–AAO synchronization extends from the troposphere to the stratosphere, stratospheric variations may be responsible for the synchronization. This finding of AO–AAO synchronization points the way to a better understanding of past, present, and future pole-to-pole climatic relationships and improvements in long-term weather forecasts.

Keywords: Arctic Oscillation, Antarctic Oscillation, sudden stratospheric warming

©2019. Japan Geoscience Union. All Right Reserved. 

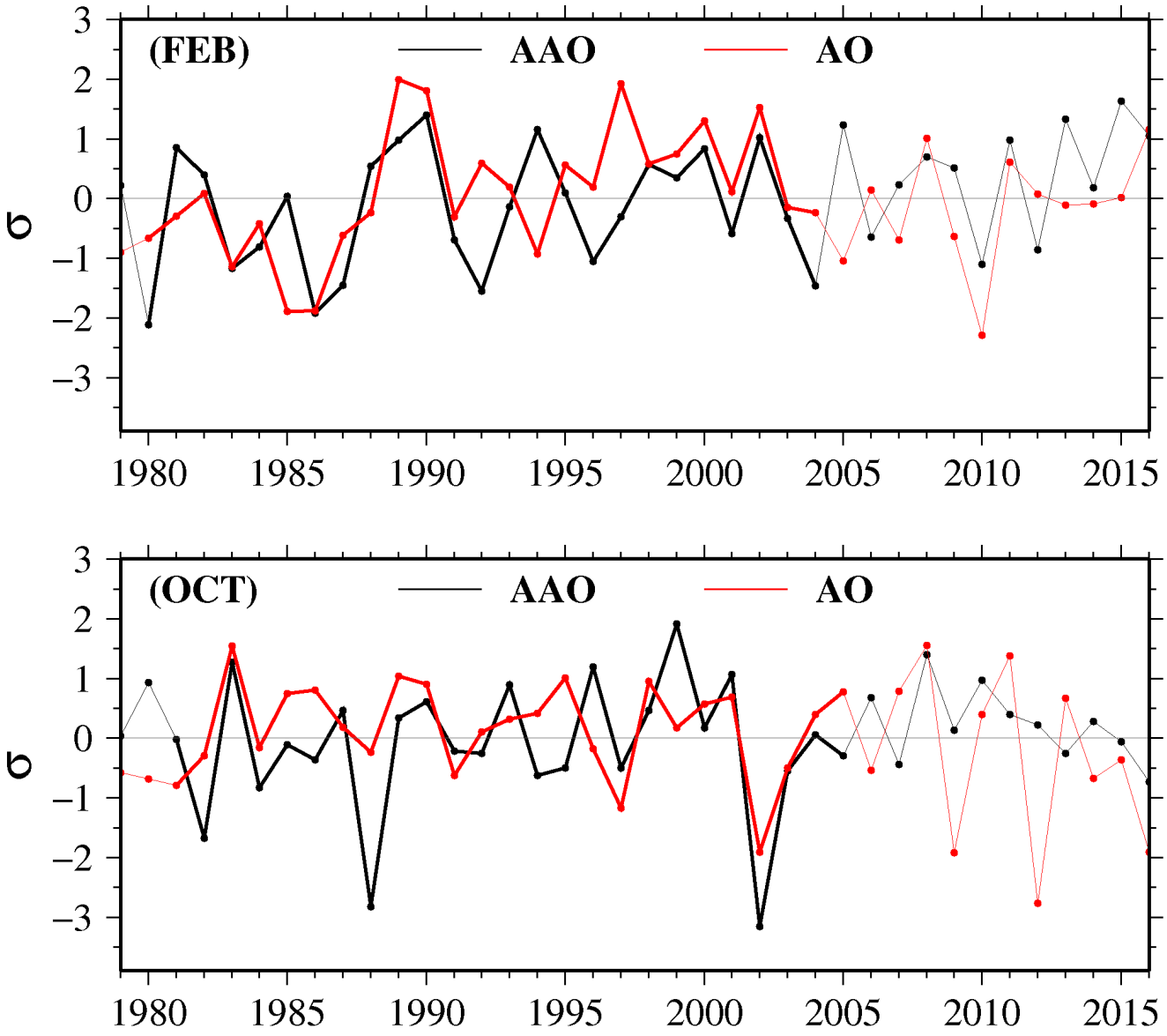


©2019. Japan Geoscience Union. All Right Reserved. 

# Marginal ice zone sea ice observations in the refreezing Chukchi Sea

*Takehiko Nose[1], Tsubasa Kodaira[1], Takuji Waseda[1], Jun Inoue[2]

1. The university of Tokyo, 2. National Institute of Polar Research

Regions in the Arctic Ocean that were inaccessible in November are now open for navigation, even for non-icebreakers, and R/V Mirai, a Polar Class 6 vessel, carried out a late autumn voyage in 2018. It conducted a 12-day sea ice observation campaign during the 9th–20th of November along a fixed Marginal Ice Zone (MIZ) transect in the eastern Chukchi Sea and obtained first-hand observations at a time when research vessels are rarely in the sea. Satellite sea ice data were compared with the shipboard observations and compared relatively well. A sequence of events to describe the observations are grouped and described in four phases: 9th–13th, “Sea ice growth under relatively calm wind conditions”; 14th–16th, “the on-ice wave event, sea ice break up, and subsequent sea ice advance”; 17th–18th, “sea ice retreat or a mass shift under moderate easterly winds”; and 19th–20th, “warming sea surface temperature (SST) under strengthening cold off-ice winds and air temperatures below -10 ˚C”. Shipboard and ERA5 reanalysis data were analysed to identify physical processes that affect the Chukchi Sea refreezing process. Sea ice conditions during the first two phases appear to be influenced primarily by surface winds whereas the analysis suggests a driver of sea ice conditions in the latter phases were due to ocean interior processes. The MIZ transect waters became heavily ice covered within five days after R/V Mirai began its return voyage, so the observation period covered most of the refreezing process along the transect water.

Keywords: R/V Mirai, Marginal Ice Zone, sea ice, refreezing ocean, the Chukchi Sea

©2019. Japan Geoscience Union. All Right Reserved. 

# Prediction of wildfire and air pollution with machine learning over the five domains of Eastern Eurasia

*Teppei J Yasunari[1,2], Ichigaku Takigawa[3], Kyu-Myong Kim[4], Arlindo M da Silva[4]

1. Faculty of Engineering, Hokkaido University, 2. Arctic Research Center, Hokkaido University, 3. Graduate School of Information Science and Technology, Hokkaido University, 4. NASA Goddard Space Flight Center

Under the ongoing global warming, necessity of better forecasting on wildfires and its air pollutions is increasing. In the last year, we carried out a preliminary wildfire prediction using the areal-averaged monthly mean data over a large Siberian domain (Yasunari et al., 2018, presented at AGU Fall Meeting 2018: http://bit.ly/2PG1bmK). Here we extend our previous analysis of machine learning and prediction into the five separated domains over the Arctic and sub-Arctic regions over Eastern Eurasia including Siberia, East Asia, Far East, etc. We use the same monthly mean dataset during 2003-2017 as we did in the last year above (i.e., NASA's FEER fire data, MODIS Snow Cover Fraction, SCF, Modern-Era Retrospective analysis for Research and Applications, Version 2, MERRA-2). The time periods of 2003–2014 and 2015–2017 focus on learning and prediction. Areal averaged data for objective (i.e., wildfire and air pollution variables) and explanatory variables (i.e., snow, temperature, wind, surface soil wetness, precipitation, geopotential height, etc.) over the defined five domains over Eastern Eurasia (Domain 1: 57°–70°N, 60°–90°E; Domain 2: 57°–70°N, 90°–140°E; Domain 3: 60°–70°N, 140°–180°E; Domain 4: 42.5°–57°N, 60°–90°E; Domain 5: 42.5°–57°N, 90°–140°E) are calculated, together with producing monthly time-lagged data for explanatory variables up to six months (i.e., total 174-month data available during 2003 and 2017). In addition, we made different areal-averaged fire pixel count data in which some smaller fires were removed with defined thresholds to remove expected human-made fires such as bonfires (i.e., assumed natural fire cases). If the areal-averaged fire data under the thresholds on a specific month showed no fire, we replaced that data to zero (i.e., used for our analyses but treated as zero fire data on that month).
Using Random Forest Regression, for example, in the machine learning, except for Domain 5, all the fire-included case showed the worse prediction score than those of the assumed natural fire cases. This implies that smaller fire cases, which were likely ignited by human activities or others, would be one of the causes for making wildfire predictions worse. However, over Domain 5, all the fire-included case showed the best probably because the assumed natural fire case was probably affected by the unusual large-scale wildfire events (i.e., outliers). These significantly large-scale wildfire cases also likely to make predictions worse because of not enough such cases existing in the training data (i.e., not frequent). In addition, these outliers might happen under unusual climatic and environmental conditions. How to include more large-scale fire cases in training data would be one of the important future targets on wildfire prediction with machine learning. On the day of the presentation, we'll also show the results for air pollution prediction.

Keywords: Arctic, wildfire, air pollution, PM2.5, machine learning, Siberia

©2019. Japan Geoscience Union. All Right Reserved. 

# Hydrological Changes in the Four Largest Siberian Arctic River Basins

*Kazuyoshi Suzuki[1], Tetsuya Hiyama[2], Kazuhito Ichii[3], Yoshihiro Iijima[4], Koji Matsuo[5], Dai Yamazaki[6,1]

1. Japan Agency for Marine-Earth Science and Technology, 2. Institute for Space-Earth Environmental Research, Nagoya University, 3. Chiba University, 4. Graduate School of Bioresources, Mie University, 5. Geospatial Information Authority of Japan, 6. Institute of Industrial Sciences, The University of Tokyo

The Arctic freshwater budget affects global climate and is critical for understanding the climate in polar regions. However, the hydrology of the largest Eurasian Arctic rivers is still not understood well. In this paper, we analyze spatiotemporal variations in hydro-climatological factors related to four of the largest Siberian Arctic river basins (Ob, Yenisey, Lena, and Kolyma). To examine recent hydro-climatological changes in these river basins, we utilize monthly observation-based gridded meteorological and evapotranspiration data, Moderate Resolution Imaging Spectroradiometer (MODIS)-based products such as the snow area fraction (SAF) and normalized vegetation index (NDVI), global land data assimilation system products, and Gravity Recovery and Climate Experiment (GRACE) data from 2000 to 2016. Combining these with river runoff data, we identify how river runoff shifted from June to May during the study period. River runoff in May significantly increased although there was no clear trend in annual discharge. In addition, SAF decreased drastically in April and this is evidence that spring snow coverage in Siberian basins is shrinking and snowmelt is shifting toward earlier. On the other hand, we found the positive trend in summer NDVI. Focusing on permafrost distribution, this paper will discuss the correlation in the temporal lag between the water cycle and vegetation activity.

Keywords: Snow, Vegetation, Premafrost

©2019. Japan Geoscience Union. All Right Reserved. 

# Mapping thermokarst subsidence in Central Yakutia using L-band SAR interferometry

*Takahiro Abe[1], Go Iwahana[2,3], Takeo Tadono[1]

1. Earth Observation Research Center, Japan Aerospace Exploration Agency, 2. International Arctic Research Center, University of Alaska, Fairbanks, 3. Arctic Research Center, Hokkaido University

Thermokarst is an irreversible phenomenon with geomorphological change, resulted from the thawing of ice-rich permafrost or the melting of massive ice. The formation of large depressions in the ground surface by thermokarst processes results in surface inundation, and causes damages on infrastructure. Central Yakutia in Eastern Siberia is one of the regions where ice-rich permafrost is broadly distributed. The remarkable surface subsidence due to thermokarst has been observed in recent years, which could cause destruction of building and infrastructure in this area (Shiklomanov et al., 2017; Hjort et al., 2018). The thermokarst settlement are frequently observed in continuous permafrost zones in arctic regions, especially in Alaska and the Northeastern Siberia. However, it is so difficult to know where and how surface deforms in vast permafrost zones.

Remote sensing technique, especially Interferometric Synthetic Aperture Radar (InSAR), has a great potential to monitor the thermokarst subsidence, and seasonal permafrost melting and heaving. SAR sends microwave toward ground, and receive the reflected and scatter signals under all-weather and day-and-night condition without any instrument on ground. Thus, InSAR can provide essential information to understand thawing process of ice-rich permafrost and to predict the future stage over arctic permafrost region. Many studies about permafrost dynamics using SAR images have been reported so far (e.g., Liu et al., 2010; Iwahana et al., 2016; Antonova et al., 2018; Strozzi et al., 2018), but there is no study using SAR in Central Yakutia.

In this study, we used ALOS/PALSAR (2007-2010) and ALOS-2/PALSAR-2 (2014-2018) images to examine ground subsidence caused by thermokarst development. GAMMA software was used to generate Single Look Complex data from Lv1.0 data in ALOS/PALSAR and Lv1.1 data in ALOS-2/PALSAR-2. ALOS world DEM derived from ALOS/PRISM was used to simulate and remove topographic effect. We generated many interferograms, selected some of them, and applied stacking procedure weighted on period between two SAR data acquisition time, estimating the mean change rate along line of sight (LOS). Assuming ground displacement is only vertical component, the LOS change was converted to vertical displacement using incidence angle.

At the last JpGU, we reported ground subsidence in Mayya, on the right bank of Rena River, Central Yakutia, derived from ALOS/ALOS-2 InSAR stacking. To validate the InSAR signals, we carried out the ground observation in Mayya at the end of September, 2018. As a result, the subsidence rate of 2-3 cm/yr was obtained at the two measurement points in 2017-2018. The result of ground observation is consistent with that of InSAR result from ALOS-2. We also went to some places where there are subsidence signals in the ALOS-2 results. As a consequence, the two large subsidence signals were found in alasses. Alas is considered as a final geomorphological stage of old thermokarst development. Significant amount of the subsidence may be due to consolidation settlement associated with soil desiccation under recent dry climate conditions. However, judging from new developments of polygonal subsidence in the bottom areas of alasses, ground ice still remains under the alasses, which may cause further thermokarst progress.

©2019. Japan Geoscience Union. All Right Reserved. 

Moreover, we extended our target to other cities, Amga, and Churapcha, where thermokarst has been also developing (e.g., Saito et al. 2018). The similar subsidence signals were obtained in the two cities, where it is in area of many polygons. It suggests that the signals be presumably due to thermokarst development.

Keywords: Permafrost, Thermokarst, Synthetic Aperture Radar (SAR), SAR Interferometry, ALOS-2, ALOS

©2019. Japan Geoscience Union. All Right Reserved. 

[J] Oral | A (Atmospheric and Hydrospheric Sciences)：A-CG Complex & General

Thu. May 30, 2019 10:45 AM - 12:15 PM JST | Thu. May 30, 2019 1:45 AM - 3:15 AM UTC | 303 3F

## [A-CG37] Science in the Arctic Region

convener:NAOYA KANNA(Arctic Research Center, Hokkaido University), Masashi Niwano(Meteorological Research Institute), Tetsu Nakamura(Faculty of Environmental Earth Science, Hokkaido University), Shunsuke Tei(Arctic Research Center, Hokkaido University), Chairperson:Shunsuke Tei(Arctic Research Center, Hokkaido University), Masashi Niwano(Meteorological Research Institute)

The Arctic and circumpolar region is the key area for the study of global change because the anthropogenic impact is projected to be the largest in this area due to the complicated feedback processes of the nature. A number of international and interdisciplinary research projects have been conducted for the studies on the land-atmosphere-ocean system. In order to understand the feedback processes occurring in the Arctic and to project the global warming in the future, we need to establish the intense observational network and to exchange the knowledge and information by combining the different scientific communities under the common interest of the Arctic. The objectives of this session are 1) to exchange our knowledge on the observational facts and integrated modelling and 2) to deepen our understanding on wide range of natural sciences related to the Arctic and the circumpolar region. Studies on humanities, social sciences, and interdisciplinary fields are also welcomed.

10:45 AM - 11:00 AM JST | 1:45 AM - 2:00 AM UTC

### [ACG37-07] Spatiotemporal variation of thaw subsidence and frost heave of permafrost caused by wildfire around Batagay, East Siberia

*Kazuki Yanagiya[1], Masato Furuya[2] (1.Graduate School of Science, Hokkiado University, 2.Faculty of Science, Hokkaido University)

11:00 AM - 11:15 AM JST | 2:00 AM - 2:15 AM UTC

### [ACG37-08] Influence of recent climate change on permafrost coast dynamics in the Kara Sea, Russian Arctic Ocean

*A. Kioka[1,2], V. S. Isaev[2], A. V. Koshurnikov[2], A. Pogorelov[2], R. M. Amangurov[2], O. Podchasov[2], D. O. Sergeev[3], S. N. Buldovich[2], D. M. Aleksyutina[4], E. A. Grishakina[5] (1.Institut für Geologie, Leopold-Franzens-Universität Innsbruck, Austria, 2.Department of Geocryology, Lomonosov Moscow State University, Russia, 3.Sergeev Institute of Environmental Geoscience, Russian Academy of Science, Russia, 4.Research Laboratory of Geoecology of the Northern Territories, Lomonosov Moscow State University, Russia, 5.Vernadsky Institute of Geochemistry and Analytical Chemistry, Russian Academy of Science, Russia)

11:15 AM - 11:30 AM JST | 2:15 AM - 2:30 AM UTC

### [ACG37-09] Ice front variations of Heilprin Glacier in northwestern Greenland controlled by the ocean and glacier bed geometries

*Izumi Asaji[1,2], Daiki Sakakibara[3], Takuto Ando[3], Shin Sugiyama[1] (1.Institute of Low Temperature Science, Hokkaido University, 2.Graduate School of Environmental Science, Hokkaido University, 3.Arctic Research Center, Hokkaido University)

11:30 AM - 11:45 AM JST | 2:30 AM - 2:45 AM UTC

### [ACG37-10] Meltwater discharge and flooding of the outlet stream of Qaanaaq Glacier, northwestern Greenland

*Ken Kondo[1,2], Daiki Sakakibara[3,2], Shungo Fukumoto[1,2], Shin Sugiyama[2] (1.Graduate School of Environmental Science, Hokkaido University, 2.Institute of Low Temperature Science, Hokkaido University, 3.Arctic Research Center, Hokkaido University)

11:45 AM - 12:00 PM JST | 2:45 AM - 3:00 AM UTC

### [ACG37-11] Occurrence frequency of lee-side downslope winds near Siorapaluk in northwest Greenland

*Akihiro Hashimoto[1], Tetsuhide Yamasaki[2], Teruo Aoki[3,1], Masashi Niwano[1], Satoru Yamaguchi[4] (1.Meteorological Research Institute, 2.Avangnaq, 3.The Graduate School of Natural Science and Technology, Okayama University, 4.Snow and Ice Research Center, National Research Institute for Earth Science and Disaster Resilience)

---

12:00 PM - 12:15 PM JST | 3:00 AM - 3:15 AM UTC

## [ACG37-12] Impacts of clouds on the Greenland ice sheet surface melt and mass balance

*Masashi Niwano[1], Akihiro Hashimoto[1], Teruo Aoki[2] (1.Meteorological Research Institute, 2.Graduate School of Natural Science and Technology, Okayama University)

# Spatiotemporal variation of thaw subsidence and frost heave of permafrost caused by wildfire around Batagay, East Siberia

*Kazuki Yanagiya[1], Masato Furuya[2]

1. Graduate School of Science, Hokkiado University, 2. Faculty of Science, Hokkaido University

Thawing permafrost release soil organic carbon as a greenhouse gases, and it can be positive feedback on global warming (Shuur et al. 2015). To estimate terrestrial carbon budget precisely, permafrost degradation should be observed in the entire circumpolar region. However, it is impractical to perform field observation over all the permafrost areas in northern hemisphere. Especially in Siberia, observation sites by the international network (e.g. GTN-P, CALM) is very few despite the largest area in terms of permafrost distribution. Therefore, remote sensing techniques to cover wide areas are indispensable. Observing ground deformation by InSAR (Interferometric Synthetic Aperture Radar) can tell us the state of permafrost with high spatiotemporal resolution. Some previous studies are conducted in a part of Alaska, Canada and Siberia that can be easy to compare with field work (Liu et al. 2010; Short et al. 2011; Antonova et al. 2018).

We focused on East Siberia, where no previous studies by InSAR are conducted. Study area is around Batagay town (67’ 39N, 134’ 39E). At ~10 km southeast of Batagay, there is a well-known and one of the largest slump terrains caused by thawing of permafrost (Murton et al. 2017). Processing ALOS and ALOS2 InSAR images, we found the deformation signal due to wildfire at the hill to the 20 km northwest of Batagay. Loss of surficial vegetation layer by wildfire accelerates permafrost thawing, and the degradation continues for several years to decades after a fire (Yoshikawa et al. 2002). Furthermore, given the fact that the frequency and intensity of wildfires are increasing in the Arctic region with global warming (Alexander et al. 2018; Gibson et al. 2018; Masrur et al. 2018), it is important to reveal the spatiotemporal variation of the ground deformation in the post-wildfire area.

Here, we report our detection of the post-wildfire ground deformation in the place where the fire occurred in 2014. We used SAR images obtained from ALOS 2 (L-band) and Sentinel-1 (C-band) satellites from 2014 to 2018. Secular deformation is detected by ALOS2 data. The results indicated that thawing subsidence up to 10cm in the satellite line of sight direction continued after 2-3 years after the fire. Seasonal deformation from 2017 to 2018 is detected and compared with both satellites data. The magnitude and spatial patterns of subsidence and uplift was consistent in both satellites. Especially, short-term InSAR images with Sentinel-1 data revealed detailed temporal variation from the start to the end of thawing and freezing. Estimation of permafrost thawing amount from ground deformation amount detected by InSAR can contribute to reducing uncertainty of terrestrial carbon budget. Those physical models are under discussion (Liu et al. 2014; Hu et al. 2018; Molan et al. 2018). In this study, we verified the Molan model in our study area, and developed it taking into account the deformation in the slope direction.

Keywords: permafrost, InSAR, ALOS2, Sentinel-1, wildfire, Batagay

©2019. Japan Geoscience Union. All Right Reserved. 

# Influence of recent climate change on permafrost coast dynamics in the Kara Sea, Russian Arctic Ocean

*A. Kioka[1,2], V. S. Isaev[2], A. V. Koshurnikov[2], A. Pogorelov[2], R. M. Amangurov[2], O. Podchasov[2], D. O. Sergeev[3], S. N. Buldovich[2], D. M. Aleksyutina[4], E. A. Grishakina[5]

1. Institut für Geologie, Leopold-Franzens-Universität Innsbruck, Austria, 2. Department of Geocryology, Lomonosov Moscow State University, Russia, 3. Sergeev Institute of Environmental Geoscience, Russian Academy of Science, Russia, 4. Research Laboratory of Geoecology of the Northern Territories, Lomonosov Moscow State University, Russia, 5. Vernadsky Institute of Geochemistry and Analytical Chemistry, Russian Academy of Science, Russia

Recent years of increasing air temperature in the Arctic have known to lead a significant increase in the retreat speed of permafrost coast, which has threatened livelihoods and infrastructure along the coasts. The Kara Sea hosts more than 25% of the total length of Arctic coasts. Despite many works for more than six decades, little is known about how the Kara Sea coasts, affected by permafrost and sea-ice, may have changed through time and what the climatic and environmental drivers are. To understand the dominant climatic factors influencing the dynamic processes along the permafrost and sea-ice affected coastline, we study dynamics of permafrost coast along the Baydaratskaya Bay of Kara Sea, Western Siberia, during the rapidly retreated period 2005–2016, by handheld differential GPS mapping, satellite imagery, measurements of ground temperature and subsurface resistivity, and meteorological data. These multidisciplinary data reveal that the activity of wind-driven ocean wave during the sea ice-free (open water) days influences the magnitude of coastal retreat in the study area, while that recent temperature rise less contributes to enhancing coastal retreat during the study period. This suggests that the magnitude of wave activity over the sea ice-free days controls the quantities of the eroded sediment and the associated release of nutrient to the nearshore zone, which might result in influencing infrastructure along the permafrost coast and marine ecosystem in the proximal ocean.

Keywords: Permafrost coast, Kara Sea, Sea ice, Wind-driven ocean wave

©2019. Japan Geoscience Union. All Right Reserved. 

# Ice front variations of Heilprin Glacier in northwestern Greenland controlled by the ocean and glacier bed geometries

*Izumi Asaji[1,2], Daiki Sakakibara[3], Takuto Ando[3], Shin Sugiyama[1]

1. Institute of Low Temperature Science, Hokkaido University, 2. Graduate School of Environmental Science, Hokkaido University, 3. Arctic Research Center, Hokkaido University

The Greenland ice sheet is losing mass under the influence of increasing surface melting and ice discharge from marine-terminating outlet glaciers. Better understanding of mechanisms controlling ice dynamics of marine-terminating glaciers is crucial for predicting future mass loss from the ice sheet. However, processes controlling rapid retreat of the glaciers are not well explained. As many Greenlandic glaciers thinned recent years, ice thickness near the current front position is possibly close to the hydrostatic equilibrium condition. Therefore, we hypothesize that a possible cause of recent rapid retreat of marine-terminating glaciers is surface lowering below the flotation level (ice surface elevation at which buoyancy and gravitational forces balance). Validation of this hypothesis requires detailed ice surface and bed elevation data near the calving front.

In this study, we measured bed topography and surface elevation of Heilprin Glacier in northwestern Greenland. Heilprin Glacier has a 6 km-wide terminus, which is currently separated to three calving fronts. The front position advanced by 800 m from 1990 to 2000, and retreated by 1 km from 2000 to 2009. We measured the ocean bed topography near the one of the calving front situated in the north, using a sonar fixed on a boat from 13 to 15 August, 2018. The surface elevation change from 2001 to 2012 was analyzed by using digital elevation models generated from satellite images acquired by an optical sensor ASTER (Advanced Spaceborne Thermal Emission and Reflection Radiometer) mounted on the Terra satellite. We computed the flotation level from the bed elevation, and compared it with glacier surface elevation before and after the rapid retreat.

Near the studied glacier front, the fjord is deeper in the northern side of the glacier, and the maximum water depth in the region was 340 m. The glacier retreated by 1 km over this deepest area from 1998 to 2008. Analysis of the data showed that the glacier surface near the front in 2000 was 10 m below the flotation level, suggesting significant ice thinning prior to the rapid retreat. It is likely that the retreat of northern front of Heilprin Glacier was driven by thinning and ice flotation at the deepest area of the fjord.

Keywords: Greenland, Calving glacier, Bed topography

©2019. Japan Geoscience Union. All Right Reserved. 

# Meltwater discharge and flooding of the outlet stream of Qaanaaq Glacier, northwestern Greenland

*Ken Kondo[1,2], Daiki Sakakibara[3,2], Shungo Fukumoto[1,2], Shin Sugiyama[2]

1. Graduate School of Environmental Science, Hokkaido University, 2. Institute of Low Temperature Science, Hokkaido University, 3. Arctic Research Center, Hokkaido University

Glacial meltwater discharge is increasing in Greenalnd under recent warming climate. As a consequence, floods and damages on infrastructures are reported at outlet streams of land terminating glaciers. For instance, discharge from Qaanaaq Glacier in northwestern Greenland rapidly increased on 21 July 2015 and 2 August 2016, leading to floods of a proglacial stream and destruction of a road between a settlement and Qaanaaq Airport. To better understand the mechanisms of the flood events at Qaanaaq Glacier, we investigated meteorological conditions during the 2015 and 2016 events by using AWS operated on the ice cap at 944 m a.s.l. (SIGMA-B) (Aoki et al., 2014). We performed field measurements in the summer 2017 and 2018 to investigate melting process of Qaanaaq Glacier and the response of the outlet discharge. These data were combined with surface mass balance of Qaanaaq Glacier observed from 2012 to 2018 to analyse the cause of floods in 2015 and 2016.

Surface mass balance was significantly more negative in 2015 and 2016 as compared to the other years. Glacier wide mass balance was −0.76±0.13 m w.e. in 2014/2015 and -0.28±0.7 m w.e. in 2015/2016. Before the floods, daily mean temperature rose above 5 ˚C for 5 days in 2015 and above freezing for almost a month in 2016 at SIGMA-B. Such warm conditions caused intensive melting over the entire glacier, resulting in saturation and disappearance of snowpack from the glacier below 950 m a.s.l. In addition to large exposure of ice surface, heavy rainfall (90 mm $d^{-1}$) occurred on the date of the flood in 2016. we assume that the exposed ice surface helped immediate runoff of a large amount of rainwater. These analyses suggested the loss of snow cover played a key role in the flood events in 2015 and 2016.

We measured discharge from Qaanaaq Glacier from 21 July to 3 August 2017. Stream discharge rapidly increased on 28 July 2017, leading to a peak value of 8.11 $m^3$ $s^{-1}$. From 21 to 28 July, snowline elevation rose from 500 to 650 m a.s.l. after intensive melting. Runoff measured before the peak discharge accounted for only 60 % of the estimated total glacier melt, indicating the rest of meltwater remained in snowpack on the glacier. These data suggested snowpack was saturated with meltwater, and rapidly released water during the period of rapid melting and upglacier snowline migration. Together with data obtained by similar measurements in 2018, we conclude that saturation and disappearance of snowpack are the key to predict rapid increase in stream discharge and flooding.

Reference:
Aoki, T., S. Matoba, J. Uetake, N. Takeuchi, and H. Motoyama (2014), Field activities of the “Snow Impurity and Glacial Microbe effects on abrupt warming in the Arctic” (SIGMA) Project in Greenland in 2011-2013, Bull. Glaciol. Res., 32, 3–20.

Keywords: Glacier, Greenland, Surface mass balance, Freshwater runoff

©2019. Japan Geoscience Union. All Right Reserved. 

# Occurrence frequency of lee-side downslope winds near Siorapaluk in northwest Greenland

*Akihiro Hashimoto[1], Tetsuhide Yamasaki[2], Teruo Aoki[3,1], Masashi Niwano[1], Satoru Yamaguchi[4]

1. Meteorological Research Institute, 2. Avangnaq, 3. The Graduate School of Natural Science and Technology, Okayama University, 4. Snow and Ice Research Center, National Research Institute for Earth Science and Disaster Resilience

In early April 2018, Niwano et al. (2018) conducted the scientific traverse expedition “Snow impurity and glacial microbe effect on the abrupt warming in the Arctic (SIGMA) Traverse 2018”. The expedition crews had initially planned to depart Siorapaluk on April 2, 2018. However, their departure was delayed by four days because of strong winds and snow blocking the way. Numerical experiment showed that the strong wind had characteristics of a lee-side downslope wind (Hashimoto et al., 2018). Matoba and Yamasaki (2018) reported a sea ice outflow event and its damage to fishery along the coast of Qaanaaq (50-km southeast of Siorapaluk) in early December 2016, which was the first time experience for residents of Qaanaaq over the last 30 years. They assumed that northeasterly winds of more than 30 $ms^{-1}$ on 6-hour average dispersed sea ice from the coast, based on observation data at Qaanaaq airport.

These strong wind events seriously affected the scientific activity and residents’ living, which motivate the authors to study occurrence characteristics of strong winds in the northwest Greenland. According to observation performed during 2016-2017 and 2017-2018 winter seasons in Siorapaluk, strong winds more than 15 $ms^{-1}$ occur in several times. These winds are always from the north-northeast to the observation point, which means that these winds blow beyond the ridgeline in the north of Siorapaluk. Year-round observation in Qaanaaq shows that strong winds appear also in summer as well as in winter. Some strong wind events are found to occur simultaneously in Siorapaluk and Qaanaaq. Numerical simulations are conducted for the period from May 2017 to April 2018 by using the Japan Meteorological Agency’s non-hydrostatic model (JMA-NHM) with the 1-km horizontal resolution to reveal temporal and spatial distributions of strong winds and mechanisms causing them. Statistical features of strong winds and dynamical connections between synoptic and local wind systems will be presented in the meeting.

References

Matoba, S. and T. Yamasaki, 2018: Sea ice outflow damage to fishery in Qaanaaq, northwestern Greenland in December 2016. –Changes of the livelihood associated with social and environmental changes –. *Snow and Ice in Hokkaido*, **37**, 51-54.(in Japanese)

Niwano, M., T. Yamasaki and S. Yamaguchi, 2018: Arctic dog-sled expedition 2018, *Seppyo*, **80**, 588-592. (in Japanese)

Hashimoto, A., M. Niwano, S. Yamaguchi, T. Yamasaki and T. Aoki, 2018: Numerical simulation of lee-side downslope winds near Siorapaluk in northwest Greenland. *CAS/JSC WGNE Research Activities in Atmospheric and Oceanic Modelling*, **48**, 5.05-5.06.

Acknowledgements

This work was partly supported by the Joint Research Program of the Institute of Low Temperature Science, Hokkaido University, Japan, and JSPS KAKENHI Grant Numbers, JP15H01733, JP16H01772, and JP17K12817.

©2019. Japan Geoscience Union. All Right Reserved. 

Keywords: Greenland, lee-side downslope wind, Non-hydrostatic model

©2019. Japan Geoscience Union. All Right Reserved. 

# Impacts of clouds on the Greenland ice sheet surface melt and mass balance

*Masashi Niwano[1], Akihiro Hashimoto[1], Teruo Aoki[2]

1. Meteorological Research Institute, 2. Graduate School of Natural Science and Technology, Okayama University

Clouds have been recognized to enhance surface melt on the Greenland Ice Sheet (GrIS). However, quantitative estimates of the effects of clouds on the GrIS melt area enhancement and resultant ice-sheet-wide surface mass balance modulations are still lacking. Here we assessed the effects of clouds with the state-of-the-art regional climate model NHM-SMAP (Niwano et al., 2018), conducting a numerical sensitivity test in which clear-sky downward radiations and adiabatic atmospheric conditions were assumed, although the precipitation rate was the same as in the control all-sky simulation. By including or excluding cloud effects, we quantified time-integrated feedbacks for the first time. We found that the surface melt area extent increased by 3.1%, 0.3%, and 0.7% (of the total GrIS area) by the presence of clouds during summer (June to August) in 2012, 2013, and 2014, respectively. During the same periods, clouds reduced solar heating and thus daily runoff by 1.6, 0.8, and 1.0 Gt $day^{-1}$, respectively: clouds did not enhance the GrIS surface mass loss. In the ablation area, the presence of clouds results in a reduction of downward latent heat flux at the snow/ice surface so that much less energy is available for the surface melt, which highlights the importance of indirect effects of clouds.

References:
Niwano, M., Aoki, T., Hashimoto, A., Matoba, S., Yamaguchi, S., Tanikawa, T., Fujita, K., Tsushima, A., Iizuka, Y., Shimada, R., and Hori, M. (2018): NHM–SMAP: spatially and temporally high-resolution nonhydrostatic atmospheric model coupled with detailed snow process model for Greenland Ice Sheet. The Cryosphere, 12, 635-655, doi:10.5194/tc-12-635-2018.

Keywords: Greenland ice sheet, surface mass balance, NHM-SMAP, clouds

©2019. Japan Geoscience Union. All Right Reserved. 

[J] Poster | A (Atmospheric and Hydrospheric Sciences )：A-CG Complex & General

Thu. May 30, 2019 1:45 PM - 3:15 PM JST | Thu. May 30, 2019 4:45 AM - 6:15 AM UTC | Poster Hall International Exhibition Hall8, Makuhari Messe_4

## [A-CG37] Science in the Arctic Region

convener:NAOYA KANNA(Arctic Research Center, Hokkaido University), Masashi Niwano(Meteorological Research Institute), Tetsu Nakamura(Faculty of Environmental Earth Science, Hokkaido University), Shunsuke Tei(Arctic Research Center, Hokkaido University)

The Arctic and circumpolar region is the key area for the study of global change because the anthropogenic impact is projected to be the largest in this area due to the complicated feedback processes of the nature. A number of international and interdisciplinary research projects have been conducted for the studies on the land-atmosphere-ocean system. In order to understand the feedback processes occurring in the Arctic and to project the global warming in the future, we need to establish the intense observational network and to exchange the knowledge and information by combining the different scientific communities under the common interest of the Arctic. The objectives of this session are 1) to exchange our knowledge on the observational facts and integrated modelling and 2) to deepen our understanding on wide range of natural sciences related to the Arctic and the circumpolar region. Studies on humanities, social sciences, and interdisciplinary fields are also welcomed.

[ACG37-P01] Increasing trend of downward long-wave radiation at the surface in the winter Arctic

*Yuta Miwa[1], Toru Nozawa[2] (1.Faculty of Science, Okayama University , 2.Graduate School of Natural Science and Technology, Okayama University)

[ACG37-P02] **Climate memory of the Eurasian land process for the Arctic amplification**

*Tetsu Nakamura[1], Koji Yamazaki[1], Tomonori Sato[1], Jinro Ukita[2] (1.Faculty of Environmental Earth Science, Hokkaido University, 2.Faculty of Science , Niigata University)

[ACG37-P03] Interannual variation of summer precipitation and atmospheric water circulation over and around Alaska

*Shohei Morino[1], Tetsuya Hiyama[2], Hatsuki Fujinami[2], Hironari Kanamori[2], Masahito Ueyama[3] (1. Graduate School of Environmental Studies, Nagoya University, 2.Institute for Space-Earth Environmental Research, Nagoya University, 3.Graduate School of Life and Environmental Sciences, Osaka Prefecture University)

[ACG37-P04] Detection of a climatological short break in the polar night jet in early winter and its relation to cooling over Siberia

*Yuta Ando[1], Koji Yamazaki[2], Yoshihiro Tachibana[1], Masayo Ogi[3], Jinro Ukita[4] (1.Graduate School of Bioresources, Mie University, 2.Hokkaido University, 3.Centre for Earth Observation Science, University of Manitoba, 4.Faculty of Science, Niigata University)

[ACG37-P05] Recent breakdown of the seasonal linkage between the winter North Atlantic Oscillation/Northern Annular Mode and summer Northern Annular Mode

*Koji Yamazaki[1], Yoshihiro Tachibana[2], Masayo Ogi[1], Tetsu Nakamura[1], Kazuhiro Oshima[3] (1.Hokkaido University, 2.Mie University, 3.Institute of Environmental Sciences)

[ACG37-P06] Did an Arctic sea-ice hole cause hemispheric extreme cold winter in 2017/18?

*Keisuke Ota[1], Yoshihiro Tachibana[1], Kensuke K. Komatsu[1], Alexeev A. Vladimir[2], Cai Lei[2], Yuta Ando[1] (1.Graduate School of Bioresources, Mie University, 2.International Arctic Research Center, University of Alaska Fairbanks)

[ACG37-P07] Flood affects vegetation at plant species level to regional level: *Arctagrostis latifolia* increased one year after flooding in Indigirka lowland, northeastern Siberia

*Tomoki Morozumi[1,2], Shihong Zhong[1], Ryo Shingubara[5,1], Shunsuke Tei[2], Shinya Takano[1], Rong Fan[1,2], Yumiko Miyamoto[2], Ruslan Shakhmatov[1], Shin Nagai[3], Hideki Kobayashi[3], Rikie Suzuki[3], Trofim C Maximov[4,6], Atsuko Sugimoto[2,7] (1.Graduate School of Environmental Science, Hokkaido University, 2.Arctic Research Center, Hokkaido University, 3.Japan Agency for Marine-Earth Science and Technology, 4.Institute for Biological Problems of Cryolithozone SB RAS, 5.Graduate School of Environmental Studies, Nagoya University, 6.North Eastern Federal University, 7.Station for Arctic Research, Global Institution for Collaborative Research and Education, Hokkaido University)

[ACG37-P08] Extent and cause of an extreme flooding occurred in spring - summer 2017 over the Indigirka River lowland in Northeastern Siberia

*Shunsuke Tei[1], Tomoki Morozumi[2], Shin Nagai[3], Shinya Takano[2], Atsuko Sugimoto[1], Ryo Shingubara[4], RONG FAN[2], Alexander Fedorov[5], Trofim Maximov[6] (1.Arctic Research Center, Hokkaido University, 2.Graduate School of Environmental Science, Hokkaido University, 3.Japan Agency for Marine Earth Science and Technology, 4.Graduate School of Environmental studies, Nagoya University, 5.Melnikov Permafrost Institute, 6.North-Eastern Federal University)

[ACG37-P09] Monitoring of the light absorbing aerosols and the impact on radiation budget of atmosphere and snow

*Masahiro Hosaka[1], Hiroshi Ishimoto[1], Tomonori Tanikawa[1], Masashi Niwano[1], Kouji Adachi[1], Naga Oshima[1], Mizuo Kajino[1], Taichu Y Tanaka[1], Sumito Matoba[2] (1.Meteorological Research Institute, 2.Hokkaido University)

[ACG37-P10] Mass concertation and particle number of black carbon on glaciers in the eastern Alaskan Range, Alaska USA

*Keiko Konya[1], Takuma Miyakawa[1], Masayuki Takigawa[1], Masahiro Yamaguchi[1], Shad O'neel[2], Martin Truffer[3] (1.Japan Agency for Marine-Earth Science and Technology, 2.USGS, 3.University of Alaska, Fairbanks)

[ACG37-P11] Remote estimation of phenological shifts in phytoplankton community in the Pacific Arctic Region

*Hisatomo Waga[1], Toru Hirawake[1] (1.Hokkaido University)

[ACG37-P12] Seasonality of diatom and silicoflagellate assemblages observed in settling particles of the western Arctic Ocean

*Jonaotaro Onodera[1,2], EIJI WATANABE[2], Naomi Harada[1,2] (1.Research and Development Center for Global Change, JAMSTEC, 2.Institute of Arctic Climate and Environment Change Research, JAMSTEC)

[ACG37-P13] Iron and macronutrient distributions near the fronts of marine-terminating glaciers in Inglefield Gulf, northwestern Greenland

*NAOYA KANNA[1], Shin Sugiyama[2], Takuto Ando[1], Izumi Asaji[3,2], Yoshiki Fujishi[3,2], Jun Nishioka[2] (1.Arctic Research Center, Hokkaido University, 2.Institute of Low Temperature Science, Hokkaido University, 3.Graduate School of Environmental Science, Hokkaido University)

[ACG37-P14] Paleoenvironmental reconstruction from sediments of Bowdoin fjord, northwestern Greenland

*Takuto Ando[1], NAOYA KANNA[1], Izumi Asaji[2,3], Yoshiki Fujishi[2,3], Shin Sugiyama[1,2,3] (1.Arctic Research Center, Hokkaido University, 2.Institute of Low Temperature Science, Hokkaido University, 3.Graduate School of Environmental Science, Hokkaido University)

[ACG37-P15] A large-eddy simulation of upwelling meltwater plume at marine-terminating glacier fronts

*Yoshimasa Matsumura[1], Naoya Kanna[2], Shin Sugiyama[3,2] (1.Atmosphere and Ocean Research Institute, University of Tokyo, 2.Arctic Research Center, Hokkaido University, 3.Institute of Low Temperature Science, Hokkaido University)

---

## [ACG37-P16] Impact of observation-based snow/ice albedo with starting temperature of −2°C for surface melting effect on a global ocean simulation

*Takahiro Toyoda[1], Teruo Aoki[1,2], Masashi Niwano[1], Tomonori Tanikawa[1], Shogo Urakawa[1], Hiroyuki Tsujino[1], Hideyuki Nakano[1], Kei Sakamoto[1], Nariaki Hirose[1], Goro Yamanaka[1] (1.Meteorological Research Institute, Japan Meteorological Agency, 2.Graduate School of Natural Science and Technology, Okayama University)

# Increasing trend of downward long-wave radiation at the surface in the winter Arctic

*Yuta Miwa[1], Toru Nozawa[2]

1. Faculty of Science, Okayama University , 2. Graduate School of Natural Science and Technology, Okayama University

In recent years, observations show that warming in the Arctic is remarkable and rate of the warming after the 1950s is about twice that of the global average. This feature is called "Arctic amplification", and the Arctic warming is especially significant in autumn and winter. According to the previous studies, analysis based on the thermal energy balance on the surface suggests that the warming in the Arctic winter has the largest influence of the downward longwave radiation. On the other hand, factors that increase downward longwave radiation are not necessarily clearly shown. In this study, after analyzing the same as the previous studies, we considered the factor that causes downward longwave radiation increase in winter Arctic warming.

We used the Japanese 55-year Reanalysis (JRA-55) dataset. We analyzed the 30 winter season from 1988 to 2018, taking the average for the three months from November to January, where the influence of solar radiation can be ignored for the Arctic region north of 60 ˚N. It was found that, although it is different dataset and different period from the previous studies, increases in the downward longwave radiation has the largest influence on the surface warming. The downward longwave radiation can be divided into the following two components: clear-sky radiation and cloud radiative forcing (CRF), both of which are consistent with the trend pattern of the surface warming, and the clear-sky radiation has relatively larger influence on the surface warming than the CRF. Increase in clear-sky radiation is brought about by increase either in atmospheric water vapor or well-mixed greenhouse gases. From the diagnosis of radiative forcing due to an increase in greenhouse gas concentration, however, it is suggested that the increase in water vapor dominates. Trend pattern of the precipitable water is also consistent with that of the downward longwave radiation in the clear-sky. In addition, it is suggested that an increase in the CRF is due to that in the low-level clouds. It is also suggested that decreases in sea ice area and increases in net evaporation over the ice-retreated area may cause increases in the atmospheric water vapor and low-level clouds, but due to a problem of the JRA-55, further analysis is necessary.

Keywords: Arctic Amplification, JRA-55

©2019. Japan Geoscience Union. All Right Reserved. 

# Climate memory of the Eurasian land process for the Arctic amplification

*Tetsu Nakamura[1], Koji Yamazaki[1], Tomonori Sato[1], Jinro Ukita[2]

1. Faculty of Environmental Earth Science, Hokkaido University, 2. Faculty of Science , Niigata University

Amplified warming over the Arctic region, so called Arctic amplification (AA), and its relevance to the mid-latitude cooling in winter have recently been intensively studied. Recognizing rapid decline of the Arctic sea ice as to coincide with AA, sea ice-climate impacts have been examined in both observational and modeling studies. However, there is a serious gap between diverged simulation results among models/studies and observational evidence showing strong relevance of sea ice variation to AA signals on the interannual to decadal timescales. To fill the gap, we assume the climate memory effect of the land process that achieves amplification and recurrence of the sea ice-climate impacts. Here we designed and performed a set of general circulation model experiments that is able to extract the memory effect of land process. The memory of the northern Eurasian cooling anomalies that originally induced by sea ice loss are stored as snow amount and soil temperature. Memorized anomalies could induce the atmospheric circulation resembling the negative Arctic oscillation and amplify the Arctic warming in the later years. Estimated atmospheric circulation change due to this memory effect is comparable with that directly induced by sea ice loss. Reducing uncertainty of the land process operated in the climate models, which is expected to have large model dependency, would be a major choice to achieve the robust simulation results to evaluate sea ice-induced AA.

Keywords: Arctic amplification, Arctic sea ice retreat, Arctic Oscillation, Climate memory, land process

©2019. Japan Geoscience Union. All Right Reserved. 

# Interannual variation of summer precipitation and atmospheric water circulation over and around Alaska

*Shohei Morino[1], Tetsuya Hiyama[2], Hatsuki Fujinami[2], Hironari Kanamori[2], Masahito Ueyama[3]

1. Graduate School of Environmental Studies, Nagoya University, 2. Institute for Space-Earth Environmental Research, Nagoya University, 3. Graduate School of Life and Environmental Sciences, Osaka Prefecture University

Arctic warming is more apparent than global average. Water cycle in the region is also changing due to the climate warming. The variation of atmospheric water circulation influences terrestrial ecosystems through precipitation and soil water content. Hiyama et al. (2016) revealed the atmospheric circulation associated with the increase in summer precipitation from 2005 to 2008 in eastern Siberia. Ohta et al. (2014) indicated that increased precipitation in eastern Siberia caused waterlogging and damaged the larch forest. On the other hand, a recent observational research indicated that recent increased summer precipitation caused increase in methane emission from the black spruce forest in the interior of Alaska. Therefore, this study investigated interannual variability of summer precipitation and associated atmospheric water circulation in the interior of Alaska using ERA-Interim reanalysis data and rain gauge observation data in Fairbanks from 2003 to 2017. We extracted dry and wet years based on summer precipitation time series and then conducted composite analyses. Geopotential height and horizontal wind at 850 hPa and vertically integrated moisture flux were composited. We found that the change in low-level westerly wind and moisture flux blowing into the interior of Alaska was a primary factor to induce the interannual variation of summer precipitation in the region. This westerly moisture flux is associated with the atmospheric circulation pattern with cyclonic and anticyclonic anomalies around and over the Alaska. Moreover, the anomaly pattern is related to cyclone activity. More cyclones are detected in the region of the cyclonic anomaly, while less cyclones in the region of the anticyclonic anomaly. Sea surface temperature may partly contribute to the cyclone activity. A planetary wave might influence precipitation variability in the interior of Alaska through a teleconnection in these latitudes.

Keywords: Atmospheric water circulation, Summer precipitation, Anticyclonic anomaly, Cyclonic anomaly

©2019. Japan Geoscience Union. All Right Reserved. 

# Detection of a climatological short break in the polar night jet in early winter and its relation to cooling over Siberia

*Yuta Ando[1], Koji Yamazaki[2], Yoshihiro Tachibana[1], Masayo Ogi[3], Jinro Ukita[4]

1. Graduate School of Bioresources, Mie University, 2. Hokkaido University, 3. Centre for Earth Observation Science, University of Manitoba, 4. Faculty of Science, Niigata University

The polar night jet (PNJ) is a strong stratospheric westerly circumpolar wind in winter, and the strength of the climatological PNJ is widely recognized to increase from October through late December. We found the PNJ stops increasing temporarily during late November, when the upward propagation of Rossby waves from the troposphere increases. The upward propagation of Rossby waves, which is strongest over Siberia, is related to strengthening of the low pressure over Siberia. We suggest that longitudinally asymmetric forcing by land–sea heating contrasts caused by their different heat capacities might cause the strengthening of the low pressure.

Keywords: Stratosphere, Rossby wave, Land–sea heating contrast, Seasonal evolution

©2019. Japan Geoscience Union. All Right Reserved. 

# Deviation of WAFz100 (16 NOV–30 NOV)

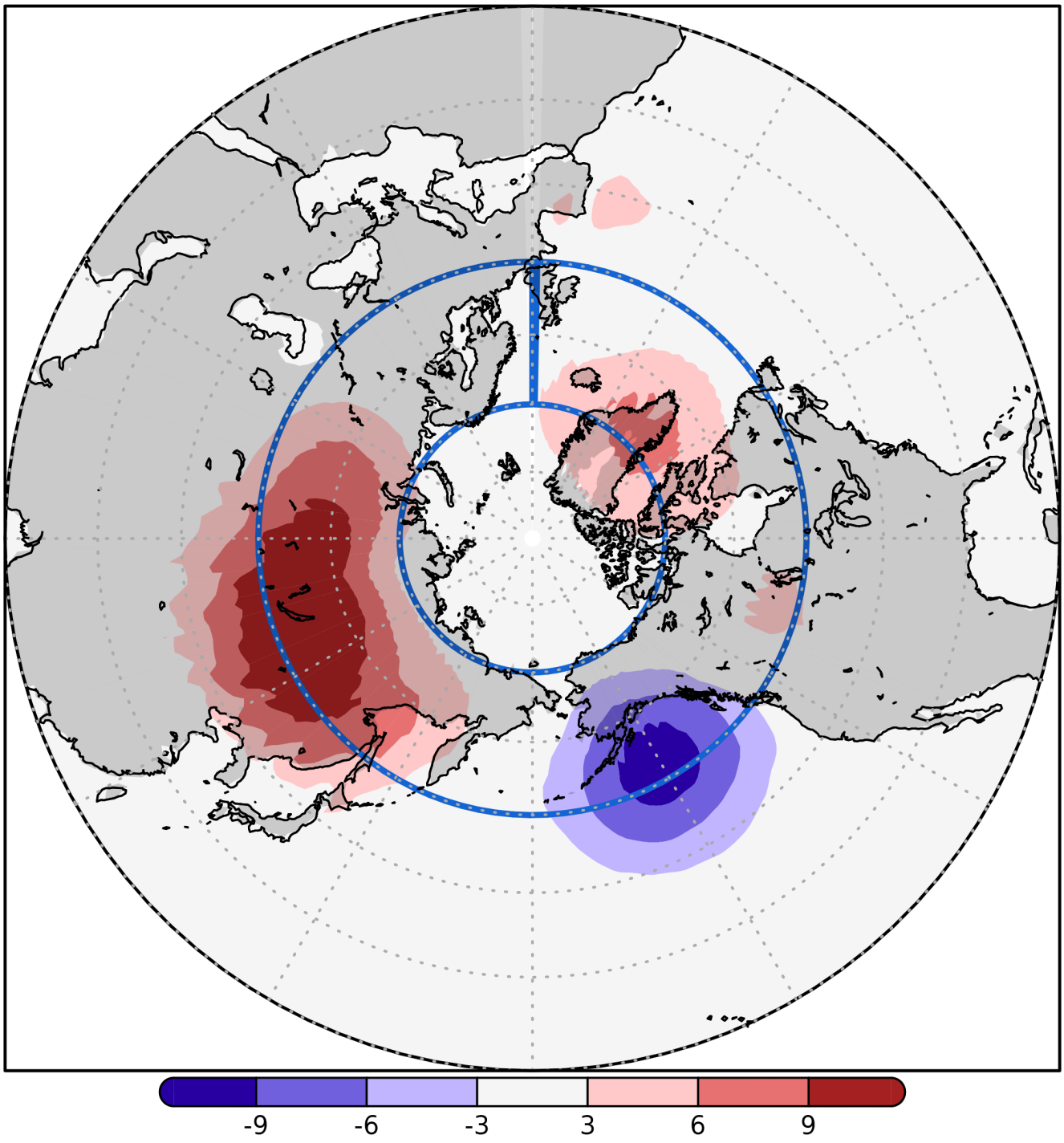


©2019. Japan Geoscience Union. All Right Reserved.

# Recent breakdown of the seasonal linkage between the winter North Atlantic Oscillation/Northern Annular Mode and summer Northern Annular Mode

*Koji Yamazaki[1], Yoshihiro Tachibana[2], Masayo Ogi[1], Tetsu Nakamura[1], Kazuhiro Oshima[3]

1. Hokkaido University, 2. Mie University, 3. Institute of Environmental Sciences

The summer Northern Annular Mode (NAM) and the winter North Atlantic Oscillation (NAO)/winter NAM have a positive correlation from the mid-1960s to the 1980s. Namely, when the winter NAO/NAM is in a positive phase, the following summer NAM tended to be a positive phase. During the period from the mid-1960s to 1980s, the NAO/NAM signals extended to the stratosphere in winter. Also, lower tropospheric warm anomaly over northern Eurasia in winter associated with the positive phase of NAO/NAM continued to spring. In summer, the annular anomalies in the temperature and 500-hPa height fields appeared and high-latitude westerly was enhanced following the winter positive NAO/NAM. However, after circa 1990, the seasonal linkage was broken, i.e., the winter-to-summer correlation became insignificant. The stratospheric signal in the winter NAO/NAM became weak and summer signals associated with the winter NAO/NAM almost disappeared. Seasonal evolutions of atmospheric circulation and sea surface temperature (SST) anomalies associated with the winter NAO are examined for early good linkage period and recent poor linkage period. We discuss the possible causes of the linkage breakdown such as stratospheric ozone, North Atlantic SST, and Atlantic multidecadal oscillation, besides chaotic internal variability in the climate system. Simulations with the Community Earth System model suggest that the ocean and/or sea ice with inter-seasonal memories possibly cause the linkage, besides large internal variability through which the linkage can take place by chance.

Keywords: North Atlantic Oscillation, Arctic Oscillation, Atlantic Multidecadal Oscillation, Ozone depletion, Arctic sea ice

©2019. Japan Geoscience Union. All Right Reserved. 

# Did an Arctic sea-ice hole cause hemispheric extreme cold winter in 2017/18?

*Keisuke Ota[1], Yoshihiro Tachibana[1], Kensuke K. Komatsu[1], Alexeev A. Vladimir[2], Cai Lei[2], Yuta Ando[1]

1. Graduate School of Bioresources, Mie University, 2. International Arctic Research Center, University of Alaska Fairbanks

While unprecedented cold weather characterized the American and Asian winter of 2017/18, the Pacific side of the Arctic experienced largely ice-free ocean, referred to as a “sea-ice hole.” The jet stream dividing cold Arctic air from warm persistently meandered northward with intrusion into the sea-ice hole. Large southward streams over Asia and America were also persistent, allowing cold air to spread there. We hypothesise that the sea-ice hole and Pacific atmospheric rivers were responsible for the cold winter, using data analyses and numerical experiments. We argue that the presence of the sea-ice hole resulted in formation of atmospheric rivers that penetrated into the Arctic with anomalous south winds toward the sea-ice hole, which led to more warm water injected into the sea-ice hole by the wind-driven current through Bering Strait. Poleward propagation of the atmospheric rivers made upper air warm, leading to their upgliding, which further heated the overlying air, causing poleward jet meanders. As a part of the response the jet meandered southward over Asia and North America, resulting in cold intrusions. This winter may be the first year when the sea-ice hole shifted the dynamics of hemispheric climate to the new state, with potential for self-sustainability.

Keywords: Chukchi Sea, Sea-ice

©2019. Japan Geoscience Union. All Right Reserved. 

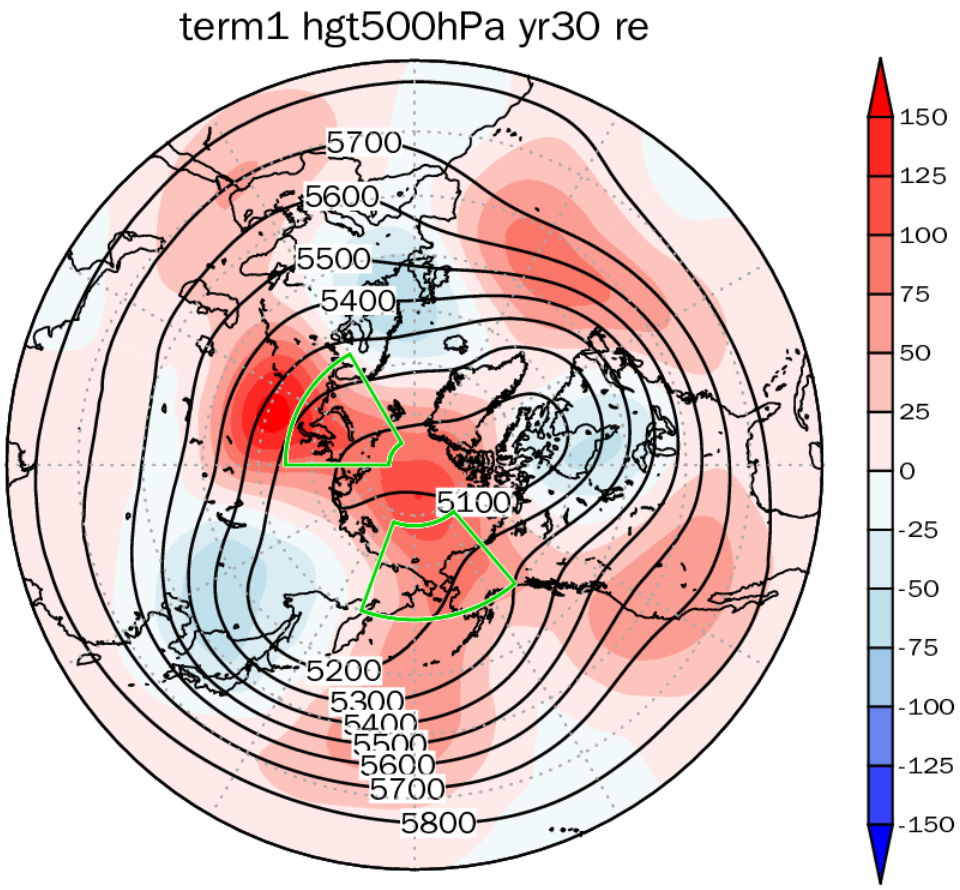


©2019. Japan Geoscience Union. All Right Reserved. 

# Flood affects vegetation at plant species level to regional level: *Arctagrostis latifolia* increased one year after flooding in Indigirka lowland, northeastern Siberia

*Tomoki Morozumi[1,2], Shihong Zhong[1], Ryo Shingubara[5,1], Shunsuke Tei[2], Shinya Takano[1], Rong Fan[1,2], Yumiko Miyamoto[2], Ruslan Shakhmatov[1], Shin Nagai[3], Hideki Kobayashi[3], Rikie Suzuki[3], Trofim C Maximov[4,6], Atsuko Sugimoto[2,7]

1. Graduate School of Environmental Science, Hokkaido University, 2. Arctic Research Center, Hokkaido University, 3. Japan Agency for Marine-Earth Science and Technology, 4. Institute for Biological Problems of Cryolithozone SB RAS, 5. Graduate School of Environmental Studies, Nagoya University, 6. North Eastern Federal University, 7. Station for Arctic Research, Global Institution for Collaborative Research and Education, Hokkaido University

In June-July 2017, unusual extensive (~10000 $km^2$) and long-time (~2 months) river floods were observed at coastal lowlands in northeastern Siberia. We focused on vegetation covered with dwarf shrub, sparse larch and polygonal wetlands, which were affected by the extreme flooding. We investigated plant species composition and in-situ phenology at site, and clarify the vegetation change after the flood in Indigirka river lowland, eastern Siberia (70°N, 148°E) for 2009-2018 July summer. We also recorded timing of leaf opening (greening) after flooding by digital time-lapse camera (GardenWatchCam, Brinno), and visible-near-infrared band satellite images (Landsat 8 OLI, USGS). In the field, forbs and graminoids (e.g. *Arctagrostis latifolia* as indicator of disturbance in arctic tundra) were increased among plots after the flood. On the other hand, dwarf shrubs (i.e. *Vaccinium vitis-idaea*) and moss species (i.e. *Hylocomium splendens*) were declined. The timing of leaf opening was delayed in the field. Fraction of leaf coverage per plot surface area were estimated from photo images. Leaf coverage on shrub were significantly smaller in 2017 summer (5.6%) than those in 2012-2016 (37%) in the plots (n=3, $p < 0.005$). Satellite images also supported that the greening of vegetation was delayed, and vegetation cover was declined in the region in 2017. Damaged moss cover and organic layers were remained to be exposed mud / bare soil in August 2018 (1 year after flood). However, leaf covers were even increased in some sedge-wetland plots, because of the increased growth of graminoids (e.g. *Arctagrostis latifolia*), forbs and sedges. Replacing to more graminoid might affect carbon and energy balances, and even might triggering permafrost thaw in some parts. Therefore, process changing and recovering from flood should be monitored in temporary and spatially multiscale.

Keywords: Vegetation, Environmental monitoring, Leaf Area, Flood, Tundra

©2019. Japan Geoscience Union. All Right Reserved. 

# Extent and cause of an extreme flooding occurred in spring - summer 2017 over the Indigirka River lowland in Northeastern Siberia

*Shunsuke Tei[1], Tomoki Morozumi[2], Shin Nagai[3], Shinya Takano[2], Atsuko Sugimoto[1], Ryo Shingubara[4], RONG FAN[2], Alexander Fedorov[5], Trofim Maximov[6]

1. Arctic Research Center, Hokkaido University, 2. Graduate School of Environmental Science, Hokkaido University, 3. Japan Agency for Marine Earth Science and Technology, 4. Graduate School of Environmental studies, Nagoya University, 5. Melnikov Permafrost Institute, 6. North-Eastern Federal University

Flooding is one of the greatest disasters that produce strong effects on the ecosystem and livelihoods of local population. It is expected that the flood frequency will increase globally making its risk assessment an urgent issue. In spring - summer (June - July) 2017, an extreme flooding occurred in the Indigirka River lowland of Northeastern Siberia that covered a large area with water. In this study, the extent and cause of the flooding were determined using the results of field observations, satellite images, and climate re-analysis datasets, and its possible effects on the ecosystem were discussed. It was found that the flooding covered a significant lowland area equal to about 9530 $km^2$ and that the rise in the relative Indigirka River water level with respect to the average value determined for the period of nine years spanning from 2009 to 2017 amounted to about 350 cm. The largest annual maximum snow depth (snow water equivalent: SWE) in the lowland was observed in 2017 over the same period (2009-2017), and the surface of the lower reach of the lowland was partially covered with snow even in the end of June due to the extreme snowfall that occurred in fall - winter 2016. The climate re-analysis dataset obtained for temporal-spatial variations in SWE, snowmelt, and runoff over the lowland during 2015-2017 revealed that a large amount of snow-melted water had flown into the river system in June 2017, resulting in the extreme flooding. The latter also waterlogged most trees over the lowland, which caused serious ecosystem devastation and changes in the material cycling in the studied region.

Keywords: extreme flooding, Indigirka River lowland, Northeastern Siberia, material cycling, water level, snowfall

©2019. Japan Geoscience Union. All Right Reserved. 

# Monitoring of the light absorbing aerosols and the impact on radiation budget of atmosphere and snow

*Masahiro Hosaka[1], Hiroshi Ishimoto[1], Tomonori Tanikawa[1], Masashi Niwano[1], Kouji Adachi[1], Naga Oshima[1], Mizuo Kajino[1], Taichu Y Tanaka[1], Sumito Matoba[2]

1. Meteorological Research Institute, 2. Hokkaido University

The cryosphere is one of the most vulnerable regions to climate change. Snow/ice rapidly melts in the Arctic region under global warming. The light absorbing aerosols (black carbon and mineral dust) contribute to it by absorbing solar radiation and heating the atmosphere, and the deposition of these aerosols reduces the snow/ice surface albedo. In addition, snow grain size tends to increase in the warmer environment, which further reduces snow surface albedo. Therefore, we started the project, entitled "Monitoring of the light absorbing aerosols and the impact on radiation budget of atmosphere and snow ice (FY2017-2021)", which is supported by Ministry of the Environment.

In this research project, we will monitor the snow impurities originating from the light absorbing aerosols, the snow grain size, and the related surface albedo variations. These are to be accomplished by ground-based measurements and satellite remote sensing with special focuses on East Asia, one of the major sources of the light absorbing aerosols, and the Arctic region most affected by them. Field observation of weather, radiation and snowpack in Japan and the Arctic regions will be continued to create longer datasets while observation sites are added. We will implement new measurements and devices for analysis. The results of the observation measured in more detail will be utilized to improve the process models as well as the remote sensing algorithm. Such improvements should allow us to create longer-term datasets (i.e., shape advancement of snow particle and snow impurity particle) by remote sensing over the entire Northern Hemisphere.

The numerical models should allow us to assess the impact of physical processes described above on global warming. We will improve the MRI-ESM (Meteorological Research Institute - Earth System Model) and a new model NHM-Chem-SMAP which is a regional atmospheric model that incorporates chemical processes and snow physical processes. We will also investigate the dynamics and the radiation absorption of light absorbing aerosols and the influence of its deposition and snow grain size on albedo.

This research project is composed of three sub-projects. The results of them in FY 2017 are the followings:

(1) Monitoring by ground-based observation measurements: We continued observation of the weather, radiation and snowpack in winter at three stations in Japan. In addition to the continuous observation of weather and radiation by the automatic weather station (AWS; Automatic Weather Station), periodic snow pit observation with snow sampling was performed. Snow impurity concentration was measured by analysis of the snow samples. We visited Qaanaaq in northwest Greenland and Ny-Alesund in the Arctic Ocean. In addition to continuously obtaining valuable observation data with maintenance, we started the sampling of aerosol in the Arctic atmosphere and carried out the observation of sea ice albedo. By introducing a sublimation device, we developed a method to directly observe and analyze snow impurities in snow samples with a microscope without melting snow. The results will be used for the improvement of the remote sensing algorithm.

©2019. Japan Geoscience Union. All Right Reserved. 

(2) Monitoring by satellite remote sensing: Shape of real snow particles and their scattering characteristics were investigated. It was confirmed that they were consistent with those of virtual particles used for the algorithm. Using Himawari 8 with high temporal-spatial resolution, we developed an algorithm to improve the detection method of snow cover and sea ice. Therefore, high accuracy monitoring in the East Asian region including Japan became possible.

(3) Evaluation by numerical models: We improved the MRI-ESM results including the black carbon representation. The radiation effects were also investigated. We also improved the aerosol expression of NHM-Chem and investigated its effect. We also succeeded in coupling NHM-Chem with SMAP, so that we can now proceed with our research using this coupled model.

Keywords: light absorbing aerosols, snow grain size, snow albedo, in situ observations, remote sensing, climate model

©2019. Japan Geoscience Union. All Right Reserved. 

# Mass concertation and particle number of black carbon on glaciers in the eastern Alaskan Range, Alaska USA

*Keiko Konya[1], Takuma Miyakawa[1], Masayuki Takigawa[1], Masahiro Yamaguchi[1], Shad O'neel[2], Martin Truffer[3]

1. Japan Agency for Marine-Earth Science and Technology, 2. USGS, 3. University of Alaska, Fairbanks

Black Carbon (BC) on snow reduces albedo lower and accelerates ablation. The Arctic demonstrates susceptibility to albedo feedbacks from non-local sources. We have estimated BC mass concentrations in snow from glacier surfaces (0-2 cm depth) and at subsurface (2-10 cm depth) in the Alaska range.
During April 2017, snow sampling was conducted on Gulkana, Black Rapids and Jarvis glaciers, which are all located within 50 km of each other. Between one and four sampling sites were selected at each glacier, at approximately 1500 m elevations. BC mass concentrations and particle size distributions was measured with a Single Particle Soot Photometer (SP2).
Measured BC mass concentrations are similar but less than previous studies. The mean value was about 6 $\mu$g/L and size distribution shows two modes around 0.3 and 0.7 $\mu$m. We have also measured the number of all aerosols by coulter counter and revealed that BC particles are about 1% of all aerosols.
We compared our measurements results to simulated BC deposition using the Weather Research and Forecasting model coupled to Chemistry (WRF-Chem). The simulated BC mass concentration agreed well with observed. We also reveaed by model result that contribution rate of biomass burning in Siberia was about 25 %. We will also estimate increase of surface melt rate caused by BC deposition.

Keywords: black carbon, snow, glacier, Arctic, Alaska, aerosol

©2019. Japan Geoscience Union. All Right Reserved. 

# Remote estimation of phenological shifts in phytoplankton community in the Pacific Arctic Region

*Hisatomo Waga[1], Toru Hirawake[1]

1. Hokkaido University

Phytoplankton blooms in the Pacific Arctic Region (PAR) has been characterized as a huge single bloom in spring when light availability is high, the mixed layer is shallow and nutrients are abundant due to winter deep mixing. However, several studies have reported that recent increases in occurrence of a relatively small but evident second bloom in fall when light availability is still relatively high and storm-driven mixing replenishes nutrients in the upper well-lit layer. Here we explored interannual variations in phytoplankton phenology in PAR by focusing on biomass and size structure of phytoplankton community based on satellite data. In this study, phenology of phytoplankton community was divided into three types based on time-series chlorophyll-*a* (chl*a*) variations using a nonlinear least squares optimization function: fall bloom (FB), flat high (FH), and flat low (FL). The simple model for FH and FL was a straight line with slope 0, and FH and FL are divided by the chl*a* threshold of 2.5 mg $m^{-3}$. The complex parameterization of the time-series chl*a* variation for FB was a Gaussian model superimposed over a background concentration of phytoplankton. During our study period of 2003–2017, FB was dominant in the middle (65–67 ˚N) and southern PAR (62–65 ˚N), and accounted for 49.1 and 66.8%, respectively. On the other hand, FL was dominant and accounted for 45.9% in the northern PAR (67–70 ˚N). The proportions of FB and FL showed significant ($p < 0.05$) increasing and decreasing trends in northern PAR (67–70 ˚N), whereas both middle and southern PAR didn’ t show any significant trend for temporal variations in these proportions. In addition, the amplitudes of FB in northern and southern PAR exhibited increasing and decreasing trends, respectively. When we compared the phytoplankton size structure during each phenology, the largest phytoplankton size structure was found in FH, followed by FB and then FL. Moreover, higher amplitude was consisted by larger phytoplankton size structure, suggesting the phytoplankton size structure during the bloom period directly influenced on the amplitude of FB. Since the phytoplankton size structure determines the sinking rate of phytoplankton, these results indicate that benthic organisms in northern and southern PAR would receive more and less fresh phytoplankton during fall. Our findings suggest that the spatiotemporal monitoring of phytoplankton community not only in spring bloom period but also after the period is important for understanding of variations in PAR, because even small changes in the phytoplankton community would have cascading effects on the higher trophic levels via the short and efficient energy pathways in this region. Overall, satellite monitoring of phytoplankton community could improve our understanding about processes of marine ecosystem variations which occurred and/or would occur in PAR.

Keywords: Arctic, Satellite, Phytoplankton

©2019. Japan Geoscience Union. All Right Reserved. 

# Seasonality of diatom and silicoflagellate assemblages observed in settling particles of the western Arctic Ocean

*Jonaotaro Onodera[1,2], EIJI WATANABE[2], Naomi Harada[1,2]

1. Research and Development Center for Global Change, JAMSTEC, 2. Institute of Arctic Climate and Environment Change Research, JAMSTEC

Under the changing hydrographic condition of Arctic Ocean, production, species composition and the phenology of phytoplankton and ice-algae assemblages has been influenced. In order to observe the relationship between changing environmental condition and siliceous phytoplankton (diatoms and silicoflagellates), settling particle samples obtained by bottom tethered moorings with sediment trap were studied in the southern Chukchi Borderland and the southwestern Canada Basin from October 2010 to September 2014 and from September 2015 to September 2017, respectively. Settling flux of diatom valves increased in summer and occasional events of shelf matter advection. Settling flux of ice algae was relatively abundant around late July-early August probably reflecting seasonal sea-ice retreat. However, ice algae and planktic diatoms did not increase in summer 2012 when oligotrophic sea-surface water covered around the mooring station. Settling fluxes of silicoflagellate skeleton increased in July (with high dominance of Stephanocha speculum commonly observed in cold waters) and November-January (with S. medianoctisol which is relatively abundant in polar ocean with sea-ice).

Keywords: Arctic Ocean, Settling particles, Diatom, Silicoflagellate

©2019. Japan Geoscience Union. All Right Reserved. 

# Iron and macronutrient distributions near the fronts of marine-terminating glaciers in Inglefield Gulf, northwestern Greenland

*NAOYA KANNA[1], Shin Sugiyama[2], Takuto Ando[1], Izumi Asaji[3,2], Yoshiki Fujishi[3,2], Jun Nishioka[2]

1. Arctic Research Center, Hokkaido University, 2. Institute of Low Temperature Science, Hokkaido University, 3. Graduate School of Environmental Science, Hokkaido University

The Greenland Ice Sheet drains freshwater into the ocean through land- and marine-terminating glaciers. Runoff from land-terminating glaciers is assumed to be iron (Fe) and silicate source to the ocean. However, influence of discharge from marine-terminating glaciers on Fe or macronutrient enrichment is poorly understood due to the difficulty of oceanographic observations in a proglacial fjord. Here we present Fe and macronutrient dataset obtained in Inglefield Gulf region of northwestern Greenland, which is fed by ~10 marine-terminating glaciers.

In the summers of 2016-18, we collected meltwater samples on Bowdoin Glacier, one of marine-terminating glaciers feeding Inglefield Gulf. Seawater was sampled in Inglefield Gulf with acid-cleaned Teflon-coated Niskin-X samplers and a Teflon coating messenger suspended on a Kevlar wire. Dissolved Fe (DFe, passes 0.2 $\mu$m acid-cleaned filters) in the seawater samplers was pre-concentrated using NOBIAS Chelate PA-1 resin (Hitachi High-Tech. Corp.). The DFe in the seawater and the glacial meltwater were analyzed with and without pre-concentration on a Graphite Furnace Atomic Absorption Spectrometer (Hitachi High-Tech. Corp.). Macronutrient in these water samplers was analyzed using an auto-analyzer (QuAAtro, BL TEC Inc.) with a continuous flow system.
Near the terminus of three marine-terminating glaciers (Melvill, Sharp, and Hart Glaciers), relatively cold (1~2°C) and fresh (as low as 28) waters were distributed in the upper 50 m. We deduce that the water masses in the upper 50 m have been modified by interaction with these glaciers, as previously reported. The DFe in the glacially modified waters ranged from 1.5 to 4.3 nmol/kg. On the Bowdoin Glacier, DFe in the meltwater ranged from 15.6 to 636 nmol/kg, with an average of 197 ±179 nmol/kg (n = 13). The glacial meltwater was significantly enriched in DFe, and thus discharge from marine-terminating glaciers is a potentially important DFe source of the glacially modified waters. The DFe:nitrate ($NO_3^-$) ratios in the glacially modified waters varied from 0.7 to 147 mmol/mol, which were notably higher than phytoplankton cellular Fe:N ratios (~0.02 mmol/mol, Sunda and Huntsman, 1995). This suggests that phytoplankton in the glacially modified waters were under Fe replete conditions in Inglefield Gulf.

Keywords: Greenland, Marine-terminating glacier, Nutrient, Iron

©2019. Japan Geoscience Union. All Right Reserved. 

# Paleoenvironmental reconstruction from sediments of Bowdoin fjord, northwestern Greenland

*Takuto Ando[1], NAOYA KANNA[1], Izumi Asaji[2,3], Yoshiki Fujishi[2,3], Shin Sugiyama[1,2,3]

1. Arctic Research Center, Hokkaido University, 2. Institute of Low Temperature Science, Hokkaido University, 3. Graduate School of Environmental Science, Hokkaido University

Evaluating impact of Arctic amplification on sea ice extent and the Greenland ice sheet is seriously important for predicting future environmental change. Calving glaciers that flow directly into the ocean are widely distributed in the north Greenland. In the ocean nearby calving glaciers, obvious seasonal variation results sea ice cover in winter and upwelling of deep water associated with the glacial meltwater in summer. Especially, freshwater plumes in summer season enhance primary production due to entrainment of nutrient-rich deep water and distribute glacial sediments in front of the glacier terminus. The present conditions of marine environment near the glacier terminus has been investigated in recent studies. However, it is necessary to reconstruct the variations in marine and depositional environments near the glacial terminus in the past for more accurate prediction of future environmental changes. In the Arctic regions, only a few researches have been performed on paleoclimate reconstruction from fjord sediments, while ice cores and lake sediment cores have often been used for the same purpose. We collected surface sediments and sediment cores from Bowdoin fjord in northwestern Greenland, which is in front of the carving glacier, in July 2018. In this presentation, we show preliminary results about sedimentation process and marine ecosystem in Bowdoin fjord, which are reconstructed from the sediments.

Keywords: Greenland, glacial sediment, biomarker, palynomorph, primary producer, sediment core

©2019. Japan Geoscience Union. All Right Reserved. 

# A large-eddy simulation of upwelling meltwater plume at marine-terminating glacier fronts

*Yoshimasa Matsumura[1], Naoya Kanna[2], Shin Sugiyama[3,2]

1. Atmosphere and Ocean Research Institute, University of Tokyo, 2. Arctic Research Center, Hokkaido University, 3. Institute of Low Temperature Science, Hokkaido University

To investigate the behavior of subglacier discharge of meltwater and its impact on the oceanic environment in Greenland fjords, large-eddy simulations of upwelling meltwater plume were performed using a three-dimensional non-hydrostatic ocean model.

The model setup was idealized based on in-situ measurements at the glacier front in the Bowdoin fjold, northwestern Greenland. The model resolution was 2.0 m horizontally and vertically and the time step interval was less than 0.1 second, which were sufficiently fine to capture the turbulent nature of upwelling plume and its high frequency disturbance recorded in the in-situ data.

The buoyancy supply caused by the underwater discharge of fresh meltwater induced immediate and strong upwelling, then the plume reached the surface with vertical momentum that radially pushed out the surface water and clearly formed semicircular structure of ~200 m adjoined to the glacier front, which was visualized by high turbidity in reality.
Since the turbulent plume entrains the saline and nutrient-rich water of Atlantic origin below thermocline, the underwater meltwater discharge acts as a pump for providing nutrients to the photic layer, that may support primary production and ecosystem in the fjold.

In the presentation, we will introduce results of sensitivity experiments with different shapes of glacier front cavity and discharge conduit, and quantitative comparison with in-situ observations will be discussed.

Keywords: meltwater discharge, large-eddy simulation

©2019. Japan Geoscience Union. All Right Reserved. 

# Impact of observation-based snow/ice albedo with starting temperature of −2˚C for surface melting effect on a global ocean simulation

*Takahiro Toyoda[1], Teruo Aoki[1,2], Masashi Niwano[1], Tomonori Tanikawa[1], Shogo Urakawa[1], Hiroyuki Tsujino[1], Hideyuki Nakano[1], Kei Sakamoto[1], Nariaki Hirose[1], Goro Yamanaka[1]

1. Meteorological Research Institute, Japan Meteorological Agency, 2. Graduate School of Natural Science and Technology, Okayama University

Based on detailed field observations, we conducted global ocean simulation experiments with modification of starting temperature for surface melting effect from −1˚C to −2˚C in the snow/ice albedo parameterization. An ensemble mean field of five experiments with the modified parameterization starting from December 1989–January 1990 were compared with the original experiment. Significance of the impact of the modification was evaluated by using the ensemble spread, which measures the internal variability.

In the Arctic Ocean, the mean albedo was reduced by up to 0.015 in June–July by the modification of the parameterization (i.e. lower albedo in the ensemble mean of the modified experiements than in the original experiment), which resulted comparably from both direct effect of the modification and indirect effect via changes of the snow and ice distributions by the albedo reduction. Snow thickness on the sea ice was reduced by up to 1.5 cm in June–July but afterward impact of the modification was diminished as the snow mostly melted away. Impact of the modification on the sea ice firstly appeared in the rim regions of the snow cover with the bare ice fraction extended and, in August–September, ice thickness decreases by 1.5 cm were achieved over most of the Arctic Ocean. On the other hand, ice thickness increases were seen in some marginal ice zones, which were attributed to reduced ocean surface circulation, such as in the Beaufort Gyre, resulting from reduced surface stresses with reduced ice cover.

In the Southern Ocean, the albedo reduction by up to 0.015 in December–January resulted from comparable contributions of the direct effect of the modification of the parameterization and the indirect effect via the snow thickness decrease, as in the Arctic Ocean. In contrast to the Arctic Ocean, the decrease impact of the snow thickness by up to 2.5 cm in the Weddell Sea partly remained through year. In addition, increases of the ice thickness were widely distributed in December–January. A detailed analysis revealed that the warming effect of the albedo reduction by the modification enhanced the reduction of the sea ice concentration, in particular that of thinner ice, which weakened the ice pressure and enhanced thicker ice formation via the rheology, leading to the increases of the ice thickness. Note that thicker ice is less affected by thermodynamical melting effect than thinner ice. This thickening impact of the sea ice remained through year in the Weddell Sea. These changes by the modification of the parameterization were robust compared with the ensemble spread.

Although the above experiments and results might be rather preliminary, we believe that our demonstration of the potential impact of the new observational insight on ocean general circulation model simulations would be of value for further enhancing both observation and modelling/prediction activities and their collaborative study.

©2019. Japan Geoscience Union. All Right Reserved. 

Keywords: snow/ice albedo, OGCM, Arctic Ocean, Southern Ocean, sea ice model

©2019. Japan Geoscience Union. All Right Reserved. 

[J] Poster | A (Atmospheric and Hydrospheric Sciences )：A-CG Complex & General

Thu. May 30, 2019 5:15 PM - 6:30 PM JST | Thu. May 30, 2019 8:15 AM - 9:30 AM UTC | Poster Hall International Exhibition Hall8, Makuhari Messe_14

## [A-CG37] Science in the Arctic Region

convener:NAOYA KANNA(Arctic Research Center, Hokkaido University), Masashi Niwano(Meteorological Research Institute), Tetsu Nakamura(Faculty of Environmental Earth Science, Hokkaido University), Shunsuke Tei(Arctic Research Center, Hokkaido University)

The Arctic and circumpolar region is the key area for the study of global change because the anthropogenic impact is projected to be the largest in this area due to the complicated feedback processes of the nature. A number of international and interdisciplinary research projects have been conducted for the studies on the land-atmosphere-ocean system. In order to understand the feedback processes occurring in the Arctic and to project the global warming in the future, we need to establish the intense observational network and to exchange the knowledge and information by combining the different scientific communities under the common interest of the Arctic. The objectives of this session are 1) to exchange our knowledge on the observational facts and integrated modelling and 2) to deepen our understanding on wide range of natural sciences related to the Arctic and the circumpolar region. Studies on humanities, social sciences, and interdisciplinary fields are also welcomed.

[ACG37-P01] Increasing trend of downward long-wave radiation at the surface in the winter Arctic

*Yuta Miwa[1], Toru Nozawa[2] (1.Faculty of Science, Okayama University , 2.Graduate School of Natural Science and Technology, Okayama University)

[ACG37-P02] **Climate memory of the Eurasian land process for the Arctic amplification**

*Tetsu Nakamura[1], Koji Yamazaki[1], Tomonori Sato[1], Jinro Ukita[2] (1.Faculty of Environmental Earth Science, Hokkaido University, 2.Faculty of Science , Niigata University)

[ACG37-P03] Interannual variation of summer precipitation and atmospheric water circulation over and around Alaska

*Shohei Morino[1], Tetsuya Hiyama[2], Hatsuki Fujinami[2], Hironari Kanamori[2], Masahito Ueyama[3] (1. Graduate School of Environmental Studies, Nagoya University, 2.Institute for Space-Earth Environmental Research, Nagoya University, 3.Graduate School of Life and Environmental Sciences, Osaka Prefecture University)

[ACG37-P04] Detection of a climatological short break in the polar night jet in early winter and its relation to cooling over Siberia

*Yuta Ando[1], Koji Yamazaki[2], Yoshihiro Tachibana[1], Masayo Ogi[3], Jinro Ukita[4] (1.Graduate School of Bioresources, Mie University, 2.Hokkaido University, 3.Centre for Earth Observation Science, University of Manitoba, 4.Faculty of Science, Niigata University)

[ACG37-P05] Recent breakdown of the seasonal linkage between the winter North Atlantic Oscillation/Northern Annular Mode and summer Northern Annular Mode

*Koji Yamazaki[1], Yoshihiro Tachibana[2], Masayo Ogi[1], Tetsu Nakamura[1], Kazuhiro Oshima[3] (1.Hokkaido University, 2.Mie University, 3.Institute of Environmental Sciences)

[ACG37-P06] Did an Arctic sea-ice hole cause hemispheric extreme cold winter in 2017/18?

*Keisuke Ota[1], Yoshihiro Tachibana[1], Kensuke K. Komatsu[1], Alexeev A. Vladimir[2], Cai Lei[2], Yuta Ando[1] (1.Graduate School of Bioresources, Mie University, 2.International Arctic Research Center, University of Alaska Fairbanks)

[ACG37-P07] Flood affects vegetation at plant species level to regional level: *Arctagrostis latifolia* increased one year after flooding in Indigirka lowland, northeastern Siberia

*Tomoki Morozumi[1,2], Shihong Zhong[1], Ryo Shingubara[5,1], Shunsuke Tei[2], Shinya Takano[1], Rong Fan[1,2], Yumiko Miyamoto[2], Ruslan Shakhmatov[1], Shin Nagai[3], Hideki Kobayashi[3], Rikie Suzuki[3], Trofim C Maximov[4,6], Atsuko Sugimoto[2,7] (1.Graduate School of Environmental Science, Hokkaido University, 2.Arctic Research Center, Hokkaido University, 3.Japan Agency for Marine-Earth Science and Technology, 4.Institute for Biological Problems of Cryolithozone SB RAS, 5.Graduate School of Environmental Studies, Nagoya University, 6.North Eastern Federal University, 7.Station for Arctic Research, Global Institution for Collaborative Research and Education, Hokkaido University)

[ACG37-P08] Extent and cause of an extreme flooding occurred in spring - summer 2017 over the Indigirka River lowland in Northeastern Siberia

*Shunsuke Tei[1], Tomoki Morozumi[2], Shin Nagai[3], Shinya Takano[2], Atsuko Sugimoto[1], Ryo Shingubara[4], RONG FAN[2], Alexander Fedorov[5], Trofim Maximov[6] (1.Arctic Research Center, Hokkaido University, 2.Graduate School of Environmental Science, Hokkaido University, 3.Japan Agency for Marine Earth Science and Technology, 4.Graduate School of Environmental studies, Nagoya University, 5.Melnikov Permafrost Institute, 6.North-Eastern Federal University)

[ACG37-P09] Monitoring of the light absorbing aerosols and the impact on radiation budget of atmosphere and snow

*Masahiro Hosaka[1], Hiroshi Ishimoto[1], Tomonori Tanikawa[1], Masashi Niwano[1], Kouji Adachi[1], Naga Oshima[1], Mizuo Kajino[1], Taichu Y Tanaka[1], Sumito Matoba[2] (1.Meteorological Research Institute, 2.Hokkaido University)

[ACG37-P10] Mass concertation and particle number of black carbon on glaciers in the eastern Alaskan Range, Alaska USA

*Keiko Konya[1], Takuma Miyakawa[1], Masayuki Takigawa[1], Masahiro Yamaguchi[1], Shad O'neel[2], Martin Truffer[3] (1.Japan Agency for Marine-Earth Science and Technology, 2.USGS, 3.University of Alaska, Fairbanks)

[ACG37-P11] Remote estimation of phenological shifts in phytoplankton community in the Pacific Arctic Region

*Hisatomo Waga[1], Toru Hirawake[1] (1.Hokkaido University)

[ACG37-P12] Seasonality of diatom and silicoflagellate assemblages observed in settling particles of the western Arctic Ocean

*Jonaotaro Onodera[1,2], EIJI WATANABE[2], Naomi Harada[1,2] (1.Research and Development Center for Global Change, JAMSTEC, 2.Institute of Arctic Climate and Environment Change Research, JAMSTEC)

[ACG37-P13] Iron and macronutrient distributions near the fronts of marine-terminating glaciers in Inglefield Gulf, northwestern Greenland

*NAOYA KANNA[1], Shin Sugiyama[2], Takuto Ando[1], Izumi Asaji[3,2], Yoshiki Fujishi[3,2], Jun Nishioka[2] (1.Arctic Research Center, Hokkaido University, 2.Institute of Low Temperature Science, Hokkaido University, 3.Graduate School of Environmental Science, Hokkaido University)

[ACG37-P14] Paleoenvironmental reconstruction from sediments of Bowdoin fjord, northwestern Greenland

*Takuto Ando[1], NAOYA KANNA[1], Izumi Asaji[2,3], Yoshiki Fujishi[2,3], Shin Sugiyama[1,2,3] (1.Arctic Research Center, Hokkaido University, 2.Institute of Low Temperature Science, Hokkaido University, 3.Graduate School of Environmental Science, Hokkaido University)

[ACG37-P15] A large-eddy simulation of upwelling meltwater plume at marine-terminating glacier fronts

*Yoshimasa Matsumura[1], Naoya Kanna[2], Shin Sugiyama[3,2] (1.Atmosphere and Ocean Research Institute, University of Tokyo, 2.Arctic Research Center, Hokkaido University, 3.Institute of Low Temperature Science, Hokkaido University)

---

## [ACG37-P16] Impact of observation-based snow/ice albedo with starting temperature of −2°C for surface melting effect on a global ocean simulation

*Takahiro Toyoda[1], Teruo Aoki[1,2], Masashi Niwano[1], Tomonori Tanikawa[1], Shogo Urakawa[1], Hiroyuki Tsujino[1], Hideyuki Nakano[1], Kei Sakamoto[1], Nariaki Hirose[1], Goro Yamanaka[1] (1.Meteorological Research Institute, Japan Meteorological Agency, 2.Graduate School of Natural Science and Technology, Okayama University)

# Increasing trend of downward long-wave radiation at the surface in the winter Arctic

*Yuta Miwa[1], Toru Nozawa[2]

1. Faculty of Science, Okayama University , 2. Graduate School of Natural Science and Technology, Okayama University

In recent years, observations show that warming in the Arctic is remarkable and rate of the warming after the 1950s is about twice that of the global average. This feature is called "Arctic amplification", and the Arctic warming is especially significant in autumn and winter. According to the previous studies, analysis based on the thermal energy balance on the surface suggests that the warming in the Arctic winter has the largest influence of the downward longwave radiation. On the other hand, factors that increase downward longwave radiation are not necessarily clearly shown. In this study, after analyzing the same as the previous studies, we considered the factor that causes downward longwave radiation increase in winter Arctic warming.

We used the Japanese 55-year Reanalysis (JRA-55) dataset. We analyzed the 30 winter season from 1988 to 2018, taking the average for the three months from November to January, where the influence of solar radiation can be ignored for the Arctic region north of 60 ˚N. It was found that, although it is different dataset and different period from the previous studies, increases in the downward longwave radiation has the largest influence on the surface warming. The downward longwave radiation can be divided into the following two components: clear-sky radiation and cloud radiative forcing (CRF), both of which are consistent with the trend pattern of the surface warming, and the clear-sky radiation has relatively larger influence on the surface warming than the CRF. Increase in clear-sky radiation is brought about by increase either in atmospheric water vapor or well-mixed greenhouse gases. From the diagnosis of radiative forcing due to an increase in greenhouse gas concentration, however, it is suggested that the increase in water vapor dominates. Trend pattern of the precipitable water is also consistent with that of the downward longwave radiation in the clear-sky. In addition, it is suggested that an increase in the CRF is due to that in the low-level clouds. It is also suggested that decreases in sea ice area and increases in net evaporation over the ice-retreated area may cause increases in the atmospheric water vapor and low-level clouds, but due to a problem of the JRA-55, further analysis is necessary.

Keywords: Arctic Amplification, JRA-55

©2019. Japan Geoscience Union. All Right Reserved. 

# Climate memory of the Eurasian land process for the Arctic amplification

*Tetsu Nakamura[1], Koji Yamazaki[1], Tomonori Sato[1], Jinro Ukita[2]

1. Faculty of Environmental Earth Science, Hokkaido University, 2. Faculty of Science , Niigata University

Amplified warming over the Arctic region, so called Arctic amplification (AA), and its relevance to the mid-latitude cooling in winter have recently been intensively studied. Recognizing rapid decline of the Arctic sea ice as to coincide with AA, sea ice-climate impacts have been examined in both observational and modeling studies. However, there is a serious gap between diverged simulation results among models/studies and observational evidence showing strong relevance of sea ice variation to AA signals on the interannual to decadal timescales. To fill the gap, we assume the climate memory effect of the land process that achieves amplification and recurrence of the sea ice-climate impacts. Here we designed and performed a set of general circulation model experiments that is able to extract the memory effect of land process. The memory of the northern Eurasian cooling anomalies that originally induced by sea ice loss are stored as snow amount and soil temperature. Memorized anomalies could induce the atmospheric circulation resembling the negative Arctic oscillation and amplify the Arctic warming in the later years. Estimated atmospheric circulation change due to this memory effect is comparable with that directly induced by sea ice loss. Reducing uncertainty of the land process operated in the climate models, which is expected to have large model dependency, would be a major choice to achieve the robust simulation results to evaluate sea ice-induced AA.

Keywords: Arctic amplification, Arctic sea ice retreat, Arctic Oscillation, Climate memory, land process

©2019. Japan Geoscience Union. All Right Reserved. 

# Interannual variation of summer precipitation and atmospheric water circulation over and around Alaska

*Shohei Morino[1], Tetsuya Hiyama[2], Hatsuki Fujinami[2], Hironari Kanamori[2], Masahito Ueyama[3]

1. Graduate School of Environmental Studies, Nagoya University, 2. Institute for Space-Earth Environmental Research, Nagoya University, 3. Graduate School of Life and Environmental Sciences, Osaka Prefecture University

Arctic warming is more apparent than global average. Water cycle in the region is also changing due to the climate warming. The variation of atmospheric water circulation influences terrestrial ecosystems through precipitation and soil water content. Hiyama et al. (2016) revealed the atmospheric circulation associated with the increase in summer precipitation from 2005 to 2008 in eastern Siberia. Ohta et al. (2014) indicated that increased precipitation in eastern Siberia caused waterlogging and damaged the larch forest. On the other hand, a recent observational research indicated that recent increased summer precipitation caused increase in methane emission from the black spruce forest in the interior of Alaska. Therefore, this study investigated interannual variability of summer precipitation and associated atmospheric water circulation in the interior of Alaska using ERA-Interim reanalysis data and rain gauge observation data in Fairbanks from 2003 to 2017. We extracted dry and wet years based on summer precipitation time series and then conducted composite analyses. Geopotential height and horizontal wind at 850 hPa and vertically integrated moisture flux were composited. We found that the change in low-level westerly wind and moisture flux blowing into the interior of Alaska was a primary factor to induce the interannual variation of summer precipitation in the region. This westerly moisture flux is associated with the atmospheric circulation pattern with cyclonic and anticyclonic anomalies around and over the Alaska. Moreover, the anomaly pattern is related to cyclone activity. More cyclones are detected in the region of the cyclonic anomaly, while less cyclones in the region of the anticyclonic anomaly. Sea surface temperature may partly contribute to the cyclone activity. A planetary wave might influence precipitation variability in the interior of Alaska through a teleconnection in these latitudes.

Keywords: Atmospheric water circulation, Summer precipitation, Anticyclonic anomaly, Cyclonic anomaly

©2019. Japan Geoscience Union. All Right Reserved. 

# Detection of a climatological short break in the polar night jet in early winter and its relation to cooling over Siberia

*Yuta Ando[1], Koji Yamazaki[2], Yoshihiro Tachibana[1], Masayo Ogi[3], Jinro Ukita[4]

1. Graduate School of Bioresources, Mie University, 2. Hokkaido University, 3. Centre for Earth Observation Science, University of Manitoba, 4. Faculty of Science, Niigata University

The polar night jet (PNJ) is a strong stratospheric westerly circumpolar wind in winter, and the strength of the climatological PNJ is widely recognized to increase from October through late December. We found the PNJ stops increasing temporarily during late November, when the upward propagation of Rossby waves from the troposphere increases. The upward propagation of Rossby waves, which is strongest over Siberia, is related to strengthening of the low pressure over Siberia. We suggest that longitudinally asymmetric forcing by land–sea heating contrasts caused by their different heat capacities might cause the strengthening of the low pressure.

Keywords: Stratosphere, Rossby wave, Land–sea heating contrast, Seasonal evolution

©2019. Japan Geoscience Union. All Right Reserved. 

# Deviation of WAFz100 (16 NOV–30 NOV)

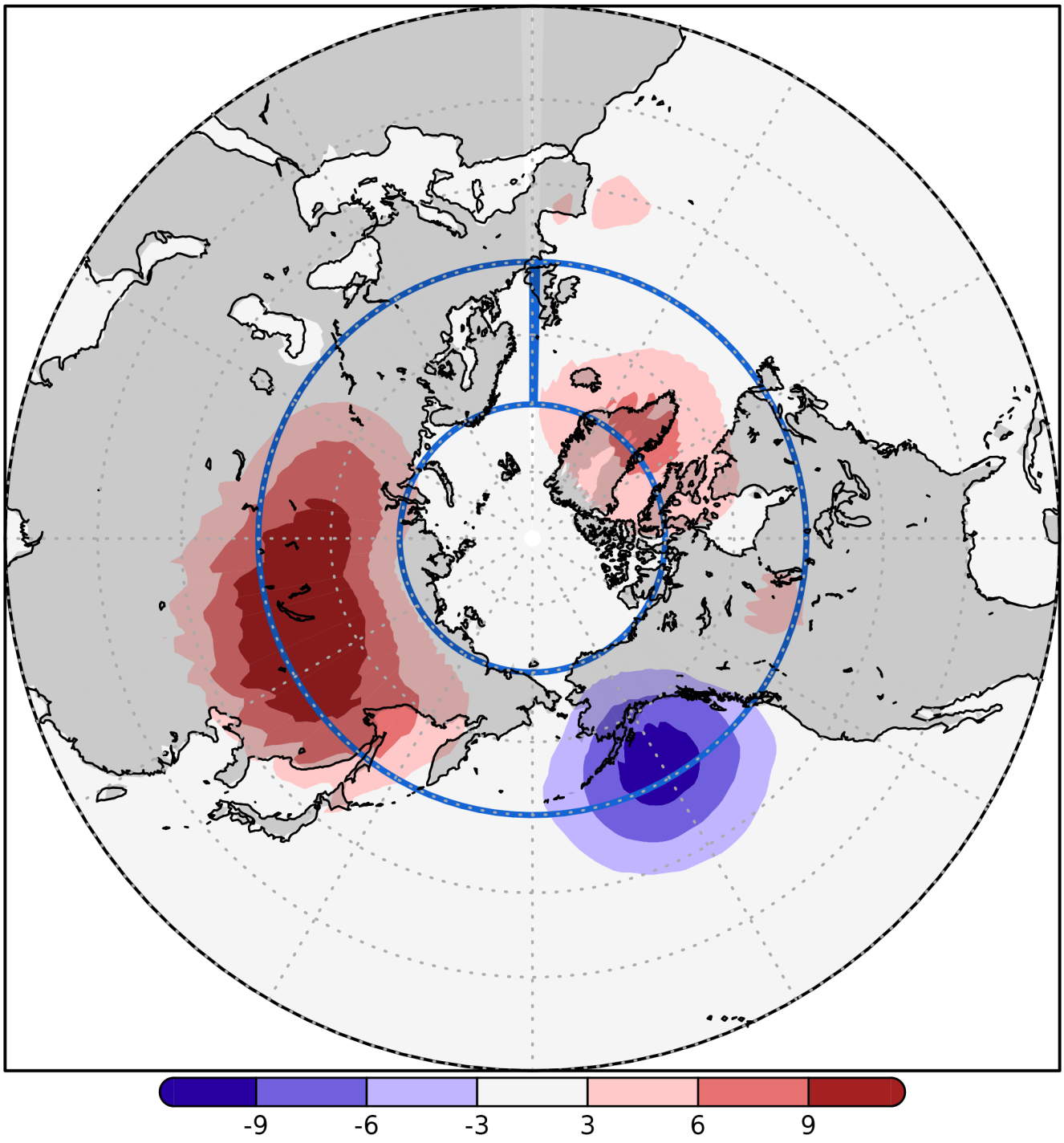


©2019. Japan Geoscience Union. All Right Reserved.

# Recent breakdown of the seasonal linkage between the winter North Atlantic Oscillation/Northern Annular Mode and summer Northern Annular Mode

*Koji Yamazaki[1], Yoshihiro Tachibana[2], Masayo Ogi[1], Tetsu Nakamura[1], Kazuhiro Oshima[3]

1. Hokkaido University, 2. Mie University, 3. Institute of Environmental Sciences

The summer Northern Annular Mode (NAM) and the winter North Atlantic Oscillation (NAO)/winter NAM have a positive correlation from the mid-1960s to the 1980s. Namely, when the winter NAO/NAM is in a positive phase, the following summer NAM tended to be a positive phase. During the period from the mid-1960s to 1980s, the NAO/NAM signals extended to the stratosphere in winter. Also, lower tropospheric warm anomaly over northern Eurasia in winter associated with the positive phase of NAO/NAM continued to spring. In summer, the annular anomalies in the temperature and 500-hPa height fields appeared and high-latitude westerly was enhanced following the winter positive NAO/NAM. However, after circa 1990, the seasonal linkage was broken, i.e., the winter-to-summer correlation became insignificant. The stratospheric signal in the winter NAO/NAM became weak and summer signals associated with the winter NAO/NAM almost disappeared. Seasonal evolutions of atmospheric circulation and sea surface temperature (SST) anomalies associated with the winter NAO are examined for early good linkage period and recent poor linkage period. We discuss the possible causes of the linkage breakdown such as stratospheric ozone, North Atlantic SST, and Atlantic multidecadal oscillation, besides chaotic internal variability in the climate system. Simulations with the Community Earth System model suggest that the ocean and/or sea ice with inter-seasonal memories possibly cause the linkage, besides large internal variability through which the linkage can take place by chance.

Keywords: North Atlantic Oscillation, Arctic Oscillation, Atlantic Multidecadal Oscillation, Ozone depletion, Arctic sea ice

©2019. Japan Geoscience Union. All Right Reserved. 

# Did an Arctic sea-ice hole cause hemispheric extreme cold winter in 2017/18?

*Keisuke Ota[1], Yoshihiro Tachibana[1], Kensuke K. Komatsu[1], Alexeev A. Vladimir[2], Cai Lei[2], Yuta Ando[1]

1. Graduate School of Bioresources, Mie University, 2. International Arctic Research Center, University of Alaska Fairbanks

While unprecedented cold weather characterized the American and Asian winter of 2017/18, the Pacific side of the Arctic experienced largely ice-free ocean, referred to as a “sea-ice hole.” The jet stream dividing cold Arctic air from warm persistently meandered northward with intrusion into the sea-ice hole. Large southward streams over Asia and America were also persistent, allowing cold air to spread there. We hypothesise that the sea-ice hole and Pacific atmospheric rivers were responsible for the cold winter, using data analyses and numerical experiments. We argue that the presence of the sea-ice hole resulted in formation of atmospheric rivers that penetrated into the Arctic with anomalous south winds toward the sea-ice hole, which led to more warm water injected into the sea-ice hole by the wind-driven current through Bering Strait. Poleward propagation of the atmospheric rivers made upper air warm, leading to their upgliding, which further heated the overlying air, causing poleward jet meanders. As a part of the response the jet meandered southward over Asia and North America, resulting in cold intrusions. This winter may be the first year when the sea-ice hole shifted the dynamics of hemispheric climate to the new state, with potential for self-sustainability.

Keywords: Chukchi Sea, Sea-ice

©2019. Japan Geoscience Union. All Right Reserved. 

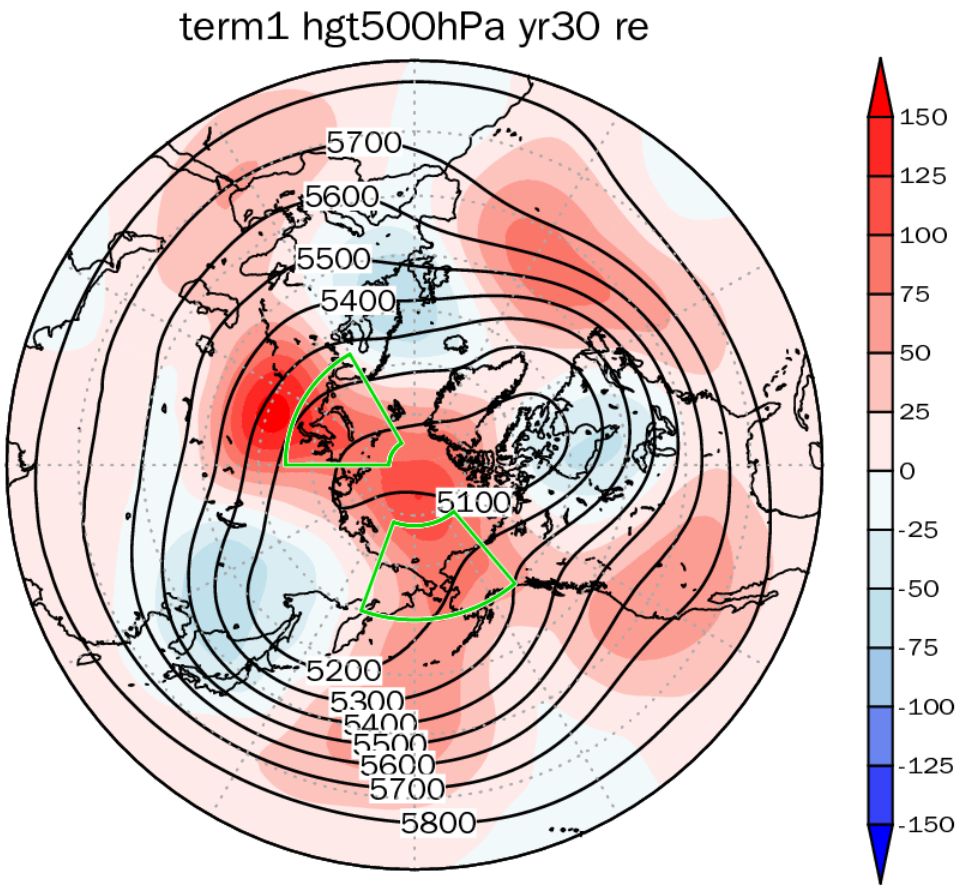


©2019. Japan Geoscience Union. All Right Reserved. 

# Flood affects vegetation at plant species level to regional level: *Arctagrostis latifolia* increased one year after flooding in Indigirka lowland, northeastern Siberia

*Tomoki Morozumi[1,2], Shihong Zhong[1], Ryo Shingubara[5,1], Shunsuke Tei[2], Shinya Takano[1], Rong Fan[1,2], Yumiko Miyamoto[2], Ruslan Shakhmatov[1], Shin Nagai[3], Hideki Kobayashi[3], Rikie Suzuki[3], Trofim C Maximov[4,6], Atsuko Sugimoto[2,7]

1. Graduate School of Environmental Science, Hokkaido University, 2. Arctic Research Center, Hokkaido University, 3. Japan Agency for Marine-Earth Science and Technology, 4. Institute for Biological Problems of Cryolithozone SB RAS, 5. Graduate School of Environmental Studies, Nagoya University, 6. North Eastern Federal University, 7. Station for Arctic Research, Global Institution for Collaborative Research and Education, Hokkaido University

In June-July 2017, unusual extensive (~10000 $km^2$) and long-time (~2 months) river floods were observed at coastal lowlands in northeastern Siberia. We focused on vegetation covered with dwarf shrub, sparse larch and polygonal wetlands, which were affected by the extreme flooding. We investigated plant species composition and in-situ phenology at site, and clarify the vegetation change after the flood in Indigirka river lowland, eastern Siberia (70°N, 148°E) for 2009-2018 July summer. We also recorded timing of leaf opening (greening) after flooding by digital time-lapse camera (GardenWatchCam, Brinno), and visible-near-infrared band satellite images (Landsat 8 OLI, USGS). In the field, forbs and graminoids (e.g. *Arctagrostis latifolia* as indicator of disturbance in arctic tundra) were increased among plots after the flood. On the other hand, dwarf shrubs (i.e. *Vaccinium vitis-idaea*) and moss species (i.e. *Hylocomium splendens*) were declined. The timing of leaf opening was delayed in the field. Fraction of leaf coverage per plot surface area were estimated from photo images. Leaf coverage on shrub were significantly smaller in 2017 summer (5.6%) than those in 2012-2016 (37%) in the plots (n=3, $p < 0.005$). Satellite images also supported that the greening of vegetation was delayed, and vegetation cover was declined in the region in 2017. Damaged moss cover and organic layers were remained to be exposed mud / bare soil in August 2018 (1 year after flood). However, leaf covers were even increased in some sedge-wetland plots, because of the increased growth of graminoids (e.g. *Arctagrostis latifolia*), forbs and sedges. Replacing to more graminoid might affect carbon and energy balances, and even might triggering permafrost thaw in some parts. Therefore, process changing and recovering from flood should be monitored in temporary and spatially multiscale.

Keywords: Vegetation, Environmental monitoring, Leaf Area, Flood, Tundra

©2019. Japan Geoscience Union. All Right Reserved. 

# Extent and cause of an extreme flooding occurred in spring - summer 2017 over the Indigirka River lowland in Northeastern Siberia

*Shunsuke Tei[1], Tomoki Morozumi[2], Shin Nagai[3], Shinya Takano[2], Atsuko Sugimoto[1], Ryo Shingubara[4], RONG FAN[2], Alexander Fedorov[5], Trofim Maximov[6]

1. Arctic Research Center, Hokkaido University, 2. Graduate School of Environmental Science, Hokkaido University, 3. Japan Agency for Marine Earth Science and Technology, 4. Graduate School of Environmental studies, Nagoya University, 5. Melnikov Permafrost Institute, 6. North-Eastern Federal University

Flooding is one of the greatest disasters that produce strong effects on the ecosystem and livelihoods of local population. It is expected that the flood frequency will increase globally making its risk assessment an urgent issue. In spring - summer (June - July) 2017, an extreme flooding occurred in the Indigirka River lowland of Northeastern Siberia that covered a large area with water. In this study, the extent and cause of the flooding were determined using the results of field observations, satellite images, and climate re-analysis datasets, and its possible effects on the ecosystem were discussed. It was found that the flooding covered a significant lowland area equal to about 9530 $km^2$ and that the rise in the relative Indigirka River water level with respect to the average value determined for the period of nine years spanning from 2009 to 2017 amounted to about 350 cm. The largest annual maximum snow depth (snow water equivalent: SWE) in the lowland was observed in 2017 over the same period (2009-2017), and the surface of the lower reach of the lowland was partially covered with snow even in the end of June due to the extreme snowfall that occurred in fall - winter 2016. The climate re-analysis dataset obtained for temporal-spatial variations in SWE, snowmelt, and runoff over the lowland during 2015-2017 revealed that a large amount of snow-melted water had flown into the river system in June 2017, resulting in the extreme flooding. The latter also waterlogged most trees over the lowland, which caused serious ecosystem devastation and changes in the material cycling in the studied region.

Keywords: extreme flooding, Indigirka River lowland, Northeastern Siberia, material cycling, water level, snowfall

©2019. Japan Geoscience Union. All Right Reserved. 

# Monitoring of the light absorbing aerosols and the impact on radiation budget of atmosphere and snow

*Masahiro Hosaka[1], Hiroshi Ishimoto[1], Tomonori Tanikawa[1], Masashi Niwano[1], Kouji Adachi[1], Naga Oshima[1], Mizuo Kajino[1], Taichu Y Tanaka[1], Sumito Matoba[2]

1. Meteorological Research Institute, 2. Hokkaido University

The cryosphere is one of the most vulnerable regions to climate change. Snow/ice rapidly melts in the Arctic region under global warming. The light absorbing aerosols (black carbon and mineral dust) contribute to it by absorbing solar radiation and heating the atmosphere, and the deposition of these aerosols reduces the snow/ice surface albedo. In addition, snow grain size tends to increase in the warmer environment, which further reduces snow surface albedo. Therefore, we started the project, entitled "Monitoring of the light absorbing aerosols and the impact on radiation budget of atmosphere and snow ice (FY2017-2021)", which is supported by Ministry of the Environment.

In this research project, we will monitor the snow impurities originating from the light absorbing aerosols, the snow grain size, and the related surface albedo variations. These are to be accomplished by ground-based measurements and satellite remote sensing with special focuses on East Asia, one of the major sources of the light absorbing aerosols, and the Arctic region most affected by them. Field observation of weather, radiation and snowpack in Japan and the Arctic regions will be continued to create longer datasets while observation sites are added. We will implement new measurements and devices for analysis. The results of the observation measured in more detail will be utilized to improve the process models as well as the remote sensing algorithm. Such improvements should allow us to create longer-term datasets (i.e., shape advancement of snow particle and snow impurity particle) by remote sensing over the entire Northern Hemisphere.

The numerical models should allow us to assess the impact of physical processes described above on global warming. We will improve the MRI-ESM (Meteorological Research Institute - Earth System Model) and a new model NHM-Chem-SMAP which is a regional atmospheric model that incorporates chemical processes and snow physical processes. We will also investigate the dynamics and the radiation absorption of light absorbing aerosols and the influence of its deposition and snow grain size on albedo.

This research project is composed of three sub-projects. The results of them in FY 2017 are the followings:

(1) Monitoring by ground-based observation measurements: We continued observation of the weather, radiation and snowpack in winter at three stations in Japan. In addition to the continuous observation of weather and radiation by the automatic weather station (AWS; Automatic Weather Station), periodic snow pit observation with snow sampling was performed. Snow impurity concentration was measured by analysis of the snow samples. We visited Qaanaaq in northwest Greenland and Ny-Alesund in the Arctic Ocean. In addition to continuously obtaining valuable observation data with maintenance, we started the sampling of aerosol in the Arctic atmosphere and carried out the observation of sea ice albedo. By introducing a sublimation device, we developed a method to directly observe and analyze snow impurities in snow samples with a microscope without melting snow. The results will be used for the improvement of the remote sensing algorithm.

©2019. Japan Geoscience Union. All Right Reserved. 

(2) Monitoring by satellite remote sensing: Shape of real snow particles and their scattering characteristics were investigated. It was confirmed that they were consistent with those of virtual particles used for the algorithm. Using Himawari 8 with high temporal-spatial resolution, we developed an algorithm to improve the detection method of snow cover and sea ice. Therefore, high accuracy monitoring in the East Asian region including Japan became possible.

(3) Evaluation by numerical models: We improved the MRI-ESM results including the black carbon representation. The radiation effects were also investigated. We also improved the aerosol expression of NHM-Chem and investigated its effect. We also succeeded in coupling NHM-Chem with SMAP, so that we can now proceed with our research using this coupled model.

Keywords: light absorbing aerosols, snow grain size, snow albedo, in situ observations, remote sensing, climate model

©2019. Japan Geoscience Union. All Right Reserved. 

# Mass concertation and particle number of black carbon on glaciers in the eastern Alaskan Range, Alaska USA

*Keiko Konya[1], Takuma Miyakawa[1], Masayuki Takigawa[1], Masahiro Yamaguchi[1], Shad O'neel[2], Martin Truffer[3]

1. Japan Agency for Marine-Earth Science and Technology, 2. USGS, 3. University of Alaska, Fairbanks

Black Carbon (BC) on snow reduces albedo lower and accelerates ablation. The Arctic demonstrates susceptibility to albedo feedbacks from non-local sources. We have estimated BC mass concentrations in snow from glacier surfaces (0-2 cm depth) and at subsurface (2-10 cm depth) in the Alaska range.
During April 2017, snow sampling was conducted on Gulkana, Black Rapids and Jarvis glaciers, which are all located within 50 km of each other. Between one and four sampling sites were selected at each glacier, at approximately 1500 m elevations. BC mass concentrations and particle size distributions was measured with a Single Particle Soot Photometer (SP2).
Measured BC mass concentrations are similar but less than previous studies. The mean value was about 6 $\mu$g/L and size distribution shows two modes around 0.3 and 0.7 $\mu$m. We have also measured the number of all aerosols by coulter counter and revealed that BC particles are about 1% of all aerosols.
We compared our measurements results to simulated BC deposition using the Weather Research and Forecasting model coupled to Chemistry (WRF-Chem). The simulated BC mass concentration agreed well with observed. We also reveaed by model result that contribution rate of biomass burning in Siberia was about 25 %. We will also estimate increase of surface melt rate caused by BC deposition.

Keywords: black carbon, snow, glacier, Arctic, Alaska, aerosol

©2019. Japan Geoscience Union. All Right Reserved. 

# Remote estimation of phenological shifts in phytoplankton community in the Pacific Arctic Region

*Hisatomo Waga[1], Toru Hirawake[1]

1. Hokkaido University

Phytoplankton blooms in the Pacific Arctic Region (PAR) has been characterized as a huge single bloom in spring when light availability is high, the mixed layer is shallow and nutrients are abundant due to winter deep mixing. However, several studies have reported that recent increases in occurrence of a relatively small but evident second bloom in fall when light availability is still relatively high and storm-driven mixing replenishes nutrients in the upper well-lit layer. Here we explored interannual variations in phytoplankton phenology in PAR by focusing on biomass and size structure of phytoplankton community based on satellite data. In this study, phenology of phytoplankton community was divided into three types based on time-series chlorophyll-*a* (chl*a*) variations using a nonlinear least squares optimization function: fall bloom (FB), flat high (FH), and flat low (FL). The simple model for FH and FL was a straight line with slope 0, and FH and FL are divided by the chl*a* threshold of 2.5 mg $m^{-3}$. The complex parameterization of the time-series chl*a* variation for FB was a Gaussian model superimposed over a background concentration of phytoplankton. During our study period of 2003–2017, FB was dominant in the middle (65–67 ˚N) and southern PAR (62–65 ˚N), and accounted for 49.1 and 66.8%, respectively. On the other hand, FL was dominant and accounted for 45.9% in the northern PAR (67–70 ˚N). The proportions of FB and FL showed significant ($p < 0.05$) increasing and decreasing trends in northern PAR (67–70 ˚N), whereas both middle and southern PAR didn’ t show any significant trend for temporal variations in these proportions. In addition, the amplitudes of FB in northern and southern PAR exhibited increasing and decreasing trends, respectively. When we compared the phytoplankton size structure during each phenology, the largest phytoplankton size structure was found in FH, followed by FB and then FL. Moreover, higher amplitude was consisted by larger phytoplankton size structure, suggesting the phytoplankton size structure during the bloom period directly influenced on the amplitude of FB. Since the phytoplankton size structure determines the sinking rate of phytoplankton, these results indicate that benthic organisms in northern and southern PAR would receive more and less fresh phytoplankton during fall. Our findings suggest that the spatiotemporal monitoring of phytoplankton community not only in spring bloom period but also after the period is important for understanding of variations in PAR, because even small changes in the phytoplankton community would have cascading effects on the higher trophic levels via the short and efficient energy pathways in this region. Overall, satellite monitoring of phytoplankton community could improve our understanding about processes of marine ecosystem variations which occurred and/or would occur in PAR.

Keywords: Arctic, Satellite, Phytoplankton

©2019. Japan Geoscience Union. All Right Reserved. 

# Seasonality of diatom and silicoflagellate assemblages observed in settling particles of the western Arctic Ocean

*Jonaotaro Onodera[1,2], EIJI WATANABE[2], Naomi Harada[1,2]

1. Research and Development Center for Global Change, JAMSTEC, 2. Institute of Arctic Climate and Environment Change Research, JAMSTEC

Under the changing hydrographic condition of Arctic Ocean, production, species composition and the phenology of phytoplankton and ice-algae assemblages has been influenced. In order to observe the relationship between changing environmental condition and siliceous phytoplankton (diatoms and silicoflagellates), settling particle samples obtained by bottom tethered moorings with sediment trap were studied in the southern Chukchi Borderland and the southwestern Canada Basin from October 2010 to September 2014 and from September 2015 to September 2017, respectively. Settling flux of diatom valves increased in summer and occasional events of shelf matter advection. Settling flux of ice algae was relatively abundant around late July-early August probably reflecting seasonal sea-ice retreat. However, ice algae and planktic diatoms did not increase in summer 2012 when oligotrophic sea-surface water covered around the mooring station. Settling fluxes of silicoflagellate skeleton increased in July (with high dominance of Stephanocha speculum commonly observed in cold waters) and November-January (with S. medianoctisol which is relatively abundant in polar ocean with sea-ice).

Keywords: Arctic Ocean, Settling particles, Diatom, Silicoflagellate

©2019. Japan Geoscience Union. All Right Reserved. 

# Iron and macronutrient distributions near the fronts of marine-terminating glaciers in Inglefield Gulf, northwestern Greenland

*NAOYA KANNA[1], Shin Sugiyama[2], Takuto Ando[1], Izumi Asaji[3,2], Yoshiki Fujishi[3,2], Jun Nishioka[2]

1. Arctic Research Center, Hokkaido University, 2. Institute of Low Temperature Science, Hokkaido University, 3. Graduate School of Environmental Science, Hokkaido University

The Greenland Ice Sheet drains freshwater into the ocean through land- and marine-terminating glaciers. Runoff from land-terminating glaciers is assumed to be iron (Fe) and silicate source to the ocean. However, influence of discharge from marine-terminating glaciers on Fe or macronutrient enrichment is poorly understood due to the difficulty of oceanographic observations in a proglacial fjord. Here we present Fe and macronutrient dataset obtained in Inglefield Gulf region of northwestern Greenland, which is fed by ~10 marine-terminating glaciers.

In the summers of 2016-18, we collected meltwater samples on Bowdoin Glacier, one of marine-terminating glaciers feeding Inglefield Gulf. Seawater was sampled in Inglefield Gulf with acid-cleaned Teflon-coated Niskin-X samplers and a Teflon coating messenger suspended on a Kevlar wire. Dissolved Fe (DFe, passes 0.2 $\mu$m acid-cleaned filters) in the seawater samplers was pre-concentrated using NOBIAS Chelate PA-1 resin (Hitachi High-Tech. Corp.). The DFe in the seawater and the glacial meltwater were analyzed with and without pre-concentration on a Graphite Furnace Atomic Absorption Spectrometer (Hitachi High-Tech. Corp.). Macronutrient in these water samplers was analyzed using an auto-analyzer (QuAAtro, BL TEC Inc.) with a continuous flow system.
Near the terminus of three marine-terminating glaciers (Melvill, Sharp, and Hart Glaciers), relatively cold (1~2°C) and fresh (as low as 28) waters were distributed in the upper 50 m. We deduce that the water masses in the upper 50 m have been modified by interaction with these glaciers, as previously reported. The DFe in the glacially modified waters ranged from 1.5 to 4.3 nmol/kg. On the Bowdoin Glacier, DFe in the meltwater ranged from 15.6 to 636 nmol/kg, with an average of 197 ±179 nmol/kg (n = 13). The glacial meltwater was significantly enriched in DFe, and thus discharge from marine-terminating glaciers is a potentially important DFe source of the glacially modified waters. The DFe:nitrate ($NO_3^-$) ratios in the glacially modified waters varied from 0.7 to 147 mmol/mol, which were notably higher than phytoplankton cellular Fe:N ratios (~0.02 mmol/mol, Sunda and Huntsman, 1995). This suggests that phytoplankton in the glacially modified waters were under Fe replete conditions in Inglefield Gulf.

Keywords: Greenland, Marine-terminating glacier, Nutrient, Iron

©2019. Japan Geoscience Union. All Right Reserved. 

# Paleoenvironmental reconstruction from sediments of Bowdoin fjord, northwestern Greenland

*Takuto Ando[1], NAOYA KANNA[1], Izumi Asaji[2,3], Yoshiki Fujishi[2,3], Shin Sugiyama[1,2,3]

1. Arctic Research Center, Hokkaido University, 2. Institute of Low Temperature Science, Hokkaido University, 3. Graduate School of Environmental Science, Hokkaido University

Evaluating impact of Arctic amplification on sea ice extent and the Greenland ice sheet is seriously important for predicting future environmental change. Calving glaciers that flow directly into the ocean are widely distributed in the north Greenland. In the ocean nearby calving glaciers, obvious seasonal variation results sea ice cover in winter and upwelling of deep water associated with the glacial meltwater in summer. Especially, freshwater plumes in summer season enhance primary production due to entrainment of nutrient-rich deep water and distribute glacial sediments in front of the glacier terminus. The present conditions of marine environment near the glacier terminus has been investigated in recent studies. However, it is necessary to reconstruct the variations in marine and depositional environments near the glacial terminus in the past for more accurate prediction of future environmental changes. In the Arctic regions, only a few researches have been performed on paleoclimate reconstruction from fjord sediments, while ice cores and lake sediment cores have often been used for the same purpose. We collected surface sediments and sediment cores from Bowdoin fjord in northwestern Greenland, which is in front of the carving glacier, in July 2018. In this presentation, we show preliminary results about sedimentation process and marine ecosystem in Bowdoin fjord, which are reconstructed from the sediments.

Keywords: Greenland, glacial sediment, biomarker, palynomorph, primary producer, sediment core

©2019. Japan Geoscience Union. All Right Reserved. 

# A large-eddy simulation of upwelling meltwater plume at marine-terminating glacier fronts

*Yoshimasa Matsumura[1], Naoya Kanna[2], Shin Sugiyama[3,2]

1. Atmosphere and Ocean Research Institute, University of Tokyo, 2. Arctic Research Center, Hokkaido University, 3. Institute of Low Temperature Science, Hokkaido University

To investigate the behavior of subglacier discharge of meltwater and its impact on the oceanic environment in Greenland fjords, large-eddy simulations of upwelling meltwater plume were performed using a three-dimensional non-hydrostatic ocean model.

The model setup was idealized based on in-situ measurements at the glacier front in the Bowdoin fjold, northwestern Greenland. The model resolution was 2.0 m horizontally and vertically and the time step interval was less than 0.1 second, which were sufficiently fine to capture the turbulent nature of upwelling plume and its high frequency disturbance recorded in the in-situ data.

The buoyancy supply caused by the underwater discharge of fresh meltwater induced immediate and strong upwelling, then the plume reached the surface with vertical momentum that radially pushed out the surface water and clearly formed semicircular structure of ~200 m adjoined to the glacier front, which was visualized by high turbidity in reality.
Since the turbulent plume entrains the saline and nutrient-rich water of Atlantic origin below thermocline, the underwater meltwater discharge acts as a pump for providing nutrients to the photic layer, that may support primary production and ecosystem in the fjold.

In the presentation, we will introduce results of sensitivity experiments with different shapes of glacier front cavity and discharge conduit, and quantitative comparison with in-situ observations will be discussed.

Keywords: meltwater discharge, large-eddy simulation

©2019. Japan Geoscience Union. All Right Reserved. 

# Impact of observation-based snow/ice albedo with starting temperature of −2˚C for surface melting effect on a global ocean simulation

*Takahiro Toyoda[1], Teruo Aoki[1,2], Masashi Niwano[1], Tomonori Tanikawa[1], Shogo Urakawa[1], Hiroyuki Tsujino[1], Hideyuki Nakano[1], Kei Sakamoto[1], Nariaki Hirose[1], Goro Yamanaka[1]

1. Meteorological Research Institute, Japan Meteorological Agency, 2. Graduate School of Natural Science and Technology, Okayama University

Based on detailed field observations, we conducted global ocean simulation experiments with modification of starting temperature for surface melting effect from −1˚C to −2˚C in the snow/ice albedo parameterization. An ensemble mean field of five experiments with the modified parameterization starting from December 1989–January 1990 were compared with the original experiment. Significance of the impact of the modification was evaluated by using the ensemble spread, which measures the internal variability.

In the Arctic Ocean, the mean albedo was reduced by up to 0.015 in June–July by the modification of the parameterization (i.e. lower albedo in the ensemble mean of the modified experiements than in the original experiment), which resulted comparably from both direct effect of the modification and indirect effect via changes of the snow and ice distributions by the albedo reduction. Snow thickness on the sea ice was reduced by up to 1.5 cm in June–July but afterward impact of the modification was diminished as the snow mostly melted away. Impact of the modification on the sea ice firstly appeared in the rim regions of the snow cover with the bare ice fraction extended and, in August–September, ice thickness decreases by 1.5 cm were achieved over most of the Arctic Ocean. On the other hand, ice thickness increases were seen in some marginal ice zones, which were attributed to reduced ocean surface circulation, such as in the Beaufort Gyre, resulting from reduced surface stresses with reduced ice cover.

In the Southern Ocean, the albedo reduction by up to 0.015 in December–January resulted from comparable contributions of the direct effect of the modification of the parameterization and the indirect effect via the snow thickness decrease, as in the Arctic Ocean. In contrast to the Arctic Ocean, the decrease impact of the snow thickness by up to 2.5 cm in the Weddell Sea partly remained through year. In addition, increases of the ice thickness were widely distributed in December–January. A detailed analysis revealed that the warming effect of the albedo reduction by the modification enhanced the reduction of the sea ice concentration, in particular that of thinner ice, which weakened the ice pressure and enhanced thicker ice formation via the rheology, leading to the increases of the ice thickness. Note that thicker ice is less affected by thermodynamical melting effect than thinner ice. This thickening impact of the sea ice remained through year in the Weddell Sea. These changes by the modification of the parameterization were robust compared with the ensemble spread.

Although the above experiments and results might be rather preliminary, we believe that our demonstration of the potential impact of the new observational insight on ocean general circulation model simulations would be of value for further enhancing both observation and modelling/prediction activities and their collaborative study.

©2019. Japan Geoscience Union. All Right Reserved. 

Keywords: snow/ice albedo, OGCM, Arctic Ocean, Southern Ocean, sea ice model

©2019. Japan Geoscience Union. All Right Reserved. 

[J] Oral | A (Atmospheric and Hydrospheric Sciences)：A-CG Complex & General

Thu. May 30, 2019 3:30 PM - 5:00 PM JST | Thu. May 30, 2019 6:30 AM - 8:00 AM UTC | 303 3F

## [A-CG37] Science in the Arctic Region

convener:NAOYA KANNA(Arctic Research Center, Hokkaido University), Masashi Niwano(Meteorological Research Institute), Tetsu Nakamura(Faculty of Environmental Earth Science, Hokkaido University), Shunsuke Tei(Arctic Research Center, Hokkaido University), Chairperson:Naoya Kanna(Arctic Research Center, Hokkaido University)

The Arctic and circumpolar region is the key area for the study of global change because the anthropogenic impact is projected to be the largest in this area due to the complicated feedback processes of the nature. A number of international and interdisciplinary research projects have been conducted for the studies on the land-atmosphere-ocean system. In order to understand the feedback processes occurring in the Arctic and to project the global warming in the future, we need to establish the intense observational network and to exchange the knowledge and information by combining the different scientific communities under the common interest of the Arctic. The objectives of this session are 1) to exchange our knowledge on the observational facts and integrated modelling and 2) to deepen our understanding on wide range of natural sciences related to the Arctic and the circumpolar region. Studies on humanities, social sciences, and interdisciplinary fields are also welcomed.

3:30 PM - 3:45 PM JST | 6:30 AM - 6:45 AM UTC

[ACG37-13] Introduction of the IASC project "T-MOSAiC"

Masaki Uchida[1], *Tetsuo Sueyoshi[1] (1.National Institute of Polar Research)

---

3:45 PM - 4:00 PM JST | 6:45 AM - 7:00 AM UTC

[ACG37-14] Estimation of ice thickness and volume in the Sea of Okhotsk using ICESat and CryoSat-2 data

*Sohey Nihashi[1], Nathan T. Kurtz[2], Takenobu Toyota[3] (1.National Institute of Technology, Tomakomai College, 2.NASA GSFC, 3.Institute of Low Temperature Science, Hokkaido University)

---

4:00 PM - 4:15 PM JST | 7:00 AM - 7:15 AM UTC

[ACG37-15] Arctic Sea Ice Changes in the DAMIP experiments using the MRI Earth System Model

*Takuro Aizawa[1], Masayoshi Ishii[2], Naga Oshima[2], Seiji Yukimoto[2], Hiroyasu Hasumi[1] (1.Atmosphere and Ocean Research Institute, The University of Tokyo, 2.Meteorological Reseaerch Institute)

---

4:15 PM - 4:30 PM JST | 7:15 AM - 7:30 AM UTC

[ACG37-16] **Oceanographic Observation in the Refreezing Warm Chukchi Sea during 2018 Mirai Cruise**

*Tsubasa Kodaira[1], Takehiko Nose[1], Takuji Waseda[1], Jun Inoue[2] (1.The University of Tokyo, 2.National Institute of Polar Research)

---

4:30 PM - 4:45 PM JST | 7:30 AM - 7:45 AM UTC

[ACG37-17] **Observed Waves in the refreezing eastern Chukchi Sea during 2018 Mirai Cruise**

*Takuji Waseda[1], Takehiko Nose[1], Tsubasa Kodaira[1], Alison Kohout[2], Johannes Gemmrich[3], Hui Shen[4], Jun Inoue[5] (1.The University of Tokyo, 2.National Institute of Water and Atmospheric Research, 3.University of Victoria, 4.Bedford Institute of Oceanography, 5.National Institute for Polar Research)

---

4:45 PM - 5:00 PM JST | 7:45 AM - 8:00 AM UTC

[ACG37-18] Mooring measurement near a marine-terminating glacier in Bowdoin Fjord in northwestern Greenland

*Yoshiki Fujishi[1,2], Yasushi Fukamachi[1,3], NAOYA KANNA[3], Shin Sugiyama[1,3] (1.Institute of Low Temperature Science, Hokkaido University, 2.Graduate School of Environmental Science, Hokkaido University , 3.Arctic Research Center, Hokkaido University)

# Introduction of the IASC project "T-MOSAiC"

Masaki Uchida[1], *Tetsuo Sueyoshi[1]

1. National Institute of Polar Research

Terrestrial Multidisciplinary distributed Observatories for the Study of Arctic Connections (T-MOSAiC) is one of the IASC (International Arctic Science Committee) projects. T-MOSAiC has been formulated as a research and synthesis project to provide an integrated, cross-disciplinary evaluation of how the changing Arctic Ocean affects terrestrial environments, from the coastal zone to the continental interior. The project will focus on connecting studies which take place throughout the Arctic and across disciplines in order to generate new findings into Arctic geosystems, ecosystems and human systems. There are key aspects to be addressed include connectivity, gradients, discontinuities, thresholds, extreme events and emergent properties, with specific questions that bridge sites and disciplines. Data sets will be available via open access repositories. T-MOSAiC will run in parallel to the ocean-based project Multidisciplinary drifting Observatory for the Study of Arctic Climate (MOSAiC), with temporal overlap in 2019-2020 and exchange of data sets such as climate observations from land and ocean stations.

Participating in T-MOSAiC has several advantages to your research. Join an international project across disciplines that targets key physical, ecological and societal issues affecting the Arctic and the world, at this critical time of rapid change and international decision-making. Contribute to fill key observational data in gaps identified by the T-MOSAiC Science Plan. Assure laboratory and project visibility at the international level. Benefit from T-MOSAiC and IASC grants for early career researchers for networking. Link with large T-MOSAiC partners such as MOSAiC (https://www.mosaic-expedition.org/), INTERACT (https://eu-interact.org/), Sentinel North (https://sentinelnorth.ulaval.ca/en), Nunataryuk (https://nunataryuk.org/) and others. Develop new collaborations, including across disciplines. Please visit the T-MOSAiC web site and get more information (https://www.t-mosaic.com/).

Keywords: Arctic, Terretrial, Observations, International Collaborative Study

©2019. Japan Geoscience Union. All Right Reserved. 

# Estimation of ice thickness and volume in the Sea of Okhotsk using ICESat and CryoSat-2 data

*Sohey Nihashi[1], Nathan T. Kurtz[2], Takenobu Toyota[3]

1. National Institute of Technology, Tomakomai College, 2. NASA GSFC, 3. Institute of Low Temperature Science, Hokkaido University

Sea-ice thickness in the Sea of Okhotsk is estimated from freeboard derived from satellite altimeter data. Ice thickness is estimated by assuming densities of sea ice, snow, and seawater based on in-situ observations (Toyota et al., 2007; Ohshima et al., 2001). Snow depth is assumed 10% of ice thickness by referring to in-situ observation (Toyota et al., 2007). Ice freeboard (thickness) derived from a laser altimeter GLAS on ICESat is used for 2004-08 (Nihashi et al., 2018). After 2011 to 2018, data from radar altimeter SIRAL-2 on CryoSat-2 is used. CryoSat-2 freeboard is obtained by a method of Kurtz et al. (2014). Comparison with ice thickness observed hourly aboard icebreaker Soya by visual observation suggests that ice thickness derived from ICESat and CryoSat-2 are almost consistent. Total ice thickness (ice thickness including snow depth) in February and March, when the sea-ice area is maximum, averaged over the entire sea-ice zone ranges from 77.5 cm (2008) to 123.0 cm (2017). The mode of total ice thickness ranges from 50-60 cm (2007; 2008; 2017) to 90-100 cm (2013). Ice volume in the Sea of Okhotsk is estimated from the total ice thickness and ice concentration derived from AMSR-E (2004-11), SSMI (2012), and AMSR2 (2013-18). Ice volume is estimated by interpolating these sea-ice datasets onto an NSIDC polar stereographic grid at a spatial resolution of about 12 km. The maximum ice volume is $8.3\times10^{11}$ $m^3$ (2016), while the minimum is $5.4\times10^{11}$ $m^3$ (2015). The interannual variability is shown to be mainly determined by the sea-ice area, although ice thickness seemed to be effective in 2008. It has been shown that the maximum sea-ice area and ice production in the Sea of Okhotsk can be explained from atmospheric and oceanographic conditions (e.g., Ohshima et al., 2006; Nakanowatari et al., 2010; Kashiwase et al., 2014). Based on these studies, we compare the ice volume with the atmospheric and oceanographic data. And then we find that the ice volume can be explained to some extent by the air temperature in the northwest and north of the sea just before the freezing season (November-December), the air temperature in the northwest of the sea during active freezing period (February-March), and the wind toward the offshore during the ice advance season (January-March). Multiple regression analysis is performed on the ice volume using these atmospheric conditions. And we try to reproduce the ice volume in the Sea of Okhotsk since the 1950s when the satellite data does not exist from the atmospheric data by using the regression line.

Keywords: Sea of Okhotsk, sea-ice thickness, satellite altimeter

©2019. Japan Geoscience Union. All Right Reserved. 

# Arctic Sea Ice Changes in the DAMIP experiments using the MRI Earth System Model

*Takuro Aizawa[1], Masayoshi Ishii[2], Naga Oshima[2], Seiji Yukimoto[2], Hiroyasu Hasumi[1]

1. Atmosphere and Ocean Reseaerch Institute, The University of Tokyo, 2. Meteorological Reseaerch Institute

Arctic sea ice decreases rapidly with a temperature rise by Arctic amplification which is caused by an increase of the greenhouse gases. According to some studies, the Arctic Ocean is projected to become ice-free Ocean in the nature future. As sea ice melts due to the effect of sensible heat, it has a close relationship with air temperature. Although the historical temperature in the Arctic is well known by the previous observational studies, the historical sea ice variability hasn’ t still understood sufficiently because of the lack of observations in pre-satellite era. Therefore, the modeling study will greatly contribute to the understanding of the Arctic climate change.

Meteorological Research Institute (MRI) has developed a new version of MRI Earth System Model (MRI-ESM2) for participating in the various Model Intercomparison Project (MIP), especially CMIP6 (Coupled Model Intercomparison Project Phase 6). We conducted the CMIP6 historical experiment (1850-2014) and the DAMIP (Detection and Attribution MIP) experiments by MRI-ESM2. The DAMIP experiments consist of hist-GHG (Well-mixed greenhouse-gas-only historical simulations), hist-aer (Anthropogenic-aerosol-only historical simulations) and hist-nat (Natural-only historical simulations). The DAMIP experiments make it possible to the clarify the impacts of anthropogenic and natural forcing on the global warming. And the experiment will be able to estimate how the sea ice variability was influenced by the external anthropogenic and the natural forcing. The decadal to multi-decadal variability of the Arctic sea ice is seen in all experiments, but each experiment indicates some characteristic changes. The hist-GHG experiment shows a strongly decrease in the sea ice extent due to the rapid increase of the greenhouse gases. The hist-aer experiment indicates an expansion in the summer sea ice extent over the period to 1980 when the concentration of sulphate aerosols is peak out, which lead to the global and Arctic cooling. But over the period from 1980 to now, the summer sea ice extent shows a decrease. The hist-nat experiment shows a weakly decrease in the summer sea ice extent over the period from 1880 to 1940, since then the summer sea ice extent remains at the same level. Thus, our simulations show the historical summer Arctic sea ice extent and the contributions of the external anthropogenic and the natural forcing to the sea ice changes.

Keywords: Arctic sea ice change, Global warming, Aerosol

©2019. Japan Geoscience Union. All Right Reserved. 

# Oceanographic Observation in the Refreezing Warm Chukchi Sea during 2018 Mirai Cruise

*Tsubasa Kodaira[1], Takehiko Nose[1], Takuji Waseda[1], Jun Inoue[2]

1. The University of Tokyo, 2. National Institute of Polar Research

In November 2018, R/V Mirai entered Chukchi Sea to conduct observations with special attention to the Marginal Ice Zone (MIZ). Based on satellite SST measurements over Chukchi Sea, it is found that Chukchi Sea has a clear warming trend in the last decade. The warm Chukchi Sea enabled R/V Mirai to conduct rare observations in November to measure the refreezing ocean. The preliminary results of the hydrographic and velocity observation are presented. The repeated measurements along an observation line toward MIZ north of Hana Shoal showed temperature and salinity changes largely over the Chukchi slope compared to the shallow shelf.

Keywords: R/V Mirai, MIZ

©2019. Japan Geoscience Union. All Right Reserved. 

# Observed Waves in the refreezing eastern Chukchi Sea during 2018 Mirai Cruise

*Takuji Waseda[1], Takehiko Nose[1], Tsubasa Kodaira[1], Alison Kohout[2], Johannes Gemmrich[3], Hui Shen[4], Jun Inoue[5]

1. The University of Tokyo, 2. National Institute of Water and Atmospheric Research, 3. University of Victoria, 4. Bedford Institute of Oceanography, 5. National Institute for Polar Research

The sea ice in the Pacific side of the Arctic Ocean starts to melt in August, retreats the most in September, and advances again in October. In November, in typical years, most of the Chukchi Sea is covered by ice. Waves generated in the open waters is largest in October. During the R/V Mirai (JAMSTEC) expedition in November 2018 (MR18–05C, PI J. Inoue), anomalously warm surface waters delayed freezing of Chukchi Sea providing a unique opportunity to observe ocean waves in the freezing period. A drifting wave buoy, ship-borne wave gauge, and satellite synthetic aperture radar data were analyzed to characterize the waves during that period. The drifting wave buoy was deployed at the edge of the Marginal Ice Zone, gradually migrated to the west, and eventually got trapped in the sea ice. During this period, the largest significant wave height observed by a buoy was 2.6 m. Once trapped in ice, the buoy-detected wave energy significantly reduced from the open water wave height detected by ship-borne wave gauge. The possible generation, decay, and propagation of waves in the ice-covered sea for on-ice and off-ice conditions will be discussed in conjunction with the obtained satellite SAR images.

Keywords: wave-ice interaction, Marginal Ice Zone, Chukchi Sea, R/V Mirai, SAR

©2019. Japan Geoscience Union. All Right Reserved. 

# Mooring measurement near a marine-terminating glacier in Bowdoin Fjord in northwestern Greenland

*Yoshiki Fujishi[1,2], Yasushi Fukamachi[1,3], NAOYA KANNA[3], Shin Sugiyama[1,3]

1. Institute of Low Temperature Science, Hokkaido University, 2. Graduate School of Environmental Science, Hokkaido University , 3. Arctic Research Center, Hokkaido University

Submarine melting of calving glaciers is considered as an important process in the mass loss of the Greenland ice sheet (Straneo et al., 2013). Moreover, freshwater runoff has been increasing in recent years and its impact on marine ecosystem is recognized. Bowdoin Glacier, a marine-terminating outlet glacier in northwestern Greenland, has experienced rapid retreat since 2008 (Sakakibara et al., 2018). However, oceanographic observations are sparse in Greenlandic fjords, especially near the calving front of glaciers. The lack of a long-term in-situ data makes it difficult to quantify submarine melting. To better understand seasonal variability in current, temperature, and salinity in this proglacial fjord, mooring measurement was performed in Bowdoin Fjord, a 20-km-long fjord in front of Bowdoin Glacier.
Two moorings were deployed in Bowdoin Fjord, one at 17 km from the glacier front (BF17) and another at approximately 1 km from the glacier front (BF01), respectively. The ocean depth was 540 m at BF17 and 186 m at BF01. The moorings were equipped with a pressure sensor (DEFI2-D50HG, JFE Advantech), thermistors (NWT-SN, Nichiyu Giken and SBE56, Seabird), current meters (INFINITY-EM, JFE Advantech) and conductivity-temperature sensors (SBE-37SM, Seabird). At BF17, a current meter and a conductivity-temperature sensor were at the depths 527 m and 530 m, respectively. A pressure sensor and seven thermistors were at 220 m and 222, 246, 268, 318, 368, 418, and 468 m, respectively. At BF01, a current meter and a conductivity-temperature sensor were at the depths of 167 m and 170 m, respectively. The instruments were operated from August 2016 to July 2018 at BF17 and from July 2017 to July 2018 at BF01.
At BF17, temperature near the bottom was lower during northward current (towards the glacier). Temperature variations corresponded well with that of salinity throughout the year, i.e. temperature increased when salinity decreased. From August to October, we observed fortnightly temperature variations suggesting the influence of tide on water exchange in the fjord. In early August, water near the bottom at BF01 flowed towards the glacier and temperature near the bottom rapidly decreased. This event occurred when the daily mean air temperature measured at Qaanaaq Airport exceeded 0 ˚C, indicating the initiation of subglacial discharge. Temperature variations near the bottom at BF01 correlated with salinity, i.e. temperature and salinity increased at similar timings. Both at BF17 and BF01, temperature variations were small in winter and spring, which we attribute to sea ice cover usually observed in Bowdoin Fjord from November to June. Our data suggested that tide plays a key role in water exchange in the fjord, whereas water property near the glacier front was strongly influenced by meltwater discharge. In the presentation, water property variations and fjord circulation are discussed with weather conditions, and the data obtained at BF17 are compared with those at BF01.

ACKNOWLEDGEMENTS
This research was funded by the Arctic research project Arctic Challenge for Sustainability (ArCS).

REFERENCE
Straneo F., et al., (2013): Challenges to understanding the dynamic response of Greenland’ s marine terminating glaciers to oceanic and atmospheric forcing. *Amer. Meteor. Soc.*, 94, 1131–1144

©2019. Japan Geoscience Union. All Right Reserved. 

Sakakibara D., et al. (2018) Ice front and flow speed variations of marine-terminating outlet glaciers along the coast of Prudhoe Land, northwestern Greenland. J. Glaciol., 64(244), 300–310

Keywords: Greenland, Fjord, Marine-terminating glacier

©2019. Japan Geoscience Union. All Right Reserved. 

[J] Oral | H (Human Geosciences )：H-DS Disaster geosciences

Thu. May 30, 2019 1:45 PM - 3:15 PM JST | Thu. May 30, 2019 4:45 AM - 6:15 AM UTC | 106 1F

## [H-DS15] Human environment and disaster risk

convener:Tatsuto Aoki(School of Regional Development Studies, Kanazawa University), Hisao Kondo(Geological Survey of Japan, National Institute of Advanced Industrial Science and Technology), Chairperson:Tatsuto Aoki(金沢大学地域創造学類)

This session discusses disaster risks being inherent in the natural and human environment, which sometimes happen to appear at a disaster, from the viewpoint of not only natural sciences but also social and human sciences. Examples of discussion subjects are as follows: uncertainty of forecasting disaster and problems of huge disaster with low frequency that raised from the 2011 Tohoku earthquake, the methodology for improving hazard maps, national recovery plans considering probable changes or sustainability of the society, international cooperation for disaster mitigation, problems of active faults or liquefaction, adjusting disaster mitigation plan to the regional characteristics, technical development for supporting disaster prevention, education for the disaster mitigation.

1:45 PM - 2:00 PM JST | 4:45 AM - 5:00 AM UTC

[HDS15-01] Influence of inhomogeneous structure in surficial reclaimed body traced by aerial photos and delineated by near surface geophysical survey at Makuhari-Kaihin Park liquefied by the 2011 off the Pacific coast of Tohoku earthquake.

*Tomio INAZAKI[1], Takanori Ogahara[1] (1.Public Works Research Institute, Tsukuba Central Institute)

2:00 PM - 2:15 PM JST | 5:00 AM - 5:15 AM UTC

[HDS15-02] Distribution morphology of deformed reclaimed valley associated with the 2018 Hokkaido Eastern Iburi Earthquake

*Takayuki Nakano[1], Satoshi Fujiwara[1], Hiroshi Une[1] (1.GSI of Japan)

2:15 PM - 2:30 PM JST | 5:15 AM - 5:30 AM UTC

[HDS15-03] Liquefaction risk evaluation using relative height data of natural levee

*Mamoru Koarai[1], Kouta Uchiyama[1], Takayuki Nakano[2] (1.Earth Science course, College of Science, Ibaraki University, 2.Geospatial Information Authority of Japan)

2:30 PM - 2:45 PM JST | 5:30 AM - 5:45 AM UTC

[HDS15-04] **Spatial Analysis of Social Vulnerability to large-scale flood: a case study on the Katsushika Ward, Tokyo**

*LIAN XIAO[1] (1.University of Tsukuba)

2:45 PM - 3:00 PM JST | 5:45 AM - 6:00 AM UTC

[HDS15-05] Importance and method of visualization of future occurrence possibilities of giant earthquakes along the Nankai trough

*Yo Fukushima[1] (1.International Research Institute of Disaster Science, Tohoku University)

3:00 PM - 3:15 PM JST | 6:00 AM - 6:15 AM UTC

[HDS15-06] Investigation of efficient tsunami evacuation using real-time disaster information

*Yusuke Oishi[1,2,3], Takashi Furumura[2], Fumihiko Imamura[3], Yoshiteru Mihara[4], Fumiyasu Makinoshima[3], Yamashita Kei[3], Takao Higashiyama[5], Tomonori Goto[5], Makoto Oomura[4], Mitsuyuki Nagayama[4] (1.Fujitsu Laboratories Ltd., 2.Earthquake Research Institute, the University of Tokyo, 3.IRIDeS, Tohoku University, 4.Kawasaki City, 5.Fujitsu Ltd.)

# Influence of inhomogeneous structure in surficial reclaimed body traced by aerial photos and delineated by near surface geophysical survey at Makuhari-Kaihin Park liquefied by the 2011 off the Pacific coast of Tohoku earthquake.

*Tomio INAZAKI[1], Takanori Ogahara[1]

1. Public Works Research Institute, Tsukuba Central Institute

We reanalyzed the comprehensive geoscientific investigation data obtained at a site where outstanding liquefaction took place just after the 2011 off the Pacific coast of Tohoku earthquake. The studied site, Makuhari-Kaihin Park, Chiba Prefecture, faces the Tokyo Bay and is situated on a reclaimed land constructed through 1973 to 1987. The field surveys were composed of high-resolution seismic surveys along two short lines, core boring at 4 points, suspension PS logging, CPTs at 7 points, and dynamic cone penetration tests. Core descriptions and detailed grain size analyses were quite helpful to discriminate man-made strata from natural layers and classify them into wet deposits, dry soils and surface cover soils. A time series of aerial photos of the site was interpreted to reconstruct the reclamation process of the site. Our interpretation is as follows; 1) Northern block was first reclaimed since 1973 and the southern block was followed since 1976. Reclamation was completed till 1987 and then the surface was covered with improved soils to form a loan park surrounded by a planted zone. The boundary between the reclamation blocks was buried in the northern part of the park. Aerial photos clearly recorded dendritic sand dunes in the southern block spread by using aligned sand pipes. Wet deposits were overlain with 1 to 2 m thick dry soils toward the offshore.
Based on the time and spatial history of the reclamation process at the site, we implemented a geoscientific interpretation of liquefaction process of the site. 1) The cover soils acted as a cap layer which controlled the mode of occurrence of the surface fissures and sand boil chains caused by liquefaction. 2) Sand dominant parts in the wet deposits first liquefied during the earthquake, and it caused segmentation of man-made strata into several fragments and differential oscillations during the earthquake. Liquefaction resulted in fluidization of fine-grained parts in the wet deposits. No trace of liquefaction was recognized in the underlying natural layers. In contrast, characteristic structure associated with liquefaction and fluidization was obvious in the wet deposits in the whole points of the site. It means that the surface fissures and sand boil chains were inappropriate to explain liquefaction process because liquefaction inherently takes place in the subsurface.

Keywords: 2011 off the Pacific Coast Tohoku Earthquake, reclaimed land, liquefaction, fluidization, near surface geophysics, aerial photo interpretation

©2019. Japan Geoscience Union. All Right Reserved. 

# Distribution morphology of deformed reclaimed valley associated with the 2018 Hokkaido Eastern Iburi Earthquake

*Takayuki Nakano[1], Satoshi Fujiwara[1], Hiroshi Une[1]

1. GSI of Japan

## 1. Introduction

In the 2018 Hokkaido Eastern Iburi Earthquake (M6.7) that occurred on September 6, 2018 (Japan Society of Erosion Control Engineering, 2018 etc.), the fluidization phenomenon of filled land caused by liquefaction etc. in reclaimed valley on Kiyota Ward, Sapporo City seriously damaged residential land and social infrastructures (Japanese Geotechnical Society and Japan Society of Civil Engineers, 2018 etc.). In order to discuss this fluidization phenomenon of reclaimed valley, it is necessary to know the reclaimed valley distribution morphology. Therefore, we disclosed the distribution morphology of the reclaimed valley created by the difference between the pseudo DEM generated from aerial photos using the SfM-MVS technique and the post-construction DEM. Also, we extracted the surface deformation in this area from SAR interferogram and compared it with reclaimed valley distribution.

## 2. Target area and study method

Reclaimed valley distribution maps were created in Kiyota Ward, Sapporo City (Kiyota site) and Atsuma Town (Atsuma site). Pre-construction DSMs were generated from 44 aerial photos of the 1960s and 1970s taken by the GSI of Japan, respectively. The DSMs were generated by using the SfM-MVS technique and the DSMs were converted to a pseudo DEM by filtering (Nakano, 2017). On the SfM analysis, we established 35 and 20 ground control points (GCPs) respectively. A 5-m grid DEM of the fundamental geospatial data was used for the post-construction DEM. The used SAR interferogram is an image by a pair of August 23, 2018 and September 6, 2018 analyzed by the GSI of Japan using the ALOS-2 data of JAXA.

## 3. Result & Discussion

We acquired the reclaimed valley distribution map more detail than the past distribution map in the Kiyota site. The reclaimed thickness at the Satozuka district where ground damage was serious in the Kiyota site was ca. 15 m at the maximum. Since the RMSE of vertical residual of GCPs on the SfM analysis was ca. 1.2 m, the value of reclaimed thickness has an error equivalent to that. Comparing this reclaimed valley distribution map with the SAR interferogram, we could identify surface deformations moving away from the satellite or non-interference areas in the reclaimed valley area. This non-interference areas correspond the serious damage areas and the surface deformations area has the potential to show the subsidence or sliding-like deformation of reclaimed valley.

In the Atsuma site, we confirmed small reclaimed valley which the thickness is less than 10 m. The RMSE of vertical residual of GCPs on the SfM analysis was ca. 0.8 m. Surface fissures in this site were discovered on site (Iiba and Nagai, 2018 etc.), and it is estimated that the sliding-like deformation of reclaimed valley occurred.

## 4. Challenges

We identified the reclaimed valley distribution morphology easily and quickly by using SfM-MVS and filtering analysis with aerial photo. Also, InSAR indicated the possibility of quickly detecting the surface deformation immediately after the disaster. However, we should be careful since the pseudo DEM created from DSM generated by the SfM analysis will have large errors when the area was forest land before construction. It is necessary to examine a more effective and prompt filtering method. Finally, I would like

©2019. Japan Geoscience Union. All Right Reserved. 

to offer my sincere sympathy to the people living in the damaged regions by the earthquake.

**Acknowledgements:** PALSAR-2 data are provided from JAXA through joint cooperative agreement between GSI and JAXA. The ownership of PALSAR-2 data belongs to JAXA.

**References:**

Iiba and Nagai (2018): Damage investigation report of the Hokkaido Eastern Iburi Earthquake (prompt report), foundation ground related.
Japanese Geotechnical Society and Japan Society of Civil Engineers (2018): Liquefaction damage by the Hokkaido Eastern Iburi Eartuquake.
Nakano (2017): Research result report of KAKENHI, 15K16288.

Keywords: The 2018 Hokkaido Eastern Iburi Earthquake, reclaimed valley, SfM-MVS, InSAR

©2019. Japan Geoscience Union. All Right Reserved. 

# Liquefaction risk evaluation using relative height data of natural levee

*Mamoru Koarai[1], Kouta Uchiyama[1], Takayuki Nakano[2]

1. Earth Science course, College of Science, Ibaraki University, 2. Geospatial Information Authority of Japan

The liquefaction risk evaluation of the natural levee has been divided in two by a border of relative height 5m in the liquefaction evaluation standard of Nakano et.al. (2015).But it is necessary to reconsider evaluation division, because almost no natural levee with over 5m relative height exists in the Naka River low land and the Tone River downstream.
In this study, land condition map, 5m grid DEM and liquefaction occurrence area by The 2011 off the Pacific coast of Tohoku Earthquake in downstream of the Tone River were overlaid by GIS. The relative height of natural levee was calculated from an elevation of the natural levee liquefaction generated and an elevation of other neighbor landform such as back marsh, coastal plain and delta.
After the liquefaction occurrence rate of the natural levee was calculated every relative height difference of the 0.5m unit, the liquefaction occurrence rate decreased suddenly between 1.5 m-2.5 m of relative height or the liquefaction occurrence rate gradually decreased over 1.5 m-2.5m of relative height. It is appropriate to establish a border of relative elevation of a natural levee by 2m or 3m.

Keywords: liquefaction hazard map, natural levee, relative height

©2019. Japan Geoscience Union. All Right Reserved. 

# Spatial Analysis of Social Vulnerability to large-scale flood: a case study on the Katsushika Ward, Tokyo

*LIAN XIAO[1]

1. University of Tsukuba

Due to global climate change, the scalability and frequency of flooding is increasing. On the other hand, population aging and family structural changes, as well as the lack of adaptation measures, accelerate vulnerability to flooding. It is necessary to reduce the vulnerability to floods and to accelerate adaptive capacity. Therefore, assessing social vulnerability to flooding disasters is an important step in reducing flooding vulnerability and accelerating resilience.

In this study, we refer to the MOVE framework (a disaster vulnerability assessment framework) and analyze social vulnerability from three perspectives: exposure to a flood, susceptibility, and resilience. We subsequently develop an index system to evaluate the social vulnerability using 14 indicators. Spatial distribution of the social vulnerability of floods in the Katsushika Ward, Tokyo, is revealed based on the collected data using the information entropy method and geographic information system (GIS).

Keywords: GIS, large-scale flood, Social Vulnerability

©2019. Japan Geoscience Union. All Right Reserved. 

# Importance and method of visualization of future occurrence possibilities of giant earthquakes along the Nankai trough

*Yo Fukushima[1]

1. International Research Institute of Disaster Science, Tohoku University

Earthquakes occur in a diverse fashon and we can only make probabilistic forecasts on their occurrence. In a future, we might be able to make deterministic forecasts for certain earthquakes, but at the current status we do not foresee a realization of such a type of forecast.

Currently, discussion on how to take countermeasures on the anticipated giant Nankai trough earthquakes based on forecast information is going on in Japan, led by a Japanese governmental working group. On the giant Nankai trough earthquakes, it has been known mainly from historic documents and seismological observations that 1) the mean recurrence interval of giant Nankai trough earthquakes is 100–150 years, 2) there are two segments, west and east of the Kii peninsula, and they tend to generate earthquakes one after another with a short time interval (within a few years) or rupture simultaneously, 3) normally there are few interplate earthquakes along the Nankai subduction.

Based on such current knowledge, the report by the governmental working group issued in December 2018 emphasizes on the case where a magnitude ~8 earthquake rupturing only one side (west or east) and another earthquake is strongly anticipated on the other side. The report also mentions the cases where a smaller earthquake (magnitude ~7) or an unusual slow slip occur, but with conservative descriptions on the countermeasures for such cases. In short, the report focuses on relatively certain and presumably impending case of what to do in case of the “half-rupture”.

While, at the standpoint of the national government, the framework of the report is appropriate, there seems to be potential motivation on local government, public organizations and private companies to make own flexible decisions depending on their circumstances. There may be cases where some anomalous geophysical phenomenon, even without an eventual occurrence of a giant earthquake, would lead to social reactions and the organizations should take some countermeasures. It seems thus useful for the organizations to understand the possibilities of anomalous natural phenomena that might lead to an earthquake (and social phenomena that follows). Event tree diagrams used in volcanology and other fields can be useful for that purpose. It would be important that experts collaborate with the stakeholders (potential users) and know their needs and opinions in developing them.

Keywords: Nankai Trough Giant Earthquakes, Earthquake Forecast

©2019. Japan Geoscience Union. All Right Reserved. 

# Investigation of efficient tsunami evacuation using real-time disaster information

*Yusuke Oishi[1,2,3], Takashi Furumura[2], Fumihiko Imamura[3], Yoshiteru Mihara[4], Fumiyasu Makinoshima[3], Yamashita Kei[3], Takao Higashiyama[5], Tomonori Goto[5], Makoto Oomura[4], Mitsuyuki Nagayama[4]

1. Fujitsu Laboratories Ltd., 2. Earthquake Research Institute, the University of Tokyo, 3. IRIDeS, Tohoku University, 4. Kawasaki City, 5. Fujitsu Ltd.

## 1. Introduction

In recent years, due to the expansion of the offshore tsunami observation network in Japan and the development of high-speed analysis techniques to utilize the observed data, it is becoming possible to transmit more detailed real-time disaster prediction information. Just after the 2011 Tohoku-Oki Earthquake occurred, while the majority of voice calls were regulated, packet communication continued to be relatively connected and smartphones played an important role in information sharing. Therefore, it is expected that real-time disaster information obtained through smartphones can realize safer evacuation in the near future. In this study, in order to evaluate the effect and the challenge of providing real-time disaster information through smartphone in tsunami evacuation, a demonstration experiment was carried out.

## 2. Tsunami evacuation demonstration experiment

In the demonstration experiment conducted in the opportunity of the Kawasaki city’ s annual tsunami evacuation drill on December 9, 2018, we set up points where passing through was not permitted due to assumed damages caused by strong shake of earthquake, e.g., building collapse, fire, liquefaction, etc., and staff members were located with panels that said “impassable”. When participants of the demonstration experiment encountered the impassable points, they posted the location of these points through a smartphone application, and the posted information was shared in real time on the application screen of other participants. The smartphone application was developed for this experiment and was distributed before the experiment. The number of participants who used the provided smartphone application was 84.

Evacuation behaviors were measured as time series data of position information by the position measurement function of smartphones. In the experiment, in order to evaluate the effect of real-time disaster information about the locations of above-mentioned impassable points on evacuation behaviors, 24 participants from the organizations conducting the demonstration experiment were divided into two groups. One of the two groups were not provided the posted information. As a result, in the group with disaster information, multiple evacuees succeeded in choosing an efficient evacuation route by reducing the number of encounters to the impassable points, and the effectiveness of the real-time disaster information was confirmed. However, when comparing the average value for each group, although the evacuation distance was slightly shorten in the group with the information, it did not lead to reduction in evacuation time, because the average walking speed was slower than the group without the information. The average walking speed that takes the standstill time into account was 4.9 km/h for the group without the real-time disaster information and was 4.7 km/h for the group with the information.

©2019. Japan Geoscience Union. All Right Reserved. 

One of the estimated factors that lower the average walking speed is the standstill time to consider evacuation routes using the smartphone application at the branching points and at the places near the impassable points, or the action to post the impossible points. In the group with the real-time disaster information, among twelve people, nine people stopped for more than 10 seconds during the evacuation action.

### 3. Future work

One of the reasons why the average evacuation speed was decreased in the group with the real-time information is that the accuracy of the posted information was rather low and the standstill time to consider evacuation route was prolonged. In the questionnaire conducted after the evacuation drill, there were multiple opinions such as "With the wrong information, there were no passible road leading to the evacuation site". Among the 74 postings about the impassable points, 40 posts (54.8% of the whole) were accurate with an error of 20 m or less. In order to realize evacuation effectively utilizing real-time disaster information, it is important to evaluate the quality of information and consider information providing means that are easy-to-understand and lead to immediate determination of the next action.

Keywords: tsunami, evacuation, smartphone application

©2019. Japan Geoscience Union. All Right Reserved. 

[J] Poster | H (Human Geosciences )：H-DS Disaster geosciences

Thu. May 30, 2019 3:30 PM - 5:00 PM JST | Thu. May 30, 2019 6:30 AM - 8:00 AM UTC | Poster Hall International Exhibition Hall8, Makuhari Messe_7

## [H-DS15] Human environment and disaster risk

convener:Tatsuto Aoki(School of Regional Development Studies, Kanazawa University), Hisao Kondo(Geological Survey of Japan, National Institute of Advanced Industrial Science and Technology)

This session discusses disaster risks being inherent in the natural and human environment, which sometimes happen to appear at a disaster, from the viewpoint of not only natural sciences but also social and human sciences. Examples of discussion subjects are as follows: uncertainty of forecasting disaster and problems of huge disaster with low frequency that raised from the 2011 Tohoku earthquake, the methodology for improving hazard maps, national recovery plans considering probable changes or sustainability of the society, international cooperation for disaster mitigation, problems of active faults or liquefaction, adjusting disaster mitigation plan to the regional characteristics, technical development for supporting disaster prevention, education for the disaster mitigation.

[HDS15-P01] Validity Verification in Typhoon Disaster Prevention Model for Typhoon Damage Reduction– GUST Wind Speed, Maximum Wind Speed -

*Woo-Sik JUNG[1], Hana Na[1] (1.Department of Atmospheric Environment Information Engineering, Atmospheric Environment Information Research Center, Inje University, Gimhae 50834, Korea)

[HDS15-P02] A Study on the Assimilation of Meteorological Data and Sea Surface Temperature Data for Improving the Accuracy of WRF Prediction during Typhoon periods on the Korean Peninsula

*Woo-Sik JUNG[1], Hana Na[1] (1.Department of Atmospheric Environment Information Engineering, Atmospheric Environment Information Research Center, Inje University, Gimhae 50834, Korea)

[HDS15-P03] Validation and application of a finite element approach on field mechanically stabilized earth walls with secondary reinforcement

*BING-RU WU[1], CHIH-HSUAN LIU[1], CHING HUNG[1] (1.National Cheng Kung University)

[HDS15-P04] **EXPERIMENTAL STUDY ON POLYUREA-COATED RC SLAB SUBJECTED TO CONTACT EXPLOSIONS**

*Minghsien Wu[1], Yingkuan Tsai[1], Chien-Hsien Liu[1], Pang-Ting Pai[1], Feng-Cheng Yang[1], Chun-Chia Huang[1] (1.Chung Cheng Institute of Technology National Defense University)

[HDS15-P05] Simulation and field investigation of scour and sediment transport after Dam removal in the mountainous creek in Central Taiwan

*Chunhung WU[1] (1.Feng Chia University)

[HDS15-P06] Examination and systematization of predispositions to floods in the Heavy Rain in July 2018

*Kanako Kimura[1], Toshihiko Sugai[2] (1.The University of Tokyo, 2.Graduate School of Frontier Sciences, the University of Tokyo)

[HDS15-P07] Expand various disaster risk information and sophisticate methods to disseminate on the Hazard Map Portal Site

*Takuya Ueshiba[1], Yumeka Fujii[1], Naoki Yoshimatsu[1], Noriyuki Takakuwa[1], Wataru Yamasaki[1], Jun Suwabe[1] (1.GSI of Japan)

[HDS15-P08] A study on evaluation formulae of the principal fault in PFDHA- In consideration of a relevance to known active faults-

*Tsuyoshi Kanda[1], Makoto Takao[1], Toshimichi Kaneto[1], Takehisa Arakawa[1] (1.Tokyo Electoric Power Company Holdings, Inc)

[HDS15-P09] Characteristics of sediment deposition distribution in debris flow disasters in caused by heavy rain in August 2014 Hiroshima, Japan

*Shoichiro Uchiyama[1], Toshihiko Sugai[2] (1.National Research Institute for Earth Science and Disaster Resilience, 2.The University of Tokyo)

[HDS15-P10] Land use change after tsunami and its problems in Kii peninsula

*Kenta Okidate[1], Tatsuto Aoki[2] (1.School of Humanities, Kanazawa University, 2.School of Regional Development Studies, Kanazawa University)

[HDS15-P11] Reconstruction of the building damages caused by the Typhoon Kathleen and analyses of their land conditions at the southern foot of the Akagi Volcano using U.S. military aerial photographs

*Masafumi Aoyama[1], Yoshiki Saito[2] (1.Faculty of Education, Gunma University, 2.Graduate Student, Gunma University)

# Validity Verification in Typhoon Disaster Prevention Model for Typhoon Damage Reduction –GUST Wind Speed, Maximum Wind Speed -

*Woo-Sik JUNG[1], Hana Na[1]

1. Department of Atmospheric Environment Information Engineering, Atmospheric Environment Information Research Center, Inje University, Gimhae 50834, Korea

In recent years, as the intensity of typhoons affecting the Korean peninsula has become stronger due to global warming resulting from climate change, studies on typhoons attacking the Korean peninsula are being increasingly carried out. Many previous studies have constructed typhoon disaster prevention models for estimating the maximum wind speed of the 3-second gust that can occur during a typhoon. In addition, such studies have enabled the establishment of foundational materials for the typhoon disaster prevention system. However, there have been few studies on the validity of the maximum possible wind speed of the 3-second gust, as estimated by the typhoon disaster prevention model. Therefore, in this study, validity analysis was carried out via verification using the observed 3-second gust values. For the verification, the GUST wind speed data from marine meteorological buoys (which serves as the basis of maximum wind speed) monitored by the Korea Meteorological Administration, and maximum instantaneous wind speed data from lighthouse observation, were used. In addition, this study compared and analyzed the 3-second gust values observed at points located within the radius of the maximum wind speed, and at points located outside the radius of the maximum wind speed during the typhoon season. The points within the radius of the maximum wind speed showed a more similar trend to the observed values than the points outside the radius. In addition, the points within the radius better simulated the maximum wind speed. Moreover, the 3-second gust values calculated by the typhoon disaster prevention model were slightly greater than the observed values at almost all points. From the viewpoint that the calculated value is the maximum possible wind speed, it is considered to provide useful information in terms of pre-disaster prevention regarding typhoon damage. As a result of comparing the wind speeds at the 10 m altitude (which were obtained from the typhoon prevention model by categorizing the Korean peninsula into inland, coastal, and island regions), with the observed values, the island region, showed the best results (due to the presence of fewest obstacles on the ground), followed by the coastal, and inland regions. This study suggests that the 3-second gust is a justified parameter to be used in the typhoon disaster prevention model. Therefore, the typhoon disaster prevention model can be efficiently applied to the typhoon disaster prevention system.

This research was supported by Basic Science Research Program through the National Research Foundation of Korea(NRF) funded by the Ministry of Education(2017R1D1A3B03036152)

Keywords: Typhoon Disaster Prevention Model, Gust, Maximum WInd Speed

©2019. Japan Geoscience Union. All Right Reserved. 

# Validity Verification in Typhoon Disaster Prevention Model for Typhoon Damage Reduction – GUST Wind Speed, Maximum Wind Speed -

Woo-Sik Jung, Hana Na

In recent years, as the intensity of typhoons affecting the Korean peninsula has become stronger due to global warming resulting from climate change, studies on typhoons attacking the Korean peninsula are being increasingly carried out. Many previous studies have constructed typhoon disaster prevention models for estimating the maximum wind speed of the 3-second gust that can occur during a typhoon. In addition, such studies have enabled the establishment of foundational materials for the typhoon disaster prevention system. However, there have been few studies on the validity of the maximum possible wind speed of the 3-second gust, as estimated by the typhoon disaster prevention model. Therefore, in this study, validity analysis was carried out via verification using the observed 3-second gust values. For the verification, the GUST wind speed data from marine meteorological buoys (which serves as the basis of maximum wind speed) monitored by the Korea Meteorological Administration, and maximum instantaneous wind speed data from lighthouse observation, were used. In addition, this study compared and analyzed the 3-second gust values observed at points located within the radius of the maximum wind speed, and at points located outside the radius of the maximum wind speed during the typhoon season. The points within the radius of the maximum wind speed showed a more similar trend to the observed values than the points outside the radius. In addition, the points within the radius better simulated the maximum wind speed. Moreover, the 3-second gust values calculated by the typhoon disaster prevention model were slightly greater than the observed values at almost all points. From the viewpoint that the calculated value is the maximum possible wind speed, it is considered to provide useful information in terms of pre-disaster prevention regarding typhoon damage. As a result of comparing the wind speeds at the 10 m altitude (which were obtained from the typhoon prevention model by categorizing the Korean peninsula into inland, coastal, and island regions), with the observed values, the island region, showed the best results (due to the presence of fewest obstacles on the ground), followed by the coastal, and inland regions. This study suggests that the 3-second gust is a justified parameter to be used in the typhoon disaster prevention model. Therefore, the typhoon disaster prevention model can be efficiently applied to the typhoon disaster prevention system.

Acknowledgement

This research was supported by Basic Science Research Program through the National Research Foundation of Korea(NRF) funded by the Ministry of Education(2017R1D1A3B03036152)

©2019. Japan Geoscience Union. All Right Reserved. 

# A Study on the Assimilation of Meteorological Data and Sea Surface Temperature Data for Improving the Accuracy of WRF Prediction during Typhoon periods on the Korean Peninsula

*Woo-Sik JUNG[1], Hana Na[1]

1. Department of Atmospheric Environment Information Engineering, Atmospheric Environment Information Research Center, Inje University, Gimhae 50834, Korea

Typhoons affecting the Korean peninsula and the surrounding regions originate in the Western Pacific Ocean. The SST around Korean peninsula are increasing at a more rapid rate than the rate of global SST. Consequently, the intensity of typhoons affecting the Korean peninsula will become stronger. Therefore, studies on the implementation of the typhoon disaster prevention system, to minimize the damage by predicting the maximum possible wind speed at the time of the influence of the typhoon, were carried out. In addition, recent studies have used the WRF model, which is useful for work-site operation and research. It is suitable for work-site operation as well as research to emulate the high-resolution data of the typhoon disaster prevention model. In this study, SST data and FDDA data were assimilated to produce the optimal WRF results. The results obtained were used as input data to the typhoon disaster prevention model, which is part of the typhoon disaster prevention system. This study selected Typhoon Bolaven (that moved north to the Yellow Sea and greatly damaged the metropolitan area in the Korean peninsula), and used WRF 3.5.1 version for data evaluation. The RDAPS numerical model data of the Korea Meteorological Administration were used as the model input data, and the OSTIA data were used as the SST data. For the FDDA data assimilation (OBS nudging), the sensitivity test was performed using the wind speed and temperature data of vertical and synoptic observations in the Korean peninsula region. As a results of time series analysis and statistical analysis, the maximum wind speed difference was about 5 m/s when the input data were applied differently. High-resolution sea surface temperature data assimilation yielded better results than the meteorological data assimilation. When the meteorological data assimilation and high-resolution sea surface temperature data assimilation were applied simultaneously, better results were obtained than under individual data assimilation cases. If the maximum possible wind speed of the 3-second gust that can occur during a typhoon is estimated using the optimal high-resolution results, the damage due to the typhoon will be effectively reduced through accurate prediction.

This research was supported by Basic Science Research Program through the National Research Foundation of Korea(NRF) funded by the Ministry of Education(2017R1D1A3B03036152)

Keywords: WRF, Typhoon, SST

©2019. Japan Geoscience Union. All Right Reserved. 

# A Study on the Assimilation of Meteorological Data and Sea Surface Temperature Data for Improving the Accuracy of WRF Prediction during Typhoon periods on the Korean Peninsula

Woo-Sik Jung, Hana Na

Typhoons affecting the Korean peninsula and the surrounding regions originate in the Western Pacific Ocean. The SST around Korean peninsula are increasing at a more rapid rate than the rate of global SST. Consequently, the intensity of typhoons affecting the Korean peninsula will become stronger. Therefore, studies on the implementation of the typhoon disaster prevention system, to minimize the damage by predicting the maximum possible wind speed at the time of the influence of the typhoon, were carried out. In addition, recent studies have used the WRF model, which is useful for work-site operation and research. It is suitable for work-site operation as well as research to emulate the high-resolution data of the typhoon disaster prevention model. In this study, SST data and FDDA data were assimilated to produce the optimal WRF results. The results obtained were used as input data to the typhoon disaster prevention model, which is part of the typhoon disaster prevention system. This study selected Typhoon Bolaven (that moved north to the Yellow Sea and greatly damaged the metropolitan area in the Korean peninsula), and used WRF 3.5.1 version for data evaluation. The RDAPS numerical model data of the Korea Meteorological Administration were used as the model input data, and the OSTIA data were used as the SST data. For the FDDA data assimilation (OBS nudging), the sensitivity test was performed using the wind speed and temperature data of vertical and synoptic observations in the Korean peninsula region. As a results of time series analysis and statistical analysis, the maximum wind speed difference was about 5 m/s when the input data were applied differently. High-resolution sea surface temperature data assimilation yielded better results than the meteorological data assimilation. When the meteorological data assimilation and high-resolution sea surface temperature data assimilation were applied simultaneously, better results were obtained than under individual data assimilation cases. If the maximum possible wind speed of the 3-second gust that can occur during a typhoon is estimated using the optimal high-resolution results, the damage due to the typhoon will be effectively reduced through accurate prediction.

Acknowledgement

This research was supported by Basic Science Research Program through the National Research Foundation of Korea(NRF) funded by the Ministry of Education(2017R1D1A3B03036152)

©2019. Japan Geoscience Union. All Right Reserved. 

# Validation and application of a finite element approach on field mechanically stabilized earth walls with secondary reinforcement

*BING-RU WU[1], CHIH-HSUAN LIU[1], CHING HUNG[1]

1. National Cheng Kung University

Mechanically stabilized earth (MSE) walls have been used widely to prevent slopes from natural disasters around the world. The typical vertical spacing of geosynthetic reinforcement used in the practical MSE wall may cause high reinforcement connection strength and lead to wall-facing bulging. Previous studies show that installing short (secondary) reinforcement layers in-between primary reinforcement layers could mitigate these problems by reducing wall facing deflection and primary reinforcement strains, increasing the wall internal stability, alleviating down-drag forces behind the wall facing, and so on. Although the performance of the secondary reinforcement has been widely examined, its controlling factors (i.e., length, spacing, distribution) on the behavior of MSE wall are scarcely studied. In this study, a finite element approach was validated via a benchmark field case and was applied to understand the effect of the controlling factors on the behavior of MSE wall as well as giving a guidance on the design of MSE wall with secondary reinforcement.

Keywords: retaining structure, MSE wall, controlling factors, secondary reinforcement, finite element

©2019. Japan Geoscience Union. All Right Reserved. 

# EXPERIMENTAL STUDY ON POLYUREA-COATED RC SLAB SUBJECTED TO CONTACT EXPLOSIONS

*Minghsien Wu[1], Yingkuan Tsai[1], Chien-Hsien Liu[1], Pang-Ting Pai[1], Feng-Cheng Yang[1], Chun-Chia Huang[1]

1. Chung Cheng Institute of Technology National Defense University

Global terrorism is on the rise as the number of attacks soared, puts the world under the threat of car bomb, suicide bomb and so forth, and causes a huge amount of loss of life and property. Current buildings and infrastructures are mostly constructed using reinforced concrete, due to the brittleness of concrete material, when a structure subjected to blast loadings, the phenomena such as cracking and spalling at the proximal face of the target, and the ejection of fragments from the distal face of the loaded surface can be observed. These types of damage or failure could severely harm to the structural stability and the safety of people and equipment inside the building. Thus, the blast resistance of buildings has become an important issue in structural design and evaluation. Considering the high tensile strength and excellent impact resistance of polyurea materials, it is expected that the blast performance of a reinforced concrete element can be enhanced by coating this material onto its surface.

The purpose of this study is to investigate the blast performance of the polyurea coating on reinforced concrete slabs by conducting a series of filed explosion tests. The size of the specimen is 50cm×50cm×15cm. Four pieces of RC slabs were tested: RC slab without coating, RC slabs with coating on the front face, coating on the back face, and coating on the both faces. The thickness of coating is 3 mm. The specimens were fixed on a steel frame and detonated at the center of the test surface with a size of 5cm×5cm×2.5cm of 100g C4 rectangular explosive. The size and depth of the damage area on the front and back of the RC slabs were measured and evaluated by developing 3D models with point clouds from photographs.

The results show that when the unreinforced RC slabs is subjected to contact explosion, cratering will occur on the front side of the specimen and spalling will occur on the back side of the specimen; and when the RC slabs is coated on the front side of the specimen, the polyurea reinforcing layer at the contact explosion site is destroyed, but the damage degree were reduced; and in the case of the back-explosive surface reinforcement, the damage range of the cratering is also reduced, and the polyurea coated with the back-explosive surface has no crack, damage and blow-through. When the coating layer is removed, the back surface of the test piece is observed, and only cracks are generated but no obvious spalling. It is obvious that polyurea produces good adhesion due to its material properties and tightly constrains the fragments. Therefore, it has been shown by experiments that the use of polyurea elastic coatings to reinforce the explosion surface or the back explosion surface of the RC slabs can enhance the explosion-proof capability and reduce or protect from spalling, thereby achieving the purpose of protecting the internal life and property of the building. It is known from this test that the polyurea coating with a thickness of 3 mm can effectively and significantly reduce or avoid the occurrence of spalling when applied to the back surface of RC slabs.

Keywords: polyurea coatings, contact explosions, cratering, spalling

©2019. Japan Geoscience Union. All Right Reserved. 

# Simulation and field investigation of scour and sediment transport after Dam removal in the mountainous creek in Central Taiwan

*Chunhung WU[1]

1. Feng Chia University

The research focuses on using the flume experiments to observe the head-erosion phenomena caused by dam removal and simulate the channel evolution in the upstream and downstream of dam after dam removal by using CCHE2D model. The research area is in the Landaw river watershed in Huisun National Forest Area in the Central Taiwan. Two silts of silt dam build in the Landaw river had been lowered down 2.5 m height to release the deposited sediment to transport to downstream in 2013, and the research proceeded long term observation of the head-erosion in the upstream of the silt dam by using UAV and field investigation.
The research proceeded the flume experiments to simulate the sediment transport from the upstream of the dam and simulate the channel evolution in the upstream and downstream of dam by using CCHE2D model after dam removal. The control factors in the flume experiments are the sediment size, the discharge, the channel slope, and the removal area of check dams. The sediment size settings in this research include totally 0.9 mm, half 0.9 mm and half 0.5 mm, and totally 0.5mm, while the discharge settings include 3.4, 83.0, and 102.6 cubic centimeter per second. The channel slope settings include 4.4, 8.7 and 13 degree. The research records the sediment yield volume, the geomorphologic changes and the knickpoints evolution in the longitudinal sections after removing different area of dams in 27 flume experiments. Based on the dominant factors for the bank erosion scouring, 27 flume experiments can be classified into 3 types, including infiltration-dominated bank erosion experiments, surface runoff-dominated bank erosion experiments, and infiltration and surface runoff co-exist bank erosion experiments.
Furthermore, the research also uses CCHE2D model to simulate the sediment transport after the dam removal process of the silt dam in the upstream of Landaw river watershed. The research uses the river discharge in the day with the maximum 24 hours accumulated rainfall from 2015 to 2018, and the original DSMs in 2010, 2016, 2018 as the topographic models to simulate the scouring process in the upstream of the silt dam after dam removal. The research also proceeded the field investigation to verify the simulation result.
The accumulated rainfall setting for the simulation of CCHE2D model is 585 mm in 24 hours, and this is the accumulated rainfall with return period years of 50 year in the Landaw river watershed. Based on the simulation result by using CCHE2D model with the accumulated rainfall of 585 mm in 24 hours, the elevation of main river has been lowered down 5.4 m, and the maximum width of the head-erosion in the upstream od the silt dam is around 5.24 m. The total erosion sediment volume is estimated as 1370 cubic meter. The slope in the longitudinal profile along the main river can be classified into two sections. The slope from the silt dam to 23 m upward in the upstream is estimated as 0.31, while that from the 23 m upward in the upstream to the 200 m upward in the upstream is estimated as 0.151. This means that the knickpoint is in the 23 m upward in the upstream of the silt dam. The result will be the basis for developing the assessment model for assess the feasibility of dam removal in the rivers.

Keywords: Dam Removal, CCHE-2D, sediment transport

©2019. Japan Geoscience Union. All Right Reserved. 

# Examination and systematization of predispositions to floods in the Heavy Rain in July 2018

*Kanako Kimura[1], Toshihiko Sugai[2]

1. The University of Tokyo, 2. Graduate School of Frontier Sciences, the University of Tokyo

## Introduction

Though predispositions to floods have been mentioned in the studies of river engineering, geography and geomorphology, the relationship between flood and topography / geology is dealt with as self-evident in most of them. Hence, this study focuses on the predispositions to floods.
The floods in the Heavy Rain in July 2018, especially those of the Oda River (the Takahashi River System) are the subjects of this study. The purposes of this study are (1) to create a database on the floods, (2) to examine predispositions for each space scale, taking into account the influence of artificiality, (3) to acquire knowledge contributing to high accuracy of flood risk assessment.

## Fields & Methods

In the Chugoku district, 3 denudation surfaces are seen. And, the plains on the Setouchi side have been formed by the rivers flowing down from the Chugoku mountains. These rivers are characterized by weathering granitoids distributed upstream.
The Oda River is a first-class river which joins the Takahashi River in Kurashiki city. Since the Oda River has a gentler river bed than that of the Takahashi River, it is affected by the backwater from the Takahashi River.
The Association of Japanese Geographers has released the map of the flood points caused by the heavy rain on the Web (http://ajg-disaster.blogspot.com/). The characteristics of the river channels on the flood points on this map (mainly those of the Oda River) were investigated and compiled into a matrix.
On 9 dike break points of 4 rivers, the aerial photos were interpreted, and the classification maps of flood landforms were created.
Besides, the downstream change graph of the river bed height, the bed slope…etc. of the Oda River were created.

## Results

Many dike break points lie in the administrative sections of the prefectures, and raised beds are seen on 9 of the 10 points in the tributaries to the Oda River. There are sluice gates on 2 dike break points and 5 slope failure points reported in the Council for Social Infrastructure (2018). At the outer bank of the large river curve in Fukuhara, where the overflows and the slope failures were occurred this time, dike breaks were also occurred in the past.
Although alluvial ridges have been regarded as safe against floods, the largest dike breaks occurred on the alluvial ridge.
The downstream change graphs show that floods didn’ t occur in a downstream section of a weir with a relatively steep river bed but occur in a further downstream section where a river bed becomes gentle.

## Discussion

On the point scale, a sluice gates and a raised bed section is one of the predispositions to floods. From comparing dike break points and non-dike break points, it is suggested that steep slope gradient affects dike break, too. And it is necessary to update the flood risk assessment on alluvial ridges.
On the section scale, compared the downstream section of a weir with a steep river bed, the further

©2019. Japan Geoscience Union. All Right Reserved. 

downstream section with a gentle bed is dangerous.
On the regional scale, it is considered that the bed slope difference of the Oda River and the Takahashi River is affected by the denudation surfaces. It is also one of the predispositions that granitoids is widely distributed in Chugoku district.
Regarding artificiality, it turned out that the river maintenance has not kept up. However, there is the more serious issue that the Mabi-cho area, where many floods occurred this time, has become a bedroom town. Therefore, it is necessary to reconsider how to use land.

## References

Council for Social Infrastructure, The Ministry of Land, Infrastructure, Transport and Tourism (2018), About the Heavy Rain in July 2018
Izumida, A. (2018), Crevasse splay formation and contribution to the development of alluvial ridges in the lower Kinu River, central Japan, Master's thesis of Graduate School of Frontier Sciences, The University of Tokyo
Uchida, K. (2011), Activities of the flood prevention unions in the Oda River basin in Okayama prefecture, Water Utilization Science No.320, pp.40-55

Keywords: the Oda River, raised bed river, alluvial ridge, crevasse splay, channel slope

©2019. Japan Geoscience Union. All Right Reserved. 

| | 地点 | 種類 | 確かさ 海津ほか | 直後写真 | 確かさ 総合 | 支流名 | 岸 | 河道植生 | 砂州 | 河床材料 | 河道幅 (m) | 低水路幅 水面幅(m) | 狭窄 (m) | /河道幅 (広) | 堤防高 堤外地 | 堤防高 堤内地 | 横幅 堤内地 | 傾斜 堤内地 |
|---|---|---|---|---|---|---|---|---|---|---|---|---|---|---|---|---|---|---|
| 小田川 | 4 | 破堤 | ほぼ正確 | × | △ | 尾坂川 | 左 | 草（2014） | 上216-85mに（2014） | 砂 | 27 | (7) | - | - | 2.1 | 1.7 | 9 | 0.189 |
| | 5 | 破堤 | ほぼ正確 | × | △ | - | 左 | 草（2007） | - | - | 142 | (30) | - | - | 6.3 | 3.1 | 17 | 0.182 |
| | 6 | 破堤 | ほぼ正確 | × | △ | - | 右 | ～草（2014） | 下15m左岸，固定化（2014） | 砂 | 155 | (35) | - | - | 5.1 | 2.6 | 22 | 0.118 |
| | 7 | 破堤 | ほぼ正確 | × | △ | - | 左 | 草（2014） | - | 砂 | 180 | (20-37) | 100 | 0.42 | 5.7 | 2.5 | 13 | 0.192 |
| | 8 | 破堤 | ほぼ正確 | ○ | ○ | (水路) | 左 | - | - | - | 5 | 2 | - | - | 1.3 | 1.8 | 9 | 0.200 |
| | 9 | 越水 | ほぼ正確 | ○ | ○ | - | 右 | 草（～樹木） | 両岸 | 砂 | 181 | 38-47 | - | - | 7.3 | (山) | - | - |
| | 10 | 破堤 | 不正確 | ○ | ○ | 大武谷川 | 右 | ～草 | - | - | 13 | 1-2 | - | - | 1.5-2.1 | 2.2 | 8 | 0.275 |
| | 11 | 破堤 | ほぼ正確 | ○ | ○ | - | 左 | 草～樹木 | 左（内）岸に30m | 砂 | 206 | 58 | 28 | 0.14 | 5.8 | 4.0 | 12 | 0.333 |
| | 12 | 破堤 | ほぼ正確 | ○ | ○ | 真谷川 | 左 | 草（～樹木） | - | - | 37 | 1-2 | - | - | 6.0 | 5.4 | 13 | 0.415 |
| | 13 | 越水 | ほぼ正確 | ○ | ○ | - | 右 | 草～樹木 | 樹林化中州 | 砂 | 233 | 複数本 | - | - | 7.8 | 3.4 | 13 | 0.262 |
| | 14 | 破堤 | ほぼ正確 | ○ | ○ | 高馬川 | 右 | 草 | - | - | 13 | 7 | - | - | 1.5 | 4.0 | 14 | 0.286 |
| | 15 | 破堤 | ほぼ正確 | ○ | ○ | 高馬川 | 左 | 草 | - | - | 13 | 7 | - | - | 3.0 | 5.8 | 13 | 0.446 |
| | 16 | 破堤 | ほぼ正確 | ○ | ○ | - | 左 | 草～樹木 | 樹林化中州 | 砂 | 217 | 複数本 | - | - | 8.2 | 6.0 | 18 | 0.333 |
| | 17 | 越水 | ほぼ正確 | ○ | ○ | - | 右 | 樹木 | 樹林化中州 | 砂 | 227 | 複数本 | - | - | 7.2 | 2.6 | 16 | 0.163 |
| | 18 | 破堤 | ほぼ正確 | ○ | ○ | 末政川 | 右 | ～草 | - | - | 12 | 1-2 | - | - | 1.6 | - | - | - |
| | 19 | 破堤 | ほぼ正確 | ○ | ○ | 末政川 | 左 | ～草 | - | - | 12 | 1-2 | - | - | 2.1 | - | - | - |
| | 20 | 破堤 | ほぼ正確 | ○ | ○ | 末政川 | 右 | ～草 | - | - | 30 | 1-2 | 6 | 0.20 | 5.1 | 6.5 | 18 | 0.361 |
| | 21 | 破堤 | ほぼ正確 | ○ | ○ | 末政川 | 左 | ～草 | - | - | 32 | 1-2 | 6 | 0.19 | 5.5 | 6.2 | 19 | 0.326 |
| 高梁川 | 1 | 破堤 | - | ○ | ○ | - | 右 | 樹木多い | 右（内）に80m | 砂 | 240 | 65 | 70（緩やか） | - | 10.3 | 3.0 | 11 | 0.273 |
| | 2 | 破堤 | - | ○ | ○ | - | 右 | 樹木多い | 右（内） | 砂 | 190 | 80 | 同上 | - | 9.7 | 2.2 | 9 | 0.244 |
| 砂川 | | 破堤 | ほぼ正確 | × | △ | - | 左 | 草～樹木（2007） | 右岸(2007) | 砂 | 58 | 5 | - | - | 4.5 | 4.5 | 15 | 0.300 |
| 旭川 | | 破堤 | ほぼ正確 | × | △ | - | 左 | 草～（2007） | 80m下から(2007) | 粗砂～ | 175 | 116 | 80m下から54減 | 0.31 | 5.3 | - | - | - |
| 芦田川 | | 破堤 | 不正確 | ○ | ○ | 吉野川 | 右 | ～草 | - | - | 9 | 0-1 | - | - | 0.3 | 1.9 | 8 | 0.238 |
| 賀茂川 | | 破堤 | 不正確 | ○ | ○ | - | 右 | ～草 | 右岸に17m | 砂 | 37 | 16 | - | - | - | 2.5 | 10 | 0.250 |

**Fig. 1** A part of flood point matrix.

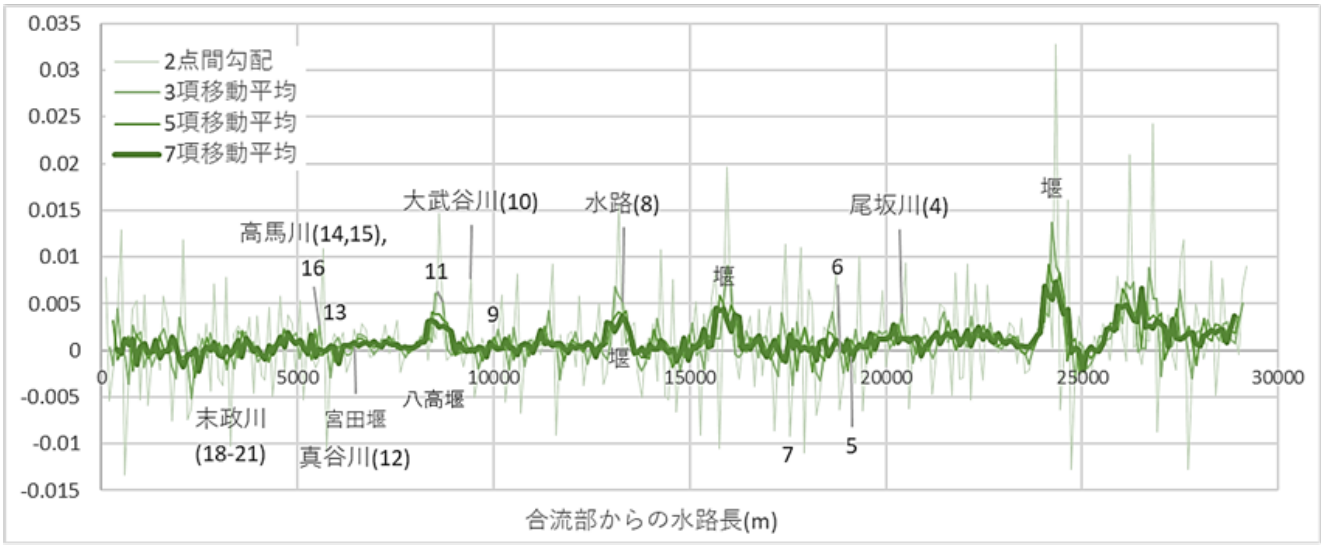


**Fig. 2** The downstream change graph of the river bed slope.

©2019. Japan Geoscience Union. All Right Reserved. 

# Expand various disaster risk information and sophisticate methods to disseminate on the Hazard Map Portal Site

*Takuya Ueshiba[1], Yumeka Fujii[1], Naoki Yoshimatsu[1], Noriyuki Takakuwa[1], Wataru Yamasaki[1], Jun Suwabe[1]

1. GSI of Japan

I. Introduction
In June 2006, it was necessary to prepare the portal site about hazard maps which anyone can search on the internet, according to the policy established by Ministry of Land, Infrastructure Transport and Tourism. Geospatial Information Authority of Japan, in cooperation with Water and Disaster Management Bureau and so on, began to operate Hazard Map Portal Site since April 2007. This latest site has two main contents. One is Layered Hazard Map which enables users to layer various maps and disaster risks, and another is Published Hazard Map showing links to hazard maps made by each local government.

II. Questionnaire about Hazard Map Portal Site
A questionnaire was conducted in 2015 for 18 local governments and about 1,000 residents to figure out these things: how much they recognize and use it, needs, and to know the problems of this site. Various needs and requests were made clear, for example, the addition of the function displaying all disaster risk information by clicking map, implementation of browsing feature by mobile device, preparation of download page published data on this site, expanding the data about disaster risk information and evacuation facilities, making the data open for public on the Internet and machine-readable (hereinafter referred to “Open Data”) and so on.

III. Three activities
Three activities were carried out based on this questionnaire.
1. Improvement of function
Three functions were mainly added on this site. One is the function displaying multiple risks, which were inundation, landslide, sediment disaster and so on, at arbitrary point on Layered Hazard Map, another is the compatibility with smartphones which enable to access this site away from home, and the other is function of downloading list files of URL linking to Published Hazard Map.
2. Expanding Data
Designated Emergency Evacuation Area (flood from river, storm surges, tsunami, debris flow, steep slope failure / landslide, fire disasters), expected inundation areas of ministry-controlled river due to statistical heaviest rainfall, expected inundation areas of tsunami, and landform classification of Fundamental Land Classification Survey were released.
3. Open Data
Raster tiles of expected inundation areas of ministry-controlled river due to statistical heaviest rainfall, Landslide Prone Areas and dangerous site by sediment and landslide disaster was added to Open Data list. Furthermore, these raster tiles data started to be converted to vector tiles data and will be distributed as Open Data by June 2019.

IV. Future perspective
We carried out improvement of this site system, expansion data of disaster risk information and Open Date of raster tiles covered on Layered Hazard Map. Due to this effort, tasks revealed in 2015 questionnaire survey were solved and this site became more useful. This result led to further publicize

©2019. Japan Geoscience Union. All Right Reserved. 

disaster risk and contributed to raise awareness of disaster prevention.
In order to expand data and make the site more useful, various information including expected inundation area maps classified by duration time and expected inundation areas by reservoir break will be disclosed and more functions, for example 3D page of Layered Hazard Map, will be added.

Keywords: disaster risk, hazard map, web map, open data

©2019. Japan Geoscience Union. All Right Reserved. 

# A study on evaluation formulae of the principal fault in PFDHA- In consideration of a relevance to known active faults-

*Tsuyoshi Kanda[1], Makoto Takao[1], Toshimichi Kaneto[1], Takehisa Arakawa[1]

1. Tokyo Electoric Power Company Holdings, Inc

Takao et al. (2013) proposed some evaluation formulae for probabilistic fault displacement hazard analysis (PFDHA) based on data on surface earthquake faults in Japan.

As for the formulae in terms of the principal fault, Takao et al. (2013) did not discriminate between (1) an earthquake that occurred in an area where an active fault exists, and (2) an earthquake that occurred in an area where no cumulative deformation or active fault exists, in the same way as Youngs et al. (2003).

In this study, we re-examined the aforementioned evaluation formulae by discriminating between (1) and (2) for the 107 hypocenters described in Takao et al. (2003).

The results show that the differences in the P1p between (1) and (2) are distinct and that the P1p is closely correlated to the distance between the active fault and the hypocenter, so discrimination between (1) and (2) is useful for these evaluation formulae.

Therefore, it is suggested that the results of this study can be a powerful tool for applying the idea of diffuse seismicity in the probabilistic seismic hazard analysis (PSHA) to the PFDHA.

There are some differences in the evaluation formula for the fault displacement between (1) and (2), whereas it was confirmed that there is no clear correlation between the threshold value (boundary between (1) and (2)) and the predicted displacement using the regression equation.

We strongly recommend that these evaluation formulae should be examined in future by gathering more data on surface earthquake faults because the present data may be insufficient to consider the correlation between threshold value and fault displacement.

Keywords: PFDHA, probability of surface rupture of the principal fault, fault displacement, a relevance to an active fault

©2019. Japan Geoscience Union. All Right Reserved. 

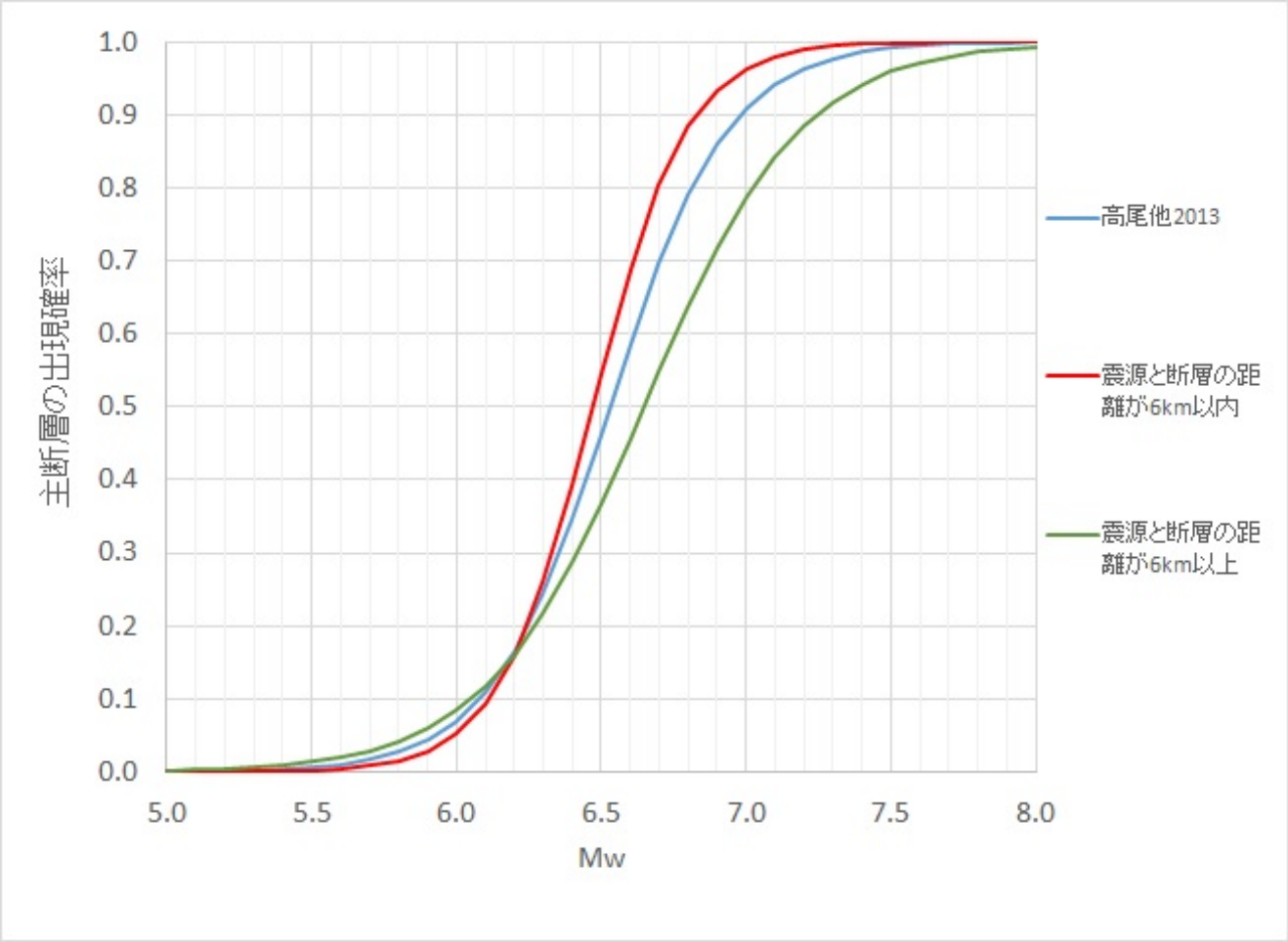


©2019. Japan Geoscience Union. All Right Reserved. 

# Characteristics of sediment deposition distribution in debris flow disasters in caused by heavy rain in August 2014 Hiroshima, Japan

*Shoichiro Uchiyama[1], Toshihiko Sugai[2]

1. National Research Institute for Earth Science and Disaster Resilience, 2. The University of Tokyo

1. Background
Post-war sediment disaster countermeasures have been promoted mainly by the development of structural measures. However, disaster prone areas are expanding annually owing to the development of residential areas. Owing to the difficulty involved in preventing sediment disasters by taking structural measures alone, nonstructural measures are being promoted. However, many of the victims of the sediment damage caused by the Heavy Rain Event of July 2018 were located in sediment disaster-prone areas. From these facts, we can see that the preliminary evacuation is inadequately performed.

2. Purpose and significance
For autonomous evacuation to be conducted when the risk of the disaster is identified, it is necessary to anticipate the extent of damage possible in the inhabited areas. For example, the damage owing to debris flow can be predicted using knowledge of the behavior of debris flow and the relationship between debris flow and buildings or vegetation in the flow path. Therefore, in this study, the volume of sediment deposition by debris flow was measured, and its distribution characteristics were analyzed in six districts of Asaminami-ku, Hiroshima, which was damaged by the debris flow on August 20, 2014.

3. Method
There were 23 digital aerial photographs (Geospatial Information Authority of Japan) taken on May 21, 2008. Further, approximately four days after the disaster, unmanned aerial vehicles were used to capture aerial photographs, which comprised 700 vertical images. 30 points were measured by conducting a GNSS survey; 10 ground reference and 14 accuracy verification points were used. The spatial resolution of DSM and orthoimage created by SfM photogrammetry were 20.0 cm and 3.5 cm before and after the disaster, respectively. As a result of the accuracy verification of the DSM, the three-dimensional RMSEs at the accuracy verification point that employed 14 points were 26.2 cm (2008 DSM value) and 11.5 cm (2014 DSM value). The change in the height of the ground was obtained by subtracting the 2008 DSM elevation from the 2014 DSM value calculated using GIS. Next, the sediment deposition areas were interpreted from the orthoimage after the disaster, and polygon data were created using GIS.
In the surface height change data, a mesh having a positive value corresponds to sediment deposition inside the sediment deposition area polygon. At this time, we considered the error of the DSM at 2 periods as follows: the square root of the sum of the squares (28.6 cm) of RMSE values (26.2 cm before disaster, 11.5 cm after disaster) at each time were obtained as mentioned above, and only the mesh with a height change larger than this value was targeted.

4. Result
Of the results obtained, Yagi 3 districts were figured. There were two blue falling water lines near the center, and the main flow path widened to approximately 25 m. Within the range 70 m above and below the flow path, seven buildings were lost, resulting in 20 casualties (A). In the housing at the most downstream part of this row, a portion of the building moved downward while remaining intact, resulting in two casualties. In addition, the apartment that was in the center of this row of houses was lost in the debris flow; however, because it was a vacant lot in the pre-disaster aerial photograph, the apparent

©2019. Japan Geoscience Union. All Right Reserved. 

change in the DSM appears to be sedimentary (B). In the public housing building located on the falling water line, sediment flowed, resulting in one casualty (C). Among the vegetation growing adjacent to the main flow path, the side close to the flow path was eroded (D). There was an area in which the sediment deposition thickness was in the main flow path thin (E). A sediment layer exceeding 2 m in thickness accumulated in the parking lot at the end of the main flow path. In the orthorectified images, the sediments exhibited a mud-like texture (F).

Keywords: debris flow, heavy rain in August 2014, volume of sediment deposition, UAV, SfM-MVS Photogrammetry

©2019. Japan Geoscience Union. All Right Reserved. 

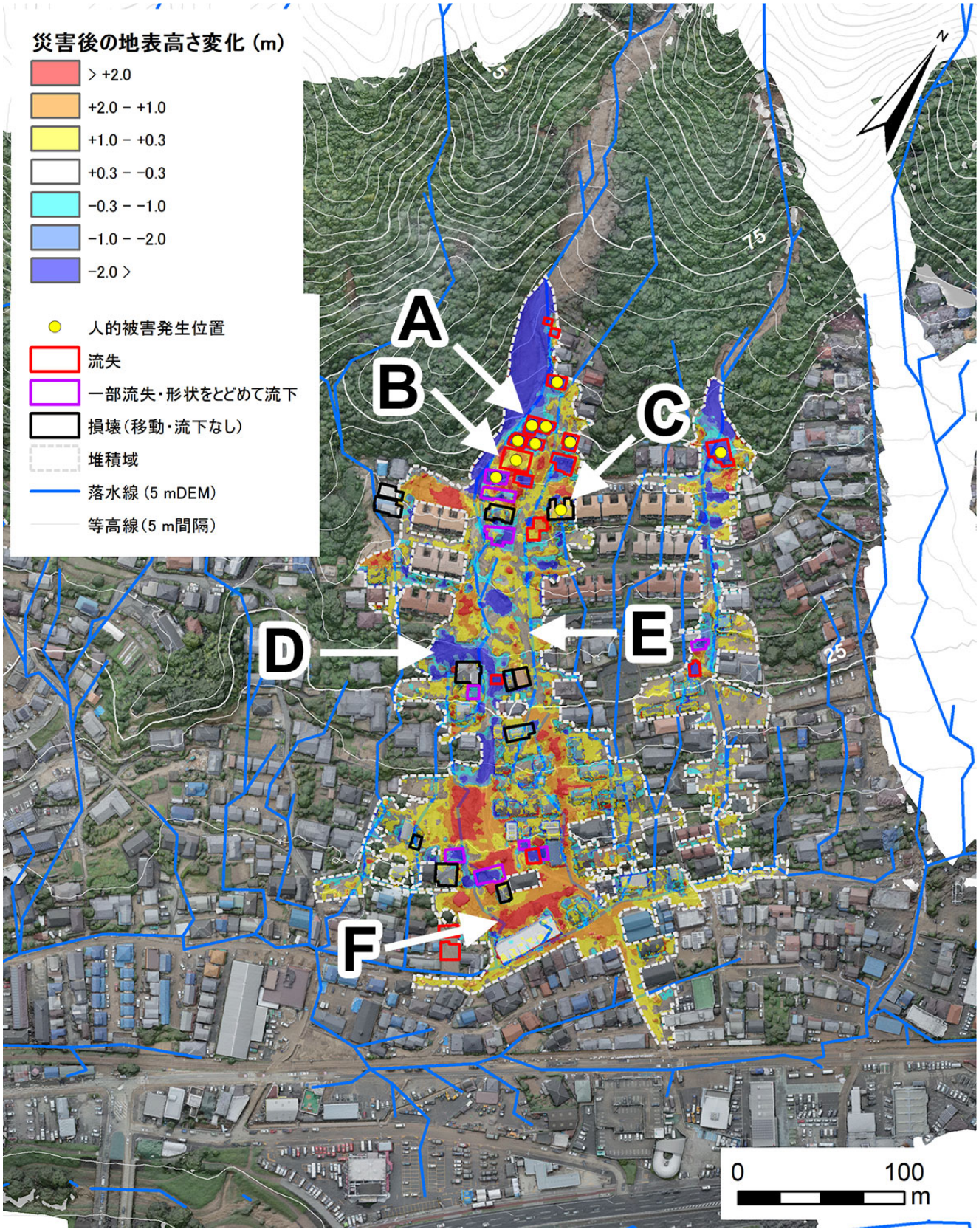


©2019. Japan Geoscience Union. All Right Reserved. 

# Land use change after tsunami and its problems in Kii peninsula

*Kenta Okidate[1], Tatsuto Aoki[2]

1. School of Humanities, Kanazawa University, 2. School of Regional Development Studies, Kanazawa University

Disaster prevention against tsunami is paid attention socially. In Japan, many cities are located in the coast and have a possibilities of damage by tsunami. This paper presents the results of quantitative analyzing land use changes in region have few researches and clarifying its regional characteristics and problem.

Three study areas, Shirahama area, Kushimoto area, Nachiwan surrounding area, were damaged by tsunami in 1944 and 1946. After the disaster, these regions were restored disorderly.

By analyzing Geographic Information System (GIS) data with QGIS, Interview, and field survey, land use changes in study areas were clarified.

Housing/Building increased greatly by converting Wasteland/Farmland and Forest. Especially, from 1947 to 1965, converting flooded vacant lot by tsunami into Housing/Building was prominent. Increasing of Housing/Building, Wasteland/Farmland and port facilities by reclamation were seen. Also, building lot increased in tsunami inundated areas and these areas for itself increased by reclamation in all study areas. Large buildings are increased in the coast with the passing of the years.

As a result of analysis, expanding building lot, building port facilities and so on were clarified as regional characteristics. These are geomorphological limitation, tourism development, increasing demand of building lot and economic structure as its factors. 3 problems, crowded building lot in the coast, increasing building lot and port facilities by reclamation, large buildings in the coast, were also clarified. These problems may disturb refuge from tsunami. A long-term plan for safe land use is necessary to solve problems.

Keywords: Disaster prevention, Nankai Trough Earthquake, land use, GIS

©2019. Japan Geoscience Union. All Right Reserved. 

# Reconstruction of the building damages caused by the Typhoon Kathleen and analyses of their land conditions at the southern foot of the Akagi Volcano using U.S. military aerial photographs

*Masafumi Aoyama[1], Yoshiki Saito[2]

1. Faculty of Education, Gunma University, 2. Graduate Student, Gunma University

We reconstructed building damages caused by the Typhoon Kathleen and analyses of their land conditions at the southern foot of the Akagi Volcano using U.S. military aerial photographs and GIS. Flood inundation area were identified based on the building damages and flood deposits by using U.S. military aerial photos. Building damages due to the flood concentrated in the former river channel and valley bottom plain. Several schools (25%) in the study area located in the inundation area of the Typhoon Kathleen.

Keywords: Typhoon Kathleen, flood risk assessment, building damage, U.S. military aerial photographs, southern foot of the Akagi Volcano

©2019. Japan Geoscience Union. All Right Reserved. 

[J] Poster | H (Human Geosciences )：H-DS Disaster geosciences

Thu. May 30, 2019 5:15 PM - 6:30 PM JST | Thu. May 30, 2019 8:15 AM - 9:30 AM UTC | Poster Hall International Exhibition Hall8, Makuhari Messe_15

## [H-DS15] Human environment and disaster risk

convener:Tatsuto Aoki(School of Regional Development Studies, Kanazawa University), Hisao Kondo(Geological Survey of Japan, National Institute of Advanced Industrial Science and Technology)

This session discusses disaster risks being inherent in the natural and human environment, which sometimes happen to appear at a disaster, from the viewpoint of not only natural sciences but also social and human sciences. Examples of discussion subjects are as follows: uncertainty of forecasting disaster and problems of huge disaster with low frequency that raised from the 2011 Tohoku earthquake, the methodology for improving hazard maps, national recovery plans considering probable changes or sustainability of the society, international cooperation for disaster mitigation, problems of active faults or liquefaction, adjusting disaster mitigation plan to the regional characteristics, technical development for supporting disaster prevention, education for the disaster mitigation.

[HDS15-P01] Validity Verification in Typhoon Disaster Prevention Model for Typhoon Damage Reduction– GUST Wind Speed, Maximum Wind Speed -

*Woo-Sik JUNG[1], Hana Na[1] (1.Department of Atmospheric Environment Information Engineering, Atmospheric Environment Information Research Center, Inje University, Gimhae 50834, Korea)

[HDS15-P02] A Study on the Assimilation of Meteorological Data and Sea Surface Temperature Data for Improving the Accuracy of WRF Prediction during Typhoon periods on the Korean Peninsula

*Woo-Sik JUNG[1], Hana Na[1] (1.Department of Atmospheric Environment Information Engineering, Atmospheric Environment Information Research Center, Inje University, Gimhae 50834, Korea)

[HDS15-P03] Validation and application of a finite element approach on field mechanically stabilized earth walls with secondary reinforcement

*BING-RU WU[1], CHIH-HSUAN LIU[1], CHING HUNG[1] (1.National Cheng Kung University)

[HDS15-P04] **EXPERIMENTAL STUDY ON POLYUREA-COATED RC SLAB SUBJECTED TO CONTACT EXPLOSIONS**

*Minghsien Wu[1], Yingkuan Tsai[1], Chien-Hsien Liu[1], Pang-Ting Pai[1], Feng-Cheng Yang[1], Chun-Chia Huang[1] (1.Chung Cheng Institute of Technology National Defense University)

[HDS15-P05] Simulation and field investigation of scour and sediment transport after Dam removal in the mountainous creek in Central Taiwan

*Chunhung WU[1] (1.Feng Chia University)

[HDS15-P06] Examination and systematization of predispositions to floods in the Heavy Rain in July 2018

*Kanako Kimura[1], Toshihiko Sugai[2] (1.The University of Tokyo, 2.Graduate School of Frontier Sciences, the University of Tokyo)

[HDS15-P07] Expand various disaster risk information and sophisticate methods to disseminate on the Hazard Map Portal Site

*Takuya Ueshiba[1], Yumeka Fujii[1], Naoki Yoshimatsu[1], Noriyuki Takakuwa[1], Wataru Yamasaki[1], Jun Suwabe[1] (1.GSI of Japan)

[HDS15-P08] A study on evaluation formulae of the principal fault in PFDHA- In consideration of a relevance to known active faults-

*Tsuyoshi Kanda[1], Makoto Takao[1], Toshimichi Kaneto[1], Takehisa Arakawa[1] (1.Tokyo Electoric Power Company Holdings, Inc)

[HDS15-P09] Characteristics of sediment deposition distribution in debris flow disasters in caused by heavy rain in August 2014 Hiroshima, Japan

*Shoichiro Uchiyama[1], Toshihiko Sugai[2] (1.National Research Institute for Earth Science and Disaster Resilience, 2.The University of Tokyo)

[HDS15-P10] Land use change after tsunami and its problems in Kii peninsula

*Kenta Okidate[1], Tatsuto Aoki[2] (1.School of Humanities, Kanazawa University, 2.School of Regional Development Studies, Kanazawa University)

[HDS15-P11] Reconstruction of the building damages caused by the Typhoon Kathleen and analyses of their land conditions at the southern foot of the Akagi Volcano using U.S. military aerial photographs

*Masafumi Aoyama[1], Yoshiki Saito[2] (1.Faculty of Education, Gunma University, 2.Graduate Student, Gunma University)

# Validity Verification in Typhoon Disaster Prevention Model for Typhoon Damage Reduction –GUST Wind Speed, Maximum Wind Speed -

*Woo-Sik JUNG[1], Hana Na[1]

1. Department of Atmospheric Environment Information Engineering, Atmospheric Environment Information Research Center, Inje University, Gimhae 50834, Korea

In recent years, as the intensity of typhoons affecting the Korean peninsula has become stronger due to global warming resulting from climate change, studies on typhoons attacking the Korean peninsula are being increasingly carried out. Many previous studies have constructed typhoon disaster prevention models for estimating the maximum wind speed of the 3-second gust that can occur during a typhoon. In addition, such studies have enabled the establishment of foundational materials for the typhoon disaster prevention system. However, there have been few studies on the validity of the maximum possible wind speed of the 3-second gust, as estimated by the typhoon disaster prevention model. Therefore, in this study, validity analysis was carried out via verification using the observed 3-second gust values. For the verification, the GUST wind speed data from marine meteorological buoys (which serves as the basis of maximum wind speed) monitored by the Korea Meteorological Administration, and maximum instantaneous wind speed data from lighthouse observation, were used. In addition, this study compared and analyzed the 3-second gust values observed at points located within the radius of the maximum wind speed, and at points located outside the radius of the maximum wind speed during the typhoon season. The points within the radius of the maximum wind speed showed a more similar trend to the observed values than the points outside the radius. In addition, the points within the radius better simulated the maximum wind speed. Moreover, the 3-second gust values calculated by the typhoon disaster prevention model were slightly greater than the observed values at almost all points. From the viewpoint that the calculated value is the maximum possible wind speed, it is considered to provide useful information in terms of pre-disaster prevention regarding typhoon damage. As a result of comparing the wind speeds at the 10 m altitude (which were obtained from the typhoon prevention model by categorizing the Korean peninsula into inland, coastal, and island regions), with the observed values, the island region, showed the best results (due to the presence of fewest obstacles on the ground), followed by the coastal, and inland regions. This study suggests that the 3-second gust is a justified parameter to be used in the typhoon disaster prevention model. Therefore, the typhoon disaster prevention model can be efficiently applied to the typhoon disaster prevention system.

This research was supported by Basic Science Research Program through the National Research Foundation of Korea(NRF) funded by the Ministry of Education(2017R1D1A3B03036152)

Keywords: Typhoon Disaster Prevention Model, Gust, Maximum WInd Speed

©2019. Japan Geoscience Union. All Right Reserved. 

# Validity Verification in Typhoon Disaster Prevention Model for Typhoon Damage Reduction – GUST Wind Speed, Maximum Wind Speed -

Woo-Sik Jung, Hana Na

In recent years, as the intensity of typhoons affecting the Korean peninsula has become stronger due to global warming resulting from climate change, studies on typhoons attacking the Korean peninsula are being increasingly carried out. Many previous studies have constructed typhoon disaster prevention models for estimating the maximum wind speed of the 3-second gust that can occur during a typhoon. In addition, such studies have enabled the establishment of foundational materials for the typhoon disaster prevention system. However, there have been few studies on the validity of the maximum possible wind speed of the 3-second gust, as estimated by the typhoon disaster prevention model. Therefore, in this study, validity analysis was carried out via verification using the observed 3-second gust values. For the verification, the GUST wind speed data from marine meteorological buoys (which serves as the basis of maximum wind speed) monitored by the Korea Meteorological Administration, and maximum instantaneous wind speed data from lighthouse observation, were used. In addition, this study compared and analyzed the 3-second gust values observed at points located within the radius of the maximum wind speed, and at points located outside the radius of the maximum wind speed during the typhoon season. The points within the radius of the maximum wind speed showed a more similar trend to the observed values than the points outside the radius. In addition, the points within the radius better simulated the maximum wind speed. Moreover, the 3-second gust values calculated by the typhoon disaster prevention model were slightly greater than the observed values at almost all points. From the viewpoint that the calculated value is the maximum possible wind speed, it is considered to provide useful information in terms of pre-disaster prevention regarding typhoon damage. As a result of comparing the wind speeds at the 10 m altitude (which were obtained from the typhoon prevention model by categorizing the Korean peninsula into inland, coastal, and island regions), with the observed values, the island region, showed the best results (due to the presence of fewest obstacles on the ground), followed by the coastal, and inland regions. This study suggests that the 3-second gust is a justified parameter to be used in the typhoon disaster prevention model. Therefore, the typhoon disaster prevention model can be efficiently applied to the typhoon disaster prevention system.

Acknowledgement

This research was supported by Basic Science Research Program through the National Research Foundation of Korea(NRF) funded by the Ministry of Education(2017R1D1A3B03036152)

©2019. Japan Geoscience Union. All Right Reserved. 

# A Study on the Assimilation of Meteorological Data and Sea Surface Temperature Data for Improving the Accuracy of WRF Prediction during Typhoon periods on the Korean Peninsula

*Woo-Sik JUNG[1], Hana Na[1]

1. Department of Atmospheric Environment Information Engineering, Atmospheric Environment Information Research Center, Inje University, Gimhae 50834, Korea

Typhoons affecting the Korean peninsula and the surrounding regions originate in the Western Pacific Ocean. The SST around Korean peninsula are increasing at a more rapid rate than the rate of global SST. Consequently, the intensity of typhoons affecting the Korean peninsula will become stronger. Therefore, studies on the implementation of the typhoon disaster prevention system, to minimize the damage by predicting the maximum possible wind speed at the time of the influence of the typhoon, were carried out. In addition, recent studies have used the WRF model, which is useful for work-site operation and research. It is suitable for work-site operation as well as research to emulate the high-resolution data of the typhoon disaster prevention model. In this study, SST data and FDDA data were assimilated to produce the optimal WRF results. The results obtained were used as input data to the typhoon disaster prevention model, which is part of the typhoon disaster prevention system. This study selected Typhoon Bolaven (that moved north to the Yellow Sea and greatly damaged the metropolitan area in the Korean peninsula), and used WRF 3.5.1 version for data evaluation. The RDAPS numerical model data of the Korea Meteorological Administration were used as the model input data, and the OSTIA data were used as the SST data. For the FDDA data assimilation (OBS nudging), the sensitivity test was performed using the wind speed and temperature data of vertical and synoptic observations in the Korean peninsula region. As a results of time series analysis and statistical analysis, the maximum wind speed difference was about 5 m/s when the input data were applied differently. High-resolution sea surface temperature data assimilation yielded better results than the meteorological data assimilation. When the meteorological data assimilation and high-resolution sea surface temperature data assimilation were applied simultaneously, better results were obtained than under individual data assimilation cases. If the maximum possible wind speed of the 3-second gust that can occur during a typhoon is estimated using the optimal high-resolution results, the damage due to the typhoon will be effectively reduced through accurate prediction.

This research was supported by Basic Science Research Program through the National Research Foundation of Korea(NRF) funded by the Ministry of Education(2017R1D1A3B03036152)

Keywords: WRF, Typhoon, SST

©2019. Japan Geoscience Union. All Right Reserved. 

# A Study on the Assimilation of Meteorological Data and Sea Surface Temperature Data for Improving the Accuracy of WRF Prediction during Typhoon periods on the Korean Peninsula

Woo-Sik Jung, Hana Na

Typhoons affecting the Korean peninsula and the surrounding regions originate in the Western Pacific Ocean. The SST around Korean peninsula are increasing at a more rapid rate than the rate of global SST. Consequently, the intensity of typhoons affecting the Korean peninsula will become stronger. Therefore, studies on the implementation of the typhoon disaster prevention system, to minimize the damage by predicting the maximum possible wind speed at the time of the influence of the typhoon, were carried out. In addition, recent studies have used the WRF model, which is useful for work-site operation and research. It is suitable for work-site operation as well as research to emulate the high-resolution data of the typhoon disaster prevention model. In this study, SST data and FDDA data were assimilated to produce the optimal WRF results. The results obtained were used as input data to the typhoon disaster prevention model, which is part of the typhoon disaster prevention system. This study selected Typhoon Bolaven (that moved north to the Yellow Sea and greatly damaged the metropolitan area in the Korean peninsula), and used WRF 3.5.1 version for data evaluation. The RDAPS numerical model data of the Korea Meteorological Administration were used as the model input data, and the OSTIA data were used as the SST data. For the FDDA data assimilation (OBS nudging), the sensitivity test was performed using the wind speed and temperature data of vertical and synoptic observations in the Korean peninsula region. As a results of time series analysis and statistical analysis, the maximum wind speed difference was about 5 m/s when the input data were applied differently. High-resolution sea surface temperature data assimilation yielded better results than the meteorological data assimilation. When the meteorological data assimilation and high-resolution sea surface temperature data assimilation were applied simultaneously, better results were obtained than under individual data assimilation cases. If the maximum possible wind speed of the 3-second gust that can occur during a typhoon is estimated using the optimal high-resolution results, the damage due to the typhoon will be effectively reduced through accurate prediction.

Acknowledgement

This research was supported by Basic Science Research Program through the National Research Foundation of Korea(NRF) funded by the Ministry of Education(2017R1D1A3B03036152)

©2019. Japan Geoscience Union. All Right Reserved. 

# Validation and application of a finite element approach on field mechanically stabilized earth walls with secondary reinforcement

*BING-RU WU[1], CHIH-HSUAN LIU[1], CHING HUNG[1]

1. National Cheng Kung University

Mechanically stabilized earth (MSE) walls have been used widely to prevent slopes from natural disasters around the world. The typical vertical spacing of geosynthetic reinforcement used in the practical MSE wall may cause high reinforcement connection strength and lead to wall-facing bulging. Previous studies show that installing short (secondary) reinforcement layers in-between primary reinforcement layers could mitigate these problems by reducing wall facing deflection and primary reinforcement strains, increasing the wall internal stability, alleviating down-drag forces behind the wall facing, and so on. Although the performance of the secondary reinforcement has been widely examined, its controlling factors (i.e., length, spacing, distribution) on the behavior of MSE wall are scarcely studied. In this study, a finite element approach was validated via a benchmark field case and was applied to understand the effect of the controlling factors on the behavior of MSE wall as well as giving a guidance on the design of MSE wall with secondary reinforcement.

Keywords: retaining structure, MSE wall, controlling factors, secondary reinforcement, finite element

©2019. Japan Geoscience Union. All Right Reserved. 

# EXPERIMENTAL STUDY ON POLYUREA-COATED RC SLAB SUBJECTED TO CONTACT EXPLOSIONS

*Minghsien Wu[1], Yingkuan Tsai[1], Chien-Hsien Liu[1], Pang-Ting Pai[1], Feng-Cheng Yang[1], Chun-Chia Huang[1]

1. Chung Cheng Institute of Technology National Defense University

Global terrorism is on the rise as the number of attacks soared, puts the world under the threat of car bomb, suicide bomb and so forth, and causes a huge amount of loss of life and property. Current buildings and infrastructures are mostly constructed using reinforced concrete, due to the brittleness of concrete material, when a structure subjected to blast loadings, the phenomena such as cracking and spalling at the proximal face of the target, and the ejection of fragments from the distal face of the loaded surface can be observed. These types of damage or failure could severely harm to the structural stability and the safety of people and equipment inside the building. Thus, the blast resistance of buildings has become an important issue in structural design and evaluation. Considering the high tensile strength and excellent impact resistance of polyurea materials, it is expected that the blast performance of a reinforced concrete element can be enhanced by coating this material onto its surface.

The purpose of this study is to investigate the blast performance of the polyurea coating on reinforced concrete slabs by conducting a series of filed explosion tests. The size of the specimen is 50cm×50cm×15cm. Four pieces of RC slabs were tested: RC slab without coating, RC slabs with coating on the front face, coating on the back face, and coating on the both faces. The thickness of coating is 3 mm. The specimens were fixed on a steel frame and detonated at the center of the test surface with a size of 5cm×5cm×2.5cm of 100g C4 rectangular explosive. The size and depth of the damage area on the front and back of the RC slabs were measured and evaluated by developing 3D models with point clouds from photographs.

The results show that when the unreinforced RC slabs is subjected to contact explosion, cratering will occur on the front side of the specimen and spalling will occur on the back side of the specimen; and when the RC slabs is coated on the front side of the specimen, the polyurea reinforcing layer at the contact explosion site is destroyed, but the damage degree were reduced; and in the case of the back-explosive surface reinforcement, the damage range of the cratering is also reduced, and the polyurea coated with the back-explosive surface has no crack, damage and blow-through. When the coating layer is removed, the back surface of the test piece is observed, and only cracks are generated but no obvious spalling. It is obvious that polyurea produces good adhesion due to its material properties and tightly constrains the fragments. Therefore, it has been shown by experiments that the use of polyurea elastic coatings to reinforce the explosion surface or the back explosion surface of the RC slabs can enhance the explosion-proof capability and reduce or protect from spalling, thereby achieving the purpose of protecting the internal life and property of the building. It is known from this test that the polyurea coating with a thickness of 3 mm can effectively and significantly reduce or avoid the occurrence of spalling when applied to the back surface of RC slabs.

Keywords: polyurea coatings, contact explosions, cratering, spalling

©2019. Japan Geoscience Union. All Right Reserved. 

# Simulation and field investigation of scour and sediment transport after Dam removal in the mountainous creek in Central Taiwan

*Chunhung WU[1]

1. Feng Chia University

The research focuses on using the flume experiments to observe the head-erosion phenomena caused by dam removal and simulate the channel evolution in the upstream and downstream of dam after dam removal by using CCHE2D model. The research area is in the Landaw river watershed in Huisun National Forest Area in the Central Taiwan. Two silts of silt dam build in the Landaw river had been lowered down 2.5 m height to release the deposited sediment to transport to downstream in 2013, and the research proceeded long term observation of the head-erosion in the upstream of the silt dam by using UAV and field investigation.
The research proceeded the flume experiments to simulate the sediment transport from the upstream of the dam and simulate the channel evolution in the upstream and downstream of dam by using CCHE2D model after dam removal. The control factors in the flume experiments are the sediment size, the discharge, the channel slope, and the removal area of check dams. The sediment size settings in this research include totally 0.9 mm, half 0.9 mm and half 0.5 mm, and totally 0.5mm, while the discharge settings include 3.4, 83.0, and 102.6 cubic centimeter per second. The channel slope settings include 4.4, 8.7 and 13 degree. The research records the sediment yield volume, the geomorphologic changes and the knickpoints evolution in the longitudinal sections after removing different area of dams in 27 flume experiments. Based on the dominant factors for the bank erosion scouring, 27 flume experiments can be classified into 3 types, including infiltration-dominated bank erosion experiments, surface runoff-dominated bank erosion experiments, and infiltration and surface runoff co-exist bank erosion experiments.
Furthermore, the research also uses CCHE2D model to simulate the sediment transport after the dam removal process of the silt dam in the upstream of Landaw river watershed. The research uses the river discharge in the day with the maximum 24 hours accumulated rainfall from 2015 to 2018, and the original DSMs in 2010, 2016, 2018 as the topographic models to simulate the scouring process in the upstream of the silt dam after dam removal. The research also proceeded the field investigation to verify the simulation result.
The accumulated rainfall setting for the simulation of CCHE2D model is 585 mm in 24 hours, and this is the accumulated rainfall with return period years of 50 year in the Landaw river watershed. Based on the simulation result by using CCHE2D model with the accumulated rainfall of 585 mm in 24 hours, the elevation of main river has been lowered down 5.4 m, and the maximum width of the head-erosion in the upstream od the silt dam is around 5.24 m. The total erosion sediment volume is estimated as 1370 cubic meter. The slope in the longitudinal profile along the main river can be classified into two sections. The slope from the silt dam to 23 m upward in the upstream is estimated as 0.31, while that from the 23 m upward in the upstream to the 200 m upward in the upstream is estimated as 0.151. This means that the knickpoint is in the 23 m upward in the upstream of the silt dam. The result will be the basis for developing the assessment model for assess the feasibility of dam removal in the rivers.

Keywords: Dam Removal, CCHE-2D, sediment transport

©2019. Japan Geoscience Union. All Right Reserved. 

# Examination and systematization of predispositions to floods in the Heavy Rain in July 2018

*Kanako Kimura[1], Toshihiko Sugai[2]

1. The University of Tokyo, 2. Graduate School of Frontier Sciences, the University of Tokyo

## Introduction

Though predispositions to floods have been mentioned in the studies of river engineering, geography and geomorphology, the relationship between flood and topography / geology is dealt with as self-evident in most of them. Hence, this study focuses on the predispositions to floods.
The floods in the Heavy Rain in July 2018, especially those of the Oda River (the Takahashi River System) are the subjects of this study. The purposes of this study are (1) to create a database on the floods, (2) to examine predispositions for each space scale, taking into account the influence of artificiality, (3) to acquire knowledge contributing to high accuracy of flood risk assessment.

## Fields & Methods

In the Chugoku district, 3 denudation surfaces are seen. And, the plains on the Setouchi side have been formed by the rivers flowing down from the Chugoku mountains. These rivers are characterized by weathering granitoids distributed upstream.
The Oda River is a first-class river which joins the Takahashi River in Kurashiki city. Since the Oda River has a gentler river bed than that of the Takahashi River, it is affected by the backwater from the Takahashi River.
The Association of Japanese Geographers has released the map of the flood points caused by the heavy rain on the Web (http://ajg-disaster.blogspot.com/). The characteristics of the river channels on the flood points on this map (mainly those of the Oda River) were investigated and compiled into a matrix.
On 9 dike break points of 4 rivers, the aerial photos were interpreted, and the classification maps of flood landforms were created.
Besides, the downstream change graph of the river bed height, the bed slope…etc. of the Oda River were created.

## Results

Many dike break points lie in the administrative sections of the prefectures, and raised beds are seen on 9 of the 10 points in the tributaries to the Oda River. There are sluice gates on 2 dike break points and 5 slope failure points reported in the Council for Social Infrastructure (2018). At the outer bank of the large river curve in Fukuhara, where the overflows and the slope failures were occurred this time, dike breaks were also occurred in the past.
Although alluvial ridges have been regarded as safe against floods, the largest dike breaks occurred on the alluvial ridge.
The downstream change graphs show that floods didn’ t occur in a downstream section of a weir with a relatively steep river bed but occur in a further downstream section where a river bed becomes gentle.

## Discussion

On the point scale, a sluice gates and a raised bed section is one of the predispositions to floods. From comparing dike break points and non-dike break points, it is suggested that steep slope gradient affects dike break, too. And it is necessary to update the flood risk assessment on alluvial ridges.
On the section scale, compared the downstream section of a weir with a steep river bed, the further

©2019. Japan Geoscience Union. All Right Reserved. 

downstream section with a gentle bed is dangerous.
On the regional scale, it is considered that the bed slope difference of the Oda River and the Takahashi River is affected by the denudation surfaces. It is also one of the predispositions that granitoids is widely distributed in Chugoku district.
Regarding artificiality, it turned out that the river maintenance has not kept up. However, there is the more serious issue that the Mabi-cho area, where many floods occurred this time, has become a bedroom town. Therefore, it is necessary to reconsider how to use land.

## References

Council for Social Infrastructure, The Ministry of Land, Infrastructure, Transport and Tourism (2018), About the Heavy Rain in July 2018
Izumida, A. (2018), Crevasse splay formation and contribution to the development of alluvial ridges in the lower Kinu River, central Japan, Master's thesis of Graduate School of Frontier Sciences, The University of Tokyo
Uchida, K. (2011), Activities of the flood prevention unions in the Oda River basin in Okayama prefecture, Water Utilization Science No.320, pp.40-55

Keywords: the Oda River, raised bed river, alluvial ridge, crevasse splay, channel slope

©2019. Japan Geoscience Union. All Right Reserved. 

| | 地点 | 種類 | 確かさ 海津ほか | 直後写真 | 確かさ 総合 | 支流名 | 岸 | 河道植生 | 砂州 | 河床材料 | 河道幅 (m) | 低水路幅 水面幅(m) | 狭窄 (m) | /河道幅 (広) | 堤防高 堤外地 | 堤防高 堤内地 | 横幅 堤内地 | 傾斜 堤内地 |
|---|---|---|---|---|---|---|---|---|---|---|---|---|---|---|---|---|---|---|
| 小田川 | 4 | 破堤 | ほぼ正確 | × | △ | 尾坂川 | 左 | 草（2014） | 上216-85mに（2014） | 砂 | 27 | (7) | - | - | 2.1 | 1.7 | 9 | 0.189 |
| | 5 | 破堤 | ほぼ正確 | × | △ | - | 左 | 草（2007） | - | - | 142 | (30) | - | - | 6.3 | 3.1 | 17 | 0.182 |
| | 6 | 破堤 | ほぼ正確 | × | △ | - | 右 | ～草（2014） | 下15m左岸，固定化（2014） | 砂 | 155 | (35) | - | - | 5.1 | 2.6 | 22 | 0.118 |
| | 7 | 破堤 | ほぼ正確 | × | △ | - | 左 | 草（2014） | - | 砂 | 180 | (20-37) | 100 | 0.42 | 5.7 | 2.5 | 13 | 0.192 |
| | 8 | 破堤 | ほぼ正確 | ○ | ○ | (水路) | 左 | - | - | - | 5 | 2 | - | - | 1.3 | 1.8 | 9 | 0.200 |
| | 9 | 越水 | ほぼ正確 | ○ | ○ | - | 右 | 草（～樹木） | 両岸 | 砂 | 181 | 38-47 | - | - | 7.3 | (山) | - | - |
| | 10 | 破堤 | 不正確 | ○ | ○ | 大武谷川 | 右 | ～草 | - | - | 13 | 1-2 | - | - | 1.5-2.1 | 2.2 | 8 | 0.275 |
| | 11 | 破堤 | ほぼ正確 | ○ | ○ | - | 左 | 草～樹木 | 左（内）岸に30m | 砂 | 206 | 58 | 28 | 0.14 | 5.8 | 4.0 | 12 | 0.333 |
| | 12 | 破堤 | ほぼ正確 | ○ | ○ | 真谷川 | 左 | 草（～樹木） | - | - | 37 | 1-2 | - | - | 6.0 | 5.4 | 13 | 0.415 |
| | 13 | 越水 | ほぼ正確 | ○ | ○ | - | 右 | 草～樹木 | 樹林化中州 | 砂 | 233 | 複数本 | - | - | 7.8 | 3.4 | 13 | 0.262 |
| | 14 | 破堤 | ほぼ正確 | ○ | ○ | 高馬川 | 右 | 草 | - | - | 13 | 7 | - | - | 1.5 | 4.0 | 14 | 0.286 |
| | 15 | 破堤 | ほぼ正確 | ○ | ○ | 高馬川 | 左 | 草 | - | - | 13 | 7 | - | - | 3.0 | 5.8 | 13 | 0.446 |
| | 16 | 破堤 | ほぼ正確 | ○ | ○ | - | 左 | 草～樹木 | 樹林化中州 | 砂 | 217 | 複数本 | - | - | 8.2 | 6.0 | 18 | 0.333 |
| | 17 | 越水 | ほぼ正確 | ○ | ○ | - | 右 | 樹木 | 樹林化中州 | 砂 | 227 | 複数本 | - | - | 7.2 | 2.6 | 16 | 0.163 |
| | 18 | 破堤 | ほぼ正確 | ○ | ○ | 末政川 | 右 | ～草 | - | - | 12 | 1-2 | - | - | 1.6 | - | - | - |
| | 19 | 破堤 | ほぼ正確 | ○ | ○ | 末政川 | 左 | ～草 | - | - | 12 | 1-2 | - | - | 2.1 | - | - | - |
| | 20 | 破堤 | ほぼ正確 | ○ | ○ | 末政川 | 右 | ～草 | - | - | 30 | 1-2 | 6 | 0.20 | 5.1 | 6.5 | 18 | 0.361 |
| | 21 | 破堤 | ほぼ正確 | ○ | ○ | 末政川 | 左 | ～草 | - | - | 32 | 1-2 | 6 | 0.19 | 5.5 | 6.2 | 19 | 0.326 |
| 高梁川 | 1 | 破堤 | - | ○ | ○ | - | 右 | 樹木多い | 右（内）に80m | 砂 | 240 | 65 | 70（緩やか） | - | 10.3 | 3.0 | 11 | 0.273 |
| | 2 | 破堤 | - | ○ | ○ | - | 右 | 樹木多い | 右（内） | 砂 | 190 | 80 | 同上 | - | 9.7 | 2.2 | 9 | 0.244 |
| 砂川 | | 破堤 | ほぼ正確 | × | △ | - | 左 | 草～樹木（2007） | 右岸(2007) | 砂 | 58 | 5 | - | - | 4.5 | 4.5 | 15 | 0.300 |
| 旭川 | | 破堤 | ほぼ正確 | × | △ | - | 左 | 草～（2007） | 80m下から(2007) | 粗砂～ | 175 | 116 | 80m下から54減 | 0.31 | 5.3 | - | - | - |
| 芦田川 | | 破堤 | 不正確 | ○ | ○ | 吉野川 | 右 | ～草 | - | - | 9 | 0-1 | - | - | 0.3 | 1.9 | 8 | 0.238 |
| 賀茂川 | | 破堤 | 不正確 | ○ | ○ | - | 右 | ～草 | 右岸に17m | 砂 | 37 | 16 | - | - | - | 2.5 | 10 | 0.250 |

**Fig. 1** A part of flood point matrix.

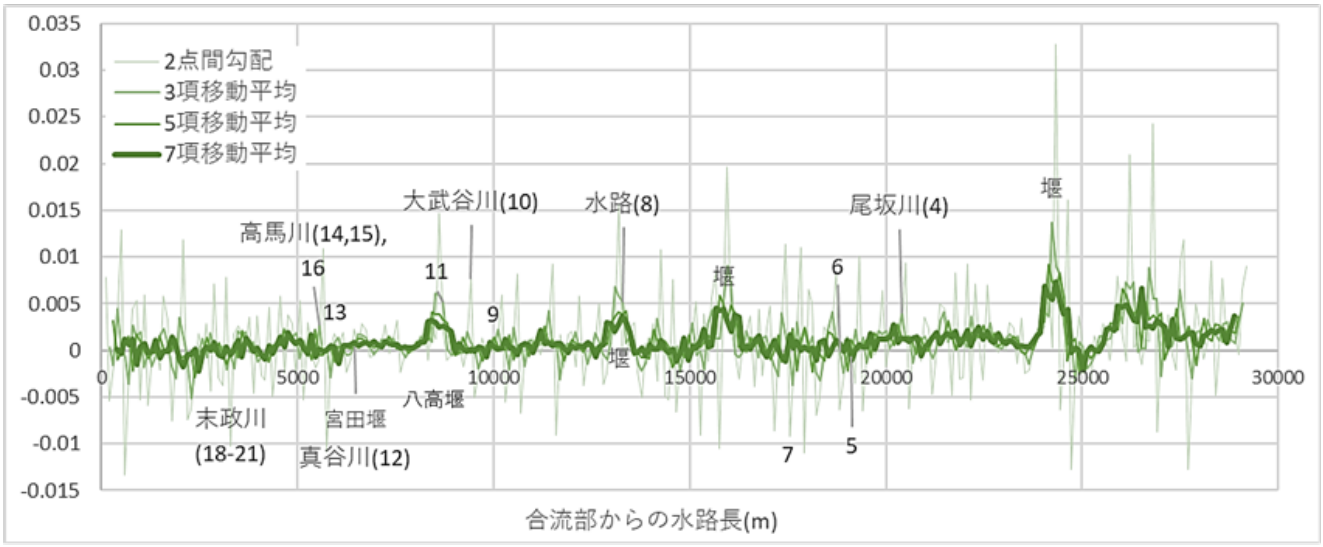


**Fig. 2** The downstream change graph of the river bed slope.

©2019. Japan Geoscience Union. All Right Reserved. 

# Expand various disaster risk information and sophisticate methods to disseminate on the Hazard Map Portal Site

*Takuya Ueshiba[1], Yumeka Fujii[1], Naoki Yoshimatsu[1], Noriyuki Takakuwa[1], Wataru Yamasaki[1], Jun Suwabe[1]

1. GSI of Japan

I. Introduction
In June 2006, it was necessary to prepare the portal site about hazard maps which anyone can search on the internet, according to the policy established by Ministry of Land, Infrastructure Transport and Tourism. Geospatial Information Authority of Japan, in cooperation with Water and Disaster Management Bureau and so on, began to operate Hazard Map Portal Site since April 2007. This latest site has two main contents. One is Layered Hazard Map which enables users to layer various maps and disaster risks, and another is Published Hazard Map showing links to hazard maps made by each local government.

II. Questionnaire about Hazard Map Portal Site
A questionnaire was conducted in 2015 for 18 local governments and about 1,000 residents to figure out these things: how much they recognize and use it, needs, and to know the problems of this site. Various needs and requests were made clear, for example, the addition of the function displaying all disaster risk information by clicking map, implementation of browsing feature by mobile device, preparation of download page published data on this site, expanding the data about disaster risk information and evacuation facilities, making the data open for public on the Internet and machine-readable (hereinafter referred to “Open Data”) and so on.

III. Three activities
Three activities were carried out based on this questionnaire.
1. Improvement of function
Three functions were mainly added on this site. One is the function displaying multiple risks, which were inundation, landslide, sediment disaster and so on, at arbitrary point on Layered Hazard Map, another is the compatibility with smartphones which enable to access this site away from home, and the other is function of downloading list files of URL linking to Published Hazard Map.
2. Expanding Data
Designated Emergency Evacuation Area (flood from river, storm surges, tsunami, debris flow, steep slope failure / landslide, fire disasters), expected inundation areas of ministry-controlled river due to statistical heaviest rainfall, expected inundation areas of tsunami, and landform classification of Fundamental Land Classification Survey were released.
3. Open Data
Raster tiles of expected inundation areas of ministry-controlled river due to statistical heaviest rainfall, Landslide Prone Areas and dangerous site by sediment and landslide disaster was added to Open Data list. Furthermore, these raster tiles data started to be converted to vector tiles data and will be distributed as Open Data by June 2019.

IV. Future perspective
We carried out improvement of this site system, expansion data of disaster risk information and Open Date of raster tiles covered on Layered Hazard Map. Due to this effort, tasks revealed in 2015 questionnaire survey were solved and this site became more useful. This result led to further publicize

©2019. Japan Geoscience Union. All Right Reserved. 

disaster risk and contributed to raise awareness of disaster prevention.
In order to expand data and make the site more useful, various information including expected inundation area maps classified by duration time and expected inundation areas by reservoir break will be disclosed and more functions, for example 3D page of Layered Hazard Map, will be added.

Keywords: disaster risk, hazard map, web map, open data

©2019. Japan Geoscience Union. All Right Reserved. 

# A study on evaluation formulae of the principal fault in PFDHA- In consideration of a relevance to known active faults-

*Tsuyoshi Kanda[1], Makoto Takao[1], Toshimichi Kaneto[1], Takehisa Arakawa[1]

1. Tokyo Electoric Power Company Holdings, Inc

Takao et al. (2013) proposed some evaluation formulae for probabilistic fault displacement hazard analysis (PFDHA) based on data on surface earthquake faults in Japan.

As for the formulae in terms of the principal fault, Takao et al. (2013) did not discriminate between (1) an earthquake that occurred in an area where an active fault exists, and (2) an earthquake that occurred in an area where no cumulative deformation or active fault exists, in the same way as Youngs et al. (2003).

In this study, we re-examined the aforementioned evaluation formulae by discriminating between (1) and (2) for the 107 hypocenters described in Takao et al. (2003).

The results show that the differences in the P1p between (1) and (2) are distinct and that the P1p is closely correlated to the distance between the active fault and the hypocenter, so discrimination between (1) and (2) is useful for these evaluation formulae.

Therefore, it is suggested that the results of this study can be a powerful tool for applying the idea of diffuse seismicity in the probabilistic seismic hazard analysis (PSHA) to the PFDHA.

There are some differences in the evaluation formula for the fault displacement between (1) and (2), whereas it was confirmed that there is no clear correlation between the threshold value (boundary between (1) and (2)) and the predicted displacement using the regression equation.

We strongly recommend that these evaluation formulae should be examined in future by gathering more data on surface earthquake faults because the present data may be insufficient to consider the correlation between threshold value and fault displacement.

Keywords: PFDHA, probability of surface rupture of the principal fault, fault displacement, a relevance to an active fault

©2019. Japan Geoscience Union. All Right Reserved. 

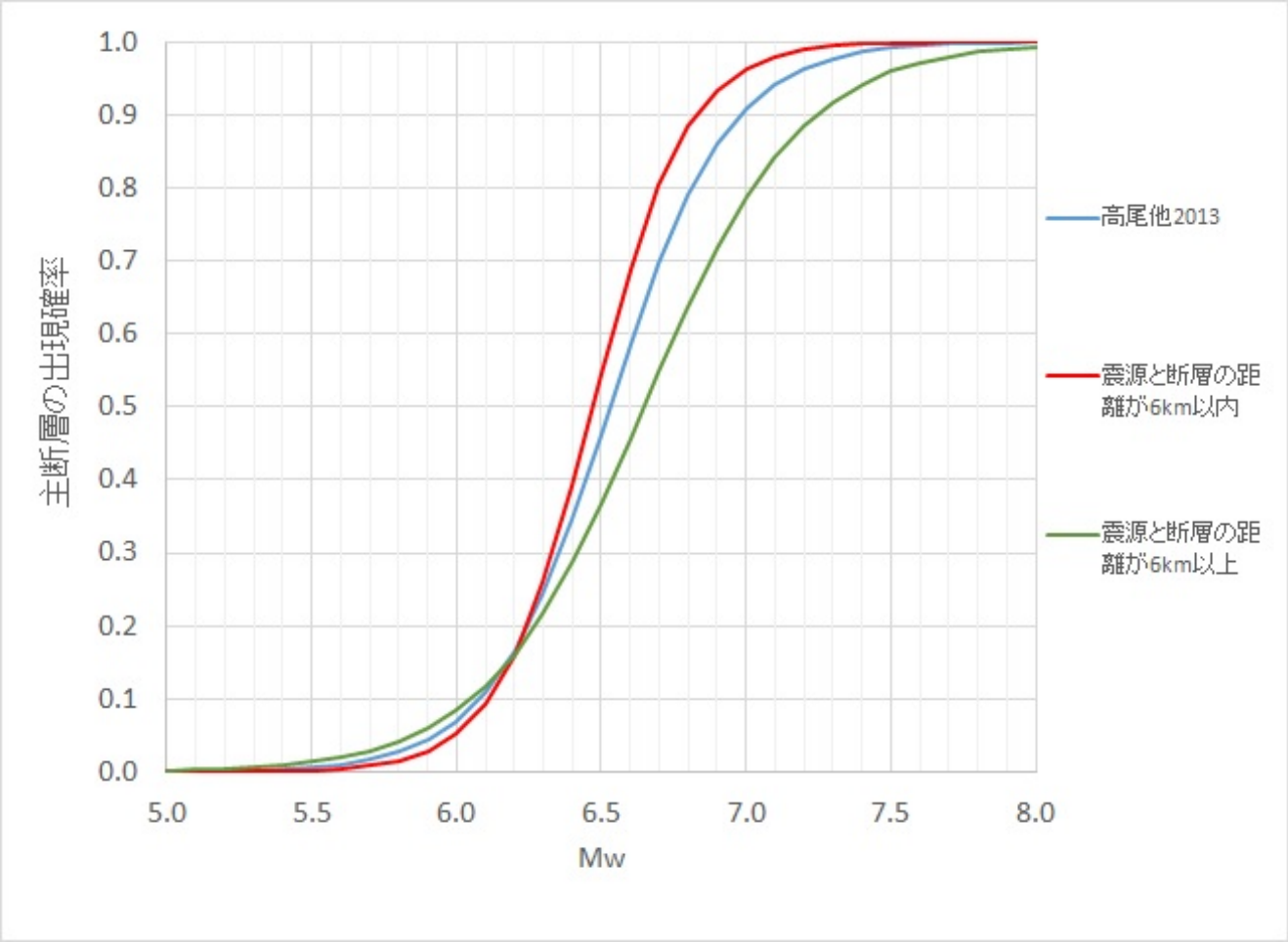


©2019. Japan Geoscience Union. All Right Reserved. 

# Characteristics of sediment deposition distribution in debris flow disasters in caused by heavy rain in August 2014 Hiroshima, Japan

*Shoichiro Uchiyama[1], Toshihiko Sugai[2]

1. National Research Institute for Earth Science and Disaster Resilience, 2. The University of Tokyo

1. Background
Post-war sediment disaster countermeasures have been promoted mainly by the development of structural measures. However, disaster prone areas are expanding annually owing to the development of residential areas. Owing to the difficulty involved in preventing sediment disasters by taking structural measures alone, nonstructural measures are being promoted. However, many of the victims of the sediment damage caused by the Heavy Rain Event of July 2018 were located in sediment disaster-prone areas. From these facts, we can see that the preliminary evacuation is inadequately performed.

2. Purpose and significance
For autonomous evacuation to be conducted when the risk of the disaster is identified, it is necessary to anticipate the extent of damage possible in the inhabited areas. For example, the damage owing to debris flow can be predicted using knowledge of the behavior of debris flow and the relationship between debris flow and buildings or vegetation in the flow path. Therefore, in this study, the volume of sediment deposition by debris flow was measured, and its distribution characteristics were analyzed in six districts of Asaminami-ku, Hiroshima, which was damaged by the debris flow on August 20, 2014.

3. Method
There were 23 digital aerial photographs (Geospatial Information Authority of Japan) taken on May 21, 2008. Further, approximately four days after the disaster, unmanned aerial vehicles were used to capture aerial photographs, which comprised 700 vertical images. 30 points were measured by conducting a GNSS survey; 10 ground reference and 14 accuracy verification points were used. The spatial resolution of DSM and orthoimage created by SfM photogrammetry were 20.0 cm and 3.5 cm before and after the disaster, respectively. As a result of the accuracy verification of the DSM, the three-dimensional RMSEs at the accuracy verification point that employed 14 points were 26.2 cm (2008 DSM value) and 11.5 cm (2014 DSM value). The change in the height of the ground was obtained by subtracting the 2008 DSM elevation from the 2014 DSM value calculated using GIS. Next, the sediment deposition areas were interpreted from the orthoimage after the disaster, and polygon data were created using GIS.
In the surface height change data, a mesh having a positive value corresponds to sediment deposition inside the sediment deposition area polygon. At this time, we considered the error of the DSM at 2 periods as follows: the square root of the sum of the squares (28.6 cm) of RMSE values (26.2 cm before disaster, 11.5 cm after disaster) at each time were obtained as mentioned above, and only the mesh with a height change larger than this value was targeted.

4. Result
Of the results obtained, Yagi 3 districts were figured. There were two blue falling water lines near the center, and the main flow path widened to approximately 25 m. Within the range 70 m above and below the flow path, seven buildings were lost, resulting in 20 casualties (A). In the housing at the most downstream part of this row, a portion of the building moved downward while remaining intact, resulting in two casualties. In addition, the apartment that was in the center of this row of houses was lost in the debris flow; however, because it was a vacant lot in the pre-disaster aerial photograph, the apparent

©2019. Japan Geoscience Union. All Right Reserved. 

change in the DSM appears to be sedimentary (B). In the public housing building located on the falling water line, sediment flowed, resulting in one casualty (C). Among the vegetation growing adjacent to the main flow path, the side close to the flow path was eroded (D). There was an area in which the sediment deposition thickness was in the main flow path thin (E). A sediment layer exceeding 2 m in thickness accumulated in the parking lot at the end of the main flow path. In the orthorectified images, the sediments exhibited a mud-like texture (F).

Keywords: debris flow, heavy rain in August 2014, volume of sediment deposition, UAV, SfM-MVS Photogrammetry

©2019. Japan Geoscience Union. All Right Reserved. 

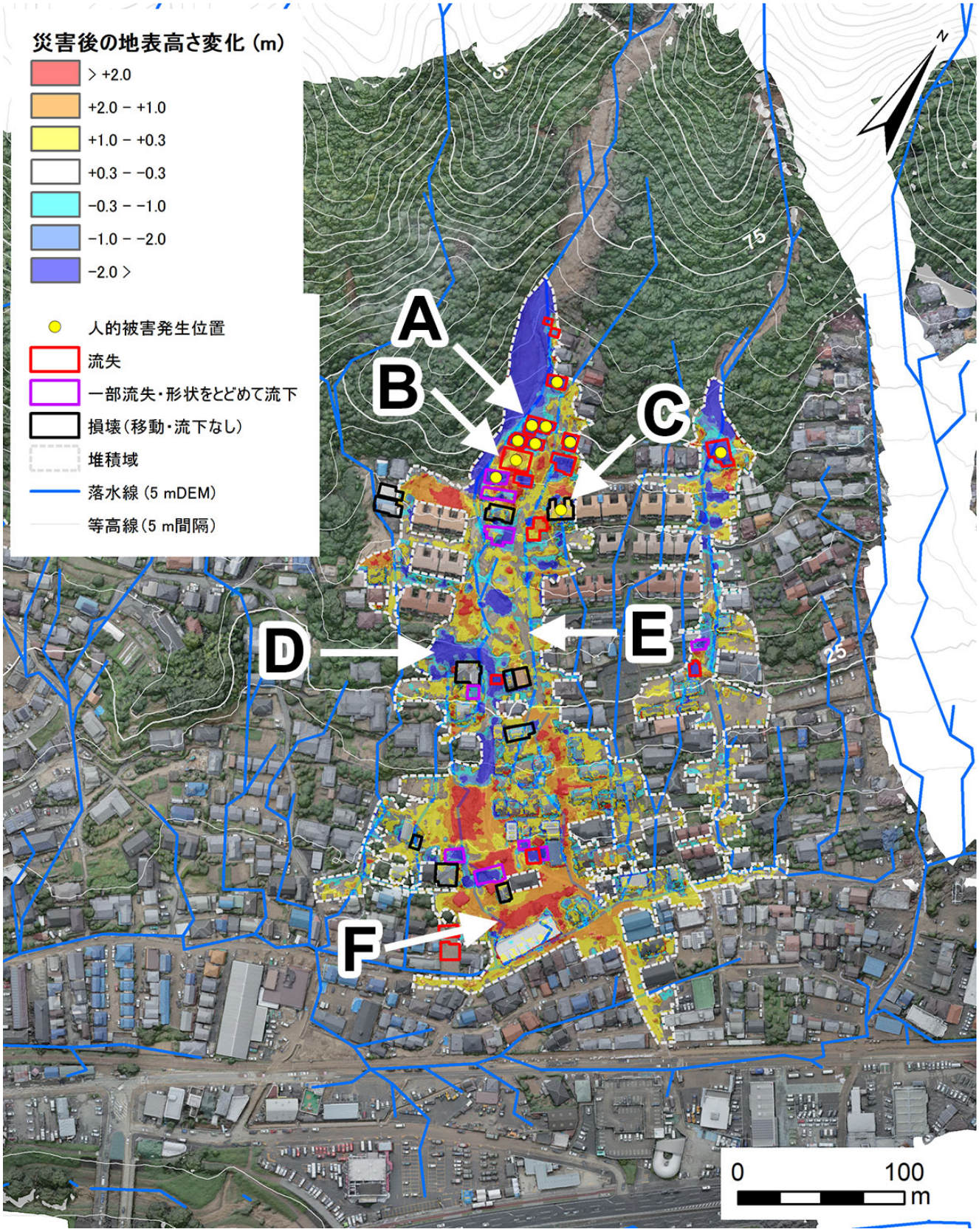


©2019. Japan Geoscience Union. All Right Reserved. 

# Land use change after tsunami and its problems in Kii peninsula

*Kenta Okidate[1], Tatsuto Aoki[2]

1. School of Humanities, Kanazawa University, 2. School of Regional Development Studies, Kanazawa University

Disaster prevention against tsunami is paid attention socially. In Japan, many cities are located in the coast and have a possibilities of damage by tsunami. This paper presents the results of quantitative analyzing land use changes in region have few researches and clarifying its regional characteristics and problem.

Three study areas, Shirahama area, Kushimoto area, Nachiwan surrounding area, were damaged by tsunami in 1944 and 1946. After the disaster, these regions were restored disorderly.

By analyzing Geographic Information System (GIS) data with QGIS, Interview, and field survey, land use changes in study areas were clarified.

Housing/Building increased greatly by converting Wasteland/Farmland and Forest. Especially, from 1947 to 1965, converting flooded vacant lot by tsunami into Housing/Building was prominent. Increasing of Housing/Building, Wasteland/Farmland and port facilities by reclamation were seen. Also, building lot increased in tsunami inundated areas and these areas for itself increased by reclamation in all study areas. Large buildings are increased in the coast with the passing of the years.

As a result of analysis, expanding building lot, building port facilities and so on were clarified as regional characteristics. These are geomorphological limitation, tourism development, increasing demand of building lot and economic structure as its factors. 3 problems, crowded building lot in the coast, increasing building lot and port facilities by reclamation, large buildings in the coast, were also clarified. These problems may disturb refuge from tsunami. A long-term plan for safe land use is necessary to solve problems.

Keywords: Disaster prevention, Nankai Trough Earthquake, land use, GIS

©2019. Japan Geoscience Union. All Right Reserved. 

# Reconstruction of the building damages caused by the Typhoon Kathleen and analyses of their land conditions at the southern foot of the Akagi Volcano using U.S. military aerial photographs

*Masafumi Aoyama[1], Yoshiki Saito[2]

1. Faculty of Education, Gunma University, 2. Graduate Student, Gunma University

We reconstructed building damages caused by the Typhoon Kathleen and analyses of their land conditions at the southern foot of the Akagi Volcano using U.S. military aerial photographs and GIS. Flood inundation area were identified based on the building damages and flood deposits by using U.S. military aerial photos. Building damages due to the flood concentrated in the former river channel and valley bottom plain. Several schools (25%) in the study area located in the inundation area of the Typhoon Kathleen.

Keywords: Typhoon Kathleen, flood risk assessment, building damage, U.S. military aerial photographs, southern foot of the Akagi Volcano

©2019. Japan Geoscience Union. All Right Reserved. 

[E] Poster | H (Human Geosciences )：H-TT Technology & Techniques

Thu. May 30, 2019 10:45 AM - 12:15 PM JST | Thu. May 30, 2019 1:45 AM - 3:15 AM UTC | Poster Hall International Exhibition Hall8, Makuhari Messe_3

## [H-TT19] Geographic Information Systems and Cartography

convener:Takashi Oguchi(Center for Spatial Information Science, The University of Tokyo), Yuji Murayama(Graduate School of Life and Environmental Sciences), Yoshiki Wakabayashi(Graduate School of Urban Environmental Sciences, Tokyo Metropolitan University)

This session discusses various methods which acquire, store, analyze and visualize geospatial data, and presents the outcomes of empirical studies using GIS or mapping methods. The session also deals with applications of digital data, and GIS, and mapping to various fields of earth and planetary science and human society. All presentations and discussion of this session are made in English.

### [HTT19-P01] Monitoring and Simulating Land Use/Cover Changes and its Impact on Land Surface Temperature in Sapporo City, Japan

*RUCI WANG[1], YUJI MURAYAMA[1] (1.University of Tsukuba)

### [HTT19-P02] Spatiotemporal Variations of Land Cover/Use and Sustainable Urban Heat Island (UHI) Mitigation Strategies: A Case Study of Chinese Bay Megacities

★Invited Papers

*Fei LIU[1], Yuji MURAYAMA[1] (1. University of Tsukuba)

### [HTT19-P03] A LST Study of the Seoul Metropolitan City, South Korea, Based on Landsat Data (1996 – 2017)

*Prabath Priyankara[1,3], Manjula Ranagalage[1,4], DMSLB Dissanayake[1,4], Takehiro Morimoto[1,2], Yuji Murayama[1,2] (1.Graduate School of Life and Environmental Sciences, University of Tsukuba, Japan, 2.Faculty of Life and Environmental Sciences, University of Tsukuba, Japan, 3.Faculty of Agriculture, University of Ruhuna, Sri Lanka, 4.Faculty of Social Sciences and Humanities, Rajarata University of Sri Lanka, Sri Lanka)

### [HTT19-P04] Improvement of GIS exercise classes using the GIS open educational resources based on questionnaire surveys

★Invited Papers

*Hiroyuki Yamauchi[1], Takashi Oguchi[1], Yuichi S. Hayakawa[2,1], Kotaro Iizuka[1] (1.Center for Spatial Information Science, The University of Tokyo, 2.Environmental Geography, Faculty of Environmental Earth Science, Hokkaido University)

### [HTT19-P05] The Development of COP for Tzu Chi Disaster Prevention System by Using QGIS-Taking 2018 Hualien Earthquake as an Example

*kuan-wen tseng[1], Ming-Ta Tsai[1], Yun-Ching Wang[1], Ming-Chih Wang[1], Chien-Hsien Liu[1] (1.03-3809093)

### [HTT19-P06] Comparative study on shape and distribution of landslides caused by the 2012 Northern Kyushu heavy rainfall and the 2016 Kumamoto earthquake in the Aso region, Kumamoto, Japan

*Yasutaka Haneda[1], Takashi Oguchi[2], Kotaro Iizuka[2], Hitoshi SAITO[3,2], Yuichi S. Hayakawa[4,2], Shoichiro Uchiyama[5] (1.Graduate School of Frontier Science, The University of Tokyo, 2.Center for Spatial Information Science, The University of Tokyo, 3.College of Economics, Kanto Gakuin University, 4.Faculty of Environmental Earth Science, Hokkaido University, 5.National Research Institute for Earth Science and Disaster Resilience)

### [HTT19-P07] Using GIS and remote sensing to assess relationships between landslides and land cover changes in the Sanbagawa and Mikabu Belts, Shikoku, Japan

*Roxanne Lai[1], Takashi Oguchi[1] (1.University of Tokyo)

[HTT19-P08] **Analysis of Morphometric Parameters for Mountains Ranges and Landslides due to the July 2018 Heavy Rain in Western Japan Using GIS Data**

*Toshikazu Fukuba[1], Takashi Oguchi[2] (1.Department of Earth and Planetary Environmental Science, The University of Tokyo, 2.Center for Spatial Information Science, The University of Tokyo)

---

[HTT19-P09] Analyzing short-term topographic change in coastal sand dunes using UAS-SfM photogrammetry: A case study in Northern Kujukuri, Japan

*Seulgi Lee[1], Yasutaka Nakata[2], Kotaro Iizuka[3], Takashi Oguchi[3] (1.Graduate School of Frontier Sciences, The University of Tokyo, 2.Forest Research Department, Forestry Research Institute, Hokkaido Research Organization, 3.Center for Spatial Information Science, The University of Tokyo)

---

[HTT19-P10] **Responses of suspended sediment yield to precipitation, topography and dam control in the Yellow River Basin, China**

*Ruiqi Zhang[1], Takashi Oguchi[2] (1. Department of Natural Environmental Studies, Graduate School of Frontier Sciences, The University of Tokyo, 2.Center for Spatial Information Science, The University of Tokyo)

# Monitoring and Simulating Land Use/Cover Changes and its Impact on Land Surface Temperature in Sapporo City, Japan

*RUCI WANG[1], YUJI MURAYAMA[1]

1. University of Tsukuba

In recent years, urban heat island phenomenon (UHI) which prevails in many cities worldwide has caused broad public concern. UHI phenomenon impairs healthy urban development and causes excessive energy consumption, climatic and environmental deterioration. Land use/cover changes are one of the most crucial variables influencing on UHI. Therefore, monitoring and simulating land use/cover changes and analyzing its effects on LST are essential for healthy urban development. This study aims to capture the impact of land use/cover on LST and simulate the LST under various land use/cover scenarios in Sapporo city, Japan. At first, we monitored the land use/cover changes from 1985 to 2015 and detect the change of LST concerning land use/cover distribution. Then, we predicted the future conditions of LST based on various land use/cover scenarios. The results show that the LST differs according to land use/cover types, and the proportion of land use/cover types is the most significant factor affecting LST. The findings also indicate that the built-up area and paddy field have the highest average LST, while the green space and water area help cool the city. In the future, the green area such as urban green parks and grassland should be planned in the city to mitigate the UHI phenomenon. It reveals the spatial characterization of LST which provides significant insights for government and city planners.

Keywords: Geographical information science, Urban heat island, Land surface temperature, Land use/cover change, Sapporo city

©2019. Japan Geoscience Union. All Right Reserved. 

# Spatiotemporal Variations of Land Cover/Use and Sustainable Urban Heat Island (UHI) Mitigation Strategies: A Case Study of Chinese Bay Megacities

*Fei LIU[1], Yuji MURAYAMA[1]

1. University of Tsukuba

Rapid urbanization significantly affects the urban thermal environment in the context of global climate change. The assessment of surface urban heat island (SUHI) and development of mitigation strategies in megacities have become frontier issues on human health and urban sustainability. In this study, taking of the three Chinese bay megacities, we attempt to 1) disclose the relationship between land surface temperature (LST) and land cover using remote sensing quantified analysis, 2) to clarify the mechanism and characteristics of SUHI formation based on bi-temporal patterns and variations of land cover, and 3) to sustainably regulate and optimize the urban environment and further create urban planning and policies for relieving urban thermal effect. The study target is Guangzhou metropolitan area (GMA), Hangzhou metropolitan area (HMA) and Shanghai Metropolitan area (SMA) in China. The result of this study indicated remarkably different characteristics, arrangement, and variations among different bay thermal environments. Overall, spatial layouts and changes in the thermal environment of these three megacities were substantially identical with their land cover pattern and tendency. Although land covers significantly influenced the LST as a whole, the different areas had different magnitudes of SUHI coming from different land cover compositions and differentials. The results would provide a valuable reference to disentangle spatiotemporal variation of the bay urban thermal environments, and the urbanization-induced land covers temperature dynamics. This study would contribute to the development of future SUHI mitigation solutions.

Keywords: Land Cover/Use , Urban Heat Island (UHI), Mitigation Strategies

©2019. Japan Geoscience Union. All Right Reserved. 

# A LST Study of the Seoul Metropolitan City, South Korea, Based on Landsat Data (1996 –2017)

*Prabath Priyankara[1,3], Manjula Ranagalage[1,4], DMSLB Dissanayake[1,4], Takehiro Morimoto[1,2], Yuji Murayama[1,2]

1. Graduate School of Life and Environmental Sciences, University of Tsukuba, Japan, 2. Faculty of Life and Environmental Sciences, University of Tsukuba, Japan, 3. Faculty of Agriculture, University of Ruhuna, Sri Lanka, 4. Faculty of Social Sciences and Humanities, Rajarata University of Sri Lanka, Sri Lanka

Rapid urban growth often replaced urban vegetation with impervious surfaces which leads to increase land surface temperature (LST) periodically and tends to form urban heat islands (UHI). This is a serious issue of urbanized cities and the increase of LST badly affects the well-being of the life and environments of the cities. The Seoul Metropolitan City (SMC), South Korea, is one of the developed and rapidly urbanizing metropolitan city in Asia. The aim of this study was to examine the spatiotemporal variations of LST in the SMC and surroundings in the context of the UHI using Landsat data. The study examined the relationship of LST with the normalized difference vegetation index (NDVI) and the normalized difference built-up index (NDBI) at three time periods 1996, 2006, and 2017. Also, the study was investigated the environmentally critical areas based on LST and NDVI by modeling environmental criticality index (ECI). According to the results of the study, there is a negative correlation between LST with NDVI and positive correlation of LST with NDBI across all three time periods. In SMC, most of the environmentally critical areas are located in the central business district (CBD), near the harbor, and along the main transportation network. According to the results of the study, it is recommended that the identified environmentally critical areas to be considered in the urban planning of the city. Green spaces of the city will help to improve the life and environmental well-being of the SMC.

Keywords: Urban Heat Island, Land Surface Temperature, NDVI, NDBI, Environmental Criticality Index, Seoul Metropolitan City

©2019. Japan Geoscience Union. All Right Reserved. 

# Improvement of GIS exercise classes using the GIS open educational resources based on questionnaire surveys

*Hiroyuki Yamauchi[1], Takashi Oguchi[1], Yuichi S. Hayakawa[2,1], Kotaro Iizuka[1]

1. Center for Spatial Information Science, The University of Tokyo, 2. Environmental Geography, Faculty of Environmental Earth Science, Hokkaido University

Free and open source GIS software has been utilized for GIS education all over the world. However, as far as we recognize, GIS education in many Japanese universities underutilize such software packages. Therefore, we developed GIS exercise materials explaining spatial data analyses using free and open-source GIS. We have been providing these materials for higher education and designated them as the GIS Open Educational Resources. We used the materials in a university exercise class, which was held as an intensive course for three days at The University of Tokyo. During the exercise, we have conducted questionnaire surveys to clarify the three criteria: difficulty, understanding and satisfactory levels of the students. The results showed that the students felt difficulty in some situations such as the utilization of GIS for the first time and complex operations using different types of data. The contents of the exercise syllabus and materials were improved based on the feedback. We conducted another GIS exercise class at the university to verify the utility of improvements. In this presentation, we show the improvements in the exercise syllabus and the comparison of educational effects on students before and after the improvements.

Keywords: GIS education, exercise, Open Educational Resources, Free and open-source GIS

©2019. Japan Geoscience Union. All Right Reserved. 

# The Development of COP for Tzu Chi Disaster Prevention System by Using QGIS-Taking 2018 Hualien Earthquake as an Example

*kuan-wen tseng[1], Ming-Ta Tsai[1], Yun-Ching Wang[1], Ming-Chih Wang[1], Chien-Hsien Liu[1]

1. 03-3809093

The Hualien earthquake occurred at 23:50 and 41.6 seconds on February 6, 2018. The epicenter was located in the coastal area of Hualien County. The earthquake scale was 6.2 and the Seismic source depth was 6.3 kilometers. The earthquake disaster along the Milun fault was mainly concentrated in Hualien City, and collapsed the first and second floors of the “Tongshuai” building. The “Yunmen Cuidi” Building showed a 45-degree tilt. The lower floors of the residential community building "Baijin Shuangxing" and “Wuzhu Wusu” at Guosheng Sixth Street were destroyed. This study mainly uses the powerful geospatial analysis capabilities of Geographic Information System (GIS) to provide Tzu Chi's plans for disaster mitigation. The projects include: (1) humanitarian cares; (2) visiting and reporting of damage situations around main disaster areas and (3) “Reassuring Homes Visits” in order to provide assistance to Tzu Chi people for operations of disaster mitigation.

Keywords: Millun fault, geographic information system, spatial analysis, Tzu Chi Foundation

©2019. Japan Geoscience Union. All Right Reserved. 

# Comparative study on shape and distribution of landslides caused by the 2012 Northern Kyushu heavy rainfall and the 2016 Kumamoto earthquake in the Aso region, Kumamoto, Japan

*Yasutaka Haneda[1], Takashi Oguchi[2], Kotaro Iizuka[2], Hitoshi SAITO[3,2], Yuichi S. Hayakawa[4,2], Shoichiro Uchiyama[5]

1. Graduate School of Frontier Science, The University of Tokyo, 2. Center for Spatial Information Science, The University of Tokyo, 3. College of Economics, Kanto Gakuin University, 4. Faculty of Environmental Earth Science, Hokkaido University, 5. National Research Institute for Earth Science and Disaster Resilience

The 2016 Kumamoto earthquake triggered many landslides in the Aso region, southwestern Japan. Previous studies have revealed the processes of some large representative landslides in the western Aso region, but they have not comprehensively dealt with lots of small landslides. Other studies have discussed landslide distribution and relationships with that of the heavy rainfall events in July 2012 in the northern part of the Central Cones of the Aso volcano. However, they have not been investigated the western part of the Aso region which has various topographical and geological characteristics. Therefore, this study compares the formation and distribution of landslides caused by the heavy rainfall and earthquake events in both the central and western part of the Aso region.

The study areas are the western part of the Aso region and the Sensuikyo region at the northern part of the Central Cones (Fig. 1). The western part was divided into three sites: site P (caldera walls and the outer rim), Q (western part of Central Cones), and R (river terrace and talus) based on geomorphological and geological characteristics. The Sensuikyo region is referred to as site S. This study utilized multi-temporal datasets derived from airborne lidar and photogrammetry using UAV photographs: (i) before the heavy rainfall, (ii) between the heavy rainfall and the earthquake, and (iii) after the earthquake. By using digital elevation data and a sediment transportation map, elevation lowering spots caused by the landslides were identified. Then terrain information and the indexes of shape and spatial distribution were analyzed at the elevation lowering spots.

From the analysis, it was found that the heavy rainfall induced 374 landslides and the earthquake triggered 440 landslides. Landslides affected by the two different events were recognized in sites P and S. In site S, the indexes of spatial distribution showed that the earthquake caused the displacement of regolith remained on the upper convex part of the slope. In site P, the shape indexes indicated that the former event led to removal of topsoil, whereas the latter event induced the failure of lava and pyroclastic rocks. In site Q, failed slopes are not as steep as locations where landslides occurred due to past heavy rainfall events, and remained thick unconsolidated topsoil is composed of volcanic ash. It slipped deeply in 2016 due to strong seismic shaking strengthened by topographic site effects on the convex part of the slope. In site R, landslide shapes and comparison with those in site P suggest that collapsed soil directly fell into rivers without erosion of topsoil.

This study has revealed that the distribution of landslides due to the earthquake is related to that by the heavy rainfall in the Sensuikyo region. On the other hand, in the western part of the Aso region, differences in shape and distribution are found between landslides caused by the two events. Moreover, there are differences in the formation of earthquake-induced landslides among the different study sites.

©2019. Japan Geoscience Union. All Right Reserved. 

Keywords: The 2016 Kumamoto Earthquake, July 2012 Northern Kyushu Heavy rainfall, landslides

©2019. Japan Geoscience Union. All Right Reserved. 

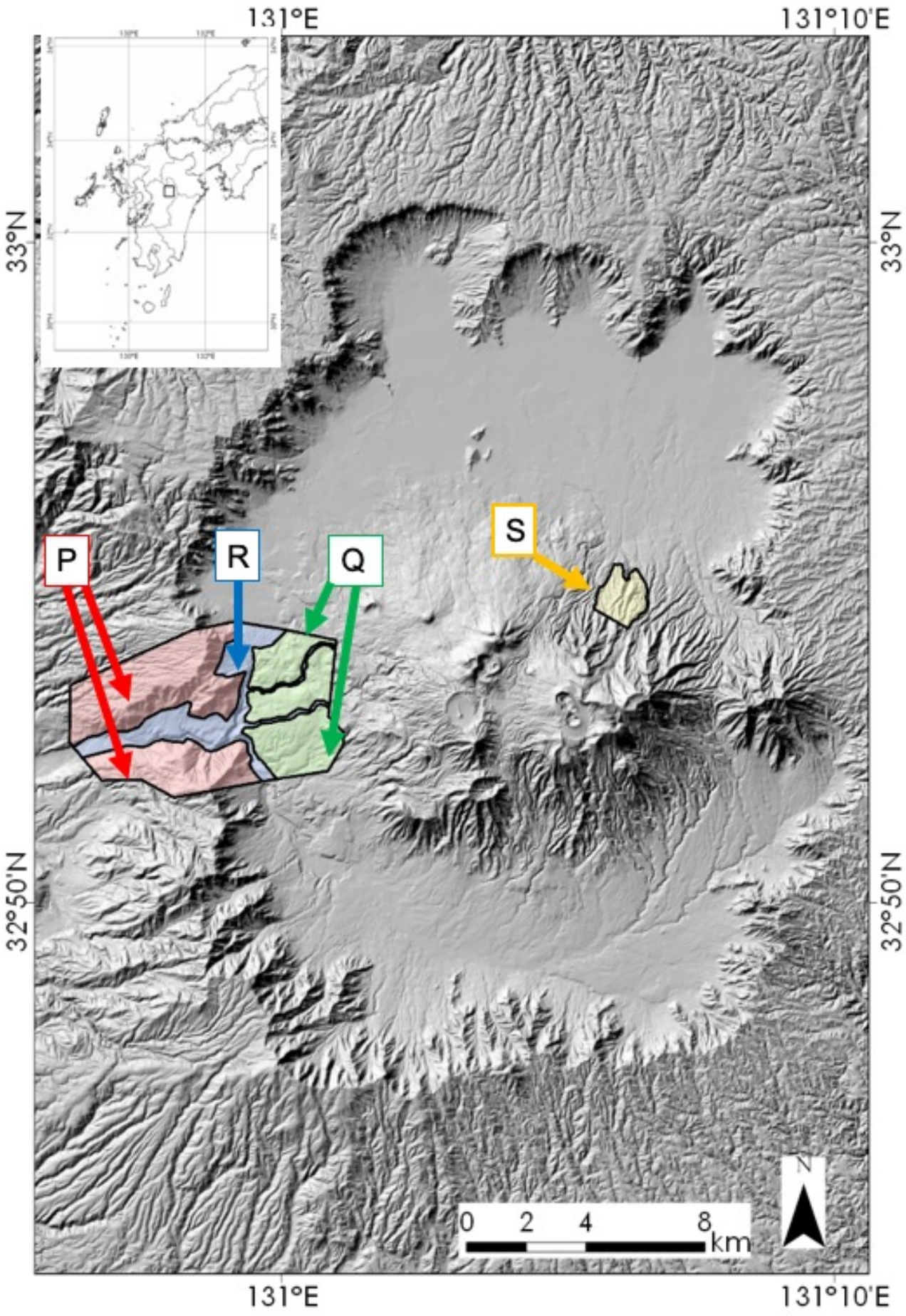


©2019. Japan Geoscience Union. All Right Reserved. 

# Using GIS and remote sensing to assess relationships between landslides and land cover changes in the Sanbagawa and Mikabu Belts, Shikoku, Japan

*Roxanne Lai[1], Takashi Oguchi[1]

1. University of Tokyo

The Sanbagawa and Mikabu Belts are metamorphic belts that run across Southwest Japan, and are home to numerous large crystalline schist landslides, including the widely-studied slow but continuously moving Zentoku landslide. Villages and communities have been built on these landslide areas due to historical and cultural factors, as well as the fertility of the soil. With changing human needs and social trends, however, changing land uses is becoming an increasingly important issue. In Japan, movement of the population from rural to urban areas have resulted in much land and agricultural land abandonment. As vegetation cover changes after land abandonment, this temporal and spatial effect may have important effects on geomorphic processes such as landslide susceptibility and landslide kinematics.

Here we track long-term land cover changes over vegetated landslide areas of the Sanbagawa and Mikabu Belts of Shikoku Island, Japan, and conduct spatio-temporal analyses to assess relationships between landslides and land cover changes. Given changing land uses, including land abandonment in these landslide areas over time, we use long-term high-resolution land cover vegetation datasets to examine first the long-term land use changes, and then use statistical methods to explore their relationships with landslide susceptibility and kinematics. Mapping of spatial data and their analysis using GIS constitute a core part of the research. The results suggest interconnections between land use changes and land movement.

Keywords: Landslides, Shikoku, GIS , Remote Sensing

©2019. Japan Geoscience Union. All Right Reserved. 

# Analysis of Morphometric Parameters for Mountains Ranges and Landslides due to the July 2018 Heavy Rain in Western Japan Using GIS Data

*Toshikazu Fukuba[1], Takashi Oguchi[2]

1. Department of Earth and Planetary Environmental Science, The University of Tokyo, 2. Center for Spatial Information Science, The University of Tokyo

Morphometric parameters for mountains ranges have been analyzed in many studies. These studies in recent years used Digital Elevation Models (DEMs) to calculate values of morphometric parameters within mountains and provided consideration on landform evolution. In addition, morphometric parameters calculated by DEMs have been used for producing landslide hazard maps. This study investigates geomorphometric parameters within the Chugoku and Shikoku Mountains, Japan, and the relationships among the parameters. In addition, landslides caused by the July 2018 heavy rain in western Japan is also investigated and the relationships between the landforms of the mountains and the landslides are discussed. Altitude, slope angle, slope aspect and slope curvature are chosen for morphometric parameters to be investigated.

Morphometric parameters for the Chugoku and in Shikoku Mountains computed using DEMs and GIS have some characteristics common to the Japanese Alps. For example, for wide altitudinal zones, slope angle tends to be constant around 30 to 40 degrees even if altitude changes. However, the values of the constant slope angle are not the same, which may be due to geological differences or the difference in the formation age of mountains. Although the frequency distribution of slope aspect is similar to the Chugoku and Shikoku Mountains, anisotropy of slope aspect is different between the two mountains. This may be caused by differences in the formation age, formation mechanism, or geology of the mountains.

Analysis of landslides caused by the July 2018 heavy rain in Hiroshima using landslide data and DEMs revealed that landslides mostly occurred around 300 m in altitude, at 15 to 30 degrees in slope angle, and on concave slopes. Although the characteristics slope angles higher than 30 degrees point to frequent slope failures at high and steep mountain slopes in the Chugoku and Shikoku Mountains, landslides corresponding to one rainfall event do not necessarily follow this, because they depend on the distribution of rainfall during the event. Therefore, possibility of landslides in low and gentle mountains close to populated areas needs to be considered seriously for mitigating landslide disasters.

Keywords: GIS, Mountain landform, Landslide, Morphometric parameters

©2019. Japan Geoscience Union. All Right Reserved. 

# Analyzing short-term topographic change in coastal sand dunes using UAS-SfM photogrammetry: A case study in Northern Kujukuri, Japan

*Seulgi Lee[1], Yasutaka Nakata[2], Kotaro Iizuka[3], Takashi Oguchi[3]

1. Graduate School of Frontier Sciences, The University of Tokyo, 2. Forest Research Department, Forestry Research Institute, Hokkaido Research Organization, 3. Center for Spatial Information Science, The University of Tokyo

Collection of spatial data is critical for the identification of coastlines and coastal zones and related studies in coastal geomorphology. It is particularly important to obtain high-resolution elevation data in order to observe topographical changes of coastal sand dunes with frequent dynamic movements during a short period of time. Unmanned Aerial System (UAS) photogrammetry combined with Structure from Motion (SfM) offers an effective solution to the acquisition of such data. Kujukuri, facing the Pacific Ocean in Chiba Prefecture, Japan, is a region with a long coastal zone of about 60 km. Although the development of this area since the 1960s has destroyed many natural landscapes, they are relatively preserved in Northern Kujukuri. This study focuses on short-term topographic changes in coastal sand dunes there and discusses the effects of vegetation and wind.
UAV-SfM surveys were conducted seven times from September 2016 to December 2018, and the obtained topographic data were analyzed using GIS software (ArcGIS Pro) to evaluate changes in terrain conditions by season and year. We also analyzed the wind direction data provided by the Japan Meteorological Agency. Vegetation data were obtained from the field surveys and the green-red vegetation index extracted from the UAS images. The following three characteristics were identified: 1) Short-term topographic changes tend to be influenced by specific events such as storm events, and therefore terrain conditions in the same season may be different from year to year. 2) General wind conditions represented by the meteorological data corresponding to the overall change of sand dune topography, especially at seasonal or longer scales. 3) Formation of small sand dunes is affected by vegetation distribution. This study has suggested factors affecting short-term topographic changes of coastal sand dunes based on frequent data acquisition in the field and geospatial technologies.

Keywords: GIS, Coastal sand dunes, UAV, SfM

©2019. Japan Geoscience Union. All Right Reserved. 

# Responses of suspended sediment yield to precipitation, topography and dam control in the Yellow River Basin, China

*Ruiqi Zhang[1], Takashi Oguchi[2]

1. Department of Natural Environmental Studies, Graduate School of Frontier Sciences, The University of Tokyo, 2. Center for Spatial Information Science, The University of Tokyo

Soil erosion has long been a serious problem in the Yellow River Basin in China. The high sediment load carried by the Yellow River results in deposition along its path, raising the riverbed and increasing the flood risk in the lower reaches. To mitigate this situation, large-scale soil conservation measures have been put into practice such as the construction of dams to effectively trap fluvial sediments. Previous studies on this topic focused on the interannual fluctuation of sediment yield caused by dams and reservoirs. However, few studies focused on their effects on the seasonal variation of sediment yield. In 2002, the Yellow River Conservancy Committee began to implement the water-sediment regulation (WSR) scheme to regulate the river water, which further strengthen the impact of dam control on the seasonality of sediment yield. Therefore, this research aims to integrate natural contributing factors such as topography and precipitation with the WSR-based dam control to analyze the seasonal and spatial variations of sediment yield in the Yellow River, for the years 2008 to 2012. Data of daily suspended sediment concentration, water discharge, and precipitation were downloaded from the Chinese Data Sharing Infrastructure of Earth System Science, and the ASTER GLOBAL DEMs with a resolution of 1 arc-second were downloaded from the U.S. Geological Survey web site. ArcGIS and R software packages are used to analyze the obtained data. Inspection of data quality revealed that consecutive sediment yield and precipitation data for 97 watersheds are usable.

Data analysis indicated the following four basic hydrological characteristics of the watersheds. 1) Water discharge within each watershed is not stable both interannually and seasonally, because it has been affected by the implementation of dam regulation as well as low discharge conditions mostly in spring and winter especially in some small watersheds. 2) The variation of sediment yield in some natural watersheds reflects change in precipitation, leading to sediment yield peaks in summer. 3) In other watersheds, the variation of sediment yield tends to be independent of precipitation. Instead, some artificial conservation measures such as dam control effectively intercept sediments from the upstream area. 4) The correlation between suspended sediment yield and water discharge varies among watersheds, and the correlation coefficient can be used as a parameter representing hydrological characteristics. The DEMs have been also analyzed to relate hydrology and climate with geomorphology. The obtained results may help the policy makers better understand the erosion situations in the Yellow River Basin and regulate the soil conservation measures.

Keywords: Suspended sediment yield, the Yellow River basin, seasonality, precipitation, topography, dam control

©2019. Japan Geoscience Union. All Right Reserved. 

[E] Poster | H (Human Geosciences )：H-TT Technology & Techniques

Thu. May 30, 2019 5:15 PM - 6:30 PM JST | Thu. May 30, 2019 8:15 AM - 9:30 AM UTC | Poster Hall International Exhibition Hall8, Makuhari Messe_16

## [H-TT19] Geographic Information Systems and Cartography

convener:Takashi Oguchi(Center for Spatial Information Science, The University of Tokyo), Yuji Murayama(Graduate School of Life and Environmental Sciences), Yoshiki Wakabayashi(Graduate School of Urban Environmental Sciences, Tokyo Metropolitan University)

This session discusses various methods which acquire, store, analyze and visualize geospatial data, and presents the outcomes of empirical studies using GIS or mapping methods. The session also deals with applications of digital data, and GIS, and mapping to various fields of earth and planetary science and human society. All presentations and discussion of this session are made in English.

### [HTT19-P01] Monitoring and Simulating Land Use/Cover Changes and its Impact on Land Surface Temperature in Sapporo City, Japan

*RUCI WANG[1], YUJI MURAYAMA[1] (1.University of Tsukuba)

### [HTT19-P02] Spatiotemporal Variations of Land Cover/Use and Sustainable Urban Heat Island (UHI) Mitigation Strategies: A Case Study of Chinese Bay Megacities

★Invited Papers

*Fei LIU[1], Yuji MURAYAMA[1] (1. University of Tsukuba)

### [HTT19-P03] A LST Study of the Seoul Metropolitan City, South Korea, Based on Landsat Data (1996 – 2017)

*Prabath Priyankara[1,3], Manjula Ranagalage[1,4], DMSLB Dissanayake[1,4], Takehiro Morimoto[1,2], Yuji Murayama[1,2] (1.Graduate School of Life and Environmental Sciences, University of Tsukuba, Japan, 2.Faculty of Life and Environmental Sciences, University of Tsukuba, Japan, 3.Faculty of Agriculture, University of Ruhuna, Sri Lanka, 4.Faculty of Social Sciences and Humanities, Rajarata University of Sri Lanka, Sri Lanka)

### [HTT19-P04] Improvement of GIS exercise classes using the GIS open educational resources based on questionnaire surveys

★Invited Papers

*Hiroyuki Yamauchi[1], Takashi Oguchi[1], Yuichi S. Hayakawa[2,1], Kotaro Iizuka[1] (1.Center for Spatial Information Science, The University of Tokyo, 2.Environmental Geography, Faculty of Environmental Earth Science, Hokkaido University)

### [HTT19-P05] The Development of COP for Tzu Chi Disaster Prevention System by Using QGIS-Taking 2018 Hualien Earthquake as an Example

*kuan-wen tseng[1], Ming-Ta Tsai[1], Yun-Ching Wang[1], Ming-Chih Wang[1], Chien-Hsien Liu[1] (1.03-3809093)

### [HTT19-P06] Comparative study on shape and distribution of landslides caused by the 2012 Northern Kyushu heavy rainfall and the 2016 Kumamoto earthquake in the Aso region, Kumamoto, Japan

*Yasutaka Haneda[1], Takashi Oguchi[2], Kotaro Iizuka[2], Hitoshi SAITO[3,2], Yuichi S. Hayakawa[4,2], Shoichiro Uchiyama[5] (1.Graduate School of Frontier Science, The University of Tokyo, 2.Center for Spatial Information Science, The University of Tokyo, 3.College of Economics, Kanto Gakuin University, 4.Faculty of Environmental Earth Science, Hokkaido University, 5.National Research Institute for Earth Science and Disaster Resilience)

### [HTT19-P07] Using GIS and remote sensing to assess relationships between landslides and land cover changes in the Sanbagawa and Mikabu Belts, Shikoku, Japan

*Roxanne Lai[1], Takashi Oguchi[1] (1.University of Tokyo)

[HTT19-P08] **Analysis of Morphometric Parameters for Mountains Ranges and Landslides due to the July 2018 Heavy Rain in Western Japan Using GIS Data**

*Toshikazu Fukuba[1], Takashi Oguchi[2] (1.Department of Earth and Planetary Environmental Science, The University of Tokyo, 2.Center for Spatial Information Science, The University of Tokyo)

---

[HTT19-P09] Analyzing short-term topographic change in coastal sand dunes using UAS-SfM photogrammetry: A case study in Northern Kujukuri, Japan

*Seulgi Lee[1], Yasutaka Nakata[2], Kotaro Iizuka[3], Takashi Oguchi[3] (1.Graduate School of Frontier Sciences, The University of Tokyo, 2.Forest Research Department, Forestry Research Institute, Hokkaido Research Organization, 3.Center for Spatial Information Science, The University of Tokyo)

---

[HTT19-P10] **Responses of suspended sediment yield to precipitation, topography and dam control in the Yellow River Basin, China**

*Ruiqi Zhang[1], Takashi Oguchi[2] (1. Department of Natural Environmental Studies, Graduate School of Frontier Sciences, The University of Tokyo, 2.Center for Spatial Information Science, The University of Tokyo)

# Monitoring and Simulating Land Use/Cover Changes and its Impact on Land Surface Temperature in Sapporo City, Japan

*RUCI WANG[1], YUJI MURAYAMA[1]

1. University of Tsukuba

In recent years, urban heat island phenomenon (UHI) which prevails in many cities worldwide has caused broad public concern. UHI phenomenon impairs healthy urban development and causes excessive energy consumption, climatic and environmental deterioration. Land use/cover changes are one of the most crucial variables influencing on UHI. Therefore, monitoring and simulating land use/cover changes and analyzing its effects on LST are essential for healthy urban development. This study aims to capture the impact of land use/cover on LST and simulate the LST under various land use/cover scenarios in Sapporo city, Japan. At first, we monitored the land use/cover changes from 1985 to 2015 and detect the change of LST concerning land use/cover distribution. Then, we predicted the future conditions of LST based on various land use/cover scenarios. The results show that the LST differs according to land use/cover types, and the proportion of land use/cover types is the most significant factor affecting LST. The findings also indicate that the built-up area and paddy field have the highest average LST, while the green space and water area help cool the city. In the future, the green area such as urban green parks and grassland should be planned in the city to mitigate the UHI phenomenon. It reveals the spatial characterization of LST which provides significant insights for government and city planners.

Keywords: Geographical information science, Urban heat island, Land surface temperature, Land use/cover change, Sapporo city

©2019. Japan Geoscience Union. All Right Reserved. 

# Spatiotemporal Variations of Land Cover/Use and Sustainable Urban Heat Island (UHI) Mitigation Strategies: A Case Study of Chinese Bay Megacities

*Fei LIU[1], Yuji MURAYAMA[1]

1. University of Tsukuba

Rapid urbanization significantly affects the urban thermal environment in the context of global climate change. The assessment of surface urban heat island (SUHI) and development of mitigation strategies in megacities have become frontier issues on human health and urban sustainability. In this study, taking of the three Chinese bay megacities, we attempt to 1) disclose the relationship between land surface temperature (LST) and land cover using remote sensing quantified analysis, 2) to clarify the mechanism and characteristics of SUHI formation based on bi-temporal patterns and variations of land cover, and 3) to sustainably regulate and optimize the urban environment and further create urban planning and policies for relieving urban thermal effect. The study target is Guangzhou metropolitan area (GMA), Hangzhou metropolitan area (HMA) and Shanghai Metropolitan area (SMA) in China. The result of this study indicated remarkably different characteristics, arrangement, and variations among different bay thermal environments. Overall, spatial layouts and changes in the thermal environment of these three megacities were substantially identical with their land cover pattern and tendency. Although land covers significantly influenced the LST as a whole, the different areas had different magnitudes of SUHI coming from different land cover compositions and differentials. The results would provide a valuable reference to disentangle spatiotemporal variation of the bay urban thermal environments, and the urbanization-induced land covers temperature dynamics. This study would contribute to the development of future SUHI mitigation solutions.

Keywords: Land Cover/Use , Urban Heat Island (UHI), Mitigation Strategies

©2019. Japan Geoscience Union. All Right Reserved. 

# A LST Study of the Seoul Metropolitan City, South Korea, Based on Landsat Data (1996 –2017)

*Prabath Priyankara[1,3], Manjula Ranagalage[1,4], DMSLB Dissanayake[1,4], Takehiro Morimoto[1,2], Yuji Murayama[1,2]

1. Graduate School of Life and Environmental Sciences, University of Tsukuba, Japan, 2. Faculty of Life and Environmental Sciences, University of Tsukuba, Japan, 3. Faculty of Agriculture, University of Ruhuna, Sri Lanka, 4. Faculty of Social Sciences and Humanities, Rajarata University of Sri Lanka, Sri Lanka

Rapid urban growth often replaced urban vegetation with impervious surfaces which leads to increase land surface temperature (LST) periodically and tends to form urban heat islands (UHI). This is a serious issue of urbanized cities and the increase of LST badly affects the well-being of the life and environments of the cities. The Seoul Metropolitan City (SMC), South Korea, is one of the developed and rapidly urbanizing metropolitan city in Asia. The aim of this study was to examine the spatiotemporal variations of LST in the SMC and surroundings in the context of the UHI using Landsat data. The study examined the relationship of LST with the normalized difference vegetation index (NDVI) and the normalized difference built-up index (NDBI) at three time periods 1996, 2006, and 2017. Also, the study was investigated the environmentally critical areas based on LST and NDVI by modeling environmental criticality index (ECI). According to the results of the study, there is a negative correlation between LST with NDVI and positive correlation of LST with NDBI across all three time periods. In SMC, most of the environmentally critical areas are located in the central business district (CBD), near the harbor, and along the main transportation network. According to the results of the study, it is recommended that the identified environmentally critical areas to be considered in the urban planning of the city. Green spaces of the city will help to improve the life and environmental well-being of the SMC.

Keywords: Urban Heat Island, Land Surface Temperature, NDVI, NDBI, Environmental Criticality Index, Seoul Metropolitan City

©2019. Japan Geoscience Union. All Right Reserved. 

# Improvement of GIS exercise classes using the GIS open educational resources based on questionnaire surveys

*Hiroyuki Yamauchi[1], Takashi Oguchi[1], Yuichi S. Hayakawa[2,1], Kotaro Iizuka[1]

1. Center for Spatial Information Science, The University of Tokyo, 2. Environmental Geography, Faculty of Environmental Earth Science, Hokkaido University

Free and open source GIS software has been utilized for GIS education all over the world. However, as far as we recognize, GIS education in many Japanese universities underutilize such software packages. Therefore, we developed GIS exercise materials explaining spatial data analyses using free and open-source GIS. We have been providing these materials for higher education and designated them as the GIS Open Educational Resources. We used the materials in a university exercise class, which was held as an intensive course for three days at The University of Tokyo. During the exercise, we have conducted questionnaire surveys to clarify the three criteria: difficulty, understanding and satisfactory levels of the students. The results showed that the students felt difficulty in some situations such as the utilization of GIS for the first time and complex operations using different types of data. The contents of the exercise syllabus and materials were improved based on the feedback. We conducted another GIS exercise class at the university to verify the utility of improvements. In this presentation, we show the improvements in the exercise syllabus and the comparison of educational effects on students before and after the improvements.

Keywords: GIS education, exercise, Open Educational Resources, Free and open-source GIS

©2019. Japan Geoscience Union. All Right Reserved. 

# The Development of COP for Tzu Chi Disaster Prevention System by Using QGIS-Taking 2018 Hualien Earthquake as an Example

*kuan-wen tseng[1], Ming-Ta Tsai[1], Yun-Ching Wang[1], Ming-Chih Wang[1], Chien-Hsien Liu[1]

1. 03-3809093

The Hualien earthquake occurred at 23:50 and 41.6 seconds on February 6, 2018. The epicenter was located in the coastal area of Hualien County. The earthquake scale was 6.2 and the Seismic source depth was 6.3 kilometers. The earthquake disaster along the Milun fault was mainly concentrated in Hualien City, and collapsed the first and second floors of the “Tongshuai” building. The “Yunmen Cuidi” Building showed a 45-degree tilt. The lower floors of the residential community building "Baijin Shuangxing" and “Wuzhu Wusu” at Guosheng Sixth Street were destroyed. This study mainly uses the powerful geospatial analysis capabilities of Geographic Information System (GIS) to provide Tzu Chi's plans for disaster mitigation. The projects include: (1) humanitarian cares; (2) visiting and reporting of damage situations around main disaster areas and (3) “Reassuring Homes Visits” in order to provide assistance to Tzu Chi people for operations of disaster mitigation.

Keywords: Millun fault, geographic information system, spatial analysis, Tzu Chi Foundation

©2019. Japan Geoscience Union. All Right Reserved. 

# Comparative study on shape and distribution of landslides caused by the 2012 Northern Kyushu heavy rainfall and the 2016 Kumamoto earthquake in the Aso region, Kumamoto, Japan

*Yasutaka Haneda[1], Takashi Oguchi[2], Kotaro Iizuka[2], Hitoshi SAITO[3,2], Yuichi S. Hayakawa[4,2], Shoichiro Uchiyama[5]

1. Graduate School of Frontier Science, The University of Tokyo, 2. Center for Spatial Information Science, The University of Tokyo, 3. College of Economics, Kanto Gakuin University, 4. Faculty of Environmental Earth Science, Hokkaido University, 5. National Research Institute for Earth Science and Disaster Resilience

The 2016 Kumamoto earthquake triggered many landslides in the Aso region, southwestern Japan. Previous studies have revealed the processes of some large representative landslides in the western Aso region, but they have not comprehensively dealt with lots of small landslides. Other studies have discussed landslide distribution and relationships with that of the heavy rainfall events in July 2012 in the northern part of the Central Cones of the Aso volcano. However, they have not been investigated the western part of the Aso region which has various topographical and geological characteristics. Therefore, this study compares the formation and distribution of landslides caused by the heavy rainfall and earthquake events in both the central and western part of the Aso region.

The study areas are the western part of the Aso region and the Sensuikyo region at the northern part of the Central Cones (Fig. 1). The western part was divided into three sites: site P (caldera walls and the outer rim), Q (western part of Central Cones), and R (river terrace and talus) based on geomorphological and geological characteristics. The Sensuikyo region is referred to as site S. This study utilized multi-temporal datasets derived from airborne lidar and photogrammetry using UAV photographs: (i) before the heavy rainfall, (ii) between the heavy rainfall and the earthquake, and (iii) after the earthquake. By using digital elevation data and a sediment transportation map, elevation lowering spots caused by the landslides were identified. Then terrain information and the indexes of shape and spatial distribution were analyzed at the elevation lowering spots.

From the analysis, it was found that the heavy rainfall induced 374 landslides and the earthquake triggered 440 landslides. Landslides affected by the two different events were recognized in sites P and S. In site S, the indexes of spatial distribution showed that the earthquake caused the displacement of regolith remained on the upper convex part of the slope. In site P, the shape indexes indicated that the former event led to removal of topsoil, whereas the latter event induced the failure of lava and pyroclastic rocks. In site Q, failed slopes are not as steep as locations where landslides occurred due to past heavy rainfall events, and remained thick unconsolidated topsoil is composed of volcanic ash. It slipped deeply in 2016 due to strong seismic shaking strengthened by topographic site effects on the convex part of the slope. In site R, landslide shapes and comparison with those in site P suggest that collapsed soil directly fell into rivers without erosion of topsoil.

This study has revealed that the distribution of landslides due to the earthquake is related to that by the heavy rainfall in the Sensuikyo region. On the other hand, in the western part of the Aso region, differences in shape and distribution are found between landslides caused by the two events. Moreover, there are differences in the formation of earthquake-induced landslides among the different study sites.

©2019. Japan Geoscience Union. All Right Reserved. 

Keywords: The 2016 Kumamoto Earthquake, July 2012 Northern Kyushu Heavy rainfall, landslides

©2019. Japan Geoscience Union. All Right Reserved. 

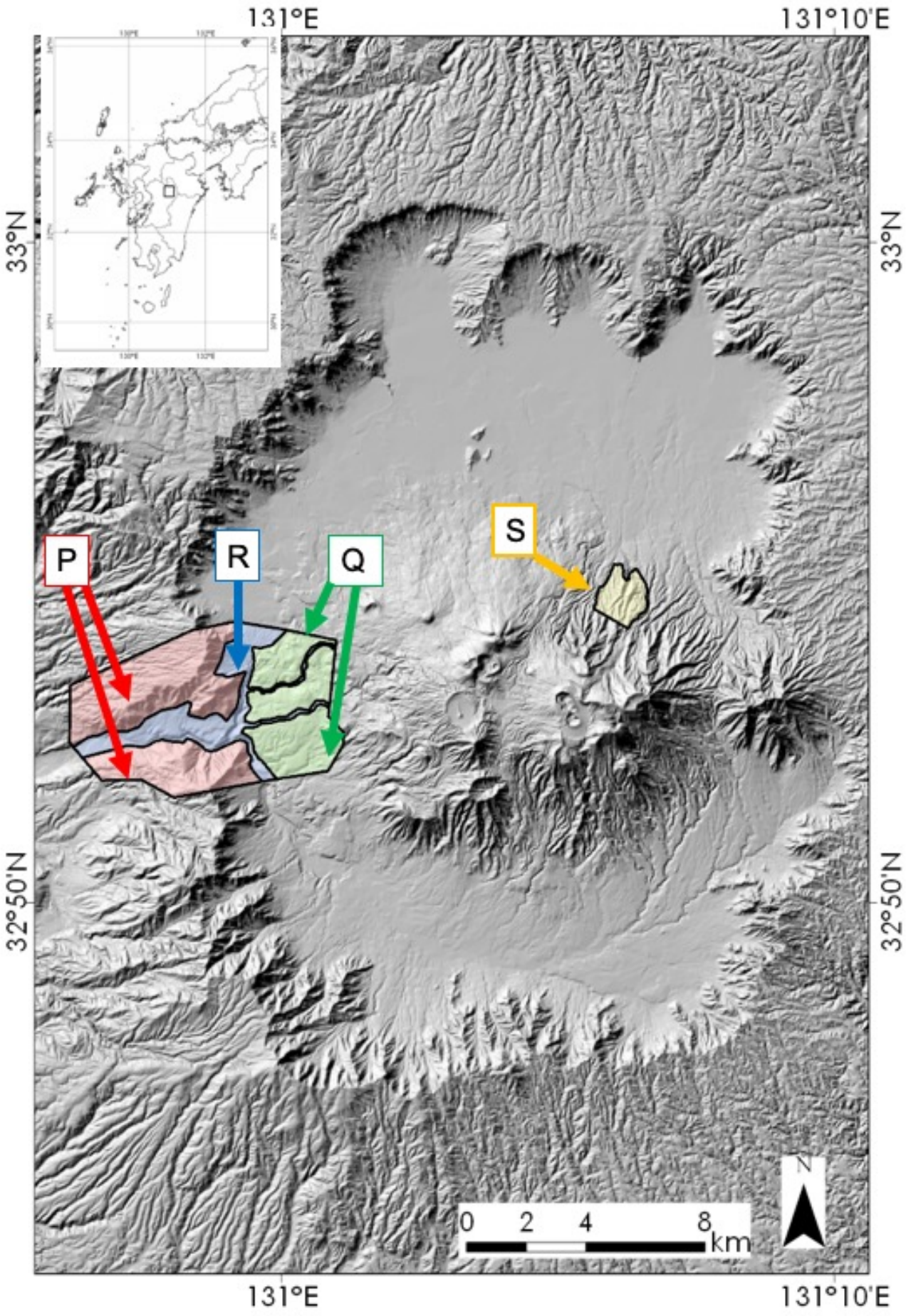


©2019. Japan Geoscience Union. All Right Reserved. 

# Using GIS and remote sensing to assess relationships between landslides and land cover changes in the Sanbagawa and Mikabu Belts, Shikoku, Japan

*Roxanne Lai[1], Takashi Oguchi[1]

1. University of Tokyo

The Sanbagawa and Mikabu Belts are metamorphic belts that run across Southwest Japan, and are home to numerous large crystalline schist landslides, including the widely-studied slow but continuously moving Zentoku landslide. Villages and communities have been built on these landslide areas due to historical and cultural factors, as well as the fertility of the soil. With changing human needs and social trends, however, changing land uses is becoming an increasingly important issue. In Japan, movement of the population from rural to urban areas have resulted in much land and agricultural land abandonment. As vegetation cover changes after land abandonment, this temporal and spatial effect may have important effects on geomorphic processes such as landslide susceptibility and landslide kinematics.

Here we track long-term land cover changes over vegetated landslide areas of the Sanbagawa and Mikabu Belts of Shikoku Island, Japan, and conduct spatio-temporal analyses to assess relationships between landslides and land cover changes. Given changing land uses, including land abandonment in these landslide areas over time, we use long-term high-resolution land cover vegetation datasets to examine first the long-term land use changes, and then use statistical methods to explore their relationships with landslide susceptibility and kinematics. Mapping of spatial data and their analysis using GIS constitute a core part of the research. The results suggest interconnections between land use changes and land movement.

Keywords: Landslides, Shikoku, GIS , Remote Sensing

©2019. Japan Geoscience Union. All Right Reserved. 

# Analysis of Morphometric Parameters for Mountains Ranges and Landslides due to the July 2018 Heavy Rain in Western Japan Using GIS Data

*Toshikazu Fukuba[1], Takashi Oguchi[2]

1. Department of Earth and Planetary Environmental Science, The University of Tokyo, 2. Center for Spatial Information Science, The University of Tokyo

Morphometric parameters for mountains ranges have been analyzed in many studies. These studies in recent years used Digital Elevation Models (DEMs) to calculate values of morphometric parameters within mountains and provided consideration on landform evolution. In addition, morphometric parameters calculated by DEMs have been used for producing landslide hazard maps. This study investigates geomorphometric parameters within the Chugoku and Shikoku Mountains, Japan, and the relationships among the parameters. In addition, landslides caused by the July 2018 heavy rain in western Japan is also investigated and the relationships between the landforms of the mountains and the landslides are discussed. Altitude, slope angle, slope aspect and slope curvature are chosen for morphometric parameters to be investigated.

Morphometric parameters for the Chugoku and in Shikoku Mountains computed using DEMs and GIS have some characteristics common to the Japanese Alps. For example, for wide altitudinal zones, slope angle tends to be constant around 30 to 40 degrees even if altitude changes. However, the values of the constant slope angle are not the same, which may be due to geological differences or the difference in the formation age of mountains. Although the frequency distribution of slope aspect is similar to the Chugoku and Shikoku Mountains, anisotropy of slope aspect is different between the two mountains. This may be caused by differences in the formation age, formation mechanism, or geology of the mountains.

Analysis of landslides caused by the July 2018 heavy rain in Hiroshima using landslide data and DEMs revealed that landslides mostly occurred around 300 m in altitude, at 15 to 30 degrees in slope angle, and on concave slopes. Although the characteristics slope angles higher than 30 degrees point to frequent slope failures at high and steep mountain slopes in the Chugoku and Shikoku Mountains, landslides corresponding to one rainfall event do not necessarily follow this, because they depend on the distribution of rainfall during the event. Therefore, possibility of landslides in low and gentle mountains close to populated areas needs to be considered seriously for mitigating landslide disasters.

Keywords: GIS, Mountain landform, Landslide, Morphometric parameters

©2019. Japan Geoscience Union. All Right Reserved. 

# Analyzing short-term topographic change in coastal sand dunes using UAS-SfM photogrammetry: A case study in Northern Kujukuri, Japan

*Seulgi Lee[1], Yasutaka Nakata[2], Kotaro Iizuka[3], Takashi Oguchi[3]

1. Graduate School of Frontier Sciences, The University of Tokyo, 2. Forest Research Department, Forestry Research Institute, Hokkaido Research Organization, 3. Center for Spatial Information Science, The University of Tokyo

Collection of spatial data is critical for the identification of coastlines and coastal zones and related studies in coastal geomorphology. It is particularly important to obtain high-resolution elevation data in order to observe topographical changes of coastal sand dunes with frequent dynamic movements during a short period of time. Unmanned Aerial System (UAS) photogrammetry combined with Structure from Motion (SfM) offers an effective solution to the acquisition of such data. Kujukuri, facing the Pacific Ocean in Chiba Prefecture, Japan, is a region with a long coastal zone of about 60 km. Although the development of this area since the 1960s has destroyed many natural landscapes, they are relatively preserved in Northern Kujukuri. This study focuses on short-term topographic changes in coastal sand dunes there and discusses the effects of vegetation and wind.
UAV-SfM surveys were conducted seven times from September 2016 to December 2018, and the obtained topographic data were analyzed using GIS software (ArcGIS Pro) to evaluate changes in terrain conditions by season and year. We also analyzed the wind direction data provided by the Japan Meteorological Agency. Vegetation data were obtained from the field surveys and the green-red vegetation index extracted from the UAS images. The following three characteristics were identified: 1) Short-term topographic changes tend to be influenced by specific events such as storm events, and therefore terrain conditions in the same season may be different from year to year. 2) General wind conditions represented by the meteorological data corresponding to the overall change of sand dune topography, especially at seasonal or longer scales. 3) Formation of small sand dunes is affected by vegetation distribution. This study has suggested factors affecting short-term topographic changes of coastal sand dunes based on frequent data acquisition in the field and geospatial technologies.

Keywords: GIS, Coastal sand dunes, UAV, SfM

©2019. Japan Geoscience Union. All Right Reserved. 

# Responses of suspended sediment yield to precipitation, topography and dam control in the Yellow River Basin, China

*Ruiqi Zhang[1], Takashi Oguchi[2]

1. Department of Natural Environmental Studies, Graduate School of Frontier Sciences, The University of Tokyo, 2. Center for Spatial Information Science, The University of Tokyo

Soil erosion has long been a serious problem in the Yellow River Basin in China. The high sediment load carried by the Yellow River results in deposition along its path, raising the riverbed and increasing the flood risk in the lower reaches. To mitigate this situation, large-scale soil conservation measures have been put into practice such as the construction of dams to effectively trap fluvial sediments. Previous studies on this topic focused on the interannual fluctuation of sediment yield caused by dams and reservoirs. However, few studies focused on their effects on the seasonal variation of sediment yield. In 2002, the Yellow River Conservancy Committee began to implement the water-sediment regulation (WSR) scheme to regulate the river water, which further strengthen the impact of dam control on the seasonality of sediment yield. Therefore, this research aims to integrate natural contributing factors such as topography and precipitation with the WSR-based dam control to analyze the seasonal and spatial variations of sediment yield in the Yellow River, for the years 2008 to 2012. Data of daily suspended sediment concentration, water discharge, and precipitation were downloaded from the Chinese Data Sharing Infrastructure of Earth System Science, and the ASTER GLOBAL DEMs with a resolution of 1 arc-second were downloaded from the U.S. Geological Survey web site. ArcGIS and R software packages are used to analyze the obtained data. Inspection of data quality revealed that consecutive sediment yield and precipitation data for 97 watersheds are usable.

Data analysis indicated the following four basic hydrological characteristics of the watersheds. 1) Water discharge within each watershed is not stable both interannually and seasonally, because it has been affected by the implementation of dam regulation as well as low discharge conditions mostly in spring and winter especially in some small watersheds. 2) The variation of sediment yield in some natural watersheds reflects change in precipitation, leading to sediment yield peaks in summer. 3) In other watersheds, the variation of sediment yield tends to be independent of precipitation. Instead, some artificial conservation measures such as dam control effectively intercept sediments from the upstream area. 4) The correlation between suspended sediment yield and water discharge varies among watersheds, and the correlation coefficient can be used as a parameter representing hydrological characteristics. The DEMs have been also analyzed to relate hydrology and climate with geomorphology. The obtained results may help the policy makers better understand the erosion situations in the Yellow River Basin and regulate the soil conservation measures.

Keywords: Suspended sediment yield, the Yellow River basin, seasonality, precipitation, topography, dam control

©2019. Japan Geoscience Union. All Right Reserved. 

[E] Oral | H (Human Geosciences )：H-TT Technology & Techniques

Thu. May 30, 2019 1:45 PM - 3:15 PM JST | Thu. May 30, 2019 4:45 AM - 6:15 AM UTC | 301B 3F

## [H-TT19] Geographic Information Systems and Cartography

convener:Takashi Oguchi(Center for Spatial Information Science, The University of Tokyo), Yuji Murayama(Graduate School of Life and Environmental Sciences), Yoshiki Wakabayashi(Graduate School of Urban Environmental Sciences, Tokyo Metropolitan University), Chairperson:Yuji Murayama, Yoshiki Wakabayashi

This session discusses various methods which acquire, store, analyze and visualize geospatial data, and presents the outcomes of empirical studies using GIS or mapping methods. The session also deals with applications of digital data, and GIS, and mapping to various fields of earth and planetary science and human society. All presentations and discussion of this session are made in English.

1:45 PM - 2:00 PM JST | 4:45 AM - 5:00 AM UTC

### [HTT19-01] A study on geographical changes in main roads and coastlines in the 200 years in Japan

*Yuki IWAI[1], Yuji Murayama[1] (1.Graduate School of Life and Environmental Sciences, University of Tsukuba)

2:00 PM - 2:15 PM JST | 5:00 AM - 5:15 AM UTC

### [HTT19-02] Comparative analysis of foreign tourists' spatial behavior in Tokyo using locational data from the photo-sharing service of Flickr

*Bochra Bettaieb[1], Yoshiki Wakabayashi[1] (1.Tokyo Metropolitan University)

2:15 PM - 2:30 PM JST | 5:15 AM - 5:30 AM UTC

### [HTT19-03] Neighborhood Walkability and its Potential Associations with Residents' Walking Habits

★Invited Papers

*Ikuho Yamada[1], Keiichiro Sanada[2] (1.Faculty of Science and Engineering, Chuo University, 2.Graduate School of Science and Engineering, Chuo University)

2:30 PM - 2:45 PM JST | 5:30 AM - 5:45 AM UTC

### [HTT19-04] THE STUDY OF USING PARTICLE FILTER METHOD COMBINED INDOOR MAGNETIC MAP AND PEDESTRIAN DEAD RECKONING FOR INDOOR POSITIONING.

*Yu-Chun Chen[1] (1.Department of Land Economics, National Chengchi University)

2:45 PM - 3:00 PM JST | 5:45 AM - 6:00 AM UTC

### [HTT19-05] Assessing the Agriculture Sustainability based on Geospatial Technique in a Tropical Mountain Area : A Case Study in Kotmale Catchment in Sri Lanka.

*DM Sanjeewa Lasantha Bandara[1], Takehiro Morimoto [2] (1.Division of Spatial Information Science, Graduate School of Life and Environmental Sciences, University of Tsukuba, 2.Faculty of Life and Environmental Sciences, University of Tsukuba)

3:00 PM - 3:15 PM JST | 6:00 AM - 6:15 AM UTC

### [HTT19-06] Spatial Evaluation of Potential Tsunami Vertical Evacuation: A Case Study of the Western Coastal Belt in Sri Lanka

*Ranagalage Mahinda Manjula[1], Yuji Murayama[1] (1.Division of Spatial Science, Graduate School of Life and Environmental Sciences, University of Tsukuba, Japan)

# A study on geographical changes in main roads and coastlines in the 200 years in Japan

*Yuki IWAI[1], Yuji Murayama[1]

1. Graduate School of Life and Environmental Sciences, University of Tsukuba

This study analyzed the changes in the spatial distribution of main roads and coastlines and its determining factors between 1818 and 2018. These changes are important social and natural foundations for the Japanese national land formation, and the knowledge of the spatial changes is useful for promoting the sustainable society. Previous studies have focused on the regional transformation using aerial photographs, drilling surveys, and some old paper maps. They used the geographical data after modernization and targeted the specific region. In our study, an attempt is made to compare the long term of 200 years on the national scale by using INŌ's digital map.
Digital data of main roads and coastlines on the INŌ's map are included in the “Digital INŌ's Map, Professional Edition”. This is digitized by using the INŌ's large paper map which is the largest scale in the INŌ's map. In the analysis of the changes in main roads, we used the attribute information of Digital INŌ's Map. The changes in coastlines were derived by overlay analysis with coastlines of Digital INŌ's Map and the present national land. In the overlay analysis, each section of coastlines which did not overlap with the present national land was defined as the section changed by the backward movement of the coastline. On the other hand, each section of coastlines which overlapped with the present national land contained both the section changed by the reclamation and the section almost unchanged. In analyzing the determining factors, land use data (100m gridded area) and coastal ocean data (1km gridded area) were mainly used.
As a result, it was found that the route changes in main roads were 18.3% of the total (Fig.1), and the changes in coastlines were 28.9% of the whole length. In the changed coastlines, the changed section by the backward movement was 66.3% (Fig.2A), and the changed section due to the reclamation was 33.7% (Fig.2B). Main roads drawn on the INŌ's large map had different density depending on the region, because only main roads surveyed by INŌ's team were drawn on the INŌ's large map. Therefore, the distance of the changed section was summarized at the regional level. The rate of the change was the largest in Kyushu region (27.8%), and the smallest in Shikoku region (2.8%). On the other hand, coastlines drawn on the INŌ's large map distribute uniformly at the national scale. The rate of the change was the largest in the eastern Japan (Fig.2A) and the industrial areas (Fig.2B). Details on determining factors of changes will be discussed on the day of the presentation.

Keywords: Changes in Roads, Changes in Coastlines, INŌ's Map , GIS, Japan

©2019. Japan Geoscience Union. All Right Reserved. 

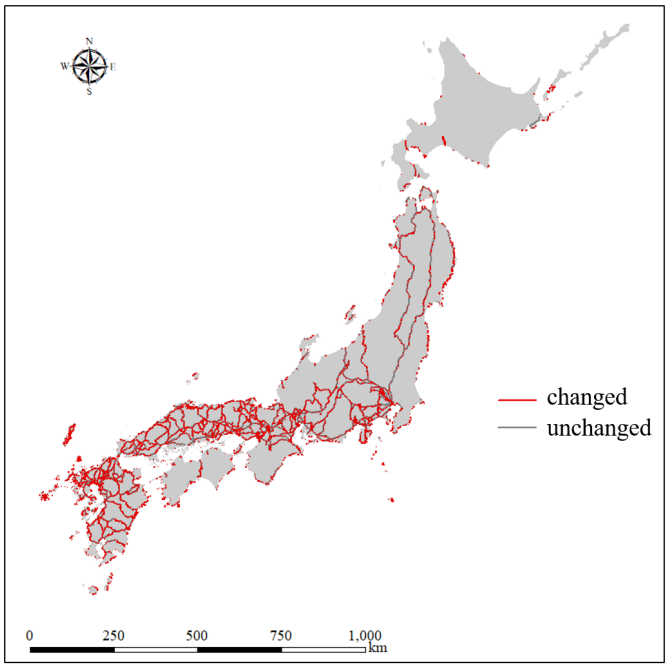


**Figure 1 The main roads drawn in the INŌ's large map**

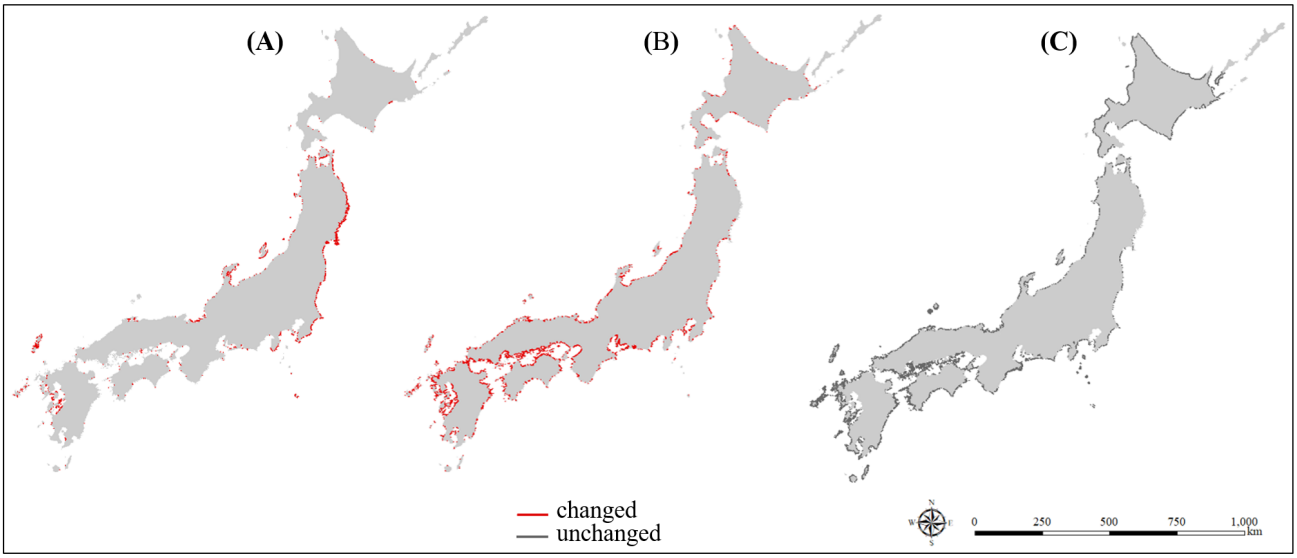


**Figure 2 The coastlines drawn in the INŌ's large map; (A) coastlines occurred by backward movement, (B) coastlines occurred by reclamation, (C) coastlines unchanged**

©2019. Japan Geoscience Union. All Right Reserved. 

# Comparative analysis of foreign tourists' spatial behavior in Tokyo using locational data from the photo-sharing service of Flickr

*Bochra Bettaieb[1], Yoshiki Wakabayashi[1]

1. Tokyo Metropolitan University

These new sources of geospatial data, such as smartphones, global positioning systems, and travel cards, provide the possibility of analyzing high-resolution big data to capture patterns of human spatial behavior across space and time. This study analyzes the geocoded photos from a photo-sharing service to make a comparison of the tourist behavior in Tokyo between countries of foreign visitors.

We selected three places (Shinjuku, Asakusa, and Ginza) as study districts. The data were downloaded from Flickr, one of the most popular online platforms for people to share their travel experiences by uploading photos. We used the data of geocoded photos from 2014, taken within 1.5 km from Shinjuku, Ginza, and Asakusa stations. Information on the nationality of contributors recorded in the Flickr data was used to compare the tourist spots of foreign visitors. To summarize the distribution of the points of photos, we aggregated the point features into a rectangular polygon feature with 100 meter grid square, then we made dot maps and mesh maps to capture the overall distribution of the photos.

The obtained results showed that some tourist spots common to foreign visitors in three study areas, namely, places close to railroad stations. However, spatial patterns of tourist spots varied with the study district in question. In Shinjuku and Ginza, there are differences in tourist spots between Asians and Europeans. Particularly, European tourists' hot spots tend to be more scattered than Asians. However, such differences are not observed in Asakusa, where tourists' hot spots are concentrated around Sensoji Temple and Tokyo Sky Tree. The reason for this is that tourist attractions are concentrated in and around specific facilities in the Asakusa district. Hence, the variations of tourist spots obtained by analyzing the geotagged photographs on Flickr can be explained by the difference in behavior and interest of foreign tourists between countries, as well as the spatial distribution of tourist attractions.

Keywords: social media, Flickr, spatial behavior, mesh map, Tokyo

©2019. Japan Geoscience Union. All Right Reserved. 

# Neighborhood Walkability and its Potential Associations with Residents' Walking Habits

*Ikuho Yamada[1], Keiichiro Sanada[2]

1. Faculty of Science and Engineering, Chuo University, 2. Graduate School of Science and Engineering, Chuo University

Walkability is a concept that embraces various aspects of physical neighborhood environments that may support and promote walking in a neighborhood. Walkable neighborhoods are expected to improve residents' physical activity level and thus health because such environments may be able to implicitly encourage residents to choose walking over driving as a daily transportation mode. While research on walkability originated in western countries, where obesity and lifestyle-related illnesses has been a longstanding public health problem, such research in Japan is also useful and necessary because improving healthy life expectancy among the elderly in an undemanding way is critical in our super-aging society. The concept of walkability is also closely related to that of the compact city, which is considered to be a promising form of sustainable cities in the field of urban planning, as walking is expected to be a major transportation mode in such cities.

This research therefore aims to investigate potential associations between neighborhood walkability and residents' walking habits with specific consideration to characteristics of Japanese cities. Here, we consider two types of walking, namely walking for transportation and walking for leisure, separately because they may relate to neighborhood walkability in different ways. Moreover, we assess neighborhood walkability both subjectively and objectively so as to capture the neighborhood situations in a more comprehensive manner.

An Internet-based questionnaire survey was conducted in January 2018 in order to collect information about residents' walking habits, subjective evaluations of neighborhood environments, and health in selected 49 municipalities in Tokyo. The survey was implemented via an Internet research company, and about 4000 individuals who had registered as a panel of the ompany responded. Questions related to the residents' subjective evaluations of neighborhoods were based on an internationally used standard questionnaire named ANEWS (Abbreviated Neighborhood Environment Walkability Scale). In addition, objective measures of neighborhood walkability were computed using various GIS datasets such as the small area statistics of 2015 Population Census, road network data, and facility location data. Then, statistical analysis was conducted to assess potential associations between residents' walking habits and both subjectively and objectively measured neighborhood walkability.
Results indicated that the two types of walking habits related to different aspects of neighborhood walkability. For example, neighborhood community was found to have positive association with walking for leisure, but no such association was found with walking for transportation. Further, it was suggested that the associations between residents' walking habits and neighborhood walkability would potentially vary depending on neighborhood settings such as urban and suburban regions. Our results also suggested that subjective and objective measures of walkability might have different associations with the two types of walking even when they were assumed to measure the same aspect of neighborhood environments.

Keywords: walkability, neighborhood environments, walking for transportation, walking for leisure, ANEWS (Abbreviated Neighborhood Environment Walkability Scale)

©2019. Japan Geoscience Union. All Right Reserved. 

©2019. Japan Geoscience Union. All Right Reserved. 

# THE STUDY OF USING PARTICLE FILTER METHOD COMBINED INDOOR MAGNETIC MAP AND PEDESTRIAN DEAD RECKONING FOR INDOOR POSITIONING.

*Yu-Chun Chen[1]

1. Department of Land Economics, National Chengchi University

In the past, we often needed a map to find out the destination in an unfamiliar environment. With the appearance of Global Positioning System, the outdoor positioning performance has approached perfection. However, due to the environment obstruction, the indoor signal will reduce the positioning accuracy. Therefore, indoor positioning technology has become the focus of research and development in recent years.
In the history of indoor positioning technology, target positions were detected by sensors, radio signals and image or Pedestrian Dead Reckoning (PDR). All the technologies above have their own advantages and disadvantages, like costly or low accuracy. It is necessary to combine the different technologies to achieve a comprehensive consideration of cost, efficiency and accuracy. This study used the built-in magnetometer of the smart phones to build the magnetic field maps of the floor and also accelerometer as an aid to achieve indoor positioning. This study effectively improved the accuracy and efficiency of indoor positioning by using the particle filter method combine PDR with the magnetic positioning.

Keywords: Indoor positioning, Magnetic field map, Pedestrian Dead Reckoning, Particle filter

©2019. Japan Geoscience Union. All Right Reserved. 

# THE STUDY OF USING PARTICLE FILTER METHOD COMBINED INDOOR MAGNETIC MAP AND PEDESTRIAN DEAD RECKONING FOR INDOOR POSITIONING.

Yu-Chun Chen , Fang-Shii Ning

Department of Land Economics, National Chengchi University,
NO.64, Sec.2, ZhiNan Rd., Wenshan District,Taipei City 11605, Taiwan (R.O.C)
Email: 106257031@nccu.edu.tw; fsn@nccu.edu.tw

**Abstract:** In the past, we often needed a map to find out the destination in an unfamiliar environment. With the appearance of Global Positioning System, the outdoor positioning performance has approached perfection. However, due to the environment obstruction, the indoor signal will reduce the positioning accuracy. Therefore, indoor positioning technology has become the focus of research and development in recent years.

In the history of indoor positioning technology, target positions were detected by sensors, radio signals and image or Pedestrian Dead Reckoning (PDR). All the technologies above have their own advantages and disadvantages, like costly or low accuracy. It is necessary to combine the different technologies to achieve a comprehensive consideration of cost, efficiency and accuracy. This study used the built-in magnetometer of the smart phones to build the magnetic field maps of the floor and also accelerometer as an aid to achieve indoor positioning. This study effectively improved the accuracy and efficiency of indoor positioning by using the particle filter method combine PDR with the magnetic positioning.

**Keywords**: Indoor positioning, Magnetic field map, Pedestrian Dead Reckoning, Particle filter

©2019. Japan Geoscience Union. All Right Reserved. 

# Assessing the Agriculture Sustainability based on Geospatial Technique in a Tropical Mountain Area : A Case Study in Kotmale Catchment in Sri Lanka.

*DM Sanjeewa Lasantha Bandara[1], Takehiro Morimoto [2]

1. Division of Spatial Information Science, Graduate School of Life and Environmental Sciences, University of Tsukuba,
2. Faculty of Life and Environmental Sciences, University of Tsukuba

Sustainable agricultural systems aim at developing new farming practices that do not degrade the environment. It should be catering to the future societal needs for food and feed, ecosystem services and human health, maximizing the net benefit for people, without compromising the ability of future generations to meet their own needs. The agricultural land where located in the tropical mountain area has been becoming a dilapidated situation due to the unplanned agricultural practices coupled with the physical properties of the area and socioeconomic factors. The Kotmale catchment area is located in the central highland of Sri Lanka and covers 572 $km^2$ with altitude ranges from 681 to 2,505 meters above mean sea level. It is extended from latitude 7˚6'32.80"N to 6˚47'33.12"N and from longitude 80˚ 50'21.26"E to 80˚34'31.34"E which encompasses in the south-central mountainous. The primary objective of this study is to assess the sustainability of agriculture based on the environmental and socioeconomic indicators in the Kotmale catchment using geospatial techniques. The Analytic Hierarchy Process (AHP) combined with Multi-Criteria Decision Making (MCDM) methods was used as data computation method, and both spatial and non-spatial data were used under the three main criteria, such as environment, social and economic. The results of the analysis show that soil erosion is one of the major issues and it is reported as mean erosion is 9.8 t $ha^{-1}$ $yr^{-1}$. The mean annual rainfall in this area has decreased over the study period (1986-2016) while temperature has increased up to 2-3 $^0$C. In view of socioeconomic factors, education level of the farmers, lack of labor force, fluctuation of the unit price of the agricultural production, insufficient income of the farmers was negatively affected to the current agricultural activities of the research area. The result would be an aid and sources for assessing the sustainability of agricultural land and decision makers will be able to use this result for future planning.

Keywords: Kotmale watershed, Soil erosion, Agriculture land sustainability , MCDA , AHP

©2019. Japan Geoscience Union. All Right Reserved. 

# Spatial Evaluation of Potential Tsunami Vertical Evacuation: A Case Study of the Western Coastal Belt in Sri Lanka

*Ranagalage Mahinda Manjula[1], Yuji Murayama[1]

1. Division of Spatial Science, Graduate School of Life and Environmental Sciences, University of Tsukuba, Japan

On December 26, 2004, a massive tsunami resulted to recode extensive damages in the Indian Ocean. The recorded death toll was more than 35,000, and approximately one million people were affected in Sri Lanka. Lack of awareness was the main reason for massive damage. After this tsunami incident, Sri Lanka was also categorized as a tsunami-vulnerable country. Several past studies have contributed to introducing proper mechanisms that would minimize the damages from the next tsunami incident. Most tsunami-vulnerable areas have been covered by horizontal tsunami evacuation after 2004, and people need to travel great distances to reach tsunami evacuation centers due to the lower elevation profile of the coastal area. The purpose of this study was to spatially evaluate the potential for tsunami vertical evacuation in the western coastal belt in Sri Lanka. The western coastal belt selected by considering the existing urban structure and tsunami vulnerability. Several criteria and assumptions have been computed to achieve the goal of the study. In this analysis, three tsunami scenarios 4 m, 8 m, and 12 m were used to identify potential vertical evacuation sites. According to the results of the inundation ratio, the category of critical buildings can be increased to 1.7% and 67.0% in 4 m and 12 m scenarios, respectively. It was indicated that the 12 m scenario consisted of more damage than the other two scenarios. Tsunami evacuation sites were selected based on the three tsunami scenarios and 220, 232 and 122 sites were selected for the 4 m, 8 m and 12 m tsunami scenarios, respectively. According to the calculations of the capacity of each site, the selected 220 sites will facilitate 17,594 people during the 4 m tsunami scenario. The selected 232 sites will accommodate 25,677 people during the 8 m scenarios. All selected sites are capable of accommodating the affected population in both the 4 m and the 8 m scenarios. However, the selected evacuation sites are not sufficient for accommodating the affected population in the 12 m scenario. In the 12 m scenario, 12,221 people are affected. However, the evacuation sites can only accommodate 10,165 people. The finding of vertical evacuation by considering the existing urban structure of the city is essential to save human lives during the next tsunami incident. The adopted methodology can be used as an example for other lowland coastal cities to select vertical evacuation to protect human life.

Keywords: tsunami scenario, building volume, vertical evacuation, tsunami , Sri Lanka

©2019. Japan Geoscience Union. All Right Reserved. 

[E] Oral | H (Human Geosciences )：H-TT Technology & Techniques

Thu. May 30, 2019 3:30 PM - 5:00 PM JST | Thu. May 30, 2019 6:30 AM - 8:00 AM UTC | 301B 3F

## [H-TT19] Geographic Information Systems and Cartography

convener:Takashi Oguchi(Center for Spatial Information Science, The University of Tokyo), Yuji Murayama(Graduate School of Life and Environmental Sciences), Yoshiki Wakabayashi(Graduate School of Urban Environmental Sciences, Tokyo Metropolitan University), Chairperson:Takashi Oguchi, Ikuho Yamada(Chuo University)

This session discusses various methods which acquire, store, analyze and visualize geospatial data, and presents the outcomes of empirical studies using GIS or mapping methods. The session also deals with applications of digital data, and GIS, and mapping to various fields of earth and planetary science and human society. All presentations and discussion of this session are made in English.

3:30 PM - 3:45 PM JST | 6:30 AM - 6:45 AM UTC

[HTT19-07] A Framework for Assessing the Spatial Distribution of Vulnerability of Communities to Landslides in Tropical Mountainous Region: A Case study from Kegalle District – Sri Lanka.

★Invited Papers

*Nimala Chinthake Perera[1] (1.SANASA CAMPUS - SRI LANKA, IHRA - UNIVERSITY OF COLOMBO - SRI LANKA)

3:45 PM - 4:00 PM JST | 6:45 AM - 7:00 AM UTC

[HTT19-08] Applications of WebGIS to Educating Disaster Risk Reduction for Chinese and Japanese Students

*Jiali SONG[1], Takashi Oguchi[2], Hiroyuki Yamauchi[2], Takuro Ogura[1] (1.Graduate School of Frontier Sciences, The University of Tokyo, 2.Center for Spatial Information Science, The University of Tokyo)

4:00 PM - 4:15 PM JST | 7:00 AM - 7:15 AM UTC

[HTT19-09] Solar System Treks - GIS that provides interactive visualization and analysis for planetary science and exploration

★Invited Papers

*Emily Law[1], Brian Hamilton Day[2] (1.NASA Jet Propulsion Laboratory, 2.NASA Ames Research Center)

4:15 PM - 4:30 PM JST | 7:15 AM - 7:30 AM UTC

[HTT19-10] **Landslide Recognition using Remote Sensing Images and PCANet**

*Yimei Wei[1], Takashi Oguchi[1] (1.Graduate School of Frontier Science, the University of Tokyo)

4:30 PM - 4:45 PM JST | 7:30 AM - 7:45 AM UTC

[HTT19-11] Estimating the fractional vegetation cover using fixed-wing drone and multiple vegetation indices

★Invited Papers

*Kotaro Iizuka[1] (1.Center for Spatial Information Science, The University of Tokyo)

4:45 PM - 5:00 PM JST | 7:45 AM - 8:00 AM UTC

[HTT19-12] Topographic surveys in Ny-Alesund, Svalbard, and improvement of mapping methods

*Jaeyong Lee[1], Takashi Oguchi[2] (1.Department of Environmental Studies, Graduate School of Frontier Sciences, The University of Tokyo, 2.Center for Spatial Information Science, The University of Tokyo)

# A Framework for Assessing the Spatial Distribution of Vulnerability of Communities to Landslides in Tropical Mountainous Region: A Case study from Kegalle District –Sri Lanka.

*Nimala Chinthake Perera[1]

1. SANASA CAMPUS - SRI LANKA, IHRA - UNIVERSITY OF COLOMBO - SRI LANKA

Landslide vulnerability refers to the degree of loss to a given element at risk due to the occurrence of a landslide event. The concept of vulnerability is difficult to quantify due to the involvement of some social and physical indicators to determine vulnerability to a landslide in a given location. Therefore, limited research has been carried out to determine the spatial distribution of landslide vulnerability. This study attempt to map the spatial distribution of vulnerability to landslide using vulnerability index developed by entropy method abstracting information from fourteen indicators. The study was based on primary sources of data, obtained from 402 elements including associated human capital from Kegalle District-Sri Lanka. Then the Entropy method was used to estimate the level of vulnerability in sample locations (elements). Computed vulnerably vales were imported into Geodatabase which was used to evaluate element at vulnerability and map the spatial distribution of vulnerability. The spatial distribution of vulnerability was obtained from interpolating vulnerability values of sample locations (elements) by using Kriging interpolation method. Results were expressed on maps on which different spatial patterns of levels of vulnerability were found for the study area. According to the map, landslide vulnerabilities in the study area demonstrate notable regional specification. In general, vulnerability reflects expected degree of damage to the considered element or location by the adjacent to occurred landslides. Also, the spatial distribution of vulnerability has shown a close relationship with the rural-urban divide. According to landslide vulnerability analyses, 14.6% (247 sq Km) of the entire area is found to be the highest vulnerable zone for a landslide.

Further, 32% (544 sq Km) of the total land area categorized under very high or high vulnerable zones. Moderately vulnerable zones take part 13.4% (227 sq Km) of the total area. However, 26.4% (448 sq Km) of land area categorized as low or very low vulnerability, while 13.4% (227 sq Km) area categorize under the lowest zone it can be concluding that entropy method has a sufficient level of capacity to defined weigh for indicators which use for vulnerability assessment

Keywords: Element at risk , Entropy method, Spatial distribution, Vulnerability

©2019. Japan Geoscience Union. All Right Reserved. 

# Applications of WebGIS to Educating Disaster Risk Reduction for Chinese and Japanese Students

*Jiali SONG[1], Takashi Oguchi[2], Hiroyuki Yamauchi[2], Takuro Ogura[1]

1. Graduate School of Frontier Sciences, The University of Tokyo, 2. Center for Spatial Information Science, The University of Tokyo

In this world of globalization and information explosion, WebGIS (Web Geographic Information Systems) can effectively support education in natural and social sciences. We should utilize this technology and for better human life. Research on mortality due to natural disasters has shown that nations with higher levels of education experience lower levels of mortality. This suggests that young students are knowledgeable and will contribute to future disaster risk reduction (DRR) if they are well educated. Hence, it is important to introduce DRR into high school education such as classes of geography. At present Chinese researchers are preparing disaster-related compulsory curricula for high school DDR education, and are designing special textbooks for this purpose. In Japan, some researchers have already constructed online WebGIS systems for DRR education using hazard maps available on the Internet. However, such DRR activities tend to be insufficient because of limited cognition of citizens about information related to hazards and risks. This study aims to construct an improved online DRR system for high school education using WebGIS technology along with hazard information including maps for China and Japan. In August 2018, Japanese students used the system in an event funded by the Japan Society for the Promotion of Science. After that, a similar educational event was held in a high school in China. During these activities, students compared paper hazard maps with electronic hazard maps and used both of them for consideration. At the end of each event, the feasibility and effectiveness of the system were surveyed by questionnaires to evaluate the understanding of students about WebGIS and relevant knowledge. The results indicate that students in both countries prefer teaching materials like the constructed DRR system for school classes. However, there are some differences between the two countries. For example, the Chinese students thought that analysis of dangerous areas using the layer of flooding areas was more difficult than the Japanese students, reflecting differences in DDR knowledge. To improve the applicability of the system, further educational activities will be conducted in the near future.

Keywords: WebGIS, Disaster risk reduction, Geography education

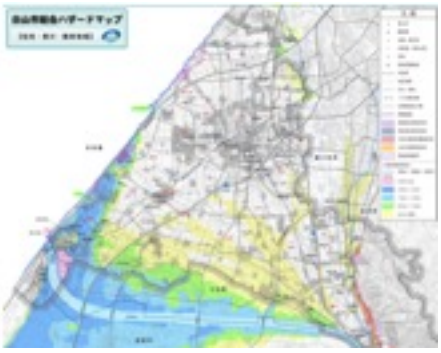

©2019. Japan Geoscience Union. All Right Reserved. 

# Solar System Treks - GIS that provides interactive visualization and analysis for planetary science and exploration

*Emily Law[1], Brian Hamilton Day[2]

1. NASA Jet Propulsion Laboratory, 2. NASA Ames Research Center

Meeting the challenges of space exploration has resulted in new knowledge that has kept NASA and JPL world leaders in big data science and technology. We, NASA’s Solar System Treks Project (SSTP – https://trek.nasa.gov) development team at JPL, under the management of Solar System Exploration Virtual Research Institute (SSERVI, https://sservi.nasa.gov/), have developed a Geographic Information Sysetms (GIS) based system that includes a set of web-based portals that provide a suite of interactive visualization and analysis tools to enable mission planners, scientists, and engineers to access a large volume of cartographic products and models from a growing number of spacecraft. Currently, various web-based portals are available for discovering and exploring the Moon, Mars, Vesta, Ceres, Titan and Icy Moons of Saturn, and hydrology on Earth. This presentation will provide an overview of this GIS-based system highlighting its high level architecture, technologies and capabilities that was designed and developed specifically for exploration of any Solar System bodies. We will also describe its uses, features and capabilities, highlighting visualization and analysis innovations.

Keywords: GIS, Visualization, Analysis, Solar System

©2019. Japan Geoscience Union. All Right Reserved. 

# Landslide Recognition using Remote Sensing Images and PCANet

*Yimei Wei[1], Takashi Oguchi[1]

1. Graduate School of Frontier Science, the University of Tokyo

Landslides are complex geological phenomena that can cause serious damage to the natural and social environments and may result in a significant loss of lives and properties. Consequently, landslide recognition, mapping, and monitoring are important for the prevention of secondary disasters and post-disaster relief. Since various remote sensing images have become more accessible in recent years, the use of satellite and aerial imagery for geological disasters has become a hot research topic. When remote sensing images are used to recognize landslides, image feature extraction is the main technical issue, and inefficiency in extracting ground object features has been a major challenge. This study explores the use of a simplified deep learning network structure, PCANet, to learn image features from post-disaster remote sensing images and train the classifier. This approach reduces the computation time of feature extraction and improves the efficiency of landslide recognition. The materials for training PCANet are image data sets for several areas in Japan including both landslide and non-landslide samples. They were collected from vertical aerial photographs and orthophotographs provided by the Geospatial Information Authority of Japan (GSI). In addition, post-disaster landslide distribution maps provided by the National Institute of Geosciences and Disaster Recovery (NIED) and GSI were utilized in the selection of sample images. As the analyzed remote sensing images were taken in a short time after a serious geological disaster, this research also contributes to future rapid responses to landslide hazards.

Keywords: Landslide recognition, Image feature extraction, PCANet, Machine learning

©2019. Japan Geoscience Union. All Right Reserved. 

# Estimating the fractional vegetation cover using fixed-wing drone and multiple vegetation indices

*Kotaro Iizuka[1]

1. Center for Spatial Information Science, The University of Tokyo

Fractional vegetation cover (percentage of vegetation cover) plays a key role in characterizing the conditions of the terrestrial environment. To analyze the distribution of the vegetation conditions, several methods and models can be found for estimating its coverage. Remote sensing techniques, especially utilizing the satellite imagery is one of the major approaches due to its applicability in larger spatial extent and multiple channels observed from different electromagnetic spectra. Although, in cases of high frequent cloud covering regions such as the tropical regions, usually this is difficult to conduct. Thus, in this work, we seek in alternatively collecting a remotely sensed imagery from a fixed-wing drone and analyze to estimate the fractional vegetation cover of the study site. Normal RGB camera and multispectral sensors were carried onboard the fixed-wing drone, and multiple images were collected. The Structure from Motion method was implemented to develop an ortho image of the whole study site. The imageries were used to further develop a general land use/land cover (LULC) map of the site, and within the determined gridded area, the fraction of each LULC types were examined with different vegetation indices (VIs) computed from the multispectral data. Clear positive trend was found with increasing VIs and increasing fractional cover of healthy trees, and clear negative trend was found with decreasing VIs and increasing fractional cover of soils. This approach demonstrates that it is possible to analyze the coverage information through the utilization of drones, which can be also used as ground truthing, moreover, the findings would play an important role in further simulating such as the water cycles.

Keywords: Drone, Forests, Remote Sensing, Vegetation Index, Land Cover, Structure from Motion

©2019. Japan Geoscience Union. All Right Reserved. 

# Topographic surveys in Ny-Alesund, Svalbard, and improvement of mapping methods

*Jaeyong Lee[1], Takashi Oguchi[2]

1. Department of Environmental Studies, Graduate School of Frontier Sciences, The University of Tokyo, 2. Center for Spatial Information Science, The University of Tokyo

In Ny-Alesund, Svalbard in the Arctic, frozen layers with the active layer that melts only in the summer and the impermeable permanently frozen layer distribute widely. The vertical structure affects the distribution of groundwater as well as the surface environment and sediment movement. In addition, patterned-ground formed by repeated freezing and thawing and associated vegetation are the basis of polar ecosystems. Recent global warming alters the surface environments especially the expansion of the active layer and increased groundwater flow. In order to quantitatively understand such changes in the surface environment, we developed the technique of high-resolution mapping in Ny-Alesund. As field surveys in the polar regions have limitations in terms of site accessibility and duration, we utilized data from not only our fieldwork but also past fieldwork, along with satellite/aerial images and other geospatial data.
We analyzed altitude slope, aspect, curvature, and solar radiation for the area near the Ny-Alesund Science Village using DEMs produced by the Norwegian Polar Institute. We evaluated the reliability of the terrain analysis using TopoSvalbard satellite images and aerial photographs. We also utilized ground photographs and high-resolution ground mapping with the SfM-MVS method to produce a topographic map of the area. Since legal restrictions on the use of radio frequency in Ny-Alesund limit the use of UAVs, we made a pole camera with stabilizer function, which provides photographs with about 3 mm resolution. Such photographs are useful for very high-resolution mapping for small areas.

Keywords: Ny-Alesund, Permafrost, High-resolution mapping

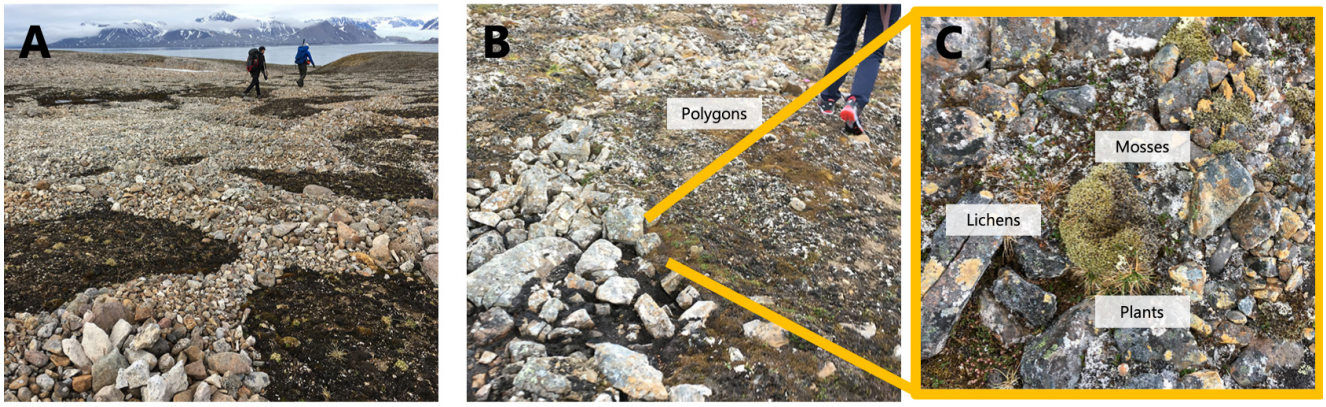


The images of frozen layer taken in field survey in Ny-Alesund, 2017.
**A)** Well-developed polygon shape patterned ground., **B)**, **C)** Vegetation on the polygons.

©2019. Japan Geoscience Union. All Right Reserved. 

[J] Oral | H (Human Geosciences )：H-TT Technology & Techniques

Thu. May 30, 2019 10:45 AM - 12:15 PM JST | Thu. May 30, 2019 1:45 AM - 3:15 AM UTC | 301B 3F

## [H-TT23] Geographic Information System and Cartography

convener:Mamoru Koarai(Earth Science course, College of Science, Ibaraki University), Kazunari Tanka(Department of Civil Engineering and Urban Design, Faculty of Engineering, Osaka Institute of Technology), Kazuhiko Nakamura(The University of Tokyo), Chairperson:Mamoru KOARAI(Ibaraki University), Kazunari Tanaka(大阪工業大学)

This session discusses various methods which acquire, store, analyze and visualize geospatial data, and presents the outcomes of empirical studies using GIS or mapping methods. The session also deals with applications of digital data, GIS, and mapping to various fields of earth and planetary science and human society. All presentations and discussion of this session are made in Japanese.

10:45 AM - 11:00 AM JST | 1:45 AM - 2:00 AM UTC

[HTT23-01] **An analysis of the year-round distribution of $PM_{2.5}$ and Oxidant by (Web)GIS and R**

★Invited Papers

*Junji Yamakawa[1] (1.Graduate School of Natural Science and Technology, Okayama University)

---

11:00 AM - 11:15 AM JST | 2:00 AM - 2:15 AM UTC

[HTT23-02] Development Process and Spatial Structure of Urban Villages in Shenzhen City China

*YARONG LUAN

---

11:15 AM - 11:30 AM JST | 2:15 AM - 2:30 AM UTC

[HTT23-03] An analysis on the location characteristic of alley spaces in Tokyo

*Ryo Taniguchi[1], Go Ishikawa[1], Mayumi Oka[2] (1.Tokyo Map Research Inc., 2.Research Organization of Information and Systems The Institute of Statistical Mathematics)

---

11:30 AM - 11:45 AM JST | 2:30 AM - 2:45 AM UTC

[HTT23-04] Image analysis of night scape using lyrics

*Hiroki Komai[1], Kazunari Tanaka[1] (1.Osaka Institute of Technology)

---

11:45 AM - 12:00 PM JST | 2:45 AM - 3:00 AM UTC

[HTT23-05] On the Method to Evaluate Signboards based on the Relationship with the Surrounding Space

*Akihiro Kishikawa[1], Kazunari Tanaka[1] (1.Osaka Institute of Technology)

---

12:00 PM - 12:15 PM JST | 3:00 AM - 3:15 AM UTC

[HTT23-06] ON THE LANDSCAPES ELEMENTS FROM A BIRD’S-EYE VIEW SCAPE

*Nobuaki Tanaka[1], kazunari Tanaka[1] (1.Osaka Institute of Technology)

# An analysis of the year-round distribution of $PM_{2.5}$ and Oxidant by (Web)GIS and R

*Junji Yamakawa[1]

1. Graduate School of Natural Science and Technology, Okayama University

The year-round concentration distribution of $PM_{2.5}$ and Oxidant in Okayama City, Okayama Prefecture, Japan were estimated by using the geostatistics method and expressed by the (Web)GIS.

The observed concentration data of those environmental substances were obtained from the Website of the National Institute for Environmental Studies. The target year of $PM_{2.5}$ was 2015, and the year of the oxidant was 2006. GNU R (R core team, 2018) was used for geostatistics analysis. The JPGIS (Geographical Survey Institute, 2018), which is government-based open data, was used for geostatistics analysis. The On-premise type GIS and the WebGIS were used in the research. The QGIS (QGIS Development Team, FOSS4G, 2018), and the jSTAT MAP (Statistics Bureau, Ministry of Internal Affairs and Communications, 2019) were used for the each type of the GIS.

First, the variogram of the observed concentration data of the environmental substances, were calculated for the estimation of the spatial dependence, then the prediction of the concentration distribution on the target area were carried out by using the Kriging method. The estimated concentration data were examined together with other geographic information data using (Web)GIS. The expression scheme of the accuracy of the estimation were investigated on the QGIS. Furthermore, transformation of the coordinates that was required on the using of the jSTAT MAP was also investigated.

The year-round mean concentration distribution of $PM_{2.5}$ and oxidant in Okayama city were estimated with certain accuracy. It was also possible to qualitative analysis of the coefficient of variation of estimated distributions of $PM_{2.5}$ and oxidant by GIS and WebGIS. The minor error on the conversion from the rectangular coordinate system to the regional mesh code requires further consideration.

GIS is effective for analysis and mapping of the global environmental data and geographic information data. WebGIS is also becoming capable of executing these analysis with only by the Web browser. Further utilization is expected in the study field of the Earth and planetary science.

Keywords: GIS, jSTAT MAP, Kriging, FOSS4G, PM2.5, Oxidant

©2019. Japan Geoscience Union. All Right Reserved. 

# Development Process and Spatial Structure of Urban Villages in Shenzhen City China

*YARONG LUAN

During the 30 years of the reform and opening-up policy, economically developed cities and regions have expanded rapidly in China. Villages which originally surrounded the city before their expansion were rapidly submerged by the expanded city areas and surrounded by high-rise buildings. They are turned into the "urban villages". In the rapidly urbanized regions, urban villages are common phenomena. This problem becomes extremely serious in the Pearl River Delta region in China.

In the present study, Shenzhen City was selected as the research area. Field work was performed on the 18 sample urban villages selected from total 320 urban villages of Shenzhen City. Based on the changes in their internal spatial structures, the development of the urban villages is divided into three stages, e.g., embryonic stage, growth stage, reformed stage. After analyzing the spatial structures, different characteristic features were found in each stage. And the main factors of the spatial structural changes arising from different stages were summarized.

It was found that the traffic condition was the key factor for the embryonic stage; rental price was the key factor for the growth stage and the regulatory power of the government was the key factor for the reformed stage.

Keywords: Urban Village, Shenzhen City

©2019. Japan Geoscience Union. All Right Reserved. 

# An analysis on the location characteristic of alley spaces in Tokyo

*Ryo Taniguchi[1], Go Ishikawa[1], Mayumi Oka[2]

1. Tokyo Map Research Inc., 2. Research Organization of Information and Systems The Institute of Statistical Mathematics

The number of alley spaces in urban areas is rapidly decreasing due to road transportation plans centered on automobiles and large-scale development. In recent years, however, aspects of the alley as a common space are being reconsidered, and town planning with the alley was also promoted throughout the country. The alley is considered to be an important factor characterizing urban spaces, but it is difficult to grasp its location as special information. So than before, we devised "Alley Estimation Logic" which extracts block areas where the existence of allays is presumed by using GIS, and have checked the accuracy of logic through field survey in Tokyo and Tokushima prefectures.
In this study, we conducted "Alley Estimation Logic" for Tokyo and estimated the alley location. For the analysis, we used “Foundation Geographical Data” (scale level 2500) made by Geographical Survey Institute and “ArcGIS Pro 2.2” by Esri. Furthermore, we calculated "Alley Ratio" from the estimation result and considered the location characteristics of the alley through comparison with the number of wooden buildings and the use district etc. In addition, we estimate the "Alley Ratio" of municipalities in Mie prefecture as a whole, and we will verify regional differences due to differences in prefectures.

Keywords: Geospatial information Data, Alleys, GIS

©2019. Japan Geoscience Union. All Right Reserved. 

# Image analysis of night scape using lyrics

*Hiroki Komai[1], Kazunari Tanaka[1]

1. Osaka Institute of Technology

**Night scape has a beauty that attracts people. In recent years, due to the spread of cameras and SNS, there are many new trends and new popular spots. As a byproduct, this seems to attract tourist. In this research, the characteristics of the night scape were analyzed using the photos and post contents from SNS. As a result, by the analysis to evaluate a part of the values, the examples: the perseverance, the painfulness and the merriment are appeared of the night scape.**

Keywords: Image analysis, Night scape, SNS

©2019. Japan Geoscience Union. All Right Reserved. 

# On the Method to Evaluate Signboards based on the Relationship with the Surrounding Space

*Akihiro Kishikawa[1], Kazunari Tanaka[1]

1. Osaka Institute of Technology

The street space in the city is an important space to impress visitors with the image of the city.

However, in recent years, miscellaneous and townscapes are being formed due to the enlargement of buildings and the diversification of size, forms and colors of signboards.

The signboard design combines size, color, and letters together to create a signboard.

In this research, we aim at grasping the degree of group signs by checking the placement and colors appropriate to the characteristics of the place for Kyoto city.

Based on these relationships, we try to design a signboard suitable for the street.

Keywords: Outdoor Advertisement, Regulation, Kyoto

©2019. Japan Geoscience Union. All Right Reserved. 

# ON THE LANDSCAPES ELEMENTS FROM A BIRD’S-EYE VIEW SCAPE

*Nobuaki Tanaka[1], kazunari Tanaka[1]

1. Osaka Institute of Technology

When it comes to landscapes, beautiful landscapes are formed from local climates such as history and customs by elements such as varying nature and demographic structures. A feature that creates these beautiful landscapes is the linear landscape element. This linear element is characterized as being beautiful because landscape elements that can be continuously viewed form a beautiful landscape such as a building that looks continuous due to the shape and color, in addition to linear landscape elements such as rivers and roads. Hypotheses concerning continuity and image are present not only in urban landscapes, but also in the landscape of rural areas and mountainous regions. Therefore, in this research, focusing on a bird's eye view from high vantage points, we aim to examine urban landscapes by analyzing their elements, shape, view and area. As for the examination method, analyzed and expressed the continuity of streets, rivers, green roads etc, using image analysis and GIS. From the results, extract and consider the relationship between the position and shape of elements with regards to continuity and the beauty of urban landscapes.

Keywords: High-rise building, Bird's eye view Landscape , Continuity

©2019. Japan Geoscience Union. All Right Reserved. 

[J] Poster | H (Human Geosciences )：H-TT Technology & Techniques

Thu. May 30, 2019 3:30 PM - 5:00 PM JST | Thu. May 30, 2019 6:30 AM - 8:00 AM UTC | Poster Hall International Exhibition Hall8, Makuhari Messe_8

## [H-TT23] Geographic Information System and Cartography

convener:Mamoru Koarai(Earth Science course, College of Science, Ibaraki University), Kazunari Tanka(Department of Civil Engineering and Urban Design, Faculty of Engineering, Osaka Institute of Technology), Kazuhiko Nakamura(The University of Tokyo)

This session discusses various methods which acquire, store, analyze and visualize geospatial data, and presents the outcomes of empirical studies using GIS or mapping methods. The session also deals with applications of digital data, GIS, and mapping to various fields of earth and planetary science and human society. All presentations and discussion of this session are made in Japanese.

### [HTT23-P01] Development of 3D Web map making service, MyMap3D

★Invited Papers

*Yoshiharu Nishioka[1], Kaoru Kitao[2] (1.National Insititute of Advanced Industrial Science and Technology, 2.CubeWorks Inc.)

### [HTT23-P02] Experimental hazard map for accurate communication

*Ryo Endo[1], Takayuki Nakano[1] (1.GSI of Japan)

### [HTT23-P03] Effectiveness of color hillshade with multiple light sources for geopark guide maps : A case of the North Ibaraki Geopark Project

*Keiko SUZUKI[1], Go ISHIKAWA[1], Mamoru KOARAI[2], Rika IMAIZUMI[3], Naoki TAKEDA[4] (1.Tokyo Map Research Inc., 2.Ibaraki University, 3.Aero Asahi Co., Ltd., 4.Association for Promotion of North Ibaraki Geopark Project)

### [HTT23-P04] Estimation of three-dimensional structure of forest using LiDAR data in Abukuma mountainous region

Akane Narikiyo[1], *Mamoru Koarai[1], Wataru Murakami[2], Yasuhiro Ogawa[2] (1.Earth Science course, College of Science, Ibaraki University, 2.Forest Research Institute)

### [HTT23-P05] Disaster information sharing of welfare service workers based on knowledge from experience in a tsunami disaster area

*ARISA INOUE[1], Yoshiki Wakabayashi[1] (1.Graduate School of Urban Environmental Sciences, Tokyo Metropolitan University)

### [HTT23-P06] Spatial analysis of children's commuting space - a case study of Toyama city elementary school -

*Koji Ohnishi[1] (1.Department of Humanities, University of Toyama)

# Development of 3D Web map making service, MyMap3D

*Yoshiharu Nishioka[1], Kaoru Kitao[2]

1. National Insititute of Advanced Industrial Science and Technology, 2. CubeWorks Inc.

We have developed MyMap3D as the service by which the user can make a 3D web map freely. The elevation data used for topography making, basically, using elevation tiles of the PNG format Geographical Survey Institute offers, when, everyone is without charge and it can be used. This service is designed in order to change most items of the indication setting, and it's designated using a query parameter of URL. A 3D rendering is performed using WebGL through three.js.

Keywords: 3D, map, WebGL, Elevation, PNG Elevation tile

©2019. Japan Geoscience Union. All Right Reserved. 

# Experimental hazard map for accurate communication

*Ryo Endo[1], Takayuki Nakano[1]

1. GSI of Japan

Hazard maps have been prepared and published in each local government in order to utilize them for disaster prevention measures and evacuation in the event of a disaster. Color representation is often used for the map representation of the hazard map. However, there are some cases in which visibility deteriorates due to excessive information and mixed colors. In this report, we tried to create a hazard map considering the following matters, with the aim of improving the accuracy and understanding of hazard map information. The prototype is a paper hazard map of liquefaction.

1. Background map
A lot of kinds of maps are used as background maps of hazard maps. However, some background maps are difficult to read because of low-resolution. In order to ensure the legibility of the background diagram, we use vector data.

2. Information
Disaster related organizations (e.g. government offices, fire departments, police), evacuation routes / evacuation centers, hospitals, etc. are usually listed in hazard maps. but in order to prevent deterioration of visibility due to excessive information, we only list risk information of each hazard on the area and nformation on evacuation .

3. Color scheme
In the hazard map, many colors are used for map expression including disaster risk. However, there are individual differences in the characteristics of color vision, not everyone recognizes the color in the same way. For example, it has been pointed out that about 5% of men and about 0.2% of women have color vision characteristics that are difficult to distinguish between red and green (for example, Ito (2012)). Therefore, avoiding combinations of red and green, focusing on expressions of disaster risk degree, we tried to make a hazard map with attention to lightness and saturation etc. We confirmed whether people with color vision abnormality can properly read information of prototype hazard map using simulation images created with Adobe photoshop CC 2018.

Keywords: hazard map, universal design, color scheme

©2019. Japan Geoscience Union. All Right Reserved. 

# Effectiveness of color hillshade with multiple light sources for geopark guide maps : A case of the North Ibaraki Geopark Project

*Keiko SUZUKI[1], Go ISHIKAWA[1], Mamoru KOARAI[2], Rika IMAIZUMI[3], Naoki TAKEDA[4]

1. Tokyo Map Research Inc., 2. Ibaraki University, 3. Aero Asahi Co., Ltd., 4. Association for Promotion of North Ibaraki Geopark Project

Until 2018, 44 geoparks were certified In Japan, and in each geopark, they use a large number of guide maps with geosite which to introduce the characteristic topography and geology of the area for education and sightseeing. For those guide maps topographic features and geological information that is easier for users to understand are emphasized. And there are also guide maps that use various topographic representation with high-precision elevation data and geographical analysis by GIS.

In the North Ibaraki Geopark Project of northern Ibaraki prefecture, they have created geosite maps, but the topography and geological representation were not necessarily sufficient. Therefore, we attempted to create a topographic representation that easy to understand topographic features and geological phenomena spatially for this new geosite guide maps in the project. Topographic representation is to express geo information practically and easily understand and for guide maps, we use color hillshade to make it artistic. According to the reduced scale, and regional features, three kinds of light source were examined, single light source, multiple light sources, multiple light sources with pseudo-shade. In this presentation, we describeits effectiveness, topographic representation and map representation.

*This research is supported by Ibaraki University Geological Information Utilizing Project and KAKENHI (16K01213).

Keywords: Color hillshade with multiple light sources, North Ibaraki Geopark Project, Guide map

©2019. Japan Geoscience Union. All Right Reserved. 

# Estimation of three-dimensional structure of forest using LiDAR data in Abukuma mountainous region

Akane Narikiyo[1], *Mamoru Koarai[1], Wataru Murakami[2], Yasuhiro Ogawa[2]

1. Earth Science course, College of Science, Ibaraki University, 2. Forest Research Institute

Many shallow slope failure has occurred in granite area. The root of tree has effects of suppressing collapse. However, it is difficult to study using a method to dig roots. The tendency that root width is larger as stump diameter is larger as the results of field survey in southern part of Abukuma Mountains. In the meantime, Okatani et al., (2013) reports that it is possible to understand the 3D structure of forest by using LiDAR data. This study has two goals in Abukuma Mountains central area. The first is surveying the relationship with weathering layer of granite and root system development, the second is considering usefulness of LiDAR data for detection of the 3D structure of forest.

Research method for the first goal are field survey and data analysis. In 75 points in survey area, root system data (stump diameter, root width and root depth), weathered layer, slope topography (upper or under of slope, ridge or valley), slope orientation and inclination were surveyed. And the relationship of those data was analyzed using GIS. Investigation method for the second goal are every tree survey in two square zone and the forest zone, and analysis LiDAR data. Those data were superimposed, and number, tree height and total cross-sectional area sum was compared whether match or not using GIS.

In the first result, a positive correlation was found between stump diameter and root width, and between stump diameter and root depth. Also, the thinner soil layer thickness is the wider root width. In the second result, about the number, the estimated value by LiDAR data was significantly lower than the measured value in both square sections. But compared by two squares, the magnitude relation of the estimated value was the same as the measured value. In the forest zone, the actual measurement value of 7 out of 10 points didn’t differ the estimated tree height. Also, a positive correlation was found between stump diameter and tree height.

From there results, in a wide range, there is a possibility that the depth of the root can be estimated by the 3D structure of forest detected using LiDAR data.

Keywords: LiDAR data, three dimensional structure of forest, granite, Abukuma Mountainous region

©2019. Japan Geoscience Union. All Right Reserved. 

# Disaster information sharing of welfare service workers based on knowledge from experience in a tsunami disaster area

*ARISA INOUE[1], Yoshiki Wakabayashi[1]

1. Graduate School of Urban Environmental Sciences, Tokyo Metropolitan University

In Great East Japan Earthquake occurred on March 11, 2011, welfare service facilities suffered great damage. Hence, improvement of evacuation plans for welfare service facilities having many elderly people who need assistance in the event of a disaster is an urgent issue. The aim of this study is to we can clarify what kind of information should be shared with their successors based on the disaster knowledge possessed by the staffs of the welfare service facilities.

To this end, I conducted the following research and analysis. First, I identified what kind of disaster knowledge acquired from the Great East Japan Earthquake. Second, I asked the responsible officials of the facilities about tsunami inundation area and evacuation dangerous area at the time of disaster. Third, I explored the current issues of disaster information sharing.

The study area is Oarai-machi, Higashi Ibaraki-gun, Ibaraki prefecture, that suffered the tsunami disaster at the time of the Great East Japan Earthquake. I chose five respondents from welfare facilities in Oarai-machi by employing a semi-structured interview.

The results of this study are summarized as follows. The evacuation behavior of the welfare service facility is not necessarily related to the location of the facility. The interview survey revealed that the staff did not trust the information of the tsunami hazard map issued by the administration nor the evacuation manual but they rely on the disaster knowledge. Concerning the tsunami inundation range considered by the responsible stuffs at the time of the disaster, the information varied with experience of the Great East Japan Great Earthquake.

In the evacuation dangerous area considered by the staff responsible for earthquake response, the dangerous places considered depend on the site of the facility location. Reasons for answering the dangerous area can be divided into two types: natural and artificial. The accuracy of disaster knowledge as for the tsunami inundation range depends on the experience of the Great East Japan Earthquake.

These findings suggest that the staff responsible for the disaster response is likely to take evacuation decision and evacuation behaviors based on their disaster knowledge in the future. Nevertheless, they do not share and make correction of disaster knowledge with staffs of other facilities. Hence transmission of knowledge from experience was not done. A cause of it can be the high turnover rate of welfare service staff; the staffs are too busy with, day-to-day correspondence, there is no time to think about the disaster. In addition, weak relationship between facilities can prevent information sharing. In the future, it is important to inherit knowledge from experience to staff who have no disaster experience and to share and modify knowledge among peers in welfare facilities.

Keywords: disaster information, tsunami, welfare facilities, hazard map, Oarai-machi

©2019. Japan Geoscience Union. All Right Reserved. 

# Spatial analysis of children's commuting space - a case study of Toyama city elementary school -

*Koji Ohnishi[1]

1. Department of Humanities, University of Toyama

Social attention to the safety and security of children has become high since the 1990s. Children use the outdoor space to move between school and home. Watching activities and urban maintenance have been done to protect children from crimes and traffic accidents. It is necessary to grasp the outdoor activities of children for these effective efforts. Currently, the progress of information and communication technology (ITC) makes it possible to research using child's location information with GNSS. In Toyama City, LPWA network covers 98% of the residential area as a Smart City infrastructure building project. So we used the location information from the LoRaWAN position information. This research was conducted in two school districts, Shibazono Elementary School District and the Hayahoshi Elementary School District. GPS position information (latitude / longitude) is transmitted at 1 minute intervals from the position information acquisition sensor device. The implementation period was from January 21 to February 15, 2019, 267 participants in Shibazono elementary school district and 550 participants in Hayahoshi elementary school district. Analysis was done from the viewpoint of distribution and density. As a result, it was found that a high-density point distribution can be seen along the set school road, and it was found that the school-established school road is prominently used. However, cases where unexpected small diameters are also used at high density from routes of movement to school childcare such as on routes not designated by the school were also collected. Also, the number of children going to school and returning to home is the same, but there was a big difference in density. It is due to the diversity of movement of children by afterschool activities. Looking at the point distribution by time, the time of passing through the danger points became clear. These information is effective for the local community. The differences in grade, the distribution has spread the lower grade than higher grade. It is due to autonomous movement and going out after returning home in higher grade, while lower grades move to various places depending on the guardian's car movement.

Keywords: elementary school children, commuting, position information, ICT

©2019. Japan Geoscience Union. All Right Reserved. 

[J] Poster | H (Human Geosciences )：H-TT Technology & Techniques

Thu. May 30, 2019 5:15 PM - 6:30 PM JST | Thu. May 30, 2019 8:15 AM - 9:30 AM UTC | Poster Hall International Exhibition Hall8, Makuhari Messe_17

## [H-TT23] Geographic Information System and Cartography

convener:Mamoru Koarai(Earth Science course, College of Science, Ibaraki University), Kazunari Tanka(Department of Civil Engineering and Urban Design, Faculty of Engineering, Osaka Institute of Technology), Kazuhiko Nakamura(The University of Tokyo)

This session discusses various methods which acquire, store, analyze and visualize geospatial data, and presents the outcomes of empirical studies using GIS or mapping methods. The session also deals with applications of digital data, GIS, and mapping to various fields of earth and planetary science and human society. All presentations and discussion of this session are made in Japanese.

### [HTT23-P01] Development of 3D Web map making service, MyMap3D

★Invited Papers

*Yoshiharu Nishioka[1], Kaoru Kitao[2] (1.National Insititute of Advanced Industrial Science and Technology, 2.CubeWorks Inc.)

### [HTT23-P02] Experimental hazard map for accurate communication

*Ryo Endo[1], Takayuki Nakano[1] (1.GSI of Japan)

### [HTT23-P03] Effectiveness of color hillshade with multiple light sources for geopark guide maps : A case of the North Ibaraki Geopark Project

*Keiko SUZUKI[1], Go ISHIKAWA[1], Mamoru KOARAI[2], Rika IMAIZUMI[3], Naoki TAKEDA[4] (1.Tokyo Map Research Inc., 2.Ibaraki University, 3.Aero Asahi Co., Ltd., 4.Association for Promotion of North Ibaraki Geopark Project)

### [HTT23-P04] Estimation of three-dimensional structure of forest using LiDAR data in Abukuma mountainous region

Akane Narikiyo[1], *Mamoru Koarai[1], Wataru Murakami[2], Yasuhiro Ogawa[2] (1.Earth Science course, College of Science, Ibaraki University, 2.Forest Research Institute)

### [HTT23-P05] Disaster information sharing of welfare service workers based on knowledge from experience in a tsunami disaster area

*ARISA INOUE[1], Yoshiki Wakabayashi[1] (1.Graduate School of Urban Environmental Sciences, Tokyo Metropolitan University)

### [HTT23-P06] Spatial analysis of children's commuting space - a case study of Toyama city elementary school -

*Koji Ohnishi[1] (1.Department of Humanities, University of Toyama)

# Development of 3D Web map making service, MyMap3D

*Yoshiharu Nishioka[1], Kaoru Kitao[2]

1. National Insititute of Advanced Industrial Science and Technology, 2. CubeWorks Inc.

We have developed MyMap3D as the service by which the user can make a 3D web map freely. The elevation data used for topography making, basically, using elevation tiles of the PNG format Geographical Survey Institute offers, when, everyone is without charge and it can be used. This service is designed in order to change most items of the indication setting, and it's designated using a query parameter of URL. A 3D rendering is performed using WebGL through three.js.

Keywords: 3D, map, WebGL, Elevation, PNG Elevation tile

©2019. Japan Geoscience Union. All Right Reserved. 

# Experimental hazard map for accurate communication

*Ryo Endo[1], Takayuki Nakano[1]

1. GSI of Japan

Hazard maps have been prepared and published in each local government in order to utilize them for disaster prevention measures and evacuation in the event of a disaster. Color representation is often used for the map representation of the hazard map. However, there are some cases in which visibility deteriorates due to excessive information and mixed colors. In this report, we tried to create a hazard map considering the following matters, with the aim of improving the accuracy and understanding of hazard map information. The prototype is a paper hazard map of liquefaction.

1. Background map
A lot of kinds of maps are used as background maps of hazard maps. However, some background maps are difficult to read because of low-resolution. In order to ensure the legibility of the background diagram, we use vector data.

2. Information
Disaster related organizations (e.g. government offices, fire departments, police), evacuation routes / evacuation centers, hospitals, etc. are usually listed in hazard maps. but in order to prevent deterioration of visibility due to excessive information, we only list risk information of each hazard on the area and nformation on evacuation .

3. Color scheme
In the hazard map, many colors are used for map expression including disaster risk. However, there are individual differences in the characteristics of color vision, not everyone recognizes the color in the same way. For example, it has been pointed out that about 5% of men and about 0.2% of women have color vision characteristics that are difficult to distinguish between red and green (for example, Ito (2012)). Therefore, avoiding combinations of red and green, focusing on expressions of disaster risk degree, we tried to make a hazard map with attention to lightness and saturation etc. We confirmed whether people with color vision abnormality can properly read information of prototype hazard map using simulation images created with Adobe photoshop CC 2018.

Keywords: hazard map, universal design, color scheme

©2019. Japan Geoscience Union. All Right Reserved. 

# Effectiveness of color hillshade with multiple light sources for geopark guide maps : A case of the North Ibaraki Geopark Project

*Keiko SUZUKI[1], Go ISHIKAWA[1], Mamoru KOARAI[2], Rika IMAIZUMI[3], Naoki TAKEDA[4]

1. Tokyo Map Research Inc., 2. Ibaraki University, 3. Aero Asahi Co., Ltd., 4. Association for Promotion of North Ibaraki Geopark Project

Until 2018, 44 geoparks were certified In Japan, and in each geopark, they use a large number of guide maps with geosite which to introduce the characteristic topography and geology of the area for education and sightseeing. For those guide maps topographic features and geological information that is easier for users to understand are emphasized. And there are also guide maps that use various topographic representation with high-precision elevation data and geographical analysis by GIS.

In the North Ibaraki Geopark Project of northern Ibaraki prefecture, they have created geosite maps, but the topography and geological representation were not necessarily sufficient. Therefore, we attempted to create a topographic representation that easy to understand topographic features and geological phenomena spatially for this new geosite guide maps in the project. Topographic representation is to express geo information practically and easily understand and for guide maps, we use color hillshade to make it artistic. According to the reduced scale, and regional features, three kinds of light source were examined, single light source, multiple light sources, multiple light sources with pseudo-shade. In this presentation, we describeits effectiveness, topographic representation and map representation.

*This research is supported by Ibaraki University Geological Information Utilizing Project and KAKENHI (16K01213).

Keywords: Color hillshade with multiple light sources, North Ibaraki Geopark Project, Guide map

©2019. Japan Geoscience Union. All Right Reserved. 

# Estimation of three-dimensional structure of forest using LiDAR data in Abukuma mountainous region

Akane Narikiyo[1], *Mamoru Koarai[1], Wataru Murakami[2], Yasuhiro Ogawa[2]

1. Earth Science course, College of Science, Ibaraki University, 2. Forest Research Institute

Many shallow slope failure has occurred in granite area. The root of tree has effects of suppressing collapse. However, it is difficult to study using a method to dig roots. The tendency that root width is larger as stump diameter is larger as the results of field survey in southern part of Abukuma Mountains. In the meantime, Okatani et al., (2013) reports that it is possible to understand the 3D structure of forest by using LiDAR data. This study has two goals in Abukuma Mountains central area. The first is surveying the relationship with weathering layer of granite and root system development, the second is considering usefulness of LiDAR data for detection of the 3D structure of forest.

Research method for the first goal are field survey and data analysis. In 75 points in survey area, root system data (stump diameter, root width and root depth), weathered layer, slope topography (upper or under of slope, ridge or valley), slope orientation and inclination were surveyed. And the relationship of those data was analyzed using GIS. Investigation method for the second goal are every tree survey in two square zone and the forest zone, and analysis LiDAR data. Those data were superimposed, and number, tree height and total cross-sectional area sum was compared whether match or not using GIS.

In the first result, a positive correlation was found between stump diameter and root width, and between stump diameter and root depth. Also, the thinner soil layer thickness is the wider root width. In the second result, about the number, the estimated value by LiDAR data was significantly lower than the measured value in both square sections. But compared by two squares, the magnitude relation of the estimated value was the same as the measured value. In the forest zone, the actual measurement value of 7 out of 10 points didn’t differ the estimated tree height. Also, a positive correlation was found between stump diameter and tree height.

From there results, in a wide range, there is a possibility that the depth of the root can be estimated by the 3D structure of forest detected using LiDAR data.

Keywords: LiDAR data, three dimensional structure of forest, granite, Abukuma Mountainous region

©2019. Japan Geoscience Union. All Right Reserved. 

# Disaster information sharing of welfare service workers based on knowledge from experience in a tsunami disaster area

*ARISA INOUE[1], Yoshiki Wakabayashi[1]

1. Graduate School of Urban Environmental Sciences, Tokyo Metropolitan University

In Great East Japan Earthquake occurred on March 11, 2011, welfare service facilities suffered great damage. Hence, improvement of evacuation plans for welfare service facilities having many elderly people who need assistance in the event of a disaster is an urgent issue. The aim of this study is to we can clarify what kind of information should be shared with their successors based on the disaster knowledge possessed by the staffs of the welfare service facilities.

To this end, I conducted the following research and analysis. First, I identified what kind of disaster knowledge acquired from the Great East Japan Earthquake. Second, I asked the responsible officials of the facilities about tsunami inundation area and evacuation dangerous area at the time of disaster. Third, I explored the current issues of disaster information sharing.

The study area is Oarai-machi, Higashi Ibaraki-gun, Ibaraki prefecture, that suffered the tsunami disaster at the time of the Great East Japan Earthquake. I chose five respondents from welfare facilities in Oarai-machi by employing a semi-structured interview.

The results of this study are summarized as follows. The evacuation behavior of the welfare service facility is not necessarily related to the location of the facility. The interview survey revealed that the staff did not trust the information of the tsunami hazard map issued by the administration nor the evacuation manual but they rely on the disaster knowledge. Concerning the tsunami inundation range considered by the responsible stuffs at the time of the disaster, the information varied with experience of the Great East Japan Great Earthquake.

In the evacuation dangerous area considered by the staff responsible for earthquake response, the dangerous places considered depend on the site of the facility location. Reasons for answering the dangerous area can be divided into two types: natural and artificial. The accuracy of disaster knowledge as for the tsunami inundation range depends on the experience of the Great East Japan Earthquake.

These findings suggest that the staff responsible for the disaster response is likely to take evacuation decision and evacuation behaviors based on their disaster knowledge in the future. Nevertheless, they do not share and make correction of disaster knowledge with staffs of other facilities. Hence transmission of knowledge from experience was not done. A cause of it can be the high turnover rate of welfare service staff; the staffs are too busy with, day-to-day correspondence, there is no time to think about the disaster. In addition, weak relationship between facilities can prevent information sharing. In the future, it is important to inherit knowledge from experience to staff who have no disaster experience and to share and modify knowledge among peers in welfare facilities.

Keywords: disaster information, tsunami, welfare facilities, hazard map, Oarai-machi

©2019. Japan Geoscience Union. All Right Reserved. 

# Spatial analysis of children's commuting space - a case study of Toyama city elementary school -

*Koji Ohnishi[1]

1. Department of Humanities, University of Toyama

Social attention to the safety and security of children has become high since the 1990s. Children use the outdoor space to move between school and home. Watching activities and urban maintenance have been done to protect children from crimes and traffic accidents. It is necessary to grasp the outdoor activities of children for these effective efforts. Currently, the progress of information and communication technology (ITC) makes it possible to research using child's location information with GNSS. In Toyama City, LPWA network covers 98% of the residential area as a Smart City infrastructure building project. So we used the location information from the LoRaWAN position information. This research was conducted in two school districts, Shibazono Elementary School District and the Hayahoshi Elementary School District. GPS position information (latitude / longitude) is transmitted at 1 minute intervals from the position information acquisition sensor device. The implementation period was from January 21 to February 15, 2019, 267 participants in Shibazono elementary school district and 550 participants in Hayahoshi elementary school district. Analysis was done from the viewpoint of distribution and density. As a result, it was found that a high-density point distribution can be seen along the set school road, and it was found that the school-established school road is prominently used. However, cases where unexpected small diameters are also used at high density from routes of movement to school childcare such as on routes not designated by the school were also collected. Also, the number of children going to school and returning to home is the same, but there was a big difference in density. It is due to the diversity of movement of children by afterschool activities. Looking at the point distribution by time, the time of passing through the danger points became clear. These information is effective for the local community. The differences in grade, the distribution has spread the lower grade than higher grade. It is due to autonomous movement and going out after returning home in higher grade, while lower grades move to various places depending on the guardian's car movement.

Keywords: elementary school children, commuting, position information, ICT

©2019. Japan Geoscience Union. All Right Reserved. 

[J] Oral | H (Human Geosciences )：H-CG Complex & General

Thu. May 30, 2019 9:00 AM - 10:30 AM JST | Thu. May 30, 2019 12:00 AM - 1:30 AM UTC | 101 1F

## [H-CG31] Nuclear Energy and Geoscience

convener:Eiji Sasao(Tono Geoscience Center, Japan Atomic Energy Agency), Ryuta Hataya(Central Research Institute of Electric Power Industry), Shinji Takeuchi(Department of Earth and Environmental Sciences, College of Humanities & Sciences, Nihon University), Chairperson:Tadafumi Niizato

Handling of geological hazard assessments represent a major environmental concern in the modern society due to constructing nuclear facilities and their radioactive wastes, and also related to the management of contaminated biosphere after nuclear disasters of Fukushima-Daiichi Nuclear Power Plant. The session rational is to provide a forum to deal with various aspects of scientific and engineering aspects of nuclear power. The session in this year focuses on radioactive waste disposal and covers not only scientific aspect such as characterization of geological environment but also engineering aspects such as microbe-nuclide, mineral-water, and cement-water interactions. In addition to this, themes on seismic hazards at nuclear facilities, environmental behavior of radionuclides emitted from disabled nuclear plants, and volume reduction and reuse of cesium contaminated soils are welcomed. Through these presentations, we aim to promote intercultural communication and collaboration between science, engineering and social science.

9:00 AM - 9:15 AM JST | 12:00 AM - 12:15 AM UTC

### [HCG31-01] Uplift estimation in coastal sea area by extrapolation of the land area model and its uncertainty

*Ryuta Hataya[1], Takaomi Hamada[1], Yohei Shimizu[1] (1.Central Research Institute of Electric Power Industry)

9:15 AM - 9:30 AM JST | 12:15 AM - 12:30 AM UTC

### [HCG31-02] Deep groundwater mobility at costal area estimated by groundwater dating

*Takuma HASEGAWA[1], Kotaro NAKATA[1], Yuichi Tomioka[1], Tomoko Ota[1], Atsunao Marui[2], Isao Machida[2], Reo Ikawa[2], Masahiko Ono[2], Shinji Matsumoto[2] (1.Central Research Institute of Electric Power Industry, 2.The National Institute of Advanced Industrial Science and Technology)

9:30 AM - 9:45 AM JST | 12:30 AM - 12:45 AM UTC

### [HCG31-03] Attempt to Estimate permeability of rock mass based on elasticity and resistivity measurement in underground tunnel

*Sota Kawaguchi[1], Tada-nori Goto[1], Koki Kashiwaya[1] (1.Graduate School of Engineering, Kyoto University)

9:45 AM - 10:00 AM JST | 12:45 AM - 1:00 AM UTC

### [HCG31-04] Study on relationship between pathway of groundwater and mass transport, and cooling process of granitic rock

*Eiji Sasao[1], Takashi Yuguchi[2], Masayuki Ishibashi[1] (1.Tono Geoscience Center, Japan Atomic Energy Agency, 2.Faculty of Science, Yamagata University)

10:00 AM - 10:15 AM JST | 1:00 AM - 1:15 AM UTC

### [HCG31-05] Fracture characterization in the accretionary complex from the view point of mass transfer

*Shinji Takeuchi[1], Chikara Kurata[1], Masakazu Niwa[2], Tadamasa Ueki[2] (1.Department of Earth and Environmental Sciences, College of Humanities & Sciences, Nihon University, 2.Japan Atomic Energy Agency)

10:15 AM - 10:30 AM JST | 1:15 AM - 1:30 AM UTC

### [HCG31-06] Retardation of Cs and Sr leachings by geopolymer matrices with zeolte and titanate adsorbent

*Kazuma Kuroda[1], Soonthornwiphat Natatsawas[1], Chaerun Raudhatul Islam[1], Hnin Wint Wint Two[1], Kanako Toda[1], Yutaro Kobayashi[1], Tsutomu Sato[2], Tsubasa Otake[2] (1.Graduate school of Engineering, Hokkaido University, 2.Faculty of Engineering, Hokkaido University)

# Uplift estimation in coastal sea area by extrapolation of the land area model and its uncertainty

*Ryuta Hataya[1], Takaomi Hamada[1], Yohei Shimizu[1]

1. Central Research Institute of Electric Power Industry

## 1. Introduction

The research meeting of the METI in 2015-2016 discussed research issues of geological disposal in the coastal area [1]. After that, we began this study in August 2016[2]. In this study, finally, we’ d like to estimate the downward erosion under the coastal seafloor.

## 2. Method

We use the conventional method considering the future preliminary investigation for geological disposal siting [2, 3, 4, 5 etc.]. We drew the distribution map of the late Pleistocene uplift in the land using these data. Then, we construct a model of uplift motion after late Pleistocene in three dimensions on the basis of the uplift distribution and extrapolate it to the sea. Next, we have verified the model by discussing the uplift history from the tertiary to the recent. Furthermore, we’ ve discussed uncertainty of the extrapolation of uplift late from the land to the sea by the sensitivity analysis.

## 3. Case study

We have conducted the case study on the Miyazaki plain, which is known to have terraces widely distributed and the amount of uplift after the late Pleistocene is relatively large.

### (1) Basic uplift model

Our basic model of the uplift in the case study area is a flat plate approximation model, which means monotonous tilting in one direction [2].

### (2) Verification of uplift model by discussing the uplift history

The geological structure of the Neogene system shows tilting movement in the ESE direction [6]. The geomorphology and geological distribution of Pleistocene suggest tilting movement in the ENE direction. In addition, it is now rotating counterclockwise in North Kyusu district [7]. From these, the tilting direction in the late Pleistocene is considered to be in the ENE direction.

### (3) Discussed uncertainty of the extrapolation of uplift late from the land to the sea

In addition to the basic data set, we have created multiple possible data sets reflecting the uncertainty of the survey. These are saved data of some areas from the basic data set, and some data are replaced based on working hypotheses of terrace chronology. We constructed models from each data set and compare the average uplift rate distribution models of the late Pleistocene of coastal sea area. In this examination, the difference in uplift estimation due to the amount of data was larger than the difference of terrace chronology.

## 4. Summary and future tasks

©2019. Japan Geoscience Union. All Right Reserved. 

Needless to say, the uplift model in the land depends on the data set of the uplift, and discussion on geological history is useful for verification of the model. Also, in this presentation, we showed how to evaluate the effect of uncertainty deriving from data set and models (working hypothesis). We would like to continue case studies.

**Acknowledgments:**
This study was conducted as a project of the Ministry of Economy, Trade and Industry. Tono Geoscience Centre of Japan Atomic Energy Agency, DIA Consultant and Kawasaki Geological Engineering greatly helped us. For the survey of the sea area, we used the sea acoustic wave exploration records disclosed by the National Institute of Advanced Industrial Science and Technology. We express our deep thanks to their participants.

**Reference:**
[1] Research group on technical issues of geological disposal in the Ministry of Economy, Trade and Industry, Coastal Submarine Bottom
http: //www.meti.go.jp/committee/kenkyukai/energy_environment.html#engan_kaiteika
[2] Hataya et al., 2018, JPGU meeting 2018, HCG27-02.
[3] Machida and Koike, 2001, Atlas of Quaternary marine terraces in the Japanese islands, Tokyo University Press.
[4] Nagaoka et al., 2010, J. Geography, 119, 632-667.
[5] Yoshiyama and Yanagida, 1995, J. Geography, 104, 809-826.
[6] Suzuki, 1986, Contributions from the Institute of Geology and Paleontology Tohoku University, 90, 24p.
[7] Earthquake Research Committee, 2018, Long-term evaluation of active faults in the Kyushu area (Ver.1).

Keywords: high level radioactive waste, geological disposal, coastal area, uplift, Quaternary

©2019. Japan Geoscience Union. All Right Reserved. 

# Deep groundwater mobility at costal area estimated by groundwater dating

*Takuma HASEGAWA[1], Kotaro NAKATA[1], Yuichi Tomioka[1], Tomoko Ota[1], Atsunao Marui[2], Isao Machida[2], Reo Ikawa[2], Masahiko Ono[2], Shinji Matsumoto[2]

1. Central Research Institute of Electric Power Industry, 2. The National Institute of Advanced Industrial Science and Technology

On high-level radioactive waste disposal, “Nationwide map of Scientific Features for Geological Disposal” was published and costal area is the favorable from transportation point of view. To evaluate deep groundwater mobility at coastal area, groundwater was sampled from deep borehole at the order of 1000 m in depth. Major ions, tritium, carbon-14, chorine-36 were measured. Based on these results, the groundwaters were categorized into four groups, which are modern meteoric water, modern seawater, glacial meteoric water, fossil sea water. Meteoric water and seawater was divided by 1900 mg/l of Cl concentration. Modern and old groundwater was divided by 10 pMC of $^{14}C$ concentration. The type of seawaters was well categorized into modern seawater and fossil seawater by $^{14}C$ concentration because residence times of modern seawater and fossil seawater are quite different. $^{36}Cl/Cl$ of Modern sea water is equivalent to that of present seawater ($\fallingdotseq 0.7\times10^{-15}$), and that of fossil sea water is higher than that of present seawater. It indicates that $^{36}C/Cl$ of fossil seawater influenced by in-situ production, which takes at least a few ten thousand years. Thus, the category of modern seawater and fossil seawater was validated by not only $^{14}C$ but also $^{36}Cl$. Due to the lack of information, which are shallow groundwater and surface investigation, it could not be confirmed that modern meteoric water and glacial meteoric water was categorized by water isotopes and noble gas temperature. However, it is deduced the origin of Cl of meteoric water is from modern seawater and that of glacial meteoric water is from fossil sea water. It is though that the age of mixing water reflects the groundwater age.

As a result, the deep groundwaters at costal area were categorized into modern meteoric water and modern seawater about 40%, glacial and fossil seawater about 60%.

This study was performed under contracts “Development and Improvement on waste disposal system at coastal area” awarded by the Japanese Ministry of Economy, Trade and Industry.

Keywords: groundwater dating, costal area, radioactive isotopes

©2019. Japan Geoscience Union. All Right Reserved. 

# Attempt to Estimate permeability of rock mass based on elasticity and resistivity measurement in underground tunnel

*Sota Kawaguchi[1], Tada-nori Goto[1], Koki Kashiwaya[1]

1. Graduate School of Engineering, Kyoto University

Fracture distribution in the rock has a great influence on the groundwater flow. So, it is necessary to grasp its characteristics for resource exploration and geological disposal of radioactive waste. Previous studies have been attempting to grasp the hydraulic characteristics on a local scale using boreholes and the like, but it is considered difficult to grasp the hydraulic characteristics in undrilled areas. In this study, we tried to estimate the permeability of rocks in deep underground from physical property values like resistivity and Young's modulus in order to grasp macroscopic hydraulic characteristics of rock including fracture. The validity of the present estimation method was examined, by comparing this estimated value with the measured value.

The survey area is the research tunnel exposed bedrock (depth 300 m, 500 m) of the Mizunami underground research labolatory of the Japan Atomic Energy Agency, located in Mizunami-city, Gifu Prefecture. In this area, a lot of logging data is published and the fracture distribution in the gallery is also examined in detail.(eg. Ishibashi et al.,2016) Furthermore, permeability of the same rock is measured in 2015 (Sato, 2015). In this study, we measured resistivity using a small electric surveying device (4 pole method with electrode interval of about 10 cm) in addition to these. Young's modulus was measured using a Schmidt-lock hammer.

In this study, the permeability was estimated using a rock physics model. The resistivity was expressed as follows using modified archie’ s law (Katsube and Hume,1983)(1).

$\sigma_{eff}=a\,\sigma_w\,\Phi^m+\sigma_c c$(1)

Where $\sigma_{eff}$ is electrical conductivity of rock, $a$is toriosity, $\sigma_w$ is relectrical conductivity of pore water, $\Phi$is porosity, m is cementation factor, $\sigma_c$ is clay reistivity.The elasticity of rock, was expressed as follows using Gassmann’ s Relation (Gassmann, 1951) added clay effect (2).

$1/K=1/K_m+\Phi/K_w+c/K_c$(2)

Where K is bulk module of rock, $K_m$ is bulk module of mineral, $\Phi$is porosity, $K_w$ is bulk module of pore water, $c$ is clay content, $K_c$ is bulk module of clay. Where K is bulk module of rock, Km is bulk module of mineral, $\Phi$is porosity, $Kw$ is bulk module of pore water, $c$ is clay content, $Kc$ is bulk module of clay. The porosity and the clay content rate were two unknown parameter, and these were determined from the measured values of resistivity and bulk modulus by Nelder-Mead method. Permeability was estimated from Kozeny-Carman's equation (Carman, 1961) for plane crack (3).

$k=\Phi t^2/8\,\tau^2$

k is permeability, $\Phi$is porosity, t is opening width, $\tau$ is tortuosity.

Estimated value of pemeability and measured value are consistent with estimated value and error of about one digit in many rock parts.

We will use other rock physics models like unsaturated pore and data obtained from laboratory experiments and loggingdate to further improve the estimation accuracy of permeability.

©2019. Japan Geoscience Union. All Right Reserved. 

# Study on relationship between pathway of groundwater and mass transport, and cooling process of granitic rock

*Eiji Sasao[1], Takashi Yuguchi[2], Masayuki Ishibashi[1]

1. Tono Geoscience Center, Japan Atomic Energy Agency, 2. Faculty of Science, Yamagata University

Fractures in the crystalline rock (e.g. granite) can act as the pathways for groundwater flow and mass transport. Therefore, understanding of the fracture distribution is an important subject for the disposal of high-level nuclear waste. The authors studied the relation between the formation of fracture and infilling mineral, and geological history from the emplacement to present in the Toki granite, Tono district, central Japan (Sasao et al., 2015). Ishibashi et al. (2016a) found that the micropores are selectively formed in plagioclases due to deuteric alteration and that those have the potential of acting as matrix diffusion paths. These results suggest that the magma cooling process played a significant role for the formation and development of the pathways for groundwater flow and mass transport.

The authors studied cooling process of granitic magma in the Toki granite, distributed in the southwestern part of Gifu Prefecture, central Japan, based on petrological, mineralogical and themochronological methodologies. We also discussed the relationship between magma cooling process, and fracture distribution and alteration of biotite and plagioclase (Yuguchi et al., 2019a, 2019b, 2015, 2012, Ishibashi et al., 2016a, 2016b, 2014). In this study, We present the relationship between formation of the pathway of groundwater and mass transport, and cooling process of granitic rock.

Reference

Ishibashi et a., 2014; J. Japan Soc. Eng. Geol., 55, 156-165.
Ishibashi et al., 2016a; Eng. Geol., 208, 114-127.
Ishibashi et al., 2016b; J. Nucl. Fuel Cycle Environ., 23, 121-129.
Sasao et al., 2015; JpGU2015, HCG34-01.
Yuguchi et al., 2011a; J. Mineral. Petrol. Sci., 106, 61-78.
Yuguchi et al., 2011b; J. Mineral. Petrol. Sci., 106, 130-141.
Yuguchi et al., 2012; Eng. Geol. 149-150, 35-46.
Yuguchi et al., 2015; Am. Mineral., 100, 1134-1152.
Yuguchi et al., 2019a; J. Asian Earth Sci., 169, 47-66.
Yuguchi et al., 2019b; Am. Mineral., in press.

Keywords: granite, cooling process of granitic magma, fracture, micropore

©2019. Japan Geoscience Union. All Right Reserved. 

# Fracture characterization in the accretionary complex from the view point of mass transfer

*Shinji Takeuchi[1], Chikara Kurata[1], Masakazu Niwa[2], Tadamasa Ueki[2]

1. Department of Earth and Environmental Sciences, College of Humanities & Sciences, Nihon University, 2. Japan Atomic Energy Agency

Introduction
As most of the basement rock of Japan is thought to be composed of accretionary complexes (Kano et al., 1998), accretionary prisms should not be ignored for the site selection of geological disposal of high-level radioactive waste. Because of many discontinuous structures such as faults and fractures formed due to the subduction of the plate in the accretionary complex, radioactive materials may migrate in the discontinuous structure together with the groundwater flow. Therefore, it is important to understand the characteristics of the mass transfer in along the discontinuous structure in the accretionary complex. In this study, we have carried out geological observation, permeability test in the laboratory, etc. using the samples containing discontinuous structures in the Neogene and Pre-Neogene accretionary complex (Takeuchi et al. 2018).

The study areas are Chichibu Belt (Akiruno City, Tokyo) for the Pre-Neogene accretionary complex, and Miura Group Misaki Formation (Miura City, Kanagawa Prefecture) for the Neogene accretionary complex. In the Misaki Formation, plain-less fault (Ijiri et al., 1955) in the mudstone are widely distributed. On the other hand, argillaceous matrix rock in the mélange which characterizes the accretionary complex are widely distributed. An optical microscope, scanning electron microscope (SEM) observation, X-ray fluorescence micro-scanner (XGT) analysis, permeability test, etc. have been were carried out using those samples.

2. Neogene accretionary complex

In the Miura Group Misaki Formation exposed to the southern tip of Miura Peninsula, plain-less faults are widely distributed. It was confirmed by SEM observation and XGT observation that there has been no change in the element distribution, although the host rock was granulated due to a cataclastic fracturing in the fault zone (Takeuchi et al. 2018). The porosity of the host rock and faults has been measured using SEM images. As a result of measurement, the porosity in the fault zone is about 1.2%, and that of the host rock is about 2.7%. In addition, hydraulic conductivity of the host rock without plain-less fault and the specimen perpendicular to the plain-less fault is estimated by the permeability test. As a result, the former is about 6 E - 9 (m / s), and in the latter is about 2E - 8 (m / s). This suggests hydraulic anisotropy in the formation with plain-less fault. From the above results, it is expected that a barrier effect on the mass transfer within the area surrounded by the plain-less fault.

3. Pre-Neogene accretionary complex

As a result of observation of thin sections, scaly cleavage due to shear deformation can be observed in the mudstone. In addition, concentrations of Fe have been confirmed along the cleavage from the XGT analysis. The concentration of Fe (the count number of XGT analysis) perpendicular to the cleavage shows almost restricted to the cleavage part, and diffusion has not been observed in the adjacent area. As a result of permeability test in the laboratory, the hydraulic conductivity parallel to the cleavage is estimated

©2019. Japan Geoscience Union. All Right Reserved. 

about 4E - 8 (m / s), on the other hand, that perpendicular to the cleavage is about 2.5 E-8 (m / s). From the result above, it is assumed that faint hydraulic anisotropy exists in the mudstone matrix part. The reason for the small difference in hydraulic conductivity is thought to be connectivity of the curvature scaly cleavage or the weathering at the surface.

From the above results, it is considered that cleavage planes in the mudstone matrix can be selective migration pathways for mass transfer.

4. Summary

From this study, we have constructed a conceptual model showing the characteristics of material transfer in discontinuous structures in Neogene and Pre-Neogene accretionary complex. In the future, we have to improve the conceptual model from the mass transfer point of view properly by using deeper samples.

Keywords: Geological disposal, Accretionary complex, Neogene, Pre-Neogene, Mass transfer

©2019. Japan Geoscience Union. All Right Reserved. 

# Retardation of Cs and Sr leachings by geopolymer matrices with zeolte and titanate adsorbent

*Kazuma Kuroda[1], Soonthornwiphat Natatsawas[1], Chaerun Raudhatul Islam[1], Hnin Wint Wint Two[1], Kanako Toda[1], Yutaro Kobayashi[1], Tsutomu Sato[2], Tsubasa Otake[2]

1. Graduate school of Engineering, Hokkaido University, 2. Faculty of Engineering, Hokkaido University

After the accident at the Fukushima Daiichi Nuclear Power Station (FDNPS) that occurred due to the Tohoku big earthquake in 2011, contaminated water with radioactive nuclides such as cesium (Cs) and strontium (Sr) have been continuously generated due to cooling of fuel debris by water. Zeolite or titanate adsorbents have been used for removing Cs or Sr from the contaminated water. The spent adsorbents would probably be solidified for the safety storage and disposal. Glass and cement have been proposed for solidifying binder. However, they have some disadvantages such as generation of secondary radioactive waste during vitrification and large amount of waste volume limited by bigger free water volume. Recently, geopolymer is considered as new binder which has potential to solve the above disadvantages for safety disposal of the spent adsorbent. Geopolymer has the potential to decrease total volume of solidified substances comparing cement because amount of containing free water is less than that containing cement. Primary phases of geopolymer such as calcium silicate hydrate (C-S-H) or potassium alumino silicate hydrate (K-A-S-H) may have property for sorbing radioactive nuclides. Furthermore, it is possible to obtain the desirable phases by changing the type and ratio of the starting materials. So, the appropriate primary phases could be designed depending on the type of the radioactive nuclide in disposed radioactive waste. However, there are few data about leaching behavior of radioactive nuclides from geopolymer in real disposal condition. In this context, this study was conducted leaching and sorption experiments to understand the leaching behavior from geopolymer with zeolite or titanate containing Cs or Sr.

In this study, geopolymer samples from mixing of KOH, metakaoline and water glass were investigated in leaching experiments. From the leaching experiments of Cs and Sr from geopolymer with titanate, most of Sr was tightly remained after 90 days even without titanate. This means that K-A-S-H matrix formed after the mixing has high capacity for Sr storage. On the other hand, small part of Cs (around 4%) was leached out after 90 days. However, although it is well known that Cs and Sr are easily leached out from cement matrix (A. El-Kamash, et al., 2006, and M. Takaoka, et al., 2015), K-A-S-H matrix is better in terms of Cs and Ss storage. From sorption experiments of Cs and Sr by using powder C-S-H and K-A-S-H samples as matrix components of cement and geopolymer, it is cleared that K-A-S-H has higher sorption capacity than that of C-S-H. From desorption experiment of Cs and Sr using deionized water from the C-S-H and K-A-S-H, it is cleared that almost of Cs was desorbed from C-S-H even for one day, while 90% of Cs was remained in K-A-S-H under the same condition. Consequently, K-A-S-H matrix in geopolymer has higher retention capacity than that of C-S-H matrix in cement. We conducted safety assessment for geopolymer and cement waste form in pit type disposal system using leaching ratio obtained in this study. From results of the assessment, K-geopolymer would be applicable for safety encapsulation and disposal of Cs and Sr as waste form.

Keywords: Geopolymer, Disposal of radioactive waste, Potassium almino silicate hydrate, Calcium silicate hydrate

©2019. Japan Geoscience Union. All Right Reserved. 

[J] Oral | H (Human Geosciences )：H-CG Complex & General

Thu. May 30, 2019 10:45 AM - 12:15 PM JST | Thu. May 30, 2019 1:45 AM - 3:15 AM UTC | 101 1F

## [H-CG31] Nuclear Energy and Geoscience

convener:Eiji Sasao(Tono Geoscience Center, Japan Atomic Energy Agency), Ryuta Hataya(Central Research Institute of Electric Power Industry), Shinji Takeuchi(Department of Earth and Environmental Sciences, College of Humanities & Sciences, Nihon University), Chairperson:Shinji Takeuchi

Handling of geological hazard assessments represent a major environmental concern in the modern society due to constructing nuclear facilities and their radioactive wastes, and also related to the management of contaminated biosphere after nuclear disasters of Fukushima-Daiichi Nuclear Power Plant. The session rational is to provide a forum to deal with various aspects of scientific and engineering aspects of nuclear power. The session in this year focuses on radioactive waste disposal and covers not only scientific aspect such as characterization of geological environment but also engineering aspects such as microbe-nuclide, mineral-water, and cement-water interactions. In addition to this, themes on seismic hazards at nuclear facilities, environmental behavior of radionuclides emitted from disabled nuclear plants, and volume reduction and reuse of cesium contaminated soils are welcomed. Through these presentations, we aim to promote intercultural communication and collaboration between science, engineering and social science.

10:45 AM - 11:00 AM JST | 1:45 AM - 2:00 AM UTC

[HCG31-07] Focus points of post-closure monitoring in geological disposal

*Hiroaki Murakami[1], Yusuke Watanabe[1], Kenji Fukuda[1], Teruki Iwatsuki[1] (1.Japan Atomic Energy Agency)

---

11:00 AM - 11:15 AM JST | 2:00 AM - 2:15 AM UTC

[HCG31-08] 5 years monitoring results for the environmental dynamics of radiocesium in mountainous forest of the Abukuma Mountains, Fukushima

*Tadafumi Niizato[1], Takayoshi Watanabe[1], Yoshito Sasaki[1], Katsuaki Mitachi[2], Satomi Ito[1], Hironobu Abe[1] (1.Japan Atomic Energy Agency, 2.ATOM TRANSPORT SERVICE CO., LTD)

---

11:15 AM - 11:30 AM JST | 2:15 AM - 2:30 AM UTC

[HCG31-09] Problems of geological disposal based on the contaminated water issues at Fukushima Daiichi NPS

*Naoaki Shibasaki[1] (1.Fukushima University)

---

11:30 AM - 11:45 AM JST | 2:30 AM - 2:45 AM UTC

[HCG31-10] Examination of "Nationalwide Map of Scientific Features" for HLRW geological disposal in case of Niigata Prefecture and fundamental problems in the fair discussion on this task

*Junji Akai[1], Ryuichiro Ohno (1.Emeritus Professor of Niigata University)

---

11:45 AM - 12:00 PM JST | 2:45 AM - 3:00 AM UTC

[HCG31-11] Problems of the "Nationwide Map of Scientific Features for Geological Disposal" in Saitama prefecture and storage method of High-level Radioactive Waste (HLW)

*Kazuaki SEKINE[1], Kazuyuki SUENAGA[2], Tadao KOBAYASHI (1.Saitama Prefectural Chichibu High School, 2.SUENAGA Environmental Geology)

---

12:00 PM - 12:15 PM JST | 3:00 AM - 3:15 AM UTC

Discussion

# Focus points of post-closure monitoring in geological disposal

*Hiroaki Murakami[1], Yusuke Watanabe[1], Kenji Fukuda[1], Teruki Iwatsuki[1]

1. Japan Atomic Energy Agency

To understand geological-environment stability at the deep underground, it is important to understand the hydrochemical disturbance process and its recovery process due to construction, operation and closure of the underground facility. Monitoring after closure of underground facility is effective method to understand the EdZ recovery process, however few studies have been reported on post-closure monitoring. We considered about focus points of post-closure monitoring by using hydrochemical data of groundwater in/around Mizunami Underground Research Laboratory.

As the groundwater level declined due to the construction and operation of the Mizunami URL, mixing of deep high-salinity groundwater and shallow low-salinity groundwater occurred in the monitoring section of conglomerate layer. In this section, groundwater flow will change again as water pressure recovers after closure of the Mizunami URL. Therefore, we should extract hydrogeologically important sections such as the conglomerate layer and select it as the observation section of post-closure monitoring.

Keywords: Groundwater, Closure of underground facility, monitoring

©2019. Japan Geoscience Union. All Right Reserved. 

# 5 years monitoring results for the environmental dynamics of radiocesium in mountainous forest of the Abukuma Mountains, Fukushima

*Tadafumi Niizato[1], Takayoshi Watanabe[1], Yoshito Sasaki[1], Katsuaki Mitachi[2], Satomi Ito[1], Hironobu Abe[1]

1. Japan Atomic Energy Agency, 2. ATOM TRANSPORT SERVICE CO., LTD

An understanding of long-term environmental dynamics of radiocesium, which is released by the TEPCO’s Fukushima Dai-ichi Nuclear Power Plant accident, is a key issue for predicting the future radiocesium distribution and forest products radioactivity in a forested environment, especially $^{137}Cs$ with half-life of 30 years. We compiled the five-years monitoring results of radiocesium input-output budgets in broad-leaved deciduous forests and Japanese cedar evergreen forests of the Abukuma Mountains, Fukushima, Japan. The input-output rates were a few percent of the radiocesium inventory of the monitoring site. In addition, both rates have been decreasing with time. Belowground radiocesium occupied 90% of the total inventory in the Japanese cedar forest on October 2015. The belowground radiocesium was distributed mainly in the topsoil of 0-6 cm depth, approximately 70-80% of the underground inventory on August 2016. These results indicate that the distribution of radiocesium in the forest is similar to the distribution of tree rootlet responsible for absorption of inorganic elements, nutrients, and water. This means long residence time of radiocesium in rooting zone. In the condition of the limited amount of radiocesium input-output rates in the forest, estimation of the migration flux of radiocesium from forest floor to the forest products are considered to be most important issues in the present.

Keywords: TEPCO’s Fukushima Dai-ichi Nuclear Power Plant accident, radiocesium, input-output budgets, mountainous forest

©2019. Japan Geoscience Union. All Right Reserved. 

# Problems of geological disposal based on the contaminated water issues at Fukushima Daiichi NPS

*Naoaki Shibasaki[1]

1. Fukushima University

The contaminated water issues at the Fukushima Daiichi Nuclear Power Station (NPS) have not been solved yet even after 8 years since the severe nuclear accident. Many countermeasures against the issues have been implemented, however, the groundwater bypass and frozen soil wall are not effective as expected. This is due to lack of investigations and understanding on the complex geology and hydrogeology at the site. Based on the experience, the author examined the Nationwide Map of Scientific Features for Geological Disposal published in July 2017 by the Ministry of Economy, Trade and Industry, Japan. The map does not show detailed information on groundwater and hydrogeology. The author presents crucial points for geological disposal from the viewpoints of hydrogeology and groundwater flow system.

Keywords: Fukushima Daiichi NPS, contaminated water issues, groundwater, geological disposal, Nationwide Map of Scientific Features for Geological Disposal

©2019. Japan Geoscience Union. All Right Reserved. 

# Examination of "Nationalwide Map of Scientific Features" for HLRW geological disposal in case of Niigata Prefecture and fundamental problems in the fair discussion on this task

*Junji Akai[1], Ryuichiro Ohno

1. Emeritus Professor of Niigata University

" Natinalwide Map of Scientific Features" for HLRW geological disposal in Niigata Prefecture region was critically examined from the standpoint of geoscience. Furthermore, Fundamental problems on the fair process of discussion of this task are discussed.

Keywords: High Level Radioactive Waste (HLRW), Nationalwide Map of Scientific Features, Niigata, Fundamental problem, unscientific, fair discussion

©2019. Japan Geoscience Union. All Right Reserved. 

# Problems of the "Nationwide Map of Scientific Features for Geological Disposal" in Saitama prefecture and storage method of High-level Radioactive Waste (HLW)

*Kazuaki SEKINE[1], Kazuyuki SUENAGA[2], Tadao KOBAYASHI

1. Saitama Prefectural Chichibu High School, 2. SUENAGA Environmental Geology

The "Nationwide Map of Scientific Features for Geological Disposal" was announced by the Agency for Natural Resources and Energy in 2017. Candidate sites for suitable places and inappropriate places for geological disposal are shown by each color. In Saitama prefecture, the linear yellow part extending from the northwest end to the southeast direction is the most prominent unsuitable place. Other areas are mostly suitable.

In the northern part of Saitama Prefecture, there is the Kanto Plain Northwest Rim Fault Zone. The main one is the fault zone represented by the Fukaya fault and the fault zone represented by the Ayasegawa fault. This fault zone is evaluated as follows. The dip is southwest inclination of 50 ˚to 70 ˚(depth less than 500 m) , the width is about 20 to 25 km, the average slip speed is 20 to 40cm / 1,000 years, The latest activity period is after 6,200 years ago, before about 2,500 years ago. When this fault caused an earthquake, the predicted seismic intensity is the maximum magnitude 8.0 (The Headquarters for Earthquake Research Promotion Committee,2005).

The length of the Fukaya fault system is about 80 km (Sugiyama, 2000). According to the criteria of the "Nationwide Map of Scientific Features for Geological Disposal", since the inappropriate place related to the active fault is one hundredth of the length of the fault, the width of the inappropriate area of the Fukaya fault system is about 800 m. Since there is a possibility that the dip of the fault plane is 50 ˚, considering the horizontal spread, there is no sufficient basis for the width of the inappropriate area.

The depth of the epicenter of the earthquake caused by the Fukaya fault and the Ayasegawa fault is estimated to be 17 to 19 km and the magnitude of the earthquake is to be the maximum magnitude of 8.0. The area with seismic intensity of 7 is distributed in Honjo City, Yoshimi Town, etc. Also the intensity 6 is expected to be distributed in wide area in the prefecture. These areas are much wider than the areas that are regarded as inappropriate in the "Nationwide Map of Scientific Features for Geological Disposal". Since the depth of the epicenter is expected to be 17 to 19 km, there is a high possibility that a wide area suffers a strong shake.

Since the geological disposal site could be kept for more than tens of thousands of years, there is a possibility that a new active fault will destroy the site. As a result, the radioactive material leaks out and it is possible that it can be carried to the ground by groundwater. It is pointed out that groundwater flow is the most important requirement for geological disposal of radioactive waste (IAEA, 1977) , but the matter of groundwater flow is not reflected in the " Nationwide Map of Scientific Features for Geological Disposal ". Since the behavior of groundwater is not well understood in deep underground, classification of suitable sites by the "Nationwide Map of Scientific Features for Geological Disposal" requires detailed study of groundwater.

As the "Nationwide Map of Scientific Features for Geological Disposal" has many problems, construction

©2019. Japan Geoscience Union. All Right Reserved. 

of the geological disposal site is not carried out until sufficient safety and understanding of the people are obtained, and it is appropriate to temporarily keep the radioactive waste on the ground etc. (Science Council of Japan, 2012). It seems necessary to seriously consider options other than geological disposal.

Keywords: Nationwide Map of Scientific Features for Geological Disposal, Kanto Plain Northwest Rim Fault Zone, groundwater, storage method

©2019. Japan Geoscience Union. All Right Reserved. 

[J] Poster | H (Human Geosciences )：H-CG Complex & General

Thu. May 30, 2019 3:30 PM - 5:00 PM JST | Thu. May 30, 2019 6:30 AM - 8:00 AM UTC | Poster Hall International Exhibition Hall8, Makuhari Messe_9

## [H-CG31] Nuclear Energy and Geoscience

convener:Eiji Sasao(Tono Geoscience Center, Japan Atomic Energy Agency), Ryuta Hataya(Central Research Institute of Electric Power Industry), Shinji Takeuchi(Department of Earth and Environmental Sciences, College of Humanities & Sciences, Nihon University)

Handling of geological hazard assessments represent a major environmental concern in the modern society due to constructing nuclear facilities and their radioactive wastes, and also related to the management of contaminated biosphere after nuclear disasters of Fukushima-Daiichi Nuclear Power Plant. The session rational is to provide a forum to deal with various aspects of scientific and engineering aspects of nuclear power. The session in this year focuses on radioactive waste disposal and covers not only scientific aspect such as characterization of geological environment but also engineering aspects such as microbe-nuclide, mineral-water, and cement-water interactions. In addition to this, themes on seismic hazards at nuclear facilities, environmental behavior of radionuclides emitted from disabled nuclear plants, and volume reduction and reuse of cesium contaminated soils are welcomed. Through these presentations, we aim to promote intercultural communication and collaboration between science, engineering and social science.

[HCG31-P01] Better identification of submerged terraces based on digital terrain analysis

*Hiura Yuki[1], Tetsuya Komatsu[1], Toshihiko Sugai[2] (1.Japan Atomic Energy Agency, 2.Graduate School of Frontier Sciences, The University of Tokyo)

[HCG31-P02] Advanced examination technique for river erosion in inland area – a case study of the Kii Peninsula, Japan –

*Nakanishi Toshimichi[1], Tetsuya Komatsu[1], Manabu Ogata[1], Takashi Hosoya[2], Takumi Kaga[2] (1.Japan Atomic Energy Agency, 2.Chuo Kaihatsu Corporation)

[HCG31-P03] Hydrothermal experiment on quartz hydration: Toward a development of new dating method for natural phenomena

*Masakazu Niwa[1], Koji Shimada[1] (1.Japan Atomic Energy Agency)

[HCG31-P04] **Diffusion Coefficient and Porosity of Granite for Evaluation of Mobility Parameter**

*Kenji Fukuda[1], Hiroaki Murakami[1], Kaori Itai[2], Masayuki Ishibashi[1], Eiji Sasao[1] (1.Japan Atomic Energy Agency, 2.C･TECH corporation)

[HCG31-P05] Hydrogeological structure of hydraulic conductive fractures in gallery scale and their rock matrix

*Ai Hamada[1] (1.Central Research Institute of Electric Power Industry)

# Better identification of submerged terraces based on digital terrain analysis

*Hiura Yuki[1], Tetsuya Komatsu[1], Toshihiko Sugai[2]

1. Japan Atomic Energy Agency, 2. Graduate School of Frontier Sciences, The University of Tokyo

One of the primary issues of the geological disposal technology is to advance the techniques associated with investigation/assessment for long-term uplift and erosion in terrestrial-marine transitional zone in Japan. To examine this issue, it is essential to understand the distribution of seafloor landforms indicating uplift and erosion in the continental shelf, which widely emerged during glacial periods. This study introduces a method for better identification of submerged terraces, some of which are expected to be an indicator of regional tectonics, based on analysis of depth-area distribution of seafloor using digital elevation models constructed from digital bathymetric charts of Japan Hydrographic Association (M7000 series). Case studies of 18 sea areas in Japan show the analysis of depth-area distribution of seafloor works effectively to identify submerged terraces in the continental shelfs dominated by slopes less than 1 degree.
Acknowledgments: This study was carried out under a contract with METI (Ministry of Economy, Trade and Industry) as part of its R&D supporting program for developing geological disposal technology.

Keywords: geological disposal, seafloor landform, submerged terrace, depth-area distribution

©2019. Japan Geoscience Union. All Right Reserved. 

# Advanced examination technique for river erosion in inland area –a case study of the Kii Peninsula, Japan –

*Nakanishi Toshimichi[1], Tetsuya Komatsu[1], Manabu Ogata[1], Takashi Hosoya[2], Takumi Kaga[2]

1. Japan Atomic Energy Agency, 2. Chuo Kaihatsu Corporation

Yasue et al. (2014) focused on detached meander cores to estimate an erosional rate in alluvial region with few terraces. However, two subjects, 1) chronology of emergence age, 2) applicability of this method to other region, should be improved. To examine above, this research was conducted along the Totsugawa River in the Kii Peninsula, central Japan. This research contributes to evaluate uplift and erosion during Late Quaternary for site selection and safety assessment of a geological disposal of high-level radioactive waste.

Four sediment cores were collected from three sites of detached meander cores, located at 100 to 120 m above from the river surface, where was suitable for optically stimulated luminescence dating using feldspar (pIRIR) and identification of fluvial channel sediments by main stream. Field survey and sample collection for pIRIR and terrestrial cosmogenic nuclide (TCN) dating, microfossil and tephra analyses were performed at outcrops of alluvial terraces at elevation of 90 to 100 m, located at the downstream of detached meander cores and 40 to 50 m above from the river surface. Moreover, sample collection for pIRIR dating and microfossil analysis was performed at outcrops of marine terraces at elevation of 40 m, located around the river mouth.

Cross-laminated sand bed with rounded gravels was recognized at only one detached meander core at ca 100 m from the river surface. This sediment was interpreted as a fluvial channel sediment by main stream because the well-sorted sand layers indicated stable bed load environments. Sand and gravel beds including weathering angular gravels were mainly composed the other drilling sites. They were interpreted as slope deposits because the matrix, mixture of silt to conglomerate, implied that were provided from small water catchments. Thick (more than 54 m) slope deposits were recognized under the detached meander core at ca 120 m from the river surface. It clearly suggests that this topographic flat surface of detached meander core was not originate by the old fluvial channel.

We would like to conduct pIRIR and TCN dating on the sand samples obtained from drilling cores and outcrops. In addition, we would like to discuss the timing of emergence from river channels by conducting volcanic ash and microfossil analysis in muddy sediments. The integration will improve the estimation of the erosional rate in inland region.

Acknowledgments: This study was carried out under a contract with the Agency of Natural Resources and Energy, part of the Ministry of Economy, Trade and Industry of Japan as part of its R&D program supporting development of technology for geological disposal of high-level radioactive waste.

Reference:

Yasue, K., Takatori, R., Tanigawa, S., Ninomiya, A., Tanase, A., Furusawa, A., Tajikara M. (2014) Study on index of erosion rate in inland mountains: Case study using old river valley around detached meander cone. *Jour. Geol. Soc. Japan*, 120(12), 435-445.

©2019. Japan Geoscience Union. All Right Reserved. 

Keywords: Terrace, Detached meander core, Chronology, Late Quaternary, Kii Peninsula

©2019. Japan Geoscience Union. All Right Reserved. 

# Hydrothermal experiment on quartz hydration: Toward a development of new dating method for natural phenomena

*Masakazu Niwa[1], Koji Shimada[1]

1. Japan Atomic Energy Agency

In the field of archaeology, the diffusion of water into quartz exposed to the natural environment has been proposed as a dating method (quartz hydration dating: QHD) applicable to archaeological artifacts. We examined application of QHD to geologic materials to understand natural phenomena crucial for safety assessment of geological disposal, such as uplift and erosion, faulting, and hydrothermal activity.

In this study, hydrothermal experiments were conducted to understand the degree of the diffusion of water into natural quartz included in an exposed rock body. Intact granite samples (Late Cretaceous Kojaku Granite, central Japan) were mirror polished and immersed in deionized water in an autoclave apparatus. We held the samples in the apparatus at controlled temperatures (150˚C or 250˚C) and controlled pressures (9.8 MPa or 25.5 MPa) for 100 hours. The pressurization was performed by $CO_2$ gas (pH in the water is 3.2 to 3.6), or $N_2$ gas. After the experiment, secondary ion intensity of $H^+$ from the quartz surface in the samples was measured by secondary ion mass spectrometry (SIMS). We estimated thickness of hydration layer based on depth profile of $H^+$ intensity.

According to the SIMS measurement, clear increase of $H^+$ concentration within 2 $\mu$m depth from the surface was identified in the experiment at 250˚C and 25.5 MPa. The $H^+$ concentration increased more in the case of the pressurization by $CO_2$ gas than by $N_2$ gas. Based on Ericson et al. (2004, J. Archaeol. Sci.), diffusion coefficient on water uptake of quartz was calculated from the depth profile of $H^+$ concentration by fitting with complementary error function. The calculated diffusion coefficient was consistent with values from archaeological artifacts and synthetic crystals reported by previous studies. Development of hydration layer of maximum thickness several $\mu$m in quartz is possible for a ten thousand year, according to the estimation from diffusion coefficient at ambient temperature calculated by extrapolation based on the Arrhenius equation. Thus, the QHD can be promising as a new tool to understand natural phenomena.

In contrast, no clear increase of $H^+$ concentration was identified in the experiment at 150˚C. According to the estimation from diffusion coefficient at 150˚C calculated by extrapolation based on the Arrhenius equation, this infers that the hydration layer was too thin to detect by SIMS.

This study was carried out under a contract with Ministry of Economy, Trade and Industry of Japan as part of its R&D supporting program for developing geological disposal technology.

Keywords: natural phenomena, quartz, hydration, hydrothermal experiment, dating

©2019. Japan Geoscience Union. All Right Reserved. 

# Diffusion Coefficient and Porosity of Granite for Evaluation of Mobility Parameter

*Kenji Fukuda[1], Hiroaki Murakami[1], Kaori Itai[2], Masayuki Ishibashi[1], Eiji Sasao[1]

1. Japan Atomic Energy Agency, 2. C・TECH corporation

Matrix diffusion is one of the important for evaluating solute transport in granite. Diffusion of ions in granite pore water was studied in order to evaluate diffusivity in rock. Effective diffusion coefficient of uranine was measured using a diffusion cell. The effective diffusion coefficient of uranine in granite without fissure and alteration was found to be in the range $10^{-15}$ to $10^{-13}$ $m^2$ $s^{-1}$. The porosities of the granite samples were determined by observation of petrographic thin sections using entity fluorescence microscope. There was a positive correlation between the porosity larger than 1% and the effective diffusion coefficient.

Keywords: granite, Effective diffusion coefficient, uranine, porosity

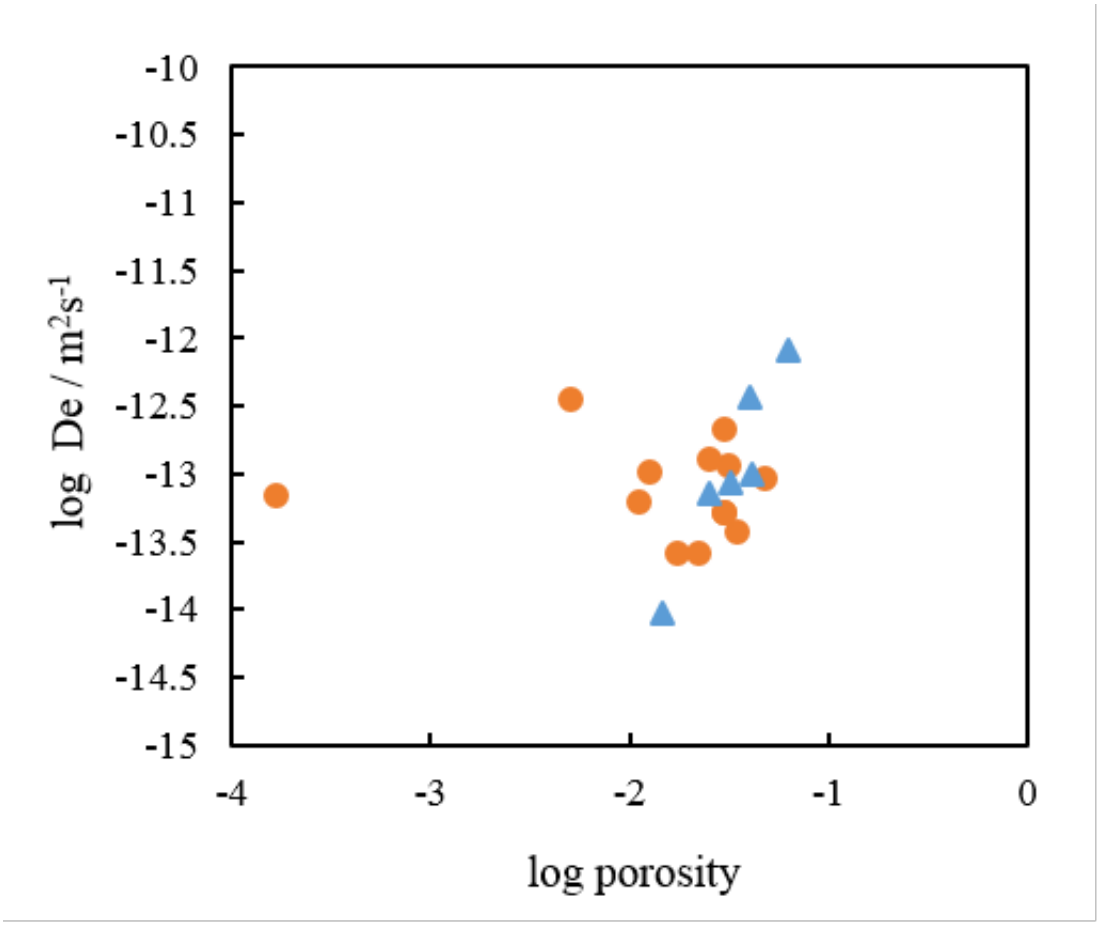


Figure 1 Relationship of logarithmic value of effective diffusion coefficient of uranine versus logarithmic value of the porosity. ●: This work and ▲: Reference value (Ishibashi, 2017).

©2019. Japan Geoscience Union. All Right Reserved. 

# Hydrogeological structure of hydraulic conductive fractures in gallery scale and their rock matrix

*Ai Hamada[1]

1. Central Research Institute of Electric Power Industry

In geological disposal of high-level nuclear waste, hydraulic conductive fractures in crystalline rock such as granite have been considered as a main pathway for radionuclides. Diffusion and absorption of radionuclide through microstructure in rock matrix can make mass transport to retard. Because the change of the characteristics of microstructure in rock matrix by structural movement and hydrothermal alteration have an effect on mass transport, it is important to understand the distribution and the structures of hydrogeological continuity of fractures as well as their characteristics of microstructure in rock matrix.
The characteristics of hydraulic conductive fractures and their microstructure in rock matrix across multiple boreholes to the west side of the gallery at 300 m depth of Mizunami Underground Laboratory are summarized as follows, hydraulic conductive fractures, which mainly show NW strike and high dip angle, have two types of characteristics: calcite-filled fractures with highly matrix chloritization and fractures with poor filling minerals which is formed along cataclastic texture. The transmissibility coefficients in both types of fractures are measured about $10^{-7}$-$10^{-5}m^2/s$. They make hydraulic conductive zone connected by low dip angle fractures, which is distributed around the Upper fracture zone in Toki Granite. On the other hand, hydraulic conductive fractures on the east side of the gallery at 300 m depth, according to the investigation of 2 boreholes about 40 m each, tend to have smaller inflow, higher alteration in rock matrix and filling minerals in fractures compared to the west side. According to the result of borehole TV observation of the borehole which has larger inflow, the direction of fractures shows NW and NE strike with high dip angle and also low dip angle fractures the same as the west side of the gallery. As a result of scanning with the X-ray CT, a higher density mineral than the surroundings is filling the fractures with partly opened part. The distribution of fracture-filling minerals can be caused a low permeability at the east side of the gallery compared to the west.
This study is commissioned by the Agency for Natural Resources and Energy in the Ministry of Economy, Trade and Industry. Core sampling were conducted as a part of a collaborative research with JAEA.

Keywords: high-level radioactive waste, microstructure, X-ray CT scannar, Toki Granite, Mizunami Underground Laboratory

©2019. Japan Geoscience Union. All Right Reserved. 

[J] Poster | H (Human Geosciences )：H-CG Complex & General

Thu. May 30, 2019 5:15 PM - 6:30 PM JST | Thu. May 30, 2019 8:15 AM - 9:30 AM UTC | Poster Hall International Exhibition Hall8, Makuhari Messe_18

## [H-CG31] Nuclear Energy and Geoscience

convener:Eiji Sasao(Tono Geoscience Center, Japan Atomic Energy Agency), Ryuta Hataya(Central Research Institute of Electric Power Industry), Shinji Takeuchi(Department of Earth and Environmental Sciences, College of Humanities & Sciences, Nihon University)

Handling of geological hazard assessments represent a major environmental concern in the modern society due to constructing nuclear facilities and their radioactive wastes, and also related to the management of contaminated biosphere after nuclear disasters of Fukushima-Daiichi Nuclear Power Plant. The session rational is to provide a forum to deal with various aspects of scientific and engineering aspects of nuclear power. The session in this year focuses on radioactive waste disposal and covers not only scientific aspect such as characterization of geological environment but also engineering aspects such as microbe-nuclide, mineral-water, and cement-water interactions. In addition to this, themes on seismic hazards at nuclear facilities, environmental behavior of radionuclides emitted from disabled nuclear plants, and volume reduction and reuse of cesium contaminated soils are welcomed. Through these presentations, we aim to promote intercultural communication and collaboration between science, engineering and social science.

[HCG31-P01] Better identification of submerged terraces based on digital terrain analysis

*Hiura Yuki[1], Tetsuya Komatsu[1], Toshihiko Sugai[2] (1.Japan Atomic Energy Agency, 2.Graduate School of Frontier Sciences, The University of Tokyo)

[HCG31-P02] Advanced examination technique for river erosion in inland area – a case study of the Kii Peninsula, Japan –

*Nakanishi Toshimichi[1], Tetsuya Komatsu[1], Manabu Ogata[1], Takashi Hosoya[2], Takumi Kaga[2] (1.Japan Atomic Energy Agency, 2.Chuo Kaihatsu Corporation)

[HCG31-P03] Hydrothermal experiment on quartz hydration: Toward a development of new dating method for natural phenomena

*Masakazu Niwa[1], Koji Shimada[1] (1.Japan Atomic Energy Agency)

[HCG31-P04] **Diffusion Coefficient and Porosity of Granite for Evaluation of Mobility Parameter**

*Kenji Fukuda[1], Hiroaki Murakami[1], Kaori Itai[2], Masayuki Ishibashi[1], Eiji Sasao[1] (1.Japan Atomic Energy Agency, 2.C･TECH corporation)

[HCG31-P05] Hydrogeological structure of hydraulic conductive fractures in gallery scale and their rock matrix

*Ai Hamada[1] (1.Central Research Institute of Electric Power Industry)

# Better identification of submerged terraces based on digital terrain analysis

*Hiura Yuki[1], Tetsuya Komatsu[1], Toshihiko Sugai[2]

1. Japan Atomic Energy Agency, 2. Graduate School of Frontier Sciences, The University of Tokyo

One of the primary issues of the geological disposal technology is to advance the techniques associated with investigation/assessment for long-term uplift and erosion in terrestrial-marine transitional zone in Japan. To examine this issue, it is essential to understand the distribution of seafloor landforms indicating uplift and erosion in the continental shelf, which widely emerged during glacial periods. This study introduces a method for better identification of submerged terraces, some of which are expected to be an indicator of regional tectonics, based on analysis of depth-area distribution of seafloor using digital elevation models constructed from digital bathymetric charts of Japan Hydrographic Association (M7000 series). Case studies of 18 sea areas in Japan show the analysis of depth-area distribution of seafloor works effectively to identify submerged terraces in the continental shelfs dominated by slopes less than 1 degree.
Acknowledgments: This study was carried out under a contract with METI (Ministry of Economy, Trade and Industry) as part of its R&D supporting program for developing geological disposal technology.

Keywords: geological disposal, seafloor landform, submerged terrace, depth-area distribution

©2019. Japan Geoscience Union. All Right Reserved. 

# Advanced examination technique for river erosion in inland area –a case study of the Kii Peninsula, Japan –

*Nakanishi Toshimichi[1], Tetsuya Komatsu[1], Manabu Ogata[1], Takashi Hosoya[2], Takumi Kaga[2]

1. Japan Atomic Energy Agency, 2. Chuo Kaihatsu Corporation

Yasue et al. (2014) focused on detached meander cores to estimate an erosional rate in alluvial region with few terraces. However, two subjects, 1) chronology of emergence age, 2) applicability of this method to other region, should be improved. To examine above, this research was conducted along the Totsugawa River in the Kii Peninsula, central Japan. This research contributes to evaluate uplift and erosion during Late Quaternary for site selection and safety assessment of a geological disposal of high-level radioactive waste.

Four sediment cores were collected from three sites of detached meander cores, located at 100 to 120 m above from the river surface, where was suitable for optically stimulated luminescence dating using feldspar (pIRIR) and identification of fluvial channel sediments by main stream. Field survey and sample collection for pIRIR and terrestrial cosmogenic nuclide (TCN) dating, microfossil and tephra analyses were performed at outcrops of alluvial terraces at elevation of 90 to 100 m, located at the downstream of detached meander cores and 40 to 50 m above from the river surface. Moreover, sample collection for pIRIR dating and microfossil analysis was performed at outcrops of marine terraces at elevation of 40 m, located around the river mouth.

Cross-laminated sand bed with rounded gravels was recognized at only one detached meander core at ca 100 m from the river surface. This sediment was interpreted as a fluvial channel sediment by main stream because the well-sorted sand layers indicated stable bed load environments. Sand and gravel beds including weathering angular gravels were mainly composed the other drilling sites. They were interpreted as slope deposits because the matrix, mixture of silt to conglomerate, implied that were provided from small water catchments. Thick (more than 54 m) slope deposits were recognized under the detached meander core at ca 120 m from the river surface. It clearly suggests that this topographic flat surface of detached meander core was not originate by the old fluvial channel.

We would like to conduct pIRIR and TCN dating on the sand samples obtained from drilling cores and outcrops. In addition, we would like to discuss the timing of emergence from river channels by conducting volcanic ash and microfossil analysis in muddy sediments. The integration will improve the estimation of the erosional rate in inland region.

Acknowledgments: This study was carried out under a contract with the Agency of Natural Resources and Energy, part of the Ministry of Economy, Trade and Industry of Japan as part of its R&D program supporting development of technology for geological disposal of high-level radioactive waste.

Reference:

Yasue, K., Takatori, R., Tanigawa, S., Ninomiya, A., Tanase, A., Furusawa, A., Tajikara M. (2014) Study on index of erosion rate in inland mountains: Case study using old river valley around detached meander cone. *Jour. Geol. Soc. Japan*, 120(12), 435-445.

©2019. Japan Geoscience Union. All Right Reserved. 

Keywords: Terrace, Detached meander core, Chronology, Late Quaternary, Kii Peninsula

©2019. Japan Geoscience Union. All Right Reserved. 

# Hydrothermal experiment on quartz hydration: Toward a development of new dating method for natural phenomena

*Masakazu Niwa[1], Koji Shimada[1]

1. Japan Atomic Energy Agency

In the field of archaeology, the diffusion of water into quartz exposed to the natural environment has been proposed as a dating method (quartz hydration dating: QHD) applicable to archaeological artifacts. We examined application of QHD to geologic materials to understand natural phenomena crucial for safety assessment of geological disposal, such as uplift and erosion, faulting, and hydrothermal activity.

In this study, hydrothermal experiments were conducted to understand the degree of the diffusion of water into natural quartz included in an exposed rock body. Intact granite samples (Late Cretaceous Kojaku Granite, central Japan) were mirror polished and immersed in deionized water in an autoclave apparatus. We held the samples in the apparatus at controlled temperatures (150˚C or 250˚C) and controlled pressures (9.8 MPa or 25.5 MPa) for 100 hours. The pressurization was performed by $CO_2$ gas (pH in the water is 3.2 to 3.6), or $N_2$ gas. After the experiment, secondary ion intensity of $H^+$ from the quartz surface in the samples was measured by secondary ion mass spectrometry (SIMS). We estimated thickness of hydration layer based on depth profile of $H^+$ intensity.

According to the SIMS measurement, clear increase of $H^+$ concentration within 2 $\mu$m depth from the surface was identified in the experiment at 250˚C and 25.5 MPa. The $H^+$ concentration increased more in the case of the pressurization by $CO_2$ gas than by $N_2$ gas. Based on Ericson et al. (2004, J. Archaeol. Sci.), diffusion coefficient on water uptake of quartz was calculated from the depth profile of $H^+$ concentration by fitting with complementary error function. The calculated diffusion coefficient was consistent with values from archaeological artifacts and synthetic crystals reported by previous studies. Development of hydration layer of maximum thickness several $\mu$m in quartz is possible for a ten thousand year, according to the estimation from diffusion coefficient at ambient temperature calculated by extrapolation based on the Arrhenius equation. Thus, the QHD can be promising as a new tool to understand natural phenomena.

In contrast, no clear increase of $H^+$ concentration was identified in the experiment at 150˚C. According to the estimation from diffusion coefficient at 150˚C calculated by extrapolation based on the Arrhenius equation, this infers that the hydration layer was too thin to detect by SIMS.

This study was carried out under a contract with Ministry of Economy, Trade and Industry of Japan as part of its R&D supporting program for developing geological disposal technology.

Keywords: natural phenomena, quartz, hydration, hydrothermal experiment, dating

©2019. Japan Geoscience Union. All Right Reserved. 

# Diffusion Coefficient and Porosity of Granite for Evaluation of Mobility Parameter

*Kenji Fukuda[1], Hiroaki Murakami[1], Kaori Itai[2], Masayuki Ishibashi[1], Eiji Sasao[1]

1. Japan Atomic Energy Agency, 2. C・TECH corporation

Matrix diffusion is one of the important for evaluating solute transport in granite. Diffusion of ions in granite pore water was studied in order to evaluate diffusivity in rock. Effective diffusion coefficient of uranine was measured using a diffusion cell. The effective diffusion coefficient of uranine in granite without fissure and alteration was found to be in the range $10^{-15}$ to $10^{-13}$ $m^2$ $s^{-1}$. The porosities of the granite samples were determined by observation of petrographic thin sections using entity fluorescence microscope. There was a positive correlation between the porosity larger than 1% and the effective diffusion coefficient.

Keywords: granite, Effective diffusion coefficient, uranine, porosity

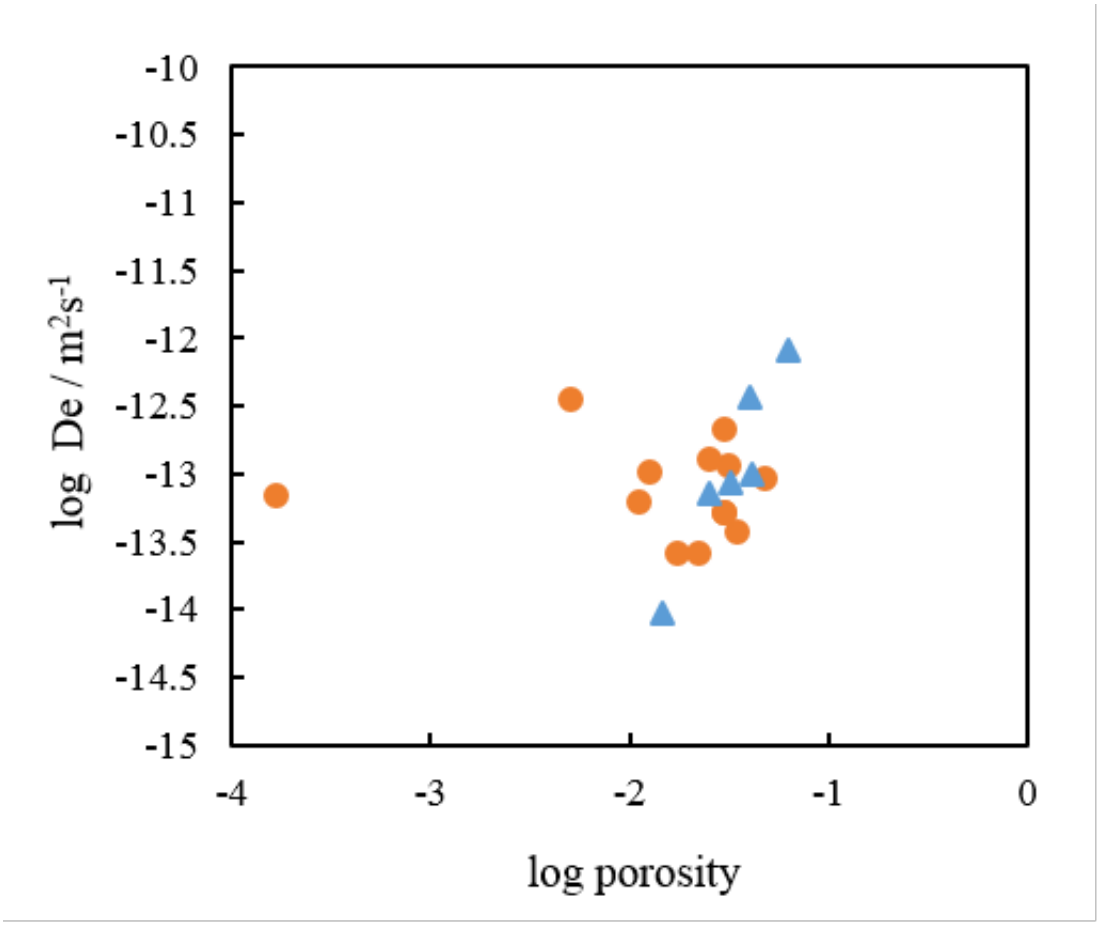


Figure 1 Relationship of logarithmic value of effective diffusion coefficient of uranine versus logarithmic value of the porosity. ●: This work and ▲: Reference value (Ishibashi, 2017).

©2019. Japan Geoscience Union. All Right Reserved. 

# Hydrogeological structure of hydraulic conductive fractures in gallery scale and their rock matrix

*Ai Hamada[1]

1. Central Research Institute of Electric Power Industry

In geological disposal of high-level nuclear waste, hydraulic conductive fractures in crystalline rock such as granite have been considered as a main pathway for radionuclides. Diffusion and absorption of radionuclide through microstructure in rock matrix can make mass transport to retard. Because the change of the characteristics of microstructure in rock matrix by structural movement and hydrothermal alteration have an effect on mass transport, it is important to understand the distribution and the structures of hydrogeological continuity of fractures as well as their characteristics of microstructure in rock matrix.
The characteristics of hydraulic conductive fractures and their microstructure in rock matrix across multiple boreholes to the west side of the gallery at 300 m depth of Mizunami Underground Laboratory are summarized as follows, hydraulic conductive fractures, which mainly show NW strike and high dip angle, have two types of characteristics: calcite-filled fractures with highly matrix chloritization and fractures with poor filling minerals which is formed along cataclastic texture. The transmissibility coefficients in both types of fractures are measured about $10^{-7}$-$10^{-5}m^2/s$. They make hydraulic conductive zone connected by low dip angle fractures, which is distributed around the Upper fracture zone in Toki Granite. On the other hand, hydraulic conductive fractures on the east side of the gallery at 300 m depth, according to the investigation of 2 boreholes about 40 m each, tend to have smaller inflow, higher alteration in rock matrix and filling minerals in fractures compared to the west side. According to the result of borehole TV observation of the borehole which has larger inflow, the direction of fractures shows NW and NE strike with high dip angle and also low dip angle fractures the same as the west side of the gallery. As a result of scanning with the X-ray CT, a higher density mineral than the surroundings is filling the fractures with partly opened part. The distribution of fracture-filling minerals can be caused a low permeability at the east side of the gallery compared to the west.
This study is commissioned by the Agency for Natural Resources and Energy in the Ministry of Economy, Trade and Industry. Core sampling were conducted as a part of a collaborative research with JAEA.

Keywords: high-level radioactive waste, microstructure, X-ray CT scannar, Toki Granite, Mizunami Underground Laboratory

©2019. Japan Geoscience Union. All Right Reserved. 

[J] Poster | H (Human Geosciences )：H-CG Complex & General

Thu. May 30, 2019 1:45 PM - 3:15 PM JST | Thu. May 30, 2019 4:45 AM - 6:15 AM UTC | Poster Hall International Exhibition Hall8, Makuhari Messe_5

## [H-CG34] Education and research for rehabilitation of agriculture against harmful rumors in nuclear disaster areas

convener:Masaru Mizoguchi(Graduate school of Agricultural and Life Sciences, The University of Tokyo)

Since the eastern Japan earthquake, various universities are carrying out educational programs that take students to the field and let the students recognize the importance of picking up on-site needs from the real field. This session convener also went to Iitate Village in Fukushima Prefecture three months after the nuclear accident, and continues a unique activities in cooperation with NPO and farmers. In this session, university's teachers will report changes in student's consciousness observed through on-site education and field research, and discuss social value of university.

[HCG34-P01] Calculation of water and sediment discharge from a small forested catchment for evaluating load of the particulate radioactive cesium

*Takuhei Yamasaki[1], Shoichiro Hamamoto[1], Taku Nishimura[1] (1.University of Tokyo)

[HCG34-P02] Radiocesium Inter-Annual Variations and Spatial Dynamics in Watershed in Iitate, Fukushima, Japan

*Saito Mari[1], Kazutoshi Osawa[1], Naoto Nihei[2] (1.Utsunomiya University, 2.Tokyuo University)

[HCG34-P03] Efforts in university to keep consciousness of disaster caused by The Great East Japan Earthquake for resurrection of agriculture at Iitate village

*Junko NISHIWAKI[1], Masaru Mizoguchi[2] (1.College of Agriculture, Ibaraki University, 2.Graduate School of Agricultural and Life Sciences, The University of Tokyo)

[HCG34-P04] Effects of remaining radiocesium in bunds and slopes of paddy fields on ambient dose and downstream environment.

*Yoshida Shuichiro[1], Kazuhiro Nishida[1], Taku Fukui[1] (1.The University of Tokyo)

# Calculation of water and sediment discharge from a small forested catchment for evaluating load of the particulate radioactive cesium

*Takuhei Yamasaki[1], Shoichiro Hamamoto[1], Taku Nishimura[1]

1. University of Tokyo

Vast amount of radionuclides was released into the environments by the accident of the Fukushima Dai-ichi Nuclear Power Plant (FDNPP) on March 2011. By 2018, decontamination of deposited radionuclides in the agricultural and residential areas has completed except for a zone with high air-dose rate near the FDNPP. Forested areas, however, are not planned to decontaminate radionuclides. Hence, dynamics of radionuclides, especially radioactive cesium (RCs), in forests are major concern for not only human health (external exposure), but also recontamination in the decontaminated areas (downstream migration).
Total RCs discharge for a year from the forested areas was generally small, less than 1% of the catchment deposition. However, once a large storm event occurs, RCs adsorbing on the fine sediments such as clay and silt particles and organic matter (called particulate RCs) was eroded and released into the river. Production and movement of particulate RCs were controlled by the soil erosion process, which has been well studied for a long time. Hence, it is expected that RCs discharge from a catchment can be estimated by evaluating the sediment runoff from the catchment. The aim of our study is to verify our hypothesis.

Method
Study site is located at the southeast part of the Iitate village, Fukushima Prefecture. Catchment area is 56 ha. Catchment geology was weathered granite, and whole catchment is covered with mixed forest. At the basin outlet, we measured water runoff and turbidity in every 10 min, and sampled channel water when water level exceeds threshold value due to rainfall events.
We used process based soil erosion model, GeoWEPP (Renschler, 2003), to evaluate sediment yield from the catchment. This model requires four types of input data, climate, topography, land use, and soil data. Climate data was based on the observed temperature and rainfall depth at the study site. The other weather data, daily solar radiation, wind velocity and dew point, was collected from the AMeDAS Iitate or Fukushima. Topography data was made with DEM provided by Geospatial Information Authority of Japan. Land use was set to “forest”, pre-set parameter set in GeoWEPP. Soil hydraulic parameter was fitted to reproduce observed daily direct runoff, since soil erosion mainly occurs during high flow periods just after the rainfall event. Soil erodibility was set as a granitic forest soil and channel calibrated by the gauged station with granitic rock in central Japan. Calibration was done using observed data in 2016, and fitted parameters were validated with 2017 data.

Results and Discussion
GeoWEPP well reproduced the daily channel discharge for most rainfall events in both calibration and validation year. At the typhoon event in 2017, however, model overestimated the observed runoff. This is partly because GeoWEPP is not a flood runoff model.
In calculation, sediment yield at the outlet occurred during middle to large storm events. However, sediment production during small events was not well reproduced, though SS load at the small rainfall event was small for annual total load. Since sediment production process may depend on the scale of the rainfall event, we should set the another soil erodibility to reproduce the sediment production for the small rainfall events.
Sediment production mainly occurred at the channel section. In hillslope section, soil loss area was

©2019. Japan Geoscience Union. All Right Reserved. 

limited near the channel section. This implies that RCs in most forested areas is immobile due to the low soil erodibility in the forested area. However, once vegetation at the forest floor and surface organic matter were removed by the inappropriate forest management, RCs mobility in the catchment would increase.

Keywords: radioactive cesium, particulate form, soil erosion, GeoWEPP

©2019. Japan Geoscience Union. All Right Reserved. 

# Radiocesium Inter-Annual Variations and Spatial Dynamics in Watershed in Iitate, Fukushima, Japan

*Saito Mari[1], Kazutoshi Osawa[1], Naoto Nihei[2]

1. Utsunomiya University, 2. Tokyuo University

A large amount of radiocesium, $^{137}$Cs and $^{134}$Cs, were released and deposited on the soil surface due to the accident at Fukushima Daiichi Nuclear Power Plant, FDNPP, due to the Great East Japan Earthquake that occurred on March 11, 2011. Among them, $^{137}$Cs is easily absorbed by clay minerals and soil organic matter, and its physical half-life is 30.2 years. $^{137}$Cs are redistributed to waterways, rivers, lakes and coastal areas by rainfall-runoff process, so long-term influences on residents' lives and agricultural, forestry and fishery products in the area surrounding the accident are concerned. In order to evaluate the influence of secondary contamination of $^{137}$Cs, it is necessary to grasp the temporal and spatial dynamics in the watershed including areas with high $^{137}$Cs deposits.

In this study, fixed point observations was conducted on two rivers, Hiso river and Mano river, in Iitate village, Fukushima Prefecture from 2013 to 2018. In addition, multiple observation points were set up in watersheds, and simultaneous water sampling was done at multiple points. We measured SS concentration and $^{137}$Cs concentration from water samples, grasped the long-term change in $^{137}$Cs runoff, and identified the catchment area where $^{137}$Cs runoff was noticeable.

The $^{137}$Cs concentration of SS dropped drastically with extreme large flood due to Typhoon Etau in 2015, and the concentration remained low until 2018. The same result was obtained in 2018. In Hiso river, $^{137}$Cs concentration of SS in 2018 increased slightly compared to 2017. This is thought to be the effect of the decontamination work in the Nagadoro district.

As a result of simultaneous multipoint observation, spatial distribution of $^{137}$Cs concentration in the watershed was changing as merging the branch streams into the main stream. In addition, it was revealed that sediment with high $^{137}$Cs concentration flowed in from Nagadoro district where decontamination works was incomplete.

Keywords: Radiocesium, Soil erosion, Annual Variations, Spatial Dynamics

©2019. Japan Geoscience Union. All Right Reserved. 

# Efforts in university to keep consciousness of disaster caused by The Great East Japan Earthquake for resurrection of agriculture at Iitate village

*Junko NISHIWAKI[1], Masaru Mizoguchi[2]

1. College of Agriculture, Ibaraki University, 2. Graduate School of Agricultural and Life Sciences, The University of Tokyo

After the Great East Japan Earthquake, the revival of agriculture, the various countermeasures have been conducted for resurrection of agriculture and rural community at the disaster area. On the other hand, the consciousness of the damage caused by the disaster is decreasing, and a lot of people tended not to consider disaster area and the life in such area. The recovery on the mental side of people who live in disaster area is important to the revival from the disaster in addition to recovery of the hardware such as the infrastructure. For that reason, the actual information should be sharing between inside and outside the disaster area, and it is necessary to push forward mutual understanding to get rid of the feeling of being estranged that the inhabitants of the disaster area feel. In addition, to prevent weathering of the consciousness is important for without forgetting disaster prevention awareness to a possible disaster in future.
Authors have held some field trips and rice planting and harvesting events in Iitate village, Fukushima to be able to grasp the situation of the earthquake disaster and really feel efforts of the reconstruction of the area for the people who attended the events by a meeting and cooperation of local farmers and the authorized NPO corporation Resurrection of Fukushima. As university staffs, we are inviting the student participants in the field trips and events to have a young generation know the tragic situation after the disaster and strength of inhabitants overcoming the damage. We want students to think about what could we do and what should we do for recovering this situation as an own problem. We also assign a report problem to think what agricultural science can do for solving the problems in Fukushima for students, after our classes about the actions of the experts in the disaster area from the field of agriculture.
The events in Iitate village had planned since 2013 with farmers in Iitate to listen the real story from those farmers. In our classes, we introduce the soil physical and agricultural engineering way to remove radioactive materials and efforts by other specialized fields. Various useful opinions for resurrection of Iitate agriculture are suggested by students. In this presentation, we introduce the contents of field trips and events, class lecture and some feelings and opinions from students.

Keywords: disaster area by Great East Japan Earthquake, decreasing of damage consciousness, agriculture, field trip

©2019. Japan Geoscience Union. All Right Reserved. 

# Effects of remaining radiocesium in bunds and slopes of paddy fields on ambient dose and downstream environment.

*Yoshida Shuichiro[1], Kazuhiro Nishida[1], Taku Fukui[1]

1. The University of Tokyo

After the devastating contamination by radionuclides in Iltate Village, removal of the contaminated surface soil from the farmlands was performed over the village. However, the paddy bunds, banks or slopes of the irrigation/drainage canals have not been subject to the removal of contaminated surface soil because of the cost to recover them. This study aimed to show the quantitative influence of these 'semi-contaminated ground' as the source of gamma beam and the contamination of downstream water.

First, we analyzed the dose rates regularly monitored by Iitate village every two weeks since 2011 at 18 points within the village, where the decontamination works were conducted during the period. From the temporal change of the dose rate, the decrease in dose rate due to the decontamination work was evaluated at each point. The spherical views around the monitoring points of dose rate was captured by a 360-degree camera (Ricoh Theta), to evaluate the ratio of solid angle for the contaminated and decontaminated surface. The woods, paddy bunds, banks or slopes were regarded as the contaminated surface, while the buildings, farmlands or paved roads were classified to the decontaminated surface.

The percentage of the dose rate reduction by the decontamination works ranged between 31% and 83% depending on the land use around the points. The dose rate reduction is negatively correlated to the ratio of the solid angle of the contaminated surfaces from the monitoring points. Thus, the bunds, banks, or slopes, where the decontamination have not covered, are functioning as the ambient source of gamma beam to the monitoring points.

Second, we measured radiocesium effluence from the slopes of a drainage canal beside paddy fields in Iitate Village. The four of five slopes were covered with weeds which have been regularly cut; the other is bushed and has trees. The contaminated surface soil of the all slopes was not removed. The total radiocesium inventory estimated by scintillation survey meter ranged between 350 and 400 $kBqm^{-2}$. The radiocesium was mainly distributed within upper 5cm of the mineral soil layer. Metal gutters were installed at the bottom of the slopes, from which the water flowing over the slopes was collected and led to the storing tanks. The water in the tank was collected to the other tanks and taken to the laboratory on 10 Aug. 2018 and 26 Oct 2018. The water samples containing contaminated sediments were filtrated by glass filters with 440 $\mu$m opening followed by membrane filter with 0.45 $\mu$m opening. The dissolved form of radiocesium in the filtrates were removed by the special cartridge. After drying and weighing, the radiocesium on the filters and cartridges were measured by Ge semi-conductor detector run by RI Research and Education Center in the Graduate School of Agricultural and Life Sciences, The University of Tokyo.

The radiocesium effluence rate from the slopes under 550 mm of total rainfall during the measured period ranged from 0.13 to 1.50 $Bqm^{-2}$. The effluence rate of suspended particles ranged as little as 0.08 $gm^{-2}$. Corresponding to this result, the ratio of particulate form of radiocesium tended to be less although the water flow over the slopes probably occurred under the intense rainfalls. Although the measured radiocesium effluence rate was too little to affect the radiocesium concentration in the downstream river

©2019. Japan Geoscience Union. All Right Reserved. 

water, it should be noted that we should monitor the radiocesium effluence from bared or collapsing slopes which can be the potential source of radiocesium to the downstream area.

Keywords: Radiocesium, Dose rate, Effluence from slope

©2019. Japan Geoscience Union. All Right Reserved.

©2019. Japan Geoscience Union. All Right Reserved. 

[J] Poster | H (Human Geosciences )：H-CG Complex & General

Thu. May 30, 2019 5:15 PM - 6:30 PM JST | Thu. May 30, 2019 8:15 AM - 9:30 AM UTC | Poster Hall International Exhibition Hall8, Makuhari Messe_19

## [H-CG34] Education and research for rehabilitation of agriculture against harmful rumors in nuclear disaster areas

convener:Masaru Mizoguchi(Graduate school of Agricultural and Life Sciences, The University of Tokyo)

Since the eastern Japan earthquake, various universities are carrying out educational programs that take students to the field and let the students recognize the importance of picking up on-site needs from the real field. This session convener also went to Iitate Village in Fukushima Prefecture three months after the nuclear accident, and continues a unique activities in cooperation with NPO and farmers. In this session, university's teachers will report changes in student's consciousness observed through on-site education and field research, and discuss social value of university.

### [HCG34-P01] Calculation of water and sediment discharge from a small forested catchment for evaluating load of the particulate radioactive cesium

*Takuhei Yamasaki[1], Shoichiro Hamamoto[1], Taku Nishimura[1] (1.University of Tokyo)

### [HCG34-P02] Radiocesium Inter-Annual Variations and Spatial Dynamics in Watershed in Iitate, Fukushima, Japan

*Saito Mari[1], Kazutoshi Osawa[1], Naoto Nihei[2] (1.Utsunomiya University, 2.Tokyuo University)

### [HCG34-P03] Efforts in university to keep consciousness of disaster caused by The Great East Japan Earthquake for resurrection of agriculture at Iitate village

*Junko NISHIWAKI[1], Masaru Mizoguchi[2] (1.College of Agriculture, Ibaraki University, 2.Graduate School of Agricultural and Life Sciences, The University of Tokyo)

### [HCG34-P04] Effects of remaining radiocesium in bunds and slopes of paddy fields on ambient dose and downstream environment.

*Yoshida Shuichiro[1], Kazuhiro Nishida[1], Taku Fukui[1] (1.The University of Tokyo)

# Calculation of water and sediment discharge from a small forested catchment for evaluating load of the particulate radioactive cesium

*Takuhei Yamasaki[1], Shoichiro Hamamoto[1], Taku Nishimura[1]

1. University of Tokyo

Vast amount of radionuclides was released into the environments by the accident of the Fukushima Dai-ichi Nuclear Power Plant (FDNPP) on March 2011. By 2018, decontamination of deposited radionuclides in the agricultural and residential areas has completed except for a zone with high air-dose rate near the FDNPP. Forested areas, however, are not planned to decontaminate radionuclides. Hence, dynamics of radionuclides, especially radioactive cesium (RCs), in forests are major concern for not only human health (external exposure), but also recontamination in the decontaminated areas (downstream migration).
Total RCs discharge for a year from the forested areas was generally small, less than 1% of the catchment deposition. However, once a large storm event occurs, RCs adsorbing on the fine sediments such as clay and silt particles and organic matter (called particulate RCs) was eroded and released into the river. Production and movement of particulate RCs were controlled by the soil erosion process, which has been well studied for a long time. Hence, it is expected that RCs discharge from a catchment can be estimated by evaluating the sediment runoff from the catchment. The aim of our study is to verify our hypothesis.

Method
Study site is located at the southeast part of the Iitate village, Fukushima Prefecture. Catchment area is 56 ha. Catchment geology was weathered granite, and whole catchment is covered with mixed forest. At the basin outlet, we measured water runoff and turbidity in every 10 min, and sampled channel water when water level exceeds threshold value due to rainfall events.
We used process based soil erosion model, GeoWEPP (Renschler, 2003), to evaluate sediment yield from the catchment. This model requires four types of input data, climate, topography, land use, and soil data. Climate data was based on the observed temperature and rainfall depth at the study site. The other weather data, daily solar radiation, wind velocity and dew point, was collected from the AMeDAS Iitate or Fukushima. Topography data was made with DEM provided by Geospatial Information Authority of Japan. Land use was set to “forest”, pre-set parameter set in GeoWEPP. Soil hydraulic parameter was fitted to reproduce observed daily direct runoff, since soil erosion mainly occurs during high flow periods just after the rainfall event. Soil erodibility was set as a granitic forest soil and channel calibrated by the gauged station with granitic rock in central Japan. Calibration was done using observed data in 2016, and fitted parameters were validated with 2017 data.

Results and Discussion
GeoWEPP well reproduced the daily channel discharge for most rainfall events in both calibration and validation year. At the typhoon event in 2017, however, model overestimated the observed runoff. This is partly because GeoWEPP is not a flood runoff model.
In calculation, sediment yield at the outlet occurred during middle to large storm events. However, sediment production during small events was not well reproduced, though SS load at the small rainfall event was small for annual total load. Since sediment production process may depend on the scale of the rainfall event, we should set the another soil erodibility to reproduce the sediment production for the small rainfall events.
Sediment production mainly occurred at the channel section. In hillslope section, soil loss area was

©2019. Japan Geoscience Union. All Right Reserved. 

limited near the channel section. This implies that RCs in most forested areas is immobile due to the low soil erodibility in the forested area. However, once vegetation at the forest floor and surface organic matter were removed by the inappropriate forest management, RCs mobility in the catchment would increase.

Keywords: radioactive cesium, particulate form, soil erosion, GeoWEPP

©2019. Japan Geoscience Union. All Right Reserved. 

# Radiocesium Inter-Annual Variations and Spatial Dynamics in Watershed in Iitate, Fukushima, Japan

*Saito Mari[1], Kazutoshi Osawa[1], Naoto Nihei[2]

1. Utsunomiya University, 2. Tokyuo University

A large amount of radiocesium, $^{137}$Cs and $^{134}$Cs, were released and deposited on the soil surface due to the accident at Fukushima Daiichi Nuclear Power Plant, FDNPP, due to the Great East Japan Earthquake that occurred on March 11, 2011. Among them, $^{137}$Cs is easily absorbed by clay minerals and soil organic matter, and its physical half-life is 30.2 years. $^{137}$Cs are redistributed to waterways, rivers, lakes and coastal areas by rainfall-runoff process, so long-term influences on residents' lives and agricultural, forestry and fishery products in the area surrounding the accident are concerned. In order to evaluate the influence of secondary contamination of $^{137}$Cs, it is necessary to grasp the temporal and spatial dynamics in the watershed including areas with high $^{137}$Cs deposits.

In this study, fixed point observations was conducted on two rivers, Hiso river and Mano river, in Iitate village, Fukushima Prefecture from 2013 to 2018. In addition, multiple observation points were set up in watersheds, and simultaneous water sampling was done at multiple points. We measured SS concentration and $^{137}$Cs concentration from water samples, grasped the long-term change in $^{137}$Cs runoff, and identified the catchment area where $^{137}$Cs runoff was noticeable.

The $^{137}$Cs concentration of SS dropped drastically with extreme large flood due to Typhoon Etau in 2015, and the concentration remained low until 2018. The same result was obtained in 2018. In Hiso river, $^{137}$Cs concentration of SS in 2018 increased slightly compared to 2017. This is thought to be the effect of the decontamination work in the Nagadoro district.

As a result of simultaneous multipoint observation, spatial distribution of $^{137}$Cs concentration in the watershed was changing as merging the branch streams into the main stream. In addition, it was revealed that sediment with high $^{137}$Cs concentration flowed in from Nagadoro district where decontamination works was incomplete.

Keywords: Radiocesium, Soil erosion, Annual Variations, Spatial Dynamics

©2019. Japan Geoscience Union. All Right Reserved. 

# Efforts in university to keep consciousness of disaster caused by The Great East Japan Earthquake for resurrection of agriculture at Iitate village

*Junko NISHIWAKI[1], Masaru Mizoguchi[2]

1. College of Agriculture, Ibaraki University, 2. Graduate School of Agricultural and Life Sciences, The University of Tokyo

After the Great East Japan Earthquake, the revival of agriculture, the various countermeasures have been conducted for resurrection of agriculture and rural community at the disaster area. On the other hand, the consciousness of the damage caused by the disaster is decreasing, and a lot of people tended not to consider disaster area and the life in such area. The recovery on the mental side of people who live in disaster area is important to the revival from the disaster in addition to recovery of the hardware such as the infrastructure. For that reason, the actual information should be sharing between inside and outside the disaster area, and it is necessary to push forward mutual understanding to get rid of the feeling of being estranged that the inhabitants of the disaster area feel. In addition, to prevent weathering of the consciousness is important for without forgetting disaster prevention awareness to a possible disaster in future.
Authors have held some field trips and rice planting and harvesting events in Iitate village, Fukushima to be able to grasp the situation of the earthquake disaster and really feel efforts of the reconstruction of the area for the people who attended the events by a meeting and cooperation of local farmers and the authorized NPO corporation Resurrection of Fukushima. As university staffs, we are inviting the student participants in the field trips and events to have a young generation know the tragic situation after the disaster and strength of inhabitants overcoming the damage. We want students to think about what could we do and what should we do for recovering this situation as an own problem. We also assign a report problem to think what agricultural science can do for solving the problems in Fukushima for students, after our classes about the actions of the experts in the disaster area from the field of agriculture.
The events in Iitate village had planned since 2013 with farmers in Iitate to listen the real story from those farmers. In our classes, we introduce the soil physical and agricultural engineering way to remove radioactive materials and efforts by other specialized fields. Various useful opinions for resurrection of Iitate agriculture are suggested by students. In this presentation, we introduce the contents of field trips and events, class lecture and some feelings and opinions from students.

Keywords: disaster area by Great East Japan Earthquake, decreasing of damage consciousness, agriculture, field trip

©2019. Japan Geoscience Union. All Right Reserved. 

# Effects of remaining radiocesium in bunds and slopes of paddy fields on ambient dose and downstream environment.

*Yoshida Shuichiro[1], Kazuhiro Nishida[1], Taku Fukui[1]

1. The University of Tokyo

After the devastating contamination by radionuclides in Iltate Village, removal of the contaminated surface soil from the farmlands was performed over the village. However, the paddy bunds, banks or slopes of the irrigation/drainage canals have not been subject to the removal of contaminated surface soil because of the cost to recover them. This study aimed to show the quantitative influence of these 'semi-contaminated ground' as the source of gamma beam and the contamination of downstream water.

First, we analyzed the dose rates regularly monitored by Iitate village every two weeks since 2011 at 18 points within the village, where the decontamination works were conducted during the period. From the temporal change of the dose rate, the decrease in dose rate due to the decontamination work was evaluated at each point. The spherical views around the monitoring points of dose rate was captured by a 360-degree camera (Ricoh Theta), to evaluate the ratio of solid angle for the contaminated and decontaminated surface. The woods, paddy bunds, banks or slopes were regarded as the contaminated surface, while the buildings, farmlands or paved roads were classified to the decontaminated surface.

The percentage of the dose rate reduction by the decontamination works ranged between 31% and 83% depending on the land use around the points. The dose rate reduction is negatively correlated to the ratio of the solid angle of the contaminated surfaces from the monitoring points. Thus, the bunds, banks, or slopes, where the decontamination have not covered, are functioning as the ambient source of gamma beam to the monitoring points.

Second, we measured radiocesium effluence from the slopes of a drainage canal beside paddy fields in Iitate Village. The four of five slopes were covered with weeds which have been regularly cut; the other is bushed and has trees. The contaminated surface soil of the all slopes was not removed. The total radiocesium inventory estimated by scintillation survey meter ranged between 350 and 400 $kBqm^{-2}$. The radiocesium was mainly distributed within upper 5cm of the mineral soil layer. Metal gutters were installed at the bottom of the slopes, from which the water flowing over the slopes was collected and led to the storing tanks. The water in the tank was collected to the other tanks and taken to the laboratory on 10 Aug. 2018 and 26 Oct 2018. The water samples containing contaminated sediments were filtrated by glass filters with 440 $\mu$m opening followed by membrane filter with 0.45 $\mu$m opening. The dissolved form of radiocesium in the filtrates were removed by the special cartridge. After drying and weighing, the radiocesium on the filters and cartridges were measured by Ge semi-conductor detector run by RI Research and Education Center in the Graduate School of Agricultural and Life Sciences, The University of Tokyo.

The radiocesium effluence rate from the slopes under 550 mm of total rainfall during the measured period ranged from 0.13 to 1.50 $Bqm^{-2}$. The effluence rate of suspended particles ranged as little as 0.08 $gm^{-2}$. Corresponding to this result, the ratio of particulate form of radiocesium tended to be less although the water flow over the slopes probably occurred under the intense rainfalls. Although the measured radiocesium effluence rate was too little to affect the radiocesium concentration in the downstream river

©2019. Japan Geoscience Union. All Right Reserved. 

water, it should be noted that we should monitor the radiocesium effluence from bared or collapsing slopes which can be the potential source of radiocesium to the downstream area.

Keywords: Radiocesium, Dose rate, Effluence from slope

©2019. Japan Geoscience Union. All Right Reserved.

©2019. Japan Geoscience Union. All Right Reserved. 

[J] Oral | H (Human Geosciences )：H-CG Complex & General

Thu. May 30, 2019 3:30 PM - 5:00 PM JST | Thu. May 30, 2019 6:30 AM - 8:00 AM UTC | 202 2F

## [H-CG34] Education and research for rehabilitation of agriculture against harmful rumors in nuclear disaster areas

convener:Masaru Mizoguchi(Graduate school of Agricultural and Life Sciences, The University of Tokyo), Chairperson:Masaru Mizoguchi(The University of Tokyo), Kousuke Noborio(School of Agricultural Science, Meiji University)

Since the eastern Japan earthquake, various universities are carrying out educational programs that take students to the field and let the students recognize the importance of picking up on-site needs from the real field. This session convener also went to Iitate Village in Fukushima Prefecture three months after the nuclear accident, and continues a unique activities in cooperation with NPO and farmers. In this session, university's teachers will report changes in student's consciousness observed through on-site education and field research, and discuss social value of university.

3:30 PM - 3:45 PM JST | 6:30 AM - 6:45 AM UTC

[HCG34-01] Education and research for rehabilitation of agriculture against harmful rumors in nuclear disaster areas

*Masaru Mizoguchi[1] (1.Graduate school of Agricultural and Life Sciences, The University of Tokyo)

---

3:45 PM - 4:00 PM JST | 6:45 AM - 7:00 AM UTC

[HCG34-02] Towards the reborn of Iitate village 'Agriculture'

★Invited Papers

Makoto Sugisoka[2], *Masaru Mizoguchi[1] (1.Graduate school of Agricultural and Life Sciences, The University of Tokyo, 2.Division of Reconstruction Measures, Iitate Village)

---

4:00 PM - 4:15 PM JST | 7:00 AM - 7:15 AM UTC

[HCG34-03] Difference among crop species by radiocesium absorption from different soil fractions

*Nihei Naoto[1], Yoshimi Ohmae[1], Makoto Furukawa[1], Syuichiro Yoshida[1] (1.The University of Tokyo, Graduate School of Agricultural and Life Sciences)

---

4:15 PM - 4:30 PM JST | 7:15 AM - 7:30 AM UTC

[HCG34-04] Wild vegetables and mushrooms retrieving agriculter in Iitate Village, Fukushima Prefecture

*Kosuke Noborio[1], Yudai Fukuyama[2], Satoko Fujita[1], Hiroaki Sugino[2], Masaru Mizoguchi[2] (1.Meiji University, 2.the Univewrsity of Tokyo)

---

4:30 PM - 4:45 PM JST | 7:30 AM - 7:45 AM UTC

[HCG34-05] Effect of Study Tour toward Participants' Attachment on the Study Site - Case Study of University Student Tour to
Iitate Village, Fukushiima Prefecture -

*Natsumi Ebitani[1], Masaru Mizoguchi[1], Hiroaki Sugino[1] (1.Graduate school of Agricultural and Life Sciences, The University of Tokyo)

---

4:45 PM - 5:00 PM JST | 7:45 AM - 8:00 AM UTC

Discussion

# Education and research for rehabilitation of agriculture against harmful rumors in nuclear disaster areas

*Masaru Mizoguchi[1]

1. Graduate school of Agricultural and Life Sciences, The University of Tokyo

Since the eastern Japan earthquake of 2011, various universities are carrying out educational programs that take students to the field and let the students recognize the importance of picking up on-site needs from the real field. This session convener also went to Iitate Village in Fukushima Prefecture three months after the nuclear accident, developed a unique agricultural land decontamination method in cooperation with NPO corporations and farmers, and has been experimentally cultivating crops. Also, since 2012, we have held students' field tours and have witnessed changes in student's awareness before and after the local visit. Through these experiences, we have come to the idea that it is necessary to nurture young people who will challenge the creation of a new Japanese type agriculture in Fukushima. "Educational research program for revitalizing agriculture and elimination of bad rumor in Iitate village" is being carried out at the Ministry of Education, Culture, Sports, Science and Technology's "Fukushima Innovation Coast Concept Promotion Project. In this session, members of the Japanese Society of Soil Physics will report changes in student’s consciousness observed through on-site education and field research, and discuss social value of university.

Keywords: nuclear disaster, agriculture reborn, against harmful rumor

©2019. Japan Geoscience Union. All Right Reserved. 

# Towards the reborn of Iitate village 'Agriculture'

Makoto Sugisoka[2], *Masaru Mizoguchi[1]

1. Graduate school of Agricultural and Life Sciences, The University of Tokyo, 2. Division of Reconstruction Measures, Iitate Village

In Iitate Village where all villagers were evacuated due to the accident of TEPCO Fukushima Daiichi Nuclear Power Plant, evacuation order were canceled in March 2017 except for some areas. Because of lack of living environment and anxiety about radioactivity in the environment, the number of people who actually settle in Iitate village is less than 10%. However, the Iitate Village Office has proposed four agricultural plans (For protecting agricultural lands, For fun-to -live, For livelihood, For challenging new agriculture) according to the wishes of farmers, and is striving for the revival of "agriculture". In this presentation, I will introduce such efforts.

Keywords: Iitate Village, agriculture, reborn

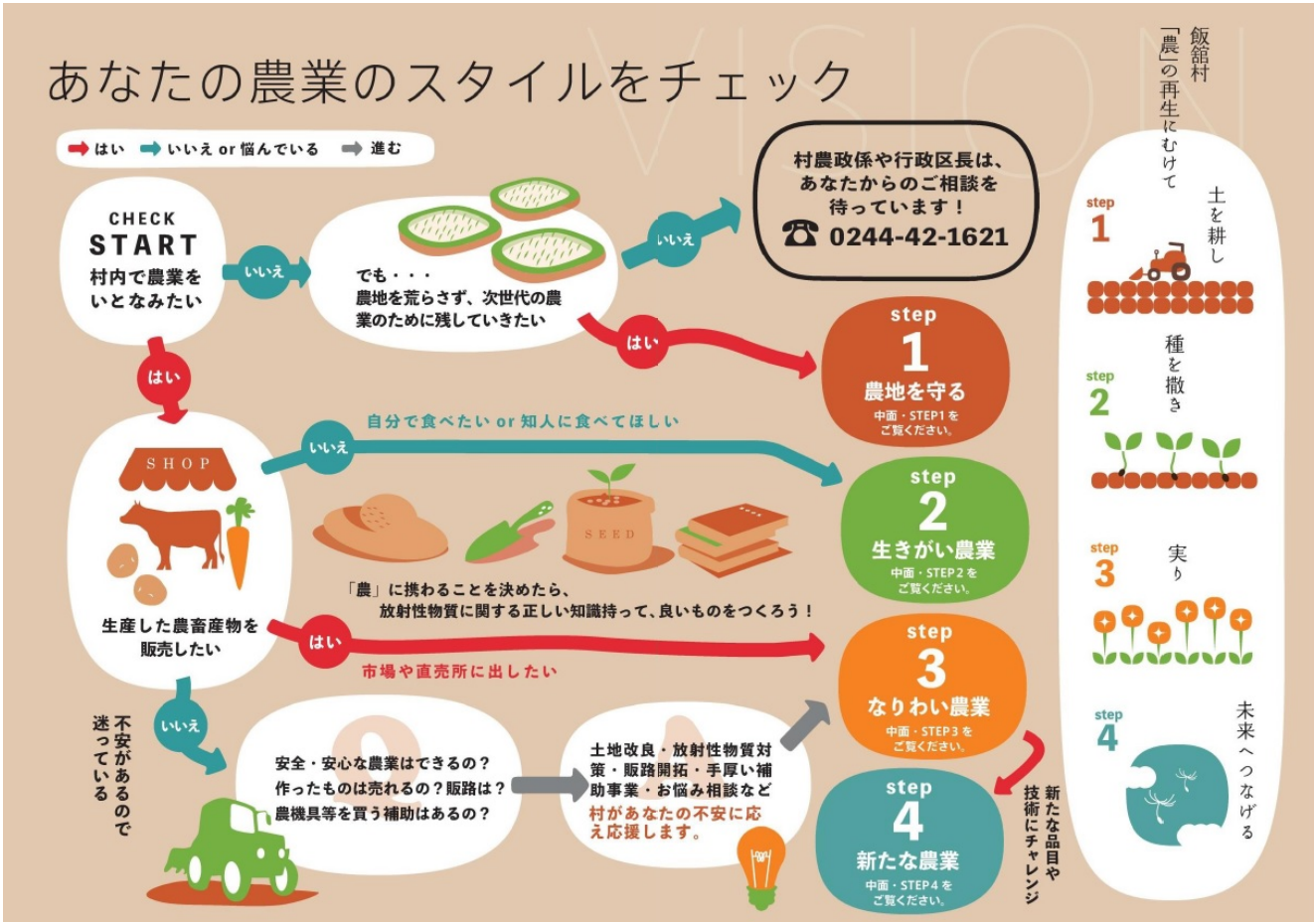


©2019. Japan Geoscience Union. All Right Reserved. 

# Difference among crop species by radiocesium absorption from different soil fractions

*Nihei Naoto[1], Yoshimi Ohmae[1], Makoto Furukawa[1], Syuichiro Yoshida[1]

1. The University of Tokyo, Graduate School of Agricultural and Life Sciences

Radioactive cesium (137 Cs) contaminated widely due to Fukushima Daiichi Nuclear Power Plant accident. The presence form of 137 Cs in soil can be divided into a fraction (adsorbed to ion exchange state or organic matter, defined as f 1 fraction) which crops are considered to be easy to absorb and utilize, and the another fraction (strong acid extraction and total decomposition component by hydrofluoric acid, defined as f2 fraction) which crops are considered to be difficult to absorb and utilize.

If we know how much 137 Cs will be absorbed from which soil fraction, we can grasp the Cs absorption characteristics of a crop. However, there has been no research report on a method showing 137 Cs absorption from each soil fraction. In this study, to grasp the soil fraction absorbing 137 Cs of the crop, the transfer factor (defined as TFf 1 and TFf 2) from each soil fraction were investigated by using the naturally occurring stable isotope cesium (133 Cs) . In addition, absorption ratios (defined as $\lambda$ 1 and $\lambda$ 2) in crops derived from each soil fraction were calculated.

Soybean, buckwheat and rice were cultivated for 30 days in a pot, and the 133 Cs and 137 Cs concentrations in the aerial part were measured. Contaminated soil (137 Cs approx 22 kBq / kg, 133 Cs approx. 3.4 mg / kg) obtained by topsoil stripping due to decontamination in Fukushima prefecture was used for soil. The soil after cultivation was successively extracted (ammonium acetate extraction, hydrogen peroxide decomposition, nitric acid decomposition, total decomposition by hydrofluoric acid), and the concentrations of 133 Cs and 137 Cs contained in each fraction were measured. In order to simplify the calculation, the soil fraction was set to two fractions of f1 (ammonium acetate extraction, hydrogen peroxide decomposition) and f2 (nitric acid decomposition, total decomposition by hydrofluoric acid). Measurement of 133 Cs was measured by ICP mass spectrometer (Perkin Elmer, Nex ION 350 S), measurement of 137 Cs by NaI scintillation counter (Perkin Elmer, Wizard). Judgment of each soil fraction absorbed by crops was calculated by 133 Cf 1 ×TFf 1 + 133 Cf 2 ×TFf 2 = 133 Ccrops, 137 Cf 1 ×TFf 1 + 137 Cf 2 ×TF f 2 = 137 Ccrops.

Cf1 or Cf2 is the Cs concentration of the soil in f1 or f2 fraction, TFf1 or TFf2 is Cs transfer factor from f1 fraction or f2 fractionation soil to crop, and Ccrop shows Cs concentration of crop.

TFf 1 and TFf 2 were different depending on the crop, soybean had higher absorption from f 2 fraction than buckwheat. Absorption from f1 fraction in 137 Cs of crops was 66% for soybean, 89% for buckwheat, 76% for rice, confirming the difference between crops. Furthermore, the effect of suppressing Cs absorption by potassium fertilization was shown to be different for each crop. By devising and defining these indices, it was possible to grasp the absorption capacity of crops.

Keywords: Radiocesium, soil fraction, soybean

©2019. Japan Geoscience Union. All Right Reserved. 

# Wild vegetables and mushrooms retrieving agriculter in Iitate Village, Fukushima Prefecture

*Kosuke Noborio[1], Yudai Fukuyama[2], Satoko Fujita[1], Hiroaki Sugino[2], Masaru Mizoguchi[2]

1. Meiji University, 2. the Univewrsity of Tokyo

Wild vegetables and mushroom at mountaineous slopes could be key agricultural products in Iitate Village in the future. Radiocesium fallout from the Fukushima Daiichi Nuclear Powerplant contaminated surface soils in its vicinities. Removal of contaminated surface soils was recently completed in agricultural fields, but not in forest areas where wild vegetables and mushrooms were grown. Pine mushroom is one of the precious wild mushrooms in Japan because it has not been successfully grown under controlled environments. We thought pine mushroom could be a key agricultural product for retrieving agriculture in Iitate Villege. Soil and air temperatures in a litter layer were measured to know environmental condidition of growing pine mushroom. We report the preliminary results of the environmental conditions.

Keywords: pine mushroom, sensing environmental factors, soil environment

©2019. Japan Geoscience Union. All Right Reserved.

©2019. Japan Geoscience Union. All Right Reserved. 

# Effect of Study Tour toward Participants' Attachment on the Study Site - Case Study of University Student Tour to Iitate Village, Fukushiima Prefecture -

*Natsumi Ebitani[1], Masaru Mizoguchi[1], Hiroaki Sugino[1]

1. Graduate school of Agricultural and Life Sciences, The University of Tokyo

Reconstruction in the affected areas of the Great East Japan Earthquake is progressing, but now there have been many people who feel less interested in understanding of the current situation and remained damage. In order to advance the further development after the basic reconstruction with lessons learned from the disaster, it is necessary to communicate the charm of the area to people outside of the affected area and make opportunities for rural exchange. Therefore, the authors are considering regularly holding study tours to the affected area. This presentation introduces a one-night two-day study tour as a case study for Iitate Village in Fukushima Prefecture held three times from October to November 2018. Before and after the tour, we conducted a questionnaire survey on a total of 44 participants (university students) who are mainly majoring in agriculture, and analyzed the obtained data by co-occurrence network analysis and factor analysis. In the end, this study discusses the effect of the tour on students' attachment to the tour site, and examined how future study tours should be.

Keywords: study tour, rural exchange, place attachment

©2019. Japan Geoscience Union. All Right Reserved. 

[J] Poster | S (Solid Earth Sciences)：S-SS Seismology

Thu. May 30, 2019 10:45 AM - 12:15 PM JST | Thu. May 30, 2019 1:45 AM - 3:15 AM UTC | Poster Hall International Exhibition Hall8, Makuhari Messe_4

## [S-SS12] Crustal Structure

convener:Kazuo Nakahigashi(Tokyo University of Marine Science and Technology)

The aim of this session is to cover seismological and geophysical studies on the Earth's crust. Contribution on seismological and geophysical structure of the crust, processes that develop in the crust which include earthquakes, volcanoes and geological descriptions of the crust are welcomed. We also welcome theoretical and methodological studies that will serve as basics in such explorations.

[SSS12-P01] Regional difference in long period surface wave phase velocity by an explosive phenomenon generated in North Korea on September 3, 2017

*Koji Yamada[1] (1.Hanshin Consultants co., ltd.)

[SSS12-P02] Phase velocity estimation based on spatial gradient of surface wave arrival time of teleseismic earthquakes observed by S-net

*Akira Ishigami[1], Ryota Takagi[1] (1.Research Center for Prediction of Earthquakes and Volcanic Eruptions, Graduate School of Science)

[SSS12-P03] Crustal seismic velocity structure in the Japanese Islands from receiver function analysis using similar earthquakes

*Toshihiro Igarashi[1] (1.Earthquake Research Institute, University of Tokyo)

[SSS12-P04] **Estimation of the Crustal Structure beneath the Broadband Seismic Network in the Eskisehir Region, Turkey, by Using Receiver Function Method**

*Pinar Duran[1], Asim Oguz Ozel[1], Hiroaki Yamanaka[2] (1.ISTANBUL UNIVERSITY-CERRAHPASA, 2.TOKYO INSTITUTE OF TECHNOLOGY)

[SSS12-P05] Three-dimensional S-wave attenuation structure in and around Hokkaido, Japan

*Ryoichi Nakamura[1], Takahiro Shiina[1] (1.Earthquake Research Institute, The University of Tokyo)

[SSS12-P06] Reexamination for the subsurface structure beneath the southern part of the Hidaka
Collision Zone, Hokkaido, Japan by using a numerical test of wave propagation

*Masahiro Shimazaki[1], Noriko Tsumura[2] (1.Graduate School of Science and Engineering, Chiba University, 2.Graduate School of Science, Chiba University)

[SSS12-P07] High resolution seismic surveys in the Kuril trench off Hokkaido

*Yasuyuki Nakamura[1], Shuichi Kodaira[1], Mikiya Yamashita[1], Seiichi Miura[1], Gou Fujie[1] (1.Japan Agency for Marine Earth Science and Technology)

[SSS12-P08] Subsurface Structure at the North of the Yokosuka Fault by Seismic Reflection Survey

*Shinobu Ito[1] (1.Geological Survey of Japan, AIST)

[SSS12-P09] **Crust and Uppermost mantle P-wave velocity structure of the Ordos block and its neighbors based on travel time tomography**

*Yaning Liu[1], Jianping Wu[1], Shuxian Bao[1], Xiaohong Meng[2] (1.Institute of Geophysics, China Earthquake Administration, 2.China University of Geosciences (Beijing))

[SSS12-P10] Seismic imaging of the 2016 Kumamoto earthquake area using P and PmP data

*Dapeng Zhao[1], Haibo Wang[2], Zhouchuan Huang[2], Mingjie Xu[2], Liangshu Wang[2] (1.Department of Geophysics, Tohoku University, 2.School of Earth Sciences and Engineering, Nanjing University)

[SSS12-P11] Estimation of 3D velocity structure in Kyushu region by the seismic tomography

*Toya Mitsuhiro[1], Koji Yamada[1] (1.Hanshin Consultants Co., Ltd.)

[SSS12-P12] Estimation of the structure of the Philippine Sea slab under south Kyushu using receiver function analysis

*Masaki Uchida[1], Takahiro Ohkura[1], Takuo Shibutani[1], Yuki Abe[2], Shintaro Komatsu[1], Ken'ichi Yamazaki[1], Yusuke Yamashita[1], Shin Yoshikawa[1], Masato Iguchi[1], Takeshi Tameguri[1], Tadaomi Sonoda[1] (1.Kyoto Univ., 2.Hot Springs Research Institute)

[SSS12-P13] Imaging subduction structure beneath the eastern part of Kii Peninsula, SW Japan, using an earthquake reflection method

*Eiji Kurashimo[1], Takashi Iidaka[1], Noriko Tsumura[2], Takaya Iwasaki[1] (1.Earthquake Research Institute, the University of Tokyo, 2.Chiba University)

[SSS12-P14] **Tomography of Mejillones Peninsula using cross-correlation of ambient seismic noise**

*Kellen Azua Quezada[1], Sergio Ruiz[1], Francisco Pasten-Araya[2,3], José Salomón[4], Pablo Salazar[2,3], Miguel Saez[1], César Pastén[4], Felipe Leyton[5], Wasja Bloch[6] (1.DGF, UChile, 2.DG, UCN, 3.CIGIDEN, 4.DIC, UChile, 5.CSN, Chile, 6.GFZ)

[SSS12-P15] **Crustal thickness beneath Central Indonesia by the cross-correlation analysis of seismic ambient noise (2)**

*Masyitha Retno Budiati[1], Genti Toyokuni[1], Tomomi Okada[1], Toru Matsuzawa[1] (1.Graduate School of Science, Geophysics Department, Tohoku University)

[SSS12-P16] Subsurface structure below the southernmost area of South Japanese Alps estimated by seismic interferometry imaging

*Toshiki Watanabe[1], Hasegawa Daima[1], Tanio Ito[2], Ken'ichi Kano[3], Susumu Abe[4], Akira Fujiwara[5], Yoshinori Kouchi[6] (1.Graduate School of Environmental Studies, Nagoya University, 2.Association for the Development of Earthquake Prediction, 3.Shizuoka Univertity, 4.JAPEX, Co. Ltd., 5.JOGMEC, 6.Geosys, Inc.)

[SSS12-P17] Strong variations of near-surface seismic anisotropy of Taiwan revealed by coda interferometry

*Hsin-Yu Lee[1], Yuancheng Gung[1], Li-Wei Chen[2], Ling-Yun Chiao[3] (1.Department of Geosciences, National Taiwan University, Taiwan, 2.Department of Earth and Planetary Science, University of California at Berkeley, CA, USA, 3.Institute of Oceanography, National Taiwan University, Taiwan)

[SSS12-P18] Investigating anomalous crustal structures along the convergent zone in eastern Taiwan with the new airborne magnetic survey and updated seismic tomographic models

*Chi-Hsuan Chen[1], Hsin-Hua Huang[2], Lun-Tao Tong[3], Wayne Lin[3], Po-Tsun Lee[1], Shou-Fang Chang[1], Jin-Fa Lee[1] (1.Cntrl. Geo. Surv., MOEA, Taiwan, 2.Inst. Earth. Sc., Acad. Sinica, Taiwan , 3.Industr. Technol. Res. Inst., Taiwan)

# Regional difference in long period surface wave phase velocity by an explosive phenomenon generated in North Korea on September 3, 2017

*Koji Yamada[1]

1. Hanshin Consultants co., ltd.

An explosive phenomenon to assume the Democratic People's Republic of Korea cause at past 12:30 of September 3, 2017 was observed in each place. The position of the seismic center is considered to be 41.3 degrees N, 129.1 degrees E, 0 kilometers in depth by Japan Meteorological Agency and almost assumes surface of the earth neighborhood cause. Because it is an explosive phenomenon generated in an earth surface, Rayleigh wave is observed other than P wave, and can considered the observed wave mortion to be an observation record of huge size surface wave exploration.

The observed Rayleigh wave shows strong dispersibility at around 0.03-0.1Hz. After performing MASW (Multichannel Analysis of Surface Wave) for the Kinki districts where P-wave velocity structure is estimated using data of the large blast observation, the provided phase velocity almost matching with the one dimension S-wave velocity structure that I set in reference to Hirose& Ito (2006). Yamada(2018) thought that the observed phase velocity dependend on velocity structure to the Moho.

Because after doing MASW at a suitable angle based on the direction from the seismic center about each domestic area, a local difference was seen in provided phase velocity, I report it.

Acknownledgement:

In this study, I used the observation record of broadband Seismograph network (F-net), high sensitivity seismograph network (Hi-net) by NIED, each national university, and Japan Meteorological Agency.

Keywords: Explosive phenomenon generated in North Korea, Long period surface wave, Homo, Multichannel Analysis of Surface Wave

©2019. Japan Geoscience Union. All Right Reserved. 

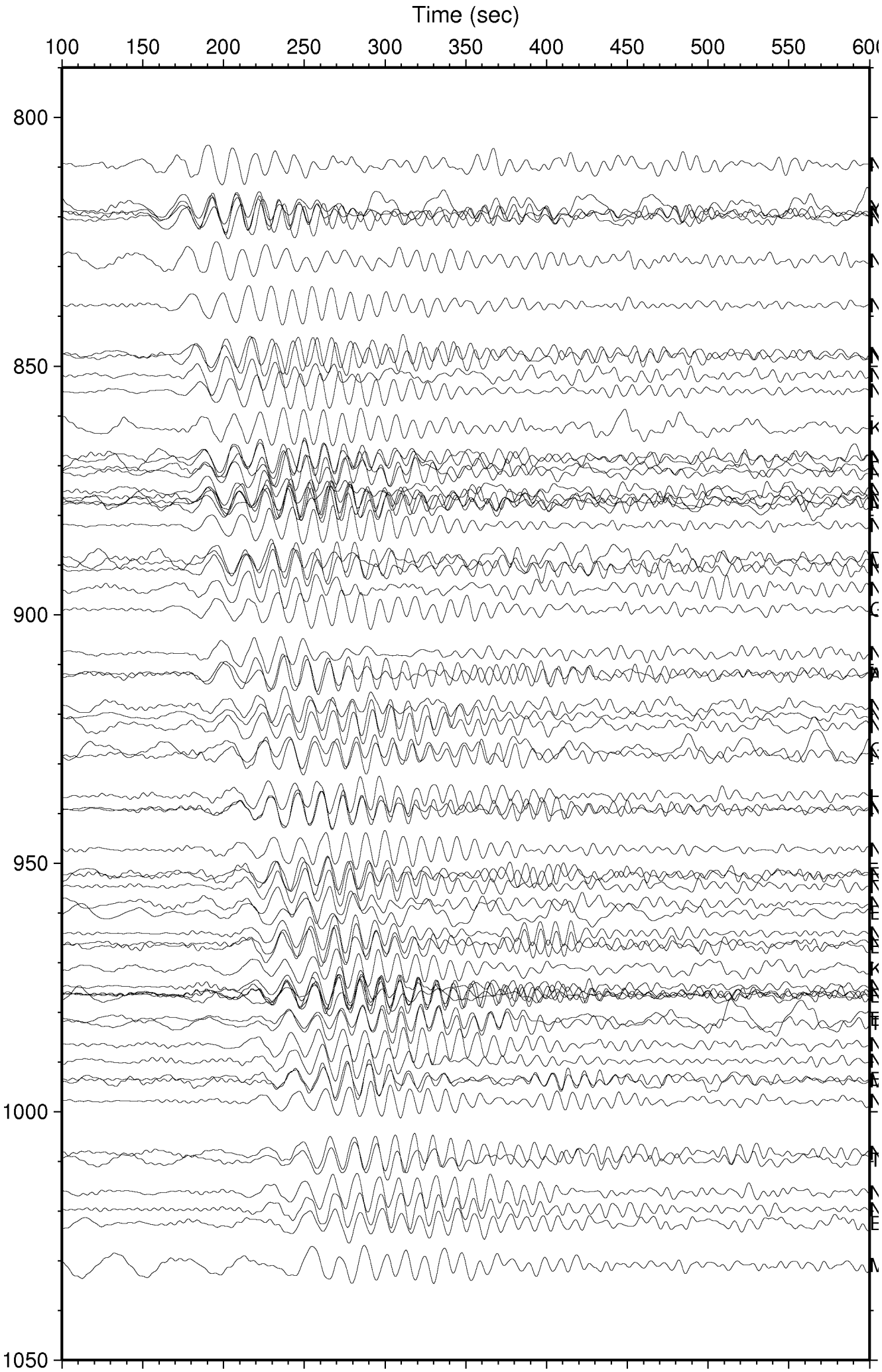


©2019. Japan Geoscience Union. All Right Reserved.

©2019. Japan Geoscience Union. All Right Reserved. 

# Phase velocity estimation based on spatial gradient of surface wave arrival time of teleseismic earthquakes observed by S-net

*Akira Ishigami[1], Ryota Takagi[1]

1. Research Center for Prediction of Earthquakes and Volcanic Eruptions, Graduate School of Science

Seismice velocity structure is fundamental information to understand environmental cause of earthquakes and slip behavior on the plate interface. In addition, recent developments of dense seismic network enable us to catch seismic waveforms as seismic wavefield. In the present study, we use S-net data to estimate phase velocity map by calculating spatial gradient of surface wave arrival time of teleseismic earthquakes.

We used long-period accelerometer records of teleseismic earthquakes. We analyzed a teleseismic earthquake occurred in Alaska Bay on January 23, 2018 (depth: 25km, Mw 7.9). We used vertical records to estimate Rayleigh wave phase velocity after converting observed records from XYZ to UNE components. To estimate phase velocity map, we followed Lin et al. (2009). We first applied frequency-time analysis (FTAN) to waveform data of each station to get phase velocity dispersion curve. We then picked surface wave arrival times at certain period and spatially interpolated to get arrival time map. Finally, we obtained phase velocity map by calculating spatial gradient of the arrival time map. We estimated phase velocity maps at 20-50 s by intervals of 5 s.

When we estimate the phase velocity curve, there is the $2\pi$ phase ambiguity. Although a reference phase velocity curve allows us to estimate the number of cycles, the discrepancy from the real phase velocity curve and the initial phase effect causes misestimation of the cycle number. Thus, we solved this problem by iteratively update the reference dispersion curve. First, we used PREM 1D model to estimate dispersion curve at each station. In the next step, we used average of the estimated dispersion curves as the reference model. We repeated the procedure until we can obtain a consistent cycle number within the all S-net stations.

The phase velocity is estimated within 3.6-3.9 km and consistent with general phase velocity of Rayleigh wave. We found high velocity anomaly which may be attributed to the subducting slab at the period of 45 s. We also found high velocity anomaly off Miyagi and Fukushima.

To confirm the spatial pattern of the phase velocity, we need to analyze other teleseismic events. We can also estimate azimuthal anisotropy of phase velocity by using several earthquakes of which surface waves propagate in different direction. In addition, we need to examine the method of spatial interpolation for robust estimation of phase velocity map.

Keywords: S-net, surface wave, tomography, Tohoku-oki earthquake, phase velocity

©2019. Japan Geoscience Union. All Right Reserved. 

# Crustal seismic velocity structure in the Japanese Islands from receiver function analysis using similar earthquakes

*Toshihiro Igarashi[1]

1. Earthquake Research Institute, University of Tokyo

The stress and strain changes due to the recurrence process on the inter-plate great earthquakes of the subducting plate should have a significant effect on shallow inland seismicity and velocity structure in the overriding plate. In this study, we applied receiver function analysis using similar earthquakes, which repeatedly occurred at almost the same location, to investigate the spatiotemporal change of the crustal seismic velocity structure beneath the Japanese Islands. Similar earthquakes used as data were extracted from the seismograms of medium-sized earthquakes, which observed in the seismic network of Japan and occurred in the epicentral distances between 30 degrees and 90 degrees in the periods from September 1989 to February 2016. We estimated temporal changes of crustal seismic velocity structure by receiver function analysis from the selection of pairs of similar earthquakes occurred before and after the 2011 Tohoku-Oki earthquake (M9.0). In this analysis, we assumed that the depths of the Moho discontinuity, which estimated using all available data for the above period, do not change within the analysis period. As a result, we detected areas of decreased crustal velocity to the west of the source region of the Tohoku-Oki earthquake. We suggest that the stress change by a great inter-plate earthquake affected the velocity reduction or velocity polarization. On the other hand, the crustal velocity increased to the north of the source region. This change may be caused by the effect of the postseismic deformation after the 2003 Tokachi-Oki earthquake (M8.0). However, it is difficult to specify the accurate timing of the change because of long-term data stack. The impact of the great earthquakes has been widespread for a long time. The further studies of the seismic velocity structure in arbitrary period will clarify the cause of changes.

©2019. Japan Geoscience Union. All Right Reserved. 

# Estimation of the Crustal Structure beneath the Broadband Seismic Network in the Eskisehir Region, Turkey, by Using Receiver Function Method

*Pinar Duran[1], Asim Oguz Ozel[1], Hiroaki Yamanaka[2]

1. ISTANBUL UNIVERSITY-CERRAHPASA, 2. TOKYO INSTITUTE OF TECHNOLOGY

Receiver function imaging is an important tool for the investigation of the crust and upper mantle structure. The P to S conversion (Ps) from the Moho is typically one of the most prominent phase on the P-wave receiver funtions. The time delay between the Ps converted phase and direct P wave is sensitive to the depth of the velocity discontinuities, and the average S wave velocity above it. Estimates of the depth and thickness of the Moho and $V_P$ /$V_S$ ratio of the crust are important goals of many receiver funtion investigations. In the frame of the Turkey-Japan joint project, we attempt to determine S-wave velocity structure of the crust beneath Eskisehir Region, described by various tectonic settings. The teleseismic events are recorded by broadband three-component seismic stations of ANA-NET Seismic Network, which is operated by the Eskisehir Anadolu University since 2010. The seismograms from these events, whose epicenters lay at distances greater than 30$^o$, were deconvolved in the time domain to remove the unwanted noise and then stacked to obtain better receiver functions. This information will be used to establish a linear relationship between thickness and $V_P$ /$V_S$ ratio, each of which is stacked for a given station to identify a best-fit estimate for depth to the Moho and Vp/Vs ratio. To determine their accuracy, these results will be compared with other geophysical studies performed in the region, 1-D crustal models will be presented at the conference. This study is supported by the Joint Research Project under the Bilateral Program of the Japan Society for the Promotion of Science (JSPS) and The Scientific and Technological Research Council of Turkey (TUBITAK) under Grant TUBITAK 116Y524.

Keywords: Receiver Function Analysis, Crustal structure, P-receiver functions, Waveform inversion, Eskisehir Fault Zone

©2019. Japan Geoscience Union. All Right Reserved. 

# Three-dimensional S-wave attenuation structure in and around Hokkaido, Japan

*Ryoichi Nakamura[1], Takahiro Shiina[1]

1. Earthquake Research Institute, The University of Tokyo

## 1. Introduction

At Hokkaido, Japan, the collision between the Kuril and the NE Japan arcs occur (e.g., Kimura, 1994, JGR), and thus complicated crustal structure would be developed. According to Kita et al. (2012), the arc-crust is subducted by the collision and reaches deep up to near the upper part of the mantle. Additionally, the 2018 Eastern Iburi Earthquake (M6.7, depth 37 km) and its aftershocks occurred at considerably deep as a crustal earthquake. This activity at the deep crust is thought to link to the complicated geologic structure in Hokkaido.

Several detailed tomographic studies of seismic velocity and Qp structures have been done in this region (e.g., Kita et al., 2014, JGR; Shiina et al., 2018, JGR). These studies showed low Qp, low Vp, low Vs, and high Vp/Vs at a depth of 10 km in the west side of the Hidaka mountain range and that these anomalous structures distribute to the depth of 50 km which comparable to the upper surface of the subducting Pacific plate. On the other hand, the Qs structure in this area has not been well investigated. Therefore, in this study, we estimate the detailed Qs structure of Hokkaido by using the 3D spectrum inversion method.

## 2. Method and Data

In this study, we adopt the 3D spectral inversion method (Nakamura and Uetake, 2002) to strong motion records observed around the Hokkaido. In the method, we estimate source spectrums, site factors, and Qs value of each block. The study area is 138 ˚- 148 ˚E and 39 ˚- 46 ˚N, and is discretized by blocks of which size is 0.1 ˚in latitude and longitude and 10 km in depth direction.

The strong motion records are collected from on the K-net and the KiK-net stations deployed near the surface. Periods collecting the records are to Nov. 2019 from operation beginnings of each station. The magnitude of earthquakes is 4.0 - 7.5. We limit stations by epicentral distances: < 100 km and < 500 km for earthquakes occurred at depths of 0-30 km and 30-200 km, respectively. Moreover, we exclude strong motion records with 100 Gal or stronger to reduce influences of ground nonlinearity effects as possible. Fourier spectrum amplitudes are computed from the strong motion records of NS component at 1-10 Hz with every 1 Hz.

## 3. Results

We show the estimated Qs structure in and around the Hokkaido obtained at 10 Hz in Figure 1. In this study, we examine the CKB resolution test and, in Figure 1, we display only the results where the assumed structures are well recovered in the resolution test. The obtained Qs structure reveal the high-attenuation (low-Qs) zones beneath the volcanoes at depths of 30-40 km and the Pacific slab with low-attenuation (high-Qs), as well as tomographic images in Tohoku district (e.g., Nakamura and Uetake, 2004; Liu et al., 2014).

©2019. Japan Geoscience Union. All Right Reserved. 

At the west side of the Hidaka mountain range, the remarkable high-attenuation zone is estimated at depths of 0-20 km and there seem to continuously distribute by about 40 km. This high-attenuation anomaly is consistent with that estimated in Qp (Kita et al., 2014). Additionally, the belt-like distribution of low-attenuation area along the Hidaka mountain range can be revealed in this study. These structures would represent heterogeneity resulted from the collision between Kuril and NE Japan arcs.
Around the source area of the 2018 Hokkaido Eastern Iburi Earthquake, high S-wave attenuation is imaged. The high-attenuation zone is extended from near the Hidaka mountain range (the result at 30-40 km in Figure 1) and the contrast of between high- and low-attenuation property clearly identified along the north-south direction. This is comparable to distributions of aftershocks of the Eastern Iburi earthquake. Therefore, we consider that the heterogeneous structures which are developed in the collision zone would closely link to the occurrence of the Eastern Iburi earthquake and its aftershocks.

Keywords: Hokkaido, Collision zone, S wave attenuation structure, the 2018 Eastern Iburi Earthquake

©2019. Japan Geoscience Union. All Right Reserved. 

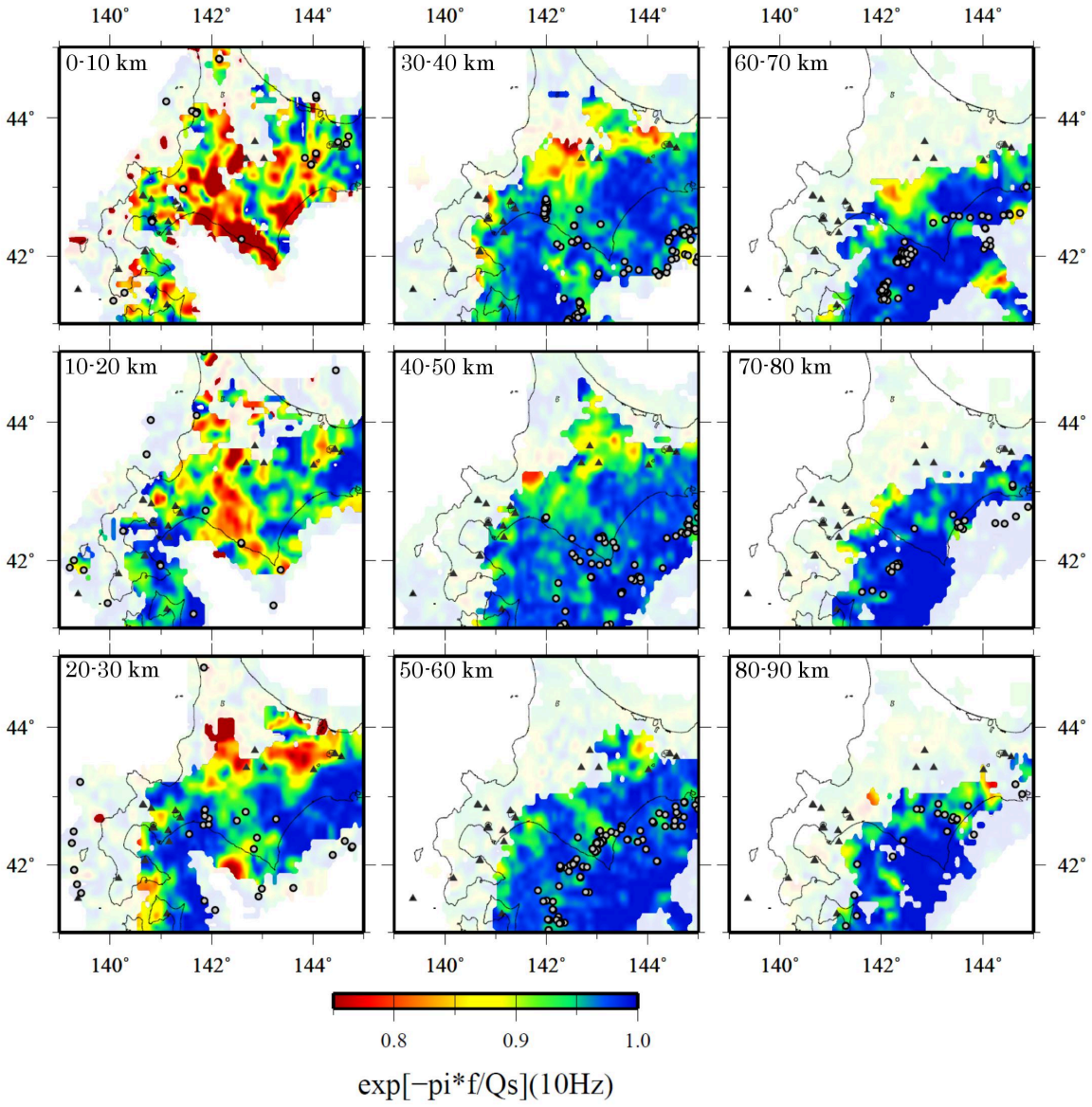


Fig.1 Qs structure in and around the Hokkaido, Japan, obtained at 10 Hz. Less resolved area are masked in the figure. White circles denote the locations of earthquakes used in this study. Black triangles is active volcanoes.



©2019. Japan Geoscience Union. All Right Reserved. 

# Reexamination for the subsurface structure beneath the southern part of the Hidaka Collision Zone, Hokkaido, Japan by using a numerical test of wave propagation

*Masahiro Shimazaki[1], Noriko Tsumura[2]

1. Graduate School of Science and Engineering, Chiba University, 2. Graduate School of Science, Chiba University

Hidaka Collision Zone (HCZ) is located in the central and southern part of Hokkaido where the Kuril forearc dragged by oblique subduction of the Pacific plate collided with the northeastern Japan arc. The Kuril arc’ s middle crust and its shallower part have been thrusted up along the Hidaka Main Thrust (HMT) and are exposed to the surface. Various seismic reflection surveys have been conducted for the purpose of investigating the subsurface structure of this region.
At the southernmost part of the HCZ, researchers of Hokkaido university, university of Tokyo and Chiba university conducted three seismic reflection surveys whose lines were settled across the HCZ in 1994, 1996, and 1997, respectively. From obtained time section, Tsumura et al. (1999) showed that the lower crust of the Kuril arc is divided into a northeast-dipping ascending layer and a southwest-dipping descending layer at a depth of 23km and interpreted it as delamination structure. Seismic profiles which were obtained by integrating three survey lines [Ito et al.,2000] and by applying new analysis technique of CRS / MDRS method [Ito et al.,2013] also supported the delamination structure.
Meanwhile, Kita et al. (2012) estimated the three-dimensional P wave velocity structure in the same region by travel time tomography. They suggested that a shallower part than 23km indicates the similar structure to that of Ito et al. (2000), but at deeper than 23 km, crustal material of the northeastern Japan arc reaches the plate boundary of the Pacific plate.
If delamination has occurred beneath the HCZ, it is expected that the length of southwest-dipping descending layer corresponds to the one of ascending layer having northeast inclination. Although two parallel reflectors can be recognized at the depth from 23 km to 38 km, deeper extension more than 38km cannot be found in the depth cross section of Ito et al. (2013). Then, in this study, we conducted a numerical test to know what kind of reflected waves can be observed when shots are performed with the same specification of actual surveys using analysis software Madagascar.
For the numerical test, we prepared two kind of subsurface structure models: One is a “Delami” model in which delamination occurs and lower part of the lower crust are descending into the depths deeper than 38km; and the other one is a “Non-Delami” model based on the interpretation of Kita et al. (2012). Both of the models consist of upper crust, lower crust, mantle and oceanic plate, and the average density of each material was set as density. Velocity of each layer was given referring to the result of Kita et al. (2012).
For the “Delami” model, only the reflected waves from the tip of wedge like structure of the subducting layer reached within the survey lines, whereas reflected waves from the deeper part reached the southwestern outside of the survey line. For the “Non-Delami” model, no reflected waves were seen around the arrival times which correspond to those of reflected waves from the depths at 23 km to 38 km.

©2019. Japan Geoscience Union. All Right Reserved. 

Keywords: Collision zone, Hidaka, Subsurface structure, Reflection survey

©2019. Japan Geoscience Union. All Right Reserved. 

# High resolution seismic surveys in the Kuril trench off Hokkaido

*Yasuyuki Nakamura[1], Shuichi Kodaira[1], Mikiya Yamashita[1], Seiichi Miura[1], Gou Fujie[1]

1. Japan Agency for Marine Earth Science and Technology

In the Kuril trench subduction zone, several large earthquakes (e.g., Tokachi-oki earthquakes) have occurred, which caused the earthquake and tsunami hazards in the Hokkaido and Tohoku region. Because the earthquake and tsunami risk was evaluated to be high in this region, more investigation and studies are required to contribute to the mitigation of those risks. In 2016 and 2018, we conducted high resolution seismic surveys in the Kuril trench from Erimo Seamount to off Kushiro by R/V *Yokosuka*. Approximately 35 km long 24 seismic profiles with ~ 6 km line separation were acquired using a 1.2 km long streamer cable and 380 inch$^3$ cluster guns. Obtained profiles demonstrate the detailed geological structure in the trench axis region. Subducting Pacific plate is deformed by the bend-related normal faults. The throw of the faults is up to ~ 300 –400 ms TWT. The thickness of the incoming sediments is > 500 ms maximum in the survey area and becomes thinner near the seamounts. Thick trench-fill sediment is deposited in the trench axis west of the Kushiro canyon, and the thickness is up to ~ 800 ms. Some profiles show weak landward dipping reflections within the hanging wall sediments. Possible slope failure is suggested in the lowermost landward slope near the Erimo Seamount.

Keywords: Kuril trench, seismic imaging, seamount, sediments

©2019. Japan Geoscience Union. All Right Reserved. 

# Subsurface Structure at the North of the Yokosuka Fault by Seismic Reflection Survey

*Shinobu Ito[1]

1. Geological Survey of Japan, AIST

The rupture of the Mikawa Earthquake on January 13, 1945 is considered to be on the Fukozu and the Yokosuka Faults. The Fukozu Fault is located relatively south and reverse L-shaped. On the other hand, the Yokosuka Fault is located relatively north and L-shaped. Ando (1974) mentioned that the NS strike section of the Yokosuka Fault in the fault zone was caused by a secondary deformation. Sugito and Okada (2004) investigated surface displacement in detail along the fault zone. They concluded that the NS strike section of the Yokosuka fault is the upper extension of the earthquake source fault although they referred to the possibility of the secondary deformation. Sugito and Okada (2004) referred that the surface earthquake fault of the Mikawa Earthquake is inconsistent with the source model of the earthquake estimated by Kikuchi et. al. (2003) from seismograms. In this way, the NS strike section of the Yokosuka Fault is not understood clearly. We carried out the P-wave seismic reflection survey at Shikoya-cho, Nishio, Aichi; at the north end of the Yokosuka Fault, in order to investigate lower extension of the Yokosuka Fault.

Not only the survey at the north of the Yokosuka Fault (GS-NSO2) but also the other survey at the south east extension of the Takahama Fault (GS-NSO1) were carried out from September 27 to October 2 in 2018. The length of the survey line GS-NSO2 is 1810m. We used one EnviroVibe manufactured by IVI. Sweep frequency is 10 to 120Hz, and sweep duration is 16S. Standard shot interval is 5m, and exceptionally 2.5m. Total shot points are 421, and we shot 3 to 5 times for each point. We used 3 string geophones of OMNI-2400 ($f_0$=15Hz) by Geospace. We used offline seismic recorder GSX system also by Geospace. Receiver interval is 5m, and total receiver points are 342. We made seismic profile by CMP stack.

We cannot see any obvious faults or signs related to the faults in the profile. Trenching survey indicate that the Mikawa Earthquake was preceded by one earthquake 2000 years ago. Total displacement of the Mikawa Earthquake and the preceding event is not more than 2m. It is impossible to detect the displacement in case of 2m displacement. However, it is possible in case that the displacement increase with depth. At least, we cannot detect the cumulative displacement in the survey.

Keywords: Yokosuka Fault, fault, seismic reflection survey

©2019. Japan Geoscience Union. All Right Reserved. 

# Crust and Uppermost mantle P-wave velocity structure of the Ordos block and its neighbors based on travel time tomography

*Yaning Liu[1], Jianping Wu[1], Shuxian Bao[1], Xiaohong Meng[2]

1. Institute of Geophysics, China Earthquake Administration, 2. China University of Geosciences (Beijing)

The Ordos block is located on the west side of the North China Carton, adjacent to the northeastern part of the Tibetan Plateau, with the Yinshan organic belt to the north and the South China block to the south. And the tectonic evolution of Ordos block is controlled by the North China basin extension caused with subduction of the Pacific plate and the extrusion and sheared from the northeastern margin of the Tibet Plateau follow the collision of the Indian-Eurasian plate.

The study area spans from 32˚N to 42˚N and 108˚E to 114˚E , which includes the Ordos block and its adjacent structures . The seismic data we used for inversion were recorded by 1244 stations including: 198 permanent stations and 1043 temporary stations (ChinArray II and III), from November 2013 to August 2017. The study uses local-seismic for inversion. After manual labeled the seismic phase, we select events with more than ten phase records of individual seismic events. The epicentral distance is less than 200km. Finally, we obtained about 22,500 phase records of 1882 local seismic events.

Our preliminary research results are consistent with previous studies and surface structures of a wide range of velocity distributions. However, in the middle-upper crust under the Liupan Mountain, the low-speed anomaly extending downward is shown, which may be caused by the horizontal extrusion caused by the eastward asthenosphere flow driven by the continuous compression of the northeastern margin of the Qinghai-Tibet Plateau during the Cenozoic. While, in the middle crust of the Ordos Basin, there are weak high-speed anomalies that divide the low-speed disturbances in the basin into three parts, showing the fluctuation of the crystalline basement of the basin. In the Taihang Mountains in the west of the study area, low-velocity anomalies extending to the upper layer of the mantle are shown. We initially believe that this anomaly is related to the volcanic thermal motion that once existed on the area.

Keywords: P-wave velocity structure, Ordos block

©2019. Japan Geoscience Union. All Right Reserved. 

# Seismic imaging of the 2016 Kumamoto earthquake area using P and PmP data

*Dapeng Zhao[1], Haibo Wang[2], Zhouchuan Huang[2], Mingjie Xu[2], Liangshu Wang[2]

1. Department of Geophysics, Tohoku University, 2. School of Earth Sciences and Engineering, Nanjing University

We determined a high-resolution model of 3-D P-wave velocity (Vp) tomography of the crust in the source zone of the 2016 Kumamoto earthquake (M 7.3) in Kyushu, SW Japan using a large number of arrival times of first P-waves and reflected P-waves from the Moho discontinuity (PmP). The PmP data are collected from original seismograms of the Kumamoto aftershocks and other local crustal events in Kyushu. Detailed resolution tests show that the addition of the PmP data can significantly improve the resolution of the crustal tomography, especially that of the lower crust. Our results show that significant low-velocity (low-Vp) anomalies exist in the entire crust beneath the active volcanoes, which may reflect the pathway of arc magma. The 2016 Kumamoto earthquake occurred at the edge of a small low-Vp zone in the upper crust. A significant low-Vp anomaly is revealed in the lower crust beneath the source zone, which may reflect the arc magma and fluids ascending from the mantle wedge. These results suggest that the rupture nucleation of the 2016 Kumamoto earthquake was affected by fluids and arc magma.

Keywords: Kumamoto earthquake, crustal reflected wave, seismic tomography

©2019. Japan Geoscience Union. All Right Reserved. 

# Estimation of 3D velocity structure in Kyushu region by the seismic tomography

*Toya Mitsuhiro[1], Koji Yamada[1]

1. Hanshin Consultants Co., Ltd.

## 1. Introduction

A high-resolution crustal structure in the volcanic zone is basic information for prediction of volcanic activity in the future. Therefore, in this study, we carry out preliminary research in Kyushu region aiming at the estimation of three-dimensional (3D) velocity structure in the volcanic zone by the 3D seismic tomography. In this region, it is suitable for this study because a large number of earthquake records of the main shock and aftershocks of the Kumamoto earthquake that occurred in April 2016 can be used and there are many volcanoes such as Mt. Aso and Mt. Unzen. Thus, we perform the 3D seismic tomography in Kyushu region for the estimation of 3D velocity structure, and consider problems on application to the volcanic zone.

## 2. Data and Method

We used arrival time data downloaded from the website of National Research Institute for Earth Science and Disaster Resilience (NIED). We selected 59011 earthquakes observed at 141 stations from April 2016 to March 2017. The selected area is 129.3˚E ~ 132.1˚E, 30.9˚N~ 34.0˚N, 0 ~ 50 km in depth. And, for P-wave arrivals, we added 804 earthquakes observed at 4 V-net stations at Mt. Aso and travel time data obtained by explosion seismic observations in the Hinagu fault area, Kyushu (The Research Group for the 2003 Hinagu Fault Seismic Expedition, 2008) and Eastern Kyushu (RESEARCH GROUP FOR EXPLOSION SEISMOLOGY, 1999). In total, our selection result in 871,690 P-wave arrivals and 840,633 S-wave arrivals.

We estimate 3D seismic velocity structure using the Fast Marching Tomography (FMTOMO) method of Rawlinson et al. (2006). This program uses the fast marching method via finite difference solution of the eikonal equation (Sethian, 1996) for calculation of synthetic travel times. The model area is 129.2˚E ~ 132.2˚E, 30.8˚N~ 34.1˚N, -4 ~ 52 km in depth. The horizontal grid spacing is 0.1˚(about 10 km) and the vertical is 4 km (the number of grids is 34×31×15 for three coordinate axis). An initial velocity structure model is JMA2001 (Ueno et al. 2002) and we set six iterations of the tomographic inversion scheme. Then, we examined the resolution of the tomographic inversion using a checkerboard resolution test (CRT). The size of checker is 2×2×2 in grid number, and the velocity perturbation for the initial velocity structure model is ±0.1 km/s. As a result of the CRT, we confirmed that checkerboard pattern is well resolved up to about 20 km deep in the Kumamoto area.

## 3. Results

Figure 1 shows plan views of the P-wave velocity and the S-wave velocity structures obtained here at 4 km depth. The pattern of velocity variation is similar to each other and pronounced low velocity area exists in the southern Kumamoto. At 0 ~ 1 km depth, low velocity area exists in the Kumamoto Plain. However, in this study, pronounced velocity variation is not seen beneath Mt. Aso and other volcanic zones. So, for improving the resolution, we are going to add earthquakes in the area with less them and stations (K-net, V-net and so on).

## Acknowledgments

We would like to thank the National Research Institute for Earth Science and Disaster Resilience (NIED)

©2019. Japan Geoscience Union. All Right Reserved. 

for the use of the arrival time and the seismic data. All figures are made using the free software GMT (Wessel & Smith 1998).

Keywords: seismic tomography, velocity structure, Kyushu

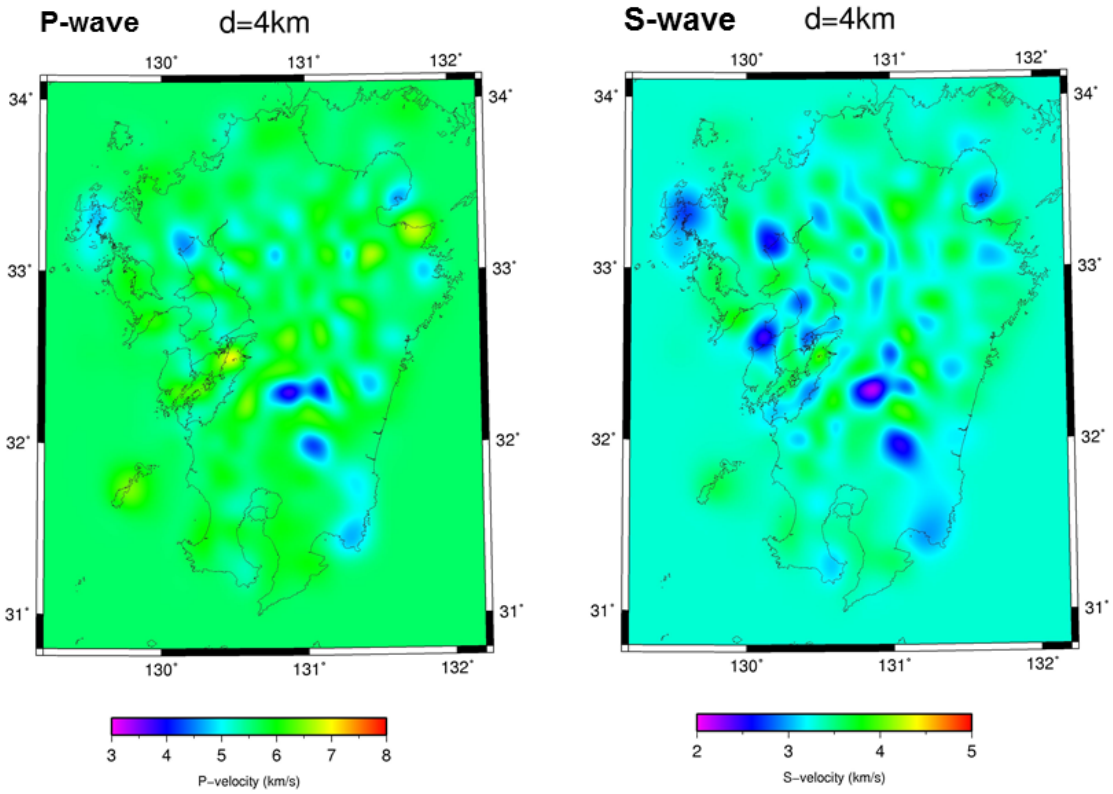


Fig. 1. Plan views of velocity structure for Vp (left), velocity structure for Vs (right)

©2019. Japan Geoscience Union. All Right Reserved. 

# Estimation of the structure of the Philippine Sea slab under south Kyushu using receiver function analysis

*Masaki Uchida[1], Takahiro Ohkura[1], Takuo Shibutani[1], Yuki Abe[2], Shintaro Komatsu[1], Ken'ichi Yamazaki[1], Yusuke Yamashita[1], Shin Yoshikawa[1], Masato Iguchi[1], Takeshi Tameguri[1], Tadaomi Sonoda[1]

1. Kyoto Univ., 2. Hot Springs Research Institute

In the subduction zone, it is considered that magmatism is caused by fluid transported to the upper mantle from the subducting slab [Tatsumi, 1986, GRL]. In order to clarify the relation between the magmatism and the subsurface structure of Sakurajima and Kirishima volocanoes, we investigate seismic velocity discontinuities beneath these regions by receiver function analyses of the teleseismic waveform.

A Receiver function (RF) is calculated by deconvolving the vertical component of a waveform of a teleseismic P-wave from its horizontal component, and phases converted at seismic velocity discontinuities in its coda can be detected with RFs [Langston, 1979, JGR]. In order to estimate the geometry of steeply dipping discontinuities, such as the upper boundary of the subducting Philippine Sea plate, with RFs, refraction of the seismic rays at the dipping discontinuities should be taken into account. For this purpose, we apply the method for stacking RFs using the multi-stage fast marching method developed by Abe et al. [2011, GJI].

Abe et al. [2013, JGR] revealed the regional variation of S wave velocity discontinuity across the Philippine Sea plate, which is divided by the Kyushu - Palau Ridge, from RF analyses of the waveform data obtained at the permanent stations. In this research, we use waveform data obtained at dense observation networks along Miyazaki-Akune and Miyazaki-Sakurajima lines from teleseismic earthquakes with magnitude greater than 5.5 occurred from November 2009 to March 2017. We use 3-D seismic velocity model [Matsubara et al. 2007, Tectonophysics] for stacking RFS, although Abe et al. [2013] used one dimensional IASP91 model.

Beneath the south Kyushu where the Western Philippine Basin formed at about 50 Ma subducts [Hilde and Lee, 1984, Tectonophysics], it is suggested that the fluid dehydrated from the Philippine Sea slab is transported to the back-arc and may cause arc volcanism activity by Abe et al. [2013]. In addition, low velocity zone of mantle wedge is detected, and this zone is considered to correspond to a serpentinized mantle by a fluid derived from oceanic crust [Bostock et al. 2002, Nature], based on the S wave velocity of serpentinite estimated by Hacker et al. [2003, JGR] and Christensen [2004, Int Geol Rev].

We obtain more precise receiver function images using dense network data and discuss the seisimic structure of Sakurajima and Kirishima volcanoes.

Keywords: Receiver function analyses, Southern Kyushu, Philippine Sea slab

©2019. Japan Geoscience Union. All Right Reserved. 

# Imaging subduction structure beneath the eastern part of Kii Peninsula, SW Japan, using an earthquake reflection method

*Eiji Kurashimo[1], Takashi Iidaka[1], Noriko Tsumura[2], Takaya Iwasaki[1]

1. Earthquake Research Institute, the University of Tokyo, 2. Chiba University

The Nankai trough region, where the Philippine Sea Plate (PHS) subducts beneath SW Japan arc, is a well-known seismogenic zone of interplate earthquakes. The most recent great earthquakes occurred in 1944 (Tonankai Earthquake, M=7.9) and 1946 (Nankai Earthquake, M=8.0). In recent years, various slip motions with a different time scale have been recognized at or near the updip and downdip limits of seismogenic zone [e.g., Obara, 2002; Ito and Obara, 2006]. Revealing structural factors that control the fault slip behavior is important to understand the earthquake rupture dynamics. Seismic reflection characteristics and seismic velocity variations can provide important information on the heterogeneous structure around plate interface. Recent seismic experiments reveal the relation between the crustal structure and the fault slip behavior. However, little is known about the deeper part of the plate boundary, especially the down-dip side of the seismogenic zone. In 2015, seismic array observation was conducted to obtain the subduction structure beneath the eastern part of the Kii Peninsula [Kurashimo et al., 2016]. Ninety 3-component portable seismographs were installed on a 90-km-long line nearly parallel to the direction of the subduction of the PHS. Waveforms were continuously recorded during a six-month period. During the seismic array observation, Japan Meteorological Agency determined 45 events within 10 km of our survey line. Prominent late arrivals, probably reflected waves from the deeper part of the crust can be recognized on the record sections. Earthquake data is useful to obtain a deep image. So, in order to clarify the spatial distribution of the reflectors, we applied the reflection method to the earthquake data. We used horizontal-component seismograms, because high amplitude S-wave reflection can be recognized on the record sections. Conventional common mid-point processing cannot be applied to earthquake data because the reflection point does not lie at the mid-point between source and receiver, so, we applied the Common Reflection Point (CRP) transformation [e.g., Quiros et al., 2016] to the earthquake data set using a tomography-derived 3D S-wave velocity model [Kurashimo et al., 2016]. Reflection points and their relevant travel-time from earthquake to receiver were calculated using a 3D finite difference travel-time algorithm [Hole and Zelt, 1995]. Before applying the CRP transformation, the waveform data were filtered by a band-pass filter (1 -8 Hz). After applying the CRP transformation and the stacking process, we applied a post-stack migration technique. The migrated shear wave reflection image shows that the northward dipping reflective zone interpreted to be the upper boundary of the PHS can be recognized at a depth range of about 25 -30 km. The top of the low-frequency earthquakes (LFEs) occurrence zone well corresponds to the high amplitude S-wave reflective zone. LFEs are also located in and around the low Vp and high Vp/Vs zone [Kurashimo et al., 2016]. These results suggest the occurrence of the LFEs may be associated with fluids.

Keywords: Philippine Sea plate, earthquake reflection method, Low-frequency earthquake

©2019. Japan Geoscience Union. All Right Reserved. 

# Tomography of Mejillones Peninsula using cross-correlation of ambient seismic noise

*Kellen Azua Quezada[1], Sergio Ruiz[1], Francisco Pasten-Araya[2,3], José Salomón[4], Pablo Salazar[2,3], Miguel Saez[1], César Pastén[4], Felipe Leyton[5], Wasja Bloch[6]

1. DGF, UChile, 2. DG, UCN, 3. CIGIDEN, 4. DIC, UChile, 5. CSN, Chile, 6. GFZ

The Mejillones Peninsula (MP) is locate in northern Chile (-23.28º, -70.5º). MP is a geomorphic atypical uplifted block of the coastal platform of 100 km length. This structure has been proposed as a segment boundary for large subduction earthquakes, as the case of Mw 8.0 Antofagasta (1995) and Mw 7.7 Tocopilla (2007) events. Additionally, the Peninsula presents a wide and deep layer of sediments that could enhance site effects. For this reason, in this work we study the shallow structure of MP basin. We deployed a dense temporary seismic network in the MP, which registered in continuous time from July 2013 to September 2015. From the continuous records, we built a local tomography using the spectral ambient seismic noise. We use vertical component of seismograms to obtain the Green function from cross-correlation between station pairs. The frequency domain method allows determine of phase velocity relating the zero-crossing of the real part of cross-correlation spectrum with the zero crossing of the zero-order Bessel function of the first order. The Rayleigh wave phase velocities are inverted by means of a non-linear iterative 2-D tomographic technique; finally we recover phase velocity maps at different frequencies. The tomographic maps present significant features that correlate with surface geology. We found in the West part of the MP lower velocities that East zone. We can associate this with fractured metamorphic rock. Higher velocities in the Eastern part of the peninsula are associated with the presence of intrusive rocks. The difference in velocity of these two anomalies is maintained at differents depth.

Keywords: Tomography, Ambient Seismic Noise

©2019. Japan Geoscience Union. All Right Reserved. 

# Crustal thickness beneath Central Indonesia by the cross-correlation analysis of seismic ambient noise (2)

*Masyitha Retno Budiati[1], Genti Toyokuni[1], Tomomi Okada[1], Toru Matsuzawa[1]

1. Graduate School of Science, Geophysics Department, Tohoku University

Central Indonesia has complex tectonic structures where is characterized by several subduction zones at northern and eastern part and also active faults (e.g., Palu Koro, Matano and Hamilton faults). These complexities affect crustal structures around the region. In this study, we estimated spatial variation of crustal thickness and their relation with active tectonics. We used waveform data recorded at 10 BMKG broadband stations around Sulawesi Island. Firstly, the continuous data were divided into 20 minutes segments with time shift in every 5 minutes. Once the pre-processing steps for each segment were done, we calculated the CCFs between two contemporaneous segments from two stations and stacked the daily-averaged CCFs over 5 months. We further compressed the two-sided signal into one-sided signal by taking the average of positive and negative lag part of the CCFs in order to stabilize the dispersion curves of group velocities. To fit the synthetic and the observed group velocities, we adjusted the two layers crustal velocity model from CRUST 1.0 (Laske et al., 2013) corresponding to the observation group velocities. The velocity model that is faster than the observation was subtracted 5% and 10% to find the best crustal thickness with minimum RMS between observations and synthetics at period of 20s –30s. To confirm our procedure above, we currently apply the similar procedure to estimate the well-known Moho discontinuity in Tohoku region, Japan. We collected 5 months continuous waveform data from vertical components of 10 F-net stations around Tohoku region. The results showed that the slower velocity models makes the crustal thickness shallower. The estimated depth of Moho discontinuity beneath Tohoku region is about 20km –30km using subtracted velocity models. This is almost consistent with previous studies (e.g. Zhao et al., 1990). While the estimated depth of Moho discontinuity at eastern part of Central Indonesia is about 27km –35km which is related to the ocean crust, Batui and Sula thrust and at the continent of Sulawesi Island the estimated depth of Moho is about 35km –45km.

Keywords: Central Indonesia, Tohoku Region, Crustal structure

©2019. Japan Geoscience Union. All Right Reserved. 

# Subsurface structure below the southernmost area of South Japanese Alps estimated by seismic interferometry imaging

*Toshiki Watanabe[1], Hasegawa Daima[1], Tanio Ito[2], Ken'ichi Kano[3], Susumu Abe[4], Akira Fujiwara[5], Yoshinori Kouchi[6]

1. Graduate School of Environmental Studies, Nagoya University, 2. Association for the Development of Earthquake Prediction, 3. Shizuoka Univertity, 4. JAPEX, Co. Ltd., 5. JOGMEC, 6. Geosys, Inc.

In the Tokai area, seismological events, such as low frequency events and slow slip events as well as large earthquakes, are occurred caused by subduction of the Philippine Sea (PHS) plate. The eastern Tokai area is a transition zone from the collision zone of Izu arc to the subduction area. To understand the subsurface structure in this area and fill the gap between the previous seismic surveys, a seismic observation using a dense seismic linear array composed of 34 receivers was conducted in 2013.
In this study, we applied seismic interferometry imaging to the seismic records of the array observation. Seismic interferometry can retrieve the reflection response between two receivers as if one receiver is a virtual shot and the other is a receiver by calculating the cross-correlation of the transmission responses recorded at the two receivers. For a single receiver, the reflection response recorded at the receiver from a source at the same location is retrieved by calculating the autocorrelation of the transmission response recorded at the receiver. In this study, we used regional deep earthquakes occurred in the Pacific Oceanic slab as the seismic sources to image the PHS plate and crustal structures. We conducted autocorrelation analysis and created reflection profiles for both P- and S-waves. We projected the cross-correlation between two adjacent stations to their mid-point to improve the spatial density of the stations. After migration using the velocity structure obtained by the tomography analysis, we obtained the P- and S-wave reflection depth profiles.
In the S-wave depth profile, the shallower area above 25 km shows reflective, while the deeper area is less reflective. The boundary becomes shallower to the north-east of the profile. By comparing this profile with the result of other seismic surveys and with pre-existing plate models, we interpreted that the strong reflectors shown at the depth about 25 km in the southwest of this profile are the plate boundary. This interpretation is consistent with the result of Hirose et al. (2008) showing that the basaltic oceanic crust of the PHS plate shows low Vs and high Vp/Vs. In the eastern half of the profile lacks reflectors that correspond to the plate boundary. This may be attributed to a weak contrast of physical properties between the felsic island arc crust proposed by Kodaira et al. (2004) and the Japanese island arc crust, or complicated geological structure due to the collision of Izu arc.

Keywords: seismic array observation, seismic interferometry, reflection depth profile, plate boundary

©2019. Japan Geoscience Union. All Right Reserved. 

# Strong variations of near-surface seismic anisotropy of Taiwan revealed by coda interferometry

*Hsin-Yu Lee[1], Yuancheng Gung[1], Li-Wei Chen[2], Ling-Yun Chiao[3]

1. Department of Geosciences, National Taiwan University, Taiwan, 2. Department of Earth and Planetary Science, University of California at Berkeley, CA, USA, 3. Institute of Oceanography, National Taiwan University, Taiwan

We report the near-surface (<500 m) seismic structure, Vs, Vp and Vs anisotropy, of Taiwan using the empirical Green’ s function of body waves extracted by applying coda interferometry to the vertical station pairs at 56 borehole sites. We find clear characteristic cos2θ dependence of Vs in all the determinations of Vs azimuthal anisotropy. Because the borehole sites are located at very diverse geological structures of Taiwan, we are able to notice the following interesting features about the near-surface Vs anisotropy: (1) The patterns of the observed anisotropy fall into two categories, OPA (Orogeny-Parallel Anisotropy) and SAA (Stress-Aligned Anisotropy), and both types of anisotropy fit well the local geological fabrics and/or the ambient stress. (2) About half of the amplitudes of anisotropy are larger than 10 %. The site with the largest amplitude of anisotropy (34%) is located in the slate belt of the Central Ranges, while the sites with weak anisotropy (~1%) are associated with low Vs and/or small strain rate. (3) The amplitudes of OPA are generally stronger than SAA, and the types of anisotropy are closely related to the Poisson’ s ratios at the borehole sites. (4) The strong variations of the OPA amplitudes can be explained by the rock types in the well body with the metamorphic rocks carrying stronger anisotropy than the sedimentary rocks. (5) The strong near-surface anisotropy also implies that delay times contributed by the shallow crust might have been underestimated in studies of shear-wave splitting measurements using the direct arrivals of earthquakes waves.

Keywords: coda interferometry, near-surface seismic anisotropy, Taiwan

©2019. Japan Geoscience Union. All Right Reserved. 

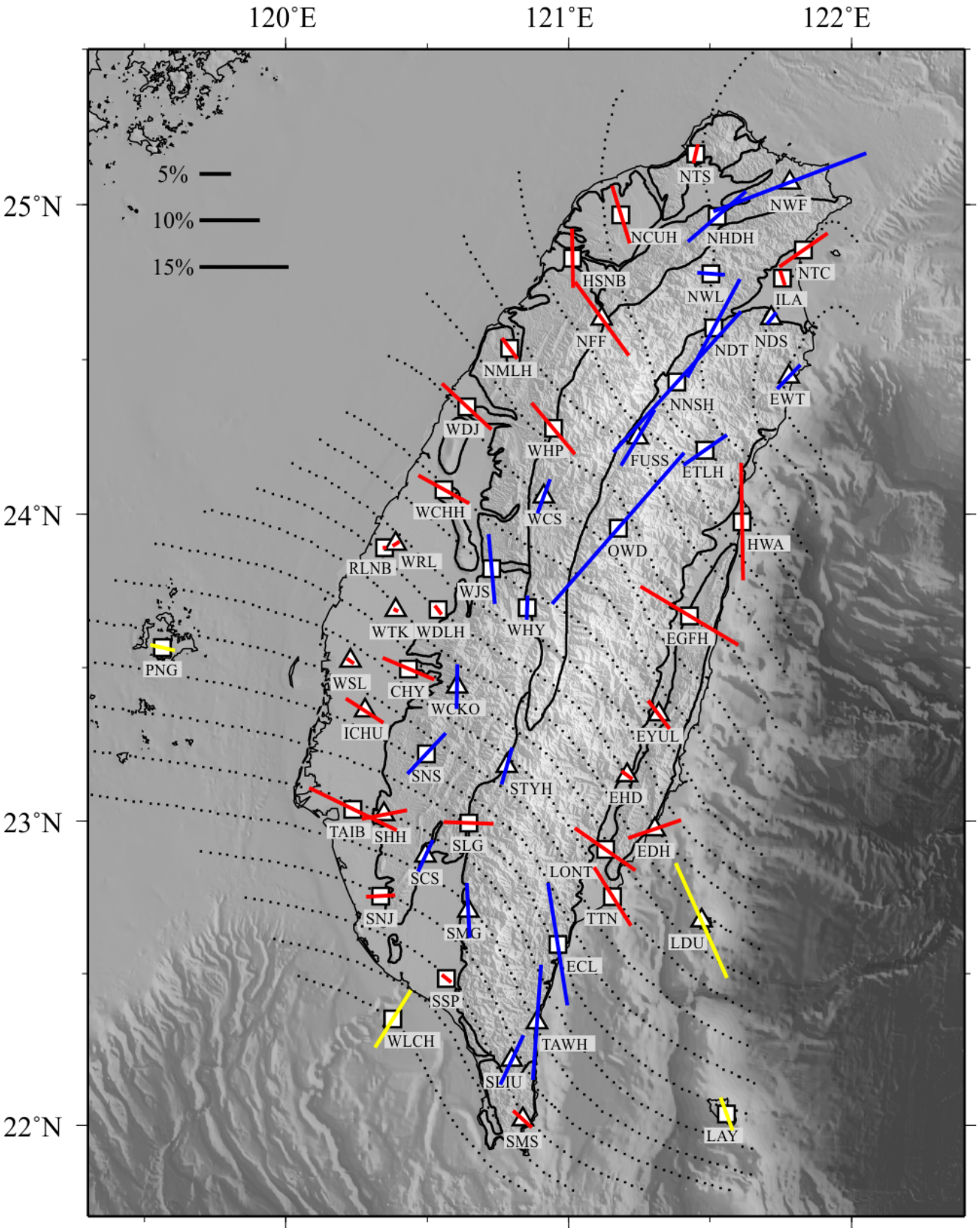


©2019. Japan Geoscience Union. All Right Reserved. 

# Investigating anomalous crustal structures along the convergent zone in eastern Taiwan with the new airborne magnetic survey and updated seismic tomographic models

*Chi-Hsuan Chen[1], Hsin-Hua Huang[2], Lun-Tao Tong[3], Wayne Lin[3], Po-Tsun Lee[1], Shou-Fang Chang[1], Jin-Fa Lee[1]

1. Cntrl. Geo. Surv., MOEA, Taiwan, 2. Inst. Earth. Sc., Acad. Sinica, Taiwan , 3. Industr. Technol. Res. Inst., Taiwan

The convergence between Eurasian plate and Philippine sea plate produces the tectonically and geodynamically complex regions of Taiwan. The orogeny has been suggested as from ancient oceanic-oceanic plate subduction transforming to the continental-oceanic plate collision as the proceeding of the accreted volcanic arcs. The major suture of the plate boundary in eastern Taiwan, the Longitudinal Valley, contributes most of the seismic activities and absorbed about half of the plate convergence. How the shortening and disappearance of the oceanic plate provoked multidisciplinary researches in discussing the kinematics and the related earthquake structures.

Local seismic tomography is a useful technique for unraveling the subsurface structures. The Taiwan seismic tomographic studies that are advanced by large projects or by integrating multiple data sets have been proposed in recent years. Furthermore, since 2012 the seismic signal digitization of the Central Weather Bureau (CWB) seismic network was upgraded from 12 to 24 bit, and the potential timing issue of telemetry delays has been eliminated with onsite GPS time system. Additionally, the new airborne magnetic survey has been carried out in eastern Taiwan by the Central Geological Survey (CGS) and the Industrial Technology Research Institute (ITRI) recently. High magnetic anomalies were detected not only in the volcanic arc but also in the eastern Central Range along the north-south trending Longitudinal Valley. These observations motivate us to revisit the subsurface structures with updated seismic tomographic models using new CWB data sets from 2012 to 2015.

The iso-velocity contours of the updated model keep similar structures with the previous model at first order but furtherly reveal more details. A continuous high-Vp and high-Vp/Vs bulge which extends to the shallow depths of the eastern Central Range has been interpreted as a high-pressure rock exhumation along the subduction of South China sea plate or an obducted Luzon forearc sliver. On the other hand, the new airborne magnetic survey reveals two individual high magnetic stripes that share the same high magnetic characteristics with the oceanic crust. However, the magnetization vectors behave oppositely in the direction at both flanks of the Longitudinal Valley. Such findings of these integrated geophysical analyses enable us to discuss the anomalous crustal structures and their tectonic implications.

Keywords: Airborne magnetic Survey, Seismic tomography, Forearc obduction, Exhumation, Oceanic crust

©2019. Japan Geoscience Union. All Right Reserved. 

[J] Poster | S (Solid Earth Sciences)：S-SS Seismology

Thu. May 30, 2019 5:15 PM - 6:30 PM JST | Thu. May 30, 2019 8:15 AM - 9:30 AM UTC | Poster Hall International Exhibition Hall8, Makuhari Messe_20

## [S-SS12] Crustal Structure

convener:Kazuo Nakahigashi(Tokyo University of Marine Science and Technology)

The aim of this session is to cover seismological and geophysical studies on the Earth's crust. Contribution on seismological and geophysical structure of the crust, processes that develop in the crust which include earthquakes, volcanoes and geological descriptions of the crust are welcomed. We also welcome theoretical and methodological studies that will serve as basics in such explorations.

[SSS12-P01] Regional difference in long period surface wave phase velocity by an explosive phenomenon generated in North Korea on September 3, 2017

*Koji Yamada[1] (1.Hanshin Consultants co., ltd.)

[SSS12-P02] Phase velocity estimation based on spatial gradient of surface wave arrival time of teleseismic earthquakes observed by S-net

*Akira Ishigami[1], Ryota Takagi[1] (1.Research Center for Prediction of Earthquakes and Volcanic Eruptions, Graduate School of Science)

[SSS12-P03] Crustal seismic velocity structure in the Japanese Islands from receiver function analysis using similar earthquakes

*Toshihiro Igarashi[1] (1.Earthquake Research Institute, University of Tokyo)

[SSS12-P04] **Estimation of the Crustal Structure beneath the Broadband Seismic Network in the Eskisehir Region, Turkey, by Using Receiver Function Method**

*Pinar Duran[1], Asim Oguz Ozel[1], Hiroaki Yamanaka[2] (1.ISTANBUL UNIVERSITY-CERRAHPASA, 2.TOKYO INSTITUTE OF TECHNOLOGY)

[SSS12-P05] Three-dimensional S-wave attenuation structure in and around Hokkaido, Japan

*Ryoichi Nakamura[1], Takahiro Shiina[1] (1.Earthquake Research Institute, The University of Tokyo)

[SSS12-P06] Reexamination for the subsurface structure beneath the southern part of the Hidaka
Collision Zone, Hokkaido, Japan by using a numerical test of wave propagation

*Masahiro Shimazaki[1], Noriko Tsumura[2] (1.Graduate School of Science and Engineering, Chiba University, 2.Graduate School of Science, Chiba University)

[SSS12-P07] High resolution seismic surveys in the Kuril trench off Hokkaido

*Yasuyuki Nakamura[1], Shuichi Kodaira[1], Mikiya Yamashita[1], Seiichi Miura[1], Gou Fujie[1] (1.Japan Agency for Marine Earth Science and Technology)

[SSS12-P08] Subsurface Structure at the North of the Yokosuka Fault by Seismic Reflection Survey

*Shinobu Ito[1] (1.Geological Survey of Japan, AIST)

[SSS12-P09] **Crust and Uppermost mantle P-wave velocity structure of the Ordos block and its neighbors based on travel time tomography**

*Yaning Liu[1], Jianping Wu[1], Shuxian Bao[1], Xiaohong Meng[2] (1.Institute of Geophysics, China Earthquake Administration, 2.China University of Geosciences (Beijing))

[SSS12-P10] Seismic imaging of the 2016 Kumamoto earthquake area using P and PmP data

*Dapeng Zhao[1], Haibo Wang[2], Zhouchuan Huang[2], Mingjie Xu[2], Liangshu Wang[2] (1.Department of Geophysics, Tohoku University, 2.School of Earth Sciences and Engineering, Nanjing University)

[SSS12-P11] Estimation of 3D velocity structure in Kyushu region by the seismic tomography

*Toya Mitsuhiro[1], Koji Yamada[1] (1.Hanshin Consultants Co., Ltd.)

[SSS12-P12] Estimation of the structure of the Philippine Sea slab under south Kyushu using receiver function analysis

*Masaki Uchida[1], Takahiro Ohkura[1], Takuo Shibutani[1], Yuki Abe[2], Shintaro Komatsu[1], Ken'ichi Yamazaki[1], Yusuke Yamashita[1], Shin Yoshikawa[1], Masato Iguchi[1], Takeshi Tameguri[1], Tadaomi Sonoda[1] (1.Kyoto Univ., 2.Hot Springs Research Institute)

[SSS12-P13] Imaging subduction structure beneath the eastern part of Kii Peninsula, SW Japan, using an earthquake reflection method

*Eiji Kurashimo[1], Takashi Iidaka[1], Noriko Tsumura[2], Takaya Iwasaki[1] (1.Earthquake Research Institute, the University of Tokyo, 2.Chiba University)

[SSS12-P14] **Tomography of Mejillones Peninsula using cross-correlation of ambient seismic noise**

*Kellen Azua Quezada[1], Sergio Ruiz[1], Francisco Pasten-Araya[2,3], José Salomón[4], Pablo Salazar[2,3], Miguel Saez[1], César Pastén[4], Felipe Leyton[5], Wasja Bloch[6] (1.DGF, UChile, 2.DG, UCN, 3.CIGIDEN, 4.DIC, UChile, 5.CSN, Chile, 6.GFZ)

[SSS12-P15] **Crustal thickness beneath Central Indonesia by the cross-correlation analysis of seismic ambient noise (2)**

*Masyitha Retno Budiati[1], Genti Toyokuni[1], Tomomi Okada[1], Toru Matsuzawa[1] (1.Graduate School of Science, Geophysics Department, Tohoku University)

[SSS12-P16] Subsurface structure below the southernmost area of South Japanese Alps estimated by seismic interferometry imaging

*Toshiki Watanabe[1], Hasegawa Daima[1], Tanio Ito[2], Ken'ichi Kano[3], Susumu Abe[4], Akira Fujiwara[5], Yoshinori Kouchi[6] (1.Graduate School of Environmental Studies, Nagoya University, 2.Association for the Development of Earthquake Prediction, 3.Shizuoka Univertity, 4.JAPEX, Co. Ltd., 5.JOGMEC, 6.Geosys, Inc.)

[SSS12-P17] Strong variations of near-surface seismic anisotropy of Taiwan revealed by coda interferometry

*Hsin-Yu Lee[1], Yuancheng Gung[1], Li-Wei Chen[2], Ling-Yun Chiao[3] (1.Department of Geosciences, National Taiwan University, Taiwan, 2.Department of Earth and Planetary Science, University of California at Berkeley, CA, USA, 3.Institute of Oceanography, National Taiwan University, Taiwan)

[SSS12-P18] Investigating anomalous crustal structures along the convergent zone in eastern Taiwan with the new airborne magnetic survey and updated seismic tomographic models

*Chi-Hsuan Chen[1], Hsin-Hua Huang[2], Lun-Tao Tong[3], Wayne Lin[3], Po-Tsun Lee[1], Shou-Fang Chang[1], Jin-Fa Lee[1] (1.Cntrl. Geo. Surv., MOEA, Taiwan, 2.Inst. Earth. Sc., Acad. Sinica, Taiwan , 3.Industr. Technol. Res. Inst., Taiwan)

# Regional difference in long period surface wave phase velocity by an explosive phenomenon generated in North Korea on September 3, 2017

*Koji Yamada[1]

1. Hanshin Consultants co., ltd.

An explosive phenomenon to assume the Democratic People's Republic of Korea cause at past 12:30 of September 3, 2017 was observed in each place. The position of the seismic center is considered to be 41.3 degrees N, 129.1 degrees E, 0 kilometers in depth by Japan Meteorological Agency and almost assumes surface of the earth neighborhood cause. Because it is an explosive phenomenon generated in an earth surface, Rayleigh wave is observed other than P wave, and can considered the observed wave mortion to be an observation record of huge size surface wave exploration.

The observed Rayleigh wave shows strong dispersibility at around 0.03-0.1Hz. After performing MASW (Multichannel Analysis of Surface Wave) for the Kinki districts where P-wave velocity structure is estimated using data of the large blast observation, the provided phase velocity almost matching with the one dimension S-wave velocity structure that I set in reference to Hirose& Ito (2006). Yamada(2018) thought that the observed phase velocity dependend on velocity structure to the Moho.

Because after doing MASW at a suitable angle based on the direction from the seismic center about each domestic area, a local difference was seen in provided phase velocity, I report it.

Acknownledgement:

In this study, I used the observation record of broadband Seismograph network (F-net), high sensitivity seismograph network (Hi-net) by NIED, each national university, and Japan Meteorological Agency.

Keywords: Explosive phenomenon generated in North Korea, Long period surface wave, Homo, Multichannel Analysis of Surface Wave

©2019. Japan Geoscience Union. All Right Reserved. 

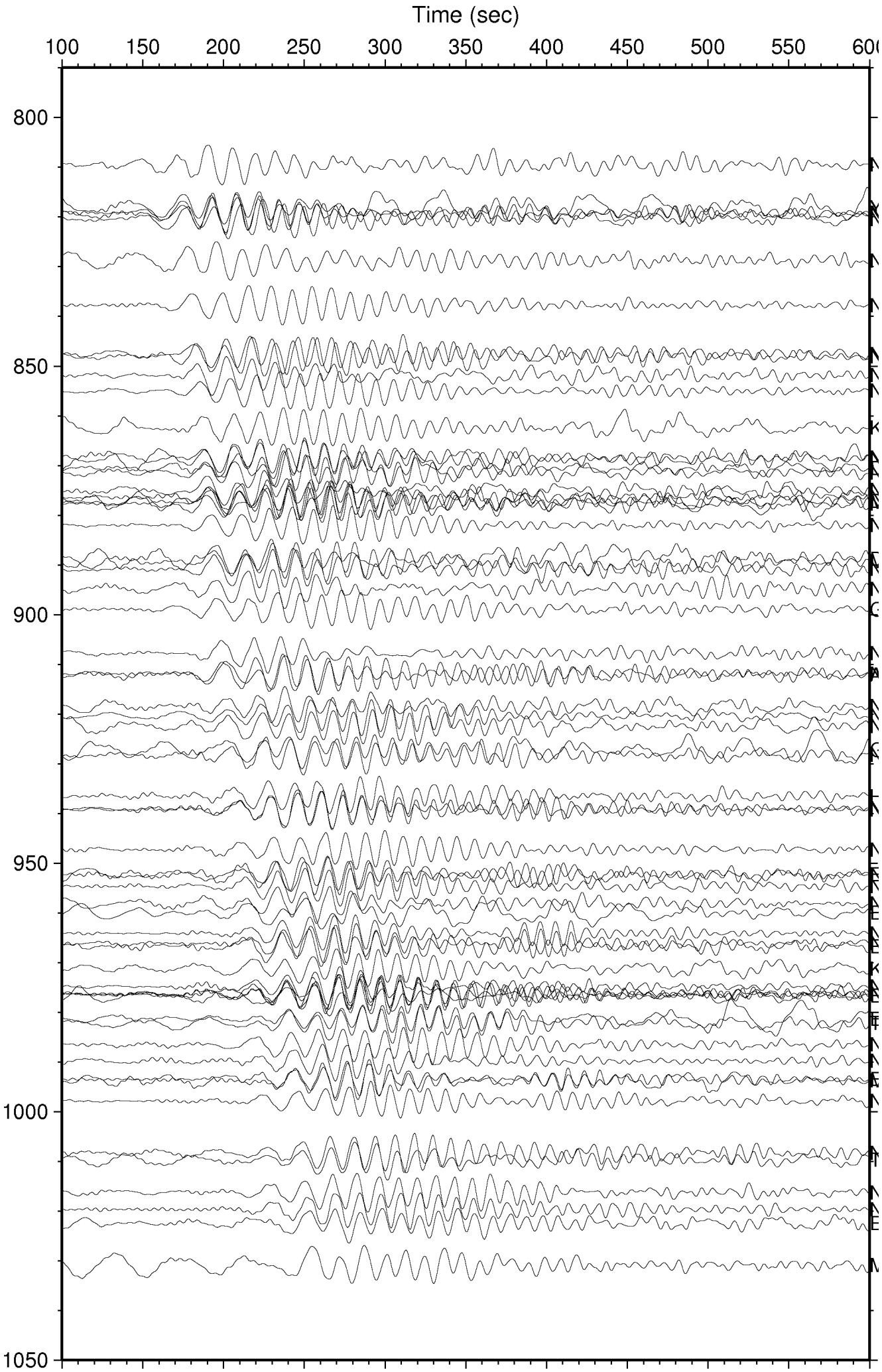


©2019. Japan Geoscience Union. All Right Reserved.

©2019. Japan Geoscience Union. All Right Reserved. 

# Phase velocity estimation based on spatial gradient of surface wave arrival time of teleseismic earthquakes observed by S-net

*Akira Ishigami[1], Ryota Takagi[1]

1. Research Center for Prediction of Earthquakes and Volcanic Eruptions, Graduate School of Science

Seismice velocity structure is fundamental information to understand environmental cause of earthquakes and slip behavior on the plate interface. In addition, recent developments of dense seismic network enable us to catch seismic waveforms as seismic wavefield. In the present study, we use S-net data to estimate phase velocity map by calculating spatial gradient of surface wave arrival time of teleseismic earthquakes.

We used long-period accelerometer records of teleseismic earthquakes. We analyzed a teleseismic earthquake occurred in Alaska Bay on January 23, 2018 (depth: 25km, Mw 7.9). We used vertical records to estimate Rayleigh wave phase velocity after converting observed records from XYZ to UNE components. To estimate phase velocity map, we followed Lin et al. (2009). We first applied frequency-time analysis (FTAN) to waveform data of each station to get phase velocity dispersion curve. We then picked surface wave arrival times at certain period and spatially interpolated to get arrival time map. Finally, we obtained phase velocity map by calculating spatial gradient of the arrival time map. We estimated phase velocity maps at 20-50 s by intervals of 5 s.

When we estimate the phase velocity curve, there is the $2\pi$ phase ambiguity. Although a reference phase velocity curve allows us to estimate the number of cycles, the discrepancy from the real phase velocity curve and the initial phase effect causes misestimation of the cycle number. Thus, we solved this problem by iteratively update the reference dispersion curve. First, we used PREM 1D model to estimate dispersion curve at each station. In the next step, we used average of the estimated dispersion curves as the reference model. We repeated the procedure until we can obtain a consistent cycle number within the all S-net stations.

The phase velocity is estimated within 3.6-3.9 km and consistent with general phase velocity of Rayleigh wave. We found high velocity anomaly which may be attributed to the subducting slab at the period of 45 s. We also found high velocity anomaly off Miyagi and Fukushima.

To confirm the spatial pattern of the phase velocity, we need to analyze other teleseismic events. We can also estimate azimuthal anisotropy of phase velocity by using several earthquakes of which surface waves propagate in different direction. In addition, we need to examine the method of spatial interpolation for robust estimation of phase velocity map.

Keywords: S-net, surface wave, tomography, Tohoku-oki earthquake, phase velocity

©2019. Japan Geoscience Union. All Right Reserved. 

# Crustal seismic velocity structure in the Japanese Islands from receiver function analysis using similar earthquakes

*Toshihiro Igarashi[1]

1. Earthquake Research Institute, University of Tokyo

The stress and strain changes due to the recurrence process on the inter-plate great earthquakes of the subducting plate should have a significant effect on shallow inland seismicity and velocity structure in the overriding plate. In this study, we applied receiver function analysis using similar earthquakes, which repeatedly occurred at almost the same location, to investigate the spatiotemporal change of the crustal seismic velocity structure beneath the Japanese Islands. Similar earthquakes used as data were extracted from the seismograms of medium-sized earthquakes, which observed in the seismic network of Japan and occurred in the epicentral distances between 30 degrees and 90 degrees in the periods from September 1989 to February 2016. We estimated temporal changes of crustal seismic velocity structure by receiver function analysis from the selection of pairs of similar earthquakes occurred before and after the 2011 Tohoku-Oki earthquake (M9.0). In this analysis, we assumed that the depths of the Moho discontinuity, which estimated using all available data for the above period, do not change within the analysis period. As a result, we detected areas of decreased crustal velocity to the west of the source region of the Tohoku-Oki earthquake. We suggest that the stress change by a great inter-plate earthquake affected the velocity reduction or velocity polarization. On the other hand, the crustal velocity increased to the north of the source region. This change may be caused by the effect of the postseismic deformation after the 2003 Tokachi-Oki earthquake (M8.0). However, it is difficult to specify the accurate timing of the change because of long-term data stack. The impact of the great earthquakes has been widespread for a long time. The further studies of the seismic velocity structure in arbitrary period will clarify the cause of changes.

©2019. Japan Geoscience Union. All Right Reserved. 

# Estimation of the Crustal Structure beneath the Broadband Seismic Network in the Eskisehir Region, Turkey, by Using Receiver Function Method

*Pinar Duran[1], Asim Oguz Ozel[1], Hiroaki Yamanaka[2]

1. ISTANBUL UNIVERSITY-CERRAHPASA, 2. TOKYO INSTITUTE OF TECHNOLOGY

Receiver function imaging is an important tool for the investigation of the crust and upper mantle structure. The P to S conversion (Ps) from the Moho is typically one of the most prominent phase on the P-wave receiver funtions. The time delay between the Ps converted phase and direct P wave is sensitive to the depth of the velocity discontinuities, and the average S wave velocity above it. Estimates of the depth and thickness of the Moho and $V_P$ /$V_S$ ratio of the crust are important goals of many receiver funtion investigations. In the frame of the Turkey-Japan joint project, we attempt to determine S-wave velocity structure of the crust beneath Eskisehir Region, described by various tectonic settings. The teleseismic events are recorded by broadband three-component seismic stations of ANA-NET Seismic Network, which is operated by the Eskisehir Anadolu University since 2010. The seismograms from these events, whose epicenters lay at distances greater than 30$^o$, were deconvolved in the time domain to remove the unwanted noise and then stacked to obtain better receiver functions. This information will be used to establish a linear relationship between thickness and $V_P$ /$V_S$ ratio, each of which is stacked for a given station to identify a best-fit estimate for depth to the Moho and Vp/Vs ratio. To determine their accuracy, these results will be compared with other geophysical studies performed in the region, 1-D crustal models will be presented at the conference. This study is supported by the Joint Research Project under the Bilateral Program of the Japan Society for the Promotion of Science (JSPS) and The Scientific and Technological Research Council of Turkey (TUBITAK) under Grant TUBITAK 116Y524.

Keywords: Receiver Function Analysis, Crustal structure, P-receiver functions, Waveform inversion, Eskisehir Fault Zone

©2019. Japan Geoscience Union. All Right Reserved. 

# Three-dimensional S-wave attenuation structure in and around Hokkaido, Japan

*Ryoichi Nakamura[1], Takahiro Shiina[1]

1. Earthquake Research Institute, The University of Tokyo

## 1. Introduction

At Hokkaido, Japan, the collision between the Kuril and the NE Japan arcs occur (e.g., Kimura, 1994, JGR), and thus complicated crustal structure would be developed. According to Kita et al. (2012), the arc-crust is subducted by the collision and reaches deep up to near the upper part of the mantle. Additionally, the 2018 Eastern Iburi Earthquake (M6.7, depth 37 km) and its aftershocks occurred at considerably deep as a crustal earthquake. This activity at the deep crust is thought to link to the complicated geologic structure in Hokkaido.

Several detailed tomographic studies of seismic velocity and Qp structures have been done in this region (e.g., Kita et al., 2014, JGR; Shiina et al., 2018, JGR). These studies showed low Qp, low Vp, low Vs, and high Vp/Vs at a depth of 10 km in the west side of the Hidaka mountain range and that these anomalous structures distribute to the depth of 50 km which comparable to the upper surface of the subducting Pacific plate. On the other hand, the Qs structure in this area has not been well investigated. Therefore, in this study, we estimate the detailed Qs structure of Hokkaido by using the 3D spectrum inversion method.

## 2. Method and Data

In this study, we adopt the 3D spectral inversion method (Nakamura and Uetake, 2002) to strong motion records observed around the Hokkaido. In the method, we estimate source spectrums, site factors, and Qs value of each block. The study area is 138 ˚- 148 ˚E and 39 ˚- 46 ˚N, and is discretized by blocks of which size is 0.1 ˚in latitude and longitude and 10 km in depth direction.

The strong motion records are collected from on the K-net and the KiK-net stations deployed near the surface. Periods collecting the records are to Nov. 2019 from operation beginnings of each station. The magnitude of earthquakes is 4.0 - 7.5. We limit stations by epicentral distances: < 100 km and < 500 km for earthquakes occurred at depths of 0-30 km and 30-200 km, respectively. Moreover, we exclude strong motion records with 100 Gal or stronger to reduce influences of ground nonlinearity effects as possible. Fourier spectrum amplitudes are computed from the strong motion records of NS component at 1-10 Hz with every 1 Hz.

## 3. Results

We show the estimated Qs structure in and around the Hokkaido obtained at 10 Hz in Figure 1. In this study, we examine the CKB resolution test and, in Figure 1, we display only the results where the assumed structures are well recovered in the resolution test. The obtained Qs structure reveal the high-attenuation (low-Qs) zones beneath the volcanoes at depths of 30-40 km and the Pacific slab with low-attenuation (high-Qs), as well as tomographic images in Tohoku district (e.g., Nakamura and Uetake, 2004; Liu et al., 2014).

©2019. Japan Geoscience Union. All Right Reserved. 

At the west side of the Hidaka mountain range, the remarkable high-attenuation zone is estimated at depths of 0-20 km and there seem to continuously distribute by about 40 km. This high-attenuation anomaly is consistent with that estimated in Qp (Kita et al., 2014). Additionally, the belt-like distribution of low-attenuation area along the Hidaka mountain range can be revealed in this study. These structures would represent heterogeneity resulted from the collision between Kuril and NE Japan arcs.
Around the source area of the 2018 Hokkaido Eastern Iburi Earthquake, high S-wave attenuation is imaged. The high-attenuation zone is extended from near the Hidaka mountain range (the result at 30-40 km in Figure 1) and the contrast of between high- and low-attenuation property clearly identified along the north-south direction. This is comparable to distributions of aftershocks of the Eastern Iburi earthquake. Therefore, we consider that the heterogeneous structures which are developed in the collision zone would closely link to the occurrence of the Eastern Iburi earthquake and its aftershocks.

Keywords: Hokkaido, Collision zone, S wave attenuation structure, the 2018 Eastern Iburi Earthquake

©2019. Japan Geoscience Union. All Right Reserved. 

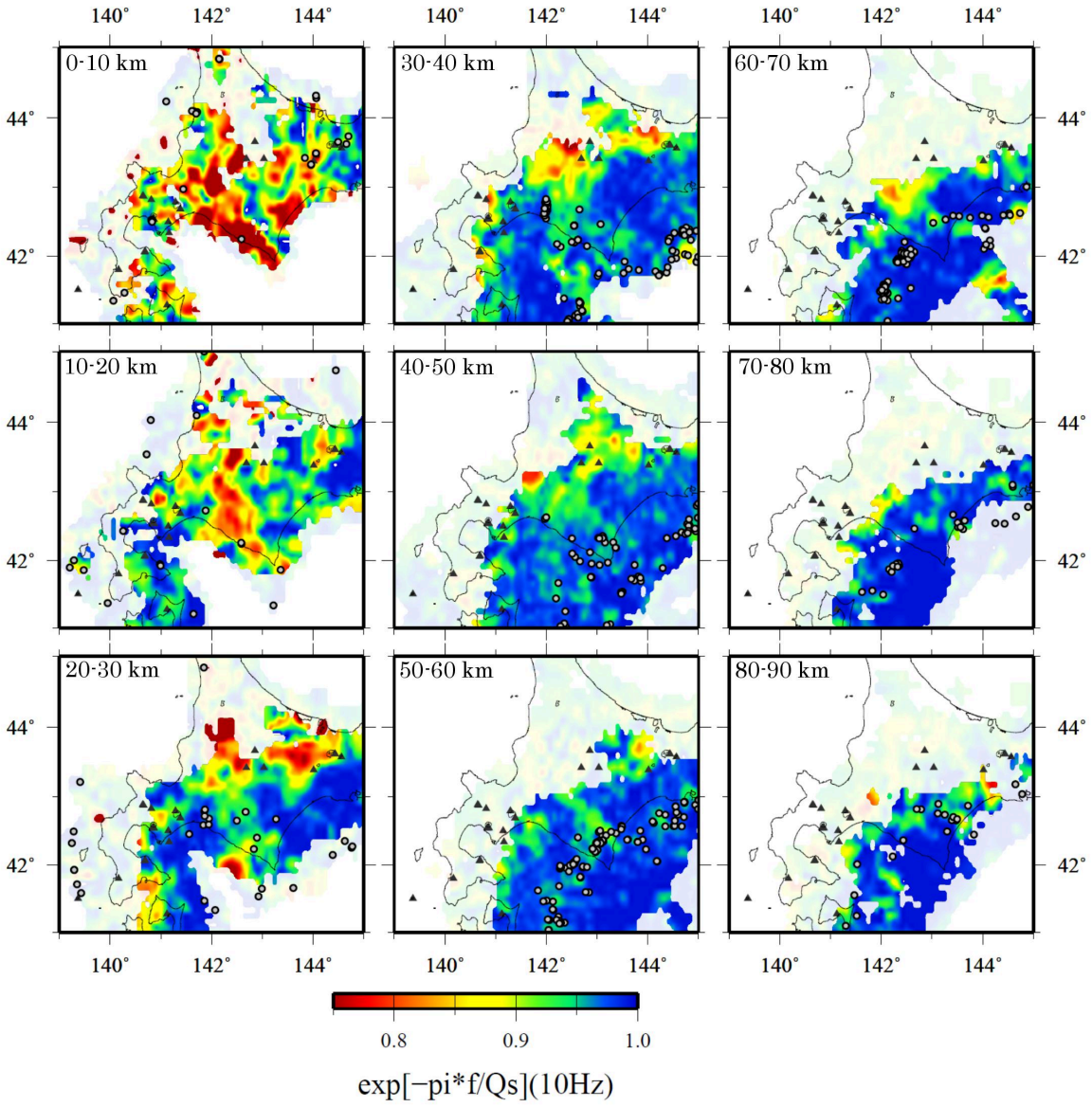


Fig.1 Qs structure in and around the Hokkaido, Japan, obtained at 10 Hz. Less resolved area are masked in the figure. White circles denote the locations of earthquakes used in this study. Black triangles is active volcanoes.



©2019. Japan Geoscience Union. All Right Reserved. 

# Reexamination for the subsurface structure beneath the southern part of the Hidaka Collision Zone, Hokkaido, Japan by using a numerical test of wave propagation

*Masahiro Shimazaki[1], Noriko Tsumura[2]

1. Graduate School of Science and Engineering, Chiba University, 2. Graduate School of Science, Chiba University

Hidaka Collision Zone (HCZ) is located in the central and southern part of Hokkaido where the Kuril forearc dragged by oblique subduction of the Pacific plate collided with the northeastern Japan arc. The Kuril arc’ s middle crust and its shallower part have been thrusted up along the Hidaka Main Thrust (HMT) and are exposed to the surface. Various seismic reflection surveys have been conducted for the purpose of investigating the subsurface structure of this region.
At the southernmost part of the HCZ, researchers of Hokkaido university, university of Tokyo and Chiba university conducted three seismic reflection surveys whose lines were settled across the HCZ in 1994, 1996, and 1997, respectively. From obtained time section, Tsumura et al. (1999) showed that the lower crust of the Kuril arc is divided into a northeast-dipping ascending layer and a southwest-dipping descending layer at a depth of 23km and interpreted it as delamination structure. Seismic profiles which were obtained by integrating three survey lines [Ito et al.,2000] and by applying new analysis technique of CRS / MDRS method [Ito et al.,2013] also supported the delamination structure.
Meanwhile, Kita et al. (2012) estimated the three-dimensional P wave velocity structure in the same region by travel time tomography. They suggested that a shallower part than 23km indicates the similar structure to that of Ito et al. (2000), but at deeper than 23 km, crustal material of the northeastern Japan arc reaches the plate boundary of the Pacific plate.
If delamination has occurred beneath the HCZ, it is expected that the length of southwest-dipping descending layer corresponds to the one of ascending layer having northeast inclination. Although two parallel reflectors can be recognized at the depth from 23 km to 38 km, deeper extension more than 38km cannot be found in the depth cross section of Ito et al. (2013). Then, in this study, we conducted a numerical test to know what kind of reflected waves can be observed when shots are performed with the same specification of actual surveys using analysis software Madagascar.
For the numerical test, we prepared two kind of subsurface structure models: One is a “Delami” model in which delamination occurs and lower part of the lower crust are descending into the depths deeper than 38km; and the other one is a “Non-Delami” model based on the interpretation of Kita et al. (2012). Both of the models consist of upper crust, lower crust, mantle and oceanic plate, and the average density of each material was set as density. Velocity of each layer was given referring to the result of Kita et al. (2012).
For the “Delami” model, only the reflected waves from the tip of wedge like structure of the subducting layer reached within the survey lines, whereas reflected waves from the deeper part reached the southwestern outside of the survey line. For the “Non-Delami” model, no reflected waves were seen around the arrival times which correspond to those of reflected waves from the depths at 23 km to 38 km.

©2019. Japan Geoscience Union. All Right Reserved. 

Keywords: Collision zone, Hidaka, Subsurface structure, Reflection survey

©2019. Japan Geoscience Union. All Right Reserved. 

# High resolution seismic surveys in the Kuril trench off Hokkaido

*Yasuyuki Nakamura[1], Shuichi Kodaira[1], Mikiya Yamashita[1], Seiichi Miura[1], Gou Fujie[1]

1. Japan Agency for Marine Earth Science and Technology

In the Kuril trench subduction zone, several large earthquakes (e.g., Tokachi-oki earthquakes) have occurred, which caused the earthquake and tsunami hazards in the Hokkaido and Tohoku region. Because the earthquake and tsunami risk was evaluated to be high in this region, more investigation and studies are required to contribute to the mitigation of those risks. In 2016 and 2018, we conducted high resolution seismic surveys in the Kuril trench from Erimo Seamount to off Kushiro by R/V *Yokosuka*. Approximately 35 km long 24 seismic profiles with ~ 6 km line separation were acquired using a 1.2 km long streamer cable and 380 inch$^3$ cluster guns. Obtained profiles demonstrate the detailed geological structure in the trench axis region. Subducting Pacific plate is deformed by the bend-related normal faults. The throw of the faults is up to ~ 300 –400 ms TWT. The thickness of the incoming sediments is > 500 ms maximum in the survey area and becomes thinner near the seamounts. Thick trench-fill sediment is deposited in the trench axis west of the Kushiro canyon, and the thickness is up to ~ 800 ms. Some profiles show weak landward dipping reflections within the hanging wall sediments. Possible slope failure is suggested in the lowermost landward slope near the Erimo Seamount.

Keywords: Kuril trench, seismic imaging, seamount, sediments

©2019. Japan Geoscience Union. All Right Reserved. 

# Subsurface Structure at the North of the Yokosuka Fault by Seismic Reflection Survey

*Shinobu Ito[1]

1. Geological Survey of Japan, AIST

The rupture of the Mikawa Earthquake on January 13, 1945 is considered to be on the Fukozu and the Yokosuka Faults. The Fukozu Fault is located relatively south and reverse L-shaped. On the other hand, the Yokosuka Fault is located relatively north and L-shaped. Ando (1974) mentioned that the NS strike section of the Yokosuka Fault in the fault zone was caused by a secondary deformation. Sugito and Okada (2004) investigated surface displacement in detail along the fault zone. They concluded that the NS strike section of the Yokosuka fault is the upper extension of the earthquake source fault although they referred to the possibility of the secondary deformation. Sugito and Okada (2004) referred that the surface earthquake fault of the Mikawa Earthquake is inconsistent with the source model of the earthquake estimated by Kikuchi et. al. (2003) from seismograms. In this way, the NS strike section of the Yokosuka Fault is not understood clearly. We carried out the P-wave seismic reflection survey at Shikoya-cho, Nishio, Aichi; at the north end of the Yokosuka Fault, in order to investigate lower extension of the Yokosuka Fault.

Not only the survey at the north of the Yokosuka Fault (GS-NSO2) but also the other survey at the south east extension of the Takahama Fault (GS-NSO1) were carried out from September 27 to October 2 in 2018. The length of the survey line GS-NSO2 is 1810m. We used one EnviroVibe manufactured by IVI. Sweep frequency is 10 to 120Hz, and sweep duration is 16S. Standard shot interval is 5m, and exceptionally 2.5m. Total shot points are 421, and we shot 3 to 5 times for each point. We used 3 string geophones of OMNI-2400 ($f_0$=15Hz) by Geospace. We used offline seismic recorder GSX system also by Geospace. Receiver interval is 5m, and total receiver points are 342. We made seismic profile by CMP stack.

We cannot see any obvious faults or signs related to the faults in the profile. Trenching survey indicate that the Mikawa Earthquake was preceded by one earthquake 2000 years ago. Total displacement of the Mikawa Earthquake and the preceding event is not more than 2m. It is impossible to detect the displacement in case of 2m displacement. However, it is possible in case that the displacement increase with depth. At least, we cannot detect the cumulative displacement in the survey.

Keywords: Yokosuka Fault, fault, seismic reflection survey

©2019. Japan Geoscience Union. All Right Reserved. 

# Crust and Uppermost mantle P-wave velocity structure of the Ordos block and its neighbors based on travel time tomography

*Yaning Liu[1], Jianping Wu[1], Shuxian Bao[1], Xiaohong Meng[2]

1. Institute of Geophysics, China Earthquake Administration, 2. China University of Geosciences (Beijing)

The Ordos block is located on the west side of the North China Carton, adjacent to the northeastern part of the Tibetan Plateau, with the Yinshan organic belt to the north and the South China block to the south. And the tectonic evolution of Ordos block is controlled by the North China basin extension caused with subduction of the Pacific plate and the extrusion and sheared from the northeastern margin of the Tibet Plateau follow the collision of the Indian-Eurasian plate.

The study area spans from 32˚N to 42˚N and 108˚E to 114˚E , which includes the Ordos block and its adjacent structures . The seismic data we used for inversion were recorded by 1244 stations including: 198 permanent stations and 1043 temporary stations (ChinArray II and III), from November 2013 to August 2017. The study uses local-seismic for inversion. After manual labeled the seismic phase, we select events with more than ten phase records of individual seismic events. The epicentral distance is less than 200km. Finally, we obtained about 22,500 phase records of 1882 local seismic events.

Our preliminary research results are consistent with previous studies and surface structures of a wide range of velocity distributions. However, in the middle-upper crust under the Liupan Mountain, the low-speed anomaly extending downward is shown, which may be caused by the horizontal extrusion caused by the eastward asthenosphere flow driven by the continuous compression of the northeastern margin of the Qinghai-Tibet Plateau during the Cenozoic. While, in the middle crust of the Ordos Basin, there are weak high-speed anomalies that divide the low-speed disturbances in the basin into three parts, showing the fluctuation of the crystalline basement of the basin. In the Taihang Mountains in the west of the study area, low-velocity anomalies extending to the upper layer of the mantle are shown. We initially believe that this anomaly is related to the volcanic thermal motion that once existed on the area.

Keywords: P-wave velocity structure, Ordos block

©2019. Japan Geoscience Union. All Right Reserved. 

# Seismic imaging of the 2016 Kumamoto earthquake area using P and PmP data

*Dapeng Zhao[1], Haibo Wang[2], Zhouchuan Huang[2], Mingjie Xu[2], Liangshu Wang[2]

1. Department of Geophysics, Tohoku University, 2. School of Earth Sciences and Engineering, Nanjing University

We determined a high-resolution model of 3-D P-wave velocity (Vp) tomography of the crust in the source zone of the 2016 Kumamoto earthquake (M 7.3) in Kyushu, SW Japan using a large number of arrival times of first P-waves and reflected P-waves from the Moho discontinuity (PmP). The PmP data are collected from original seismograms of the Kumamoto aftershocks and other local crustal events in Kyushu. Detailed resolution tests show that the addition of the PmP data can significantly improve the resolution of the crustal tomography, especially that of the lower crust. Our results show that significant low-velocity (low-Vp) anomalies exist in the entire crust beneath the active volcanoes, which may reflect the pathway of arc magma. The 2016 Kumamoto earthquake occurred at the edge of a small low-Vp zone in the upper crust. A significant low-Vp anomaly is revealed in the lower crust beneath the source zone, which may reflect the arc magma and fluids ascending from the mantle wedge. These results suggest that the rupture nucleation of the 2016 Kumamoto earthquake was affected by fluids and arc magma.

Keywords: Kumamoto earthquake, crustal reflected wave, seismic tomography

©2019. Japan Geoscience Union. All Right Reserved. 

# Estimation of 3D velocity structure in Kyushu region by the seismic tomography

*Toya Mitsuhiro[1], Koji Yamada[1]

1. Hanshin Consultants Co., Ltd.

## 1. Introduction

A high-resolution crustal structure in the volcanic zone is basic information for prediction of volcanic activity in the future. Therefore, in this study, we carry out preliminary research in Kyushu region aiming at the estimation of three-dimensional (3D) velocity structure in the volcanic zone by the 3D seismic tomography. In this region, it is suitable for this study because a large number of earthquake records of the main shock and aftershocks of the Kumamoto earthquake that occurred in April 2016 can be used and there are many volcanoes such as Mt. Aso and Mt. Unzen. Thus, we perform the 3D seismic tomography in Kyushu region for the estimation of 3D velocity structure, and consider problems on application to the volcanic zone.

## 2. Data and Method

We used arrival time data downloaded from the website of National Research Institute for Earth Science and Disaster Resilience (NIED). We selected 59011 earthquakes observed at 141 stations from April 2016 to March 2017. The selected area is 129.3˚E ~ 132.1˚E, 30.9˚N~ 34.0˚N, 0 ~ 50 km in depth. And, for P-wave arrivals, we added 804 earthquakes observed at 4 V-net stations at Mt. Aso and travel time data obtained by explosion seismic observations in the Hinagu fault area, Kyushu (The Research Group for the 2003 Hinagu Fault Seismic Expedition, 2008) and Eastern Kyushu (RESEARCH GROUP FOR EXPLOSION SEISMOLOGY, 1999). In total, our selection result in 871,690 P-wave arrivals and 840,633 S-wave arrivals.

We estimate 3D seismic velocity structure using the Fast Marching Tomography (FMTOMO) method of Rawlinson et al. (2006). This program uses the fast marching method via finite difference solution of the eikonal equation (Sethian, 1996) for calculation of synthetic travel times. The model area is 129.2˚E ~ 132.2˚E, 30.8˚N~ 34.1˚N, -4 ~ 52 km in depth. The horizontal grid spacing is 0.1˚(about 10 km) and the vertical is 4 km (the number of grids is 34×31×15 for three coordinate axis). An initial velocity structure model is JMA2001 (Ueno et al. 2002) and we set six iterations of the tomographic inversion scheme. Then, we examined the resolution of the tomographic inversion using a checkerboard resolution test (CRT). The size of checker is 2×2×2 in grid number, and the velocity perturbation for the initial velocity structure model is ±0.1 km/s. As a result of the CRT, we confirmed that checkerboard pattern is well resolved up to about 20 km deep in the Kumamoto area.

## 3. Results

Figure 1 shows plan views of the P-wave velocity and the S-wave velocity structures obtained here at 4 km depth. The pattern of velocity variation is similar to each other and pronounced low velocity area exists in the southern Kumamoto. At 0 ~ 1 km depth, low velocity area exists in the Kumamoto Plain. However, in this study, pronounced velocity variation is not seen beneath Mt. Aso and other volcanic zones. So, for improving the resolution, we are going to add earthquakes in the area with less them and stations (K-net, V-net and so on).

## Acknowledgments

We would like to thank the National Research Institute for Earth Science and Disaster Resilience (NIED)

©2019. Japan Geoscience Union. All Right Reserved. 

for the use of the arrival time and the seismic data. All figures are made using the free software GMT (Wessel & Smith 1998).

Keywords: seismic tomography, velocity structure, Kyushu

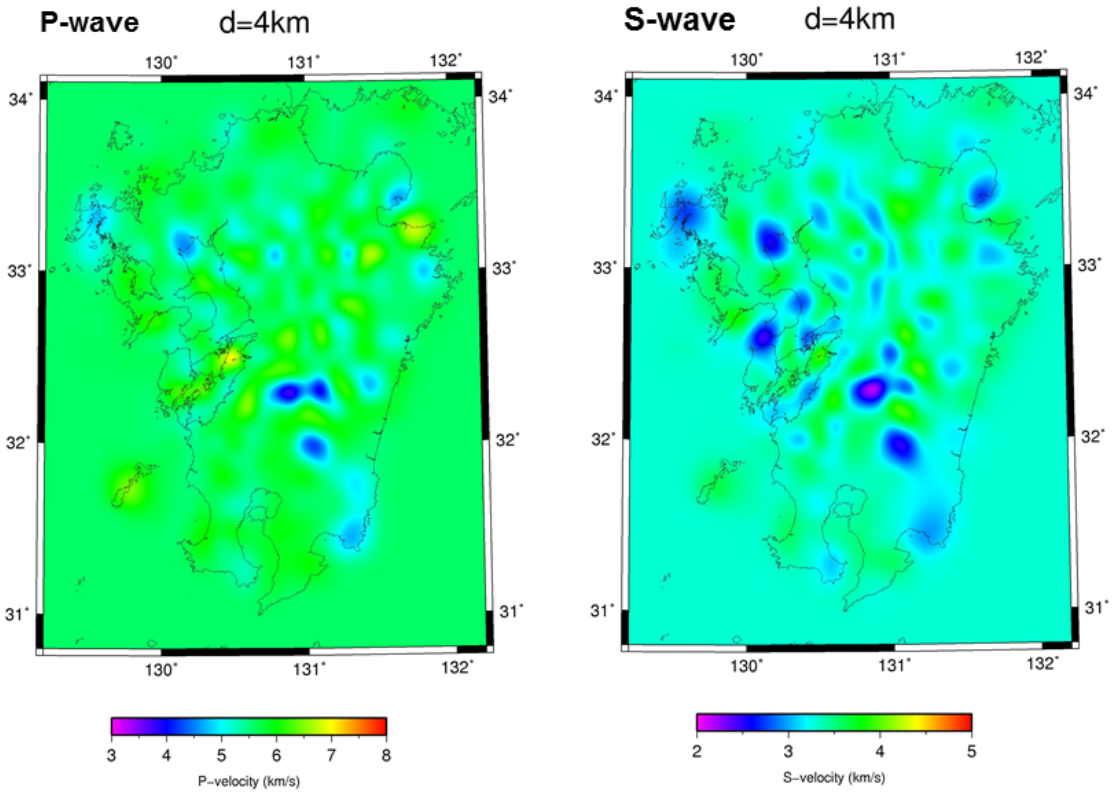


Fig. 1. Plan views of velocity structure for Vp (left), velocity structure for Vs (right)

©2019. Japan Geoscience Union. All Right Reserved. 

# Estimation of the structure of the Philippine Sea slab under south Kyushu using receiver function analysis

*Masaki Uchida[1], Takahiro Ohkura[1], Takuo Shibutani[1], Yuki Abe[2], Shintaro Komatsu[1], Ken'ichi Yamazaki[1], Yusuke Yamashita[1], Shin Yoshikawa[1], Masato Iguchi[1], Takeshi Tameguri[1], Tadaomi Sonoda[1]

1. Kyoto Univ., 2. Hot Springs Research Institute

In the subduction zone, it is considered that magmatism is caused by fluid transported to the upper mantle from the subducting slab [Tatsumi, 1986, GRL]. In order to clarify the relation between the magmatism and the subsurface structure of Sakurajima and Kirishima volocanoes, we investigate seismic velocity discontinuities beneath these regions by receiver function analyses of the teleseismic waveform.

A Receiver function (RF) is calculated by deconvolving the vertical component of a waveform of a teleseismic P-wave from its horizontal component, and phases converted at seismic velocity discontinuities in its coda can be detected with RFs [Langston, 1979, JGR]. In order to estimate the geometry of steeply dipping discontinuities, such as the upper boundary of the subducting Philippine Sea plate, with RFs, refraction of the seismic rays at the dipping discontinuities should be taken into account. For this purpose, we apply the method for stacking RFs using the multi-stage fast marching method developed by Abe et al. [2011, GJI].

Abe et al. [2013, JGR] revealed the regional variation of S wave velocity discontinuity across the Philippine Sea plate, which is divided by the Kyushu - Palau Ridge, from RF analyses of the waveform data obtained at the permanent stations. In this research, we use waveform data obtained at dense observation networks along Miyazaki-Akune and Miyazaki-Sakurajima lines from teleseismic earthquakes with magnitude greater than 5.5 occurred from November 2009 to March 2017. We use 3-D seismic velocity model [Matsubara et al. 2007, Tectonophysics] for stacking RFS, although Abe et al. [2013] used one dimensional IASP91 model.

Beneath the south Kyushu where the Western Philippine Basin formed at about 50 Ma subducts [Hilde and Lee, 1984, Tectonophysics], it is suggested that the fluid dehydrated from the Philippine Sea slab is transported to the back-arc and may cause arc volcanism activity by Abe et al. [2013]. In addition, low velocity zone of mantle wedge is detected, and this zone is considered to correspond to a serpentinized mantle by a fluid derived from oceanic crust [Bostock et al. 2002, Nature], based on the S wave velocity of serpentinite estimated by Hacker et al. [2003, JGR] and Christensen [2004, Int Geol Rev].

We obtain more precise receiver function images using dense network data and discuss the seisimic structure of Sakurajima and Kirishima volcanoes.

Keywords: Receiver function analyses, Southern Kyushu, Philippine Sea slab

©2019. Japan Geoscience Union. All Right Reserved. 

# Imaging subduction structure beneath the eastern part of Kii Peninsula, SW Japan, using an earthquake reflection method

*Eiji Kurashimo[1], Takashi Iidaka[1], Noriko Tsumura[2], Takaya Iwasaki[1]

1. Earthquake Research Institute, the University of Tokyo, 2. Chiba University

The Nankai trough region, where the Philippine Sea Plate (PHS) subducts beneath SW Japan arc, is a well-known seismogenic zone of interplate earthquakes. The most recent great earthquakes occurred in 1944 (Tonankai Earthquake, M=7.9) and 1946 (Nankai Earthquake, M=8.0). In recent years, various slip motions with a different time scale have been recognized at or near the updip and downdip limits of seismogenic zone [e.g., Obara, 2002; Ito and Obara, 2006]. Revealing structural factors that control the fault slip behavior is important to understand the earthquake rupture dynamics. Seismic reflection characteristics and seismic velocity variations can provide important information on the heterogeneous structure around plate interface. Recent seismic experiments reveal the relation between the crustal structure and the fault slip behavior. However, little is known about the deeper part of the plate boundary, especially the down-dip side of the seismogenic zone. In 2015, seismic array observation was conducted to obtain the subduction structure beneath the eastern part of the Kii Peninsula [Kurashimo et al., 2016]. Ninety 3-component portable seismographs were installed on a 90-km-long line nearly parallel to the direction of the subduction of the PHS. Waveforms were continuously recorded during a six-month period. During the seismic array observation, Japan Meteorological Agency determined 45 events within 10 km of our survey line. Prominent late arrivals, probably reflected waves from the deeper part of the crust can be recognized on the record sections. Earthquake data is useful to obtain a deep image. So, in order to clarify the spatial distribution of the reflectors, we applied the reflection method to the earthquake data. We used horizontal-component seismograms, because high amplitude S-wave reflection can be recognized on the record sections. Conventional common mid-point processing cannot be applied to earthquake data because the reflection point does not lie at the mid-point between source and receiver, so, we applied the Common Reflection Point (CRP) transformation [e.g., Quiros et al., 2016] to the earthquake data set using a tomography-derived 3D S-wave velocity model [Kurashimo et al., 2016]. Reflection points and their relevant travel-time from earthquake to receiver were calculated using a 3D finite difference travel-time algorithm [Hole and Zelt, 1995]. Before applying the CRP transformation, the waveform data were filtered by a band-pass filter (1 -8 Hz). After applying the CRP transformation and the stacking process, we applied a post-stack migration technique. The migrated shear wave reflection image shows that the northward dipping reflective zone interpreted to be the upper boundary of the PHS can be recognized at a depth range of about 25 -30 km. The top of the low-frequency earthquakes (LFEs) occurrence zone well corresponds to the high amplitude S-wave reflective zone. LFEs are also located in and around the low Vp and high Vp/Vs zone [Kurashimo et al., 2016]. These results suggest the occurrence of the LFEs may be associated with fluids.

Keywords: Philippine Sea plate, earthquake reflection method, Low-frequency earthquake

©2019. Japan Geoscience Union. All Right Reserved. 

# Tomography of Mejillones Peninsula using cross-correlation of ambient seismic noise

*Kellen Azua Quezada[1], Sergio Ruiz[1], Francisco Pasten-Araya[2,3], José Salomón[4], Pablo Salazar[2,3], Miguel Saez[1], César Pastén[4], Felipe Leyton[5], Wasja Bloch[6]

1. DGF, UChile, 2. DG, UCN, 3. CIGIDEN, 4. DIC, UChile, 5. CSN, Chile, 6. GFZ

The Mejillones Peninsula (MP) is locate in northern Chile (-23.28º, -70.5º). MP is a geomorphic atypical uplifted block of the coastal platform of 100 km length. This structure has been proposed as a segment boundary for large subduction earthquakes, as the case of Mw 8.0 Antofagasta (1995) and Mw 7.7 Tocopilla (2007) events. Additionally, the Peninsula presents a wide and deep layer of sediments that could enhance site effects. For this reason, in this work we study the shallow structure of MP basin. We deployed a dense temporary seismic network in the MP, which registered in continuous time from July 2013 to September 2015. From the continuous records, we built a local tomography using the spectral ambient seismic noise. We use vertical component of seismograms to obtain the Green function from cross-correlation between station pairs. The frequency domain method allows determine of phase velocity relating the zero-crossing of the real part of cross-correlation spectrum with the zero crossing of the zero-order Bessel function of the first order. The Rayleigh wave phase velocities are inverted by means of a non-linear iterative 2-D tomographic technique; finally we recover phase velocity maps at different frequencies. The tomographic maps present significant features that correlate with surface geology. We found in the West part of the MP lower velocities that East zone. We can associate this with fractured metamorphic rock. Higher velocities in the Eastern part of the peninsula are associated with the presence of intrusive rocks. The difference in velocity of these two anomalies is maintained at differents depth.

Keywords: Tomography, Ambient Seismic Noise

©2019. Japan Geoscience Union. All Right Reserved. 

# Crustal thickness beneath Central Indonesia by the cross-correlation analysis of seismic ambient noise (2)

*Masyitha Retno Budiati[1], Genti Toyokuni[1], Tomomi Okada[1], Toru Matsuzawa[1]

1. Graduate School of Science, Geophysics Department, Tohoku University

Central Indonesia has complex tectonic structures where is characterized by several subduction zones at northern and eastern part and also active faults (e.g., Palu Koro, Matano and Hamilton faults). These complexities affect crustal structures around the region. In this study, we estimated spatial variation of crustal thickness and their relation with active tectonics. We used waveform data recorded at 10 BMKG broadband stations around Sulawesi Island. Firstly, the continuous data were divided into 20 minutes segments with time shift in every 5 minutes. Once the pre-processing steps for each segment were done, we calculated the CCFs between two contemporaneous segments from two stations and stacked the daily-averaged CCFs over 5 months. We further compressed the two-sided signal into one-sided signal by taking the average of positive and negative lag part of the CCFs in order to stabilize the dispersion curves of group velocities. To fit the synthetic and the observed group velocities, we adjusted the two layers crustal velocity model from CRUST 1.0 (Laske et al., 2013) corresponding to the observation group velocities. The velocity model that is faster than the observation was subtracted 5% and 10% to find the best crustal thickness with minimum RMS between observations and synthetics at period of 20s –30s. To confirm our procedure above, we currently apply the similar procedure to estimate the well-known Moho discontinuity in Tohoku region, Japan. We collected 5 months continuous waveform data from vertical components of 10 F-net stations around Tohoku region. The results showed that the slower velocity models makes the crustal thickness shallower. The estimated depth of Moho discontinuity beneath Tohoku region is about 20km –30km using subtracted velocity models. This is almost consistent with previous studies (e.g. Zhao et al., 1990). While the estimated depth of Moho discontinuity at eastern part of Central Indonesia is about 27km –35km which is related to the ocean crust, Batui and Sula thrust and at the continent of Sulawesi Island the estimated depth of Moho is about 35km –45km.

Keywords: Central Indonesia, Tohoku Region, Crustal structure

©2019. Japan Geoscience Union. All Right Reserved. 

# Subsurface structure below the southernmost area of South Japanese Alps estimated by seismic interferometry imaging

*Toshiki Watanabe[1], Hasegawa Daima[1], Tanio Ito[2], Ken'ichi Kano[3], Susumu Abe[4], Akira Fujiwara[5], Yoshinori Kouchi[6]

1. Graduate School of Environmental Studies, Nagoya University, 2. Association for the Development of Earthquake Prediction, 3. Shizuoka Univertity, 4. JAPEX, Co. Ltd., 5. JOGMEC, 6. Geosys, Inc.

In the Tokai area, seismological events, such as low frequency events and slow slip events as well as large earthquakes, are occurred caused by subduction of the Philippine Sea (PHS) plate. The eastern Tokai area is a transition zone from the collision zone of Izu arc to the subduction area. To understand the subsurface structure in this area and fill the gap between the previous seismic surveys, a seismic observation using a dense seismic linear array composed of 34 receivers was conducted in 2013.
In this study, we applied seismic interferometry imaging to the seismic records of the array observation. Seismic interferometry can retrieve the reflection response between two receivers as if one receiver is a virtual shot and the other is a receiver by calculating the cross-correlation of the transmission responses recorded at the two receivers. For a single receiver, the reflection response recorded at the receiver from a source at the same location is retrieved by calculating the autocorrelation of the transmission response recorded at the receiver. In this study, we used regional deep earthquakes occurred in the Pacific Oceanic slab as the seismic sources to image the PHS plate and crustal structures. We conducted autocorrelation analysis and created reflection profiles for both P- and S-waves. We projected the cross-correlation between two adjacent stations to their mid-point to improve the spatial density of the stations. After migration using the velocity structure obtained by the tomography analysis, we obtained the P- and S-wave reflection depth profiles.
In the S-wave depth profile, the shallower area above 25 km shows reflective, while the deeper area is less reflective. The boundary becomes shallower to the north-east of the profile. By comparing this profile with the result of other seismic surveys and with pre-existing plate models, we interpreted that the strong reflectors shown at the depth about 25 km in the southwest of this profile are the plate boundary. This interpretation is consistent with the result of Hirose et al. (2008) showing that the basaltic oceanic crust of the PHS plate shows low Vs and high Vp/Vs. In the eastern half of the profile lacks reflectors that correspond to the plate boundary. This may be attributed to a weak contrast of physical properties between the felsic island arc crust proposed by Kodaira et al. (2004) and the Japanese island arc crust, or complicated geological structure due to the collision of Izu arc.

Keywords: seismic array observation, seismic interferometry, reflection depth profile, plate boundary

©2019. Japan Geoscience Union. All Right Reserved. 

# Strong variations of near-surface seismic anisotropy of Taiwan revealed by coda interferometry

*Hsin-Yu Lee[1], Yuancheng Gung[1], Li-Wei Chen[2], Ling-Yun Chiao[3]

1. Department of Geosciences, National Taiwan University, Taiwan, 2. Department of Earth and Planetary Science, University of California at Berkeley, CA, USA, 3. Institute of Oceanography, National Taiwan University, Taiwan

We report the near-surface (<500 m) seismic structure, Vs, Vp and Vs anisotropy, of Taiwan using the empirical Green’ s function of body waves extracted by applying coda interferometry to the vertical station pairs at 56 borehole sites. We find clear characteristic cos2θ dependence of Vs in all the determinations of Vs azimuthal anisotropy. Because the borehole sites are located at very diverse geological structures of Taiwan, we are able to notice the following interesting features about the near-surface Vs anisotropy: (1) The patterns of the observed anisotropy fall into two categories, OPA (Orogeny-Parallel Anisotropy) and SAA (Stress-Aligned Anisotropy), and both types of anisotropy fit well the local geological fabrics and/or the ambient stress. (2) About half of the amplitudes of anisotropy are larger than 10 %. The site with the largest amplitude of anisotropy (34%) is located in the slate belt of the Central Ranges, while the sites with weak anisotropy (~1%) are associated with low Vs and/or small strain rate. (3) The amplitudes of OPA are generally stronger than SAA, and the types of anisotropy are closely related to the Poisson’ s ratios at the borehole sites. (4) The strong variations of the OPA amplitudes can be explained by the rock types in the well body with the metamorphic rocks carrying stronger anisotropy than the sedimentary rocks. (5) The strong near-surface anisotropy also implies that delay times contributed by the shallow crust might have been underestimated in studies of shear-wave splitting measurements using the direct arrivals of earthquakes waves.

Keywords: coda interferometry, near-surface seismic anisotropy, Taiwan

©2019. Japan Geoscience Union. All Right Reserved. 

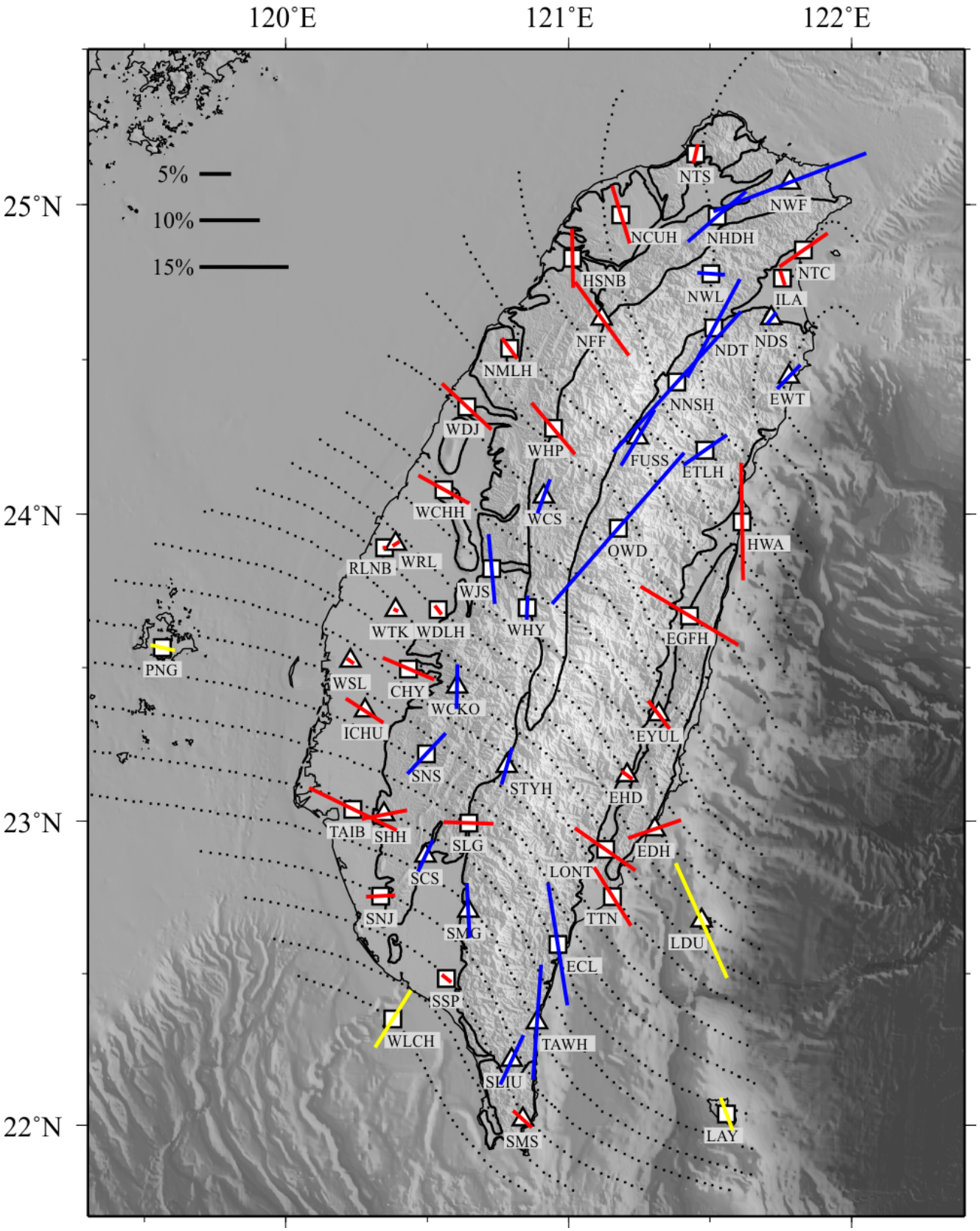


©2019. Japan Geoscience Union. All Right Reserved. 

# Investigating anomalous crustal structures along the convergent zone in eastern Taiwan with the new airborne magnetic survey and updated seismic tomographic models

*Chi-Hsuan Chen[1], Hsin-Hua Huang[2], Lun-Tao Tong[3], Wayne Lin[3], Po-Tsun Lee[1], Shou-Fang Chang[1], Jin-Fa Lee[1]

1. Cntrl. Geo. Surv., MOEA, Taiwan, 2. Inst. Earth. Sc., Acad. Sinica, Taiwan , 3. Industr. Technol. Res. Inst., Taiwan

The convergence between Eurasian plate and Philippine sea plate produces the tectonically and geodynamically complex regions of Taiwan. The orogeny has been suggested as from ancient oceanic-oceanic plate subduction transforming to the continental-oceanic plate collision as the proceeding of the accreted volcanic arcs. The major suture of the plate boundary in eastern Taiwan, the Longitudinal Valley, contributes most of the seismic activities and absorbed about half of the plate convergence. How the shortening and disappearance of the oceanic plate provoked multidisciplinary researches in discussing the kinematics and the related earthquake structures.

Local seismic tomography is a useful technique for unraveling the subsurface structures. The Taiwan seismic tomographic studies that are advanced by large projects or by integrating multiple data sets have been proposed in recent years. Furthermore, since 2012 the seismic signal digitization of the Central Weather Bureau (CWB) seismic network was upgraded from 12 to 24 bit, and the potential timing issue of telemetry delays has been eliminated with onsite GPS time system. Additionally, the new airborne magnetic survey has been carried out in eastern Taiwan by the Central Geological Survey (CGS) and the Industrial Technology Research Institute (ITRI) recently. High magnetic anomalies were detected not only in the volcanic arc but also in the eastern Central Range along the north-south trending Longitudinal Valley. These observations motivate us to revisit the subsurface structures with updated seismic tomographic models using new CWB data sets from 2012 to 2015.

The iso-velocity contours of the updated model keep similar structures with the previous model at first order but furtherly reveal more details. A continuous high-Vp and high-Vp/Vs bulge which extends to the shallow depths of the eastern Central Range has been interpreted as a high-pressure rock exhumation along the subduction of South China sea plate or an obducted Luzon forearc sliver. On the other hand, the new airborne magnetic survey reveals two individual high magnetic stripes that share the same high magnetic characteristics with the oceanic crust. However, the magnetization vectors behave oppositely in the direction at both flanks of the Longitudinal Valley. Such findings of these integrated geophysical analyses enable us to discuss the anomalous crustal structures and their tectonic implications.

Keywords: Airborne magnetic Survey, Seismic tomography, Forearc obduction, Exhumation, Oceanic crust

©2019. Japan Geoscience Union. All Right Reserved. 

[J] Oral | S (Solid Earth Sciences)：S-SS Seismology

Thu. May 30, 2019 1:45 PM - 3:15 PM JST | Thu. May 30, 2019 4:45 AM - 6:15 AM UTC | A05 TOKYO BAY MAKUHARI HALL

## [S-SS12] Crustal Structure

convener:Kazuo Nakahigashi(Tokyo University of Marine Science and Technology), Chairperson:Yoshio Murai(Hokkaido University), Genti Toyokuni(東北大学)

The aim of this session is to cover seismological and geophysical studies on the Earth's crust. Contribution on seismological and geophysical structure of the crust, processes that develop in the crust which include earthquakes, volcanoes and geological descriptions of the crust are welcomed. We also welcome theoretical and methodological studies that will serve as basics in such explorations.

1:45 PM - 2:00 PM JST | 4:45 AM - 5:00 AM UTC

### [SSS12-01] Shrinking and draining continental lower crust: its binary effects of stress and fluid on crustal activities

*Takehito Koyama[1] (1.Institute of Industrial Science, the University of Tokyo)

2:00 PM - 2:15 PM JST | 5:00 AM - 5:15 AM UTC

### [SSS12-02] Seismic velocity structure in southern Hokkaido deduced from ocean-bottom seismographic and land observations

*Yoshio Murai[1], Kei Katsumata[1], Tetsuo Takanami[2], Tomoki Watanabe[3], Tadashi Yamashina[4], Ikuo Cho[5], Masayuki Tanaka[6], Ryosuke Azuma[7] (1.Institute of Seismology and Volcanology, Faculty of Science, Hokkaido University, 2.Department of Terrestrial Magnetism, Carnegie Institution of Washington, 3.Marine Works Japan LTD, 4.Kochi University, 5.National Institute of Advanced Industrial Science and Technology, 6.Meteorological Research Institute, 7.Research Center for Prediction of Earthquakes and Volcanic Eruptions, Graduate School of Science, Tohoku University)

2:15 PM - 2:30 PM JST | 5:15 AM - 5:30 AM UTC

### [SSS12-03] Structural Complexity Associated with Arc-Arc Collision in Hokkaido Island, Japan - Review on Controlled-Source Seismic Researches in Western and Central Hokkaido -

★Invited Papers

*Takaya Iwasaki[1], Noriko Tsumura[2], Tanio Ito[3], Kazunori Arita[4], Hiroshi Sato[1] (1.Eathquake Research Institute, the University of Tokyo, 2.Graduate School of Science, Chiba University, 3.Association for the Development of Earthquake Prediction, 4.Hokkaido Research Center of Geology)

2:30 PM - 2:45 PM JST | 5:30 AM - 5:45 AM UTC

### [SSS12-04] Seismic imaging of the eastern Japan forearc region using S-net data

*Genti Toyokuni[1], Dapeng Zhao[1], Naoki Uchida[1], Takashi NAKAYAMA[1] (1.RCPEVE, Tohoku Univ.)

2:45 PM - 3:00 PM JST | 5:45 AM - 6:00 AM UTC

### [SSS12-05] The relationship between the location of the mid crustal reflector and seismicity in Iwaki area, northeastern Japan

*Takashi Iidaka[1], Shin'ichi Sakai[1], Toshihiro Igarashi[1], Kazushige Obara[1], Aitaro Kato[1], Tetsuya Takeda[2], Shigeki Nakagawa[1] (1.Earthquake Research Institute, University of Tokyo, 2.National Research Institute for Earth Science and Disaster Resilience)

3:00 PM - 3:15 PM JST | 6:00 AM - 6:15 AM UTC

### [SSS12-06] Abnormal Seismic Anisotropy beneath the Tokyo Metropolitan Area (1) Mantle of the Philippine Sea Slab

*Motoko Ishise[1], Shin'ichi Sakai[1], Aitaro Kato[1], Shin Aoi[2], Makoto MATSUBARA[2] (1.Earthquake Reseach Institute, University of Tokyo, 2.National Research Institute for EarthScience and Disaster Resillience)

# Shrinking and draining continental lower crust: its binary effects of stress and fluid on crustal activities

*Takehito Koyama[1]

1. Institute of Industrial Science, the University of Tokyo

Basically, the continental crust itself is presumed to be static passive polycrystalline rocks with its ductility in the aseismic deep. However, this ductility seems difficult to explain crustal activities still debated: not only the long-standing stability (the resistivity to the isostatic decay) but also the short-term activities, e.g., inland horizontal compressive state (Zoback, et al. (1989)), intracrustal seismicity (Calais, et al. (2016)), and rare lower crustal earthquakes (Simpson (1999)).

Then, can we rethink the crust, especially its controversial lower? Actually, I presented a possibility of the shrinking and draining of the continental crust through “phase separation or phase demixing” at JpGU in 2012. Thus, I will propose a new lower crust causing the deformation, qualitatively but comprehensively discussing the activities.

As basic components of the lower crust, I consider $SiO_2$ and $H_2O$ (with other elements and volatiles). Their melt mixtures cause phase separation under lower crustal temperatures and pressures (Kawamoto (2006), Hack, et al. (2007)). Furthermore, melt $SiO_2$ forms 3-dimensional macromolecular network (Stebbins (2016)). Thus, I regard this process as the volume shrinking of this elastic $SiO_2$ network separating from an aqueous fluid (Tanaka (2012), Koyama, et al. (2009), Koyama and Tanaka (2018); also the shrinking $SiO_2$ in Tognonvi, et al. (2011)): This network macroscopically behaves as a phase-separating glass (before crystallization) or an elastically hard self-squeezing wet sponge.

Then, the new lower crust, constructed by the shrinking $SiO_2$ network draining the $H_2O$ fluid, combines and interacts with the usual upper crust (Figure): The elastic shrinking laterally compress the upper crust from below, bringing the long-term stability and intermittent drained-fluid injections triggering the intra-upper-crustal earthquakes. Importantly, this lower crust, aiming at shrinking, must follow some degree of external compression: the aseismicity or the apparent ductility. However, when the elastic $SiO_2$ network suffers a large local differential stresses under the stress/fluid interlayer interactions, the brittleness should arise as lower crustal seismicity.

Therefore, assuming the lower crust to be not monistic solid but dualistic solid/fluid coexisting during their phase separation, we can qualitatively explain the crustal movements using the actively shrinkable/drainable lower crust mechanically/materially interacting with the upper crust.

Keywords: Continental crust, Stability, Stress, Seismicity, Phase separation

©2019. Japan Geoscience Union. All Right Reserved. 

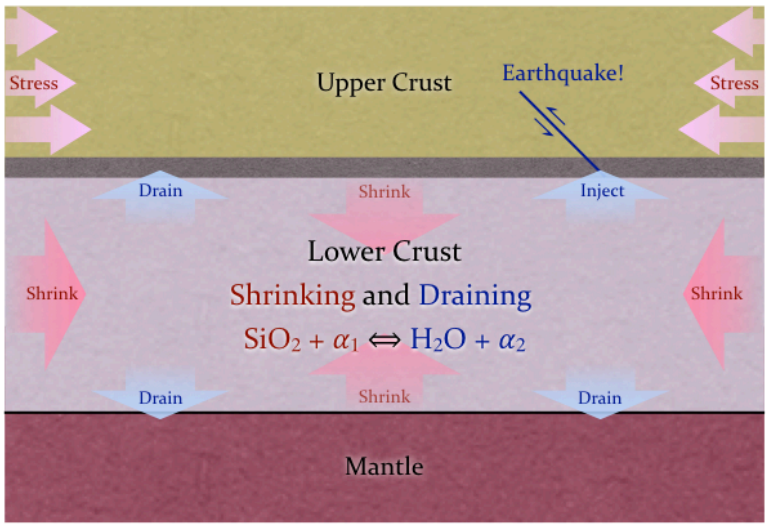


Figure: Self-squeezing lower crust mechanically and materially affecting the static and passive upper crust above.

©2019. Japan Geoscience Union. All Right Reserved.

# Seismic velocity structure in southern Hokkaido deduced from ocean-bottom seismographic and land observations

*Yoshio Murai[1], Kei Katsumata[1], Tetsuo Takanami[2], Tomoki Watanabe[3], Tadashi Yamashina[4], Ikuo Cho[5], Masayuki Tanaka[6], Ryosuke Azuma[7]

1. Institute of Seismology and Volcanology, Faculty of Science, Hokkaido University, 2. Department of Terrestrial Magnetism, Carnegie Institution of Washington, 3. Marine Works Japan LTD, 4. Kochi University, 5. National Institute of Advanced Industrial Science and Technology, 6. Meteorological Research Institute, 7. Research Center for Prediction of Earthquakes and Volcanic Eruptions, Graduate School of Science, Tohoku University

The Kuril arc collides with the northeast Japan arc in the southern part of Hokkaido, Japan. Such a collision results in building the Hidaka Mountains and is related to the seismic activity and large earthquake occurrence such as the Urakawa-Oki earthquake (Ms 6.8) on March 21, 1982. It is important to image the three-dimensional crustal structure in order to clarify the collision tectonics and understand the patterns of earthquake occurrence and the mechanism of large earthquake occurrence. A group of seismologists from eleven universities operated a dense temporary network of land stations from 1999 to 2001 in and around the Hidaka Collision Zone [Katsumata *et al.* (2002, Bull. Earthq. Res. Inst., **77**)]. In addition, we conducted ocean-bottom seismographic observations in 1999 and 2000 in the south off Hokkaido region. Murai *et al.* (2003, GRL **30**) estimated P-wave velocity (Vp) structure by the 3-D tomographic inversion [Zhao *et al.* (1992, JGR **97**)] of seismic travel time data obtained from networks of ocean-bottom seismographs (OBSs) and land stations in 1999. However, their spatial resolution was poor for the deep crustal structure and they could not obtain S-wave velocity (Vs) structure because of limitation of the number of data. Murai *et al.* (2016, JpGU) estimated structure of both Vp and Vs by the tomographic inversion of travel time data from OBSs and land stations in 1999 and 2000. We found a problem in the reduction of the travel time residuals due to errors of station corrections in their analysis. Here we estimate Vp and Vs structure again after correcting their errors.

The results from the tomographic analysis are as follows.

1. A high-velocity body seems to be obducted toward the crest of the Hidaka Mountains from east beneath the land area, which is interpreted as the obducted lower crust of the Kuril arc. The high-velocity region extends to the east of the Hidaka Mountains at depths of 15-35 km. A low-velocity region is located to the west of the Hidaka Mountains so as to contact with the high-velocity region at the Hidaka main thrust. It is interpreted as the northeast Japan arc. These results are consistent with those obtained by previous tomographic studies.

2. We found a distinct low velocity region dipping southwestward from beneath the Hidaka Mountains to the source area of the 1982 Urakawa-oki earthquake at depths of 35-45 km which was imaged only by the tomographic analysis using the data from OBSs. It is interpreted as the lower part of the delaminated Kuril arc lower crust, which has an area of about 50 km wide by 50 km long.

3. The colliding low-velocity crustal material disappears in the southeast of Cape Erimo. Moreover many microearthquakes occurred in the low-velocity region whereas the seismic activity was low outside it. These results suggest the effect of arc-arc collision is reduced abruptly in the offshore area as the southeastward extension of the Hidaka Mountains.

©2019. Japan Geoscience Union. All Right Reserved. 

4. The hypocenter of the 1970 Hidaka earthquake (M 6.7) is located at the boundary between the high and low velocity regions. The fault plane of the 1982 Urakawa-oki earthquake is located at the western boundary of the high Vp anomaly faster than 8.0 km/s. Thus these M7 class inland earthquakes occurred at material boundaries, which is consistent with Kita *et al.* (2012, JGR **117**).

5. The overriding plate above the seismogenic asperity of the 2003 Tokachi-oki earthquake (M 8.0) is characterized by high Vp/Vs on the northeast side of Cape Erimo. This result is consistent with Machida *et al.* (2009, Tectonophysics **465**).

Acknowledgments
We thank the crew of the R/V Kofu Maru of the former Hakodate Marine Observatory for their cooperation during deployment of OBSs. We thank D. Zhao for permitting us to use his computer program for 3-D tomographic inversion.

Keywords: ocean-bottom seismograph (OBS), seismicity, tomography, Hidaka Collision Zone, delamination, Hokkaido

©2019. Japan Geoscience Union. All Right Reserved. 

# Structural Complexity Associated with Arc-Arc Collision in Hokkaido Island, Japan - Review on Controlled-Source Seismic Researches in Western and Central Hokkaido -

*Takaya Iwasaki[1], Noriko Tsumura[2], Tanio Ito[3], Kazunori Arita[4], Hiroshi Sato[1]

1. Eathquake Research Institute, the University of Tokyo, 2. Graduate School of Science, Chiba University, 3. Association for the Development of Earthquake Prediction, 4. Hokkaido Research Center of Geology

Hokkaido Island has a complicated crustal structure reflecting subduction, accretion and collision processes from Late Jurassic to the present (e.g. Niida and Kito, 1986; Kimura, 1986; Ueda 2016). Central Hokkaido is composed of almost N-S trending geological units of the Sorachi-Yezo Belt (SYB), Hidaka Belt (HB) and Tokoro Belt (TB) from west to east. This region has been highly deformed under the dextral oblique collision between the Eurasia and North America (Okhotsk) Plates and the following westward movement of the Kuril Arc due to the oblique subduction of the Pacific Plate. The latter event has formed the Hidaka Collision Zone (HCZ) with the uplift of the Hidaka metamorphic rocks along the Hidaka Main Thrust (HMT) and the development of the west-verging fold-and-thrust belt with thick sedimentary package on the SYB.

In this paper, we review the previous controlled-source seismic studies in western and central Hokkaido, focusing the structural complexity formed by the arc-arc collision. The first seismic refraction study was undertaken in western Hokkaido in 1968-1969 (Okada et al., 1973). The crust obtained is 20-30 km thick, consisting of 5.9 and 6.6 km/s layers overlying the uppermost mantle of 7.5 km/s. Seismic refraction studies in 1984 and 1992 revealed the complicated structure in central Hokkaido (Iwasaki et al., 1998). The result from the 1984 profile along the Pacific coast is characterized by a rather thick (> 7 km) sedimentary package with a velocity of 2.5-5.5 km/s in SYB. The 1992 refraction/wide-angle reflection profile, which was extended from the western SYB to the eastern TB with SW-NE direction, also show a thick (~8 km) sedimentary package with a velocity of 2.6-5.8 km/s in the southwestern part of SYB, The upper crustal velocity show significant increase from 5.6 km in HB to 5.7-6.15 km in TB.

In 1990’s, several seismic reflection and refraction/wide-angle refraction experiments were undertaken in the southern HCZ (Arita et al., 1998; Tsumura et al., 1999; Ito et al., 2000) and the northern HCZ (Iwasaki et al., 2004, 2016). In the southern HCZ, the crustal delamination by the collision was clearly imaged from the reflection data by applying an advanced method of CRS/MDRS stacking (Tsumura et al., 2014). Namely, the upper 22-23 km crust in the Kuril Arc side is obducted along the HMT, while the lower part of the crust is descending almost to reach the Pacific plate. In the northern part of the HCZ, the detailed structure was obtained along the 227-km profile with E-W direction. In the fold-and-thrust belt of SYB, there exists a very thick (> 10-12 km) sediments including two or three velocity reversals. East of this package, several west-verging events are recognized down to a depth of 7-8 km, probably corresponding to the faults and structural boundaries formed by the collision process. The HMT was well imaged both by seismic reflection processing and refraction/wide-angle reflection analysis, along which the crystalline basement is almost outcropped. Beneath these complicated structures, we succeeded in imaging the NE Japan Arc crust which descends eastward to a depth of about 40 km under the hinterland side.

In the northern HCZ, the clear crustal delamination is not seen. The obduction of the upper Kuril crust starts at a deeper crustal level of at least 27-30 km and more easterly (~20 km) of the HMT as compared

©2019. Japan Geoscience Union. All Right Reserved. 

with the case in the southern HCZ. If the metamorphic rocks outcropped east of the HMT are the same crustal materials at depths shallower than 23 km as in the case of the southern HCZ, the deeper crustal portion originally situated at 23-27~30 km depth must exist in the western side of the present HMT. The very strong and deep reflectors found west of the HMT might result from the mixture of upper crustal (low velocity) materials of the NE Japan Arc and middle/lower crustal (high velocity) materials of the Kuril Arc.

Keywords: crustal and upper mantle structure, Hokkaido Island, Controlled-source seismic experiments, Arc-arc collision, Hidaka, Delamination of crust

©2019. Japan Geoscience Union. All Right Reserved. 

# Seismic imaging of the eastern Japan forearc region using S-net data

*Genti Toyokuni[1], Dapeng Zhao[1], Naoki Uchida[1], Takashi NAKAYAMA[1]

1. RCPEVE, Tohoku Univ.

The great 2011 Tohoku-oki earthquake (Mw 9.0) occurred off the Pacific coast of Northeast Japan, where the Pacific plate is subducting beneath the Okhotsk plate. The S-net (the Seafloor observation network for earthquakes and tsunamis along the Japan Trench), initiated in 2016, is a large-scale, permanent, ocean-floor seismograph network with cabled 150 stations, which covers a wide oceanic region off Northeast Japan (Kanazawa, 2013). In this study, we aim to reveal the 3-D seismic velocity structure beneath the forearc region covered by the S-net.

We carefully picked 3754 first P-wave arrival times of 63 local earthquakes (M3.5–6.2) in the Tohoku forearc region from the continuous S-net records. Then, the newly picked data are integrated with the existing arrival-time data (Zhao et al., 2012) of 360 teleseismic and 1,180 local earthquakes recorded at 3,205 Hi-net stations on the Japanese land areas. These combined data are inverted to obtain a new 3-D P-wave velocity (Vp) model beneath the entire Northeast Japan arc by using the seismic tomography method of Zhao et al. (2012).

In this work we focus on the obtained 3-D images at depths < 40 km below the region covered by the S-net. The major results are summarized as follows.
(1) Prominent low-Vp anomalies are revealed in the off-Iwate and off-Fukushima areas. These features are consistent with those revealed by previous works (e.g., Zhao et al., 2011; Huang & Zhao, 2013; Liu and Zhao, 2018), indicating that our hand-picked arrival-time data are quite accurate and robust.
(2) A significant high-Vp anomaly is revealed along the Japan Trench especially beneath the off-Miyagi region where the 2011 Tohoku-oki earthquake (Mw 9.0) occurred, which may reflect that the sedimentary layer is very thin above the subducting Pacific plate.

References
Huang, Z., D. Zhao (2013) JAES, 70–71, 160–168.
Kanazawa, T. (2013) Underwater Technology Symposium (UT), 2013 IEEE International.
Liu, X., D. Zhao (2018) Science Advances 4, eaat4396.
Zhao, D. et al. (2011) GRL 38, L17308.
Zhao, D. et al. (2012) GJI 190, 816–828.

Keywords: Seismic tomography, Offshore Northeast Japan, S-net, 3-D velocity structure

©2019. Japan Geoscience Union. All Right Reserved. 

# The relationship between the location of the mid crustal reflector and seismicity in Iwaki area, northeastern Japan

*Takashi Iidaka[1], Shin'ichi Sakai[1], Toshihiro Igarashi[1], Kazushige Obara[1], Aitaro Kato[1], Tetsuya Takeda[2], Shigeki Nakagawa[1]

1. Earthquake Research Institute, University of Tokyo, 2. National Research Institute for Earth Science and Disaster Resilience

The Tohoku-Oki earthquake occurred on March 11, 2011. After the 2011 Tohoku-Oki earthquake, the seismicity in Japan changed. The seismicity increased in some areas. The seismicity decreased areas also exist. It has been considered that the change of the seismicity is related to the change of the stress field caused by the large slip at the plate boundary. The Iwaki area, northeastern part of Japan, is one of the areas that the seismicity changed. The seismicity in this area increased drastically. Before the 2011 Tohoku-Oki earthquake, the seismicity was very low. But, the seismicity increased after the Tohoku-Oki earthquake. The cause of the changes of seismicity was not clear. It is very important to survey the crustal structure in order to understand the mechanism of the seismicity in this region. The characteristics of the seismicity of the area are following. The earthquakes were occurred within a triangle area. The size of the one side of the triangle was around 50 km. The crustal seismicity in the area divided into two depth range. The seismicity in the shallower area is less than 15 km. The depth range of the other group is 15–25 km.

A temporary dense seismic array (63 seismometers) has been deployed to know the seismicity and mechanism in this area. Usuda (Master thesis 2018) studied the crustal structure using this data. The crustal structure was studied with a reversed VSP (Vertical Seismic Profile) method. The clear two later phases were detected. One of the later phases was the reflected wave at the Moho boundary. The other phase was the reflected phase at the middle of crust. The location of the boundary of the middle of the crust was consistent with that of seismic activity area inside the crust. The amplitude of the reflected wave was very large. It was expected that the reflected wave was caused by the reflector with fluid.

We researched that the relationship between the seismicity in this area and location of the mid-crustal reflector. In this area, the seismicity increases from March, 11, 2011. The seismicity started at the southern part the reflector. The seismicity increased in and around reflector area from Mar., 11 to Apr. 10, 2011. At the northern part of the reflector, a relatively low-seismicity area appeared. On the Apr., 11, 2011, the Hamadori earthquake occurred in the low-seismicity area. We suppose that there is some relationship between the seismicity of the area and reflector. If the reflector is caused by the crustal fluid, the increase of the seismicity in Iwaki area might be related to the crustal fluid.
The outline of reflector obtained by Usuda (Master thesis 2018) is related to the location of the temporally seismic stations. In Iwaki region, the earthquakes are located at the north of the reflector. We want to know the true size of the reflector. We researched the waveforms of the seismic stations located in the north of the reflector area. Hi-net and F-net stations were used. The later phase with large amplitude was found at the seismic stations. We found the reflector at the north of the reflector of Usuda (2018).

Keywords: Iwaki area, seismicity, reflector

©2019. Japan Geoscience Union. All Right Reserved. 

# Abnormal Seismic Anisotropy beneath the Tokyo Metropolitan Area (1) Mantle of the Philippine Sea Slab

*Motoko Ishise[1], Shin'ichi Sakai[1], Aitaro Kato[1], Shin Aoi[2], Makoto MATSUBARA[2]

1. Earthquake Reseach Institute, University of Tokyo, 2. National Research Institute for EarthScience and Disaster Resillience

## 1. Introduction

The Tokyo metropolitan area is located on a unique convergence zone associated with the North American (NA) plate: beneath the metropolitan area, dual subduction system was formed by the Pacific (PAC) and Philippine Sea (PHS) plates. Furthermore, subduction of the PHS slab brings a collision zone between the NA plate and the Izu-Ogasawara islands arc, which is on the PHS slab, in the vicinity of the metropolitan area. Therefore, the metropolitan area is seismically active and has various types of earthquakes. However, the relationship between the configuration of plates (the NA, PAC, and PHS plates) and the seismicity remains unknown, although seismo-tectonics of the region has been studied from the various points of view, such as earthquake mechanism, hypocenter distribution, and seismic velocity structure. Thus, we focus on seismic anisotropy that could provide useful information on dynamics and tectonic. In this study, we investigate the three-dimensional (3D) structure of P-wave azimuthal anisotropy beneath the Tokyo metropolitan area.

## 2. Data and Method

The modeling space is the Tokyo metropolitan area (34.7 - 36.8˚N, 138.5 - 141.5˚E, 0 - 150 km). In order to determine 3D P-wave azimuthal anisotropy velocity structure, seismic anisotropy tomography method of Ishise and Oda [2008] was applied to 442960 P wave arrival time data from 1859 local earthquakes recorded at 500 seismic stations, including 296 Meso-net stations. Initial source parameters (location and origin time of earthquake) used in this analysis were determined independently by NIED. The 3D velocity structure in the modeling space is described by velocity parameters assigned to a 3D grid structure. The grid structure was composed of 0.1˚ - 0.2˚ grid spacing in the latitude and longitude directions. In the vertical direction, grid nodes were spaced at 5 - 20 km.

## 3. Results

As a result of the tomographic analysis, we found a unique anisotropy region in the lower edge of the PHS slab mantle, or rather the contact zone between the PHS and PAC slabs. The region has strong anisotropy, and the fast axes are uniformly oriented in the N-S trending direction. Generally, anisotropy in the slab can be explained by lattice preferred orientation of mantle minerals or alignments of cracks and faults. However, any mechanism cannot explain the N-S trending anisotropy in the PHS slab beneath the study area. It might suggest that the modeling under the assumption of azimuthal anisotropy would be inappropriate for the study area. Alternatively, it is possible that we have to change our basic idea of the subduction zone.

Acknowledgments: We used Hi-net seismological data. This study was supported by the Tokyo metropolitan project.

©2019. Japan Geoscience Union. All Right Reserved. 

Keywords: seismic anisotropy tomography, Tokyo metropolitan area, Philippine Sea slab, Pacific slab

©2019. Japan Geoscience Union. All Right Reserved. 

[J] Oral | S (Solid Earth Sciences)：S-SS Seismology

Thu. May 30, 2019 3:30 PM - 5:00 PM JST | Thu. May 30, 2019 6:30 AM - 8:00 AM UTC | A05 TOKYO BAY MAKUHARI HALL

## [S-SS12] Crustal Structure

convener:Kazuo Nakahigashi(Tokyo University of Marine Science and Technology), Chairperson:Tsuruga Kayoko(Tokyo University of Marine Science and Technology), Yojiro Yamamoto(Japan Agency for Marine-Earth Science and Technology)

The aim of this session is to cover seismological and geophysical studies on the Earth's crust. Contribution on seismological and geophysical structure of the crust, processes that develop in the crust which include earthquakes, volcanoes and geological descriptions of the crust are welcomed. We also welcome theoretical and methodological studies that will serve as basics in such explorations.

3:30 PM - 3:45 PM JST | 6:30 AM - 6:45 AM UTC

### [SSS12-07] Deep seismic reflection profiling across the Suruga trough, Shizuoka, Japan

*Hiroshi Sato[1], Kayoko Tsuruga[2], Hisatoshi Baba[3], Tatsuya Ishiyama[1], Shinji Kawasaki[4], Yasuhisa Tanaka[4], Toshifumi Hayashi[2], Yoshihiro Sekino[2], Masanao Shinohara[1], Takaya Iwasaki[1], Makoto MATSUBARA[5], Naoshi Hirata[1,5] (1.Earthquake Research Institute, The University of Tokyo, 2.Tokyo University of Marine Science and Technology, 3.Tokai Univerisity, 4.JGI Inc., 5.National Research Institute for Earth Science and Disaster Resilience)

3:45 PM - 4:00 PM JST | 6:45 AM - 7:00 AM UTC

### [SSS12-08] Multi-channel seismic profiling in the northern part of Suruga bay using the Shiyomaru-vessel of Tokyo University of Marine Science and Technology (Preliminary report)

*Kayoko Tsuruga[1], Hiroshi Sato[2], Hisatoshi Baba[3], Yoshihiro Sekino[1], Toshifumi Hayashi[1], Hayato Kondotec[1], Chiharu Aoyama[1], Tetsutaro Aikawa[1], Tatsuya Ishiyama[2], Masanao Shinohara[2], Shinji Kawasaki[4], Yasuhisa Tanaka[4] (1.Tokyo University of Marine Science and Technology, 2.University of Tokyo, 3.Tokai University, 4.JGI, Inc.)

4:00 PM - 4:15 PM JST | 7:00 AM - 7:15 AM UTC

### [SSS12-09] Crustal structure refraction survey using Airgun-OBS in the northern part of Suruga Bay -Fujikawa fault zone- (Preliminary Report)

*Hisatoshi Baba[1], Kayoko Tsuruga[2], Hiroshi Sato[3], Tatsuya Ishiyama[3], Masanao Shinohara[3], Takahito Nishimiya[4], Shintaro Abe[5] (1.Department of Marine and Earth Science, Tokai University, 2.Tokyo University of Marine Science and Technology, 3.Earthquake Research Institute, University of Tokyo, 4.Meteorological Research Institute, Japan Meteorological Agency, 5.Association for the Development of Earthquake Prediction)

4:15 PM - 4:30 PM JST | 7:15 AM - 7:30 AM UTC

### [SSS12-10] 3D seismic attenuation profiling for imaging an active fault in Uchiura wan

*Tetsuro Tsuru[1], Shio Shimizu[1], Mayu Ogawa[1], Jin-Oh Park[2], Seishiro Furuyama[1], Kosaku Arai[3], Takahiko Inoue[3], Chen Guo[2] (1.Tokyo University of Marine Science and Technology, 2.Atmosphere and Ocean Research Institute, The University of Tokyo, 3.National Institute of Advanced Industrial Science and Technology)

4:30 PM - 4:45 PM JST | 7:30 AM - 7:45 AM UTC

### [SSS12-11] Gravity survey at the extension of the Takahama fault and the Yokosuka fault in Nishio City, Aichi Prefecture

*Tokunosuke Tatsuzawa[1,2], Tatsuya Sumita[2], Shinobu Ito[2], Tomoya Abe[2] (1.Department of Earth Sciences, Resources and Environmental Engineering, Creative Science and Engineering, Faculty of Science and Engineering, Waseda University, 2.National Institute of Advanced Industrial Science and Technology)

4:45 PM - 5:00 PM JST | 7:45 AM - 8:00 AM UTC

[SSS12-12] Subduction geometry and seismicity around northern Ryukyu subduction zone

*Yojiro Yamamoto[1], Tsutomu Takahashi[1], Yasushi Ishihara[1], Koichiro Obana[1], Seiichi Miura[1], Shuichi Kodaira[1], Yoshiyuki Kaneda[2] (1.Japan Agency for Marine-Earth Science and Technology (JAMSTEC), 2.Kagawa University)

# Deep seismic reflection profiling across the Suruga trough, Shizuoka, Japan

*Hiroshi Sato[1], Kayoko Tsuruga[2], Hisatoshi Baba[3], Tatsuya Ishiyama[1], Shinji Kawasaki[4], Yasuhisa Tanaka[4], Toshifumi Hayashi[2], Yoshihiro Sekino[2], Masanao Shinohara[1], Takaya Iwasaki[1], Makoto MATSUBARA[5], Naoshi Hirata[1,5]

1. Earthquake Research Institute, The University of Tokyo, 2. Tokyo University of Marine Science and Technology, 3. Tokai Univerisity, 4. JGI Inc., 5. National Research Institute for Earth Science and Disaster Resilience

An onshore-offshore seismic data set was collected across the Suruga bay in 2018 to determine the deep structure of the subducting Philippine Sea plate (PHS), whose upper surface is estimated to be a seismogenic source fault of the Fujikawa fault system. Three-component of land seismometers (GSX) were deployed with a spacing 100 –200 m from the southern range of Akaishi Mountains to Yui and western part of Izu Peninsula along the seismic lines using total 300 seismometers along the 40-km-long seismic lines. Three-component of ocean bottom seismometers (OBSs) were deployed with spacing of 1 km on the sea bottom deeper than 500 m along the 18 km-long marine part. Five shallow marine ocean bottom seismometers (OBXs) were deployed at the shallow marine western part of Suruga Bay along the 2-km-long interval. They recorded seismic shots generated from four, 200 kg dynamite shots and air gun array with a total volume of 1950 cu. inch. Total number of shots by air gun array was 1479 and shot spacing was 25 m. Data quality is good, allowing the identification of clear refraction by air gun array in the integrated shot gathers. Multi-channel seismic data were also collected towing a 600-m-long streamer cable with 96-ch hydrophones (Tsuruga et al., 2019 JpGU). The redatumed seismic data were produced using interferometric OBS imaging method (Shiraishi et al., 2016). All seismic data were processed according to a standard common-midpoint (CMP) stacking and a post stack time migration. We used refraction tomography to determine the P-wave velocity structure, that revealed down to 10 km in depth beneath the central part of the seismic line. Obtained post-migrated time section portrays the west-dipping reflectors from 3.5 sec (TWT) to 7 sec beneath the eastern part of the Suruga bay, from 5 to 11 sec beneath thesouthern range of Akaishi Mountains. The migrated time section was depth converted using the velocity structure obtained by earthquake tomography based on Hi-net data. On the depth section the depth to an estimated upper surface of PHS is 7 km beneath Yui, western coast of Suruga bay, and 15 km in beneath the central part of land seismic line in the Shizuoka side. The p-wave velocity structure deduced by refraction tomography reveal the wedge-shaped low-velocity area beneath the western part of Suruga bay. The velocity structure accords well to the subduction of PHS and distribution of hypocenters.

The onshore-offshore seismic survey was performed under the Integrated Research Project on the Fujikawa-kako fault zone funded by MEXT. This survey also supported by the research fund of ERI, Univ. Tokyo.

Keywords: plate boundary megathrust, deep seismic reflection profiling, Izu collision zone

©2019. Japan Geoscience Union. All Right Reserved. 

# Multi-channel seismic profiling in the northern part of Suruga bay using the Shiyomaru-vessel of Tokyo University of Marine Science and Technology (Preliminary report)

*Kayoko Tsuruga[1], Hiroshi Sato[2], Hisatoshi Baba[3], Yoshihiro Sekino[1], Toshifumi Hayashi[1], Hayato Kondotec[1], Chiharu Aoyama[1], Tetsutaro Aikawa[1], Tatsuya Ishiyama[2], Masanao Shinohara[2], Shinji Kawasaki[4], Yasuhisa Tanaka[4]

1. Tokyo University of Marine Science and Technology, 2. University of Tokyo, 3. Tokai University, 4. JGI, Inc.

There is few detail observations and studies about the subduction structure in Suruga trough area as a plate boundary between the Philippine sea plate and Eurasia plate. It is very important to understand the detail structure of Fujigawa fault system to prevent and reduce earthquake disaster by future Tokai earthquake. We have been trying to clarify a shallow structure in this important area by means of both seismic reflection and refraction surveys since 2016 and 2017 (Tsuruga *et al.*, 2016, 2017, 2018). In this report, we show the preliminary results of the seismic reflection and refraction surveys in Suruga Bay, Central Japan, conducted by Shiyomaru-vessel of Tokyo University of Marine Science and Technology (TUMSAT) cooperated with University of Tokyo and Tokai University.

We conducted the 2-D seismic reflection and refraction survey with air-guns and streamer cable system in Suruga Bay, from Oct. 1 to 9, 2018, along three surrey lines (*i.e.*, H30-L00/R00, H30-L01 and H30-L02 lines) which were located in the northern part of Suruga bay with the length of 19.5 km, 20.0 km and 16.1 km, respectively. We used two Bolt air-gun source systems of ‘Tri-Gun’ 1500LL (350 cu.in x 3) and 1500LL (300cu.in x 3) with a total air volume of 1,950 cu.in for H30-L00/R00 and H30-L02 survey lines with a shot interval of 50 m while we used Tri-Gun 1500LL (350cu.in x 3 ) with a volume of 1050cu.in with a shot interval of 25 m along H30-L01 line. Total shot number was 2717. Hydrophone receivers array consisted of Hydroscience digital streamer cable including 96 channel sensors with an interval of 6.25 m inside a cable of 600 m long, and a small tailbouy. TUMSAT research vessel ‘Shinyomaru’ has the following principle specifications: length, beam, and gross tonnage are 65 m, 12.5m, and 986 tons, respectively. Details of the refraction survey across a land area and oceanic area will be shown by Sato *et al*. and Baba *et al*. (in this meeting, 2019).

Preliminary results show some important features as follows: Reflection section of H30-L00 indicates a continuous west-tilting reflection phase which may be located around an upper boundary of the sedimentary layers over the subducting oceanic plate toward west. These reflection phases might be continued to the those along H29-L02 located in the northern area and H30-L02 and H28-L03 located in the southern area. We have not found the dominant characteristics of subduction boundary in these observations. Along H30-L01 we might find an interesting feature as a boundary between Honshu block and Izu peninsula. The details of our result will be shown in the presentation.

This study was supported by fond from the Ministry of Education, Culture, Sports, Science and Technology. We appreciate the big cooperation by Shizuoka prefecture Federation of Fisheries Cooperative Associations and many Fishery Cooperatives around Suruga Bay to understand our study. We thank Tokai University for helping us in an ocean by a vessel ‘Hokuto’. Finally, we greatly thank Shinyomaru's crews and many staffs of our university for their encouragement and helps.

©2019. Japan Geoscience Union. All Right Reserved. 

Keywords: Plate boundary, Seismic reflection and refraction survey, Suruga Trough

©2019. Japan Geoscience Union. All Right Reserved. 

# Crustal structure refraction survey using Airgun-OBS in the northern part of Suruga Bay -Fujikawa fault zone- (Preliminary Report)

*Hisatoshi Baba[1], Kayoko Tsuruga[2], Hiroshi Sato[3], Tatsuya Ishiyama[3], Masanao Shinohara[3], Takahito Nishimiya[4], Shintaro Abe[5]

1. Department of Marine and Earth Science, Tokai University, 2. Tokyo University of Marine Science and Technology, 3. Earthquake Research Institute, University of Tokyo, 4. Meteorological Research Institute, Japan Meteorological Agency, 5. Association for the Development of Earthquake Prediction

As part of the exploration of the crustal structure of the Ministry of Education, Culture, Sports, Science and Technology "Priority investigation observation in the Fujikawa fault zone" (Sato et al., 2019 (the present Society); Tsuruga et al., 2019 (the present Society)), in Suruga Bay Reflection and refraction seismic survey by the Tokyo University of Marine Science and Technology, practice ship "Shinyo Maru (986 tons)" was carried out at a survey line of about 19 km (H30 - L00 main line) traversing north to east and west. In this our presentation, we present a preliminary report on the outline of Airgun-OBS structure exploration (refraction seismic survey) and the results obtained.

The H30 - L00 main line starts at the water depth of 485 m in Shizuoka, Shimizu, Okitsu City coastal area, the deepest part is 1320 m in the vicinity of the central part of Suruga Trough and the eastern end is over 500 m in the coastal area of Numazu, Heda City. It is a survey line of trough topography sandwiched by slopes. Since the distance between east and west distances in the northern part of Suruga Bay is short and the coastal area is also a fishing ground, the length of the survey line is limited to about 19 km.

For the refraction seismic survey in the main line, two sets of Tri-Gun by Bolt Co., Ltd. (total capacity 1950 $in^3$) were towed, and at about 50 m intervals (since the shooting points were adjusted so as to be interposed between practically approximately blast occurred at intervals of 25 m), 18 sets OBS were deployed at about 980 m intervals. Typhoon 24 passed around Suruga Bay on the day of the exploration, so six of the 18 OBSs caused abnormal floating and so on, and they stranded to the coast (Nakao et al., 2019 (the present Society)), so data could not be obtained near the Suruga trough central axis. However, good records were obtained with 12 OBS.

Analysis is ongoing. Looking at the state of each Record Section obtained, the first arrival data can be clearly confirmed throughout the survey line, but a complex structure is presumed because it is also a line surrounding the plate boundary. The earliest layer of apparent velocity is about 6.8 km / sec, and the velocity structure model is estimated to be roughly 5-layer structure. The sedimentary layer of the first, the second and the third layer (acoustic basement layer) are inclined to the west side towards the Suruga Bay central axis, and the reflection cross section (Tsuruga et al., 2019 (the present Society)) and Match. Detailed structure model results will be reported in this presentation.

We have greatly cooperated and inconvenienced the Yui Port Fishery Cooperative Association, Shimizu Fisher Cooperative Cooperative Association and Toda Fisher Cooperative Cooperative Association for the establishment of OBS.

Keywords: Suruga Bay, OBS, Crustal Structure

©2019. Japan Geoscience Union. All Right Reserved. 

# 3D seismic attenuation profiling for imaging an active fault in Uchiura wan

*Tetsuro Tsuru[1], Shio Shimizu[1], Mayu Ogawa[1], Jin-Oh Park[2], Seishiro Furuyama[1], Kosaku Arai[3], Takahiko Inoue[3], Chen Guo[2]

1. Tokyo University of Marine Science and Technology, 2. Atmosphere and Ocean Research Institute, The University of Tokyo, 3. National Institute of Advanced Industrial Science and Technology

We tested seismic attenuation profiling (SAP) to image active faults on a mini-3D seismic reflection dataset observed at Uchiura wan in 2018. Seismic reflection surveys are often conducted to investigate not only geological structures but also development of faults in sedimentary basins, because the past activities of faults are recorded as offsets of geological formations at their locations. However, it is sometimes difficult to specify the existence of faults within highly faulted/fractured areas because seismic reflections are inherently invisible there. SAP has been, therefore, applied to image faults as well as fractures and investigate their activities in poorly reflective areas: the igneous oceanic crust and volcanic areas.

SAP is a method to map seismic attenuation property using seismic reflection data. The authors use the spectral ratio method to estimate Q from seismic reflection data in frequency domain, because the method can be robustly applied in poorly reflective area. Reversely, Q-estimation methods in time domain are not stable in such areas because no reliable amplitude information is available there. However, SAP using the spectral ratio method has not been applied to image faults and fractures developed in sedimentary units (e.g. Tsuru et al, 2017; 2018), because the accuracy in Q-estimation decreases due to spectrum distortions. The spectrum distortions are mostly caused by interruption between primary reflections and interbed multiples within the sedimentary layers. Shimizu (2019) investigated the influences of several Q-estimation methods to interbed multiples by numerical experiments and then improved some processing parameters in the estimation of Q in the frequency domain. As a result, the authors successfully imaged a trend of an active fault on SAP time-slices (Q-slices) from a mini-3D seismic reflection dataset.

A high-resolution mini-3D seismic survey was conducted at Uciura wan in Suruga Bay on August 7$^{th}$ in 2018, by chartering R/V Daini Ikoi Maru of Oki Seatec Co., Ltd. During the survey, twenty of seismic lines were collected with sampling rate of 1 ms. An underwater speaker was adopted as an energy source in consideration of mitigating impact on marine ecosystem. Shot records were collected every 10 s (equivalent to about 10 m with the vessel speed of 2 knots) with a streamer cable of 16 channels. The source and the streamer cable were towed at 0.5 and about 1 m depths, respectively.

As a result of seismic data processing, including band-pass filter, NMO corrections and stacking with one velocity of 1500 m/s, a 3D seismic cube was created. The seismic cube was used for input data of SAP analysis. The data processing was conducted by MATLAB. On the other hand, as a result of the SAP analysis, a 3D cube of average Q was created. An active fault, which cuts seafloor, was clearly demonstrated over several seismic reflection profiles. However, its trend was not clear on seismic time-slices. Reversely, the trend of active fault was clearly figured out on several Q-slices as high attenuation anomalies. In this paper, we would like to show the results of SAP analysis from the mini 3D seismic reflection data observed in Uchiura wan.

©2019. Japan Geoscience Union. All Right Reserved. 

Keywords: seismic attenuation, active fault, 3D seismic data

©2019. Japan Geoscience Union. All Right Reserved. 

# Gravity survey at the extension of the Takahama fault and the Yokosuka fault in Nishio City, Aichi Prefecture

*Tokunosuke Tatsuzawa[1,2], Tatsuya Sumita[2], Shinobu Ito[2], Tomoya Abe[2]

1. Department of Earth Sciences, Resources and Environmental Engineering, Creative Science and Engineering, Faculty of Science and Engineering, Waseda University, 2. National Institute of Advanced Industrial Science and Technology

We conducted a gravity survey in Nishio city, Aichi Prefecture to clarify the subsurface structure related to the Takahama fault and the Yokosuka fault (Fig.1). Seismic reflection survey was held in that area in September 2018 (Ito, 2019) and the velocity structure was also obtained by refraction analysis. Then, we consider that we can clarify more detailed subsurface structure by conducting gravity survey on the seismic survey lines and their extensions (Line1 and Line2) and also by comparing gravity survey results with the seismic survey results. We also conducted gravity survey along the Yahagi Furukawa river (Line 3) that is supposed to cross the northern extension of the Yokosuka fault in the active fault map “Gamagori” (Okada et al., 2004) issued by Geospatial Information Authority of Japan and that is also crossing the concealed fault inferred by Sugito and Okada(2004).
In this survey, a total of 150 points of relative gravity was measured by the Lacoste D-type gravimeter (D68) and the Lacoste G-type gravimeter (G304). Measurement distance intervals were about 50m or 100m on Line1 and Line 2, about 30m or 50m on Line 3. The location coordinates of each gravity measurement point were mainly measured by GNSS(network type RTK-VRS), while some points were also measured by Total Station. Gravity anomaly was calculated by the standard procedure SPECG1988 (GSJ Gravity Survey Group, 1989). We performed terrain correction with 50m mesh DEM (Murata et al., 1996) for the Bouguer anomaly calculation. The contribution of terrain on gravity anomaly is small because the surveyed area is nearly flat. In fact, the maximum difference between simple Bouguer anomaly and the Bouguer anomaly calculated with 50m mesh DEM is 0.074mGal, and the pattern of the anomaly profile does not differ greatly between them.
As a result of gravity survey, the pattern of the Bouguer anomaly profile on Line1 and Line 2 is well related to the contour line of 3000m/s in P wave velocity section by the refraction analysis. On Line3, the Bouguer anomaly shows significant change around the point where the presence of the concealed fault of the Yokosuka fault was estimated (Sugito and Okada, 2004; Imaizumi et al., 2018). In addition, the Bouguer anomaly shows complex change on the eastern part of Line 2, where the P wave velocity is also lower than surrounding area by the result of the refraction analysis. In the coming months, we are going to make the density structure model by using the reflection boundary of the seismic profile and the gravity anomaly to reveal the details.

Reference

GSJ Gravity Survey Group (1989) On the standard procedure SPECG1988 for evaluating the correction of gravity at the Geological Survey of Japan. Bull. Geol. Surv. Japan, vol.40(11), p.601-611
Ito, S., (2019), Subsurface Structure at the North of the Yokosuka Fault by Seismic Reflection Survey, this meeting
Imaizumi, T., Miyauchi, T., Tsutsumi, H., Nakata, T. (2018) Digital Active Fault Map of Japan [Revised Edition], 154p
Murata, Y., Makino, M., Endo, H., Watanabe, K., Watanabe, S., Urabe, A. (1996) Microgravity survey in Kobe, Ashiya and Nishinomiya cities, Kinki district, Japan(1)-Bouguer anomaly and concealed faults-. Bull. Geol. Surv. Japan, vol.47(2/3), p.109-132

©2019. Japan Geoscience Union. All Right Reserved. 

Okada, A., Suzuki, Y., Tsutsumi, H., Togo, M. (2004) 1:25,000 The active fault map “Gamagori”, Geospatial Information Authority of Japan
Sugito, N., Okada, A. (2004) Surface rupture associated with the 1945 Mikawa Earthquake, Active Fault Research, vol.24, p.103-127

Keywords: active fault, gravity anomaly, subsurface structure, density structure, seismic reflection survey, Lacoste gravimeter

©2019. Japan Geoscience Union. All Right Reserved. 

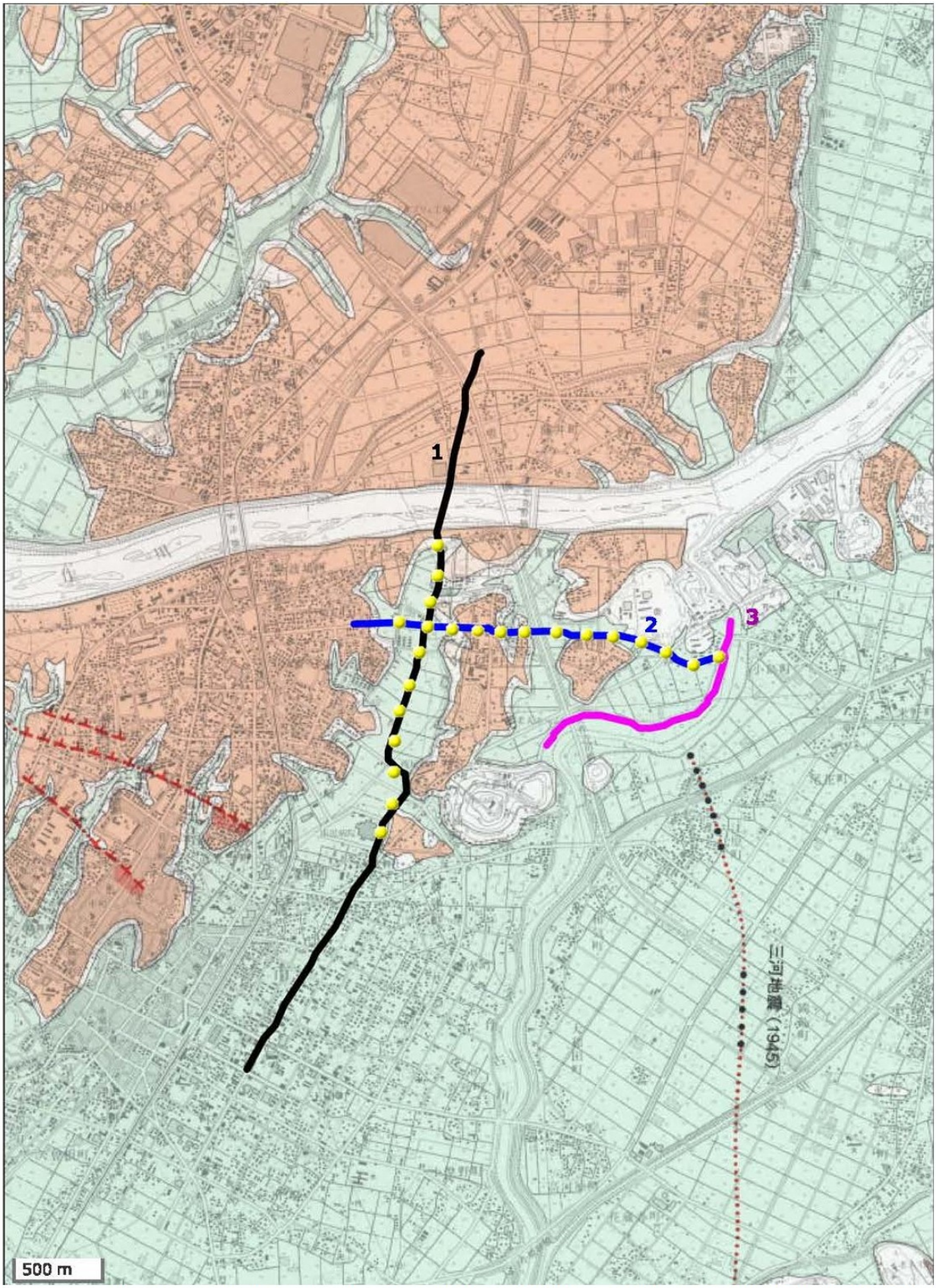


図1　愛知県西尾市における重力探査測線。都市圏活断層図「蒲郡」（岡田ほか、2004）をもとに加工して作成。
黒線が測線1、青線が測線2、紫線が測線3、を示す。測線1及び測線2の一部では反射法地震探査（2019、伊藤）が実施された。黄点線はその地震探査測線を示す。赤線は活断層、赤点は活断層(伏在部)、黒点は地震断層を示す。

©2019. Japan Geoscience Union. All Right Reserved. 

©2019. Japan Geoscience Union. All Right Reserved. 

# Subduction geometry and seismicity around northern Ryukyu subduction zone

*Yojiro Yamamoto[1], Tsutomu Takahashi[1], Yasushi Ishihara[1], Koichiro Obana[1], Seiichi Miura[1], Shuichi Kodaira[1], Yoshiyuki Kaneda[2]

1. Japan Agency for Marine-Earth Science and Technology (JAMSTEC), 2. Kagawa University

At the Ryukyu subduction zone, located forearc region of Japan’ s Southwest Islands, the Philippine Sea plate is subducting beneath the Eurasian plate toward northwest direction. Due to the subduction, not only active seismicity but also short-term slow slip event (SSE) (Nishimura, 2014) and low frequency tremor (LFT) activity (Yamashita et al., 2015) were observed in the forearc region of Ryukyu arc. However, the subduction geometry is still unclear since seismic and geodetic stations are limited to the sparsely distributed islands. To know the seismicity, lithospheric structures and subduction geometry, Japan Agency for Marine-Earth Science and Technology (JAMSTEC) launched a series of seismic observations and active-source seismic surveys at the Ryukyu arc from 2013, as a part of research project funded by Ministry of Education, Culture, Sports, Science and Technology, Japan. In FY2016, we have conducted a passive source observation in the northern Ryukyu forearc region. We have deployed 47 seismic stations including 43 ocean bottom seismographs (OBS) and 4 onshore stations at Tanegashima (two stations), Nakano-shima, and Akuseki-jima. The observation period of OBS is about 4 months, from September to December 2016.

In this study, we conduct double-difference seismic tomography (Zhang and Thurber, 2006) to obtain both precious hypocenter location and structural information around plate boundary. We combine 1,303 events detect from our observation data with 454 events from Japan Meteorological Agency (JMA) with our data set. To improve the spatial resolution and ray coverage, we also used the arrival time data at 33 permanent stations from JMA seismic catalogue and dataset of a part of previous OBS observation in Hyuga-nada (Yamamoto et al., 2013; 161 events and 27 OBSs). After the tomographic inversion, we estimate the focal mechanisms by using P-wave first arrival polarity data. Then, we establish the subduction geometry model with reference to the velocity model, distribution of low-angle thrust type earthquakes, previous geometry model based on active source surveys (Nishizawa et al., 2009, 2017; Nakanishi et al., 2018).

Estimated subduction geometry indicates that there is no obvious roughness in this study area. Interplate earthquake, defined as earthquakes within 5 km from plate boundary of this study, is active at depth between 15 and 30 km especially in the southern part. The down-dip limit of interplate earthquakes is corresponding to the high Vp/Vs just above the plate boundary, suggesting that the existence of serpentinized mantle wedge. In addition, LFT, SSE, and interplate earthquake seem to be separately occurred along the plate boundary. Intraslab earthquake is also active. Some of them occurred in the seaward of trench axis. The separation between intraslab earthquakes and plate boundary is larger (25 ~ 30 km) in northern part than that in southern part (15 ~ 20 km). This regionality might be relate to the subduction of Amami Plateau.

Keywords: Ryukyu Trench subduction zone, Philippine Sea Plate, seismicity, tomography

©2019. Japan Geoscience Union. All Right Reserved. 

[E] Oral | S (Solid Earth Sciences )：S-IT Science of the Earth's Interior & Techtonophysics

Thu. May 30, 2019 9:00 AM - 10:30 AM JST | Thu. May 30, 2019 12:00 AM - 1:30 AM UTC | A09 TOKYO BAY MAKUHARI HALL

## [S-IT25] Planetary cores: Structure, formation, and evolution

convener:Hidenori Terasaki(Graduate School of Science, Osaka University), Eiji Ohtani(Department of Earth and Planetary Materials Science, Graduate School of Science, Tohoku University), William F McDonough(University of Maryland College Park), George Helffrich(Earth-Life Science Institute, Tokyo Institute of Technology), Chairperson:George Helffrich(ELSI, Tokyo Institute of Technology), Hidenori Terasaki

There are fundamental links between the formation and evolution of planets and their satellites to that of their cores. Defining the physical and chemical properties of the cores of these terrestrial bodies are fundamental for understanding their internal structures and thermal profile. Recent advances in experimental and theoretical studies provide new insights and applications to the Earth's cores and other terrestrial bodies. Near-future exploration missions will obtain data on the internal structure of terrestrial planets (e.g., Mars and Mercury) and planet-satellite systems. We anticipate presentations on recent advances on the physical and chemical properties of cores and discussions regarding the latest views of their formation and evolution. We welcome contributions from mineral/rock physics, geophysics, geochemistry, geodynamics, and planetary science.

9:00 AM - 9:15 AM JST | 12:00 AM - 12:15 AM UTC

[SIT25-01] **High-pressure Equation of State of Schreibersite $Fe_{2.15}Ni_{0.85}P$: Implications for the Martian Core**

*Xuejing He[1], Jiazeng Guo[2], Xiang Wu[3], Shengxuan Huang[1], Fei Qin[1], Xiangping Gu[4], Shan Qin[1] (1.Peking Univ., 2.Nanyang Normal Univ., 3.China Univ. of Geosciences, 4.Central South Univ.)

9:15 AM - 9:30 AM JST | 12:15 AM - 12:30 AM UTC

[SIT25-02] Bottom-up solidification versus top-down solidification of the liquid core of the relatively small planetary bodies

*Satoru Urakawa[1], Hidenori Terasaki[2] (1.Department of Earth Sciences, Okayama University, 2.Department of Earth and Space Science, Osaka University)

9:30 AM - 9:45 AM JST | 12:30 AM - 12:45 AM UTC

[SIT25-03] P-wave velocity of $Fe_3S$ under high pressure and temperature

*Seiji Kamada[1,2], Hidenori Terasaki[3], Hiroshi Fukui[4,5], Tatsuya Sakamaki[2], Hiroshi Uchiyama[6], Satoshi Tsutsui[6], Eiji Ohtani[2], Alfred Q.R. Baron[5] (1.Frontier Research Institute for Interdisciplinary Sciences, Tohoku University, 2.Department of Earth Science, Graduate School of Science, Tohoku University, 3.Department of Earth and Space Science, Graduate School of Science, Osaka University, 4.Graduate School of Material Science, University of Hyogo, 5.RIKEN, 6.JASRI)

9:45 AM - 10:00 AM JST | 12:45 AM - 1:00 AM UTC

[SIT25-04] The sound velocity of liquid Fe-Ni-S-Si alloys under Mercury’s core condition

*Iori Yamada[1], Hidenori Terasaki[1], Asaka Kamiya[1], Ryo Tsuruoka[1], Yuji Higo[2], Akihiko Machida[3] (1.Graduate School of Science, Osaka University, 2.Japan Synchrotron Radiation Research Institute, 3.National Institute for Quantum and Radiological Science and Technology)

10:00 AM - 10:15 AM JST | 1:00 AM - 1:15 AM UTC

[SIT25-05] In situ observation of Rayleigh–Taylor instability growth of liquid Fe-Si using laser shock

*Hidenori Terasaki[1], Tatsuhiro Sakaiya[1], Keisuke Shigemori[2], Hiroki Kato[2], Yoichiro Hironaka[2], Tadashi Kondo[1] (1.Graduate School of Science, Osaka University, 2.Institute of Laser Engineering, Osaka University)

10:15 AM - 10:30 AM JST | 1:15 AM - 1:30 AM UTC
Discussion

# High-pressure Equation of State of Schreibersite $Fe_{2.15}Ni_{0.85}P$: Implications for the Martian Core

*Xuejing He[1], Jiazeng Guo[2], Xiang Wu[3], Shengxuan Huang[1], Fei Qin[1], Xiangping Gu[4], Shan Qin[1]

1. Peking Univ., 2. Nanyang Normal Univ., 3. China Univ. of Geosciences, 4. Central South Univ.

Phosphorus is thought to be an important light element existing in planetary cores. The phosphorus abundance is evaluated to be ~0.20 wt% in the Earth's core, and ~0.32 wt% in the Martian core. To fully understand its existence in planetary cores, structural and physical properties of iron-nickel phosphides should be investigated under high pressure and high temperature. $(Fe,Ni)_3P$-schreibersite is observed as a common accessory in the veinlet of iron and stony-iron meteorites, so that it is of significance to discuss and constrain the properties of planetary cores. The equation of state of a natural single-crystal schreibersite, $Fe_{2.15}Ni_{0.85}P$, has been studied up to ~50 GPa at room temperature in a diamond anvil cell using *in situ* synchrotron-radiation X-ray diffraction. The sample kept its tetragonal structure ($I\bar{4}$) up to the highest pressure with no observation of phase transition. Experimental results have shown that the magnetic collapse of $Fe_{2.15}Ni_{0.85}P$ is weakened because of the substitution of nickel, leading to an isotropic axial compressibility. The pressure-volume data were fitted by the third-order Birch-Murnaghan equation of state, yielding $K_0$ = 184(4) GPa, $K_0'$ = 4.1(2), $V_0$ = 365.9(1) $Å^3$. The density of $Fe_{2.15}Ni_{0.85}P$, along with several iron sulfides and iron phosphides has been calculated under relative pressure-temperature conditions of the Martian core. The comparison with that of $\gamma$-Fe and a density model of the Martian core evidences that nickel and phosphorus dopant would result in density reduction of iron sulfides, suggesting that $(Fe,Ni)_3(S,P)$ might be a possible compound existing in the Martian core.

Keywords: schreibersite, high pressure, equation of state, Martian core

©2019. Japan Geoscience Union. All Right Reserved. 

# Bottom-up solidification versus top-down solidification of the liquid core of the relatively small planetary bodies

*Satoru Urakawa[1], Hidenori Terasaki[2]

1. Department of Earth Sciences, Okayama University, 2. Department of Earth and Space Science, Osaka University

Some planetary bodies, such as Mercury and Ganymede, have their own magnetic fields and other bodies, such as the Moon and Mars, once had a magnetic field. These magnetic fields of the relatively small bodies are thought to be originated from core dynamo driven by compositional convection. Compositional convection is related to the density fluctuation due to partial crystallization of liquid core. The phenomenon that iron solidified at the upper part of the core settles is called ‘Fe snowing’ and it is considered as the main cause of compositional convection in the core of the small planetary bodies. However, crystallization of iron occurs from the top of the core in some cases and from the bottom of the core in another case, due to the complexity of melting relationships of iron-light element system under pressure. Whether the top-down freezing occurs or the bottom-up freezing occurs depends on the adiabat in the liquid core and the melting slope of the constituent substance of the core. We have investigated the adiabatic temperature gradient of the Fe-S liquid core based on the thermal expansivity which is determined by X-ray absorption density measurements at high pressures. Then, we divided the pressure-composition space for the Fe-FeS system into the bottom-up solidification field and the top-down solidification field at the pressures up to 10 GPa. These would contribute to understand the generation of magnetic field in the relatively small bodies.

Keywords: Planetary magnetic field, planetary core, compositional convection, adiabat, Fe-S liquid

©2019. Japan Geoscience Union. All Right Reserved. 

# P-wave velocity of $Fe_3S$ under high pressure and temperature

*Seiji Kamada[1,2], Hidenori Terasaki[3], Hiroshi Fukui[4,5], Tatsuya Sakamaki[2], Hiroshi Uchiyama[6], Satoshi Tsutsui[6], Eiji Ohtani[2], Alfred Q.R. Baron[5]

1. Frontier Research Institute for Interdisciplinary Sciences, Tohoku University, 2. Department of Earth Science, Graduate School of Science, Tohoku University, 3. Department of Earth and Space Science, Graduate School of Science, Osaka University, 4. Graduate School of Material Science, University of Hyogo, 5. RIKEN, 6. JASRI

Martian cores have been thought to include a certain amount of sulfur as a light element. Sohl and Spohn (1997) proposed seismic wave velocity and density profiles of the interior of Mars based on equations of state of core matrials although seismic wave velocities of core materials are needed for presice estimation. However, there have been only a limited number of works for $V_P$ of Fe alloys with sulfur. In the Fe-FeS system, $V_P$ of FeS and $FeS_2$ have been studied (e.g. Badro et al. 2007) but these compounds are not appropriate for the core materials of Mars because $Fe_3S$ is a stable phase above 20 GPa corresponding to Martian core conditions (Fei et al., 1997, 2000) up to at least 200 GPa (Kamada et al., 2010, 2012). Therefore, $Fe_3S$ is a subsolidus phase together with $\varepsilon$ -Fe in the Fe-$Fe_3S$ system at Martian core conditions and it is essential to study $V_P$ of $Fe_3S$ to understand seismic properties of the Martian core. We have measured sound $V_P$ of $Fe_3S$ under high temperature and pressure at BL35XU of SPring-8.
In this study, a synthesized $Fe_3S$ was used as a starting material. A symmetric diamond anvil cell was used to generate high pressures. IXS(Inelastic X-ray Scattering) and XRD experiments were performed at the beamline 35XU of SPring-8, Japan (Baron et al., 2000). $V_P$ of $Fe_3S$ were measured up to 100 GPa and 2000 K. We will discuss temperature effect on the $V_P$ of $Fe_3S$ and the Birch's law and seismic wave velocity profile of the Martian core.

Keywords: Inelastic X-ray scattering, diamond anvil cell, laser heateting

©2019. Japan Geoscience Union. All Right Reserved. 

# The sound velocity of liquid Fe-Ni-S-Si alloys under Mercury’s core condition

*Iori Yamada[1], Hidenori Terasaki[1], Asaka Kamiya[1], Ryo Tsuruoka[1], Yuji Higo[2], Akihiko Machida[3]

1. Graduate School of Science, Osaka University, 2. Japan Synchrotron Radiation Research Institute, 3. National Institute for Quantum and Radiological Science and Technology

Mercury has a large liquid core and it mainly consists of Fe-Ni and possibly contains some light elements. The X-ray spectroscopy measurements by the MESSENGER spacecraft indicates that surface on Mercury contains 1-4wt% S (Nittler et al. 2011). When silicate containing 1-4 wt%S coexists with liquid metal, S and Si tend to dissolve into liquid metal based on partitioning of S and Si between metal and silicate melts. This suggests that both S and Si are likely to be included in the outer core of Mercury (Chabot et al. 2014). Thus, elastic properties of liquid Fe-Ni-S-Si at BL04B1 and BL22XU beamlines, SPring-8 Facility. High pressure was generated using 1500ton Kawai-type or 180 ton cubic multianvi press. The sound velocity was measured using the pulse-echo overlap method. We used two kinds of compositions (Fe-11wt%Ni-6wt%S-4wt%Si and Fe-11wt%Ni-3wt%S-8wt%Si) for Fe-Ni-S-Si sample. The P-wave velocity ($V_P$) was measured up to 16 GPa and 2000 K and it increases with pressure. Temperature dependence on the $V_P$ of liquid Fe-Ni (Kuwabara et al. 2016), the $V_P$ of liquid Fe-Ni decreases approximately 1.6 % by addition of 6 wt%S and 4 wt%Si and increases approximately 3.1 % by addition of 3wt%S and 8wt%Si. This suggests that the effect of S reduces the $V_P$ effectively also in the Fe-Ni-S-Si system.

Keywords: Mercury, Core, Sound velocity, Light element

©2019. Japan Geoscience Union. All Right Reserved. 

# In situ observation of Rayleigh–Taylor instability growth of liquid Fe-Si using laser shock

*Hidenori Terasaki[1], Tatsuhiro Sakaiya[1], Keisuke Shigemori[2], Hiroki Kato[2], Yoichiro Hironaka[2], Tadashi Kondo[1]

1. Graduate School of Science, Osaka University, 2. Institute of Laser Engineering, Osaka University

Rayleigh–Taylor instability occurs at the interface between two fluids with different densities when a heavy fluid overlies a light one in a gravitational field. The RT instability is considered as one of the important core formation mechanism beneath the magma ocean. This mechanism has been discussed from simulations (e.g., Honda et al. 1993, Ricard et al. 2009) and analog experiment (e.g., Olson and Weeraratne, 2008). However, experimental approach using liquid Fe-alloys for this mechanism has never been performed under high pressure. In this study, we applied the laser-shock technique to observe *in situ* the Rayleigh–Taylor instability of liquid Fe-Si alloy under high pressure. The growth of the Rayleigh–Taylor instability was successfully observed using *in situ* x-ray radiography under shock compression. The growth rate of the Rayleigh–Taylor instability was estimated to 0.3 $ns^{-1}$. The present results provide useful information to constrain the time scale of the Earth’ s and planetary core formation.

Keywords: Core formation, Rayleigh–Taylor instability, liquid Fe-alloy

©2019. Japan Geoscience Union. All Right Reserved. 

[E] Oral | S (Solid Earth Sciences )：S-IT Science of the Earth's Interior & Techtonophysics

Thu. May 30, 2019 10:45 AM - 12:15 PM JST | Thu. May 30, 2019 1:45 AM - 3:15 AM UTC | A09 TOKYO BAY MAKUHARI HALL

## [S-IT25] Planetary cores: Structure, formation, and evolution

convener:Hidenori Terasaki(Graduate School of Science, Osaka University), Eiji Ohtani(Department of Earth and Planetary Materials Science, Graduate School of Science, Tohoku University), William F McDonough(University of Maryland College Park), George Helffrich(Earth-Life Science Institute, Tokyo Institute of Technology), Chairperson:William McDonough(University of Maryland / Tohoku University), Eiji Ohtani(Tohoku University)

There are fundamental links between the formation and evolution of planets and their satellites to that of their cores. Defining the physical and chemical properties of the cores of these terrestrial bodies are fundamental for understanding their internal structures and thermal profile. Recent advances in experimental and theoretical studies provide new insights and applications to the Earth's cores and other terrestrial bodies. Near-future exploration missions will obtain data on the internal structure of terrestrial planets (e.g., Mars and Mercury) and planet-satellite systems. We anticipate presentations on recent advances on the physical and chemical properties of cores and discussions regarding the latest views of their formation and evolution. We welcome contributions from mineral/rock physics, geophysics, geochemistry, geodynamics, and planetary science.

10:45 AM - 11:00 AM JST | 1:45 AM - 2:00 AM UTC

[SIT25-06] *P-V-T* equation-of-state of liquid Fe from *ab-initio* simulations to the TPa regime

*Gerd Steinle-Neumann[1], Fabian Wagle[1] (1.Bayerisches Geoinstitut, University of Bayreuth, Germany)

11:00 AM - 11:15 AM JST | 2:00 AM - 2:15 AM UTC

[SIT25-07] ***Ab initio* study of Iron-Nickel alloys in Super-Earths cores**

*Francois Soubiran[1], Razvan Caracas[1] (1.Ecole normale superieure de Lyon, Laboratoire de Géologie de Lyon, Université Lyon 1, CNRS UMR 5276, Lyon, France)

11:15 AM - 11:30 AM JST | 2:15 AM - 2:30 AM UTC

[SIT25-08] **Impurity effect on the iron's transport properties at Earth's core conditions: A key constraint for the evolution of the Earth's core**

*Youjun Zhang[1], Mingqiang Hou[2], Nilesh Salke[2], Jung-Fu Lin[3] (1.Sichuan University, 2.HPSTAR, 3.University of Texas at Austin)

11:30 AM - 11:45 AM JST | 2:30 AM - 2:45 AM UTC

[SIT25-09] Melting in the Fe-FeO system to 214 GPa

*Kenta Oka[1], Yuto Kidokoro, Kei Hirose[1], Yoichi Nakajima[2], Guillaume Morard[3], Guillaume Fiquet[3], Nicolas Coudurier[3] (1.Department of Earth and Planetary Science, The University of Tokyo, 2.Priority Organization for Innobation and Excellence, 3.Sorbonne Université)

11:45 AM - 12:00 PM JST | 2:45 AM - 3:00 AM UTC

[SIT25-10] B2 phase in the inner core: constraints from high pressure experiments

*Eiji Ohtani[1], Daijo Ikuta[1], Seiji Kamada[2], Tatsuya Sakamaki[1], Naohisa Hirao[3] (1.Department of Earth and Planetary Materials Science, Graduate School of Science, Tohoku University, 2.Frontier Institute for Interdisciplinary Research, Tohoku University, 3.SRring-8, Japan Synchrotron Research Institute)

12:00 PM - 12:15 PM JST | 3:00 AM - 3:15 AM UTC

Discussion

# *P-V-T* equation-of-state of liquid Fe from *ab-initio* simulations to the TPa regime

*Gerd Steinle-Neumann[1], Fabian Wagle[1]

1. Bayerisches Geoinstitut, University of Bayreuth, Germany

The pressure-volume-temperature (*P-V-T*) equation-of-state (EoS) of liquid iron provides important information (reference adiabat, density $\rho$, and higher order thermodynamic parameters) in the modelling of the internal structure of planetary bodies with Fe-based cores. Relevant P-conditions range from a few GPa (Moon, Mercury) through the Mbar range (Earth) to several TPa (super-Earth exoplanets). Experimental data on $\rho$ in the liquid stability field are scarce and a thermodynamic assessment of $\rho$ depends on matching Gibbs energy along the melting line which remains controversial to this day. The alternative determination of a *P-V-T* EoS based on ab-initio simulations, on the other hand, suffer from the fact that $\rho$ at ambient P is predicted too large by as much as 20% in the simulations [e.g., 1]. Here, we have fitted *P-V-T* triplets from *ab-initio* molecular dynamics simulations with an EoS formulation that is thermodynamically self-consistent [2] and combined it with a correction formalism that accounts for the known $\rho$-mismatch at ambient *P* [3]. As the correction is additive to the Helmholtz potential and shows the correct limiting behavior at high and low $\rho$, the thermodynamic self-consistency of the results is not affected. Using this combination, the EoS we have developed reproduces $\rho$ from shock-wave experiments as well as previous models, but shows a significantly improved agreement at ambient *P*, the critical point and the sole low $\rho$ measurement at 4.3 GPa [4] (T11 in Figure). We explore the performance of our thermodynamic potential and various previously published models [1,5,6] for liquid iron over a wide range of conditions: (i) at ambient pressure as a function of temperature, (ii) along the melting curve of Fe to 40 GPa, relevant for the cores of smaller terrestrial bodies in our solar system (Figure), (iii) along isentropes in the Earth's outer core and (iv) for the core of super-Earth Kepler-36b. The correction term significantly improves the agreement of computed properties with experiments and other thermodynamic models that are based on an assessment of the phase diagram at ambient and moderate pressure, showing how *ab-initio* molecular dynamics simulations can be used at par with other thermodynamic techniques. For the Earth's core, densities from the various models are similar, but higher-order derivatives (acoustic velocities and Grüneisen parameter) show significant differences. Evaluated along a core-temperature profile in Kepler-36b, differences in density from various models are negligible, for core mass they do not exceed 2%, showing robust extrapolation of all equation of state models.

[1] Ichikawa et al., JGR 119, 240 (2014) (I14); [2] Vlček et al., PRB 85, 184201 (2012); [3] French & Mattsson, JAP 116, 013510 (2014); [4] Tateyama et al., PCM 38, 801 (2011) (T11); [5] Komabayashi, JGR 119, 4164 (2014) (K14); [6] Dorogokupets et al., SciRep 7, 41,863 (2017) (D17); [7] Nishida et al., PEPI 257, 230 (2016) (N16); [8] Jing et al., EPSL 396, 78 (2014) (J14); [9] Assael et al., JPCRD 35, 285 (2006) (A06); [10] Morard et al., AmMin 103, 1770 (2018) (M18); [11] Tsu et al., BRIMDM 41, 1 (1985) (T85).

Keywords: planetary cores, iron, equation of state

©2019. Japan Geoscience Union. All Right Reserved. 

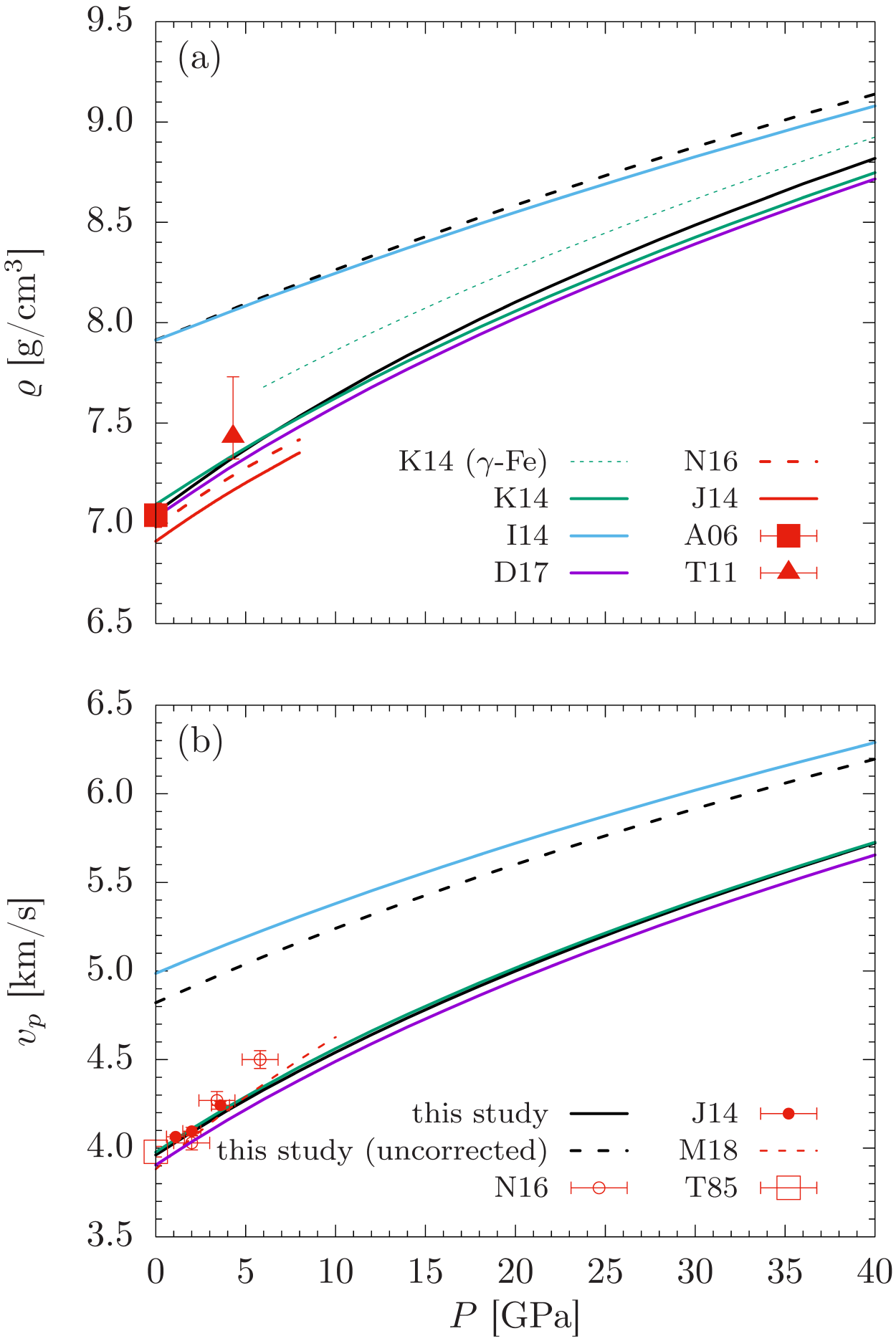


©2019. Japan Geoscience Union. All Right Reserved.

# *Ab initio* study of Iron-Nickel alloys in Super-Earths cores

*Francois Soubiran[1], Razvan Caracas[1]

1. Ecole normale superieure de Lyon, Laboratoire de Géologie de Lyon, Université Lyon 1, CNRS UMR 5276, Lyon, France

Iron-nickel alloys are considered the main components of Earth and Super-Earth cores, which make them crucial systems in order to comprehend the properties of these planets. While the relative nickel content is anticipated to be around 10% in the Earth, this value could differ slightly in other planets because of different host star metallicity and formation history. It is thus important to understand the properties of iron-nickel systems with various compositions in the multi-megabar regime.

While pure iron is anticipated to have hexagonal close packing at high pressure, nickel is expected to have face-centered cubic packing. This means there is a structural change as the composition is modified, which can also mean a limited stability of the solid solutions of iron-nickel.

We will discuss the properties of iron-nickel alloys in the megabar regime as predicted by *ab initio* simulations. We will examine the relative stability of different iron-nickel solid solution compositions and the interplay of the spin states. After characterizing the properties of these alloys at pressure-temperature conditions relevant for Super-Earth, we will discuss possible consequences their cores.

Keywords: Super-Earth, iron core, Ab initio simulations

©2019. Japan Geoscience Union. All Right Reserved. 

# Impurity effect on the iron’s transport properties at Earth’s core conditions: A key constraint for the evolution of the Earth’s core

*Youjun Zhang[1], Mingqiang Hou[2], Nilesh Salke[2], Jung-Fu Lin[3]

1. Sichuan University, 2. HPSTAR, 3. University of Texas at Austin

The Earth’s core is mainly composed of Fe-Ni alloyed with some light elements, such as Si, S, O and C [1]. The transport properties of Fe alloys at Earth’s core conditions constrain the heat flow from the core into mantle, which governs the geodynamo, dynamics and thermal evolution of Earth’s core [2,3]. While, this property is still not well understood and remains controversial in previous work due to the experimental challenging at very high pressure and temperature [4,5]. Here, we directly measure the electrical resistivity of hcp-Fe-Ni and hcp-Fe-Si alloys at the relevant conditions of Earth’s core using double-side laser-heated Diamond Anvil Cells. Our results show a quasi-linear relation between temperature and resistivity in hcp-Fe-Ni and hcp-Fe-Si at the core pressures. Compared with hcp-Fe [6], the impurities like Ni and Si can elevate iron’s resistivity but they show different magnitude. Thermal conductivity of an Fe-Ni-Si alloy as a candidate core composition was modelled via the Wiedemann-Franz law based on our measured resistivity. Our results show that the core’s thermal conductivity could be strongly reduced by impurities, supporting a Mesoproterozoic inner core age and a self-consistent convection-driven geodynamo.

Refs:
[1] Li and Fei. Treat. Geochem., 527-557 (2014)
[2] Davies et al. Nat. Geosci. 8, 678-685 (2015)
[3] Williams. Annu. Rev. Earth Planet. Sci. 46: 47-66 (2018)
[4] Ohta et al. Nature 534, 95-98 (2016)
[5] Konôpková et al. Nature 534, 99-101 (2016)
[6] Zhang et al. Submitted, (2019)

Keywords: Fe alloys, Transport properties, High pressure-temperature, Geodynamo, Thermal evolution of the core

©2019. Japan Geoscience Union. All Right Reserved. 

# Melting in the Fe-FeO system to 214 GPa

*Kenta Oka[1], Yuto Kidokoro, Kei Hirose[1], Yoichi Nakajima[2], Guillaume Morard[3], Guillaume Fiquet[3], Nicolas Coudurier[3]

1. Department of Earth and Planetary Science, The University of Tokyo, 2. Priority Organization for Innobation and Excellence, 3. Sorbonne Université

Oxygen is one of the likely candidates as the light elements in the Earth’ s core. If oxygen is the primary one, the oxygen content in the outer core should be less than that of the eutectic liquid composition in the Fe-FeO system, which is required to explain the dense solid inner core compared to the liquid outer core. The eutectic liquid composition in the Fe-FeO system has been estimated under high pressures, on the basis of thermodynamic calculations and high-pressure experiments. However, large inconsistency is found among these previous studies, especially below 100 GPa.
In this study, we have conducted high-temperature and high-pressure experiments up to 214 GPa and 3650 K. Liquidus phase relations were determined from textural and chemical characterizations of recovered samples using FIB/FE-EDS/FE-EPMA. Liquid-liquid immiscibility reported below 21 GPa in previous multi-anvil studies (Tsuno et al., 2007) was not observed above 42 GPa in the present DAC experiments. Our results demonstrate that the eutectic liquid composition in the Fe-FeO binary system changed largely from Fe+1.3wt.%O at 15 GPa (Tsuno et al., 2007) to >8 wt.% O at 42 GPa. It then further increased gradually to ~13 wt.% O with increasing pressure to 214 GPa.
These results are in reasonably good agreement with the previous DAC experiments by Seagle et al. (2008) based on XRD measurements and the earlier thermodynamic model by Komabayashi (2014) that considered non-ideal mixing between liquid Fe and FeO. Our data also showed contamination by variable amounts of carbon in liquid, which may explain the difference from the results by Morard et al. (2017) below 80 GPa. The large change in the liquidus phase relations in the Fe-FeO system observed between 15 and 42 GPa is likely related to the disappearance of liquid-liquid immiscibility.
The outer core may include 5.5 wt.% O if oxygen is a sole light element (Badro et al., 2014). When extrapolating our data to 330 GPa, the eutectic liquid in the Fe-FeO binary system includes about 15 wt.% O, which is much higher than the 5.5 wt.% O and therefore allows the outer core liquid containing oxygen as one of important light elements to crystallize solid Fe at the ICB. These results support the presence of oxygen in the core.

Keywords: outer core, light elements, melting experiment, Fe-FeO System

©2019. Japan Geoscience Union. All Right Reserved. 

# B2 phase in the inner core: constraints from high pressure experiments

*Eiji Ohtani[1], Daijo Ikuta[1], Seiji Kamada[2], Tatsuya Sakamaki[1], Naohisa Hirao[3]

1. Department of Earth and Planetary Materials Science, Graduate School of Science, Tohoku University, 2. Frontier Institute for Interdisciplinary Research, Tohoku University, 3. SRring-8, Japan Synchrotron Research Institute

The Earth inner core is considered to be composed of hcp-iron alloy with small amounts of light elements, and intensive efforts have been made to clarify the physical properties of hcp-iron. On the other hand, there are many seismological observations on existence of heterogeneities, layering, and anisotropy in the inner core, which cannot be accounted for only by hcp-iron.

It has been suggested that B2 or bcc phase can exit in the inner core mainly by theoretical calculations (e.g., Belonoshko et al., 2003). Therefore, it has been a debated matter on the existence of a stable B2 structure of iron alloys in the inner core. There is experimental reports suggesting existence of B2 phase in Fe-Si alloy (Fischer et al., 2013). Coexistence of hcp+B2 is observed by Fishcer et al. (2013) in the Fe-Si system with silicon greater than 6 wt. %.

Nickel is an important metallic component in meteorites, and it can modify the phase relations of iron alloy systems significantly. In order to clarify the stability of B2 phase in the inner core, we studied the phase relations of the Fe-Ni-Si system at high pressure and temperature relevant in the core. The in-situ X-ray observations of the Fe-Ni-Si alloys at high pressure and temperature were conducted at BL10XU of SPring-8 by using the double sided laser heating diamond anvil cell. We observed a wide stability field of coexistence of B2 phase and hcp at high pressure and temperature above 100 GPa and 2500 K in the composition of Fe7wt%Ni5wt%Si alloy.

The nickel and silicon contents in the inner core were estimated to be 0~8 wt% and 3-6 wt% respectively in order to account for the PREM inner core based on the equation of state of hcpFe-Ni-Si alloy (Asanuma et al., 2013) and the sound velocity of hcpFe-Si alloy (Sakairi et al., 2018). Combined with the phase relations together with the sound velocity measurements, we can suggest that the inner core is mainly composed of hcp-iron with a small amount of B2 phase. Coexistence of B2 phase with hcp-Fe alloy in the inner core can explain the heterogeneity and fine structure of the inner core reported in seismology.

Reference: Belonoshki et al. (2003) Nature, 466, 744-747. Fischer et al. (2015) Am Min, 100, 2718-2724. Asanuma et al. (2011) EPSL, 310, 113-118. Sakairi et al. (2018), Am Min., 102, 85-90.

Keywords: inner core, bcc, hcp, Fe-Ni-Si alloy, phase relation, sound velocity

©2019. Japan Geoscience Union. All Right Reserved. 

[E] Poster | S (Solid Earth Sciences )：S-IT Science of the Earth's Interior & Techtonophysics

Thu. May 30, 2019 3:30 PM - 5:00 PM JST | Thu. May 30, 2019 6:30 AM - 8:00 AM UTC | Poster Hall International Exhibition Hall8, Makuhari Messe_10

## [S-IT25] Planetary cores: Structure, formation, and evolution

convener:Hidenori Terasaki(Graduate School of Science, Osaka University), Eiji Ohtani(Department of Earth and Planetary Materials Science, Graduate School of Science, Tohoku University), William F McDonough(University of Maryland College Park), George Helffrich(Earth-Life Science Institute, Tokyo Institute of Technology)

There are fundamental links between the formation and evolution of planets and their satellites to that of their cores. Defining the physical and chemical properties of the cores of these terrestrial bodies are fundamental for understanding their internal structures and thermal profile. Recent advances in experimental and theoretical studies provide new insights and applications to the Earth's cores and other terrestrial bodies. Near-future exploration missions will obtain data on the internal structure of terrestrial planets (e.g., Mars and Mercury) and planet-satellite systems. We anticipate presentations on recent advances on the physical and chemical properties of cores and discussions regarding the latest views of their formation and evolution. We welcome contributions from mineral/rock physics, geophysics, geochemistry, geodynamics, and planetary science.

### [SIT25-P01] Stratification of the Earth’s core by $SiO_2$ crystallisation

*George Helffrich[1], Satoshi Kaneshima[2], Kei Hirose[1,3] (1.Earth-Life Science Institute, Tokyo Institute of Technology, 2.Earth and Planetary Sciences, Kyushu University, 3.Earth and Planetary Sciences Department, University of Tokyo)

### [SIT25-P02] Relation between sound velocity and density for liquid iron alloys under Earth’s core pressures by laser-shock compression

*Tatsuhiro Sakaiya[1], Tadashi Kondo[1], Hidenori Terasaki[1], Keisuke Shigemori[2], Yoichiro Hironaka[2] (1.Graduate School of Science, Osaka University, 2.Institute of Laser Engineering, Osaka University)

### [SIT25-P03] Geochemical estimates of Earth's core heat content at the end of accretion

*Vincent Clesi[1], Renaud Deguen[1] (1.Laboratoire de Geologie de Lyon - Terre, Planètes, Environnement, Université Claude Bernard Lyon 1, CNRS, ENS-Lyon, 69622 Villeurbanne, France.)

### [SIT25-P04] The effect of temperature on density of solid metals

*Asaka Kamiya[1], Hidenori Terasaki[1], Tadashi Kondo[1] (1.Osaka University)

### [SIT25-P05] Phase relations in the Fe-Ni-Si system at high pressures and high temperatures

*Daijo Ikuta[1], Eiji Ohtani[1], Saori Kawaguchi[2], Naohisa Hirao[2], Yasuo Ohishi[2] (1.Department of Earth Science, Tohoku University, 2.JASRI)

# Stratification of the Earth's core by $SiO_2$ crystallisation

*George Helffrich[1], Satoshi Kaneshima[2], Kei Hirose[1,3]

1. Earth-Life Science Institute, Tokyo Institute of Technology, 2. Earth and Planetary Sciences, Kyushu University, 3. Earth and Planetary Sciences Department, University of Tokyo

Based on various studies reporting seismic wavespeed deviations from PREM in the outermost outer core, the core appears to be stratified. Compositional layering, where liquids of different densities overlie one another is one stratification possibility. This mechanism, however, inhibits vertical flows in the liquid near the surface of the core implied by models of secular variation of the Earth's magnetic field. To avoid this limitation, we propose a mechanism by which the layering arises in an analogous way to atmospheric cloud formation. If liquid metal containing dissolved Si+O reaches a saturation level in the outermost outer core, $SiO_2$ will crystallize and rise to the core-mantle boundary (CMB), causing density changes in the liquid by release of latent heat and changing composition. We present an physical model for this process and show that it explains the observed outer core wavespeed variations better than previous parameterizations. For a CMB temperature of 3800 K and a core light element content of 5 wt% Si+O, $SiO_2$ begins crystallizing 260 km below the CMB through an interval about 160 km thick, yet core liquid can flow freely through the crystallization interval, facilitating magnetic field changes on decadal to century time scales.

©2019. Japan Geoscience Union. All Right Reserved. 

# Relation between sound velocity and density for liquid iron alloys under Earth's core pressures by laser-shock compression

*Tatsuhiro Sakaiya[1], Tadashi Kondo[1], Hidenori Terasaki[1], Keisuke Shigemori[2], Yoichiro Hironaka[2]

1. Graduate School of Science, Osaka University, 2. Institute of Laser Engineering, Osaka University

Sound velocity at Earth's core conditions are one of the most important physical properties in Earth science because it can be directly compared with the seismological Earth model (PREM: Preliminary Reference Earth Model) [1]. The composition of solid inner core is estimated from the comparison of the model [1] and the extrapolation of sound velocities as a function of density of iron and iron alloys obtained by the static compression experiment [2, 3]. Birch's law, a linear sound velocity–density relation [4], is used to extrapolate sound velocities to densities in the core condition. On the other hand, the composition of liquid outer core is estimated from the partitioning and solubility data in the inner core boundary condition for the composition of solid core. There has been some works for the sound velocity of iron and iron alloys on the Earth's core condition by dynamic techniques using explosive [5], gas gun [5-11], and laser [12-14]. In this study, we measure the sound velocity and density of liquid iron alloys by shock-compression method using high-power laser.
We conducted shock-compression experiments using a High Intensity Plasma Experimental Research (HIPER) system at the GEKKO-XII laser irradiation facility [15] at the Institute of Laser Engineering, Osaka University. The samples were Fe-Ni alloys, pure nickel, Fe-Si alloys, pure silicon, and pyrrhotite. The sound velocities and densities of shock-compressed iron alloys using the high-power laser were measured by x-ray radiography [12-14] at pressures up to 1000 GPa.
Part of this work was performed under the joint research project of the Institute of Laser Engineering, Osaka University and supported by JSPS KAKENHI Grant Number JP16K05541.

References
[1] A. M. Dziewonski and D. L. Anderson, Phys. Earth Planet. Inter. 25, 297-356 (1981).
[2] J. Badro et al., Earth Planet. Sci. Lett. 254, 233-238 (2007).
[3] G. Fiquet et al., Phys. Earth Planet. Inter. 172, 125-129 (2009).
[4] F. Birch, Geophys. J. R. Astron. Soc. 4, 295-311 (1961).
[5] J. M. Brown and R. G. McQueen, J. Geophys. Res. 91, 7485-7494 (1986).
[6] J. H. Nguyen and N. C. Holmes, Nature 427, 339-342 (2004).
[7] J. W. Shaner et al., Shock Waves in Condensed Matter, 135-138 (1988).
[8] H. Huang et al., J. Geophys. Res. 116, B04201 (2010).
[9] H. Huang et al., Nature 479, 513-516 (2011).
[10] Y. Zhang et al., Sci. Rep. 6, 22473 (2016).
[11] H. Huang et al., J. Geophys. Res. 123, 4730 (2018).
[12] K. Shigemori et al., Eur. Phys. J. D 44, 301-305 (2007).
[13] K. Shigemori et al., Rev. Sci. Instrum. 83, 10E529 (2012).
[14] T. Sakaiya et al., Earth Planet. Sci. Lett. 392, 80-85 (2014).
[15] C. Yamanaka et al., Nucl. Fusion 27, 19-30 (1987).

Keywords: sound velocity, shock compression, iron alloy, Earth's core, Birch's law

©2019. Japan Geoscience Union. All Right Reserved. 

# Geochemical estimates of Earth's core heat content at the end of accretion

*Vincent Clesi[1], Renaud Deguen[1]

1. Laboratoire de Geologie de Lyon - Terre, Planètes, Environnement, Université Claude Bernard Lyon 1, CNRS, ENS-Lyon, 69622 Villeurbanne, France.

The composition of Earth's mantle, when compared to experimentally determined partitioning coefficients, can be used to constrain the conditions of equilibration - pressure *P*, temperature *T*, and oxygen fugacity $fO_2$ - of the metal and silicates during core-mantle differentiation.
This places constraints on the thermal state of the planet during its accretion, and it is tempting to try to use these data to estimate the heat content of the core at the end of accretion.
To do so, we develop an analytical model of the thermal evolution of the metal phase during its descent through the solid mantle toward the growing core, taking into account compression heating, viscous dissipation heating, and heat exchange with the surrounding silicates. For each impact, the model takes as initial condition the pressure and temperature at the base of the magma ocean, and gives the temperature of the metal when it reaches the core. The growth of the planet results in additional pressure increase and compression heating of the core.
The thermal model is coupled to a Monte-Carlo inversion of the metal/silicates equilibration conditions ($P$, $T$, $fO_2$) in the course of accretion from the abundance of Ni, Co, V and Cr in the mantle, and provides an estimate of the core heat content at the end of accretion for each geochemically successful accretion.
The core heat content depends on the mean degree of metal-silicates equilibration, on the mode of metal/silicates separation in the mantle (diapirism, percolation, or dyking), but also very significantly on the shape of the equilibration conditions curve (equilibration *P* and *T* vs. fraction of Earth accreted).
We find that many accretion histories which are successful in reproducing the mantle composition yield a core that is colder than its current state.
Imposing that the temperature of the core at the end of accretion is higher than its current values therefore provides strong constraints on the accretion history.
In particular, we find that the core heat content depends significantly on the last stages of accretion

Keywords: Core formation, Model

©2019. Japan Geoscience Union. All Right Reserved. 

# The effect of temperature on density of solid metals

*Asaka Kamiya[1], Hidenori Terasaki[1], Tadashi Kondo[1]

1. Osaka University

It is reported that sound velocities of several solid metals show drastic non-linear reduction at near the melting temperature. This is called premelting effect. Nadal and Le Poac (2013) reported that the sound velocity (P-wave and S-wave velocities) of solid tin (Sn) decreased drastically just before melting ($T/T_m$ ~0.99) at ambient pressure. They suggested that this decrease is due to reduction of elastic moduli (bulk and shear moduli). To understand the premelting effect more accurately, density data of tin near the melting temperature is also required in addition to sound velocity data. However, the precise density behavior of tin around the melting temperature is still missing. In this study, we measured the density of solid metals (tin and nickel) at ambient pressure and studied the effect of temperature on the density near melting temperature. The densities of solid metals were measured from optical image of the sample in the high-temperature furnace up to 673 K for Sn and 1873 K for fcc-Ni. The densities in this study were measured with error of 0.07 % for Sn and 0.4 % for Ni. Density of Sn decreases linearly with increasing temperature up to 490 K and reduced drastically above 490 K (at $T/T_m$~0.97). This drastic decrease in density of Sn is likely to relate to the premelting effect suggested from sound velocity measurement. In contrast, density of Ni decreases almost linearly with increasing temperature up to melting point and no drastic density change was observed in solid state.

Keywords: premelting effect, Tin, Ni, density, high temperature, electric furnace

©2019. Japan Geoscience Union. All Right Reserved. 

# Phase relations in the Fe-Ni-Si system at high pressures and high temperatures

*Daijo Ikuta[1], Eiji Ohtani[1], Saori Kawaguchi[2], Naohisa Hirao[2], Yasuo Ohishi[2]

1. Department of Earth Science, Tohoku University, 2. JASRI

The Earth's core has supposed to be constituted by iron-nickel alloys with some light elements. Silicon is one of the most convincing candidates among the light elements. Therefore, the study of high pressure and high temperature properties and behaviors for the Fi-Ni-Si system is important in understanding and constraining to the properties of the Earth's core. In this study, high pressure and high temperature properties for three different contents of Fe-Ni-Si alloys were investigated by using laser heated diamond anvil cells and in situ X-ray diffraction with synchrotron radiation. We determined the phase relations of $Fe_{(0.94-x)}Ni_{0.06}Si_x$ ($x$ = 0.10, 0.17, 0.26) up to 166 GPa and 2800 K, respectively. According to previous Fe-Si system studies, $Fe_{0.83}Si_{0.17}$ alloys transform from hcp to hcp+B2 and fcc+hcp+B2 phases with increasing temperature in isobaric conditions. We observed the change in temperature increase and positive slope of these boundaries due to the nickel containing effect and the difference in silicon content. We report the details of phase relations in the Fe-Ni-Si system and discuss with the differences from the Fe-Si system.

Keywords: Fe-Ni-Si system, phase relation, high pressure

©2019. Japan Geoscience Union. All Right Reserved. 

[E] Poster | S (Solid Earth Sciences )：S-IT Science of the Earth's Interior & Techtonophysics

Thu. May 30, 2019 5:15 PM - 6:30 PM JST | Thu. May 30, 2019 8:15 AM - 9:30 AM UTC | Poster Hall International Exhibition Hall8, Makuhari Messe_21

## [S-IT25] Planetary cores: Structure, formation, and evolution

convener:Hidenori Terasaki(Graduate School of Science, Osaka University), Eiji Ohtani(Department of Earth and Planetary Materials Science, Graduate School of Science, Tohoku University), William F McDonough(University of Maryland College Park), George Helffrich(Earth-Life Science Institute, Tokyo Institute of Technology)

There are fundamental links between the formation and evolution of planets and their satellites to that of their cores. Defining the physical and chemical properties of the cores of these terrestrial bodies are fundamental for understanding their internal structures and thermal profile. Recent advances in experimental and theoretical studies provide new insights and applications to the Earth's cores and other terrestrial bodies. Near-future exploration missions will obtain data on the internal structure of terrestrial planets (e.g., Mars and Mercury) and planet-satellite systems. We anticipate presentations on recent advances on the physical and chemical properties of cores and discussions regarding the latest views of their formation and evolution. We welcome contributions from mineral/rock physics, geophysics, geochemistry, geodynamics, and planetary science.

### [SIT25-P01] Stratification of the Earth’s core by $SiO_2$ crystallisation

*George Helffrich[1], Satoshi Kaneshima[2], Kei Hirose[1,3] (1.Earth-Life Science Institute, Tokyo Institute of Technology, 2.Earth and Planetary Sciences, Kyushu University, 3.Earth and Planetary Sciences Department, University of Tokyo)

### [SIT25-P02] Relation between sound velocity and density for liquid iron alloys under Earth’s core pressures by laser-shock compression

*Tatsuhiro Sakaiya[1], Tadashi Kondo[1], Hidenori Terasaki[1], Keisuke Shigemori[2], Yoichiro Hironaka[2] (1.Graduate School of Science, Osaka University, 2.Institute of Laser Engineering, Osaka University)

### [SIT25-P03] Geochemical estimates of Earth's core heat content at the end of accretion

*Vincent Clesi[1], Renaud Deguen[1] (1.Laboratoire de Geologie de Lyon - Terre, Planètes, Environnement, Université Claude Bernard Lyon 1, CNRS, ENS-Lyon, 69622 Villeurbanne, France.)

### [SIT25-P04] The effect of temperature on density of solid metals

*Asaka Kamiya[1], Hidenori Terasaki[1], Tadashi Kondo[1] (1.Osaka University)

### [SIT25-P05] Phase relations in the Fe-Ni-Si system at high pressures and high temperatures

*Daijo Ikuta[1], Eiji Ohtani[1], Saori Kawaguchi[2], Naohisa Hirao[2], Yasuo Ohishi[2] (1.Department of Earth Science, Tohoku University, 2.JASRI)

# Stratification of the Earth's core by $SiO_2$ crystallisation

*George Helffrich[1], Satoshi Kaneshima[2], Kei Hirose[1,3]

1. Earth-Life Science Institute, Tokyo Institute of Technology, 2. Earth and Planetary Sciences, Kyushu University, 3. Earth and Planetary Sciences Department, University of Tokyo

Based on various studies reporting seismic wavespeed deviations from PREM in the outermost outer core, the core appears to be stratified. Compositional layering, where liquids of different densities overlie one another is one stratification possibility. This mechanism, however, inhibits vertical flows in the liquid near the surface of the core implied by models of secular variation of the Earth's magnetic field. To avoid this limitation, we propose a mechanism by which the layering arises in an analogous way to atmospheric cloud formation. If liquid metal containing dissolved Si+O reaches a saturation level in the outermost outer core, $SiO_2$ will crystallize and rise to the core-mantle boundary (CMB), causing density changes in the liquid by release of latent heat and changing composition. We present an physical model for this process and show that it explains the observed outer core wavespeed variations better than previous parameterizations. For a CMB temperature of 3800 K and a core light element content of 5 wt% Si+O, $SiO_2$ begins crystallizing 260 km below the CMB through an interval about 160 km thick, yet core liquid can flow freely through the crystallization interval, facilitating magnetic field changes on decadal to century time scales.

©2019. Japan Geoscience Union. All Right Reserved. 

# Relation between sound velocity and density for liquid iron alloys under Earth's core pressures by laser-shock compression

*Tatsuhiro Sakaiya[1], Tadashi Kondo[1], Hidenori Terasaki[1], Keisuke Shigemori[2], Yoichiro Hironaka[2]

1. Graduate School of Science, Osaka University, 2. Institute of Laser Engineering, Osaka University

Sound velocity at Earth's core conditions are one of the most important physical properties in Earth science because it can be directly compared with the seismological Earth model (PREM: Preliminary Reference Earth Model) [1]. The composition of solid inner core is estimated from the comparison of the model [1] and the extrapolation of sound velocities as a function of density of iron and iron alloys obtained by the static compression experiment [2, 3]. Birch's law, a linear sound velocity–density relation [4], is used to extrapolate sound velocities to densities in the core condition. On the other hand, the composition of liquid outer core is estimated from the partitioning and solubility data in the inner core boundary condition for the composition of solid core. There has been some works for the sound velocity of iron and iron alloys on the Earth's core condition by dynamic techniques using explosive [5], gas gun [5-11], and laser [12-14]. In this study, we measure the sound velocity and density of liquid iron alloys by shock-compression method using high-power laser.
We conducted shock-compression experiments using a High Intensity Plasma Experimental Research (HIPER) system at the GEKKO-XII laser irradiation facility [15] at the Institute of Laser Engineering, Osaka University. The samples were Fe-Ni alloys, pure nickel, Fe-Si alloys, pure silicon, and pyrrhotite. The sound velocities and densities of shock-compressed iron alloys using the high-power laser were measured by x-ray radiography [12-14] at pressures up to 1000 GPa.
Part of this work was performed under the joint research project of the Institute of Laser Engineering, Osaka University and supported by JSPS KAKENHI Grant Number JP16K05541.

References
[1] A. M. Dziewonski and D. L. Anderson, Phys. Earth Planet. Inter. 25, 297-356 (1981).
[2] J. Badro et al., Earth Planet. Sci. Lett. 254, 233-238 (2007).
[3] G. Fiquet et al., Phys. Earth Planet. Inter. 172, 125-129 (2009).
[4] F. Birch, Geophys. J. R. Astron. Soc. 4, 295-311 (1961).
[5] J. M. Brown and R. G. McQueen, J. Geophys. Res. 91, 7485-7494 (1986).
[6] J. H. Nguyen and N. C. Holmes, Nature 427, 339-342 (2004).
[7] J. W. Shaner et al., Shock Waves in Condensed Matter, 135-138 (1988).
[8] H. Huang et al., J. Geophys. Res. 116, B04201 (2010).
[9] H. Huang et al., Nature 479, 513-516 (2011).
[10] Y. Zhang et al., Sci. Rep. 6, 22473 (2016).
[11] H. Huang et al., J. Geophys. Res. 123, 4730 (2018).
[12] K. Shigemori et al., Eur. Phys. J. D 44, 301-305 (2007).
[13] K. Shigemori et al., Rev. Sci. Instrum. 83, 10E529 (2012).
[14] T. Sakaiya et al., Earth Planet. Sci. Lett. 392, 80-85 (2014).
[15] C. Yamanaka et al., Nucl. Fusion 27, 19-30 (1987).

Keywords: sound velocity, shock compression, iron alloy, Earth's core, Birch's law

©2019. Japan Geoscience Union. All Right Reserved. 

# Geochemical estimates of Earth's core heat content at the end of accretion

*Vincent Clesi[1], Renaud Deguen[1]

1. Laboratoire de Geologie de Lyon - Terre, Planètes, Environnement, Université Claude Bernard Lyon 1, CNRS, ENS-Lyon, 69622 Villeurbanne, France.

The composition of Earth's mantle, when compared to experimentally determined partitioning coefficients, can be used to constrain the conditions of equilibration - pressure *P*, temperature *T*, and oxygen fugacity $fO_2$ - of the metal and silicates during core-mantle differentiation.
This places constraints on the thermal state of the planet during its accretion, and it is tempting to try to use these data to estimate the heat content of the core at the end of accretion.
To do so, we develop an analytical model of the thermal evolution of the metal phase during its descent through the solid mantle toward the growing core, taking into account compression heating, viscous dissipation heating, and heat exchange with the surrounding silicates. For each impact, the model takes as initial condition the pressure and temperature at the base of the magma ocean, and gives the temperature of the metal when it reaches the core. The growth of the planet results in additional pressure increase and compression heating of the core.
The thermal model is coupled to a Monte-Carlo inversion of the metal/silicates equilibration conditions ($P$, $T$, $fO_2$) in the course of accretion from the abundance of Ni, Co, V and Cr in the mantle, and provides an estimate of the core heat content at the end of accretion for each geochemically successful accretion.
The core heat content depends on the mean degree of metal-silicates equilibration, on the mode of metal/silicates separation in the mantle (diapirism, percolation, or dyking), but also very significantly on the shape of the equilibration conditions curve (equilibration *P* and *T* vs. fraction of Earth accreted).
We find that many accretion histories which are successful in reproducing the mantle composition yield a core that is colder than its current state.
Imposing that the temperature of the core at the end of accretion is higher than its current values therefore provides strong constraints on the accretion history.
In particular, we find that the core heat content depends significantly on the last stages of accretion

Keywords: Core formation, Model

©2019. Japan Geoscience Union. All Right Reserved. 

# The effect of temperature on density of solid metals

*Asaka Kamiya[1], Hidenori Terasaki[1], Tadashi Kondo[1]

1. Osaka University

It is reported that sound velocities of several solid metals show drastic non-linear reduction at near the melting temperature. This is called premelting effect. Nadal and Le Poac (2013) reported that the sound velocity (P-wave and S-wave velocities) of solid tin (Sn) decreased drastically just before melting ($T/T_m$ ~0.99) at ambient pressure. They suggested that this decrease is due to reduction of elastic moduli (bulk and shear moduli). To understand the premelting effect more accurately, density data of tin near the melting temperature is also required in addition to sound velocity data. However, the precise density behavior of tin around the melting temperature is still missing. In this study, we measured the density of solid metals (tin and nickel) at ambient pressure and studied the effect of temperature on the density near melting temperature. The densities of solid metals were measured from optical image of the sample in the high-temperature furnace up to 673 K for Sn and 1873 K for fcc-Ni. The densities in this study were measured with error of 0.07 % for Sn and 0.4 % for Ni. Density of Sn decreases linearly with increasing temperature up to 490 K and reduced drastically above 490 K (at $T/T_m$~0.97). This drastic decrease in density of Sn is likely to relate to the premelting effect suggested from sound velocity measurement. In contrast, density of Ni decreases almost linearly with increasing temperature up to melting point and no drastic density change was observed in solid state.

Keywords: premelting effect, Tin, Ni, density, high temperature, electric furnace

©2019. Japan Geoscience Union. All Right Reserved. 

# Phase relations in the Fe-Ni-Si system at high pressures and high temperatures

*Daijo Ikuta[1], Eiji Ohtani[1], Saori Kawaguchi[2], Naohisa Hirao[2], Yasuo Ohishi[2]

1. Department of Earth Science, Tohoku University, 2. JASRI

The Earth's core has supposed to be constituted by iron-nickel alloys with some light elements. Silicon is one of the most convincing candidates among the light elements. Therefore, the study of high pressure and high temperature properties and behaviors for the Fi-Ni-Si system is important in understanding and constraining to the properties of the Earth's core. In this study, high pressure and high temperature properties for three different contents of Fe-Ni-Si alloys were investigated by using laser heated diamond anvil cells and in situ X-ray diffraction with synchrotron radiation. We determined the phase relations of $Fe_{(0.94-x)}Ni_{0.06}Si_x$ ($x$ = 0.10, 0.17, 0.26) up to 166 GPa and 2800 K, respectively. According to previous Fe-Si system studies, $Fe_{0.83}Si_{0.17}$ alloys transform from hcp to hcp+B2 and fcc+hcp+B2 phases with increasing temperature in isobaric conditions. We observed the change in temperature increase and positive slope of these boundaries due to the nickel containing effect and the difference in silicon content. We report the details of phase relations in the Fe-Ni-Si system and discuss with the differences from the Fe-Si system.

Keywords: Fe-Ni-Si system, phase relation, high pressure

©2019. Japan Geoscience Union. All Right Reserved. 

[J] Oral | S (Solid Earth Sciences)：S-GL Geology

Thu. May 30, 2019 9:00 AM - 10:30 AM JST | Thu. May 30, 2019 12:00 AM - 1:30 AM UTC | A10 TOKYO BAY MAKUHARI HALL

## [S-GL27] Geochronology and Isotope Geology

convener:Takahiro Tagami(Graduate School of Science, Kyoto University), Yuji Sano(Division of Ocean and Earth Systems, Atmosphere and Ocean Research Institute, University of Tokyo),
Chairperson:Takahiro Tagami, Yuji Sano

Reliable reconstruction of geohistory is of primary importance to better envision the present and future of the Earth. Geochronology and isotope geology play major roles in the reconstruction. This session offers an opportunity to present the results of fundamental studies, including the developments / improvements of analytical methods and age calibration, as well as applications to the Earth and planetary materials. We particularly focus on: (1) radiometric dating, bio-stratigraphy, magneto-stratigraphy and stable isotopic time series that provide the age information, (2) radioisotopes and stable isotopes widely employed for analyzing the Earth and planetary systems and (3) hypothesis and numerical modeling that utilize / assimilate the age and isotopic data. We also welcome contributions that integrate a variety of relevant disciplines.

9:00 AM - 9:30 AM JST | 12:00 AM - 12:30 AM UTC

### [SGL27-01] Terrestrial cosmogenic nuclides as a dating tool of landforms and near-surface materials: applicability and limitations

★Invited Papers

*Yuki Matsushi[1] (1.Disaster Prevention Research Institute, Kyoto University)

9:30 AM - 9:45 AM JST | 12:30 AM - 12:45 AM UTC

### [SGL27-02] Dating of marine erosional terraces using cosmogenic nuclides: A case study of the Hyuga City, Miyazaki Prefecture, southwest Japan (preliminary results)

*Shigeru Sueoka[1], Tetsuya Komatsu[1], Yuki Matsushi[2], Yusuke Yonaga[1], Naomi Sano[1], Noriaki Hirao[1], Tadamasa Ueki[1], Natsuko Fujita[1], Yoko Kokubu[1], Masakazu Niwa[1] (1.Japan Atomic Energy Agency, 2.Disaster Prevention Research Institute, Kyoto University)

9:45 AM - 10:00 AM JST | 12:45 AM - 1:00 AM UTC

### [SGL27-03] Estimation of thermal history of Toki granite over 0.1Myr timescale by Multi-OSL-thermochronometry

*Manabu Ogata[1], Georgina E King[2], Frédéric Herman[2], Shigeru Sueoka[1] (1.Tono Geoscience Center, Japan Atomic Energy Agency, 2.University of Lausanne)

10:00 AM - 10:15 AM JST | 1:00 AM - 1:15 AM UTC

### [SGL27-04] Depth condition under which OSL signal of quartz gouge experiences coseismic zeroing

*Yuki Minomo[1], Kiyokazu Oohashi[1], Noriko Hasebe[2], Kazumasa Miura[3] (1.Graduate School of science and Technology for Innovation, Yamaguchi University , 2.Institute of Nature and Environmental Technology, Kanazawa University, 3.Kanazawa University)

10:15 AM - 10:30 AM JST | 1:15 AM - 1:30 AM UTC

### [SGL27-05] Result of age determination of samples from Hokuriku Group

*Noriko Hasebe[1], Ryo Kamiguchi[2] (1.Institute of Nature and Environmental Technology, Kanazawa University, 2.Department of Earth Sciences, Kanazawa University)

# Terrestrial cosmogenic nuclides as a dating tool of landforms and near-surface materials: applicability and limitations

*Yuki Matsushi[1]

1. Disaster Prevention Research Institute, Kyoto University

This study overviews methodology for application of terrestrial cosmogenic nuclides for dating of diverse types of landforms and near-surface materials. Accumulation of the nuclides in the bedrock or sediment on land surfaces enables us to determine exposure ages of the landform. This methodology targets reconstruction of environmental changes in mountainous areas due to climatic transition, timings of large landslide occurrence, and formation ages of fluvial or marine terraces. In this application, post-event erosion or sedimentation, and/or pre-event irradiation of cosmic rays enlarge uncertainty in the model ages. The nuclide concentration in an eroding bedrock or current sediment reflects residence time of the material near the land surface, which then can be converted to denudation rates of the landform. This application has revealed rates of carbonate denudation as a function of climatic conditions of the sites, soil production and catchment-wide denudation rates in silicate areas, which corresponds to topography of the terrain. For samples of deeply-buried sediments, ratio of paired nuclides in identical mineral grains indicates ages of burying of the debris. The pair of $^{10}$Be and $^{26}$Al in quartz has been used for dating sediments in caves, for a timescale of $10^6$ years. Analysis of such samples provides also a clue to reconstruct paleo denudation rates of the source areas of the debris. In this presentation, applicability and limitations of this method will be discussed with several actual data and outputs from various models of nuclide accumulation.

Keywords: Terrestrial cosmogenic nuclides, Exposure age, Denudation rate, Burial age, Landscape evolution

©2019. Japan Geoscience Union. All Right Reserved. 

# Dating of marine erosional terraces using cosmogenic nuclides: A case study of the Hyuga City, Miyazaki Prefecture, southwest Japan (preliminary results)

*Shigeru Sueoka[1], Tetsuya Komatsu[1], Yuki Matsushi[2], Yusuke Yonaga[1], Naomi Sano[1], Noriaki Hirao[1], Tadamasa Ueki[1], Natsuko Fujita[1], Yoko Kokubu[1], Masakazu Niwa[1]

1. Japan Atomic Energy Agency, 2. Disaster Prevention Research Institute, Kyoto University

Uplift rate in an inland region and coastal region in the past $10^4$ to $10^5$ years can be estimated based on the elevation and emergent age of marine terraces (e.g., Ota and Omura, 1991). Marine depositional terraces in Japan have been dated by using radioactive carbon dating, tephrochronology, and recently developed optically stimulated luminescence dating (especially pIRIR dating for feldspar; e.g., Ito et al., 2015). On the other hand, it is difficult to date marine erosional terraces which lack sedimentary layers on the surfaces to apply these dating methods.

This study attempted to date marine erosional terraces by using terrestrial cosmogenic nuclide (TCN) dating methods, especially $^{10}$Be and $^{26}$Al methods. The $^{10}$Be and $^{26}$Al methods can reconstruct an exposure age and/or erosion rate of a rock based on the contents of $^{10}$Be and $^{26}$Al which are produced by irradiations of cosmic rays to oxygen and silicon in the rock (Wakasa et al., 2004; Matsushi et al., 2007). The production rates of $^{10}$Be and $^{26}$Al at the surface or at a certain depth depend on the cosmic-ray intensity (related to the latitude and altitude), density of the covering materials, and depth of the rock. The cosmic-ray intensity is computed theoretically, and the density of the covering materials can be also measured or assumed. Therefore, time-depth process of the rock, namely erosion and deposition history at the site, can be constrained by measuring the $^{10}$Be and $^{26}$Al contents.

We studied marine erosional terraces in Hyuga City, Miyazaki Prefecture, southwest Japan. Three groups of marine terraces were identified in this region, which are hereinafter named M1, M2 and L surfaces, respectively. The elevations of the surfaces are 30-50 m for M1 surface, 19-30 m for M2 surfaces, and sea-level to ~8 m for L surface. Considering the elevation, M1 and M2 surfaces can be correlated to the Sanzaibaru surface and Nyutabaru surface (Nagaoka et al., 2010), respectively, whereas L surface is thought to be the Holocene terraces. We collected rock samples for TCN dating by excavating three pits on M2 surface. The cross-sections of the pits consist of the basement rock, angular to subangular gravel layer interpreted as *in-situ* weathered basement rock, and soil from the base to the top. Rock samples were collected from the top of the gravel layer (depth: ~50 cm to 1 m) which is thought to be the surface of the former wave-cut benches. The lithology of the samples is the granite porphyry of the Osuzuyama acidic rocks formed in the middle Miocene (Nakata, 1978). The samples were processed by following the procedures of Kohl and Nishizumi (1992) and the $^{10}$Be and $^{26}$Al contents were measured using JAEA-AMS-TONO, an accelerator mass spectrometer at the Tono Geoscience Center, Japan Atomic Energy Agency (Saito-Kokubu et al., 2013).

The $^{26}$Al contents measured were rejected because these values were lower than the theoretical values. The $^{10}$Be contents yielded ~100 to 70 ka of the minimum exposure ages. More realistic erosion/deposition scenarios were adopted for better dating of the terrace surfaces, in which sedimentary layers were assumed to be deposited at a constant rate after the emergent of the surface. Consequently, M2 surface is thought to be emerged in MIS 5a although the correlated Nyutabaru surface emerged in

©2019. Japan Geoscience Union. All Right Reserved. 

MIS 5c. We are planning to determine more accurate age of the surfaces by tuning model parameters and by obtaining depth profiles of TCN contents.

Acknowledgements: This study was carried out under a contract with METI (Ministry of Economy, Trade and Industry) as part of its R&D supporting program for developing geological disposal technology.

Keywords: cosmogenic nuclide dating, marine erosional terrace

©2019. Japan Geoscience Union. All Right Reserved. 

# Estimation of thermal history of Toki granite over 0.1Myr timescale by Multi-OSL-thermochronometry

*Manabu Ogata[1], Georgina E King[2], Frédéric Herman[2], Shigeru Sueoka[1]

1. Tono Geoscience Center, Japan Atomic Energy Agency, 2. University of Lausanne

Estimation of denudation history is important for geological disposal of high-level radioactive waste because denudation influences underground water flow and distance between the surface and underground facility. Terrestrial cosmogenic nuclide ($^{10}$Be, $^{26}$Al) dating is used to evaluate denudation rate in a few meters, whereas low-temperature thermochronology, such as fission-track and (U-Th)/He methods, is applied to estimate denudation histories for a few to several kilometers in the last $10^6$-$10^8$ years. However, the middle-term ($10^4$-$10^5$ years) denudation history over several hundred meters is more important for geological disposal because it takes tens of thousands of years to reduce the radioactivity of radioactive waste to the level of that of natural uranium ore.
Recently, multi- OSL-thermochronometry has been proposed as a tool that offers the potential for tight constraint of cooling histories in the low-temperature domain (< 75℃) over recent (0.1-0.2 Myr) timescales. This method determines the timing and rate at which electrons are trapped and thermally released in minerals, in response to in situ radiation and rock cooling. The technique of OSL thermochronometry is able to be used to unravel denudation histories.
Application of OSL thermochronometry is currently limited to regions that have experienced denudation rates higher than 3 mm/year, assuming a general geothermal gradient and surface temperature; luminescence signals saturate before the rocks are exhumed to the surface in a slowly-denuded region. Given such limitations on the cooling/denudation rate, previous researches on OSL themochronometry has focused on tectonically active mountain ranges, such as the Himalayas, the Southern Alps of New Zealand and Hida range in Japan.
We attempt to apply multi-OSL-thermochronometry to the tectonics that have experienced slowly denudation rate using long borehole. We used the borehole MIZ-1 which was drilled at Mino plateau, Gifu, Japan. The denudation rate in this area is expected to be around 0.1 mm/year or less from the denudation rate since ~40 Ma estimated by the apatite fission track method and uplift rate between MIS6 and MIS2 based on elevations and emergent ages of the fluvial terraces. This borehole consists mainly of the Cretaceous Toki granite pluton which is located at the Sanyo Belt in the Inner zone of the South west Japan Arc. The total length of MIZ-1 is about 1,300 mabh (meter along borehole) and Toki granite ranges from 110 to 1,300 mabh. We collected the samples at 159, 449, 751 mabh for multi-OSL-thermochronometry.
Cooling histories of all samples are similar. Their temperatures decreased to the present ambient temperature at each depth before 0.1 Ma and have then been stable. These results correspond to the expected slow denudation rate. Our results indicate that, by using long borehole, multi-OSL-thermochronometry can be applied to slowly-denuded regions.
This study was carried out under a contract with METI (Ministry of Economy, Trade and Industry) as part of its R&D supporting program for advanced research on long-term stability of geological environment.

Keywords: luminescence, thermochronometry, feldspar

©2019. Japan Geoscience Union. All Right Reserved. 

# Depth condition under which OSL signal of quartz gouge experiences coseismic zeroing

*Yuki Minomo[1], Kiyokazu Oohashi[1], Noriko Hasebe[2], Kazumasa Miura[3]

1. Graduate School of science and Technology for Innovation, Yamaguchi University , 2. Institute of Nature and Environmental Technology, Kanazawa University, 3. Kanazawa University

Attempts to determine the age of faulting recorded on a fault rock have been made using methods such as the K-Ar dating, FT dating, and ESR dating (e.g., Murakami & Tagami, 2004, GRL). Among the proposed methods, the luminescence dating method has an applicable time range of few decades to few hundred thousand years ago, and hence it is suitable for dating an active fault. Early trial demonstrated a successful determination of the latest earthquake event along the active fault in central Japan (Ganzawa et al., 2013, JGSJ). The slip rate dependence of the condition that optically-stimulated luminescence (OSL) signal of quartz gouge resets was experimentally verified, so that the signal start to decrease from the slip rate of 0.25 m/s and becomes zero at slip rate ≧ 0.65 m/s (Minomo et al., 2018, JPGU). Here we show the clear reduction (zeroing) of OSL signal of quartz gouge after the laboratory experiments and estimate depth condition required to occur age resetting in natural fault zones. In the experiments, we used quartz powder with a particle size of <150 μm which is extracted from Tsushigawa granite, located in Awaji island, Hyogo Prefecture. We irradiated 400 Gy of gamma-ray for the quartz powder before the experiments to simulate natural radiation damage. Friction experiments were conducted under the following conditions in darkroom environment using a rotary-shear, high-velocity friction apparatus in Yamaguchi University; normal stress of 0.5–5.0 MPa and slip rate of 0.65 m/s (constant from starts to finish). To eliminate the effect of crushing on OSL signal, we measured coarse grains (75–150 μm) extracted from recovered sample.As a result of the measurement, OSL signal intensity start to decrease from the normal stress of 0.5 MPa. We found “partial resetting” which is characterized by coexistence of both particles with signal and without signal at normal stress of 0.5 and 1.0 MPa, and then frequency of the signal intensity for each aliquot is bimodal distribution.On the other hand, complete resetting of the signal was observed in all particles at normal stress ≧ 2.0 MPa.. Assuming a coseismic fault slip rate of 0.6 m/s, depth conditions required for operating partial and complete resetting of OSL age expected to be 18~36 m and 72 m respectively.

[Acknowledgements] This work was supported by grants from the Nuclear Regulation Authority (FY 2015-2018).

Keywords: optically-stimulated luminescence, active fault

©2019. Japan Geoscience Union. All Right Reserved. 

# Result of age determination of samples from Hokuriku Group

*Noriko Hasebe[1], Ryo Kamiguchi[2]

1. Institute of Nature and Environmental Technology, Kanazawa University, 2. Department of Earth Sciences, Kanazawa University

The Hokuriku Group is distributed from the southern part of Ishikawa Prefecture to the eastern part of Toyama prefecture and deposited in the Neogene period (about 25 Ma to 2.5 Ma). This study reports zircon fission track (ZFT) and U-Pb ages from several volcanic rocks distributed in the Tsurugi district, the southern part of Ishikawa Prefecture, Kanazawa University district, and Uozu area in Toyama prefecture. The Iozen Formation in Tsurugi district show ZFT ages between 12.2 ±1.9 to 15.7 ±2.8 Ma (error, 2 sigma) and U-Pb ages between 17.2 ±0.5 to 21.0 ±0.9 Ma. U-Pb ages coincide with the Japan Sea opening event, and eruption age by ZFT is about 5 mys after zircon crystallization. One sample from Otogawa Formation shows an equivalent age with the Iozen Formation, suggesting a rapid volcanic sedimentation for both formations. The sample from a quarry, which we thought is from TR1 (Ohkubo, 1999), therefore estimated age is about 4.4 Ma (Tamura and Yamazaki, 2004) by the correlation, shows much older age of ZFT 33.2 ±4.6 Ma and U-Pb 65.3 ±2.0 Ma, and further investigation, especially on the sample identification, is necessary. For Uozu area, ZFT ages of 3.4 ±0.7 to 9.7 ±1.4 Ma and U-Pb ages of 2.9 ±0.8 to 71.7 ±2.8 Ma are obtained, and eruption ages are equivalent to tephra found in Yatsuo district (Sumii, 1986)

Keywords: Hokuriku Group, TR1 tephra, Tng tephra

©2019. Japan Geoscience Union. All Right Reserved. 

[J] Oral | S (Solid Earth Sciences)：S-GL Geology

Thu. May 30, 2019 10:45 AM - 12:15 PM JST | Thu. May 30, 2019 1:45 AM - 3:15 AM UTC | A10 TOKYO BAY MAKUHARI HALL

## [S-GL27] Geochronology and Isotope Geology

convener:Takahiro Tagami(Graduate School of Science, Kyoto University), Yuji Sano(Division of Ocean and Earth Systems, Atmosphere and Ocean Research Institute, University of Tokyo), Chairperson:Yuji Sano, Takahiro Tagami

Reliable reconstruction of geohistory is of primary importance to better envision the present and future of the Earth. Geochronology and isotope geology play major roles in the reconstruction. This session offers an opportunity to present the results of fundamental studies, including the developments / improvements of analytical methods and age calibration, as well as applications to the Earth and planetary materials. We particularly focus on: (1) radiometric dating, bio-stratigraphy, magneto-stratigraphy and stable isotopic time series that provide the age information, (2) radioisotopes and stable isotopes widely employed for analyzing the Earth and planetary systems and (3) hypothesis and numerical modeling that utilize / assimilate the age and isotopic data. We also welcome contributions that integrate a variety of relevant disciplines.

10:45 AM - 11:15 AM JST | 1:45 AM - 2:15 AM UTC

[SGL27-06] **Geochemical origin/cycle analysis with isotopologues and isotopomers**

★Invited Papers

*Naohiro Yoshida[1] (1.Department of Chemical Science and Engineering, Earth-Life Science Institute, Tokyo Institute of Technology)

---

11:15 AM - 11:30 AM JST | 2:15 AM - 2:30 AM UTC

[SGL27-07] Estimation of Paleoenvironment by sedimentary rocks in Labrador, Cacada

*katsutaka sudo[1], Yuji Sano[1], Tsuyoshi Komiya[1], Bakert David[2], Michael Broadley[2], Bernard Marty[2] (1.University of Tokyo, 2.CRPG-CNRS, Université de Lorraine)

---

11:30 AM - 11:45 AM JST | 2:30 AM - 2:45 AM UTC

[SGL27-08] Hf-W dating of zircons from mesosiderites with high-pressure sintered sample

*Yuta Koyama[1], Naoto Takahata[1], Yuji Sano[1], Naoji Sugiura[1], Mizuho Koike[2], Makiko K. Haba[3], Sakata Shuhei[4], Hideharu Kuwahara[5], Tetsuo Irifune[5] (1.the University of Tokyo, 2.Japan Aerospace Exploration Agency, 3.Tokyo Institute of Technology, 4.Gakushuin University, 5.Geodynamics Research Center, Ehime University)

---

11:45 AM - 12:15 PM JST | 2:45 AM - 3:15 AM UTC

[SGL27-09] Radiometric ages *vs.* astrophysical ages -with regard to the numerical age in the International Stratigraphic Chart

★Invited Papers

*Ichiro Kaneoka[1] (1.Earthquake Research Institute, University of Tokyo)

# Geochemical origin/cycle analysis with isotopologues and isotopomers

*Naohiro Yoshida[1]

1. Department of Chemical Science and Engineering, Earth-Life Science Institute, Tokyo Institute of Technology

Since the 1950's, the stable isotope composition of natural samples has proved to be a unique tool for the study of geological and biological processes, their evolution and effect on Earth's surface environment. However, due to technical and conceptual limitations, the complete set of information potentially contained in the different modes of isotopic substitution remains largely unexplored. In this study, using new methodological developments that allow analysis of more isotopically substituted molecules, we are developing new tracers in 3 modes of isotopic substitution, fully integrated in the study of geological, biological and anthropogenic processes which affect the origin and evolution of the Earth's surface environment.

3 modes of substitution of stable isotopes in a single molecular species are;

1) Position specific isotope abundance (PSIA): Our group has pioneered PSIA of $N_2O$[1,2] and organic molecules using classic isotope mass spectrometry[3] and nuclear magnetic resonance[4,5]. We have shown that PSIA of hydrocarbons and organic acids allows to distinguish between biological and non-biological processes[4,6].

2) Mass-independent fractionation (MIF): The discovery of MIF of sulfur and oxygen in terrestrial samples has revolutionized environmental geochemistry and our understanding of the evolutionary history of the Earth's environment and life[7-9].

3) Clumped isotopes (i.e. isotopologues and isotopomers with 2 minor isotopes) provide unique information about the temperature history of molecules such as carbonates[10] or organic compounds[11-13].

We are currently developing new and improved tracers of environmental and biogeochemical processes and applying them to the environmental diagnosis. We are establishing and standardizing new methods for the analyses of every 3 complex modes of isotopic substitution, and unifying them to develop ultimate environmental diagnosis.

The development and application of these new isotopic tools to the environment evolution, in modern and more ancient eras, represents an important conceptual advance in Earth and life sciences. This will open new areas of research about, for example, the geological production of some atmospheric gases, metabolic processes and the biological fixation of atmospheric $CO_2$, the production and cycling of pollutant gas by industrial processes. As a whole, these new tracers will be integrated together for diagnosis of the Earth's environment.

References:

1)Yoshida & Toyoda, 2000 *Nature*; 2)Yamazaki, Toyoda, Yoshida, et al., 2014 *Biogeosciences*; 3)Yamada, Yoshida, et al., 2002 *RCM*; 4)Gilbert, Yamada, Yoshida, 2013 *Anal. Chem.*, and 5) 2014 *Anal. Chim. Acta*; 6)Gilbert, Yamada, Ueno, Yoshida 2016 *Geochim. Cosmochim. Acta*; 7)Danielache, Ueno, Yoshida et al.,

©2019. Japan Geoscience Union. All Right Reserved. 

2008 *J. Geophys. Res.*; 8)Hattori, Danielache, Ueno, Yoshida et al., 2013 *PNAS*, 9)Ueno, 2015 *Science*; 10) Yoshida, Abe, Yamada et al., RCM, 2013; 11)Tsuji, Yamada, Yoshida et al., 2012 *Sensor;*: 12)Ono et al., 2014 *Anal. Chem.*; 13)Stolper et al., 2014 *Science*.

Keywords: isotopomer, isotopologue, geochemical cycle, light element stable isotopes

©2019. Japan Geoscience Union. All Right Reserved. 

# Estimation of Paleoenvironment by sedimentary rocks in Labrador, Cacada

*katsutaka sudo[1], Yuji Sano[1], Tsuyoshi Komiya[1], Bakert David[2], Michael Broadley[2], Bernard Marty[2]

1. University of Tokyo, 2. CRPG-CNRS, Université de Lorraine

In the previous research, we reported isotopic compositions of graphite and carbonate in the 3.95Ga metasedimentary rocks from northern Labrador, Canada (Tashiro et al., 2017). Based on the isotopic shift of 20-30‰, we claimed a carbonate fixation by the Earth’ s earliest life. In this work, we picked up graphite from the very old rocks collected in Labrador and Nuvvuagittuq, and measured volatile isotope compositions by the step-wise heating method. We analyzed nitrogen isotopes to investigate whether the organic carbon was producted by cyanobacteria or methanobacteria, and noble gas (argon, krypton, xenon) isotopes to determine the age of rocks. We have used two types of gas mass spectrometer; VG3600 for nitrogen, Helix-MC for noble gases. The obtained data together with experimental method will be given in the presentation.

©2019. Japan Geoscience Union. All Right Reserved. 

# Hf-W dating of zircons from mesosiderites with high-pressure sintered sample

*Yuta Koyama[1], Naoto Takahata[1], Yuji Sano[1], Naoji Sugiura[1], Mizuho Koike[2], Makiko K. Haba[3], Sakata Shuhei[4], Hideharu Kuwahara[5], Tetsuo Irifune[5]

1. the University of Tokyo, 2. Japan Aerospace Exploration Agency, 3. Tokyo Institute of Technology, 4. Gakushuin University, 5. Geodynamics Research Center, Ehime University

Hf-W dating is a chronometer based on the decay of $^{182}$Hf to stable $^{182}$W with a half-life of 8.9 Myr (Vockenhuber et al., 2004). This radiometric dating method is important for discussing the timing of core formation in protoplanets and meteorites' parent bodies because hafnium is a lithophile element while tungsten is a siderophile one. In-situ analysis of Hf/W ratio on zircon ($ZrSiO_4$) mineral shows several difficulties, whereas meteoritic zircons have been often used to acquire the information of the early solar system due to their high resistance to thermal metamorphism and great aptitude for U-Th-Pb chronology. Generally, in-situ analysis needs standard materials which have well documented concentrations of target elements and the same matrix as the sample in order to avoid the change of sensitivity depending on major components (matrix effects) during an analysis using a secondary ion mass spectrometer (SIMS). There are no available standard zircons which include abundant and homogeneous tungsten because of its incompatibility with zircon crystal. Therefore, the previous studies determining the relative sensitivity factor (RSF) of Hf and W (Hf/W) for Hf-W dating of zircons using SIMS have been based on several assumptions (e.g., Ireland & Bukovanská,2003; Koike et al., 2017). These methods for measuring Hf/W ratios are indirect ways in terms of lacking standard zircons with known amount of W. In this study, we created new standard zircons which have abundant Hf and W concentrations. High purity zircon powder was mixed with hafnium and tungsten oxide. They were well crushed and mixed by a high energy ball mill and solidified by high-pressure sintering method with multi-anvil apparatus (ORANGE-3000, Geodynamics Research Center, Ehime University) in order to establish the direct way to determine the RSF of Hf/W ratio on zircons for in-situ analyses. Moreover, we applied these standards to Hf-W dating of zircons from a couple of mesosiderites with NanoSIMS (Atmosphere and Ocean Research Institute, the University of Tokyo) at approximately 30 $\mu$m scale. As a result of these analyses, we obtained the Hf-W age consistent with Koike et al. (2017) for the mesosiderite Asuka 882023.

Keywords: Hf-W dating, zircon, mesosiderite, sintering, NanoSIMS, RSF

©2019. Japan Geoscience Union. All Right Reserved. 

# Radiometric ages *vs.* astrophysical ages -with regard to the numerical age in the International Stratigraphic Chart

*Ichiro Kaneoka[1]

1. Earthquake Research Institute, University of Tokyo

In July, 2018, ICS(International Stratigraphy Commission) of IUGS published the new International Stratigraphic Chart (ISC: v.2018/07). The author drew an attention to the public about some issues to be cautioned on the usage of numerical ages in the ISC based on the 2009 version(v.2009/08) at the JpGU before (Kaneoka, 2016). The essential points do not change between the two versions of ISC, but there are some differences in the representation of numerical ages in the new ISC. Here, the author comments some points about them and discuss issues of astrophysical and radiometric ages used in the ISC.

Keywords: International Stratigraphic Chart, numerical age value, effective numerical value, astrophysical age, radiometric age

©2019. Japan Geoscience Union. All Right Reserved. 

[J] Poster | S (Solid Earth Sciences)：S-GL Geology

Thu. May 30, 2019 3:30 PM - 5:00 PM JST | Thu. May 30, 2019 6:30 AM - 8:00 AM UTC | Poster Hall International Exhibition Hall8, Makuhari Messe_11

## [S-GL27] Geochronology and Isotope Geology

convener:Takahiro Tagami(Graduate School of Science, Kyoto University), Yuji Sano(Division of Ocean and Earth Systems, Atmosphere and Ocean Research Institute, University of Tokyo)

Reliable reconstruction of geohistory is of primary importance to better envision the present and future of the Earth. Geochronology and isotope geology play major roles in the reconstruction. This session offers an opportunity to present the results of fundamental studies, including the developments / improvements of analytical methods and age calibration, as well as applications to the Earth and planetary materials. We particularly focus on: (1) radiometric dating, bio-stratigraphy, magneto-stratigraphy and stable isotopic time series that provide the age information, (2) radioisotopes and stable isotopes widely employed for analyzing the Earth and planetary systems and (3) hypothesis and numerical modeling that utilize / assimilate the age and isotopic data. We also welcome contributions that integrate a variety of relevant disciplines.

[SGL27-P01] Research report on long-term stability of geological environments and LA-ICP-MS-based age dating

★Invited Papers

*Tatsunori Yokoyama[1], Takehiro Mitsucuchi[1], Shigeru Sueoka[1] (1.Japan Atomic Energy Agency)

[SGL27-P02] **U-Pb detrital zircon age dating from the Aileu Formation of Timor-Leste; Estimate depositional age and provenance of the sediment**

*Jovita Elisa Fatima da Costa[1], Shoichi Kiyokawa[1], Yukiyasu Tsutsumi[2] (1.Kyushu University, 2.National Museum of Nature and Science)

[SGL27-P03] Petrological, geochemical, and geochronological characteristics of the Oritate travertine from Unazuki area, Toyama, Japan: possibility of U-Pb geochronology of carbonates with high common Pb.

*Mayuko Fukuyama[1], Masatsugu Ogasawara[2] (1.Graduate School of Engineering Science, Akita University, 2.Geological Survey of Japan, National Institute of Advanced Industrial Science and Technology)

[SGL27-P04] Zircon U-Pb age and tectonics of shirakamidake granitic complex

*Hiroki Sato[1], Koji Umeda[1] (1.Hirosaki University)

[SGL27-P05] Zircon U-Pb dating of plutonic rocks from Yamizo Area, northeast Japan

*Terumi Ejima[1,2], Yoshiaki Kon[2], Daisuke Araoka[2], Shigenori Kawano[3], Yutaka Takahashi[2] (1.Shinshu University, 2.Geological Survey of Japan, 3.Tochigi Prefectural Museum)

[SGL27-P06] Denudation history of the Higher Himalayan Crystallines in West-Central Nepal: insights from zircon fission-track dating and thermokinematic modeling

*Nakajima Toru[1], Harutaka Sakai[1], Hideki Iwano[2], Tohru Danhara[2], Takafumi Hirata[3] (1.Division of Earth and Planetary Sciences, Graduate School of Science, Kyoto University, 2.Kyoto Fission-Track Co., Ltd., 3. Geochemical Research Center, The University of Tokyo)

[SGL27-P07] Thermochronology on the fore-arc side of Northeast Japan Arc

*Yuya Kajita[1], Shigeru Sueoka[2], Shoma Fukuda[1], Noriko Hasebe[3], Akihiro Tomoaki[4], Tomoaki Morishita[4], Barry P. Kohn[5], Tatsunori Yokoyama[2], Takahiro Tagami[1] (1.Graduate School of Science, Kyoto University , 2.Japan Atomic Energy Agency, 3.Institute of Nature and Environmental Technology, Kanazawa University, 4.Department of Sciences, Kanazawa University, 5.School of Earth Sciences, University of Melbourne)

[SGL27-P08] Argon diffusion in rocks - classical approach in view of heating and relaxation

Horst Zwingmann[1], *Hironobu Hyodo[2] (1.KUEPS, Kyoto University, 2.Research Institute of Natural Sciences, Okayama University of Science)

---

[SGL27-P09] $^{4}$He/U-Th dating of pore waters from Quaternary sediments in Switzerland: potential and challenges

*Yama Tomonaga[1], Edith Horstmann[1], Gaudenz Deplazes[2], Rolf Kipfer[1] (1.Swiss Federal Institute of Aquatic Science and Technology (Eawag), 2.National Cooperative for the Disposal of Radioactive Waste (Nagra))

---

[SGL27-P10] Compound-specific radiocarbon analysis of lipid biomarkers in surface sediment from Lake Kawaguchi, central Japan

*Shinya Yamamoto[1], Yosuke Miyairi[2], Yusuke Yokoyama[2], Hisami Suga[3], Nanako O. Ogawa[3], Naohiko Ohkouchi[3] (1.Mount Fuji Research Institute, Yamanashi Prefectural Government, 2.Atmosphere and Ocean Research Institute, The University of Tokyo, 3.Japan Agency for Marine-Earth Science and Technology)

---

[SGL27-P11] Reestablishment of the Mesozoic and Cenozoic Stratigraphic Events of the Fergana Basin, Uzbekistan

*OTABEK ULUGBEK OGLI ANVAROV[1], Ken-ichiro Hisada[1], Teruyuki Maruoka[1], Junichiro Kuroda[2], Sherzod Makhmudov[3] (1.UNIVERSITY OF TSUKUBA, 2.Atmosphere and Ocean Research Institute, the University of Tokyo , 3.State Comittee of Geology and Mineral Resources of Uzbekistan)

# Research report on long-term stability of geological environments and LA-ICP-MS-based age dating

*Tatsunori Yokoyama[1], Takehiro Mitsucuchi[1], Shigeru Sueoka[1]

1. Japan Atomic Energy Agency

In recent years, it has become possible to carry out high-precision microscale age dating of geological samples (with a spatial resolution of less than several tens of micrometers) using developed micro-analytical techniques such as secondary ion mass spectrometry (SIMS), laser ablation inductively coupled plasma mass spectrometry (LA-ICP-MS), etc. Application of LA-ICP-MS-based microscale U-Pb dating is extending from U-rich heavy minerals such as zircon, apatite and monazite to U-depleted minerals such as calcite. This kind of method enables age determination of several types of mineral grains (and their internal zoning structures) occurring within rock bodies, and thereby reveals chronological changes in chemical composition of source materials from which the minerals were crystallized, with some cases in which thermal history of the crystal formation system can be reconstructed.

For research and development of geological disposal techniques for high-level radioactive wastes, we develop and facilitate geochronological dating techniques for evaluation of long-term stability in geological environments, at Tono Geoscience Center, Japan Atomic Energy Agency. Elucidating past long-term variations of geological environments leads to predicting the future of the environments and is essential for the geological disposal, because the radioactive wastes need to be buried in deep underground and isolated far from the human living sphere for more than tens of thousands of years. Geochronological dating techniques are necessary for this purpose. LA-ICP-MS U-Pb dating of zircon provides reliable information about igneous activities such as magmatic differentiation and is also useful for provenance analysis if the mineral is found in sediments. Additionally, dating techniques using $^{10}Be$ and $^{26}Al$, which are generated by cosmic rays reaching the ground, can be applied to quantitative estimation of the amount of uplift and erosion. Combining these various dating methods has great potential to elucidate past long-term variations of geological environments.

In our presentation, we introduce the current status of our development for research on long-term stability of geological environments, U-Pb dating of calcite, U-Pb dating of young zircon and trace element analysis by using LA-ICP-MS.

This study was carried out under a contract with METI as part of its R&D supporting program for developing geological disposal technology.

Keywords: long-term stability in geological environments, LA-ICP Mass Spectrometry, U-Pb dating

©2019. Japan Geoscience Union. All Right Reserved. 

# U-Pb detrital zircon age dating from the Aileu Formation of Timor-Leste; Estimate depositional age and provenance of the sediment

*Jovita Elisa Fatima da Costa[1], Shoichi Kiyokawa[1], Yukiyasu Tsutsumi[2]

1. Kyushu University, 2. National Museum of Nature and Science

The Aileu Formation is a part of allochthonous metamorphic complexes distributed a 110km long and 40 km wide in Timor-Leste. It occupies most of the north-west of Timor-Leste and crops out along the north coast from Manatutu to the West Timor border and passing through to the south (Audley Charles, 1968). It is considerable lithological variation and metamorphic grade varies between lower greenschist to upper amphibolite facies (Beery and Grady, 1981). Our research area is affected by greenschist metamorphism and comprises an extensive succession of mostly terrigenous metasedimentary rock. The previous study of the north coast suggests that detrital zircon U-Pb from metasandstone, shows three groups at 270-440Ma, 860-1240, and 1480-1870Ma, and the metamorphic age also identified by 40Ar/39Ar of hornblende cooling ages of 10–6 Ma (Elly et al, (2014)). The Aileu Formation contain east-west foliation and north-south widely distributed. However, it's not a well-known south area of metasedimentary origin and depositional age. This study, we collect 3 samples of meta-sandstone transect north-south about 20 km wide. We analyzed U-Pb detrital zircon by using LA-ICP-MS.

Petrographically the 3 samples composed majorities of fine, fine medium grain of quartz-rich sandstone weakly deform and foliated. The three samples composed less than 2% muscovite, biotite, plagioclase, and another accessory mineral include zircon. Texturally immature characterized by sub-angular to sub-rounded and fresh of mica. These three samples are almost consisting of the same morphological characteristic of zircon grain.

The U-Pb age distribution of detrital zircon result from the concordant dataset reflected similar characteristic for all three samples and shows 270-420 Ma 900-1300Ma and 1400-1900 Ma. Grain younger than 270 Ma and older than 1900 Ma makes up 4% of the population. The most significant age peak, at 283-290 Ma indicated that the distribution of sediment coming from early Permian source rocks. The youngest zircon and main peaks are 239.87 Ma and 283-290 Ma, we consider this for maximum deposition age in the south which is the same as the north area. We suggest that the Sedimentation age of the south area of Aileu Formation after middle Triassic. These age from the previous study (north coast) and this study (north-south) shows the similarity characteristic for all samples. The Aileu Formation might be formed a fold and thrust belt and resemble sequences stacked north to south. Source sediment for Aileu Formation is compatible with a sediment source located in South East Asia as part of the now fragmented Sula Spur (Ely 2014). Sula spur is containing a Paleozoic granite and metamorphic basement which is extending from west of New Guinee and include the Bangai and Sula island.

Keywords: U/Pb Age of detrital zircon, Aileu Formation , Metasandstone

©2019. Japan Geoscience Union. All Right Reserved. 

# Petrological, geochemical, and geochronological characteristics of the Oritate travertine from Unazuki area, Toyama, Japan: possibility of U-Pb geochronology of carbonates with high common Pb.

*Mayuko Fukuyama[1], Masatsugu Ogasawara[2]

1. Graduate School of Engineering Science, Akita University, 2. Geological Survey of Japan, National Institute of Advanced Industrial Science and Technology

U-Pb dating of carbonate minerals can be widely applied to understand the timing of vein-type mineralization, fault movements, and other geological events forming calcites, which are difficult to be dated by other methods. Reference materials for U-Pb dating of calcite, such as WC-1 (254.4 ±6.4 Ma, Roberts *et al.*, 2017) and ASH-15D (3.001 ±0.012 Ma, Mason *et al.*, 2013; Vaks *et al.*, 2013), are available from several laboratories. However, it is often difficult to obtain reliable estimated ages of calcite because calcite usually contains high common Pb content.

In this study, we present the petrological, geochemical, and geochronological characteristic of the Oritate travertine from Unazuki area, Toyama, Japan. Typically, travertines are formed by a precipitation of carbonate minerals from hot spring. Thus, the U-Pb dating of calcite provides the timing of hydrothermal fluid activity. The Oritate travertine is called as ‘Onyx Marble’ by its texture. It shows layered texture with different colors from gray, white, to brown. It consists of aragonite and calcite. The chondrite normalized REE patterns of travertines show the flat and positive Eu anomalies which are different characteristics from oceanic limestones.

High initial $^{238}U/^{204}Pb$ ($\mu$) content is requirement for precise U-Pb dating of calcite (Rasbury & Cole, 2009), because calcite generally contains significant amount of common Pb. It is also better to contain high U in the order of several tens of ppm for U-Ob dating. U/Pb ratio of the Oritate travertines range from 1.1 to 2.2. The U and Pb concentration of Oritate travertines are very low which is less than 1 ppm. The brownish colored layers in travertines contain relatively high U concentrations. Although the chemical compositions of Oritate travertine imply the difficulty to apply U-Pb method, we examined U-Pb dating of calcite with high common Pb. We analyzed travertines with relatively high U/Pb ratio and U contents parts of the travertines for U-Pb dating. U-Pb dating was attempted with the solution ICP-MS as well as the LA-ICP-MS utilize a New Wave Research 193UC excimer laser ablation system, coupled to a Nu Instruments Nu Plasma II multi-collector ICP-MS or Agilent 7700 quadru-pole ICP-MS at Akita University. We discuss and evaluate the U-Pb dating method for calcite with high common Pb.

Keywords: U-Pb dating, carbonate mineral, travertine, ICP-MS, Oritate

©2019. Japan Geoscience Union. All Right Reserved. 

# Zircon U-Pb age and tectonics of shirakamidake granitic complex

*Hiroki Sato[1], Koji Umeda[1]

1. Hirosaki University

The Shirakamidake granitic complex in the Southwest of Aomori prefecture, is divided into the East, Central and West bodies. The East body and the Central bodies are mainly composed of coarse to medium grained hornblende biotite granodiorite and coarse to medium grained granite, respectively. The West body consists of schistose medium to coarse grained hornblende biotite granodiorite and light color schistose medium to coarse grained hornblende biotite granodiorite with mylonite zone (hujimoto, 2010). A large number of petrological studies have investigated the cooling history of the Shirakamidake granitic complex. Apatite (U-Th)/He age of 4.2±2.0 Ma, biotite K-Ar age of 86-100 Ma, amphibole K-Ar age of 89-94 Ma and whole-rock Rb-Sr age of 110.1±6.0 Ma have been reported. Generally, the ages of the West body are younger than those of the East body.

In this study, we describe geological and petrological features each bodies by polarizing microscopy, XRF spectrometry and EPMA analysis. We also present geochronological data utilizing laser ablation ICP mass spectrometry technique on the zircons that provides zircon U-pb age of 107.7±1.4Ma.
Thermochronological data suggests two distinctive cooling stages for the Shirakamidake granitic complex; 1) a first rapid cooling stage in which the granitic magma was cooled to the temperature of host rock soon after intrusion, and 2) second slow cooling stage associated with the uplift and subsequent erosion of the granite intrusion after ~90 Ma.

Keywords: The Shirakamidake granitic complex , Zircon, U-Pb age

©2019. Japan Geoscience Union. All Right Reserved. 

# Zircon U-Pb dating of plutonic rocks from Yamizo Area, northeast Japan

*Terumi Ejima[1,2], Yoshiaki Kon[2], Daisuke Araoka[2], Shigenori Kawano[3], Yutaka Takahashi[2]

1. Shinshu University, 2. Geological Survey of Japan, 3. Tochigi Prefectural Museum

To investigate the timing of the tectonothermal events of Yamizo plutonic suite, U-Pb dating of zircon was carried out using laser ablation inductively coupled plasma mass spectrometry combined with cathodoluminescence imaging on zircon grains separated from the Yamizo plutons.

In the Yamizo mountain areas, K-Ar ages of Ozasa (67.5Ma), Fukuroda (101 Ma), Iwafune (64.5 Ma), Kamehis (64.9 Ma) and Ooyamada plutons (71.8 Ma and 108 Ma) have been reported by Shibata et al. (1973). Basically, the K-Ar ages are sometimes younger than actual intrusive ages because the closure temperature of K-Ar ages are lower than that of the solidus of granitic rocks. The closure temperature of the U-Pb age of zircon was higher than that of K-Ar age and more suitable for investigating intrusive age of magma.

Nagasaka, Hatajyuku, Yamagiwa, Nomisawa, Ozasayama, Kizami, Kamehisa and Hanatatetouge plutons are distributed in the northern part of the Yamizo area. Zircon U-Pb ages of these plutons were 69–63 Ma. In the southern part of the Yamizo area, Ooyamada, Fukuroda and Korofuji plutons are distributed. The zircon U-Pb ages of these plutons were 104–102 Ma.

According to the results in this study, U-Pb ages correspond to the K-Ar ages previously reported. This result indicated that cooling rates after intrusion of the plutons in the Yamizo area were relatively fast. Moreover, U-Pb ages of plutons in the southern part of the Yamizo area were same as those of the Bato pluton (109–106 Ma: Ejima et al., 2017) and of Abukuma plutons (121–97 Ma: Kon and Takagi, 2012; Ishihara and Orihashi, 2015; Kon et al., 2015; Takahashi et al., 2016). On the other hand, U-Pb ages of plutons in the northern part of the Yamizo area were same as those of plutons around Tsukuba mountain (80 Ma, 63–58 Ma: Koike and Tsutsumi, 2018).

Keywords: Yamizo area, U-Pb age of zircon, plutons

©2019. Japan Geoscience Union. All Right Reserved. 

# Denudation history of the Higher Himalayan Crystallines in West-Central Nepal: insights from zircon fission-track dating and thermokinematic modeling

*Nakajima Toru[1], Harutaka Sakai[1], Hideki Iwano[2], Tohru Danhara[2], Takafumi Hirata[3]

1. Division of Earth and Planetary Sciences, Graduate School of Science, Kyoto University, 2. Kyoto Fission-Track Co., Ltd., 3. Geochemical Research Center, The University of Tokyo

Zircon Fission-Track (FT) dating and thermochronological inverse calculation were used to indentify the denudation history of the Higher Himalayan Crystalline (HHC) in west-central Nepal. We newly obtained 17 zircon and 4 apatite FT ages from Higher Himalayan Crystallines (HHC), the overlying Tibetan Tethys Sediments (TTS) and the underlying Lesser Himalayan Sediments (LHS) along 80km long transect across the Himalaya.
The ZFT age from the underlyng sediments displayed northward younging linear distribution of the oldest age in the frontal part of the Lesser Hilamaya (13.4 ±1.0 Ma) to the youngest age in the root zone near the Main Central Thrust (1.5 ±0.2 Ma). On the other hand, the ZFT ages from the HHC and the overlying sediments ranged from 10.9 ±0.8 Ma to 1.7 ±0.4 Ma, and showed southward younging distribution. The ZFT age distribution along NNE-SSW transect displayed a concave upward pattern with the youngest FT age located near the Main Central Thrust (MCT). This distribution pattern is well corresponded to present uplift rate, indicating that the FT age distribution pattern reflects the tectonically driven exhumation.
Thermochronological invert calculation showed two rapid cooling (<100 ℃/Myr) phases of the HHC and the LHS in the late Miocene and the Pleistocene. With respect to this result, rapid exhumation is not only suggested in the Pleistocene, but also in the late Miocene. The former implies rapid exhumation of the HHC accompanied by reactivation of the MCT in the late Miocene, the latter implies rapid denudation accompanied by overthrusting of the hanging wall of the Main Himalayan Thrust (MHT).
Thermo-kinematic calculation results also suggest that the distribution of FT ages is well explained by exhumation process accompanied by the activity of the MHT. Furthermore, the kinematic model considering reactivation of the MCT in the late Miocene yields a better fit between predicted and observed ages than the model without reactivation, indicating agreement with reactivation of the MCT in late Miocene.

Keywords: Himalaya, thermochronology, fission-track age, denudation history, Higher Himalayan Crystallilne

©2019. Japan Geoscience Union. All Right Reserved. 

# Thermochronology on the fore-arc side of Northeast Japan Arc

*Yuya Kajita[1], Shigeru Sueoka[2], Shoma Fukuda[1], Noriko Hasebe[3], Akihiro Tomoaki[4], Tomoaki Morishita[4], Barry P. Kohn[5], Tatsunori Yokoyama[2], Takahiro Tagami[1]

1. Graduate School of Science, Kyoto University , 2. Japan Atomic Energy Agency, 3. Institute of Nature and Environmental Technology, Kanazawa University, 4. Department of Sciences, Kanazawa University, 5. School of Earth Sciences, University of Melbourne

An arc trench system is composed of a topographically high land and a trench along a subduction zone. An arc trench system is grouped into continental arc and island arc. The latter has a back-arc basin. Island arcs are tectonically active regions where a lot of volcanic activities and earthquakes occur, providing keys to solve the formation and evolution processes of orogenic zones and continents (Toriumi et al., 2018).

Northeast (NE) Japan is one of the best regions to study tectonics of island arc because NE Japan has comparatively obvious island arc components, i.e., fore-arc, volcanic front, back-arc and back-arc basin. Therefore, many studies have focused on the tectonic evolution of NE Japan (e.g. Amano and Sato, 1989; Sato, 1992; Nakajima, 2013). However, there are a few quantitative investigations of the mountain uplift and denudation histories which are important for estimating tectonics of island arcs.

For measuring uplift or denudation rates, some techniques are available (e.g., GPS survey, elevation of terraces, and thermochronology). To estimate million-year-scale mountain uplift and denudation rates, thermochronology is among the most appropriate methods. Thermochronology can reconstruct the time-temperature relationship of rock/mineral samples, based on radiometric ages and closure temperatures specific to the combination of radiometric dating methods and target minerals. Furthermore, some assumptions enable discussion of mountain uplift and denudation histories. Although thermochronology has been successfully applied to orogens worldwide (Hermam et al., 2013), a small number of thermochronometric studies have been attempted in NE Japan (e.g. Sueoka et al., 2017, Fukuda et al., in press). Moreover, these previous studies focused on the denudation histories of the across-arc scale rather than individual geologic component, namely fore-arc, Ou backbone range and back-arc.

In this study, we focus on fore-arc side of NE Japan, i.e., Kitakami Mountains and Abukuma Mountains, at which granitic rocks are distributed extensively, providing preferable study areas to apply thermochronology. We adopted apatite fission-track (AFT), apatite (U-Th-Sm)/He (AHe) and zircon (Zr) U-Pb analyses. AFT ages were estimated at 66.8-39.1 Ma in Kitakami and 61.0-40.5 Ma in Abukuma. AHe ages were obtained at 51.2-36.1 Ma in Kitakami and 75.9-60.1 Ma in Abukuma. Zr U-Pb ages were calculated at 110.3-104.3 Ma in Abukuma. With our results and the ages obtained by the previous studies, we discuss age trend and denudation history.

In Kitakami Mountains, AFT ages become younger to the east. On the other hand, all AHe ages are approximately comparable with each other except for the oldest age obtained at the westernmost locality. In Abukuma Mountains, both AFT and AHe age trends change across Hatagawa fault zone (HFZ); the ages were younger at the west side of HFZ than at the east side. Assuming that geothermal gradient is uniform at all localities, westerly tilting uplift and subsequent change of the uplift style were suggested in Kitakami Mountains. In Abukuma Mountains, our age data can constrain the faulting history of HFZ.

©2019. Japan Geoscience Union. All Right Reserved. 

As future subjects, we are planning to conduct 1) improvement of accuracy and precision by further analyzing, 2) increasing number of sampling localities and employing other methods (e.g., cosmogenic nuclides analysis and ESR thermochronology), 3) applying thermal inverse modeling of AFT data to estimate more detailed thermal histories, 4) discussion of geothermal gradient, uplift model and tectonics model in Kitakami Mountains and Abukuma Mountains.

Acknowledgements: This study was carried out under a contract with METI (Ministry of Economy, Trade and Industry) as part of its R&D supporting program for developing geological disposal technology. This work was supported by the Grant-in-Aid for Scientific Research on Innovative Areas (KAKENHI No. 26109003) from the Ministry of Education, Culture, Sports, Science and Technology (MEXT).

Keywords: Thermochronology, Northeast Japan Arc, Abukuma, Kitakami

©2019. Japan Geoscience Union. All Right Reserved. 

# Argon diffusion in rocks - classical approach in view of heating and relaxation

Horst Zwingmann[1], *Hironobu Hyodo[2]

1. KUEPS, Kyoto University, 2. Research Institute of Natural Sciences, Okayama University of Science

Since the development of the conventional K-Ar and subsequent 40Ar-39Ar dating methods fundamental noble gas diffusion processes in rocks were investigated including complex multi-scale and multi-path aspects in polyphase materials. Traditional models interpret the loss of radiogenic Argon due to an increase of temperatures. Hyodo (2017) proposed a new approach investigating the relaxation time and temperature relation within an “unclosure temperature” model. This model regards duration of a heating event as time for relaxation in a diffusion system at specific temperature. The model applies a functional form of mathematical approximation on fractional loss by diffusion. It allows fractional loss of certain amount of radiogenic 40Ar as long as the step heating model spectra in 40Ar-39Ar dating (plateau) maintains its original age within its age error. This new model approach is compared to a classical heating diffusion model (Huon et al., 1993) focusing on clay minerals (<10 and <2 μm) and larger muscovite grains (200 and 100 μm). The classical diffusion heating models applies three main parameters comprising a. grainsize (μm), b. temperature range (°C) and c. time scale (Ma). The obtained results provide a unique insight to compare an active heating versus passive cooling time and temperature path of clay minerals and muscovite with applications for general earth sciences and economic geology such as hydrocarbon exploration.

Huon, S. et al., 1993. Mise en évidence au Maroc d'événements thermiques d'âge triascico-liasique liés à l'ouverture de l'Atlantique. Bulletin de la societe géologique de France, 164/2, 165–176.

Hyodo, H., 2017. Unclosure temperature of a mineral: Cylinder and plane geometry. Bull. Res. Inst. Nat. Sci. Okayama Univ. Sci., No.43, 13-18.

Keywords: K-Ar dating, diffusion, reheating

©2019. Japan Geoscience Union. All Right Reserved. 

# $^{4}$He/U-Th dating of pore waters from Quaternary sediments in Switzerland: potential and challenges

*Yama Tomonaga[1], Edith Horstmann[1], Gaudenz Deplazes[2], Rolf Kipfer[1]

1. Swiss Federal Institute of Aquatic Science and Technology (Eawag), 2. National Cooperative for the Disposal of Radioactive Waste (Nagra)

Dating based on the $^{4}$He/U-Th method is used to estimate the residence time of pore waters in very low-permeable rocks and consolidated sediments. The residence time is inferred from the time necessary to accumulate radiogenic $^{4}$He measured in the pore water being produced by the decay of U and Th in the sediment matrix [1].
In the Jurassic Opalinus Clay, the pore water still contains remnants of the original marine formation water that was entrapped during sediment deposition. The pore water composition was altered only by diffusive processes [2,3]. The fact that even ~100-Ma-old water signatures can be preserved in their original pore space suggests that such preservation might also be possible in much younger dense glacial deposits. The $^{4}$He concentrations measured in the pore waters of glacial tills were translated into mean residence times of 15-25 kyrs [4] that agree rather well with the expected depositional ages of 25-31 kyrs [5]. These observations, as well as evidence from lacustrine sediments [6,7], suggest that, if the solute transport in the pore space is sufficiently attenuated, even unconsolidated sediments can "store" and host "old" pore waters.
In the present work we investigate if the $^{4}$He/U-Th dating of pore waters can be used as a novel tool to complement the luminescence dating of unconsolidated Quaternary sediments. We applied the $^{4}$He/U-Th method to date pore waters in the time range of 10 to 100 thousands of years which covers the age range of the sedimentary depositions targeted by the Quaternary drillings (QBOs) managed by the National Cooperative for the Disposal of Radioactive Waste (Nagra) in Switzerland. In particular, we focus on fine-grained lacustrine sediment layers that might provide low-permeability conditions suitable for the preservation of radiogenic $^{4}$He concentrations in the pore space.
We report the preliminary results of the $^{4}$He/U-Th dating based on the measurements conducted in sediment samples from the first QBOs, highlighting potential and challenges of the method with respect to the studied glaciofluvial sediments of the Swiss Midland.

References

[1] Torgersen, T., Clarke, W.B. (1985). Helium accumulation in groundwater, I: an evaluation of sources and the continental flux of crustal $^{4}$He in the Great Artesian Basin, Australia. *Geochim. Cosmochim. Acta 49*, 1211–1218.
[2] Gimmi T., Waber H. N., Gautschi A., Rübel A. (2007). Stable water isotopes in pore water of Jurassic argillaceous rocks as tracers for solute transport over large spatial and temporal scales. *Water Resour. Res. 43*(4).
[3] Mazurek, M., Alt-Epping, P., Bath, A., Gimmi, T., Niklaus Waber, H., Buschaert, S., et al. (2011). Natural tracer profiles across argillaceous formations. *Appl. Geochem. 26*(7), 1035–1064.
[4] Hendry, M. J., Kotzer, T. G., Solomon, D. K. (2005). Sources of radiogenic helium in a clay till aquitard and its use to evaluate the timing of geologic events. *Geochim. Cosmochim. Acta 69*(2), 475–483.
[5] Wassenaar L.I., Hendry M.J. (2000). Mechanisms Controlling the Distribution and Transport of $^{14}$C in a Clay-Rich Till Aquitard. *Groundwater 38*(3), 343–349.

©2019. Japan Geoscience Union. All Right Reserved. 

[6] Tomonaga, Y., Brennwald, M. S., Meydan, A. F., Kipfer, R. (2014). Noble gases in the sediments of Lake Van - Solute transport and palaeoenvironmental reconstruction. *Quat. Sci. Rev. 104*, 117–126.
[7] Tomonaga, Y., Brennwald, M. S., Kipfer, R. (2015). Attenuation of noble-gas transport in laminated sediments of the Stockholm Archipelago. *Limnol. Oceanogr. 60*(2), 497–511.

Keywords: pore water, noble gases, unconsolidated sediments

©2019. Japan Geoscience Union. All Right Reserved. 

# Compound-specific radiocarbon analysis of lipid biomarkers in surface sediment from Lake Kawaguchi, central Japan

*Shinya Yamamoto[1], Yosuke Miyairi[2], Yusuke Yokoyama[2], Hisami Suga[3], Nanako O. Ogawa[3], Naohiko Ohkouchi[3]

1. Mount Fuji Research Institute, Yamanashi Prefectural Government, 2. Atmosphere and Ocean Research Institute, The University of Tokyo, 3. Japan Agency for Marine-Earth Science and Technology

Lake sediment in volcanic regions contains valuable information on past eruptive history, as well as environmental consequences that took place in the catchment along with volcanisms. In this study, we performed compound-specific radiocarbon analysis (CSRA) of lipid biomarkers in surface sediment from Lake Kawaguchi situated northern proximal to Mount Fuji, central Japan, including short-chain ($C_{16}$) and long-chain ($C_{24}$, $C_{26}$ and $C_{28}$) fatty acids. The results are compared with the $^{14}C$ content of TOC, plant macrofossils (plant leaf and wood) and lake surface water in order to access their potential for dating tool in the lake sediment. The $^{14}C$ concentration of the long-chain ($C_{24}$, $C_{26}$ and $C_{28}$) fatty acids ranged from −43 to −183‰, corresponding to $^{14}C$ ages between 288 to 1554 years BP. This indicates that these acids contain substantial pre-aged materials in addition to those emitted from contemporary plant leaf waxes. In contrast, the short-chain ($C_{16}$) fatty acids showed a good agreement with the $^{14}C$ concentration of lake surface water, suggesting that they are most likely derived from primary producers (diatom) in the present lake and have a potential to improve chronologies in the sedimentary sequence in which the occurrence of fossil leaves is rather limited.

Keywords: compound-specific radiocarbon analysis, lake sediment, fatty acid

©2019. Japan Geoscience Union. All Right Reserved. 

# Reestablishment of the Mesozoic and Cenozoic Stratigraphic Events of the Fergana Basin, Uzbekistan

*OTABEK ULUGBEK OGLI ANVAROV[1], Ken-ichiro Hisada[1], Teruyuki Maruoka[1], Junichiro Kuroda[2], Sherzod Makhmudov[3]

1. UNIVERSITY OF TSUKUBA, 2. Atmosphere and Ocean Research Institute, the University of Tokyo , 3. State Comittee of Geology and Mineral Resources of Uzbekistan

Despite the fact that the Fergana Basin is being the important geologic and tectonic region in Central Asia, for more than a century of research represented that different views have been formed on its geological structure and history of development. Although, it is the least studied intermountain depressions within the Tien-Shan, and lies at the northeastern part of Uzbekistan, covering the 22.000 km $^2$ area. The first attempts on the basins geological investigations dates back to 1916’ s research by A.D. Arkhangelskiy which he started the descriptions of the preliminary stratigraphy of the Cretaceous deposits of the basin and adjacent areas. So far, the scientific debates got interrupted after the explorations of the important industrial resources as oil, gas, gold, uranium and so on, from the 50’ s during the Soviet Period, where all geological investigations concentrated only on broad explorations of resources. Yet, after the collapse of the Soviet Union, the studies still remained as minor and all works were referenced back to the old data, where the most studies were lack of the reliability. The purpose of this study is to reconstruct the stratigraphy of the Fergana Basin.

Generally, three stratigraphic units are involved in the stratigraphy of the basin. The lower one is represented by the Paleozoic formations. The second unit includes Mesozoic to Paleogene sediments. The third is composed of a thick unit of the Cenozoic molasses and the Quaternary sediments covering them. Five geological sections around Chust City, northern part of the Fergana Basin at the foothills of Northwestern Tien-Shan and Chatkal-Kurama Mountain Ranges in the Republic of Uzbekistan were selected and preliminary observations were carried out. The study area were represented by very well exposed deposits starting from the Permian andesites, trachytes and tuffs, the Triassic trachytes, the Cretaceous red beds of conglomerates, paleosols and sandstone shell beds of oyster and bivalve fossils, and the Paleogene grey limestones, sandstones and conglomerates with oyster fossils. At the sections from the Cretaceous to Paleogene, the transitions from terrestrial to marine environment were observed with alluvial, lagoon and costal-marine deposits. But, at the Cretaceous deposits the Upper Cretaceous sections were not observed, where documented as observable by the study of Abduazimova et al. (2012).

The preliminary results showed that the analyzed samples from the Cretaceous, just boundary to the Paleogene beds were the Aptian age of the Lower Cretaceous, therefore this study does not agree with Abduazimova et al. (2012), which documented the existence of the Upper Cretaceous deposits. The Paleogene samples showed the Eocene time. Therefore, the preliminary results of this study can suggest that the existence of disconformity between the Cretaceous and Paleogene sections, which suggests the Paleogene regression following the Late Cretaceous transgression.

Keywords: Fergana Basin, Stable Isotope Stratigraphy, Shell bed, Cretaceous, Paleogene

©2019. Japan Geoscience Union. All Right Reserved. 

[J] Poster | S (Solid Earth Sciences)：S-GL Geology

Thu. May 30, 2019 5:15 PM - 6:30 PM JST | Thu. May 30, 2019 8:15 AM - 9:30 AM UTC | Poster Hall International Exhibition Hall8, Makuhari Messe_22

## [S-GL27] Geochronology and Isotope Geology

convener:Takahiro Tagami(Graduate School of Science, Kyoto University), Yuji Sano(Division of Ocean and Earth Systems, Atmosphere and Ocean Research Institute, University of Tokyo)

Reliable reconstruction of geohistory is of primary importance to better envision the present and future of the Earth. Geochronology and isotope geology play major roles in the reconstruction. This session offers an opportunity to present the results of fundamental studies, including the developments / improvements of analytical methods and age calibration, as well as applications to the Earth and planetary materials. We particularly focus on: (1) radiometric dating, bio-stratigraphy, magneto-stratigraphy and stable isotopic time series that provide the age information, (2) radioisotopes and stable isotopes widely employed for analyzing the Earth and planetary systems and (3) hypothesis and numerical modeling that utilize / assimilate the age and isotopic data. We also welcome contributions that integrate a variety of relevant disciplines.

[SGL27-P01] Research report on long-term stability of geological environments and LA-ICP-MS-based age dating

★Invited Papers

*Tatsunori Yokoyama[1], Takehiro Mitsucuchi[1], Shigeru Sueoka[1] (1.Japan Atomic Energy Agency)

[SGL27-P02] **U-Pb detrital zircon age dating from the Aileu Formation of Timor-Leste; Estimate depositional age and provenance of the sediment**

*Jovita Elisa Fatima da Costa[1], Shoichi Kiyokawa[1], Yukiyasu Tsutsumi[2] (1.Kyushu University, 2.National Museum of Nature and Science)

[SGL27-P03] Petrological, geochemical, and geochronological characteristics of the Oritate travertine from Unazuki area, Toyama, Japan: possibility of U-Pb geochronology of carbonates with high common Pb.

*Mayuko Fukuyama[1], Masatsugu Ogasawara[2] (1.Graduate School of Engineering Science, Akita University, 2.Geological Survey of Japan, National Institute of Advanced Industrial Science and Technology)

[SGL27-P04] Zircon U-Pb age and tectonics of shirakamidake granitic complex

*Hiroki Sato[1], Koji Umeda[1] (1.Hirosaki University)

[SGL27-P05] Zircon U-Pb dating of plutonic rocks from Yamizo Area, northeast Japan

*Terumi Ejima[1,2], Yoshiaki Kon[2], Daisuke Araoka[2], Shigenori Kawano[3], Yutaka Takahashi[2] (1.Shinshu University, 2.Geological Survey of Japan, 3.Tochigi Prefectural Museum)

[SGL27-P06] Denudation history of the Higher Himalayan Crystallines in West-Central Nepal: insights from zircon fission-track dating and thermokinematic modeling

*Nakajima Toru[1], Harutaka Sakai[1], Hideki Iwano[2], Tohru Danhara[2], Takafumi Hirata[3] (1.Division of Earth and Planetary Sciences, Graduate School of Science, Kyoto University, 2.Kyoto Fission-Track Co., Ltd., 3. Geochemical Research Center, The University of Tokyo)

[SGL27-P07] Thermochronology on the fore-arc side of Northeast Japan Arc

*Yuya Kajita[1], Shigeru Sueoka[2], Shoma Fukuda[1], Noriko Hasebe[3], Akihiro Tomoaki[4], Tomoaki Morishita[4], Barry P. Kohn[5], Tatsunori Yokoyama[2], Takahiro Tagami[1] (1.Graduate School of Science, Kyoto University , 2.Japan Atomic Energy Agency, 3.Institute of Nature and Environmental Technology, Kanazawa University, 4.Department of Sciences, Kanazawa University, 5.School of Earth Sciences, University of Melbourne)

[SGL27-P08] Argon diffusion in rocks - classical approach in view of heating and relaxation

Horst Zwingmann[1], *Hironobu Hyodo[2] (1.KUEPS, Kyoto University, 2.Research Institute of Natural Sciences, Okayama University of Science)

## [SGL27-P09] $^{4}$He/U-Th dating of pore waters from Quaternary sediments in Switzerland: potential and challenges

*Yama Tomonaga[1], Edith Horstmann[1], Gaudenz Deplazes[2], Rolf Kipfer[1] (1.Swiss Federal Institute of Aquatic Science and Technology (Eawag), 2.National Cooperative for the Disposal of Radioactive Waste (Nagra))

## [SGL27-P10] Compound-specific radiocarbon analysis of lipid biomarkers in surface sediment from Lake Kawaguchi, central Japan

*Shinya Yamamoto[1], Yosuke Miyairi[2], Yusuke Yokoyama[2], Hisami Suga[3], Nanako O. Ogawa[3], Naohiko Ohkouchi[3] (1.Mount Fuji Research Institute, Yamanashi Prefectural Government, 2.Atmosphere and Ocean Research Institute, The University of Tokyo, 3.Japan Agency for Marine-Earth Science and Technology)

# Research report on long-term stability of geological environments and LA-ICP-MS-based age dating

*Tatsunori Yokoyama[1], Takehiro Mitsucuchi[1], Shigeru Sueoka[1]

1. Japan Atomic Energy Agency

In recent years, it has become possible to carry out high-precision microscale age dating of geological samples (with a spatial resolution of less than several tens of micrometers) using developed micro-analytical techniques such as secondary ion mass spectrometry (SIMS), laser ablation inductively coupled plasma mass spectrometry (LA-ICP-MS), etc. Application of LA-ICP-MS-based microscale U-Pb dating is extending from U-rich heavy minerals such as zircon, apatite and monazite to U-depleted minerals such as calcite. This kind of method enables age determination of several types of mineral grains (and their internal zoning structures) occurring within rock bodies, and thereby reveals chronological changes in chemical composition of source materials from which the minerals were crystallized, with some cases in which thermal history of the crystal formation system can be reconstructed.

For research and development of geological disposal techniques for high-level radioactive wastes, we develop and facilitate geochronological dating techniques for evaluation of long-term stability in geological environments, at Tono Geoscience Center, Japan Atomic Energy Agency. Elucidating past long-term variations of geological environments leads to predicting the future of the environments and is essential for the geological disposal, because the radioactive wastes need to be buried in deep underground and isolated far from the human living sphere for more than tens of thousands of years. Geochronological dating techniques are necessary for this purpose. LA-ICP-MS U-Pb dating of zircon provides reliable information about igneous activities such as magmatic differentiation and is also useful for provenance analysis if the mineral is found in sediments. Additionally, dating techniques using $^{10}Be$ and $^{26}Al$, which are generated by cosmic rays reaching the ground, can be applied to quantitative estimation of the amount of uplift and erosion. Combining these various dating methods has great potential to elucidate past long-term variations of geological environments.

In our presentation, we introduce the current status of our development for research on long-term stability of geological environments, U-Pb dating of calcite, U-Pb dating of young zircon and trace element analysis by using LA-ICP-MS.

This study was carried out under a contract with METI as part of its R&D supporting program for developing geological disposal technology.

Keywords: long-term stability in geological environments, LA-ICP Mass Spectrometry, U-Pb dating

©2019. Japan Geoscience Union. All Right Reserved. 

# U-Pb detrital zircon age dating from the Aileu Formation of Timor-Leste; Estimate depositional age and provenance of the sediment

*Jovita Elisa Fatima da Costa[1], Shoichi Kiyokawa[1], Yukiyasu Tsutsumi[2]

1. Kyushu University, 2. National Museum of Nature and Science

The Aileu Formation is a part of allochthonous metamorphic complexes distributed a 110km long and 40 km wide in Timor-Leste. It occupies most of the north-west of Timor-Leste and crops out along the north coast from Manatutu to the West Timor border and passing through to the south (Audley Charles, 1968). It is considerable lithological variation and metamorphic grade varies between lower greenschist to upper amphibolite facies (Beery and Grady, 1981). Our research area is affected by greenschist metamorphism and comprises an extensive succession of mostly terrigenous metasedimentary rock. The previous study of the north coast suggests that detrital zircon U-Pb from metasandstone, shows three groups at 270-440Ma, 860-1240, and 1480-1870Ma, and the metamorphic age also identified by 40Ar/39Ar of hornblende cooling ages of 10–6 Ma (Elly et al, (2014)). The Aileu Formation contain east-west foliation and north-south widely distributed. However, it's not a well-known south area of metasedimentary origin and depositional age. This study, we collect 3 samples of meta-sandstone transect north-south about 20 km wide. We analyzed U-Pb detrital zircon by using LA-ICP-MS.

Petrographically the 3 samples composed majorities of fine, fine medium grain of quartz-rich sandstone weakly deform and foliated. The three samples composed less than 2% muscovite, biotite, plagioclase, and another accessory mineral include zircon. Texturally immature characterized by sub-angular to sub-rounded and fresh of mica. These three samples are almost consisting of the same morphological characteristic of zircon grain.

The U-Pb age distribution of detrital zircon result from the concordant dataset reflected similar characteristic for all three samples and shows 270-420 Ma 900-1300Ma and 1400-1900 Ma. Grain younger than 270 Ma and older than 1900 Ma makes up 4% of the population. The most significant age peak, at 283-290 Ma indicated that the distribution of sediment coming from early Permian source rocks. The youngest zircon and main peaks are 239.87 Ma and 283-290 Ma, we consider this for maximum deposition age in the south which is the same as the north area. We suggest that the Sedimentation age of the south area of Aileu Formation after middle Triassic. These age from the previous study (north coast) and this study (north-south) shows the similarity characteristic for all samples. The Aileu Formation might be formed a fold and thrust belt and resemble sequences stacked north to south. Source sediment for Aileu Formation is compatible with a sediment source located in South East Asia as part of the now fragmented Sula Spur (Ely 2014). Sula spur is containing a Paleozoic granite and metamorphic basement which is extending from west of New Guinee and include the Bangai and Sula island.

Keywords: U/Pb Age of detrital zircon, Aileu Formation , Metasandstone

©2019. Japan Geoscience Union. All Right Reserved. 

# Petrological, geochemical, and geochronological characteristics of the Oritate travertine from Unazuki area, Toyama, Japan: possibility of U-Pb geochronology of carbonates with high common Pb.

*Mayuko Fukuyama[1], Masatsugu Ogasawara[2]

1. Graduate School of Engineering Science, Akita University, 2. Geological Survey of Japan, National Institute of Advanced Industrial Science and Technology

U-Pb dating of carbonate minerals can be widely applied to understand the timing of vein-type mineralization, fault movements, and other geological events forming calcites, which are difficult to be dated by other methods. Reference materials for U-Pb dating of calcite, such as WC-1 (254.4 ±6.4 Ma, Roberts *et al.*, 2017) and ASH-15D (3.001 ±0.012 Ma, Mason *et al.*, 2013; Vaks *et al.*, 2013), are available from several laboratories. However, it is often difficult to obtain reliable estimated ages of calcite because calcite usually contains high common Pb content.

In this study, we present the petrological, geochemical, and geochronological characteristic of the Oritate travertine from Unazuki area, Toyama, Japan. Typically, travertines are formed by a precipitation of carbonate minerals from hot spring. Thus, the U-Pb dating of calcite provides the timing of hydrothermal fluid activity. The Oritate travertine is called as ‘Onyx Marble’ by its texture. It shows layered texture with different colors from gray, white, to brown. It consists of aragonite and calcite. The chondrite normalized REE patterns of travertines show the flat and positive Eu anomalies which are different characteristics from oceanic limestones.

High initial $^{238}U/^{204}Pb$ ($\mu$) content is requirement for precise U-Pb dating of calcite (Rasbury & Cole, 2009), because calcite generally contains significant amount of common Pb. It is also better to contain high U in the order of several tens of ppm for U-Ob dating. U/Pb ratio of the Oritate travertines range from 1.1 to 2.2. The U and Pb concentration of Oritate travertines are very low which is less than 1 ppm. The brownish colored layers in travertines contain relatively high U concentrations. Although the chemical compositions of Oritate travertine imply the difficulty to apply U-Pb method, we examined U-Pb dating of calcite with high common Pb. We analyzed travertines with relatively high U/Pb ratio and U contents parts of the travertines for U-Pb dating. U-Pb dating was attempted with the solution ICP-MS as well as the LA-ICP-MS utilize a New Wave Research 193UC excimer laser ablation system, coupled to a Nu Instruments Nu Plasma II multi-collector ICP-MS or Agilent 7700 quadru-pole ICP-MS at Akita University. We discuss and evaluate the U-Pb dating method for calcite with high common Pb.

Keywords: U-Pb dating, carbonate mineral, travertine, ICP-MS, Oritate

©2019. Japan Geoscience Union. All Right Reserved. 

# Zircon U-Pb age and tectonics of shirakamidake granitic complex

*Hiroki Sato[1], Koji Umeda[1]

1. Hirosaki University

The Shirakamidake granitic complex in the Southwest of Aomori prefecture, is divided into the East, Central and West bodies. The East body and the Central bodies are mainly composed of coarse to medium grained hornblende biotite granodiorite and coarse to medium grained granite, respectively. The West body consists of schistose medium to coarse grained hornblende biotite granodiorite and light color schistose medium to coarse grained hornblende biotite granodiorite with mylonite zone (hujimoto, 2010). A large number of petrological studies have investigated the cooling history of the Shirakamidake granitic complex. Apatite (U-Th)/He age of 4.2±2.0 Ma, biotite K-Ar age of 86-100 Ma, amphibole K-Ar age of 89-94 Ma and whole-rock Rb-Sr age of 110.1±6.0 Ma have been reported. Generally, the ages of the West body are younger than those of the East body.

In this study, we describe geological and petrological features each bodies by polarizing microscopy, XRF spectrometry and EPMA analysis. We also present geochronological data utilizing laser ablation ICP mass spectrometry technique on the zircons that provides zircon U-pb age of 107.7±1.4Ma.
Thermochronological data suggests two distinctive cooling stages for the Shirakamidake granitic complex; 1) a first rapid cooling stage in which the granitic magma was cooled to the temperature of host rock soon after intrusion, and 2) second slow cooling stage associated with the uplift and subsequent erosion of the granite intrusion after ~90 Ma.

Keywords: The Shirakamidake granitic complex , Zircon, U-Pb age

©2019. Japan Geoscience Union. All Right Reserved. 

# Zircon U-Pb dating of plutonic rocks from Yamizo Area, northeast Japan

*Terumi Ejima[1,2], Yoshiaki Kon[2], Daisuke Araoka[2], Shigenori Kawano[3], Yutaka Takahashi[2]

1. Shinshu University, 2. Geological Survey of Japan, 3. Tochigi Prefectural Museum

To investigate the timing of the tectonothermal events of Yamizo plutonic suite, U-Pb dating of zircon was carried out using laser ablation inductively coupled plasma mass spectrometry combined with cathodoluminescence imaging on zircon grains separated from the Yamizo plutons.

In the Yamizo mountain areas, K-Ar ages of Ozasa (67.5Ma), Fukuroda (101 Ma), Iwafune (64.5 Ma), Kamehis (64.9 Ma) and Ooyamada plutons (71.8 Ma and 108 Ma) have been reported by Shibata et al. (1973). Basically, the K-Ar ages are sometimes younger than actual intrusive ages because the closure temperature of K-Ar ages are lower than that of the solidus of granitic rocks. The closure temperature of the U-Pb age of zircon was higher than that of K-Ar age and more suitable for investigating intrusive age of magma.

Nagasaka, Hatajyuku, Yamagiwa, Nomisawa, Ozasayama, Kizami, Kamehisa and Hanatatetouge plutons are distributed in the northern part of the Yamizo area. Zircon U-Pb ages of these plutons were 69–63 Ma. In the southern part of the Yamizo area, Ooyamada, Fukuroda and Korofuji plutons are distributed. The zircon U-Pb ages of these plutons were 104–102 Ma.

According to the results in this study, U-Pb ages correspond to the K-Ar ages previously reported. This result indicated that cooling rates after intrusion of the plutons in the Yamizo area were relatively fast. Moreover, U-Pb ages of plutons in the southern part of the Yamizo area were same as those of the Bato pluton (109–106 Ma: Ejima et al., 2017) and of Abukuma plutons (121–97 Ma: Kon and Takagi, 2012; Ishihara and Orihashi, 2015; Kon et al., 2015; Takahashi et al., 2016). On the other hand, U-Pb ages of plutons in the northern part of the Yamizo area were same as those of plutons around Tsukuba mountain (80 Ma, 63–58 Ma: Koike and Tsutsumi, 2018).

Keywords: Yamizo area, U-Pb age of zircon, plutons

©2019. Japan Geoscience Union. All Right Reserved. 

# Denudation history of the Higher Himalayan Crystallines in West-Central Nepal: insights from zircon fission-track dating and thermokinematic modeling

*Nakajima Toru[1], Harutaka Sakai[1], Hideki Iwano[2], Tohru Danhara[2], Takafumi Hirata[3]

1. Division of Earth and Planetary Sciences, Graduate School of Science, Kyoto University, 2. Kyoto Fission-Track Co., Ltd., 3. Geochemical Research Center, The University of Tokyo

Zircon Fission-Track (FT) dating and thermochronological inverse calculation were used to indentify the denudation history of the Higher Himalayan Crystalline (HHC) in west-central Nepal. We newly obtained 17 zircon and 4 apatite FT ages from Higher Himalayan Crystallines (HHC), the overlying Tibetan Tethys Sediments (TTS) and the underlying Lesser Himalayan Sediments (LHS) along 80km long transect across the Himalaya.
The ZFT age from the underlyng sediments displayed northward younging linear distribution of the oldest age in the frontal part of the Lesser Hilamaya (13.4 ±1.0 Ma) to the youngest age in the root zone near the Main Central Thrust (1.5 ±0.2 Ma). On the other hand, the ZFT ages from the HHC and the overlying sediments ranged from 10.9 ±0.8 Ma to 1.7 ±0.4 Ma, and showed southward younging distribution. The ZFT age distribution along NNE-SSW transect displayed a concave upward pattern with the youngest FT age located near the Main Central Thrust (MCT). This distribution pattern is well corresponded to present uplift rate, indicating that the FT age distribution pattern reflects the tectonically driven exhumation.
Thermochronological invert calculation showed two rapid cooling (<100 ℃/Myr) phases of the HHC and the LHS in the late Miocene and the Pleistocene. With respect to this result, rapid exhumation is not only suggested in the Pleistocene, but also in the late Miocene. The former implies rapid exhumation of the HHC accompanied by reactivation of the MCT in the late Miocene, the latter implies rapid denudation accompanied by overthrusting of the hanging wall of the Main Himalayan Thrust (MHT).
Thermo-kinematic calculation results also suggest that the distribution of FT ages is well explained by exhumation process accompanied by the activity of the MHT. Furthermore, the kinematic model considering reactivation of the MCT in the late Miocene yields a better fit between predicted and observed ages than the model without reactivation, indicating agreement with reactivation of the MCT in late Miocene.

Keywords: Himalaya, thermochronology, fission-track age, denudation history, Higher Himalayan Crystallilne

©2019. Japan Geoscience Union. All Right Reserved. 

# Thermochronology on the fore-arc side of Northeast Japan Arc

*Yuya Kajita[1], Shigeru Sueoka[2], Shoma Fukuda[1], Noriko Hasebe[3], Akihiro Tomoaki[4], Tomoaki Morishita[4], Barry P. Kohn[5], Tatsunori Yokoyama[2], Takahiro Tagami[1]

1. Graduate School of Science, Kyoto University , 2. Japan Atomic Energy Agency, 3. Institute of Nature and Environmental Technology, Kanazawa University, 4. Department of Sciences, Kanazawa University, 5. School of Earth Sciences, University of Melbourne

An arc trench system is composed of a topographically high land and a trench along a subduction zone. An arc trench system is grouped into continental arc and island arc. The latter has a back-arc basin. Island arcs are tectonically active regions where a lot of volcanic activities and earthquakes occur, providing keys to solve the formation and evolution processes of orogenic zones and continents (Toriumi et al., 2018).

Northeast (NE) Japan is one of the best regions to study tectonics of island arc because NE Japan has comparatively obvious island arc components, i.e., fore-arc, volcanic front, back-arc and back-arc basin. Therefore, many studies have focused on the tectonic evolution of NE Japan (e.g. Amano and Sato, 1989; Sato, 1992; Nakajima, 2013). However, there are a few quantitative investigations of the mountain uplift and denudation histories which are important for estimating tectonics of island arcs.

For measuring uplift or denudation rates, some techniques are available (e.g., GPS survey, elevation of terraces, and thermochronology). To estimate million-year-scale mountain uplift and denudation rates, thermochronology is among the most appropriate methods. Thermochronology can reconstruct the time-temperature relationship of rock/mineral samples, based on radiometric ages and closure temperatures specific to the combination of radiometric dating methods and target minerals. Furthermore, some assumptions enable discussion of mountain uplift and denudation histories. Although thermochronology has been successfully applied to orogens worldwide (Hermam et al., 2013), a small number of thermochronometric studies have been attempted in NE Japan (e.g. Sueoka et al., 2017, Fukuda et al., in press). Moreover, these previous studies focused on the denudation histories of the across-arc scale rather than individual geologic component, namely fore-arc, Ou backbone range and back-arc.

In this study, we focus on fore-arc side of NE Japan, i.e., Kitakami Mountains and Abukuma Mountains, at which granitic rocks are distributed extensively, providing preferable study areas to apply thermochronology. We adopted apatite fission-track (AFT), apatite (U-Th-Sm)/He (AHe) and zircon (Zr) U-Pb analyses. AFT ages were estimated at 66.8-39.1 Ma in Kitakami and 61.0-40.5 Ma in Abukuma. AHe ages were obtained at 51.2-36.1 Ma in Kitakami and 75.9-60.1 Ma in Abukuma. Zr U-Pb ages were calculated at 110.3-104.3 Ma in Abukuma. With our results and the ages obtained by the previous studies, we discuss age trend and denudation history.

In Kitakami Mountains, AFT ages become younger to the east. On the other hand, all AHe ages are approximately comparable with each other except for the oldest age obtained at the westernmost locality. In Abukuma Mountains, both AFT and AHe age trends change across Hatagawa fault zone (HFZ); the ages were younger at the west side of HFZ than at the east side. Assuming that geothermal gradient is uniform at all localities, westerly tilting uplift and subsequent change of the uplift style were suggested in Kitakami Mountains. In Abukuma Mountains, our age data can constrain the faulting history of HFZ.

©2019. Japan Geoscience Union. All Right Reserved. 

As future subjects, we are planning to conduct 1) improvement of accuracy and precision by further analyzing, 2) increasing number of sampling localities and employing other methods (e.g., cosmogenic nuclides analysis and ESR thermochronology), 3) applying thermal inverse modeling of AFT data to estimate more detailed thermal histories, 4) discussion of geothermal gradient, uplift model and tectonics model in Kitakami Mountains and Abukuma Mountains.

Acknowledgements: This study was carried out under a contract with METI (Ministry of Economy, Trade and Industry) as part of its R&D supporting program for developing geological disposal technology. This work was supported by the Grant-in-Aid for Scientific Research on Innovative Areas (KAKENHI No. 26109003) from the Ministry of Education, Culture, Sports, Science and Technology (MEXT).

Keywords: Thermochronology, Northeast Japan Arc, Abukuma, Kitakami

©2019. Japan Geoscience Union. All Right Reserved. 

# Argon diffusion in rocks - classical approach in view of heating and relaxation

Horst Zwingmann[1], *Hironobu Hyodo[2]

1. KUEPS, Kyoto University, 2. Research Institute of Natural Sciences, Okayama University of Science

Since the development of the conventional K-Ar and subsequent 40Ar-39Ar dating methods fundamental noble gas diffusion processes in rocks were investigated including complex multi-scale and multi-path aspects in polyphase materials. Traditional models interpret the loss of radiogenic Argon due to an increase of temperatures. Hyodo (2017) proposed a new approach investigating the relaxation time and temperature relation within an “unclosure temperature” model. This model regards duration of a heating event as time for relaxation in a diffusion system at specific temperature. The model applies a functional form of mathematical approximation on fractional loss by diffusion. It allows fractional loss of certain amount of radiogenic 40Ar as long as the step heating model spectra in 40Ar-39Ar dating (plateau) maintains its original age within its age error. This new model approach is compared to a classical heating diffusion model (Huon et al., 1993) focusing on clay minerals (<10 and <2 μm) and larger muscovite grains (200 and 100 μm). The classical diffusion heating models applies three main parameters comprising a. grainsize (μm), b. temperature range (°C) and c. time scale (Ma). The obtained results provide a unique insight to compare an active heating versus passive cooling time and temperature path of clay minerals and muscovite with applications for general earth sciences and economic geology such as hydrocarbon exploration.

Huon, S. et al., 1993. Mise en évidence au Maroc d'événements thermiques d'âge triascico-liasique liés à l'ouverture de l'Atlantique. Bulletin de la societe géologique de France, 164/2, 165–176.

Hyodo, H., 2017. Unclosure temperature of a mineral: Cylinder and plane geometry. Bull. Res. Inst. Nat. Sci. Okayama Univ. Sci., No.43, 13-18.

Keywords: K-Ar dating, diffusion, reheating

©2019. Japan Geoscience Union. All Right Reserved. 

# $^{4}$He/U-Th dating of pore waters from Quaternary sediments in Switzerland: potential and challenges

*Yama Tomonaga[1], Edith Horstmann[1], Gaudenz Deplazes[2], Rolf Kipfer[1]

1. Swiss Federal Institute of Aquatic Science and Technology (Eawag), 2. National Cooperative for the Disposal of Radioactive Waste (Nagra)

Dating based on the $^{4}$He/U-Th method is used to estimate the residence time of pore waters in very low-permeable rocks and consolidated sediments. The residence time is inferred from the time necessary to accumulate radiogenic $^{4}$He measured in the pore water being produced by the decay of U and Th in the sediment matrix [1].
In the Jurassic Opalinus Clay, the pore water still contains remnants of the original marine formation water that was entrapped during sediment deposition. The pore water composition was altered only by diffusive processes [2,3]. The fact that even ~100-Ma-old water signatures can be preserved in their original pore space suggests that such preservation might also be possible in much younger dense glacial deposits. The $^{4}$He concentrations measured in the pore waters of glacial tills were translated into mean residence times of 15-25 kyrs [4] that agree rather well with the expected depositional ages of 25-31 kyrs [5]. These observations, as well as evidence from lacustrine sediments [6,7], suggest that, if the solute transport in the pore space is sufficiently attenuated, even unconsolidated sediments can "store" and host "old" pore waters.
In the present work we investigate if the $^{4}$He/U-Th dating of pore waters can be used as a novel tool to complement the luminescence dating of unconsolidated Quaternary sediments. We applied the $^{4}$He/U-Th method to date pore waters in the time range of 10 to 100 thousands of years which covers the age range of the sedimentary depositions targeted by the Quaternary drillings (QBOs) managed by the National Cooperative for the Disposal of Radioactive Waste (Nagra) in Switzerland. In particular, we focus on fine-grained lacustrine sediment layers that might provide low-permeability conditions suitable for the preservation of radiogenic $^{4}$He concentrations in the pore space.
We report the preliminary results of the $^{4}$He/U-Th dating based on the measurements conducted in sediment samples from the first QBOs, highlighting potential and challenges of the method with respect to the studied glaciofluvial sediments of the Swiss Midland.

References

[1] Torgersen, T., Clarke, W.B. (1985). Helium accumulation in groundwater, I: an evaluation of sources and the continental flux of crustal $^{4}$He in the Great Artesian Basin, Australia. *Geochim. Cosmochim. Acta 49*, 1211–1218.
[2] Gimmi T., Waber H. N., Gautschi A., Rübel A. (2007). Stable water isotopes in pore water of Jurassic argillaceous rocks as tracers for solute transport over large spatial and temporal scales. *Water Resour. Res. 43*(4).
[3] Mazurek, M., Alt-Epping, P., Bath, A., Gimmi, T., Niklaus Waber, H., Buschaert, S., et al. (2011). Natural tracer profiles across argillaceous formations. *Appl. Geochem. 26*(7), 1035–1064.
[4] Hendry, M. J., Kotzer, T. G., Solomon, D. K. (2005). Sources of radiogenic helium in a clay till aquitard and its use to evaluate the timing of geologic events. *Geochim. Cosmochim. Acta 69*(2), 475–483.
[5] Wassenaar L.I., Hendry M.J. (2000). Mechanisms Controlling the Distribution and Transport of $^{14}$C in a Clay-Rich Till Aquitard. *Groundwater 38*(3), 343–349.

©2019. Japan Geoscience Union. All Right Reserved. 

[6] Tomonaga, Y., Brennwald, M. S., Meydan, A. F., Kipfer, R. (2014). Noble gases in the sediments of Lake Van - Solute transport and palaeoenvironmental reconstruction. *Quat. Sci. Rev. 104*, 117–126.
[7] Tomonaga, Y., Brennwald, M. S., Kipfer, R. (2015). Attenuation of noble-gas transport in laminated sediments of the Stockholm Archipelago. *Limnol. Oceanogr. 60*(2), 497–511.

Keywords: pore water, noble gases, unconsolidated sediments

©2019. Japan Geoscience Union. All Right Reserved. 

# Compound-specific radiocarbon analysis of lipid biomarkers in surface sediment from Lake Kawaguchi, central Japan

*Shinya Yamamoto[1], Yosuke Miyairi[2], Yusuke Yokoyama[2], Hisami Suga[3], Nanako O. Ogawa[3], Naohiko Ohkouchi[3]

1. Mount Fuji Research Institute, Yamanashi Prefectural Government, 2. Atmosphere and Ocean Research Institute, The University of Tokyo, 3. Japan Agency for Marine-Earth Science and Technology

Lake sediment in volcanic regions contains valuable information on past eruptive history, as well as environmental consequences that took place in the catchment along with volcanisms. In this study, we performed compound-specific radiocarbon analysis (CSRA) of lipid biomarkers in surface sediment from Lake Kawaguchi situated northern proximal to Mount Fuji, central Japan, including short-chain ($C_{16}$) and long-chain ($C_{24}$, $C_{26}$ and $C_{28}$) fatty acids. The results are compared with the $^{14}C$ content of TOC, plant macrofossils (plant leaf and wood) and lake surface water in order to access their potential for dating tool in the lake sediment. The $^{14}C$ concentration of the long-chain ($C_{24}$, $C_{26}$ and $C_{28}$) fatty acids ranged from −43 to −183‰, corresponding to $^{14}C$ ages between 288 to 1554 years BP. This indicates that these acids contain substantial pre-aged materials in addition to those emitted from contemporary plant leaf waxes. In contrast, the short-chain ($C_{16}$) fatty acids showed a good agreement with the $^{14}C$ concentration of lake surface water, suggesting that they are most likely derived from primary producers (diatom) in the present lake and have a potential to improve chronologies in the sedimentary sequence in which the occurrence of fossil leaves is rather limited.

Keywords: compound-specific radiocarbon analysis, lake sediment, fatty acid

©2019. Japan Geoscience Union. All Right Reserved. 

[J] Oral | S (Solid Earth Sciences )：S-MP Mineralogy & Petrology

Thu. May 30, 2019 9:00 AM - 10:30 AM JST | Thu. May 30, 2019 12:00 AM - 1:30 AM UTC | 301B 3F

## [S-MP32] Deformed rocks, Metamorphic rocks and Tectonics

convener:Yumiko Harigane(Geological Survey of Japan, National Institute of Advanced Industrial Science and Technology (AIST)), Yoshihiro Nakamura(Geological Survey of Japan, National Institute of Advanced Industrial Science and Technology), Chairperson:Yoshihiro Nakamura(産総研), Yumiko Harigane(産総研)

We invite all researchers who aim to understand the dynamics of the earth's crust and mantle at the plate boundaries, to discuss the latest results from various viewpoints. The scope will include contributions through petrology and structural geology as well as various techniques including rheology and transformation of heat and mass.

9:00 AM - 9:15 AM JST | 12:00 AM - 12:15 AM UTC

[SMP32-19] Thermal interaction of the lithosphere and asthenosphere revealed from internal variations of pressure-temperature history in orogenic peridotite complexes

*Kazuhito Ozawa[1], Carlos J. Garrido[2], Karoly Hidas[2], Jean-Louis Bodinier[3] (1.Department of Earth and Planetary Science, Graduate School of Science, University of Tokyo, 2.Instituto Andaluz de Ciencias de la Tierra (IACT), CSIC – UGR, Armilla, Granada, Spain, 3.Geosciences Montpellier, Montpellier, France)

9:15 AM - 9:30 AM JST | 12:15 AM - 12:30 AM UTC

[SMP32-20] **Hydration and Ca-metasomatism in Mantle Wedge: An evidence from the Alag Khadny Accretionary Wedge, Western Mongolia**

*OTGONBAYAR DANDAR[1], Atsushi Okamoto[1], Masaoki Uno[1], Noriyoshi Tsuchiya[1] (1.Graduate School of Environmental Studies, Tohoku University)

9:30 AM - 9:45 AM JST | 12:30 AM - 12:45 AM UTC

[SMP32-21] **Attenuated Total Reflection Infrared (ATR-IR) Spectroscopy of Antigorite, Chrysotile and Lizardite**

*Ilona Talvikki Sakaguchi[1] (1.Nagoya University)

9:45 AM - 10:00 AM JST | 12:45 AM - 1:00 AM UTC

[SMP32-22] Fabric and petrological characteristics of sheared peridotites in Marion transform fault, Southwest Indian Ridge

*Kakihata Yuki[1], Katsuyoshi Michibayashi[2], Henry Dick[3] (1.Shizuoka University Graduate School of Science, 2.Nagoya University Graduate School of Environmental Studies, 3.Woods Hole Oceanographic Institution)

10:00 AM - 10:15 AM JST | 1:00 AM - 1:15 AM UTC

[SMP32-23] Structure and formation mechanism of lithosphere-asthenosphere boundary decoded from Ichinomegata peridotite xenoliths

*Yuto Sato[1], Kazuhito Ozawa[1] (1.Department of Earth and Planetary Science, Graduate School of Science, The University of Tokyo)

10:15 AM - 10:30 AM JST | 1:15 AM - 1:30 AM UTC

[SMP32-24] Metasomatic banding and deformation instability in the metamorphic rocks

*mitsuhiro toriumi[1] (1.Japan agency of marine science and technology)

# Thermal interaction of the lithosphere and asthenosphere revealed from internal variations of pressure-temperature history in orogenic peridotite complexes

*Kazuhito Ozawa[1], Carlos J. Garrido[2], Karoly Hidas[2], Jean-Louis Bodinier[3]

1. Department of Earth and Planetary Science, Graduate School of Science, University of Tokyo, 2. Instituto Andaluz de Ciencias de la Tierra (IACT), CSIC –UGR, Armilla, Granada, Spain, 3. Geosciences Montpellier, Montpellier, France

Dynamics of interaction between lithosphere and asthenosphere in their boundary zones (LABZ) plays an important role in transferring heat, material, and momentum from the earth’ s interior to the surface. Orogenic peridotites provide direct and high-resolution information for better understanding mantle processes taking place in the boundary zone. However, their exhumation obscure the information on dynamics operating in LABZ, while they could be driven and affected by processes taking place in and beneath the LABZ. This issue leads to ambiguity in the link between magmatism, relevant to whole-rock chemical characteristics, and exhumation of peridotite complexes, relevant to deformation and subsolidus reactions. Bodinier et al. (2008) actually pointed out two possible formation scenarios for plagioclase peridotites in orogenic peridotite complexes: subsolidus reaction from spinel peridotites and open magmatic processes in the plagioclase peridotite facies in the shallow mantle. In the context of lithosphere-asthenosphere interaction, it is crucial to discriminate these two possibilities. Spatial and temporal changes of pressure and temperature within an orogenic peridotite complex can be used to better constrain its history of decompression and magmatism. By exploiting the advantage of size of orogenic peridotite complexes, these data may provide valuable constraints on the LABZ dynamics.

Here, we examine internal variations of thermal and decompression history of three orogenic peridotite complexes: Ronda, Pyrénées, and Horoman. They exhibit diverse geological and petrologic characteristics providing an excellent chance of comparative study. The common feature of these orogenic peridotites is decompression from the garnet peridotite facies deeper than ~50km. In this study, we focus on garnet-related reaction microstructures, which are powerful tools to resolve pressure-temperature history because of their high hysteresis as compared with suppressed hysteresis of chemical zoning in minerals. Garnet and its breakdown products show contrasting features among the three. (1) Garnet was completely decomposed in both peridotite and pyroxenite lithologies in Horoman with formation of symplectite in slightly depleted peridotites; garnet rarely remains in both peridotite and pyroxenite lithologies with extensive formation of symplectite and kelyphite in Ronda; and garnet is completely decomposed into two-pyroxene spinel symplectite in peridotites but well preserved with partial formation of kelyphite rim and veinlets in pyroxenites in Pyrénées. (2) Coarse-grained granular olivine-plagioclase assemblage in both fertile peridotite and pyroxenites is common in Horoman; formation of olivine-plagioclase assemblage forming fine-grained intergrowth in fertile peridotites and pyroxenites is common with its extent being spatially variable in Ronda; and formation of olivine-plagioclase assemblage rarely in pyroxenites and very rarely in fertile peridotites in Pyrénées. These contrasts suggest: (1) high-temperature decompression path all through its ascent in Horoman; (2) low-temperature in deeper levels but relatively high-temperature decompression path in shallower levels in Ronda; and (3) high-temperature decompression path in deeper levels followed by rapid cooling in shallower levels in Pyrénées. Combined with pressure-temperature path deduced from chemical zoning and microstructure related to exsolution and dissolution in pyroxenes, we propose that the shallow high-temperature decompression of Ronda was caused by heating in the plagioclase peridotite facies and that the

©2019. Japan Geoscience Union. All Right Reserved. 

high-temperature decompression of Horoman by heating over a wide depth range deeper than the plagioclase peridotite facies. Pyrénées is probably intermediate of these two cases. The contrasting modes of thermal perturbation may imply different mechanisms of lithosphere-asthenosphere interaction, such as active upwelling vs. passive upwelling.

Keywords: lithosphere-asthenosphere boundary, pressure-temperature history, orogenic peridotite

©2019. Japan Geoscience Union. All Right Reserved. 

# Hydration and Ca-metasomatism in Mantle Wedge: An evidence from the Alag Khadny Accretionary Wedge, Western Mongolia

*OTGONBAYAR DANDAR[1], Atsushi Okamoto[1], Masaoki Uno[1], Noriyoshi Tsuchiya[1]

1. Graduate School of Environmental Studies, Tohoku University

Hydration and metasomatic reactions of mantle wedge play important roles on global material circulation and changes in physical properties along the plate interface within the subduction zone. Metasomatism is caused by specific components of fluids such as silica; however, our understanding on the relationship between hydration and metasomatism in mantle wedge is still limited. In this study, we report outstanding alteration textures of orthopyroxene as an evidence for significant Ca metasomatism within the mantle wedge, and its relation to the hydration processes.

The Alag Khadny accretionary wedge is located in the Chandman area, western Mongolia, Central Asian Orogenic Belt. The accretionary wedge is subdivided into northern and southern belts. The northern belt is consisted of orthogneiss bodies with layers of mica schists and paragneisses, including amphibolized eclogite, marble, and serpentinite bodies. The southern belt is composed mainly of serpentinized peridotite with minor ophicarbonates and limestone layer including lenses of epidote amphibolites. The ultramafic body mainly consists of harzburgite and lherzolite with minor dunite and its origin is interpreted as mantle wedge.

We collected 17 samples from the ultramafic body in southern belt of the Alag Khadny accretionary wedge in the Chandman area. The peridotites contain primary olivine (Ol), orthopyroxene (Opx), clinopyroxene (Cpx), and spinel. The peridotites were suffered from various extents of metasomatism and hydration. P-Olivine was replaced by antigorite with various extent, whereas primary Cpx was preserved without reactions. One of the notable features that is common in the peridotite is intense replacement of orthopyroxene (>60 vol.% was replaced). The mineralogy of the orthopyroxene replacement is divided into three types: secondary Cpx (S-Cpx) + tremolite (Tr), S-Cpx + tremolite (Tr) + S-olivine, S-Cpx. S-olivine shows lower Mg# (0.85-0.91) than the primary ones (Mg#=0.90-0.91), and S-Cpx shows the lower Al content and higher Mg# than the primary Cpx. Mass-balance calculation for the Opx pseudomorph showed the gains of Ca and water, and losses of silica, Mg and Fe. Due to the lack of Ca source in the primary minerals, significant amount of Ca metasomatism occurred induced by infiltration of the external fluids. The products of Ca metasomatism (S-Cpx, Tr) are commonly cut by antigorite veins, indicating that main hydration (antigorite formation) occurred after Ca metasomatism. The stability field of mineral assemblage of the Opx replacement was consistent with the P-T conditions of eclogite bodies in the Chandman area (T= 590-630 ˚C and P=11-16 kbar), implying that the hydration and metasomatism were caused by mantle wedge due to a supply of fluids derived from dehydration of the subducting slab.

Keywords: Ca metasomatism, Mantle Wedge, Orthopyroxene, Alag Khadny accretionary wedge

©2019. Japan Geoscience Union. All Right Reserved. 

# Attenuated Total Reflection Infrared (ATR-IR) Spectroscopy of Antigorite, Chrysotile and Lizardite

*Ilona Talvikki Sakaguchi[1]

1. Nagoya University

Ilona Sakaguchi[1], Yui Kouketsu[1], Katsuyoshi Michibayashi[1], Simon Wallis[2]

[1]Graduate School of Environmental Studies, Nagoya University, [2]Department of Earth and Planetary Science, The University of Tokyo

Distinguishing serpentine minerals antigorite, chrysotile and lizardite from a thin section can be challenging due to the similarity of their optical properties and chemical composition. Infrared spectroscopy (IR) is a method based on the characteristic absorption of infrared radiation by different chemical bonds. Since each serpentine mineral has a distinct crystal structure, infrared spectroscopy can be applied in serpentine mineral identification. Infrared radiation is also particularly strong in polar bonds making IR spectroscopy a powerful tool in studying serpentine mineral hydroxyl groups. Transmission infrared spectroscopy is the most widely used IR method but it requires time-consuming and arduous sample preparation. Using a newer method known as attenuated total reflection infrared spectroscopy (ATR-IR) can significantly reduce the sample preparation time since the measurements can be made directly from the surface of a normal thin section.

We applied the ATR-IR method to characterize antigorite, chrysotile and lizardite from samples from Mt. Shiraga serpentinite body, located in central Shikoku, SW Japan. The ATR-IR method proved to be a reliable and simple method to measure the infrared spectrum of serpentine minerals as there were clear differences in the absorbance band positions of the three serpentine minerals. However, we observed notable differences in the absorbance band positions and absorbance intensities of serpentine minerals between the ATR-IR measurements and transmission IR measurements published in previous studies. These results reflect the fact that the ATR-IR method is susceptible to spectral distortions that are caused by the dependence of absorbance intensity to wavelength and by anomalous dispersion of infrared radiation. On the other hand, spectral mapping is much more convenient in the ATR-IR method as measurements can be done from normal thin sections. We also used the ATR-IR method to map a sample with three co-existing serpentine minerals with interesting reaction textures.

ATR-IR spectroscopy, and especially ATR-IR mapping, has a lot of potential in the field of mineral spectroscopy and it could be applied in the study of a wide variety of serpentinite microstructures, such as veining and faulting. One possible research avenue would be to combine ATR-IR mapping of serpentinite microstructures to quantitative analysis of serpentine mineral hydroxyl group absorbance intensities.

Keywords: Attenuated total reflection infrared (ATR-IR) spectroscopy , Fourier-transform infrared spectroscopy (FTIR), Sanbagawa metamorphic belt, Antigorite, Chrysotile, Lizardite

©2019. Japan Geoscience Union. All Right Reserved. 

# Fabric and petrological characteristics of sheared peridotites in Marion transform fault, Southwest Indian Ridge

*Kakihata Yuki[1], Katsuyoshi Michibayashi[2], Henry Dick[3]

1. Shizuoka University Graduate School of Science, 2. Nagoya University Graduate School of Environmental Studies, 3. Woods Hole Oceanographic Institution

The ultraslow spreading (14 mm/yr) Southwest Indian Ridge (SWIR) lies between the Bouvet and Rodriguez Triple Junctions. The SWIR is volcanically inactive, possibly reflecting poor advection of heat and intensive conductive cooling. Accordingly, there are only partly thin basaltic crusts, and peridotites exposed to the sea floor. Dredge surveys have been performed along the SWIR, and basalt, gabbro and peridotite specimens have been derived since 1980s.

In this study, we studied the microstructural development of 7 peridotite samples obtained from Marion Fracture Zone of the SWIR by the PROTEA cruise Leg.5 in 1983. The peridotites consisted of olivine, orthopyroxene and clinopyroxene with amphibole, plagioclase and chlorite, as well as secondary minerals such as serpentine and magnetite. The peridotites were classified into two groups based on their microstructures: 2 ultramylonites consisting of extremely fine grains (3-5 $\mu$m) with several porphyroclasts (~15 $\mu$m) and 5 heterogeneous tectonites consisting of deformed coarse-granular textures with subsequently developed fine-grained textures. In both types of peridotites, some of olivine grains had subgrain boundaries, whereas phase mixing occurred. These textural features suggest that heterogeneous textures of tectonites had been developed as lowering temperature and decreasing grain size, and subsequently became to ultramylonites.

Major element compositions of olivine and spinel indicated that these peridotites had fertile to moderately depleted mantle composition. Amphibole grains have the chemical compositions of tremolite, magnesio-hornblende and pargasite.

The ultramylonites have intensely deformed amphibole grains, whereas the heterogeneous tectonites have amphibole ranging from undeformed to highly deformed grains, indicating that amphibole formed before and/or during intensive shearing in the mantle. Moreover, olivine crystal-fabrics within the deformed amphibole bearing peridotites have B and E types developed under hydrous conditions. Consequently, the petrophysical characteristics of peridotites indicate that the uppermost mantle below the Marion transform fault has been hydrated during shearing.

Fine olivine grains in heterogeneous tectonites showed weak crystallographic preferred orientation (CPO) patterns. In contrast, those in the ultramylonites exhibited strongly concentrated CPOs. Furthermore, olivine grains were distorted more strongly in the ultramylonites than in the tectonites. These textural characteristics imply that fine-grained textures within the tectonites were deformed by mainly grain boundary sliding/diffusion creep under relatively low differential stress, whereas the ultramylonites were mainly deformed by dislocation creep under high differential stress.

Keywords: transform fault, peridotite, deformation mechanism

©2019. Japan Geoscience Union. All Right Reserved. 

# Structure and formation mechanism of lithosphere-asthenosphere boundary decoded from Ichinomegata peridotite xenoliths

*Yuto Sato[1], Kazuhito Ozawa[1]

1. Department of Earth and Planetary Science, Graduate School of Science, The University of Tokyo

Lithosphere-asthenosphere boundary (LAB) is one of the largest discontinuities in mantle where heat transfer mechanisms change from conduction to convection (Sleep, 2005, 2006). Various formation mechanisms of LAB have been proposed and still controversial (Green et al., 2010; Hirschmann, 2010; Hirth & Kohlstedt, 1996; Karato, 2010, 2012; O' Reilly & Griffin, 2006). Mantle xenoliths are fragments of mantle material (Nixon, 1987) and could have derived from the LAB zone and are useful to reconstruct its internal structure and to understand the ultimate cause of LAB zone and dynamic processes operated there. We have examined spinel peridotite xenoliths from Ichinomegata maar located in the back-arc side of NE Japan to address this issue (Sato & Ozawa, submitting to Ame. Min.; Sato & Ozawa, 2017, 2018, JpGU meeting; Sato & Ozawa, 2016, 2017, AGU fall meeting). We succeeded in reconstructing the structures and clarifying the formation mechanism of the LAB zone beneath Ichinomegata.

Ichinomegata maar is a latest Pleistocene andesitic-dacitic volcano yielding spinel peridotite xenoliths (Katsui et al., 1979). Diversities of thermal, chemical, rheological, and petrological features of the xenoliths have been documented by previous studies (e.g., Kuno, 1967; Kuno & Aoki, 1970; Takahashi 1980, 1986; Koyaguchi, 1986; Tanaka & Aoki, 1981; Abe et al., 1992, 1998; Abe & Yamamoto, 1999; Satsukawa & Michibayashi, 2014; Satsukawa et al., 2017). Despite the numerous data, the derivation depths of the xenoliths have never been seriously examined. We devoted our effort to geothermobarometry of spinel peridotite xenoliths, and successfully estimated derivation pressures and temperatures ranging 0.7-1.6 GPa and 828-1081 ˚C for 8 of the 9 examined xenoliths by examining the time scale of development of every chemical zoning to identify minerals, mineral portions, and chemical species attaining equilibrium as close as possible just before the xenolith extraction.

Various depth variations were clarified. The shallow mantle, ranging from 28 to 32 km, is characterized by low temperature, granular, and plagioclase- and amphibole-bearing mantle, and the deep mantle, from 41 to 55 km, by high temperature, porphyroclastic, and plagioclase- and amphibole-free and melt-bearing mantle. It is notable that the sample-derived solidus condition coincides with the depth of change of deformation microstructures. This indicates that the wet solidus controls rheological LAB zone beneath Ichinomegata. We infer that the shallow zone corresponds to lithospheric mantle and the deep zone to LAB zone.

Intimate correlations between the depth variations of absence or presence of plagioclase and amphibole and geochemical data obtained by previous studies (e.g., Tanaka & Aoki, 1981; Abe et al., 1998) enable us to reconstruct geochemical depth variation; clinopyroxene and whole-rock of plagioclase- and amphibole-bearing shallower peridotites are characterized by light rare earth element (LREE) depleted patterns, low $^{87}Sr/^{86}Sr$ ratios (~0.7027-0.7030), and high $^{143}Nd/^{144}Nd$ ratios (~0.5133-0.5134); in contrast, those of plagioclase- and amphibole-free and melt-bearing deeper peridotites by LREE enriched patterns, high $^{87}Sr/^{86}Sr$ ratios (~0.7033-0.7047), and low $^{143}Nd/^{144}Nd$ ratios (~0.5125-0.5130).

Previous studies attributed geochemical diversity to local magma-related processes beneath MOHO (e.g., Takahashi, 1980; Abe et al., 1992). However, the systematic depth variations of geochemistry indicate a

©2019. Japan Geoscience Union. All Right Reserved. 

larger-scale stratification of the upper mantle beneath Ichinomegata. We infer that the shallower geochemically depleted mantle represents oceanic lithosphere formed during Japan Sea opening and that the deeper enriched mantle represents LAB zone which formed recently through lithosphere thinning by asthenospheric upwelling. A similar scenario was proposed by Ohki et al. (1994) on the basis of temporal variations of Nd-Sr isotopes from Middle Miocene.

Keywords: lithosphere-asthenosphere boundary zone, geothermobarometry, spinel peridotite xenolith, mantle structure

©2019. Japan Geoscience Union. All Right Reserved. 

# Metasomatic banding and deformation instability in the metamorphic rocks

*mitsuhiro toriumi[1]

1. Japan agency of marine science and technology

Low grade metamorphic rocks formed in the plate boundary commonly show mineral bands composed of albite, amphiboles, chlorite and epidote in basic schists, and of chlorite, albite and quartz in pelitic schists. These bands are almost monomineralic and bimineralic and parallel to subparallel against schistosity plane. Judging from the orientation of bands nearly normal to the maximum stress direction, it seems that the banding is derived from compaction banding/porosity banding induced from the non-linearity of microcrack plasticity (Toriumi and Hara, 1995), elastic modulus (Fortin et al., 2009) and preferred orientation growth of chlorite and actinolite.
In this model, the low grade metamorphic rocks deform accompanied with progressive banding of low porosity and with migration of water vertical to the banding, and it induces stability change of solution and metamorphic minerals. Chlorite may favor the compaction bands but albite does porous bands. This type of yielding shoud lower the yield stress and then the deformation instability may occur in the metasomatic process in the plate boundary rocks.
Toriumi, M., and Hara, E., 1995, Tectonophysics, 245,249-261
Fortin, J., Stanchits,S., Dresen, G., Gueguen, Y., 2009, PAGEO, Doi 10.1007/s00024-009-0479-0

Keywords: metamorphic banding, compaction banding, deformation instability

©2019. Japan Geoscience Union. All Right Reserved. 

[E] Oral | S (Solid Earth Sciences )：S-VC Volcanology

Thu. May 30, 2019 9:00 AM - 10:30 AM JST | Thu. May 30, 2019 12:00 AM - 1:30 AM UTC | A07 TOKYO BAY MAKUHARI HALL

## [S-VC34] Connecting magma dynamics in vent-conduit system with surface expression of volcanic eruption

convener:Takahiro Miwa(National research institute for earth science and disaster prevention), Nobuo Geshi(Geological Survey of Japan, The National Institute of Advanced Industrial Science and Technology), Chairperson:Takahiro Miwa, Jacopo Taddeucci

Magma dynamics within a shallow conduit system control the diversity of behavior of volcanic eruptions. Recent advancements in geophysical, airborne and ground-based observation techniques provide quantitative data about the dynamic behavior of volcanic eruptions. New analytical methods of the macro and microtextures of eruptive products also open new insights on detailed dynamics of magmas within conduit. The aim of this session is the integration of these new techniques to approach the dynamics of magma ascending from a shallow part of conduit to vent. This session seeks submissions that explore magma dynamics controlling the behaviors of volcanic eruption by integrated investigation of 1) degassing, outgassing, crystallization, and fragmentation of ascending magma, 2) emission and recycling of eruptive product, and 3) morphological characterization of the vent-conduit system. We encourage contributions based on textural-petrological analyses of eruptive product, experimental study reproducing magma in the conduit, geophysical observation on surface expression of volcanic eruption, and related numerical modeling.

9:00 AM - 9:15 AM JST | 12:00 AM - 12:15 AM UTC

[SVC34-01] An experimental basis for estimating particle properties following volcanic ash emissions

★Invited Papers

*Adrian Hornby[1], Ulrich Kueppers[1], Hanna Horsch[2], Paul Ayris[1], Nick Varley[3], Daniele Andronico[4], Boris Behncke[4], Yan Lavallée[5], Jackie E Kendrick[5], James Utley[5], Amy Hughes[5], David Damby[6], Benedikt Maurer[1], Marlin Juchem[1], Donald B Dingwell[1] (1.Ludwig-Maximilians-Universität München, DE, 2.Hazen Research, Golden, USA, 3.University of Colima, MX, 4.INGV Catania, IT, 5.University of Liverpool, UK, 6.USGS Cascades Volcano Observatory, USA)

9:15 AM - 9:30 AM JST | 12:15 AM - 12:30 AM UTC

[SVC34-02] **Vapor transport in shallow intruded magmas: insights from diktytaxitic texture**

*Ryosuke Sakurai[1], Michihiko Nakamura[2], Satoshi Okumura[2], Mayumi Mujin[2], Takayuki Nakatani[2] (1.Division of Earth and Planetary Materials Science, Faculty of Science, Tohoku University, 2.Division of Earth and Planetary Materials Science, Department of Earth Science, Graduate School of Science, Tohoku University)

9:30 AM - 9:45 AM JST | 12:30 AM - 12:45 AM UTC

[SVC34-03] First observation of nanolites and ultrananolites in alkaline volcanic glasses (Eifel, Germany)

*Marija Putak Juricek[1], Michihiko Nakamura[2], Mayumi Mujin[2], Hans-Ulrich Schmincke[3], Mari Sumita[3], Nobuyoshi Miyajima[1] (1.BGI, 2.Tohoku Univ., 3.GEOMAR)

9:45 AM - 10:00 AM JST | 12:45 AM - 1:00 AM UTC

[SVC34-04] Textural Study of Pumice Clasts from The Youngest Toba Tuff Eruption

*Gabriela Nogo Retnaningtyas Bunga Naen[1], Atsushi Toramaru[1], Tomoharu Miyamoto[1], Haryo Edi Wibowo[2] (1.Department Earth and Planetary Sciences, Graduate School of Sciences, Kyushu University, Nishiku, 744, Motooka, Fukuoka, 819-0395, Japan, 2.Geological Engineering Department, Universitas Gadjah Mada, 55284, Yogyakarta, Indonesia)

10:00 AM - 10:15 AM JST | 1:00 AM - 1:15 AM UTC

[SVC34-05] **Oomurodashi volcano: Past effusive and phreatomagmatic activity revealed by submarine and subaerial deposits**

*Iona McIntosh[1], Kenichiro Tani[2], Alexander Nichols[3], Qing Chang[1], Jun-Ichi Kimura[1] (1.Japan Agency for Marine-Earth Science and Technology, Yokosuka, 2.National Museum of Nature and Science, Tsukuba, 3.University of Canterbury, Christchurch, New Zealand)

---

10:15 AM - 10:30 AM JST | 1:15 AM - 1:30 AM UTC

[SVC34-06] Mechanism of volatile transport from mafic to silicic magma upon mixing

*Shumpei Yoshimura[1], Akiko Matsumoto[1], Mitsuhiro Nakagawa[1] (1.Department of Earth and Planetary Sciences, Hokkaido University)

# An experimental basis for estimating particle properties following volcanic ash emissions

*Adrian Hornby[1], Ulrich Kueppers[1], Hanna Horsch[2], Paul Ayris[1], Nick Varley[3], Daniele Andronico[4], Boris Behncke[4], Yan Lavallée[5], Jackie E Kendrick[5], James Utley[5], Amy Hughes[5], David Damby[6], Benedikt Maurer[1], Marlin Juchem[1], Donald B Dingwell[1]

1. Ludwig-Maximilians-Universität München, DE, 2. Hazen Research, Golden, USA, 3. University of Colima, MX, 4. INGV Catania, IT, 5. University of Liverpool, UK, 6. USGS Cascades Volcano Observatory, USA

In recent years, mitigating the impact of volcanic ash emissions has risen up political and research agendas. Despite intense research efforts, challenges remain as to the detection and forecasting of emissions, and subsequent interactions in the earth system. Monitoring instruments and ash dispersal models usually require the input of volcanic ash properties in order to operate effectively, however forensic methods are poorly suited to volcanic eruptions where near-real-time data is required, and default values are commonly used. Here, we take an experimental approach to demonstrate that the surface composition and the initial size and shape distribution of volcanic ash particles depends upon (i) the initial rock texture, chemistry and mineralogy and (ii) the fragmentation processes that produced the particles.

We compare natural pyroclasts produced during recent eruptive activity at Volcán de Colima, Mt Etna, Santiaguito, Mt Agung and Tungurahua, with particles produced in fragmentation experiments using fresh rock samples from Volcán de Colima and Mt Etna. Sets of experiments were conducted under varying conditions in shock tube, tumbling and fault friction apparatuses to simulate natural eruption processes. Using QEMSCAN, an SEM-based automated mineralogy technique, we produce micron-scale maps showing the size, shape and phase distribution of thousands of ash particles in each sample. We measure particle size-, shape- and phase distribution in each sample and show that particle sizes and shapes show characteristic variation between different experimental methods and eruptive activity. Some phases, particularly groundmass glass (or tachylite), feldspars and pyroxenes are found to vary significantly at particles boundaries compared to the bulk. The pattern of enrichment and depletion of phases is shown to relate to the fragmentation mechanism and the rock texture at the macro- and micro-scale, and correlations between experimental and natural samples indicate a robust signal.

Volcanic ash presents unique hazards to aviation, health and the environment and better constraints on ash particle properties immediately following activity may improve estimations of the intensity and spatial extent of ash-related hazards. Our results may benefit local hazard management, monitoring and forecasting efforts at the case study volcanoes.

Keywords: Volcanic ash, Fragmentation processes, Experimental volcanology, Hazards, Ash dispersal and monitoring, QEMSCAN

©2019. Japan Geoscience Union. All Right Reserved. 

# Vapor transport in shallow intruded magmas: insights from diktytaxitic texture

*Ryosuke Sakurai[1], Michihiko Nakamura[2], Satoshi Okumura[2], Mayumi Mujin[2], Takayuki Nakatani[2]

1. Division of Earth and Planetary Materials Science, Faculty of Science, Tohoku University, 2. Division of Earth and Planetary Materials Science, Department of Earth Science, Graduate School of Science, Tohoku University

Volcanic ashes from Vulcanian explosions derived from shallow-intruded magmas and dome lavas often include microporous and glass-free groundmass in which lath-shaped plagioclase microlites form angular voids. Such texture, generally described as diktytaxitic texture, is known to control the permeability of bulk rock significantly when the connected porosity of bubbles and cracks is small (Kushnir et al., 2016). How and under what conditions diktytaxitic texture is formed is, however, not precisely known. In this study we simulated the formation of diktytaxitic groundmass through a series of isobaric-isothermal (IBIT) crystallization experiments in order to clarify its formation kinetics. As a result, diktytaxitic texture was formed at 850 and 900℃ and at 10 and 20 MPa, and almost entire groundmass became diktytaxitic (i.e. glass-free) in the experiment kept at 850℃ and 20 MPa for 189 h. At 850℃ and 10 MPa for >24 h, interstitial melt completely disappeared to form the groundmass composed of feldspar microlites with angular voids. Cristobalite crystals were found in the groundmass and on the interior walls of capsules. The glass compositions form liner trends between the plagioclase microlites and the precipitated silica on the $SiO_2$-$Al_2O_3$ diagram. These observations indicate that evaporation of $SiO_2$-rich melt and condensation of cristobalite are the dominant process for the formation of microporous groundmass characteristic of dixtytaxitic texture. The wide range of $K_2O$ contents in the glass can be explained as a result of vapor-phase growth of ~10 $\mu$m K-feldspar microlites in the diktytaxitic groundmass. Hence, we conclude that diktytaxitic texture is formed through (1) enrichment of silicon and potassium in the melt by microlite crystallization, (2) evaporation of $SiO_2$-rich constituents from the melt accompanied by breakage of Si-O covalent bond, and (3) precipitation of cristobalite and K-feldspar from vapor. The present study indicates that the late stage magma crystallization in shallow intrusions and lava domes proceeds dominantly through a vapor phase.

Keywords: crystallization experiment, evaporation-condensation, cristobalite, diktytaxitic texture, vapor-phase growth, lava dome

©2019. Japan Geoscience Union. All Right Reserved. 

# First observation of nanolites and ultrananolites in alkaline volcanic glasses (Eifel, Germany)

*Marija Putak Juricek[1], Michihiko Nakamura[2], Mayumi Mujin[2], Hans-Ulrich Schmincke[3], Mari Sumita[3], Nobuyoshi Miyajima[1]

1. BGI, 2. Tohoku Univ., 3. GEOMAR

Nanolites are the smallest, less than <1 μm wide, crystals observed in groundmass of volcanic rocks. They are believed to be the last solid phases that crystallize from the melt during eruptions. Understanding mechanisms of nucleation and subsequent growth of nanolites could potentially provide information about the physiochemical conditions of magma just prior to eruption.

Since nanolite studies are scarce in literature and experimental observation of crystal nucleation and growth is challenging, few constraints on kinetics of nanolite crystallization are available at present. Furthermore, previous studies have investigated nanolites from exclusively calc-alkaline volcanic products. Since melt composition may have a significant effect on crystal nucleation and growth, detailed and systematic descriptions of nanolites occurring in eruptive products of different magma series are required.

The purpose of this study is to present a preliminary overview of nanolite nucleation and growth mechanisms in alkaline melts. Due to high concentrations of network modifying Na and K atoms and considerable volatile budgets, alkaline magmas have very low viscosities. As chemical diffusion is highly dependent on viscosity, nucleation and growth of nanolites in alkaline melts may be governed by different mechanisms from those observed in previous studies.

Variously differentiated samples produced by different eruption styles were collected from West and East Eifel Volcanic Fields (Germany). Samples were observed using a combination of polarized microscopy, FE-SEM and TEM.

Preliminary observation suggests that average nanolite nucleation density in mafic and ultramafic Eifel samples is noticeably higher in comparison to calc-alkaline rocks. In general, nanolites in alkaline eruptive products display a wide range of morphologies with a tendency towards acicular and dendritic habits. Examples of both homogeneous and heterogeneous nucleation were observed. The most abundant phase in the nanolite population of mafic and ultramafic samples is magnetite. The only highly differentiated sample, a phonolitic glass, contained very few nanolites.

In a recently published experimental study it was suggested that precipitation of magnetite nano-crystals may increase magma viscosity by modifying the melt composition. Considering the abundance of magnetite nanolites in Eifel scoria fragments, these magmas may have experienced a severe viscosity increase at shallow crustal levels. We suspect that the presence of extensive interconnected networks of acicular and dendritic magnetite nanolites may have mechanically impeded magma flow as well, contributing to the explosive nature of Eifel eruptions that was previously attributed to magma-water mixing.

Keywords: nanolites, alkaline, nucleation, dendrites

©2019. Japan Geoscience Union. All Right Reserved. 

©2019. Japan Geoscience Union. All Right Reserved. 

# Textural Study of Pumice Clasts from The Youngest Toba Tuff Eruption

*Gabriela Nogo Retnaningtyas Bunga Naen[1], Atsushi Toramaru[1], Tomoharu Miyamoto[1], Haryo Edi Wibowo[2]

1. Department Earth and Planetary Sciences, Graduate School of Sciences, Kyushu University, Nishiku, 744, Motooka, Fukuoka, 819-0395, Japan, 2. Geological Engineering Department, Universitas Gadjah Mada, 55284, Yogyakarta, Indonesia

Toba Caldera Complex, North Sumatra, Indonesia is well known as the largest Quaternary caldera (87×33 km) that formed by four major eruptions with magnitude of VEI 8 among which the biggest one is the latest eruption of the Youngest Toba Tuff (YTT) about 74,000 years ago. The conduit dynamics of Toba caldera forming eruption is still poorly understood. Bubbles in pumice, which are produced by an explosive eruption possibly record dynamic processes in the conduit during eruption. This textural study aims to estimate the decompression rate of the biggest event of Toba eruption (YTT) by using textural data from Bubble Number Density (BND) together with geochemical, petrographical, grain size distribution (GSD), and bulk density data. In general, only a few data of decompression rate from caldera forming eruption events are available because the products were mostly welded and the original texture has been erased. Meanwhile, Toba eruption produced non-welded to welded deposit. Therefore, we focus on the nonwelded part of the biggest Quaternary caldera forming eruption localized on the northern part of the caldera in order to extract the original condition of the bubble formation. Samples from three different locations were employed for the analyses. Whole rock geochemical data of pumices were obtained by XRF. Petrography analysis for 21 thin sections were conducted using optical microscope. Bulk density measurement for 338 individual pumices with the size range of 4-8 mm and 8-16 mm were conducted using Laser 3D scanner. Textural analysis was carried out for 6 particles of 3 selected thin sections using microphotographs taken by SEM and further analyzed using image processing software. Geochemical data showed that the YTT magma is rhyodacitic to rhyolitic in whole rock compositions with the narrow range of $SiO_2$ (69.15 - 72.17 wt. %). Phenocrysts are plagioclase, biotite, quartz, and sanidine, most of which are fractured. The vesicle has a variety in size from 2.5 $\mu$m to 97 $\mu$m and in shape from rounded, elongated, to complex. GSD for each location are dominated by fine size (phi=1). Bulk density of individual pumice ranges from 0.4 to 1.1 $gcm^{-3}$. BND calculation were done in carefully selected area where is uniform in size of bubbles to represent samples in estimating the decompression rate in the conduit. BND value ranges from $10^5$ - $10^7$ $mm^{-3}$ showing a wide range of BND magnitude. Qualitatively, higher magnitude of BND is correlated with higher silica content, higher frequency of crystal fracture, complex vesicle shape, smaller vesicle size, and lower bulk density, and vice versa . The decompression rate was calculated using the BND decompression rate meter from Toramaru (2006). The result showed that Toba caldera forming eruption has high decompression rate ranging from $10^7$ –$10^8$ Pa/s. Those fact shows that Toba experienced with rapid decrease of pressure in the conduit. Moreover, this idea could be an important factor to reveals the conduit dynamic system of YTT super eruption.

Keywords: Toba Caldera, Pumice of the Youngest Toba Tuff (YTT), Textural Study, Conduit Dynamics, Bubble Number Density, High Decompression Rate

©2019. Japan Geoscience Union. All Right Reserved. 

# Oomurodashi volcano: Past effusive and phreatomagmatic activity revealed by submarine and subaerial deposits

*Iona McIntosh[1], Kenichiro Tani[2], Alexander Nichols[3], Qing Chang[1], Jun-Ichi Kimura[1]

1. Japan Agency for Marine-Earth Science and Technology, Yokosuka, 2. National Museum of Nature and Science, Tsukuba, 3. University of Canterbury, Christchurch, New Zealand

Oomurodashi is a recently discovered active, shallow (~140 mbsl), silicic submarine volcano in the northern Izu-Bonin arc, only 60 km from the entrance to Tokyo Bay. Past activity at Oomurodashi spans a wide range of eruption styles and includes small lava effusions, submarine pumice, and subaerial tephra deposits on nearby Izu-Oshima and Toshima islands. Here we present volatile and textural data that reveal contrasting degassing, quench and fragmentation processes occurring in the shallow conduit and overlying water column.

$H_2O$ data for pumiceous pyroclasts and lavas were obtained using new Fourier Transform Infrared spectroscopy (FTIR) analytical techniques for vesicular and hydrated glasses. Although the Oomurodashi glasses are extensively hydrated, the interconversion of $H_2O$ species (i.e. molecular water, $H_2O_m$, and hydroxyl groups, OH) stops at the glass transition temperature, and low temperature hydration occurs via diffusive addition of $H_2O_m$ only, leaving OH contents unchanged. OH data can therefore be interpreted according to the known pressure-dependence of $H_2O$ solubility and temperature dependence of $H_2O$ speciation.

Pumice clasts within the subaerial tephra layer have OH contents that are consistent with quench fragmentation at depths of ~60 –150 m depth within the shallow edifice. Moreover, the majority of this tephra deposit consists of ‘mosslike’ particles formed by annealing of extremely fine-grained material, which are typically formed by explosive phreatomagmatic activity. We therefore propose that this tephra represents the distal deposits from the explosive formation of the shallow (~100 m depth) summit crater by a shallow submarine, phreatomagmatic maar-type eruption.

By contrast, two in situ submarine lavas have lower OH contents than expected for their current water depths. Comparison with past sea level variation suggests that these effusive eruptions occurred at ~8-9 and ~12 ka during times of lower sea level. Loose submarine pumice also sampled from the edifice has a range of OH contents and vesicularities, reflecting different quench depths and dispersal histories within the water column.

Keywords: Submarine volcanism, FTIR, Volatiles, Magma fragmentation

©2019. Japan Geoscience Union. All Right Reserved. 

# Mechanism of volatile transport from mafic to silicic magma upon mixing

*Shumpei Yoshimura[1], Akiko Matsumoto[1], Mitsuhiro Nakagawa[1]

1. Department of Earth and Planetary Sciences, Hokkaido University

Introduction
Deep-derived, high-temperature mafic magma often injects into shallow-stored, low-temperature silicic magma, producing either well-mixed intermediate magma or mafic enclaves floating in host magma. Volatile transport from mafic to silicic magma accompanies magma mixing, and it may control volcanic activity (e.g., Roberge et al., 2009). However, the detailed mechanism of such volatile transport is unclear. In this study, we investigated how the gas was generated in mafic magma and transported to the silicic magma based on S and Cl analysis of Atchiyama rhyolitic lava that contains abundant basaltic enclaves.

Method
We observed Atchiyama biotite-rhyolite lava that erupted 1600 BP in Niijima Island (Isshiki, 1997), and analysed compositions of host rhyolite and basaltic enclaves. Cl mapping analysis was also performed on the area of enclave-host boundary to track the volatile transfer paths.

Results and discussion
Basaltic enclaves exhibited fine-grained groundmass composed of dendritic crystals, rhyolitic interstitial melt, and bubbles. The interstitial melt, which was compositionally distinguishable from the host rhyolite, was S-free (<50 ppm) and Cl-rich (1200 ppm). Melt inclusion analysis showed that the initial basaltic melt before mixing was S-rich (~4000 ppm) and Cl-poor (~430 ppm). These observations indicate that the basaltic magma cooled and crystallised rapidly upon injection, and the interstitial rhyolitic melt was produced as a result of crystallisation fractionation. Crystallisation-induced vesiculation (second boiling) occurred and S degassed completely, while Cl was concentrated in the interstitial melt.
Groundmass glass of host rhyolite was S-free and Cl-poor (~800 ppm). However, Cl mapping analysis revealed that the Cl content increased to 1200 ppm near the enclave margin. In addition, finger-like veins containing vapour-phase crystals developed from the enclave to far afield in host rhyolite, and the Cl content was also high near such veins. All these observations indicate that S- and Cl-rich gas was generated in crystallising enclave, and it was transported to the host rhyolitic magma via gas flow and diffusion.

Keywords: magma, mixing, volatile

©2019. Japan Geoscience Union. All Right Reserved. 

[E] Oral | S (Solid Earth Sciences )：S-VC Volcanology

Thu. May 30, 2019 10:45 AM - 12:15 PM JST | Thu. May 30, 2019 1:45 AM - 3:15 AM UTC | A07 TOKYO BAY MAKUHARI HALL

## [S-VC34] Connecting magma dynamics in vent-conduit system with surface expression of volcanic eruption

convener:Takahiro Miwa(National research institute for earth science and disaster prevention), Nobuo Geshi(Geological Survey of Japan, The National Institute of Advanced Industrial Science and Technology), Chairperson:Nobuo Geshi(GSJ/AIST), Adrian Hornby(Ludwig-Maximilians-University Munich)

Magma dynamics within a shallow conduit system control the diversity of behavior of volcanic eruptions. Recent advancements in geophysical, airborne and ground-based observation techniques provide quantitative data about the dynamic behavior of volcanic eruptions. New analytical methods of the macro and microtextures of eruptive products also open new insights on detailed dynamics of magmas within conduit. The aim of this session is the integration of these new techniques to approach the dynamics of magma ascending from a shallow part of conduit to vent. This session seeks submissions that explore magma dynamics controlling the behaviors of volcanic eruption by integrated investigation of 1) degassing, outgassing, crystallization, and fragmentation of ascending magma, 2) emission and recycling of eruptive product, and 3) morphological characterization of the vent-conduit system. We encourage contributions based on textural-petrological analyses of eruptive product, experimental study reproducing magma in the conduit, geophysical observation on surface expression of volcanic eruption, and related numerical modeling.

10:45 AM - 11:00 AM JST | 1:45 AM - 2:00 AM UTC

[SVC34-07] The in-flight grain size distribution of lapilli and bombs from Strombolian explosions

*Jacopo Taddeucci[1], Piergiorgio Scarlato[1], Elisabetta Del Bello[1], Tullio Ricci[1], Ulrich Kueppers[2], Bruce Houghton[3] (1.Istituto Nazionale di Geofisica e Vulcanologia, Rome, Italy, 2.Department of Earth and Environmental Sciences. Ludwig-Maximilians-Universität (LMU). Munich, Germany, 3.Department of Earth Sciences, University of Hawai‘i at Mānoa, Honolulu, USA)

11:00 AM - 11:15 AM JST | 2:00 AM - 2:15 AM UTC

[SVC34-08] **Pyrrotite oxidation as a proxy for air entrainment in eruption columns**

*Keiko Matsumoto[1], Michihiko Nakamura[2] (1.Geological Survey of Japan, The National Institute of Advanced Industrial Science and Technology, 2.Faculty of Science, Tohoku University)

11:15 AM - 11:30 AM JST | 2:15 AM - 2:30 AM UTC

[SVC34-09] **Thermal signals in volcano monitoring: combining MODIS-MIROVA data with ground-based measurements at Aso Volcano, Japan**

*Corrado CIGOLINI[1], Akihiko Yokoo[2], Diego Coppola[1], Marco Laiolo[1] (1.Department of Earth Sciences, University of Torino, Italy, 2.Aso Volcanological Laboratory, Institute for Geothermal Sciences, Kyoto University, Japan)

11:30 AM - 11:45 AM JST | 2:30 AM - 2:45 AM UTC

[SVC34-10] Magma transfer processes in the NE Japan arc: insights from crustal ambient noise tomography combined with volcanic eruption records

*Georg F Zellmer[1], Kai-Xun Chen[2], Yuancheng Gung[2], Ban-Yuan Kuo[3], Takeyoshi Yoshida[4] (1.Massey University, Palmerston North, New Zealand, 2.National Taiwan University, Taipei, Taiwan, 3.Academia Sinica, Taipei, Taiwan, 4.Tohoku University, Sendai, Japan)

11:45 AM - 12:00 PM JST | 2:45 AM - 3:00 AM UTC

[SVC34-11] **STRATIGRAPHY RENEWAL, MAGMA CHAMBER STRATIFICATION, AND CONDUIT PROCESS OF THE 1815 TAMBORA CALDERA FORMING ERUPTION**

*Indranova Suhendro[1], Atsushi Toramaru[1], Yasuo Miyabuchi[2], Tomoharu Miyamoto[1] (1.Department of Earth and Planetary Sciences, Graduate School of Sciences, Kyushu University, Japan, 2.Faculty of Advanced Science and Technology, Kumamoto University, Kurokami 2-40-1, Chuo-ku, Kumamoto 860-8555, Japan)

12:00 PM - 12:15 PM JST | 3:00 AM - 3:15 AM UTC

Discussion

# The in-flight grain size distribution of lapilli and bombs from Strombolian explosions

*Jacopo Taddeucci[1], Piergiorgio Scarlato[1], Elisabetta Del Bello[1], Tullio Ricci[1], Ulrich Kueppers[2], Bruce Houghton[3]

1. Istituto Nazionale di Geofisica e Vulcanologia, Rome, Italy, 2. Department of Earth and Environmental Sciences. Ludwig-Maximilians-Universität (LMU). Munich, Germany, 3. Department of Earth Sciences, University of Hawai ʻi at Mānoa, Honolulu, USA

Grain size distribution is one of the fundamental physical parameters of pyroclastic deposits, key to understanding both magma fragmentation and tephra emplacement processes during an explosive eruption. Most commonly, the grain size distribution of pyroclasts from one eruption is obtained from field sampling and analysis of the resulting tephra deposit; integration of multiple analyses gives a total grain size distribution. In this process it is often assumed that the grain size distribution of the deposit reflects that of the assemblage of pyroclasts that left the eruptive vent. However, observations suggest that multiple processes may act to change the size of erupted pyroclasts during their emplacement, so that the grain size distribution of a deposit may differ, to a variable degree, from that at the vent. Here, we use high-speed imaging to measure the in-flight grain size distribution of pyroclasts for the first tens of meters above an eruptive vent.

We focus on lapilli and bombs from Strombolian- explosions at Stromboli volcano (Italy) in September 2018. At that time, multiple, well-collimated jets with incandescent pyroclasts and no visible ash erupted from a vent about one meter in diameter and in plain view. The activity was recorded by using a high-speed camera filming with a temporal and spatial resolution of 500 frames per second and 0.012 m/pixel, respectively. The high-speed videos were pre-processed for background subtraction, then thresholded for gray level intensity, and finally the individual particles measured for their 2-D size and shape by using image processing. Particle velocity and size was also measured using particle tracking algorithms.

In a parametric study, the effect of different thresholding levels and frame sampling has been investigated. The results define the best parameters and the most effective truncation limits of the measured grain size distributions. Modal values of the grain size are broadly centered around the phi -4 to -5 size classes (16-32 mm) by particle number and the phi -5 to -6 size classes (32 to 64) by particle mass, respectively. The grain size distribution of erupted pyroclasts shifts considerably over time, with smaller clasts being ejected at the beginning of an explosion, and larger median diameters recorded at instants of higher pyroclast volume fluxes.

These results highlight the complexity and variability of the erupted size distributions at the vent, but also the need for a careful assessment of analytical error and methodological limitations.

Keywords: strombolian, explosion, grain size distribution

©2019. Japan Geoscience Union. All Right Reserved. 

# Pyrrotite oxidation as a proxy for air entrainment in eruption columns

*Keiko Matsumoto[1], Michihiko Nakamura[2]

1. Geological Survey of Japan, The National Institute of Advanced Industrial Science and Technology, 2. Faculty of Science, Tohoku University

Entrainment of air by turbulent mixing into eruption columns is a primary control of explosive eruption styles. Pyrrhotite (Po; $Fe_{1-x}S$) in erupted materials is oxidized to form magnetite (Mt) and hematite (Hm) at the oxygen fugacity ($fO_2$) on the Earth's surface and at magmatic temperature. Degree of Po breakdown has been proposed as a proxy for magma oxidation and cooling by entrained air through examination of the Plinian pumice and lavas from the 1914 eruption at Sakurajima volcano (VEI4). To verify and further investigate the potential use of Po oxidation for estimating eruption intensities from pyroclasts, we have examined the pumice clasts from three andesitic explosive eruptions with similar magmatic temperature and different eruption intensity: the 1783 Plinian eruption of the Asama volcano (VEI4), the 2011 sub-Plinian eruption of the Shinmoedake volcano (VEI2) and the 2010 Vulcanian explosion of the Sakurajima volcano (VEI1).

Mineral phases of magmatic sulfide and occurrence of pseudomorph (Mt and Hm) are different among the three eruption samples. Po is observed in the groundmass of the pumice from the Asama 1783 eruption and the Sakurajima 2010 eruption, whereas the sulfide in the Shinmoedake 2011 groundmass is intermediate solid solution (iss; $Cu_{1-x}Fe_{2+y}S_{2-z}$). Po is sometimes replaced to form pseudomorph, while iss shows no replacement. The porous texture of the Po pseudomorph, which indicates a reaction of Po with air, is similar to that observed for the oxidation product having columnar microstructure reported in the pumice from the Sakurajima 1914 eruption (Matsumoto and Nakamura, 2017). Approximately half of the Po grains are partly or entirely replaced by the pseudomorph in the Asama 1783 pumice, as observed in the Sakurajima 1914 samples. On the other hand, proportion of the pseudomorphic Po grains is less than 20% in the Sakurajima 2010 pumice. This difference indicates that the Asama 1783 pumice, together with the Sakurajima 1914 pumice, has been more efficiently oxidized than the Sakurajima 2010 pumice. The preservation of iss in the Shinmoedake 2011 pumice is probably due to the difference in oxidation mechanism between iss and Po. The efficient oxidation of Po during the two Plinian eruptions (i.e., the Asama 1783 and the Sakurajima 1914 eruptions) can be attributed to the longer duration in which temperature of pumice were kept high in the eruption columns than that in the Vulcanian column. These results underscore the potential use of Po oxidation for the purpose of constraining the temperature and $fO_2$ of eruption columns that reflect eruption intensity of explosive eruptions.

Keywords: pyrrhotite, oxidation, explosive eruption, eruption column

©2019. Japan Geoscience Union. All Right Reserved. 

# Thermal signals in volcano monitoring: combining MODIS-MIROVA data with ground-based measurements at Aso Volcano, Japan

*Corrado CIGOLINI[1], Akihiko Yokoo[2], Diego Coppola[1], Marco Laiolo[1]

1. Department of Earth Sciences, University of Torino, Italy, 2. Aso Volcanological Laboratory, Institute for Geothermal Sciences, Kyoto University, Japan

Active volcanoes bearing crater lakes are rather challenging targets for thermal monitoring since their anomalies are rather small when compared to lava flows and/or domes. Thus, we have combined satellite data with ground-based measurements at Aso Volcano during its recent activity.
The thermal signals of Aso Volcano (Nakadake) during unrest episodes have been analyzed by means of the MODIS-MIROVA data set and high resolution images (LANDSAT 8 OLI and Sentinel 2) cross-checked with ground-based thermal observations. The Volcanic Radiative Power (VRP) detected by nighttime satellite data during the time span considered was mainly below 3 MW. This value is a thermal threshold that marks the transition from high fumarole activity (HFA) to Strombolian eruptions (SE). Periods with the occurrence of sporadic phreatic eruptions (PE, eventually bearing phreatomagmatic episodes), is the dominant phase during unrest episodes, with VRP values around 0.5 MW. However, during sustained Strombolian phases (November-December 2014) the radiative power was higher than 4 MW, reaching peak values up to 15.6 MW (on December 7, 2014, 10 days after the major Strombolian explosion of November 27). Ground-based measurements, recorded by FLIR T440 Thermo-camera on the fumarole field of the South Area, shows that the heat-flux stabilized around 2 MW until February 2015. Apparent temperatures measured on the fumarole field were around 490-575˚C before the major Strombolian explosive event, whereas those recorded at the active vent (Central Pit) reached their maxima around 600 ˚C. In the following days they both exhibited a decreasing trend. However, during the Strombolian phase the crater lake dried out and was then replenished by early July, 2016. Then volcanic activity shifted back to phreatic-phreatomagmatic and the eruptive cycle was completed; in this period ground measurements were fluctuating around 1 MW. Following the major phreatic explosion of October 8, 2016 satellite VRP were moderately above 2 MW and then progressively decreased. During 2018, they were essentially below 1 MW (with a mean of 0.75 Mw and few peaks above 1 MW).
We estimated the total amount of Magma Equivalent Volume (MEV) responsible for satellite thermal anomalies during the Strombolian phase (from the end of November 2014 to May 2015). The cumulative volume involved in this phase reached 4.5 x $10^5$ $m^3$, which is two order of magnitude lower than the total volume of magma undergoing degassing (estimated by means of the petrologic models based on $SO_2$ degassing). This indicates that thermal anomalies during the Strombolian phases detect the magma that is reaching the surface and through a feeder dike, or conduit, connected at depth with a major reservoir.

Keywords: Aso Volcano, unrest episodes, thermal anomalies, Strombolian activity, major explosions

©2019. Japan Geoscience Union. All Right Reserved. 

# Magma transfer processes in the NE Japan arc: insights from crustal ambient noise tomography combined with volcanic eruption records

*Georg F Zellmer[1], Kai-Xun Chen[2], Yuancheng Gung[2], Ban-Yuan Kuo[3], Takeyoshi Yoshida[4]

1. Massey University, Palmerston North, New Zealand, 2. National Taiwan University, Taipei, Taiwan, 3. Academia Sinica, Taipei, Taiwan, 4. Tohoku University, Sendai, Japan

Subduction zone magmatic budgets and crustal growth processes depend on poorly constrained intrusive : extrusive ratios of arc magmas. Published ambient noise tomography data from northeast Japan reveal upper crustal low-$V_S$ bodies, indicating elevated temperatures of plutonic rocks, beneath most sites of active arc-front volcanoes, with the exception of Zao volcano. Strikingly, when small eruptions (VEI 1 to VEI 3) from arc-front volcanoes in the last 2 kyr are considered, Zao has erupted most frequently and has produced a more than three times greater tephra volume than any of the other volcanoes. We propose that the frequent low-volume volcanism at Zao is fed by dikes that traverse the crustal section rapidly, fracturing through brittle lithologies. Beneath the other volcanoes, hotter and more ductile plutonic bodies have developed through repeated intrusive activity, hindering magma transport to the surface. This positive feedback mechanism ultimately results in cataclysmic caldera-forming events. We show that the number of late Cenozoic calderas is higher above the imaged low-$V_S$ crust, consistent with this interpretation. We propose that generation of plutonic bodies is facilitated by volcaniclastic materials buried in a Miocene rift graben, which dampen fracture propagation and promote repeated sill intrusion. In contrast, transcurrent faulting has moved cold Cretaceous basement of the fore-arc range into the arc-front beneath Zao. These brittle rocks instead provide fracture pathways explored by magmas rapidly rising to the surface. The combined data imply that millions of years of crustal growth and tectonic history have a direct control on present-day volcanic eruption style.

Keywords: heat incubation, crustal magma ascent, crustal growth history, volcanic eruption style, Tohoku volcanism, brittle-ductile transition

©2019. Japan Geoscience Union. All Right Reserved. 

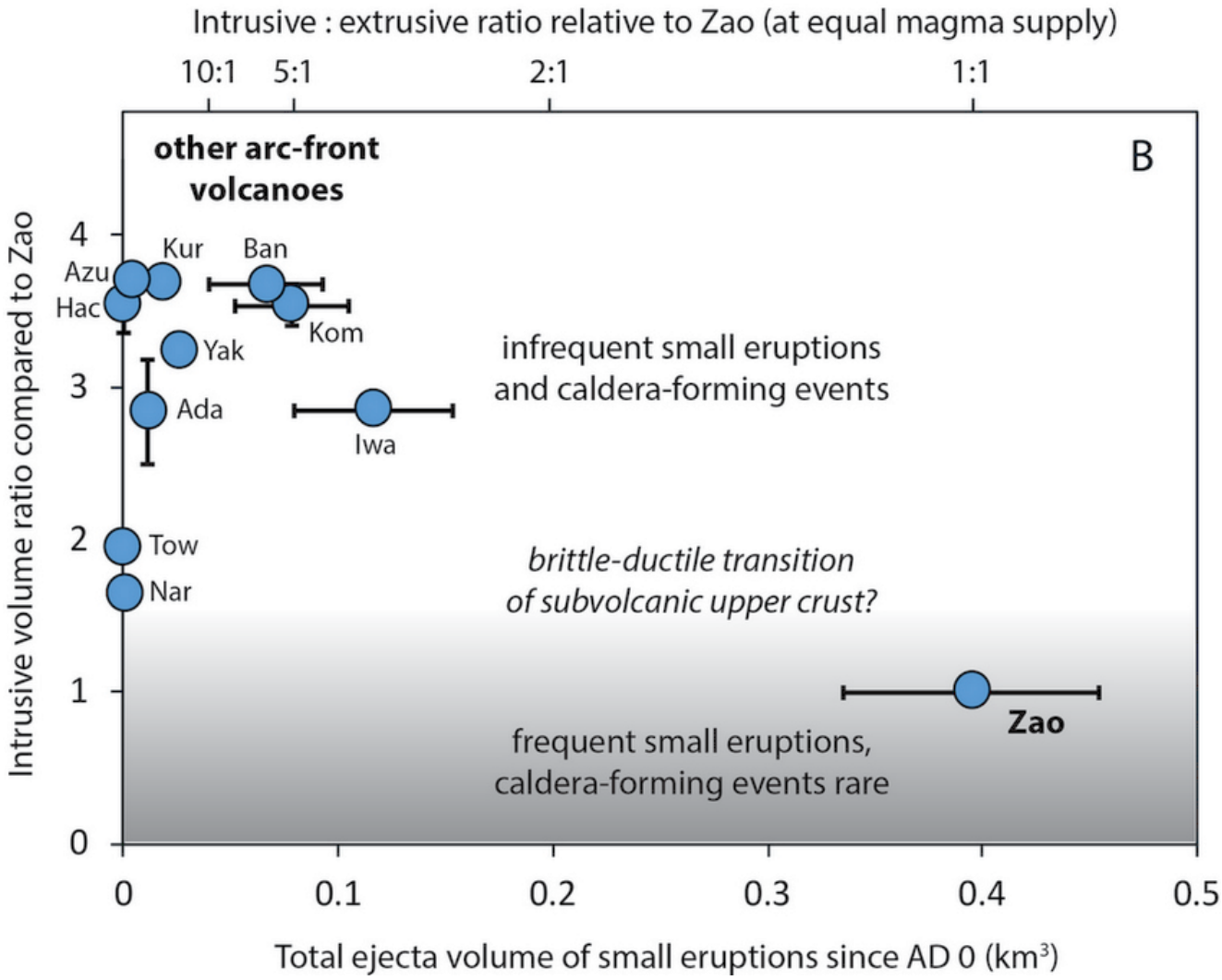


©2019. Japan Geoscience Union. All Right Reserved. 

# STRATIGRAPHY RENEWAL, MAGMA CHAMBER STRATIFICATION, AND CONDUIT PROCESS OF THE 1815 TAMBORA CALDERA FORMING ERUPTION

*Indranova Suhendro[1], Atsushi Toramaru[1], Yasuo Miyabuchi[2], Tomoharu Miyamoto[1]

1. Department of Earth and Planetary Sciences, Graduate School of Sciences, Kyushu University, Japan, 2. Faculty of Advanced Science and Technology, Kumamoto University, Kurokami 2-40-1, Chuo-ku, Kumamoto 860-8555, Japan

The 1815 eruption of Tambora volcano was initiated by two precursory Plinian falls and terminated by pyroclastic density current (PDC) deposits. Although the occurrence of fall deposits and pumice rich PDC has been well-described by previous researchers, we discover scoria rich PDC deposits. However, the presence and relationship of scoria rich PDC with another well-described 1815 eruption deposit has never been discussed in detail. Moreover, several aspects of the magma chamber and conduit dynamics are still poorly understood. In order to that, we conducted petrography by optical microscope, chemical anlyses by XRF, SEM-EDS, and FE-EPMA, and textural analyses of BND and MND. Systematic change in the phenocryst, vesicle, microlite, and chemical compositions also observed through the stratigraphic position. Plinian fall units are characterized by relatively low crystal abundance and small average phenocryst size (0.44 - 0.52 mm) with higher silica content (56.8-58.05 wt.% $SiO_2$). In contrast, PDC deposits are characterized by relatively higher crystal abundance and greater average phenocryst size (0.53 - 0.59 mm) with lower silica content (56.5-57.5 wt.% $SiO_2$). There is no evidence of magma mixing because no bimodal distribution in anorthite content and no reverse zoning pattern in plagioclase phenocryst. Large phenocrysts (>1 mm) have less variation than small phenocrysts (<1 mm) in chemistry. Core compositions of large phenocrysts are $An_{70}$-$_{90,}$ while those of small phenocrysts are $An_{40}$-$_{95}$. The correlation between crystal size, chemical composition, and stratigraphic position suggests that stratification of crystals and chemical compositions in the magma chamber was established prior to 1815 eruption. Juveniles from Plinian eruption are composed of higher BND and lower MND value, compared to juveniles from PDC. As a result, we explained negative correlation of BND and MND by the control of decompression rate ($dP/dt$). Namely, high decompression rate will induce high nucleation rate of bubble thus facilitate magma to ascent rapidly and limiting the growth of microlite. The increase of lithic population from precursory Plinian towards PDC can be regarded as vent-widening process. Therefore, the decrease of decompression rate accompanied by conduit widening during the early to later phase has shifted the eruption style, from buoyant Plinian column to PDC. Finally, rapid and voluminous magma withdrawal from the chamber has led to the formation of caldera.

Keywords: Tambora, caldera forming eruption, textural analyses, detailed stratigraphy, bubble number density, microlite number density

©2019. Japan Geoscience Union. All Right Reserved. 

[E] Poster | S (Solid Earth Sciences)：S-VC Volcanology

Thu. May 30, 2019 3:30 PM - 5:00 PM JST | Thu. May 30, 2019 6:30 AM - 8:00 AM UTC | Poster Hall International Exhibition Hall8, Makuhari Messe_12

## [S-VC34] Connecting magma dynamics in vent-conduit system with surface expression of volcanic eruption

convener:Takahiro Miwa(National research institute for earth science and disaster prevention), Nobuo Geshi(Geological Survey of Japan, The National Institute of Advanced Industrial Science and Technology)

Magma dynamics within a shallow conduit system control the diversity of behavior of volcanic eruptions. Recent advancements in geophysical, airborne and ground-based observation techniques provide quantitative data about the dynamic behavior of volcanic eruptions. New analytical methods of the macro and microtextures of eruptive products also open new insights on detailed dynamics of magmas within conduit. The aim of this session is the integration of these new techniques to approach the dynamics of magma ascending from a shallow part of conduit to vent. This session seeks submissions that explore magma dynamics controlling the behaviors of volcanic eruption by integrated investigation of 1) degassing, outgassing, crystallization, and fragmentation of ascending magma, 2) emission and recycling of eruptive product, and 3) morphological characterization of the vent-conduit system. We encourage contributions based on textural-petrological analyses of eruptive product, experimental study reproducing magma in the conduit, geophysical observation on surface expression of volcanic eruption, and related numerical modeling.

[SVC34-P01] A new formulation of viscosity-included bubble nucleation rate in ascending magmas and re-estimation of bubble number density (2)

*Mizuki Nishiwaki[1], Atsushi Toramaru[2] (1.Department of Earth and Planetary Sciences, Graduate School of Sciences, Kyushu University, 2.Department of Earth and Planetary Sciences, Faculty of Sciences, Kyushu University)

[SVC34-P02] Kinetic delay of crystal growth controls plagioclase-basaltic melt apparent disequilibrium

*Ryoya Oida[1], Hidemi Ishibashi[1], ATSUSHI YASUDA[2], Natsumi Hokanishi[2] (1.Faculty of Science, Shizuoka University, 2.Earthquake Research Institute, University of Tokyo)

[SVC34-P03] **Eruptive trends and dynamics of remote volcanoes detected form space-based thermal data and $SO_2$ emissions: a comparative analysis of Stromboli, Batu Tara and Tinakula volcanoes**

*Corrado CIGOLINI[1], Marco Laiolo[1], Francesco Massimetti[1,2], Maurizio Ripepe[2], Diego Coppola[1] (1.Department of Earth Sciences, University of Torino, Italy, 2.Department of Earth Sciences, University of Firenze, Italy)

[SVC34-P04] The source depth of Strombolian explosions: a multiparametric approach and comparison

*Jacopo Taddeucci[1], Miguel Angel Alatorre-Ibarguengoitia[2], Valeria Cigala[3], Elisabetta Del Bello[1], Damien Gaudin[4], Ulrich Kueppers[4], Tullio Ricci[1], Valentino Salvatore[5], Piergiorgio Scarlato[1] (1.Istituto Nazionale di Geofisica e Vulcanologia, Rome, Italy, 2.Centro de Investigación en Gestión de Riesgo y Cambio Climático, Universidad de Ciencias y Artes de Chiapas, Tuxtla Gutiérrez, Mexico, 3.Department of Geosciences, Università degli Studi di Padova, Padua, Italy, 4.Department of Earth and Environmental Sciences. Ludwig-Maximilians-Universität (LMU). Munich, Germany, 5.Dipartimento di Scienze della Terra, Sapienza Università di Roma, Rome, Italy)

[SVC34-P05] Magmatic aggregate of basaltic ash particles

*Takahiro Miwa[1], Nobuo Geshi[2] (1.National research institute for earth science and disaster prevention, 2.National Institute of Advanced Industrial Science and Technology)

[SVC34-P06] Melt inclusion study on the eruption process of Izu-Omuroyama monogenetic volcano, Japan

Risako Hatada[1], *Hidemi Ishibashi[1], Yusuke Suzuki[2], ATSUSHI YASUDA[3], Natsumi Hokanishi[3] (1.Faculty of Science, Shizuoka University, 2.Izu Peninsula Geopark, 3.Earthquake Research Institute, University of Tokyo)

---

[SVC34-P07] Time-series variation in the textures of ejecta of the An'ei eruption, Izu-Oshima

*Yuya Ikenaga[1], Fukashi Maeno[1], ATSUSHI YASUDA[1] (1.Earthquake Research Institute, The University of Tokyo)

---

[SVC34-P08] The textural analysis of pumice from the Plinian eruption of Taupo volcano: implications for tube pumice

*Masatoshi Ohashi[1], Mie Ichihara[2], Fukashi Maeno[2], Ben Kennedy[3], Darren Gravley[3] (1.Department of Earth and Planetary Science, Graduate School of Science, The University of Tokyo, 2.Earthquake Research Institute, The University of Tokyo, 3.Department of Geological Sciences, The University of Canterbury)

# A new formulation of viscosity-included bubble nucleation rate in ascending magmas and re-estimation of bubble number density (2)

*Mizuki Nishiwaki[1], Atsushi Toramaru[2]

1. Department of Earth and Planetary Sciences, Graduate School of Sciences, Kyushu University, 2. Department of Earth and Planetary Sciences, Faculty of Sciences, Kyushu University

To evaluate the effect of melt viscosity on bubble nucleation, we newly formulate homogeneous nucleation rate of water bubbles to explicitly include melt viscosity. The viscosity appears in the pre-exponential factor of the nucleation rate in terms of the Péclet number: the ratio of bubble growth timescale by molecular diffusion and viscous relaxation timescale. The pre-exponential factor linearly decreases with increasing viscosity (or decreasing Péclet number) under a given supersaturation. We numerically solve the evolution of bubble nucleation and growth processes in ascending magmas by using the new formula of nucleation rate and a precise approximation of moment equations of bubble size distribution function. In high viscosity or high decompression rate region, the effect of melt viscosity reduces bubble number density by several orders of magnitude compared with the previous study. Because of the lack of experimental data in this high-viscous regime, the reality of this regime will be verified by future experiments.

Keywords: bubble nucleation, bubble growth, BND (Bubble Number Density), BSD (Bubble Size Distribution), Péclet number

©2019. Japan Geoscience Union. All Right Reserved. 

# Kinetic delay of crystal growth controls plagioclase-basaltic melt apparent disequilibrium

*Ryoya Oida[1], Hidemi Ishibashi[1], ATSUSHI YASUDA[2], Natsumi Hokanishi[2]

1. Faculty of Science, Shizuoka University, 2. Earthquake Research Institute, University of Tokyo

Plagioclase-melt compositional relations sensitively depend on temperature, T, and water content, $X_W$, of melt. Therefore, the relations are formulated as functions of T and $X_W$ and used as geothermohygrometer (e.g., Putirka, 2008). Plagioclase-melt equilibrium is postulated for applying the thermohygrometer models. However, validity of the assumption is unobvious for microlite crystallization driven by degassing and/or cooling during eruption. Can we apply the thermohygrometers to the plagioclase-melt pairs formed by dynamic crystallization? To examine the issue, the cooling crystallization experiments of the high-Al basaltic melt were carried out and textural and chemical analyses were performed the run samples.

We used the high-Al basalt lava from Waianae, Hawaii Oahu as the starting material for the cooling crystallization experiments. This experiment was conducted using the 1atm $fO_2$-controlled furnace at University of Hawaii at Manoa. After 3 hours pre-heating at 1180℃, ~30K higher than the liquidus, the samples were cooled at cooling rates, $R_c$, of 0.1, 0.3, 1, 3, and 10K/min, and then quenched in water at four target temperatures, $T_q$, of 1150, 1120, 1090, and 1060℃. We used FE-EPMA (JEOL-JXA-8530FPlus) and EPMA (JEOL8800R) at Earthquake Research Institute, University of Tokyo, for textural and chemical analyses of the run samples.

As $R_c$ and/or $T_q$ increase, the abundance and size of plagioclase crystals decrease. As $R_c$ increases, the shape of plagioclase changes from euhedral to dendritic. The $R_c$-dependent shape change is more obvious at lower $T_q$. Pyroxene crystallization was suppressed in the run samples coolied at higher $R_c$. In addition, melt boundary layers are observed around pyroxene in the samples cooled at 0.3-1K/min, quenched at 1090℃ and cooled at 0.3-3K/min, quenched at 1060℃, and around plagioclase in the samples cooled at >3K/min, quenched at <1120℃. Lower diffusivity of $Al_2O_3$ compared to those of FeO and MgO is responsible for lower threshold cooling rate of melt boundary layer formation around pyroxene.

The maximum An# [=100Ca/(Ca + Na)] of plagioclase was almost the same among all run samples. We applied both plagioclase liquidus and plagioclase-melt An-partitioning thermometers of Putirka (2008) to the pairs of plagioclase rim-boundary layer melt (BLM) and plagioclase rim-far field melt (FFM) to estimate temperatures recorded in their phase compositions. At $T_q$=1150℃, the estimated temperatures well represent $T_q$ for both BLM and FFM. However, at lower $T_q$, both of the thermometers estimate temperatures higher than $T_q$; difference between estimated temperature and $T_q$, $\Delta T$, increases as decreasing $T_q$. The two thermometers estimate similar temperatures for each sample, and the differences between the two estimated temperatures do not depend on $R_c$. These results suggest that the plagioclase-melt partition coefficient of An component does not depend on the $R_c$. Therefore, the increase of $\Delta T$ at lower $T_q$ is not due to the $R_c$-dependence of the partition coefficient. It is attributed to the kinetic delay of the crystal growth at lower temperature. On the other hand, the coincidence between calculated temperatures and $T_q$ at 1150℃ suggests that kinetic delay of plagioclase crystal growth is small at near liquidus temperature.

©2019. Japan Geoscience Union. All Right Reserved. 

Present results show that plagioclase-melt thermometers can be applied regardless of the $R_c$ at higher temperatures, while magmatic temperature tends to be overestimated due to kinetic delay of crystal growth at lower temperature.

Keywords: plagioclase, crystallization, kinetics, basalt, geothermometry

©2019. Japan Geoscience Union. All Right Reserved. 

# Eruptive trends and dynamics of remote volcanoes detected form space-based thermal data and $SO_2$ emissions: a comparative analysis of Stromboli, Batu Tara and Tinakula volcanoes

*Corrado CIGOLINI[1], Marco Laiolo[1], Francesco Massimetti[1,2], Maurizio Ripepe[2], Diego Coppola[1]

1. Department of Earth Sciences, University of Torino, Italy, 2. Department of Earth Sciences, University of Firenze, Italy

South-Eastern Pacific has a large number of unmonitored volcanoes that may potentially produce large-scale eruptive events capable to affect highly-populated areas. Therefore, forecasting changes in volcanic activity in the light of historical time-series is a rather intriguing challenge for the space-based earth observations.
Batu Tara (Indonesia) and Tinakula (Solomon Island) are two poorly known volcanic islands with morphologies and reported short-term activities rather similar to the ones observed at Stromboli volcano (Italy). However, thanks to over a decade-long satellite data we are able to effectively compare the activity occurring at Stromboli (a unique natural laboratory and “open-vent” system) with those taking place at the above volcanoes.
We process and analyse the radiant flux (thermal activity) coupled with $SO_2$ emissions (degassing activity) at these three volcanoes for over a decade. The combined analysis of Volcanic Radiant Power (from MODIS data) and $SO_2$ burden (from OMI data) reveals different long-term eruptive trends, and contrasting ratio of gas vs. thermal emissions. In fact, the persistent open-vent explosive activity of Stromboli volcano is interrupted by flank effusions that periodically drain the degassed magma stored at shallow levels. On the other hand, the long-lasting exponential decay of both thermal and gas emissions observed at Batu Tara is consistent with the eruption of an “undegassed magma” from a deep, and likely a “closed” magma chamber. Finally, Tinakula volcano exhibits multiple year-long eruptive phases, characterised by evolving gas vs. thermal ratio correlated with an increasing eruptive intensity: thus suggesting the involvement of a volatile-zoned magma chamber with periodic phases of gas/magma accumulations.
Our results suggest that the combined analysis of satellite thermal/gas data is a useful tool for better understanding long-term volcanic dynamics and interpreting volcanic processes occurring at a shorter time-scale. We also stress that large satellite datasets on active volcanoes, available from different platforms, greatly enhance the opportunity to efficiently monitor remote volcanic targets in the attempt to mitigate volcanic risk.

Keywords: Remote volcanoes, satellite datasets, Volcanic Radiative Power, SO2 emissions, volcanic risk

©2019. Japan Geoscience Union. All Right Reserved. 

# The source depth of Strombolian explosions: a multiparametric approach and comparison

*Jacopo Taddeucci[1], Miguel Angel Alatorre-Ibarguengoitia[2], Valeria Cigala[3], Elisabetta Del Bello[1], Damien Gaudin[4], Ulrich Kueppers[4], Tullio Ricci[1], Valentino Salvatore[5], Piergiorgio Scarlato[1]

1. Istituto Nazionale di Geofisica e Vulcanologia, Rome, Italy, 2. Centro de Investigación en Gestión de Riesgo y Cambio Climático, Universidad de Ciencias y Artes de Chiapas, Tuxtla Gutiérrez, Mexico, 3. Department of Geosciences, Università degli Studi di Padova, Padua, Italy, 4. Department of Earth and Environmental Sciences. Ludwig-Maximilians-Universität (LMU). Munich, Germany, 5. Dipartimento di Scienze della Terra, Sapienza Università di Roma, Rome, Italy

The source depth of an individual explosion during Strombolian-style explosive volcanic activity can be defined as the depth of the region within the volcanic conduit where magma fragmentation occurs and the acceleration of pyroclasts by the expanding gas continuum begins. Source depth is thought to exert a first-order control on the final ejection dynamics of the pyroclasts and the ensuing eruptive styles and hazards. As such, different methods to estimate source depth have been developed in the past.

Here, we used three independent methods to estimate the source depth of some Strombolian explosions from Stromboli and Etna volcanoes (Italy). The first method uses the back-tracking of the trajectories of pyroclasts leaving the vent to infer their minimum release depth. It is a purely geometric method relying on the assumption that pyroclasts follow linear trajectories after fragmentation. The second method uses the time delay between the appearance of pyroclasts at the vent and the arrival of acoustic waves at a recording station at a known distance from the vent. This method relies on several assumptions, including (i) the sound velocity inside the conduit, (ii) the co-location of source depth of pyroclasts and acoustic waves, and (iii) a constant velocity of pyroclasts in the conduit, following the initial acceleration. The third method uses the velocity of pyroclasts progressively exiting the vent. This velocity decays following a non-linear trend which is function of the source depth, as illustrated by previous experimental and theoretical studies. As for the second method, also this last one assumes a constant velocity of pyroclasts rising in the conduit.

For the Etna case, the three methods provide consistent results and a shallow (<20 m) source depth of the explosions. For the Stromboli case, the first and third methods provide shallow (around 6 and 15 m, respectively) source depths while the second method provides depths of around 60 m. The incompatibility of such large depths with the first two methods, and given the relative assumptions, we believe that in the Stromboli case the co-location of the particles and acoustic source is probably the least strong assumption. These results suggest that caution should be used in assessing source depth from a single methodology, and that more investigations are required on the source of acoustic signals from the explosions and on the motion (specifically the acceleration and deceleration) of pyroclasts ascending along the conduit.

Keywords: strombolian, explosion, depth

©2019. Japan Geoscience Union. All Right Reserved. 

# Magmatic aggregate of basaltic ash particles

*Takahiro Miwa[1], Nobuo Geshi[2]

1. National research institute for earth science and disaster prevention, 2. National Institute of Advanced Industrial Science and Technology

Dynamics of volcanic cloud and jet at the vent is largely controled by a grain size of pyroclast. The grain size is considered to be determined by primary fragmentation of magma, and subsequent breakup of pyroclasts due to therir collsions in upper conduit (Dufek et al. 2012). However, whether the breakup occurs or not depend on viscoelastic responce of magma (Dingwell and Webb, 1989).
In this study, we report aggregate of ash particles which is formed in magmatic temperature. We observed basaltic ash samples from Stromboli volcano, Italy, and Aso volcano, Japan. The “magmatic aggretate” shows texture that numerous small guest particles (< 200 $\mu$m) adhere or stick on a host particle (> 1 mm). All the host particles are catergorized to sideromelane having fluidal morphology. The guest particles are on fluidal surface of the host particle, and show fluidal and dense morphology. These characteristics found in the magmatic aggregate can be explaned by collision and aggretation of ash particles in high temperature condition. Here we model formation of the magmatic aggregates as passing of two frying particles bearing viscoelastic nature, by using viscosity of magma estimated ($10^4$-$10^5$ Pa s). When the relative velocity of the two particles falls the critical value, the two particles behave as viscous material, coalsece each other, and then form the magmatic aggregate. The result of calculation demonstrates that the critical relative velocity is approximately $10^{-2}$ m/s, and implies the magmatic aggregation is difficult to occur for silisic magma with highly viscosity. Thus we conclude that the collision can increase average grain size of pyroclast in basaltic system.

Keywords: Eruptive dynamics, Interaction of ash particles, Viscoelastic response of magma

©2019. Japan Geoscience Union. All Right Reserved. 

# Melt inclusion study on the eruption process of Izu-Omuroyama monogenetic volcano, Japan

Risako Hatada[1], *Hidemi Ishibashi[1], Yusuke Suzuki[2], ATSUSHI YASUDA[3], Natsumi Hokanishi[3]

1. Faculty of Science, Shizuoka University, 2. Izu Peninsula Geopark, 3. Earthquake Research Institute, University of Tokyo

Izu-Omuroyama is one of monogenetic volcanoes in Izu-Tobu volcanic field, which is the largest pyroclastic cone formed by ~4ka eruption with ~450 million tons of tephra and lava (Koyano et al., 1996). Because a monogenetic volcano such as Omuroyama is built by the first eruption of a newly-formed magma plumbing system, phenocrysts and melt inclusions (MIs) in its volcanic products may record information about the initial process of formation of the magma plumbing system. In this study, textural and chemical analyses were performed for phenocrysts and MIs in Strombolian scoria of the Omuroyama eruption to clarify the eruption process of the monogenetic volcano.

According to Koyano et al. (1996), Omuroyama eruption started from sub-plinian phase (stage-A), followed by weak ash-eruption phase (stage-B), and then shifted to the main phase of Strombolian eruption (stage-C). Omuroyama pyroclastic cone was built during the stage-C. In this study, we performed textural and chemical analyses for phenocrysts and MIs in the fall scoria erupted during the stage-C, by using FE-EPMA and EPMA at ERI, Univ. Tokyo, Japan.

The scoria contain ~3.3 vol.% of olivine and ~5.4 vol.% of plagioclase as phenocrysts, and their groundmass include olivine and plagioclase microphenocsyts (MPs) of several tens-100 microns sizes embedded in almost glassy or microlite-rich matrix. Olivine phenocrysts are homogeneous (Fo~74-83 with concentration at 83-84) in each grain except for normal zoned rim. Olivine MPs has compositions similar to Fo-poor phenocrysts. Most of plagioclase phenocrysts show reverse zoning with cores of An~30-60 and rims of An~84 and dusty zones are often found. Plagioclase MPs have compositions identical to those of phenocryst rims. Olivine- and plagioclase-hosted MIs have $SiO_2$ contents of ~52-60 wt.% and 57-78 wt.%, respectively. Compositions of both olivine- and plagioclase-hosted MIs with $SiO_2$~57-60 wt.% are identical with glass in microlite-poor groundmass, indicating that the melt was saturated with olivine and plagioclase. Based on the olivine-plagioclase-melt compositional relation, temperature and $H_2O$ content conditions of the melt is estimated to be ~1080ºC and ~2 wt.% (H2O-saturated depth of ~2km), respectively. Majority of MIs in plagioclase phenocrysts are rhyolitic with SiO2~70-74wt.%. FeO content of host plagioclase crystals are consistent with those in equilibrium with the MIs. $H_2O$ contents of the MIs are estimated by melt-plagioclase hygrometer to be ~6.2-9.2 wt.% ($H_2O$-saturated depth of ~8-14km), under assumption of temperature of 800-850 ºC. In addition, olivine-hosted MIs with $SiO_2 < 57$ wt.% are enriched in $SO_3$ (~0.3-0.5 wt.%), indicating their origin deeper than those of more evolved MIs ($SO_3 < 0.1$ wt.%).

Present results suggest that (1) deep-derived, olivine-bearing mafc melt ascent, captured plagioclase phenocrysts and rhyolitic melt and mixed with them at 11km depth, and crystallized MPs at 2km depth before the eruption, and (2) rhyolitic melt existed at ~11km depth beneath the volcanic field at ca. 800 years before the first eruption of rhyolitic magma at Kawagodaira volcano.

Keywords: melt inclusion, monogenetic volcano, rhyolite, Izu-Omuroyama, plagioclase

©2019. Japan Geoscience Union. All Right Reserved. 

©2019. Japan Geoscience Union. All Right Reserved. 

# Time-series variation in the textures of ejecta of the An'ei eruption, Izu-Oshima

*Yuya Ikenaga[1], Fukashi Maeno[1], ATSUSHI YASUDA[1]

1. Earthquake Research Institute, The University of Tokyo

In Izu-Oshima, a large-scale eruption called the An’ ei eruption began in 1777. This eruption lasted for 15 years, and scoria and lava flows were strongly ejected before ash eruption period (Nakamura, 1964; Isshiki, 1984; Koyama and Hayakawa, 1996, Tsukui et al, 2009). As for scoria eruption, the transition of the intensity of eruption was unveiled (Ikenaga et al., 2018). Scoria eruption in the initial stage (Unit A) was somewhat weak and scoria is poor in plagioclase phenocrysts (Pl). After the small-scale scoria eruption (Unit B, rich in Pl), the climax stage (Unit C) occurred. Scoria in Unit C is richest in Pl and eruption column height of this unit is inferred to be approximately 10km. The change in the textures of scoriae among these 3 units, however, has not been investigated yet. It becomes clear in this study that there are differences in the textures of scoriae.

The scoria of Unit A (A-scoria) is rich in microlites and the groundmass glass has low transparency. The surface of bubbles is rough and many bubbles are connected each other. On the other hand, the scoria of Unit C (C-scoria) has almost no microlites and the glass is transparent. The shape of bubbles is spherical or ellipsoid, and the surface of bubbles is smooth. The connectivity of bubbles is low. The characteristics of the scoria of Unit B (B-scoria) are intermediate between those of A- and C-scoria. Considering the transition in the intensity of eruption, magma ascent rate of Unit A is expected to have been low than that of Unit C, and the crystallization of microlites and connection of bubbles in Unit A were probably caused because of low decompression rate.

The compositions of Pl, groundmass glass and melt inclusions in Pl of scoriae were measured using EPMA, and there are no difference in these compositions among 3 units. It is inferred from this result that the change in the intensity of 3 units was not caused by injection of undifferentiated magma into magma chamber, but caused by other processes, such as decompression of magma chamber after the eruption of Unit A. It is a future issue to reveal the cause of the change in intensity.

Keywords: Izu-Oshima, Transition in texture, Composition of eruption products

©2019. Japan Geoscience Union. All Right Reserved. 

# The textural analysis of pumice from the Plinian eruption of Taupo volcano: implications for tube pumice

*Masatoshi Ohashi[1], Mie Ichihara[2], Fukashi Maeno[2], Ben Kennedy[3], Darren Gravley[3]

1. Department of Earth and Planetary Science, Graduate School of Science, The University of Tokyo, 2. Earthquake Research Institute, The University of Tokyo, 3. Department of Geological Sciences, The University of Canterbury

Tube pumice is characterized by aligned highly elongated bubbles and is a common product of explosive silicic eruptions. This bubble texture is thought to reflect shear deformations during flow in a conduit (Marti et al., 1999). Therefore, quantitative measurements of tube pumice texture can inform conduit flow models. Recent development in X-ray tomography allows us to measure bubble shapes in 3D pumice accurately (e.g., Dingwell et al., 2016). In addition to the microscopic structures of individual pumices, the abundance of tube and non-tube pumices in the stratigraphy is important in inferring temporal and spatial variations in a conduit flow. This study aims at quantifying micro-structural and stratigraphic features of pumice from the 1.8 ka eruption of Taupo volcano, New Zealand.

The 1.8 ka eruption is the most recent large eruptive event from Taupo volcano. It is characterized by various eruptive styles, including three phreatomagmatic fall deposits (units 1, 3, 4), Hatepe plinian fall deposit (unit 2), Taupo plinian fall deposit (unit 5), and Taupo ignimbrite (unit 6) (Houghton et al., 2010). Since those deposits show chemically uniform pumices and melt inclusions, the great diversity of bubble textures in pumices may reflect purely physical processes in the eruption. We collected samples from the units of the two plinian eruptions (units 2 and 5) and the ignimbrite (unit 6), and measured bubble textures and vesicularities. Among those units, we focused on unit 5 to investigate the transition from plinian fall to ignimbrite. For this purpose, a detailed sampling of unit 5 was conducted at an outcrop about 25 km away from the vent, where the unit consists of a fine lower part (40 cm) and a coarse upper part (180 cm). We sampled clasts from the bottom to top of the unit 5 layer at 20cm interval. The bubble textures of more than 1000 pumice samples were measured by a digital microscope (VHX-1000, Keyence) with variable illumination function. The illumination was optimized to make good luminance contrast between the flat surface and bubbles for image analysis.

The image analysis shows that bubbles in unit 5 are more elongated than those in unit 2 and less elongated than those in unit 6. The average values of bubble elongation in unit 2 and 6 are proportional to those of vesicularity. In contrast, bubble elongation and vesicularity are uniform within unit 5. The component analysis over unit 5 shows that the weight percentage of lithics is also uniform except in the lowest part. The relatively high lithic content in the lowest part suggests vent widened or shifted location at the beginning of the Taupo plinian event.

Previous studies in other volcanoes suggest that bubbles in the pre-ignimbrite phase become more elongated toward the flow stage (Taddeucci and Wohletz 2001, Polacci et al., 2003). The increased amount of tube pumice is thought to reflect a gradual transition from fallout to ignimbrite, and it was interpreted as a result of increased erosive activity near the conduit wall, or a greater conduit area available for shearing (Polacci et al., 2003). In contrast, no such variation of bubble texture is observed in Taupo plinian event (unit 5), which implies that a steady conduit flow was sustained during the pre-ignimbrite fallout eruption. The ignimbrite (unit 6) might not simply be the result of a collapsing plinian eruption column. It is also possible that the topmost part of unit 5 had been eroded by and/or mixed with the pyroclastic flow that deposited the subsequent ignimbrite (unit 6).

©2019. Japan Geoscience Union. All Right Reserved. 

Keywords: bubble texture, tube pumice, Taupo

©2019. Japan Geoscience Union. All Right Reserved. 

[E] Poster | S (Solid Earth Sciences)：S-VC Volcanology

Thu. May 30, 2019 5:15 PM - 6:30 PM JST | Thu. May 30, 2019 8:15 AM - 9:30 AM UTC | Poster Hall International Exhibition Hall8, Makuhari Messe_23

## [S-VC34] Connecting magma dynamics in vent-conduit system with surface expression of volcanic eruption

convener:Takahiro Miwa(National research institute for earth science and disaster prevention), Nobuo Geshi(Geological Survey of Japan, The National Institute of Advanced Industrial Science and Technology)

Magma dynamics within a shallow conduit system control the diversity of behavior of volcanic eruptions. Recent advancements in geophysical, airborne and ground-based observation techniques provide quantitative data about the dynamic behavior of volcanic eruptions. New analytical methods of the macro and microtextures of eruptive products also open new insights on detailed dynamics of magmas within conduit. The aim of this session is the integration of these new techniques to approach the dynamics of magma ascending from a shallow part of conduit to vent. This session seeks submissions that explore magma dynamics controlling the behaviors of volcanic eruption by integrated investigation of 1) degassing, outgassing, crystallization, and fragmentation of ascending magma, 2) emission and recycling of eruptive product, and 3) morphological characterization of the vent-conduit system. We encourage contributions based on textural-petrological analyses of eruptive product, experimental study reproducing magma in the conduit, geophysical observation on surface expression of volcanic eruption, and related numerical modeling.

### [SVC34-P01] A new formulation of viscosity-included bubble nucleation rate in ascending magmas and re-estimation of bubble number density (2)

*Mizuki Nishiwaki[1], Atsushi Toramaru[2] (1.Department of Earth and Planetary Sciences, Graduate School of Sciences, Kyushu University, 2.Department of Earth and Planetary Sciences, Faculty of Sciences, Kyushu University)

### [SVC34-P02] Kinetic delay of crystal growth controls plagioclase-basaltic melt apparent disequilibrium

*Ryoya Oida[1], Hidemi Ishibashi[1], ATSUSHI YASUDA[2], Natsumi Hokanishi[2] (1.Faculty of Science, Shizuoka University, 2.Earthquake Research Institute, University of Tokyo)

### [SVC34-P03] Eruptive trends and dynamics of remote volcanoes detected form space-based thermal data and $SO_2$ emissions: a comparative analysis of Stromboli, Batu Tara and Tinakula volcanoes

*Corrado CIGOLINI[1], Marco Laiolo[1], Francesco Massimetti[1,2], Maurizio Ripepe[2], Diego Coppola[1] (1.Department of Earth Sciences, University of Torino, Italy, 2.Department of Earth Sciences, University of Firenze, Italy)

### [SVC34-P04] The source depth of Strombolian explosions: a multiparametric approach and comparison

*Jacopo Taddeucci[1], Miguel Angel Alatorre-Ibarguengoitia[2], Valeria Cigala[3], Elisabetta Del Bello[1], Damien Gaudin[4], Ulrich Kueppers[4], Tullio Ricci[1], Valentino Salvatore[5], Piergiorgio Scarlato[1] (1.Istituto Nazionale di Geofisica e Vulcanologia, Rome, Italy, 2.Centro de Investigación en Gestión de Riesgo y Cambio Climático, Universidad de Ciencias y Artes de Chiapas, Tuxtla Gutiérrez, Mexico, 3.Department of Geosciences, Università degli Studi di Padova, Padua, Italy, 4.Department of Earth and Environmental Sciences. Ludwig-Maximilians-Universität (LMU). Munich, Germany, 5.Dipartimento di Scienze della Terra, Sapienza Università di Roma, Rome, Italy)

### [SVC34-P05] Magmatic aggregate of basaltic ash particles

*Takahiro Miwa[1], Nobuo Geshi[2] (1.National research institute for earth science and disaster prevention, 2.National Institute of Advanced Industrial Science and Technology)

[SVC34-P06] Melt inclusion study on the eruption process of Izu-Omuroyama monogenetic volcano, Japan

Risako Hatada[1], *Hidemi Ishibashi[1], Yusuke Suzuki[2], ATSUSHI YASUDA[3], Natsumi Hokanishi[3] (1.Faculty of Science, Shizuoka University, 2.Izu Peninsula Geopark, 3.Earthquake Research Institute, University of Tokyo)

---

[SVC34-P07] Time-series variation in the textures of ejecta of the An'ei eruption, Izu-Oshima

*Yuya Ikenaga[1], Fukashi Maeno[1], ATSUSHI YASUDA[1] (1.Earthquake Research Institute, The University of Tokyo)

---

[SVC34-P08] The textural analysis of pumice from the Plinian eruption of Taupo volcano: implications for tube pumice

*Masatoshi Ohashi[1], Mie Ichihara[2], Fukashi Maeno[2], Ben Kennedy[3], Darren Gravley[3] (1.Department of Earth and Planetary Science, Graduate School of Science, The University of Tokyo, 2.Earthquake Research Institute, The University of Tokyo, 3.Department of Geological Sciences, The University of Canterbury)

# A new formulation of viscosity-included bubble nucleation rate in ascending magmas and re-estimation of bubble number density (2)

*Mizuki Nishiwaki[1], Atsushi Toramaru[2]

1. Department of Earth and Planetary Sciences, Graduate School of Sciences, Kyushu University, 2. Department of Earth and Planetary Sciences, Faculty of Sciences, Kyushu University

To evaluate the effect of melt viscosity on bubble nucleation, we newly formulate homogeneous nucleation rate of water bubbles to explicitly include melt viscosity. The viscosity appears in the pre-exponential factor of the nucleation rate in terms of the Péclet number: the ratio of bubble growth timescale by molecular diffusion and viscous relaxation timescale. The pre-exponential factor linearly decreases with increasing viscosity (or decreasing Péclet number) under a given supersaturation. We numerically solve the evolution of bubble nucleation and growth processes in ascending magmas by using the new formula of nucleation rate and a precise approximation of moment equations of bubble size distribution function. In high viscosity or high decompression rate region, the effect of melt viscosity reduces bubble number density by several orders of magnitude compared with the previous study. Because of the lack of experimental data in this high-viscous regime, the reality of this regime will be verified by future experiments.

Keywords: bubble nucleation, bubble growth, BND (Bubble Number Density), BSD (Bubble Size Distribution), Péclet number

©2019. Japan Geoscience Union. All Right Reserved. 

# Kinetic delay of crystal growth controls plagioclase-basaltic melt apparent disequilibrium

*Ryoya Oida[1], Hidemi Ishibashi[1], ATSUSHI YASUDA[2], Natsumi Hokanishi[2]

1. Faculty of Science, Shizuoka University, 2. Earthquake Research Institute, University of Tokyo

Plagioclase-melt compositional relations sensitively depend on temperature, T, and water content, $X_W$, of melt. Therefore, the relations are formulated as functions of T and $X_W$ and used as geothermohygrometer (e.g., Putirka, 2008). Plagioclase-melt equilibrium is postulated for applying the thermohygrometer models. However, validity of the assumption is unobvious for microlite crystallization driven by degassing and/or cooling during eruption. Can we apply the thermohygrometers to the plagioclase-melt pairs formed by dynamic crystallization? To examine the issue, the cooling crystallization experiments of the high-Al basaltic melt were carried out and textural and chemical analyses were performed the run samples.

We used the high-Al basalt lava from Waianae, Hawaii Oahu as the starting material for the cooling crystallization experiments. This experiment was conducted using the 1atm $fO_2$-controlled furnace at University of Hawaii at Manoa. After 3 hours pre-heating at 1180℃, ~30K higher than the liquidus, the samples were cooled at cooling rates, $R_c$, of 0.1, 0.3, 1, 3, and 10K/min, and then quenched in water at four target temperatures, $T_q$, of 1150, 1120, 1090, and 1060℃. We used FE-EPMA (JEOL-JXA-8530FPlus) and EPMA (JEOL8800R) at Earthquake Research Institute, University of Tokyo, for textural and chemical analyses of the run samples.

As $R_c$ and/or $T_q$ increase, the abundance and size of plagioclase crystals decrease. As $R_c$ increases, the shape of plagioclase changes from euhedral to dendritic. The $R_c$-dependent shape change is more obvious at lower $T_q$. Pyroxene crystallization was suppressed in the run samples coolied at higher $R_c$. In addition, melt boundary layers are observed around pyroxene in the samples cooled at 0.3-1K/min, quenched at 1090℃ and cooled at 0.3-3K/min, quenched at 1060℃, and around plagioclase in the samples cooled at >3K/min, quenched at <1120℃. Lower diffusivity of $Al_2O_3$ compared to those of FeO and MgO is responsible for lower threshold cooling rate of melt boundary layer formation around pyroxene.

The maximum An# [=100Ca/(Ca + Na)] of plagioclase was almost the same among all run samples. We applied both plagioclase liquidus and plagioclase-melt An-partitioning thermometers of Putirka (2008) to the pairs of plagioclase rim-boundary layer melt (BLM) and plagioclase rim-far field melt (FFM) to estimate temperatures recorded in their phase compositions. At $T_q$=1150℃, the estimated temperatures well represent $T_q$ for both BLM and FFM. However, at lower $T_q$, both of the thermometers estimate temperatures higher than $T_q$; difference between estimated temperature and $T_q$, $\Delta T$, increases as decreasing $T_q$. The two thermometers estimate similar temperatures for each sample, and the differences between the two estimated temperatures do not depend on $R_c$. These results suggest that the plagioclase-melt partition coefficient of An component does not depend on the $R_c$. Therefore, the increase of $\Delta T$ at lower $T_q$ is not due to the $R_c$-dependence of the partition coefficient. It is attributed to the kinetic delay of the crystal growth at lower temperature. On the other hand, the coincidence between calculated temperatures and $T_q$ at 1150℃ suggests that kinetic delay of plagioclase crystal growth is small at near liquidus temperature.

©2019. Japan Geoscience Union. All Right Reserved. 

Present results show that plagioclase-melt thermometers can be applied regardless of the $R_c$ at higher temperatures, while magmatic temperature tends to be overestimated due to kinetic delay of crystal growth at lower temperature.

Keywords: plagioclase, crystallization, kinetics, basalt, geothermometry

©2019. Japan Geoscience Union. All Right Reserved. 

# Eruptive trends and dynamics of remote volcanoes detected form space-based thermal data and $SO_2$ emissions: a comparative analysis of Stromboli, Batu Tara and Tinakula volcanoes

*Corrado CIGOLINI[1], Marco Laiolo[1], Francesco Massimetti[1,2], Maurizio Ripepe[2], Diego Coppola[1]

1. Department of Earth Sciences, University of Torino, Italy, 2. Department of Earth Sciences, University of Firenze, Italy

South-Eastern Pacific has a large number of unmonitored volcanoes that may potentially produce large-scale eruptive events capable to affect highly-populated areas. Therefore, forecasting changes in volcanic activity in the light of historical time-series is a rather intriguing challenge for the space-based earth observations.
Batu Tara (Indonesia) and Tinakula (Solomon Island) are two poorly known volcanic islands with morphologies and reported short-term activities rather similar to the ones observed at Stromboli volcano (Italy). However, thanks to over a decade-long satellite data we are able to effectively compare the activity occurring at Stromboli (a unique natural laboratory and “open-vent” system) with those taking place at the above volcanoes.
We process and analyse the radiant flux (thermal activity) coupled with $SO_2$ emissions (degassing activity) at these three volcanoes for over a decade. The combined analysis of Volcanic Radiant Power (from MODIS data) and $SO_2$ burden (from OMI data) reveals different long-term eruptive trends, and contrasting ratio of gas vs. thermal emissions. In fact, the persistent open-vent explosive activity of Stromboli volcano is interrupted by flank effusions that periodically drain the degassed magma stored at shallow levels. On the other hand, the long-lasting exponential decay of both thermal and gas emissions observed at Batu Tara is consistent with the eruption of an “undegassed magma” from a deep, and likely a “closed” magma chamber. Finally, Tinakula volcano exhibits multiple year-long eruptive phases, characterised by evolving gas vs. thermal ratio correlated with an increasing eruptive intensity: thus suggesting the involvement of a volatile-zoned magma chamber with periodic phases of gas/magma accumulations.
Our results suggest that the combined analysis of satellite thermal/gas data is a useful tool for better understanding long-term volcanic dynamics and interpreting volcanic processes occurring at a shorter time-scale. We also stress that large satellite datasets on active volcanoes, available from different platforms, greatly enhance the opportunity to efficiently monitor remote volcanic targets in the attempt to mitigate volcanic risk.

Keywords: Remote volcanoes, satellite datasets, Volcanic Radiative Power, SO2 emissions, volcanic risk

©2019. Japan Geoscience Union. All Right Reserved. 

# The source depth of Strombolian explosions: a multiparametric approach and comparison

*Jacopo Taddeucci[1], Miguel Angel Alatorre-Ibarguengoitia[2], Valeria Cigala[3], Elisabetta Del Bello[1], Damien Gaudin[4], Ulrich Kueppers[4], Tullio Ricci[1], Valentino Salvatore[5], Piergiorgio Scarlato[1]

1. Istituto Nazionale di Geofisica e Vulcanologia, Rome, Italy, 2. Centro de Investigación en Gestión de Riesgo y Cambio Climático, Universidad de Ciencias y Artes de Chiapas, Tuxtla Gutiérrez, Mexico, 3. Department of Geosciences, Università degli Studi di Padova, Padua, Italy, 4. Department of Earth and Environmental Sciences. Ludwig-Maximilians-Universität (LMU). Munich, Germany, 5. Dipartimento di Scienze della Terra, Sapienza Università di Roma, Rome, Italy

The source depth of an individual explosion during Strombolian-style explosive volcanic activity can be defined as the depth of the region within the volcanic conduit where magma fragmentation occurs and the acceleration of pyroclasts by the expanding gas continuum begins. Source depth is thought to exert a first-order control on the final ejection dynamics of the pyroclasts and the ensuing eruptive styles and hazards. As such, different methods to estimate source depth have been developed in the past.

Here, we used three independent methods to estimate the source depth of some Strombolian explosions from Stromboli and Etna volcanoes (Italy). The first method uses the back-tracking of the trajectories of pyroclasts leaving the vent to infer their minimum release depth. It is a purely geometric method relying on the assumption that pyroclasts follow linear trajectories after fragmentation. The second method uses the time delay between the appearance of pyroclasts at the vent and the arrival of acoustic waves at a recording station at a known distance from the vent. This method relies on several assumptions, including (i) the sound velocity inside the conduit, (ii) the co-location of source depth of pyroclasts and acoustic waves, and (iii) a constant velocity of pyroclasts in the conduit, following the initial acceleration. The third method uses the velocity of pyroclasts progressively exiting the vent. This velocity decays following a non-linear trend which is function of the source depth, as illustrated by previous experimental and theoretical studies. As for the second method, also this last one assumes a constant velocity of pyroclasts rising in the conduit.

For the Etna case, the three methods provide consistent results and a shallow (<20 m) source depth of the explosions. For the Stromboli case, the first and third methods provide shallow (around 6 and 15 m, respectively) source depths while the second method provides depths of around 60 m. The incompatibility of such large depths with the first two methods, and given the relative assumptions, we believe that in the Stromboli case the co-location of the particles and acoustic source is probably the least strong assumption. These results suggest that caution should be used in assessing source depth from a single methodology, and that more investigations are required on the source of acoustic signals from the explosions and on the motion (specifically the acceleration and deceleration) of pyroclasts ascending along the conduit.

Keywords: strombolian, explosion, depth

©2019. Japan Geoscience Union. All Right Reserved. 

# Magmatic aggregate of basaltic ash particles

*Takahiro Miwa[1], Nobuo Geshi[2]

1. National research institute for earth science and disaster prevention, 2. National Institute of Advanced Industrial Science and Technology

Dynamics of volcanic cloud and jet at the vent is largely controled by a grain size of pyroclast. The grain size is considered to be determined by primary fragmentation of magma, and subsequent breakup of pyroclasts due to therir collsions in upper conduit (Dufek et al. 2012). However, whether the breakup occurs or not depend on viscoelastic responce of magma (Dingwell and Webb, 1989).
In this study, we report aggregate of ash particles which is formed in magmatic temperature. We observed basaltic ash samples from Stromboli volcano, Italy, and Aso volcano, Japan. The “magmatic aggretate” shows texture that numerous small guest particles (< 200 $\mu$m) adhere or stick on a host particle (> 1 mm). All the host particles are catergorized to sideromelane having fluidal morphology. The guest particles are on fluidal surface of the host particle, and show fluidal and dense morphology. These characteristics found in the magmatic aggregate can be explaned by collision and aggretation of ash particles in high temperature condition. Here we model formation of the magmatic aggregates as passing of two frying particles bearing viscoelastic nature, by using viscosity of magma estimated ($10^4$-$10^5$ Pa s). When the relative velocity of the two particles falls the critical value, the two particles behave as viscous material, coalsece each other, and then form the magmatic aggregate. The result of calculation demonstrates that the critical relative velocity is approximately $10^{-2}$ m/s, and implies the magmatic aggregation is difficult to occur for silisic magma with highly viscosity. Thus we conclude that the collision can increase average grain size of pyroclast in basaltic system.

Keywords: Eruptive dynamics, Interaction of ash particles, Viscoelastic response of magma

©2019. Japan Geoscience Union. All Right Reserved. 

# Melt inclusion study on the eruption process of Izu-Omuroyama monogenetic volcano, Japan

Risako Hatada[1], *Hidemi Ishibashi[1], Yusuke Suzuki[2], ATSUSHI YASUDA[3], Natsumi Hokanishi[3]

1. Faculty of Science, Shizuoka University, 2. Izu Peninsula Geopark, 3. Earthquake Research Institute, University of Tokyo

Izu-Omuroyama is one of monogenetic volcanoes in Izu-Tobu volcanic field, which is the largest pyroclastic cone formed by ~4ka eruption with ~450 million tons of tephra and lava (Koyano et al., 1996). Because a monogenetic volcano such as Omuroyama is built by the first eruption of a newly-formed magma plumbing system, phenocrysts and melt inclusions (MIs) in its volcanic products may record information about the initial process of formation of the magma plumbing system. In this study, textural and chemical analyses were performed for phenocrysts and MIs in Strombolian scoria of the Omuroyama eruption to clarify the eruption process of the monogenetic volcano.

According to Koyano et al. (1996), Omuroyama eruption started from sub-plinian phase (stage-A), followed by weak ash-eruption phase (stage-B), and then shifted to the main phase of Strombolian eruption (stage-C). Omuroyama pyroclastic cone was built during the stage-C. In this study, we performed textural and chemical analyses for phenocrysts and MIs in the fall scoria erupted during the stage-C, by using FE-EPMA and EPMA at ERI, Univ. Tokyo, Japan.

The scoria contain ~3.3 vol.% of olivine and ~5.4 vol.% of plagioclase as phenocrysts, and their groundmass include olivine and plagioclase microphenocsyts (MPs) of several tens-100 microns sizes embedded in almost glassy or microlite-rich matrix. Olivine phenocrysts are homogeneous (Fo~74-83 with concentration at 83-84) in each grain except for normal zoned rim. Olivine MPs has compositions similar to Fo-poor phenocrysts. Most of plagioclase phenocrysts show reverse zoning with cores of An~30-60 and rims of An~84 and dusty zones are often found. Plagioclase MPs have compositions identical to those of phenocryst rims. Olivine- and plagioclase-hosted MIs have $SiO_2$ contents of ~52-60 wt.% and 57-78 wt.%, respectively. Compositions of both olivine- and plagioclase-hosted MIs with $SiO_2$~57-60 wt.% are identical with glass in microlite-poor groundmass, indicating that the melt was saturated with olivine and plagioclase. Based on the olivine-plagioclase-melt compositional relation, temperature and $H_2O$ content conditions of the melt is estimated to be ~1080ºC and ~2 wt.% (H2O-saturated depth of ~2km), respectively. Majority of MIs in plagioclase phenocrysts are rhyolitic with SiO2~70-74wt.%. FeO content of host plagioclase crystals are consistent with those in equilibrium with the MIs. $H_2O$ contents of the MIs are estimated by melt-plagioclase hygrometer to be ~6.2-9.2 wt.% ($H_2O$-saturated depth of ~8-14km), under assumption of temperature of 800-850 ºC. In addition, olivine-hosted MIs with $SiO_2 < 57$ wt.% are enriched in $SO_3$ (~0.3-0.5 wt.%), indicating their origin deeper than those of more evolved MIs ($SO_3 < 0.1$ wt.%).

Present results suggest that (1) deep-derived, olivine-bearing mafc melt ascent, captured plagioclase phenocrysts and rhyolitic melt and mixed with them at 11km depth, and crystallized MPs at 2km depth before the eruption, and (2) rhyolitic melt existed at ~11km depth beneath the volcanic field at ca. 800 years before the first eruption of rhyolitic magma at Kawagodaira volcano.

Keywords: melt inclusion, monogenetic volcano, rhyolite, Izu-Omuroyama, plagioclase

©2019. Japan Geoscience Union. All Right Reserved. 

©2019. Japan Geoscience Union. All Right Reserved. 

# Time-series variation in the textures of ejecta of the An'ei eruption, Izu-Oshima

*Yuya Ikenaga[1], Fukashi Maeno[1], ATSUSHI YASUDA[1]

1. Earthquake Research Institute, The University of Tokyo

In Izu-Oshima, a large-scale eruption called the An’ ei eruption began in 1777. This eruption lasted for 15 years, and scoria and lava flows were strongly ejected before ash eruption period (Nakamura, 1964; Isshiki, 1984; Koyama and Hayakawa, 1996, Tsukui et al, 2009). As for scoria eruption, the transition of the intensity of eruption was unveiled (Ikenaga et al., 2018). Scoria eruption in the initial stage (Unit A) was somewhat weak and scoria is poor in plagioclase phenocrysts (Pl). After the small-scale scoria eruption (Unit B, rich in Pl), the climax stage (Unit C) occurred. Scoria in Unit C is richest in Pl and eruption column height of this unit is inferred to be approximately 10km. The change in the textures of scoriae among these 3 units, however, has not been investigated yet. It becomes clear in this study that there are differences in the textures of scoriae.

The scoria of Unit A (A-scoria) is rich in microlites and the groundmass glass has low transparency. The surface of bubbles is rough and many bubbles are connected each other. On the other hand, the scoria of Unit C (C-scoria) has almost no microlites and the glass is transparent. The shape of bubbles is spherical or ellipsoid, and the surface of bubbles is smooth. The connectivity of bubbles is low. The characteristics of the scoria of Unit B (B-scoria) are intermediate between those of A- and C-scoria. Considering the transition in the intensity of eruption, magma ascent rate of Unit A is expected to have been low than that of Unit C, and the crystallization of microlites and connection of bubbles in Unit A were probably caused because of low decompression rate.

The compositions of Pl, groundmass glass and melt inclusions in Pl of scoriae were measured using EPMA, and there are no difference in these compositions among 3 units. It is inferred from this result that the change in the intensity of 3 units was not caused by injection of undifferentiated magma into magma chamber, but caused by other processes, such as decompression of magma chamber after the eruption of Unit A. It is a future issue to reveal the cause of the change in intensity.

Keywords: Izu-Oshima, Transition in texture, Composition of eruption products

©2019. Japan Geoscience Union. All Right Reserved. 

# The textural analysis of pumice from the Plinian eruption of Taupo volcano: implications for tube pumice

*Masatoshi Ohashi[1], Mie Ichihara[2], Fukashi Maeno[2], Ben Kennedy[3], Darren Gravley[3]

1. Department of Earth and Planetary Science, Graduate School of Science, The University of Tokyo, 2. Earthquake Research Institute, The University of Tokyo, 3. Department of Geological Sciences, The University of Canterbury

Tube pumice is characterized by aligned highly elongated bubbles and is a common product of explosive silicic eruptions. This bubble texture is thought to reflect shear deformations during flow in a conduit (Marti et al., 1999). Therefore, quantitative measurements of tube pumice texture can inform conduit flow models. Recent development in X-ray tomography allows us to measure bubble shapes in 3D pumice accurately (e.g., Dingwell et al., 2016). In addition to the microscopic structures of individual pumices, the abundance of tube and non-tube pumices in the stratigraphy is important in inferring temporal and spatial variations in a conduit flow. This study aims at quantifying micro-structural and stratigraphic features of pumice from the 1.8 ka eruption of Taupo volcano, New Zealand.

The 1.8 ka eruption is the most recent large eruptive event from Taupo volcano. It is characterized by various eruptive styles, including three phreatomagmatic fall deposits (units 1, 3, 4), Hatepe plinian fall deposit (unit 2), Taupo plinian fall deposit (unit 5), and Taupo ignimbrite (unit 6) (Houghton et al., 2010). Since those deposits show chemically uniform pumices and melt inclusions, the great diversity of bubble textures in pumices may reflect purely physical processes in the eruption. We collected samples from the units of the two plinian eruptions (units 2 and 5) and the ignimbrite (unit 6), and measured bubble textures and vesicularities. Among those units, we focused on unit 5 to investigate the transition from plinian fall to ignimbrite. For this purpose, a detailed sampling of unit 5 was conducted at an outcrop about 25 km away from the vent, where the unit consists of a fine lower part (40 cm) and a coarse upper part (180 cm). We sampled clasts from the bottom to top of the unit 5 layer at 20cm interval. The bubble textures of more than 1000 pumice samples were measured by a digital microscope (VHX-1000, Keyence) with variable illumination function. The illumination was optimized to make good luminance contrast between the flat surface and bubbles for image analysis.

The image analysis shows that bubbles in unit 5 are more elongated than those in unit 2 and less elongated than those in unit 6. The average values of bubble elongation in unit 2 and 6 are proportional to those of vesicularity. In contrast, bubble elongation and vesicularity are uniform within unit 5. The component analysis over unit 5 shows that the weight percentage of lithics is also uniform except in the lowest part. The relatively high lithic content in the lowest part suggests vent widened or shifted location at the beginning of the Taupo plinian event.

Previous studies in other volcanoes suggest that bubbles in the pre-ignimbrite phase become more elongated toward the flow stage (Taddeucci and Wohletz 2001, Polacci et al., 2003). The increased amount of tube pumice is thought to reflect a gradual transition from fallout to ignimbrite, and it was interpreted as a result of increased erosive activity near the conduit wall, or a greater conduit area available for shearing (Polacci et al., 2003). In contrast, no such variation of bubble texture is observed in Taupo plinian event (unit 5), which implies that a steady conduit flow was sustained during the pre-ignimbrite fallout eruption. The ignimbrite (unit 6) might not simply be the result of a collapsing plinian eruption column. It is also possible that the topmost part of unit 5 had been eroded by and/or mixed with the pyroclastic flow that deposited the subsequent ignimbrite (unit 6).

©2019. Japan Geoscience Union. All Right Reserved. 

Keywords: bubble texture, tube pumice, Taupo

©2019. Japan Geoscience Union. All Right Reserved. 

[J] Poster | S (Solid Earth Sciences)：S-VC Volcanology

Thu. May 30, 2019 10:45 AM - 12:15 PM JST | Thu. May 30, 2019 1:45 AM - 3:15 AM UTC | Poster Hall International Exhibition Hall8, Makuhari Messe_5

## [S-VC37] Dynamics of volcanic eruptions and their physical and chemical processes

convener:Yujiro Suzuki(Earthquake Research Institute, The University of Tokyo)

This session discusses the dynamics of volcanic and igneous activities such as magma accumulation, magma ascent in volcanic conduits, and dispersion of volcanic products. In order to understand such multi-scale phenomena, the researches of microscopic and macroscopic scales and the techniques that combine the different scales are required. We aim to discuss the latest approaches based on the recent observations, laboratory experiments and numerical simulations, from the viewpoint of cross-cutting research.

### [SVC37-P01] Geochemical interpretation of Ulleung Island volcanic rocks: Implication for the new magmatic model for plume-slab interaction in East Asia

*Chungwan LIM[1], Dohyun Kim[1] (1.Kongju National University)

### [SVC37-P02] 1D particle model for vertiacal non-uniform bubble coalescence

*Maruishi Takafumi[1] (1.Department of Earth and Planetary Sciences, Faculty of Sciences, Kyushu University)

### [SVC37-P03] The formation process of a 100m thick basaltic lava flow in the Kitamatsuura basalts, northwestern Kyushu

*Ryotaro Araki[1], Tetsuya Sakuyama[1] (1.Osaka City University)

### [SVC37-P04] An introduction to the observation method of imaging volcanoes by using cosmic-ray muons

*Seigo Miyamoto[1] (1.Earth Reasearch Institute, University of Tokyo)

### [SVC37-P05] Simulation and test observation for omni-directional muography at Omuro-yama

*Shogo Nagahara[1], Seigo Miyamoto[1], Kunihiro Morishima[2], Toshiyuki Nakano[2], Masato Koyama[3], Yusuke Suzuki[4] (1.Earthquake Research Institute,the University of Tokyo, 2.Nagoya University, 3.Shizuoka University, 4.Izu Peninsula Geopark Promotion Council)

### [SVC37-P06] Estimation of pressure source occurring volcanic crustal deformation with FEM considering topography

*Shinya Yamada[1], Tomokazu Kobayashi[1] (1.GSI of Japan)

# Geochemical interpretation of Ulleung Island volcanic rocks: Implication for the new magmatic model for plume-slab interaction in East Asia

*Chungwan LIM[1], Dohyun Kim[1]

1. Kongju National University

Ulleung Island has been considered as an intraplate volcanic island located in the East Sea/Japan Sea. The alkaline tephra originated from Ulleung Island has played an important role in understanding of the intraplate alkaline volcanism during the Quaternary. Ulleung Island on volcanism that occurs far from plate margins is abstruse with the current paradigm of plate tectonics. The Ulleung Island volcanic complex is unlikely to result from a mantle plume rising at the base of the mantle.

Ulleung Island is consisted of basaltic lava, agglomerate succession, and trachytic/phonolitic pumiceous tephra. The analyses of chemical compositions of glass shards in Ulleung tephras is necessary to identify each unit. During the Quaternary, at least six pumiceous tephras (UT-1~6) covered the island for this research. Based on the relationships of $SiO_2$, the $Al_2O_3$, $Na_2O$, $K_2O$, and $Fe_2O_3$ contents of the tephras increase as $SiO_2$ increases and decrease MgO as $SiO_2$ increases in Ulleung tephras. The trace elements in tephra show intra-plate type characteristics. Sr-Nd-Pb isotopic data from the literature of volcanic glass shards suggest that the mix in magma source might have involved EM1 and EM2-components of Quaternary tephras from Ulleung Island, South Korea.

This study has two principal objectives: First, multiple Ulleung tephras are expected to detect and identify the Ulleung Island. In order to accurately identify and correlate the tephras, it is necessary to consider stratigraphic position as well as geochemical characteristics. The chemical composition of volcanic glass shards is a useful tool for evaluating mixtures of multiple layers. The heavy mineral composition can also be used to identify tephra units. In order to reveal the distribution of each tephra unit to a high degree of certainty, characteristics such as heavy mineral and chemical compositions of each unit must be determined in greater detail itself. Second, we propose that the anomaly represents lithospheric mantle that had been accompanied by beneath the sinking lithosphere of the Philippine Sea Plate and was erupted through a slab-tear in the subducting slab. We suggest that this subduction-induced upwelling process produces mantle-upwelling that feeds the Ulleung Island volcanoes. Subduction-induced upwelling may also may explain back-arc volcanism at other subduction zones in East Asia.

Keywords: Ulleung Island volcano, intraplate, plume-slab interaction

©2019. Japan Geoscience Union. All Right Reserved. 

# 1D particle model for vertiacal non-uniform bubble coalescence

*Maruishi Takafumi[1]

1. Department of Earth and Planetary Sciences, Faculty of Sciences, Kyushu University

Bubble coalescence deeply affects the dynamics of conduit flow during volcanic eruption.

Previously, the theory assuming nonuniform coalescence has been used.(Macini et al., 2016, etc.). However, in the outgassing process, non-uniform bubble coalescence is considered important in the radial direction and vertical direction of the conduit, the model cannot deal with the coalescence process.

In this study, we construct a simple model that describe a bubble as a particle moving on a one-dimensional line, particle coalesces when particles contact with each other, and calculates the bubble size distribution in a nonuniform coalescence process in the vertical direction.

The particles have a speed corresponding to the size (buoyancy), and the size increases with the altitude and time (expansion / growth). Note that this model is equivalent to the model by Meakin (1989) when bubble growth and advection are not considered. The particles are fed to the lower end of the system at a constant rate (foaming).

Numerical calculation was carried out by broadly controlling the time scale of foaming, rising buoyancy, expansion and growth.

As a result, there was a parameter range where foaming and coalescence are balanced, and it was found that the size distribution shows a dynamic scaling rule regardless of the fluctuation of the radius and number of particles to be supplied.

The relational expression between the expansion and growth exponential law and the vertical scaling index is derived from the conservation law under the assumption that the size distribution is self-similar.

Keywords: bubble coalescence

©2019. Japan Geoscience Union. All Right Reserved. 

# The formation process of a 100m thick basaltic lava flow in the Kitamatsuura basalts, northwestern Kyushu

*Ryotaro Araki[1], Tetsuya Sakuyama[1]

1. Osaka City University

Kita Matsuura basalts cover the Northwest Kyushu Kitamatsuura Peninsula widely and they were the eruption activities of basaltic lavas which were one of the largest in the Cenozoic in Southwest Japan. The volcanic activity of this basaltic rock had erupted sub-alkaline basalt lavas from multiple sources from the late stage of activity, and ended at about 6.5 Ma. There is a mountain composed of basaltic lavas called Senryu Shiradake that was formed at the end of the eruption in the Senryu Area (Matsui et al., 1989; Sakuyama et al., 2009). Although Senryu Shiradake has a specific height of about 100 m, the boundary of the flow unit has not been confirmed (Fukuyama, 1960, 1961; Kurasawa, 1967). The lapilli tuff layers are sandwiched between this basaltic lava and the lower basalt plateau widely cover the upper surface of the lower basalt plateau and are distributed in a narrower area above it (Matsui et al. 1989). It is difficult to think that basaltic lava which are thought to be more robust against weathering and erosion than erosion of the lapilli tuff are selectively eroded, and that valley buried basaltic lava was eroded Selectively, It is unlikely that the mountain body had remained. From this, it can be considered that Senryu Shiradake is a single basaltic lava flow.

The thickness and length of the lava flow forming the volcanoes are systematically varied in general depending on the chemical composition. Basaltic lavas have low viscosity, so the run length of the basaltic lava flows are longer than that of the andesitic and rhyolitic lava flows, and the average thickness is at most about 30 m (Walker et al., 1973). On the other hand, Senryu Shiradake is formed a basaltic lava flow but its height is about 100 m. In this study, we investigated the lava flow that formed the mountain body of Senryu Shiradake from a petrological point of view.

Analysis of whole rock chemical composition of samples taken from Senryu Shiradake was performed by a fluorescent X-ray analyzer. It was confirmed that Senryu Shiradake basaltic lava has $SiO_2$ = 50 to 53 wt%, MgO = 7 to 11 wt%, FeO * / MgO = 0.87 to 1.5, and it is formed of undifferentiated basalt. The phenocrysts are predominant in olivine and contain a small amount of clinopyroxene, orthopyroxene, and the total phenocryst amount was 3 to 15 vol%. There was a correlation between the sampling altitude and the total rock chemical composition. As the height from the foot increased, the total rock SiO2 amount tended to increased and the MgO amount tended to decrease.

First, assuming that only the phenocrysts were crystallized at the time of lava eruption, the viscosity of lava flow was calculated using the model of Pinkerton & Stevenson (1992) for the effect of crystals on magma viscosity and the model of Hui & Zhang (2007) for the influence of the viscosity of melt. Melt composition was estimated using total rock chemical composition, phenocryst mode composition, and mineral composition. We assumed that all the water in the magma was volatilized and the magma temperature at the time of squirting was 1320 K estimated using pyroxene thermometer. the lava flow model used the flow of magma is stopped by solid shell formation by cooling by Griffiths & Fink (1993).

In this study, we investigated the conditions that can explain the thickness and radius of circulation of the basaltic lava of Senryu Shiradake, considering three variables of volume of erupting magma, time change rate of eruption volume and magma temperature. As a result, even if the rate of change of the first eruption amount and the eruption rate were changed, the thickness was only about 20 m at most which did not reproduce 100 m thick lava flow of Senryu Shiradake. Next, the same study as above was carried out assuming that the degree of crystallization at the time of erupting was 50%, but the thickness was about 30 m at most. From this, it is possible that a 100m thick basaltic lava flow was formed by erupting at

©2019. Japan Geoscience Union. All Right Reserved. 

a lower temperature.

Keywords: Kita-matsuura Basalts, lava flow thickness, magma viscosity

©2019. Japan Geoscience Union. All Right Reserved. 

# An introduction to the observation method of imaging volcanoes by using cosmic-ray muons

*Seigo Miyamoto[1]

1. Earth Reasearch Institute, University of Tokyo

The purpose of this presentation is widely to inform a method of exploring the density structure inside a gigantic structure such as a volcano, by using high evergy muons included in cosmic rays. It is considered that there are some reasons for low awareness. For example, the history of this method which is applied to Earth and planetary science is still short, knowledge about "Muon" which is one of "cosmic rays" or "elementary particles" is not known widely. To improve such a situation, we will review the fundamental principles to evaluate the internal density of volcanoes using cosmic-ray muons, past and going-on observation examples of volcanoes, and technological developments stories in this presentation.

Keywords: volcano, cosmic-ray, muon, imaging

©2019. Japan Geoscience Union. All Right Reserved. 

# Simulation and test observation for omni-directional muography at Omuro-yama

*Shogo Nagahara[1], Seigo Miyamoto[1], Kunihiro Morishima[2], Toshiyuki Nakano[2], Masato Koyama[3], Yusuke Suzuki[4]

1. Earthquake Research Institute,the University of Tokyo, 2. Nagoya University, 3. Shizuoka University, 4. Izu Peninsula Geopark Promotion Council

In the understanding of the eruption of the volcano, the size and the shape of the volcanic vent close to the crater are important. Generally, the size is several to hundreds of meters, and the shape is not simple cylinder. When we consider the largest vent, we need spatial resolution of several tens of meters to measure the shape of vent.

“Muography” is the technique to observe two-dimensional the inner density structure with high spatial resolution. In previous study, they attempted to reconstruct the three-dimensional (3D) density structure by observing the volcano from multiple directions, but they got three-dimensional density structure with only several hundreds of meters spatial resolution because of a few observation points. To improve the spatial resolution, we are planning “omni-directional muography”, putting ten or more observation points to surround the volcano.

We are planning to demonstrate omni-directional muography at Omuro-yama, located in Shizuoka pref., Japan. We have two reasons that we choose this volcano. First, Omuro-yama is a scoria cone formed by a single eruption, so simple structure is expected and it is easy to obtain significant result. Second, there are no objects around near it. In addition, there are no observation of muography at scoria cone.

We carried out the feasibility check of demonstration observation at Omuro-yama by simulation and test observation by using 3 points muography before full observation. In this simulation, we used a method applying Filtered Back Projection. As a result of simulation, it was found that it is necessary to ensure the minimum S / N ratio for the number of muons observed at each observation point. As a result of test observation, it was found that there was a high density part in the west part of crater rim.

In this publication, we will show the detail of simulation of feasibility check and the result of test observation.

Keywords: volcano, three-dimensional, cosmic-ray, muon

©2019. Japan Geoscience Union. All Right Reserved. 

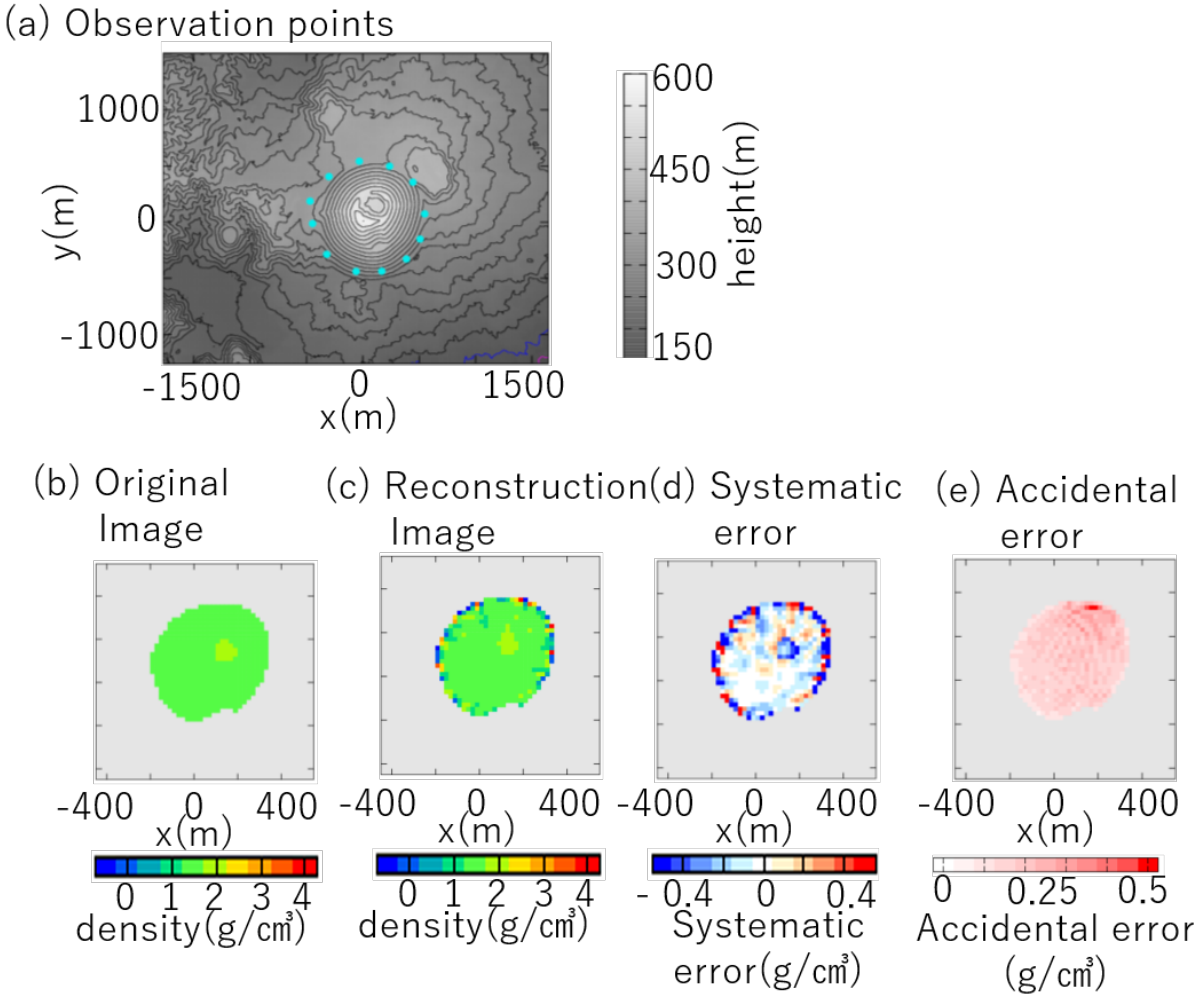


Simulation results when we set 12 observation points and use the detectors which are 0.04㎡ for 90 days. (a) DEM (Digital Elevation Map) near Omuro-yama and observation points (blue dots) in this simulation. (b)-(e) Density structure and error at 490m height in this simulation.

©2019. Japan Geoscience Union. All Right Reserved. 

# Estimation of pressure source occurring volcanic crustal deformation with FEM considering topography

*Shinya Yamada[1], Tomokazu Kobayashi[1]

1. GSI of Japan

In order to grasp the activity of the volcano and evaluate it, it is necessary to grasp the behavior of the magma and the like. When volcanic disasters such as eruption occurred, we estimated the deformation source assuming volume change of the spherical pressure source or opening displacement of the dike using observation results of crustal deformation obtained by GNSS and InSAR . Conventionally, when calculating the crustal deformation, calculation was carried out based on a model assuming a semi-infinite homogeneous elastic body. However, if there is a deformation source especially in the shallow part of the volcano, the influence of the topography cannot be ignored. In recent years, along with the development of the technology of InSAR, crustal movement at the crater and its surroundings can be observed in a planar manner, and detailed analysis has become possible. Therefore, in order to more accurately estimate the deformation source, it is necessary to estimate with the topography added.

Based on this background, we developed a crustal deformation calculation system that incorporates the Finite Element Method (FEM) that divides elastic bodies into minute meshes and calculates displacement for each mesh. As a result, it became possible to analyze taking model topography and underground structure into account. In this study, we compare the deformation source estimated using the FEM with the deformation source estimated by the conventional method. In this presentation, we mainly examined the eruption of Mt.Ontake in Nagano Prefecture in 2014. We detected about 10cm crustal deformation in the crater and its surroundings with InSAR analysis by ALOS-2 satellite on the eruption (Yamada et al., 2014). Based on this observation result, we estimated the deformation source with a model assuming a conventional semi-infinite homogeneous elastic body, and we obtained the result that the almost vertical crack opened 45 cm. However, since the topography of the region where the crustal deformation was observed by this eruption is steep and it is thought that the deformation is also influenced by the topography, in this presentation we report the results of comparison of the conventional estimation and the estimation considering the influence of the topography.

Keywords: FEM, Mt.Ontake, GNSS, InSAR, ALOS-2

©2019. Japan Geoscience Union. All Right Reserved. 

[J] Poster | S (Solid Earth Sciences )：S-VC Volcanology

Thu. May 30, 2019 5:15 PM - 6:30 PM JST | Thu. May 30, 2019 8:15 AM - 9:30 AM UTC | Poster Hall International Exhibition Hall8, Makuhari Messe_24

## [S-VC37] Dynamics of volcanic eruptions and their physical and chemical processes

convener:Yujiro Suzuki(Earthquake Research Institute, The University of Tokyo)

This session discusses the dynamics of volcanic and igneous activities such as magma accumulation, magma ascent in volcanic conduits, and dispersion of volcanic products. In order to understand such multi-scale phenomena, the researches of microscopic and macroscopic scales and the techniques that combine the different scales are required. We aim to discuss the latest approaches based on the recent observations, laboratory experiments and numerical simulations, from the viewpoint of cross-cutting research.

### [SVC37-P01] Geochemical interpretation of Ulleung Island volcanic rocks: Implication for the new magmatic model for plume-slab interaction in East Asia

*Chungwan LIM[1], Dohyun Kim[1] (1.Kongju National University)

### [SVC37-P02] 1D particle model for vertiacal non-uniform bubble coalescence

*Maruishi Takafumi[1] (1.Department of Earth and Planetary Sciences, Faculty of Sciences, Kyushu University)

### [SVC37-P03] The formation process of a 100m thick basaltic lava flow in the Kitamatsuura basalts, northwestern Kyushu

*Ryotaro Araki[1], Tetsuya Sakuyama[1] (1.Osaka City University)

### [SVC37-P04] An introduction to the observation method of imaging volcanoes by using cosmic-ray muons

*Seigo Miyamoto[1] (1.Earth Reasearch Institute, University of Tokyo)

### [SVC37-P05] Simulation and test observation for omni-directional muography at Omuro-yama

*Shogo Nagahara[1], Seigo Miyamoto[1], Kunihiro Morishima[2], Toshiyuki Nakano[2], Masato Koyama[3], Yusuke Suzuki[4] (1.Earthquake Research Institute,the University of Tokyo, 2.Nagoya University, 3.Shizuoka University, 4.Izu Peninsula Geopark Promotion Council)

### [SVC37-P06] Estimation of pressure source occurring volcanic crustal deformation with FEM considering topography

*Shinya Yamada[1], Tomokazu Kobayashi[1] (1.GSI of Japan)

# Geochemical interpretation of Ulleung Island volcanic rocks: Implication for the new magmatic model for plume-slab interaction in East Asia

*Chungwan LIM[1], Dohyun Kim[1]

1. Kongju National University

Ulleung Island has been considered as an intraplate volcanic island located in the East Sea/Japan Sea. The alkaline tephra originated from Ulleung Island has played an important role in understanding of the intraplate alkaline volcanism during the Quaternary. Ulleung Island on volcanism that occurs far from plate margins is abstruse with the current paradigm of plate tectonics. The Ulleung Island volcanic complex is unlikely to result from a mantle plume rising at the base of the mantle.

Ulleung Island is consisted of basaltic lava, agglomerate succession, and trachytic/phonolitic pumiceous tephra. The analyses of chemical compositions of glass shards in Ulleung tephras is necessary to identify each unit. During the Quaternary, at least six pumiceous tephras (UT-1~6) covered the island for this research. Based on the relationships of $SiO_2$, the $Al_2O_3$, $Na_2O$, $K_2O$, and $Fe_2O_3$ contents of the tephras increase as $SiO_2$ increases and decrease MgO as $SiO_2$ increases in Ulleung tephras. The trace elements in tephra show intra-plate type characteristics. Sr-Nd-Pb isotopic data from the literature of volcanic glass shards suggest that the mix in magma source might have involved EM1 and EM2-components of Quaternary tephras from Ulleung Island, South Korea.

This study has two principal objectives: First, multiple Ulleung tephras are expected to detect and identify the Ulleung Island. In order to accurately identify and correlate the tephras, it is necessary to consider stratigraphic position as well as geochemical characteristics. The chemical composition of volcanic glass shards is a useful tool for evaluating mixtures of multiple layers. The heavy mineral composition can also be used to identify tephra units. In order to reveal the distribution of each tephra unit to a high degree of certainty, characteristics such as heavy mineral and chemical compositions of each unit must be determined in greater detail itself. Second, we propose that the anomaly represents lithospheric mantle that had been accompanied by beneath the sinking lithosphere of the Philippine Sea Plate and was erupted through a slab-tear in the subducting slab. We suggest that this subduction-induced upwelling process produces mantle-upwelling that feeds the Ulleung Island volcanoes. Subduction-induced upwelling may also may explain back-arc volcanism at other subduction zones in East Asia.

Keywords: Ulleung Island volcano, intraplate, plume-slab interaction

©2019. Japan Geoscience Union. All Right Reserved. 

# 1D particle model for vertiacal non-uniform bubble coalescence

*Maruishi Takafumi[1]

1. Department of Earth and Planetary Sciences, Faculty of Sciences, Kyushu University

Bubble coalescence deeply affects the dynamics of conduit flow during volcanic eruption.

Previously, the theory assuming nonuniform coalescence has been used.(Macini et al., 2016, etc.). However, in the outgassing process, non-uniform bubble coalescence is considered important in the radial direction and vertical direction of the conduit, the model cannot deal with the coalescence process.

In this study, we construct a simple model that describe a bubble as a particle moving on a one-dimensional line, particle coalesces when particles contact with each other, and calculates the bubble size distribution in a nonuniform coalescence process in the vertical direction.

The particles have a speed corresponding to the size (buoyancy), and the size increases with the altitude and time (expansion / growth). Note that this model is equivalent to the model by Meakin (1989) when bubble growth and advection are not considered. The particles are fed to the lower end of the system at a constant rate (foaming).

Numerical calculation was carried out by broadly controlling the time scale of foaming, rising buoyancy, expansion and growth.

As a result, there was a parameter range where foaming and coalescence are balanced, and it was found that the size distribution shows a dynamic scaling rule regardless of the fluctuation of the radius and number of particles to be supplied.

The relational expression between the expansion and growth exponential law and the vertical scaling index is derived from the conservation law under the assumption that the size distribution is self-similar.

Keywords: bubble coalescence

©2019. Japan Geoscience Union. All Right Reserved. 

# The formation process of a 100m thick basaltic lava flow in the Kitamatsuura basalts, northwestern Kyushu

*Ryotaro Araki[1], Tetsuya Sakuyama[1]

1. Osaka City University

Kita Matsuura basalts cover the Northwest Kyushu Kitamatsuura Peninsula widely and they were the eruption activities of basaltic lavas which were one of the largest in the Cenozoic in Southwest Japan. The volcanic activity of this basaltic rock had erupted sub-alkaline basalt lavas from multiple sources from the late stage of activity, and ended at about 6.5 Ma. There is a mountain composed of basaltic lavas called Senryu Shiradake that was formed at the end of the eruption in the Senryu Area (Matsui et al., 1989; Sakuyama et al., 2009). Although Senryu Shiradake has a specific height of about 100 m, the boundary of the flow unit has not been confirmed (Fukuyama, 1960, 1961; Kurasawa, 1967). The lapilli tuff layers are sandwiched between this basaltic lava and the lower basalt plateau widely cover the upper surface of the lower basalt plateau and are distributed in a narrower area above it (Matsui et al. 1989). It is difficult to think that basaltic lava which are thought to be more robust against weathering and erosion than erosion of the lapilli tuff are selectively eroded, and that valley buried basaltic lava was eroded Selectively, It is unlikely that the mountain body had remained. From this, it can be considered that Senryu Shiradake is a single basaltic lava flow.

The thickness and length of the lava flow forming the volcanoes are systematically varied in general depending on the chemical composition. Basaltic lavas have low viscosity, so the run length of the basaltic lava flows are longer than that of the andesitic and rhyolitic lava flows, and the average thickness is at most about 30 m (Walker et al., 1973). On the other hand, Senryu Shiradake is formed a basaltic lava flow but its height is about 100 m. In this study, we investigated the lava flow that formed the mountain body of Senryu Shiradake from a petrological point of view.

Analysis of whole rock chemical composition of samples taken from Senryu Shiradake was performed by a fluorescent X-ray analyzer. It was confirmed that Senryu Shiradake basaltic lava has $SiO_2$ = 50 to 53 wt%, MgO = 7 to 11 wt%, FeO * / MgO = 0.87 to 1.5, and it is formed of undifferentiated basalt. The phenocrysts are predominant in olivine and contain a small amount of clinopyroxene, orthopyroxene, and the total phenocryst amount was 3 to 15 vol%. There was a correlation between the sampling altitude and the total rock chemical composition. As the height from the foot increased, the total rock SiO2 amount tended to increased and the MgO amount tended to decrease.

First, assuming that only the phenocrysts were crystallized at the time of lava eruption, the viscosity of lava flow was calculated using the model of Pinkerton & Stevenson (1992) for the effect of crystals on magma viscosity and the model of Hui & Zhang (2007) for the influence of the viscosity of melt. Melt composition was estimated using total rock chemical composition, phenocryst mode composition, and mineral composition. We assumed that all the water in the magma was volatilized and the magma temperature at the time of squirting was 1320 K estimated using pyroxene thermometer. the lava flow model used the flow of magma is stopped by solid shell formation by cooling by Griffiths & Fink (1993).

In this study, we investigated the conditions that can explain the thickness and radius of circulation of the basaltic lava of Senryu Shiradake, considering three variables of volume of erupting magma, time change rate of eruption volume and magma temperature. As a result, even if the rate of change of the first eruption amount and the eruption rate were changed, the thickness was only about 20 m at most which did not reproduce 100 m thick lava flow of Senryu Shiradake. Next, the same study as above was carried out assuming that the degree of crystallization at the time of erupting was 50%, but the thickness was about 30 m at most. From this, it is possible that a 100m thick basaltic lava flow was formed by erupting at

©2019. Japan Geoscience Union. All Right Reserved. 

a lower temperature.

Keywords: Kita-matsuura Basalts, lava flow thickness, magma viscosity

©2019. Japan Geoscience Union. All Right Reserved. 

# An introduction to the observation method of imaging volcanoes by using cosmic-ray muons

*Seigo Miyamoto[1]

1. Earth Reasearch Institute, University of Tokyo

The purpose of this presentation is widely to inform a method of exploring the density structure inside a gigantic structure such as a volcano, by using high evergy muons included in cosmic rays. It is considered that there are some reasons for low awareness. For example, the history of this method which is applied to Earth and planetary science is still short, knowledge about "Muon" which is one of "cosmic rays" or "elementary particles" is not known widely. To improve such a situation, we will review the fundamental principles to evaluate the internal density of volcanoes using cosmic-ray muons, past and going-on observation examples of volcanoes, and technological developments stories in this presentation.

Keywords: volcano, cosmic-ray, muon, imaging

©2019. Japan Geoscience Union. All Right Reserved. 

# Simulation and test observation for omni-directional muography at Omuro-yama

*Shogo Nagahara[1], Seigo Miyamoto[1], Kunihiro Morishima[2], Toshiyuki Nakano[2], Masato Koyama[3], Yusuke Suzuki[4]

1. Earthquake Research Institute,the University of Tokyo, 2. Nagoya University, 3. Shizuoka University, 4. Izu Peninsula Geopark Promotion Council

In the understanding of the eruption of the volcano, the size and the shape of the volcanic vent close to the crater are important. Generally, the size is several to hundreds of meters, and the shape is not simple cylinder. When we consider the largest vent, we need spatial resolution of several tens of meters to measure the shape of vent.

“Muography” is the technique to observe two-dimensional the inner density structure with high spatial resolution. In previous study, they attempted to reconstruct the three-dimensional (3D) density structure by observing the volcano from multiple directions, but they got three-dimensional density structure with only several hundreds of meters spatial resolution because of a few observation points. To improve the spatial resolution, we are planning “omni-directional muography”, putting ten or more observation points to surround the volcano.

We are planning to demonstrate omni-directional muography at Omuro-yama, located in Shizuoka pref., Japan. We have two reasons that we choose this volcano. First, Omuro-yama is a scoria cone formed by a single eruption, so simple structure is expected and it is easy to obtain significant result. Second, there are no objects around near it. In addition, there are no observation of muography at scoria cone.

We carried out the feasibility check of demonstration observation at Omuro-yama by simulation and test observation by using 3 points muography before full observation. In this simulation, we used a method applying Filtered Back Projection. As a result of simulation, it was found that it is necessary to ensure the minimum S / N ratio for the number of muons observed at each observation point. As a result of test observation, it was found that there was a high density part in the west part of crater rim.

In this publication, we will show the detail of simulation of feasibility check and the result of test observation.

Keywords: volcano, three-dimensional, cosmic-ray, muon

©2019. Japan Geoscience Union. All Right Reserved. 

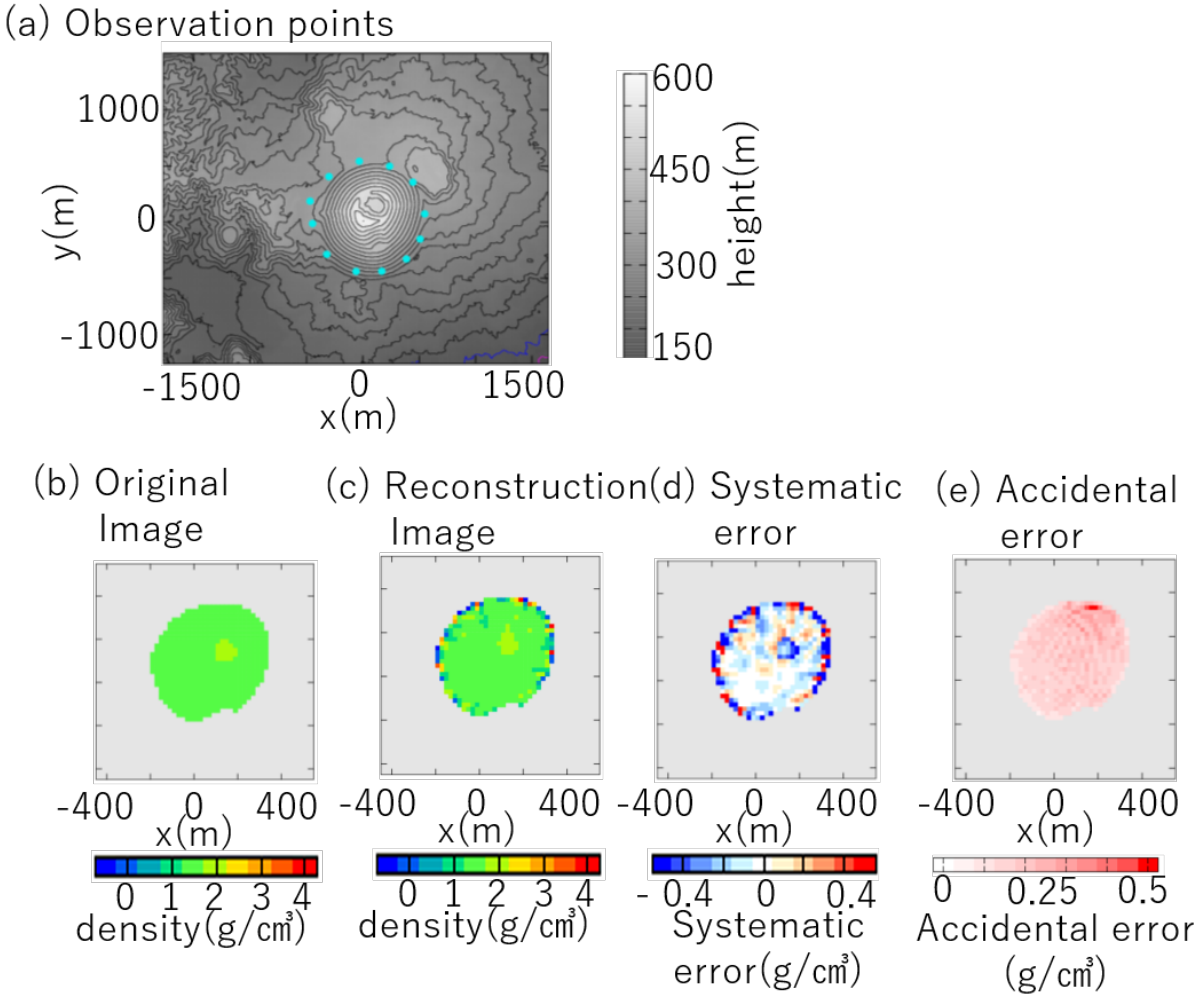


Simulation results when we set 12 observation points and use the detectors which are 0.04㎡ for 90 days. (a) DEM (Digital Elevation Map) near Omuro-yama and observation points (blue dots) in this simulation. (b)-(e) Density structure and error at 490m height in this simulation.

©2019. Japan Geoscience Union. All Right Reserved. 

# Estimation of pressure source occurring volcanic crustal deformation with FEM considering topography

*Shinya Yamada[1], Tomokazu Kobayashi[1]

1. GSI of Japan

In order to grasp the activity of the volcano and evaluate it, it is necessary to grasp the behavior of the magma and the like. When volcanic disasters such as eruption occurred, we estimated the deformation source assuming volume change of the spherical pressure source or opening displacement of the dike using observation results of crustal deformation obtained by GNSS and InSAR . Conventionally, when calculating the crustal deformation, calculation was carried out based on a model assuming a semi-infinite homogeneous elastic body. However, if there is a deformation source especially in the shallow part of the volcano, the influence of the topography cannot be ignored. In recent years, along with the development of the technology of InSAR, crustal movement at the crater and its surroundings can be observed in a planar manner, and detailed analysis has become possible. Therefore, in order to more accurately estimate the deformation source, it is necessary to estimate with the topography added.

Based on this background, we developed a crustal deformation calculation system that incorporates the Finite Element Method (FEM) that divides elastic bodies into minute meshes and calculates displacement for each mesh. As a result, it became possible to analyze taking model topography and underground structure into account. In this study, we compare the deformation source estimated using the FEM with the deformation source estimated by the conventional method. In this presentation, we mainly examined the eruption of Mt.Ontake in Nagano Prefecture in 2014. We detected about 10cm crustal deformation in the crater and its surroundings with InSAR analysis by ALOS-2 satellite on the eruption (Yamada et al., 2014). Based on this observation result, we estimated the deformation source with a model assuming a conventional semi-infinite homogeneous elastic body, and we obtained the result that the almost vertical crack opened 45 cm. However, since the topography of the region where the crustal deformation was observed by this eruption is steep and it is thought that the deformation is also influenced by the topography, in this presentation we report the results of comparison of the conventional estimation and the estimation considering the influence of the topography.

Keywords: FEM, Mt.Ontake, GNSS, InSAR, ALOS-2

©2019. Japan Geoscience Union. All Right Reserved. 

[J] Oral | S (Solid Earth Sciences)：S-VC Volcanology

Thu. May 30, 2019 1:45 PM - 3:15 PM JST | Thu. May 30, 2019 4:45 AM - 6:15 AM UTC | A07 TOKYO BAY MAKUHARI HALL

## [S-VC37] Dynamics of volcanic eruptions and their physical and chemical processes

convener:Yujiro Suzuki(Earthquake Research Institute, The University of Tokyo), Chairperson:Yujiro Suzuki(Earthquake Research Institute, The University of Tokyo), Hiroyuki Shimizu(Earthquake Research Institute, The University of Tokyo)

This session discusses the dynamics of volcanic and igneous activities such as magma accumulation, magma ascent in volcanic conduits, and dispersion of volcanic products. In order to understand such multi-scale phenomena, the researches of microscopic and macroscopic scales and the techniques that combine the different scales are required. We aim to discuss the latest approaches based on the recent observations, laboratory experiments and numerical simulations, from the viewpoint of cross-cutting research.

1:45 PM - 2:00 PM JST | 4:45 AM - 5:00 AM UTC

[SVC37-01] Volcanic activities triggered or inhibited by resonance of volcanic edifices to large earthquakes

*Atsuko Namiki[1], Eleonora Rivalta[2], Heiko Woith[2], Timothy Willey[2], Stefano Parolai[3], Thomas R Walter[2] (1.Graduate School of Integrated Arts and Sciences, Hiroshima University, 2.GFZ, 3.OGS)

2:00 PM - 2:15 PM JST | 5:00 AM - 5:15 AM UTC

[SVC37-02] **Groundmass crystallization experiments of an andesitic pumice under low vapor pressure.**

*Yasukawa Hiroki[1], Mayumi Mujin[1], Michihiko Nakamura[1], Shizuka Otsuki[2] (1.Division of Earth and Planetary Materials Science, Department of Earth Science, Graduate School of Science, Tohoku University., 2.National Institute of Advanced Industrial Science and Technology)

2:15 PM - 2:30 PM JST | 5:15 AM - 5:30 AM UTC

[SVC37-03] Decoding pre-eruptive magma evolution and water behavior from plagioclase phenocrysts: Application to the Hoei eruption of Mt. Fuji

*Tsuyoshi Iizuka[1], Chiyo Harada[1], Kenji Shimizu[2], Takayuki Ushikubo[2], Morihisa Hamada[2], Mitsuhiro Yoshimoto[3] (1.University of Tokyo, 2.JAMSTEC, 3.Mount Fuji Research Institute)

2:30 PM - 2:45 PM JST | 5:30 AM - 5:45 AM UTC

[SVC37-04] Probing magmatic processes just prior to historic eruptions at Sakurajima volcano: Toward understanding “magma pre-charge”

*Naoki Araya[1], Michihiko Nakamura[1], Satoshi Okumura[1] (1.Division of Earth and Planetary Materials Science, Department of Earth Science, Graduate School of Science, Tohoku UniversityUniversity)

2:45 PM - 3:00 PM JST | 5:45 AM - 6:00 AM UTC

[SVC37-05] Magmatic processes prior to the Vulcanian eruptions of Sakurajima volcano: A combined petrologic and geophysical approach

*Sakauchi Nono[2], Michihiko Nakamura[2], ATSUSHI YASUDA[1], Satoshi Okumura[2], Naoki Araya[2], Masato Iguchi[3], Daisuke Miki[3], Nobuo Geshi[4] (1.Earthquake Research Institute, University of Tokyo, 2.Division of Earth and Planetary Materials Science, Department of Earth Science, Graduate School of Science, Tohoku University, 3.Sakurajima Volcano Research Center, Disaster Prevention Research Institute, Kyoto University, 4.Geological Survey of Japan, The National Institute of Advanced Industrial Science and Technology)

3:00 PM - 3:15 PM JST | 6:00 AM - 6:15 AM UTC

[SVC37-06] Cyclic degassing behavior accompanying dome-forming lava effusion at Shinmoedake volcano in the 2018 eruption

★Invited Papers

*Taishi Yamada[1], Hideki Ueda[1], Toshiya Mori[2], Toshikazu Tanada[1] (1.National Research Institute for Earth Science and Disaster Resilience, 2.Geochemical Research Center, Graduate School of Science, The University of Tokyo)

# Volcanic activities triggered or inhibited by resonance of volcanic edifices to large earthquakes

*Atsuko Namiki[1], Eleonora Rivalta[2], Heiko Woith[2], Timothy Willey[2], Stefano Parolai[3], Thomas R Walter[2]

1. Graduate School of Integrated Arts and Sciences, Hiroshima University, 2. GFZ, 3. OGS

The existence of a causal link between large earthquakes and volcanic unrest is widely accepted. Recent observations have also revealed counterintuitive negative responses of volcanoes to large earthquakes, including decreased gas emissions and subsidence in volcanic areas. In order to explore the mechanisms that could simultaneously explain both the positive and negative responses of volcanic activity to earthquakes, we here focus on the role played by topography. In the laboratory, we shook a volcanic edifice analogue, made of gel, previously injected with a buoyant fluid. We find that shaking triggers rapid migration of the buoyant fluid upward, downward, or laterally, depending on the fluid’ s buoyancy and storage depth; bubbly fluids stored at shallow depth ascend, while low-buoyancy fluids descend or migrate laterally. The migration of fluids induced by shaking is two orders of magnitude faster than without shaking. Downward or lateral fluid migration may decrease volcanic gas emissions and cause subsidence as a negative response, while upward migration is consistent both with an increase in volcanic activity and immediate unrest (deformation and seismicity) after large earthquakes. The fluid migration is more efficient when the oscillation frequency is close to the resonance frequency of the edifice. The resonance frequency for a 30-km-wide volcanic mountain range, such as those where subsidence was observed, is ~0.07 Hz. Only large earthquakes are able to cause oscillation at such low frequencies.

Reference:
Namiki et al., Geology (2018) 47 (1): 67-70.

Keywords: Resonance

©2019. Japan Geoscience Union. All Right Reserved. 

# Groundmass crystallization experiments of an andesitic pumice under low vapor pressure.

*Yasukawa Hiroki[1], Mayumi Mujin[1], Michihiko Nakamura[1], Shizuka Otsuki[2]

1. Division of Earth and Planetary Materials Science, Department of Earth Science, Graduate School of Science, Tohoku University., 2. National Institute of Advanced Industrial Science and Technology

Recently, nanoscale crystals (ultrananolite and nanolite) have been found in groundmass glasses of volcanic rocks. These crystals are thought to crystallize at very shallow part of conduit or inside lava dome. It is suggested that nanoscale crystals recorded information about eruption style transition in shallow conduit. In addition, the eruption style is assumed to be change with viscosity increase due to crystallization of nanoscale crystals. Therefore, it is imoprtant to clarify the nucleation and growth condition of nanoscale crystals for understanding volcanic eruption dynamics . Kinetics of nanoscale crystallization is, however, poorly understood compared to that of microlites. In this study, we performed the series of crystallization experiments that simulate dehydration-induced crystallization in shallow conduit and near surface conditions and investigated the crystallization condition of ultrananolite and nanolite.

As a starting material for the experiments, we used almost microlite-free andesitic pumice clasts from the 1914 (Taisho) Plinian eruption of Sakurajima volcano. The water content in the groundmass glass is approximately 0.5 wt.%. The samples were sealed in a silica glass tube and heated instantaneously to temperatures of 800, 900, 930, and 1000˚C for 3 and 30 minutes, and 2, 8 and 32 hours. When the silica glass tube was evaluated and welded shut, vapor pressure produced via degassing of the starting material is calculated to be of 0.07 (Low Vapor Pressure runs: LVPs). The higher vapor pressures were conducted at 2, 4, and 6 MPa by dehydration of brucite powder.

The mineral assemblage of the crystallized nanolite includes magnetite and pyroxene. The crystallization mode of the groundmass crystals is mostly classified into 5 types; 1) homogeneous nucleation of pyroxene in whole the sample and following growth to the size up to nanolite and occasionally microlite, 2) homogeneous nucleation of ultrananolite in whole the sample, 3) homogeneous nucleation of pyroxene and magnetite crystallization in the vicinity of plagioclase, 4) heterogeneous nucleation of pyroxene on the surface of plagioclase phenocrysts and microlites, and 5) heterogeneous crystallization of pyroxene and magnetite on the bubble surface. Appearance of these types was dependent on the experimental conditions. Magnetite nanolite crystallized under relatively high supercooling, i.e. at low $H_2O$ vapor pressure. Pyroxene nanolite crystallized under wide temperature and pressure conditions. Ultrananolite crystallized in all the runs at 800˚C and at LVP. This indicates that ultrananolite appears under high supercooling. These results on nanoscale crystallization can be used to constrain the pressure-temperature-time paths of volcanic pyroclasts in a shallow conduit.

Keywords: nanolite, ultrananolite

©2019. Japan Geoscience Union. All Right Reserved. 

# Decoding pre-eruptive magma evolution and water behavior from plagioclase phenocrysts: Application to the Hoei eruption of Mt. Fuji

*Tsuyoshi Iizuka[1], Chiyo Harada[1], Kenji Shimizu[2], Takayuki Ushikubo[2], Morihisa Hamada[2], Mitsuhiro Yoshimoto[3]

1. University of Tokyo, 2. JAMSTEC, 3. Mount Fuji Research Institute

Explosive eruptions are often accompanied by signs of mixing of felsic and mafic magmas in their eruptive products, suggesting the potential link between explosive eruptions and magma mixing. Yet, the underlying mechanism of such eruptions remains elusive. The key to this debate is understanding pre-eruptive magma evolution including water behavior in the magma and the time lag between the magma mixing and eruption.

Water behavior in pre-eruptive magma has been widely studied using melt-inclusions in phenocrysts. More recently, it has been shown that hydrogen concentration in plagioclase phenocryst can be used as a hygrometer of pre-eruptive magma (Hamada et al., 2013). Furthermore, zoning of hydrogen content in the phenocryst can be used as a high-resolution chronometer, as hydrogen diffusion in plagioclase is sufficiently fast.

Here we report the first study that combines in-situ measurements of the contents of major and trace elements, including hydrogen, in plagioclase phenocrysts using the EPMA, LA-ICP-QMS, and SIMS, respectively. These analyses were carried out on sequential eruptive products of the 1707 Hoei eruption at Mt. Fuji. The Hoei eruption is characterized by its explosivity and wide chemical variation in the eruptive products (e.g., $SiO_2$=50~70 wt%), and the interaction of mafic and felsic magmas has been considered as playing a role in triggering the explosive eruption (Fujii et al., 2002).

We found that the light REE concentrations of plagioclase phenocrysts split in two clusters. These results suggest that there were at least two magma reservoirs underneath Fuji volcano in which magma differentiation had individually proceeded before the Hoei eruption, and also that plagioclase phenocrysts crystallized from these individual magmas were partly mixed before or during the eruption.

Our results further reveal that most melt inclusions have lower water contents than those estimated from hydrogen contents of the host plagioclase phenocrysts and the plagioclase-melt hydrogen partitioning. This suggests that water in melt inclusion could be more easly lost by secondary events than hydrogen in plagioclase phenocryst. Measured hydrogen contents in plagioclase phenocrysts suggest that the early-erupted felsic magma contained water up to 17wt%, whereas the late-erupted mafic magma had lower contents of ~5 wt%. Moreover, the combination of REE and hydrogen contents in the plagioclase phenocrysts (Figure) revealed that the higher water contents, Ce contents, and lower Anorthite contents in the evolved magma can be attributed to fractional crystallization. Moreover, intra-grain chemical variations suggest that rapid crystallization of plagioclase likely driven by decompression accompanied by the exsolution of water occurred in the felsic magma several hours before the explosive eruption. The decompression and water exsolution may result from the convection of the felsic magma caused by the injection of the hot and water-poor mafic magma.

Keywords: plagioclase, hygrometer, magma mixing, explosive eruption, Mt. Fuji

©2019. Japan Geoscience Union. All Right Reserved. 

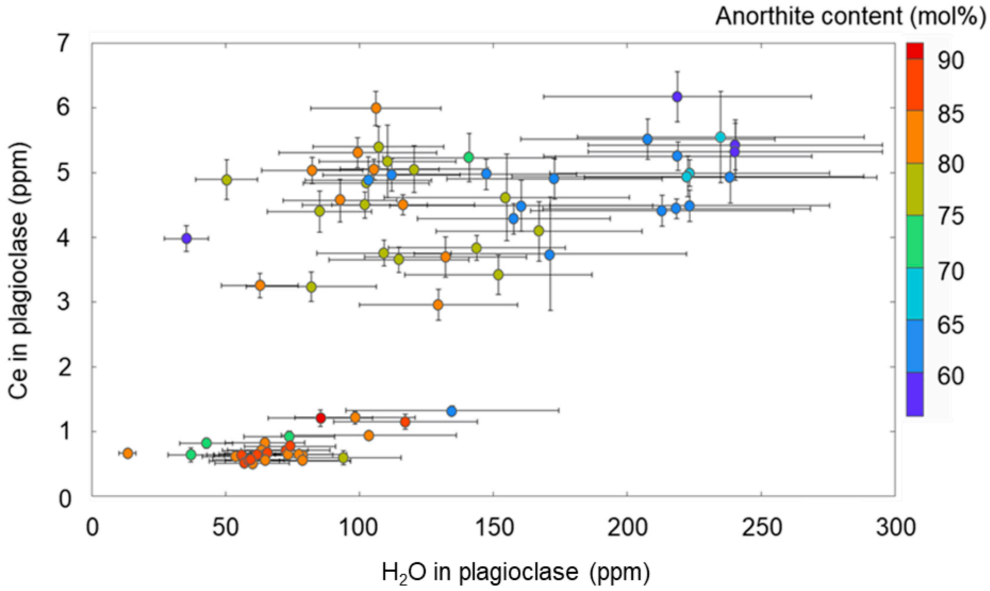


Figure: Cerium versus water contents in plagioclase phenocrysts. The plots are color-coded according to anorthite content. The water contents were calculated from the measured hydrogen concentrations in the phenocrysts.

©2019. Japan Geoscience Union. All Right Reserved. 

# Probing magmatic processes just prior to historic eruptions at Sakurajima volcano: Toward understanding “magma pre-charge”

*Naoki Araya[1], Michihiko Nakamura[1], Satoshi Okumura[1]

1. Division of Earth and Planetary Materials Science, Department of Earth Science, Graduate School of Science, Tohoku UniversityUniversity

Based on the pressure at which volatiles within phenocryst-hosted melt inclusions and plagioclase rims were finally equilibrated, Araya et al. (2019, Scientific Reports) reported that the magma storage depths immediately prior to the historic Plinian eruptions at the Sakurajima volcano (AD 1471, 1779, 1914) were much shallower (0.9–3.2 km) than those of the present magma reservoirs beneath Aira Caldera (~10 km) and Sakurajima (~4–6 km). They proposed that the Plinian eruptions were fed from a thick shallow conduit pre-charged from the magma reservoirs. How this process, “magma pre-charge”, has occurred is poorly understood because the Sakurajima case is the first report. As magma pre-charge is assumed to have occurred at least a few tens of days before each eruption, probing magmatic processes just prior to the eruptions is a key to prepare for the possible future eruption.

Magnetite is a mineral suitable for investigating short-timescale pre-eruptive processes because of its fast element diffusion (i.e., high time resolution) compared to common phenocrystic silicates. We have analysed chemical compositions of more than 300 magnetite phenocrysts in pumices and lavas from the historic eruptions. The magnetite phenocrysts showed scarce zoning in each crystal (mostly within 1 Usp mol%), while their compositional range is wide (e.g., 27–45 Usp mol% for the 1914–1915 eruption). This indicates that the eruptions had initiated from a magma reservoir heterogeneous in at least either temperature, melt composition, or oxygen fugacity, and that this heterogeneity had not been perturbed prior to the eruptions. Therefore, widely accepted models for eruption trigger, such as new magma injection and overturn of stratified magma reservoir are not likely to apply to these historic Plinian eruptions.

Keywords: Sakurajima volcano, magnetite, diffusion

©2019. Japan Geoscience Union. All Right Reserved. 

# Magmatic processes prior to the Vulcanian eruptions of Sakurajima volcano: A combined petrologic and geophysical approach

*Sakauchi Nono[2], Michihiko Nakamura[2], ATSUSHI YASUDA[1], Satoshi Okumura[2], Naoki Araya[2], Masato Iguchi[3], Daisuke Miki[3], Nobuo Geshi[4]

1. Earthquake Research Institute, University of Tokyo, 2. Division of Earth and Planetary Materials Science, Department of Earth Science, Graduate School of Science, Tohoku University, 3. Sakurajima Volcano Research Center, Disaster Prevention Research Institute, Kyoto University, 4. Geological Survey of Japan, The National Institute of Advanced Industrial Science and Technology

We analyzed water contents of phenocryst melt inclusions (= MIs) in the erupted materials of Vulcanian explosions from Sakurajima volcano in a period from October 30, 1975 to February 18, 2015. The 11 typical and characteristic Vulcanian explosions were selected with respect to the seismic and geodetic behaviors prior to the explosions. The water contents of 153 MIs were analyzed with FT-IR micro-reflectance spectroscopy (Yasuda, 2014). We then observed the texture of MIs and analyzed the major chemical element compositions with EMPA.

Most of the MI s have dacitic to rhyolitic compositions. The MIs in lava-type pyroclasts have lower water contents (0–1.9wt.%) than those in the scoria type (0–4.1 wt.%). This is consistent with a general view that the lava-type pyroclasts are derived from degassed and compacted magmas in a very shallow conduit. The MIs with high water contents were quenched and fragmented at deeper parts of the conduit or within short time insufficient for water re-equilibrium with surrounding melt in the shallow conduit.

The MIs in pyroclasts from the Minamidake crater have higher water contents than those from the Showa crater. The average water content of MIs in the samples from the Showa crater is 1.4 wt.%, while that from the Minamidake crater is 0.6 wt.%. This shows that the magma was ejected from the shallower part of conduit or their residence time in the shallow conduit was longer during the activity of the Showa crater, being consistent with the fact that Vulcanian explosions from the Minamidake crater were more vigorous than those from the Showa crater.

The water contents of MIs contained in the pyroclasts erupted on August 24, 1995 from the Minamidake crater were 1.9–4.3 wt.% (2.5 wt.% on average). This range of water contents is similar to those of the three historical Plinian eruptions of Sakurajima (Araya et al., 2019). This indicates that the magma ascended nearly as fast as in the Plinian eruptions, and that magma ascent rate does not solely determine the difference between Vulcanian and Plinian eruptions.

The eruption on August 24, 1995 occurred after approximately 3 months low-activity period. As a precursory phenomenon of the explosion, raid and large intrusion of magma was detected through inflation of the volcanic edifice observed with an extensometer. Five hours after the expansion started (at the time the tiltmeter scaled-out), the eruption began concurrently with the beginning of the BL swarm. In the early stage, the eruption was not accompanied by air shocks, and a fire fountain 100–200 m in height was observed, then later the activity shifted to the Vulcanian explosions with repeated air shocks. The volume of magma intruded prior to the eruption was estimated from the amount of crustal inflation to be more than 5 times as much as that of the average value for the explosions at Minamidake crater. Such a sub-Plinian-like eruption sequence on August 24, 1995 seems to be consistent with the result that the magma ascent rate was close to those of the Plinian eruptions.

©2019. Japan Geoscience Union. All Right Reserved. 

Keywords: Vulcanian explosion, Melt inclusion, Sakurajima volcano

©2019. Japan Geoscience Union. All Right Reserved. 

# Cyclic degassing behavior accompanying dome-forming lava effusion at Shinmoedake volcano in the 2018 eruption

*Taishi Yamada[1], Hideki Ueda[1], Toshiya Mori[2], Toshikazu Tanada[1]

1. National Research Institute for Earth Science and Disaster Resilience, 2. Geochemical Research Center, Graduate School of Science, The University of Tokyo

Shinmoedake volcano, one of the most active volcanoes in the Kirishima complex in Japan, had a series of eruption in 2018. At the beginning of the eruption sequence in March 2018, Shinmoedake had a dome-forming effusive eruption. Observation networks of the National Institute for Earth Science and Disaster Resilience (NIED, V-net), the Japan Meteorological Agency (JMA), and the Geospatial Information Authority of Japan (GSJ, GEONET) around the Kirishima area detected significant ground deformation accompanying the lava effusion. The deformation can be explained by assuming a pressure source located at the same position (7 km NW from Shinmoedake, depth of 10 km) that is adopted to explain syn-eruptive ground deformation in the 2011 eruption (Ueda, 2018, VSJ). The time series of the magma chamber contraction obtained by geodetic observations provides remarkable insight to constrain the macroscopic behavior of the eruption mechanism. Here, we examine characteristics of volcanic earthquake catalogue, seismic, acoustic, tilt, SO2 gas flux measurement, and visual observation data obtained by observation networks of NIED, JMA, and University of Tokyo, to constrain detail aspects of the effusive eruption such as the magma flow regimes inside the conduit.

Hypocenters of low-frequency earthquakes accompanying the lava effusion are distributed almost vertically in the range of 0.1–3.2 km from the surface. Therefore, we assume vertical elongated conduit geometry. Syn-eruptive seismic waveforms record cyclic tremor signals with a peak frequency of about 0.8 Hz, with a duration of 5–20 minutes as well as repose time. The tremor is accompanied with explosive degassing from the crater, which is recorded by infrasound, SO2 gas flux measurement, and visual camera data. Tilt data with a bandpass filter of 250–2000 s show inflation-deflation cycles of the Shinmoedake edifice accompanying the cyclic degassing. Both inflation and deflation of the filtered tilt data correspond to the repose time and amplitude increasing of the tremor.

Some features of the cyclic degassing at Shinmoedake from our data set are summarized as follows: (1) Inflation of the volcano edifice (2) Beginning of degassing and deflation of the volcano edifice (3) End of degassing and repose time until next inflation. Such an inflation-deflation cycle is reported by Takeo et al. (2013) from observation data of lava effusion in the 2011 eruption. Dome-forming lava effusion at Santiaguito also produces such a cyclic degassing and related ground deformation (Johnson et al., 2014). The inflation prior to the degassing may have similar source physics to that related Strombolian and Vulcanian eruptions. Next our challenge is to quantify the source of those signals to estimate the amount of relating gas or magma, and relationship with the time series of the magma chamber contraction.

Acknowledgement: We appreciate the JMA to provide observation data at Kirishima area.

Keywords: Lava dome, Shinmoedake

©2019. Japan Geoscience Union. All Right Reserved. 

[J] Oral | S (Solid Earth Sciences)：S-VC Volcanology

Thu. May 30, 2019 3:30 PM - 5:00 PM JST | Thu. May 30, 2019 6:30 AM - 8:00 AM UTC | A07 TOKYO BAY MAKUHARI HALL

## [S-VC37] Dynamics of volcanic eruptions and their physical and chemical processes

convener:Yujiro Suzuki(Earthquake Research Institute, The University of Tokyo), Chairperson:Yujiro Suzuki(Earthquake Research Institute, The University of Tokyo), Taishi Yamada

This session discusses the dynamics of volcanic and igneous activities such as magma accumulation, magma ascent in volcanic conduits, and dispersion of volcanic products. In order to understand such multi-scale phenomena, the researches of microscopic and macroscopic scales and the techniques that combine the different scales are required. We aim to discuss the latest approaches based on the recent observations, laboratory experiments and numerical simulations, from the viewpoint of cross-cutting research.

3:30 PM - 3:45 PM JST | 6:30 AM - 6:45 AM UTC

[SVC37-07] Estimation of the amplitude of infrasoundsignal based on sound diffraction

*Kyoka Ishii[1], Akihiko Yokoo[1] (1.Graduate School of Science, Kyoto University)

---

3:45 PM - 4:00 PM JST | 6:45 AM - 7:00 AM UTC

[SVC37-08] Mechanism and frequency change of pressure oscillation in the laboratory geyser system

*Noriko Teshima[1], Atsushi Toramaru[2] (1.Department of Earth and Planetary Sciences, Graduate School of Sciences, Kyushu University, 2.Department of Earth and Planetary Sciences, Faculty of Sciences, Kyushu University)

---

4:00 PM - 4:15 PM JST | 7:00 AM - 7:15 AM UTC

[SVC37-09] Effects of temperature on the run-out distance of large-scale pyroclastic density currents: Numerical simulation of a two-layer depth-averaged model

*Hiroyuki A. Shimizu[1], Takehiro Koyaguchi[1], Yujiro J. Suzuki[1] (1.Earthquake Research Institute, The University of Tokyo)

---

4:15 PM - 4:30 PM JST | 7:15 AM - 7:30 AM UTC

[SVC37-10] **Total grain-size distribution of pumice fallout deposits (Kj-P1) from 54 ka plinian eruption at Kuju Volcano**

*Tomohiro Tsuji[1], Kishimoto Hiroshi[2], Fujita Kouji[2], Chisato Nakamura[3], Nagata Tomohiro[3], Kimura Kazunari[3], Michiharu Ikeda[1], Naoki Nishizaka[4], Kozo Onishi[4] (1.Shikoku Research Institute Inc., 2.Asia Air Survey Co. Ltd., 3.Naiba, 4.Shikoku Electric Power Co. Inc.)

---

4:30 PM - 4:45 PM JST | 7:30 AM - 7:45 AM UTC

[SVC37-11] Estimating ashfall volumes for the 2018 Shinmoedake eruptions using the Ellipse Approximated Isopach (EAI) method - How to quantify ashfall volumes from limited ashfall observation locations

*Yasuhisa Tajima[1], Setsuya Nakada[2], Masashi NAGAI[2], Fukashi Maeno[3], Jun Oikawa[3], Teruki Oikawa[4], Yasuo Miyabuchi[5], Toshiaki Hasenaka[5], Masataka Kawaguchi[5] (1.NIPPON KOEI CO.,LTD., 2.NIED, 3.ERI, the Univ. Tokyo, 4.Geological Survey of Japan, AIST, 5.Kumamoto Univ.)

---

4:45 PM - 5:00 PM JST | 7:45 AM - 8:00 AM UTC

[SVC37-12] Optical disdrometer measurement of tephra fall: Constraints on radar parameters for eruption cloud observations

★Invited Papers

*Tomofumi Kozono[1], Masato Iguchi[2], Takahiro Miwa[3], Masayuki Maki[4], Takeshi Maesaka[3], Daisuke Miki[2], Takeshi Nishimura[1] (1.Department of Geophysics, Graduate School of Science, Tohoku University, 2.Sakurajima Volcano Research Center, Disaster Prevention Research Institute, Kyoto University,

3.National Research Institute for Earth Science and Disaster Resilience, 4.Research and Education Center for Natural Hazards, Kagoshima University)

# Estimation of the amplitude of infrasoundsignal based on sound diffraction

*Kyoka Ishii[1], Akihiko Yokoo[1]

1. Graduate School of Science, Kyoto University

Observation of infrasound signals generated from volcano eruptions provides us with important information directly reflecting explosion processes at the source. How to determine the locations of stations for acquiring clear signals has been one of the most fundamental problems for researchers. The best way to solve this problem should be a numerical simulation of infrasound wave propagation considering the propagation effect of topography (e.g., Kim & Lees, 2011; Lacanna & Ripepe, 2013). However, we have to take time and cost money to perform numerical simulations. In this study, we attempt to estimate the amplitude of infrasound signal by an easier method applying the sound diffraction theory. We replaced the cross-section of topography from the source to the station by an equivalent single screen and calculated the attenuation of the amplitude due to diffraction by the thin screen based on Macdonald's exact solution (1915). Then, our results were compared with the calculated amplitudes from 3D-FDTD simulation (Kim et al., 2015) and the observed amplitudes of 31 explosive events occurring at Showa crater, Sakurajima in September 2017. For comparison, the amplitude value was converted to the amplitude ratio with respect to the amplitude of the KUR station in the line-of-sight with the source. As a result, the amplitude ratios estimated by our method were determined at an accuracy of ±30% of the amplitude from the FDTD simulation at all stations. The amplitude ratio of our method was included in the range of the observed amplitude ratio at five stations. On the other hand, at one station, where the azimuth and distance from the source is almost similar to those of the KUR station, observation results cannot agree with the result of our method. This discrepancy suggests that the infrasound signal is affected by other effects than diffraction, such as reflection at the ground, and further study is required in the future.

Keywords: infrasound , diffraction, FDTD simulation

©2019. Japan Geoscience Union. All Right Reserved. 

# Mechanism and frequency change of pressure oscillation in the laboratory geyser system

*Noriko Teshima[1], Atsushi Toramaru[2]

1. Department of Earth and Planetary Sciences, Graduate School of Sciences, Kyushu University, 2. Department of Earth and Planetary Sciences, Faculty of Sciences, Kyushu University

Geysers are hydrothermal activities seen in volcanic areas, which have the similarities with volcanos in seismicity. It is known that the pressure pulses occurring inside geyser's conduit excite tremors, but the source and mechanism of the pressure pulses are still unclear. Because phenomena of natural geysers are complex due to additional factors such as the influence of atmospheric conditions, and because their interiors are hardly observed directly, simplified laboratory experiments which allow us to directly observe what are happening in the interior may be useful. In this study, we tried to reveal the mechanism of the pressure oscillation and factors controlling its dominant frequency using our fluid oscillation model and pressure and temperature data measured in our laboratory experiments.

We designed an experimental setup which reproduces cyclic eruptions of natural geysers. The setup mainly consisted of a flask and a glass tube, which correspond to natural hot water chamber and conduit, respectively. Heating the flask by the hotplate, we measured pressure and temperature in the flask, and erupted mass of each eruption. We also took video images of flask interior and water surface in the conduit with normal-speed and high-speed video cameras. From the movies of the water surface, we digitalized the vertical water column movement in the conduit using a video analysis software. We examined the effects of experimental conditions on characteristics of pressure oscillation by varying three geometric parameters of the experimental system: (i) inner flask volume, (ii) initial water level in the conduit, and (iii) cross-sectional area of the conduit.

In interpreting experimental results, we used the model proposed by Toramaru et al. (Volcanological Society of Japan 2010 Fall Meeting), in which the frequency of pressure oscillation is represented in terms of geometric parameters of the experimental system and the effective bulk modulus K* of fluid in the flask. In our experiments, it was difficult to determine correctly the effective bulk modulus K* from the movie analysis or another measurement, so we calculated the values of K* using a model to relate the pressure variation in the flask $\Delta P$ and water level in the conduit $\Delta L$, by $AK^*/Vo = \Delta P/\Delta L$, where, A is cross-sectional area of glass tube, Vo is inner flask volume, respectively. The values other than K* were obtained from our experimental measurements. From these expressions, we calculated theoretical values of the resonance frequency and compared it with the measured values of dominant frequency of pressure oscillation.

The results showed that the measured pressure oscillation in the flask consisted of high-frequency pulses and subsequent low-frequency damped oscillation. The damped pressure oscillation had a strong inverse correlation with vertical water column movement in the conduit. From the observation of video images synchronized with pressure record, we found that the bubble formations in the flask bottom caused the pressure pulses. From an eruption to the next eruption, the dominant frequency of pressure oscillation decreased systematically. This monotonic decrease in the dominant frequency was explained by the reduction of K*, as a result of increase in the gas volume in the flask by heating. We found that the dominant frequency of pressure oscillation varied depending on experimental conditions. The variations in temporal behavior of dominant frequency could be interpreted by differences in the setting of

©2019. Japan Geoscience Union. All Right Reserved. 

geometric parameters and in the initial values of K* just after eruptions due to various erupted masses of the preceding eruptions.

In conclusion, the pressure oscillation in the experimental geyser system is caused by bubble formations in the flask and vertical water column movement in the conduit. The dominant frequency of pressure oscillation is controlled by the geometric parameters of the experimental system and the erupted mass of the preceding eruption.

Keywords: Laboratory experiment, Geyser, Pressure oscillation, Fluid oscillation, Frequency change

©2019. Japan Geoscience Union. All Right Reserved. 

# Effects of temperature on the run-out distance of large-scale pyroclastic density currents: Numerical simulation of a two-layer depth-averaged model

*Hiroyuki A. Shimizu[1], Takehiro Koyaguchi[1], Yujiro J. Suzuki[1]

1. Earthquake Research Institute, The University of Tokyo

During large-scale explosive volcanic eruptions, a mixture of volcanic particles and gas is continuously ejected from the volcanic vent and can flow along the ground surface as a pyroclastic density current (PDC). Understanding the relationship between the run-out distance of PDC (i.e., the extent of PDC deposits) and the eruption conditions (e.g., the magma discharge rate and the temperature of erupted mixture) is desired to mitigate volcanic hazard associated with explosive eruptions. This study aims to clarify the effect of temperature on the run-out distance of large-scale PDCs on the basis of numerical simulations. The effect of temperature is a key issue, because it closely relates to the eruption style; the temperature ranges from less than 500 K for phreatomagmatic eruptions to more than 1000 K for magmatic eruptions.

Generally, the run-out distance of PDC is affected by the vertical stratification of particle concentration in PDC; it is determined by lift-off of the upper dilute part (particle concentrations < 1 vol.%) or deposition of the lower dense part (~ 10—50 vol.%). To reproduce the run-out distance of a density current with a strong density stratification, we have developed a new two-layer depth-averaged model. In order to evaluate the effects of temperature on the PDC dynamics, our model considers entrainment of ambient air into the upper dilute current, and thermal expansion of the entrained air. We assumed that a homogeneous dilute current is steadily supplied during time > 0 from the source vent on a horizontal ground surface. We performed a parametric study for various temperatures of the dilute current at the source (400—1200 K).

The numerical results show that, as a dilute current spreads radially from the source, the current density decreases through particle settling, air entrainment, and thermal expansion of the entrained air. When the frontal region of the dilute current becomes lighter than the ambient air to reverse buoyancy and lift off, the dilute current stops forward propagation and converges to a steady state (the distance between whose front position and the source position is referred to as $r_{\infty U}$). Particles settling from the base of the dilute current form a thin dense current, which also spreads radially. As the radial mass flux of the dense current at the front balances the basal deposition rate, the dense current stops forward propagation and converges to a steady state (the distance between whose front position and the source position is referred to as $r_{\infty L}$). The result of the parametric study shows that the relative magnitude between $r_{\infty U}$ and $r_{\infty L}$ depends on the temperature: $r_{\infty U}$ is shorter than $r_{\infty L}$ in high-temperature cases (> 600 K) whereas $r_{\infty U}$ is longer than $r_{\infty L}$ in low-temperature cases (< 600 K). This variation comes from the fact that the lift-off distance of the dilute current (i.e., $r_{\infty U}$) significantly increases as the temperature decreases, because thermal expansion of entrained air is suppressed with the decreasing temperature. The results of the low-temperature cases (i.e., $r_{\infty U} > r_{\infty L}$) explain the observation that stratified surge deposits originated from dilute PDCs are widely observed in the deposits of phreatomagmatic eruptions.

Keywords: Pyroclastic density current, Two-layer model, Run-out distance, Temperature of erupted material, Magmatic eruption, Phreatomagmatic eruption

©2019. Japan Geoscience Union. All Right Reserved. 

©2019. Japan Geoscience Union. All Right Reserved. 

# Total grain-size distribution of pumice fallout deposits (Kj-P1) from 54 ka plinian eruption at Kuju Volcano

*Tomohiro Tsuji[1], Kishimoto Hiroshi[2], Fujita Kouji[2], Chisato Nakamura[3], Nagata Tomohiro[3], Kimura Kazunari[3], Michiharu Ikeda[1], Naoki Nishizaka[4], Kozo Onishi[4]

1. Shikoku Research Institute Inc., 2. Asia Air Survey Co. Ltd., 3. Naiba, 4. Shikoku Electric Power Co. Inc.

Constraining physical parameters (e.g. Total grain-size distribution; TGSD) of tephra dispersion and deposition from explosive volcanic eruptions have been studied using observation and analyses of deposits of recent eruptions. However, TGSD of old tephra deposit is a significant challenge and has been rarely studied, because of the difficulty of measuring grain size of altered pumice particles and lack of observation. In this study, to estimate TGSD of VEI5 dacitic plinian explosive eruption occurred at 54 ka at Kuju volcano, we conducted geological survey and grain size analyses for the Kj-P1 pumice fall deposit.

Based on grain-size distribution, maximum pumice size and components, Kj-P1 pumice fall deposit is divided into finer lower and coarser upper layer. We analyzed each grain-size distribution for the lower and upper layers.

Generally, sieving and laser-diffraction analysis have been used for measuring grain-size of tephra and we also used these methods. However, because the upper layer of Kj-P1 has been altered and lumped, it can be hardly separated. In addition, because the altered pumice particle could be broken into finer particles under water, we cannot measure accurate grain sizes. Then, we challenged a new method, image analysis, outlining pumice particles on photographs of outcrops and measure the sizes and area ratio of each pumice particles. We combined the results of the image analyses, sieving and laser-diffraction analyses at 15 and 20 localities for the lower and the upper layers. Using volonoi distribution, Md phi and sigma phi are calculated to be -1.5 and 2.5 for the upper layer and 0.5 and 2.6 for the lower layer. The result fit the observation of altered pumice particles at the outcrops better than the result without the image analyses. To verify this method, analytical methods such as numerical simulation are needed.

Keywords: grain size distribution, Kuju Volcano, plinian eruption, pumice fall deposit

©2019. Japan Geoscience Union. All Right Reserved. 

# Estimating ashfall volumes for the 2018 Shinmoedake eruptions using the Ellipse Approximated Isopach (EAI) method - How to quantify ashfall volumes from limited ashfall observation locations

*Yasuhisa Tajima[1], Setsuya Nakada[2], Masashi NAGAI[2], Fukashi Maeno[3], Jun Oikawa[3], Teruki Oikawa[4], Yasuo Miyabuchi[5], Toshiaki Hasenaka[5], Masataka Kawaguchi[5]

1. NIPPON KOEI CO.,LTD., 2. NIED, 3. ERI, the Univ. Tokyo, 4. Geological Survey of Japan, AIST, 5. Kumamoto Univ.

A volcanic ash eruption began on March 3, 2018 at the Shinmoedake Volcano, in the Kirishima Volcanoes Group. Eruption activity increased to March 5, and lava flow was observed on March 6. Eruptions continued until June 27. We observed volcanic ashfall amounts around the Shinmoedake Volcano and analyzed volcanic ashfall volumes for each eruption using the EAI method (EAI ashfall volume) proposed by Tajima et al. (2013). The EAI method can be used in four different ways. Firstly, ashfall volume is estimated based on one ashfall deposit data point. Second, the estimation is undertaken using two ashfall deposit data points. Third, the estimation is based on three ashfall deposit data points. Fourth, the estimation is based over four ashfall deposit data points.

Tajima et al. (2013) suggest that if an accurate calculation axis and an accurate aspect ratio of a distribution are determined, we can calculate the total volume of ashfall deposit using the EAI method using only one ashfall deposit data point. The calculation axis for the ellipse must be accurate, but it is difficult to determine an accurate calculation axis from the observation. Tajima et al. (2013) determined the lower threshold of detectable ashfall as 0.1 $g/m^2$ for an eruption of the Sakurajima Volcano. This lower threshold of detectable ashfall value is used in this calculation. The EAI method is used based on one data point calculation, and we have taken a suitable aspect ratio of the ellipse which is fitted between the EAI isopach from 0.1 $g/m^2$ and a limit location of detectable ashfall. We calculated ashfall deposit volumes for the period of eruption from 11 am on March 1 to 7 am on March 2.

Next, we demonstrate a calculation using two data points. Tajima et al. (2013) suggest, if an accurate axis of the ellipse distribution is determined, we can calculate an EAI ashfall volume of the deposit using two ashfall data points. In this case, we would need a limit location of a detectable ashfall deposit, because it is difficult to determine an accurate calculation axis. In this case we select two ashfall deposit data points for the EAI calculation, then we determine a suitable axis which is fitted between the EAI isopach as 0.1 $g/m^2$ and a limit location of visible ashfall. In this way, we estimated the EAI ashfall volume of the eruption at 15:58 pm on March 9. For comparison, we observed a limit location of visible ashfall on a car.

We show a calculation procedure for three ashfall deposit data points. This is a normal calculation case shown by Tajima et al (2013). We select two ashfall deposit data values for the EAI calculation, and determine a suitable axis to fit the observation points and the calculated distribution. However, sometimes it is take the over or under estimated volume from the calculation, because estimation of EAI ashfall volume can be influenced by environmental variables, such as wind direction changes, depositional conditions of ash-fall, and other research conditions. Lastly, we demonstrate the estimation of ashfall deposit volumes using four ashfall deposit data points. In this case, we select two ash-fall values for the EAI calculation. We determined a suitable axis which best fits the observation points and the calculated distribution. Using four ashfall deposit data points improves accuracy.

©2019. Japan Geoscience Union. All Right Reserved. 

It is determined the EAI ashfall volumes of over 10 eruptions of the 2018 Shinmoedake eruptions. We assume that the eruption rate of each volumes per an hour increased before the lava flow producing. We will discuss the accuracy of the EAI method and the practical applications of this method.

Keywords: Shinmoedake, ash fall, EAI

©2019. Japan Geoscience Union. All Right Reserved. 

# Optical disdrometer measurement of tephra fall: Constraints on radar parameters for eruption cloud observations

*Tomofumi Kozono[1], Masato Iguchi[2], Takahiro Miwa[3], Masayuki Maki[4], Takeshi Maesaka[3], Daisuke Miki[2], Takeshi Nishimura[1]

1. Department of Geophysics, Graduate School of Science, Tohoku University, 2. Sakurajima Volcano Research Center, Disaster Prevention Research Institute, Kyoto University, 3. National Research Institute for Earth Science and Disaster Resilience, 4. Research and Education Center for Natural Hazards, Kagoshima University

A tephra fallout process during a volcanic eruption has mainly been investigated by geological method such as based on measurement of mass and grain size distribution on tephra deposits. Recently, a combination of the tephra fallout deposit data with numerical simulations of tephra dispersal and fallout contributes to understanding the detail of the eruption dynamics. In order to further promote the combination between the simulations and the observations, we need multi-parameter observations of the eruptive phenomena with high-time resolution which is comparable with the timescale of the eruption. One of the methods for the high-resolution observations is to apply techniques already used in other fields, such as precipitation measurements by weather radar and disdrometer in meteorology. In this study, we investigated the main characteristics of tephra fall from the eruptions at Sakurajima volcano in southern Kyushu, Japan by using a laser based optical disdrometer, Parsivel.

The disdrometer measurements were carried out for two years at one station located 2.5 km south of Showa crater of Sakurajima volcano, and made it possible to detect 76 tephra fall events, in which particle size and fall velocity were simultaneously measured with one-minute sampling interval. We found that the tephra fall can be easily distinguished from precipitation because of a notable feature of the tephra fall that both the particle size and the fall velocity gradually decrease with time during each event. The detected events were compared with the information about the direction of eruption cloud which is reported in eruption list by JMA, and it was found that the detection rate of the tephra fall during the eruptions with south-directed eruption cloud is about 7 times higher than that with other directions. Furthermore, the feature of the temporal changes in the size and the velocity was also most obvious in the case of south-directed eruption cloud. These indicate that the disdrometer can successfully measure the tephra fall directly reaching from the crater location to the station, and that the disdrometer measurements at multiple stations covering all directions may provide valuable information about the tephra dispersion and eruption cloud dynamics.

By using the tephra fall events, we obtained a quantitative relationship between the particle size and fall velocity. The cumulative weight of the tephra fall during one event was also measured by digital electric scale set close to the disdrometer, which enabled us to calculate the density of the particles. On the basis of the size-velocity relationship and the particle density data, we can estimate morphological parameters of volcanic particles in models of terminal fall velocity in previous studies. Furthermore, the tephra size and fall velocity data enabled us to calculate a particle size distribution per unit volume and size class, and we found that this distribution is well explained by exponential distribution. In the case of precipitation, the value of exponent is modeled as a function of the amount of rain fall. When we estimate the exponent as a function of the amount of the tephra fall using the same manner as precipitation, it was found that the exponent is smaller than that for precipitation. Because the size-velocity relationship and the particle size distribution are important parameters for radar analysis, the formulation and parametrization for its relationship and distribution in this study can be utilized for eruption cloud observations by weather radar.

©2019. Japan Geoscience Union. All Right Reserved. 

Keywords: Tephra size , Tephra fall velocity, Parsivel, Particle size distribution, Vulcanian eruption

©2019. Japan Geoscience Union. All Right Reserved. 

[J] Oral | S (Solid Earth Sciences)：S-TT Technology & Techniques

Thu. May 30, 2019 10:45 AM - 12:15 PM JST | Thu. May 30, 2019 1:45 AM - 3:15 AM UTC | A11 TOKYO BAY MAKUHARI HALL

## [S-TT43] seismic monitoring and processing system

convener:Takahiro Maeda(National Research Institute for Earth Science and Disaster Resilience), Chairperson:Masanao Shinohara(Earthquake Research Institute, The University of Tokyo)

This session covers scientific and technical issues in seismic monitoring or data processing systems for earthquakes or explosions observation. This includes development or improvement of seismic observation networks, innovative techniques in observation and monitoring, cutting-edge data acquisition and processing techniques in geophysical explorations. Other topics related to geophysical observation are also welcome.

10:45 AM - 11:00 AM JST | 1:45 AM - 2:00 AM UTC

### [STT43-01] Summary and Considerations about Characteristics of Borehole Stress Meter for Continuous Observation

*Hiroshi Ishii[1], Yasuhiro Asai[1] (1.Tono Research Institute of Earthquake Science, Association for the Development of Earthquake Prediction)

11:00 AM - 11:15 AM JST | 2:00 AM - 2:15 AM UTC

### [STT43-02] Seismic monitoring by an autonomous robotic float equipped with a hydrophone: MERMAID

*Masayuki Obayashi[1], Hiroko Sugioka[2] (1.Japan Agency for Marine-Earth Science and Technology, 2.Department of Planetology, Kobe University)

11:15 AM - 11:30 AM JST | 2:15 AM - 2:30 AM UTC

### [STT43-03] Earthquake observation in a borehole over 250 °C using high temperature optical fiber and DAS technology

*Tsunehisa KIMURA[1] (1.Schlumberger)

11:30 AM - 11:45 AM JST | 2:30 AM - 2:45 AM UTC

### [STT43-04] Distributed Acoustic Sensing measurement by using seafloor optical fiber cable system off Sanriku for dense seismic observation

*Masanao Shinohara[1], Tomoaki Yamada[1], Takeshi Akuhara[1], Kimihiro Mochizuki[1], Takeo Kasajima[2], Takahiro Arioka[2], Masayuki Hamakawa[3], Shunsuke Kubota[4] (1.Earthquake Research Institute, University of Tokyo, 2.Fujitsu Laboratories Ltd., 3.Fujitsu Limited, 4.YK Giken Co., Ltd.)

11:45 AM - 12:00 PM JST | 2:45 AM - 3:00 AM UTC

Discussion

12:00 PM - 12:15 PM JST | 3:00 AM - 3:15 AM UTC

Discussion

# Summary and Considerations about Characteristics of Borehole Stress Meter for Continuous Observation

*Hiroshi Ishii[1], Yasuhiro Asai[1]

1. Tono Research Institute of Earthquake Science, Association for the Development of Earthquake Prediction

Summary and Considerations about Borehole Stress Meter for Continuous Observation

We will explain the following items
1. Stress Meter can Observe both Stress and Strain
2. Stress unlike Strain can be Derived without Knowing an Elastic Constant
3. Why is Observed Elastic Invariants Similar with Vertical Component ?
4. How High Resolution Does a Stress Meter Have ?
5.How Wide Observation Range Does a Stress Meter Have ?

Keywords: Borehole Stress Meter for Continuous Observation, Observation of both Stress and Strain, Wide Observation Range, Similarity of Elastic Invariants and Vertical Component , High Resolution

©2019. Japan Geoscience Union. All Right Reserved. 

# Seismic monitoring by an autonomous robotic float equipped with a hydrophone: MERMAID

*Masayuki Obayashi[1], Hiroko Sugioka[2]

1. Japan Agency for Marine-Earth Science and Technology, 2. Department of Planetology, Kobe University

Seismic monitoring in the oceans has been limited to rather localized experiments such as ocean bottom seismometers (OBSs) and moored hydrophones. Because about 70% of the Earth is covered by water, advances in seismic monitoring depend on the development of radically new instruments, capable of providing seismic data all over the ocean. Recently a new instrument, named MERMAID (Mobile Earthquake Recording in Marine Areas by Independent Divers), was developed to measure acoustic signals converted from seismic waves at the seafloor. The MERMAID is an autonomous robotic float equipped with a hydrophone and drifts passively at 1,500 −2,000 m depth until an earthquake signal is detected. If this is identified as a strong P wave, the MERMAID ascends at speed of 10 cm/s for transmission of the recorded waveform within time window of a hundred seconds before and after the P wave arrival as well as its global positioning system coordinates at the surface. After transmitting the data via satellite links, the MERMAID descends at speed of 5 cm/s to monitor earthquake signals at 1,500 −2,000 m depth again. Therefore we are able to obtain seismograms from the ocean in quasi-real time. Under an international project collaborated among Japan, France, United States and China, we planed to deploy more than 40 drifting buoys with hydrophone to image the detail of the South Pacific mantle plume that is one of two huge mantle plumes from the base of the mantle. As part of this project, we deployed drifting floats in the South Pacific during the 1st leg of MR18-06 cruise. We will show the obtained seismograms and discuss their quality.

Keywords: seismic monitoring in the ocean, underwater acoustic wave, float, hydrophone

©2019. Japan Geoscience Union. All Right Reserved. 

# Earthquake observation in a borehole over 250 ˚C using high temperature optical fiber and DAS technology

*Tsunehisa KIMURA[1]

1. Schlumberger

DAS (Distributed Acoustic Sensing) technology has been used to meet the demands of pipeline monitoring and intrusion detection in Oil & Gas business since 2011. The latest optical fiber sensing technology using differential phase data called “hDVS” (heterodyne Distributed Vibration Sensing), now enables DAS to record seismic signal including VSP (Vertical Seismic Profiling)[1)]. Three-dimensional imaging can also be performed by a 3DVSP method[2)]. We have introduced the observation of natural earthquakes and waves, targeting the tsunami detection, using the hDVS device at recent meetings of JpGU and the seismological society of Japan (SSJ)[3)].

Late 2018, we conducted an experiment of natural earthquake observation using the hDVS system at the geothermal well in Japan. A high temperature optical fiber logging cable with 300 ˚C rating was run in a deviated well having a maximum depth of about 1,600 m and connected the third generation hDVS acquisition system to the optical fiber (single mode fiber) and recorded natural earthquake events for 5 days. The maximum temperature recorded at a depth of about 900 m was more than 250 ˚C. Under such a high temperature environment, almost all electronic, electric and magnetic sensors including seismometers cannot operate for a long time. Even with the use of DAS equipment, there is no precedent as far as I know, at least it is the first attempt in Japan.

A weight of 2 m length and 25 kg weight was attached to the high temperature optical fiber logging cable, and the observation was started by lowering the weight to the depth of 977 m inside the casing in order to avoid the weight becoming stuck in the open hole section of the well. With continuous recording with 60 seconds as one file, data of 975 m section from the surface was recorded for 5 days. In this paper, we report on the result of verifying how much observation of natural earthquake waves can be performed by using continuous measurement data.

During the observation period, we succeeded in capturing six natural earthquake events. Two of them were medium-scale earthquakes published in the earthquake information of the Japan Meteorological Agency (JMA). An example of this was recorded as follows.

**(21st of November, 2018 04:09:49.9 Latitude 30˚24.0'N Longitude 130˚9.0'E 123km depth M5.2)**

Earthquake data recorded by hDVS is shown in Fig. 1.

The arrival time of the P-wave analyzed from the waveform is 4:10:12.2 JST on 21st of November at the deepest part of the borehole and 4:10:12.5 JST near surface. Measurement parameters were gauge length 4 m, spatial sampling 1 m, and sampling period 1 msec. We also conducted reprocessing to change the gauge length and confirmed that data with higher S/N can be obtained. Reprocessing the raw data for an optimized gauge length is a capability that is unique to hDVS amongst the available DAS techniques.

We also compared it with continuous seismometer records by NIED (Hi-net). The nearest Hi-net station

©2019. Japan Geoscience Union. All Right Reserved. 

from the wellsite (just about 4km away), is compared with the recorded hDVS data, and it was found that they match well. For small earthquake events, S/N was higher in the measurement data of hDVS in some cases, which will be shown during the presentation.

It was confirmed that hDVS/DAS system can be used to monitor natural earthquake events while monitoring the reservoir or other purpose under very high-temperature condition such as geothermal well or very deep well that reaches a mantle, if the condition of the optical fiber is good.

Acknowledgements: JMA and NIRD data are used as a reference earthquake data for comparison. We thank these organizations.

References:

1) Kimura, T., Lees, G., and Hartog, A., Optical Fiber Vertical Seismic Profile using DAS Technology, JpGU 2016 (RAEG 2016, STT17-12) Extended Abstract.

2) Kimura, T. et al, Hybrid 3D VSP Using Fiber-Optic Technology and a Conventional Borehole Seismic Array Tool, EAGE Copenhagen 2018 (Th H 10) Extended Abstract.

3) Kimura, T., Kobayashi, Y., Naruse, R., and Xue, Z., Earthquake events monitoring in a well using Optical Fiber and DAS Technology, JpGU 2018 (STT50-04), Kimura, T., Summary of Earthquake Events Recorded in Japan using DAS Technology, and Future Vision, SSJ 2018 (S02-P12).

Keywords: DAS, hDVS, optical fiber, high temperature, seismic monitoring, earthquake

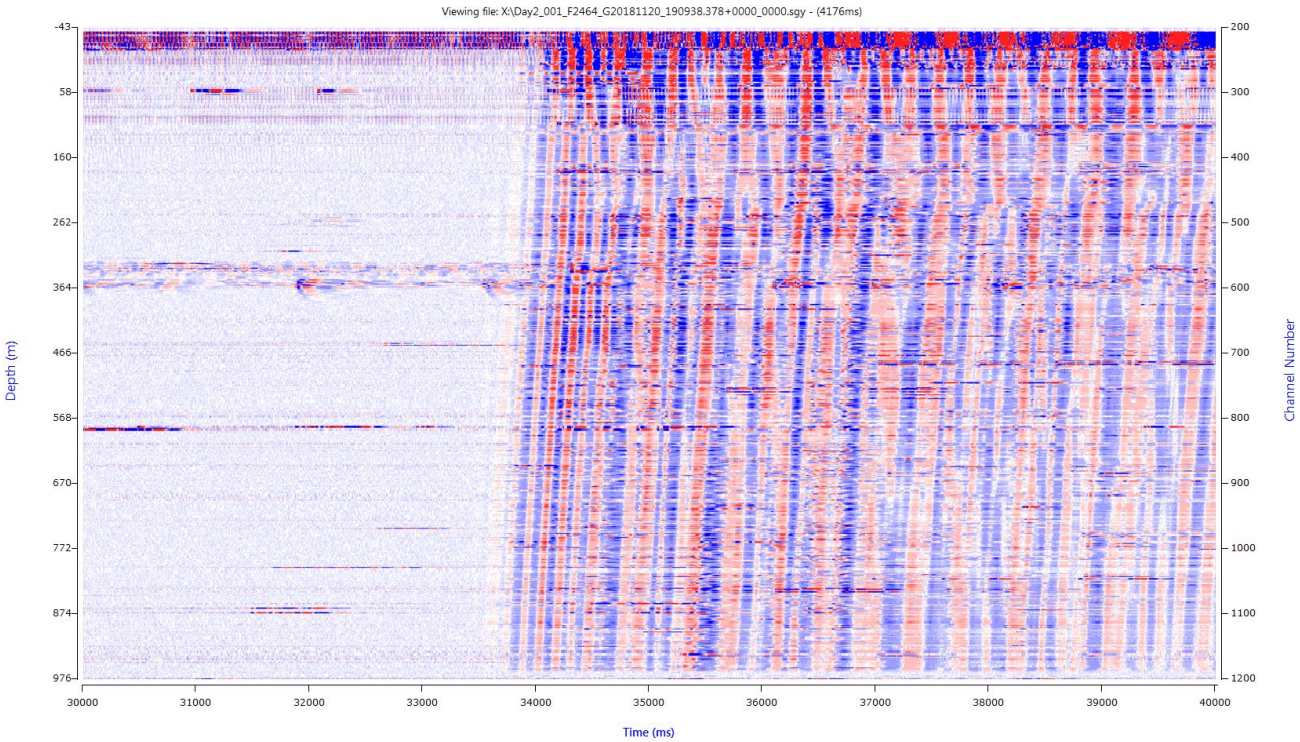


©2019. Japan Geoscience Union. All Right Reserved. 

# Distributed Acoustic Sensing measurement by using seafloor optical fiber cable system off Sanriku for dense seismic observation

*Masanao Shinohara[1], Tomoaki Yamada[1], Takeshi Akuhara[1], Kimihiro Mochizuki[1], Takeo Kasajima[2], Takahiro Arioka[2], Masayuki Hamakawa[3], Shunsuke Kubota[4]

1. Earthquake Research Institute, University of Tokyo, 2. Fujitsu Laboratories Ltd., 3. Fujitsu Limited, 4. YK Giken Co., Ltd.

Recently Distributed Acoustic Sensing (DAS) measurement which utilizes an optical fiber itself as a sensor becomes popular for security surveillance, monitoring of oil pipe line system. etc. In addition, DAS measurement begins to be applied to seismic prospecting such as vertical seismic profiling for an exploration of energy resources. As DAS measurement is thought to be useful for earthquake observation, there is a trial to observe an earthquake using a seafloor optical fiber. DAS measurement is one of optical fiber sensing technologies. A coherent laser pulse with short duration is transmitted continuously to a single mode optical fiber, and backscattered light is observed. When a small deformation of a fiber occurs by a vibration near fiber, a pattern change of the backscattered light is observed. Travel time of light and pulse length correspond to distance of measurement point and spatially resolution, respectively. Spatially resolution is 1 - 20 m in the highest case. From these characteristics, DAS measurement enables a linear array seismic observation. A length of the array with short sensor interval corresponds to that of a deployed optical fiber. Using the present technology, the maximum length of a DAS measurement reaches more than 70 km. On the other hand, development of data processing is needed because the principle of measurement by the DAS differs from that of conventional seismic measurement using a pendulum. In 1996, a seafloor seismic tsunami observation system using an optical fiber cable was deployed off Sanriku by Earthquake Research Institute, the University of Tokyo. The system still continues the observations experiencing an interruption by a damage of the 2011 Tohoku-oki earthquake. The system has six spare (dark) optical fibers for future extension. The length of dark fibers is about 120 km without a repeater. The dark fibers are suitable for DAS measurement due to dispersion shifted single mode fiber. Therefore we start development of a seafloor seismic observation system by the DAS technology with Sanriku cable observation system as a next generation of marine seismic observation system. The observation system using the DAS measurement can increase spatial resolution on seafloor seismic observation. In February 2019, we made a pilot observation of DAS measurement using a dark fiber of Sanriku seafloor observation system. An interrogator was installed in the landing station temporarily, data were recorded continuously for 100 km length with spatial resolution of 10 m or 40 m and sampling frequency of about 500 Hz. As a result, earthquakes including small local earthquakes occurring near the cable system, deep earthquakes were recorded. We will develop data processing using the obtained data.

Keywords: Seafloor optical cabled observation system off Sanriku, Distributed Acoustic Sensing (DAS) measurement, High dense seafloor seismic observation

©2019. Japan Geoscience Union. All Right Reserved. 

[J] Poster | S (Solid Earth Sciences )：S-TT Technology & Techniques

Thu. May 30, 2019 3:30 PM - 5:00 PM JST | Thu. May 30, 2019 6:30 AM - 8:00 AM UTC | Poster Hall International Exhibition Hall8, Makuhari Messe_13

## [S-TT43] seismic monitoring and processing system

convener:Takahiro Maeda(National Research Institute for Earth Science and Disaster Resilience)

This session covers scientific and technical issues in seismic monitoring or data processing systems for earthquakes or explosions observation. This includes development or improvement of seismic observation networks, innovative techniques in observation and monitoring, cutting-edge data acquisition and processing techniques in geophysical explorations. Other topics related to geophysical observation are also welcome.

### [STT43-P01] Proposal of the low cost seismometer network system

*Takamori Ito[1], Takashi Akazawa[2], Koichi Kusunoki[3], Masato Yazawa[4] (1.aLab Inc., 2.Geo-Research Institute, 3.ERI, The University of Tokyo, 4.MAD Lab.)

### [STT43-P02] Experimental observation toward the realization of low-cost and high-density strong-motion observation network

*Takashi Akazawa[1], Takamori Ito[2] (1.Geo-Research Institute, 2.aLab Inc.)

### [STT43-P03] Comparison of noise levels of the JMA and F-net broadband seismographs / strong motion velocity-type seismographs in long-period range for the purpose of magnitude estimation of tsunami earthquakes

*Masayuki Tanaka[1], Akio Katsumata[1] (1.Meteorological Research Institute)

### [STT43-P04] Estimation of seismic wave velocity of seafloor surface and installation orientation at S-net station based on observed waveform of air gun: Toward sound source localization of large baleen whale

*Ryoichi Iwase[1] (1.National Research and Development Agency, Japan Agency for Marine-Earth Science and Technology)

### [STT43-P05] Parametric time series – video sincronization tool

*Gerardo Manuel Mendo Pérez[1], Alejandra Arciniega Ceballos[1,2], Alejandro Rosado Fuentes[1] (1.Earth Science Graduate Program, National Autonomous University of Mexico, 2.Department of Volcanology, Institute of Geophysics, National Autonomus University of Mexico)

# Proposal of the low cost seismometer network system

*Takamori Ito[1], Takashi Akazawa[2], Koichi Kusunoki[3], Masato Yazawa[4]

1. aLab Inc., 2. Geo-Research Institute, 3. ERI, The University of Tokyo, 4. MAD Lab.

In the IT strong-motion seismometer (Takano et al. 2004), we aimed at realizing "the earthquake disaster prevention information system which can be offered for grassroots organizing" at first. The development as the general-purpose seismometer network does not advance. One of these causes is that operative cost of the whole system including a network was not low conventionally. We regarded a method to build a seismometer network in a low price as VPS(virtual private server) using VPN(virtual private network) and began examination use.
http://itk.seism.jp/
We use WIN system as a telemeter system. It is a stable system and is used widely. However, the transfer method of the WIN system is weak to use it on the Internet. The VPN router to deal with it is expensive. We can cut the cost of this part by realizing VPN by usable free software. In the WIN system, X-Window is used in display basically and is difficult to approach other than some researchers. In the prototype IT strong-motion seismometer, we realized display via the Web using CGI and Java applet. Because support of the Java applet was broken off, we realized waveform display by the Web using a JavaScript.
We use VPS of the SAKURA Internet Inc. for a core server. Virtual machine with a fixed global IP address is offered in 685 yen / month. We use OpenVPN as VPN. We use RaspberryPi for other construction apparatuses. The global addresses are unnecessary for them. The seismometer can raise a low price by connecting ADXL355 of the MEMS acceleration sensor of Analog Devices, Inc. to RaspberryPi. Because WIN system is carried out on RaspberryPi, existing win output logger can do this network connection through RaspberryPi.
We continue examination use and will push forward development of the application that made use of this network in future.

Keywords: seismic network

©2019. Japan Geoscience Union. All Right Reserved. 

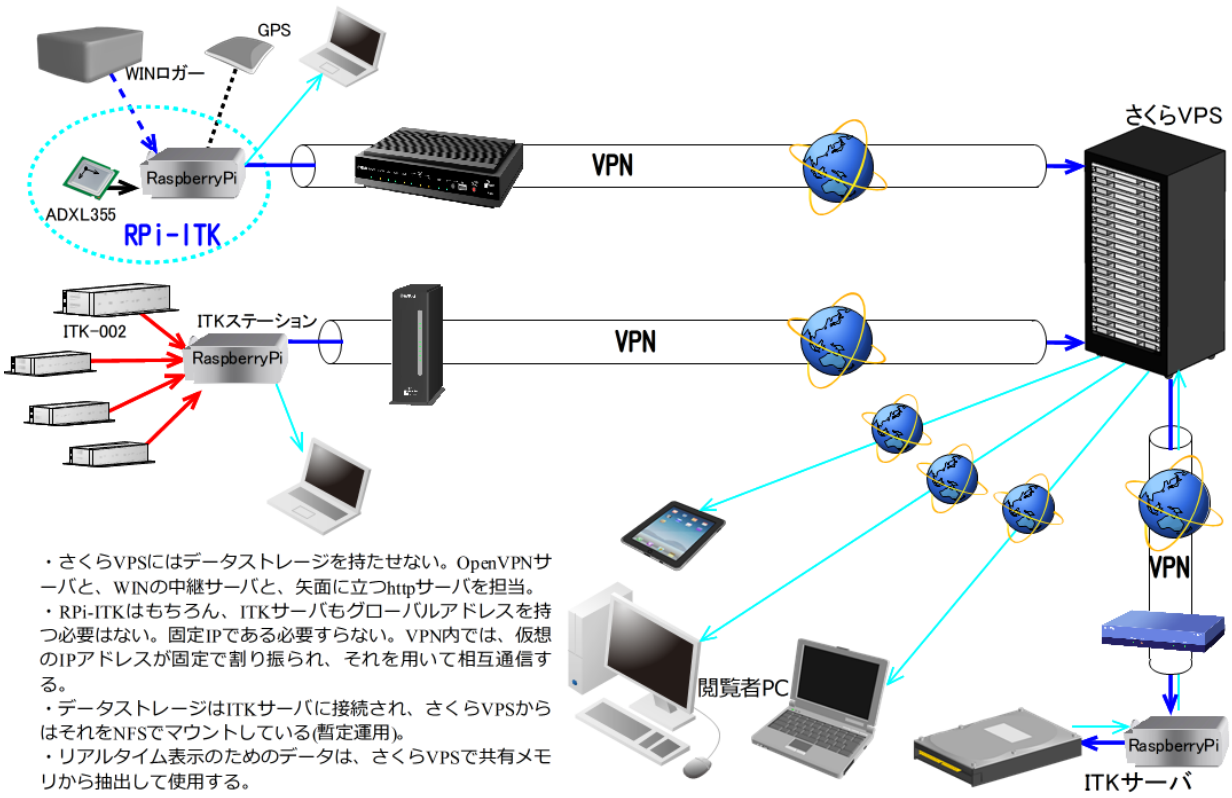


・さくらVPSにはデータストレージを持たせない。OpenVPNサーバと、WINの中継サーバと、矢面に立つhttpサーバを担当。
・RPi-ITKはもちろん、ITKサーバもグローバルアドレスを持つ必要はない。固定IPである必要すらない。VPN内では、仮想のIPアドレスが固定で割り振られ、それを用いて相互通信する。
・データストレージはITKサーバに接続され、さくらVPSからはそれをNFSでマウントしている(暫定運用)。
・リアルタイム表示のためのデータは、さくらVPSで共有メモリから抽出して使用する。

©2019. Japan Geoscience Union. All Right Reserved. 

# Experimental observation toward the realization of low-cost and high-density strong-motion observation network

*Takashi Akazawa[1], Takamori Ito[2]

1. Geo-Research Institute, 2. aLab Inc.

After the 1995 Kobe earthquake, high-density strong-motion observation network without parallel in the world has been improved in Japan. For example, the National Research Institute for Earth Science and Disaster Resilience (NIED) built K-NET (Kyoshin network), which consists of more than 1,000 seismic observation stations distributed every 20 km uniformly covering Japan. In Kansai area, together with the network, The Committee of Earthquake Observation and Research in the Kansai Area (CEORKA) has built one’ s own strong-motion observation network since 1994. However, under the existing observation density, there is a limit to comprehend the seismic ground motion. To solve the problem, there is a method of increasing the number of seismic observation station furthermore. However, the method requires a huge amount of money.
We developed a prototype of a low-cost ITK sensor, which is composed of Raspberry Pi (small single-board computer) and ADXL355 (MEMS acceleration sensor), corresponded to the IT strong-motion seismometer and began experimental observation using the sensor for evaluating the performance as a strong-motion seismometer, in parallel with the experimental operation of the low-cost seismometer network using VPS (Virtual Private Server) and VPN (Virtual Private Network) (Ito et al. (2019)). We will continue the experimental observation and will conduct further examination toward the realization of low-cost and high-density strong-motion observation network.

Keywords: Strong-motion observation, Strong-motion seismometer

©2019. Japan Geoscience Union. All Right Reserved. 

# Comparison of noise levels of the JMA and F-net broadband seismographs / strong motion velocity-type seismographs in long-period range for the purpose of magnitude estimation of tsunami earthquakes

*Masayuki Tanaka[1], Akio Katsumata[1]

1. Meteorological Research Institute

Slow tsunami earthquakes generate tsunamis higher than those expected from conventional magnitude such as surface wave magnitude $M_s$ or the Japan Meteorological Agency (JMA) magnitude $M_J$ (Kanamori, 1972). The 1992 Nicaragua earthquake ($M_s$ :7.2, $M_w$ :7.6) is considered as a typical slow tsunami earthquake because the rupture duration exceeded 100 seconds (e.g., Satake *et al.*, 1993). Therefore, the observation data from the broadband seismograph is very promising in the analyses of mechanism and the magnitude estimation of such an earthquake. In Japan, data from the Full Range Seismograph Network of Japan (F-net) operated by the National Research Institute for Earth Science and Disaster Resilience is utilized. The broadband seismographs are susceptible to temperature changes. Seismometers of the F-net are installed in vaults. According to previous studies, the strong motion velocity-type seismograph of F-net would be helpful for estimating size of tsunami earthquakes (e.g., Tanaka and Katsumata, 2017 SSJ Fall Meeting, Tanaka and Katsumata, JpGU Meeting 2018, Tanaka and Katsumata, 2018 SSJ Fall Meeting). The JMA also installed the broadband seismographs and the strong motion velocity-type seismographs, but it is not necessarily together at the same site. However, the observation environments of the JMA stations are not as good as these of the F-net stations, for example they are not installed in the vaults. We examined the background noise level from the observed continuous waveform data of JMA and F-net. The power spectral densities are calculated for the 1-day length time-window data with moving it with a step of the half day (e.g., McNamara and Buland, 2004). From the results, we investigate whether the broadband seismographs and the strong motion velocity-type seismograph of the JMA can be used for magnitude estimation of tsunami earthquakes. Figure 1 shows the power spectral densities of the vertical component of the strong motion velocity-type seismograph at the Nemuro Toyosato station of the JMA (Red line) and the nearby F-net Nemuro station (Blue line). The period is one hour from 00:00 January 1, 2019. The noise levels of the two recordings are approximately the same.

Acknowledgment
We used waveform data of F-net (NIED).

Keywords: Broadband Seismograph, Strong Motion Velocity-type Seismograph, Power Spectral Density, Noise Level

©2019. Japan Geoscience Union. All Right Reserved. 

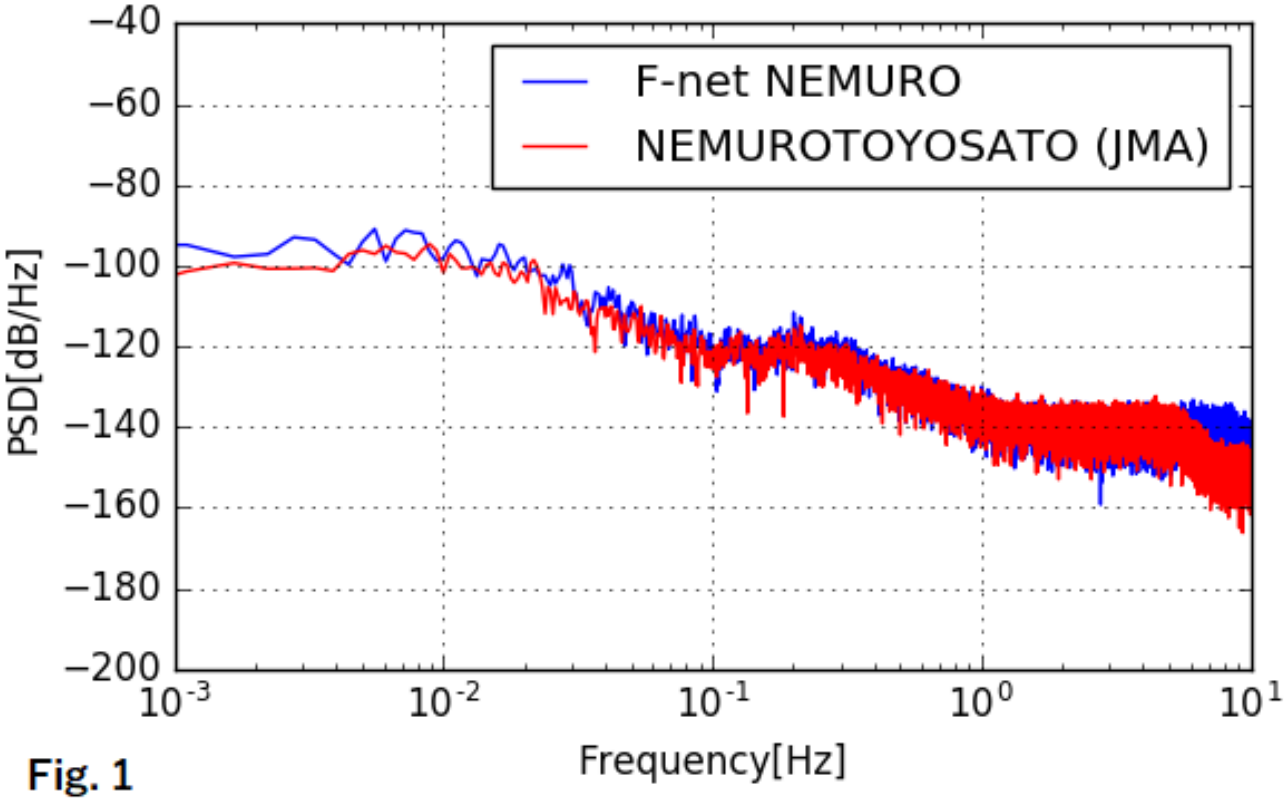


**Fig. 1**

©2019. Japan Geoscience Union. All Right Reserved. 

# Estimation of seismic wave velocity of seafloor surface and installation orientation at S-net station based on observed waveform of air gun: Toward sound source localization of large baleen whale

*Ryoichi Iwase[1]

1. National Research and Development Agency, Japan Agency for Marine-Earth Science and Technology

The vocalization of fin whale, one of the large baleen whales, has been detected with hydrophones and ocean bottom seismometers (OBSs) which are equipped with submarine cabled observatories off Kushiro-Tokachi in Hokkaido, off Sanriku, and off Boso Peninsula (Iwase, 2015). In recent years, a large cabled observatory "S-net"(Seafloor observation network for earthquakes and tsunamis along the Japan Trench), consisting of 150 stations in the vast range from Hokkaido to Chiba in the Pacific Ocean off the east coast of Japan, was deployed by National Research Institute for Earth Science and Disaster Resilience (NIED). The waveform data of the observatory are open to public. Not only for the observation and early detection of earthquakes and tsunamis, “S-net" would expand the capability of the vocalization detection area that had been limited to local to the one in a vast ocean area, It is expected that it will contribute to the elucidation of migratory behaviors of the baleen whales in the West Pacific, which has been a mostly unknown area, especially in the waters of Japan.
Meanwhile, in order to elucidate these behaviors, it is desirable that not only to detect whale vocalization but also to know individual movement based on sound source localization becomes possible. However, unlike earthquakes, the source sound pressure level of the whale vocalization is usually not so large as to be detected at multiple stations constituting the cabled observatory. It is necessary to localize the sound source with waveform data at a single station. As a sound source localization method using a single three component seismometer, there is a method of using the incident angle of the underwater sound at seafloor based on particle motion for the horizontal distance estimation, in addition to the estimation of the azimuth, of sound source. However, the OBS can only observe the apparent emergence angle of the transmitted wave, which is a composite of a pressure wave (P-wave) and a vertical shear wave (SV wave), which are both converted at the seafloor provided that the incidence angle is less than the critical angle. Therefore, the relationship between the incidence angle and the apparent emergence angle depends not only on the difference in P-wave velocity between the water and the sediment of the seafloor surface but also on the S-wave velocity in the sediment. Thus, both the P-wave velocity and the S-wave velocity in the sediment are necessary. In Iwase (2016), the seismic wave velocities in sediment were estimated *in situ* based on the observation of the transmitted wave of an air gun signal, whose sound source location is known, using an OBS at the cabled observatory offshore of Kamaishi in Sanriku which was deployed by Earthquake Research Institute (ERI), the University of Tokyo. Specifically, the seismic velocities were estimated by comparing the apparent emergence angle of the transmitted wave, which was obtained from the observed particle motion, with the theoretical emergence angle based on the Zoeppritz equation assuming plane-wave incidence at fluid-solid boundary.
With regard to S-net, JAMSTEC's research vessel "Kaimei", whose track line data are published on the web, passed through in the vicinity of some stations while oscillating the air gun. The same method in Iwase (2016) is applicable.
This time, the estimated results of seismic wave velocities of seafloor surface and installation orientation at S-net station will be reported based on the open data of NIED and JAMSTEC.

References

©2019. Japan Geoscience Union. All Right Reserved. 

R.Iwase, Jpn. Jour. App. Phys, 54, 07HG03, 2015.
R.Iwase, Jpn. Jour. App. Phys, 55, 07KG01, 2016.

Keywords: Ocean bottom seismometer (OBS), transmitted wave, particle motion

©2019. Japan Geoscience Union. All Right Reserved. 

# Parametric time series –video sincronization tool

*Gerardo Manuel Mendo Pérez[1], Alejandra Arciniega Ceballos[1,2], Alejandro Rosado Fuentes[1]

1. Earth Science Graduate Program, National Autonomous University of Mexico, 2. Department of Volcanology, Institute of Geophysics, National Autonomus University of Mexico

In recent years, the development of experimental methodologies and techniques have facilitated the study of volcano-conduit dynamics through high-sensitive laboratory experiments; in which parametric time series and high-resolution videos have been analyzed separately. We present a computational tool that synchronizes parametric time series with high-resolution videos in cases where the experimental setup allows the physical phenomena to be filmed. The open-access program has been writen in Python using ObsPy (time series processing) and OpenCV3.0 (image processing) libraries and runs in different operating systems. It scales parametric time series and video frames in order to run both at same time and correlate characteristics of interest. In addition, the program can display multiple-parameter time series in one frame to study and interpret them together. We present some examples where elastic signals were sincronized with high-resolution videos in experiments that aim to understand elasto-dynamic behavior of conduits and the fluid-rock interaction. Our results display good correlation between the elastic characteristics shown in signals and the physical phenomena observed in the video. This program is an alternative tool for processing experimental data of parametric time series correlated with video frames. The program will be available under request to the main author's email.

©2019. Japan Geoscience Union. All Right Reserved. 

[J] Poster | S (Solid Earth Sciences )：S-TT Technology & Techniques

Thu. May 30, 2019 5:15 PM - 6:30 PM JST | Thu. May 30, 2019 8:15 AM - 9:30 AM UTC | Poster Hall International Exhibition Hall8, Makuhari Messe_25

## [S-TT43] seismic monitoring and processing system

convener:Takahiro Maeda(National Research Institute for Earth Science and Disaster Resilience)

This session covers scientific and technical issues in seismic monitoring or data processing systems for earthquakes or explosions observation. This includes development or improvement of seismic observation networks, innovative techniques in observation and monitoring, cutting-edge data acquisition and processing techniques in geophysical explorations. Other topics related to geophysical observation are also welcome.

### [STT43-P01] Proposal of the low cost seismometer network system

*Takamori Ito[1], Takashi Akazawa[2], Koichi Kusunoki[3], Masato Yazawa[4] (1.aLab Inc., 2.Geo-Research Institute, 3.ERI, The University of Tokyo, 4.MAD Lab.)

### [STT43-P02] Experimental observation toward the realization of low-cost and high-density strong-motion observation network

*Takashi Akazawa[1], Takamori Ito[2] (1.Geo-Research Institute, 2.aLab Inc.)

### [STT43-P03] Comparison of noise levels of the JMA and F-net broadband seismographs / strong motion velocity-type seismographs in long-period range for the purpose of magnitude estimation of tsunami earthquakes

*Masayuki Tanaka[1], Akio Katsumata[1] (1.Meteorological Research Institute)

### [STT43-P04] Estimation of seismic wave velocity of seafloor surface and installation orientation at S-net station based on observed waveform of air gun: Toward sound source localization of large baleen whale

*Ryoichi Iwase[1] (1.National Research and Development Agency, Japan Agency for Marine-Earth Science and Technology)

### [STT43-P05] Parametric time series – video sincronization tool

*Gerardo Manuel Mendo Pérez[1], Alejandra Arciniega Ceballos[1,2], Alejandro Rosado Fuentes[1] (1.Earth Science Graduate Program, National Autonomous University of Mexico, 2.Department of Volcanology, Institute of Geophysics, National Autonomus University of Mexico)

# Proposal of the low cost seismometer network system

*Takamori Ito[1], Takashi Akazawa[2], Koichi Kusunoki[3], Masato Yazawa[4]

1. aLab Inc., 2. Geo-Research Institute, 3. ERI, The University of Tokyo, 4. MAD Lab.

In the IT strong-motion seismometer (Takano et al. 2004), we aimed at realizing "the earthquake disaster prevention information system which can be offered for grassroots organizing" at first. The development as the general-purpose seismometer network does not advance. One of these causes is that operative cost of the whole system including a network was not low conventionally. We regarded a method to build a seismometer network in a low price as VPS(virtual private server) using VPN(virtual private network) and began examination use.
http://itk.seism.jp/
We use WIN system as a telemeter system. It is a stable system and is used widely. However, the transfer method of the WIN system is weak to use it on the Internet. The VPN router to deal with it is expensive. We can cut the cost of this part by realizing VPN by usable free software. In the WIN system, X-Window is used in display basically and is difficult to approach other than some researchers. In the prototype IT strong-motion seismometer, we realized display via the Web using CGI and Java applet. Because support of the Java applet was broken off, we realized waveform display by the Web using a JavaScript.
We use VPS of the SAKURA Internet Inc. for a core server. Virtual machine with a fixed global IP address is offered in 685 yen / month. We use OpenVPN as VPN. We use RaspberryPi for other construction apparatuses. The global addresses are unnecessary for them. The seismometer can raise a low price by connecting ADXL355 of the MEMS acceleration sensor of Analog Devices, Inc. to RaspberryPi. Because WIN system is carried out on RaspberryPi, existing win output logger can do this network connection through RaspberryPi.
We continue examination use and will push forward development of the application that made use of this network in future.

Keywords: seismic network

©2019. Japan Geoscience Union. All Right Reserved. 

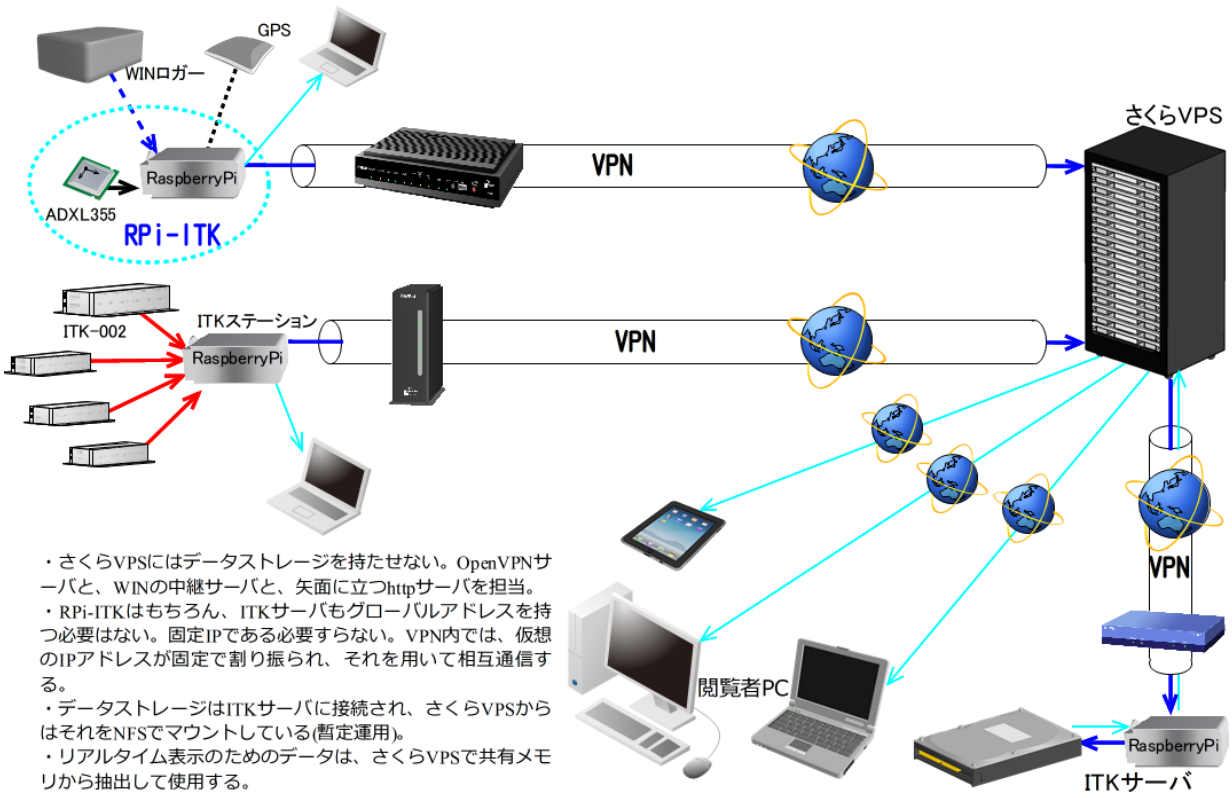


・さくらVPSにはデータストレージを持たせない。OpenVPNサーバと、WINの中継サーバと、矢面に立つhttpサーバを担当。
・RPi-ITKはもちろん、ITKサーバもグローバルアドレスを持つ必要はない。固定IPである必要すらない。VPN内では、仮想のIPアドレスが固定で割り振られ、それを用いて相互通信する。
・データストレージはITKサーバに接続され、さくらVPSからはそれをNFSでマウントしている(暫定運用)。
・リアルタイム表示のためのデータは、さくらVPSで共有メモリから抽出して使用する。

©2019. Japan Geoscience Union. All Right Reserved. 

# Experimental observation toward the realization of low-cost and high-density strong-motion observation network

*Takashi Akazawa[1], Takamori Ito[2]

1. Geo-Research Institute, 2. aLab Inc.

After the 1995 Kobe earthquake, high-density strong-motion observation network without parallel in the world has been improved in Japan. For example, the National Research Institute for Earth Science and Disaster Resilience (NIED) built K-NET (Kyoshin network), which consists of more than 1,000 seismic observation stations distributed every 20 km uniformly covering Japan. In Kansai area, together with the network, The Committee of Earthquake Observation and Research in the Kansai Area (CEORKA) has built one’ s own strong-motion observation network since 1994. However, under the existing observation density, there is a limit to comprehend the seismic ground motion. To solve the problem, there is a method of increasing the number of seismic observation station furthermore. However, the method requires a huge amount of money.
We developed a prototype of a low-cost ITK sensor, which is composed of Raspberry Pi (small single-board computer) and ADXL355 (MEMS acceleration sensor), corresponded to the IT strong-motion seismometer and began experimental observation using the sensor for evaluating the performance as a strong-motion seismometer, in parallel with the experimental operation of the low-cost seismometer network using VPS (Virtual Private Server) and VPN (Virtual Private Network) (Ito et al. (2019)). We will continue the experimental observation and will conduct further examination toward the realization of low-cost and high-density strong-motion observation network.

Keywords: Strong-motion observation, Strong-motion seismometer

©2019. Japan Geoscience Union. All Right Reserved. 

# Comparison of noise levels of the JMA and F-net broadband seismographs / strong motion velocity-type seismographs in long-period range for the purpose of magnitude estimation of tsunami earthquakes

*Masayuki Tanaka[1], Akio Katsumata[1]

1. Meteorological Research Institute

Slow tsunami earthquakes generate tsunamis higher than those expected from conventional magnitude such as surface wave magnitude $M_s$ or the Japan Meteorological Agency (JMA) magnitude $M_J$ (Kanamori, 1972). The 1992 Nicaragua earthquake ($M_s$ :7.2, $M_w$ :7.6) is considered as a typical slow tsunami earthquake because the rupture duration exceeded 100 seconds (e.g., Satake *et al.*, 1993). Therefore, the observation data from the broadband seismograph is very promising in the analyses of mechanism and the magnitude estimation of such an earthquake. In Japan, data from the Full Range Seismograph Network of Japan (F-net) operated by the National Research Institute for Earth Science and Disaster Resilience is utilized. The broadband seismographs are susceptible to temperature changes. Seismometers of the F-net are installed in vaults. According to previous studies, the strong motion velocity-type seismograph of F-net would be helpful for estimating size of tsunami earthquakes (e.g., Tanaka and Katsumata, 2017 SSJ Fall Meeting, Tanaka and Katsumata, JpGU Meeting 2018, Tanaka and Katsumata, 2018 SSJ Fall Meeting). The JMA also installed the broadband seismographs and the strong motion velocity-type seismographs, but it is not necessarily together at the same site. However, the observation environments of the JMA stations are not as good as these of the F-net stations, for example they are not installed in the vaults. We examined the background noise level from the observed continuous waveform data of JMA and F-net. The power spectral densities are calculated for the 1-day length time-window data with moving it with a step of the half day (e.g., McNamara and Buland, 2004). From the results, we investigate whether the broadband seismographs and the strong motion velocity-type seismograph of the JMA can be used for magnitude estimation of tsunami earthquakes. Figure 1 shows the power spectral densities of the vertical component of the strong motion velocity-type seismograph at the Nemuro Toyosato station of the JMA (Red line) and the nearby F-net Nemuro station (Blue line). The period is one hour from 00:00 January 1, 2019. The noise levels of the two recordings are approximately the same.

Acknowledgment
We used waveform data of F-net (NIED).

Keywords: Broadband Seismograph, Strong Motion Velocity-type Seismograph, Power Spectral Density, Noise Level

©2019. Japan Geoscience Union. All Right Reserved. 

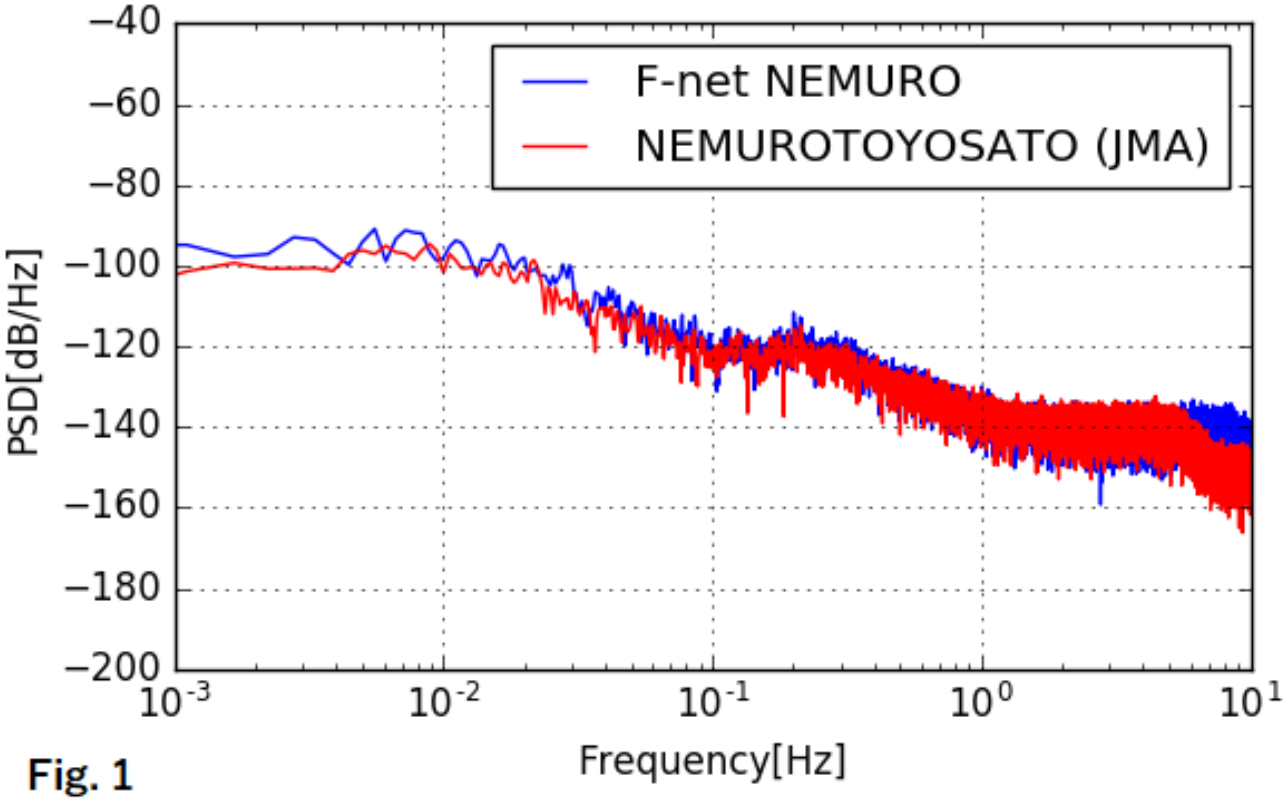


**Fig. 1**

©2019. Japan Geoscience Union. All Right Reserved. 

# Estimation of seismic wave velocity of seafloor surface and installation orientation at S-net station based on observed waveform of air gun: Toward sound source localization of large baleen whale

*Ryoichi Iwase[1]

1. National Research and Development Agency, Japan Agency for Marine-Earth Science and Technology

The vocalization of fin whale, one of the large baleen whales, has been detected with hydrophones and ocean bottom seismometers (OBSs) which are equipped with submarine cabled observatories off Kushiro-Tokachi in Hokkaido, off Sanriku, and off Boso Peninsula (Iwase, 2015). In recent years, a large cabled observatory "S-net"(Seafloor observation network for earthquakes and tsunamis along the Japan Trench), consisting of 150 stations in the vast range from Hokkaido to Chiba in the Pacific Ocean off the east coast of Japan, was deployed by National Research Institute for Earth Science and Disaster Resilience (NIED). The waveform data of the observatory are open to public. Not only for the observation and early detection of earthquakes and tsunamis, “S-net" would expand the capability of the vocalization detection area that had been limited to local to the one in a vast ocean area, It is expected that it will contribute to the elucidation of migratory behaviors of the baleen whales in the West Pacific, which has been a mostly unknown area, especially in the waters of Japan.
Meanwhile, in order to elucidate these behaviors, it is desirable that not only to detect whale vocalization but also to know individual movement based on sound source localization becomes possible. However, unlike earthquakes, the source sound pressure level of the whale vocalization is usually not so large as to be detected at multiple stations constituting the cabled observatory. It is necessary to localize the sound source with waveform data at a single station. As a sound source localization method using a single three component seismometer, there is a method of using the incident angle of the underwater sound at seafloor based on particle motion for the horizontal distance estimation, in addition to the estimation of the azimuth, of sound source. However, the OBS can only observe the apparent emergence angle of the transmitted wave, which is a composite of a pressure wave (P-wave) and a vertical shear wave (SV wave), which are both converted at the seafloor provided that the incidence angle is less than the critical angle. Therefore, the relationship between the incidence angle and the apparent emergence angle depends not only on the difference in P-wave velocity between the water and the sediment of the seafloor surface but also on the S-wave velocity in the sediment. Thus, both the P-wave velocity and the S-wave velocity in the sediment are necessary. In Iwase (2016), the seismic wave velocities in sediment were estimated *in situ* based on the observation of the transmitted wave of an air gun signal, whose sound source location is known, using an OBS at the cabled observatory offshore of Kamaishi in Sanriku which was deployed by Earthquake Research Institute (ERI), the University of Tokyo. Specifically, the seismic velocities were estimated by comparing the apparent emergence angle of the transmitted wave, which was obtained from the observed particle motion, with the theoretical emergence angle based on the Zoeppritz equation assuming plane-wave incidence at fluid-solid boundary.
With regard to S-net, JAMSTEC's research vessel "Kaimei", whose track line data are published on the web, passed through in the vicinity of some stations while oscillating the air gun. The same method in Iwase (2016) is applicable.
This time, the estimated results of seismic wave velocities of seafloor surface and installation orientation at S-net station will be reported based on the open data of NIED and JAMSTEC.

References

©2019. Japan Geoscience Union. All Right Reserved. 

R.Iwase, Jpn. Jour. App. Phys, 54, 07HG03, 2015.
R.Iwase, Jpn. Jour. App. Phys, 55, 07KG01, 2016.

Keywords: Ocean bottom seismometer (OBS), transmitted wave, particle motion

©2019. Japan Geoscience Union. All Right Reserved. 

# Parametric time series –video sincronization tool

*Gerardo Manuel Mendo Pérez[1], Alejandra Arciniega Ceballos[1,2], Alejandro Rosado Fuentes[1]

1. Earth Science Graduate Program, National Autonomous University of Mexico, 2. Department of Volcanology, Institute of Geophysics, National Autonomus University of Mexico

In recent years, the development of experimental methodologies and techniques have facilitated the study of volcano-conduit dynamics through high-sensitive laboratory experiments; in which parametric time series and high-resolution videos have been analyzed separately. We present a computational tool that synchronizes parametric time series with high-resolution videos in cases where the experimental setup allows the physical phenomena to be filmed. The open-access program has been writen in Python using ObsPy (time series processing) and OpenCV3.0 (image processing) libraries and runs in different operating systems. It scales parametric time series and video frames in order to run both at same time and correlate characteristics of interest. In addition, the program can display multiple-parameter time series in one frame to study and interpret them together. We present some examples where elastic signals were sincronized with high-resolution videos in experiments that aim to understand elasto-dynamic behavior of conduits and the fluid-rock interaction. Our results display good correlation between the elastic characteristics shown in signals and the physical phenomena observed in the video. This program is an alternative tool for processing experimental data of parametric time series correlated with video frames. The program will be available under request to the main author's email.

©2019. Japan Geoscience Union. All Right Reserved. 

[E] Oral | S (Solid Earth Sciences )：S-CG Complex & General

Thu. May 30, 2019 9:00 AM - 10:30 AM JST | Thu. May 30, 2019 12:00 AM - 1:30 AM UTC | Convention Hall A 2F

## [S-CG48] Science of slow earthquakes: Toward unified understandings of whole earthquake process

convener:Satoshi Ide(Department of Earth an Planetary Science, University of Tokyo), Hitoshi Hirose(Research Center for Urban Safety and Security, Kobe University), Kohtaro Ujiie(Graduate School of Life and Environmental Sciences, University of Tsukuba), Takahiro Hatano(Earthquake Research Institute, University of Tokyo), Chairperson:Kimihiro Mochizuki(Earthquake Research Institute, University of Tokyo), Ryuta Arai

Accumulating observational studies on various types of slow deformation events, such as tectonic tremors, very low frequency events, and slow slip events, portrays some universal characteristics in generally complex behavior, including interaction among events and influence by various outer loadings. Some of these phenomena seem to have causal relation with the occurrence of very large earthquakes. A unified understanding of these slow and fast earthquake processes requires an approach integrating geophysics, seismology, geodesy, geology, and non-equilibrium statistical physics. We welcome presentations based on, but not limited to, geophysical observation, data analysis, analytical theory, numerical simulation, field study, and laboratory experiments.

9:00 AM - 9:15 AM JST | 12:00 AM - 12:15 AM UTC

[SCG48-17] Three-dimensional seismic structure of the shallow plate boundary in the northern Hikurangi margin from NZ3D OBS data

*Ryuta Arai[1], Shuichi Kodaira[1], Richard Kellett[2], Valerie Stucker[2], Dan Bassett[2], Stuart Henrys[2], Koichiro Obana[1], Nathan Bangs[3], Dan Barker[2], Rebecca Bell[4], Kimihiro Mochizuki[5], Gou Fujie[1], Seiichi Miura[1], Bill Fry[2], team NZ3D (1.Japan Agency for Marine-Earth Science and Technology, 2.GNS Science, 3.University of Texas Institute for Geophysics, 4.Imperial College London, 5.Earthquake Research Institute, University of Tokyo)

9:15 AM - 9:45 AM JST | 12:15 AM - 12:45 AM UTC

[SCG48-18] **Using earthquake focal mechanisms to investigate slow slip driving forces in the northern Hikurangi**

★Invited Papers

*Emily Warren-Smith[1], Bill Fry[1], Laura Wallace[1] (1.GNS Science)

9:45 AM - 10:00 AM JST | 12:45 AM - 1:00 AM UTC

[SCG48-19] Seismological structural changes around source regions of slow earthquakes in Nankai subduction zone inferred from broadband receiver functions

*Yasunori Sawaki[1], Yoshihiro Ito[2], Kazuaki Ohta[2], Takuo Shibutani[2], Tomotaka Iwata[2] (1.Graduate School of Science, Kyoto University , 2.Disaster Prevention Research Institute, Kyoto University)

10:00 AM - 10:15 AM JST | 1:00 AM - 1:15 AM UTC

[SCG48-20] Slip tendency maps for compressional and extensional stress states on a shallow decollement in Nankai Trough

*Yoshitaka Hashimoto[1], Shigeyuki Sato[1], Gregory F Moore[2], Masataka Kinoshita[3], Gaku Kimura[4], Ayumu Miyakawa[5], Kazuya Shiraishi[6], Yasuhiro Yamada[6] (1.Kochi University, 2.University of Hawaii, 3.University of Tokyo, 4.Tokyo University of Marine Science and Technology, 5.AIST, 6.JAMSTEC)

10:15 AM - 10:30 AM JST | 1:15 AM - 1:30 AM UTC

[SCG48-21] Permeability and its anisotropy on creeping Chihshang Fault, Taiwan

*Tyas Dwi Aprilniadi[1], Wen-Jie Wu[1], Li-Wei Kuo[1], Jian-Cheng Lee[2], Jia-Jyun Dong[3] (1.Department of Earth Sciences, National Central University, 2.Institute of Earth Sciences, Academia Sinica, 3.Graduate Institute of Applied Geology, National Central University)

# Three-dimensional seismic structure of the shallow plate boundary in the northern Hikurangi margin from NZ3D OBS data

*Ryuta Arai[1], Shuichi Kodaira[1], Richard Kellett[2], Valerie Stucker[2], Dan Bassett[2], Stuart Henrys[2], Koichiro Obana[1], Nathan Bangs[3], Dan Barker[2], Rebecca Bell[4], Kimihiro Mochizuki[5], Gou Fujie[1], Seiichi Miura[1], Bill Fry[2], team NZ3D

1. Japan Agency for Marine-Earth Science and Technology, 2. GNS Science, 3. University of Texas Institute for Geophysics, 4. Imperial College London, 5. Earthquake Research Institute, University of Tokyo

Slow earthquakes occur around the seismogenic zones of the plate boundary faults and they have so far been largely studied on the deep portions of the plate interface based on land-based geophysical observations. On the other hand, recent marine studies reveal that shallow slow earthquakes at the up-dip portions of seismogenic zones are also common in subduction zones. These shallow slow earthquakes have been found to occur from near the trench to ~10 km depth of the plate interface and their genesis is thought to be closely linked to fluid pressures and effective stresses at the fault. However, primary controls on seismogenesis at these depths, such as fault structures and stratigraphic/hydrogeologic properties around the subduction megathrust faults, are highly complex in three dimensions and poorly understood.

In order to refine our understanding of structural characteristics regulating slow earthquakes occurring at shallow plate boundaries, we collected 3-D seismic refraction/wide-angle reflection data from offshore Gisborne at the northern Hikurangi subduction margin, New Zealand, as part of an international collaborative project, NZ3D. The dataset covers an area of 60 km x 14 km ranging from the northern Tuaheni landslide complex and the easterly forearc slope to the subduction trench and was recorded on 97 ocean bottom seismographs deployed with an average spacing of 2 km on 4 parallel lines with over 140,000 airgun sources. In the study area, shallow slow slip events and tectonic tremor have been well documented (Wallace et al., 2016; Todd et al., 2018). Previous 2-D seismic reflection studies also show that the subduction of large-scale seamounts facilitates the transport of fluid-rich sediments deep into the subduction zone and produces conditions of high fluid pressures along the plate interface and pathways for fluid migration into the overriding plate (Bell et al., 2010; Barker et al., 2018).

Using the very dense airgun-OBS data, we constructed a preliminary three-dimensional P-wave velocity structure model of the accretionary forearc and the plate boundary from first arrival tomography. The velocity images from over 250,000 first arrivals revealed a thick low-velocity (Vp < 5.0 km/s) volume along the plate interface down to a depth of at least ~10 km. This velocity structure may represent a thick subduction channel filled with fluid-rich sediments associated with seamount subduction.

Keywords: Shallow plate boundary, Hikurangi margin, 3-D seismic structure

©2019. Japan Geoscience Union. All Right Reserved. 

# Using earthquake focal mechanisms to investigate slow slip driving forces in the northern Hikurangi

*Emily Warren-Smith[1], Bill Fry[1], Laura Wallace[1]

1. GNS Science

Understanding the processes that drive slow slip events (SSEs) may assist in improving our understanding of the physics of both slow and fast earthquakes. Recent work has shown that the stress ratio, R, retrieved by focal mechanism inversion systematically decreases prior to SSEs in New Zealand's northern Hikurangi subduction zone, and subsequently increases during the evolution of each SSE. These R fluctuations are proposed to represent slow, precursory increases and fast concurrent decreases in fluid pressure within overpressured subducting oceanic crust during the SSE cycle.

These observations represent an exciting opportunity to improve forecasts of SSE occurrence via monitoring of R changes. Thus far, this cyclic behaviour has only been observed over a short time-period (9 months, 4 SSE cycles) when ocean-bottom seismographs were deployed.

Here we present the results of a waveform cross-correlation study that aims to extend the catalogue in time and reduce the magnitude of completeness for focal mechanisms of northern Hikurangi seismicity. This enables improved temporal coverage and statistical analysis of stress tensor changes across multiple SSE cycles. By using well constrained focal mechanisms of events recorded on >30 OBS and land stations as templates, we automatically assign correlation-derived relative polarities to waveforms and subsequently invert for focal mechanisms and R using many more earthquakes complete to a lower magnitude. This approach offers an important step towards accurate SSE forecasting and an improved understanding of the physical processes leading to slow rupture nucleation.

Keywords: slow slip, seismology, focal mechanisms, stress inversions, Hikurangi, fluid pressure

©2019. Japan Geoscience Union. All Right Reserved. 

# Seismological structural changes around source regions of slow earthquakes in Nankai subduction zone inferred from broadband receiver functions

*Yasunori Sawaki[1], Yoshihiro Ito[2], Kazuaki Ohta[2], Takuo Shibutani[2], Tomotaka Iwata[2]

1. Graduate School of Science, Kyoto University , 2. Disaster Prevention Research Institute, Kyoto University

Coupled phenomena of tremors accompanying short-term slow slip events and very low frequency earthquakes (Ito et al., 2007) have been detected at deeper parts of seismogenic regions on the Nankai Subduction Zone in southwestern Japan. Elucidating detailed seismological structures on plate interfaces hosting slow earthquakes is very important to understand mechanisms and relationships of slow earthquakes and megathrust earthquakes. Few studies, however, have proposed detailed velocity structure models and their spatio-temporal variations with high resolution receiver functions (RFs) on plate interfaces. In this study, we calculate broadband RFs around source regions with slow earthquake events in the Nankai Subduction Zone. We also investigate frequency dependency of RFs to constrain detailed physical features near the plate interface.
RF method is one of the best approaches to estimate the velocity structure beneath seismic stations by extracting P-to-S phases converted on velocity discontinuity from teleseismic waveforms. In southwestern Japan, Shiomi et al. (2008) confirmed the oceanic Moho discontinuity in the Philippine Sea Slab. In usual cases, high cut filter (e.g. 0.6Hz: Shiomi et al., 2008) is used when deconvoluting vertical component waveforms from horizontal ones in order to avoid instability on calculation. Akuhara et al. (2017) recently calculated high frequency RFs up to 4 Hz using ocean bottom seismometers equipped off the Kii peninsula, and confirmed the existence of a thin low velocity zone composed of a fluid-rich sediment layer along the Nankai trough megathrust fault. In this study, we calculate RFs applying the Extended-Time Multitaper method modified by Shibutani et al. (2008) and the frequency dependency of RFs is examined by taking different frequency ranges up to 0.5, 1, 2, 3 and 4 Hz.
We have used Hi-net and F-net seismograms provided by National Research Institute for Earth Science and Disaster Resilience in Japan. We confirm that spectra of teleseismic waveforms have sufficient SN ratios up to 3 or 4 Hz. Fig.1 shows an example of the RFs at NKTH located on the Kii peninsula. The RFs at most of the stations contain positive and negative phases around 3-4 s after P-wave arrival, which correspond to oceanic Moho discontinuity and the plate interface, respectively. The amplitude and the arrival time of these phases depend on backazimuth, suggesting that dependency on the incident angle of a ray to the subducting plate interface. In case of a downdip for the subducting slab, incoming P-waves have lower incident angles and generate smaller convert S-waves. On the contrary, an updip case, incoming P-waves have higher incident angles and generate larger convert S-waves.
At higher frequency RFs (Fig.1, right), the phases from the plate interface are generally sharper than those at lower frequency, whereas the phases corresponding to oceanic Moho seems to tend to be broader or split into several phases, suggesting that the oceanic Moho is not a simple velocity discontinuity but would consists of several layers. The split positive phase just after the negative phase from the plate interface may relate to the thin low velocity zone inferred from Akuhara et al. (2017).

Keywords: Receiver function, Broadband receiver function, Slow earthquake, Nankai subduction zone

©2019. Japan Geoscience Union. All Right Reserved. 

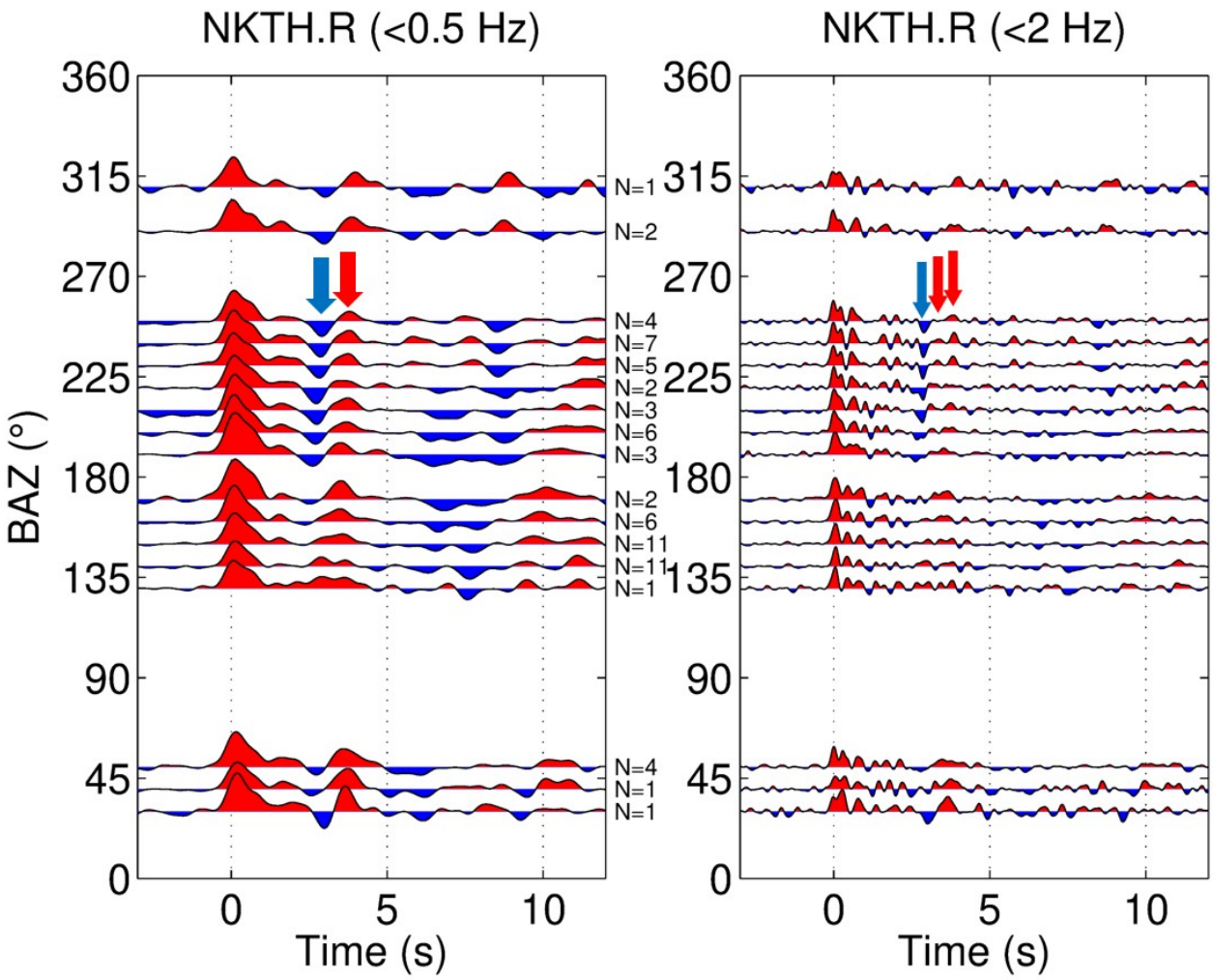


**Fig. 1** Radial receiver functions (RFs) on NKTH with frequency ranges up to (left) 0.5 Hz and (right) 2 Hz. The vertical and horizontal axes denote delay time from P-wave arrival [s] and backazimuth [degree], respectively. Areas colored in red and blue show the positive and negative amplitudes, respectively. N is the number of RFs stacked every 10 degrees. Red and blue arrows indicate later phases from the oceanic Moho and the plate interface, respectively.

©2019. Japan Geoscience Union. All Right Reserved. 

# Slip tendency maps for compressional and extensional stress states on a shallow decollement in Nankai Trough

*Yoshitaka Hashimoto[1], Shigeyuki Sato[1], Gregory F Moore[2], Masataka Kinoshita[3], Gaku Kimura[4], Ayumu Miyakawa[5], Kazuya Shiraishi[6], Yasuhiro Yamada[6]

1. Kochi University, 2. University of Hawaii, 3. University of Tokyo, 4. Tokyo University of Marine Science and Technology, 5. AIST, 6. JAMSTEC

Stress state along a subduction plate interface is one of important controls for wedge architectures, fault activations and seismogenic behaviors. In a shallow portion of a subduction plate interface, a large displacement along decollement could be expected for tsunamigenic events (Fujiwara et al., 2012) as well as slow earthquakes such as very low frequency earthquakes and slow slips have been observed (Araki et al., 2017, Nakano et al., 2018). Paleo-stress state has been estimated using micro-fault inversion method from exhumed accretionary complexes and oceanic accretionary wedges, which shows the stress state changes between compression and extension states with almost horizontal and vertical principal stress axes. The stress change could be related to seismic cycle.

In this study, we examined geographical features of a shallow decollement using 3D seismic profiles and mapped slip tendencies on the decollement with compressional and extensional stress state to discuss an effect of distribution of slip tendency on the fault slip behaviors. Slip tendency is a shear stress ratio to normal stress on a fault surface when a regional stress state is applied on a fault surface.

The target transect of the 3D seismic profiles is located at the Nankai Trough off Kii Peninsula, SW Japan where Philippine Sea Plate subducted into Eurasian Plate, and IODP NantroSEIZE project has been operated. The 3D seismic profiles had been reprocessed to make reflectors clear using an updated technology. We traced the shallow decollement to make geographic features (3D surface) by Petrel. We analyzed dip angle and dip azimuth for 50 m mesh of the surface. The characteristics of geographic features of the shallow decollement are 1) almost horizontal with dip angle ranging 5-15, 2) dip azimuth directing 300-350˚ (NW-NWN) in average. In addition, some narrow zones with dip azimuth directing 50-150˚ (SE-SES) are identified, which shows a relatively high frequency reliefs striking NE-SW direction. Some of these are related to the geography of oceanic basement.

Compressional and extensional stress states were applied on the surface to examine a change in slip tendency with change in stress state. We assumed that compressional one has (150, 0) sigma 1 and (90, 90) sigma 3 and others has (150, 0) sigma 3 and (90, 90) sigma 1. The 0.6 of friction coefficient was assumed as the maximum value. We calculated differential stresses for compressional and extensional stress states to make a plane with idealized attitude to applied stress state reactivated. This assumption implies that the estimated slip tendency is the maximum value.

Resulted slip tendency represents a strong relationship with geomorphic features. In compressional stress state, large slip tendency (0.4-0.5) distributes on the surface with dip azimuth directing 300-350˚ whereas small slip tendency (0.1-0.2) corresponds to the surface with dip azimuth directing 50-150˚. In extensional stress state, the similar distribution with that in compressional stress state is identified but the difference between the dip azimuths is very small; slip tendency ranges 0.1-0.2. The differences between slip tendencies in compressional and extensional stress states is almost similar to that for compressional stress state because slip tendency for extensional stress state is almost 0.1-0.2.

©2019. Japan Geoscience Union. All Right Reserved. 

If we take the difference in slip tendency as a kind of stress drop, relatively small stress drop are observed on the surface with dip azimuth directing 50-150˚, which is distributed in NE-SW zones. Nakano et al. (2018) found that VLFs in the region migrates toward NE, which is consistent with the directions of zones with stress drop is small. The area for VLFEs could be limited in these zones where the slip tendency is small both in compressional and extensional stress states, implying that the material with very low friction coefficient and/or high pore fluid pressure are expected to make a plane reactivated with small slip tendency.

Keywords: Slip tendency, seismic cycle, Nankai Trough, very low frequency earthquake

©2019. Japan Geoscience Union. All Right Reserved. 

# Permeability and its anisotropy on creeping Chihshang Fault, Taiwan

*Tyas Dwi Aprilniadi[1], Wen-Jie Wu[1], Li-Wei Kuo[1], Jian-Cheng Lee[2], Jia-Jyun Dong[3]

1. Department of Earth Sciences, National Central University, 2. Institute of Earth Sciences, Academia Sinica, 3. Graduate Institute of Applied Geology, National Central University

The Chihshang Fault in eastern Taiwan is a 20-km-long segment of the Longitudinal Valley Fault that a plate-suture boundary fault between the Eurasian continental margin and the Philippine Sea Plate has fastest shallow creep in the world and infrequently occurs earthquakes (Magnitude greater than 6). Here we performed permeability measurements on Lichi Mélange and conglomerate with an intra-vessel oil pressure apparatus (YOKO2) at room temperature at isotropic confining pressure, using helium as pore fluid. We made samples, with dip and normal direction of fault, from retrieved rock cores in WAN-2 borehole and attempted to build the permeability structure across creeping Chihshang Fault. Generally, intrinsic permeabilities of Lichi Mélange were lower than that of conglomerate and intrinsic permeabilities in dip direction were higher than that in normal direction. But the permeability differed in rock type and was associated with shear structures that fault zone architecture is not typical as simple mode suggested by Caine et al. (1996). The results show Lichi Mélange was a natural aquifuge blocking the fluid flow that may be responsible for fluid-rock interaction and seasonal fluctuation on creeping Chihshang Fault. The heterogeneous Lichi Mélange has complicated composition as other Mélange that the microstructural observation would be conducted for investigating the relationship between microstructures and permeability in creeping Chihshang Fault. Taking microstructures, permeability anisotropy and the fault zone architecture into consideration, we may depict the permeability structures of Chihshang Fault and further provide the information of matrix permeability for hydraulic properties in the field.

Keywords: creeping Chihshang Fault, Lichi Mélange, permeability anisotropy

©2019. Japan Geoscience Union. All Right Reserved. 

[E] Oral | S (Solid Earth Sciences )：S-CG Complex & General

Thu. May 30, 2019 10:45 AM - 12:15 PM JST | Thu. May 30, 2019 1:45 AM - 3:15 AM UTC | Convention Hall A 2F

## [S-CG48] Science of slow earthquakes: Toward unified understandings of whole earthquake process

convener:Satoshi Ide(Department of Earth an Planetary Science, University of Tokyo), Hitoshi Hirose(Research Center for Urban Safety and Security, Kobe University), Kohtaro Ujiie(Graduate School of Life and Environmental Sciences, University of Tsukuba), Takahiro Hatano(Earthquake Research Institute, University of Tokyo), Chairperson:Kohtaro Ujiie(Graduate School of Life and Environmental Sciences, University of Tsukuba), Simon Wallis(Nagoya University)

Accumulating observational studies on various types of slow deformation events, such as tectonic tremors, very low frequency events, and slow slip events, portrays some universal characteristics in generally complex behavior, including interaction among events and influence by various outer loadings. Some of these phenomena seem to have causal relation with the occurrence of very large earthquakes. A unified understanding of these slow and fast earthquake processes requires an approach integrating geophysics, seismology, geodesy, geology, and non-equilibrium statistical physics. We welcome presentations based on, but not limited to, geophysical observation, data analysis, analytical theory, numerical simulation, field study, and laboratory experiments.

10:45 AM - 11:00 AM JST | 1:45 AM - 2:00 AM UTC

[SCG48-22] Short fluid infiltration events in the low permeable metamorphic rocks triggered by crustal fracturing at amphibolite–granulite facies conditions

*Diana Mindaleva[1], Masaoki Uno[1], Fumiko Higashino[1], Atsushi Okamoto[1], Noriyoshi Tsuchiya[1] (1.Graduate school of environmental studies, Tohoku University)

11:00 AM - 11:15 AM JST | 2:00 AM - 2:15 AM UTC

[SCG48-23] Generation of high fluid pressure at the base of the shallow mantle wedge—evidence from serpentinite of the Sanbagawa belt, SW Japan

*Simon Richard Wallis[1], Yui Kouketsu[2], Mari Yokota[1,2] (1.University of Tokyo, 2.Nagoya University)

11:15 AM - 11:30 AM JST | 2:15 AM - 2:30 AM UTC

[SCG48-24] **Overpressured subduction plate boundary caused by infiltration of mantle-derived fluids: Evidence from helium isotope analysis on veins in subduction mélange**

*Naoki Nishiyama[1], Kohtaro Ujiie[1], Hirochika Sumino[2] (1.University of Tsukuba, 2.The University of Tokyo)

11:30 AM - 11:45 AM JST | 2:30 AM - 2:45 AM UTC

[SCG48-25] **Geological and rheological conditions of subduction plate boundary between the seismogenic zone and the ETS zone in warm-slab environments**

*Kohtaro Ujiie[1], Kazuya Noro[1], Norio Shigematsu[2], Ake Fagereng[3], Naoki Nishiyama[1], Christopher Tulley[3], Haruna MASUYAMA[1], Yasushi Mori[4] (1.Graduate School of Life and Environmental Sciences, University of Tsukuba, 2.Research Institute of Earthquake and Volcano Geology, National Institute of Advanced Industrial Science and Technology, Japan, 3.Cardiff University, 4.Kitakyushu Museum of Natural History and Human History)

11:45 AM - 12:00 PM JST | 2:45 AM - 3:00 AM UTC

[SCG48-26] Temperature variation in tectonic mélanges of the Shimanto Belt, SW Japan

*Tsai-Wei Chen[1], Donald M Fisher[1], Andrew J Smye[1], Yoshitaka Hashimoto[2] (1.Penn State Univ., 2.Kochi Univ.)

12:00 PM - 12:15 PM JST | 3:00 AM - 3:15 AM UTC

## [SCG48-27] Frictional properties of opal gouge at low-temperature hydrothermal conditions and their implications for seismogenic faulting along subduction-zone megathrusts

*Kyuichi Kanagawa[1], Tomoya Nakanishi[2], Morito Kuwana[3], Michiyo Sawai[1], Takehiro Hirose[4] (1.School of Science, Chiba University, 2.Graduate School of Science and Engineering, Chiba University, 3.Faculty of Science, Chiba University, 4.Kochi Institute for Core Sample Research, Japan Agency for Marine-Earth Science and Technology)

# Short fluid infiltration events in the low permeable metamorphic rocks triggered by crustal fracturing at amphibolite–granulite facies conditions

*Diana Mindaleva[1], Masaoki Uno[1], Fumiko Higashino[1], Atsushi Okamoto[1], Noriyoshi Tsuchiya[1]

1. Graduate school of environmental studies, Tohoku University

Aqueous fluids flow could be responsible for changing hydrologic and thermodynamic properties of rocks. It is generally accepted that fluids play a key role in the generation of earthquakes, tremors, and slow slip events. For example, it was suggested that tremors are related to fluids released during dehydration processes in the subduction slab (e.g., Abers et al., 2009; Katsumata and Kamaya, 2003; Obara et al., 2004). Hydrous minerals in subducting slabs release $H_2O$ due to dehydration reactions. Released water increases fluid pressure rapidly. However, fluid pressure gradients within the crust remain poorly constrained due to their heterogeneity. Therefore, it is important to constrain timescales of fluid infiltration to understand fluid pressure gradient, permeability, and tectonic evolution.

We have investigated fluid-rock reaction zones in mafic granulite and amphibolite samples from Mefjell, south-central part of the Sør Rondane Mountains (SRM), East Antarctica, and constrained pressure gradient and permeability. Mafic granulite and amphibolite samples are cut by numerous randomly-oriented veins. Samples are partially hydrated along veins associated with mm-scale hydration reactions zones. Reaction zones fingerprint relationship between fluid infiltration and rock response. We divide samples into several reaction zones increasing distance from the vein center by modal amount of minerals, reaction textures, and trace elements concentrations distributions profiles in apatite. The P-T conditions for the fluid infiltration in mafic granulite were estimated to be 0.65 GPa, 650˚C , and that for peak P-T conditions were 850˚C, 0.55-1.0 GPa. On the other hand, P-T conditions for the fluid infiltration in amphibolite were estimated to be around 500˚C.

Trace elements concentrations (Cl, Sr, and some REE) measured by EPMA and LA-ICP-MS in several apatite grains were gradually decreasing with distance from the vein. Cl distributions profiles were analyzed by a reactive-transport model to define transport mechanism by fitting to Peclet number (Pe#=vL/D, where v is pore velocity, L is length of reaction zone, D is self-diffusion coefficient) and time-scales of fluid infiltration. For mafic granulite Pe# is 0.025, for amphibolite is 90. Whereas diffusion transport is revealed to be dominant for mafic granulite, advection transport is likely for amphibolite. Duration of fluid infiltration was estimated to be 5.5 h for mafic granulite and 1-3 h for amphibolite, which is very short in geological timescales. This suggests rapid and intense fluid flux through the mantle wedge and onto overlying crust. Short timescales of fluid infiltration may reflect linkage to the seismic events.

To estimate permeability, the pressure gradient for the reaction zones was calculated from the water and other elements activities constrained by pseudosection analysis for different reaction zones. Bulk compositions at each reaction zone were used to create pseudosections. Permeability was calculated from the estimated pressure gradient and total flux $q=-\kappa(\partial P/\partial x)/\eta$, where q is total flux, k is permeability, $\eta$ is viscosity, and $(\partial P/\partial x)$ is pressure gradient. Results suggest low and contrasting permeability between mafic granulite dominated by diffusion and amphibolite dominated by advection mass transport mechanisms. This difference may be explained by different P-T conditions for fluid infiltration and heterogeneity of the pressure gradients. Therefore, it suggest that fluid infiltration in low

©2019. Japan Geoscience Union. All Right Reserved. 

permeable rocks caused fracturing and formed narrow reaction zones, which released fluid pressure in a short time. Above results of our study suggest importance of fluid transport phenomena in relation to the evolution of rocks hydrological properties.

Abers G. A. et al. Geology 37.12 (2009): 1119-1122.

Katsumata A., Kamaya N. Geophysical Research Letters 30.1 (2003): 20-1.

Obara K. et al. Geophysical Research Letters 31.23 (2004).

Keywords: Pressure gradient, Permeability, Water-rock interaction

©2019. Japan Geoscience Union. All Right Reserved. 

# Generation of high fluid pressure at the base of the shallow mantle wedge—evidence from serpentinite of the Sanbagawa belt, SW Japan

*Simon Richard Wallis[1], Yui Kouketsu[2], Mari Yokota[1,2]

1. University of Tokyo, 2. Nagoya University

Serpentinite units derived from the mantle wedge in the Sanbagawa subduction-type metamorphic belt record interaction between the shallow mantle-wedge and the flow of SiO2-bearing fluids at two different depths in the paleo subduction zone. The mineralogy and geochemistry of two units indicate there was a major increase in the fluid flow perpendicular to the subduction boundary with decreasing pressure. The rate of flow can be related to the presence or absence of a thick shear zone. Estimates of fluid flux from subducted slabs combined with experimentally determined permeability of serpentinite suggests that the presence of a zone of gently dipping strongly foliated serpentinite is a key component of developing high fluid pressures at depths of 30–50 km in subduction zones—a key requirement for the development of slow earthquakes. Most of the SiO2 in these subduction fluids will be absorbed in the serpentinite and is unlikely to be available for precipitation and formation of an impermeable cap at higher levels in the system.

Keywords: Fluid pressure, Deep slow earthquakes, Serpentinite, Sanbagawa belt

©2019. Japan Geoscience Union. All Right Reserved. 

# Overpressured subduction plate boundary caused by infiltration of mantle-derived fluids: Evidence from helium isotope analysis on veins in subduction mélange

*Naoki Nishiyama[1], Kohtaro Ujiie[1], Hirochika Sumino[2]

1. University of Tsukuba, 2. The University of Tokyo

Fluid overpressures have been invoked as one of the key factors controlling slow earthquakes in subduction zones. The generation of fluid overpressures has been thought to occur by in-situ processes such as compaction disequilibrium and mineral dehydration in sediment and oceanic crust. To determine the origin of fluid responsible for overpressured subduction plate boundary, we examined noble gas and microthermometric analyses on quartz-calcite veins in the subduction mélange deformed at ~10–15 km depth.

The analyzed veins are sigmoidal extension vein arrays and shear veins. The former represents Riedel shear zones formed during subduction under vertical $\sigma_1$. The latter records the numerous low-angle brittle thrusting at very small shear strength with recurrence time comparable to that of slow earthquakes, which could account for the generation of tectonic tremors [1]. Homogenization and ice melting temperatures of fluid inclusions indicate that the both types of veins recorded the fluids with salinity of 3–7 wt% and near-lithostatic fluid pressures at 10–15 km depth. The measured $^{3}He/^{4}He$ range 1.6–2.5 Ra (Ra is the $^{3}He/^{4}He$ of air) regardless of types of veins, indicating the presence of mantle helium. The ratios of non-radiogenic heavy noble gas isotopes ($^{36}Ar$, $^{84}Kr$, and $^{130}Xe$) are similar to those of seawater and serpentinite in slab mantle [2]. Because porosity in sediments already decreased to <1 % at depths of 4–5 km [3], seawater captured in the pores would be completely expelled from the subducting sediments before reaching to 10–15 km depth, and thus the serpentinized slab mantle is the likely origin of the $^{36}Ar$, $^{84}Kr$, and $^{130}Xe$. The measured $^{3}He/^{4}He$, non-radiogenic heavy noble gas ratios, and salinity are consistent with those of slab-derived fluids observed in mantle wedge peridotites from subduction zones [4, 5], suggesting that fluids released from subducted serpentinite to the mantle wedge migrate toward shallow depths along subduction boundary. From a mixing calculation using $^{36}Ar$, $^{84}Kr$, and $^{130}Xe$ data, more than 64% of vein-forming fluids were originated from the subducted serpentinite. Therefore, the migration of mantle-derived fluids has a potential to induce brittle failures in plate boundaries via increasing fluid pressures.

[1] Ujiie *et al.* (2018) *Geophys. Res. Lett.* **45**, 5371–5379. [2] Kendrick *et al.* (2013) *Earth Planet. Sci. Lett.* **365**, 86–96. [3] Kato *et al.* (2004) *Geophys. Res. Lett.* **31**, L06602. [4] Sumino *et al.* (2010) *Earth Planet. Sci. Lett.* **294**, 163–172. [5] Kobayashi *et al.* (2017) *Earth Planet. Sci. Lett.* **457**, 106–116.

Keywords: Fluid overpressure, Mantle-derived fluids, Helium isotopes, Crack-seal vein

©2019. Japan Geoscience Union. All Right Reserved. 

# Geological and rheological conditions of subduction plate boundary between the seismogenic zone and the ETS zone in warm-slab environments

*Kohtaro Ujiie[1], Kazuya Noro[1], Norio Shigematsu[2], Ake Fagereng[3], Naoki Nishiyama[1], Christopher Tulley[3], Haruna MASUYAMA[1], Yasushi Mori[4]

1. Graduate School of Life and Environmental Sciences, University of Tsukuba, 2. Research Institute of Earthquake and Volcano Geology, National Institute of Advanced Industrial Science and Technology, Japan, 3. Cardiff University, 4. Kitakyushu Museum of Natural History and Human History

In subduction zones particularly under warm-slab environments, the transition zone between the locked seismogenic zone and the deeper, stably sliding zone is the site of slow earthquakes such as episodic tremor and slip (ETS) and long-term slow slip events (L-SSEs). Exhumed subduction mélanges on Kyushu Island, Japan, were deformed at depths of ~15–30 km and temperatures of ~370–500 ˚C under warm-slab environments and thus provide an invaluable opportunity to examine geological and rheological conditions that may responsible for slow earthquakes. The mélanges record low-angle thrust sense, viscous shear associated with metasomatic reactions. The metasomatism is caused by the infiltration of sodium-bearing fluid between pelitic schist and mafic to ultramafic rocks, resulting in albitization of pelitic schist. Microstructural observations and electron backscatter diffraction analysis show that viscous shear was accommodated by dislocation creep, mechanical rotation, and possible diffusion creep, resulting in dynamic recrystallization of quartz, strong shape and crystal preferred orientations of actinolite and chlorite, and random orientation of albite, respectively. Strain rate of viscous shear zones, estimated from the recrystallized grain size piezometer and flow law for quartz, increases with depth from ~$10^{-13}s^{-1}$to ~$10^{-10}s^{-1}$. The upper value of strain rate is consistent with the strain rate of L-SSEs in subduction zones, when the thickness of viscous shear zone is orders of 10–100 m, compatible with our field observation. Lattice-preferred orientation patterns of quartz c-axes also changes with depth from Type I crossed girdle to c-axis maximum subparallel to shear direction, showing a shear sense consistent with low-angle thrust faulting. Albitized pelitic schist formed by metasomatic reactions and associated viscous shear zones are absent in the mélange deformed at temperatures less than ~330 ˚C. In total, viscous shear associated with metasomatic reactions may account for strain rate, kinematics, and lower limit temperature of L-SSEs zone.

Keywords: subduction mélange, metasomatism, viscous shear

©2019. Japan Geoscience Union. All Right Reserved. 

# Temperature variation in tectonic mélanges of the Shimanto Belt, SW Japan

*Tsai-Wei Chen[1], Donald M Fisher[1], Andrew J Smye[1], Yoshitaka Hashimoto[2]

1. Penn State Univ., 2. Kochi Univ.

Silica redistribution along plate interfaces is a fault zone aging process likely to affect the slip behavior of subduction interfaces. Numerical modeling for slip according to the rate law based on silica kinetics reproduces the characteristics of real-world subduction zones, such as an updip limit to the seismogenic zone, earthquake clustering, and a power-law size distribution of earthquake magnitudes. In the field, the structure of subduction fault zones is typically marked by veined sandstone blocks within mudstones with scaly fabric, with mudstones providing a local source of silica and other elements that precipitate as minerals veins, which act as a sink for mobile elements. The silica kinetics related to diffusion from shearing mudstones to cracking sandstone blocks in mélange provides a temperature dependent mechanism for fault zone aging whereby the contact area across the fault zone increases in the time between slip instabilities. In the Shimanto belt of Japan, scaly fabric and vein microstructures show textural variability as a function of temperature. There is a gradient in the age of paleosubducting oceanic crust from north to south within the inner Shimanto belt, from the Yokonami mélange, with a thick pelagic chert section and older basalt and younger mélanges in the south (Okitsu, Hyuga, and Mugi) with little or no chert section, suggesting younger subducting crust. Thus, the mélanges of the Shimanto belt were accreted at different temperatures and depths along the interface, and there also may have been differences in the subduction geotherm. We suggest that these variations in temperature are likely to lead to different silica kinetics and rates of mineral redistribution, recorded in microstructural variations that may reflect different frictional properties along the plate interface. The slip behavior of the plate interface depends on temperature as evidenced by down dip variations in slip mode and differences in earthquake size distributions for subduction zones with different age crust. We therefore have undertaken a study of oxygen isotope thermometry using coexisting mineral pairs of quartz-albite-calcite observed in the tectonic mélanges from the Shimanto belt at a variety of estimated temperatures. This data provides an independent method for evaluating the temperature during mineral redistribution that can be compared with current estimates based on vitrinite reflectance and fluid inclusion analyses.

Keywords: Subduction zone processes, Shimanto Belt , Silica redistribution, Oxygen isotope thermometry

©2019. Japan Geoscience Union. All Right Reserved. 

# Frictional properties of opal gouge at low-temperature hydrothermal conditions and their implications for seismogenic faulting along subduction-zone megathrusts

*Kyuichi Kanagawa[1], Tomoya Nakanishi[2], Morito Kuwana[3], Michiyo Sawai[1], Takehiro Hirose[4]

1. School of Science, Chiba University, 2. Graduate School of Science and Engineering, Chiba University, 3. Faculty of Science, Chiba University, 4. Kochi Institute for Core Sample Research, Japan Agency for Marine-Earth Science and Technology

We conducted a series of triaxial friction experiments on opal gouge at low-temperature (≦200˚C) hydrothermal conditions, in order to address the change in frictional stability along subduction-zone megathrusts. The results revealed frictional properties of opal gouge dependent on temperature ($T$), displacement ($V$) or pore water presure ($P_p$), as described below.

When fitted by the rate- and state-friction constitutive law, friction parameter $a$ does not change much with $T$, $V$ or $P_p$, while friction parameter $b$ increases, and resultantly ($a-b$) value decreases with increasing $T$, decreasing $V$ or increasing $P_p$. Microstructural observations revealed that densification and coalescence of gouge particles occurred at higher $T$, suggesting the operation of pressure solution. Thus increasing activity of thermally activated pressure solution with increasing $T$, decreasing $V$ or increasing $P_p$ promotes gouge lithification to increase frictional strength, by which ($a-b$) value decreases to <0, and thereby the transition from aseismic faulting to seismic faulting along subduction-zone megathrusts. Our results also imply that increasing $P_p$ at that transition region where ($a-b$) ≈0 would decrease ($a-b$) value to <0, and hence promote slow seismic faulting with small negative ($a-b$) values, which is consistent with high $V_P/V_S$ ratios observed in the regions of slow earthquakes.

Keywords: frictional properties, opal gouge, low-temperature hydrothermal conditions

©2019. Japan Geoscience Union. All Right Reserved. 

[E] Oral | S (Solid Earth Sciences )：S-CG Complex & General

Thu. May 30, 2019 1:45 PM - 3:15 PM JST | Thu. May 30, 2019 4:45 AM - 6:15 AM UTC | Convention Hall A 2F

## [S-CG48] Science of slow earthquakes: Toward unified understandings of whole earthquake process

convener:Satoshi Ide(Department of Earth an Planetary Science, University of Tokyo), Hitoshi Hirose(Research Center for Urban Safety and Security, Kobe University), Kohtaro Ujiie(Graduate School of Life and Environmental Sciences, University of Tsukuba), Takahiro Hatano(Earthquake Research Institute, University of Tokyo), Chairperson:Takahiro Hatano, Takehito Suzuki

Accumulating observational studies on various types of slow deformation events, such as tectonic tremors, very low frequency events, and slow slip events, portrays some universal characteristics in generally complex behavior, including interaction among events and influence by various outer loadings. Some of these phenomena seem to have causal relation with the occurrence of very large earthquakes. A unified understanding of these slow and fast earthquake processes requires an approach integrating geophysics, seismology, geodesy, geology, and non-equilibrium statistical physics. We welcome presentations based on, but not limited to, geophysical observation, data analysis, analytical theory, numerical simulation, field study, and laboratory experiments.

1:45 PM - 2:00 PM JST | 4:45 AM - 5:00 AM UTC

[SCG48-28] **Rate and State Dependent Friction Law and Static Friction Force**

*Hiroshi Matsukawa [1] (1.Aoyama Gakuin University)

---

2:00 PM - 2:30 PM JST | 5:00 AM - 5:30 AM UTC

[SCG48-29] **Stable sliding, slow and silent slip events and laboratory earthquakes across the brittle ductile transition**

★Invited Papers

*Alexandre Schubnel[1], Aubry Jérôme[1], François Passelègue[2] (1.Laboratoire de Géologie, ENS, PARIS, France, 2.EPFL, Switzerland)

---

2:30 PM - 2:45 PM JST | 5:30 AM - 5:45 AM UTC

[SCG48-30] Dramatic velocity weakening of dry quartz friction at relatively slow slip velocities

*Akito Tsutsumi[1], Hirotaka Iida[2], Yuko Onoe[1] (1.Graduate School of Science, Kyoto University, 2.Geothermal Engineering. Co. Ltd.)

---

2:45 PM - 3:00 PM JST | 5:45 AM - 6:00 AM UTC

[SCG48-31] Rupture nucleation processes accompanying tremor and slow slip in gel friction experiments

*Tetsuo Yamaguchi[1] (1.Graduate school of Engineering, Kyushu University)

---

3:00 PM - 3:15 PM JST | 6:00 AM - 6:15 AM UTC

[SCG48-32] Solution Orbit for k and epsilon Model for Turbulent Flow in Porous Media

*Takehito Suzuki[1] (1.Department of Physics and Mathematics, Aoyama Gakuin University)

# Rate and State Dependent Friction Law and Static Friction Force

*Hiroshi Matsukawa [1]

1. Aoyama Gakuin University

It is well known that the Rate and State Dependent Friction Law (RSF) plays an important role in the study of earthquake including slow-earthquake [1, 2]. RSF was introduced by Dietrich [3] and Ruina [4] based on the laboratory experiments and describes the sliding velocity and state-variable dependences of the friction coefficient. The dependences are analyzed by the thermal activation process of the deformation and detachment of actual contact points [5-7]. The thermal activation of the deformation of actual contact points, which is called the indirect process, cause the increase of the actual contact area and then the friction force with increasing contact time of actual contact point, which is inversely proportional to the sliding velocity. The thermal activation of the detachment of actual contact points, which is called the direct process, cause the increase of the friction force with increasing sliding velocity. Such analysis discuss the change of friction coefficient depending on the sliding velocity and state-variable. Here we extend the analysis and discuss the absolute value of the friction coefficient. In the case that the direct process overwhelm the indirect process, the friction coefficient can vanish in the limit of vanishing sliding velocity, that means the vanishing static friction force. The vanishing static friction force results from the thermal activation of the detachment of the actual contact points. The velocity dependence of the friction coefficient in the low velocity regime is investigated. It is also shown that even in the case that the indirect process overwhelm the direct process in the usual velocity regime, the direct process overwhelm the indirect process in the law velocity limit. In this case the steady state friction coefficient once increase from zero in the low velocity regime, shows a peak and then decreases with increasing sliding velocity. The relations with the laboratory experiment [8] and slow earthquake are discussed.

References

1, Scholz, C., “*Earthquakes and friction laws*”, Nature **391**, 37 (1998).

2, Saito, T., Ujiie, K., Tsutsumi, A., & Kameda, J., “*Geological and frictional aspects of very-low-frequency earthquakes in an accretionary prism*”, Geophysical Research Letters **40**, 703 (2013).

3, Dieterich, J., “*Modeling of rock friction 1. Experimental results and constitutive equations*” and “*Modeling of rock friction 2. Simulation of preseismic slip”*, Journal of Geophysical Research **80,** 2161 and 2169 (1979).

4, Ruina, A. , “*Slip instability and state variable friction law*”, Journal of Geophysical Research: Solid Earth **88,** 10359 (1983).

5, Heslot, F., Baumberger, T., Perrin, B., Caroli, B., & Caroli, C. *“Creep, stick-slip, and dry-friction dynamics: Experiments and a heuristic model”*, Physical Review E **49**, 4973 (1994).

6, Hatano T., “*Rate and state friction law as derived from atomistic processes at Asperities*”, arXiv:1512.05078v1 (2015).

©2019. Japan Geoscience Union. All Right Reserved. 

7. Aharonv, E., & Scholz, C.H., “*A physics based rock friction constitutive law: Steady state friction*”, Journal of Geophysical Research: Solid Earth **123**, 1591 (2018).

8. Yamaguchi, T., private communication.

Keywords: Rate and State Dependent Friction Law, Static Friction Force

©2019. Japan Geoscience Union. All Right Reserved. 

# Stable sliding, slow and silent slip events and laboratory earthquakes across the brittle ductile transition

*Alexandre Schubnel[1], Aubry Jérôme[1], François Passelègue[2]

1. Laboratoire de Géologie, ENS, PARIS, France, 2. EPFL, Switzerland

The transition from brittle to plastic deformation corresponds to the regime where brittle fracturing and plastic flow co-exist. This transition is of fundamental importance to understand how natural faults behave differently at the bottom of the seismogenic zone, at PT conditions where the deformation regime is not fully brittle anymore.

Here, we reproduced the complete spectrum of natural faulting at laboratory scale, from stable slip to slow earthquakes and up to fast instabilities, on samples of dolostones and carbonates. Transitions from creep to slow ruptures and from slow to fast ruptures, are obtained by increasing both pressure and temperature up to conditions encountered at 3 km depth (i.e. 100 MPa confining pressure and 100 ˚C), which corresponds to the onset of seismicity in nature. Increasing confining pressure and temperature augments the fault elastic stiffness, which decreases the nucleation length and enhances the slip velocities during the nucleation to values allowing flash weakening and decarbonation processes.

From our experimental results, we conclude that: (i) laboratory earthquakes may nucleate on inherited fault interfaces at brittle-ductile transition conditions; (ii) in this regime where plastic deformation of the bulk and dynamic fault slip may co-exist, laboratory earthquakes are promoted when the interface is smooth, or when the loading rate is slow; (iii) stable sliding tends to produce mirror-like surface, while stick-slips is associated with matte surfaces, on which the size of the asperities grows with increasing confining pressure, (iv) slower loading rates and higher confining pressures promote the occurrence of laboratory earthquakes associated with increasing plastic deformation, while increasing initial roughness promotes stable sliding and slow stick-slip.

Keywords: slow and silent earthquakes, stick slip, brittle ductile transition

©2019. Japan Geoscience Union. All Right Reserved. 

# Dramatic velocity weakening of dry quartz friction at relatively slow slip velocities

*Akito Tsutsumi[1], Hirotaka Iida[2], Yuko Onoe[1]

1. Graduate School of Science, Kyoto University, 2. Geothermal Engineering. Co. Ltd.

Understanding the frictional properties of subduction-zone fault materials is crucial to understanding subduction-zone seismogenesis. Previous experimental studies have demonstrated that fault weakening in siliceous rocks occurred at relatively low slip velocities ($V > 0.01$ mm/s) [Goldsby and Tullis, 2002; Di Toro et al., 2004; Hayashi and Tsutsumi, 2010], under which conditions transformation reactions are unable to proceed because of low temperatures. Formation of a silica gel layer has been suggested as a possible cause of the weakening behavior [Goldsby and Tullis, 2002]. However, there exists only limited information on the frictionally generated material and little is known about the weakening mechanism. To study the effect of moisture on the fault zone process in siliceous material, we have performed friction experiments on a synthetic quartz sample under two different humidity conditions: in room humidity (relative humidity RH = 20 to 75%) and in dry (RH < 3%) conditions. to

Three types of friction experiments were performed using a rotary-type testing machine on a pair of hollow-cylindrical specimens of quartz with outer and inner diameter of 25 and 5 mm, respectively, at a constant normal stress of 1.5 MPa. Constant velocity tests and velocity stepping tests were conducted under a range of slip velocities from 0.005 to 105 mm/s. In slide-hold-slide (SHS) tests, samples were first slid at $v = 105$ mm/s, by which sliding friction coefficient $f$ decreases to attain a steady-state value of about $f = 0.2$. Then, rotation of the sample was stopped for periods of 1 to 10000s, after which rotation of the sample at the same rate was restarted.

In room humidity conditions, steady state friction shows velocity weakening at $v > 0.01$ mm/s, which is consistent to the previous studies. We find that steady-state friction values measured at the dry condition are almost constant at $f = 0.2$ for slip velocities $v$ from 0.1 to 100 mm/s. SHS tests show that time-dependent frictional healing is observed for hold time duration $t > 10$s in room humidity condition. On the contrary, the time-dependent frictional healing is negligible when tested in the dry condition.

Our results imply that the moisture-absorption strengthening, which has been proposed to be an effective mechanism for time-dependent healing of high-velocity friction of gabbro (Mizoguchi et al. 2006) is an important underlying mechanism of the frictional weakening of quartz rocks observed in ambient humidity conditions.

Keywords: high-velicity friction, velocity weakening, gel lubrication

©2019. Japan Geoscience Union. All Right Reserved. 

# Rupture nucleation processes accompanying tremor and slow slip in gel friction experiments

*Tetsuo Yamaguchi[1]

1. Graduate school of Engineering, Kyushu University

We have been elucidating similarities between our analogue experiments and earthquakes through some examples, such as coexistence of fast and slow slip, GR relation, size-duration scaling, and supershear rupture. In this study, we observed rupture nucleation processes for large events. As a result, we found the occurrence of tremor in coincident with slow slip. We also found that the duration of a slow event is proportional to the minus one-third power to the driving velocity. This power law behavior suggests that the slow slip process is determined independently of the characteristic velocity scale of the system. We will elucidate the relationship between frictional constitutive law and the macroscopic behavior. We will also discuss the realistic geological setup for our lab systems.

Keywords: Slow slip, Tremor, Analogue experiment, Gel

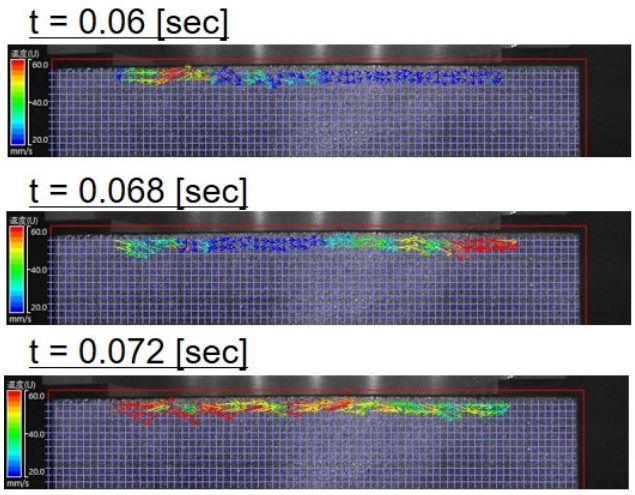


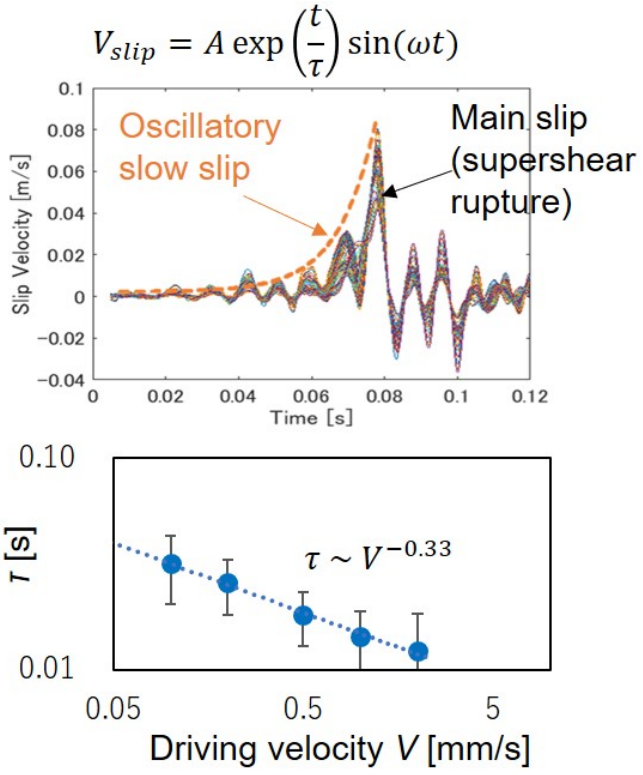


©2019. Japan Geoscience Union. All Right Reserved. 

# Solution Orbit for k and epsilon Model for Turbulent Flow in Porous Media

*Takehito Suzuki[1]

1. Department of Physics and Mathematics, Aoyama Gakuin University

Turbulent flow within porous media such as fault rocks can affect dynamic earthquake rupture processes and has attracted interests of many researchers. Among models treating the turbulent flow, the k-epsilon model has widely been employed, where k is the turbulent kinetic energy and epsilon is the dissipation rate of k. However, analytical treatment associated with the effect of the initial values of k and epsilon on the final state has not been performed.

We assume a one-dimensional homogeneous porous medium and isotropic turbulence. We also assume that the density of the fluid, rho, and the porosity, phi, are constant, and the ensemble averages of phi k and phi epsilon will be written as k and epsilon below, respectively. With these assumptions, it should be emphasized that exactly the same straight line given by the equation epsilon=$c_k$ $u_D$ k /\sqrt{*K*} is a nullcline common to both variables on the k-epsilon phase space, where $c_k$ is a constant number, $u_D$ is averaged Darcy velocity, and *K* is permeability. We can regard this line as a line attractor or repeller as observed in other systems such as Suzuki (2017). Moreover, the straight line epsilon=0 (k axis) is also a nullcline for epsilon.

Actually, the analytical form of solution orbits is given by epsilon=epsilon$_0$ (k/$k_0$)^$C_2$, where $C_2$ is a constant, 1.9. Using this, we show below that the common nullcline epsilon=$c_k$ phi $u_D$ k/\sqrt{*K*} is a line attractor for this solution orbit. First, we define Region I as the region 0< epsilon < $c_k$ $u_D$ k /\sqrt{*K*} on the phase space, and Region II as the region epsilon > $c_k$ $u_D$ k/\sqrt{K}>0. We also define the point ($k_f$, epsilon$_f$ ) as the point where the solution orbit passing the point ($k_0$, epsilon$_0$) crosses the nullcline. With these definitions, we have relations $k_0$f and epsilon$_0$f if ($k_0$, epsilon$_0$) is in the Region I. This occurs because epsilon is proportional to k on the nullcline, while epsilon is proportional to k^$C_2$ on the solution orbit and $C_2$ >1. We can also conclude $k_0$>$k_f$ and epsilon$_0$>epsilon$_f$ if ($k_0$, epsilon$_0$) is in the Region II. Second, we should emphasize that k and epsilon increase (decrease) with increasing time in the Region I (II), since \partial k/\partial t and \partial epsilon/\partial t are positive (negative). Therefore, if ($k_0$, epsilon$_0$) is in the Region I (II), the solution moves to the upper right (lower left), and is absorbed into the nullcline with the limit t \to \infty. We can conclude that the nullcline is a line attractor, not a repeller. The steady stable solution is given by (k, epsilon)=($k_f$, epsilon$_f$).

Note that k and epsilon vanish with the limit t \to \infty for usual isotropic turbulent flow, even though the solution orbit for such flow is the same as one obtained here. Actually, the usual turbulent flow is described by the limit *K* \to \infty in the present model. The nullcline is k axis in such a case, and the Region I vanishes. Therefore, all the solutions are absorbed into the origin. The finite *K* enables the turbulence to be survive with t \to \infty for the homogeneous state.

Keywords: porous media, k-epsilon model, solution orbit

©2019. Japan Geoscience Union. All Right Reserved. 

[E] Oral | S (Solid Earth Sciences )：S-CG Complex & General

Thu. May 30, 2019 3:30 PM - 5:00 PM JST | Thu. May 30, 2019 6:30 AM - 8:00 AM UTC | Convention Hall A 2F

## [S-CG48] Science of slow earthquakes: Toward unified understandings of whole earthquake process

convener:Satoshi Ide(Department of Earth an Planetary Science, University of Tokyo), Hitoshi Hirose(Research Center for Urban Safety and Security, Kobe University), Kohtaro Ujiie(Graduate School of Life and Environmental Sciences, University of Tsukuba), Takahiro Hatano(Earthquake Research Institute, University of Tokyo), Chairperson:Naofumi Aso, Takahiro Hatano

Accumulating observational studies on various types of slow deformation events, such as tectonic tremors, very low frequency events, and slow slip events, portrays some universal characteristics in generally complex behavior, including interaction among events and influence by various outer loadings. Some of these phenomena seem to have causal relation with the occurrence of very large earthquakes. A unified understanding of these slow and fast earthquake processes requires an approach integrating geophysics, seismology, geodesy, geology, and non-equilibrium statistical physics. We welcome presentations based on, but not limited to, geophysical observation, data analysis, analytical theory, numerical simulation, field study, and laboratory experiments.

3:30 PM - 4:00 PM JST | 6:30 AM - 7:00 AM UTC

[SCG48-33] **Modelling precursory seismicity in the laboratory using a roughness derived rate and state friction model**

★Invited Papers

*Paul A Selvadurai[1], Percy Galvez[2], Stefan Wiemer[1], P. Martin Mai[2] (1.Swiss Seismological service, ETH Zurich, Switzerland, 2.King Abdullah University of Science and Technology, Thuwal, Saudi Arabia)

4:00 PM - 4:15 PM JST | 7:00 AM - 7:15 AM UTC

[SCG48-34] Exponential dependence on perturbation stress of earthquake nucleation

*Saito Takuya[1], Takahiro Hatano[1] (1.The University of Tokyo)

4:15 PM - 4:30 PM JST | 7:15 AM - 7:30 AM UTC

[SCG48-35] Stochastic modeling of slow earthquakes comparable to observations

*Naofumi Aso[1], Ryosuke Ando[2], Satoshi Ide[2] (1.Tokyo Institute of Technology, 2.University of Tokyo)

4:30 PM - 4:45 PM JST | 7:30 AM - 7:45 AM UTC

[SCG48-36] Migration of aqueous fluid near the subducting plate interface

*Manabu Morishige[1] (1.Japan Agency for Marine-Earth Science and Technology)

4:45 PM - 5:00 PM JST | 7:45 AM - 8:00 AM UTC

[SCG48-37] EnKF estimation of frictional properties and slip evolution on a LSSE fault and the changing slip deficit rate on a megathrust fault

*Kazuro Hirahara[1,2] (1.Institute of Education, Research and Regional Cooperation for crisis Management Shikoku, Kagawa University , 2.Riken, AIP center)

# Modelling precursory seismicity in the laboratory using a roughness derived rate and state friction model

*Paul A Selvadurai[1], Percy Galvez[2], Stefan Wiemer[1], P. Martin Mai[2]

1. Swiss Seismological service, ETH Zurich, Switzerland, 2. King Abdullah University of Science and Technology, Thuwal, Saudi Arabia

Growing amounts of seismologic observations appear to be capturing a larger diversity in slip behavior along natural faults. One such behavior is the appearance of localized high-frequency events occurring within a larger preparatory region of accelerated preslip. A mechanism explaining this phenomenon is that fault zones have contrasting strength, which may affect the spatial variability of seismic coupling. Recent numerical studies of faults governed by rate-and-state (RS) friction, show that systematic variations in the strength heterogeneity could explain diverse slip behaviors, such as, stable sliding without spontaneous slip transients, or unstable with spontaneous rupture [Liu and Ampuero, 2017].

Here we detail results from a direct shear friction experiment where a well-instrumented fault was formed by pressing together mature (worn) surfaces of poly(methyl methacrylate), then subjecting it to shear, until gross ‘stick-slip’ failure occurred. Prior to failure, spontaneous ruptures were found to nucleate within a region of accelerated slip, but *arrested locally within a seismogenic section* of the interface. Seismic waves produced by these high-frequency events were measured by an array of calibrated piezoelectric transducers. The seismogenic section was found to form where a slow slip front propagated into a relatively locked region [Selvadurai and Glaser, 2015].

To model the behavior of this lab-scale seismogenic region, we use multi-cycle simulations and linear stability analysis in the open source software QDYN, which utilizes boundary element method and adaptive time-stepping [Luo et al., 2017]. We studied the postmortem surfaces and found that the worn fault displayed a clear bimodal Gaussian distribution of surface height. This unique distribution of surface roughness was determined to be a proxy for a heterogeneous description of the critical slip distance $D_c$ used in numerical calculation that modelled the seismogenic region as a VW section with constant normal stress that obeyed the slip law in terms of RS friction.

Our model showed that it was capable of producing the same diversity in slip behaviors from stable sliding to unstable with localized spontaneous ruptures and this was dependent on parameter selection. Preferentially smooth (polished) sections of fault exhibited low $D_c$ and were susceptible to rupture nucleation. However, the extent to which they propagated along the fault depended on the level strength heterogeneity. Wearing of the fault also led to a natural periodicity in the spatial distribution of strength, which produced numerical estimates of source characteristics that matched those made from an independent analysis of seismic waves. Matching numerical and experimental estimates of source characteristics (seismic moment, source length scale and stress drop) was used a calibration tool to accurately tune the model behavior and better understand conditions leading to the production of seismicity attributed to the interaction of a slow slip front into a relatively locked section of fault.

References:

Luo, Y., Ampuero, J.-P. (2017), Stability of faults with heterogeneous friction properties and effective normal stress, *Tectonophysics*, doi:10.1016/j.tecto.2017.11.006

©2019. Japan Geoscience Union. All Right Reserved. 

Luo, Y., Ampuero, J.P., Galvez, P., Ende, M., Idini, B., (2017). *QDYN: a Quasi-DYNamic Earthquake simulator (V1.1).* http://dx.doi.org/10.5281/zenodo.322459.

Selvadurai, P. A., and S. D. Glaser (2015), Laboratory-developed contact models controlling instability on frictional faults, *J. Geophys. Res. Solid Earth*, 120, doi:10.1002/2014JB011690.

Keywords: Foreshocks, Linear stability analysis, Strength heterogeneity, Laboratory studies

©2019. Japan Geoscience Union. All Right Reserved. 

# Exponential dependence on perturbation stress of earthquake nucleation

*Saito Takuya[1], Takahiro Hatano[1]

1. The University of Tokyo

Recent observations have reported that some tremors in slow earthquake are sensitive to stress perturbations caused by ocean tides [1]. According to the preceding studies [1], occurrence frequencies of the susceptible tremors display exponential dependence on the stress magnitude. This study numerically investigates effects on earthquake nucleation growths of the periodic stress perturbations to see if the nucleation developed under the rate-and-state friction law reproduces the stress dependence. The numerical results suggest the exponential dependence on the perturbation stress magnitudes even in the presence of superimposed sinusoidal waves with the different periods. In addition, the exponential rates are found not to be sensitive to a change in the perturbation period or the superposition components of the sinusoidal perturbations, which implies the critical stresses magnitude are independent of a variety of the perturbations.

[1] S. Ide and Y. Tanaka, Geophys. Res. Lett. 41, 3842 (2014); S. Ide, S. Yabe, H.-J. Tai, and K. H. Chen, Geophys. Res. Lett., 42, 3248 (2015).

©2019. Japan Geoscience Union. All Right Reserved. 

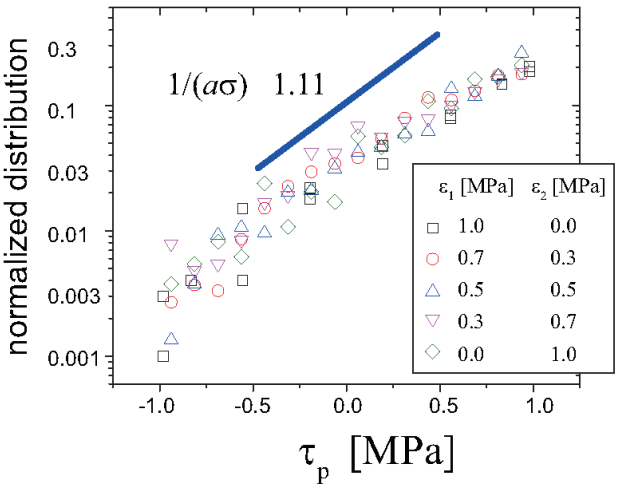


FIG. 1: Numerical results of stress dependence of the nucleation growth under the perturbation $\tau_p = \epsilon_1 \sin(\omega_1 t) + \epsilon_2 \sin(\omega_2 t + \phi_{2,ini})$. Horizontal or vertical axes represents stress magnitude or the normalized distribution, respectively. For each parameter condition, we measured the stresses of 1000 nucleation samples, which grow from randomly generated initial conditions, when the nucleation slip reaches the threshold velocity $V_{thr} = 1.0$ mm/s.



©2019. Japan Geoscience Union. All Right Reserved. 

# Stochastic modeling of slow earthquakes comparable to observations

*Naofumi Aso[1], Ryosuke Ando[2], Satoshi Ide[2]

1. Tokyo Institute of Technology, 2. University of Tokyo

Slow earthquakes are often modeled using rate-and-state friction law with heterogeneously distributed parameters. However, we never know the exact friction law nor the perfect distribution of frictional parameters. Also, other physics are also proposed to contribute to the slow process, including pore fluid. Since any deterministic approaches cannot adequately capture the temporal stress change at a specific site because of the inherent unpredictability caused by various nonlinear processes, we instead focus on the stochastic approach to model slow earthquakes.
In stochastic modeling, we artificially add stochastic fluctuations in numerical simulations. When the result agrees with observations, the stochastic fluctuations are found to represent underlying physics. Then, we can make some predictions that could be evaluated by further observations. After capturing many characteristics of the stochasticity, we could finally approach physics. Although the deductive approach based on specific physics is often taken in earthquake source physics, the experimental approach has the potential to fill the gap between modeling and observations.
Here, we demonstrate that the consideration of stochastic stress fluctuations in ordinary crack simulations can reproduce a variety of observations of slow earthquakes, including burst-like tremor initiation, the existence of tremor front, decelerating tremor migration, and precursory slow earthquakes. The identical model can also reproduce both crack-like and pulse-like ordinary earthquakes by simply changing the strength drop and initial stress level.

©2019. Japan Geoscience Union. All Right Reserved. 

# Migration of aqueous fluid near the subducting plate interface

*Manabu Morishige[1]

1. Japan Agency for Marine-Earth Science and Technology

At least in several subduction zones including Tohoku, Japan, and Cascadia, low surface heat flow has been observed in the forearc, which suggests the existence of a cold fore-arc mantle. This low heat flow has been explained by a thin, low-viscosity layer (LVL) on top of the subducting slab that decouples the movement between the slab and the overriding mantle wedge. Although the formation mechanism of the LVL remains unclear, hydrous minerals such as serpentine may play an essential role in it. The effects of the LVL on solid (or rock) velocity have been extensively investigated. However, little is known of aqueous fluid migration in and around the LVL, despite its importance to our understanding of seismic activity along the subducting plate interface which includes slow earthquakes. In this presentation, I propose a mechanism of fluid flow through the LVL based on a numerical modeling of two-phase flow.

It has been shown that the equations for the solid and fluid phases can be decoupled if porosity is small. I therefore take the following two-step approach based on this assumption. I first solve for solid velocity and the dynamic pressure gradient in and around the LVL. These results are then used to solve for the porosity and compaction pressure in this region.

Preliminary results show that a large amount of fluid is trapped within the LVL by the effects of compaction, that is, the fluid cannot easily flow into the overriding mantle wedge with high viscosity. Dynamic pressure gradient within the LVL becomes large when a thin LVL or high solid viscosity within the LVL is assumed, which leads to a faster fluid flow in the updip direction. These findings suggest that the effects of compaction and dynamic pressure gradient are critical to understand the fluid flow near the subducting plate interface. I also find that the fluid tends to stay near the basal region of the LVL when a non-linear solid viscosity is applied.

Keywords: slow earthquakes, aqueous fluid, subduction zones, low-viscosity layer

©2019. Japan Geoscience Union. All Right Reserved. 

# EnKF estimation of frictional properties and slip evolution on a LSSE fault and the changing slip deficit rate on a megathrust fault

*Kazuro Hirahara[1,2]

1. Institute of Education, Research and Regional Cooperation for crisis Management Shikoku, Kagawa University , 2. Riken, AIP center

With EnKF(Ensemble Kalman Filter), we are developing a system of real-time estimation of frictional properties and slip evolution on LSSE(long-term slow slip event) faults together with the slip deficit rate of the megathrust existing at the up-dip portion of the LSSE faults from the observed GNSS data, through numerical experiments. In the present system, the state vector to be forecasted and updated includes slip rates, state variables and frictional parameters on a LSSE fault, and the slip deficit rate in the megathrust fault. The first 3 parameters are constrained by a RSF(rate and state friction) law and data, but the last one is only by data in a kinematic way. Nishikiori and Hirahara (2017) have shown that the system with EnKF has successfully estimated the slip deficit rate together with frictional properties and slip evolution on the assumed Bungo-Channel LSSE fault for the station distribution corresponding to the GEONET one. So far, we have mainly examined the case of the constant slip deficit rate of the locked megathrust fault, assuming a short and stationary period in the Nankai earthquake cycle.
Several simulation studies have suggested the activity of LSSE is changing during the megaquake cycle, and the real-time monitoring of LSSE activity is important for understanding the stress state of the megaquake fault. Hirahara and Nishikiori (2018) have preliminarily examined the effect of changing deficit rate of the locked region. This study is an extension of theirs. A time series of slip deficit rate derived from a simple simulation of the Nankai earthquake cycle with a RSF law produces shorter reoccurrence time and larger slip rate of the Bungo-Channel LSSE fault toward the occurrence of Nankai megaquake. Based on this simulation model, we produce the simulated deformation rate data at GEONET stations. Then we try to estimate the changing slip deficit rate of the Nankai earthquake fault together with frictional parameters and slip evolution on the LSSE fault. Here, we define v_lock=V_lock -Vpl, and assign Vpl=6.5cm/yr. We can correctly trace the v_lock around -6cm/y during almost locked period. However, when v_lock is larger than -4 cm/yr, our system can not trace v_lock and underestimate the value. Then other parameters become to be also estimated as values deviated from the true ones. Therefore, we try to apply covariance inflation to enlarge the error covariance of the forecast state vector. There are two types of covariance inflation to enlarge the error covariance of the forecast vector. One is multiplicative inflation, where the forecast vector is artificially enlarged. Another is additive inflation, where we add random perturbation to the analysis vector in the previous time step, and obtain the forecast one in the next time step. In the latter one, the perturbation is not added directly to the forecast vector but to the analyzed one in the previous time step, so that the dynamical balances are kept when the next forecast is obtained. We use the approach of additive inflation of covariance. Then, we can correctly estimate the value of v_lock as well as other parameters up to a high value of v_lock around 25 cm/yr. We discuss such problems of abrupt breaks when we encounter in applying our system in numerical experiments.

Keywords: Ensemble Kalman Filter, Slow Slip Events, Rate and State Friction, Megaquake, Covariance Inflation

©2019. Japan Geoscience Union. All Right Reserved. 

[E] Oral | S (Solid Earth Sciences )：S-CG Complex & General

Thu. May 30, 2019 9:00 AM - 10:30 AM JST | Thu. May 30, 2019 12:00 AM - 1:30 AM UTC | A02 TOKYO BAY MAKUHARI HALL

## [S-CG50] Intraslab and intraplate earthquakes

convener:Saeko Kita(International Institute of Seismology and Earthquake Engineering, BRI), Tomohiro Ohuchi(Geodynamics Research Center, Ehime University), Marcel Thielmann(Bavarian Geoinstitute, University of Bayreuth), Ryo Okuwaki(Research Institute of Earthquake and Volcano Geology, Geological Survey of Japan, National Institute of Advanced Industrial Science and Technology), Chairperson:Saeko Kita(Building Research Insitute), Tomohiro Ohuchi(Geodynamics Research Center, Ehime University), Marcel Thielmann(University of Bayreuth), Ryo Okuwaki(筑波大学), Thomas Ferrand(UC San Diego)

The purpose of this session is to share recent advances of geo-scientifical studies for intraslab and shallow-depth intraplate earthquakes. We seek to formulate future directions of the interdisciplinary study of the occurrence of intermediate-depth and deep earthquakes from the viewpoint of seismology, geodynamics and mineral physics. We welcome presentations from a wide variety of scientific disciplines, including seismology, seismotectonics, geodynamics, mineral and rock physics, other geophysics, geology, and numerical modeling.

9:00 AM - 9:15 AM JST | 12:00 AM - 12:15 AM UTC

### [SCG50-01] On a reversely-dipping low-velocity layer in the Tohoku-slab beneath the forearc: unbending induced fluid pathway?

★Invited Papers
# Cancelled

*Hitoshi Kawakatsu[1], HyeJeong Kim[1] (1.Earthquake Research Institute, University of Tokyo)

9:15 AM - 9:30 AM JST | 12:15 AM - 12:30 AM UTC

### [SCG50-02] Evidence for transient fluid pathways in the mantle of the subducting Nazca slab from seismological observations and modeling of the Poisson's ratio

★Invited Papers

*Wasja Bloch[1,2], Timm John[2], Jörn Kummerow[2], Bernd Schurr[1], Pablo Salazar[3,4], Serge A. Shapiro[2] (1.GeoForschungszentrum GFZ, Potsdam, Germany, 2.Freie Universität Berlin, Germany, 3.Universidád Católica del Norte, Antofagasta, Chile, 4.National Research Center for Integrated Natural Disasters Management (CIGIDEN), Santiago, Chile)

9:30 AM - 9:45 AM JST | 12:30 AM - 12:45 AM UTC

### [SCG50-03] Numerical simulation of water transportation along subducting slabs and implications for intraslab earthquakes

★Invited Papers

*Atsushi Nakao[1], Hikaru Iwamori[1,2,3], Tomoeki Nakakuki[4], Yujiro Suzuki[1], Takashi Nakagawa[5], Hitomi Nakamura[2,3,6,7] (1.Earthquake Research Institute, University of Tokyo, 2.Department of Solid Earth Geochemistry, Japan Agency for Marine-Earth Science and Technology, 3.Department of Earth and Planetary Sciences, Tokyo Institute of Technology, 4.Department of Earth and Planetary Systems Science, Hiroshima University, 5.Department of Earth Sciences, The University of Hong Kong, 6.Geological Survey of Japan, National Institute of Advanced Industrial Science and Technology, 7.Ocean Resource Research Center for Next Generation, Chiba Institute of Technology)

9:45 AM - 10:00 AM JST | 12:45 AM - 1:00 AM UTC

### [SCG50-04] Subduction of serpentinized fracture zone and intraslab earthquakes in southern Mexico

★Invited Papers

*Marina Manea[1,2] (1.Computational Geodynamics Laboratory, Geosciences Center, National Autonomous University of Mexico, 2.Institute of Astronomy, Romanian Academy)

10:00 AM - 10:15 AM JST | 1:00 AM - 1:15 AM UTC

[SCG50-05] Reaction-induced embrittlement of the lower continental crust

*Alexandre Schubnel[1], Sarah Incel[2], Julien Gasc[1], Nadège Hilairet[5], Yanbin Wang[3], Feng Shi[3], Loic Labrousse[4] (1.Laboratoire de Géologie, ENS, 2.University of Oslo, 3.GCECARS, University of Chicago, 4.ISTEP, Sorbonne Université, 5.UMET, Université de Lille)

---

10:15 AM - 10:30 AM JST | 1:15 AM - 1:30 AM UTC

[SCG50-06] **Transformation-induced, melt-enhanced faulting in orthoenstatite: implications for global intermediate-depth earthquakes**

Feng Shi[1], Jianguo Wen[2], Tony Yu[1], Lupei Zhu[3], *Yanbin Wang[1] (1.Center for Advanced Radiation Sources, University of Chicago, Chicago, IL, USA, 2.Center for Nanoscale Materials, Argonne National Laboratory, Argonne, IL, USA, 3.Department of Earth & Atmospheric Sciences, Saint Louis University, St. Louis, MO, USA)

# On a reversely-dipping low-velocity layer in the Tohoku-slab beneath the forearc: unbending induced fluid pathway?

*Hitoshi Kawakatsu[1], HyeJeong Kim[1]

1. Earthquake Research Institute, University of Tokyo

Kawakatsu & Kim (2018, SSJ) have recently updated the receiver function reflectivity images beneath the Japanese islands reported earlier in a series of papers by Kawakatsu and others(e.g., Kawakatsu & Watada, 2007, Science). We collected data from recent 14 years (April 2004 to April 2018) of Hi-net recordings; the resulting new dataset is 2.4, 6.4 and 4.8 times larger in terms of the time period, the number of earthquakes, and the number of RF waveforms compared to the earlier works. New images obtained are generally consistent with the previous ones; as the data quantity increases, the covered area widens and images tend to be clearer and smoother. One exception is that there is a glimpse of reversely-dipping low-velocity layer (LVL) within the slab beneath the forearc region dipping toward the Japan trench. When compared with the recent tomographic model that incorporates data from a seafloor cable seismic network S-net, the LVL appears to correspond to a strong P-wave LVL dipping also toward the trench that is imaged from the slab surface at around a depth of 40km to at least 60km. As this LVL is observed along the entire Tohoku Japan arc, it might be a representation of some mechanical process associated with subduction, unless some systematic bias is introduced in tomography (e.g., mis-location of off-shore earthquake depths). We speculate that this structure may continue to the bottom of the slab as imaged by the tomography though not resolved, and be related with the slab unbending that straightens the slab in the mantle (e.g., Kawakatsu, 1986, JGR). Tensile stress caused by unbending near the slab bottom may open a pathway for the sub-slab fluid to migrate upwards all the way to the slab top to further supply fluids around the slab surface, as well as to hydrate the lower-layer of the double seismic zone as suggested by Seno & Yamanaka (1996, AGU Monograph). Geophysical and geochemical consequences of this hypothesis that might be testable via various ways may be discussed.

Keywords: unbending, slab, fluid

©2019. Japan Geoscience Union. All Right Reserved. 

# Evidence for transient fluid pathways in the mantle of the subducting Nazca slab from seismological observations and modeling of the Poisson's ratio

*Wasja Bloch[1,2], Timm John[2], Jörn Kummerow[2], Bernd Schurr[1], Pablo Salazar[3,4], Serge A. Shapiro[2]

1. GeoForschungszentrum GFZ, Potsdam, Germany, 2. Freie Universität Berlin, Germany, 3. Universidád Católica del Norte, Antofagasta, Chile, 4. National Research Center for Integrated Natural Disasters Management (CIGIDEN), Santiago, Chile

Subduction zones worldwide show the common pattern of a lower seismicity plane, where earthquakes occur at intermediate depth within the mantle of the subducting slab. In order to explain the occurrence of these earthquakes different earthquake nucleation mechanisms have been proposed. Some of them attribute seismicity to different transient phenomena that accompany the metamorphic breakdown of water bearing mineral phases. Event though such mechanisms can well explain the distinct shape of the lower seismicity plane and can well be reproduced in laboratory experiments, they are based on the assumption that the subducting plate is hydrated tens of kilometers below the oceanic Moho. Direct evidence for this assumption is scarce.

To detect the possible presence of fluids in the slab mantle, as predicted by the dehydration hypotheses, we estimated the Poisson's ratio of a small rock volume that hosts intra-slab earthquakes by employing a non-tomographic seismic method that has its greatest sensitivity in the direct vicinity of the earthquakes and delivers unique results. We interpret our results by means of a state-of-the-art coupled thermodynamic-poroelastic model. We additionally determine focal mechanisms in the lower seismicity plane to gain information about the prevailing stresses.

The joint interpretation yields a picture in which seismicity occurs at a low rate at 50km depth in a dehydrating but not over-pressured environment at low, overall tensile differential stresses. The modeling results indicate that the fluid occupies a minor volume fraction in the order of only 0.1% and constitutes an interconnected, vein-shaped and therefore transient pore network. These findings are in agreement with results from laboratory experiments, numerical simulations and outcrop studies. They imply that the oceanic mantle of the subducting Nazca slab must be at least weakly hydrated to a depth of 20-30km below the seafloor. Our interpretation can also be applied to tomographic images of other lower seismicity planes, e.g. in Japan.

Keywords: Mantle dehydration, Fluid processes, Seismology

©2019. Japan Geoscience Union. All Right Reserved. 

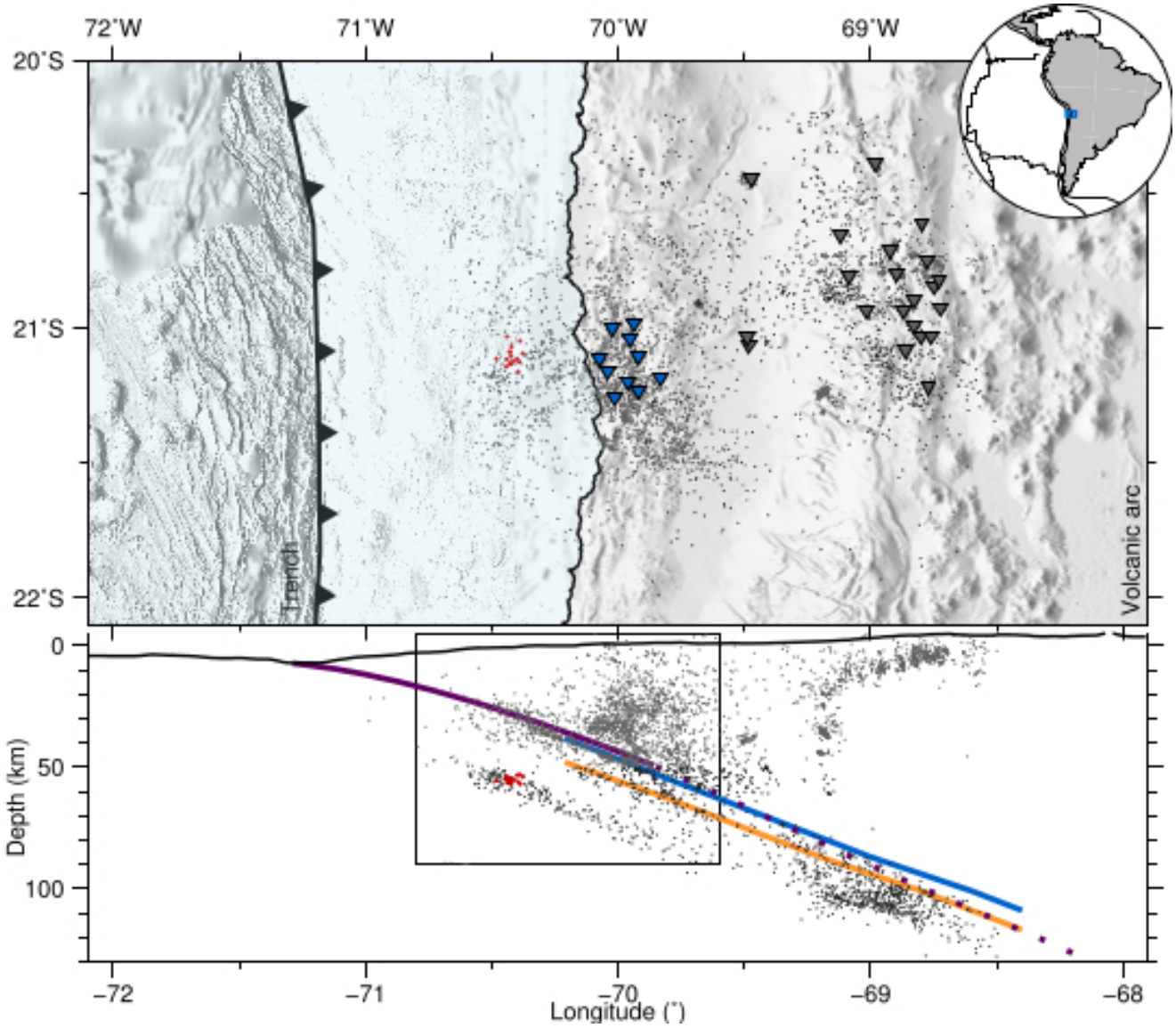


©2019. Japan Geoscience Union. All Right Reserved. 

# Numerical simulation of water transportation along subducting slabs and implications for intraslab earthquakes

*Atsushi Nakao[1], Hikaru Iwamori[1,2,3], Tomoeki Nakakuki[4], Yujiro Suzuki[1], Takashi Nakagawa[5], Hitomi Nakamura[2,3,6,7]

1. Earthquake Research Institute, University of Tokyo, 2. Department of Solid Earth Geochemistry, Japan Agency for Marine-Earth Science and Technology, 3. Department of Earth and Planetary Sciences, Tokyo Institute of Technology, 4. Department of Earth and Planetary Systems Science, Hiroshima University, 5. Department of Earth Sciences, The University of Hong Kong, 6. Geological Survey of Japan, National Institute of Advanced Industrial Science and Technology, 7. Ocean Resource Research Center for Next Generation, Chiba Institute of Technology

It has been argued that water is abundant enough across subducting slabs to trigger lower seismic planes (i.e., >40-km-thick hydrous mantle; Peacock, 2001). Geodynamic modeling, however, suggests that the Pacific slab has a low water content beneath Northreast Japan (NEJ) (Nakao et al., 2018), despite presence of the clear lower seismic plane. The model shows that the thickly serpentinized slab mantle (>10 km for 100-Ma slab) causes slow plate convergence, stationary trenches, and slab penetration into the 660-km boundary, in contrast to the case of NEJ (Lallemand et al., 2008; Fukao & Obayashi, 2013). Moreover, seismic velocity and anisotropy structures also indicate a small amount of water around the lower plane in the Pacific slab (Zhang et al., 2004; Reynard et al., 2010). To address this discrepancy, we performed numerical simulations of water transport within and along the subducting slab of a variable age and initial water content. It is demonstrated that the loci of fluid liberation from the subducted slab of an old age (130 Ma) broadly correspond to the upper seismic plane beneath NEJ. On the other hand, loci of any dehydration reaction within the old slab may not explain the lower seismic plane. Instead, the loci of chlorite breakdown for a 36-Ma slab correspond to the lower plane beneath NEJ. In this case, the breakdown and formation of chlorite repeatedly occur, and liberated fluid forms a long curved-linear locus similar to the shape and extent of lower seismic plane in the Pacific slab beneath NEJ. We suggest that the repeated chlorite breakdown which effectively reutilizes a small amount of water contained initially in the slab may trigger the long lower seismic plane beneath NEJ.

Keywords: Wadati-Benioff zone, intermediate-depth earthquake, plate tectonics, phase relation, thermal structure

©2019. Japan Geoscience Union. All Right Reserved. 

# Subduction of serpentinized fracture zone and intraslab earthquakes in southern Mexico

*Marina Manea[1,2]

1. Computational Geodynamics Laboratory, Geosciences Center, National Autonomous University of Mexico, 2. Institute of Astronomy, Romanian Academy

Oceanic fracture zones are born where spreading centers are offset, creating strong gradients in oceanic floor age and vertical offsets in the oceanic lithosphere. Several lines of evidence, such as tectonic uplift and localized volcanic activity distributed along fracture zones, suggest that oceanic fracture zones represent zones of weakness where seawater can infiltrate several kilometers down into the lithosphere and transform mantle peridotites into serpentinites. Such major serpentinized fracture zones are often consumed into subduction zones where they release large quantities of fluids. The southern Mexican subduction zone is similarly characterized by the presence of a large fracture zone, the Tehuantepec fracture zone (TFZ), which presumably is serpentinized. Moreover, the region where TFZ enters into subduction is marked by a relatively low intraplate seismic activity and a large seismic gap where no large megathrust occurred in the last 100 years or more.

In general the physical processes associated with such seismic gaps are not well understood. However, the presence of TFZ in this area can provide a unique opportunity to advance our knowledge into earthquake mechanics linked to mantle thermal structure. The peculiar 2017 M8.2 Tehuantepec intraslab earthquake nucleated in the vicinity of TFZ, and, from analyses of regional geophysical observations, it is demonstrated that this large normal faulting event ruptured the entire ~26 Ma Cocos slab right beneath the megathrust region. The faulting most likely reactivated a bend fault fabric and ruptured to a depth well below the predicted brittle-ductile transition for the Cocos slab, including regions where temperature is expected to exceed 1000˚C, at far greater P-T conditions than previously considered. Additionally, since the rupture area also propagated laterally along the trench and stopped abruptly when encountered the subducted TFZ, we propose that large and serpentinized fracture zones can act as barriers for intraslab earthquakes. I have to acknowledge that all numerical computations were performed at the National Laboratory for Advanced Scientific Visualization at UNAM (LAVIS).

Keywords: intraslab earthquakes, fracture zone, serpentinization , southern Mexico

©2019. Japan Geoscience Union. All Right Reserved. 

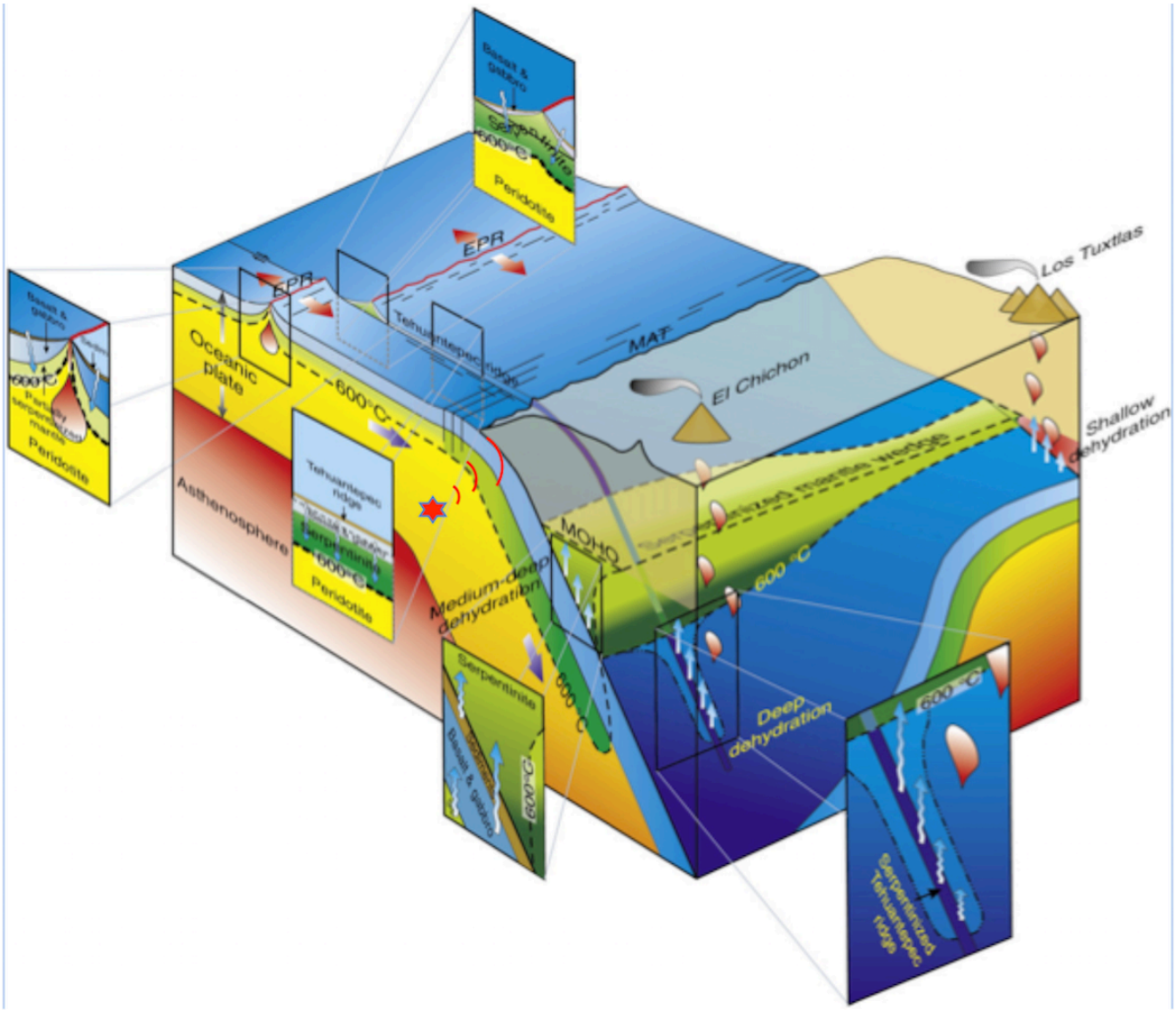


©2019. Japan Geoscience Union. All Right Reserved. 

# Reaction-induced embrittlement of the lower continental crust

*Alexandre Schubnel[1], Sarah Incel[2], Julien Gasc[1], Nadège Hilairet[5], Yanbin Wang[3], Feng Shi[3], Loic Labrousse[4]

1. Laboratoire de Géologie, ENS, 2. University of Oslo, 3. GCECARS, University of Chicago, 4. ISTEP, Sorbonne Université, 5. UMET, Université de Lille

Field observations and geophysical data reveal a causal link between brittle seismic failure and eclogitization of the lower continental crust. We present results from experimental deformation of plagioclase-rich samples at eclogite-facies conditions and quantify the link between rock rheology and the kinetics of the eclogitization reactions. The deformation was ductile both in the absence of reaction and when the progress of eclogitization was fast compared to the imposed strain rate. However, when the reaction rate was relatively slow, the breakdown of plagioclase into nanocrystalline reaction products induced a weakening that triggered seismic failure. Fluid-induced plagioclase breakdown under eclogite-facies conditions is an exothermic reaction accompanied by a negative change in solid volume. This is similar to other mineral transformations that are known to trigger transformational faulting. We demonstrate that mineral reactions lead to brittle deformation in situations where reaction rates are slow compared to the deformation rate. This reaction-induced instability may provide a generic mechanism for embrittlement at depths beyond the normal seismogenic zone.

Keywords: lower crust, Eclogitisation, Granulite

©2019. Japan Geoscience Union. All Right Reserved. 

# Transformation-induced, melt-enhanced faulting in orthoenstatite: implications for global intermediate-depth earthquakes

Feng Shi[1], Jianguo Wen[2], Tony Yu[1], Lupei Zhu[3], *Yanbin Wang[1]

1. Center for Advanced Radiation Sources, University of Chicago, Chicago, IL, USA, 2. Center for Nanoscale Materials, Argonne National Laboratory, Argonne, IL, USA, 3. Department of Earth & Atmospheric Sciences, Saint Louis University, St. Louis, MO, USA

Intermediate-depth earthquakes, which occur at ~50-300 km depths and account for ~90% of all deep earthquakes between 50 and 700 km, are ubiquitously observed along convergent plate margins and post great hazards in many regions of the world. Earthquake-depth distribution in oceanic subduction zones exhibits a prevalent secondary seismicity peak between 180 and 240 km, where major dehydration reactions are expected to have completed [1, 2]. This secondary seismcity peak is a direct manifestation of earthquake activities in the lower plane of the double seimic zone [3]. One of the main constituents of oceanic slabs is harzburgite, which consists mainly of olivine and orthoenstatite (OEn) [4]. The latter transforms to high-pressure clinoenstatite (HP-CEn) at ~120 –210 km depths, depending on aluminum content and slab temperature [5, 6]. We conducted deformation experiments on OEn at conditions corresponding to ~ 40 –250 km depths. Within its stability field, OEn deforms plastically; no brittle failure is detected with acoustic emission (AE) monitoring. In the HP-CEn stability field, metastable OEn generates numerous AEs generated, and fails by macroscopic faulting between ~773 and 1373 K. Outside this temperature range, metastable OEn flows plastically again with no AEs detected. Recovered failed samples contain large conjugated faults, with ultrafine-grained gouge layers containing melts that are more Al-rich. OEn grain boundaries are decorated with fine grained (grainsize < 1 micron) garnet and clinoenstatite (CEn). The latter is interpreted as back-transformed HP-CEn upon pressure release. Within large OEn grains, finer-grained garnet forms thin lamellae preferentially parallel to the OEn (100) twin planes. These results suggest that micro-ruptures start in metastable OEn by syn-deformational transformation, which, aided by exothermic latent heat production, results in exsolution lamellae of garnet and CEn, both along the OEn (100) planes, associated with intragranular ruptures. These micro-ruptures conglomerate along weakened grain boundaries to form intergragular faults consisting of ultrafine grained reaction and shear zones, which, through adiabatic heating and local melting, self-organize into macroscopic faults. We propose that in harzburgite, the observed OEn instability triggers shear localization in olivine, resulting in adiabatic instability, a mechanism hypothesized on theoretical grounds [7, 8] and recently observed in laboratory experiments [9].

*References*:
[1] Hacker, B.R., Peacock, S.M., Abers, G.A., Holloway, S.D., 2003. J Geophys Res 108, 2019.
[2] Syracuse, E.M., van Keken, P.E., Abers, G.A., 2010. Phys Earth Planet In 183, 73–90.
[3] Brudzinski, M.R., C.H. Thurber, B. R. Hacker, E.R. Engdahl, Science, 316, 1472-1474.
[4] Ringwood, A.E., Irifune, T., 1988. Nature 331, 131–136.
[5] Gasparik, T., 2003. Phase diagrams for geoscientists. An Atlas of the Earth's Interior.
[6] Akashi, A.,et al., 2009. J Geophys Res 114, 322.
[7] Ogawa, M., 1987. J Geophys Res 92, 13801-13810.
[8] Hoobs, B.E., Ord, A., 1988. J. Geophys Res 93, 10521-10540.
[9] Ohuchi, T., et al., 2017. Nature Geoscience 10, 771.

©2019. Japan Geoscience Union. All Right Reserved. 

[E] Oral | S (Solid Earth Sciences )：S-CG Complex & General

Thu. May 30, 2019 10:45 AM - 12:15 PM JST | Thu. May 30, 2019 1:45 AM - 3:15 AM UTC | A02 TOKYO BAY MAKUHARI HALL

## [S-CG50] Intraslab and intraplate earthquakes

convener:Saeko Kita(International Institute of Seismology and Earthquake Engineering, BRI), Tomohiro Ohuchi(Geodynamics Research Center, Ehime University), Marcel Thielmann(Bavarian Geoinstitute, University of Bayreuth), Ryo Okuwaki(Research Institute of Earthquake and Volcano Geology, Geological Survey of Japan, National Institute of Advanced Industrial Science and Technology), Chairperson:Saeko Kita(Building Research Insitute), Tomohiro Ohuchi(Geodynamics Research Center, Ehime University), Marcel Thielmann(University of Bayreuth), Ryo Okuwaki(筑波大学), Thomas Ferrand(UC San Diego)

The purpose of this session is to share recent advances of geo-scientifical studies for intraslab and shallow-depth intraplate earthquakes. We seek to formulate future directions of the interdisciplinary study of the occurrence of intermediate-depth and deep earthquakes from the viewpoint of seismology, geodynamics and mineral physics. We welcome presentations from a wide variety of scientific disciplines, including seismology, seismotectonics, geodynamics, mineral and rock physics, other geophysics, geology, and numerical modeling.

10:45 AM - 11:00 AM JST | 1:45 AM - 2:00 AM UTC

### [SCG50-07] The Isolated M7.9 Deep Earthquake of 30 May 2015 Under the Present Bonin Wadati-Benioff Zone: Evidence from the New ISC-EHB Earthquake Catalogue (1930-2015) and CMT Focal Mechanisms

*Stephen Kirby[1], E. Robert Engdahl[2], Emile Andre Okal[3] (1.United States Geological Survey, Menlo Park, 2.University of Colorado, 3.Northwestern University)

11:00 AM - 11:15 AM JST | 2:00 AM - 2:15 AM UTC

### [SCG50-08] What Can $M_W$ –4 Lab-Quakes Teach Us About Deep-Focus Earthquakes?

★Invited Papers

*Julien Gasc[1], Julien Fauconnier[1], Clémence Daigre[1], Arefeh Moarefvand[1], Damien Deldicque[1], Blandine Gardonio[1], Alexandre Schubnel[1], Pamela Burnley[2] (1.Laboratoire de Géologie, ENS-CNRS, Paris, FRANCE, 2.University of Nevada Las Vegas, Las Vegas, USA)

11:15 AM - 11:30 AM JST | 2:15 AM - 2:30 AM UTC

### [SCG50-09] Deep intraslab earthquake rupture due to grain size assisted thermal runaway

*Marcel Thielmann[1], Thibault Duretz[2] (1.Bavarian Geoinstitute, University of Bayreuth, Germany, 2.Université de Rennes, Rennes, France)

11:30 AM - 11:45 AM JST | 2:30 AM - 2:45 AM UTC

### [SCG50-10] Fault model of the 2012 off-Miyagi intraslab earthquake doublet and its implication for rheological signature of incoming Pacific plate

*Tatsuya Kubota[1], Ryota Hino[2], Syuichi Suzuki[2] (1.National Research Institute for Earth Science and Disaster Resilience, 2.Graduate School of Science, Tohoku University)

11:45 AM - 12:00 PM JST | 2:45 AM - 3:00 AM UTC

### [SCG50-11] Source-rupture process of the intraplate earthquake; its diversity related to the fault geometry and damaged fault zone

*Ryo Okuwaki[1], Yuji Yagi[1] (1.Graduate School of Life and Environmental Sciences, University of Tsukuba)

12:00 PM - 12:15 PM JST | 3:00 AM - 3:15 AM UTC

### [SCG50-12] Aftershocks of the NEXT Cascadia Intraslab Earthquake

*Paul Bodin[1,2] (1.University of Washington Seattle, 2.Pacific Northwest Seismic Network)

# The Isolated M7.9 Deep Earthquake of 30 May 2015 Under the Present Bonin Wadati-Benioff Zone: Evidence from the New ISC-EHB Earthquake Catalogue (1930-2015) and CMT Focal Mechanisms

*Stephen Kirby[1], E. Robert Engdahl[2], Emile Andre Okal[3]

1. United States Geological Survey, Menlo Park, 2. University of Colorado, 3. Northwestern University

The M7.9 deep earthquake of 30 May 2015 at a depth of about 680 km was surprising in that it occurred more that 150 km distant from any event in the main Bonin sector Wadati-Benioff Zone (WBZ) above it and more than 120 km deeper than any well-recorded event in the Bonin subduction system. We applied the recently developed ISC-EHB methodology (GJI, 2018, v. 214, 474-484) to produce a comprehensive catalogue of hypocenters for the Izu-Bonin-Marianas region from 1904 to 2015. This methodology, which utilizes only events well-recorded telesesismically along with reported depth phases, ensures that the hypocenters in any given region are relatively well constrained in both location and depth. Individual trench-normal cross sections though the Southern-Bonin/Northern-Marianas subduction systems (including the transition through the Ogasawara Plateau collision zone) display a very sharply defined Bonin inclined seismic zone with no ISC-EHB events at depths and positions between the 2015 deep event and the Izu-Bonin Wadati Benioff Zone (WBZ) above it. Moreover the 2015 deep event occurred at least 200 km north of a possible tear in the main slab at about latitude about 25-26 ˚N where the deep WBZ bends back under the intermediate-depth segment. Most of the CMT focal mechanisms deeper than 300 km within the Bonin WBZ have normal-faulting mechanisms. Some published papers have claimed that the 2015 deep Bonin earthquake occurred in a steeply-dipping sector of the Bonin slab based largely on seismic tomography, but none of these studies have demonstrated sufficient resolution for convincing evidence of high-wave-speed slab material clearly linking the 2015 hypocenter with the main Bonin WBZ. Other published papers show independent evidence that the 2105 event occurred below the Bonin WBZ. We are left with the interpretation that the 2015 event occurred in a slab fragment separated from the main Bonin WBZ. We offer a possible fragmentation scenario involving a oceanic plateau collision, a consequent slab detachment, and an eastward trench stepback. Isolated deep earthquakes in slab fragments can rupture by transformational faulting in metastable olivine (MO) where stresses can originate by the residual stresses caused by heterogeneous volume changes associated with the MO->Spinel transformation (Okal and Kirby, PEPI, 1998).

Keywords: Deep earthquakes, Bonin seismic zone, 2015 Ultra-deep earthquake, Metastable olivine

©2019. Japan Geoscience Union. All Right Reserved. 

# What Can $M_w$ −4 Lab-Quakes Teach Us About Deep-Focus Earthquakes?

*Julien Gasc[1], Julien Fauconnier[1], Clémence Daigre[1], Arefeh Moarefvand[1], Damien Deldicque[1], Blandine Gardonio[1], Alexandre Schubnel[1], Pamela Burnley[2]

1. Laboratoire de Géologie, ENS-CNRS, Paris, FRANCE, 2. University of Nevada Las Vegas, Las Vegas, USA

In recent years, several experimental studies have shed new light on possible faulting mechanisms responsible for intermediate and deep-seated earthquakes. These studies rely not only on the traditional analysis of mechanical data and recovered microstructures, but also on the in situ collection of acoustic data –in the form of Acoustic Emissions (AEs)– used to identify possible co-seismic faulting, i.e., brittle failure.

I will give an overview of this recent work and detail how, recently, deep-focus earthquakes mechanisms could be investigated at 1.5 GPa and 750-900˚C, in a new-generation Griggs-type apparatus using sintered $Mg_2GeO_4$ samples. This compound is an analogue of natural olivine for which the transition towards the high pressure phase (spinel structure) occurs at atmospheric pressure, instead of ~14 GPa for the silicate. This transition induces a mechanical instability –the so-called *transformational faulting*– that leads to macroscopic failure of the samples in a narrow temperature window. The boundaries of this brittle window, as for other reactions (quartz-coesite, antigorite dehydration, plagioclase breakdown and so on), are defined by the reaction kinetics. Here, faulting only occurs in cases where spinel nucleates but hardly grows, i.e., when reaction rates are slow.

At 900˚C mechanical data show a softening, indicative of ductile plastic flow, whereas large amounts of hardening followed by rapid stress drops (and audible stick slips) are recorded at 750˚C. AEs were detected in both cases and differences between P and S waves arrival times suggest that the majority of AEs originate inside the sample. Coherence analysis of the AEs seems to suggest that some bursts of events have similar sources. Surprisingly, AEs are more numerous (~600) at higher temperature, where deformation takes place in a ductile way, accommodated by the development of a wide mylonitic shear band. However, at 750˚C, far more energy is released acoustically upon brittle faulting despite a lower number of AEs (~100). Therefore, higher temperatures favor larger reaction rates, which, in turn, allow the growth of ductile fine-grained spinel. Our results confirm that the brittle temperature window (1) is a function of both equilibrium overstep (reaction kinetic) and strain rate and (2) seems to shift towards lower temperatures with decreasing strain rates, which may explain how earthquakes can occur in a slowly reacting metastable olivine wedge at strain rates orders of magnitude lower than in the lab.

Keywords: deep focus earthquakes, high pressure deformation experiments, transformational faulting, olivine spinel transition, acoustic emissions

©2019. Japan Geoscience Union. All Right Reserved. 

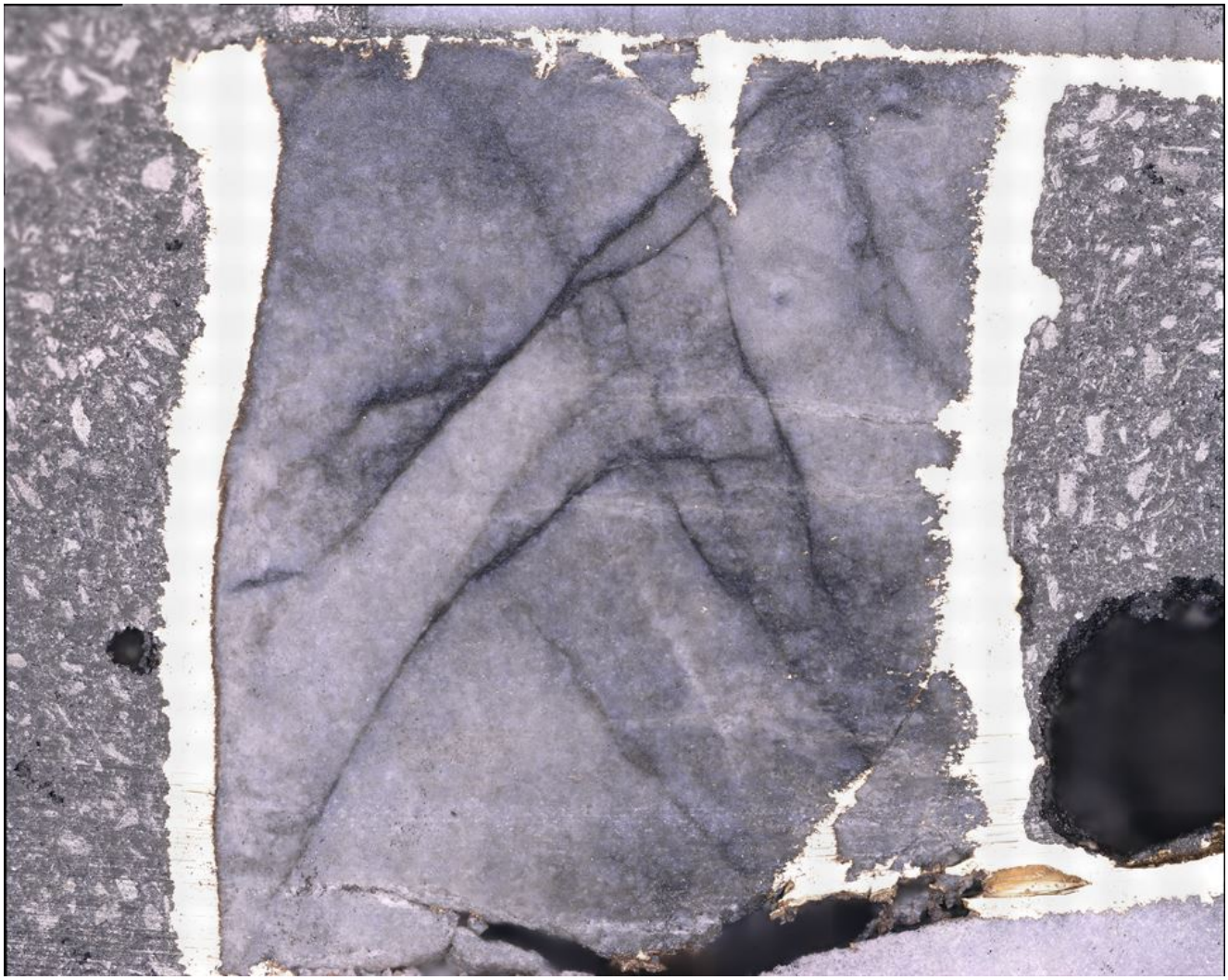

©2019. Japan Geoscience Union. All Right Reserved. 

# Deep intraslab earthquake rupture due to grain size assisted thermal runaway

*Marcel Thielmann[1], Thibault Duretz[2]

1. Bavarian Geoinstitute, University of Bayreuth, Germany, 2. Université de Rennes, Rennes, France

The rupture of the 2017 Mw 8.2 Tehuantepec earthquake has been shown to extend to temperatures above 1,000 ˚C. Ruptures penetrating to regions of such temperatures are highly unusal and raise the question whether the governing rupture mechanisms at these temperatures are comparable to shallow earthquakes. It has been suggested that dehydration embrittlement could result in deep intraslab earthquakes. However, dehydration embrittlement requires the presence of fluids. In the case of the Tehuantepec earthquake, this means that fluids would have to infiltrate the slab to depths that have not been observed.
An alternative mechanism that may lead to failure at these temperatures and depths is thermal runaway, in particular in conjunction with grain size reduction. Due to the conversion from mechanical work to heat during irreversible deformation, this mechanism weakens the rock. In certain conditions, it then results in zones of highly localized viscous creep along which a significant amount of displacement can be accumulated.
Here, we investigate the onset and formation of a ductile shear zone nucleating a cold temperatures and then propagating to regions of higher temperature using 2D numerical models with a nonlinear viscoelastic rheology. We show that it is indeed possible to form a ductile shear zone through the combined action of grain size reduction and shear heating and determine the parameter ranges where this feedback loop may result in ductile shear zone formation and thus also deep earthquake rupture.

Keywords: intraslab earthquakes, deep earthquakes, thermal runaway, grain size evolution

©2019. Japan Geoscience Union. All Right Reserved. 

# Fault model of the 2012 off-Miyagi intraslab earthquake doublet and its implication for rheological signature of incoming Pacific plate

*Tatsuya Kubota[1], Ryota Hino[2], Syuichi Suzuki[2]

1. National Research Institute for Earth Science and Disaster Resilience, 2. Graduate School of Science, Tohoku University

An Mjma 7.3 earthquake composed of a deep reverse-faulting subevent (~60km, Mw 7.2; subevent 1) and a shallow normal-faulting subevent (~20km, Mw 7.1; subevent 2) occurred on 7 December 2012, within the Pacific Plate near the Japan Trench. Since the fault mechanisms of two subevents are consistent with the stress field within the incoming plate near the trench, characterized by the deep compressional and shallow tensile stresses due to the bending of the subducting plate (bending stress, e.g., Chapple and Forsyth, 1979 JGR), we have estimated the finite fault model of this earthquake to discuss the intraplate stress field in this region (Kubota, 2017 PhD thesis, Tohoku Univ). In this study, we conducted more comprehensive discussions for the intraplate stress state, the physical properties, and the relationship between the 2012 earthquake and the Tohoku-Oki earthquake.

We first estimated the initial sea-surface height distribution by inverting the tsunami records and compared it with the vertical deformation expected from the Global CMT solution, to find that the subsided area was generated only by subevent 2 and the uplift area was by both subevents. Then we estimated the optimum fault model for subevent 2, which explains the subsided area of the initial height distribution and the aftershock distribution determined by Obana et al. (2015 AGU FM). Finally, based on the the teleseismic records and the residual displacement between the initial height and the vertical displacement expected from the subevent 2 fault model, we estimated the subevent 1 fault model. We also evaluated the estimation error of our fault model based on the models which had relatively good reproductivity of the sea-surface deformation. As a result, the depth range of the faults of subevents 1 and 2 fell into ~ 45 –70 km and ~ 5 (seafloor) –35 km, respectively.

The down-dip edge of the shallow normal-faulting seismicity in 2012 (~35 km) significantly deepened compared to that in 2007 (~25 km, Hino et al., 2009 G3). However, consideringthe vertical stress gradient of the bending stress (~15 MPa/km), the coseismic stress change by the 2011 Tohoku-Oki earthquake around the normal-faulting seismicity (~20 MPa) is too small to cause normal-faulting earthquakes in that depth range, suggesting that the plate down to ~ 35 km is required to have been already yielded before the Tohoku-Oki earthquake and the frictional strength in the normal-faulting depth range is required to be significantly weaker than the empirical relationship (e.g., Byerlee, 1978). Accounting for the result of the active seismic survey of Fujie et al. (2018 Nature Comm), who suggested the existence of the pore fluid at the shallow part of the subducting plate (< ~ 5 km), the strength reduction is caused by the pore fluid infiltration down to ~ 35 km, along the bending faults (e.g., Faccenda et al., 2009 Nature Geo).

We also obtained the down-dip depth of the deep reverse-faulting subevent at ~70 km, which obviously below the brittle-ductile transition depth expected for the age of the plate. The deep penetration of the fault is explained by the viscoelastic relaxation following the Tohoku-Oki earthquake (e.g., Tomita et al., 2017 Science Adv), which increases the strain rate in the deeper part of the plate. Since the increase of the strain rate makes the brittle-ductile transition depth (e.g., Scholtz, 1988), the depth range of the brittle rupture are extended deeper than that before the Tohoku-Oki earthquake. This result suggests that deep reverse-faulting earthquake in the incoming plate can grow larger after the massive interplate

©2019. Japan Geoscience Union. All Right Reserved. 

earthquake than in the interseismic period.

Keywords: The 2011 Tohoku-Oki earthquake, Intraplate earthquake, Rheology, Stress, Tsunami

©2019. Japan Geoscience Union. All Right Reserved. 

# Source-rupture process of the intraplate earthquake; its diversity related to the fault geometry and damaged fault zone

*Ryo Okuwaki[1], Yuji Yagi[1]

1. Graduate School of Life and Environmental Sciences, University of Tsukuba

Supershear rupture is one of the features that characterizes the earthquake-rupture complexity. Both the theoretical analyses and the laboratory experiments suggests that the rupture-front propagation can exceed the shear wave velocity of the medium due to the excess of the energy flux into the rupture tip. However in real earthquakes, extrinsic factor that controls the manner of supershear rupture has yet been well captured and a relationship between the geometric complexity of the fault and the supershear rupture propagation has been elusive. Geometrical complexity of the fault system is a challenging feature against a reliable estimate of kinematic slip evolution on the basis of finite-fault inversion, since the presumed, fixed rectangle-fault plane or even configuration of the multiple rectangles may not necessarily, fully represent a real fault geometry. Especially for the strike-slip (mode-II rupture) earthquake, the radiation pattern of the wave is sensitive around nodal-shear planes, and if the earthquake involves the geometric complexity in the fault system, the radiation pattern at a certain location on a fault cannot be reproduced when the presumed model fault geometry deviates from the real one. Although supershear-rupture propagation has often been observed in the large strike-slip earthquake (e.g. Mw 7.8 2001 Kunlun, Tibet and Mw 7.9 2002 Denali, Alaska earthquakes), such limitations of finite-fault modeling has prevented us to discuss a relationship between supershear rupture and the fault geometry.

Here we present a kinematic rupture model for the intraplate, Mw 7.5 2018 Palu, Indonesia, earthquake. The 2018 Palu earthquake occurred along the strike-slip Palu-Koro fault zone, which is located around the triple junction of the Australia, Eurasia, and Philippines sea plates. The trace of the surface rupture of the 2018 Palu earthquake, mapped by the Interferometric Synthetic Aperture Rader (InSAR), shows the geometric complexity around the epicenter and south of the Palu bay. We inverted the teleseismic waveforms to resolve both the spatiotemporal evolution of shear slip and the variation of fault geometry by representing slip with five-basis potency-density tensors, without forcing a shear plane to be consistent with a pre-fixed model plane. A possibility of supershear rupture was taken into account by resolving slip in a wide parametric-model space with longer duration of slip-rate function and faster maximum rupture velocity.

The resultant model showed that a rupture front persistently propagated at a high speed (~5 km/s) that exceeds the local shear wave velocity throughout 200-km long within 40 s, but also showed the transient deceleration and acceleration of slip migration, which can be seen as an inchworm walking. The transient deceleration and acceleration of the slip migration was resolved in the area where the strike angle was rotated from the reference-model strike (358˚), which also coincides with the geometric discontinuity of the surface rupture resolved by the InSAR analyses. We will then discuss possible roles of geometric discontinuity that develops inchworm-like slip evolution and damaged fault zone that enables long-lived supershear rupture propagation, which may be characteristic factors that control diverse rupture process of the intraplate earthquake.

Keywords: Intraplate earthquake, Waveform inversion, Fault geometry, Supershear rupture, source rupture process

©2019. Japan Geoscience Union. All Right Reserved. 

©2019. Japan Geoscience Union. All Right Reserved. 

# Aftershocks of the NEXT Cascadia Intraslab Earthquake

*Paul Bodin[1,2]

1. University of Washington Seattle, 2. Pacific Northwest Seismic Network

In 1949, 1965, and 2001 damaging (M6.5-M6.8) deep (~60 km) earthquakes ruptured faults within the Juan de Fuca slab beneath the Puget Sound region of the Cascadia subduction zone in the Pacific Northwest of the U.S.. Each had only a few and very small (approximately M<4) aftershocks. Immediately after the *next* such damaging intraslab earthquake shall we tell the public and first responders that there will likely be no damaging aftershocks? While this low likelihood of aftershocks seems probable based on the historical record, there is no compelling well-agreed-upon physical reason to expect this behavior. For example, recent deep intraslab earthquakes in Japan, Alaska, and Mexico have been followed by strong aftershock sequences. Is the lack of aftershocks following Cascadian intraslab earthquakes unique or extreme? And is it expected and explainable? Possible explanations for regulating the production rate of aftershocks include physical environmental characteristics such as pressure and temperature, geological differences like rock types and faulting geometry, dynamic frictional factors like slip rates, afterslip, and stress drop, and possible roles of fluids. We survey aftershock occurrence following recent smaller Cascadian intraslab earthquakes and following recent large intraslab earthquakes in a number of subduction zones and attempt to classify and distinguish between hypotheses for the lack of Cascadian deep earthquake aftershocks. Is this another possibly unique feature of Cascadia, like the nearly complete lack of instrumentally observed interface earthquakes of any size?

Keywords: intraslab, aftershock, Cascadia, intraplate

©2019. Japan Geoscience Union. All Right Reserved. 

[E] Poster | S (Solid Earth Sciences)：S-CG Complex & General

Thu. May 30, 2019 3:30 PM - 5:00 PM JST | Thu. May 30, 2019 6:30 AM - 8:00 AM UTC | Poster Hall International Exhibition Hall8, Makuhari Messe_14

## [S-CG50] Intraslab and intraplate earthquakes

convener:Saeko Kita(International Institute of Seismology and Earthquake Engineering, BRI), Tomohiro Ohuchi(Geodynamics Research Center, Ehime University), Marcel Thielmann(Bavarian Geoinstitute, University of Bayreuth), Ryo Okuwaki(Research Institute of Earthquake and Volcano Geology, Geological Survey of Japan, National Institute of Advanced Industrial Science and Technology)

The purpose of this session is to share recent advances of geo-scientifical studies for intraslab and shallow-depth intraplate earthquakes. We seek to formulate future directions of the interdisciplinary study of the occurrence of intermediate-depth and deep earthquakes from the viewpoint of seismology, geodynamics and mineral physics. We welcome presentations from a wide variety of scientific disciplines, including seismology, seismotectonics, geodynamics, mineral and rock physics, other geophysics, geology, and numerical modeling.

[SCG50-P01] Changes in seismicity rate, stress orientations, and b-values before and after ETS events in the Philippine sea plate under Kii Peninsula

*Saeko Kita[1], Heidi Houston[2], Sachiko Tanaka[3], Youichi Asano[3], Takuo Shibutani[4], Naoki Suda[5] (1.Building Research Institute, 2.USC, 3.NIED, 4.DPRI, Kyoto University, 5.Hiroshima University)

[SCG50-P02] **Inhomogeneous conduit across slab controlled by intraslab stress heterogeneity in the Nankai subduction zone**

*Makoto Otsubo[1], Ayumu Miyakawa[2], Ikuo Katayama[3], Keishi Okazaki[4] (1.Geological Survey of Japan, Research Institute of Earthquake and Volcano Geology, 2.Geological Survey of Japan, Research Institute of Geology and Geoinformation, 3.Hiroshima University, 4.JAMSTEC)

[SCG50-P03] New insights into the mechanism of deep-focus earthquakes

*Ayako Tsuchiyama[1], Junichi Nakajima[1] (1.Tokyo Institute of Technology)

[SCG50-P04] Faulting in deforming harzburgite under wet conditions

*Tomohiro Ohuchi[1], Xinglin Lei[2], Yuji Higo[3], Yoshinori Tange[3], Takeshi Sakai[1] (1.Geodynamics Research Center, Ehime University, 2.National Institute of Advanced Industrial Science and Technology, 3.Japan Synchrotron Radiation Research Institute)

[SCG50-P05] Semi-brittle behavior of olivine single crystals under the conditions of Earth's mantle transition zone

Yoshihisa Naruse[1], *Tomohiro Ohuchi[1] (1.Geodynamics Research Center, Ehime University)

[SCG50-P06] High-pressure deformation experiments on peridotite gouges under hydrothermal conditions, using a deformation-DIA apparatus

*Maki Semba[1], Ken-ichi Hirauchi[1], Tomohiro Ohuchi[2], Katsuyoshi Michibayashi[3] (1.Department of Geosciences, Faculty of Science, Shizuoka University, 2.Geodynamics Research Center, Ehime University, 3.Department of Earth and Planetary Sciences, Nagoya university)

[SCG50-P07] Stable fault slip in antigorite-olivine aggregates at high pressures

Mai Ikehara[1], *Tomoaki Kubo[1], Takuya Iwasato[2], Yuji Higo[3], Masahiro Imamura[1], Yoshinori Tange[3] (1.Kyushu University, 2.Shin-Nippon Nondestructive Inspection Co., Ltd., 3.JASRI)

[SCG50-P08] Rheology and frictional instability of lawsonite in high pressure deformation experiments

*Rei Shiraishi[1], Jun Muto[1], Akihiro Tsunoda[2], Sando Sawa[1], Akio Suzuki[1] (1.Department of Earth Science, Graduate School of Science, Tohoku University, 2.Earthquake Research Institute, University of Tokyo)

[SCG50-P09] Grain Size Dependency of Olivine-Spinel Phase Transformational Mechanism Responsible for Deep-focus Earthquakes

*Sando Sawa[1], Jun Muto[1], Nobuyoshi Miyajima[2], Hiroyuki Nagahama[1] (1.Department of Earth Science, Tohoku University, 2.Bayerisches Geoinstitut, University of Bayreuth)

[SCG50-P10] **Seismicity and mineral destabilizations in the subducting mantle up to 6 GPa, 200 km depth**

*Thomas P. Ferrand[1] (1.Earthquake Research Institute)

[SCG50-P11] Receiver function imaging of subducting Pacific plate and mantle wedge under Japanese islands using denser network of stations

*HyeJeong Kim[1], Hitoshi Kawakatsu[1], Takeshi Akuhara[1], Masanao Shinohara[1] (1.Earthquake Research Institute, The University of Tokyo)

[SCG50-P12] Strong S-wave attenuation in the mantle wedge beneath the NE Japan and interpretations of high-frequency wave propagation path of intraslab earthquakes

*Takahiro Shiina[1,2], Kei Katsumata[2], Kiyoshi Yomogida[3], Aitaro Kato[1] (1.Earthquake Research Institute, The University of Tokyo, 2.Institute of Seismology and Volcanology, Graduate School of Science, Hokkaido University, 3.Graduate School of Science, Hokkaido University)

# Changes in seismicity rate, stress orientations, and b-values before and after ETS events in the Philippine sea plate under Kii Peninsula

*Saeko Kita[1], Heidi Houston[2], Sachiko Tanaka[3], Youichi Asano[3], Takuo Shibutani[4], Naoki Suda[5]

1. Building Research Institute, 2. USC, 3. NIED, 4. DPRI, Kyoto University, 5. Hiroshima University

The slip on the plate interface has the potential to affect the stress field and seismicity within the subducting slab. Several studies have examined the interaction of slow slip phenomena with intraslab earthquakes [Nankai and Tokai regions, Han et al. 2014; Mexico, Radiguet et al. 2018, 2018 JpGU meeting; New Zealand, 2018, Warren-Smith, 2018 AGU meeting]. Kita et al. [2018, SSJ meeting] reported the stress change in the whole slab associated with ETS times based on stress tensor inversion results. However, we find a clear double seismic zone under Kii Peninsula, as also noted in a previous study [e.g. Miyoshi and Ishibashi, 2004]. Therefore, we here examine seismicity rate variations, stress changes, and b-value variations of seismicity separately for the upper plane events and oceanic mantle ones relative to ETS timings beneath the Kii Peninsula. We use the JMA earthquake catalog, the NIED tremor catalog, the upper surface of the Philippine sea plate estimated by Shibutani and Hirahara [2016], P-wave polarity data by NIED, and a stress tensor inversion code [Vavrycuk, 2014].

We determined the timings of ~30 large ETS beneath the Kii Peninsula from 2001 to 2017, and categorized slab seismicity relative to the occurrence times of nearby the ETS (i.e., 60 days before or after). We then combined or stacked the slab seismicity based on these relative occurrence times. The rate of seismicity both in the upper plane events and in the oceanic mantle ones after the ETS timings clearly decreased, compared to the rate before the ETS timings. The peaks of b-values of seismicity both in the upper plane events and oceanic mantle ones were found to occur 1.5 months before ETS. A change in stress orientations before and after the ETS was seen in the oceanic mantle, and a relatively small change was seen for the upper plane events. The stress change in the upper plane events appears to be larger in the region updip of the ETS zone. The results of our study suggest that the aseismic slip on the plate boundary may affect the stress field and the occurrence of seismicity within the subducting slab beneath the Kii Peninsula. Fluid migration from the oceanic slab into the ETS zone on the plate boundary could be related to the interaction of slow slip phenomena with intraslab earthquakes.

Keywords: Intraslab earthquake, ETS, stress change, b-value, time change, Kii peninsula

©2019. Japan Geoscience Union. All Right Reserved. 

# Inhomogeneous conduit across slab controlled by intraslab stress heterogeneity in the Nankai subduction zone

*Makoto Otsubo[1], Ayumu Miyakawa[2], Ikuo Katayama[3], Keishi Okazaki[4]

1. Geological Survey of Japan, Research Institute of Earthquake and Volcano Geology, 2. Geological Survey of Japan, Research Institute of Geology and Geoinformation, 3. Hiroshima University, 4. JAMSTEC

Non volcanic deep low-frequency tremors and slow slip events occur simultaneously in the transition zone from locked to continuously creeping fault at the down dip portion of the Nankai Trough subduction zone, southwestern Japan. The occurrence of these slow earthquakes is attributed to the effect of high pore pressures on the plate boundaries. The Nankai Trough subduction zone has a discontinuous band of occurrence of these slow earthquakes along the trench. Here we show that spatial variation of intraslab stress can control fluid migration through the subducted Philippine Sea slab to the plate boundary. The tri-axial normal faulting stress detected by the stress tensor inversion by using focal mechanisms in the slab controls anisotropies of permeability trending NNW–SSE sub-horizontal orientation from the subducted Philippine Sea slab to the plate boundary. The inhomogeneous condition controlled by the spatial stress heterogeneities in the subducted Philippine Sea slab represents the intraslab fluid pathway. The hypothesis is consistent with spatial heterogeneity of slow earthquake activities and $^{3}He/^{4}He$ ratio distributions.

Keywords: Fluid, Nankai Trough, Slab, Slow earthquake, Stress

©2019. Japan Geoscience Union. All Right Reserved. 

# New insights into the mechanism of deep-focus earthquakes

*Ayako Tsuchiyama[1], Junichi Nakajima[1]

1. Tokyo Institute of Technology

Generally, deep-focus earthquakes were generated in subducting slabs and occurred along some specific regions such as Izu-Bonin zone and Tonga-Fiji zone. We have not identified their occurrence mechanisms, even though some plausible hypotheses, dehydration embrittlement, thermal and shear plastic instability, and transformational faulting, were proposed. In this study, we try to obtain new constraints that deepen the understanding of deep-focus earthquakes through waveform analysis of earthquakes in the Izu-Bonin subduction zone.

First, we picked up 460 quakes at a depth range of 300-400 km in 2003-2015 beneath Tokai area from the catalog data provided by Japan Meteorological Agency, and relocated them with double-difference earthquake relocation algorithm (hypoDD; Waldhauser and Ellsworth, 2000). Second, we computed their coherence values between all available pairs of earthquakes with cross-spectrum analysis. Then, we were successful to identify a few earthquake clusters that had a very high coherence value over 0.9 in a long time window of 40 s including P and S waves. Moreover, we relocated these earthquakes with hypoDD again by using precisely-determined differential travel-time data derived from waveform data. As a result, we could find that earthquakes in each cluster occurred on single fault plane with complementary rapture areas.

Additionally, we implemented moment tensor inversion (Gephart and Forsyth, 1984) and estimated the stress field around the region where we discovered a few clusters showing waveform similarities. Moreover, we computed the amount of stress drop of the similar earthquakes with spectrum analysis of seismic wave. Through these waveform analyses, we interpreted that the mechanism of these similar deep-focus earthquakes could be explained by combining two possible mechanisms; dehydration embrittlement that regulates the rupture initiation and thermal and shear plastic instability that controls the rupture propagation along a pre-existing fault.

Keywords: deep-focus earthquakes, intraslab earthquakes

©2019. Japan Geoscience Union. All Right Reserved. 

# Faulting in deforming harzburgite under wet conditions

*Tomohiro Ohuchi[1], Xinglin Lei[2], Yuji Higo[3], Yoshinori Tange[3], Takeshi Sakai[1]

1. Geodynamics Research Center, Ehime University, 2. National Institute of Advanced Industrial Science and Technology, 3. Japan Synchrotron Radiation Research Institute

The subduction zone produces a major fraction of the Earth's seismic activity. The mechanisms of intermediate-depth (> 40 km depth) and deep-focus (> 300 km) earthquakes are fundamentally different from those of shallow (< 40 km) earthquakes. This is because the frictional strength of silicate rocks exceeds the upper limit of the stress level in the upper mantle (< 300 MPa: Obata and Karato, 1995) at pressures higher than 1 GPa (~30 km depth). Therefore, the cause of intraslab seismicity at intermediate depths has been attributed to dehydration of serpentinite (e.g., Peakock, 2001) because the water released during dehydration reaction of serpentinite reduces the effective confining pressure. The dehydration embrittlement model is now widely accepted, because the location of the double seismic zone in the subducting Pacific slab corresponds to the main dehydration field in the pressure-temperature diagram of the hydrous peridotite (Omori et al., 2002).

To evaluate the effect of water on semi-brittle behavior of harzburgite, we conducted in-situ uniaxial deformation experiments on as-is/water-saturated harzburgite at pressures 1.2-3.0 GPa and temperatures 770-1250 K with a constant displacement rate using a deformation-DIA apparatus. Pressure, stress, and strain were measured in situ by using x-ray diffraction patterns and radiographs. Acoustic emissions (AEs) were also recorded continuously on six sensors, and three-dimensional AE source location were determined.

Formation of throughgoing faults was observed even when differential stress is much lower than the confining pressure (i.e., > 0.3 times of confining pressure) in water-saturated harzburgite. This is contrast to the case of water-saturated dunite (Ohuchi et al., 2018), in which fracture strength exceeds the confining pressure (i.e., Goetze's criterion). Creep strength of water-saturated harzburgite was lower than that of as-is harzburgite (~0.5-1 GPa at each temperature). Weakening of the harzburgite by the aqueous fluid resulted in the reduction in the number of AE events and decrease in fault slip rate (< 3.6E-4 $s^{-1}$ at a stress of < 1.05 GPa). Stress/pressure drop around the timing of a faulting was limited at strains of 1E-4 $s^{-1}$. The aseismic faulting observed in the water-saturated harzburgite implies that silent slip events around the subduction interface is due to semi-brittle flow of water-saturated harzburgite (i.e., a dehydration product of antigorite).

Keywords: harzburgite, water, semi-brittle flow

©2019. Japan Geoscience Union. All Right Reserved. 

# Semi-brittle behavior of olivine single crystals under the conditions of Earth’s mantle transition zone

Yoshihisa Naruse[1], *Tomohiro Ohuchi[1]

1. Geodynamics Research Center, Ehime University

The origin of deep-focus earthquakes, which occur at depths of 300-700km in the subducting slabs, fundamentally differs from that of other earthquakes and has been attributed to the pressure-induced phase transition in olivine. Previous studies on $Mg_2GeO_4$ olivine have shown that grain size reduction induced by the phase transition in olivine causes shear localization (e.g., Burnley et al., 1991; Schubnel et al., 2013). Schubnel et al. (2013) reported intense acoustic emissions around the timing of a faulting which would be induced by shear localization in polycrystalline $Mg_2GeO_4$ olivine. In order to understand the relationship between fracturing and the phase transition in olivine, we conducted deformation experiments on single crystals of San Carlos olivine ($Fo_{91}$) at pressure of 10-15 GPa and temperatures of 1000-1100 degC using a deformation-DIA apparatus. Single crystal of olivine was chosen to exclude the effect of grain boundaries on nucleation of high-pressure phases of olivine (i.e., wadsleyite and ringwoodite).

Array of microcrack parallel to either (100), (010) or (110) plane was developed at an ~50 degree to the direction of uniaxial compression. Rotation of olivine axes associating the formation of subgrain boundaries was observed around the microcrack arrays, showing that plastic deformation of the olivine single crystal inevitably associated formation of the microcracks. In most samples, microcracks coalesced and then a few throughgoing fractures were developed. Particles of wadsleyite /ringwoodite having a diameter of a few micrometer or less were preferentially nucleated on the microcrack surfaces. Ultrafine-grained domains, which consist of the wadsleyite /ringwoodite particles, were formed along the throughgoing fractures. Development of a banded ultrafine-grained domain was also observed along a throughgoing fracture, implying that shear localization could occur as a result of semi-brittle flow of olivine and a transition from dislocation creep to grain-size-sensitive creep in subducting slabs at depths > 410 km.

Keywords: olivine, phase transition, semi-brittle flow, microcrack, deep-focus earthquake

©2019. Japan Geoscience Union. All Right Reserved. 

# High-pressure deformation experiments on peridotite gouges under hydrothermal conditions, using a deformation-DIA apparatus

*Maki Semba[1], Ken-ichi Hirauchi[1], Tomohiro Ohuchi[2], Katsuyoshi Michibayashi[3]

1. Department of Geosciences, Faculty of Science, Shizuoka University, 2. Geodynamics Research Center, Ehime University, 3. Department of Earth and Planetary Sciences, Nagoya university

In subducting oceanic plates, the focal depth of intraslab earthquakes is deeper (>40 km) than that of interplate earthquakes. Since the normal stress on faults (e.g., outer-rise faults) hosting the intraslab earthquakes is too high to generate brittle shear failure, there may be some mechanisms to weaken effective fault strength. In addition, the hypocenter distribution of intraslab earthquakes forms double-planed structure of the deep seismic zone, and the location of the lower plane is in accord with the stability limit of serpentine (antigorite), suggesting shear deformation of antigorite-bearing peridotite gouges in the presence of hydrothermal water. Here, in order to understand the influence of hydrous minerals on the fault strength, we performed deformation experiments on simulated peridotite gouges with compositions of dunite (100% olivine) and harzburgite (70% olivine/30% orthopyroxene) under hydrothermal conditions, using a deformation-DIA apparatus. The experiments were conducted at a temperature of 580˚C, a confining pressure of 2.5 GPa, and shear strain rates of 2.70 $\times 10^{-5}$ to 1.03 $\times 10^{-4}$ $s^{-1}$. In the deformed peridotite gouges, localized shear zones such as $R_1$ and B shears were observed, and these shears were accompanied with newly formed hydrous phases (serpentine or talc). Olivine grains have a crystal preferred orientation characterized by a slip system of [001] (010). These results indicate that semi-brittle flow is a major deformation mechanism of the peridotite gouges. Considering low coefficients of friction of serpentine and talc, we can suggest that the infiltration of seawater along outer-rise fault planes and subsequent hydrothermal alteration result in effective shear strengths low enough to produce intraslab earthquakes.

Keywords: deformation-DIA apparatus, peridotite, serpentinization, frictional strength

©2019. Japan Geoscience Union. All Right Reserved. 

# Stable fault slip in antigorite-olivine aggregates at high pressures

Mai Ikehara[1], *Tomoaki Kubo[1], Takuya Iwasato[2], Yuji Higo[3], Masahiro Imamura[1], Yoshinori Tange[3]

1. Kyushu University, 2. Shin-Nippon Nondestructive Inspection Co., Ltd., 3. JASRI

Intermediate-depth earthquakes are observed to occur within subducting oceanic plates at depths of about 60-300 km where most materials exhibit plastic deformation rather than brittle failure, owing to high pressures and temperatures. Dehydration embrittlement of hydrous minerals, particularly antigorite serpentine, is one of the most popular hypotheses for explaining shear instability under such conditions (e.g., Raleigh and Paterson, 1965). Recent high-pressure deformation experiments, monitoring Acoustic Emission (AE) activities upon syndeformational antigorite dehydration, showed that dehydration embrittlement was not observed on single-phase antigorite (Gasc et al., 2017), whereas dehydration related faulting was formed on antigorite-olivine aggregates with strong AEs (Ferrand et al., 2017). However, most of the previous high-pressure studies have been conducted in axial compression at relatively low pressures (< 3.5 GPa), insufficient to consider intermediate-depth earthquakes. Therefore, in this study, we conducted high-pressure shear deformation experiments on two-phase aggregates of antigorite and olivine, considering partially serpentinized peridotites, in order to investigate possible shear localization and shear instability up to 7 GPa.

Deformation experiments were conducted at 5-7 GPa, 350-700 ℃ using Deformation-DIA apparatuses at SPring-8 (BL04B1). Monochromatic X-rays (50-60 keV) were used to measure dehydration kinetics, shear strain and stress with recording AEs. We used three kinds of starting materials; natural cored antigorite from Kawarakoba in Nagasaki prefecture, forsterite polycrystal, and two-phase sintered mixtures of antigorite and San Carlos olivine (antigorite 10, 30, 50 vol %). The samples were cut into disks having thickness of 300 $\mu$m and used for a shear deformation study by being assembled between two 45˚-cut alumina pistons. In shear deformation experiments, the starting disk was compressed to 5 or 7 GPa at room temperature, annealed at 350 or 400 ℃ for 1 h, and then deformed with an anvil displacement rate of 200 $\mu$m/h. In some experiments, we increased temperature during shear deformation with a ramping rate of 0.1 ℃/sec to induce dehydration reaction. Microstructures of the recovered samples were examined by an optical microscope and a scanning electron microscope (SEM).

From X-ray radiography images, we observed shear localization in all two-phase samples deformed within the antigorite stability field at 5 GPa. The locallization occurred when homogeneous shear strain $\gamma$ reached 0.4-0.9 (strain rate 1.3-2.2 $\times 10^{-4}$/s), and then most strains were partitioned to the fault zone with the slip velocity of 4.6-9.1 $\times 10^{-2}$ $\mu$m/s. Because no AEs were detected from the sample region, the localized deformation is thought to occur by stable sliding. SEM observations revealed that a thin shear deformation zone was formed along the fault, where the plastic deformation of both antigorite and olivine was significant. Striation and nanograins were observed on the fault plane, suggesting the formation of nanogouge. In contrast, homogeneous deformation was developed during antigorite dehydration with temperature ramping, even in the sample showing shear localization in the antigorite stability field. Under higher pressure condition 7 GPa, shear localization did not occur in all samples regardless of temperature. These results suggest that, although AE activities were detected with the dehydration in the antigorite-olivine aggregates up to 3.5 GPa in the previous study, further increase of pressure inhibits shear instability and shear localization. Thus, other dehydration reactions and/or instability mechanisms are required to explain intermediate-depth earthquakes deeper than ~100 km.

©2019. Japan Geoscience Union. All Right Reserved. 

©2019. Japan Geoscience Union. All Right Reserved. 

# Rheology and frictional instability of lawsonite in high pressure deformation experiments

*Rei Shiraishi[1], Jun Muto[1], Akihiro Tsunoda[2], Sando Sawa[1], Akio Suzuki[1]

1. Department of Earth Science, Graduate School of Science, Tohoku University, 2. Earthquake Research Institute, University of Tokyo

The cause of intermediate-depth earthquakes (50-300 km) in subducting slabs have been proposed to be the dehydration embrittlement (e.g., Raleigh and Paterson, 1965), because there are many kinds of hydrous minerals in a subducting slab and hypocenter distribution coincides with the dehydration boundary determined by high pressure experiments (e.g., Hacker et al., 2003). Many experimental studies on antigorite have been conducted, but a few previous works about dehydration embrittlement of lawsonite-bearing rocks experimentally. Lawsonite, $CaAl_2Si_2O_7(OH)_2H_2O$, is a hydrous mineral which contains 11 wt% water in its structure as both water molecules and a hydroxy group (Cmodi and Zanazzi, 1996). Lawsonite is one of the candidate for dehydration embrittlement in cold subducting slabs, however previous works have apparently contradictory results. Okazaki and Hirth (2016) showed that lawsonite dehydration induced unstable fault slip based on deformation experiments of pure lawsonite using Griggs-type deformation apparatus at 1 GPa. On the other hand, Incel et al. (2017) also investigated deformation properties of lawsonite and glaucophane mixture at 1.5 to 3.0 GPa using deformation-DIA apparatus. They insisted that there is no evidence for a straightforward relation to the dehydration of lawsonite and the brittle failure of samples. So, we have conducted the deformation experiments of lawsonite under the cold slab conditions in order to clarify the deformation property of lawsonite and understand the relationship between dehydration and brittle failure.

Experiments were carried out using Deformation-Cubic Anvil Press (D-CAP) installed at KEK PF AR-NE7A beamline. Pure lawsonite powder (98%) was used as starting materials. Deformation experiments were carried out at a pressure of 6 GPa and temperatures of 300 - 800 ˚C. The temperature was increased at the same time as deformation started. The temperature ramping rate over the strain rate was set the ranges for the real subducting slab, which ranges from $10^2$ to $10^4$ ˚C (Chernak and Hirth, 2011; Okazaki and Hirth, 2016). During deformation stages, strain, stress and transformation rate were measured for in-situ using a monochromatic X-ray beam with an energy of 60 keV.

Four experiments showed rapid stress drop during temperature ramping before lawsonite dehydration starts. We observed microstructure of recovered samples, there are many through going faults and microcracks but no dehydration products. Our results indicate that brittle process and frictional sliding occur without dehydration of lawsonite. This suggests that the intermediate-depth earthquakes can be caused by the deformation itself of lawsonite without the dehydration of lawsonite.

Keywords: intermediate-depth earthquakes, dehydration embrittlement, Lawsonite

©2019. Japan Geoscience Union. All Right Reserved. 

# Grain Size Dependency of Olivine-Spinel Phase Transformational Mechanism Responsible for Deep-focus Earthquakes

*Sando Sawa[1], Jun Muto[1], Nobuyoshi Miyajima[2], Hiroyuki Nagahama[1]

1. Department of Earth Science, Tohoku University, 2. Bayerisches Geoinstitut, University of Bayreuth

Deep-focus earthquakes occur at the depth from 440 km to 660 km in the subducting slab. The mechanism responsible for the earthquakes is thought to be different from that of shallow earthquakes, so that previous studies have reported the various mechanisms. By the geophysical observations and deformation experiments, the phase transformational faulting mechanism is presumed as the precursor of deep-focus earthquakes (e.g., Zhan et al., 2014). The phase transformational faulting mechanism is that metastable olivine in the slab undergoes the phase transformation to fine-grained spinel and faulting occurs with strain localization into the fine-grained spinel. This shear instability depends on grain size. Furthermore, the grain size may restrict the pressure- and temperature-conditions where the shear instability occurs, that is, the region of slab where deep-focus earthquakes occur. However, previous studies have conducted deformation experiments with finer grain size than expected in the slab (e.g., Burnley et al., 1991). Hence, the results from the laboratory experiments cannot directly apply to the geophysical observation. In this study, to reveal the grain size dependency on the phase transformational faulting, we conducted the deformation experiments of germanate olivine (about 3 $\mu$m), which is an analogue material of silicate olivine, finer-grained than that in previous studies (30 $\mu$m). We used a Griggs-type solid-confining media deformation apparatus. The confining pressure, temperature and strain rate are 1.2 GPa, 400~900 ℃ and $2.0\times10^{-4}$ $s^{-1}$, respectively. Even though deformation experiments were conducted under wider temperature conditions than previous studies, we did not observe any shear instability event with apparent stress drops. Also, Raman spectroscopy clarified that the germanate olivine underwent the transformation to spinel at temperatures higher than 500 ℃. Shear instability does not occur because the difference in grain sizes between olivine and nucleated spinel in this study was smaller than those in previous studies. Also, the transformation temperature in this study was much lower than those in previous study (T > 1000 ℃ in Burnley et al., 1991). Considering the rate equation of the transformation (Chan, 1956), small grain size promotes the transformation, but these fast rates of the transformation cannot be explained only by the effect of the grain size. Therefore, the presence of water such as absorbed water in a starting material can also contribute to promote the transformation. Hence, both small initial grain size and a little amount of water promote the transformation even at lower temperature. These results indicate that the phase transformational faulting mechanism has strong grain size dependency. In summary, the pressure- and temperature-conditions where the faulting occurs depends on the grain size of olivine and amount of water. Because the grain size in the slab is larger than that in the experiments, by extrapolating from these results, we may restrict the region of slab where deep-focus earthquakes occur.

This work was supported by the JSPS Japanese-German Graduate Externship.

[Reference]
Burnley et al. (1991), JGR, vol 96, 425-443.
Chan (1956), Acta Metallurgica, vol 4, 449-459.
Zhan et al. (2014), EPSL, vol 385, 89-96.

©2019. Japan Geoscience Union. All Right Reserved. 

Keywords: Deep-focus earthquakes, Griggs type piston-cylinder apparatus, phase transformation

©2019. Japan Geoscience Union. All Right Reserved. 

# Seismicity and mineral destabilizations in the subducting mantle up to 6 GPa, 200 km depth

*Thomas P. Ferrand[1]

1. Earthquake Research Institute

In the subducting oceanic lithosphere, a significant part of the seismicity is triggered in the mantle, especially along the upper and lower Wadati-Benioff planes. Several studies have investigated the potential involvement of dehydration reactions in the triggering mechanism of mantle earthquakes. Recent experimental results reveal that, under subduction conditions, mechanical instabilities nucleate in strong stable mineral aggregates during the destabilization of minor amounts of antigorite, i.e. the high-temperature serpentine, through a stress transfer, without any fluid overpressure. Here I confront these laboratory results to seismological observations. On one hand, most of the natural hydrous magnesium silicates seem to be known, with experimentally-deduced stability limits up to 7 GPa, at least, available as relatively accurate estimates. On the other hand, recent achievements in thermal structure of subduction zones combined with precise hypocentre relocation give access to pressure and temperature conditions at earthquakes hypocentres. A series of P-T diagrams summarizes the stability limit of minerals that may be part of natural peridotite with variable compositions at pressures from 0.5 to 6 GPa and temperatures from 200 to 950˚C, and compares it with seismicity. Both hydrous and anhydrous phases are considered. A myriad of minor metamorphic reactions could participate in a transformation-driven stress transfer, even if the stability limits of serpentine minerals seem to correlate with most of the observed seismicity.

Keywords: earthquakes, intraslab, DDST, dehydration, transformation, subduction

©2019. Japan Geoscience Union. All Right Reserved. 

# Receiver function imaging of subducting Pacific plate and mantle wedge under Japanese islands using denser network of stations

*HyeJeong Kim[1], Hitoshi Kawakatsu[1], Takeshi Akuhara[1], Masanao Shinohara[1]

1. Earthquake Research Institute, The University of Tokyo

Receiver function imaging has been frequently used by different groups focusing on different depths of the Japanese subduction zone. The overlying crust (Shiomi and Park, 2008, Bianchi et al, 2015), the Pacific plate before (Kawakatsu et al., 2009) and after subduction (Kawakatsu and Watada, 2007; Wirth and Long, 2012), and the mantle transition zones (Kawakatsu and Yoshioka, 2011; Tauzin et al., 2018) were discussed using the NIED array stations (Hi-net and F-net). Recently, deployment of ocean bottom seismometers (OBSs) enabled studies of subduction zones closer to the trench (e.g., Akuhara and Mochizuki, 2015). Kawakatsu and Kim (2018, SSJ) have obtained a new version of receiver function imaging using 14-year long of Hi-net data. However, there are other land stations (e.g., J-array) that can improve the station coverage. Here, we collect data from available on-land stations deployed in north-eastern Japan to obtain a denser 2-D array of stations. Additionally, data from temporary OBS stations (Shinohara et al. 2012) are gathered to image the subducted Pacific plate in shallower depths than previously available. Continuous imaging from ocean to land will help to constrain transition of the hydrated oceanic crust along subduction that is expressed as a low velocity layer for better understanding of the hydration/dehydration processes during subduction, which might be related to the occurrence of subduction zone earthquakes.

Keywords: subduction zone, receiver function, ccp stacking

©2019. Japan Geoscience Union. All Right Reserved. 

# Strong S-wave attenuation in the mantle wedge beneath the NE Japan and interpretations of high-frequency wave propagation path of intraslab earthquakes

*Takahiro Shiina[1,2], Kei Katsumata[2], Kiyoshi Yomogida[3], Aitaro Kato[1]

1. Earthquake Research Institute, The University of Tokyo, 2. Institute of Seismology and Volcanology, Graduate School of Science, Hokkaido University, 3. Graduate School of Science, Hokkaido University

For intraslab earthquakes at intermediate-depths in NE Japan, especially at greater than about 100-km depths, it has been often recorded that high-frequency waveform higher than 8 Hz show a remarkable delay of arrival compared with S wave which predominates in a low-frequency band. The magnitude of the delay is little in the forearc region, whereas it increases up to about 40 s in the backarc region. In this study, we investigate the details in the propagation processes of the high-frequency later phase observed for the intraslab earthquakes at the intermediate-depths. To constrain the source location of the high-frequency later phase, we employ the source-scanning algorithm (SSA) [Kao and Shan, 2004] with realistic velocity and attenuation structures, assuming that the high-frequency later phase is generated by the single scattering process. Namely, we estimate a scattering point by using mean-square amplitudes which is synthesized from two horizontal components of the observed waveforms.
Results in frequency bands of 4-32 Hz show that scattering points are distributed beneath the forearc region. The scattering points can reproduce the observed delays of amplitude amplifications associating with the high-frequency later phases. Moreover, similar locations of the scattering points are imaged along the forearc region in the entire NE Japan. These results indicate that high-frequency later phase is a wave scattered at the forearc region and that short wave-length heterogeneity generally developed in the forearc region of NE Japan.
This interpretation well matches implications from previous studies [e.g., Yomogida et al., 2004; Hasemi and Horiuchi, 2010]. Additionally, the obtained distributions of scattering points which appear to surround the highly attenuating mantle wedge suggest that attenuation structure strongly controls propagation paths of seismic wave, in particular, a high-frequency wave. In other words, the identifications of high-frequency later phase may become easy because the amplitude of direct wave crossing the high-attenuation zone decreases. To confirm this consideration, we estimate *Qs* along the direct wave by using the coda-normalization method [e.g., Aki, 1980]. This estimation provides 2-3 times smaller path-averaged *Qs* in seismic records of which rays lay on the backarc and the volcanic front than that of which rays lay on the forearc region. These results support that spatial variation in *QS* produces heterogenous propagations of seismic waves emitted from intraslab earthquakes. It is thus required to take scattering and attenuation structures simultaneously into account to understand complex behaviors of high-frequency waves in a future study.

Keywords: S-wave attenuation, Intraslab earthquakes, High-frequency later phase, Scattered wave

©2019. Japan Geoscience Union. All Right Reserved. 

[E] Poster | S (Solid Earth Sciences)：S-CG Complex & General

Thu. May 30, 2019 5:15 PM - 6:30 PM JST | Thu. May 30, 2019 8:15 AM - 9:30 AM UTC | Poster Hall International Exhibition Hall8, Makuhari Messe_26

## [S-CG50] Intraslab and intraplate earthquakes

convener:Saeko Kita(International Institute of Seismology and Earthquake Engineering, BRI), Tomohiro Ohuchi(Geodynamics Research Center, Ehime University), Marcel Thielmann(Bavarian Geoinstitute, University of Bayreuth), Ryo Okuwaki(Research Institute of Earthquake and Volcano Geology, Geological Survey of Japan, National Institute of Advanced Industrial Science and Technology)

The purpose of this session is to share recent advances of geo-scientifical studies for intraslab and shallow-depth intraplate earthquakes. We seek to formulate future directions of the interdisciplinary study of the occurrence of intermediate-depth and deep earthquakes from the viewpoint of seismology, geodynamics and mineral physics. We welcome presentations from a wide variety of scientific disciplines, including seismology, seismotectonics, geodynamics, mineral and rock physics, other geophysics, geology, and numerical modeling.

[SCG50-P01] Changes in seismicity rate, stress orientations, and b-values before and after ETS events in the Philippine sea plate under Kii Peninsula

*Saeko Kita[1], Heidi Houston[2], Sachiko Tanaka[3], Youichi Asano[3], Takuo Shibutani[4], Naoki Suda[5] (1.Building Research Institute, 2.USC, 3.NIED, 4.DPRI, Kyoto University, 5.Hiroshima University)

[SCG50-P02] **Inhomogeneous conduit across slab controlled by intraslab stress heterogeneity in the Nankai subduction zone**

*Makoto Otsubo[1], Ayumu Miyakawa[2], Ikuo Katayama[3], Keishi Okazaki[4] (1.Geological Survey of Japan, Research Institute of Earthquake and Volcano Geology, 2.Geological Survey of Japan, Research Institute of Geology and Geoinformation, 3.Hiroshima University, 4.JAMSTEC)

[SCG50-P03] New insights into the mechanism of deep-focus earthquakes

*Ayako Tsuchiyama[1], Junichi Nakajima[1] (1.Tokyo Institute of Technology)

[SCG50-P04] Faulting in deforming harzburgite under wet conditions

*Tomohiro Ohuchi[1], Xinglin Lei[2], Yuji Higo[3], Yoshinori Tange[3], Takeshi Sakai[1] (1.Geodynamics Research Center, Ehime University, 2.National Institute of Advanced Industrial Science and Technology, 3.Japan Synchrotron Radiation Research Institute)

[SCG50-P05] Semi-brittle behavior of olivine single crystals under the conditions of Earth's mantle transition zone

Yoshihisa Naruse[1], *Tomohiro Ohuchi[1] (1.Geodynamics Research Center, Ehime University)

[SCG50-P06] High-pressure deformation experiments on peridotite gouges under hydrothermal conditions, using a deformation-DIA apparatus

*Maki Semba[1], Ken-ichi Hirauchi[1], Tomohiro Ohuchi[2], Katsuyoshi Michibayashi[3] (1.Department of Geosciences, Faculty of Science, Shizuoka University, 2.Geodynamics Research Center, Ehime University, 3.Department of Earth and Planetary Sciences, Nagoya university)

[SCG50-P07] Stable fault slip in antigorite-olivine aggregates at high pressures

Mai Ikehara[1], *Tomoaki Kubo[1], Takuya Iwasato[2], Yuji Higo[3], Masahiro Imamura[1], Yoshinori Tange[3] (1.Kyushu University, 2.Shin-Nippon Nondestructive Inspection Co., Ltd., 3.JASRI)

[SCG50-P08] Rheology and frictional instability of lawsonite in high pressure deformation experiments

*Rei Shiraishi[1], Jun Muto[1], Akihiro Tsunoda[2], Sando Sawa[1], Akio Suzuki[1] (1.Department of Earth Science, Graduate School of Science, Tohoku University, 2.Earthquake Research Institute, University of Tokyo)

[SCG50-P09] Grain Size Dependency of Olivine-Spinel Phase Transformational Mechanism Responsible for Deep-focus Earthquakes

*Sando Sawa[1], Jun Muto[1], Nobuyoshi Miyajima[2], Hiroyuki Nagahama[1] (1.Department of Earth Science, Tohoku University, 2.Bayerisches Geoinstitut, University of Bayreuth)

[SCG50-P10] **Seismicity and mineral destabilizations in the subducting mantle up to 6 GPa, 200 km depth**

*Thomas P. Ferrand[1] (1.Earthquake Research Institute)

[SCG50-P11] Receiver function imaging of subducting Pacific plate and mantle wedge under Japanese islands using denser network of stations

*HyeJeong Kim[1], Hitoshi Kawakatsu[1], Takeshi Akuhara[1], Masanao Shinohara[1] (1.Earthquake Research Institute, The University of Tokyo)

[SCG50-P12] Strong S-wave attenuation in the mantle wedge beneath the NE Japan and interpretations of high-frequency wave propagation path of intraslab earthquakes

*Takahiro Shiina[1,2], Kei Katsumata[2], Kiyoshi Yomogida[3], Aitaro Kato[1] (1.Earthquake Research Institute, The University of Tokyo, 2.Institute of Seismology and Volcanology, Graduate School of Science, Hokkaido University, 3.Graduate School of Science, Hokkaido University)

# Changes in seismicity rate, stress orientations, and b-values before and after ETS events in the Philippine sea plate under Kii Peninsula

*Saeko Kita[1], Heidi Houston[2], Sachiko Tanaka[3], Youichi Asano[3], Takuo Shibutani[4], Naoki Suda[5]

1. Building Research Institute, 2. USC, 3. NIED, 4. DPRI, Kyoto University, 5. Hiroshima University

The slip on the plate interface has the potential to affect the stress field and seismicity within the subducting slab. Several studies have examined the interaction of slow slip phenomena with intraslab earthquakes [Nankai and Tokai regions, Han et al. 2014; Mexico, Radiguet et al. 2018, 2018 JpGU meeting; New Zealand, 2018, Warren-Smith, 2018 AGU meeting]. Kita et al. [2018, SSJ meeting] reported the stress change in the whole slab associated with ETS times based on stress tensor inversion results. However, we find a clear double seismic zone under Kii Peninsula, as also noted in a previous study [e.g. Miyoshi and Ishibashi, 2004]. Therefore, we here examine seismicity rate variations, stress changes, and b-value variations of seismicity separately for the upper plane events and oceanic mantle ones relative to ETS timings beneath the Kii Peninsula. We use the JMA earthquake catalog, the NIED tremor catalog, the upper surface of the Philippine sea plate estimated by Shibutani and Hirahara [2016], P-wave polarity data by NIED, and a stress tensor inversion code [Vavrycuk, 2014].

We determined the timings of ~30 large ETS beneath the Kii Peninsula from 2001 to 2017, and categorized slab seismicity relative to the occurrence times of nearby the ETS (i.e., 60 days before or after). We then combined or stacked the slab seismicity based on these relative occurrence times. The rate of seismicity both in the upper plane events and in the oceanic mantle ones after the ETS timings clearly decreased, compared to the rate before the ETS timings. The peaks of b-values of seismicity both in the upper plane events and oceanic mantle ones were found to occur 1.5 months before ETS. A change in stress orientations before and after the ETS was seen in the oceanic mantle, and a relatively small change was seen for the upper plane events. The stress change in the upper plane events appears to be larger in the region updip of the ETS zone. The results of our study suggest that the aseismic slip on the plate boundary may affect the stress field and the occurrence of seismicity within the subducting slab beneath the Kii Peninsula. Fluid migration from the oceanic slab into the ETS zone on the plate boundary could be related to the interaction of slow slip phenomena with intraslab earthquakes.

Keywords: Intraslab earthquake, ETS, stress change, b-value, time change, Kii peninsula

©2019. Japan Geoscience Union. All Right Reserved. 

# Inhomogeneous conduit across slab controlled by intraslab stress heterogeneity in the Nankai subduction zone

*Makoto Otsubo[1], Ayumu Miyakawa[2], Ikuo Katayama[3], Keishi Okazaki[4]

1. Geological Survey of Japan, Research Institute of Earthquake and Volcano Geology, 2. Geological Survey of Japan, Research Institute of Geology and Geoinformation, 3. Hiroshima University, 4. JAMSTEC

Non volcanic deep low-frequency tremors and slow slip events occur simultaneously in the transition zone from locked to continuously creeping fault at the down dip portion of the Nankai Trough subduction zone, southwestern Japan. The occurrence of these slow earthquakes is attributed to the effect of high pore pressures on the plate boundaries. The Nankai Trough subduction zone has a discontinuous band of occurrence of these slow earthquakes along the trench. Here we show that spatial variation of intraslab stress can control fluid migration through the subducted Philippine Sea slab to the plate boundary. The tri-axial normal faulting stress detected by the stress tensor inversion by using focal mechanisms in the slab controls anisotropies of permeability trending NNW–SSE sub-horizontal orientation from the subducted Philippine Sea slab to the plate boundary. The inhomogeneous condition controlled by the spatial stress heterogeneities in the subducted Philippine Sea slab represents the intraslab fluid pathway. The hypothesis is consistent with spatial heterogeneity of slow earthquake activities and $^{3}He/^{4}He$ ratio distributions.

Keywords: Fluid, Nankai Trough, Slab, Slow earthquake, Stress

©2019. Japan Geoscience Union. All Right Reserved. 

# New insights into the mechanism of deep-focus earthquakes

*Ayako Tsuchiyama[1], Junichi Nakajima[1]

1. Tokyo Institute of Technology

Generally, deep-focus earthquakes were generated in subducting slabs and occurred along some specific regions such as Izu-Bonin zone and Tonga-Fiji zone. We have not identified their occurrence mechanisms, even though some plausible hypotheses, dehydration embrittlement, thermal and shear plastic instability, and transformational faulting, were proposed. In this study, we try to obtain new constraints that deepen the understanding of deep-focus earthquakes through waveform analysis of earthquakes in the Izu-Bonin subduction zone.

First, we picked up 460 quakes at a depth range of 300-400 km in 2003-2015 beneath Tokai area from the catalog data provided by Japan Meteorological Agency, and relocated them with double-difference earthquake relocation algorithm (hypoDD; Waldhauser and Ellsworth, 2000). Second, we computed their coherence values between all available pairs of earthquakes with cross-spectrum analysis. Then, we were successful to identify a few earthquake clusters that had a very high coherence value over 0.9 in a long time window of 40 s including P and S waves. Moreover, we relocated these earthquakes with hypoDD again by using precisely-determined differential travel-time data derived from waveform data. As a result, we could find that earthquakes in each cluster occurred on single fault plane with complementary rapture areas.

Additionally, we implemented moment tensor inversion (Gephart and Forsyth, 1984) and estimated the stress field around the region where we discovered a few clusters showing waveform similarities. Moreover, we computed the amount of stress drop of the similar earthquakes with spectrum analysis of seismic wave. Through these waveform analyses, we interpreted that the mechanism of these similar deep-focus earthquakes could be explained by combining two possible mechanisms; dehydration embrittlement that regulates the rupture initiation and thermal and shear plastic instability that controls the rupture propagation along a pre-existing fault.

Keywords: deep-focus earthquakes, intraslab earthquakes

©2019. Japan Geoscience Union. All Right Reserved. 

# Faulting in deforming harzburgite under wet conditions

*Tomohiro Ohuchi[1], Xinglin Lei[2], Yuji Higo[3], Yoshinori Tange[3], Takeshi Sakai[1]

1. Geodynamics Research Center, Ehime University, 2. National Institute of Advanced Industrial Science and Technology, 3. Japan Synchrotron Radiation Research Institute

The subduction zone produces a major fraction of the Earth's seismic activity. The mechanisms of intermediate-depth (> 40 km depth) and deep-focus (> 300 km) earthquakes are fundamentally different from those of shallow (< 40 km) earthquakes. This is because the frictional strength of silicate rocks exceeds the upper limit of the stress level in the upper mantle (< 300 MPa: Obata and Karato, 1995) at pressures higher than 1 GPa (~30 km depth). Therefore, the cause of intraslab seismicity at intermediate depths has been attributed to dehydration of serpentinite (e.g., Peakock, 2001) because the water released during dehydration reaction of serpentinite reduces the effective confining pressure. The dehydration embrittlement model is now widely accepted, because the location of the double seismic zone in the subducting Pacific slab corresponds to the main dehydration field in the pressure-temperature diagram of the hydrous peridotite (Omori et al., 2002).

To evaluate the effect of water on semi-brittle behavior of harzburgite, we conducted in-situ uniaxial deformation experiments on as-is/water-saturated harzburgite at pressures 1.2-3.0 GPa and temperatures 770-1250 K with a constant displacement rate using a deformation-DIA apparatus. Pressure, stress, and strain were measured in situ by using x-ray diffraction patterns and radiographs. Acoustic emissions (AEs) were also recorded continuously on six sensors, and three-dimensional AE source location were determined.

Formation of throughgoing faults was observed even when differential stress is much lower than the confining pressure (i.e., > 0.3 times of confining pressure) in water-saturated harzburgite. This is contrast to the case of water-saturated dunite (Ohuchi et al., 2018), in which fracture strength exceeds the confining pressure (i.e., Goetze's criterion). Creep strength of water-saturated harzburgite was lower than that of as-is harzburgite (~0.5-1 GPa at each temperature). Weakening of the harzburgite by the aqueous fluid resulted in the reduction in the number of AE events and decrease in fault slip rate (< 3.6E-4 $s^{-1}$ at a stress of < 1.05 GPa). Stress/pressure drop around the timing of a faulting was limited at strains of 1E-4 $s^{-1}$. The aseismic faulting observed in the water-saturated harzburgite implies that silent slip events around the subduction interface is due to semi-brittle flow of water-saturated harzburgite (i.e., a dehydration product of antigorite).

Keywords: harzburgite, water, semi-brittle flow

©2019. Japan Geoscience Union. All Right Reserved. 

# Semi-brittle behavior of olivine single crystals under the conditions of Earth’s mantle transition zone

Yoshihisa Naruse[1], *Tomohiro Ohuchi[1]

1. Geodynamics Research Center, Ehime University

The origin of deep-focus earthquakes, which occur at depths of 300-700km in the subducting slabs, fundamentally differs from that of other earthquakes and has been attributed to the pressure-induced phase transition in olivine. Previous studies on $Mg_2GeO_4$ olivine have shown that grain size reduction induced by the phase transition in olivine causes shear localization (e.g., Burnley et al., 1991; Schubnel et al., 2013). Schubnel et al. (2013) reported intense acoustic emissions around the timing of a faulting which would be induced by shear localization in polycrystalline $Mg_2GeO_4$ olivine. In order to understand the relationship between fracturing and the phase transition in olivine, we conducted deformation experiments on single crystals of San Carlos olivine ($Fo_{91}$) at pressure of 10-15 GPa and temperatures of 1000-1100 degC using a deformation-DIA apparatus. Single crystal of olivine was chosen to exclude the effect of grain boundaries on nucleation of high-pressure phases of olivine (i.e., wadsleyite and ringwoodite).

Array of microcrack parallel to either (100), (010) or (110) plane was developed at an ~50 degree to the direction of uniaxial compression. Rotation of olivine axes associating the formation of subgrain boundaries was observed around the microcrack arrays, showing that plastic deformation of the olivine single crystal inevitably associated formation of the microcracks. In most samples, microcracks coalesced and then a few throughgoing fractures were developed. Particles of wadsleyite /ringwoodite having a diameter of a few micrometer or less were preferentially nucleated on the microcrack surfaces. Ultrafine-grained domains, which consist of the wadsleyite /ringwoodite particles, were formed along the throughgoing fractures. Development of a banded ultrafine-grained domain was also observed along a throughgoing fracture, implying that shear localization could occur as a result of semi-brittle flow of olivine and a transition from dislocation creep to grain-size-sensitive creep in subducting slabs at depths > 410 km.

Keywords: olivine, phase transition, semi-brittle flow, microcrack, deep-focus earthquake

©2019. Japan Geoscience Union. All Right Reserved. 

# High-pressure deformation experiments on peridotite gouges under hydrothermal conditions, using a deformation-DIA apparatus

*Maki Semba[1], Ken-ichi Hirauchi[1], Tomohiro Ohuchi[2], Katsuyoshi Michibayashi[3]

1. Department of Geosciences, Faculty of Science, Shizuoka University, 2. Geodynamics Research Center, Ehime University, 3. Department of Earth and Planetary Sciences, Nagoya university

In subducting oceanic plates, the focal depth of intraslab earthquakes is deeper (>40 km) than that of interplate earthquakes. Since the normal stress on faults (e.g., outer-rise faults) hosting the intraslab earthquakes is too high to generate brittle shear failure, there may be some mechanisms to weaken effective fault strength. In addition, the hypocenter distribution of intraslab earthquakes forms double-planed structure of the deep seismic zone, and the location of the lower plane is in accord with the stability limit of serpentine (antigorite), suggesting shear deformation of antigorite-bearing peridotite gouges in the presence of hydrothermal water. Here, in order to understand the influence of hydrous minerals on the fault strength, we performed deformation experiments on simulated peridotite gouges with compositions of dunite (100% olivine) and harzburgite (70% olivine/30% orthopyroxene) under hydrothermal conditions, using a deformation-DIA apparatus. The experiments were conducted at a temperature of 580˚C, a confining pressure of 2.5 GPa, and shear strain rates of 2.70 $\times 10^{-5}$ to 1.03 $\times 10^{-4}$ $s^{-1}$. In the deformed peridotite gouges, localized shear zones such as $R_1$ and B shears were observed, and these shears were accompanied with newly formed hydrous phases (serpentine or talc). Olivine grains have a crystal preferred orientation characterized by a slip system of [001] (010). These results indicate that semi-brittle flow is a major deformation mechanism of the peridotite gouges. Considering low coefficients of friction of serpentine and talc, we can suggest that the infiltration of seawater along outer-rise fault planes and subsequent hydrothermal alteration result in effective shear strengths low enough to produce intraslab earthquakes.

Keywords: deformation-DIA apparatus, peridotite, serpentinization, frictional strength

©2019. Japan Geoscience Union. All Right Reserved. 

# Stable fault slip in antigorite-olivine aggregates at high pressures

Mai Ikehara[1], *Tomoaki Kubo[1], Takuya Iwasato[2], Yuji Higo[3], Masahiro Imamura[1], Yoshinori Tange[3]

1. Kyushu University, 2. Shin-Nippon Nondestructive Inspection Co., Ltd., 3. JASRI

Intermediate-depth earthquakes are observed to occur within subducting oceanic plates at depths of about 60-300 km where most materials exhibit plastic deformation rather than brittle failure, owing to high pressures and temperatures. Dehydration embrittlement of hydrous minerals, particularly antigorite serpentine, is one of the most popular hypotheses for explaining shear instability under such conditions (e.g., Raleigh and Paterson, 1965). Recent high-pressure deformation experiments, monitoring Acoustic Emission (AE) activities upon syndeformational antigorite dehydration, showed that dehydration embrittlement was not observed on single-phase antigorite (Gasc et al., 2017), whereas dehydration related faulting was formed on antigorite-olivine aggregates with strong AEs (Ferrand et al., 2017). However, most of the previous high-pressure studies have been conducted in axial compression at relatively low pressures (< 3.5 GPa), insufficient to consider intermediate-depth earthquakes. Therefore, in this study, we conducted high-pressure shear deformation experiments on two-phase aggregates of antigorite and olivine, considering partially serpentinized peridotites, in order to investigate possible shear localization and shear instability up to 7 GPa.

Deformation experiments were conducted at 5-7 GPa, 350-700 ℃ using Deformation-DIA apparatuses at SPring-8 (BL04B1). Monochromatic X-rays (50-60 keV) were used to measure dehydration kinetics, shear strain and stress with recording AEs. We used three kinds of starting materials; natural cored antigorite from Kawarakoba in Nagasaki prefecture, forsterite polycrystal, and two-phase sintered mixtures of antigorite and San Carlos olivine (antigorite 10, 30, 50 vol %). The samples were cut into disks having thickness of 300 $\mu$m and used for a shear deformation study by being assembled between two 45˚-cut alumina pistons. In shear deformation experiments, the starting disk was compressed to 5 or 7 GPa at room temperature, annealed at 350 or 400 ℃ for 1 h, and then deformed with an anvil displacement rate of 200 $\mu$m/h. In some experiments, we increased temperature during shear deformation with a ramping rate of 0.1 ℃/sec to induce dehydration reaction. Microstructures of the recovered samples were examined by an optical microscope and a scanning electron microscope (SEM).

From X-ray radiography images, we observed shear localization in all two-phase samples deformed within the antigorite stability field at 5 GPa. The locallization occurred when homogeneous shear strain $\gamma$ reached 0.4-0.9 (strain rate 1.3-2.2 $\times 10^{-4}$/s), and then most strains were partitioned to the fault zone with the slip velocity of 4.6-9.1 $\times 10^{-2}$ $\mu$m/s. Because no AEs were detected from the sample region, the localized deformation is thought to occur by stable sliding. SEM observations revealed that a thin shear deformation zone was formed along the fault, where the plastic deformation of both antigorite and olivine was significant. Striation and nanograins were observed on the fault plane, suggesting the formation of nanogouge. In contrast, homogeneous deformation was developed during antigorite dehydration with temperature ramping, even in the sample showing shear localization in the antigorite stability field. Under higher pressure condition 7 GPa, shear localization did not occur in all samples regardless of temperature. These results suggest that, although AE activities were detected with the dehydration in the antigorite-olivine aggregates up to 3.5 GPa in the previous study, further increase of pressure inhibits shear instability and shear localization. Thus, other dehydration reactions and/or instability mechanisms are required to explain intermediate-depth earthquakes deeper than ~100 km.

©2019. Japan Geoscience Union. All Right Reserved. 

©2019. Japan Geoscience Union. All Right Reserved. 

# Rheology and frictional instability of lawsonite in high pressure deformation experiments

*Rei Shiraishi[1], Jun Muto[1], Akihiro Tsunoda[2], Sando Sawa[1], Akio Suzuki[1]

1. Department of Earth Science, Graduate School of Science, Tohoku University, 2. Earthquake Research Institute, University of Tokyo

The cause of intermediate-depth earthquakes (50-300 km) in subducting slabs have been proposed to be the dehydration embrittlement (e.g., Raleigh and Paterson, 1965), because there are many kinds of hydrous minerals in a subducting slab and hypocenter distribution coincides with the dehydration boundary determined by high pressure experiments (e.g., Hacker et al., 2003). Many experimental studies on antigorite have been conducted, but a few previous works about dehydration embrittlement of lawsonite-bearing rocks experimentally. Lawsonite, $CaAl_2Si_2O_7(OH)_2H_2O$, is a hydrous mineral which contains 11 wt% water in its structure as both water molecules and a hydroxy group (Cmodi and Zanazzi, 1996). Lawsonite is one of the candidate for dehydration embrittlement in cold subducting slabs, however previous works have apparently contradictory results. Okazaki and Hirth (2016) showed that lawsonite dehydration induced unstable fault slip based on deformation experiments of pure lawsonite using Griggs-type deformation apparatus at 1 GPa. On the other hand, Incel et al. (2017) also investigated deformation properties of lawsonite and glaucophane mixture at 1.5 to 3.0 GPa using deformation-DIA apparatus. They insisted that there is no evidence for a straightforward relation to the dehydration of lawsonite and the brittle failure of samples. So, we have conducted the deformation experiments of lawsonite under the cold slab conditions in order to clarify the deformation property of lawsonite and understand the relationship between dehydration and brittle failure.

Experiments were carried out using Deformation-Cubic Anvil Press (D-CAP) installed at KEK PF AR-NE7A beamline. Pure lawsonite powder (98%) was used as starting materials. Deformation experiments were carried out at a pressure of 6 GPa and temperatures of 300 - 800 ˚C. The temperature was increased at the same time as deformation started. The temperature ramping rate over the strain rate was set the ranges for the real subducting slab, which ranges from $10^2$ to $10^4$ ˚C (Chernak and Hirth, 2011; Okazaki and Hirth, 2016). During deformation stages, strain, stress and transformation rate were measured for in-situ using a monochromatic X-ray beam with an energy of 60 keV.

Four experiments showed rapid stress drop during temperature ramping before lawsonite dehydration starts. We observed microstructure of recovered samples, there are many through going faults and microcracks but no dehydration products. Our results indicate that brittle process and frictional sliding occur without dehydration of lawsonite. This suggests that the intermediate-depth earthquakes can be caused by the deformation itself of lawsonite without the dehydration of lawsonite.

Keywords: intermediate-depth earthquakes, dehydration embrittlement, Lawsonite

©2019. Japan Geoscience Union. All Right Reserved. 

# Grain Size Dependency of Olivine-Spinel Phase Transformational Mechanism Responsible for Deep-focus Earthquakes

*Sando Sawa[1], Jun Muto[1], Nobuyoshi Miyajima[2], Hiroyuki Nagahama[1]

1. Department of Earth Science, Tohoku University, 2. Bayerisches Geoinstitut, University of Bayreuth

Deep-focus earthquakes occur at the depth from 440 km to 660 km in the subducting slab. The mechanism responsible for the earthquakes is thought to be different from that of shallow earthquakes, so that previous studies have reported the various mechanisms. By the geophysical observations and deformation experiments, the phase transformational faulting mechanism is presumed as the precursor of deep-focus earthquakes (e.g., Zhan et al., 2014). The phase transformational faulting mechanism is that metastable olivine in the slab undergoes the phase transformation to fine-grained spinel and faulting occurs with strain localization into the fine-grained spinel. This shear instability depends on grain size. Furthermore, the grain size may restrict the pressure- and temperature-conditions where the shear instability occurs, that is, the region of slab where deep-focus earthquakes occur. However, previous studies have conducted deformation experiments with finer grain size than expected in the slab (e.g., Burnley et al., 1991). Hence, the results from the laboratory experiments cannot directly apply to the geophysical observation. In this study, to reveal the grain size dependency on the phase transformational faulting, we conducted the deformation experiments of germanate olivine (about 3 $\mu$m), which is an analogue material of silicate olivine, finer-grained than that in previous studies (30 $\mu$m). We used a Griggs-type solid-confining media deformation apparatus. The confining pressure, temperature and strain rate are 1.2 GPa, 400~900 ℃ and $2.0\times10^{-4}$ $s^{-1}$, respectively. Even though deformation experiments were conducted under wider temperature conditions than previous studies, we did not observe any shear instability event with apparent stress drops. Also, Raman spectroscopy clarified that the germanate olivine underwent the transformation to spinel at temperatures higher than 500 ℃. Shear instability does not occur because the difference in grain sizes between olivine and nucleated spinel in this study was smaller than those in previous studies. Also, the transformation temperature in this study was much lower than those in previous study (T > 1000 ℃ in Burnley et al., 1991). Considering the rate equation of the transformation (Chan, 1956), small grain size promotes the transformation, but these fast rates of the transformation cannot be explained only by the effect of the grain size. Therefore, the presence of water such as absorbed water in a starting material can also contribute to promote the transformation. Hence, both small initial grain size and a little amount of water promote the transformation even at lower temperature. These results indicate that the phase transformational faulting mechanism has strong grain size dependency. In summary, the pressure- and temperature-conditions where the faulting occurs depends on the grain size of olivine and amount of water. Because the grain size in the slab is larger than that in the experiments, by extrapolating from these results, we may restrict the region of slab where deep-focus earthquakes occur.

This work was supported by the JSPS Japanese-German Graduate Externship.

[Reference]
Burnley et al. (1991), JGR, vol 96, 425-443.
Chan (1956), Acta Metallurgica, vol 4, 449-459.
Zhan et al. (2014), EPSL, vol 385, 89-96.

©2019. Japan Geoscience Union. All Right Reserved. 

Keywords: Deep-focus earthquakes, Griggs type piston-cylinder apparatus, phase transformation

©2019. Japan Geoscience Union. All Right Reserved. 

# Seismicity and mineral destabilizations in the subducting mantle up to 6 GPa, 200 km depth

*Thomas P. Ferrand[1]

1. Earthquake Research Institute

In the subducting oceanic lithosphere, a significant part of the seismicity is triggered in the mantle, especially along the upper and lower Wadati-Benioff planes. Several studies have investigated the potential involvement of dehydration reactions in the triggering mechanism of mantle earthquakes. Recent experimental results reveal that, under subduction conditions, mechanical instabilities nucleate in strong stable mineral aggregates during the destabilization of minor amounts of antigorite, i.e. the high-temperature serpentine, through a stress transfer, without any fluid overpressure. Here I confront these laboratory results to seismological observations. On one hand, most of the natural hydrous magnesium silicates seem to be known, with experimentally-deduced stability limits up to 7 GPa, at least, available as relatively accurate estimates. On the other hand, recent achievements in thermal structure of subduction zones combined with precise hypocentre relocation give access to pressure and temperature conditions at earthquakes hypocentres. A series of P-T diagrams summarizes the stability limit of minerals that may be part of natural peridotite with variable compositions at pressures from 0.5 to 6 GPa and temperatures from 200 to 950˚C, and compares it with seismicity. Both hydrous and anhydrous phases are considered. A myriad of minor metamorphic reactions could participate in a transformation-driven stress transfer, even if the stability limits of serpentine minerals seem to correlate with most of the observed seismicity.

Keywords: earthquakes, intraslab, DDST, dehydration, transformation, subduction

©2019. Japan Geoscience Union. All Right Reserved. 

# Receiver function imaging of subducting Pacific plate and mantle wedge under Japanese islands using denser network of stations

*HyeJeong Kim[1], Hitoshi Kawakatsu[1], Takeshi Akuhara[1], Masanao Shinohara[1]

1. Earthquake Research Institute, The University of Tokyo

Receiver function imaging has been frequently used by different groups focusing on different depths of the Japanese subduction zone. The overlying crust (Shiomi and Park, 2008, Bianchi et al, 2015), the Pacific plate before (Kawakatsu et al., 2009) and after subduction (Kawakatsu and Watada, 2007; Wirth and Long, 2012), and the mantle transition zones (Kawakatsu and Yoshioka, 2011; Tauzin et al., 2018) were discussed using the NIED array stations (Hi-net and F-net). Recently, deployment of ocean bottom seismometers (OBSs) enabled studies of subduction zones closer to the trench (e.g., Akuhara and Mochizuki, 2015). Kawakatsu and Kim (2018, SSJ) have obtained a new version of receiver function imaging using 14-year long of Hi-net data. However, there are other land stations (e.g., J-array) that can improve the station coverage. Here, we collect data from available on-land stations deployed in north-eastern Japan to obtain a denser 2-D array of stations. Additionally, data from temporary OBS stations (Shinohara et al. 2012) are gathered to image the subducted Pacific plate in shallower depths than previously available. Continuous imaging from ocean to land will help to constrain transition of the hydrated oceanic crust along subduction that is expressed as a low velocity layer for better understanding of the hydration/dehydration processes during subduction, which might be related to the occurrence of subduction zone earthquakes.

Keywords: subduction zone, receiver function, ccp stacking

©2019. Japan Geoscience Union. All Right Reserved. 

# Strong S-wave attenuation in the mantle wedge beneath the NE Japan and interpretations of high-frequency wave propagation path of intraslab earthquakes

*Takahiro Shiina[1,2], Kei Katsumata[2], Kiyoshi Yomogida[3], Aitaro Kato[1]

1. Earthquake Research Institute, The University of Tokyo, 2. Institute of Seismology and Volcanology, Graduate School of Science, Hokkaido University, 3. Graduate School of Science, Hokkaido University

For intraslab earthquakes at intermediate-depths in NE Japan, especially at greater than about 100-km depths, it has been often recorded that high-frequency waveform higher than 8 Hz show a remarkable delay of arrival compared with S wave which predominates in a low-frequency band. The magnitude of the delay is little in the forearc region, whereas it increases up to about 40 s in the backarc region. In this study, we investigate the details in the propagation processes of the high-frequency later phase observed for the intraslab earthquakes at the intermediate-depths. To constrain the source location of the high-frequency later phase, we employ the source-scanning algorithm (SSA) [Kao and Shan, 2004] with realistic velocity and attenuation structures, assuming that the high-frequency later phase is generated by the single scattering process. Namely, we estimate a scattering point by using mean-square amplitudes which is synthesized from two horizontal components of the observed waveforms.
Results in frequency bands of 4-32 Hz show that scattering points are distributed beneath the forearc region. The scattering points can reproduce the observed delays of amplitude amplifications associating with the high-frequency later phases. Moreover, similar locations of the scattering points are imaged along the forearc region in the entire NE Japan. These results indicate that high-frequency later phase is a wave scattered at the forearc region and that short wave-length heterogeneity generally developed in the forearc region of NE Japan.
This interpretation well matches implications from previous studies [e.g., Yomogida et al., 2004; Hasemi and Horiuchi, 2010]. Additionally, the obtained distributions of scattering points which appear to surround the highly attenuating mantle wedge suggest that attenuation structure strongly controls propagation paths of seismic wave, in particular, a high-frequency wave. In other words, the identifications of high-frequency later phase may become easy because the amplitude of direct wave crossing the high-attenuation zone decreases. To confirm this consideration, we estimate *Qs* along the direct wave by using the coda-normalization method [e.g., Aki, 1980]. This estimation provides 2-3 times smaller path-averaged *Qs* in seismic records of which rays lay on the backarc and the volcanic front than that of which rays lay on the forearc region. These results support that spatial variation in *QS* produces heterogenous propagations of seismic waves emitted from intraslab earthquakes. It is thus required to take scattering and attenuation structures simultaneously into account to understand complex behaviors of high-frequency waves in a future study.

Keywords: S-wave attenuation, Intraslab earthquakes, High-frequency later phase, Scattered wave

©2019. Japan Geoscience Union. All Right Reserved. 

[E] Poster | S (Solid Earth Sciences)：S-CG Complex & General

Thu. May 30, 2019 10:45 AM - 12:15 PM JST | Thu. May 30, 2019 1:45 AM - 3:15 AM UTC | Poster Hall International Exhibition Hall8, Makuhari Messe_6

## [S-CG51] Role of volatiles on Earth and planetary dynamics

convener:Takayuki Ishii(Bavarian Research Institute, University of Bayreuth), Eiji Ohtani(Department of Earth and Planetary Materials Science, Graduate School of Science, Tohoku University), Michihiko Nakamura(Division of Earth and Planetary Materials Science, Department of Earth Science, Graduate School of Science, Tohoku University), Bjorn Mysen(Geophysical Laboratory, Carnegie Inst. Washington)

This session addresses how volatile species affect dynamics of the<br/>Earth and planets from natural observations, laboratory experiments, and<br/>numerical modeling in the temperature, pressure, and oxygen activity<br/>range from the early stage of the planet formation to the present. The<br/>volatiles can be critical in zones of magma storage and ascent, mantle<br/>upwelling and melting in the fluid-enriched subduction zones, in the<br/>mantle transition zone, in the lower mantle, in the core-mantle boundary,<br/>and in Earth and planetary cores. However, volatiles affect properties<br/>and processes differently depending on their pressure, temperature, and<br/>redox conditions, which vary in time and space. <br/> This session aims to address how volatiles control the dynamic<br/>processes of the Earth and planets, governed by their geophysical and<br/>geochemical properties. We welcome papers dealing with geological and<br/>laboratory observations coupled with numerical modeling on the role of<br/>volatiles. The topics include (1) Stability relations, chemical and<br/>physical properties of crystalline, molten and fluid phases,<br/>partitioning of volatiles among these phases, (2) Rheological and other<br/>physical properties of minerals, and the effects of intergranular fluid<br/>on the properties, (3) Volatiles and dehydration induced seismicity and<br/>volcanism in various tectonic regions including subduction zones, and (4)<br/>Effects of volatiles in numerical simulation of geo-tectonics, and (5)<br/>Magma outgassing and its control of volcanic eruption dynamics.

[SCG51-P01] Permeability prediction of porous media with the finite difference Stokes solver LaMEM

*Philipp Eichheimer[1], Wakana Fujita[2], Marcel Thielmann[1], Anton Popov[3], Gregor Golabek[1], Boris Kaus[3], Maximilian Kottwitz[3] (1.Bayerisches Geoinstitut, University of Bayreuth, 2.Department of Earth Science, Tohoku University, Sendai, 3.Institute of Geosciences, Johannes Gutenberg University Mainz)

[SCG51-P02] Grain growth-induced fluid localization and permeability reduction

*Wakana Fujita[1], Michihiko Nakamura[1], Kentaro Uesugi[2] (1.Graduate School of Science, Tohoku University, 2.JASRI/SPring-8)

[SCG51-P03] Pargasite stability in the upper mantle at $H_2O$-undersaturated conditions

*Marija Putak Juricek[1], Hans Keppler[1] (1.BGI)

[SCG51-P04] **Constraining the water content at the top of the mantle transition zone with the elasticity of wadsleyite and olivine**

*Zhongqing Wu[1] (1.University of Science and Technology of China)

[SCG51-P05] ***Single crystal elasticity of Fe-bearing phase E by Brillouin spectroscopy***

*Niccolo Satta[1], Hauke Marquardt [2], Alexander Kurnosov[1], Tiziana Boffa Ballaran [1], Johannes Buchen[3], Catherine McCammon[1], Takaaki Kawazoe[4] (1.Bayerisches Geoinstitut, University of Bayreuth, 95440 Bayreuth, Germany, 2.Department of Earth Sciences, University of Oxford, South Parks Road, Oxford, UK., 3.Seismological Laboratory, California Institute of Technology, Pasadena, CA 91125, USA., 4.Department of Earth and Planetary Systems Science, Hiroshima University, Hiroshima 739-8526, Japan.)

[SCG51-P06] Discovery of two hexagonal phases in (Fe,Al)OOH under the P-T conditions of the deep lower mantle

*Lu Liu[1,2], Li Zhang[1], Hongsheng Yuan[1] (1.Center for High Pressure Science and Technology Advanced Research, 2.University of Science and Technology of China)

[SCG51-P07] **Effect of grid resolution on tectonic regimes in global-scale convection models**

*Enrico Marzotto[1], Marcel Thielmann[1], Gregor Golabek[1] (1.Bayerisches Geoinstitut)

[SCG51-P08] A 3-D crust and uppermost mantle electrical conductivity model of subduction zone beneath NE Japan

*Masahiro Ichiki[1,2], Toshiki Kaida[1], Yasuo Ogawa[3] (1.Graduate School of Science, Tohoku University, 2.International Research Institute of Disaster Science, 3.School of Science, Tokyo Institute of Technology)

[SCG51-P09] *The conditions of sublithospheric diamond formation constrained from ferric iron-rich exsolution from ferropericlase inclusions.*

*Caterina Melai[1], Daniel Frost[1], Tiziana Boffa Ballaran[1], Catherine McCammon[1] (1.Bayerisches Geoinstitute)

[SCG51-P10] **Probing the variation of the oxygen fugacity in diamond anvil cells using the Fe-Ir alloy as redox sensor**

*Serena Dominijanni[1], Catherine McCammon[1], Leonid Dubrovinsky[1], Dan Frost[1], Nobuyoshi Miyajima[1] (1.Bayerisches Geoinstitut)

[SCG51-P11] Goethite behavior at Earth's lower mantle conditions

*Egor Gennadievich Koemets[1], Maxim Bykov[1], George Aprilis[2], Timofey Fedotenko[2], Stella Chariton[1], Saiana Khandarkhaeva[1], Iuliia Koemets[1], Marcel Thielmann[1], Natalia Dubrovinsaia[2], Leonid Dubrovinsky[1] (1.BGI (Bayerisches Geoinstitut), Universität Bayreuth, Germany, 2.Material Physics and Technology at Extreme Conditions, Laboratory of Crystallography, Universität Bayreuth, Germany)

[SCG51-P12] The oxygen content of sulphides in the mantle and a geothermometer for diamond formation

*Sumith Abeykoon[1], Dan Frost[1], Vera Laurenz[1] (1.Bayerisches Geoinstitut, University of Bayreuth)

# Permeability prediction of porous media with the finite difference Stokes solver LaMEM

*Philipp Eichheimer[1], Wakana Fujita[2], Marcel Thielmann[1], Anton Popov[3], Gregor Golabek[1], Boris Kaus[3], Maximilian Kottwitz[3]

1. Bayerisches Geoinstitut, University of Bayreuth, 2. Department of Earth Science, Tohoku University, Sendai, 3. Institute of Geosciences, Johannes Gutenberg University Mainz

The flow of fluids through porous media such as groundwater flow or magma migration is one of the most important processes in geological sciences. The property controlling the efficiency of the flow is the permeability of the rock, thus an accurate determination and prediction of its value is of crucial importance. For this reason, permeability of rocks has been measured across different scales. As laboratory measurements exhibit a range of limitations, the numerical prediction of permeability at conditions where laboratory experiments struggle has become an important method to complement laboratory approaches. At high resolutions, this prediction becomes computationally very expensive, which makes it crucial to develop methods that maximize accuracy. In this work we introduce the open-source finite difference solver LaMEM that can be used to numerically predict the permeability of porous media under laminar conditions. We employ a stencil rescaling method to increase accuracy due to a better description of the solid-fluid interface, thus reducing the computational cost. To validate the method, we perform a series of tests employing both analytical solutions for simplified geometries as well as results from other numerical approaches for more complicated geometries. Furthermore we compare our numerical results to laboratory measurements on glass bead samples with porosities ranging from 20% to 2.5%, showing good agreement.

Keywords: Permeability, Numerical modelling, Digital Rock Physics

©2019. Japan Geoscience Union. All Right Reserved. 

# Grain growth-induced fluid localization and permeability reduction

*Wakana Fujita[1], Michihiko Nakamura[1], Kentaro Uesugi[2]

1. Graduate School of Science, Tohoku University, 2. JASRI/SPring-8

Efficiency of segregation of geological fluids such as aqueous fluids and melts is an essential elementary process for volatile cycles in subduction zones. Permeability is an intrinsic rock property that controls flow rate of fluid. Various permeability models have been presented by numerical models of textually equilibrated rocks (e.g. 1, 2), laboratory measurements on synthetic rocks (e.g. 3) and estimation from cross-sectional area of synthetic rocks (4). However, there exist discrepancies among those models. Because permeability is very sensitive to microscopic geometry of pore fluid, those disagreements may arise from lack of understanding toward three-dimensional (3D) microstructure of fluid network.

Dihedral angle has been considered to be a critical parameter that controls fluid geometry and thus permeability. Beside, some previous studies shed light on the effect of grain growth on fluid distribution because it could induce pore fluid distortion and coalescence (5, 6). These studies suggest that in the actual systems where the microstructure of rocks evolve in dynamic processes, grain growth would be important along with the dihedral angle.

To investigate the effect of grain growth on the fluid distribution and permeability, we present 3D images of quartz–CHO fluid aggregates, containing nominal fluid fractions between 0.03 and 0.10. Samples were synthesized from a powdered mixture of Arkansus quartz and amorphous silica prepared by sol-gel method and hot-pressed in a piston–cylinder apparatus at 900˚C and 1.0 GPa for 192h. The fluid fractions and the dihedral angles were controlled using brucite added in the capsule bottom and oxalic acid dihydrate mixed with $SiO_2$ powder. 3D images were obtained using synchrotron X-ray microtomography at BL20XU experimental hutch2 of SPring-8. Regardless of dihedral angles ($CO_2$ content in fluids), both cross-sectional area and 3D images of samples showed grain-scale fluid localization which would be formed by pore fluid coalescence induced by grain growth. Computed permeabilities using numerical model, LaMEM (7) were almost consistent with laboratory measurements by (3) but more than one order of magnitude lower than a numerical model by (2). This would indicate that localized fluids extensively reduce permeability by reducing the diameter of fluid tubes along grain edges, which would suggest transport of water into Earth’ s deep interior by the subducting slab.

Reference:
1. von Bargen and Waff. 1986, J. Geophys. Res. 91, 9261–9276.
2. Rudge, J.F. 2018, Proc. R. Soc. Lond. A 474, 20170639.
3. Wark and Watson. 1998, Earth Planet. Sci. Lett. 164, 591–605.
4. Faul, U.H. 1997, J. Geophys. Res. 102, 10299–10311.
5. Walte et al. 2003, Geology 2003 31, 1009-1012.
6. Yoshino and Watson. 2005, Earth Planet. Sci. Lett. 235, 453–468.
7. Kaus et al. 2016, NIC Symposium 2016

Keywords: Permeability, Quartz, Grain growth, Dihedral angle, Fluid segregation

©2019. Japan Geoscience Union. All Right Reserved. 

# Pargasite stability in the upper mantle at $H_2O$-undersaturated conditions

*Marija Putak Juricek[1], Hans Keppler[1]

1. BGI

Amphibole is the most commonly occurring hydrous mineral in mantle xenoliths and the majority of upper mantle amphiboles have compositions close to pargasite end member. Previous experimental work has demonstrated that pargasite stability is sensitive to variations in bulk alkali and water content of the starting material. While it has been successfully shown that addition of more alkali leads to stabilization of pargasite to higher P and T, the effect of water on amphibole stability is not so straightforward.

At $H_2O$-saturated conditions, alkali elements partition strongly into aqueous fluid and become less available for crystallization of amphibole. As a result, amphibole seemingly becomes stable at higher P and T when less $H_2O$ is added to the starting material. This observation led to the hypothesis that pargasite may be a ubiquitous phase in the upper mantle, which is believed to contain only several hundred ppm of $H_2O$. However, most of the previous studies determined pargasite stability at $H_2$ O-saturated conditions where solid phases coexist with an aqueous fluid during experiments. Since such environments are not representative of the nearly dry upper mantle, the purpose of this study is to investigate pargasite stability at $H_2O$-undersaturated conditions.

Because of the high specific surface area of powders, adsorption of atmospheric $H_2O$ on fine grained starting materials prevents attaining $H_2O$-undersaturation by adding small amounts of water to the sample. Instead, $H_2O$-undersaturated conditions may be precisely controlled by diluting the water in the sample with another component. Under such conditions, solid phases are expected to coexist with a low water activity fluid throughout the experiment. As molecular nitrogen is mostly insoluble in upper mantle minerals, it can be used to adjust the water activity of the fluid to a desired low value.

All experiments were performed in a piston cylinder apparatus. The samples for $H_2O$-undersaturated experiments were prepared by adding silver azide ($AgN_3$) and brucite to a synthetic peridotite mixture. In several experiments water was added directly as $H_2O_{(l)}$. The amount of water was kept constant in all experiments (1 wt. percent) and the molar fraction of water in the $N_2$-$H_2O$ fluid was adjusted to the desired value by weighing an appropriate amount of $AgN_3$, which decomposed to metallic silver and molecular nitrogen during heating. In $H_2O$-saturated experiments, no silver azide was added to the peridotite mixture. Experimental products were analyzed using JEOL JXA-8200 electron microprobe.

Preliminary results show that pargasite is not stable in equilibrium with fluids diluted to $X_{H2O}$=0.1 at pressures above 1 GPa. At $H_2O$-saturated conditions pargasite stability field can extend to pressures of 4 GPa and above 1100 ℃, depending on bulk alkali and water contents. Results from experiments at $X_{H2O}$ =0.1 and $X_{H2O}$=1 suggest that pargasite can exist only in regions of the upper mantle which have been affected by high water activity fluids, such as areas in the vicinity of subduction zones. The ambient nominally anhydrous upper mantle, better represented by experiments at $H_2O$-undersaturated conditions, is not expected to contain pargasite.

Keywords: pargasite, stability, upper, mantle

©2019. Japan Geoscience Union. All Right Reserved. 

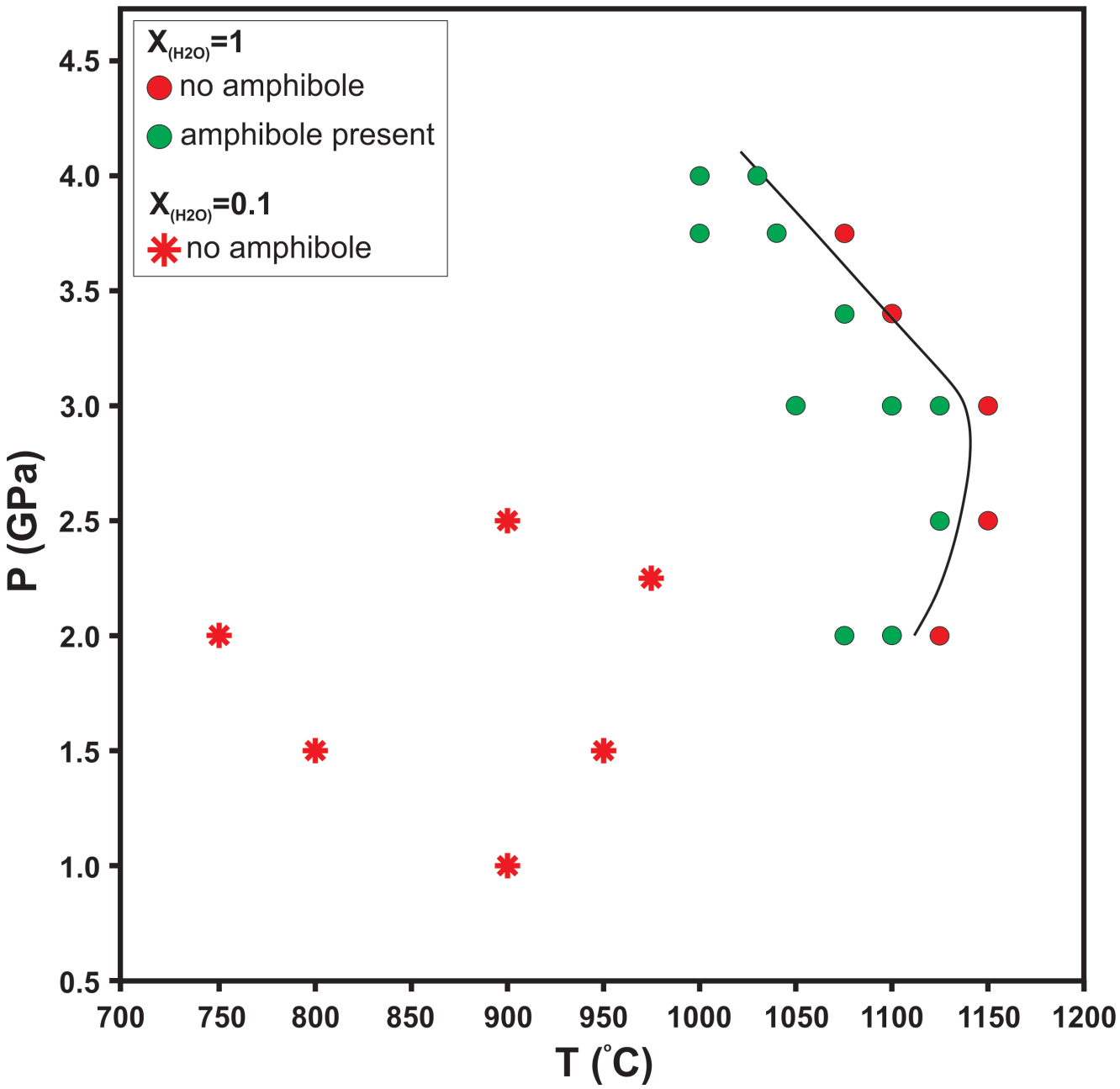


©2019. Japan Geoscience Union. All Right Reserved. 

# Constraining the water content at the top of the mantle transition zone with the elasticity of wadsleyite and olivine

*Zhongqing Wu[1]

1. University of Science and Technology of China

Zhongqing Wu[a,b,*], Wenzhong Wang[a,b], Michael J. Walter[c] ,Ye Peng[a,b], Simon Redfern[d],

[a] Laboratory of Seismology and Physics of Earth’ s Interior, School of Earth and Space Sciences, University of Science and Technology of China, Hefei, Anhui 230026, China

[b] Mengcheng National Geophysical Observatory, Anhui, China

[c]School of Earth Sciences, University of Bristol, Bristol BS8 1RJ, UK

[d]Department of Earth Science, University of Cambridge, Cambridge CB2 3EQ, UK

The water content in the mantle transition zone (MTZ) exerts a controlling influence on the dynamical and chemical evolution of Earth, but is poorly known. In principle the water content at the top of the transition zone can be inferred by comparing the velocity and density contrasts across the 410-km seismic discontinuity with predictions based on the phase transition of olivine to wadsleyite. The high-quality elastic data of at pressure and temperature (PT) conditions of the transition zone are crucial but are very challenge for experiments to obtain. Calculating these elastic data at high PT conditions in conventional method are also very expensive. Instead, these elastic data were calculated using the method of Wu and Wentzcovitch (2011), which reduces the computational workload to tenth of the conventional method. All calculations for two phases were conducted using the same computational details as far as possible, which guarantees that the velocity and density differences between two phases have very high precise. All these calculated elastic data agree well with the available experimental data. The iron and water effect on the elasticity are also well described.

With these high-quality elastic data covered the PT condition of the transition zone, we analyze the water and wadsleyite content at the top of the transition zone. We found that the water content of wadsleyite at the top of the transition zone can be well constrained when density and velocities jumps are considered together. For a pyrolitic mantle composition with ~60% olivine, our best fit is ~ 0.5 wt% water at the top of the transition zone. If the transition zone is dry, as suggested by some electrical conductivity models, the upper mantle may only contain ~ 50% olivine.

Wu, Z., Wentzcovitch, R.M., 2011. Quasiharmonic thermal elasticity of crystals: An analytical approach. Phys. Rev. B - Condens. Matter Mater. Phys. 83, 1–8. doi:10.1103/PhysRevB.83.184115

©2019. Japan Geoscience Union. All Right Reserved. 

# *Single crystal elasticity of Fe-bearing phase E by Brillouin spectroscopy*

*Niccolo Satta[1], Hauke Marquardt [2], Alexander Kurnosov[1], Tiziana Boffa Ballaran [1], Johannes Buchen[3], Catherine McCammon[1], Takaaki Kawazoe[4]

1. Bayerisches Geoinstitut, University of Bayreuth, 95440 Bayreuth, Germany, 2. Department of Earth Sciences, University of Oxford, South Parks Road, Oxford, UK., 3. Seismological Laboratory, California Institute of Technology, Pasadena, CA 91125, USA., 4. Department of Earth and Planetary Systems Science, Hiroshima University, Hiroshima 739-8526, Japan.

Earth’s deep water cycle plays a key role for the dynamic evolution of our planet and the development of habitable conditions. Surface water can be transported to Earth’s mantle by subduction of oceanic lithosphere. Experimental investigations have shown that water can be efficiently stored in Dense Hydrous Magnesium Silicates (DHMS) in cold subducting slabs. However, quantification of the incoming water budget based on the interpretation of seismological observations is hampered by a lack of elasticity measurements of DHMSs. Here, we report single-crystal elasticity measurements of Fe-bearing phase E, a DHMS that is stable at pressures and temperature of Earth’s mantle transition zone. A very low bulk modulus has been reported for phase E, suggesting that it might produce seismic velocity heterogeneities detectable by seismological investigations. However, the shear modulus of phase E has not been quantified.

We synthesized Fe-bearing phase E single crystals in a multi-anvil apparatus. Chemical composition as well as crystal structure have been determined using electron microprobe analysis, Mössbauer spectroscopy, and single-crystal X-ray diffraction. We derived the full elastic stiffness tensor by Brillouin spectroscopy on two single crystals of selected orientations. We found phase E to have both the lowest bulk modulus and shear modulus among the DHMSs at ambient conditions. Phase E shows very low compressional and shear velocities especially when compared to the other principal minerals likely present in subducting slabs after serpentine breakdown. Modelling of seismic velocities in dry and hydrated upper mantle and transition zone rocks suggests that the presence of even small amounts of phase E can appreciably lower seismic wave velocities. Phase E could be used as seismological indicator for water stored at depth in subducting scenarios. The elasticity of phase E under mantle conditions will be explored in future research.

Keywords: Brillouin scattering, Phase E, Seismic wave velocities

©2019. Japan Geoscience Union. All Right Reserved. 

# Discovery of two hexagonal phases in (Fe,Al)OOH under the P-T conditions of the deep lower mantle

*Lu Liu[1,2], Li Zhang[1], Hongsheng Yuan[1]

1. Center for High Pressure Science and Technology Advanced Research, 2. University of Science and Technology of China

Deep water can cause a series of complex seismological phenomena by changing the density and thermal stability of lower mantle components. δ-H solid solution phase (AlOOH-$MgSiO_2(OH)$) is stable at lower mantle conditions[1],because the crystallographic frameworks of the phase H is similar to that of the δ-AlOOH phase, with very strong hydrogen bonds[2,3]. δ-AlOOH and ε-FeOOH can also form solid solution[4] (δ - ε solution). It is reasonable to infer that δ - ε solid solution may have similar thermal stability as that of H- δ solution, considering their similar crystal structure[5]. In our experiments, we synthesized the δ - ε solution at 79GPa and 1600K in a laser-heated diamond anvil cell. As the temperature increases to 2100k, the orthorhombic δ - ε solution transformed into a hexagonal-structured phase. By combining powder X-ray diffraction techniques with multigrain indexation[6], we determined its hexagonal lattice with a=b=10.019Å and c=2.614Å. At 79GPa and 2400K, the hexagonal phase transforms into another hexagonal phase, with the lattice parameters of a=b=2.733Å and c=9.343Å. The discovery of these two new phases may provide new insights into the deep-water storage.

References
1.Ohira I, Ohtani E, Sakai T, et al. Stability of a hydrous δ-phase, AlOOH-$MgSiO_2(OH)_2$, and a mechanism for water transport into the base of lower mantle[J].Earth and Planetary Science Letters, 2014, 401: 12-17.
2.Ohtani, E., Amaike, Y., Kamada, S., Sakamaki, T. and Hirao, N. Stability of hydrous phase H $MgSiO_4H_2$ under lower mantle conditions. Geophys. Res. Lett. 41, -8287 (2014).
3.Nishi M,Kuwayama Y,Tsuchiya J,et al.The pyrite-type high-pressure form of FeOOH[J]. Nature,2017,54(7662):205-208.
4.T Kawazoe,I Ohira,T Ishii et al. Single crystal synthesis of δ-(Al,Fe)OOH American Mineralogist. Volume 102, pages 1953–1956, (2017)
5.Gleason A E,Quiroga C E,Suzuki A,et al.Symmetrization driven spin transition in ε-FeOOH at high pressure[J]. Earth and Planetary Science Letters, 2013, 379: 49-55.
6.Zhang L,Yuan H,Meng Y,et al.Discovery of a hexagonal ultradense hydrous phase in (Fe, Al) OOH[J]. Proceedings of the National Academy of Sciences,2018,115(12):2908-2911.

Keywords: High temperature and high pressure experiment, hydrous phase, diamond anvil cell

©2019. Japan Geoscience Union. All Right Reserved. 

# Effect of grid resolution on tectonic regimes in global-scale convection models

*Enrico Marzotto[1], Marcel Thielmann[1], Gregor Golabek[1]

1. Bayerisches Geoinstitut

Global-scale convection models using a visco-plastic rheology coupled with a temperature-dependent viscosity usually show different tectonic regimes: mobile, episodic or stagnant lid.

In the mobilelidregime, the lid is continuously subducting into the mantle (plate-like behavior). The episodic lid regime is characterized by the stability of the lid until sufficiently large lithospheric stresses break it, causing rapid resurfacing. Finally the stagnant lid regime is defined by an undeformable lid that does not participate in convection

In numerical simulations these three types of regimes can be obtained by varying some target parameters such as: temperature-dependency of viscosity and yield stress.

The yield stress in particular is a key parameter because it sets the stress necessary to cause plastic yielding, hence, in a visco-plastic rheology, the stress necessary to break the cold surface regions. A high yield stress will result in a stagnant lid. On the other hand, a low yield stress causes a weak lid that is constantly broken and sinks into the mantle.Despite the key importance of physical parameters, also numerical parameters have an effect on the tectonic regime, determining different outcomes justby changing the grid resolution.

Here we use the code StagYY (*Tackley, 2008*) in a 2D spherical annulus geometry (*Hernlund & Tackley, 2008*) to determine the resolution-dependent tectonic regime for different yield stresses in global-scale convection models. To assess the effect of grid resolution on lid behavior we use 16 different resolutions keeping all physical parameters unchanged. To make sure that steady state has been reached each simulation is run for 15 Gyrs. Tested resolutions vary from 128x32 to 1024x256 grid points. To understand this influence on the tectonic regime we study the resolution within the lid requiring an appropriate lid definition, based on the thermal and velocity field. Our results show that there is a correspondence between low radial resolution and mobile lid regime and that low aspect ratio cells (azimuthal to radial grid spacing) favor a plate-like behavior of the lid, while for large aspect ratios the mobile lid regime is persistent.

This work is the first part of a larger project, aiming to studyslab stagnation and hydration of the mantle transition zone (MTZ) using self-consistent global-scale mantle convection models, where subducting slabs carry water from the surface into the Earth’ s interior and potentially hydrate the MTZ. We expect that our previous work packages will help us to obtain realistic slab ponding in the MTZ, so we can study the hydration state of this region over time.

References:

Tackley, P. J. (2008). Modelling compressible mantle convection with large viscosity contrasts in a

©2019. Japan Geoscience Union. All Right Reserved. 

three-dimensional spherical shell using the yin-yang grid. *Phys. Earth Planet. Int.* 171, 7-18.

Hernlund, J. W. and P. J. Tackley (2008). Modeling mantle convection in the spherical annulus. *Phys. Earth Planet. Int.* 171, 48-54

Keywords: Geodynamical Modelling, StagYY, Grid Resolution

©2019. Japan Geoscience Union. All Right Reserved. 

# A 3-D crust and uppermost mantle electrical conductivity model of subduction zone beneath NE Japan

*Masahiro Ichiki[1,2], Toshiki Kaida[1], Yasuo Ogawa[3]

1. Graduate School of Science, Tohoku University, 2. International Research Institute of Disaster Science, 3. School of Science, Tokyo Institute of Technology

The crustal fluids beneath NE Japan is originated from dehydration of subducting Pacific slab or from convection in the backarc mantle, as is shown by seismic tomography [e.g. Zhao, 2017]. We investigated the fluid transportation paths from upper mantle to crust of subduction zone using electrical conductivity exploration.

We expanded electromagnetic field observation sites (96 sites) to northern part of NE Japan and obtained magnetotelluric responses and geomagnetic transfer functions in the period range of 20 –30720 seconds (22 periods) by BIRRP code [Chave and Thomson, 2004]. We used WSINV3D [Siripunvaraporn and Egbert, 2009] to invert those responses into three dimensional electrical resistivity model.

The preliminary model gives normalized root mean square misfit 5.87. A prominent conductor appears in the crust to uppermost mantle and the conductor spreads towards backarc direction. In our previous model [Ichiki et al., 2015], we found the overturned shape conductor towards backarc direction in the mantle wedge beneath central part of NE Japan. This study has found it beneath northern part NE Japan as well.

Those imply the crustal fluid and/or melt is transported along the pathway that is the plate boundary beneath the volcanic front to the backarc crust. The fluid transportation can explain the presence of enigmatic backarc volcano in the NE Japan. In this presenation, we speculate and discuss evolution of this pathway in geological time on the basis of the chlonological data of igneous rocks [Yoshida et al., 2013].

Acknouwledgement: This study is financially supported by KAKEN-HI No.26109006.

Keywords: electrical conductivity, resistivity, magnetotelluric, subduction zone

©2019. Japan Geoscience Union. All Right Reserved. 

# *The conditions of sublithospheric diamond formation constrained from ferric iron-rich exsolution from ferropericlase inclusions.*

*Caterina Melai[1], Daniel Frost[1], Tiziana Boffa Ballaran[1], Catherine McCammon[1]

1. Bayerisches Geoinstitute

Ferropericlase is apparently one of the more common inclusions to be found in sub-lithospheric diamonds, which are considered to form in the convecting mantle. Although relatively rare, these inclusions have been examined in a number of studies in the hope of providing information on the formation conditions of such deep diamonds, which could potentially be in the transition zone or lower mantle. The wide range of oxide Fe/(Fe+Mg) ratios found has raised the idea that they may form through the oxidation of iron metal. During TEM investigations, however, evidence for the exsolution of $Fe_2O_3$-rich phases such as magnesioferrite have been found, which implies that a more complex scenario may be involved. Ferropericlase-magnesiowüstite diamond inclusions are most likely some of the deepest available samples from the mantle and they potentially provide the most direct evidence for deep mantle carbon transport processes. The ferric iron contents of such inclusions alone may not provide a direct estimate for the oxygen fugacity at which the inclusions were trapped, particularly if pressure has a strong effect on the $fo_2$ - $Fe^{3+}/Fe_{tot}$ relationship. However, using experimental data it is possible to determine the oxygen fugacity at which the exsolution observed in the diamond inclusions occurred and coupled with the oxide $Fe^{3+}/Fe_{tot}$ ratio this could be used to estimate the pressure of formation.

The ferropericlase- magnesioferrite system has been investigated by several studies at room pressure but the stability field of the two components has been shown to become more complicated at high pressure due to the formation of mixed valence oxides. We have combined experimental measurements with thermodynamic modelling in order to address two main questions: at which P, T, $fO_2$ conditions do $Fe_2O_3$ -rich phases exsolve from ferropericlase? And what is the maximum $Fe^{3+}/Fe_{tot}$ ratio of ferropericlase. To answer these questions, multianvil experiments have been performed between 6 –25 GPa and 1200-1800˚C using a starting composition of $(Mg_{86}Fe_{14})O$ plus 20 % $Fe_2O_3$. Pt powder was added to the experiments to act as a redox sensor and minor amounts of Ni, Cr, Mn and Na were also added. Samples were then analyzed with the scanning electron microscope, electron microprobe, Mössbauer spectroscopy and X-ray diffraction. In the recovered experiments ferropericlase coexists with magnetite-magnesioferrite solid solution up to 10 GPa and $Mg_2Fe_2O_5$-$Fe_4O_5$ solid solution at higher pressures. In the calculation of the oxygen fugacity a ferropericlase model in the FeO-$Fe_{2/3}O$-MgO system was employed and exchange of Mg and $Fe^{2+}$ in magnetite was accounted for. Oxygen fugacities at which the phases coexist can be calculated in the magnetite-magnesioferrite field using three different equilibria and a quite simple ferropericlase mixing model results in calculated oxygen fugacities that are within 0.1 log units of each other for all three equilibria. The results show that magnetite-magnesioferrite solid solution should not be in equilibrium with ferropericlase in the diamond stability field. Our results imply that the exsolution of $Fe^{3+}$ rich phases observed in natural samples likely occurred at pressures corresponding to the transition zone or deeper.

©2019. Japan Geoscience Union. All Right Reserved. 

# Probing the variation of the oxygen fugacity in diamond anvil cells using the Fe-Ir alloy as redox sensor

*Serena Dominijanni[1], Catherine McCammon[1], Leonid Dubrovinsky[1], Dan Frost[1], Nobuyoshi Miyajima[1]

1. Bayerisches Geoinstitut

Understanding the oxygen fugacity ($fO_2$) in diamond anvil cells (DACs) is an important issue for many reasons, among them reconciling contradictory results that have been obtained for carbonate studies (Cerantola et al., 2017; Dorfman et al., 2018) that might be due to different redox conditions during the experiments. We therefore investigated the $fO_2$ conditions during DAC experiments using powder X-ray diffraction (beamlines ID15b and ID27) and energy-domain Synchrotron Mössbauer Source (SMS) spectroscopy (beamline ID18) at the European Synchrotron Radiation Facility (Grenoble, France). Double sided laser heating experiments (Aprilis et al., 2017) were carried out at high pressure and temperature using a mixture of synthetic ferropericlase ($Mg_{0.75}Fe_{0.25}$)O and pure iridium powder as a sliding redox sensor (Borisov and Palme, 2000; Swartzendruber, 1984; Taylor et al., 1992). The Fe content in the Fe-Ir alloy, together with the amount of FeO in ferropericlase, allows a calculation of $fO_2$ during the experiments (Stagno et al., 2011; Woodland and O'Neill, 1997). Preliminary results from powder X-ray diffraction data show that, after heating, an Fe-Ir metal alloy that can be indexed in the Fm-3m space group is formed by the reaction of pure Ir and Fe from ferropericlase according to the reaction:

(Mg,Fe)O + Ir --> (Mg,Fe)O + (Fe,Ir)

The compressibility of the Fe-Ir alloy and ferropericlase was measured up to ~ 60 GPa and SMS data were collected before and after heating. X-ray diffraction results coupled with energy-dispersive X-ray spectroscopy (EDS) measurements and a simple thermodynamic model indicate that the redox conditions during the DAC experiments were close to the iron-wüstite (IW) buffer, although some inhomogeneity was observed. Further chemical analyses and additional experiments are ongoing to understand the variation of oxygen fugacity in a DAC during laser heating.

Keywords: oxygen fugacity , redox sensor, diamond anvil cell

©2019. Japan Geoscience Union. All Right Reserved. 

# Goethite behavior at Earth's lower mantle conditions

*Egor Gennadievich Koemets[1], Maxim Bykov[1], George Aprilis[2], Timofey Fedotenko[2], Stella Chariton[1], Saiana Khandarkhaeva[1], Iuliia Koemets[1], Marcel Thielmann[1], Natalia Dubrovinsaia[2], Leonid Dubrovinsky[1]

1. BGI (Bayerisches Geoinstitut), Universität Bayreuth, Germany, 2. Material Physics and Technology at Extreme Conditions, Laboratory of Crystallography, Universität Bayreuth, Germany

Water and water-bearing species have a strong impact on numerous processes in Earth’ s interiors. Presence of water affects chemical and physical properties of mantle minerals, changes melting temperatures, sound velocities and viscosity of materials, and causing different global phenomena such as, for example, arc volcanism and plate tectonics. Thereby, the deep Earth’ s regions enriched with water are crucial for understanding our planet’ s geodynamics and geochemistry. Still, mechanisms of water circulation between geospheres remain poorly understood. Recent studies suggest that goethite present in Banded Iron Formations (BIFs) may transfer some quantities of water to the deep Earth interiors with subducting slabs. It was reported that goethite remains stable in the sinking slab until it reaches the base of a lower mantle. By the meaning of in situ powder XRD it was revealed that at pressures corresponding to the depths ~1500-1800 km and moderately high temperatures goethite undergoes a phase transition to form a novel stable pyrite-type phase $FeO_2H_x$ with $0 \leqq x \leqq 1$ (named as Py-phase). Thus, goethite and its HP pyrite-type form became a candidate for water and/or hydrogen transfer and storage to the lower mantle and the core-mantle boundary. Using laser-heating in diamond anvil cells we performed a series of experiments on an investigation of goethite (as a starting material) stability at P-T conditions covering possible range in subducting slabs. By the meaning of sensitive in situ single-crystal XRD in DACs we registered decomposition of goethite and formation of known (such as $\iota$-$Fe_2O_3$, $\eta$-$Fe_2O_3$, a high-pressure orthorhombic form of $Fe_3O_4$, $Fe_5O_7$) and novel iron-oxygen compounds. Results of structure solution and refinement established these compounds to be orthorhombic $Fe_7O_{10}$ and hexagonal non-stoichiometric phase $Fe_{6.31}O_9$. Our results suggest that FeOOH cannot transport water into the deep of Earth’ s mantle.

Keywords: Goethite, Diamond anvil cell, High Pressure, Single-crystal XRD, Subducting slabs

©2019. Japan Geoscience Union. All Right Reserved. 

# The oxygen content of sulphides in the mantle and a geothermometer for diamond formation

*Sumith Abeykoon[1], Dan Frost[1], Vera Laurenz[1]

1. Bayerisches Geoinstitut, University of Bayreuth

Sulphides are ubiquitous accessory minerals in mantle rocks and form the most prevalent type of inclusion in diamonds. Diamond sulphide inclusions are trapped as sulphide melts that crystallise on cooling to form Fe-Ni monosulphide solid solution (MSS) and ultimately recrystallizes to assemblages containing pyrrhotite, $Fe_{(1-x)}S$ (x = 0 to 0.2), pentlandite, $(Fe,Ni)_9S_8$, and sometimes pyrite ($FeS_2$). Sulphide inclusions are also found in many xenoliths but those which are hosted by diamonds provide potentially the most pristine samples from the lithospheric mantle and deeper. Previous experiments indicate that oxygen partitions into sulphide melts and although sparse, some measurements of natural sulphide inclusions from mantle xenoliths indeed show measurable and in some cases relatively high oxygen concentrations. If the parameters that control sulphide oxygen concentration can be determined then they could be potentially used to understand conditions in the mantle and in particular in sublithospheric diamonds. The oxygen content of sulphides separating to the core during core formation could have also influenced the oxygen fugacity of the early mantle.
We have measured the oxygen contents of sulphide melts within experimentally produced mantle assemblages at high pressures and temperatures. A series of multi-anvil experiments were conducted to equilibrate a peridotite assemblage with molten sulphide (FeS) at pressures between 3 –11 GPa and temperatures of 1300 ˚C –1700 ˚C. The effects of pressure, temperature, oxygen fugacity and composition have been investigated. Oxygen fugacity was determined in some experiments by saturating the sulphide in Ir to produce a separate Ir-Fe metal alloy, for which the Fe content is a function of oxygen fugacity. The results show that sulphide melt oxygen contents can range up to 16 weight % FeO, at mantle conditions. Moreover, the content of oxygen in the sulphide is found to be not controlled by $fO_2$ or $fS_2$, which is in disagreement with previous experimental studies conducted at ambient pressure conditions. The experiments indicate that the oxygen concentration is mainly controlled by the FeO activity in coexisting silicates phases and the temperature, although further work is still required to calibrate effects of Ni and Cu. In order to fit the data and to account for the FeO dependence, we developed a thermodynamic model using an end-member equilibrium between olivine, pyroxene and FeO in the sulphide melt. The resulting relationship can be used as a geothermometer based on sulphide inclusion oxygen contents and could be particularly useful for determining diamond formation temperatures for sub lithospheric diamonds.

Keywords: Sulfide, Oxygen, Geothermometer

©2019. Japan Geoscience Union. All Right Reserved. 

[E] Poster | S (Solid Earth Sciences )：S-CG Complex & General

Thu. May 30, 2019 5:15 PM - 6:30 PM JST | Thu. May 30, 2019 8:15 AM - 9:30 AM UTC | Poster Hall International Exhibition Hall8, Makuhari Messe_27

## [S-CG51] Role of volatiles on Earth and planetary dynamics

convener:Takayuki Ishii(Bavarian Research Institute, University of Bayreuth), Eiji Ohtani(Department of Earth and Planetary Materials Science, Graduate School of Science, Tohoku University), Michihiko Nakamura(Division of Earth and Planetary Materials Science, Department of Earth Science, Graduate School of Science, Tohoku University), Bjorn Mysen(Geophysical Laboratory, Carnegie Inst. Washington)

This session addresses how volatile species affect dynamics of the<br/>Earth and planets from natural observations, laboratory experiments, and<br/>numerical modeling in the temperature, pressure, and oxygen activity<br/>range from the early stage of the planet formation to the present. The<br/>volatiles can be critical in zones of magma storage and ascent, mantle<br/>upwelling and melting in the fluid-enriched subduction zones, in the<br/>mantle transition zone, in the lower mantle, in the core-mantle boundary,<br/>and in Earth and planetary cores. However, volatiles affect properties<br/>and processes differently depending on their pressure, temperature, and<br/>redox conditions, which vary in time and space. <br/> This session aims to address how volatiles control the dynamic<br/>processes of the Earth and planets, governed by their geophysical and<br/>geochemical properties. We welcome papers dealing with geological and<br/>laboratory observations coupled with numerical modeling on the role of<br/>volatiles. The topics include (1) Stability relations, chemical and<br/>physical properties of crystalline, molten and fluid phases,<br/>partitioning of volatiles among these phases, (2) Rheological and other<br/>physical properties of minerals, and the effects of intergranular fluid<br/>on the properties, (3) Volatiles and dehydration induced seismicity and<br/>volcanism in various tectonic regions including subduction zones, and (4)<br/>Effects of volatiles in numerical simulation of geo-tectonics, and (5)<br/>Magma outgassing and its control of volcanic eruption dynamics.

[SCG51-P01] Permeability prediction of porous media with the finite difference Stokes solver LaMEM

*Philipp Eichheimer[1], Wakana Fujita[2], Marcel Thielmann[1], Anton Popov[3], Gregor Golabek[1], Boris Kaus[3], Maximilian Kottwitz[3] (1.Bayerisches Geoinstitut, University of Bayreuth, 2.Department of Earth Science, Tohoku University, Sendai, 3.Institute of Geosciences, Johannes Gutenberg University Mainz)

[SCG51-P02] Grain growth-induced fluid localization and permeability reduction

*Wakana Fujita[1], Michihiko Nakamura[1], Kentaro Uesugi[2] (1.Graduate School of Science, Tohoku University, 2.JASRI/SPring-8)

[SCG51-P03] Pargasite stability in the upper mantle at $H_2O$-undersaturated conditions

*Marija Putak Juricek[1], Hans Keppler[1] (1.BGI)

[SCG51-P04] **Constraining the water content at the top of the mantle transition zone with the elasticity of wadsleyite and olivine**

*Zhongqing Wu[1] (1.University of Science and Technology of China)

[SCG51-P05] ***Single crystal elasticity of Fe-bearing phase E by Brillouin spectroscopy***

*Niccolo Satta[1], Hauke Marquardt [2], Alexander Kurnosov[1], Tiziana Boffa Ballaran [1], Johannes Buchen[3], Catherine McCammon[1], Takaaki Kawazoe[4] (1.Bayerisches Geoinstitut, University of Bayreuth, 95440 Bayreuth, Germany, 2.Department of Earth Sciences, University of Oxford, South Parks Road, Oxford, UK., 3.Seismological Laboratory, California Institute of Technology, Pasadena, CA 91125, USA., 4.Department of Earth and Planetary Systems Science, Hiroshima University, Hiroshima 739-8526, Japan.)

[SCG51-P06] Discovery of two hexagonal phases in (Fe,Al)OOH under the P-T conditions of the deep lower mantle

*Lu Liu[1,2], Li Zhang[1], Hongsheng Yuan[1] (1.Center for High Pressure Science and Technology Advanced Research, 2.University of Science and Technology of China)

[SCG51-P07] **Effect of grid resolution on tectonic regimes in global-scale convection models**

*Enrico Marzotto[1], Marcel Thielmann[1], Gregor Golabek[1] (1.Bayerisches Geoinstitut)

[SCG51-P08] A 3-D crust and uppermost mantle electrical conductivity model of subduction zone beneath NE Japan

*Masahiro Ichiki[1,2], Toshiki Kaida[1], Yasuo Ogawa[3] (1.Graduate School of Science, Tohoku University, 2.International Research Institute of Disaster Science, 3.School of Science, Tokyo Institute of Technology)

[SCG51-P09] *The conditions of sublithospheric diamond formation constrained from ferric iron-rich exsolution from ferropericlase inclusions.*

*Caterina Melai[1], Daniel Frost[1], Tiziana Boffa Ballaran[1], Catherine McCammon[1] (1.Bayerisches Geoinstitute)

[SCG51-P10] **Probing the variation of the oxygen fugacity in diamond anvil cells using the Fe-Ir alloy as redox sensor**

*Serena Dominijanni[1], Catherine McCammon[1], Leonid Dubrovinsky[1], Dan Frost[1], Nobuyoshi Miyajima[1] (1.Bayerisches Geoinstitut)

[SCG51-P11] Goethite behavior at Earth's lower mantle conditions

*Egor Gennadievich Koemets[1], Maxim Bykov[1], George Aprilis[2], Timofey Fedotenko[2], Stella Chariton[1], Saiana Khandarkhaeva[1], Iuliia Koemets[1], Marcel Thielmann[1], Natalia Dubrovinsaia[2], Leonid Dubrovinsky[1] (1.BGI (Bayerisches Geoinstitut), Universität Bayreuth, Germany, 2.Material Physics and Technology at Extreme Conditions, Laboratory of Crystallography, Universität Bayreuth, Germany)

[SCG51-P12] The oxygen content of sulphides in the mantle and a geothermometer for diamond formation

*Sumith Abeykoon[1], Dan Frost[1], Vera Laurenz[1] (1.Bayerisches Geoinstitut, University of Bayreuth)

# Permeability prediction of porous media with the finite difference Stokes solver LaMEM

*Philipp Eichheimer[1], Wakana Fujita[2], Marcel Thielmann[1], Anton Popov[3], Gregor Golabek[1], Boris Kaus[3], Maximilian Kottwitz[3]

1. Bayerisches Geoinstitut, University of Bayreuth, 2. Department of Earth Science, Tohoku University, Sendai, 3. Institute of Geosciences, Johannes Gutenberg University Mainz

The flow of fluids through porous media such as groundwater flow or magma migration is one of the most important processes in geological sciences. The property controlling the efficiency of the flow is the permeability of the rock, thus an accurate determination and prediction of its value is of crucial importance. For this reason, permeability of rocks has been measured across different scales. As laboratory measurements exhibit a range of limitations, the numerical prediction of permeability at conditions where laboratory experiments struggle has become an important method to complement laboratory approaches. At high resolutions, this prediction becomes computationally very expensive, which makes it crucial to develop methods that maximize accuracy. In this work we introduce the open-source finite difference solver LaMEM that can be used to numerically predict the permeability of porous media under laminar conditions. We employ a stencil rescaling method to increase accuracy due to a better description of the solid-fluid interface, thus reducing the computational cost. To validate the method, we perform a series of tests employing both analytical solutions for simplified geometries as well as results from other numerical approaches for more complicated geometries. Furthermore we compare our numerical results to laboratory measurements on glass bead samples with porosities ranging from 20% to 2.5%, showing good agreement.

Keywords: Permeability, Numerical modelling, Digital Rock Physics

©2019. Japan Geoscience Union. All Right Reserved. 

# Grain growth-induced fluid localization and permeability reduction

*Wakana Fujita[1], Michihiko Nakamura[1], Kentaro Uesugi[2]

1. Graduate School of Science, Tohoku University, 2. JASRI/SPring-8

Efficiency of segregation of geological fluids such as aqueous fluids and melts is an essential elementary process for volatile cycles in subduction zones. Permeability is an intrinsic rock property that controls flow rate of fluid. Various permeability models have been presented by numerical models of textually equilibrated rocks (e.g. 1, 2), laboratory measurements on synthetic rocks (e.g. 3) and estimation from cross-sectional area of synthetic rocks (4). However, there exist discrepancies among those models. Because permeability is very sensitive to microscopic geometry of pore fluid, those disagreements may arise from lack of understanding toward three-dimensional (3D) microstructure of fluid network.

Dihedral angle has been considered to be a critical parameter that controls fluid geometry and thus permeability. Beside, some previous studies shed light on the effect of grain growth on fluid distribution because it could induce pore fluid distortion and coalescence (5, 6). These studies suggest that in the actual systems where the microstructure of rocks evolve in dynamic processes, grain growth would be important along with the dihedral angle.

To investigate the effect of grain growth on the fluid distribution and permeability, we present 3D images of quartz–CHO fluid aggregates, containing nominal fluid fractions between 0.03 and 0.10. Samples were synthesized from a powdered mixture of Arkansus quartz and amorphous silica prepared by sol-gel method and hot-pressed in a piston–cylinder apparatus at 900˚C and 1.0 GPa for 192h. The fluid fractions and the dihedral angles were controlled using brucite added in the capsule bottom and oxalic acid dihydrate mixed with $SiO_2$ powder. 3D images were obtained using synchrotron X-ray microtomography at BL20XU experimental hutch2 of SPring-8. Regardless of dihedral angles ($CO_2$ content in fluids), both cross-sectional area and 3D images of samples showed grain-scale fluid localization which would be formed by pore fluid coalescence induced by grain growth. Computed permeabilities using numerical model, LaMEM (7) were almost consistent with laboratory measurements by (3) but more than one order of magnitude lower than a numerical model by (2). This would indicate that localized fluids extensively reduce permeability by reducing the diameter of fluid tubes along grain edges, which would suggest transport of water into Earth’ s deep interior by the subducting slab.

Reference:
1. von Bargen and Waff. 1986, J. Geophys. Res. 91, 9261–9276.
2. Rudge, J.F. 2018, Proc. R. Soc. Lond. A 474, 20170639.
3. Wark and Watson. 1998, Earth Planet. Sci. Lett. 164, 591–605.
4. Faul, U.H. 1997, J. Geophys. Res. 102, 10299–10311.
5. Walte et al. 2003, Geology 2003 31, 1009-1012.
6. Yoshino and Watson. 2005, Earth Planet. Sci. Lett. 235, 453–468.
7. Kaus et al. 2016, NIC Symposium 2016

Keywords: Permeability, Quartz, Grain growth, Dihedral angle, Fluid segregation

©2019. Japan Geoscience Union. All Right Reserved. 

# Pargasite stability in the upper mantle at $H_2O$-undersaturated conditions

*Marija Putak Juricek[1], Hans Keppler[1]

1. BGI

Amphibole is the most commonly occurring hydrous mineral in mantle xenoliths and the majority of upper mantle amphiboles have compositions close to pargasite end member. Previous experimental work has demonstrated that pargasite stability is sensitive to variations in bulk alkali and water content of the starting material. While it has been successfully shown that addition of more alkali leads to stabilization of pargasite to higher P and T, the effect of water on amphibole stability is not so straightforward.

At $H_2O$-saturated conditions, alkali elements partition strongly into aqueous fluid and become less available for crystallization of amphibole. As a result, amphibole seemingly becomes stable at higher P and T when less $H_2O$ is added to the starting material. This observation led to the hypothesis that pargasite may be a ubiquitous phase in the upper mantle, which is believed to contain only several hundred ppm of $H_2O$. However, most of the previous studies determined pargasite stability at $H_2$ O-saturated conditions where solid phases coexist with an aqueous fluid during experiments. Since such environments are not representative of the nearly dry upper mantle, the purpose of this study is to investigate pargasite stability at $H_2O$-undersaturated conditions.

Because of the high specific surface area of powders, adsorption of atmospheric $H_2O$ on fine grained starting materials prevents attaining $H_2O$-undersaturation by adding small amounts of water to the sample. Instead, $H_2O$-undersaturated conditions may be precisely controlled by diluting the water in the sample with another component. Under such conditions, solid phases are expected to coexist with a low water activity fluid throughout the experiment. As molecular nitrogen is mostly insoluble in upper mantle minerals, it can be used to adjust the water activity of the fluid to a desired low value.

All experiments were performed in a piston cylinder apparatus. The samples for $H_2O$-undersaturated experiments were prepared by adding silver azide ($AgN_3$) and brucite to a synthetic peridotite mixture. In several experiments water was added directly as $H_2O_{(l)}$. The amount of water was kept constant in all experiments (1 wt. percent) and the molar fraction of water in the $N_2$-$H_2O$ fluid was adjusted to the desired value by weighing an appropriate amount of $AgN_3$, which decomposed to metallic silver and molecular nitrogen during heating. In $H_2O$-saturated experiments, no silver azide was added to the peridotite mixture. Experimental products were analyzed using JEOL JXA-8200 electron microprobe.

Preliminary results show that pargasite is not stable in equilibrium with fluids diluted to $X_{H2O}$=0.1 at pressures above 1 GPa. At $H_2O$-saturated conditions pargasite stability field can extend to pressures of 4 GPa and above 1100 ℃, depending on bulk alkali and water contents. Results from experiments at $X_{H2O}$ =0.1 and $X_{H2O}$=1 suggest that pargasite can exist only in regions of the upper mantle which have been affected by high water activity fluids, such as areas in the vicinity of subduction zones. The ambient nominally anhydrous upper mantle, better represented by experiments at $H_2O$-undersaturated conditions, is not expected to contain pargasite.

Keywords: pargasite, stability, upper, mantle

©2019. Japan Geoscience Union. All Right Reserved. 

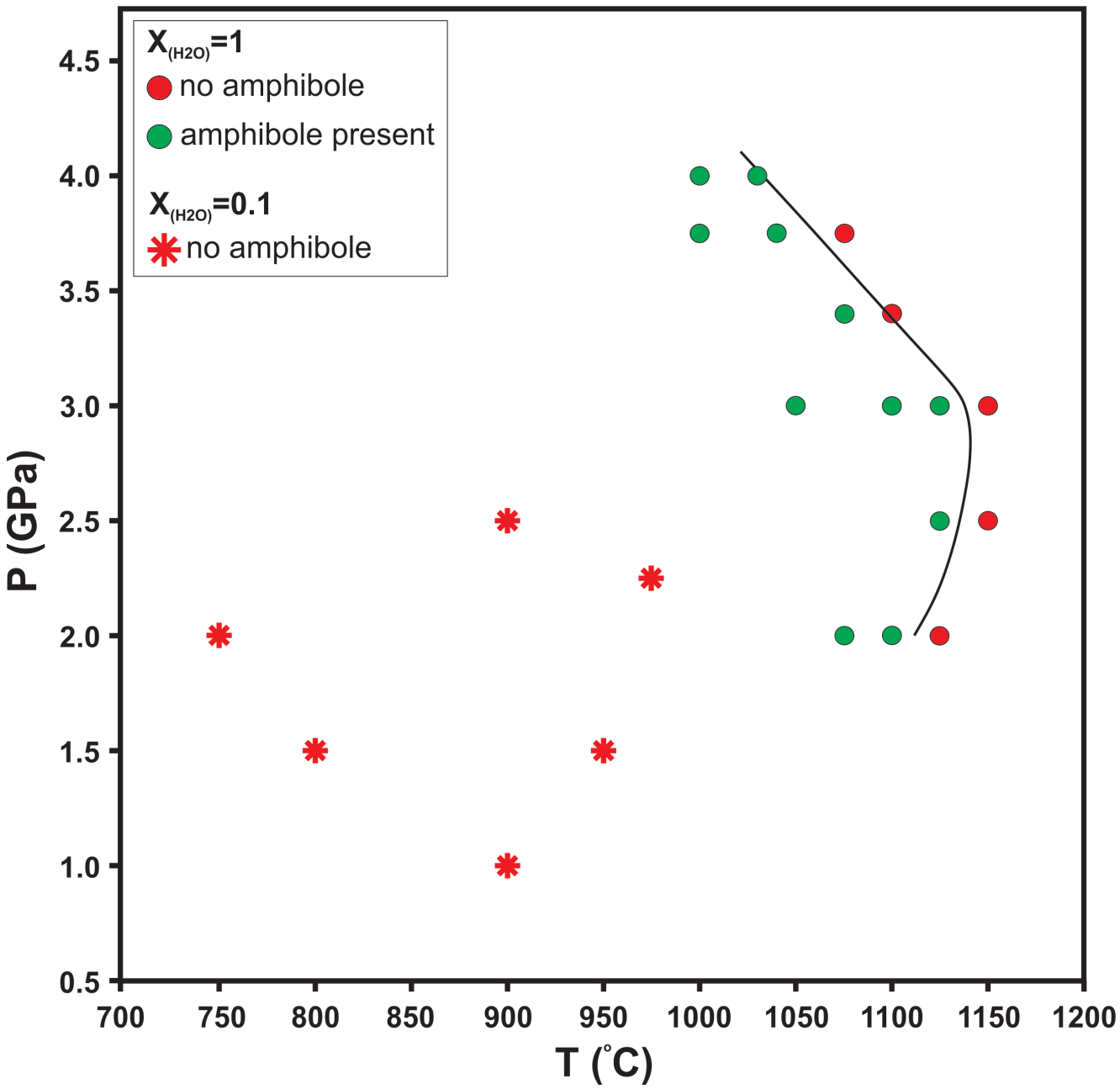


©2019. Japan Geoscience Union. All Right Reserved. 

# Constraining the water content at the top of the mantle transition zone with the elasticity of wadsleyite and olivine

*Zhongqing Wu[1]

1. University of Science and Technology of China

Zhongqing Wu[a,b,*], Wenzhong Wang[a,b], Michael J. Walter[c] ,Ye Peng[a,b], Simon Redfern[d],

[a] Laboratory of Seismology and Physics of Earth’ s Interior, School of Earth and Space Sciences, University of Science and Technology of China, Hefei, Anhui 230026, China

[b] Mengcheng National Geophysical Observatory, Anhui, China

[c]School of Earth Sciences, University of Bristol, Bristol BS8 1RJ, UK

[d]Department of Earth Science, University of Cambridge, Cambridge CB2 3EQ, UK

The water content in the mantle transition zone (MTZ) exerts a controlling influence on the dynamical and chemical evolution of Earth, but is poorly known. In principle the water content at the top of the transition zone can be inferred by comparing the velocity and density contrasts across the 410-km seismic discontinuity with predictions based on the phase transition of olivine to wadsleyite. The high-quality elastic data of at pressure and temperature (PT) conditions of the transition zone are crucial but are very challenge for experiments to obtain. Calculating these elastic data at high PT conditions in conventional method are also very expensive. Instead, these elastic data were calculated using the method of Wu and Wentzcovitch (2011), which reduces the computational workload to tenth of the conventional method. All calculations for two phases were conducted using the same computational details as far as possible, which guarantees that the velocity and density differences between two phases have very high precise. All these calculated elastic data agree well with the available experimental data. The iron and water effect on the elasticity are also well described.

With these high-quality elastic data covered the PT condition of the transition zone, we analyze the water and wadsleyite content at the top of the transition zone. We found that the water content of wadsleyite at the top of the transition zone can be well constrained when density and velocities jumps are considered together. For a pyrolitic mantle composition with ~60% olivine, our best fit is ~ 0.5 wt% water at the top of the transition zone. If the transition zone is dry, as suggested by some electrical conductivity models, the upper mantle may only contain ~ 50% olivine.

Wu, Z., Wentzcovitch, R.M., 2011. Quasiharmonic thermal elasticity of crystals: An analytical approach. Phys. Rev. B - Condens. Matter Mater. Phys. 83, 1–8. doi:10.1103/PhysRevB.83.184115

©2019. Japan Geoscience Union. All Right Reserved. 

# *Single crystal elasticity of Fe-bearing phase E by Brillouin spectroscopy*

*Niccolo Satta[1], Hauke Marquardt [2], Alexander Kurnosov[1], Tiziana Boffa Ballaran [1], Johannes Buchen[3], Catherine McCammon[1], Takaaki Kawazoe[4]

1. Bayerisches Geoinstitut, University of Bayreuth, 95440 Bayreuth, Germany, 2. Department of Earth Sciences, University of Oxford, South Parks Road, Oxford, UK., 3. Seismological Laboratory, California Institute of Technology, Pasadena, CA 91125, USA., 4. Department of Earth and Planetary Systems Science, Hiroshima University, Hiroshima 739-8526, Japan.

Earth’s deep water cycle plays a key role for the dynamic evolution of our planet and the development of habitable conditions. Surface water can be transported to Earth’s mantle by subduction of oceanic lithosphere. Experimental investigations have shown that water can be efficiently stored in Dense Hydrous Magnesium Silicates (DHMS) in cold subducting slabs. However, quantification of the incoming water budget based on the interpretation of seismological observations is hampered by a lack of elasticity measurements of DHMSs. Here, we report single-crystal elasticity measurements of Fe-bearing phase E, a DHMS that is stable at pressures and temperature of Earth’s mantle transition zone. A very low bulk modulus has been reported for phase E, suggesting that it might produce seismic velocity heterogeneities detectable by seismological investigations. However, the shear modulus of phase E has not been quantified.

We synthesized Fe-bearing phase E single crystals in a multi-anvil apparatus. Chemical composition as well as crystal structure have been determined using electron microprobe analysis, Mössbauer spectroscopy, and single-crystal X-ray diffraction. We derived the full elastic stiffness tensor by Brillouin spectroscopy on two single crystals of selected orientations. We found phase E to have both the lowest bulk modulus and shear modulus among the DHMSs at ambient conditions. Phase E shows very low compressional and shear velocities especially when compared to the other principal minerals likely present in subducting slabs after serpentine breakdown. Modelling of seismic velocities in dry and hydrated upper mantle and transition zone rocks suggests that the presence of even small amounts of phase E can appreciably lower seismic wave velocities. Phase E could be used as seismological indicator for water stored at depth in subducting scenarios. The elasticity of phase E under mantle conditions will be explored in future research.

Keywords: Brillouin scattering, Phase E, Seismic wave velocities

©2019. Japan Geoscience Union. All Right Reserved. 

# Discovery of two hexagonal phases in (Fe,Al)OOH under the P-T conditions of the deep lower mantle

*Lu Liu[1,2], Li Zhang[1], Hongsheng Yuan[1]

1. Center for High Pressure Science and Technology Advanced Research, 2. University of Science and Technology of China

Deep water can cause a series of complex seismological phenomena by changing the density and thermal stability of lower mantle components. δ-H solid solution phase (AlOOH-$MgSiO_2(OH)$) is stable at lower mantle conditions[1],because the crystallographic frameworks of the phase H is similar to that of the δ-AlOOH phase, with very strong hydrogen bonds[2,3]. δ-AlOOH and ε-FeOOH can also form solid solution[4] (δ - ε solution). It is reasonable to infer that δ - ε solid solution may have similar thermal stability as that of H- δ solution, considering their similar crystal structure[5]. In our experiments, we synthesized the δ - ε solution at 79GPa and 1600K in a laser-heated diamond anvil cell. As the temperature increases to 2100k, the orthorhombic δ - ε solution transformed into a hexagonal-structured phase. By combining powder X-ray diffraction techniques with multigrain indexation[6], we determined its hexagonal lattice with a=b=10.019Å and c=2.614Å. At 79GPa and 2400K, the hexagonal phase transforms into another hexagonal phase, with the lattice parameters of a=b=2.733Å and c=9.343Å. The discovery of these two new phases may provide new insights into the deep-water storage.

References
1.Ohira I, Ohtani E, Sakai T, et al. Stability of a hydrous δ-phase, AlOOH-$MgSiO_2(OH)_2$, and a mechanism for water transport into the base of lower mantle[J].Earth and Planetary Science Letters, 2014, 401: 12-17.
2.Ohtani, E., Amaike, Y., Kamada, S., Sakamaki, T. and Hirao, N. Stability of hydrous phase H $MgSiO_4H_2$ under lower mantle conditions. Geophys. Res. Lett. 41, -8287 (2014).
3.Nishi M,Kuwayama Y,Tsuchiya J,et al.The pyrite-type high-pressure form of FeOOH[J]. Nature,2017,54(7662):205-208.
4.T Kawazoe,I Ohira,T Ishii et al. Single crystal synthesis of δ-(Al,Fe)OOH American Mineralogist. Volume 102, pages 1953–1956, (2017)
5.Gleason A E,Quiroga C E,Suzuki A,et al.Symmetrization driven spin transition in ε-FeOOH at high pressure[J]. Earth and Planetary Science Letters, 2013, 379: 49-55.
6.Zhang L,Yuan H,Meng Y,et al.Discovery of a hexagonal ultradense hydrous phase in (Fe, Al) OOH[J]. Proceedings of the National Academy of Sciences,2018,115(12):2908-2911.

Keywords: High temperature and high pressure experiment, hydrous phase, diamond anvil cell

©2019. Japan Geoscience Union. All Right Reserved. 

# Effect of grid resolution on tectonic regimes in global-scale convection models

*Enrico Marzotto[1], Marcel Thielmann[1], Gregor Golabek[1]

1. Bayerisches Geoinstitut

Global-scale convection models using a visco-plastic rheology coupled with a temperature-dependent viscosity usually show different tectonic regimes: mobile, episodic or stagnant lid.

In the mobilelidregime, the lid is continuously subducting into the mantle (plate-like behavior). The episodic lid regime is characterized by the stability of the lid until sufficiently large lithospheric stresses break it, causing rapid resurfacing. Finally the stagnant lid regime is defined by an undeformable lid that does not participate in convection

In numerical simulations these three types of regimes can be obtained by varying some target parameters such as: temperature-dependency of viscosity and yield stress.

The yield stress in particular is a key parameter because it sets the stress necessary to cause plastic yielding, hence, in a visco-plastic rheology, the stress necessary to break the cold surface regions. A high yield stress will result in a stagnant lid. On the other hand, a low yield stress causes a weak lid that is constantly broken and sinks into the mantle.Despite the key importance of physical parameters, also numerical parameters have an effect on the tectonic regime, determining different outcomes justby changing the grid resolution.

Here we use the code StagYY (*Tackley, 2008*) in a 2D spherical annulus geometry (*Hernlund & Tackley, 2008*) to determine the resolution-dependent tectonic regime for different yield stresses in global-scale convection models. To assess the effect of grid resolution on lid behavior we use 16 different resolutions keeping all physical parameters unchanged. To make sure that steady state has been reached each simulation is run for 15 Gyrs. Tested resolutions vary from 128x32 to 1024x256 grid points. To understand this influence on the tectonic regime we study the resolution within the lid requiring an appropriate lid definition, based on the thermal and velocity field. Our results show that there is a correspondence between low radial resolution and mobile lid regime and that low aspect ratio cells (azimuthal to radial grid spacing) favor a plate-like behavior of the lid, while for large aspect ratios the mobile lid regime is persistent.

This work is the first part of a larger project, aiming to studyslab stagnation and hydration of the mantle transition zone (MTZ) using self-consistent global-scale mantle convection models, where subducting slabs carry water from the surface into the Earth’ s interior and potentially hydrate the MTZ. We expect that our previous work packages will help us to obtain realistic slab ponding in the MTZ, so we can study the hydration state of this region over time.

References:

Tackley, P. J. (2008). Modelling compressible mantle convection with large viscosity contrasts in a

©2019. Japan Geoscience Union. All Right Reserved. 

three-dimensional spherical shell using the yin-yang grid. *Phys. Earth Planet. Int.* 171, 7-18.

Hernlund, J. W. and P. J. Tackley (2008). Modeling mantle convection in the spherical annulus. *Phys. Earth Planet. Int.* 171, 48-54

Keywords: Geodynamical Modelling, StagYY, Grid Resolution

©2019. Japan Geoscience Union. All Right Reserved. 

# A 3-D crust and uppermost mantle electrical conductivity model of subduction zone beneath NE Japan

*Masahiro Ichiki[1,2], Toshiki Kaida[1], Yasuo Ogawa[3]

1. Graduate School of Science, Tohoku University, 2. International Research Institute of Disaster Science, 3. School of Science, Tokyo Institute of Technology

The crustal fluids beneath NE Japan is originated from dehydration of subducting Pacific slab or from convection in the backarc mantle, as is shown by seismic tomography [e.g. Zhao, 2017]. We investigated the fluid transportation paths from upper mantle to crust of subduction zone using electrical conductivity exploration.

We expanded electromagnetic field observation sites (96 sites) to northern part of NE Japan and obtained magnetotelluric responses and geomagnetic transfer functions in the period range of 20 –30720 seconds (22 periods) by BIRRP code [Chave and Thomson, 2004]. We used WSINV3D [Siripunvaraporn and Egbert, 2009] to invert those responses into three dimensional electrical resistivity model.

The preliminary model gives normalized root mean square misfit 5.87. A prominent conductor appears in the crust to uppermost mantle and the conductor spreads towards backarc direction. In our previous model [Ichiki et al., 2015], we found the overturned shape conductor towards backarc direction in the mantle wedge beneath central part of NE Japan. This study has found it beneath northern part NE Japan as well.

Those imply the crustal fluid and/or melt is transported along the pathway that is the plate boundary beneath the volcanic front to the backarc crust. The fluid transportation can explain the presence of enigmatic backarc volcano in the NE Japan. In this presenation, we speculate and discuss evolution of this pathway in geological time on the basis of the chlonological data of igneous rocks [Yoshida et al., 2013].

Acknouwledgement: This study is financially supported by KAKEN-HI No.26109006.

Keywords: electrical conductivity, resistivity, magnetotelluric, subduction zone

©2019. Japan Geoscience Union. All Right Reserved. 

# *The conditions of sublithospheric diamond formation constrained from ferric iron-rich exsolution from ferropericlase inclusions.*

*Caterina Melai[1], Daniel Frost[1], Tiziana Boffa Ballaran[1], Catherine McCammon[1]

1. Bayerisches Geoinstitute

Ferropericlase is apparently one of the more common inclusions to be found in sub-lithospheric diamonds, which are considered to form in the convecting mantle. Although relatively rare, these inclusions have been examined in a number of studies in the hope of providing information on the formation conditions of such deep diamonds, which could potentially be in the transition zone or lower mantle. The wide range of oxide Fe/(Fe+Mg) ratios found has raised the idea that they may form through the oxidation of iron metal. During TEM investigations, however, evidence for the exsolution of $Fe_2O_3$-rich phases such as magnesioferrite have been found, which implies that a more complex scenario may be involved. Ferropericlase-magnesiowüstite diamond inclusions are most likely some of the deepest available samples from the mantle and they potentially provide the most direct evidence for deep mantle carbon transport processes. The ferric iron contents of such inclusions alone may not provide a direct estimate for the oxygen fugacity at which the inclusions were trapped, particularly if pressure has a strong effect on the $fo_2$ - $Fe^{3+}/Fe_{tot}$ relationship. However, using experimental data it is possible to determine the oxygen fugacity at which the exsolution observed in the diamond inclusions occurred and coupled with the oxide $Fe^{3+}/Fe_{tot}$ ratio this could be used to estimate the pressure of formation.

The ferropericlase- magnesioferrite system has been investigated by several studies at room pressure but the stability field of the two components has been shown to become more complicated at high pressure due to the formation of mixed valence oxides. We have combined experimental measurements with thermodynamic modelling in order to address two main questions: at which P, T, $fO_2$ conditions do $Fe_2O_3$ -rich phases exsolve from ferropericlase? And what is the maximum $Fe^{3+}/Fe_{tot}$ ratio of ferropericlase. To answer these questions, multianvil experiments have been performed between 6 –25 GPa and 1200-1800˚C using a starting composition of $(Mg_{86}Fe_{14})O$ plus 20 % $Fe_2O_3$. Pt powder was added to the experiments to act as a redox sensor and minor amounts of Ni, Cr, Mn and Na were also added. Samples were then analyzed with the scanning electron microscope, electron microprobe, Mössbauer spectroscopy and X-ray diffraction. In the recovered experiments ferropericlase coexists with magnetite-magnesioferrite solid solution up to 10 GPa and $Mg_2Fe_2O_5$-$Fe_4O_5$ solid solution at higher pressures. In the calculation of the oxygen fugacity a ferropericlase model in the FeO-$Fe_{2/3}O$-MgO system was employed and exchange of Mg and $Fe^{2+}$ in magnetite was accounted for. Oxygen fugacities at which the phases coexist can be calculated in the magnetite-magnesioferrite field using three different equilibria and a quite simple ferropericlase mixing model results in calculated oxygen fugacities that are within 0.1 log units of each other for all three equilibria. The results show that magnetite-magnesioferrite solid solution should not be in equilibrium with ferropericlase in the diamond stability field. Our results imply that the exsolution of $Fe^{3+}$ rich phases observed in natural samples likely occurred at pressures corresponding to the transition zone or deeper.

©2019. Japan Geoscience Union. All Right Reserved. 

# Probing the variation of the oxygen fugacity in diamond anvil cells using the Fe-Ir alloy as redox sensor

*Serena Dominijanni[1], Catherine McCammon[1], Leonid Dubrovinsky[1], Dan Frost[1], Nobuyoshi Miyajima[1]

1. Bayerisches Geoinstitut

Understanding the oxygen fugacity ($fO_2$) in diamond anvil cells (DACs) is an important issue for many reasons, among them reconciling contradictory results that have been obtained for carbonate studies (Cerantola et al., 2017; Dorfman et al., 2018) that might be due to different redox conditions during the experiments. We therefore investigated the $fO_2$ conditions during DAC experiments using powder X-ray diffraction (beamlines ID15b and ID27) and energy-domain Synchrotron Mössbauer Source (SMS) spectroscopy (beamline ID18) at the European Synchrotron Radiation Facility (Grenoble, France). Double sided laser heating experiments (Aprilis et al., 2017) were carried out at high pressure and temperature using a mixture of synthetic ferropericlase ($Mg_{0.75}Fe_{0.25}$)O and pure iridium powder as a sliding redox sensor (Borisov and Palme, 2000; Swartzendruber, 1984; Taylor et al., 1992). The Fe content in the Fe-Ir alloy, together with the amount of FeO in ferropericlase, allows a calculation of $fO_2$ during the experiments (Stagno et al., 2011; Woodland and O'Neill, 1997). Preliminary results from powder X-ray diffraction data show that, after heating, an Fe-Ir metal alloy that can be indexed in the Fm-3m space group is formed by the reaction of pure Ir and Fe from ferropericlase according to the reaction:

(Mg,Fe)O + Ir --> (Mg,Fe)O + (Fe,Ir)

The compressibility of the Fe-Ir alloy and ferropericlase was measured up to ~ 60 GPa and SMS data were collected before and after heating. X-ray diffraction results coupled with energy-dispersive X-ray spectroscopy (EDS) measurements and a simple thermodynamic model indicate that the redox conditions during the DAC experiments were close to the iron-wüstite (IW) buffer, although some inhomogeneity was observed. Further chemical analyses and additional experiments are ongoing to understand the variation of oxygen fugacity in a DAC during laser heating.

Keywords: oxygen fugacity , redox sensor, diamond anvil cell

©2019. Japan Geoscience Union. All Right Reserved. 

# Goethite behavior at Earth's lower mantle conditions

*Egor Gennadievich Koemets[1], Maxim Bykov[1], George Aprilis[2], Timofey Fedotenko[2], Stella Chariton[1], Saiana Khandarkhaeva[1], Iuliia Koemets[1], Marcel Thielmann[1], Natalia Dubrovinsaia[2], Leonid Dubrovinsky[1]

1. BGI (Bayerisches Geoinstitut), Universität Bayreuth, Germany, 2. Material Physics and Technology at Extreme Conditions, Laboratory of Crystallography, Universität Bayreuth, Germany

Water and water-bearing species have a strong impact on numerous processes in Earth’ s interiors. Presence of water affects chemical and physical properties of mantle minerals, changes melting temperatures, sound velocities and viscosity of materials, and causing different global phenomena such as, for example, arc volcanism and plate tectonics. Thereby, the deep Earth’ s regions enriched with water are crucial for understanding our planet’ s geodynamics and geochemistry. Still, mechanisms of water circulation between geospheres remain poorly understood. Recent studies suggest that goethite present in Banded Iron Formations (BIFs) may transfer some quantities of water to the deep Earth interiors with subducting slabs. It was reported that goethite remains stable in the sinking slab until it reaches the base of a lower mantle. By the meaning of in situ powder XRD it was revealed that at pressures corresponding to the depths ~1500-1800 km and moderately high temperatures goethite undergoes a phase transition to form a novel stable pyrite-type phase $FeO_2H_x$ with $0 \leqq x \leqq 1$ (named as Py-phase). Thus, goethite and its HP pyrite-type form became a candidate for water and/or hydrogen transfer and storage to the lower mantle and the core-mantle boundary. Using laser-heating in diamond anvil cells we performed a series of experiments on an investigation of goethite (as a starting material) stability at P-T conditions covering possible range in subducting slabs. By the meaning of sensitive in situ single-crystal XRD in DACs we registered decomposition of goethite and formation of known (such as $\iota$-$Fe_2O_3$, $\eta$-$Fe_2O_3$, a high-pressure orthorhombic form of $Fe_3O_4$, $Fe_5O_7$) and novel iron-oxygen compounds. Results of structure solution and refinement established these compounds to be orthorhombic $Fe_7O_{10}$ and hexagonal non-stoichiometric phase $Fe_{6.31}O_9$. Our results suggest that FeOOH cannot transport water into the deep of Earth’ s mantle.

Keywords: Goethite, Diamond anvil cell, High Pressure, Single-crystal XRD, Subducting slabs

©2019. Japan Geoscience Union. All Right Reserved. 

# The oxygen content of sulphides in the mantle and a geothermometer for diamond formation

*Sumith Abeykoon[1], Dan Frost[1], Vera Laurenz[1]

1. Bayerisches Geoinstitut, University of Bayreuth

Sulphides are ubiquitous accessory minerals in mantle rocks and form the most prevalent type of inclusion in diamonds. Diamond sulphide inclusions are trapped as sulphide melts that crystallise on cooling to form Fe-Ni monosulphide solid solution (MSS) and ultimately recrystallizes to assemblages containing pyrrhotite, $Fe_{(1-x)}S$ (x = 0 to 0.2), pentlandite, $(Fe,Ni)_9S_8$, and sometimes pyrite ($FeS_2$). Sulphide inclusions are also found in many xenoliths but those which are hosted by diamonds provide potentially the most pristine samples from the lithospheric mantle and deeper. Previous experiments indicate that oxygen partitions into sulphide melts and although sparse, some measurements of natural sulphide inclusions from mantle xenoliths indeed show measurable and in some cases relatively high oxygen concentrations. If the parameters that control sulphide oxygen concentration can be determined then they could be potentially used to understand conditions in the mantle and in particular in sublithospheric diamonds. The oxygen content of sulphides separating to the core during core formation could have also influenced the oxygen fugacity of the early mantle.
We have measured the oxygen contents of sulphide melts within experimentally produced mantle assemblages at high pressures and temperatures. A series of multi-anvil experiments were conducted to equilibrate a peridotite assemblage with molten sulphide (FeS) at pressures between 3 –11 GPa and temperatures of 1300 ˚C –1700 ˚C. The effects of pressure, temperature, oxygen fugacity and composition have been investigated. Oxygen fugacity was determined in some experiments by saturating the sulphide in Ir to produce a separate Ir-Fe metal alloy, for which the Fe content is a function of oxygen fugacity. The results show that sulphide melt oxygen contents can range up to 16 weight % FeO, at mantle conditions. Moreover, the content of oxygen in the sulphide is found to be not controlled by $fO_2$ or $fS_2$, which is in disagreement with previous experimental studies conducted at ambient pressure conditions. The experiments indicate that the oxygen concentration is mainly controlled by the FeO activity in coexisting silicates phases and the temperature, although further work is still required to calibrate effects of Ni and Cu. In order to fit the data and to account for the FeO dependence, we developed a thermodynamic model using an end-member equilibrium between olivine, pyroxene and FeO in the sulphide melt. The resulting relationship can be used as a geothermometer based on sulphide inclusion oxygen contents and could be particularly useful for determining diamond formation temperatures for sub lithospheric diamonds.

Keywords: Sulfide, Oxygen, Geothermometer

©2019. Japan Geoscience Union. All Right Reserved. 

[E] Oral | S (Solid Earth Sciences )：S-CG Complex & General

Thu. May 30, 2019 1:45 PM - 3:15 PM JST | Thu. May 30, 2019 4:45 AM - 6:15 AM UTC | A11 TOKYO BAY MAKUHARI HALL

## [S-CG51] Role of volatiles on Earth and planetary dynamics

convener:Takayuki Ishii(Bavarian Research Institute, University of Bayreuth), Eiji Ohtani(Department of Earth and Planetary Materials Science, Graduate School of Science, Tohoku University), Michihiko Nakamura(Division of Earth and Planetary Materials Science, Department of Earth Science, Graduate School of Science, Tohoku University), Bjorn Mysen(Geophysical Laboratory, Carnegie Inst. Washington), Chairperson:Michihiko Nakamura, Eiji Ohtani(Tohoku University)

This session addresses how volatile species affect dynamics of the<br/>Earth and planets from natural observations, laboratory experiments, and<br/>numerical modeling in the temperature, pressure, and oxygen activity<br/>range from the early stage of the planet formation to the present. The<br/>volatiles can be critical in zones of magma storage and ascent, mantle<br/>upwelling and melting in the fluid-enriched subduction zones, in the<br/>mantle transition zone, in the lower mantle, in the core-mantle boundary,<br/>and in Earth and planetary cores. However, volatiles affect properties<br/>and processes differently depending on their pressure, temperature, and<br/>redox conditions, which vary in time and space. <br/> This session aims to address how volatiles control the dynamic<br/>processes of the Earth and planets, governed by their geophysical and<br/>geochemical properties. We welcome papers dealing with geological and<br/>laboratory observations coupled with numerical modeling on the role of<br/>volatiles. The topics include (1) Stability relations, chemical and<br/>physical properties of crystalline, molten and fluid phases,<br/>partitioning of volatiles among these phases, (2) Rheological and other<br/>physical properties of minerals, and the effects of intergranular fluid<br/>on the properties, (3) Volatiles and dehydration induced seismicity and<br/>volcanism in various tectonic regions including subduction zones, and (4)<br/>Effects of volatiles in numerical simulation of geo-tectonics, and (5)<br/>Magma outgassing and its control of volcanic eruption dynamics.

1:45 PM - 2:00 PM JST | 4:45 AM - 5:00 AM UTC

### [SCG51-01] Constraining the degassing rate of the mantle since 3 Ga using the deficit of xenon-129 in the ancient atmosphere

★Invited Papers

*Bernard Marty[1], David Bekaert[1], Michael Broadley[1] (1.Centre de Recherches Pétrographiques et Géochimiques/ CNRS - Universite de Lorraine France)

2:00 PM - 2:15 PM JST | 5:00 AM - 5:15 AM UTC

### [SCG51-02] Investigating volatile cycles in the terrestrial mantle by incorporating He and Ar isotopes into geodynamical models of mantle convection

★Invited Papers

*Rosie Ellen Jones[1], Peter van Keken[2], Jonathan M Tucker[2], Chris J Ballentine[1] (1.Department of Earth Sciences, University of Oxford, Oxford, UK, 2.Department of Terrestrial Magnetism, Carnegie Institution of Washington, Washington, USA)

2:15 PM - 2:30 PM JST | 5:15 AM - 5:30 AM UTC

### [SCG51-03] Fluid circulation in the forearc mantle wedge inferred from the dihedral angle in an olivine-$H_2O$-NaCl system

*Yongsheng HUANG[1], Takayuki Nakatani[1], Michihiko Nakamura[1], Catherine McCammon[2] (1.Graduate School of Science, Tohoku University, 2.Byerisches Geoinstitut, University of Bayreuth)

2:30 PM - 2:45 PM JST | 5:30 AM - 5:45 AM UTC

### [SCG51-04] The oxygen fugacity of serpentinites: implications for subduction zone redox evolution

*Lisa Eberhard[1], Dan Frost[1], Catherine McCammon[1] (1.BGI)

2:45 PM - 3:00 PM JST | 5:45 AM - 6:00 AM UTC

[SCG51-05] Experimental study of the effect of composition on water solubility in natural silicate melts

*Shigeru Yamashita[1] (1.Institute for Planetary Materials, Okayama University)

3:00 PM - 3:15 PM JST | 6:00 AM - 6:15 AM UTC

[SCG51-06] Deep mantle volatile cycle and plate tectonics: Impact to the climate evolution

*Takashi Nakagawa[1], Shintaro Kadoya[2], Eiichi Tajika[3] (1.Department of Earth Sciences, The University of Hong Kong, 2.Department of Earth and Space Sciences, University of Washington, 3.Department of Earth and Planetary Sciences, The University of Tokyo)

# Constraining the degassing rate of the mantle since 3 Ga using the deficit of xenon-129 in the ancient atmosphere

*Bernard Marty[1], David Bekaert[1], Michael Broadley[1]

1. Centre de Recherches Pétrographiques et Géochimiques/ CNRS - Universite de Lorraine France

Degassing of volatile elements from the mantle to the atmosphere requires decompression melting, magma generation and degassing, and is therefore linked to mantle convection. Mantle convection is a physical process that tends to minimize temperature contrasts between the Earth's surface and the deep regions of the mantle. Hence its strength was variable through geological periods of time as it depended on heat generation within the Earth as well as heat dissipation to space. Convection of planetary mantles is a key driver of the evolution of planets and on Earth has been modulating the generation and stabilization of the continental crust. Still the thermal regime of the Earth, and notably the radiogenic/total heat production ratio (the Urey number) are not precisely known. It is related to the distribution of radioactive isotopes (mainly $^{238,235}$U, $^{232}$Th, $^{40}$K) among Earth's reservoirs which varied through time, on the latent heat of core crystallization, on the residual energy of accretion, and on the heat dissipation from the Earth's interior, which depends on mantle convection, a self-regulating process. Geological and geochemical observations have the potential to set constraints on variations of mantle convection in the distant time. Atmospheric xenon presents excesses in $^{129}$Xe, an isotope contributed by the decay of extinct iodine-129 ($T_{1/2}$ = 16 Ma). Part of this excess resulted from early degassing of the mantle and, possibily from contributions of comet to early Earth. Mantle degassing also contributed $^{129}$Xe to the atmosphere through time since the solid Earth is rich in $^{129}$Xe compared to the atmosphere. In agreement with this possibility, remnants of the Archean atmosphere trapped in fluid inclusions (Avice et al *Nature Comm*, 2017, GCA 2018) and in organic matter (Bekaert et al Science Adv 2018) show that xenon in Archean air was depleted in $^{129}$Xe compared to the modern composition (see Figure; error bars at 2 s; the grey area represents the reproducibility of air standards at the 2 slevel). However, this deficit cannot be accounted for by the modern degassing rate (as estimated from noble gas fluxes from the mantle), and requires degassing rates two orders of magnitude larger in the distant past than at present. This discrepancy implies a more vigorously convecting Archean-Proterozoic Earth, and suggests a potential impact on the composition of the Archean atmosphere. It also leads credence to models advocating a magmatic origin for drastic environmental changes like the great oxidation event.

Keywords: mantle degassing, Archean, noble gases

©2019. Japan Geoscience Union. All Right Reserved. 

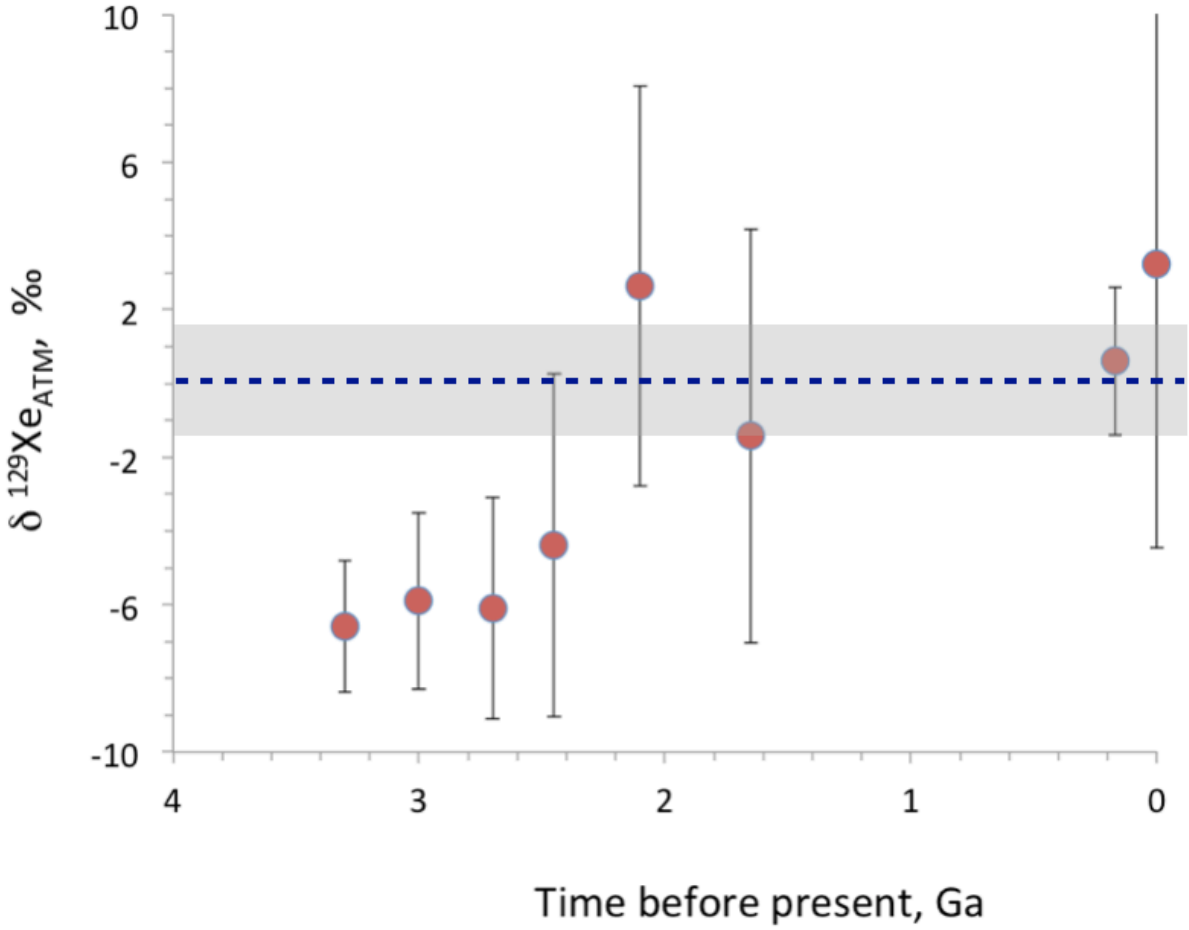


©2019. Japan Geoscience Union. All Right Reserved. 

# Investigating volatile cycles in the terrestrial mantle by incorporating He and Ar isotopes into geodynamical models of mantle convection

*Rosie Ellen Jones[1], Peter van Keken[2], Jonathan M Tucker[2], Chris J Ballentine[1]

1. Department of Earth Sciences, University of Oxford, Oxford, UK, 2. Department of Terrestrial Magnetism, Carnegie Institution of Washington, Washington, USA

The dichotomy in $^{3}He/^{4}He$ isotopes ratios between mid ocean ridge and ocean island basalt samples (MORB and OIB) has provided a fundamental cornerstone in defining the need for a long-lived, volatile rich, and possibly primordial, geochemical reservoir within the deep mantle. However, this is somewhat at odds with evidence from other radiogenic isotope systems (e.g., U-Th-Pb, Lu-Hf, Sm-Nd, Rb-Sr), as well as geophysical evidence, for recycled surficial/crustal material in the deep mantle. Geodynamic models of mantle convection have been developed to incorporate earth-like phase and viscosity changes and can reproduce earth-like surface heat flow and plate motion. When such models take into account the higher density of the subducting oceanic crust, compared to the surrounding mantle, it provides a mechanism of retarding convection in the deepest mantle and reproduces observed geochemical distributions in multiple isotope systems (U-Th-Pb, Rb-Sr, Sm-Nd, Lu-Hf and Re-Os) that define the DMM, HIMU and EMI mantle endmembers (Brandenburg et al., 2008, Jones et al., 2017). Here we use a geodynamical model of mantle convection (Brandenburg et al., 2008), and combine it with geochemical input parameters, to investigate whether the subduction of dense eclogite can retard lower mantle convection sufficiently to explain the observed differences in $^{3}He/^{4}He$ obtained for MORB and OIB. We go on to analyse the effect of $^{3}He$ outgassing from the Earth's core and early recycling of extra-terrestrial material containing high $^{3}He$ (e.g., interplanetary dust particles (IDPs)) into the mantle. The K-Ar system is also incorporated into the model and earth-like $^{40}Ar$ planetary degassing from the mantle is reproduced. We explore the impact of $^{36}Ar$ recycling on the $^{40}Ar/^{36}Ar$ compositions of MORB and OIB. The results suggest recycling of atmospheric Ar can produce the observed $^{40}Ar/^{36}Ar$ compositions of the upper and lower mantle.

Brandenburg, J.P., Hauri, E.H., van Keken, P.E., Ballentine, C.J., 2008. Earth and Planetary Science Letters 276, 1-13.

Jones, R., van Keken, P. E., Hauri, E., Vervoort, J. D., & Ballentine, C. J., 2017. AGU Fall Meeting Abstracts.

Keywords: He isotopes, Ar isotopes, Mantle convection, Geodynamic model, Geochemistry, Volatiles

©2019. Japan Geoscience Union. All Right Reserved. 

# Fluid circulation in the forearc mantle wedge inferred from the dihedral angle in an olivine-$H_2O$-NaCl system

*Yongsheng HUANG[1], Takayuki Nakatani[1], Michihiko Nakamura[1], Catherine McCammon[2]

1. Graduate School of Science, Tohoku University, 2. Byerisches Geoinstitut, University of Bayreuth

In subduction zones, the circulation of slab-released aqueous fluids is crucial to understand the generation of arc magma and recycle of materials, and further to constrain the global geodynamics. The infiltration of aqueous fluids plays an important role in controlling geophysical properties of the mantle wedge such as elasticity, permeability and electrical conductivity. Recently, magnetotellulic studies found a high electrical conductor beneath the fore-arc region which was interpreted as a storage of voluminous slab-derived fluid, implying the presence of permeable mantle wedge at fore-arc depths. By contrast, experimental constraints on dihedral (wetting) angle ( $\theta$ ) in the olivine-$H_2O$ system indicated the fluid is once trapped in isolated pores ( $\theta > 60^\circ$) within the down-dragging mantle matrixat fore-arc depths and finally released just beneath the arc volcano where $\theta < 60^\circ$. Here we present the precisely determined dihedral angles in the olivine and NaCl-bearing aqueous fluid (5–27.5 wt% NaCl) system at 1–4 GPa and 800–1100˚C to reveal the influence of NaCl on the fluid connectivity because the NaCl is now recognized to be an important constituent of subduction zone fluids. We found that NaCl significantly decreases $\theta$ down to below 60˚ at all the investigated temperature and pressure conditions even at 5 wt% NaCl. Our results suggest that released NaCl-bearing aqueous fluid begins to form an interconnected network in the mantle at relatively shallow depths of ~80 km and can partly penetrate the fore-arc crust without causing mantle melting, which could account for the high electrical conductivity anomalies beneath the for-are region. Our model also emphasizes that partial melting of peridotite triggered by the addition of aqueous fluid can occur more widely than that previously thought, and implies that the release depth of aqueous fluid is not a primary control on the volcanic front position. This work was supported by the JSPS Japanese-German Graduate Externship.

Keywords: dihedral angle, NaCl-bearing, fluid network, mantle wedge, subduction zone

©2019. Japan Geoscience Union. All Right Reserved. 

# The oxygen fugacity of serpentinites: implications for subduction zone redox evolution

*Lisa Eberhard[1], Dan Frost[1], Catherine McCammon[1]

1. BGI

At subduction zones $H_2O$ and $CO_2$ are returned to the Earth’ s mantle, bound within hydrous and carbonate minerals. Serpentinites are considered to be major carriers of $H_2O$ into the mantle but natural exposures indicate that some sections of serpentinized mantle also contain significant amounts of carbonate minerals. Determining the fate of so called ophicarbonate rocks presents an important challenge because it involves the interaction between both $H_2O$- and $CO_2$- bearing fluids. A further aspect however is that serpentine minerals also contain ferric in addition to ferrous iron. Natural serpentinites record in fact a very wide range of $Fe^{3+}/Fe^{tot}$ ratio but the effect of this ratio on the high pressure stability of serpentine and the relationship with the speciation of coexisting C-O-H fluid phases is unknown.

We have examined the stability of the serpentinite mineral antigorite within ophicabonate assemblages at subarc conditions as a function of P, T and $fO_2$. Multi-anvil experiments were performed both inside the stability field of antigorite, but also at conditions where antigorite starts to dehydrate. Natural serpentinites are used as starting materials with initially high and low $Fe^{3+}/Fe^{tot}$ ratios. Calcium carbonate was then added to these assemblages to simulate ophicarbonate composition. Iridium metal was added to some nominally unbuffered experiments to allow the oxygen fugacity to be determined, whereas in other experiments the oxygen fugacity was fixed using powders of Ru + $RuO_2$ and Re + $ReO_2$ distributed throughout the sample. Ferrous Fe is located in the octahedral site of antigorite whereas ferric Fe may additionally occupy the tetrahedral site of the trioctahedral 1:1 sheet silicates, providing charge balance. We have determined the location and speciation of the Fe atoms in serpentinites as a function of $fO_2$, P and T by using Mössbauer spectroscopy to examine the run products of the multi-anvil experiments.

The experiments were run for approximately 3 days during which it was possible to change the $Fe^{3+}/Fe^{tot}$ ratios of the starting materials to both higher and lower ratios depending on the redox buffers employed. We found that the relationship between the $Fe^{3+}/Fe^{tot}$ ratio of antigorite and the oxygen fugacity is very temperature dependent with antigorite $Fe^{3+}/Fe^{tot}$ ratios decreasing sharply at the same oxygen fugacity as dehydration commences. This behaviour should cause the oxygen fugacity within subducting lithosphere to increase as dehydration takes place, which will have important implications for fluid speciation. On the other hand the stabilisation of ferric iron in antigorite at high oxygen fugacities appears to have a minimal effect on the temperature of dehydration.

Keywords: Serpentine, subduction zone, f(O2), Multi-anvil, Mössbauer spectroscopy

©2019. Japan Geoscience Union. All Right Reserved. 

# Experimental study of the effect of composition on water solubility in natural silicate melts

*Shigeru Yamashita[1]

1. Institute for Planetary Materials, Okayama University

Water is the first dominant volatile dissolved in magmas. Oversaturation and exsolution of the water in magmas affects the buoyancy and excess vapor pressure of the system, and hence the water solubility in silicate melts is fundamental in controlling magma transport beneath volcanoes. Many experimental studies of the solubility for water in natural silicate melts are now available, but most of them were performed over a limited range of composition. For example, published solubility data for water are rather sparse for the natural silicate melts having moderate $SiO_2$ contents. This has resulted in insufficient data coverage of composition space, which makes difficult to precisely model if a melt is subject of compositional change due to partial crystallization, assimilation, or magma hybridization. This study presents results from experimental determinations of the solubility for water in a natural dacitic melt at near-the liquidus and the superheated conditions.

The starting material for the experiments was the natural subalkaline dacite JA1 (GSJ standard reference material, ~65 wt% $SiO_2$). A nominally anhydrous glass was prepared from the starting material, and the glass was equilibrated with water in an internally heated pressure vessel for ~24 hours at 1000-1200 ˚C and 100-200 MPa. Double capsule technique was employed to control the oxygen fugacity in the sample along Ni-NiO buffer during the experiments. The water content in the quenched glass was determined from the near infrared absorption intensities of the hydroxyl groups band at ~4500 $cm^{-1}$ and the molecular water band at ~5200 $cm^{-1}$ using the molar absorption coefficients of Ohlhost et al. (2001).

Results of this study are overall consistent with previous determinations of pressure- and temperature-dependence of water solubility in rhyolitic melts. Water solubility in the dacitic melt increases with pressure at a fixed temperature, and decreases with temperature at a fixed pressure. On the other hand, the water solubility in the dacitic melt was found to be 10-20 % (relative, on the mole fraction basis) greater than those previously determined by Holtz et al. (1992; 1995) and Yamashita (1999) for the rhyolitic melts when compared at the same pressure and temperature condition. This advocates that the effect of melt composition play a noticeable role in controlling the degree of water oversaturation during magmatic processes. When a hotter basaltic magma is injected to a colder rhyolitic magma body, a purely thermal effect on water solubility enhances formation of vapor bubbles in the rhyolitic magma (e.g., Yamashita, 1999). Once hybridization between the melt portions of the two magmas proceeds, the effect of melt composition on water solubility becomes important, i.e., already present, sub-millimeter size bubbles (thus their buoyant separation is limited) can be resorbed by the hybridized melt which has an intermediate composition.

References: Holtz et al., Chem. Geol., 96, 289-302, 1992; Holtz et al., Amer. Mineral., 80, 94-108, 1995; Ohlhost et al., Chem. Geol., 174, 5-20, 2001; Yamashita, J. Petrol., 40, 1497-1507, 1999.

Keywords: magma, water solubility, composition dependence

©2019. Japan Geoscience Union. All Right Reserved. 

# Deep mantle volatile cycle and plate tectonics: Impact to the climate evolution

*Takashi Nakagawa[1], Shintaro Kadoya[2], Eiichi Tajika[3]

1. Department of Earth Sciences, The University of Hong Kong, 2. Department of Earth and Space Sciences, University of Washington, 3. Department of Earth and Planetary Sciences, The University of Tokyo

We investigate the deep mantle volatile (water and carbon) cycle and its impact to plate tectonics and climate evolution in the numerical mantle convection simulations couping with the energy balance model of the surface climate model. To calculate the mantle water cycle, the storage capacity model of water in each mantle minerals as functions of temperature and pressure is incorporated into numerical mantle convection simulations so that the dehydration process can be included in the numerical model of mantle water cycling as well as the regassing and degassing processes. However, the decarbonation process cannot be included because the storage capacity model of carbon is not well-established. In three migration processes of mantle volatiles, the volcanic degassing plays a significant role because the volatile composition of the atmosphere-ocean system can be described as a balance between degassing flux and silicate weathering effects as uptake of the volatile components. As a result, the optical properties of the atmosphere-ocean system such as the Albedo and planetary radiation are changed with the volcanic degassing. Other two migration processes may be worked for regulating the volatile content stored in the deep planetary interior and inventory of surface volatile reservoir. The style of plate tectonics driven by mantle convection may strongly affect the style of climate evolution and inventory of surface volatile reservoir. In the stagnant lid mode of mantle convection, the snowball climate is dominated for over a few billion years because the strong radiative cooling is controlled due to less amount of volcanic degassing associated with the stagnant lid convection. Whereas, the continuous carbon degassing is expected in the continuous surface plate motions so that the mild climate can be found, which allows having the liquid water over a few billion years on the planetary surface. In order to preserve the amount of surface seawater on the planetary surface as the present-day amount of surface seawater on the Earth, the required amount of the water in the entire planetary system may be around 10 to 12 Ocean Masses of present-day Earth's water ocean. Therefore, the mantle volatile cycle concerning with the plate tectonics driven by mantle convection may control the habitability of the rocky planets such as the Earth.

Keywords: plate tectonics, volatile cycle, climate evolution

©2019. Japan Geoscience Union. All Right Reserved. 

[E] Oral | S (Solid Earth Sciences )：S-CG Complex & General

Thu. May 30, 2019 3:30 PM - 5:00 PM JST | Thu. May 30, 2019 6:30 AM - 8:00 AM UTC | A11 TOKYO BAY MAKUHARI HALL

## [S-CG51] Role of volatiles on Earth and planetary dynamics

convener:Takayuki Ishii(Bavarian Research Institute, University of Bayreuth), Eiji Ohtani(Department of Earth and Planetary Materials Science, Graduate School of Science, Tohoku University), Michihiko Nakamura(Division of Earth and Planetary Materials Science, Department of Earth Science, Graduate School of Science, Tohoku University), Bjorn Mysen(Geophysical Laboratory, Carnegie Inst. Washington), Chairperson:Takayuki Ishii(Bavarian Research Institute, University of Bayreuth), Bjorn Mysen(Carnegie Institution of Washington)

This session addresses how volatile species affect dynamics of the<br/>Earth and planets from natural observations, laboratory experiments, and<br/>numerical modeling in the temperature, pressure, and oxygen activity<br/>range from the early stage of the planet formation to the present. The<br/>volatiles can be critical in zones of magma storage and ascent, mantle<br/>upwelling and melting in the fluid-enriched subduction zones, in the<br/>mantle transition zone, in the lower mantle, in the core-mantle boundary,<br/>and in Earth and planetary cores. However, volatiles affect properties<br/>and processes differently depending on their pressure, temperature, and<br/>redox conditions, which vary in time and space. <br/> This session aims to address how volatiles control the dynamic<br/>processes of the Earth and planets, governed by their geophysical and<br/>geochemical properties. We welcome papers dealing with geological and<br/>laboratory observations coupled with numerical modeling on the role of<br/>volatiles. The topics include (1) Stability relations, chemical and<br/>physical properties of crystalline, molten and fluid phases,<br/>partitioning of volatiles among these phases, (2) Rheological and other<br/>physical properties of minerals, and the effects of intergranular fluid<br/>on the properties, (3) Volatiles and dehydration induced seismicity and<br/>volcanism in various tectonic regions including subduction zones, and (4)<br/>Effects of volatiles in numerical simulation of geo-tectonics, and (5)<br/>Magma outgassing and its control of volcanic eruption dynamics.

3:30 PM - 3:45 PM JST | 6:30 AM - 6:45 AM UTC

[SCG51-07] The nature of water induced small degree melts in the deep mantle

★Invited Papers

*Daniel James Frost[1], Pierre Condamine[3], Davide Novella[2], Rong Huang[1] (1.University of Bayreuth, 2.University of Cambridge, 3.Université de Lorraine)

3:45 PM - 4:00 PM JST | 6:45 AM - 7:00 AM UTC

[SCG51-08] **Phase separation of hydrous Vesuvius melt: vesicle nucleation or spinodal decomposition?**

★Invited Papers

*Anja Allabar[1], Marcus Nowak[1] (1.University of Tuebingen)

4:00 PM - 4:15 PM JST | 7:00 AM - 7:15 AM UTC

[SCG51-09] Role of water on dynamics in the lower mantle and core-mantle boundary regions

*Eiji Ohtani[1], Takayuki Ishii[2], Liang Yuan[1], Daijo Ikuta[1], Tomoo Katsura[2], Dan Frost[2] (1.Department of Earth and Planetary Materials Science, Graduate School of Science, Tohoku University, 2.Bavarian Research Institute, University of Bayreuth)

4:15 PM - 4:30 PM JST | 7:15 AM - 7:30 AM UTC

[SCG51-10] Stability of Fe-bearing hydrous phases and element partitioning in the system $MgO$-$Al_2O_3$-$Fe_2O_3$-$SiO_2$-$H_2O$ in Earth's lowermost mantle

*Hongsheng Yuan[1], Li Zhang[1], Eiji Ohtani[2], Yue Meng[3], Eran Greenberg[4], Vitali B. Prakapenka [4] (1.Center for High Pressure Science and Technology Advanced Research, 2.Department of Earth Science, Graduate School of Science, Tohoku University, 3.HPCAT, X-Ray Science Division, Argonne National Laboratory, 4.Center for Advanced Radiation Sources, University of Chicago)

4:30 PM - 4:45 PM JST | 7:30 AM - 7:45 AM UTC

[SCG51-11] **Laboratory Micro-Seismicity during Serpentinite Deformation as a Potential Analogue for Lower Wadati-Benioff Plane Seismicity**

*Julien Gasc[1,3], Nadège Hilairet[2], Tony Yu[3], Yanbin Wang[3], Thomas P. Ferrand[1], Alexandre Schubnel[1] (1.Laboratoire de Géologie, CNRS - ENS, Paris, FRANCE, 2.Unité Matériaux et Transformations, CNRS - Lille University, Villeneuve d'Ascq, FRANCE, 3.GeoSoilEnviro-CARS, University of Chicago, Argonne IL, USA)

---

4:45 PM - 5:00 PM JST | 7:45 AM - 8:00 AM UTC

[SCG51-12] Water transport and mixing in the whole-mantle scale convection

*Takeo Kaneko[1], Tomoeki Nakakuki[1], Masanori Kameyama[2], Hikaru Iwamori[3] (1.Department of Earth and Planetary Systems Science, Graduate School of Science, Hiroshima University, 2.Geodynamics Research Center, Ehime University, 3.Earthquake Research Institute, University of Tokyo)

# The nature of water induced small degree melts in the deep mantle

*Daniel James Frost[1], Pierre Condamine[3], Davide Novella[2], Rong Huang[1]

1. University of Bayreuth, 2. University of Cambridge, 3. Université de Lorraine

Slow S-wave velocities in the deep mantle have been used to argue for the presence of hydrous silicate melts. Small degree partial melts could potentially be formed due to a reduction in the $H_2O$ storage capacity of mantle minerals due to pressure induced phase transitions or as a result of redox processes. Hydrous melt layers could accumulate at certain depths in the mantle due to neutral buoyancy. Water concentrations in the ambient mantle are at most likely to lead to only small degrees of melting. Such incipient melts would be in equilibrium with a peridotite assemblage containing minerals that would be practically identical in major elements as the unmelted assemblage. The compositions of such melts are important because their water contents constrain the relationship between melt fraction and the bulk water content. Furthermore, the water content and the iron content would mainly determine their buoyancy. To assess if neutrally buoyant small degree hydrous melt layers exist in the mantle and to determine how much water would need to be present to create them requires experimental determination of their compositions.

Determining the chemical composition of low degree melts and particularly their water contents is experimentally very challenging. At pressures higher than 2 GPa melts no longer quench to form glasses and can therefore not be analyzed to determine water contents. Small melt fractions are very hard to analyze due to their very small volume and due to modification through reaction with solid phases during quenching. One way to overcome these problems and produce an analyzable portion of incipient melt composition is by performing sandwich experiments. In this method an initial first guess melt composition is equilibrated with a sub-equal proportion of peridotite. The resulting melt is then re- equilibrated with peridotite in a series of iterative experiments until a composition is obtained that is in equilibrium with the entire peridotite assemblage.

We have used this procedure to determine the compositions of incipient melts at depths equivalent to around 200 and 400 km in the mantle at adiabatic temperatures. The sandwich technique has to be modified in a number of ways when used at very high pressures, mainly to ensure that water contents can be accurately determined through mass balance. The resulting melts have affinities with the major classes of kimberlite magmas and their compositions can be used to assess their buoyancy in the deep mantle.

Keywords: Pressure, Transition zone

©2019. Japan Geoscience Union. All Right Reserved. 

# Phase separation of hydrous Vesuvius melt: vesicle nucleation or spinodal decomposition?

*Anja Allabar[1], Marcus Nowak[1]

1. University of Tuebingen

The phase separation of $H_2O$ fluids from supersaturated hydrous silicate melts determines the starting point of explosive volcanic eruptions. The number of fluid vesicles per unit volume of silicate melt (*VND*) is a basic property that controls the efficiency of fluid-melt separation and as a result the acceleration of magma ascent. To simulate the phase separation of single phase hydrous silicate melts during ascent, continuous decompression experiments were performed at superliquidus temperatures with AD79 Vesuvius white pumice composition. This pumice buried Herculaneum and Pompeii and is representative of other catastrophic phonolitic and trachytic explosive eruptions like the violent 39 ka Campi Flegrei and the 1815 AD Tambora eruption.
Experiments were conducted in an internally heated pressure vessel equipped with a high-pressure valve that facilitates continuous decompression. 5.3 wt% $H_2O$ were dissolved in the melts at 200 MPa and 1523 K for 96 h. Subsequently, the slightly $H_2O$ undersaturated melts were isothermally decompressed at 1323 or 1373 K with rates of 0.024-1.7 MPa·s$^{-1}$. At final pressures ($P_{final}$) between 110 and 70 MPa, the samples were isobarically quenched with ~150 K·s$^{-1}$ to room temperature. The *VND* of the vitreous samples were determined with optical microscopy and quantitative backscattered electron image analysis combined with computational 2D to 3D transformation.
Homogeneously dispersed vesicles are observed in the samples decompressed to a $P_{final}$ ≦100 MPa which corresponds to a $\Delta P$ of ~95 MPa that is necessary to induce homogeneous phase separation. High log *VND*'*s* of ~5.2 (in mm$^{-3}$), corresponding to average vesicle distances of 10 $\mu$m, are observed irrespective of decompression rate within the investigated range. A nucleation theory based decompression rate meter (Toramaru, 2006), which is commonly used to estimate magma ascent velocity from *VND* of volcanic ejecta, fails to explain the experimentally observed decompression rate independent *VND*. Alternatively, decompression induced $H_2O$-silicate melt phase separation may be described by the theory of spinodal decomposition (Cahn, 1965) at the limit of thermodynamic stability. Critical behavior of hydrous silicate melt has already been evidenced experimentally by e.g. Shen and Keppler (1997) and is attributed to spinodal decomposition.
Irrespective of the phase separation mechanism, a decompression rate independent *VND* has profound consequences for the degassing dynamics of natural polyphase hydrous magma, that contain crystals and pre-existing fluid vesicles. During ascent, $H_2O$ supersaturation is decreased in melt shells surrounding pre-existing vesicles by $H_2O$ diffusion. Homogeneous phase separation occurs in interstitial melt volumes in which sufficient supersaturation is still preserved. If the decompression rate is fast enough to maintain such supersaturated volumes, the formation of vesicles with high log*VND* of 5.2 inevitably causes efficient melt degassing within seconds due to short $H_2O$ diffusion distances on a 10 $\mu$m scale from the melt into fluid vesicles. This causes rapid density decrease accompanied by sudden increase of magma buoyancy required for explosive volcanism.

Cahn, J.W., 1965. J. Chem. Phys. 42, 93–99.
Shen, A.H., Keppler, H., 1997. Nature 385, 710–712.
Toramaru, A., 2006. J. Volcanol. Geotherm. Res. 154, 303–316.

©2019. Japan Geoscience Union. All Right Reserved. 

Keywords: magma degassing, magma ascent rate, vesicle number density, spinodal decomposition, phase separation

©2019. Japan Geoscience Union. All Right Reserved. 

# Role of water on dynamics in the lower mantle and core-mantle boundary regions

*Eiji Ohtani[1], Takayuki Ishii[2], Liang Yuan[1], Daijo Ikuta[1], Tomoo Katsura[2], Dan Frost[2]

1. Department of Earth and Planetary Materials Science, Graduate School of Science, Tohoku University, 2. Bavarian Research Institute, University of Bayreuth

Recent experimental evidence indicated that the Earth’ s transition zone contains some amount of water at least locally. Subduction of the slabs into the lower mantle can transport water further into the lower mantle. One of the most important candidates of the water carrier into the lower mantle is hydrous phase delta-AlOOH and phase H-$MgSiO_4H_2$ solid solution. Our works on the stability of this solid solution revealed that it coexists with bridgmanite under the lower mantle conditions [1, 2].

We studied the hydrogen and aluminum partitioning between alumina and hydrogen between the delta-H solid solution and aluminous bridgmanite at high pressure and temperature. We observed that bridgmanite under the wet conditions depleted in aluminum, and it contains almost no water under the wet lower mantle conditions at 28 GPa and 800-1400°C. This partitioning of H and Al can provide significant effect on lower mantle dynamics through the change of the garnet-bridgmanite phase boundary, the pressure of the spin transition of both bridgmanite and delta-H solid solution, and bridganite-postperovskite transition.

The supply of water to the core-mantle boundary can create a reaction of water and iron in the core to produce $FeO_2H$ and its reaction product postperovskite $Fe_2O_3$. These phases together with the delta-H solid solution can play important roles at the bottom of the lower mantle. Physical properties of these phases can account for the sound velocity and density anomalies in the regions such as ULVZ (ultra-low velocity zone) and LLSVP (large low shear velocity province) [3].

References:

[1] Ohira et al. (2014) Earth Planet. Sci. Lett., 401: 12–17, [2] Ohtani et al. (2018) Jour. Asian Earth Sci. 2018, [3] Yuan et al. (2018) Geophys. Res. Lett.,45. doi.org/10.1002/2017GL0757

Keywords: Water, lower mantle, hydrous mineral, phase delta, phase H, bridgmanite

©2019. Japan Geoscience Union. All Right Reserved. 

# Stability of Fe-bearing hydrous phases and element partitioning in the system MgO-$Al_2O_3$-$Fe_2O_3$-$SiO_2$-$H_2O$ in Earth's lowermost mantle

*Hongsheng Yuan[1], Li Zhang[1], Eiji Ohtani[2], Yue Meng[3], Eran Greenberg[4], Vitali B. Prakapenka [4]

1. Center for High Pressure Science and Technology Advanced Research, 2. Department of Earth Science, Graduate School of Science, Tohoku University, 3. HPCAT, X-Ray Science Division, Argonne National Laboratory, 4. Center for Advanced Radiation Sources, University of Chicago

We performed experiments on a synthetic hydrous gel consisting of a model composition of subducted slabs in the MgO–$Al_2O_3$–$Fe_2O_3$–$SiO_2$–$H_2O$ system and containing ~7 wt.% water. The experiments were conducted in laser-heated diamond anvil cells under high pressure–temperature (*P-T*) conditions corresponding to the lowermost mantle using *in situ* synchrotron X-ray diffraction and *ex situ* transmission electron microscope techniques. The hydrous δ-phase AlOOH–FeOOH–$MgSiO_2(OH)_2$–$SiO_2$ (with an orthorhombic symmetry and the space group of *Pnnm*) coexists with bridgmanite (Bdg), post-perovskite (pPv), or both in a broad *P-T* range of 104–126 GPa and 1900–2500 K, whereas the pyrite-type (py) $FeOOH_x$ phase was only observed to coexist with the pPv phase by *in situ* XRD. Chemical analysis on recovered samples showed that (i) in the Bdg-bearing assemblage quenched from 104 GPa and 1900 K, the Bdg phase contains ~8 at.% Al and ~11 at.% Fe, and the coexisting hydrous δ-phase contains ~70 at.% Al and ~14 at.% Fe; (ii) in the pPv-bearing assemblage quenched from 117 GPa and 2050 K, the pPv phase contains ~7 at.% Al and ~16 at.% Fe, and the coexisting hydrous δ-phase contains ~81 at.% Al and ~9 at.% Fe. The considerable $Fe_2O_2(OH)_2$ (8–13 mol%) and $SiO_2$ (9–13 mol%) content in the δ-phase does not reduce its thermal stability; therefore, the Fe-bearing δ-phase can transport water to the lowermost mantle along the mantle geotherm. The dense py-phase may accumulate in the lowermost mantle in the presence of the pPv phase. In a hydrous system, $Al_2O_3$ depletion in both the Bdg and pPv phases can significantly reduce the width of the Bdg to pPv transition compared with the width in a dry system. On the other hand, significant Fe enrichment in pPv relative to the coexisting Bdg lowers the transition pressure to the depth of the D'' discontinuity. Accordingly, the depth and thickness of the Bdg to pPv transition in subducted hydrous basaltic crustal materials might explain the seismically detected D'' discontinuity. The formation of the dense hydrous py-phase in subducted slabs may contribute to chemical heterogeneities in the lowermost mantle.

Keywords: deep lower mantle, hydrous phase, bridgmanite to post-perovskite transition, synchrotron X-ray diffraction, multigrain analysis

©2019. Japan Geoscience Union. All Right Reserved. 

# Laboratory Micro-Seismicity during Serpentinite Deformation as a Potential Analogue for Lower Wadati-Benioff Plane Seismicity

*Julien Gasc[1,3], Nadège Hilairet[2], Tony Yu[3], Yanbin Wang[3], Thomas P. Ferrand[1], Alexandre Schubnel[1]

1. Laboratoire de Géologie, CNRS - ENS, Paris, FRANCE, 2. Unité Matériaux et Transformations, CNRS - Lille University, Villeneuve d'Ascq, FRANCE, 3. GeoSoilEnviro-CARS, University of Chicago, Argonne IL, USA

The origin of intermediate-depth earthquakes, which occur at depths of 60-300 km along subducting slabs, remains somehow enigmatic. In the pressure and temperature conditions involved, rocks should indeed deform in a ductile fashion. Dehydration embrittlement, due to serpentine breakdown, was long considered a good candidate to explain lower Wadati-Benioff plane seismicity. However, unlike in the classic dehydration embrittlement theory, dehydration induced volume changes are negative at such depths and cannot trigger instabilities via pore pressure buildup. Accordingly, some experimental studies have shown that faulting of serpentinites related to dehydration, occurs in a stable and aseismic way (Chernak and Hirth, 2011; Gasc et al., 2011). Nevertheless, tremendous progress was recently made in understanding the mechanics of intermediate earthquakes, notably thanks to the combination of high pressure deformation experiments and in-situ synchrotron techniques. In order to assess the seismic potential of serpentinites, micro-seismicity was monitored during high pressure experiments by recording Acoustic Emissions (AE's) –or labquakes. A D-DIA apparatus was used to deform natural antigorite-rich samples at pressures of 1-5 GPa, both within and outside antigorite's stability field.

Below 400˚C, the deformation of fully hydrated serpentinite samples involves aseismic ductile cataclastic flow. Above 600˚C, despite conditions propitious to dehydration embrittlement (i.e., with fast strain rates and reaction kinetics), joint deformation and dehydration also lead to ductile shear, without generation of AE's. However, samples show a brittle temperature window around 500˚C that seems to correlate with the very onset of the mineral's breakdown, and is therefore not associated to significant release of water. In this latter case, AE's are consistently collected upon faulting and extremely sharp strain localization is observed (Gasc et al., 2017). In addition, brittle faulting of partly hydrated samples (a mixture of olivine and antigorite) can also occur with minor amounts of antigorite, due to stress percolation upon antigorite breakdown. Unlike for low-pressure dehydration embrittlement, faulting is also enabled here by the metastability of the solid phase rather than by fluid overpressure and dynamic fault propagation occurs concomitantly with the appearance of pseudotachylites along the fault plane (Ferrand et al., 2017).
Both brittle failure mechanisms identified in these studies share major similarities with the now-classic concept of transformational faulting (Burnley et al., 1991), often invoked for deep-focus earthquakes, and both may be a source of seismicity in subducting slabs. We provide evidence that destabilizing antigorite at mantle depths can initiate faulting and thus be involved in intermediate-depth earthquakes. However, analysis of the acoustic signal shows that it is relatively weaker than its real-earth counterpart, once scaled relative to standard brittle faulting. This suggests that other mechanisms are responsible for large intermediate-depth earthquakes, which may reflect fault propagation in the adjacent peridotitic mantle.

Keywords: intermediate-depth earthquakes, serpentinite, high pressure, deformation experiments, acoustic emissions

©2019. Japan Geoscience Union. All Right Reserved. 

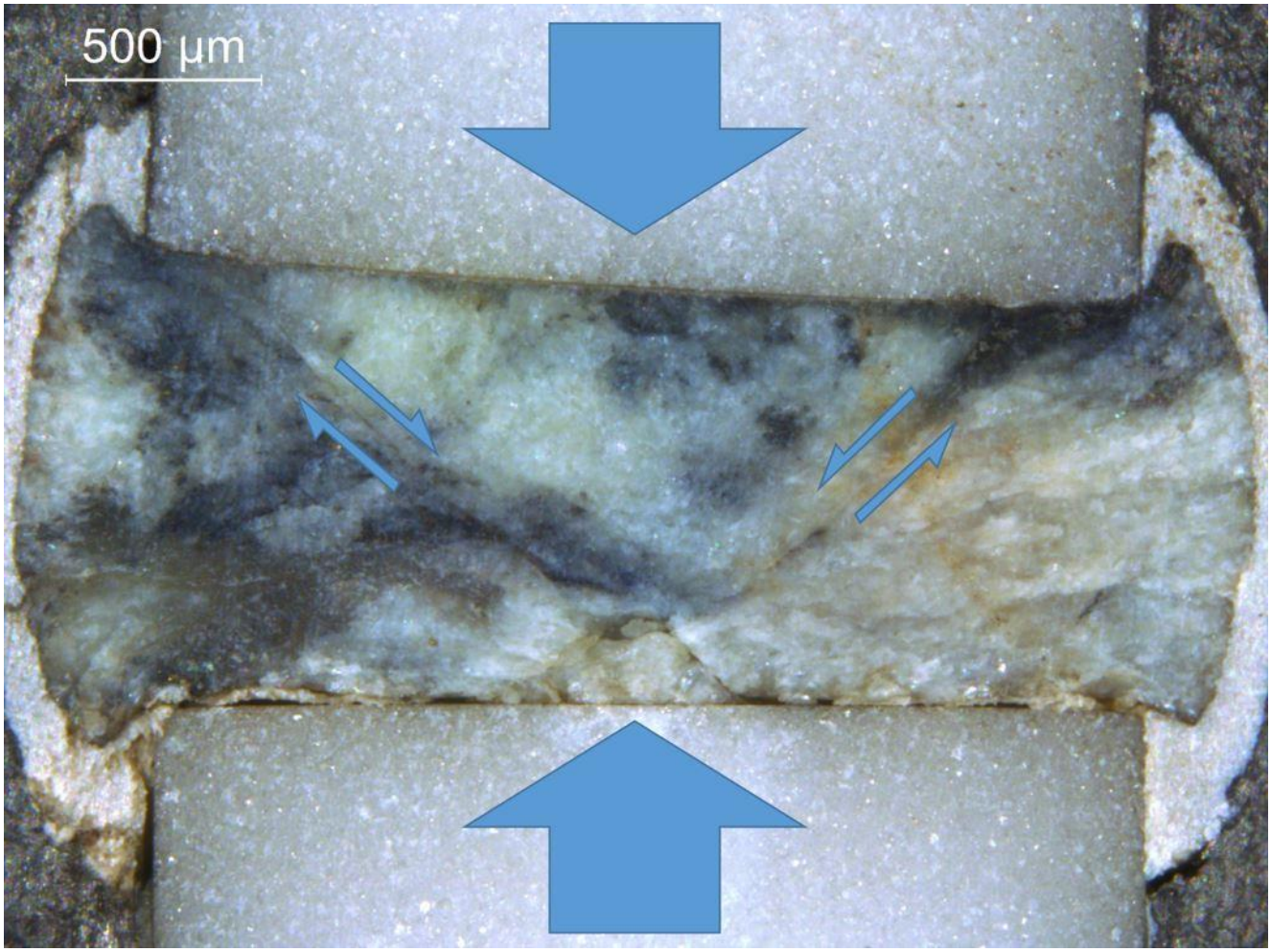


©2019. Japan Geoscience Union. All Right Reserved. 

# Water transport and mixing in the whole-mantle scale convection

*Takeo Kaneko[1], Tomoeki Nakakuki[1], Masanori Kameyama[2], Hikaru Iwamori[3]

1. Department of Earth and Planetary Systems Science, Graduate School of Science, Hiroshima University, 2. Geodynamics Research Center, Ehime University, 3. Earthquake Research Institute, University of Tokyo

The subduction of oceanic plates transports sea water with the basaltic crust to the Earth’ s interior. High-pressures experiments reveal that nominally anhydrous minerals (NAMs) contain the water of a few thousands ppm in the weight fraction. On the other hand, numerical simulations show that the NAMs layer above the subducted slab plays an important role in water transport into the deep mantle. However, the details of the water circulation and distribution processes on the whole mantle has still not been understood well.
We perform numerical simulations of isoviscous mantle convection in a two-dimensional cylinder in which hydrous-mineral phase changes and the hydration-dehydration reaction are considered. We systematically examined the effects of parameters that control activity and mixing efficiency of the mantle convection, i.e., the Rayleigh number, the internal heating rate, and the water storage capacity of the lower mantle, on the water transport into the deep mantle.
The distribution and total amount of the water transported into the mantle strongly depends on the convection style. When the internal heating is absent, stable cellular flow dominates the mantle convection. The stable convection does not mix water well so that the water distributes only near the convection cell boundary. When the mantle has the internal heating, the mantle flow becomes strongly time-dependent by thermal boundary layer instabilities. Migration of the convection cell boundary enhances the mixing of the water into the whole mantle. In addition, mixing efficiency increases with the Rayleigh number, which is an index indicating convective vigor. When the water storage capacity of the lower mantle is much smaller than the NAMs, the ejected water forms the regional hydrous layer with high water content over the 660 km discontinuity near the downwellings. However, these hydrous regions are hindered from globally spreading to the mantle transition zone. The water content in most of the mantle rocks becomes equal to the smaller value among water storage capacities of the NAMs in the upper mantle and the lower mantle finally, though the upper mantle can accommodate more water. The amount of the water stored in the whole mantle rocks is, therefore, smaller than the summation of their capacities. As a result, the equilibrium of the water regassing and degassing is realized more rapidly than the whole mantle rocks are completely saturated.

©2019. Japan Geoscience Union. All Right Reserved. 

[J] Oral | S (Solid Earth Sciences)：S-CG Complex & General

Thu. May 30, 2019 10:45 AM - 12:15 PM JST | Thu. May 30, 2019 1:45 AM - 3:15 AM UTC | A08 TOKYO BAY MAKUHARI HALL

## [S-CG52] Petrology, Mineralogy & Resource Geology

convener:Tatsuo Nozaki(Research and Development Center for Submarine Resources, Japan Agency for Marine-Earth Science and Technology), Satoshi SAITO(Graduate School of Science and Engineering, Ehime University), Koichi Momma(National Museum of Nature and Science), Nobutaka Tsuchiya(Department of Geology, Faculty of Education, Iwate University), Chairperson:Tatsuo Nozaki(JAMSTEC), Satoshi Saito

We widely invite presentations in the fields of petrology, mineralogy and resource geology. Especially description of minerals and rocks, investigation of their origin and evolution by field investigation and/or laboratory experiments, and development of new methods are accepted.

10:45 AM - 11:00 AM JST | 1:45 AM - 2:00 AM UTC

### [SCG52-01] Coordinated sample preparation with cryo-FIB-SEM and X-ray CT: Applications to chemical analysis for fluid inclusions in minerals

*Yu Kodama[1], Naotaka Tomioka[2], Tatsuhiko Kawamoto[3], Junichiro Kuroda[4], Masafumi MURAYAMA[5], Motoo Ito[2] (1.Marine Works Japan Ltd., 2.Kochi Institute for Core Sample Research, JAMSTEC, 3.Department of Geoscience, Faculty of Science, Shizuoka University, 4.Atmosphere and Ocean Research Institute, the University of Tokyo, 5.Faculty of Agriculture and Marine Science, Kochi University)

11:00 AM - 11:15 AM JST | 2:00 AM - 2:15 AM UTC

### [SCG52-02] Feasibility Study for Precise Particle Characterization of Fine Clay Particle Using An Automated Particle Image Analysis and Nanotrakcking Analysis.

*Daisuke Sasakura[1], Aiko Hayauchi[1], Sho Kimura[2] (1.MalvernPanalytical Japan ,Div of Spectris Co.Ltd,., 2.Faculty of Agriculture, University of the Ryukyu)

11:15 AM - 11:30 AM JST | 2:15 AM - 2:30 AM UTC

### [SCG52-03] Crystal structure and local structures of natural perovskite-type (Na,REE,Ca)(Ti, Nb)$O_3$ loparite by single crystal diffraction and XAFS analyses

*Ginga Kitahara[1], Akira Yoshiasa[1], Makoto Tokuda[1], Kazumasa Sugiyama[2] (1.Kumamoto University, 2.Tohoku University)

11:30 AM - 11:45 AM JST | 2:30 AM - 2:45 AM UTC

### [SCG52-04] Crystal Size Distributions based on crystal habit of groundmass pyroxene crystals in the ejecta of the Shinmoedake 2011 eruption

*Shota Okumura[1], Mayumi Mujin[2], Akira Tsuchiyama[1], Norimasa Shimobayashi[1], Akira Miyake[1] (1.Department of Geology and Mineralogy, Graduate School of Science, Kyoto University, 2.Division of Earth and Planetary Materials Science, Department of Earth Science, Tohoku University)

11:45 AM - 12:00 PM JST | 2:45 AM - 3:00 AM UTC

### [SCG52-05] Petrochemistry and zircon U-Pb age of ``lateritic'' metamorphic rocks from the Kitakami Mountains

*Nobutaka Tsuchiya[1], Yamato Kumagai[1], Tatsuro Adachi[2], Nobuhiko Nakano[2], Yasuhito Osanai[2] (1.Department of Geology, Faculty of Education, Iwate University, 2.Department of Earth Sciences, Faculty of Social and Cultural Studies, Kyushu University)

12:00 PM - 12:15 PM JST | 3:00 AM - 3:15 AM UTC

### [SCG52-06] How to make 'syn-plutonic dike' - - - Another story from the Ryoke granitic province, Southwest Japan

*Takashi Nakajima[1], Hiroyuki Kamiyama[2], Ian S. Williams[3] (1.Geological Survey of Japan, 2.Ueyama-Shisui, Co. Ltd., 3.Australian National University)

# Coordinated sample preparation with cryo-FIB-SEM and X-ray CT: Applications to chemical analysis for fluid inclusions in minerals

*Yu Kodama[1], Naotaka Tomioka[2], Tatsuhiko Kawamoto[3], Junichiro Kuroda[4], Masafumi MURAYAMA[5], Motoo Ito[2]

1. Marine Works Japan Ltd., 2. Kochi Institute for Core Sample Research, JAMSTEC, 3. Department of Geoscience, Faculty of Science, Shizuoka University, 4. Atmosphere and Ocean Research Institute, the University of Tokyo, 5. Faculty of Agriculture and Marine Science, Kochi University

Hydrothermal fluids and seawater are often entrapped in minerals as fluid inclusions in crustal/mantle materials, marine halites and even in rare meteorites [1, 2, 3, 4]. The chemical compositions of fluid inclusions and mineral inclusion therein are keys to decipher their origins and evolution of the geofulids. A laser-ablation inductively-coupled-plasma mass-spectrometry (LA-ICP-MS), a Raman spectrometry and an environmental SEM (cryo-SEM with EDS) are methods for chemical analysis of fluid inclusions, entrapped tiny minerals and gasses. For example, Kawamoto and coworkers recently determined Na/K ratio of fluid inclusions in olivine crystals from mantle xenoliths from the Pinatubo volcano by LA-ICP-MS in 20-$\mu$m spatial resolution [1]. The attempt successfully provided new insight on the fate of seawater subducting into the mantle in a plate convergent region. Lowenstein et al. investigated major chemistry of fluid inclusions from marine halites by a cryo-SEM with EDS system, and found systematic and oscillating changes in Phanerozoic seawater chemistry ($Na^+$ vs. $Cl^-$ and $Mg^{2+}$ vs. $Cl^-$) [3].

As unique sample preparation and analytical approach to a fluid inclusion, combined instrument of focused ion beam system and scanning electron microscope with a cryo sample stage (cryo-FIB-SEM) is recently utilized (e.g., Yoshida et al., 2018 [2]). Fluid inclusions can be exposed as ices in the vacuum sample chamber of cryo-FIB-SEM, and then the frozen fluids can be directly analyzed by EDS attached to SEM. Advantages of this approach are a direct access to fluid inclusions by precise sample milling with FIB, and simultaneous analysis for major elements with a relatively high spatial resolution (~5 $\mu$m). The method has been first applied to fluid inclusions in quartz [2].

A cryo-FIB-SEM approach is, however, time-consuming: entire processing and analysis with cryo-FIB-SEM requires several to few tens of hours for a several tens micrometer-sized sample. Descriptions of exact locations and spatial distribution of each fluid inclusion in host minerals will help to minimize a processing time with FIB. We, therefore, used a laboratory-based micro-focus XCT apparatus ($\mu$XCT) at the Center for Advanced Marine Core Research, Kochi University for acquiring an accurate three-dimensional characterization of fluid inclusions in minerals with a spatial resolution of 0.5 to 2.5 $\mu$m depending on sample size. In the present study, we aim to improve the throughput of the fluid inclusion analysis using cryo-FIB-SEM and establish a reasonable analytical flow. We have obtained spatial distributions of fluids in olivine from the Pinatubo xenoliths and those in halite in Sicilian rock by $\mu$XCT. Pretreatments for the samples have been carried out by micro-sampling system, and then microfabrication and chemical analysis of frozen fluids in the samples have been carried

©2019. Japan Geoscience Union. All Right Reserved. 

out by cryo-FIB-SEM.

In this talk, we will present the effectiveness of coordinated sample preparation utilizing cryo-FIB-SEM and $\mu$XCT, and a comprehensive microanalysis of fluid inclusions in addition to cryo-FIB-SEM. For instance, residues of fluid inclusions and associated minute minerals in FIB-processed samples can be further characterized in a higher spatial resolution by an analytical transmission electron microscope (TEM) and a secondary ion mass spectrometer (SIMS).

[1] Kawamoto, T., Kimura, J., Chang, Q., Yoshikawa, M., Okuno, M., Kobayashi, T., in prep.
[2] Yoshida, K., Orozbaev, R., Hirajima, T., Miyake, A., Tsuchiyama, A., Bakirov, A., Takasu, A., Sakiev, K. (2018). Micro-excavation and direct chemical analysis of individual fluid inclusion by cryo-FIB-SEM-EDS: Application to the UHP talc-garnet-chloritoid schist from the Makbal Metamorphic Complex, Kyrgyz Tian-Shan. Geochemical Journal, 52(1), 59-67.
[3] Lowenstein, T. K., Timofeeff, M. N., Brennan, S. T., Hardie, L. A., & Demicco, R. V. (2001). Oscillations in Phanerozoic seawater chemistry: Evidence from fluid inclusions. Science, 294(5544), 1086-1088.
[4] Zolensky, M. E., Bodnar, R. J., Gibson, E. K., Nyquist, L. E., Reese, Y., Shih, C. Y., & Wiesmann, H. (1999). Asteroidal water within fluid inclusion-bearing halite in an H5 chondrite, Monahans (1998). Science, 285(5432), 1377-1379.

Keywords: cryo-FIB-SEM-EDS, fluid inclusion, micro-focus X-ray CT

©2019. Japan Geoscience Union. All Right Reserved. 

# Feasibility Study for Precise Particle Characterization of Fine Clay Particle Using An Automated Particle Image Analysis and Nanotrakcking Analysis.

*Daisuke Sasakura[1], Aiko Hayauchi[1], Sho Kimura[2]

1. MalvernPanalytical Japan ,Div of Spectris Co.Ltd,., 2. Faculty of Agriculture, University of the Ryukyu

## Introduction

Clay minerals are very common in soils, in fine-grained sedimentary rocks such as shale, mudstone, and siltstone and in fine-grained metamorphic slate and phyllite. Typical mechanism to generation of clay is alteration of the surface on mineral rock due to affected by transfer of water on the earth surface. Behavior of generation of clay is controlled by surface of minerals be forced to transform to other mineral component due to the moment contact with water. Particle size of clay minerals are usually ultrafine-grained, such as normally considered to be less than 2 micrometers in size on standard particle size distributions. Notable properties of clay are high-affinities with water, minerals due to unique properties of possible to make intercalation in crystal structure, and possibly disperse to anywhere with moving of water on earth surface due to fine particle size range. Therefore, to understand characteristics of clay is possible to consider as a maker index parameter of material transportation on the surface of earth. Especially particle characterization of clay is promising as fundamental parameter. Existing approaches to characterize of particle are such as an electron microscope (Scanning type: SEM, Transmission type :TEM) , an optical microscope (OM) , a laser diffraction (LD), an electro zone methods (coulter counter) and a dynamic light scattering (DLS) . However, drawbacks of these methods were such as indirect method, limited work on concentration determination, time consuming to measure over than several thousand particles and requirement to highly concentration (over than 3wt%) of ionized water. Complementally analytical approach using an automated particle image analysis (APIA) and Nanotracking analysis (NTA) are promising tools to as new flamework. In this report will be discuss for feasibility and technical discussion to applicable for fine clay using this flamework.

## Material and Methods.

As model samples for clay mineral, purchased Kaolin was used. To investigate purity and chemical components using crystal structure , XRD (Aereris , MalvernPanalytical , Almero, Netherlands) was used. Profile of XRD chart suggested diffraction peaks on 9.6, 19.3, 19.9, and 29.1 degrees. These peaks were significantly suggested as Pyrophyllite using library search.To characterize micrometer particles range, APIA analyses were conducted on a Morphologi G3SE as automated image analysis system (MalvernPanalytical Instruments, Worcestershire, UK). To characterize nanometer range, NTA analyses were conducted on a NS300 as nanotracking analyzing systems (MalvernPanalytical Instruments, Worcestershire, UK) with particle concentration.

Keywords: Clay Minerals, Particle Morphology, Particle Charactarization

©2019. Japan Geoscience Union. All Right Reserved. 

# Crystal structure and local structures of natural perovskite-type (Na,REE,Ca)(Ti, Nb)$O_3$ loparite by single crystal diffraction and XAFS analyses

*Ginga Kitahara[1], Akira Yoshiasa[1], Makoto Tokuda[1], Kazumasa Sugiyama[2]

1. Kumamoto University, 2. Tohoku University

The perovskite type compound $ABX_3$ expresses various physical properties such as ferroelectricity and piezoelectricity, symmetry changes according to composition, pressure and temperature, and various deformations of framework constituted by $BX_6$ octahedral occur. Even in a solid solution, ferroelectricity, para electricity, superionic conductivity and the like are developed. Recently, it has attracted attention as a material for solar cells.

The perovskite-type minerals, which exist in the Earth’ s mantle, are one of the major host mineral of trace elements such as Th and REE. However, there are few detailed studies on rare earth elements and various heavy metals contained in naturally occurring perovskite-type minerals. In this study, we report on structural properties of solid solution, local structural characteristics of contained elements and irregularities due to radioactive elements, etc.

Analysis of chemical composition using SEM JSM-7001F manufactured by JEOL and EDS INCA SYSTEM manufactured by Oxford, and BL-9C and NW10A of KEK were used analysis of local structures and oxidation states by XAFS analysis and refinement of single crystal structure using Rigaku XtaLAB Super Nova.

The mineral produced from, Mt. Khibiny, Kola, Russia, which we treat as samples, is the solid solution with Lueshite $Na^{+}Nb^{5+}O_3$, Loparite $Na^{+}REE^{3+}Ti^{4+}{}_2O_6$, Perovskite $Ca^{2+}Ti^{4+}O_3$, Tausonite $Sr^{2+}Ti^{4+}O_3$ as end members. (Mitchell and Chakhmouradian 2000) SEM-EDS analysis reveal that there are albites mainly composed of $NaAlSi_3O_8$ at the rim. Therefore, we performed single crystal X-ray diffraction experiment with untwinned crystals picked up from the center.

Many discussions have been made on the crystal structure of Loparite. (Haggerty and Mariano 1983, Vlasov 1966, Mitchell 1996, Zubkova et al. 1998, Chakhmouradian et al. 1999, Mitchell et al. 2000) We attempted to analyze rhombohedral, tetragonal and tetragonal crystals which have been mentioned in previous research using this sample. Rhombohedral crystal: space group *R-3c*, a = 5.5077(2), c = 13.4906(5), Tetragonal crystal: space group *I4/mcm*, a = 5.5166(6), c = 7.7814(10), Ortho crystal Space group *Pbnm*, a = 5.5142(5), b = 5.5085(7), c = 7.7961(8) From more precise structural analysis, we will discuss the phase transition of Loparite structure etc.

From the shape of the XANES spectrum of Fe by spectral analysis, it turned out that the oxidation state of Fe contained is divalent, similar to the Ce-perovskite we investigated last time. In the Ti K-edge spectrum, it can be seen that the local distortion around Ti is considerably large from the peak intensity of pre-edge. With the substitution of Nb, the local strain of Ti at the octahedral site in the solid solution is larger than the $CaTiO_3$ end component, and the electron transition probability from 1s to 3d orbital is increasing. In the Th L3-edge spectrum, XANES is remarkable, and it can be interpreted that the actinoid element Th changes to U by causing radioactive decay, and irregularization corresponding to local metamictization

©2019. Japan Geoscience Union. All Right Reserved. 

occurs.

Keywords: perovskite, XAFS, structure refinement, Loparite

©2019. Japan Geoscience Union. All Right Reserved. 

# Crystal Size Distributions based on crystal habit of groundmass pyroxene crystals in the ejecta of the Shinmoedake 2011 eruption

*Shota Okumura[1], Mayumi Mujin[2], Akira Tsuchiyama[1], Norimasa Shimobayashi[1], Akira Miyake[1]

1. Department of Geology and Mineralogy, Graduate School of Science, Kyoto University, 2. Division of Earth and Planetary Materials Science, Department of Earth Science, Tohoku University

The 2011 eruption of Shinmoedake, Kirishima volcano, Japan, is characterized by the transition of eruption styles and was preceded by magma mixing (e.g., Suzuki et al., 2013). However, the condition in the volcano has not fully clarified yet, thus clarification of the transition processes needs more information about the magma ascent process from the chamber to the shallow conduit. Meanwhile, Marsh (1988) has proposed that Crystal Size Distributions (CSDs) reflect the kinetic and physical processes affecting crystallization. Mujin and Nakamura (2014) and Mujin et al. (2017) have studied the CSDs of the groundmass crystals in the products of the eruption, and found that the CSD plots exhibit kinks which divide the groundmass crystals into two groups; the coarser ones with the gentler slope and the finer ones with the steeper slope. They proposed that the CSDs reflect the difference of the physicochemical conditions of magma depending on eruption styles. In this study, we focused on pyroxene crystals in groundmass to obtain the information about the physicochemical conditions during ascent in the conduit.

The samples used were the gray pumice of sub-Plinian eruptions and Vulcanian explosions of Shinmoedake 2011 eruption. We determined the miller indices of the pyroxene groundmass crystals by X-ray CT at SPring-8 (BL47XU) and an electron backscatter diffraction (EBSD), analyzed the size and shape of them with a field emission scanning electron microscope (FE-SEM), observed their microtextures with a transmission electron microscope (TEM), and performed composition analysis by a scanning TEM with an energy dispersive X-ray spectrometer (STEM-EDS).

We found that many of the crystals were in a hexagonal or octagonal prism. The former consisted of {010} and {110} prismatic faces and the latter had {100} faces. There were more hexagonal crystals than octagonal ones in the sub-Plinian pumice. In the Vulcanian pumice, by contrast, octagonal ones were dominant and there were only a few of hexagonal ones. In both eruption styles, the hexagonal ones were distributed in finer part than the octagonal ones. The slopes of the CSD also differed according to the habits; that is, the slopes of the hexagonal ones were steeper than that of the octagonal ones. The TEM observation showed that these pyroxene crystals in groundmass were composite crystals composed of orthopyroxene (Opx) and clinopyroxene (Cpx) which was attached to both {100} faces of the Opx, and that the Cpx parts on the both sides were occasionally in twin orientation relationship each other. Their microtextures were symmetric with respect to *c*-axis, which indicated the concentric spreads of the textures.

We found that the size distributions and slopes of the hexagonal and octagonal ones were similar to those of the finer group and the coarser group in Mujin and Nakamura (2014), respectively. Marsh (1988) proposed that CSD slope is a measure of the product of growth rate and residence time. Assuming that the growth rates were almost the same regardless of habits, residence times could be estimated from the CSD slopes as similar durations to the magma ascent durations in the conduit estimated from geophysical data (Kozono et al., 2013, Sato et al., 2013). In particular, the estimated residence time of the hexagonal ones in sub-Plinian pumice was similar to the ascend duration in sub-Plinian eruption. Hence, the hexagonal habit is assumed to reflect the relatively rapid magma ascent rate, which indicates that the

©2019. Japan Geoscience Union. All Right Reserved. 

habits of pyroxene groundmass crystals may reflect the ascent rates in the conduits. Moreover, the TEM observation suggests that microtextures of the crystals may record the temporal change of conditions during the ascent, which indicates the possibility that pyroxene groundmass crystals contribute to reveal the behavior of magma.

Keywords: CSD, crystal habit, pyroxene, volcano

©2019. Japan Geoscience Union. All Right Reserved. 

# Petrochemistry and zircon U-Pb age of ``lateritic'' metamorphic rocks from the Kitakami Mountains

*Nobutaka Tsuchiya[1], Yamato Kumagai[1], Tatsuro Adachi[2], Nobuhiko Nakano[2], Yasuhito Osanai[2]

1. Department of Geology, Faculty of Education, Iwate University, 2. Department of Earth Sciences, Faculty of Social and Cultural Studies, Kyushu University

Fe- and Al-rich metamorphic rocks were discovered from the Shinkama, Ofunato City, Kitakami Mountains, Japan. These metamorphic rocks underwent contact metamorphism during the intrusion of the lower Cretaceous Goyosan granitic rocks. The rocks from Shinkama are mainly composed of Pl, Bt, Ms, Grt, Crd(+/-), Kfs, Spl(+/-), Ilm, Ap. On the other hand, the rocks from Shinkama east are Pl, Bt, Ms, Grt(+/-), Crd, Kfs, Spl, And(+/-), Sil(+/-), Crn(+/-), Ilm, Ap. These rocks are characterized by low SiO2 contents (20--47%), high FeO* contents (12--33%) and high Al2O3 contents (18--38%). Bulk rock chemistry of the metamorphic rocks are resemble those from ``lateritic'' rocks from the Abukuma Metamorphic Belt. ``Lateritic'' rocks from the Abukuma Metamorphic Belt characteristically contains staurolite, however, metamorphic rocks from Shinkama does not include staurolite. This indicates the possibility that the metamorphic rocks in the Shinkama were probalbly metamorphosed under low pressure conditions than those from the Abukuma Metamorphic Belt.

U-Pb dating of zircons were carried out using Agilent 7500cx quadrupole inductively coupled plasma mass spectrometer (ICP-MS) with a New Wave Research UP-213 Nd-YAG UV (213 nm) laser ablation system (LA) installed at the Kyushu University. The operating parameters of analyses with LA-ICP-MS system are after Adachi et al. (2012). Zircon grains from the Shinkama metamorphic rocks are euhedral crystal (ca. 0.05mm) with remarkable oscillatory zoning, and define a concordant age of 126+/- 3Ma. On the other hand, zircon grains of subhedral crystal (larger than 0.1mm) with no oscillatory zoning, and define a concordant age of 326+/- 3Ma. The former age correspond to the contact metamorphism of Early Cretaceous, on the other hand, the latter corresopond to the hydrothermal alteration event of Carboniferous.

Keywords: laterite, metamorphic rocks, zircon U-Pb age, petrochemistry

©2019. Japan Geoscience Union. All Right Reserved. 

# How to make 'syn-plutonic dike' --- Another story from the Ryoke granitic province, Southwest Japan

*Takashi Nakajima[1], Hiroyuki Kamiyama[2], Ian S. Williams[3]

1. Geological Survey of Japan, 2. Ueyama-Shisui, Co. Ltd., 3. Australian National University

Syn-plutonic dike is interpreted to express a magma chamber process with intermingling silicic and mafic magmas in fluidal state.

In the Ryoke granitoids in Southwest Japan, mafic rocks often occur in so-called syn-plutonic dikes. They are pillow-like balls in the silicic matrix (pillow-type), and dikes intruding silicic matrix with silicic back-veins into them (dike-type). We found the 14-20Ma time discrepancies between mafic and silicic rocks in above both two types of syn-plutonic dikes in the Ryoke granitoids, 90-94Ma of silicic rocks and 70-75Ma of mafic rocks in zircon U-Pb ages. The time duration of 14-20Ma seems too long to imagine that these two components of the syn-plutonic dike was generated during a lifetime of a single magma chamber.

In a silicic rock of those syn-plutonic dike, we found a partly dissolved and re-grown intrastructure of a zircon grain in the CL image, with the ages of cc.70Ma in the re-grown part and cc.90Ma in the undissolved core. The mafic rocks of the syn-plutonic dike nearby gives cc.70Ma and the host Ryoke granitoids around them give 90-96Ma. So it could be interpreted that the syn-plutonic dike was formed with injection of the mafic magma at cc.70Ma into the already solidified 90-96Ma granitoids and partially melted them, which led the physical interaction of local silicic mushy melt and mafic magma. The partly dissolved and re-grown zircon described above could tell that story of forming syn-plutonic dike.

As this type of the “syn-plutonic dikes” occur widespread in a km-sized area in the Ryoke granitoids, that process may be regarded as local and partial revival of granitic magma chamber.

Keywords: syn-plutonic dike, U-Pb ages, Ryoke granitic rocks, magma chamber process, Southwest Japan, Cretaceous

©2019. Japan Geoscience Union. All Right Reserved. 

[J] Poster | S (Solid Earth Sciences )：S-CG Complex & General

Thu. May 30, 2019 3:30 PM - 5:00 PM JST | Thu. May 30, 2019 6:30 AM - 8:00 AM UTC | Poster Hall International Exhibition Hall8, Makuhari Messe_15

## [S-CG52] Petrology, Mineralogy & Resource Geology

convener:Tatsuo Nozaki(Research and Development Center for Submarine Resources, Japan Agency for Marine-Earth Science and Technology), Satoshi SAITO(Graduate School of Science and Engineering, Ehime University), Koichi Momma(National Museum of Nature and Science), Nobutaka Tsuchiya(Department of Geology, Faculty of Education, Iwate University)

We widely invite presentations in the fields of petrology, mineralogy and resource geology. Especially description of minerals and rocks, investigation of their origin and evolution by field investigation and/or laboratory experiments, and development of new methods are accepted.

### [SCG52-P01] Combined microspectroscopic characterization of a red-colored granite rock sample

*Katsuya Okada[1], Satoru Nakashima[1] (1.Department of Earth and Space Science, Graduate School of Science, Osaka University)

### [SCG52-P02] Crystal chemistry of synthetic mukhinite, V-analogue of clinozoisite, on the join $Ca_2Al_3Si_3O_{12}(OH)$-$Ca_2Al_2VSi_3O_{12}(OH)$

*Mariko Nagashima[1], Daisuke Nishio-Hamane[2], Nobuhiko Nakano[3], Toshisuke Kawasaki[4] (1.Graduate school of Sciences and Technology for Innovation, Yamaguchi University, 2.The institute for Solid State Physics, the University of Tokyo, 3.Department of Environmental Changes, Faculty of Social and Cultural Studies, Kyushu University, 4.Faculty of Science, Ehime University)

### [SCG52-P03] High temperature In-situ TEM observation of crystallization in Sakurajima volcanic glass

*Akira Miyake[1], Shota Okumura[1] (1.Department of Geology and Mineralogy, Graduate School of Science, Kyoto University)

### [SCG52-P04] Timing of intrusion and Sr isotopic composition of granodiorite porphyrites in the Noko Island, western part of northern Kyushu

*Masaki Yuhara[1], Yoshinobu Kawano[2], Osamu Okano[3] (1.Department of Earth System Science, Faculty of Science, Fukuoka University, 2.Department of Environment Systems, Faculty of Geo-environmental Science, Rissho University, 3.Department of Earth Sciences, Faculty of Science, Okayama University)

### [SCG52-P05] Petrological study of crystallization process of a composite dike in the Ryoke belt (Mie Prefecture, SW Japan)

*Ayu Yamazaki[1], Tetsuo Kawakami[1], Fumiko Higashino[2] (1.Department of Geology and Mineralogy, Graduate school of Science, Kyoto University , 2.Graduate school of Environmental Studies, Tohoku University)

### [SCG52-P06] Petrography and Zircon U-Pb ages of the Ryoke Granitoids distributed in the Takanawa Peninsula, Ehime Prefecture.

*Kazuya Shimooka[1], Satoshi SAITO[1], Kenichiro Tani[2] (1.Graduate School of Science and Engineering, Ehime University, 2.Department of Geology and Paleontology, National Museum of Nature and Science)

### [SCG52-P07] Neoproterozoic arc magmatism and high-grade metamorphism of the basement rocks in southern Malawi

*Toshiaki Tsunogae[1], Sam Uthup[1], Mzee Wandembo Nyirongo[2], Md. Sazzadur Rahman[1], Yusuke Takamura[1], Kazuki Takahashi[1] (1.University of Tsukuba, 2.Malawi University of Science and Technology)

[SCG52-P08] Geochemical features of Quaternary rhyolitic magma and xenolith from Hime-shima volcanic group

*Takehiro Hirayama[1], Tomoyuki Shibata[1], Masako Yoshikawa[1], Yasutaka Hayasaka[1], Keiji Takemura[2] (1.Department of Earth and Planetary Systems Science, Graduate School of Science, Hiroshima University, 2.Kyoto university)

---

[SCG52-P09] Petrological study on the intrusive contact of a Setouchi volcanic rock dike in the Nakajima
Island, Ehime Prefecture

*Taiki Omori[1], Satoshi SAITO[2] (1.Department of Earth Science, Faculty of Science, Ehime University , 2.Department of Earth Science, Graduate Schoole of Science, Ehime University)

---

[SCG52-P10] **Fundamental evaluation for making simulated sea bed floc**

*AIKO HAYAUCHI[1], Daisuke Sasakura[1], Hisato Yasuda[2], Shinya Nakamura[3], Sho Kimura[3], Shohei Noda[4] (1.Malvern Panalytical division of Spectris Co., Ltd, 2.Kochi University, 3.UNIVERSITY OF THE RYUKYU, 4.TOKYO UNIVESITY OF SCIENCE)

---

[SCG52-P11] Petrology of the Morobe Granodiorite in the Kuper Range, Morobe Province, Papua New Guinea

Angela Lynett Bokuik[1], *Takashi Hoshide[1] (1.Faculty of International Resource Sciences, Akita University)

---

[SCG52-P12] Sr–Nd isotopic compositions of the San-yo Belt, Southwest Japan: Implications for the Cretaceous enriched mantle

*Shogo Kodama[1], Masaaki Owada[1], Teruyoshi Imaoka[1], Atsushi Kamei[2] (1.Yamaguchi University, 2.Shimane University)

---

[SCG52-P13] Lithological variation of massive serpentinites in marginal zone of serpentinite body in Kamuikotan belt, Hokkaido, Japan: Analysis of advanced-boring cores for tunnel construction

*Shusaku Yamazaki[1], Kenji Okazaki[1], Toshiyuki Kurahashi[1] (1.Civil Engineering Research Institute for Cold Region, Public Works Research Institute, National Research and Development Agency)

# Combined microspectroscopic characterization of a red-colored granite rock sample

*Katsuya Okada[1], Satoru Nakashima[1]

1. Department of Earth and Space Science, Graduate School of Science, Osaka University

Tenzan granite, Saga, Japan, has reddish color portions spreading from a grey prehnite vein over about 10 mm. However, origins of red coloration remain unclear. Combined microspectroscopic mapping have been conducted on a Tenzan granite sample by using an original visible/fluorescence/Raman microspectrometer together with a low vacuum scanning electron microscopy–energy dispersive spectrometry (SEM-EDS) without coating.

Visible darkfield reflectance spectra were converted to L*a*b* color values and Kubelka–Munk (KM) spectra. Large a* value (red) positions correspond to large band areas at 500–560 nm, possibly due to hematite-like iron oxide, while large b* value (yellow) positions to large band areas at 450–500 nm, due to epidote-like mineral. SEM-EDS analyses indicated that the reddish parts are Na and K-feldspars with low Fe contents (<0.5wt%). Raman microspectroscopy could not detect hematite-like minerals. Since some hematite-like minerals were identified by electron diffraction patterns under transmission electron microscope, they are considered to be submicron microcrystals disseminated in feldspar matrices.

The KM spectra for prehnite-like minerals show a weak broad band around 430 nm due possibly to a ligand field band of $Fe^{3+}$ without clear $Fe^{2+}$–$Fe^{3+}$ inter-valence charge transfer (IVCT) bands around 720nm. Therefore, Fe in prehnite is not considered to be present as hematite-like iron oxide, but can be mainly present as $Fe^{3+}$ replacing $Al^{3+}$ in the crystal structure.
Since determination of physicochemical states of Fe such as valence and coordination states ($Fe^{2+}$ or $Fe^{3+}$, oxide or in crystal lattice, etc.) and their distributions are extremely difficult, especially in complex colored rocks, the present combined microspectroscopic methods are useful for their nondestructive characterization.

Keywords: red granite, hematite, visible microspectroscopy, color values, band area map, SEM-EDS

©2019. Japan Geoscience Union. All Right Reserved. 

# Crystal chemistry of synthetic mukhinite, V-analogue of clinozoisite, on the join $Ca_2Al_3Si_3O_{12}(OH)$-$Ca_2Al_2VSi_3O_{12}(OH)$

*Mariko Nagashima[1], Daisuke Nishio-Hamane[2], Nobuhiko Nakano[3], Toshisuke Kawasaki[4]

1. Graduate school of Sciences and Technology for Innovation, Yamaguchi University, 2. The institute for Solid State Physics, the University of Tokyo, 3. Department of Environmental Changes, Faculty of Social and Cultural Studies, Kyushu University, 4. Faculty of Science, Ehime University

This is the first report of the crystal structure of mukhinite, V-analogue clinozoisite, on the join $Ca_2Al_3Si_3O_{12}(OH)$-$Ca_2Al_2V^{3+}Si_3O_{12}(OH)$ synthesized at 1.5 GPa and 800 ºC (Run 20). The study was performed to clarify the distribution of $V^{3+}$ among structurally independent octahedral M1, M2 and M3 sites, and the effect of $V^{3+}$ on the crystal structure. Although epidote-supergroup minerals occur widely in low- to medium-grade metamorphic mafic rocks, and hydrothermally altered rocks, clinozoisite- and allanite-subgroup minerals rich in $V^{3+}$ are not common, and have been reported from restricted localities. Mukhinite from the Tashelginskoye iron ore deposit, southwestern Siberia, having the composition of $Ca_{2.0}(Al_{2.1}V_{0.8}Fe_{0.1})Si_{3.1}O_{12}(OH)$ has been regarded as a $V^{3+}$-analogue of clinozoisite (Shepel and Karpenko 1969). However, its crystal structure and $V^{3+}$ distribution among octahedra have not been investigated. Several syntheses and/or phase-equilibrium studies on clinozoisite-subgroup minerals have been performed. To the best of our knowledge, there has been no investigation of synthetic V-bearing epidote-supergroup minerals.

Syntheses were performed under the conditions of 1.2-1.5 GPa and 600-800 ºC, and run duration 89-261 hours. Mukhinite and $V^{3+}$-bearing clinozoisite (Czo) in all run products are associated with zoisite (Zo), and also coexist with V-bearing phases such as vanadomalayaite, goldmanite, V-oxides and unidentified Ca-Al-bearing vanadates. Czo and Zo were distinguished by using Raman spectra. As the result of submicroscopic texture observation by TEM, Zo in Run 19 product often contain Czo lamellae with several nm thickness, and they have epitaxial relationship as Zo[010]//Cz[010]. Czo and Zo in Run 20 product are generally separated, but in a few cases, they contact each other at boundaries. However, the phases in Run 20 do not have an epitaxial relationship, and Zo intergrowth with Czo is not observed. Mukhinite and $V^{3+}$-bearing clinozoisite crystallized in the Run 20 product show a compositional gap between 0.33-0.74 V atoms per formula unit (apfu), and the V content attains 1.14 apfu. The co-existence of low $V^{3+}$- and high $V^{3+}$-clinozoisites indicates the presence of a miscibility gap at 1.5 GPa and 800 ºC. Two mukhinite crystals with 0.75 and 0.83 $V^{3+}$ apfu were used for X-ray single-crystal structure analysis (hereafter, labelled as 20d and 20k). Structure refinements of the 20d and 20k crystals converged to $R_1$ values of 4.20% and 3.33%, respectively. The unit-cell parameters are $a$ = 8.8995(2), $b$ = 5.6299(1), $c$ = 10.1532(2) Å, beta = 115.327(1)º, and $V$ = 459.81(2) Å$^3$ for 20d, and $a$ = 8.8999(1), $b$ = 5.6357(1), $c$ = 10.1499(1) Å, beta = 115.306(1)º, and $V$ = 460.24(2) Å$^3$ for 20k. The resulting $V^{3+}$ occupancies among the octahedral sites of 20d and 20k are $^{M1}(Al_{0.894(6)}V_{0.106})^{M2}(Al_{0.976(6)}V_{0.024})^{M3}(V_{0.621(6)}Al_{0.379})$ and $^{M1}(Al_{0.868(4)}V_{0.132})^{M2}(Al_{0.957(4)}V_{0.043})^{M3}(V_{0.652(2)}Al_{0.348})$, respectively. Site preference of $V^{3+}$ at the octahedral sites is M3>M1>M2 as that of $Fe^{3+}$ and $Mn^{3+}$. The intracrystalline partition coefficient of $V^{3+}$ and $Al^{3+}$ between the M1 and M3 sites, $K_D = (V^{3+}/Al)^{M1}/(V^{3+}/Al)^{M3}$, is 0.07-0.08, which is greater than those of $Fe^{3+}$ and $Al^{3+}$ (0.03-0.05) and of $Mn^{3+}$ and $Al^{3+}$ (0.04-0.06). Variations of the unit-cell parameters are strongly related to the variations of the M3-O*i* and M1-O*i* distances. The unit-cell volumes of mukhinites are similar to those of $Ca_2(Al,Fe^{3+})_3Si_3O_{12}(OH)$-epidote. However, it is noticed that the *a*-dimension is longer, and the *c*-dimensions shorter. The b angles of the mukhinites are also different from those of epidotes, but similar to those of $Cr^{3+}$-clinozoisite. Although the behavior of $V^{3+}$ and its effect on the epidote-type structure are expected to be similar to those in the case of $Fe^{3+}$ due to their similar ionic radii, some structural

©2019. Japan Geoscience Union. All Right Reserved. 

variations cannot be explained only in terms of the similarity of ionic radii between $V^{3+}$ and $Fe^{3+}$.

Keywords: mukhinite, clinozoisite, synthesis, crystal chemistry, Raman spectroscopy, TEM

©2019. Japan Geoscience Union. All Right Reserved. 

# High temperature In-situ TEM observation of crystallization in Sakurajima volcanic glass

*Akira Miyake[1], Shota Okumura[1]

1. Department of Geology and Mineralogy, Graduate School of Science, Kyoto University

Recently, it attracts attention that the enviroment TEM (transmission electron microscope) holders using MEMS (Micro electro mechanical sysytem) tecunique, which is one of the integrated technologies of semiconductor circuit and It is possible to in-situ and nanometer-scale observe and analyze using these enviroment TEM holders, e.g., heating, biasing, gas and liquid conditions.
In the present study, in-stu heating TEM experiment was carried out to observe the crystallization in volcanic glass using in-situ heating TEM holder (Wildfire D6, DENS solutions). Sample is the volcanic glass from Sakurajima volcano.
Experiment condition is that at first heating 23 degC to 1600 degC, which shows the set value, at 1 degC/sec, nextly keeping the 1160 degC for around 24 min, and finally cooling 1160 degC to 23 degC at 1 degC/sec. Because our previous temperature calbration experiments indicated that the actual temperature had the about 200 degC lower value than the setting temperature, it is thought taht 1160 degC, the setting temperature in this study, showed about 950 degC.
Many minerals crstallized in volcanic glass were observed in the in-situ experiments, although we could not observe just crystallization from glass at first unfortunately. During keeping the 1160 degC, we could observe that mineral disappeared and re-crystallization. After cooling, we identified these minerals crystallized at high temperature, and these minerals were magnetite (Fe3O4) and clinopyroxene (space group: C2/c).

Keywords: in-stu heating TEM experiment

©2019. Japan Geoscience Union. All Right Reserved. 

# Timing of intrusion and Sr isotopic composition of granodiorite porphyrites in the Noko Island, western part of northern Kyushu

*Masaki Yuhara[1], Yoshinobu Kawano[2], Osamu Okano[3]

1. Department of Earth System Science, Faculty of Science, Fukuoka University, 2. Department of Environment Systems, Faculty of Geo-environmental Science, Rissho University, 3. Department of Earth Sciences, Faculty of Science, Okayama University

The granodiorite porphyrite dykes are intruded into the Kitazaki Tonalite and metamorphic rocks distributed in Noko Island, western part of northern Kyushu. The petrological features of those dykes suggest that granodiorite porphyrite has been formed by mixing of tonalitic magma, which is differ from the Kitazaki Tonalite, and granitic magma (Yuhara, 2017).

The granodiorite porphyrite dyke includes lamprophyre (Yuhara et al., 2007), and the lamprophyre dyke cuts granodiorite porphyrite dyke. These occurrences imply that both dykes intruded at the same time. Ishibashi et al. (2007) reported K-Ar whole rock age of 90.7±1.2 Ma from lamprophyre dyke, and interpreted timing of intrusion. Thus, granodiorite porphyrite dykes intruded at about 90.7 Ma. Both dykes cut fine-grained granitic dykes intruded into the Kitazaki Tonalite.

Initial Sr isotopic ratios (SrI) of granodiorite porphyrites and mafic enclaves range from 0.70459 to 0.70487 and from 0.70430 to 0.70466, respectively. That of lamprophyre is 0.70414. Sr isotopic ratios calculated at 90.7 Ma of the Kitazaki Tonalite and fine-grained granites range from 0.70435 to 0.70480 and from 0.70512 to 0.70580, respectively. SrI of granodiorite porphyrites and mafic enclaves are lower than that of fine-grained granites, and in range of SrI of the Cretaceous granitic rocks in northern Kyusyu (Owada et al., 1999; Yuhara et al., 2005; Kawano and Yuhara, 2008). SrI of lamprophyre is lower than that of the Cretaceous granitic rocks in northern Kyusyu, but within that of the Shikanoshima basic rocks (Yuhara et al., 2016).

Keywords: granodiorite porphyrite, lamprophyre, Sr isotopic composition, Kitazaki Tonalite, Noko Island, Cretaceous granitic rocks in northern Kyusyu

©2019. Japan Geoscience Union. All Right Reserved. 

# Petrological study of crystallization process of a composite dike in the Ryoke belt (Mie Prefecture, SW Japan)

*Ayu Yamazaki[1], Tetsuo Kawakami[1], Fumiko Higashino[2]

1. Department of Geology and Mineralogy, Graduate school of Science, Kyoto University , 2. Graduate school of Environmental Studies, Tohoku University

A composite dike with a width of about 3 m discordantly intrudes to the gneissose structure of pelitic and psammitic migmatites in Hakusan-cho, Mie Prefecture (Ryoke belt, SW Japan). This composite dike has silicic margin of about 15 cm in width and mafic rocks in its center in the form of discrete pillows of about 5-30 cm in width, representing coexistence of silicic and mafic magmas. This study aims to discuss how the composition of these magmas changed through magma mingling, magma mixing and chemical diffusion by observing microtextures indicative of magma mixing and spatial change of mineral compositions.

The silicic host rock more than 3 cm distant from the mafic pillow consists of plagioclase + biotite + quartz + K-feldspar + garnet. Silicic host rock in the vicinity of the mafic pillows shows the mineral assemblage of plagioclase + biotite + quartz ±K-feldspar with minor garnet. On the other hand, the mafic pillows mainly consist of two parts, hornblende-bearing and hornblende-free domains. The hornblende-bearing domain mainly consists of plagioclase + hornblende + biotite + quartz ±K-feldspar. The hornblende-free domain, commonly developed in between the hornblende-bearing domain and the silicic host, mainly consists of plagioclase + biotite + quartz ±K-feldspar.

Some microtextures indicative of magma mixing (e.g. acicular apatites, rapakivi feldspars, “anorthite spikes” in plagioclase) (Hibbard, 1991; Baxter and Feely, 2002) were found both from the mafic pillows and from the silicic host in the vicinity of them. Especially in felsic back veins developed in the mafic pillows, coarse-grained plagioclase shows a zonal inclusion arrangement of quartz and biotite. A number of acicular apatite crystals are included in and outside the inclusion arrangement, whereas no apatite inclusion is present inside the inclusion arrangement. This microtexture is considered as evidence of local magma mixing in felsic back veins.

When focusing on one pair of a discrete pillow and its silicic host, systematic change in mineral composition is observed in the silicic host and the mafic pillow as a distance from the mafic pillow: From the silicic host to the mafic pillow, anorthite value of fine-grained plagioclase, $Mg/(Mg+Fe_{total})$ ratio, Cl and $TiO_2$ concentrations of biotite gradually approach to the value observed in the mafic pillow. These chemical trends indicate that magma composition changed prior to the crystallization of these minerals. Observation of the sharp silicic host/mafic pillow boundary and rare occurrence of magma mixing textures both in silicic and mafic rocks suggests that chemical diffusion across the interface between the two magmas played an important role before mechanical mixing.

In a larger scale, 3 different mafic pillows in different positions of the vein (about 10 cm, 20 cm and 160 cm distant from the dike wall) show different $Mg/(Mg+Fe_{total})$ ratio of biotite and hornblende. The mafic pillow at 10 cm and that at 20 cm have similar $Mg/(Mg+Fe_{total})$ ratio of biotite and hornblende, whereas mafic pillow at 160 cm-distance has higher $Mg/(Mg+Fe_{total})$ ratio than them. This indicates the difference in the degree of chemical exchange between the silicic host and the mafic pillows as a distance from the vein wall.

©2019. Japan Geoscience Union. All Right Reserved. 

# Petrography and Zircon U-Pb ages of the Ryoke Granitoids distributed in the Takanawa Peninsula, Ehime Prefecture.

*Kazuya Shimooka[1], Satoshi SAITO[1], Kenichiro Tani[2]

1. Graduate School of Science and Engineering, Ehime University, 2. Department of Geology and Paleontology, National Museum of Nature and Science

Various types of granitoids are widely distributed in the Ryoke Belt of Takanawa Peninsula, Ehime Prefecture. Based on geological and petrographic studies, Ochi (1982) has been classified the granitoids into three groups including (1) three tonalitic bodies, (2) four granodioritic bodies and (3) seven granitic bodies, and suggested that the tonalitic bodies intruded at the oldest stage, followed successively by the intrusion of the granodioritic and granitic bodies. In this study, we performed geological and petrographic investigation on the Ryoke granitoids in Takanawa Peninsula, and further obtained new zircon U-Pb ages for representative samples collected from the tonalitic, granodioritic and granitic bodies. The new zircon U-Pb ages are ca. 94 Ma for tonalite, ca. 89 Ma for granodiorite, and ca. 94 Ma for granite. The results suggest multiple intrusive activities in the study area including the older magmatism which has formed tonalites and granites at ca. 94 Ma and the younger granodiorite formation at ca. 89 Ma.

Keywords: Ryoke belt, Granitoids, Takanawa Peninsula

©2019. Japan Geoscience Union. All Right Reserved. 

# Neoproterozoic arc magmatism and high-grade metamorphism of the basement rocks in southern Malawi

*Toshiaki Tsunogae[1], Sam Uthup[1], Mzee Wandembo Nyirongo[2], Md. Sazzadur Rahman[1], Yusuke Takamura[1], Kazuki Takahashi[1]

1. University of Tsukuba, 2. Malawi University of Science and Technology

The basement rocks in southern Malawi form part of the Mozambique Belt (or the southern Irumide Belt) that correspond a typical example of Neoproterozoic collisional orogens in southeastern Africa. The dominant lithologies in Lilongwe-Zomba-Blantyre area in southern Malawi are biotite gneiss (biotite + quartz + microcline + plagioclase), charnockite (orthopyroxene + K-feldspar + quartz + plagioclase + ilmenite + magnetite), and mafic granulite (plagioclase + clinopyroxene + garnet + calcic amphibole + quartz + orthopyroxene + ilmenite) which are intruded by syenite (K-feldspar + calcic amphibole + biotite + quartz + clinopyroxene) and granite (quartz + K-feldspar + plagioclase + biotite). Garnet in the mafic granulite is often mantled by plagioclase + orthopyroxene coronae, suggesting post-peak decompression. Phase equilibria modeling of the mafic granulite in the system NCKFMASHTO yielded the peak metamorphic condition of 800-920 °C and ~10 kbar with a clockwise *P-T* evolution. Major, minor, and REE geochemical data for selected felsic orthogneisses suggest arc-magmatic signatures of the rocks. The results of this study suggest that the orthogneisses in southern Malawi corresponds to a Neoproterozoic magmatic arc unit that was probably metamorphosed at high- to ultrahigh-temperature conditions during the latest Neoproterozoic East-African and Kuunga orogens.

Keywords: Mozambique Belt, Kuunga Orogen, East African Orogen, Granulite, Phase equilibria modeling

©2019. Japan Geoscience Union. All Right Reserved. 

# Geochemical features of Quaternary rhyolitic magma and xenolith from Hime-shima volcanic group

*Takehiro Hirayama[1], Tomoyuki Shibata[1], Masako Yoshikawa[1], Yasutaka Hayasaka[1], Keiji Takemura[2]

1. Department of Earth and Planetary Systems Science, Graduate School of Science, Hiroshima University, 2. Kyoto university

The Hime-shima volcanic group is composed of seven volcanoes; Oomi, Yahazudake, Kane, Ukisu, Shiroyama, Darumayama and Inazumi volcano, and is located offing of Kunisaki Peninsula, western Seto Inland Sea. The Philippine Sea Plate (PSP) is subducting under this island. It is thought that the volcanic rocks of the Himeshima volcanic groups were formed by magma mixing of dacite magma and rhyolitic magma, on the bases of disequilibrium amphibole in rhyolite and the linear trends of major element contents with the increasing in $SiO_2$ contents. According to their high Sr/Y ratios (some 100), low Y contents (< 14.3 ppm) and low $^{87}Sr/^{86}Sr$ rations (0.7037), the source material for dacitic endmember was inferred as partial melt of subducted PSP (Shibata et al. 2014). On the other hand, contributions of crustal materials are suggested from the existence of crustal xenoliths in the dacite (Shibata et al., 2014, 2016) and residual material of metapelite in the rhyolite (Hirayama et al., 2018). However, quantitative discussion for genesis of rhyolitic endmember have not been made. Therefore, we determined trace element compositions of rhyolites and major and trace element compositions of the crustal xenoliths in order to discuss the genesis of rhyolite magma. Additionally, we determined the U-Pb zircon age of the xenoliths to know their origin.

Trace element Primitive Mantle (PM)-normalized patterns of rhyolite from Hime-shima volcanic group is characterized by negative Sr, Zr and Eu anomalies and liner trend of Nb. According to their relationship between Sr/Y ratio and Y content, rhyolite from Hime-shima volcanic group have Sr/Y ratio ( < 10) and Y content ( < 15 ppm). Rhyolite from Hime-shima volcanic group cannot be classified as adakite and island-arc andesite-dacite-rhyolite. Geochemical features of the rhyolite have high Rb/Sr ratio (> 1.0), low Zr content (30 ppm) and high Nb content (15 ppm).

Petrography of xenoliths from Hime-shima volcanic group is similar to that of basement rocks of Ryoke metamorphic rocks and granites from Kunisaki peninsula. U-Pb ages of zircon grains from metapelite are ca. 100 –110 Ma. These ages show agreement with ages of U-Pb zircon in metamorphic rocks from Ryoke metamorphic belt. Geochemical features of these xenoliths have wide Zr contents (20 –100 ppm), low Nb contents ( < 10 ppm), high Y contents (> 15 ppm) and low Sr/Y ratios (< 40 ppm), although the xenolith of basaltic andesite shows high Sr/Y ratio of 90. As results of comparing the geochemical compositions between rhyolite and xenoliths from Hime-shima volcanic group, we think that there is no genetic relationship between the xenoliths and rhyolite.

We examined the genesis of xenoliths from Hime-shima volcanic group are from rocks composed with Ryoke metamorphic belt, because Ryoke metamorphic belt, which is composed of metamorphic rocks, diorites and granites, is under Hime-shima. We compared geochemical features of granites from Ryoke metamorphic belt (Ryoke granites, Yuhara, 1994) with rhyolites from Hime-shima. Trace element PM-normalized patterns of the granites have similar to those of rhyolite from Hime-shima volcanic group, which are characterized by negative Sr, Zr and Eu anomalies and liner trend of Nb. Geochemical compositions of the Ryoke granites have high Rb/Sr ratios (0.5 - 1.5), low Sr/Y ratios (10 - 20), wide

©2019. Japan Geoscience Union. All Right Reserved. 

composition range of Y contents (12 - 35 ppm) high Nb concentrations (10 - 20 ppm) and wide composition range of Zr contents (50 - 250 ppm). The chemical features of the rhyolite from Hime-shima volcanic group have high Nb (> 15 ppm), high Rb/Sr ratio (> 1.0), low Y content (< 10 ppm), low Sr/Y ratio (< 10) and low Zr content (< 50 ppm). These chemical features share rhyolites in Hime-shima volcanic group with the Ryoke granites. Therefore, it is interpreted that the rhyolites from Hime-shima volcanic group was derived from crustal material, which compositions is similar to the Ryoke granites.

Keywords: Hime-shima volcanic group, Xenolith, Rhyolite

©2019. Japan Geoscience Union. All Right Reserved. 

# Petrological study on the intrusive contact of a Setouchi volcanic rock dike in the Nakajima Island, Ehime Prefecture

*Taiki Omori[1], Satoshi SAITO[2]

1. Department of Earth Science, Faculty of Science, Ehime University , 2. Department of Earth Science, Graduate Schoole of Science, Ehime University

We performed a detailed petrological study on the intrusive contact between a Setouchi andesitic dike and host Ryoke granitoids occurring in the Nakajima Island, Ehime Prefecture. At the intrusive contact, the andesite contains many fragments of host granitoids. The bulk $SiO_2$ contents of the marginal andesite at the intrusive contact are markedly higher than those of internal domain implying the mixing between the andesite intrusion and the host granitoids. Other bulk chemical compositions such as MgO, CaO, $Na_2O$, $K_2O$, Cr and Zr also imply mixing of the host granitoids into the andesite intrusion at the intrusive contact. However, the $Al_2O_3$ contents of the marginal andesite can not be explained by bulk mixing of the host granitoids and the andesite intrusion because the $Al_2O_3$ contents of the marginal andesite are higher than those of the host granites and internal domain of the andesite intrusion. Assuming that the marginal andesite with chilled margin texture retain original compositions of intrusive magma, we tested the major element mass-balance modeling to explain chemical compositions of internal domain of the andesite intrusion. The modeling reproduced the major element compositions of internal andesites by adding ~7 % of host granite components and ~12 % of mafic phenocryst minerals into the marginal andesite.

Keywords: Setouchi volcanic rocks, Nakajima Island, Ehime Prefecture

©2019. Japan Geoscience Union. All Right Reserved. 

# Fundamental evaluation for making simulated sea bed floc

*AIKO HAYAUCHI[1], Daisuke Sasakura[1], Hisato Yasuda[2], Shinya Nakamura[3], Sho Kimura[3], Shohei Noda[4]

1. Malvern Panalytical division of Spectris Co., Ltd, 2. Kochi University, 3. UNIVERSITY OF THE RYUKYU, 4. TOKYO UNIVESITY OF SCIENCE

1. Introduction
Flock is an aggregate in which fine particles such as clay and silt gathered loosely. It exists in the seabed for example. Research on flocs has been carried out on site and/or real samples, and many are observational approaches. There we tried analysis from a micro viewpoint for making floc simulation samples and reported about relationship between sample particle feature and how ease to be floc last year.
But we didn’ t care flocculant concentration in that report. Flocculant concentration must be important factor to discuss with making a simulated floc. Therefore we focused on influence of flocculant concentration to floc characteristic in this study.

2. Material and method
Kaolin as a model sample and Eb-a(Hayashi Co., Ltd.) as a flocculant for simulated floc preparation were used. Eb-a water solution concentration was 0%, 0.1%, 0.01%, 0.01% and 0.0001%. 0.05% sample water solution was prepared with each Eb-a water solution.
One of famous parameter of solution stability evaluation is zeta potential. Zeta potential was measured with Zetasizer nano ZSP (Malvern Instruments). Particle size distribution (incl. floc size distribution) was measured with Mastersizer 3000 (Malvern Instruments) which is laser diffraction system. Mastersizer 3000 is circulation system. In other hand, Morphologi 4 (Malvern instruments) which is a statistical particle image analysis system was also used for measuring particle size distribution. Morphologi 4 is not circulation system, so we can know original floc size distribution and we can see floc as well because Morphologi 4 is imaging system.

3. Result
Zeta potential in each flocculant concentration is shown in Table 1. In general, the system is stable when the zeta potential absolute value is over 20mV. Zeta potential in Eb-a concentration 0%, 0.001% and 0.0001% were around -60mV. It means that these systems are very stable and it indicates that it is difficult to occur flocculation in these situations. In the other hand, zeta potential absolute value in Eb-a concentration 0.01%, 0.1% and 1% were under 10mV, so that these indicate easy to occur flocculation.
The floc size measured by Mastersizer3000 is shown in Table 2. At The size was measured with 1500rpm/stirring speed at first, then was measured with change to 2500rpm/stirring speed. Comparing each Dv90 on 1500rpm, higher Eb-a concentration showed bigger floc size. In terms of toughness of floc, comparing the ratio of Dv90 on 1500rpm to Dv90 on 2500rpm was 1% Eb-a (0.54), 0.1% Eb-a (65%) and 0.01% Eb-a (75%). This is a result indicating that 0.01% Eb - a was the least fragile among these three samples. Also interestingly, Dv10 on 2500rpm was 0.01% Eb-a (18um), 0.1% Eb-a (9.6um) and 1% Eb-a (5.1um).
The floc size was measured by Morphlogi 4 as well. These data will discuss indetail on that day.

©2019. Japan Geoscience Union. All Right Reserved. 

4. Conclusions

The results show flocculation concentration is one of important factor to make simulated floc. We will continue to study to make clear which factor important to make simulated floc.

Keywords: floc, flocculation, zeta potential, particle size distribution, imaging

| Eb-a(%) | 0 | 0.0001 | 0.001 | 0.01 | 0.1 | 1 |
|---|---|---|---|---|---|---|
| Zeta Potential (mV) | -58.0 | -59.4 | -57.9 | -9.62 | -1.03 | 0.119 |

Table 1: Zeta potential in each flocculant concentration

| Eb-a(%) | stirre speed | Dv10(μm) | Dv50(μm) | Dv90(μm) |
|---|---|---|---|---|
| 1 | 1500rpm | 14.6 | 62.5 | 155 |
| 1 | 2500rpm | 5.06 | 25.0 | 83.3 |
| 0.1 | 1500rpm | 12.4 | 42.4 | 106 |
| 0.1 | 2500rpm | 9.64 | 30.3 | 68.5 |
| 0.01 | 1500rpm | 19 | 45.2 | 87.6 |
| 0.01 | 2500rpm | 17.6 | 36.3 | 65.6 |
| 0 | 1500rpm | 2.69 | 6.11 | 14.9 |

Table 2: Floc size

©2019. Japan Geoscience Union. All Right Reserved. 

# Petrology of the Morobe Granodiorite in the Kuper Range, Morobe Province, Papua New Guinea

Angela Lynett Bokuik[1], *Takashi Hoshide[1]

1. Faculty of International Resource Sciences, Akita University

The Morobe Granodiorite is a composite batholith comprising of monzodiorite, monzonite, quartz monzonite, granite, granodiorite, diorite and gabbro. Mafic Microgranular Enclaves (MME) are abundant in the intrusion. The mineral assemblage of the Morobe Granodiorite comprises of hornblende, biotite, plagioclase, alkali feldspar and quartz with accessory minerals of titanite, apatite, magnetite and ilmenite. The rocks have a variety of texture, such as poikilitic, cumulous and porphyritic. The MME also has a similar mineral assemblage and texture to its host however, it is abundant in mafic minerals hornblende and biotite.

Mineral compositions for amphibole of the granodiorite and MMEs are similar, implying similar magma environment. By the iteration calculation using a geobarometer (Anderson and Smith, 1995) and a geothermometer (Blundy and Holland, 1990), we estimated the crystallization temperature of 597-766˚C and the maximum crystallization pressure of 3.6 kbar. Crystallization conditions from the MME yield higher temperature (812˚C) and pressure (5.3 kbar) to its host, which implies MMEs represent the deeper hotter parts of the same magma chamber of which the MME and host formed.

The geochemical signature of the Morobe Granodiorite represent calc-alkaline and metaluminous nature typical of I-type granites. The variations of major elements in the Harker diagram can be best explained by fractionation mainly of hornblende and plagioclase. The interpretation is consistent with the textural variations of the rocks. Low $FeO^T/(FeO^T + MgO)$ ratios and high Mg-number for granodioritic rocks suggest magma originated from partial melting of the lower mafic crust. This magma was contaminated upon ascent wall rock assimilations of the host rock Owen Stanley Metamorphic. This can be seen as $Na_2O$ vs $SiO_2$ and $K_2O$ vs $SiO_2$ variation diagrams.

Keywords: Morobe Granodiorite, mafic microgranular enclaves, fractional crystallization

©2019. Japan Geoscience Union. All Right Reserved. 

# Sr–Nd isotopic compositions of the San-yo Belt, Southwest Japan: Implications for the Cretaceous enriched mantle

*Shogo Kodama[1], Masaaki Owada[1], Teruyoshi Imaoka[1], Atsushi Kamei[2]

1. Yamaguchi University, 2. Shimane University

Cretaceous to Paleogene igneous rocks are widely exposed in the Inner Zone of Southwest Japan where the granitic rocks have been divided into the San-in, San-yo, and Ryoke Belts on the basis of their lithologies, geochemical compositions, magnetic susceptibility and associated ore deposits (Ishihara, 1971). The San-yo and Ryoke Belts belong to the ilmenite-series granitic rocks, but the San-in Belt corresponds to the magnetite-series ones (Ishihara, 1977). According to Sr isotopic compositions, Kagami et al. (1992) classified these granitic rocks into the North Zone , South Zone, and Transitional Zone situated between the North and South Zones. The granitic rocks from the Transitional and South Zones show negative eNdI values (Kagami et al., 1992); however, the isotopic compositions of granitic rocks would serve only as proof for the bulk of the continental crust (Jahn, 2010). This means that those data are unlikely to provide us with mantle signatures. Imaoka et al. (2014) described the Early Cretaceous lamprophyer (c. 105 Ma) from the Kyoto district. The Kyoto lamprophyres geochemically show enriched signatures with positive and negative eNdI values corrected to 105 Ma. In consideration of the geochemical signatures and tectonic setting, Imaoka et al. (2014) concluded that the Kyoto lamprophyre was derived from heterogenous enriched mantle created by the subduction of the oceanic crust. Aspects of the existence of enriched mantle, however, are still unclear, such as in regard to its regional extension and duration for the Cretaceous magma activities of the Inner Zone of Southwest Japan.

Late Cretaceous igneous rocks are widely exposed in the western part of Honshu Island. These igneous rocks consist mainly of granitic rocks and felsic to intermediate volcanic rocks. We newly found a small gabbro stock (c. 1 km in diameter) with relatively primitive compositions in the central part of Yamaguchi Prefecture. The gabbro stock accompanies the Susuma-Nagaho granodiorite as coeval intrusive rocks. Therefore, we refer to both granodiorite and gabbro as the Susuma-Nagaho Plutonic Complex (SNPC, hereafter). The gabbro can be subdivided into fine-grained gabbro (Fn-gabbro) and coarse-grained cumulus gabbro (Co-gabbro). The Fn-gabbro has a high Mg-number similar to primitive basalt with negative eNd values corrected to 92 Ma although Cr and Ni contents are relatively low, which indicates that the basaltic magma may have been derived from enriched mantle. In consideration of the geochemical signatures including the Sr and Nd isotopic compositions, the enriched mantle characterized by negative eNd isotopic values would have existed underneath the Inner Zone of Southwest Japan during the Cretaceous.

Keywords: Late Cretaceous, San-yo Belt, Gabbro, Enriched mantole

©2019. Japan Geoscience Union. All Right Reserved. 

# Lithological variation of massive serpentinites in marginal zone of serpentinite body in Kamuikotan belt, Hokkaido, Japan: Analysis of advanced-boring cores for tunnel construction

*Shusaku Yamazaki[1], Kenji Okazaki[1], Toshiyuki Kurahashi[1]

1. Civil Engineering Research Institute for Cold Region, Public Works Research Institute, National Research and Development Agancy

Serpentinite body associated with high-pressure metamorphic rocks such as Kamuikotan belt in Hokkaido is very important as a key to understand a deep subduction process in subduction zone. In the field of marine geology, recent advances of sampling and analytical techniques contribute to understand of serpentinization process of abyssal peridotites. On the other hand, terrestrial serpentinite body still remain a lot of unexplained processes such as variation of serpentinization, uplifting mechanism and formation of internal structure, because of poor sampling by its fragile and fragmented rock conditions on earth surface conditions. There are over 30 tunnel construction cases drilling into a serpentinite body in Japan. Geoengineering investigation including description of tunnel drilling face, measurement of physical properties and making cross section of the tunnel route were operated in each tunnel. However, a detailed geological information such as types of source rock and degree and aspect of serpentinization has been less understood from the construction records. In addition, even in recent yeses with developed drilling technology, excavation of serpentinites often encounters serious trouble such as tunnel collapse. It indicates that more detailed classification of serpentinites for tunnel construction is necessary using recent geological insights and technique.

The authors focus on reconstruction of the tunnel geological section and the detailed classification of serpentinites of a tunnel with 1241 m into Takadomari serpentinite body of Horokanai area in Kamuikotan belt in Hokkaido, Japan. In this study, massive serpentinites, which were sampled from advanced-boring core at 50 to 100 m intervals along tunnel route, were conduct to description of core and thin section and XRD analysis to investigate lithological variation around the marginal zone of the serpentinite body contact with Kamuikotan metamorphic rocks.

The research by Igarashi et al. (1985) revealed that serpentinites of the Takadomari body were classified into massive, foliated and clay serpentinites and their source rocks were mostly harzburgite and partly dunite as band in harzburgite. There are large number of “micordiorite” and micro gabbro dikes in the body. As a result of this study, advanced-boring cores from the tunnel also have same variation of massive, foliated and clay serpentinites. The source rock types of massive serpentinites from the marginal zone are also mainly harzburgite with minor band of dunite. All samples were completely serpentinized and only Cr-spinel is survived as primary mineral. Original texture of the massive serpentinite is classified into dunitic texture without pyroxenes, harzburgitic texture with orthopyroxene, cumulate texture with euhedral orthopyroxene and foliation of spinel allay. Serpentine types in the massive serpentinites are antigorite that replaced olivine and orthopyroxene and lately formed asbestos chrysotile vein. Minor amount of brucite also appears through the tunnel. As a notable feature in the marginal zone of the body, three zones of difference serpentinization were observed. In the center of the tunnel, the serpentinites well remain the original harzburgitic and dunitic texture. In the west side with amphibolites, the massive serpentinites contain magnesite veins and patches as metasomatism. In the east side with the contact to greenschists, the original texture is completely disappeared with greenish large antigorite and massive of

©2019. Japan Geoscience Union. All Right Reserved. 

grains of magnetite with brucite. The difference of texture and mineralogy of the serpentinites in this tunnel could possibly be explained that the serpentinization process in subduction zone is difference in the both sides of marginal zone in the association with the types of the Kamuikotan metamorphic rocks.

Keywords: Serpentinite, Kamuikotan belt, Boring core

©2019. Japan Geoscience Union. All Right Reserved. 

[J] Poster | S (Solid Earth Sciences)：S-CG Complex & General

Thu. May 30, 2019 5:15 PM - 6:30 PM JST | Thu. May 30, 2019 8:15 AM - 9:30 AM UTC | Poster Hall International Exhibition Hall8, Makuhari Messe_28

## [S-CG52] Petrology, Mineralogy & Resource Geology

convener:Tatsuo Nozaki(Research and Development Center for Submarine Resources, Japan Agency for Marine-Earth Science and Technology), Satoshi SAITO(Graduate School of Science and Engineering, Ehime University), Koichi Momma(National Museum of Nature and Science), Nobutaka Tsuchiya(Department of Geology, Faculty of Education, Iwate University)

We widely invite presentations in the fields of petrology, mineralogy and resource geology. Especially description of minerals and rocks, investigation of their origin and evolution by field investigation and/or laboratory experiments, and development of new methods are accepted.

### [SCG52-P01] Combined microspectroscopic characterization of a red-colored granite rock sample

*Katsuya Okada[1], Satoru Nakashima[1] (1.Department of Earth and Space Science, Graduate School of Science, Osaka University)

### [SCG52-P02] Crystal chemistry of synthetic mukhinite, V-analogue of clinozoisite, on the join $Ca_2Al_3Si_3O_{12}(OH)$-$Ca_2Al_2VSi_3O_{12}(OH)$

*Mariko Nagashima[1], Daisuke Nishio-Hamane[2], Nobuhiko Nakano[3], Toshisuke Kawasaki[4] (1.Graduate school of Sciences and Technology for Innovation, Yamaguchi University, 2.The institute for Solid State Physics, the University of Tokyo, 3.Department of Environmental Changes, Faculty of Social and Cultural Studies, Kyushu University, 4.Faculty of Science, Ehime University)

### [SCG52-P03] High temperature In-situ TEM observation of crystallization in Sakurajima volcanic glass

*Akira Miyake[1], Shota Okumura[1] (1.Department of Geology and Mineralogy, Graduate School of Science, Kyoto University)

### [SCG52-P04] Timing of intrusion and Sr isotopic composition of granodiorite porphyrites in the Noko Island, western part of northern Kyushu

*Masaki Yuhara[1], Yoshinobu Kawano[2], Osamu Okano[3] (1.Department of Earth System Science, Faculty of Science, Fukuoka University, 2.Department of Environment Systems, Faculty of Geo-environmental Science, Rissho University, 3.Department of Earth Sciences, Faculty of Science, Okayama University)

### [SCG52-P05] Petrological study of crystallization process of a composite dike in the Ryoke belt (Mie Prefecture, SW Japan)

*Ayu Yamazaki[1], Tetsuo Kawakami[1], Fumiko Higashino[2] (1.Department of Geology and Mineralogy, Graduate school of Science, Kyoto University , 2.Graduate school of Environmental Studies, Tohoku University)

### [SCG52-P06] Petrography and Zircon U-Pb ages of the Ryoke Granitoids distributed in the Takanawa Peninsula, Ehime Prefecture.

*Kazuya Shimooka[1], Satoshi SAITO[1], Kenichiro Tani[2] (1.Graduate School of Science and Engineering, Ehime University, 2.Department of Geology and Paleontology, National Museum of Nature and Science)

### [SCG52-P07] Neoproterozoic arc magmatism and high-grade metamorphism of the basement rocks in southern Malawi

*Toshiaki Tsunogae[1], Sam Uthup[1], Mzee Wandembo Nyirongo[2], Md. Sazzadur Rahman[1], Yusuke Takamura[1], Kazuki Takahashi[1] (1.University of Tsukuba, 2.Malawi University of Science and Technology)

[SCG52-P08] Geochemical features of Quaternary rhyolitic magma and xenolith from Hime-shima volcanic group

*Takehiro Hirayama[1], Tomoyuki Shibata[1], Masako Yoshikawa[1], Yasutaka Hayasaka[1], Keiji Takemura[2] (1.Department of Earth and Planetary Systems Science, Graduate School of Science, Hiroshima University, 2.Kyoto university)

---

[SCG52-P09] Petrological study on the intrusive contact of a Setouchi volcanic rock dike in the Nakajima
Island, Ehime Prefecture

*Taiki Omori[1], Satoshi SAITO[2] (1.Department of Earth Science, Faculty of Science, Ehime University , 2.Department of Earth Science, Graduate Schoole of Science, Ehime University)

---

[SCG52-P10] **Fundamental evaluation for making simulated sea bed floc**

*AIKO HAYAUCHI[1], Daisuke Sasakura[1], Hisato Yasuda[2], Shinya Nakamura[3], Sho Kimura[3], Shohei Noda[4] (1.Malvern Panalytical division of Spectris Co., Ltd, 2.Kochi University, 3.UNIVERSITY OF THE RYUKYU, 4.TOKYO UNIVESITY OF SCIENCE)

---

[SCG52-P11] Petrology of the Morobe Granodiorite in the Kuper Range, Morobe Province, Papua New Guinea

Angela Lynett Bokuik[1], *Takashi Hoshide[1] (1.Faculty of International Resource Sciences, Akita University)

---

[SCG52-P12] Sr–Nd isotopic compositions of the San-yo Belt, Southwest Japan: Implications for the Cretaceous enriched mantle

*Shogo Kodama[1], Masaaki Owada[1], Teruyoshi Imaoka[1], Atsushi Kamei[2] (1.Yamaguchi University, 2.Shimane University)

---

[SCG52-P13] Lithological variation of massive serpentinites in marginal zone of serpentinite body in Kamuikotan belt, Hokkaido, Japan: Analysis of advanced-boring cores for tunnel construction

*Shusaku Yamazaki[1], Kenji Okazaki[1], Toshiyuki Kurahashi[1] (1.Civil Engineering Research Institute for Cold Region, Public Works Research Institute, National Research and Development Agency)

# Combined microspectroscopic characterization of a red-colored granite rock sample

*Katsuya Okada[1], Satoru Nakashima[1]

1. Department of Earth and Space Science, Graduate School of Science, Osaka University

Tenzan granite, Saga, Japan, has reddish color portions spreading from a grey prehnite vein over about 10 mm. However, origins of red coloration remain unclear. Combined microspectroscopic mapping have been conducted on a Tenzan granite sample by using an original visible/fluorescence/Raman microspectrometer together with a low vacuum scanning electron microscopy–energy dispersive spectrometry (SEM-EDS) without coating.

Visible darkfield reflectance spectra were converted to L*a*b* color values and Kubelka–Munk (KM) spectra. Large a* value (red) positions correspond to large band areas at 500–560 nm, possibly due to hematite-like iron oxide, while large b* value (yellow) positions to large band areas at 450–500 nm, due to epidote-like mineral. SEM-EDS analyses indicated that the reddish parts are Na and K-feldspars with low Fe contents (<0.5wt%). Raman microspectroscopy could not detect hematite-like minerals. Since some hematite-like minerals were identified by electron diffraction patterns under transmission electron microscope, they are considered to be submicron microcrystals disseminated in feldspar matrices.

The KM spectra for prehnite-like minerals show a weak broad band around 430 nm due possibly to a ligand field band of $Fe^{3+}$ without clear $Fe^{2+}$–$Fe^{3+}$ inter-valence charge transfer (IVCT) bands around 720nm. Therefore, Fe in prehnite is not considered to be present as hematite-like iron oxide, but can be mainly present as $Fe^{3+}$ replacing $Al^{3+}$ in the crystal structure.
Since determination of physicochemical states of Fe such as valence and coordination states ($Fe^{2+}$ or $Fe^{3+}$, oxide or in crystal lattice, etc.) and their distributions are extremely difficult, especially in complex colored rocks, the present combined microspectroscopic methods are useful for their nondestructive characterization.

Keywords: red granite, hematite, visible microspectroscopy, color values, band area map, SEM-EDS

©2019. Japan Geoscience Union. All Right Reserved. 

# Crystal chemistry of synthetic mukhinite, V-analogue of clinozoisite, on the join $Ca_2Al_3Si_3O_{12}(OH)$-$Ca_2Al_2VSi_3O_{12}(OH)$

*Mariko Nagashima[1], Daisuke Nishio-Hamane[2], Nobuhiko Nakano[3], Toshisuke Kawasaki[4]

1. Graduate school of Sciences and Technology for Innovation, Yamaguchi University, 2. The institute for Solid State Physics, the University of Tokyo, 3. Department of Environmental Changes, Faculty of Social and Cultural Studies, Kyushu University, 4. Faculty of Science, Ehime University

This is the first report of the crystal structure of mukhinite, V-analogue clinozoisite, on the join $Ca_2Al_3Si_3O_{12}(OH)$-$Ca_2Al_2V^{3+}Si_3O_{12}(OH)$ synthesized at 1.5 GPa and 800 ºC (Run 20). The study was performed to clarify the distribution of $V^{3+}$ among structurally independent octahedral M1, M2 and M3 sites, and the effect of $V^{3+}$ on the crystal structure. Although epidote-supergroup minerals occur widely in low- to medium-grade metamorphic mafic rocks, and hydrothermally altered rocks, clinozoisite- and allanite-subgroup minerals rich in $V^{3+}$ are not common, and have been reported from restricted localities. Mukhinite from the Tashelginskoye iron ore deposit, southwestern Siberia, having the composition of $Ca_{2.0}(Al_{2.1}V_{0.8}Fe_{0.1})Si_{3.1}O_{12}(OH)$ has been regarded as a $V^{3+}$-analogue of clinozoisite (Shepel and Karpenko 1969). However, its crystal structure and $V^{3+}$ distribution among octahedra have not been investigated. Several syntheses and/or phase-equilibrium studies on clinozoisite-subgroup minerals have been performed. To the best of our knowledge, there has been no investigation of synthetic V-bearing epidote-supergroup minerals.

Syntheses were performed under the conditions of 1.2-1.5 GPa and 600-800 ºC, and run duration 89-261 hours. Mukhinite and $V^{3+}$-bearing clinozoisite (Czo) in all run products are associated with zoisite (Zo), and also coexist with V-bearing phases such as vanadomalayaite, goldmanite, V-oxides and unidentified Ca-Al-bearing vanadates. Czo and Zo were distinguished by using Raman spectra. As the result of submicroscopic texture observation by TEM, Zo in Run 19 product often contain Czo lamellae with several nm thickness, and they have epitaxial relationship as Zo[010]//Cz[010]. Czo and Zo in Run 20 product are generally separated, but in a few cases, they contact each other at boundaries. However, the phases in Run 20 do not have an epitaxial relationship, and Zo intergrowth with Czo is not observed. Mukhinite and $V^{3+}$-bearing clinozoisite crystallized in the Run 20 product show a compositional gap between 0.33-0.74 V atoms per formula unit (apfu), and the V content attains 1.14 apfu. The co-existence of low $V^{3+}$- and high $V^{3+}$-clinozoisites indicates the presence of a miscibility gap at 1.5 GPa and 800 ºC. Two mukhinite crystals with 0.75 and 0.83 $V^{3+}$ apfu were used for X-ray single-crystal structure analysis (hereafter, labelled as 20d and 20k). Structure refinements of the 20d and 20k crystals converged to $R_1$ values of 4.20% and 3.33%, respectively. The unit-cell parameters are $a$ = 8.8995(2), $b$ = 5.6299(1), $c$ = 10.1532(2) Å, beta = 115.327(1)º, and $V$ = 459.81(2) Å$^3$ for 20d, and $a$ = 8.8999(1), $b$ = 5.6357(1), $c$ = 10.1499(1) Å, beta = 115.306(1)º, and $V$ = 460.24(2) Å$^3$ for 20k. The resulting $V^{3+}$ occupancies among the octahedral sites of 20d and 20k are $^{M1}(Al_{0.894(6)}V_{0.106})^{M2}(Al_{0.976(6)}V_{0.024})^{M3}(V_{0.621(6)}Al_{0.379})$ and $^{M1}(Al_{0.868(4)}V_{0.132})^{M2}(Al_{0.957(4)}V_{0.043})^{M3}(V_{0.652(2)}Al_{0.348})$, respectively. Site preference of $V^{3+}$ at the octahedral sites is M3>M1>M2 as that of $Fe^{3+}$ and $Mn^{3+}$. The intracrystalline partition coefficient of $V^{3+}$ and $Al^{3+}$ between the M1 and M3 sites, $K_D = (V^{3+}/Al)^{M1}/(V^{3+}/Al)^{M3}$, is 0.07-0.08, which is greater than those of $Fe^{3+}$ and $Al^{3+}$ (0.03-0.05) and of $Mn^{3+}$ and $Al^{3+}$ (0.04-0.06). Variations of the unit-cell parameters are strongly related to the variations of the M3-O*i* and M1-O*i* distances. The unit-cell volumes of mukhinites are similar to those of $Ca_2(Al,Fe^{3+})_3Si_3O_{12}(OH)$-epidote. However, it is noticed that the *a*-dimension is longer, and the *c*-dimensions shorter. The b angles of the mukhinites are also different from those of epidotes, but similar to those of $Cr^{3+}$-clinozoisite. Although the behavior of $V^{3+}$ and its effect on the epidote-type structure are expected to be similar to those in the case of $Fe^{3+}$ due to their similar ionic radii, some structural

©2019. Japan Geoscience Union. All Right Reserved. 

variations cannot be explained only in terms of the similarity of ionic radii between $V^{3+}$ and $Fe^{3+}$.

Keywords: mukhinite, clinozoisite, synthesis, crystal chemistry, Raman spectroscopy, TEM

©2019. Japan Geoscience Union. All Right Reserved. 

# High temperature In-situ TEM observation of crystallization in Sakurajima volcanic glass

*Akira Miyake[1], Shota Okumura[1]

1. Department of Geology and Mineralogy, Graduate School of Science, Kyoto University

Recently, it attracts attention that the enviroment TEM (transmission electron microscope) holders using MEMS (Micro electro mechanical sysytem) tecunique, which is one of the integrated technologies of semiconductor circuit and It is possible to in-situ and nanometer-scale observe and analyze using these enviroment TEM holders, e.g., heating, biasing, gas and liquid conditions.
In the present study, in-stu heating TEM experiment was carried out to observe the crystallization in volcanic glass using in-situ heating TEM holder (Wildfire D6, DENS solutions). Sample is the volcanic glass from Sakurajima volcano.
Experiment condition is that at first heating 23 degC to 1600 degC, which shows the set value, at 1 degC/sec, nextly keeping the 1160 degC for around 24 min, and finally cooling 1160 degC to 23 degC at 1 degC/sec. Because our previous temperature calbration experiments indicated that the actual temperature had the about 200 degC lower value than the setting temperature, it is thought taht 1160 degC, the setting temperature in this study, showed about 950 degC.
Many minerals crstallized in volcanic glass were observed in the in-situ experiments, although we could not observe just crystallization from glass at first unfortunately. During keeping the 1160 degC, we could observe that mineral disappeared and re-crystallization. After cooling, we identified these minerals crystallized at high temperature, and these minerals were magnetite (Fe3O4) and clinopyroxene (space group: C2/c).

Keywords: in-stu heating TEM experiment

©2019. Japan Geoscience Union. All Right Reserved. 

# Timing of intrusion and Sr isotopic composition of granodiorite porphyrites in the Noko Island, western part of northern Kyushu

*Masaki Yuhara[1], Yoshinobu Kawano[2], Osamu Okano[3]

1. Department of Earth System Science, Faculty of Science, Fukuoka University, 2. Department of Environment Systems, Faculty of Geo-environmental Science, Rissho University, 3. Department of Earth Sciences, Faculty of Science, Okayama University

The granodiorite porphyrite dykes are intruded into the Kitazaki Tonalite and metamorphic rocks distributed in Noko Island, western part of northern Kyushu. The petrological features of those dykes suggest that granodiorite porphyrite has been formed by mixing of tonalitic magma, which is differ from the Kitazaki Tonalite, and granitic magma (Yuhara, 2017).

The granodiorite porphyrite dyke includes lamprophyre (Yuhara et al., 2007), and the lamprophyre dyke cuts granodiorite porphyrite dyke. These occurrences imply that both dykes intruded at the same time. Ishibashi et al. (2007) reported K-Ar whole rock age of 90.7±1.2 Ma from lamprophyre dyke, and interpreted timing of intrusion. Thus, granodiorite porphyrite dykes intruded at about 90.7 Ma. Both dykes cut fine-grained granitic dykes intruded into the Kitazaki Tonalite.

Initial Sr isotopic ratios (SrI) of granodiorite porphyrites and mafic enclaves range from 0.70459 to 0.70487 and from 0.70430 to 0.70466, respectively. That of lamprophyre is 0.70414. Sr isotopic ratios calculated at 90.7 Ma of the Kitazaki Tonalite and fine-grained granites range from 0.70435 to 0.70480 and from 0.70512 to 0.70580, respectively. SrI of granodiorite porphyrites and mafic enclaves are lower than that of fine-grained granites, and in range of SrI of the Cretaceous granitic rocks in northern Kyusyu (Owada et al., 1999; Yuhara et al., 2005; Kawano and Yuhara, 2008). SrI of lamprophyre is lower than that of the Cretaceous granitic rocks in northern Kyusyu, but within that of the Shikanoshima basic rocks (Yuhara et al., 2016).

Keywords: granodiorite porphyrite, lamprophyre, Sr isotopic composition, Kitazaki Tonalite, Noko Island, Cretaceous granitic rocks in northern Kyusyu

©2019. Japan Geoscience Union. All Right Reserved. 

# Petrological study of crystallization process of a composite dike in the Ryoke belt (Mie Prefecture, SW Japan)

*Ayu Yamazaki[1], Tetsuo Kawakami[1], Fumiko Higashino[2]

1. Department of Geology and Mineralogy, Graduate school of Science, Kyoto University , 2. Graduate school of Environmental Studies, Tohoku University

A composite dike with a width of about 3 m discordantly intrudes to the gneissose structure of pelitic and psammitic migmatites in Hakusan-cho, Mie Prefecture (Ryoke belt, SW Japan). This composite dike has silicic margin of about 15 cm in width and mafic rocks in its center in the form of discrete pillows of about 5-30 cm in width, representing coexistence of silicic and mafic magmas. This study aims to discuss how the composition of these magmas changed through magma mingling, magma mixing and chemical diffusion by observing microtextures indicative of magma mixing and spatial change of mineral compositions.

The silicic host rock more than 3 cm distant from the mafic pillow consists of plagioclase + biotite + quartz + K-feldspar + garnet. Silicic host rock in the vicinity of the mafic pillows shows the mineral assemblage of plagioclase + biotite + quartz ±K-feldspar with minor garnet. On the other hand, the mafic pillows mainly consist of two parts, hornblende-bearing and hornblende-free domains. The hornblende-bearing domain mainly consists of plagioclase + hornblende + biotite + quartz ±K-feldspar. The hornblende-free domain, commonly developed in between the hornblende-bearing domain and the silicic host, mainly consists of plagioclase + biotite + quartz ±K-feldspar.

Some microtextures indicative of magma mixing (e.g. acicular apatites, rapakivi feldspars, “anorthite spikes” in plagioclase) (Hibbard, 1991; Baxter and Feely, 2002) were found both from the mafic pillows and from the silicic host in the vicinity of them. Especially in felsic back veins developed in the mafic pillows, coarse-grained plagioclase shows a zonal inclusion arrangement of quartz and biotite. A number of acicular apatite crystals are included in and outside the inclusion arrangement, whereas no apatite inclusion is present inside the inclusion arrangement. This microtexture is considered as evidence of local magma mixing in felsic back veins.

When focusing on one pair of a discrete pillow and its silicic host, systematic change in mineral composition is observed in the silicic host and the mafic pillow as a distance from the mafic pillow: From the silicic host to the mafic pillow, anorthite value of fine-grained plagioclase, $Mg/(Mg+Fe_{total})$ ratio, Cl and $TiO_2$ concentrations of biotite gradually approach to the value observed in the mafic pillow. These chemical trends indicate that magma composition changed prior to the crystallization of these minerals. Observation of the sharp silicic host/mafic pillow boundary and rare occurrence of magma mixing textures both in silicic and mafic rocks suggests that chemical diffusion across the interface between the two magmas played an important role before mechanical mixing.

In a larger scale, 3 different mafic pillows in different positions of the vein (about 10 cm, 20 cm and 160 cm distant from the dike wall) show different $Mg/(Mg+Fe_{total})$ ratio of biotite and hornblende. The mafic pillow at 10 cm and that at 20 cm have similar $Mg/(Mg+Fe_{total})$ ratio of biotite and hornblende, whereas mafic pillow at 160 cm-distance has higher $Mg/(Mg+Fe_{total})$ ratio than them. This indicates the difference in the degree of chemical exchange between the silicic host and the mafic pillows as a distance from the vein wall.

©2019. Japan Geoscience Union. All Right Reserved. 

# Petrography and Zircon U-Pb ages of the Ryoke Granitoids distributed in the Takanawa Peninsula, Ehime Prefecture.

*Kazuya Shimooka[1], Satoshi SAITO[1], Kenichiro Tani[2]

1. Graduate School of Science and Engineering, Ehime University, 2. Department of Geology and Paleontology, National Museum of Nature and Science

Various types of granitoids are widely distributed in the Ryoke Belt of Takanawa Peninsula, Ehime Prefecture. Based on geological and petrographic studies, Ochi (1982) has been classified the granitoids into three groups including (1) three tonalitic bodies, (2) four granodioritic bodies and (3) seven granitic bodies, and suggested that the tonalitic bodies intruded at the oldest stage, followed successively by the intrusion of the granodioritic and granitic bodies. In this study, we performed geological and petrographic investigation on the Ryoke granitoids in Takanawa Peninsula, and further obtained new zircon U-Pb ages for representative samples collected from the tonalitic, granodioritic and granitic bodies. The new zircon U-Pb ages are ca. 94 Ma for tonalite, ca. 89 Ma for granodiorite, and ca. 94 Ma for granite. The results suggest multiple intrusive activities in the study area including the older magmatism which has formed tonalites and granites at ca. 94 Ma and the younger granodiorite formation at ca. 89 Ma.

Keywords: Ryoke belt, Granitoids, Takanawa Peninsula

©2019. Japan Geoscience Union. All Right Reserved. 

# Neoproterozoic arc magmatism and high-grade metamorphism of the basement rocks in southern Malawi

*Toshiaki Tsunogae[1], Sam Uthup[1], Mzee Wandembo Nyirongo[2], Md. Sazzadur Rahman[1], Yusuke Takamura[1], Kazuki Takahashi[1]

1. University of Tsukuba, 2. Malawi University of Science and Technology

The basement rocks in southern Malawi form part of the Mozambique Belt (or the southern Irumide Belt) that correspond a typical example of Neoproterozoic collisional orogens in southeastern Africa. The dominant lithologies in Lilongwe-Zomba-Blantyre area in southern Malawi are biotite gneiss (biotite + quartz + microcline + plagioclase), charnockite (orthopyroxene + K-feldspar + quartz + plagioclase + ilmenite + magnetite), and mafic granulite (plagioclase + clinopyroxene + garnet + calcic amphibole + quartz + orthopyroxene + ilmenite) which are intruded by syenite (K-feldspar + calcic amphibole + biotite + quartz + clinopyroxene) and granite (quartz + K-feldspar + plagioclase + biotite). Garnet in the mafic granulite is often mantled by plagioclase + orthopyroxene coronae, suggesting post-peak decompression. Phase equilibria modeling of the mafic granulite in the system NCKFMASHTO yielded the peak metamorphic condition of 800-920 °C and ~10 kbar with a clockwise *P-T* evolution. Major, minor, and REE geochemical data for selected felsic orthogneisses suggest arc-magmatic signatures of the rocks. The results of this study suggest that the orthogneisses in southern Malawi corresponds to a Neoproterozoic magmatic arc unit that was probably metamorphosed at high- to ultrahigh-temperature conditions during the latest Neoproterozoic East-African and Kuunga orogens.

Keywords: Mozambique Belt, Kuunga Orogen, East African Orogen, Granulite, Phase equilibria modeling

©2019. Japan Geoscience Union. All Right Reserved. 

# Geochemical features of Quaternary rhyolitic magma and xenolith from Hime-shima volcanic group

*Takehiro Hirayama[1], Tomoyuki Shibata[1], Masako Yoshikawa[1], Yasutaka Hayasaka[1], Keiji Takemura[2]

1. Department of Earth and Planetary Systems Science, Graduate School of Science, Hiroshima University, 2. Kyoto university

The Hime-shima volcanic group is composed of seven volcanoes; Oomi, Yahazudake, Kane, Ukisu, Shiroyama, Darumayama and Inazumi volcano, and is located offing of Kunisaki Peninsula, western Seto Inland Sea. The Philippine Sea Plate (PSP) is subducting under this island. It is thought that the volcanic rocks of the Himeshima volcanic groups were formed by magma mixing of dacite magma and rhyolitic magma, on the bases of disequilibrium amphibole in rhyolite and the linear trends of major element contents with the increasing in $SiO_2$ contents. According to their high Sr/Y ratios (some 100), low Y contents (< 14.3 ppm) and low $^{87}Sr/^{86}Sr$ rations (0.7037), the source material for dacitic endmember was inferred as partial melt of subducted PSP (Shibata et al. 2014). On the other hand, contributions of crustal materials are suggested from the existence of crustal xenoliths in the dacite (Shibata et al., 2014, 2016) and residual material of metapelite in the rhyolite (Hirayama et al., 2018). However, quantitative discussion for genesis of rhyolitic endmember have not been made. Therefore, we determined trace element compositions of rhyolites and major and trace element compositions of the crustal xenoliths in order to discuss the genesis of rhyolite magma. Additionally, we determined the U-Pb zircon age of the xenoliths to know their origin.

Trace element Primitive Mantle (PM)-normalized patterns of rhyolite from Hime-shima volcanic group is characterized by negative Sr, Zr and Eu anomalies and liner trend of Nb. According to their relationship between Sr/Y ratio and Y content, rhyolite from Hime-shima volcanic group have Sr/Y ratio ( < 10) and Y content ( < 15 ppm). Rhyolite from Hime-shima volcanic group cannot be classified as adakite and island-arc andesite-dacite-rhyolite. Geochemical features of the rhyolite have high Rb/Sr ratio (> 1.0), low Zr content (30 ppm) and high Nb content (15 ppm).

Petrography of xenoliths from Hime-shima volcanic group is similar to that of basement rocks of Ryoke metamorphic rocks and granites from Kunisaki peninsula. U-Pb ages of zircon grains from metapelite are ca. 100 –110 Ma. These ages show agreement with ages of U-Pb zircon in metamorphic rocks from Ryoke metamorphic belt. Geochemical features of these xenoliths have wide Zr contents (20 –100 ppm), low Nb contents ( < 10 ppm), high Y contents (> 15 ppm) and low Sr/Y ratios (< 40 ppm), although the xenolith of basaltic andesite shows high Sr/Y ratio of 90. As results of comparing the geochemical compositions between rhyolite and xenoliths from Hime-shima volcanic group, we think that there is no genetic relationship between the xenoliths and rhyolite.

We examined the genesis of xenoliths from Hime-shima volcanic group are from rocks composed with Ryoke metamorphic belt, because Ryoke metamorphic belt, which is composed of metamorphic rocks, diorites and granites, is under Hime-shima. We compared geochemical features of granites from Ryoke metamorphic belt (Ryoke granites, Yuhara, 1994) with rhyolites from Hime-shima. Trace element PM-normalized patterns of the granites have similar to those of rhyolite from Hime-shima volcanic group, which are characterized by negative Sr, Zr and Eu anomalies and liner trend of Nb. Geochemical compositions of the Ryoke granites have high Rb/Sr ratios (0.5 - 1.5), low Sr/Y ratios (10 - 20), wide

©2019. Japan Geoscience Union. All Right Reserved. 

composition range of Y contents (12 - 35 ppm) high Nb concentrations (10 - 20 ppm) and wide composition range of Zr contents (50 - 250 ppm). The chemical features of the rhyolite from Hime-shima volcanic group have high Nb (> 15 ppm), high Rb/Sr ratio (> 1.0), low Y content (< 10 ppm), low Sr/Y ratio (< 10) and low Zr content (< 50 ppm). These chemical features share rhyolites in Hime-shima volcanic group with the Ryoke granites. Therefore, it is interpreted that the rhyolites from Hime-shima volcanic group was derived from crustal material, which compositions is similar to the Ryoke granites.

Keywords: Hime-shima volcanic group, Xenolith, Rhyolite

©2019. Japan Geoscience Union. All Right Reserved. 

# Petrological study on the intrusive contact of a Setouchi volcanic rock dike in the Nakajima Island, Ehime Prefecture

*Taiki Omori[1], Satoshi SAITO[2]

1. Department of Earth Science, Faculty of Science, Ehime University , 2. Department of Earth Science, Graduate Schoole of Science, Ehime University

We performed a detailed petrological study on the intrusive contact between a Setouchi andesitic dike and host Ryoke granitoids occurring in the Nakajima Island, Ehime Prefecture. At the intrusive contact, the andesite contains many fragments of host granitoids. The bulk $SiO_2$ contents of the marginal andesite at the intrusive contact are markedly higher than those of internal domain implying the mixing between the andesite intrusion and the host granitoids. Other bulk chemical compositions such as MgO, CaO, $Na_2O$, $K_2O$, Cr and Zr also imply mixing of the host granitoids into the andesite intrusion at the intrusive contact. However, the $Al_2O_3$ contents of the marginal andesite can not be explained by bulk mixing of the host granitoids and the andesite intrusion because the $Al_2O_3$ contents of the marginal andesite are higher than those of the host granites and internal domain of the andesite intrusion. Assuming that the marginal andesite with chilled margin texture retain original compositions of intrusive magma, we tested the major element mass-balance modeling to explain chemical compositions of internal domain of the andesite intrusion. The modeling reproduced the major element compositions of internal andesites by adding ~7 % of host granite components and ~12 % of mafic phenocryst minerals into the marginal andesite.

Keywords: Setouchi volcanic rocks, Nakajima Island, Ehime Prefecture

©2019. Japan Geoscience Union. All Right Reserved. 

# Fundamental evaluation for making simulated sea bed floc

*AIKO HAYAUCHI[1], Daisuke Sasakura[1], Hisato Yasuda[2], Shinya Nakamura[3], Sho Kimura[3], Shohei Noda[4]

1. Malvern Panalytical division of Spectris Co., Ltd, 2. Kochi University, 3. UNIVERSITY OF THE RYUKYU, 4. TOKYO UNIVESITY OF SCIENCE

1. Introduction
Flock is an aggregate in which fine particles such as clay and silt gathered loosely. It exists in the seabed for example. Research on flocs has been carried out on site and/or real samples, and many are observational approaches. There we tried analysis from a micro viewpoint for making floc simulation samples and reported about relationship between sample particle feature and how ease to be floc last year.
But we didn’ t care flocculant concentration in that report. Flocculant concentration must be important factor to discuss with making a simulated floc. Therefore we focused on influence of flocculant concentration to floc characteristic in this study.

2. Material and method
Kaolin as a model sample and Eb-a(Hayashi Co., Ltd.) as a flocculant for simulated floc preparation were used. Eb-a water solution concentration was 0%, 0.1%, 0.01%, 0.01% and 0.0001%. 0.05% sample water solution was prepared with each Eb-a water solution.
One of famous parameter of solution stability evaluation is zeta potential. Zeta potential was measured with Zetasizer nano ZSP (Malvern Instruments). Particle size distribution (incl. floc size distribution) was measured with Mastersizer 3000 (Malvern Instruments) which is laser diffraction system. Mastersizer 3000 is circulation system. In other hand, Morphologi 4 (Malvern instruments) which is a statistical particle image analysis system was also used for measuring particle size distribution. Morphologi 4 is not circulation system, so we can know original floc size distribution and we can see floc as well because Morphologi 4 is imaging system.

3. Result
Zeta potential in each flocculant concentration is shown in Table 1. In general, the system is stable when the zeta potential absolute value is over 20mV. Zeta potential in Eb-a concentration 0%, 0.001% and 0.0001% were around -60mV. It means that these systems are very stable and it indicates that it is difficult to occur flocculation in these situations. In the other hand, zeta potential absolute value in Eb-a concentration 0.01%, 0.1% and 1% were under 10mV, so that these indicate easy to occur flocculation.
The floc size measured by Mastersizer3000 is shown in Table 2. At The size was measured with 1500rpm/stirring speed at first, then was measured with change to 2500rpm/stirring speed. Comparing each Dv90 on 1500rpm, higher Eb-a concentration showed bigger floc size. In terms of toughness of floc, comparing the ratio of Dv90 on 1500rpm to Dv90 on 2500rpm was 1% Eb-a (0.54), 0.1% Eb-a (65%) and 0.01% Eb-a (75%). This is a result indicating that 0.01% Eb - a was the least fragile among these three samples. Also interestingly, Dv10 on 2500rpm was 0.01% Eb-a (18um), 0.1% Eb-a (9.6um) and 1% Eb-a (5.1um).
The floc size was measured by Morphlogi 4 as well. These data will discuss indetail on that day.

©2019. Japan Geoscience Union. All Right Reserved. 

4. Conclusions

The results show flocculation concentration is one of important factor to make simulated floc. We will continue to study to make clear which factor important to make simulated floc.

Keywords: floc, flocculation, zeta potential, particle size distribution, imaging

| Eb-a(%) | 0 | 0.0001 | 0.001 | 0.01 | 0.1 | 1 |
|---|---|---|---|---|---|---|
| Zeta Potential (mV) | -58.0 | -59.4 | -57.9 | -9.62 | -1.03 | 0.119 |

Table 1: Zeta potential in each flocculant concentration

| Eb-a(%) | stirre speed | Dv10(μm) | Dv50(μm) | Dv90(μm) |
|---|---|---|---|---|
| 1 | 1500rpm | 14.6 | 62.5 | 155 |
| 1 | 2500rpm | 5.06 | 25.0 | 83.3 |
| 0.1 | 1500rpm | 12.4 | 42.4 | 106 |
| 0.1 | 2500rpm | 9.64 | 30.3 | 68.5 |
| 0.01 | 1500rpm | 19 | 45.2 | 87.6 |
| 0.01 | 2500rpm | 17.6 | 36.3 | 65.6 |
| 0 | 1500rpm | 2.69 | 6.11 | 14.9 |

Table 2: Floc size

©2019. Japan Geoscience Union. All Right Reserved. 

# Petrology of the Morobe Granodiorite in the Kuper Range, Morobe Province, Papua New Guinea

Angela Lynett Bokuik[1], *Takashi Hoshide[1]

1. Faculty of International Resource Sciences, Akita University

The Morobe Granodiorite is a composite batholith comprising of monzodiorite, monzonite, quartz monzonite, granite, granodiorite, diorite and gabbro. Mafic Microgranular Enclaves (MME) are abundant in the intrusion. The mineral assemblage of the Morobe Granodiorite comprises of hornblende, biotite, plagioclase, alkali feldspar and quartz with accessory minerals of titanite, apatite, magnetite and ilmenite. The rocks have a variety of texture, such as poikilitic, cumulous and porphyritic. The MME also has a similar mineral assemblage and texture to its host however, it is abundant in mafic minerals hornblende and biotite.

Mineral compositions for amphibole of the granodiorite and MMEs are similar, implying similar magma environment. By the iteration calculation using a geobarometer (Anderson and Smith, 1995) and a geothermometer (Blundy and Holland, 1990), we estimated the crystallization temperature of 597-766˚C and the maximum crystallization pressure of 3.6 kbar. Crystallization conditions from the MME yield higher temperature (812˚C) and pressure (5.3 kbar) to its host, which implies MMEs represent the deeper hotter parts of the same magma chamber of which the MME and host formed.

The geochemical signature of the Morobe Granodiorite represent calc-alkaline and metaluminous nature typical of I-type granites. The variations of major elements in the Harker diagram can be best explained by fractionation mainly of hornblende and plagioclase. The interpretation is consistent with the textural variations of the rocks. Low $FeO^T/(FeO^T + MgO)$ ratios and high Mg-number for granodioritic rocks suggest magma originated from partial melting of the lower mafic crust. This magma was contaminated upon ascent wall rock assimilations of the host rock Owen Stanley Metamorphic. This can be seen as $Na_2O$ vs $SiO_2$ and $K_2O$ vs $SiO_2$ variation diagrams.

Keywords: Morobe Granodiorite, mafic microgranular enclaves, fractional crystallization

©2019. Japan Geoscience Union. All Right Reserved. 

# Sr–Nd isotopic compositions of the San-yo Belt, Southwest Japan: Implications for the Cretaceous enriched mantle

*Shogo Kodama[1], Masaaki Owada[1], Teruyoshi Imaoka[1], Atsushi Kamei[2]

1. Yamaguchi University, 2. Shimane University

Cretaceous to Paleogene igneous rocks are widely exposed in the Inner Zone of Southwest Japan where the granitic rocks have been divided into the San-in, San-yo, and Ryoke Belts on the basis of their lithologies, geochemical compositions, magnetic susceptibility and associated ore deposits (Ishihara, 1971). The San-yo and Ryoke Belts belong to the ilmenite-series granitic rocks, but the San-in Belt corresponds to the magnetite-series ones (Ishihara, 1977). According to Sr isotopic compositions, Kagami et al. (1992) classified these granitic rocks into the North Zone , South Zone, and Transitional Zone situated between the North and South Zones. The granitic rocks from the Transitional and South Zones show negative eNdI values (Kagami et al., 1992); however, the isotopic compositions of granitic rocks would serve only as proof for the bulk of the continental crust (Jahn, 2010). This means that those data are unlikely to provide us with mantle signatures. Imaoka et al. (2014) described the Early Cretaceous lamprophyer (c. 105 Ma) from the Kyoto district. The Kyoto lamprophyres geochemically show enriched signatures with positive and negative eNdI values corrected to 105 Ma. In consideration of the geochemical signatures and tectonic setting, Imaoka et al. (2014) concluded that the Kyoto lamprophyre was derived from heterogenous enriched mantle created by the subduction of the oceanic crust. Aspects of the existence of enriched mantle, however, are still unclear, such as in regard to its regional extension and duration for the Cretaceous magma activities of the Inner Zone of Southwest Japan.

Late Cretaceous igneous rocks are widely exposed in the western part of Honshu Island. These igneous rocks consist mainly of granitic rocks and felsic to intermediate volcanic rocks. We newly found a small gabbro stock (c. 1 km in diameter) with relatively primitive compositions in the central part of Yamaguchi Prefecture. The gabbro stock accompanies the Susuma-Nagaho granodiorite as coeval intrusive rocks. Therefore, we refer to both granodiorite and gabbro as the Susuma-Nagaho Plutonic Complex (SNPC, hereafter). The gabbro can be subdivided into fine-grained gabbro (Fn-gabbro) and coarse-grained cumulus gabbro (Co-gabbro). The Fn-gabbro has a high Mg-number similar to primitive basalt with negative eNd values corrected to 92 Ma although Cr and Ni contents are relatively low, which indicates that the basaltic magma may have been derived from enriched mantle. In consideration of the geochemical signatures including the Sr and Nd isotopic compositions, the enriched mantle characterized by negative eNd isotopic values would have existed underneath the Inner Zone of Southwest Japan during the Cretaceous.

Keywords: Late Cretaceous, San-yo Belt, Gabbro, Enriched mantole

©2019. Japan Geoscience Union. All Right Reserved. 

# Lithological variation of massive serpentinites in marginal zone of serpentinite body in Kamuikotan belt, Hokkaido, Japan: Analysis of advanced-boring cores for tunnel construction

*Shusaku Yamazaki[1], Kenji Okazaki[1], Toshiyuki Kurahashi[1]

1. Civil Engineering Research Institute for Cold Region, Public Works Research Institute, National Research and Development Agancy

Serpentinite body associated with high-pressure metamorphic rocks such as Kamuikotan belt in Hokkaido is very important as a key to understand a deep subduction process in subduction zone. In the field of marine geology, recent advances of sampling and analytical techniques contribute to understand of serpentinization process of abyssal peridotites. On the other hand, terrestrial serpentinite body still remain a lot of unexplained processes such as variation of serpentinization, uplifting mechanism and formation of internal structure, because of poor sampling by its fragile and fragmented rock conditions on earth surface conditions. There are over 30 tunnel construction cases drilling into a serpentinite body in Japan. Geoengineering investigation including description of tunnel drilling face, measurement of physical properties and making cross section of the tunnel route were operated in each tunnel. However, a detailed geological information such as types of source rock and degree and aspect of serpentinization has been less understood from the construction records. In addition, even in recent yeses with developed drilling technology, excavation of serpentinites often encounters serious trouble such as tunnel collapse. It indicates that more detailed classification of serpentinites for tunnel construction is necessary using recent geological insights and technique.

The authors focus on reconstruction of the tunnel geological section and the detailed classification of serpentinites of a tunnel with 1241 m into Takadomari serpentinite body of Horokanai area in Kamuikotan belt in Hokkaido, Japan. In this study, massive serpentinites, which were sampled from advanced-boring core at 50 to 100 m intervals along tunnel route, were conduct to description of core and thin section and XRD analysis to investigate lithological variation around the marginal zone of the serpentinite body contact with Kamuikotan metamorphic rocks.

The research by Igarashi et al. (1985) revealed that serpentinites of the Takadomari body were classified into massive, foliated and clay serpentinites and their source rocks were mostly harzburgite and partly dunite as band in harzburgite. There are large number of “micordiorite” and micro gabbro dikes in the body. As a result of this study, advanced-boring cores from the tunnel also have same variation of massive, foliated and clay serpentinites. The source rock types of massive serpentinites from the marginal zone are also mainly harzburgite with minor band of dunite. All samples were completely serpentinized and only Cr-spinel is survived as primary mineral. Original texture of the massive serpentinite is classified into dunitic texture without pyroxenes, harzburgitic texture with orthopyroxene, cumulate texture with euhedral orthopyroxene and foliation of spinel allay. Serpentine types in the massive serpentinites are antigorite that replaced olivine and orthopyroxene and lately formed asbestos chrysotile vein. Minor amount of brucite also appears through the tunnel. As a notable feature in the marginal zone of the body, three zones of difference serpentinization were observed. In the center of the tunnel, the serpentinites well remain the original harzburgitic and dunitic texture. In the west side with amphibolites, the massive serpentinites contain magnesite veins and patches as metasomatism. In the east side with the contact to greenschists, the original texture is completely disappeared with greenish large antigorite and massive of

©2019. Japan Geoscience Union. All Right Reserved. 

grains of magnetite with brucite. The difference of texture and mineralogy of the serpentinites in this tunnel could possibly be explained that the serpentinization process in subduction zone is difference in the both sides of marginal zone in the association with the types of the Kamuikotan metamorphic rocks.

Keywords: Serpentinite, Kamuikotan belt, Boring core

©2019. Japan Geoscience Union. All Right Reserved. 

[J] Oral | S (Solid Earth Sciences)：S-CG Complex & General

Thu. May 30, 2019 10:45 AM - 12:15 PM JST | Thu. May 30, 2019 1:45 AM - 3:15 AM UTC | A05 TOKYO BAY MAKUHARI HALL

## [S-CG53] Environment formed and maintained by active faults

convener:Naoji Koizumi(School of Environmental Science,the University of Shiga Prefecture), Makoto Yamano(Earthquake Research Institute, the University of Tokyo), Takafumi Kasaya(Japan Agency for Marine-Earth Science and Technology), Hideki Hamamoto(Center for Environmental Science in Saitama), Chairperson:NAOJI KOIZUMI, TADANORI GOTO(Graduate School of Engineering, Kyoto University)

An active fault causes a large earthquake at a very low frequency such as once every several thousand to tens of thousands years and destroys the surrounding environment. On the other hand, during the period when the large earthquake or the fault movement does not occur, the unique environments such as mountains, basins, structural lakes, hot springs and mineral deposits are formed and maintained by the topography and hydrogeological structure made by the accumulation of the fault movement. In general, the presence of active faults is recognized as a factor of environmental destruction, but it is also necessary to understand the active faults as a factor of environmental formation and maintenance. In this session, we welcome wide-ranging topics on the role of active faults as a factor for the formation and maintenance of the environment and how to investigate it.

10:45 AM - 11:00 AM JST | 1:45 AM - 2:00 AM UTC

### [SCG53-01] Effect of the Hanaore fault and Biwako-seigan fault on the water quality of the Ado river in Shiga Prefecture

*Naoji Koizumi[1], Masahiro Ueda[1], Shinsuke Minote[1], Tatsuya Tanaka[1], Masahiro Maruo[1], Kanto Mitani[2] (1.School of Environmental Science,the University of Shiga Prefecture, 2.Daikokuten Bussan Co., Ltd.)

11:00 AM - 11:15 AM JST | 2:00 AM - 2:15 AM UTC

### [SCG53-02] Hydrothermal vents in the deep basin of Lake Biwa

★Invited Papers

*Michio Kumagai[1] (1.Ritsumeikan University)

11:15 AM - 11:30 AM JST | 2:15 AM - 2:30 AM UTC

### [SCG53-03] Heat flow anomalies observed on the seafloor in the vicinity of faults: indication of fluid flow

*Makoto Yamano[1], Shusaku Goto[2], Yoshifumi Kawada[3], Hideki Hamamoto[4] (1.Earthq. Res. Inst., Univ. Tokyo, 2.Geol. Surv. Japan, AIST, 3.IRIDeS, Tohoku Univ., 4.Center Environ. Sci. Saitama)

11:30 AM - 11:45 AM JST | 2:30 AM - 2:45 AM UTC

### [SCG53-04] How can we quantify the hydraulic permeability of fault based on geophysical survey?

*Tada-nori Goto[1], Sota Kawaguchi[1] (1.Graduate School of Engineering, Kyoto University)

11:45 AM - 12:00 PM JST | 2:45 AM - 3:00 AM UTC

### [SCG53-05] Healing process of the Nojima Fault zone after 1995 Hyogo-ken Nanbu earthquake

*Hideki Murakami[1], Naoto Oshiman[2], Ryokei Yoshimura[2], Tsutomu Miura[2], Masato Kamo[2] (1.Research and Education Faculty,Kochi University, 2.Disaster Prevention Research Institute,Kyoto University)

12:00 PM - 12:15 PM JST | 3:00 AM - 3:15 AM UTC

### [SCG53-06] Discussion on the environment formed and maintained by active faults

*Naoji Koizumi[1] (1.School of Environmental Science,the University of Shiga Prefecture)

# Effect of the Hanaore fault and Biwako-seigan fault on the water quality of the Ado river in Shiga Prefecture

*Naoji Koizumi[1], Masahiro Ueda[1], Shinsuke Minote[1], Tatsuya Tanaka[1], Masahiro Maruo[1], Kanto Mitani[2]

1. School of Environmental Science,the University of Shiga Prefecture, 2. Daikokuten Bussan Co., Ltd.

1.Introduction
Along a fault plain, there is a fractured damage zone, which has high permeability. This zone is often become groundwater path from deep to shallow (Faulkner et al., 2010). As a result, the fault-related groundwater stably supplies heat and chemical materials including water itself, which make some effect on the environment in and around the fault zone. For example, hot and mineral springs tends to distribute in and around fault zones. This fault-related groundwater should also have some effect on the river in the case that the river runs along or across the fault.

The Ado river, which is located in the western part of Shiga Prefecture, is the second longest in the rivers which flow into Lake Biwa, which is the largest lake in Japan. The catchment area of the Ado river is also the largest in the rivers which flow into Lake Biwa. In the part of the upstream and most of the midstream, the Ado river runs along the Hanaore fault. In the downstream the Ado river cross the Biwako-seigan fault (Fig.1). Both of the faults are the main active faults in the western part of the Shiga Prefecture. Therefore the Ado river is suitable for investigating the effect of active faults on the river water quality.

2.Observation
We surveyed the Ado river during the period from August 12 to August 14 in 2018 (Fig.1) , which is named the spatial survey. Before this period there had been no precipitation for thirteen days at IMZ and MNM. Therefore it is considered that the river water was mainly composed of the base flow, which supplies from groundwater to river. We also surveyed the Ado river at RYD, HRS, ADG and KTG about once a month from April, 2018, which is named the temporal survey.

3.Result
In the spatial survey the water quality type was Ca-HCO3 at all the sampling points. The ion concentrations were gradually increased from AD7 to TKI although there were no systematic change in the ion concentrations at the other sampling points. Between HRS and ADG, where the Ado river crosses the Biwako-seigan fault, there was no change in the ion concentrations. In the temporal survey, there was also no no change in the ion concentrations between HRS and ADG. This shows that the Hanaore fault has some effect on the water quality of the Ado river although the Biwako-seigan fault has little effect on it.

Fig.1 The solid circles show the sampling points of the Ado river during the period from August 12 to August 14 in 2018. The solid triangles denote meteorological observation points of Japan Meteorologidal Agency. This is modified from the figure of the active fault database of Japan (Geological Survey of Japan, AIST, 2019). The background map is from Geographycal Information Authority of Japan (2019).

Keywords: Ado river, Active fault, Water quality, Permeability

©2019. Japan Geoscience Union. All Right Reserved. 

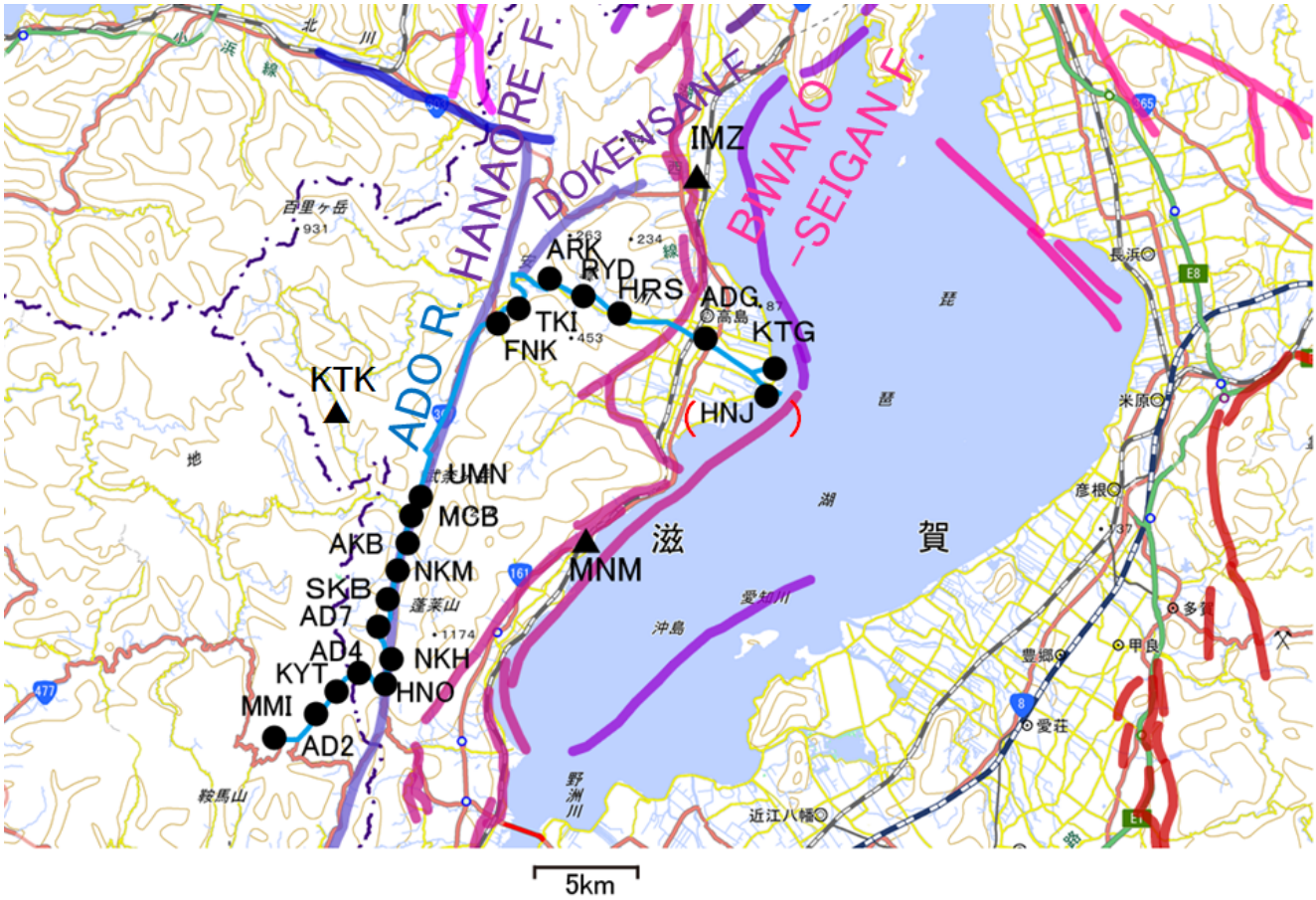


©2019. Japan Geoscience Union. All Right Reserved. 

# Hydrothermal vents in the deep basin of Lake Biwa

*Michio Kumagai[1]

1. Ritsumeikan University

The autonomous underwater vehicle (AUV) “Tantan” was constructed and first deployed in the year 2000, as the world’s first AUV conceived for lake ecosystem exploration and monitoring. Tantan (meaning “freshwater surveillance” in Japanese) was designed to move along bottom slopes keeping a constant distance above the sediments, with a payload that includes two high-definition video cameras, a digital camera, a submersible microscope and various sensors. In December 2009, Tantan identified turbid water ebullition on the deep area in the North Basin of Lake Biwa, which is a larger basin with maximum depth 104 m and 99% water volume, and follow-up investigations were conducted in April, December 2010 and January 2012. This study confirmed the existence of hydrothermal vents, and provided the evidence that their vent numbers per unit area on the lake bottom have increased from 1.0 $km^{-2}$ vent in 2009 to 54.0 vents $km^{-2}$ in 2012. We also found that those discovered vents located along the ridge of sunken mountains which form the basement of Lake Biwa with covered sediments. Some back-up investigations have been performed with a remotely operated vehicle (ROV) and several kinds of sonar devices, and all of the outputs support the existence of vents found by Tantan.

Keywords: vent, Lake Biwa, AUV

©2019. Japan Geoscience Union. All Right Reserved. 

# Heat flow anomalies observed on the seafloor in the vicinity of faults: indication of fluid flow

*Makoto Yamano[1], Shusaku Goto[2], Yoshifumi Kawada[3], Hideki Hamamoto[4]

1. Earthq. Res. Inst., Univ. Tokyo, 2. Geol. Surv. Japan, AIST, 3. IRIDeS, Tohoku Univ., 4. Center Environ. Sci. Saitama

Active fluid flow along faults may yield temperature or surface heat flow anomalies because advective heat transport by fluid flow is much more efficient than conductive transport. On land, it is rather difficult to observe such anomalies as temperature profile measurement in deep boreholes is required. On the other hand, we can conduct dense heat flow measurements on seafloor if surface sediment is soft enough to allow penetration of temperature probes. Heat flow and/or temperature anomalies in the vicinity of faults have been reported in some accretionary prisms, e.g., Cascadia and Barbados subduction zones. In this presentation, we show examples of heat flow anomalies associated with faults on the seafloor in the Nankai Trough area.

Accretionary prism developed landward of the Nankai Trough is extensively faulted in a compressional stress field due to subduction of the Philippine Sea plate. At the toe of the prism off Muroto, eastern Shikoku, closely-spaced heat flow measurements were made with a ROV and conspicuous high anomalies were found around the second frontal thrust, indicating that pore fluid flows upward along the fault (Kawada et al., 2014). Off the Kii peninsula, a large thrust fault system termed the megasplay cuts through the entire prism and its branches reach the seafloor. Yamano et al. (2014) conducted heat flow measurements with a surface ship across a branch of the megasplay and observed high heat flow values on the lower part of a fault scarp. Goto et al. (2008) made measurements with a submersible around biological communities along another branch of the megasplay and showed a sharp heat flow variation in a scale of several meters. These observations demonstrate that fluid flow along faults in various spatial scales can be detected by surface heat flow measurements.

The velocity or flux of vertical fluid flow may be estimated through long-term monitoring of temperature distribution in surface sediment. Temporal variation of the bottom water temperature propagates downward through sediment by thermal diffusion. Since this propagation process is affected by vertical fluid flow, analysis of long-term record of temperatures at multiple depths allows us to estimate fluid flow velocity (Goto et al., 2005). This method was applied to temperature records obtained in and around a biological community located a tip of the megasplay branch fault and the result indicates the existence of upward fluid flow (Kawada et al., 2013).

Keywords: heat flow anomaly, fluid flow, fault, heat transport, long-term monitoring

©2019. Japan Geoscience Union. All Right Reserved. 

# How can we quantify the hydraulic permeability of fault based on geophysical survey?

*Tada-nori Goto[1], Sota Kawaguchi[1]

1. Graduate School of Engineering, Kyoto University

For understanding impacts of faults/fractures to the Earth's environment, evaluation of hydraulic permeability along fault and fractures are required because they hydrogeologically play a role of pathway of deep groundwater and gas. Previous studies have obtained the hydraulic characteristics using boreholes and rock samples. However, such information is only valid in a local scale, and it is basically considered to be difficult to estimate the hydraulic permeability at several-hundred meter scales or more. In this study, we try to estimate the permeability in and around fractures in typical bedrocks (e.g., granitic rocks) based on the geophysical explorations: resistivity, seismic velocity and so on. The geophysical logging experiment (e.g., cross-hole tomography) can indicate both local and larger scale geophysical information. More large-scaled information can be obtained by land-surface geophysical surveys. For evaluation of permeability of large-scale fault, a rock physical modeling will be helpful since it can connect geophysical property to the hydraulic property theoretically or numerically.
Prior to the challenge of large-scale permeability estimation, we applied the rock physical modeling to the small-scale geophysical measurements. We measured DC resistivity and elastic properties (Young modulus) on the exposed fresh granite at the Mizunami Underground Research Laboratory, Japan Atomic Energy Agency. Based on the simple rock physical model, we estimated the permeability of granite with less fracturing. The in-situ permeability measurements confirmed that the estimated values are enough close to the measured ones (within the difference of half of order). The technique is also valid to the permeability measurements by pumping test at wells. We succeeded that the observed permeability obtained at Mizunami can be reproduced by only using geophysical logging data such as resistivity and seismic P-wave velocity.
Then, we applied this rock physical model to the large-scale geophysical images based on the magnetotellurics and seismic tomography. Although it is a preliminary result, the estimated permeability structure by our method is not realistic one unfortunately. In this study, we discuss on the additional information and technique how the accuracy of estimated permeability is improved.

Keywords: Permeability, Rock Physics, Resistivity

©2019. Japan Geoscience Union. All Right Reserved. 

# Healing process of the Nojima Fault zone after 1995 Hyogo-ken Nanbu earthquake

*Hideki Murakami[1], Naoto Oshiman[2], Ryokei Yoshimura[2], Tsutomu Miura[2], Masato Kamo[2]

1. Research and Education Faculty,Kochi University, 2. Disaster Prevention Research Institute,Kyoto University

Two faults of the Nojima Fault and the Higashiura Fault exist in the northeastern part of Awaji Island. Repeated activities of these faults have formed the topography of Awaji Island. In this study, we report the result of the Nojima water injection experiment of 2018 and the healing process of the Nojima Fault zone estimated from self-potential variations associated with water injection experiments. The water injection experiments were conducted 8 times between 1997 and 2018 in an 1800 m long borehole near the Nojima Fault, which is the surface earthquake fault of 1995 Hyogo-ken Nanbu earthquake, to investigate the recovery process of the fault zone after the large earthquake. We have estimated the time evolution of hydraulic parameters from self-potential variations associated with water injection. It is expected that hydraulic parameters will decrease as the healing process of the fault zone progresses. Though the Nojima Fault has repeatedly moved at a recurrence interval of ca. 2,000 years during the Late Quaternary, it is estimated from the experiment results that the healing process of the fault zone is progressing in several years after the earthquake shorter than the recurrence interval.

Keywords: Nojima Fault, healing process of a fault, water injection experiment, self-potential

©2019. Japan Geoscience Union. All Right Reserved. 

# Discussion on the environment formed and maintained by active faults

*Naoji Koizumi[1]

1. School of Environmental Science,the University of Shiga Prefecture

In this presentation we will comprehensively discuss on the environment formed and maintained by active faults.

Keywords: Active fault, Environment

©2019. Japan Geoscience Union. All Right Reserved. 

[J] Poster | S (Solid Earth Sciences )：S-CG Complex & General

Thu. May 30, 2019 3:30 PM - 5:00 PM JST | Thu. May 30, 2019 6:30 AM - 8:00 AM UTC | Poster Hall International Exhibition Hall8, Makuhari Messe_16

## [S-CG53] Environment formed and maintained by active faults

convener:Naoji Koizumi(School of Environmental Science,the University of Shiga Prefecture), Makoto Yamano(Earthquake Research Institute, the University of Tokyo), Takafumi Kasaya(Japan Agency for Marine-Earth Science and Technology), Hideki Hamamoto(Center for Environmental Science in Saitama)

An active fault causes a large earthquake at a very low frequency such as once every several thousand to tens of thousands years and destroys the surrounding environment. On the other hand, during the period when the large earthquake or the fault movement does not occur, the unique environments such as mountains, basins, structural lakes, hot springs and mineral deposits are formed and maintained by the topography and hydrogeological structure made by the accumulation of the fault movement. In general, the presence of active faults is recognized as a factor of environmental destruction, but it is also necessary to understand the active faults as a factor of environmental formation and maintenance. In this session, we welcome wide-ranging topics on the role of active faults as a factor for the formation and maintenance of the environment and how to investigate it.

### [SCG53-P01] Heat flow measurement in Lake Biwa

*Hideki Hamamoto[1], Makoto Yamano[2] (1.Center for Environmental Science in Saitama, 2.Earthquake Research Institute, University of Tokyo)

---

### [SCG53-P02] Shallow Resistivity Structure across the Futagawa-Fault Nishihara Area and the Reliability

*Tada-nori Goto[1], Hisatoshi Koji[1], Sota Kawaguchi[1], Satoru Yamaguchi[2], Yuto Yamalaka[2], Daigo Furukawa[2], Koki Aizawa[3] (1.Graduate School of Engineering, Kyoto University, 2.Graduate School of Science, Osaka City University, 3.Institute of Seismology and Volcanology, Faculty of Sciences, Kyushu University)

---

### [SCG53-P03] Detailed topography and sub-surface structure around the 2016 Fukushima Earthquake

*Takafumi Kasaya[1], Toshiya Fujiwara[1], Toshiya Kanamatsu[1], Katsunori FUJIKURA[1] (1.Japan Agency for Marine-Earth Science and Technology)

# Heat flow measurement in Lake Biwa

*Hideki Hamamoto[1], Makoto Yamano[2]

1. Center for Environmental Science in Saitama, 2. Earthquake Research Institute, University of Tokyo

Active venting of water and gas has been observed in the vicinity of a fault on the bottom of Lake Biwa. Heat flow measurement is a useful tool for investigation of such fluid flow. Previous studies reported heat flow values at two stations in Lake Biwa: one is 50 $mW/m^2$ in a borehole on the bottom of the lake and the other is 44 $mW/m^2$ in a borehole located at the lakeshore. Taking account of values measured in the surrounding area, heat flow in the Lake Biwa area not disturbed by fluid flow is estimated to be about 50 $mW/m^2$.

We conducted heat flow measurement at five stations in a deep basin in the northwestern part of Lake Biwa in 2010 using a research vessel “Hakken-gou”, which was operated by Lake Biwa Environmental Research Institute at that time. We used a conventional heat flow probe for measurement on deep seafloor. The length of probe is 1.5 or 3.0 m and seven temperature sensors are mounted along the probe. The maximum water depth of Lake Biwa is about 100 m, and bottom water temperature (BWT) variation with a large amplitude has been observed. Subsurface temperature within a few meters of the lake bottom must be affected by BWT variation. The temperature profiles we measured with the heat flow probe were apparently disturbed by BWT variations. At one station in close vicinity to fluid vents, we obtained an extremely large temperature gradient (approximately 300 mK/m). It means that heat flow at this station is anomalously high, whatever disturbance by BWT variation the temperature profile suffered. The observed high heat flow is attributable to upward fluid flow through sediment, since advective heat transport by fluid flow is very efficient.

However, we cannot measure heat flow precisely with conventional heat flow probes in shallow water areas with significant BWT variations. For obtaining reliable heat flow values, we should conduct long-term temperature monitoring and analyze the data considering influence of BWT variations. Analysis of long-term temperature data may also provide information on fluid flow velocity. We need to conduct reliable and high-density heat flow measurements for investigation of fluid flow related to faults on the bottom of Lake Biwa.

Keywords: Heat flow, Lake Biwa, Bottom water temperature variation

©2019. Japan Geoscience Union. All Right Reserved. 

# Shallow Resistivity Structure across the Futagawa-Fault Nishihara Area and the Reliability

*Tada-nori Goto[1], Hisatoshi Koji[1], Sota Kawaguchi[1], Satoru Yamaguchi[2], Yuto Yamalaka[2], Daigo Furukawa[2], Koki Aizawa[3]

1. Graduate School of Engineering, Kyoto University, 2. Graduate School of Science, Osaka City University, 3. Institute of Seismology and Volcanology, Faculty of Sciences, Kyushu University

At the 2016 Kumamoto earthquake, Japan, many surface ruptures occurred. They are distributed along the Futagwa fault already known as an active fault. In the Nishihara area, Kumamoto prefecture, the Futagwa fault consists of two parallel sub-faults with E-W strike, and large displacements were observed along the southern one. The analysis of InSAR data, a large deformation zone is presumed in the area between the two sub-faults (Fujiwara et al., 2016). InSAR results also showed a linear surface rupture located south of the Futagwa fault, which is not equivalent to the known active faults. Thus, the distribution of ground displacement/rupture at the 2016 Kumamoto earthquake is complicated, and the reason should be due to the complexity of the geological structure along the active fault. However, the shallow structure around the Futagwa fault has not been estimated in this area.

In this study, electromagnetic survey (AMT exploration) was carried out in the Nishihara area for exploration of the shallow resistivity structure. The equipment used is MTU-5A by Phoenix Geophysics. The total number of AMT sites is 14, arranged on a N-S survey profile across the Futagwa fault. High-quality AMT responses were obtained at 11 site, and a inversion scheme by Uchida and Ogawa (1993) for estimation of two-dimensional resistivity model was applied. In the correction of static shift, we focused on the spatial smoothness of Zssq phase, and applied the spatial filtering to observed apparent resistivity.

The obtained resistivity structure indicated two buried low-resistive zones along the two sub-faults, with depth from 0m to 500m or more. One of the low resistive zone along the northern one of sub-faults has a north dip with about 60 degrees, consistent with the previous geological survey. On the other hand, another low resistivity zone along the south sub-faults has a larger width (about 400 m) than the northern one, and has a south dip. The reliability of the low resistive zones was evaluated based on the principal component analysis method and the Markov chain Monte Carlo method (Koji and Goto, 2019). As a result, the sensitivity of southern low-resistive zone is high enough. The two parallel low-resistive zones, one of which has a south dip, were not reported in the previous geophysical and geological studies. However, such features are consistent with the InSAR results. As a conclusion, geophysical explorations for evaluating of shallow structure at active faults are effective to understand and predict the ground displacement and shaking at earthquakes.

Keywords: Kumamoto Earthquake, Futagawa Fault, Resistivity

©2019. Japan Geoscience Union. All Right Reserved. 

# Detailed topography and sub-surface structure around the 2016 Fukushima Earthquake

*Takafumi Kasaya[1], Toshiya Fujiwara[1], Toshiya Kanamatsu[1], Katsunori FUJIKURA[1]

1. Japan Agency for Marine-Earth Science and Technology

The large earthquake of M7.4 was occurred off Fukushima Prefecture on 22 Nov. 2017. This earthquake was not a interpolate earthquake, but normal fault type earthquake occurred in the land-side plate. However, a tsunami with a maximum wave height of 1.4 m was observed around the coastal area of Tohoku distinct. When this earthquake occurred, R/V Shinseimaru and R//V Yokosuka were under the scientific survey mission of other purpose near the focal region of this earthquake. JAMSTEC decided to carry out the immediate survey using both vessels. As the results, some small cliffs were detected. In order to obtain the further information of the succession of cliffs and sea floor condition, including the distribution of benthos, we carried out the visual observation using ROV Hyper-Dolphin (HPD) and detailed survey using the multi narrow echo-sounder and sub-bottom profiler at the KS-17-J04 cruise conducted by the project “Tohoku Ecosystem-Associated Marine Sciences”. We carried out two dives and could detect the flesh topographical cliff of about 1-2 m height difference around the cliff detected by the immediate observation. The uppermost layer under the seafloor is a soft mud layer containing concentrated layer of shells. The lower layer is formed of consolidated sedimentary layer. In near the cliff and the bottom of fissure, some white discoloration zones considered as bacteria mats were observed. At the northernmost fissure where we could arrive, the populations of benthos were observed. Furthermore, we conducted the detailed dense bathymetric survey, sub-surface structure, and the observation using a sidescan sonar with 400 kHz. As these results, we could obtain the distribution of the lineaments and faults around the focal area.

Keywords: 2016 Off Fukushima earthquake, Detailed topography, Fault, Bacteria mat

©2019. Japan Geoscience Union. All Right Reserved. 

[J] Poster | S (Solid Earth Sciences)：S-CG Complex & General

Thu. May 30, 2019 5:15 PM - 6:30 PM JST | Thu. May 30, 2019 8:15 AM - 9:30 AM UTC | Poster Hall International Exhibition Hall8, Makuhari Messe_29

## [S-CG53] Environment formed and maintained by active faults

convener:Naoji Koizumi(School of Environmental Science,the University of Shiga Prefecture), Makoto Yamano(Earthquake Research Institute, the University of Tokyo), Takafumi Kasaya(Japan Agency for Marine-Earth Science and Technology), Hideki Hamamoto(Center for Environmental Science in Saitama)

An active fault causes a large earthquake at a very low frequency such as once every several thousand to tens of thousands years and destroys the surrounding environment. On the other hand, during the period when the large earthquake or the fault movement does not occur, the unique environments such as mountains, basins, structural lakes, hot springs and mineral deposits are formed and maintained by the topography and hydrogeological structure made by the accumulation of the fault movement. In general, the presence of active faults is recognized as a factor of environmental destruction, but it is also necessary to understand the active faults as a factor of environmental formation and maintenance. In this session, we welcome wide-ranging topics on the role of active faults as a factor for the formation and maintenance of the environment and how to investigate it.

### [SCG53-P01] Heat flow measurement in Lake Biwa

*Hideki Hamamoto[1], Makoto Yamano[2] (1.Center for Environmental Science in Saitama, 2.Earthquake Research Institute, University of Tokyo)

### [SCG53-P02] Shallow Resistivity Structure across the Futagawa-Fault Nishihara Area and the Reliability

*Tada-nori Goto[1], Hisatoshi Koji[1], Sota Kawaguchi[1], Satoru Yamaguchi[2], Yuto Yamalaka[2], Daigo Furukawa[2], Koki Aizawa[3] (1.Graduate School of Engineering, Kyoto University, 2.Graduate School of Science, Osaka City University, 3.Institute of Seismology and Volcanology, Faculty of Sciences, Kyushu University)

### [SCG53-P03] Detailed topography and sub-surface structure around the 2016 Fukushima Earthquake

*Takafumi Kasaya[1], Toshiya Fujiwara[1], Toshiya Kanamatsu[1], Katsunori FUJIKURA[1] (1.Japan Agency for Marine-Earth Science and Technology)

# Heat flow measurement in Lake Biwa

*Hideki Hamamoto[1], Makoto Yamano[2]

1. Center for Environmental Science in Saitama, 2. Earthquake Research Institute, University of Tokyo

Active venting of water and gas has been observed in the vicinity of a fault on the bottom of Lake Biwa. Heat flow measurement is a useful tool for investigation of such fluid flow. Previous studies reported heat flow values at two stations in Lake Biwa: one is 50 $mW/m^2$ in a borehole on the bottom of the lake and the other is 44 $mW/m^2$ in a borehole located at the lakeshore. Taking account of values measured in the surrounding area, heat flow in the Lake Biwa area not disturbed by fluid flow is estimated to be about 50 $mW/m^2$.

We conducted heat flow measurement at five stations in a deep basin in the northwestern part of Lake Biwa in 2010 using a research vessel “Hakken-gou”, which was operated by Lake Biwa Environmental Research Institute at that time. We used a conventional heat flow probe for measurement on deep seafloor. The length of probe is 1.5 or 3.0 m and seven temperature sensors are mounted along the probe. The maximum water depth of Lake Biwa is about 100 m, and bottom water temperature (BWT) variation with a large amplitude has been observed. Subsurface temperature within a few meters of the lake bottom must be affected by BWT variation. The temperature profiles we measured with the heat flow probe were apparently disturbed by BWT variations. At one station in close vicinity to fluid vents, we obtained an extremely large temperature gradient (approximately 300 mK/m). It means that heat flow at this station is anomalously high, whatever disturbance by BWT variation the temperature profile suffered. The observed high heat flow is attributable to upward fluid flow through sediment, since advective heat transport by fluid flow is very efficient.

However, we cannot measure heat flow precisely with conventional heat flow probes in shallow water areas with significant BWT variations. For obtaining reliable heat flow values, we should conduct long-term temperature monitoring and analyze the data considering influence of BWT variations. Analysis of long-term temperature data may also provide information on fluid flow velocity. We need to conduct reliable and high-density heat flow measurements for investigation of fluid flow related to faults on the bottom of Lake Biwa.

Keywords: Heat flow, Lake Biwa, Bottom water temperature variation

©2019. Japan Geoscience Union. All Right Reserved. 

# Shallow Resistivity Structure across the Futagawa-Fault Nishihara Area and the Reliability

*Tada-nori Goto[1], Hisatoshi Koji[1], Sota Kawaguchi[1], Satoru Yamaguchi[2], Yuto Yamalaka[2], Daigo Furukawa[2], Koki Aizawa[3]

1. Graduate School of Engineering, Kyoto University, 2. Graduate School of Science, Osaka City University, 3. Institute of Seismology and Volcanology, Faculty of Sciences, Kyushu University

At the 2016 Kumamoto earthquake, Japan, many surface ruptures occurred. They are distributed along the Futagwa fault already known as an active fault. In the Nishihara area, Kumamoto prefecture, the Futagwa fault consists of two parallel sub-faults with E-W strike, and large displacements were observed along the southern one. The analysis of InSAR data, a large deformation zone is presumed in the area between the two sub-faults (Fujiwara et al., 2016). InSAR results also showed a linear surface rupture located south of the Futagwa fault, which is not equivalent to the known active faults. Thus, the distribution of ground displacement/rupture at the 2016 Kumamoto earthquake is complicated, and the reason should be due to the complexity of the geological structure along the active fault. However, the shallow structure around the Futagwa fault has not been estimated in this area.

In this study, electromagnetic survey (AMT exploration) was carried out in the Nishihara area for exploration of the shallow resistivity structure. The equipment used is MTU-5A by Phoenix Geophysics. The total number of AMT sites is 14, arranged on a N-S survey profile across the Futagwa fault. High-quality AMT responses were obtained at 11 site, and a inversion scheme by Uchida and Ogawa (1993) for estimation of two-dimensional resistivity model was applied. In the correction of static shift, we focused on the spatial smoothness of Zssq phase, and applied the spatial filtering to observed apparent resistivity.

The obtained resistivity structure indicated two buried low-resistive zones along the two sub-faults, with depth from 0m to 500m or more. One of the low resistive zone along the northern one of sub-faults has a north dip with about 60 degrees, consistent with the previous geological survey. On the other hand, another low resistivity zone along the south sub-faults has a larger width (about 400 m) than the northern one, and has a south dip. The reliability of the low resistive zones was evaluated based on the principal component analysis method and the Markov chain Monte Carlo method (Koji and Goto, 2019). As a result, the sensitivity of southern low-resistive zone is high enough. The two parallel low-resistive zones, one of which has a south dip, were not reported in the previous geophysical and geological studies. However, such features are consistent with the InSAR results. As a conclusion, geophysical explorations for evaluating of shallow structure at active faults are effective to understand and predict the ground displacement and shaking at earthquakes.

Keywords: Kumamoto Earthquake, Futagawa Fault, Resistivity

©2019. Japan Geoscience Union. All Right Reserved. 

# Detailed topography and sub-surface structure around the 2016 Fukushima Earthquake

*Takafumi Kasaya[1], Toshiya Fujiwara[1], Toshiya Kanamatsu[1], Katsunori FUJIKURA[1]

1. Japan Agency for Marine-Earth Science and Technology

The large earthquake of M7.4 was occurred off Fukushima Prefecture on 22 Nov. 2017. This earthquake was not a interpolate earthquake, but normal fault type earthquake occurred in the land-side plate. However, a tsunami with a maximum wave height of 1.4 m was observed around the coastal area of Tohoku distinct. When this earthquake occurred, R/V Shinseimaru and R//V Yokosuka were under the scientific survey mission of other purpose near the focal region of this earthquake. JAMSTEC decided to carry out the immediate survey using both vessels. As the results, some small cliffs were detected. In order to obtain the further information of the succession of cliffs and sea floor condition, including the distribution of benthos, we carried out the visual observation using ROV Hyper-Dolphin (HPD) and detailed survey using the multi narrow echo-sounder and sub-bottom profiler at the KS-17-J04 cruise conducted by the project “Tohoku Ecosystem-Associated Marine Sciences”. We carried out two dives and could detect the flesh topographical cliff of about 1-2 m height difference around the cliff detected by the immediate observation. The uppermost layer under the seafloor is a soft mud layer containing concentrated layer of shells. The lower layer is formed of consolidated sedimentary layer. In near the cliff and the bottom of fissure, some white discoloration zones considered as bacteria mats were observed. At the northernmost fissure where we could arrive, the populations of benthos were observed. Furthermore, we conducted the detailed dense bathymetric survey, sub-surface structure, and the observation using a sidescan sonar with 400 kHz. As these results, we could obtain the distribution of the lineaments and faults around the focal area.

Keywords: 2016 Off Fukushima earthquake, Detailed topography, Fault, Bacteria mat

©2019. Japan Geoscience Union. All Right Reserved. 

[J] Oral | S (Solid Earth Sciences )：S-CG Complex & General

Thu. May 30, 2019 9:00 AM - 10:30 AM JST | Thu. May 30, 2019 12:00 AM - 1:30 AM UTC | A11 TOKYO BAY MAKUHARI HALL

## [S-CG55] Crustal fluids and deformation

convener:Yuichi Kitagawa(Tectono-Hydrology Research Group, Geological Survey of Japan, National Institute of Advanced Industrial Science and Technology), Naoji Koizumi(School of Environmental Science,the University of Shiga Prefecture), Koji Umeda(Hirosaki University), Fumiaki Tsunomori(Geochemical Research Center, Graduate School of Science, University of Tokyo), Chairperson:Yuichi Kitagawa(産業技術総合研究所地質調査総合センター地震地下水研究グループ), Fumiaki Tsunomori(東京大学大学院理学系研究科地殻化学実験施設)

We will provide an opportunity to discuss about observation and modeling of crustal fluids. Topics of interests include, but not limited to (1) a field of physics and chemistry of fault fluids, which is related to earthquake occurrences and researches physical and chemical changes of the fluids caused by crustal deformation including earthquakes, (2) a field of earthquake hydrology, which estimates crustal deformation from level, pressure and chemistry of groundwater using poroelastic theory, and (3) a field of chemistry of crustal fluids, which concerns chemical and isotopic features of the crustal fluids and try to estimate the flux of them.

9:00 AM - 9:15 AM JST | 12:00 AM - 12:15 AM UTC

### [SCG55-01] Estimation of fault models of the short-term SSE using groundwater pressures at the Hokusei observation site

*Yuichi Kitagawa[1], Norio Matsumoto[1] (1.Tectono-Hydrology Research Group, Geological Survey of Japan, National Institute of Advanced Industrial Science and Technology)

---

9:15 AM - 9:35 AM JST | 12:15 AM - 12:35 AM UTC

### [SCG55-02] Groundwater level changes during the 2018 Hokkaido Eastern Iburi earthquake

★Invited Papers

*Tomo Shibata[1], Ryo Takahashi[2], Hiroaki Takahashi[3], Takanori Kagoshima[4], Yuji Sano[4], Daniele Pinti[5] (1.Graduate School of Science, Kyoto University, 2.Geological Survey of Hokkaido, Hokkaido Research Organization, 3.Graduate School of Science, Hokkaido University, 4.Atmosphere and Ocean Research Institute, The University of Tokyo, 5.GEOTOP, Université du Québec)

---

9:35 AM - 9:50 AM JST | 12:35 AM - 12:50 AM UTC

### [SCG55-03] Postseismic streamflow changes after the 2016 Kumamoto earthquake

*Naoji Koizumi[1], Shinsuke Minote[1], Tatusya Tanaka[1] (1.School of Environmental Science,the University of Shiga Prefecture)

---

9:50 AM - 10:05 AM JST | 12:50 AM - 1:05 AM UTC

### [SCG55-04] Development of Radium Concentration Monitoring System based on Gamma-Ray Spectroscopy

*Fumiaki Tsunomori[1], Shigekazu Nagai[2], Junji Yoshii[3], Yoshihide Kimura[4], Yoriyuki Kamakura[5], Yuki Inoue[5], Norihito Sato[6], Shiro Sakuragi[7], Ryuichi Shimizu[8], V N Gluchschenko[9] (1.Geochemical Research Center, Graduate School of Science, University of Tokyo, 2.Graduate School of Engineering, Mie University, 3.Advanced Clinical Research Center, Fukushima Medical University, 4.Graduate School of Engineering, Osaka University, 5.Faculty of Information Science and Technology, Osaka Institute of Technology, 6.Chiyoda Technol corp., 7.Union Material Inc., 8.Office for University-Industry Collaboration, Osaka University, 9.Institute of Nuclear Physics, Almaty, Republic of Kazakhstan)

---

10:05 AM - 10:25 AM JST | 1:05 AM - 1:25 AM UTC

### [SCG55-05] $^{222}$Rn concentration distribution in Yatsushiro Sea

★Invited Papers

*Kuniyo Kawabata[1], Fumiaki Tsunomori[2], Yujin Kitamura[1], Hakuho-Maru K18-3 scientists (1.Graduate School of Science and Engineering, KAGOSHIMA UNIVERSITY, 2.Geochemical Research Center, Graduate

School of Science, University of Tokyo)

10:25 AM - 10:30 AM JST | 1:25 AM - 1:30 AM UTC
Discussion

# Estimation of fault models of the short-term SSE using groundwater pressures at the Hokusei observation site

*Yuichi Kitagawa[1], Norio Matsumoto[1]

1. Tectono-Hydrology Research Group, Geological Survey of Japan, National Institute of Advanced Industrial Science and Technology

One of the problems is the lack of high quality crustal deformation/groundwater observation sites in the western part of Aichi prefecture and the northern part of Mie prefecture around Ise Bay, in terms of the estimation of short-term slow slip events (SSEs) occurring at the plate boundary of the Nankai Trough. One of the causes is that unconsolidated sedimentary layers such as the Tokai Group are thickly deposited in this area. In May 2016, the inner pipe of the observation well at the Hokusei observation site located in the northern part of Mie prefecture was sealed with a packer in order to improve the response of groundwater level to crustal deformation. Because the permeability of the target aquifer at this site is low, the groundwater level before the sealing was poor in response to crustal strain changes before the sealing. The groundwater pressure is observed after sealing, then tidal fluctuation clearly appeared in the groundwater pressure, therefore we found the response of the groundwater pressure to crustal deformation to be clearly improved. The response of the groundwater pressure to crustal strain after sealing improved about 10 times than that of the groundwater level before the sealing. By eliminating the tidal component, barometric pressure response, and rain response from the groundwater pressure data, short-term SSEs were detected by the changes in groundwater pressure in July 2016, November 2017 and April 2018. And then slips of the short-term SSEs were estimated to be spread to Northern Ise Bay by the data of strain, tilt and groundwater pressure. In the area around Northern Ise Bay where deep low frequency tremors are not active, it is shown that short-term SSEs repeatedly occurred. In soft sedimentary layer which is unsuitable for observation of crustal deformation by strain meter and tilt meter, it is showed that the measurement of groundwater level (pressure) is a powerful means of crustal deformation observation.

Keywords: groundwater, strain sensitivity, closed well, slow slip event

©2019. Japan Geoscience Union. All Right Reserved. 

# Groundwater level changes during the 2018 Hokkaido Eastern Iburi earthquake

*Tomo Shibata[1], Ryo Takahashi[2], Hiroaki Takahashi[3], Takanori Kagoshima[4], Yuji Sano[4], Daniele Pinti[5]

1. Graduate School of Science, Kyoto University, 2. Geological Survey of Hokkaido, Hokkaido Research Organization, 3. Graduate School of Science, Hokkaido University, 4. Atmosphere and Ocean Research Institute, The University of Tokyo, 5. GEOTOP, Université du Québec

Groundwater table level in wells can fluctuate under stress provoked by earthquakes located even thousands of kilometers away. The mechanisms of changes in groundwater level can be explained by hydrological changes such as pore-pressure response to coseismic static elastic strain, permeability changes caused by seismic waves and fluid migration along seismogenic dilatant cracks or crustal ruptures. The Geological Survey of Hokkaido, Hokkaido Research Organization (HRO), has been monitoring groundwater tables in several wells after the 2018 Hokkaido Eastern Iburi earthquake. The wells were drilled for exploiting hot spring water but have not been used in the last 20 years. The groundwater level was measured by pressure gauges with resolution about 5-10 mm in 10-minute intervals in each monitored well. After the Hokkaido Eastern Iburi earthquake, we were able to find a step-like decrease in groundwater levels in three wells. These wells are located within the region where tensile changes of the quake-induced volumetric strain can be calculated by using the fault model, suggesting that the changes in groundwater levels are qualitatively consistent with those in volumetric strain. The observed groundwater level changes are also affected by tidal and barometric effects, and we can estimate the response of groundwater level for tidal components. The tidal responses in all the wells have not changed before and after the earthquake.

Keywords: Groundwater level, Poroelastic behavior, Earthquake, Hokkaido

©2019. Japan Geoscience Union. All Right Reserved. 

# Postseismic streamflow changes after the 2016 Kumamoto earthquake

*Naoji Koizumi[1], Shinsuke Minote[1], Tatusya Tanaka[1]

1. School of Environmental Science,the University of Shiga Prefecture

It has been well known that large earthquakes sometimes cause hydrological changes widely in and around the region of strong ground motion. In several cases of those changes, stream flow and spring flow increases in lowland and water table drops in highland. It has often been explained by permeability enhancement in the region of strong ground motion (Rojstaczer et al. ,1995; Wang and Manga, 2004). Since Japan is relatively rich in water resources, people may have not paid much attention to these earthquake-related hydrological changes. But those hydrological changes are clearly one of the seismic risks and should also be examined in Japan because those changes sometimes continue for a period of several months to years (Rojstaczer et al. ,1995) .

The 2016 Kumamoto Earthquake, which occurred mainly in Kumamoto Prefecture, Japan in April 2016, caused severe damages in and around Kumamoto Prefecture. It also caused many changes in stream water and groundwater (Ichiyanagi and Ando, 2017; Sato et al., 2017). The region of strong ground motion of the main shock spreads from the coastal plain to the Aso caldera.

We analyzed the data of streamflow at fourteen flow rate observation stations of three major rivers in Kumamoto prefecture during the period from 1990s to 2017. After the 2016 Kumamoto earthquake, streamflow was increased at four of the fourteen observation stations, where the rivers flow from the Aso caldera or the foot of Mt.Aso. However the streamflow was not increased just after the 2016 Kumamoto earthquake. It was increased 2 months after the Kumamoto earthquake, when a heavy rainfall occurred. In addition it is found that (flood frow rate/precipitation amount) ratio tends to be increased when the precipitation amount is large after the 2016 Kumamoto earthquake. This can be explained not by permeability enhancement but by decrease of the soil moisture retention capacity. In and around the region of the strong ground motion of the 2016 Kumamoto earthquake there were many mudslides and landslides, which could reduce the soil moisture retention capacity. The earthquake-related decrease of the soil moisture retention capacity could have caused the streamflow increase in and around the region of the strong ground motion of the 2016 Kumamoto earthquake.

Keywords: Kumamoto earthquake, Streamflow, Permeability, Strong ground motion

©2019. Japan Geoscience Union. All Right Reserved. 

# Development of Radium Concentration Monitoring System based on Gamma-Ray Spectroscopy

*Fumiaki Tsunomori[1], Shigekazu Nagai[2], Junji Yoshii[3], Yoshihide Kimura[4], Yoriyuki Kamakura[5], Yuki Inoue[5], Norihito Sato[6], Shiro Sakuragi[7], Ryuichi Shimizu[8], V N Gluchschenko[9]

1. Geochemical Research Center, Graduate School of Science, University of Tokyo, 2. Graduate School of Engineering, Mie University, 3. Advanced Clinical Research Center, Fukushima Medical University, 4. Graduate School of Engineering, Osaka University, 5. Faculty of Information Science and Technology, Osaka Institute of Technology, 6. Chiyoda Technol corp., 7. Union Material Inc., 8. Office for University-Industry Collaboration, Osaka University, 9. Institute of Nuclear Physics, Almaty, Republic of Kazakhstan

We have developed a radium concentration monitoring system in order to analyze a radium concentration in soil samples based on a gamma-ray spectrum. A gamma-ray spectrum of a soil sample was measured by a $SrI_2$ solid scintillator equipped by a multi-pixel photon counter (hereinafter a detector). The detector was shielded by 5cm-thick lead brocks, because 214-bismuth, which is a daughter elements of radium contained in cement materials, emits strong gamma-ray. We have achieved 80% background reduction. We prepared a calibration curve in order to determine a soil radium concentration by a peak area of 214-bismuth in a gamma-ray spectrum of JG-1 geochemical reference sample (AIST, GSJ). We are going to have a discussion to improve problems of this system.

Keywords: Soil Radium Concentration, Gamma-Ray Spectroscopy

©2019. Japan Geoscience Union. All Right Reserved. 

# $^{222}$Rn concentration distribution in Yatsushiro Sea

*Kuniyo Kawabata[1], Fumiaki Tsunomori[2], Yujin Kitamura[1], Hakuho-Maru K18-3 scientists

1. Graduate School of Science and Engineering, KAGOSHIMA UNIVERSITY, 2. Geochemical Research Center, Graduate School of Science, University of Tokyo

Radon concentrations in Yatsushiro sea were surveyed to examine relationship with the submarine sediments and geological structure such as submarine active faults.

$^{222}$Rn is a radioactive noble gas and occurs naturally in earth’ s crust as an intermediate step in the normal radioactive decay chain of uranium series. Radon shows high solubility for water and thus high mobility through groundwater and fluids in earth’ s crust. Concentration of radon in crustal fluid and groundwater can provide a clue to understand geology of the aquifer and state of crustal deformation as crack formation and change in strain state, because its release rate depends mainly on rock surface area. Recently location of active faults and its activity have been examined by using the method (e.g. Malgrange and Gleeson, 2014, Tsunomori et al., 2017).

A bunch of submarine active faults underlies in Yatsushiro area sea. These faults compose the Futagawa-Hinagu Fault zone which was activated at the 2016 Kumamoto earthquake. To evaluate records of submarine landslides and changes in submarine circumstances due to historical earthquakes, R/V Hakuho-Maru sailed for research expedition (KH-1803) in Yatsushiro sea from 27th to 30th July, 2018. We collected bottom water from obtained multiple cores and piston cores, and pore waters from piston cores for the measurement of the radon concentration in the sample water on board.
The results of radon concentration distribution from multiple cores, (MC 1-12), show that higher concentration along the Line Y18a. The radon concentrations from bottom water of piston cores (PC 1-11) also show similar results while the values are larger than the results from multiple cores. A higher radon concentration is attributed to difference in (1) Radium concentration in sediments, and/or (2) properties of sediments such as porosity and/or surface area of grains which are caused by difference in types of sediment or fault activity in sediments. The Line Y18a extends across a major submarine active fault (FA1, Tanoura-Tsunagi-oki-faults) (Kagohara et al., 2011). Such a geological setting suggests that the radon concentration distribution in Yatsushiro sea might reflect the current fault activity. We discuss the contributing factor of the higher radon concentration by comparison with Ra concentration in sediment, sediment properties in each site and geological structure in Yatsushiro sea.

Keywords: Radon concentration in water, Submarine active fault, Yatsushiro sea, $\gamma$ ray analysis, The 2016 Kumamoto earthquake

©2019. Japan Geoscience Union. All Right Reserved. 

[J] Poster | S (Solid Earth Sciences )：S-CG Complex & General

Thu. May 30, 2019 3:30 PM - 5:00 PM JST | Thu. May 30, 2019 6:30 AM - 8:00 AM UTC | Poster Hall International Exhibition Hall8, Makuhari Messe_17

## [S-CG55] Crustal fluids and deformation

convener:Yuichi Kitagawa(Tectono-Hydrology Research Group, Geological Survey of Japan, National Institute of Advanced Industrial Science and Technology), Naoji Koizumi(School of Environmental Science,the University of Shiga Prefecture), Koji Umeda(Hirosaki University), Fumiaki Tsunomori(Geochemical Research Center, Graduate School of Science, University of Tokyo)

We will provide an opportunity to discuss about observation and modeling of crustal fluids. Topics of interests include, but not limited to (1) a field of physics and chemistry of fault fluids, which is related to earthquake occurrences and researches physical and chemical changes of the fluids caused by crustal deformation including earthquakes, (2) a field of earthquake hydrology, which estimates crustal deformation from level, pressure and chemistry of groundwater using poroelastic theory, and (3) a field of chemistry of crustal fluids, which concerns chemical and isotopic features of the crustal fluids and try to estimate the flux of them.

### [SCG55-P01] Application of slug test model to earthquake-related groundwater-level change in the Oi well Kanagawa Prefecture, Center Japan

*Yang Li[1], Motoo Ukawa[1], Kazuhiro Itadera[2], Masatake Harada[2] (1.Nihon University, 2.Hot Spring Research Institute of Kanagawa Prefecture)

### [SCG55-P02] Changes in groundwater level and borehole strain data associated with the 2018 Osaka Hokubu earthquake (M6.1) at the Takarazuka observatory

*Norio Matsumoto[1], Tsutomu Kiguchi[1] (1.Geological Survey of Japan, National Institute of Advanced Industrial Science and Technology (AIST))

### [SCG55-P03] Changes in groundwater level at the Kusanagi observatory

*Norio Matsumoto[1] (1.Tectono-Hydrology Research Group, Geological Survey of Japan, National Institute of Advanced Industrial Science and Technology (AIST))

### [SCG55-P04] Spatial and temporal changes of $^{3}He/^{4}He$ ratios around a source region before and after an inland earthquake

*Koji Umeda[1] (1.Hirosaki University)

# Application of slug test model to earthquake-related groundwater-level change in the Oi well Kanagawa Prefecture, Center Japan

*Yang Li[1], Motoo Ukawa[1], Kazuhiro Itadera[2], Masatake Harada[2]

1. Nihon University, 2. Hot Spring Research Institute of Kanagawa Prefecture

The sustained groundwater level changes following earthquake have been reported since the early twentieth century, and several mechanisms have been proposed for these phenomena. In this study, we applied slug test model in order to explain time constants of the sustained uplifts observed in the Ohi well, center Japan. The Ohi observation well, 300 m in depth, is one of the deep wells belonging to groundwater level monitoring system established by Hot Springs Research Institute of Kanagawa Prefecture (HSRI). The groundwater level is recorded by pressure gauge in 1 Hz sampling. In the Oi well the groundwater level changes in exponential sustained increase following earthquakes has been documented by HSRI. We selected the events in which groundwater level increased over 5 cm were observed in the period from 2011 to 2016. By fitting these changes with exponential decay function, the time constant of the Ohi well is ranging 100 to 400 s. We show, by applying slug test model, that this time constant range of the uplift of groundwater level is explained by the time constant of the system consisting of the well and the surrounding aquifer. The success of application of the slug test model strongly suggests that the pore-pressure rapidly increased just after the arrival of seismic waves. This time constant rang means the hydraulic permeability almost no change by earthquake.

Keywords: Permeability, Eeathquake, Slug test

©2019. Japan Geoscience Union. All Right Reserved. 

# Changes in groundwater level and borehole strain data associated with the 2018 Osaka Hokubu earthquake (M6.1) at the Takarazuka observatory

*Norio Matsumoto[1], Tsutomu Kiguchi[1]

1. Geological Survey of Japan, National Institute of Advanced Industrial Science and Technology (AIST)

Groundwater level sensor and the Sakata-type three-component borehole strainmeter was deployed at the Takarazuka observation well in 1996. We observed changes in groundwater level and borehole strain data associated with the 2018 Osaka Hokubu earthquake (M6.1) at the Takarazuka observatory, which is located 26 km away from the epicenter of the earthquake. Observed groundwater level change was 14 cm decrease just after the earthquake, then, we observed rapid increase: 25 cm increase after one hour and 4.2 m increase after 8 days of the earthquake. These changes in groundwater level cannot be explained by the static strain change associated with the earthquake. We compare these changes with the changes in groundwater level and borehole strain data associated with the other distant and local earthquakes in these 20 years.

Keywords: groundwater level, strain, Osaka Hokubu earthquake

©2019. Japan Geoscience Union. All Right Reserved. 

# Changes in groundwater level at the Kusanagi observatory

*Norio Matsumoto[1]

1. Tectono-Hydrology Research Group, Geological Survey of Japan, National Institute of Advanced Industrial Science and Technology (AIST)

Since 1994 groundwater level has been observed at the Kusanagi observation well. Changes in groundwater level associated with the middle –large local earthquakes and the large distant earthquakes were observed. All groundwater level changes associated with these earthquakes were increase. The relationship between these changes in groundwater level and distant and local earthquakes in these 20 years is discussed.

Keywords: groundwater level, earthquake, Kusanagi observatory

©2019. Japan Geoscience Union. All Right Reserved. 

# Spatial and temporal changes of $^{3}He/^{4}He$ ratios around a source region before and after an inland earthquake

*Koji Umeda[1]

1. Hirosaki University

Static stress change caused by the megathrust slip of the 2011 $M_w$ 9.0 Tohoku-Oki earthquake considerably affected the seismicity pattern in inland areas, resulting in the occurrence of numerous earthquakes along several active faults in Japan. On June 30, 2011, the $M_j$ 5.4 central Nagano earthquake occurred at a shallow depth of 5 km, indicating the reactivation of the Gofukuji fault in Central Japan. This study was undertaken to elucidate spatial and temporal changes of $^{3}He/^{4}He$ ratios around a source region before and after an inland earthquake using both new and existing helium isotope data from hot spring and drinking water wells. Most gas samples near the seismic source region are characterized by increase in postseismic $^{3}He/^{4}He$ ratios. In contrast, the postseismic ratios decrease by up to about 30 % away from the seismic source region. Episodic faulting could release accumulated crustal (radiogenic) helium from host rocks, or enhance the transfer of mantle volatiles through permeable fault zones, such that subsequent fluid flow proximal to the source region could then explain the spatio-temporal variations in $^{3}He/^{4}He$ ratios.

Keywords: 2011 central Nagano earthquake , helium isotopes

©2019. Japan Geoscience Union. All Right Reserved. 

[J] Poster | S (Solid Earth Sciences)：S-CG Complex & General

Thu. May 30, 2019 5:15 PM - 6:30 PM JST | Thu. May 30, 2019 8:15 AM - 9:30 AM UTC | Poster Hall International Exhibition Hall8, Makuhari Messe_30

## [S-CG55] Crustal fluids and deformation

convener:Yuichi Kitagawa(Tectono-Hydrology Research Group, Geological Survey of Japan, National Institute of Advanced Industrial Science and Technology), Naoji Koizumi(School of Environmental Science,the University of Shiga Prefecture), Koji Umeda(Hirosaki University), Fumiaki Tsunomori(Geochemical Research Center, Graduate School of Science, University of Tokyo)

We will provide an opportunity to discuss about observation and modeling of crustal fluids. Topics of interests include, but not limited to (1) a field of physics and chemistry of fault fluids, which is related to earthquake occurrences and researches physical and chemical changes of the fluids caused by crustal deformation including earthquakes, (2) a field of earthquake hydrology, which estimates crustal deformation from level, pressure and chemistry of groundwater using poroelastic theory, and (3) a field of chemistry of crustal fluids, which concerns chemical and isotopic features of the crustal fluids and try to estimate the flux of them.

### [SCG55-P01] Application of slug test model to earthquake-related groundwater-level change in the Oi well Kanagawa Prefecture, Center Japan

*Yang Li[1], Motoo Ukawa[1], Kazuhiro Itadera[2], Masatake Harada[2] (1.Nihon University, 2.Hot Spring Research Institute of Kanagawa Prefecture)

### [SCG55-P02] Changes in groundwater level and borehole strain data associated with the 2018 Osaka Hokubu earthquake (M6.1) at the Takarazuka observatory

*Norio Matsumoto[1], Tsutomu Kiguchi[1] (1.Geological Survey of Japan, National Institute of Advanced Industrial Science and Technology (AIST))

### [SCG55-P03] Changes in groundwater level at the Kusanagi observatory

*Norio Matsumoto[1] (1.Tectono-Hydrology Research Group, Geological Survey of Japan, National Institute of Advanced Industrial Science and Technology (AIST))

### [SCG55-P04] Spatial and temporal changes of $^{3}He/^{4}He$ ratios around a source region before and after an inland earthquake

*Koji Umeda[1] (1.Hirosaki University)

# Application of slug test model to earthquake-related groundwater-level change in the Oi well Kanagawa Prefecture, Center Japan

*Yang Li[1], Motoo Ukawa[1], Kazuhiro Itadera[2], Masatake Harada[2]

1. Nihon University, 2. Hot Spring Research Institute of Kanagawa Prefecture

The sustained groundwater level changes following earthquake have been reported since the early twentieth century, and several mechanisms have been proposed for these phenomena. In this study, we applied slug test model in order to explain time constants of the sustained uplifts observed in the Ohi well, center Japan. The Ohi observation well, 300 m in depth, is one of the deep wells belonging to groundwater level monitoring system established by Hot Springs Research Institute of Kanagawa Prefecture (HSRI). The groundwater level is recorded by pressure gauge in 1 Hz sampling. In the Oi well the groundwater level changes in exponential sustained increase following earthquakes has been documented by HSRI. We selected the events in which groundwater level increased over 5 cm were observed in the period from 2011 to 2016. By fitting these changes with exponential decay function, the time constant of the Ohi well is ranging 100 to 400 s. We show, by applying slug test model, that this time constant range of the uplift of groundwater level is explained by the time constant of the system consisting of the well and the surrounding aquifer. The success of application of the slug test model strongly suggests that the pore-pressure rapidly increased just after the arrival of seismic waves. This time constant rang means the hydraulic permeability almost no change by earthquake.

Keywords: Permeability, Eeathquake, Slug test

©2019. Japan Geoscience Union. All Right Reserved. 

# Changes in groundwater level and borehole strain data associated with the 2018 Osaka Hokubu earthquake (M6.1) at the Takarazuka observatory

*Norio Matsumoto[1], Tsutomu Kiguchi[1]

1. Geological Survey of Japan, National Institute of Advanced Industrial Science and Technology (AIST)

Groundwater level sensor and the Sakata-type three-component borehole strainmeter was deployed at the Takarazuka observation well in 1996. We observed changes in groundwater level and borehole strain data associated with the 2018 Osaka Hokubu earthquake (M6.1) at the Takarazuka observatory, which is located 26 km away from the epicenter of the earthquake. Observed groundwater level change was 14 cm decrease just after the earthquake, then, we observed rapid increase: 25 cm increase after one hour and 4.2 m increase after 8 days of the earthquake. These changes in groundwater level cannot be explained by the static strain change associated with the earthquake. We compare these changes with the changes in groundwater level and borehole strain data associated with the other distant and local earthquakes in these 20 years.

Keywords: groundwater level, strain, Osaka Hokubu earthquake

©2019. Japan Geoscience Union. All Right Reserved. 

# Changes in groundwater level at the Kusanagi observatory

*Norio Matsumoto[1]

1. Tectono-Hydrology Research Group, Geological Survey of Japan, National Institute of Advanced Industrial Science and Technology (AIST)

Since 1994 groundwater level has been observed at the Kusanagi observation well. Changes in groundwater level associated with the middle –large local earthquakes and the large distant earthquakes were observed. All groundwater level changes associated with these earthquakes were increase. The relationship between these changes in groundwater level and distant and local earthquakes in these 20 years is discussed.

Keywords: groundwater level, earthquake, Kusanagi observatory

©2019. Japan Geoscience Union. All Right Reserved. 

# Spatial and temporal changes of $^{3}He/^{4}He$ ratios around a source region before and after an inland earthquake

*Koji Umeda[1]

1. Hirosaki University

Static stress change caused by the megathrust slip of the 2011 $M_w$ 9.0 Tohoku-Oki earthquake considerably affected the seismicity pattern in inland areas, resulting in the occurrence of numerous earthquakes along several active faults in Japan. On June 30, 2011, the $M_j$ 5.4 central Nagano earthquake occurred at a shallow depth of 5 km, indicating the reactivation of the Gofukuji fault in Central Japan. This study was undertaken to elucidate spatial and temporal changes of $^{3}He/^{4}He$ ratios around a source region before and after an inland earthquake using both new and existing helium isotope data from hot spring and drinking water wells. Most gas samples near the seismic source region are characterized by increase in postseismic $^{3}He/^{4}He$ ratios. In contrast, the postseismic ratios decrease by up to about 30 % away from the seismic source region. Episodic faulting could release accumulated crustal (radiogenic) helium from host rocks, or enhance the transfer of mantle volatiles through permeable fault zones, such that subsequent fluid flow proximal to the source region could then explain the spatio-temporal variations in $^{3}He/^{4}He$ ratios.

Keywords: 2011 central Nagano earthquake , helium isotopes

©2019. Japan Geoscience Union. All Right Reserved. 

[J] Poster | S (Solid Earth Sciences )：S-CG Complex & General

Thu. May 30, 2019 10:45 AM - 12:15 PM JST | Thu. May 30, 2019 1:45 AM - 3:15 AM UTC | Poster Hall International Exhibition Hall8, Makuhari Messe_7

## [S-CG58] Brittle-Ductile Transition and Supercritical Geofluids for Crustal Energy in Island Arc

convener:Noriyoshi Tsuchiya(Graduate School of Environmental Studies, Tohoku University), Hiroshi Asanuma(AIST), Yasuo Ogawa(Volcanic Fluid Research Center, School of Science, Tokyo Institute of Technology), Shigemi Naganawa(Akita University)

Nature of rock mass below the brittle-ductile transition (BDT) is of great scientific interest to understand various phenomenon in the Earth's crust. We will review and discuss current understanding of characteristics the rock mass below the BDT, including composites, stress, failure mechanism induced by liquid injection and associates earthquake generation mechanism, and water rock interaction, considering engineered geothermal development in the BDT. Discussions on the possible phenomena in the geothermal development in the BDT will be followed in this session. <br/> New drilling technology is key of issues. This session will cover advanced drilling technology under high temperature conditions for energy extraction.<br/><br/>

### [SCG58-P01] Mechanical and hydrological properties of granite under supercritical fluid conditions

*Manami Kitamura[1], Miki Takahashi[1] (1.National Institute of Advanced Industrial Science and Technology)

### [SCG58-P02] Three-dimensional electrical resistivity structure of kuju Volcano, Central Kyushu, Japan revealed by Magnetotelluric survey data

*Sabry Abdallah[1], Mitsuru Utsugi [1], Koki Aizawa[2], Makoto Uyeshima[3], Wataru Kanda[4], Takao Koyama[3] (1.Institute of geothermal science, Faculty of Science, Kyoto University, 2.Institute of Seismology and Volcanology, Faculty of Sciences, Kyushu University, 3.Earthquake Research Institute, The University of Tokyo, 4.Volcanic Fluid Research Center, School of Science, Tokyo Institute of Technology)

### [SCG58-P03] Preliminary Report on Themoluminescence Geothermal Exploration in Northern Area of Mt. Kurikoma (Akayumata-River), NE Japan.

*Hiroki Okano[1], Nobuo Hirano[1], Noriyoshi Tsuchiya[1] (1.Graduate School of Environmental Studies Tohoku University)

### [SCG58-P04] Experimental Study of Critical Point Determination for Multicomponent Fluids using light-scattering Spectroscopic Method

*Nobuo Hirano[1], Yuta Oshima[1], Atsushi Okamoto[1], Noriyoshi Tsuchiya[1] (1.Graduate School of Environmental studies, Tohoku University)

### [SCG58-P05] Transport and Reaction Behavior of Supercritical Geofluid Revealed by Porphyry Copper Deposit

*Geri Agroli[1], Noriyoshi Tsuchiya[1] (1.Tohoku University)

### [SCG58-P06] Characteristics of precipitation of amorphous silica and its influences on permeability of fractured granite in superhot geothermal environments

*Hikaru Abe[1], Noriaki Watanabe[1], Kengo Nakamura[1], Atsushi Okamoto[1], Takeshi Komai[1] (1.Graduate School of Environmental Studies, Tohoku University)

### [SCG58-P07] Evolution and The Total Budget of Fluid in Granitic Magma through Magmatism and Volcanism in The Subduction Zone, NE Japan

*Fajar Febiani Amanda[1], Ryoichi Yamada[2], Satoshi Okumura[2], Masaoki Uno[1], Noriyoshi Tsuchiya[1] (1.Graduate School of Environmental Studies, Tohoku University, 2.Graduate School of Science, Tohoku

University)

[SCG58-P08] **Porosity generation during feldspar replacement as the mark of potassium-rich supercritical fluids on the top of granitic intrusion**

*Astin Nurdiana[1], Atsushi Okamoto[1], Masaoki Uno[1], Kenta Yoshida[2], Noriyoshi Tsuchiya[1] (1.Tohoku University, 2.Japan Agency for Marine-earth Science and Technology)

[SCG58-P09] Quantitative evaluation of fracture distribution in granite and the relationship between fracture distribution and physical properties

*Manami Kadono[1], Shin-ichi Uehara[2], Miki Takahashi[3], Manami Kitamura[3] (1.Department of Environment Systems, Graduate School of frontier Science, The University of Tokyo, 2.Department of Enviroment Science, Faculty of Science, Toho University, 3.National Institute of Advanced Industrial Science and Technology)

# Mechanical and hydrological properties of granite under supercritical fluid conditions

*Manami Kitamura[1], Miki Takahashi[1]

1. National Institute of Advanced Industrial Science and Technology

To extract geothermal energy effectively and safely from magma and/or adjacent hot rock, we need to tackle many issues which require new technology development. One of them we are targeting on is to develop a technology to mitigate induced-earthquakes. It is required to understand roles of factors on occurrences of the induced-earthquake (e.g., strength, crack density, and fluid-rock reaction) and their intercorrelations (e.g., *Asanuma* et al., 2012).

Our purpose of this series of experiments is to clarify a relationship between the rock strength and the fracture density under hydrothermally supercritical conditions. We conducted triaxial deformation test on intact granite rock strength under high-temperature (250 –750˚C), high-pressure (104 MPa) condition at a constant load velocity (0.1 μm/sec) using a gas-rig at GSJ, AIST. We used Oshima granite, which has initially ~0.55% of the porosity, 4.95±1.01 km/s in Vp at dry condition (dry). All experimental products showed brittle feature having several oblique fracture surfaces, but both value of peak stress and amount of stress drop became smaller at higher temperature. Additionally, Young’s modulus decreases with increasing the temperature from 57.4 GPa at 250˚C to 32.3 GPa at 750˚C. At 400˚C, the stress drop accelerated the deformation with ~98 times faster velocity than that at load-point. In contrast, at 650˚C and 750˚C, the velocity during stress drop kept the same order of the load-point velocity. Therefore, the deformation feature may start to be of ductile when the temperature exceeds 650˚C. The microstructures of samples deformed at 400˚C and 550˚C showed the shear zone with the grain reduction. In contrast, for the samples deformed at 650˚C and 750˚C, we partly observed the sintered structure at grain boundaries among feldspar gouge. The sintered structure at >650°C might be the cause of the slow stress drop. Highly dense cracked granite specimens were formed by a rapid decompression test (RDT) using an autoclave settled at Tohoku University (*Kitamura & Takahashi*, 2017AGU; *Takagi* et al., 2017GRC Trans.), caused by a reduction of the fluid pressure within 2 seconds from vapor/supercritical state pressure (10 –48 MPa, 550 ˚C) to ambient pressure. X-ray CT scanning on the specimens after RDT showed that numerous microcracks were generated in them (see details in *Takahashi & Kitamura*, 2018, annual meeting of Geological Soc. Japan). The RDT imposed the porosity increasing towards 3.91 % and Vp decreasing towards 1.46±0.22 km/s (dry). We conducted the permeability measurement on fractured granites after RDT with the porosity of 2.1 –2.7% under a combined condition of 400 ˚C in temperature, 104 MPa in confining pressure, 39 –99 MPa in pore fluid pressure ($P_p$). Permeability measured by pore pressure oscillation method decreases from $1.3\times10^{-16}$ $m^2$ at $P_p$ of 99 MPa to $2.6\times10^{-18}$ $m^2$ at $P_p$ of 39 MPa for the permeable case. Permeability on fractured granite of 2.1% in porosity at room temperature (RT) show relatively lower permeability than those at 400°C except for at $P_p$ of 99 MPa. Permeability at RT rapidly decreases from $1.0\times10^{-15}$ $m^2$ at $P_p$ of 99 MPa to $1.0\times10^{-18}$ $m^2$ at $P_p$ of 84 MPa, and then reaches $5.8\times10^{-19}$ $m^2$ at $P_p$ of 99 MPa. In the meeting, we will show additional results of permeability tests on fractured granites under various high temperature conditions.

Keywords: supercritical fluid, geothermal, granite

©2019. Japan Geoscience Union. All Right Reserved. 

# Three-dimensional electrical resistivity structure of kuju Volcano, Central Kyushu, Japan revealed by Magnetotelluric survey data

*Sabry Abdallah[1], Mitsuru Utsugi [1], Koki Aizawa[2], Makoto Uyeshima[3], Wataru Kanda[4], Takao Koyama[3]

1. Institute of geothermal science, Faculty of Science, Kyoto University, 2. Institute of Seismology and Volcanology, Faculty of Sciences, Kyushu University, 3. Earthquake Research Institute, The University of Tokyo, 4. Volcanic Fluid Research Center, School of Science, Tokyo Institute of Technology

The Kuju volcano is located in south western part of Oita prefecture, Japan , and is one of the important geothermal areas in Japan. It has began to erupt on October 11,1995 at the eastern flank of Mt. Hossho, which is in the central part of Kuju volcano. Second eruption started again in the middle of December, 1995, producing an ash volume of about 5000 $m^3$. Iwoyama is the central part Kuju Volcano and considered to be one of the most hydrothermal active hydrothermal field in Japan. Geothermal areas beneath active volcanoes may have an important role in geothermal energy development in the future. so it is important to monitor and clarify the thermal and hydrologic processes occurring beneath volcanoes. Magnetotelluric (MT) investigation is an important tool to identify the subsurface resistivity structure using natural variation in the electromagnetic field, therefore it is convenient to for the hydrothermal system investigation. We applied a Wide-band MT survey method to identify the structures associated with the hydrothermal systems beneath Kuju volcano. MT field survey data were collected at 63 observation points around the Kuju volcano from September to October 2015. Fourier Transform(FT) applied to the collected data to reduce the background noise associated with Power supply of 60 Hz and other noises associated with higher frequencies. Inverse FT was applied to the data to transform from frequency-domain to time-domain data. The 3-D resistivity structure model is obtained by inverting the MT impedance using ModEM code (Kelbert, A. et al., 2014). The primary 3-D resistivity structure model clarified that, a resistive structure (100-300 Ω.m) prevail the most of Kuju Volcano area. A very conductive structure (~1Ω.m) exists around Iowyama-Kuju area and extends with the depth towards the south-east part of Iowyama. In comparison with the previous studies, the resistive structure can be interpreted as lava and pyroclastic deposits, whereas the conductive structure around Iowyama-Kuju area is maybe corresponds to aquifers and altered layers.

Keywords: MT survey at Volcanic areas, 3D MT inversion, Hydro-thermal energy

©2019. Japan Geoscience Union. All Right Reserved. 

# Preliminary Report on Themoluminescence Geothermal Exploration in Northern Area of Mt. Kurikoma (Akayumata-River), NE Japan.

*Hiroki Okano[1], Nobuo Hirano[1], Noriyoshi Tsuchiya[1]

1. Graduate School of Environmental Studies Tohoku University

Thermoluminescence (TL) is a method to evaluate radiation dose accumulated in minerals by heating minerals and analyzing luminescence. We can evaluate geothermal manifestation through analyzing the variation of Paleodose in minerals caused by geothermal activities. In this study, geological survey waa performed around Mt. Takamatsudake in the northern area of Mt. Kurikoma, and We estimated geothermal structure of the area and relation between TL distribution and geothermal structure.

In the exploration area, the Takamatsudake lava is distributed around Mt. Takamatsudake, and in the lower part, Torageyama tuff formation is distributed , and also Doroyu fomation composed of mudstone is distributed in the lower part of the Torageyama tuff fomation. 33 samples were collected from Torageyama tuff and Doroyu fomation.

As a result of TL analysis, TL anomalies were confirmed downstream of Akayumata-river hot springs. However, no significant TL anomalies was observed around Yunomata hot springs. In Akayumata H.S(hot spring), boiling water are discharging from a few places, whereas Yunomata H.S are only spouted from one point at 50 ℃. In the earthquake hypocentral distribution from 1985 to 2015, hypocentral clusters are confirmed at shallow part arounf 2 ~ 7 km beneath Akayumata and Yunomata H.S, and it may suggest the existence of a fluid. Around Akayumata H.S, the mud layer is exposed with a local anticline structure. We suggest that hot water discharge to the surface along with cracks and faults associated with these geological structure.

As a result of alteration mineral analysis, both the Torageyama F. and the Doroyu F. were confirmed to have a Green Tuff alteration due to chlorite and sericite. In addition, kaolinite was found near the Akayumata H.S, and laumontite was found around Yunomata H.S. and upstream of Akayumata-river. TL anomaly is harmonious with the distribution of kaolinite, but the weakly related to the distribution of laumontite. From this point of view, it is predicted that TL has information on the temperature-time effect, which is different from altered minerals. By investigating more detailed underground structures in the future and conducting quantitative analysis on the temperature dependency of TL, it is expected that the accuracy of information given by the surface TL data can be improved.

Keywords: thermoluminescence, geothermal exploration, geophysical exploration

©2019. Japan Geoscience Union. All Right Reserved. 

# Experimental Study of Critical Point Determination for Multicomponent Fluids using light-scattering Spectroscopic Method

*Nobuo Hirano[1], Yuta Oshima[1], Atsushi Okamoto[1], Noriyoshi Tsuchiya[1]

1. Graduate School of Environmental studies, Tohoku University

Geofluid is a multicomponent fluid by reaction with various crustal materials, and it is in a supercritical state under high temperature and high pressure conditions inside the Earth. It is very important to know the critical point (CP) and phase state of a geo-fluid in order to know the fluid-rock reaction mechanism under high temperature and high pressure conditions. However, it is difficult to directly determine CP of multicomponent fluid such as geological fluid and sea water by calculation using state equation (EOS) using fluid components, and it is necessary to decide experimentally.
Molecules in the supercritical fluid are unevenly distributed and are known to form both high density and sparse molecular regions in the fluid. Such nonuniformity of molecular distribution is called density fluctuation, and this degree becomes maximum at CP of fluid.
Therefore, for pure material such as H 2 O and CO 2, the critical opalescence is spectroscopically observed at the subcritical to supercritical transition. Therefore, if the density variation of the multicomponent fluid can be observed by a spectroscopic method, it is possible to determine the CP value.
The objective of this study is to establish a new measurement technique / procedure for easily determining CP of multicomponent fluid using spectroscopic observation of subcritical / supercritical transition state.

Keywords: decision of critical point, multicomponent fluid, supercritical fluid, scatter spectroscopy

©2019. Japan Geoscience Union. All Right Reserved. 

# Transport and Reaction Behavior of Supercritical Geofluid Revealed by Porphyry Copper Deposit

*Geri Agroli[1], Noriyoshi Tsuchiya[1]

1. Tohoku University

Supercritical geothermal reservoir (SCGR) is a novel system in the geothermal field. Recently this geothermal system got a lot of attention from scholar since the successful of IDDP that encountered the supercritical fluid in Reykjanes and Krafla geothermal field. SCGR is promising exploited geothermal resource in the near future with several benefits in the economic and technical aspect. However the limited access to geological properties of SCGR system to optimize the potential of the system as well as to address the issue of the system lead us to investigate the natural analog that suitable with this system, Instead of we spend huge money for drilling activity. Porphyry copper deposit is a suitable candidate for SCGR analog where magma ascent from deep mantle and fluid infiltrate a ductile rock mass at ~600˚C, and stock work fracture as an important fluid pathway developed intensively.

The research was conducted on the largest porphyry copper deposit in northern Mongolia called Erdenet deposit. We used 700m depth drill core samples from an open pit. Based on texture and mineralogy, lithology of Erdenet comprises of quartz porphyry and granodiorite porphyry at shallow and deep level consecutively. Mineral assemblages of Quartz porphyry are qtz-ser-py-cp±cal and chl-plg-qtz±kfs for Granodiorite porphyry. Stockwork vein system can be well observed on certain samples and Er-22 (569.9m) reveal distinct vein generation process and evolution based on cross-cutting relationship. Qtz-Mo vein precipitated at the beginning of the process followed by the formation qtz-py±cp vein and those 2 vein type cut by qtz±cal vein. Fluid activity was investigated by several analytical techniques to measure mineral composition to further obtain thermodynamics properties (P-T conditions). Host rock crystallize at temperature 389-861˚C (measurement point from core to rim) using Ti-in-Quartz geothermometer under lithostatic pressure derived from a cotectic line in the Qz-Ab-Or ternary diagram. The similar methods perform to obtain quartz precipitation temperature of qtz-mo vein and the result show vein was precipitated at 323-678˚C (measurement point from core to rim). Fluid inclusion is a useful technique to determine the precipitation of the other two vein type. Qtz-py±cp vein homogenizes at temperature 147.8-358.9˚C with median 251.9˚C but the pressure regime and salinity of fluid are difficult to measure due to most of the inclusion size is less than 5 $\mu$m. The last fluid activity marked by the presence of qtz±cal that cut all of the previous veins. The homogenization temperature is less than 200˚C.

The distribution of vein in the granodiorite porphyry system in Erdenet revealed the evolution of fluid in order to understand the geological properties of a supercritical geothermal reservoir. The emplacement of granodiorite at >600˚C followed by formation of qtz-mo vein that interpreted to have formed in the supercritical regime at 500-600˚C under lithostatic pressure and subsequent pressure drop to hydrostatic condition induce qtz-py±cp vein formation due to drop of silica solubility. Lithostatic to hydrostatic pressure shifting indicate by the presence of pervasive sericite alteration imply meteoric water had circulated into the system. The temperature of the system keeps decrease and precipitation of qtz±cal occurred as the last product on this system. Erdenet Cu-Mo provides a lesson regarding on fluid process and development of supercritical geothermal activity and strong candidate as a natural analog for advanced scientific studied in the future.

©2019. Japan Geoscience Union. All Right Reserved. 

Keywords: supercritical geothermal reservoir, erdenet, porphyry deposit, fluid inclusion

©2019. Japan Geoscience Union. All Right Reserved. 

# Characteristics of precipitation of amorphous silica and its influences on permeability of fractured granite in superhot geothermal environments

*Hikaru Abe[1], Noriaki Watanabe[1], Kengo Nakamura[1], Atsushi Okamoto[1], Takeshi Komai[1]

1. Graduate School of Environmental Studies, Tohoku University

Superhot geothermal environments (above ca. 400˚C) represent a new geothermal energy frontier. However, the networks of permeable fractures capable of storing and transmitting fluids are likely to sealed by a rapid precipitation of amorphous silica in response to an occurrence of high-level of supersaturation for amorphous silica due to a phase change between liquid water, steam, and supercritical water. Here we report results of two sets of hydrothermal precipitation experiments at 400-500˚C and 20-35 MPa, which were respectively conducted to investigate characteristics of precipitation of amorphous silica and its influences on permeability of fractured granite in superhot geothermal environments. In the first set of the precipitation experiments, liquid water with a prescribed Si concentration, which was prepared from water that dissolved granite at 360 ˚C and 35 MPa, was injected to a stainless-steel pipe, in which amorphous silica was precipitated at a prescribed combination of temperature (400-500˚C), pressure (20-35 MPa) and degree of saturation (1.5-2.5). As a result, spherical particles of amorphous silica of <10 μm (typically, 0.2-1.0 μm) were precipitated at all conditions. These particles tended to become smaller and aggregated with increasing temperature or degree of saturation (i.e., with increasing rate of nucleation), while there was no significant influence of pressure. Based on this finding, the second set of the precipitation experiments to investigate influences of the amorphous silica particles on permeability of fractured granite was conducted at 450°C, 25 MPa, and different degrees of saturation. The above-mentioned liquid water with a prescribed Si concentration was injected into a thermally fractured granite containing multiple fractures at an effective confining stress of 10 MPa, where initial permeability of the fractured granite was relatively high (ca. $10^{-16}$ $m^2$) because of the presence of fractures having relatively large apertures of >10 μm. As a result, permeability did not decrease with time at both conditions for the formations of larger and dispersed particles, and smaller and aggregated particles. This finding indicates that precipitation of amorphous silica does not always reduce permeability of fractured granite immediately, and silica particles will move to other locations after its formation. Therefore, in producing superhot geothermal energy, amorphous silica particles will be produced via a production well or will be trapped within fractured granite having a relatively lower initial permeability, therefore relatively smaller apertures. Although the present study has not been completed yet, it is suggested that in case of a superhot geothermal reservoir with permeability aperture large enough to transmit the amorphous silica particle, the permeability may not be destroyed even if precipitation of amorphous silica occurs rapidly.

©2019. Japan Geoscience Union. All Right Reserved. 

# Evolution and The Total Budget of Fluid in Granitic Magma through Magmatism and Volcanism in The Subduction Zone, NE Japan

*Fajar Febiani Amanda[1], Ryoichi Yamada[2], Satoshi Okumura[2], Masaoki Uno[1], Noriyoshi Tsuchiya[1]

1. Graduate School of Environmental Studies, Tohoku University, 2. Graduate School of Science, Tohoku University

Fluids (especially water) are carried by oceanic plates which are subducted into the depth of the mantle and released through the dehydration process. Water migrates upward and contributes to the melting of the mantle wedge in the formation of an arc magma. The formation of volcanoes and igneous rocks as plutons in the arc magma produces geothermal energy sources and the formation of ore mineral deposits. Throughout its migration within the crust, the fluid evolves both in temperature and pressure, composition and amount. These fluid traces can be found among the minerals as melt and/or fluid inclusions in volcanic products, igneous plutons, and the veinlets. In this study, water budget estimated on the crust by determining the condition of P-T and composition of fluids in the volcanic rocks and igneous plutons including the host rock and veinlets.

Samples were taken from caldera fill sediment and porphyry copper deposits in NE Japan region. The P-T condition and fluid composition are measured from the melt inclusion in quartz from the caldera fill sediments and fluid inclusions in the granite intrusion and the veinlets. The sample is divided into several types, namely volcanic rock samples from caldera fill sediment, granite from porphyry copper deposits, and the veinlets contained in the granite body including quartz vein, glassy vein, and hydrothermal breccia vein. In volcanic rock samples, quartz crystals were picked, encased in resin and polished for major element and water content analysis. In granite samples and veinlets, the rock thin sections were made for fluid inclusion microthermometry analysis and fluid diffusion analysis using apatite mineral. Water budget in the upper crust is estimated from caldera fill sediments to be 2.3–7.6 t /yr/m. Water budget in the deeper part of the crust can then be determined from porphyry copper deposits.

Keywords: water budget, fluid evolution, melt inclusion, fluid inclusion

©2019. Japan Geoscience Union. All Right Reserved. 

# Porosity generation during feldspar replacement as the mark of potassium-rich supercritical fluids on the top of granitic intrusion

*Astin Nurdiana[1], Atsushi Okamoto[1], Masaoki Uno[1], Kenta Yoshida[2], Noriyoshi Tsuchiya[1]

1. Tohoku University, 2. Japan Agency for Marine-earth Science and Technology

Feldspar replacement is prevalent process within the crust which has been studied for decades. In particular, it is known that feldspar is texturally sensitive to an interaction with fluids, and the process often results in by the pore generation. Recently, Plümper, et al. (2017) proposed that such reaction-induced nanoporosity plays significant roles in pervasive fluid flow in the crusts, yet it is still unclear until what extent nanoporosity commonly presents and is affected by the feldspar replacement. In this study, we report novel pore structures that have been produced during feldspar replacement in the hornblende schist around the granitoid body.

The Kinkasan Island, which is part of southern Kitakami Mountains, mainly consists of the Cretaceous granitoid bodies with abundant pegmatite dikes, and metamorphic sequences, including hornblende (Hbl) schists and biotite schists. Quartz diorite, as the host plutonic body, and metamorphic rocks were formed under the conditions estimated to be 700-750˚C and 610-660˚C in 0.37-0.42 GPa, respectively. The Hbl schists are often cut by thin alkali feldspar veins in direction perpendicular to the foliation. In the matrix, primordial plagioclase grains (An48Ab52Or0) are generally replaced by patchy grains of albite (An4Ab94Or2) and alkali feldspar (An0Ab1Or99). The mass balance analyses of the plagioclase and alteration products show the gains of Si, K, and fewer Na, also loss of Ca and Al, indicating that feldspar replacement was induced by infiltration of the potassium-rich fluids (the K/Na molar ratio of 3). The detail observations by FIB-SEM reveal that the replacement process yields extensive amount of pore with throat size of ~0.1 –5 $\mu$m. These pores preferentially formed along the grain boundaries of newly-produced albite. Generally, the pores distribute throughout all the plagioclase grains without preference for matrix grain boundary, and formed 3D pore network that seems barely to continue. However, it increased the porosity of the rock up to ~2%. These features of pores related to the feldspar replacement suggests the importance of the reactive fluid infiltration through low-permeability metamorphic rocks, likewise give a new insight on how fluid propagation generate micro-to nano-scale porosity.

Reference: Plümper et al., 2017. Nature geoscience, 10, 685-690.

Keywords: feldspar replacement, pore network, potassium-rich fluids, fluid transport, FIB-SEM

©2019. Japan Geoscience Union. All Right Reserved. 

# Quantitative evaluation of fracture distribution in granite and the relationship between fracture distribution and physical properties

*Manami Kadono[1], Shin-ichi Uehara[2], Miki Takahashi[3], Manami Kitamura[3]

1. Department of Environment Systems, Graduate School of frontier Science, The University of Tokyo, 2. Department of Enviroment Science, Faculty of Science, Toho University, 3. National Institute of Advanced Industrial Science and Technology

Recently, geothermal uses in the depth below the brittle-ductile boundary have been considered for collecting geothermal energy more efficiently than conventional geothermal uses [1]. One of them is supercritical geothermal power generation, which uses supercritical fluid of higher temperature and pressure than conventional type, and therefore output per power plant is expected to be increased [2]. In this geothermal development, there is a plan to artificially create geothermal reservoirs when the geothermal fluid enough for the power generation capacity does not exist in the rock. These artificial reservoirs are planned to be created through processes such as cooling rocks by water injection, emergence of brittle region, causing hydraulic fracturing, and then emergence of high permeability region. Here, crack generation and propagation by injecting water and cooling rock have some possibility of inducing earthquakes. Therefore, it is important to elucidate properties of crack generation and propagation in the rock in this situation. However, these properties have not been understood enough. In addition, clarifying the relationship between properties of crack distributions and elastic wave velocities, which is not established so far, may be of useful for investigating the crack distributions at actual geothermal development sites by elastic wave explorations.
In this study, we generate cracks in granite specimens by heating them up to 550℃ then cooling, and we clarified the relationship between the cooling rate and the conditions of crack distributions in the specimens. We also tried to clarify the relation between the crack conditions and physical properties such as (elastic wave velocity, porosity and elastic properties derived from the elastic wave velocities) .
Cylindrical specimens (20 mm in the diameter and 40 mm in the length) of granite from Oshima, Ehime Prefecture (initial porosity: <0.38 %, P and S wave velocity ($V_P$), ($V_S$) under water saturated condition: 5.96±0.14, 3.10±0.10 km/s, respectively) were used for the experiments. After being heated the specimens, were cooled in three ways with different cooling rates for the surface temperature (approximately 3.3 ℃/min, 17.7℃/min, and 516 ℃/sec). Observations of X-ray CT images revealed that microscopic cracks were generated in the specimens after the heating-cooling processes. Cracks were extracted from this CT images and the number of cracks was measured. The number of cracks per image (20 mm×40 mm) $N$ was $600 < N < 2600$, and the faster the cooling rate was, the larger $N$ per unit area was. This is probably because faster cooling rate causes the greater temperature difference between the center and surface of specimens, which causes larger difference in the degree of shrinkage of the minerals constituting the specimens, and then the minerals are easier to be separated from each other. When $N$ is lager, the porosity is larger (0.60 - 0.82%), and $V_P$ and $V_S$ are smaller (4.63 - 4.86 and 1.69 - 2.15 km/s, respectively). Bulk modulus and shear modulus were decreased from 61 - 65 to 45 - 48 GPa and 24 - 26 to 7 - 13 GPa, respectively, through the heating-cooling processes. In the presentation, we will investigate the relationship between $p$, a parameter representing the distribution propability of cracks defined by Hestir & Long [3], and physical properties.

References

[1] Muraoka, H., Asanuma, H., Ito, H., 2013, geoscience magazine, 343 - 361.
[2] Yonekura, H., 2016, "TSC Foresight geothermal power generation" overview,

©2019. Japan Geoscience Union. All Right Reserved. 

https://www.nedo.go.jp/content/100789529.pdf, 1 - 33.
[3] Hestir, K., and Long, J., 1990, Journal of geophysical research, vol. 95, 21, 565 - 21, 581.

Keywords: Granite, Fracture, Geothermal

©2019. Japan Geoscience Union. All Right Reserved. 

[J] Poster | S (Solid Earth Sciences )：S-CG Complex & General

Thu. May 30, 2019 5:15 PM - 6:30 PM JST | Thu. May 30, 2019 8:15 AM - 9:30 AM UTC | Poster Hall International Exhibition Hall8, Makuhari Messe_31

## [S-CG58] Brittle-Ductile Transition and Supercritical Geofluids for Crustal Energy in Island Arc

convener:Noriyoshi Tsuchiya(Graduate School of Environmental Studies, Tohoku University), Hiroshi Asanuma(AIST), Yasuo Ogawa(Volcanic Fluid Research Center, School of Science, Tokyo Institute of Technology), Shigemi Naganawa(Akita University)

Nature of rock mass below the brittle-ductile transition (BDT) is of great scientific interest to understand various phenomenon in the Earth's crust. We will review and discuss current understanding of characteristics the rock mass below the BDT, including composites, stress, failure mechanism induced by liquid injection and associates earthquake generation mechanism, and water rock interaction, considering engineered geothermal development in the BDT. Discussions on the possible phenomena in the geothermal development in the BDT will be followed in this session. <br/> New drilling technology is key of issues. This session will cover advanced drilling technology under high temperature conditions for energy extraction.<br/><br/>

### [SCG58-P01] Mechanical and hydrological properties of granite under supercritical fluid conditions

*Manami Kitamura[1], Miki Takahashi[1] (1.National Institute of Advanced Industrial Science and Technology)

### [SCG58-P02] Three-dimensional electrical resistivity structure of kuju Volcano, Central Kyushu, Japan revealed by Magnetotelluric survey data

*Sabry Abdallah[1], Mitsuru Utsugi [1], Koki Aizawa[2], Makoto Uyeshima[3], Wataru Kanda[4], Takao Koyama[3] (1.Institute of geothermal science, Faculty of Science, Kyoto University, 2.Institute of Seismology and Volcanology, Faculty of Sciences, Kyushu University, 3.Earthquake Research Institute, The University of Tokyo, 4.Volcanic Fluid Research Center, School of Science, Tokyo Institute of Technology)

### [SCG58-P03] Preliminary Report on Themoluminescence Geothermal Exploration in Northern Area of Mt. Kurikoma (Akayumata-River), NE Japan.

*Hiroki Okano[1], Nobuo Hirano[1], Noriyoshi Tsuchiya[1] (1.Graduate School of Environmental Studies Tohoku University)

### [SCG58-P04] Experimental Study of Critical Point Determination for Multicomponent Fluids using light-scattering Spectroscopic Method

*Nobuo Hirano[1], Yuta Oshima[1], Atsushi Okamoto[1], Noriyoshi Tsuchiya[1] (1.Graduate School of Environmental studies, Tohoku University)

### [SCG58-P05] Transport and Reaction Behavior of Supercritical Geofluid Revealed by Porphyry Copper Deposit

*Geri Agroli[1], Noriyoshi Tsuchiya[1] (1.Tohoku University)

### [SCG58-P06] Characteristics of precipitation of amorphous silica and its influences on permeability of fractured granite in superhot geothermal environments

*Hikaru Abe[1], Noriaki Watanabe[1], Kengo Nakamura[1], Atsushi Okamoto[1], Takeshi Komai[1] (1.Graduate School of Environmental Studies, Tohoku University)

### [SCG58-P07] Evolution and The Total Budget of Fluid in Granitic Magma through Magmatism and Volcanism in The Subduction Zone, NE Japan

*Fajar Febiani Amanda[1], Ryoichi Yamada[2], Satoshi Okumura[2], Masaoki Uno[1], Noriyoshi Tsuchiya[1] (1.Graduate School of Environmental Studies, Tohoku University, 2.Graduate School of Science, Tohoku

University)

[SCG58-P08] **Porosity generation during feldspar replacement as the mark of potassium-rich supercritical fluids on the top of granitic intrusion**

*Astin Nurdiana[1], Atsushi Okamoto[1], Masaoki Uno[1], Kenta Yoshida[2], Noriyoshi Tsuchiya[1] (1.Tohoku University, 2.Japan Agency for Marine-earth Science and Technology)

[SCG58-P09] Quantitative evaluation of fracture distribution in granite and the relationship between fracture distribution and physical properties

*Manami Kadono[1], Shin-ichi Uehara[2], Miki Takahashi[3], Manami Kitamura[3] (1.Department of Environment Systems, Graduate School of frontier Science, The University of Tokyo, 2.Department of Enviroment Science, Faculty of Science, Toho University, 3.National Institute of Advanced Industrial Science and Technology)

# Mechanical and hydrological properties of granite under supercritical fluid conditions

*Manami Kitamura[1], Miki Takahashi[1]

1. National Institute of Advanced Industrial Science and Technology

To extract geothermal energy effectively and safely from magma and/or adjacent hot rock, we need to tackle many issues which require new technology development. One of them we are targeting on is to develop a technology to mitigate induced-earthquakes. It is required to understand roles of factors on occurrences of the induced-earthquake (e.g., strength, crack density, and fluid-rock reaction) and their intercorrelations (e.g., *Asanuma* et al., 2012).

Our purpose of this series of experiments is to clarify a relationship between the rock strength and the fracture density under hydrothermally supercritical conditions. We conducted triaxial deformation test on intact granite rock strength under high-temperature (250 –750˚C), high-pressure (104 MPa) condition at a constant load velocity (0.1 μm/sec) using a gas-rig at GSJ, AIST. We used Oshima granite, which has initially ~0.55% of the porosity, 4.95±1.01 km/s in Vp at dry condition (dry). All experimental products showed brittle feature having several oblique fracture surfaces, but both value of peak stress and amount of stress drop became smaller at higher temperature. Additionally, Young’s modulus decreases with increasing the temperature from 57.4 GPa at 250˚C to 32.3 GPa at 750˚C. At 400˚C, the stress drop accelerated the deformation with ~98 times faster velocity than that at load-point. In contrast, at 650˚C and 750˚C, the velocity during stress drop kept the same order of the load-point velocity. Therefore, the deformation feature may start to be of ductile when the temperature exceeds 650˚C. The microstructures of samples deformed at 400˚C and 550˚C showed the shear zone with the grain reduction. In contrast, for the samples deformed at 650˚C and 750˚C, we partly observed the sintered structure at grain boundaries among feldspar gouge. The sintered structure at >650°C might be the cause of the slow stress drop. Highly dense cracked granite specimens were formed by a rapid decompression test (RDT) using an autoclave settled at Tohoku University (*Kitamura & Takahashi*, 2017AGU; *Takagi* et al., 2017GRC Trans.), caused by a reduction of the fluid pressure within 2 seconds from vapor/supercritical state pressure (10 –48 MPa, 550 ˚C) to ambient pressure. X-ray CT scanning on the specimens after RDT showed that numerous microcracks were generated in them (see details in *Takahashi & Kitamura*, 2018, annual meeting of Geological Soc. Japan). The RDT imposed the porosity increasing towards 3.91 % and Vp decreasing towards 1.46±0.22 km/s (dry). We conducted the permeability measurement on fractured granites after RDT with the porosity of 2.1 –2.7% under a combined condition of 400 ˚C in temperature, 104 MPa in confining pressure, 39 –99 MPa in pore fluid pressure ($P_p$). Permeability measured by pore pressure oscillation method decreases from $1.3\times10^{-16}$ $m^2$ at $P_p$ of 99 MPa to $2.6\times10^{-18}$ $m^2$ at $P_p$ of 39 MPa for the permeable case. Permeability on fractured granite of 2.1% in porosity at room temperature (RT) show relatively lower permeability than those at 400°C except for at $P_p$ of 99 MPa. Permeability at RT rapidly decreases from $1.0\times10^{-15}$ $m^2$ at $P_p$ of 99 MPa to $1.0\times10^{-18}$ $m^2$ at $P_p$ of 84 MPa, and then reaches $5.8\times10^{-19}$ $m^2$ at $P_p$ of 99 MPa. In the meeting, we will show additional results of permeability tests on fractured granites under various high temperature conditions.

Keywords: supercritical fluid, geothermal, granite

©2019. Japan Geoscience Union. All Right Reserved. 

# Three-dimensional electrical resistivity structure of kuju Volcano, Central Kyushu, Japan revealed by Magnetotelluric survey data

*Sabry Abdallah[1], Mitsuru Utsugi [1], Koki Aizawa[2], Makoto Uyeshima[3], Wataru Kanda[4], Takao Koyama[3]

1. Institute of geothermal science, Faculty of Science, Kyoto University, 2. Institute of Seismology and Volcanology, Faculty of Sciences, Kyushu University, 3. Earthquake Research Institute, The University of Tokyo, 4. Volcanic Fluid Research Center, School of Science, Tokyo Institute of Technology

The Kuju volcano is located in south western part of Oita prefecture, Japan , and is one of the important geothermal areas in Japan. It has began to erupt on October 11,1995 at the eastern flank of Mt. Hossho, which is in the central part of Kuju volcano. Second eruption started again in the middle of December, 1995, producing an ash volume of about 5000 $m^3$. Iwoyama is the central part Kuju Volcano and considered to be one of the most hydrothermal active hydrothermal field in Japan. Geothermal areas beneath active volcanoes may have an important role in geothermal energy development in the future. so it is important to monitor and clarify the thermal and hydrologic processes occurring beneath volcanoes. Magnetotelluric (MT) investigation is an important tool to identify the subsurface resistivity structure using natural variation in the electromagnetic field, therefore it is convenient to for the hydrothermal system investigation. We applied a Wide-band MT survey method to identify the structures associated with the hydrothermal systems beneath Kuju volcano. MT field survey data were collected at 63 observation points around the Kuju volcano from September to October 2015. Fourier Transform(FT) applied to the collected data to reduce the background noise associated with Power supply of 60 Hz and other noises associated with higher frequencies. Inverse FT was applied to the data to transform from frequency-domain to time-domain data. The 3-D resistivity structure model is obtained by inverting the MT impedance using ModEM code (Kelbert, A. et al., 2014). The primary 3-D resistivity structure model clarified that, a resistive structure (100-300 Ω.m) prevail the most of Kuju Volcano area. A very conductive structure (~1Ω.m) exists around Iowyama-Kuju area and extends with the depth towards the south-east part of Iowyama. In comparison with the previous studies, the resistive structure can be interpreted as lava and pyroclastic deposits, whereas the conductive structure around Iowyama-Kuju area is maybe corresponds to aquifers and altered layers.

Keywords: MT survey at Volcanic areas, 3D MT inversion, Hydro-thermal energy

©2019. Japan Geoscience Union. All Right Reserved. 

# Preliminary Report on Themoluminescence Geothermal Exploration in Northern Area of Mt. Kurikoma (Akayumata-River), NE Japan.

*Hiroki Okano[1], Nobuo Hirano[1], Noriyoshi Tsuchiya[1]

1. Graduate School of Environmental Studies Tohoku University

Thermoluminescence (TL) is a method to evaluate radiation dose accumulated in minerals by heating minerals and analyzing luminescence. We can evaluate geothermal manifestation through analyzing the variation of Paleodose in minerals caused by geothermal activities. In this study, geological survey waa performed around Mt. Takamatsudake in the northern area of Mt. Kurikoma, and We estimated geothermal structure of the area and relation between TL distribution and geothermal structure.

In the exploration area, the Takamatsudake lava is distributed around Mt. Takamatsudake, and in the lower part, Torageyama tuff formation is distributed , and also Doroyu fomation composed of mudstone is distributed in the lower part of the Torageyama tuff fomation. 33 samples were collected from Torageyama tuff and Doroyu fomation.

As a result of TL analysis, TL anomalies were confirmed downstream of Akayumata-river hot springs. However, no significant TL anomalies was observed around Yunomata hot springs. In Akayumata H.S(hot spring), boiling water are discharging from a few places, whereas Yunomata H.S are only spouted from one point at 50 ℃. In the earthquake hypocentral distribution from 1985 to 2015, hypocentral clusters are confirmed at shallow part arounf 2 ~ 7 km beneath Akayumata and Yunomata H.S, and it may suggest the existence of a fluid. Around Akayumata H.S, the mud layer is exposed with a local anticline structure. We suggest that hot water discharge to the surface along with cracks and faults associated with these geological structure.

As a result of alteration mineral analysis, both the Torageyama F. and the Doroyu F. were confirmed to have a Green Tuff alteration due to chlorite and sericite. In addition, kaolinite was found near the Akayumata H.S, and laumontite was found around Yunomata H.S. and upstream of Akayumata-river. TL anomaly is harmonious with the distribution of kaolinite, but the weakly related to the distribution of laumontite. From this point of view, it is predicted that TL has information on the temperature-time effect, which is different from altered minerals. By investigating more detailed underground structures in the future and conducting quantitative analysis on the temperature dependency of TL, it is expected that the accuracy of information given by the surface TL data can be improved.

Keywords: thermoluminescence, geothermal exploration, geophysical exploration

©2019. Japan Geoscience Union. All Right Reserved. 

# Experimental Study of Critical Point Determination for Multicomponent Fluids using light-scattering Spectroscopic Method

*Nobuo Hirano[1], Yuta Oshima[1], Atsushi Okamoto[1], Noriyoshi Tsuchiya[1]

1. Graduate School of Environmental studies, Tohoku University

Geofluid is a multicomponent fluid by reaction with various crustal materials, and it is in a supercritical state under high temperature and high pressure conditions inside the Earth. It is very important to know the critical point (CP) and phase state of a geo-fluid in order to know the fluid-rock reaction mechanism under high temperature and high pressure conditions. However, it is difficult to directly determine CP of multicomponent fluid such as geological fluid and sea water by calculation using state equation (EOS) using fluid components, and it is necessary to decide experimentally.
Molecules in the supercritical fluid are unevenly distributed and are known to form both high density and sparse molecular regions in the fluid. Such nonuniformity of molecular distribution is called density fluctuation, and this degree becomes maximum at CP of fluid.
Therefore, for pure material such as H 2 O and CO 2, the critical opalescence is spectroscopically observed at the subcritical to supercritical transition. Therefore, if the density variation of the multicomponent fluid can be observed by a spectroscopic method, it is possible to determine the CP value.
The objective of this study is to establish a new measurement technique / procedure for easily determining CP of multicomponent fluid using spectroscopic observation of subcritical / supercritical transition state.

Keywords: decision of critical point, multicomponent fluid, supercritical fluid, scatter spectroscopy

©2019. Japan Geoscience Union. All Right Reserved. 

# Transport and Reaction Behavior of Supercritical Geofluid Revealed by Porphyry Copper Deposit

*Geri Agroli[1], Noriyoshi Tsuchiya[1]

1. Tohoku University

Supercritical geothermal reservoir (SCGR) is a novel system in the geothermal field. Recently this geothermal system got a lot of attention from scholar since the successful of IDDP that encountered the supercritical fluid in Reykjanes and Krafla geothermal field. SCGR is promising exploited geothermal resource in the near future with several benefits in the economic and technical aspect. However the limited access to geological properties of SCGR system to optimize the potential of the system as well as to address the issue of the system lead us to investigate the natural analog that suitable with this system, Instead of we spend huge money for drilling activity. Porphyry copper deposit is a suitable candidate for SCGR analog where magma ascent from deep mantle and fluid infiltrate a ductile rock mass at ~600˚C, and stock work fracture as an important fluid pathway developed intensively.

The research was conducted on the largest porphyry copper deposit in northern Mongolia called Erdenet deposit. We used 700m depth drill core samples from an open pit. Based on texture and mineralogy, lithology of Erdenet comprises of quartz porphyry and granodiorite porphyry at shallow and deep level consecutively. Mineral assemblages of Quartz porphyry are qtz-ser-py-cp±cal and chl-plg-qtz±kfs for Granodiorite porphyry. Stockwork vein system can be well observed on certain samples and Er-22 (569.9m) reveal distinct vein generation process and evolution based on cross-cutting relationship. Qtz-Mo vein precipitated at the beginning of the process followed by the formation qtz-py±cp vein and those 2 vein type cut by qtz±cal vein. Fluid activity was investigated by several analytical techniques to measure mineral composition to further obtain thermodynamics properties (P-T conditions). Host rock crystallize at temperature 389-861˚C (measurement point from core to rim) using Ti-in-Quartz geothermometer under lithostatic pressure derived from a cotectic line in the Qz-Ab-Or ternary diagram. The similar methods perform to obtain quartz precipitation temperature of qtz-mo vein and the result show vein was precipitated at 323-678˚C (measurement point from core to rim). Fluid inclusion is a useful technique to determine the precipitation of the other two vein type. Qtz-py±cp vein homogenizes at temperature 147.8-358.9˚C with median 251.9˚C but the pressure regime and salinity of fluid are difficult to measure due to most of the inclusion size is less than 5 $\mu$m. The last fluid activity marked by the presence of qtz±cal that cut all of the previous veins. The homogenization temperature is less than 200˚C.

The distribution of vein in the granodiorite porphyry system in Erdenet revealed the evolution of fluid in order to understand the geological properties of a supercritical geothermal reservoir. The emplacement of granodiorite at >600˚C followed by formation of qtz-mo vein that interpreted to have formed in the supercritical regime at 500-600˚C under lithostatic pressure and subsequent pressure drop to hydrostatic condition induce qtz-py±cp vein formation due to drop of silica solubility. Lithostatic to hydrostatic pressure shifting indicate by the presence of pervasive sericite alteration imply meteoric water had circulated into the system. The temperature of the system keeps decrease and precipitation of qtz±cal occurred as the last product on this system. Erdenet Cu-Mo provides a lesson regarding on fluid process and development of supercritical geothermal activity and strong candidate as a natural analog for advanced scientific studied in the future.

©2019. Japan Geoscience Union. All Right Reserved. 

Keywords: supercritical geothermal reservoir, erdenet, porphyry deposit, fluid inclusion

©2019. Japan Geoscience Union. All Right Reserved. 

# Characteristics of precipitation of amorphous silica and its influences on permeability of fractured granite in superhot geothermal environments

*Hikaru Abe[1], Noriaki Watanabe[1], Kengo Nakamura[1], Atsushi Okamoto[1], Takeshi Komai[1]

1. Graduate School of Environmental Studies, Tohoku University

Superhot geothermal environments (above ca. 400˚C) represent a new geothermal energy frontier. However, the networks of permeable fractures capable of storing and transmitting fluids are likely to sealed by a rapid precipitation of amorphous silica in response to an occurrence of high-level of supersaturation for amorphous silica due to a phase change between liquid water, steam, and supercritical water. Here we report results of two sets of hydrothermal precipitation experiments at 400-500˚C and 20-35 MPa, which were respectively conducted to investigate characteristics of precipitation of amorphous silica and its influences on permeability of fractured granite in superhot geothermal environments. In the first set of the precipitation experiments, liquid water with a prescribed Si concentration, which was prepared from water that dissolved granite at 360 ˚C and 35 MPa, was injected to a stainless-steel pipe, in which amorphous silica was precipitated at a prescribed combination of temperature (400-500˚C), pressure (20-35 MPa) and degree of saturation (1.5-2.5). As a result, spherical particles of amorphous silica of <10 μm (typically, 0.2-1.0 μm) were precipitated at all conditions. These particles tended to become smaller and aggregated with increasing temperature or degree of saturation (i.e., with increasing rate of nucleation), while there was no significant influence of pressure. Based on this finding, the second set of the precipitation experiments to investigate influences of the amorphous silica particles on permeability of fractured granite was conducted at 450°C, 25 MPa, and different degrees of saturation. The above-mentioned liquid water with a prescribed Si concentration was injected into a thermally fractured granite containing multiple fractures at an effective confining stress of 10 MPa, where initial permeability of the fractured granite was relatively high (ca. $10^{-16}$ $m^2$) because of the presence of fractures having relatively large apertures of >10 μm. As a result, permeability did not decrease with time at both conditions for the formations of larger and dispersed particles, and smaller and aggregated particles. This finding indicates that precipitation of amorphous silica does not always reduce permeability of fractured granite immediately, and silica particles will move to other locations after its formation. Therefore, in producing superhot geothermal energy, amorphous silica particles will be produced via a production well or will be trapped within fractured granite having a relatively lower initial permeability, therefore relatively smaller apertures. Although the present study has not been completed yet, it is suggested that in case of a superhot geothermal reservoir with permeability aperture large enough to transmit the amorphous silica particle, the permeability may not be destroyed even if precipitation of amorphous silica occurs rapidly.

©2019. Japan Geoscience Union. All Right Reserved. 

# Evolution and The Total Budget of Fluid in Granitic Magma through Magmatism and Volcanism in The Subduction Zone, NE Japan

*Fajar Febiani Amanda[1], Ryoichi Yamada[2], Satoshi Okumura[2], Masaoki Uno[1], Noriyoshi Tsuchiya[1]

1. Graduate School of Environmental Studies, Tohoku University, 2. Graduate School of Science, Tohoku University

Fluids (especially water) are carried by oceanic plates which are subducted into the depth of the mantle and released through the dehydration process. Water migrates upward and contributes to the melting of the mantle wedge in the formation of an arc magma. The formation of volcanoes and igneous rocks as plutons in the arc magma produces geothermal energy sources and the formation of ore mineral deposits. Throughout its migration within the crust, the fluid evolves both in temperature and pressure, composition and amount. These fluid traces can be found among the minerals as melt and/or fluid inclusions in volcanic products, igneous plutons, and the veinlets. In this study, water budget estimated on the crust by determining the condition of P-T and composition of fluids in the volcanic rocks and igneous plutons including the host rock and veinlets.

Samples were taken from caldera fill sediment and porphyry copper deposits in NE Japan region. The P-T condition and fluid composition are measured from the melt inclusion in quartz from the caldera fill sediments and fluid inclusions in the granite intrusion and the veinlets. The sample is divided into several types, namely volcanic rock samples from caldera fill sediment, granite from porphyry copper deposits, and the veinlets contained in the granite body including quartz vein, glassy vein, and hydrothermal breccia vein. In volcanic rock samples, quartz crystals were picked, encased in resin and polished for major element and water content analysis. In granite samples and veinlets, the rock thin sections were made for fluid inclusion microthermometry analysis and fluid diffusion analysis using apatite mineral. Water budget in the upper crust is estimated from caldera fill sediments to be 2.3–7.6 t /yr/m. Water budget in the deeper part of the crust can then be determined from porphyry copper deposits.

Keywords: water budget, fluid evolution, melt inclusion, fluid inclusion

©2019. Japan Geoscience Union. All Right Reserved. 

# Porosity generation during feldspar replacement as the mark of potassium-rich supercritical fluids on the top of granitic intrusion

*Astin Nurdiana[1], Atsushi Okamoto[1], Masaoki Uno[1], Kenta Yoshida[2], Noriyoshi Tsuchiya[1]

1. Tohoku University, 2. Japan Agency for Marine-earth Science and Technology

Feldspar replacement is prevalent process within the crust which has been studied for decades. In particular, it is known that feldspar is texturally sensitive to an interaction with fluids, and the process often results in by the pore generation. Recently, Plümper, et al. (2017) proposed that such reaction-induced nanoporosity plays significant roles in pervasive fluid flow in the crusts, yet it is still unclear until what extent nanoporosity commonly presents and is affected by the feldspar replacement. In this study, we report novel pore structures that have been produced during feldspar replacement in the hornblende schist around the granitoid body.

The Kinkasan Island, which is part of southern Kitakami Mountains, mainly consists of the Cretaceous granitoid bodies with abundant pegmatite dikes, and metamorphic sequences, including hornblende (Hbl) schists and biotite schists. Quartz diorite, as the host plutonic body, and metamorphic rocks were formed under the conditions estimated to be 700-750˚C and 610-660˚C in 0.37-0.42 GPa, respectively. The Hbl schists are often cut by thin alkali feldspar veins in direction perpendicular to the foliation. In the matrix, primordial plagioclase grains (An48Ab52Or0) are generally replaced by patchy grains of albite (An4Ab94Or2) and alkali feldspar (An0Ab1Or99). The mass balance analyses of the plagioclase and alteration products show the gains of Si, K, and fewer Na, also loss of Ca and Al, indicating that feldspar replacement was induced by infiltration of the potassium-rich fluids (the K/Na molar ratio of 3). The detail observations by FIB-SEM reveal that the replacement process yields extensive amount of pore with throat size of ~0.1 –5 $\mu$m. These pores preferentially formed along the grain boundaries of newly-produced albite. Generally, the pores distribute throughout all the plagioclase grains without preference for matrix grain boundary, and formed 3D pore network that seems barely to continue. However, it increased the porosity of the rock up to ~2%. These features of pores related to the feldspar replacement suggests the importance of the reactive fluid infiltration through low-permeability metamorphic rocks, likewise give a new insight on how fluid propagation generate micro-to nano-scale porosity.

Reference: Plümper et al., 2017. Nature geoscience, 10, 685-690.

Keywords: feldspar replacement, pore network, potassium-rich fluids, fluid transport, FIB-SEM

©2019. Japan Geoscience Union. All Right Reserved. 

# Quantitative evaluation of fracture distribution in granite and the relationship between fracture distribution and physical properties

*Manami Kadono[1], Shin-ichi Uehara[2], Miki Takahashi[3], Manami Kitamura[3]

1. Department of Environment Systems, Graduate School of frontier Science, The University of Tokyo, 2. Department of Enviroment Science, Faculty of Science, Toho University, 3. National Institute of Advanced Industrial Science and Technology

Recently, geothermal uses in the depth below the brittle-ductile boundary have been considered for collecting geothermal energy more efficiently than conventional geothermal uses [1]. One of them is supercritical geothermal power generation, which uses supercritical fluid of higher temperature and pressure than conventional type, and therefore output per power plant is expected to be increased [2]. In this geothermal development, there is a plan to artificially create geothermal reservoirs when the geothermal fluid enough for the power generation capacity does not exist in the rock. These artificial reservoirs are planned to be created through processes such as cooling rocks by water injection, emergence of brittle region, causing hydraulic fracturing, and then emergence of high permeability region. Here, crack generation and propagation by injecting water and cooling rock have some possibility of inducing earthquakes. Therefore, it is important to elucidate properties of crack generation and propagation in the rock in this situation. However, these properties have not been understood enough. In addition, clarifying the relationship between properties of crack distributions and elastic wave velocities, which is not established so far, may be of useful for investigating the crack distributions at actual geothermal development sites by elastic wave explorations.
In this study, we generate cracks in granite specimens by heating them up to 550℃ then cooling, and we clarified the relationship between the cooling rate and the conditions of crack distributions in the specimens. We also tried to clarify the relation between the crack conditions and physical properties such as (elastic wave velocity, porosity and elastic properties derived from the elastic wave velocities) .
Cylindrical specimens (20 mm in the diameter and 40 mm in the length) of granite from Oshima, Ehime Prefecture (initial porosity: <0.38 %, P and S wave velocity ($V_P$), ($V_S$) under water saturated condition: 5.96±0.14, 3.10±0.10 km/s, respectively) were used for the experiments. After being heated the specimens, were cooled in three ways with different cooling rates for the surface temperature (approximately 3.3 ℃/min, 17.7℃/min, and 516 ℃/sec). Observations of X-ray CT images revealed that microscopic cracks were generated in the specimens after the heating-cooling processes. Cracks were extracted from this CT images and the number of cracks was measured. The number of cracks per image (20 mm×40 mm) $N$ was $600 < N < 2600$, and the faster the cooling rate was, the larger $N$ per unit area was. This is probably because faster cooling rate causes the greater temperature difference between the center and surface of specimens, which causes larger difference in the degree of shrinkage of the minerals constituting the specimens, and then the minerals are easier to be separated from each other. When $N$ is lager, the porosity is larger (0.60 - 0.82%), and $V_P$ and $V_S$ are smaller (4.63 - 4.86 and 1.69 - 2.15 km/s, respectively). Bulk modulus and shear modulus were decreased from 61 - 65 to 45 - 48 GPa and 24 - 26 to 7 - 13 GPa, respectively, through the heating-cooling processes. In the presentation, we will investigate the relationship between $p$, a parameter representing the distribution propability of cracks defined by Hestir & Long [3], and physical properties.

References

[1] Muraoka, H., Asanuma, H., Ito, H., 2013, geoscience magazine, 343 - 361.
[2] Yonekura, H., 2016, "TSC Foresight geothermal power generation" overview,

©2019. Japan Geoscience Union. All Right Reserved. 

https://www.nedo.go.jp/content/100789529.pdf, 1 - 33.
[3] Hestir, K., and Long, J., 1990, Journal of geophysical research, vol. 95, 21, 565 - 21, 581.

Keywords: Granite, Fracture, Geothermal

©2019. Japan Geoscience Union. All Right Reserved. 

[J] Oral | S (Solid Earth Sciences)：S-CG Complex & General

Thu. May 30, 2019 1:45 PM - 3:15 PM JST | Thu. May 30, 2019 4:45 AM - 6:15 AM UTC | A09 TOKYO BAY MAKUHARI HALL

## [S-CG58] Brittle-Ductile Transition and Supercritical Geofluids for Crustal Energy in Island Arc

convener:Noriyoshi Tsuchiya(Graduate School of Environmental Studies, Tohoku University), Hiroshi Asanuma(AIST), Yasuo Ogawa(Volcanic Fluid Research Center, School of Science, Tokyo Institute of Technology), Shigemi Naganawa(Akita University), Chairperson:Noriyoshi Tsuchiya, Atsushi Okamoto

Nature of rock mass below the brittle-ductile transition (BDT) is of great scientific interest to understand various phenomenon in the Earth's crust. We will review and discuss current understanding of characteristics the rock mass below the BDT, including composites, stress, failure mechanism induced by liquid injection and associates earthquake generation mechanism, and water rock interaction, considering engineered geothermal development in the BDT. Discussions on the possible phenomena in the geothermal development in the BDT will be followed in this session. <br/>
New drilling technology is key of issues. This session will cover advanced drilling technology under high temperature conditions for energy extraction.<br/><br/>

1:45 PM - 1:55 PM JST | 4:45 AM - 4:55 AM UTC

[SCG58-01] Supercritical Geothermal Resources as a Function of Mass and Energy Transport in Subduction Zone

*Noriyoshi Tsuchiya[1] (1.Graduate School of Environmental Studies, Tohoku University)

---

1:55 PM - 2:05 PM JST | 4:55 AM - 5:05 AM UTC

[SCG58-02] Outline of NEDO Supercritical Geothermal Project

*Hiroshi Asanuma[1] (1.AIST)

---

2:05 PM - 2:30 PM JST | 5:05 AM - 5:30 AM UTC

[SCG58-03] Mineral precipitation/dissolution from water and brine with decreasing temperatures along hydrostatic pressures

★Invited Papers

*Kenichi Hoshino[1] (1.Department of Earth and Planetary Systems Science, Hiroshima University)

---

2:30 PM - 2:45 PM JST | 5:30 AM - 5:45 AM UTC

[SCG58-04] Thermodynamic data of aqueous species for supercritical water–rock interaction: dissolution experiments and density-based extrapolation

*Atsushi Okamoto[1], Hajime Ishii[1], Ryosuke Oyanagi[2], Noriyoshi Tsuchiya[1] (1.Graduate School of Environmental Studies, 2.JAMSTEC)

---

2:45 PM - 3:00 PM JST | 5:45 AM - 6:00 AM UTC

[SCG58-05] Nitrogen isotope ratios of ammonium in hypersaline hot spring waters distributed along Arima-Takatsuki fault zone.

*Kazuhiro Amita[1], Takashi Nakamura[2], Shinji Ohsawa[3] (1.Faculty of Engineering Science, Akita University, 2.International Research Center for River Basin Environment, University of YAMANASHI, 3.Institute for Geothermal Sciences, Graduate School of Science, Kyoto University)

---

3:00 PM - 3:15 PM JST | 6:00 AM - 6:15 AM UTC

[SCG58-06] **Crustal fluid pressure gradients and permeability estimated from fluid-rock reaction zones**

*Masaoki Uno[1], Diana Mindaleva[1], Noriyoshi Tsuchiya[1] (1.Graduate School of Environmental Studies, Tohoku University)

# Supercritical Geothermal Resources as a Function of Mass and Energy Transport in Subduction Zone

*Noriyoshi Tsuchiya[1]

1. Graduate School of Environmental Studies, Tohoku University

Our research group is conducting fundamental and engineering studies of “Supercritical Geothermal Development”. Fracture networks and their formation mechanisms would be studied by using petrological and fluid inclusion studies in order to understand the geological model of a supercritical geothermal reservoir. The granite-porphyry system provides useful information for understanding supercritical geothermal reservoirs and EGS technology as novel energy system in subduction zone. Hydrothermal experiments under supercritical conditions were performed by using tri-axial machine. Fracture cloud could be formed and permeability was enhanced in supercritical conditions.
Selected References as follow:
[1] Noriaki Watanabe, Kiyotoshi Sakaguchi, Ryota Goto, Takahiro Miura, Kota Yamane, Takuya Ishibashi, Youqing Chen, Komai Takeshi and Noriyoshi Tsuchiya, “Cloud-fracture networks as a means of accessing superhot geothermal energy”, Scientific Reports Scientific (2019), 10.1038/s41598-018-37634-z
[2] Fajar F Amanda, Ryoichi Yamada, Masaoki Uno, Satoshi Okumura adn Noriyoshi Tsuchiya, “Evaluation of Caldera Hosted Geothermal Potential during Vaolcanism and Magnetism in Subduction System, NE Japan” ,Geofluids (2019).
[3] Batkhishig, B., Bignall, G., Tsuchiya, N. "Hydrothermal quartz vein formation, revealed by coupled SEM-CL imaging and fluid inclusion microthermometry: Shuteen Complex, South Gobi, Mongolia." Resource Geology, (2014), 55, 1-8.
[4]Tsuchiya, N., Yamada, R., and Uno, M. "Supercritical geothermal reservoir revealed by a granite–porphyry system." Geothermics, 63, (2016), 182-194.
[5]Watanabe, N., Hirano, N. & Tsuchiya, N. "Determination of aperture structure and fluid flow in a rock fracture by a high-resolution numerical modeling on the basis of a flow-through experiment under confining pressure." Water Resource Research, 44, (2008), W06412 .
[6]Watanabe, N., Hirano, N., Tsuchiya, N. "Diversity of channeling flow in heterogeneous aperture distribution inferred from integrated experimental-numerical analysis on flow through shear fracture in granite." J. Geophysical. Research, 114, (2009), 10.1029/2008JB005959.
[7]Ishibashi, T., Watanabe, N., Asanuma, H., and Tsuchiya, N. "Linking microearthquakes to fracture permeability." Geophysical Research Letters, (2016), 10.1002/2016GL069478.
[8]Watanabe, N., Numakura, T., Sakaguchi, K., Saishu, H., Okamoto, A., Ingebritsen, S. E. and Tsuchiya, N. "Potentially exploitable supercritical geothermal resources in the ductile crust." Nature Geoscience, (2017), 10.1038/NGEO2879.
[9]Saishu, H., Okamoto, A., and Tsuchiya, N. "Mineralogical variation of silica induced by Al and Na in hydrothermal solutions." American Mineralogist, 97, (2012), 2060-2063.
[10]Saishu, H., Okamoto, A., and Tsuchiya, N. "The significance of silica precipitation on the formation of the permeable–impermeable boundary within Earth’s crust, Terra Nova, 26, (2014), 253-259.

Keywords: geothermal, subduction zone, energy transport, supercritical

©2019. Japan Geoscience Union. All Right Reserved. 

# Outline of NEDO Supercritical Geothermal Project

*Hiroshi Asanuma[1]

1. AIST

Nationalwide potential of “Supercritical Geothermal Power Generation” has been roughly estimated to reach hundreds GW, although there are a lot of scientific unknowns and necessary technological breakthroughs. NEDO has funded to survey the most promising location of the proof-of-concept drilling and to investigate detailed feasibility of the Supercritical Geothermal Power Generation from FY2018, and 6 projects are on-going. Outline of the studies in the NEDO Supercritical Geothermal Project will be presented in the session.

Keywords: Supercritical Geothermal

©2019. Japan Geoscience Union. All Right Reserved. 

# Mineral precipitation/dissolution from water and brine with decreasing temperatures along hydrostatic pressures

*Kenichi Hoshino[1]

1. Department of Earth and Planetary Systems Science, Hiroshima University

Mineral-fluid interactions with decreasing temperatures along hydrostatic pressures, from 15.84 MPa - 500°C to 6.64 MPa - 200°C, have been simulated for 0.01 molal and 1 molal NaCl solutions. The dielectric constants of the former were taken from SUPCRT92 (Johnson et al., 1992), while those of the latter has been proposed from quartz solubility data in brine as:

$$\varepsilon_b / \varepsilon_w = a / (2\pi b)^{0.5} \exp(-(T - c)^2 / (2b)) + d,$$

where, $\varepsilon_b$ is the constant of the 1 molal NaCl solution, $\varepsilon_w$ is that of water derived by SUPCRT92, $\pi$ represents the ratio of the circumference of a circle to its diameter, T is a temperature in Celsius, the parameter a depends on a pressure (P in MPa) as a = -0.9 * P + 420, and b, c and d are the constants as 13000, 300 and 0.8, respectively.

On the other hand, a difference in chemical potentials of a jth solute ($\Delta\mu^\circ_j$) in the solution and water may be expressed as:

$$\Delta\mu^\circ_j = \omega_j (1/\varepsilon_b - 1/\varepsilon_w),$$

where, $\omega_j$ is the Born coefficient of the solute. Since the coefficients of the most charged species as well as $SiO_{2(aq)}$ are positive and $\varepsilon_b$ is larger than $\varepsilon_w$ in the simulated conditions, the chemical potentials of the above solutes in brine are smaller than those in water. This causes great differences between mineral solubilities in water (0.01M NaCl) and in brine (1M NaCl) as below.

Quartz

Since quartz solubility decreases with decreasing temperatures in water and brine, quartz precipitates from the both solvents with decreasing temperatures. However, because a decreasing rate of solubility in brine is smaller at higher temperatures and larger at lower temperatures, the precipitation amount shows a maximum at around 350 - 400°C. On the other hand, the amount decreases monotonically with decreasing temperatures in water.

Feldspar

Aluminum is dissolved mostly as $AlO_2^-$ (= $Al(OH)_4^-$) in the both solvents. Equilibrium constants of dissolution reactions of K-feldspar, albite and anorthite with the above Al species decrease with decreasing temperatures. Therefore, the precipitation amounts of those feldspar from water solvent decrease monotonically with decreasing temperatures. On the other hand, it is quite interesting that they dissolve in brine at higher temperatures, while precipitate at lower.

Pyroxene and Al-free amphibole

Most pyroxene and amphibole show similar tendencies as feldspar. They gradually precipitate or dissolve small amounts with decreasing temperatures in water, while they dissolve in brine at higher temperatures and precipitate at lower.

One of the conceivable causes of the above temperature dependencies of the silicate precipitation/dissolution in brine is a great difference in activity coefficients of charged species. For

©2019. Japan Geoscience Union. All Right Reserved. 

example, the activity coefficients (Debye-Hückel terms) for a divalent element in 0.01M NaCl solutions at 450°C and 300°C are 0.34 and 0.47, respectively, while they differ largely in 1M solutions as 0.023 and 0.20, respectively.
Carbonate
$CO_{2(aq)}$ is the major dissolved species above 250°C in the both solvents. Since the equilibrium constants of dissolution reactions of calcite, dolomite and magnesite with $CO_{2(aq)}$ decrease with decreasing temperatures, they precipitate from water gradually with decreasing temperatures, while they dissolve in brine at higher temperatures and precipitate at lower as feldspar, pyroxene and amphibole.

It should be emphasized that the temperatures of brine at which the above all silicate and carbonate minerals change their modes from dissolution to precipitation are around 400°C - 300°C.

Precipitation/dissolution of solid solutions of the above minerals and alteration (hydration) of some of the above minerals will also be discussed in the presentation.

Keywords: dielectric constant, brine, mineral, precipitation, dissolution

©2019. Japan Geoscience Union. All Right Reserved. 

# Thermodynamic data of aqueous species for supercritical water–rock interaction: dissolution experiments and density-based extrapolation

*Atsushi Okamoto[1], Hajime Ishii[1], Ryosuke Oyanagi[2], Noriyoshi Tsuchiya[1]

1. Graduate School of Environmental Studies, 2. JAMSTEC

Geothermal reservoirs under the supercritical conditions (supercritical geothermal reservoirs) have been taken grater attentions as the potential renewable energy in volcanic areas in the world. The chemical and physical processes of such supercritical regions are of special importance for various geological processes including understanding the formation of hydrothermal ore deposits, hydrological properties around brittle-ductile transitions of the crusts, and metamorphic and metasomatic processes. The thermodynamic data of the aqueous species at elevated temperatures and pressures has been constructed based on the Helgeson-Kirham-Flowers (HKF) model, where molar Gibbs energy is defined as a function of dielectric constant of water and species-specific Born parameter (e.g., Tanger and Helgeson, 1988), and the most common data is available through a software SUPCRT92. However, a large issue for understanding the supercritical water-rock interaction is a lack of thermodynamic data of charged aqueous species (ions and complexes) for the region near critical point of water and low water-density region (<0.35 g/cm3). In contrast to the electrostatic model like HKF model, the empirical density model has been proposed based on the fact that the log of molar Gibbs free energy of aqueous species shows a linear relationship with log of water density. Based on this model, Caciagli and Manning (2003) proposed the extrapolation of SUPCRT log K data to the high pressure regions; however, the effectiveness of this method to the low density region is not clear. In addition, the experiments for dissolution experiments are lacking for the low-density region.

In the present study, we tried the expansion of log K data set of the speciation and mineral dissolution into the vapor-like supercritical region (400, 420 degreeC, 20-35 MPa). We also conducted the new experiments for the mineral solubility measurements. The apparatus consist of 60 ml vessel with Ti inner wall, and pressure was controlled by syringe pump. We conducted the dissolution experiments with albite power and mix powders of albite-K-feldspar-quartz. Then, for evaluating the validity of the extrapolated data, we compared the extrapolated logK of mineral dissolution equilibrium and the ion products (log Q) obtained from the solution chemistry of the experiments and extrapolated log K data set of aqueous species. The deviation of log K from log Q is systematic and less than 2 in log unit, indicating the effectiveness of this method as the first approximation.

Reference

Tanger , J.C., Helgeson, H.C., 1988. Am J Sci, 288, 19-98.

Caciagli N.C., Manning, C.E., 2003. Contrib. Mineral Petrol, 146, 275-285.

Keywords: thermodynamic data, supercritical fluids, water-rock interaction, hydrothermal experiments

©2019. Japan Geoscience Union. All Right Reserved. 

# Nitrogen isotope ratios of ammonium in hypersaline hot spring waters distributed along Arima-Takatsuki fault zone.

*Kazuhiro Amita[1], Takashi Nakamura[2], Shinji Ohsawa[3]

1. Faculty of Engineering Science, Akita University, 2. International Research Center for River Basin Environment, University of YAMANASHI, 3. Institute for Geothermal Sciences, Graduate School of Science, Kyoto University

Recently, there has been a lot of research on the relationship between hot springs and deep thermal fluids (Slab dehydrated fluids) which are thought to be released from subducting oceanic plate (eg, Kazahaya et al., 2014; Kusuda et al., 2014). These researches shown that the water of slab dehydrated fluid is a high salinity of Na-Cl type and rich in the CO2, and that the isotope ratios of helium and carbon had the similar values as that of the mantle. On the other hand, although nitrogen (ammonium ion) is a component contained in most deep fluids, it is not clear properties and behaviors. Studies on nitrogen in rocks have been conducted since the 1960's that have been obtained many knowledge on their concentrations and isotope ratios. Haendel (1986) pointed out that the concentration and isotope ratios of ammonia nitrogen in rock, change systematically with the progression of a series of metamorphism from sediment to rock. In this relation, the nitrogen concentration decreased as the degree of metamorphism progressed, and conversely the nitrogen isotopic ratio increased. Similar trends have also been confirmed in subsequent studies (eg, Gray and Marilyn, 1991, Yiefei, 2006). On the other hand, Amita et al. (2014) pointed out the possibility that metamorphism is involved in the made of deep thermal fluids. Therefore, it is expected that we can obtain knowledge about the behavior of nitrogen in deep under the earth's surface by clarifying the relationship between the nitrogen isotope ratios of rocks and deep fluids. Therefore, as a preliminary approach to the measurement of the nitrogen isotope ratios of ammonium ion contained in the hypersaline hot spring, two hot springs distributed along the Arima-Takatsuki fault zone are selected and performed sampling survey and nitrogen isotope ratios of ammonium ion were measured. Two sampling points are part of the hot springs that the authors have performed research in the past (Osawa et al., 2015) and are well-understood hot springs whose chemical and isotopic properties. Therefore, as a preliminary approach to the measurement of the nitrogen isotope ratios of ammonium ion contained in the hypersaline hot spring, two hot springs distributed along the Arima-Takatsuki fault zone are selected and performed sampling survey and nitrogen isotope ratios of ammonium ion were measured. The hot spring water samples collected at the sampling site were immediately cooled and frozen immediately to suppress biological activity and kept until just before the isotope analysis. Pretreatment for measurement of nitrogen stable isotope ratio of ammonium ion was carried out by ammonia gas diffusion method which can suppress measurement inhibition due to decomposition of dissolved organic nitrogen. The water samples were made alkaline in a sealing vial, ammonium ion was scattered as ammonia gas, and catched to a filter paper acidified with diluted sulfuric acid, and the object was analyzed using an isotope ratio mass spectrometer (ANCA-GSL with Hydra 20-20, Sercon Ltd.). As a result of the analysis, we obtained results of +13.3 (‰) and +12.8 (‰) as nitrogen isotope ratios of two hot spring water samples. Since these results are values before data correction, careful consideration is required at the evaluation. Although, it was confirmed that the measurement of nitrogen isotopic ratios can be performed even for hyper saline hot springs where the total dissolved solids exceeds tens of thousands ppm.

Keywords: Nitrogen isotope ratios, Ammonium ion, Hypersaline hot spring

©2019. Japan Geoscience Union. All Right Reserved. 

# Crustal fluid pressure gradients and permeability estimated from fluid-rock reaction zones

*Masaoki Uno[1], Diana Mindaleva[1], Noriyoshi Tsuchiya[1]

1. Graduate School of Environmental Studies, Tohoku University

High pore fluid pressure has been recognized by geophysical observations and is generally considered as triggers of earthquakes and slow–earthquakes (e.g., Audet and Bürgmann, 2014). Although such high pore fluid pressure is recognized as mineral filled fractures in geologic observations, the actual fluid pressure gradients in the crustal rock have not been evaluated quantitatively and remain largely unknown. Here we propose a new methodology estimating the fluid pressure gradients recorded in fluid-rock reaction zones, by utilizing thermodynamic analyses in conjunction with trace element profiles along the reaction zones. With numerical analysis of reactive advection-diffusion transport profiles of Cl and F in the fluid-rock reaction zones, we constrain the duration, fluid velocity and permeability of the fluid-rock reaction zones. We have analyzed amphibolite and granulite hosted fluid–rock reaction zones at Sør Rodane mountains, East Antarctica. The analyses of decimeter scale granitic dyke–crust reaction zone at 0.5 GPa, 700˚C (Uno et al., 2017) show fluid pressure gradients of ~100 MPa/10 cm or ~1 MPa/mm. mm-sized hydration reaction zones around single fracture at ~0.5 GPa, 450˚C (Mindaleva et al., in prep.) also suggest fluid pressure gradients of ~1 MPa/mm. These extremely high fluid pressure gradients represent the low permeability of the intact amphibolite and granulite host rocks without fractures. The estimated permeabilities are ~$10^{-20}$ $m^2$ for the granulite–granitic dyke reaction zones and amphibolite–fluid reaction zones, and are several orders smaller than the widely accepted crustal permeability model (~$10^{-18}$ $m^2$; e.g., Ingebritsen and Manning, 2010). On the other hand, permeability along the fractures are estimated as high as $10^{-14–15}$ $m^2$ for the granulite and amphibolite-hosted fractures, which is analogous to the permeability estimated for the hypocenter migration for the inland earthquake swarms (~$10^{-15}$ $m^2$; e.g., Okada et al., 2014). These results show the importance of low permeability of intact amphibolite/granulite-facies metamorphic rocks in conjunction with episodic high permeability of brittle fractures even at high temperature conditions of 450–700˚C, both of which affect the regional scale permeability in the deep crust.

[References]
Audet, P., Bürgmann, R., 2014. *Nature* **509**, 389–92.
Ingebritsen, S.E., Manning, C.E., 2010. *Geofluids* **10**, 193–205.
Okada, T., Matsuzawa, T., Umino, N. et al., 2015. *Geofluids* **15**, 293–309.
Uno, M., Okamoto, A., Tsuchiya, N., 2017. *Lithos* **284–285**, 625–641.

Keywords: fluid pressure gradient, permeability, time-scales of fluid infiltration, fluid-rock reaction zone

©2019. Japan Geoscience Union. All Right Reserved. 

[J] Oral | S (Solid Earth Sciences)：S-CG Complex & General

Thu. May 30, 2019 3:30 PM - 5:00 PM JST | Thu. May 30, 2019 6:30 AM - 8:00 AM UTC | A09 TOKYO BAY MAKUHARI HALL

## [S-CG58] Brittle-Ductile Transition and Supercritical Geofluids for Crustal Energy in Island Arc

convener:Noriyoshi Tsuchiya(Graduate School of Environmental Studies, Tohoku University), Hiroshi Asanuma(AIST), Yasuo Ogawa(Volcanic Fluid Research Center, School of Science, Tokyo Institute of Technology), Shigemi Naganawa(Akita University), Chairperson:Noriyoshi Tsuchiya

Nature of rock mass below the brittle-ductile transition (BDT) is of great scientific interest to understand various phenomenon in the Earth's crust. We will review and discuss current understanding of characteristics the rock mass below the BDT, including composites, stress, failure mechanism induced by liquid injection and associates earthquake generation mechanism, and water rock interaction, considering engineered geothermal development in the BDT. Discussions on the possible phenomena in the geothermal development in the BDT will be followed in this session. <br/> New drilling technology is key of issues. This session will cover advanced drilling technology under high temperature conditions for energy extraction.<br/><br/>

3:30 PM - 3:45 PM JST | 6:30 AM - 6:45 AM UTC

[SCG58-07] 3D S-wave velocity structure in volcanic region using surface-wave tomography

*Hiro Nimiya[1], Tatsunori Ikeda[1], Takeshi Tsuji[1] (1.Kyushu University)

---

3:45 PM - 4:00 PM JST | 6:45 AM - 7:00 AM UTC

[SCG58-08] Resistivity-Based Temperature and Permeability Estimation of the Kakkonda Geothermal Field, Japan, Using a Neural Network

*Ugou Tsubasa[1], Kazuya Ishitsuka[2], Toru Mogi[3] (1.Department of Socio-Environmental Engineering Scool of Engineering Hokkaido University, 2.Division of Urban Management, Grduate School of Engineering, Kyoto University, 3.Division of Sustinable Resources Enginieering, Faculty of Engineering, Hokkaido University)

---

4:00 PM - 4:15 PM JST | 7:00 AM - 7:15 AM UTC

[SCG58-09] Preliminary report on geothermal structure revealed by geological and MT surveys around Akayumatasawa river in Sanzugawa caldera, NE Japan

*Keishi Nunohara[1], Kuo Hsuan Tseng[2], Hiroki Okano[1], Yasuo Ogawa[2], Noriyoshi Tsuchiya[1] (1.Graduate school of Environmental Studies Tohoku University , 2.Graduate school of Science , Tokyo Institute of Technology)

---

4:15 PM - 4:30 PM JST | 7:15 AM - 7:30 AM UTC

[SCG58-10] Characterization of hydraulic fracturing phenomena in supercritical geothermal environments revealed by elastic wave measurements

*Miura Takahiro[1], Noriaki Watanabe[1], Kiyotoshi Sakaguchi[1], Ryota Goto, Kota Yamane, Takeshi Komai[1], Youqing CHEN[2], Takuya ISHIBASHI[3], Noriyoshi Tsuchiya[1] (1. Graduate School of Environmental Studies, Tohoku University, 2.Graduate School of Energy Science, Kyoto University, 3.AIST, FREA)

---

4:30 PM - 4:45 PM JST | 7:30 AM - 7:45 AM UTC

[SCG58-11] Experimental measurements of transport pore radius of thermally cracked granite and the relationship of pore structure to permeability

*Sueyoshi Kazumasa[1], Tadashi Yokoyama[2], Ikuo Katayama[1] (1.Department of Earth and Planetary Systems Science, Hiroshima University, 2.Graduate School of Integrated Arts and Sciences, Hiroshima University)

---

4:45 PM - 5:00 PM JST | 7:45 AM - 8:00 AM UTC

# [SCG58-12] Geothermal reservoir evaluation by using TL of Quartz and Fluid Flow Simulation Model of the Kakkonda system in Japan

*Alvaro Josue Amaya[1], Nobuo Hirano[1], Noriyoshi Tsuchiya[1] (1.Tohoku University. Graduate School of Environmental Studies)

# 3D S-wave velocity structure in volcanic region using surface-wave tomography

*Hiro Nimiya[1], Tatsunori Ikeda[1], Takeshi Tsuji[1]

1. Kyushu University

EGS (Engineered / Enhanced Geothermal System) is expected to generate significant energy and reduce CO2 emission. Although EGS could be effective in Japan where many volcanoes exist, there are still many problems to solve to run the power plant using EGS. The supercritical fluid which can exist below the brittle-ductile transition (BDT) is essential to develop the EGS. However, structures and physical properties around and below BDT are still unclear. Since the development of EGS needs long time before operation and requires high cost, it is important to evaluate the suitable area for EGS. Therefore, estimating the structure in high spatial resolution from surface to around BDT is important to develop EGS and reduce risks.

In recent years, surface-wave analysis has been widely applied to estimate underground structure from ambient noise. In this analysis, surface-wave phase velocity can be estimated from ambient noise, and S-wave velocity structures can be estimated from surface-wave phase velocity because phase velocity strongly depends on S-wave velocity. Surface-wave analysis using ambient noise does not require active sources. Therefore, this is effective to survey steep area where it is difficult to enter such as geothermal area. In addition, this method is also effective to monitor change in subsurface for a long period because we can obtain seismic ambient noise continuously only using seismometers.

We used continuous seismic data recorded by a high-sensitivity seismograph network (Hi-net) for a year. We computed cross spectra of ambient noise data between the station pairs, and extracted phase velocity dispersion curves using the frequency domain method. Since the frequency domain method can overcome the limitation of interstation distance (far-field approximation) occurred in the time domain method, we can extract phase velocity at short-interstation pairs which reflect local structures. We then estimated the 3D S-wave velocity structure by applying a direct surface-wave inversion method. Our results show the low velocity structures beneath active volcanoes such as Mt. Asama, and Mt. Nasu, that could reflect volcanic fluid. If we apply this method to dense seismometers around the geothermal fields or volcanic area, we could obtain S-wave velocity in higher spatial resolution and use the information to identify suitable reservoir for EGS.

Keywords: Surface-wave tomography, S-wave velocity structure, seismic ambient noise, volcano, geothermal

©2019. Japan Geoscience Union. All Right Reserved. 

# Resistivity-Based Temperature and Permeability Estimation of the Kakkonda Geothermal Field, Japan, Using a Neural Network

*Ugou Tsubasa[1], Kazuya Ishitsuka[2], Toru Mogi[3]

1. Department of Socio-Environmental Engineering Scool of Engineering Hokkaido University, 2. Division of Urban Management, Grduate School of Engineering, Kyoto University, 3. Division of Sustinable Resources Enginieering, Faculty of Engineering, Hokkaido University

Estimation of temperature distribution around a geothermal field is important to understand a geothermal system. Previously, temperature distributions were successfully estimated by a neural network based on temperature logs and magnetotelluric (MT) data (Ishitsuka et al., 2018). This method firstly learns the relationship between three-dimensional locations, resistivities and temperatures by a neural network or neural kriging. Then, the optimized neural network is used to estimate temperature distribution based on a resistivity structure obtained by the MT method. On the other hand, not only temperature but also permeability are important physical parameters to evaluate a geothermal system. In this study, we developed a method to estimate permeability distribution as well as temperature distribution by a neural network and neural kriging. The methodology was applied to the Kakkonda geothermal field, Japan.
Permeability along a well is not generally measured. Therefore, to create a training data of permeability, we estimated permeability along a well based on porosity deduced from resistivity log using Archie’ s law. Temperature-dependence of the resistivity of water was corrected at the processing. In addition, we assumed that the salt concentration at each depth was equal to the salt concentration of the collected fluid inclusion. Subsequently, the porosity was converted into the permeability by the Kozeny-Carman equation.
We then estimated temperature and permeability distribution around the Kakkonda geothermal field. For training data, we used temperature logs and the estimated permeability logs using resistivity profiles at the 7 wells (Hanano and Kajiwara, 1999). To estimate temperature distribution, we used the resistivity structure by Yamaya et al. (2017) using the MT method.
As for the result, the temperature rising was estimated in the deep part, and the point where the high-temperature fluid is considered to be rising from the geothermal reservoir was estimated. The permeability showed a high value, especially in the low resistivity part. The accuracy of the estimated temperature and permeability distribution was evaluated by comparing temperature data measured beneath a depth of 3100 m of WD-1 well. As a result of accuracy verification, neural networks showed the smallest temperature error when the number of the intermediate layers was 2, and the permeability error was the smallest when the number of the intermediate layers was 9. Both the temperature and the permeability of neural kriging were smaller than those of neural networks. Although further development of the methodology to increase the accuracy of the estimation is required, our results demonstrated the effectiveness of our neural network approach to estimate permeability as well as temperature distribution around a geothermal field.
This study is supported by a NEDO project.

Keywords: Neural network, Teperature, Permeability

©2019. Japan Geoscience Union. All Right Reserved. 

# Preliminary report on geothermal structure revealed by geological and MT surveys around Akayumatasawa river in Sanzugawa caldera, NE Japan

*Keishi Nunohara[1], Kuo Hsuan Tseng[2], Hiroki Okano[1], Yasuo Ogawa[2], Noriyoshi Tsuchiya[1]

1. Graduate school of Environmental Studies Tohoku University , 2. Graduate school of Science , Tokyo Institute of Technology

Inner part of Sanzugawa caldera, NE Japan, is one of the promising geothermal areas that had been found by many geological and geophysical surveys after 1970’ s. In this area, one geothermal power plant (Uenotai geothermal power plant) is currently in operation, and additional one (Wasabizawa geothermal power plant) is being constructed now.

There are a number of high-temperature hot springs along Akayumatasawa river that flows through the center of Sanzugawa caldera. This study reports the resistivity and geological structures based on MT surveys and field surveys around Akayumatasawa. In addition to these structures, the gravity structure, distribution of hot springs, and hypocenter clusters under Akayumatasawa indicate existence of geothermal fluid that is ascending from deep subsurface.

Keywords: geothermal structure, MT, geothermal fluid

©2019. Japan Geoscience Union. All Right Reserved. 

# Characterization of hydraulic fracturing phenomena in supercritical geothermal environments revealed by elastic wave measurements

*Miura Takahiro[1], Noriaki Watanabe[1], Kiyotoshi Sakaguchi[1], Ryota Goto, Kota Yamane, Takeshi Komai[1], Youqing CHEN[2], Takuya ISHIBASHI[3], Noriyoshi Tsuchiya[1]

1. Graduate School of Environmental Studies, Tohoku University, 2. Graduate School of Energy Science, Kyoto University, 3. AIST, FREA

Supercritical geothermal resources above the critical temperature of water (374℃) are expected as potential novel geothermal resources [Watanabe et al., 2017, Nat. Geosci.]. Although granitic rocks under temperature and depth conditions where supercritical geothermal resources are present are considered ductile against compression, they may be brittle against tensile, so that it is suggested that the reservoir layer may be formed. In fact, we carried out hydraulic fracturing experiments on cylindrical granite with a borehole in $\sigma_1$ direction placed under 450℃ and confining pressure triaxial stress (greatest principal stress $\sigma_1$:90MPa, intermediate principal stress $\sigma_2$ / least principal stress $\sigma_3$:40 MPa), and then three-dimensional isotropic reticulated fractures are formed with a smaller water pressure than hydraulic fracturing at low temperature, and it is found that the permeability increases by about 1000 times [Watanabe et al., 2017, Geophys. Res. Lett.]. Based on this previous study, we are currently working on clarifying the phenomenon of hydraulic fracturing under supercritical geothermal environments using a hydraulic fracturing experiment system under high stress and true triaxial stress conditions.

We have carried out hydraulic fracturing experiments on cubic granite with vertically downward borehole at 400℃ or 450℃ and true triaxial stress ($\sigma_1$:40 MPa, $\sigma_2$:15 MPa, $\sigma_3$:5 MPa), and AE (Acoustic Emission) measurement during the experiment and P-wave velocity measurement before and after the experiment have been conducted. As a result, irrespective of temperature and stress field, the P wave velocity of the rock after the experiment decreased isotropically, and it was suggested that the formation of reticulated fractures found in the previous study is mainly due to pressurization of existing microcracks which are isotropically distributed in rocks by low viscosity water. Furthermore, as a result of AE measurement during the experiment, the peak of AE occurrence was present not only at the time when the borehole pressure reached the maximum value (breakdown pressure) but also after the breakdown. Considering the deformation behavior of the rock during the experiment and the observation result of the thin sections after the experiment, it is suggested that the first peak is due to the occurrence of hydraulic fracturing but the second peak is due to the occurrence of small scale shear deformation and fracture depending on the stress field of the rock where strength has decreased by hydraulic fracturing. As a result, the possibility that the rock behavior after the breakdown also affects the ultimate fracture pattern and the change of permeability was newly found.

・Watanabe, N. et al. Potentially exploitable supercritical geothermal resources in the ductile crust. Nat. Geosci. 10(2), 140–144 (2017).

・Watanabe, N., Egawa, M., Sakaguchi, K., Ishibashi, T. & Tsuchiya, N. Hydrofracturing and permeability enhancement in granite from subcritical/brittle to supercritical/ductile conditions. Geophys. Res. Lett. 44,

©2019. Japan Geoscience Union. All Right Reserved. 

5468–5475 (2017).

Keywords: geothermal, supercritical, true-triaxial

©2019. Japan Geoscience Union. All Right Reserved. 

# Experimental measurements of transport pore radius of thermally cracked granite and the relationship of pore structure to permeability

*Sueyoshi Kazumasa[1], Tadashi Yokoyama[2], Ikuo Katayama[1]

1. Department of Earth and Planetary Systems Science, Hiroshima University, 2. Graduate School of Integrated Arts and Sciences, Hiroshima University

Fluid flow in rocks plays a key role in many geological processes such as geothermal reservoirs. Permeability is known to be dependent on porosity and pore radius (Walsh and Brace, 1984), while direct determination of pore radius is usually more difficult than determination of permeability. Water expulsion method (Yokoyama and Takeuchi, 2009) is a way to determine the radius of transport pore from gas pressure at which gas breaks through a water-saturated sample ($\Delta P_{break}$). Although several previous studies investigated the relationship between permeability and $\Delta P_{break}$ of impermeable rock such as mudstone, those of granite have not been reported. In this study, we develop the water expulsion method under confining pressure and aim to evaluate the relationship between permeability and pore characteristics such as porosity and transport pore radius under high pressure up to 30 MPa.

Thermally-cracked Aji granites were prepared to cylindrical shape (20 mm long and 20 mm in diameter). Thermal cracking was introduced by heating up to 600 ℃ and porosity of a heat-treated sample was about 2.4 % . The transport pore radius was determined by a manner similar to those reported in Yokoyama and Takeuchi (2009), which is an experimental method measuring gas pressure $\Delta P_{break}$ (Pa) at which gas breaks through a water-saturated sample. From $\Delta P_{break}$ and interfacial tension $\gamma$ (N m$^{-1}$), transport pore radius $r$ (m) can be estimated as follows: $r = 2\gamma / \Delta P_{break}$. Permeability was determined from the flow rate at a constant pore pressure ($P_p$ = 0.5 - 3 MPa). The flow rate was measured by a flow method using water as a pore fluid and permeability was calculated following Darcy’ s law. Porosity was estimated using the gas porosimeter, where the grain volume and pore volume of a sample were determined by using Boyle’ s law. Experiments were performed under confining pressure ranging 5 to 30 MPa at room temperature.

Transport pore radius and permeability of thermally-cracked Aji granite were 0.74 $\mu$m and 5.5×10$^{-17}$ m$^2$ under confining pressure of 5 MPa. These values decreased with increase in confining pressure and were 0.14 $\mu$m and 2.0×10$^{-18}$ m$^2$ under confining pressure of 30 MPa. Permeability $k$ (m$^2$) of granite can be approximated by pore radius $r$ and porosity $\phi$ according to the relation: $k = 5.32\times10^{-3}\,\phi r^2$. This indicates that permeability is primarily dependent on transport pore radius. These results are consistent with the conventional permeability model (Simpson et al., 2003) and estimation of transport pore radius is important for understanding permeability of granite.

Keywords: permeability, transport pore radius, water expulsion method

©2019. Japan Geoscience Union. All Right Reserved. 

# Geothermal reservoir evaluation by using TL of Quartz and Fluid Flow Simulation Model of the Kakkonda system in Japan

*Alvaro Josue Amaya[1], Nobuo Hirano[1], Noriyoshi Tsuchiya[1]

1. Tohoku University. Graduate School of Environmental Studies

Thermoluminescence (TL) of quartz is used in many geoscientist applications: Radiation measurements, geological dating and recently in geothermal activity prospection. After kinetic understanding, a new geothermal reservoir model has been developed based on the analysis of geological thermoluminescence surface samples and cuttings of borehole quartz samples combined with the system behavior equations. This novel methodology has been designed especially for an early stage of geothermal exploration condition and has been validated in the Kakkonda geothermal field in its initial exploration state. The system was simulated from surface to 5 Km on depth. In order to obtain the geothermal model that uses TL as a heat sensor, the sensitivity of the mineral property to natural heat has been monitored and evaluated through kinetic TL quartz decay experiments using aliquots of a standard sample rooted from same geothermal origin and subjected to different controlled conditions of temperatures taken at different time and deconvoluted by keeping constant 4 peak positions for all database; this has allowed the development of novel TL equations that have been coupled in this proposed reservoir model, which, is based on the description of the system through 3 governing equations for a specific control volume: the geothermal potential system balance, the Fourier equation, and the non-steady state heat conduction equation. Coupled with reservoir model and thermoluminescence model, we can obtain a numerical model of three-dimensional geothermal prospecting temperatures at any position (X, Y, Z) got through geoprocessing GIS tools. Finally, the 3D thermal model was used to parameterize a fluid flow simulation that considers the supercritical condition of the system at 5 Km as a heat source model and by using Hydrotherm software many scenarios of natural system evolution were gotten and a novel sustainable application for operation of the geothermal production operation in the Kakkonda Geothermal Power Plant was proposed.

Keywords: Thermoluminescence, Geothermal Reservoir Evaluation, Thermal Modeling

©2019. Japan Geoscience Union. All Right Reserved. 

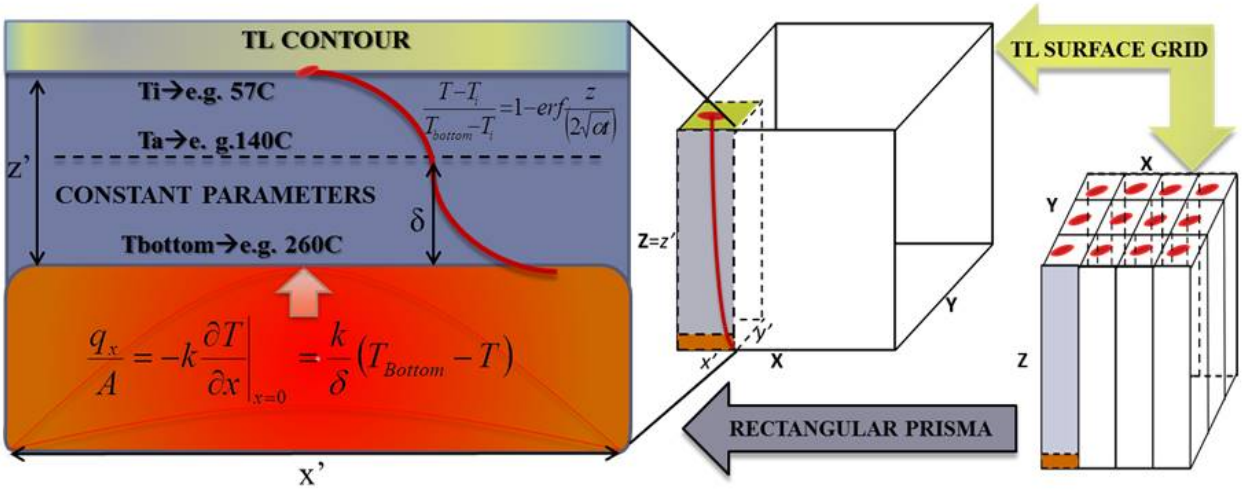


©2019. Japan Geoscience Union. All Right Reserved. 

[J] Poster | S (Solid Earth Sciences)：S-CG Complex & General

Thu. May 30, 2019 10:45 AM - 12:15 PM JST | Thu. May 30, 2019 1:45 AM - 3:15 AM UTC | Poster Hall International Exhibition Hall8, Makuhari Messe_8

## [S-CG59] Reducing risks from earthquakes, tsunamis & volcanoes: new applications of realtime geophysical data

convener:Masashi Ogiso(Meteorological Research Institute, Japan Meteorological Agency), Naotaka YAMAMOTO CHIKASADA(National Research Institute for Earth Science and Disaster Resilience), Satoshi Kawamoto(Geospatial Information Authority of Japan), Mitsuyuki Hoshiba(Meteorological Research Institute)

As the number of population centers grows in regions with earthquake, tsunami and volcano hazards, the importance of improving methods for rapid, realtime estimates of activity increases. Realtime monitoring, analysis, and prediction of seismic ground motion, crustal movement and tsunami will be powerful tools to contribute to earthquake and tsunami disaster preparedness/mitigation. Tsunami and Earthquake Early Warning systems exist today in many locations around the world. Now JMA has started to promptly provide Eruption Notices to inform people of impending and beginning volcanic eruptions. Large events like the 2011 Tohoku Earthquake (Mw9.0) have demonstrated some of the shortcomings of existing techniques. In this session, we invite presentations on new ideas, methods and applications of (near) realtime analysis of seismic, geodetic and tsunami data, to the problem of realtime prediction aimed at improving disaster preparedness/mitigation in the fields of earthquake, tsunami and volcano observation. Presentation is encouraged to bring together scientists, engineers, and practitioners from a broad range of backgrounds from around the world, and to promote collaborative communication at the leading edge of the science and technologies.

### [SCG59-P01] Numerical Shake Prediction for earthquake early warning: prediction of distant future using Green function method

*Mitsuyuki Hoshiba[1] (1.Meteorological Research Institute)

### [SCG59-P02] Introduction of forward scattering model into the Numerical Shake Prediction scheme

*Masashi Ogiso[1] (1.Meteorological Research Institute, Japan Meteorological Agency)

### [SCG59-P03] Magnitude estimation by using ocean-bottom pressure gauge data

*Takeshi Nakamura[1], Eiichiro Araki[2], Narumi Takahashi[1], Kensuke Suzuki[2], Shunroku Yamamoto[3], Masahiro Korenaga[3], Shunta Noda[3] (1.National Research Institute for Earth Science and Disaster Resilience, 2.Japan Agency for Marine-Earth Science and Technology, 3.Railway Technical Research Institute)

### [SCG59-P04] Calculation of tsunami propagation by applying ray tracing based on the shortest path method to tsunamis

*Shoji Sekiguchi[1] (1.National Research Institute for Earth Science and Disaster Prevention)

### [SCG59-P05] Derivation of the series expansion of Kajiura filter, Green's function of a tsunami

*Nobuki Kame[1], Tetsuya Kusakabe[1], Shingo Watada[1] (1.Earthquake Research Institute, the University of Tokyo)

# Numerical Shake Prediction for earthquake early warning: prediction of distant future using Green function method

*Mitsuyuki Hoshiba[1]

1. Meteorological Research Institute

Although many previous studies of earthquake early warning have focused on rapid estimation of hypocenter and magnitude, recently we proposed a method called “Numerical Shake Prediction” (Hoshiba and Aoki, 2015), in which ground motion is predicted directly from monitored ground motion skipping the process of estimation of hypocenter and magnitude. In the Numerical Shake Prediction, current wavefield is estimated precisely using data assimilation technique, and then future wavefield is predicted using physics of wave propagation. Hoshiba and Aoki (2015) investigated a method to predict envelope of seismic wave focusing on seismic intensity. Furumura et al.(2018) studied an application to long period ground motion. For Tsunami, Maeda et al.(2015) tried the method to tsunami early warning. The researches, estimation of current wavefield and then prediction of future wavefield skipping the process of source information, is now progressed for earthquake and tsunami early warning.

Recently Wang et al.(2017) proposed a method to use Green function method for tsunami early warning, in which Green function is used instead of simulation of wave propagation. Oba et al.(2018) investigated an application of the Green function technique to early warning of long period ground motion. Because future wavefield is estimated from iterative calculation of seismic wave propagation in Hoshiba and Aoki (2015), it requires more computation time for more distant future. Using Green function technique, the computation time is not different between near future prediction and distant future prediction. It is also possible to predict distant future, skipping the prediction of near future.

I will show application of the Green function method for prediction of envelope of seismic wave focusing on seismic intensity. For the physics of wave propagation, radiative transfer theory is applied as the same as Hoshiba and Aoki (2015). This is high-frequency approximation based on ray theoretical approach, and energy propagation is considered instead of wave propagation itself. Energy which arrives at location, (X, Y) at time T later is quantitatively calculated beforehand from unity energy which propagats at (xi, yi) into direction qn. That is, Green function; G(X,Y,T; xi, yi, qn). Energy at location (X, Y) at time T later can be predicted from spatial and directional integrals of multiplication of this Green function and current energy distribution, E(xi, yi, qn), which is evaluated from data assimilation.

Using the Green function, it is possible to predict distant future with less computational time if the target points are not so many. On the other hand, it requires more computational time for prediction of more target points. When the target points are not so many, the Green function is effective method for prediction, including distant future.

Keywords: Earthquake Early Warning , Data Assimilation , Green function, prediction of distant future

©2019. Japan Geoscience Union. All Right Reserved. 

# Introduction of forward scattering model into the Numerical Shake Prediction scheme

*Masashi Ogiso[1]

1. Meteorological Research Institute, Japan Meteorological Agency

A real-time ground motion prediction scheme based on a real-time monitoring of current wavefield (e.g., Hoshiba, 2013) is one of the promising approaches for an earthquake early warning (EEW) purpose. Hoshiba and Aoki (2015) implemented the idea and proposed the Numerical Shake Prediction scheme for the EEW. Hoshiba and Aoki (2015) adopted a radiative transfer theory in 2D space based on an isotropic scattering model for the prediction of future ground motion. The isotropic scattering model is suitable for the development of coda waves, however, it cannot represent an envelope broadening effect of the direct waves. The radiative transfer theory with non-isotropic (forward) scattering coefficients can model full seismogram envelopes (e.g., Wegler et al., 2006). In this study, we introduce a forward scattering model into the Numerical Shake Prediction scheme and investigate how the scattering model affects the ground motion prediction.

To introduce the forward scattering effect in the radiative transfer theory, we assume 2D exponential-type random media where the correlation distance is 1 km and the root-mean-square of the fractional random fluctuation is 0.05, then calculate non-isotropic scattering coefficients based on the Born approximation.

We compare the prediction results based on the non-isotropic scattering model with those based on the isotopic scattering model (Ogiso et al., 2018). Although the forward scattering model yields slightly larger residuals in maximum seismic intensity prediction than the isotropic scattering model, the forward scattering model results in smaller prediction residuals in whole seismogram envelope than the isotropic scattering model. The forward scattering model improves the prediction residuals, especially in the coda part. When we adopt momentum transfer scattering coefficient of the 2D random media as the scattering coefficient of isotropic scattering model, envelope prediction of the coda part is similar to that by the forward scattering model, however, residuals of maximum seismic intensity in isotropic scattering model become larger than the forward scattering model. Hence, we conclude that only the forward scattering model has a possibility to predict whole seismogram envelopes in the Numerical Shake Prediction scheme.

Acknowledgment

We used seismic waveforms recorded by K-NET/KiK-net operated by the NIED. This study was financially supported by the JSPS KAKENHI Grand No. JP17H02064 and JP18K13622.

Keywords: real-time ground motion prediction, seismic wave scattering, seismic attenuation

©2019. Japan Geoscience Union. All Right Reserved. 

# Magnitude estimation by using ocean-bottom pressure gauge data

*Takeshi Nakamura[1], Eiichiro Araki[2], Narumi Takahashi[1], Kensuke Suzuki[2], Shunroku Yamamoto[3], Masahiro Korenaga[3], Shunta Noda[3]

1. National Research Institute for Earth Science and Disaster Resilience, 2. Japan Agency for Marine-Earth Science and Technology, 3. Railway Technical Research Institute

Deployments of ocean-bottom stations such as DONET and S-net could enhance early signal detections and improvements of accuracy for hypocenter analyses of suboceanic earthquakes. However, at some accelerometer stations deployed in ocean-bottom areas, tilt and rotation motions of sensor and/or sensor hysteresis would have occurred during strong motions, which causes anomalous waveforms and analysis errors on seismic motions. At the 2016 moderate-sized suboceanic earthquake (Mjma 6.5) occurring off the Mie prefecture in southwest Japan, significant amplifications of observed amplitude to amplitude calculated from the empirical equation and their considerable spatial variations are found at the DONET stations (Nakamura et al., 2018), which would not be explained by the source radiation pattern and subsurface structures. These undesired amplifications and variations are considered to be caused by acceleration offsets that are associated with the tilt and rotation motions and/or sensor hysteresis and could contribute to the overestimation and instable estimation results of source analyses such as magnitude estimation and finite fault modeling. In this study, we attempt to estimate the amplitude magnitude by using pressure gauge (Paroscientific 8B7000-2) data at DONET stations instead of using accelerometer (Metrozet TSA-100S) data to suppress the undesired features and evaluate the stabilities. We analyzed the waveforms after integrating the observed pressure gauge data and applying a high-pass filter with a corner period of 6 s. In the case of ocean-bottom stations deployed in a water depth of more than 2,200 m, the amplitude of pressure waveforms in this period band is roughly consistent with the vertical amplitude of ocean-bottom velocity (e.g., Matsumoto et al., 2012). The period band of less than 6 s corresponds to that used for estimating the amplitude magnitude of the unified hypocenter catalogue and EEW by JMA. We constructed the empirical equation between the magnitude and the filtered amplitude data and estimated the magnitude for each event data.
Our results show that the magnitude estimated from using pressure gauge data correlates well with that in the JMA list. The deviation (two sigma) is 0.70, which is the same value as that estimated from using three component data of accelerometer. For the event data of the 2016 earthquake (Mjma 6.5), the estimated magnitudes by accelerometer data are 6.64–8.34, while those by pressure gauge data are 6.33–6.81, indicating that the magnitude estimation using the latter data provides less amplification and stable results. The pressure gauge installed at DONET stations may be relatively low sensor hysteresis and less effects of sensor rotation on short-period component of waveforms compared with those of accelerometer.

Keywords: DONET, earthquake magnitude, pressure gauge, Earthquake Early Warning

©2019. Japan Geoscience Union. All Right Reserved. 

# Calculation of tsunami propagation by applying ray tracing based on the shortest path method to tsunamis

*Shoji Sekiguchi[1]

1. National Research Institute for Earth Science and Disaster Prevention

Ray tracing of seismic surface wave was already applied to tsunami propagation (Satake,1988). Here, we apply another ray tracing method based on the shortest path method. In standard ray tracing method, the ray starts at a source point and travel to an end point. However, it is difficult to reach the end point when the ray path is sensitive to velocity distribution (bathymetry distribution). Sometimes, the calculated ray is a local minimum path, not a global minimum path. When we trace the ray based on the shortest path method, there are no such problems. We calculate rays in Pacific Ocean and Japan Sea. Using 1’ by 1’ ETOPO1 data, 1 degree by 1 degree bathymetric data are obtained for trans-Pacific tsunami by applying moving average. 0.1 degree by 0.1 degree depth data are obtained for the Japan Sea tsunami. Moving average is made with neighboring +-5 degrees for the Pacific Ocean data and +-0.5 degree for the Japan Sea data. In the shortest path method, the studied area is divided into many square cells. On the cell boundary, several nodes are evenly distributed. Paths are made by connecting all combinations of two nodes of common cell by straight lines. The path of the shortest travel time from the starting point to each node is searched. At first, the cell is same as the bathymetric data grid of each of Pacific Ocean and the Japan Sea, and node number is set to be 5. Then, the cell number and the node number are multiplied by 2, respectively. When the difference of the mean travel time is less than 60 seconds, we judge the calculation is converged. The mean travel time is obtained by averaging all travel time values at 1 degree by 1 degree data grid points for the Pacific Ocean or 0.1 degree by 0.1 degree data grid point for the Japan Sea. Tsunami sources are located off the shore of Chile and at 1983 Japan Sea earthquake. Converged (cell number, node number)’s are (1,10) and (1,5), and calculation times are about 3.14s and 0.60s, respectively. Areas of depth shallower than 1,000m are excluded in the calculation of the Pacific Ocean. It is shown that travel times of all the target area can be estimated by the shortest path method within very short calculation time.

Keywords: tsunami, shortest path method

©2019. Japan Geoscience Union. All Right Reserved. 

# Derivation of the series expansion of Kajiura filter, Green's function of a tsunami

*Nobuki Kame[1], Tetsuya Kusakabe[1], Shingo Watada[1]

1. Earthquake Research Institute, the University of Tokyo

Here we explicitly show the derivation of the series expansion of Kajiura filter, Green's function of a tsunami analytically derived in Kajiura (1963). The series expansion expression is extensively used in the numerical evaluation and we think it beneficial for tsunami researchers to show the whole derivation process in detail.

Reference: T. Kusakabe, N. Kame, S. Watada, Derivation of Series Expansion of Kajiura Filter, Green's Function of Tsunami, Zisin(2), vol. 71, 117-119, 2018, DOI: 10.4294/zisin.2017-16

Fig. 1 Plot of Kajiura filter G(r/h), the initial surface displacement due to a spatiotemporal impulsive point displacement at the bottom.
Reference:

Keywords: Tsunami, Green's Function, Kajiura Filter

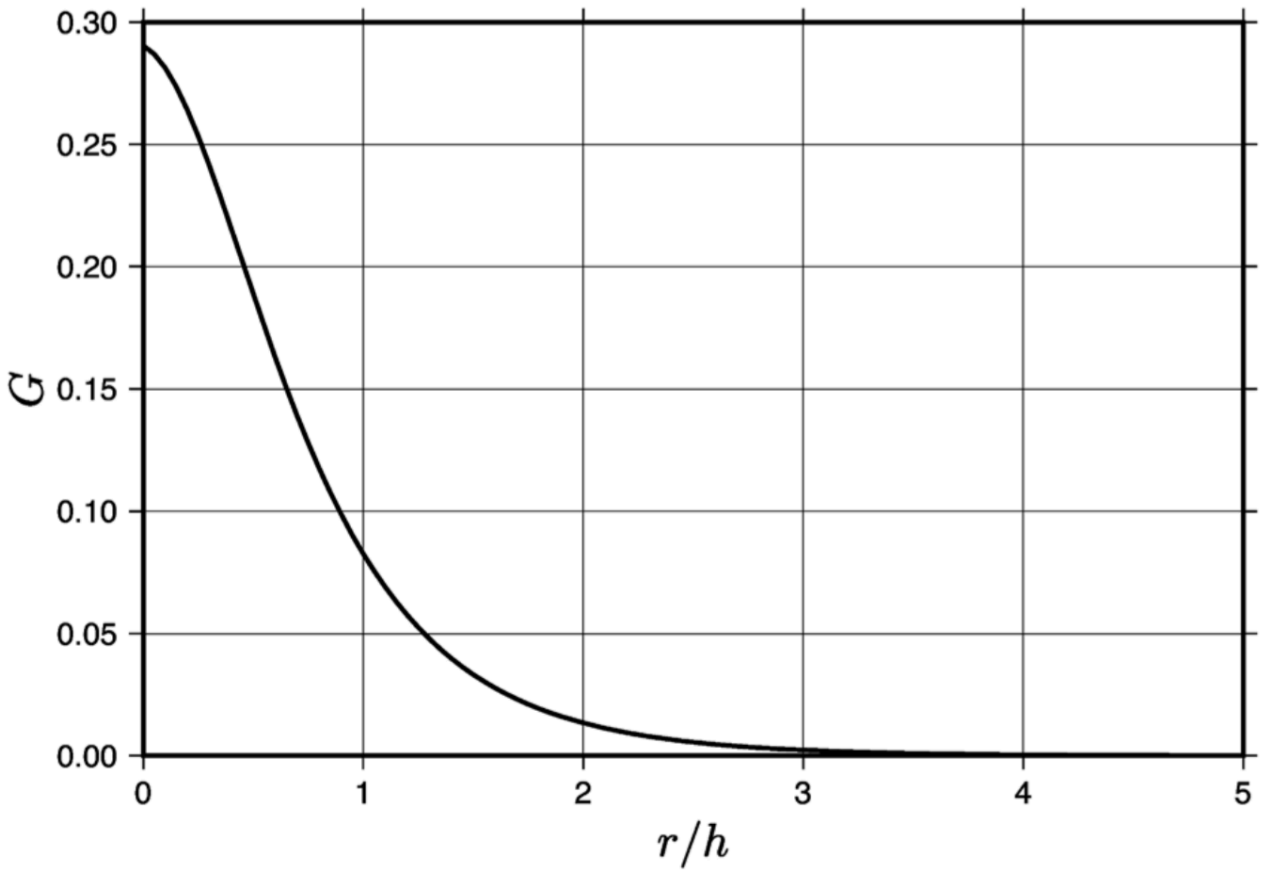


©2019. Japan Geoscience Union. All Right Reserved. 

[J] Poster | S (Solid Earth Sciences )：S-CG Complex & General

Thu. May 30, 2019 5:15 PM - 6:30 PM JST | Thu. May 30, 2019 8:15 AM - 9:30 AM UTC | Poster Hall International Exhibition Hall8, Makuhari Messe_32

## [S-CG59] Reducing risks from earthquakes, tsunamis & volcanoes: new applications of realtime geophysical data

convener:Masashi Ogiso(Meteorological Research Institute, Japan Meteorological Agency), Naotaka YAMAMOTO CHIKASADA(National Research Institute for Earth Science and Disaster Resilience), Satoshi Kawamoto(Geospatial Information Authority of Japan), Mitsuyuki Hoshiba(Meteorological Research Institute)

As the number of population centers grows in regions with earthquake, tsunami and volcano hazards, the importance of improving methods for rapid, realtime estimates of activity increases. Realtime monitoring, analysis, and prediction of seismic ground motion, crustal movement and tsunami will be powerful tools to contribute to earthquake and tsunami disaster preparedness/mitigation. Tsunami and Earthquake Early Warning systems exist today in many locations around the world. Now JMA has started to promptly provide Eruption Notices to inform people of impending and beginning volcanic eruptions. Large events like the 2011 Tohoku Earthquake (Mw9.0) have demonstrated some of the shortcomings of existing techniques. In this session, we invite presentations on new ideas, methods and applications of (near) realtime analysis of seismic, geodetic and tsunami data, to the problem of realtime prediction aimed at improving disaster preparedness/mitigation in the fields of earthquake, tsunami and volcano observation. Presentation is encouraged to bring together scientists, engineers, and practitioners from a broad range of backgrounds from around the world, and to promote collaborative communication at the leading edge of the science and technologies.

### [SCG59-P01] Numerical Shake Prediction for earthquake early warning: prediction of distant future using Green function method

*Mitsuyuki Hoshiba[1] (1.Meteorological Research Institute)

### [SCG59-P02] Introduction of forward scattering model into the Numerical Shake Prediction scheme

*Masashi Ogiso[1] (1.Meteorological Research Institute, Japan Meteorological Agency)

### [SCG59-P03] Magnitude estimation by using ocean-bottom pressure gauge data

*Takeshi Nakamura[1], Eiichiro Araki[2], Narumi Takahashi[1], Kensuke Suzuki[2], Shunroku Yamamoto[3], Masahiro Korenaga[3], Shunta Noda[3] (1.National Research Institute for Earth Science and Disaster Resilience, 2.Japan Agency for Marine-Earth Science and Technology, 3.Railway Technical Research Institute)

### [SCG59-P04] Calculation of tsunami propagation by applying ray tracing based on the shortest path method to tsunamis

*Shoji Sekiguchi[1] (1.National Research Institute for Earth Science and Disaster Prevention)

### [SCG59-P05] Derivation of the series expansion of Kajiura filter, Green's function of a tsunami

*Nobuki Kame[1], Tetsuya Kusakabe[1], Shingo Watada[1] (1.Earthquake Research Institute, the University of Tokyo)

# Numerical Shake Prediction for earthquake early warning: prediction of distant future using Green function method

*Mitsuyuki Hoshiba[1]

1. Meteorological Research Institute

Although many previous studies of earthquake early warning have focused on rapid estimation of hypocenter and magnitude, recently we proposed a method called “Numerical Shake Prediction” (Hoshiba and Aoki, 2015), in which ground motion is predicted directly from monitored ground motion skipping the process of estimation of hypocenter and magnitude. In the Numerical Shake Prediction, current wavefield is estimated precisely using data assimilation technique, and then future wavefield is predicted using physics of wave propagation. Hoshiba and Aoki (2015) investigated a method to predict envelope of seismic wave focusing on seismic intensity. Furumura et al.(2018) studied an application to long period ground motion. For Tsunami, Maeda et al.(2015) tried the method to tsunami early warning. The researches, estimation of current wavefield and then prediction of future wavefield skipping the process of source information, is now progressed for earthquake and tsunami early warning.

Recently Wang et al.(2017) proposed a method to use Green function method for tsunami early warning, in which Green function is used instead of simulation of wave propagation. Oba et al.(2018) investigated an application of the Green function technique to early warning of long period ground motion. Because future wavefield is estimated from iterative calculation of seismic wave propagation in Hoshiba and Aoki (2015), it requires more computation time for more distant future. Using Green function technique, the computation time is not different between near future prediction and distant future prediction. It is also possible to predict distant future, skipping the prediction of near future.

I will show application of the Green function method for prediction of envelope of seismic wave focusing on seismic intensity. For the physics of wave propagation, radiative transfer theory is applied as the same as Hoshiba and Aoki (2015). This is high-frequency approximation based on ray theoretical approach, and energy propagation is considered instead of wave propagation itself. Energy which arrives at location, (X, Y) at time T later is quantitatively calculated beforehand from unity energy which propagats at (xi, yi) into direction qn. That is, Green function; G(X,Y,T; xi, yi, qn). Energy at location (X, Y) at time T later can be predicted from spatial and directional integrals of multiplication of this Green function and current energy distribution, E(xi, yi, qn), which is evaluated from data assimilation.

Using the Green function, it is possible to predict distant future with less computational time if the target points are not so many. On the other hand, it requires more computational time for prediction of more target points. When the target points are not so many, the Green function is effective method for prediction, including distant future.

Keywords: Earthquake Early Warning , Data Assimilation , Green function, prediction of distant future

©2019. Japan Geoscience Union. All Right Reserved. 

# Introduction of forward scattering model into the Numerical Shake Prediction scheme

*Masashi Ogiso[1]

1. Meteorological Research Institute, Japan Meteorological Agency

A real-time ground motion prediction scheme based on a real-time monitoring of current wavefield (e.g., Hoshiba, 2013) is one of the promising approaches for an earthquake early warning (EEW) purpose. Hoshiba and Aoki (2015) implemented the idea and proposed the Numerical Shake Prediction scheme for the EEW. Hoshiba and Aoki (2015) adopted a radiative transfer theory in 2D space based on an isotropic scattering model for the prediction of future ground motion. The isotropic scattering model is suitable for the development of coda waves, however, it cannot represent an envelope broadening effect of the direct waves. The radiative transfer theory with non-isotropic (forward) scattering coefficients can model full seismogram envelopes (e.g., Wegler et al., 2006). In this study, we introduce a forward scattering model into the Numerical Shake Prediction scheme and investigate how the scattering model affects the ground motion prediction.

To introduce the forward scattering effect in the radiative transfer theory, we assume 2D exponential-type random media where the correlation distance is 1 km and the root-mean-square of the fractional random fluctuation is 0.05, then calculate non-isotropic scattering coefficients based on the Born approximation.

We compare the prediction results based on the non-isotropic scattering model with those based on the isotopic scattering model (Ogiso et al., 2018). Although the forward scattering model yields slightly larger residuals in maximum seismic intensity prediction than the isotropic scattering model, the forward scattering model results in smaller prediction residuals in whole seismogram envelope than the isotropic scattering model. The forward scattering model improves the prediction residuals, especially in the coda part. When we adopt momentum transfer scattering coefficient of the 2D random media as the scattering coefficient of isotropic scattering model, envelope prediction of the coda part is similar to that by the forward scattering model, however, residuals of maximum seismic intensity in isotropic scattering model become larger than the forward scattering model. Hence, we conclude that only the forward scattering model has a possibility to predict whole seismogram envelopes in the Numerical Shake Prediction scheme.

Acknowledgment

We used seismic waveforms recorded by K-NET/KiK-net operated by the NIED. This study was financially supported by the JSPS KAKENHI Grand No. JP17H02064 and JP18K13622.

Keywords: real-time ground motion prediction, seismic wave scattering, seismic attenuation

©2019. Japan Geoscience Union. All Right Reserved. 

# Magnitude estimation by using ocean-bottom pressure gauge data

*Takeshi Nakamura[1], Eiichiro Araki[2], Narumi Takahashi[1], Kensuke Suzuki[2], Shunroku Yamamoto[3], Masahiro Korenaga[3], Shunta Noda[3]

1. National Research Institute for Earth Science and Disaster Resilience, 2. Japan Agency for Marine-Earth Science and Technology, 3. Railway Technical Research Institute

Deployments of ocean-bottom stations such as DONET and S-net could enhance early signal detections and improvements of accuracy for hypocenter analyses of suboceanic earthquakes. However, at some accelerometer stations deployed in ocean-bottom areas, tilt and rotation motions of sensor and/or sensor hysteresis would have occurred during strong motions, which causes anomalous waveforms and analysis errors on seismic motions. At the 2016 moderate-sized suboceanic earthquake (Mjma 6.5) occurring off the Mie prefecture in southwest Japan, significant amplifications of observed amplitude to amplitude calculated from the empirical equation and their considerable spatial variations are found at the DONET stations (Nakamura et al., 2018), which would not be explained by the source radiation pattern and subsurface structures. These undesired amplifications and variations are considered to be caused by acceleration offsets that are associated with the tilt and rotation motions and/or sensor hysteresis and could contribute to the overestimation and instable estimation results of source analyses such as magnitude estimation and finite fault modeling. In this study, we attempt to estimate the amplitude magnitude by using pressure gauge (Paroscientific 8B7000-2) data at DONET stations instead of using accelerometer (Metrozet TSA-100S) data to suppress the undesired features and evaluate the stabilities. We analyzed the waveforms after integrating the observed pressure gauge data and applying a high-pass filter with a corner period of 6 s. In the case of ocean-bottom stations deployed in a water depth of more than 2,200 m, the amplitude of pressure waveforms in this period band is roughly consistent with the vertical amplitude of ocean-bottom velocity (e.g., Matsumoto et al., 2012). The period band of less than 6 s corresponds to that used for estimating the amplitude magnitude of the unified hypocenter catalogue and EEW by JMA. We constructed the empirical equation between the magnitude and the filtered amplitude data and estimated the magnitude for each event data.
Our results show that the magnitude estimated from using pressure gauge data correlates well with that in the JMA list. The deviation (two sigma) is 0.70, which is the same value as that estimated from using three component data of accelerometer. For the event data of the 2016 earthquake (Mjma 6.5), the estimated magnitudes by accelerometer data are 6.64–8.34, while those by pressure gauge data are 6.33–6.81, indicating that the magnitude estimation using the latter data provides less amplification and stable results. The pressure gauge installed at DONET stations may be relatively low sensor hysteresis and less effects of sensor rotation on short-period component of waveforms compared with those of accelerometer.

Keywords: DONET, earthquake magnitude, pressure gauge, Earthquake Early Warning

©2019. Japan Geoscience Union. All Right Reserved. 

# Calculation of tsunami propagation by applying ray tracing based on the shortest path method to tsunamis

*Shoji Sekiguchi[1]

1. National Research Institute for Earth Science and Disaster Prevention

Ray tracing of seismic surface wave was already applied to tsunami propagation (Satake,1988). Here, we apply another ray tracing method based on the shortest path method. In standard ray tracing method, the ray starts at a source point and travel to an end point. However, it is difficult to reach the end point when the ray path is sensitive to velocity distribution (bathymetry distribution). Sometimes, the calculated ray is a local minimum path, not a global minimum path. When we trace the ray based on the shortest path method, there are no such problems. We calculate rays in Pacific Ocean and Japan Sea. Using 1’ by 1’ ETOPO1 data, 1 degree by 1 degree bathymetric data are obtained for trans-Pacific tsunami by applying moving average. 0.1 degree by 0.1 degree depth data are obtained for the Japan Sea tsunami. Moving average is made with neighboring +-5 degrees for the Pacific Ocean data and +-0.5 degree for the Japan Sea data. In the shortest path method, the studied area is divided into many square cells. On the cell boundary, several nodes are evenly distributed. Paths are made by connecting all combinations of two nodes of common cell by straight lines. The path of the shortest travel time from the starting point to each node is searched. At first, the cell is same as the bathymetric data grid of each of Pacific Ocean and the Japan Sea, and node number is set to be 5. Then, the cell number and the node number are multiplied by 2, respectively. When the difference of the mean travel time is less than 60 seconds, we judge the calculation is converged. The mean travel time is obtained by averaging all travel time values at 1 degree by 1 degree data grid points for the Pacific Ocean or 0.1 degree by 0.1 degree data grid point for the Japan Sea. Tsunami sources are located off the shore of Chile and at 1983 Japan Sea earthquake. Converged (cell number, node number)’s are (1,10) and (1,5), and calculation times are about 3.14s and 0.60s, respectively. Areas of depth shallower than 1,000m are excluded in the calculation of the Pacific Ocean. It is shown that travel times of all the target area can be estimated by the shortest path method within very short calculation time.

Keywords: tsunami, shortest path method

©2019. Japan Geoscience Union. All Right Reserved. 

# Derivation of the series expansion of Kajiura filter, Green's function of a tsunami

*Nobuki Kame[1], Tetsuya Kusakabe[1], Shingo Watada[1]

1. Earthquake Research Institute, the University of Tokyo

Here we explicitly show the derivation of the series expansion of Kajiura filter, Green's function of a tsunami analytically derived in Kajiura (1963). The series expansion expression is extensively used in the numerical evaluation and we think it beneficial for tsunami researchers to show the whole derivation process in detail.

Reference: T. Kusakabe, N. Kame, S. Watada, Derivation of Series Expansion of Kajiura Filter, Green's Function of Tsunami, Zisin(2), vol. 71, 117-119, 2018, DOI: 10.4294/zisin.2017-16

Fig. 1 Plot of Kajiura filter G(r/h), the initial surface displacement due to a spatiotemporal impulsive point displacement at the bottom.
Reference:

Keywords: Tsunami, Green's Function, Kajiura Filter

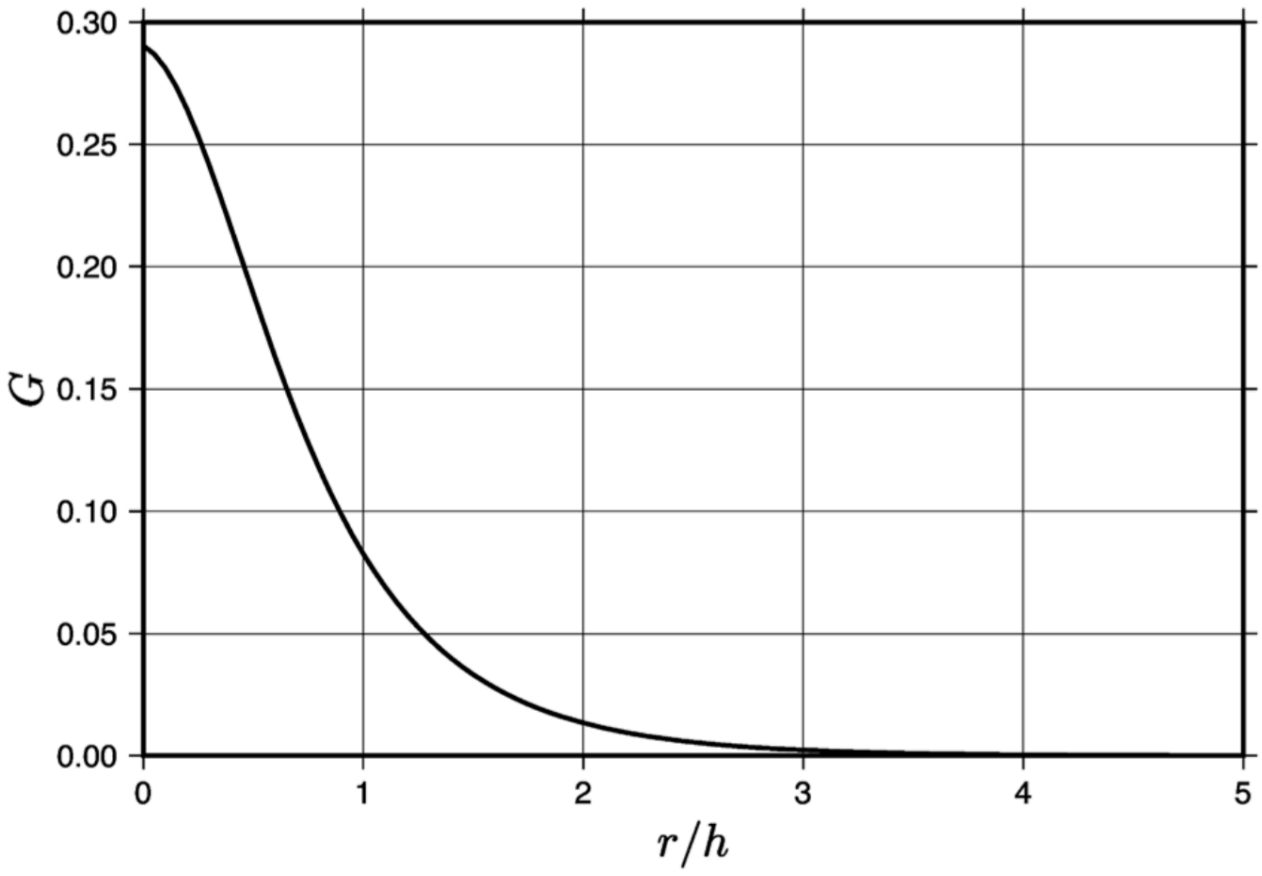


©2019. Japan Geoscience Union. All Right Reserved. 

[J] Oral | S (Solid Earth Sciences)：S-CG Complex & General

Thu. May 30, 2019 1:45 PM - 3:15 PM JST | Thu. May 30, 2019 4:45 AM - 6:15 AM UTC | A08 TOKYO BAY MAKUHARI HALL

## [S-CG59] Reducing risks from earthquakes, tsunamis & volcanoes: new applications of realtime geophysical data

convener:Masashi Ogiso(Meteorological Research Institute, Japan Meteorological Agency), Naotaka YAMAMOTO CHIKASADA(National Research Institute for Earth Science and Disaster Resilience), Satoshi Kawamoto(Geospatial Information Authority of Japan), Mitsuyuki Hoshiba(Meteorological Research Institute), Chairperson:Mitsuyuki Hoshiba(Meteorological Res. Inst., JMA, Japan), Satoshi Kawamoto(Geospatial Information Authority of Japan )

As the number of population centers grows in regions with earthquake, tsunami and volcano hazards, the importance of improving methods for rapid, realtime estimates of activity increases. Realtime monitoring, analysis, and prediction of seismic ground motion, crustal movement and tsunami will be powerful tools to contribute to earthquake and tsunami disaster preparedness/mitigation. Tsunami and Earthquake Early Warning systems exist today in many locations around the world. Now JMA has started to promptly provide Eruption Notices to inform people of impending and beginning volcanic eruptions. Large events like the 2011 Tohoku Earthquake (Mw9.0) have demonstrated some of the shortcomings of existing techniques. In this session, we invite presentations on new ideas, methods and applications of (near) realtime analysis of seismic, geodetic and tsunami data, to the problem of realtime prediction aimed at improving disaster preparedness/mitigation in the fields of earthquake, tsunami and volcano observation. Presentation is encouraged to bring together scientists, engineers, and practitioners from a broad range of backgrounds from around the world, and to promote collaborative communication at the leading edge of the science and technologies.

1:45 PM - 2:00 PM JST | 4:45 AM - 5:00 AM UTC

[SCG59-01] Earthquake early warning in the United States and beyond

★Invited Papers

*Richard M Allen[1] (1.University of California Berkeley)

---

2:00 PM - 2:15 PM JST | 5:00 AM - 5:15 AM UTC

[SCG59-02] Study on the relationship between seismometer site environment and earthquake early warning seismic parameter estimation accuracy

*Katsutomo Niwa[1], Naoyasu Iwata[1], Shunroku Yamamoto[1] (1.Railway Technical Research Institute)

---

2:15 PM - 2:30 PM JST | 5:15 AM - 5:30 AM UTC

[SCG59-03] **Prediction of surface ground motion using underground seismic records based on data assimilation (2)**

*Masaya Ishihara[1], Hisashi Nakahara[1] (1.Solid Earth Physics Laboratory, Department of Geophysics, Graduate School of Science, Tohoku University)

---

2:30 PM - 2:45 PM JST | 5:30 AM - 5:45 AM UTC

[SCG59-04] Development of Realtlime Long-Period Ground-Motion Prediction System and Demonstration Experiment

★Invited Papers

*Shin Aoi[1], Takeshi Kimura[1], Takashi Kunugi[1], Wataru Suzuki[1], Yadab Prasad Dhakal[1], Naoto Kojya[2] (1.National Research Institute for Earth Science and Disaster Resilience, 2.Japan Meteorological Agency)

---

2:45 PM - 3:00 PM JST | 5:45 AM - 6:00 AM UTC

[SCG59-05] Real-time forecasting of long-period ground motions for the Nankai Trough earthquake: The effectivity of the Green function-based data assimilation method

*Atsuki Oba[1], Takashi Furumura[1], Takuto Maeda[2] (1.Earthquake Research Institute, University of Tokyo, 2.Graduate School of Science and Technology, Hirosaki University)

---

3:00 PM - 3:15 PM JST | 6:00 AM - 6:15 AM UTC

## [SCG59-06] Development of EEW system exchanging real-time seismic intensity and seismic waveform

*Shigeki Horiuchi[1], Yuko Sato[1], Taku Urabe[2], Yamaimaiti Nizhamudong[3], Kazuo Sasaki[3] (1.Home Seismometer Corporation, 2.telemetra , 3.Challenge)

# Earthquake early warning in the United States and beyond

*Richard M Allen[1]

1. University of California Berkeley

The ShakeAlert earthquake early warning (EEW) system is now delivering alerts up and down the west-coast of the United States (California, Oregon and Washington). The warnings are being used by targeted groups including transportation, schools, hospitals and other infrastructure operators. Alert are also available to the public in some regions through smartphone apps, and there is an expectation that they will be more widely available in the coming months. The system is operated by the US Geological Survey in cooperation with UC Berkeley, Caltech, the University of Oregon and the University of Washington.

The ShakeAlerts are currently generated by seismic-only algorithms, specifically the EPIC point-source algorithm and the FINDER finite-source algorithm. A great deal of research effort is underway to determine the accuracy and reliability of the current system, and to determine what additional information could be provided by new algorithms. In particular, the use of geodetic observations to improve magnitude estimates and estimate fault finiteness for the largest events is being explored, as is the addition of the PLUM ground motion model approach.

Looking beyond traditional seismic and geodetic networks, the use of smartphones to detect earthquakes and characterize their likely impact for EEW is also being explored. The MyShake global smartphone seismic network is currently recording ground shaking using the 40,000 Android phones that have the app installed. More than 800 earthquakes around the globe have been detected, and research is underway to use these detections to generate alerts and also to improve the quality of alerts from traditional networks.

Keywords: Earthquake , Warnings

©2019. Japan Geoscience Union. All Right Reserved. 

# Study on the relationship between seismometer site environment and earthquake early warning seismic parameter estimation accuracy

*Katsutomo Niwa[1], Naoyasu Iwata[1], Shunroku Yamamoto[1]

1. Railway Technical Research Institute

When earthquakes that threaten the safety of railway facilities and running trains occur, earthquake early warning systems aim to stop the trains as soon as possible. The seismometers installed for these systems automatically detect the P-wave arrival, then using information from the initial few seconds of the P-wave estimate seismic parameters such as epicentral distance, epicentral back-azimuth and magnitude, in order to quickly issue an alarm if necessary.

In this research, in order to improve the accuracy of the seismic parameters estimation, we examined the influence of the seismometers installation environment on the accuracy. We defined as characteristics representing the site environment: the ambient noise level of the observation site, determined from 2 seconds of the waveform recorded before P-wave arrival; and the hardness of the subsurface ground, indicated by the average S-wave velocity from the depth of 30m to the surface, henceforth referred to as AVS30.

Firstly, we calculated the RMS pf the 2 seconds of data before the P-wave arrival as the noise level, and checked the relationship between the noise level and the estimation error of the seismic parameters. When the noise level is small, the error of the P-wave detection time tends to become small. When the noise level is large, the automatic P-wave detection time tends to be earlier than would be chosen manually. The epicentral distance tends to be underestimated as the noise level is larger. The estimation error of the epicentral back-azimuth tends to decrease the estimation error as the noise level decreases. However, the magnitude based on the calculated displacement is hardly affected by the noise level, because the magnitude is determined by the maximum value of the observed amplitude.

Following this, we checked the relationship between AVS30 and the estimation error of the seismic parameters. The AVS30 is calculated from the K-NET PS logging result according to a method proposed by Shi and Midorikawa (1999). Since the variation of AVS30 showed little correlation with the estimation error, it can be thought that P-wave detection is hardly affected by the hardness of the subsurface ground. Though the epicentral distance tends to be underestimated as AVS30 gets smaller, this is only to a small extent. The epicentral back-azimuth tends to be smaller as the AVS30 is larger. The magnitude estimation is not correlated with the AVS30.

According to the results outlined above, the accuracy of the seismic parameters estimation will be improved in a quiet environment where the ambient vibration is small, and the subsurface ground is relatively hard. When we select the installation site of seismometers for earthquake early warning, we should therefore give priority to site environments with these characteristics.

Keywords: Earthquake early warning, Seismic parameters estimation, Seismometers installation environment, Noise level, Averaged S-wave velocity

©2019. Japan Geoscience Union. All Right Reserved. 

# Prediction of surface ground motion using underground seismic records based on data assimilation (2)

*Masaya Ishihara[1], Hisashi Nakahara[1]

1. Solid Earth Physics Laboratory, Department of Geophysics, Graduate School of Science, Tohoku University

## Introduction

To improve Earthquake early warning (EEW), methods using data assimilation have been proposed for seismic wave field prediction (e.g. Hoshiba et al., 2015) and tsunami prediction (Maeda et al., 2015). Hoshiba et al. (2015) used radiative transfer theory to predict the spatial distribution of seismic intensity. Maeda et al. (2015) used wave equation for tsunami prediction. Recently, Furumura et al. (2018 SSJ) used wave equation for the prediction of long-period seismic ground motion. However, data assimilation based on wave equation has probably not yet used for short-period seismic waves due to restrictions on the density of observation stations, computational costs, and so on. In order to predict short period seismic waves, therefore, we started to apply data assimilation based on wave equation to one-dimensional problems for vertical boreholes such as KiK-net (Ishihara and Nakahara, 2018 SSJ). If we can reproduce surface seismic records quickly and precisely from subsurface seismic records, we will be able to speed up the issuing of alarms more quickly than with surface earthquake records alone. This research is regarded as a basic research towards the advancement of the onsite type EEW for local earthquakes.

## Data, Method

In this study, we used NIED KiK-net CHBH10 (Chiba) station. At this observation site, strong motion seismometers are installed on the surface and at a depth of 2000m. We analyzed 60 earthquakes of over M5 occurring around Chiba prefecture. In the simulation, we used the method of Tanaka & Takenaka (2004) which can solve the oblique incidence of plane waves in horizontally stratified structure efficiently by the finite difference method. We calculated the direction of arrival and the incident angle of seismic waves from the particle trajectory of the 1-second-long initial P waves on subsurface records. We simulated the wavefield based on the finite difference method using seismic velocity structure estimated from the logging information. Using the calculated incident angles and subsurface records, we simulated waveforms on the ground surface and compared them with observed waveforms.

## Results and discussion

Ishihara and Nakahara (2018 SSJ) found out two problems in this analysis. First, the degree of the fit between observed and calculated waveforms becomes worse with the lapse time. This is caused by artificial upgoing waves which occur when observed waveforms (upgoing wave + downgoing wave) and calculated waveforms (falling wave) do not match at a subsurface station. Another big problem is that the degree of the fit is deteriorated as the angle of incidence becomes larger. This is because artificial SV waves are generated due to the absence of information about stress when inputting observation values (particle velocity) of P waves at the subsurface observation station.

In this study, we calculated the ratio of artificial SV to P waves assuming only P wave input (stress input is zero) to evaluate this effect. The incident angle was varied from 0 ˚to 45 ˚with a step of 1 ˚. As a result, artificial SV waves are generated with an amplitude of about 4% of the P-wave maximum amplitude for an incident angle of 10 ˚, about 10% for 20 ˚, about 25% for 30 ˚and 50% for 45 ˚. In addition, in order to

©2019. Japan Geoscience Union. All Right Reserved. 

reduce this effect, we are repeating simulations by adding virtual stress conditions and subsurface observation stations.
In the future, we will compare our result with the wavefield calculation of Haskell (1962). In order to solve these problems and to improve the prediction accuracy, we will consider optimum arrangements of subsurface observation stations and suitable settings of appropriate stress conditions.

Keywords: earthquake early warning, data assimilation

©2019. Japan Geoscience Union. All Right Reserved. 

# Development of Realtlime Long-Period Ground-Motion Prediction System and Demonstration Experiment

*Shin Aoi[1], Takeshi Kimura[1], Takashi Kunugi[1], Wataru Suzuki[1], Yadab Prasad Dhakal[1], Naoto Kojya[2]

1. National Research Institute for Earth Science and Disaster Resilience, 2. Japan Meteorological Agency

Current technology seems to be hard to predict an occurrence of earthquakes, but is capable to deliver realtime earthquake information just after the occurrence. For railway systems, the earthquake early warning (EEW) system for Shinkansen was utilized in 1990s. For nationwide warning and alerts, Japan Meteorological Agency (JMA) has operated the EEW system since 2007, and realtime information of ground motion plays an important role in society.

On the other hand, the JMA EEW provides only seismic intensities, and not yet to alert broader ground motion information such as long-period ground motions. Long-period ground motions generated during large earthquakes shake skyscrapers in urban area and cause furniture overturning and damage of elevators in them. Recently, JMA issues the long-period ground motion levels based on 5%-damped absolute velocity response spectra in the period range of 1.6 to 7.8 s to respond beyond the seismic intensity measures. Dhakal et al. [2015] constructed a ground motion prediction equation (GMPE) for absolute velocity response spectra in the period range of 1 to 10 s using 36 earthquakes and 12,401 strong motion recordings observed at K-NET and KiK-net stations. The GMPE can provide accurate predictions with correction factors that use depths of the Vs 1.4 km/s layer beneath the sites from the subsurface velocity model provided by the Japan Seismic Hazard Information Station (J-SHIS). The GMPE has an advantage to use the JMA magnitude Mj that is available immediately after the earthquake, not moment magnitude Mw. We developed realtlime long-period ground-motion prediction system using the GMPE of Dhakal et al. [2015] and hypocenter locations and earthquake magnitudes provided by the JMA EEW.

JMA plans to deliver alerts of EEW for long-period ground motions that are similar to the current EEW for seismic intensities. A working group to investigate prediction information for various needs has been established at JMA to activate the plan. Realtime prediction information for ground motions is not allowed to open to the public based on the weather service law. Therefore, NIED collaborates with JMA, and performs demonstration experiments to deliver prediction information of long-period ground motions where NIED acts as a virtual business predictor. The demonstration experiments consist of two types. One is an experiment to use automatic processed prediction information. The other is an experiment to use spatial distribution of prediction information.

In this presentation, we introduce demonstration experiments, results, and future perspectives to deliver observation and realtime prediction information to users using long-period ground-motion prediction system and API and long-period ground-motion monitor.

Keywords: long-period ground-motion, realtlime prediction, earthquake early warning, demonstration experiment

©2019. Japan Geoscience Union. All Right Reserved. 

# Real-time forecasting of long-period ground motions for the Nankai Trough earthquake: The effectivity of the Green function-based data assimilation method

*Atsuki Oba[1], Takashi Furumura[1], Takuto Maeda[2]

1. Earthquake Research Institute, University of Tokyo, 2. Graduate School of Science and Technology, Hirosaki University

In this study, we considered the possibility of more efficient data assimilation method in order to realize real-time forecasting of Long-Period (LP) ground motions based on the assimilation of strong-motion records and simulation of seismic wave propagation.

Furumura et al. (2019) conducted the real-time forecasting experiment of LP ground motions in the metropolitan area for the 2007 Off Niigata and the 2011 Off Tohoku earthquakes based on the data assimilation of the K-NET and KiK-net records and seismic wave propagation simulation using 3-D FDM. They used optimum interpolation technique, which was also used for real-time forecasting of seismic intensity (Hoshiba and Aoki, 2015) and tsunami (Maeda et al., 2015; Gusman et al., 2016). Since the performance of the supercomputers has improved a lot for recent years, simulation for the Japanese islands scale can be done several times faster than the propagation speed of the seismic wave. However, more effort is necessary to reduce the computational time in order to attain longer lead time before the shaking.

In this study, we considered the applicability of Green's function-based data assimilation. This method is proposed by Wang et al. (2017) as Green'sFunction Tsunami Data Assimilation (GFTDA). GFTDA is the method developed for efficient data assimilation and forecast of tsunami using offshore tsunami network. The Green's functions between the target point and each station are calculated beforehand. The tsunami waveform at the target point is calculated instantaneously by convoluting these Green's functions and the residuals between observation and forecast calculated for each station. This method is proved to be mathematically equivalent to the previous data assimilation method in Wang et al. (2017).

To validate the use of this Green's function-based method for the forecast of LP ground motions, we first conducted the numerical experiment for the 2004 off the Kii Peninsula earthquake (M7.4) and forecasted the LP ground motions at Shinjuku (K-NET TKY007) using the strong-motion records observed in this event. Green's functions are calculated efficiently using reciprocity. The results showed that instant forecast can be available with its accuracy equivalent to that of the previous method. LP ground motions in the distant target point can be forecasted immediately after the assimilation of the observed data near the source, which leads to much longer lead time. Moreover, more accurate forecast and longer lead time were obtained by using offshore stations in DONET, a dense oceanfloor network system for earthquake and tsunamis.

Next, we conducted the forecast experiment for the Nankai Trough earthquake using this method. The target points were Konohana (KiK-net OSKH02), Tsushima (K-NET AIC003) and Shinjuku (K-NET TKY007) stations. For the source model, we used the 1944 Tonankai earthquake, the 1946 Nankai earthquake and the largest event expected (M9) suggested by the Cabinet Office, Japan (2016). For each event, LP ground motions were calculated by 3-D FDM and were used as the observation data. In addition to

©2019. Japan Geoscience Union. All Right Reserved. 

aforementioned networks, stations in the JMA submarine cable network and hypothetical stations of N-net, a newly-planned ocean bottom seismograph/tsunameter network off Hyuganada, were also used. The intensity of strong ground motions was evaluated by GMRotD50 (the median value of the geometric means of the response spectra for two horizontal components when rotating from 0 to 90 degree; Boore et al., 2006). For the evaluation of the duration of LP ground motions, cumulative displacement was calculated. The accuracy of the forecast improved with the assimilation time. In the experiment for the 1946 Nankai earthquake, for example, when the rupture started form the east side, the forecast at Shinjuku with velocity response spectrum and cumulative displacement 70% of the actual observation was obtained about 80 s before the large amplitude LP ground motions started. It required 70 s assimilation after the rupture started. In the case that the rupture started from the west side, the longer lead time (~120 s) was secured when the accuracy reached the same level due to the farther distance between the target point and the rupture initiation point. However, because LP ground motions developed as the fault rupture approached the metropolitan area, longer assimilation time (~100 s) was necessary. From these results, it will be suggested that assimilation should be done while the fault rupture extends and the forecasts should be updated constantly as well as the importance of the strong-motion records near the source region in order to the realize both accurate forecast and longer lead time.

Keywords: long-period ground motions, data assimilation, Green's function

©2019. Japan Geoscience Union. All Right Reserved. 

# Development of EEW system exchanging real-time seismic intensity and seismic waveform

*Shigeki Horiuchi[1], Yuko Sato[1], Taku Urabe[2], Yamaimaiti Nizhamudong[3], Kazuo Sasaki[3]

1. Home Seismometer Corporation, 2. telemetra , 3. Challenge

**1. Introduction** JMA started to issue PLUM telegram in EEW system, which delivers values of real-time intensity measured at all JMA seismic stations in addition to the values of hypocenter parameters. Since the magnitude saturates when a catastrophic earthquake occurs, JMA recommends to use the PLUM method, which uses the maximum value of intensity within 30 km from user location for the intensity estimation. Horiuchi et al. (2011) proposed a method to estimate the fault area of a catastrophic event in real time by using the spatial distribution of real-time seismic intensities. In this report, we developed a system that estimates the location of fault area, displays it on the screen of user’ s PC, and outputs the sound alarm. This system collects continuous waveform from seismic stations using MEMS sensor and delivers waveform data at a time of earthquake occurrence to users PC.

**2. Method of real-time estimation of the fault area of a catastrophic event** In the case JMA issues EEW with magnitude 7.7 or more, the present system starts to determine fault area by using the method of Horiuchi et al. (2011) with data of real-time shaking intensities. When values of observed seismic intensity is larger than the estimated values from the empirical attenuation equation by Shi and Midorikawa (1999), their method determines distances from these stations to the edge of the fault and determine the location of fault area from the distribution of the edge locations.

**3. System overview** The present system consists of center server and seismic observation stations equipped with MEMS sensor and Raspberry pi. The roles of center server are (1) receives the plum telegrams from JMA, (2) accepts user registration, (3) acquires continuous waveforms for observation stations, (4) transmits followings to the windows PC of users, 1) hypocenter parameters from JMA, 2) Real-time seismic intensities from JMA and from observation stations of Raspberry Pi, 3) Waveform data at a time of earthquake occurrence. It is required for the user to register user information such as the coordinates of the user location from the Web screen. When the EEW is delivered, the predicted seismic intensity is outputted on the screen. There is a function to issue EEW for the training. In a case a user generates an earthquake in the web site of center server, the center server sends hypocenter parameters and values of shaking intensity to him. If the testing earthquake is a catastrophic event, his PC computes and displays the spread of the fault area for the testing event.

**4. result**

(1) Since the present PC software provides shaking intensity data and the real-time waveform from the neighboring observation station, these data may be effectively used for the accurate damage prediction by a strong earthquake.

(2) We checked with using observed shaking intensity data whether the spread of the fault area are correctly obtained by the present system. We use shaking intensity data obtained by K-NET from the 17 major earthquakes for the checking. As a result, it was shown that a nearly correct fault area was estimated.

Keywords: EEW, Real-time estimation of the spread of the fault area of a Catastrophic earthquake, exchange of seismic waveform, Rasberry pi seismic station

©2019. Japan Geoscience Union. All Right Reserved. 

[J] Oral | S (Solid Earth Sciences )：S-CG Complex & General

Thu. May 30, 2019 3:30 PM - 5:00 PM JST | Thu. May 30, 2019 6:30 AM - 8:00 AM UTC | A08 TOKYO BAY MAKUHARI HALL

## [S-CG59] Reducing risks from earthquakes, tsunamis & volcanoes: new applications of realtime geophysical data

convener:Masashi Ogiso(Meteorological Research Institute, Japan Meteorological Agency), Naotaka YAMAMOTO CHIKASADA(National Research Institute for Earth Science and Disaster Resilience), Satoshi Kawamoto(Geospatial Information Authority of Japan), Mitsuyuki Hoshiba(Meteorological Research Institute), Chairperson:Naotaka Chikasada(National Res. Inst. for Earth Science and Disaster Resilience), Masashi Ogiso(Meteorological Research Institute, JMA)

As the number of population centers grows in regions with earthquake, tsunami and volcano hazards, the importance of improving methods for rapid, realtime estimates of activity increases. Realtime monitoring, analysis, and prediction of seismic ground motion, crustal movement and tsunami will be powerful tools to contribute to earthquake and tsunami disaster preparedness/mitigation. Tsunami and Earthquake Early Warning systems exist today in many locations around the world. Now JMA has started to promptly provide Eruption Notices to inform people of impending and beginning volcanic eruptions. Large events like the 2011 Tohoku Earthquake (Mw9.0) have demonstrated some of the shortcomings of existing techniques. In this session, we invite presentations on new ideas, methods and applications of (near) realtime analysis of seismic, geodetic and tsunami data, to the problem of realtime prediction aimed at improving disaster preparedness/mitigation in the fields of earthquake, tsunami and volcano observation. Presentation is encouraged to bring together scientists, engineers, and practitioners from a broad range of backgrounds from around the world, and to promote collaborative communication at the leading edge of the science and technologies.

3:30 PM - 3:45 PM JST | 6:30 AM - 6:45 AM UTC

[SCG59-07] Enhancements of real time seismic intensity estimation using seismic intensity meters maintained by a local government – Case study on Tottori prefecture -

*Takao Kagawa[1] (1.Tottori University Graduate School of Engineering)

3:45 PM - 4:00 PM JST | 6:45 AM - 7:00 AM UTC

[SCG59-08] **Drawig of the realtime seismic intesity on live screen and maximum distribution map for the Earthquak disaster prevension.**
**-Planar indication of seismic intensity using surface ground amplification factor-**

*Kenji Kanjo[1], Isao Takahashi[1], Yoshinori Shinohara[1], Rami Ibrahim[2] (1.Takamisawa cybernetics Co. Ltd, 2.Earthquake Research Institute, University of Tokyo)

4:00 PM - 4:15 PM JST | 7:00 AM - 7:15 AM UTC

[SCG59-09] Improvements of the GEONET real-time analysis system (REGARD) for more reliable operation

*Kazuyuki Ohashi[1], Satoshi Abe[1], Yasuaki Kakiage[1], Satoshi Kawamoto[1], Hiroshi Munekane[1] (1.GSI of Japan)

4:15 PM - 4:30 PM JST | 7:15 AM - 7:30 AM UTC

[SCG59-10] Development of “real-time” uncertainty evaluation algorithm for the estimated coseismic fault model using MCMC approach

*Keitaro Ohno[1], Yusaku Ohta[1] (1.Recerch Center for Prediction of Earthquakes and Volcanic Eruptions, Graduate School of Science, Tohoku University)

4:30 PM - 4:45 PM JST | 7:30 AM - 7:45 AM UTC

[SCG59-11] Drifting float measurement of pressure change by tsunami

*Masayuki Obayashi[1], Shingo Watada[2], Hiroko Sugioka[3] (1.Japan Agency for Marine-Earth Science and Technology, 2.Earthquake Research Institute, University of Tokyo, 3.Department of Planetology, Kobe University)

4:45 PM - 5:00 PM JST | 7:45 AM - 8:00 AM UTC

[SCG59-12] Development of the Real-time Forecasting for Meteorite Impact Tsunami

*Naotaka YAMAMOTO CHIKASADA[1], Toshitaka Baba[2], Tetsuharu Fuse[3] (1.NIED, 2.Tokushima University, 3.NICT)

# Enhancements of real time seismic intensity estimation using seismic intensity meters maintained by a local government –Case study on Tottori prefecture -

*Takao Kagawa[1]

1. Tottori University Graduate School of Engineering

Enhancements of real time seismic intensity estimation using seismic intensity meters maintained by a local government is demonstrated. Dense observation network is desirable for upgrading accuracy and quality of Earthquake Early Warning System. Seismic intensity meters installed in all municipalities are the most suitable equipment for the purpose. The seismic intensity meters in Tottori prefecture are improved to broadcast packets with peak ground acceleration and JMA seismic intensity at every one second. The data are received at Tottori University and PLUM method is applied to the data for estimating JMA seismic intensity distribution at 1km grid points. In this study, two additional methodologies are introduced on the system. One is attenuation of seismic intensities from observed sites and propagation from every grids for estimation. Another is introduction of P wave amplitudes for seismic intensity estimation. Using the methodologies, we can obtain rapid and detailed seismic intensity distribution than before.

Keywords: Local Government, Seismic Intensity Meter, Real Time, PLUM method, P wave

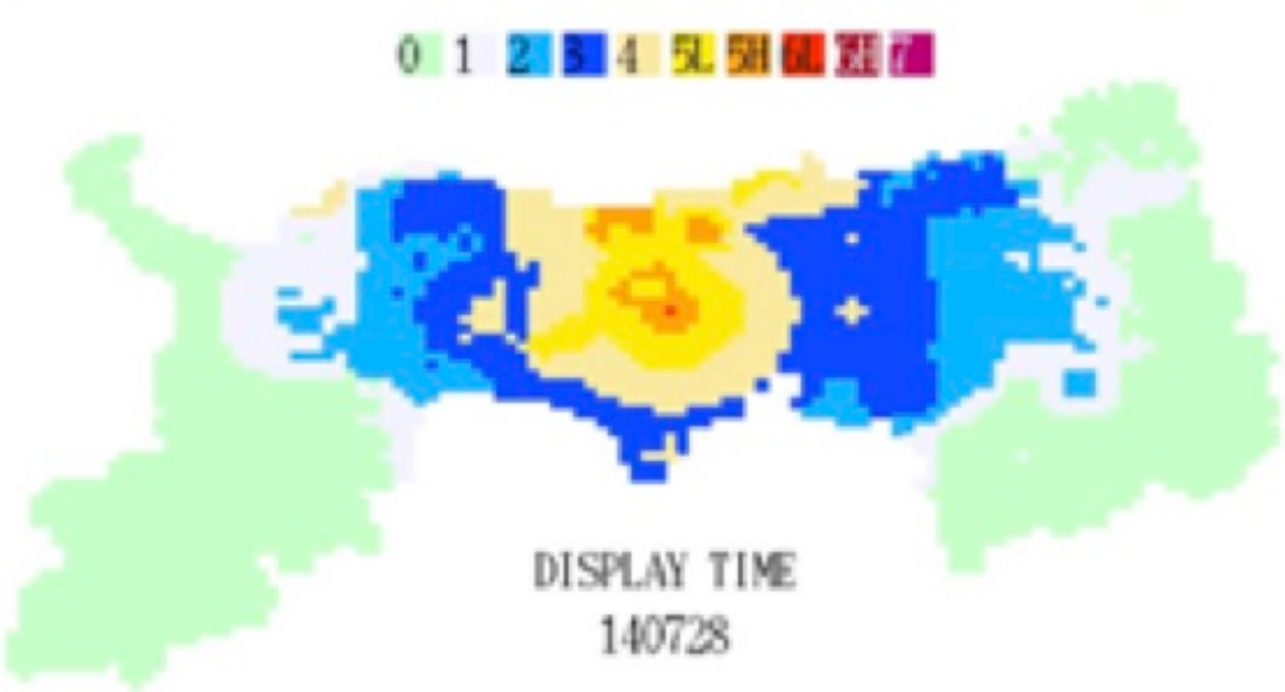


©2019. Japan Geoscience Union. All Right Reserved. 

# Drawig of the realtime seismic intesity on live screen and maximum distribution map for the Earthquak disaster prevension. -Planar indication of seismic intensity using surface ground amplification factor-

*Kenji Kanjo[1], Isao Takahashi[1], Yoshinori Shinohara[1], Rami Ibrahim[2]

1. Takamisawa cybernetics Co. Ltd, 2. Earthquake Research Institute, University of Tokyo

Earthquake damage can be caused from a small-sized earthquake (magnitude class 4.5) occurs in inland areas to a large-sized earthquake such as the 2011 Tohoku earthquake (Mw 9.1). In recent years, it is possible to estimate the amount of detailed displacement of the destruction zone from the inversion analysis of observed data. Moreover, ground motion prediction equations (GMPEs) and earthquake prediction recipes have been proposed. Those developments contributed to the earthquake disaster mitigation measures. Earthquake early warning system (EEW) of Japan has been in operation since 2007, it is very useful to issue information that have a great impact on disaster mitigation, however, some problems still exist with the information issued by EEW. For instance, the warnings are sometimes issued after S-wave arrivals, which leaves an area without alarm known as a blind zone area.

In this study, we used a dense seismic network dataset recorded during the 2016 Kumamoto (Mw 7.0), and the 2019 January 3rd (Mw 5.1) earthquakes, maximum JMA intensity of 7 and 6 upper, respectively. In spite of the difference of magnitudes and source size area the two earthquakes had close maximum intensity values. It noted that the average spacing distribution of seismic instrument in that regions is ~ 4-5 km. We here obtain the maximum peak ground acceleration (PGA) on free surface on each observed point, we then corrected PGA to engineering basement, using site effect information from J-SHIS (NIED), spaced by 1×1 $km^2$. Using PGA on engineering bedrock, we estimate the PGA on free surface by multiplying with surface amplification factor at each grid point of 1×1 $km^2$, we then evaluate the seismic intensity at each grid. We repeat this process for each observed point considering the inter-station distance and finally produce the intensity map.

Our method gives a quick information about earthquake location (close or far), hypocentral depth (shallow or deep) inferred from apparent velocity distribution maps. It also recognizes the earthquake source size (small or large) inferred from the spatial distribution of PGA. We also attempted scaling by so-called P wave detection and maximum seismic intensity distribution prediction using theoretical amplitude ratio (5 times) of S wave / P wave at the seismic source.

It is a very important issue to observe the strong-ground motion in real-time to improve the performance of EEW. We strongly recommend local government to have their own high density network, which gives a quick earthquake disaster information. The Japan Meteorological Agency will aim for speeding up and improving the precision of emergency earthquakes (eliminating the blind zone) by integrating server information of each local government (with small budget without directly telemetering observation point data covering several thousands of points).

**Acknowledgments**
We express our appreciations to the officials in Tokyo, Kyoto, Nara, Sapporo,
Kumamoto, Miyagi, Fukushima and Ibaraki prefectures uploaded the seismic intensity data used for the

©2019. Japan Geoscience Union. All Right Reserved. 

analysis to the Japan Meteorological Agency Web page.

Keywords: Local government measurement intensity meter, Engineer basement seismic intensity , Evaluate by surface amplification factor , Real time seismic intensity, Live view, Maximum seismic intensity distribution map

©2019. Japan Geoscience Union. All Right Reserved. 

# Improvements of the GEONET real-time analysis system (REGARD) for more reliable operation

*Kazuyuki Ohashi[1], Satoshi Abe[1], Yasuaki Kakiage[1], Satoshi Kawamoto[1], Hiroshi Munekane[1]

1. GSI of Japan

The displacement data produced by GNSS observations never saturate for large earthquakes in contrast to seismometer data that has a limitation of instrument saturation. Geospatial Information Authority of Japan has launched a real-time GNSS analysis system named “REGARD” which estimates finite fault models based on the Japanese nationwide GNSS network GEONET. The REGARD system has been in operation since April, 2016. The system experienced 2016 Kumamoto earthquake, and provided a single rectangular fault model with very high variance reduction (VR) of 96%. The REGARD system has been become increasingly important for rapid response to major earthquakes for providing coseismic displacements, finite model estimate, and moment magnitude rapidly. Therefore, the system must be more stable. So we try to implement other positioning procedure to REGARD system.

The REGARD system conduct relative positioning by using reference station data and rover station data. If reference station data lacked, we can’t obtain the coordinates of all other station. So we focus on Precise Point Positioning(PPP). Real-time PPP analysis needs correction data of Ionospheric delay, Tropospheric delay, satellite clock and so on. We implement as follow system. (1) Collect real time observation data from about 100 worldwide GNSS station. (2) Estimate ephemeris and collection data by using MADOCA(Multi-GNSS Advanced Demonstration tool for Orbit and Clock Analysis) developed by JAXA. (3) Conduct real time PPP analysis.

As a results of accuracy evaluation of real time PPP analysis, the accuracy is less than REGARD system. If we subtract one station results from other station(PPP-differential), the accuracy is improvement as well as REGRAD system. Therefore, real time PPP analysis system is expected to be useful for improving redundancy and robustness of REGARD system.

Keywords: REGARD, GNSS, PPP

©2019. Japan Geoscience Union. All Right Reserved. 

# Development of “real-time” uncertainty evaluation algorithm for the estimated coseismic fault model using MCMC approach

*Keitaro Ohno[1], Yusaku Ohta[1]

1. Recerch Center for Prediction of Earthquakes and Volcanic Eruptions, Graduate School of Science, Tohoku University

Rapid understanding of the magnitude of large earthquakes and their associated fault dimensions are extremely important. Since September 2012, Geospatial Information Authority of Japan (GSI) and Tohoku University are jointly developing the GEONET real-time analysis system (REGARD). REGARD system rapidly estimates two types of coseismic fault models, which are slip distribution along the plate interface and single rectangular fault model, using permanent displacement field based on the real-time GNSS tine series. Currently, REGARD adopted the maximum likelihood approach to estimate the optimum model. The system has two points to be improved. As first point, it is difficult to estimate the quantitative uncertainty estimation of the obtained result because of the estimated result should contain both of the observation error of the real time GNSS and modeling error caused by the model settings. Understanding of such uncertainties quantitatively based on the data is important for evaluation of the result for disaster response. Second point, the problem is non-linear to estimate the single rectangular fault model in REGARD. Thus, the result strongly may depend on the initial values of the fault parameters. It is necessary to find the global minimum quickly for real-time use.

Based on these backgrounds, we are developing coseismic fault model estimation system using MCMC (Markov Chain Monte Carlo methods), which is probabilistic approach based on Bayesian statistics. MCMC does not specify one maximum likelihood value, but estimates the posterior probability density function (PDF). In addition, dependency on the initial value is relatively small by searching unknown parameters over a wide range randomly. In this study, we focus on the development the algorithm to estimate the single rectangular fault model deduced from permanent coseismic displacement field in real-time. We adopted basic Metropolis Hasting method as sampler and utilized parallel tempering approach to improve the sampling efficiency. One of the challenges for using MCMC in real time is how to make search settings, such as initial value, walk distance, variance of likelihood function, and Burn-in, which are generally decided by the try and error. We suggest a method of deciding these values automatically using scaling law and original sampling flow. Other challenging issue is calculation time. In generally, the calculation cost of MCMC is problem for the real-time purpose. To improve the performance of the MCMC we adopted OpenMP for the parallelization of the computing.

We applied this approach to the 2011 Tohoku-Oki earthquake, 2016 Kumamoto earthquake, and 2016 Fukushima-Oki earthquake using the actual permanent displacement time series from REGARD. In each estimations, we got $1\times10^6$ samples and obtained posterior PDF within 30 seconds. To emphasize, this algorithm could estimate the magnitude as distributions based on the data. Especially in Tohoku-Oki earthquake, obtained results clearly shows the tradeoff between the fault area and the slip amount. This result suggests that the onshore GNSS data cannot constrain them, which are extremely important factors for precise near-field tsunami forecasting.
In our presentation, we will show the more detail characteristic of the algorithm. We are working on development of it for single rectangular fault model aiming at actual operation. Furthermore, we will expand this approach to not only the single rectangular fault but also the slip distribution along the plate interface.

©2019. Japan Geoscience Union. All Right Reserved. 

Keywords: MCMC, GNSS, real-rime, rapid prediction, bayesian, uncertainty

©2019. Japan Geoscience Union. All Right Reserved. 

# Drifting float measurement of pressure change by tsunami

*Masayuki Obayashi[1], Shingo Watada[2], Hiroko Sugioka[3]

1. Japan Agency for Marine-Earth Science and Technology, 2. Earthquake Research Institute, University of Tokyo, 3. Department of Planetology, Kobe University

Recently a new instrument, named MERMAID (Mobile Earthquake Recording in Marine Areas by Independent Divers), was developed to measure acoustic signals converted from seismic waves at the seafloor. The MERMAID is a Lagrangian drifter equipped with a hydrophone and drifts passively at 1,500 –2,000 m depth until an earthquake signal is detected. If this is identified as a strong P wave, the MERMAID ascends at speed of 10 cm/s for transmission of the recorded waveform within time window of a hundred seconds before and after the P wave arrival as well as its global positioning system (GPS) coordinates at the surface. After transmitting the data via satellite links, the MERMAID descends at speed of 5 cm/s to monitor earthquake signals at 1,500 –2,000 m depth again.
It was reported that tsunamis were recorded by hydrophones (e.g. Okal et al., 2007), notably in frequency bands extending outside the range of the Shallow Water Approximation. If MERMAID floats can cover the oceans as dense as the Argo project of which almost 4000 floats are now drifting to measure temperature and salinity in the oceans, we acquire valuable tsunami data. Here we estimate what signals are observed by a MERMAID, by comparing to the pressure change of the 2010 Chile Tsunami measured by a differential pressure gauge (DPG) at about 4800 m deep seafloor.
We assume linearized water wave with period $T$, amplitude $H$, and phase velocity $c$ as shown in Figure 1. Phase velocity $c$ is given by $c = (g \tanh(kD) / k)^{1/2}$, where $k$ is horizontal wavenumber $k = \omega / c$, $\omega = 2\pi / T$ is angular frequency and $g$ is gravity. The wavenumber $k(\omega, D)$ of the water waves in a constant depth ocean as a function of a wave period is obtained by the recursion equation. The water wave height $W(x, t)$ as the function of time $t$ and horizontal position $x$ is expressed as
$W(x,t) = H e^{i(kx-\omega t)}$
The MERMAID is Lagrangian float drifting at a depth of $z$ ($0 > z > -D$) and measures Lagrangian pressure of water, where $D$ is water depth.
Lagrangian pressure $\delta p(x, z, t)$ is given by
$\delta p(x, z, t) = -\{H \rho_o g \sinh(kz) / (\sinh(kD) \cosh(kD))\} e^{i(kx-\omega t)}$
Eulerian pressure is given by
$p'(x, z, t) = \{H \rho_o g \cosh(k(D+z)) / \cosh(kD)\} e^{i(kx-\omega t)}$
Therefore, pressure measured by a DPG at seafloor is expressed as
$p'(x,-D, t) = \{H \rho_o g / \cosh(kD)\} e^{i(kx-\omega t)}$
and the pressure $\delta p(z)$ measured by a MERMAID at $z$ depth can be related
with the DPG pressure $p'(D)$ by
$\delta p(z) = R\, p'(-D)$, $R = -\sinh(kz) / \sinh(kD)$
If $T$ is large enough that $k$ is close to 0, $R$ becomes close to $z/D$. Figure 2 shows the $R$ as the function of $T$ for floats at 1000 (blue) and 2000 (red) m depth, suggesting the $R$ acts as a low-pass filter. Figure 3 shows the predicted pressure changes observed floats drifting at 1000 (blue) and 2000 (red) m depth. In the presentation, we will discuss availability of tsunami measurement by a float.

Keywords: tsunami, float, hydrophone, differential pressure gauge

©2019. Japan Geoscience Union. All Right Reserved. 

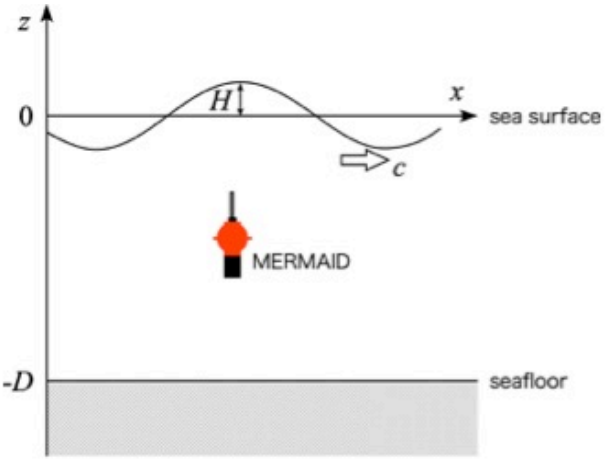


Figure 1. Problem setting

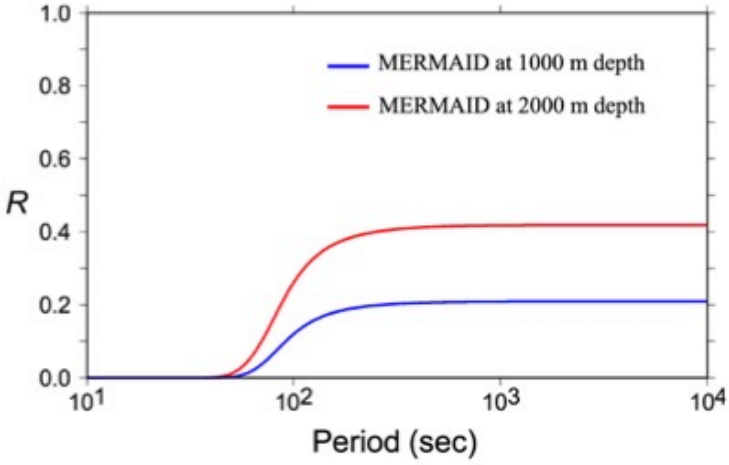


Figure 2. $R$ as the function of period $T$

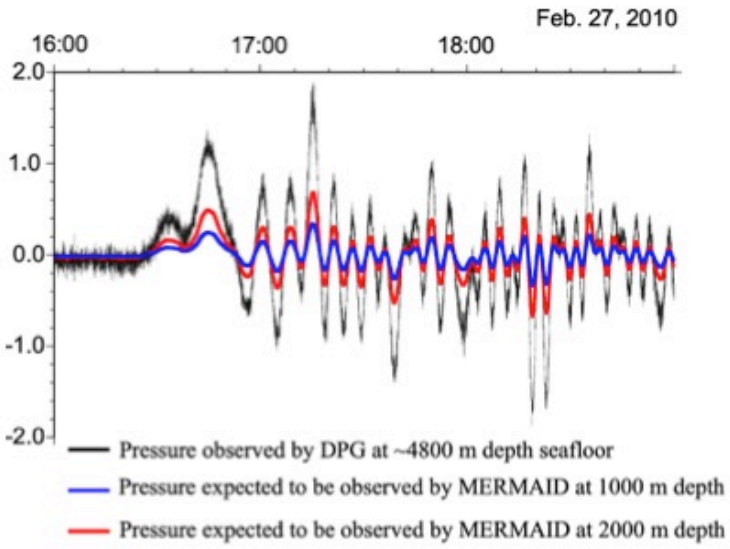


Figure 3. Predicted pressure changes observed by MERMAIDs at 1000 and 2000 m depth.

©2019. Japan Geoscience Union. All Right Reserved. 

# Development of the Real-time Forecasting for Meteorite Impact Tsunami

*Naotaka YAMAMOTO CHIKASADA[1], Toshitaka Baba[2], Tetsuharu Fuse[3]

1. NIED, 2. Tokushima University, 3. NICT

Tsunami induced by earthquakes, submarine landslides, volcanic eruption in submarine and coastal area and meteorological phenomena is one of the most devastating natural disasters. A meteorite impact into the oceans spawn large tsunami depending on the size and velocity of the meteorite and the sea depth at the location of the impact as well. However, we do not have a numerical model to reproduce both of meteorite impacts and tsunami propagations. We have started to develop a new numerical model to simulate tsunamis generated by the meteorite impact combining iSALE (Wünnemann et al., 2006) for simulating impact phenomena and JAGURS (Baba et al., 2017) for simulating tsunami. The iSALE is a multi-material and multi-rheology shock physics code for simulating impact phenomena. JAGURS is a parallelized tsunami simulation code to solve two-dimensional non-linear long-wave equation with Boussinesq terms for representing observed tsunami waveforms, tsunami height and inundation. We set sea-floor deformation, sea-surface disturbance and velocity of gravity wave which is the output from iSALE to the input of JAGURS. We then calculate tsunami height along the coastlines in any place using ASTER GDEM version 2 (Fujisada et al., 2012) and GEBCO_2014 Grid. ASTER GDEM has one arcsecond (about 30 m) spatial resolution and covers land between 56S and 60N latitude as a topographic data. GEBCO’s gridded bathymetric data has thirty arcseconds (about 1 km) spatial resolution for the worldwide.
We first investigate the tsunami generation using iSALE code for creating tsunami source model depending on the meteor size, the velocity of impact, the size of cavity, the width and depth of crater and tsunami propagation speed. We also investigate probabilistic hazard of meteorite impact tsunami using simplified cavity curves with developed JAGURS built-in. Finally, we construct a new numerical model of meteorite impact tsunami combining iSALE and JAGURS. Additionally, we consider the way of automatic detection of meteorite impact using the recode of the highly sensitive seismograph network in real-time.
We gratefully acknowledge the developers of iSALE, including Gareth Collins, Kai Wünnemann, Boris Ivanov, H. Jay Melosh and Dirk Elbeshausen. Data analysis and visualizations of iSALE were carried out on PC cluster and computers at Center for Computational Astrophysics, National Astronomical Observatory of Japan. This work was partially supported by JSPS KAKENHI Grant Number JP18K04674.

Keywords: Real-time forecast, Tsunami, Meteorite impact

©2019. Japan Geoscience Union. All Right Reserved. 

[J] Oral | B (Biogeosciences)：B-PT Paleontology

Thu. May 30, 2019 1:45 PM - 3:15 PM JST | Thu. May 30, 2019 4:45 AM - 6:15 AM UTC | 201A 2F

## [B-PT05] Biotic History

convener:Isao Motoyama(Department of Earth and Environmental Sciences, Yamagata University), Takao Ubukata(Division of Geology & Mineralogy, Department of Earth & Planetary Sciences, Kyoto University), Kazuyoshi Moriya(Department of Earth Sciences, Faculty of Education and Integrated Arts and Sciences, Waseda University), Chairperson:Isao Motoyama, Takao Ubukata, Kazuyoshi Moriya

The Biotic History session covers all aspects of ancient life and the history of biosphere through the geologic time. The study of ancient life is essential for unveiling mysteries of our planet earth. It also provides evidence for evolution of oceans, continents and island arcs. Modern progress in this field has been enhanced by interdisciplinary collaboration with allied sciences, such as paleoceanography and evolutionary biology. Our session intends to be a hub of communication amongst all earth scientists studying the biosphere; we welcome biological and biogeochemical approaches toward the understanding of the history of life.

1:45 PM - 2:00 PM JST | 4:45 AM - 5:00 AM UTC

### [BPT05-01] Cause of accelerated evolution of Earth's life; four-layered underground robust bio-communities played a critical role for the accelerated genome evolution as a response of mass extinction

*Shigenori Maruyama[1], Akio Kanai[2], Issay Narumi[3] (1.Earth-Life Science Institute, Tokyo Institute of Technology, 2.keio University, 3.Toyo University)

2:00 PM - 2:15 PM JST | 5:00 AM - 5:15 AM UTC

### [BPT05-02] Amino acid composition in molluscan shells and its relation to taxa and shell microstructure ~ Toward reconstruction of ancient trophic level using compound specific isotope analysis of amino acids ~

*Naoki Yugami[1], Akiko Goto[2], Robert Jenkins[2] (1.Graduate School of Natural Science & Technology. Kanazawa Univercity, 2.Institute of Science & Engineering . Kanazawa Univercity)

2:15 PM - 2:30 PM JST | 5:15 AM - 5:30 AM UTC

### [BPT05-03] Relation of shell form to rocking motion in planispiral cephalopods

*Takao Ubukata[1] (1.Division of Geology & Mineralogy, Department of Earth & Planetary Sciences, Kyoto University)

2:30 PM - 2:45 PM JST | 5:30 AM - 5:45 AM UTC

### [BPT05-04] Paleoenvironment aross the Meddle Eocene Climatic Optimum

Hiroki Masui[1], *Kazuyoshi Moriya[1] (1.Department of Earth Sciences, Faculty of Education and Integrated Arts and Sciences, Waseda University)

2:45 PM - 3:00 PM JST | 5:45 AM - 6:00 AM UTC

### [BPT05-05] Reconstruction of the North Pacific subtropical gyre from the Middle to Late Miocene as inferred from radiolarian assemblages

*Shin-ichi Kamikuri[1], Isao Motoyama[2], Taiki Sawada[3] (1.Faculty of Education, Ibaraki University, 2.Faculty of Science, Yamagata University, 3.Japan Petroleum Exploration Co.,Ltd.)

3:00 PM - 3:15 PM JST | 6:00 AM - 6:15 AM UTC

### [BPT05-06] Fossilization processes of Pliocene tree fossils from the Yasu River, Shiga Prefecture, Japan: Organic geochemical approach

*Jinya Nakamura[1], Ken Sawada[2], Masashi A Ikeda[1], Hideto Nakamura[3], Minoru Tsukagoshi[4] (1.Graduate School of Science, Hokkaido University, 2.Department of Earth and Planetary Sciences, Faculty of Science, Hokkaido University, 3.Faculty of Science, Osaka City Univerisity, 4.Osaka Museum of Natural History)

# Cause of accelerated evolution of Earth’s life; four-layered underground robust bio-communities played a critical role for the accelerated genome evolution as a response of mass extinction

*Shigenori Maruyama[1], Akio Kanai[2], Issay Narumi[3]

1. Earth-Life Science Institute, Tokyo Institute of Technology, 2. keio University, 3. Toyo University

It has long been recognized the concept of five kingdom or six kingdom model which shows the life with difference of function and size. If believing Darwinian Evolution, how can we interpret the diversified distribution with primitive small microbes to the most evolved types of large life. If we consider the most evolved metazoans such as human being to be the result of increased free oxygen in atmosphere, why do the anoxic microbes remain on the surface.
We have engaged in the decoding Earth history Program over 30 years, and obtained the following six results, (1)Since the birth of life until 4.0Ga, three times of Great Evolution of Life (GEL) occurred, (2)Those evolutions were predominantly controlled by the $pO_2$ increase in the environments, (3)Underground bio-communities are present forming 4-layers with boundary layers, (4)Each layer corresponds to different $pO_2$ levels; the older the lower $pO_2$ , (5)In between the two, where two-way genome biomes are present, although speculative, and (6)These four layers could have been formed during the 3 GEL times, accompanying many mass extinctions. Those were remained as fossil environments where evolution stopped, because of no significant environmental changes, in spite of extremely severe surface environments with frequent mass extinction and resultant accelerated evolution of life.
The result corresponds to the concept of 5-6 Kingdom which suggests the preservation of biological communities with different level of $pO_2$ in environments. Through the Earth history, new GEC occurred with great change of $pO_2$ , the advanced life on the surface suffered mass extinctions due to exponentially decreased $pO_2$, instead the underground microbes invaded to the surface, and evolved there again. This is the entity of evolution of life on the earth. Therefore, the presence of robust 4 layered underground biological communities must have contributed to evolving life on this planet, in spite of severe environmental change of planets over 4.0 billion of years in the Universe, not by death, but evolved thorough GEL at 4.0Ga, 2.2Ga and 0.6Ga.

Keywords: oxygen level, underground bio-community, accelaration of life's evolution

©2019. Japan Geoscience Union. All Right Reserved. 

# Amino acid composition in molluscan shells and its relation to taxa and shell microstructure ~ Toward reconstruction of ancient trophic level using compound specific isotope analysis of amino acids ~

*Naoki Yugami[1], Akiko Goto[2], Robert Jenkins[2]

1. Graduate School of Natural Science & Technology. Kanazawa Univercity, 2. Institute of Science & Engineering . Kanazawa Univercity

We may clarify the trophic level of fossils applying “trophic level estimation method using compound specific isotope analysis of amino acids” (Chikaraishi et al., 2009). When applying the method to fossils, we must pay attention to whether amino acids in fossils are original or not, so screening of fossil samples is important. We can apply "amino acid composition conforming to shell microstructure" to the screening of fossi samples. This depends on a study showing the amino acid composition is different for each shell microstructure in the present bivalve (Kobayashi and Samata, 2006). We may determine whether amino acids present in the fossil shell are original or not by confirming “whether there is an amino acid composition specific to the shell microstructure observed in the fossil”. However, Kobayashi and Samata (2006) showed only the difference in amino acid composition each shell microstructures in the bivalvia, and not showed stability in the lineage relationship of the same microstructure. Moreover, there are problems such as the fraction of the amino acid composition, the method used, and the equipment to be used are different for each article, so it is difficult to compare for each article easily. In addition, there are no papers showing amino acid composition of Protbranchia of bivalvia. From the above, the stability of the amino acid composition for each shell microstructures in the lineage is unknown. Therefore, we set the pupose of this research that clarifying the stability of the amino acid composition of each shell microstructure in molluscan from the present raw sample. In this study, we focus on nacreous structure because this structure contain a lot of organic matter and it is primitive structure. We will clarify the stability of the amino acid composition of each taxa and shell microstructure, comparing within each taxa and lineage of bivalve, gastropod, and cephalopod.

As a result of cluster analysis, we found that the amino acid composition can be roughly divided into two groups, "primitive group" and "derivative group", in both the gastropoda and bivalvia. The amino acid composition of *Turbo sazae, Turbo mamoratus* and *Lunella coreensis* of gastropoda belonging to the same family were stable. Moreover, in the bivalvia, the amino acid composition is stable in the Pteriomorpha and Palaeoheterodonta, and in the Protobranchia, respectively. We could find the differences in the amount of alanine etc. in the Pteriomorpha- Palaeoheterodonta lineage and Protobranchia lineage. From this, it can be said that the amino acid composition of the nacreous structure is stable in family in gastropoda and stable in subclass in bivalvia. Cluster analysis showed that "gastropoda group" and "bivalvia group" have relatively close relationships, and their amino acid composition is similar in that alanine and glycine are abundantly included. However, it has been suggested that proteins used for shell formation in bivalvia and gastropoda may have been obtained independently in the process of evolution (Mann et al., 2018). Since amino acids which are likely to be included depending on the function of the protein are determined, it is thought that the amino acid composition converges evolutionarily and is similar even if it has different proteins.

Through this study, both bivalvia and gastropoda are roughly divided into two groups, "primitive group" and "derivative group", and furthermore, we could set the amino acid compositions used for screening of

©2019. Japan Geoscience Union. All Right Reserved. 

fossil samples of nacreous structure to five, "Nautilus", "primitive of Vetigastropoda", "derivative of Vetigastropoda", "primitive of Bivalvia (Protobranchia)", "derivative of Bivalvia (Pteriomorpha, Palaeoheterodonta)". Therefore, we will be able to screen fossil samples of nacreous structure more precisely by using "amino acid composition conforming to lineage-shell microstructure" for trophic level estimation.

Keywords: amino acids, Phylogenetic relationships, trophic level, molluscs

©2019. Japan Geoscience Union. All Right Reserved. 

# Relation of shell form to rocking motion in planispiral cephalopods

*Takao Ubukata[1]

1. Division of Geology & Mineralogy, Department of Earth & Planetary Sciences, Kyoto University

In Recent *Nautilus*, thrust force produced by the hyponomic jet acts to rotate the shell resulting in a rocking motion during swimming. This instability is a potential problem for any other ectoconchleate cephalopods with planispiral conchs when they swim. A smaller distance between the center of gravity and center of buoyancy tends to cause a large rotation of the shell. For this reason, it has long been imagined that ammonoids with long body chambers are less stable than *Nautilus* during swimming. In contrast, it has also been considered that a long body chamber places the aperture higher and positions the hyponome at the same level of the center of gravity so that the hyponomic jet can act directly through the center of gravity. Previous discussions on static stability of ectoconchleate cephalopods largely focused on indirect assessment based on the aperture orientation and the position of the center of gravity and center of buoyancy. The present study assessed the angle of rocking motion for various shell forms of planispiral cephalopods to generalize the relationship between conch geometry and static stability. The angle of rocking motion was computed for theoretical morphologic models based on force and moment balance presuming a neutrally buoyant condition. The thrust force of hyponomic jet was assumed to be expelled from the ventral edge of the aperture and to generate a moment which is opposed by the restorative moment produced by inclination of segment between the center of gravity and center of buoyancy. Form drag and shear stress acting on the shell moving with respect to surrounding water were ignored in calculating the opposing moment. The inclination angle of the segment between the center of gravity and center of buoyancy was regarded as the angle of rocking motion and was computed for each theoretical model with given values of whorl expansion rate, relative umbilical width, and relative whorl breadth. The result revealed following: (1) The angle of rocking motion fluctuates with changes in the whorl expansion rate (*W*) if the value of *W* is small enough so that the body chamber is more than one whorl in length. In this condition, the rocking angle varies sensitively to the change in *W*. (2) The rocking angle is large when the shell is slender. (3) The rocking angle does not highly depend on the relative umbilical width. These results indicate that the long body chamber resulting from a small *W* does not always allow the animal stable swimming and a slight intraspecific or ontogenetic variation in *W* may cause drastic change in static stability in such form. The result suggests that such static instability limits swimming ability in some ammonoids with tightly coiled conchs.

Keywords: cephalopods, hydrostatics, stability

©2019. Japan Geoscience Union. All Right Reserved. 

# Paleoenvironment aross the Meddle Eocene Climatic Optimum

Hiroki Masui[1], *Kazuyoshi Moriya[1]

1. Department of Earth Sciences, Faculty of Education and Integrated Arts and Sciences, Waseda University

The Middle Eocene Climatic Optimum (MECO) is an abrupt short-term global warming event that occurred about 40 Ma. Although this event is now reported from all across the world, the environmental impacts and biotic responses accompanying the event are still poorly understood. Since we are now faced with the threat of global warming, deeper understanding of past global warming events like the MECO is critical.

We present bulk carbonate stable isotope data, coarse fraction accumulation rates (CFAR), and planktic foraminiferal assemblage data spanning the MECO interval from International Ocean Discovery Program (IODP) Site U1408 in the Northwest Atlantic to assess environmental changes and biotic responses across the event. A negative shift in bulk $d^{18}O$ was observed from 40.6 Ma (the MECO onset) to 40.0 Ma (the peak MECO), followed by a sudden return to the background level by 39.9 Ma (the termination). A significant decline of CFAR was observed near the peak of the MECO (40.3 Ma–40.0 Ma). This may reflect a decline in planktic foraminiferal production due to starving caused by elevated metabolism coupled by limited availability of nutrients. In contrast, a sudden increase in bulk $d^{13}C$, CFAR, and eutrophic planktic foraminiferal genus, *Pseudohastigerina*, was observed immediately after the peak of the MECO (40.0-39.9Ma). This may indicate a sudden switch to the eutrophic environment and an increase in primary and planktic foraminiferal production. The termination of the warming might have caused continental aridification and resulted in an increased input of aeolian dust to the ocean. In addition, the relative abundance of photosymbiotic planktic foraminiferal genus, *Acarinina*, declined toward the peak of the MECO, while the relative abundance of another photosymbiotic genus, *Globigerinatheka* remained almost constant throughout the MECO. This may indicate the loss of photosymbiotic algae exclusively affected *Acarinina* during the event.

Keywords: Planktic foraminifers

©2019. Japan Geoscience Union. All Right Reserved. 

# Reconstruction of the North Pacific subtropical gyre from the Middle to Late Miocene as inferred from radiolarian assemblages

*Shin-ichi Kamikuri[1], Isao Motoyama[2], Taiki Sawada[3]

1. Faculty of Education, Ibaraki University, 2. Faculty of Science, Yamagata University, 3. Japan Petroleum Exploration Co.,Ltd.

A major objective of the present study is to reconstruct gyral circulation patterns of the subtropical North Pacific from the middle to late Miocene based on the radiolarian assemblages. We collected the mudstones from ODP Site 1021 of the California margin in the northern area of the California Current, and from outcrops of the Boso Peninsula (Japan) in the northern area of the Kuroshio.
The middle Miocene subtropical Pacific was dominated by warm-water taxa, and similar taxa in the eastern and western areas. The distribution pattern of radiolarian faunas in the subtropical North Pacific was due to be similar in the surface water structure and temperature, and indicates that the general gyral circulation system was only weakly developed in the middle Miocene. During the late Miocene the cool-water taxa increased and the warm-water taxa declined overall in the subtropical Pacific. At the same time the east-west faunal provincialism increased. This faunal change has been associated with the resultant strengthening of the general gyral circulation in the subtropical Pacific due to the significant high latitude cooling and the closing of the Indo-Pacific Seaway at that time.

Keywords: North Pacific subtropical gyre, Miocene, radiolarian assemblage

©2019. Japan Geoscience Union. All Right Reserved. 

# Fossilization processes of Pliocene tree fossils from the Yasu River, Shiga Prefecture, Japan: Organic geochemical approach

*Jinya Nakamura[1], Ken Sawada[2], Masashi A Ikeda[1], Hideto Nakamura[3], Minoru Tsukagoshi[4]

1. Graduate School of Science, Hokkaido University, 2. Department of Earth and Planetary Sciences, Faculty of Science, Hokkaido University, 3. Faculty of Science, Osaka City Univerisity, 4. Osaka Museum of Natural History

The Pliocene fossil forest (ca. 2.7 Ma) is known to be distributed in the Yasu River, Shiga Prefecture, Japan. The tree fossils in the forest are characterized by blackish coal-like tissues in the surface but living tree-like fresh lignite in their inner part. In the present study, we investigate by organic geochemical analyses to identify the taxonomy and to examine fossilization, diagenesis, and taphonomy of the tree fossil.

The tree fossils used was separated to three parts; surface (outer), intermediate, and inner parts. The outer part is blackish coal-like tissue, but inner part is brownish lignite. The intermediate part is dark brownish lignite-like tissue. Lipids were extracted with dichloromethane/methanol, and separated to aliphatic, aromatic and polar fractions. Lipids were identified and quantified by GC-MS. The residues after extraction were used for pyrolysis and thermochemolysis by GC-MS equipped a Curie-point pyrolyzer. Thermochemolysis was performed with tetramethylammonium hydroxide (TMAH)

By the thermochemolysis, vanillic phenols are predominantly detected in all parts of the tree fossils. Phyllocladane and cuparane were identified as major plant-derived terpenoids in fee (extractable) components of the fossil samples. The phyllocladane is conifer-derived diterpenoid, and cuparane is a specific sesquiterpenoid produced by subfamily Cupressaceae. In addition, sugiol, which originated from family Taxodiaceae, were not detected in the fossil samples. Thus, the tree fossil can be presumably identified as subfamily Cupressaceae.

Polyaromatic hydrocarbon (PAH), which are generated by combustion at high temperature, were hardly detected in the blackish outer sample. Thus, the fossil did not experience burning by wild fire etc. The relative abundances of aldehyde-type lignin phenols are clearly lower in the outer sample, implying that degradation of woody tissues took place in the outer parts of fossil. Interestingly, aromatic and A-ring degraded (des-A) terpenoids were identified as free compounds in the outer sample. The aromatic and des-A terpenoids were reported to be compounds generated by microbial degradation during early diagenesis. The facts indicate that the woody tissues might be degraded by microbial activity in the outer part of the tree fossil. Moreover, the relative abundances of methoxy phenols decrease in the outer part, so that gelification of the degraded woody tissues occurred in the parts.

Keywords: tree fossil, fossilization processe, microbial degradation, plant terpenoid, lignin phenol

©2019. Japan Geoscience Union. All Right Reserved. 

[J] Poster | B (Biogeosciences )：B-PT Paleontology

Thu. May 30, 2019 3:30 PM - 5:00 PM JST | Thu. May 30, 2019 6:30 AM - 8:00 AM UTC | Poster Hall International Exhibition Hall8, Makuhari Messe_18

## [B-PT05] Biotic History

convener:Isao Motoyama(Department of Earth and Environmental Sciences, Yamagata University), Takao Ubukata(Division of Geology & Mineralogy, Department of Earth & Planetary Sciences, Kyoto University), Kazuyoshi Moriya(Department of Earth Sciences, Faculty of Education and Integrated Arts and Sciences, Waseda University)

The Biotic History session covers all aspects of ancient life and the history of biosphere through the geologic time. The study of ancient life is essential for unveiling mysteries of our planet earth. It also provides evidence for evolution of oceans, continents and island arcs. Modern progress in this field has been enhanced by interdisciplinary collaboration with allied sciences, such as paleoceanography and evolutionary biology. Our session intends to be a hub of communication amongst all earth scientists studying the biosphere; we welcome biological and biogeochemical approaches toward the understanding of the history of life.

### [BPT05-P01] Simultaneous observations of both hard and soft tissues of *Oulastrea crispata* (Cnidaria: Scleractinia)

*Rie Tajiri[1], Yuki Tokuda[2], Yoichi Ezaki[1] (1.Osaka City University, 2.Tottori University of Environment Studies)

### [BPT05-P02] Coral-based paleoenvironmental interpretation and depositional history of the late middle Pleistocene Minatogawa Formation, southern Okinawa-jima, Japan

*Riho Tomatsu[1], Marc Humblet[1], Kazuhiko Fujita[2] (1.Graduate School of Environmental Studies, Nagoya University, 2.Department of Physics and Earth Sciences, University of the Ryukyus)

### [BPT05-P03] Calcareous nannofossil biostratigraphy and oxygen isotope stratigraphy of the lower part of the Pleistocene formation distributed in the central part of the Pacific side of Japan

*Daisuke Kuwano[1], Yoshimi Kubota[2], Kanako Mantoku[2], Koji Kameo[3] (1.Division of Earth and Environmental Sciences, Graduate School of Science and Engineering, Chiba University, 2.National Museum of Nature and Science, 3.Department of Earth Sciences, faculty of Science, Chiba University)

### [BPT05-P04] Cretaceous and Miocene geology and paleontology of the Tounai River region, Biratori, Hokkaido

*Isao Motoyama[1], Kotaro Uchimura[2], Tomohiro Nishimura[3], Yojiro Taketani (1.Department of Earth and Environmental Sciences, Yamagata University, 2.JCE Co.,LTD, 3.Hobetsu Museum)

### [BPT05-P05] Response of benthic organisms to oceanic anoxic event in the Early Jurasic (T-OAE): Insights from quantitative analysis of the trace fossil Phycosiphon from the Nishinakayama Formation, Toyora Group

*Kyosuke Kitabatake[1,2], Kentaro Izumi[3], Kenji Okoshi[1] (1.Department of Environmental Science, Faculty of Science, Toho University, 2.Department of Earth Sciences, College of Science, Ibaraki University, 3.Faculty & Graduate School of Education, Chiba University)

# Simultaneous observations of both hard and soft tissues of *Oulastrea crispata* (Cnidaria: Scleractinia)

*Rie Tajiri[1], Yuki Tokuda[2], Yoichi Ezaki[1]

1. Osaka City University, 2. Tottori University of Environment Studies

*Oulastrea crispata* is a zooxanthellate colonial Scleractinia with a black skeleton. This coral inhabits areas of very shallow water where mud accumulates, and occupies the northernmost range of Japanese zooxanthellate corals. In this study, the hard and soft tissues of *O. crispata* were observed simultaneously by transmitted-light binocular microscope, fluorescence microscope, and scanning electron microscope by using the resin penetration technique (Tajiri and Fujita 2013) and the dehydration method (Tajiri and Ezaki 2018). Symbiotic algae are considered to play a key role in the life of *O. crispata*; however, the spatial distribution of such algae within the coral remains unknown. The present observations indicate that algal density is extremely high in the outer layers of polyps, and algae are densely distributed adjacent to the radial septa that partition the inner parts of polyps. The algal density is lower in deeper parts of polyps, and algae are scarce in the deepest part (up to 1 cm in depth), suggesting that little sunlight, if any, is available for photosynthesis. The hard skeletons of *O. crispata* are locally bored by euendoliths, which include microorganisms such as cyanobacteria, Chlorophyta, Rhodophyta, and fungi. These organisms erode not only the postmortem skeletal remains but also the living skeletons (e.g. Le Campion-Alsumard et al. 1995; Tribollet 2007). In living *Oulastrea*, skeletons located near the underlying hard substrate are intensively bored by euendoliths, mainly cyanobacteria and Chlorophyta. Endolithic filaments invade the soft parts of the coral, and the density of endolithic traces is lower near the upper part of skeletons and rare in upper peripheral areas. In contrast, both the lower and upper parts of dead skeletons are affected by intense endolithic activity. *O. crispata* manages to survive the prolonged biotic attack, especially the effects on its lower parts near the substrate that are subjected to a severe environment of intensive sedimentation and mechanical erosion.

Keywords: Oulastrea crispata, thin section, soft tissue, zooxanthella, euendolith, cyanobacteria

©2019. Japan Geoscience Union. All Right Reserved. 

# Coral-based paleoenvironmental interpretation and depositional history of the late middle Pleistocene Minatogawa Formation, southern Okinawa-jima, Japan

*Riho Tomatsu[1], Marc Humblet[1], Kazuhiko Fujita[2]

1. Graduate School of Environmental Studies, Nagoya University, 2. Department of Physics and Earth Sciences, University of the Ryukyus

Reef-complex deposits exposed in the Ryukyu Archipelago, southwestern Japan, offer a unique record of Quaternary reef growth and sea-level changes close to the northern limit of modern coral reef distribution. Among these deposits, the Minatogawa Formation belongs to the so-called “younger limestone” (<0.4 Ma), and crops out in southern Okinawa-jima and on nearby small islands. The deposition of the Minatogawa Formation marks a major change in depositional style in the Ryukyu Islands, from subsidence-dominated, aggrading and retrograding sequences (>0.4 Ma) to uplift-dominated deposits offlaping older limestone (<0.4 Ma). Although their age has not been determined precisely yet, the limestones of the Minatogawa Formation are thought to have deposited during Marine Isotope Stage (MIS) 5 or the older MIS 7. The Minatogawa Formation is composed of two main lithologies: coral limestone (boundstone) and well-sorted detrital limestone (mainly foraminifer-rich grainstone). The coral limestones of the Minatogawa Formation contain abundant and diverse in situ fossil corals, but no detailed taxonomic study has been carried out so far despite their paleo-ecological importance. In this study, we examine the taxonomic composition and the spatio-temporal distribution of fossil coral assemblages in two stratigraphic units (Unit 2 and 3) of the Minatogawa Formation exposed in the Horikawa quarry, southern Okinawa island, and reconstruct their depositional history. Five coral assemblages are identified in the coral limestone, each indicating a particular reef environment. The depositional history of Unit 3, inferred from the analysis of coral assemblages and of the boundary between the coral boundstone and adjacent well-sorted detrital limestone in this unit, reveals at least two transgressive/regressive cycles of sea-level change, several meters in amplitude, resulting in an unconformity (dissolution surface) between the coral boundstone and adjacent well-sorted detrital limestone. In contrast, the coral limestone and well-sorted detrital limestone in Unit 2 formed concomitantly in the same reef setting, a lower reef slope, or perhaps a shallower but turbitid environment. In addition, the discovery of a syn-depositional fault suggests that small-amplitude relative sea-level changes were caused by tectonic activity and may have influenced reef growth and community structure during the deposition of the Minatogawa Formation.

Keywords: fossil coral communities, late middle Pleistocene, environmental and sea level changes, tectonic uplift, Minatogawa Formation, Okinawa-jima

©2019. Japan Geoscience Union. All Right Reserved. 

# Calcareous nannofossil biostratigraphy and oxygen isotope stratigraphy of the lower part of the Pleistocene formation distributed in the central part of the Pacific side of Japan

*Daisuke Kuwano[1], Yoshimi Kubota[2], Kanako Mantoku[2], Koji Kameo[3]

1. Division of Earth and Environmental Sciences, Graduate School of Science and Engineering, Chiba University, 2. National Museum of Nature and Science, 3. Department of Earth Sciences, faculty of Science, Chiba University

Calcareous nannofossils, tiny calcite shells produced by calcareous nannoplankton, have been utilized to correlate marine strata and to determine their geologic ages. In the Quaternary, traceable sixteen nannofossil biohorizons were recognized (e.g., Sato et al., 1991) and some chronological studies have been done in order to test whether they were synchronous events or not based on comparative studies with astronomically tuned timescale in the equatorial Atlantic, the equatorial Pacific and the Mediterranean (e.g., Gradstein et al., 2012). This study aims at establishing the early Pleistocene age model based on oxygen isotopes in the central part of the Pacific side of Japan and evaluating synchrony of the early Pleistocene nannofossil biohorizons detected by Kuwano et al. (2019). We analyzed stable oxygen isotopes of a planktonic foraminifera, *Globorotalia inflata* from the upper part of Kiwada Formation in the Kazusa Group, a lower Pleistocene formation in the Pacific side of Japan. Isotopic measurements were performed by MAT253 Isotope mass spectrometer coupled with a Kiel IV carbonate device in the National Museum of Nature and Science.

An oxygen isotope curve obtained from 44 samples was correlated with the LR04 stack curve (Lisiecki and Raymo, 2005) and Marine Isotope Stages (MIS) 40 to 36 were recognized in the formation. Two calcareous nannofossil biohorizons, the last occurrences (LO) of large forms of *Gephyrocapsa* (>5.5 μm) and *Helicosphaera sellii* coincide with MIS 37/38 boundary and MIS 40, respectively. The LO of large forms of *Gephyrocapsa* is slightly older than those in other areas because this biohorizon is mostly situated in the early part of MIS 37 (Raffi et al., 2006). On the other hand, the LO of *Helicosphaera sellii* is found in MIS 38 in the northeastern Atlantic (Sato et al., 2009) and MIS 42 in the eastern equatorial Pacific (Wei, 1993). This biohorizon is possibly diachronous bioevent due to sporadic occurrences of this species.

Reference

Kuwano et al, 2019, Micropaleontological Reference Center Meeting 2019, O-4., Gradstein et al., 2012, The Geologic Time Scale 2012. Boston, USA, Elsevier, 1083-1127., Lisiecki and Raymo, 2005, Paleoceanography, 20, PA1003., Raffi et al., 2006, Quaternary Science Reviews, 25, 3113-3137., Sato et al., 1991, Scientific Results, ODP, 117, 37-54., Sato et al., 2009, Date Report, IODP, 303/306., Wei, 1993, Paleoceanography, 8, 85-99.

Keywords: Calcareous nannofossil, Biohorizon, Quaternary, Oxygen isotope stratigraphy

©2019. Japan Geoscience Union. All Right Reserved. 

# Cretaceous and Miocene geology and paleontology of the Tounai River region, Biratori, Hokkaido

*Isao Motoyama[1], Kotaro Uchimura[2], Tomohiro Nishimura[3], Yojiro Taketani

1. Department of Earth and Environmental Sciences, Yamagata University, 2. JCE Co.,LTD, 3. Hobetsu Museum

The Cretaceous rocks of the Yezo Group exposed in the Hobetsu district are richly fossiliferous containing marine mollusks (mainly inoceramids and ammonites), reptiles (mosasaurs, plesiosaurs and turtles) and echinoids and, therefore, many geological and paleontological works have been done so far. The Cretaceous rocks extend to the south, adjacent Biratori district, but works were less common there. We have carried out mapping to provide a revised geological map in the Tounai River area, Biratori Town, and analyzed molluscan and radiolarian fossils to estimate depositional ages. This is the first report of radiolarians from this area.

The Cretaceous Yezo Group in this area is subdivided into the Kashima and Hakobuchi Formations in ascending order and is cut by some faults. The Kashima Formation comprises fairly monotonous, hemipelagic mudstone intercalating with many acidic tuff beds. The Hakobuchi Formation is composed mainly of sandstone, conglomerate and sandy mudstone. Cross-bedded sandstone and minor coal beds suggest shallow-marine depositional environments for the Hakobuchi Formation. As a result, it has been recognized that the Kashima Formation distributes in the western part of the studied area and probably extends north to the neighboring region where the distribution of the Kashima Formation was discovered in 2015 by Negishi and coworkers. It is previously estimated that the Kashima Formation forms an anticlinal structure in the northern part of the Tounai River area. However, our investigation about facies and structures of tuff beds does not support such fold structure.

Fossils occurred throughout the Cretaceous sequence concerned here. Molluscan fossils, including *Inoceramus amakusensis*, *Inoceramus japonicus* and *Eupachydiscus haradai*, collected from the Kashima Formation of the studied section indicate ages of Santonian to Campanian. Radiolarian assemblages include *Amphipyndax stocki*, *Lithocampe manifesta* and *Spongotripus morenoensis*, suggesting ages of Coniacian to Maastrichtian for the Kashima Formation.

Miocene rocks distribute in the western margin of the studied area and are bounded from the Cretaceous rocks by a fault. The Miocene rocks subdivided into the Takinoue and Kawabata Formations in ascending order. The Takinoue Formation consists of mudstone and sandstone. Strata of the Kawabata Formation are dominated by interbedded mudstone and sandstone representing turbidite facies of deep-sea fans. In the studied area, the lower part of the Kawabata Formation crops out. Radiolarians were almost absent from the samples collected from these Miocene formations.

Keywords: Yezo Group, Ammonoid, Inoceramus, Radiolaria

©2019. Japan Geoscience Union. All Right Reserved. 

# Response of benthic organisms to oceanic anoxic event in the Early Jurasic (T-OAE): Insights from quantitative analysis of the trace fossil Phycosiphon from the Nishinakayama Formation, Toyora Group

*Kyosuke Kitabatake[1,2], Kentaro Izumi[3], Kenji Okoshi[1]

1. Department of Environmental Science, Faculty of Science, Toho University, 2. Department of Earth Sciences, College of Science, Ibaraki University, 3. Faculty & Graduate School of Education, Chiba University

Paleontological researches on the early Toarcian (Early Jurassic) oceanic anoxic event (T-OAE) have mostly focused on body fossils including marine microfossils. However, marine trace fossils, which are important for understanding the paleoecology of trace-making soft bodied marine benthos, have relatively less been investigated. Therefore, in this study, to evaluate the response of benthos to the T-OAE, we quantitatively measured the occurrence, fractal dimension, and maximum diameter of the trace fossil *Phycosiphon*, which is interpreted to have been produced by small benthos, from the Lower Jurassic shallow-marine Nishinakayama Formation of the Toyora Group (Shimonoseki City, Yamaguchi Prefecture, southwest Japan). Furthermore, to estimate the oceanic redox conditions during the early Toarcian, in addition to the consideration based on available geochemical data, we newly analyzed the size distributions of the pyrite framboids from the mudstones of the Nishinakayama Formation. As a result of our analysis, occurrence percentage and fractal dimension of *Phycosiphon* diminished in the T-OAE interval, and the maximum size also decreased. In addition, the size distribution of the pyrite framboids suggested that the euxinic conditionoccurred in the ocean at least several times during the T-OAE interval. Available geochemical data suggests that dysoxic benthic condition generally prevailed at the time of deposition of the Nishinakayama Formation. Taken together, it is possible that oceanic redox conditions may have been negatively affected to the ecology and body size of small marine benthos, although small organisms are generally less susceptible to environmental changes than large organisms.

Keywords: Trace fossil, Phycosiphon, Toarcian, Oceanic Anoxic Event, Toyora Group, Nishinakayama Formation

©2019. Japan Geoscience Union. All Right Reserved. 

[J] Poster | B (Biogeosciences )：B-PT Paleontology

Thu. May 30, 2019 5:15 PM - 6:30 PM JST | Thu. May 30, 2019 8:15 AM - 9:30 AM UTC | Poster Hall International Exhibition Hall8, Makuhari Messe_33

## [B-PT05] Biotic History

convener:Isao Motoyama(Department of Earth and Environmental Sciences, Yamagata University), Takao Ubukata(Division of Geology & Mineralogy, Department of Earth & Planetary Sciences, Kyoto University), Kazuyoshi Moriya(Department of Earth Sciences, Faculty of Education and Integrated Arts and Sciences, Waseda University)

The Biotic History session covers all aspects of ancient life and the history of biosphere through the geologic time. The study of ancient life is essential for unveiling mysteries of our planet earth. It also provides evidence for evolution of oceans, continents and island arcs. Modern progress in this field has been enhanced by interdisciplinary collaboration with allied sciences, such as paleoceanography and evolutionary biology. Our session intends to be a hub of communication amongst all earth scientists studying the biosphere; we welcome biological and biogeochemical approaches toward the understanding of the history of life.

### [BPT05-P01] Simultaneous observations of both hard and soft tissues of *Oulastrea crispata* (Cnidaria: Scleractinia)

*Rie Tajiri[1], Yuki Tokuda[2], Yoichi Ezaki[1] (1.Osaka City University, 2.Tottori University of Environment Studies)

### [BPT05-P02] Coral-based paleoenvironmental interpretation and depositional history of the late middle Pleistocene Minatogawa Formation, southern Okinawa-jima, Japan

*Riho Tomatsu[1], Marc Humblet[1], Kazuhiko Fujita[2] (1.Graduate School of Environmental Studies, Nagoya University, 2.Department of Physics and Earth Sciences, University of the Ryukyus)

### [BPT05-P03] Calcareous nannofossil biostratigraphy and oxygen isotope stratigraphy of the lower part of the Pleistocene formation distributed in the central part of the Pacific side of Japan

*Daisuke Kuwano[1], Yoshimi Kubota[2], Kanako Mantoku[2], Koji Kameo[3] (1.Division of Earth and Environmental Sciences, Graduate School of Science and Engineering, Chiba University, 2.National Museum of Nature and Science, 3.Department of Earth Sciences, faculty of Science, Chiba University)

### [BPT05-P04] Cretaceous and Miocene geology and paleontology of the Tounai River region, Biratori, Hokkaido

*Isao Motoyama[1], Kotaro Uchimura[2], Tomohiro Nishimura[3], Yojiro Taketani (1.Department of Earth and Environmental Sciences, Yamagata University, 2.JCE Co.,LTD, 3.Hobetsu Museum)

### [BPT05-P05] Response of benthic organisms to oceanic anoxic event in the Early Jurasic (T-OAE): Insights from quantitative analysis of the trace fossil Phycosiphon from the Nishinakayama Formation, Toyora Group

*Kyosuke Kitabatake[1,2], Kentaro Izumi[3], Kenji Okoshi[1] (1.Department of Environmental Science, Faculty of Science, Toho University, 2.Department of Earth Sciences, College of Science, Ibaraki University, 3.Faculty & Graduate School of Education, Chiba University)

# Simultaneous observations of both hard and soft tissues of *Oulastrea crispata* (Cnidaria: Scleractinia)

*Rie Tajiri[1], Yuki Tokuda[2], Yoichi Ezaki[1]

1. Osaka City University, 2. Tottori University of Environment Studies

*Oulastrea crispata* is a zooxanthellate colonial Scleractinia with a black skeleton. This coral inhabits areas of very shallow water where mud accumulates, and occupies the northernmost range of Japanese zooxanthellate corals. In this study, the hard and soft tissues of *O. crispata* were observed simultaneously by transmitted-light binocular microscope, fluorescence microscope, and scanning electron microscope by using the resin penetration technique (Tajiri and Fujita 2013) and the dehydration method (Tajiri and Ezaki 2018). Symbiotic algae are considered to play a key role in the life of *O. crispata*; however, the spatial distribution of such algae within the coral remains unknown. The present observations indicate that algal density is extremely high in the outer layers of polyps, and algae are densely distributed adjacent to the radial septa that partition the inner parts of polyps. The algal density is lower in deeper parts of polyps, and algae are scarce in the deepest part (up to 1 cm in depth), suggesting that little sunlight, if any, is available for photosynthesis. The hard skeletons of *O. crispata* are locally bored by euendoliths, which include microorganisms such as cyanobacteria, Chlorophyta, Rhodophyta, and fungi. These organisms erode not only the postmortem skeletal remains but also the living skeletons (e.g. Le Campion-Alsumard et al. 1995; Tribollet 2007). In living *Oulastrea*, skeletons located near the underlying hard substrate are intensively bored by euendoliths, mainly cyanobacteria and Chlorophyta. Endolithic filaments invade the soft parts of the coral, and the density of endolithic traces is lower near the upper part of skeletons and rare in upper peripheral areas. In contrast, both the lower and upper parts of dead skeletons are affected by intense endolithic activity. *O. crispata* manages to survive the prolonged biotic attack, especially the effects on its lower parts near the substrate that are subjected to a severe environment of intensive sedimentation and mechanical erosion.

Keywords: Oulastrea crispata, thin section, soft tissue, zooxanthella, euendolith, cyanobacteria

©2019. Japan Geoscience Union. All Right Reserved. 

# Coral-based paleoenvironmental interpretation and depositional history of the late middle Pleistocene Minatogawa Formation, southern Okinawa-jima, Japan

*Riho Tomatsu[1], Marc Humblet[1], Kazuhiko Fujita[2]

1. Graduate School of Environmental Studies, Nagoya University, 2. Department of Physics and Earth Sciences, University of the Ryukyus

Reef-complex deposits exposed in the Ryukyu Archipelago, southwestern Japan, offer a unique record of Quaternary reef growth and sea-level changes close to the northern limit of modern coral reef distribution. Among these deposits, the Minatogawa Formation belongs to the so-called “younger limestone” (<0.4 Ma), and crops out in southern Okinawa-jima and on nearby small islands. The deposition of the Minatogawa Formation marks a major change in depositional style in the Ryukyu Islands, from subsidence-dominated, aggrading and retrograding sequences (>0.4 Ma) to uplift-dominated deposits offlaping older limestone (<0.4 Ma). Although their age has not been determined precisely yet, the limestones of the Minatogawa Formation are thought to have deposited during Marine Isotope Stage (MIS) 5 or the older MIS 7. The Minatogawa Formation is composed of two main lithologies: coral limestone (boundstone) and well-sorted detrital limestone (mainly foraminifer-rich grainstone). The coral limestones of the Minatogawa Formation contain abundant and diverse in situ fossil corals, but no detailed taxonomic study has been carried out so far despite their paleo-ecological importance. In this study, we examine the taxonomic composition and the spatio-temporal distribution of fossil coral assemblages in two stratigraphic units (Unit 2 and 3) of the Minatogawa Formation exposed in the Horikawa quarry, southern Okinawa island, and reconstruct their depositional history. Five coral assemblages are identified in the coral limestone, each indicating a particular reef environment. The depositional history of Unit 3, inferred from the analysis of coral assemblages and of the boundary between the coral boundstone and adjacent well-sorted detrital limestone in this unit, reveals at least two transgressive/regressive cycles of sea-level change, several meters in amplitude, resulting in an unconformity (dissolution surface) between the coral boundstone and adjacent well-sorted detrital limestone. In contrast, the coral limestone and well-sorted detrital limestone in Unit 2 formed concomitantly in the same reef setting, a lower reef slope, or perhaps a shallower but turbitid environment. In addition, the discovery of a syn-depositional fault suggests that small-amplitude relative sea-level changes were caused by tectonic activity and may have influenced reef growth and community structure during the deposition of the Minatogawa Formation.

Keywords: fossil coral communities, late middle Pleistocene, environmental and sea level changes, tectonic uplift, Minatogawa Formation, Okinawa-jima

©2019. Japan Geoscience Union. All Right Reserved. 

# Calcareous nannofossil biostratigraphy and oxygen isotope stratigraphy of the lower part of the Pleistocene formation distributed in the central part of the Pacific side of Japan

*Daisuke Kuwano[1], Yoshimi Kubota[2], Kanako Mantoku[2], Koji Kameo[3]

1. Division of Earth and Environmental Sciences, Graduate School of Science and Engineering, Chiba University, 2. National Museum of Nature and Science, 3. Department of Earth Sciences, faculty of Science, Chiba University

Calcareous nannofossils, tiny calcite shells produced by calcareous nannoplankton, have been utilized to correlate marine strata and to determine their geologic ages. In the Quaternary, traceable sixteen nannofossil biohorizons were recognized (e.g., Sato et al., 1991) and some chronological studies have been done in order to test whether they were synchronous events or not based on comparative studies with astronomically tuned timescale in the equatorial Atlantic, the equatorial Pacific and the Mediterranean (e.g., Gradstein et al., 2012). This study aims at establishing the early Pleistocene age model based on oxygen isotopes in the central part of the Pacific side of Japan and evaluating synchrony of the early Pleistocene nannofossil biohorizons detected by Kuwano et al. (2019). We analyzed stable oxygen isotopes of a planktonic foraminifera, *Globorotalia inflata* from the upper part of Kiwada Formation in the Kazusa Group, a lower Pleistocene formation in the Pacific side of Japan. Isotopic measurements were performed by MAT253 Isotope mass spectrometer coupled with a Kiel IV carbonate device in the National Museum of Nature and Science.

An oxygen isotope curve obtained from 44 samples was correlated with the LR04 stack curve (Lisiecki and Raymo, 2005) and Marine Isotope Stages (MIS) 40 to 36 were recognized in the formation. Two calcareous nannofossil biohorizons, the last occurrences (LO) of large forms of *Gephyrocapsa* (>5.5 μm) and *Helicosphaera sellii* coincide with MIS 37/38 boundary and MIS 40, respectively. The LO of large forms of *Gephyrocapsa* is slightly older than those in other areas because this biohorizon is mostly situated in the early part of MIS 37 (Raffi et al., 2006). On the other hand, the LO of *Helicosphaera sellii* is found in MIS 38 in the northeastern Atlantic (Sato et al., 2009) and MIS 42 in the eastern equatorial Pacific (Wei, 1993). This biohorizon is possibly diachronous bioevent due to sporadic occurrences of this species.

Reference

Kuwano et al, 2019, Micropaleontological Reference Center Meeting 2019, O-4., Gradstein et al., 2012, The Geologic Time Scale 2012. Boston, USA, Elsevier, 1083-1127., Lisiecki and Raymo, 2005, Paleoceanography, 20, PA1003., Raffi et al., 2006, Quaternary Science Reviews, 25, 3113-3137., Sato et al., 1991, Scientific Results, ODP, 117, 37-54., Sato et al., 2009, Date Report, IODP, 303/306., Wei, 1993, Paleoceanography, 8, 85-99.

Keywords: Calcareous nannofossil, Biohorizon, Quaternary, Oxygen isotope stratigraphy

©2019. Japan Geoscience Union. All Right Reserved. 

# Cretaceous and Miocene geology and paleontology of the Tounai River region, Biratori, Hokkaido

*Isao Motoyama[1], Kotaro Uchimura[2], Tomohiro Nishimura[3], Yojiro Taketani

1. Department of Earth and Environmental Sciences, Yamagata University, 2. JCE Co.,LTD, 3. Hobetsu Museum

The Cretaceous rocks of the Yezo Group exposed in the Hobetsu district are richly fossiliferous containing marine mollusks (mainly inoceramids and ammonites), reptiles (mosasaurs, plesiosaurs and turtles) and echinoids and, therefore, many geological and paleontological works have been done so far. The Cretaceous rocks extend to the south, adjacent Biratori district, but works were less common there. We have carried out mapping to provide a revised geological map in the Tounai River area, Biratori Town, and analyzed molluscan and radiolarian fossils to estimate depositional ages. This is the first report of radiolarians from this area.

The Cretaceous Yezo Group in this area is subdivided into the Kashima and Hakobuchi Formations in ascending order and is cut by some faults. The Kashima Formation comprises fairly monotonous, hemipelagic mudstone intercalating with many acidic tuff beds. The Hakobuchi Formation is composed mainly of sandstone, conglomerate and sandy mudstone. Cross-bedded sandstone and minor coal beds suggest shallow-marine depositional environments for the Hakobuchi Formation. As a result, it has been recognized that the Kashima Formation distributes in the western part of the studied area and probably extends north to the neighboring region where the distribution of the Kashima Formation was discovered in 2015 by Negishi and coworkers. It is previously estimated that the Kashima Formation forms an anticlinal structure in the northern part of the Tounai River area. However, our investigation about facies and structures of tuff beds does not support such fold structure.

Fossils occurred throughout the Cretaceous sequence concerned here. Molluscan fossils, including *Inoceramus amakusensis*, *Inoceramus japonicus* and *Eupachydiscus haradai*, collected from the Kashima Formation of the studied section indicate ages of Santonian to Campanian. Radiolarian assemblages include *Amphipyndax stocki*, *Lithocampe manifesta* and *Spongotripus morenoensis*, suggesting ages of Coniacian to Maastrichtian for the Kashima Formation.

Miocene rocks distribute in the western margin of the studied area and are bounded from the Cretaceous rocks by a fault. The Miocene rocks subdivided into the Takinoue and Kawabata Formations in ascending order. The Takinoue Formation consists of mudstone and sandstone. Strata of the Kawabata Formation are dominated by interbedded mudstone and sandstone representing turbidite facies of deep-sea fans. In the studied area, the lower part of the Kawabata Formation crops out. Radiolarians were almost absent from the samples collected from these Miocene formations.

Keywords: Yezo Group, Ammonoid, Inoceramus, Radiolaria

©2019. Japan Geoscience Union. All Right Reserved. 

# Response of benthic organisms to oceanic anoxic event in the Early Jurasic (T-OAE): Insights from quantitative analysis of the trace fossil Phycosiphon from the Nishinakayama Formation, Toyora Group

*Kyosuke Kitabatake[1,2], Kentaro Izumi[3], Kenji Okoshi[1]

1. Department of Environmental Science, Faculty of Science, Toho University, 2. Department of Earth Sciences, College of Science, Ibaraki University, 3. Faculty & Graduate School of Education, Chiba University

Paleontological researches on the early Toarcian (Early Jurassic) oceanic anoxic event (T-OAE) have mostly focused on body fossils including marine microfossils. However, marine trace fossils, which are important for understanding the paleoecology of trace-making soft bodied marine benthos, have relatively less been investigated. Therefore, in this study, to evaluate the response of benthos to the T-OAE, we quantitatively measured the occurrence, fractal dimension, and maximum diameter of the trace fossil *Phycosiphon*, which is interpreted to have been produced by small benthos, from the Lower Jurassic shallow-marine Nishinakayama Formation of the Toyora Group (Shimonoseki City, Yamaguchi Prefecture, southwest Japan). Furthermore, to estimate the oceanic redox conditions during the early Toarcian, in addition to the consideration based on available geochemical data, we newly analyzed the size distributions of the pyrite framboids from the mudstones of the Nishinakayama Formation. As a result of our analysis, occurrence percentage and fractal dimension of *Phycosiphon* diminished in the T-OAE interval, and the maximum size also decreased. In addition, the size distribution of the pyrite framboids suggested that the euxinic conditionoccurred in the ocean at least several times during the T-OAE interval. Available geochemical data suggests that dysoxic benthic condition generally prevailed at the time of deposition of the Nishinakayama Formation. Taken together, it is possible that oceanic redox conditions may have been negatively affected to the ecology and body size of small marine benthos, although small organisms are generally less susceptible to environmental changes than large organisms.

Keywords: Trace fossil, Phycosiphon, Toarcian, Oceanic Anoxic Event, Toyora Group, Nishinakayama Formation

©2019. Japan Geoscience Union. All Right Reserved. 

[E] Poster | M (Multidisciplinary and Interdisciplinary)：M-IS Intersection

Thu. May 30, 2019 10:45 AM - 12:15 PM JST | Thu. May 30, 2019 1:45 AM - 3:15 AM UTC | Poster Hall International Exhibition Hall8, Makuhari Messe_9

## [M-IS03] Evolution and variability of the Asian monsoon in Cenozoic global climate changes

convener:Masanobu Yamamoto(Faculty of Environmental Earth Science, Hokkaido University), Ryuji Tada(Department of Earth and Planetary Science, Graduate School of Science, The Univeristy of Tokyo)

The Asian Monsoon (AM) is a part of interhemispheric atmospheric phenomena that is driven by the thermal gradient between ocean and land. Contrasts of insolation, heat content and latent heat transfer between ocean and land may have affected the behavior of the AM in the past, but the proxy records are occasionally controversial and do not show a clear picture of the AM variability. Recent proxy and modeling studies suggest that glacial pCO2 cycles could be related to the position of southern westerlies, which is sensitive to interhemispheric heat imbalance. Because monsoon is driven by the heat imbalance, knowledge on the variability of the AM is important to understand the behavior of the global climate system. In this session, presentations on the reconstruction of long-term AM variability from various archives such as IODP expedition cores, discussion on its forcing, and the roles of the AM in global climate changes are welcome.

[MIS03-P01] Asian dust source variability since 10 Ma based on grain size specific mineral composition at IODP Site U1425 in the Japan Sea

*Mui Fa Alison Lee[1], Tomohisa Irino[1] (1.Faculty of Environmental Earth Science, Hokkaido University)

[MIS03-P02] Sources and formation environment of biomass burning products in Pliocene and Pleistocene marine sediments in the Japan Sea

*Song Lu[1], Youhei Yamashita[2], Tomohisa Irino[2] (1.Graduate School of Environmental Science, Hokkaido University , 2.Faculty of Environmental Earth Science, Hokkaido University)

[MIS03-P03] Variation of mineral dust flux in peat at a high moor on the Mt. Daisetsu during Holocene

*Tomohisa Irino[1], Keisuke Hirai[1], Osamu Seki[1], James Hooper[2], Samuel Marx[2] (1.Hokkaido University, 2.University of Wollongong)

[MIS03-P04] Variations in sea surface environments recorded by algal biomarkers in the Japan Sea off the western coast of Hokkaido (IODP Site U1422) over the last 250 ka

*Asako Suzuki[1], Ken Sawada[2], Satoshi Furota[3], Yaeko Igarashi[4], Tomohisa Irino[5] (1.Graduate School of Science, Hokkaido University, 2.Department of Earth and Planetary Sciences, Faculty of Science, Hokkaido University, 3.Japan Agency for Marine-Earth Science and Technology, 4.Institute for Paleoenvironment of Northern Regions, 5.Faculty of Environmental Earth Science, Hokkaido University)

[MIS03-P05] **Decadal oscillation in hydrogen stable isotope ratio of long chain fatty acids in Lake Suigetsu sediment core**

*Masaya Inagaki[1], Masanobu Yamamoto[1,2], Takeshi Nakagawa[3] (1.Graduate School of Environmental Science, Hokkaido University, 2.Faculty of Environmental Earth Science, Hokkaido University, 3.Research Center for Palaeoclimatology, Ritsumeikan University)

[MIS03-P06] **Amplitude modulation of sea surface temperature variability in the Bay of Bengal by 400-kyr eccentricity cycle**

*Masanobu Yamamoto[1], Yuko Tsuchiya[1], Steven Clemens[2] (1.Faculty of Environmental Earth Science, Hokkaido University, 2.Department of Earth, Planetary and Environmental Sciences, Brown University)

# Asian dust source variability since 10 Ma based on grain size specific mineral composition at IODP Site U1425 in the Japan Sea

*Mui Fa Alison Lee[1], Tomohisa Irino[1]

1. Faculty of Environmental Earth Science, Hokkaido University

Sediments at Integrated Ocean Drilling Program (IODP) Site U1425 in the Japan Sea is under the strong influence of westerly jet stream and winter monsoon wind which transporting a significant amount of aeolian dust from both Taklamakan deserts and Gobi deserts. Aeolian dust from Taklamakan showed very high content of quartz (60-90%) and less plagioclase (5-40%) than from NE Chinese deserts and Loess (Gobi). The lower value of half height width (FWHM) of illite peak in X-ray diffraction (XRD) profile can be used as an indicator higher illite crystallinity. A decreasing trend of illite FWHM (increasing trend of the crystalinity) towards the core of the fold and thrust anticline has been recognized (Robinson et al. 1990; Orozco et al. 1998). Illite is also predominant component of the Chinese loess, and its highly crystallized nature has been interpreted to indicate that the illite was not formed at surface temperature and may have originated from a low temperature metamorphic environment.

In order to reconstruct a long-term changes in dust sources and transport pathways of Asian dust utilizing knowledges above, we examined mineral composition of IODP Site U1425 located at the central Japan Sea. The sediment samples were separated into >4 $\mu$m (silt) and <4 $\mu$m (clay) fractions by repeated pipette method. Both fractions were used for powder XRD analysis and peak heights of diagnostic peaks of major minerals were regarded as relative abundance of the minerals. FWHM and chemical index of illite were also examined.

In general, a very high quartz content found at Site U1425 may indicate sediments are aeolian source from Taklamakan deserts and higher plagioclase (albite) may infer dust source from Gobi deserts. Intervals around 9.5 Ma, 8.3 Ma, 7.9 Ma and 4.5 Ma showed very high quartz content and less albite at Site U1425, which indicate increases in dust supplied from Taklamakan than Gobi deserts due to stronger westerly wind. During Pliocene to early Pleistocene (4.2-2Ma), Taklamakan dust is still dominant, however the increasing influence of Gobi dust is recognized at 4.1 and 3.4Ma. On the other hand, an abrupt increase of the ratio of albite to quartz from 0.2 at 4.5 Ma to 0.8 at 4.1 Ma is found, which also shows another maximum at 0.6 Ma. In general, increase of albite abundance in sediments at Site U1425 during Pleistocene indicates the increasing dust supplied from NE China and Gobi deserts and the strengthened winter monsoon.

FWHM (crystallinity) of illite in silt fraction at Site U1425 showed low values (high crystallinity) with narrow range around 0.2˚2$\theta$ during Pleistocene. The illite chemistry index showed values below 0.4 and genrerally around 0.3 during Pleistocene, which represents (Fe, Mg)-rich illites (biotite) characterized for physically eroded or unweathered rocks. The highly crystallized and Fe–Mg rich illites in the silt fraction at Site U1425 in the Japan Sea suggests their aeolian origin which may be derived from pre-existing sediments which eroded from low-grade metamorphic rocks in the northern regions of the Tibetan Plateau. In a longer time-scale, higher crystallinity and lower chemistry index of illite in silt fractions occurred in similar timing at 9.3 Ma and 6.6-2.7 Ma which could be correlated with the active regional uplift and tectonic activities of the northeastern margin of the Tibetan Plateau. Possible changes in source of illite indicates frequent plate tectonic activities near the Taklamakan deserts of North Tibet plateau especially from 6.6-2.7Ma.

©2019. Japan Geoscience Union. All Right Reserved. 

Keywords: Aeolian dust, Taklamakan deserts, Quartz, Feldspar , Illite, Gobi deserts

©2019. Japan Geoscience Union. All Right Reserved. 

# Sources and formation environment of biomass burning products in Pliocene and Pleistocene marine sediments in the Japan Sea

*Song Lu[1], Youhei Yamashita[2], Tomohisa Irino[2]

1. Graduate School of Environmental Science, Hokkaido University , 2. Faculty of Environmental Earth Science, Hokkaido University

Behavior of black carbon (BC) is crucial for the earth surface environment because it could cause global warming by absorbing sunlight in the atmosphere. BC is originated from incomplete combustion of biomass or fossil fuels. Combustion in natural processes is incomplete due to local limitation of oxygen during the fire, which leads to the formation of organic fire residues. Robustness of BC to degradation in the natural environment enables us to use BC as a proxy to study the driving force of frequency and burning temperatures of past wildfire events. But the previous fire researches (paleoclimate rather than modern ecology) did not discuss the control factors for burning temperature or try to rebuild the fire temperature. Objective of this study is to understand factors controlling the thermal/optical/chemical characters of BC with burning temperature, provenance and aging in relation to the variabilities of vegetation in the hinterland. For these purposes, BC was quantified as elemental carbon (EC) in coarse (>2 $\mu$m) and fine (<2 $\mu$m) fractions of sediment samples using a thermal optical transmittance (TOT) method, and their burning temperatures were estimated for bulk samples through measurement of composition of benzene polycarboxylic acids (BPCAs), molecular markers of fire residues, determined with High Performance Liquid Chromatography (HPLC). In order to examine the relationship between burning temperature and BPCA composition, selected plants were experimentally charred to obtain standard charcoal samples. We also applied TOT and BPCA methods to marine sediments such as the surface sediments collected during KR15-10 cruise off the Wakasa Bay and 63 samples between 0 and 203 m CCSF-D were selected from IODP Site U1423 in the northeastern Japan Sea which covered the last 4.3 Myr. Size dependencies of EC contents and thermal properties will be compared with the contents and composition of BPCAs to examine the influence of sources, transport pathways, and burning temperatures of BCs contained in marine sediments.

Keywords: biomass burning, elemental carbon, benzene polycarboxylic acid

©2019. Japan Geoscience Union. All Right Reserved. 

# Variation of mineral dust flux in peat at a high moor on the Mt. Daisetsu during Holocene

*Tomohisa Irino[1], Keisuke Hirai[1], Osamu Seki[1], James Hooper[2], Samuel Marx[2]

1. Hokkaido University, 2. University of Wollongong

Mt. Daisetsu, Hokkaido, Japan is located just below the northern route of Asian dust transport and receives a significant amount of dust which dies snow surface brown in spring time every year. This area is also characterized by well-developed high moors on the mountains covering the last 4000 - 7500 yrs, which would continuously record the history of climate change during the middle to late Holocene. Peat collected from these high moor could be also a suitable material for a precise age determination using the radio carbon, and its inorganic fraction might consist of aeolian dust of continental origin and volcanic materials of the local origin which could be easily distinguished from each other.

Asian dust transported to the northern Japan may have a different source from those transported to the southwestern Japan. In spite of this, many of previous dust studies for Asian dust deposition in Japan have been conducted for the paleo-archives collected from the southern area. Therefore, it is necessary to reconstruct the composition and flux of Asian dust transported to the northern Japan in order to understand the spatio-temporal variability of westerly that could have significant influence on the climate in east Asia.

We collected peat cores from the high moor in Mt. Daisetsuzan area, and measured the mineral composition contained in peat. After heat treatment of peat samples, we conducted X-ray diffraction (XRD) analysis on the ash fraction and semi-quantified the minerals. Quartz, illite, and chlorite showed positive correlation among others, while various feldspars showed another positive correlation among others independent from quartz. Amorphous materials exhibited a variability different from quartz or feldspars. High ash content was associated with high feldspars or amorphous. Comparing these mineral compositions with those of aeolian dust deposited in this area and the local riverbed materials, we judged that the inorganic fraction could be explained by mixtures of aeolian dust and two kinds (crystalline and amorphous) of local volcanic materials.

We applied statistical unmixing of these mineral assemblage using PARAFAC algorithm on XRD profiles. Quantification of subcomponents such as Asian dust and local volcanic materials enabled us to estimate the variation of dust flux to this northern region for the last 5000 years. Comparison of our results with previous works for dust depositional history in southwestern region around Japan shows an antiphase variation of dust fluxes between north and south, which suggests the change in meandering pattern or pathway of westerly jet trasporting Asian dust.

Keywords: Asian dust, peat, Mt. Daisetsu, Holocene

©2019. Japan Geoscience Union. All Right Reserved. 

# Variations in sea surface environments recorded by algal biomarkers in the Japan Sea off the western coast of Hokkaido (IODP Site U1422) over the last 250 ka

*Asako Suzuki[1], Ken Sawada[2], Satoshi Furota[3], Yaeko Igarashi[4], Tomohisa Irino[5]

1. Graduate School of Science, Hokkaido University, 2. Department of Earth and Planetary Sciences, Faculty of Science, Hokkaido University, 3. Japan Agency for Marine-Earth Science and Technology, 4. Institute for Paleoenvironment of Northern Regions, 5. Faculty of Environmental Earth Science, Hokkaido University

The Japan Sea is a marginal sea that is closed by four straits, and the surface and deep waters are characterized by the Tsushima Warm Current (TWC), and Japan Sea Proper Water, respectively. In glacial-interglacial cycle, the sea surface environment in the Japan Sea has repeatedly changed by sea level fluctuation. It is reported that intense cooling of surface waters in the northern Japan Sea occurred caused by intensification of the East Asian Winter Monsoon (EAWM), but there have been few researches in this area. Thus, we analyzed algal biomarkers of a sediment core from the site U1422 (northern Japan Sea) of IODP Exp. 346 for the last 250ka. In particular, we apply the paleothermometer using long-chain alkyl diols, which are thought to be produced by diatoms and eustigmatophyte algae in addition to a proxy for sea surface temperature (SST based on alkenones, which are produced by haptophyte algae. The long-chain alkyl diols were also used as the proxies for upwelling intensity and inflow of fresh water, and thus, can provide multiple information for reconstruction of marine paleoenvironment.

The sediment cores studied were recovered at Site U1422 in the northern part of the Japan Basin (the Japan Sea off the western coast of Hokkaido) at 43°45.99’ N, 138°49.99’ E by Integrated Ocean Drilling Program (IODP) Expedition 346. We focus the duration from the MIS 8 to the present (-ca. 250ka). Lipids were extracted with dichloromethane/methanol, and separated to aliphatic, aromatic and polar fractions. Lipids were identified and quantified by GC-MS and GC-FID.

The SSTs based on alkenones and alkyl diols basically fluctuated along the glacial-interglacial cycles. The alkenone-based SSTs were found to be much higher than the diol-based SSTs during the MIS 2-3. The reasons of the differences are likely to be high contribution of distinctive alkenone producer during these stages. In our study, we calculated not only $U^{K'}_{37}$ but also the index containing tetra-unsaturated alkenone ($U^{K}_{37}$) in the SST estimate, because the tetra-unsaturated alkenone is abundantly detected in several samples. The $U^{K}_{37}$-based SSTs generally tend to be lower than those estimated by $U^{K'}_{37}$.

Diol Indices 1 and 2, which are proxies of upwelling intensity, are overall low levels. These results indicate that consistent upwelling system is hardly developed in the northern Japan Sea. However, the indices increase in the MIS 2, implying that vertical mixing was promoted as a result of the surface cooling in this stage. Moreover, the $C_{32}$ 1, 15-diol ratio, which is considered as an indicator of fresh water input into marine environment, tended to increase at the transition periods, such as the glacial to interglacial periods. These results suggest that fresh water arisen by melting of snows and ices accumulated on lands was flowing into the Japan Sea through the rivers during these transitions. The increasing spikes of the diol-based fresh water index are also observed during the glacial periods. This can be attributed to the fresh waters arisen by sea ice melting that came from the northward and/or affected by the inflow of TWC as a result of sea-level falling.

©2019. Japan Geoscience Union. All Right Reserved. 

Keywords: Northern Japan Sea, Algal biomarker, Alkenone, Diol, East Asian Monsoon, Quaternary

©2019. Japan Geoscience Union. All Right Reserved. 

# Decadal oscillation in hydrogen stable isotope ratio of long chain fatty acids in Lake Suigetsu sediment core

*Masaya Inagaki[1], Masanobu Yamamoto[1,2], Takeshi Nakagawa[3]

1. Graduate School of Environmental Science, Hokkaido University, 2. Faculty of Environmental Earth Science, Hokkaido University, 3. Research Center for Palaeoclimatology, Ritsumeikan University

Japanese weathers are affected by the Pacific Decadal Oscillation (PDO), monsoon, and El Niño Southern Oscillation. In this study, we analyzed the hydrogen isotopes of long chain n-fatty acids in sediment cores from Lake Suigetsu in Fukui Prefecture, and reconstructed variability in the isotopic ratio of precipitation from 1362 to 1662 CE and from1852 to 2017 CE. Hydrogen isotopic composition ( δ D) showed decadal oscillation ranging from ~-170‰ to ~-120‰. Between 1362 and 1662 CE, this oscillation corresponded to the decadal oscillation seen in the UK37’ -based sea surface temperature (SST) in Beppu Bay. Higher SST corresponded to higher δ D. Because the SST in Beppu Bay corresponds to the PDO, we suppose that variability in the δ D of long chain n-fatty acids in Lake Suigetsu reflected the isotopic ratio of precipitation that responded to the PDO. In Nagoya, the isotope ratio of precipitation is governed by the position of Baiu front. When Baiu front is developed north of Nagoya, the isotope ratio is high. When Baiu front is south of Nagoya, isotope ratio is low (Kurita et al., 2015 Climate of the Past). This suggest that the position of the Baiu front was linked to the PDO from 1362 to 1662 CE. In the conditions of the negative PDO (high SST in Beppu Bay), the Baiu front was tended to be located north of Lake Suigetsu.

Keywords: PDO, isotopic ratio of precipitation, climate change

©2019. Japan Geoscience Union. All Right Reserved. 

# Amplitude modulation of sea surface temperature variability in the Bay of Bengal by 400-kyr eccentricity cycle

*Masanobu Yamamoto[1], Yuko Tsuchiya[1], Steven Clemens[2]

1. Faculty of Environmental Earth Science, Hokkaido University, 2. Department of Earth, Planetary and Environmental Sciences, Brown University

We generated a 1.7 kyr-resolution $TEX_{86}$-based sea surface temperature (SST) record from the International Ocean Discovery Program Site U1446 in the Bay of Bengal during the last 1.46 Myr. The SST varied synchronously with LR04 benthic foraminifera $\delta^{18}O$ and deep water $\delta^{13}C$. The cyclicity changed from 41-kyr to 100-kyr around 900 ka. The amplitude of SST variation responded to the 400-kyr cycles of eccentricity. Higher amplitude corresponded to low eccentricity. This suggests that eccentricity forced climate variability independently of the shift of cyclicity of glacial cycles across the Mid-Pleistocene Transition.

Keywords: Bay of Bengal, Sea surface temperature, Mid-Pleistocene Transition

©2019. Japan Geoscience Union. All Right Reserved. 

[E] Poster | M (Multidisciplinary and Interdisciplinary)：M-IS Intersection

Thu. May 30, 2019 5:15 PM - 6:30 PM JST | Thu. May 30, 2019 8:15 AM - 9:30 AM UTC | Poster Hall International Exhibition Hall8, Makuhari Messe_34

## [M-IS03] Evolution and variability of the Asian monsoon in Cenozoic global climate changes

convener:Masanobu Yamamoto(Faculty of Environmental Earth Science, Hokkaido University), Ryuji Tada(Department of Earth and Planetary Science, Graduate School of Science, The Univeristy of Tokyo)

The Asian Monsoon (AM) is a part of interhemispheric atmospheric phenomena that is driven by the thermal gradient between ocean and land. Contrasts of insolation, heat content and latent heat transfer between ocean and land may have affected the behavior of the AM in the past, but the proxy records are occasionally controversial and do not show a clear picture of the AM variability. Recent proxy and modeling studies suggest that glacial pCO2 cycles could be related to the position of southern westerlies, which is sensitive to interhemispheric heat imbalance. Because monsoon is driven by the heat imbalance, knowledge on the variability of the AM is important to understand the behavior of the global climate system. In this session, presentations on the reconstruction of long-term AM variability from various archives such as IODP expedition cores, discussion on its forcing, and the roles of the AM in global climate changes are welcome.

[MIS03-P01] Asian dust source variability since 10 Ma based on grain size specific mineral composition at IODP Site U1425 in the Japan Sea

*Mui Fa Alison Lee[1], Tomohisa Irino[1] (1.Faculty of Environmental Earth Science, Hokkaido University)

[MIS03-P02] Sources and formation environment of biomass burning products in Pliocene and Pleistocene marine sediments in the Japan Sea

*Song Lu[1], Youhei Yamashita[2], Tomohisa Irino[2] (1.Graduate School of Environmental Science, Hokkaido University , 2.Faculty of Environmental Earth Science, Hokkaido University)

[MIS03-P03] Variation of mineral dust flux in peat at a high moor on the Mt. Daisetsu during Holocene

*Tomohisa Irino[1], Keisuke Hirai[1], Osamu Seki[1], James Hooper[2], Samuel Marx[2] (1.Hokkaido University, 2.University of Wollongong)

[MIS03-P04] Variations in sea surface environments recorded by algal biomarkers in the Japan Sea off the western coast of Hokkaido (IODP Site U1422) over the last 250 ka

*Asako Suzuki[1], Ken Sawada[2], Satoshi Furota[3], Yaeko Igarashi[4], Tomohisa Irino[5] (1.Graduate School of Science, Hokkaido University, 2.Department of Earth and Planetary Sciences, Faculty of Science, Hokkaido University, 3.Japan Agency for Marine-Earth Science and Technology, 4.Institute for Paleoenvironment of Northern Regions, 5.Faculty of Environmental Earth Science, Hokkaido University)

[MIS03-P05] **Decadal oscillation in hydrogen stable isotope ratio of long chain fatty acids in Lake Suigetsu sediment core**

*Masaya Inagaki[1], Masanobu Yamamoto[1,2], Takeshi Nakagawa[3] (1.Graduate School of Environmental Science, Hokkaido University, 2.Faculty of Environmental Earth Science, Hokkaido University, 3.Research Center for Palaeoclimatology, Ritsumeikan University)

[MIS03-P06] **Amplitude modulation of sea surface temperature variability in the Bay of Bengal by 400-kyr eccentricity cycle**

*Masanobu Yamamoto[1], Yuko Tsuchiya[1], Steven Clemens[2] (1.Faculty of Environmental Earth Science, Hokkaido University, 2.Department of Earth, Planetary and Environmental Sciences, Brown University)

# Asian dust source variability since 10 Ma based on grain size specific mineral composition at IODP Site U1425 in the Japan Sea

*Mui Fa Alison Lee[1], Tomohisa Irino[1]

1. Faculty of Environmental Earth Science, Hokkaido University

Sediments at Integrated Ocean Drilling Program (IODP) Site U1425 in the Japan Sea is under the strong influence of westerly jet stream and winter monsoon wind which transporting a significant amount of aeolian dust from both Taklamakan deserts and Gobi deserts. Aeolian dust from Taklamakan showed very high content of quartz (60-90%) and less plagioclase (5-40%) than from NE Chinese deserts and Loess (Gobi). The lower value of half height width (FWHM) of illite peak in X-ray diffraction (XRD) profile can be used as an indicator higher illite crystallinity. A decreasing trend of illite FWHM (increasing trend of the crystalinity) towards the core of the fold and thrust anticline has been recognized (Robinson et al. 1990; Orozco et al. 1998). Illite is also predominant component of the Chinese loess, and its highly crystallized nature has been interpreted to indicate that the illite was not formed at surface temperature and may have originated from a low temperature metamorphic environment.

In order to reconstruct a long-term changes in dust sources and transport pathways of Asian dust utilizing knowledges above, we examined mineral composition of IODP Site U1425 located at the central Japan Sea. The sediment samples were separated into >4 $\mu$m (silt) and <4 $\mu$m (clay) fractions by repeated pipette method. Both fractions were used for powder XRD analysis and peak heights of diagnostic peaks of major minerals were regarded as relative abundance of the minerals. FWHM and chemical index of illite were also examined.

In general, a very high quartz content found at Site U1425 may indicate sediments are aeolian source from Taklamakan deserts and higher plagioclase (albite) may infer dust source from Gobi deserts. Intervals around 9.5 Ma, 8.3 Ma, 7.9 Ma and 4.5 Ma showed very high quartz content and less albite at Site U1425, which indicate increases in dust supplied from Taklamakan than Gobi deserts due to stronger westerly wind. During Pliocene to early Pleistocene (4.2-2Ma), Taklamakan dust is still dominant, however the increasing influence of Gobi dust is recognized at 4.1 and 3.4Ma. On the other hand, an abrupt increase of the ratio of albite to quartz from 0.2 at 4.5 Ma to 0.8 at 4.1 Ma is found, which also shows another maximum at 0.6 Ma. In general, increase of albite abundance in sediments at Site U1425 during Pleistocene indicates the increasing dust supplied from NE China and Gobi deserts and the strengthened winter monsoon.

FWHM (crystallinity) of illite in silt fraction at Site U1425 showed low values (high crystallinity) with narrow range around 0.2˚2$\theta$ during Pleistocene. The illite chemistry index showed values below 0.4 and genrerally around 0.3 during Pleistocene, which represents (Fe, Mg)-rich illites (biotite) characterized for physically eroded or unweathered rocks. The highly crystallized and Fe–Mg rich illites in the silt fraction at Site U1425 in the Japan Sea suggests their aeolian origin which may be derived from pre-existing sediments which eroded from low-grade metamorphic rocks in the northern regions of the Tibetan Plateau. In a longer time-scale, higher crystallinity and lower chemistry index of illite in silt fractions occurred in similar timing at 9.3 Ma and 6.6-2.7 Ma which could be correlated with the active regional uplift and tectonic activities of the northeastern margin of the Tibetan Plateau. Possible changes in source of illite indicates frequent plate tectonic activities near the Taklamakan deserts of North Tibet plateau especially from 6.6-2.7Ma.

©2019. Japan Geoscience Union. All Right Reserved. 

Keywords: Aeolian dust, Taklamakan deserts, Quartz, Feldspar , Illite, Gobi deserts

©2019. Japan Geoscience Union. All Right Reserved. 

# Sources and formation environment of biomass burning products in Pliocene and Pleistocene marine sediments in the Japan Sea

*Song Lu[1], Youhei Yamashita[2], Tomohisa Irino[2]

1. Graduate School of Environmental Science, Hokkaido University , 2. Faculty of Environmental Earth Science, Hokkaido University

Behavior of black carbon (BC) is crucial for the earth surface environment because it could cause global warming by absorbing sunlight in the atmosphere. BC is originated from incomplete combustion of biomass or fossil fuels. Combustion in natural processes is incomplete due to local limitation of oxygen during the fire, which leads to the formation of organic fire residues. Robustness of BC to degradation in the natural environment enables us to use BC as a proxy to study the driving force of frequency and burning temperatures of past wildfire events. But the previous fire researches (paleoclimate rather than modern ecology) did not discuss the control factors for burning temperature or try to rebuild the fire temperature. Objective of this study is to understand factors controlling the thermal/optical/chemical characters of BC with burning temperature, provenance and aging in relation to the variabilities of vegetation in the hinterland. For these purposes, BC was quantified as elemental carbon (EC) in coarse (>2 $\mu$m) and fine (<2 $\mu$m) fractions of sediment samples using a thermal optical transmittance (TOT) method, and their burning temperatures were estimated for bulk samples through measurement of composition of benzene polycarboxylic acids (BPCAs), molecular markers of fire residues, determined with High Performance Liquid Chromatography (HPLC). In order to examine the relationship between burning temperature and BPCA composition, selected plants were experimentally charred to obtain standard charcoal samples. We also applied TOT and BPCA methods to marine sediments such as the surface sediments collected during KR15-10 cruise off the Wakasa Bay and 63 samples between 0 and 203 m CCSF-D were selected from IODP Site U1423 in the northeastern Japan Sea which covered the last 4.3 Myr. Size dependencies of EC contents and thermal properties will be compared with the contents and composition of BPCAs to examine the influence of sources, transport pathways, and burning temperatures of BCs contained in marine sediments.

Keywords: biomass burning, elemental carbon, benzene polycarboxylic acid

©2019. Japan Geoscience Union. All Right Reserved. 

# Variation of mineral dust flux in peat at a high moor on the Mt. Daisetsu during Holocene

*Tomohisa Irino[1], Keisuke Hirai[1], Osamu Seki[1], James Hooper[2], Samuel Marx[2]

1. Hokkaido University, 2. University of Wollongong

Mt. Daisetsu, Hokkaido, Japan is located just below the northern route of Asian dust transport and receives a significant amount of dust which dies snow surface brown in spring time every year. This area is also characterized by well-developed high moors on the mountains covering the last 4000 - 7500 yrs, which would continuously record the history of climate change during the middle to late Holocene. Peat collected from these high moor could be also a suitable material for a precise age determination using the radio carbon, and its inorganic fraction might consist of aeolian dust of continental origin and volcanic materials of the local origin which could be easily distinguished from each other.

Asian dust transported to the northern Japan may have a different source from those transported to the southwestern Japan. In spite of this, many of previous dust studies for Asian dust deposition in Japan have been conducted for the paleo-archives collected from the southern area. Therefore, it is necessary to reconstruct the composition and flux of Asian dust transported to the northern Japan in order to understand the spatio-temporal variability of westerly that could have significant influence on the climate in east Asia.

We collected peat cores from the high moor in Mt. Daisetsuzan area, and measured the mineral composition contained in peat. After heat treatment of peat samples, we conducted X-ray diffraction (XRD) analysis on the ash fraction and semi-quantified the minerals. Quartz, illite, and chlorite showed positive correlation among others, while various feldspars showed another positive correlation among others independent from quartz. Amorphous materials exhibited a variability different from quartz or feldspars. High ash content was associated with high feldspars or amorphous. Comparing these mineral compositions with those of aeolian dust deposited in this area and the local riverbed materials, we judged that the inorganic fraction could be explained by mixtures of aeolian dust and two kinds (crystalline and amorphous) of local volcanic materials.

We applied statistical unmixing of these mineral assemblage using PARAFAC algorithm on XRD profiles. Quantification of subcomponents such as Asian dust and local volcanic materials enabled us to estimate the variation of dust flux to this northern region for the last 5000 years. Comparison of our results with previous works for dust depositional history in southwestern region around Japan shows an antiphase variation of dust fluxes between north and south, which suggests the change in meandering pattern or pathway of westerly jet trasporting Asian dust.

Keywords: Asian dust, peat, Mt. Daisetsu, Holocene

©2019. Japan Geoscience Union. All Right Reserved. 

# Variations in sea surface environments recorded by algal biomarkers in the Japan Sea off the western coast of Hokkaido (IODP Site U1422) over the last 250 ka

*Asako Suzuki[1], Ken Sawada[2], Satoshi Furota[3], Yaeko Igarashi[4], Tomohisa Irino[5]

1. Graduate School of Science, Hokkaido University, 2. Department of Earth and Planetary Sciences, Faculty of Science, Hokkaido University, 3. Japan Agency for Marine-Earth Science and Technology, 4. Institute for Paleoenvironment of Northern Regions, 5. Faculty of Environmental Earth Science, Hokkaido University

The Japan Sea is a marginal sea that is closed by four straits, and the surface and deep waters are characterized by the Tsushima Warm Current (TWC), and Japan Sea Proper Water, respectively. In glacial-interglacial cycle, the sea surface environment in the Japan Sea has repeatedly changed by sea level fluctuation. It is reported that intense cooling of surface waters in the northern Japan Sea occurred caused by intensification of the East Asian Winter Monsoon (EAWM), but there have been few researches in this area. Thus, we analyzed algal biomarkers of a sediment core from the site U1422 (northern Japan Sea) of IODP Exp. 346 for the last 250ka. In particular, we apply the paleothermometer using long-chain alkyl diols, which are thought to be produced by diatoms and eustigmatophyte algae in addition to a proxy for sea surface temperature (SST based on alkenones, which are produced by haptophyte algae. The long-chain alkyl diols were also used as the proxies for upwelling intensity and inflow of fresh water, and thus, can provide multiple information for reconstruction of marine paleoenvironment.

The sediment cores studied were recovered at Site U1422 in the northern part of the Japan Basin (the Japan Sea off the western coast of Hokkaido) at 43°45.99’ N, 138°49.99’ E by Integrated Ocean Drilling Program (IODP) Expedition 346. We focus the duration from the MIS 8 to the present (-ca. 250ka). Lipids were extracted with dichloromethane/methanol, and separated to aliphatic, aromatic and polar fractions. Lipids were identified and quantified by GC-MS and GC-FID.

The SSTs based on alkenones and alkyl diols basically fluctuated along the glacial-interglacial cycles. The alkenone-based SSTs were found to be much higher than the diol-based SSTs during the MIS 2-3. The reasons of the differences are likely to be high contribution of distinctive alkenone producer during these stages. In our study, we calculated not only $U^{K'}_{37}$ but also the index containing tetra-unsaturated alkenone ($U^{K}_{37}$) in the SST estimate, because the tetra-unsaturated alkenone is abundantly detected in several samples. The $U^{K}_{37}$-based SSTs generally tend to be lower than those estimated by $U^{K'}_{37}$.

Diol Indices 1 and 2, which are proxies of upwelling intensity, are overall low levels. These results indicate that consistent upwelling system is hardly developed in the northern Japan Sea. However, the indices increase in the MIS 2, implying that vertical mixing was promoted as a result of the surface cooling in this stage. Moreover, the $C_{32}$ 1, 15-diol ratio, which is considered as an indicator of fresh water input into marine environment, tended to increase at the transition periods, such as the glacial to interglacial periods. These results suggest that fresh water arisen by melting of snows and ices accumulated on lands was flowing into the Japan Sea through the rivers during these transitions. The increasing spikes of the diol-based fresh water index are also observed during the glacial periods. This can be attributed to the fresh waters arisen by sea ice melting that came from the northward and/or affected by the inflow of TWC as a result of sea-level falling.

©2019. Japan Geoscience Union. All Right Reserved. 

Keywords: Northern Japan Sea, Algal biomarker, Alkenone, Diol, East Asian Monsoon, Quaternary

©2019. Japan Geoscience Union. All Right Reserved. 

# Decadal oscillation in hydrogen stable isotope ratio of long chain fatty acids in Lake Suigetsu sediment core

*Masaya Inagaki[1], Masanobu Yamamoto[1,2], Takeshi Nakagawa[3]

1. Graduate School of Environmental Science, Hokkaido University, 2. Faculty of Environmental Earth Science, Hokkaido University, 3. Research Center for Palaeoclimatology, Ritsumeikan University

Japanese weathers are affected by the Pacific Decadal Oscillation (PDO), monsoon, and El Niño Southern Oscillation. In this study, we analyzed the hydrogen isotopes of long chain n-fatty acids in sediment cores from Lake Suigetsu in Fukui Prefecture, and reconstructed variability in the isotopic ratio of precipitation from 1362 to 1662 CE and from1852 to 2017 CE. Hydrogen isotopic composition ( δ D) showed decadal oscillation ranging from ~-170‰ to ~-120‰. Between 1362 and 1662 CE, this oscillation corresponded to the decadal oscillation seen in the UK37’ -based sea surface temperature (SST) in Beppu Bay. Higher SST corresponded to higher δ D. Because the SST in Beppu Bay corresponds to the PDO, we suppose that variability in the δ D of long chain n-fatty acids in Lake Suigetsu reflected the isotopic ratio of precipitation that responded to the PDO. In Nagoya, the isotope ratio of precipitation is governed by the position of Baiu front. When Baiu front is developed north of Nagoya, the isotope ratio is high. When Baiu front is south of Nagoya, isotope ratio is low (Kurita et al., 2015 Climate of the Past). This suggest that the position of the Baiu front was linked to the PDO from 1362 to 1662 CE. In the conditions of the negative PDO (high SST in Beppu Bay), the Baiu front was tended to be located north of Lake Suigetsu.

Keywords: PDO, isotopic ratio of precipitation, climate change

©2019. Japan Geoscience Union. All Right Reserved. 

# Amplitude modulation of sea surface temperature variability in the Bay of Bengal by 400-kyr eccentricity cycle

*Masanobu Yamamoto[1], Yuko Tsuchiya[1], Steven Clemens[2]

1. Faculty of Environmental Earth Science, Hokkaido University, 2. Department of Earth, Planetary and Environmental Sciences, Brown University

We generated a 1.7 kyr-resolution $TEX_{86}$-based sea surface temperature (SST) record from the International Ocean Discovery Program Site U1446 in the Bay of Bengal during the last 1.46 Myr. The SST varied synchronously with LR04 benthic foraminifera $\delta^{18}O$ and deep water $\delta^{13}C$. The cyclicity changed from 41-kyr to 100-kyr around 900 ka. The amplitude of SST variation responded to the 400-kyr cycles of eccentricity. Higher amplitude corresponded to low eccentricity. This suggests that eccentricity forced climate variability independently of the shift of cyclicity of glacial cycles across the Mid-Pleistocene Transition.

Keywords: Bay of Bengal, Sea surface temperature, Mid-Pleistocene Transition

©2019. Japan Geoscience Union. All Right Reserved. 

[E] Oral | M (Multidisciplinary and Interdisciplinary)：M-IS Intersection

Thu. May 30, 2019 1:45 PM - 3:15 PM JST | Thu. May 30, 2019 4:45 AM - 6:15 AM UTC | 304 3F

## [M-IS03] Evolution and variability of the Asian monsoon in Cenozoic global climate changes

convener:Masanobu Yamamoto(Faculty of Environmental Earth Science, Hokkaido University), Ryuji Tada(Department of Earth and Planetary Science, Graduate School of Science, The Univeristy of Tokyo), Chairperson:Masanobu Yamamoto(Hokkaido University), Tomohisa Irino, Yoshimi Kubota(National Science Museum), Ryuji Tada(The University of Tokyo)

The Asian Monsoon (AM) is a part of interhemispheric atmospheric phenomena that is driven by the thermal gradient between ocean and land. Contrasts of insolation, heat content and latent heat transfer between ocean and land may have affected the behavior of the AM in the past, but the proxy records are occasionally controversial and do not show a clear picture of the AM variability. Recent proxy and modeling studies suggest that glacial pCO2 cycles could be related to the position of southern westerlies, which is sensitive to interhemispheric heat imbalance. Because monsoon is driven by the heat imbalance, knowledge on the variability of the AM is important to understand the behavior of the global climate system. In this session, presentations on the reconstruction of long-term AM variability from various archives such as IODP expedition cores, discussion on its forcing, and the roles of the AM in global climate changes are welcome.

1:45 PM - 2:00 PM JST | 4:45 AM - 5:00 AM UTC

### [MIS03-01] Reconstruction of Indian summer monsoon variability during the last 1,460,000 years

*Masanobu Yamamoto[1], Steven Clemens[2] (1.Faculty of Environmental Earth Science, Hokkaido University, 2.Department of Earth, Environmental and Planetary Sciences, Brown University)

2:00 PM - 2:20 PM JST | 5:00 AM - 5:20 AM UTC

### [MIS03-02] Pleistocene Seawater $\delta^{18}O$ reconstructions from the Indian and East Asian Monsoon Regions

★Invited Papers

*Steven C Clemens[1], Masanobu Yamamoto[2] (1.Brown University, 2.Hokkaido University)

2:20 PM - 2:40 PM JST | 5:20 AM - 5:40 AM UTC

### [MIS03-03] The Monsoon Erosion Pump

★Invited Papers
# Cancelled

*Liviu Giosan[1] (1.Woods Hole Oceanographic Institution)

2:40 PM - 3:00 PM JST | 5:40 AM - 6:00 AM UTC

### [MIS03-04] East Asian winter monsoon intensity in the Pleistocene based on seasonal land snail shell stable isotope ratios

★Invited Papers

*David L Dettman[1,3], Xin Wang[2], Mi Wang[2], Junhui Zhang[2] (1.University of Arizona, Geosciences Dept., Environmental Isotope Lab., 2.Lanzhou University, Key Laboratory of Western China's Environmental Systems, College of Earth and Environmental Sciences, 3.Shimane University, Estuary Research Center)

3:00 PM - 3:15 PM JST | 6:00 AM - 6:15 AM UTC

### [MIS03-05] Reconstruction of ventilation history of the Japan Sea based on physical properties data collected during IODP Exp. 346

*Tomohisa Irino[1], Liviu Giosan[2], Ryuji Tada[3], Ken Ikehara[4] (1.Faculty of Environmental Earth Science, Hokkaido University, 2.Woods Hole Oceanographic Institution, 3.Graduate School of Science, University of Tokyo, 4.Institute of Geology and Geoinformation, National Institute of Advanced Industrial Science and Technology)

# Reconstruction of Indian summer monsoon variability during the last 1,460,000 years

*Masanobu Yamamoto[1], Steven Clemens[2]

1. Faculty of Environmental Earth Science, Hokkaido University, 2. Department of Earth, Environmental and Planetary Sciences, Brown University

Monsoon is an atmospheric phenomenon dominant in low and mid-latitudes and determines the temporal and spatial distributions of rainfall that govern vegetation. A classical model assumes that monsoon responds to precession-controlled changes in seasonal insolation. Speleothem records show a precession cycle in oxygen isotope variation consistent with this model, but marine and loess records generally do not show strong precession variation. This mismatch has long been debated. Key approach is the precipitation reconstruction to understand past changes in summer monsoon. In this study, we generated an Indian summer monsoon (ISM) record by evaluating riverine discharge. We used GDGT indices, i.e., CBT and MBT, as a proxy of soil organic matter contribution and generated a 1,700-year resolution record of Mahanadi River soil discharge in IODP Site U1446 to understand changes in the ISM rainfall during the last 1,460,000 years. The CBT and BIT show a similar variation according to glacial-interglacial cycles. Maxima appeared after the peak of interglacial. Minima appeared during deglaciations. Their variations are reversely correlated with the sea water $\delta^{18}O$ obtained based on *G. ruber* $\delta^{18}O$, global $\delta^{18}O$ and $TEX_{86}$-based SST. The records are consistent with previously-reported ISM records from marine archives and Borneo speleothems in the overlap periods and different from Chinese speleothem records. Spectral analysis indicates that BIT and CBT show 100,000, 41,000, 30,000, 23,000 and 19,000-year cycles during the last 800,000 years, the variation was out of phase with variation in northern hemisphere summer insolation. This suggests that the ISM did not respond directly to orbital forcing, in contrast to the classical hypothesis, but was driven by internal feedback processes. Orbital cycles were not clearly shown prior to 800,000 years ago. This suggests that the strong response of the ISM to orbital forcing was initiated around 800,000 years ago, which coincided with the onset of glacial 100,000 year cycles.

Keywords: Indian summer monsoon, Pleistocene, IODP

©2019. Japan Geoscience Union. All Right Reserved. 

# Pleistocene Seawater $\delta^{18}O$ reconstructions from the Indian and East Asian Monsoon Regions

*Steven C Clemens[1], Masanobu Yamamoto[2]

1. Brown University, 2. Hokkaido University

The study of orbital-scale climate change during the late Pleistocene is unique in that the signal-to-noise ratio is large, the external forcing (insolation) is known, and the critical internal forcings (greenhouse gases and terrestrial ice volume) are well constrained. As such, it should be possible to assess the underlying mechanisms driving climate change at this time scale, as well as the relative sensitivity to these forcing mechanisms.

We present three reconstructions of local seawater $\delta^{18}O$, including previously published records from the East China Sea (U1429)[*S. C. Clemens et al.*, 2018], the Andaman Sea (NGHP 17)[*Gebregiorgis et al.*, 2018], and our new work from the northeast Indian Margin, Bay of Bengal (U1446). Local seawater $\delta^{18}O$ is based on removal of the SST and global seawater $\delta^{18}O$ from planktonic foraminifer $\delta^{18}O$ and reflects changes in surface salinity driven by rainfall and runoff from surrounding catchment basins. This proxy offers an independent reconstruction for comparison to speleothem $\delta^{18}O$ and other proxies in order to assess driving mechanisms and the extent to which the Indian and East Asian subsystems covary with one another.

In the northern East China Sea, *G. ruber* $\delta^{18}O$ has the same precession- and millennial-scale structure as the onshore speleothem $\delta^{18}O$ record from the Yangtze River Valley[*Cheng et al.*, 2016]. However, after removing the temperature and global seawater $\delta^{18}O$ signals, the offshore seawater $\delta^{18}O$ has almost no precession-scale (23 kyr) variance)[*S. C. Clemens et al.*, 2018]. This result contrasts with the speleothem record, which is almost exclusively dominated by precession-scale variance, and argues against external insolation as the primary driver of East Asian monsoon rainfall in the Yangtze River Valley region.

The Andaman Sea record monitors direct rainfall and runoff from the Irrawaddy and Salween catchment basins. The precession-band timing of low seawater $\delta^{18}O$ (increased rainfall, low mixed-layer salinity) indicates that strong monsoonal rainfall lags maximum northern hemisphere insolation by ~9 kyrs at the precession band[*Gebregiorgis et al.*, 2018]. Our new Indian Margin record resides within the low-salinity East India Coastal Current fed by runoff from the Ganges-Brahmaputra complex, the Mahanadi Basin, and direct rainfall. The Indian Margin seawater $\delta^{18}O$ reconstruction also demonstrates this large lag. The lag in both these records agrees with that of the summer-season (southwest) monsoon wind strength records from the NW Arabian Sea[*S.C. Clemens and Prell*, 2003; *S.C. Clemens et al.*, 1991].

This precession-band timing (lagging minimum precession by 7-9 kyrs) precludes insolation as a direct forcing for Indian monsoon rainfall and wind strength, pointing instead to decreased high-latitude ice volume, increased greenhouse gasses, and latent heat export from the southern hemisphere as the primary drivers of monsoon circulation at these time scales[*S.C. Clemens and Prell*, 2003].

©2019. Japan Geoscience Union. All Right Reserved. 

Cheng, H., et al. (2016), The Asian monsoon over the past 640,000 years and ice age terminations, Nature, 534(7609), 640-646, doi: 10.1038/nature18591

Clemens, S. C., and W. L. Prell (2003), A 350,000 year summer-monsoon multi-proxy stack from the Owen Ridge, Northern Arabian Sea, Marine Geology, 201, 35-51.

Clemens, S. C., W. L. Prell, D. Murray, G. Shimmield, and G. Weedon (1991), Forcing mechanisms of the Indian Ocean monsoon, Nature, 353, 720-725.

Clemens, S. C., A. Holbourn, Y. Kubota, K. E. Lee, Z. Liu, G. Chen, A. Nelson, and B. Fox-Kemper (2018), Precession-band variance missing from East Asian monsoon runoff, Nature Communications, 9(1), 3364, doi: 10.1038/s41467-018-05814-0.

Gebregiorgis, D., E. C. Hathorne, L. Giosan, S. Clemens, D. Nürnberg, and M. Frank (2018), Southern Hemisphere forcing of South Asian monsoon precipitation over the past ~1 million years, Nature Communications, 9(1), 4702, doi: 10.1038/s41467-018-07076-2.

Keywords: East Asian Monsoon, Indian Monsoon, East China Sea, Bay of Bengal, Paleoclimate, Greenhouse Gas

©2019. Japan Geoscience Union. All Right Reserved. 

# The Monsoon Erosion Pump

*Liviu Giosan[1]

1. Woods Hole Oceanographic Institution

Understanding the factors controlling the flux of materials from land to oceans has key implications for global biogeochemical cycling and the links between the sedimentary record and landscape evolution. Monsoonal climates are recognized as prodigious sediment producers but conflicting proxy reconstructions limit assessing their influence on land-sea material transfers at various timescales. Here I discuss the concept of a monsoon erosion pump based on terrestrial and oceanic records reconstructed from recent Indian National Gas Hydrate Program and IODP drilling in the Bay of Bengal, Arabian and Andaman Seas. From millennial to orbital to tectonic timescales, these records suggest that vegetation land cover interacts and modulates the regime of erosion and weathering under perennial but variable monsoonal rain conditions. Under this new proposed interpretation the Indian monsoon exhibits two distinct flavours during the Cenozoic that can be largely explained by its heartbeat, or astronomical forcing. This erosional regime is mediated by the global glacial state and attendant sea level and by limiting conditions imposed by the paleogeography of Asia.

Keywords: monsoon, India, erosion

©2019. Japan Geoscience Union. All Right Reserved. 

# East Asian winter monsoon intensity in the Pleistocene based on seasonal land snail shell stable isotope ratios

*David L Dettman[1,3], Xin Wang[2], Mi Wang[2], Junhui Zhang[2]

1. University of Arizona, Geosciences Dept., Environmental Isotope Lab., 2. Lanzhou University, Key Laboratory of Western China's Environmental Systems, College of Earth and Environmental Sciences, 3. Shimane University, Estuary Research Center

Monsoon climates are characterized by strong seasonal oscillations between a very wet season and very dry conditions. The study of ancient variation in monsoon climate strength and its impact on regional environments is difficult because geological materials rarely record individual seasons. It is difficult to infer seasonal change through time when working with oxygen isotope records that average multiple years or centuries. One solution is to use high-resolution sampling of land snail shells as monitors of wet-season and dry-season differences. Although land snail fossils are often rare, in many cases they are well preserved and widely distributed across the planet. We subsampled shells along the spiral growth axis, producing 15 to 35 samples per shell to document maximum and minimum oxygen and carbon stable isotope ratios. The most robust signal in land snail shell oxygen isotope records is connected to evaporation. The arid dry-season leads to significant evaporation in the land snail body water, which elevates the δ18O values recorded in the shell. Wet-season oxygen isotope ratios are more negative and can be tied roughly to the δ18O of wet season precipitation and summer temperatures. Carbon isotope ratios are tied to the diet of the animals, and reveal the proportion of C3 and C4 plants in the landscape.

Larger land snail (> 1.5 cm diameter) taxa have behaviors that can lead to significant evaporation of body water, as they are willing to range away from local water sources. Modern samples show that the total amplitude in oxygen isotope variation in a shell can be related to the intensity and duration of the dry season. This suggests that amplitudes in ancient shells are indicators of the winter monsoon strength. Although under extremely arid conditions snail growth occurs only when surface water is available and d18O amplitudes collapse in desert conditions. The most negative δ18O values are not correlated with the intensity of the summer monsoon, suggesting that δ18O values are not good indicators of summer monsoon strength.

Data from one genus of land snail (*Cathaica* species) living on the Chinese loess plateau throughout the late Pleistocene allow us to make some generalizations about monsoon climate in this region. In general, the oxygen isotope amplitude in shells from glacial periods are larger than those from the interglacial periods. This suggests that the East Asian Winter Monsoon was strongest during glacial intervals on the Loess Plateau. The largest δ18O amplitude observed was 19.2 ‰. Marine Isotope Stages 2, 6, and 8 have the largest amplitudes and, by inference, the strongest winter monsoons in our record. Older glacial intervals seem to have weaker winter monsoons. However, glacial amplitudes were not always larger, just as climate undergoes significant short-term variation in glacial intervals (such as D-O cycles and Heinrich events) oxygen isotope amplitudes show large amounts of variability in glacial times. In contrast, interglacial intervals tend to have smaller δ18O amplitudes, pointing to warmer and wetter winters in interglacial times. But like the glacial data, some interglacial amplitudes are larger than some glacial records. These data show that the differences in high frequency climate variability is as large as the differences between glacial and interglacial climates.

©2019. Japan Geoscience Union. All Right Reserved. 

Keywords: Winter Monsoon, Seasonality, Oxygen isotopes, Land Snails

©2019. Japan Geoscience Union. All Right Reserved. 

# Reconstruction of ventilation history of the Japan Sea based on physical properties data collected during IODP Exp. 346

*Tomohisa Irino[1], Liviu Giosan[2], Ryuji Tada[3], Ken Ikehara[4]

1. Faculty of Environmental Earth Science, Hokkaido University, 2. Woods Hole Oceanographic Institution, 3. Graduate School of Science, University of Tokyo, 4. Institute of Geology and Geoinformation, National Institute of Advanced Industrial Science and Technology

The Japan Sea is a semi-enclosed marginal sea located at the eastern edge of Asian continent and under the influence of east Asian monsoon. The primary production is controlled by nutrient supply from the East China Sea by summer monsoon, while deep water ventilation is promoted by winter monsoon cooling of the surface water of the Japan Sea. Perfectly continuous sediment splice sequences were established at Sites U1422-U1427 and U1430 which have been correlated among others using apparent dark-light cycles. The coverage of water depths are, in ascending order, 330 m at Site U1427, 903 m at Site U1426, 1072 m at Site U1430, 1785 m at Site U1423, 1909 m at Site U1425, 2808 m at Site U1424, and 3429 m at Site U1422, which enable us to reconstruct the temporal variation of depth distribution of organic carbon flux related to the past primary production and deep water ventilation in the Japan Sea.

For calculation of the mass accumulation of organic carbon (OC flux) at each site, we used the perfectly continuous records of dry bulk density (DBD) and total organic carbon content (TOC) calculated from shipboard measurements such as gamma-ray attenuation (GRA) density with grain density and a strong negative correlation between TOC and photo RGB values, respectively. Linear sedimentation rate (LSR) of each site was estimated based on the projection of the age model established at Site U1424 by tuning the GRA variation onto LR04 benthic oxygen isotope curve. Based on the consistent correlation among sites, depth distribution of OC flux was reconstructed for 1 ky step during the last 1.5 million years.

Princple component analysis for depth-temporal OC flux distribuion suggests that three princple component explain 74% of the total variance. Principle component (PC) 1 loading was positively correlated with all the sites except for the U1427 (330 m), while PC2 loading was correlated positively with sites shallower than 1000 m and negatively with those deeper than 2000 m. PC3 loading was correlated negatively with sites around 1000 m and positively with other sites. Such depth dependent patterns suggest that primary production (PC2) and ventilation (PC1) at middle to deeper depth were primary controls on the OC deposition. PC3 may indicate stronger middle depth ventilation or (oppositely) formation of oxygen minimum zone.

We also examined the color variation of these sediments using metric hue. Sediment color varies between dull green (higher hue) and olive (lower hue). Average metric hue is about 88 degree for all the site and variability is smaller for shallower sites. The metric hue at Site U1425 (1909 m) varies in harmony with the score of PC1, and lower metric hue is associated with larger PC1 score. Namely, higher OC flux (a lower oxygenation level) was associated with more olive color, which could be interpreted that dull green background (detritus) color was overridden by olive color reduced iron. Such an agreement between independently estimated variables suggests that the deep water ventilation intensity in the Japan Sea could be independently reconstructed as a proxy of winter monsoon intensity.

Keywords: Japan Sea, Organic carbon flux, Ventilation, IODP Expedition 346

©2019. Japan Geoscience Union. All Right Reserved. 

©2019. Japan Geoscience Union. All Right Reserved. 

[E] Oral | M (Multidisciplinary and Interdisciplinary)：M-IS Intersection

Thu. May 30, 2019 3:30 PM - 5:00 PM JST | Thu. May 30, 2019 6:30 AM - 8:00 AM UTC | 304 3F

## [M-IS03] Evolution and variability of the Asian monsoon in Cenozoic global climate changes

convener:Masanobu Yamamoto(Faculty of Environmental Earth Science, Hokkaido University), Ryuji Tada(Department of Earth and Planetary Science, Graduate School of Science, The Univeristy of Tokyo), Chairperson:Ryuji Tada(The University of Tokyo), Yoshimi Kubota(National Science Museum), Masanobu Yamamoto(Hokkaido University)

The Asian Monsoon (AM) is a part of interhemispheric atmospheric phenomena that is driven by the thermal gradient between ocean and land. Contrasts of insolation, heat content and latent heat transfer between ocean and land may have affected the behavior of the AM in the past, but the proxy records are occasionally controversial and do not show a clear picture of the AM variability. Recent proxy and modeling studies suggest that glacial pCO2 cycles could be related to the position of southern westerlies, which is sensitive to interhemispheric heat imbalance. Because monsoon is driven by the heat imbalance, knowledge on the variability of the AM is important to understand the behavior of the global climate system. In this session, presentations on the reconstruction of long-term AM variability from various archives such as IODP expedition cores, discussion on its forcing, and the roles of the AM in global climate changes are welcome.

3:30 PM - 3:45 PM JST | 6:30 AM - 6:45 AM UTC

[MIS03-06] The spatial-temporal patterns of Indian monsoonal variations during the past 80 kyr recorded in NGHP-02 Hole 19B, western Bay of Bengal: Implications from chemical and mineral properties

*Yuki Ota[1,2,3,4], Hodaka Kawahata[4], Junichiro Kuroda[4,3], Atsushi Suzuki[2], Daisuke Araoka[2], Asuka Yamaguchi[4], Ayako Abe-Ouchi[4] (1.Department of Earth and Planetary Science, The University of Tokyo, 2.Geological Survey of Japan, National Institute of Advanced Industrial Science and Technology, 3.Department of Biogeochemistry, Japan Agency for Marine-Earth Science and Technology, 4.Atmosphere and Ocean Research Institute, The University of Tokyo)

3:45 PM - 4:05 PM JST | 6:45 AM - 7:05 AM UTC

[MIS03-07] **400,000 years millennial scale temperature and rainfall in East Asia deduced from paired Mg/Ca and oxygen isotope of planktic foraminifera from the East China Sea**

★Invited Papers

*Yoshimi Kubota[1], Steven Clemens[2], Kyung-Eun Lee[3], Ann Holbourn[4], Etsuko Wakisaka[5], Keiji Horikawa[5], Ryuji Tada[6], Katsunori Kimoto[7] (1.National Museum of Nature and Science, 2.Brown University, 3.Korea Maritime and Ocean University, 4.Christian-Albrechts-University, 5.University of Toyama, 6.The University of Tokyo, 7.Japan Agency for Marine-Earth Science and Technology)

4:05 PM - 4:20 PM JST | 7:05 AM - 7:20 AM UTC

[MIS03-08] Onset and evolution of millennial-scale variability of East Asian Monsoon recorded in the Japan Sea sediments: New data with new interpretation

*Ryuji Tada[1], Tomohisa Irino[2], Arisa Seki[3], Masafumi Murayama[4], Kaz Mitake[1], Masayuki Ikeda[5] (1.Department of Earth and Planetary Science, Graduate School of Science, The Univeristy of Tokyo, 2.Faculty of Environmental Earth Science, Hokkaido University, 3.Faculty of Science, Shinshu University, 4.Faculty of Agriculture and Marine Science, 5.Shizuoka University)

4:20 PM - 4:40 PM JST | 7:20 AM - 7:40 AM UTC

[MIS03-09] Interhemispheric linkages of Australian and Asian monsoons on a warmer-than-modern Earth

★Invited Papers

*Ann E Holbourn[1], Wolfgang Kuhnt[1], Janika Joehnck[1], Sebastian Beil[1], Julia Luebbers[1], Kenji Marc Raymond Matsuzaki[2], Yair Rosenthal[3], Denise Kulhanek[4], IODP Expedition 363 Scientists (1.University of Kiel, 2.University of Tokyo, 3.Rutgers University, 4.Texas A&M University)

4:40 PM - 5:00 PM JST | 7:40 AM - 8:00 AM UTC

[MIS03-10] **Miocene evolution of the Asian Monsoon from climate and productivity proxies in the Bay of Bengal and South China Sea**

★Invited Papers

*Wolfgang Kuhnt[1], Julia Luebbers[1], Ann Holbourn[1], Karlos GD Kochhann[2], Steven C Clemens[3], Clara T Bolton[4], Yoichi Usui[5] (1.University of Kiel, 2.UNISINOS University, 3.Brown University, 4.Aix-Marseille Université, 5.Japan Agency for Marine-Earth Science and Technology)

# The spatial-temporal patterns of Indian monsoonal variations during the past 80 kyr recorded in NGHP-02 Hole 19B, western Bay of Bengal: Implications from chemical and mineral properties

*Yuki Ota[1,2,3,4], Hodaka Kawahata[4], Junichiro Kuroda[4,3], Atsushi Suzuki[2], Daisuke Araoka[2], Asuka Yamaguchi[4], Ayako Abe-Ouchi[4]

1. Department of Earth and Planetary Science, The University of Tokyo, 2. Geological Survey of Japan, National Institute of Advanced Industrial Science and Technology, 3. Department of Biogeochemistry, Japan Agency for Marine-Earth Science and Technology, 4. Atmosphere and Ocean Research Institute, The University of Tokyo

Detailed reconstruction of Indian summer monsoons is necessary to better understand the late Quaternary climate history of the Bay of Bengal and Indian peninsula. We established a chronostratigraphy for a sediment core from Hole 19B in the western Bay of Bengal, extending to approximately 80 kyr BP, and examined major and trace element compositions and clay mineral components of the sediments. Lower lithogenic matter flux, higher $\delta^{18}O$ values, and weaker weathering in the sediment source area during marine isotope stages (MIS) 2 and 4 compared to MIS 1, 3, and 5 are explained by increased Indian summer monsoonal precipitation and river discharge around the western Bay of Bengal. Chemical components indicate a felsic sediment source, suggesting the Precambrian gneissic complex of the eastern Indian peninsula as the dominant sediment source at this site since 80 kyr. Trace element ratios indicate increased sediment contributions from mafic rocks during MIS 2 and 4. We interpret these results as reflecting the changing influences of the eastern and western branches of the Indian summer monsoon, and a greater decrease in rainfall in the eastern and northeastern parts of the Indian peninsula than in the western part during MIS 2 and 4.

Keywords: Indian Monsoon, Bay of Bengal sediments, late Quaternary

©2019. Japan Geoscience Union. All Right Reserved. 

# 400,000 years millennial scale temperature and rainfall in East Asia deduced from paired Mg/Ca and oxygen isotope of planktic foraminifera from the East China Sea

*Yoshimi Kubota[1], Steven Clemens[2], Kyung-Eun Lee[3], Ann Holbourn[4], Etsuko Wakisaka[5], Keiji Horikawa[5], Ryuji Tada[6], Katsunori Kimoto[7]

1. National Museum of Nature and Science, 2. Brown University, 3. Korea Maritime and Ocean University, 4. Christian-Albrechts-University, 5. University of Toyama, 6. The University of Tokyo, 7. Japan Agency for Marine-Earth Science and Technology

Abrupt millennial-scale climate changes during the late Quaternary were widely recognized in the East Asian monsoon region from deep-sea sediments in the Japan Sea and more recently from oxygen isotope ($\delta^{18}O$) variability in Chinese speleothems ($\delta^{18}O_{sp}$). The finely $^{230}Th$-dating method on the speleothems enables comparison to climate records from other regions on millennial scale, and there is little doubt that the variability of these $\delta^{18}O_{sp}$ records is synchronized with climate perturbation in the North Atlantic high latitude, known as Heinrich events and with Dansgaard-Oeschger (D-O) oscillations in Greenland. However, mechanisms of the climate response in East Asia remain unclear due to the lack of fundamental agreement on what the $\delta^{18}O_{sp}$ climate signal represents. A primary impediment to interpreting the variability in $\delta^{18}O_{sp}$ is the lack of the means to decompose $\delta^{18}O_{sp}$ into constituent components. By contrast, the $\delta^{18}O$ of calcite planktic foraminifers ($\delta^{18}O_{p}$) from nearshore marine sediments can be quantitatively partitioned into sea surface temperature (SST) and $\delta^{18}O_{w}$ of seawater ($\delta^{18}O_{w}$), a function of sea surface salinity (SSS). In this study, millennial-scale climate variability in East Asia is investigated using 400,000-yr records of SST, $\delta^{18}O_{p}$, and $\delta^{18}O_{w}$ from the East China Sea (IODP Site U1429). $\delta^{18}O_{w}$ can be interpreted as reflecting SSS, hence rainfall, as the monsoonal runoff from the Yangtze River determines summer SSS in the northern East China Sea. As a result, SST and $\delta^{18}O_{w}$ variability accounts for 58% and 35% of the total variability of $\delta^{18}O_{p}$ and the rest (6%) is the ice volume component or noise; the primary contributor to $\delta^{18}O_{p}$ variations is SST, and the secondary is $\delta^{18}O_{w}$. Foraminiferal $\delta^{18}O_{p}$ shows the strongest similarly with Chinese $\delta^{18}O_{sp}$, indicating that $\delta^{18}O_{sp}$ is best interpreted as the combination of changes in surface temperature and monsoon rainfall; it is not indicative of summer monsoon rainfall alone. Partitioning of variance between temperature and rainfall does not change on glacial-interglacial timescales indicating that the hemispheric teleconnection mechanism between the Atlantic and East Asia does not depend on the global climate background status ($CO_2$, ice volume). In comparison with the millennial scale Greenland temperature, the East China Sea SST decreases and $\delta^{18}O_{w}$ increases (rainfall deceases) in most of the North Atlantic cold events (e.g., Heinrichs). However, SST and $\delta^{18}O_{w}$ exhibit overall poor coherence, revealing that these climate parameters fundamentally behave differently on the millennial scale, but tend to respond in the manner described above (decrease in temperature and rainfall) once a severe cold event occurs in the North Atlantic.

Keywords: Asian Monsoon, East China Sea, Millennial-scale climate variability, oxygen isotope, Mg/Ca, IODP Exp.346

©2019. Japan Geoscience Union. All Right Reserved. 

# Onset and evolution of millennial-scale variability of East Asian Monsoon recorded in the Japan Sea sediments: New data with new interpretation

*Ryuji Tada[1], Tomohisa Irino[2], Arisa Seki[3], Masafumi Murayama[4], Kaz Mitake[1], Masayuki Ikeda[5]

1. Department of Earth and Planetary Science, Graduate School of Science, The Univeristy of Tokyo, 2. Faculty of Environmental Earth Science, Hokkaido University, 3. Faculty of Science, Shinshu University, 4. Faculty of Agriculture and Marine Science, 5. Shizuoka University

New XRF scanner data from U1426 on Oki Ridge and comparison with those of the deeper sites U1424 and 1425 revealed Br (MOC proxy) profile of deeper sites are significantly influenced by post-depositional oxidation during the early diagenesis while Br profile of shallower site (U1426) better preserve surface productivity signal. Thus we use Br profile of U1426 during the last 3 Ma to analyze past changes in millennial-scale variability of East Asian Summer Monsoon intensity and the response of the Japan Sea to such changes. The result suggests several new information which will be presented at 2019JpGU.

Keywords: East Asian Summer Monsoon, Japan Sea

©2019. Japan Geoscience Union. All Right Reserved. 

# Interhemispheric linkages of Australian and Asian monsoons on a warmer-than-modern Earth

*Ann E Holbourn[1], Wolfgang Kuhnt[1], Janika Joehnck[1], Sebastian Beil[1], Julia Luebbers[1], Kenji Marc Raymond Matsuzaki[2], Yair Rosenthal[3], Denise Kulhanek[4], IODP Expedition 363 Scientists -

1. University of Kiel, 2. University of Tokyo, 3. Rutgers University, 4. Texas A&M University

The large-scale Asian-Australian monsoon system consists of several regional subsystems that are dynamically linked through the annual migration of the Intertropical Convergence Zone across the equator, but exhibit distinct responses to external (local insolation) and internal (e.g., ice volume, greenhouse gas concentrations) forcings. Here we provide a long-term perspective of regional variability under different mean-state climate conditions. We focus on the 8 to 5 Ma period, which was characterized by warmer-than-modern climate conditions, but was also marked by distinct reversals in climate trends including transient cooling events exhibiting similarities to late Pleistocene Heinrich stadials. Extended sediment archives recovered by the Ocean Drilling Program (ODP) and the International Ocean Discovery Program (IODP) in the South China Sea, Bay of Bengal and off Northwest Australia allow direct comparison of Northern and Southern Hemisphere monsoonal subsystems on orbital timescales. High-resolution XRF-scanner derived estimates of terrigenous discharge, foraminiferal Mg/Ca derived mixed layer temperatures and stable isotopes reveal cooling and strengthening of the Northern Hemisphere winter monsoon starting at ~7 Ma. This intensification occurred synchronously with an increase in monsoonal seasonality in the Southern Hemisphere. In all regions, summer monsoonal precipitation intensified after ~5.5 Ma in tandem with globally rising sea surface temperatures. Our results suggest that changes in latitudinal temperature gradients, greenhouse gas concentrations and moisture budgets strongly influenced the long-term evolution of the Australian and Asian monsoons during the transition from a unipolar to a bipolar glaciated Earth.

Keywords: Asian-Australian Monsoon, late Miocene, International Ocean Discovery Program, Foraminiferal stable isotopes, Foraminiferal Mg/Ca, X-ray fluorescence scanner elemental data

©2019. Japan Geoscience Union. All Right Reserved. 

# Miocene evolution of the Asian Monsoon from climate and productivity proxies in the Bay of Bengal and South China Sea

*Wolfgang Kuhnt[1], Julia Luebbers[1], Ann Holbourn[1], Karlos GD Kochhann[2], Steven C Clemens[3], Clara T Bolton[4], Yoichi Usui[5]

1. University of Kiel, 2. UNISINOS University, 3. Brown University, 4. Aix-Marseille Université, 5. Japan Agency for Marine-Earth Science and Technology

Export particle flux from primary production and terrigenous input in combination with planktic and benthic foraminiferal isotope records were used to monitor monsoon-related paleoceanographic changes in the Bay of Bengal (Indian Monsoon) and South China Sea (East Asian Monsoon) through the middle to late Miocene. Proxy indicators of carbon export flux to the seafloor and carbonate accumulation rates at International Ocean Discovery Program (IODP) Site U1443 located in 2925 m water depth at the northern end of the Ninetyeast Ridge closely track changes in the carbonate budget of the deep Indian Ocean. Prolonged intervals of low carbonate concentrations and accumulation rates from ~17 to 15 Ma and from ~13.2 to 8.7 Ma indicate episodes of reduced carbonate deposition, which correlate with the globally recognized early to middle Miocene “Carbonate Drought” and the middle to late Miocene “Carbonate Crash”. The global occurrence of these events implies that changes in chemical weathering and in the riverine input of calcium and alkalinity into the ocean reservoir (rather than changes in circulation or inter-ocean carbonate fractionation) drove carbonate accumulation in the deep Indian Ocean. Higher XRF-scanner derived Log(Ba/Ti) together with a change in the redox state of deep sea sediments at ~11.2 Ma indicate a rise in biological production and export flux to the sea floor. A contemporaneous stepwise steepening of the gradient between mixed layer and deep ocean $\delta^{13}C$ starting from a minimum at ~11 Ma also indicates intensification of the biological pump at Ocean Drilling Program (ODP) Site 1146 (2091 m water depth) in the South China Sea. We suggest that the attendant increase in carbonate accumulation in the Indian Ocean was linked to increased nutrient flux and intensification of upper ocean mixing, associated with changes in the seasonality and intensity of the Asian monsoon.

Keywords: Asian Monsoon, Miocene, International Ocean Discovery Program , Foraminiferal stable isotopes, Foraminiferal Mg/Ca, X-ray fluorescence scanning elemental data

©2019. Japan Geoscience Union. All Right Reserved. 

[E] Poster | M (Multidisciplinary and Interdisciplinary)：M-IS Intersection

Thu. May 30, 2019 10:45 AM - 12:15 PM JST | Thu. May 30, 2019 1:45 AM - 3:15 AM UTC | Poster Hall International Exhibition Hall8, Makuhari Messe_10

## [M-IS04] Interdisciplinary studies on pre-earthquake processes

convener:Katsumi Hattori(Department of Earth Sciences, Graduate School of Science, Chiba University), JANN-YENQ Liu(Institute of Space Science, National Central University, Taiwan), Dimitar Ouzounov(Center of Excellence in Earth Systems Modeling & Observations (CEESMO) , Schmid College of Science & Technology Chapman University, Orange, California, USA), Qinghua Huang(Peking University)

This session expands the interdisciplinary discussions on preparation process of earthquake and earthquake predictability by presenting the latest progress in studying the physically based pre-earthquake phenomena. New observations from space and ground have provided<br/>evidences, which may enhance better understanding of tectonic activity. The session anticipates talks that include but not limited to observations and analyses of seismic, electrical, electromagnetic, electro-chemical and thermodynamic processes related to stress changes in the lithosphere along with their statistical and physical validation. Presentations on the latest observational results associated with major earthquakes obtained by different methodologies are welcomed. The topics of the session are as follows but not limited.<br/><br/>-General discussion on earthquake preparation process and the physics of pre-earthquake signals<br/><br/>- Theory, modeling, laboratory experiments, computational simulation for generation and propagation of pre-earthquake signals and their connection with seismic cycle<br/><br/> - Multi-parameter observations, detection, and validation of pre-earthquake signals<br/><br/> - Cross-disciplinary studies, practical and technical approaches for better understanding of earthquake preparation processes and their connection with seismicity

### [MIS04-P01] Statistical analysis and Evaluation of ULF seismo-magnetic phenomena at Kakioka, Japan, during 1983-2017

*Kei Takahashi[1], Katsumi Hattori[2], Peng Han[3] (1.Faculty of Science, Chiba University, 2.Graduate School of Science, Chiba University, 3.Southern University of Science and Technology, China)

### [MIS04-P02] Pre-seismic anomalies on Earth’s magnetic field and ionosphere electron density using Swarm data

*Amune Yamazaki[1], Katsumi Hattori[1], Rui Song[1] (1.Chiba University)

### [MIS04-P03] Measurement of radon density in the atmosphere at Okayama, Kochi, Choshi and Kiyosumi, II

*Tohru Okabayashi[1], Kiyotaka Ninagawa[2], Isao Yamamoto[3], Katsumi Hattori[4], Chie Yoshino[4], Haruna Kojima[4], Nobuhiro Maeda (1.Department of Merical Risk and Crisis Management, Faculty of Risk and Crisis Management, Chiba Institute of Science, 2.Faculty of Science, Okayama University of Science, 3.Falcuty of Engineering, Okayama University of Science, 4.Graduate school of Science, Chiba University)

### [MIS04-P04] Possible anomalous changes in solar quiet-daily geomagnetic variation *Sq* related to the 2011 off the Pacific coast of Tohoku earthquake (Mw 9.0)

*Xiaocan Liu[1], Katsumi Hattori[2,3], Peng Han[4], Huaran Chen[1] (1.Institute of geophysics China Earthquake Administrition, 2.Graduate School of Science, Chiba University, Chiba, Japan, 3. Center for Environmental Remote Sensing, Chiba University, Chiba, Japan, 4.Department of Earth and Space Sciences, Southern University of Science and Technology, ShenZhen, China)

### [MIS04-P05] Co-seismic geomagnetic fluctuations and atmospheric disturbances during the 2018 M6.2 Hualien Earthquake

*Chun-Rong Chen[1], JANN-YENQ Liu[1] (1.Graduate Institute of Space Science, National Central University)

### [MIS04-P06] Multi-sensor monitoring network for earthquake precursor study near subduction zone at Boso, Japan

*Katsumi Hattori[1], Chie Yoshino[1], WEIYUN XIE[2], Sanaka Saito[2], Haruna Kojima[2], Rui Song[2], Peng Han[3], Toru Mogi[4], Tada-nori Goto[5], Ichi Takumi[6], Hiroshi Yasukawa[7], Motoaki Mouri[8], Jun Izutsu[9], Tadashi Takano[10], Chihiro Yamanaka[11], Masashi Kamogawa[12], Yoshiaki Ando[13], JANN-YENQ Liu[14], Dimitar Ouzounov[15], Valery Tramutoli[16] (1.Department of Earth Sciences, Graduate School of Science, Chiba University, 2.Graduate School of Science and Engineering, Chiba University, 3.Southern University of Science and Technology, China, 4.Hokkaido University, 5.Kyoto University, 6.Nagoya Institute of Technology, 7.Aichi Prefectural University, 8.Aichi University, 9.Chubu University, 10.Nihon University, 11.Osaka University, 12.Tokyo Gakugei University, 13.The University of Electro-Communications, 14.National Central University, Taiwan, 15.Chapman University, US, 16.University of Basilicagta, Italy)

---

[MIS04-P07] Transient Effects in Atmosphere and Ionosphere Associated with 2018 Mw 7.5 Sulawesi Indonesia Earthquake and Triggered Tsunami and Volcano Activities

★Invited Papers

*Dimitar Ouzounov[1], Sergey Pulinets[2], Dmitry Davidenko[2], Alexander Rozhnoi[3], Maria Solovieva[3], Tiger Liu[4] (1.Center of Excellence in Earth Systems Modeling & Observations (CEESMO) , Schmid College of Science & Technology Chapman University, Orange, California, USA, 2.Space Research Institute, RAS, Moscow, Russia, 3.The Schmidt Institute of Physics of the Earth, RAS, Moscow, Russia, 4.Center for Astronautical Physics and Engineering, National Central University, Taoyuan City, Taiwan)

---

[MIS04-P08] Seismicity change and b value variation prior to the Wenchuan earthquake (*Ms 8.0*)

*Peng Han[1], Rui Wang[1], Ying Chang[1], Miao Miao[1], Haixia Shi[2], Lingyuan Meng[2], Xuemei Zhang[2], Weiyun Xie[3], Katsumi Hattori[3] (1.Southern University of Science and Technology, Shenzhen, China, 2.China Earthquake Networks Center, Beijing 100045, China, 3.Chiba University, Chiba, Japan)

# Statistical analysis and Evaluation of ULF seismo-magnetic phenomena at Kakioka, Japan, during 1983-2017

*Kei Takahashi[1], Katsumi Hattori[2], Peng Han[3]

1. Faculty of Science, Chiba University, 2. Graduate School of Science, Chiba University, 3. Southern University of Science and Technology, China

To clarify and verify the ultralow frequency (ULF) seismo-magnetic phenomena, we have performed statistical studies on the geomagnetic data observed at the Kakioka (KAK) station, Japan, during 1983-2017. We investigated the energy of ULF geomagnetic signals of the frequency around 0.01 Hz using wavelet transform analysis. To minimize the influences of artificial noises and global magnetic perturbations, we used only the geomagnetic data observed at midnight time (LT 2:30 A.M. to 4:00 A.M.).We define the geomagnetic anomalies when the Z components of geomagnetic data exceeds median + 1.5 IQR, where IQR is the interquartile range. Considering that ionospheric disturbances may also lead to enhancements in the Z component, we exclude the anomaly when the energy of H component exceeds median + 3.0 IQR. Statistical analysis of superposed epoch analysis have indicated that ULF magnetic anomalies are more likely to appear before sizable isolated earthquake events (Es parameter which is higher than 8th power of 10 and no earthquake events during ±45 days ) rather than after them, especially 6-10 days before the events. Finally, we have evaluated the precursory information of ULF geomagnetic signals for local sizable earthquakes using Molchan’ s error diagram. The above results have indicated that the ULF seismo-magnetic phenomena at Kakioka clearly contain precursory information and have a possibility of improving forecasting of large earthquakes.

©2019. Japan Geoscience Union. All Right Reserved. 

# Pre-seismic anomalies on Earth’s magnetic field and ionosphere electron density using Swarm data

*Amune Yamazaki[1], Katsumi Hattori[1], Rui Song[1]

1. Chiba University

An earthquake is a rapid release of stress in the lithosphere and often leads to serious damages on human lives and society. Even though the short-time forecast of earthquake is important, it is not achieved yet. However, many electromagnetic phenomena that may be related to seismic activity have been reported recently. The satellite, one of the useful tools to observe these phenomena, can cover the global areas and can collect a large amount of data related to earthquakes which have large magnitude worldwide in short time. The Swarm satellites mission started to operate on November 22, 2013 by European Space Agency, with the constellation of three satellites (A, B, C) The anomalies preceded to the Ecuador earthquake in 2016 have been reported using the Swarm data. In this paper, in order to validate these results using the magnetic vector Y data by VFM and electron density data by Langmuir probe, we have analyzed the Swarm data related the M6.3~6.9 earthquakes occurred at Lombok Island, Indonesia, in July 28, August 5, and 19, 2018. The study area is a 1000 km square from the epicenter of 20180805 earthquake and the analyzed period is from May 28 to September 27, 2018. In this paper we report night-time orbit data at 18:00-6:00 LT.

As results, we found the following tendencies; (1) positive anomalies on magnetic Y vector about 1-2 weeks before the earthquakes and (2) negative anomalies on electron density from 1 week to 1 month before the earthquakes. We performed the same analysis to the data on the same period in 2016 and 2017 for reference when there were no M6+ earthquakes. We found that the number of anomaly track is only abruptly increased in the short period from the end of June to July in 2018, and that the trend is not able to be found in 2016 and 2017. From this unique trend in 2018, it is suggestive of the existence of the relation between the local seismic activity and in-situ satellite anomalies in the magnetic field and electron density in Lombok area.

©2019. Japan Geoscience Union. All Right Reserved. 

# Measurement of radon density in the atmosphere at Okayama, Kochi, Choshi and Kiyosumi, II

*Tohru Okabayashi[1], Kiyotaka Ninagawa[2], Isao Yamamoto[3], Katsumi Hattori[4], Chie Yoshino[4], Haruna Kojima[4], Nobuhiro Maeda

1. Department of Merical Risk and Crisis Management, Faculty of Risk and Crisis Management, Chiba Institute of Science, 2. Faculty of Science, Okayama University of Science, 3. Falcuty of Engineering, Okayama University of Science, 4. Graduate school of Science, Chiba University

We report continuous measurement of radon density in atmosphere at Okayama for three years, Kochi, Choshi and Kiyosumi for two years. An increase of radon density in groundwater at Nishinomiya city [1] and in atmosphere [2] at the southern part of Hyogo Prefecture Earthquake in 1995 were reported, respectively. In the case of Tohoku Region Pacific Coast Earthquake, the data obtained the exhaust air monitor that peak duration was long and the peak decreased rapidly before earthquake has been reported at the radiation facility of Fukushima Medical College in Fukushima [3]. On the other hand, a PIN photodiode have been developed and used as a high sensitive alpha ray detector in Super Kamiokande [4]. Since 2016, we also made an experimental setup using PIN photodiode, and measured the radon density in atmosphere. Using a Si PIN photodiode (S3204-09, unsealed, Hamamatsu Photodiode K.K.) as an alpha ray detector, we constructed radon detection setup combined with aluminum pot as an air accumulator, H4083 (Hamamatsu) as a charge amplifier, C4900-01 (Hamamatsu) as a high voltage power supply module, a pulse shaped amplifier with time constant of 10 msec, a multi channel analyzer (MCA-LiteN), and a PC as a data analysis. Obtained alpha spectra of atmosphere showed 4 peaks originated from $^{218}$Po, $^{214}$Po and $^{210}$Po of U series, and $^{212}$Po of Th series. Since 2017, we newly started to measure at Kochi, Choshi and Kiyosumi using our apparatus. Details of observed data are discussed in addition the data at Okayama since 2016.

[1] Igarashi G., Saeki S., Takahata N., Sumikawa K., Tasaka S., Sasaki Y., Takahashi M. and Sano Y. : Ground-water radon anomaly before the Kobe earthquake in Japan, Science, 269, 60-61, 1995.
[2] Yasuoka, Y. and Shinogi, M.: Anomaly in atmospheric radon concentration: a possible precursor of the 1995 Kobe, Japan, earthquake. Health Physics, 72, 759-761, 1997.
[3] Nagahama H., Yasuoka Y., Suzuki T., and Homma Y.: Radon Variation in the Air Before the 2011 Tohoku Earthquake (Mw =9.0), Programme and Abstracts, A32-09, The Seismological Society of Japan. 2011, Fall Meeting.
[4] Nemoto, M., Tasaka S., Hori H., Okumura K., Kajita T., and Takeuchi Y. : Development of High Sensitive Radon Detector with Electrostatic Collection. Radioisotopes, 46, 710-719, 1997 (Japanese).

Keywords: radon, atmosphere, earthquake prediction

©2019. Japan Geoscience Union. All Right Reserved. 

# Possible anomalous changes in solar quiet-daily geomagnetic variation *Sq* related to the 2011 off the Pacific coast of Tohoku earthquake (Mw 9.0)

*Xiaocan Liu[1], Katsumi Hattori[2,3], Peng Han[4], Huaran Chen[1]

1. Institute of geophysics China Earthquake Administrition, 2. Graduate School of Science, Chiba University, Chiba, Japan, 3. Center for Environmental Remote Sensing, Chiba University, Chiba, Japan, 4. Department of Earth and Space Sciences, Southern University of Science and Technology, ShenZhen, China

Seismo-electromagnetic researches have been studied for decades (e.g. Hayakawa and Fujinawa, 1994; Hayakawa and Molchanov, 2002, 2008,2013; Hattori, 2004, Hattori, et al., 2004a, 2004b; Hayakawa et al., 2007;, Hattori et al., 2013; Han et al., 2011, 2014, 2015, 2016, 2017; Huang QH et al., 2011, 2015; Du A, Huang Q et al., 2002, Rong YM et al., 2012, Yuan G.P., Zhang X.M. et al. 2015), and the geomagnetic diurnal variation (GDV) is a stable variation of the geomagnetic field that can be used to detect possible anomalous changes associated with large earthquakes.

We investigated data observed at 20 geomagnetic observatories at longitudes of 130˚E to 150˚E between 2009 and 2012 to detect possible anomalous changes in the geomagnetic solar quiet daily variation (Sq) related to the 2011 off the Pacific coast of Tohoku earthquake (Mw 9.0) occurred on March 11, 2011 in Japan. We selected the 5 quiet days every month and analyzed three component magnetic data with 1 min resolution using the natural orthogonal component (NOC) method to identify Sq variations from observations, and performed the spherical harmonic analysis (SHA) to separate the internal and the external equivalent Sq current systems of Je and Ji. We obtained that, Je and Ji are distorted near the epicenter area on two geomagnetic quiet days of January 23 and 27, 2011. They are about two months before the earthquake. Then, we made backward computation on the external and internal parts of the SHA model geomagnetic fields, Be and Bi, to determine the possible anomalous magnetic field variations at each station. Results show significant differences in daily variation for all components on January 23 and 27, 2011. The other days, we could not recognize any apparent anomalous behaviors, except known secular, seasonal, and solar activity dependences. A possible connection between this anomaly and the very strong Tohoku earthquake, which followed only one and half month after the geomagnetic anomaly is of highest interest for the research on earthquake precursors.

Keywords: geomagnetic solar quiet daily variation (Sq), natural orthogonal component (NOC) method, spherical harmonic analysis (SHA), the 2011 off the Pacific coast of Tohoku earthquak

©2019. Japan Geoscience Union. All Right Reserved. 

# Co-seismic geomagnetic fluctuations and atmospheric disturbances during the 2018 M6.2 Hualien Earthquake

*Chun-Rong Chen[1], JANN-YENQ Liu[1]

1. Graduate Institute of Space Science, National Central University

The strong ground motion of 6 February 2018 M6.2 Hualien Earthquake triggered a series of co-seismic geomagnetic fluctuations and seismo-traveling atmospheric disturbances (STADs) signatures in infrasonic waves and micro-pressures upon the seismic wave arrival. Networks of 9 QuakeFinder systems, 3 infrasound systems, 2 tiltmeters, 2 micro-barometers, and 11 co-located seismometers are used in this study. Each QuakeFinder system consists of a 3-axes induction magnetometer, an air conductivity sensor, a geophone, and temperature/relative humidity sensors. Co-seismic signatures clearly appear in the induction magnetometers, infrasound systems, and micro-barometers data. The magnetometers register both high- and low-frequency pulsations. Geomagnetic fluctuations occur upon the seismic wave arrival but last a longer duration, while the STADs lag their co-located seismic waves by about 15-45 seconds. The long-lasting fluctuations recorded by both induction and fluxgate magnetometers suggest that the ground/underground water motion play an important role, which is further conformed by low-frequency fluctuations in the tiltmeter data. In general, the amplitude of geomagnetic fluctuations decays as away from the epicenter. However, unusual large co-seismic geomagnetic fluctuations are detected over areas of the abnormal seismic intensity level and/or the magnetic underground structure with anomalously high susceptibilities.

Keywords: Geomagnetic, QuakeFinder, Infrasound, micro-Barometer, Tiltmeter

©2019. Japan Geoscience Union. All Right Reserved. 

# Multi-sensor monitoring network for earthquake precursor study near subduction zone at Boso, Japan

*Katsumi Hattori[1], Chie Yoshino[1], WEIYUN XIE[2], Sanaka Saito[2], Haruna Kojima[2], Rui Song[2], Peng Han[3], Toru Mogi[4], Tada-nori Goto[5], Ichi Takumi[6], Hiroshi Yasukawa[7], Motoaki Mouri[8], Jun Izutsu[9], Tadashi Takano[10], Chihiro Yamanaka[11], Masashi Kamogawa[12], Yoshiaki Ando[13], JANN-YENQ Liu[14], Dimitar Ouzounov[15], Valery Tramutoli[16]

1. Department of Earth Sciences, Graduate School of Science, Chiba University, 2. Graduate School of Science and Engineering, Chiba University, 3. Southern University of Science and Technology, China, 4. Hokkaido University, 5. Kyoto University, 6. Nagoya Institute of Technology, 7. Aichi Prefectural University, 8. Aichi University, 9. Chubu University, 10. Nihon University, 11. Osaka University, 12. Tokyo Gakugei University, 13. The University of Electro-Communications, 14. National Central University, Taiwan, 15. Chapman University, US, 16. University of Basilicagta, Italy

New observations from ground and space have provided multiple evidences of pre-earthquake signals and the latest studies show their statistical significance, repeatability, and universality. In this project, to understand the preparation process of large earthquakes and slow-slip events in subduction zone, especially to clarify the nucleation stage of the earthquake cycle, we plan to establish a dense observation network in Boso, Japan, where large subduction earthquakes are expected soon. Since the subsurface fluid flow may play an important role in the preparation process of subduction activities, we intend to employ electromagnetic approaches including oceanic and continental MT survey to monitor the underground resistivity structure which is sensitive to the dynamics of fluid. Other geophysical monitoring such as ULF geomagnetic and geoelectrical observations, radon measurements, and inland GPS movements, TIR, and OLR will be incorporated to help to understand the preparation process and evaluate the applicability of various pre-earthquake signals towards short term earthquake forecasting. We call this idea “sensor WEB”. We will show the state of the art and some results in our presentation.
This study is supported by Grand-in-Aids for Scientific Research of Japan Society for Promotion of Science (26249060).

©2019. Japan Geoscience Union. All Right Reserved. 

# Transient Effects in Atmosphere and Ionosphere Associated with 2018 Mw 7.5 Sulawesi Indonesia Earthquake and Triggered Tsunami and Volcano Activities

*Dimitar Ouzounov[1], Sergey Pulinets[2], Dmitry Davidenko[2], Alexander Rozhnoi[3], Maria Solovieva[3], Tiger Liu[4]

1. Center of Excellence in Earth Systems Modeling & Observations (CEESMO) , Schmid College of Science & Technology Chapman University, Orange, California, USA, 2. Space Research Institute, RAS, Moscow, Russia, 3. The Schmidt Institute of Physics of the Earth, RAS, Moscow, Russia, 4. Center for Astronautical Physics and Engineering, National Central University, Taoyuan City, Taiwan

We analyze retrospectively the transient variations of four different physical parameters of atmosphere/ionosphere during the time of M7.5 od Sept 28, 2018 in Indonesia namely: (i) thermodynamic proprieties in the lower atmosphere, (ii) outgoing earth radiation (OLR) at the TOA, (ii) GPS/TEC and (iv) the very-low-frequency (VLF/LF) signals at the receiving station in Petropavlovsk-Kamchatski (RTK, Russia). We found that in the second part of September 2018 a rapid augment of satellite observed earth radiation in the atmosphere and the anomaly located in close vicinity to the future M7.5 epicenter reached the maximum on Sept 21-22. The GPS/TEC data analysis indicates an augment and variation in electron density reaching a maximum value during the Sept 26-27 periods. Two VLF/LF crossing wave paths - NWC-RTK and JJY-RTK, have shown abnormal behavior of signals during on days Sept 26-28 two days before the earthquake. Our results show coherence between the appearance of pre-earthquake transient’ s effects in atmosphere and ionosphere (with a short time-lag, from hours up to a few days) and the occurrence of 2018 M7.5 in Indonesia. Traveling ionospheric tsunami disturbances (TITDs) in the total electron content (TEC) induced by tsunami waves of the 28 September 2018 Mw 7.5 Sulawesi Indonesia earthquake are detected by of seven ground-based receivers of the global positioning system (GPS) in South Asia, Oceanic, Pacific areas. It is found that the origin is about 100 km North of the epicenter and the horizontal speed is of about 187 m/s.

The pre-earthquake nature of the signals in atmosphere and ionosphere were revealed by simultaneous analysis of satellite, GPS/TEC and VLF/LF observations and suggest that they follow a general temporal-spatial evolution pattern, which has been seen in other large earthquakes worldwide.

Keywords: earthquake, tsunami, volcano, precursor, GPS/TEC, thermal anomaly

©2019. Japan Geoscience Union. All Right Reserved. 

# Seismicity change and b value variation prior to the Wenchuan earthquake (*Ms 8.0*)

*Peng Han[1], Rui Wang[1], Ying Chang[1], Miao Miao[1], Haixia Shi[2], Lingyuan Meng[2], Xuemei Zhang[2], Weiyun Xie[3], Katsumi Hattori[3]

1. Southern University of Science and Technology, Shenzhen, China, 2. China Earthquake Networks Center, Beijing 100045, China, 3. Chiba University, Chiba, Japan

The Gutenberg-Richter Law describes frequency-magnitude distribution of earthquakes. A number of studies have shown that the slope (b value) of the relationship between frequency and magnitude decreased before large earthquakes. Based on the analysis of the earthquake catalog from January, 2000 to April, 2008, we have investigated seismicity change and b value variation prior to the *Ms* 8.0 Wenchuan earthquake. The results show clear drops of both monthly and quarterly frequency of earthquakes during 2005-2006. The b value exhibits a long-term decrease trend since 2002, and reaches to the minimum just before the onset of the main shock. The temporal variation of b value is quite similar to that prior to the *Mw* 9.0 Tohoku earthquake in Japan, which may reflect the stress evolution during the preparation process of large earthquakes. These results indicate that the b value is an important indicator of an impending great earthquake, and has high potential in terms of predicting a future large quake.

Keywords: Wenchuan earthquake, b value, seismicity

©2019. Japan Geoscience Union. All Right Reserved. 

[E] Poster | M (Multidisciplinary and Interdisciplinary)：M-IS Intersection

Thu. May 30, 2019 5:15 PM - 6:30 PM JST | Thu. May 30, 2019 8:15 AM - 9:30 AM UTC | Poster Hall International Exhibition Hall8, Makuhari Messe_35

## [M-IS04] Interdisciplinary studies on pre-earthquake processes

convener:Katsumi Hattori(Department of Earth Sciences, Graduate School of Science, Chiba University), JANN-YENQ Liu(Institute of Space Science, National Central University, Taiwan), Dimitar Ouzounov(Center of Excellence in Earth Systems Modeling & Observations (CEESMO) , Schmid College of Science & Technology Chapman University, Orange, California, USA), Qinghua Huang(Peking University)

This session expands the interdisciplinary discussions on preparation process of earthquake and earthquake predictability by presenting the latest progress in studying the physically based pre-earthquake phenomena. New observations from space and ground have provided<br/>evidences, which may enhance better understanding of tectonic activity. The session anticipates talks that include but not limited to observations and analyses of seismic, electrical, electromagnetic, electro-chemical and thermodynamic processes related to stress changes in the lithosphere along with their statistical and physical validation. Presentations on the latest observational results associated with major earthquakes obtained by different methodologies are welcomed. The topics of the session are as follows but not limited.<br/><br/>-General discussion on earthquake preparation process and the physics of pre-earthquake signals<br/><br/>- Theory, modeling, laboratory experiments, computational simulation for generation and propagation of pre-earthquake signals and their connection with seismic cycle<br/><br/> - Multi-parameter observations, detection, and validation of pre-earthquake signals<br/><br/> - Cross-disciplinary studies, practical and technical approaches for better understanding of earthquake preparation processes and their connection with seismicity

### [MIS04-P01] Statistical analysis and Evaluation of ULF seismo-magnetic phenomena at Kakioka, Japan, during 1983-2017

*Kei Takahashi[1], Katsumi Hattori[2], Peng Han[3] (1.Faculty of Science, Chiba University, 2.Graduate School of Science, Chiba University, 3.Southern University of Science and Technology, China)

### [MIS04-P02] Pre-seismic anomalies on Earth's magnetic field and ionosphere electron density using Swarm data

*Amune Yamazaki[1], Katsumi Hattori[1], Rui Song[1] (1.Chiba University)

### [MIS04-P03] Measurement of radon density in the atmosphere at Okayama, Kochi, Choshi and Kiyosumi, II

*Tohru Okabayashi[1], Kiyotaka Ninagawa[2], Isao Yamamoto[3], Katsumi Hattori[4], Chie Yoshino[4], Haruna Kojima[4], Nobuhiro Maeda (1.Department of Merical Risk and Crisis Management, Faculty of Risk and Crisis Management, Chiba Institute of Science, 2.Faculty of Science, Okayama University of Science, 3.Falcuty of Engineering, Okayama University of Science, 4.Graduate school of Science, Chiba University)

### [MIS04-P04] Possible anomalous changes in solar quiet-daily geomagnetic variation *Sq* related to the 2011 off the Pacific coast of Tohoku earthquake (Mw 9.0)

*Xiaocan Liu[1], Katsumi Hattori[2,3], Peng Han[4], Huaran Chen[1] (1.Institute of geophysics China Earthquake Administrition, 2.Graduate School of Science, Chiba University, Chiba, Japan, 3. Center for Environmental Remote Sensing, Chiba University, Chiba, Japan, 4.Department of Earth and Space Sciences, Southern University of Science and Technology, ShenZhen, China)

### [MIS04-P05] Co-seismic geomagnetic fluctuations and atmospheric disturbances during the 2018 M6.2 Hualien Earthquake

*Chun-Rong Chen[1], JANN-YENQ Liu[1] (1.Graduate Institute of Space Science, National Central University)

### [MIS04-P06] Multi-sensor monitoring network for earthquake precursor study near subduction zone at Boso, Japan

*Katsumi Hattori[1], Chie Yoshino[1], WEIYUN XIE[2], Sanaka Saito[2], Haruna Kojima[2], Rui Song[2], Peng Han[3], Toru Mogi[4], Tada-nori Goto[5], Ichi Takumi[6], Hiroshi Yasukawa[7], Motoaki Mouri[8], Jun Izutsu[9], Tadashi Takano[10], Chihiro Yamanaka[11], Masashi Kamogawa[12], Yoshiaki Ando[13], JANN-YENQ Liu[14], Dimitar Ouzounov[15], Valery Tramutoli[16] (1.Department of Earth Sciences, Graduate School of Science, Chiba University, 2.Graduate School of Science and Engineering, Chiba University, 3.Southern University of Science and Technology, China, 4.Hokkaido University, 5.Kyoto University, 6.Nagoya Institute of Technology, 7.Aichi Prefectural University, 8.Aichi University, 9.Chubu University, 10.Nihon University, 11.Osaka University, 12.Tokyo Gakugei University, 13.The University of Electro-Communications, 14.National Central University, Taiwan, 15.Chapman University, US, 16.University of Basilicagta, Italy)

---

[MIS04-P07] Transient Effects in Atmosphere and Ionosphere Associated with 2018 Mw 7.5 Sulawesi Indonesia Earthquake and Triggered Tsunami and Volcano Activities

★Invited Papers

*Dimitar Ouzounov[1], Sergey Pulinets[2], Dmitry Davidenko[2], Alexander Rozhnoi[3], Maria Solovieva[3], Tiger Liu[4] (1.Center of Excellence in Earth Systems Modeling & Observations (CEESMO) , Schmid College of Science & Technology Chapman University, Orange, California, USA, 2.Space Research Institute, RAS, Moscow, Russia, 3.The Schmidt Institute of Physics of the Earth, RAS, Moscow, Russia, 4.Center for Astronautical Physics and Engineering, National Central University, Taoyuan City, Taiwan)

---

[MIS04-P08] Seismicity change and b value variation prior to the Wenchuan earthquake (*Ms 8.0*)

*Peng Han[1], Rui Wang[1], Ying Chang[1], Miao Miao[1], Haixia Shi[2], Lingyuan Meng[2], Xuemei Zhang[2], Weiyun Xie[3], Katsumi Hattori[3] (1.Southern University of Science and Technology, Shenzhen, China, 2.China Earthquake Networks Center, Beijing 100045, China, 3.Chiba University, Chiba, Japan)

# Statistical analysis and Evaluation of ULF seismo-magnetic phenomena at Kakioka, Japan, during 1983-2017

*Kei Takahashi[1], Katsumi Hattori[2], Peng Han[3]

1. Faculty of Science, Chiba University, 2. Graduate School of Science, Chiba University, 3. Southern University of Science and Technology, China

To clarify and verify the ultralow frequency (ULF) seismo-magnetic phenomena, we have performed statistical studies on the geomagnetic data observed at the Kakioka (KAK) station, Japan, during 1983-2017. We investigated the energy of ULF geomagnetic signals of the frequency around 0.01 Hz using wavelet transform analysis. To minimize the influences of artificial noises and global magnetic perturbations, we used only the geomagnetic data observed at midnight time (LT 2:30 A.M. to 4:00 A.M.).We define the geomagnetic anomalies when the Z components of geomagnetic data exceeds median + 1.5 IQR, where IQR is the interquartile range. Considering that ionospheric disturbances may also lead to enhancements in the Z component, we exclude the anomaly when the energy of H component exceeds median + 3.0 IQR. Statistical analysis of superposed epoch analysis have indicated that ULF magnetic anomalies are more likely to appear before sizable isolated earthquake events (Es parameter which is higher than 8th power of 10 and no earthquake events during ±45 days ) rather than after them, especially 6-10 days before the events. Finally, we have evaluated the precursory information of ULF geomagnetic signals for local sizable earthquakes using Molchan’ s error diagram. The above results have indicated that the ULF seismo-magnetic phenomena at Kakioka clearly contain precursory information and have a possibility of improving forecasting of large earthquakes.

©2019. Japan Geoscience Union. All Right Reserved. 

# Pre-seismic anomalies on Earth’s magnetic field and ionosphere electron density using Swarm data

*Amune Yamazaki[1], Katsumi Hattori[1], Rui Song[1]

1. Chiba University

An earthquake is a rapid release of stress in the lithosphere and often leads to serious damages on human lives and society. Even though the short-time forecast of earthquake is important, it is not achieved yet. However, many electromagnetic phenomena that may be related to seismic activity have been reported recently. The satellite, one of the useful tools to observe these phenomena, can cover the global areas and can collect a large amount of data related to earthquakes which have large magnitude worldwide in short time. The Swarm satellites mission started to operate on November 22, 2013 by European Space Agency, with the constellation of three satellites (A, B, C) The anomalies preceded to the Ecuador earthquake in 2016 have been reported using the Swarm data. In this paper, in order to validate these results using the magnetic vector Y data by VFM and electron density data by Langmuir probe, we have analyzed the Swarm data related the M6.3~6.9 earthquakes occurred at Lombok Island, Indonesia, in July 28, August 5, and 19, 2018. The study area is a 1000 km square from the epicenter of 20180805 earthquake and the analyzed period is from May 28 to September 27, 2018. In this paper we report night-time orbit data at 18:00-6:00 LT.

As results, we found the following tendencies; (1) positive anomalies on magnetic Y vector about 1-2 weeks before the earthquakes and (2) negative anomalies on electron density from 1 week to 1 month before the earthquakes. We performed the same analysis to the data on the same period in 2016 and 2017 for reference when there were no M6+ earthquakes. We found that the number of anomaly track is only abruptly increased in the short period from the end of June to July in 2018, and that the trend is not able to be found in 2016 and 2017. From this unique trend in 2018, it is suggestive of the existence of the relation between the local seismic activity and in-situ satellite anomalies in the magnetic field and electron density in Lombok area.

©2019. Japan Geoscience Union. All Right Reserved. 

# Measurement of radon density in the atmosphere at Okayama, Kochi, Choshi and Kiyosumi, II

*Tohru Okabayashi[1], Kiyotaka Ninagawa[2], Isao Yamamoto[3], Katsumi Hattori[4], Chie Yoshino[4], Haruna Kojima[4], Nobuhiro Maeda

1. Department of Merical Risk and Crisis Management, Faculty of Risk and Crisis Management, Chiba Institute of Science, 2. Faculty of Science, Okayama University of Science, 3. Falcuty of Engineering, Okayama University of Science, 4. Graduate school of Science, Chiba University

We report continuous measurement of radon density in atmosphere at Okayama for three years, Kochi, Choshi and Kiyosumi for two years. An increase of radon density in groundwater at Nishinomiya city [1] and in atmosphere [2] at the southern part of Hyogo Prefecture Earthquake in 1995 were reported, respectively. In the case of Tohoku Region Pacific Coast Earthquake, the data obtained the exhaust air monitor that peak duration was long and the peak decreased rapidly before earthquake has been reported at the radiation facility of Fukushima Medical College in Fukushima [3]. On the other hand, a PIN photodiode have been developed and used as a high sensitive alpha ray detector in Super Kamiokande [4]. Since 2016, we also made an experimental setup using PIN photodiode, and measured the radon density in atmosphere. Using a Si PIN photodiode (S3204-09, unsealed, Hamamatsu Photodiode K.K.) as an alpha ray detector, we constructed radon detection setup combined with aluminum pot as an air accumulator, H4083 (Hamamatsu) as a charge amplifier, C4900-01 (Hamamatsu) as a high voltage power supply module, a pulse shaped amplifier with time constant of 10 msec, a multi channel analyzer (MCA-LiteN), and a PC as a data analysis. Obtained alpha spectra of atmosphere showed 4 peaks originated from $^{218}$Po, $^{214}$Po and $^{210}$Po of U series, and $^{212}$Po of Th series. Since 2017, we newly started to measure at Kochi, Choshi and Kiyosumi using our apparatus. Details of observed data are discussed in addition the data at Okayama since 2016.

[1] Igarashi G., Saeki S., Takahata N., Sumikawa K., Tasaka S., Sasaki Y., Takahashi M. and Sano Y. : Ground-water radon anomaly before the Kobe earthquake in Japan, Science, 269, 60-61, 1995.
[2] Yasuoka, Y. and Shinogi, M.: Anomaly in atmospheric radon concentration: a possible precursor of the 1995 Kobe, Japan, earthquake. Health Physics, 72, 759-761, 1997.
[3] Nagahama H., Yasuoka Y., Suzuki T., and Homma Y.: Radon Variation in the Air Before the 2011 Tohoku Earthquake (Mw =9.0), Programme and Abstracts, A32-09, The Seismological Society of Japan. 2011, Fall Meeting.
[4] Nemoto, M., Tasaka S., Hori H., Okumura K., Kajita T., and Takeuchi Y. : Development of High Sensitive Radon Detector with Electrostatic Collection. Radioisotopes, 46, 710-719, 1997 (Japanese).

Keywords: radon, atmosphere, earthquake prediction

©2019. Japan Geoscience Union. All Right Reserved. 

# Possible anomalous changes in solar quiet-daily geomagnetic variation *Sq* related to the 2011 off the Pacific coast of Tohoku earthquake (Mw 9.0)

*Xiaocan Liu[1], Katsumi Hattori[2,3], Peng Han[4], Huaran Chen[1]

1. Institute of geophysics China Earthquake Administrition, 2. Graduate School of Science, Chiba University, Chiba, Japan, 3. Center for Environmental Remote Sensing, Chiba University, Chiba, Japan, 4. Department of Earth and Space Sciences, Southern University of Science and Technology, ShenZhen, China

Seismo-electromagnetic researches have been studied for decades (e.g. Hayakawa and Fujinawa, 1994; Hayakawa and Molchanov, 2002, 2008,2013; Hattori, 2004, Hattori, et al., 2004a, 2004b; Hayakawa et al., 2007;, Hattori et al., 2013; Han et al., 2011, 2014, 2015, 2016, 2017; Huang QH et al., 2011, 2015; Du A, Huang Q et al., 2002, Rong YM et al., 2012, Yuan G.P., Zhang X.M. et al. 2015), and the geomagnetic diurnal variation (GDV) is a stable variation of the geomagnetic field that can be used to detect possible anomalous changes associated with large earthquakes.

We investigated data observed at 20 geomagnetic observatories at longitudes of 130˚E to 150˚E between 2009 and 2012 to detect possible anomalous changes in the geomagnetic solar quiet daily variation (Sq) related to the 2011 off the Pacific coast of Tohoku earthquake (Mw 9.0) occurred on March 11, 2011 in Japan. We selected the 5 quiet days every month and analyzed three component magnetic data with 1 min resolution using the natural orthogonal component (NOC) method to identify Sq variations from observations, and performed the spherical harmonic analysis (SHA) to separate the internal and the external equivalent Sq current systems of Je and Ji. We obtained that, Je and Ji are distorted near the epicenter area on two geomagnetic quiet days of January 23 and 27, 2011. They are about two months before the earthquake. Then, we made backward computation on the external and internal parts of the SHA model geomagnetic fields, Be and Bi, to determine the possible anomalous magnetic field variations at each station. Results show significant differences in daily variation for all components on January 23 and 27, 2011. The other days, we could not recognize any apparent anomalous behaviors, except known secular, seasonal, and solar activity dependences. A possible connection between this anomaly and the very strong Tohoku earthquake, which followed only one and half month after the geomagnetic anomaly is of highest interest for the research on earthquake precursors.

Keywords: geomagnetic solar quiet daily variation (Sq), natural orthogonal component (NOC) method, spherical harmonic analysis (SHA), the 2011 off the Pacific coast of Tohoku earthquak

©2019. Japan Geoscience Union. All Right Reserved. 

# Co-seismic geomagnetic fluctuations and atmospheric disturbances during the 2018 M6.2 Hualien Earthquake

*Chun-Rong Chen[1], JANN-YENQ Liu[1]

1. Graduate Institute of Space Science, National Central University

The strong ground motion of 6 February 2018 M6.2 Hualien Earthquake triggered a series of co-seismic geomagnetic fluctuations and seismo-traveling atmospheric disturbances (STADs) signatures in infrasonic waves and micro-pressures upon the seismic wave arrival. Networks of 9 QuakeFinder systems, 3 infrasound systems, 2 tiltmeters, 2 micro-barometers, and 11 co-located seismometers are used in this study. Each QuakeFinder system consists of a 3-axes induction magnetometer, an air conductivity sensor, a geophone, and temperature/relative humidity sensors. Co-seismic signatures clearly appear in the induction magnetometers, infrasound systems, and micro-barometers data. The magnetometers register both high- and low-frequency pulsations. Geomagnetic fluctuations occur upon the seismic wave arrival but last a longer duration, while the STADs lag their co-located seismic waves by about 15-45 seconds. The long-lasting fluctuations recorded by both induction and fluxgate magnetometers suggest that the ground/underground water motion play an important role, which is further conformed by low-frequency fluctuations in the tiltmeter data. In general, the amplitude of geomagnetic fluctuations decays as away from the epicenter. However, unusual large co-seismic geomagnetic fluctuations are detected over areas of the abnormal seismic intensity level and/or the magnetic underground structure with anomalously high susceptibilities.

Keywords: Geomagnetic, QuakeFinder, Infrasound, micro-Barometer, Tiltmeter

©2019. Japan Geoscience Union. All Right Reserved. 

# Multi-sensor monitoring network for earthquake precursor study near subduction zone at Boso, Japan

*Katsumi Hattori[1], Chie Yoshino[1], WEIYUN XIE[2], Sanaka Saito[2], Haruna Kojima[2], Rui Song[2], Peng Han[3], Toru Mogi[4], Tada-nori Goto[5], Ichi Takumi[6], Hiroshi Yasukawa[7], Motoaki Mouri[8], Jun Izutsu[9], Tadashi Takano[10], Chihiro Yamanaka[11], Masashi Kamogawa[12], Yoshiaki Ando[13], JANN-YENQ Liu[14], Dimitar Ouzounov[15], Valery Tramutoli[16]

1. Department of Earth Sciences, Graduate School of Science, Chiba University, 2. Graduate School of Science and Engineering, Chiba University, 3. Southern University of Science and Technology, China, 4. Hokkaido University, 5. Kyoto University, 6. Nagoya Institute of Technology, 7. Aichi Prefectural University, 8. Aichi University, 9. Chubu University, 10. Nihon University, 11. Osaka University, 12. Tokyo Gakugei University, 13. The University of Electro-Communications, 14. National Central University, Taiwan, 15. Chapman University, US, 16. University of Basilicagta, Italy

New observations from ground and space have provided multiple evidences of pre-earthquake signals and the latest studies show their statistical significance, repeatability, and universality. In this project, to understand the preparation process of large earthquakes and slow-slip events in subduction zone, especially to clarify the nucleation stage of the earthquake cycle, we plan to establish a dense observation network in Boso, Japan, where large subduction earthquakes are expected soon. Since the subsurface fluid flow may play an important role in the preparation process of subduction activities, we intend to employ electromagnetic approaches including oceanic and continental MT survey to monitor the underground resistivity structure which is sensitive to the dynamics of fluid. Other geophysical monitoring such as ULF geomagnetic and geoelectrical observations, radon measurements, and inland GPS movements, TIR, and OLR will be incorporated to help to understand the preparation process and evaluate the applicability of various pre-earthquake signals towards short term earthquake forecasting. We call this idea “sensor WEB”. We will show the state of the art and some results in our presentation.
This study is supported by Grand-in-Aids for Scientific Research of Japan Society for Promotion of Science (26249060).

©2019. Japan Geoscience Union. All Right Reserved. 

# Transient Effects in Atmosphere and Ionosphere Associated with 2018 Mw 7.5 Sulawesi Indonesia Earthquake and Triggered Tsunami and Volcano Activities

*Dimitar Ouzounov[1], Sergey Pulinets[2], Dmitry Davidenko[2], Alexander Rozhnoi[3], Maria Solovieva[3], Tiger Liu[4]

1. Center of Excellence in Earth Systems Modeling & Observations (CEESMO) , Schmid College of Science & Technology Chapman University, Orange, California, USA, 2. Space Research Institute, RAS, Moscow, Russia, 3. The Schmidt Institute of Physics of the Earth, RAS, Moscow, Russia, 4. Center for Astronautical Physics and Engineering, National Central University, Taoyuan City, Taiwan

We analyze retrospectively the transient variations of four different physical parameters of atmosphere/ionosphere during the time of M7.5 od Sept 28, 2018 in Indonesia namely: (i) thermodynamic proprieties in the lower atmosphere, (ii) outgoing earth radiation (OLR) at the TOA, (ii) GPS/TEC and (iv) the very-low-frequency (VLF/LF) signals at the receiving station in Petropavlovsk-Kamchatski (RTK, Russia). We found that in the second part of September 2018 a rapid augment of satellite observed earth radiation in the atmosphere and the anomaly located in close vicinity to the future M7.5 epicenter reached the maximum on Sept 21-22. The GPS/TEC data analysis indicates an augment and variation in electron density reaching a maximum value during the Sept 26-27 periods. Two VLF/LF crossing wave paths - NWC-RTK and JJY-RTK, have shown abnormal behavior of signals during on days Sept 26-28 two days before the earthquake. Our results show coherence between the appearance of pre-earthquake transient’ s effects in atmosphere and ionosphere (with a short time-lag, from hours up to a few days) and the occurrence of 2018 M7.5 in Indonesia. Traveling ionospheric tsunami disturbances (TITDs) in the total electron content (TEC) induced by tsunami waves of the 28 September 2018 Mw 7.5 Sulawesi Indonesia earthquake are detected by of seven ground-based receivers of the global positioning system (GPS) in South Asia, Oceanic, Pacific areas. It is found that the origin is about 100 km North of the epicenter and the horizontal speed is of about 187 m/s.

The pre-earthquake nature of the signals in atmosphere and ionosphere were revealed by simultaneous analysis of satellite, GPS/TEC and VLF/LF observations and suggest that they follow a general temporal-spatial evolution pattern, which has been seen in other large earthquakes worldwide.

Keywords: earthquake, tsunami, volcano, precursor, GPS/TEC, thermal anomaly

©2019. Japan Geoscience Union. All Right Reserved. 

# Seismicity change and b value variation prior to the Wenchuan earthquake (*Ms 8.0*)

*Peng Han[1], Rui Wang[1], Ying Chang[1], Miao Miao[1], Haixia Shi[2], Lingyuan Meng[2], Xuemei Zhang[2], Weiyun Xie[3], Katsumi Hattori[3]

1. Southern University of Science and Technology, Shenzhen, China, 2. China Earthquake Networks Center, Beijing 100045, China, 3. Chiba University, Chiba, Japan

The Gutenberg-Richter Law describes frequency-magnitude distribution of earthquakes. A number of studies have shown that the slope (b value) of the relationship between frequency and magnitude decreased before large earthquakes. Based on the analysis of the earthquake catalog from January, 2000 to April, 2008, we have investigated seismicity change and b value variation prior to the *Ms* 8.0 Wenchuan earthquake. The results show clear drops of both monthly and quarterly frequency of earthquakes during 2005-2006. The b value exhibits a long-term decrease trend since 2002, and reaches to the minimum just before the onset of the main shock. The temporal variation of b value is quite similar to that prior to the *Mw* 9.0 Tohoku earthquake in Japan, which may reflect the stress evolution during the preparation process of large earthquakes. These results indicate that the b value is an important indicator of an impending great earthquake, and has high potential in terms of predicting a future large quake.

Keywords: Wenchuan earthquake, b value, seismicity

©2019. Japan Geoscience Union. All Right Reserved. 

[E] Oral | M (Multidisciplinary and Interdisciplinary)：M-IS Intersection

Thu. May 30, 2019 1:45 PM - 3:15 PM JST | Thu. May 30, 2019 4:45 AM - 6:15 AM UTC | A02 TOKYO BAY MAKUHARI HALL

## [M-IS04] Interdisciplinary studies on pre-earthquake processes

convener:Katsumi Hattori(Department of Earth Sciences, Graduate School of Science, Chiba University), JANN-YENQ Liu(Institute of Space Science, National Central University, Taiwan), Dimitar Ouzounov(Center of Excellence in Earth Systems Modeling & Observations (CEESMO) , Schmid College of Science & Technology Chapman University, Orange, California, USA), Qinghua Huang(Peking University), Chairperson:Jann-Yenq Liu(National Central University, Taiwan), Toshiyasu Nagao

This session expands the interdisciplinary discussions on preparation process of earthquake and earthquake predictability by presenting the latest progress in studying the physically based pre-earthquake phenomena. New observations from space and ground have provided<br/>evidences, which may enhance better understanding of tectonic activity. The session anticipates talks that include but not limited to observations and analyses of seismic, electrical, electromagnetic, electro-chemical and thermodynamic processes related to stress changes in the lithosphere along with their statistical and physical validation. Presentations on the latest observational results associated with major earthquakes obtained by different methodologies are welcomed. The topics of the session are as follows but not limited.<br/><br/>-General discussion on earthquake preparation process and the physics of pre-earthquake signals<br/><br/>- Theory, modeling, laboratory experiments, computational simulation for generation and propagation of pre-earthquake signals and their connection with seismic cycle<br/><br/> - Multi-parameter observations, detection, and validation of pre-earthquake signals<br/><br/> - Cross-disciplinary studies, practical and technical approaches for better understanding of earthquake preparation processes and their connection with seismicity

1:45 PM - 2:00 PM JST | 4:45 AM - 5:00 AM UTC

### [MIS04-01] Application of blind source separation method in seismo-magnetic data analysis

★Invited Papers

*Peng Han[1], Yi Zhong[1], Yuanyuan Zhou[1], Yonghui Ma[2], Chengliang Xie[3], Katsumi Hattori[4], Chie Yoshino[4] (1.Southern University of Science and Technology, Shenzhen, China, 2.Harbin Institute of Technology (Shenzhen), Shenzhen 518055, China, 3.China University of Geosciences (Beijing), Beijing, 100083, China, 4.Chiba University, Chiba, Japan)

2:00 PM - 2:15 PM JST | 5:00 AM - 5:15 AM UTC

### [MIS04-02] Rn flux anomaly and local seiemicity around Asahi station,Boso,Japan

*Haruna Kojima[1], Katsumi Hattori[2], Chie Yoshino[2], Michikuni Shimo[3], Toshiharu Konishi[4], Ryuichi Furuya[5] (1.Graduate School of Science and Engineering,Chiba University, 2.Department of Earth Sciences,Graduate School of Science,Chiba University, 3.Fujita Hearth University, 4.OHYO KOKEN KOGYO Co.,Ltd, 5.COM SYSTEM ,INC.)

2:15 PM - 2:30 PM JST | 5:15 AM - 5:30 AM UTC

### [MIS04-03] Geochemical evidence for the occurrence of 2018 Hualien earthquake triggered by earlier earthquake swarm

*Ching-Chou Fu[1], Lou-Chuang Lee[1], Cheng-Horng Lin[1], Vivek Walia[2], Dimitar Ouzounov[3] (1.Institute of Earth Sciences, Academia Sinica, 2.National Center for Research on Earthquake Engineering, NARL, Taiwan, 3.Chapman University, One University Drive, Orange, CA, USA)

2:30 PM - 2:45 PM JST | 5:30 AM - 5:45 AM UTC

### [MIS04-04] Temporal Variation and Statistical Assessment of b value

*weiyun xie[1], Katsumi Hattori[1], Peng Han[2] (1.chiba university, 2. Southern University of Science and Technology)

2:45 PM - 3:00 PM JST | 5:45 AM - 6:00 AM UTC

[MIS04-05] The S-K characteristics of the borehole areal strains associated with the Ms 8.0 Wenchuan and Ms 7.0 Lushan earthquakes

★Invited Papers

*Kaiguang Zhu[1], Zining Yu[1], Chenquan Chi[1], Mengxuan Fan[1], Kaiyan Lii[1] (1.Jilin University)

---

3:00 PM - 3:15 PM JST | 6:00 AM - 6:15 AM UTC

[MIS04-06] The Relationship between Earthquakes and Lightning Events of the globe during 2009-2017

*Ching-Chung Cheng[1], JANN-YENQ Liu[1,2,3] (1.Graduate Institute of Space Science, National Central University, TAIWAN, 2.Center for Astronautical Physics and Engineering, National Central University, TAIWAN, 3.Center for Space and Remote Sensing Research, National Central University, TAIWAN)

# Application of blind source separation method in seismo-magnetic data analysis

*Peng Han[1], Yi Zhong[1], Yuanyuan Zhou[1], Yonghui Ma[2], Chengliang Xie[3], Katsumi Hattori[4], Chie Yoshino[4]

1. Southern University of Science and Technology, Shenzhen, China, 2. Harbin Institute of Technology (Shenzhen), Shenzhen 518055, China, 3. China University of Geosciences (Beijing), Beijing, 100083, China, 4. Chiba University, Chiba, Japan

Along with the development of urban constructions, artificial disturbances in geomagnetic observations are becoming more and more tremendous. The near-field noises produced by human activities such as vehicles, subway and high-speed railways make it difficult to precisely measure geomagnetic pulsations on the ground, thus reducing the practical application value of geomagnetic data. Therefore, suppressing near-field noises has scientific significance and application value. In this study, by combining remote reference and blind source separation analysis methods, we proposed a new signal processing approach which is able to separate geomagnetic pulsation from near-field noise. First, we demonstrated the effectiveness of the new approach by separating signals of different sources in the simulation analysis. Then, we applied this method to geomagnetic field data observed in Chiba, Japan where DC-driven train noises were intense. The results showed that geomagnetic pulsations and train noises are separated clearly, and near-field train noise could be reduced effectively on that basis. It is concluded that the reference-based blind source separation analysis is useful in extracting geomagnetic pulsations and suppressing near-field noises, and may have potential application value in electromagnetic exploration.

Keywords: blind source separation, seismo-magnetic data analysis, Boso, Japan

©2019. Japan Geoscience Union. All Right Reserved. 

# Rn flux anomaly and local seiemicity around Asahi station,Boso,Japan

*Haruna Kojima[1], Katsumi Hattori[2], Chie Yoshino[2], Michikuni Shimo[3], Toshiharu Konishi[4], Ryuichi Furuya[5]

1. Graduate School of Science and Engineering,Chiba University, 2. Department of Earth Sciences,Graduate School of Science,Chiba University, 3. Fujita Hearth University, 4. OHYO KOKEN KOGYO Co.,Ltd, 5. COM SYSTEM ,INC.

In recent years, there are many studies reported electromagnetic phenomena preceding earthquakes such as ionospheric anomalies. Lithosphere-Atmosphere-Ionosphere Coupling (LAIC) model has been proposed to explain these phenomena. In this study, to explain the possibility of the chemical channel of LAIC, we have installed sensors for atmospheric electric field (AEF), atmospheric ion concentration (AIC), atmospheric Rn concentration (ARC), ground Rn concentration (GRC), and weather elements at Asahi station, Boso Peninsula, Japan. Because the atmospheric electricity parameters could be mainly influenced by weather factors, it is necessary to remove these influences as much as possible. In this sense, we apply the MSSA (Multi-channel Singular Spectral Analysis) to remove these influences from the GRC variation and estimate the Rn flux from the ground. Then, we investigate the correlation between the changes in the Rn flux and seismicity around the station. As a result, we found the correlation between Rn flux and regional cumulative seismic moment and/or Es index, which indicates the daily seismic energy near the station received at the station. It is highly suggestive of the effectiveness of GRC monitoring in regional seismicity around the station. Further researches such as network observations will be required for the detailed consideration on the correlation between Rn flux and seismicity such as magnitude and distance dependences.

Keywords: Lithosphere-Atmosphere-Ionosphere Coupling, atmospheric electric field, atmospheric ion concentration, ground Rn concentration

©2019. Japan Geoscience Union. All Right Reserved. 

# Geochemical evidence for the occurrence of 2018 Hualien earthquake triggered by earlier earthquake swarm

*Ching-Chou Fu[1], Lou-Chuang Lee[1], Cheng-Horng Lin[1], Vivek Walia[2], Dimitar Ouzounov[3]

1. Institute of Earth Sciences, Academia Sinica, 2. National Center for Research on Earthquake Engineering, NARL, Taiwan, 3. Chapman University, One University Drive, Orange, CA, USA

The continuous observations of soil radon for earthquake studies at the Tapingti station (TPT) have been recorded and are compared with the data from gamma rays observations at the Taiwan Volcano Observation station (YMSG), located north to the TPT station. The previous significant increases of gamma rays and radon were observed at both stations before the earthquakes, which occurred in eastern and northeastern Taiwan, suggest that anomalies in gamma and radon may provide the good indicator for exploring earthquake precursor in eastern Taiwan. A Mw 6.4 Hualien earthquake struck eastern Taiwan on 6 February 2018. Based on seismological studies, this earthquake may be triggered by the earthquake swarm that shook eastern Taiwan on 4 February 2018. In this study, both stations recorded significant changes about two weeks before the Hualien Earthquake. However, we provide the possible evidences from geochemical data for the occurrence of 2018 Hualien earthquake was triggered by earlier earthquake swarm. The continuous monitoring on the multiple parameters can improve our understanding of the relationship between the observed radon and gamma-ray variations and the regional crustal stress/strain in the area.

©2019. Japan Geoscience Union. All Right Reserved. 

# Temporal Variation and Statistical Assessment of b value

*weiyun xie[1], Katsumi Hattori[1], Peng Han[2]

1. chiba university, 2. Southern University of Science and Technology

The Gutenberg-Richter Law describes frequency-magnitude distribution of earthquakes. A number of studies have shown that the slope (b value) of the relationship between frequency and magnitude decreased before large earthquakes. In this paper, we investigate the temporal variation of the b value in the Hokkaido and Tohoku regions, Japan and the Wenchuan region, China, respectively, where M 8.0+ earthquakes occurred in the new century. The magnitude of completeness (Mc) in the catalog is evaluated by combining the maximum curvature (MAXC) technique and the bootstrap approach. Then, the b value and its uncertainty is computed by using the maximum likelihood estimation. The Akaike Information Criterion (AIC) with the bootstrap approach is introduced to statistically assess the temporal variation of b values and quantify the significance level. The results show decrease trends of the b value prior to the 2003 Tokachi Earthquake (M8.0) in Hokkaido, the 2011 Tohoku Earthquake (M9.0), and the 2008 Wenchuan Earthquake in China. In addition, the decrease of b values shows certain statistical significance few months before the three M8.0+ great earthquakes. It is concluded that the b value with statistical assessment may contain potential information for future large earthquake preparation.

Keywords: b-value, AIC

©2019. Japan Geoscience Union. All Right Reserved. 

# The S-K characteristics of the borehole areal strains associated with the Ms 8.0 Wenchuan and Ms 7.0 Lushan earthquakes

*Kaiguang Zhu[1], Zining Yu[1], Chenquan Chi[1], Mengxuan Fan[1], Kaiyan Lii[1]

1. Jilin University

The skewness and kurtosis of daily borehole areal strain at Guza station are jointly analysed on the S-K plane for the Wenchuan and Lushan earthquakes. We define a crustal stationary background to distinguish possible anomalies related to the earthquakes on the assumption that the background exhibits a quasi-Gaussian distribution. By calculating the S-K biases of the daily areal strain from the crustal stationary background, we found that before the Wenchuan earthquake, the large S-K bias anomalies were always negative, implying that the crust was compressed near the station. Whereas for the Lushan earthquake, clustered positive bias anomalies appeared within two time periods, revealing tensile changes in the crust. In addition, the S-K distributions of two arthquakes are separated on the S-K plane, further indicating differences in the associated deformation. These results demonstrate that the S-K characteristics of borehole areal strain data are potentially promising as earthquake precursors.

Keywords: borehole areal strain, S-K biases, S-K distributions, Wenchuan and Lushan earthquakes

©2019. Japan Geoscience Union. All Right Reserved. 

# The Relationship between Earthquakes and Lightning Events of the globe during 2009-2017

*Ching-Chung Cheng[1], JANN-YENQ Liu[1,2,3]

1. Graduate Institute of Space Science, National Central University, TAIWAN, 2. Center for Astronautical Physics and Engineering, National Central University, TAIWAN, 3. Center for Space and Remote Sensing Research, National Central University, TAIWAN

Lightning activities observed by WWLLN (World-Wide Lightning Location Networks) and 95 magnitude greater than 7.0 earthquakes within 30 degrees north and south latitude during 2009 - Nov. 2017 have been statistically examineed. In particular, we investigate how the lightning activities relate to the magnitude, depth, and distance to the epicenter of the earthquakes. Results show that the lightning events 12-22 days before the magnitude greater than 7.9 earthquakes significantly increase around the epicenter. Furthermore, the area size around the epicenter with the statistical significance of lightning activity enhancements is proportional to the earthquake magnitude. These results suggest that lightning activities can be used to find the possible location of forthcoming large earthquakes.

Keywords: Earthquake, Lightning

©2019. Japan Geoscience Union. All Right Reserved. 

[E] Oral | M (Multidisciplinary and Interdisciplinary)：M-IS Intersection

Thu. May 30, 2019 3:30 PM - 5:00 PM JST | Thu. May 30, 2019 6:30 AM - 8:00 AM UTC | A02 TOKYO BAY MAKUHARI HALL

## [M-IS04] Interdisciplinary studies on pre-earthquake processes

convener:Katsumi Hattori(Department of Earth Sciences, Graduate School of Science, Chiba University), JANN-YENQ Liu(Institute of Space Science, National Central University, Taiwan), Dimitar Ouzounov(Center of Excellence in Earth Systems Modeling & Observations (CEESMO) , Schmid College of Science & Technology Chapman University, Orange, California, USA), Qinghua Huang(Peking University), Chairperson:Peng Han, Katsumi Hattori

This session expands the interdisciplinary discussions on preparation process of earthquake and earthquake predictability by presenting the latest progress in studying the physically based pre-earthquake phenomena. New observations from space and ground have provided<br/>evidences, which may enhance better understanding of tectonic activity. The session anticipates talks that include but not limited to observations and analyses of seismic, electrical, electromagnetic, electro-chemical and thermodynamic processes related to stress changes in the lithosphere along with their statistical and physical validation. Presentations on the latest observational results associated with major earthquakes obtained by different methodologies are welcomed. The topics of the session are as follows but not limited.<br/><br/>-General discussion on earthquake preparation process and the physics of pre-earthquake signals<br/><br/>- Theory, modeling, laboratory experiments, computational simulation for generation and propagation of pre-earthquake signals and their connection with seismic cycle<br/><br/> - Multi-parameter observations, detection, and validation of pre-earthquake signals<br/><br/> - Cross-disciplinary studies, practical and technical approaches for better understanding of earthquake preparation processes and their connection with seismicity

3:30 PM - 3:45 PM JST | 6:30 AM - 6:45 AM UTC

[MIS04-07] 3D-Tomography of the Ionospheric Anomalies Preceding the 2011 Tohoku-Oki ($M_W$9.0) Earthquake

*Ihsan Naufal Muafiry[1,2], Kosuke Heki[1] (1.Hokkaido University, Japan, 2.Universitas Esa Unggul, Indonesia)

3:45 PM - 4:00 PM JST | 6:45 AM - 7:00 AM UTC

[MIS04-08] Statistical Analysis of Pre-seismic Ionospheric Electron Density Anomalies and Investigation of Precursor

*Sanaka Saito[1], Chie Yoshino[1], Katsumi Hattori[1] (1.Chiba University)

4:00 PM - 4:15 PM JST | 7:00 AM - 7:15 AM UTC

[MIS04-09] Spatial clustering of pre-earthquake anomalies as an indicator of the preparation/activation zone

*Dimitar Ouzounov[1], Sergey Pulinets[2], Tiger Liu[3], Katsumi Hattori[4] (1.Center of Excellence in Earth Systems Modeling & Observations (CEESMO) , Schmid College of Science & Technology Chapman University, Orange, California, USA, 2.Space Research Institute, RAS, Moscow, Russia, 3.National Central University, Taoyuan City, Taiwan, 4. Chiba University, Chiba, Japan)

4:15 PM - 4:30 PM JST | 7:15 AM - 7:30 AM UTC

[MIS04-10] **Application of the ionospheric parameters on the seismic research**- -Seismic-ionospheric effect detected from China Seismo-Electromagnetic Satellite

★Invited Papers

*Rui Song[1], Hattori Katsumi[2], Xuemin Zhang[3] (1.Graduate School of Science and Engeering, Chiba University, 2.Graduate School of Science, Chiba University, 3.Institute of Earthquake Science, China Earthquake Administration)

4:30 PM - 4:45 PM JST | 7:30 AM - 7:45 AM UTC

[MIS04-11] ROC curve analyses on the ionospheric TEC of M>=6.0 earthquakes in Japan during 1998-2015

★Invited Papers

*JANN-YENQ Liu[1], Yuh-Ing Chen[2], Pei-Jung Lee[1] (1.Center for Astronautical Physics and Engineering; Graduate Institute of Space Science, National Central University, Taiwan, 2.Graduate Institute of Statistics, National Central University, Taiwan)

---

4:45 PM - 5:00 PM JST | 7:45 AM - 8:00 AM UTC

[MIS04-12] FORMOSAT-5/AIP observes seismo-ionospheric precursors

*JANN-YENQ Liu[1], Chi-Kuang Chao[1] (1.Center for Astronautical Physics and Engineering; and Graduate Institute of Space Science, National Central University, TAIWAN)

# 3D-Tomography of the Ionospheric Anomalies Preceding the 2011 Tohoku-Oki ($M_w$9.0) Earthquake

*Ihsan Naufal Muafiry[1,2], Kosuke Heki[1]

1. Hokkaido University, Japan, 2. Universitas Esa Unggul, Indonesia

The vertical deformation of solid earth could trigger direct acoustic wave propagating upward and will reach the F-layer of the ionosphere ~10 minutes after earthquakes (Cahyadi & Heki, 2015). Such an acoustic disturbance may also make long-lasting electron depletion (Shinagawa et al., 2013). These phenomena can be studied through Total Electron Content (TEC) data using Global Navigation Satellite System (GNSS) receivers. The GNSS phase difference can be converted to slant TEC (STEC) integrated along its line-of-sight (LoS), which are further converted to absolute vertical TEC (VTEC) by removing inter-frequency biases and multiplying with the cosine of the incidence angle of LoS to the ionosphere.

Shortly after the 2011 Tohoku-Oki $M_w$9.0 earthquake, Heki (2011) reported a significant positive anomaly in TEC starting ~40 minutes before the earthquake above the focal area, and He & Heki (2017) found similar TEC enhancements before 18 earthquakes with $M_w$ 7.3-9.2. He & Heki (2016; 2018) investigated the spatial structure of the electron density anomalies before the 2015 Illapel earthquake, Chile ($M_w$8.3) using three-dimensional (3D) tomography technique. The result showed that positive electron density anomaly at ~200 km and negative anomalies at high altitudes line up along the geomagnetic field. This suggests their origin by electron redistribution caused by electric field made by surface positive electric charge (e.g. Freund, 2011).

Here, we report the 3D structure of the ionospheric electron density anomalies immediately before the 2011 Tohoku-Oki Earthquake using data from GEONET, a dense GNSS arrays in Japan, and the dense network in South Korea, with the 3D tomography technique similar to He & Heki (2018) and Muafiry et al. (2018). We set up more than 1500 blocks over the region covering the whole Japanese Islands, the Japan Sea, and the Korean Peninsula, with the size of 1.0° (E-W) x 0.9° (N-S) x 60 km (U-D) up to 900 km altitude. By using STEC residuals of pairs of thousand stations and 8 GPS satellites from reference curves, carefully determined by the L-curve method, as the input, we estimated the number of electron density anomalies within individual blocks. To stabilize and regularize the solution, we applied two types of constraints, i.e. continuity constraint and altitude-dependent absolute value constraint assuming the Chapman distribution. Before using the real data, we performed various tests to confirm the reliability of the solution including the checkerboard test, the test assuming realistic preseismic anomaly pattern, and comparing observed STEC anomalies of 10 % of the observation data with those calculated using the electron density anomalies estimated from the remaining 90% of data. These tests showed that our tomography results are robust with its difference is below 0.5 total electron content unit (TECU).

The attached figure shows the map view of our result at a height of 350 km with longitudinal and latitudinal profiles at three different epochs. The results show that positive electron density anomalies occurred at ~300 km altitude. They become large without spatial drifts as the main-shock approaches. Negative anomalies surround this compact and strong positive anomaly. The anomaly is situated just above to the focal area, suggesting its origin as the concentration of ionospheric electrons in response to surface positive electric charges appearing immediately before the 2011 Tohoku-Oki earthquake.

©2019. Japan Geoscience Union. All Right Reserved. 

Keywords: Ionosphere-Anomalies, Earthquake Precursor, GPS-TEC, 3D-tomography

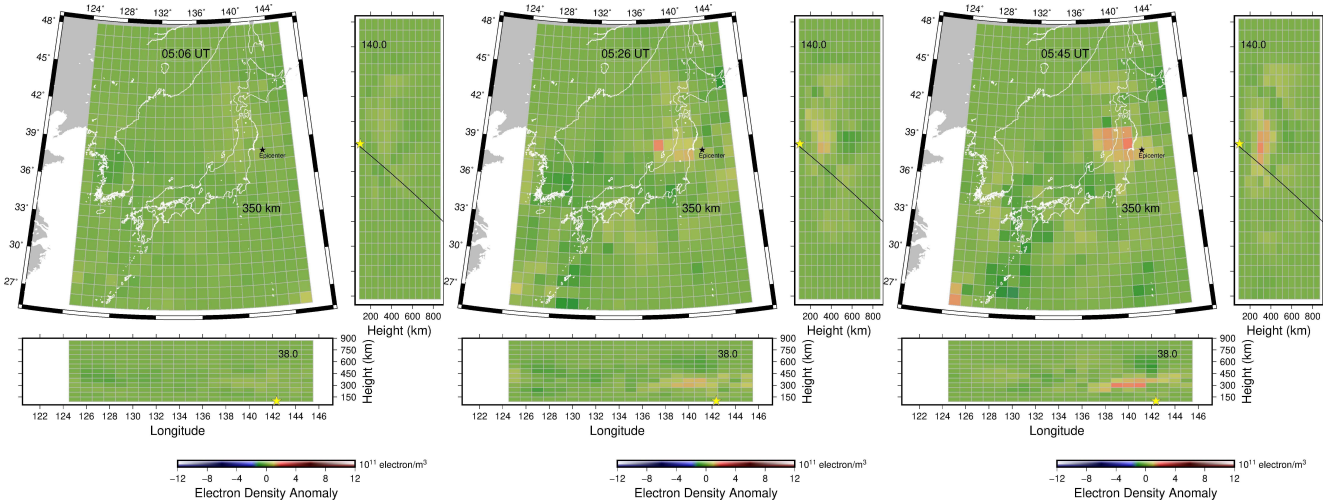


©2019. Japan Geoscience Union. All Right Reserved. 

# Statistical Analysis of Pre-seismic Ionospheric Electron Density Anomalies and Investigation of Precursor

*Sanaka Saito[1], Chie Yoshino[1], Katsumi Hattori[1]

1. Chiba University

Recently, many papers have been published on the earthquake-related ionospheric anomalies. In particular, event studies and statistical studies on Ionospheric electrons using Ionosonde and GPS TEC (total electron content) indicate the pre-seismic anomalies. In Japan region, the previous statistical study during 1998-2010 shows that there is an increase anomaly 1-5 days before the earthquake with M>=6 D<=40 km. In this study, we performed statistical analysis on ionosonde data observed at Kokubunji (35.71N, 139.49E), Japan over 60 years of 1958 ~ 2017 in order to investigate the earthquake-related ionospheric anomalies. The ionosonde is operated by the National Institute of Information and Communication Technology, Japan. The studied parameters are NmF2, which indicates the maximum electron density in the F2 layer, hmF2, which shows the NmF2 altitude, and foEs which is the critical frequency of the Es layer. We select earthquakes occurred within 1000 km and 350 km radius from the ionosonde station, and M >= 6 and D <= 40 km. There are 352 and 148 earthquakes. Ionospheric anomalies are also induced by geomagnetic storm. Therefore, to remove the geomagnetic storm effects, we adopt the Dst index. We divided the values into some classes by onset time and intensity. For each class, we performed statistical processes to calculate duration of ionospheric anomalies triggered by a geomagnetic storm. We found these anomalies last about 1-3 days, and we remove the data based on results. To investigate the correlation between ionospheric anomalies and earthquakes, we perform the Superposed Epoch Analysis (SEA). We define the anomaly as 15 days backward median value ±1.5 IQR and an anomalous day has the anomaly with more than 10 hours. Then, we make up the binary time series data on the earthquake-related anomaly. We extract dataset 30 days before and after the earthquake day for the all selected earthquakes and perform SEA. To evaluate the statistical significance, we compute the random test. SEA results show that there is a significant positive anomalies 1-10 days before the earthquakes in NmF2 data. For hmF2 data, we can find there are no clear correlation. As for foEs, we need further investigation. For NmF2, we checked Molchan’ s Error Diagram (MED). From the results of MED, NmF2 may be precursor for earthquakes. The detailed will be given in the presentation.

©2019. Japan Geoscience Union. All Right Reserved. 

# Spatial clustering of pre-earthquake anomalies as an indicator of the preparation/activation zone

*Dimitar Ouzounov[1], Sergey Pulinets[2], Tiger Liu[3], Katsumi Hattori[4]

1. Center of Excellence in Earth Systems Modeling & Observations (CEESMO) , Schmid College of Science & Technology Chapman University, Orange, California, USA, 2. Space Research Institute, RAS, Moscow, Russia, 3. National Central University, Taoyuan City, Taiwan, 4. Chiba University, Chiba, Japan

We present an interdisciplinary study of observations of pre-earthquake processes associated with major earthquakes based on integrating space and ground- data. We are exploring the general temporal-spatial and evolution patterns of these pre-earthquake signals as a function of both their type and the earthquake magnitude. We examined the possible correlation between the spatial clustering of pre-Earthquake anomalies and the size of earthquake preparation/activation ( Dobrovolsky-Bowman zone) in the framework of the Lithosphere-Atmosphere-Ionosphere Coupling (LAIC) concept. For this analysis we selected six most massive earthquakes from the last decade with differing geographic and seismo-tectonics regions: (1) M9.3, Off the West Coast of Northern Sumatra, Dec 26, 2004; (2) M9.0 Great Tohoku Earthquake, , Japan, March 11, 2011; (3 and (4) M7.8 and M7.3 Gorkha, Nepal, 2015; (5); M8.2 Tehuantepec, Mexico, September 8, 2017 and; (6) M7.1, Puebla central Mexico earthquakes, Mexico, September 19, 2017.
Four physical parameters were measured from ground and satellite were used in the temporal-spatial patterns: 1) Ground Radon variation; 2) Outgoing Long-wavelength Radiation (OLR obtained from NPOESS, NASA/AQUA) on top of the atmosphere (TOA); 3) Atmospheric Chemical Potential (ACP) obtained from NASA assimilation models and; 4) electron density variations in the ionosphere via GPS Total Electron Content (GPS/TEC).

Our preliminary results of temporal-evolution patterns indicate an enhancement of radon (about a week to ten days prior) followed by the increase in the atmospheric chemical potential measured near the epicenter from both satellite and subsequently with an increase of OLR observed on the TOA from NOAA/NASA (a week in advance). Finally, GPS/TEC data indicate an increase in electron concentration 1-4 days before the earthquakes. Although the radon variations, some of satellite OLR and GPS/TEC anomalies were observed far (>2000km) from the epicenter areas, the anomalies were always inside the estimates of the Dobrovolsky-Bowman area of preparation. This finding provides new metrics in the assessment of pre-earthquake signals according to LAIC for both sea and land earthquakes possible only by integrating satellite and ground observations. A detailed summary of our approach to this study of pre-earthquake research has just been published as AGU/Wiley Geophysical Monograph Series No. 234.

Keywords: earthquake forecasting, pre-earthquake, LAIC, GPS/TEC, satellite thermal anomaly, radon

©2019. Japan Geoscience Union. All Right Reserved. 

# Application of the ionospheric parameters on the seismic research --Seismic-ionospheric effect detected from China Seismo-Electromagnetic Satellite

*Rui Song[1], Hattori Katsumi[2], Xuemin Zhang[3]

1. Graduate School of Science and Engeering, Chiba University, 2. Graduate School of Science, Chiba University, 3. Institute of Earthquake Science, China Earthquake Administration

The ionosphere is located at the altitude of 60 kilometers above the earth surface and the top of the ionosphere is about 500km. Figure 1 shows the basic structure of the ionosphere, where D, E and F layers are all clearly concluded. In addition, F layer can be divided into F1 and F2 layers. F1 layers and D region always disppear in nighttime. The seismic-ionospheric research began in 1960s, when American scientists studied the Alaska M8.5 earthquake in 1964, they first found that the disturbance of plasma density before this earthquake. Since then, many researchers engaged in this field. Based on the promising seismic-ionospheric research, China government launched the Seismo-electromagnetic satellite, CSES for short, on February, 2018 for both the earthquake observation and geophysical research. As the data is available now, in this research we adopt the observed data from CSES. The basic information of this satellite is listed in Table 1. There are four consecutive shallow focus earthquakes in a short period in Indonesia during July to Augst, 2018, where Table 2 shows the detailed information about these four earthquakes, and figure 2 shows the specific locations of four epicenters on the map. As for the data sources, there are mainly three kinds of data. The first kind is the Ionospheric Electron density (Ne for short) from CSES satellite. Figure 3 shows the launch and flight status of CSES satellite where a total of 8 payloads concluded, and we adopted the electron density from Langmuir Probe PayloadIn this research. The second kind of data is Ne corresponding with the observed data from International Reference Ionosphere model 2016 (IRI 2016). The third kind is the global ionosphere map from CODE whose time resolution is 1 hour, spatial resolution is 2.5deg*5deg. We adopt these data to evaluate the reliability of the CSES satellite data. First, we used the following formula to calculate the percent disturbance of electron density from CSES satellite. After calculation, we found that there are mainly four significant anomalies on July 27, 31, August 07, and 14 respectively, shown as figure 3. Compared with the earthquake time listed in table 2, these four disturbances just happened before the four earthquakes, which maybe the seismic-ionospheric effect. And the red star in these figures represent the epicenter. After checking different kinds of space weather index, we can exclude that the disturbance is caused by space weather. As for the IRI 2016 model can be seen as the background data without any seismic factors, so we adopt the corresponding Ne from IRI model to evaluate the reliability of CSES data. From figure 4, it is clear the abnormal orbits in figure 3 also show the similar disturbance. As the orbit revisiting period is 5 days, figure 5 shows the comparison between the revisiting orbits of CSES on July 31 and August 14, the other two orbits go through the same location 5 or 10 days before. From this figure, the electron density shows obvious swelling on the abnormal days while the electron temperature shows the opposite trend. Then we used the grid data from CODE to calculate the disturbance about VTEC. Figure 6 (a) shows the percent disturbance of VTEC on August 1, 2018, from 5:00UT the abnormal around the epicenter is gradually increased, till 15:00UT the abnormal area disappeared. It is worth noting that the anomaly did not change with time, which means it is not triggered by sun activity. The percent disturbance of VTEC on Aug. 14, 2018 also shows the similar results from figure 6 (b). In the following research, we counted all the earthquakes that occurred in Indonesia over a 10-year period during 2007-2017 between 106.45 E-126.45 E and 8.3 S-1.7 N from USGS to check the anomalies of

©2019. Japan Geoscience Union. All Right Reserved. 

ionospheric vertical TEC from CODE. After selecting the earthquake accidents whose depth is less than 50km, and magnitude is greater than M5.8, there are a total of 35 earthquakes in the end, shown as figure 7. Figure 8 shows the statistical results of the count of TEC anomalies 15 days before and after these 35 earthquakes. It is obvious that 1-7 days before one earthquake in Indonesian region, the number of ionospheric parameter anomalies is more than other time.

Keywords: Seismic-ionospheric effect, Electron density, Total electron contents, CSES satellite

©2019. Japan Geoscience Union. All Right Reserved. 

# ROC curve analyses on the ionospheric TEC of M>=6.0 earthquakes in Japan during 1998-2015

*JANN-YENQ Liu[1], Yuh-Ing Chen[2], Pei-Jung Lee[1]

1. Center for Astronautical Physics and Engineering; Graduate Institute of Space Science, National Central University, Taiwan, 2. Graduate Institute of Statistics, National Central University, Taiwan

To verify the pre-earthquake ionospheric anomaly (PEIA), statistical analyses are implemented on the relationship between the total electron content (TEC) of global ionosphere map (GIM) and M>=6.0 earthquakes in Japan during 1998-2018. A median-based method together with z test is employed to find the criteria and/or characteristics of TEC anomalies related to earthquakes. It is found that the GIM TEC over the Japan significantly increases 1-3 days before the earthquakes. The receiver operating characteristic (ROC) curve is used to compare the TEC anomaly-based method with some competitive alternatives for predicting the earthquakes under study. We find, based on possible TEC anomalies, that the observed PEIAs are significantly earthquake-related. Moreover, the results of regression analyses show that the PEIA strength is associated with the magnitude of earthquakes.

Keywords: pre-earthquake ionospheric anomaly (PEIA), total electron content (TEC), earthquake, receiver operating characteristic (ROC)

©2019. Japan Geoscience Union. All Right Reserved. 

# FORMOSAT-5/AIP observes seismo-ionospheric precursors

*JANN-YENQ Liu[1], Chi-Kuang Chao[1]

1. Center for Astronautical Physics and Engineering; and Graduate Institute of Space Science, National Central University, TAIWAN

FORMOSAT-5 (F5) was launched at 18:51 UT (universal time) on 24 August 2017 with a sun-synchronous orbit at 720 km altitude and 98.28° inclination, which passes at almost the same local time everywhere in the daytime of about 10:30 LT and the nighttime of about 22:30 LT. It carries a primary payload, optical RSI (Remote Sensing Instrument), and a science payload, AIP (Advanced Ionospheric Probe), which are normally operating in the daytime and nighttime, respectively. The AIP mission is to monitor seismo-ionospheric precursors (SIPs) and observe ionospheric space weather. It is basically a multi-grid planar ion probe integrated with a planar Langmuir probe within a 10 cm ×10 cm aperture, which consists of Retarding Potential Analyzer (RPA), and Ion Drift Meter (IDM)/Ion Trap (IT) to maximize the total availability of ionospheric ion concentration (or density), ion velocities, and ion/electron temperatures at a sample rate up to 8192 Hz over a wide range of spatial scales in ionospheric plasma. The electroformed gold grids used has almost no hysteresis in sweeping current-voltage curves, and results in that the AIP can accurately probe plasma quantities in the ionosphere. The RPA and IDM/IT have been alternatively operating on every other orbit since end of October 2017. The RPA probes the ion density, while the IDM/IT derives the ion density and ion drift velocity. This paper combines in situ plasma measurements of F5/AIP and remote sensing of the TEC (total electron content) derived by ground-based GNSS (global navigation satellite system) receivers to three-dimensionally study SIPs of the 12 November 2017 M7.3 Iran-Iraq Border Earthquake and disturbances of ionospheric storms on 1 and 21 November 2017. The F5/AIP ion density is employed to confirm the SIP signatures and storm signatures being observed, while the F5/AIP ion velocity is employed to find electric fields associated with the SIPs and the ionospheric storms.

Keywords: FORMOSAT-5, AIP (Advanced Ionospheric Probe), seismo-ionospheric precursors

©2019. Japan Geoscience Union. All Right Reserved. 

[E] Oral | M (Multidisciplinary and Interdisciplinary)：M-IS Intersection

Thu. May 30, 2019 1:45 PM - 3:15 PM JST | Thu. May 30, 2019 4:45 AM - 6:15 AM UTC | 202 2F

## [M-IS06] Conservation of geoparks, natural geosites and cultural heritage: weathering process and damage assessment

convener:Chiaki T. Oguchi(Institute for Environmental Science and Technology, Graduate School of Science and Engineering, Saitama University), Tetsuya Waragai(Graduate School of Science and Engineering, Nihon University), Kuniyasu Mokudai(Tohoku Gakuin University), Magdalini Theodoridou(School of Engineering, Cardiff University), Chairperson:Tetsuya Waragai(日本大学大学院理工学研究科), Kuniyasu Mokudai(Japan Geoservicee)

Geoparks, world heritage sites, natural geosites and cultural heritage structures are considered important natural and/or cultural heritage properties. They have been exposed to weathering not only in geologic time frame but also in human time scale, thus rocks and geological materials are often facing deterioration. In order to preserve these sites conservation measures should be considered. Several studies have taken place on this topic involving a wide range of research fields, such as geomorphology, engineering geology, geoarchaeology, conservation science, geoconservation, materials science, petrophysics, geochemistry, geotechnical engineering etc. However, our knowledge on many aspects is still limited. The session welcomes contributions, presenting original research, discussions as well as case studies on documentation, measurement and monitoring techniques, experimental procedures, predictive models, damage assessment, etc. Papers from all research fields are invited dealing with the broad topic of geosites and cultural heritage.

1:45 PM - 2:00 PM JST | 4:45 AM - 5:00 AM UTC

[MIS06-01] Geopark's response to conservation of geosites from natural hazards

*Kuniyasu Mokudai[1], Shuichi Hasegawa[2] (1.Japan Geoservice Incorporated, 2.Kagawa Univ.)

2:00 PM - 2:15 PM JST | 5:00 AM - 5:15 AM UTC

[MIS06-02] Physical and mechanical properties for damage assesment of Taya Cave rocks, central Japan

*Chiaki T. Oguchi[1], Yurina Akimoto[2], Yasuhiko TAMURA[3], Kaisei Sakane[1] (1.Institute for Environmental Science and Technology, Graduate School of Science and Engineering, Saitama University, 2.Faculty of Engineering, Saitama University, 3.The Exective Committee for the Preservation of TAYA CAVERN)

2:15 PM - 2:30 PM JST | 5:15 AM - 5:30 AM UTC

[MIS06-03] Interdisciplinary approaches on conservation of underground geoheritage for community development of Taya Cave and its adjacent area

★Invited Papers

*Yasuhiko TAMURA[1,2], Chiaki T. Oguchi[4], Yuichi S. Hayakawa[5,2], Takuro Ogura[2], OGATA KEISUKE[6], Masashi MORITA[3] (1.The Executive Committee for the Preservation of TAYA CAVERN , 2.The University of Tokyo, Center for Spatial Information Science, 3.Yokohama National University, Institute of Urban Innovation, 4.Saitama University, Graduate School of Science and Engineering, 5.Hokkaido University, Faculty of Environmental Earth Science, 6.Tsurumi University, The Department of Cultural Properties)

2:30 PM - 2:45 PM JST | 5:30 AM - 5:45 AM UTC

[MIS06-04] Italian underground cultural heritage: from monitoring to enhancement

★Invited Papers

*Mario Parise[1], Tiziana Vitolo[2], Roberta Varriale[2] (1.Univ. Aldo Moro, Dept. Earth and Environmental Sciences, Bari, Italy, 2.CNR-ISSM, Italy)

2:45 PM - 3:00 PM JST | 5:45 AM - 6:00 AM UTC

[MIS06-05] Possibility of insolation weathering of sandstone blocks composing Angkor temples, Cambodia

*Tetsuya Waragai[1] (1.Graduate School of Science and Engineering, Nihon University)

3:00 PM - 3:15 PM JST | 6:00 AM - 6:15 AM UTC

[MIS06-06] **Durability evaluation of pyroclastic rocks used in the historical built environment of Hungary**

*Luigi Germinario[1,2], Ákos Török[1] (1.Budapest University of Technology and Economics, Hungary, 2.Saitama University, Japan)

# Geopark's response to conservation of geosites from natural hazards

*Kuniyasu Mokudai[1], Shuichi Hasegawa[2]

1. Japan Geoservice Incorporated, 2. Kagawa Univ.

Various natural hazards such as floods, slope failures, earthquake motions, etc. occur in the Japanese islands. Such natural hazards greatly affect the state of geosite. The Geopark performs activities in the event of a natural hazard, but its know-how has not accumulated. At Shikoku Seiyo Geopark, the Seiyo City needed to do disaster restoration work during the western Japan heavy rain in 2018. Therefore, it was difficult to transmit information and preserve the geosite as a geopark.

Keywords: geopark, geoconservation, natural hazard

©2019. Japan Geoscience Union. All Right Reserved. 

# Physical and mechanical properties for damage assesment of Taya Cave rocks, central Japan

*Chiaki T. Oguchi[1], Yurina Akimoto[2], Yasuhiko TAMURA[3], Kaisei Sakane[1]

1. Institute for Environmental Science and Technology, Graduate School of Science and Engineering, Saitama University, 2. Faculty of Engineering, Saitama University, 3. The Exective Committee for the Preservation of TAYA CAVERN

Taya cave, an artificial cave in a hill in south Yokohama, was excavated from the Kamakura period through the late Edo period. There are many sculptures and bas-reliefs on the surface of the cave wall made of soft rock which deposited in Pleistocene. Those sculptures has been suffering from weathering and deterioration, especially exfoliation of the wall and ceiling. In this study, for the purpose of conservation and restoration of sculptural murals, rock physical properties were investigated to assess the current situation. As a result, the possibility of surface exfoliation is considered to be affected by moisture difference, whereas the possibility of collapse of ceilings or floors between stairs becomes higher if too much water infiltrate.

Keywords: Phisical property, Mechanical property, Taya Cave

©2019. Japan Geoscience Union. All Right Reserved. 

# Interdisciplinary approaches on conservation of underground geoheritage for community development of Taya Cave and its adjacent area

*Yasuhiko TAMURA[1,2], Chiaki T. Oguchi[4], Yuichi S. Hayakawa[5,2], Takuro Ogura[2], OGATA KEISUKE[6], Masashi MORITA[3]

1. The Executive Committee for the Preservation of TAYA CAVERN , 2. The University of Tokyo, Center for Spatial Information Science, 3. Yokohama National University, Institute of Urban Innovation, 4. Saitama University, Graduate School of Science and Engineering, 5. Hokkaido University, Faculty of Environmental Earth Science, 6. Tsurumi University, The Department of Cultural Properties

TAYA Cave is an underground geoheritage locating in a Buddhism temple of Shingon sect, Josen-ji, south Yokohama, Japan. The cave is supposed to have its origin in the Kamakura period about 800 years ago, and then been used for religious trainings for priests. After opened to public in Edo era, a certain number of general people visited there. It was registered as a cultural property of Yokohama City in 1990. The cave originates in Kamakura period over 800 years ago. It was made by digging with human hands to shape a tunnel-like three-layer structure. More than 300 beautiful bas-reliefs are existed on the walls. However, those artifacts have been damaged due to deterioration or weathering. We are facing to urgent problem to preserve it to inherit in the future.
The authors have been trying to preserve this cave for four years. *The Executive Committee for the Preservation of Taya Cave* was established to make 3D digital data of this underground cultural property. In order to outline the approaches, three practical trials were carried out. The first one is dissemination of basic conditions of the cave from the viewpoints of earth science such as geology, geography and geotechnics to local people. Throughout of this activity, environmental characteristics of Taya Cave will be understood quantitatively. The second one is to understand regional culture and environment by interpreting regional history appearing on fundamental survey of bas-relief. The third one is to consider the possibilities of city planning with considering various regulations existed in the real society and environmental regulations. By comprehensively advancing these activities, urban rural area will be able to develop and gain vitality. The present study reports the results of these multidisciplinary practical trials carried out so far.

Keywords: Preservation of cultural property, underground heritage, multi-field joint basic survey, regional cooperation, Elementary school - University collaboration, TAYA Cave

©2019. Japan Geoscience Union. All Right Reserved.

©2019. Japan Geoscience Union. All Right Reserved. 

# Italian underground cultural heritage: from monitoring to enhancement

*Mario Parise[1], Tiziana Vitolo[2], Roberta Varriale[2]

1. Univ. Aldo Moro, Dept. Earth and Environmental Sciences, Bari, Italy, 2. CNR-ISSM, Italy

Italy is among the European countries with the highest number of artificial cavities, many of which represent a precious testimony of past civilizations and cultures, and of the continuous link between town development and the underground as well. The Italian underground has historically managed several environmental conflicts and social interactions, in both urban and rural settings. Nowadays the artificial cavities represent a significant segment within the local cultural heritage and have become in the last decades the object of strategic planning addressed towards their regeneration, valorization and public fruition. All these actions, however, need to be based on sound studies and researches aimed at evaluating the opportunity to open to the public sites that could potentially be unsafe. At this regard, monitoring plans and activities, and careful assessment of the susceptibility to failure and collapses, must be performed. Only after the stability conditions have been positively ascertained, underground sites might be considered for valorization, public visits and other activities.
In such a framework, we present in this contribution some case studies (including the underground tanks Cisternone in Formia, Latium, and Palombaro in Matera, Basilicata), also to describe their use at the time of realization, and to illustrate the related "sense of place". Environmental, social, historical and economic reconstructions have been carried out to generate and manage the knowledge of the places selected in order to facilitate their use and contribute to their development, in direct link with the cities where they are hosted. The methodology adopted aims at highlighting the cultural vitality and the identity of these places for the benefit of the local populations, and of tourists as well.

Keywords: artificial cavity, underground, stability, monitoring, enhancement

©2019. Japan Geoscience Union. All Right Reserved. 

# Possibility of insolation weathering of sandstone blocks composing Angkor temples, Cambodia

*Tetsuya Waragai[1]

1. Graduate School of Science and Engineering, Nihon University

Angkor temples such as Angkor Wat and Bayon temples built from 9$^{th}$ to 13$^{th}$ century are mainly composed of sandstone blocks. However, as a result of tree cutting that has been proceeded to protect the temples from rootwedging processes, most of temples are exposed to direct insolation. Possibility of insolation weathering of the sandstone blocks are pointed out, since the sandstone blocks can keep high temperature condition during daytime. Therefore, this study carried out field experiments that expose a sandstone cylindrical specimen in a dry season as a trial experiment using an acoustic emission (AE) method that may detect microcracks in the specimen by temperature changes. The experiment was carried out at the test site of Angkor Wat temple by measuring surface temperatures and AE signals of the specimen in December 2018. As the results, the surface temperatures of the specimen were 51.5 ˚C in maximum and 20.8 ˚C in minimum, and diurnal difference was 30.3 ˚C. In addition, the maximum elevation rate of the temperature was 1.50 ˚C/min and the minimum descending rate of the temperature was -1.88 ˚C/min. Although the surface temperature measurement could not synchronize to the AE measurement, an AE signal that is 40% bigger than ordinal value, was detected at the time of 0.43 ˚C/min of the elevation rate of temperature. This is though that sandstone blocks maybe deteriorate due to temperature changes by insolation.

Keywords: Angkor temples, sandstone, insolation weathering, acoustic emission

©2019. Japan Geoscience Union. All Right Reserved. 

# Durability evaluation of pyroclastic rocks used in the historical built environment of Hungary

*Luigi Germinario[1,2], Ákos Török[1]

1. Budapest University of Technology and Economics, Hungary, 2. Saitama University, Japan

Pyroclastic rocks of diverse composition have experienced a broad historical usage in the built environment of Hungary, especially from the Middle Ages. In the northern regions, for instance, acid ignimbrites have been widely used as building stones in monumental construction, e.g., churches and castles, Ottoman architectures like mosques and spas, as well as common dwellings. Their characterization reveals a small-scale inconstancy of their physico-mechanical performance and petrographic features, which affects weathering susceptibility. That involves most significantly porosity, pore-size distribution, and tensile strength, considering the technical properties; on the other hand, texture must be accounted for in terms of changing quantity and size of pumice clasts, phenocrysts, and crystals, and amount of the weak and porous groundmass. The behavior of the ignimbrites when subjected to artificial weathering, by freeze-thaw and salt attack tests, alters accordingly. The variability of open porosity represents the most important factor marking a possible dramatically diverse durability. It turns out to be proportional to water absorption, controlling the amount of infiltrating water or salt solutions, at the base of potential rock failure due to ice or salt crystallization. The sole high moisture may also lead to an extreme and hazardous deterioration of the mechanical properties. Finally, high porosity is correlated with low welding degree and, in turn, low strength. Such outcomes suggest criteria for evaluating the vulnerability of these volcanic rocks in cultural heritage, and directing reasonable material selections for stonework restorations.

Keywords: Stone decay, Freeze-thaw, Salt weathering, Petrophysical properties, Mechanical properties, Rhyolite tuff

©2019. Japan Geoscience Union. All Right Reserved. 

[E] Poster | M (Multidisciplinary and Interdisciplinary)：M-IS Intersection

Thu. May 30, 2019 3:30 PM - 5:00 PM JST | Thu. May 30, 2019 6:30 AM - 8:00 AM UTC | Poster Hall International Exhibition Hall8, Makuhari Messe_19

## [M-IS06] Conservation of geoparks, natural geosites and cultural heritage: weathering process and damage assessment

convener:Chiaki T. Oguchi(Institute for Environmental Science and Technology, Graduate School of Science and Engineering, Saitama University), Tetsuya Waragai(Graduate School of Science and Engineering, Nihon University), Kuniyasu Mokudai(Tohoku Gakuin University), Magdalini Theodoridou(School of Engineering, Cardiff University)

Geoparks, world heritage sites, natural geosites and cultural heritage structures are considered important natural and/or cultural heritage properties. They have been exposed to weathering not only in geologic time frame but also in human time scale, thus rocks and geological materials are often facing deterioration. In order to preserve these sites conservation measures should be considered. Several studies have taken place on this topic involving a wide range of research fields, such as geomorphology, engineering geology, geoarchaeology, conservation science, geoconservation, materials science, petrophysics, geochemistry, geotechnical engineering etc. However, our knowledge on many aspects is still limited. The session welcomes contributions, presenting original research, discussions as well as case studies on documentation, measurement and monitoring techniques, experimental procedures, predictive models, damage assessment, etc. Papers from all research fields are invited dealing with the broad topic of geosites and cultural heritage.

[MIS06-P01] The artistic qualities of religion reliefs in Taya-cave.Japan

*OGATA KEISUKE[1] (1.TSURUMI UNIVERSITY)

[MIS06-P02] Effect of stress concentration on the Weathering Mechanism of Sandstone Pillars of Angkor Wat, Cambodia by means of numerical simulation

*Takato Takemura[1], Tetsuya Waragai[2] (1.Nihon Univ., 2.Nihon University)

[MIS06-P03] Meaning to preserve evidence of large scale landslide

*Kuniyasu Mokudai[1], Hidekazu Sato[2] (1.Japan Geoservice Incorporated, 2.Mt. Kurikoma Area Geopark)

# The artistic qualities of religion reliefs in Taya-cave.Japan

*OGATA KEISUKE[1]

1. TSURUMI UNIVERSITY

The Yaya-csve is located within the Jōsenji-Temle in Taya Town,Sakae ward,Yokohama-shi,Kanagawa Prefecture.The cave is called “Yuga-dou”,which is thought to be the present form in the Edo period, when the Kamakura period entered monks drills as a training ground. As for the religious relief carved in the cave, it is presumed from the record of “Koukoku-chishi” that it was produced for about 20years from 1842 to1862. In addition, “Sekiguchi diary” contains articles on visiting caves in 1859.

Subjects of reliefs are divided into the following areas in order of the route, and about 300 are engraved over 250 meters in total length.

First area:A and Un lions, Up and Doun dragon, Gold wing bird. Ceiling family crest.

Second area:Zodiac image. Ceiling three bats.

Third area:Chichibu 33 Kannon sacred place. Karyou-binga.

Fourth area:Asahina-benzaiten.

Fifth area:Saigoku 33 Kannon sacred place.

Sixth area:Sone Tenman-gū shrine and Takasago pine.

Seventh area:Yakuyoke Kobō-daishi master.

Eighth area:Taizōkai-shugi-mandala. Ceiling crane hemp leaf pattern.

Ninth area:Ichigan Kobō-daishi master. Shikoku 88 sacred place.

Tenth area:Shikoku 88 sacred place. 49in-shugi-mandala. Four Gorin tower.

Eleventh area:Godai-myouou.

Twelfth area:Water Kobō-daishi master. Sadasan one Turtle. Kouya-san Ishidoumaru. Unchū-kuyou bodhisattva.

Thirteenth area:18Rakan.

Fourteenth area:Iwaya-Fudou.

Fifteenth area:Bandou 33 Kannon sacred place.

Regrading the style, religious subjecks such as the Saigoku, bandou, Chichibu 33 Kannon sacred place,

©2019. Japan Geoscience Union. All Right Reserved. 

Shikoku 88 sacred place and shugi-mandala are also perfunctory aspects, but “Sone Tenman-gū shrine and Takasago pine” and “Sadasan one Turtle” and 18-Rakan etc are the sculptures with high artistic and strong paintertly elements.

The faith in the 18th century was diverse, especially the common people went around the whole countey sacred place. Also for each of those who can not visit the sacred place a mini sacred place of each sacred place was established in various places. The Taya-cave near the Tokaido must also have collected the faith of the common people as a mini sacred place.

Taya-cave is currently designated as a registered cultural property of Yokohama City as a historic site in 1990. However, due to years of deterioration, it is becoming difficult to preserve and maintain the current situation. Therefore, in 2017 the Taya-cave preservation execution committee was established, we aim to conduct a basic survey in each department of cultural property, engineering and environmental studies, revalidate its value, preserve it as VR digital data in the future, to make it public and utilize.
In 2018, under the auspices of the Japan Society for the Promotion of Science(JSPS), collaborative research with the Italian ISSM/CNR Laboratory began, and in 2019 the research was continued with the subsidy of the Asahi Shimbun Cultural Foundation.

Keywords: History of Jōsenji-Temle and Taya-cave., On the time of religion haut-reliefs prodactionin in Taya-cave., Types and artistic religious reliefs in Taya-cave., From of common people’s belief in Japan in the 18th century., Preservation of Taya-cave and its future use.

©2019. Japan Geoscience Union. All Right Reserved. 

# Effect of stress concentration on the Weathering Mechanism of Sandstone Pillars of Angkor Wat, Cambodia by means of numerical simulation

*Takato Takemura[1], Tetsuya Waragai[2]

1. Nihon Univ., 2. Nihon University

Since Angkor Wat is located in a tropical monsoon climate, the sandstone building materials are strongly affected by weathering related to high temperatures, heavy rainfall and intense solar radiation. Weathering damage can be observed on a number of pillars, however, the outer pillars exhibit little weathering damage compared to the inner pillars, even though the outer pillars are more exposed to the rain and sunlight than the inner pillars. To understand the effect of stress concentration on the weathering sandstone pillars, we carried out the measurement of the degree of weathering damage of pillars, in-situ measurement of humidity and temperature change near the pillar and the numerical simulation for structural analysis.As a result, the weathering damage is not necessarily only due to the wetting-drying cycle. Since relatively large compressive stress is applied to the base of the inner pillar where the weathering damage is large, therefore, the weathering rate could be accelerated by the compressive stress concentration.

Keywords: Angkor Wat, Stress concentration

©2019. Japan Geoscience Union. All Right Reserved. 

# Meaning to preserve evidence of large scale landslide

*Kuniyasu Mokudai[1], Hidekazu Sato[2]

1. Japan Geoservice Incorporated, 2. Mt. Kurikoma Area Geopark

There are many mountainous area in Japanese islands. In mountainous area, many natural hazards occured. Visualization of landslide is necessary in order to understand the slope process in the mountains to non-experts. At Mt. Kurikoma Mountain area Geopark, we have been engaged in conservation of large-scale landslide landform, education and information dissemination activities. In order to preserve the landslide phenomenon which is the cause of the slope disaster, a scientific understanding of the landform is necessary. Furthermore, it is necessary to restructure the view of nature of the concerned parties.

Keywords: large scale landslide, geopark, geoconservation

©2019. Japan Geoscience Union. All Right Reserved. 

[E] Poster | M (Multidisciplinary and Interdisciplinary)：M-IS Intersection

Thu. May 30, 2019 5:15 PM - 6:30 PM JST | Thu. May 30, 2019 8:15 AM - 9:30 AM UTC | Poster Hall International Exhibition Hall8, Makuhari Messe_36

## [M-IS06] Conservation of geoparks, natural geosites and cultural heritage: weathering process and damage assessment

convener:Chiaki T. Oguchi(Institute for Environmental Science and Technology, Graduate School of Science and Engineering, Saitama University), Tetsuya Waragai(Graduate School of Science and Engineering, Nihon University), Kuniyasu Mokudai(Tohoku Gakuin University), Magdalini Theodoridou(School of Engineering, Cardiff University)

Geoparks, world heritage sites, natural geosites and cultural heritage structures are considered important natural and/or cultural heritage properties. They have been exposed to weathering not only in geologic time frame but also in human time scale, thus rocks and geological materials are often facing deterioration. In order to preserve these sites conservation measures should be considered. Several studies have taken place on this topic involving a wide range of research fields, such as geomorphology, engineering geology, geoarchaeology, conservation science, geoconservation, materials science, petrophysics, geochemistry, geotechnical engineering etc. However, our knowledge on many aspects is still limited. The session welcomes contributions, presenting original research, discussions as well as case studies on documentation, measurement and monitoring techniques, experimental procedures, predictive models, damage assessment, etc. Papers from all research fields are invited dealing with the broad topic of geosites and cultural heritage.

[MIS06-P01] The artistic qualities of religion reliefs in Taya-cave.Japan

*OGATA KEISUKE[1] (1.TSURUMI UNIVERSITY)

[MIS06-P02] Effect of stress concentration on the Weathering Mechanism of Sandstone Pillars of Angkor Wat, Cambodia by means of numerical simulation

*Takato Takemura[1], Tetsuya Waragai[2] (1.Nihon Univ., 2.Nihon University)

[MIS06-P03] Meaning to preserve evidence of large scale landslide

*Kuniyasu Mokudai[1], Hidekazu Sato[2] (1.Japan Geoservice Incorporated, 2.Mt. Kurikoma Area Geopark)

# The artistic qualities of religion reliefs in Taya-cave.Japan

*OGATA KEISUKE[1]

1. TSURUMI UNIVERSITY

The Yaya-csve is located within the Jōsenji-Temle in Taya Town,Sakae ward,Yokohama-shi,Kanagawa Prefecture.The cave is called “Yuga-dou”,which is thought to be the present form in the Edo period, when the Kamakura period entered monks drills as a training ground. As for the religious relief carved in the cave, it is presumed from the record of “Koukoku-chishi” that it was produced for about 20years from 1842 to1862. In addition, “Sekiguchi diary” contains articles on visiting caves in 1859.

Subjects of reliefs are divided into the following areas in order of the route, and about 300 are engraved over 250 meters in total length.

First area:A and Un lions, Up and Doun dragon, Gold wing bird. Ceiling family crest.

Second area:Zodiac image. Ceiling three bats.

Third area:Chichibu 33 Kannon sacred place. Karyou-binga.

Fourth area:Asahina-benzaiten.

Fifth area:Saigoku 33 Kannon sacred place.

Sixth area:Sone Tenman-gū shrine and Takasago pine.

Seventh area:Yakuyoke Kobō-daishi master.

Eighth area:Taizōkai-shugi-mandala. Ceiling crane hemp leaf pattern.

Ninth area:Ichigan Kobō-daishi master. Shikoku 88 sacred place.

Tenth area:Shikoku 88 sacred place. 49in-shugi-mandala. Four Gorin tower.

Eleventh area:Godai-myouou.

Twelfth area:Water Kobō-daishi master. Sadasan one Turtle. Kouya-san Ishidoumaru. Unchū-kuyou bodhisattva.

Thirteenth area:18Rakan.

Fourteenth area:Iwaya-Fudou.

Fifteenth area:Bandou 33 Kannon sacred place.

Regrading the style, religious subjecks such as the Saigoku, bandou, Chichibu 33 Kannon sacred place,

©2019. Japan Geoscience Union. All Right Reserved. 

Shikoku 88 sacred place and shugi-mandala are also perfunctory aspects, but “Sone Tenman-gū shrine and Takasago pine” and “Sadasan one Turtle” and 18-Rakan etc are the sculptures with high artistic and strong paintertly elements.

The faith in the 18th century was diverse, especially the common people went around the whole countey sacred place. Also for each of those who can not visit the sacred place a mini sacred place of each sacred place was established in various places. The Taya-cave near the Tokaido must also have collected the faith of the common people as a mini sacred place.

Taya-cave is currently designated as a registered cultural property of Yokohama City as a historic site in 1990. However, due to years of deterioration, it is becoming difficult to preserve and maintain the current situation. Therefore, in 2017 the Taya-cave preservation execution committee was established, we aim to conduct a basic survey in each department of cultural property, engineering and environmental studies, revalidate its value, preserve it as VR digital data in the future, to make it public and utilize.
In 2018, under the auspices of the Japan Society for the Promotion of Science(JSPS), collaborative research with the Italian ISSM/CNR Laboratory began, and in 2019 the research was continued with the subsidy of the Asahi Shimbun Cultural Foundation.

Keywords: History of Jōsenji-Temle and Taya-cave., On the time of religion haut-reliefs prodactionin in Taya-cave., Types and artistic religious reliefs in Taya-cave., From of common people’s belief in Japan in the 18th century., Preservation of Taya-cave and its future use.

©2019. Japan Geoscience Union. All Right Reserved. 

# Effect of stress concentration on the Weathering Mechanism of Sandstone Pillars of Angkor Wat, Cambodia by means of numerical simulation

*Takato Takemura[1], Tetsuya Waragai[2]

1. Nihon Univ., 2. Nihon University

Since Angkor Wat is located in a tropical monsoon climate, the sandstone building materials are strongly affected by weathering related to high temperatures, heavy rainfall and intense solar radiation. Weathering damage can be observed on a number of pillars, however, the outer pillars exhibit little weathering damage compared to the inner pillars, even though the outer pillars are more exposed to the rain and sunlight than the inner pillars. To understand the effect of stress concentration on the weathering sandstone pillars, we carried out the measurement of the degree of weathering damage of pillars, in-situ measurement of humidity and temperature change near the pillar and the numerical simulation for structural analysis.As a result, the weathering damage is not necessarily only due to the wetting-drying cycle. Since relatively large compressive stress is applied to the base of the inner pillar where the weathering damage is large, therefore, the weathering rate could be accelerated by the compressive stress concentration.

Keywords: Angkor Wat, Stress concentration

©2019. Japan Geoscience Union. All Right Reserved. 

# Meaning to preserve evidence of large scale landslide

*Kuniyasu Mokudai[1], Hidekazu Sato[2]

1. Japan Geoservice Incorporated, 2. Mt. Kurikoma Area Geopark

There are many mountainous area in Japanese islands. In mountainous area, many natural hazards occured. Visualization of landslide is necessary in order to understand the slope process in the mountains to non-experts. At Mt. Kurikoma Mountain area Geopark, we have been engaged in conservation of large-scale landslide landform, education and information dissemination activities. In order to preserve the landslide phenomenon which is the cause of the slope disaster, a scientific understanding of the landform is necessary. Furthermore, it is necessary to restructure the view of nature of the concerned parties.

Keywords: large scale landslide, geopark, geoconservation

©2019. Japan Geoscience Union. All Right Reserved. 

[E] Oral | M (Multidisciplinary and Interdisciplinary)：M-IS Intersection

Thu. May 30, 2019 9:00 AM - 10:30 AM JST | Thu. May 30, 2019 12:00 AM - 1:30 AM UTC | 201A 2F

## [M-IS07] Astrobiology

convener:Hikaru Yabuta(Hiroshima University, Department of Earth and Planetary Systems Science), Seiji Sugita(Department of Earth and Planetary Science, Graduate School of Science Sciece, The University of Tokyo), Misato Fukagawa(National Astronomical Observatory of Japan), Fujishima Kosuke(Tokyo Institute of Technology, Earth-Life Science Institute), Chairperson:Hikaru Yabuta(Hiroshima University), Seiji Sugita(東京大学大学院 理学系研究科), Misato Fukagawa(名古屋大学大学院 理学研究科), Kosuke Fujishima(ELSI 地球生命研究所)

Twenty years have passed since when the field of Astrobiology, which aims to unveil the origins, evolution, and habitability of life by integrating multidisciplinary fields, was established. Individual themes related to Astrobiology, such as chemical evolution in the early Solar System, formation of planetary system, prebiotic chemistry in the early Earth, evolution of life in the Earth's history, extremophile, and habitable planetary environments, has been studied by the knowledge and methods from the multiple fields, which has enabled us to explain "Where we came from" in some ways. However, despite an overwhelming number of investigations and discussions through gathering of the scientists from different fields, there has remained the long-standing unsolved question: How did abiotic materials gain biological function in the Earth and elsewhere in universe? There is still a large gap between prebiotic organic chemistry and biochemistry toward Origins of Life and planetary habitability. Therefore, the JpGU Astrobiology session focuses on pathfinding of "integration of astronomy, geoscience, and biochemistry", which will face an increasing need for the future Astrobiology. In order to enhance our understanding of "What is life", we propose to discuss the biochemical events linked with planetary systems, which is beyond the knowledge in a test tube, by an integration of exoplanets and molecular biology, etc. Through this approach, we will lead the discussions and developments of life-detection strategies for the future exploration of life in universe.

9:00 AM - 9:20 AM JST | 12:00 AM - 12:20 AM UTC

[MIS07-06] How to find and characterize nearby habitable exoplanets

★Invited Papers

*Norio Narita[1] (1.Astrobiology Center)

9:20 AM - 9:40 AM JST | 12:20 AM - 12:40 AM UTC

[MIS07-07] **Organic Matter Preserved in Mudstones of a 3-Billion-Year-Old Lake Deposit in Gale Crater, Mars**

★Invited Papers

*Jennifer L Eigenbrode[1], Roger E Summons[2], Andrew Steele[3], Caroline Freissinet[4], Maëva Millan[5], Rafael Navarro-González[6], Paul Mahaffy[1] (1.NASA Goddard Space Flight Center, 2.Massachusetts Institute of Technology, 3.Carnegie Institution of Washington, 4.Institut Pierre Simon Laplace, CNRS, 5.Georgetown University, 6.Universidad Nacional Autónoma de México)

9:40 AM - 9:55 AM JST | 12:40 AM - 12:55 AM UTC

[MIS07-08] **The third year sample return of Tanpopo: Capture and Exposure Experiment of Micrometeorite and Microbes on Exposure Facility of International Space Station**

*Akihiko Yamagishi[1], Hirofumi Hashimoto[2], Hajime Yano[2], Shin-ichi Yokobori[3], Kensei Kobayashi[4], Hajime Mita[5], Hikaru Yabuta[6], Masumi Higashide[7], Makoto Tabata[8], Hideyuki Kawai[8], Eiichi Imai[9] (1.Tokyo University of Pharmacy and Life Science, Department of Molecular Biology, 2.ISAS/JAXA, Sagamihara, Japan, 3.Tokyo University of Pharmacy and Life Science, Tokyo, Japan, 4.Yokohama National University, Yokohama, Japan, 5.Fukuoka Institute of Technology, Fukuoka, Japan, 6.Hiroshima University, Hirosima, Japan, 7.Japan Aerospace Exploration Agency (JAXA), Tokyo, Japan, 8.Chiba University, Chiba, Japan, 9.Nagaoka University of Technology, Nagaoka, Japan)

9:55 AM - 10:10 AM JST | 12:55 AM - 1:10 AM UTC

[MIS07-09] Theoretical search for photosynthetic pigments applicable around low temperature stars: Modulation of physical-chemical properties by central metals

*Yu Komatsu[1,2], Kenji Takizawa[1,3] (1.Astrobiology Center, 2.National Astronomical Observatory of Japan, 3.National Institute for Basic Biology)

10:10 AM - 10:25 AM JST | 1:10 AM - 1:25 AM UTC

[MIS07-10] Effects of the formation of hydrocarbon aerosols on the climate stability of Earth-like planets and their habitability

*Yasuto Watanabe[1], Eiichi Tajika[1], Kazumi Ozaki[2], Peng Hong[3] (1.The University of Tokyo, 2.Toho University, 3.Chiba Institute of Technology)

10:25 AM - 10:30 AM JST | 1:25 AM - 1:30 AM UTC

Discussion

# How to find and characterize nearby habitable exoplanets

*Norio Narita[1]

1. Astrobiology Center

In this review, I will summarize previous and ongoing efforts to find habitable exoplanets in the vicinity of the Solar system and future prospects to characterize such planets with next generation telescopes and instruments. In addition, I will talk about the importance and some examples of interdisciplinary studies of astrobiology to consider future missions.

Keywords: Exoplanets, Astrobiology

©2019. Japan Geoscience Union. All Right Reserved. 

# Organic Matter Preserved in Mudstones of a 3-Billion-Year-Old Lake Deposit in Gale Crater, Mars

*Jennifer L Eigenbrode[1], Roger E Summons[2], Andrew Steele[3], Caroline Freissinet[4], Maëva Millan[5], Rafael Navarro-González[6], Paul Mahaffy[1]

1. NASA Goddard Space Flight Center, 2. Massachusetts Institute of Technology, 3. Carnegie Institution of Washington, 4. Institut Pierre Simon Laplace, CNRS, 5. Georgetown University, 6. Universidad Nacional Autónoma de México

*In situ* analyses of lake-deposited mudstones of the Murray formation at Pahrump Hills, Gale crater, Mars show the presence of aliphatic, aromatic, and sulfur-bearing organic gases upon heating to 500-860˚C, as detected by the Sample Analysis at Mars (SAM) instrument suite on the Mars Science Laboratory's (MSL's) Curiosity rover. Organic-sulfur compounds, including thiophenes, dimethylsulfide and thiols were identified by gas chromatography-mass spectrometry (GCMS) and observed in evolved gas analyses (EGA). Other aromatic and aliphatic hydrocarbon components were also indicated by EGA. The distributions of organic molecules observed were specific to samples and cannot be from SAM's instrument background. The temperatures these organic volatiles were released is consistent with the pyrolytic cleavage of organic fragments from large molecules (macromolecules) indigenous to the mudstones. Some portion may also be derived from the thermal release of organics entrained within minerals.

The release of organic-sulfur compounds occurs at high temperatures in the SAM oven; thus, these compounds are most likely derived from sulfurized organics in the sediments and are not an artifact of sulfurization reactions in the oven. On Earth, sulfurization is a key process that facilitates organic matter preservation over geological time-scales by transforming individual organic molecules into recalcitrant macromolecules. Organic matter at the base of the Murray formation probably underwent sulfurization prior to deposition or during early diagenesis. Multiple factors likely contribute to the organic preservation in the Gale crater mudstones, however, sulfurization may be largely responsible for the greater abundance and the molecular diversity observed in the lower Murray formation.

Keywords: Mars, organic matter, lacustrine, Curiosity rover, Mars Science Laboratory (MSL) mission, Sample Analysis at Mars (SAM)

©2019. Japan Geoscience Union. All Right Reserved. 

# The third year sample return of Tanpopo: Capture and Exposure Experiment of Micrometeorite and Microbes on Exposure Facility of International Space Station

*Akihiko Yamagishi[1], Hirofumi Hashimoto[2], Hajime Yano[2], Shin-ichi Yokobori[3], Kensei Kobayashi[4], Hajime Mita[5], Hikaru Yabuta[6], Masumi Higashide[7], Makoto Tabata[8], Hideyuki Kawai[8], Eiichi Imai[9]

1. Tokyo University of Pharmacy and Life Science, Department of Molecular Biology, 2. ISAS/JAXA, Sagamihara, Japan, 3. Tokyo University of Pharmacy and Life Science, Tokyo, Japan, 4. Yokohama National University, Yokohama, Japan, 5. Fukuoka Institute of Technology, Fukuoka, Japan, 6. Hiroshima University, Hirosima, Japan, 7. Japan Aerospace Exploration Agency (JAXA), Tokyo, Japan, 8. Chiba University, Chiba, Japan, 9. Nagaoka University of Technology, Nagaoka, Japan

### Purpose of Tanpopo mission

Tanpopo, a dandelion in Japanese, is a plant species whose seeds with floss are spread by wind. We proposed this mission to examine possible interplanetary migration of microbes, and organic compounds at the Exposure Facility of Japan Experimental Module (JEM: KIBO) of the International Space Station (ISS).
We are testing the panspermia hypothesis, which proposes the interplanetary transfer of life. We are also testing if the organic compound may be transferred from space before the origin of life on the earth.
The Tanpopo mission consists of six subthemes: Capture of microbes in space (Subtheme 1), exposure of microbes in space (Subtheme 2), analysis of organic compounds in interplanetary dust (Subtheme 3), exposure of organic compounds in space (Subtheme 4), measurement of space debris at the ISS orbit (Subtheme 5), and evaluation of ultra low-density aerogel developed for the Tanpopo mission (Subtheme 6).

### Apparatus developed for Tanpopo mission

We have developed two types of apparatus used for Tanpopo mission: Capture Panels for aerogel to capture micro-particles and Exposure Panels for exposure of microbes and organic materials.
Each Capture Panel contains a silica aerogel block in an aluminum mesh container. Silica aerogel, which is the lowest density solid material, is used to capture micro particles, which may include, micrometeorite, artificial space debris and earth-originated natural particles. We are going to analyze if the particles contain terrestrial microbial cells or not, and if the micrometeorite contains organic compounds or not.
Exposure Panels have been developed to expose microbes and organic compounds to the space environment. Several microbial species including, *Deinococcus radiodurans, Deinococcus aerius, Deinococcus aetherius, Nostoc sp., Schizosaccharomyces pombe,* have been exposed to the space environment. These species are expected to be resistant against space environment, vacuum, desiccation, temperature-cycle, UV and ionization radiation. We have tested the survival of these species after one-, two- and three-year exposure in space. Organic compound such as amino acids and the precursors have also been exposed.

### Schedule of Tanpopo mission

Tanpopo apparatus was launched in April 2015. The Panels were placed on the Exposed Experiment Handrail Attachment Mechanism (ExHAM) in the ISS. The ExHAM with Panels were placed on the Exposure Facility of KIBO (JEM) with the Japanese robotic arms through the airlock of KIBO in May 2015.
The first set of Capture Panels and an Exposure Panel were retrieved in June 2016, contained in plastic

©2019. Japan Geoscience Union. All Right Reserved. 

bags, and stored in the pressurized area of the International Space Station. They have returned to the ground in the space capsule, and returned to JAXA in September 2016. The second set of Capture Panels and an Exposure Panel were detached in July 2017 and returned to JAXA in October 2017. The third set were detached in June 2018, the Exposure Panel and the Capture Panels were returned to JAXA in September 2018 and in February 2019, respectively.
Exposure Panel was separated into Exposure Units, each harboring either microbe or organic compound was handed over to the scientist in charge of each microbe or organic compound. Some of the Units are dedicated to the UV or radiation dose measurement.
Each aerogel block of each Capture Panel was examined for the particles captured and the tracks made upon the impact, which were extracted from the aerogel block and handed over to the scientists. The analysis includes, fluorescence microscopic inspection to test if there are microbial cells or not. Particles and tracks will be used for the mineral analysis as well as the analysis of organic compounds.
The first report has been published and the following results will be reported.
**References:** 1) A. Yamagishi, et al. “TANPOPO: astrobiology exposure and micrometeoroid capture experiments.” International Symposium on Space Technology and Science (ISTS) Web Paper Archives. 2008-k-05 , 2008. 2) Y. Kawaguchi, et a. “Investigation of the interplanetary transfer of microbes in the Tanpopo mission at the Exposed Facility of the International Space Station,” *Astrobiolgy* Vol. 16, pp. 1-14, 2016 .
3) A. Yamagishi, et al. Environmental data and survival data of *Deinococcus aetherius* from the Exposure Facility of the Japan Experimental Module of the International Space Station obtained by the Tanpopo Mission. *Astrobiology* Vol. 18, pp. 1369-1374., 2018.

Keywords: Micrometeotite, Microbes, Organics, Debris, Aerogel

©2019. Japan Geoscience Union. All Right Reserved. 

# Theoretical search for photosynthetic pigments applicable around low temperature stars: Modulation of physical-chemical properties by central metals

*Yu Komatsu[1,2], Kenji Takizawa[1,3]

1. Astrobiology Center, 2. National Astronomical Observatory of Japan, 3. National Institute for Basic Biology

A lot of extrasolar planets have been discovered in the habitable zone, and the number of samples will be increasing in future. In order to discover planets which harbour lives, it will be a significant achievement to identify potential biosignatures, which are traces of life from planetary spectra. Gaseous molecules such as oxygen and ozone and spectral features in surface vegetation called as "vegetation red edge (VRE)" are considered as biosignatures. In current observations, planets around M dwarfs, lower temperature stars than the Sun, have been focused, and there are large uncertainties in how assumed photosynthetic organisms evolve in the planets and how they would exhibit spectral features. Recently, it has been shown that the Earth-type photosynthesis can be evolved even around M dwarfs, considered lighting conditions in shallow water and how phototrophs can adapt to it (Takizawa, K., et al.: 2017, *Scientific Reports*, **7**, 7561). Moreover, an interesting example has been discovered that a cyanobacteria, which are categorized into oxygenic photosynthetic bacteria, becomes to utilize longer wavelength radiation for photochemistry than previously known, after grown under near infrared light, 750 nm (Nürnberg, D. J. et al.: 2018, *Science*, **360**, 1210.). Accumulating such knowledges and benchmarks from various points of view would lead to implications for future observations.

We investigate thoroughly by quantum chemical calculations the properties of photosynthetic pigments like and artificial pigments which might form on early Earth or other planets to unravel the red limit of the pigment. Photosynthetic pigments play a central role to convert available light energies into chemical energies. Chlorophyll has a tetrapyrrole ring with a metal ion such as Mg in the center of the ring. The ring structure can encapsulate a variety of metals to have a modulation of physical-chemical properties. Starting with the tetrapyrrole, we search for the pigments which are applicable around M dwarfs by calculating their basic structures, functional groups, central metals and solvents to determine the absorption wavelength and other properties. At first, we focused on the role of the central metal. Metals *M={H2, Mg, Ca, Ni, Cu, Zn, Sr, Cd, Hg, Pb, ...}* are put in the center of rings and are evaluated. According to our calculations, the wavelength of the first excited state is slight long in *M=Ni* in chlorophylls *a* and *b* and bacteriochlorophylls *a* and *b*. Additionally, binding eneries for metals into the rings in solvent conditions, molecular orbitals and reactivities (ionization potential and electron affinity) are analyzed for each pigment.

Keywords: Extrasolar planet, Biosignatures, Photosynthesis, Quantum Chemistry

©2019. Japan Geoscience Union. All Right Reserved. 

# Effects of the formation of hydrocarbon aerosols on the climate stability of Earth-like planets and their habitability

*Yasuto Watanabe[1], Eiichi Tajika[1], Kazumi Ozaki[2], Peng Hong[3]

1. The University of Tokyo, 2. Toho University, 3. Chiba Institute of Technology

It is known that the haze particles composed of hydrocarbons can form in an anoxic atmosphere in which the $CH_4/CO_2$ ratio exceeds the critical level (~0.2), as observed in Titan's atmosphere. The haze particles have characteristic optical properties that could affect the planetary climate as discussed in the context of the anoxic early Earth before the rise of atmospheric oxygen owing to the activity of oxygen-producing photosynthetic bacteria. Under low $pO_2$ condition, $CO_2$ and $CH_4$ can be photochemically broken up to form CO, and the excess CO reacts with OH radical to form $CO_2$. If primitive anaerobic microbial ecosystem exists on the Earth-like planet as in the early Earth, it can also affect the balance between $CO_2$, $CH_4$, and CO. Primitive marine microbial ecosystem may produce $CH_4$ to the atmosphere-ocean system via methanogenesis. The primitive microbial ecosystem consumes $CO_2$ from the atmosphere-ocean system via anoxygenic photosynthesis, but it also provides $CO_2$ via decomposition of organic matters and methanogenesis, and/or other abiotic processes. This implies that the balance between $CO_2$, $CH_4$, and CO in the early Earth must have been significantly different from that at present. Photochemical reactions and biological processes in the ocean may affect the stability of the planetary climate through the formation of the haze particles.

Here we developed a coupled atmospheric photochemistry-marine microbial ecosystem-global carbon cycle model to explore how the atmospheric photochemistry and the primitive marine microbial ecosystem can affect the carbon cycle and $CO_2$ budget on the Earth-like planet. We found that when the primitive biosphere produces large $CH_4$ flux (~$10^{11}$ $cm^{-2}$ $s^{-1}$), OH radicals should be consumed in the lower atmosphere through the reaction with $CH_4$. As a result, the reaction between CO and OH, which produces $CO_2$, cannot compensate the photolysis of $CO_2$ in the upper atmosphere. This means that photochemical reactions may work as a net $CO_2$ consumption process in the atmosphere-ocean system. The excess CO in the atmosphere is considered to have been converted to $CO_2$ and $CH_4$ through the CO-using chemosynthesis and methanogenesis in the oceans on the early Earth. Therefore, marine microbial reactions can work as a net $CO_2$ production process in the atmosphere-ocean system. We also found that, when the $CO_2$ level is so low that the hydrocarbon haze can form, the photochemical net consumption of $CO_2$ exceeds the biospheric net production. In this case, $CO_2$ is removed from the atmosphere-ocean system as the haze particle. As a result, the climate with the hydrocarbon haze should be unstable, and the climate is expected to change to the snowball state with low $pCO_2$ or to the hot climate state (> ~310 K on the $CO_2$ degassing rate of the present Earth) with high $pCO_2$ and $pCH_4$ on the planets with anoxic environment and primitive microbial ecosystem in the ocean.

Our result would put a theoretical constraint on the existence of life on extrasolar Earth-like planets and their habitability.

Keywords: Habitability, Climate stability

©2019. Japan Geoscience Union. All Right Reserved. 

[E] Oral | M (Multidisciplinary and Interdisciplinary)：M-IS Intersection

Thu. May 30, 2019 10:45 AM - 12:15 PM JST | Thu. May 30, 2019 1:45 AM - 3:15 AM UTC | 201A 2F

## [M-IS07] Astrobiology

convener:Hikaru Yabuta(Hiroshima University, Department of Earth and Planetary Systems Science), Seiji Sugita(Department of Earth and Planetary Science, Graduate School of Science Sciece, The University of Tokyo), Misato Fukagawa(National Astronomical Observatory of Japan), Fujishima Kosuke(Tokyo Institute of Technology, Earth-Life Science Institute), Chairperson:Kosuke Fujishima(ELSI 地球生命研究所), Misato Fukagawa(名古屋大学大学院 理学研究科), Seiji Sugita(東京大学大学院 理学系研究科), Hikaru Yabuta(Hiroshima University)

Twenty years have passed since when the field of Astrobiology, which aims to unveil the origins, evolution, and habitability of life by integrating multidisciplinary fields, was established. Individual themes related to Astrobiology, such as chemical evolution in the early Solar System, formation of planetary system, prebiotic chemistry in the early Earth, evolution of life in the Earth's history, extremophile, and habitable planetary environments, has been studied by the knowledge and methods from the multiple fields, which has enabled us to explain "Where we came from" in some ways. However, despite an overwhelming number of investigations and discussions through gathering of the scientists from different fields, there has remained the long-standing unsolved question: How did abiotic materials gain biological function in the Earth and elsewhere in universe? There is still a large gap between prebiotic organic chemistry and biochemistry toward Origins of Life and planetary habitability. Therefore, the JpGU Astrobiology session focuses on pathfinding of "integration of astronomy, geoscience, and biochemistry", which will face an increasing need for the future Astrobiology. In order to enhance our understanding of "What is life", we propose to discuss the biochemical events linked with planetary systems, which is beyond the knowledge in a test tube, by an integration of exoplanets and molecular biology, etc. Through this approach, we will lead the discussions and developments of life-detection strategies for the future exploration of life in universe.

10:45 AM - 11:05 AM JST | 1:45 AM - 2:05 AM UTC

### [MIS07-11] the emergence of iron-sulfur protometabolism

★Invited Papers

*Sheref Mansy[1] (1.University of Trento)

11:05 AM - 11:25 AM JST | 2:05 AM - 2:25 AM UTC

### [MIS07-12] Life-water-mineral interactions and their products

★Invited Papers

*Fumito Shiraishi[1] (1.Hiroshima University)

11:25 AM - 11:40 AM JST | 2:25 AM - 2:40 AM UTC

### [MIS07-13] How much can we learn about ancient cells from sequence analysis? New metrics on an old problem.

*Shawn E McGlynn[1], Sarah J Berkemer[2,3] (1.Earth-Life Science Institute, Tokyo Institute of Technology, 2.Bioinformatics Group, Department of Computer Science, Interdisciplinary Center for Bioinformatics, University of Leipzig, 3.Max Planck Institute for Mathematics in the Sciences, Leipzig, Germany)

11:40 AM - 11:55 AM JST | 2:40 AM - 2:55 AM UTC

### [MIS07-14] Scientific significance of searching living cells on Mars surface by Life Detection Microscope (LDM )

*Yoshitaka Yoshimura[1], Akihiko Yamagishi[2], Takehiko Satoh[3], Atsuo Miyakawa[2], Eiichi Imai[4], Satoshi Sasaki[5], Kensei Kobayashi[6], Yoko Kebukawa[6], Tomoka Okada[6], Keigo Enya[3], Hikaru Yabuta[7], Takeshi Naganuma[7], Hajime Mita[8], Kazuhisa Fujita[3], Tomohiro Usui[3] (1.College of Agriculture, Tamagawa University, 2.Tokyo University of Pharmacy and Life Science, 3.Japan Aerospace Exploration Agency, 4.Nagaoka University of Technology, 5.Tokyo University of Technology, 6.Yokohama National University, 7.Hiroshima University, 8.Fukuoka Institute of Technology)

11:55 AM - 12:10 PM JST | 2:55 AM - 3:10 AM UTC

[MIS07-15] Civilization-bearing planets in the Milky-Way Galaxy; 50 necessary conditions must be satisfied in order

*Shigenori Maruyama[1] (1.Earth-Life Science Institute, Tokyo Institute of Technology)

12:10 PM - 12:15 PM JST | 3:10 AM - 3:15 AM UTC

Discussion

# the emergence of iron-sulfur protometabolism

*Sheref Mansy[1]

1. University of Trento

Iron-sulfur clusters are considered to be one of life's most ancient cofactors. Traditionally, the reliance of extant biology on iron-sulfur proteins has been interpreted to mean that iron-sulfur clusters of some type actively participated in the prebiotic chemistry that led to life. Since globular proteins were likely not present on the prebiotic Earth, most investigations into the early roles of iron-sulfur clusters have centered upon the potential activity of minerals, such as greigite and pyrite. Although minerals undoubtedly heavily impacted prebiotic chemistry and likely participated in the synthesis of molecules necessary for the emergence of life, it is unclear how minerals could have been later superseded by protein enzymes. Here we discuss our efforts in understanding the plausibility of synthesizing iron-sulfur clusters coordinated to prebiotically plausible peptides. We find that the solution conditions impact the type of iron-sulfur cluster formed, that UV light facilitates the synthesis of iron-sulfur clusters, and that iron-sulfur peptides can mediate the types of electron transfer reactions needed to sustain an early form of metabolism.

Keywords: iron-sulfur cluster, protocell, prebiotic chemistry, origins of life

©2019. Japan Geoscience Union. All Right Reserved. 

# Life-water-mineral interactions and their products

*Fumito Shiraishi[1]

1. Hiroshima University

Studies of modern and ancient microbial deposits on the Earth have demonstrated that the traces of microbial life are preserved as various kinds of minerals via life-water-mineral interactions. They include carbonates, phosphates, iron oxides, and manganese oxides, and their recent knowledge is introduced in the presentation.

For carbonates, cyanobacterial photosynthesis can produce $CaCO_3$ minerals to form deposits like stromatolites. However, their depositional fabrics are strongly influenced by the acidity of EPS (extracellular polymeric substances) secreted by cyanobacteria. In some cases, $CaCO_3$ minerals formed by cyanobacteria exhibit specific traces.

For phosphates, phosphorites are generally produced via degradation of organic matter during diagenesis. In the case of high phosphorus concentration in the euphotic zone, however, microbial photosynthesis potentially produces phosphate minerals to form phosphate stromatolites. Such process may occur after the snowball Earth glaciations in the Neoproterozoic as well as in the Paleoproterozoic.

For iron oxides, microbial Fe(II) oxidation is effective only when $O_2$ concentration is below ca. 50 $\mu$M, and inorganic process prevails above this level. The trace of iron-oxidizing bacteria is potentially preserved in the structure of iron oxide minerals.

For manganese oxides, substantial Mn(II) oxidation does not occur inorganically even under $O_2$ concentration equilibrated with the modern atmospheric level, and microbial processes are essential for it. In addition, manganese oxides adsorb various metals that potentially sustain metal-dependent microbial ecosystems in organic matter-deficient settings.

The knowledge about microbial traces on the Earth would provide valuable information for exploring extraterrestrial life.

©2019. Japan Geoscience Union. All Right Reserved. 

# How much can we learn about ancient cells from sequence analysis? New metrics on an old problem.

*Shawn E McGlynn[1], Sarah J Berkemer[2,3]

1. Earth-Life Science Institute, Tokyo Institute of Technology, 2. Bioinformatics Group, Department of Computer Science, Interdisciplinary Center for Bioinformatics, University of Leipzig, 3. Max Planck Institute for Mathematics in the Sciences, Leipzig, Germany

A longstanding goal is to apply molecular phylogenetics to understanding ancient physiological and evolutionary states (*e.g.* [1]). With the current explosion of molecular sequencing data (e.g. [2]), it is a good time to consider how far back we can peer with the comparative molecular lens, and ask if we can understand life in its nascent years. A standard test for inferring ancient genes is to look for conservation in microbial genomes, and to analyze phylogenetic branch positions and determine if a gene separates the archaea and the bacteria. However, many phylogenetic trees are cluttered by phenomena such as horizontal gene transfer and non-orthologous displacement [3], making inferences difficult.

In this presentation, we will give an overview of recent work in this area [4, 5], and also present new analyses which help identify ancient proteins. Using the COG database, we built phylogenetic trees for all protein families and analyzed the number of interdomain gene transfer events for each family. We find that proteins assigned to COGs exhibit widely variable amounts of interdomain gene transfer. By using distance matrices which relate *intra*-domain sequence similarity to *inter*-domain similarity, we find that protein families exhibiting numerous inter domain gene transfer events are also most self-similar between domains. Integrating this observation with previous analyses, ancient proteins appear to have large branch lengths separating the domains, but recent proteins are more bushy in tree shape. These findings will be discussed in the context of inferring the characteristics of the most ancient cells. Although this work provides new dimensions to analyze protein families with, more work is needed to definitively identify the proteins in the last common ancestor of the bacteria and archaea.

REFERENCES CITED

*1. Woese, C.R.: Bacterial evolution. Microbiol. Rev. 51, 221–271 (1987)*
*2. Castelle, C.J., Banfield, J.F.: Major New Microbial Groups Expand Diversity and Alter our Understanding of the Tree of Life. Cell. 172, 1181–1197 (2018). doi:10.1016/j.cell.2018.02.016*
*3. Koonin, E.V.: Comparative genomics, minimal gene-sets and the last universal common ancestor. Nat. Rev. Microbiol. 1, 127–136 (2003). doi:10.1038/nrmicro751*
*4. Forterre, P.: The universal tree of life: an update. Front. Microbiol. 6, (2015). doi:10.3389/fmicb.2015.00717*
*5. Weiss, M.C., Sousa, F.L., Mrnjavac, N., Neukirchen, S., Roettger, M., Nelson-Sathi, S., Martin, W.F.: The physiology and habitat of the last universal common ancestor. Nat. Microbiol. 1, 16116 (2016). doi:10.1038/nmicrobiol.2016.116*

Keywords: LUCA, Early life, Phylogenetics , Bioinformatics

©2019. Japan Geoscience Union. All Right Reserved. 

# Scientific significance of searching living cells on Mars surface by Life Detection Microscope (LDM )

*Yoshitaka Yoshimura[1], Akihiko Yamagishi[2], Takehiko Satoh[3], Atsuo Miyakawa[2], Eiichi Imai[4], Satoshi Sasaki[5], Kensei Kobayashi[6], Yoko Kebukawa[6], Tomoka Okada[6], Keigo Enya[3], Hikaru Yabuta[7], Takeshi Naganuma[7], Hajime Mita[8], Kazuhisa Fujita[3], Tomohiro Usui[3]

1. College of Agriculture, Tamagawa University, 2. Tokyo University of Pharmacy and Life Science, 3. Japan Aerospace Exploration Agency, 4. Nagaoka University of Technology, 5. Tokyo University of Technology, 6. Yokohama National University, 7. Hiroshima University, 8. Fukuoka Institute of Technology

Past trial of direct detection of life on Mars by 1970's Viking mission ended up with a negative conclusion [1]. Whereas, numbers of new finding provided by Mars exploration missions in the last decade indicate that there are good reasons to perform another life detection program. The sensitivity of the gas chromatograph mass spectrometer onboard the Viking mission was not very high, and was not able to detect the microbes $10^6$ cells in 1 gram clay [2,3].

Recent findings on Mars tend to support the possible presence of living microbes near the surface of Mars. MSL Curiosity has found organic compounds [4], the temporal increase of methane concentration in Martian atmosphere [5] and reduced sulfur compounds such as pyrite in Martian soil [6]. Methane and reduced sulfur compounds can be energy sources to support the growth of chemoautotrophic microbes [7]. Possible presence of liquid water at Recurring Slope Lineae has been supported by the detection of hydrated salts [8]. These evidences tend to support the possible presence of living microbes near the surface of Mars and indicate that another life detection program is necessary.

The Life Detection Microscope (LDM) that we have proposed [7, 9] has the potential sensitivity much higher than the Viking instrument. Microscopes directly image life forms and identify their shapes, sizes, and other morphological structures and have the potential to detect a single cell in field of view. Therefore, the sensitivity can be as high as desired just by increasing the volume of sample to be scanned in a reasonable duration of experiment. LDM scans about 1 $mm^3$ and detects less than $10^4$ cells in 1 gram soil at a spatial resolution of 1 $\mu$m [9]. LDM differentiates among organic compounds surrounded by membranes or with enzyme activity by staining the samples with fluorescent pigments. This technique is especially useful for the detection of living microorganisms.

The search for living microorganisms is important not only for scientific interest but for planetary protection. Before future human missions begin, surveys investigating the presence of living microorganisms should be conducted to mitigate the risk of human contact with Martian microorganisms, which may be harmful to human health. Scientific significance the development of LDM will be addressed in this report.

References

[1] Margulis, L. et al. *J. Mol. Evol.* 14 (1979)

[2] Glavin, et al, *Earth Planet. Sci. Let.*, 185 (2001)

©2019. Japan Geoscience Union. All Right Reserved. 

[3] Navarro-González, et al., *Proc. Natl. Acad. Sci. USA.*, 103 (2006)

[4] Eigenbrode, J. L., et al., *Science*, 360 (2018).

[5] Webster, C. R., et al., *Science*, 360 (2018).

[6] Ming, D., et al., *Science*, 343 (2014)

[7] Yamagishi, A. et al. *Biol. Sci. Space*, 24 (2010)

[8] Ojha, L. et al. *Nature Geosci.*, 8 (2015)

[9] Yamagishi, A., et al., *Trans. JSASS, Aerospace Tech. Japan*, 16 (2018).

Keywords: fluorescent microscope, extraterrestrial life

©2019. Japan Geoscience Union. All Right Reserved. 

# Civilization-bearing planets in the Milky-Way Galaxy; 50 necessary conditions must be satisfied in order

*Shigenori Maruyama[1]

1. Earth-Life Science Institute, Tokyo Institute of Technology

**<Purpose>**

Is there any life in the Universe, or specifically civilization-bearing planets? Recent popular answer for this basic question is easy-going “Yes”, which was also trendy answer 100 years ago. They think there are so many stars in the Universe, e.g., $10^{11}$, so it is reasonable to think the possibility of the presence of life in the Universe. However, is it right scientifically?

**<Method>**

If the number of necessary conditions to make civilization-bearing planet is 50, simple estimate of presence or absence is $(1/2)^{50}=1/(10^{11})$, indicating that it is only one in the Milky Way Galaxy. To discuss the presence of life in the Universe, the best example with the most detailed research information is the Earth and its history. Other examples are planets, asteroid and meteorites in the solar system. Applying those data to the Universe, we can lead to general aspects of necessary conditions to infer life in the Universe.

**<Result>**

Based on the data set inferred from the research of Earth and life, 48 requirements are listed up. Those necessary conditions are mainly categorized into the following four. First group has 11 planetary conditions to be a life-sustaining planet; for example, “Chemical composition of central star”, “Mass of central star”, and “Circular orbit”. Second Group has 14 conditions of rocky planets to prepare the cradle of life; such as “Formation of bimodal continental and oceanic lithospheres to initiate plate tectonics”, “Restricted amount of initial mass of ocean to supply of nutrients for life”. Third group has 9 conditions to emerge and evolve life; such as “continuous and strong outer energy by natural geyser”, and “well-balanced nutrients source of landmass”. Forth group has 10 conditions to evolve into civilization bearing planet; such as “Survival over 2 billion years until birth of Eukaryote”, “A way to Eukaryote from Prokaryotes”, “A way to metazoans and Plant”, “Acceleration of life evolution”. There are other important 4 conditions; such as “Galactic habitable Zone”

**<Discussion>**

If we simply calculate the probability of presence of life in the Universe, civilization-bearing planet is only one (Earth). It is also emphasized that the requirements mentioned above is treated as presence of absence for all requirements, but several requirements are definitely less than 50% probability, e.g., extremely strict constraint for the amount of ocean volume 3km±1km. Moreover, it is emphasized that the number 51 is combinations and not permutations. This strongly indicates that we are alone in the Universe, even including whole Universe beyond our Milky Way Galaxy.

Keywords: habitable planet, civilization bearing planet, condition

©2019. Japan Geoscience Union. All Right Reserved. 

©2019. Japan Geoscience Union. All Right Reserved. 

[E] Poster | M (Multidisciplinary and Interdisciplinary) : M-IS Intersection

Thu. May 30, 2019 3:30 PM - 5:00 PM JST | Thu. May 30, 2019 6:30 AM - 8:00 AM UTC | Poster Hall International Exhibition Hall8, Makuhari Messe_20

## [M-IS07] Astrobiology

convener:Hikaru Yabuta(Hiroshima University, Department of Earth and Planetary Systems Science), Seiji Sugita(Department of Earth and Planetary Science, Graduate School of Science Sciece, The University of Tokyo), Misato Fukagawa(National Astronomical Observatory of Japan), Fujishima Kosuke(Tokyo Institute of Technology, Earth-Life Science Institute)

Twenty years have passed since when the field of Astrobiology, which aims to unveil the origins, evolution, and habitability of life by integrating multidisciplinary fields, was established. Individual themes related to Astrobiology, such as chemical evolution in the early Solar System, formation of planetary system, prebiotic chemistry in the early Earth, evolution of life in the Earth's history, extremophile, and habitable planetary environments, has been studied by the knowledge and methods from the multiple fields, which has enabled us to explain "Where we came from" in some ways. However, despite an overwhelming number of investigations and discussions through gathering of the scientists from different fields, there has remained the long-standing unsolved question: How did abiotic materials gain biological function in the Earth and elsewhere in universe? There is still a large gap between prebiotic organic chemistry and biochemistry toward Origins of Life and planetary habitability. Therefore, the JpGU Astrobiology session focuses on pathfinding of "integration of astronomy, geoscience, and biochemistry", which will face an increasing need for the future Astrobiology. In order to enhance our understanding of "What is life", we propose to discuss the biochemical events linked with planetary systems, which is beyond the knowledge in a test tube, by an integration of exoplanets and molecular biology, etc. Through this approach, we will lead the discussions and developments of life-detection strategies for the future exploration of life in universe.

### [MIS07-P01] Exoplanets Revealed by High-Precision Infrared Doppler Technique Using IRD: Large Exploration for Planets around Cool M-type Stars Begins

*Masayuki Kuzuhara[1,3], Bunei Sato[4], Motohide Tamura[2,1,3], Takayuki Kotani[1,3,5], Nagayoshi Ohashi[3,6], Masashi Omiya[1,3], Teruyuki Hirano[4], Hiroki Harakawa[6,3,1], Wako Aoki[3,5], Norio Narita[2,1], Yasunori Hori[1,3], Akitoshi Ueda[3,5], Akihiko Fukui[2], Hiroyuki Tako Ishikawa[5,3], Ishizuka Masato[2], Takashi Kurokawa[1,7], Nobuhiko Kusakabe[1,3], Tomoyuki Kudo[6,3,1], Eiichiro Kokubo[3], Mihoko Konishi[1,3], Tadashi Nakajima[1,3,5], Jun Nishikawa[3,5,1], Masahiro Ogihara[3], Takuma Serizawa[7] (1.Astrobiology Center of NINS, 2.The University of Tokyo, Graduate School of Science, 3.National Astronomical Observatory of Japan, 4.Tokyo Institute of Technology, 5.SOKENDAI, 6.Subaru Telescope, 7.Tokyo University of Agriculture and Technology)

### [MIS07-P02] Discrimination of organic compounds and mineral particles by fluorescent microscopy for the detection of Martian life.

*Tomoka Okada[1], Yoshitaka Yoshimura[2], Atsuo Miyakawa[3], Yuka Murano[3], Shin-ichi Yokobori[3], Akihiko Yamagishi[3], Kensei Kobayashi[1], Yoko Kebukawa[1] (1.YOKOHAMA National university, 2.Tamagawa University, 3.Tokyo University of Pharmacy and Life Sciences)

### [MIS07-P03] Morphological and spectroscopic characteristics of organic matter in Banded Iron Formation, Barberton Greenstone Belt, South Africa

*Hiroki Amemiya[1], Ryo Nakajima[1], Yoko Ohtomo[1], Tsubasa Otake[1], Tsutomu Sato[1] (1.Division of sustainable Resources Engineering, Faculty of Engineering, Hokkaido University)

### [MIS07-P04] Understanding peptide sequence selectivity on iron sulfide (FeS) nanoparticle surfaces

*Fujishima Kosuke[1], Norio Kitadai[1], Kenji Kasama[1] (1.Earth-Life Science Institute, Tokyo Institute of Technology)

### [MIS07-P05] A process model of L-homochiral peptides formation initiated with L-alanine

*Toratane Munegumi[1], Taisuke Yamaga[1] (1.Department of Science Education, Naruto University of Education)

[MIS07-P06] Possible Formation of Amino Acids and Carboxylic Acids in Slightly-Reducing Primitive Earth Atmospheres

*Miei Kinoshita[1], Shintaro Ikeda[1], Kimitaka Kawamura[2], Bhagawati Kunwar[2], Hitoshi Fukuda[3], Yoshiyuki Oguri[3], Hiromi Shibata[4], Junichi Takahashi[1], Vladimir Airapetian[5], Yoko Kebukawa[1], Kensei Kobayashi[1] (1.Yokohama National University, 2.Chubu University, 3.Tokyo Institute of Technology, 4.Osaka University, 5.NASA Goddard SFC)

[MIS07-P07] Application of Machine learning and software development for initial analysis in the TANPOPO mission

*Kyoko Okudaira[1], Yuto Toda[1], Takashi Sonoke[1], Yuichi Yaguchi[1], Masashi Yoshida[1], Junya Imani[2], Satoshi Sasaki[3], Hajime Yano[4], Hirohide Demura[1], Makoto Tabata[5], Akihiko Yamagishi[6] (1.The University of Aizu, 2.YUKI Precision, 3.Tokyo University of Technology, 4.JAXA, 5.Chiba University, 6.Tokyo University of Pharmacy and Life Science)

[MIS07-P08] Structure analysis of the hyper velocity impact tracks of the particles captured by silica aerogel on the International Space Station

*Mizuho Nishi[1], Akira Tsuchiyama[1], Hajime Yano[2], Hikaru Yabuta[3], Kyoko Okudaira[4], Junya Matsuno[1], Masayuki Uesugi[5], Uesugi Kentaro[5], Nakano Tukasa[6], Takaaki Noguchi[7], MITA Hajime[8], Akihiko Yamagishi[9] (1.Kyoto University, 2.Institute of Space and Astronautical Science, Japan Aerospace Exploration Agency, 3.Hiroshima University, 4.The University of Aizu, 5.JASRI/SPring-8, 6.National Institute of Advanced Industrial Science and Technology, 7.Kyusyu University, 8.Fukuoka Institute of Technology, 9.Tokyo University of Pharmacy and Life Science)

[MIS07-P09] High-Angular-Resolution Observations of Protoplanetary Disks

*Misato Fukagawa[1] (1.National Astronomical Observatory of Japan)

[MIS07-P10] Characterization of high molecular weight amino acid precursors formed in interstellar ice analog

*Soushi Kuramoto[1], Tomohito Sato[1], Hitoshi Fukuda[2], Yoshiyuki Oguri[2], Kotaro Kondo[2], Hiromi Shibata[3], Yoko Kebukawa[1], Kensei Kobayashi[1], Satoshi Yoshida[4] (1.Yokohama National University, 2.Tokyo Institute of Technology, 3.University of Osaka, 4.National Institutes for Quantum Radiological Science and Technology)

[MIS07-P11] Theoretical elucidation of prebiotic formation processes into nucleobases

*Yu Komatsu[1,2], Taiki Suzuki[1,2] (1.Astrobiology Center, 2.National Astronomical Observatory of Japan)

[MIS07-P12] Formation Process of A Glycine's Precursor Candidate, CH3NH2

*Taiki Suzuki[1,2], Liton Majumdar[3], Masatoshi Ohishi[2] (1.National Institutes of Natural Sciences Astrobiology Center, 2.National Astronomical Observatory of Japan, 3.NASA Jet Propulsion Laboratory (JPL))

[MIS07-P13] Numerical study on the stellar atmosphere & wind of Cool Stars

*Takahito Sakaue[1], Kazunari Shibata[1] (1.Kyoto University)

[MIS07-P14] Design of space exposure experiments of organic matter in Tanpopo 2

*Takuya Yokoo[1], tomohito sato[1], Itsuki Sakon[2], Kazumichi Nakagawa[3], Hajime Yano[4], Miki Nakayama[5], Hajime Mita[5], Yoko Kebukawa[1], Kensei Kobayashi[1] (1.Yokohama National University, 2.University of Tokyo, 3.Kobe University, 4.JAXA, 5.Fukuoka Institute of Technology)

# Exoplanets Revealed by High-Precision Infrared Doppler Technique Using IRD: Large Exploration for Planets around Cool M-type Stars Begins

*Masayuki Kuzuhara[1,3], Bunei Sato[4], Motohide Tamura[2,1,3], Takayuki Kotani[1,3,5], Nagayoshi Ohashi[3,6], Masashi Omiya[1,3], Teruyuki Hirano[4], Hiroki Harakawa[6,3,1], Wako Aoki[3,5], Norio Narita[2,1], Yasunori Hori[1,3], Akitoshi Ueda[3,5], Akihiko Fukui[2], Hiroyuki Tako Ishikawa[5,3], Ishizuka Masato[2], Takashi Kurokawa[1,7], Nobuhiko Kusakabe[1,3], Tomoyuki Kudo[6,3,1], Eiichiro Kokubo[3], Mihoko Konishi[1,3], Tadashi Nakajima[1,3,5], Jun Nishikawa[3,5,1], Masahiro Ogihara[3], Takuma Serizawa[7]

1. Astrobiology Center of NINS, 2. The University of Tokyo, Graduate School of Science, 3. National Astronomical Observatory of Japan, 4. Tokyo Institute of Technology, 5. SOKENDAI, 6. Subaru Telescope, 7. Tokyo University of Agriculture and Technology

Planets outside the Solar system, so-called exoplanets, are promising as a new window for astrobiology. Among those, planets orbiting cool M-type stars (main-sequence stars with effective temperatures less than about 3000 K) have the great potential to push forward astrobiological studies on exoplanets. The habitable zone (HZ) is the zone where liquid water is sustainable on the surfaces of planets. It is expected that the HZs around cooler stars come closer to the parent stars (Kopparapu et al. 2013, ApJ 765, 131). In addition, the recent exoplanet observations performed by the *Kepler* space telescope have revealed that the occurrence rate of small exoplanets similar to Earth increases as the effective temperatures of stars decrease (e.g., Mulders et al. 2015, ApJ 798, 112). Furthermore, the Doppler technique, one of primary methods for exoplanet observations, can more easily find a planet with the orbit closer to its parent star. Accordingly, targeting cool M-type stars provides a significant advantage in the observations of rocky planets in HZs based on the Doppler technique. Also, the snow line around a cool M-type star is close to the star; this is intriguing in terms of the planet formation process.
Nevertheless, the exoplanet observations for cool M-type stars have not been advanced compared with those for hotter stars, due to their faintness. In particular, the low brightness of a cool M-type star at optical wavelengths makes it problematic to observe its planet based on visible light, which has been mostly used in exoplanet observations. We have therefore developed the InfraRed Doppler (IRD) instrument, which is a high-dispersion spectrograph to enable the exoplanet observations using the high-precision Doppler technique at near-infrared (Kotani et al. 2018, Proc. of the SPIE 10702, 1070211). Near-infrared light is suited for observing cool M-type stars, since their peak flux is located in a near-infrared region. One of bottlenecks to achieve high-precision measurements using the near-infrared Doppler technique is the lack of a reference source that enables us to correctly calibrate a measurement fluctuation caused by the instability of an observation instrument. We use a laser frequency comb (LFC) generated by the system that has been newly developed for IRD as a reference source to calibrate IRD measurements. An LFC spectrum has a number of emission lines with fine sampling intervals and is observed simultaneously with a stellar spectrum, so it works as a correct wavelength calibrator for the stellar spectrum. After our laboratory performance verifications of IRD with its LFC system (Kuzuhara et al. 2018, Proc. of the SPIE 10702, 1070260), the IRD operation started on the Subaru Telescope, whose large primary mirror enables high-sensitivity observations even for cool M-type stars. The use of IRD with the Subaru Telescope significantly helps the discoveries and characterizations of exoplanets around cool M-type stars.
We have planned a large survey for planets around cool M-type stars with IRD on the Subaru Telescope, which actually begins on February, 2019. In this survey, we monitor 60 M-type stars over 175 nights

©2019. Japan Geoscience Union. All Right Reserved. 

allocated for 5 years. Our pre-survey simulation prospects more than 60 planet detections; those discoveries include a few dozen Earth-like planets, among which some are expected to locate within HZs. Thus, the IRD survey provides important contributions on improving our current understanding of planet formation models for low-mass stars like cool M-type stars, as well as the provisions of samples for exoplanet characterizations using the future large telescopes such as TMT. Here, we report the result of our ongoing on-sky tests to evaluate the IRD performances such as its measurement precision and stability. Furthermore, we explain the above large program in detail: our science goals, and the target selection and observation strategy for the goals are provided.

Keywords: Exoplanet, Doppler technique, Habitable Zone, IRD, planet formation, M-type star

©2019. Japan Geoscience Union. All Right Reserved. 

# Discrimination of organic compounds and mineral particles by fluorescent microscopy for the detection of Martian life.

*Tomoka Okada[1], Yoshitaka Yoshimura[2], Atsuo Miyakawa[3], Yuka Murano[3], Shin-ichi Yokobori[3], Akihiko Yamagishi[3], Kensei Kobayashi[1], Yoko Kebukawa[1]

1. YOKOHAMA National university, 2. Tamagawa University, 3. Tokyo University of Pharmacy and Life Sciences

The Viking mission searched life on Mars in 1976, but did not find apparent biological activities[1)]. However, the detection sensitivity of the Viking instrument (GC-MS) has been found to be low, suggesting that organic compounds could exist on Martian surface. Recently the MSL Curiosity by NASA detected organic compounds[2)]. The Phoenix mission discovered $H_2O$ ice[3)] and possible liquid water flows were found at RSL (Recurring Slope Lineae) by MRO (Mars Reconnaissance Orbiter)[4)]. These findings suggested that life might exist on Martian surface.

We have proposed a life search program on the surface of Mars with a fluorescence microscope[5)]. This microscope is called Life detection Microscope (LDM) which detects microorganisms in more than 100 times higher sensitivity than the Viking GC-MS. In this program, we plan to use two fluorescent dyes SYTO 24 and propidium iodide (PI) in LDM. SYTO24 permeates cell membrane and stains organic compounds. PI also stains organic compounds such as nucleic acids, but it doesn’t permeate cell membrane. Therefore, the combination of these two dyes makes it possible to differentiate the organic compounds surrounded by membranes (living cells) and dead cells.

However, there are some mineral particles have autofluorescence, possibly detected as false positives. In this research, in order to discriminate organic compounds from mineral particles, the autofluorescence of minerals were measured under various conditions.

Various kind of mineral specimens were finely ground with a glass pen washed with ethanol. Fluorescent images were obtained with a fluorescence microscope and a digital camera and their fluorescent intensities were measured by image analysis. We also examined fluorescent spectra of mineral particles using a diffraction grating. The results showed the fluorescent intensities and spectra of mineral particles were clearly different from the stained organic compounds. These methods would be useful to detect organic compounds among mineral particles.

1) Navarro-Gonzalez, R., *et al.,* 2006, *PNAS*, 103: 16089-16094. 2) Freissient, C., *et al*., 2015, *J. Geophys. Res. Planets,* 120: 495-514. 3) Feldman, W. C., *et al.,* 2002. *Science*, 297, 75-78. 4) McEwen A. S, *et al.,* 2011, *Science,* 333: 740-743. 5) Yamagishi, A., *et al*., 2010, *Bio. Sci. Space,* 24: 67-82.

Keywords: Mars, Fluorescent microscope, Life Detection

©2019. Japan Geoscience Union. All Right Reserved. 

# Morphological and spectroscopic characteristics of organic matter in Banded Iron Formation, Barberton Greenstone Belt, South Africa

*Hiroki Amemiya[1], Ryo Nakajima[1], Yoko Ohtomo[1], Tsubasa Otake[1], Tsutomu Sato[1]

1. Division of sustainable Resources Engineering, Faculty of Engineering, Hokkaido University

The emergence of cyanobacteria has been postulated to cause an increase in Earth’ s atmospheric oxygen concentration ~2.45 Ga and oxidation of ferrous iron in a seawater, facilitating the formation of Banded Iron Formations (BIFs) in the Proterozoic era. On the other hand, iron precipitation process in the Archean is still controversial. Previous studies suggest that anoxygenic iron-oxidizing bacteria and/or free oxygen produced by cyanobacteria, was responsible for iron oxidation before ~2.45 Ga. Organic matter preserved in BIFs may provide insights into the iron oxidation process and biological evolution in Archean. However, authenticity of Archaean organic matter has to be first clarified for further investigations due to possible later contamination. Here, we investigated morphological and spectroscopic characteristics of organic matter in ~3.2 Ga BIFs in Sheba mine, Moodies Group, Barberton Green stone Belt, South Africa to estimate the chemical structure combined with a contamination check using Raman spectroscopy.

Organic matter was collected by two different methods: extraction by acid treatment of powder samples and pick up with a micro-manipulator from thin sections. When Raman spectra were obtained using 532 nm wavelength laser, acid-treated organic matter showed two peaks ~1350 and ~1580 $cm^{-1}$ corresponding to disordered and ordered carbon structures, whereas micro-sampled organic matter shows no detectable peak with a high background. Because yellow-green fluorescence was observed in micro-sampled organic matter using a Fluorescence microscope, the fluorescence likely causes a high background in the Raman spectra. Therefore, 785 nm wavelength laser was applied for micro-sampled organic matter. Calculated metamorphic temperature from the Raman spectra obtained by acid-treated and micro-sampled organic matter was from 400 to 540˚C, which is consist with greenschist facies of the Barberton Greenstone Belt. This indicates that the organic matter is not a later contamination. Chemical mapping with an Electron Probe Micro Analyzer shows that micro-sampled organic matter is predominately comprised of carbon with slight contribution of nitrogen (< 0.1wt%). Infrared spectra of the organic matter show absorption peaks corresponding to N-O, C-O, and C=O bonds, suggesting that organic matter remains their functional groups in the structure. Based on the morphology and microstructure observed by Field Emission- Scanning Electron Microscope, the organic matter may have been derived from biofilm because of similarity in the morphology as well as the large size (20 –50 $\mu$m). Furthermore, the micro-sampled organic matter has a rough surface while the acid-treated organic matter has a smooth one, which may be due to damages by acid-treatment. Our results suggest that micro-sampling is suitable to observe the detailed morphological and structural features of organic matter preserved in Archean sedimentary rocks.

Keywords: Archean, Microfossils, Barberton Greenstone Belt, Raman spectroscopy, Infrared spectroscopy

©2019. Japan Geoscience Union. All Right Reserved. 

# Understanding peptide sequence selectivity on iron sulfide (FeS) nanoparticle surfaces

*Fujishima Kosuke[1], Norio Kitadai[1], Kenji Kasama[1]

1. Earth-Life Science Institute, Tokyo Institute of Technology

The emergence and evolution of functional biopolymers on Earth is one of the unsolved key questions regarding the origin of life. Amongst various building blocks of polymers, amino acids are prebiotically abundant and different plausible paths toward forming polypeptides have been previously shown in the context of early Earth environment. However, relationship between a specific geochemical environment and the types of biopolymers that could retain or to propergate in that condition is not yet fully systematically explored. Hence, we have prepared random octapeptide library with a combination of limited set of amino acids (Gly, Ile, His, Asp, Cys, Arg) as a probe to explore the sequence selectivity of iron sulfide (FeS) nanoparticles as a simulant of the geochemical settings that once existed at the deep-sea floor or the surface of early Earth. Experiment was carried out by mixing the FeS nanoparticles and random peptides in pure $H_2O$ solution inside the anoxic chamber to allow adsorption under moderate temperature/pH condition. After extensive rinsing step, peptides that remain bound to the FeS nanoparticles were analyzed directly by MALDI-MS/MS to retrieve sequence information. We will discuss the latest sequence results obtained from screening and discuss sequence selective feature of FeS and its relevance to the iron-sulfur cluster known as a fundamental cofactor in biology.

Keywords: Iron sulfide, peptide adsorption, MALDI-MS/MS, iron-sulfur cluster

©2019. Japan Geoscience Union. All Right Reserved. 

# A process model of L-homochiral peptides formation initiated with L-alanine

*Toratane Munegumi[1], Taisuke Yamaga[1]

1. Department of Science Education, Naruto University of Education

Hydrogen abstraction from L-alanine by hydroxy radical facilitates alkylation on $\beta$-carbon of alanine as well as retention of L-chirality. The reaction rate constant of hydrogen abstraction ($k=6.21\times10^{7}\ M^{-1}s^{-1}$) on $\beta$-carbon was about 3.7 times faster than that ($k=1.7\times10^{7}\ M^{-1}s^{-1}$) on $\alpha$-carbon. The fact supports that alkylation proceeds faster than racemization, and the chirality of product amino acids will be hold. Similar alkylation of oligopeptides will also proceed with a lower level epimerization than alkylation. This research discusses how the lower reaction rate of epimerization than alkylation lead homochiral peptides.

Keywords: L-alanine, peptides, homochirality

©2019. Japan Geoscience Union. All Right Reserved. 

# Possible Formation of Amino Acids and Carboxylic Acids in Slightly-Reducing Primitive Earth Atmospheres

*Miei Kinoshita[1], Shintaro Ikeda[1], Kimitaka Kawamura[2], Bhagawati Kunwar[2], Hitoshi Fukuda[3], Yoshiyuki Oguri[3], Hiromi Shibata[4], Junichi Takahashi[1], Vladimir Airapetian[5], Yoko Kebukawa[1], Kensei Kobayashi[1]

1. Yokohama National University, 2. Chubu University, 3. Tokyo Institute of Technology, 4. Osaka University, 5. NASA Goddard SFC

Since 1950s, a large number of laboratory experiments have been performed to examine possible formation of bioorganic compounds such as amino acids in primitive Earth atmosphere. Earlier experiments with strongly reducing gas mixtures containing large molar ratio of methane and ammonia, and it was reported that efficient production of amino acids and other important organics were formed in it by spark discharges and other energy sources. It is now estimated, however, that the early Earth atmosphere was only slightly reducing [1]: $N_2$ and $CO_2$were the major atmospheric constituents, together with some small amount of reducing carbon species like $CH_4$ and/or CO. Simulation experiments suggested, however, that amino acid formation was restricted under these conditions [2]. We reported that cosmic rays could facilitate chemical reactions with less reducing model of primitive atmosphere such as a mixture of $CO_2$, CO, $N_2$and $H_2O$ [3]. However these energy sources have been ignored in experiments with initiation of prebiotic chemistry [4]. Here, we examine possible formation of amino acids from slightly reducing gas mixtures by applying high-energy protons to simulate the action of cosmic rays.

We conducted three sets of laboratory experiments using energetic particles, spark discharge and UV light as dominant energy sources. In these sets of experiments we used 400 mL of gas mixture of $N_2$, $CO_2$and $CH_4$introduced to a Pyrex tube together with 5 mL of pure water under 350 Torr of N2 and 350 Torr of mixtures with varied mixing ratios of $CH_4$and $CO_2$. In order to simulate possible roles of cosmic rays, the gas mixture was irradiated with 2.5 MeV proton beam produced in the Tandem accelerator at Tokyo Tech, Japan. We also exposed the same composition of gas mixtures to spark discharges by using a Tesla coil to simulate lightning. The gas mixtures were also irradiated with UV light (l> 190 nm) from a xenon lamp. Each product was acid-hydrolyzed and was subjected to amino acid analysis by HPLC and GC/MS, both after derivatization. Carboxylic acids were determined by GC/MS after derivatization. Starting and resulting gas mixtures were analyzed with a quadrupole mass spectrometer.

Amino acids were detected in the hydrolyzed products when gas mixtures of $N_2$, $CO_2$, $CH_4$and $H_2O$ were irradiated with 2.5 MeV protons at the initial the molar ratio of methane ($r_{CH4}$) in the starting gas mixture as low as 0.5 %. On the other hand, amino acids were detected only when $r_{CH4}$was greater than 15 % in the case of spark discharges. The experiments with UV irradiation source did not yield amino acids or their precursors even when $r_{CH4}$was 50 %. Very little amino acids were detected in all the products before hydrolysis. It was shown that not free amino acids but amino acid precursors were formed in selected experiments.

Carboxylic acids including formic acid, oxalic acid and glyoxylic acid were detected from unhydrolized products derived from $N_2$-$CO_2$gas mixtures exposed to spark discharges and proton irradiation. We show that some free carboxylic acids could be formed in non-reducing atmospheres as well as slightly reducing atmospheres either by proton irradiation or by spark discharges. It was suggested that the mechanism of formation of amino acid precursors from $N_2$-$CO_2$-$CH_4$-$H_2O$ mixtures was quite different from that of

©2019. Japan Geoscience Union. All Right Reserved. 

carboxylic acids.

Lightning and solar UV have been considered important energy sources for prebiotic synthesis in primitive Earth atmosphere. We here showed that lightning and solar UV could not singularly synthesize important N-containing organics such as amino acids from slightly reducing primitive Earth atmosphere. On the other hand, cosmic ray could have been an important energy source to synthesize amino acid precursors even if primitive Earth atmosphere was only slightly reducing. It would be of interest to examine whether there are synergetic effects among cosmic rays, UV and thundering.

**References:**

[1] H. Kuwahara and S. Sugita, *Icarus,* **257**,290-301 (2015).

[2] H. Kuwahara *et al.,Orig. Life Evol. Biosph.,* **42**,533-541(2012).

[3] K. Kobayashi *et al.*, *Orig. Life Evol. Biosph.* **28**, 155-165 (1998).

[4] S. L. Miller and H. C. Urey, *Science,* **130**,245-251 (1957).

Keywords: Primitive Earth Atmospheres, Amino Acids, Solar Energetic Particles

©2019. Japan Geoscience Union. All Right Reserved. 

# Application of Machine learning and software development for initial analysis in the TANPOPO mission

*Kyoko Okudaira[1], Yuto Toda[1], Takashi Sonoke[1], Yuichi Yaguchi[1], Masashi Yoshida[1], Junya Imani[2], Satoshi Sasaki[3], Hajime Yano[4], Hirohide Demura[1], Makoto Tabata[5], Akihiko Yamagishi[6]

1. The University of Aizu, 2. YUKI Precision, 3. Tokyo University of Technology, 4. JAXA, 5. Chiba University, 6. Tokyo University of Pharmacy and Life Science

One of the goals of the TANPOPO mission is collecting cosmic dust and space debris on the International Space Station [1]. Ultra-low density material “silica aerogel” panels are used as capture media [2]. These panels retrieved from the space are sent to the laboratory and initial analysis has been conducted by a system called “CLOXS”.

CLOXS efficiently covers the processes (1) Automatic imaging the entire panel, 2) Search for penetration track candidates, 3) Mapping of track candidates, 4) Shape data acquisition of tracks, and 5) Automatic sample cutting) up to sample allocation to researchers. However, to reduce researchers’ time and effort, improvement of the software and automation of some processes are required.

In this study, application of machine learning in discrimination of objects in aerogel images taken by CLOXS is mainly reported. The research goal is to classify objects in the images into tracks and dirt using machine learning.

There are morphological varieties in the objects. As for both tracks and dirt, they are classified into 4 types respectively in this study.

Since the contrast of the images are low, the first step of our approach is preprocessing of the images. We compared the results of *Contrast Stretching* and *CLAHE* (Contrast Limited Adaptive Histogram Equalization).

Learning data and test data are prepared respectively, to compare the case that the images are categorized into 4 types and the case that the images of all types are dealt altogether.

*Convolutional Neural Network* (CNN) is used as a method of machine learning. *Python* is used as programing Language.

In conclusion, as for image processing, *CLAHE* showed higher accuracy when tracks were judged to be tracks, and *Contrast Stretching* was found to yield a better result for dirt. It is probably because, in *Contrast Stretching*, *CNN* was not sufficiently highlighted to capture features, and *CLAHE* was able to improve the contrast sufficiently.

Regarding separating the types of tracks and dirt, the accuracy rate was higher when tracks were categorized into different types and learned.

Although further evaluation and improvements might be needed, our accuracy rates meet the mission requirements, that is, the percentage of identifying track as track should be more than 95 %, while the percentage of identifying dirt as dirt should be more than 70 % (that of NOT identifying true track as dirt

©2019. Japan Geoscience Union. All Right Reserved. 

should be less than 30 %).

[1] A. Yamagishi et al., “Tanpopo: Astrobiology exposure and micrometeoroid capture experiments - proposed experiments at the exposure facility of ISS-JEM”, *Trans. JSASS. Aerospace Tech. Jpn.* vol. 12, No. ists29, p. Tk_49-Tk_55, 2014.

[2] M. Tabata, et al. “Ultralow-density double-layer silica aerogel fabrication for the intact capture of cosmic dust in low-Earth orbits” *J. Sol-Gel Sci. Technol.* 77(2), 325-334, 2016.

Keywords: TANPOPO mission, Astrobiology, Initial analysis, Machine learning, Software development

©2019. Japan Geoscience Union. All Right Reserved. 

# Structure analysis of the hyper velocity impact tracks of the particles captured by silica aerogel on the International Space Station

*Mizuho Nishi[1], Akira Tsuchiyama[1], Hajime Yano[2], Hikaru Yabuta[3], Kyoko Okudaira[4], Junya Matsuno[1], Masayuki Uesugi[5], Uesugi Kentaro[5], Nakano Tukasa[6], Takaaki Noguchi[7], MITA Hajime[8], Akihiko Yamagishi[9]

1. Kyoto University, 2. Institute of Space and Astronautical Science, Japan Aerospace Exploration Agency, 3. Hiroshima University, 4. The University of Aizu, 5. JASRI/SPring-8, 6. National Institute of Advanced Industrial Science and Technology, 7. Kyusyu University, 8. Fukuoka Institute of Technology, 9. Tokyo University of Pharmacy and Life Science

In Japan's first astrobiology experiment “Tanpopo”, attempts have been made to capture cosmic dust by installing ultra-low-density silica aerogel at the Japanese Experiment Module “Kibo” of the International Space Station (ISS) [1]. This mission was conducted with the aim of verifying the hypothesis that the origin of life was supplied from outside the earth [2]. Silica aerogel had been used in NASA’s cometary dust sample return mission “Stardust” [3]. Impact tracks formed by collision of cometary dust against aerogel were classified into 3 types, A, B and C, based on their shapes [4]. The track shapes have useful information for estimating the size and density of dust particles [5]. The purposes of this research are (1) to find impact tracks formed by cosmic dust in Tanpopo aerogel and (2) to describe the three-dimensional shapes of impact tracks with different origins (cosmic dust and space debris) and finally to clarify the relation between the track shape and the origin.

At SPring-8 BL47XU, three-dimensional shapes were obtained with imaging absorption tomography for 8 impact tracks (D1-231, D1-298, D1-362, E1-200, E1-304, F1-328, F1-389, F1-623), which were found in Tanpopo aerogel faced to the space direction. The imaging experiments were made at 7, 8, 9 keV with the voxel size of 0.24 or 0.465 $\mu$m. CT images at 8 keV were used to extract track shapes. Track length ($L_t$), maximum track diameter ($D_m$), aspect ratio, and other shape properties were obtained. These values were compared with Stardust tracks. Dual-energy tomography (DET) [6] was applied to estimate the materials of particles captured in the tracks. Another track (E2-000) was observed only with an optical microscope. For D1-231, D1-298, D1-362 and E2-000, the aerogel was compressed and real solid particles in the tracks were searched with an optical microscope.

The 9 tracks in total were classified into 5 types based on their shapes. Type 1 (E2-000) is a track formed by cosmic dust, where two pyroxene particles were identified at the tip of the track [7]. The track shape resembles Stardust type B track, but its entrance widely spreads. Type 2 (D1-231) is somewhat similar to Stardust type A track. Type 3 (E1-200 and E1-304) is a track having abundant cracks developed on the wall with a narrow entrance. Type 4 (F1-328 and F1-389) is extremely asymmetrical in its shape and has cracks similar to Type 3. Type 5 (D1-362 and F1-623) is a bowl-shaped track with a large entrance. The relationship between $L_t$ and $D_m$ of these tracks was almost the same as that of Stardust tracks except for Type 5. However, their specific shapes of Types 2, 3 and 4 are significantly different from Stardust tracks. The cracks of these tracks are similar to those seen at the end of Stardust type A and B tracks, indicating that they were formed by a relatively low-speed impact. Similar tracks to Type 5 were reported in the aerogel in the exposure experiment on the Mir Station. They may be due to high-speed collision of weakly-adhered aggregates [8]. From the quantitative analysis of such impact tracks, there is a possibility of obtaining knowledge about new parameter areas which could not be obtained by conventional research. DET results showed that most of fine particles in the tracks do not contain Fe and Ni. Low values of their

©2019. Japan Geoscience Union. All Right Reserved. 

linear absorption coefficients are smaller than that of cosmic dust. They should be formed by impact of weekly-adhered aggregates that were broken into very small pieces by the impact and mixed with condensed aerogel. Two particles with relatively high linear absorption coefficient were confirmed in D1-231 and D1-362. They were confirmed by and optical microscope after compressing.

[1] Yamagishi A. et al. 2012. Space Utiliz Res, 28, 220. [2] Chyba C. & Sagan C. 1992. Nature, 355, 125. [3] Brownlee D. et al. 2006. Science, 314, 1711. [4] Hörz et al. 2006. Science, 314, 1716. [5] Tsuchiyama A. et al. 2009. Meteoritics & Planetary Science, 44, 1203. [6] Tsuchiyama A. 2013. Geochimica et Cosmochimica Acta 116, 5. [7] Noguchi T., 2018, Private message. [8] Hörz and Zolensky, 2000, Icarus 147, 559.

Keywords: Tanpopo mission, Cosmic dust

©2019. Japan Geoscience Union. All Right Reserved. 

# High-Angular-Resolution Observations of Protoplanetary Disks

*Misato Fukagawa[1]

1. National Astronomical Observatory of Japan

The recent progress in understanding of planet-formation process will be reviewed based on the results obtained at high angular resolution with astronomical facilities such as the Atacama Large Millimeter/submillimeter Array (ALMA). Circumstellar disk structures around young stars are birthplaces of planets. The physical and chemical condition in such protoplanetary disks can be linked to some extent to the planetary environment (e.g., atmospheric composition) where further chemical reactions might lead to formation of building blocks of life. This presentation includes the topics on detailed disk density structures at ~5-au or better resolution, gas detections in the later stages of disks where the collisional events in the planetary systems may happen, detections of organic molecules, and the prospects on disk observations in future.

Keywords: Exoplanets, Astronomy

©2019. Japan Geoscience Union. All Right Reserved. 

# Characterization of high molecular weight amino acid precursors formed in interstellar ice analog

*Soushi Kuramoto[1], Tomohito Sato[1], Hitoshi Fukuda[2], Yoshiyuki Oguri[2], Kotaro Kondo[2], Hiromi Shibata[3], Yoko Kebukawa[1], Kensei Kobayashi[1], Satoshi Yoshida[4]

1. Yokohama National University, 2. Tokyo Institute of Technology, 3. University of Osaka, 4. National Institutes for Quantum Radiological Science and Technology

It is suggested that extraterrestrial organic compounds are important for chemical evolution toward the generation of the first life on the Earth. Bioorganic compounds such as amino acids were found in hydrolyzed extracts of meteorite [1]. The products before hydrolysis referred to as “amino acid precursors” were, however, little known. It has been sometimes claimed that a-amino acids found in meteorites were formed by the Strecker synthesis. If so, aminonitriles and amino acid amides are the precursors, but they have not identified as major precursors yet. Extraterrestrial amino acid precursors were probably synthesized in molecular cloud environments or small celestial bodies. We irradiated possible interstellar media, such as mixture of carbon monoxide, ammonia and water to simulate possible reactions among interstellar media in dense clouds. The irradiation products were analyzed by HPLC and mass spectrometry.

A gaseous mixture (CO and $NH_3$) was sealed in a Pyrex glass tube with liquid water. The gaseous mixture was irradiated with 2.5 MeV protons from a Tandem accelerator at Tokyo Institute of Technology. Total quantity of electricity was 2 mC. The name of the irradiation products is hereafter called CAW. CAW was fractionated by cation exchange HPLC into several fractions to discriminate the fractions with glycine amide or aminoacetonitrile (the Strecker-type precursors) and those without them. Each fraction was hydrolyzed with 6M HCl at 110 ˚C for 24h and was subjected to amino acid analysis. Molecular weights of CAW were estimated by ultrafiltration (molecular weight cut off: 3000), gel filtration (column: Shodex OHpak SB-802.5 HQ) and mass spectrometry by ESI-TOF-MS.

It was shown that glycine was rarely detected in the fractions with the Strecker-type simple amino acid precursors (aminoacetonitrile, glycine amide). It was suggested that the CAW (an interstellar organics analogue) contained complex amino acid precursors with molecular weights of some thousands. Compared with molecular weights standards (authentic proteins), molecular weights of CAW were estimated 6000 or more by gel filtration chromatography. Peaks of $m/z$ = 1000 or over were detected by mass spectrometry. These results strongly suggested that complex amino acid precursors with large molecular weights could be directly generated from small molecules such as CO in interstellar environments. We are now trying to characterize amino acid precursors formed in interstellar ice analogue (frozen mixture of CH3OH, NH3 and H2O [2]) by heavy ions irradiation.

[1] K. A. Kvenvolden *et al.*, *Nature* 228, 923 (1970).

[2] K. Kobayashi *et al.*, *Electr. Commun.* Jpn. 91, 293 (2008).

Keywords: Chemical evolution, interstellar ice, the Strecker synthesis, amino acid precursor

©2019. Japan Geoscience Union. All Right Reserved. 

# Theoretical elucidation of prebiotic formation processes into nucleobases

*Yu Komatsu[1,2], Taiki Suzuki[1,2]

1. Astrobiology Center, 2. National Astronomical Observatory of Japan

As argued [1], the comets and meteorites may have provided a large amount of prebiotic molecules to the Early Earth. However, where and how such organic molecules were built is still controversial.

Recently, volatile glycine (NH2CH2COOH) has been detected in the coma of comet 67P/Churyumov-Gerasimenko by the ROSINA mass spectrometer [2], with giving us clues to glycine's interstellar origin. Moreover, in addition to various amino acids, nucleobases, such as purine, uracil, guanine, and xanthine have been identified in the meteorite (e.g., [3]). These studies suggest the formation of prebiotic molecules in the extreme condition prior to the early Earth chemistry.

If prebiotic molecules are built from small atoms or radicals in the cold ISM, the prebiotic molecules must have almost barrier-less formation paths. On the other hand, the bombardment of comets and/or asteroids would have provided very high temperature condition for chemical reactions, which may have led to the decomposition and formation of further complex prebiotic molecules. To understand the formation processes, the quantum chemical calculation is a powerful tool. The previous quantum chemical calculation has already reported the promising chemical paths to amino acids and nucleobases (e.g., [4]).

Here we investigated the possible pathway of pyrimidine, purine, uracil and thymine by the automated exploration of chemical reaction pathways. We have already discovered key dissociations for each molecule. For example, uracil and thymine, the pyrimidine type of nucleobase, have lower barriers to dissociate into an isocyanic acid, which corresponds to the previous laboratory experience, and the rest molecule. Pyrimidine and purine, which are skeleton structures of nucleobases and do not poses any oxygen atoms, have high barriers, implying to require high temperature environment like the bombardment, even though we did not exclude all possibilities of radical reactions. Detailed discussions will be provided on our poster.

References

[1] Ehrenfreund (2002), Rep. Prog. Phys. 65 1427

[2] Altwegg et al. (2016), Sci, 2, e1600285

[3] Simomiya et al. (1990), Geo, 24,343

[4] Ferus et al. (2015), PNAS, 112, 7109

Keywords: Prebiotic Chemistry, Quantum Chemistry, DNA /RNA, Interstellar Chemistry

©2019. Japan Geoscience Union. All Right Reserved. 

©2019. Japan Geoscience Union. All Right Reserved. 

# Formation Process of A Glycine's Precursor Candidate, CH3NH2

*Taiki Suzuki[1,2], Liton Majumdar[3], Masatoshi Ohishi[2]

1. National Institutes of Natural Sciences Astrobiology Center, 2. National Astronomical Observatory of Japan, 3. NASA Jet Propulsion Laboratory (JPL)

As [1] argued, the comets and meteorites may have provided a large amount of prebiotic molecules to the early Earth. An attempt to understand the origins of life must necessarily begin with detailed studies of the formation and evolution of complex organic molecules (COMs), products of complex chemistry that most likely starts in molecular clouds and continues within the protoplanetary disk.
Since the amino acids are the essential building blocks of life, the search for amino acids and their complex organic precursors at different stages of star and planet formation is one of the exciting topics in modern astronomy. Recently, volatile glycine ($NH_2CH_2COOH$) was detected in the coma of comet 67P/Churyumov-Gerasimenko by the ROSINA mass spectrometer [2], also giving clues about glycine's interstellar origin. However, the survey observations of glycine toward ISM have been not successful. Therefore, revealing the formation pathways to glycine is important for astrochemistry and astrobiology not only to know the promising glycine-rich sources for future surveys but also to understand the general chemical evolution of N-bearing molecules in the ISM.
In this context, we performed the chemical modeling study for the high-mass star, with the possible formation processes of glycine with theoretically and/or experimentally suggested formation paths [3]. We suggested that glycine was efficiently formed through the following reactions: First, the hydrogenation process to HCN leads to the formation of $CH_2NH$ and $CH_3NH_2$ on interstellar grain surface (HCN + 2H => $CH_2NH$, and then $CH_2NH$ + 2H => $CH_3NH_2$). Then, the destruction of $CH_3NH_2$ by radicals will form $CH_2NH_2$. Finally, $CH_2NH_2$ and COOH radical react to form glycine. For this test, a key molecule would be $CH_3OH$, whose formation process is well known. Both experiments and theoretical works suggested that $CH_3OH$ is built via grain surface hydrogenation processes to CO (CO + 2H => $H_2CO$, and then $H_2CO$ + 2H => $CH_3OH$). If $CH_3NH_2$ is also produced through hydrogenation process, “$CH_3NH_2/CH_3OH$” ratio should be well reproduced by the modeling. However, it was difficult to test this formation process due to the very limited number of previous CH3NH2 observations.
With this motivation, we performed the observation of $CH_3NH_2$ and $CH_3OH$ with ALMA toward high mass star-forming regions, G10.47+0.03, NGC6334I, W51 e1/e2, and G31.41+0.3. As a result, both of $CH_3OH$ and $CH_3NH_2$ were detected toward all sources. The molecular abundances were derived with rotation diagram method. The high excitation temperatures of 100 and 200 K and compact distributions suggest that $CH_3NH_2$ emissions originate from the hot and dense regions. The observed molecular abundance ratio, “$CH_3NH_2/CH_3OH$” ranges from 0.2 to 2.1. The low “$CH_3NH_2/CH_3OH$” ratio of 0.2 is close to our modeling, supporting that $CH_3NH_2$ is the product of the hydrogenation process in those sources. However, the higher “$CH_3NH_2/CH_3OH$” ratio of nearly two, observed toward NGC6334I MM1, could not be reproduced with our modeling under the possible parameter range. Thus, our chemical modeling would not correctly reproduce the physics or chemistry of such $CH_3NH_2$-rich sources. Further studies of such sources will enable us to promote our knowledge of glycine chemistry and provide us with promising sources for future glycine surveys.

Citations:
[1] Ehrenfreund (2002), Rep. Prog. Phys. 65 1427

©2019. Japan Geoscience Union. All Right Reserved. 

[2] Altwegg et al. (2016), Sci, 2, e1600285
[3] Suzuki et al, (2018), ApJ, 825, 51

Keywords: radio astronomy, chemical modeling, prebiotic molecules

©2019. Japan Geoscience Union. All Right Reserved. 

# Numerical study on the stellar atmosphere & wind of Cool Stars

*Takahito Sakaue[1], Kazunari Shibata[1]

1. Kyoto University

Cool stars offer the good opportunities to investigate what environments the Earth-like exoplanets are in, and how they are affected by the host star. TRAPPIST-1 is an ultracool dwarf; the spectral type is M8V ($T_{eff}$ =2559K) with the lower mass of 0.08$M_{sun}$ (radius = 0.11$R_{sun}$). The star is confirmed to have seven planets (Gillon et al. 2017) and thus greatly interested in not only by stellar astrophysics but also by astrobiology. Here, we report the results of one-dimensional magnetohydrodynamic (MHD) simulation of the stellar wind from TRAPPIST-1. Several solar wind theories, which have been examined observationally, are applied to the case of TRAPPIST-1. Among them, it is the plausible idea that the dissipation of the incompressible MHD wave leads to the heating and driving the stellar wind. For instance, Garraffo et al. 2017 succeeded in the three-dimensional MHD simulation of the stellar wind from TRAPPIST-1, by extending their solar wind model in which the incompressible MHD wave is exhausted by the turbulent dissipation. The incompressible MHD wave, on the other hand, is also affected not only by the turbulent dissipation but also by the nonlinear mode coupling, which leads to the formation of the shock wave and consequently contribute to heating the wind. This nonlinear process has been well investigated to account for the dynamics of the lower solar atmosphere (Kudoh & Shibata 1999) and driving the solar wind (Suzuki & Inutsuka 2005), but not discussed for the stellar wind from TRAPPIST-1. In this study, therefore, we performed the one-dimensional MHD simulation to consider the nonlinear process of the incompressible MHD wave leading to the shock formation, and succeeded in reproducing the stellar wind from TRAPPIST-1.

Keywords: stellar wind, cool stars, TRAPPIST-1

©2019. Japan Geoscience Union. All Right Reserved. 

# Design of space exposure experiments of organic matter in Tanpopo 2

*Takuya Yokoo[1], tomohito sato[1], Itsuki Sakon[2], Kazumichi Nakagawa[3], Hajime Yano[4], Miki Nakayama[5], Hajime Mita[5], Yoko Kebukawa[1], Kensei Kobayashi[1]

1. Yokohama National University, 2. University of Tokyo, 3. Kobe University, 4. JAXA, 5. Fukuoka Institute of Technology

## 1. Introduction

Large number of organic compounds have been discovered in molecular clouds and in meteorites. Some of organic compounds required for emergence of life are thought to be synthesized in space. Then, meteorites and interplanetary dust particles could deliver them to the Earth. The first Japanese astrobiology space experiment called “Tanpopo” was conducted to study this hypothesis[1].
The objective of the Tanpopo Mission is to understand bi-directional propagation of microorganisms and organic matter between the Earth and space. In other words, in the Tanpopo Mission, we examine whether life exists only on the earth by evaluating whether microorganisms can escape into space and whether organic matter can reach to the Earth from outer space.
As one of subthemes in this project, amino acids and their precursor compounds including complex interstellar organic matter analog were directly exposed to outer space by utilizing the International Space Station (ISS), and recoveries of these organics were measured to understand degradation of organic compounds under the environment of the outer space. In the Tanpopo experiment, hexatriacontane (HTC) was used to prevent the sample from sublimation during exposure to space at the ISS. However, HTC absorbs ultraviolet light with a wavelength of 160 nm or less. To understand the effects of shorter wavelength UV, the next space experiment "Tanpopo 2" applies a new design for direct exposure of organic compounds without HTC and optical windows. In addition to the aluminum plate same as the one used in Tanpopo, the silicon substrates are also used for exposure the sample to space, in the organic matter exposure experiment of “Tanpopo 2 “. In the Tanpopo Mission, glycine, hydantoin, isovaline, ethylmethylhydantoin, CAW (complex organic matter produced from proton beam irradiation to CO, $NH_3$, $H_2O$ mixture) were used, and glycine and CAW showed relatively high recoveries [2]. In "Tanpopo 2", glycine and CA (proton beam irradiation product to CO, $NH_3$ mixture) on the silicon substrates will be directly exposed to space in addition to the same compounds on the same aluminum plate used in the Tanpopo. The recovered samples will be analyzed by FT-IR, XANES, and SEM, in addition to amino acid analysis.
Here we report the design of the space experiment such as preparation method of the space experiment sample.

## 2. Experimental

(1) A gas mixture of CO (350 Torr) and $NH_3$ (350 Torr) and a silicon plate (10 mm$\phi$) were placed in a glass container, and the gas mixture was irradiated with 2.5 MeV proton beam from a tandem accelerator to deposit organic matter on the plate.
(2) The thickness of the organic matter (CA) film on the silicon plate was measured using a three-dimensional microscope.
(3) Structural analysis of organic matter (CA) on the silicon plate was also carried out using FT-IR.
(4) Amino acid analysis was carried out by cation exchange HPLC after hydrolyzing silicon plate with CA with 6 M hydrochloric acid at 110 ˚C for 24 hours.

©2019. Japan Geoscience Union. All Right Reserved. 

(5) Glycine is planned to be deposited on a silicon substrate by a vacuum vapor deposition equipment (Fukuoka Institute of Technology).

3. Results and Discussion

The CA deposition thickness was approximately 8 μm, but more sample thickness would be required due to potential loss of the organic materials by atomic oxygen present in low Earth orbit during exposure. Thus, we decided to use non-polished Si substrates instead of polished Si substrate. Because the sample can be kept in the bottom of indentations on the rough surface of non-polished substrate, even if a part of sample surface is lost.
Amino acid analyses of CA by cation exchanged HPLC showed, various amino acids including aspartic acid, threonine, glycine, alanine, -aminoisobutyric acid and serine were detected after acid hydrolysis. Glycine was particularly abundant, whose yield was 827 ±7 nmol from a single CA deposited Si substrate.

4. Conclusions

We will conduct the durability test of our samples on the silicon substrate including the vibration test, cooling test, heating test before launch in 2019 with the space X company to the ISS. We are planning to conduct various analyses from recovered samples. The recovery and degradation of these samples will make a further leap forward our understanding of the possible delivery of organic matter from interplanetary dust particles to the early Earth.

5. References

[1] A. Yamagishi, H. Yano, K. Okudaira, K. Kobayashi, S. Yokobori, M. Tabata, H. Kawai, *Biol. Sci. Space*, **21** : 67-75 (2007).
[2] K. Kobayashi *et al.*, 2018 JpGU meeting, Chiba (2018).

©2019. Japan Geoscience Union. All Right Reserved. 

[E] Poster | M (Multidisciplinary and Interdisciplinary) : M-IS Intersection

Thu. May 30, 2019 5:15 PM - 6:30 PM JST | Thu. May 30, 2019 8:15 AM - 9:30 AM UTC | Poster Hall International Exhibition Hall8, Makuhari Messe_37

## [M-IS07] Astrobiology

convener:Hikaru Yabuta(Hiroshima University, Department of Earth and Planetary Systems Science), Seiji Sugita(Department of Earth and Planetary Science, Graduate School of Science Sciece, The University of Tokyo), Misato Fukagawa(National Astronomical Observatory of Japan), Fujishima Kosuke(Tokyo Institute of Technology, Earth-Life Science Institute)

Twenty years have passed since when the field of Astrobiology, which aims to unveil the origins, evolution, and habitability of life by integrating multidisciplinary fields, was established. Individual themes related to Astrobiology, such as chemical evolution in the early Solar System, formation of planetary system, prebiotic chemistry in the early Earth, evolution of life in the Earth's history, extremophile, and habitable planetary environments, has been studied by the knowledge and methods from the multiple fields, which has enabled us to explain "Where we came from" in some ways. However, despite an overwhelming number of investigations and discussions through gathering of the scientists from different fields, there has remained the long-standing unsolved question: How did abiotic materials gain biological function in the Earth and elsewhere in universe? There is still a large gap between prebiotic organic chemistry and biochemistry toward Origins of Life and planetary habitability. Therefore, the JpGU Astrobiology session focuses on pathfinding of "integration of astronomy, geoscience, and biochemistry", which will face an increasing need for the future Astrobiology. In order to enhance our understanding of "What is life", we propose to discuss the biochemical events linked with planetary systems, which is beyond the knowledge in a test tube, by an integration of exoplanets and molecular biology, etc. Through this approach, we will lead the discussions and developments of life-detection strategies for the future exploration of life in universe.

### [MIS07-P01] Exoplanets Revealed by High-Precision Infrared Doppler Technique Using IRD: Large Exploration for Planets around Cool M-type Stars Begins

*Masayuki Kuzuhara[1,3], Bunei Sato[4], Motohide Tamura[2,1,3], Takayuki Kotani[1,3,5], Nagayoshi Ohashi[3,6], Masashi Omiya[1,3], Teruyuki Hirano[4], Hiroki Harakawa[6,3,1], Wako Aoki[3,5], Norio Narita[2,1], Yasunori Hori[1,3], Akitoshi Ueda[3,5], Akihiko Fukui[2], Hiroyuki Tako Ishikawa[5,3], Ishizuka Masato[2], Takashi Kurokawa[1,7], Nobuhiko Kusakabe[1,3], Tomoyuki Kudo[6,3,1], Eiichiro Kokubo[3], Mihoko Konishi[1,3], Tadashi Nakajima[1,3,5], Jun Nishikawa[3,5,1], Masahiro Ogihara[3], Takuma Serizawa[7] (1.Astrobiology Center of NINS, 2.The University of Tokyo, Graduate School of Science, 3.National Astronomical Observatory of Japan, 4.Tokyo Institute of Technology, 5.SOKENDAI, 6.Subaru Telescope, 7.Tokyo University of Agriculture and Technology)

### [MIS07-P02] Discrimination of organic compounds and mineral particles by fluorescent microscopy for the detection of Martian life.

*Tomoka Okada[1], Yoshitaka Yoshimura[2], Atsuo Miyakawa[3], Yuka Murano[3], Shin-ichi Yokobori[3], Akihiko Yamagishi[3], Kensei Kobayashi[1], Yoko Kebukawa[1] (1.YOKOHAMA National university, 2.Tamagawa University, 3.Tokyo University of Pharmacy and Life Sciences)

### [MIS07-P03] Morphological and spectroscopic characteristics of organic matter in Banded Iron Formation, Barberton Greenstone Belt, South Africa

*Hiroki Amemiya[1], Ryo Nakajima[1], Yoko Ohtomo[1], Tsubasa Otake[1], Tsutomu Sato[1] (1.Division of sustainable Resources Engineering, Faculty of Engineering, Hokkaido University)

### [MIS07-P04] Understanding peptide sequence selectivity on iron sulfide (FeS) nanoparticle surfaces

*Fujishima Kosuke[1], Norio Kitadai[1], Kenji Kasama[1] (1.Earth-Life Science Institute, Tokyo Institute of Technology)

### [MIS07-P05] A process model of L-homochiral peptides formation initiated with L-alanine

*Toratane Munegumi[1], Taisuke Yamaga[1] (1.Department of Science Education, Naruto University of Education)

[MIS07-P06] Possible Formation of Amino Acids and Carboxylic Acids in Slightly-Reducing Primitive Earth Atmospheres

*Miei Kinoshita[1], Shintaro Ikeda[1], Kimitaka Kawamura[2], Bhagawati Kunwar[2], Hitoshi Fukuda[3], Yoshiyuki Oguri[3], Hiromi Shibata[4], Junichi Takahashi[1], Vladimir Airapetian[5], Yoko Kebukawa[1], Kensei Kobayashi[1] (1.Yokohama National University, 2.Chubu University, 3.Tokyo Institute of Technology, 4.Osaka University, 5.NASA Goddard SFC)

[MIS07-P07] Application of Machine learning and software development for initial analysis in the TANPOPO mission

*Kyoko Okudaira[1], Yuto Toda[1], Takashi Sonoke[1], Yuichi Yaguchi[1], Masashi Yoshida[1], Junya Imani[2], Satoshi Sasaki[3], Hajime Yano[4], Hirohide Demura[1], Makoto Tabata[5], Akihiko Yamagishi[6] (1.The University of Aizu, 2.YUKI Precision, 3.Tokyo University of Technology, 4.JAXA, 5.Chiba University, 6.Tokyo University of Pharmacy and Life Science)

[MIS07-P08] Structure analysis of the hyper velocity impact tracks of the particles captured by silica aerogel on the International Space Station

*Mizuho Nishi[1], Akira Tsuchiyama[1], Hajime Yano[2], Hikaru Yabuta[3], Kyoko Okudaira[4], Junya Matsuno[1], Masayuki Uesugi[5], Uesugi Kentaro[5], Nakano Tukasa[6], Takaaki Noguchi[7], MITA Hajime[8], Akihiko Yamagishi[9] (1.Kyoto University, 2.Institute of Space and Astronautical Science, Japan Aerospace Exploration Agency, 3.Hiroshima University, 4.The University of Aizu, 5.JASRI/SPring-8, 6.National Institute of Advanced Industrial Science and Technology, 7.Kyusyu University, 8.Fukuoka Institute of Technology, 9.Tokyo University of Pharmacy and Life Science)

[MIS07-P09] High-Angular-Resolution Observations of Protoplanetary Disks

*Misato Fukagawa[1] (1.National Astronomical Observatory of Japan)

[MIS07-P10] Characterization of high molecular weight amino acid precursors formed in interstellar ice analog

*Soushi Kuramoto[1], Tomohito Sato[1], Hitoshi Fukuda[2], Yoshiyuki Oguri[2], Kotaro Kondo[2], Hiromi Shibata[3], Yoko Kebukawa[1], Kensei Kobayashi[1], Satoshi Yoshida[4] (1.Yokohama National University, 2.Tokyo Institute of Technology, 3.University of Osaka, 4.National Institutes for Quantum Radiological Science and Technology)

[MIS07-P11] Theoretical elucidation of prebiotic formation processes into nucleobases

*Yu Komatsu[1,2], Taiki Suzuki[1,2] (1.Astrobiology Center, 2.National Astronomical Observatory of Japan)

[MIS07-P12] Formation Process of A Glycine's Precursor Candidate, CH3NH2

*Taiki Suzuki[1,2], Liton Majumdar[3], Masatoshi Ohishi[2] (1.National Institutes of Natural Sciences Astrobiology Center, 2.National Astronomical Observatory of Japan, 3.NASA Jet Propulsion Laboratory (JPL))

[MIS07-P13] Numerical study on the stellar atmosphere & wind of Cool Stars

*Takahito Sakaue[1], Kazunari Shibata[1] (1.Kyoto University)

[MIS07-P14] Design of space exposure experiments of organic matter in Tanpopo 2

*Takuya Yokoo[1], tomohito sato[1], Itsuki Sakon[2], Kazumichi Nakagawa[3], Hajime Yano[4], Miki Nakayama[5], Hajime Mita[5], Yoko Kebukawa[1], Kensei Kobayashi[1] (1.Yokohama National University, 2.University of Tokyo, 3.Kobe University, 4.JAXA, 5.Fukuoka Institute of Technology)

# Exoplanets Revealed by High-Precision Infrared Doppler Technique Using IRD: Large Exploration for Planets around Cool M-type Stars Begins

*Masayuki Kuzuhara[1,3], Bunei Sato[4], Motohide Tamura[2,1,3], Takayuki Kotani[1,3,5], Nagayoshi Ohashi[3,6], Masashi Omiya[1,3], Teruyuki Hirano[4], Hiroki Harakawa[6,3,1], Wako Aoki[3,5], Norio Narita[2,1], Yasunori Hori[1,3], Akitoshi Ueda[3,5], Akihiko Fukui[2], Hiroyuki Tako Ishikawa[5,3], Ishizuka Masato[2], Takashi Kurokawa[1,7], Nobuhiko Kusakabe[1,3], Tomoyuki Kudo[6,3,1], Eiichiro Kokubo[3], Mihoko Konishi[1,3], Tadashi Nakajima[1,3,5], Jun Nishikawa[3,5,1], Masahiro Ogihara[3], Takuma Serizawa[7]

1. Astrobiology Center of NINS, 2. The University of Tokyo, Graduate School of Science, 3. National Astronomical Observatory of Japan, 4. Tokyo Institute of Technology, 5. SOKENDAI, 6. Subaru Telescope, 7. Tokyo University of Agriculture and Technology

Planets outside the Solar system, so-called exoplanets, are promising as a new window for astrobiology. Among those, planets orbiting cool M-type stars (main-sequence stars with effective temperatures less than about 3000 K) have the great potential to push forward astrobiological studies on exoplanets. The habitable zone (HZ) is the zone where liquid water is sustainable on the surfaces of planets. It is expected that the HZs around cooler stars come closer to the parent stars (Kopparapu et al. 2013, ApJ 765, 131). In addition, the recent exoplanet observations performed by the *Kepler* space telescope have revealed that the occurrence rate of small exoplanets similar to Earth increases as the effective temperatures of stars decrease (e.g., Mulders et al. 2015, ApJ 798, 112). Furthermore, the Doppler technique, one of primary methods for exoplanet observations, can more easily find a planet with the orbit closer to its parent star. Accordingly, targeting cool M-type stars provides a significant advantage in the observations of rocky planets in HZs based on the Doppler technique. Also, the snow line around a cool M-type star is close to the star; this is intriguing in terms of the planet formation process.
Nevertheless, the exoplanet observations for cool M-type stars have not been advanced compared with those for hotter stars, due to their faintness. In particular, the low brightness of a cool M-type star at optical wavelengths makes it problematic to observe its planet based on visible light, which has been mostly used in exoplanet observations. We have therefore developed the InfraRed Doppler (IRD) instrument, which is a high-dispersion spectrograph to enable the exoplanet observations using the high-precision Doppler technique at near-infrared (Kotani et al. 2018, Proc. of the SPIE 10702, 1070211). Near-infrared light is suited for observing cool M-type stars, since their peak flux is located in a near-infrared region. One of bottlenecks to achieve high-precision measurements using the near-infrared Doppler technique is the lack of a reference source that enables us to correctly calibrate a measurement fluctuation caused by the instability of an observation instrument. We use a laser frequency comb (LFC) generated by the system that has been newly developed for IRD as a reference source to calibrate IRD measurements. An LFC spectrum has a number of emission lines with fine sampling intervals and is observed simultaneously with a stellar spectrum, so it works as a correct wavelength calibrator for the stellar spectrum. After our laboratory performance verifications of IRD with its LFC system (Kuzuhara et al. 2018, Proc. of the SPIE 10702, 1070260), the IRD operation started on the Subaru Telescope, whose large primary mirror enables high-sensitivity observations even for cool M-type stars. The use of IRD with the Subaru Telescope significantly helps the discoveries and characterizations of exoplanets around cool M-type stars.
We have planned a large survey for planets around cool M-type stars with IRD on the Subaru Telescope, which actually begins on February, 2019. In this survey, we monitor 60 M-type stars over 175 nights

©2019. Japan Geoscience Union. All Right Reserved. 

allocated for 5 years. Our pre-survey simulation prospects more than 60 planet detections; those discoveries include a few dozen Earth-like planets, among which some are expected to locate within HZs. Thus, the IRD survey provides important contributions on improving our current understanding of planet formation models for low-mass stars like cool M-type stars, as well as the provisions of samples for exoplanet characterizations using the future large telescopes such as TMT. Here, we report the result of our ongoing on-sky tests to evaluate the IRD performances such as its measurement precision and stability. Furthermore, we explain the above large program in detail: our science goals, and the target selection and observation strategy for the goals are provided.

Keywords: Exoplanet, Doppler technique, Habitable Zone, IRD, planet formation, M-type star

©2019. Japan Geoscience Union. All Right Reserved. 

# Discrimination of organic compounds and mineral particles by fluorescent microscopy for the detection of Martian life.

*Tomoka Okada[1], Yoshitaka Yoshimura[2], Atsuo Miyakawa[3], Yuka Murano[3], Shin-ichi Yokobori[3], Akihiko Yamagishi[3], Kensei Kobayashi[1], Yoko Kebukawa[1]

1. YOKOHAMA National university, 2. Tamagawa University, 3. Tokyo University of Pharmacy and Life Sciences

The Viking mission searched life on Mars in 1976, but did not find apparent biological activities[1)]. However, the detection sensitivity of the Viking instrument (GC-MS) has been found to be low, suggesting that organic compounds could exist on Martian surface. Recently the MSL Curiosity by NASA detected organic compounds[2)]. The Phoenix mission discovered $H_2O$ ice[3)] and possible liquid water flows were found at RSL (Recurring Slope Lineae) by MRO (Mars Reconnaissance Orbiter)[4)]. These findings suggested that life might exist on Martian surface.

We have proposed a life search program on the surface of Mars with a fluorescence microscope[5)]. This microscope is called Life detection Microscope (LDM) which detects microorganisms in more than 100 times higher sensitivity than the Viking GC-MS. In this program, we plan to use two fluorescent dyes SYTO 24 and propidium iodide (PI) in LDM. SYTO24 permeates cell membrane and stains organic compounds. PI also stains organic compounds such as nucleic acids, but it doesn’t permeate cell membrane. Therefore, the combination of these two dyes makes it possible to differentiate the organic compounds surrounded by membranes (living cells) and dead cells.

However, there are some mineral particles have autofluorescence, possibly detected as false positives. In this research, in order to discriminate organic compounds from mineral particles, the autofluorescence of minerals were measured under various conditions.

Various kind of mineral specimens were finely ground with a glass pen washed with ethanol. Fluorescent images were obtained with a fluorescence microscope and a digital camera and their fluorescent intensities were measured by image analysis. We also examined fluorescent spectra of mineral particles using a diffraction grating. The results showed the fluorescent intensities and spectra of mineral particles were clearly different from the stained organic compounds. These methods would be useful to detect organic compounds among mineral particles.

1) Navarro-Gonzalez, R., *et al.,* 2006, *PNAS*, 103: 16089-16094. 2) Freissient, C., *et al*., 2015, *J. Geophys. Res. Planets,* 120: 495-514. 3) Feldman, W. C., *et al.,* 2002. *Science*, 297, 75-78. 4) McEwen A. S, *et al.,* 2011, *Science,* 333: 740-743. 5) Yamagishi, A., *et al*., 2010, *Bio. Sci. Space,* 24: 67-82.

Keywords: Mars, Fluorescent microscope, Life Detection

©2019. Japan Geoscience Union. All Right Reserved. 

# Morphological and spectroscopic characteristics of organic matter in Banded Iron Formation, Barberton Greenstone Belt, South Africa

*Hiroki Amemiya[1], Ryo Nakajima[1], Yoko Ohtomo[1], Tsubasa Otake[1], Tsutomu Sato[1]

1. Division of sustainable Resources Engineering, Faculty of Engineering, Hokkaido University

The emergence of cyanobacteria has been postulated to cause an increase in Earth’ s atmospheric oxygen concentration ~2.45 Ga and oxidation of ferrous iron in a seawater, facilitating the formation of Banded Iron Formations (BIFs) in the Proterozoic era. On the other hand, iron precipitation process in the Archean is still controversial. Previous studies suggest that anoxygenic iron-oxidizing bacteria and/or free oxygen produced by cyanobacteria, was responsible for iron oxidation before ~2.45 Ga. Organic matter preserved in BIFs may provide insights into the iron oxidation process and biological evolution in Archean. However, authenticity of Archaean organic matter has to be first clarified for further investigations due to possible later contamination. Here, we investigated morphological and spectroscopic characteristics of organic matter in ~3.2 Ga BIFs in Sheba mine, Moodies Group, Barberton Green stone Belt, South Africa to estimate the chemical structure combined with a contamination check using Raman spectroscopy.

Organic matter was collected by two different methods: extraction by acid treatment of powder samples and pick up with a micro-manipulator from thin sections. When Raman spectra were obtained using 532 nm wavelength laser, acid-treated organic matter showed two peaks ~1350 and ~1580 $cm^{-1}$ corresponding to disordered and ordered carbon structures, whereas micro-sampled organic matter shows no detectable peak with a high background. Because yellow-green fluorescence was observed in micro-sampled organic matter using a Fluorescence microscope, the fluorescence likely causes a high background in the Raman spectra. Therefore, 785 nm wavelength laser was applied for micro-sampled organic matter. Calculated metamorphic temperature from the Raman spectra obtained by acid-treated and micro-sampled organic matter was from 400 to 540˚C, which is consist with greenschist facies of the Barberton Greenstone Belt. This indicates that the organic matter is not a later contamination. Chemical mapping with an Electron Probe Micro Analyzer shows that micro-sampled organic matter is predominately comprised of carbon with slight contribution of nitrogen (< 0.1wt%). Infrared spectra of the organic matter show absorption peaks corresponding to N-O, C-O, and C=O bonds, suggesting that organic matter remains their functional groups in the structure. Based on the morphology and microstructure observed by Field Emission- Scanning Electron Microscope, the organic matter may have been derived from biofilm because of similarity in the morphology as well as the large size (20 –50 $\mu$m). Furthermore, the micro-sampled organic matter has a rough surface while the acid-treated organic matter has a smooth one, which may be due to damages by acid-treatment. Our results suggest that micro-sampling is suitable to observe the detailed morphological and structural features of organic matter preserved in Archean sedimentary rocks.

Keywords: Archean, Microfossils, Barberton Greenstone Belt, Raman spectroscopy, Infrared spectroscopy

©2019. Japan Geoscience Union. All Right Reserved. 

# Understanding peptide sequence selectivity on iron sulfide (FeS) nanoparticle surfaces

*Fujishima Kosuke[1], Norio Kitadai[1], Kenji Kasama[1]

1. Earth-Life Science Institute, Tokyo Institute of Technology

The emergence and evolution of functional biopolymers on Earth is one of the unsolved key questions regarding the origin of life. Amongst various building blocks of polymers, amino acids are prebiotically abundant and different plausible paths toward forming polypeptides have been previously shown in the context of early Earth environment. However, relationship between a specific geochemical environment and the types of biopolymers that could retain or to propergate in that condition is not yet fully systematically explored. Hence, we have prepared random octapeptide library with a combination of limited set of amino acids (Gly, Ile, His, Asp, Cys, Arg) as a probe to explore the sequence selectivity of iron sulfide (FeS) nanoparticles as a simulant of the geochemical settings that once existed at the deep-sea floor or the surface of early Earth. Experiment was carried out by mixing the FeS nanoparticles and random peptides in pure $H_2O$ solution inside the anoxic chamber to allow adsorption under moderate temperature/pH condition. After extensive rinsing step, peptides that remain bound to the FeS nanoparticles were analyzed directly by MALDI-MS/MS to retrieve sequence information. We will discuss the latest sequence results obtained from screening and discuss sequence selective feature of FeS and its relevance to the iron-sulfur cluster known as a fundamental cofactor in biology.

Keywords: Iron sulfide, peptide adsorption, MALDI-MS/MS, iron-sulfur cluster

©2019. Japan Geoscience Union. All Right Reserved. 

# A process model of L-homochiral peptides formation initiated with L-alanine

*Toratane Munegumi[1], Taisuke Yamaga[1]

1. Department of Science Education, Naruto University of Education

Hydrogen abstraction from L-alanine by hydroxy radical facilitates alkylation on $\beta$-carbon of alanine as well as retention of L-chirality. The reaction rate constant of hydrogen abstraction ($k=6.21\times10^{7}\ M^{-1}s^{-1}$) on $\beta$-carbon was about 3.7 times faster than that ($k=1.7\times10^{7}\ M^{-1}s^{-1}$) on $\alpha$-carbon. The fact supports that alkylation proceeds faster than racemization, and the chirality of product amino acids will be hold. Similar alkylation of oligopeptides will also proceed with a lower level epimerization than alkylation. This research discusses how the lower reaction rate of epimerization than alkylation lead homochiral peptides.

Keywords: L-alanine, peptides, homochirality

©2019. Japan Geoscience Union. All Right Reserved. 

# Possible Formation of Amino Acids and Carboxylic Acids in Slightly-Reducing Primitive Earth Atmospheres

*Miei Kinoshita[1], Shintaro Ikeda[1], Kimitaka Kawamura[2], Bhagawati Kunwar[2], Hitoshi Fukuda[3], Yoshiyuki Oguri[3], Hiromi Shibata[4], Junichi Takahashi[1], Vladimir Airapetian[5], Yoko Kebukawa[1], Kensei Kobayashi[1]

1. Yokohama National University, 2. Chubu University, 3. Tokyo Institute of Technology, 4. Osaka University, 5. NASA Goddard SFC

Since 1950s, a large number of laboratory experiments have been performed to examine possible formation of bioorganic compounds such as amino acids in primitive Earth atmosphere. Earlier experiments with strongly reducing gas mixtures containing large molar ratio of methane and ammonia, and it was reported that efficient production of amino acids and other important organics were formed in it by spark discharges and other energy sources. It is now estimated, however, that the early Earth atmosphere was only slightly reducing [1]: $N_2$ and $CO_2$were the major atmospheric constituents, together with some small amount of reducing carbon species like $CH_4$ and/or CO. Simulation experiments suggested, however, that amino acid formation was restricted under these conditions [2]. We reported that cosmic rays could facilitate chemical reactions with less reducing model of primitive atmosphere such as a mixture of $CO_2$, CO, $N_2$and $H_2O$ [3]. However these energy sources have been ignored in experiments with initiation of prebiotic chemistry [4]. Here, we examine possible formation of amino acids from slightly reducing gas mixtures by applying high-energy protons to simulate the action of cosmic rays.

We conducted three sets of laboratory experiments using energetic particles, spark discharge and UV light as dominant energy sources. In these sets of experiments we used 400 mL of gas mixture of $N_2$, $CO_2$and $CH_4$introduced to a Pyrex tube together with 5 mL of pure water under 350 Torr of N2 and 350 Torr of mixtures with varied mixing ratios of $CH_4$and $CO_2$. In order to simulate possible roles of cosmic rays, the gas mixture was irradiated with 2.5 MeV proton beam produced in the Tandem accelerator at Tokyo Tech, Japan. We also exposed the same composition of gas mixtures to spark discharges by using a Tesla coil to simulate lightning. The gas mixtures were also irradiated with UV light (l> 190 nm) from a xenon lamp. Each product was acid-hydrolyzed and was subjected to amino acid analysis by HPLC and GC/MS, both after derivatization. Carboxylic acids were determined by GC/MS after derivatization. Starting and resulting gas mixtures were analyzed with a quadrupole mass spectrometer.

Amino acids were detected in the hydrolyzed products when gas mixtures of $N_2$, $CO_2$, $CH_4$and $H_2O$ were irradiated with 2.5 MeV protons at the initial the molar ratio of methane ($r_{CH4}$) in the starting gas mixture as low as 0.5 %. On the other hand, amino acids were detected only when $r_{CH4}$was greater than 15 % in the case of spark discharges. The experiments with UV irradiation source did not yield amino acids or their precursors even when $r_{CH4}$was 50 %. Very little amino acids were detected in all the products before hydrolysis. It was shown that not free amino acids but amino acid precursors were formed in selected experiments.

Carboxylic acids including formic acid, oxalic acid and glyoxylic acid were detected from unhydrolized products derived from $N_2$-$CO_2$gas mixtures exposed to spark discharges and proton irradiation. We show that some free carboxylic acids could be formed in non-reducing atmospheres as well as slightly reducing atmospheres either by proton irradiation or by spark discharges. It was suggested that the mechanism of formation of amino acid precursors from $N_2$-$CO_2$-$CH_4$-$H_2O$ mixtures was quite different from that of

©2019. Japan Geoscience Union. All Right Reserved. 

carboxylic acids.

Lightning and solar UV have been considered important energy sources for prebiotic synthesis in primitive Earth atmosphere. We here showed that lightning and solar UV could not singularly synthesize important N-containing organics such as amino acids from slightly reducing primitive Earth atmosphere. On the other hand, cosmic ray could have been an important energy source to synthesize amino acid precursors even if primitive Earth atmosphere was only slightly reducing. It would be of interest to examine whether there are synergetic effects among cosmic rays, UV and thundering.

**References:**

[1] H. Kuwahara and S. Sugita, *Icarus,* **257**,290-301 (2015).

[2] H. Kuwahara *et al.,Orig. Life Evol. Biosph.,* **42**,533-541(2012).

[3] K. Kobayashi *et al.*, *Orig. Life Evol. Biosph.* **28**, 155-165 (1998).

[4] S. L. Miller and H. C. Urey, *Science,* **130**,245-251 (1957).

Keywords: Primitive Earth Atmospheres, Amino Acids, Solar Energetic Particles

©2019. Japan Geoscience Union. All Right Reserved. 

# Application of Machine learning and software development for initial analysis in the TANPOPO mission

*Kyoko Okudaira[1], Yuto Toda[1], Takashi Sonoke[1], Yuichi Yaguchi[1], Masashi Yoshida[1], Junya Imani[2], Satoshi Sasaki[3], Hajime Yano[4], Hirohide Demura[1], Makoto Tabata[5], Akihiko Yamagishi[6]

1. The University of Aizu, 2. YUKI Precision, 3. Tokyo University of Technology, 4. JAXA, 5. Chiba University, 6. Tokyo University of Pharmacy and Life Science

One of the goals of the TANPOPO mission is collecting cosmic dust and space debris on the International Space Station [1]. Ultra-low density material “silica aerogel” panels are used as capture media [2]. These panels retrieved from the space are sent to the laboratory and initial analysis has been conducted by a system called “CLOXS”.

CLOXS efficiently covers the processes (1) Automatic imaging the entire panel, 2) Search for penetration track candidates, 3) Mapping of track candidates, 4) Shape data acquisition of tracks, and 5) Automatic sample cutting) up to sample allocation to researchers. However, to reduce researchers’ time and effort, improvement of the software and automation of some processes are required.

In this study, application of machine learning in discrimination of objects in aerogel images taken by CLOXS is mainly reported. The research goal is to classify objects in the images into tracks and dirt using machine learning.

There are morphological varieties in the objects. As for both tracks and dirt, they are classified into 4 types respectively in this study.

Since the contrast of the images are low, the first step of our approach is preprocessing of the images. We compared the results of *Contrast Stretching* and *CLAHE* (Contrast Limited Adaptive Histogram Equalization).

Learning data and test data are prepared respectively, to compare the case that the images are categorized into 4 types and the case that the images of all types are dealt altogether.

*Convolutional Neural Network* (CNN) is used as a method of machine learning. *Python* is used as programing Language.

In conclusion, as for image processing, *CLAHE* showed higher accuracy when tracks were judged to be tracks, and *Contrast Stretching* was found to yield a better result for dirt. It is probably because, in *Contrast Stretching*, *CNN* was not sufficiently highlighted to capture features, and *CLAHE* was able to improve the contrast sufficiently.

Regarding separating the types of tracks and dirt, the accuracy rate was higher when tracks were categorized into different types and learned.

Although further evaluation and improvements might be needed, our accuracy rates meet the mission requirements, that is, the percentage of identifying track as track should be more than 95 %, while the percentage of identifying dirt as dirt should be more than 70 % (that of NOT identifying true track as dirt

©2019. Japan Geoscience Union. All Right Reserved. 

should be less than 30 %).

[1] A. Yamagishi et al., “Tanpopo: Astrobiology exposure and micrometeoroid capture experiments - proposed experiments at the exposure facility of ISS-JEM”, *Trans. JSASS. Aerospace Tech. Jpn.* vol. 12, No. ists29, p. Tk_49-Tk_55, 2014.

[2] M. Tabata, et al. “Ultralow-density double-layer silica aerogel fabrication for the intact capture of cosmic dust in low-Earth orbits” *J. Sol-Gel Sci. Technol.* 77(2), 325-334, 2016.

Keywords: TANPOPO mission, Astrobiology, Initial analysis, Machine learning, Software development

©2019. Japan Geoscience Union. All Right Reserved. 

# Structure analysis of the hyper velocity impact tracks of the particles captured by silica aerogel on the International Space Station

*Mizuho Nishi[1], Akira Tsuchiyama[1], Hajime Yano[2], Hikaru Yabuta[3], Kyoko Okudaira[4], Junya Matsuno[1], Masayuki Uesugi[5], Uesugi Kentaro[5], Nakano Tukasa[6], Takaaki Noguchi[7], MITA Hajime[8], Akihiko Yamagishi[9]

1. Kyoto University, 2. Institute of Space and Astronautical Science, Japan Aerospace Exploration Agency, 3. Hiroshima University, 4. The University of Aizu, 5. JASRI/SPring-8, 6. National Institute of Advanced Industrial Science and Technology, 7. Kyusyu University, 8. Fukuoka Institute of Technology, 9. Tokyo University of Pharmacy and Life Science

In Japan's first astrobiology experiment “Tanpopo”, attempts have been made to capture cosmic dust by installing ultra-low-density silica aerogel at the Japanese Experiment Module “Kibo” of the International Space Station (ISS) [1]. This mission was conducted with the aim of verifying the hypothesis that the origin of life was supplied from outside the earth [2]. Silica aerogel had been used in NASA’s cometary dust sample return mission “Stardust” [3]. Impact tracks formed by collision of cometary dust against aerogel were classified into 3 types, A, B and C, based on their shapes [4]. The track shapes have useful information for estimating the size and density of dust particles [5]. The purposes of this research are (1) to find impact tracks formed by cosmic dust in Tanpopo aerogel and (2) to describe the three-dimensional shapes of impact tracks with different origins (cosmic dust and space debris) and finally to clarify the relation between the track shape and the origin.

At SPring-8 BL47XU, three-dimensional shapes were obtained with imaging absorption tomography for 8 impact tracks (D1-231, D1-298, D1-362, E1-200, E1-304, F1-328, F1-389, F1-623), which were found in Tanpopo aerogel faced to the space direction. The imaging experiments were made at 7, 8, 9 keV with the voxel size of 0.24 or 0.465 $\mu$m. CT images at 8 keV were used to extract track shapes. Track length ($L_t$), maximum track diameter ($D_m$), aspect ratio, and other shape properties were obtained. These values were compared with Stardust tracks. Dual-energy tomography (DET) [6] was applied to estimate the materials of particles captured in the tracks. Another track (E2-000) was observed only with an optical microscope. For D1-231, D1-298, D1-362 and E2-000, the aerogel was compressed and real solid particles in the tracks were searched with an optical microscope.

The 9 tracks in total were classified into 5 types based on their shapes. Type 1 (E2-000) is a track formed by cosmic dust, where two pyroxene particles were identified at the tip of the track [7]. The track shape resembles Stardust type B track, but its entrance widely spreads. Type 2 (D1-231) is somewhat similar to Stardust type A track. Type 3 (E1-200 and E1-304) is a track having abundant cracks developed on the wall with a narrow entrance. Type 4 (F1-328 and F1-389) is extremely asymmetrical in its shape and has cracks similar to Type 3. Type 5 (D1-362 and F1-623) is a bowl-shaped track with a large entrance. The relationship between $L_t$ and $D_m$ of these tracks was almost the same as that of Stardust tracks except for Type 5. However, their specific shapes of Types 2, 3 and 4 are significantly different from Stardust tracks. The cracks of these tracks are similar to those seen at the end of Stardust type A and B tracks, indicating that they were formed by a relatively low-speed impact. Similar tracks to Type 5 were reported in the aerogel in the exposure experiment on the Mir Station. They may be due to high-speed collision of weakly-adhered aggregates [8]. From the quantitative analysis of such impact tracks, there is a possibility of obtaining knowledge about new parameter areas which could not be obtained by conventional research. DET results showed that most of fine particles in the tracks do not contain Fe and Ni. Low values of their

©2019. Japan Geoscience Union. All Right Reserved. 

linear absorption coefficients are smaller than that of cosmic dust. They should be formed by impact of weekly-adhered aggregates that were broken into very small pieces by the impact and mixed with condensed aerogel. Two particles with relatively high linear absorption coefficient were confirmed in D1-231 and D1-362. They were confirmed by and optical microscope after compressing.

[1] Yamagishi A. et al. 2012. Space Utiliz Res, 28, 220. [2] Chyba C. & Sagan C. 1992. Nature, 355, 125. [3] Brownlee D. et al. 2006. Science, 314, 1711. [4] Hörz et al. 2006. Science, 314, 1716. [5] Tsuchiyama A. et al. 2009. Meteoritics & Planetary Science, 44, 1203. [6] Tsuchiyama A. 2013. Geochimica et Cosmochimica Acta 116, 5. [7] Noguchi T., 2018, Private message. [8] Hörz and Zolensky, 2000, Icarus 147, 559.

Keywords: Tanpopo mission, Cosmic dust

©2019. Japan Geoscience Union. All Right Reserved. 

# High-Angular-Resolution Observations of Protoplanetary Disks

*Misato Fukagawa[1]

1. National Astronomical Observatory of Japan

The recent progress in understanding of planet-formation process will be reviewed based on the results obtained at high angular resolution with astronomical facilities such as the Atacama Large Millimeter/submillimeter Array (ALMA). Circumstellar disk structures around young stars are birthplaces of planets. The physical and chemical condition in such protoplanetary disks can be linked to some extent to the planetary environment (e.g., atmospheric composition) where further chemical reactions might lead to formation of building blocks of life. This presentation includes the topics on detailed disk density structures at ~5-au or better resolution, gas detections in the later stages of disks where the collisional events in the planetary systems may happen, detections of organic molecules, and the prospects on disk observations in future.

Keywords: Exoplanets, Astronomy

©2019. Japan Geoscience Union. All Right Reserved. 

# Characterization of high molecular weight amino acid precursors formed in interstellar ice analog

*Soushi Kuramoto[1], Tomohito Sato[1], Hitoshi Fukuda[2], Yoshiyuki Oguri[2], Kotaro Kondo[2], Hiromi Shibata[3], Yoko Kebukawa[1], Kensei Kobayashi[1], Satoshi Yoshida[4]

1. Yokohama National University, 2. Tokyo Institute of Technology, 3. University of Osaka, 4. National Institutes for Quantum Radiological Science and Technology

It is suggested that extraterrestrial organic compounds are important for chemical evolution toward the generation of the first life on the Earth. Bioorganic compounds such as amino acids were found in hydrolyzed extracts of meteorite [1]. The products before hydrolysis referred to as “amino acid precursors” were, however, little known. It has been sometimes claimed that a-amino acids found in meteorites were formed by the Strecker synthesis. If so, aminonitriles and amino acid amides are the precursors, but they have not identified as major precursors yet. Extraterrestrial amino acid precursors were probably synthesized in molecular cloud environments or small celestial bodies. We irradiated possible interstellar media, such as mixture of carbon monoxide, ammonia and water to simulate possible reactions among interstellar media in dense clouds. The irradiation products were analyzed by HPLC and mass spectrometry.

A gaseous mixture (CO and $NH_3$) was sealed in a Pyrex glass tube with liquid water. The gaseous mixture was irradiated with 2.5 MeV protons from a Tandem accelerator at Tokyo Institute of Technology. Total quantity of electricity was 2 mC. The name of the irradiation products is hereafter called CAW. CAW was fractionated by cation exchange HPLC into several fractions to discriminate the fractions with glycine amide or aminoacetonitrile (the Strecker-type precursors) and those without them. Each fraction was hydrolyzed with 6M HCl at 110 ˚C for 24h and was subjected to amino acid analysis. Molecular weights of CAW were estimated by ultrafiltration (molecular weight cut off: 3000), gel filtration (column: Shodex OHpak SB-802.5 HQ) and mass spectrometry by ESI-TOF-MS.

It was shown that glycine was rarely detected in the fractions with the Strecker-type simple amino acid precursors (aminoacetonitrile, glycine amide). It was suggested that the CAW (an interstellar organics analogue) contained complex amino acid precursors with molecular weights of some thousands. Compared with molecular weights standards (authentic proteins), molecular weights of CAW were estimated 6000 or more by gel filtration chromatography. Peaks of $m/z$ = 1000 or over were detected by mass spectrometry. These results strongly suggested that complex amino acid precursors with large molecular weights could be directly generated from small molecules such as CO in interstellar environments. We are now trying to characterize amino acid precursors formed in interstellar ice analogue (frozen mixture of CH3OH, NH3 and H2O [2]) by heavy ions irradiation.

[1] K. A. Kvenvolden *et al.*, *Nature* 228, 923 (1970).

[2] K. Kobayashi *et al.*, *Electr. Commun.* Jpn. 91, 293 (2008).

Keywords: Chemical evolution, interstellar ice, the Strecker synthesis, amino acid precursor

©2019. Japan Geoscience Union. All Right Reserved. 

# Theoretical elucidation of prebiotic formation processes into nucleobases

*Yu Komatsu[1,2], Taiki Suzuki[1,2]

1. Astrobiology Center, 2. National Astronomical Observatory of Japan

As argued [1], the comets and meteorites may have provided a large amount of prebiotic molecules to the Early Earth. However, where and how such organic molecules were built is still controversial.

Recently, volatile glycine (NH2CH2COOH) has been detected in the coma of comet 67P/Churyumov-Gerasimenko by the ROSINA mass spectrometer [2], with giving us clues to glycine's interstellar origin. Moreover, in addition to various amino acids, nucleobases, such as purine, uracil, guanine, and xanthine have been identified in the meteorite (e.g., [3]). These studies suggest the formation of prebiotic molecules in the extreme condition prior to the early Earth chemistry.

If prebiotic molecules are built from small atoms or radicals in the cold ISM, the prebiotic molecules must have almost barrier-less formation paths. On the other hand, the bombardment of comets and/or asteroids would have provided very high temperature condition for chemical reactions, which may have led to the decomposition and formation of further complex prebiotic molecules. To understand the formation processes, the quantum chemical calculation is a powerful tool. The previous quantum chemical calculation has already reported the promising chemical paths to amino acids and nucleobases (e.g., [4]).

Here we investigated the possible pathway of pyrimidine, purine, uracil and thymine by the automated exploration of chemical reaction pathways. We have already discovered key dissociations for each molecule. For example, uracil and thymine, the pyrimidine type of nucleobase, have lower barriers to dissociate into an isocyanic acid, which corresponds to the previous laboratory experience, and the rest molecule. Pyrimidine and purine, which are skeleton structures of nucleobases and do not poses any oxygen atoms, have high barriers, implying to require high temperature environment like the bombardment, even though we did not exclude all possibilities of radical reactions. Detailed discussions will be provided on our poster.

References

[1] Ehrenfreund (2002), Rep. Prog. Phys. 65 1427

[2] Altwegg et al. (2016), Sci, 2, e1600285

[3] Simomiya et al. (1990), Geo, 24,343

[4] Ferus et al. (2015), PNAS, 112, 7109

Keywords: Prebiotic Chemistry, Quantum Chemistry, DNA /RNA, Interstellar Chemistry

©2019. Japan Geoscience Union. All Right Reserved. 

©2019. Japan Geoscience Union. All Right Reserved. 

# Formation Process of A Glycine's Precursor Candidate, CH3NH2

*Taiki Suzuki[1,2], Liton Majumdar[3], Masatoshi Ohishi[2]

1. National Institutes of Natural Sciences Astrobiology Center, 2. National Astronomical Observatory of Japan, 3. NASA Jet Propulsion Laboratory (JPL)

As [1] argued, the comets and meteorites may have provided a large amount of prebiotic molecules to the early Earth. An attempt to understand the origins of life must necessarily begin with detailed studies of the formation and evolution of complex organic molecules (COMs), products of complex chemistry that most likely starts in molecular clouds and continues within the protoplanetary disk.
Since the amino acids are the essential building blocks of life, the search for amino acids and their complex organic precursors at different stages of star and planet formation is one of the exciting topics in modern astronomy. Recently, volatile glycine ($NH_2CH_2COOH$) was detected in the coma of comet 67P/Churyumov-Gerasimenko by the ROSINA mass spectrometer [2], also giving clues about glycine's interstellar origin. However, the survey observations of glycine toward ISM have been not successful. Therefore, revealing the formation pathways to glycine is important for astrochemistry and astrobiology not only to know the promising glycine-rich sources for future surveys but also to understand the general chemical evolution of N-bearing molecules in the ISM.
In this context, we performed the chemical modeling study for the high-mass star, with the possible formation processes of glycine with theoretically and/or experimentally suggested formation paths [3]. We suggested that glycine was efficiently formed through the following reactions: First, the hydrogenation process to HCN leads to the formation of $CH_2NH$ and $CH_3NH_2$ on interstellar grain surface (HCN + 2H => $CH_2NH$, and then $CH_2NH$ + 2H => $CH_3NH_2$). Then, the destruction of $CH_3NH_2$ by radicals will form $CH_2NH_2$. Finally, $CH_2NH_2$ and COOH radical react to form glycine. For this test, a key molecule would be $CH_3OH$, whose formation process is well known. Both experiments and theoretical works suggested that $CH_3OH$ is built via grain surface hydrogenation processes to CO (CO + 2H => $H_2CO$, and then $H_2CO$ + 2H => $CH_3OH$). If $CH_3NH_2$ is also produced through hydrogenation process, “$CH_3NH_2/CH_3OH$” ratio should be well reproduced by the modeling. However, it was difficult to test this formation process due to the very limited number of previous CH3NH2 observations.
With this motivation, we performed the observation of $CH_3NH_2$ and $CH_3OH$ with ALMA toward high mass star-forming regions, G10.47+0.03, NGC6334I, W51 e1/e2, and G31.41+0.3. As a result, both of $CH_3OH$ and $CH_3NH_2$ were detected toward all sources. The molecular abundances were derived with rotation diagram method. The high excitation temperatures of 100 and 200 K and compact distributions suggest that $CH_3NH_2$ emissions originate from the hot and dense regions. The observed molecular abundance ratio, “$CH_3NH_2/CH_3OH$” ranges from 0.2 to 2.1. The low “$CH_3NH_2/CH_3OH$” ratio of 0.2 is close to our modeling, supporting that $CH_3NH_2$ is the product of the hydrogenation process in those sources. However, the higher “$CH_3NH_2/CH_3OH$” ratio of nearly two, observed toward NGC6334I MM1, could not be reproduced with our modeling under the possible parameter range. Thus, our chemical modeling would not correctly reproduce the physics or chemistry of such $CH_3NH_2$-rich sources. Further studies of such sources will enable us to promote our knowledge of glycine chemistry and provide us with promising sources for future glycine surveys.

Citations:
[1] Ehrenfreund (2002), Rep. Prog. Phys. 65 1427

©2019. Japan Geoscience Union. All Right Reserved. 

[2] Altwegg et al. (2016), Sci, 2, e1600285
[3] Suzuki et al, (2018), ApJ, 825, 51

Keywords: radio astronomy, chemical modeling, prebiotic molecules

©2019. Japan Geoscience Union. All Right Reserved. 

# Numerical study on the stellar atmosphere & wind of Cool Stars

*Takahito Sakaue[1], Kazunari Shibata[1]

1. Kyoto University

Cool stars offer the good opportunities to investigate what environments the Earth-like exoplanets are in, and how they are affected by the host star. TRAPPIST-1 is an ultracool dwarf; the spectral type is M8V ($T_{eff}$ =2559K) with the lower mass of 0.08$M_{sun}$ (radius = 0.11$R_{sun}$). The star is confirmed to have seven planets (Gillon et al. 2017) and thus greatly interested in not only by stellar astrophysics but also by astrobiology. Here, we report the results of one-dimensional magnetohydrodynamic (MHD) simulation of the stellar wind from TRAPPIST-1. Several solar wind theories, which have been examined observationally, are applied to the case of TRAPPIST-1. Among them, it is the plausible idea that the dissipation of the incompressible MHD wave leads to the heating and driving the stellar wind. For instance, Garraffo et al. 2017 succeeded in the three-dimensional MHD simulation of the stellar wind from TRAPPIST-1, by extending their solar wind model in which the incompressible MHD wave is exhausted by the turbulent dissipation. The incompressible MHD wave, on the other hand, is also affected not only by the turbulent dissipation but also by the nonlinear mode coupling, which leads to the formation of the shock wave and consequently contribute to heating the wind. This nonlinear process has been well investigated to account for the dynamics of the lower solar atmosphere (Kudoh & Shibata 1999) and driving the solar wind (Suzuki & Inutsuka 2005), but not discussed for the stellar wind from TRAPPIST-1. In this study, therefore, we performed the one-dimensional MHD simulation to consider the nonlinear process of the incompressible MHD wave leading to the shock formation, and succeeded in reproducing the stellar wind from TRAPPIST-1.

Keywords: stellar wind, cool stars, TRAPPIST-1

©2019. Japan Geoscience Union. All Right Reserved. 

# Design of space exposure experiments of organic matter in Tanpopo 2

*Takuya Yokoo[1], tomohito sato[1], Itsuki Sakon[2], Kazumichi Nakagawa[3], Hajime Yano[4], Miki Nakayama[5], Hajime Mita[5], Yoko Kebukawa[1], Kensei Kobayashi[1]

1. Yokohama National University, 2. University of Tokyo, 3. Kobe University, 4. JAXA, 5. Fukuoka Institute of Technology

## 1. Introduction

Large number of organic compounds have been discovered in molecular clouds and in meteorites. Some of organic compounds required for emergence of life are thought to be synthesized in space. Then, meteorites and interplanetary dust particles could deliver them to the Earth. The first Japanese astrobiology space experiment called “Tanpopo” was conducted to study this hypothesis[1].
The objective of the Tanpopo Mission is to understand bi-directional propagation of microorganisms and organic matter between the Earth and space. In other words, in the Tanpopo Mission, we examine whether life exists only on the earth by evaluating whether microorganisms can escape into space and whether organic matter can reach to the Earth from outer space.
As one of subthemes in this project, amino acids and their precursor compounds including complex interstellar organic matter analog were directly exposed to outer space by utilizing the International Space Station (ISS), and recoveries of these organics were measured to understand degradation of organic compounds under the environment of the outer space. In the Tanpopo experiment, hexatriacontane (HTC) was used to prevent the sample from sublimation during exposure to space at the ISS. However, HTC absorbs ultraviolet light with a wavelength of 160 nm or less. To understand the effects of shorter wavelength UV, the next space experiment "Tanpopo 2" applies a new design for direct exposure of organic compounds without HTC and optical windows. In addition to the aluminum plate same as the one used in Tanpopo, the silicon substrates are also used for exposure the sample to space, in the organic matter exposure experiment of “Tanpopo 2 “. In the Tanpopo Mission, glycine, hydantoin, isovaline, ethylmethylhydantoin, CAW (complex organic matter produced from proton beam irradiation to CO, $NH_3$, $H_2O$ mixture) were used, and glycine and CAW showed relatively high recoveries [2]. In "Tanpopo 2", glycine and CA (proton beam irradiation product to CO, $NH_3$ mixture) on the silicon substrates will be directly exposed to space in addition to the same compounds on the same aluminum plate used in the Tanpopo. The recovered samples will be analyzed by FT-IR, XANES, and SEM, in addition to amino acid analysis.
Here we report the design of the space experiment such as preparation method of the space experiment sample.

## 2. Experimental

(1) A gas mixture of CO (350 Torr) and $NH_3$ (350 Torr) and a silicon plate (10 mm$\phi$) were placed in a glass container, and the gas mixture was irradiated with 2.5 MeV proton beam from a tandem accelerator to deposit organic matter on the plate.
(2) The thickness of the organic matter (CA) film on the silicon plate was measured using a three-dimensional microscope.
(3) Structural analysis of organic matter (CA) on the silicon plate was also carried out using FT-IR.
(4) Amino acid analysis was carried out by cation exchange HPLC after hydrolyzing silicon plate with CA with 6 M hydrochloric acid at 110 ˚C for 24 hours.

©2019. Japan Geoscience Union. All Right Reserved. 

(5) Glycine is planned to be deposited on a silicon substrate by a vacuum vapor deposition equipment (Fukuoka Institute of Technology).

3. Results and Discussion

The CA deposition thickness was approximately 8 μm, but more sample thickness would be required due to potential loss of the organic materials by atomic oxygen present in low Earth orbit during exposure. Thus, we decided to use non-polished Si substrates instead of polished Si substrate. Because the sample can be kept in the bottom of indentations on the rough surface of non-polished substrate, even if a part of sample surface is lost.
Amino acid analyses of CA by cation exchanged HPLC showed, various amino acids including aspartic acid, threonine, glycine, alanine, -aminoisobutyric acid and serine were detected after acid hydrolysis. Glycine was particularly abundant, whose yield was 827 ±7 nmol from a single CA deposited Si substrate.

4. Conclusions

We will conduct the durability test of our samples on the silicon substrate including the vibration test, cooling test, heating test before launch in 2019 with the space X company to the ISS. We are planning to conduct various analyses from recovered samples. The recovery and degradation of these samples will make a further leap forward our understanding of the possible delivery of organic matter from interplanetary dust particles to the early Earth.

5. References

[1] A. Yamagishi, H. Yano, K. Okudaira, K. Kobayashi, S. Yokobori, M. Tabata, H. Kawai, *Biol. Sci. Space*, **21** : 67-75 (2007).
[2] K. Kobayashi *et al.*, 2018 JpGU meeting, Chiba (2018).

©2019. Japan Geoscience Union. All Right Reserved. 

[J] Oral | M (Multidisciplinary and Interdisciplinary) : M-IS Intersection

Thu. May 30, 2019 1:45 PM - 3:15 PM JST | Thu. May 30, 2019 4:45 AM - 6:15 AM UTC | 102 1F

## [M-IS09] dust

convener:Ishizuka Masahide(Kagawa University), Yasunori Kurosaki(Arid Land Research Center, Tottori University), Thomas Sekiyama(Meteorological Research Institute), Kana Nagashima(Japan Agency for Marine-Earth Science and Technology, Research and Development Center for Global Change), Chairperson:Tsuyoshi Sekiyama

Mineral dust is generated from the ground surface by strong winds, and it transports long distance over the earth. In the process, cloud formation and absorption and scattering of solar radiation cause weather and climate changes. Also, when deposited in the ocean, feeding nutrients to phytoplankton, promoting photosynthesis, and when deposited on snow and ice causes albedo change. This is known as the yellow dust (Asian dust) phenomenon in Asia region including Japan. In order to understand this, integration in a wide range of academic areas is necessary. <br/> In the emission process, the amount of dust changes greatly depending on the surface condition in dryland area, and in order to know the conditions, it deals with areas such as soil, topography, vegetation, precipitation, desert and soil deterioration. In the transport process, we deal with areas such as weather, atmospheric aerosol, radiation. In the deposition process, we deal with areas such as ocean, snow ice, health to people and livestock. Drying and changes in vegetation also have social scientific aspects such as national policies, management of livestock, and population increase. Dust and sand dunes are common phenomena not only to the Earth but also to other planets such as Mars and Saturn. In this way, it is impossible to understand the dust phenomenon only in one field, it is important for researchers in many areas to discuss and share information through this session, and advance exchange of researchers.

1:45 PM - 1:55 PM JST | 4:45 AM - 4:55 AM UTC

Introduction

---

1:55 PM - 2:15 PM JST | 4:55 AM - 5:15 AM UTC

[MIS09-01] Global modeling study of atmospheric supply of lithogenic and pyrogenic Fe-containing aerosols to the ocean

★Invited Papers

*Akinori Ito[1], Akitomo Yamamoto[1], Michio Watanabe[1], Maki Noguchi Aita[1], Ying Ye[2] (1.Japan Agency for Marine-Earth Science and Technology, 2.Alfred Wegener Institute for Polar and Marine Research)

---

2:15 PM - 2:30 PM JST | 5:15 AM - 5:30 AM UTC

[MIS09-02] Regional variations in the elemental and mineral compositions of solid particles in rainwater in Iran

*Yoriko Yokoo[1], Chihiro Sakamoto[1], Atsushi Kitamura[1], Ryo Anma[2], Shiva Mehrabani[3] (1.Faculty of Science and Engineering, Doshisha University, 2.Tokushima University, 3.Kurdistan University)

---

2:30 PM - 2:45 PM JST | 5:30 AM - 5:45 AM UTC

[MIS09-03] Comparison of airborne microbial variations in air samples from Asian-dust source and arrival regions

*Teruya Maki[1], Tatsuyuki Fujita[1], Yuuma Mastuba[1], Yasunori Kurosaki[2], Masahide Ishizuka[3], Kei Kawai[4], Yasunobu Iwasaka[5] (1.College of Science and Engineering, Kanazawa University, 2.Arid Land Research Center, Tottori University, Tottori University, 3.Faculty of Engineering, Kagawa University, 4.Graduate School of Environmental Studies, Nagoya Universit, 5.Center for Environmental Creative Studies)

---

2:45 PM - 3:00 PM JST | 5:45 AM - 6:00 AM UTC

[MIS09-04] Prediction of health effects of cross-border atmospheric pollutants using the Model of Aerosol Species in the Global Atmosphere (MASINGAR)

*Kazunari Onishi[1], Thomas Sekiyama[2], Yasunori Kurosaki[3], Masato Shinoda[4] (1.Graduate School of Public Health, Support Unit for Conducting Clinically Essential Studies, St.Luke's International University,

2.Meteorological Research Institute, 3.Arid Land Research Center, Tottori University, 4.Graduate School of Environmental Studies Nagoya University)

3:00 PM - 3:15 PM JST | 6:00 AM - 6:15 AM UTC

## [MIS09-05] Dust layer captured by an inversion layer over the Gobi Desert on 29–30 April 2015

*Kei Kawai[1], Yuta Nishio[2], Kenji Kai[1,3], Jun Noda[4], Erdenebadrakh Munkhjargal[1,5], Masato Shinoda[1], Nobuo Sugimoto[6], Atsushi Shimizu[6], Enkhbaatar Davaanyam[5,7], Dashdondog Batdorj[8] (1.Nagoya University, 2.Japan Meteorological Agency, 3.Ibaraki University, 4.Rakuno Gakuen University, 5.Information and Research Institute of Meteorology, Hydrology and Environment, Mongolia, 6.National Institute for Environmental Studies, 7.University of Tsukuba, 8.National Agency for Meteorology and Environmental Monitoring, Mongolia)

# Global modeling study of atmospheric supply of lithogenic and pyrogenic Fe-containing aerosols to the ocean

*Akinori Ito[1], Akitomo Yamamoto[1], Michio Watanabe[1], Maki Noguchi Aita[1], Ying Ye[2]

1. Japan Agency for Marine-Earth Science and Technology, 2. Alfred Wegener Institute for Polar and Marine Research

Atmospheric supply of iron (Fe) to the ocean has been suggested to increase the marine primary productivity in large parts of the ocean. However, there are still large uncertainties regarding the effects of atmospheric aerosols on Fe dissolved in the surface ocean and marine productivity. Here, we use an atmospheric chemistry model and two ocean biogeochemistry models to explore the sensitivity to the atmospheric input of dissolved Fe.

The atmospheric model considered the deposition of both lithogenic and pyrogenic Fe-containing aerosols and their chemical transformation due to reactions with gaseous species. Sensitivity simulations are carried out with the deposition of lithogenic Fe only, and both Fe content in mineral dust of 3.5% and solubility of 2% are prescribed in the ocean models.

The results from the sensitivity simulations show that additional sources of dust and combustion aerosols increased the marine phytoplankton biomass in the subarctic north Pacific. The two ocean biogeochemistry models show similar spatial patterns but substantially different magnitude of responses to the atmospheric input of dissolved Fe. Moreover, the atmospheric model underestimated dissolved Fe concentration in aerosols over the North Pacific, although more observations are needed before drawing any firm conclusions on the model performance over the Pacific. Thus, further investigations of processes in emission of Fe from East Asia and transformation of dissolved Fe in the atmosphere and the ocean are needed.

Keywords: Mineral dust, Combustion aerosols, Iron deposition

©2019. Japan Geoscience Union. All Right Reserved. 

# Regional variations in the elemental and mineral compositions of solid particles in rainwater in Iran

*Yoriko Yokoo[1], Chihiro Sakamoto[1], Atsushi Kitamura[1], Ryo Anma[2], Shiva Mehrabani[3]

1. Faculty of Science and Engineering, Doshisha University, 2. Tokushima University, 3. Kurdistan University

We collected monthly solid particles (air dust; > 0.2 $\mu$m) in rainwater samples in four western cities (Hamedan, Ilam, Shiraz, Ahvaz) from October 2014 to July 2015 and three eastern cities (Mashhad, Birjand, Zahedan) from January 2016 to January 2017 in Iran, and determined their elemental and mineral compositions in order to elucidate the regional variation and to consider their provenance. In no-rainfall months, we rinsed the sampler with ultrapure water and collected the trapped air dust. Mineral composition of the collected dust was determined using an XRD. We dissolved the same dust samples using mixed-acids and measured elemental compositions using an ICP-MS.
The amount of dust in eastern cities were higher than those in western cities, especially the samples collected in Birjand. Samples from Mashhad and Zahedan had high amount of dust during dry season. These results suggest that aeolian dust from surrounding deserts such as Dasht-e Kavir and Dasht-e Lut affected atmospheric deposition in eastern Iran.
All of dust samples contained quartz and feldspar. Most of the dust samples in western cities also contained calcite. The concentrations of Ca, Na and K in the dust of western cities were 0.45-29.33%, 0.24-0.82% and 0.49-1.94%, respectively. Those in the dust of eastern cities were 0.97-6.23%, 0.59-2.74% and 0.88-3.15%, respectively. The concentration of Ca in the dust of western cities were higher, and Na and K concentrations were lower than those of eastern cities. High calcite contents were observed in western cities and Birjand : thus, high-Ca in the dust is attributed to calcite originated from the arid area. A part of Ca in the dust of eastern cities could also be attributed to feldspars.
Cd, Sb, Pb and As in the dust of western cities and Ni, Zn, As, Cd and Sb in those of eastern cities had the maximum values of the enrichment factor (EF): $(X/Al)_{sample}/(X/Al)_{crust}$ over ten. These results suggest a part of the dust were originated from anthropogenic substances such as road dust and petroleum industry. The EF values of Pb and As of dust samples in western cities showed higher than those in eastern cities, suggesting that the atmospheric deposition were influenced by anthropogenic substances from petroleum industry, which is generally high in Pb and As.

Keywords: insoluble substance, elemental composition, mineral composition, West Aisa

©2019. Japan Geoscience Union. All Right Reserved. 

# Comparison of airborne microbial variations in air samples from Asian-dust source and arrival regions

*Teruya Maki[1], Tatsuyuki Fujita[1], Yuuma Mastuba[1], Yasunori Kurosaki[2], Masahide Ishizuka[3], Kei Kawai[4], Yasunobu Iwasaka[5]

1. College of Science and Engineering, Kanazawa University, 2. Arid Land Research Center, Tottori University, Tottori University, 3. Faculty of Engineering, Kagawa University, 4. Graduate School of Environmental Studies, Nagoya Universit, 5. Center for Environmental Creative Studies

Aerosol dust is emerging as a significant vehicle for long-range transport of microorganisms. Nonetheless, many factors relating to this highly influential dispersal mechanisms remain unresolved, including the variation in dispersal bacterial communities during stochastic desert dust events, and the effect of aerosol transit over continental and oceanic surfaces to these communities. Here we elucidated bacterial 16S rRNA gene and fungal ITS-defined changes in airborne microbial communities at Asian-dust source regions (Gobi) and arrival regions (Japan) both lying along the trajectory for dust-event transport. Aerosols collected in the both regions generally reflected local origin from freshwater, marine, plant, or animal sources. In particular, dust events in the Gobi Desert increased these microbial cells and mineral particles to more than ten folds of concentrations. After dust-events occurrences in desert areas, the spore-forming microorganisms (bacteria: Bacillaceae, fungi: Davidiellaceae) and organic-aggregating bacteria (Cytophagaceae) showed high relative abundances, suggesting the survival of some microbes against strict atmospheric stressors over desert. These stress-resistance microbial populations were frequently dominated during Asian-dust evens over Japan, which are located cross China industrial area and Japan Sea. Presumably, atmospheric stressors over desert transit over deserts, anthropogenic polluted areas and oceanic waters strongly selects for airborne microbial populations through atmospheric stressors.

Keywords: bioaerosol, long range transport, microorganisms

©2019. Japan Geoscience Union. All Right Reserved. 

# Prediction of health effects of cross-border atmospheric pollutants using the Model of Aerosol Species in the Global Atmosphere (MASINGAR)

*Kazunari Onishi[1], Thomas Sekiyama[2], Yasunori Kurosaki[3], Masato Shinoda[4]

1. Graduate School of Public Health, Support Unit for Conducting Clinically Essential Studies, St.Luke's International University, 2. Meteorological Research Institute, 3. Arid Land Research Center, Tottori University, 4. Graduate School of Environmental Studies Nagoya University

Health effects of cross-border air pollutants and Asian dust are of significant concern in Japan. Currently, models predicting the arrival of aerosols have not investigated the association between arrival predictions and health effects. We investigated the association between subjective health symptoms and unreleased aerosol data from the Model of Aerosol Species in the Global Atmosphere (MASINGAR) acquired from the Japan meteorological agency, with the objective of ascertaining if these data could be applied to predicting health effects.
Subjective symptom scores were collected via self-administered questionnaires and, along with modeled surface aerosol concentration data, were used to conduct a risk evaluation using generalized estimating equations between October and November 2011.
Altogether, 29 individuals provided 1670 responses. Spearman's correlation coefficients were determined for the relationship between the proportion of the participants reporting the maximum score of two or more for each symptom and the surface concentrations for each considered aerosol species calculated using MASINGAR; the coefficients showed significant intermediate correlations between surface sulfate aerosol concentration and respiratory, throat, and fever symptoms (R=0.557, 0.454, and 0.470, respectively; $p < 0.01$). In the general estimation equation (logit link) analyses, a significant linear association of surface sulfate aerosol concentration, with an endpoint determined by reported respiratory symptom scores of two or more,was observed (P trend=0.001, odds ratio [OR] of the highest quartile [Q4] vs. the lowest[Q1]=5.31, 95% CI=2.18 to 12.96), with adjustment for potential confounding. The surface sulfate aerosol concentration was also associated with throat and fever symptoms. Association of surface dust aerosol concentration and respiratory symptom were odds ratio [OR] of the highest quartile [Q4] vs. the lowest[Q1]=3.32, 95% CI=0.90 to 12.27).
In conclusion, our findings suggest that modeled data are potentially useful for predicting health risks of cross-border aerosol arrivals.

Keywords: Atmospheric air pollution, Health forecast, Aerosol forecast

©2019. Japan Geoscience Union. All Right Reserved. 

# Dust layer captured by an inversion layer over the Gobi Desert on 29–30 April 2015

*Kei Kawai[1], Yuta Nishio[2], Kenji Kai[1,3], Jun Noda[4], Erdenebadrakh Munkhjargal[1,5], Masato Shinoda[1], Nobuo Sugimoto[6], Atsushi Shimizu[6], Enkhbaatar Davaanyam[5,7], Dashdondog Batdorj[8]

1. Nagoya University, 2. Japan Meteorological Agency, 3. Ibaraki University, 4. Rakuno Gakuen University, 5. Information and Research Institute of Meteorology, Hydrology and Environment, Mongolia, 6. National Institute for Environmental Studies, 7. University of Tsukuba, 8. National Agency for Meteorology and Environmental Monitoring, Mongolia

Asian dust originates in arid and semi-arid regions of East Asia, such as the Gobi Desert and the Taklimakan Desert. If the dust emitted from the ground surface reaches the free troposphere, it can be transported toward the Pacific Ocean over a long range by the westerlies. Therefore, the vertical distribution of dust over the source region is a key factor of the long-range transport of dust. In the Gobi Desert, a ceilometer (compact lidar) observation has been conducted at Dalanzadgad, Mongolia, since the end of April 2013. The ceilometer observed a developed dust storm over the ground and a dust layer at a height of 1.2–1.8 km on 29–30 April 2015. According to SYNOP reports, this dust storm had already developed in the upwind region before arriving at Dalanzadgad. This feature was consistent with the sudden increase of the ceilometer observation values. Then, the dust was lifted to a height of 1.2–1.8 km, and the dust layer was observed at almost the same height for 12 hours by the ceilometer. During this dust event, radiosonde observation at Dalanzadgad showed an inversion layer at a height of 1.2–1.5 km over cold air. These results suggest that the dust layer was captured by the inversion layer, which prevented the dust from reaching the free troposphere and restrained the long-range transport of the dust by the westerlies. This study was supported by Research Fellowships of Japan Society for the Promotion of Science (JSPS) for Young Scientists and by Grants-in-Aid for Scientific Research from the JSPS (16H02703, 17H01616, and 18J12795).

Keywords: Asian dust, dust storm, long-range transport, ceilometer, lidar, Gobi Desert

©2019. Japan Geoscience Union. All Right Reserved. 

[J] Oral | M (Multidisciplinary and Interdisciplinary)：M-IS Intersection

Thu. May 30, 2019 3:30 PM - 5:00 PM JST | Thu. May 30, 2019 6:30 AM - 8:00 AM UTC | 102 1F

## [M-IS09] dust

convener:Ishizuka Masahide(Kagawa University), Yasunori Kurosaki(Arid Land Research Center, Tottori University), Thomas Sekiyama(Meteorological Research Institute), Kana Nagashima(Japan Agency for Marine-Earth Science and Technology, Research and Development Center for Global Change), Chairperson:Kana Nagashima

Mineral dust is generated from the ground surface by strong winds, and it transports long distance over the earth. In the process, cloud formation and absorption and scattering of solar radiation cause weather and climate changes. Also, when deposited in the ocean, feeding nutrients to phytoplankton, promoting photosynthesis, and when deposited on snow and ice causes albedo change. This is known as the yellow dust (Asian dust) phenomenon in Asia region including Japan. In order to understand this, integration in a wide range of academic areas is necessary.
In the emission process, the amount of dust changes greatly depending on the surface condition in dryland area, and in order to know the conditions, it deals with areas such as soil, topography, vegetation, precipitation, desert and soil deterioration. In the transport process, we deal with areas such as weather, atmospheric aerosol, radiation. In the deposition process, we deal with areas such as ocean, snow ice, health to people and livestock. Drying and changes in vegetation also have social scientific aspects such as national policies, management of livestock, and population increase. Dust and sand dunes are common phenomena not only to the Earth but also to other planets such as Mars and Saturn. In this way, it is impossible to understand the dust phenomenon only in one field, it is important for researchers in many areas to discuss and share information through this session, and advance exchange of researchers.

3:30 PM - 3:45 PM JST | 6:30 AM - 6:45 AM UTC

### [MIS09-06] Favorable regions for dust haze transport revealed by ensemble simulations

*Kazunori Ogohara[1], Shogo Isoda[1] (1.School of Engineering, University of Shiga Prefecture)

3:45 PM - 4:00 PM JST | 6:45 AM - 7:00 AM UTC

### [MIS09-07] Measurement of adhesion force of individual aerosol particles by atomic force microscopy

*Kohei Ono[1], Yuki Mizushima[4], Ayumi Iwata[3], Furuya Masaki[1], Nozomu Tsuchiya[1], Atsushi Matsuki[2] (1.Graduate School of Natural Science and Technology, Kanazawa University, 2.Institute of Nature and Environmental Technology, Kanazawa University, 3.Faculty of Science and Technology, Keio University, 4.College of Science and Technology, Kanazawa University)

4:00 PM - 4:15 PM JST | 7:00 AM - 7:15 AM UTC

### [MIS09-08] Occurrence of micro-meso scale dust storms and its relationship to the vegetation and topography in Mongolian grassland and Gobi Desert

*Kenji Kai[1], Kei Kawai[2], Teruya Maki[3], Jun Noda[4] (1.College of Education, Ibaraki University , 2.Nagoya University, 3.Kanazawa University, 4.Rakuno-Gakuen University)

4:15 PM - 4:30 PM JST | 7:15 AM - 7:30 AM UTC

### [MIS09-09] A trial of elucidation for dust emission conditions in East Asia by synoptic data analyses and a field observation

*Yasunori Kurosaki[1], Jing Wu[1], Batjargal Buyantogtokh[1], Ishizuka Masahide[2], Batdelger Gantsetseg[3] (1.Tottori University, 2.Kagawa University, 3.IRIMHE, Mongolia)

4:30 PM - 4:45 PM JST | 7:30 AM - 7:45 AM UTC

### [MIS09-10] Monitoring and assessing aeolian desertification processes based on a dust erodibility index – A case study in the Xilingol grassland, China

*Jing Wu[1], Yasunori Kurosaki[1], Chunling Du[2], Tao Wang[3] (1. Arid Land Research Center, Tottori University, 2.School of Economics and Management, Inner Mongolia Agricultural University, 3.Northwest Institute of

Eco-Environment and Resources, Chinese Academy of Sciences)

4:45 PM - 5:00 PM JST | 7:45 AM - 8:00 AM UTC

## [MIS09-11] Influences of land surface conditions and human activities on dust events in Inner Mongolian grasslands, China

*Mei Yong[1], Masato Shinoda[2], Nandintsetseg Banzragch[2] (1.Inner Mongolia normal university, 2.Nagoya university)

# Favorable regions for dust haze transport revealed by ensemble simulations

*Kazunori Ogohara[1], Shogo Isoda[1]

1. School of Engineering, University of Shiga Prefecture

Dust is the major source of the solar heating in the Martian atmosphere and then drives the circulation of dust itself. Dust events (dust storms, dust devils and dust haze) are disasters in the Mars atmosphere near the surface because they can generate strong winds and block sunlight almost completely. Statistics of dust events have been studied by analyzing atmospheric temperature, dust optical depth and visible images observed by successive orbiters, landers and rovers. Active areas of local dust storms, including curvilinear and textured storms have been identified observationally. The tendency of such small scale dust events should be affected by the large scale atmospheric conditions such as thermal or dynamical stabilities. Activity of regional dust storms has been investigated using the vast number of images observed by Mars Orbiter Camera onboard Mars Global Surveyor (MGS/MOC) and MARs Color Imager onboard Mars Reconnaissance Orbiter (MRO/MARCI). They tend to break out near the storm zones in the northern mid-latitudes and are probably very linked to baroclinic instability and the fronts. Although mechanisms of the growth, maintenance and decay of global dust storms have not been well investigated, most of global dust storms started in the southern spring to summer seasons as regional storms were merging with each other.
Questions about the mechanisms of dust storms and haze are as follow:
- Why does a dust storm/haze break out?
- Why does the dust storm/haze expand?
Mechanisms of initiation and maintenance of local dust storms will be understood and categorized into a few types in the near future by statistical studies. They can be also inferred from observations and theories of terrestrial dust storms. However, there are local dust storms also in the northern mid-latitudes. Why do not the local storms grow into regional dust storms? Why do not all regional dust storms merge with each other? Ogohara and Satomura (2011) found five favorable regions for expansion of local dust haze (FRs) and revealed what kind of the atmospheric phenomena controls the dust haze transport around such regions. However, it still remains unclear whether these five FRs are also favorable for dust haze transport climatologically because they performed just a single year calculation. Thus, we identify the climatologically robust FRs in this study by ensemble simulations. If such FRs were found, atmospheric phenomena characteristic of the FRs would govern the dust transport around there.
Each ensemble simulation is performed in the same manner as that by Ogohara and Satomura (2011). Although they could not separate injected dust from the background dust due to the model architecture, wee modify the model in this study so that I can treat the injected and background dust separately. The first spin-up run started from an isothermal (220 K) condition with constant surface pressure (6.4 hPa) and no wind over the entire planet. Fifty kinds of small disturbances are added to the temperature output data of the first spin-up run. The small disturbances of temperature at each sigma level are normal random numbers. The standard deviation of the distribution function is 0.01 times of the standard deviation of temperature at the sigma level of the first spin-up result. The second spin-up runs are performed for 1 MY from $L_s$=180 independently using the 50 kinds of the output data of the first spin-up run with small disturbances as the initial data. After these spin-up runs, fifty global maps of dust haze expansion potential are made using the output data from the 50 kinds of the second spin-up runs as the initial data. The maps of dust haze expansion potential clearly show that there are a few robust FRs in the northern fall season. Also, it turns out that standard deviations of dust haze expansion are significantly

©2019. Japan Geoscience Union. All Right Reserved. 

higher in the northern high latitudes than in the low latitudes. The reasons why dust tends to expand around the robust FRs are the same as those explained by Ogohara and Satomura (2011). However, high ensemble standard deviation in dust haze expansion is clearly shown at the first time by this study. In the presentation, we will show when dust haze tends to spread extensively and when it does not.

Keywords: Mars, dust storm, ensemble simulation

©2019. Japan Geoscience Union. All Right Reserved. 

# Measurement of adhesion force of individual aerosol particles by atomic force microscopy

*Kohei Ono[1], Yuki Mizushima[4], Ayumi Iwata[3], Furuya Masaki[1], Nozomu Tsuchiya[1], Atsushi Matsuki[2]

1. Graduate School of Natural Science and Technology, Kanazawa University, 2. Institute of Nature and Environmental Technology, Kanazawa University, 3. Faculty of Science and Technology, Keio University, 4. College of Science and Technology, Kanazawa University

A new method was developed to quantitatively evaluate the adhesion force of individual aerosol particles. The method involves force-curve-mapping by atomic force microscopy. Firstly, adhesion force of particle surrogates (PSL, ammonium sulfate, quartz) were measured to evaluate the applicability of the new method on individual particles. Spatial distribution and representative adhesion force was successfully obtained. The force-curve-mapping method was then applied on actual ambient samples. The aged Asian dust particles following long-range transport were collected within Kanazawa University campus. The same dust particles were identified under both AFM and SEM-EDX and analyzed for their morphology, adhesion force distribution and elemental composition. It was found that the adhesion force of aged silicate Asian dust was greater than that of fresh dust collected near the source in China. It was suggested that the adhesion force of aged silicate dust increases and becomes comparable to those of inorganic salts (i.e. ammonium sulfate and sea salt particles). Ca-rich Asian dust exhibited even stronger adhesion force. The result revealed difference of adhesion forces between silicate and Ca-rich Asian dust following atmospheric processing during long-range transport. This study also spotted few carbonaceous particles with exceptionally high adhesion force, suggesting certain organic aerosols may be particularly adhesive. This work successfully demonstrated the importance of adhesion force measurement on individual particle basis, and applicability of force-curve-mapping method for characterizing adhesivity of internally mixed particles.

Keywords: Asian dust, Atomic Force Microscopy(AFM), adhesion force, long-range transport, deposition, aging

©2019. Japan Geoscience Union. All Right Reserved. 

# Occurrence of micro-meso scale dust storms and its relationship to the vegetation and topography in Mongolian grassland and Gobi Desert

*Kenji Kai[1], Kei Kawai[2], Teruya Maki[3], Jun Noda[4]

1. College of Education, Ibaraki University , 2. Nagoya University, 3. Kanazawa University, 4. Rakuno-Gakuen University

Gobi Desert and Mongolian grassland are one of the main sources of the Asian dust. In order to investigate the occurrence of micro-meso scale dust storms and its relationship to the vegetation and topography, we conducted moving observations running across the Gobi Desert from Ulaanbaatar to Dalanzadgad in springs of 2015-2017. An optical particle counter (OPC: Aerotrak 9306-V2), a sunphotometer (Microtops II) and meteorological instrument were installed in a car.

The vegetation had a suppression effect on the dust emission. Number concentrations of coarse particles (1-10 $\mu$m) decreased from the desert to the grassland. They had significant negative correlations with the vegetation (NDVI) from 3 $\mu$m to 10 $\mu$m, but the number concentration at 0.3 –0.5 $\mu$m had little correlation to the vegetation.

During the moving observations, we found a hotspot of dust storms in the Gobi Desert. An analysis of Himawari-8 Dust RGB clearly shows that the hotspot appeared at a jointing point of two valleys, a bottleneck and an exit of a valley.

In summary, the horizontal distribution of number concentrations of aerosol particles reflected the surface vegetation. Locations of the hotspot were determined by a local topography such a jointing point of two valleys.

Keywords: Asian dust, Himawari-8 Dust RGB, Hotspot of dust storms

©2019. Japan Geoscience Union. All Right Reserved. 

# A trial of elucidation for dust emission conditions in East Asia by synoptic data analyses and a field observation

*Yasunori Kurosaki[1], Jing Wu[1], Batjargal Buyantogtokh[1], Ishizuka Masahide[2], Batdelger Gantsetseg[3]

1. Tottori University, 2. Kagawa University, 3. IRIMHE, Mongolia

Mineral dust particles are blown up into the free atmosphere by sand-dust storm (SDS) in drylands, and they are broadly distributed by wind in the upper atmosphere. SDS is a type of disaster in drylands, which sometimes kills people and animal, destroys infrastructure, reduces merchandise value of livestock etc. In downwind regions like Japan, there is reports on its health effect. In the global scale, there are many reports about their effects on climate via direct and indirect effects of radiation. Many researchers have developed numerical dust model to avoid such damages, but their accuracy is still low, especially in its emission phase (Uno et al. 2006; Carmichael et al. 2008).

We can divide causes of dust emission (in other words, wind erosion) into erosivity (i.e., ability of wind to cause erosion) and erodibility (i.e., susceptibility of soil and land surface to wind erosion represented by the threshold wind speed for dust emission). Erosivity can be expressed by one parameter, which is wind speed and accuracy for its observation and its forecast is relatively reliable. On the other hand, erodibility has many parameters relating with soil and land surface such as soil particle size, soil wetness, crust, soil freeze, snow cover, vegetation cover, and we have a very big hurdles for monitoring all with high accuracy. This can be a big reason of low accuracy of dust emission modeling.

Tottori University set up a dust monitoring system at Tsogt-Ovoo, Mongolia, which is located in a northern part of the Gobi Desert. We have clarified that effects of soil crust (Ishizuka et al. 2012 SOLA), vegetation cover in topographic depression (Gantsetseg et al. 2017 J. of Arid Land), stone (Buyantogtokh et al. 2019 in preparation), dead leaves on erodibility. We also have conducted analyses of wind and present weather data included in synoptic report to elucidate dust emission conditions, which differs place by place. Kurosaki et al. (2011 GRL) clarified that dust emission frequencies increased at many synoptic meteorological observatories in East Asia from 1990s to 2000s and the major causes are in increased erodibility, which can be shown by reductions of threshold wind speed. Wu et al. (2016 SOLA) clarified that the major causes for dust emission are different station by station in East Asia. Wu et al. (2019 in preparation) clarified that effect of livestock number at Abaga Qi, which is located at Xilingol Grassland, China.

Keywords: drylands, aeolian dust, wind erosion, erosivity, erodibility

©2019. Japan Geoscience Union. All Right Reserved. 

# Monitoring and assessing aeolian desertification processes based on a dust erodibility index –A case study in the Xilingol grassland, China

*Jing Wu[1], Yasunori Kurosaki[1], Chunling Du[2], Tao Wang[3]

1. Arid Land Research Center, Tottori University, 2. School of Economics and Management, Inner Mongolia Agricultural University, 3. Northwest Institute of Eco-Environment and Resources, Chinese Academy of Sciences

Aeolian desertification is land degradation characterized by wind erosion, which is dependent on erosivity and erodibility. Progressive aeolian desertification causes dust to occur frequently, which has negative impacts on the environment and human health. To effectively prevent the expansion of aeolian desertification, it is crucial to monitor the processes of aeolian desertification and understand its mechanism(s). However, due to its complexity, it is difficult to apply a common indicator for monitoring desertification status.
In this study, we assessed aeolian desertification by using a dust erodibility index as an indicator that reflects the vulnerability of the land surface to wind erosion. We used dust occurrence ratio (DOR), which was calculated as the ratio of the frequency of dust occurrence to the frequency of strong winds, to represent the status of aeolian desertification. We evaluted aeolian desertification procesess at one site (Abaga-Qi) in the Xilingol grassland during the period 1974–2013. DOR values during 2001–2013 were notably higher than those in 1974–2000, indicating that land surface conditions became vulnerable to wind erosion in recent years. However, the DOR values trended lower from 2001 to 2013, corresponding to periods in which restoration projects were implemented aimed at combating desertification in China. To understand the mechanism(s) underlying aeolian desertification after the implementation of restoration projects, we conducted multiple regression analysis of climatic variables (precipitation and temperature) and an anthropogenic variable (livestock number) on recent variations (2001–2013) in aeolian desertification. Stepwise multiple regression results indicate that the recent decline in DOR values was associated with abundant precipitation and low temperature during summer of the previous year and a small livestock population at the end of the previous year. Livestock reduction made the greatest contribution. Our results suggest that aeolian desertification can be effectively reversed by reducing the number of livestock in the Xilingol grassland.

Keywords: desertification, erodibility, climate change, human activity, livestock

©2019. Japan Geoscience Union. All Right Reserved. 

# Influences of land surface conditions and human activities on dust events in Inner Mongolian grasslands, China

*Mei Yong[1], Masato Shinoda[2], Nandintsetseg Banzragch[2]

1. Inner Mongolia normal university, 2. Nagoya university

Aeolian processes in temperate grasslands (TGs) are unique in that the plant growth–decay cycle, soil moisture, and land-use interactivity affect seasonal and interannual variations of dust events. When compared with Mongolian TGs, Inner Mongolian TGs are characterized by unique land-uses (settle grazing and grass mowing). Since 2003, to prevent desertification and dust storms, land-uses have been controlled by the grassland protection law. We used process-based ecosystem (DAYCENT) and statistical models as well as dust event observations during March–June 1981–2015 to (1) identify critical land surface factors that control dust emission (soil moisture and vegetation components; live grasses, standing dead grasses and litter) in Inner Mongolian steppe and desert steppe sites, and (2) estimate the impacts of the controlled land-use law on dust events. The DAYCENT model realistically simulated dynamics of the vegetation components and soil moisture that were captured by observations (2005–2015). Results showed that at both sites, the spring dust events had a similar amplitude of significant correlation with wind speed and a combination of all the surface factors that retained anomalies (memory) of the preceding year. Among the surface factors, vegetation was a critical dust suppressing factor in Inner Mongolian TGs, similar to Mongolian TGs. Importantly, in the desert steppe, the standing dead grasses had the strongest memory and simultaneous significant correlation with the dust events, while no significant correlations were found in the steppe. This suggests that in the steppe, intensive grazing and mowing resulted in smaller dead grasses and a negligible effect on dust events. Moreover, simulations of dust events under controlled land-use (light grazing) and uncontrolled conditions (heavy grazing) showed that since 2003, the grassland protection law resulted in reduced dust events by 25% and 40% in the steppe and desert steppe, respectively.

Keywords: Dust events, DAYCENT model, Vegetation components, Soil moisture, Xilingol grassland

©2019. Japan Geoscience Union. All Right Reserved. 

[J] Poster | M (Multidisciplinary and Interdisciplinary)：M-IS Intersection

Thu. May 30, 2019 5:15 PM - 6:30 PM JST | Thu. May 30, 2019 8:15 AM - 9:30 AM UTC | Poster Hall International Exhibition Hall8, Makuhari Messe_38

## [M-IS09] dust

convener:Ishizuka Masahide(Kagawa University), Yasunori Kurosaki(Arid Land Research Center, Tottori University), Thomas Sekiyama(Meteorological Research Institute), Kana Nagashima(Japan Agency for Marine-Earth Science and Technology, Research and Development Center for Global Change)

Mineral dust is generated from the ground surface by strong winds, and it transports long distance over the earth. In the process, cloud formation and absorption and scattering of solar radiation cause weather and climate changes. Also, when deposited in the ocean, feeding nutrients to phytoplankton, promoting photosynthesis, and when deposited on snow and ice causes albedo change. This is known as the yellow dust (Asian dust) phenomenon in Asia region including Japan. In order to understand this, integration in a wide range of academic areas is necessary.
In the emission process, the amount of dust changes greatly depending on the surface condition in dryland area, and in order to know the conditions, it deals with areas such as soil, topography, vegetation, precipitation, desert and soil deterioration. In the transport process, we deal with areas such as weather, atmospheric aerosol, radiation. In the deposition process, we deal with areas such as ocean, snow ice, health to people and livestock. Drying and changes in vegetation also have social scientific aspects such as national policies, management of livestock, and population increase. Dust and sand dunes are common phenomena not only to the Earth but also to other planets such as Mars and Saturn. In this way, it is impossible to understand the dust phenomenon only in one field, it is important for researchers in many areas to discuss and share information through this session, and advance exchange of researchers.

### [MIS09-P01] Study on decadal influencing of the teleconnection pattern EA and SCAND on major atmospheric circulation systems of the northern China dust storms during the past 65 years (1954-2018)

*Gao Tao[1], Mei Yong[2] (1.Inner Mongolia Meteorological Institute, 2.Inner Mongolia Normal University)

### [MIS09-P02] Effects of freeze-thaw and land-surface processes on dust occurrence in the Mongolian desert steppe

*Kaman kong[1], Masato Shinoda[1], Banzragch Nandintsetseg[1,2,3], Yasunori Kurosaki[4] (1.Nagoya Unviserity, 2.Information and Research Institute of Meteorology, Hydrology, and Environment, 3.National University of Mongolia, 4.Tottori University)

### [MIS09-P03] Mineral particles suspending in the surface waters of the North Pacific and its marginal seas – atmospheric dust deposition as investigated from seawater analysis

*Yoko Iwamoto[1], Mitsuo Uematsu[2] (1.Graduate School of Biosphere Science, Hiroshima University, 2.Atmosphere and Ocean Research Institute, the University of Tokyo)

### [MIS09-P04] Seasonal change of the Asian dust provenance within the Canadian ice core estimated from cathodoluminescence spectra of single quartz grains

*Kana Nagashima[1], Kumiko Goto-Azuma[2] (1.Japan Agency for Marine-Earth Science and Technology, Research and Development Center for Global Change, 2.National Institute of Polar Research)

### [MIS09-P05] Wind tunnel experiments for saltation and dust emission under weak crusted Mongolian soil

*Ishizuka Masahide[1], Yusuke Nakahara[5], Hitomi Masaoka[6], Genki Nakao[6], Tomoyuki Ishii[6], Yasunori Kurosaki[2], Hagino Hiroaki[3], Kouichi Nakamura[7], Batdelger Gantsetseg[4], Kazuki Nanko[9], Eiji Nishihara[8], Satoru Suzuki[9] (1.Kagawa University, Faculty of Engineering and Design, 2.Tottori University, Arid land research center, 3.Forestry and Forest Products Research Institute, Tohoku Research Center, 4.Information and Research Institute of Meteorology Hydrology and Environment, 5.Kagawa University, Graduate school of Engineering, 6.Kagawa University, Faculty of Engineering, 7.Tottori University, Faculty of

Engineering, 8.Tottori University, Faculty of Agriculture, 9.Forestry and Forest Products Research Institute, Meteorology and Hydrology)

---

## [MIS09-P06] Effect of stone on sand saltation in Tsogt-Ovoo, Mongolia: Observation and Model simulation

*Batjargal Buyantogtokh[1], Yasunori Kurosaki[1], Masahide Ishizuka[2], Tsuyoshi Sekiyama[3] (1.Arid Land Research Center, Tottori University, 2.Faculty of Engineering and Design, Kagawa University, 3.Japan Meteorological Agency, Meteorological Research Institute)

# Study on decadal influencing of the teleconnection pattern EA and SCAND on major atmospheric circulation systems of the northern China dust storms during the past 65 years (1954-2018)

*Gao Tao[1], Mei Yong[2]

1. Inner Mongolia Meteorological Institute, 2. Inner Mongolia Normal University

Frequent cold-air attacks with less precipitation and aired surface conditions are mainly direct causes of more dust storm occurrences over the dust-source-areas during winter-spring season. In this study, the observation records of the horizontal visibility at 65 stations dotted in northern China (35˚-45˚N, 94˚-120˚E) for 65 years (1954-2018) were collected and used to investigate the frequencies of dust storm (DS) and severe dust storm (SDS) events during the term of February-June. As a whole, declining trends were appeared for both DS and SDS during the past several decades. A dust storm frequently occurrence term is confirmed from 1950s to 1970s, with decadal means of 7.1 and 2.5 events for both DS and SDS. From 1980s to 2010s, the DS and SDS decreased significantly with decadal means of 3.8 and 1.1 events, separately. The 1970s is the most frequent dust storm decade, during which 81 DS events have been recorded. Oppositely, the 1990s is the most infrequent decade with totally 25 DS events. Comparing spring precipitation and snow events of the previous winter, the precipitation anomaly of the 1970s is -13.3% and for 1990s, it is 15.9%. Decadal mean of the prior winter snow events are 3.6 and 4.8 respectively for 1970s and 1990s. That means 1970s has less than normal precipitation during winter-spring. The climate was dry. In turn, it had more precipitation during the 1990s, the climate was wet and the dust storm decreased.

By comparing the major atmospheric circulation systems relating to frequent and infrequent dust storm springs, it has been identified that a weak West Pacific subtropical high (WPSH), a strong North Polar vortex (NPV) and a strong and western position East Asian trough (EAT), in general, corresponding to less precipitation and dry climate, and then, a frequent dust storm spring. Contrarily, it is opposite.

Indices of the atmospheric teleconnection pattern EA and SCAND (also named EU1) were issued on the website of the Climate Prediction Center of USA. Influence of these two teleconnection patterns on the major atmospheric circulation systems and dust storms was studied in this work. Analyzed outcomes indicate that the EA has a closely positive connection with the WPSH and the westerly for winter-spring season. A strong WPSH is benefit to the sea vapor transportation for the dust source regions where located in northern China, bring more rainfalls to there. Additionally, a strong westerly over Eurasia confines the extension of the NPV, and the cold air from the Polar decreases, corresponding to an infrequent DS spring. It is opposite when the EA is weak. The SCAND displays a significantly negative relationship with the westerly and a converse variation trend with the DS frequency. The westerly not only has an impact on the NPV, but also affects the EAT as well. The westerly may become weak when the SCAND is strong, at the same term, the meridionality varied big and the polar cold air attacks may increase, lead to more DS weathers. The EAT may becomes strong and moves to more western position while the westerly is weak. This EAT condition is unfavorable to the vapor transferred to the focused area from the East Sea, results in less precipitation and dry climate, DS may increase during the springtime. Conversely, the westerly may become strong when the SCAND is in weak phases. The NPV, in general, is weak and the cold air attacks decrease. The EAT varies weak and move to eastern than normal position, favoring to the vapor transportation and more rainfall moistening the surface soil, the DS may decrease.

©2019. Japan Geoscience Union. All Right Reserved. 

Keywords: Dust storm, Teleconnection pattern, Atmospheric circulation, Northern China

©2019. Japan Geoscience Union. All Right Reserved. 

# Effects of freeze-thaw and land-surface processes on dust occurrence in the Mongolian desert steppe

*Kaman kong[1], Masato Shinoda[1], Banzragch Nandintsetseg[1,2,3], Yasunori Kurosaki[4]

1. Nagoya Unviserity, 2. Information and Research Institute of Meteorology, Hydrology, and Environment, 3. National University of Mongolia, 4. Tottori University

Dust storms not only cause serious environmental problems, but also influence social and economic activities. They depend on the relationships between erosivity (wind speed) and erodibility (e.g., soil moisture, freeze-thaw cycle, and vegetation). However, in the Mongolian desert steppe (MDS), these relationships have not fully been investigated, particularly the effect of freeze-thaw cycles on dust events. Here, we investigated the impacts of freeze-thaw and land surface processes on dust occurrence at Tsogt-Ovoo in the MDS during 2012–2017. This study uses the saltation number and dust concentration measurements, and modelled land-surface variables by an ecosystem (DAYCENT) model, which was validated with field measurements. Results showed that interannual variations in wind speed and dust concentration were not significantly different within springs (April–June) of 2012–2017. However, large interannual variability of saltation events observed at the same time. Saltation events were high in springs of 2012 and 2015 because small threshold wind speed that was related to dry soil and less vegetation, which were, in turn, the result of less precipitation in the preceding summer. Additionally, saltation events tended to occur after near-surface soil temperature rose above the freezing point. This freeze-thaw process likely plays an important role in increasing the susceptibility of soil to erosion.

Keywords: Mongolian desert steppe, freeze-thaw cycles, land-surface processes, dust occurrence, DAYCENT model

©2019. Japan Geoscience Union. All Right Reserved. 

# Mineral particles suspending in the surface waters of the North Pacific and its marginal seas –atmospheric dust deposition as investigated from seawater analysis

*Yoko Iwamoto[1], Mitsuo Uematsu[2]

1. Graduate School of Biosphere Science, Hiroshima University, 2. Atmosphere and Ocean Research Institute, the University of Tokyo

Suspended particulate matter (SPM) in the ocean consists of a variety of components from both biogenic and crustal sources. The mineral particles from crustal sources are brought to the oceans mainly via river run-off and atmospheric deposition. The atmospheric pathway becomes important especially in the open ocean far from the continents. In addition, atmospheric dust contains iron which can be used as nutrients for marine phytoplankton. Therefore, it is important to understand the size and chemical characteristics of the mineral particles that deposit to the ocean in understanding the linkage between atmosphere and marine ecosystem.

This study presents the properties of mineral particles in the SPM collected in the North Pacific and its marginal seas (the Sea of Okhotsk, the Bering Sea and the Chukchi Sea) based on bulk and individual particle analyses.

The mineral particles were distributed ubiquitously in the North Pacific even during summer when the influence of atmospheric Asian dust transport is small. Their relative abundances in the total SPM was 5 to15% by number and about 2 to 7% by volume. The size distribution of the suspended mineral particles in the SPM was similar to that of the atmospheric dust aerosols, indicating that mineral dust of background level occurs in the marine boundary layer even in summer.

The shipboard observation during a Kosa (Asian dust) season showed that atmoepheric dust settled onto the ocean surface, and resulted in increase in the mineral particles' concentration four to five times in surface water of the western subarctic North Pacific. The deposition flux of atmospheric dust into the ocean surface by a Kosa-event was calculated to be 270 mg $m^{-2}$ $event^{-1}$. The dissolve iron flux at the Kosa-event was also estimated at 130-230 $\mu$g $m^{-2}$ $event^{-1}$, and is found to have a potential to supply enough iron to lead the phytoplankton bloom in HNLC waters. This result confirms that a sporadic supply of dissolved iron that leading to phytoplankton bloom can naturally occur in the western subarctic North Pacific.

Keywords: the North Pacific, Marginal seas, Suspended particulate matters in seawater, Kosa, Iron, Geographical distribution

©2019. Japan Geoscience Union. All Right Reserved. 

# Seasonal change of the Asian dust provenance within the Canadian ice core estimated from cathodoluminescence spectra of single quartz grains

*Kana Nagashima[1], Kumiko Goto-Azuma[2]

1. Japan Agency for Marine-Earth Science and Technology, Research and Development Center for Global Change, 2. National Institute of Polar Research

Mineral dust is considered to have a great effect on the natural environment of the Earth by altering the global radiative balance, cloud properties (Intergovernmental Panel on Climate Change (IPCC) AR5, 2014) and ocean primary productivity (Maher et al., 2010). At present, a large amount of aeolian dust is emitted from the huge dry areas of East Asia, typically the Taklimakan Desert in western China and Gobi in southern Mongolia and northern China (Sun et al., 2001). The dust particles derived from such deserts are transported to China, Korea, Japan, and the northwestern North Pacific by the westerlies and is sometimes transported more than one full circuit around the globe through the westerly jet (Uno et al., 2009). Hence, the Asian dust affects climate/environments throughout the northern hemisphere. For the further investigation and evaluation of Asian dust impacts on global environment, it is critical to determine the amount and main sources of Asian dust transported over long distances.
Ice cores from Mt. Logan (60N, 141E), Canada, are the ideal recorder of seasonal to decadal-scale changes in dust transport over a long distance (Zdanowicz et al., 2006). Hence here we examine the past seasonal change of dust provenance using an ice core from King col (4135m above sea level) at Mt. Logan by utilizing a new provenance-tracing method, cathodoluminescence (CL) spectral analysis of “single” quartz grains (Nagashima et al., 2017). CL spectroscopy can detect crystal-chemical features in quartz such as impurities and intrinsic imperfections that depend on the conditions affecting quartz from its formation onward, which are useful to identify the quartz from two major Asian deserts, the Taklimakan Desert and Mongolian Gobi. The CL analysis was performed on quartz grains within ice core samples corresponding to 1941, 1951, 1967, 1983, and 1986 A.D. (6–7 samples/year). We found most quartz grains from ice core samples show two CL emission bands in red and blue regions, which were deconvolved to at most five emission components, each of which represents a specific defect due to an impurity or imperfection. The statistical analysis using the ratios of emission components exhibits ratios of clusters of each sample, which are mostly between those of quartz from Taklimakan Desert and Mongolian Gobi, suggesting the mixing of quartz from the two deserts. Furthermore, the cluster compositions of ice core samples suggest seasonal and possible decadal-scale changes of the dust provenance transported over a long distance, of which detail will discuss in the presentation.

Keywords: Asian dust, provenance, ice core

©2019. Japan Geoscience Union. All Right Reserved. 

# Wind tunnel experiments for saltation and dust emission under weak crusted Mongolian soil

*Ishizuka Masahide[1], Yusuke Nakahara[5], Hitomi Masaoka[6], Genki Nakao[6], Tomoyuki Ishii[6], Yasunori Kurosaki[2], Hagino Hiroaki[3], Kouichi Nakamura[7], Batdelger Gantsetseg[4], Kazuki Nanko[9], Eiji Nishihara[8], Satoru Suzuki[9]

1. Kagawa University, Faculty of Engineering and Design, 2. Tottori University, Arid land research center, 3. Forestry and Forest Products Research Institute, Tohoku Research Center, 4. Information and Research Institute of Meteorology Hydrology and Environment, 5. Kagawa University, Graduate school of Engineering, 6. Kagawa University, Faculty of Engineering, 7. Tottori University, Faculty of Engineering, 8. Tottori University, Faculty of Agriculture, 9. Forestry and Forest Products Research Institute, Meteorology and Hydrology

Dryland area is enlarging and its environment is changing in the globe. Mineral dust is generated from such dry area and causes various problems such as health damage which is caused by well-known air pollutants such as $PM_{2.5}$, traffics stoppage due to low visibility, and a reduction of agricultural productivity due to loss of nitrogen and phosphorus contained in surface soil. The nutrients and soil minerals make algal blooms in ocean and its photosynthesis makes $CO_2$ absorption from atmosphere. Mineral dust itself acts as an ice nuclei primarily and effects cloud formation, and absorbs and/or diffuses solar and infrared radiations secondary. In addition, it transports biological gene of microorganism and bacteria attached to the soil surfaces. Like this, mineral dust gives large influences for various fields and is important to understand the natural and social changes.

This study focuses on the emission process of dust, especially, soil crust effect on the saltation and dust emission. Soil crust is one of the ground surface conditions, which affects dust generation largely due to strong soil aggregation. But it is well not understood how much soil crust effects saltation and dust emission amount yet. To clarify this, wind tunnel experiment was conducted in a laboratory of Forestry and Forest Products Research Institute, Tsukaba, Japan. Toyoura sand is used as saltating grains and Mongol soil which has both finer and larger particles (Loam) sampled at Tsogt-Ovoo in the northern Gobi Desert is used as a target soil. The water ratio is set 0-15 % for making artificial soil crust.

PTV (Particle Tracking Velocimetry) analysis by using a high-speed camera (30000 fps) shows the reduction of kinetic energy of saltation particle after it hits the ground surface. The crusted surface soil was not much erodible under the higher water ratio. Dust concentration decreases under the crusted condition. These findings are fundamental for elucidating the process of dust emission and will link to improve dust forecasting accuracy by atmospheric models.

Keywords: KOSA, Asian dust, dryland, water ratio, PM2.5

©2019. Japan Geoscience Union. All Right Reserved. 

# Effect of stone on sand saltation in Tsogt-Ovoo, Mongolia: Observation and Model simulation

*Batjargal Buyantogtokh[1], Yasunori Kurosaki[1], Masahide Ishizuka[2], Tsuyoshi Sekiyama[3]

1. Arid Land Research Center, Tottori University, 2. Faculty of Engineering and Design, Kagawa University, 3. Japan Meteorological Agency, Meteorological Research Institute

Non-erodible elements (i.e., pebble, stone, bedrock, vegetation, dead leaf) are key factors to control wind erosion. The non-erodible elements can protect the underlining surface by absorbing the wind momentum, thus increasing the threshold velocity for sand movement on the intervening surface (Tan et al., 2013). According to Haustein et al. (2015), however, all results of box models, which are 0-dimensional dust emission models installing schemes of Marticorena and Bergametti (1995), Shao (2004), and Alfero and Gomes (2001), overestimate the horizontal sand flux due to lack of consideration in the surface coverage by the non-erodible elements. This suggests current global and regional dust models don’ t consider the effects of them well. We will show observation and box models result of sand saltation at different land surface characteristics at Tsogt-Ovoo located in a northern part of the Gobi Desert, Mongolia.

An analysis of meteorological observatory data showed that the frequency of dust storms was the highest at Tsogt-Ovoo in East Asia (Kurosaki and Mikami, 2007). There is a topographic depression, whose sizes are about 10 km and 20 km in NE-SW and NW-SE directions, respectively. Such topography makes spatially different soil and land surface characteristics such as bedrock coverage, stone coverage, parent soil particle size and vegetation coverage. We made a measurement of sand saltation and wind speed at 7 sites during 31 April –5 May 2018. We installed ud-101 (Udo 2009; Sherman 2011) at 0.1 m height for sand saltation and anemometer (S-WSA-M003, Onset Company) at 1.7 m height at each site.

Our observation shows the sand saltation counts and threshold wind speed differs very much site-by-site due to differences in non-erodible elements like stone, dead leaf and soil crust. Even though wind speed is high, small counts of sand saltation were observed at Sub18A and Sub18C sites which are highly covered by bedrock and stone, whose coverages (hereafter, BSC) are 76.9% and 50.6%, respectively. Our sand saltation box model, which is based on Shao's dust emission scheme, also showed small sand flux under such high BSC like those sites. Big sand saltation counts were observed at Main and Sub14B sites, those stone coverages are 18.2 % and 17.6 %, respectively. The threshold wind speeds of sand flux with stone effect are similar with observation in the result of model. The observation and model simulations showed that BSC effect is a major controlling factor for sand saltation counts and flux for Sub18A, Sub18C, Main and Sub14B sites.
At Sub14A and Sub18D sites, even though stone coverages are small (2.1% and 6.4%, respectively), our observations show very small sand saltation counts even under strong wind conditions. These results suggest a hypothesis that other non-erodible elements such as standing dead leaves and soil crusts majorly suppress sand saltation, though we could find them by our eyes but we don't have their quantitative data. Our simulations show sand saltation fluxes increase with wind speed. One reason of it is the BSC effect doesn't work very much due to small stone coverages at sites. Another possible reason is effects of other non-erodible elements such as standing dead leaves and soil crusts are not installed in our model but they work very much in reality.

©2019. Japan Geoscience Union. All Right Reserved. 

Keywords: Non-erodible elements, sand saltation, stone effect, box model

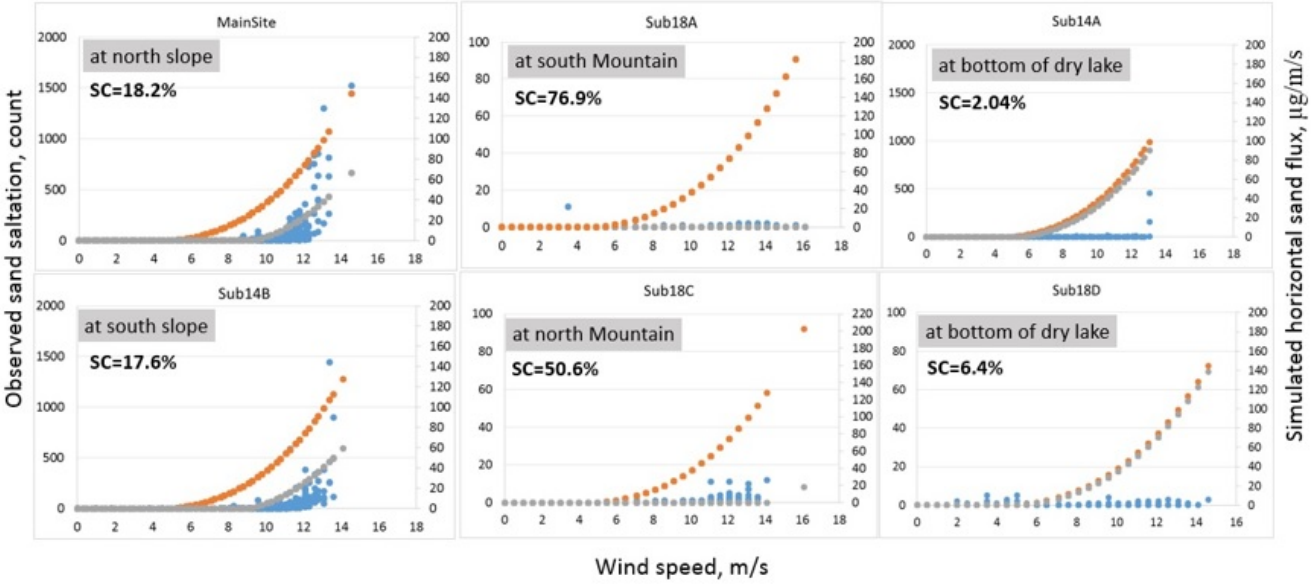


Fig. 1 Observed wind speed (x-axis) and observed sand saltation counts (left axis) (shown by blue dots) at sites which different stone coverage (SC) during the period of May 1-5, 2018 at Tsogt-Ovoo, Mongolia. Simulated wind speed (x-axis) and simulated sand fluxes (right axis) without BSC effect (BSC=0%) (orange dots) and same for with BSC effect (observed BSC value) (gray dots) for same sites and for same period.

©2019. Japan Geoscience Union. All Right Reserved. 

[J] Oral | M (Multidisciplinary and Interdisciplinary) : M-IS Intersection

Thu. May 30, 2019 9:00 AM - 10:30 AM JST | Thu. May 30, 2019 12:00 AM - 1:30 AM UTC | Convention Hall B 2F

## [M-IS12] tsunami deposit

convener:Takashi Chiba(Faculty of Bioresource Sciences, Akita Prefectural University), Tetsuya Shinozaki(Center for Research in Isotopes and Environmental Dynamics (CRiED), University of Tsukuba), Daisuke Ishimura(Department of Geography, Tokyo Metropolitan University), Chairperson:Daisuke Ishimura(Department of Geography, Tokyo Metropolitan University)

The 2011 off the Pacific coast of Tohoku Earthquake and tsunami have an influence on the development of tsunami deposit research. After the tsunami, a lot of findings have been reported on various research fields. However, identification criteria of the tsunami deposit are not yet established. Moreover, it is still uncertain how to use the tsunami deposit in the risk assessment. In this session, we welcome researches from all aspect of sedimentary records of modern and paleo tsunamis both onshore and offshore, and numerical and experimental modeling studies for risk assessment. In addition, we also welcome other event deposits, such as flooding and storm surge, that they are considered to be important for discrimination of tsunami deposit.

9:00 AM - 9:15 AM JST | 12:00 AM - 12:15 AM UTC

### [MIS12-01] Geological Record of Tsunamis and Storms Influenced by Relative Sea-Level Change, Southern Hidaka Coast, Hokkaido, Japan.

*RYO NAKANISHI[1], Satoshi Okamura[1,2], Tsumoru Sagayama[3], Yusuke Yokoyama[4], Yosuke Miyairi[4] (1.Hokkaido Edu. Univ., 2.Hokkaido Soil Res. Co-op., 3.HRCG, 4.Univ. Tokyo)

9:15 AM - 9:30 AM JST | 12:15 AM - 12:30 AM UTC

### [MIS12-02] Before and after relationship between the seismic uplift and the large tsunami due to the seventeenth-century giant earthquake observed in the seismic barrier systems around the Kuril subduction zone

*Futoshi Nanayama[1,5], Kazuaki Watanabe[1], Keita Fukatsu[2], Takeshi Hasegawa[4], Kiyoyuki Shigeno[3], Masayuki Ishii[6], Kazuhito Ishiwata[7], Shigeto Inokuma[8] (1.Geological Survey of Japan, AIST, 2.Notsuke Peninsula Nature Center, 3.Meiji consultant Co., Ltd., 4.Ibaraki University, 5.CWMD, Kumamoto Univ., 6.Ishii Professional Engineer Office, 7.Betsukai municipal museum, 8.Nemuro City museum history and nature)

9:30 AM - 9:45 AM JST | 12:30 AM - 12:45 AM UTC

### [MIS12-03] Coastal landform changes and Washover deposits due to high waves generated by anatmospheric low-pressure system in June 2016 at Horokayanto, Hokkaido, Japan

*Takashi Chiba[1], Yuichi Nishimura[2] (1.Faculty of Bioresource Sciences, Akita Prefectural University, 2.Graduate School of Science, Hokkaido University)

9:45 AM - 10:00 AM JST | 12:45 AM - 1:00 AM UTC

### [MIS12-04] Survey of tsunami deposits in Kunashiri Island: Results obtained in the 2015-2018 projects

*Yuichi Nishimura[1], Yasuhiro Takashimizu[2], Daisuke Sugawara[3], Takafumi Enya[4], Takashi Chiba[5], Ryo Nakanishi[6], Alexander Shishkin[7], Alexey Gorbunov[8], Victor Kaistrenko[8], Asuka Takahashi[9], Hiroki Muramatsu[10], Yasuyuki Kawazoe[11], Naofumi Takamatsu[11] (1.Graduate School of Science, Hokkaido University, 2.Institute of Humanities, Social Sciences and Education, Niigata University, 3.Museum of Natural and Environmental History, Shizuoka, 4.Hokkaido Museum, 5.Faculty of Bioresource Sciences, Akita Prefectural University, 6.Hokkaido Education University, 7.Shikotan Geophysical Observatory, 8.Institute of Marine Geology and Geophysics, Russian Academy of Sciences, 9.Japan Meteorological Agency, 10.Geospatial Information Authority of Japan, 11.Ministry of Education, Culture, Sports, Science and Technology)

10:00 AM - 10:15 AM JST | 1:00 AM - 1:15 AM UTC

[MIS12-05] Deposit-based assessment of tsunami size: example from Nankai-Trough earthquakes

*Daisuke Sugawara[1], Kentaro Imai[2], Shinsuke Okada[3], Takuto Maeda[4] (1.Museum of Natural and Environmental History, Shizuoka, 2.JAMSTEC, 3.Tohoku University, 4.Hirosaki University)

10:15 AM - 10:30 AM JST | 1:15 AM - 1:30 AM UTC

[MIS12-06] Flume experiments for understanding variety of tsunami deposit

★Invited Papers

*Naofumi Yamaguchi[1] (1.Center for Water Environment Studies, Ibaraki University)

# Geological Record of Tsunamis and Storms Influenced by Relative Sea-Level Change, Southern Hidaka Coast, Hokkaido, Japan.

*RYO NAKANISHI[1], Satoshi Okamura[1,2], Tsumoru Sagayama[3], Yusuke Yokoyama[4], Yosuke Miyairi[4]

1. Hokkaido Edu. Univ., 2. Hokkaido Soil Res. Co-op., 3. HRCG, 4. Univ. Tokyo

In the last a few hundred years, southern Hidaka coast in Hokkaido was suffered from large tsunamis by subduction of the Pacific Plate along the southern Kuril Trench. 2003 Tokachi-oki earthquake left traces at maximum altitude 4 m in Hyakunin Hama in the eastern part of Cape Erimo, also maximum altitude 3 m in western part of Cape Erimo. It was caused by the edge wave propagating from Cape Erimo along the west coast of the Hidaka area (Tanioka et al., 2004) . On the other hand, geological studies in eastern part of Hokkaido revealed that intervals of outsized tsunamis by Kuril subduction inferred average nearly 400 years but range widely from about 100 to about 800 years (Sawai et al., 2009), and these probably reached western part of Cape Erimo. However, the only 17th century tsunami deposits reported in the western part of Cape Erimo are said to be unknown the trigger. Thus, This study conducted Simple boring survey to reveal tsunamis cycle and age of emergence in Northern Hidaka coast. Consequently, we compared western part and eastern part of Cape Erimo about scale of tsunamis, also examined the relationship with the paleo environment.

As a result of boring survey by a geoslicer in the peat swamp behind the beach, we found three volcanic ash layers and nine event sand layers in the humus and the peat. In order from the top, it was AD 1663 Us-b tephra, AD946 B-Tm tephra, two sand layer (Us1, U1), 2700-2500BP Ta-c2 tephra, seven sand layer (U2-8). Peat layers change to remarkably undegraded humus from the U4 layer downward. The number of sand layers decreased landward, finally being zero at about 500 m from coastline. U1-8 sand layers were similar in particle size and gray color to beach sands, and sorting very well. These common characteristics were from inverse to normal grading and contain rip-up clasts. Also, grain size and thickness were inverse correlation with distance from coastline, but no correlation with distance from river. Because the diatom assemblages from event sand layers contained marine, brackish and terrestrial species in contrast peat occupied by freshwater species, these turn out to derive from seaward. Conversely, the Us1 layer had limited distribution several tens meter from paleo beach ridge, the thickness changed from 20 cm to very thin at only 20m landward. Grain size of the Us1 layer was fine - very coarse, including Φ1cm flat gravel. The Us1 layer can be supposedly distinguished from U1-8 layers from these features similar to storm deposits. A result of measuring ages for the time of sand deposition by AMS radiocarbon dating, we obtained the age of about 5500BP from under the U8 layer, about 2000BP from above the U1 layer. The average recurrence intervals of event is nearly 400 years, the interval is sometime shorter (50 years) or longer (550 years) than the average, so the U1-8 event layers are probably tsunami deposits by subduction earthquakes like seen in eastern Hokkaido.

The U7 layer is the thickest in all sand layers, thickness of event layers tend to become thinner as the upper stratigraphy. The U7 layer is most widely distributed inland, it deposited in about 4900BP, when high-standard period in eastern Hokkaido (Dura et al., 2016). It was found from the result of continuous chemical analysis of peat samples in the vertical direction that Fe and S increased as deeper at the depth deeper than the U5 layer (about 3800BP). In this site, considering the humus layer shows undegraded under the U4 layer, this chemical characteristic imply that the peat was reductive and the sea-level was high at that time. We inferred that tsunamis inundated over the sand ridge in this area only for 5500BP to

©2019. Japan Geoscience Union. All Right Reserved. 

2000BP, because didn’ t find tsunami deposits from the stratigraphy since 2000BP. In conclusion, when restoration of paleo tsunami record, it necessary to consider that changing sea-level and associated topographic change.

Dura, T. et al. (2016) The role of Holocene relative sea-level change in preserving records of subduction zone earthquakes. Curr. Clim. Change. Rep. 2, 86–100.

Sawai, Y., Kamataki, T., Shishikura, M., Nasu, H., Okamura, Y., Satake, K.,… Aung T. T., 2009, Aperiodic recurrence of geologically recorded tsunamis during the past 5500 years in eastern Hokkaido, Japan. Jour. Geophys. Res., 114, B01319.

Tanioka, Y., Nishimura, Y., Hirakawa, K., Imamura, F., Abe, I., Abe, Y……Masaka, S., 2004, Tsunami run-up heights of the 2003 Tokachi-oki earthquake. Earth Planets Space, 56, 359-365.

Keywords: Tsunami deposits, Storm deposits, Kuril subduction, Radiocarbon dating, Paleo environment restoration, Holocene High Standard

©2019. Japan Geoscience Union. All Right Reserved. 

# Before and after relationship between the seismic uplift and the large tsunami due to the seventeenth-century giant earthquake observed in the seismic barrier systems around the Kuril subduction zone

*Futoshi Nanayama[1,5], Kazuaki Watanabe[1], Keita Fukatsu[2], Takeshi Hasegawa[4], Kiyoyuki Shigeno[3], Masayuki Ishii[6], Kazuhito Ishiwata[7], Shigeto Inokuma[8]

1. Geological Survey of Japan, AIST, 2. Notsuke Peninsula Nature Center, 3. Meiji consultant Co., Ltd., 4. Ibaraki University, 5. CWMD, Kumamoto Univ., 6. Ishii Professional Engineer Office, 7. Betsukai municipal museum, 8. Nemuro City museum history and nature

The Kuril subduction zone is one of the most frequent earthquakes in Japan. There are many undeveloped plains in this area, unspoiled nature is left, and many barrier coasts and tsunami deposits due to the giant earthquake (17th century type) repeatedly generated at 400 to 500 years intervals can be widely observed around this area. However, the relationship between the timing of both is not clear yet. Especially two tsunami deposits, which are occurred in the 17th century, can be observed in many places around the eastern Pacific coast of Hokkaido. On the other hand, there are many active barrier systems around the coast of Nemuro Strait and Konsen ~ Tokachi coast, and it has recently become evident that a 17th century giant earthquake occurred as a trigger. Our research group examined the relationship between the occurence timing of these uprifting barrier systems and the 17th century tsunami in several areas in detail, and some interesting facts have been found, so we will report the outline in this meeting.

This work was supported by JSPS KAKENHI Grant Number 18K03767.

Keywords: Seventeenth-century giant earthquake, Tsunami, Regional crustal movement, Barrier system, eastern Hokkaido, Kuril subduction zone

©2019. Japan Geoscience Union. All Right Reserved. 

# Coastal landform changes and Washover deposits due to high waves generated by anatmospheric low-pressure system in June 2016 at Horokayanto, Hokkaido, Japan

*Takashi Chiba[1], Yuichi Nishimura[2]

1. Faculty of Bioresource Sciences, Akita Prefectural University, 2. Graduate School of Science, Hokkaido University

The lake bottom of Horokayanto, one of the lagoons in eastern Hokkaido, Japan, was partly exposed as a result of sandbar breaching during severe weather in June 2016. The mean lake level fell from approximately 3.1 to 1.2 m above TP, which is equivalent to the height of the MHHTL in the Tokachi area by the breached sandbar. Some erosion forms were recognized in the southwestern breached point of the sandbar. However, the washover fan formed by the high waves from the seaward to the lakeward sides was recognized in the northeastern part of the sandbar. Moreover, characteristic diatom assemblages resulting from coastal environmental changes were also recognized around the lake. The high-tide-level indicator *Pseudopodosira kosugii* was recognized in the emerged lake bottom assemblage together with freshwater–brackish and brackish–marine species. Water pressure or moisture changes caused by either the emergence, the changes in light quantum density and ultraviolet rays, the changes in water quality such as salinity and pH, or a mixture of these factors, may have influenced the increase in *P. kosugii*. Reworked Neogene marine diatoms such as *Denticulopsis* spp. that were presumably derived from nearby Neogene basement rocks were also detected–albeit infrequently–in the modern assemblages. The fossil diatoms were eroded by current inflows into the lake during the severe weather. During the period of emergence, seawater may have been transported into Horokayanto Lagoon by high waves generated by an atmospheric low-pressure system. However, the height of the waves was below that of the central part of the sandbar.

Keywords: washover deposit, sandbar breach, emerged lake bottom, diatom assemblage, Horokayanto

©2019. Japan Geoscience Union. All Right Reserved. 

# Survey of tsunami deposits in Kunashiri Island: Results obtained in the 2015-2018 projects

*Yuichi Nishimura[1], Yasuhiro Takashimizu[2], Daisuke Sugawara[3], Takafumi Enya[4], Takashi Chiba[5], Ryo Nakanishi[6], Alexander Shishkin[7], Alexey Gorbunov[8], Victor Kaistrenko[8], Asuka Takahashi[9], Hiroki Muramatsu[10], Yasuyuki Kawazoe[11], Naofumi Takamatsu[11]

1. Graduate School of Science, Hokkaido University, 2. Institute of Humanities, Social Sciences and Education, Niigata University, 3. Museum of Natural and Environmental History, Shizuoka, 4. Hokkaido Museum, 5. Faculty of Bioresource Sciences, Akita Prefectural University, 6. Hokkaido Education University, 7. Shikotan Geophysical Observatory, 8. Institute of Marine Geology and Geophysics, Russian Academy of Sciences, 9. Japan Meteorological Agency, 10. Geospatial Information Authority of Japan, 11. Ministry of Education, Culture, Sports, Science and Technology

Historical and prehistorical tsunami deposits in Kunashir Island, the Northern Territories, were studied as parts of visa-free exchange programs of Japan and Russia. The reconnaissance survey was conducted for 30 days for 4 years from 2015 to 2018, and 105 sites in the ca. 50 km area along the Pacific coastline was examined. As a result, it was confirmed that the sand layer, which can be regarded as a trace of the 1994 Hokkaido Toho-Oki tsunami is well preserved near the surface layer in the eastern lowland from Furukamappu to Ruyobetsu. The 1994 tsunami run-up, estimated from the distribution of the deposits, is 50-150 m from the coast and 3-4 m in height. Furthermore, the chemical composition of the volcanic glass was analyzed for as many as 30 volcanic tephras. Examining the results together with the stratigraphy, it was found that known tephra from volcanoes of Hokkaido, such as Ko-c1 (1856), Ta-a (1739), Ko-c2 (1694), Ta-b (1667), Ma-b (10th Century) and Ta-c (2,700 BP) are deposited at multiple sites on the island. With these volcanic deposits as the key layer, we could estimate the age of the candidates of tsunami deposits. For example, in the wetland of Furukamappu, there is one event in the 17th and 10th centuries, and two in the 10th century and 2700 years ago. It is inferred that the large tsunami that would leave the deposit in Kunashiri occurred at a frequency of once in 1000 years.

Keywords: the Northern Territories, Kunashiri Island, tsunami deposit, paleo earthquake, volcanic tephra

©2019. Japan Geoscience Union. All Right Reserved. 

# Deposit-based assessment of tsunami size: example from Nankai-Trough earthquakes

*Daisuke Sugawara[1], Kentaro Imai[2], Shinsuke Okada[3], Takuto Maeda[4]

1. Museum of Natural and Environmental History, Shizuoka, 2. JAMSTEC, 3. Tohoku University, 4. Hirosaki University

Researches on historical documents and geological records, such as tsunami deposits, have clarified the recurrence of the Nankai-Trough earthquakes and tsunamis during the past 6000 years. Magnitudes and source parameters of some historical tsunamigenic earthquakes, such as the 1707 Hoei and 1854 Ansei events, have been examined based on numerical modeling of coseismic crustal deformation and tsunami propagation and inundation. For example, the extent of the rupture area of the Hoei earthquake was revised based on the numerical modeling of tsunami inundation, considering tsunami heights from historical records and tsunami deposits in the Ryujin-ike pond in the eastern coast of Kyushu island (Furumura et al., 2011). The revised rupture area of the Hoei earthquake was extended to the Hyuga-nada, 70 km beyond the previously estimated rupture area.

The magnitude of the presumed largest (Mw=9.0) earthquake which may occur in the Nankai Trough (Disaster Management of Cabinet Office, 2012) is much greater than the size of known historical events. To validate the assumptions of the largest earthquake, information from tsunami deposits, which may record tsunamigenic earthquakes in longer time span, will play an important role. However, most tsunami deposits in the Nankai Trough region have been found from coastal lakes and narrow lowlands. In this region, spatial distribution of tsunami deposits cannot be a good indicator of tsunami inundation. Explorations are needed to correlate spatially-limited data of tsunami deposit with the magnitude information and source parameters of earthquake and tsunami.

In this presentation, deposit-based assessment of the size of earthquake and tsunami will be discussed based on numerical modeling of tsunami and sediment transport in the Ryujin-ike pond. Main interest of the research is that whether or not we can correlate the formation processes, distribution and thickness of tsunami deposit with the source parameters of the tsunami. In addition, results of the modeling will be compared with field observations of the deposits, to discuss the relationship with the historical earthquakes.

Acknowledgement

This research was supported by MEXT (“Research project for compound disaster mitigation on the great earthquakes and tsunamis around the Nankai Trough region”) and JSPS KAKENHI Grant Numbers 16H03146,

References

Furumura, T., Imai, K., Maeda, T. (2011) A revised tsunami source model for the 1707 Hoei earthquake and simulation of tsunami inundation of Ryujin Lake, Kyushu, Japan. Journal of Geophysical Research,

©2019. Japan Geoscience Union. All Right Reserved. 

116, B02308. doi:10.1029/2010JB007918

Disaster Management of Cabinet Office (2012). Investigative commission of great earthquakes in Nankai Trough. http://www.bousai.go.jp/jishin/nankai/model/index.html (Retrieved on Feb. 17, 2019)

Keywords: Nankai Trough, Tsunami, Deposit

©2019. Japan Geoscience Union. All Right Reserved. 

# Flume experiments for understanding variety of tsunami deposit

*Naofumi Yamaguchi[1]

1. Center for Water Environment Studies, Ibaraki University

Flume experiments, in which sedimentary conditions can be easily controlled, are expected to provide insights into the sedimentary process under tsunami flow. The previous studies using flume experiments have contributed to improvement of numerical models of tsunami sediment transport. By contrast, there is not enough experimental studies to examine sedimentary process in order to improve the identification and interpretation of (paleo) tsunami deposits in geological record. In this presentation, I will summarize previous studies of tsunami deposit using flume experiment, and show the potential for better understanding of sedimentary process of tsunami deposits.

Keywords: Tsunami deposit, Flume experiment, Sedimentary process

©2019. Japan Geoscience Union. All Right Reserved. 

[J] Oral | M (Multidisciplinary and Interdisciplinary)：M-IS Intersection

Thu. May 30, 2019 10:45 AM - 12:15 PM JST | Thu. May 30, 2019 1:45 AM - 3:15 AM UTC | Convention Hall B 2F

## [M-IS12] tsunami deposit

convener:Takashi Chiba(Faculty of Bioresource Sciences, Akita Prefectural University), Tetsuya Shinozaki(Center for Research in Isotopes and Environmental Dynamics (CRiED), University of Tsukuba), Daisuke Ishimura(Department of Geography, Tokyo Metropolitan University), Chairperson:Tetsuya Shinozaki(Center for Research in Isotopes and Environmental Dynamics, University of Tsukuba)

The 2011 off the Pacific coast of Tohoku Earthquake and tsunami have an influence on the development of tsunami deposit research. After the tsunami, a lot of findings have been reported on various research fields. However, identification criteria of the tsunami deposit are not yet established. Moreover, it is still uncertain how to use the tsunami deposit in the risk assessment. In this session, we welcome researches from all aspect of sedimentary records of modern and paleo tsunamis both onshore and offshore, and numerical and experimental modeling studies for risk assessment. In addition, we also welcome other event deposits, such as flooding and storm surge, that they are considered to be important for discrimination of tsunami deposit.

10:45 AM - 11:00 AM JST | 1:45 AM - 2:00 AM UTC

[MIS12-07] **Inverse modeling of Tsunami deposit using Deep Learning Neural Network**

*Rimali Mitra[1], Hajime Naruse[1] (1.Kyoto University, Graduate School of Science)

11:00 AM - 11:15 AM JST | 2:00 AM - 2:15 AM UTC

[MIS12-08] Numerical estimation of tsunami size using boulders deposited by the 2011 Tohoku-oki tsunami at Settai, Miyako city, Japan

*Tatsuya Takei[1,4], Kazuhisa Goto[2], Masaki Yamada[3] (1.Department of Earth Sciences, Graduate School of Science, Tohoku University, 2.International Research Institute of Disaster Science (IRIDeS), Tohoku University, 3.Earthquake Research Institute, University of Tokyo, 4.Department of Complexity Science and Engineering, Graduate School of Frontier Sciences, Tokyo University)

11:15 AM - 11:30 AM JST | 2:15 AM - 2:30 AM UTC

[MIS12-09] Constraint of the ages of historical tsunami deposits on the Ishinomaki Plain

*Hiroshi Tetsuka[1], Kazuhisa Goto[2], Takashi Ishizawa[1], Daisuke Sugawara[3], Yusuke Yokoyama[4], Yosuke Miyairi[4] (1.Department of Earth Science, Tohoku University, 2.International Research Institute of Disaster Science, Tohoku University, 3.Museum of Natural and Environmental History, Shizuoka, 4.Atmosphere and Ocean Research Institute, University of Tokyo)

11:30 AM - 11:45 AM JST | 2:30 AM - 2:45 AM UTC

[MIS12-10] Non-destructive analyzes of sediments to discern tsunami-related mud cap and overlying muds to improve age determination of tsunami deposits

*Takashi Ishizawa[1], Kazuhisa Goto[2], Yusuke Yokoyama[3], Yosuke Miyairi[3] (1.Department of Earth Science, Tohoku University, 2.International Research Institute of Disaster Science, Tohoku University, 3.Atmosphere and Ocean Research Institute, The University of Tokyo)

11:45 AM - 12:00 PM JST | 2:45 AM - 3:00 AM UTC

[MIS12-11] Sedimentological and paleontological studies of storm surge deposits in intertidal mud floor -case study of Ena Bay on Miura Peninsula, Central Japan.

*Akihisa Kitamura[1], yamamoto yuka[1], Takashi Toyofuku[2] (1.Institute of Geosciences, Faculty of Science, Shizuoka University, 2.Japan Agency for Marine-Earth Science and Technology (JAMSTEC))

12:00 PM - 12:15 PM JST | 3:00 AM - 3:15 AM UTC

[MIS12-12] Shallow marine tsunami deposits and bioturbation

★Invited Papers

*Koji Seike[1] (1.Geological Survey of Japan, AIST)

# Inverse modeling of Tsunami deposit using Deep Learning Neural Network

*Rimali Mitra[1], Hajime Naruse[1]

1. Kyoto University, Graduate School of Science

Tsunami is one of the most catastrophic disasters along coastal zones, and tsunami deposits are layers of sediment formed by hydrodynamic activities of tsunami. These event deposits provide clues to estimate the recurrence intervals and relative magnitude of prehistoric tsunamis that serve as a tool for future tsunami hazard evaluation. Towards the quantitative assessment of hydraulic conditions of tsunamis from deposits, this study applies the inverse model using deep learning neural network (DNN) for tsunami deposit. In order to conduct machine learning of DNN, forward model calculation was repeated at random initial flow conditions (e.g. maximum inundation height, flow velocity, concentration, etc.) to produce artificial training data sets which represent depositional characteristics such as thickness and grain-size distribution. The model serves as the modified version of previously proposed FITTNUSS model, which incorporates nonuniform and unsteady transport of suspended sediment and also turbulent mixing. Then, DNN was trained for establishing the inverse model on the basis of artificial data sets. SGD (Stochastic gradient descent) is used as an optimizer for this DNN model. Tests using artificial data sets successfully indicated that the established DNN can reconstruct the original flow conditions from the characteristics of deposits. Finally, the model was applied to natural data sets taken from the 2011 Tohoku-Oki Tsunami deposit. The deep learning neural network showed promising result for natural data sets. Comparing to existing inverse models, deep learning neural network enables the inversion to employ a forward model that requires higher computational costs, and to avoid a local optimum. The further applicability and validation of this method will be checked with other parameters, and natural data set from different field visits in future endeavour.

Keywords: Tsunami Deposits, Inverse Modeling, Machine Learning

©2019. Japan Geoscience Union. All Right Reserved. 

# Numerical estimation of tsunami size using boulders deposited by the 2011 Tohoku-oki tsunami at Settai, Miyako city, Japan

*Tatsuya Takei[1,4], Kazuhisa Goto[2], Masaki Yamada[3]

1. Department of Earth Sciences, Graduate School of Science, Tohoku University, 2. International Research Institute of Disaster Science (IRIDeS), Tohoku University, 3. Earthquake Research Institute, University of Tokyo, 4. Department of Complexity Science and Engineering, Graduate School of Frontier Sciences, Tokyo University

Tsunami boulders are important geological evidence to understand paleotsunami activity. Previous studies have intended to extract the information about tsunami size from the distribution of tsunami boulders. However, although several numerical methods have been proposed to estimate tsunami size using tsunami boulders, there have been no studies validating the estimated tsunami size by comparing with the actual tsunami size. Also, it is important to consider the methodology of the estimation of tsunami size using boulders. In this study, we estimated local size of the 2011 Tohoku-oki tsunami at Settai, Miyako City, Japan based on the numerical modeling of boulder transport. We seaerch an incident wave condition of sin waves which could explain the distribution of boulders well. We then compared the estimated results with the tsunami size calculated by existing well-validated tsunami source model. As a result of the simulation, we estimated that the tsunami size was ranging from 9 m to 21 m in wave height and from 60 s to 300 s in period at the point of 5200 m offshore of Settai.This range covers the actual tsunami size; so the tsunami size can be estimated from the boulders in Settai. According to the above results, the method that we proposed was effective. On the other hand, we found that assumption of the initial position of boulders are critically important and it should be constrained by multiple information such as topographic condition and composition of the boulders.

Keywords: Tsunami boulder, Tsunami size, numerical model, simulation

©2019. Japan Geoscience Union. All Right Reserved. 

# Constraint of the ages of historical tsunami deposits on the Ishinomaki Plain

*Hiroshi Tetsuka[1], Kazuhisa Goto[2], Takashi Ishizawa[1], Daisuke Sugawara[3], Yusuke Yokoyama[4], Yosuke Miyairi[4]

1. Department of Earth Science, Tohoku University, 2. International Research Institute of Disaster Science, Tohoku University, 3. Museum of Natural and Environmental History, Shizuoka, 4. Atmosphere and Ocean Research Institute, University of Tokyo

The research of tsunami deposit has an important role for understanding the paleo-tsunami history. On the Ishinomaki Plain, where the AD 2011 Tohoku-Oki tsunami inundated widely, at least six paleo-event deposits were found by previous studies (Shishikura et al., 2007; Sawai et al., 2012; Takeda et al., 2017). Sawai et al. (2012) correlate the latest three event deposits (Sand K, A, and B) with the tsunamis generated by the AD 1611 Keicho Ohsyu earthquake, the AD 1454 Kyotoku earthquake, and the AD 869 Jogan earthquake, respectively. Among them, the event age of Sand B is well constrained by the To-a tephra of AD 915 and radiocarbon ages, which ensure the validity of correlation with the historical record. However, the event ages of Sands K and A were not well constrained because accurate estimation of these event ages by radiocarbon dating is theoretically difficult. There remains a need to improve the accuracy of these event ages for understanding recurrence interval of tsunamis and comparing with the age of tsunami events in other sites. Therefore, we conducted multi-proxy analyses including radiocarbon dating, and analyses of diatom and pollens for the samples taken from the Ishinomaki Plain and then discuss the age of event deposits formed during the last 700 years.

The field survey was carried out on the coast area of Higashi-Matsushima City, Miyagi Prefecture. Cultivated soil, silt, and peat layers were found in the core samples. In some sites, one or two medium sand layers were found. Diatom analysis, pollen analysis, X-ray CT scan, and radiocarbon dating were conducted for the clearly identified two sand layers. The radiocarbon dating results were calibrated by OxCal Ver. 4.3.2 (Bronk Ramsey, 2009) with IntCal13 (Reimer et al., 2013) and constrained by stratigraphy (Bronk Ramsey, 2008).
Two sand layers (hereafter we call, Sands 1 and 2 for the upper and lower sand layers, respectively) are closely spaced with sandy silt layer of approximately 1–3 cm between them. Two hypotheses can be considered for the formation of these sand layers; they were deposited by different events, or a single event. Eyewitness observation and X-ray CT scan analysis imply that the sandy silt deposits in between these two sand layers contain many sand grains, and clearly different from the peat layer below Sand 2. The radiocarbon dating revealed that the age of sandy silt layer is intermediate between silt above Sand 1 and peat below Sand 2. In addition, sandy silt includes many freshwater diatoms but does not include marine and marine-brackish diatoms; diatom assemblage is clearly different from peat below Sand 2 that contains marine-brackish diatoms but few freshwater diatoms. Thus, sandy silt between Sands 1 and 2 is probably deposited as normal sediment so that Sands 1 and 2 should have been formed by different events.

The ages of Sands 1 and 2 can be constrained as 11 to 408 cal BP and 357 to 538 cal BP ($2\sigma$), respectively. These event ages are consistent with the AD 1611 Keicho Ohsyu earthquake and the AD 1454 Kyotoku earthquake, as interpreted by Sawai et al. (2012). The pollen analysis further shows the extensive increase of *Pinus sp.* and *Cryptomeria sp.* in the sediment above Sand 1. This result can be correlated with the afforestation policy by Sendai Domain after mid-17th century as planting Japanese

©2019. Japan Geoscience Union. All Right Reserved. 

pine and cedar was encouraged by the AD 1621 Sendai domain’ s law (Hanso Date Masamune kensho-kai, 1938). Therefore, Sand 1 has most likely been formed by the AD 1611 tsunami.

Keywords: earthquake, tsunami, AD 1611 Keicho ohsyu earthquake

©2019. Japan Geoscience Union. All Right Reserved. 

# Non-destructive analyzes of sediments to discern tsunami-related mud cap and overlying muds to improve age determination of tsunami deposits

*Takashi Ishizawa[1], Kazuhisa Goto[2], Yusuke Yokoyama[3], Yosuke Miyairi[3]

1. Department of Earth Science, Tohoku University, 2. International Research Institute of Disaster Science, Tohoku University, 3. Atmosphere and Ocean Research Institute, The University of Tokyo

Age of tsunami deposit is usually determined from dating results of sediments above and below the tsunami derived layers. However, determining the upper boundary of tsunami deposit is often difficult, because the top of tsunami deposit is sometimes comprised of mud-dominated sediment (mud cap) which can be indistinguishable from overlying muddy sediment deposited under normal sedimentary condition. This ambiguity may cause serious problem determining true tsunami ages.

Here we present an examples of non-destructive and destructive analyses of core sample taken from Okirai, Iwate prefecture. Our results indicated that X-CT (X-ray Computed Tomography), XRF (X-ray Fluorescence), and grain size analyses were useful to identify tsunami-related mud cap from overlying muds deposited after tsunami events. Since X-CT and XRF analyses are non-destructive analyses, it is highly recommended to conduct these analyses before subsampling of the sediments for further analyses including radiocarbon dating. Such careful sampling for dating will contribute to improve age estimation of tsunami deposits.

Keywords: Tsunami deposit, Mud cap, Non-destructive analyzes

©2019. Japan Geoscience Union. All Right Reserved. 

# Sedimentological and paleontological studies of storm surge deposits in intertidal mud floor -case study of Ena Bay on Miura Peninsula, Central Japan.

*Akihisa Kitamura[1], yamamoto yuka[1], Takashi Toyofuku[2]

1. Institute of Geosciences, Faculty of Science, Shizuoka University, 2. Japan Agency for Marine-Earth Science and Technology (JAMSTEC)

Storm surges and tsunamis deposits provide essential information for disaster assessments of coastal lowlands in low- and middle-latitude regions and active margins. However, studying these coastal lowland strata is becoming increasingly difficult, particularly in residential regions, due to extensive anthropogenic disturbances. Consequently, the focus of research has had to extend to shallow marine deposits such as bay sediments, although few studies have examined storm surge deposits related to recent storm events. This study identified storm surge deposits within tidal flat sediments in Ena bay, located in the southern coastal area of metropolitan Tokyo, Central Japan. Identification of the deposits was based on a comparison of surveys undertaken before and after Typhoon Lan (lowest pressure of 915 hPa), which struck the area on 23 October 2017. The results indicate that the storm surge deposits are limited to the supratidal and intertidal zones, demonstrating that the distal extent of sand beds deposited by storm surges is less than that of sand beds typically deposited by larger tsunamis.

Keywords: storm surges deposits, recent muddy tidal flat sediments, benthic foraminifer

©2019. Japan Geoscience Union. All Right Reserved. 

# Shallow marine tsunami deposits and bioturbation

*Koji Seike[1]

1. Geological Survey of Japan, AIST

The huge tsunami waves induced by the 2011 off the Pacific coast of Tohoku Earthquake severely affected shallow marine ecosystems along the Pacific coast of northeastern Japan. Among shallow marine settings, subtidal seafloor ecosystems composed of fine-grained sediments are the most heavily disturbed by tsunami waves as they are greatly altered by rapid erosion and deposition processes (Seike et al., 2013). In order to discuss preservation potential of the tsunami deposits in relation to sediment mixing by recolonizing benthic animals, we have monitored temporal changes in the sedimentary structures of the tsunami affected area (Seike et al., 2016, 2017a). Tsunami deposits also provide useful information on the nature of bioturbation because there are no pre-existing burrows in the sediments. We revealed the nature of bioturbation such as burrowing depth, substrate-softening effect by echinoid bioturbation on the basis of observations on the 2011 tsunami deposit (Seike et al., 2017b, 2018).

## References

Seike et al. (2013) PLoS One 8, e65417.
Seike et al. (2016) Journal of Oceanography, 72, 141–149.
Seike et al. (2017a) Island Arc, 26, e12174
Seike et al. (2017b) PLoS One,12, e0182753
Seike et al. (2018) Journal of Geophysical Research - Oceans, 123, 1376-1392

Keywords: tsunami deposits, bioturbation, Sanriku

©2019. Japan Geoscience Union. All Right Reserved. 

[J] Poster | M (Multidisciplinary and Interdisciplinary)：M-IS Intersection

Thu. May 30, 2019 3:30 PM - 5:00 PM JST | Thu. May 30, 2019 6:30 AM - 8:00 AM UTC | Poster Hall International Exhibition Hall8, Makuhari Messe_21

## [M-IS12] tsunami deposit

convener:Takashi Chiba(Faculty of Bioresource Sciences, Akita Prefectural University), Tetsuya Shinozaki(Center for Research in Isotopes and Environmental Dynamics (CRiED), University of Tsukuba), Daisuke Ishimura(Department of Geography, Tokyo Metropolitan University)

The 2011 off the Pacific coast of Tohoku Earthquake and tsunami have an influence on the development of tsunami deposit research. After the tsunami, a lot of findings have been reported on various research fields. However, identification criteria of the tsunami deposit are not yet established. Moreover, it is still uncertain how to use the tsunami deposit in the risk assessment. In this session, we welcome researches from all aspect of sedimentary records of modern and paleo tsunamis both onshore and offshore, and numerical and experimental modeling studies for risk assessment. In addition, we also welcome other event deposits, such as flooding and storm surge, that they are considered to be important for discrimination of tsunami deposit.

[MIS12-P01] Discussion of tsunami age estimation using coralline tsunami deposits

*Ryosuke Fujita[1], Kazuhisa Goto[1], Yasufumi Iryu[1], Takashi Ishizawa[1], Yusuke Yokoyama[2], Yosuke Miyairi[2] (1.TOHOKU University, 2.Atmosphere and Ocean Research Institute, the University of Tokyo)

[MIS12-P02] Identification method of event deposits caused by natural hazards

*Takumi Yoshii[1], Shiro Tanaka[1], Yuki Ito[1], Takaomi Hamada[1], Masafumi Matsuyama[1] (1.Central Research Institute of Electric Power Industry)

[MIS12-P03] Investigation of event deposits for construction of tsunami deposit discriminating method

*Shiro Tanaka[1], Takumi Yoshii[1], Yasuto Hirata[1], Takaomi Hamada[1], Masafumi Matsuyama[1], Yuki Ito[1] (1.Central Research Institute of Electric Power Industry)

[MIS12-P04] Lateral variation of mud clasts in onshore tsunami deposits

*Yasuhiro Takashimizu[1], Daichi Ito (1.Niigata University)

[MIS12-P05] Examination of model validity and sensitivity of tsunami sediment transport modeling using the 2011 Tohoku tsunami deposits in Iwate, Miyagi, and Fukushima Prefectures

*Satoshi Kusumoto[1], Aditya Gusman[2], Kenji Satake[1] (1.Earthquake Research Institute, the Univ. of Tokyo, 2.GNS Science)

[MIS12-P06] Paleotsunami History in Hachinohe, Aomori Prefecture, northern Japan

*Erick Velasco R.[1], Kazuhisa Goto[2], Takahiro Shinohara[1], Daisuke Sugawara[3], Yuichi Nishimura[4], Takashi Chiba[5] (1.Earth Science Department, Graduate Faculty of Science, Tohoku Univ., 2.International Research Institute of Disaster Science (IRIDeS), Tohoku Univ., 3.Museum of Natural and Environmental History, Shizuoka, 4.Graduate School of Science, Hokkaido Univ., 5.Faculty of Bioresource Sciences, Akita Prefectural Univ.)

[MIS12-P07] Characteristics of event deposits and their source in Sekine-hama, Mutsu city, Aomori prefecture

# Cancelled

*Daisuke Ishimura[1], Kaori Aoki[2] (1.Department of Geography, Tokyo Metropolitan University, 2.Research Center for Volcanic Hazards and Their Mitigation, Tokyo Metropolitan University)

[MIS12-P08] **Sedimentary structure and composition of sand blows and sand dikes formed by the 2018 Iburi-Tobu Earthquake, Hokkaido, Japan**

*Yuichi Nishimura[1], Takashi Chiba[2] (1.Graduate School of Science, Hokkaido University, 2.Faculty of Bioresource Sciences, Akita Prefectural University)

---

[MIS12-P09] Tsunami deposits and tsunami wave source of the southern part of Okushiri Island, Hokkaido

*Atsushi Urabe[1], Yoshihiro Kase[2], Gentaro Kawakami[2], Kenji Nishina[2], Hiromichi Koyasu[2] (1.Research Institute for Natural Hazards and Disaster Recovery, Niigata University, 2.Geological Survey of Hokkaido, Hokkaido Research Organization)

---

[MIS12-P10] Inter-seismic and post-seismic tectonic movements detected during the 17th century earthquake and inferred from diatom analysis in Tokachi area, Hokkaido, Japan

*Takashi Chiba[1], Yuichi Nishimura[2] (1.Faculty of Bioresource Sciences, Akita Prefectural University, 2.Graduate School of Science, Hokkaido University)

# Discussion of tsunami age estimation using coralline tsunami deposits

*Ryosuke Fujita[1], Kazuhisa Goto[1], Yasufumi Iryu[1], Takashi Ishizawa[1], Yusuke Yokoyama[2], Yosuke Miyairi[2]

1. TOHOKU University, 2. Atmosphere and Ocean Research Institute, the University of Tokyo

To estimate the age of tsunami deposit, we usually do not use the tsunami sediment itself but organic matters in the soil layers above and below the tsunami deposit. However, this method is not suitable to the deposits in subtropical areas with lots of disturbance by vegetation such as Okinawa prefecture. Thus it is necessary to develop a methodology to estimate tsunami age using samples in the tsunami sediments. Also, statistical analysis based on ages of multiple samples is required for estimating the event age using reworked sediments. In this study, we preliminarily performed radiocarbon dating of 12 marine organism samples in the single sandy tsunami deposit layer of Minna Island, Okinawa prefecture.
The dating results tend to focus on 3 age ranges: around A.D. 1000–1200 (Group A, 7 samples), around A.D. 750–1000 (Group B, 3 samples) and around B.C. 1000–700 (Group C, 2 samples). According to the XRD and SEM results, we identified that samples in Groups A and B are relatively fresh, while a sample with great abrasion and the one with less abrasion belong to Group C.
It is highly likely that the age of the tsunami deposit is around A.D. 1000–1200 based on the Group A samples. On the other hand, samples in Group B has as much abrasion as samples in Group A despite the radiocarbon ages are slightly older than the presumed tsunami age. It may indicate that samples in Group B died and deposited on the top of the shallow lagoon in the reef before the tsunami event and are transported by the tsunami toward the island. Samples in Group C, which died at significantly older time than the presumed tsunami, might have been transported from the coast or reef and redeposited inland by the tsunami.
Our results suggest that if we can select appropriate samples for radiocarbon dating, it is possible to estimate the appropriate tsunami age even by the reworked sediments. We will further discuss the method of sample selection for dating and statistical analysis.

Keywords: tsunami deposit

©2019. Japan Geoscience Union. All Right Reserved. 

# Identification method of event deposits caused by natural hazards

*Takumi Yoshii[1], Shiro Tanaka[1], Yuki Ito[1], Takaomi Hamada[1], Masafumi Matsuyama[1]

1. Central Research Institute of Electric Power Industry

Geological survey of event deposits can be a powerful technique for unveiling the history of natural hazards. For example, many unrecorded tsunamis have been investigated by utilizing tsunami deposits. Although the identification criteria for tsunami deposits have been developed, the criteria for other hazards such as high tide, storm, and flood were not fully discussed. The identification method of event deposits for multiple hazards is needed for disaster planning.

We present the identification method of event deposits which can take account of uncertainties of geological information and scale of natural hazards. First, we classified the natural hazards which can make event deposits on land based on their scales and characteristics. Then, we organized sedimentary, geochemical, paleontological survey items by information that we can retrieve from event deposits. We evaluated uncertainties of geological information by assuming the probability distributions for each information. The probabilities of event deposits being made by each natural hazard were presented with the uncertainties. In the presentation, we will show some examples of this identification method and discuss its effectiveness compared with the existing identification methods.

Keywords: Natural hazard, Tsunami deposit, uncertainty

©2019. Japan Geoscience Union. All Right Reserved. 

# Investigation of event deposits for construction of tsunami deposit discriminating method

*Shiro Tanaka[1], Takumi Yoshii[1], Yasuto Hirata[1], Takaomi Hamada[1], Masafumi Matsuyama[1], Yuki Ito[1]

1. Central Research Institute of Electric Power Industry

In order to establish a method to certify tsunami deposit, we investigated event deposits not due to the tsunami to be compared. Targets of survey are debris flow deposits due to torrential rains in Chugoku region in July 2018 and storm deposits due to September No.21 typhoon in Kansai region. Major survey points are debris flow generated at the slope facing the Hiroshima International University, debris flow generated behind JR Mizushiri Station, and debris flow generated on the upstream slope of JR Yano station in Hiroshima Prefecture. Debris flow deposits are distinguishable from tsunami deposits since they are mainly composed of huge rock masses near the source. On the other hand, at the end of the debris flow, it becomes a deposit having a layer structure mainly composed of sand size particles. Therefore, in this survey, we investigated and sampled deposits at the end of the debris flows. Surveys of storm surge deposits were conducted at Ashiyahama Beach and Omaehama Park in Hyogo Prefecture and at Nishikinohama Beach in Osaka Prefecture. The survey was conducted about 10 days after the storm surge occurrence, it was difficult to collect storm deposits at the Ashiyahama Beach and the Omaehama Park, but deposits possibly formed by storm surge could be collected at the Nishikinohama Beach. In the presentation, we will introduce mainly the particle size distribution of these deposits.

Keywords: tsunami deposit, debris flow deposit, storm surge deposit

©2019. Japan Geoscience Union. All Right Reserved. 

# Lateral variation of mud clasts in onshore tsunami deposits

*Yasuhiro Takashimizu[1], Daichi Ito

1. Niigata University

The lower part of the 2011 Tohoku-oki tsunami deposits in the region of Odaka in the Minami-Soma city, Japan well contains many mud clasts. This study focused on the features of mud clasts taken from two sites: the Z07 site which is 760 m from the coast and the T07 site which is 1140 m from the coast. Sedimentary analyses of both mud clast layers were conducted and lateral variations in the mud clasts were examined. The mud clast section of site T07 was composed of one unit, while site Z07 was composed of three units, which were units 1, 2, and 3 in ascending order.
The basal surface of the mud clast section of the site Z07 sample was generally flat and inclined slightly seawards. It displayed small and circular-shaped reliefs. However, the surface of the site T07 sample displayed a strongly irregular surface with clear reliefs of approximately 5 cm in depth.
The median grain size of the mud clasts of site T07 was -2.9$\phi$ and the mud clast grain sizes of Z07 were -1.7$\phi$, -2.5$\phi$, and 2.6$\phi$ for units 1, 2 and 3, respectively. The median grain size of the mud clasts of T07 was -2.9$\phi$ and for the mud clasts of Z07 were -1.7$\phi$, -2.5$\phi$, and -2.6$\phi$ for units 1, 2, and 3, respectively. This indicated that the mud clasts of T07 were coarser than the Z07 sample. Conversely, the roundness parameter ($R$) of site T07 was 0.74 and for site Z07 it was 0.74, 0.78, and 0.74 for units 1, 2, and 3, respectively. There were no clear differences between those units, although unit 2 of site Z07 displayed a slightly higher value. Moreover, the relationship between grain size and roundness did not show a clear correlation. From the results of the sedimentary analyses, it was confirmed that mud clasts were not fined and abraded under the tsunami inflow at sites Z07 and T07. The inflow at site T07 had a more strongly eroded ground surface than site Z07.

Keywords: tsunami deposits, mud clasts, roundness

©2019. Japan Geoscience Union. All Right Reserved. 

# Examination of model validity and sensitivity of tsunami sediment transport modeling using the 2011 Tohoku tsunami deposits in Iwate, Miyagi, and Fukushima Prefectures

*Satoshi Kusumoto[1], Aditya Gusman[2], Kenji Satake[1]

1. Earthquake Research Institute, the Univ. of Tokyo, 2. GNS Science

Sediment transport numerical models due to tsunami are continuously developed (e.g., Takahashi et al., 1999; 2011; Gusman et al., 2012; 2018). However, there are only few studies evaluating the tsunami sediment transport model validity and sensitivity. In this study, to examine the model validity and sensitivity of tsunami sediment transport simulation, we applied it to the 2011 Tohoku tsunami deposits at Numanohama marsh in Iwate Prefecture, Sendai plain in Miyagi Prefecture, and Idagawa lowland in Fukushima Prefecture.

One-dimensional sediment transport simulations with a single grain size and multiple grain sizes were used in this study. To consider the multiple-sized sediment transport, three representative diameters were selected based on a grain size distribution measured from tsunami deposits. The calculated sediment thickness for multiple grain sizes was defined as the sum of the computed sediment thickness for each single grain size with an assumption that the interaction between different particles is negligible. To examine the model sensitivity, a total of 11 tsunami source scenarios (Models 1 to 11) were also evaluated by modified Satake *et al*. (2013).

For Idagawa lowland and Sendai plain, the calculated results for a single grain size were much thinner than the observation. By considering the multiple grain sizes, the results computed from previously estimated models (Models 1 and 2) agreed with the observation, whereas the other models were underestimated or overestimated the observation. For Numanohama marsh, the agreement indexes for simulation using a single grain size was better than that for simulation using multiple grain sizes. This is probably because the 2011 Tohoku tsunami deposit in Numanohama marsh was generally coarser than those in Idagawa lowland and Sendai plain.

Our results show that the sediment transport modeling has a certain validity. Additionally, it is more effective and has higher sensitivity to constrain tsunami source model, than the technique that compares the maximum extent of tsunami deposit with the computed tsunami inundation distance (e.g., Satake *et al*., 2008; Namegaya *et al*., 2010; Namegaya and Satake, 2014). We are planning to further verify for the application to paleo-tsunami deposits.

Keywords: tsunami deposit, sediment transport modeling, 2011 Tohoku earthquake

©2019. Japan Geoscience Union. All Right Reserved. 

# Paleotsunami History in Hachinohe, Aomori Prefecture, northern Japan

*Erick Velasco R.[1], Kazuhisa Goto[2], Takahiro Shinohara[1], Daisuke Sugawara[3], Yuichi Nishimura[4], Takashi Chiba[5]

1. Earth Science Department, Graduate Faculty of Science, Tohoku Univ., 2. International Research Institute of Disaster Science (IRIDeS), Tohoku Univ., 3. Museum of Natural and Environmental History, Shizuoka, 4. Graduate School of Science, Hokkaido Univ., 5. Faculty of Bioresource Sciences, Akita Prefectural Univ.

Along the history, the Pacific coast of the Tohoku region has been characterized for facing a vast number of tsunamis associated with the highly active subduction of the Japan Trench. Most of the paleotsunami research has been focused on the south and central third of the Pacific coast of Tohoku, while in the northern third the number of this kind of studies is reduced; on the other hand, on the Pacific coast of Hokkaido paleotsunami research has been conducted to establish the recurrence linked to the Kuril trench (Minoura et al., 2013; Chagué-Goff et al., 2017; Inoue et al., 2017; Sawai, 2017). In Hachinohe, this type of research has not been done, being the results of Inoue et al., 2017 the closest at just 60 km southeastward and where the tsunami heights of the 2011 event were similar (Haraguchi & Iwamatsu, 2011). Because of this paleotsunami studies in Hachinohe are of enormous importance since its position could show tsunami activity related to both Kuril and Pacific trenches and its junction, where large tsunamigenic earthquakes have not been historically registered, hence, being this the primary objective of the present research.

The study site is located on a marine terrace surface elevated between 5-10 MAMSL, on the Kamikita coastal plain (Miyauchi, 1985) and 1.2 km inland from the present shoreline; at the same time, this surface is positioned between the Oirase and Gonohe rivers. We have identified eight sand layers, interbedded with mud and occasional tephra layers. Based on tephra analysis, some of them were possible to confirm as the To-a and To-cu tephra at the top and bottom of the sequence, respectively, giving a range of 6 thousand years of geological history, while the last 1000 years has been apparently eroded, removed or disturbed by human activity. To-a tephra layer contained many diatoms, which implies a water flow or shallow water body as deposition environment. Soils from the top of the section.

The stratigraphic correlation shows that four of the eight sand layers can be well traced landward, and grain analysis shows upward and landward fining. Diatom analysis reveals the presence of marine spices in some sand layers, on the other hand, freshwater and reworked freshwater extinct species were found in the uppermost sand layer (under To-a), suggesting a freshwater inundation event as a genetical source for that. CT number profiles (Hounsfield Units) evidence density changes related to lithological variations between the sand and mud layers. Moreover, XRF core scanner (ITRAX) shows that most of the sand layers are strongly related to a marine origin and exposes concentration of Ti that could be related to heavy minerals concentration and, in consequence, suggesting a sedimentary environment of high energy. Therefore, described evidence suggest a marine origin to the seven sand sheets.

In order to clarify the origin of the sand layers, we performed the numerical simulation to differentiate tsunami sands from storm sands proposed by Watanabe et al. (2018), by comparing wave penetration capacity for each phenomenon; the calculation showed that the only way to carry marine sediments on such further inland is with a tsunami event, if we assume present topography.

©2019. Japan Geoscience Union. All Right Reserved. 

Keywords: Paleotsunami research, Tsunami sedimentology, Numerical simulation, Geochemistry

©2019. Japan Geoscience Union. All Right Reserved. 

# Characteristics of event deposits and their source in Sekine-hama, Mutsu city, Aomori prefecture

*Daisuke Ishimura[1], Kaori Aoki[2]

1. Department of Geography, Tokyo Metropolitan University, 2. Research Center for Volcanic Hazards and Their Mitigation, Tokyo Metropolitan University

Tsunami deposit research is progressing in Japan after the 2011 Tohoku-oki earthquake. Especially, along the Pacific coast in the Tohoku region, many event deposits related with paleo-tsunamis were found by geological surveys. Their survey sites were concentrated from the Sanriku coast to Sendai plain (Sawai et al., 2007; Shishikura et al., 2007; Ishimura and Miyauchi, 2015, 2017; Goto et al., 2015; Inoue et al., 2017; Takada et al., 2016) and, but the number of surveys in the northern part of the Sanriku coast and southern part of the Sendai plain is small due to the limitation of the appropriate site for tsunami deposit research. This study reports the event deposits found at Sekinehama, Mutsu city, Aomori prefecture, which is the northernmost part of the Pacific coast of Honshu Island.

Our study site, Sekinehama, is located between Omazaki and Shiriyazaki and late Pleistocene marine terraces and sand dune were distributed near the coast. In the 2011 Tohoku-oki earthquake, tsunami runup height of 2 to 6 m was reported (The 2011 Tohoku Earthquake Tsunami Joint Survey (TTJS) Group (http://www.coastal.jp/ttjt/)). The outcrop is exposed about 50 m far from coastline and its height is 2 m. Sampled event deposits were used for grain size analysis. Moreover, we conducted radiocarbon dating (five samples) and tephra analysis (one sample).

As a result, we found 18 sandy event deposits interbedded within the soil, marsh, and marine sediments. One of them is the Baegdusan-Tomakomai tephra (AD946; Oppenheimer et al., 2017) including a small number of volcanic glass shards originating in Towada-a tephra (AD915; Machida and Arai, 2003). We estimated the origin of sands in event deposits by comparing with the grain size distribution of modern beach and sand dune sediments, resulted in that 14 event deposits are composed of beach sands. Thus, the source of these 14 event deposits is beach sediments and this indicates that they are transported by a kind of coastal events (e.g., storm, high tide, tsunami). Additionally, some of them showed sedimentary structures (erosional contact and lateral distribution) like tsunami deposits. Thus, we thought that some of them, at least, are tsunami deposits. As for radiocarbon dating, we are measuring now, and thus will show the event ages in our presentation.

Keywords: Event deposits, Shimokita peninsula, B-Tm tephra

©2019. Japan Geoscience Union. All Right Reserved. 

# Sedimentary structure and composition of sand blows and sand dikes formed by the 2018 Iburi-Tobu Earthquake, Hokkaido, Japan

*Yuichi Nishimura[1], Takashi Chiba[2]

1. Graduate School of Science, Hokkaido University, 2. Faculty of Bioresource Sciences, Akita Prefectural University

The M6.7 Hokkaido Iburi-Tobu Earthquake of September 6th, 2018, left sand blows and sand dikes result from liquefaction at Tomakomai, Atsuma, and Mukawa. We investigated distribution, shape, sedimentary structure and composition of the new deposits. Sand blows are mainly observed in flat areas on coast and estuaries that have undergone artificial modification. Size of the sand blows varies from several tens of centimeters to several meters in diameter. Each sand blow has a vent or vent system that aligned along a fissure. Sand blows are composed by fine to coast sand, mud, pebbles and various size of pumice. A layered structure is commonly seen in the cross-section. In most of the case, mud, pumice, and sand are deposited in order from the bottom to the top of the deposit. It seems that the mixed layer of sand and pumice in the landfill soil liquefied and sand and pumice separated in the layer. Then they ejected with mud from the accumulated light particles near to the vent. The sand dikes are observed by trenching or by using a handy geo-slicer. Most of the dikes are not straight, they are curved or bent along the boundary of the inhomogeneous medium around them. The width of the dikes vary from 1 mm to 10 cm, and they are filled with sand or pebbles that are the same materials as those came out at the final stage of the ejection. There are dikes that are clogged from the bottom with pumice and coarse sand. In those dikes, the size of the particle filling the dike decreased upward with the clogged location as the boundary. Thus, a feature of sand blow and sand dike can be complicated reflecting the size and density characteristics of the particles constituting the liquefaction layer. The precise description of the new sand blows and sand dikes can provide a better understanding of the liquefaction process and also can be useful for the identification and evaluation of paleo liquefaction deposits.

Keywords: liquefaction, sand blow, paleo-eathquake

©2019. Japan Geoscience Union. All Right Reserved. 

# Tsunami deposits and tsunami wave source of the southern part of Okushiri Island, Hokkaido

*Atsushi Urabe[1], Yoshihiro Kase[2], Gentaro Kawakami[2], Kenji Nishina[2], Hiromichi Koyasu[2]

1. Research Institute for Natural Hazards and Disaster Recovery, Niigata University, 2. Geological Survey of Hokkaido, Hokkaido Research Organization

In the Okushiri area of South Hokkaido, a tsunami history approximately 3,000 years before is clarified based on an investigation of tsunami deposits. On the other hand, the tsunami history before approximately 3,000 years ago is unclear. In this study, boring exploration was carried out at the Wasabiyachi area for the purpose of analysis of the previous tsunami deposit. As a result, the event sand layer which suggested the beach origin was recognized in twenty horizons after approximately 7,400 years ago. As a result of examined the change of the sedimentary facies etc., in several horizons, this area may uplift at the same time as tsunami.

Keywords: tsunami deposit, okushiri island

©2019. Japan Geoscience Union. All Right Reserved. 

# Inter-seismic and post-seismic tectonic movements detected during the 17th century earthquake and inferred from diatom analysis in Tokachi area, Hokkaido, Japan

*Takashi Chiba[1], Yuichi Nishimura[2]

1. Faculty of Bioresource Sciences, Akita Prefectural University, 2. Graduate School of Science, Hokkaido University

It has been evidenced from geological records that paleo-earthquakes accompanied by huge tsunamis occurred at least twice in the last millennium at the southern part of the Kuril Trench. The first of the two tsunamis is supposed to have occurred in the 12-13th century, while the other is supposed to have occurred in the 17th century. The paleo-earthquake and successive tsunami of the 17th century have been particularly investigated by previous studies in the area between Akkeshi to Nemuro at the Hokkaido, Japan. However, the crustal movements due to the earthquake in the area at western side of the Akkeshi such as Tokachi area is still unknown. This lack of substantive information is an obstacle for the studies attempting to calculate the actual impact of the paleo-earthquake and estimating its source region. We conducted a survey using a geo-slicer and GPS. We also performed paleo-environmental reconstruction by diatom analysis for the core samples obtained from the Toberi River mouth area, in Tokachi area to derive indicative data about the crustal movements. Since massive Neogene diatomaceous siltstones sediments containing fossil marine diatoms are widely distributed in the study area, we identified the reworked fossil marine species and excluded it from the diatom analysis in the paleo-environmental reconstruction.As a result of the geo-slicer survey, the tsunami deposits from the coast to the inland up to a distance of 1.8 km in a straight line could be detected. Changes in diatom assemblages which are reflective of inter-seismic subsidence and post-seismic uplift caused by the earthquake were also recognized. On the other hand, inferences derived from diatom analysis of geo-slicer core samples showed that the vertical crustal movement estimated by the elevation of the freshwater-brackish boundary of the core sample was maximum 2.3 m. The freshwater-brackish boundary was identified to be extending up to 1.9 km inland at 3.9 m altitude from the seashore, however it was not conspicuous in the inland and above the elevation at more than 4.0 m. This observation confirmed the relationship between the vertical crustal movements generated by the earthquake and the elevation of pale-sea level. Although it is difficult to reconstruct the crustal movements caused by the 12-13th century earthquake, in light of the above observations it can be concluded that they might possibly have risen up to tens of centimeters at least after the earthquake and then began to change to the inter-seismic subsidence.

Keywords: tsunami deposit, tectonic movement, diatom analysis, Tokachi area

©2019. Japan Geoscience Union. All Right Reserved. 

[J] Poster | M (Multidisciplinary and Interdisciplinary)：M-IS Intersection

Thu. May 30, 2019 5:15 PM - 6:30 PM JST | Thu. May 30, 2019 8:15 AM - 9:30 AM UTC | Poster Hall International Exhibition Hall8, Makuhari Messe_39

## [M-IS12] tsunami deposit

convener:Takashi Chiba(Faculty of Bioresource Sciences, Akita Prefectural University), Tetsuya Shinozaki(Center for Research in Isotopes and Environmental Dynamics (CRiED), University of Tsukuba), Daisuke Ishimura(Department of Geography, Tokyo Metropolitan University)

The 2011 off the Pacific coast of Tohoku Earthquake and tsunami have an influence on the development of tsunami deposit research. After the tsunami, a lot of findings have been reported on various research fields. However, identification criteria of the tsunami deposit are not yet established. Moreover, it is still uncertain how to use the tsunami deposit in the risk assessment. In this session, we welcome researches from all aspect of sedimentary records of modern and paleo tsunamis both onshore and offshore, and numerical and experimental modeling studies for risk assessment. In addition, we also welcome other event deposits, such as flooding and storm surge, that they are considered to be important for discrimination of tsunami deposit.

[MIS12-P01] Discussion of tsunami age estimation using coralline tsunami deposits

*Ryosuke Fujita[1], Kazuhisa Goto[1], Yasufumi Iryu[1], Takashi Ishizawa[1], Yusuke Yokoyama[2], Yosuke Miyairi[2] (1.TOHOKU University, 2.Atmosphere and Ocean Research Institute, the University of Tokyo)

[MIS12-P02] Identification method of event deposits caused by natural hazards

*Takumi Yoshii[1], Shiro Tanaka[1], Yuki Ito[1], Takaomi Hamada[1], Masafumi Matsuyama[1] (1.Central Research Institute of Electric Power Industry)

[MIS12-P03] Investigation of event deposits for construction of tsunami deposit discriminating method

*Shiro Tanaka[1], Takumi Yoshii[1], Yasuto Hirata[1], Takaomi Hamada[1], Masafumi Matsuyama[1], Yuki Ito[1] (1.Central Research Institute of Electric Power Industry)

[MIS12-P04] Lateral variation of mud clasts in onshore tsunami deposits

*Yasuhiro Takashimizu[1], Daichi Ito (1.Niigata University)

[MIS12-P05] Examination of model validity and sensitivity of tsunami sediment transport modeling using the 2011 Tohoku tsunami deposits in Iwate, Miyagi, and Fukushima Prefectures

*Satoshi Kusumoto[1], Aditya Gusman[2], Kenji Satake[1] (1.Earthquake Research Institute, the Univ. of Tokyo, 2.GNS Science)

[MIS12-P06] Paleotsunami History in Hachinohe, Aomori Prefecture, northern Japan

*Erick Velasco R.[1], Kazuhisa Goto[2], Takahiro Shinohara[1], Daisuke Sugawara[3], Yuichi Nishimura[4], Takashi Chiba[5] (1.Earth Science Department, Graduate Faculty of Science, Tohoku Univ., 2.International Research Institute of Disaster Science (IRIDeS), Tohoku Univ., 3.Museum of Natural and Environmental History, Shizuoka, 4.Graduate School of Science, Hokkaido Univ., 5.Faculty of Bioresource Sciences, Akita Prefectural Univ.)

[MIS12-P07] Characteristics of event deposits and their source in Sekine-hama, Mutsu city, Aomori prefecture

*Daisuke Ishimura[1], Kaori Aoki[2] (1.Department of Geography, Tokyo Metropolitan University, 2.Research Center for Volcanic Hazards and Their Mitigation, Tokyo Metropolitan University)

[MIS12-P08] **Sedimentary structure and composition of sand blows and sand dikes formed by the 2018 Iburi-Tobu Earthquake, Hokkaido, Japan**

*Yuichi Nishimura[1], Takashi Chiba[2] (1.Graduate School of Science, Hokkaido University, 2.Faculty of Bioresource Sciences, Akita Prefectural University)

---

[MIS12-P09] Tsunami deposits and tsunami wave source of the southern part of Okushiri Island, Hokkaido

*Atsushi Urabe[1], Yoshihiro Kase[2], Gentaro Kawakami[2], Kenji Nishina[2], Hiromichi Koyasu[2] (1.Research Institute for Natural Hazards and Disaster Recovery, Niigata University, 2.Geological Survey of Hokkaido, Hokkaido Research Organization)

---

[MIS12-P10] Inter-seismic and post-seismic tectonic movements detected during the 17th century earthquake and inferred from diatom analysis in Tokachi area, Hokkaido, Japan

*Takashi Chiba[1], Yuichi Nishimura[2] (1.Faculty of Bioresource Sciences, Akita Prefectural University, 2.Graduate School of Science, Hokkaido University)

# Discussion of tsunami age estimation using coralline tsunami deposits

*Ryosuke Fujita[1], Kazuhisa Goto[1], Yasufumi Iryu[1], Takashi Ishizawa[1], Yusuke Yokoyama[2], Yosuke Miyairi[2]

1. TOHOKU University, 2. Atmosphere and Ocean Research Institute, the University of Tokyo

To estimate the age of tsunami deposit, we usually do not use the tsunami sediment itself but organic matters in the soil layers above and below the tsunami deposit. However, this method is not suitable to the deposits in subtropical areas with lots of disturbance by vegetation such as Okinawa prefecture. Thus it is necessary to develop a methodology to estimate tsunami age using samples in the tsunami sediments. Also, statistical analysis based on ages of multiple samples is required for estimating the event age using reworked sediments. In this study, we preliminarily performed radiocarbon dating of 12 marine organism samples in the single sandy tsunami deposit layer of Minna Island, Okinawa prefecture.
The dating results tend to focus on 3 age ranges: around A.D. 1000–1200 (Group A, 7 samples), around A.D. 750–1000 (Group B, 3 samples) and around B.C. 1000–700 (Group C, 2 samples). According to the XRD and SEM results, we identified that samples in Groups A and B are relatively fresh, while a sample with great abrasion and the one with less abrasion belong to Group C.
It is highly likely that the age of the tsunami deposit is around A.D. 1000–1200 based on the Group A samples. On the other hand, samples in Group B has as much abrasion as samples in Group A despite the radiocarbon ages are slightly older than the presumed tsunami age. It may indicate that samples in Group B died and deposited on the top of the shallow lagoon in the reef before the tsunami event and are transported by the tsunami toward the island. Samples in Group C, which died at significantly older time than the presumed tsunami, might have been transported from the coast or reef and redeposited inland by the tsunami.
Our results suggest that if we can select appropriate samples for radiocarbon dating, it is possible to estimate the appropriate tsunami age even by the reworked sediments. We will further discuss the method of sample selection for dating and statistical analysis.

Keywords: tsunami deposit

©2019. Japan Geoscience Union. All Right Reserved. 

# Identification method of event deposits caused by natural hazards

*Takumi Yoshii[1], Shiro Tanaka[1], Yuki Ito[1], Takaomi Hamada[1], Masafumi Matsuyama[1]

1. Central Research Institute of Electric Power Industry

Geological survey of event deposits can be a powerful technique for unveiling the history of natural hazards. For example, many unrecorded tsunamis have been investigated by utilizing tsunami deposits. Although the identification criteria for tsunami deposits have been developed, the criteria for other hazards such as high tide, storm, and flood were not fully discussed. The identification method of event deposits for multiple hazards is needed for disaster planning.

We present the identification method of event deposits which can take account of uncertainties of geological information and scale of natural hazards. First, we classified the natural hazards which can make event deposits on land based on their scales and characteristics. Then, we organized sedimentary, geochemical, paleontological survey items by information that we can retrieve from event deposits. We evaluated uncertainties of geological information by assuming the probability distributions for each information. The probabilities of event deposits being made by each natural hazard were presented with the uncertainties. In the presentation, we will show some examples of this identification method and discuss its effectiveness compared with the existing identification methods.

Keywords: Natural hazard, Tsunami deposit, uncertainty

©2019. Japan Geoscience Union. All Right Reserved. 

# Investigation of event deposits for construction of tsunami deposit discriminating method

*Shiro Tanaka[1], Takumi Yoshii[1], Yasuto Hirata[1], Takaomi Hamada[1], Masafumi Matsuyama[1], Yuki Ito[1]

1. Central Research Institute of Electric Power Industry

In order to establish a method to certify tsunami deposit, we investigated event deposits not due to the tsunami to be compared. Targets of survey are debris flow deposits due to torrential rains in Chugoku region in July 2018 and storm deposits due to September No.21 typhoon in Kansai region. Major survey points are debris flow generated at the slope facing the Hiroshima International University, debris flow generated behind JR Mizushiri Station, and debris flow generated on the upstream slope of JR Yano station in Hiroshima Prefecture. Debris flow deposits are distinguishable from tsunami deposits since they are mainly composed of huge rock masses near the source. On the other hand, at the end of the debris flow, it becomes a deposit having a layer structure mainly composed of sand size particles. Therefore, in this survey, we investigated and sampled deposits at the end of the debris flows. Surveys of storm surge deposits were conducted at Ashiyahama Beach and Omaehama Park in Hyogo Prefecture and at Nishikinohama Beach in Osaka Prefecture. The survey was conducted about 10 days after the storm surge occurrence, it was difficult to collect storm deposits at the Ashiyahama Beach and the Omaehama Park, but deposits possibly formed by storm surge could be collected at the Nishikinohama Beach. In the presentation, we will introduce mainly the particle size distribution of these deposits.

Keywords: tsunami deposit, debris flow deposit, storm surge deposit

©2019. Japan Geoscience Union. All Right Reserved. 

# Lateral variation of mud clasts in onshore tsunami deposits

*Yasuhiro Takashimizu[1], Daichi Ito

1. Niigata University

The lower part of the 2011 Tohoku-oki tsunami deposits in the region of Odaka in the Minami-Soma city, Japan well contains many mud clasts. This study focused on the features of mud clasts taken from two sites: the Z07 site which is 760 m from the coast and the T07 site which is 1140 m from the coast. Sedimentary analyses of both mud clast layers were conducted and lateral variations in the mud clasts were examined. The mud clast section of site T07 was composed of one unit, while site Z07 was composed of three units, which were units 1, 2, and 3 in ascending order.
The basal surface of the mud clast section of the site Z07 sample was generally flat and inclined slightly seawards. It displayed small and circular-shaped reliefs. However, the surface of the site T07 sample displayed a strongly irregular surface with clear reliefs of approximately 5 cm in depth.
The median grain size of the mud clasts of site T07 was -2.9$\phi$ and the mud clast grain sizes of Z07 were -1.7$\phi$, -2.5$\phi$, and 2.6$\phi$ for units 1, 2 and 3, respectively. The median grain size of the mud clasts of T07 was -2.9$\phi$ and for the mud clasts of Z07 were -1.7$\phi$, -2.5$\phi$, and -2.6$\phi$ for units 1, 2, and 3, respectively. This indicated that the mud clasts of T07 were coarser than the Z07 sample. Conversely, the roundness parameter ($R$) of site T07 was 0.74 and for site Z07 it was 0.74, 0.78, and 0.74 for units 1, 2, and 3, respectively. There were no clear differences between those units, although unit 2 of site Z07 displayed a slightly higher value. Moreover, the relationship between grain size and roundness did not show a clear correlation. From the results of the sedimentary analyses, it was confirmed that mud clasts were not fined and abraded under the tsunami inflow at sites Z07 and T07. The inflow at site T07 had a more strongly eroded ground surface than site Z07.

Keywords: tsunami deposits, mud clasts, roundness

©2019. Japan Geoscience Union. All Right Reserved. 

# Examination of model validity and sensitivity of tsunami sediment transport modeling using the 2011 Tohoku tsunami deposits in Iwate, Miyagi, and Fukushima Prefectures

*Satoshi Kusumoto[1], Aditya Gusman[2], Kenji Satake[1]

1. Earthquake Research Institute, the Univ. of Tokyo, 2. GNS Science

Sediment transport numerical models due to tsunami are continuously developed (e.g., Takahashi et al., 1999; 2011; Gusman et al., 2012; 2018). However, there are only few studies evaluating the tsunami sediment transport model validity and sensitivity. In this study, to examine the model validity and sensitivity of tsunami sediment transport simulation, we applied it to the 2011 Tohoku tsunami deposits at Numanohama marsh in Iwate Prefecture, Sendai plain in Miyagi Prefecture, and Idagawa lowland in Fukushima Prefecture.

One-dimensional sediment transport simulations with a single grain size and multiple grain sizes were used in this study. To consider the multiple-sized sediment transport, three representative diameters were selected based on a grain size distribution measured from tsunami deposits. The calculated sediment thickness for multiple grain sizes was defined as the sum of the computed sediment thickness for each single grain size with an assumption that the interaction between different particles is negligible. To examine the model sensitivity, a total of 11 tsunami source scenarios (Models 1 to 11) were also evaluated by modified Satake *et al*. (2013).

For Idagawa lowland and Sendai plain, the calculated results for a single grain size were much thinner than the observation. By considering the multiple grain sizes, the results computed from previously estimated models (Models 1 and 2) agreed with the observation, whereas the other models were underestimated or overestimated the observation. For Numanohama marsh, the agreement indexes for simulation using a single grain size was better than that for simulation using multiple grain sizes. This is probably because the 2011 Tohoku tsunami deposit in Numanohama marsh was generally coarser than those in Idagawa lowland and Sendai plain.

Our results show that the sediment transport modeling has a certain validity. Additionally, it is more effective and has higher sensitivity to constrain tsunami source model, than the technique that compares the maximum extent of tsunami deposit with the computed tsunami inundation distance (e.g., Satake *et al*., 2008; Namegaya *et al*., 2010; Namegaya and Satake, 2014). We are planning to further verify for the application to paleo-tsunami deposits.

Keywords: tsunami deposit, sediment transport modeling, 2011 Tohoku earthquake

©2019. Japan Geoscience Union. All Right Reserved. 

# Paleotsunami History in Hachinohe, Aomori Prefecture, northern Japan

*Erick Velasco R.[1], Kazuhisa Goto[2], Takahiro Shinohara[1], Daisuke Sugawara[3], Yuichi Nishimura[4], Takashi Chiba[5]

1. Earth Science Department, Graduate Faculty of Science, Tohoku Univ., 2. International Research Institute of Disaster Science (IRIDeS), Tohoku Univ., 3. Museum of Natural and Environmental History, Shizuoka, 4. Graduate School of Science, Hokkaido Univ., 5. Faculty of Bioresource Sciences, Akita Prefectural Univ.

Along the history, the Pacific coast of the Tohoku region has been characterized for facing a vast number of tsunamis associated with the highly active subduction of the Japan Trench. Most of the paleotsunami research has been focused on the south and central third of the Pacific coast of Tohoku, while in the northern third the number of this kind of studies is reduced; on the other hand, on the Pacific coast of Hokkaido paleotsunami research has been conducted to establish the recurrence linked to the Kuril trench (Minoura et al., 2013; Chagué-Goff et al., 2017; Inoue et al., 2017; Sawai, 2017). In Hachinohe, this type of research has not been done, being the results of Inoue et al., 2017 the closest at just 60 km southeastward and where the tsunami heights of the 2011 event were similar (Haraguchi & Iwamatsu, 2011). Because of this paleotsunami studies in Hachinohe are of enormous importance since its position could show tsunami activity related to both Kuril and Pacific trenches and its junction, where large tsunamigenic earthquakes have not been historically registered, hence, being this the primary objective of the present research.

The study site is located on a marine terrace surface elevated between 5-10 MAMSL, on the Kamikita coastal plain (Miyauchi, 1985) and 1.2 km inland from the present shoreline; at the same time, this surface is positioned between the Oirase and Gonohe rivers. We have identified eight sand layers, interbedded with mud and occasional tephra layers. Based on tephra analysis, some of them were possible to confirm as the To-a and To-cu tephra at the top and bottom of the sequence, respectively, giving a range of 6 thousand years of geological history, while the last 1000 years has been apparently eroded, removed or disturbed by human activity. To-a tephra layer contained many diatoms, which implies a water flow or shallow water body as deposition environment. Soils from the top of the section.

The stratigraphic correlation shows that four of the eight sand layers can be well traced landward, and grain analysis shows upward and landward fining. Diatom analysis reveals the presence of marine spices in some sand layers, on the other hand, freshwater and reworked freshwater extinct species were found in the uppermost sand layer (under To-a), suggesting a freshwater inundation event as a genetical source for that. CT number profiles (Hounsfield Units) evidence density changes related to lithological variations between the sand and mud layers. Moreover, XRF core scanner (ITRAX) shows that most of the sand layers are strongly related to a marine origin and exposes concentration of Ti that could be related to heavy minerals concentration and, in consequence, suggesting a sedimentary environment of high energy. Therefore, described evidence suggest a marine origin to the seven sand sheets.

In order to clarify the origin of the sand layers, we performed the numerical simulation to differentiate tsunami sands from storm sands proposed by Watanabe et al. (2018), by comparing wave penetration capacity for each phenomenon; the calculation showed that the only way to carry marine sediments on such further inland is with a tsunami event, if we assume present topography.

©2019. Japan Geoscience Union. All Right Reserved. 

Keywords: Paleotsunami research, Tsunami sedimentology, Numerical simulation, Geochemistry

©2019. Japan Geoscience Union. All Right Reserved. 

# Characteristics of event deposits and their source in Sekine-hama, Mutsu city, Aomori prefecture

*Daisuke Ishimura[1], Kaori Aoki[2]

1. Department of Geography, Tokyo Metropolitan University, 2. Research Center for Volcanic Hazards and Their Mitigation, Tokyo Metropolitan University

Tsunami deposit research is progressing in Japan after the 2011 Tohoku-oki earthquake. Especially, along the Pacific coast in the Tohoku region, many event deposits related with paleo-tsunamis were found by geological surveys. Their survey sites were concentrated from the Sanriku coast to Sendai plain (Sawai et al., 2007; Shishikura et al., 2007; Ishimura and Miyauchi, 2015, 2017; Goto et al., 2015; Inoue et al., 2017; Takada et al., 2016) and, but the number of surveys in the northern part of the Sanriku coast and southern part of the Sendai plain is small due to the limitation of the appropriate site for tsunami deposit research. This study reports the event deposits found at Sekinehama, Mutsu city, Aomori prefecture, which is the northernmost part of the Pacific coast of Honshu Island.

Our study site, Sekinehama, is located between Omazaki and Shiriyazaki and late Pleistocene marine terraces and sand dune were distributed near the coast. In the 2011 Tohoku-oki earthquake, tsunami runup height of 2 to 6 m was reported (The 2011 Tohoku Earthquake Tsunami Joint Survey (TTJS) Group (http://www.coastal.jp/ttjt/)). The outcrop is exposed about 50 m far from coastline and its height is 2 m. Sampled event deposits were used for grain size analysis. Moreover, we conducted radiocarbon dating (five samples) and tephra analysis (one sample).

As a result, we found 18 sandy event deposits interbedded within the soil, marsh, and marine sediments. One of them is the Baegdusan-Tomakomai tephra (AD946; Oppenheimer et al., 2017) including a small number of volcanic glass shards originating in Towada-a tephra (AD915; Machida and Arai, 2003). We estimated the origin of sands in event deposits by comparing with the grain size distribution of modern beach and sand dune sediments, resulted in that 14 event deposits are composed of beach sands. Thus, the source of these 14 event deposits is beach sediments and this indicates that they are transported by a kind of coastal events (e.g., storm, high tide, tsunami). Additionally, some of them showed sedimentary structures (erosional contact and lateral distribution) like tsunami deposits. Thus, we thought that some of them, at least, are tsunami deposits. As for radiocarbon dating, we are measuring now, and thus will show the event ages in our presentation.

Keywords: Event deposits, Shimokita peninsula, B-Tm tephra

©2019. Japan Geoscience Union. All Right Reserved. 

# Sedimentary structure and composition of sand blows and sand dikes formed by the 2018 Iburi-Tobu Earthquake, Hokkaido, Japan

*Yuichi Nishimura[1], Takashi Chiba[2]

1. Graduate School of Science, Hokkaido University, 2. Faculty of Bioresource Sciences, Akita Prefectural University

The M6.7 Hokkaido Iburi-Tobu Earthquake of September 6th, 2018, left sand blows and sand dikes result from liquefaction at Tomakomai, Atsuma, and Mukawa. We investigated distribution, shape, sedimentary structure and composition of the new deposits. Sand blows are mainly observed in flat areas on coast and estuaries that have undergone artificial modification. Size of the sand blows varies from several tens of centimeters to several meters in diameter. Each sand blow has a vent or vent system that aligned along a fissure. Sand blows are composed by fine to coast sand, mud, pebbles and various size of pumice. A layered structure is commonly seen in the cross-section. In most of the case, mud, pumice, and sand are deposited in order from the bottom to the top of the deposit. It seems that the mixed layer of sand and pumice in the landfill soil liquefied and sand and pumice separated in the layer. Then they ejected with mud from the accumulated light particles near to the vent. The sand dikes are observed by trenching or by using a handy geo-slicer. Most of the dikes are not straight, they are curved or bent along the boundary of the inhomogeneous medium around them. The width of the dikes vary from 1 mm to 10 cm, and they are filled with sand or pebbles that are the same materials as those came out at the final stage of the ejection. There are dikes that are clogged from the bottom with pumice and coarse sand. In those dikes, the size of the particle filling the dike decreased upward with the clogged location as the boundary. Thus, a feature of sand blow and sand dike can be complicated reflecting the size and density characteristics of the particles constituting the liquefaction layer. The precise description of the new sand blows and sand dikes can provide a better understanding of the liquefaction process and also can be useful for the identification and evaluation of paleo liquefaction deposits.

Keywords: liquefaction, sand blow, paleo-eathquake

©2019. Japan Geoscience Union. All Right Reserved. 

# Tsunami deposits and tsunami wave source of the southern part of Okushiri Island, Hokkaido

*Atsushi Urabe[1], Yoshihiro Kase[2], Gentaro Kawakami[2], Kenji Nishina[2], Hiromichi Koyasu[2]

1. Research Institute for Natural Hazards and Disaster Recovery, Niigata University, 2. Geological Survey of Hokkaido, Hokkaido Research Organization

In the Okushiri area of South Hokkaido, a tsunami history approximately 3,000 years before is clarified based on an investigation of tsunami deposits. On the other hand, the tsunami history before approximately 3,000 years ago is unclear. In this study, boring exploration was carried out at the Wasabiyachi area for the purpose of analysis of the previous tsunami deposit. As a result, the event sand layer which suggested the beach origin was recognized in twenty horizons after approximately 7,400 years ago. As a result of examined the change of the sedimentary facies etc., in several horizons, this area may uplift at the same time as tsunami.

Keywords: tsunami deposit, okushiri island

©2019. Japan Geoscience Union. All Right Reserved. 

# Inter-seismic and post-seismic tectonic movements detected during the 17th century earthquake and inferred from diatom analysis in Tokachi area, Hokkaido, Japan

*Takashi Chiba[1], Yuichi Nishimura[2]

1. Faculty of Bioresource Sciences, Akita Prefectural University, 2. Graduate School of Science, Hokkaido University

It has been evidenced from geological records that paleo-earthquakes accompanied by huge tsunamis occurred at least twice in the last millennium at the southern part of the Kuril Trench. The first of the two tsunamis is supposed to have occurred in the 12-13th century, while the other is supposed to have occurred in the 17th century. The paleo-earthquake and successive tsunami of the 17th century have been particularly investigated by previous studies in the area between Akkeshi to Nemuro at the Hokkaido, Japan. However, the crustal movements due to the earthquake in the area at western side of the Akkeshi such as Tokachi area is still unknown. This lack of substantive information is an obstacle for the studies attempting to calculate the actual impact of the paleo-earthquake and estimating its source region. We conducted a survey using a geo-slicer and GPS. We also performed paleo-environmental reconstruction by diatom analysis for the core samples obtained from the Toberi River mouth area, in Tokachi area to derive indicative data about the crustal movements. Since massive Neogene diatomaceous siltstones sediments containing fossil marine diatoms are widely distributed in the study area, we identified the reworked fossil marine species and excluded it from the diatom analysis in the paleo-environmental reconstruction.As a result of the geo-slicer survey, the tsunami deposits from the coast to the inland up to a distance of 1.8 km in a straight line could be detected. Changes in diatom assemblages which are reflective of inter-seismic subsidence and post-seismic uplift caused by the earthquake were also recognized. On the other hand, inferences derived from diatom analysis of geo-slicer core samples showed that the vertical crustal movement estimated by the elevation of the freshwater-brackish boundary of the core sample was maximum 2.3 m. The freshwater-brackish boundary was identified to be extending up to 1.9 km inland at 3.9 m altitude from the seashore, however it was not conspicuous in the inland and above the elevation at more than 4.0 m. This observation confirmed the relationship between the vertical crustal movements generated by the earthquake and the elevation of pale-sea level. Although it is difficult to reconstruct the crustal movements caused by the 12-13th century earthquake, in light of the above observations it can be concluded that they might possibly have risen up to tens of centimeters at least after the earthquake and then began to change to the inter-seismic subsidence.

Keywords: tsunami deposit, tectonic movement, diatom analysis, Tokachi area

©2019. Japan Geoscience Union. All Right Reserved. 

[J] Oral | M (Multidisciplinary and Interdisciplinary)：M-IS Intersection

Thu. May 30, 2019 9:00 AM - 10:30 AM JST | Thu. May 30, 2019 12:00 AM - 1:30 AM UTC | A05 TOKYO BAY MAKUHARI HALL

## [M-IS16] Dynamics of eruption cloud and cumulonimbus; modelling and observation

convener:Eiichi Sato(Meteorological Research Institute), Fukashi Maeno(Earthquake Research Institute, University of Tokyo), Takeshi Maesaka(National Research Institute for Earth Science and Disaster Resilience), Chairperson:Eiichi Sato(Meteorological Research Institute)

Volcanic eruption clouds (eruption column, pyroclastic flow, and umbrella cloud) and cumulonimbus are similar phenomena in the atmosphere. Models that can precisely reproduce the physical processes in such phenomena, and accurate observations have been required. Recently, the development of remote sensing techniques such as weather radar and weather satellite are remarkable, and they are being adopted for volcanic eruption monitoring. However, it is indispensable to verify the results of modeling and remote sensing using in-situ observations. In this session, we will discuss the modelling and the observations of eruption clouds and cumulonimbus from the viewpoint of meteorology, volcanology, geology, and other related fields. The related phenomena such as ashfall, rainfall, snowfall, hail and volcanic block will also be discussed.

9:00 AM - 9:15 AM JST | 12:00 AM - 12:15 AM UTC

### [MIS16-01] Observations of Volcanic Eruption Columns with Different Types of Weather Radars

★Invited Papers

*Masayuki Maki[1], Takehiko KOBORI[1], Yura Kim[1], Yasushi Fujiyoshi[2], Eiichi Sato[3], Hidehiko Tokushima[4], Masato Iguchi[5] (1.Kagoshima University, 2.Hokkaido University, 3.Meteorological Research Institute, 4.Field Researchers Corporation, 5.Kyoto University)

9:15 AM - 9:30 AM JST | 12:15 AM - 12:30 AM UTC

### [MIS16-02] Observation of Eruption Plumes by X-Band MP radar and Lidar at Sakurajima and Kuchinoerabujima

*Haruhisa Nakamichi[1], Atsushi Shimizu[2], Makoto Shimomura[1], Magfira Syarifuddin[1], Masato Iguchi[1] (1.Sakurajima Volcano Research Center, Disaster Prevention Research Institute, Kyoto University, 2.National Institute for Environmental Studies)

9:30 AM - 9:45 AM JST | 12:30 AM - 12:45 AM UTC

### [MIS16-03] 2018-2019 Kuchinoerabu-jima eruption plume/cloud echoes observed by JMA weather radar network

*Eiichi Sato[1], Keiichi Fukui[2], Toshiki Shimbori[1] (1.Meteorological Research Institute, 2.Japan Meteorological Agency)

9:45 AM - 10:00 AM JST | 12:45 AM - 1:00 AM UTC

### [MIS16-04] Numerical Study on the Ejection Conditions of Ash Clouds during Recent Eruptions of Kuchinoerabujima Volcano

*Yasuhiro Ishimine[1], Teruki Oikawa[2], Nobuo Geshi[2] (1.Research and Education Center for Natural Hazards, Kagoshima University, 2.Geological Survey of Japan, AIST)

10:00 AM - 10:15 AM JST | 1:00 AM - 1:15 AM UTC

### [MIS16-05] Image analysis of volcanic clouds during the 2011 Kirishima Shinmoedake eruption

*Takehiko KOBORI[1], Kisei KINOSHITA[1], Naoko IINO[2], Masayuki MAKI[1], Seiji FUKUSHIMA[1] (1.Kagoshima University, 2.Kumamoto University)

10:15 AM - 10:30 AM JST | 1:15 AM - 1:30 AM UTC

### [MIS16-06] Cloud Radar Network for Early Detection of Cumulonimbus Generation

*Takeshi Maesaka[1], Tadayasu Ohigashi[1], Koyuru Iwanami[1], Shin-Ichi Suzuki[1], Yukari Shusse[1], Namiko Sakurai[1] (1.National Research Institute for Earth Science and Disaster Resilience)

# Observations of Volcanic Eruption Columns with Different Types of Weather Radars

*Masayuki Maki[1], Takehiko KOBORI[1], Yura Kim[1], Yasushi Fujiyoshi[2], Eiichi Sato[3], Hidehiko Tokushima[4], Masato Iguchi[5]

1. Kagoshima University, 2. Hokkaido University, 3. Meteorological Research Institute, 4. Field Researchers Corporation, 5. Kyoto University

The present paper describes the results of observational studies of volcanic ash columns using different types of weather radars: X-band marine radar, bi-static Ku-band radar, Ka-band Doppler radar, and operational X-band polarimetric radar. In order to observe eruption columns with extremely fine temporal resolution, an X-band marine radar was set up during three months in 2018 at the Kurokami observatory of Kyoto University located about 4km from the vent of Sakurajima volcano. The marine radar has a slot antenna that has the PPI scanning speed of 48 rpm, with a vertical beam width of 22˚ and a horizontal beam width of 1.2˚, and a range resolution of 8m. We carried out observations by physically changing the rotational axis of the slot antenna from vertical (PPI) to horizontal (RHI) to achieve an elevation angle resolution of 1.2˚. The MRI Ku-band radar and Kagoshima University Ku- band radar set up in 2017 in Sakurajima have Luneberg antenna with a horizontal and vertical beam width of 3˚. The antenna rotates spirally from an elevation angle of 0˚ to 90˚ to obtain hemispherical volume data in one minute. The Ka-band Doppler radar of NIED was operating at the Kurokami observatory during 3 months in 2015 to investigate the inner structure with the RHI antenna scanning. The MLIT operational X-band polarimetric radar located approximately 11km from the vent of the Sakurajima volcano can measure volcanic ash columns three-dimensionally at 5-minute intervals, even though it is an operational radar aiming to measure heavy rainfalls in Sakurajima.

Utilizing these different types of radar data, we perform detailed analysis of eruption columns. The marine radar succeeded in detecting eruptions and at the same time detecting falling pyroclastic particles (Fig. 1). The radar also reveals the fine structure of an ascending eruption column at 1.25-second intervals. While the marine radar observes volcanic ash columns with the wider azimuth angel resolution 22˚ due to its fan beam antenna, Ka-band Doppler radar can observe the targets with finer azimuthal resolution using RHI scanning of the parabolic antenna. The Ka-band radar RHI observations also reveal the upward speed of the ash echo top at 2-minute intervals. While both the marine radar and the Ku-band Doppler radar measure eruption column vertically at a fixed azimuthal direction, the Ku-band Doppler radar measures all azimuth and elevation angles every 1 minute. Using this scanning strategy, we can clarify the temporal change of the eruption column during its downwind movement: the radar reflectivity factor of the upper part of the eruption column becomes high 5-minute after the eruption, which is probably due to the aggregation process in water clouds (Fig. 2). The operational X-band MP radar collects 20 tilts PPI scan data at 5-minute interval. We can construct three-dimensional data of ash clouds with time and spatial interpolation method. Then we can obtain the wide-area ash fall distributions.

In conclusion, as mentioned above, different types of weather radars are now available for studying volcanic eruption columns and their applications to disaster prevention are promising.

Keywords: X-band marine radar, Ku-band rapid scanning Doppler radar, X-band polarimetric radar

©2019. Japan Geoscience Union. All Right Reserved. 

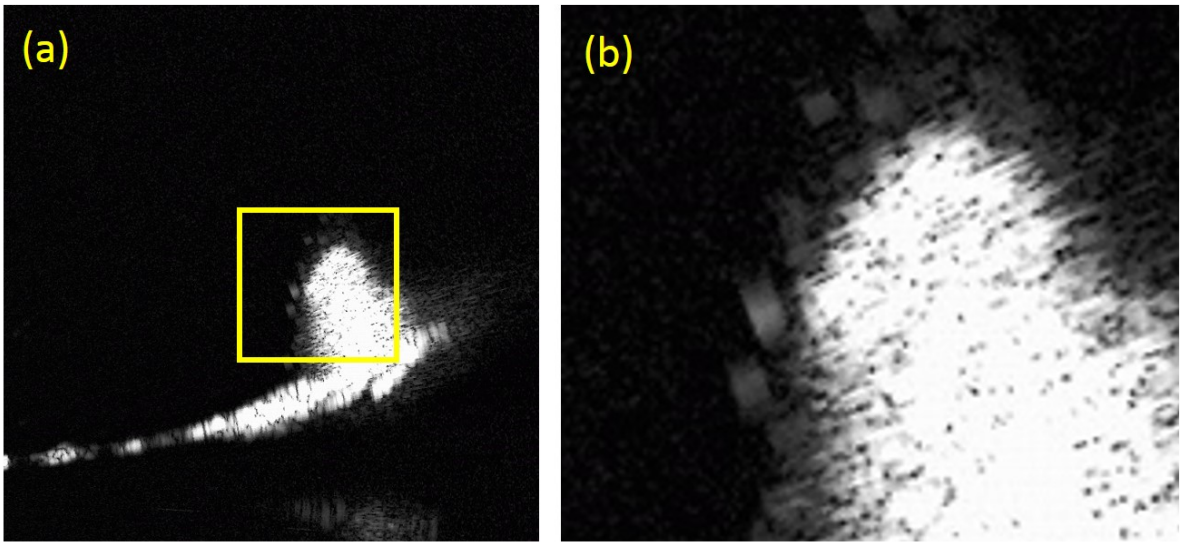


Fig. 1 Volcanic eruption column 2 minute after eruption observed by X-band marine radar. 22:11 LST, May 4, 2018.

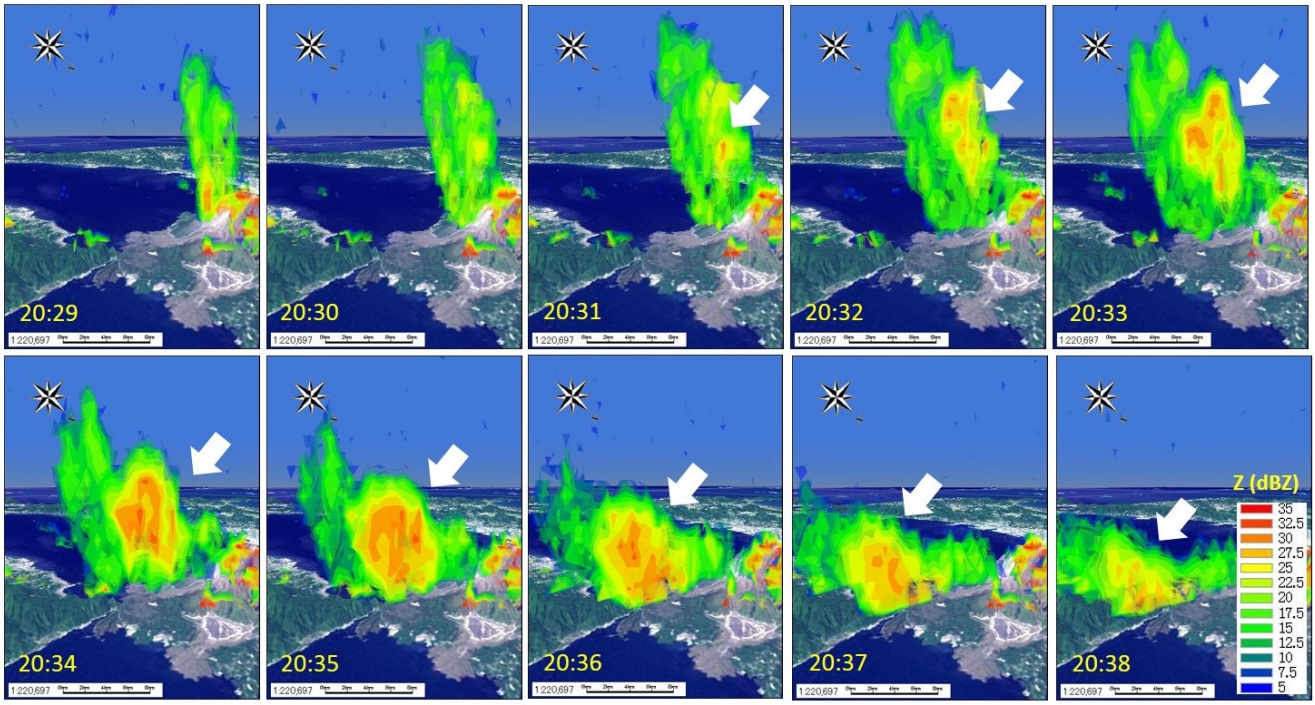


Fig. 2 Temporal change of inner structures of volcanic eruption clouds observed by KuRAD. 20:29-20:38 LST, March 5, 2018.

©2019. Japan Geoscience Union. All Right Reserved. 

# Observation of Eruption Plumes by X-Band MP radar and Lidar at Sakurajima and Kuchinoerabujima

*Haruhisa Nakamichi[1], Atsushi Shimizu[2], Makoto Shimomura[1], Magfira Syarifuddin[1], Masato Iguchi[1]

1. Sakurajima Volcano Research Center, Disaster Prevention Research Institute, Kyoto University, 2. National Institute for Environmental Studies

We report the comparison between results by radar and lidar observations of Minamidake eruption on June 16, 2018, at Sakurajima, and the radar observation results of Kuchinoerabujima eruptions since December 2018. The radar reflectivity factor data distribution showed that the plume reached 3,300 m height within 1 min after the onset of the Minamidake eruption and increased to be 5,000 m height, after 3 min from the onset of the eruption. At the same time, it was confirmed from the radar reflectivity factor data that the eruption column shifted 1 km to the west direction. The radar reflectivity factor reincreased vertically above the crater at about 3,000 m height, 5 min after the starting of the eruption, which is corresponding to the second eruption. In the lidar observation, changes corresponding to the movement in the west direction of the eruption column were observed from 3 min after the start of the eruption to 8 min afterward, and the scattering peak corresponded well with the enhancement of the radar reflectivity factor. After 15 min from the onset of the eruption, there was no change in the radar reflectivity factor corresponding to the ash plume, but the significant scattering intensity of the lidar was found at a distance less than 2 km and continued for more than 20 minutes. It reflects that the lidar outperforms the radar in terms of detecting the finer particles exist in the atmosphere. The lidar observation showed that volcanic ash was diffused and moved by the wind. Next, we observed the increase in the radar reflectivity factor corresponding to the eruption columns of the eruptions on December 18, 2018, and January 17 and 29, 2019 at Kuchinoerabujima. One minute after the eruption on December 28, the radar reflectivity factor showed a rise to 3,000 m of ash plume and reached the maximum height at about 5,000 m, 3 min after the onset of the eruption. It was found from the radar reflectivity factor that the maximum height of the plume was 4,000 m, 2 min after the onset of the eruption on January 17. Five minutes after the onset of eruption, the reflectivity factor of the plume reached 4,000 m and did not raise any further. From these facts, we can suggest that by grasping the temporal change of the plume height given by the temporal changes in radar reflectivity factor, we can extract the information of the eruption intensity.

Keywords: X-band MP Radar, Lidar, Eruption, Sakurajima, Kuchinoerabujima

©2019. Japan Geoscience Union. All Right Reserved. 

# 2018-2019 Kuchinoerabu-jima eruption plume/cloud echoes observed by JMA weather radar network

*Eiichi Sato[1], Keiichi Fukui[2], Toshiki Shimbori[1]

1. Meteorological Research Institute, 2. Japan Meteorological Agency

At Shindake crater of Kuchinoerabu-jima volcano, a very small eruption occurred on October 21, 2018, and then continued intermittently until December 13. After that, three eruptions accompanied by pyroclastic flow occurred on December 18, 2018, January 17 and 29, 2019. Although Japan Meteorological Agency (JMA) failed to visually confirm the top of the former two eruption plumes, they were observed by Himawari-8, a meteorological satellite of JMA, and X-band MP radar of Disaster Prevention Research Institute (DPRI), Kyoto University. Meanwhile, the eruptions were also observed by JMA's weather radar network. In this presentation, we will report on the analyses using them.
Eruption plume/cloud echo associated with the eruption on January 17, 2019 was observed by Tanegashima radar and Naze radar. The plume echo height observed by Tanegashima radar was about 6.7 km above sea level (ASL), and about 6.5 km ASL by Naze radar. These are consistent with about 6 km above the crater edge (about 6.6km ASL), the result of the analysis with Himawari 8. On the other hand, the eruption plume echo height observed by the DPRI radar was about 4 km above the sea level. This may be due to the vertical wind shear. In other words, the authors think that the 125-degree RHI observation, i.e., vertical cross section observation by DPRI radar, did not capture the top of the plume, because the wind direction observed by the JMA wind profiler at Yakushima was northwesterly or north-northwesterly in the lower troposphere (2km or less), however, the wind was westerly in the middle troposphere (about 3-6km).
Meanwhile, in other cases including eruption cases on December 18, 2018 and January 29, 2019, the JMA radar network did not properly capture the eruption plume/cloud echoes. It is considered that the volcanic ash density especially near the top of the plume was low, and the mismatch occurred between the scan sequence of the radar and the rising process of the plume.
As a result of analysis by weather radar, we captured some of the eruption activity, however, there were many cases that could not be properly caught. We will show the limits of the observation method with weather radar, and show some possible countermeasures.

**References**

Fukuoka Regional Volcanic Observation and Warning Center and Kagoshima Local Office (2019) Activities of Kuchinoerabu-jima volcano in January, 2019, < https://www.data.jma.go.jp/svd/vois/data/tokyo/STOCK/monthly_v-act_doc/fukuoka/19m01/509_19m01.pdf>. Accessed February 18, 2019.
Disaster Prevention Research Institute, Kyoto University (2019) Radar observation of volcanic eruption on January 17, 2019, < http://www.svo.dpri.kyoto-u.ac.jp/new/wp-content/uploads/2019/01/RadarKuchinoerabu20190117.pdf>. Accessed February 18, 2019

Keywords: volcanic eruption, Kuchinoerabu-jima, weather radar

©2019. Japan Geoscience Union. All Right Reserved. 

# Numerical Study on the Ejection Conditions of Ash Clouds during Recent Eruptions of Kuchinoerabujima Volcano

*Yasuhiro Ishimine[1], Teruki Oikawa[2], Nobuo Geshi[2]

1. Research and Education Center for Natural Hazards, Kagoshima University, 2. Geological Survey of Japan, AIST

Kuchinoerabujima Volcano in Kyushu, Japan have erupted in 2014 and 2015. The volcanic activities intensified again since October 2018 and generated explosive eruptions accompanying pyroclastic density currents on 18 December 2018, 17 and 29 January 2019. The pyroclastic density currents are so hazardous that it is crucial to assess the risk that residential area near the volcano could be affected by the currents.

We performed a series of numerical simulations on the ejection of volcanic ash clods and subsequent density currents with the parameter settings, which were based on the observational data acquired during the explosive eruptions of Kuchinoerabujima volcano from 2014 to 2018. The supercomputer system HOKUSAI, RIKEN was used (Project number: Q18431).

We assumed that the initial temperature, density and ejection speed of ash clouds significantly affect the dynamics of the ash clouds, and thus, we searched plausible combinations of the parameter set of the thee variables by conducting a series of numerical simulations. Some of the simulations yielded the results that are comparable with the observed eruptions accompanying pyroclastic density currents. In particular, the results implies that the pyroclastic density currents are prone to occur when the initial temperature of the ejected ash clouds is lower than 800K.

In addition, the numerical simulations exhibited that the small north-south trending ridge on the east of the volcanic vent of Kuchinoerabujima volcano had the main part of the pyroclastic density currents spread over the western flank of the volcanic edifice. This is consistent with our observation at Kuchinoerabujma volcano.

Keywords: Kuchinoerabujima volcano, Pyroclastic Density Current, Numerical Simulation

©2019. Japan Geoscience Union. All Right Reserved. 

# Image analysis of volcanic clouds during the 2011 Kirishima Shinmoedake eruption

*Takehiko KOBORI[1], Kisei KINOSHITA[1], Naoko IINO[2], Masayuki MAKI[1], Seiji FUKUSHIMA[1]

1. Kagoshima University, 2. Kumamoto University

We report the development and spatial scale of the sub-plinian eruption of Kirishima Shinmoedake in January 26-27, 2011. In addition to the multipoint image observation and the cloud diffusion analysis of satellite images in the previous reports [1-3], we analyze Ohnami-ike volcano monitoring camera images [4] and the photographs published.
For the image analysis of the plume, we improved the photo analysis program [5] and developed a method fitting the skyline created from the elevation tile [6] to the image. By considering the curvature of the earth when creating skyline, accurate altitude estimation became possible.
Since 2008, fumes and white vaporous clouds were often observed at Shinmoedake. Then, volcanic ash containing fresh magma was confirmed at the small eruption on January 19, 2011 at 01:27 [7]. After that, it changed to continuous discharge of ash cloud as observed on January 22 and 25. The plume flowed and rose to about 5-7 km downstream, with its top reaching 1700 to 2200 m above sea level, and flowed horizontally. Discharge of the plume continued until around 14:00 on January 26, and reached the highest point of 1700-1900 m above sea level at the downstream 3-4 km. Despite poor visibility due to atmospheric turbidity on January 26th, near-infrared video images and photographs from the observation point of 50 km south-southwest of Shinmoedake, captured the whole plume shape and developmental process of the sub-plinian eruption started at 15:29 on January 26th. The upper part of the large-scale ash cloud was also observed from a southern point of Kagoshima City located in 58 km southwest of Shinmoedake, and the visible web camera in the Hitoyoshi Basin located in 38 km north of Shinmoedake. By sharpening and analyzing these images, the plume height was obtained. On January 26, the plume rose to 7-8 km downstream, the altitude above sea level was 5000-6000 m, rarely 7000 m. This is close to sea level altitude 7000 m (accuracy 1 km) [8] obtained from radar analysis of the Tanegashima and Fukuoka data. On January 27, continuous magmatic clouds were observed since the morning. At the explosion at 15:30 and 15:41, sub-plinian type eruption restarted, and heavy ash cloud reaching 7000-8000 m above sea level was seen from each observation point.
Acknowledgement: We are very grateful to Aira-Isa Promotion Bureau of Development, Kagoshima Pref., for providing us the movie files of the highlight scenes of the 2011 Shinmoedake eruption.

[1] K.Kinoshita et al., Volcanic eruption clouds in southwest Japan observed from the ground and satellites. IAVCEI 2013 Sci. Assembry, Kagoshima, 4A1_2E-O8.
[2] K.Kinoshita, Eruption of Mt.Shinmoedake in Kirishima volcanoes and crisis management, J.Japanese Scientists, 46,1120-1126, 2011 (in J.).
[3] N.Iino et al., Ground observation and advection analysis of the 2011 Shinmoe-dake eruption clouds of Kirishima volcano, Bull. Fuc. Ed. Kumamoto Univ., Nat. Sci., 60, 69-76, 2011 (in J.).
[4] Aira-Isa Promotion Bureau of Development, Kagoshima Pref., http://kirishima-live.jpn.org/ (in J.).
[5] K.Kinoshita and K.Yoshida, Photo analysis of volcanic plumes from Mt.Sakurajima, Bull. Fac. Ed. Kagoshima Univ., Nat. Sci., 42, 1-19, 1990 (in J.).
[6] Geospacial Information Authority of Japan (https://maps.gsi.go.jp/development/ichiran.html#dem)
[7] S.Nakada et al., The outline of the 2011 eruption at Shinmoe-dake (Kirishima), Japan, Earth Planets Space, 65, 475-488, 2013.
[8] T.Shimbori et al., Observation of eruption clouds with weather radars and meteorological satellites,

©2019. Japan Geoscience Union. All Right Reserved. 

Quart. J. Seismol., 77, 139-214, 2013 (in J.).

Keywords: Volcanic Clouds, Image Analysis, Digital Elevation Model

©2019. Japan Geoscience Union. All Right Reserved. 

# Cloud Radar Network for Early Detection of Cumulonimbus Generation

*Takeshi Maesaka[1], Tadayasu Ohigashi[1], Koyuru Iwanami[1], Shin-Ichi Suzuki[1], Yukari Shusse[1], Namiko Sakurai[1]

1. National Research Institute for Earth Science and Disaster Resilience

Recently municipal engineers point out that urban city is vulnerable for localized heavy rainfall, and that rainfall monitoring and forecasting are important for water management. A weather radar is a powerful tool for that purpose; however it is only precipitation particles (hydrometeors excluding cloud particles) that current operational radars (S-, C- and X-band) can detect. This means that when the radar catches the echo, the rainfall may have already started. Meanwhile, the heavy rainfall is caused by a mature cumulonimbus which develops from a cumulus. So the detection of the cumulous is expected to make the lead time of heavy rainfall forecasting longer. But the current radar cannot observe the cumulus which consists of the cloud particles. For an early warning of heavy rainfall, we developed the cloud radar network around Tokyo metropolitan area.
The network consists of five Ka-band (35 GHz) radars whose specifications are as follows: azimuth-/elevation-scanning Cassegrain antenna with a diameter of 2 m, 3 kW Extended Interaction Klystron (EIK) as a microwave amplifier, pulse compression by linear frequency modulation, and dual polarimetric capability (simultaneous transmission and reception of H and V; only three of the five radars). The minimum sensitivity we need is -17 dBZ (-20 dBZ) at 20 km range for dual (single) polarimetric type, respectively, because our target is the detection of a conversion from cloud droplets to raindrops. These radars were just deployed in February 2015. We would like to present preliminary results of our cloud radar and to discuss the availability to the early monitoring of cumulonimbus generation.

Keywords: Cloud Radar, Cumulonimbus, Early Detection

©2019. Japan Geoscience Union. All Right Reserved. 

[J] Poster | M (Multidisciplinary and Interdisciplinary)：M-IS Intersection

Thu. May 30, 2019 3:30 PM - 5:00 PM JST | Thu. May 30, 2019 6:30 AM - 8:00 AM UTC | Poster Hall International Exhibition Hall8, Makuhari Messe_22

## [M-IS16] Dynamics of eruption cloud and cumulonimbus; modelling and observation

convener:Eiichi Sato(Meteorological Research Institute), Fukashi Maeno(Earthquake Research Institute, University of Tokyo), Takeshi Maesaka(National Research Institute for Earth Science and Disaster Resilience)

Volcanic eruption clouds (eruption column, pyroclastic flow, and umbrella cloud) and cumulonimbus are similar phenomena in the atmosphere. Models that can precisely reproduce the physical processes in such phenomena, and accurate observations have been required. Recently, the development of remote sensing techniques such as weather radar and weather satellite are remarkable, and they are being adopted for volcanic eruption monitoring. However, it is indispensable to verify the results of modeling and remote sensing using in-situ observations. In this session, we will discuss the modelling and the observations of eruption clouds and cumulonimbus from the viewpoint of meteorology, volcanology, geology, and other related fields. The related phenomena such as ashfall, rainfall, snowfall, hail and volcanic block will also be discussed.

### [MIS16-P01] Redesign of the Japan Meteorological Agency Atmospheric Transport Model

*Toshiki Shimbori[1], Kensuke Ishii[1] (1.Volcanology Research Department, Meteorological Research Institute)

### [MIS16-P02] Mathematical mechanism of an inverse problem for tephra transport and dispersal model

*Kensuke Ishii[1], Takehiro Koyaguchi[2] (1.Meteorological Research Institute, 2.Earthquake Research Institute, the University of Tokyo)

### [MIS16-P03] Development of the plume source model for inversion of tephra fallout

*Akira Nishijo[1], Takehiro Koyaguchi[1], Yujiro Suzuki[1] (1.The University of Tokyo Earthquake Research Institute)

### [MIS16-P04] Segregation height and size distribution of volcanic ash of Sakurajima eruptions inferred by observed settling velocity

*Kosei Takishita[1], Masato Iguchi[2], Tadaomi Sonoda[2] (1.Graduate School of Science, Kyoto Univ., 2.DPRI, Kyoto Univ.)

### [MIS16-P05] Distant tracking of maximum pumice diameter in pumice-fall of the Tenmei eruption of Asama volcano: An attempt to draw isopleth lines of mm scale-maximum pumice diameter in the Kanto Plain

*Shingo Takeuchi[1], Shimpei Uesawa[1] (1.Central Research Institute of Electric Power Industry, Civil Engineering Research Laboratory, Geosphere Sciences)

### [MIS16-P06] Degassing activity of Aso volcano, Japan, before the 8 October 2016 eruption measured by satellite and ground-based remote sensing techniques

*Masaaki Morita[1] (1.Geological Survey of Japan, AIST)

### [MIS16-P07] Characteristics of polarimetric radar parameters of dry volcanic ash clouds

*Yura Kim[1], Masayuki Maki[1], Masato Iguchi[2], Dong-In Lee[3] (1.Research and Education Center for Natural Hazards, Kagoshima University, Korimoto, Kagoshima, Japan, 2.Sakurajima Volcano Research Center/DPRI, Kyoto University, Sakurajima, Kagoshima, Japan, 3.Department of Atmospheric Sciences, Pukyong National University, Namgu, Busan, Republic of Korea)

### [MIS16-P08] Development of easy tools for volcanic eruption plume/cloud analysis using weather radars

*Eiichi Sato[1], Ryutaro Senba[2] (1.Meteorological Research Institute, 2.Fukuoka Regional Headquarter, Japan Meteorological Agency)

# Redesign of the Japan Meteorological Agency Atmospheric Transport Model

*Toshiki Shimbori[1], Kensuke Ishii[1]

1. Volcanology Research Department, Meteorological Research Institute

The Meteorological Research Institute (MRI) of the Japan Meteorological Agency (JMA) will develop a new Atmospheric Transport Model (ATM) called the JMA-ATM.

The JMA is currently operating the Global ATM (JMA-GATM) and Regional ATM (JMA-RATM) to issue Volcanic Ash Advisories (VAAs) and Volcanic Ash Fall Forecasts (VAFFs). The JMA-GATM and RATM are driven by the grid point values of Global Spectral Model (GSM) and Meso-Scale Model (MSM) or Local Forecast Model (LFM) based on the nonhydrostatic model ASUCA (Forecast Department, 2014), respectively. The MRI is planning to renew the JMA's ATM and join a volcanic ash data assimilation system (Ishii *et al.*, 2017) under one of the MRI research plans which start in April 2019.

The new JMA-ATM is designed from the point of view of robustness, promptness, flexibility and manageability. *Robustness*: To avoid any abnormal ends in operation, the JMA-ATM takes Lagrangian description. *Promptness*: To issue VAAs and VAFFs immediately, the JMA-ATM calculate offline. Further, element conversion of grid point values executes in preprocess and main ATM calculation runs parallel processing using Message Passing Interface (MPI) on high performance computers. *Flexibility*: ATM tracers are not limited to volcanic ash generated by an eruption column model as initial condition and the ATM coordinate is not customized only for the input data of GSM, MSM or LFM. *Manageability*: In order to review and share source codes within the JMA, project management and version control systems are used in the ATM development. With regard to the above design, the offline Lagrangian model is the same as current ATMs. Whereas the vertical coordinate of JMA-GATM is $\sigma$-$p$ hybrid of GSM and that of JMA-RATM (Shimbori *et al.*, 2016) is hybrid terrain-following of ASUCA, the JMA-ATM takes identical $z$-coordinate of the converted grid point values. Therefore two current ATMs can be unified to the single ATM (see Fig. 1). For readability, the JMA-ATM are written in the Fortran in accordance with the standard coding rule (Muroi *et al.*, 2002) and all subroutines are modularized. In order that dynamical and physical processes are commutative in a timestep of the JMA-ATM, time tendency of tracer variables is calculated in each process and integrated at the last timestep. The JMA-ATM project is managed with Redmine and its source code version is controlled with Subversion (SVN) which have been installed in JMA (Forecast Department, 2017).

A first object of the new ATM as an operational model is to maintain the same accuracy of JMA-GATM and RATM predictions. In particular, to precisely predict the atmospheric transport phenomena near ground surface, suitable treatments of model terrain in terms of $z$-coordinate are primary subjects. A technical platform, such as visualization and verification tools, is also needed. We are going to publish the documentation of the JMA-ATM in the Technical Reports of the MRI in 2020. Furthermore, for the purpose of accuracy improvement of the JMA-ATM prediction, we are planning to implement processes of aggregation and resuspension, in addition to joining the data assimilation system for volcanic ash that observed by weather radars (*e.g.*, Sato *et al.*, 2019) and so on.

## References

Ishii, K., T. Shimbori, E. Sato, Y. Hayashi, T. Tokumoto, K. Fukui, A. Hashimoto, 2017: Development of a

©2019. Japan Geoscience Union. All Right Reserved. 

volcanic ash data assimilation system for atmospheric transport model. *Proc. JpGU-AGU Joint Meeting*, MIS02-P02.
Forecast Department/JMA, 2014: *Separate Volume of Annual Report of Numerical Prediction Division*, **60**, 151 p. https://www.jma.go.jp/jma/kishou/books/nwpreport/60/No60_all.pdf
Forecast Department/JMA, 2017: *Separate Volume of Annual Report of Numerical Prediction Division*, **63**, 108 p. https://www.jma.go.jp/jma/kishou/books/nwpreport/63/No63_all.pdf
Muroi, C., E. Toyoda, H. Yoshimura, M. Hosaka and M. Sugi, 2002: Standard coding rule. *Tenki*, **49**, 91-95.
Sato, E., R. Semba, K. Fukui and T. Shimbori, 2019: Volcanic ash plume observation by polarimetric radar on cloudy/rainy conditions. Part II. *Proc. Meteor. Soc. Japan*.
Shimbori, T., 2016: Tephra Transport: Modeling and Forecasting. *Bull. Volcanol. Soc. Japan*, **61**, 399-427.
Shimbori, T., Y. Hayashi, Y. Fujiwara, K. Matsuda, K. Ishii, E. Sato and T. Tokumoto, 2016: Applying the ASUCA GPVs to the JMA Regional Atmospheric Transport Model for the operational Volcanic Ash Fall Forecasts. *Proc. Volcanol. Soc. Japan*, 189.

Keywords: Atmospheric Transport Model, JMA-ATM, volcanic ash, lapilli, VAFF, VAA

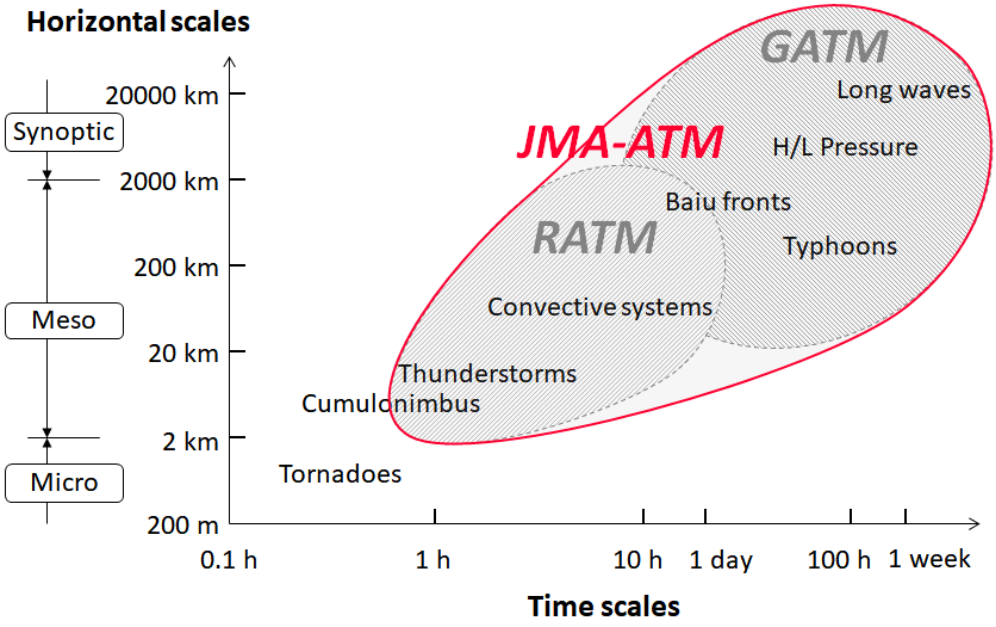


Fig. 1 Horizontal and time scales of atmospheric phenomena covered by the JMA 's ATMs (after Shimbori, 2016).

©2019. Japan Geoscience Union. All Right Reserved. 

# Mathematical mechanism of an inverse problem for tephra transport and dispersal model

*Kensuke Ishii[1], Takehiro Koyaguchi[2]

1. Meteorological Research Institute, 2. Earthquake Research Institute, the University of Tokyo

Estimation of tephra mass released along the eruption column is crucial for the characterization of explosive volcanic eruptions systems and for the volcanic hazard mitigations. For example, the uncertainties of assumed tephra mass distribution as the source term for tephra transport and dispersal models critically influence the accuracy of the tephra forecast. In addition, the estimated tephra mass distribution can be used for verification and comprehension of some eruption column models which have been developed in previous studies (e.g. Woods & Bursik, 1991) .

We are studying an inverse problem of a model which relates the tephra mass distribution along the eruption column to the tephra fallout deposits. The model is expressed as a linear system which builds on the advection-fall-dispersion-sedimentation equation. The inverse problem is, therefore reduced to a ‘linear inverse problem’. In this study, we investigated the properties of this linear inverse problem on the basis of the singular value decomposition (SVD) using numerical experiments that generate pseudo-observations.

The SVD analysis indicates that present inverse problem is that of an ‘ill-conditioned’ system, where most of singular values are nearly zero. This characteristic comes from the fact that tephra particles released from high altitudes tend to lose the information of their sources because of diffusion. The small singular values cause an unstable and non-physical inverse solution to be completely dominated by small amount of observation error (referred to as over-fitting). Therefore, the present inverse problem requires careful consideration to obtain stable and meaningful solutions. In our study, the regularization and the optimization of the vertical grid are applied to produce such solutions. In the regularization, we do not include singular vectors with small singular value as the basis function expressing the inverse solution, such that the solution can be less sensitive to observation error. In the optimization of the vertical grids, we reduce the number of vertical grids of the model parameters using linear interpolation to avoid singular vectors with small singular values. Combining these two methods, we successfully find approximate solutions without over-fitting. In the presentation, we also discuss how the eruption conditions (e.g., magma discharge rate) are constrained by the model parameters estimated from the present method.

Keywords: inverse problem, singurar value, singurar value decomposition, eruption column, tephra fallout deposit, volcanic eruption

©2019. Japan Geoscience Union. All Right Reserved. 

# Development of the plume source model for inversion of tephra fallout

*Akira Nishijo[1], Takehiro Koyaguchi[1], Yujiro Suzuki[1]

1. The University of Tokyo Earthquake Research Institute

During an explosive volcanic eruption, tephra falls out from eruption cloud to ground surface and forms tephra deposits. The characteristics of tephra deposits (e.g. their thickness and spatial distribution) reflect the eruption source conditions. When an eruption source condition is specified by parameters, tephra transport and deposition can be calculated using the advection-diffusion model. Based on this forward model, we can inversely search for an optimal set of parameters that explain the observed characteristics of tephra deposits (e.g. Conner & Conner 2006). In practice, we estimate the supply rate of tephra particles from the eruption cloud into the atmosphere as a function of height and grain size (referred to as “supply rate function”) from the inversion analysis. The form of supply rate function is determined by the physical processes of particle separation from the eruption cloud, and hence it must depend on the dynamics of eruption column. In previous studies, however, the form of supply rate function was assumed to be a certain mathematical function without physical considerations (White et al 2017). In this study, we developed a physical model to obtain the supply rate function.
The physical model is a combination of a particle sedimentation model and a cloud dynamics model. The sedimentation model describes the process of particle fallout from the cloud. The cloud dynamics model is subdivided into 2 models: the 1-D plume model and the gravity current model. The 1-D plume model describes the dynamics of eruption columns below the neutral buoyancy level (NBL), and the gravity current model describes the dynamics of spreading cloud around NBL. We used the 1-D plume model of Bursik (2001), which considers bending by windy air and the effects of particle sedimentation. We also take into account the geometrical effects of plume bending on the sedimentation model.
From a parametric study using the above physical model, we obtained the supply rate function for each grain size. The supply rate function is composed of two functions: “plume supply rate function” and “gravity-current supply rate function”. The plume supply rate function represents the mass loss of particles from the edge of a rising plume below NBL. It is convex downward and monotonically decreasing against height regardless of grain size. The gravity-current supply rate function describes the mass flux of particles at NBL in the cloud (i.e., at the top of the rising plume), and it is used as the source term for the gravity current model. The characteristics of the supply rate function depend on grain size. Because most of coarse particles (>10 mm) fallout from the lower part of rising plume, their plume supply rate function decreases rapidly with height, and the value of their gravity-current supply rate function is nearly zero. Because most of fine particles (< 1 mm) carried by rising plume up to NBL, their plume supply rate function has small values throughout the plume, and their gravity-current supply rate function is approximately equal to the supply rate at the vent. The plume supply rate function of intermediate particles (1~10 mm) is a mildly decreasing function, and it has larger values than that of fine particles; therefore, it has greater values than those of coarse or fine particles for the upper part of the plume. The value of the gravity-current supply rate function for intermediate particles remarkably decreases with the increasing grain size. In the presentation, we compare these results based on our plume source model with the mathematical functions used in previous inversion analyses.

Keywords: explosive volcanic eruption, inversion of tephra fallout, 1-D eruption model, particle sedimentation, advection-diffusion model

©2019. Japan Geoscience Union. All Right Reserved. 

# Segregation height and size distribution of volcanic ash of Sakurajima eruptions inferred by observed settling velocity

*Kosei Takishita[1], Masato Iguchi[2], Tadaomi Sonoda[2]

1. Graduate School of Science, Kyoto Univ., 2. DPRI, Kyoto Univ.

## 1. Introduction

The most important input values of a volcanic ash dispersion model are mass eruption rate and wind. Aiming more precise estimation, ash segregation pattern from plumes is also important. Mannen [2014] estimated the segregation height of ash particles of 1986B sub-Plinian eruption of Izu-Oshima volcano, with a column of 10km high, using Tephra2, an advection-diffusion model. Using a method similar to Mannen [2014], we investigate features of particle segregation height and size distribution (PSD), based on the observation of the settling velocity of ash particles released by many Vulcanian eruptions of Sakurajima Volcano.

## 2. Observation method and Data

We install Parsivel$^2$, a laser-optical rain gauge (OTT Co.) at 13 sites in Sakurajima. The instrument classifies particles into 32 diameters (0.2-24.5mm) and 32 settling velocities (0.2-20.8m/s), and records particle count every minute. We analyze the data from May to December in 2018. Ash particles were detected at a total of 261 sites from 156 eruptions among 346 events. The size ranges from 0.25mm to 20mm, and the volume-based mode diameter is 0.625mm - 0.75mm. The settling velocity is less than 12.8m/s and slower than the terminal velocity of sphere in each diameter [Wilson and Huang, 1973].

## 3. Analysis method

Ash particles from a plume reach the ground through combination process of advection, diffusion, and dropping. We estimate back trajectory of ash particles from the ground to the plume based on wind data measured by JMA, in order to determine the nearest point to the plume as the segregation height. Horizontal wind field is obtained at the time of eruptions by the interpolation in time and altitude, and vertical wind is neglected. We assume the 2D Gaussian distribution [Suzuki, 1983] for diffusion, a constant settling velocity determined by observation for dropping, and a vertical line source for plume.

## 4. Particle segregation and PSD

Segregation mass and PSD are obtained for 17 eruptions using the data of ash particles estimated to have segregated within 10 minutes from the eruption. The plume height ranges from 400 to 4700m, and the mass and PSD are estimated at heights interval of 150m - 990m. The largest height interval is obtained at 1260m –2250m above sea level (asl) for the eruption which occurred at 15:09, June 9$^{th}$ in 2018. Its plume height was 1400m above the crater (2400m asl), and $4.4\times10^3$ tons of ash is estimated to be released from the range. Here we define $\alpha$ as the logarithm of the segregation density [t/m]. In the eruption, $\alpha$ ranges from -1 to 0 and there was no correlation between $\alpha$ and height. As for PSD, there was a strong inverse correlation (R=-0.94) between height and volume fraction of particles smaller than 0.75mm.

The plume of the eruption on July 16$^{th}$ in 2018 reached an elevation of 4600m above the crater. Segregation mass is $3.6\times10^3$ tons at the altitude range of 1290m –1710m and 2070m –2570m asl. $\alpha$ ranges from -2 to 0, and there is no correlation with $\alpha$ and height. As for PSD, there is no strong correlation (R=-0.39) between height and volume fraction of particles smaller than 0.75mm.

While most of eruptions don’t have correlation between height and PSD, some have strong inverse correlation (R<-0.9; 4 events) and another has strong positive correlation (R>0.9; 1 event). Mannen [2014] also showed similar inverse correlation.

## 5. Examination of the method

©2019. Japan Geoscience Union. All Right Reserved. 

The mean $\alpha$ during the same period is obtained, 0.46, from the total mass of volcanic ash sampled continuously at wider area in Kagoshima pref. The mean $\alpha$ in this study, -0.18, is smaller than this because we treat the data for 10 minutes from the beginning.
Some segregation heights were obtained below the crater (1000m asl). This may be due to negligence of downward wind. Vertical wind will be taken into account later.

Keywords: segregation from a volcanic plume, Sakurajima volcano, tephra fall, Parsivel

©2019. Japan Geoscience Union. All Right Reserved. 

# Distant tracking of maximum pumice diameter in pumice-fall of the Tenmei eruption of Asama volcano: An attempt to draw isopleth lines of mm scale-maximum pumice diameter in the Kanto Plain

*Shingo Takeuchi[1], Shimpei Uesawa[1]

1. Central Research Institute of Electric Power Industry, Civil Engineering Research Laboratory, Geosphere Sciences

Volcanic ash-fall reaches distant areas and has great adverse effects on human health and society. Therefore, it is important to investigate properties of volcanic ash-fall of past eruption in distant areas for volcanic hazard assessment. However, thin ash-fall deposit in a distant point is not preserved as a visible geological layer. Instead, particles of ash-fall are mixed in soil. The characteristics of distal ash-fall particles in soil is an important geological evidence to assess volcanic ash hazard and constrain modelling of volcanic ash-fall processes in distant areas. Takeuchi and Uesawa (2018, JpGU) studied the Tenmei eruption (AD1783 eruption) of Asama volcano and detected pumice particles in the topsoil at areas along ash dispersal axis with distance up to ca. 170 km in the Kanto plain, and correlated the pumice particles to the pumice-fall of Tenmei eruption. They tracked the maximum pumice diameter (MP) along the dispersal axis and obtained the MP variation with distance which can be consistently linked with the data with distance up to ca. 55 km of Minakami (1942). In this study, same soil survey has been performed in areas away from the dispersal axis to track the maximum pumice diameter (MP). The preliminary result suggests that we can draw isopleth lines of MP down to 1 mm in diameter in the middle to the southern area of the Kanto Plain. In addition, we have investigated characteristics of ash fall of Tennin eruption (AD1108 eruption), because ash dispersal areas of Tennin eruption partly overlaps those of Temmei eruption in the northern Kanto Plain, at which pumice particles originated from the Tennin eruption are also found in topsoil. In the future analysis, we need to distinguish pumice particles from those of Tennin eruption to determine the MP of Temmei eruption.

Keywords: volcanic ash-fall, maximum pumice size, Tenmei eruption of Asama volcano

©2019. Japan Geoscience Union. All Right Reserved. 

# Degassing activity of Aso volcano, Japan, before the 8 October 2016 eruption measured by satellite and ground-based remote sensing techniques

*Masaaki Morita[1]

1. Geological Survey of Japan, AIST

The flux of volcanic gases has been monitored as sulfur dioxide ($SO_2$) flux at many volcanoes by ground-based remote sensing measurements using a miniature spectrometer such as Mini-DOAS. A recent advance in satellite remote sensing techniques has also enabled for $SO_2$ amounts emitted by persistent degassing to be monitored at sufficient temporal resolution. In this study, we combined these two techniques with ground-based visible camera images to constrain the degassing activity before the 8 October 2016 phreatomagmatic eruption of Aso volcano, Japan. We compared the time series of atmospheric $SO_2$ mass in the lower troposphere above the volcano measured by the Ozone Mapping and Profiler Suite (OMPS) nadir mapper instrument to those of the ground-based $SO_2$ flux and plume height measured by the Japan Meteorological Agency. Our results between April and October 2016 showed similar temporal variations among these values. The $SO_2$ mass and the plume height increased to, respectively, about 1000 tons and 900 m above the crater rim two months before the eruption, and then gradually decreased. Both values again increased about a week before the eruption and reached their maximum values (> 1200 tons and 1010 m above the crater rim, respectively). These similar temporal variations between the $SO_2$ emissions and the plume height likely indicate that, although the degassing system of the volcano has been stable during the study period, the accumulation of volcanic gases in the shallow part of the volcanic conduit might trigger the phreatomagmatic eruption. Our result suggests that the satellite remote sensing techniques can be sufficient for monitoring $SO_2$ flux of the volcanic plume at low altitude.

Keywords: Volcanic gas, Aso volcano, Remote sensing, Sulfur dioxide flux, OMPS

©2019. Japan Geoscience Union. All Right Reserved. 

# Characteristics of polarimetric radar parameters of dry volcanic ash clouds

*Yura Kim[1], Masayuki Maki[1], Masato Iguchi[2], Dong-In Lee[3]

1. Research and Education Center for Natural Hazards, Kagoshima University, Korimoto, Kagoshima, Japan, 2. Sakurajima Volcano Research Center/DPRI, Kyoto University, Sakurajima, Kagoshima, Japan, 3. Department of Atmospheric Sciences, Pukyong National University, Namgu, Busan, Republic of Korea

We analyzed statistically the polarimetric radar data of 9 Sakurajima volcanic eruption clouds in 2013. All eruption clouds have a height exceeding 3000m. According to the results, $Z_H$ has positively skewed distributions (Skewness of 1.6; mean $Z_H$ of 9.77 dBZ and median of 7.4 dBZ), $Z_{DR}$ has normal distributions (Skewness of 0.02; mean $Z_{DR}$ of 1.58 dB and median of 1.6 dB), $K_{DP}$ has positively skewed distributions (Skewness of 7.12; mean $K_{DP}$ of 0.03 deg/km and median of 0.0 deg/km), and $\rho_{hv}$ has negatively skewed distributions (Skewness of -1.02; mean $\rho_{hv}$ of 0.77 and median of 0.8). Depending on time after the eruption, the average $Z_H$ decreased from 22.3 dBZ to 6.75 dBZ while the average $Z_{DR}$ and $\rho_{hv}$ tended to increase from 1.24 dB to 1.67 dB, and from 0.47 to 0.83, respectively.

Keywords: polarimetric radar parameters, volcanic ash, statistical analysis

©2019. Japan Geoscience Union. All Right Reserved. 

# Development of easy tools for volcanic eruption plume/cloud analysis using weather radars

*Eiichi Sato[1], Ryutaro Senba[2]

1. Meteorological Research Institute, 2. Fukuoka Regional Headquarter, Japan Meteorological Agency

Meteorological Research Institute and Kagoshima Local Meteorological Office, Japan Meteorological Agency (JMA) have been cooperatively working on research on simple analysis methods of volcanic eruption plume using weather radars. In volcanology, since researchers of radar analysis whose target is volcanic eruption plume/cloud are minority, we are developing simple analysis tools especially for beginners of radar meteorology. As visible images of cameras were used to monitor volcano, operational analysis of volcanic eruption plume/cloud by JMA become impossible if the visibility is poor. If analysis using radar data became easier, immediate analysis of volcanic eruption cloud in all-weathers would be possible, and, as a result, we can make a database of “hidden” eruptions. In this presentation, outline of the tool development and results of a case study will be shown.
In the tool development, we use the software named “Draft” developed by MRI. This software consists of many commands, e.g., format conversion, analysis of radar data, and drawing results. Although it is possible to analyze the radar echo of volcanic eruption cloud using these commands, it may be difficult for beginners of radar meteorology and “Draft”. Hence, we started to create some shell scripts that the users can perceive the shapes of volcanic eruption plumes easily with radar data. Our goal is to make easy-to-use tools that enable us to do everything, from collecting radar data to drawing the results, automatically.
As a case study, we chose the eruption from the Minamidake summit crater of Sakurajima occurred on November 11, 2017. In this case, we couldn’t see the eruption plume by cloud around the summit. Considering the amount of ground deformation detected by extensometer in an observation tunnel in Arimura, Sakurajima, it's no wonder that the volcanic ash and the gas spewed to more than 5,000m with this eruption. It is because the amount of strain change associated with the eruption is almost the same with the case on June 16, 2018, whose eruption cloud height was 5,700m. In this case, we used the data of two (Fukuoka and Tanegashima) weather radars which belong to JMA operational weather radar network (JMA-RDN). As a result, we revealed that the eruption cloud was about 4,500 to 6,000m, and kept this height for about 10 minutes. In 2017, this eruption may be one of the largest eruptions, because the eruption occurred from Showa crater on May 2 is the only one eruption whose volcanic ash rose more than 5,000m.
Interestingly, we found two peaks in the radar echo distribution by the Tanegashima radar. We consider that one peak is due to the dense ash above the summit, and the other peak was made by aggregates and water coated ash. We are planning to carry out further analysis using different types of radar, e.g., polarimetric weather radar.
As a conclusion, effectiveness of the analysis tools using weather radars was confirmed in this study. It is expected that the tools enable us immediate analysis of volcanic eruption cloud in all-weathers. However, there are some problems. One of them is that we may not be able to analyze an accurate eruption cloud altitude especially in the case whose amount of ash is small and the duration is a few minutes, since the time resolution of the JMA-RDN is about 5minutes. We will continuously develop the analysis tools and improve the analysis methods through analyzing more cases.

Keywords: volcanic eruption plume/cloud, weather radar, Sakurajima volcano

©2019. Japan Geoscience Union. All Right Reserved. 

©2019. Japan Geoscience Union. All Right Reserved. 

[J] Poster | M (Multidisciplinary and Interdisciplinary)：M-IS Intersection

Thu. May 30, 2019 5:15 PM - 6:30 PM JST | Thu. May 30, 2019 8:15 AM - 9:30 AM UTC | Poster Hall International Exhibition Hall8, Makuhari Messe_40

## [M-IS16] Dynamics of eruption cloud and cumulonimbus; modelling and observation

convener:Eiichi Sato(Meteorological Research Institute), Fukashi Maeno(Earthquake Research Institute, University of Tokyo), Takeshi Maesaka(National Research Institute for Earth Science and Disaster Resilience)

Volcanic eruption clouds (eruption column, pyroclastic flow, and umbrella cloud) and cumulonimbus are similar phenomena in the atmosphere. Models that can precisely reproduce the physical processes in such phenomena, and accurate observations have been required. Recently, the development of remote sensing techniques such as weather radar and weather satellite are remarkable, and they are being adopted for volcanic eruption monitoring. However, it is indispensable to verify the results of modeling and remote sensing using in-situ observations. In this session, we will discuss the modelling and the observations of eruption clouds and cumulonimbus from the viewpoint of meteorology, volcanology, geology, and other related fields. The related phenomena such as ashfall, rainfall, snowfall, hail and volcanic block will also be discussed.

### [MIS16-P01] Redesign of the Japan Meteorological Agency Atmospheric Transport Model

*Toshiki Shimbori[1], Kensuke Ishii[1] (1.Volcanology Research Department, Meteorological Research Institute)

### [MIS16-P02] Mathematical mechanism of an inverse problem for tephra transport and dispersal model

*Kensuke Ishii[1], Takehiro Koyaguchi[2] (1.Meteorological Research Institute, 2.Earthquake Research Institute, the University of Tokyo)

### [MIS16-P03] Development of the plume source model for inversion of tephra fallout

*Akira Nishijo[1], Takehiro Koyaguchi[1], Yujiro Suzuki[1] (1.The University of Tokyo Earthquake Research Institute)

### [MIS16-P04] Segregation height and size distribution of volcanic ash of Sakurajima eruptions inferred by observed settling velocity

*Kosei Takishita[1], Masato Iguchi[2], Tadaomi Sonoda[2] (1.Graduate School of Science, Kyoto Univ., 2.DPRI, Kyoto Univ.)

### [MIS16-P05] Distant tracking of maximum pumice diameter in pumice-fall of the Tenmei eruption of Asama volcano: An attempt to draw isopleth lines of mm scale-maximum pumice diameter in the Kanto Plain

*Shingo Takeuchi[1], Shimpei Uesawa[1] (1.Central Research Institute of Electric Power Industry, Civil Engineering Research Laboratory, Geosphere Sciences)

### [MIS16-P06] Degassing activity of Aso volcano, Japan, before the 8 October 2016 eruption measured by satellite and ground-based remote sensing techniques

*Masaaki Morita[1] (1.Geological Survey of Japan, AIST)

### [MIS16-P07] Characteristics of polarimetric radar parameters of dry volcanic ash clouds

*Yura Kim[1], Masayuki Maki[1], Masato Iguchi[2], Dong-In Lee[3] (1.Research and Education Center for Natural Hazards, Kagoshima University, Korimoto, Kagoshima, Japan, 2.Sakurajima Volcano Research Center/DPRI, Kyoto University, Sakurajima, Kagoshima, Japan, 3.Department of Atmospheric Sciences, Pukyong National University, Namgu, Busan, Republic of Korea)

### [MIS16-P08] Development of easy tools for volcanic eruption plume/cloud analysis using weather radars

*Eiichi Sato[1], Ryutaro Senba[2] (1.Meteorological Research Institute, 2.Fukuoka Regional Headquarter, Japan Meteorological Agency)

# Redesign of the Japan Meteorological Agency Atmospheric Transport Model

*Toshiki Shimbori[1], Kensuke Ishii[1]

1. Volcanology Research Department, Meteorological Research Institute

The Meteorological Research Institute (MRI) of the Japan Meteorological Agency (JMA) will develop a new Atmospheric Transport Model (ATM) called the JMA-ATM.

The JMA is currently operating the Global ATM (JMA-GATM) and Regional ATM (JMA-RATM) to issue Volcanic Ash Advisories (VAAs) and Volcanic Ash Fall Forecasts (VAFFs). The JMA-GATM and RATM are driven by the grid point values of Global Spectral Model (GSM) and Meso-Scale Model (MSM) or Local Forecast Model (LFM) based on the nonhydrostatic model ASUCA (Forecast Department, 2014), respectively. The MRI is planning to renew the JMA's ATM and join a volcanic ash data assimilation system (Ishii *et al.*, 2017) under one of the MRI research plans which start in April 2019.

The new JMA-ATM is designed from the point of view of robustness, promptness, flexibility and manageability. *Robustness*: To avoid any abnormal ends in operation, the JMA-ATM takes Lagrangian description. *Promptness*: To issue VAAs and VAFFs immediately, the JMA-ATM calculate offline. Further, element conversion of grid point values executes in preprocess and main ATM calculation runs parallel processing using Message Passing Interface (MPI) on high performance computers. *Flexibility*: ATM tracers are not limited to volcanic ash generated by an eruption column model as initial condition and the ATM coordinate is not customized only for the input data of GSM, MSM or LFM. *Manageability*: In order to review and share source codes within the JMA, project management and version control systems are used in the ATM development. With regard to the above design, the offline Lagrangian model is the same as current ATMs. Whereas the vertical coordinate of JMA-GATM is $\sigma$-$p$ hybrid of GSM and that of JMA-RATM (Shimbori *et al.*, 2016) is hybrid terrain-following of ASUCA, the JMA-ATM takes identical $z$-coordinate of the converted grid point values. Therefore two current ATMs can be unified to the single ATM (see Fig. 1). For readability, the JMA-ATM are written in the Fortran in accordance with the standard coding rule (Muroi *et al.*, 2002) and all subroutines are modularized. In order that dynamical and physical processes are commutative in a timestep of the JMA-ATM, time tendency of tracer variables is calculated in each process and integrated at the last timestep. The JMA-ATM project is managed with Redmine and its source code version is controlled with Subversion (SVN) which have been installed in JMA (Forecast Department, 2017).

A first object of the new ATM as an operational model is to maintain the same accuracy of JMA-GATM and RATM predictions. In particular, to precisely predict the atmospheric transport phenomena near ground surface, suitable treatments of model terrain in terms of $z$-coordinate are primary subjects. A technical platform, such as visualization and verification tools, is also needed. We are going to publish the documentation of the JMA-ATM in the Technical Reports of the MRI in 2020. Furthermore, for the purpose of accuracy improvement of the JMA-ATM prediction, we are planning to implement processes of aggregation and resuspension, in addition to joining the data assimilation system for volcanic ash that observed by weather radars (*e.g.*, Sato *et al.*, 2019) and so on.

## References

Ishii, K., T. Shimbori, E. Sato, Y. Hayashi, T. Tokumoto, K. Fukui, A. Hashimoto, 2017: Development of a

©2019. Japan Geoscience Union. All Right Reserved. 

volcanic ash data assimilation system for atmospheric transport model. *Proc. JpGU-AGU Joint Meeting*, MIS02-P02.
Forecast Department/JMA, 2014: *Separate Volume of Annual Report of Numerical Prediction Division*, **60**, 151 p. https://www.jma.go.jp/jma/kishou/books/nwpreport/60/No60_all.pdf
Forecast Department/JMA, 2017: *Separate Volume of Annual Report of Numerical Prediction Division*, **63**, 108 p. https://www.jma.go.jp/jma/kishou/books/nwpreport/63/No63_all.pdf
Muroi, C., E. Toyoda, H. Yoshimura, M. Hosaka and M. Sugi, 2002: Standard coding rule. *Tenki*, **49**, 91-95.
Sato, E., R. Semba, K. Fukui and T. Shimbori, 2019: Volcanic ash plume observation by polarimetric radar on cloudy/rainy conditions. Part II. *Proc. Meteor. Soc. Japan*.
Shimbori, T., 2016: Tephra Transport: Modeling and Forecasting. *Bull. Volcanol. Soc. Japan*, **61**, 399-427.
Shimbori, T., Y. Hayashi, Y. Fujiwara, K. Matsuda, K. Ishii, E. Sato and T. Tokumoto, 2016: Applying the ASUCA GPVs to the JMA Regional Atmospheric Transport Model for the operational Volcanic Ash Fall Forecasts. *Proc. Volcanol. Soc. Japan*, 189.

Keywords: Atmospheric Transport Model, JMA-ATM, volcanic ash, lapilli, VAFF, VAA

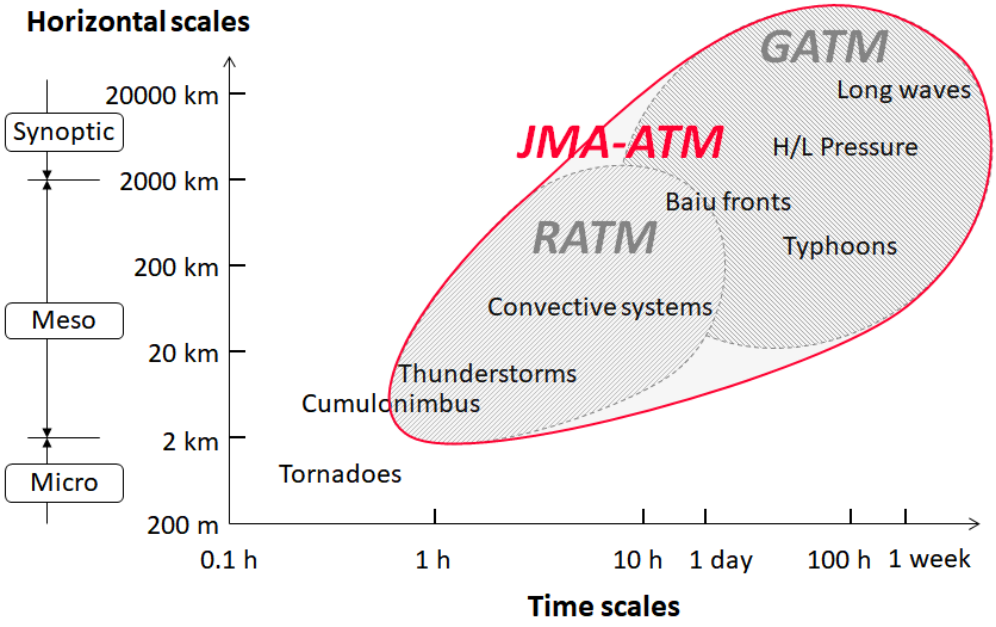


Fig. 1 Horizontal and time scales of atmospheric phenomena covered by the JMA 's ATMs (after Shimbori, 2016).

©2019. Japan Geoscience Union. All Right Reserved. 

# Mathematical mechanism of an inverse problem for tephra transport and dispersal model

*Kensuke Ishii[1], Takehiro Koyaguchi[2]

1. Meteorological Research Institute, 2. Earthquake Research Institute, the University of Tokyo

Estimation of tephra mass released along the eruption column is crucial for the characterization of explosive volcanic eruptions systems and for the volcanic hazard mitigations. For example, the uncertainties of assumed tephra mass distribution as the source term for tephra transport and dispersal models critically influence the accuracy of the tephra forecast. In addition, the estimated tephra mass distribution can be used for verification and comprehension of some eruption column models which have been developed in previous studies (e.g. Woods & Bursik, 1991) .

We are studying an inverse problem of a model which relates the tephra mass distribution along the eruption column to the tephra fallout deposits. The model is expressed as a linear system which builds on the advection-fall-dispersion-sedimentation equation. The inverse problem is, therefore reduced to a ‘linear inverse problem’. In this study, we investigated the properties of this linear inverse problem on the basis of the singular value decomposition (SVD) using numerical experiments that generate pseudo-observations.

The SVD analysis indicates that present inverse problem is that of an ‘ill-conditioned’ system, where most of singular values are nearly zero. This characteristic comes from the fact that tephra particles released from high altitudes tend to lose the information of their sources because of diffusion. The small singular values cause an unstable and non-physical inverse solution to be completely dominated by small amount of observation error (referred to as over-fitting). Therefore, the present inverse problem requires careful consideration to obtain stable and meaningful solutions. In our study, the regularization and the optimization of the vertical grid are applied to produce such solutions. In the regularization, we do not include singular vectors with small singular value as the basis function expressing the inverse solution, such that the solution can be less sensitive to observation error. In the optimization of the vertical grids, we reduce the number of vertical grids of the model parameters using linear interpolation to avoid singular vectors with small singular values. Combining these two methods, we successfully find approximate solutions without over-fitting. In the presentation, we also discuss how the eruption conditions (e.g., magma discharge rate) are constrained by the model parameters estimated from the present method.

Keywords: inverse problem, singurar value, singurar value decomposition, eruption column, tephra fallout deposit, volcanic eruption

©2019. Japan Geoscience Union. All Right Reserved. 

# Development of the plume source model for inversion of tephra fallout

*Akira Nishijo[1], Takehiro Koyaguchi[1], Yujiro Suzuki[1]

1. The University of Tokyo Earthquake Research Institute

During an explosive volcanic eruption, tephra falls out from eruption cloud to ground surface and forms tephra deposits. The characteristics of tephra deposits (e.g. their thickness and spatial distribution) reflect the eruption source conditions. When an eruption source condition is specified by parameters, tephra transport and deposition can be calculated using the advection-diffusion model. Based on this forward model, we can inversely search for an optimal set of parameters that explain the observed characteristics of tephra deposits (e.g. Conner & Conner 2006). In practice, we estimate the supply rate of tephra particles from the eruption cloud into the atmosphere as a function of height and grain size (referred to as “supply rate function”) from the inversion analysis. The form of supply rate function is determined by the physical processes of particle separation from the eruption cloud, and hence it must depend on the dynamics of eruption column. In previous studies, however, the form of supply rate function was assumed to be a certain mathematical function without physical considerations (White et al 2017). In this study, we developed a physical model to obtain the supply rate function.
The physical model is a combination of a particle sedimentation model and a cloud dynamics model. The sedimentation model describes the process of particle fallout from the cloud. The cloud dynamics model is subdivided into 2 models: the 1-D plume model and the gravity current model. The 1-D plume model describes the dynamics of eruption columns below the neutral buoyancy level (NBL), and the gravity current model describes the dynamics of spreading cloud around NBL. We used the 1-D plume model of Bursik (2001), which considers bending by windy air and the effects of particle sedimentation. We also take into account the geometrical effects of plume bending on the sedimentation model.
From a parametric study using the above physical model, we obtained the supply rate function for each grain size. The supply rate function is composed of two functions: “plume supply rate function” and “gravity-current supply rate function”. The plume supply rate function represents the mass loss of particles from the edge of a rising plume below NBL. It is convex downward and monotonically decreasing against height regardless of grain size. The gravity-current supply rate function describes the mass flux of particles at NBL in the cloud (i.e., at the top of the rising plume), and it is used as the source term for the gravity current model. The characteristics of the supply rate function depend on grain size. Because most of coarse particles (>10 mm) fallout from the lower part of rising plume, their plume supply rate function decreases rapidly with height, and the value of their gravity-current supply rate function is nearly zero. Because most of fine particles (< 1 mm) carried by rising plume up to NBL, their plume supply rate function has small values throughout the plume, and their gravity-current supply rate function is approximately equal to the supply rate at the vent. The plume supply rate function of intermediate particles (1~10 mm) is a mildly decreasing function, and it has larger values than that of fine particles; therefore, it has greater values than those of coarse or fine particles for the upper part of the plume. The value of the gravity-current supply rate function for intermediate particles remarkably decreases with the increasing grain size. In the presentation, we compare these results based on our plume source model with the mathematical functions used in previous inversion analyses.

Keywords: explosive volcanic eruption, inversion of tephra fallout, 1-D eruption model, particle sedimentation, advection-diffusion model

©2019. Japan Geoscience Union. All Right Reserved. 

# Segregation height and size distribution of volcanic ash of Sakurajima eruptions inferred by observed settling velocity

*Kosei Takishita[1], Masato Iguchi[2], Tadaomi Sonoda[2]

1. Graduate School of Science, Kyoto Univ., 2. DPRI, Kyoto Univ.

## 1. Introduction

The most important input values of a volcanic ash dispersion model are mass eruption rate and wind. Aiming more precise estimation, ash segregation pattern from plumes is also important. Mannen [2014] estimated the segregation height of ash particles of 1986B sub-Plinian eruption of Izu-Oshima volcano, with a column of 10km high, using Tephra2, an advection-diffusion model. Using a method similar to Mannen [2014], we investigate features of particle segregation height and size distribution (PSD), based on the observation of the settling velocity of ash particles released by many Vulcanian eruptions of Sakurajima Volcano.

## 2. Observation method and Data

We install Parsivel$^2$, a laser-optical rain gauge (OTT Co.) at 13 sites in Sakurajima. The instrument classifies particles into 32 diameters (0.2-24.5mm) and 32 settling velocities (0.2-20.8m/s), and records particle count every minute. We analyze the data from May to December in 2018. Ash particles were detected at a total of 261 sites from 156 eruptions among 346 events. The size ranges from 0.25mm to 20mm, and the volume-based mode diameter is 0.625mm - 0.75mm. The settling velocity is less than 12.8m/s and slower than the terminal velocity of sphere in each diameter [Wilson and Huang, 1973].

## 3. Analysis method

Ash particles from a plume reach the ground through combination process of advection, diffusion, and dropping. We estimate back trajectory of ash particles from the ground to the plume based on wind data measured by JMA, in order to determine the nearest point to the plume as the segregation height. Horizontal wind field is obtained at the time of eruptions by the interpolation in time and altitude, and vertical wind is neglected. We assume the 2D Gaussian distribution [Suzuki, 1983] for diffusion, a constant settling velocity determined by observation for dropping, and a vertical line source for plume.

## 4. Particle segregation and PSD

Segregation mass and PSD are obtained for 17 eruptions using the data of ash particles estimated to have segregated within 10 minutes from the eruption. The plume height ranges from 400 to 4700m, and the mass and PSD are estimated at heights interval of 150m - 990m. The largest height interval is obtained at 1260m –2250m above sea level (asl) for the eruption which occurred at 15:09, June 9$^{th}$ in 2018. Its plume height was 1400m above the crater (2400m asl), and $4.4\times10^3$ tons of ash is estimated to be released from the range. Here we define $\alpha$ as the logarithm of the segregation density [t/m]. In the eruption, $\alpha$ ranges from -1 to 0 and there was no correlation between $\alpha$ and height. As for PSD, there was a strong inverse correlation (R=-0.94) between height and volume fraction of particles smaller than 0.75mm.

The plume of the eruption on July 16$^{th}$ in 2018 reached an elevation of 4600m above the crater. Segregation mass is $3.6\times10^3$ tons at the altitude range of 1290m –1710m and 2070m –2570m asl. $\alpha$ ranges from -2 to 0, and there is no correlation with $\alpha$ and height. As for PSD, there is no strong correlation (R=-0.39) between height and volume fraction of particles smaller than 0.75mm.

While most of eruptions don’t have correlation between height and PSD, some have strong inverse correlation (R<-0.9; 4 events) and another has strong positive correlation (R>0.9; 1 event). Mannen [2014] also showed similar inverse correlation.

## 5. Examination of the method

©2019. Japan Geoscience Union. All Right Reserved. 

The mean $\alpha$ during the same period is obtained, 0.46, from the total mass of volcanic ash sampled continuously at wider area in Kagoshima pref. The mean $\alpha$ in this study, -0.18, is smaller than this because we treat the data for 10 minutes from the beginning.
Some segregation heights were obtained below the crater (1000m asl). This may be due to negligence of downward wind. Vertical wind will be taken into account later.

Keywords: segregation from a volcanic plume, Sakurajima volcano, tephra fall, Parsivel

©2019. Japan Geoscience Union. All Right Reserved. 

# Distant tracking of maximum pumice diameter in pumice-fall of the Tenmei eruption of Asama volcano: An attempt to draw isopleth lines of mm scale-maximum pumice diameter in the Kanto Plain

*Shingo Takeuchi[1], Shimpei Uesawa[1]

1. Central Research Institute of Electric Power Industry, Civil Engineering Research Laboratory, Geosphere Sciences

Volcanic ash-fall reaches distant areas and has great adverse effects on human health and society. Therefore, it is important to investigate properties of volcanic ash-fall of past eruption in distant areas for volcanic hazard assessment. However, thin ash-fall deposit in a distant point is not preserved as a visible geological layer. Instead, particles of ash-fall are mixed in soil. The characteristics of distal ash-fall particles in soil is an important geological evidence to assess volcanic ash hazard and constrain modelling of volcanic ash-fall processes in distant areas. Takeuchi and Uesawa (2018, JpGU) studied the Tenmei eruption (AD1783 eruption) of Asama volcano and detected pumice particles in the topsoil at areas along ash dispersal axis with distance up to ca. 170 km in the Kanto plain, and correlated the pumice particles to the pumice-fall of Tenmei eruption. They tracked the maximum pumice diameter (MP) along the dispersal axis and obtained the MP variation with distance which can be consistently linked with the data with distance up to ca. 55 km of Minakami (1942). In this study, same soil survey has been performed in areas away from the dispersal axis to track the maximum pumice diameter (MP). The preliminary result suggests that we can draw isopleth lines of MP down to 1 mm in diameter in the middle to the southern area of the Kanto Plain. In addition, we have investigated characteristics of ash fall of Tennin eruption (AD1108 eruption), because ash dispersal areas of Tennin eruption partly overlaps those of Temmei eruption in the northern Kanto Plain, at which pumice particles originated from the Tennin eruption are also found in topsoil. In the future analysis, we need to distinguish pumice particles from those of Tennin eruption to determine the MP of Temmei eruption.

Keywords: volcanic ash-fall, maximum pumice size, Tenmei eruption of Asama volcano

©2019. Japan Geoscience Union. All Right Reserved. 

# Degassing activity of Aso volcano, Japan, before the 8 October 2016 eruption measured by satellite and ground-based remote sensing techniques

*Masaaki Morita[1]

1. Geological Survey of Japan, AIST

The flux of volcanic gases has been monitored as sulfur dioxide ($SO_2$) flux at many volcanoes by ground-based remote sensing measurements using a miniature spectrometer such as Mini-DOAS. A recent advance in satellite remote sensing techniques has also enabled for $SO_2$ amounts emitted by persistent degassing to be monitored at sufficient temporal resolution. In this study, we combined these two techniques with ground-based visible camera images to constrain the degassing activity before the 8 October 2016 phreatomagmatic eruption of Aso volcano, Japan. We compared the time series of atmospheric $SO_2$ mass in the lower troposphere above the volcano measured by the Ozone Mapping and Profiler Suite (OMPS) nadir mapper instrument to those of the ground-based $SO_2$ flux and plume height measured by the Japan Meteorological Agency. Our results between April and October 2016 showed similar temporal variations among these values. The $SO_2$ mass and the plume height increased to, respectively, about 1000 tons and 900 m above the crater rim two months before the eruption, and then gradually decreased. Both values again increased about a week before the eruption and reached their maximum values (> 1200 tons and 1010 m above the crater rim, respectively). These similar temporal variations between the $SO_2$ emissions and the plume height likely indicate that, although the degassing system of the volcano has been stable during the study period, the accumulation of volcanic gases in the shallow part of the volcanic conduit might trigger the phreatomagmatic eruption. Our result suggests that the satellite remote sensing techniques can be sufficient for monitoring $SO_2$ flux of the volcanic plume at low altitude.

Keywords: Volcanic gas, Aso volcano, Remote sensing, Sulfur dioxide flux, OMPS

©2019. Japan Geoscience Union. All Right Reserved. 

# Characteristics of polarimetric radar parameters of dry volcanic ash clouds

*Yura Kim[1], Masayuki Maki[1], Masato Iguchi[2], Dong-In Lee[3]

1. Research and Education Center for Natural Hazards, Kagoshima University, Korimoto, Kagoshima, Japan, 2. Sakurajima Volcano Research Center/DPRI, Kyoto University, Sakurajima, Kagoshima, Japan, 3. Department of Atmospheric Sciences, Pukyong National University, Namgu, Busan, Republic of Korea

We analyzed statistically the polarimetric radar data of 9 Sakurajima volcanic eruption clouds in 2013. All eruption clouds have a height exceeding 3000m. According to the results, $Z_H$ has positively skewed distributions (Skewness of 1.6; mean $Z_H$ of 9.77 dBZ and median of 7.4 dBZ), $Z_{DR}$ has normal distributions (Skewness of 0.02; mean $Z_{DR}$ of 1.58 dB and median of 1.6 dB), $K_{DP}$ has positively skewed distributions (Skewness of 7.12; mean $K_{DP}$ of 0.03 deg/km and median of 0.0 deg/km), and $\rho_{hv}$ has negatively skewed distributions (Skewness of -1.02; mean $\rho_{hv}$ of 0.77 and median of 0.8). Depending on time after the eruption, the average $Z_H$ decreased from 22.3 dBZ to 6.75 dBZ while the average $Z_{DR}$ and $\rho_{hv}$ tended to increase from 1.24 dB to 1.67 dB, and from 0.47 to 0.83, respectively.

Keywords: polarimetric radar parameters, volcanic ash, statistical analysis

©2019. Japan Geoscience Union. All Right Reserved. 

# Development of easy tools for volcanic eruption plume/cloud analysis using weather radars

*Eiichi Sato[1], Ryutaro Senba[2]

1. Meteorological Research Institute, 2. Fukuoka Regional Headquarter, Japan Meteorological Agency

Meteorological Research Institute and Kagoshima Local Meteorological Office, Japan Meteorological Agency (JMA) have been cooperatively working on research on simple analysis methods of volcanic eruption plume using weather radars. In volcanology, since researchers of radar analysis whose target is volcanic eruption plume/cloud are minority, we are developing simple analysis tools especially for beginners of radar meteorology. As visible images of cameras were used to monitor volcano, operational analysis of volcanic eruption plume/cloud by JMA become impossible if the visibility is poor. If analysis using radar data became easier, immediate analysis of volcanic eruption cloud in all-weathers would be possible, and, as a result, we can make a database of “hidden” eruptions. In this presentation, outline of the tool development and results of a case study will be shown.
In the tool development, we use the software named “Draft” developed by MRI. This software consists of many commands, e.g., format conversion, analysis of radar data, and drawing results. Although it is possible to analyze the radar echo of volcanic eruption cloud using these commands, it may be difficult for beginners of radar meteorology and “Draft”. Hence, we started to create some shell scripts that the users can perceive the shapes of volcanic eruption plumes easily with radar data. Our goal is to make easy-to-use tools that enable us to do everything, from collecting radar data to drawing the results, automatically.
As a case study, we chose the eruption from the Minamidake summit crater of Sakurajima occurred on November 11, 2017. In this case, we couldn’t see the eruption plume by cloud around the summit. Considering the amount of ground deformation detected by extensometer in an observation tunnel in Arimura, Sakurajima, it's no wonder that the volcanic ash and the gas spewed to more than 5,000m with this eruption. It is because the amount of strain change associated with the eruption is almost the same with the case on June 16, 2018, whose eruption cloud height was 5,700m. In this case, we used the data of two (Fukuoka and Tanegashima) weather radars which belong to JMA operational weather radar network (JMA-RDN). As a result, we revealed that the eruption cloud was about 4,500 to 6,000m, and kept this height for about 10 minutes. In 2017, this eruption may be one of the largest eruptions, because the eruption occurred from Showa crater on May 2 is the only one eruption whose volcanic ash rose more than 5,000m.
Interestingly, we found two peaks in the radar echo distribution by the Tanegashima radar. We consider that one peak is due to the dense ash above the summit, and the other peak was made by aggregates and water coated ash. We are planning to carry out further analysis using different types of radar, e.g., polarimetric weather radar.
As a conclusion, effectiveness of the analysis tools using weather radars was confirmed in this study. It is expected that the tools enable us immediate analysis of volcanic eruption cloud in all-weathers. However, there are some problems. One of them is that we may not be able to analyze an accurate eruption cloud altitude especially in the case whose amount of ash is small and the duration is a few minutes, since the time resolution of the JMA-RDN is about 5minutes. We will continuously develop the analysis tools and improve the analysis methods through analyzing more cases.

Keywords: volcanic eruption plume/cloud, weather radar, Sakurajima volcano

©2019. Japan Geoscience Union. All Right Reserved. 

©2019. Japan Geoscience Union. All Right Reserved. 

[J] Oral | M (Multidisciplinary and Interdisciplinary)：M-IS Intersection

Thu. May 30, 2019 9:00 AM - 10:30 AM JST | Thu. May 30, 2019 12:00 AM - 1:30 AM UTC | 304 3F

## [M-IS19] Paleoclimatology and paleoceanography

convener:Yusuke Okazaki(Department of Earth and Planetary Sciences, Graduate School of Science, Kyushu University), Akira Oka(Atmosphere and Ocean Research Institute, The University of Tokyo), Michinobu Kuwae(Center for Marine Environmental Studies), Hitoshi Hasegawa(Faculty of Science and Technology, Kochi University), Chairperson:Hitoshi Hasegawa

Past environmental changes and events at multi-decadal to tectonic timescale toward an understanding of Earth climate system by an integration of terrestrial and marine proxy studies and numerical modeling will be discussed. At JpGU2019, a series of presentations on present and future climate and environmental changes from paleo-perspective will be held. We welcome a variety of paleo-environmental studies from a wide range of background. We hope that this session will provide an opportunity to promote communication between participants from multidisciplinary field.

9:00 AM - 9:15 AM JST | 12:00 AM - 12:15 AM UTC

### [MIS19-17] Paleotemperature and precipitation history (18.1–4.5 ka) in stalagmite bulk and clumped isotopes from Hiroshima, Japan

*Hirokazu Kato[1], Shota Amekawa[1], Akihiro Kano[1] (1.Department of Earth and Planetary Science, The University of Tokyo)

9:15 AM - 9:30 AM JST | 12:15 AM - 12:30 AM UTC

### [MIS19-18] Terrestrial paleoclimate since 80 ka recorded in stable and clumped isotopes of two stalagmites obtained from the Pacific side of the Japanese islands

*Shota Amekawa[1], Hirokazu Kato[1], Akihiro Kano[1], Kenji Kashiwagi[2], Taiki Mori[3], Ryoko Senda[3], Chuan–Chou Shen[4] (1.Graduate School of Science, The University of Tokyo, 2.Graduate School of Science and Engineering for Research, University of Toyama, 3.Graduate School of Integrated Sciences for Global Society, Kyushu University, 4.Department of Geosciences, National Taiwan University)

9:30 AM - 9:45 AM JST | 12:30 AM - 12:45 AM UTC

### [MIS19-19] Seasonal changes in Li/Ca ratio and inferred phytoplankton abundance as analyzed by daily growth increments of *Pecten albicans* (Bivalvia)

*Kondo Yasuo[1], Hondo Shutaro, Hasegawa Hitoshi[1], Nshio Yoshiro[1], Hirota Takayoshi (1.National University Corporation Kochi University)

9:45 AM - 10:00 AM JST | 12:45 AM - 1:00 AM UTC

### [MIS19-20] Geological reconstruction of Antarctic Ice Sheet deglaciation on Soya Coast, East Antarctica since the Last Glacial Maximum

*Moto Kawamata[1], Yusuke Suganuma[2,1], Koichiro Doi[2,1], Takanobu Sawagaki[3], Akihisa Hattori[1] (1.Department of Polar Science, School of Multidisciplinary Science, SOKENDAI (The Graduate Unversity for Advanced Studies), 2.National Institute of Polar Research, 3.Hosei University)

10:00 AM - 10:15 AM JST | 1:00 AM - 1:15 AM UTC

### [MIS19-21] Os isotope record of the Quaternary seawater derived from pelagic sediment in the Lau Basin, western South Pacific Ocean, and its implications for global climate changes

*Yusuke Kuwahara[1], Kazutaka Yasukawa[1,2], Koichiro Fujinaga[2,3], Tatsuo Nozaki[4,3,5,2], Junichiro Ohta[2,6,3], Honami Sato[2,4], Jun-Ichi Kimura[6], Kentaro Nakamura[1], Yasuhiro Kato[3,1,2] (1.Department of Systems Innovation, School of Engineering, The University of Tokyo, 2.Ocean Resources Research Center for Next Generation, Chiba Institute of Technology, 3.Frontier Research Center for Energy and Resources, School of Engineering, The University of Tokyo, 4.Research and Development Center for Submarine Resources, Japan Agency for Marine-Earth Science and Technology , 5.Department of Planetology, Graduate School of Science, Kobe University, 6.Department of Solid Earth Geochemistry, Japan Agency for Marine-Earth Science and Technology)

10:15 AM - 10:30 AM JST | 1:15 AM - 1:30 AM UTC

## [MIS19-22] Rapid glaciation and sea level changes during the Last Glacial Maximum and the deglaciation

*Yusuke Yokoyama[1], Tezer M Esat[9], William G Thompson[10], Alexandar L Thomas[11], Jody W Webster[2], Yosuke Miyairi[1], Chikako Sawada[1], Takahiro AZE[1], Hiroyuki Matsuzaki[1], Jun'ichi Okuno[3], Stewart Fallon[9], Juan-Carlos Braga[12], Marc Humblet[4], Yasufumi Iryu[5], Donald C Potts[13], Kazuhiko Fujita[6], Atsushi Suzuki[7], Hironobu Kan[8] (1.Atmosphere and Ocean Research Institute, University of Tokyo, 2.University of Sydney, Australia, 3.National Institute of Polar Research, 4.Nagoya University, 5.Tohoku University, 6.University of the Ryukyus, 7.The Geological Survey of Japan, AIST, 8.Kyushu University, 9.Research School of Earth Sciences, The Australian National University, Australia, 10.Woods Hole Oceanographic Institute, USA, 11.University of Edinburgh, UK, 12.Universidad de Granada, Spain, 13.University of California Santa Cruise, USA)

# Paleotemperature and precipitation history (18.1–4.5 ka) in stalagmite bulk and clumped isotopes from Hiroshima, Japan

*Hirokazu Kato[1], Shota Amekawa[1], Akihiro Kano[1]

1. Department of Earth and Planetary Science, The University of Tokyo

Variation in stalagmite $\delta^{18}O$ is basically controlled by two major factors, temperature and isotopic composition of cave dripwater derived from the local precipitation. It is however not easy to separate relative impacts from these two fundamental controls by conventional oxygen isotope alone.
A possible solution is applying carbonate clumped isotope thermometry that can reconstruct the temperature without information of the isotopic compositions of the environmental water. The principle of the clumped isotope thermometry is based on the temperature-dependency of the abundance anomaly of $^{13}C^{18}O^{16}O$ ($\Delta_{47}$) from acid digestion of carbonate.
In this study, carbonate clumped isotope ($\Delta_{47}$) was measured from 50 layers of Hiro-1 stalagmite from Hiroshima Prefecture by purification line and MAT 253 settled at Kyushu University. The growth interval of the stalagmite is from 18.1 to 4.5 ka and includes two hiatuses in 10.8–7.7 ka and 12.8–11.4 ka.
The $\Delta_{47}$ values of 50 layers in Hiro-1 range from 0.683 to 0.741‰, which correspond to 3.2–23.4 ºC by temperature calibration on the basis of tufa measurements (Kato *et al.*, 2019).The temperature range of each time-series is 5.2–12.5 ºC (7.4 ºC in average; 18.0–16.0 ka), 10.4–12.8 ºC (11.9 ºC in average; 15.9–14.5 ka), 3.2–9.4 ºC (6.1 ºC in average; 14.2–12.6 ka), 6.8–12.4ºC (9.2 ºC in average; 11.0–10.7 ka), 7.6–23.4 ºC (15.7 ºC in average; 7.7–4.9 ka) and 3.9–9.7 ºC (8.2 ºC in average; 4.9–4.5 ka).
The $\Delta_{47}$ temperature record from Hiro-1 is broadly consistent with already-known climatic stages. For instance, the temperature recovery from LGM, lowering around Younger-Dryas, increase into Holocene and the peak of warming around Hypsithermal. Temperature difference between LGM (18.0–16.0 ka) and mid-Holocene (7.7–4.9 ka) is 8.3 ºC. Isotopic data in the period of 15.9–14.5 ka, and also at 10.7 ka has the features from the kinetic effect, i.e., high $\delta^{18}O$ values and low $\Delta_{47}$ values comparing to the data of adjacent intervals. These intervals are characteristic in high prior calcite precipitation (PCP) of Hiro-1 stalagmite as suggested by Hori *et al.* (2013) and this shift was likely caused by some disequilibrium effect.
The $\delta^{18}O_{Hiro\text{-}1}$ profile can be corrected by subtraction of temperature effect and $\delta^{18}O_{MW}$ which represents isotopic composition of past meteoric water was obtained. The reconstructed $\delta^{18}O_{MW}$ value shows 1–2‰ rising from the last glacial period to Holocene. The shift has probably reflected an increase of summer precipitation by strengthened EASM in Holocene and the lowering of continentality by advance of Seto Island Sea.

Reference

Kato H., Amekawa S., Kano A., Mori T., Kuwahara Y., Quade J. (2019) Seasonal temperature changes obtained from carbonate clumped isotopes of annually laminated tufas from Japan: Discrepancy between natural and synthetic calcites. *GCA* **244**, 548–564.
Hori M., Ishikawa T., Nagaishi K., Lin K., Wang B.-S., You C.-F., Shen C.-C., Kano A. (2013) Prior calcite precipitation and source mixing process influence Sr/Ca, Ba/Ca and $^{87}Sr/^{86}Sr$ of a stalagmite developed in southwestern Japan during 18.0 4.5 ka. *Chem. Geol.* **347**, 190–198.

Keywords: stalagmite, carbonate clumped isotope, temperature reconstruction, last glacial period, Holocene, paleoclimate

©2019. Japan Geoscience Union. All Right Reserved. 

©2019. Japan Geoscience Union. All Right Reserved. 

# Terrestrial paleoclimate since 80 ka recorded in stable and clumped isotopes of two stalagmites obtained from the Pacific side of the Japanese islands

*Shota Amekawa[1], Hirokazu Kato[1], Akihiro Kano[1], Kenji Kashiwagi[2], Taiki Mori[3], Ryoko Senda[3], Chuan-Chou Shen[4]

1. Graduate School of Science, The University of Tokyo, 2. Graduate School of Science and Engineering for Research, University of Toyama, 3. Graduate School of Integrated Sciences for Global Society, Kyushu University, 4. Department of Geosciences, National Taiwan University

Terrestrial paleoclimate during late Quaternary has been broadly reconstructed by oxygen isotope ($\delta^{18}O$) of stalagmites. Previous studies have pointed out that stalagmite $\delta^{18}O$ is largely associated with change in $\delta^{18}O$ of meteoric water due to amount effect and shift of vapor sources, but also can be influenced by temperature change. One of solutions for evaluating the temperature effect is carbonate clumped isotope thermometer. Clumped isotopes are isotopologues in which rare isotopes are doubly or multiply substituted. In case of $CO_2$ generated from reaction of carbonate and phosphoric acis, the measuring target is $^{13}C^{18}O^{16}O$ (mass of 47). Previous studies have shown that measured abundance of clumped isotopes is slightly more than the stochastic abundance and its excess or "clumping" ($\Delta_{47}$) comes from thermodynamic stability, which allows us to reconstruct temperature during carbonate precipitation only by $\Delta_{47}$ of the generated $CO_2$. In this study, $\Delta_{47}$ and stable isotopes are applied to two stalagmites from the Pacific side of the Japanese islands, which should not be affected by vapor from Indian Ocean and Japan Sea.
Two analyzed stalagmites (KA01 and 03) were obtained from Taiki town, Mie prefecture, Japan. 32 U-Th age points determined at National Taiwan University reveal that KA01 was dated from ca. 14 ka to ca. 1 ka and KA03 (Mori et al., 2018) was from ca. 80 ka to ca. 20 ka as well as the Holocene. $\delta^{18}O$ changes of KA01 and KA03 show similar trends with the cave records in south Chinese (e.g. Hulu cave), but the amplitude of the $\delta^{18}O$ changes was reduced in half.
Results of our $\Delta_{47}$ values require reconsideration of the previous interpretation for the Chinese stalagmite $\delta^{18}O$, dominant control by $\delta^{18}O$ of meteoric water. A reconstructed temperature at the top of KA01 is consistent with modern temperature at the cave. The whole trend of reconstructed temperature combined with $\delta^{18}O$ of modern rainfall indicates that $\delta^{18}O$ changes of KA01 are mainly controlled by temperature changes instead of rainfall $\delta^{18}O$. $\Delta_{47}$ of KA03 yields higher temperature during cool periods of Heinrich events (HE), which apparently contradicts with previous studies. Before and after HEs, the carbon isotopic value increases by 0.5–1 ‰, indicating degassing of $^{13}C$-depleted $CO_2$ from dripwater and carbonate precipitation in the conduit of the host rock because of reduced water supply. Drying during HEs could have made the surface of the stalagmite dry and resulted in apparent contradictory temperature. This study verifies that $\delta^{18}O$ change should be used together with $\Delta_{47}$ for robust interpretation of the stalagmite records.

Keywords: clumped isotope, speleothem paleoclimatology

©2019. Japan Geoscience Union. All Right Reserved. 

# Seasonal changes in Li/Ca ratio and inferred phytoplankton abundance as analyzed by daily growth increments of *Pecten albicans* (Bivalvia)

*Kondo Yasuo[1], Hondo Shutaro, Hasegawa Hitoshi[1], Nshio Yoshiro[1], Hirota Takayoshi

1. National University Corporation Kochi University

To evaluate the potentials of scallop shells as paleoenvironmental archives, Li/Ca ratio and other geochemical data were obtained using LA-ICP-MS for the *Pecten albicans* specimen (KSG-th001) collected alive on April 29, 2011, from Tosa Bay, and was analyzed in relation to the seasonal changes of environmental parameters including water temperature and Chlorophyll *a* (Hirota and Ichikawa, 2012). In the analysis, fine striae on the left valve of *P. albicans*, were used as daily growth marker.
As a result, the analyzed specimen displayed overall higher rate of shell growth from spring to summer, while shell growth slowed down in fall and winter in 2010. A white band (annual ring) on the generally brown left valve corresponds to the lower rate interval of shell growth. However, another lower shell growth interval is recognized between spring (ca. 50 days) and late summer (ca. 20 days). This corresponds to the lower water temperature interval in late June and early July at 100 m depth in Tosa Bay, which is interpreted as representing upwelling associated with anticlockwise rotational current in Tosa Bay when the Kuroshio current became close to the shore.
These microgrowth patterns of the shell of *Pecten albicans* displayed a close similarity to the Li/Ca profile. Li enrichment in scallop shells is considered to have originated from the frustules of edible species in the digestive tract of scallops, and Li/Ca ratio of *P. maximus* in a bay in France was proposed as a proxy of timing and magnitude of diatom bloom (Thébault and Chauvaud, 2013). Our study confirms the validity of Li/Ca in scallop shells as a proxy of diatom bloom for different scallop species in a distant biogeographic province.
This study was performed under the cooperative research program of Center for Advanced Marine Core Research (CMCR), Kochi University Accept No.18B060 .

Keywords: Li/Ca, Pecten albicans, daily growth increment, seasonal change, plankton bloom

©2019. Japan Geoscience Union. All Right Reserved. 

# Geological reconstruction of Antarctic Ice Sheet deglaciation on Soya Coast, East Antarctica since the Last Glacial Maximum

*Moto Kawamata[1], Yusuke Suganuma[2,1], Koichiro Doi[2,1], Takanobu Sawagaki[3], Akihisa Hattori[1]

1. Department of Polar Science, School of Multidisciplinary Science, SOKENDAI (The Graduate Unversity for Advanced Studies), 2. National Institute of Polar Research, 3. Hosei University

A robust understanding of the history of ice retreat in East Antarctica since the Last Glacial Maximum (LGM) is important in order to validate ice sheet and glacial-isostatic adjustment models and to anticipate their contribution to global sea-level rise. Geomorphological studies and surface exposure dating (SED) will provide direct evidence of the timing and the history of ice retreat on coastal oases and nunatak regions in East Antarctica. Recent studies have reported retreat ages based on surface exposure dating (SED) in Skarvsnes, southern part of Soya Coast, East Antarctica. However, the history of ice retreat remains unclear, because a limited number of surface exposure ages were reported by a previous study, and the results were not interpreted based on field-based geomorphological survey In this study, we reconstruct the last history of ice retreat of the Skarvsnes based on the field-based geomorphological survey and newly obtained SED samples. As results of the field survey, we distinguish three Phase of the ice sheet retreat at the Skarvsnes. The basement rocks at the highest peak (ca. 400 masl) to ca. 250 masl area of the Skarvsnes was weathered extensively, whereas weathering of the basement rocks below ca. 250 masl was relatively weak. The extensively weathered basement rock feature is quite similar to that of the northern part of Soya Coast, where $^{14}C$ dating of fossil shells in the raised beaches suggests that the area had remained ice-free throughout the LGM. Therefore, the differences in weathering feature are thought to indicate the upper limit of ice sheet height at LGM at the Skarvsnes (Phase 1). In the other area of Skarvsnes, glacial striations including cross-cutting set were clearly observed. That is, the ice sheet flow direction was changed with ice sheet thickness thinning under the influence of the basement topography after the LGM (Phase 2). Eventually, the ice sheet was flowing down divided in North and South obstructed by the 362 masl mountain (Shirasuso-Yama) near the current ice sheet margin (Phase 3). Several surface exposure ages were obtained from rocks sampled at sites of different altitudes and distances from the current ice margin. These ages are consistent with the above geomorphological interpretation and it suggests that near current ice sheet margin has been exposed from ice about 9 ka. These data are almost consistent with retreat ages at Mac. Robertson Land in East Antarctica.

Keywords: Glacial geomorphology, surface exposure dating

©2019. Japan Geoscience Union. All Right Reserved. 

# Os isotope record of the Quaternary seawater derived from pelagic sediment in the Lau Basin, western South Pacific Ocean, and its implications for global climate changes

*Yusuke Kuwahara[1], Kazutaka Yasukawa[1,2], Koichiro Fujinaga[2,3], Tatsuo Nozaki[4,3,5,2], Junichiro Ohta[2,6,3], Honami Sato[2,4], Jun-Ichi Kimura[6], Kentaro Nakamura[1], Yasuhiro Kato[3,1,2]

1. Department of Systems Innovation, School of Engineering, The University of Tokyo, 2. Ocean Resources Research Center for Next Generation, Chiba Institute of Technology, 3. Frontier Research Center for Energy and Resources, School of Engineering, The University of Tokyo, 4. Research and Development Center for Submarine Resources, Japan Agency for Marine-Earth Science and Technology , 5. Department of Planetology, Graduate School of Science, Kobe University, 6. Department of Solid Earth Geochemistry, Japan Agency for Marine-Earth Science and Technology

Silicate weathering on land has been considered to play an important role in controlling global climate change through the consumption of atmospheric $CO_2$ on long timescales (>$10^6$ yr). This process has been working as a negative feedback mechanism, which has prevented the Earth system from runaway warming or cooling. However, whether this system works on even shorter-term global climate changes on the timescale of $10^4$–$10^5$ yr such as Quaternary glacial-interglacial cycles is still controversial. In order to constrain the response time of the solid earth to global climate change, we employed the marine Os isotopic ratios ($^{187}Os/^{188}Os$) as a proxy of continental weathering. The marine Os isotopic ratio reflects the relative intensity of two dominant influxes to the ocean; radiogenic continental-derived materials ($^{187}Os/^{188}Os$ = 1.0–1.4) and unradiogenic mantle-like materials (i.e. hydrothermal fluids and cosmic dust) ($^{187}Os/^{188}Os$ = ~0.12). Owing to the contrasting $^{187}Os/^{188}Os$ values between these two influxes, and short residence time of Os in the ocean (~$10^4$ yr), the variability in $^{187}Os/^{188}Os$ of seawater constitutes a sensitive tracer for mantle and continental input into the marine environment. By assuming that the fluxes of mantle-derived materials into the ocean were constant during the Quaternary, we can obtain the fluctuation in the intensity of continental silicate weathering on glacial-interglacial timescales from the marine Os isotope record. Here, we report the marine Os isotopic variations during the glacial-interglacial cycles derived from the pelagic sediment in the Lau Basin, western South Pacific Ocean. In the present work, we targeted metalliferous carbonate as the most suitable media preserving marine Os isotope records at the timing of deposition. This sediment is enriched in hydrothermal Fe-oxyhydroxides that absorb Os in seawater efficiently and deposits rapidly without significant contamination of detrital materials from continents. As the result, we observed a clear fluctuation of the marine $^{187}Os/^{188}Os$ value along with the glacial–interglacial cycles. Based on the marine $^{187}Os/^{188}Os$ record, we also present the fluctuation of riverine Os flux calculated by simple 1-box mass-balance modeling, and its implications for the Quaternary climate change.

Keywords: Glacial–interglacial cycle, Global warming, Osmium isotopic ratio, Carbon cycle, Hydrothermal sediment

©2019. Japan Geoscience Union. All Right Reserved. 

# Rapid glaciation and sea level changes during the Last Glacial Maximum and the deglaciation

*Yusuke Yokoyama[1], Tezer M Esat[9], William G Thompson[10], Alexandar L Thomas[11], Jody W Webster[2], Yosuke Miyairi[1], Chikako Sawada[1], Takahiro AZE[1], Hiroyuki Matsuzaki[1], Jun'ichi Okuno[3], Stewart Fallon[9], Juan-Carlos Braga[12], Marc Humblet[4], Yasufumi Iryu[5], Donald C Potts[13], Kazuhiko Fujita[6], Atsushi Suzuki[7], Hironobu Kan[8]

1. Atmosphere and Ocean Research Institute, University of Tokyo, 2. University of Sydney, Australia, 3. National Institute of Polar Research, 4. Nagoya University, 5. Tohoku University, 6. University of the Ryukyus, 7. The Geological Survey of Japan, AIST, 8. Kyushu University, 9. Research School of Earth Sciences, The Australian National University, Australia, 10. Woods Hole Oceanographic Institute, USA, 11. University of Edinburgh, UK, 12. Universidad de Granada, Spain, 13. University of California Santa Cruise, USA

Studying changes in rates and magnitudes of glaciations/deglaciations during the past is a key to understand global climate system. The Last Glacial Maximum (LGM), centered around 20,000 years ago, as well as period after the LGM, therefore, represents key period to investigate. Sea level observations from sites far from the former ice sheets (far-field) are well suited due to the relatively small influence of surface deformation caused by glacio-hydro-isostatic adjustments (GIA). Australian coastlines are located in such regions and were targeted in this study of sea level changes over the past 30,000 years. The sites are situated off the North Eastern and North Western coasts of Australia respectively the Great Barrier Reef (GBR) and Bonaparte Gulf. Over thirty fossil reef cores were obtained from GBR shelf edge and two transects in northern and southern sites and >1,000 radiometric dating were conducted, in combination with detailed sedimentogic and biologic studies (Yokoyama et al., 2018). GIA modeling was also conducted to deduce global mean sea level (GMSL) from relative sea level records obtained from these regions. The results show that the LGM started when GMSL abruptly dropped by about 40 metres at around 31,000 years ago. The sea level at the shelf edge of the Great Barrier Reef then dropped by around 20 metres between 22,000 and 21,500 years ago, to -118 metres below the present and similar changes are observed in Bonaparte Gulf samples. Sea level began to rise just after the full extent of the LGM, consistent with previous studies. The LGM GMSL obtained from our study is about -125 to -130 metres. Sea level records from the North Australian coasts suggest that glaciers may have behaved more dynamically during the LGM than previously thought. The GBR had been existed despite from severe environmental changes during the last 30,000 years (Webster et al., 2018).

References:
Yokoyama et al. (2018) Nature, v559, p603-607
Webster, Yokoyama et al (2018) Nature Geoscience, v11, p426-432

Keywords: Sea level, ice sheet, the last glacial maximum

©2019. Japan Geoscience Union. All Right Reserved. 

[J] Oral | M (Multidisciplinary and Interdisciplinary)：M-IS Intersection

Thu. May 30, 2019 10:45 AM - 12:15 PM JST | Thu. May 30, 2019 1:45 AM - 3:15 AM UTC | 304 3F

## [M-IS19] Paleoclimatology and paleoceanography

convener:Yusuke Okazaki(Department of Earth and Planetary Sciences, Graduate School of Science, Kyushu University), Akira Oka(Atmosphere and Ocean Research Institute, The University of Tokyo), Michinobu Kuwae(Center for Marine Environmental Studies), Hitoshi Hasegawa(Faculty of Science and Technology, Kochi University), Chairperson:Yusuke Okazaki

Past environmental changes and events at multi-decadal to tectonic timescale toward an understanding of Earth climate system by an integration of terrestrial and marine proxy studies and numerical modeling will be discussed. At JpGU2019, a series of presentations on present and future climate and environmental changes from paleo-perspective will be held. We welcome a variety of paleo-environmental studies from a wide range of background. We hope that this session will provide an opportunity to promote communication between participants from multidisciplinary field.

10:45 AM - 11:00 AM JST | 1:45 AM - 2:00 AM UTC

[MIS19-23] Long-chain alkenediones found from marine sediments and their unsaturation ratios: key compounds to study the evolution of alkenone biosynthetic pathway?

*Satoshi Furota[1], Hideto Nakamura[2], Ken Sawada[3] (1.Department of Biogeochemistry, Japan Agency for Marine-Earth Science and Technology (JAMSTEC), 2.Faculty of Science, Osaka City University, 3.Department of Earth and Planetary Sciences, Faculty of Science, Hokkaido University)

11:00 AM - 11:15 AM JST | 2:00 AM - 2:15 AM UTC

[MIS19-24] **Geomorphic and pedogenic forcing on the distribution of organic matter from vegetation to soil- a concern for paleoenvironment studies**

*Biswajit Roy[1], Kanva Goyal[1], Prasanta Sanyal[1] (1.Indian Institute of Science Education Research Kolkata)

11:15 AM - 11:30 AM JST | 2:15 AM - 2:30 AM UTC

[MIS19-25] Sea surface salinity of the Kuroshio Current along the Nansei Islands in the mid-Holocene inferred from fossil corals

*Kohki Sowa[1], Chuki Hongo[2], Kentaro Tanaka[3], Takuma Fujii[4], Saburo Sakai[1], Kosei E. Yamaguchi[6,5] (1.Japan Agency for Marine-Earth Science and Technology, 2.Ryukyu University, 3.The University of Tokyo , 4.Kagoshima University, 5.Toho University, 6.NASA Astrobiology Institute)

11:30 AM - 11:45 AM JST | 2:30 AM - 2:45 AM UTC

[MIS19-26] An ocean-dynamic model for the periodic inflow of Tsushima Current in the early Holocene

*Atsuhiko Isobe[1] (1.Research Institute for Applied Mechanics, Kyushu University)

11:45 AM - 12:00 PM JST | 2:45 AM - 3:00 AM UTC

[MIS19-27] Centennial to millennial scale variability of the Aleutian Low and Westerly Jet during the Holocene

*Kana Nagashima[1], Naomi Harada[1] (1.Japan Agency for Marine-Earth Science and Technology, Research and Development Center for Global Change)

12:00 PM - 12:15 PM JST | 3:00 AM - 3:15 AM UTC

[MIS19-28] **Monsoon-related errors in paleotemperature estimation based on leaf margin analysis in central Japan**

*Yuqing Wang[1], Arata Momohara[1], Yongjiang Huang[2] (1.Graduate School of Horticulture, Chiba University, 2.Key Laboratory for Plant Diversity and Biogeography of East Asia, Kunming Institute of Botany, CAS)

# Long-chain alkenediones found from marine sediments and their unsaturation ratios: key compounds to study the evolution of alkenone biosynthetic pathway?

*Satoshi Furota[1], Hideto Nakamura[2], Ken Sawada[3]

1. Department of Biogeochemistry, Japan Agency for Marine-Earth Science and Technology (JAMSTEC), 2. Faculty of Science, Osaka City University, 3. Department of Earth and Planetary Sciences, Faculty of Science, Hokkaido University

Long-chain alkenones ($C_{37}$ to $C_{39}$ alkenones) are characteristic compounds produced by haptophyte, and their unsaturation ratios in marine sediments have been used as a proxy for sea surface temperature (SST). Paleocenographic studies using the alkenone proxies are based on the physiological features of the modern alkenone producers such as *Emiliania huxleyi* and *Gephyrocapsa oceanica*. However, these species firstly occurred at ca. 0.29 Ma and ca. 1.85 Ma, respectively, and thus, understandings of the evolutional variations in the alkenone biosynthetic pathway is important to apply the alkenone proxies to the older age. In our recent study, $C_{38:2}$ alkenedione was found in the Miocene to Pliocene marine sediments (Furota et al., 2016). This compound was interpreted to be produced by ancient alkenone producers, because (1) the molecular structure resembles to those of the alkenones, (2) it has not been detected from the extant alkenone producers and sediments, and (3) the relative abundance of the alkenedione to alkenones were significantly higher in the older sediments. Therefore, the alkenedione presumably is a key compound to study the evolutional changes in the biosynthetic pathway of alkenones.
We analyzed the alkenones and alkenediones in the hemipelagic sediments recovered from the NE Atlantic during the IODP exp. 339 to evaluate the variations in their compositions at 100,000-year scale from the late Miocene to Pleistocene. We measured using gas chromatography–flame ionization detector (GC–FID) and GC–mass spectrometry (GC–MS) equipping with a mid-polarity capillary column (VF-200 ms). The GC analysis using the mid-polarity column makes the peak shapes sharp and achieves the well chromatographic separations in the analyses of long-chain alkenones, and thus, several recent studies applied this technique (Longo et al., 2013; Furota et al., 2016).
The long-chain alkenones and the $C_{38}$ alkenediones were detected from all the study samples. Interestingly, the carbon numbers of the alkenediones are only $C_{38}$ in contrast to the alkenones. Mass fragmentogram shows that the $C_{38}$ alkenedione has a methyl-ketone and ethyl-ketone groups at the each terminals of the carbon chain. In addition to $C_{38:2}$ alkenedione as reported previously, we firstly identified tri-unsaturated ($C_{38:3}$) alkenedione in the late Pliocene–Pleistocene sediments.
The relative abundances of the $C_{38}$ alkenediones to alkenones were significantly higher in older sediments, and gradually decreased from the Miocene to Pleistocene. These results support the interpretation that the alkenediones could be produced by the ancient alkenone producers, and imply that those producers decreased from the Miocene to Pleistocene. The unsaturation ratios of $C_{38}$ alkenediones, defines as $C_{38:2}/(C_{38:2} + C_{38:3})$, highly correlate with the unsaturation ratios of the $C_{37}$ alkenones ($U^{K'}_{37}$) ($R^2 = 0.85$). This fact strongly suggests that the alkenediones had a similar biological function and biosynthetic pathway related to the alkenones. Furthermore, the carbon number of alkenediones ($C_{38}$) is averaged one for those of alkenones ($C_{37}$–$C_{39}$), and the positions of ketone groups are equal to those of alkenones. From these results, we conclude that the $C_{38}$ alkenedione had the similar functions with the alkenones, and might be produced by primitive alkenone biosynthetic pathway.

References

Furota et al. (2016) Org. Geochem. 101, 166–175.

©2019. Japan Geoscience Union. All Right Reserved. 

Longo et al. (2013) Org. Geochem. 65, 94-102.

Keywords: Alkenone, Alkenedione, Paleoceanography

©2019. Japan Geoscience Union. All Right Reserved. 

# Geomorphic and pedogenic forcing on the distribution of organic matter from vegetation to soil- a concern for paleoenvironment studies

*Biswajit Roy[1], Kanva Goyal[1], Prasanta Sanyal[1]

1. Indian Institute of Science Education Research Kolkata

The $\delta^{13}C$ values of soil organic matter (SOM) have been used to reconstruct the abundance of $C_3$ and $C_4$ plants. However, the intimate connection of distribution of vegetation with geomorphic processes and landforms may impart different $\delta^{13}C$ value in the contemporaneous vegetation. Such variation would also get registered in the organic matter composition of the soil, with an erroneous assumption of a significant change in $C_3$ and $C_4$ abundance. Therefore, it is important to understand the effect of lateral variation in riverine geomorphic architecture and its impact on the $\delta^{13}C$ value of vegetation and soil. In this study, a lateral transect (6 km) of an undulatory geomorphic surface of north-south trending lateritic alluvium of South Bengal (India) was considered to unveil the effect of topography, and active channel distance on the contemporaneous vegetation and soil. A variation of ca. 50‰ is observed in the n-alkane H-isotopic composition ($\delta D_{C31}$) of the dominating tropical deciduous species (Sal- *Shorearo busta*). The $\delta^{18}O$ value of the groundwater and the river water was analysed to understand the source of water for the tropical trees. The D/H ratio suggests that the vegetation near the active channel was mostly influenced by the river water (enriched) and in distal areas by the groundwater (depleted). Preliminary study on the $\delta^{13}C$ values of the Sal species suggests an enrichment of ca. 7‰ away from the active river channel. The difference is attributed to the change in water-availability, canopy, topography, and vegetation density that varied along the transect. Disparity in the efficiency of water use was observed in the long chain n-alkane average chain length (ACL) and carbon preference index (CPI) distribution. The higher ACL (>29) and CPI (>2) values are mostly associated with the badlands or upland soil environment with very low moisture availability. Preservation of the contemporaneous vegetation signals in the litter layer was regulated by the geomorphology, vegetation density, and the soil texture. The upland, and the distal areas with sparse vegetation tend to preserve more positive $^{13}C/^{12}C$ ratio (−24‰) compared to the lowland with well-developed soils (−28‰). The upland and distal soils, with a coarser texture, suggests faster decomposition of OM (TOC% <0.2) due to higher percolation and soil aeration; whereas in fine-textured lowland soils depleted (−4‰) and high TOC% (>0.5) is observed. Further, due to continuous abrasion by the riverine process, the TOC is also low in the soils adjacent to the active river. The nitrogen isotopic composition ($\delta^{15}N_{SOM}$) increases as alteration/decay or leaching of SOM proceeds. The faster decomposition and microbial processing of SOM in upland and distal area soils registered higher $\delta^{15}N$ (+4‰) values whereas lower values are registered in low-lying areas. This geomorphic and pedogenic effect on the plant-soil system may result in ambiguous interpretation about the past vegetation and thus warrants detail vegetation, geomorphic and physical or chemical characterisation of the soil before employing it as a paleo-record archive.

Keywords: Vegetation, Soil organic matter, Geomorphology, Pedogenesis

©2019. Japan Geoscience Union. All Right Reserved. 

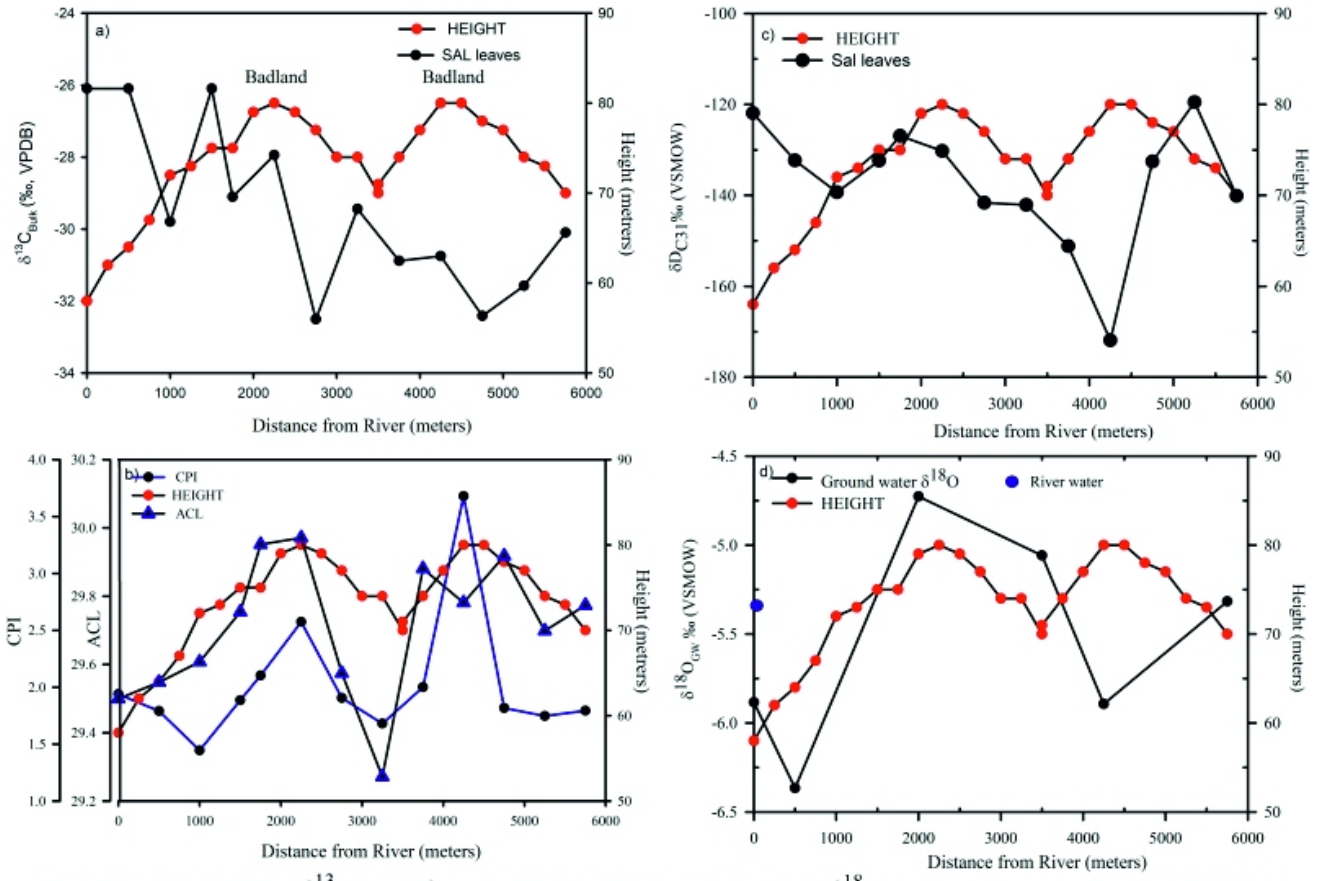


Fig. 1. Variation in the: SAL a) $\delta^{13}C_{Bulk}$ , b) $\delta D_{C31}$, c)CPI and ACL value; and Groundwater $\delta^{18}O_{GW}$ value along the lateral transect of the river.

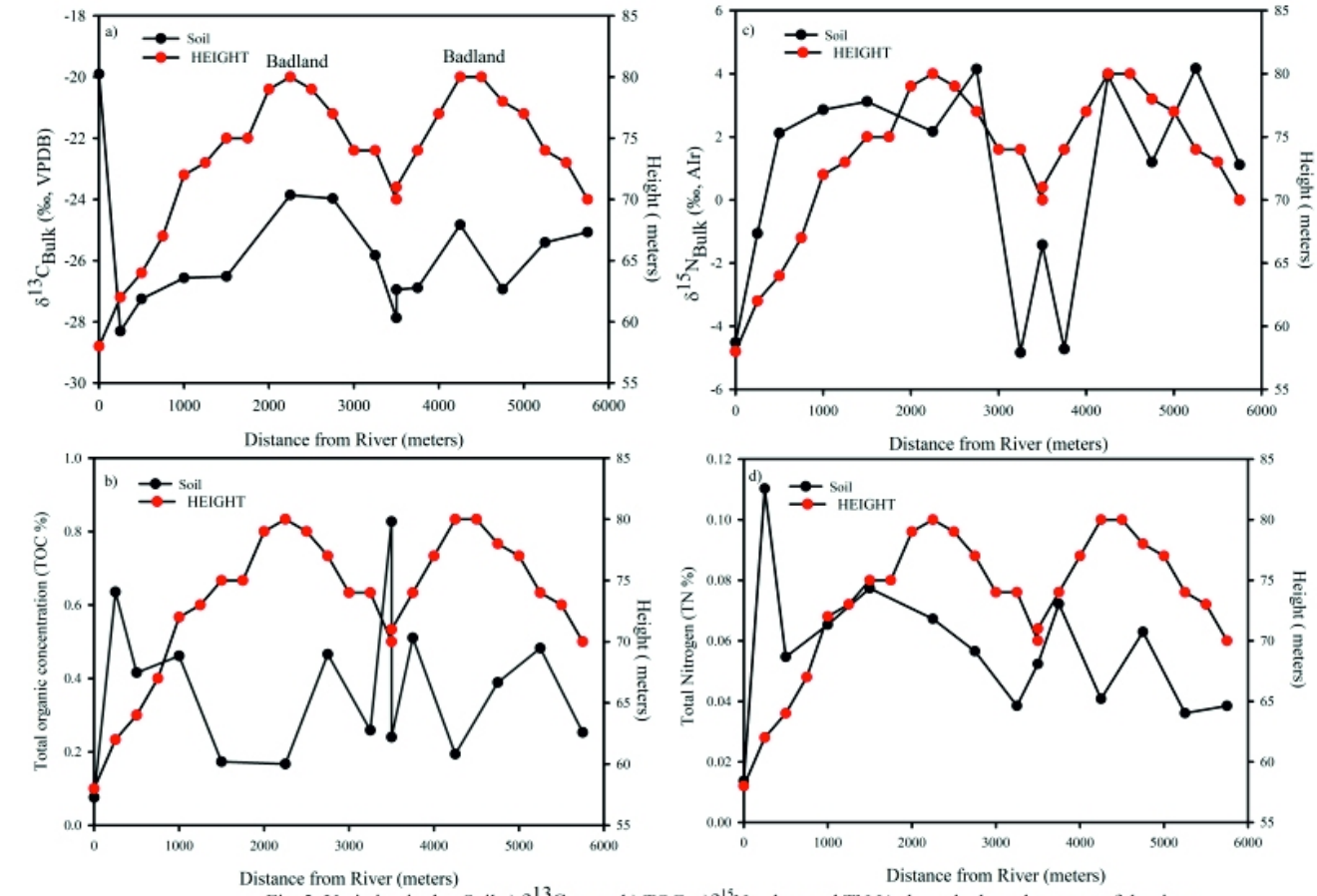


Fig. 2. Variation in the: Soil a) $\delta^{13}C_{Bulk}$ , b) TOC, c)$\delta^{15}N$ value; and TN % along the lateral transect of the river.

©2019. Japan Geoscience Union. All Right Reserved. 

# Sea surface salinity of the Kuroshio Current along the Nansei Islands in the mid-Holocene inferred from fossil corals

*Kohki Sowa[1], Chuki Hongo[2], Kentaro Tanaka[3], Takuma Fujii[4], Saburo Sakai[1], Kosei E. Yamaguchi[6,5]

1. Japan Agency for Marine-Earth Science and Technology, 2. Ryukyu University, 3. The University of Tokyo , 4. Kagoshima University, 5. Toho University, 6. NASA Astrobiology Institute

Sea surface salinity (SSS), which is the parameters of water mass properties, is one of the crucial tracers for reconstructing water motion and climate system. After the mid-Holocene, a period roughly from 7000 to 5000 years ago, freshening of seawater in the Western Pacific has been reported, and the cause of the salinity variation is under discussion (e.g. Stott *et al.*, 2004). The distribution of annual-mean salinity in the Northwest Pacific is space-dependent on factors such as depth, longitude, and latitude. Therefore, to understand the cause of the freshening, more constraining salinity conditions in time and space are needed. However, most research was limited to tropical areas.

The Kuroshio Current comes from the North Equatorial Current and cultivates the coral ecosystems of the subtropical, temperate area along the Nansei Islands (N24°-31°). Therefore, the Nansei Islands provide a latitudinal constraint to the paleo SSS variation. The $\delta^{18}O_{seawater}$ estimated from $\delta^{18}O$ and Sr/Ca in coral skeletons enables reconstruction of the seasonal SSS for shallow areas. Previous studies reconstruct SSS at Kuroshio Current only for Kikai Island (28°N, 130°E), which is off the main Kuroshio Current. To discuss spatial distribution of SSS during the mid-Holocene, further SSS data at different latitudes along the main Kuroshio Current area of the Nansei Islands are useful.

This study shows SSS for Okinawa Island (26°N, 128°E) and Takara Island (29°N, 129°E) during the mid-Holocene using modern and fossil coral cores. The $^{14}C$ age is 5400±140 cal. yr BP (Okinawa Island) from fossil *Porites* coral and 6180±180 cal. yr BP (Takara Island) from *Acropora* coral, which was collected near the coring site of the fossil *Porites* coral. For Okinawa Island, the seasonal $\delta^{18}O$ of fossil *Porites* coral (~26-year, N=1) averages -4.36‰, which is ~0.54‰ higher than that of modern coral (~5-year, N=2). XRD analysis and SEM observation imply good preservation of coral skeletons. The average extension rate > 6 mm suggests minor kinetic isotopic effect related to skeletal growth. Previous studies suggested that sea surface temperatures of the Kuroshio Current have been consistent during the past 7500 years, inferred from research on sediment cores (e.g. Lo *et al.* 2013). These imply that SSS was slightly higher in the mid-Holocene than today, at Okinawa Island. In this presentation, we will discuss SSS along the Nansei Island in the mid-Holocene using additional $\delta^{18}O$ and Sr/Ca analyses at Okinawa and Takara Island.

*References*

Stott *et al.* (2004) Decline of surface temperature and salinity in the western tropical Pacific Ocean in the Holocene epoch. *Nature* 431, 56-59.

Lo *et al.* (2013) Persistent sea surface temperature and declined sea surface salinity in the northwestern tropical Pacific over the past 7500 years. *Journal of Asian Earth Sciences* 66, 234-239.

Keywords: Salinity, Kuroshio Current, Mid-Holocene, Fossil coral, Nansei Islands

©2019. Japan Geoscience Union. All Right Reserved. 

# An ocean-dynamic model for the periodic inflow of Tsushima Current in the early Holocene

*Atsuhiko Isobe[1]

1. Research Institute for Applied Mechanics, Kyushu University

In the early Holocene, the Tsushima Current was a periodic inflow into the Sea of Japan opened to the North Pacific, and thereafter became a steady throughflow after 8,000 years from the present (Oba et al., 1991, Oba, 2006). However, we met some resistance to accept this periodic-inflow idea from ocean dynamics, because the Tsushima Current has been recognized as a linear bypass flow which separates from the subtropical gyre (Minato & Kimura, 1980). Thus, the Tsushima Current could not be a periodic flow unless the subtropical gyre had fluctuated, or unless the Tsushima Strait was periodically opened and closed to the North Pacific. We here proposed an ocean dynamic model in which a periodic inflow generated from the steady subtropical gyre by using a non-linear model based on an island rule in Kida & Qiu (2013). We demonstrate that the volume transport of the Tsushima Current has two solutions which were alternatively revealed in line with the transition of the environment which might appear around the shallow Tsushima Strait in the early Holocene.

Keywords: Tsushima Current, periodic inflow, nonlinear model

©2019. Japan Geoscience Union. All Right Reserved. 

# Centennial to millennial scale variability of the Aleutian Low and Westerly Jet during the Holocene

*Kana Nagashima[1], Naomi Harada[1]

1. Japan Agency for Marine-Earth Science and Technology, Research and Development Center for Global Change

The Aleutian Low (AL), the semi-permanent low-pressure system located over the Gulf of Alaska, is critically linked to environmental change in the North Pacific and surrounding continental areas. At timescales that exceed the recent instrumental record of the last 100 years, the AL intensity has been reported to vary on centennial to millennial scales from various proxy records (e.g., Anderson et al., 2005, 2016; Fisher et al., 2008; Jones et al., 2014). However, the ultimate trigger of these intensity changes has not been systematically studied.

Recent meteorological records showed that the Westerly Jet (WJ) over East Asia and the North Pacific links strongly to the AL intensity and position through changes in cyclogenesis, monsoon, and storm track activity (e.g. Lau, 1998; Nakamura et al., 2002; Nakamura and Shimpo, 2004). According to Lau (1988), southward displacement of the WJ axis and associated storm track path over the North Pacific results in a southeastward shift and intensification of the AL. At longer timescales, however, the interactions between the AL and the WJ are virtually unknown. This study examines millennial- and centennial-scale linkages between the AL and WJ during the Holocene to better understand the long-term nature of their interaction. We also introduce WJ records from the Southern Hemisphere, because the WJ path in both the Northern and Southern Hemispheres trace the expansion and shrinkage of the Hadley Cell circulation, which helps to understand changes in North Pacific atmospheric circulation.

The proxy records of the AL and WJ revealed millennial-scale coupling of the AL-WJ path with weakened AL and poleward WJ shifts in both hemispheres during 7–5.2 and 2.8–1.2 ka, and an intensified AL and equatorward shift of the WJ path during 5.2–2.8 ka and 1.2 ka onward (Nagashima et al., submitted to Quaternary Research). Centennial scale AL intensification and equatorward shifts of the WJ path in both hemispheres also appeared in the proxy records. Periods of centennial and millennial-scale AL maxima and equatorward shifts of the WJ correlate well with periods of solar activity minima, suggesting solar activity has played a primary role in the generation of the atmospheric circulation changes, possibly through dynamic Hadley cell changes (Nagashima et al., submitted to Quaternary Research).

Keywords: Holocene, Aleutian Low, Westerly Jet, Solar activity

©2019. Japan Geoscience Union. All Right Reserved. 

# Monsoon-related errors in paleotemperature estimation based on leaf margin analysis in central Japan

*Yuqing Wang[1], Arata Momohara[1], Yongjiang Huang[2]

1. Graduate School of Horticulture, Chiba University, 2. Key Laboratory for Plant Diversity and Biogeography of East Asia, Kunming Institute of Botany, CAS

Paleotemperature reconstruction has important implications for a better understanding of present climate change. Among various paleotemperature estimation methods, Leaf Margin Analysis is a method that has been widely used by paleobotanist. In the modern flora, former researchers found that the percentage of the species with untoothed leaf margin in total woody dicot species of a flora (untoothed%) is strongly correlated to mean annual temperature (MAT). Based on this phenomenon, equations showing relationships between untoothed% and MAT have been used in paleotemperature estimation proposed as the Leaf Margin Analysis. However, untoothed%-MAT relationships are inconsistent among different regions according to previous studies. To date, eight different untoothed%-MAT equations have been proposed for different regions, although several samples from Japan are included, these sites were only obtained from limited areas close to the Pacific Ocean. However, considering various local climate conditions caused by the complex topography in Japan along with the different influence of summer and winter monsoon, the untoothed%-MAT relationship may vary among different areas in Japan, which cannot be reflected in the formerly published equations.

In this study, we aim to detect the untoothed%-MAT relationship in woody floras of central Japan. Two research areas with different climate conditions were chosen: The Pacific Ocean coastal areas and the Sea of Japan coastal areas. Based on the climate data, the Pacific Ocean coastal areas are characterized by less snow condition and higher summer precipitation affected by the activity of the East Asian Summer Monsoon. While the Sea of Japan coastal areas are characterized by heavy snow in winter, which is formed under the influence of Tsushima warm current in the Sea of Japan with East Asian Winter Monsoon, and grown season precipitation in this zone is much lower than the Pacific Ocean coastal areas.

We found that the untoothed%-MAT relationships of the two research areas are obviously different. In the Pacific Ocean coastal areas, a significant positive untoothed%-MAT relationship was detected. Compare to the other regions of the world, floras from central Japan include more species characterized by toothed-margin leaf at a given mean annual temperature. While in deep snow areas along the Sea of Japan, the untoothed%-MAT relationship becomes unclear with the effect of deep snow cover.

According to our results, paleotemperature estimated by the Leaf Margin Analysis of Japanese fossil floras may include inadequacy. The heavy snow condition along the Sea of Japan began since the middle Early Pleistocene, thus fossil floras of interglacial stages younger than that of these areas is not suitable to do the Leaf Margin Analysis. For Japanese fossil localities from areas without thick snow cover, because the untoothed%-MAT relationship of Japanese flora deviates from other regions of the world, applying these fossil floras into the formerly published untoothed%-MAT relationships will receive inaccurate paleotemperature data.

©2019. Japan Geoscience Union. All Right Reserved. 

[J] Poster | M (Multidisciplinary and Interdisciplinary)：M-IS Intersection

Thu. May 30, 2019 3:30 PM - 5:00 PM JST | Thu. May 30, 2019 6:30 AM - 8:00 AM UTC | Poster Hall International Exhibition Hall8, Makuhari Messe_23

## [M-IS19] Paleoclimatology and paleoceanography

convener:Yusuke Okazaki(Department of Earth and Planetary Sciences, Graduate School of Science, Kyushu University), Akira Oka(Atmosphere and Ocean Research Institute, The University of Tokyo), Michinobu Kuwae(Center for Marine Environmental Studies), Hitoshi Hasegawa(Faculty of Science and Technology, Kochi University)

Past environmental changes and events at multi-decadal to tectonic timescale toward an understanding of Earth climate system by an integration of terrestrial and marine proxy studies and numerical modeling will be discussed. At JpGU2019, a series of presentations on present and future climate and environmental changes from paleo-perspective will be held. We welcome a variety of paleo-environmental studies from a wide range of background. We hope that this session will provide an opportunity to promote communication between participants from multidisciplinary field.

### [MIS19-P01] Orbital-scale changes in redox condition and biogenic silica/detrital fluxes of the Jurassic Radiolarite: Possible link with glaciation?

*Masayuki Ikeda[1] (1.Shizuoka University)

### [MIS19-P02] Evaluation of hinterland weathering and paleoclimate of the Cretaceous strata in the Sichuan basin, central China

*Tenichi Cho[1], Hideaki Mantani[1], Tohru Ohta[1], Gang Li[2] (1.Waseda University, 2.Nanjing Institute of Geology and Paleontology)

### [MIS19-P03] Productivity-induced lacustrine bedded chert formation in the Eocene Green River Formation

*Ryusei Kuma[1], Hitoshi Hasegawa[2], Koshi Yamamoto[1], Hidekazu Yoshida[1], Masayuki Ikeda[3], Nagayoshi Katsuta[4], J. Whiteside[5] (1.Nagoya University, 2.Kochi University, 3.Shizuoka University, 4.Gifu University, 5.Southampton University)

### [MIS19-P04] Extraction of the sedimentary cycles and application of cyclostratigraphy to the Middle Miocene Onnagawa Formation in Yashima District, Akita Prefecture, Japan

*Jumpei Yoshioka[1], Ryuji Tada[1,3], Kenji Marc Raymond Matsuzaki[2], Toshihiro Tada[1], Aki Sakuma[1], Yusuke Umemiya[1], Shunsuke Kurokawa (1.Department of Earth and Planetary Science, the University of Tokyo, 2.Atmosphere and Ocean Research Institute, the University of Tokyo, 3.Yunnan University)

### [MIS19-P05] Pliocene magneto–oxygen isotope stratigraphy from the Anno Formation, Awa Group, central Japan

*Yuki Haneda[1], Makoto Okada[1] (1.College of Science, Ibaraki University)

### [MIS19-P06] Planktonic foraminiferal assemblage and paleoceanography of the Plio-Pleistocene sequence at IODP Site U1499 in the northern South China Sea

*Mizuki Kitamura[1], Akira Furusawa[1], Hiroki Hayashi[1] (1.SHIMANE University)

### [MIS19-P07] Reconstruction of the surface water mass fluctuation during the late Pliocene to early Pleistocene based on planktonic foraminiferal fossils from the Mera Formation, Chikura Group, in the southernmost part of the Boso Peninsula

*Makoto Okada[1], Daisuke Hasegawa[2] (1.Department of Earth Sciences, Faculty of Science, Ibaraki University, 2.Graduate School of Scinece and Engineering, Ibaraki University)

### [MIS19-P08] Centennial-scale bioproductivity changes during the earliest Middle-Pleistocene

*Waka Fujii[1], Masayuki Hyodo[1], Shigehiro Katoh[2], Yosuke Miyairi[3], Haruka Yamaguchi[1], Yusuke Yokoyama[3] (1.Kobe University, 2.Hyogo Museum of Nature and Human Activities, 3.University of Tokyo)

[MIS19-P09] Development of new-paleoceanographic proxies based on oxygen isotope analysis of sponge spicule

*Hitomi Uchimura Wakaki[1], Akira Ijiri[2], Minoru Ikehara[1], Sangmin Hyun[3] (1.Center for Advanced Marine Core Research, Kochi University, 2.Japan Agency for Marine-Earth Science and Technology, 3.Korea Institute of Ocean Science & Technology)

[MIS19-P10] A system for automatic collection of specific microfossil species using a deep learning classification

*Takuya Itaki[1], Yosuke Taira[2], Naoki Kuwamori[2], Toshinori Maebayashi[3], Satoshi Takeshima[4], Kenji Toya[4] (1.Geological Survey of Japan, AIST, 2.NEC Corporation, 3.Microsupport Co.Ltd, 4.Mitani-Corporation)

[MIS19-P11] Towards reconstructing environmental conditions related to Australian Great Barrier Reef initiation

*Stephen Obrochta[1], Wataru Miwa[1], Kotaro Shirai[2], Yusuke Yokoyama[2], Yosuke Miyairi[2], Jody Webster[2,3], Albert Hine[4] (1.Akita University, 2.University of Tokyo Atmosphere and Ocean Research Institute, 3.University of Sydney, 4.University of South Florida College of Marine Science)

[MIS19-P12] An 8,000-year climate record from Lake Motosu, Japan: Implications for the East Asian Monsoon

Sarah McDonlad[3], Jonathan Tyler[3], *Stephen Obrochta[1], Yusuke Yokoyama[2], Yosuke Miyairi[2], Kosuke Ota[2] (1.Akita University, 2.University of Tokyo Atmosphere and Ocean Research Institute, 3.Department of Earth Sciences, The University of Adelaide)

[MIS19-P13] Environmental changes in northern Mongolia in During the Late Pleistocene: chemical analyses of lacustrine sedimentary sequences in Darhad basin

Yumiko Ohno[1], Sayuri Naito[1], *Nagayoshi Katsuta[1], Takuma Murakami[3], Shinya Ochiai[2], Noriko Hasebe[2], Shin-ichi kawaka[4] (1.Faculty of Education, Gifu University, 2.Institute of Natural and Environmental Technology, Kanazawa University, 3.Horonobe Research Inst. for the Subsurface Environment, 4.Faculty of Education, Gifu Shotoku Gakuen University)

[MIS19-P14] Paleoenvironmental changes recorded in Orog Lake, southwestern Mongolia during MIS 3 and its relationship with *Homo sapiens*'s migration into northern Asia

*Hitoshi Hasegawa[1], Nanase Noma[1], Nagayoshi Katsuta[2], Masafumi MURAYAMA[3], Toru Tamura[4], Masami Izuho[5], Niiden Ichinnorov[6], Davaasuren Davaadorj[7], Noriko Hasebe[8], Miho Sasaoka[9], Masao Iwai[9] (1.Faculty of Science and Technology, Kochi Univ., 2.Faculty of Education, Gifu Univ., 3.Faculty of Agriculture and Marine Science, Kochi Univ., 4.Geological Survey of Japan, AIST, 5.Faculty of Social Sciences and Humanities, Tokyo Metropolitan Univ., 6.Mongolian Academy of Sciences, 7.National University of Mongolia, 8.Institute of Nature and Environmental Technology, Kanazawa Univ., 9.Center for Advanced Marine Core Research, Kochi Univ.)

[MIS19-P15] Reconstruction for water-mass structure of the Okhotsk Sea for the past 1.5 million years based on radiolarian assemblages

*Tatuya Sakamoto[1], Yusuke Okazaki[1] (1.Department of Earth and Planetary Sciences, School of Science, Kyushu University)

[MIS19-P16] Silicoflagellate assemblages in the Okhotsk Sea during the interglacial periods

*Kazuki Egashira[1], Yusuke Okazaki[2], Tatsuhiko Sakamoto[3] (1.Department of Earth and Planetary Sciences, Kyushu University, 2.Department of Earth and Planetary Sciences, Graduate School of Science, Kyushu University , 3.Mie University)

[MIS19-P17] Role of wind stress and sea surface thermal forcing in the formation of the Atlantic meridional overturning circulation at the Last Glacial Maximum

*Akira Oka[1], Kazuki Togawa[1] (1.Atmosphere and Ocean Research Institute, The University of Tokyo)

[MIS19-P18] Comparison of the Kuroshio during LGM simulated by an ocean general circulation model driven by multiple paleoclimate models

*Kensho Ichikawa[1], Haiyan Yang[2], Xinyu Guo[2], Yasumasa Miyazawa[3] (1.Graduate School of Science and Engineering,Ehime University, 2.Center for Marine Environmental Studies,Ehime University, 3.Japan Agency for Marine-Earth Science and Technology)

[MIS19-P19] The changes of the Kuroshio path in the Northwest Pacific since 35ka

*Haiyan Yang[1], Xinyu Guo[1], Ayako Abe-Ouchi[2], Yasumasa Miyazawa[3], Sergey Varlamov[4], Wing-Le Chan[2] (1.Center for Marine Environmental Studies, Ehime University, 2.Atmosphere and Ocean Research Institute, University of Tokyo, 3.Research Institute for Global Change, Japan Agency for Marine-Earth Science and Technology, 4.Application Laboratory, Japan Agency for Marine-Earth Science and Technology)

[MIS19-P20] Temperature reconstruction in the late Pleistocene using fossil terrestrial snails and a stalagmite from an archaeological cave in Okinawa

*Ryuji Asami[1], Rikuto Hondoh[2], Ryu Uemura[3], Ryuichi Shinjo[3], Akihiro Kano[4], Masaki Fujita[5], Shinji Yamasaki[6], Hideko Takayanagi[1], Yasufumi Iryu[1] (1.Graduate School of Science, Tohoku University, 2.Faculty of Science, Tohoku University, 3.Faculty of Science, University of the Ryukyus, 4.School of Science, the University of Tokyo, 5.National Museum of Nature and Science, 6.Okinawa Prefectural Museum and Art Museum)

[MIS19-P21] Silicoflagellate and *Actiniscus* response to meltwater during the last deglaciation in the Alaska margin

*Asuka Tomokawa[1], Yusuke Okazaki[1], Jonaotaro Onodera[2], Keiji Horikawa[3] (1.Department of Earth and Planetary Sciences, Kyushu University, 2.Research and Development Center for Global Change, JAMSTEC, 3.Graduate School of Engineer and Science, University of Toyama)

[MIS19-P22] Application of the ramped pyrolysis $^{14}C$ dating to postglacial sediments from the Alaskan margin, Arctic Ocean

*Kenta Suzuki[1], Masanobu Yamamoto[1,2], Brad Rosenheim[3], Takayuki Omori[4], Leonid Polyak[5] (1.Graduate School of Environmental Science, Hokkaido University, 2.Faculty of Environmental Earth Science, Hokkaido University, 3.College of Marine Science, University of South Florida, 4.The University Museum, The University of Tokyo, 5.Bard Polar and Climate Research Center, Ohio State University)

[MIS19-P23] Utility of sedimentary environmental DNA for indices of past pelagic fish species populations

*Hiromichi Tamai[1], Michinobu Kuwae[2], Hideyuki Doi[3], Toshihumi Minamoto[4] (1.Graduate School of Science and Engineering, Ehime university, 2.Center for Marine Environmental Studies, Ehime university, 3.Graduate School of Simulation Studies, University of Hyogo, 4.Graduate School of Human Development and Environment, Kobe University)

[MIS19-P24] Improvements of extraction methods of sedimentary fish-origin DNA for reconstruction of marine fish communities

*Jun Kurata[1], Hiromichi Tamai[2], Hideyuki Doi[3], Toshihumi Minamoto[4], Michinobu Kuwae[5] (1. department of earth science, Ehime university, 2.Graduate School of Science and Engineering, Ehime university, 3.Graduate School of Simulation Studies, University of Hyogo, 4.Graduate School of Human Development and Environment, Kobe University, 5.Center for Marine Environmental Studies, Ehime university)

[MIS19-P25] The paleotemperature reconstruction during the late-Holocene using the sediment core recovered from the Tokyo Bay, Japan

*Hiroto Kajita[1,2,3,4], Naomi Harada[5], Miyako Sato[5], Nanako Ogawa[1], Yusuke Yokoyama[1,2,4], Chikako Sawada[1], Yosuke Miyairi[1], Masayuki Utsunomiya[3], Atsushi Suzuki[3], Hodaka Kawahata[1,2,3] (1.Atmosphere and Ocean Research Institute, The University of Tokyo, Japan, 2.Department of Earth and Planetary Science, Graduate school of Science, The University of Tokyo, Japan, 3. Research Institute of Geology and Geoinformation, Geological Survey of Japan, National Institute of Advanced Industrial Science and Technology (AIST), Japan, 4.Department of Biochemistry, Japan Agency for Marine-Earth Science and Technology (JAMSTEC), Japan, 5.Research and Development Center for Global Change, Japan Agency for Marine-Earth Science and Technology (JAMSTEC), Japan)

[MIS19-P26] Summer monsoon variability over the past 400 years in Tateyama, Japan, as reconstructed from tree-ring oxygen isotope data

*Masaki Sano[1], Kota Mori[1], Akane Tsushima[2], Zhen Li[3], Koh Yasue[4], Takeshi Nakatsuka[2,3] (1.Faculty of Human Sciences, Waseda University, 2.Nagoya University, 3.Research Institute for Humanity and Nature, 4.Shinshu University)

[MIS19-P27] Eventural Layers of anciant disasters during these 4500 years at Lake Ikeda (Lake Daijya), western coast of Kyushu Island presumed by diatom assemblages in lake deposits

*Kaoru Kashima[1], Tomokazu Mita[1], Yu Fukumoto[3], Tsuyoshi Haraguchi[2], Kazuyoshi Yamada[4] (1.Department of Earth and Planetary Sciences, Kyushu University, 2.Department of Geosicneces, Graduate School of Science, Osaka City University, 3.Ritsumeikan University, 4.Museum of Natural and Environmental History, Shizuoka)

[MIS19-P28] Variability of hemipelagic and event depositions in the Beppu Bay during Holocene

*Tomohisa Irino[1], Airi Maruyama[1], Ken Ikehara[2], Masanobu Yamamoto[1], Michinobu Kuwae[3] (1.Graduate School of Environmental Science, Hokkaido University, 2.Institute of Geology and Geoinformation, National Institute of Advanced Industrial Science and Technology, 3. Center for Marine Environmental Studies, Ehime University)

[MIS19-P29] The composition of laminae in the sediment of Beppu-Bay and potential as annual laminations

*Yoshiaki Suzuki[1], Michinobu Kuwae[2], Kazuno Arai[3], Ken Ikehara[4], Masafumi MURAYAMA[3] (1.Waseda University, 2.Ehime University, 3.Kochi University, 4.AIST)

[MIS19-P30] Simulation of global distribution of Pa/Th using an ocean general circulation model

*Yusuke Sasaki[1], Akira Oka[1] (1.Atmosphere and Ocean Research Institute, The University of Tokyo)

[MIS19-P31] Construction of modern silicoflagellate assemblage dataset in the North Pacific for paleo sea-surface temperature and its application for sediment cores

*Yusuke Okazaki[1], fumiaki nishizono[1], Tanizaki Kyohei[1] (1.Department of Earth and Planetary Sciences, Graduate School of Science, Kyushu University)

[MIS19-P32] Microplastics in surface sediments of the Ariake Bay

Hiroki Sonoda[1], *Yusuke Okazaki[1], Atsuhiko Isobe[2] (1.Department of Earth and Planetary Sciences, Graduate School of Science, Kyushu University, 2.Research Institute for Applied Mechanics, Kyushu University)

# Orbital-scale changes in redox condition and biogenic silica/detrital fluxes of the Jurassic Radiolarite: Possible link with glaciation?

*Masayuki Ikeda[1]

1. Shizuoka University

Orbital forcing has been shown to be a fundamental driver of climate change through both icehouse and greenhouse periods. To reveal the impact of orbital-forcing on the oceanic environment through a greenhouse-icehouse transition, we established ~ 4 Myr-long cyclostratigraphy of the Bajocian-Callovian (Middle Jurassic; ~ 160 Ma) Basal Radiolarites at the Torre De Busi and Corre Di Sogno sections in the Lombardian Basin, N-Italy. Stratigraphic changes in chertabundance (chert/shale thickness ratio) and color (darkness) of Radiolarites show hierarchal periodicities of 8 cm, 16 cm, 40 cm, 160 cm, and ~ 4 m, corresponding to ~ 20 kyr, 40 kyr, 100 kyr, 400 kyr, and ~ 1 Myr cycles based on the biostratigraphic age model. Black cherts in intervals with high chert abundance might reflect oxygen-depleted conditions due to orbital-scale high productivity. On the other hand, black cherts in intervals with low chert abundance (high detrital input) might reflect oxygen-depleted conditions, probably due to orbital-scale sea-level drop and stratification. On 40 kyr and 100 kyr cycles, the anoxic condition occurred in low chert abundance intervals across ~ 8 m above (~ 2 Myr after) the base of the Radiolarites. These results imply that the formation of the restricted basin resulted from tectonic and/or eustatic sea-level drop, which is consistent with increased black chert deposition and redox-sensitive elements abundances (Mo/TOC, Mo/U). Their out-of-phase relationships on the 405 kyr cycle throughout the sequence (~ 4 Myr-long) with increasing amplitude above −8 M level would be caused possibly by tectonic activity, or more likely by glacio-eustatic sea-level changes reported from sequence stratigraphy, similar to those of the Oligocene to Pliocene glacial cycles, but probably with less amplitude.

Keywords: icehouse, greenhouse, orbital cycle

©2019. Japan Geoscience Union. All Right Reserved. 

# Evaluation of hinterland weathering and paleoclimate of the Cretaceous strata in the Sichuan basin, central China

*Tenichi Cho[1], Hideaki Mantani[1], Tohru Ohta[1], Gang Li[2]

1. Waseda University, 2. Nanjing Institute of Geology and Paleontology

Reconstruction of paleoclimate during the Cretaceous Period is important for the understanding of the Earth system operating during the greenhouse conditions. However, information of paleoclimate from continental inland-basins is scarce compared to continental margin marine-basins. This situation is also true in the Asian continent; Cretaceous ecosystem and paleoclimate data are accumulating in the Pacific side, while those of the Asian continental side is lacking. Paleoclimate conditions in Asian inland basins are considered to be equally important in order to elucidate the land-ocean climate system operated during the Cretaceous. In this regard, the present study investigates the geochemistry and clay mineralogy of the Cretaceous mudstones distributed in the Sichuan basin, central China, for the aim of paleoclimate evaluation. The depositional age of studied strata ranges from Berriasian to Maastrichtian. Sediments are mostly fluvial to lacustrine origin, however recently, a broad distribution of aeolian dune sandstones was identified from the Cenomanian to Turonian interval (Li et al., 2016). Before discussing hinterland weathering and paleoclimate, the effect of diagenesis was evaluated, which can alter the geochemical signatures of paleoclimate. The illite crystallinity index indicates that diagenetic effect was moderately high for the analyzed mudstones, and the degree of diagenesis has a high correlation with CaCO3 abundance. Accordingly, CaO wt% abundances are mostly of post-depositional carbonate origin, and thus, CaO derived from carbonates was subtracted from the following discussion of hinterland weathering evaluation. Geochemical weathering indices (e.g., W value) demonstrate a significant increase in hinterland paleoweathering from Berriasian (W=70) to Cenomanian-Turonian (W=95), and then slightly decrease towards the Maastrichtian (W=80). This fluctuation pattern of the weathering indices is concordant with the Cretaceous paleotemperature estimates (e.g., O’ Brien et al., 2017). Therefore, the present result suggests that the hinterland paleoweathering rate in the Sichuan basin was governed by the global temperature changes. The weathering index reached the maximum value of 95 in Cenomanian-Turonian stages. Furthermore, sediments of Cenomanian-Turonian horizons contained abundant kaolinite mineral, which is a product of hydrolysis decomposition of rock-forming minerals. Both lines of evidence suggest that the Sichuan basin was under the tropical and pluvious climate during the Cenomanian-Turonian. However, as mentioned before, the previous study identified aeolian sand dunes from the Cenomanian-Turonian strata. Note that Li et al. (2016) elucidated an arid climate from amalgamated sandstone facies, while the present pluvious climate interpretation is derived from the analysis of intervening piled mudstone facies. When these geological evidences are integrated together, it is reasonable to suggest the development of an alternating pluvious and arid paleoclimate during the Cenomanian-Turonian. The nature and trigger of this extremely oscillating pluvious/arid climate cannot be deduced solely from the present study. However, the timing of this renewed climate system matches with the Cretaceous greenhouse optimum (Cenomanian-Turonian). The development of monsoon-like pluvious/arid paleoclimate in the Sichuan basin is possibly related to the mid-Cretaceous re-configuration in the global climate system.

Keywords: Cretaceous, Continental weathering, Alluval deposits, Desert deposits, XRF, W index

©2019. Japan Geoscience Union. All Right Reserved. 

# Productivity-induced lacustrine bedded chert formation in the Eocene Green River Formation

*Ryusei Kuma[1], Hitoshi Hasegawa[2], Koshi Yamamoto[1], Hidekazu Yoshida[1], Masayuki Ikeda[3], Nagayoshi Katsuta[4], J. Whiteside[5]

1. Nagoya University, 2. Kochi University, 3. Shizuoka University, 4. Gifu University, 5. Southampton University

Rhythmically alternated beds of chert and shale, also called as bedded chert, are commonly observed in marine sedimentary rocks. Recent studies revealed that changes in bed thickness of chert represent orbitally-paced variations in marine productivity and silicate weathering rate (Hori et al., 1993; Ikeda et al., 2017). On the other hand, bedded cherts are occasionally found in lacustrine deposits. Previous study interpreted that formational mechanism of lacustrine bedded chert is linked to the interplay between silica dissolution in alkaline lake waters and its precipitation due to the conversion of lake water’ s pH (e.g. Hesse, 1989). Some studies suggested that the pH of saline and alkaline lake water could have changed by the freshwater input (Eugster, 1967; Eugster 1969). Other study implied that the metabolic processes of cyanobacteria modified the pH of lake water and influenced to the silica precipitation (Behr and Rohricht, 2000). However, convincing evidence of chertification mechanism in lacustrine deposits have not been clarified yet.

In order to elucidate the formation mechanism of lacustrine chert, the present study examined a lacustrine bedded chert succession in the Eocene Green River Formation in northern Utah, USA. We have conducted detailed field survey in the Indian Canyon section in northern Utah. Bedded cherts occur in shallow lake level stage and alternated with dolomite beds with every 5–10 cm in thickness. Elemental mapping by Scanning X-ray analytical microscope (SXAM) reveals that the Ca concentration in dolomite layer, while Si concentration in chert layer, with sharp boundary coincide with lithofacies boundary. Elemental distribution also shows that alternation of chert and dolomite occur in every 1–2 cm in thickness. In addition, fluorescent microscopic inspection reveals that the distribution of Si concentration coincides with the dense accumulation of spherical organic matter. These spheres show the brightest fluorescence carbon shell with similar size (30–40 $\mu$m). The morphology of these spherical organic matter resembles to green algae, such as *Botryococcus braunii*, which are also abundantly preserved in the Green River Formation. Occurrences of algal organic matters in chert layer imply that deposition of algal organic matter could be related with the formation of lacustrine chert.

It is noteworthy that the lake water alkalinity of the Green River Formation is considered to be high (pH>9) because of extensive volcanic activity around Colorado Plateau. These lines of evidence suggested that silica precipitation is possibly caused by decreased pH due to the decaying organic matter (increasing $CO_2$ and/or organic acid) in sediment pore water. Deposition of organic matter can be related to changes in the lake algal productivity. Given that sedimentation rate of the formation in Indian Canyon section is estimated as ca. 10–15 cm/kyr (Smith et al., 2008), observed chert occurrence (1–2 cm and 5–10 cm) yields 67–200 and 333–1000 year’ s cyclicities. Therefore, periodic occurrences of chert beds in the Green River Formation are possibly linked to the centennial-scale changes in the lake algal productivity.

Keywords: lake sediments, Eocene, productivity, chert, silica, pH

©2019. Japan Geoscience Union. All Right Reserved. 

# Extraction of the sedimentary cycles and application of cyclostratigraphy to the Middle Miocene Onnagawa Formation in Yashima District, Akita Prefecture, Japan

*Jumpei Yoshioka[1], Ryuji Tada[1,3], Kenji Marc Raymond Matsuzaki[2], Toshihiro Tada[1], Aki Sakuma[1], Yusuke Umemiya[1], Shunsuke Kurokawa

1. Department of Earth and Planetary Science, the University of Tokyo, 2. Atmosphere and Ocean Research Institute, the University of Tokyo, 3. Yunnan University

Middle Miocene (16.0-11.6Ma) is the time of the second of the three cooling steps during Cenozoic. In this cooling event, siliceous sediments with high organic contents were widely deposited along the North Pacific rim because of high productivity and/or preservation of diatoms. In the northern Japan Sea, those sediments are known as the Onnagawa Formation. It was reported that siliceous rocks in the Onnagawa Fm. showed meter-scale rhythmical bedding reflecting fluctuations in productivity of diatoms and flux of detrital materials. Furthermore, it was also reported that parts of highly siliceous rocks in the Onnagawa Fm. showed centimeter-scale black bands. However, the age and the cause of their occurrence has not been understood.

In this study, we tried to construct a high-resolution and precise age model of the Onnagawa Fm. in the Yashima District by applying cyclostratigraphy to the m-scale rhythmical bedding, that is attributable to the fluctuation of biogenic silica content.

Firstly, a ca. 130m-long continuous composite columnar section was constructed by correlation of 6 sections. This composite columnar section is divided into 5 lithological units, cyclic alternations of marl and interbedded mudstone (Unit A), mudstone with cyclic siliceous rocks intercalations (Unit B), siliceous-mudstone with muddy-porcelanite intercalations (Unit C), bedded muddy-porcelanite with cm-scale black bands (Unit D) and siliceous-mudstone and hard siliceous-mudstone alternations (Unit E).

“Silica rank”, which is defined as degree of siliceousness and divided into 5 grades based on hardness of the siliceous rocks observed in the field and confirmed by XRD analysis, was determined every 10cm for Unit B, Unit C and Unit D. It showed obvious m-scale cyclicities. The silica rank variation for Unit B and Unit C was obviously different from that for Unit D, and it is considered that this difference may reflect either the change in the sedimentation rate or the change in response of sedimentation mechanism to the orbital forcing that results in the lithological change. In order to construct an age model, the silica rank was tuned to $\delta^{18}O$ of benthic foraminifera with age constraints given by microfossil biostratigraphy.

Keywords: the Onnagawa Fm., Miocene, silica rank, cyclostratigraphy

©2019. Japan Geoscience Union. All Right Reserved. 

# Pliocene magneto–oxygen isotope stratigraphy from the Anno Formation, Awa Group, central Japan

*Yuki Haneda[1], Makoto Okada[1]

1. College of Science, Ibaraki University

The Pliocene climate is one of the best analogs for the climate of a globally warmer future. Here, we present a new Pliocene integrated chronostratigraphy from the Anno Formation in the uppermost Awa Group, which is distributed throughout the Boso Peninsula, central Japan, based on paleomagnetic and benthic foraminiferal oxygen isotope records. This new chronostratigraphy provides valuable constraints for paleoceanographic and paleoclimatic studies in the northwestern Pacific Ocean, where the number of paleoceanographic records is limited due to the lack of calcareous microfossils from deep-sea sediment cores, with the exception of some plateaus at water depths above the calcite compensation depth (CCD).

We performed progressive Alternating field and thermal demagnetizations for each specimen in order to remove secondary remanence. Additionally, we conducted thermomagnetic, low-temperature magnetic, magnetic hysteresis, and FORC analyses as rock-magnetic experiments to assess stability of paleomagnetic signal which specimens have acquired. The paleomagnetic and rock-magnetic experiments indicate that primary remanences are carried by magnetite in pseudo-single domain size as detrital remanent magnetization. The progressive AF demagnetization is, however, unsuitable to remove secondary remanence in specimens from polarity transitional horizons due to magnetically hard mineral, such as goethite. Therefore, thermal demagnetization is necessary to obtain primary remanence from the Anno Formation.

Paleomagnetic results by the thermal demagnetization indicate that the Anno Formation corresponds to the period extending from the Nunivak normal polarity subchronozone (4.493–4.631 Ma) to Chron C2An.2n (3.116–3.207 Ma). Although foraminifera are not found in the middle Anno Formation, our oxygen isotope records from the upper and lower Anno Formation demonstrate the recording of glacial–interglacial cycles. However, the amplitude of our $\delta^{18}O$ profile is much larger than that of the LR04 stack, with similar to slightly lower glacial values and much lower interglacial values. This trend is suppressed after 3.4 Ma. These observations imply that the bottom water had lower $\delta^{18}O$ values and/or a warmer water mass during interglacials until 3.4 Ma compared with global average deep-water regions.

Keywords: Pliocene, Boso Peninsula, Anno Formation, Benthic foraminifera, Oxygen isotope stratigraphy, Magnetostratigraphy

©2019. Japan Geoscience Union. All Right Reserved. 

# Planktonic foraminiferal assemblage and paleoceanography of the Plio-Pleistocene sequence at IODP Site U1499 in the northern South China Sea

*Mizuki Kitamura[1], Akira Furusawa[1], Hiroki Hayashi[1]

1. SHIMANE University

The South China Sea (SCS) is a marginal sea located in the tropical zone of the western Pacific with an average depth of ca. 1,140 m. The East Asian monsoon affects the climate system in this area by the prevailing seasonal winds. Such influence of the East Asian monsoon is expected to be stronger during the glacial period and weaker during the interglacial period.
During Internatinal Ocean Discovery Program (IODP) Expedition 367, drilling of Site U1499 was conducted near the outer shelf of the northern SCS in 2017. As an onboard result of this site, sediments from Oligocene to Present were recovered and the upper sequence especially contains abundant foraminiferal fossils. The purpose of the present study is to clarify temporal changes of planktonic foraminiferal assemblage in the northern SCS from approximately 4 to 1 Ma.
As a result, 80 species belonging to 19 genera of planktonic foraminifera were detected. According to multivariate analyses of the foraminiferal assemblage, we determined the temporal change into four stages: Stage A (ca. 4.1 to 3.4 Ma), Stage B (ca. 3.4 to 1.8 Ma), Stage C (ca. 1.8 to 1.45 Ma) and Stage D (ca. 1.4 to 1 Ma). During Stage A, SCS had been stratified by oligotrophic tropical surface water and relatively cold subsurface water with a shallow thermocline. At the next Stage B, the thermocline was deepened and SCS was occupied by a subtropical oligotorophic water. In turn, the thermocline shoaled and subsurface species of planktonic foraminifera were increased during the Stage C. After that, the Stage D is characterized by alternative changes between subtropical surface components and cold-temperate components caused by the glacial-interglacial changes.

Keywords: South China Sea, Planktonic foraminifera, Pliocene, Pleistocene, International Ocean Discovery Program

©2019. Japan Geoscience Union. All Right Reserved. 

# Reconstruction of the surface water mass fluctuation during the late Pliocene to early Pleistocene based on planktonic foraminiferal fossils from the Mera Formation, Chikura Group, in the southernmost part of the Boso Peninsula

*Makoto Okada[1], Daisuke Hasegawa[2]

1. Department of Earth Sciences, Faculty of Science, Ibaraki University, 2. Graduate School of Scinece and Engineering, Ibaraki University

The purpose of this study is to examine whether the cooling event has occurred associate with the NHG (Northern Hemisphere Glaciation) off the Boso peninsula and how the surface water mass has changed with the glacial-interglacial cycle. We carried out analysis of planktonic foraminiferal assemblages at the 57 horizons corresponding to period from 3.0 Ma to 2.2 Ma. We propose 6 phases including the following three distinctive phases based on relative abundance of environmental indicator species.
Phase Ⅱ (2.75-2.65Ma): Transitional water species increased up to 50%. It was a cold environment where the influence of mixed water was strong.
Phase Ⅴ (2.42-2.35Ma): Kuroshio species increased up to 40%, which is the highest value in this study
PhaseⅥ (2.35Ma~):Transitional water species increased to about 50% while repeating amplitude. Therefore, cooling was gradually strengthened in this phase.
Cooling did not proceed unilaterally after 2.7Ma, it occurs again from 2.35Ma after the period when the influence of Kuroshio became temporarily stronger. In addition the glacial-interglacial cycles seem to be affecting composition of planktonic foraminiferal assemblages.

Keywords: Planktonic foraminiferal assemblages, Chikura Group, Northern Hemisphere Glaciation

©2019. Japan Geoscience Union. All Right Reserved. 

# Centennial-scale bioproductivity changes during the earliest Middle-Pleistocene

*Waka Fujii[1], Masayuki Hyodo[1], Shigehiro Katoh[2], Yosuke Miyairi[3], Haruka Yamaguchi[1], Yusuke Yokoyama[3]

1. Kobe University, 2. Hyogo Museum of Nature and Human Activities, 3. University of Tokyo

Elucidation of the mechanism of global warming in the geological time is important, which may lead to understanding of the present global warming. In this study, we conducted paleoenvironmental analyses of sediments to reveal the rapid climate changes across the warmest interval in the Marine Isotope Stage (MIS) 19 interglacial, which is known as an orbital analogue of the Holocene. In particular, we aim at elucidating the mechanism of the repeated bioproductivity proxy (Ca/Ti ratio) changes dominated by bicentennial cycles for a span from about 777 to 775 ka, which was observed in core TB2 from the Chiba Section. Focused on the time span, we conducted pollen analyses using the Osaka Bay 1,700 m core with abundant pollen fossils, and measurements of $^{10}$Be using core TB2. Both cores are stratigraphically correlated with the centennial to millennial scale resolution. The result of pollen analyses revealed that the proportion of evergreen *Quercus* (*Cyclobalanopsis*), a warm proxy, began at about 777 ka to increase with bicentennial oscillations, followed by a sudden drop within 1 kyr. These changes are quite consistent with those in the bioproductivity in core TB2. Therefore, the bioproductivity changed affected by the climate. The $^{10}$Be content, an index of the galactic cosmic ray flux, generally showed similar changes with the bioproductivity except some intervals, one of which showed a large disagreement between the $^{10}$Be flux and the bioproductivity, coincided with the iceberg discharge event in the North Atlantic. These results suggest that the centennial-scale bioproductivity changes observed in core TB2 probably reflect climate variations, and may be affected by solar activity. Solar activity can affect climate through galactic cosmic rays that control the low cloud (Svensmark effect), in addition to the direct influence through solar radiation.

©2019. Japan Geoscience Union. All Right Reserved. 

# Development of new-paleoceanographic proxies based on oxygen isotope analysis of sponge spicule

*Hitomi Uchimura Wakaki[1], Akira Ijiri[2], Minoru Ikehara[1], Sangmin Hyun[3]

1. Center for Advanced Marine Core Research, Kochi University, 2. Japan Agency for Marine-Earth Science and Technology, 3. Korea Institute of Ocean Science & Technology

The objective of this study is to construct the new-paleoceanographic proxy based on the oxygen isotope ratio of sponge spicule. To examine the variations in water depth and temperature, we selected GH08 surface sediment samples ranging from a water depth of 216 m to 2679 m in the Northwest Pacific. These samples were obtained from the area off eastern Okinawa Island during the GH08 cruise in 2008 by Geological Survey of Japan, AIST. The upper 0–2 cm of each surface sediment was sampled. The sediment samples were washed in a 250-mesh sieve and dried in the oven. In this study, we also analyzed the oxygen isotope ratio of sea-bottom water by laser spectroscopic analysis of Liquid Water Isotope Analyzer (LWIA).

We chose two benthic foraminifers' species *Cibicidoides* sp. and *Cibicidoides wuellerstorfi* to analyze the oxygen isotope ratio. Benthic foraminifer was analyzed by phosphoric acid digestion to carbon dioxide gas and the measurement of the oxygen isotope ratio by IsoPrime at Kochi University. We can recognize that the result of the foraminifera between the oxygen isotope ratio and temperature has a negative trend. In other words, the oxygen isotope ratio of benthic foraminifera in this study shows temperature dependence. Our results agree with those obtained by the previous studies (Marchitto et al., 2014). These results can be regarded as the data of benthic foraminifera in this study is considered appropriate for the reference.

We also analyzed the oxygen isotope ratio of sponge spicule by a new method of iHTR (inductive high-temperature carbon reduction) and CF-IRMS (continuous-flow isotope ratio mass spectrometry) (Ijiri et al., 2014). Some the oxygen isotope ratio values of sponge spicule are consistent with previous reported data (Brandriss et al., 1998, Moschen et al., 2005), which were analyzed the oxygen isotope ratio of biogenic opal (diatom). However, some of the oxygen isotope ratio of sponge spicule don't have any trends. These irregular date has possibility to be influenced by the acid treatment and the difference of gas pressure, and should be evaluated the validity in future experiment used based on additional samples.

Keywords: sponge spicule, benthic foraminifera, stable oxygen isotope, temperature dependence

©2019. Japan Geoscience Union. All Right Reserved. 

# A system for automatic collection of specific microfossil species using a deep learning classification

*Takuya Itaki[1], Yosuke Taira[2], Naoki Kuwamori[2], Toshinori Maebayashi[3], Satoshi Takeshima[4], Kenji Toya[4]

1. Geological Survey of Japan, AIST, 2. NEC Corporation, 3. Microsupport Co.Ltd, 4. Mitani-Corporation

For geochemical analysis such as stable isotope ratio, radiocarbon age and minor elements for a single species of microfossils, a large number of their skeletons is required to pick up one by one with enormous time and effort by a person under a microscope. In this study, we have developed a device that automates these efforts. Even if experts are absent, microfossils are accurately classified their taxonomic species level using deep learning which is one of the learning methods of artificial intelligence, and they are picked up using a micromanipulator installed in the microscope with motorized X-Y stage. It is possible to collect a large number of particles with speed and accuracy that could not be achieved with human hands. This technology to accumulate only specific species of microfossils contributes not only to greatly reduce hand work of picking up, but also to be enable chemical analysis such as isotope ratios and minor elements for small microfossil species that hitherto difficult because the necessary measurement amount cannot be collected.In addition to microfossils, it can be applied to various particles, and it is also expected to be utilized in various fields such as medical, food, horticulture and materials.

Keywords: Microfossil, AI, Automatic classification

©2019. Japan Geoscience Union. All Right Reserved. 

# Towards reconstructing environmental conditions related to Australian Great Barrier Reef initiation

*Stephen Obrochta[1], Wataru Miwa[1], Kotaro Shirai[2], Yusuke Yokoyama[2], Yosuke Miyairi[2], Jody Webster[2,3], Albert Hine[4]

1. Akita University, 2. University of Tokyo Atmosphere and Ocean Research Institute, 3. University of Sydney, 4. University of South Florida College of Marine Science

Previous work exploited the unique mixed carbonate-siliciclastic environment of Northeast Australia to identify the timing of changes in off-shelf sediment transport with respect to sea-level variation. Because sediment transport from the continental shelf to slope is strongly controlled by the presence/absence of a rimmed morphology, this provides a means for indirectly estimating the age of the Great Barrier Reef (GBR). Preliminary results indicate that a change in the timing of maximum off-shelf terrigenous sediment accumulation occurred during the glacial termination of MIS 20. This in turn suggests that an effective barrier morphology was emplaced during the MIS 21 interglacial. Instead of being deposited directly to the continental slope by incised rivers, terrigenous material first accumulated behind the barrier during the MIS 20 sea-level lowstand and was then redoposited as rising sea level reflooded the shelf.

Here we present initial results attempting to understand if and how changing environmental conditions promoted enhanced reef growth. The results include a higher-resolution isotope stratigraphy for improved chronological control, additional terrigenous mass accumulation rate measurements, and initial results of Mg/Ca analyses, which allow for calculating sea surface temperature changes and the oxygen isotopic composition of sea water that is expected to better resolve glacial-interglacial cycles. In the future we expect to add additional information from micro and/or nanofossil faunal assemblage data.

Keywords: Mixed Carbonate-Siliciclastic Sedimentary Systems, Great Barrier Reef

©2019. Japan Geoscience Union. All Right Reserved. 

# An 8,000-year climate record from Lake Motosu, Japan: Implications for the East Asian Monsoon

Sarah McDonlad[3], Jonathan Tyler[3], *Stephen Obrochta[1], Yusuke Yokoyama[2], Yosuke Miyairi[2], Kosuke Ota[2]

1. Akita University, 2. University of Tokyo Atmosphere and Ocean Research Institute, 3. Department of Earth Sciences, The University of Adelaide

The East Asian Summer Monsoon controls the timing and amount of rainfall for around a third of the world’ s population. An understanding of past changes in monsoon strength is thus crucial for placing current events in context and for characterising future climate risk. Whilst many monsoon records have been developed for continental Asia, fewer records exist from the north-eastern edge of the monsoon region. We present a new monsoon record for central Japan based on an 8,000-year lacustrine sedimentary sequence from Lake Motosu, located at the northern foot of Mt Fuji. Lake Motosu is a hydrologically closed lake and is therefore expected to be sensitive to changes in monsoon strength. Additional macrofossil radiocarbon dates are used to refine an existing high-fidelity age model. This age model is then applied to constrain the timing of changes in bulk sediment geochemistry (TC, TN, C/N, $\delta^{13}C$, $\delta^{15}N$) and the oxygen isotopic composition of sedimentary cellulose ($\delta^{18}O$). Changes in sediment chemistry reflect shifts in the sources of organic matter to the sediments, variations in lake hydrology and changes to the local catchment. In turn, these changes are linked to regional variations in monsoon strength. However, their interpretation is complicated by the impact of local seismic and volcanic activity.

Keywords: monsoon, Lake Mostosu, geochemistry

©2019. Japan Geoscience Union. All Right Reserved. 

# Environmental changes in northern Mongolia in During the Late Pleistocene: chemical analyses of lacustrine sedimentary sequences in Darhad basin

Yumiko Ohno[1], Sayuri Naito[1], *Nagayoshi Katsuta[1], Takuma Murakami[3], Shinya Ochiai[2], Noriko Hasebe[2], Shin-ichi kawaka[4]

1. Faculty of Education, Gifu University, 2. Institute of Natural and Environmental Technology, Kanazawa University, 3. Horonobe Research Inst. for the Subsurface Environment, 4. Faculty of Education, Gifu Shotoku Gakuen University

Spread of modern human (*Homo sapiens*) from Africa to Eurasia seems to have occurred in the periods from ca. 60 kyrs ago to ca. 50 kyrs ago via two routes from western Asia into northern Eurasia and across Arabia into southern Asia. To understand relationship between environmental changes and human migration in central Eurasia, we reconstructed a 120-kyr sediment record of environmental change using the Darhad basin (northern Mogolia) sediment core with a nondestructive $\mu$-XRF techniques of Horiba SXAM, XRD analysis, and petrolograhic observation.

Keywords: north Mongolia, sediment, paleoglacial lake

©2019. Japan Geoscience Union. All Right Reserved. 

# Paleoenvironmental changes recorded in Orog Lake, southwestern Mongolia during MIS 3 and its relationship with *Homo sapiens*' migration into northern Asia

*Hitoshi Hasegawa[1], Nanase Noma[1], Nagayoshi Katsuta[2], Masafumi MURAYAMA[3], Toru Tamura[4], Masami Izuho[5], Niiden Ichinnorov[6], Davaasuren Davaadorj[7], Noriko Hasebe[8], Miho Sasaoka[9], Masao Iwai[9]

1. Faculty of Science and Technology, Kochi Univ., 2. Faculty of Education, Gifu Univ., 3. Faculty of Agriculture and Marine Science, Kochi Univ., 4. Geological Survey of Japan, AIST, 5. Faculty of Social Sciences and Humanities, Tokyo Metropolitan Univ., 6. Mongolian Academy of Sciences, 7. National University of Mongolia, 8. Institute of Nature and Environmental Technology, Kanazawa Univ., 9. Center for Advanced Marine Core Research, Kochi Univ.

An aim of the present study is to understand detailed paleoenvironmental changes in Mongolia, situated at a key crossroad for *Homo sapiens*'s migration between central, eastern, and northern Asia during the Initial and Early Upper Paleolithic (IUP-EUP). Available archaeological evidences have suggested the emergence of IUP at around ca. 45-40 ka (e.g., Zwyns *et al.*, 2014; Rybin *et al.*, 2016; Izuho *et al.*, 2018). However, yet the paleoenvironmental changes of this period in Mongolia is largely unclear, preventing us to understand whether the possible environmental changes were significant as a major driving forth for modern human's lifeway.

In this paper, we present a new record of paleoenvironmental changes in southwestern Mongolia during MIS 3. In January 2017, we took two parallel cores (OROG01, 24 m; OROG02, 21 m) from Orog Lake, a shallow saline lake located in northwestern margin of Gobi Desert. The high-resolution major and minor element composition changes were obtained using μXRF core scanner (Cox, Itrax) at Center for Advanced Marine Core Research, Kochi University. Based on the preliminary results of OSL and 14C age dating, basal age of sediment core OROG01 yielded ca. 38 ±4 ka, nearly accordant with the basal age of ~45 ka reported in the previous study (Yu *et al.*, 2019). On the basis of our high-resolution elemental composition data, in conjunction with previous sedimentological and palynological data (Yu *et al.*, 2019), the paleoenvironments of southwestern Mongolia were more humid with higher lake levels during MIS 3 than Holocene. Our results also suggest periodic and higher amplitude paleoenvironmental changes in this region, which likely correspond to Dansgaard-Oeschger events. This new record would allow us to discuss potential relationship between paleoenvironmental changes and ecosystem changes in Mongolia during the IUP-EUP.

Keywords: Lake sediments, Saline lake, Paleoenvironmental changes, Dansgaad event, Homo sapiens, Initial and Early Upper Paleolithic

©2019. Japan Geoscience Union. All Right Reserved. 

# Reconstruction for water-mass structure of the Okhotsk Sea for the past 1.5 million years based on radiolarian assemblages

*Tatuya Sakamoto[1], Yusuke Okazaki[1]

1. Department of Earth and Planetary Sciences, School of Science, Kyushu University

The North Pacific Intermediate Water (NPIW) play an important role in transporting heat and freshwater. NPIW originates from the Okhotsk Sea where is the southernmost seasonal ice area in the northern hemisphere. Sea-ice in the Okhotsk Sea is formed mainly in the northwestern shelf area and moved south by the seasonal wind. Brine water rejected during sea-ice formation sinks to the intermediate layer and forms the Okhotsk Sea Intermediate Water (OSIW) characterized by abundant particulate organic carbon, low temperature, and rich in oxygen. OSIW is a source water of NPIW. Radiolarians are zooplankton with biogenic opal skeletons, and various species distribute from sea-surface to deep-sea. *Cycladophora davisiana* is a radiolarian species that favors well-ventilated intermediate water masses, therefore, *C. davisiana* is used as indicator of OSIW. In this study, we conducted radiolarian assemblage analysis for a giant piston core sample (MD01-2414, water depth 1123 m) to reconstruct the water-mass structure change for the past 1.5 million years. Size fraction greater 45 micrometers were used for slide preparation for light microscope observation. In general, total radiolarian skeletons during interglacials were 10 to 100 times greater than that during the glacial periods. *Cycladophora davisiana* was abundant during interglacials, suggesting enhanced OSIW formation. However, during MIS 11 and 31 known as the super interglacials, much less C. davisiana abundances were observed, suggesting weaken OSIW formation due to significant sea-ice retreat. Four radiolarian biostratigraphic markers in the North Pacific region were identified: *Amphimelissa setosa*, *Lychnocanomma sakaii*, and *Spongodiscidae* sp. In addition, two radiolarian species *Ceratospyris borealis* and *Zygocircus productus* indicated high productivity during interglacials.

Keywords: Radiolarian, Okhotsk Sea, Intermediate water, Sea ice

©2019. Japan Geoscience Union. All Right Reserved. 

# Silicoflagellate assemblages in the Okhotsk Sea during the interglacial periods

*Kazuki Egashira[1], Yusuke Okazaki[2], Tatsuhiko Sakamoto[3]

1. Department of Earth and Planetary Sciences, Kyushu University, 2. Department of Earth and Planetary Sciences, Graduate School of Science, Kyushu University , 3. Mie University

Silicoflagellate is a phytoplankton with a skeleton of biogenic opal. There are two major genera for modern silicoflagellates: *Dictyocha* mainly dwelling in tropical to temperate regions and *Stephanocha* mainly dwelling in subarctic region. The *Dictyocha*/*Stephanocha* ratio has been used as a paleotemperature proxy. Earth’s climate for the past 800,000 years is characterized by the glacial and interglacial cycles with a frequency of 100,000 years. Oxygen isotope ratios of benthic foraminifera mainly reflect continental ice-sheet volume fluctuations, lighter in the interglacials and heavier in the glacials. This fluctuation is called as Marine Isotope Stage (MIS), odd numbers correspond to interglacials and even numbers correspond to glacials. Among the interglacials, the oxygen isotope ratios were lighter than that of the present: MIS 5e (120,000 years ago), 9 (330,000 years ago), and 11 (400,000 years ago). Pollen assemblages in Lake El’gygytgyn sediment from the Far East Russiat in the Arctic Circle indicates pronounced warming during MIS 11. Because atmospheric carbon dioxide concentrations during the past interglacials were comparable to the preindustrial level, it is important to know the status of warming climate during interglacials. The purpose of this study is to reconstruct sea-surface conditions of the Okhotsk Sea during the past interglacials based on silicoflagellate assemblages preserved in sediments. By comparing silicoflagellate assemblages during MIS 1, 5e, 9 and 11, we test the extent of warming during interglacials. The Okhotsk Sea is a marginal sea of the western North Pacific located south of Lake El’gygytgyn, known as southernmost sea-ice covered area in the Northern Hemisphere. A piston core YK07-12 PC-3B (water depth: 1049 m, core length: 14.09 m). Age model of core YK07-12 PC-3B is established by benthic foraminiferal oxygen isotope stratigraphy and the estimate bottom age is 450,000 years ago. Silicoflagellate assemblage analysis was performed by using sediment samples collected from sedimentary horizons corresponding to MIS 1, 5e, 9, and 11. For each interglacials, three samples from peaks of biogenic opal content, maximum calcium carbonate content and minimum benthic foraminiferal oxygen isotope ratio were picked up, consequently, a total of 12 samples were selected. 100 silicoflagellate specimens were counted for each slide under light microscope. Almost all encountered silicoflagellate species during core YK07-12 PC-3B microscopic observation were belonging to genus *Stephanocha*. During MIS 11, *Stephanocha speculum*(particularly, *S. speculum minuta*) was the most abundant silicoflagellate taxa. Because *Stephanocha speculum*is known as a representative silicoflagellate species in the subarctic Pacific dwelling cold and nutrient rich environments, this result indicates that there is no evidence of significant warming in the Okhotsk Sea during MIS 11. Another abundant silicoflagellate species in core YK07-12 PC-3B was *Stephanocha octangulata*, also known as subarctic taxa. This species was dominant during MIS 1 and 5e. Unique oceanic environments such as seasonal sea-ice coverage and influence of low salinity water originating from the Amur River may have influenced on the silicoflagellate assemblages of core YK07-12 PC-3B.

©2019. Japan Geoscience Union. All Right Reserved. 

# Role of wind stress and sea surface thermal forcing in the formation of the Atlantic meridional overturning circulation at the Last Glacial Maximum

*Akira Oka[1], Kazuki Togawa[1]

1. Atmosphere and Ocean Research Institute, The University of Tokyo

In Previous Paleoclimate Model Intercomparison Project (PMIP) simulations of the Last Gracial Maximum (LGM) Atlantic Meridional Overturning Circulation (AMOC), the most of PMIP2 and PMIP3 models reproduced the 'deeper and stronger' AMOC than preindustrial simulations, in contrast to some reconstructions from paleo proxy data.Prior researches pointed out three factors controling the strength of AMOC in LGM climate: the cooling of the oceans in the Southern hemisphere, cooling in the North Atlantic, and the surface wind stresses in the North Atlantic. However, in the above-mentioned prior researches, the influences of these three factors on AMOC were only independently evaluated and the combined influences are still largely unknown. Here we emphasize the relative evaluation of combined influences of above- mentioned three factors on the AMOC. For this purpose, various ocean model experiments with our general ocean circulation model (COCO) were conducted; wind stress and thermal boundary conditions taken from PMIP experiments are replied to our ocean general circulation model. As a result, it was found that the difference of thermal boundary condition in the southern hemisphere most affects the strength of AMOC, and this cooling in the southern hemisphere is a necessary condition for reproducing the ‘shallower and weaker’ AMOC, but not a sufficient condition. From these results, it is implied that the stronger glacial AMOC reported in the PMIP models was possibly caused by the insufficient cooling in the southern hemisphere in LGM experiment, and this insufficient cooling possibly comes from warm bias there in the present state experiment and the associated underestimation of ice albedo feedback of sea ice.

Keywords: The Atlantic Meridional Overturning Circulation(AMOC), Ocean General Circulation Model(OGCM), Last Glacial Maximum(LGM)

©2019. Japan Geoscience Union. All Right Reserved. 

# Comparison of the Kuroshio during LGM simulated by an ocean general circulation model driven by multiple paleoclimate models

*Kensho Ichikawa[1], Haiyan Yang[2], Xinyu Guo[2], Yasumasa Miyazawa[3]

1. Graduate School of Science and Engineering,Ehime University, 2. Center for Marine Environmental Studies,Ehime University, 3. Japan Agency for Marine-Earth Science and Technology

The Kuroshio that flows south of Japan has an important role in the climate of East Asia and Japan. In modern days, the Kuroshio presents a stable path and contributes to maintenance of warm climate. However, this stable condition is considered to be different in Last Glacial Maximum (LGM) when different environment conditions from the present day were reported. During the LGM, the sea surface level was lower than present by about 130 m and the westerlies shifted southward. In addition, the air-sea heat flux was also expected to be different from present. Therefore, it is necessary for the simulation for the Kuroshio in LGM to consider the changes in above three factors (sea level, westerly, and air-sea heat flux). The Kuroshio in LGM was calculated by a numerical model that included the above mentioned three factors in Muto (2018). The model results presented the southward shifting of the Kuroshio path and decreasing of the Kuroshio intensity. However, this result was obtained from one paleoclimate model (IPSL). Therefore, it is necessary to use more paleoclimate models to confirm the results given by Muto (2018).

In this study, we performed similar calculations for the Kuroshio in LGM using four additional paleoclimate models (CNRM, GISS, MIROC, MRI) as driven forcing of ocean model. Before calculation, we compared the vorticity of wind stress given by these paleoclimate models and obtained the Sverdrup transport that is also an index of Kuroshio intensity.

Among all the five paleoclimate models, the position of zero vorticity, which corresponds roughly the position of Kuroshio, shifted to the most southward in IPSL. At the same time, the Sverdrup transport was the lowest in IPSL. Therefore, the southward shifting of the Kuroshio path and the weakening of the Kuroshio intensity given by Muto (2018) are likely an extreme case among five paleoclimate models.

Keywords: Last Glacial Maximum, Kuroshio, paleoclimate models

©2019. Japan Geoscience Union. All Right Reserved. 

# The changes of the Kuroshio path in the Northwest Pacific since 35ka

*Haiyan Yang[1], Xinyu Guo[1], Ayako Abe-Ouchi[2], Yasumasa Miyazawa[3], Sergey Varlamov[4], Wing-Le Chan[2]

1. Center for Marine Environmental Studies, Ehime University, 2. Atmosphere and Ocean Research Institute, University of Tokyo, 3. Research Institute for Global Change, Japan Agency for Marine-Earth Science and Technology, 4. Application Laboratory, Japan Agency for Marine-Earth Science and Technology

Kuroshio, a strong western boundary current in the subtropical North Pacific, has strong influences on the climate of Japan and East Asia. Global sea level rises and falls when ice sheets and glaciers melt and grow. The Last Glacial Maximum (LGM, 21ka) is the most recent interval in Earth history when global ice sheets reached their maximum integrated volume. The expansion of the ice sheets at the LGM resulted in a sea-level lowering of about 130 m and a cold phase compared to present. Under the circumstance of sea level, Kuroshio did not bifurcate into the Japan Sea and form the Tsushima Current. As the sea level rises, the Tsushima Current flowed into the Japan Sea at about 10ka (Gallagher et al., 2015), and the sea-level reached the present level at 7ka~6ka (Zheng et al., 1994). However, how the Kuroshio and Tsushima Current pathway evolved in the conditions of different sea level and climate remains unclear.

In Okinawa and southern Korea, some archaeologists have found evidences of people drifting on the Kuroshio from Taiwan to northern regions. According to studies by Japanese anthropologists, the first person that set foot on Okinawa probably sailed there on bamboo rafts from Taiwan more than 30,000 years ago. However, this hypothesis needs more evidences because sailing across the Kuroshio is a difficult thing if the Kuroshio 30,000 years ago had the same surface velocity as present. Therefore, clarifying the strength and path of Kuroshio is also helpful to the understanding on human migration.

In this study, we used the model of Japan Coastal Ocean Predictability Experiment (JCOPE) to simulate the changes of the Kuroshio path under the combined influences of sea level, the air-sea heat flux, and wind stresses in five historical regimes (35ka, 30ka, LGM, 6ka, and 0ka). The meteorological and oceanic data are provided by the climate model MIROC4m (Chan et al., 2011) which is a fully coupled atmosphere-ocean general circulation model (AOGCM).

Keywords: Kurosio, Path, Evolution

©2019. Japan Geoscience Union. All Right Reserved. 

# Temperature reconstruction in the late Pleistocene using fossil terrestrial snails and a stalagmite from an archaeological cave in Okinawa

*Ryuji Asami[1], Rikuto Hondoh[2], Ryu Uemura[3], Ryuichi Shinjo[3], Akihiro Kano[4], Masaki Fujita[5], Shinji Yamasaki[6], Hideko Takayanagi[1], Yasufumi Iryu[1]

1. Graduate School of Science, Tohoku University, 2. Faculty of Science, Tohoku University, 3. Faculty of Science, University of the Ryukyus, 4. School of Science, the University of Tokyo, 5. National Museum of Nature and Science, 6. Okinawa Prefectural Museum and Art Museum

Freshwater snails are useful for a paleoclimate proxy. For example, stable oxygen isotope composition of mollusck’ s aragonite shells depends on temperature and oxygen isotope composition of water at the time of their growth. The Ryukyu Island Arc, bounded by the East China Sea to the northwest and by the Pacific Ocean to the southeast, is an important area in climatology because its environment is highly associated with the East Asian monsoon (EAM), typhoon, and the Kuroshio current. However, terrestrial paleoclimate records such as tree rings and stalagmites are little in the Ryukyu Island Arc unlike the East Asia Continent. Meanwhile, Okinawa is widely known as a hotspot in archaeology and a lot of ancient remains and digs have been excavated for recent years. Sakitari Cave, where world’ s oldest fishhooks were discovered, is one of the most famous archaeological sites in Okinawa.
In this study, fossil shells of a freshwater snail *Semisulcospira libertina* excavated at Sakitari Cave in Okinawa-jima were investigated. These samples were from two sediment layers dated to 13-16 ka and 23 ka in the cave. We measured stable carbon and oxygen isotope ratios and trace element concentrations at intervals of 1 mm along the growth direction of the snails to reconstruct seasonal temperature variations during the Last Glacial Maximum and the last deglaciation. To estimate paleo-temperature and -oxygen isotope composition of precipitation accurately, we also measured oxygen isotope composition of fluid inclusion water in a stalagmite collected near the archaeological site. Comparing with chemical composition of living *S. libertina* shells collected around the site, estimated annual mean temperature was about 8 ˚C and 6˚C lower at 23 ka and 13-16 ka than at the present. Summer temperature has largely increased from 23 ka to 13-16 ka relative to winter temperature, which is consistent with North Hemisphere insolation changes in summer and winter. Our results indicate that the increase of mean air temperature around Okinawa-jima was larger than that of seawater temperature in the northwestern Pacific Ocean during the last deglaciation. This inconsistency is a significant finding for better understanding of past climate changes associated with the East Asian Monsoon.

Keywords: fossil snail, stalagmite, oxygen isotope composition, paleo-temperature, Okinawa, archaeological cave

©2019. Japan Geoscience Union. All Right Reserved. 

# Silicoflagellate and *Actiniscus* response to meltwater during the last deglaciation in the Alaska margin

*Asuka Tomokawa[1], Yusuke Okazaki[1], Jonaotaro Onodera[2], Keiji Horikawa[3]

1. Department of Earth and Planetary Sciences, Kyushu University, 2. Research and Development Center for Global Change, JAMSTEC, 3. Graduate School of Engineer and Science, University of Toyama

Silicoflagellate is a phytoplankton with biogenic opal skeleton, and its fossil assemblage is used for reconstruction of paleoenvironment. There are two major genera for modern silicoflagellates: *Dictyocha* mainly dwelling in tropical to temperate zone and *Stephanocha* mainly dwelling in subarctic zone. The *Dictyocha*/*Stephanocha* ratio has been used as a paleotemperature proxy. *Actiniscus pentasterias* is a species of Dinoflagellata with biogenic opal skeleton, indicator of coastal and low salinity environments. Gulf of Alaska is located eastern North Pacific. The southern Alaska margin has fjord created by the Cordilleran Ice Sheet. The purpose of this study is to clarify the silicoflagellate and *Actiniscus* assemblages to meltwater input from the Cordilleran Ice Sheet at the last deglaciation in the southern Alaska margin. A piston core KH17-3 CL14 was obtained from the southern Alaska margin (59° 33.350’ N, 144° 09.344’ E, water depth: 695 m). Age model of core KH17-3 CL14 is established by planktic foraminiferal radiocarbon dates and the bottom of the core is estimated to be ~17 ka. We used 48 samples for Silicoflagellate and *Actiniscus* analyses. 100 silicoflagellate specimens were counted for each slide and all *Actiniscus pentasterias* specimens were counted for each slide under light microscope. 7 species and 2 subspecies of genus *Dictyocha* and 4 species of genus *Stephanocha* were identified. Relative abundances of genus *Dictyocha* accounted for greater than 50% since Younger Dryas (YD), whereas genus *Stephanocha* (particularly *S. speculum*) was abundant during Bolling-Allerod (BA). This suggests that *Dictyocha*/*Stephanocha* ratio didn’t simply reflect cold (YD) and warm (BA) events during the last deglaciation. Two *Actiniscus pentasterias* peaks were observed during the last deglaciation which were coincident with Meltwater Pulse 1A and 1B. This suggests salinity decline due to meltwater from the Cordilleran Ice Sheet. The meltwater into the subarctic Pacific may have leaded to enhanced productivity during BA. Because *Stephanocha speculum* is suggested to be an indicator of high productivity from modern sediment trap observation, high abundances of *S. speculum* in core KH17-3 CL14 during BA can be explained by the enhanced productivity driven by meltwater from the Cordilleran Ice Sheet.

Keywords: Silicoflgellate, Gulf of Alaska

©2019. Japan Geoscience Union. All Right Reserved. 

# Application of the ramped pyrolysis $^{14}C$ dating to postglacial sediments from the Alaskan margin, Arctic Ocean

*Kenta Suzuki[1], Masanobu Yamamoto[1,2], Brad Rosenheim[3], Takayuki Omori[4], Leonid Polyak[5]

1. Graduate School of Environmental Science, Hokkaido University, 2. Faculty of Environmental Earth Science, Hokkaido University, 3. College of Marine Science, University of South Florida, 4. The University Museum, The University of Tokyo, 5. Bard Polar and Climate Research Center, Ohio State University

Radiocarbon dating of biogenic carbonates, such as foraminiferal tests, is commonly used for dating marine sediments up to 50 ka old. However, in carbonate-poor environments, such as typical for polar seas, direct dating of carbonaceous material is difficult, while bulk organic matter (OM) may contain a mixture of carbon with different ages. Rosenheim et al. (2008) developed the ramped pyrolysis $^{14}C$ dating of the bulk OM based on incremental generation of $CO_2$ from a range of carbon fractions, from highly reactive to more thermochemically stable. Application of this approach to Southern Ocean sediments showed that ages of highly-reactive, lower temperature fractions were considerably younger than other fractions and the bulk $^{14}C$ age. In this study, we explore ramped pyrolysis $^{14}C$ dating in Arctic Ocean sediments from the Alaskan margin to determine if the same relationships hold true.
Samples were taken from two sediment cores collected on the 2005 HOTRAX expedition and comprising Holocene marine and older glaciomarine strata (Darby et al., 2009a). Several $^{14}C$ ages have been generated on the Holocene biogenic carbonates (Darby et al., 2009b). New samples from both the Holocene and older sediments were pyrolyzed from room temperature to 900 ˚C, and the released, purified $CO_2$ fractions were sealed in borosilicate glass ampoules at the University of South Florida. Measurement of $\Delta^{14}C$ was conducted at the University of Tokyo.
Pyrolysis followed by oxidation generated three peaks of $CO_2$ at ~300 ˚C, ~400 ˚C and ~540 ˚C, which were deconvolved into three Gaussian peaks (G1 to G3). These peaks were interpreted to reflect the consecutive degradation of oxygen-containing OM functional groups, cleavage of carbon-carbon bonds, and cleavage of aromatic ring carbon, respectively. In this scenario G1 contains most of the autochthonous carbon from the sediment. We found that the slopes of the G1-G3 $^{14}C$ ages plotted against temperature of the Gaussian centroid are proportional to the offset between $^{14}C$ ages of G1 and earlier analyzed biogenic carbonates from the same core levels. Assuming that this relationship is a constant function of the overall measured age spectra, we propose to use it for estimating sediment ages from the ramped pyrolysis $^{14}C$ data. The estimated G1 age offsets range from 800 to 3,000 years in the Holocene and from 4,000 to possibly as high as 5,000 years in the older glaciomarine sediments.

©2019. Japan Geoscience Union. All Right Reserved. 

# Utility of sedimentary environmental DNA for indices of past pelagic fish species populations

*Hiromichi Tamai[1], Michinobu Kuwae[2], Hideyuki Doi[3], Toshihumi Minamoto[4]

1. Graduate School of Science and Engineering, Ehime university, 2. Center for Marine Environmental Studies, Ehime university, 3. Graduate School of Simulation Studies, University of Hyogo, 4. Graduate School of Human Development and Environment, Kobe University

Far little is known about long-term dynamics of almost all of fish species populations in the ocean during pre-instrumental era. Here we focused on environmental DNA in marine sediments as a potential tool to elucidate past fish population dynamics and tested its utility to reconstruct fish abundance in Japanese coastal waters. Based on quantitative PCR method applied to the sediment samples collected from anoxic bottom sediments in Beppu Bay, Japan, we found environmental DNA of Japanese anchovy, Japanese sardine, and Jack mackerel in the 1-meter sediment sequences spanning over the last 250 years, which is the first detection of sedimentary marine fish DNA. The observed temporal changes in sedimentary DNA abundances are consistent with those in fish scale abundances and catch in Japan, suggesting the utility of the sedimentary fish environmental DNA to track past changes in fish abundance in waters from the bottom sediment sequences. DNA analyses of five fractions of sediment samples including coarse and fine particle fractions, pore water, fish scales, and bones suggested that a main source of fish DNA in the sediments is derived from fine the particle fraction.

Keywords: eDNA, sediment core, Quantitative polymerase chain reaction, pelagic fish

©2019. Japan Geoscience Union. All Right Reserved. 

# Improvements of extraction methods of sedimentary fish-origin DNA for reconstruction of marine fish communities

*Jun Kurata[1], Hiromichi Tamai[2], Hideyuki Doi[3], Toshihumi Minamoto[4], Michinobu Kuwae[5]

1. department of earth science, Ehime university, 2. Graduate School of Science and Engineering, Ehime university, 3. Graduate School of Simulation Studies, University of Hyogo, 4. Graduate School of Human Development and Environment, Kobe University, 5. Center for Marine Environmental Studies, Ehime university

Environmental DNA is DNA fragments derived from body fluids or skin fragments of macro organisms contained in water or soil. It is expected to can be a technology to reveal long-term fish community changes which still remains unknown in the world ocean. However, DNA in the sediments has a low concentration, therefore, it is difficult to detect for a various kind of fish species. The purpose of this research is to elucidate the method that can take sedimentary DNA more efficiently. At this time, we tested five DNA extraction methods including the conventional one together with beads beating time. Quantitative PCA results showed that Power Soil had the best yield in the replications. In addition, DNA extraction of *Truchurus japonicus* figured out a better yield by increasing the amount of sediment sample. There was a significant difference between 10 min. and 30 sec. of beads beating time, it is possible that there is a higher yield with short time beating. Our future works is to test whether DNA yield improves by shortening or eliminating bead beating, effectively removal of PCR inhibitors, and an utility of PCR inhibitor.

Keywords: Environmental DNA, ocean sediment

©2019. Japan Geoscience Union. All Right Reserved. 

# The paleotemperature reconstruction during the late-Holocene using the sediment core recovered from the Tokyo Bay, Japan

*Hiroto Kajita[1,2,3,4], Naomi Harada[5], Miyako Sato[5], Nanako Ogawa[1], Yusuke Yokoyama[1,2,4], Chikako Sawada[1], Yosuke Miyairi[1], Masayuki Utsunomiya[3], Atsushi Suzuki[3], Hodaka Kawahata[1,2,3]

1. Atmosphere and Ocean Research Institute, The University of Tokyo, Japan, 2. Department of Earth and Planetary Science, Graduate school of Science, The University of Tokyo, Japan, 3. Research Institute of Geology and Geoinformation, Geological Survey of Japan, National Institute of Advanced Industrial Science and Technology (AIST), Japan, 4. Department of Biochemistry, Japan Agency for Marine-Earth Science and Technology (JAMSTEC), Japan, 5. Research and Development Center for Global Change, Japan Agency for Marine-Earth Science and Technology (JAMSTEC), Japan

Recently, investigations of Holocene climatic variability and its socioeconomic impacts have received increasing attention with regard to the prediction of future climatic change and the evaluation of its impact on human society. The Kanto area around the Tokyo Bay, Japan had a large population in the Neolithic Jomon age. After the establish of centralized system, this area has been a stage of major change in Japanese history for many times. The paleoenvironment around the Tokyo Bay has been estimated based on the analysis of the shell mounds along the coast or historical documents. However, the continuous and high time resolution paleotemperature record has not existed yet.

A piston core KT12-06-2B (8.99m) were recovered from the Tokyo Bay during the Tansei-maru KT12-06 cruise. An age model for the core, determined by the AMS$^{14}$C dating for 22 molluscan shells and the scoria layer of Hoei eruption, showed that it has the continuous records from about 4, 500 years ago. We analyzed the content of total organic carbon (TOC), alkenone unsaturation ratio ($U^{k'}_{37}$), and coccolith assemblages for this core in order to reconstruct the paleoenvironment in the Toyo Bay.

The constant TOC values (1.3-1.7 wt.%) before 1700AD suggested the stable biological production at the core site. We converted $U^{k'}_{37}$ into alkenone-SST using the conversion formula, proposed by the culture experiment of *G. oceanica* because most of coccolith contained in the sediments were *G. oceanica* based on the polarizing microscope observations. From 400 AD to the present, the alkenone-SST ranged from 20.5˚C to 22.4˚C (21.6˚C on average), including several cold periods around 1700 AD, 1420 AD, 1280 AD, and 1010 AD, which corresponded approximately to the Maunder, Spörer, Wolf, and Oort Minimum, respectively. The SSTs before 400 AD largely fluctuated between 19.5˚C and 25.3 ˚C, and its average value was 22.6˚C, which was 1 ˚C higher than the average after 400 AD. Especially large cold periods were detected around 520-440 BC (with a minimum value of 20.0℃) and 2360-2280 BC (with a minimum value of 19.5℃). The former cold period, which was also reported by the several previous studies in East Asia, might be caused by the other large minimum of solar activity around 500BC. The latter cold period corresponds to the global cooling/drying event accompanied by the monsoon retreat. In the mid- to late-Jomon age, the Neolithic Jomon society around the Tokyo Bay based on hunting and gathering, not paddy rice cultivation. We assume that they lived in warm but unstable climate, which might be disadvantageous for them to start agriculture.

Keywords: Paleoclimate, the Tokyo Bay, late-Holocene, Alkenone

©2019. Japan Geoscience Union. All Right Reserved. 

# Summer monsoon variability over the past 400 years in Tateyama, Japan, as reconstructed from tree-ring oxygen isotope data

*Masaki Sano[1], Kota Mori[1], Akane Tsushima[2], Zhen Li[3], Koh Yasue[4], Takeshi Nakatsuka[2,3]

1. Faculty of Human Sciences, Waseda University, 2. Nagoya University, 3. Research Institute for Humanity and Nature, 4. Shinshu University

With its high sensitivity to hydroclimate variability, tree-ring oxygen isotope composition has been widely used for dendroclimatology over monsoon Asia in recent years. Here we built a 400-year tree-ring oxygen isotope chronology from Tateyama, Japan to reconstruct summer hydroclimate in the region, and compared it with other tree-ring data to explore spatio-temporal variations in hydroclimate. We collected tree-ring core samples from *Pinus parviflora* var. *pentaphylla* at an altitude of 1500 m above sea level in 2016 and 2017 in Tateyama, Japan. After cross-dating each ring of the sampled cores based on ring-width patterns, a total of 5 trees were selected for isotopic analysis. Cellulose was extracted directly from 1 mm thick plates using the standard methodology. Each annual ring was separated using a blade under microscope. Oxygen isotope ratio of each ring was then measured using an isotope ratio mass spectrometer. The resultant 5 tree-ring oxygen isotope series were highly correlated with each other, indicating that the oxygen isotope ratio was governed by common climatic factors. Climatic response analysis revealed that the oxygen isotope ratio was primarily controlled by relative humidity in the early summer season (April–June), with a highest correlation appearing in June. Therefore, the tree-ring chronology can be considered to be a proxy of hydroclimate related to Meiyu-Baiu variability. The oxygen isotope data in our chronology showed an overall positive correlation with those in a tree-ring oxygen isotope record from Yakushima island, southwestern Japan. However, the correlations often became lower or negative during the positive PDO phases, implying that the PDO played a role in modulating spatial patterns of hydroclimate in the early summer season over western Japan.

Keywords: Oxygen isotope, East Asian monsoon, Pacific Decadal Oscillation

©2019. Japan Geoscience Union. All Right Reserved. 

# Eventural Layers of anciant disasters during these 4500 years at Lake Ikeda (Lake Daijya), western coast of Kyushu Island presumed by diatom assemblages in lake deposits

*Kaoru Kashima[1], Tomokazu Mita[1], Yu Fukumoto[3], Tsuyoshi Haraguchi[2], Kazuyoshi Yamada[4]

1. Department of Earth and Planetary Sciences, Kyushu University, 2. Department of Geosicneces, Graduate School of Science, Osaka City University, 3. Ritsumeikan University, 4. Museum of Natural and Environmental History, Shizuoka

Lake Ikeda (Lake Daijya) is a small coastal freshwater lake of about 200m NE and WE, located at Amakusa Island, Western part of Kyushu Area. It was a coastal lagoon, but after the eruption of Akahoya Ash (about 7.3ka), the lake was closed by a sand dune, and changed to be a freshwater environment.
Woodruff et.al. (2014) found the two Typhoon layers at 1.9-2.1m depth of the lake deposit, and presumed those were the trace of Kamikaze Typhoons, the huge typhoons on AD1274, AD1281. But their age control data were limited, and the processes to discussions to decide the Kamikaze Typhoon deposits were necessary to add multidiscipline methods.
Therefore, Haraguchi took undisturbed cores at Lake Ikeda (Lake Daijya) in 2016. It was 26m long, and covered about 8000 years presumed by C14 ages and Akahoya Ash (about 7.3ka) layer. In this presentation, we took the analysis of diatom assemblages in the lake deposits of top 9m long core dated about these 4500 years. We found the five “Event Layers” in the 9 m core. Huge typhoons like the Kamikaze Typhoon had continuously attacked the Western part of Kyushu.
The results of diatom assemblages in the core were compiled as follows:
(1)Surface deposits of the lake were composed by a lot of small fugal pellets by small animals. The pellet contained a lot of diatoms. The diatom assemblages were very simple and were dominated by freshwater plankton species (*Aulacoseira* and others), and freshwater semi-plankton species (*Staurosira* and others).
(2)Lake Ikeda (Lake Daijya) has continued as shallow freshwater for 4500 years, and freshwater plankton species (*Aulacoseira* and others), and freshwater semi-plankton species (*Staurosira* and others) were dominated in the lake deposit.
(3)But diatom assemblages were changed suddenly at the following five layers. They were caused by the invasion of marine water and slope falls surrounding the lake, presumably by the ancient huge typhoons.
(4)The depth and ages of event layers were compiled as follows. Event1 (7.26-8.26m): 4200-3800 yBP, Event2 (4.32-4.40m): 2000 yBP, Event3 (3.20-3.28m): 1400 yBP, Event4 (2.64-2.72m): 1000 yBP, Event5 (1.22-1.90 m): 500-700 yBP.
(5) To presume the detail process of each “Event Layer”, we have to analyze using multidiscipline methods and to compare the results surrounding Kyushu Area.

Keywords: Diatom Assemblages, Typhoon Deposit, Coastal lake, Lake Ikeda (Lake Daijya)

©2019. Japan Geoscience Union. All Right Reserved. 

# Variability of hemipelagic and event depositions in the Beppu Bay during Holocene

*Tomohisa Irino[1], Airi Maruyama[1], Ken Ikehara[2], Masanobu Yamamoto[1], Michinobu Kuwae[3]

1. Graduate School of Environmental Science, Hokkaido University, 2. Institute of Geology and Geoinformation, National Institute of Advanced Industrial Science and Technology, 3. Center for Marine Environmental Studies, Ehime University

The Beppu Bay located in the northeast Kyushu Island, the southwestern Japan receives detrital materials mainly from two drainage systems, the Ohno River and the Oita River. The Ohno River has the head water region at the Mt. Kuju and Mt. Aso, flows eastward combining some tributaries from the south, and then flows northward to the Beppu Bay. Surface geology of the drainage area is roughly divided into two as intermediate to felsic volcanic area covered with andosol in the northeast and Paleozoic to Mesozoic sedimentary rocks covered with brown forest soil in the south. The drainage basin of the Oita River is located in the north of the Ohno River drainage, which is characterized by mafic volcanic rocks in the headwater region. Since the provenance of the Beppu Bay sediments has such geologically contrasted drainage systems, the temporal changes in the provenance for the sediment can be utilize to seek for the interrelationship among the western Pacific paleoceanography, East Asian monsoon, ecological response (fishery, vegetation, land use), and the erosion and sediment supply from hinterland basin. For this purpose, we examined mineral composition of BP09-3 core collected from the center of Beppu Bay as well as sediment from surface soils and river beds using X-ray powder diffraction.

As a result, quartz / feldspars ratio of the Beppu Bay sediment was within the range of surface soils in the drainage of Ohno River and Oita River. Detailed examination of peak shape of feldspar in X-ray diffractogram suggests grain size dependency of feldspar composition. Feldspars in finer materials showed more “mafic” composition suggesting that fine materials are dominantly supplied from Oita River drainage and / or mafic rock is more easily weathered and forms fine materials. We also applied statistical unmixing of mineral assemblage using PARAFAC algorithm on XRD profiles. Statistically distinguished subcomponents could be attributed to biogenic subcomponents, detrital subcomponents from the Ohno and Oita Rivers in hemipelagic mud as well as two detrital subcomponents in event sands with different origin.

Temporal variation of these statistical subcomponents in hemipelagic mud suggests that vegetation and / or land use change in the drainage area affected the relative importance of suspension loads from the Ohno River associated with the increase of detrital flux for the last 3,000 yrs. Composition of event sands also shows a consistent compositional change characterized by the relative increase of contribution from sandy material of the Ohno River bed. Increase in surface erosion in the Ohno River drainage may have been responsible for increases of fine and coarse materials supply and development of the delta at the river mouth.

Keywords: Beppu Bay, Sediment, Detrital component, X-ray diffraction analysis

©2019. Japan Geoscience Union. All Right Reserved. 

# The composition of laminae in the sediment of Beppu-Bay and potential as annual laminations

*Yoshiaki Suzuki[1], Michinobu Kuwae[2], Kazuno Arai[3], Ken Ikehara[4], Masafumi MURAYAMA[3]

1. Waseda University, 2. Ehime University, 3. Kochi University, 4. AIST

The sediment of Beppu Bay in Pref. Oita is consisted of hemipelagic mud and contains many eventually deposited layers (event layers). These layers are considered to be caused by the occurrence of flood, earthquake or eruption. To reveal the mechanism of deposition of minor event layers (less than 1cm thickness), we tried to correlate the sediment with the observational record based on high-resolution age model using sediment cores obtained from four sites in Beppu Bay.
Surface sediment cores were CT-scanned and analyzed by micro XRF scanner (ITRAX). Pb and Cs isotopes were also measured by 4cm intervals for age determination.
In the deepest part of Beppu Bay(more than 60m depth), clear lamination is seen in several cores. In the shallower part, lamination cannot be observed. Based on the result of ITRAX measurement and Soft-X images, it is revealed that lamination is caused by the change of the amount of detrital material. Amount and composition of detrital material also show several positive spikes. Some of them can be observed by naked eyes as light gray or reddish brown colored thin layers (minor event layers) suggesting that they were supplied from different provenance than usual.
The results of Pb and Cs measurements agree with the age of Ev-1a which is considered to be caused by Hyuga-Nada earthquake in 1968 (Kuwae et al., 2013). Counting of lamination also agrees with Pb and Cs based age model when unclear lamination is interpolated by the average thickness of laminations. Therefore, it is strongly suggested that lamination in the bottom of Beppu Bay is annual lamination, varve. If the lamination is verified as a varve, high-resolution age model could be established and it enables detailed correlation of the sediment and observational record.

Keywords: Beppu Bay, annual lamination

©2019. Japan Geoscience Union. All Right Reserved. 

# Simulation of global distribution of Pa/Th using an ocean general circulation model

*Yusuke Sasaki[1], Akira Oka[1]

1. Atmosphere and Ocean Research Institute, The University of Tokyo

The sediment 231Pa/230Th ratio is an important major proxy for studying paleo ocean circulation. However, even in the modern ocean, the only limited data about the distribution of dissolved 231Pa and 230Th was available, and it was insufficient to understand the process that controls the oceanic distribution of 231Pa and 230Th. In addition, some of previous modeling studies did not reproduce the observation data sufficiently. Recently, number of available observation data about dissolved 231Pa and 230Th is rapidly increasing owing to the recent projects like GEOTRACES. In this study, we performed simulation of 231Pa and 230Th with an ocean general circulation model (OGCM) and discussed how well dissolved 231Pa and 230Th profile of GEOTRACES data set is reproduced by the model. First, based on the previous model that incorporates reversible scavenging processes of 231Pa and 230Th by sinking ocean particles (Siddall et al., 2005), we improved the model by taking into account of additional sink at the sea floor (bottom scavenging; Okubo et al., 2012; Roy-Barman, 2009) and the dependency of scavenging efficiency on particle concentration following Henderson et al. (1999) . Second, as for our best reproduced simulation (Control simulation), we discuss processes which control the oceanic distribution of 231Pa and 230Th into three parts; the one-dimensional reversible scavenging process, the contribution from ocean advection and diffusion, and bottom scavenging. Through this analysis, we clarified how these processes effect on the global distribution of the sediment 231Pa/230Th ratio.

As a result of the improvement of model and tuning of the parameter, we simulated the distribution of 231Pa and 230Th reported from GEOTRACES dataset successfully. First, I confirmed that the profile of both dissolved 231Pa and 230Th in the deep ocean was improved by considering bottom scavenging as suggested by Rempfer et al. (2017). While the distribution of 231Pa is reproduced realistically by considering bottom scavenging, it is found to be difficult to simulate the depth profile of dissolved 230Th consistent with observations only by considering bottom scavenging. Hence, I tried to reproduce the dissolved 230Th profile by changing parameter values which control the strength of reversible scavenging by sinking ocean particles from the case in Siddall et al. (2005), and also by incorporating the dependency of scavenging efficiency on particle concentration following Henderson et al. (1999). As a result, I also reproduced the distribution of 230Th successfully.

In the latter part of this study, we discussed the process that controls the distribution of the sediment 231Pa/230Th ratio by analyzing the Control simulation. Through this analysis it was confirmed that the process that controls the distribution of the sediment 231Pa/230Th activity ratio is largely determined by the stronger influence of advection and diffusion on 231Pa than 230Th; advection and diffusion effect only on 231Pa can reproduce overall pattern of the distribution of the sediment 231Pa/230Th activity ratio similar to observation. Our analysis revealed that the bottom scavenging effect weakens the influence of advection and diffusion on 231Pa, and tends to make the contrast of 231Pa/230Th distribution smaller. We also found that the advection and diffusion of 230Th is small but not negligible, which also contributed to decrease the advection and diffusion effect on 231Pa.

This model is useful not only for reproducing 231Pa/230Th ratio in the present-day ocean but also for that in different climate such as glacial periods. Simulation of 231Pa/230Th ratio under the glacial

©2019. Japan Geoscience Union. All Right Reserved. 

climate is an interesting future study. Such a study is an important step for discussing glacial changes in the ocean circulation more quantitatively.

Keywords: 231Pa/230Th ratio, proxy of ocean circulation, bottom scavenging, ocean general circulation model

©2019. Japan Geoscience Union. All Right Reserved. 

# Construction of modern silicoflagellate assemblage dataset in the North Pacific for paleo sea-surface temperature and its application for sediment cores

*Yusuke Okazaki[1], fumiaki nishizono[1], Tanizaki Kyohei[1]

1. Department of Earth and Planetary Sciences, Graduate School of Science, Kyushu University

Silicoflagellate is a marine phytoplankton with biogenic opal skeletons. Most of the modern silicoflagellates are belonging to two genera: *Dictyocha* mainly distributing tropical to temperate regions and *Stephanocha* mainly distributing polar to subpolar regions. Here we construct modern silicoflagellate assemblage dataset in the North Pacific for modern analog technique to reconstruct paleo sea-surface temperature (SST). The modern silicoflagellate assemblage dataset is composed of seven species in surface sediment samples from (1) wide-area of North Pacific by Poelchau (1976) and (2) newly obtained western North Pacific near Japan. A total of 174 surface sediment samples were compiled as the modern silicoflagellate assemblage dataset. Each sample site is linked with 0.25-degree grid data of annual mean SST data by World Ocean Atlas 2013. Modern analog technique analysis was performed by using Polygon 2.4.4. and applied to sediment cores from the Japan and East China Seas. Reconstructed SST of the Japan Sea off Wakasa was ~6-degree C during LGM whereas ~15-degree C during Holocene. Deglacial warming was observed between 12 and 14.5 ka. For the East China Sea core from the Danjo Basin, reconstructed SST was ranging from 10-15 degree C during LGM to 20-25 degree C during late Holocene. The reconstructed silicoflagellate based SST (10 to 25-degree C) were in between planktic foraminiferal Mg/Ca based one (20 to 25-degree C) and TEX 86 based one (7 to 20-degree C). However, deglacial rapid SST changes based on silicoflagellate was not observed in both planktic foraminiferal Mg/Ca and TEX 86 based ones.

Keywords: Silicoflagellate, Modern analog technique, paleo temperature, Last glaciation, Japan Sea, East China Sea

©2019. Japan Geoscience Union. All Right Reserved. 

# Microplastics in surface sediments of the Ariake Bay

Hiroki Sonoda[1], *Yusuke Okazaki[1], Atsuhiko Isobe[2]

1. Department of Earth and Planetary Sciences, Graduate School of Science, Kyushu University, 2. Research Institute for Applied Mechanics, Kyushu University

Microplastics are small plastic pieces less than five *millimeters* long. Numbers of microplastics floating around Japan are much greater than those of global ocean average. Microplastic cycle in the ocean is not well understood, but their final destinations are sediments. Here we investigate microplastics deposited in surface sediments of the Ariake Bay. We obtained surface sediment samples at 11 sites off Kumamoto city in the Ariake Bay by using Ekman-Berge grab in December 2016. In addition, we collected surface samples from the river mouths of Shirakawa and Midorikawa Rivers. Sediment samples were freeze-dried, weighed ~50 g and washed on a stainless-steel screen with 63 micrometers mesh. The floating and sunken residues were recovered separately by filter paper and treated with 1N HCl and 10% hydrogen peroxide on a hot plate at 200-degree C for an hour. After reaction completed, residues were washed by pure water on a nylon screen with 63 micrometers mesh, recovered by filter paper and dried in an oven overnight at 40-degree C. We picked up potential microplastic particles greater than 150 micrometers under stereomicroscope. Identification of microplastics were performed by fourier transform infrared spectroscopy (FT-IR) using FT-IR alpha spectrometry. A total of 18 and 8 microplastics were identified in 11 surface sediment samples off Kumamoto in the Ariake Bay and 3 surface sediment samples from the river mouths, respectively. Most of identified microplastics were polypropylene (PP) and polyethylene (PE). Averaged microplastic contents at the 11 sites off Kumamoto was 29 pieces per kg of dry sediment. No clear trend between geographic distribution pattern of microplastics and distance from the Kumamoto coast/river mouths. Rough estimate for microplastic deposition rate off Kumamoto in the Ariake Bay (120 square kilometers) was ranging from 5 to 10 billion pieces per year. This suggests relatively rapid removal of microplastics from water column though their specific gravities are less than one.

Keywords: Microplastics, Marine sediments, Ariake Bay

©2019. Japan Geoscience Union. All Right Reserved. 

[J] Poster | M (Multidisciplinary and Interdisciplinary)：M-IS Intersection

Thu. May 30, 2019 5:15 PM - 6:30 PM JST | Thu. May 30, 2019 8:15 AM - 9:30 AM UTC | Poster Hall International Exhibition Hall8, Makuhari Messe_41

## [M-IS19] Paleoclimatology and paleoceanography

convener:Yusuke Okazaki(Department of Earth and Planetary Sciences, Graduate School of Science, Kyushu University), Akira Oka(Atmosphere and Ocean Research Institute, The University of Tokyo), Michinobu Kuwae(Center for Marine Environmental Studies), Hitoshi Hasegawa(Faculty of Science and Technology, Kochi University)

Past environmental changes and events at multi-decadal to tectonic timescale toward an understanding of Earth climate system by an integration of terrestrial and marine proxy studies and numerical modeling will be discussed. At JpGU2019, a series of presentations on present and future climate and environmental changes from paleo-perspective will be held. We welcome a variety of paleo-environmental studies from a wide range of background. We hope that this session will provide an opportunity to promote communication between participants from multidisciplinary field.

### [MIS19-P01] Orbital-scale changes in redox condition and biogenic silica/detrital fluxes of the Jurassic Radiolarite: Possible link with glaciation?

*Masayuki Ikeda[1] (1.Shizuoka University)

### [MIS19-P02] Evaluation of hinterland weathering and paleoclimate of the Cretaceous strata in the Sichuan basin, central China

*Tenichi Cho[1], Hideaki Mantani[1], Tohru Ohta[1], Gang Li[2] (1.Waseda University, 2.Nanjing Institute of Geology and Paleontology)

### [MIS19-P03] Productivity-induced lacustrine bedded chert formation in the Eocene Green River Formation

*Ryusei Kuma[1], Hitoshi Hasegawa[2], Koshi Yamamoto[1], Hidekazu Yoshida[1], Masayuki Ikeda[3], Nagayoshi Katsuta[4], J. Whiteside[5] (1.Nagoya University, 2.Kochi University, 3.Shizuoka University, 4.Gifu University, 5.Southampton University)

### [MIS19-P04] Extraction of the sedimentary cycles and application of cyclostratigraphy to the Middle Miocene Onnagawa Formation in Yashima District, Akita Prefecture, Japan

*Jumpei Yoshioka[1], Ryuji Tada[1,3], Kenji Marc Raymond Matsuzaki[2], Toshihiro Tada[1], Aki Sakuma[1], Yusuke Umemiya[1], Shunsuke Kurokawa (1.Department of Earth and Planetary Science, the University of Tokyo, 2.Atmosphere and Ocean Research Institute, the University of Tokyo, 3.Yunnan University)

### [MIS19-P05] Pliocene magneto–oxygen isotope stratigraphy from the Anno Formation, Awa Group, central Japan

*Yuki Haneda[1], Makoto Okada[1] (1.College of Science, Ibaraki University)

### [MIS19-P06] Planktonic foraminiferal assemblage and paleoceanography of the Plio-Pleistocene sequence at IODP Site U1499 in the northern South China Sea

*Mizuki Kitamura[1], Akira Furusawa[1], Hiroki Hayashi[1] (1.SHIMANE University)

### [MIS19-P07] Reconstruction of the surface water mass fluctuation during the late Pliocene to early Pleistocene based on planktonic foraminiferal fossils from the Mera Formation, Chikura Group, in the southernmost part of the Boso Peninsula

*Makoto Okada[1], Daisuke Hasegawa[2] (1.Department of Earth Sciences, Faculty of Science, Ibaraki University, 2.Graduate School of Scinece and Engineering, Ibaraki University)

### [MIS19-P08] Centennial-scale bioproductivity changes during the earliest Middle-Pleistocene

*Waka Fujii[1], Masayuki Hyodo[1], Shigehiro Katoh[2], Yosuke Miyairi[3], Haruka Yamaguchi[1], Yusuke Yokoyama[3] (1.Kobe University, 2.Hyogo Museum of Nature and Human Activities, 3.University of Tokyo)

[MIS19-P09] Development of new-paleoceanographic proxies based on oxygen isotope analysis of sponge spicule

*Hitomi Uchimura Wakaki[1], Akira Ijiri[2], Minoru Ikehara[1], Sangmin Hyun[3] (1.Center for Advanced Marine Core Research, Kochi University, 2.Japan Agency for Marine-Earth Science and Technology, 3.Korea Institute of Ocean Science & Technology)

[MIS19-P10] A system for automatic collection of specific microfossil species using a deep learning classification

*Takuya Itaki[1], Yosuke Taira[2], Naoki Kuwamori[2], Toshinori Maebayashi[3], Satoshi Takeshima[4], Kenji Toya[4] (1.Geological Survey of Japan, AIST, 2.NEC Corporation, 3.Microsupport Co.Ltd, 4.Mitani-Corporation)

[MIS19-P11] Towards reconstructing environmental conditions related to Australian Great Barrier Reef initiation

*Stephen Obrochta[1], Wataru Miwa[1], Kotaro Shirai[2], Yusuke Yokoyama[2], Yosuke Miyairi[2], Jody Webster[2,3], Albert Hine[4] (1.Akita University, 2.University of Tokyo Atmosphere and Ocean Research Institute, 3.University of Sydney, 4.University of South Florida College of Marine Science)

[MIS19-P12] An 8,000-year climate record from Lake Motosu, Japan: Implications for the East Asian Monsoon

Sarah McDonlad[3], Jonathan Tyler[3], *Stephen Obrochta[1], Yusuke Yokoyama[2], Yosuke Miyairi[2], Kosuke Ota[2] (1.Akita University, 2.University of Tokyo Atmosphere and Ocean Research Institute, 3.Department of Earth Sciences, The University of Adelaide)

[MIS19-P13] Environmental changes in northern Mongolia in During the Late Pleistocene: chemical analyses of lacustrine sedimentary sequences in Darhad basin

Yumiko Ohno[1], Sayuri Naito[1], *Nagayoshi Katsuta[1], Takuma Murakami[3], Shinya Ochiai[2], Noriko Hasebe[2], Shin-ichi kawaka[4] (1.Faculty of Education, Gifu University, 2.Institute of Natural and Environmental Technology, Kanazawa University, 3.Horonobe Research Inst. for the Subsurface Environment, 4.Faculty of Education, Gifu Shotoku Gakuen University)

[MIS19-P14] Paleoenvironmental changes recorded in Orog Lake, southwestern Mongolia during MIS 3 and its relationship with *Homo sapiens*'s migration into northern Asia

*Hitoshi Hasegawa[1], Nanase Noma[1], Nagayoshi Katsuta[2], Masafumi MURAYAMA[3], Toru Tamura[4], Masami Izuho[5], Niiden Ichinnorov[6], Davaasuren Davaadorj[7], Noriko Hasebe[8], Miho Sasaoka[9], Masao Iwai[9] (1.Faculty of Science and Technology, Kochi Univ., 2.Faculty of Education, Gifu Univ., 3.Faculty of Agriculture and Marine Science, Kochi Univ., 4.Geological Survey of Japan, AIST, 5.Faculty of Social Sciences and Humanities, Tokyo Metropolitan Univ., 6.Mongolian Academy of Sciences, 7.National University of Mongolia, 8.Institute of Nature and Environmental Technology, Kanazawa Univ., 9.Center for Advanced Marine Core Research, Kochi Univ.)

[MIS19-P15] Reconstruction for water-mass structure of the Okhotsk Sea for the past 1.5 million years based on radiolarian assemblages

*Tatuya Sakamoto[1], Yusuke Okazaki[1] (1.Department of Earth and Planetary Sciences, School of Science, Kyushu University)

[MIS19-P16] Silicoflagellate assemblages in the Okhotsk Sea during the interglacial periods

*Kazuki Egashira[1], Yusuke Okazaki[2], Tatsuhiko Sakamoto[3] (1.Department of Earth and Planetary Sciences, Kyushu University, 2.Department of Earth and Planetary Sciences, Graduate School of Science, Kyushu University , 3.Mie University)

[MIS19-P17] Role of wind stress and sea surface thermal forcing in the formation of the Atlantic meridional overturning circulation at the Last Glacial Maximum

*Akira Oka[1], Kazuki Togawa[1] (1.Atmosphere and Ocean Research Institute, The University of Tokyo)

[MIS19-P18] Comparison of the Kuroshio during LGM simulated by an ocean general circulation model driven by multiple paleoclimate models

*Kensho Ichikawa[1], Haiyan Yang[2], Xinyu Guo[2], Yasumasa Miyazawa[3] (1.Graduate School of Science and Engineering,Ehime University, 2.Center for Marine Environmental Studies,Ehime University, 3.Japan Agency for Marine-Earth Science and Technology)

[MIS19-P19] The changes of the Kuroshio path in the Northwest Pacific since 35ka

*Haiyan Yang[1], Xinyu Guo[1], Ayako Abe-Ouchi[2], Yasumasa Miyazawa[3], Sergey Varlamov[4], Wing-Le Chan[2] (1.Center for Marine Environmental Studies, Ehime University, 2.Atmosphere and Ocean Research Institute, University of Tokyo, 3.Research Institute for Global Change, Japan Agency for Marine-Earth Science and Technology, 4.Application Laboratory, Japan Agency for Marine-Earth Science and Technology)

[MIS19-P20] Temperature reconstruction in the late Pleistocene using fossil terrestrial snails and a stalagmite from an archaeological cave in Okinawa

*Ryuji Asami[1], Rikuto Hondoh[2], Ryu Uemura[3], Ryuichi Shinjo[3], Akihiro Kano[4], Masaki Fujita[5], Shinji Yamasaki[6], Hideko Takayanagi[1], Yasufumi Iryu[1] (1.Graduate School of Science, Tohoku University, 2.Faculty of Science, Tohoku University, 3.Faculty of Science, University of the Ryukyus, 4.School of Science, the University of Tokyo, 5.National Museum of Nature and Science, 6.Okinawa Prefectural Museum and Art Museum)

[MIS19-P21] Silicoflagellate and *Actiniscus* response to meltwater during the last deglaciation in the Alaska margin

*Asuka Tomokawa[1], Yusuke Okazaki[1], Jonaotaro Onodera[2], Keiji Horikawa[3] (1.Department of Earth and Planetary Sciences, Kyushu University, 2.Research and Development Center for Global Change, JAMSTEC, 3.Graduate School of Engineer and Science, University of Toyama)

[MIS19-P22] Application of the ramped pyrolysis $^{14}C$ dating to postglacial sediments from the Alaskan margin, Arctic Ocean

*Kenta Suzuki[1], Masanobu Yamamoto[1,2], Brad Rosenheim[3], Takayuki Omori[4], Leonid Polyak[5] (1.Graduate School of Environmental Science, Hokkaido University, 2.Faculty of Environmental Earth Science, Hokkaido University, 3.College of Marine Science, University of South Florida, 4.The University Museum, The University of Tokyo, 5.Bard Polar and Climate Research Center, Ohio State University)

[MIS19-P23] Utility of sedimentary environmental DNA for indices of past pelagic fish species populations

*Hiromichi Tamai[1], Michinobu Kuwae[2], Hideyuki Doi[3], Toshihumi Minamoto[4] (1.Graduate School of Science and Engineering, Ehime university, 2.Center for Marine Environmental Studies, Ehime university, 3.Graduate School of Simulation Studies, University of Hyogo, 4.Graduate School of Human Development and Environment, Kobe University)

[MIS19-P24] Improvements of extraction methods of sedimentary fish-origin DNA for reconstruction of marine fish communities

*Jun Kurata[1], Hiromichi Tamai[2], Hideyuki Doi[3], Toshihumi Minamoto[4], Michinobu Kuwae[5] (1. department of earth science, Ehime university, 2.Graduate School of Science and Engineering, Ehime university, 3.Graduate School of Simulation Studies, University of Hyogo, 4.Graduate School of Human Development and Environment, Kobe University, 5.Center for Marine Environmental Studies, Ehime university)

[MIS19-P25] The paleotemperature reconstruction during the late-Holocene using the sediment core recovered from the Tokyo Bay, Japan

*Hiroto Kajita[1,2,3,4], Naomi Harada[5], Miyako Sato[5], Nanako Ogawa[1], Yusuke Yokoyama[1,2,4], Chikako Sawada[1], Yosuke Miyairi[1], Masayuki Utsunomiya[3], Atsushi Suzuki[3], Hodaka Kawahata[1,2,3] (1.Atmosphere and Ocean Research Institute, The University of Tokyo, Japan, 2.Department of Earth and Planetary Science, Graduate school of Science, The University of Tokyo, Japan, 3. Research Institute of Geology and Geoinformation, Geological Survey of Japan, National Institute of Advanced Industrial Science and Technology (AIST), Japan, 4.Department of Biochemistry, Japan Agency for Marine-Earth Science and Technology (JAMSTEC), Japan, 5.Research and Development Center for Global Change, Japan Agency for Marine-Earth Science and Technology (JAMSTEC), Japan)

[MIS19-P26] Summer monsoon variability over the past 400 years in Tateyama, Japan, as reconstructed from tree-ring oxygen isotope data

*Masaki Sano[1], Kota Mori[1], Akane Tsushima[2], Zhen Li[3], Koh Yasue[4], Takeshi Nakatsuka[2,3] (1.Faculty of Human Sciences, Waseda University, 2.Nagoya University, 3.Research Institute for Humanity and Nature, 4.Shinshu University)

[MIS19-P27] Eventural Layers of anciant disasters during these 4500 years at Lake Ikeda (Lake Daijya), western coast of Kyushu Island presumed by diatom assemblages in lake deposits

*Kaoru Kashima[1], Tomokazu Mita[1], Yu Fukumoto[3], Tsuyoshi Haraguchi[2], Kazuyoshi Yamada[4] (1.Department of Earth and Planetary Sciences, Kyushu University, 2.Department of Geosicneces, Graduate School of Science, Osaka City University, 3.Ritsumeikan University, 4.Museum of Natural and Environmental History, Shizuoka)

[MIS19-P28] Variability of hemipelagic and event depositions in the Beppu Bay during Holocene

*Tomohisa Irino[1], Airi Maruyama[1], Ken Ikehara[2], Masanobu Yamamoto[1], Michinobu Kuwae[3] (1.Graduate School of Environmental Science, Hokkaido University, 2.Institute of Geology and Geoinformation, National Institute of Advanced Industrial Science and Technology, 3. Center for Marine Environmental Studies, Ehime University)

[MIS19-P29] The composition of laminae in the sediment of Beppu-Bay and potential as annual laminations

*Yoshiaki Suzuki[1], Michinobu Kuwae[2], Kazuno Arai[3], Ken Ikehara[4], Masafumi MURAYAMA[3] (1.Waseda University, 2.Ehime University, 3.Kochi University, 4.AIST)

[MIS19-P30] Simulation of global distribution of Pa/Th using an ocean general circulation model

*Yusuke Sasaki[1], Akira Oka[1] (1.Atmosphere and Ocean Research Institute, The University of Tokyo)

[MIS19-P31] Construction of modern silicoflagellate assemblage dataset in the North Pacific for paleo sea-surface temperature and its application for sediment cores

*Yusuke Okazaki[1], fumiaki nishizono[1], Tanizaki Kyohei[1] (1.Department of Earth and Planetary Sciences, Graduate School of Science, Kyushu University)

[MIS19-P32] Microplastics in surface sediments of the Ariake Bay

Hiroki Sonoda[1], *Yusuke Okazaki[1], Atsuhiko Isobe[2] (1.Department of Earth and Planetary Sciences, Graduate School of Science, Kyushu University, 2.Research Institute for Applied Mechanics, Kyushu University)

# Orbital-scale changes in redox condition and biogenic silica/detrital fluxes of the Jurassic Radiolarite: Possible link with glaciation?

*Masayuki Ikeda[1]

1. Shizuoka University

Orbital forcing has been shown to be a fundamental driver of climate change through both icehouse and greenhouse periods. To reveal the impact of orbital-forcing on the oceanic environment through a greenhouse-icehouse transition, we established ~ 4 Myr-long cyclostratigraphy of the Bajocian-Callovian (Middle Jurassic; ~ 160 Ma) Basal Radiolarites at the Torre De Busi and Corre Di Sogno sections in the Lombardian Basin, N-Italy. Stratigraphic changes in chertabundance (chert/shale thickness ratio) and color (darkness) of Radiolarites show hierarchal periodicities of 8 cm, 16 cm, 40 cm, 160 cm, and ~ 4 m, corresponding to ~ 20 kyr, 40 kyr, 100 kyr, 400 kyr, and ~ 1 Myr cycles based on the biostratigraphic age model. Black cherts in intervals with high chert abundance might reflect oxygen-depleted conditions due to orbital-scale high productivity. On the other hand, black cherts in intervals with low chert abundance (high detrital input) might reflect oxygen-depleted conditions, probably due to orbital-scale sea-level drop and stratification. On 40 kyr and 100 kyr cycles, the anoxic condition occurred in low chert abundance intervals across ~ 8 m above (~ 2 Myr after) the base of the Radiolarites. These results imply that the formation of the restricted basin resulted from tectonic and/or eustatic sea-level drop, which is consistent with increased black chert deposition and redox-sensitive elements abundances (Mo/TOC, Mo/U). Their out-of-phase relationships on the 405 kyr cycle throughout the sequence (~ 4 Myr-long) with increasing amplitude above −8 M level would be caused possibly by tectonic activity, or more likely by glacio-eustatic sea-level changes reported from sequence stratigraphy, similar to those of the Oligocene to Pliocene glacial cycles, but probably with less amplitude.

Keywords: icehouse, greenhouse, orbital cycle

©2019. Japan Geoscience Union. All Right Reserved. 

# Evaluation of hinterland weathering and paleoclimate of the Cretaceous strata in the Sichuan basin, central China

*Tenichi Cho[1], Hideaki Mantani[1], Tohru Ohta[1], Gang Li[2]

1. Waseda University, 2. Nanjing Institute of Geology and Paleontology

Reconstruction of paleoclimate during the Cretaceous Period is important for the understanding of the Earth system operating during the greenhouse conditions. However, information of paleoclimate from continental inland-basins is scarce compared to continental margin marine-basins. This situation is also true in the Asian continent; Cretaceous ecosystem and paleoclimate data are accumulating in the Pacific side, while those of the Asian continental side is lacking. Paleoclimate conditions in Asian inland basins are considered to be equally important in order to elucidate the land-ocean climate system operated during the Cretaceous. In this regard, the present study investigates the geochemistry and clay mineralogy of the Cretaceous mudstones distributed in the Sichuan basin, central China, for the aim of paleoclimate evaluation. The depositional age of studied strata ranges from Berriasian to Maastrichtian. Sediments are mostly fluvial to lacustrine origin, however recently, a broad distribution of aeolian dune sandstones was identified from the Cenomanian to Turonian interval (Li et al., 2016). Before discussing hinterland weathering and paleoclimate, the effect of diagenesis was evaluated, which can alter the geochemical signatures of paleoclimate. The illite crystallinity index indicates that diagenetic effect was moderately high for the analyzed mudstones, and the degree of diagenesis has a high correlation with CaCO3 abundance. Accordingly, CaO wt% abundances are mostly of post-depositional carbonate origin, and thus, CaO derived from carbonates was subtracted from the following discussion of hinterland weathering evaluation. Geochemical weathering indices (e.g., W value) demonstrate a significant increase in hinterland paleoweathering from Berriasian (W=70) to Cenomanian-Turonian (W=95), and then slightly decrease towards the Maastrichtian (W=80). This fluctuation pattern of the weathering indices is concordant with the Cretaceous paleotemperature estimates (e.g., O’ Brien et al., 2017). Therefore, the present result suggests that the hinterland paleoweathering rate in the Sichuan basin was governed by the global temperature changes. The weathering index reached the maximum value of 95 in Cenomanian-Turonian stages. Furthermore, sediments of Cenomanian-Turonian horizons contained abundant kaolinite mineral, which is a product of hydrolysis decomposition of rock-forming minerals. Both lines of evidence suggest that the Sichuan basin was under the tropical and pluvious climate during the Cenomanian-Turonian. However, as mentioned before, the previous study identified aeolian sand dunes from the Cenomanian-Turonian strata. Note that Li et al. (2016) elucidated an arid climate from amalgamated sandstone facies, while the present pluvious climate interpretation is derived from the analysis of intervening piled mudstone facies. When these geological evidences are integrated together, it is reasonable to suggest the development of an alternating pluvious and arid paleoclimate during the Cenomanian-Turonian. The nature and trigger of this extremely oscillating pluvious/arid climate cannot be deduced solely from the present study. However, the timing of this renewed climate system matches with the Cretaceous greenhouse optimum (Cenomanian-Turonian). The development of monsoon-like pluvious/arid paleoclimate in the Sichuan basin is possibly related to the mid-Cretaceous re-configuration in the global climate system.

Keywords: Cretaceous, Continental weathering, Alluval deposits, Desert deposits, XRF, W index

©2019. Japan Geoscience Union. All Right Reserved. 

# Productivity-induced lacustrine bedded chert formation in the Eocene Green River Formation

*Ryusei Kuma[1], Hitoshi Hasegawa[2], Koshi Yamamoto[1], Hidekazu Yoshida[1], Masayuki Ikeda[3], Nagayoshi Katsuta[4], J. Whiteside[5]

1. Nagoya University, 2. Kochi University, 3. Shizuoka University, 4. Gifu University, 5. Southampton University

Rhythmically alternated beds of chert and shale, also called as bedded chert, are commonly observed in marine sedimentary rocks. Recent studies revealed that changes in bed thickness of chert represent orbitally-paced variations in marine productivity and silicate weathering rate (Hori et al., 1993; Ikeda et al., 2017). On the other hand, bedded cherts are occasionally found in lacustrine deposits. Previous study interpreted that formational mechanism of lacustrine bedded chert is linked to the interplay between silica dissolution in alkaline lake waters and its precipitation due to the conversion of lake water’ s pH (e.g. Hesse, 1989). Some studies suggested that the pH of saline and alkaline lake water could have changed by the freshwater input (Eugster, 1967; Eugster 1969). Other study implied that the metabolic processes of cyanobacteria modified the pH of lake water and influenced to the silica precipitation (Behr and Rohricht, 2000). However, convincing evidence of chertification mechanism in lacustrine deposits have not been clarified yet.

In order to elucidate the formation mechanism of lacustrine chert, the present study examined a lacustrine bedded chert succession in the Eocene Green River Formation in northern Utah, USA. We have conducted detailed field survey in the Indian Canyon section in northern Utah. Bedded cherts occur in shallow lake level stage and alternated with dolomite beds with every 5–10 cm in thickness. Elemental mapping by Scanning X-ray analytical microscope (SXAM) reveals that the Ca concentration in dolomite layer, while Si concentration in chert layer, with sharp boundary coincide with lithofacies boundary. Elemental distribution also shows that alternation of chert and dolomite occur in every 1–2 cm in thickness. In addition, fluorescent microscopic inspection reveals that the distribution of Si concentration coincides with the dense accumulation of spherical organic matter. These spheres show the brightest fluorescence carbon shell with similar size (30–40 $\mu$m). The morphology of these spherical organic matter resembles to green algae, such as *Botryococcus braunii*, which are also abundantly preserved in the Green River Formation. Occurrences of algal organic matters in chert layer imply that deposition of algal organic matter could be related with the formation of lacustrine chert.

It is noteworthy that the lake water alkalinity of the Green River Formation is considered to be high (pH>9) because of extensive volcanic activity around Colorado Plateau. These lines of evidence suggested that silica precipitation is possibly caused by decreased pH due to the decaying organic matter (increasing $CO_2$ and/or organic acid) in sediment pore water. Deposition of organic matter can be related to changes in the lake algal productivity. Given that sedimentation rate of the formation in Indian Canyon section is estimated as ca. 10–15 cm/kyr (Smith et al., 2008), observed chert occurrence (1–2 cm and 5–10 cm) yields 67–200 and 333–1000 year’ s cyclicities. Therefore, periodic occurrences of chert beds in the Green River Formation are possibly linked to the centennial-scale changes in the lake algal productivity.

Keywords: lake sediments, Eocene, productivity, chert, silica, pH

©2019. Japan Geoscience Union. All Right Reserved. 

# Extraction of the sedimentary cycles and application of cyclostratigraphy to the Middle Miocene Onnagawa Formation in Yashima District, Akita Prefecture, Japan

*Jumpei Yoshioka[1], Ryuji Tada[1,3], Kenji Marc Raymond Matsuzaki[2], Toshihiro Tada[1], Aki Sakuma[1], Yusuke Umemiya[1], Shunsuke Kurokawa

1. Department of Earth and Planetary Science, the University of Tokyo, 2. Atmosphere and Ocean Research Institute, the University of Tokyo, 3. Yunnan University

Middle Miocene (16.0-11.6Ma) is the time of the second of the three cooling steps during Cenozoic. In this cooling event, siliceous sediments with high organic contents were widely deposited along the North Pacific rim because of high productivity and/or preservation of diatoms. In the northern Japan Sea, those sediments are known as the Onnagawa Formation. It was reported that siliceous rocks in the Onnagawa Fm. showed meter-scale rhythmical bedding reflecting fluctuations in productivity of diatoms and flux of detrital materials. Furthermore, it was also reported that parts of highly siliceous rocks in the Onnagawa Fm. showed centimeter-scale black bands. However, the age and the cause of their occurrence has not been understood.

In this study, we tried to construct a high-resolution and precise age model of the Onnagawa Fm. in the Yashima District by applying cyclostratigraphy to the m-scale rhythmical bedding, that is attributable to the fluctuation of biogenic silica content.

Firstly, a ca. 130m-long continuous composite columnar section was constructed by correlation of 6 sections. This composite columnar section is divided into 5 lithological units, cyclic alternations of marl and interbedded mudstone (Unit A), mudstone with cyclic siliceous rocks intercalations (Unit B), siliceous-mudstone with muddy-porcelanite intercalations (Unit C), bedded muddy-porcelanite with cm-scale black bands (Unit D) and siliceous-mudstone and hard siliceous-mudstone alternations (Unit E).

“Silica rank”, which is defined as degree of siliceousness and divided into 5 grades based on hardness of the siliceous rocks observed in the field and confirmed by XRD analysis, was determined every 10cm for Unit B, Unit C and Unit D. It showed obvious m-scale cyclicities. The silica rank variation for Unit B and Unit C was obviously different from that for Unit D, and it is considered that this difference may reflect either the change in the sedimentation rate or the change in response of sedimentation mechanism to the orbital forcing that results in the lithological change. In order to construct an age model, the silica rank was tuned to $\delta^{18}O$ of benthic foraminifera with age constraints given by microfossil biostratigraphy.

Keywords: the Onnagawa Fm., Miocene, silica rank, cyclostratigraphy

©2019. Japan Geoscience Union. All Right Reserved. 

# Pliocene magneto–oxygen isotope stratigraphy from the Anno Formation, Awa Group, central Japan

*Yuki Haneda[1], Makoto Okada[1]

1. College of Science, Ibaraki University

The Pliocene climate is one of the best analogs for the climate of a globally warmer future. Here, we present a new Pliocene integrated chronostratigraphy from the Anno Formation in the uppermost Awa Group, which is distributed throughout the Boso Peninsula, central Japan, based on paleomagnetic and benthic foraminiferal oxygen isotope records. This new chronostratigraphy provides valuable constraints for paleoceanographic and paleoclimatic studies in the northwestern Pacific Ocean, where the number of paleoceanographic records is limited due to the lack of calcareous microfossils from deep-sea sediment cores, with the exception of some plateaus at water depths above the calcite compensation depth (CCD).

We performed progressive Alternating field and thermal demagnetizations for each specimen in order to remove secondary remanence. Additionally, we conducted thermomagnetic, low-temperature magnetic, magnetic hysteresis, and FORC analyses as rock-magnetic experiments to assess stability of paleomagnetic signal which specimens have acquired. The paleomagnetic and rock-magnetic experiments indicate that primary remanences are carried by magnetite in pseudo-single domain size as detrital remanent magnetization. The progressive AF demagnetization is, however, unsuitable to remove secondary remanence in specimens from polarity transitional horizons due to magnetically hard mineral, such as goethite. Therefore, thermal demagnetization is necessary to obtain primary remanence from the Anno Formation.

Paleomagnetic results by the thermal demagnetization indicate that the Anno Formation corresponds to the period extending from the Nunivak normal polarity subchronozone (4.493–4.631 Ma) to Chron C2An.2n (3.116–3.207 Ma). Although foraminifera are not found in the middle Anno Formation, our oxygen isotope records from the upper and lower Anno Formation demonstrate the recording of glacial–interglacial cycles. However, the amplitude of our $\delta^{18}O$ profile is much larger than that of the LR04 stack, with similar to slightly lower glacial values and much lower interglacial values. This trend is suppressed after 3.4 Ma. These observations imply that the bottom water had lower $\delta^{18}O$ values and/or a warmer water mass during interglacials until 3.4 Ma compared with global average deep-water regions.

Keywords: Pliocene, Boso Peninsula, Anno Formation, Benthic foraminifera, Oxygen isotope stratigraphy, Magnetostratigraphy

©2019. Japan Geoscience Union. All Right Reserved. 

# Planktonic foraminiferal assemblage and paleoceanography of the Plio-Pleistocene sequence at IODP Site U1499 in the northern South China Sea

*Mizuki Kitamura[1], Akira Furusawa[1], Hiroki Hayashi[1]

1. SHIMANE University

The South China Sea (SCS) is a marginal sea located in the tropical zone of the western Pacific with an average depth of ca. 1,140 m. The East Asian monsoon affects the climate system in this area by the prevailing seasonal winds. Such influence of the East Asian monsoon is expected to be stronger during the glacial period and weaker during the interglacial period.
During Internatinal Ocean Discovery Program (IODP) Expedition 367, drilling of Site U1499 was conducted near the outer shelf of the northern SCS in 2017. As an onboard result of this site, sediments from Oligocene to Present were recovered and the upper sequence especially contains abundant foraminiferal fossils. The purpose of the present study is to clarify temporal changes of planktonic foraminiferal assemblage in the northern SCS from approximately 4 to 1 Ma.
As a result, 80 species belonging to 19 genera of planktonic foraminifera were detected. According to multivariate analyses of the foraminiferal assemblage, we determined the temporal change into four stages: Stage A (ca. 4.1 to 3.4 Ma), Stage B (ca. 3.4 to 1.8 Ma), Stage C (ca. 1.8 to 1.45 Ma) and Stage D (ca. 1.4 to 1 Ma). During Stage A, SCS had been stratified by oligotrophic tropical surface water and relatively cold subsurface water with a shallow thermocline. At the next Stage B, the thermocline was deepened and SCS was occupied by a subtropical oligotorophic water. In turn, the thermocline shoaled and subsurface species of planktonic foraminifera were increased during the Stage C. After that, the Stage D is characterized by alternative changes between subtropical surface components and cold-temperate components caused by the glacial-interglacial changes.

Keywords: South China Sea, Planktonic foraminifera, Pliocene, Pleistocene, International Ocean Discovery Program

©2019. Japan Geoscience Union. All Right Reserved. 

# Reconstruction of the surface water mass fluctuation during the late Pliocene to early Pleistocene based on planktonic foraminiferal fossils from the Mera Formation, Chikura Group, in the southernmost part of the Boso Peninsula

*Makoto Okada[1], Daisuke Hasegawa[2]

1. Department of Earth Sciences, Faculty of Science, Ibaraki University, 2. Graduate School of Scinece and Engineering, Ibaraki University

The purpose of this study is to examine whether the cooling event has occurred associate with the NHG (Northern Hemisphere Glaciation) off the Boso peninsula and how the surface water mass has changed with the glacial-interglacial cycle. We carried out analysis of planktonic foraminiferal assemblages at the 57 horizons corresponding to period from 3.0 Ma to 2.2 Ma. We propose 6 phases including the following three distinctive phases based on relative abundance of environmental indicator species.
Phase Ⅱ (2.75-2.65Ma): Transitional water species increased up to 50%. It was a cold environment where the influence of mixed water was strong.
Phase Ⅴ (2.42-2.35Ma): Kuroshio species increased up to 40%, which is the highest value in this study
PhaseⅥ (2.35Ma~):Transitional water species increased to about 50% while repeating amplitude. Therefore, cooling was gradually strengthened in this phase.
Cooling did not proceed unilaterally after 2.7Ma, it occurs again from 2.35Ma after the period when the influence of Kuroshio became temporarily stronger. In addition the glacial-interglacial cycles seem to be affecting composition of planktonic foraminiferal assemblages.

Keywords: Planktonic foraminiferal assemblages, Chikura Group, Northern Hemisphere Glaciation

©2019. Japan Geoscience Union. All Right Reserved. 

# Centennial-scale bioproductivity changes during the earliest Middle-Pleistocene

*Waka Fujii[1], Masayuki Hyodo[1], Shigehiro Katoh[2], Yosuke Miyairi[3], Haruka Yamaguchi[1], Yusuke Yokoyama[3]

1. Kobe University, 2. Hyogo Museum of Nature and Human Activities, 3. University of Tokyo

Elucidation of the mechanism of global warming in the geological time is important, which may lead to understanding of the present global warming. In this study, we conducted paleoenvironmental analyses of sediments to reveal the rapid climate changes across the warmest interval in the Marine Isotope Stage (MIS) 19 interglacial, which is known as an orbital analogue of the Holocene. In particular, we aim at elucidating the mechanism of the repeated bioproductivity proxy (Ca/Ti ratio) changes dominated by bicentennial cycles for a span from about 777 to 775 ka, which was observed in core TB2 from the Chiba Section. Focused on the time span, we conducted pollen analyses using the Osaka Bay 1,700 m core with abundant pollen fossils, and measurements of $^{10}$Be using core TB2. Both cores are stratigraphically correlated with the centennial to millennial scale resolution. The result of pollen analyses revealed that the proportion of evergreen *Quercus* (*Cyclobalanopsis*), a warm proxy, began at about 777 ka to increase with bicentennial oscillations, followed by a sudden drop within 1 kyr. These changes are quite consistent with those in the bioproductivity in core TB2. Therefore, the bioproductivity changed affected by the climate. The $^{10}$Be content, an index of the galactic cosmic ray flux, generally showed similar changes with the bioproductivity except some intervals, one of which showed a large disagreement between the $^{10}$Be flux and the bioproductivity, coincided with the iceberg discharge event in the North Atlantic. These results suggest that the centennial-scale bioproductivity changes observed in core TB2 probably reflect climate variations, and may be affected by solar activity. Solar activity can affect climate through galactic cosmic rays that control the low cloud (Svensmark effect), in addition to the direct influence through solar radiation.

©2019. Japan Geoscience Union. All Right Reserved. 

# Development of new-paleoceanographic proxies based on oxygen isotope analysis of sponge spicule

*Hitomi Uchimura Wakaki[1], Akira Ijiri[2], Minoru Ikehara[1], Sangmin Hyun[3]

1. Center for Advanced Marine Core Research, Kochi University, 2. Japan Agency for Marine-Earth Science and Technology, 3. Korea Institute of Ocean Science & Technology

The objective of this study is to construct the new-paleoceanographic proxy based on the oxygen isotope ratio of sponge spicule. To examine the variations in water depth and temperature, we selected GH08 surface sediment samples ranging from a water depth of 216 m to 2679 m in the Northwest Pacific. These samples were obtained from the area off eastern Okinawa Island during the GH08 cruise in 2008 by Geological Survey of Japan, AIST. The upper 0–2 cm of each surface sediment was sampled. The sediment samples were washed in a 250-mesh sieve and dried in the oven. In this study, we also analyzed the oxygen isotope ratio of sea-bottom water by laser spectroscopic analysis of Liquid Water Isotope Analyzer (LWIA).

We chose two benthic foraminifers' species *Cibicidoides* sp. and *Cibicidoides wuellerstorfi* to analyze the oxygen isotope ratio. Benthic foraminifer was analyzed by phosphoric acid digestion to carbon dioxide gas and the measurement of the oxygen isotope ratio by IsoPrime at Kochi University. We can recognize that the result of the foraminifera between the oxygen isotope ratio and temperature has a negative trend. In other words, the oxygen isotope ratio of benthic foraminifera in this study shows temperature dependence. Our results agree with those obtained by the previous studies (Marchitto et al., 2014). These results can be regarded as the data of benthic foraminifera in this study is considered appropriate for the reference.

We also analyzed the oxygen isotope ratio of sponge spicule by a new method of iHTR (inductive high-temperature carbon reduction) and CF-IRMS (continuous-flow isotope ratio mass spectrometry) (Ijiri et al., 2014). Some the oxygen isotope ratio values of sponge spicule are consistent with previous reported data (Brandriss et al., 1998, Moschen et al., 2005), which were analyzed the oxygen isotope ratio of biogenic opal (diatom). However, some of the oxygen isotope ratio of sponge spicule don't have any trends. These irregular date has possibility to be influenced by the acid treatment and the difference of gas pressure, and should be evaluated the validity in future experiment used based on additional samples.

Keywords: sponge spicule, benthic foraminifera, stable oxygen isotope, temperature dependence

©2019. Japan Geoscience Union. All Right Reserved. 

# A system for automatic collection of specific microfossil species using a deep learning classification

*Takuya Itaki[1], Yosuke Taira[2], Naoki Kuwamori[2], Toshinori Maebayashi[3], Satoshi Takeshima[4], Kenji Toya[4]

1. Geological Survey of Japan, AIST, 2. NEC Corporation, 3. Microsupport Co.Ltd, 4. Mitani-Corporation

For geochemical analysis such as stable isotope ratio, radiocarbon age and minor elements for a single species of microfossils, a large number of their skeletons is required to pick up one by one with enormous time and effort by a person under a microscope. In this study, we have developed a device that automates these efforts. Even if experts are absent, microfossils are accurately classified their taxonomic species level using deep learning which is one of the learning methods of artificial intelligence, and they are picked up using a micromanipulator installed in the microscope with motorized X-Y stage. It is possible to collect a large number of particles with speed and accuracy that could not be achieved with human hands. This technology to accumulate only specific species of microfossils contributes not only to greatly reduce hand work of picking up, but also to be enable chemical analysis such as isotope ratios and minor elements for small microfossil species that hitherto difficult because the necessary measurement amount cannot be collected.In addition to microfossils, it can be applied to various particles, and it is also expected to be utilized in various fields such as medical, food, horticulture and materials.

Keywords: Microfossil, AI, Automatic classification

©2019. Japan Geoscience Union. All Right Reserved. 

# Towards reconstructing environmental conditions related to Australian Great Barrier Reef initiation

*Stephen Obrochta[1], Wataru Miwa[1], Kotaro Shirai[2], Yusuke Yokoyama[2], Yosuke Miyairi[2], Jody Webster[2,3], Albert Hine[4]

1. Akita University, 2. University of Tokyo Atmosphere and Ocean Research Institute, 3. University of Sydney, 4. University of South Florida College of Marine Science

Previous work exploited the unique mixed carbonate-siliciclastic environment of Northeast Australia to identify the timing of changes in off-shelf sediment transport with respect to sea-level variation. Because sediment transport from the continental shelf to slope is strongly controlled by the presence/absence of a rimmed morphology, this provides a means for indirectly estimating the age of the Great Barrier Reef (GBR). Preliminary results indicate that a change in the timing of maximum off-shelf terrigenous sediment accumulation occurred during the glacial termination of MIS 20. This in turn suggests that an effective barrier morphology was emplaced during the MIS 21 interglacial. Instead of being deposited directly to the continental slope by incised rivers, terrigenous material first accumulated behind the barrier during the MIS 20 sea-level lowstand and was then redoposited as rising sea level reflooded the shelf.

Here we present initial results attempting to understand if and how changing environmental conditions promoted enhanced reef growth. The results include a higher-resolution isotope stratigraphy for improved chronological control, additional terrigenous mass accumulation rate measurements, and initial results of Mg/Ca analyses, which allow for calculating sea surface temperature changes and the oxygen isotopic composition of sea water that is expected to better resolve glacial-interglacial cycles. In the future we expect to add additional information from micro and/or nanofossil faunal assemblage data.

Keywords: Mixed Carbonate-Siliciclastic Sedimentary Systems, Great Barrier Reef

©2019. Japan Geoscience Union. All Right Reserved. 

# An 8,000-year climate record from Lake Motosu, Japan: Implications for the East Asian Monsoon

Sarah McDonlad[3], Jonathan Tyler[3], *Stephen Obrochta[1], Yusuke Yokoyama[2], Yosuke Miyairi[2], Kosuke Ota[2]

1. Akita University, 2. University of Tokyo Atmosphere and Ocean Research Institute, 3. Department of Earth Sciences, The University of Adelaide

The East Asian Summer Monsoon controls the timing and amount of rainfall for around a third of the world’ s population. An understanding of past changes in monsoon strength is thus crucial for placing current events in context and for characterising future climate risk. Whilst many monsoon records have been developed for continental Asia, fewer records exist from the north-eastern edge of the monsoon region. We present a new monsoon record for central Japan based on an 8,000-year lacustrine sedimentary sequence from Lake Motosu, located at the northern foot of Mt Fuji. Lake Motosu is a hydrologically closed lake and is therefore expected to be sensitive to changes in monsoon strength. Additional macrofossil radiocarbon dates are used to refine an existing high-fidelity age model. This age model is then applied to constrain the timing of changes in bulk sediment geochemistry (TC, TN, C/N, $\delta^{13}C$, $\delta^{15}N$) and the oxygen isotopic composition of sedimentary cellulose ($\delta^{18}O$). Changes in sediment chemistry reflect shifts in the sources of organic matter to the sediments, variations in lake hydrology and changes to the local catchment. In turn, these changes are linked to regional variations in monsoon strength. However, their interpretation is complicated by the impact of local seismic and volcanic activity.

Keywords: monsoon, Lake Mostosu, geochemistry

©2019. Japan Geoscience Union. All Right Reserved. 

# Environmental changes in northern Mongolia in During the Late Pleistocene: chemical analyses of lacustrine sedimentary sequences in Darhad basin

Yumiko Ohno[1], Sayuri Naito[1], *Nagayoshi Katsuta[1], Takuma Murakami[3], Shinya Ochiai[2], Noriko Hasebe[2], Shin-ichi kawaka[4]

1. Faculty of Education, Gifu University, 2. Institute of Natural and Environmental Technology, Kanazawa University, 3. Horonobe Research Inst. for the Subsurface Environment, 4. Faculty of Education, Gifu Shotoku Gakuen University

Spread of modern human (*Homo sapiens*) from Africa to Eurasia seems to have occurred in the periods from ca. 60 kyrs ago to ca. 50 kyrs ago via two routes from western Asia into northern Eurasia and across Arabia into southern Asia. To understand relationship between environmental changes and human migration in central Eurasia, we reconstructed a 120-kyr sediment record of environmental change using the Darhad basin (northern Mogolia) sediment core with a nondestructive $\mu$-XRF techniques of Horiba SXAM, XRD analysis, and petrolograhic observation.

Keywords: north Mongolia, sediment, paleoglacial lake

©2019. Japan Geoscience Union. All Right Reserved. 

# Paleoenvironmental changes recorded in Orog Lake, southwestern Mongolia during MIS 3 and its relationship with *Homo sapiens*' migration into northern Asia

*Hitoshi Hasegawa[1], Nanase Noma[1], Nagayoshi Katsuta[2], Masafumi MURAYAMA[3], Toru Tamura[4], Masami Izuho[5], Niiden Ichinnorov[6], Davaasuren Davaadorj[7], Noriko Hasebe[8], Miho Sasaoka[9], Masao Iwai[9]

1. Faculty of Science and Technology, Kochi Univ., 2. Faculty of Education, Gifu Univ., 3. Faculty of Agriculture and Marine Science, Kochi Univ., 4. Geological Survey of Japan, AIST, 5. Faculty of Social Sciences and Humanities, Tokyo Metropolitan Univ., 6. Mongolian Academy of Sciences, 7. National University of Mongolia, 8. Institute of Nature and Environmental Technology, Kanazawa Univ., 9. Center for Advanced Marine Core Research, Kochi Univ.

An aim of the present study is to understand detailed paleoenvironmental changes in Mongolia, situated at a key crossroad for *Homo sapiens*'s migration between central, eastern, and northern Asia during the Initial and Early Upper Paleolithic (IUP-EUP). Available archaeological evidences have suggested the emergence of IUP at around ca. 45-40 ka (e.g., Zwyns *et al.*, 2014; Rybin *et al.*, 2016; Izuho *et al.*, 2018). However, yet the paleoenvironmental changes of this period in Mongolia is largely unclear, preventing us to understand whether the possible environmental changes were significant as a major driving forth for modern human's lifeway.

In this paper, we present a new record of paleoenvironmental changes in southwestern Mongolia during MIS 3. In January 2017, we took two parallel cores (OROG01, 24 m; OROG02, 21 m) from Orog Lake, a shallow saline lake located in northwestern margin of Gobi Desert. The high-resolution major and minor element composition changes were obtained using μXRF core scanner (Cox, Itrax) at Center for Advanced Marine Core Research, Kochi University. Based on the preliminary results of OSL and 14C age dating, basal age of sediment core OROG01 yielded ca. 38 ±4 ka, nearly accordant with the basal age of ~45 ka reported in the previous study (Yu *et al.*, 2019). On the basis of our high-resolution elemental composition data, in conjunction with previous sedimentological and palynological data (Yu *et al.*, 2019), the paleoenvironments of southwestern Mongolia were more humid with higher lake levels during MIS 3 than Holocene. Our results also suggest periodic and higher amplitude paleoenvironmental changes in this region, which likely correspond to Dansgaard-Oeschger events. This new record would allow us to discuss potential relationship between paleoenvironmental changes and ecosystem changes in Mongolia during the IUP-EUP.

Keywords: Lake sediments, Saline lake, Paleoenvironmental changes, Dansgaad event, Homo sapiens, Initial and Early Upper Paleolithic

©2019. Japan Geoscience Union. All Right Reserved. 

# Reconstruction for water-mass structure of the Okhotsk Sea for the past 1.5 million years based on radiolarian assemblages

*Tatuya Sakamoto[1], Yusuke Okazaki[1]

1. Department of Earth and Planetary Sciences, School of Science, Kyushu University

The North Pacific Intermediate Water (NPIW) play an important role in transporting heat and freshwater. NPIW originates from the Okhotsk Sea where is the southernmost seasonal ice area in the northern hemisphere. Sea-ice in the Okhotsk Sea is formed mainly in the northwestern shelf area and moved south by the seasonal wind. Brine water rejected during sea-ice formation sinks to the intermediate layer and forms the Okhotsk Sea Intermediate Water (OSIW) characterized by abundant particulate organic carbon, low temperature, and rich in oxygen. OSIW is a source water of NPIW. Radiolarians are zooplankton with biogenic opal skeletons, and various species distribute from sea-surface to deep-sea. *Cycladophora davisiana* is a radiolarian species that favors well-ventilated intermediate water masses, therefore, *C. davisiana* is used as indicator of OSIW. In this study, we conducted radiolarian assemblage analysis for a giant piston core sample (MD01-2414, water depth 1123 m) to reconstruct the water-mass structure change for the past 1.5 million years. Size fraction greater 45 micrometers were used for slide preparation for light microscope observation. In general, total radiolarian skeletons during interglacials were 10 to 100 times greater than that during the glacial periods. *Cycladophora davisiana* was abundant during interglacials, suggesting enhanced OSIW formation. However, during MIS 11 and 31 known as the super interglacials, much less C. davisiana abundances were observed, suggesting weaken OSIW formation due to significant sea-ice retreat. Four radiolarian biostratigraphic markers in the North Pacific region were identified: *Amphimelissa setosa*, *Lychnocanomma sakaii*, and *Spongodiscidae* sp. In addition, two radiolarian species *Ceratospyris borealis* and *Zygocircus productus* indicated high productivity during interglacials.

Keywords: Radiolarian, Okhotsk Sea, Intermediate water, Sea ice

©2019. Japan Geoscience Union. All Right Reserved. 

# Silicoflagellate assemblages in the Okhotsk Sea during the interglacial periods

*Kazuki Egashira[1], Yusuke Okazaki[2], Tatsuhiko Sakamoto[3]

1. Department of Earth and Planetary Sciences, Kyushu University, 2. Department of Earth and Planetary Sciences, Graduate School of Science, Kyushu University , 3. Mie University

Silicoflagellate is a phytoplankton with a skeleton of biogenic opal. There are two major genera for modern silicoflagellates: *Dictyocha* mainly dwelling in tropical to temperate regions and *Stephanocha* mainly dwelling in subarctic region. The *Dictyocha*/*Stephanocha* ratio has been used as a paleotemperature proxy. Earth’s climate for the past 800,000 years is characterized by the glacial and interglacial cycles with a frequency of 100,000 years. Oxygen isotope ratios of benthic foraminifera mainly reflect continental ice-sheet volume fluctuations, lighter in the interglacials and heavier in the glacials. This fluctuation is called as Marine Isotope Stage (MIS), odd numbers correspond to interglacials and even numbers correspond to glacials. Among the interglacials, the oxygen isotope ratios were lighter than that of the present: MIS 5e (120,000 years ago), 9 (330,000 years ago), and 11 (400,000 years ago). Pollen assemblages in Lake El’gygytgyn sediment from the Far East Russiat in the Arctic Circle indicates pronounced warming during MIS 11. Because atmospheric carbon dioxide concentrations during the past interglacials were comparable to the preindustrial level, it is important to know the status of warming climate during interglacials. The purpose of this study is to reconstruct sea-surface conditions of the Okhotsk Sea during the past interglacials based on silicoflagellate assemblages preserved in sediments. By comparing silicoflagellate assemblages during MIS 1, 5e, 9 and 11, we test the extent of warming during interglacials. The Okhotsk Sea is a marginal sea of the western North Pacific located south of Lake El’gygytgyn, known as southernmost sea-ice covered area in the Northern Hemisphere. A piston core YK07-12 PC-3B (water depth: 1049 m, core length: 14.09 m). Age model of core YK07-12 PC-3B is established by benthic foraminiferal oxygen isotope stratigraphy and the estimate bottom age is 450,000 years ago. Silicoflagellate assemblage analysis was performed by using sediment samples collected from sedimentary horizons corresponding to MIS 1, 5e, 9, and 11. For each interglacials, three samples from peaks of biogenic opal content, maximum calcium carbonate content and minimum benthic foraminiferal oxygen isotope ratio were picked up, consequently, a total of 12 samples were selected. 100 silicoflagellate specimens were counted for each slide under light microscope. Almost all encountered silicoflagellate species during core YK07-12 PC-3B microscopic observation were belonging to genus *Stephanocha*. During MIS 11, *Stephanocha speculum*(particularly, *S. speculum minuta*) was the most abundant silicoflagellate taxa. Because *Stephanocha speculum*is known as a representative silicoflagellate species in the subarctic Pacific dwelling cold and nutrient rich environments, this result indicates that there is no evidence of significant warming in the Okhotsk Sea during MIS 11. Another abundant silicoflagellate species in core YK07-12 PC-3B was *Stephanocha octangulata*, also known as subarctic taxa. This species was dominant during MIS 1 and 5e. Unique oceanic environments such as seasonal sea-ice coverage and influence of low salinity water originating from the Amur River may have influenced on the silicoflagellate assemblages of core YK07-12 PC-3B.

©2019. Japan Geoscience Union. All Right Reserved. 

# Role of wind stress and sea surface thermal forcing in the formation of the Atlantic meridional overturning circulation at the Last Glacial Maximum

*Akira Oka[1], Kazuki Togawa[1]

1. Atmosphere and Ocean Research Institute, The University of Tokyo

In Previous Paleoclimate Model Intercomparison Project (PMIP) simulations of the Last Gracial Maximum (LGM) Atlantic Meridional Overturning Circulation (AMOC), the most of PMIP2 and PMIP3 models reproduced the 'deeper and stronger' AMOC than preindustrial simulations, in contrast to some reconstructions from paleo proxy data.Prior researches pointed out three factors controling the strength of AMOC in LGM climate: the cooling of the oceans in the Southern hemisphere, cooling in the North Atlantic, and the surface wind stresses in the North Atlantic. However, in the above-mentioned prior researches, the influences of these three factors on AMOC were only independently evaluated and the combined influences are still largely unknown. Here we emphasize the relative evaluation of combined influences of above- mentioned three factors on the AMOC. For this purpose, various ocean model experiments with our general ocean circulation model (COCO) were conducted; wind stress and thermal boundary conditions taken from PMIP experiments are replied to our ocean general circulation model. As a result, it was found that the difference of thermal boundary condition in the southern hemisphere most affects the strength of AMOC, and this cooling in the southern hemisphere is a necessary condition for reproducing the ‘shallower and weaker’ AMOC, but not a sufficient condition. From these results, it is implied that the stronger glacial AMOC reported in the PMIP models was possibly caused by the insufficient cooling in the southern hemisphere in LGM experiment, and this insufficient cooling possibly comes from warm bias there in the present state experiment and the associated underestimation of ice albedo feedback of sea ice.

Keywords: The Atlantic Meridional Overturning Circulation(AMOC), Ocean General Circulation Model(OGCM), Last Glacial Maximum(LGM)

©2019. Japan Geoscience Union. All Right Reserved. 

# Comparison of the Kuroshio during LGM simulated by an ocean general circulation model driven by multiple paleoclimate models

*Kensho Ichikawa[1], Haiyan Yang[2], Xinyu Guo[2], Yasumasa Miyazawa[3]

1. Graduate School of Science and Engineering,Ehime University, 2. Center for Marine Environmental Studies,Ehime University, 3. Japan Agency for Marine-Earth Science and Technology

The Kuroshio that flows south of Japan has an important role in the climate of East Asia and Japan. In modern days, the Kuroshio presents a stable path and contributes to maintenance of warm climate. However, this stable condition is considered to be different in Last Glacial Maximum (LGM) when different environment conditions from the present day were reported. During the LGM, the sea surface level was lower than present by about 130 m and the westerlies shifted southward. In addition, the air-sea heat flux was also expected to be different from present. Therefore, it is necessary for the simulation for the Kuroshio in LGM to consider the changes in above three factors (sea level, westerly, and air-sea heat flux). The Kuroshio in LGM was calculated by a numerical model that included the above mentioned three factors in Muto (2018). The model results presented the southward shifting of the Kuroshio path and decreasing of the Kuroshio intensity. However, this result was obtained from one paleoclimate model (IPSL). Therefore, it is necessary to use more paleoclimate models to confirm the results given by Muto (2018).

In this study, we performed similar calculations for the Kuroshio in LGM using four additional paleoclimate models (CNRM, GISS, MIROC, MRI) as driven forcing of ocean model. Before calculation, we compared the vorticity of wind stress given by these paleoclimate models and obtained the Sverdrup transport that is also an index of Kuroshio intensity.

Among all the five paleoclimate models, the position of zero vorticity, which corresponds roughly the position of Kuroshio, shifted to the most southward in IPSL. At the same time, the Sverdrup transport was the lowest in IPSL. Therefore, the southward shifting of the Kuroshio path and the weakening of the Kuroshio intensity given by Muto (2018) are likely an extreme case among five paleoclimate models.

Keywords: Last Glacial Maximum, Kuroshio, paleoclimate models

©2019. Japan Geoscience Union. All Right Reserved. 

# The changes of the Kuroshio path in the Northwest Pacific since 35ka

*Haiyan Yang[1], Xinyu Guo[1], Ayako Abe-Ouchi[2], Yasumasa Miyazawa[3], Sergey Varlamov[4], Wing-Le Chan[2]

1. Center for Marine Environmental Studies, Ehime University, 2. Atmosphere and Ocean Research Institute, University of Tokyo, 3. Research Institute for Global Change, Japan Agency for Marine-Earth Science and Technology, 4. Application Laboratory, Japan Agency for Marine-Earth Science and Technology

Kuroshio, a strong western boundary current in the subtropical North Pacific, has strong influences on the climate of Japan and East Asia. Global sea level rises and falls when ice sheets and glaciers melt and grow. The Last Glacial Maximum (LGM, 21ka) is the most recent interval in Earth history when global ice sheets reached their maximum integrated volume. The expansion of the ice sheets at the LGM resulted in a sea-level lowering of about 130 m and a cold phase compared to present. Under the circumstance of sea level, Kuroshio did not bifurcate into the Japan Sea and form the Tsushima Current. As the sea level rises, the Tsushima Current flowed into the Japan Sea at about 10ka (Gallagher et al., 2015), and the sea-level reached the present level at 7ka~6ka (Zheng et al., 1994). However, how the Kuroshio and Tsushima Current pathway evolved in the conditions of different sea level and climate remains unclear.

In Okinawa and southern Korea, some archaeologists have found evidences of people drifting on the Kuroshio from Taiwan to northern regions. According to studies by Japanese anthropologists, the first person that set foot on Okinawa probably sailed there on bamboo rafts from Taiwan more than 30,000 years ago. However, this hypothesis needs more evidences because sailing across the Kuroshio is a difficult thing if the Kuroshio 30,000 years ago had the same surface velocity as present. Therefore, clarifying the strength and path of Kuroshio is also helpful to the understanding on human migration.

In this study, we used the model of Japan Coastal Ocean Predictability Experiment (JCOPE) to simulate the changes of the Kuroshio path under the combined influences of sea level, the air-sea heat flux, and wind stresses in five historical regimes (35ka, 30ka, LGM, 6ka, and 0ka). The meteorological and oceanic data are provided by the climate model MIROC4m (Chan et al., 2011) which is a fully coupled atmosphere-ocean general circulation model (AOGCM).

Keywords: Kurosio, Path, Evolution

©2019. Japan Geoscience Union. All Right Reserved. 

# Temperature reconstruction in the late Pleistocene using fossil terrestrial snails and a stalagmite from an archaeological cave in Okinawa

*Ryuji Asami[1], Rikuto Hondoh[2], Ryu Uemura[3], Ryuichi Shinjo[3], Akihiro Kano[4], Masaki Fujita[5], Shinji Yamasaki[6], Hideko Takayanagi[1], Yasufumi Iryu[1]

1. Graduate School of Science, Tohoku University, 2. Faculty of Science, Tohoku University, 3. Faculty of Science, University of the Ryukyus, 4. School of Science, the University of Tokyo, 5. National Museum of Nature and Science, 6. Okinawa Prefectural Museum and Art Museum

Freshwater snails are useful for a paleoclimate proxy. For example, stable oxygen isotope composition of mollusck’ s aragonite shells depends on temperature and oxygen isotope composition of water at the time of their growth. The Ryukyu Island Arc, bounded by the East China Sea to the northwest and by the Pacific Ocean to the southeast, is an important area in climatology because its environment is highly associated with the East Asian monsoon (EAM), typhoon, and the Kuroshio current. However, terrestrial paleoclimate records such as tree rings and stalagmites are little in the Ryukyu Island Arc unlike the East Asia Continent. Meanwhile, Okinawa is widely known as a hotspot in archaeology and a lot of ancient remains and digs have been excavated for recent years. Sakitari Cave, where world’ s oldest fishhooks were discovered, is one of the most famous archaeological sites in Okinawa.
In this study, fossil shells of a freshwater snail *Semisulcospira libertina* excavated at Sakitari Cave in Okinawa-jima were investigated. These samples were from two sediment layers dated to 13-16 ka and 23 ka in the cave. We measured stable carbon and oxygen isotope ratios and trace element concentrations at intervals of 1 mm along the growth direction of the snails to reconstruct seasonal temperature variations during the Last Glacial Maximum and the last deglaciation. To estimate paleo-temperature and -oxygen isotope composition of precipitation accurately, we also measured oxygen isotope composition of fluid inclusion water in a stalagmite collected near the archaeological site. Comparing with chemical composition of living *S. libertina* shells collected around the site, estimated annual mean temperature was about 8 ˚C and 6˚C lower at 23 ka and 13-16 ka than at the present. Summer temperature has largely increased from 23 ka to 13-16 ka relative to winter temperature, which is consistent with North Hemisphere insolation changes in summer and winter. Our results indicate that the increase of mean air temperature around Okinawa-jima was larger than that of seawater temperature in the northwestern Pacific Ocean during the last deglaciation. This inconsistency is a significant finding for better understanding of past climate changes associated with the East Asian Monsoon.

Keywords: fossil snail, stalagmite, oxygen isotope composition, paleo-temperature, Okinawa, archaeological cave

©2019. Japan Geoscience Union. All Right Reserved. 

# Silicoflagellate and *Actiniscus* response to meltwater during the last deglaciation in the Alaska margin

*Asuka Tomokawa[1], Yusuke Okazaki[1], Jonaotaro Onodera[2], Keiji Horikawa[3]

1. Department of Earth and Planetary Sciences, Kyushu University, 2. Research and Development Center for Global Change, JAMSTEC, 3. Graduate School of Engineer and Science, University of Toyama

Silicoflagellate is a phytoplankton with biogenic opal skeleton, and its fossil assemblage is used for reconstruction of paleoenvironment. There are two major genera for modern silicoflagellates: *Dictyocha* mainly dwelling in tropical to temperate zone and *Stephanocha* mainly dwelling in subarctic zone. The *Dictyocha*/*Stephanocha* ratio has been used as a paleotemperature proxy. *Actiniscus pentasterias* is a species of Dinoflagellata with biogenic opal skeleton, indicator of coastal and low salinity environments. Gulf of Alaska is located eastern North Pacific. The southern Alaska margin has fjord created by the Cordilleran Ice Sheet. The purpose of this study is to clarify the silicoflagellate and *Actiniscus* assemblages to meltwater input from the Cordilleran Ice Sheet at the last deglaciation in the southern Alaska margin. A piston core KH17-3 CL14 was obtained from the southern Alaska margin (59° 33.350’ N, 144° 09.344’ E, water depth: 695 m). Age model of core KH17-3 CL14 is established by planktic foraminiferal radiocarbon dates and the bottom of the core is estimated to be ~17 ka. We used 48 samples for Silicoflagellate and *Actiniscus* analyses. 100 silicoflagellate specimens were counted for each slide and all *Actiniscus pentasterias* specimens were counted for each slide under light microscope. 7 species and 2 subspecies of genus *Dictyocha* and 4 species of genus *Stephanocha* were identified. Relative abundances of genus *Dictyocha* accounted for greater than 50% since Younger Dryas (YD), whereas genus *Stephanocha* (particularly *S. speculum*) was abundant during Bolling-Allerod (BA). This suggests that *Dictyocha*/*Stephanocha* ratio didn’t simply reflect cold (YD) and warm (BA) events during the last deglaciation. Two *Actiniscus pentasterias* peaks were observed during the last deglaciation which were coincident with Meltwater Pulse 1A and 1B. This suggests salinity decline due to meltwater from the Cordilleran Ice Sheet. The meltwater into the subarctic Pacific may have leaded to enhanced productivity during BA. Because *Stephanocha speculum* is suggested to be an indicator of high productivity from modern sediment trap observation, high abundances of *S. speculum* in core KH17-3 CL14 during BA can be explained by the enhanced productivity driven by meltwater from the Cordilleran Ice Sheet.

Keywords: Silicoflgellate, Gulf of Alaska

©2019. Japan Geoscience Union. All Right Reserved. 

# Application of the ramped pyrolysis $^{14}C$ dating to postglacial sediments from the Alaskan margin, Arctic Ocean

*Kenta Suzuki[1], Masanobu Yamamoto[1,2], Brad Rosenheim[3], Takayuki Omori[4], Leonid Polyak[5]

1. Graduate School of Environmental Science, Hokkaido University, 2. Faculty of Environmental Earth Science, Hokkaido University, 3. College of Marine Science, University of South Florida, 4. The University Museum, The University of Tokyo, 5. Bard Polar and Climate Research Center, Ohio State University

Radiocarbon dating of biogenic carbonates, such as foraminiferal tests, is commonly used for dating marine sediments up to 50 ka old. However, in carbonate-poor environments, such as typical for polar seas, direct dating of carbonaceous material is difficult, while bulk organic matter (OM) may contain a mixture of carbon with different ages. Rosenheim et al. (2008) developed the ramped pyrolysis $^{14}C$ dating of the bulk OM based on incremental generation of $CO_2$ from a range of carbon fractions, from highly reactive to more thermochemically stable. Application of this approach to Southern Ocean sediments showed that ages of highly-reactive, lower temperature fractions were considerably younger than other fractions and the bulk $^{14}C$ age. In this study, we explore ramped pyrolysis $^{14}C$ dating in Arctic Ocean sediments from the Alaskan margin to determine if the same relationships hold true.
Samples were taken from two sediment cores collected on the 2005 HOTRAX expedition and comprising Holocene marine and older glaciomarine strata (Darby et al., 2009a). Several $^{14}C$ ages have been generated on the Holocene biogenic carbonates (Darby et al., 2009b). New samples from both the Holocene and older sediments were pyrolyzed from room temperature to 900 ˚C, and the released, purified $CO_2$ fractions were sealed in borosilicate glass ampoules at the University of South Florida. Measurement of $\Delta^{14}C$ was conducted at the University of Tokyo.
Pyrolysis followed by oxidation generated three peaks of $CO_2$ at ~300 ˚C, ~400 ˚C and ~540 ˚C, which were deconvolved into three Gaussian peaks (G1 to G3). These peaks were interpreted to reflect the consecutive degradation of oxygen-containing OM functional groups, cleavage of carbon-carbon bonds, and cleavage of aromatic ring carbon, respectively. In this scenario G1 contains most of the autochthonous carbon from the sediment. We found that the slopes of the G1-G3 $^{14}C$ ages plotted against temperature of the Gaussian centroid are proportional to the offset between $^{14}C$ ages of G1 and earlier analyzed biogenic carbonates from the same core levels. Assuming that this relationship is a constant function of the overall measured age spectra, we propose to use it for estimating sediment ages from the ramped pyrolysis $^{14}C$ data. The estimated G1 age offsets range from 800 to 3,000 years in the Holocene and from 4,000 to possibly as high as 5,000 years in the older glaciomarine sediments.

©2019. Japan Geoscience Union. All Right Reserved. 

# Utility of sedimentary environmental DNA for indices of past pelagic fish species populations

*Hiromichi Tamai[1], Michinobu Kuwae[2], Hideyuki Doi[3], Toshihumi Minamoto[4]

1. Graduate School of Science and Engineering, Ehime university, 2. Center for Marine Environmental Studies, Ehime university, 3. Graduate School of Simulation Studies, University of Hyogo, 4. Graduate School of Human Development and Environment, Kobe University

Far little is known about long-term dynamics of almost all of fish species populations in the ocean during pre-instrumental era. Here we focused on environmental DNA in marine sediments as a potential tool to elucidate past fish population dynamics and tested its utility to reconstruct fish abundance in Japanese coastal waters. Based on quantitative PCR method applied to the sediment samples collected from anoxic bottom sediments in Beppu Bay, Japan, we found environmental DNA of Japanese anchovy, Japanese sardine, and Jack mackerel in the 1-meter sediment sequences spanning over the last 250 years, which is the first detection of sedimentary marine fish DNA. The observed temporal changes in sedimentary DNA abundances are consistent with those in fish scale abundances and catch in Japan, suggesting the utility of the sedimentary fish environmental DNA to track past changes in fish abundance in waters from the bottom sediment sequences. DNA analyses of five fractions of sediment samples including coarse and fine particle fractions, pore water, fish scales, and bones suggested that a main source of fish DNA in the sediments is derived from fine the particle fraction.

Keywords: eDNA, sediment core, Quantitative polymerase chain reaction, pelagic fish

©2019. Japan Geoscience Union. All Right Reserved. 

# Improvements of extraction methods of sedimentary fish-origin DNA for reconstruction of marine fish communities

*Jun Kurata[1], Hiromichi Tamai[2], Hideyuki Doi[3], Toshihumi Minamoto[4], Michinobu Kuwae[5]

1. department of earth science, Ehime university, 2. Graduate School of Science and Engineering, Ehime university, 3. Graduate School of Simulation Studies, University of Hyogo, 4. Graduate School of Human Development and Environment, Kobe University, 5. Center for Marine Environmental Studies, Ehime university

Environmental DNA is DNA fragments derived from body fluids or skin fragments of macro organisms contained in water or soil. It is expected to can be a technology to reveal long-term fish community changes which still remains unknown in the world ocean. However, DNA in the sediments has a low concentration, therefore, it is difficult to detect for a various kind of fish species. The purpose of this research is to elucidate the method that can take sedimentary DNA more efficiently. At this time, we tested five DNA extraction methods including the conventional one together with beads beating time. Quantitative PCA results showed that Power Soil had the best yield in the replications. In addition, DNA extraction of *Truchurus japonicus* figured out a better yield by increasing the amount of sediment sample. There was a significant difference between 10 min. and 30 sec. of beads beating time, it is possible that there is a higher yield with short time beating. Our future works is to test whether DNA yield improves by shortening or eliminating bead beating, effectively removal of PCR inhibitors, and an utility of PCR inhibitor.

Keywords: Environmental DNA, ocean sediment

©2019. Japan Geoscience Union. All Right Reserved. 

# The paleotemperature reconstruction during the late-Holocene using the sediment core recovered from the Tokyo Bay, Japan

*Hiroto Kajita[1,2,3,4], Naomi Harada[5], Miyako Sato[5], Nanako Ogawa[1], Yusuke Yokoyama[1,2,4], Chikako Sawada[1], Yosuke Miyairi[1], Masayuki Utsunomiya[3], Atsushi Suzuki[3], Hodaka Kawahata[1,2,3]

1. Atmosphere and Ocean Research Institute, The University of Tokyo, Japan, 2. Department of Earth and Planetary Science, Graduate school of Science, The University of Tokyo, Japan, 3. Research Institute of Geology and Geoinformation, Geological Survey of Japan, National Institute of Advanced Industrial Science and Technology (AIST), Japan, 4. Department of Biochemistry, Japan Agency for Marine-Earth Science and Technology (JAMSTEC), Japan, 5. Research and Development Center for Global Change, Japan Agency for Marine-Earth Science and Technology (JAMSTEC), Japan

Recently, investigations of Holocene climatic variability and its socioeconomic impacts have received increasing attention with regard to the prediction of future climatic change and the evaluation of its impact on human society. The Kanto area around the Tokyo Bay, Japan had a large population in the Neolithic Jomon age. After the establish of centralized system, this area has been a stage of major change in Japanese history for many times. The paleoenvironment around the Tokyo Bay has been estimated based on the analysis of the shell mounds along the coast or historical documents. However, the continuous and high time resolution paleotemperature record has not existed yet.

A piston core KT12-06-2B (8.99m) were recovered from the Tokyo Bay during the Tansei-maru KT12-06 cruise. An age model for the core, determined by the AMS$^{14}$C dating for 22 molluscan shells and the scoria layer of Hoei eruption, showed that it has the continuous records from about 4, 500 years ago. We analyzed the content of total organic carbon (TOC), alkenone unsaturation ratio ($U^{k'}_{37}$), and coccolith assemblages for this core in order to reconstruct the paleoenvironment in the Toyo Bay.

The constant TOC values (1.3-1.7 wt.%) before 1700AD suggested the stable biological production at the core site. We converted $U^{k'}_{37}$ into alkenone-SST using the conversion formula, proposed by the culture experiment of *G. oceanica* because most of coccolith contained in the sediments were *G. oceanica* based on the polarizing microscope observations. From 400 AD to the present, the alkenone-SST ranged from 20.5˚C to 22.4˚C (21.6˚C on average), including several cold periods around 1700 AD, 1420 AD, 1280 AD, and 1010 AD, which corresponded approximately to the Maunder, Spörer, Wolf, and Oort Minimum, respectively. The SSTs before 400 AD largely fluctuated between 19.5˚C and 25.3 ˚C, and its average value was 22.6˚C, which was 1 ˚C higher than the average after 400 AD. Especially large cold periods were detected around 520-440 BC (with a minimum value of 20.0℃) and 2360-2280 BC (with a minimum value of 19.5℃). The former cold period, which was also reported by the several previous studies in East Asia, might be caused by the other large minimum of solar activity around 500BC. The latter cold period corresponds to the global cooling/drying event accompanied by the monsoon retreat. In the mid- to late-Jomon age, the Neolithic Jomon society around the Tokyo Bay based on hunting and gathering, not paddy rice cultivation. We assume that they lived in warm but unstable climate, which might be disadvantageous for them to start agriculture.

Keywords: Paleoclimate, the Tokyo Bay, late-Holocene, Alkenone

©2019. Japan Geoscience Union. All Right Reserved. 

# Summer monsoon variability over the past 400 years in Tateyama, Japan, as reconstructed from tree-ring oxygen isotope data

*Masaki Sano[1], Kota Mori[1], Akane Tsushima[2], Zhen Li[3], Koh Yasue[4], Takeshi Nakatsuka[2,3]

1. Faculty of Human Sciences, Waseda University, 2. Nagoya University, 3. Research Institute for Humanity and Nature, 4. Shinshu University

With its high sensitivity to hydroclimate variability, tree-ring oxygen isotope composition has been widely used for dendroclimatology over monsoon Asia in recent years. Here we built a 400-year tree-ring oxygen isotope chronology from Tateyama, Japan to reconstruct summer hydroclimate in the region, and compared it with other tree-ring data to explore spatio-temporal variations in hydroclimate. We collected tree-ring core samples from *Pinus parviflora* var. *pentaphylla* at an altitude of 1500 m above sea level in 2016 and 2017 in Tateyama, Japan. After cross-dating each ring of the sampled cores based on ring-width patterns, a total of 5 trees were selected for isotopic analysis. Cellulose was extracted directly from 1 mm thick plates using the standard methodology. Each annual ring was separated using a blade under microscope. Oxygen isotope ratio of each ring was then measured using an isotope ratio mass spectrometer. The resultant 5 tree-ring oxygen isotope series were highly correlated with each other, indicating that the oxygen isotope ratio was governed by common climatic factors. Climatic response analysis revealed that the oxygen isotope ratio was primarily controlled by relative humidity in the early summer season (April–June), with a highest correlation appearing in June. Therefore, the tree-ring chronology can be considered to be a proxy of hydroclimate related to Meiyu-Baiu variability. The oxygen isotope data in our chronology showed an overall positive correlation with those in a tree-ring oxygen isotope record from Yakushima island, southwestern Japan. However, the correlations often became lower or negative during the positive PDO phases, implying that the PDO played a role in modulating spatial patterns of hydroclimate in the early summer season over western Japan.

Keywords: Oxygen isotope, East Asian monsoon, Pacific Decadal Oscillation

©2019. Japan Geoscience Union. All Right Reserved. 

# Eventural Layers of anciant disasters during these 4500 years at Lake Ikeda (Lake Daijya), western coast of Kyushu Island presumed by diatom assemblages in lake deposits

*Kaoru Kashima[1], Tomokazu Mita[1], Yu Fukumoto[3], Tsuyoshi Haraguchi[2], Kazuyoshi Yamada[4]

1. Department of Earth and Planetary Sciences, Kyushu University, 2. Department of Geosicneces, Graduate School of Science, Osaka City University, 3. Ritsumeikan University, 4. Museum of Natural and Environmental History, Shizuoka

Lake Ikeda (Lake Daijya) is a small coastal freshwater lake of about 200m NE and WE, located at Amakusa Island, Western part of Kyushu Area. It was a coastal lagoon, but after the eruption of Akahoya Ash (about 7.3ka), the lake was closed by a sand dune, and changed to be a freshwater environment.
Woodruff et.al. (2014) found the two Typhoon layers at 1.9-2.1m depth of the lake deposit, and presumed those were the trace of Kamikaze Typhoons, the huge typhoons on AD1274, AD1281. But their age control data were limited, and the processes to discussions to decide the Kamikaze Typhoon deposits were necessary to add multidiscipline methods.
Therefore, Haraguchi took undisturbed cores at Lake Ikeda (Lake Daijya) in 2016. It was 26m long, and covered about 8000 years presumed by C14 ages and Akahoya Ash (about 7.3ka) layer. In this presentation, we took the analysis of diatom assemblages in the lake deposits of top 9m long core dated about these 4500 years. We found the five “Event Layers” in the 9 m core. Huge typhoons like the Kamikaze Typhoon had continuously attacked the Western part of Kyushu.
The results of diatom assemblages in the core were compiled as follows:
(1)Surface deposits of the lake were composed by a lot of small fugal pellets by small animals. The pellet contained a lot of diatoms. The diatom assemblages were very simple and were dominated by freshwater plankton species (*Aulacoseira* and others), and freshwater semi-plankton species (*Staurosira* and others).
(2)Lake Ikeda (Lake Daijya) has continued as shallow freshwater for 4500 years, and freshwater plankton species (*Aulacoseira* and others), and freshwater semi-plankton species (*Staurosira* and others) were dominated in the lake deposit.
(3)But diatom assemblages were changed suddenly at the following five layers. They were caused by the invasion of marine water and slope falls surrounding the lake, presumably by the ancient huge typhoons.
(4)The depth and ages of event layers were compiled as follows. Event1 (7.26-8.26m): 4200-3800 yBP, Event2 (4.32-4.40m): 2000 yBP, Event3 (3.20-3.28m): 1400 yBP, Event4 (2.64-2.72m): 1000 yBP, Event5 (1.22-1.90 m): 500-700 yBP.
(5) To presume the detail process of each “Event Layer”, we have to analyze using multidiscipline methods and to compare the results surrounding Kyushu Area.

Keywords: Diatom Assemblages, Typhoon Deposit, Coastal lake, Lake Ikeda (Lake Daijya)

©2019. Japan Geoscience Union. All Right Reserved. 

# Variability of hemipelagic and event depositions in the Beppu Bay during Holocene

*Tomohisa Irino[1], Airi Maruyama[1], Ken Ikehara[2], Masanobu Yamamoto[1], Michinobu Kuwae[3]

1. Graduate School of Environmental Science, Hokkaido University, 2. Institute of Geology and Geoinformation, National Institute of Advanced Industrial Science and Technology, 3. Center for Marine Environmental Studies, Ehime University

The Beppu Bay located in the northeast Kyushu Island, the southwestern Japan receives detrital materials mainly from two drainage systems, the Ohno River and the Oita River. The Ohno River has the head water region at the Mt. Kuju and Mt. Aso, flows eastward combining some tributaries from the south, and then flows northward to the Beppu Bay. Surface geology of the drainage area is roughly divided into two as intermediate to felsic volcanic area covered with andosol in the northeast and Paleozoic to Mesozoic sedimentary rocks covered with brown forest soil in the south. The drainage basin of the Oita River is located in the north of the Ohno River drainage, which is characterized by mafic volcanic rocks in the headwater region. Since the provenance of the Beppu Bay sediments has such geologically contrasted drainage systems, the temporal changes in the provenance for the sediment can be utilize to seek for the interrelationship among the western Pacific paleoceanography, East Asian monsoon, ecological response (fishery, vegetation, land use), and the erosion and sediment supply from hinterland basin. For this purpose, we examined mineral composition of BP09-3 core collected from the center of Beppu Bay as well as sediment from surface soils and river beds using X-ray powder diffraction.

As a result, quartz / feldspars ratio of the Beppu Bay sediment was within the range of surface soils in the drainage of Ohno River and Oita River. Detailed examination of peak shape of feldspar in X-ray diffractogram suggests grain size dependency of feldspar composition. Feldspars in finer materials showed more “mafic” composition suggesting that fine materials are dominantly supplied from Oita River drainage and / or mafic rock is more easily weathered and forms fine materials. We also applied statistical unmixing of mineral assemblage using PARAFAC algorithm on XRD profiles. Statistically distinguished subcomponents could be attributed to biogenic subcomponents, detrital subcomponents from the Ohno and Oita Rivers in hemipelagic mud as well as two detrital subcomponents in event sands with different origin.

Temporal variation of these statistical subcomponents in hemipelagic mud suggests that vegetation and / or land use change in the drainage area affected the relative importance of suspension loads from the Ohno River associated with the increase of detrital flux for the last 3,000 yrs. Composition of event sands also shows a consistent compositional change characterized by the relative increase of contribution from sandy material of the Ohno River bed. Increase in surface erosion in the Ohno River drainage may have been responsible for increases of fine and coarse materials supply and development of the delta at the river mouth.

Keywords: Beppu Bay, Sediment, Detrital component, X-ray diffraction analysis

©2019. Japan Geoscience Union. All Right Reserved. 

# The composition of laminae in the sediment of Beppu-Bay and potential as annual laminations

*Yoshiaki Suzuki[1], Michinobu Kuwae[2], Kazuno Arai[3], Ken Ikehara[4], Masafumi MURAYAMA[3]

1. Waseda University, 2. Ehime University, 3. Kochi University, 4. AIST

The sediment of Beppu Bay in Pref. Oita is consisted of hemipelagic mud and contains many eventually deposited layers (event layers). These layers are considered to be caused by the occurrence of flood, earthquake or eruption. To reveal the mechanism of deposition of minor event layers (less than 1cm thickness), we tried to correlate the sediment with the observational record based on high-resolution age model using sediment cores obtained from four sites in Beppu Bay.
Surface sediment cores were CT-scanned and analyzed by micro XRF scanner (ITRAX). Pb and Cs isotopes were also measured by 4cm intervals for age determination.
In the deepest part of Beppu Bay(more than 60m depth), clear lamination is seen in several cores. In the shallower part, lamination cannot be observed. Based on the result of ITRAX measurement and Soft-X images, it is revealed that lamination is caused by the change of the amount of detrital material. Amount and composition of detrital material also show several positive spikes. Some of them can be observed by naked eyes as light gray or reddish brown colored thin layers (minor event layers) suggesting that they were supplied from different provenance than usual.
The results of Pb and Cs measurements agree with the age of Ev-1a which is considered to be caused by Hyuga-Nada earthquake in 1968 (Kuwae et al., 2013). Counting of lamination also agrees with Pb and Cs based age model when unclear lamination is interpolated by the average thickness of laminations. Therefore, it is strongly suggested that lamination in the bottom of Beppu Bay is annual lamination, varve. If the lamination is verified as a varve, high-resolution age model could be established and it enables detailed correlation of the sediment and observational record.

Keywords: Beppu Bay, annual lamination

©2019. Japan Geoscience Union. All Right Reserved. 

# Simulation of global distribution of Pa/Th using an ocean general circulation model

*Yusuke Sasaki[1], Akira Oka[1]

1. Atmosphere and Ocean Research Institute, The University of Tokyo

The sediment 231Pa/230Th ratio is an important major proxy for studying paleo ocean circulation. However, even in the modern ocean, the only limited data about the distribution of dissolved 231Pa and 230Th was available, and it was insufficient to understand the process that controls the oceanic distribution of 231Pa and 230Th. In addition, some of previous modeling studies did not reproduce the observation data sufficiently. Recently, number of available observation data about dissolved 231Pa and 230Th is rapidly increasing owing to the recent projects like GEOTRACES. In this study, we performed simulation of 231Pa and 230Th with an ocean general circulation model (OGCM) and discussed how well dissolved 231Pa and 230Th profile of GEOTRACES data set is reproduced by the model. First, based on the previous model that incorporates reversible scavenging processes of 231Pa and 230Th by sinking ocean particles (Siddall et al., 2005), we improved the model by taking into account of additional sink at the sea floor (bottom scavenging; Okubo et al., 2012; Roy-Barman, 2009) and the dependency of scavenging efficiency on particle concentration following Henderson et al. (1999) . Second, as for our best reproduced simulation (Control simulation), we discuss processes which control the oceanic distribution of 231Pa and 230Th into three parts; the one-dimensional reversible scavenging process, the contribution from ocean advection and diffusion, and bottom scavenging. Through this analysis, we clarified how these processes effect on the global distribution of the sediment 231Pa/230Th ratio.

As a result of the improvement of model and tuning of the parameter, we simulated the distribution of 231Pa and 230Th reported from GEOTRACES dataset successfully. First, I confirmed that the profile of both dissolved 231Pa and 230Th in the deep ocean was improved by considering bottom scavenging as suggested by Rempfer et al. (2017). While the distribution of 231Pa is reproduced realistically by considering bottom scavenging, it is found to be difficult to simulate the depth profile of dissolved 230Th consistent with observations only by considering bottom scavenging. Hence, I tried to reproduce the dissolved 230Th profile by changing parameter values which control the strength of reversible scavenging by sinking ocean particles from the case in Siddall et al. (2005), and also by incorporating the dependency of scavenging efficiency on particle concentration following Henderson et al. (1999). As a result, I also reproduced the distribution of 230Th successfully.

In the latter part of this study, we discussed the process that controls the distribution of the sediment 231Pa/230Th ratio by analyzing the Control simulation. Through this analysis it was confirmed that the process that controls the distribution of the sediment 231Pa/230Th activity ratio is largely determined by the stronger influence of advection and diffusion on 231Pa than 230Th; advection and diffusion effect only on 231Pa can reproduce overall pattern of the distribution of the sediment 231Pa/230Th activity ratio similar to observation. Our analysis revealed that the bottom scavenging effect weakens the influence of advection and diffusion on 231Pa, and tends to make the contrast of 231Pa/230Th distribution smaller. We also found that the advection and diffusion of 230Th is small but not negligible, which also contributed to decrease the advection and diffusion effect on 231Pa.

This model is useful not only for reproducing 231Pa/230Th ratio in the present-day ocean but also for that in different climate such as glacial periods. Simulation of 231Pa/230Th ratio under the glacial

©2019. Japan Geoscience Union. All Right Reserved. 

climate is an interesting future study. Such a study is an important step for discussing glacial changes in the ocean circulation more quantitatively.

Keywords: 231Pa/230Th ratio, proxy of ocean circulation, bottom scavenging, ocean general circulation model

©2019. Japan Geoscience Union. All Right Reserved. 

# Construction of modern silicoflagellate assemblage dataset in the North Pacific for paleo sea-surface temperature and its application for sediment cores

*Yusuke Okazaki[1], fumiaki nishizono[1], Tanizaki Kyohei[1]

1. Department of Earth and Planetary Sciences, Graduate School of Science, Kyushu University

Silicoflagellate is a marine phytoplankton with biogenic opal skeletons. Most of the modern silicoflagellates are belonging to two genera: *Dictyocha* mainly distributing tropical to temperate regions and *Stephanocha* mainly distributing polar to subpolar regions. Here we construct modern silicoflagellate assemblage dataset in the North Pacific for modern analog technique to reconstruct paleo sea-surface temperature (SST). The modern silicoflagellate assemblage dataset is composed of seven species in surface sediment samples from (1) wide-area of North Pacific by Poelchau (1976) and (2) newly obtained western North Pacific near Japan. A total of 174 surface sediment samples were compiled as the modern silicoflagellate assemblage dataset. Each sample site is linked with 0.25-degree grid data of annual mean SST data by World Ocean Atlas 2013. Modern analog technique analysis was performed by using Polygon 2.4.4. and applied to sediment cores from the Japan and East China Seas. Reconstructed SST of the Japan Sea off Wakasa was ~6-degree C during LGM whereas ~15-degree C during Holocene. Deglacial warming was observed between 12 and 14.5 ka. For the East China Sea core from the Danjo Basin, reconstructed SST was ranging from 10-15 degree C during LGM to 20-25 degree C during late Holocene. The reconstructed silicoflagellate based SST (10 to 25-degree C) were in between planktic foraminiferal Mg/Ca based one (20 to 25-degree C) and TEX 86 based one (7 to 20-degree C). However, deglacial rapid SST changes based on silicoflagellate was not observed in both planktic foraminiferal Mg/Ca and TEX 86 based ones.

Keywords: Silicoflagellate, Modern analog technique, paleo temperature, Last glaciation, Japan Sea, East China Sea

©2019. Japan Geoscience Union. All Right Reserved. 

# Microplastics in surface sediments of the Ariake Bay

Hiroki Sonoda[1], *Yusuke Okazaki[1], Atsuhiko Isobe[2]

1. Department of Earth and Planetary Sciences, Graduate School of Science, Kyushu University, 2. Research Institute for Applied Mechanics, Kyushu University

Microplastics are small plastic pieces less than five *millimeters* long. Numbers of microplastics floating around Japan are much greater than those of global ocean average. Microplastic cycle in the ocean is not well understood, but their final destinations are sediments. Here we investigate microplastics deposited in surface sediments of the Ariake Bay. We obtained surface sediment samples at 11 sites off Kumamoto city in the Ariake Bay by using Ekman-Berge grab in December 2016. In addition, we collected surface samples from the river mouths of Shirakawa and Midorikawa Rivers. Sediment samples were freeze-dried, weighed ~50 g and washed on a stainless-steel screen with 63 micrometers mesh. The floating and sunken residues were recovered separately by filter paper and treated with 1N HCl and 10% hydrogen peroxide on a hot plate at 200-degree C for an hour. After reaction completed, residues were washed by pure water on a nylon screen with 63 micrometers mesh, recovered by filter paper and dried in an oven overnight at 40-degree C. We picked up potential microplastic particles greater than 150 micrometers under stereomicroscope. Identification of microplastics were performed by fourier transform infrared spectroscopy (FT-IR) using FT-IR alpha spectrometry. A total of 18 and 8 microplastics were identified in 11 surface sediment samples off Kumamoto in the Ariake Bay and 3 surface sediment samples from the river mouths, respectively. Most of identified microplastics were polypropylene (PP) and polyethylene (PE). Averaged microplastic contents at the 11 sites off Kumamoto was 29 pieces per kg of dry sediment. No clear trend between geographic distribution pattern of microplastics and distance from the Kumamoto coast/river mouths. Rough estimate for microplastic deposition rate off Kumamoto in the Ariake Bay (120 square kilometers) was ranging from 5 to 10 billion pieces per year. This suggests relatively rapid removal of microplastics from water column though their specific gravities are less than one.

Keywords: Microplastics, Marine sediments, Ariake Bay

©2019. Japan Geoscience Union. All Right Reserved. 

[J] Oral | M (Multidisciplinary and Interdisciplinary)：M-IS Intersection

Thu. May 30, 2019 1:45 PM - 3:15 PM JST | Thu. May 30, 2019 4:45 AM - 6:15 AM UTC | 303 3F

## [M-IS26] Arctic and Antarctic Science and Future Plan

convener:Yoshifumi Nogi(National Institute of Polar Research), Takuji Nakamura(National Institute of Polar Research), Atsuko Sugimoto(Arctic Research Center, Hokkaido University), Shin Sugiyama(Institute of Low Temperature Science, Hokkaido University), Chairperson:Tetsuo Sueyoshi(National Institute of Polar Research), Yoshifumi Nogi(National Institute of Polar Research)

This session will be a forum to discuss the scientific program and the framework of the future integrated multidisciplinary study focused on the polar regions, and to consider how a large-scale science plan for Polar Science should be formulated. One of the focus of the discussion will be on the importance in the Master Plan 2020, which will be announced by the Science Council of Japan. <br/>The changes in the polar regions are essential for future projection of the Earth system. The Antarctic and Greenland ice sheet holds most of the ice and is the largest freshwater reservoir on the Earth, which is equivalent to about 70 m height of sea level. Moreover, dense seawater is produced in the polar regions and formed bottom water that drives the thermohaline circulation. Changes in the thermohaline circulation are considered to be a large impact on the global environment. Therefore, the polar regions are the key components that control global climate and sea level changes. However, the polar regions are still poorly unknown components in the Earth system and the systematic various field of scientific observations is required. From such background, the convener believes that polar science is one of the important topics which should be proposed to the Master Plan 2020.

1:45 PM - 2:00 PM JST | 4:45 AM - 5:00 AM UTC

### [MIS26-01] Antarctic Circumpolar Interdisciplinary Survey - ACIS

★Invited Papers

*Robin Elizabeth Bell[1], Kirsteen Tinto[1], Xiaojun Yuan[1] (1.Lamont Doherty Earth Observatory of Columbia University)

2:00 PM - 2:15 PM JST | 5:00 AM - 5:15 AM UTC

### [MIS26-02] Proposal of Polar Science to Master Plan 2020

*Takuji Nakamura[1], Atsuko Sugimoto[2], Shin Sugiyama[2], Yoshifumi Nogi[1], Tetsuo Sueyoshi[1] (1.National Institute of Polar Research, 2.Hokkaido University)

2:15 PM - 2:30 PM JST | 5:15 AM - 5:30 AM UTC

### [MIS26-03] Towards the understanding of mass balance variation of Arctic and Antarctic ice sheets

Teruo Aoki[1,2,4], Masashi Niwano[4], *Tetsuo Sueyoshi[2,3] (1.Okayama Univ., 2.National Institute of Polar Research, 3.Japan Agency for Marine-Earth Science and Technology, 4.Meteorological Research Institute)

2:30 PM - 2:45 PM JST | 5:30 AM - 5:45 AM UTC

### [MIS26-04] Modelling Perspective for the Past and Future tipping points of ice-sheets and climate

*Ayako Abe-Ouchi[1,2,3], Fuyuki SAITO[2], Takashi Obase[1], Ralf Greve[4], Sam Sherriff-Tadano[1] (1.Atmosphere and Ocean Research Institute, The University of Tokyo, 2.JAMSTEC, 3.NIPR, 4.Hokkaido University)

2:45 PM - 3:00 PM JST | 5:45 AM - 6:00 AM UTC

### [MIS26-05] Prediction of sea level rise caused by ice sheet melt

*Takeshi Tamura[1], Junichi Okuno[1], Yusuke Suganuma[1], Tetsuo Sueyoshi[1], Yoshifumi Nogi[1], Takuji Nakamura[1] (1.NIPR National Institute of Polar Research)

3:00 PM - 3:15 PM JST | 6:00 AM - 6:15 AM UTC

### [MIS26-06] Future Research Plan in the Polar region

*Yoshifumi Nogi[1], Tetsuo Sueyoshi[1], Takuji Nakamura[1] (1.National Institute of Polar Research)

# Antarctic Circumpolar Interdisciplinary Survey - ACIS

*Robin Elizabeth Bell[1], Kirsteen Tinto[1], Xiaojun Yuan[1]

1. Lamont Doherty Earth Observatory of Columbia University

Constraining how fast sea levels will rise around the globe in the coming decade requires a vastly improved interdisciplinary understanding of how the heat from the warming circumpolar ocean waters will cause rapid change in the Antarctic ice sheets. Advancing our knowledge of the rates of change requires improved observations of the ice, the ocean and the solid earth and bringing together scientists from these disciplines to address the key questions: (i) How much ice passes over the Antarctic grounding line each year? (ii) How does ocean circulation influence ice flow over the grounding line, and how will it change? And (iii) How will changes in ice mass affect sea level around the world? Like many major problems facing humans, the constraining the future rate of change of the Antarctic ice sheets is a problem that must be addressed through shared resources and coordinated science –across nations and across disciplines.

Here we present the vision of the Antarctic Circumpolar Interdisciplinary Survey that will allow us to better project future sea level rise from Antarctica. To address the questions requires data from all around the Antarctic ice sheet on the thickness of the ice entering the global oceans across the grounding line, the bathymetry surrounding the ice sheets and the dynamics of the warming ocean. Key observations cannot be obtained from space and require collaborative work on the ice sheet and the circumpolar Antarctic ocean. Together the international community has the capacity to address this question. Ongoing international efforts and technological advances have developed a wide range of capabilities for direct and remote sensing of the ice, ocean and rock around Antarctica. Understanding how much ice is flowing across the grounding line can be measured with using small aircraft based at permanent bases or field camps around the continent, long range aircraft based off continent and from drones launched form ships. The water depth close to the ice sheet can be obtained with ground-based explorations, airborne observation submersibles or gliders. Salinity and temperature are measured from a broad span of instruments, with additional sensors measuring current velocity, tidal variation and biogeochemical markers also deployed. Most oceanographic work operates from ships, but coastal sites also provide platforms for ocean observations, and profiling floats can successfully be deployed from aircraft. Like the International Polar Years and other large collaborative project this effort can serve as a future focal point for Antarctic Science through SCAR and other international programs.

Keywords: Antarctica, sea level, interdisciplinary

©2019. Japan Geoscience Union. All Right Reserved. 

# Proposal of Polar Science to Master Plan 2020

*Takuji Nakamura[1], Atsuko Sugimoto[2], Shin Sugiyama[2], Yoshifumi Nogi[1], Tetsuo Sueyoshi[1]

1. National Institute of Polar Research, 2. Hokkaido University

The academic large-scale research master plan of the Science Council of Japan is a collection of large-scale research plans that should be tackled in about 10 years, regardless of the field. After the discussion during past two years, we submitted in March 2019 as a proposal to Master Plan 2020 "Prediction of sea level fluctuation caused by ice sheet fluctuation" on behalf of the polar science field.

In the "Frontier of Polar Regions Science" for masterplan 2017, we have proposed a comprehensive and interdisciplinary research plan covering important processes and data acquisition of polar regions, which records the past global environmental changes with high accuracy, having multiple tipping points and great impact on the global environment. There were some critical comments that the focus was not clear enough, and also about stractural issue whether it should be a mission of the National Institute of Polar Research or a national academic projects.

In the master plan of 2020, we have restructured the proposal from a differentiated view point from the recent Arctic environmental research and Antarctic observation projects, as a comprehensive study of the ice sheet change, by setting the future sea level change for the main outcome of the project.

In this presentation we will introduce the situation of large-scale research projects, review the efforts for masterplan of polar science so far, explain the background of examination of this proposal. The aim is to stimulate the discussion at the session and future studies. The Antarctic / Arctic is an important research field that various topics such as space and planetary science, atmospheric and ocean science, solid earth science etc. should collaborate. It is also essential to obtain public understanding on its importance by stakeholders.

Keywords: Antactic, arctic, Sea level rise

©2019. Japan Geoscience Union. All Right Reserved. 

# Towards the understanding of mass balance variation of Arctic and Antarctic ice sheets

Teruo Aoki[1,2,4], Masashi Niwano[4], *Tetsuo Sueyoshi[2,3]

1. Okayama Univ., 2. National Institute of Polar Research, 3. Japan Agency for Marine-Earth Science and Technology, 4. Meteorological Research Institute

Greenland and East- and West- Antarctic ice sheets are the largest storage of fresh water on earth. The variation of these ice sheets can effect not only the sea level, but also on global climate through the modulation of the deep water formation in the ocean. The study on ice sheets have therefore a significant importance on studies and projections of global environental change.

In the Arctic, most significant signal of global warming appears by polar amplification, which results in the rapid mass loss of the Greenland ice sheet. The extreme melt event across the entire ice sheet was also observed first time ever in 2012. The cause of mass loss can be attributed to the temperature increase, albedo decrease by snow impurities, and also to the ocean wariming which induces the enhanced melt at the marginal glaciers (Box, 2013; Fettweis et al., 2013). In the Antarctic, while the West Antarctic Ice Sheet is losing its mass rapidly, the signal in the East Antarctic Ice Sheet is not yet clear (Steig et al., 2009, etc.) .

Considering such backgrounds, the following studies are needed to make a breakthrough on our understanding of the surface process of the ice sheets (Aoki, 2015): Expanding and maintenance of the AWS network, Process study by in-situ observations, Modelling efforts of physical processes such as near-surface radiation or snow metamorphose, and Development of the regional polar system model including these processes. Validation of the model performance using satellite observation is further needed. As Japanese research community already has activities on these topics, such studies on snow and ice sheets should be an effective orientation taking an advantage of ongoing research.

Keywords: Arctic, Antarctic, Ice sheet, Surface mass balance, Regional climate system model

©2019. Japan Geoscience Union. All Right Reserved. 

# Modelling Perspective for the Past and Future tipping points of ice-sheets and climate

*Ayako Abe-Ouchi[1,2,3], Fuyuki SAITO[2], Takashi Obase[1], Ralf Greve[4], Sam Sherriff-Tadano[1]

1. Atmosphere and Ocean Research Institute, The University of Tokyo, 2. JAMSTEC, 3. NIPR, 4. Hokkaido University

Ice sheet volume changes are the largest potential source of sea level change in the past and future. Since ice sheets are vulnerable under climate changes, it is important to carefully understand its dynamics and identify its irreversible behaveour, and critical threshold under climate change. Here I show modeling studies that simulate the past ice sheet change as well as climate change and discuss the implication for the studies needed to understand the tipping points both in past and future.

Keywords: climate, ice sheet, modelling

©2019. Japan Geoscience Union. All Right Reserved. 

# Prediction of sea level rise caused by ice sheet melt

*Takeshi Tamura[1], Junichi Okuno[1], Yusuke Suganuma[1], Tetsuo Sueyoshi[1], Yoshifumi Nogi[1], Takuji Nakamura[1]

1. NIPR National Institute of Polar Research

The polar climate system, consisting of atmosphere, ocean, and cryosphere, plays important roles in shaping the global environments through its vast exchange and storage of heat and freshwater. The accelerating ice mass loss in the Greenland and West Antarctica is a significant process affecting the global climate and the understanding of the ice-ocean interaction there is of primary importance. In contrast, the status of ice mass change in East Antarctica is still in debates. Recent studies show some fingerprints of huge mass loss in the past warming world and the ice mass loss from the glaciers including Totten Glacier in East Antarctica is increasing. However, the processes of heat supply and sequent ice-ocean interaction are poorly known for both continental ice sheets.
Now, we need to understand their individual processes in polar regions through observation and modeling, and to investigate the actual states and mechanisms of various interactions. In addition, integrated researches need to be conducted, contributing to the future projection of the global environmental change driven by the polar oceans and continental ice sheets. Toward these goals, we need to clarify the state and interactions between the ocean, ice sheet, crust, ecological system, greenhouse gases, etc. and their variations from the past to the future through the field observations and analyses of samples and conduct various kinds of modeling in cooperation with the observations.

©2019. Japan Geoscience Union. All Right Reserved. 

# Future Research Plan in the Polar region

*Yoshifumi Nogi[1], Tetsuo Sueyoshi[1], Takuji Nakamura[1]

1. National Institute of Polar Research

The changes in the polar regions most likely indicate the precursor and driving force of the global environmental changes, and these changes are essential for future projection of the Earth system. The Antarctic and Greenland ice sheet that holds most of the ice is the largest freshwater reservoir on the Earth, equivalent to about 70 m height of sea level. On the other hand, dense seawater produced in the polar regions formed bottom water that drives the thermohaline circulation. Changes in the thermohaline circulation are considered to be significant impacts on the global environment. Therefore, the polar regions are the key to global climate and sea level changes. However, the polar regions are still poorly unknown components in the Earth system due to the harsh weather conditions in these areas.
The interaction among the atmosphere, ice sheet, solid earth, and the ocean is vital to understand the system in the polar regions, and the various systematic field of scientific observations is required to elucidate the interaction. The scientific program and the framework of the integrated multidisciplinary study focused on the polar regions must be developed from the viewpoints of the global climate and sea level changes. Present scientific activities and plans in the polar region are summarized, and the future integrated multidisciplinary research plans in the polar region are discussed.

Keywords: Arctic, Antarctic, ice sheet, ocean circulation, global environment

©2019. Japan Geoscience Union. All Right Reserved. 

[J] Poster | M (Multidisciplinary and Interdisciplinary)：M-IS Intersection

Thu. May 30, 2019 3:30 PM - 5:00 PM JST | Thu. May 30, 2019 6:30 AM - 8:00 AM UTC | Poster Hall International Exhibition Hall8, Makuhari Messe_24

## [M-IS26] Arctic and Antarctic Science and Future Plan

convener:Yoshifumi Nogi(National Institute of Polar Research), Takuji Nakamura(National Institute of Polar Research), Atsuko Sugimoto(Arctic Research Center, Hokkaido University), Shin Sugiyama(Institute of Low Temperature Science, Hokkaido University)

This session will be a forum to discuss the scientific program and the framework of the future integrated multidisciplinary study focused on the polar regions, and to consider how a large-scale science plan for Polar Science should be formulated. One of the focus of the discussion will be on the importance in the Master Plan 2020, which will be announced by the Science Council of Japan. <br/>The changes in the polar regions are essential for future projection of the Earth system. The Antarctic and Greenland ice sheet holds most of the ice and is the largest freshwater reservoir on the Earth, which is equivalent to about 70 m height of sea level. Moreover, dense seawater is produced in the polar regions and formed bottom water that drives the thermohaline circulation. Changes in the thermohaline circulation are considered to be a large impact on the global environment. Therefore, the polar regions are the key components that control global climate and sea level changes. However, the polar regions are still poorly unknown components in the Earth system and the systematic various field of scientific observations is required. From such background, the convener believes that polar science is one of the important topics which should be proposed to the Master Plan 2020.

[MIS26-P01] Towards sustained ice–ocean observation network of East Antarctica

*Shigeru Aoki[1], Takeshi Tamura[2], Toshihiro Maki[3], Shin Sugiyama[1] (1.Hokkaido University, 2.National Institute of Polar Research, 3.The University of Tokyo)

[MIS26-P02] Deep ice corings in Antarctica and Greenland

*Kenji Kawamura[1,2,3], Kumiko Goto-Azuma[1,2], Shuji Fujita[1,2], Fumio Nakazawa[1,2], Ikumi Oyabu[1], Hideaki Motoyama[1,2], Ayako Abe-Ouchi[4,3] (1.National Institute of Polar Research, Research Organization of Information and Systems, 2.SOKENDAI (The Graduate University of Advanced Studies), 3.JAMSTEC, 4.University of Tokyo)

[MIS26-P03] **Understanding of whole history of Antarctic ice sheet, sea ice, and bottom water based on core-seismic integrated investigation from Antarctic continental shelf to deep sea floor**

*Minoru Ikehara[1], Takuya Itaki[2], Masakazu Fujii[3] (1.Center for Advanced Marine Core Research, Kochi University, 2.GSJ, AIST, 3.National Institute of Polar Research)

[MIS26-P04] Impacts of the interaction between ice sheets and solid Earth on the prediction of sea-level change

*Jun'ichi Okuno[1,2], Yoshifumi Nogi[1,2] (1.National Institute of Polar Research, 2.SOKENDAI)

[MIS26-P05] International organization's science plan and Japan's Arctic policy

*Yuji Kodama[1], Tetsuo Ohata[1] (1.National Institute of Polar Research)

# Towards sustained ice–ocean observation network of East Antarctica

*Shigeru Aoki[1], Takeshi Tamura[2], Toshihiro Maki[3], Shin Sugiyama[1]

1. Hokkaido University, 2. National Institute of Polar Research, 3. The University of Tokyo

Along with the anthropogenic climate change, changes in overturning circulations and ice mass of the Southern Ocean and Antarctic Ice Sheet are listed as the problems with huge social implications. In Amundsen Sea, West Antarctica, accelerations of basal melting of ice shelves and loss of ice mass have been observed. More recently, ice discharge of the Totten Glacier, East Antarctica, is shown to be accelerating, and a pathway of substantially warm water access has been discovered beneath the ice shelf. The ice mass behind the Totten Glacier is estimated to be 3.5 m of global sea level equivalent, and the bed rock configuration reveals a vulnerability of the maritime ice sheet instability. The acceleration of freshwater discharge can affect sea ice production and subsequent dense water formation. With the growing awareness on the importance of ice-ocean interaction and long-term variabilities off the East Antarctic Coast, observations at the ice-ocean boundaries above and underneath the sea ice and continental ice are indispensable.

Under the project called ROBOTICA for the 9th six-year plan (2016-2022) of the Japanese Antarctic Research Expedition, we are implementing broad oceanographic and cryospheric surveys using new technologies like tethered/moored profiling platforms, Remotely Operated Vehicle (ROV) and ice radars, together with the conventional observational methods. The observations here will help revealing the ongoing oceanic and cryospheric changes and set the baselines for the future changes.

Under the GRAntarctic (2017-2022) frame work, we start developing a new Autonomous Underwater Vehicle (AUV), suitable for under-ice survey of Antarctica. The AUV is designed to operate in the following 3 modes; Seafloor Tracking mode (bathymetry, imagery), Ice Tracking mode (ice shape, imagery), and Constant Depth mode (water survey).

Development of appropriate instruments and platforms of this kind is an urgent task, given the rapid progress of the environmental changes in the ice-covered ocean. To fully utilize this instruments, the basic ability required for a mother icebreaker is high, since she needs to cope with the requirements as a platform of various state-of-the art technologies in ice-covered ocean. Moreover, flexible operation from a long-term perspective such as revisiting the sites some years later will be effective.

Keywords: ice-ocean interaction, Antarctic Ice Sheet, Southern Ocean, AUV, ice radar

©2019. Japan Geoscience Union. All Right Reserved. 

# Deep ice corings in Antarctica and Greenland

*Kenji Kawamura[1,2,3], Kumiko Goto-Azuma[1,2], Shuji Fujita[1,2], Fumio Nakazawa[1,2], Ikumi Oyabu[1], Hideaki Motoyama[1,2], Ayako Abe-Ouchi[4,3]

1. National Institute of Polar Research, Research Organization of Information and Systems, 2. SOKENDAI (The Graduate University of Advanced Studies), 3. JAMSTEC, 4. University of Tokyo

The studies of deep ice cores and boreholes have provided records of past climatic and environmental changes on various time scales, as well as evidences on how the both polar regions have interacted through atmosphere and ocean to affect global climate. Understanding the processes and sensitivities that underlie the changes, through the ice-core analyses as well as in combination with climate and ice-sheet modeling, will underpin better understanding of the climate system and projections of its future change. In the next phases of Antarctic glaciological research, National Institute of Polar Research together with Dome Fuji Ice Core Consortium (ICC) and Third Dome Fuji Drilling Project plans to perform various activities related to the third deep ice-core drilling in the vicinity of Dome Fuji, in order to obtain an ice core with age much older than 800 kyr. This is also a contribution to International Partnership in Ice Core Sciences (IPICS) “Oldest ice core project”. During the JARE Phase IX, we have been investigating glaciological conditions (ice sheet surface, englacial and subglacial conditions) of the candidate area, and we will determine the exact location of the drilling site and start pilot hole drilling and casing to enable deep drilling. The deep drilling must then follow to actually recover the old ice. In Greenland, we currently participate in the East Greenland Ice Core Project (EGRIP) to better understand the dynamics and past changes of the fastest-flowing Northeast ice stream and to reconstruct the climate and environment changes during the past warm periods and during abrupt warmings during the last glacial period. After the EGRIP drilling is finished, the next Greenland deep ice coring will be carried out to obtain spatial variabilities of climate and ice sheet changes. By studying the ice core records from both polar regions, we can understand the mechanisms and global impacts of the polar climate changes such as glacial-interglacial transition and abrupt climate changes.

Keywords: Antarctica, Greenland, Ice core

©2019. Japan Geoscience Union. All Right Reserved. 

# Understanding of whole history of Antarctic ice sheet, sea ice, and bottom water based on core-seismic integrated investigation from Antarctic continental shelf to deep sea floor

*Minoru Ikehara[1], Takuya Itaki[2], Masakazu Fujii[3]

1. Center for Advanced Marine Core Research, Kochi University, 2. GSJ, AIST, 3. National Institute of Polar Research

On the shelf slope from the continental shelf of Antarctica, there are characteristic seafloor topographic features and sediments potentially influenced by the Antarctic ice sheet and the Antarctic bottom water. Gully-like submarine valleys have remarkably observed on the shelf edge off the coast of Cape Darnley, where the Antarctic bottom water is presently formed, by using marine geophysical methods such as multibeam echo sounding, sub-bottom profiling, and multichannel seismic reflection surveys. Our latest survey during the R/V Hakuho-maru KH-19-1 cruise in the early 2019 completed obtaining new exciting data which clearly shows complex submarine channels from shallow to deep seafloor and surrounding sedimentations. Although these up-to-date observations in unexplored area provided new clues for understanding origin and formation of Antarctic bottom water, currently obtained detailed seafloor topography and submarine geological structures have been essentially limited because of insufficient spatial coverage. This is mainly because of the difficulty to explore Antarctic continental shelf where sea ice and iceberg exist. Integrated promotion of marine geophysical and geological investigations as well as sediment coring in this area will allow us to develop a new science for revealing the relationship between Antarctica and Earth history which has not been clarified in the past research.

Keywords: Antarctic, Southern Ocean, sea ice, Antarctic bottom water, submarine channel, seismic reflection survey

©2019. Japan Geoscience Union. All Right Reserved. 

# Impacts of the interaction between ice sheets and solid Earth on the prediction of sea-level change

*Jun'ichi Okuno[1,2], Yoshifumi Nogi[1,2]

1. National Institute of Polar Research, 2. SOKENDAI

Ice sheet, sea water, and terrestrial water storage act as surface mass loads on the solid Earth. Past and present variations of these loads make the solid Earth deform as the elastic and the viscous responses. These deformations have been clearly observed by geodetic, geomorphological and geological methods based on the field survey and the satellite measurement. To reconstruct the sea-level change associated with the surface mass changes and the solid Earth's response based on these observations, we need to apply the numerical modeling described by the Glacial Isostatic Adjustment (GIA) theory. GIA modeling results indicate that the predicted sea-level changes in any sites are spatially non-uniform because of the crustal deformation due to the GIA depending on the geometry of the surface mass loads, namely distribution of ice and water. Therefore, the precise evaluation of the GIA is vital to elucidate present and past sea-level changes. In this presentation, we show the crustal deformation derived from GIA due to present and past surface load changes and illustrate the importance of GIA component for precise projection of the sea-level change.

Keywords: polar ice sheets, Glacial Isostatic Adjustment, sea-level change

©2019. Japan Geoscience Union. All Right Reserved. 

# International organization's science plan and Japan's Arctic policy

*Yuji Kodama[1], Tetsuo Ohata[1]

1. National Institute of Polar Research

Planning of post-ArCS is in progress. International collaboration is a “must” for Japanese Arctic (polar region) research, and it is important to be able to demonstrate Japan's strength internationally. There are several international science plan published recently and they could be a hint for one way to formulate the plan of Post ArCS. Japanese Arctic policies must be also referenced for the plan. Then, the international organization 's Science Plan on Arctic Research, Japanese Arctic Policy, Overseas Arctic Research Program are introduced.

Keywords: Srctic, Arctic Research Program, Arctic Policy

©2019. Japan Geoscience Union. All Right Reserved. 

[J] Poster | M (Multidisciplinary and Interdisciplinary)：M-IS Intersection

Thu. May 30, 2019 5:15 PM - 6:30 PM JST | Thu. May 30, 2019 8:15 AM - 9:30 AM UTC | Poster Hall International Exhibition Hall8, Makuhari Messe_42

## [M-IS26] Arctic and Antarctic Science and Future Plan

convener:Yoshifumi Nogi(National Institute of Polar Research), Takuji Nakamura(National Institute of Polar Research), Atsuko Sugimoto(Arctic Research Center, Hokkaido University), Shin Sugiyama(Institute of Low Temperature Science, Hokkaido University)

This session will be a forum to discuss the scientific program and the framework of the future integrated multidisciplinary study focused on the polar regions, and to consider how a large-scale science plan for Polar Science should be formulated. One of the focus of the discussion will be on the importance in the Master Plan 2020, which will be announced by the Science Council of Japan. <br/>The changes in the polar regions are essential for future projection of the Earth system. The Antarctic and Greenland ice sheet holds most of the ice and is the largest freshwater reservoir on the Earth, which is equivalent to about 70 m height of sea level. Moreover, dense seawater is produced in the polar regions and formed bottom water that drives the thermohaline circulation. Changes in the thermohaline circulation are considered to be a large impact on the global environment. Therefore, the polar regions are the key components that control global climate and sea level changes. However, the polar regions are still poorly unknown components in the Earth system and the systematic various field of scientific observations is required. From such background, the convener believes that polar science is one of the important topics which should be proposed to the Master Plan 2020.

[MIS26-P01] Towards sustained ice–ocean observation network of East Antarctica

*Shigeru Aoki[1], Takeshi Tamura[2], Toshihiro Maki[3], Shin Sugiyama[1] (1.Hokkaido University, 2.National Institute of Polar Research, 3.The University of Tokyo)

[MIS26-P02] Deep ice corings in Antarctica and Greenland

*Kenji Kawamura[1,2,3], Kumiko Goto-Azuma[1,2], Shuji Fujita[1,2], Fumio Nakazawa[1,2], Ikumi Oyabu[1], Hideaki Motoyama[1,2], Ayako Abe-Ouchi[4,3] (1.National Institute of Polar Research, Research Organization of Information and Systems, 2.SOKENDAI (The Graduate University of Advanced Studies), 3.JAMSTEC, 4.University of Tokyo)

[MIS26-P03] **Understanding of whole history of Antarctic ice sheet, sea ice, and bottom water based on core-seismic integrated investigation from Antarctic continental shelf to deep sea floor**

*Minoru Ikehara[1], Takuya Itaki[2], Masakazu Fujii[3] (1.Center for Advanced Marine Core Research, Kochi University, 2.GSJ, AIST, 3.National Institute of Polar Research)

[MIS26-P04] Impacts of the interaction between ice sheets and solid Earth on the prediction of sea-level change

*Jun'ichi Okuno[1,2], Yoshifumi Nogi[1,2] (1.National Institute of Polar Research, 2.SOKENDAI)

[MIS26-P05] International organization's science plan and Japan's Arctic policy

*Yuji Kodama[1], Tetsuo Ohata[1] (1.National Institute of Polar Research)

# Towards sustained ice–ocean observation network of East Antarctica

*Shigeru Aoki[1], Takeshi Tamura[2], Toshihiro Maki[3], Shin Sugiyama[1]

1. Hokkaido University, 2. National Institute of Polar Research, 3. The University of Tokyo

Along with the anthropogenic climate change, changes in overturning circulations and ice mass of the Southern Ocean and Antarctic Ice Sheet are listed as the problems with huge social implications. In Amundsen Sea, West Antarctica, accelerations of basal melting of ice shelves and loss of ice mass have been observed. More recently, ice discharge of the Totten Glacier, East Antarctica, is shown to be accelerating, and a pathway of substantially warm water access has been discovered beneath the ice shelf. The ice mass behind the Totten Glacier is estimated to be 3.5 m of global sea level equivalent, and the bed rock configuration reveals a vulnerability of the maritime ice sheet instability. The acceleration of freshwater discharge can affect sea ice production and subsequent dense water formation. With the growing awareness on the importance of ice-ocean interaction and long-term variabilities off the East Antarctic Coast, observations at the ice-ocean boundaries above and underneath the sea ice and continental ice are indispensable.

Under the project called ROBOTICA for the 9th six-year plan (2016-2022) of the Japanese Antarctic Research Expedition, we are implementing broad oceanographic and cryospheric surveys using new technologies like tethered/moored profiling platforms, Remotely Operated Vehicle (ROV) and ice radars, together with the conventional observational methods. The observations here will help revealing the ongoing oceanic and cryospheric changes and set the baselines for the future changes.

Under the GRAntarctic (2017-2022) frame work, we start developing a new Autonomous Underwater Vehicle (AUV), suitable for under-ice survey of Antarctica. The AUV is designed to operate in the following 3 modes; Seafloor Tracking mode (bathymetry, imagery), Ice Tracking mode (ice shape, imagery), and Constant Depth mode (water survey).

Development of appropriate instruments and platforms of this kind is an urgent task, given the rapid progress of the environmental changes in the ice-covered ocean. To fully utilize this instruments, the basic ability required for a mother icebreaker is high, since she needs to cope with the requirements as a platform of various state-of-the art technologies in ice-covered ocean. Moreover, flexible operation from a long-term perspective such as revisiting the sites some years later will be effective.

Keywords: ice-ocean interaction, Antarctic Ice Sheet, Southern Ocean, AUV, ice radar

©2019. Japan Geoscience Union. All Right Reserved. 

# Deep ice corings in Antarctica and Greenland

*Kenji Kawamura[1,2,3], Kumiko Goto-Azuma[1,2], Shuji Fujita[1,2], Fumio Nakazawa[1,2], Ikumi Oyabu[1], Hideaki Motoyama[1,2], Ayako Abe-Ouchi[4,3]

1. National Institute of Polar Research, Research Organization of Information and Systems, 2. SOKENDAI (The Graduate University of Advanced Studies), 3. JAMSTEC, 4. University of Tokyo

The studies of deep ice cores and boreholes have provided records of past climatic and environmental changes on various time scales, as well as evidences on how the both polar regions have interacted through atmosphere and ocean to affect global climate. Understanding the processes and sensitivities that underlie the changes, through the ice-core analyses as well as in combination with climate and ice-sheet modeling, will underpin better understanding of the climate system and projections of its future change. In the next phases of Antarctic glaciological research, National Institute of Polar Research together with Dome Fuji Ice Core Consortium (ICC) and Third Dome Fuji Drilling Project plans to perform various activities related to the third deep ice-core drilling in the vicinity of Dome Fuji, in order to obtain an ice core with age much older than 800 kyr. This is also a contribution to International Partnership in Ice Core Sciences (IPICS) “Oldest ice core project”. During the JARE Phase IX, we have been investigating glaciological conditions (ice sheet surface, englacial and subglacial conditions) of the candidate area, and we will determine the exact location of the drilling site and start pilot hole drilling and casing to enable deep drilling. The deep drilling must then follow to actually recover the old ice. In Greenland, we currently participate in the East Greenland Ice Core Project (EGRIP) to better understand the dynamics and past changes of the fastest-flowing Northeast ice stream and to reconstruct the climate and environment changes during the past warm periods and during abrupt warmings during the last glacial period. After the EGRIP drilling is finished, the next Greenland deep ice coring will be carried out to obtain spatial variabilities of climate and ice sheet changes. By studying the ice core records from both polar regions, we can understand the mechanisms and global impacts of the polar climate changes such as glacial-interglacial transition and abrupt climate changes.

Keywords: Antarctica, Greenland, Ice core

©2019. Japan Geoscience Union. All Right Reserved. 

# Understanding of whole history of Antarctic ice sheet, sea ice, and bottom water based on core-seismic integrated investigation from Antarctic continental shelf to deep sea floor

*Minoru Ikehara[1], Takuya Itaki[2], Masakazu Fujii[3]

1. Center for Advanced Marine Core Research, Kochi University, 2. GSJ, AIST, 3. National Institute of Polar Research

On the shelf slope from the continental shelf of Antarctica, there are characteristic seafloor topographic features and sediments potentially influenced by the Antarctic ice sheet and the Antarctic bottom water. Gully-like submarine valleys have remarkably observed on the shelf edge off the coast of Cape Darnley, where the Antarctic bottom water is presently formed, by using marine geophysical methods such as multibeam echo sounding, sub-bottom profiling, and multichannel seismic reflection surveys. Our latest survey during the R/V Hakuho-maru KH-19-1 cruise in the early 2019 completed obtaining new exciting data which clearly shows complex submarine channels from shallow to deep seafloor and surrounding sedimentations. Although these up-to-date observations in unexplored area provided new clues for understanding origin and formation of Antarctic bottom water, currently obtained detailed seafloor topography and submarine geological structures have been essentially limited because of insufficient spatial coverage. This is mainly because of the difficulty to explore Antarctic continental shelf where sea ice and iceberg exist. Integrated promotion of marine geophysical and geological investigations as well as sediment coring in this area will allow us to develop a new science for revealing the relationship between Antarctica and Earth history which has not been clarified in the past research.

Keywords: Antarctic, Southern Ocean, sea ice, Antarctic bottom water, submarine channel, seismic reflection survey

©2019. Japan Geoscience Union. All Right Reserved. 

# Impacts of the interaction between ice sheets and solid Earth on the prediction of sea-level change

*Jun'ichi Okuno[1,2], Yoshifumi Nogi[1,2]

1. National Institute of Polar Research, 2. SOKENDAI

Ice sheet, sea water, and terrestrial water storage act as surface mass loads on the solid Earth. Past and present variations of these loads make the solid Earth deform as the elastic and the viscous responses. These deformations have been clearly observed by geodetic, geomorphological and geological methods based on the field survey and the satellite measurement. To reconstruct the sea-level change associated with the surface mass changes and the solid Earth's response based on these observations, we need to apply the numerical modeling described by the Glacial Isostatic Adjustment (GIA) theory. GIA modeling results indicate that the predicted sea-level changes in any sites are spatially non-uniform because of the crustal deformation due to the GIA depending on the geometry of the surface mass loads, namely distribution of ice and water. Therefore, the precise evaluation of the GIA is vital to elucidate present and past sea-level changes. In this presentation, we show the crustal deformation derived from GIA due to present and past surface load changes and illustrate the importance of GIA component for precise projection of the sea-level change.

Keywords: polar ice sheets, Glacial Isostatic Adjustment, sea-level change

©2019. Japan Geoscience Union. All Right Reserved. 

# International organization's science plan and Japan's Arctic policy

*Yuji Kodama[1], Tetsuo Ohata[1]

1. National Institute of Polar Research

Planning of post-ArCS is in progress. International collaboration is a “must” for Japanese Arctic (polar region) research, and it is important to be able to demonstrate Japan's strength internationally. There are several international science plan published recently and they could be a hint for one way to formulate the plan of Post ArCS. Japanese Arctic policies must be also referenced for the plan. Then, the international organization 's Science Plan on Arctic Research, Japanese Arctic Policy, Overseas Arctic Research Program are introduced.

Keywords: Srctic, Arctic Research Program, Arctic Policy

©2019. Japan Geoscience Union. All Right Reserved. 

[E] Poster | M (Multidisciplinary and Interdisciplinary)：M-AG Applied Geosciences

Thu. May 30, 2019 10:45 AM - 12:15 PM JST | Thu. May 30, 2019 1:45 AM - 3:15 AM UTC | Poster Hall International Exhibition Hall8, Makuhari Messe_11

## [M-AG38] Satellite Land Physical Processes Monitoring at Medium/High/Very High Resolution

convener:Jean-Claude Roger(University of Maryland College Park), Shinichi Sobue(Japan Aerospace Exploration Agency), Eric Vermote(NASA Goddard Space Flight Center)

We solicit papers on the land physical processes monitoring. In particular, it will include the inversion and use of land products from medium, high, and very high spatial resolution. For the last years, medium, high, and very high resolutions became a useful and a powerful toll for Earth studies. Topics of interest mainly include (not limited to):
- New developments for data processing, including atmospheric correction and cloud screening;
- Analysis and correction of directional effects in land surface reflectances;
- Use of time series of surface reflectances for land monitoring, including land cover classification and crop yield prediction (including data integration and data harmonization);
- Development and use of new vegetation indices (i.e. red edge) and other products for agriculture applications;
- Theoretical studies for sensors capabilities enhancements to future sensors at high/medium resolutions;
- Use of products in agricultural monitoring applications (such as crop area, crop type, crop growing, yield estimation and prediction, damage assessment);
- Agriculture monitoring algorithm description;
- Evaluation or validation of potential products with ground measurements, official statistics;
- International initiative to enhance Earth-Observing-based agricultural information.

Depending on outcome, we think about a special issue.

### [MAG38-P01] Improving the AVHRR LTDR BRDF correction

*Jose Luis Villaescusa[1,2], Belen Franch[1,2], Jean-Claude Roger[1,2], Eric Vermote[2] (1.University of Maryland College Park, 2.NASA Goddard Space Flight Center)

### [MAG38-P02] Winter wheat yield model based on remote sensing data

*Belen Franch[1,2], Eric Vermote[2,1], Sergii Skakun[1,2], Jean-Claude Roger[1,2], Inbal Becker-Reshef[1], Chris Justice[1] (1.Department of Geographical Sciences, University of Maryland, 2.NASA Goddard Space Flight Center)

### [MAG38-P03] Agricultural monitoring from Optical and SAR data

*Andrés Eduardo Santamaría-Artigas[1,2], Sergii Skakun[1,2], Belen Franch[1,2], Jean-Claude Roger[1,2], Eric Vermote[2] (1.University of Maryland College Park, 2.NASA Goddard Space Flight Center)

### [MAG38-P04] Eco-hydrological modeling using field-based and Earth Observations to assess water use efficiency and support agricultural water resources management

pierre Guillevic[2,1], *Jean-Claude Roger[1,2] (1.University of Maryland, College Park, USA, 2.NASA Goddard Space flight Center, Greenbelt, USA)

### [MAG38-P05] Detecting and quantifying forest dynamics using SAR time-series data in Indonesia

*Pedro Rodriguez-Veiga[1,2,3], Narumasa Tsutsumida[3] (1.Centre for Landscape and Climate Research, University of Leicester, Leicester, UK, 2.NERC National Centre for Earth Observation (NCEO), Leicester, UK, 3.Graduate School of Global Environmental Studies, Kyoto University, Japan)

# Improving the AVHRR LTDR BRDF correction

*Jose Luis Villaescusa[1,2], Belen Franch[1,2], Jean-Claude Roger[1,2], Eric Vermote[2]

1. University of Maryland College Park, 2. NASA Goddard Space Flight Center

The Advanced Very High Resolution Radiometer (AVHRR) sensors aboard the different NOAA satellites provide a unique global remote sensing dataset that ranges from the 1980s to the present. Using these data, the NASA funded Long Term Data Record (LTDR) project aims to develop a quality and consistent Climate Data Record (CDR) of AVHRR data with the use of the Moderate Resolution Imaging Spectrometer (MODIS) instrument as a reference. This product retrieves the BRDF corrected land surface reflectance using the VJB method (Vermote et al., 2009), which corrects the anisotropic effects by obtaining Volumetric (V) and Geometrical (R) parameters, defined in the Roujean model (Roujean et al., 1992), as a function of the Normalized Difference Vegetation Index (NDVI). Inaccuracies regarding the AVHRR atmospheric correction and calibration in the red band for the pre-MODIS era (1982-2000), propagate towards the surface reflectance’ s BRDF correction. However, with the use of the less noisy Near-Infrared (NIR) band we can reduce said errors by finding an empirical relationship between the red-NIR V and R parameters. This study aims to find said relationship using the MODIS sensor, which is an already established and accurate product (Justice et al., 2002; Liang et al., 2002), to then apply it to the noisy AVHRR data and reduce the BRDF errors in the red band.

Keywords: AVHRR, VJB, MODIS, BRDF, LTDR

©2019. Japan Geoscience Union. All Right Reserved. 

# Winter wheat yield model based on remote sensing data

*Belen Franch[1,2], Eric Vermote[2,1], Sergii Skakun[1,2], Jean-Claude Roger[1,2], Inbal Becker-Reshef[1], Chris Justice[1]

1. Department of Geographical Sciences, University of Maryland, 2. NASA Goddard Space Flight Center

Accurate and timely crop yield forecasts are critical for making informed agricultural policies and investments, as well as increasing market efficiency and stability. Earth observation data from space can contribute to agricultural monitoring, including crop yield assessment and forecasting. This work presents a new EO-based empirical winter wheat yield model. It is based on the un-mixing of the wheat signal from a coarse resolution EO data at 1 km by using yearly crop type masks to a pure wheat signal (100% of wheat within the pixel). *This wheat signal is used to calibrate the model using as inputs the seasonal amplitude and length of the Difference Vegetation Index (DVI) peak extracted from Moderate Resolution Imaging Spectroradiometer (MODIS) data and the average of the evaporative fraction (EF) 30 days after the peak. The three regressors proposed are focused on the reproduction stage of the wheat (DVI amplitude and length) and the grain filling process (EF 30-days average). The model is calibrated at subnational level using historical statistics from 2001 to 2016. In each administrative unit, a different calibration coefficient (based on all possible combination of the three regressors in a linear model) is selected depending on the statistical significance of each variable. The model was applied to estimate the national and subnational winter wheat yield in the United States, Ukraine, Russia and France from 2001 to 2017. At the subnational level the model shows very good performance with a coefficient of determination higher than 0.7 and Root Mean Square Error (RMSE) lower than 15%. At the national level the model provides a strong coefficient of determination higher than 0.8 and a RMSE lower than 8%, which demonstrates good performance of the models at this scale. Additionally, it was also able to capture low winter wheat yields during years with extreme weather events, for example 2002 in US and 2003 in Ukraine.*

Keywords: Yield model, MODIS , agriculture

©2019. Japan Geoscience Union. All Right Reserved. 

# Agricultural monitoring from Optical and SAR data

*Andrés Eduardo Santamaría-Artigas[1,2], Sergii Skakun[1,2], Belen Franch[1,2], Jean-Claude Roger[1,2], Eric Vermote[2]

1. University of Maryland College Park, 2. NASA Goddard Space Flight Center

Vegetation indices derived from optical remote sensing data are a valuable source of information for agricultural monitoring. However, cloud cover over some areas reduces the number of valid observations, which can difficult the detection of changes in crop condition. In this context, synthetic aperture radar (SAR) systems are an interesting alternative due to their low sensitivity to clouds. In this work, we analyze the relationship between SAR backscatter from Sentinel-1 and vegetation indices derived from the Harmonized Landsat-8 Sentinel-2 (HLS) product with data from the year 2017 over 6 land cover classes in Ukraine: Winter crops, summer crops, bare land, grasslands, forest, and water. Results show that SAR data from Sentinel-1 could be used to complement optical indices for certain land covers. In the case of winter crops (rapeseed and wheat), the ratio between Sigma-0 VV and VH polarization showed the highest relationship with the Normalized Difference Vegetation Index (NDVI) while for summer crops (maize, sugar beet, sunflower, and soybean) the highest relationship was shown by the Sigma-0 VH polarization and NDVI. Further work is being developed to exploit more complex SAR models which account for other variables that affect the backscatter signal such as soil moisture.

Keywords: agricultural monitoring, crop condition, synthetic aperture radar, HLS, normalized difference vegetation index

©2019. Japan Geoscience Union. All Right Reserved. 

# Eco-hydrological modeling using field-based and Earth Observations to assess water use efficiency and support agricultural water resources management

pierre Guillevic[2,1], *Jean-Claude Roger[1,2]

1. University of Maryland, College Park, USA, 2. NASA Goddard Space flight Center, Greenbelt, USA

The objective of this NASA project is to develop an integrated modeling platform using Earth Observations to simulate large-scale hydrological processes and food production in support of water use decision and agricultural policy. The decision tool will provide timely and relevant assessments of crop growth, agricultural water use and available water supply from local to regional scales, with the capability to predict the impact of different climate and water resources management scenarios on food production. The approach is based on the use of field and Earth observations to calibrate an eco-hydrological model, and climate simulations to forecast crop condition and yield through the crop season. The expected primary outcomes and results for stakeholders is potential best water management practices to improve water use efficiency and prevent excessive losses of water and nitrogen to the environment. These will be provided to in-country end-users within various relevant Ministries and Departments, in order to inform regional and national decisions. Changing precipitation patterns, droughts of increasing duration and severity and growing demand for food have significant implications on water management practices, spurring an increased need for irrigation in a sustainable manner and better monitoring of water resources for the agricultural sector in general. Understanding the context and water resource constraints that stakeholders and smallholder farmers face in climate sensitive regions is critical to target and understand the potential impact of water use management. We focus on a diverse set of regional pilot cases in Argentina, South Africa, Tanzania and the United States that are representative of a range of agricultural systems, water issues and climate impacts. The application is integrated in the GEOGLAM project, an existing widely-used web-based platform which will aid synthesizing the project outcomes and expert domain knowledge to provide timely and actionable water resources and crop condition information to assist local, regional and national water management decisions. At the end, the application will be interactive and will offer the end-user organizations the possibility to submit new water resource management scenarios online for impact evaluation.

Earth Observations are critical to characterize and monitor the different components of agricultural ecosystems and change (forests, croplands and marginal lands availability, for example) across temporal and spatial scales. Satellite data in the shortwave, thermal infrared and microwave spectral domains from US (MODIS, VIIRS, Landsat, SMAP) and European (Sentinel 1 and 2) sensors will be used to characterize changes in land surfaces and water use from 2000 to the present in support of agricultural planning decisions. In a research context, the potential of new satellite missions (i.e., ECOSTRESS, SWOT and SAOACOM) to derive surface hydrology information will be evaluated. The Agricultural Policy/Environmental eXtender (APEX) watershed model is proposed as the modeling tool to understand the biophysical and human-decision processes associated with the food-energy-water nexus. Model simulations will use climate data from the NASA Goddard Earth Observing System Model (GEOS-5) Atmosphere-Ocean General Circulation Model: MERRA-2 for simulation of past conditions and seasonal (6-month) forecasts for projections in the future. The study focus on large, key agricultural regions where agricultural ecosystems are vulnerable to demographic expansion and/or climate variability and change including drought and flood events.

©2019. Japan Geoscience Union. All Right Reserved. 

Keywords: water resources, hydrologycal modelling , remote sensing

©2019. Japan Geoscience Union. All Right Reserved. 

# Detecting and quantifying forest dynamics using SAR time-series data in Indonesia

*Pedro Rodriguez-Veiga[1,2,3], Narumasa Tsutsumida[3]

1. Centre for Landscape and Climate Research, University of Leicester, Leicester, UK, 2. NERC National Centre for Earth Observation (NCEO), Leicester, UK, 3. Graduate School of Global Environmental Studies, Kyoto University, Japan

Satellite Earth Observation (EO) data allows the generation of forest disturbance maps that can improve greenhouse gas (GHG) monitoring at local and national scales, and provide information that can be used for land use planning and management. Mapping forest biomass stocks, deforestation, forest degradation and enhancement is crucial in order to determine the loss of carbon stocks due to disturbances (e.g. deforestation, fires) or the gain due to new forest or growth. Time-series observations identify decreasing or increasing trends of aboveground biomass carbon, and separate anthropogenic related changes from seasonal changes of vegetation. This is important for understanding the terrestrial carbon cycle and for supporting better forest management and policies. This study uses time-series data from L-band Synthetic Aperture Radar (SAR) JAXA’s ALOS PALSAR and ALOS-2 PALSAR-2 to quantify carbon loss and gain trajectories (emission / sequestration) of existing forests in West Java (Indonesia).

Keywords: deforestation, SAR, time-series, forest dynamics

©2019. Japan Geoscience Union. All Right Reserved. 

[E] Poster | M (Multidisciplinary and Interdisciplinary)：M-AG Applied Geosciences

Thu. May 30, 2019 5:15 PM - 6:30 PM JST | Thu. May 30, 2019 8:15 AM - 9:30 AM UTC | Poster Hall International Exhibition Hall8, Makuhari Messe_43

## [M-AG38] Satellite Land Physical Processes Monitoring at Medium/High/Very High Resolution

convener:Jean-Claude Roger(University of Maryland College Park), Shinichi Sobue(Japan Aerospace Exploration Agency), Eric Vermote(NASA Goddard Space Flight Center)

We solicit papers on the land physical processes monitoring. In particular, it will include the inversion and use of land products from medium, high, and very high spatial resolution. For the last years, medium, high, and very high resolutions became a useful and a powerful toll for Earth studies. Topics of interest mainly include (not limited to):
- New developments for data processing, including atmospheric correction and cloud screening;
- Analysis and correction of directional effects in land surface reflectances;
- Use of time series of surface reflectances for land monitoring, including land cover classification and crop yield prediction (including data integration and data harmonization);
- Development and use of new vegetation indices (i.e. red edge) and other products for agriculture applications;
- Theoretical studies for sensors capabilities enhancements to future sensors at high/medium resolutions;
- Use of products in agricultural monitoring applications (such as crop area, crop type, crop growing, yield estimation and prediction, damage assessment);
- Agriculture monitoring algorithm description;
- Evaluation or validation of potential products with ground measurements, official statistics;
- International initiative to enhance Earth-Observing-based agricultural information.

Depending on outcome, we think about a special issue.

### [MAG38-P01] Improving the AVHRR LTDR BRDF correction

*Jose Luis Villaescusa[1,2], Belen Franch[1,2], Jean-Claude Roger[1,2], Eric Vermote[2] (1.University of Maryland College Park, 2.NASA Goddard Space Flight Center)

### [MAG38-P02] Winter wheat yield model based on remote sensing data

*Belen Franch[1,2], Eric Vermote[2,1], Sergii Skakun[1,2], Jean-Claude Roger[1,2], Inbal Becker-Reshef[1], Chris Justice[1] (1.Department of Geographical Sciences, University of Maryland, 2.NASA Goddard Space Flight Center)

### [MAG38-P03] Agricultural monitoring from Optical and SAR data

*Andrés Eduardo Santamaría-Artigas[1,2], Sergii Skakun[1,2], Belen Franch[1,2], Jean-Claude Roger[1,2], Eric Vermote[2] (1.University of Maryland College Park, 2.NASA Goddard Space Flight Center)

### [MAG38-P04] Eco-hydrological modeling using field-based and Earth Observations to assess water use efficiency and support agricultural water resources management

pierre Guillevic[2,1], *Jean-Claude Roger[1,2] (1.University of Maryland, College Park, USA, 2.NASA Goddard Space flight Center, Greenbelt, USA)

### [MAG38-P05] Detecting and quantifying forest dynamics using SAR time-series data in Indonesia

*Pedro Rodriguez-Veiga[1,2,3], Narumasa Tsutsumida[3] (1.Centre for Landscape and Climate Research, University of Leicester, Leicester, UK, 2.NERC National Centre for Earth Observation (NCEO), Leicester, UK, 3.Graduate School of Global Environmental Studies, Kyoto University, Japan)

# Improving the AVHRR LTDR BRDF correction

*Jose Luis Villaescusa[1,2], Belen Franch[1,2], Jean-Claude Roger[1,2], Eric Vermote[2]

1. University of Maryland College Park, 2. NASA Goddard Space Flight Center

The Advanced Very High Resolution Radiometer (AVHRR) sensors aboard the different NOAA satellites provide a unique global remote sensing dataset that ranges from the 1980s to the present. Using these data, the NASA funded Long Term Data Record (LTDR) project aims to develop a quality and consistent Climate Data Record (CDR) of AVHRR data with the use of the Moderate Resolution Imaging Spectrometer (MODIS) instrument as a reference. This product retrieves the BRDF corrected land surface reflectance using the VJB method (Vermote et al., 2009), which corrects the anisotropic effects by obtaining Volumetric (V) and Geometrical (R) parameters, defined in the Roujean model (Roujean et al., 1992), as a function of the Normalized Difference Vegetation Index (NDVI). Inaccuracies regarding the AVHRR atmospheric correction and calibration in the red band for the pre-MODIS era (1982-2000), propagate towards the surface reflectance’ s BRDF correction. However, with the use of the less noisy Near-Infrared (NIR) band we can reduce said errors by finding an empirical relationship between the red-NIR V and R parameters. This study aims to find said relationship using the MODIS sensor, which is an already established and accurate product (Justice et al., 2002; Liang et al., 2002), to then apply it to the noisy AVHRR data and reduce the BRDF errors in the red band.

Keywords: AVHRR, VJB, MODIS, BRDF, LTDR

©2019. Japan Geoscience Union. All Right Reserved. 

# Winter wheat yield model based on remote sensing data

*Belen Franch[1,2], Eric Vermote[2,1], Sergii Skakun[1,2], Jean-Claude Roger[1,2], Inbal Becker-Reshef[1], Chris Justice[1]

1. Department of Geographical Sciences, University of Maryland, 2. NASA Goddard Space Flight Center

Accurate and timely crop yield forecasts are critical for making informed agricultural policies and investments, as well as increasing market efficiency and stability. Earth observation data from space can contribute to agricultural monitoring, including crop yield assessment and forecasting. This work presents a new EO-based empirical winter wheat yield model. It is based on the un-mixing of the wheat signal from a coarse resolution EO data at 1 km by using yearly crop type masks to a pure wheat signal (100% of wheat within the pixel). *This wheat signal is used to calibrate the model using as inputs the seasonal amplitude and length of the Difference Vegetation Index (DVI) peak extracted from Moderate Resolution Imaging Spectroradiometer (MODIS) data and the average of the evaporative fraction (EF) 30 days after the peak. The three regressors proposed are focused on the reproduction stage of the wheat (DVI amplitude and length) and the grain filling process (EF 30-days average). The model is calibrated at subnational level using historical statistics from 2001 to 2016. In each administrative unit, a different calibration coefficient (based on all possible combination of the three regressors in a linear model) is selected depending on the statistical significance of each variable. The model was applied to estimate the national and subnational winter wheat yield in the United States, Ukraine, Russia and France from 2001 to 2017. At the subnational level the model shows very good performance with a coefficient of determination higher than 0.7 and Root Mean Square Error (RMSE) lower than 15%. At the national level the model provides a strong coefficient of determination higher than 0.8 and a RMSE lower than 8%, which demonstrates good performance of the models at this scale. Additionally, it was also able to capture low winter wheat yields during years with extreme weather events, for example 2002 in US and 2003 in Ukraine.*

Keywords: Yield model, MODIS , agriculture

©2019. Japan Geoscience Union. All Right Reserved. 

# Agricultural monitoring from Optical and SAR data

*Andrés Eduardo Santamaría-Artigas[1,2], Sergii Skakun[1,2], Belen Franch[1,2], Jean-Claude Roger[1,2], Eric Vermote[2]

1. University of Maryland College Park, 2. NASA Goddard Space Flight Center

Vegetation indices derived from optical remote sensing data are a valuable source of information for agricultural monitoring. However, cloud cover over some areas reduces the number of valid observations, which can difficult the detection of changes in crop condition. In this context, synthetic aperture radar (SAR) systems are an interesting alternative due to their low sensitivity to clouds. In this work, we analyze the relationship between SAR backscatter from Sentinel-1 and vegetation indices derived from the Harmonized Landsat-8 Sentinel-2 (HLS) product with data from the year 2017 over 6 land cover classes in Ukraine: Winter crops, summer crops, bare land, grasslands, forest, and water. Results show that SAR data from Sentinel-1 could be used to complement optical indices for certain land covers. In the case of winter crops (rapeseed and wheat), the ratio between Sigma-0 VV and VH polarization showed the highest relationship with the Normalized Difference Vegetation Index (NDVI) while for summer crops (maize, sugar beet, sunflower, and soybean) the highest relationship was shown by the Sigma-0 VH polarization and NDVI. Further work is being developed to exploit more complex SAR models which account for other variables that affect the backscatter signal such as soil moisture.

Keywords: agricultural monitoring, crop condition, synthetic aperture radar, HLS, normalized difference vegetation index

©2019. Japan Geoscience Union. All Right Reserved. 

# Eco-hydrological modeling using field-based and Earth Observations to assess water use efficiency and support agricultural water resources management

pierre Guillevic[2,1], *Jean-Claude Roger[1,2]

1. University of Maryland, College Park, USA, 2. NASA Goddard Space flight Center, Greenbelt, USA

The objective of this NASA project is to develop an integrated modeling platform using Earth Observations to simulate large-scale hydrological processes and food production in support of water use decision and agricultural policy. The decision tool will provide timely and relevant assessments of crop growth, agricultural water use and available water supply from local to regional scales, with the capability to predict the impact of different climate and water resources management scenarios on food production. The approach is based on the use of field and Earth observations to calibrate an eco-hydrological model, and climate simulations to forecast crop condition and yield through the crop season. The expected primary outcomes and results for stakeholders is potential best water management practices to improve water use efficiency and prevent excessive losses of water and nitrogen to the environment. These will be provided to in-country end-users within various relevant Ministries and Departments, in order to inform regional and national decisions. Changing precipitation patterns, droughts of increasing duration and severity and growing demand for food have significant implications on water management practices, spurring an increased need for irrigation in a sustainable manner and better monitoring of water resources for the agricultural sector in general. Understanding the context and water resource constraints that stakeholders and smallholder farmers face in climate sensitive regions is critical to target and understand the potential impact of water use management. We focus on a diverse set of regional pilot cases in Argentina, South Africa, Tanzania and the United States that are representative of a range of agricultural systems, water issues and climate impacts. The application is integrated in the GEOGLAM project, an existing widely-used web-based platform which will aid synthesizing the project outcomes and expert domain knowledge to provide timely and actionable water resources and crop condition information to assist local, regional and national water management decisions. At the end, the application will be interactive and will offer the end-user organizations the possibility to submit new water resource management scenarios online for impact evaluation.

Earth Observations are critical to characterize and monitor the different components of agricultural ecosystems and change (forests, croplands and marginal lands availability, for example) across temporal and spatial scales. Satellite data in the shortwave, thermal infrared and microwave spectral domains from US (MODIS, VIIRS, Landsat, SMAP) and European (Sentinel 1 and 2) sensors will be used to characterize changes in land surfaces and water use from 2000 to the present in support of agricultural planning decisions. In a research context, the potential of new satellite missions (i.e., ECOSTRESS, SWOT and SAOACOM) to derive surface hydrology information will be evaluated. The Agricultural Policy/Environmental eXtender (APEX) watershed model is proposed as the modeling tool to understand the biophysical and human-decision processes associated with the food-energy-water nexus. Model simulations will use climate data from the NASA Goddard Earth Observing System Model (GEOS-5) Atmosphere-Ocean General Circulation Model: MERRA-2 for simulation of past conditions and seasonal (6-month) forecasts for projections in the future. The study focus on large, key agricultural regions where agricultural ecosystems are vulnerable to demographic expansion and/or climate variability and change including drought and flood events.

©2019. Japan Geoscience Union. All Right Reserved. 

Keywords: water resources, hydrologycal modelling , remote sensing

©2019. Japan Geoscience Union. All Right Reserved. 

# Detecting and quantifying forest dynamics using SAR time-series data in Indonesia

*Pedro Rodriguez-Veiga[1,2,3], Narumasa Tsutsumida[3]

1. Centre for Landscape and Climate Research, University of Leicester, Leicester, UK, 2. NERC National Centre for Earth Observation (NCEO), Leicester, UK, 3. Graduate School of Global Environmental Studies, Kyoto University, Japan

Satellite Earth Observation (EO) data allows the generation of forest disturbance maps that can improve greenhouse gas (GHG) monitoring at local and national scales, and provide information that can be used for land use planning and management. Mapping forest biomass stocks, deforestation, forest degradation and enhancement is crucial in order to determine the loss of carbon stocks due to disturbances (e.g. deforestation, fires) or the gain due to new forest or growth. Time-series observations identify decreasing or increasing trends of aboveground biomass carbon, and separate anthropogenic related changes from seasonal changes of vegetation. This is important for understanding the terrestrial carbon cycle and for supporting better forest management and policies. This study uses time-series data from L-band Synthetic Aperture Radar (SAR) JAXA’s ALOS PALSAR and ALOS-2 PALSAR-2 to quantify carbon loss and gain trajectories (emission / sequestration) of existing forests in West Java (Indonesia).

Keywords: deforestation, SAR, time-series, forest dynamics

©2019. Japan Geoscience Union. All Right Reserved. 

[E] Oral | M (Multidisciplinary and Interdisciplinary)：M-AG Applied Geosciences

Thu. May 30, 2019 1:45 PM - 3:15 PM JST | Thu. May 30, 2019 4:45 AM - 6:15 AM UTC | 302 3F

## [M-AG38] Satellite Land Physical Processes Monitoring at Medium/High/Very High Resolution

convener:Jean-Claude Roger(University of Maryland College Park), Shinichi Sobue(Japan Aerospace Exploration Agency), Eric Vermote(NASA Goddard Space Flight Center), Chairperson:Jean-Claude Roger, Eric Vermote

We solicit papers on the land physical processes monitoring. In particular, it will include the inversion and use of land products from medium, high, and very high spatial resolution. For the last years, medium, high, and very high resolutions became a useful and a powerful toll for Earth studies. Topics of interest mainly include (not limited to):<br/>- New developments for data processing, including atmospheric correction and cloud screening;<br/>- Analysis and correction of directional effects in land surface reflectances;<br/>- Use of time series of surface reflectances for land monitoring, including land cover classification and crop yield prediction (including data integration and data harmonization);<br/>- Development and use of new vegetation indices (i.e. red edge) and other products for agriculture applications;<br/>- Theoretical studies for sensors capabilities enhancements to future sensors at high/medium resolutions;<br/>- Use of products in agricultural monitoring applications (such as crop area, crop type, crop growing, yield estimation and prediction, damage assessment);<br/>- Agriculture monitoring algorithm description;<br/>- Evaluation or validation of potential products with ground measurements, official statistics;<br/>- International initiative to enhance Earth-Observing-based agricultural information.<br/><br/>Depending on outcome, we think about a special issue.

1:45 PM - 1:50 PM JST | 4:45 AM - 4:50 AM UTC

Introduction

---

1:50 PM - 2:05 PM JST | 4:50 AM - 5:05 AM UTC

[MAG38-01] 15-years of LSA-SAF/Eumetsat satellite-derived albedo products: method for retrieval validation, and recent advances using neural networks during spectral integration

*Florian Pinault[1], Dominique Carrer[1], Xavier Ceamanos[1], Gabriel Lellouch[1], Catherine Meurey[1], Suman Moparthy[1], Chloé Vincent[1], Sandra Coelho[2], Isabel Trigo[2] (1.Météo France, CNRM-GAME, UMR3589, Toulouse, France, 2.IPMA, Lisbon, Portugal)

---

2:05 PM - 2:20 PM JST | 5:05 AM - 5:20 AM UTC

[MAG38-02] **Toward a Consistent Land Long Term Climate Data Records from Large Field of View Polar Orbiting Earth Observation Satellites**

*Eric Vermote[1], Jean-Claude Roger[1,2], Belen Franch[1,2], Christopher Justice[2], Ivan Csiszar[3], Sadashiva Devadiga[1], Edward Masuoka[1] (1.NASA Goddard Space Flight Center, 2.University of Maryland, Dept. of Geographical Sciences, 3.NOAA/NESDIS/STAR)

---

2:20 PM - 2:35 PM JST | 5:20 AM - 5:35 AM UTC

[MAG38-03] **LaSRC Cloud Detection Algorithm for Landsat 8 and Sentinel-2 Data**

*Sergii Skakun[1], Eric Vermote[2], Jean-Claude Roger[1] (1.University of Maryland College Park, 2.NASA Goddard Space Flight Center)

---

2:35 PM - 2:50 PM JST | 5:35 AM - 5:50 AM UTC

[MAG38-04] **Aerosol models for the validation of Surface Reflectances for MODIS, VIIRS, Landsat-8, Sentinel-2 from LaSRC**

*Jean-Claude Roger[1,2], Eric Vermote[2], Sergii Skakun[1,2], Belen Franch[1,2], Georgia Doxani[4], William Rountree[1,2], Ferran Gascon[4], chris justice[1], oleg dubovik[3], Brent holben[2] (1.University of Maryland, College Park, USA, 2.NASA Goddard Space flight Center, Greenbelt, USA, 3.LOA, University of Lille, Villeneuve d'Ascq, France, 4.ESA, Frascati, Italy)

---

2:50 PM - 3:05 PM JST | 5:50 AM - 6:05 AM UTC

## [MAG38-05] Quantity and spatial distribution of aboveground biomass carbon in Colombia's forest

*Pedro Rodriguez-Veiga[1,2], Adriana Paola Barbosa-Herrera[3], Edersson Cabrera[3], Gustavo Galindo[3], Valentin Louis[1], Pilar Lozano[3], Pacheco-Pascagaza Ana Maria[1], Indira Pachon-Cendales[3], Salinas Nelso Ricardo[3], Heiko Balzter[1,2] (1.Centre for Landscape and Climate Research, University of Leicester, Leicester, UK, 2.NERC National Centre for Earth Observation (NCEO), Leicester, UK, 3.Institute of Hydrology, Meteorology and Environmental Studies (IDEAM), Bogota, Colombia)

---

3:05 PM - 3:15 PM JST | 6:05 AM - 6:15 AM UTC

Discussion

# 15-years of LSA-SAF/Eumetsat satellite-derived albedo products: method for retrieval validation, and recent advances using neural networks during spectral integration

*Florian Pinault[1], Dominique Carrer[1], Xavier Ceamanos[1], Gabriel Lellouch[1], Catherine Meurey[1], Suman Moparthy[1], Chloé Vincent[1], Sandra Coelho[2], Isabel Trigo[2]

1. Météo France, CNRM-GAME, UMR3589, Toulouse, France, 2. IPMA, Lisbon, Portugal

Using two sets of Eumetsat satellite sensors (geostationary MSG with SEVIRI sensor, polar orbiting Metop/EPS with AVHRR sensors), the Land Surface Analysis (LSA-SAF) team provides to the community several remote sensing products related to the land surface properties (http://lsa-saf.eumetsat.int/). The long-term continuity and consistency of these products is ensured from 2004 to at least 2022 thanks to the Eumetsat funding. In this contribution, we are focus on the various albedo products, presenting their properties, algorithms (from the L1 Top-Of-Atmosphere reflectance data to the L3 albedo), and validation results.

The main albedo retrieval algorithm is based on three steps. First, atmospheric correction is performed using a Smac approximation of a 6S off-line model. Second, the surface interaction is modeled by a kernel-based BRDF (Ross-thick-Li-sparse kernels), with an additional Kalman filter. Third, angular and spectral integrations are performed to compute spectral albedos (white-sky and black-sky) and broadband albedos (visible and NIR and total-shortwave).Validation results show a good match when comparing albedos with other sensors (MODIS) or with in-situ measurements. And performances are here analyzed in details with regards to the user requirements.

Finally we discuss the potential added value of using machine learning techniques in the scope of the launch of the next generation of European satellites which will provide observations in more spectral bands (as for instance MTG/FCI which characteristics are close to HIMAWARI 8/9: 5 visible bands and 3 NIR bands). In the third step of the albedo algorithm (spectral integration), non-convolutional neural networks seem to offer a promising way forward.

Keywords: brdf, albedo, satellite, remote sensing, neural network, machine learning

©2019. Japan Geoscience Union. All Right Reserved. 

# Toward a Consistent Land Long Term Climate Data Records from Large Field of View Polar Orbiting Earth Observation Satellites

*Eric Vermote[1], Jean-Claude Roger[1,2], Belen Franch[1,2], Christopher Justice[2], Ivan Csiszar[3], Sadashiva Devadiga[1], Edward Masuoka[1]

1. NASA Goddard Space Flight Center, 2. University of Maryland, Dept. of Geographical Sciences, 3. NOAA/NESDIS/STAR

Surface reflectance is one of the key products used in developing several higher-order land products, such as Vegetation Indices, Albedo and LAI/FPAR, it is therefore seminal to detecting trends in the biosphere and land surface and has been classed by NOAA as a “Fundamental Climate Data Record (FDCR) for Land”. Building a long-term surface reflectance data record of climate quality implies combining different instruments, sensors and satellites, accounting for different spatial resolutions and spectral characteristics, assuring consistent calibration, and correcting for atmospheric and directional effects. As the spatial resolution issue is addressed by aggregating the original data to a resolution still suitable for climate studies (e.g. 0.05 degree latitude, longitude), the instrument calibration becomes the first major hurdle one has to go through before being able to proceed any further.

In this work, we are using robust reflectance data records and inter-comparison methods that we have developed over the past several years (consisting of atmospheric correction, directional effect correction and spectral normalization) to establish and verify the inter-consistency of the reflectance products from the AVHRR sensors on-board NOAA 7, 9, 11, 14, 16, 17 and 18, the MODIS sensors on-board Aqua and Terra and the VIIRS sensors on-board Suomi-NPP and JPSS1. The resulting dataset being the 35+ years surface reflectance product and vegetation indices from 1981 to present.

Several other calibration techniques are also be applied that have been developed in the past by our team, in particular combining the cloud spectral band inter-calibration with BELMANIP cross sensor calibration in the near-infrared, using Landsat 5, 7 and 8 calibration to bridge between AVHRR and MODIS.

Keywords: surface reflectance, land climate data record, earth observations satellites

©2019. Japan Geoscience Union. All Right Reserved. 

# LaSRC Cloud Detection Algorithm for Landsat 8 and Sentinel-2 Data

*Sergii Skakun[1], Eric Vermote[2], Jean-Claude Roger[1]

1. University of Maryland College Park, 2. NASA Goddard Space Flight Center

This study aims at introducing and validating the cloud mask produced by the Land Surface Reflectance Code (LaSRC) for Landsat 8 and Sentinel-2 data. To detect clouds in optical satellite imagery, LaSRC uses quality assurance (QA) layers, which are produced during the atmospheric correction process. Validation is performed using two reference datasets. The former is the “L8 Biome” cloud validation dataset, which is produced by the US Geological Survey (USGS), and consists of 96 Landsat 8 scenes distributed globally over 12 different biomes. The latter is the dataset, which is produced over NASA GSFC assisted by ground photos of the sky and available for Landsat 8 and Sentinel-2A/B. We show that the LaSRC cloud detection algorithm reliably identifies thick clouds with commission and omission errors less than 4%. Large overdetection occurs for thin clouds. We conclude the study with recommendations on using the LaSRC QA layers, and provide an outlook on the need of acquiring objective reference cloud datasets.

Keywords: cloud, Landsat 8, Sentinel-2, LaSRC

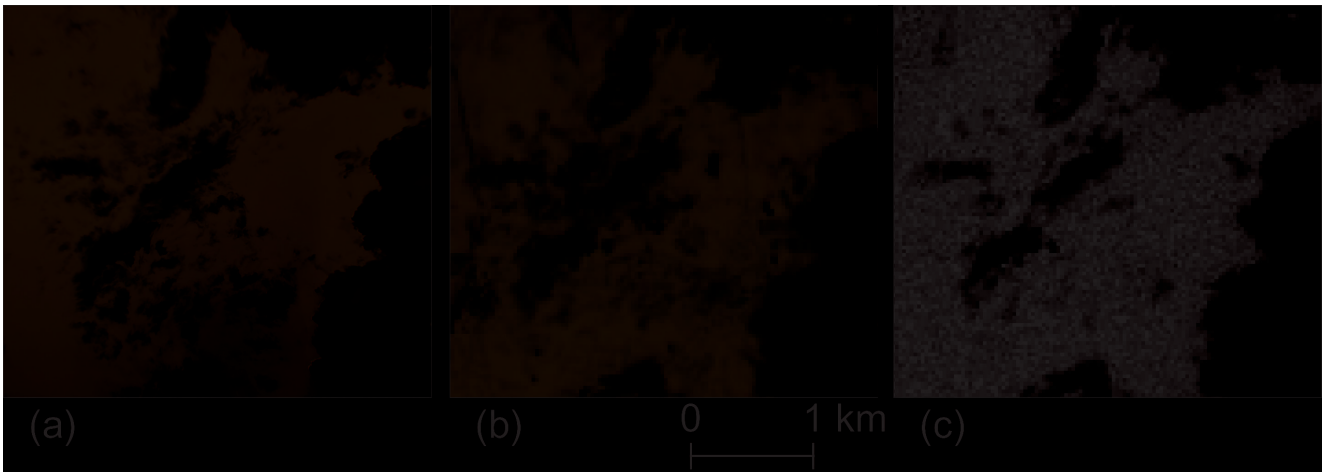


©2019. Japan Geoscience Union. All Right Reserved. 

# Aerosol models for the validation of Surface Reflectances for MODIS, VIIRS, Landsat-8, Sentinel-2 from LaSRC

*Jean-Claude Roger[1,2], Eric Vermote[2], Sergii Skakun[1,2], Belen Franch[1,2], Georgia Doxani[4], William Rountree[1,2], Ferran Gascon[4], chris justice[1], oleg dubovik[3], Brent holben[2]

1. University of Maryland, College Park, USA, 2. NASA Goddard Space flight Center, Greenbelt, USA, 3. LOA, University of Lille, Villeneuve d'Ascq, France, 4. ESA, Frascati, Italy

The land surface reflectance is a fundamental climate data record at the basis of the derivation of other climate data records (Albedo, LAI/Fpar, Vegetation indices) and has been recognized as a key parameter in the understanding of the land-surface-climate processes.

This work relies on a generic approach developed to derive surface reflectance over land from a variety of sensors. The approach is based on the inversion of the radiative transfer equation in the Lambertian case, with no adjacency effects, that account for a simplified coupling of the absorption by atmospheric gases and scattering by molecules and aerosols as implemented in the 6SV radiative transfer code. The processing code relies on look-up tables generated by 6SV, for which the accuracy (~1%) has been well documented in several papers. The LaSRC code uses ancillary data such as pressure and gas concentrations but relies on a per pixel inversion of the aerosol properties to assure the best possible accuracy for the surface reflectance, as aerosols can be highly variable both in space and time. This new aerosol inversion builds on the extensive dataset acquired by the Terra platform, combining MODIS and MISR to derive an explicit and dynamic map of band ratio’ s between blue and red channels and is a refinement of the operational approach used for MODIS and LANDSAT over the past 15 years. The aerosol inversion is generic and applicable to a variety of sensors. We use this basic approach to derive Landsat 8 and Sentinel 2 surface reflectance products for medium, high and very high spatial resolution (MODIS, VIIRS, LANDSAT, SENTINEL-2, WORLD VIEW 3…). The validation scheme is based on using aerosol models developed for each AERONET sites. We will present here the methodology to get these models. We will also show comparison of surface reflectance products with field measurements done by an instrument developed by us.
Finally, we will presents performances of LaSRC inter-compared with other operational approaches in the framework of the CEOS-ACIX (Atmospheric Correction Intercomparison eXercise) Calibration Validation Task co-Lead by ESA and NASA.

Keywords: Aerosol model, Atmospheric correction, Validation, Medium and High spatial resolution

©2019. Japan Geoscience Union. All Right Reserved. 

# Quantity and spatial distribution of aboveground biomass carbon in Colombia’s forest

*Pedro Rodriguez-Veiga[1,2], Adriana Paola Barbosa-Herrera[3], Edersson Cabrera[3], Gustavo Galindo[3], Valentin Louis[1], Pilar Lozano[3], Pacheco-Pascagaza Ana Maria[1], Indira Pachon-Cendales[3], Salinas Nelso Ricardo[3], Heiko Balzter[1,2]

1. Centre for Landscape and Climate Research, University of Leicester, Leicester, UK, 2. NERC National Centre for Earth Observation (NCEO), Leicester, UK, 3. Institute of Hydrology, Meteorology and Environmental Studies (IDEAM), Bogota, Colombia

In-situ national forest inventory data - NFI (IDEAM, 2018) as well as multispectral optical and synthetic aperture radar (SAR) satellite imagery were used to characterize the spatial distribution of forest aboveground biomass carbon (AGBC) stocks in Colombia. ALOS-2 PALSAR-2 gamma-0 backscatter annual mosaics (2015-2017) provided by JAXA were normalised and corrected using previous ALOS PALSAR annual mosaics (2007-2010) as reference. A multi-temporal Landsat 7 & 8 composite over the whole of Colombia was used for the year 2016 ±1. The national forest inventory in-situ plots used to train our model consisted of 5-subplots each and were collected during the period 2015-2017 in the main biomes of the country. A sample of permanent 1ha plots (PPMs) were also measured. Pan-tropical allometries (Chave et al, 2014) using diameter, height and specific wood gravity (type I) and a biomass-to-carbon ratio of 0.5 were used to estimate AGBC. A non-parametric random forests (RF) algorithm was used within a k-fold framework to retrieve AGBC at 30m spatial resolution for the whole of Colombia. The algorithm was trained using forest inventory plots and validated at plot (0.35 ha) and PPM level (1 ha). The accuracy assessment found coefficients of determination ($R^2$) of 0.70 and 0.68, and root mean square errors (RMSE) of 29.93 t C $ha^{-1}$ and 24.79 t C $ha^{-1}$ at plot and at PPM level, respectively. The results were also compared to the NFI estimates, and to current pantropical and global aboveground biomass carbon maps.

Keywords: biomass, carbon, SAR, machine-learning, multispectral, forest inventory

©2019. Japan Geoscience Union. All Right Reserved. 

[E] Oral | M (Multidisciplinary and Interdisciplinary)：M-AG Applied Geosciences

Thu. May 30, 2019 3:30 PM - 5:00 PM JST | Thu. May 30, 2019 6:30 AM - 8:00 AM UTC | 201B 2F

## [M-AG38] Satellite Land Physical Processes Monitoring at Medium/High/Very High Resolution

convener:Jean-Claude Roger(University of Maryland College Park), Shinichi Sobue(Japan Aerospace Exploration Agency), Eric Vermote(NASA Goddard Space Flight Center), Chairperson:Sergii Skakun(University of Mrayland, USA), Eric Vermote

We solicit papers on the land physical processes monitoring. In particular, it will include the inversion and use of land products from medium, high, and very high spatial resolution. For the last years, medium, high, and very high resolutions became a useful and a powerful toll for Earth studies. Topics of interest mainly include (not limited to):
- New developments for data processing, including atmospheric correction and cloud screening;
- Analysis and correction of directional effects in land surface reflectances;
- Use of time series of surface reflectances for land monitoring, including land cover classification and crop yield prediction (including data integration and data harmonization);
- Development and use of new vegetation indices (i.e. red edge) and other products for agriculture applications;
- Theoretical studies for sensors capabilities enhancements to future sensors at high/medium resolutions;
- Use of products in agricultural monitoring applications (such as crop area, crop type, crop growing, yield estimation and prediction, damage assessment);
- Agriculture monitoring algorithm description;
- Evaluation or validation of potential products with ground measurements, official statistics;
- International initiative to enhance Earth-Observing-based agricultural information.
Depending on outcome, we think about a special issue.

3:30 PM - 3:35 PM JST | 6:30 AM - 6:35 AM UTC

Introduction

---

3:35 PM - 3:50 PM JST | 6:35 AM - 6:50 AM UTC

[MAG38-06] Introduction of GCOM-C/SGLI Leaf Area Index & Fraction of Absorbed Photosynthetically Active Radiation products

*Toshiyuki Kobayashi[1], Yoshiaki HONDA[2], Yuhsaku Ono[2], Hideki Kobayashi[3], Wei Yang[2], Shin Nagai[3], Tomoko Akitsu[4], Kenlo Nasahara[4], Risa Miyazaki[1], Masahiro Hori[1], Hiroshi Murakami[1] (1.Japan Aerospace Exploration Agency, 2.Center for Environmental Remote Sensing, Chiba University, 3.Japan Agency for Marine-Earth Science and Technology, 4.University of Tsukuba)

---

3:50 PM - 4:05 PM JST | 6:50 AM - 7:05 AM UTC

[MAG38-07] **35-years of Land Surface Albedo and 15-years of Down-Welling Short-Wave Radiation Retrievals from Satellites through the EUMETSAT/LSA-SAF and ECMWF/C3S projects**

*Dominique Carrer[1], Florian Pinault[1], Iskander Benhadj[2], Xavier Ceamanos[1], Sandra Coelho[3], Gabriel Lellouch[1], Catherine Meurey[1], Suman Moparthy[1], Else Swinnen[2], Chloé Vincent[1], Isabel Trigo[3] (1.Meteo France, CNRM, France, 2.VITO, Belgium, 3.IPMA, Portugal)

---

4:05 PM - 4:20 PM JST | 7:05 AM - 7:20 AM UTC

[MAG38-08] **Integrating the satellite-based biophysical model and environmental zonation scheme to estimate rice yield gap in Northeast China**

*Jiahua Zhang[1,3], Jingwen Wang[1,2,3] (1.Institute of Remote Sensing and Digital Earth, Chinese Academy of Sciences, 2.University of Chinese Academy of Sciences, 3.Aerospace Information Research Institute, Chinese Academy of Sciences)

---

4:20 PM - 4:35 PM JST | 7:20 AM - 7:35 AM UTC

[MAG38-09] Landsat-based Phenological Classification Mapping in Japan

*Narumasa Tsutsumida[1], Shin Nagai[2], Pedro Rodriguez-Veiga[3,4,1], Tomoaki Miura[5] (1.Graduate School of Global Environmental Studies, Kyoto Univeristy, 2.Research and Development Center for Global Change, Japan Agency for Marine-Earth Science and Technology, 3.Centre for Landscape and Climate Research, University of Leicester, 4. National Centre for Earth Observation, University of Leicester, 5.Department of Natural Resources and Environmental Management University of Hawaii at Manoa)

---

4:35 PM - 4:50 PM JST | 7:35 AM - 7:50 AM UTC

[MAG38-10] **Incorporating satellite-retrieved canopy nitrogen content into the biophysical process model for estimating crop yield and N fertilizer recommendation**

*Jingwen Wang[1,2,3], Jiahua Zhang[1,3] (1.Institute of Remote Sensing and Digital Earth, Chinese Academy of Sciences, 2.University of Chinese Academy of Sciences, 3.Aerospace Information Research Institute, Chinese Academy of Sciences)

---

4:50 PM - 5:00 PM JST | 7:50 AM - 8:00 AM UTC

Discussion

# Introduction of GCOM-C/SGLI Leaf Area Index & Fraction of Absorbed Photosynthetically Active Radiation products

*Toshiyuki Kobayashi[1], Yoshiaki HONDA[2], Yuhsaku Ono[2], Hideki Kobayashi[3], Wei Yang[2], Shin Nagai[3], Tomoko Akitsu[4], Kenlo Nasahara[4], Risa Miyazaki[1], Masahiro Hori[1], Hiroshi Murakami[1]

1. Japan Aerospace Exploration Agency, 2. Center for Environmental Remote Sensing, Chiba University, 3. Japan Agency for Marine-Earth Science and Technology, 4. University of Tsukuba

The Japan Aerospace Exploration Agency (JAXA) launched the Global Change Observation Mission - Climate (GCOM-C) satellite on December 23rd, 2017. The Leaf Area Index (LAI) and the fraction of Absorbed Photosynthetically Active Radiation (fAPAR) product (Algorithm ID: T2B) is one of the GCOM-C standard land products. The dataset is being produced from Second Generation Global Imager (SGLI) at 250-m resolution on a daily basis. At the present time, there are several limitations on the product. In this research, we summarize the early results and limitations of the T2B products.

The LAI is defined as one half of the total green leaf area per unit ground surface area. In the GCOM-C product, LAI is estimated for overstory leaves. The information for understory vegetation is added as understory NDVI. The fAPAR is defined as the proportion of the effectively absorbed solar radiation by plants in the photosynthetically active wavelengths (the spectral region from 400 to 700 nm). LAI and fAPAR were estimated based on the Look-Up Tables (LUTs) showing the relationships between the multi-angle atmospherically-corrected land surface reflectance data and the LAI or fAPAR. The LUTs were produced to fit with the field-observed reference data collected from literatures using a radiative transfer simulator, the Forest Light Environmental Simulator (FLiES) [1]. It simulates radiative transfers in the forests and grasslands based on the Monte Carlo method.

The accuracy of the retrieved LAI and fAPAR was assessed using the in-situ observation data which was collected at several sites. The product has the tendency of overestimating LAI especially at the needle-leaved forests. One of the reasons is that the current algorithm cannot distinguish the difference between the overstory LAI and the understory vegetation well at the forested areas with sparse trees. The accuracy of the T2B product should be improved by revising the algorithm and the LUTs for retrieving LAI. We are planning to revise the land cover datasets which are the basis of retrieving LAI. The LUTs will be revised by fitting the vegetation parameters for FLiES with the SGLI data.

[1] H. Kobayashi *et al.*, A coupled 1-D atmosphere and 3-D canopy radiative transfer model for canopy reflectance, light environment, and photosynthesis simulation in a heterogeneous landscape, *Remote Sensing of Environment*, **112** (2008), 173-185.

Keywords: LAI, fAPAR, GCOM-C

©2019. Japan Geoscience Union. All Right Reserved. 

# 35-years of Land Surface Albedo and 15-years of Down-Welling Short-Wave Radiation Retrievals from Satellites through the EUMETSAT/LSA-SAF and ECMWF/C3S projects

*Dominique Carrer[1], Florian Pinault[1], Iskander Benhadj[2], Xavier Ceamanos[1], Sandra Coelho[3], Gabriel Lellouch[1], Catherine Meurey[1], Suman Moparthy[1], Else Swinnen[2], Chloé Vincent[1], Isabel Trigo[3]

1. Meteo France, CNRM, France, 2. VITO, Belgium, 3. IPMA, Portugal

The space program of EUMETSAT (project CDOP3, LSA-SAF) and the Copernicus Climate Change program (managed by ECMWF) provide (or will provide) added-value satellite products for the meteorological and environmental science communities, especially in the fields of climate modelling, environmental management, natural hazards management, and climate change detection.

The EUMETSAT/LSA-SAF project started in 1999 with research and development activities. The delivered operational products include land surface albedos, temperature, short-wave and long-wave downwelling radiation fluxes, and many others. After twenty years (1999-2019) of research, development, and progressive operational activities, Meteo-France built on a strong expertise on satellite retrieval of the surface albedo and down-welling short-wave radiation variables. Based on that experience, we started in 2016 within the framework of the COPERNICUS/C3S_312 project to develop consistent surface albedo products from the 80’s until now using multiple sensors from the past to the current generation of instrument. This will complete the EUMETSAT/LSA-SAF albedo archive for the past period. This work will lead in 2019 to more than 35 years of products characterizing the albedo properties of the surface and 15 years of short-wave downwelling radiation fluxes from different satellite sensors. First C3S collection will be available in autumn 2019 whereas more than 10 different albedos and short-wave downwelling radiation fluxes are already operational in EUMETSAT/LSA-SAF (http://lsa-saf.eumetsat.int/). Product characteristics, and performances are presented here. The next scientific challenges related to the next generation of European satellites and the emergence of artificial intelligence are also discussed.

Finally, it is important to emphasize that these programs provide a great opportunity to monitor human-induced climate change since consistent production of data sets is ensured until at least 2022. In this perspective, our effort will be in the development of open source scientific code in order to share our expertise in the remote sensing of the Earth.

Keywords: satellite, surface albedo, short-wave radiation

©2019. Japan Geoscience Union. All Right Reserved. 

# Integrating the satellite-based biophysical model and environmental zonation scheme to estimate rice yield gap in Northeast China

*Jiahua Zhang[1,3], Jingwen Wang[1,2,3]

1. Institute of Remote Sensing and Digital Earth, Chinese Academy of Sciences, 2. University of Chinese Academy of Sciences, 3. Aerospace Information Research Institute, Chinese Academy of Sciences

Yield gap analysis is a powerful method to reveal the difference between the actual crop yield and yield potential, and to understand the possible yield increase for fulfilling the growing food demand. It used to be restricted to small geographic areas in previous studies, and thus the scope of untapped yield often remains unclear at macro scale. To this end, we proposed an improved remote sensing approach to better assess the regional rice yield gap in northeast China. A biophysical model based on satellite-retrieved LAI and crop classification map was used to derive the actual yield and its spatial patterns. In addition, a machine-learning zonation scheme was developed to further evaluate the attainable potential yield for farmers within domains having similar climatic, geomorphic, and edaphic context. Results indicated that the satellite-based biophysical model can provide reliable estimates of rice yields, with RMSE all below 20 percent at the county level from 2006 to 2017; and the zonation scheme enabled better portrayal of the spatial variation in potential yield. To identify areas with the greatest potential for narrowing the yield gap, northeast China was divided into four parts with different priorities for future yield improvement. In general, south of northeast China possessed substantial yield gaps with the primary priority to be explored; whereas in the north, the actual yield already approximating yield potential, further yield increase was limited and challenging. Quantile regression model provided a complete view of relationships between natural factors and potential yield, and revealed the significant limiting effects of growing degree days, cumulative solar radiation and elevation. This study demonstrates the potential of remote sensing for agricultural decisions, and will aid planners to recognize the macro-scale food production capacity and security situation, to prioritize regions and needs for research and exploitation, and to evaluate the impact of future scenarios such as climate change.

Keywords: remote sensing, crop yield, yield gap, biophysical process model, environmental zonation scheme, Northeast China

©2019. Japan Geoscience Union. All Right Reserved. 

# Landsat-based Phenological Classification Mapping in Japan

*Narumasa Tsutsumida[1], Shin Nagai[2], Pedro Rodriguez-Veiga[3,4,1], Tomoaki Miura[5]

1. Graduate School of Global Environmental Studies, Kyoto Univeristy, 2. Research and Development Center for Global Change, Japan Agency for Marine-Earth Science and Technology, 3. Centre for Landscape and Climate Research, University of Leicester, 4. National Centre for Earth Observation, University of Leicester, 5. Department of Natural Resources and Environmental Management University of Hawaii at Manoa

Land surface phenology (LSP) is associated with climate and terrestrial conditions over space and time, and the monitoring of LSP helps understandings of the terrestrial environments. The LSP is often inferred by satellite observations, and long-term and regularly-composited satellite imagery is now freely available. Due to its complex interactions with geographical and environmental factors, it is often difficult to characterise phenological cycles by LSP. In order to understand the baseline of the phenological cycle which would be expected as the principal vegetation seasonal activity, we aim at classifying LSP temporal patterns over the entire territory of Japan. Normalised Vegetation Difference Index (NDVI) time series during the period of 2014 to 2017 with the spatial resolution of 30m calculated from Landsat 8 surface reflectance were decomposed into three harmonic terms by harmonic analysis with removing of the temporal trend. Then amplitudes and phases of these three harmonic terms were classified into 36 classes according to their orders. Considering tall vegetation (e.g., tree covers) and short vegetation (e.g., agricultural lands), while excluding other land covers, two types of phenological classification maps with 36 classes for each were produced. The phenological classification proposed in this study is a new terrestrial map which provides new important information for land cover studies regarding climate change, environmental degradation, and human impact assessment. This simple unsupervised classification approach can have diverse advantages such as i) only one specific variable (in this case NDVI) was used, yielding a consistent result compared to models with multivariate analysis, ii) complex temporal profiles can be considered, suggesting better descriptions of LSP than using phenological parameters such as start-of-season, peak-of-season, end-of-season, and length of greening period (In particular, our approach can classify temporal profiles with multiple peaks in the seasonal cycle), iii) the unsupervised classification approach do not need reference samples, which would require reliable observations of phenological events for a supervised classification scheme (such datasets are often limited), and iv) the non-thematic way of classification can avoid mislabelling problems. Interpretation of the classification map can be done by the users, making it easy to utilise towards further climate / environmental studies.

Keywords: Phenology, Earth Observation, Landsat

©2019. Japan Geoscience Union. All Right Reserved. 

# Incorporating satellite-retrieved canopy nitrogen content into the biophysical process model for estimating crop yield and N fertilizer recommendation

*Jingwen Wang[1,2,3], Jiahua Zhang[1,3]

1. Institute of Remote Sensing and Digital Earth, Chinese Academy of Sciences, 2. University of Chinese Academy of Sciences, 3. Aerospace Information Research Institute, Chinese Academy of Sciences

Remote sensing-based biophysical process models (RSBPM) are powerful and indispensable tools for estimating crop productivity over field and landscape scales. However, due to the lack of regional fertilization data, nitrogen stress is often poorly parameterized in these models, which may lead to considerable biases in crop yield simulation. To address this issue, current study improves the representation of nitrogen constraints on photosynthetic capacity in the RSBPM. Canopy nitrogen content retrieved from the newly available high-resolution Sentinel-2 spectral bands is integrated into the model to constrain nitrogen availability in the vital photosynthetic enzyme. And a two-leaf upscaling scheme is used to account for the vertically varying nitrogen content inside canopies and the associated physiological differences between leaves. Measurement data was collected for 32 field-years that spans major crops including wheat, maize, soybean and rice from 2016 to 2017 in China. The satellite-retrieved canopy nitrogen content partially reflects the field fertilization, and identifies seasonality of Rubiso-limited photosynthetic capacity. The new representation of nitrogen constraints significantly reduces the bias of estimated crop yields, and improves the temporal correlations between the simulated and the measured biomass, relative to the commonly employed cases of using specified constant nitrogen stress factor, default fertilization schemes, and the big-leaf nitrogen-constrained model. The improved RSBPM also enables the remote estimation of nitrogen nutrient index, which indicates the status of actual N absorbed versus critical N requirement in the crop. This model improvement on nitrogen constraints has significant implications for better assessment and prediction of crop yield and nitrogen use efficiency and for studying human-environment interactions.

Keywords: canopy nitrogen content, crop yield, biophysical process model, Sentinel-2, fertilization, nitrogen nutrient index

©2019. Japan Geoscience Union. All Right Reserved. 

[J] Poster | M (Multidisciplinary and Interdisciplinary)：M-AG Applied Geosciences

Thu. May 30, 2019 10:45 AM - 12:15 PM JST | Thu. May 30, 2019 1:45 AM - 3:15 AM UTC | Poster Hall International Exhibition Hall8, Makuhari Messe_12

## [M-AG39] Marine-Earth Informatics

convener:Seiji Tsuboi(JAMSTEC, Center for Earth Information Science and Technology), Keiko Takahashi(Japan Agency for Marine and Earth Science and Technology), Masaki Kanao(National Institute of Polar Research), Daisuke Matsuoka(Japan Agency for Marine-Earth Science and Technology)

In advancing the research of marine Earth science, observation and computer simulation is an essential element. In recent years, the performance of the observation apparatus is dramatically improved, along with the means of observation is diversified. It is becoming possible to observe in a resolution, which was not imaginable so far. Such data to be generated from the observation is tremendously large in quantity and its quality is drastically improved. To handle these huge and high quality dataset for data analysis, we need to have a high speed and large memory computer system but such a system now becomes within reach in our hands by the recent dramatic improvement of high performance computer system. On the other hand, researchers who can use this kind of large-scale computer in their studies are still quite limited. In this session, we try to review the situation of observation data that has undergone a dramatic change regarded with both quality and quantity in recent years of marine Earth science research. We also try to review the situation from a professional standpoint of simulation about the status of the high performance computer system to analyze these big data. Also we focus on the state of the art data analysis technique and aim to share the outlook from the professional standpoint of computational science and professional position of observation science about the future direction of the marine Earth informatics research.<br/>

### [MAG39-P01] A bottleneck against industrial distribution of atmosphere-ocean product from the Earth Simulator

*Shinya Kakuta[1], Hajime Nishimura[1] (1.JAMSTEC Japan Agency for Marine-Earth Science and Technology)

### [MAG39-P02] GANSEKI: Long-Term Strategy of JAMSTEC Deep Seafloor Rock Sample Curation

*Takayuki Tomiyama[1] (1.Japan Agency for Marine-Earth Science and Technology)

### [MAG39-P03] Running global seismic waveform simulation on Windows10

*Seiji Tsuboi[1] (1.JAMSTEC, Center for Earth Information Science and Technology)

### [MAG39-P04] Synthetic seismograms of explosive sources calculated by the Earth Simulator

*Seiji Tsuboi[1] (1.JAMSTEC, Center for Earth Information Science and Technology)

# A bottleneck against industrial distribution of atmosphere-ocean product from the Earth Simulator

*Shinya Kakuta[1], Hajime Nishimura[1]

1. JAMSTEC Japan Agency for Marine-Earth Science and Technology

For public organizations to expand research and development activities into socio-economic ripple effect, this presentation discusses strategy to generate business utilizing the Earth Simulator and its outputs under cooperation with private sectors. To solve social problems, it is necessary not only to create successful cases but also to roll them out and continue operating them for a long term. More and more public funding requires prospects for social application by private sectors to supplement itself. On the other hand, public research organizations, also required to improve socio-economic outcomes from research results, are too short of human resources to meet the requirement, occupied with on-going national projects.

The fundamental bottleneck against social application is the shortage of experts with skills to utilize environmental data, in particular, super-large volumes of meteorological data. We propose a platform to be built so that the bottleneck can be widened by division of data processing to lighten burdens on such a limited number of experts as university researchers, assigning the statistical analysis and assessment after dynamical down-scaling to data scientists or weather forecasters estimated to number around 10,000 in total in Japan, respectively. Down-scaling experts are shorter than data scientists or weather forecasters. Most of data scientists can be assumed to use such scripts as Python. On the other hand, approximately 150 weather forecasters are additionally licensed every year. In addition, private sectors should cooperate with many local governments to specify to utilize the super-large volumes, to set up small servers of in-situ data taken by local governments, and to transform the data into geographical information system.

In a long run, human resources should be developed. Every year, private sectors can headhunt or develop approximately 10 experts for assessment on extreme phenomena in collaboration with national research institutes, advanced local institutes, or universities.

Keywords: industrial distribution, bottleneck, atmosphere and ocean simulation

©2019. Japan Geoscience Union. All Right Reserved. 

# 気象プロダクトを社会データと相関解析するまでの工程

Process to correlation analyses between meteorological products & social data

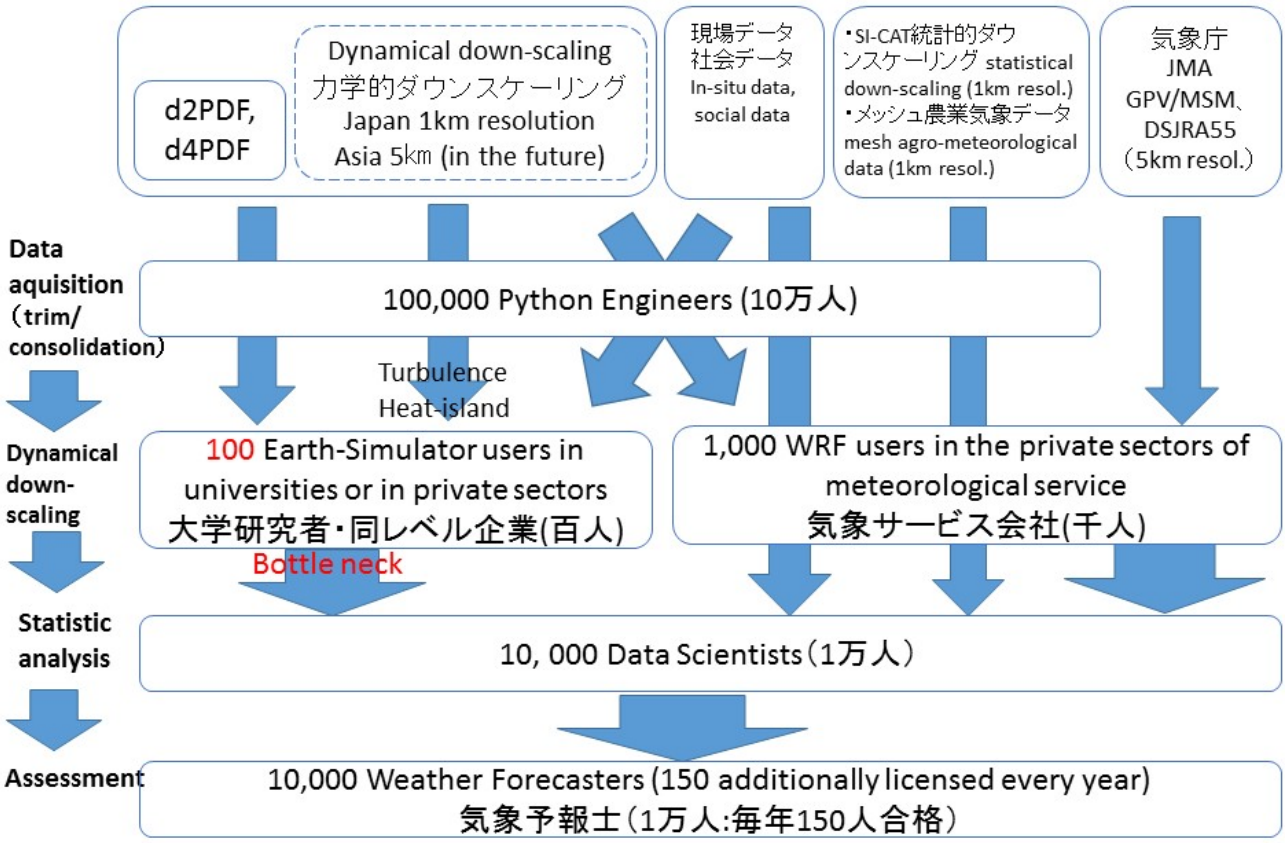


©2019. Japan Geoscience Union. All Right Reserved. 

# GANSEKI: Long-Term Strategy of JAMSTEC Deep Seafloor Rock Sample Curation

*Takayuki Tomiyama[1]

1. Japan Agency for Marine-Earth Science and Technology

More than 10 years have passed since Japan Agency for Marine-Earth Science and Technology (JAMSTEC) started the curatorial management of observation data and samples under the current JAMSTEC Data Policy [1]. This means that some of them have aged more than their minimum storage periods that are defined as 10 years. JAMSTEC Rock Sample curation is now passing one of the milestones for sustainable sample management.
JAMSTEC Rock Sample Curation has been continuously changed since it was established. As for the sample storage, JAMSTEC has come to equip fixed rock sample storage rooms in 2019, after repeated (re-)installations of mobile storage containers for every 1~2 years, however they are still considered as temporary storages. It is under planning to acquire a sample storage building, that is supposed to be the permanent rock sample storage. Some efforts, such as reduce of individual sample volumes, will become inevitable within next several years to make enough room for growing sample collections. As for the data management, the rock sample database “GANSEKI" has experienced several updates and the user-side interface was integrated into the DARWIN database [2] on 2017. Its management-side system is under remodeling for integrating databases for rock, sediment core and biological samples into one system. The variation of publishable data has been getting wider; geochemistry data, isochron ages, thin-section and closeup-texture photos, and literature information are currently publishable and more data types will be available in the future.
For years, JAMSTEC Rock Sample Curation has been operated only under JAMSTC Data Policy [1]. However, it will have to deal with the parallel existence of additional policy of JURCAOS-AORI-JAMSTEC Cooperative Research cruises [3], which will be enforced in 2019. In this presentation, the author will summarize the management history and current situations of JAMSTEC Rock Sample Curation, and discuss its future strategy.

**References:** [1] JAMSTEC (2007) “Basic Policies on the Handling of Data and Samples by Japan Agency for Marine-Earth Science and Technology”, https://www.jamstec.go.jp/e/database/data_policy.html. [2] JAMSTEC ”Data and Sample Research System for Whole Cruise Information in JAMSTEC”, http://www.godac.jamstec.go.jp/darwin/e. [3] Atmosphere and Ocean Research Institute, The University of Tokyo, “Cooperative Research System”, http://www.aori.u-tokyo.ac.jp/english/coop/.

Keywords: rock sample, curation, marine geology, database

©2019. Japan Geoscience Union. All Right Reserved. 

# Running global seismic waveform simulation on Windows10

*Seiji Tsuboi[1]

1. JAMSTEC, Center for Earth Information Science and Technology

Latest version of Windows10, which is Fall Creators Update, supports Windows Subsystem for Linux (WSL). This enables to use linux, such as Ubuntu, directly from Windows. Here we show examples of how we can use this system to run spectral-element method to calculate global seismic waveform on Windows PC and its performance of typical simulation. We use Ubuntu 18.04 available from Windows store and installed it on the latest version of Windows 10. Then we install gcc 5.4.0, gfortran 5.4.0, and OpenMPI 4.0.0 on Ubuntu. We also install SPECFEM3D_GLOBE 7.0.0 and configured under the above linux environment. We use Windows PC equipped with Core i7-3840QM CPU (2.8GHz) and 16GB memory. Since this CPU has four cores, we use one chunk simulation of SPECFEM3D_GLOBE and set the angular distance of the chunk to be 20 degree with NPROC=2. We set NEX=128, which enables to get synthetics with the accuracy of about 30 second and longer. Preliminary results of this simulation show that it takes about 4hours to compute 5 minutes synthetic seismograms over the chunk by using four cores of this CPU. We will show if this performance may be improved with further optimization of the compilation.

Keywords: Spectral Element Method, Numerical Simulation, theoretical seismograms

©2019. Japan Geoscience Union. All Right Reserved. 

# Synthetic seismograms of explosive sources calculated by the Earth Simulator

*Seiji Tsuboi[1]

1. JAMSTEC, Center for Earth Information Science and Technology

We have calculated broadband synthetic seismograms using the spectral-element method (Komatitsch et al., 2005) for realistic Earth model. Recent progress in supercomputers makes it possible to compute the synthetic seismograms with the accuracy of 1.2 second and longer (Tsuboi et al., 2016a) . Here we have used one chunk of spectral element method to compute synthetics with 1.5 second accuracy using the Earth Simulator. We calculate synthetics for Sep. 3, 2017 (MB(USGS) 6.3). The simulations are performed on 8,100 processors, which require 2,025 nodes of the Earth Simulator. We use one chunk with the angular distance 40 degrees to compute synthetic seismograms. On this number of nodes, a simulation of 5 minutes of wave propagation accurate at periods of 1.5 seconds and longer requires about 9 hours of CPU time (Tsuboi et al., 2016b) . We use CMT solution of Dreger (2017) as a source model for this event. This source model has 24% CLVD component, 34% double couple component and 42% isotropic component. The hypocenter depth of this solution is 1.4 km but we put the hypocenter at the surface for this computation. Comparisons of the synthetic waveforms with the observation at station MDJ(Mudanjiang) in China show that the arrival time of Pn and Pg waves matches well with the observation, which demonstrates that the crustal structure we have used for this computation models the actual structure well. The surface waves observed at this station are also modeled well in the synthetics, which shows that the CMT solution we have used for this computation correctly grasps the source characteristics of this event. However, the amplitudes of Pn and Pg waves in the synthetics are smaller than the observations, which indicates that the amplitude of short period components is not enough in this computation. The result also shows that crustal structure around source region should be improved to get better agreement between the synthetics and observation.

Keywords: Spectral Element Method, Numerical Simulation, explosive source

©2019. Japan Geoscience Union. All Right Reserved. 

[J] Poster | M (Multidisciplinary and Interdisciplinary)：M-AG Applied Geosciences

Thu. May 30, 2019 5:15 PM - 6:30 PM JST | Thu. May 30, 2019 8:15 AM - 9:30 AM UTC | Poster Hall International Exhibition Hall8, Makuhari Messe_44

## [M-AG39] Marine-Earth Informatics

convener:Seiji Tsuboi(JAMSTEC, Center for Earth Information Science and Technology), Keiko Takahashi(Japan Agency for Marine and Earth Science and Technology), Masaki Kanao(National Institute of Polar Research), Daisuke Matsuoka(Japan Agency for Marine-Earth Science and Technology)

In advancing the research of marine Earth science, observation and computer simulation is an essential element. In recent years, the performance of the observation apparatus is dramatically improved, along with the means of observation is diversified. It is becoming possible to observe in a resolution, which was not imaginable so far. Such data to be generated from the observation is tremendously large in quantity and its quality is drastically improved. To handle these huge and high quality dataset for data analysis, we need to have a high speed and large memory computer system but such a system now becomes within reach in our hands by the recent dramatic improvement of high performance computer system. On the other hand, researchers who can use this kind of large-scale computer in their studies are still quite limited. In this session, we try to review the situation of observation data that has undergone a dramatic change regarded with both quality and quantity in recent years of marine Earth science research. We also try to review the situation from a professional standpoint of simulation about the status of the high performance computer system to analyze these big data. Also we focus on the state of the art data analysis technique and aim to share the outlook from the professional standpoint of computational science and professional position of observation science about the future direction of the marine Earth informatics research.<br/>

### [MAG39-P01] A bottleneck against industrial distribution of atmosphere-ocean product from the Earth Simulator

*Shinya Kakuta[1], Hajime Nishimura[1] (1.JAMSTEC Japan Agency for Marine-Earth Science and Technology)

### [MAG39-P02] GANSEKI: Long-Term Strategy of JAMSTEC Deep Seafloor Rock Sample Curation

*Takayuki Tomiyama[1] (1.Japan Agency for Marine-Earth Science and Technology)

### [MAG39-P03] Running global seismic waveform simulation on Windows10

*Seiji Tsuboi[1] (1.JAMSTEC, Center for Earth Information Science and Technology)

### [MAG39-P04] Synthetic seismograms of explosive sources calculated by the Earth Simulator

*Seiji Tsuboi[1] (1.JAMSTEC, Center for Earth Information Science and Technology)

# A bottleneck against industrial distribution of atmosphere-ocean product from the Earth Simulator

*Shinya Kakuta[1], Hajime Nishimura[1]

1. JAMSTEC Japan Agency for Marine-Earth Science and Technology

For public organizations to expand research and development activities into socio-economic ripple effect, this presentation discusses strategy to generate business utilizing the Earth Simulator and its outputs under cooperation with private sectors. To solve social problems, it is necessary not only to create successful cases but also to roll them out and continue operating them for a long term. More and more public funding requires prospects for social application by private sectors to supplement itself. On the other hand, public research organizations, also required to improve socio-economic outcomes from research results, are too short of human resources to meet the requirement, occupied with on-going national projects.

The fundamental bottleneck against social application is the shortage of experts with skills to utilize environmental data, in particular, super-large volumes of meteorological data. We propose a platform to be built so that the bottleneck can be widened by division of data processing to lighten burdens on such a limited number of experts as university researchers, assigning the statistical analysis and assessment after dynamical down-scaling to data scientists or weather forecasters estimated to number around 10,000 in total in Japan, respectively. Down-scaling experts are shorter than data scientists or weather forecasters. Most of data scientists can be assumed to use such scripts as Python. On the other hand, approximately 150 weather forecasters are additionally licensed every year. In addition, private sectors should cooperate with many local governments to specify to utilize the super-large volumes, to set up small servers of in-situ data taken by local governments, and to transform the data into geographical information system.

In a long run, human resources should be developed. Every year, private sectors can headhunt or develop approximately 10 experts for assessment on extreme phenomena in collaboration with national research institutes, advanced local institutes, or universities.

Keywords: industrial distribution, bottleneck, atmosphere and ocean simulation

©2019. Japan Geoscience Union. All Right Reserved. 

# 気象プロダクトを社会データと相関解析するまでの工程

Process to correlation analyses between meteorological products & social data

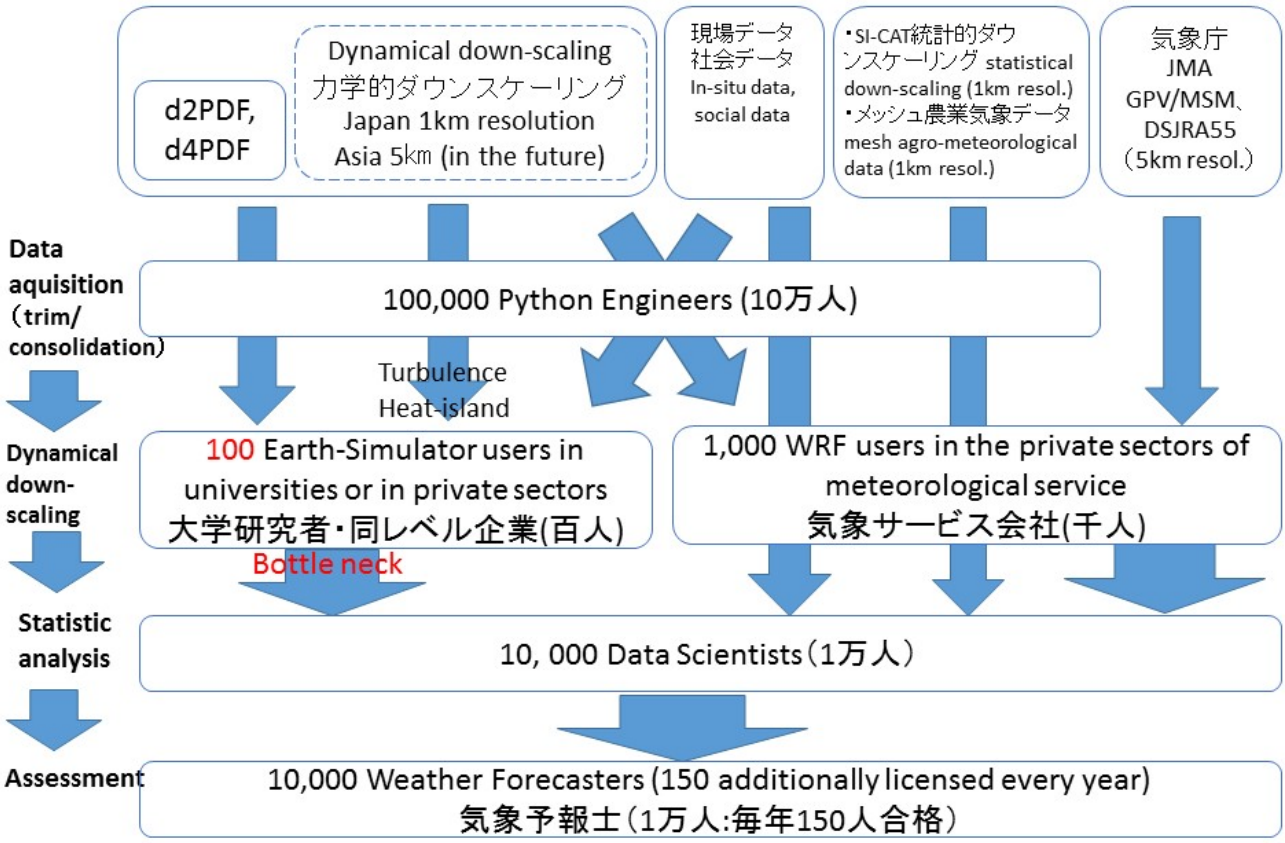


©2019. Japan Geoscience Union. All Right Reserved. 

# GANSEKI: Long-Term Strategy of JAMSTEC Deep Seafloor Rock Sample Curation

*Takayuki Tomiyama[1]

1. Japan Agency for Marine-Earth Science and Technology

More than 10 years have passed since Japan Agency for Marine-Earth Science and Technology (JAMSTEC) started the curatorial management of observation data and samples under the current JAMSTEC Data Policy [1]. This means that some of them have aged more than their minimum storage periods that are defined as 10 years. JAMSTEC Rock Sample curation is now passing one of the milestones for sustainable sample management.
JAMSTEC Rock Sample Curation has been continuously changed since it was established. As for the sample storage, JAMSTEC has come to equip fixed rock sample storage rooms in 2019, after repeated (re-)installations of mobile storage containers for every 1~2 years, however they are still considered as temporary storages. It is under planning to acquire a sample storage building, that is supposed to be the permanent rock sample storage. Some efforts, such as reduce of individual sample volumes, will become inevitable within next several years to make enough room for growing sample collections. As for the data management, the rock sample database “GANSEKI" has experienced several updates and the user-side interface was integrated into the DARWIN database [2] on 2017. Its management-side system is under remodeling for integrating databases for rock, sediment core and biological samples into one system. The variation of publishable data has been getting wider; geochemistry data, isochron ages, thin-section and closeup-texture photos, and literature information are currently publishable and more data types will be available in the future.
For years, JAMSTEC Rock Sample Curation has been operated only under JAMSTC Data Policy [1]. However, it will have to deal with the parallel existence of additional policy of JURCAOS-AORI-JAMSTEC Cooperative Research cruises [3], which will be enforced in 2019. In this presentation, the author will summarize the management history and current situations of JAMSTEC Rock Sample Curation, and discuss its future strategy.

**References:** [1] JAMSTEC (2007) “Basic Policies on the Handling of Data and Samples by Japan Agency for Marine-Earth Science and Technology”, https://www.jamstec.go.jp/e/database/data_policy.html. [2] JAMSTEC ”Data and Sample Research System for Whole Cruise Information in JAMSTEC”, http://www.godac.jamstec.go.jp/darwin/e. [3] Atmosphere and Ocean Research Institute, The University of Tokyo, “Cooperative Research System”, http://www.aori.u-tokyo.ac.jp/english/coop/.

Keywords: rock sample, curation, marine geology, database

©2019. Japan Geoscience Union. All Right Reserved. 

# Running global seismic waveform simulation on Windows10

*Seiji Tsuboi[1]

1. JAMSTEC, Center for Earth Information Science and Technology

Latest version of Windows10, which is Fall Creators Update, supports Windows Subsystem for Linux (WSL). This enables to use linux, such as Ubuntu, directly from Windows. Here we show examples of how we can use this system to run spectral-element method to calculate global seismic waveform on Windows PC and its performance of typical simulation. We use Ubuntu 18.04 available from Windows store and installed it on the latest version of Windows 10. Then we install gcc 5.4.0, gfortran 5.4.0, and OpenMPI 4.0.0 on Ubuntu. We also install SPECFEM3D_GLOBE 7.0.0 and configured under the above linux environment. We use Windows PC equipped with Core i7-3840QM CPU (2.8GHz) and 16GB memory. Since this CPU has four cores, we use one chunk simulation of SPECFEM3D_GLOBE and set the angular distance of the chunk to be 20 degree with NPROC=2. We set NEX=128, which enables to get synthetics with the accuracy of about 30 second and longer. Preliminary results of this simulation show that it takes about 4hours to compute 5 minutes synthetic seismograms over the chunk by using four cores of this CPU. We will show if this performance may be improved with further optimization of the compilation.

Keywords: Spectral Element Method, Numerical Simulation, theoretical seismograms

©2019. Japan Geoscience Union. All Right Reserved. 

# Synthetic seismograms of explosive sources calculated by the Earth Simulator

*Seiji Tsuboi[1]

1. JAMSTEC, Center for Earth Information Science and Technology

We have calculated broadband synthetic seismograms using the spectral-element method (Komatitsch et al., 2005) for realistic Earth model. Recent progress in supercomputers makes it possible to compute the synthetic seismograms with the accuracy of 1.2 second and longer (Tsuboi et al., 2016a) . Here we have used one chunk of spectral element method to compute synthetics with 1.5 second accuracy using the Earth Simulator. We calculate synthetics for Sep. 3, 2017 (MB(USGS) 6.3). The simulations are performed on 8,100 processors, which require 2,025 nodes of the Earth Simulator. We use one chunk with the angular distance 40 degrees to compute synthetic seismograms. On this number of nodes, a simulation of 5 minutes of wave propagation accurate at periods of 1.5 seconds and longer requires about 9 hours of CPU time (Tsuboi et al., 2016b) . We use CMT solution of Dreger (2017) as a source model for this event. This source model has 24% CLVD component, 34% double couple component and 42% isotropic component. The hypocenter depth of this solution is 1.4 km but we put the hypocenter at the surface for this computation. Comparisons of the synthetic waveforms with the observation at station MDJ(Mudanjiang) in China show that the arrival time of Pn and Pg waves matches well with the observation, which demonstrates that the crustal structure we have used for this computation models the actual structure well. The surface waves observed at this station are also modeled well in the synthetics, which shows that the CMT solution we have used for this computation correctly grasps the source characteristics of this event. However, the amplitudes of Pn and Pg waves in the synthetics are smaller than the observations, which indicates that the amplitude of short period components is not enough in this computation. The result also shows that crustal structure around source region should be improved to get better agreement between the synthetics and observation.

Keywords: Spectral Element Method, Numerical Simulation, explosive source

©2019. Japan Geoscience Union. All Right Reserved. 

[J] Oral | M (Multidisciplinary and Interdisciplinary)：M-AG Applied Geosciences

Thu. May 30, 2019 1:45 PM - 3:15 PM JST | Thu. May 30, 2019 4:45 AM - 6:15 AM UTC | A10 TOKYO BAY MAKUHARI HALL

## [M-AG39] Marine-Earth Informatics

convener:Seiji Tsuboi(JAMSTEC, Center for Earth Information Science and Technology), Keiko Takahashi(Japan Agency for Marine and Earth Science and Technology), Masaki Kanao(National Institute of Polar Research), Daisuke Matsuoka(Japan Agency for Marine-Earth Science and Technology), Chairperson:Daisuke Matsuoka, Seiji Tsuboi

In advancing the research of marine Earth science, observation and computer simulation is an essential element. In recent years, the performance of the observation apparatus is dramatically improved, along with the means of observation is diversified. It is becoming possible to observe in a resolution, which was not imaginable so far. Such data to be generated from the observation is tremendously large in quantity and its quality is drastically improved. To handle these huge and high quality dataset for data analysis, we need to have a high speed and large memory computer system but such a system now becomes within reach in our hands by the recent dramatic improvement of high performance computer system. On the other hand, researchers who can use this kind of large-scale computer in their studies are still quite limited. In this session, we try to review the situation of observation data that has undergone a dramatic change regarded with both quality and quantity in recent years of marine Earth science research. We also try to review the situation from a professional standpoint of simulation about the status of the high performance computer system to analyze these big data. Also we focus on the state of the art data analysis technique and aim to share the outlook from the professional standpoint of computational science and professional position of observation science about the future direction of the marine Earth informatics research.<br/>

1:45 PM - 2:00 PM JST | 4:45 AM - 5:00 AM UTC

### [MAG39-01] Future direction of Marine Earth Informatics

*Keiko Takahashi[1] (1.Japan Agency for Marine and Earth Science and Technology)

---

2:00 PM - 2:15 PM JST | 5:00 AM - 5:15 AM UTC

### [MAG39-02] Extraction method of weather informations from camera image using Deep Neural Network

*DAISUKE SUGIYAMA[1], RYO ONISHI[1], HIDENORI FUDEYASU[2] (1.Japan Agency for Marine-Earth Science and Technology, 2.Yokohama National University)

---

2:15 PM - 2:30 PM JST | 5:15 AM - 5:30 AM UTC

### [MAG39-03] Automatic detection of weather front around Japan using deep convolutional neural network

*Daisuke Matsuoka[1,2], Shiori Sugimoto[1], Yujin Nakagawa[1], Fumiaki Araki[1], Shintaro Kawahara[1], Yosuke Onoue[4], Masaaki Iiyama[3], Koji Koyamada[3] (1.Japan Agency for Marine-Earth Science and Technology, 2.Japan Science and Technology Agency, 3.Nihon University, 4.Kyoto University)

---

2:30 PM - 2:45 PM JST | 5:30 AM - 5:45 AM UTC

### [MAG39-04] Detection of multiple earthquakes by using theoretical seismograms as training dataset of machine learning

*Seiji Tsuboi[1], DAISUKE SUGIYAMA[1] (1.JAMSTEC, Center for Earth Information Science and Technology)

---

2:45 PM - 3:00 PM JST | 5:45 AM - 6:00 AM UTC

### [MAG39-05] Classification with imbalanced cloud data using deep convolutional neural network

*Daisuke Matsuoka[1,2], Masuo Nakano[1], Daisuke Sugiyama[1], Seiichi Uchida[3] (1.Japan Agency for Marine-Earth Science and Technology, 2.Japan Science and Technology Agency, 3.Kyushu University)

---

3:00 PM - 3:15 PM JST | 6:00 AM - 6:15 AM UTC

[MAG39-06] discussion

*Seiji Tsuboi[1] (1.JAMSTEC, Center for Earth Information Science and Technology)

# Future direction of Marine Earth Informatics

*Keiko Takahashi[1]

1. Japan Agency for Marine and Earth Science and Technology

In advancing the research of marine Earth science, observation and computer simulation is an essential element. In recent years, the performance of the observation apparatus is dramatically improved, along with the means of observation is diversified. It is becoming possible to observe in a resolution, which was not imaginable so far. Such data to be generated from the observation is tremendously large in quantity and its quality is drastically improved. To handle these huge and high quality dataset for data analysis, we need to have a high speed and large memory computer system but such a system now becomes within reach in our hands by the recent dramatic improvement of high performance computer system. On the other hand, researchers who can use this kind of large-scale computer in their studies are still quite limited. In this session, we try to review the situation of observation data that has undergone a dramatic change regarded with both quality and quantity in recent years of marine Earth science research. We also try to review the situation from a professional standpoint of simulation about the status of the high performance computer system to analyze these “big data”. We focus on the state of the art data analysis technique and aim to share the outlook from the professional standpoint of computational science and professional position of observation science about the future direction of the marine Earth informatics research.

©2019. Japan Geoscience Union. All Right Reserved. 

# Extraction method of weather informations from camera image using Deep Neural Network

*DAISUKE SUGIYAMA[1], RYO ONISHI[1], HIDENORI FUDEYASU[2]

1. Japan Agency for Marine-Earth Science and Technology, 2. Yokohama National University

In order to further improve precision of numerical forecasts, it is expected to utilize high-density weather information by various IoT (Internet of Things) sensor equipment networks capable of real-time acquisition via the Internet. However, the IoT sensors are installed on the ground, so we can not observe weather information in the sky simply by using the IoT sensor normally. In this study, we used artificial intelligence technology for image recognition, and worked on the development of a system that extracts cloud amount and solar radiation from images of inexpensive consumer cameras. Our method becomes possible to operate low-price camera-equipped devices as remote sensing equipment without using expensive observation equipment. The weather information extracted is not only input values for numerical simulation but also expected to be utilized in, for example, agriculture. In addition, the society of security camera network is spreading in China and others. Our method can be a fundamental technology of high-density weather observation in such society.
In this study, we first constructed a 5-layer convolutional neural network (CNN) model that predicts cloud cover amount from the image. As data to train this network, we used data labeled cloud cover on about 2,000 sky images from the Internet. The cloud cover in this study means the rate of the clouds in the sky area shown in the camera image in 11 steps from 0 to 10. On the other hand, the Japan Meteorological Agency defines the rate of the cloud region to the whole sky as the cloud amount. Attention should be paid to difference in this definition. We used the 80% data as the training data, and the remaining 20% was used for cross validation. Finally, we compared to the MSE: mean square error, of our method to the existing method. It became clear that cloud cover can be estimated with the overwhelmingly small MSE of 3.0 for this CNN, more than the existing segmentation method of 12.7.
Secondly, as training data, this model use long-term high-frequency observation data for 1 minute, observed by Yokohama National University. We chose solar radiation amount, fixed camera image in this data. The model extracts the amount of solar radiation from the sky image in the range of several tens of kilometers ahead of the fixed camera's photographing direction. With 6 years of this data, the number of images reaches max about 3 million images in one direction, and this big training data is used to train Deep Neural Network. Now, intuitively, a high brightness image tends to be considered to have a high solar radiation amount. However, consumer cameras usually have automatic brightness and contrast adjustment functions. Also, such as the slightly cloudy days are almost high brightness value. The correlation coefficient of brightness value and solar radiation, is not large. On the other hand, we can calculate the theoretical maximum solar radiation from the latitude, longitude and time of image's shooting position (Nakajima et al. 2000). Focusing on this point, we constructed a new Multimodal Deep Learning model with image + theoretical maximum solar radiation as input layers. This model estimates the attenuation value from theoretical maximum solar radiation with images of training data. It was clarified that the amount of solar radiation can be estimated with high accuracy by training this model from the image, position and time.

Keywords: Deep Learning, IoT, High-density Weather Observations

©2019. Japan Geoscience Union. All Right Reserved. 

# Automatic detection of weather front around Japan using deep convolutional neural network

*Daisuke Matsuoka[1,2], Shiori Sugimoto[1], Yujin Nakagawa[1], Fumiaki Araki[1], Shintaro Kawahara[1], Yosuke Onoue[4], Masaaki Iiyama[3], Koji Koyamada[3]

1. Japan Agency for Marine-Earth Science and Technology, 2. Japan Science and Technology Agency, 3. Nihon University, 4. Kyoto University

In this study, we automatically detect stationary front from weather forecast simulation data (GPV/MSM) using U-Net deep convolutional neural network. Our U-Net trains ten years weather data (precipitation, sea level pressure, relative humidity, air temperature, and wind velocity) and the position of weather front as the ground truth. As a result of applying the trained U-Net to the untrained one year data, our approach succeeded in accurately detecting Baiu front and autumn rain front except when Typhoon occurred. Moreover, wind velocity (zonal and meridional component) and relative humidity at 1000 hPa play an important role to obtain high detection performance. Our approach is also able to apply to weather simulation data which the weather front is not associated with.

Keywords: Deep learning, Convolutional neural network, Weather front detection

©2019. Japan Geoscience Union. All Right Reserved. 

# Detection of multiple earthquakes by using theoretical seismograms as training dataset of machine learning

*Seiji Tsuboi[1], DAISUKE SUGIYAMA[1]

1. JAMSTEC, Center for Earth Information Science and Technology

Earthquake Early Warning (EEW) is now routinely used for hazard mitigation purpose in various countries. One of the causes which results false alarm of EEW is earthquakes which happen concurrently in different location. On January 5$^{th}$, 2018, two earthquakes with magnitude around 5, which separate about 400 km, happened concurrently in Japan and false EEW was issued by JMA. Here we combine numerically computed theoretical seismograms and deep machine learning to properly identify multiple earthquakes to avoid false alarm. We calculate theoretical seismograms for realistic three-dimensional Earth model and use these seismograms to create snapshots of seismic wave propagation images at the surface of the Earth. Then we use these snapshots as training dataset of convolutional neural network. We build neural networks to identify multiple earthquakes and found that this networks may identify multiple earthquakes with 99% accuracy. Advantage of using this approach to identify multiple earthquakes is that we may include any earthquakes in our training dataset and accuracy of hypocenter parameters can be increased by accumulating theoretical seismograms for various earthquake location and size as learning dataset of deep machine learning. We also apply this technique for determination of hypocentral parameters, such as epicenter, depth, origin time and magnitude. We have applied these networks to actual seismograms to show that this procedure works successfully to locate earthquake and determine magnitude.

Keywords: earthquake location, machine learning, synthetic seismograms

©2019. Japan Geoscience Union. All Right Reserved. 

# Classification with imbalanced cloud data using deep convolutional neural network

*Daisuke Matsuoka[1,2], Masuo Nakano[1], Daisuke Sugiyama[1], Seiichi Uchida[3]

1. Japan Agency for Marine-Earth Science and Technology, 2. Japan Science and Technology Agency, 3. Kyushu University

Image classification using deep convolutional neural network is effective technique to detect extreme phenomenafrom climate data. However, the number of extreme phenomena such as tropical cyclone (TC) is overwhelmingly small compared with others. It is knon that classification performance decline du to this imbalance between positive (TCs) and negative examples (non-TCs). In the present study, we developed a new negative data selection method for binary classification for cloud images. We analyze the relationship between the ease of classification and the characteristics of data, and optimize the training data in order to decrease the false alarm ratio (FAR). As the results, we succeeded in decrease FAR from 32.8–53.4% to 60.0–70.0% in the western North Pacific in the period from July to November.

Keywords: Deep learning, Classification, Tropical cyclone

©2019. Japan Geoscience Union. All Right Reserved. 

# discussion

*Seiji Tsuboi[1]

1. JAMSTEC, Center for Earth Information Science and Technology

Discuss current and future direction of Marine Earth Informatics.

©2019. Japan Geoscience Union. All Right Reserved. 

[J] Oral | M (Multidisciplinary and Interdisciplinary)：M-AG Applied Geosciences

Thu. May 30, 2019 3:30 PM - 5:00 PM JST | Thu. May 30, 2019 6:30 AM - 8:00 AM UTC | A10 TOKYO BAY MAKUHARI HALL

## [M-AG39] Marine-Earth Informatics

convener:Seiji Tsuboi(JAMSTEC, Center for Earth Information Science and Technology), Keiko Takahashi(Japan Agency for Marine and Earth Science and Technology), Masaki Kanao(National Institute of Polar Research), Daisuke Matsuoka(Japan Agency for Marine-Earth Science and Technology), Chairperson:Seiji Tsuboi, Daisuke Matsuoka

In advancing the research of marine Earth science, observation and computer simulation is an essential element. In recent years, the performance of the observation apparatus is dramatically improved, along with the means of observation is diversified. It is becoming possible to observe in a resolution, which was not imaginable so far. Such data to be generated from the observation is tremendously large in quantity and its quality is drastically improved. To handle these huge and high quality dataset for data analysis, we need to have a high speed and large memory computer system but such a system now becomes within reach in our hands by the recent dramatic improvement of high performance computer system. On the other hand, researchers who can use this kind of large-scale computer in their studies are still quite limited. In this session, we try to review the situation of observation data that has undergone a dramatic change regarded with both quality and quantity in recent years of marine Earth science research. We also try to review the situation from a professional standpoint of simulation about the status of the high performance computer system to analyze these big data. Also we focus on the state of the art data analysis technique and aim to share the outlook from the professional standpoint of computational science and professional position of observation science about the future direction of the marine Earth informatics research.<br/>

3:30 PM - 3:50 PM JST | 6:30 AM - 6:50 AM UTC

[MAG39-07] Farmed fish management: integration of observation and simulation

★Invited Papers

*Haruka Nishikawa[1] (1.Japan Agency for Marine-Earth Science and Technology)

3:50 PM - 4:05 PM JST | 6:50 AM - 7:05 AM UTC

[MAG39-08] **Q-factor estimation for Greenland ice sheet using 3-D seismic waveform modeling**

*Genti Toyokuni[1], Hiroshi Takenaka[2], Masanao Komatsu[2], Ryota Takagi[1], Masaki Kanao[3], Seiji Tsuboi[4] (1.RCPEVE, Tohoku Univ., 2.Okayama Univ., 3.NIPR, 4.JAMSTEC)

4:05 PM - 4:20 PM JST | 7:05 AM - 7:20 AM UTC

[MAG39-09] CLCL: CAVELib Compatible Library for Head-mounted Displays

*Shintaro Kawahara[1] (1.Japan Agency for Marine-Earth Science and Technology)

4:20 PM - 4:35 PM JST | 7:20 AM - 7:35 AM UTC

[MAG39-10] Super-Resolution Simulation for Real-Time Prediction of Urban Micrometeorology

*Ryo Onishi[1], DAISUKE SUGIYAMA[1], Keigo Matsuda[1] (1.Japan Agency for Marine-Earth Science and Technology)

4:35 PM - 4:50 PM JST | 7:35 AM - 7:50 AM UTC

[MAG39-11] Proposal of adaptation measures for the anthropogenic heat release to improve the summer heat environment in a district

*Toru Sugiyama[1], Xiaoran Tong[2], Satoshi Yoshida[2], Satoru Sadohara[2] (1.Japan Agency for Marine-Earth Science and Technology Center for Earth Information Science and Technology, 2.Yokohama National Univercity Institute of Urban Innovation)

4:50 PM - 5:00 PM JST | 7:50 AM - 8:00 AM UTC

Discussion

# Farmed fish management: integration of observation and simulation

*Haruka Nishikawa[1]

1. Japan Agency for Marine-Earth Science and Technology

Since the natural fish resource is constantly decreasing, the importance of fish farming further increases. However, the technique is still depending on the skill of artisans. The feed quantity is determined by looking. Is it truly the best feed quantity? I plan to develop a fish growth simulation model based on observation and to estimate the best feed quantity by using its simulation. This technique will reduce labor cost and enhance the new entry. I will discuss the future fish farming system that is developed by an integration of observation and simulation.

Keywords: Fish farming

©2019. Japan Geoscience Union. All Right Reserved. 

# Q-factor estimation for Greenland ice sheet using 3-D seismic waveform modeling

*Genti Toyokuni[1], Hiroshi Takenaka[2], Masanao Komatsu[2], Ryota Takagi[1], Masaki Kanao[3], Seiji Tsuboi[4]

1. RCPEVE, Tohoku Univ., 2. Okayama Univ., 3. NIPR, 4. JAMSTEC

In and around Greenland, 33 seismographs are now in operation by the project “GLISN” (Greenland Ice Sheet Monitoring Network) as an international cooperation with 11 countries. Since the initiation of this project in 2009, broadband and continuous seismic waveform data have been accumulating, and data analyses using seismic interferometry have actively been conducted. For example, Toyokuni et al. (2018) detected a Rayleigh-wave phase-velocity changes over 4.5 years beneath 90 station pairs throughout Greenland, and suggested that the thermal condition (freezing or melting) of the ice-sheet base might be detected using the pattern of the velocity changes. However, the seismic interferometry is a method based on the assumption that the cross-correlation of noise waveforms from two stations yields Green’s function between them, when averaged over a long period. However, it is suggested that this assumption sometimes fails due to inhomogeneous distribution of noise sources, etc.

This study first aims to investigate whether this assumption holds for the cross-correlation waveforms from GLISN stations using 3-D seismic waveform modeling. Furthermore, we estimate the seismic Q factors of the ice sheet which explains observations the best, by performing computations several times with different structural parameters.

The scheme we used for the 3-D modeling is “Quasi-Cartesian FDM” proposed by Takenaka et al. (2017). It numerically solves 3-D elastodynamic equation by the finite-difference method (FDM), taking into account the earth's curvature, topography, sea water layer, and 3-D structures of density, seismic wavespeeds, and attenuation. We used realistic ice sheet / basal rock topography data (ETOPO 1) and 3-D crustal / mantle structures (Crist 1.0). We used FX10 Supercomputer System in Univ. Tokyo (216 nodes, 432 processor, 8 threads).

The results are as follows:
(1) The cross-correlation waveforms obtained by the seismic interferometry show good agreement with synthetic Green’s functions for almost all the pairs, showing validity of the seismic interferometry on this region.
(2) Computations with various Q factors of the ice sheet revealed that (Qp, Qs) = (20, 20) explains the cross-correlation waveforms the best. This is the first example that the high attenuation characteristic of the ice sheet is confirmed for long propagation distance (>100 km).

References:
Takenaka, H. et al. (2017) EPS, 69, 67.
Toyokuni, G. et al. (2018) PEPI, 277, 81-98.

Keywords: Q factor, Greenland ice sheet, 3-D seismic waveform modeling, finite-difference method (FDM)

©2019. Japan Geoscience Union. All Right Reserved. 

# CLCL: CAVELib Compatible Library for Head-mounted Displays

*Shintaro Kawahara[1]

1. Japan Agency for Marine-Earth Science and Technology

Head-mounted displays (HMDs) are becoming a practical platform for three-dimensional scientific visualization. To reuse existing software assets that have been developed for CAVE-type VR systems (CAVEs), I developed a C++ library called "***CLCL*** (CAVELib Compatible Library)" for porting the application software for CAVEs to HMDs. CLCL emulates the function calls of CAVELib, which is a commercial library for developing application software executable on CAVEs, and it enables us to easily port CAVELib application software to HMDs with minor modifications to the original source code. Executable files built using CLCL are able to launch on major HMDs which are Oculus Rift, HTC VIVE and Windows Mixed Reality devices. Sharing the source code also leads to an improvement in the VR software development efficiency, which is executable on both CAVEs and HMDs.

Keywords: Scientific visualization, Virtual reality, Software development

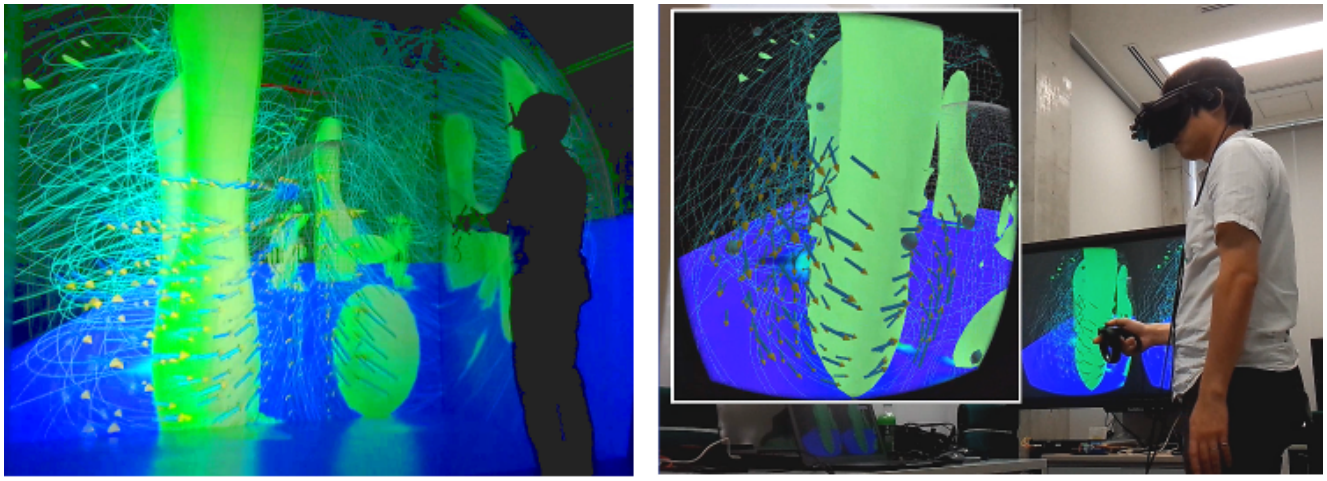

Fig.1 A CAVELib program executed on VR devices.
(Left: CAVE, Right: HMD)

©2019. Japan Geoscience Union. All Right Reserved. 

# Super-Resolution Simulation for Real-Time Prediction of Urban Micrometeorology

*Ryo Onishi[1], DAISUKE SUGIYAMA[1], Keigo Matsuda[1]

1. Japan Agency for Marine-Earth Science and Technology

We propose a super-resolution (SR) simulation system that consists of a physics-based meteorological simulation and an SR method based on a deep convolutional neural network (CNN). The CNN is trained using pairs of high-resolution (HR) and low-resolution (LR) images created from meteorological simulation results for different resolutions so that it can map LR simulation images to HR ones. The proposed SR simulation system, which performs LR simulations, can provide HR prediction results in much shorter operating cycles than those required for corresponding HR simulation prediction system. We apply the SR simulation system to urban micrometeorology, which is strongly affected by buildings and human activity. Urban micrometeorology simulations that need to resolve urban buildings are computationally costly and thus cannot be used for operational real-time predictions even when run on supercomputers. We performed HR micrometeorology simulations on a supercomputer to obtain datasets for training the CNN in the SR method. It is shown that the proposed SR method can be used with a spatial scaling factor of 4 and that it outperforms conventional interpolation methods by a large margin. It is also shown that the proposed SR simulation system has the potential to be used for operational urban micrometeorology predictions.

Keywords: super-resolution, deep learning, building-resolving urban micrometeorology, multi-scale data assimilation, IoT

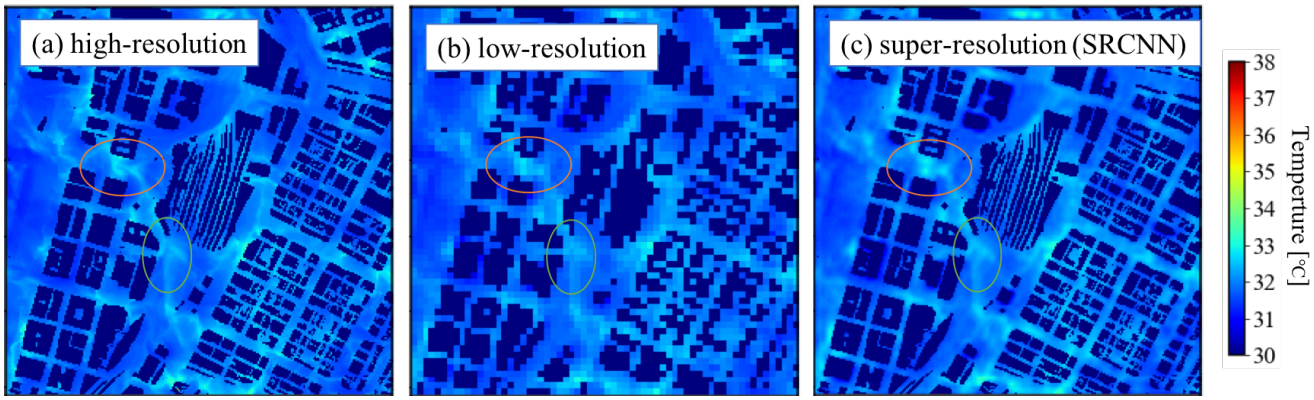


©2019. Japan Geoscience Union. All Right Reserved. 

# Proposal of adaptation measures for the anthropogenic heat release to improve the summer heat environment in a district

*Toru Sugiyama[1], Xiaoran Tong[2], Satoshi Yoshida[2], Satoru Sadohara[2]

1. Japan Agency for Marine-Earth Science and Technology Center for Earth Information Science and Technology, 2. Yokohama National Univercity Institute of Urban Innovation

As release technique of the anthropogenic exhaust heat, we propose following cases to produce comfortable districts in the forthcoming climate change era. We have performed numerical simulations to compare the thermal conditions quantitatively.

Keywords: Thermal environment, Numerical simulations, Anthropogenic heat, Energy local production for local consumption, Earth Simulator, MSSG model

©2019. Japan Geoscience Union. All Right Reserved. 

[E] Oral | M (Multidisciplinary and Interdisciplinary)：M-AG Applied Geosciences

Thu. May 30, 2019 9:00 AM - 10:30 AM JST | Thu. May 30, 2019 12:00 AM - 1:30 AM UTC | 202 2F

## [M-AG40] CTBT IMS Technologies for Detecting Nuclear Explosion and Their Applications to Earth Science

convener:Nurcan Meral Ozel(Comprehensive Nuclear-Test-Ban Treaty Organization), Hiroyuki Matsumoto(Japan Agency for Marine-Earth Science and Technology), Yosuke Naoi(Japan Atomic Energy Agency), Chairperson:Nurcan Meral Özel(Comprehensive Nuclear-Test-Ban Treaty Organization), Hiroyuki Matsumoto(JAMSTEC), Noriko Kamaya(ERI, University of Tokyo)

The Comprehensive Nuclear-Test-Ban Treaty Organization (CTBTO) was founded in 1996 in response to the adaption of the Treaty in 1996 by the United Nations General Assembly, which bans nuclear explosions on the Earth's surface, in the atmosphere, underwater and underground. The Treaty has a unique and comprehensive verification regime to make sure that no nuclear explosion goes undetected. The regime is supported by International Monitoring Systems (IMS) composed of the four state-of-art technologies; 1) Seismic, 2) Hydroacoustic, 3) Infrasound, and 4) Radionuclide, by the International Data Centre (IDC), and by the On-Site Inspections (OSI).<br/>IMS will, when complete, consists of 337 facilities worldwide to monitor the planet for signs of nuclear explosion. Around 90 % of the facilities are in operation and sending the data to the IDC in Vienna, Austria. <br/>The huge amount of data collected by the stations can be used for other purposes such as civil and scientific applications in addition to detecting nuclear explosions. They can provide Tsunami Warning centres with near real-time information about an underwater earthquake. During the Fukushima Daiichi Power Plant accident, in March 2011, the IMS network's radionuclide stations tracked the dispersion of radioactivity on a global scale. The data could also help better understand the oceans, volcanos, climate change, the movement of marine mammals, and many other issues.<br/>This session will provide the overview of CTBTO and its IMS, the scientific discussion on each technology, and its outcomes. The session welcomes young scientists and engineers who are interested in four IMS technologies.<br/>

9:00 AM - 9:15 AM JST | 12:00 AM - 12:15 AM UTC

### [MAG40-01] Japanese Contributions and Collaborations for IMS Technologies and the Verification Regime

*Nurcan Meral Ozel[1], David Jepsen[1], Naoko Nakashima[1], Hideaki Komiyama[1], Hiroyuki Matsumoto[1,2] (1.Comprehensive Nuclear-Test-Ban Treaty Organization (CTBTO), 2.Japan Agency for Marine-Earth Science and Technology (JAMSTEC))

9:15 AM - 9:30 AM JST | 12:15 AM - 12:30 AM UTC

### [MAG40-02] Review: Researches on detection of nuclear tests by seismic waves in Japan

★Invited Papers

*Noriko Kamaya[1] (1.Earthquake Research Institute, the University of Tokyo)

9:30 AM - 9:45 AM JST | 12:30 AM - 12:45 AM UTC

### [MAG40-03] Waveform Analysis on Induced Earthquakes after the 2017 Nuclear Test and Detected Mining Events in DPRK

*Masashi Motohashi[1], Takanari Fujii[1], Takayuki Otsu[1] (1.Japan Weather Association)

9:45 AM - 10:00 AM JST | 12:45 AM - 1:00 AM UTC

### [MAG40-04] Submarine volcanoes and where to find them: Harnessing IMS hydroacoustic data

★Invited Papers

*Dirk Metz[1] (1.Japan Agency for Marine-Earth Science and Technology)

10:00 AM - 10:15 AM JST | 1:00 AM - 1:15 AM UTC

### [MAG40-05] Importance of noble gas monitoring in CTBT verification technology and observation results in Takasaki radionuclide monitoring station

*Yoichi Yamamoto[1], Yuichi Kijima[1], Yutaka Tomita[1] (1.Japan Atomic Energy Agency)

10:15 AM - 10:30 AM JST | 1:15 AM - 1:30 AM UTC

[MAG40-06] ATM analysis results on radioxenons detected in Japan

*Yuichi Kijima[1], Yoichi Yamamoto[1], Yutaka Tomita[1] (1.Japan Atomic Energy Agency)

# Japanese Contributions and Collaborations for IMS Technologies and the Verification Regime

*Nurcan Meral Ozel[1], David Jepsen[1], Naoko Nakashima[1], Hideaki Komiyama[1], Hiroyuki Matsumoto[1,2]

1. Comprehensive Nuclear-Test-Ban Treaty Organization (CTBTO), 2. Japan Agency for Marine-Earth Science and Technology (JAMSTEC)

The CTBT verification regime is supported by the cooperation of member states who host monitoring stations and laboratories of the International Monitoring System (IMS) network. The proactive collaboration with state governments and research institutions hosting IMS facilities is crucial for improvement of the technologies for the verification regime.

Japan has contributed for many years in establishing and maintaining these facilities and in improving the verification technologies and regime, in a variety of aspects. Japan hosts stations for three of the technologies: seismic, infrasound and radionuclide. The technical contributions by Japan in projects for the improvement and enhancement of the radionuclide monitoring/detection capability are highlighted in this presentation.

In addition to the contributions through the operation of two IMS radionuclide monitoring stations in Japan, Okinawa, and Takasaki, two additional radionuclide measurement campaigns have been initiated at Horonobe and Mutsu, through financial support from the government of Japan (GoJ) in 2017. These campaigns started in early 2018, with the collaborations of Japan Atomic Energy Agency (JAEA). A new campaign in Fukuoka is being initiated, using another existing mobile system, aiming to configure a high dense measurement network for the evaluation and the calibration of the current noble gas system network of the IMS.

Another collaboration in the radionuclide sector is the air sampling for Ar-37 analysis and the new sampler testing at Takasaki station, in order to enhance the capability for On-site Inspection (OSI). Ar-37 is produced naturally by cosmic rays and exists in the atmosphere as background. Thus, it is also important to know its behavior in the environment. A 2-year sampling campaign was conducted at Takasaki in collaboration with JAEA in 2016-2018 utilizing their expertise.

The government of Japan (GoJ) has strongly supported to establish these collaborations, especially through voluntary contribution, in 2012, 2013 and 2017. They were used for enhancement of atmospheric transport modeling project, noble gas measurement campaign at Horonobe and Mutsu mentioned above, and sending Cost-free Experts (CFEs) of IMS HA Technology.

Keywords: Comprehensive Nuclear-Test-Ban Treaty (CTBT), International Monitoring System (IMS)

©2019. Japan Geoscience Union. All Right Reserved. 

# Review: Researches on detection of nuclear tests by seismic waves in Japan

*Noriko Kamaya[1]

1. Earthquake Research Institute, the University of Tokyo

## 1. Introduction

In Japan, if the Japan Meteorological Agency (JMA) observes a seismic wave that may not be a natural earthquake with epicenters around North Korea, the JMA immediately contacts the Prime Minister's Office and have press conferences and announces the parameters of that event. Then, with showing both waveforms of the North Korea's underground nuclear test and a natural earthquake, based on the characteristics of the waveform such as the S wave being ambiguous, JMA states there is a possibility that it is not a natural earthquake. The materials of these press conferences will be published on JMA’s website. However, because the detection of nuclear tests is not the original task of the JMA, no more analysis is not published. In addition, Japan Weather Association, which is responsible for monitoring nuclear tests based on the waveform data of the CTBTO (Comprehensive Nuclear Test Ban Treaty Organization), analyzes data, but only simple report is published on the website. It is important for Japan’s security to study detection technology of nuclear test by Japanese researchers. In this paper, we will review about Japanese researches on detection of nuclear tests by seismic waves which was published in Japanese papers.

## 2. Reports of observed events

The oldest paper would be written by Kubodera and Okano (1960). They reported long-period seismic waves with periods of 9 minutes to 1 minute were recorded at the same time that small atmospheric pressure change reached, when a hydrogen bomb test was conducted by the United States at Bikini Atoll in 1958. JMA (1972) published collection book of seismic waves recorded at underground nuclear test conducted by the US in the Amchitka Island on November 7, 1971.

## 3. Study on discrimination from natural earthquakes

Researches for discrimination nuclear tests from natural earthquakes were mainly conducted by using seismic waveforms at the Matsushiro Earthquake Observatory. Yamagishi et al. (1973) reported that the P wave of the nuclear tests were dominated by short-period waves. Also, they concluded that discrimination was possible by comparing Ms and mb. Seki et al. (1980) pointed out that S waves and surface waves were observed when large tests were conducted. Wakui and Kakishita (1986) pointed out that the discrimination method using the ratio of Mb and MS could only be applied to large-scale tests. Kamaya (1998) analyzed the waveforms of nuclear tests and natural earthquakes at Nevada and Xinjiang. She concluded the Complexity was the most effective method for discrimination. Okamoto and Kanjo (2007) analyzed waveforms of Matsushiro, Mudanjiang and Incheon of IRIS at the nuclear test by North Korea on October 9, 2006. They showed P wave radiation pattern had isotropic pattern. Koyama (2007) calculated the Complexity and the Spectral ratio of waveform in Matsushiro for the same test, and reported that the Spectral ratio was better than the Complexity for discrimination.

Kikuchi (1997) calculated the moment tensor for nuclear tests conducted by China and France from 1995

©2019. Japan Geoscience Union. All Right Reserved. 

to 1996 by waveform of the IRIS. He showed that the combination of the three main values of the moment tensor were clearly different from those of the natural earthquake. In addition, he estimated that shape of epicenters of Chinese tests were acicular and French were disk-shaped.

4. Toward the Future
It is necessary for us to learn recent research in the world in cooperation with the CTBTO. In addition, our (Japanese researchers') continuous research on detection of nuclear tests by analyzing seismic waveforms around the world is important.

Keywords: Nuclear Test, Nuclear Explosion, Seismic waves, Complexity, Spectral Ratio, Moment Tensor

©2019. Japan Geoscience Union. All Right Reserved. 

# Waveform Analysis on Induced Earthquakes after the 2017 Nuclear Test and Detected Mining Events in DPRK

*Masashi Motohashi[1], Takanari Fujii[1], Takayuki Otsu[1]

1. Japan Weather Association

After the DPRK September 2017 nuclear test event, several earthquakes were occurred near the test site. The scale of these induced earthquake events was fairly very small, therefore there were a few CTBT IMS seismic stations (e.g. KSRS, USRK, KLR) which could detect earthquake signals. Japan NDC-1 (National Data Center-1) tried to locate and discriminate these events utilizing non-IMS data such as IRIS (Incorporated Research Institutions for Seismology).

Analyzing waveform data of these events, S-wave (Sn, Lg-Phase) amplitude of waveform at close stations is larger than that of P-wave (Pn, Pg-Phase) and the feature of these events is presumed to be natural earthquake rather than man-made explosion. Near the DPRK test site, there are two open-pit mines at Chung-gang city and Musan city which locates DPRK-China border. We also compared with past mining explosion event there and we discriminated events with the indexes such as regional P/S ratio, P/S Spectral Ratio.

It was quite difficult to make event discrimination using only IMS seismic waveform data. IMS seismic network is not designed for detecting small-scale nuclear test far less than 1kt. Therefore, local and non-IMS seismic network data could largely contribute to refine event location and event discrimination.

Keywords: Waveform Analysis, Event Discrimination, Nuclear Test, Induced Earthquake

©2019. Japan Geoscience Union. All Right Reserved. 

# Submarine volcanoes and where to find them: Harnessing IMS hydroacoustic data

*Dirk Metz[1]

1. Japan Agency for Marine-Earth Science and Technology

Low-frequency underwater sound waves are a key feature of the hydroacoustic waveform component of the International Monitoring System (IMS), a global sensor network maintained by the Comprehensive Nuclear-Test-Ban Treaty Organization in an effort to detect clandestine nuclear explosions in the ocean, in the atmosphere, and underground. However, the potential of IMS data extends beyond test-ban monitoring, for instance, when studying sound phases generated by remote natural sources that otherwise would be difficult to detect, such as submarine earthquakes or volcanic eruptions. Here, we focus on IMS hydrophone recordings of Monowai, a volcanic center in the Kermadec Arc, and Ahyi volcano, located in the Northern Mariana Islands. Tripatite array data are processed using standard cross-correlation and time-difference-of-arrival techniques. Density-based clustering of arrivals at station H03, Juan Fernández Islands, reveals 82 discrete episodes of unrest at Monowai over the course of 3.5-years, making it one of the most active arc volcanoes currently known. IMS data suggests further volcanic activity at both known and unknown sites in the Tonga-Kermadec Arc region. Hydroacoustic recordings of the 2014 eruption at Ahyi show how data analysis can be advanced and streamlined, for example, to determine spectral parameters and acoustic energy release, which has implications for studying volcanic source processes and their respective impact on the ocean soundscape. IMS hydrophone arrays register volcanic seismicity as low as ~2.5 $m_b$ even at megameter distances, thus exceeding the resolution of most regional, land-based networks by more than one order of magnitude. Detectability strongly depends on frequency, source depth, and ray path geometry, which is illustrated by 2D transmission loss modeling for a range of synthetic scenarios. The findings presented here highlight the capabilities of the IMS hydrophone network for remotely detecting and studying volcanic activity in the global ocean.

Keywords: CTBTO, IMS, Submarine volcanoes, Hydroacoustics

©2019. Japan Geoscience Union. All Right Reserved. 

# Importance of noble gas monitoring in CTBT verification technology and observation results in Takasaki radionuclide monitoring station

*Yoichi Yamamoto[1], Yuichi Kijima[1], Yutaka Tomita[1]

1. Japan Atomic Energy Agency

Radionuclide monitoring for CTBT verification is the only way to judge whether the target explosion event was a nuclear test. Among the radionuclides produced by the nuclear explosion, the noble gases are particularly important because they are inert and more likely to leak to the ground rather than other substances in an underground nuclear test. Only 4 radioxenon isotopes as the noble gases are monitored for the CTBT verification. After the first nuclear test of North Korea in October 2006, a radioxenon monitoring system installed at the Takasaki radionuclide monitoring station in Japan and the radioxenon monitoring has been carried out since January 2007. We report on the past observation results of the radioxenon at the Takasaki radionuclide monitoring station and the characteristics of radioxenon background.

Keywords: CTBT, international monitoring system, noble gas, xenon, Takasaki radionuclide monitoring station

©2019. Japan Geoscience Union. All Right Reserved. 

# ATM analysis results on radioxenons detected in Japan

*Yuichi Kijima[1], Yoichi Yamamoto[1], Yutaka Tomita[1]

1. Japan Atomic Energy Agency

The Japan Atomic Energy Agency installed transportable xenon laboratories (TXLs) in collaboration with the CTBT Organization at Horonobe, Hokkaido and Mutsu, Aomori, respectively and has been measuring radioxenon since 2018. Therefore, the measurements of radioxenon for CTBT verification in Japan are currently conducted at total 3 measuring points adding the CTBT Takasaki radionuclide monitoring station. The analyses of estimation of emission source location by atmospheric transport modelling (ATM) were carried out to investigate the emission source of the radioxenons detected at these measuring points. We report the measurement results of radioxenons at 3 measuring points and the ATM analysis results.

©2019. Japan Geoscience Union. All Right Reserved. 

[E] Poster | M (Multidisciplinary and Interdisciplinary)：M-AG Applied Geosciences

Thu. May 30, 2019 3:30 PM - 5:00 PM JST | Thu. May 30, 2019 6:30 AM - 8:00 AM UTC | Poster Hall International Exhibition Hall8, Makuhari Messe_25

## [M-AG40] CTBT IMS Technologies for Detecting Nuclear Explosion and Their Applications to Earth Science

convener:Nurcan Meral Ozel(Comprehensive Nuclear-Test-Ban Treaty Organization), Hiroyuki Matsumoto(Japan Agency for Marine-Earth Science and Technology), Yosuke Naoi(Japan Atomic Energy Agency)

The Comprehensive Nuclear-Test-Ban Treaty Organization (CTBTO) was founded in 1996 in response to the adaption of the Treaty in 1996 by the United Nations General Assembly, which bans nuclear explosions on the Earth's surface, in the atmosphere, underwater and underground. The Treaty has a unique and comprehensive verification regime to make sure that no nuclear explosion goes undetected. The regime is supported by International Monitoring Systems (IMS) composed of the four state-of-art technologies; 1) Seismic, 2) Hydroacoustic, 3) Infrasound, and 4) Radionuclide, by the International Data Centre (IDC), and by the On-Site Inspections (OSI).<br/>IMS will, when complete, consists of 337 facilities worldwide to monitor the planet for signs of nuclear explosion. Around 90 % of the facilities are in operation and sending the data to the IDC in Vienna, Austria. <br/>The huge amount of data collected by the stations can be used for other purposes such as civil and scientific applications in addition to detecting nuclear explosions. They can provide Tsunami Warning centres with near real-time information about an underwater earthquake. During the Fukushima Daiichi Power Plant accident, in March 2011, the IMS network's radionuclide stations tracked the dispersion of radioactivity on a global scale. The data could also help better understand the oceans, volcanos, climate change, the movement of marine mammals, and many other issues.<br/>This session will provide the overview of CTBTO and its IMS, the scientific discussion on each technology, and its outcomes. The session welcomes young scientists and engineers who are interested in four IMS technologies.<br/>

### [MAG40-P01] Overview of the Japanese National Data Centre-1 (NDC-1)

*RYOHEI EMURA[1], Takayuki Otsu[1], Toyomi Sakamoto[1], Soshi Iwata[1], Takanari Fujii[1], Mami Nogami[1], Makiko Iwakuni[1], Masashi Motohashi[1] (1.Japan Weather Association)

### [MAG40-P02] Challenging to utilize the infrasound technologies for civil and science application

*Masashi Motohashi[1], Nobuo Arai[2], Takayuki Otsu[1], Mami Nogami[1], Makiko Iwakuni[1], Ryohei Emura[1] (1.Japan Weather Association, 2.Disaster Mitigation Research Center, Nagoya Unicersity)

### [MAG40-P03] CTBT IMS hydroacoustic signal detections from the Ioto volcanic island in the northwest Pacific Ocean

*Hiroyuki Matsumoto[1,2], Mario Zampolli[1], Georgios Haralabus[1], Jerry Stanley[1], James Mattila[1], Nurcan Meral Ozel[1] (1.Comprehensive Nuclear-Test-Ban Treaty Organization (CTBTO), 2.Japan Agency for Marine-Earth Science and Technology (JAMSTEC))

### [MAG40-P04] Installation of a floating hydrophone system within the SOFAR channel

*Hiroko Sugioka[1], Masayuki Obayashi[2] (1.Kobe University, 2.JAMSTEC)

### [MAG40-P05] Fin whale signals observed at S-net seismic stations

*Takeshi Nakamura[1], Ryoichi Iwase[2] (1.National Research Institute for Earth Science and Disaster Resilience, 2.Japan Agency for Marine-Earth Science and Technology)

### [MAG40-P06] Implementation of integrated observation from seafloor through atmosphere – past, current, and future plans

*Keisuke Ariyoshi[1], Akira Nagano[1], Hiroyuki Matsumoto[1], Nurcan Meral Ozel[2] (1.Japan Agency for Marine-Earth Science and Technology, 2.Comprehensive Nuclear-Test-Ban Treaty Organization)

# Overview of the Japanese National Data Centre-1 (NDC-1)

*RYOHEI EMURA[1], Takayuki Otsu[1], Toyomi Sakamoto[1], Soshi Iwata[1], Takanari Fujii[1], Mami Nogami[1], Makiko Iwakuni[1], Masashi Motohashi[1]

1. Japan Weather Association

Japan Weather Association (JWA) is working as the Comprehensive Nuclear-Test-Ban Treaty (CTBT) National Data Centre-1 (NDC-1) of Japan which is in charge of analysis on waveform data, operation and maintenance of seismic and infrasound stations in Japan. There are two main roles of NDC-1: 1: technical adviser to the national authority (MOFA) from the view point of seismic and infrasound analysis, and 2: station operator of IMS stations (PS22, AS51-AS55 and IS30). And there are three main activities of NDC-1 as technical adviser: 1: if the suspicious event would occur, we would try to clarify its characteristics and report its results to the MOFA via the secretariat, 2: we sometimes do 1-week integrated operational exercise hosted by the secretariat on the assumption that the situation would be, and 3: we are paying efforts to improve our analytical capability of SHI data and explanation capability by using the national exercises.

This poster introduces the integrated operational exercise and the event discrimination analysis results of the 6$^{th}$ DPRK nuclear test as of the real analysis results in particular.

The integrated operational exercise is conducted by NDCs, integrating the data and analysis addressed by NDCs, and reporting to the CTBT National Operating System of Japan. These exercises have been implemented 27 times since 2009 and 30areas were selected for regions and countries. And our event discrimination analysis takes mainly three methods: 1: regional P/S ratio, 2: P/S spectral ratio and 3: mb: Ms.

Keywords: CTBT, National Data Centre, seismic, infrasound, waveform analysis, event discrimination analysis

©2019. Japan Geoscience Union. All Right Reserved. 

# Challenging to utilize the infrasound technologies for civil and science application

*Masashi Motohashi[1], Nobuo Arai[2], Takayuki Otsu[1], Mami Nogami[1], Makiko Iwakuni[1], Ryohei Emura[1]

1. Japan Weather Association, 2. Disaster Mitigation Research Center, Nagoya Unicersity

Japan Weather Association (JWA) is working as the Comprehensive Nuclear-Test-Ban Treaty (CTBT) National Data Centre-1 (NDC-1) of Japan which is in charge of analysis on waveform data, operation and maintenance of infrasound and seismic stations in Japan.

We observed infrasonic signals two times from underground nuclear test in DPRK. From the perspective of nuclear test monitoring, it is important to analyze and study the infrasonic signals from a variety of natural phenomena to discriminate the signal from explosion. On the other hand, that kind of studies are also important for civil and science application of infrasound technologies. We also observed infrasound from large tsunami at the time of 2011 off the Pacific coast of Tohoku Earthquake. If the signals from such hazardous phenomena can be detected immediately, it will be very helpful to alert the occurrence of disaster or approach of hazardous phenomena.

This triggered us to build our own observation network in Japan. We are challenging to utilize the infrasound technologies for civil and science application as well as nuclear test monitoring.

Keywords: Barometer, Infrasound, CTBT

©2019. Japan Geoscience Union. All Right Reserved. 

# CTBT IMS hydroacoustic signal detections from the Ioto volcanic island in the northwest Pacific Ocean

*Hiroyuki Matsumoto[1,2], Mario Zampolli[1], Georgios Haralabus[1], Jerry Stanley[1], James Mattila[1], Nurcan Meral Ozel[1]

1. Comprehensive Nuclear-Test-Ban Treaty Organization (CTBTO), 2. Japan Agency for Marine-Earth Science and Technology (JAMSTEC)

*In-situ* observation in terms of seismicity suggested that the volcanic activity of Ioto (formerly Iwojima), a volcanic island offshore Japan in the northwest Pacific Ocean increased in early September in 2018. Discolored waters and a splash were confirmed in the nearshore by a local flyover observation. Although these visual signs evidenced a connection between undersea eruptions and recorded seismic activity, there still remained uncertainty as to what portion of the *in-situ* recorded seismic activity was associated with volcanic tremors vs. undersea eruptive events.
During the same period, a large number of underwater acoustic (hydroacoustic) signals were recorded by the Comprehensive Nuclear-Test-Ban Treaty’s (CTBT) International Monitoring System (IMS) hydroacoustic (HA) station HA11 Wake Island. A set of three hydrophone sensors forming a triplet makes it possible to compute the back-azimuth uniquely for wave packets with a good signal-to-noise ratio. We analyzed the data of the IMS hydrophone triplets during the month of September 2018 and compared them with *in-situ* seismic observations in Ioto for the same period.
The IMS hydrophone triplet data made it possible to discriminate the hydroacoustic signals associated with the Ioto volcanic activity. The direction-of-arrival (DOA) was estimated during the entire period of relatively high volcanic activity using cross-correlation analysis. The arrivals from Ioto at the IMS HA station and the *in-situ* observations showed good correlation. The present study suggests that two-thirds of the arrivals of hydroacoustec signals were associated with volcanic tremors and one-third with the undersea eruptions.

Keywords: Internataional Monitoring System (IMS), Hydrophone triplet, Ioto

©2019. Japan Geoscience Union. All Right Reserved. 

# Installation of a floating hydrophone system within the SOFAR channel

*Hiroko Sugioka[1], Masayuki Obayashi[2]

1. Kobe University, 2. JAMSTEC

Unequal geographical data coverage continues to fundamentally limit the quality of tomographic reconstructions of seismic wave speeds in the interior of the Earth. Only at great cost can geophysicists overcome the difficulties of placing seismographs on the two thirds of the Earth’ s surface that is covered by oceans. The lack of spatial data coverage strongly hampers the determination of the structure of the Earth in the uncovered regions. Therefore, three-dimensional Earth models are marked by blank spots in areas where little or no information can be obtained. Improving this problem requires the observation of seismic waves in the oceans. Ocean bottom seismometers are capable of addressing the coverage gap, but they are expensive to manufacture and deploy using vessels.

Oceanographers had designed robotic floating instruments, floats that spend their lives at depth but surface periodically, using a pump and bladder, to make temperature and salinity profile measurements (the large-scale international Argo project). Such low-cost Sounding Oceanographic Lagrangian Observers (SOLO) (Davis et al., 2001) could be equipped with a hydrophone to record water pressure variations induced by compressional waves. Such a floating seismometer would surface upon detection of a useful seismic event, determine a GPS location, and transmit the waveforms to a satellite, which is nicknamed MERMAID for ‘mobile earthquake recorder in marine areas by independent divers’. The great promise of this technology has been demonstrated since the first voyage in 2003, clearly illustrates its contributions to global seismology.

We installed five MERMAID floats in the South Pacific Ocean in late December of 2018 to early January of 2019 during the MR18-06 Leg 1 cruise from Japan to Chile using the R/V Mirai of JAMSTEC under an international project of SPPIM (South Pacific Plume Imaging with MERMAIDs). The launching locations for MERMAIDs are (01-42.256N,146-12.472W), (03-19.696S, 139-31.973W), (15-55.626S, 120-07.688W), (18-31.285S, 114-57.378W) and (20-59.832S, 109-59.513W), respectively. All floats have been drifting to almost west since the deployment as recording to transfer the land at sea surface every 10 days. So far, MERMAID detected several seismic events, for example, the Mw 6.8 Brazil deep focus earthquake at depth of 575 km on January 5. MERMAID recorded a clear incoming P-wave whose precise arrival time can be determined to within a fraction of a second. In addition to recording teleseismic P-waves, they would pick up hydroacoustic phases (T-waves) trapped waves propagating in the SOFAR (Sound Fixing and Ranging) channel. They might be complementary to the global seismic network including CTBTO stations to recognize unknown enigmatic events.

Keywords: SOFAR channel, Hydroacoustic waves

©2019. Japan Geoscience Union. All Right Reserved. 

# Fin whale signals observed at S-net seismic stations

*Takeshi Nakamura[1], Ryoichi Iwase[2]

1. National Research Institute for Earth Science and Disaster Resilience, 2. Japan Agency for Marine-Earth Science and Technology

Real-time earthquake and tsunami seafloor station network called “S-net” (Seafloor observation network for earthquakes and tsunamis along the Japan Trench) was developed by National Research Institute for Earth Science and Disaster Resilience (NIED) in water depths of 100-7,830 m in northeastern Japan. The network consists of 150 observation stations off Boso to Kushiro and Aomori areas (Kanazawa et al., 2016; Uehira et al. 2016; Mochizuki et al., 2016). Each station has seismic sensors and pressure gauges to observe broadband signals from seismic event and tsunami. In this study, we show fin whale signals detected from the S-net data and present the seasonal variation of the signals and the migratory behavior of the whales.

We analyzed seismic station data of S-net from 2016 to 2018. We found characteristic signals with the spectral peak in the frequency bands of 15-25 Hz. One of remarkable features in the signals is that the band width that can be identified as signal is limited in a very narrow range; the signal level is very low or below the noise level in the frequency bands of less than 10 Hz that are typical bands in seismic waves and T-phases. Another feature is that the signals have a short duration of about 1 second and are repeatedly found at regular intervals of several tens of seconds. These are consistent with the features of acoustic signals from fin whales as found in observation data at IMS hydroacoustic stations (e.g., Lawrence, 2004) and also as shown in previous studies such as Iwase (2014) and Sugioka et al. (2015) that analyzed seafloor station data off the Kushiro-Tokachi cable sensor system. We thus assume that the characteristic signals observed at S-net stations are ones associated with fin whale activities. Most of the signals were detected at stations off Kushiro and Aomori areas in cold winter. The signals were also detected at stations deployed in the outer rise area. We suppose that integrated scientific studies across marine biology to geophysics using S-net data could contribute to developing our understandings of various signal sources observed in seafloor areas and of ecological behavior of marine mammals and also to real-time monitoring of their activities and safe navigation of ships by the monitoring.

Keywords: seafloor observation, S-net, fin whale

©2019. Japan Geoscience Union. All Right Reserved. 

# Implementation of integrated observation from seafloor through atmosphere –past, current, and future plans

*Keisuke Ariyoshi[1], Akira Nagano[1], Hiroyuki Matsumoto[1], Nurcan Meral Ozel[2]

1. Japan Agency for Marine-Earth Science and Technology, 2. Comprehensive Nuclear-Test-Ban Treaty Organization

The authors have challenged to promote our understandings of global dynamics associated with ocean physics particularly by the simultaneous observation through the seafloor to the atmosphere. We have initiated the total station using both D/V ‘Chikyu’ and the seafloor observatory network ‘DONET’ in the Nankai trough. This total station has clarified the Kuroshio current variation in this region by using both the ambient pressure at DONET and the surface current measurement at D/V ‘Chikyu’. This observation performed at the point where D/V ‘Chikyu’ was in operation for a few months, and therefore there still remained some difficulties to extend to areal and long-term observation. Now, we try to extend our proposed total station to the nearshore network from the point of view of not only scientific application but also civil use for natural disaster mitigation such as earthquake, tsunami, and high-tide caused by storm. On the other hand, a global permanent observation network has been developed and operated by the Comprehensive Nuclear-Test-Ban Treaty Organization (CTBTO) since the 2000s as the International Monitoring System (IMS) regime for the real-time monitoring of nuclear explosion’s test in the underground, underwater, and above surface up to the atmosphere. Four technologies with over 330 stations will cover the entire Earth after certification of all of stations. Three categories of geophysical observations of four technologies such as seismic (50 primary and 120 auxiliary stations), infrasound (60 stations), and hydro-acoustic (11 stations) network operated globally may be beneficial and of interest for our proposed integrated observations. In the presentation, we introduce the preliminary results on our integrated observation of total stations and our drawing blue print of future plans.

Keywords: seismic observation, seafloor cabled network, disaster mitigation

©2019. Japan Geoscience Union. All Right Reserved. 

[E] Poster | M (Multidisciplinary and Interdisciplinary)：M-AG Applied Geosciences

Thu. May 30, 2019 5:15 PM - 6:30 PM JST | Thu. May 30, 2019 8:15 AM - 9:30 AM UTC | Poster Hall International Exhibition Hall8, Makuhari Messe_45

## [M-AG40] CTBT IMS Technologies for Detecting Nuclear Explosion and Their Applications to Earth Science

convener:Nurcan Meral Ozel(Comprehensive Nuclear-Test-Ban Treaty Organization), Hiroyuki Matsumoto(Japan Agency for Marine-Earth Science and Technology), Yosuke Naoi(Japan Atomic Energy Agency)

The Comprehensive Nuclear-Test-Ban Treaty Organization (CTBTO) was founded in 1996 in response to the adaption of the Treaty in 1996 by the United Nations General Assembly, which bans nuclear explosions on the Earth's surface, in the atmosphere, underwater and underground. The Treaty has a unique and comprehensive verification regime to make sure that no nuclear explosion goes undetected. The regime is supported by International Monitoring Systems (IMS) composed of the four state-of-art technologies; 1) Seismic, 2) Hydroacoustic, 3) Infrasound, and 4) Radionuclide, by the International Data Centre (IDC), and by the On-Site Inspections (OSI).<br/>IMS will, when complete, consists of 337 facilities worldwide to monitor the planet for signs of nuclear explosion. Around 90 % of the facilities are in operation and sending the data to the IDC in Vienna, Austria. <br/>The huge amount of data collected by the stations can be used for other purposes such as civil and scientific applications in addition to detecting nuclear explosions. They can provide Tsunami Warning centres with near real-time information about an underwater earthquake. During the Fukushima Daiichi Power Plant accident, in March 2011, the IMS network's radionuclide stations tracked the dispersion of radioactivity on a global scale. The data could also help better understand the oceans, volcanos, climate change, the movement of marine mammals, and many other issues.<br/>This session will provide the overview of CTBTO and its IMS, the scientific discussion on each technology, and its outcomes. The session welcomes young scientists and engineers who are interested in four IMS technologies.<br/>

### [MAG40-P01] Overview of the Japanese National Data Centre-1 (NDC-1)

*RYOHEI EMURA[1], Takayuki Otsu[1], Toyomi Sakamoto[1], Soshi Iwata[1], Takanari Fujii[1], Mami Nogami[1], Makiko Iwakuni[1], Masashi Motohashi[1] (1.Japan Weather Association)

### [MAG40-P02] Challenging to utilize the infrasound technologies for civil and science application

*Masashi Motohashi[1], Nobuo Arai[2], Takayuki Otsu[1], Mami Nogami[1], Makiko Iwakuni[1], Ryohei Emura[1] (1.Japan Weather Association, 2.Disaster Mitigation Research Center, Nagoya Unicersity)

### [MAG40-P03] CTBT IMS hydroacoustic signal detections from the Ioto volcanic island in the northwest Pacific Ocean

*Hiroyuki Matsumoto[1,2], Mario Zampolli[1], Georgios Haralabus[1], Jerry Stanley[1], James Mattila[1], Nurcan Meral Ozel[1] (1.Comprehensive Nuclear-Test-Ban Treaty Organization (CTBTO), 2.Japan Agency for Marine-Earth Science and Technology (JAMSTEC))

### [MAG40-P04] Installation of a floating hydrophone system within the SOFAR channel

*Hiroko Sugioka[1], Masayuki Obayashi[2] (1.Kobe University, 2.JAMSTEC)

### [MAG40-P05] Fin whale signals observed at S-net seismic stations

*Takeshi Nakamura[1], Ryoichi Iwase[2] (1.National Research Institute for Earth Science and Disaster Resilience, 2.Japan Agency for Marine-Earth Science and Technology)

### [MAG40-P06] Implementation of integrated observation from seafloor through atmosphere – past, current, and future plans

*Keisuke Ariyoshi[1], Akira Nagano[1], Hiroyuki Matsumoto[1], Nurcan Meral Ozel[2] (1.Japan Agency for Marine-Earth Science and Technology, 2.Comprehensive Nuclear-Test-Ban Treaty Organization)

# Overview of the Japanese National Data Centre-1 (NDC-1)

*RYOHEI EMURA[1], Takayuki Otsu[1], Toyomi Sakamoto[1], Soshi Iwata[1], Takanari Fujii[1], Mami Nogami[1], Makiko Iwakuni[1], Masashi Motohashi[1]

1. Japan Weather Association

Japan Weather Association (JWA) is working as the Comprehensive Nuclear-Test-Ban Treaty (CTBT) National Data Centre-1 (NDC-1) of Japan which is in charge of analysis on waveform data, operation and maintenance of seismic and infrasound stations in Japan. There are two main roles of NDC-1: 1: technical adviser to the national authority (MOFA) from the view point of seismic and infrasound analysis, and 2: station operator of IMS stations (PS22, AS51-AS55 and IS30). And there are three main activities of NDC-1 as technical adviser: 1: if the suspicious event would occur, we would try to clarify its characteristics and report its results to the MOFA via the secretariat, 2: we sometimes do 1-week integrated operational exercise hosted by the secretariat on the assumption that the situation would be, and 3: we are paying efforts to improve our analytical capability of SHI data and explanation capability by using the national exercises.

This poster introduces the integrated operational exercise and the event discrimination analysis results of the 6$^{th}$ DPRK nuclear test as of the real analysis results in particular.

The integrated operational exercise is conducted by NDCs, integrating the data and analysis addressed by NDCs, and reporting to the CTBT National Operating System of Japan. These exercises have been implemented 27 times since 2009 and 30areas were selected for regions and countries. And our event discrimination analysis takes mainly three methods: 1: regional P/S ratio, 2: P/S spectral ratio and 3: mb: Ms.

Keywords: CTBT, National Data Centre, seismic, infrasound, waveform analysis, event discrimination analysis

©2019. Japan Geoscience Union. All Right Reserved. 

# Challenging to utilize the infrasound technologies for civil and science application

*Masashi Motohashi[1], Nobuo Arai[2], Takayuki Otsu[1], Mami Nogami[1], Makiko Iwakuni[1], Ryohei Emura[1]

1. Japan Weather Association, 2. Disaster Mitigation Research Center, Nagoya Unicersity

Japan Weather Association (JWA) is working as the Comprehensive Nuclear-Test-Ban Treaty (CTBT) National Data Centre-1 (NDC-1) of Japan which is in charge of analysis on waveform data, operation and maintenance of infrasound and seismic stations in Japan.

We observed infrasonic signals two times from underground nuclear test in DPRK. From the perspective of nuclear test monitoring, it is important to analyze and study the infrasonic signals from a variety of natural phenomena to discriminate the signal from explosion. On the other hand, that kind of studies are also important for civil and science application of infrasound technologies. We also observed infrasound from large tsunami at the time of 2011 off the Pacific coast of Tohoku Earthquake. If the signals from such hazardous phenomena can be detected immediately, it will be very helpful to alert the occurrence of disaster or approach of hazardous phenomena.

This triggered us to build our own observation network in Japan. We are challenging to utilize the infrasound technologies for civil and science application as well as nuclear test monitoring.

Keywords: Barometer, Infrasound, CTBT

©2019. Japan Geoscience Union. All Right Reserved. 

# CTBT IMS hydroacoustic signal detections from the Ioto volcanic island in the northwest Pacific Ocean

*Hiroyuki Matsumoto[1,2], Mario Zampolli[1], Georgios Haralabus[1], Jerry Stanley[1], James Mattila[1], Nurcan Meral Ozel[1]

1. Comprehensive Nuclear-Test-Ban Treaty Organization (CTBTO), 2. Japan Agency for Marine-Earth Science and Technology (JAMSTEC)

*In-situ* observation in terms of seismicity suggested that the volcanic activity of Ioto (formerly Iwojima), a volcanic island offshore Japan in the northwest Pacific Ocean increased in early September in 2018. Discolored waters and a splash were confirmed in the nearshore by a local flyover observation. Although these visual signs evidenced a connection between undersea eruptions and recorded seismic activity, there still remained uncertainty as to what portion of the *in-situ* recorded seismic activity was associated with volcanic tremors vs. undersea eruptive events.
During the same period, a large number of underwater acoustic (hydroacoustic) signals were recorded by the Comprehensive Nuclear-Test-Ban Treaty’s (CTBT) International Monitoring System (IMS) hydroacoustic (HA) station HA11 Wake Island. A set of three hydrophone sensors forming a triplet makes it possible to compute the back-azimuth uniquely for wave packets with a good signal-to-noise ratio. We analyzed the data of the IMS hydrophone triplets during the month of September 2018 and compared them with *in-situ* seismic observations in Ioto for the same period.
The IMS hydrophone triplet data made it possible to discriminate the hydroacoustic signals associated with the Ioto volcanic activity. The direction-of-arrival (DOA) was estimated during the entire period of relatively high volcanic activity using cross-correlation analysis. The arrivals from Ioto at the IMS HA station and the *in-situ* observations showed good correlation. The present study suggests that two-thirds of the arrivals of hydroacoustec signals were associated with volcanic tremors and one-third with the undersea eruptions.

Keywords: Internataional Monitoring System (IMS), Hydrophone triplet, Ioto

©2019. Japan Geoscience Union. All Right Reserved. 

# Installation of a floating hydrophone system within the SOFAR channel

*Hiroko Sugioka[1], Masayuki Obayashi[2]

1. Kobe University, 2. JAMSTEC

Unequal geographical data coverage continues to fundamentally limit the quality of tomographic reconstructions of seismic wave speeds in the interior of the Earth. Only at great cost can geophysicists overcome the difficulties of placing seismographs on the two thirds of the Earth’ s surface that is covered by oceans. The lack of spatial data coverage strongly hampers the determination of the structure of the Earth in the uncovered regions. Therefore, three-dimensional Earth models are marked by blank spots in areas where little or no information can be obtained. Improving this problem requires the observation of seismic waves in the oceans. Ocean bottom seismometers are capable of addressing the coverage gap, but they are expensive to manufacture and deploy using vessels.

Oceanographers had designed robotic floating instruments, floats that spend their lives at depth but surface periodically, using a pump and bladder, to make temperature and salinity profile measurements (the large-scale international Argo project). Such low-cost Sounding Oceanographic Lagrangian Observers (SOLO) (Davis et al., 2001) could be equipped with a hydrophone to record water pressure variations induced by compressional waves. Such a floating seismometer would surface upon detection of a useful seismic event, determine a GPS location, and transmit the waveforms to a satellite, which is nicknamed MERMAID for ‘mobile earthquake recorder in marine areas by independent divers’. The great promise of this technology has been demonstrated since the first voyage in 2003, clearly illustrates its contributions to global seismology.

We installed five MERMAID floats in the South Pacific Ocean in late December of 2018 to early January of 2019 during the MR18-06 Leg 1 cruise from Japan to Chile using the R/V Mirai of JAMSTEC under an international project of SPPIM (South Pacific Plume Imaging with MERMAIDs). The launching locations for MERMAIDs are (01-42.256N,146-12.472W), (03-19.696S, 139-31.973W), (15-55.626S, 120-07.688W), (18-31.285S, 114-57.378W) and (20-59.832S, 109-59.513W), respectively. All floats have been drifting to almost west since the deployment as recording to transfer the land at sea surface every 10 days. So far, MERMAID detected several seismic events, for example, the Mw 6.8 Brazil deep focus earthquake at depth of 575 km on January 5. MERMAID recorded a clear incoming P-wave whose precise arrival time can be determined to within a fraction of a second. In addition to recording teleseismic P-waves, they would pick up hydroacoustic phases (T-waves) trapped waves propagating in the SOFAR (Sound Fixing and Ranging) channel. They might be complementary to the global seismic network including CTBTO stations to recognize unknown enigmatic events.

Keywords: SOFAR channel, Hydroacoustic waves

©2019. Japan Geoscience Union. All Right Reserved. 

# Fin whale signals observed at S-net seismic stations

*Takeshi Nakamura[1], Ryoichi Iwase[2]

1. National Research Institute for Earth Science and Disaster Resilience, 2. Japan Agency for Marine-Earth Science and Technology

Real-time earthquake and tsunami seafloor station network called “S-net” (Seafloor observation network for earthquakes and tsunamis along the Japan Trench) was developed by National Research Institute for Earth Science and Disaster Resilience (NIED) in water depths of 100-7,830 m in northeastern Japan. The network consists of 150 observation stations off Boso to Kushiro and Aomori areas (Kanazawa et al., 2016; Uehira et al. 2016; Mochizuki et al., 2016). Each station has seismic sensors and pressure gauges to observe broadband signals from seismic event and tsunami. In this study, we show fin whale signals detected from the S-net data and present the seasonal variation of the signals and the migratory behavior of the whales.

We analyzed seismic station data of S-net from 2016 to 2018. We found characteristic signals with the spectral peak in the frequency bands of 15-25 Hz. One of remarkable features in the signals is that the band width that can be identified as signal is limited in a very narrow range; the signal level is very low or below the noise level in the frequency bands of less than 10 Hz that are typical bands in seismic waves and T-phases. Another feature is that the signals have a short duration of about 1 second and are repeatedly found at regular intervals of several tens of seconds. These are consistent with the features of acoustic signals from fin whales as found in observation data at IMS hydroacoustic stations (e.g., Lawrence, 2004) and also as shown in previous studies such as Iwase (2014) and Sugioka et al. (2015) that analyzed seafloor station data off the Kushiro-Tokachi cable sensor system. We thus assume that the characteristic signals observed at S-net stations are ones associated with fin whale activities. Most of the signals were detected at stations off Kushiro and Aomori areas in cold winter. The signals were also detected at stations deployed in the outer rise area. We suppose that integrated scientific studies across marine biology to geophysics using S-net data could contribute to developing our understandings of various signal sources observed in seafloor areas and of ecological behavior of marine mammals and also to real-time monitoring of their activities and safe navigation of ships by the monitoring.

Keywords: seafloor observation, S-net, fin whale

©2019. Japan Geoscience Union. All Right Reserved. 

# Implementation of integrated observation from seafloor through atmosphere –past, current, and future plans

*Keisuke Ariyoshi[1], Akira Nagano[1], Hiroyuki Matsumoto[1], Nurcan Meral Ozel[2]

1. Japan Agency for Marine-Earth Science and Technology, 2. Comprehensive Nuclear-Test-Ban Treaty Organization

The authors have challenged to promote our understandings of global dynamics associated with ocean physics particularly by the simultaneous observation through the seafloor to the atmosphere. We have initiated the total station using both D/V ‘Chikyu’ and the seafloor observatory network ‘DONET’ in the Nankai trough. This total station has clarified the Kuroshio current variation in this region by using both the ambient pressure at DONET and the surface current measurement at D/V ‘Chikyu’. This observation performed at the point where D/V ‘Chikyu’ was in operation for a few months, and therefore there still remained some difficulties to extend to areal and long-term observation. Now, we try to extend our proposed total station to the nearshore network from the point of view of not only scientific application but also civil use for natural disaster mitigation such as earthquake, tsunami, and high-tide caused by storm. On the other hand, a global permanent observation network has been developed and operated by the Comprehensive Nuclear-Test-Ban Treaty Organization (CTBTO) since the 2000s as the International Monitoring System (IMS) regime for the real-time monitoring of nuclear explosion’s test in the underground, underwater, and above surface up to the atmosphere. Four technologies with over 330 stations will cover the entire Earth after certification of all of stations. Three categories of geophysical observations of four technologies such as seismic (50 primary and 120 auxiliary stations), infrasound (60 stations), and hydro-acoustic (11 stations) network operated globally may be beneficial and of interest for our proposed integrated observations. In the presentation, we introduce the preliminary results on our integrated observation of total stations and our drawing blue print of future plans.

Keywords: seismic observation, seafloor cabled network, disaster mitigation

©2019. Japan Geoscience Union. All Right Reserved. 

[J] Oral | M (Multidisciplinary and Interdisciplinary)：M-TT Technology & Techniques

Thu. May 30, 2019 10:45 AM - 12:15 PM JST | Thu. May 30, 2019 1:45 AM - 3:15 AM UTC | 202 2F

## [M-TT49] Brand-new scope of coupling geophysics being established by infrasound and associated waves

convener:Masa-yuki Yamamoto(Department of systems engineering, Kochi University of Technology), Mie Ichihara(Earthquake Research Institute, University of Tokyo), Nobuo Arai(Disaster Mitigation Research Center, Nagoya University), Chairperson:Masa-yuki Yamamoto(Kochi University of Technology), Hiroaki Saito(Kochi University of Technology)

Infrasound and associated wave studies are recently focused on coupling waves with long-distance and vertical propagation characteristics. Such kinds of waves, having with coupling process between the atmosphere and the surface of ground and ocean, are linked with elastic waves in lithosphere and oceanic sphere, as well as to atmospheric regions up to the upper atmosphere, playing a role of generating many kinds of wavelike turbulences in thermosphere. Moreover, whole on the globe, these waves excited depending on the latitude regions, as well as on the environmental regions, such as snow ice, desert, rainforest, mountain, ocean, etc., have their own characteristics. These waves can be excited by large-scale geophysical events like volcanic eruptions, tsunami, thunderstorms, etc. as well as artificial explosions, propagating with long distance. In this session, we would like to discuss such "coupling geophysics" by using many new or well-known investigated data and simulations of infrasound and associated low frequency waves. It can combine multiple spheres in geophysics and bring a brand-new scope of geophysics. Your contributions from many regions are welcome!

10:45 AM - 11:00 AM JST | 1:45 AM - 2:00 AM UTC

### [MTT49-01] A two-step amplification mechanism of infrasound waves in the ocean-atmosphere system

★Invited Papers

*Hiroyuki Shinagawa[1] (1.National Institute of Information and Communications Technology)

11:00 AM - 11:15 AM JST | 2:00 AM - 2:15 AM UTC

### [MTT49-02] Propagation of infrasound generated by an explosive eruption of Mt. Shinmoedake on 10 March 2018

*Hiroaki Saito[1], Tetsuo Yamamoto[2], Masa-yuki Yamamoto[1] (1.School of Systems Engineering, Kochi University of Technology, 2.Hokkaido University)

11:15 AM - 11:30 AM JST | 2:15 AM - 2:30 AM UTC

### [MTT49-03] Infrasound observations of atmospheric disturbances due to a sequence of 2018 explosive volcano eruptions in Japan.

*Mario Batubara[1], Masa-yuki Yamamoto[1], Saito Hiroaki[1] (1.Kochi University of Technology)

11:30 AM - 11:45 AM JST | 2:30 AM - 2:45 AM UTC

### [MTT49-04] Comparison of seismic waveforms observed by co-located seismometer and barometer installed indoors 2nd report

*Makiko Iwakuni[1], Nobuo Arai[2], Takayuki Otsu[1], Masashi Motohashi[1], Toyomi Sakamoto[1], Takanari Fujii[1], Ryohei Emura[1], Mami Nogami[1], Takahiko Murayama[1], Takuma Oi[3] (1.Japan Weather Association, 2.Disaster Mitigation Research Center, Nagoya University, 3.Toho Mercantile co., Ltd.)

11:45 AM - 12:00 PM JST | 2:45 AM - 3:00 AM UTC

### [MTT49-05] Ionospheric disturbances associated with typhoons and a tornado observed by HF doppler sounding

★Invited Papers

*Hiroyuki Nakata[1], Ryuichi Mashiko[1], Hiroyo Ohya[1], Toshiaki Takano[1], Keisuke Hosokawa[2], Ichiro Tomizawa[3], Hiromichi Nagao[4] (1.Graduate School of Science and Engineering, Chiba University, 2.Graduate School of Communication Engineering and Informatics, the University of Electro-

Communications, 3.Center for Space Science and Radio Engineering, the University of Electro-Communications, 4.Earthquake Research Institute, the University of Tokyo.)

12:00 PM - 12:15 PM JST | 3:00 AM - 3:15 AM UTC

## [MTT49-06] Two-year infrasound monitoring by using a prefectural-level sensor network in Kochi

*Masa-yuki Yamamoto[1] (1.Department of systems engineering, Kochi University of Technology)

# A two-step amplification mechanism of infrasound waves in the ocean-atmosphere system

*Hiroyuki Shinagawa[1]

1. National Institute of Information and Communications Technology

It is widely recognized that atmospheric acoustic waves (infrasound waves) are generated by seismic waves, propagating upward up to the upper atmosphere. The amplitude of seismically excited acoustic waves in the thermosphere is about $10^4$ –$10^5$ times larger than the amplitude of seismic waves on the ground [Shinagawa et al., 2013; Maruyama and Shinagawa, 2014]. In the ocean, compressibility of water becomes important for seismic waves with a period of 10 seconds or less, and acoustic waves are generated by sudden motion at the sea bottom, propagating upward up to the sea surface. Resonance of the acoustic wave in the vertical direction can occur depending on the period of the acoustic wave, and can result in large oscillations at the sea surface. Previous theoretical studies suggest that the amplitude of sea surface oscillation at resonant frequencies could reach about 100 times larger than the sea bottom oscillation [Williams and Guo, 1991; Izumiya et al., 1996]. The large amplitude oscillation driven by resonant acoustic waves generate atmospheric acoustic waves, which propagate upward into the upper atmosphere, resulting in the amplitude of acoustic waves of about $10^6$ –$10^7$ times larger than the sea bottom oscillation. Therefore, oscillations of micrometer amplitudes at the sea bottom become meter-order oscillations in the thermosphere, and may generate significant variations in the ionosphere. In this talk, I will discuss and present possible effects of the resonant amplification of acoustic waves in the ocean on the upper atmosphere.

References

(1) Shinagawa, H., T. Tsugawa, M. Matsumura, T. Iyemori, A. Saito, T. Maruyama, H. Jin, M. Nishioka, and Y. Otsuka, A simulation study of ionospheric variations in the vicinity of the epicenter of the Tohoku-oki earthquake on 11 March 2011, Geophys. Res. Lett., 40, 5009–5013, doi:10.1002/2013GL057627, 2013.
(2) Maruyama, T., and H. Shinagawa, Infrasonic sounds excited by seismic waves of the 2011 Tohoku-oki earthquake as visualized in ionograms, J. Geophys. Res. Space Physics, 119, doi:10.1002/2013JA019707, 2014.
(3) Izumiya, T., and H. Abe, Amplification mechanism of sea level fluctuation by compressibility of sea water and vertical resonance (in Japanese), Annual Journal of Coastal Engineering, JSCE, 43, 421-425, 1996.
(4) Williams, J. E., and Guo, Y. P., Standing waves on a compressible ocean, in "Mathematical Approach in Hydrodynamics" edited by Touvia Miloh, 128-138, 1991.

Keywords: acoustic waves, ocean-atmosphere system, amplification, resonance, ionospheric variation

©2019. Japan Geoscience Union. All Right Reserved. 

# Propagation of infrasound generated by an explosive eruption of Mt. Shinmoedake on 10 March 2018

*Hiroaki Saito[1], Tetsuo Yamamoto[2], Masa-yuki Yamamoto[1]

1. School of Systems Engineering, Kochi University of Technology, 2. Hokkaido University

Mt. Shinmoedake is a part of the Mt. Kirishima cluster of volcanoes in Kyushu Island, Japan. It is located at 31.54 N, 130.53 E and its elevation is 1412 m. Explosive eruptions were observed more than 40 times in March 2018. In these events, air vibrations stronger than 100 Pa were observed several times at an air vibration sensor installed by Japan Meteorological Agency at the site within ~3 km from Mt. Shinmoedake. We focus on the explosive eruption at 1:54 (JST) on 10 March 2018. This event is the most significant air vibration (~272 Pa) observed on 10 March 2018. The infrasound sensors in Shikoku Island deployed by Kochi University of Technology detected the infrasound signals from Mt. Shinmoedake. We detected major signals three times at each of the sites 1 to 3, and four times at each of the sites 4 to 6.

We developed a new formulation for three-dimensional wave propagation in a stratified atmosphere and apply it to the analysis of the detected signals. The present formulation is based on the dispersion relation of the wave, which corresponds to Hamiltonian in particle mechanics, and Hamilton equations describing time variations of group velocity of the wave and wavevector. We adopt the dispersion relation $\omega = c_s k + \boldsymbol{u} \cdot \boldsymbol{k}$, where $\omega$ is angular frequency of the wave, $c_s$ is sound speed, $\boldsymbol{k}$ is the wavevector, and $\boldsymbol{u}$ is wind velocity. Using the vertical temperature profiles provided by NRL-MSISE00(Picone et al., 2002) and the zonal and meridional wind profiles by HWM14 (Drob et al., 2015), we made ray tracing of the waves emitted at the explosive eruption observed on 10 March 2018. We show results of the ray tracing calculations and compare them with the signals detected by our infrasound sensors deployed in Shikoku Island(see the figure). Discussion is given on the origin and nature of the observed signals.

Keywords: infrasound, ray tracing, volcanic eruption

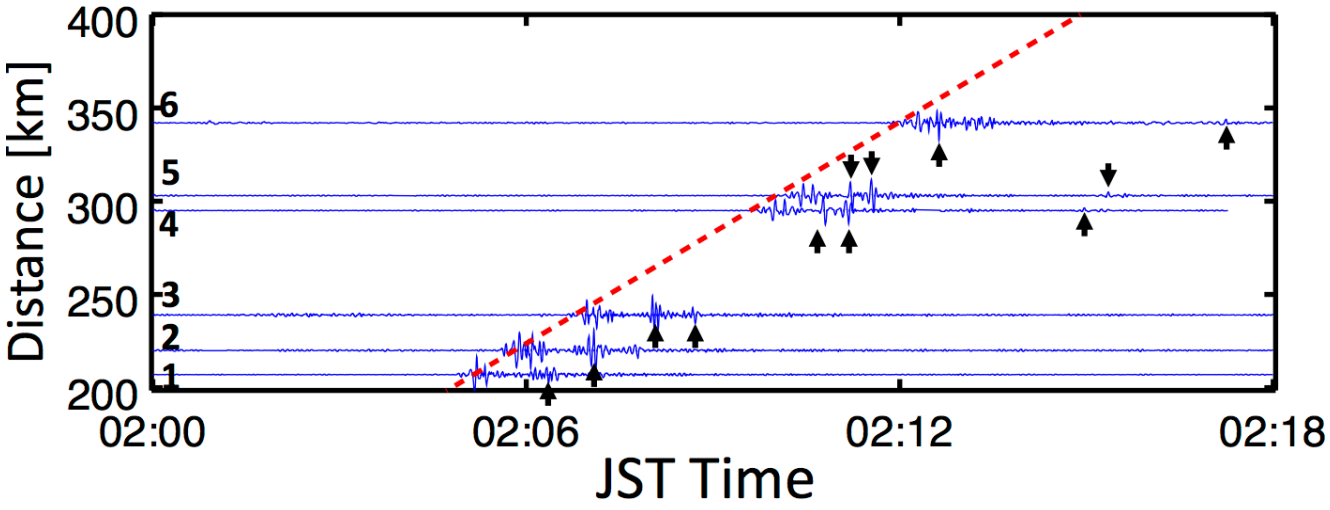


©2019. Japan Geoscience Union. All Right Reserved. 

# Infrasound observations of atmospheric disturbances due to a sequence of 2018 explosive volcano eruptions in Japan.

*Mario Batubara[1], Masa-yuki Yamamoto[1], Saito Hiroaki[1]

1. Kochi University of Technology

In this opportunity, we describe our quantitaive approach for investigating the potential atmospheric effects caused by a sequence of Japanese volcano eruptions in 2018. We used data from a number of infrasound sensors located on Shikoku Island, Japan, to detect the long wave traveling air disturbances likely to have been caused by the explosive eruptions of the volcano. We then identified certain characteristic signatures of the disturbances in individual infrasound pressure records. Based on their arrival times, we have found that the overall propagation speed of the disturbances is in the range of standard sound propagation in the atmospheric boundary layer.

Keywords: Infrasound, propagation speed, irregular array processing

©2019. Japan Geoscience Union. All Right Reserved. 

# Comparison of seismic waveforms observed by co-located seismometer and barometer installed indoors 2nd report

*Makiko Iwakuni[1], Nobuo Arai[2], Takayuki Otsu[1], Masashi Motohashi[1], Toyomi Sakamoto[1], Takanari Fujii[1], Ryohei Emura[1], Mami Nogami[1], Takahiko Murayama[1], Takuma Oi[3]

1. Japan Weather Association, 2. Disaster Mitigation Research Center, Nagoya University, 3. Toho Mercantile co., Ltd.

Surface vertical vibration due to earthquake is considered to excite sound, and it has been observed by barometer or microphone. Recorded pressure change response to seismic ground motion is considered to be due to difference of gravitational pressure observed by barograph moving up and down, air vibration (compressional wave) excited by earthquake ground motion around barograph, and internal mechanical response to acceleration by earthquake.

We started observation with co-located seismometer and barometer in Isumi, Chiba-prefecture (I30JP in The IMS Infrasound Network of CTBTO). This time one of barometer's port is close. A magnitude 4.5 earthquake occurred off south of Chiba-prefecture at a depth 44km. The seismic intensity scale in Isumi was 2. The port open barometer recorded pressure change due to the earthquake. Whereas, the port close barometer did not record pressure change due to the earthquake. It seems that the gravitational pressure change and barometer's internal mechanical response is very little at the seismic intensity 2 earthquake.

Keywords: Barometer, Seismometer, Barometer's Internal Mechanical Response by Earthquake

©2019. Japan Geoscience Union. All Right Reserved. 

# Ionospheric disturbances associated with typhoons and a tornado observed by HF doppler sounding

*Hiroyuki Nakata[1], Ryuichi Mashiko[1], Hiroyo Ohya[1], Toshiaki Takano[1], Keisuke Hosokawa[2], Ichiro Tomizawa[3], Hiromichi Nagao[4]

1. Graduate School of Science and Engineering, Chiba University, 2. Graduate School of Communication Engineering and Informatics, the University of Electro-Communications, 3. Center for Space Science and Radio Engineering, the University of Electro-Communications, 4. Earthquake Research Institute, the University of Tokyo.

It is reported that ionospheric disturbances are excited in association with natural hazards, such as earthquakes, volcanic eruptions, because the atmospheric waves generated by these natural hazards propagate upward to the ionosphere. Although the extreme weather events, such as typhoons and tornados, also excite the strong atmospheric waves, the ionospheric disturbances associated with these extreme events are not fully examined. In this study, therefore, we have examined ionospheric disturbances associated with typhoons and a tornado using HF doppler sounding system (HFD) and wind data observed by AMeDAS data provided by Japan Meteorological Agency.
We have examined the ionospheric disturbance associated with a tornado occurred on May 5, 2012 which is the largest event in Japan. The fluctuations of Doppler shifts were observed and the spectral intensities at the frequencies of 5-20 mHz were enhanced. However, the ionospheric fluctuations continued after the disappearance of the tornado. The enhancement of the doppler shift had a good correlation with a wind speed below the ground of the reflection point.
The ionospheric disturbances associated with typhoons were also correlated with the wind speed on the ground. Examining typhoons that come closer to Japan in 2013-2017, it is found that spectral intensities of the disturbances of HFD data at the frequencies from 5 mHz to 45 mHz were enhanced. The frequencies of the atmospheric disturbances observed on the ground were also the same as those of HFD disturbances. The spectral intensities of HFD and atmospheric disturbances are proportional to each other and the correlation coefficient between them is larger for higher-frequency disturbance.
From these results, the ground weather condition, especially wind data, is very important to examine the mechanism of the ionospheric disturbances associated with these extreme weather events.

Keywords: ionospheric disturbance, typhoon, tornade, infrasound wave, neutral wind

©2019. Japan Geoscience Union. All Right Reserved. 

# Two-year infrasound monitoring by using a prefectural-level sensor network in Kochi

*Masa-yuki Yamamoto[1]

1. Department of systems engineering, Kochi University of Technology

Infrasound, known as pressure waves in atmosphere with its frequency lower than the human audible limit of 20 Hz, can be used as one of the useful remote-sensing methods for atmospheric phenomena especially for large geophysical events such as tsunami, volcanic eruptions, typhoons, etc. In order to construct a dense sensor network in a model region for testing such capabilities and confirming noise level at each site on ground, an infrasound observation network has been installed in Kochi prefecture since 2016, taking account mainly for tsunami disasters. As for the pilot arrangement, we installed 5 sensors in Kuroshio Town in west part of Kochi pref. with a separation of about 2 and 8 km, making two-sized triangle arrays there. Then in 2017, 10 more sensors were added on wider area in whole of prefecture, constructing 25 km scale arrayed deployment in 2 cape areas of Muroto and Ashizuri.
During two years since the sensor network establishment, we have been tested the capability of remote-sensing by using as much as the observed datasets with comparing with the other observations of weather, seismic, optical measurements operated by the other research institutes/agencies.
Tsunami is one of the most dangerous geophysical phenomena for human life and the Japanese originated word of TSUNAMI shows Japan is one of the most dangerous regions for tsunami disasters in the world. Kochi prefecture is located in Shikoku island along its southern coast, namely, in Kochi pref., we have many dangerous sites of tsunami invasion once a huge earthquake happens in Nankai Trough in the pacific ocean. However, in normal situation, no such signals can be detected when we can live there safely from tsunami. We do not need such disaster anymore, but without having phenomena, we cannot check the disaster-mitigation performance in reality.
Thus, we have to investigate the capability of infrasound sensing by using the other geophysical/artificial phenomena such as typhoons, volcanic eruptions, thunders, fireballs (large meteors), and rocket launches. As it is one of the densest infrasound observation networks in prefecture-level area in a nation, we need another analyzing method than that applied for usual arrayed infrasound sensors. Therefore, we tried to develop some methods for getting information from the infrasound datasets, to be useful for future alert system for disaster mitigation.
Recently, multiple typhoon passages, multiple eruption signals from a few volcanoes in Kyushu area, and a bright fireball seen over shikoku island on Jan. 3, 2019 were successfully detected by multiple sensors. In this talk, we will introduce the sensor network in Kochi as a model case and the obtained datasets in consideration of geophysical phenomena.

Keywords: Infrasound, Sensor network, Remote sensing

©2019. Japan Geoscience Union. All Right Reserved. 

[J] Poster | M (Multidisciplinary and Interdisciplinary)：M-TT Technology & Techniques

Thu. May 30, 2019 3:30 PM - 5:00 PM JST | Thu. May 30, 2019 6:30 AM - 8:00 AM UTC | Poster Hall International Exhibition Hall8, Makuhari Messe_26

## [M-TT49] Brand-new scope of coupling geophysics being established by infrasound and associated waves

convener:Masa-yuki Yamamoto(Department of systems engineering, Kochi University of Technology), Mie Ichihara(Earthquake Research Institute, University of Tokyo), Nobuo Arai(Disaster Mitigation Research Center, Nagoya University)

Infrasound and associated wave studies are recently focused on coupling waves with long-distance and vertical propagation characteristics. Such kinds of waves, having with coupling process between the atmosphere and the surface of ground and ocean, are linked with elastic waves in lithosphere and oceanic sphere, as well as to atmospheric regions up to the upper atmosphere, playing a role of generating many kinds of wavelike turbulences in thermosphere. Moreover, whole on the globe, these waves excited depending on the latitude regions, as well as on the environmental regions, such as snow ice, desert, rainforest, mountain, ocean, etc., have their own characteristics. These waves can be excited by large-scale geophysical events like volcanic eruptions, tsunami, thunderstorms, etc. as well as artificial explosions, propagating with long distance. In this session, we would like to discuss such "coupling geophysics" by using many new or well-known investigated data and simulations of infrasound and associated low frequency waves. It can combine multiple spheres in geophysics and bring a brand-new scope of geophysics. Your contributions from many regions are welcome!

### [MTT49-P01] Infrasound signals in Cocos Islands (I06AU) associated with eruption or volcanic body collapse of the Anak Krakatau Volcano or tsunami

*Makiko Iwakuni[1], Nobuo Arai[2], Takayuki Otsu[1], Masashi Motohashi[1], Takanari Fujii[1], Mami Nogami[1], Takahiko Murayama[1], Takuma Oi[3] (1.Japan Weather Association, 2.Disaster Mitigation Research Center, Nagoya University, 3.Toho Mercantile co., Ltd.)

### [MTT49-P02] A try of origin identification estimated from 2 CTBTO stations detected infrasound signals excited by “The 2018 Hokkaido Eastern Iburi Earthquake”

*Mami Nogami[1], Takayuki Otsu[1], Takahiko Murayama[1], Masashi Motohashi[1], Makiko Iwakuni[1] (1.Japan Weather Association)

### [MTT49-P03] Quantitative evaluation of blast pressure in the atmosphere and direct measurement of infrasonic/acoustic wave propagation characteristics

*Yusuke Yasukochi[1], Masa-yuki Yamamoto[1], Hiroaki Saito[1] (1.Kochi University of Technology)

### [MTT49-P04] A case study on relationship with infrasonic wave and auroral activity in the polar region

*Ohata Haruka[1], Masa-yuki Yamamoto[1] (1.KOCHI UNIVERSITY OF TECHNOLOGY)

### [MTT49-P05] Development of a data-handling platform for simultaneous observation using multiple-type infrasound sensors

*Yuichiro Inoue[1], Masa-yuki Yamamoto[1] (1.Kochi University of Technology)

# Infrasound signals in Cocos Islands (I06AU) associated with eruption or volcanic body collapse of the Anak Krakatau Volcano or tsunami

*Makiko Iwakuni[1], Nobuo Arai[2], Takayuki Otsu[1], Masashi Motohashi[1], Takanari Fujii[1], Mami Nogami[1], Takahiko Murayama[1], Takuma Oi[3]

1. Japan Weather Association, 2. Disaster Mitigation Research Center, Nagoya University, 3. Toho Mercantile co., Ltd.

Severe tsunami occurred on December 22, 2018, and it was clarified by SAR analysis of GSI (Geospatial Information Authority of Japan) or visual observation by PVMBG (Pusat Vulkanologi dan Mitigasi Bencana Geologi, Indonesia) that southwest area of The Anak Krakatau collapsed. The infrasound array of the Cocos Islands (CTBTO IMS Infrasound Network: I06AU) locate about 1160 km southwest of The Anak Krakatau Volcano. Travel time of infrasound waves is estimated approximately 58 minutes. I06AU started to detect infrasound signals which came from the direction of The Anak Krakatau Volcano and recorded some remarkable infrasound wave-trains at 15:01:20-15:02:00UTC.

Keywords: Infrasound, Volcano

©2019. Japan Geoscience Union. All Right Reserved. 

# A try of origin identification estimated from 2 CTBTO stations detected infrasound signals excited by “The 2018 Hokkaido Eastern Iburi Earthquake”

*Mami Nogami[1], Takayuki Otsu[1], Takahiko Murayama[1], Masashi Motohashi[1], Makiko Iwakuni[1]

1. Japan Weather Association

A big earthquake occurred at 18:07 5th September 2018 (UTC) at eastern Iburi, Hokkaido, Japan, which recorded maximum seismic intensity 7. Large quake was observed at all of Hokkaido, many large-scale landslides occurred in mountainous area near the origin.

Infrasound excited by mountains or something shaken a lot, I45RU and I30JP which are CTBTO stations detected signals of a wave group assumed to infrasound from the earthquake. The duration of groups are 15 min to 20min long, These analysis are not constant azimuth, but have a little dispersion.

The analysis of azimuth detected I45RU and I30JP are pointing to the origin in perspective, however azimuths in each short term are not constant. While considering analysis error, we assume the dispersion is the each infrasound signals excited in the place shaken a lot while seismic wave propagates in all directions. Therefore we tried an origin identification used the intersection search method derived from azimuths analyzed in 2 stations.

Keywords: Infrasound, Origin identification, Earthquake

©2019. Japan Geoscience Union. All Right Reserved. 

# Quantitative evaluation of blast pressure in the atmosphere and direct measurement of infrasonic/acoustic wave propagation characteristics

*Yusuke Yasukochi[1], Masa-yuki Yamamoto[1], Hiroaki Saito[1]

1. Kochi University of Technology

The space industry has grown as a national strategy of each country. In recent years, space industry is rapidly growing by supporting mainly as a country when private companies in the U,S and Europe get into the rocket industry. However, there are still many mysteries in the environment of the outer space near the Earth, for example vibration by infrasound waves from the ground can shake the upper atmosphere and affect the operation of satellites. For this reason, research on the Earth's upper atmosphere is becoming increasingly important. In this research, acoustic propagation characteristics are investigated and compared with the atmospheric model of acoustic wave propagation path and verified. In addition, to ensure rocket safety is essential and important issue for private rocket companies. The explosion of the rocket affects and damages not only for the surroundings by originating equipment but also from the splashing of the debris and destruction by the blast.

From the observed value detected by the acoustic wave sensors installed on the ground, the energy from explosion can be calculated and the influence of the blast on the distance from the blast hypocenter can be evaluated. We aimed to verify the acoustic propagation path of the blast using data obtained by unexpected rocket explosion, calculating the blast wind attenuation using numerical analysis, and to obtain the blast propagation process.

MOMO3rocket experiment is scheduled to be held in 2019. If it is successful, by using the sound sources of the firework blasts and the rocket launch, propagation characteristics of audible sound and infrastructure sound in middle to upper atmosphere, the comparison between the ground observation and the direct measurement data by rocket-mounted equipment can be determined and verified with the comparison between the ground observation and the direct measurement data, as well as comparison with the atmospheric model of acoustic propagation path.

For MOMO2 rocket experiments conducted in Taiki Town, Hokkaido, we installed multiple sensors at multiple points on ground. Sensors used for ground observation were Nano loggers, SAYA infrasound sensors, condenser microphones, IC recorders and cameras, and placed at nine points in the range between 50 m and 4 km from the launch point. A set of the same type of condenser microphone for rocket experiment was also installed at 600 m on ground. Figure, shows the positional relationship of each observation point.

IST (Interstellar Technologies) launched the Momo2 rocket at 5:30 on June 30, 2018 but failed to maintain thrust due to engine trouble and crashed and the launch experiment was failed. Although the original purpose could not be achieved due to the rocket trouble, we succeeded in observing the blast pressure of the rocket by conducting simultaneous ground observation. Measurement result by a sensor with the highest precision near the blast hypocenter is shown in the figure. The blast over pressure observed at 50 m from the launch/blast point was a pressure change of 170 Pa(p-p). The blast pressure values were also recorded at all observation points.

The attenuation curve of blast pressure obtained at every observed point is shown in the figure. The

©2019. Japan Geoscience Union. All Right Reserved. 

attenuation of the sound pressure is comparatively gentle compared to the case [1] at the time of rocket firing, and it can be understood that the low frequency sound characteristic was affected.

Using the observed blast pressure as the energy per unit area, estimate the energy of this explosion from the total area of the space. The sound intensity is the energy amount passing through the unit area per unit time and is expressed by the following equation.
$I_{(t)} = P^2_{(t)} / \rho c$ [W/m$^2$], where $P_{(t)}$ is sound pressure, $\rho$ is air density, and $c$ is sound velocity. Here, we assumed that $P_{(t)}$=P$_0$sin $\omega t$ [Pa]. Hence we can estimate total energy which is given by $E = 4\pi r^2 \int I_{(t)}$ dt [J]. From the above formula, it is found that the energy at the 50 m point which is not much affected by the attenuation is 0.0084 kg in terms of TNT, this the explosion scale was weaker than expected by the reported video images.

From now on, we would like to calculate more quantitative data by carrying out numerical analysis using by precious blast pressure data. Also we will prepare for MOMO3 experiment planned to be launched in 2019.

References
[1] Kihara Oshiro, direct measurement of sound wave propagation characteristics in the development and middle-upper atmosphere of the S-310-41 Rocket equipped with PDI, FY2013 Kochi University of Technology graduate research report, 2013.

Keywords: Blast pressure, Direct measurement, infrasonic

©2019. Japan Geoscience Union. All Right Reserved. 

# A case study on relationship with infrasonic wave and auroral activity in the polar region

*Ohata Haruka[1], Masa-yuki Yamamoto[1]

1. KOCHI UNIVERSITY OF TECHNOLOGY

Overview

A comparative analysis of the auroral activity and infrasound was conducted from the data obtained from the infrasound sensors installed at Syowa Station in the Antarctica and its surroundings with an all-sky camera installed at Syowa Station. In this presentation, we will discuss about the possibility that infrasound was generated from the aurora in a frequency range between 0.01 Hz and 0.03 Hz.

When a sound is generated from the aurora in the upper atmosphere, it is highly considered that very low frequency sound (infrasound) that is difficult to attenuate with respect to the sound in various frequency ranges can be propagated on to the ground. Therefore, by using the infrasound sensor installed at Syowa Station (69 ˚0 '22 "S, 39 ˚35' 24" E) and its surroundings located beneath the aurora belt, there is possibility to observe the infrasound generated from the aurora. In this research, in order to identify the infrasound that is generated from aurora. we conduct a case study on the relationship between infrasound observed at Syowa Station and auroral activities in the sky.

Data of three cases satisfying the condition of large scale auroral activity and satisfying the condition of wind velocity of 5 m/s or less were extracted, then among these data of infrasound sensors capable of observing frequencies of 0.1 Hz or less were used. As a result, comparative analysis between the dataset of visible wavelength all-sky camera image and the infrasound sensors was performed on June 10 to 11, 2016 which satisfy the above conditions. For comparative analysis, we created and used a program to derive the rate of change of images for all-sky camera images, and we will convert win format infrasound data into plain text of csv format and some filters were applied to identify infrasound signal in a specific frequency band.

From the data obtained from the infrasound sensor from June 10 to 11 2016, it was possible to identify a specific infrasound waveform around 0:02. In addition, by using the all-sky camera images, changing from a static aurora to a dynamic aurora at around 23:50 on June 10 was confirmed. It takes about 5 minutes from the 100 km altitude where the aurora occurs to the ground before the infrasound reaches the ground [1], and the infrasound wavelength considered to be generated from the aurora is from 0.01 to 0.1 Hz [2]. Since the large amplitude change of the infrasound was seen at around 0.02 Hz when the auroral explosion (break-up) occurred on June 10, 2016, there is a possibility that the observation data of the infrasound was generated from the aurora.

References

[1] CHARLES R. WILSON, Auroral Infrasonic waves, Journal of geophysical research, space physics, 74, pp. 1812-1836, 1969.
[2] CHARLES R. WILSON, Infrasonic wave generation by aurora, Journal of Atmospheric and Terrestrial Physics, 33, pp. 973-988, 1975.

©2019. Japan Geoscience Union. All Right Reserved. 

Keywords: aurora, Infrasonic wave, polar region

©2019. Japan Geoscience Union. All Right Reserved. 

# Development of a data-handling platform for simultaneous observation using multiple-type infrasound sensors

*Yuichiro Inoue[1], Masa-yuki Yamamoto[1]

1. Kochi University of Technology

Infrasound, which is a low-frequency pressure wave with a frequency of 20 Hz or less, is hard to be attenuated when propagated through the atmosphere and has characteristics that is easy to propagate over long distances.

In Kochi University of Technology, our Laboratory succeeded in producing a low cost and high-performance infrasound sensor by joint development with companies.

In this research, own propose is to develop a new data format of infrasound observation that fills up the difference between multiple file formats between sensors, conversion software from existing data format to a new data format, and a website that performs simultaneous real-time graph drawing of two kinds of infrasound sensors.

The suggested format name is "infs", where information necessary for analysis is to be saved in the header block as 256 bytes. Then, the observation data is stored in the following successive 21 bytes data blocks. We developed software to convert the existing WIN format to the infs format by using Go language.

The created website converts observation data transmitted from two types of infrasound sensors installed at two remote locations into a laboratory data, and converts the saved data into an output format that can be displayed on a web browser, creating graphs on the browser.

The proposed new data format “infs” will be used in the laboratory in near future. In addition, we created a repository on infs format on GitHub web site that supplies exchanging anonymous information for programmers so as to be used outside the laboratory.

In the server side program developed for creating the Web site, in addition to collecting and managing the observation data collected about every 14 minutes was reduced into about every 13 seconds, the function to determine the simple 5-level alert system from the collected observation data was equipped.

In this research, we proposed a new data format for infrasound observation, conversion software from WIN format, creating of a web page with drawing quasi real-time graph of the observed data with developing, and operation of all the functions is confirmed.

Keywords: Infrasound, Data handling

©2019. Japan Geoscience Union. All Right Reserved. 

[J] Poster | M (Multidisciplinary and Interdisciplinary)：M-TT Technology & Techniques

Thu. May 30, 2019 5:15 PM - 6:30 PM JST | Thu. May 30, 2019 8:15 AM - 9:30 AM UTC | Poster Hall International Exhibition Hall8, Makuhari Messe_46

## [M-TT49] Brand-new scope of coupling geophysics being established by infrasound and associated waves

convener:Masa-yuki Yamamoto(Department of systems engineering, Kochi University of Technology), Mie Ichihara(Earthquake Research Institute, University of Tokyo), Nobuo Arai(Disaster Mitigation Research Center, Nagoya University)

Infrasound and associated wave studies are recently focused on coupling waves with long-distance and vertical propagation characteristics. Such kinds of waves, having with coupling process between the atmosphere and the surface of ground and ocean, are linked with elastic waves in lithosphere and oceanic sphere, as well as to atmospheric regions up to the upper atmosphere, playing a role of generating many kinds of wavelike turbulences in thermosphere. Moreover, whole on the globe, these waves excited depending on the latitude regions, as well as on the environmental regions, such as snow ice, desert, rainforest, mountain, ocean, etc., have their own characteristics. These waves can be excited by large-scale geophysical events like volcanic eruptions, tsunami, thunderstorms, etc. as well as artificial explosions, propagating with long distance. In this session, we would like to discuss such "coupling geophysics" by using many new or well-known investigated data and simulations of infrasound and associated low frequency waves. It can combine multiple spheres in geophysics and bring a brand-new scope of geophysics. Your contributions from many regions are welcome!

### [MTT49-P01] Infrasound signals in Cocos Islands (I06AU) associated with eruption or volcanic body collapse of the Anak Krakatau Volcano or tsunami

*Makiko Iwakuni[1], Nobuo Arai[2], Takayuki Otsu[1], Masashi Motohashi[1], Takanari Fujii[1], Mami Nogami[1], Takahiko Murayama[1], Takuma Oi[3] (1.Japan Weather Association, 2.Disaster Mitigation Research Center, Nagoya University, 3.Toho Mercantile co., Ltd.)

### [MTT49-P02] A try of origin identification estimated from 2 CTBTO stations detected infrasound signals excited by “The 2018 Hokkaido Eastern Iburi Earthquake”

*Mami Nogami[1], Takayuki Otsu[1], Takahiko Murayama[1], Masashi Motohashi[1], Makiko Iwakuni[1] (1.Japan Weather Association)

### [MTT49-P03] Quantitative evaluation of blast pressure in the atmosphere and direct measurement of infrasonic/acoustic wave propagation characteristics

*Yusuke Yasukochi[1], Masa-yuki Yamamoto[1], Hiroaki Saito[1] (1.Kochi University of Technology)

### [MTT49-P04] A case study on relationship with infrasonic wave and auroral activity in the polar region

*Ohata Haruka[1], Masa-yuki Yamamoto[1] (1.KOCHI UNIVERSITY OF TECHNOLOGY)

### [MTT49-P05] Development of a data-handling platform for simultaneous observation using multiple-type infrasound sensors

*Yuichiro Inoue[1], Masa-yuki Yamamoto[1] (1.Kochi University of Technology)

# Infrasound signals in Cocos Islands (I06AU) associated with eruption or volcanic body collapse of the Anak Krakatau Volcano or tsunami

*Makiko Iwakuni[1], Nobuo Arai[2], Takayuki Otsu[1], Masashi Motohashi[1], Takanari Fujii[1], Mami Nogami[1], Takahiko Murayama[1], Takuma Oi[3]

1. Japan Weather Association, 2. Disaster Mitigation Research Center, Nagoya University, 3. Toho Mercantile co., Ltd.

Severe tsunami occurred on December 22, 2018, and it was clarified by SAR analysis of GSI (Geospatial Information Authority of Japan) or visual observation by PVMBG (Pusat Vulkanologi dan Mitigasi Bencana Geologi, Indonesia) that southwest area of The Anak Krakatau collapsed. The infrasound array of the Cocos Islands (CTBTO IMS Infrasound Network: I06AU) locate about 1160 km southwest of The Anak Krakatau Volcano. Travel time of infrasound waves is estimated approximately 58 minutes. I06AU started to detect infrasound signals which came from the direction of The Anak Krakatau Volcano and recorded some remarkable infrasound wave-trains at 15:01:20-15:02:00UTC.

Keywords: Infrasound, Volcano

©2019. Japan Geoscience Union. All Right Reserved. 

# A try of origin identification estimated from 2 CTBTO stations detected infrasound signals excited by “The 2018 Hokkaido Eastern Iburi Earthquake”

*Mami Nogami[1], Takayuki Otsu[1], Takahiko Murayama[1], Masashi Motohashi[1], Makiko Iwakuni[1]

1. Japan Weather Association

A big earthquake occurred at 18:07 5th September 2018 (UTC) at eastern Iburi, Hokkaido, Japan, which recorded maximum seismic intensity 7. Large quake was observed at all of Hokkaido, many large-scale landslides occurred in mountainous area near the origin.

Infrasound excited by mountains or something shaken a lot, I45RU and I30JP which are CTBTO stations detected signals of a wave group assumed to infrasound from the earthquake. The duration of groups are 15 min to 20min long, These analysis are not constant azimuth, but have a little dispersion.

The analysis of azimuth detected I45RU and I30JP are pointing to the origin in perspective, however azimuths in each short term are not constant. While considering analysis error, we assume the dispersion is the each infrasound signals excited in the place shaken a lot while seismic wave propagates in all directions. Therefore we tried an origin identification used the intersection search method derived from azimuths analyzed in 2 stations.

Keywords: Infrasound, Origin identification, Earthquake

©2019. Japan Geoscience Union. All Right Reserved. 

# Quantitative evaluation of blast pressure in the atmosphere and direct measurement of infrasonic/acoustic wave propagation characteristics

*Yusuke Yasukochi[1], Masa-yuki Yamamoto[1], Hiroaki Saito[1]

1. Kochi University of Technology

The space industry has grown as a national strategy of each country. In recent years, space industry is rapidly growing by supporting mainly as a country when private companies in the U,S and Europe get into the rocket industry. However, there are still many mysteries in the environment of the outer space near the Earth, for example vibration by infrasound waves from the ground can shake the upper atmosphere and affect the operation of satellites. For this reason, research on the Earth's upper atmosphere is becoming increasingly important. In this research, acoustic propagation characteristics are investigated and compared with the atmospheric model of acoustic wave propagation path and verified. In addition, to ensure rocket safety is essential and important issue for private rocket companies. The explosion of the rocket affects and damages not only for the surroundings by originating equipment but also from the splashing of the debris and destruction by the blast.

From the observed value detected by the acoustic wave sensors installed on the ground, the energy from explosion can be calculated and the influence of the blast on the distance from the blast hypocenter can be evaluated. We aimed to verify the acoustic propagation path of the blast using data obtained by unexpected rocket explosion, calculating the blast wind attenuation using numerical analysis, and to obtain the blast propagation process.

MOMO3rocket experiment is scheduled to be held in 2019. If it is successful, by using the sound sources of the firework blasts and the rocket launch, propagation characteristics of audible sound and infrastructure sound in middle to upper atmosphere, the comparison between the ground observation and the direct measurement data by rocket-mounted equipment can be determined and verified with the comparison between the ground observation and the direct measurement data, as well as comparison with the atmospheric model of acoustic propagation path.

For MOMO2 rocket experiments conducted in Taiki Town, Hokkaido, we installed multiple sensors at multiple points on ground. Sensors used for ground observation were Nano loggers, SAYA infrasound sensors, condenser microphones, IC recorders and cameras, and placed at nine points in the range between 50 m and 4 km from the launch point. A set of the same type of condenser microphone for rocket experiment was also installed at 600 m on ground. Figure, shows the positional relationship of each observation point.

IST (Interstellar Technologies) launched the Momo2 rocket at 5:30 on June 30, 2018 but failed to maintain thrust due to engine trouble and crashed and the launch experiment was failed. Although the original purpose could not be achieved due to the rocket trouble, we succeeded in observing the blast pressure of the rocket by conducting simultaneous ground observation. Measurement result by a sensor with the highest precision near the blast hypocenter is shown in the figure. The blast over pressure observed at 50 m from the launch/blast point was a pressure change of 170 Pa(p-p). The blast pressure values were also recorded at all observation points.

The attenuation curve of blast pressure obtained at every observed point is shown in the figure. The

©2019. Japan Geoscience Union. All Right Reserved. 

attenuation of the sound pressure is comparatively gentle compared to the case [1] at the time of rocket firing, and it can be understood that the low frequency sound characteristic was affected.

Using the observed blast pressure as the energy per unit area, estimate the energy of this explosion from the total area of the space. The sound intensity is the energy amount passing through the unit area per unit time and is expressed by the following equation.
$I_{(t)} = P^2_{(t)} / \rho c$ [W/m$^2$], where $P_{(t)}$ is sound pressure, $\rho$ is air density, and $c$ is sound velocity. Here, we assumed that $P_{(t)}$=P$_0$sin $\omega t$ [Pa]. Hence we can estimate total energy which is given by $E = 4\pi r^2 \int I_{(t)}$ dt [J]. From the above formula, it is found that the energy at the 50 m point which is not much affected by the attenuation is 0.0084 kg in terms of TNT, this the explosion scale was weaker than expected by the reported video images.

From now on, we would like to calculate more quantitative data by carrying out numerical analysis using by precious blast pressure data. Also we will prepare for MOMO3 experiment planned to be launched in 2019.

References
[1] Kihara Oshiro, direct measurement of sound wave propagation characteristics in the development and middle-upper atmosphere of the S-310-41 Rocket equipped with PDI, FY2013 Kochi University of Technology graduate research report, 2013.

Keywords: Blast pressure, Direct measurement, infrasonic

©2019. Japan Geoscience Union. All Right Reserved. 

# A case study on relationship with infrasonic wave and auroral activity in the polar region

*Ohata Haruka[1], Masa-yuki Yamamoto[1]

1. KOCHI UNIVERSITY OF TECHNOLOGY

Overview

A comparative analysis of the auroral activity and infrasound was conducted from the data obtained from the infrasound sensors installed at Syowa Station in the Antarctica and its surroundings with an all-sky camera installed at Syowa Station. In this presentation, we will discuss about the possibility that infrasound was generated from the aurora in a frequency range between 0.01 Hz and 0.03 Hz.

When a sound is generated from the aurora in the upper atmosphere, it is highly considered that very low frequency sound (infrasound) that is difficult to attenuate with respect to the sound in various frequency ranges can be propagated on to the ground. Therefore, by using the infrasound sensor installed at Syowa Station (69 ˚0 '22 "S, 39 ˚35' 24" E) and its surroundings located beneath the aurora belt, there is possibility to observe the infrasound generated from the aurora. In this research, in order to identify the infrasound that is generated from aurora. we conduct a case study on the relationship between infrasound observed at Syowa Station and auroral activities in the sky.

Data of three cases satisfying the condition of large scale auroral activity and satisfying the condition of wind velocity of 5 m/s or less were extracted, then among these data of infrasound sensors capable of observing frequencies of 0.1 Hz or less were used. As a result, comparative analysis between the dataset of visible wavelength all-sky camera image and the infrasound sensors was performed on June 10 to 11, 2016 which satisfy the above conditions. For comparative analysis, we created and used a program to derive the rate of change of images for all-sky camera images, and we will convert win format infrasound data into plain text of csv format and some filters were applied to identify infrasound signal in a specific frequency band.

From the data obtained from the infrasound sensor from June 10 to 11 2016, it was possible to identify a specific infrasound waveform around 0:02. In addition, by using the all-sky camera images, changing from a static aurora to a dynamic aurora at around 23:50 on June 10 was confirmed. It takes about 5 minutes from the 100 km altitude where the aurora occurs to the ground before the infrasound reaches the ground [1], and the infrasound wavelength considered to be generated from the aurora is from 0.01 to 0.1 Hz [2]. Since the large amplitude change of the infrasound was seen at around 0.02 Hz when the auroral explosion (break-up) occurred on June 10, 2016, there is a possibility that the observation data of the infrasound was generated from the aurora.

References

[1] CHARLES R. WILSON, Auroral Infrasonic waves, Journal of geophysical research, space physics, 74, pp. 1812-1836, 1969.
[2] CHARLES R. WILSON, Infrasonic wave generation by aurora, Journal of Atmospheric and Terrestrial Physics, 33, pp. 973-988, 1975.

©2019. Japan Geoscience Union. All Right Reserved. 

Keywords: aurora, Infrasonic wave, polar region

©2019. Japan Geoscience Union. All Right Reserved. 

# Development of a data-handling platform for simultaneous observation using multiple-type infrasound sensors

*Yuichiro Inoue[1], Masa-yuki Yamamoto[1]

1. Kochi University of Technology

Infrasound, which is a low-frequency pressure wave with a frequency of 20 Hz or less, is hard to be attenuated when propagated through the atmosphere and has characteristics that is easy to propagate over long distances.

In Kochi University of Technology, our Laboratory succeeded in producing a low cost and high-performance infrasound sensor by joint development with companies.

In this research, own propose is to develop a new data format of infrasound observation that fills up the difference between multiple file formats between sensors, conversion software from existing data format to a new data format, and a website that performs simultaneous real-time graph drawing of two kinds of infrasound sensors.

The suggested format name is "infs", where information necessary for analysis is to be saved in the header block as 256 bytes. Then, the observation data is stored in the following successive 21 bytes data blocks. We developed software to convert the existing WIN format to the infs format by using Go language.

The created website converts observation data transmitted from two types of infrasound sensors installed at two remote locations into a laboratory data, and converts the saved data into an output format that can be displayed on a web browser, creating graphs on the browser.

The proposed new data format “infs” will be used in the laboratory in near future. In addition, we created a repository on infs format on GitHub web site that supplies exchanging anonymous information for programmers so as to be used outside the laboratory.

In the server side program developed for creating the Web site, in addition to collecting and managing the observation data collected about every 14 minutes was reduced into about every 13 seconds, the function to determine the simple 5-level alert system from the collected observation data was equipped.

In this research, we proposed a new data format for infrasound observation, conversion software from WIN format, creating of a web page with drawing quasi real-time graph of the observed data with developing, and operation of all the functions is confirmed.

Keywords: Infrasound, Data handling

©2019. Japan Geoscience Union. All Right Reserved. 